

HIGH-PRESSURE LIQUID CHROMATOGRAPHIC DETERMINATION OF SOME 1,4-BENZODIAZEPINES AND THEIR METABOLITES IN BIOLOGICAL FLUIDS: A REVIEW

ANIL C. MEHTA

Department of Pharmacy, The General Infirmary, Leeds, Yorkshire, England

(Received 6 June 1983. Accepted 30 July 1983)

Summary—In recent years the need for rapid, sensitive and specific assays for benzodiazepines has resulted in the publication of a number of high-pressure liquid chromatographic (HPLC) methods for their determination. This paper reviews the methods available to date for the determination of chlordiazepoxide, clonazepam, diazepam, flurazepam, lorazepam, nitrazepam, oxazepam and their metabolites in biological fluids.

The benzodiazepines are an important class of psychotherapeutic agents. They act on the central nervous system and have hypnotic, tranquilizing and anticonvulsant properties. Since there are wide differences in selectivity among these drugs, their usefulness varies considerably. They are among the most frequently prescribed drugs for the treatment of anxiety, sleep disturbance and status epilepticus. They are also used in the treatment of alcohol withdrawal, and both to relieve tension in the pre-operative period and to induce amnesia in surgical procedures.

For the clinical, toxicological and biopharmaceutical study of the benzodiazepines, rapid methods for their determination in various biological fluids are required. The benzodiazepines are clinically effective at low doses ranging from 1 to 30 mg, resulting in blood concentrations in the 10–500 ng/ml range. They also undergo extensive metabolism¹⁻⁴ and many of the metabolites are pharmacologically active.¹ Thus it is essential that the assay methods be sensitive and specific, *i.e.*, capable of separating and determining the parent drug as well as its major metabolites.

Benzodiazepines in biological fluids are determined by various techniques,⁵ of which gas-liquid chromatography (GLC)^{4,6-9} and polarography^{7,10-13} are dominant. The GLC methods, though extremely sensitive, require lengthy clean-up procedures and in some cases formation of more volatile derivatives. Furthermore, if high temperatures are used in the GLC they may cause the decomposition of certain benzodiazepines such as chlordiazepoxide, oxazepam, lorazepam and their metabolites. Polarography, despite the advantage of convenience and speed, lacks the sensitivity and specificity of GLC and requires large amounts of sample. For these reasons attention has shifted to development of HPLC methods for the determination of these drugs in body fluids. HPLC offers several advantages. The extrac-

tion procedures are relatively simple, formation of derivatives is not necessary (though there are exceptions), and operation at ambient temperature allows the determination of thermally labile benzodiazepines. The strong absorption in the 230–260 nm region gives sensitivity in the nanogram range and linearity over a wide concentration range. Moreover, since the technique is non-destructive, the eluted drugs can be recovered for further examination.

PHYSICOCHEMICAL PROPERTIES

The 1,4-benzodiazepines can be structurally generalized by the formula shown in Fig. 1. All the important benzodiazepines contain a 5-phenyl ring, a halogen or nitro group in the 7-position, and in many cases an additional halogen in the R₄-position. The substituents at key positions are shown in Table 1. Chlordiazepoxide (Fig. 2) differs from other benzodiazepines in that it is an *N*-oxide with a methylamino group at position 2 and no alkyl group at position 1.

Benzodiazepines are basic drugs and as free bases are lipid-soluble and water-insoluble. In contrast, the salts (*e.g.*, chlordiazepoxide and flurazepam hydrochlorides, dipotassium clorazepate) are water-soluble. Stock solutions of benzodiazepines are more stable (several weeks) in alcohol than in water.⁵ Howard¹⁴ and Kelly *et al.*¹⁵ have studied the stability of diazepam and nitrazepam plasma samples respectively, under various conditions. Diazepam was found to be stable for 3 weeks at room temperature, 8 weeks at 4°, and 1 year at –20°. Nitrazepam in plasma was stable for at least 3 weeks at 4° in the dark, and more than 3 weeks in a deep-frozen sample; in contrast, there was a significant decrease in nitrazepam content in samples stored at room temperature in the dark. Analysts would welcome similar stability information on other benzodiazepines. Protein binding varies from a few per cent

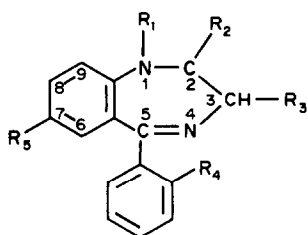


Fig. 1. Benzodiazepine structure.

with flurazepam to over 90% with diazepam.¹⁶⁻¹⁸ Plasma protein binding of benzodiazepines has been found to be concentration-independent¹⁸ and pH-dependent.¹⁹⁻²¹ The pK_a values of benzodiazepines are listed by Clifford and Smyth⁵ and in Martindale.²² Hulshoff and Perrin²³ have determined the partition coefficients of benzodiazepines in the aqueous oleyl alcohol system.

SAMPLE PREPARATION

Benzodiazepines and their metabolites are usually extracted as the neutral molecules from biofluids with a range of organic solvents under weakly alkaline conditions,⁵ with recoveries in excess of 80%. Some workers⁹ find it unnecessary to alkalinize samples since the pK_1 values of benzodiazepines are considerably below the physiological pH. There seems to be no preference for a particular solvent and the normal extraction solvents are employed either alone or in combination. Some workers choose diethyl ether, ethyl acetate and chloroform, in that order,⁵ while others⁹ prefer a relatively non-polar solvent such as heptane, benzene or toluene, to which is added a small amount of a more polar solvent such as isoamyl alcohol or methylene chloride. One advantage of low boiling solvents is they can be readily evaporated for recovery of the drug(s). A single extraction step is sufficient for all benzodiazepines except oxazepam and lorazepam. Owing to their lower lipid solubility, they need a double extraction, and the combined extracts are evaporated to dryness before chromatography.⁹ Smyth and Groves²⁴ have devised a scheme for the extraction of flurazepam and its metabolites, based on the distribution ratios for different pH values and various solvents.

Some investigators prefer enzymatic digestion (hydrolysis) of plasma,²⁵ urine²⁵⁻²⁸ or tissue²⁹ samples of benzodiazepines before extraction to liberate the conjugated fraction of the drug. Hammond *et al.*³⁰ have described two procedures (enzymatic and non-enzymatic) for the extraction of benzodiazepines from cloth or paper. The enzymatic extraction is

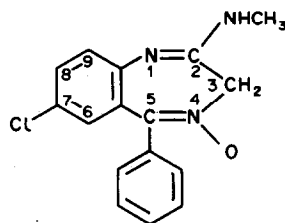


Fig. 2. Chlordiazepoxide structure.

preferred, especially for old stains strongly bound to the material.

Recently, commercially available C_{18} bonded-phase extraction columns (*e.g.*, Bond-Elut) have been used for the rapid sample preparation of diazepam,^{31,32} chlordiazepoxide³¹ and their metabolites. These columns selectively adsorb benzodiazepines and their metabolites from biofluids at a pH of 9.0. The compounds are then eluted with methanol, making sample preparation quicker than the traditional solvent extraction procedure. This procedure can also be applied to the extraction of other benzodiazepines. Missen³³ compared three adsorption methods, which included the use of activated charcoal, Amberlite XAD-2 ion-exchange resin and Celite to extract nitrazepam, diazepam and desmethyldiazepam. The Celite extraction was rapid but a large amount of cholesterol was also extracted from blood samples, whereas the other two procedures extracted much less. The Celite extraction method was used for rapidly screening blood samples. For trace analytical work the XAD-2 resin method was preferred. Balkon *et al.*³⁴ have used the Du Pont Prep I system equipped with an Amberlite XAD-2 resin column for the isolation of diazepam from biological samples.

For rapid toxicological analysis Kabra *et al.*³⁵ have used serum protein precipitation by acetonitrile followed by centrifugation, as the only means of sample preparation. A suitable aliquot of the supernatant liquid is injected onto the HPLC column for drug screening.

Lensmeyer *et al.*³⁶ have tested commercially available blood collection tubes for substances that could leach into the blood samples and adversely affect the benzodiazepine assay. None of the tubes tested affected the extraction or the chromatography of chlordiazepoxide, diazepam, flurazepam and their metabolites.

HPLC METHODS

Columns

In the early days of HPLC (early and middle seventies), the benzodiazepine drug mixtures were

Table 1. Positions of various substituents in benzodiazepine structures

Drug	R ₁	R ₂	R ₃	R ₄	R ₅
Clonazepam	-H	=O	-H	-Cl	-NO ₂
Diazepam	-CH ₃	=O	-H	-H	-Cl
Flurazepam	-(CH ₂) ₂ N(C ₂ H ₅) ₂	=O	-H	-F	-Cl
Lorazepam	-H	=O	-OH	-Cl	-Cl
Nitrazepam	-H	=O	-H	-H	-NO ₂
Oxazepam	-H	=O	-OH	-H	-Cl

separated at μg levels on columns containing silica,^{37,38} anion-exchanger,³⁹ cation-exchanger,⁴⁰ Dupapak OPN^{41,42} and Carbowax 400 coated support⁴³ and detected by single-wavelength (254 nm) ultraviolet detectors. These methods are not sensitive and selective enough to analyse ng quantities of benzodiazepines and their metabolites in biological samples. More recently reversed-phase columns have become the columns of choice because a wide variety of drugs of varied polarity can be separated. They require relatively little maintenance and perform equally well with eluent gradients. Their use also facilitates injection of aqueous samples. In most of the current HPLC methods for benzodiazepines, reversed-phase columns are employed along with ultraviolet detectors and mobile phases consisting of organic solvents mixed with water or weakly acidic buffers.

The most popular reversed-phase column packing material for benzodiazepine analysis is chemically bonded silica containing octadecyl (C_{18}) groups, followed by silica containing octyl (C_8) groups. Hexyl (C_6) and cyano-bonded reversed-phase columns as well as ordinary (silical gel) columns have also been used, but less frequently. The chromatography is generally performed at room temperature under isocratic conditions, but there are exceptions where it is performed at elevated temperature,⁴⁴⁻⁴⁷ or under gradient elution conditions,⁴⁸ or both.^{35,36}

Kinberger and Wahrgren⁴⁹ have used a reversed-phase (C_{18}) radial compression column (Waters Associates Ltd.) for the determination of diazepam and its metabolites. The column, which is made of a flexible polyethylene tube, is compressed in a specially designed holder (radial compression module) during use. The compression presumably reduces wall effects, thereby eliminating channels in the column packing. Radial compression columns afford shorter analysis time and can be operated at lower pressures, but they do not permit use of temperature programming.

Mobile phases

The most common solvent system for the reversed-phase HPLC of benzodiazepines is a mixture of acetonitrile or methanol and an aqueous acetate or phosphate buffer or water. Combinations of two organic solvents and an aqueous buffer have also been employed as mobile phases to achieve optimum conditions for the separation of closely related solutes such as diazepam,^{25,49,50} chlordiazepoxide^{50,51} and their metabolites. Lensmeyer *et al.*³⁶ have used a ternary solvent gradient system for the reversed-phase separation of diazepam, chlordiazepoxide, flurazepam and their metabolites. Three separate solutions (ammonium acetate, acetic acid and acetonitrile) were mixed so as to give pH and solvent-composition gradients. The chromatography was performed at 50° and complete resolution of benzodiazepines resulted in 15 min.

Detectors

Ultraviolet detection is still the most popular mode for HPLC benzodiazepine assays. The sensitivity is not as good as that of electron-capture GLC but can be improved by using a variable-wavelength detector. For example, monitoring at the absorbance maximum of the drug (approximately 240 nm for most benzodiazepines) frequently improves the detection limit by a factor of two compared to detection at 254 nm.⁵² Furthermore, use of the variable-wavelength detector may permit the reduction of sample volume. The sensitivity and specificity of detection can further be improved by the use of a fluorescence detector. Although benzodiazepines do not yield intense room-temperature fluorescence, they can be converted into highly fluorescent derivatives⁵ or made to luminesce at low temperature.^{53,54} These properties can be utilized in their fluorimetric HPLC determination provided that practical difficulties are overcome. It should be remembered that on-line derivative formation or low-temperature luminescence is not as easy as an ultraviolet or fluorescence detector to incorporate in an HPLC apparatus.

The presence of easily reducible nitro and/or azomethine ($>\text{C}=\text{N}-$) groups in benzodiazepines allows polarographic determination;¹² hence the development of a sensitive electrochemical detector operating in the reduction mode would extend the potential of HPLC.⁷ This is a relatively new area and very few reports are so far available. Advances in electrode design should encourage wider applications in the future. Lund *et al.*⁵⁵ have studied a simple flow-through cell with interchangeable working electrodes constructed from vitreous carbon, carbon paste and mercury. Nitrazepam, diazepam and chlordiazepoxide were studied as model compounds, and a detection limit of 3 ng was achieved for nitrazepam and 300 ng for diazepam and chlordiazepoxide. Hanekemp *et al.*^{56,57} have used a pulse-polarographic detector incorporating a dropping mercury electrode (DME) for the determination of nitrazepam in serum⁵⁶ and for the detection of bromazepam, nitrazepam, diazepam and clonazepam in a mixture.⁵⁷ Hackman and Brooks⁵⁸ have described a dual detector system for the reversed-phase HPLC determination of chlordiazepoxide and desmethylchlordiazepoxide in plasma. The eluate was first passed through an ultraviolet detector (254 nm), then through a pulse-damper to a reductive amperometric detector equipped with a DME. The electrode was operated in the differential-pulse mode. The amperometric and ultraviolet detectors were found to be of equal sensitivity and precision. The limit of detection was 50 ng/ml for chlordiazepoxide and its metabolite. Recently a similar approach (a dual detector system) has been used to determine hydroxyethylflurazepam glucuronide, a major metabolite of flurazepam in urine.²⁸ The DME has the distinct advantage of presenting a continuously renewable fresh surface during the chromatography

Table 2. HPLC methods for the determination of 1,4-benzodiazepines in biological fluids

Drug	Sample	Separation mode	Internal standard	Detection wavelength, nm	Metabolites measured	Limit of detection (parent drug), ng/ml	Limit of detection (metabolites), ng/ml	Reference
Chlordiazepoxide	B	RP, C ₁₈ , gradient	Chlorpromazine	254	Desmethylchlordiazepoxide	100	100	48
	P	RP, C ₁₈	Halazepam	254	Desmethylchlordiazepoxide, demoxepam, desmethyldiazepam	50	50	71
	P, U	RP, C ₁₈	Diazepam or prazepam	254	Desmethylchlordiazepoxide, demoxepam	50	50	72
	P	RP, C ₈	Nitrazepam	260	Desmethylchlordiazepoxide, demoxepam, desmethyldiazepam	30	30	73
	T (mouse brain)	RP, C ₁₈	Diazepam	254	Desmethylchlordiazepoxide	0.5 ng/mg	50 for desmethyldiazepam 0.5 ng/mg	74
	P	RP, C ₁₈	Medazepam	254*	Desmethylchlordiazepoxide	50	50	58
	P, U	RP, C ₈	Diazepam	240	Desmethylchlordiazepoxide, demoxepam, desmethyldiazepam, oxazepam	20	20	51
	S	RP, C ₁₈	Nitrazepam	242	Desmethylchlordiazepoxide, demoxepam, desmethyldiazepam	25	25	31
	B, P	RP, C ₁₈	Flunitrazepam	254	Desmethylchlordiazepoxide	—	—	60
	S	RP, C ₁₈	5-(<i>p</i> -Methylphenyl)-5-phenylhydantoin	240	Desmethylchlordiazepoxide, demoxepam, desmethyldiazepam	80	80	50
Clonazepam	P	RP, C ₁₈	Nitrazepam	254	Desmethylchlordiazepoxide, demoxepam, desmethyldiazepam	—	40 for demoxepam	75
	S	RP, C ₁₈ , 50°, gradient	2-Amino-2,5-dichlorobenzophenone	254	Desmethylchlordiazepoxide, demoxepam, desmethyldiazepam	50	50	36
	S, P	RP, C ₁₈ , 50°, Gradient	Hexobarbital	210	—	200	—	35
	P	RP, C ₁₈	Chlorodesmethyldiazepam	254	Desmethylchlordiazepoxide, demoxepam	50	50	76
	S	NP	Nitrazepam	313	—	—	—	77
	P	NP	4,5-Dihydrodiazepam hydrochloride	254	—	5	—	78
	P	RP, C ₆	—	306	—	2.5	—	79
	P	RP, C ₆ , 20°	Flunitrazepam	306	—	2	—	44
	B	NP	—	232	Desmethyldiazepam, oxazepam	25	25	80
	B	RP, C ₁₈	Prazepam	240	Desmethyldiazepam, oxazepam	40	30	52
Diazepam	P	NP	4,5-Dihydrodiazepam hydrochloride	254	Desmethyldiazepam	5	5	78
	S, U, Sa	RP, CH ₃	—	254	Desmethyldiazepam, oxazepam, hydroxydiazepam	0.2 ng	0.2 ng	26
	P, U (man and dog)	RP, C ₈	Flunitrazepam	230	Desmethyldiazepam, oxazepam, hydroxydiazepam	30	30	25
	S, P	RP, CN	Chlordiazepoxide	254	Desmethyldiazepam, oxazepam	20	20	81
	P	RP, C ₁₈	Prazepam	254	Desmethyldiazepam	50	50	68
	S, U	RP, C ₁₈	Prazepam	254	Desmethyldiazepam	—	—	45
	†							
	§							
	‡							
	#							
¶								
**								

Diazepam	B,P,U (man and cat)	RP,C ₁₈	—	254	Desmethyl(diazepam, oxazepam, hydroxydiazepam	50	50	27
††	S	RP,C ₁₈	5-(<i>p</i> -Methylphenyl)- 5-phenylhydantoin	240	Desmethyl(diazepam	80	80	50
	T (eye lens)	RP,C ₈ ,40°	—	232	—	400 ng	—	46
	S	RP,C ₁₈	Prazepam	254	Desmethyl(diazepam, oxazepam	—	—	82
	S	RP,C ₁₈	Nitrazepam	242	Desmethyl(diazepam	25	25	31
	S	RP,C ₁₈	Prazepam	254	Desmethyl(diazepam, oxazepam	50	50	49
	P	RP,C ₁₈	Nitrazepam	254	Desmethyl(diazepam	—	—	67
	P	RP,C ₁₈	Prazepam	254	Desmethyl(diazepam	10	2	83
	B	RP,C ₈	Methylnitrazepam and medazepam	240	Desmethyl(diazepam, oxazepam, hydroxydiazepam	25	25	32
§§	S	RP,C ₁₈ ,50° gradient	2-Amino-2,5-dich- lorobenzophenone	254	Desmethyl(diazepam, oxazepam	50	50 for desmethyl- diazepam, 75 for oxazepam	36
	P,S	RP,C ₁₈ ,50° gradient	Hexobarbital	210	Desmethyl(diazepam	200	200	35
Flurazepam	U	NP	1-(2-Methylamino- ethyl)flurazepam	254	1-(2-Hydroxyethyl)- flurazepam	—	500	84
††	P,S	RP,C ₁₈ ,50° gradient	Hexobarbital	210	—	2000	—	35
#	S	RP,C ₁₈ ,50° gradient	2-Amino-2,5-dich- lorobenzophenone	254	Desalkylflurazepam	—	50	36
Lorazepam	P (monkey)	RP,C ₁₈	Diazepam	230	—	2	—	85
Nitrazepam	U	AE	—	260	7-Aminonitrazepam, 7-acetamidonitrazepam	400	400	39
	P	NP	Prazepam	280	7-Aminonitrazepam, 7-acetamidonitrazepam	5	50 for 7-aminonitrazepam, 5 for 7-acetamidonitrazepam	15
†††	P,S	RP,C ₁₈ ,50° gradient	Hexobarbital	210	7-acetamidonitrazepam	2000	—	35
Oxazepam	P S,U,§a	RP,C ₁₈ ,50° RP,CH ₃	Desmethyl(diazepam	235 254	Oxazepam glucuronide	50 0.2 ng	—	47 26

B, blood; P, plasma; S, serum; §a, saliva; T, tissue; U, urine; NP, normal-phase; RP, reversed-phase; AE, anion-exchange.

*Electrochemical detector was also used; no change in limit of detection.

†Codeine interferes.

‡Methqualone and phenytoin interfere.

§Phenytoin, amobarbitone and methaqualone interfere.

Chlordiazepoxide interferes.

††Carbamazepine and amitriptyline interfere.

**Carbamazepine and lorazepam interfere.

††Methaqualone interferes.

§§Phenytoin, methaqualone, thiopental, carbamazepine, nitrazepam, procainamide and *N*-acetylprocainamide interfere.

†††Desmethyldoxepin interferes.

Ibuprofen interferes

†††Oxazepam interferes.

and so is not subject to poisoning, as solid electrodes are.⁵⁸

Screening procedures

Benzodiazepines have considerable potential for abuse and overdosage is very common. For their rapid identification and determination, screening procedures are required in clinical, toxicological and forensic laboratories. To this end many HPLC procedures have been published which use reversed-phase separation and ultraviolet detection.^{26,29,35,36,59-63} The drugs are detected either intact^{26,29,35,36,59-61} or as their benzophenone hydrolysis products.^{59,62,63} Tjaden *et al.*²⁶ have reported capacity factors and separation coefficients for 16 benzodiazepines and have established optimum conditions for separating 9 of them in 12 min. A reversed-phase system with a methanol-based mobile phase and an ultraviolet detector (254 nm) was used for this purpose. Osselton *et al.*²⁹ have reported a reversed-phase HPLC method for the determination of benzodiazepines and their metabolites in human and animal tissues. An aqueous methanolic mobile phase and detection at 254 nm was used in the separation of drugs on a C₁₈ column. Retention volumes and detection limits for various benzodiazepines were reported and the method was successfully applied in finding the concentrations of these drugs in cases of human self-poisoning. Kabra *et al.*³⁵ have published a rapid reversed-phase HPLC method for screening toxic drugs in serum, including chlordiazepoxide, diazepam, desmethyldiazepam, flurazepam and nitrazepam. In this method an acetonitrile-phosphate buffer (pH 3.2) is used as mobile phase and the ultraviolet detector is set at 210 nm. The separation is based on gradient elution at 50°. A complete analysis is achieved in 45 min. A normal-phase HPLC method described by Vree *et al.*⁶⁴ for the determination of flunitrazepam in body fluids also permits the separation of diazepam, desmethyldiazepam, nitrazepam and clonazepam. The drugs are eluted from a silica column with a mobile phase consisting of a mixture of hexane and ethanol and detected by their absorption at 230 nm.

Individual drugs

The HPLC methods currently available for benzodiazepines and their metabolites are summarized in Table 2. It is evident from the table that chlordiazepoxide and diazepam are the most frequently studied members of the series. Those methods in which other benzodiazepines are used as internal standards may have wider applications since one drug may be used as an internal standard for another. There are some methods in which no internal standards are used. There is a growing trend towards doing away with internal standards, particularly if a fixed-volume sample loop is used in a sample-injection system. Although the precision of such a device is very good, it will not account for the procedural drug losses in a multi-step assay.

McAllister⁶⁵ has recommended prazepam as a possible internal standard for the estimation of diazepam in plasma. Though the end analysis was done by GLC, the information (extraction, recovery, *etc.*) contained in the paper is equally useful for HPLC work. The limits of detection are governed by instrumental and procedural factors, and the values given in Table 2 should therefore be taken only as relative guidelines. It would also be sensible to reinvestigate a method before putting it to a new use, particularly with regard to specificity, since a method which works in one situation may give rise to problems (or even fail) in another. A drug assay should always be dynamic in nature and subject to continuous modification and improvement during its application.⁶⁶

CONCLUSION

This review has shown that there is a wide choice of HPLC methods available for the determination of benzodiazepines and their metabolites in biological samples. Most methods have an acceptable sensitivity for routine and research applications and should provide a useful alternative to GLC. It has been demonstrated in the case of diazepam and desmethyldiazepam that the HPLC results show an excellent correlation with those generated by GLC.^{27,45,67,68} The HPLC results have also been compared with those of homogeneous enzyme immunoassay (EMIT)⁴⁵ which was used to measure total diazepam and desmethyldiazepam. For serum levels there was very good agreement between the two methods, but EMIT urine assays gave higher results, presumably because of the sensitivity of the EMIT reagents to another urinary metabolite of diazepam, *viz.* oxazepam glucuronide, which is not measured by HPLC.

It must be emphasized that for certain benzodiazepines, HPLC still lacks the sensitivity of GLC, particularly if the sensitivity range of the ultraviolet detector is restricted to 0.01 absorbance units full scale (AUFS). Availability of more sensitive detectors (maximum sensitivity 0.001 AUFS)⁶⁹ should solve the sensitivity problems for those drugs which are more potent and given in low doses (clonazepam, flunitrazepam, lorazepam). There is also a dearth of HPLC methods for flurazepam, clorazepate dipotassium, medazepam and their active metabolites. Some promising results have been obtained by using electrochemical detectors,^{28,55-58} but further work is required to see how these detectors compare with the well-established ultraviolet detectors, in terms of overall performance. The reader's attention is drawn to recent reviews on the metabolism^{1,2} and pharmacokinetics^{1,2,16,70} of benzodiazepines, which provide up-to-date information in these fields.

With the introduction of more sensitive detectors, novel column systems and automation of the equipment, the use of HPLC in benzodiazepine analysis is likely to increase. In particular, coupling of HPLC

with mass spectrometry may allow identification of new metabolites of these drugs.

REFERENCES

- P. R. M. Bittencourt and S. Dhillon, in *Therapeutic Drug Monitoring*, A. Richens and V. Marks (eds.), p. 255. Churchill Livingstone, Edinburgh, 1981.
- H. Schütz, *Benzodiazepines: A Handbook, Basic Data, Analytical Methods, Pharmacokinetics and Comprehensive Literature*. Springer Verlag, Berlin, 1982.
- P. C. Hirom and R. L. Smith, in *Isolation and Identification of Drugs*, E. G. C. Clarke (ed.). Vol. 2, p. 979. Pharmaceutical Press, London, 1975.
- D. M. Hailey, *J. Chromatog.*, 1974, **98**, 527.
- J. M. Clifford and W. F. Smyth, *Analyst*, 1974, **99**, 241.
- C. M. Kaye, in *Progress in Drug Metabolism*, J. W. Bridges and L. F. Chasseud (eds.), Vol. 4, p. 165. Wiley, Chichester, 1980.
- J. A. F. de Silva, in *Blood Drugs and other Analytical Challenges*, E. Reid (ed.), p. 7. Horwood, Chichester, 1978.
- H. Schuetz and V. Westenberger, *J. Chromatog.*, 1979, **169**, 409.
- D. J. Greenblatt and R. I. Shader, in *Therapeutic Drug Monitoring*, A. Richens and V. Marks (eds.), p. 272. Churchill Livingstone, Edinburgh, 1981.
- J. M. Clifford and W. F. Smyth, *Anal. Proc.*, 1977, **14**, 325.
- M. A. Brooks, in *Polarography of Molecules of Biological Significance*, W. F. Smyth (ed.), p. 79. Academic Press, London, 1979.
- M. A. Brooks and J. A. F. de Silva, *Talanta*, 1975, **22**, 849.
- M. M. Ellaithy, J. Volke and O. Manoušek, *ibid.*, 1977, **24**, 137.
- P. J. Howard, *J. Pharm. Pharmacol.*, 1978, **30**, 136.
- H. Kelly, A. Huggett and S. Dawling, *Clin. Chem.*, 1982, **28**, 1478.
- S. C. Harvey, in *Pharmacological Basis of Therapeutics*, A. G. Gilman, L. S. Goodman and A. Gilman (eds.), 6th Ed., p. 339. Macmillan, New York, 1980.
- R. F. Johnson, S. Schenker, R. K. Roberts, P. V. Desmond and G. R. Wilkinson, *J. Pharm. Sci.*, 1979, **68**, 1320.
- L. J. Moschitto and D. J. Greenblatt, *J. Pharm. Pharmacol.*, 1983, **35**, 179.
- W. Müller and U. Wollert, *Arch. Pharmacol.*, 1974, **283**, 67.
- Idem*, *Biochem. Pharmacol.*, 1976, **25**, 141.
- Idem*, *ibid.*, 1976, **25**, 147.
- Martindale, *The Extra Pharmacopoeia*, 27th Ed., p. XXVII. Pharmaceutical Press, London, 1977.
- A. Hulshoff and J. H. Perrin, *J. Chromatog.*, 1976, **129**, 263.
- W. F. Smyth and J. A. Groves, *Anal. Chim. Acta*, 1981, **123**, 175.
- T. B. Vree, A. M. Baars, Y. A. Hekster, E. Van der Kleijn and W. J. O'Reilly, *J. Chromatog.*, 1979, **162**, 605.
- U. R. Tjaden, M. T. H. A. Meeles, C. P. Thys and M. Van der Kaay, *ibid.*, 1980, **181**, 227.
- S. Cötler, C. V. Puglisi and J. H. Gustafson, *ibid.*, 1981, **222**, 95.
- J. A. F. de Silva, *ibid.*, 1983, **273**, 19.
- M. D. Osselton, M. D. Hammond and P. J. Twitchett, *J. Pharm. Pharmacol.*, 1977, **29**, 460.
- M. D. Hammond, M. D. Osselton and A. C. Moffat, *J. Forensic Sci. Soc.*, 1979, **19**, 193.
- T. J. Good and J. S. Andrews, *J. Chromatog. Sci.*, 1981, **19**, 562.
- S. N. Rao, A. K. Dhar, H. Kutt and M. Okamoto, *J. Chromatog.*, 1982, **231**, 341.
- A. W. Missen, *Clin. Chem.*, 1976, **22**, 927.
- J. Balkon, B. Donnelly and D. Prendes, *J. Forensic Sci.*, 1982, **27**, 23.
- P. M. Kabra, B. E. Stafford and L. J. Marton, *J. Anal. Toxicol.*, 1981, **5**, 177.
- G. L. Lensmeyer, C. Rajani and M. A. Evenson, *Clin. Chem.*, 1982, **28**, 2274.
- C. Gonnet and J. L. Rocca, *J. Chromatog.*, 1976, **120**, 419.
- D. H. Rodgers, *J. Chromatog. Sci.*, 1974, **12**, 742.
- B. Moore, G. Nickless, C. Hallett and A. G. Howard, *J. Chromatog.*, 1977, **137**, 215.
- P. J. Twitchett, A. E. P. Gorvin and A. C. Moffat, *ibid.*, 1976, **120**, 359.
- C. G. Scott and P. Bommer, *J. Chromatog. Sci.*, 1970, **8**, 446.
- D. J. Weber, *J. Pharm. Sci.*, 1972, **61**, 1797.
- K. Macek and V. Reháč, *J. Chromatog.*, 1975, **105**, 182.
- V. Rovei and M. Sanjuan, *Ther. Drug Monit.*, 1980, **2**, 283.
- J. E. Wallace, S. C. Harris and E. L. Shimek, Jr., *Clin. Chem.*, 1980, **26**, 1905.
- H. Haberstumpf, U. Mayer and K. Gossler, *Z. Anal. Chem.*, 1981, **307**, 400.
- W. Roth and F. W. Koss, *Pharm. Ind.*, 1980, **42**, 633.
- H. B. Greizerstein and C. Wojtowicz, *Anal. Chem.*, 1977, **49**, 2235.
- B. Kinberger and P. Wahrgren, *Anal. Lett.*, 1982, **15**, 549.
- J. M. Foreman, W. M. Griffiths, P. G. Dextraze and I. Diamond, *Clin. Biochem.*, 1980, **13**, 122.
- T. B. Vree, A. M. Baars, Y. A. Hekster and E. Van der Kleijn, *J. Chromatog.*, 1981, **224**, 519.
- P. M. Kabra, G. L. Stevens and L. J. Marton, *ibid.*, 1978, **150**, 355.
- L. A. Gifford, J. N. Miller, J. W. Bridges and D. T. Burns, *Talanta*, 1977, **24**, 273.
- J. A. F. de Silva, N. Strojny and K. Stika, *Anal. Chem.*, 1976, **48**, 144.
- W. Lund, M. Hannisdal and T. Greibrokk, *J. Chromatog.*, 1979, **173**, 249.
- H. B. Hanekamp, W. H. Voogt, P. Bos and R. W. Frei, *J. Liq. Chromatog.*, 1980, **3**, 1205.
- Idem*, *Anal. Chem.*, 1981, **53**, 1362.
- M. R. Hackman and M. A. Brooks, *J. Chromatog.*, 1981, **222**, 179.
- K. Harzer and R. Barchet, *ibid.*, 1977, **132**, 83.
- M. A. Peat and L. Kopjak, *J. Forensic Sci.*, 1979, **24**, 46.
- F. T. Noggle and C. R. Clark, *J. Assoc. Off. Anal. Chem.*, 1979, **62**, 799.
- C. Violon and A. Vercurysse, *J. Chromatog.*, 1980, **189**, 94.
- C. Violon, L. Pessemier and A. Vercurysse, *ibid.*, 1982, **236**, 157.
- T. B. Vree, B. Lenselink, E. Van der Kleijn and G. M. M. Nijhuis, *ibid.*, 1977, **143**, 530.
- C. B. McAllister, *ibid.*, 1978, **151**, 62.
- A. P. De Leenheer and H. J. C. F. Nelis, *Analyst*, 1981, **106**, 1025.
- V. A. Raiseys, P. N. Friel, P. R. Graaff, K. E. Opheim and A. J. Wilensky, *J. Chromatog.*, 1980, **183**, 441.
- J. E. Wallace, H. A. Schwertner and E. L. Shimek, Jr., *Clin. Chem.*, 1979, **25**, 1296.
- A. Basey and R. W. A. Oliver, *Lab. Pract.*, 1982, **31**, 553.
- C. Bellantuono, V. Reggi, G. Tognoni and S. Garattini, *Drugs*, 1980, **19**, 195.
- N. Strojny, C. V. Puglisi and J. A. F. de Silva, *Anal. Lett.*, 1978, **11**, 135.
- M. A. Peat, B. S. Finkle and M. E. Deyman, *J. Pharm. Sci.*, 1979, **68**, 1467.

73. V. Ascalone, *J. Chromatog.*, 1980, **181**, 141.
74. H. B. Greizerstein and I. G. McLaughlin, *J. Liq. Chromatog.*, 1980, **3**, 1023.
75. G. G. Skellern, J. Meier, B. I. Knight and B. Whiting, *Br. J. Clin. Pharmacol.*, 1978, **5**, 483.
76. M. Divoll, D. J. Greenblatt and R. I. Shader, *Pharmacology*, 1982, **24**, 261.
77. D. R. A. Uges and P. Bouma, *Pharm. Weekbl.*, 1978, **113**, 1156.
78. R. J. Perchalski and B. J. Wilder, *Anal. Chem.*, 1978, **50**, 554.
79. M. Sanjuan and V. Rovei, *Lyon Med.*, 1979, **242**, 545.
80. A. Bugge, *J. Chromatog.*, 1976, **128**, 111.
81. J. J. MacKichan, W. J. Jusko, P. K. Duffner and M. E. Cohen, *Clin. Chem.*, 1979, **25**, 856.
82. N. Ratnaraj, V. D. Goldberg, A. Elyas and P. T. Lascelles, *Analyst*, 1981, **106**, 1001.
83. R. R. Brodie, L. F. Chasseaud and T. Taylor, *J. Chromatog.*, 1978, **150**, 361.
84. R. E. Weinfeld and K. F. Miller, *ibid.*, 1981, **223**, 123.
85. L. M. Walmsley and L. F. Chasseaud, *ibid.*, 1981, **226**, 155.

A CONTINUOUS-DILUTION CALIBRATION TECHNIQUE FOR FLAME ATOMIC-ABSORPTION SPECTROPHOTOMETRY

J. F. TYSON and J. M. H. APPLETON

Department of Chemistry, University of Technology, Loughborough, Leicestershire, England

(Received 15 August 1983. Accepted 5 September 1983)

Summary—Calibration in atomic-absorption spectrometry is achieved by means of a concentration-gradient chamber using a single concentrated standard solution. Calibration is rapid and extends over the entire working concentration range of the analyte, irrespective of the shape of the conventionally obtained calibration curve. No curve-fitting approximations are involved. With well-designed apparatus, deviations are less than 1%.

In most instrumental analytical techniques no absolute mathematical relationship exists between the magnitude of the quantity observed and the quantity of determinand. The relationship is generally a complex function of instrumental parameters which rarely have long-term stability, and the chemical environment of the analyte. The latter often has a profound effect on instrument response, so it is then not possible to ignore the chemical matrix when relating signal to analyte. Accordingly, most instruments require calibration immediately before analytical determinations are made. This is certainly true of atomic-absorption spectrometry. Variation in cleanliness, optical alignment, and performance of the line-source, causes day-to-day changes in instrument response. During operation, baseline drift may arise from the gradual stabilization of electrical circuits and variations in source intensity, whilst overall sensitivity may be influenced by changes in nebulizer efficiency, sample flow-rate, and flame chemistry (resulting from changes in fuel-to-oxidant ratio and sample matrix). Certainly, whenever such operational parameters are changed, recalibration is necessary.

Calibration in atomic-absorption spectrometry is usually done by stepwise dilution of a concentrated stock solution to produce a range of standard solutions for analysis. The resulting set of points on the plot of absorbance *vs.* concentration is used as the basis of the calibration curve. In many modern instruments, a microcomputer fits an equation to the calibration data. Thus the development of microprocessor technology has allowed the calibration data-processing step to be incorporated within the instrument itself. The preparation of standards, however, remains a tedious and time-consuming task which greatly reduces sample throughput. Automated calibration is therefore an attractive prospect for atomic absorption.

In considering prospects for automated calibration procedures, the so-called "flow-injection" techniques¹ developed over the last eight years or so, look

promising. The basis of flow injection is the controlled, reproducible, flow-induced dispersion obtainable when a plug of sample is injected into a reagent carrier stream as it flows through narrow-bore tubing. The changing concentration profile of the sample solution may be monitored by downstream detectors, though usually it is the concentration of reaction product that is monitored as the basis of the analysis. The modification, by stages, of the sample concentration profile, from rectangular, through skew peak, to Gaussian peak, has been described by several authors.¹⁻³ Růžička and Hansen⁴ defined the dispersion, *D*, by the equation:

$$D = C_m/C_p \quad (1)$$

where C_m is the concentration of the injected sample and C_p is the concentration at the peak maximum.

These authors have described the dependence of dispersion on flow-rate and tube dimensions. The degree of dispersion may thus be preselected to match the requirements of a particular analytical procedure. The versatility and reproducibility of the dispersion process were such that Růžička and Hansen⁴ were able to state, "We can replace beakers, pipettes and volumetric flasks with small open-ended tubes through which we pump the solutions." This is just the basis required for the automation of calibration procedures and it should be possible to produce a range of standards from a single stock solution by varying the dispersion to which it is subjected. Systems based on this concept are presently being studied.⁵

Methods of producing concentration gradients by using mixing-chambers and differential flow-rates have been described by Block and Ling.⁶ Early work with continuous-flow titration techniques employed magnetically-stirred mixing-chambers.⁷ Whilst the predictable, reproducible performance of mixing-chambers is well-known and understood, certain associated properties, notably sample hold-up and excessive sample dispersion, render them unsuitable

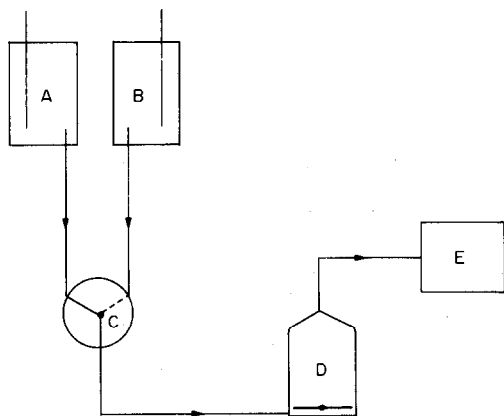


Fig. 1. Schematic diagram of basic apparatus for generating an exponential concentration gradient. A and B are constant-head reservoirs (Marriott bottles) containing water and concentrated stock solution, respectively. C is a rotary valve allowing rapid switching between one solution and the other. D is the mixing-chamber. E represents the detector and recording system.

for general use in flow-injection systems.² Their elimination was brought about by a recent return to a true flow-injection technique⁸ wherein the mixing-chamber function was achieved by means of a carefully designed flow manifold equivalent to one theoretical mixing stage. The removal of the mixing-chamber enabled the realization of high-speed continuous-flow titrations.

Electrochemists studying continuous-flow titrations have employed concentration-gradient programming, achieved by the merging of a constant-flow carrier stream with either a constant-flow reagent stream of increasing concentration⁹ or a reagent stream of constant concentration and increasing flow-rate. The practice of making measurements on alternately increasing and decreasing concentration profiles has been called the "Triangle-Programmed Titration" technique.¹⁰

Mixing-chambers have also long found favour amongst electrochemists,¹¹ who continue to defend the merits of the device.¹² Similar arguments may be advanced for the application of the mixing-chamber gradient technique to atomic-absorption calibration, namely, precise, reproducible performance described by exact mathematical equations readily related to the system parameters, and a smooth concentration profile compatible with the relatively slow response characteristics of the detection system, together with the fact that all this is achieved with simple, readily available apparatus.

The basic system, shown in Fig. 1, consists of a water-filled ideally-stirred tank into which a stream of stock solution is switched to produce an effluent concentration which is an exponential function of the time elapsed after switching. The use of this system for continuous-flow atomic-absorption calibration has previously been suggested.^{13,14} In this paper, the

results of a preliminary study of the system represented in Fig. 1 are reported. The objectives were to assess the viability of such a calibration technique and to identify the experimental conditions necessary for its successful application.

PRINCIPLE OF THE METHOD

An arrangement of the type illustrated in Fig. 1 is used to generate an exponential concentration-time profile of the type described by the equation

$$C = C_m [1 - \exp(-ut/V)] \quad (2)$$

where C is the effluent concentration at time t after the start of the concentration gradient, C_m is the concentration of stock calibrant solution, u is the flow-rate, and V is the volume of the mixing-chamber.

This equation may be derived from a consideration of the mass balance in the mixing-chamber (see *e.g.*, Danckwerts¹⁵ or Levenspiel¹⁶). The effluent from the mixing-chamber is led directly to the nebulizer of an atomic-absorption spectrometer, and the resultant absorbance-time profile is recorded with a rapid-response chart-recorder. Since in atomic-absorption work absorbance is generally not a linear function of concentration, this curve soon deviates from its initial simple exponential form, as shown in Fig. 2.

Used in conjunction with equation (2), Fig. 2 is a continuous calibration plot relating absorbance to concentration. In practice, instead of relabelling of the time axis, the absorbance-time profile is generated and then the sample is admitted directly to the nebulizer at the same flow-rate as the calibrant and its absorbance is noted. By interpolation (see Fig. 3), a corresponding value of t is obtained which is substituted into equation (2), giving the concentration of the sample. For fixed instrument settings, in the absence of interferences, absorbance is a function of only the concentration and flow-rate. Thus, if the absorbances of sample and calibrant (measured at

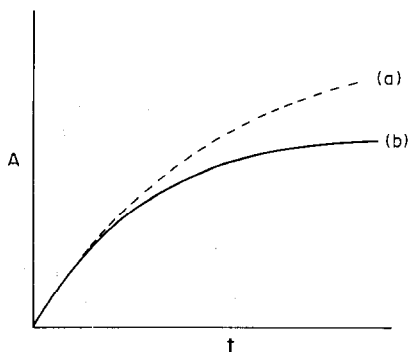


Fig. 2. Absorbance-time profile. Curve (a) corresponds to a hypothetical profile $A = A_m [1 - \exp(-ut/V)]$ where A is the absorbance at time t , and A_m the absorbance corresponding to C_m if the sensitivity were independent of concentration. Curve (b) is the profile generally observed, *i.e.*, curve (a) modified by instrument response.

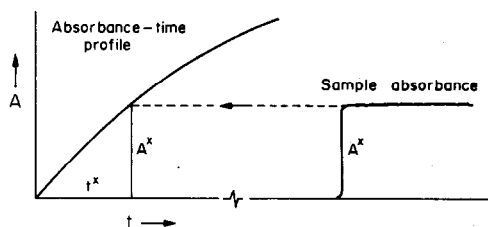


Fig. 3. Interpolation of sample absorbance on absorbance-time profile to find the characteristic time value for the sample, t^x .

the same flow-rate) are equal, their concentrations are equal and

$$C_x = C_m[1 - \exp(-ut^x/V)] \quad (3)$$

where C_x is the concentration of the sample and t^x is the time found by interpolation from the absorbance-time profile.

However, in common with other flow techniques, the creation of practical conditions under which equation (3) is valid requires careful attention to methodology. The minimum requirements are that the assumptions made in the derivation of equation (3) are valid, namely,

- (a) that mixing-chamber performance is ideal, *i.e.*, it conforms with equation (2);
- (b) that the flow-rate may be accurately determined and remains constant during the recording of both calibration and sample absorbances;
- (c) that no instrumental drift occurs between the recording of the calibration and sample absorbances;
- (d) the starting time of the absorbance-time calibration profile may be accurately located.

In addition, minimizing the length of connecting tubing, ensuring that fittings are well-matched and polished, minimizing pump noise by operating at maximum speed and minimum roller pressure, and avoiding air-bubbles, are reported¹⁷ to have a beneficial effect on precision.

EXPERIMENTAL

Apparatus

Mixing-chamber. This was constructed from borosilicate glass, as a sealed unit in the form of a vertical cylinder (diameter 2 cm, maximum height 3 cm) with a slight dome to allow the escape of air bubbles. The volume (determined by filling with water and weighing) was 8.40 ml. The inlet and outlet guides were slightly tapered to allow a push-fit of the 0.58 mm bore PTFE tubing inside a sleeve of 1.14 mm bore PTFE tubing (Corning Ltd., Laboratory Division, Stone, Staffs.). A soft-iron magnet-follower was constructed from a pin (13 × 0.5 mm) sealed inside a short piece of the 0.58 mm bore PTFE tubing.

Investigation of mixing-chamber performance. The apparatus is represented in Fig. 1, with the carrier and stock calibrant solutions gravity-fed from two constant-head vessels. The valve was a Rheodyne type 5011 six-position rotary valve and the instrument used was a Varian 634 S spectrophotometer fitted with a home-made flow-cell measuring 50 × 2 × 1 mm, mounted vertically with the largest

faces normal to the light-beam. An identical cell, filled with distilled water, was mounted in the blank cell compartment of the instrument. The instrument response was monitored by a J. J. 100 chart-recorder (J. J. Lloyd Instruments Ltd.).

Solutions

Copper(II) sulphate pentahydrate (16 g/l.) in distilled water. Magnesium, nickel and chromium, 1000-ppm stock solutions (B.D.H. Chemicals Ltd.).

Procedures

Mixing-chamber performance. With conventional cuvettes it was established that solutions of copper sulphate pentahydrate exhibited an absorption maximum at 808 nm and obeyed Beer's law up to concentrations of at least 16 g/l. A range of flow-rates was obtained by varying the head of liquid between sample reservoir and waste outlet. Flow-rate was measured by averaging the volumes of effluent collected during six 1-min intervals. Seven absorption-time growth profiles were recorded at different flow-rates over the range 3.6–8.2 ml/min.

Atomic-absorption calibration. The apparatus is shown schematically in Fig. 4. Solutions of magnesium, nickel and chromium were used. Their concentrations and the respective instrument settings employed are shown in Table 1. Magnesium was chosen for its high sensitivity and for the limited curvature of its conventional calibration plot, nickel as an element exhibiting pronounced curvature of the calibration plot, and chromium because of its reported calibration irregularities.¹⁸

The absorbance-time growth profiles were generated by using the mixing-chamber, and the time taken for 10 ml of calibrant to be consumed from the reservoir was recorded simultaneously. The mixing-chamber was then "short-circuited" by making the direct connection Z (Fig. 4), and the samples were introduced through S without changing the flow-rate. Data from the chart were analysed with the aid of a microcomputer.

RESULTS AND DISCUSSION

Mixing-chamber performance

Assuming ideal mixing-chamber performance, the growth of concentration within the chamber is ex-

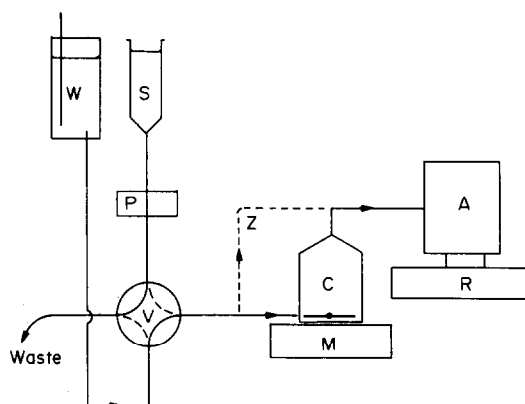


Fig. 4. Apparatus for instrument calibration. A is a Shandon Southern A3300 atomic-absorption spectrometer, C the mixing-chamber, M a Gallenkamp model SS615 combined magnetic stirrer and hot-plate, P a Gilson Minipuls 2 peristaltic pump, R a Tekmann TE200 chart-recorder, S a 10-ml Teflon non-wetting syringe barrel as sample reservoir, V an Altex model 201-25 eight-port injection valve, W a constant-head reservoir of distilled water; V and C were connected by 7.5 cm of 1.14 mm bore tubing, and C and A by 5.5 cm of 0.58 mm bore tubing.

Table 1. Solutions and instrument settings employed for atomic-absorption calibration

Setting	Magnesium	Nickel	Chromium
Monochromator, <i>nm</i>	285.2	232.0	357.9
Band-pass, <i>nm</i>	0.18	0.1	0.1
Lamp current, <i>mA</i>	3.5	5.0	3.0
Air flow, <i>arbitrary units</i>	8.0	8.2	8.65
Acetylene flow, <i>l./min</i>	2.8	2.8	5.0
Sample concentration, <i>ppm</i>	0.25–2.0	10–75	2–20
Calibrant concentrations, <i>ppm</i>	2, 5, 10	100, 200	25, 50, 75
Flow-rate, <i>ml/min</i>	8.4	8.5	8.4

Table 2. Investigation of mixing-chamber performance by solution spectrometry; data from plots of $\ln[A_m/(A_m - A)]$ against *t*

Flow-rate, <i>ml/min</i>	Gradient, <i>min</i> ⁻¹	Correlation coefficient	<i>V</i> (calculated), <i>ml</i>
3.56	0.403	0.99994	8.8
4.48	0.505	0.99998	8.9
5.07	0.599	0.99999	8.5
5.68	0.630	0.99996	9.0
6.18	0.709	0.99998	8.7
6.72	0.764	0.99997	8.8
7.50	0.886	0.99999	8.5

pressed by equation (1). Applying Beer's law, we have $C/C_m = A/A_m$, and hence

$$A = A_m [1 - \exp(-ut/V)] \quad (4)$$

and

$$\ln\left(\frac{A_m}{A_m - A}\right) = ut/V \quad (5)$$

Thus a plot of $\ln[A_m/(A_m - A)]$ against *t* should be a straight line with slope u/V , from which *V* can be calculated for a known flow-rate. The results are summarized in Table 2, and show good agreement with the predicted exponential response. The values of the flow-rates were determined with a mean relative standard deviation of 1.4% and the mean and 95% confidence interval for *V* were 8.74 ± 0.41 ml.

Observation of a theoretical chamber-volume which probably exceeds the true volume confirms Pungor's findings, which suggested that the effect

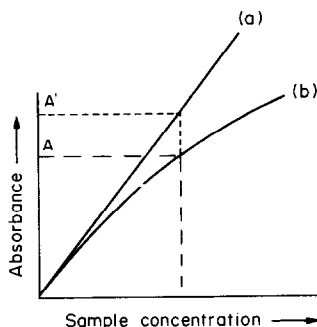


Fig. 5. "Correction" of absorbance for instrument response. (a) is a hypothetical linear calibration plot, assuming constant sensitivity, (b) is the real atomic-absorption calibration curve.

might be due to a mixing contribution within the tubes connected to the chamber. Owing to non-linear instrument response, the corresponding atomic-absorption absorbance-time profiles are not simple exponential-growth functions. Therefore they cannot normally be used directly to evaluate mixing-chamber performance. Two methods of circumventing the difficulty have been employed for test purposes. First, truly exponential absorbance-time curves can be obtained for an element of high sensitivity by use of a solution sufficiently dilute for the conventional calibration curve to be linear over the concentration range from zero to C_m (for example 0.5-ppm magnesium solution). Secondly the generally non-exponential absorbance-time curve may be "corrected" to remove the modification due to instrument response. This is accomplished by reference to the conventional calibration curve, obtained under the same experimental conditions (see Fig. 5). The exponential profile is again observed. In correcting the atomic-absorption absorbance-time profile, any absorbance *A* observed at time *t*, and corresponding to a concentration *C*, is replaced by the corresponding absorbance *A'*.

The results for a 2-ppm magnesium solution are given in Table 3. The times are measured with respect to an arbitrary zero.

A plot of $\ln[A_m/(A_m - A)]$ against *t* [equation (5)] is a straight line (correlation coefficient 0.9997). It should be noted that the use of the conventional calibration curve was confined to this preliminary investigation of mixing-chamber characteristics, which is not part of the main calibration procedure.

Ideal mixing requires that a small element of calibrant entering the chamber is instantly and uniformly dispersed throughout the chamber, and is thus recognised at the exit at the same instant. Errors are introduced if this process takes an appreciable time. Inadequate stirring causes the apparent theoretical volume of the chamber to fall,¹⁴ whilst dispersion in other parts of the apparatus causes it to rise. With such a large mixing-chamber, stirring must be vigor-

Table 3. The "correction" of absorbance for instrument response by using the conventional calibration curve

<i>t</i> , sec	0	5	10	20	30	50	70	∞
<i>A</i>	1.5	11.1	19.8	34.6	45.9	61.2	70.5	83.0
<i>A'</i>	1.5	11.1	20.3	36.3	49.2	68.2	83.6	115.0

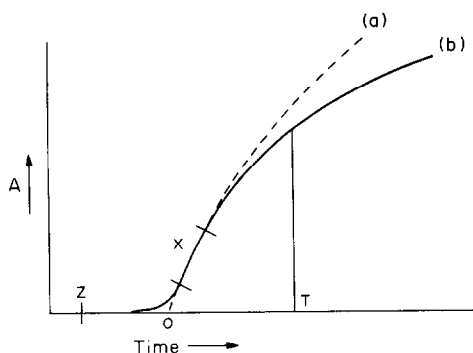


Fig. 6. Time-axis zero of the absorbance-time profile: Z = arbitrary time-zero; O = true zero; ZT = measured time, t_m ; ZO = time error, t_e ; OT = true time, t .

ous if ideal mixing is to be approached, but it must also be smooth. At very high stirring rates the magnetic-follower motion became erratic, resulting in excessive noise in the recorded calibration signal.

Atomic-absorption calibration

Flow-rate. The technique requires the flow-rates of calibrant and sample to be equal. Moreover, the flow-rate must be accurately measured, since it is required in the calibration equation. Ten replicate measurements of the time for the passage of 10 ml through the system gave a mean flow-rate of 8.37 ml/min with a standard deviation of 0.03 ml/min.

Instrumental drift. Any drift in instrument sensitivity between calibration and sample analysis causes an error. Such errors will be minimized in a fully-automated sequence in which calibration and measurement cycles can be run in close succession. The problem also arises, of course, in conventional calibration procedures.

Time-axis zero. In practice, the time-axis zero is

not sharply defined on the chart. The interconnection of the various components by tubing, no matter how short, causes some dispersion of the water-calibrant boundary. This smooths the sharp intersection of the curve with the time-axis, see Fig. 6.

The problem of locating the time-zero on the horizontal scale has been overcome by computer-assisted analysis of a small interval (X) of the curve after the point of inflection but within the linear range of the instrument response, so that the portion X has truly exponential form. An arbitrary time-zero Z is chosen, from which all times, t_m , are measured. These measured times contain a constant time error t_e , given by

$$t_e = t_m - t$$

where t_m is the time measured from the arbitrary zero and t is the time measured from the true zero.

Over the interval X, the curve is given by equation (4). Substituting for t gives

$$\begin{aligned} A &= A_m \{1 - \exp[-u(t_m - t_e)/V]\} \\ &= A_m [1 - \exp(-ut_m/V) \exp(ut_e/V)] \\ &= A_m [1 - k \exp(-ut_m/V)] \end{aligned}$$

where $k = \exp(ut_e/V)$

With time measured from the arbitrary zero, equation (2) becomes, similarly,

$$C = C_m [1 - k \exp(-ut_m/V)] \tag{6}$$

The value of k is computed by least-squares analysis of a plot of A vs. corresponding values of $\exp(-ut_m/V)$, using data from the arc X of the calibration curve; k is then the negative ratio of the slope to the absorbance intercept of this plot. An Apple II BASIC program has been written for doing the calculation. It also calculates concentrations from the time-values for the samples. Copies may be obtained from the authors by request. The results for a number of determinations are given in Table 4.

Table 4. Results obtained by continuous-dilution calibration method

Element	True concentration, ppm	Concentration found, ppm		
		C_m^*1	$C_m^\dagger2$	$C_m^\S3$
Mg	0.25 ($A = 0.19$)	0.27	0.25	0.26
	0.50	0.52	0.48	0.50
	1.00	1.03	1.00	1.01
	1.50	1.59	1.50	1.52
	2.00 ($A = 1.02$)	—	2.02	2.04
Cr	2.0 ($A = 0.16$)	1.99	2.06	2.09
	4.0	3.99	4.07	3.95
	6.0	5.94	6.10	5.86
	10.0	10.1	10.1	9.8
	15.0	15.3	15.2	15.1
Ni	20.0	20.6	20.4	20.0
	10 ($A = 0.47$)	10.3	10.3	—
	20	20.6	20.7	—
	30	31.0	30.6	—
	40	41.2	40.7	—
	50	51.5	50.4	—
	75 ($A = 1.19$)	77.7	75.8	—

*Mg 2 ppm, Cr 25 ppm, Ni 100 ppm.
 †Mg 5 ppm, Cr 75 ppm, Ni 200 ppm.
 §Mg 10 ppm, Cr 75 ppm.

The concentrations found rarely deviated by more than 4% from the sample concentrations, and in most of the analyses trends in the errors in the results were evident, suggesting that the deviations contained a contribution from systematic errors (e.g., an incorrect flow-rate or deviation from ideal performance of the mixing chamber), rather than being entirely due to random errors. It is thought that systematic errors could be reduced and the results improved by use of a carefully-designed permanent assembly of the apparatus, incorporating precise measurement techniques. A particular improvement would be to extend the role of the microcomputer to include storage and processing of the absorption-time profile and thus dispense with the chart-recorder. Ultimately, a microcomputer-controlled system is envisaged wherein a sample-input device would be switched into a "calibration" mode to record this profile, before returning to the "analysis" mode to determine sample concentrations.

CONCLUSIONS

The viability of a continuous-dilution calibration technique for atomic-absorption work has been demonstrated. The technique uses readily available or easily constructed apparatus. The results obtained suggest that less than 1% uncertainty should be attainable with a carefully-designed assembly. This is confirmed by recent results obtained by using a microcomputer interfaced with the atomic-absorption spectrometer.¹⁹

Of fundamental importance in this system is an efficiently stirred mixing-chamber having the shortest possible connecting tubes and zero dead-volume. The technique depends upon the predetermined and reproducible performance of this chamber.

In addition to eliminating the need for preparation of standards, continuous dilution calibration has

other advantages over conventional calibration. The technique is simple, easily automated, and operable with existing spectrometers. Instead of use of a limited number of data for calibration purposes, the entire calibration curve is recorded. This provides a vast amount of data suitable for computer smoothing and processing. No curve-fitting procedure is involved, and thus the technique may be applied regardless of any curvature or irregularities in the calibration plot.

Acknowledgement—Financial support for J. M. H. Appleton by the SERC is gratefully acknowledged.

REFERENCES

1. D. Betteridge, *Anal. Chem.*, 1978, **50**, 832A.
2. J. Růžička and E. H. Hansen, *Anal. Chim. Acta*, 1978, **99**, 37.
3. G. Taylor, *Proc. Roy. Soc.*, 1953, **219A**, 186.
4. J. Růžička and E. H. Hansen, *Chem. Tech.*, 1979, 756.
5. J. F. Tyson and R. Shubietah, work in progress.
6. R. M. Block and N. S. Ling, *Anal. Chem.*, 1954, **26**, 1543.
7. J. Růžička, E. H. Hansen and H. Mosbaek, *Anal. Chim. Acta*, 1977, **92**, 235.
8. A. V. Ramsing, J. Růžička and E. H. Hansen, *ibid.*, 1981, **129**, 1.
9. B. Fleet and A. Y. W. Ho, *Anal. Chem.*, 1974, **46**, 9.
10. G. Nagy, Zs. Fehér, K. Tóth and E. Pungor, *Anal. Chim. Acta*, 1977, **91**, 87.
11. G. Nagy, Zs. Fehér and E. Pungor, *ibid.*, 1970, **52**, 47.
12. E. Pungor, Zs. Fehér, G. Nagy, K. Tóth, G. Horvai and M. Gratzl, *ibid.*, 1979, **109**, 1.
13. J. F. Tyson, J. M. H. Appleton and A. B. Idris, *ibid.*, 1983, **145**, 159.
14. *Idem*, *Analyst*, 1983, **108**, 153.
15. P. V. Danckwerts, *Chem. Eng. Sci.*, 1953, **2**, 1.
16. O. Levenspiel, *Chemical Reaction Engineering*, 2nd Ed. Wiley, New York, 1972.
17. J. T. Vanderslice, K. K. Stewart, A. G. Rosenfeld and D. J. Higgs, *Talanta*, 1981, **28**, 11.
18. K. C. Thompson, *Analyst*, 1978, **103**, 1258.
19. J. M. H. Appleton and J. F. Tyson, work in progress.

INDIRECT DETERMINATION OF ORGANIC COMPOUNDS BY ATOMIC-ABSORPTION SPECTROPHOTOMETRY

E. R. CLARK and EL-SAYED A. K. YACOUB*

Department of Chemistry, University of Aston in Birmingham, Gosta Green, Birmingham B4 7ET,
England

(Received 25 August 1982. Revised 6 June 1983. Accepted 29 August 1983)

Summary—A review of the published methods for analysis of organic compounds by atomic-absorption spectrophotometry is given. Most of the applications are based on precipitation of metal compounds or solvent extraction of metal chelates or ion-association complexes. Although many of the methods offer great sensitivity, simplicity, and speed of analysis, few have been widely accepted by analysts, but some have proved to be satisfactory in field trials.

In a paper published in 1968, Christian and Feldman¹ pointed out that some inorganic anions and organic compounds could be determined indirectly by atomic-absorption spectrophotometry (AAS). In a review article in 1973, Kirkbright and Johnson² summarized the position at that time, and pointed out that much attention had been devoted to the development of indirect AAS methods in order (a) to extend the range of applications of AAS and (b) to take advantage of the inherent sensitivity of AAS. The review by Kirkbright and Johnson dealt mainly with the determination of non-metals, metals and anions, but a section was devoted to the determination of organic compounds. Since then, many more papers concerned with the indirect determination of organic compounds by AAS have been published. Pharmaceutical applications have received special attention and some comment in short reviews by Kidani,³ Miller,⁴ Rousselet and Thullier,⁵ and Ebdon.⁶ Here we give a critical discussion of developments in the organic field in the past ten years.

Procedures involving formation of copper or cobalt complexes have been particularly popular but are often non-specific. Many methods have been concerned with simulated ideal samples rather than real samples, and their authors have sometimes admitted that the results did not agree with those obtained by other techniques or recommended methods. Indirect AAS methods are limited in that the nature or composition of the sample must be known so that likely interferences can be dealt with. They should have found applications as routine methods, but few have been adopted, in spite of the many claims that they are rapid, sensitive and accurate.

Some of the methods do not distinguish between individual members of a class of compounds in a

mixture, but merely determine the total concentration of that class of compounds in terms of the reactive group. Some of these methods could be useful for comparative routine assessment of a series of samples of similar origin. This would be particularly useful if a more complete analysis would be very time-consuming or complicated. Examples will be cited later.

Many of the procedures are modifications of established spectrophotometric methods involving metal chelate formation and solvent extraction, the metal being determined by AAS. Errors can arise from contamination at the extraction stage if the metal used in the reaction is one that commonly occurs as an impurity in the solvents employed. The limitations of the original spectrophotometric methods (interferences and non-specificity) will be inherent in the procedures.

However, the indirect AAS methods may offer some advantages. They may save having to buy a particular piece of equipment required for an alternative method, or may be more rapid (and cheaper) than other procedures. The introduction of the graphite furnace has led to lower detection limits for metals, and hence for species indirectly determined.

AAS has been combined with various chromatographic techniques, including ion-exchange, and this has introduced some selectivity. The use of AAS as a detector in gas chromatography is outside the scope of this review, however.

METHODS FOR THE INDIRECT DETERMINATION OF ORGANIC COMPOUNDS BY AAS

Six approaches can be used for the AAS determination of organic species, but only two have been employed extensively—precipitation of a salt, and formation of an extractable chelate or ion-association complex. A few methods are based on the other four

*On study leave from the University of Gezira, Sudan.
Present address: Faculty of Applied Sciences, University of Oum El-Kura, Saudi Arabia.

approaches: chemical interference in the flame, chemical multiplication methods, redox methods, and direct measurement (limited to metal-containing species).

Chemical interferences in the flame

The causes of interference in flames have been widely discussed.⁷⁻⁹ An absorbance signal may be depressed owing to the formation of a species which is difficult to dissociate in the flame. For example, proteins such as glucose oxidase and ribonuclease, at concentrations below 2.5×10^{-4} % w/w cause a decrease in the absorption signal for calcium concentrations of $4-6 \times 10^{-4} M$.¹ The decrease is proportional to the protein concentration but differs from one protein to another. Glucose at concentrations of less than $10^{-6} M$ also causes a noticeable decrease in the absorption signal for $6 \times 10^{-4} M$ calcium.¹ These interferences have been attributed to alteration in the droplet-size distribution in the spray from the nebulizer.⁹

On the other hand, absorption signals may be enhanced. For example, nitrogen-containing compounds have been found to enhance the absorption signal of zirconium in a nitrous oxide-acetylene flame, the magnitude of the enhancement being proportional to the concentration of nitrogen compound.¹⁰ Aliphatic and aromatic amines and amino-acids may be determined; the enhancement has been attributed to the formation of relatively volatile and easily atomized compounds containing zirconium-nitrogen bonds.

Chemical multiplication procedures

These methods are really a subclass of the precipitation and complexation methods. They are based on formation of compounds having a high molar ratio of the element measured in the final step, to the species to be determined. For example, heteropoly acids are used as precipitants for organic bases, which can thus be determined by AAS measurement of the molybdenum content of the precipitate. Strychnine and brucine have been determined in this way, by reaction with molybdophosphoric acid (MPA) to give a precipitate;¹¹ the excess of MPA is masked with citric acid and the MPA-organic base species is extracted into methyl isobutyl ketone (MIBK), followed by stripping of the molybdenum into a basic buffer and AAS measurement at 313 nm. Alternatively, the organic phase may be aspirated directly into the flame for the molybdenum determination. Quinoline can be determined similarly. This method, which is not selective, can determine strychnine, brucine and quinoline in the ranges 0-40, 0-45 and 2-16 $\mu g/ml$ respectively.

Redox methods

In these procedures a metal is used to reduce an organic species and AAS is used to measure the amount of metal ion produced, or alternatively a

metal ion is reduced to the elemental form by the organic species and AAS is used to measure either the amount of metal produced or the decrease in the metal ion concentration. A typical method is the determination of chloramphenicol and its esters in pure form, suppositories, eye drops, capsules and oral suspensions, without prior extraction.¹² The chloramphenicol is reduced with cadmium metal, and the cadmium ions produced are determined by potentiometric titration, spectrophotometry or AAS. All three methods give consistent results, the AAS method having a 98% recovery (standard deviation 2%). An alternative is slightly more complicated; the nitro group is reduced with zinc to yield a substituted hydroxylamine, which in turn is reacted with Tollen's reagent to yield silver, which is then dissolved in nitric acid and determined by AAS.¹³ This method suffers interference from any reducing compounds present. Hassan and Eldesouki¹² claim that the cadmium reduction method is superior in some respects to other methods. For example, the argentimetric and spectrophotometric methods are not applicable to many pharmaceuticals, because of interference by excipients, whereas the cadmium method gives results in agreement with those obtained by the official method.¹⁴ The use of Tollen's reagent for determination of aldehydes by means of its reduction to silver will be discussed below, under applications.

Direct measurements

Some organic species contain metals and thus can be determined by AAS directly. The determination of cyanocobalamin (vitamin B₁₂), which contains one atom of cobalt per molecule of the vitamin, has been reported.¹⁵⁻¹⁹ Large positive errors are likely by the AAS method if the vitamin is contaminated with ionic cobalt, but some authors suggest prior extraction of the ionic cobalt with a chloroform solution of 8-hydroxyquinoline.¹⁶ Injections and liquid preparations containing cyanocobalamin may be aspirated directly into the flame, but tablets and powders must be wet-ashed first with concentrated sulphuric and nitric acids. When internal standards are used, good agreement with USP standard methods is obtained. Peck¹⁹ has developed an electrothermal atomization (ETA) method for the determination of vitamin B₁₂ in which liquid formulations or tablets are dissolved in water, acidified with hydrochloric acid and injected into a graphite furnace. A calibration graph for 0-30 ng/ml cobalt is made.

The soap content (calculated as sodium oleate) of commercial samples of refined olive oil may be determined by analysis for sodium.²⁰ The oil is treated with absolute ethanol, the mixture dissolved in ethyl methyl ketone and the solution aspirated directly into the flame. A linear calibration graph is obtained if virgin olive oil and known amounts of sodium oleate in the range 3-1000 ppm are used. Errors will occur if any other source of sodium is present.

Dimethylarsinic acid (DMAA) has been determined²¹ in sea-water after preconcentration on an ion-exchange column and chromatographic separation from other arsenicals and from Group I and II metals (which interfere in the final determination). A 20-ml sample containing a 10⁵-fold ratio of inorganic arsenic to DMAA may be analysed with a detection limit of 0.02 ng/ml and recoveries of 100–102% (standard deviation 6.3%).

The trimethylselenonium ion has been determined in urine²² after separation on a Dowex 50 W-X8 column with 4M hydrochloric acid. After digestion in a Teflon high-pressure vessel at 200°, and treatment with hydroxylammonium chloride, the selenium is extracted with dithizone in carbon tetrachloride and determined by AAS.

The speciation of some eleven mercury compounds has been studied by differential AAS.²³ The method was applicable to mercury-containing compounds in aqueous solution and in biological fluids.

Organotin compounds have been analysed for tin by direct AAS measurement,^{23a} and the same method should be suitable for the assay of the tin compounds if they occur individually and their identity is known. Organoantimony compounds have similarly been analysed.^{23b}

Precipitation procedures

The element or species of interest is precipitated in some form that contains another element determinable by AAS. This other element is then determined either in the precipitate (dissolved in a suitable solvent) or in the filtrate. Filtration is not always necessary if the precipitate is too refractory to be atomized in the flame. Thus, in the indirect AAS method for determination of sulphate by addition of barium, the barium sulphate does not yield any barium atoms in the flame. This simplified procedure does not seem to have been reported for measurement of organic species.

The metal ions used most frequently for precipitation methods are silver, and copper and nickel. Oxidation or reduction may also be involved when silver ions are used and the methods are then not specific for a particular reducing or oxidizing species. The methods using copper and nickel ions involve the formation of insoluble or extractable species with the analyte either directly or after its conversion into some suitable ligand. Many ligands form copper or nickel complexes, so the methods are non-specific and interferences are likely with real samples.

Ion-association or chelate complex formation followed by solvent extraction

The organic species (with an auxiliary species if necessary) is reacted with an excess of a metal ion to form an uncharged complex or ion-association compound which is then extracted into an organic solvent. The absorbance of the metal in the extracted species is measured in the flame, or alternatively the

unreacted metal remaining in the aqueous phase is measured and hence the organic species is determined. In another approach the species of interest acts as an interfering masking agent in the solvent extraction of a metal complex. The decrease in the concentration of metal extracted is measured by AAS and is proportional to the amount of organic analyte present in the aqueous phase.

Most chelating agents form co-ordinatively saturated neutral complexes of metals, and these are readily extracted. Ligands such as 1,10-phenanthroline form charged complexes which can be extracted into an organic solvent on neutralization of the charge with a bulky inorganic or organic anion. Hence such organic anions can be indirectly determined.

Organic solvents such as ketones, esters, alcohols, ethers, aliphatic and aromatic hydrocarbons, and nitro compounds may be used for extraction of the complexes. Electrothermal atomization possesses an advantage over flame atomization in that the range of solvents which may be used is less restricted, and the problems of toxic combustion products and other undesirable combustion characteristics are totally eliminated because very small amounts of sample solution are used. In general, the use of organic solvents in flame AAS improves the sensitivity of the metal determination and hence of the organic compound determination.

A wide range of applications has been reported, many of which are related to pharmaceutical analysis. The metal ions most frequently used are copper and cobalt. Iron, bismuth, zinc, and chromium have also been used. Most of the chromium methods involve use of Reinecke's salt [ammonium tetrathiocyanatodiamminochromate(III)].

Some indirect AAS methods involve several stages, one of which may involve conversion of the analyte into another species capable of complexation. Many of the methods are rapid and sensitive but they are often non-specific. In some cases prior separation of the components by chromatography or ion-exchange is advisable.

APPLICATIONS

The compounds or classes of compounds will be dealt with in alphabetical order. Compounds such as acids, amino-acids and amines are listed under their class names but more complex molecules or compounds of special interest such as histamine will be found under their individual names. Alkaloids are listed as bases, and thiols and thiocarbamates as sulphur-containing compounds. Chelating agents and detergents have received attention as groups of compounds, and are listed under these headings.

Acids

Aromatic carboxylic acids such as phthalic acid, anthranilic acid and β -hydroxynaphthoic acid may be determined by AAS by formation of their ion-

association compounds with a metal-phenanthroline complex. Phthalic acid^{24,25} may be determined by extraction as the ion-pair formed by biphthalate with copper(I)-neocuproine (2,9-dimethyl-1,10-phenanthroline; NC complex; $[\text{Cu}(\text{NC})_2][\text{C}_6\text{H}_4(\text{CO}_2)(\text{CO}_2\text{H})]$) into methyl isobutyl ketone (MIBK). The copper content of the organic phase is proportional to the initial concentration of the acid in the aqueous phase over the range $0-4 \times 10^{-5} M$, with a relative standard deviation of 1.0%. If isomers of phthalic acid are present, errors of up to 10% result. Anthranilic acid may be determined similarly by formation of its cobalt(II) bathophenanthroline (4,7-diphenyl-1,10-phenanthroline) ion-association complex²⁶ (linear calibration for 3–22 $\mu\text{g/ml}$; 99.5% recovery) or by formation of its iron(III) complex in acetate buffer (pH 5.9), and extraction into MIBK.²⁷ β -Hydroxynaphthoic acid at concentrations of $8 \times 10^{-5}-4 \times 10^{-4} M$ has been determined indirectly by the solvent extraction of tris(1,10-phenanthroline)nickel(II) β -hydroxynaphthoate into nitrobenzene, followed by measurement of the nickel in the organic phase.²⁸

The determination of dissolved free fatty acids has been of great interest and importance for oceanographers for many years. Treguer *et al.*²⁹ have proposed a method for the determination of total free fatty acids in sea-water, from which the acids are extracted with a chloroform-heptane mixture. A copper complex is formed when a mixture of triethanolamine, acetic acid and copper sulphate is then added. The mixture is centrifuged and an aliquot of the organic phase evaporated to dryness, then ammonium pyrrolidine dithiocarbamate in MIBK is added. The complexed copper is determined by AAS. The speed of the method (which has a precision of $\pm 10\%$) and the fact that only one litre of water is required are the main advantages. The method is also applicable to the determination of long-chain free fatty acids (longer than C_{10}) at concentrations of 10–40 $\mu\text{g/l}$. Another method for total fatty acid determinations³⁰ also involves the formation of copper complexes and extraction into a chloroform-heptane-ethanol mixture (which does not give a smoky flame). In this method the non-esterified acids in serum can be determined simply and easily, with a relative standard deviation of 4.2%.

Alcohols

Thirteen alcohols have been determined by use of a simple technique based on the chromium complexes formed when a benzene solution of the alcohols is added to a reagent solution of chromium(III) iodide and pyridine in acetic acid.³¹ The benzene phase is separated, dried with anhydrous sodium sulphate, filtered and mixed with methanol. Chromium is determined in the extract. The method is not specific and cannot be used to determine isopropyl alcohol.

Aldehydes and ketones

The determination of micromolar quantities of

aldehydes has been reported.^{32,33} Tollen's reagent is used to oxidize the aldehydes to the corresponding carboxylic acids.³² The reduced silver is filtered off, dissolved in nitric acid and the silver determined. Alternatively the silver in the filtrate is determined. This method was found to be advantageous for determining the "total aldehyde" content in many systems containing a number of aldehydes, *e.g.*, distilled liquors, flavourings, or perfumes. The working range of aldehyde concentration ($0.1-1.0 \times 10^{-4} M$) corresponds to a 2–20 $\mu\text{g/ml}$ range for silver and the relative standard deviation¹³ is 1.2–5.8% in the 1–4 $\mu\text{mole/ml}$ range. A very similar method was used by Mitsui and Kojima³⁴ for determination of aldehydes at concentrations of 0.002–0.231 g/l. Many alcohols and phenols do not interfere, but *o*- and *p*-aminophenol, resorcinol, benzoin and benzil do.

Low molecular-weight ketones and aldehydes (acetone, cyclopentanone, ethyl methyl ketone, propionaldehyde, butyraldehyde and formaldehyde) may be determined by AAS.³⁵ Copper complexes are formed by addition of thiosemicarbazide and copper acetate. The mixture is heated to 70°, then cooled, and the copper complexes are extracted into benzene. The copper content of the organic layer is determined but there are some interferences from species such as cobalt(II), nickel(II), silver(I), zinc(II), isopropylamine and chlorobenzene. No interferences from magnesium(II), ninhydrin, isatin, phenanthroquinone, phenylacetaldehyde, *p*-dimethylbenzaldehyde, cinnamaldehyde or salicylaldehyde were reported. Recoveries of 96.7–102.2% were obtained for 0.01–2.01 mg of the organic species, but the method is not specific.

Amines

This class of compound may be determined indirectly by AAS in several ways. Mitsui and Fujimura³⁶ have described a method for the determination of primary amines in amounts greater than 1 mg, based on complexation with a reagent containing triethanolamine, 5-nitrosalicylaldehyde, acetaldehyde, and copper sulphate. Copper is determined either in a solution of the precipitate in nitric acid, or in the filtrate. The method suffers from some interferences, *e.g.*, from zinc, magnesium and calcium, but secondary and tertiary amines do not interfere if they are present in not more than 20–30-fold w/w ratio to the determinand.

The reaction of secondary amines with carbon disulphide to give dialkyldithiocarbamic acids (DDTCH) has been utilized in an indirect AAS method for their determination in micromolar quantities.³⁷ The nickel complex, $\text{Ni}(\text{DDTC})_2$, resulting from the reaction between carbon disulphide and the secondary amine in the presence of an ammoniacal nickel solution, is separated from the reaction medium, and dissolved in benzene-acetone (1:1 v/v); the solvent is evaporated, then the residue is digested

with HCl-HNO₃, and diluted with water, and the nickel is determined. The calibration graph for nickel is linear over a range corresponding to 2–15 μ moles of nine secondary amines. The practical detection limit is about 0.30 μ mole/ml of secondary amine with a relative standard deviation of 7.3–12%. The reaction time is 1.5–2 hr, which is a disadvantage. Primary amines interfere and must be removed.

Hexylamine, diethylamine, triethylamine, dibutylamine, cyclohexylamine, diethanolamine and piperidine in quantities up to 0.5 mg have been determined in a procedure³⁸ based on the reaction between the protonated amine and tetrathiocyanatocobaltate(II). The complexes are formed when the reactants (in acetone) are warmed on a water-bath. After evaporation of the solvent, a few ml of benzene are added, a portion of this solution is diluted with methanol, and the cobalt content is measured by AAS. Many organic compounds do not interfere in this method and recoveries are reported to be between 96 and 103.7%.

Long-chain primary amines are sometimes added to boiler water as anti-corrosion agents. A sensitive AAS method for monitoring octadecylamine in cooling circuits of power stations is capable of determining 0.1–1.0 μ g/ml concentrations of the amine.³⁹ A mixture of 10% sulphuric acid, 5% aqueous potassium chromate, sodium sulphate and 1,4-dioxan is added to the sample containing the amine, and the whole shaken for 1 min. The ion-association complex of chromate and protonated amine is extracted into nitrobenzene and the chromium content determined by using an air-acetylene flame. The detection limit for octadecylamine is stated to be 0.02 μ g/ml. Interfering materials are normally present only in negligible concentrations in boiler waters.

Amino-acids

This class of compound has been determined by use of copper(II) solutions. A method claimed to be sensitive, reproducible, and specific has been proposed for the determination of total urinary amino-acids,⁴⁰ based on the formation of copper complexes in a borate-phosphate buffer solution. Copper is determined (air-acetylene flame) in the supernatant liquid, after centrifuging. Gawargious *et al.*⁴¹ have described a similar method for determining α -amino-acids. Glycine, valine, phenylalanine, tyrosine, tryptophan,⁴² and L-methionine and L-histidine⁴³ may be determined by reaction of the acids with salicylaldehyde in alkaline solution to give Schiff's bases which can be complexed with copper(II) and subsequently extracted into MIBK in the presence of bathophenanthroline. The copper is determined by AAS, and linear calibration graphs are obtained for 1.5–15.0 μ g/ml of glycine, and 3.0–30 μ g/ml for L-histidine and L-methionine. The last two amino-acids may both be determined in a mixture by extraction at different pH values. The relative standard deviation was about 2% and the

recovery > 97%, but the methods are not specific and not of wide applicability. The same applies to a similar procedure reported for the determination of *p*-aminobenzoic acid in pharmaceutical products, in which the acid is reacted with copper(II) to form a 2:1 complex and extracted with bathophenanthroline in MIBK.⁴⁴ The copper in the ternary complex extracted is determined. Calibration graphs are linear for 13.7–37.0 μ g/ml with a recovery of 100.6%.

Aminodeoxyhexose

This compound has been determined⁴⁵ by utilizing a reaction with pyridoxal and cobalt(II) chloride, leading to the formation of a Schiff's base complex. The unprecipitated cobalt in the filtrate is measured by AAS, enabling 0.03–0.15 mmole of the hexose to be determined, with 97.2–102.7% recovery.

Aminoquinolines

Certain aminoquinoline antimalarial compounds may be determined by formation of their ternary complexes with cobalt(II) and thiocyanate.⁴⁶ Amodiaquine (Q) and chloroquine (Q) give complexes of the type CoQ₂(SCN)_n, whereas primaquine (P) forms a CoP₄(SCN)_m ternary complex. The cobalt in the nitrobenzene extract of the complexes may be determined by spectrophotometry or AAS but the latter has higher sensitivity and may be utilized to determine the compounds in biological fluids. There is good agreement with standard methods when pharmaceutical preparations are analysed.

Barbituric acid derivatives

Barbituric acid derivatives (0.51–16.21 mg) have been determined in pharmaceutical products by precipitation as copper pyridine barbiturate complexes.⁴⁷ The copper, either in the precipitate (after dissolution in concentrated nitric acid) or in the filtrate, is determined. Although simple and rapid, the method suffers from interferences from some metals, but this may be overcome by prior precipitation of the metals with sodium carbonate solution. Sulphonal, bromovaleryl urea and bromodiethylacetyl urea do not interfere.

Another procedure for the determination of barbiturate derivatives⁴⁸ also relies on precipitation of copper complexes. Barbitol, amobarbital, phenobarbital, allobarbital, pentobarbital, and ethylhexobarbital may be determined at concentrations of 10–240 μ g/ml. The unprecipitated copper in the filtrate is determined by AAS. Sedatives such as sulphonal, bromovaleryl urea, bromodiethylacetyl urea, ethinamide and glutethimide, when present in considerable excess (19–51-fold ratio to analyte), do not interfere. Interferences from metal ions (Na⁺, K⁺, Ni²⁺, Co²⁺, Zn²⁺, and Fe²⁺) may be eliminated by extraction of the barbiturates with chloroform at pH 6.

Bases

Organic bases such as quaternary ammonium compounds,⁴⁹ azepine,⁵⁰ phenothiazines,⁵¹ and noscipine⁵² have been determined by various techniques, all of which are non-specific. Alary *et al.*⁴⁹ determined 4 μ moles of quaternary ammonium compounds by addition of sodium dioctylsulphosuccinate (DOSS) in the presence of sodium chloride, shaking the mixture, and addition of copper-1,10-phenanthroline to form a complex with the excess of DOSS. This complex is extracted with MIBK and the copper determined by flame AAS. The method is convenient for the assay of pharmaceuticals that are heavy heterocyclic compounds or contain long hydrocarbon chains. It is not recommended for pharmaceutical products containing esters, amides or hydroxy groups, even though it offers good sensitivity.⁴⁹

A number of diazepine bases may be determined by using similar procedures, all of which are unselective. At low pH (about 3), the protonated base forms a 1:1 complex with bis(2-ethylhexyl) sulphosuccinate (EHOSS). The excess of EHOSS is reacted with copper-1,10-phenanthroline, and this complex is extracted into MIBK and finally the copper is determined by AAS. One of the azepine series, opipramol, forms a 1:2 complex with EHOSS.⁵⁰ A small amount of phenothiazine (1-4 μ mole) may be determined by its reaction with DOSS at pH 3. The excess of DOSS is complexed with copper-1,10-phenanthroline and extracted with MIBK, and the copper determined. If the complex formed between DOSS and phenothiazine is not sufficiently stable, an extraction stage with chloroform is included.⁵¹

A complex can also be formed between noscipine and Reinecke's salt at pH 1.7 in the presence of tartaric acid, and extracted into chloroform, then the chromium is determined in the organic phase.⁵² Good results are claimed for synthetic and commercial samples. The method is again non-specific, since Reinecke's salt may also be utilized to determine alkaloids such as strychnine, quinine, emetine, procaine, tetracaine and ephedrine.⁵³ The complex is extracted into nitrobenzene and the chromium in it is determined by AAS. A large number of inorganic cations and anions, glutamates, starch, and sucrose do not interfere.

Benzylpenicillin

Low concentrations of benzylpenicillin (18.6-111.6 μ g/ml) have been determined by forming an ion-pair between the compound and the tris(1,10-phenanthroline)cadmium chelate, extracting into nitrobenzene and determining the cadmium.⁵⁴ The relative standard deviation is about 2%. The procedure is simple and no interference was found from compounds such as starch, lactose, dextrin and saccharin sodium.

Biuret

This compound may be determined in mixed fertilizers and urea by AAS.⁵⁵⁻⁵⁷ Singhal *et al.*⁵⁵ state that the only disadvantage is that the copper hydroxide used for complexing must be kept for 5 hr before use. The method of Woodis *et al.*⁵⁶ is based on treatment of an ethanolic solution of biuret with copper(II) in order to form the copper complex, which is filtered off and analysed for copper. The method was said to give more reliable results than the AOAC official method, in which no corrections are made for mixed fertilizers.⁵⁸ Corominas⁵⁷ studied the method of Woodis *et al.* in collaboration with ten laboratories and also concluded that the method was better than the official method for mixed fertilizers. The two methods did not differ for urea samples, and the indirect AAS method was adopted, with the AOAC method retained as an alternative for biuret in urea.

Butylscopolamine salts

Butylscopolamine bromide and butylscopolamine tannate, which are parasympathetic nerve-blocking agents have been determined in blood, urine, and faeces by formation of the ion-pair complexes with $\text{Co}(\text{SCN})_4^{2-}$ in acidic medium in the presence of tartaric acid.⁵⁹ The complexes extracted into chloroform are analysed by AAS after dilution with MIBK or ethyl acetate. The calibration graph is linear for 3-15 μ g of butylscopolamine bromide and 5-30 μ g of the tannate.

Chelating agents

Chelating agents such as ammonium pyrrolidine dithiocarbamate and 8-hydroxyquinoline may be determined by formation and extraction of their copper or cobalt chelates into MIBK at an appropriate pH.¹

Ethylenediaminetetra-acetic acid (EDTA) may be determined in two ways. The first uses the masking effect of EDTA on the extraction of the copper-oxinate complex into MIBK at pH 6.5. The decrease in the AAS signal for copper is linearly proportional to EDTA concentration over the range $0-4 \times 10^{-5} M$ in the aqueous phase.¹ The second method⁶⁰ is based on addition of excess of nickel, removal of the surplus by precipitation with dimethylglyoxime and filtration, followed by release of nickel from the EDTA complex by pH adjustment, and determination by AAS. The method has been applied to determination of EDTA added to streptomycin (during manufacture) to remove alkaline-earth metal impurities. The reproducibility is $\pm 1.3 \mu$ g/g with a detection limit of 4 μ g/g. There is no interference from phosphate, a species frequently present in pharmaceutical products.

Nitrilotriacetic acid (NTA) has also been determined by AAS,⁶¹ in an evaluation of the toxicity of aquatic systems. The method involves AAS measurement of the amount of solid lead carbonate initially dissolved by the NTA. It is claimed that the

method is easy and rapid, and no special reagents are required. However, the procedure was designed for use in controlled laboratory studies and is not recommended for field determinations. In natural and industrial waters, other complexing agents and calcium ions would interfere. The same limitations apply to a similar method which uses the complexation of copper in alkaline media for measurement of the total chelating agents.⁶² The surplus copper is precipitated, and the copper left in solution is determined by AAS. Although the method is simple and sensitive, determination of individual chelating agents requires their prior separation.

Chinoform

The drug chinoform (5-chloro-7-iodo-8-quinolinol) can be determined by extraction of its zinc chelate into MIBK⁶³ and AAS measurement of the zinc at 213.8 nm; a linear calibration graph is obtained for 6–30 $\mu\text{g/ml}$ of chinoform.

Chloropheniramine maleate

This compound forms a 1:1:1 ternary complex with the copper–zincon chelate in water at pH 4.3. The ternary complex is extracted into chloroform and the copper determined by AAS.⁶⁴ A linear relationship is found for 1.9–27.4 $\mu\text{g/ml}$ of chloropheniramine maleate in the aqueous phase, with a relative standard deviation of 2.2%. Although the method offers simplicity and good sensitivity, some species, such as methylephedrine and diphenylhydramine interfere.

Chlorprothixene

A method for the determination of chlorprothixene in drugs involves precipitation with a freshly prepared solution of ammonium reineckate.⁶⁵ The precipitate is filtered off and chromium in the filtrate determined by AAS. The calibration graph is linear for 8–10 $\mu\text{g/ml}$ of chromium and 98.6–100.9% recovery is achieved. Other basic drugs that form insoluble reineckates interfere, but tablet additives do not.

Colchicine

Colchicine in biological samples may be determined by extraction from alkaline solution with chloroform.⁶⁶ The extract is centrifuged and evaporated, and the residue dissolved in water. This solution is reacted with isonicotinohydrazide in the presence of sodium carbonate; the hydrazone produced reacts with copper acetate to form a copper complex. There are some interferences from carbonyl-containing drugs or their metabolites. The calibration curves are linear for 3–30 mg of colchicine with recoveries of 95–98%.

Detergents

Le Bihan and Courtot-Coupez^{67–71} have described several methods for the determination of anionic and cationic detergents in water. In one of these,⁶⁸ it was

possible to determine anionic detergents in water at very low concentrations (from 3 ng/ml to 2.5 $\mu\text{g/ml}$, calculated as the sodium salt). The ion-association species formed with the 1,10-phenanthroline–copper complex was extracted into MIBK, and the copper determined by AAS. Traces of cationic surfactants at the 5–200 ng/ml level have been determined⁶⁹ by formation and extraction (into benzene) of the tetrathiocyanatocobaltate ion-association complex with the surfactant, followed by determination of the cobalt in the organic phase by ETA. The same authors⁷⁰ have described a modified technique for the ETA determination of anionic and non-ionic detergents in which smaller water samples and simpler extraction processes were used, permitting determination at the 10- $\mu\text{g/l}$. level.

The benzene extraction of the tetrathiocyanatocobaltate ion-association complexes and AAS determination of the cobalt has also been used for the determination of non-ionic surfactants at concentrations down to 50 $\mu\text{g/l}$. (of Triton X-100) in the presence of up to 1 g/l. of polyoxyethylene glycol.⁷¹ The method was based on that of Greff *et al.*⁷² The relative standard deviation was found to be up to 15% and the method suffered interference from dithiocarbamates and humic acids. A method for the determination of anionic detergents at levels below 50 $\mu\text{g/l}$., reported by Crisp *et al.*,⁷³ involves solvent extraction (into chloroform) of the ion-association complex formed with bis(ethylenediamine) copper(II), followed by ETA determination of the copper in the extract. The limit of detection is 2 $\mu\text{g/l}$. for linear alkylsulphonic acids. Recoveries are 95–100% for 100 μg of the linear alkylsulphonic acids but lower for sea-water samples. Only sulphide and iron(III) interfere; the former may be destroyed by hydrogen peroxide and the addition of EDTA suppresses interference from 100 mg/l. of iron(III). The authors point out that the Methylene Blue active-substance test⁷⁴ is not adequate for concentrations below 50 $\mu\text{g/l}$. and has a detection limit of 25 $\mu\text{g/l}$. for fresh waters and poorer sensitivities with marine and estuarine waters. The selectivity of the AAS method should be an attraction, but it is not clear whether the method has been widely adopted.

Better limits of detection (0.3 $\mu\text{g/l}$.) have been achieved in a method⁷⁵ for the determination of anionic detergents in natural (fresh and saline) waters at the $\mu\text{g/l}$. level, based on the method of Crisp *et al.*⁷³ but with a lower chloroform/sample volume ratio and measurement by graphite furnace AAS. Calibration graphs were linear for 0–50 $\mu\text{g/l}$. Crisp *et al.*⁷⁶ also developed a method for determination of non-ionic surfactants at concentrations of 0.05–2 mg/l. by formation of the neutral adducts with potassium tetrathiocyanatozincate (at pH 6–8), extraction of these into 1,2-dichlorobenzene, stripping of zinc into dilute hydrochloric acid and its determination by flame AAS. Solutions of Triton X-100 were used as standards. Anionic surfactants do not produce large

errors (e.g., only the equivalent of 0.07 mg/l. when present at 5 mg/l.), but sulphides, iron(III), aluminium(III) and chromium(III) interfere at the 0.1-mg/l. level and copper(II) interferes at 10 mg/l. Soaps at 1.0 mg/l. do not interfere but cationic surfactants form extractable ion-association species with $Zn(SCN)_4^{2-}$ and interfere.

A precipitation technique has been used for the determination of 0.1–1.2 mg of non-ionic detergents in water and sewage samples.⁷⁷ A 5-litre sample is extracted with ethyl acetate by a foaming technique, the organic extract is evaporated, and the dry residue is mixed with molybdophosphoric acid solution and barium chloride. The unconsumed molybdenum present as molybdophosphoric acid after centrifugation or filtration is determined by AAS. The recoveries range from 97.3 to 102.1% and the method may be applied to samples containing proteins or calcium, magnesium or manganese salts.

Diketones

Minami *et al.*⁷⁸ have developed an indirect AAS method for the determination of 0.05–2.0 mg of biacetyl. The sample is heated with hydroxylammonium chloride and sodium acetate, then a known amount of nickel is added to precipitate the dimethylglyoxime formed and the nickel in the precipitate or the surplus nickel in the solution is determined. It is difficult to imagine applications to analysis of real samples, but the method is said to be free from interference from cations and many organic compounds such as acetone, ethyl acetate, ethanol, acetic acid and phenol. However, the method could probably be adapted for determination of hydroxylamine in water by the Pittwell method.⁷⁹

Diols

Oles and Siggia⁸⁰ have described a rapid, sensitive AAS method for the determination of micromolar quantities of 1,2-diols in the presence of 1,3-diols. The 1,2-diols are oxidized with periodic acid and the iodate formed is separated by precipitation as silver iodate which is then dissolved in ammonia solution and analysed for silver. The precision of the method is 0.9–5.0% for 0.3–4.0 μ mole of the 1,2-diol per ml. The practical limit of detection is 0.2 μ mole/ml. This procedure was found to be particularly useful for the determination of 1,2-diol impurities in compounds containing non-adjacent hydroxyl groups. The sensitivity is equal to or greater than that of other procedures.

Esters

Aliphatic esters at concentrations of 0.04–3.5 mg/ml have been determined⁸¹ by a procedure involving production of a ferric hydroxamate, followed by removal of surplus iron(III) as basic benzoate. The iron in the hydroxamate is determined by AAS. Potassium, magnesium, calcium, diethyl ether, acetone, acetic acid, aniline, nitrobenzene, pro-

pionaldehyde and phenol may be present, but there are interferences from copper and aluminium. Recoveries are between 92.4 and 105%.

Ethambutol

Up to 400 μ g/ml of ethambutol has been determined by formation of its copper complex in alkaline medium (pH 8–11.5), extraction into methyl ethyl ketone and determination of copper in the extract.⁸² The method is of limited application because so many other compounds form copper complexes.

Ethinylloestradiol

A suitable method for the determination of ethinylloestradiol in tablets⁸³ involves treatment by nitrous acid to form the *O*-nitrosoderivative, which is then converted into the cobalt chelate by treatment with sodium cobaltinitrite in acetic acid. The procedure gives a linear calibration graph for 0.5–1.0 mg of ethinylloestradiol.

Flufenamic acid

Minamikawa *et al.*⁸⁴ observed that flufenamic acid forms a chelate with copper in the presence of 2-(2-hydroxyethyl)pyridine and developed an indirect method for the determination of the compound in biological samples by extraction of the chelate into propyl acetate and AAS determination of the copper. The method is more sensitive than the thin-layer chromatographic method, and can be applied to samples without separation or preconcentration procedures.

Folic acid

Folic acid may be oxidized by potassium permanganate to 2-amino-4-hydroxypteridine-6-carboxylic acid, which reacts with nickel(II) to form a metal complex.⁸⁵ This complex, on extraction with MIBK in the presence of bathophenanthroline is converted into an ion-association complex which is then analysed for nickel. The method has been applied to pharmaceutical preparations and has a relative standard deviation of 1.8% at the 1.2–20 μ g/ml level. The method shows no interference from nicotinamide, pyridoxal phosphate, thiamine, cyanocobalamin, calcium pantothenate, retinol acetate and riboflavin.

Histamine

Histamine in animal tissues and urine may be determined⁸⁶ by formation of the histamine–copper(II) cationic chelate which can be extracted as its ion-association complex with picrate into nitrobenzene. Copper is then determined in the organic phase. Many inorganic compounds may be present in 100-fold ratio to histamine without interfering but serotonin and histidine interfere strongly, an effect which may be depressed by addition of iron(II). Catecholamines (adrenaline, noradrenaline and dopamine) do not interfere if present in less than

fivefold molar ratio to histamine (up to $2 \times 10^5 M$). In the concentration range from $5 \times 10^{-6} M$ ($0.92 \mu\text{g/ml}$) to $3 \times 10^{-5} M$ ($5.52 \mu\text{g/ml}$) the relative standard deviation is 2%.

Hyoscine-N-butylbromide

Hyoscine-*N*-butylbromide in pharmaceutical preparations⁸⁷ can be determined by extraction of its ion-association complex with tetrathiocyanatocobaltate(II), and AAS analysis for cobalt. The complex is readily soluble in most organic solvents, but 1,2-dichloroethane, in spite of its toxic combustion products, is the most suitable. A linear relationship was found for the 5×10^{-5} – $7 \times 10^{-4} M$ concentration range.

Isonicotinylhydrazine

This compound may be determined by formation of the isonicotinylhydrazine-copper chelate and extraction into MIBK.⁸⁸ The method is suitable for determination of the compound in pharmaceutical products. Determination of copper gives a linear calibration graph for concentrations of isonicotinylhydrazine in the range 0.2 – $1.7 \times 10^{-4} M$ with a relative standard deviation of 0.4%.

Malathion

The compound is hydrolysed to give dimethyl-dithiophosphate (DMDTP) which is then reacted with bismuth(III) to give a complex extractable into MIBK.⁸⁹ The bismuth-DMDTP complex is used for calibration.

Methylamphetamine hydrochloride

Methylamphetamine hydrochloride (down to $16 \mu\text{g/ml}$)⁹⁰ has been determined in drugs by precipitation as a bismuth complex, on addition of 7% hydrochloric acid and 7% potassium iodide solution saturated with bismuth(III) chloride. The unconsumed bismuth in the filtrate is determined by AAS. The determination may be done in the presence of ephedrine hydrochloride; metal ions and certain organic species do not interfere up to certain concentrations. Interferences can be eliminated by prior extraction of the methylamphetamine hydrochloride into chloroform. A more sensitive method⁹¹ has been described for the determination of methylamphetamine, and also diethylamine hydrochloride and ephedrine hydrochloride, by reacting the amines with carbon disulphide in the presence of copper(II) and ammonia solution. The copper complex is extracted into MIBK for determination of copper. Linear calibration graphs for 1.9 – $8.0 \mu\text{g/ml}$ of methylamphetamine hydrochloride, 1.1 – $6.6 \mu\text{g/ml}$ of diethylamine hydrochloride and 1.2 – $8.0 \mu\text{g/ml}$ of ephedrine hydrochloride are reported. The recoveries range from 93.3 to 103.2% and it is claimed that the method is quicker than the precipitation method with bismuth.

Nitro groups

The method involves oxidation of the nitro group to nitrate with cerium(IV) sulphate or potassium permanganate.⁹² The nitrate formed is then treated with copper-neocuproine complex to form an ion-pair which is extracted into MIBK, and the copper is determined. Tollen's reagent may also be used for the determination of some nitro-compounds.¹³ The nitro group is reduced to the substituted hydroxylamine with zinc powder, then treated with Tollen's reagent to yield metallic silver. The precipitate is dissolved in nitric acid and the silver determined by AAS. Good precision is claimed but there are interferences from resorcinol, benzoin, *p*-aminophenol and ninhydrin. Benzoic acid, aniline, benzaldehyde and *p*-nitroso-*N,N*-dimethylaniline up to 2.5 times the concentration of the nitro-compound do not interfere. Interferences from metal ions are eliminated by prior extraction of the nitro-compounds into benzene.

Oxalic acid

In recent years there has been increasing demand for a method for determination of oxalic acid in urine samples, because calcium oxalate stones can form in the urinary system and routine clinical tests are required for urine samples. Two routine AAS micro-methods are based on the precipitation of oxalate with an excess of calcium ions at pH 5.^{93,94} The calcium in the precipitate from the aliquot used is determined from the difference between the amount of calcium left in the supernatant liquid, and the total calcium in a second aliquot treated with the same amount of added calcium but at pH 2. Both methods give 95% recovery and are free from interferences from phosphate, ammonium, magnesium(II), and uric acid even at high concentration. Although the method of Koehl and Abecassis⁹⁴ gave a better precision (standard deviation 3.0 mg/l. for thirty 17-mg/l. samples) than that of Menache⁹³ (standard deviation 7.5 mg for a range of 0–40 mg), it is more time-consuming, the precipitation taking 48 hr.

Phenols

A number of phenols can be determined by forming their cobalt complexes by heating with sodium cobaltinitrite in acetic acid to 100°,⁹⁵ extracting into MIBK and analysing the organic phase for cobalt by AAS. Recoveries are 94.6–104.5%. Copper(II) and iron(III) interfere and the presence of aniline is a disadvantage. In another method,⁹⁶ catechol may be determined by extraction of its copper chelate into chloroform in the presence of trioctylmethylammonium chloride. The extract is diluted with methanol and the copper determined by AAS; a linear relationship is found for the range 11–176 $\mu\text{g/ml}$. Many cations and anions do not interfere. Pentachlorophenol (PCP) may be determined by extraction as $[\text{FePhen}_3][\text{C}_6\text{Cl}_5\text{O}]_2$ into nitrobenzene from an aqueous phase containing an excess of

tris(1,10-phenanthroline)iron(II).⁹⁷ Concentrations in the range $0-3 \times 10^{-4} M$ may be determined.

Phenylacetylene

Phenylacetylene has been determined by Smith and Bailey⁹⁸ by reaction with ammoniacal silver nitrate at room temperature to form silver acetylide. The precipitate is washed, separated and dissolved in piperidine, and the silver is determined, either in the precipitate or in the supernatant solution. In the first technique, the calibration curve was linear for 1.0–4.0 $\mu\text{g/ml}$ of silver with a mean recovery of 100.4% and a relative standard deviation of 6.5%. In the second technique the calibration curve was linear for 2.5–7.5 $\mu\text{g/ml}$ of silver with a mean recovery of 100.3% and a relative standard deviation of 2.9%.

Porphyryns

Porphyryns have been determined by separation as their copper chelates.⁹⁹ The method is claimed to be simpler and more suitable for routine use than the spectrophotometric method.

Sugars and polyhydroxy compounds

A method for the determination of sugars in plant material reported by Potter *et al.*¹⁰⁰ has the advantage of simplicity as well as good agreement with the official method. The AAS method utilizes the reduction of copper(II) in alkaline solution to insoluble copper(I) oxide, which is separated by centrifugation; the unreduced copper(II) in solution is then determined by AAS. Other reducing agents present will interfere so the method is not specific. Compounds such as glycerol, lactose, saccharose, glucose, and tartaric acid³³ have been determined in ethanol samples by utilizing their reaction with periodic acid to yield iodate, which is then precipitated by addition of silver nitrate solution. The silver iodate is washed with dilute nitric acid and water, then dissolved in ammonia solution, and the silver is determined by flame AAS. Limits of detection are 0.2–1.9 mg.

Sulphur-containing compounds

Several organic sulphur-containing compounds may be determined by precipitation of their silver compounds, followed by determination of the excess of silver in solution or in the precipitate after its dissolution in nitric acid.^{101,102} The first procedure¹⁰¹ was used to determine mercaptobenzothiazole and xanthates; good recoveries were obtained but this can be attributed to decomposition of the precipitate in the case of xanthate. The second procedure¹⁰² gives an analysis time of 15 min per sample for the determination of total thiol content at the level of 0.8–20 $\mu\text{mole/ml}$, with a relative standard deviation of 0.8–3.2%. Individual thiols cannot be determined and hydrogen sulphide interferes. Compounds not containing sulphur but giving insoluble silver salts also interfere. Hence the method has also been used

to determine iodoform, theobromine and sodium salicylate.¹⁰

Electrothermal AAS has been used for the determination of the metabolites of tetramethylthiuramdisulphide¹⁰³ and tetraethylthiuramdisulphide,¹⁰⁴ (sodium dimethyldithiocarbamate and sodium diethyldithiocarbamate respectively). The method is based on formation of the copper dithiocarbamate complex, its extraction into carbon tetrachloride, and injection of the extract into the graphite furnace. The method offers a limit of detection of 0.5 mg/l., with linear calibration graphs for 1–10 mg/l.

Tannins

Tannins in aqueous tea extracts have been determined¹⁰⁵ by precipitation with copper acetate followed by AAS determination of copper, either in the precipitate (dissolved by digestion with a mixture of nitric and sulphuric acids) or in the filtrate. The authors report that the results agreed with those obtained gravimetrically but it would appear that the AAS method offers very little advantage.

Vitamin B₁

Hassan *et al.*¹⁰⁶ have developed a simple, rapid and accurate method for the determination of vitamin B₁ in pharmaceutical preparations, based on desulphurization with potassium plumbite and precipitation of lead sulphide. The unreacted lead(II) is measured by AAS. The method takes only 15 min. It is accurate and sensitive with a linear calibration graph for 1–10 $\mu\text{g/ml}$ of lead. Recovery for pure vitamin B₁ was found to be 99.1% with a standard deviation of 0.8%. The effects of several common excipients and diluents used in the preparation of capsules, tablets and suspensions were examined. Magnesium stearate, talc, sodium citrate, carboxymethyl cellulose, Tween 80, poly(vinyl pyrrolidone), glucose and lactose in large amounts showed no interference. There was also no effect from vitamins B₂, B₆, B₁₂ and nicotinamide.

CONCLUSIONS

Many of the authors of papers dealing with indirect AAS methods for the determination of organic species have claimed that their methods are rapid, simple, accurate, and sensitive. If the nature of the matrix and the likely interferences are known, some of the methods may offer some advantages, but few have found applications for real samples. Some procedures are specific and give results which agree with those of official methods, *e.g.*, the cadmium reduction method for the determination of chloramphenicol¹² and the copper precipitation method for biuret,⁵⁶ and the latter has undergone laboratory trials that prove it to be better than the official method for mixed fertilizers.

Table 1. Principal metals used in organic analysis by AAS

Metal	Reaction or product	Applications
Chromium	Formation of reineckate	Alkaloids, ⁵³ noscapine, ⁵² chloroprothixene ⁶⁵
Cobalt	Complex formation	Alcohols, ³¹ octadecylamine ³⁹
	Tetrathiocyanatocobaltate complex	Amines, ³⁸ aminoquinoline antimalarials, ⁴⁶ butylscopolamine, ⁵⁹ detergents, ⁶⁹ hyoscine- <i>N</i> -butylbromide ⁸⁷
	Schiff's base complex	Aminodeoxyhexose ⁴⁵
	Cobalt complex	Ammonium pyrrolidine dithiocarbamate, ¹ ethinyloestradiol, ⁸³ phenols ⁹⁵
Copper	Bathophenanthroline ternary complex	Anthranilic acid ²⁶
	Ternary or ion-association complex	Amino-acids, ⁴²⁻⁴⁴ azepine, ⁵⁰ bases, ⁴⁹ chloropheniramine maleate, ⁶⁴ detergents, ^{68,70,73} diazepam, ⁵⁰ flufenamic acid, ⁸⁴ histamine, ⁸⁶ nitro compounds, ⁹² noscapine, ⁵² phenothiazines, ⁵¹ phthalic acid, ^{24,25} quaternary ammonium salts ⁴⁹
	Complex formation	Aldehydes and ketones, ³⁵ catechol, ⁹⁶ colchicine, ⁶⁶ diethylamine, ⁹¹ dithiocarbamates, ^{1,103,104} ephedrine hydrochloride, ⁹¹ ethambutol, ⁸² fatty acids, ^{29,30} 8-hydroxyquinoline, ¹ isonicotinylnyl hydrazine, ⁸⁸ methylamphetamine hydrochloride, ⁹¹ porphyrins ⁹⁹
Nickel	Masking of oxine complex	EDTA ¹
	Precipitation	Amino-acids, ^{40,41} barbiturates, ^{47,48} biuret, ⁵⁵⁻⁵⁷ primary amines, ³⁶ sugars, ¹⁰⁰ tannins, ¹⁰⁵
Silver	Precipitation	Aliphatic secondary amines, ³⁷ biacetyl, ⁷⁸ EDTA ⁶⁰
	Reduction to metal	Aldehydes, ³²⁻³⁴ nitro compounds ¹³
	Precipitation of silver iodate	Diols, ⁸⁰ sugars, ³³ tartaric acid ³³
	Precipitation of silver iodide	Iodoform ¹⁰¹
	Precipitation of silver acetylde	Phenylacetylene ⁹⁸
	Precipitation of silver salt	Salicylate, ¹⁰¹ sulphur compounds, ^{101,102} theobromine ¹⁰¹

However, many of the indirect AAS methods can be said to be notable for their ingenuity and little else. It has been pointed out that trace organic analysis presents more difficulties than does inorganic trace analysis.¹⁰⁷ Separation procedures are used extensively (except for a few cases of highly specific enzymatic methods) and the various chromatographic techniques are still the most favoured, followed by a final determination step which is specific.

For convenience in cross-reference, the main applications are listed according to the metal used in the final determination, in Table 1.

REFERENCES

- G. D. Christian and F. J. Feldman, *Anal. Chim. Acta*, 1968, **40**, 173.
- G. F. Kirkbright and H. N. Johnson, *Talanta*, 1973, **20**, 433.
- Y. Kidani, *Bunseki Kagaku*, 1981, **30**, No. 11, S59.
- J. H. M. Miller, *Intern. Lab.*, 1978, July-August, 37.
- F. Rousselet and F. Thullier, *Prog. Atom. Spectrosc.*, 1979, **1**, 353.
- L. Ebdon, in J. E. Cantle (ed.), *Atomic Absorption Spectroscopy*, p. 395. Elsevier, Amsterdam, 1982.
- W. T. Elwell and J. A. F. Gidley, *Atomic Absorption Spectrophotometry*, 2nd Ed., p. 38. Pergamon Press, Oxford, 1966.
- I. Rubeska and B. Moldan, *Atomic Absorption Spectrophotometry*, p. 97. Iliffe, London, 1967.
- M. Slavin, *Atomic Absorption Spectroscopy*, 2nd Ed., pp. 89-90. Wiley, New York, 1978.
- A. M. Bond and J. B. Willis, *Anal. Chem.*, 1968, **40**, 2087.
- S. J. Simon and D. F. Boltz, *Microchem. J.*, 1975, **20**, 468.
- S. S. M. Hassan and M. H. Eldesouki, *Talanta*, 1979, **26**, 531.
- T. Mitsui and T. Kojima, *Bunseki Kagaku*, 1977, **26**, 317; *Chem. Abstr.*, 1977, **87**, 147588p.
- U.S. Pharmacopeia XVIII*, pp. 110-112. Mack, Easton, Pa., 1970.
- D. G. Berge, R. T. Pflaum, D. A. Lehman and C. C. W. Frank, *Anal. Lett.*, 1968, **1**, 613.
- B. Mandrou and J. Bres, *J. Pharm. Belg.*, 1970, **25**, 3; *Anal. Abstr.*, 1971, **20**, 1272.
- Y. Kidani, K. Takeda and H. Koike, *Bunseki Kagaku*, 1973, **22**, 719; *Chem. Abstr.*, 1973, **79**, 97019e.
- F. J. Diaz, *Anal. Chim. Acta*, 1974, **58**, 455.

19. E. Peck, *Anal. Lett.*, 1978, **11**, 103.
20. D. Gegiou, *Analyst*, 1974, **99**, 745.
21. J. A. Persson and K. Irgum, *Anal. Chim. Acta*, 1982, **138**, 111.
22. N. Oyamada, and M. Ishizaki, *Sangyo Igaku*, 1982, **24**, 320; *Chem. Abstr.*, 1982, **97**, 209733.
23. J. W. Robinson and E. M. Skelly, *J. Environ. Sci. Health*, 1982, **A17**, 391.
- 23a. I. L. Marr and J. Anwar, *Analyst*, 1982, **107**, 260.
- 23b. I. L. Marr, J. Anwar and B. B. Sithole, *ibid.*, 1982, **107**, 1212.
24. T. Kumamaru, Y. Hayashi, N. Okamoto, E. Tao and Y. Yamamoto, *Anal. Chim. Acta*, 1966, **35**, 524.
25. T. Kumamaru, *ibid.*, 1968, **43**, 19.
26. Y. Kidani, N. Osugi, K. Inagaki and H. Koike, *Bunseki Kagaku*, 1975, **24**, 218; *Anal. Abstr.*, 1975, **29**, 5C51.
27. Y. Kidani, K. Inagaki and H. Koike, *Nagoya Shiritsu Daigaku Yakugakubu Kenkyu Nempo*, 1972, **20**, 21; *Chem. Abstr.*, 1974, **80**, 91005w.
28. Y. Yamamoto, T. Kumamaru, Y. Hayashi and S. Matsushita, *Bull. Chem. Soc. Japan*, 1969, **42**, 1774.
29. P. Treguer, P. Le Corre and P. Courtot, *J. Marine Biol. Assoc. U.K.*, 1972, **52**, 1045.
30. D. P. Le Hane and M. Werner, *Am. J. Clin. Pathol.*, 1973, **59**, 10.
31. T. Mitsui and T. Kojima, *Bunseki Kagaku*, 1977, **26**, 228; *Chem. Abstr.*, 1977, **87**, 110969b.
32. P. J. Oles and S. Siggia, *Anal. Chem.*, 1974, **46**, 911.
33. T. Mitsui and Y. Fujimura, *Bunseki Kagaku*, 1976, **25**, 429; *Chem. Abstr.*, 1977, **86**, 25666k.
34. T. Mitsui, and T. Kojima, *ibid.*, 1977, **26**, 182; *Chem. Abstr.*, 1977, **87**, 77970v.
35. Y. Minami, T. Mitsui and Y. Fujimura, *ibid.*, 1981, **30**, 566; *Chem. Abstr.*, 1981, **95**, 180334.
36. T. Mitsui and Y. Fujimura, *Bunseki Kagaku*, 1974, **23**, 1309; *Chem. Abstr.*, 1975, **82**, 38386d.
37. P. J. Oles and S. Siggia, *Anal. Chem.*, 1973, **45**, 2150.
38. T. Minami, Y. Mitsui and Y. Fujimura, *Bunseki Kagaku*, 1981, **30**, 475; *Chem. Abstr.*, 1981 **95**, 108153c.
39. E. Glaeser and L. Bartholome, *Chem. Technol. (Leipzig)*, 1978, **30**, 33; *Anal. Abstr.*, 1978, **35**, 1H29.
40. B. J. Bousquet, J. L. Bouvier and C. Dreux, *Clin. Chim. Acta*, 1972, **42**, 327.
41. Y. A. Gawargious, A. Basada and M. E. M. Hassouna, *Microchem. J.*, 1977, **22**, 96.
42. Y. Kidani, S. Uno and K. Inagaki, *Bunseki Kagaku*, 1976, **25**, 514; *Chem. Abstr.*, 1977, **86**, 21819q.
43. Y. Kidani, S. Uno and K. Inagaki, *Bunseki Kagaku*, 1977, **26**, 158; *Anal. Abstr.*, 1977, **33**, 3D143.
44. Y. Kidani, T. Saotome, K. Inagaki and H. Koike, *ibid.*, 1975, **24**, 463; *Chem. Abstr.*, 1976, **84**, 126817z.
45. Y. Minami, T. Mitsui and Y. Fujimura, *ibid.*, 1982, **31**, 334.
46. S. M. Hassan, M. E. S. Metwally and A. A. Abou Ouf, *Analyst*, 1982, **107**, 1235.
47. T. Misui and Y. Fujimura, *Bunseki Kagaku*, 1975, **24**, 575; *Chem. Abstr.*, 1975, **83**, 202424r.
48. Y. Minami, T. Mitsui and Y. Fujimura, *ibid.*, 1982, **31**, 604.
49. J. Alary, J. Rochat, A. Villet and A. Coeur, *Ann. Pharm. France.*, 1976, **34**, 345; *Anal. Abstr.*, 1977, **32**, 5E6.
50. *Idem, ibid.*, 1976, **34**, 419; *Anal. Abstr.*, 1977, **32**, 6E37.
51. *Idem, ibid.*, 1977, **35**, 439; *Anal. Abstr.*, 1978, **35**, 1E35.
52. T. Minamikawa and K. Matsumura, *Yakugaku Zasshi*, 1976, **96**, 440; *Anal. Abstr.*, 1976, **31**, 5E13.
53. Y. Minami, T. Mitsui and Y. Fujimura, *Bunseki Kagaku*, 1981, **30**, 811.
54. Y. Kidani, K. Nakamura, K. Inagaki and H. Koike, *ibid.*, 1975, **24**, 742; *Anal. Abstr.*, 1976, **31**, 1E13.
55. K. C. Singhal, R. C. P. Sinha and B. K. Banerjee, *Technology (Coimbatore, India)*, 1969, **6**, 95.
56. T. C. Woodis, G. B. Hunter and F. J. Johnson, *J. Assoc. Off. Anal. Chem.*, 1976, **59**, 22.
57. L. F. Corominas, *ibid.*, 1977, **60**, 1214.
58. *Official Methods of Analysis*, 12th Ed., 2.072-2.074. AOAC, Washington, 1978.
59. T. Minamikawa, K. Matsumura, A. Kamei and M. Yamakawa, *Bunseki Kagaku*, 1971, **20**, 1011; *Anal. Abstr.*, 1973, **25**, 312.
60. R. J. Hurtubise, *J. Pharm. Sci.*, 1974, **63**, 1131.
61. H. W. Lautenbacher and H. W. Baker, *Bull. Environ. Contam. Toxicol.*, 1974, **11**, 57.
62. R. Kunkel and S. E. Manahan, *Anal. Chem.*, 1973, **45**, 1465.
63. Y. Kidani, K. Inagaki, N. Osugi, and H. Koike, *Bunseki Kagaku*, 1973, **22**, 892; *Chem. Abstr.*, 1973, **79**, 139671u.
64. Y. Kidani, T. Saotome, M. Kato and H. Koike, *ibid.*, 1974, **23**, 265; *Chem. Abstr.*, 1974, **81**, 82461k.
65. S. Tammilehto, *Acta Pharm. Fenn.*, 1979, **88**, 25; *Anal. Abstr.*, 1980, **39**, 1E52.
66. K. V. Anastasios, M. N. Christianopoulou and V. P. Papageoriou, *Toxicol. Aspects*, 1980, **9**, 220.
67. A. Le Bihan and J. Courtot-Coupez, *Bull. Soc. Chim. France*, 1970, 406; *Anal. Abstr.*, 1971, **20**, 1346.
68. *Idem, Analysis*, 1973-1974, **2**, 695; *Anal. Abstr.*, 1975, **28**, 6H17.
69. *Idem, ibid.*, 1976, **4**, 58; *Anal. Abstr.*, 1976, **31**, 3H57.
70. *Idem, Anal. Lett.*, 1977, **10**, 759.
71. *Idem, Analysis*, 1978, **6**, 339; *Anal. Abstr.*, 1979, **36**, 6C50.
72. R. A. Greff, E. A. Setzkorn and W. D. Leslie, *J. Am. Oil Chem. Soc.*, 1965, **42**, 180.
73. P. T. Crisp, J. M. Eckert, N. A. Gibson, G. F. Kirkbright and T. S. West, *Anal. Chim. Acta*, 1976, **87**, 97.
74. *Standard Methods for the Examination of Water and Wastewater*, 13th Ed., p. 339. American Public Health Association, New York, 1971.
75. M. J. Gagnon, *Water Res.*, 1979, **13**, 53.
76. P. T. Crisp, J. M. Eckert and N. A. Gibson, *Anal. Chim. Acta*, 1979, **104**, 93.
77. J. Chlebicki and W. Garncarz, *Chem. Anal. (Warsaw)*, 1979, **24**, 675; *Anal. Abstr.*, 1980, **38**, 5H72.
78. Y. Minami, T. Mitsui and Y. Fujimura, *Bunseki Kagaku*, 1979, **28**, 717; *Anal. Abstr.*, 1980, **39**, 1C22.
79. L. R. Pittwell, *Mikrochim. Acta*, 1975 **II**, 425.
80. P. J. Oles and S. Siggia, *Anal. Chem.*, 1974, **46**, 2197.
81. Y. Minami, T. Mitsui and Y. Fujimura, *Bunseki Kagaku*, 1979, **28**, 513; *Chem. Abstr.*, 1979, **91**, 203889y.
82. A. V. Kovatsis and M. A. Tsougas, *Arzneim.-Forsch.*, 1978, **28**, 248; *Anal. Abstr.*, 1978, **35**, 2E48.
83. M. M. Amer, M. I. Walsh, I. A. Haroun and F. M. Ashour, *J. Pharm. Belg.*, 1978, **33**, 297; *Anal. Abstr.*, 1980, **38**, 6E23.
84. T. Minamikawa, K. Sakai, N. Hashitani, E. Fukushima and N. Yamagishi, *Chem. Pharm. Bull.*, 1973, **21**, 1632.
85. Y. Kidani, K. Nakamura and K. Inagaki, *Bunseki Kagaku*, 1976, **25**, 509; *Chem. Abstr.*, 1976, **85**, 182450h.
86. T. Sakai, N. Ohno, T. Wakisaka and Y. Kidani, *ibid.*, 1982, **31**, 356.
87. M. K. Park, C. Y. Shon and M. H. Shin, *Soul Taehakkyo Yakhak Nonmunjip*, 1979, **4**, 140; *Chem. Abstr.*, 1981, **94**, 162809p.
88. Y. Kidani, K. Inagaki, T. Saotome and H. Koike, *Bunseki Kagaku*, 1973, **22**, 896; *Chem. Abstr.*, 1973, **79**, 139672v.
89. I. A. Qazi, *Ph.D. Thesis*, The University of Aston in Birmingham, 1980.
90. T. Mitsui, Y. Fujimura and T. Suzuki, *Bunseki Kagaku*, 1975, **24**, 244; *Anal. Abstr.*, 1975 **29**, 5E27.

91. T. Mitsui and Y. Fujimura, *Nippon Kagaku Kaishi*, 1974, **10**, 1908; *Chem. Abstr.*, 1974, **81**, 181012w.
92. M. E. Houser and M. I. Fauth, *Microchem. J.*, 1970, **15**, 399.
93. R. Menache, *Clin. Chem.*, 1974, **20**, 1444.
94. C. Koehl and J. Abecassis, *Clin. Chim. Acta*, 1976, **70**, 71.
95. T. Mitsui and Y. Fujimura, *Bunseki Kagaku*, 1974, **23**, 1303; *Chem. Abstr.*, 1975, **82**, 38285c.
96. Y. Kidani, S. Uno, Y. Kato and H. Koike, *ibid.*, 1974, **23**, 740; *Chem. Abstr.*, 1975, **82**, 35070t.
97. Y. Yamamoto, T. Kumamaru and Y. Hayashi, *Talanta*, 1967, **14**, 611.
98. R. V. Smith and D. L. Bailey, *Anal. Chim. Acta*, 1974, **73**, 177.
99. R. Bourdon, J. Younger and M. Atoie, *Ann. Biol. Clin. (Paris)*, 1972, **30**, 427; *Chem. Abstr.*, 1973, **78**, 55024b.
100. A. L. Potter, E. D. Ducay and R. M. Macready, *J. Assoc. Off. Anal. Chem.*, 1968, **51**, 748.
101. H. K. L. Gupta and D. F. Boltz, *Microchem. J.*, 1971, **16**, 571.
102. J. S. Marhevka and S. Siggia, *Anal. Chem.*, 1979, **51**, 1259.
103. F. K. Martens and A. M. Heyndrickx, *Meded. Fed. Landbouwwet., Rijksuniv. Gent*, 1976, **41** 2(2), 1393; *Anal. Abstr.*, 1977, **33**, 5D73.
104. F. K. Martens and A. Heyndrickx, *J. Anal. Toxicol.*, 1978, **2**, 269.
105. D. Coomans, J. Silberklang, Y. Michotte, L. Dryon and D. L. Massart, *Z. Anal. Chem.*, 1979, **294**, 140; *Anal. Abstr.*, 1979, **37**, 3F34.
106. S. S. M. Hassan, M. T. Zaki, and M. H. Eldesouki, *J. Assoc. Off. Anal. Chem.*, 1979, **62**, 315.
107. K. Beyermann, *Pure Appl. Chem.*, 1978, **50**, 87.

FLUORESCENCE PROPERTIES OF SOME SCHIFF'S BASES DERIVED FROM 3-HYDROXYPYRIDINE-2-ALDEHYDE AND OF THEIR METAL CHELATES

FLUORIMETRIC DETERMINATION OF MANGANESE BASED ON ITS CATALYTIC EFFECT ON THE OXIDATION OF THESE COMPOUNDS WITH HYDROGEN PEROXIDE

J. VAZQUEZ RUIZ, A. GARCIA DE TORRES and J. M. CANO-PAVON*

Department of Analytical Chemistry, Faculty of Sciences, The University, Malaga-4, Spain

(Received 15 March 1983. Revised 10 August 1983. Accepted 17 August 1983)

Summary—The fluorimetric properties of the oxime, thiosemicarbazone, azine and 2-pyridylhydrazone of 3-hydroxypyridine-2-aldehyde have been studied; quantum yields have been measured in ethanol-water and ethanol-dimethylformamide media. Two kinetic methods are described for the determination of trace amounts of manganese(II), based on its catalytic effect on the oxidation of the thiosemicarbazone and of the azine by hydrogen peroxide. The reactions are followed by measuring the rate of change of the fluorescence. The calibration graph is linear over the manganese range 5–50 ng/ml with a precision of $\pm 3.0\%$ for the thiosemicarbazone, and 0.4–0.9 $\mu\text{g/ml}$ with a precision of $\pm 2.0\%$ for the azine. Interferences by foreign ions have been investigated.

The fluorescence of Schiff's bases derived from salicylaldehyde has been widely studied, as well as that of their metal chelates. The complexes of zinc with salicylaldehyde thiosemicarbazone, semicarbazone and acetylhydrazone have been investigated by Holzbecher,¹ although no analytical applications have been proposed. Other aromatic Schiff's bases, such as 2-hydroxyaniline-*N*-salicylidene (salicylidene-*o*-aminophenol) react with aluminium, gallium, beryllium and other metal ions to form complexes which give a fluorescent emission that can be utilized for the determination of these ions.² Recently, seventeen aromatic Schiff's base derivatives with alkyl groups *m*- or *p*- to the $-\text{CH}=\text{N}-$ group of salicylidene-*o*-aminophenol have been described,³ and the effects of the substituent groups on the fluorescence properties of their metal complexes reported.

Oxidations of Schiff's bases have been used as indicator reactions in oxido-reduction catalysis, especially when the reaction rate is determined by means of fluorimetric measurements. Kinetic fluorimetric methods for determination of traces of copper(II), mercury(II) and platinum(IV), based on their catalytic effects on aerial oxidation of 2,2'-dipyridyl ketone hydrazone have been described.^{4,5} Titanium has been determined by a similar procedure involving oxidation of picolinaldehyde nicotinoylhydrazone.⁶ A kinetic determination of traces of copper(II) by its catalytic effect on the

oxidation of 4,4'-dihydroxybenzophenone thiosemicarbazone by hydrogen peroxide has been established.⁷ Recently, a kinetic fluorimetric determination of nanogram amounts of manganese, based on its catalysis of the oxidation of 2-hydroxybenzaldehyde thiosemicarbazone with hydrogen peroxide has been described.⁸

In this paper, the fluorescence properties of the following compounds derived from 3-hydroxypyridine-2-aldehyde, as well as their metal chelates, have been studied: 3-hydroxypyridine-2-aldoxime (I), 3-hydroxypyridinaldehyde thiosemicarbazone, 3-OH-PAT (II), and 3-hydroxypyridinaldehyde azine, 3-OH-PAA (III). Results are compared with those for pyridine-2-aldehyde 2-pyridylhydrazone (IV). These compounds have been used previously in the photometric determination of diverse metal ions, and their physicochemical properties described.⁹⁻¹¹ Compound IV has been used by us in the fluorimetric determination of aluminium.¹²

EXPERIMENTAL

Apparatus

Fluorescence measurements were made with a Perkin-Elmer 204 spectrofluorimeter, equipped with a xenon-lamp source and an Ultrathermostat Colora K-5, and 1.0-cm quartz cells. Fluorescence curves were corrected with a standard solution of quinine sulphate.

Synthesis of reagents

These were synthesized as previously described⁹⁻¹² and identified by elemental analysis, melting point, and infrared and NMR spectroscopy.

Reagents and solutions

All reagents were used as $10^{-3}M$ solutions in ethanol. More dilute solutions were prepared as required from these solutions, which were stable for at least 1 week. All solvents and reagents were of analytical grade. Buffer solutions (pH 9.3 and 9.7) were prepared from $2M$ ammonium chloride and $2M$ ammonia solutions (pH 9.7: 214 ml of NH_4Cl solution and 586 ml of NH_3 solution, diluted to 1 litre; pH 9.3: 382 ml of NH_4Cl solutions and 418 ml of NH_3 solution, diluted to 1 litre).

Measurement of fluorescence quantum yields

The procedure described by Parker *et al.*¹³ was used. It is based on the integrated area (F) under the fluorescence emission spectrum being proportional to the total intensity of the fluorescence emitted by the solution, this in turn being proportional to the product $I_0\phi\epsilon cd$, where I_0 is the excitation intensity, ϕ the quantum yield, ϵ the molar absorptivity, c the concentration and d the path-length. If the fluorescence emission spectra of two solutions are measured with the same apparatus and the same excitation intensity, the ratio of the two fluorescence intensities is given by

$$\frac{F_2}{F_1} = \frac{\phi_2\epsilon_2c_2d}{\phi_1\epsilon_1c_1d} = \frac{\phi_2A_2}{\phi_1A_1}$$

where a_1 and A_2 are the absorbances of the two solutions. If one of the substances chosen has a known ϕ , the other ϕ value can be calculated very easily. In practice, quinine sulphate ($\phi = 0.55$) is used, and the areas under the curves of the corrected spectra, as well as the absorbances, are measured.

Kinetic determination of manganese with 3-OH-PAT

In a 25-ml standard flask, 2.5 ml of $10^{-3}M$ 3-OH-PAT solution in ethanol, and 3.5 ml of 0.1% hydrogen peroxide were mixed, and made up to volume with ammonia buffer (pH 9.7). Then 3.0 ml of this solution were placed in the quartz spectrofluorimeter cell and when the required temperature (25°) was reached, 50 μ l of Mn(II) solution were injected from a microsyringe. The fluorescence intensity (λ_{exc} 370 nm, λ_n 430 nm) was measured and its variation plotted *vs.* time.

Kinetic determination of manganese with 3-OH-PAA

In a 25-ml standard flask, 3.5 ml of dimethylformamide, 2 ml of 0.5% hydrogen peroxide solution and 3.5 ml of $10^{-3}M$ 3-OH-PAA solution were mixed in that order and made up to volume with ammonia buffer (pH 9.3). Then 3.0 ml of this solution were placed in the quartz spectrofluorimeter cell, and when the required temperature was reached, 50 μ l of Mn(II) solution were injected from a microsyringe. The fluorescence intensity (λ_{exc} 325 nm, λ_n 390 nm) was measured, starting 2.0 min after addition of the manganese, and plotted *vs.* time.

RESULTS AND DISCUSSION

Fluorescence of Schiff's bases and of their metal complexes

The fluorescence of the four Schiff's bases studied is quite different. Compound **I** is the most fluorescent, and the fluorescence of **III** is very small. Comparative values of the quantum yields of these compounds, in two different media (ethanol-water 1:4 and ethanol-dimethylformamide 1:4) are shown in Table 1, as well as the wavelengths of maximum excitation and fluorescence.

The influence of pH on the fluorescence intensity of these compounds in ethanol-water media was studied: **II** shows appreciable fluorescence in basic medium, and **I** only in weakly acidic medium; **IV** fluoresces in acidic and basic media, but the spectra are different.¹² Variation of fluorescence intensity with time was investigated for media of different ethanol concentrations. The most suitable concentrations were 30–40% for **II** and 35–50% for **III**.

The fluorescence properties of the metal complexes formed by **I**, **II** and **III** were investigated. Complexes formed by **I** and **III** with metal ions have similar fluorescence properties to the ligands themselves, so they are not analytically useful. **II** forms a fluorescent complex only with zinc (λ_{exc} 460 nm, λ_n 520 nm); a detailed pH study showed that this complex has its highest fluorescence intensity at pH 9.5–11.5. The stoichiometry of the zinc-**II** complex was determined by Job's method (with fluorimetric measurement), and found to be 1:3 Zn-ligand. Unfortunately, the poor sensitivity of this reaction and the effect of foreign ions preclude its use in fluorimetric analysis.

Oxidation of 3-OH-PAT with hydrogen peroxide

Only compounds **II** (3-OH-PAT) and **III** (3-OH-PAA) can be oxidized easily by hydrogen peroxide to give fluorescent compounds. 3-OH-PAT exhibits a green fluorescence in basic medium but, in the presence of hydrogen peroxide, the fluorescence changes slowly, probably owing to formation of a new compound; this compound shows an excitation band at 370 nm, and a fluorescence band at 430 nm.

Catalytic effects of metal ions on this reaction were investigated. The reaction rate increases appreciably in the presence of traces of manganese(II), but only in ammoniacal media, so a systematic study was

Table 1. Values of quantum yields of fluorescence

Compound	Ethanol-water (1:4)		Ethanol-dimethylformamide (1:4)	
	λ_{exc}/λ_n , nm	ϕ	λ_{exc}/λ_n , nm	ϕ
I	380/435	0.93	—	—
II	410/460	0.01	410/475	0.55
III	—	—	465/540	10^{-4}
IV	435/470	0.02	370/440	0.02

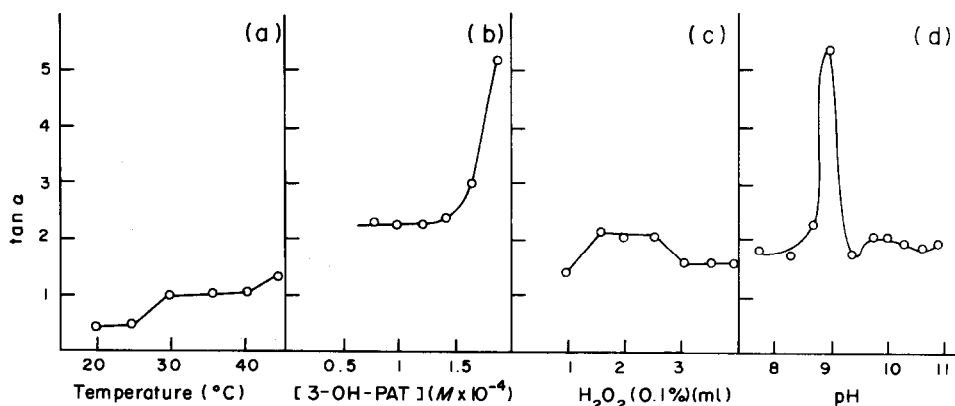


Fig. 1. Influence of experimental variables on the oxidation of 3-OH-PAT catalysed by Mn(II). (a) Variation of the initial reaction-rate with temperature. (b) Influence of the concentration of 3-OH-PAT, (c) Influence of the concentration of H_2O_2 . (d) Influence of pH. (Concentration of manganese: 50 ng/ml in all cases).

made, to determine the experimental variables involved in the oxidation of 3-OH-PAT.

Temperatures. The influence of temperature on the initial rate was determined and the results are plotted in Fig. 1(a). The range 20–25 $^{\circ}$, in which, apparently, the reaction rate obtained by fluorescence measurements remains unaltered, is the most convenient.

Reagent concentration. Results are shown in Fig. 1(b). As may be observed, the reaction order is zero with regard to the reagent for the interval $0.8\text{--}1.2 \times 10^{-4} M$. A $10^{-4} M$ concentration of 3-OH-PAT was chosen to establish the determination conditions.

Hydrogen peroxide concentration. Samples were prepared in 25-ml standard flasks with different volumes of 0.1% hydrogen peroxide solution [Fig. 1(c)]. The reaction rate remains unaltered if the volume added is ≥ 3 ml, so the optimum concentration of H_2O_2 is $\geq 3.5 \times 10^{-3} M$.

pH. Results of the optimization of pH are given in Fig. 1(d). The optimum pH (minimum reaction

order) was found to be 9.6–10.0 (ammonia buffer). For this reason, this pH interval was chosen for the present study. Other buffers are not adequate for the purpose.

Oxidation of 3-OH-PAA

3-OH-PAA exhibits a very weak fluorescence in solution (see Table 1). However, in the presence of hydrogen peroxide, a new product (much more fluorescent; $\lambda_{\text{exc}} 325$, $\lambda_{\text{fl}} 390$ nm) is formed very slowly. When traces of manganese(II) are present, in ammoniacal media, the reaction rate increases, owing to the catalytic action of this metal ion. A study of the variables involved in this oxidation was made in the same way as for 3-OH-PAT.

The results obtained on the influence of temperature, reagent concentration, oxidant concentration and pH are plotted in Fig. 2. The optimal values found are $1.2\text{--}1.6 \times 10^{-6} M$ 3-OH-PAA; $0.5\text{--}3.5$ ml of 0.5% H_2O_2 solution; temperature $30\text{--}40^{\circ}$; pH 9.4 (ammonia buffer).

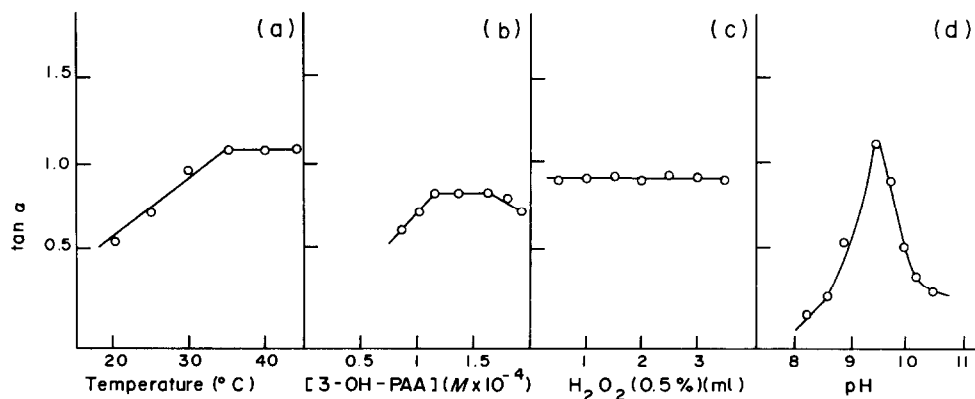


Fig. 2. Influence of experimental variables on the oxidation of 3-OH-PAA catalysed by Mn(II). (a) Variation of the initial reaction-rate with temperature. (b) Variation of the initial rate with concentration of 3-OH-PAA. (c) Influence of the concentration of H_2O_2 . (d) Influence of pH. (Concentration of manganese: 0.9 $\mu\text{g/ml}$ in all cases).

Table 2. Interference levels of foreign ions in the determination of manganese with 3-OH-PAT

Tolerance ratio ion/Mn(II), w/w	Foreign ions
100	Alkali and alkaline-earth metals
60	SCN ⁻
40	Al(III), Pb(II), Sn(II), F ⁻
20	Ga(III), Pd(II), CN ⁻
10	Ag(I), Bi(III), V(V), Os(IV), C ₂ O ₄ ²⁻
5	Mo(VI)
2.5	Ni(II), Co(II), Cu(II), Cr(III), Sb(III), Zn(II), Cd(II)
0.5	Fe(III)

Table 3. Interference levels of foreign ions on the determination of manganese with 3-OH-PAA

Tolerance ratio ion/Mn(II), w/w	Foreign ions
100	Alkali metals
50	SCN ⁻
30	Ca(II), Mg(II), Ba(II), F ⁻
25	Pb(II), CN ⁻
15	Al(III), W(VI), C ₂ O ₄ ²⁻
3	Mo(VI), Os(IV)
2	Bi(III), Sn(II), Sb(III), Ga(III), In(III), Tl(I), Zr(IV), La(III)
1	V(V), Ag(I), Cr(III)

Nature of oxidation products

Oxidation of 3-OH-PAT must be similar to the oxidation of salicylaldehyde thiosemicarbazone⁸ by hydrogen peroxide, and the corresponding semicarbazone is probably formed. 3-Hydroxypicolinaldehyde semicarbazone has been synthesized by us, and exhibits a fluorescence spectrum similar to the oxidation product of 3-OH-PAT (λ_{exc} 370, λ_{fl} 430 nm).

On the other hand, the oxidation product of 3-OH-PAA is probably 3-hydroxypyridine-2-carboxylic acid. Attempts were made to obtain this compound, but its high solubility made its isolation impossible. However, we have oxidized with hydrogen peroxide a similar compound, pyridine-2-aldehyde azine, and have isolated easily the copper salt of the pyridine-2-carboxylic acid formed. Elemental analysis confirmed its nature (found: C 46.4%, H 2.8%, N 9.5%; calculated for C₁₂H₈O₄N₂Cu: C 46.82%, H 2.68%, N 9.11%).

Kinetic determination of manganese with 3-OH-PAT

The initial-rate method was used in all determinations. The calibration curve was linear for the manganese concentration range between 5 and 50 ng/ml. The error was $\pm 3.0\%$ ($P = 0.05$; $n = 11$). The interferences are given in Table 2. The interference of iron(III) was severe, but addition of small amounts of fluoride (0.5–1.0 ppm) made possible the determination of manganese in presence of a 5-fold amount of iron. Nitrate, chloride, sulphate and perchlorate, up to at least 100 ppm, do not interfere.

Kinetic determination of manganese with 3-OH-PAA

The fixed-time method is the most convenient in this case, and was used in all determinations. In this method, a set time of 2 min is recommended; the calibration curve is linear for Mn(II) concentrations from 0.4 to 0.9 ppm. The error is $\pm 2.0\%$ ($P = 0.05$; $n = 11$).

Interferences in this method are given in Table 3 and show that the tolerance levels for anions are similar in both methods.

REFERENCES

1. Z. Holzbecher, *Chem. Listy*, 1955, **49**, 1162.
2. M. Deguchi, T. Masumoto, K. Morishige and I. Okomura, *Bunseki Kagaku*, 1979, **28**, 127.
3. K. Morishige, *Anal. Chim. Acta*, 1980, **121**, 301.
4. F. Grases, F. Garcia Sanchez and M. Valcarcel, *Anal. Chim. Acta*, 1980, **119**, 301.
5. F. Grases, J. M. Estela, F. Garcia Sanchez and M. Valcarcel, *Anal. Lett.*, 1980, **13**, 181.
6. M. D. Luque de Castro and M. Valcarcel, *Talanta*, 1980, **27**, 645.
7. J. L. Ferrer and D. Perez Bendito, *Anal. Chim. Acta*, 1981, **132**, 157.
8. A. Moreno, M. Silva, D. Perez Bendito and M. Valcarcel, *Talanta*, 1983, **30**, 107.
9. A. Garcia de Torres, E. Reina, J. M. Cano Pavon and M. Valcarcel, *Afinidad*, 1980, **37**, 51.
10. J. M. Cano Pavon, A. Lavado and F. Pino, *Mikrochim. Acta*, 1976 **II**, 233.
11. A. Garcia de Torres, M. Valcarcel and F. Pino, *Talanta*, 1973, **20**, 919.
12. J. M. Cano Pavon, M. L. Trujillo and A. Garcia de Torres, *Anal. Chim. Acta*, 1980, **117**, 319.
13. C. A. Parker and W. T. Rees, *Analyst*, 1960, **85**, 587.

SPECTROPHOTOMETRIC DETERMINATION OF CARBON MONOXIDE WITH RUTHENIUM(II) OCTAETHYLPORPHYRIN

A. CORSINI, A. CHAN and H. MEHDI*

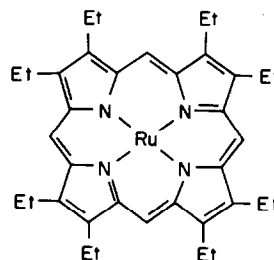
Department of Chemistry, McMaster University, Hamilton, Ontario, Canada

(Received 19 April 1982. Revised 5 August 1983. Accepted 17 August 1983)

Summary—A novel spectrophotometric method for the estimation of carbon monoxide at levels from 2 to 250 ppm is presented. The method is empirical and based on formation of a carbonyl complex of ruthenium(II) octaethylporphyrin and measurement of the difference in absorbance at 393.5 nm between this complex and the porphyrin reagent. Oxygen and nitrogen do not interfere and up to 300 ppm of sulphur dioxide and about 1500 ppm of carbon dioxide can be tolerated in determination of carbon monoxide at the 4 and 10 ppm levels. Hydrogen sulphide interferes and must be removed before the determination. The method has been tested over the range 2–45 ppm of carbon monoxide with 16 synthetic and 2 commercial standard air samples. The average error was $\pm 3\%$. Application to urban-air samples and car-exhaust gases yielded acceptable results. The main disadvantages are the tedious preparation of the initial ruthenium(III)–porphyrin compound and the decomposition of the reagent in the presence of hydrazine.

Synthetic porphyrins are being increasingly used as spectrophotometric reagents for the determination of metal ions at trace levels.¹⁻⁴ Less familiar is the use of metalloporphyrins as selective reagents for gases, especially carbon monoxide. This idea is due to Adler *et al.*⁵ and the first study, which involved the evaluation of the dipiperidine complex of iron(II) *meso*-tetraphenylporphyrin, Fe(II)TPP(pip)₂, for the determination of CO, was reported shortly thereafter.⁶ It was demonstrated that at room temperature, neither oxygen nor nitrogen reacted with Fe(II)TPP(pip)₂ in 1M piperidine and that irreversible air oxidation of Fe(II)TPP(pip)₂ to the μ -oxo-dimer was tolerably slow. The serious drawback was the poor limit of detection, about 300 ppm. Subsequent attempts to improve this limit by replacing piperidine as axial ligand by either sterically-hindered bases or pyridine were not successful.⁶

There have recently been several reports on the formation of stable carbonyl complexes of ruthenium(II) porphyrins.⁷⁻¹⁴ The CO ligand is not only more inert to displacement but also more strongly bound than in the corresponding iron(II) porphyrins.^{13,14} Indeed, Ru(II)TPP(aniline)₂ has been shown to remove carbon monoxide from acetic anhydride to form Ru(II)TPP(CO).¹¹ Also, the affinity of Ru(II)OEP (OEP = octaethylporphyrin) for CO has been demonstrated by its ability to strip CO from the surface of fused quartz.¹⁵ This CO could not be fully removed by baking under reduced pressure or by other chemical agents.



The high affinity of ruthenium(II) porphyrins for CO suggested to us that they might be more sensitive reagents than iron(II) porphyrins for CO. Thus, a study of Ru(II)OEP as a spectrophotometric reagent for CO was undertaken. The structure is shown above. Although the reaction between the Ru(II) porphyrin and CO is incomplete, the results of this study show that this empirical method is still suitable for the determination of CO in two separate ranges, 2–25 and 25–250 ppm v/v. CO₂, SO₂, O₂, N₂ and a few organic species tested do not interfere, even when present in large amounts. H₂S is an interferent and its prior removal from air samples is required. Decomposition of the Ru(II)OEP reagent occurs but the effects of this can be minimized by making the absorbance measurements at specified times.

EXPERIMENTAL

Reagents

Ru₃(CO)₁₂ and OEP were obtained from the Strem Chemical Co. Hydrazine (>95% purity, Kodak) was used fresh, several small ampoules being filled, sealed and refrigerated, and opened as required. CO from small cylinders was used to prepare air samples containing CO. Cylinders of primary-standard CO samples in air, with nominal values of 9.9 and 45 ppm v/v, were supplied by Matheson (Whitby, Canada).

*Present address: Ontario Hydro, Toronto, Ontario, Canada.

All other reagents used were of sufficient purity for the purpose intended.

The principal reagent for the determination is $K[Ru(III)OEP(CN)_2]$. The synthesis of this and of the intermediate compounds $Ru(II)OEP(CO)(CH_3OH)$ and $Ru(II)OEP(py)_2$ ($py = \text{pyridine}$) has been described previously.¹⁵

Apparatus

The gas-line assembly for preparing air samples with various CO contents was essentially that used earlier.⁶ Test mixtures of known amounts of CO in air were prepared (on a volume/volume basis) in a 2-litre gas-mixing flask as before, except that the "Ascarite" tube was not necessary. The mixture in the 2-litre flask was diluted by filling a second 2-litre flask with air to 1 atm pressure, withdrawing a calculated volume of the air through the side septum port with a gas-tight syringe, and replacing it with an equal volume of the initial stock mixture. At least 15 min were allowed for equilibration of the gas mixture in the second flask before samples were withdrawn from it.

All spectrophotometric measurements were made with a GCA McPherson double-beam spectrophotometer, Model EU-700, against methanol or distilled and demineralized water as reference. Stoppered 5-cm matched quartz cells (Helma) were used. About 4.5 ml of solution is sufficient to fill a cell. "Pressure-lok" 10-ml gas-tight syringes (Pierce Chemical Co.) were used to withdraw CO gas-samples from the 2-litre mixing flask and also as the reaction vessel for the subsequent interaction with the $Ru(II)$ porphyrin. The contents of the syringes were agitated with a wrist-action shaker (Burrell).

A portable CO analyser (ECOLYZER, Energetics Science, Inc., Elmsford, New York) was used for measurement of the CO content in urban-air samples and in car-exhaust gases. These measurements were made to provide a convenient, albeit only semi-quantitative, comparison with results obtained by the $Ru(II)OEP$ procedure.

Procedure

The following procedure was used to obtain the calibration graph for 25 ppm CO (maximum) and to test samples for CO content. Exactly 0.500 ml of a $5.0 \times 10^{-5} M$ stock solution of $K[Ru(III)OEP(CN)_2]$ in methanol was delivered into a 10-ml standard flask with a Gilmont micropipette, followed by addition of about 5 ml of methanol. Because the procedure requires critical time control for accurate results, a timetable was scheduled. At time zero, 20 μl of hydrazine (>95%) were transferred to a 10-ml standard flask with an Eppendorf pipette and diluted to the mark with methanol. Two min later, 1 ml of this hydrazine solution was pipetted into the 10-ml flask containing the $K[Ru(III)OEP(CN)_2]$ followed by dilution with methanol to the mark. This was the reagent solution (final concentration of Ru porphyrin, $2.5 \times 10^{-6} M$; of hydrazine, $6.3 \times 10^{-3} M$). Five ml of this were withdrawn into a 10-ml "Pressure-lok" syringe (sample syringe) and the remaining 5 ml were placed in a second "Pressure-lok" syringe for later measurement to provide a correction for reagent absorbance. At 7 min elapsed time, the CO sample (5 ml) was introduced into the syringe through the needle in such a manner that it bubbled through the reagent solution. (The CO sample was drawn into the syringe through the septum of the 2-litre flask, the needle being allowed to remain in the bulb atmosphere for 2 min before the syringe valve was closed). Both syringes were then mounted on the shaker and agitated at speed 7 for 45 min. The solutions were then placed in 5-cm quartz cells and 6 min after completion of the shaking the absorbance of the sample at 393.5 nm was recorded (58 min total elapsed time). The absorbance of the reagent was measured 2 min later.

For calibration graphs and samples in the 25–250 ppm range, the procedure was the same except that 1.00 ml of

$K[Ru(III)OEP(CN)_2]$ was taken, 20 μl of >95% hydrazine were added, the CO was introduced at an elapsed time of 2 or 5 min and shaking was conducted for 5, 15 or 45 min. The absorbances were taken at 11, 28 or 58 min after time zero.

Cleaning of apparatus

The quartz cells, syringes and 2-litre flasks can be cleaned adequately by thorough rinsing with methanol. Tests for possible contamination with CO through surface adsorption were performed with the $Ru(II)OEP$ reagent as described earlier¹⁵ and no memory effects were found. The occurrence of contamination in the previous study¹⁵ was the result of exposure of the surfaces to undiluted CO gas in the absence of $Ru(II)OEP$ reagent. In the present work, dilute mixtures of CO with air were used and the $Ru(II)OEP$ reagent was present. CO has a higher affinity for the reagent than for glass or quartz surfaces.

RESULTS AND DISCUSSION

Solution species and spectra

The spectrum of $K[Ru(III)OEP(CN)_2]$ has been reported previously.¹⁵ The Soret band at 390 nm and the broad less intense absorption band at about 480–560 nm are characteristic of $Ru(III)$ porphyrins.^{11,12} The addition of hydrazine to $K[Ru(III)OEP(CN)_2]$ effects reduction to $Ru(II)$. The Soret band is shifted to 394 nm, with a shoulder at 403 nm [curve (a), Fig. 1]. The 394 nm band (and bands at 498 and 526 nm, not shown in Fig. 1) are typical of $Ru(II)$ porphyrins. Other reductants such as sodium dithionite, sodium borohydride and piperidine were not as effective as hydrazine.

Curve (b) shows the Soret band (393.5 nm) after the solution yielding curve (a) has been agitated for 45 min with an air sample containing 20 ppm CO. If

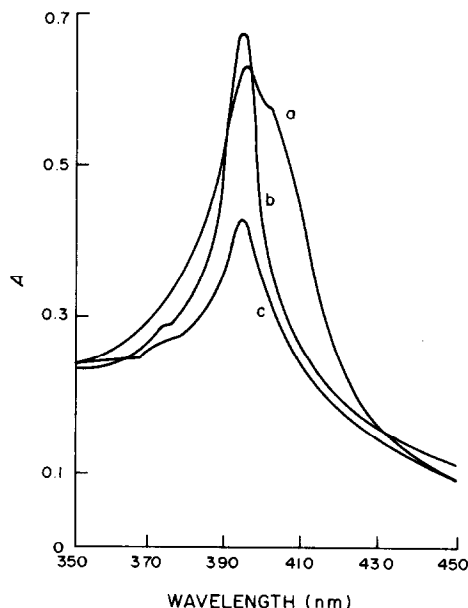


Fig. 1. Spectrum of $Ru(II)OEP(L)_2$ taken 2 min after addition of hydrazine ($6.3 \times 10^{-3} M$) to $K[Ru(III)OEP(CN)_2]$ ($2.5 \times 10^{-6} M$), curve (a); after 45-min contact with air-sample containing 20 ppm CO, curve (b); reagent solution from (a) after 58 min, curve (c).

the reagent solution that yields curve (a) is not contacted with CO but is merely allowed to stand, the absorbance at 394 nm decreases with time. Curve (c) shows the spectrum of the reagent solution after an elapsed time of 58 min. The decrease relative to curve (a), is the result of decomposition of the Ru(II)OEP(L)₂ complex (L = axial ligand) in the presence of a large excess of hydrazine. Evidence that the ligand L is hydrazine has been presented in an earlier study¹⁵ but is not conclusive. Other ligands are possible. For example, the action of hydrazine on aqueous RuCl₃ solutions is known to produce [Ru(NH₃)₅(N₂)Cl]₂. The nitrogen molecule can be replaced by a water molecule and either can be readily displaced by CO.¹⁶ Thus, the action of excess of hydrazine on K[Ru(III)OEP(CN)₂] could produce Ru(II)OEP(L)₂ or Ru(II)OEP(L)(L') in which L and L' can be NH₃, N₂H₄, CN⁻, CH₃OH or H₂O. A nitrogen molecule is a less likely ligand.¹³ Attempts to isolate and to characterize this complex were unsuccessful and were hindered by its decomposition. The decomposition itself appears to involve fragmentation of the porphyrin ring system; after 2 hr, the characteristic porphyrin bands in the Soret and visible regions are greatly reduced in intensity. In contrast to Ru(II)OEP(L)₂, the complex Ru(II)OEP(CO)(L) is stable indefinitely [curve (b)].

Calibration graphs and decomposition of the reagent

This procedure for the determination of CO involves measurement of the difference in absorbance at 393.5 nm between curve (b) and curve (c) in Fig. 1 ($\Delta A_{393.5}$). When the reagent solution is contacted with CO, two processes occur simultaneously: (i) the CO complex is formed, and (ii) the excess of reagent not bound to CO undergoes decomposition. The absorbance of the solution containing CO is at all times greater than that of the reagent solution (Fig. 2). Curve (a) depicts the decomposition of

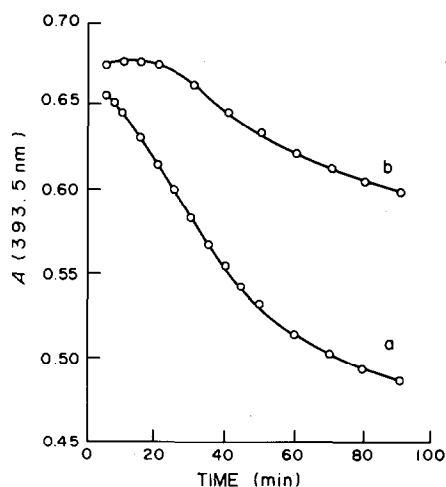


Fig. 2. Decay of absorbance of Ru(II)OEP(L)₂ ($2.5 \times 10^{-6}M$) in the presence of hydrazine ($6.3 \times 10^{-3}M$), curve (a); absorbance of identical solution (5 ml) in presence of an air-sample (5 ml) containing 16.5 ppm CO, curve (b).

Ru(II)OEP(L)₂; the decomposition is complex and the products of the reaction are not known. In the presence of CO [curve (b)], a maximum in absorbance is reached after about 15 min, indicating that the formation of the carbonyl complex is sufficiently fast to cause an overall increase in absorbance at 393.5 nm. Beyond the maximum, the formation of the carbonyl complex is slower and the absorbance decreases, being dominated by reagent decomposition. After about 55–60 min, $\Delta A_{393.5}$ becomes essentially constant. It is reasonable to assume that after this period, the reaction with CO is relatively slow and that the shape of curves is determined mainly by the slow decomposition of the reagent. In the analytical application to 2–25 ppm CO, absorbance measurements were made after 58 min total elapsed time. It was necessary to use fresh hydrazine each time to obtain satisfactory reproducibility. The reagent concentration ($2.5 \times 10^{-6}M$) represents about a 1.5-fold excess relative to 25 ppm CO. However, because only 70% of the Ru(III) compound is reduced under these conditions, and because of reagent decomposition, the effective concentration is obviously lower. The calibration graph obtained (9 points, each in triplicate) was linear up to 25 ppm CO (slope = 0.0122 absorbance per ppm CO; intercept = -0.0043 absorbance). Curvature began at 30 ppm. Each point of the calibration curve was corrected for the fact that the absorbance of the reagent solution was measured 2 min after the absorbance of the CO complex. In a separate experiment, the additional decay in reagent absorbance in this 2-min period was found to be 0.004 ± 0.002 . This amount was added to the reagent absorbance at 60 min and the sum subtracted from the sample absorbance to give $\Delta A_{393.5}$.

For the range 25–250 ppm CO, the reagent concentration was increased to $5.0 \times 10^{-6}M$ and the hydrazine concentration to $6.3 \times 10^{-2}M$. The Ru(III) complex is quantitatively reduced by this concentration of hydrazine. As in Fig. 2, the reagent solution plus CO always has a greater absorbance at 393.5 nm than the reagent solution alone. However, $\Delta A_{393.5}$ is not constant after about 60 min; for example, at 100 ppm CO, $\Delta A_{393.5} = 0.16, 0.24, 0.29$ and 0.34 after 30, 45, 60 and 80 min, respectively. Only after 100–120 min does $\Delta A_{393.5}$ become reasonably constant. Because such a long period reduces the attractiveness of an analytical method, it was decided to investigate the suitability of calibration with shorter reaction times, for the 25–250 ppm range. Agitation intervals of 5, 15 and 45 min were used, with absorbance measurement at 11, 28 and 58 min, respectively. Measurement of the reagent solutions 2 min later led to corrections of 0.009, 0.013 and 0.022, respectively. The corresponding calibration graphs are given in Fig. 3. The calibration graph for the 5-min period [curve (a)] is unsuitable because it lacks sensitivity and is very error-prone. As expected, the curve (c) for the 45-min period is the most sensitive, but the linear range is

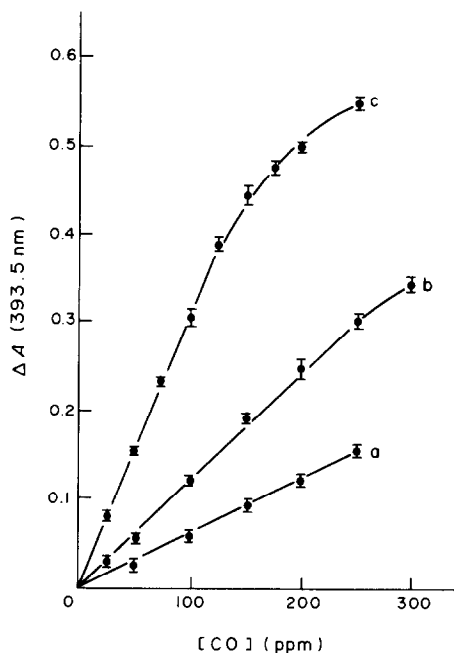


Fig. 3. $\Delta A_{393.5}$ vs. CO concentration (25–250 ppm v/v) for $\text{Ru(II)OEP(L)}_2 = 5.0 \times 10^{-6} M$, and hydrazine = $6.3 \times 10^{-2} M$, as a function of agitation ("reaction") time: 5 min, curve (a); 15 min, curve (b); 45 min, curve (c). All data points were obtained in triplicate.

more limited (25–150 ppm). The 15-min period [curve (b)] is favourable since it yields reasonably large $\Delta A_{393.5}$ values and gives a wide linear working range (25–250 ppm). Accordingly, for the 25–250 ppm range, a 15-min agitation period was used and absorbance measurements of the samples were made after 28 min elapsed time.

The curvature in curves (b) and (c) (Fig. 3) results from a combination of at least two factors: (i) subtraction of the reagent absorbance to obtain $\Delta A_{393.5}$ provides an excessive correction, particularly at the higher CO concentrations in both ranges, where consumption of the reagent by CO is greatest, and (ii) the effect of reagent decay is most sensitive at the higher CO concentrations. Although a correction for the first factor can readily be made by iterative calculation, it leads to little change in the result obtained for CO and so is not worthwhile.

For calibration curve (b), the amount of reagent present is at most only about that stoichiometrically required for 125 ppm of CO, yet the calibration curve is linear up to about 250 ppm. This is because only a fraction of the 250 ppm of CO has reacted by the end of the reaction period. The amount of CO that has reacted depends on several factors: the solubility of CO in methanol, the rate of CO transfer from the gas to the solution phase, the rate of reaction with the reagent, the concentration of reagent and of hydrazine, and the equilibrium constant for the carbonylation reaction. Furthermore, the system cannot have reached overall equilibrium as absorbance changes still occur even after 1 hr. In spite of this, if

Table 1. Determination of carbon monoxide in synthetic air-samples and in primary-standard samples

CO in sample, ppm (v/v)	CO found, ppm (v/v)
2.0	1.9
2.0	2.2
4.0	3.9
4.3	4.6
5.9	5.8
6.3	6.3
8.1	8.2
8.2	8.4
10.0	10.2
10.3	10.2
13.7	13.3
13.7	13.0
16.5	16.4
16.3	16.4
19.7	19.7
20.3	20.3
9.9*	10.1 ± 0.3
45*	45 ± 2

*Commercial primary-standard samples. The results quoted are the average and standard deviation of 10 and 9 determinations for the 9.9 and 45 ppm samples, respectively.

the conditions are rigorously controlled the system yields reliable data for the determination of CO, as shown below. In effect, the method is a fixed-time kinetic method of analysis.

Analytical application and interferences

The calibration curves proved reliable in testing 16 synthetic air-samples and two commercial primary-standard samples for CO (Table 1). The average error was 3%; the largest error was 6%. Duplicate results for the determination of CO in urban air-samples and car-exhaust gases are presented in Table 2. The readings obtained from the portable CO analyser can be regarded only as semi-quantitative; nevertheless, they lend support to the validity of the spectrophotometric method.

Calculation of the detection limit as defined by Kaiser¹⁷ is questionable for this method, as the determination of a conventional blank correction is not straightforward. Because the noise level of the instrument for low signals corresponds to an absorbance no greater than 0.003 and measurement of small $\Delta A_{393.5}$ values with good precision has been

Table 2. Determination of carbon monoxide in urban air-samples and in car-exhaust gases

CO detector reading, ppm (v/v)	CO found, ppm* (v/v)
4–6*	5.0, 4.8
5–7*	5.1, 4.9
15–20*	19.8, 18.3
100 ± 20†	91, 95
170 ± 20†	183, 167

*Air-samples, collected in central Hamilton; CO detector readings were made at the time of collection.

†Car-exhaust samples, collected in a garage, the first representing a shorter time of engine running; CO detector readings were made at the time of collection.

Table 3. Determination of carbon monoxide in synthetic air-samples containing potentially interfering gases

Gas	Conc. taken, ppm (v/v)	CO taken, ppm (v/v)	CO found,* ppm (v/v)	Recovery of CO, %
SO ₂	300	4.1, 4.3	4.2, 4.4	102
	298	10.2, 10.3	10.0, 10.5	100
CO ₂	1565	4.1, 4.3	4.2, 4.4	102
	1572	10.1, 10.2	9.5, 9.8	95
H ₂ S	197	4.1	7.8	190
	197	10.3	13.4	130
Ethane	6900	4.1	4.4, 4.1	104
<i>trans</i> -2-Butene	5700	4.1	3.8, 4.0	95
Freon-114	4670	4.1	3.8, 3.9	93

*By iterative procedure.

demonstrated (e.g., 0.004 ± 0.002), a conservative estimate for the lower limit for $\Delta A_{393.5}$ would be 0.01. This value gives a detection limit of 1 ppm CO for the low-concentration calibration. Experimentally, for 2 ppm, $\Delta A_{393.5}$ is 0.021. By contrast, for the 25–250 ppm range, 25 ppm gives $\Delta A_{393.5} = 0.032$, yielding a lower limit of application of about 8 ppm.

Ru(II)OEP is known to bind O₂ and NO.^{12,13} There is some doubt as to the existence of nitrogen complexes of Ru(II) porphyrins.¹³ Under the conditions of the present study, O₂ and N₂ do not bind to Ru(II)OEP but NO does and could cause interference. Because the background level of NO in air is only 0.0002–0.002 ppm,¹⁸ this interference is not a serious problem. SO₂ and CO₂ in large excess do not interfere, but H₂S causes serious error (Table 3). Smaller amounts of H₂S result in less serious error. If the presence of H₂S is suspected, it should be removed prior to reaction of the sample with the reagent.⁶ The interference by H₂S is not surprising, as alkanethiolate anions (RS⁻) are reported to react with Ru(II)OEP(CO) at the metal centre.¹⁹ Only a few simple hydrocarbons and halocarbons were tested and found not to have an effect at high concentration (Table 3). Formaldehyde at concentrations greater than 400 ppm caused oxidation to Ru(III). Cyclohexane (8000 ppm) and benzaldehyde (1000 ppm) added as liquids to the reagent solution did not interfere.

Limitations and advantages

The Ru(II)OEP method has two serious drawbacks. First, the preparation of K[Ru(III)OEP(CN)₂] is very tedious.¹⁵ Secondly, the Ru(II)OEP(L)₂ complexes are unstable in the presence of hydrazine. The possibility of synthesizing a stable, solid Ru(II)OEP complex (with appropriate axial ligands) that can be stored in a bottle and is sensitive to carbonylation is being pursued. In this regard, it is interesting that a methanolic solution of K[Ru(III)OEP(CN)₂] reacts directly with CO to yield Ru(II)OEP(CO)CH₃OH. Chow and Cohen¹¹ have reported a similar observation with K[Ru(III)TPP(CN)₂], but the reaction proceeds only at high CO concentrations and consequently the sensitivity for CO would be low. Otherwise, such a system would be superior to the system

described here, on account of the stability of Ru(III) compounds.

A less serious disadvantage is the fact that only a fraction of the CO in the sample has reacted by the time the measurement is made. As mentioned earlier, several factors affect the rate and extent of reaction, the solubility of CO in the solvent being one. The solubility of CO is 6 and 10 times greater in perfluorobenzene and perfluoro-*n*-heptane, respectively, than in methanol²⁰ but unfortunately, K[Ru(III)OEP(CN)₂] is insoluble in both solvents. A solid Ru(II)OEP(L)₂ complex might be sufficiently soluble, however.

Colorimetric methods for the determination of CO date back more than 50 years²¹ but are still gaining importance.^{22–27} The major drawbacks of most such methods include insufficient sensitivity, long reaction time and large sample size. The limit of detection is usually 10 ppm or higher, although in one paper²² the detection limit is reported to be 2 ppm. However, this could be achieved only at the expense of using a large sample size (125 ml) and a long reaction time (2 hr). In general, sample sizes range from 50 to 250 ml, and the average reaction time is 2 hr. Compared to the *p*-sulphaminobenzoic acid method, which has been adopted as a tentative²² and a standard method,²⁷ the Ru(II)OEP method requires a shorter time (28 or 58 min, against 2 hr) and a smaller sample (5 ml against 125 ml) and yields at least as favourable a detection limit. It also appears to be less prone to interferences.²⁴

CONCLUSION

The Ru(II)OEP(L)₂ system represents a significant improvement over the Fe(II)TPP(pip)₂ system⁶ for the determination of CO and has advantages over other spectrophotometric and colorimetric procedures. The time-consuming preparation of K[Ru(III)OEP(CN)₂] and the instability of the Ru(II)OEP(L)₂ reagent solution are limitations, however, and for good reproducibility the conditions require to be rigorously observed.

Acknowledgements—The authors wish to thank Mr. Joe Novak for his kind assistance and Dr. O. E. Hileman for

use of the gas-rack assembly. The authors also gratefully acknowledge financial support of this work from the National Science and Engineering Research Council of Canada.

REFERENCES

1. C. V. Banks and R. E. Bisque, *Anal. Chem.*, 1957, **29**, 522.
2. H. Ishii and H. Koh, *Talanta*, 1977, **24**, 417.
3. *Idem*, *Nippon Kagaku Kaishi*, 1978, 390.
4. H. Ishii, H. Koh and K. Kawamura, *ibid.*, 1979, 59.
5. A. D. Adler, V. Varadi and N. Wilson, *Ann. N.Y. Acad. Sci.*, 1975, **244**, 685.
6. S. H. Mehdi and A. Corsini, *Talanta*, 1977, **24**, 291.
7. E. B. Fleischer, R. Thorp and D. Venerable, *Chem. Commun.*, 1969, 475.
8. M. Tsutsui, D. Ostfeld and L. M. Hoffman, *J. Am. Chem. Soc.*, 1971, **93**, 1820.
9. S. S. Eaton and G. R. Eaton, *ibid.*, 1975, **97**, 235.
10. D. C. Whitten and F. R. Hopf, *ibid.*, 1976, **98**, 7422.
11. B. C. Chow and I. A. Cohen, *Bioinorg. Chem.*, 1971, **1**, 57.
12. N. Farrell, D. H. Dolphin and B. R. James, *J. Am. Chem. Soc.*, 1978, **100**, 324.
13. J. W. Buchler, *Angew. Chem. Intern. Ed. Engl.*, 1978, **17**, 407.
14. D. Dolphin, A. W. Addison, M. Cairns, R. K. Dinello, N. P. Farrell, B. R. James, D. R. Paulson and C. Welborn, *Intern. J. Quant. Chem.*, 1979, **16**, 311.
15. A. Corsini, H. Mehdi and A. Chan, *Can. J. Chem.*, 1980, **58**, 527.
16. A. D. Allen, F. Bottomley, R. O. Harris, V. P. Reinsalu and C. V. Senoff, *J. Am. Chem. Soc.*, 1967, **89**, 5595.
17. H. Kaiser and A. C. Menzies, *The Limit of Detection of a Complete Analytical Procedure*, Hilger, London, 1968.
18. G. Robinson and R. C. Robbins, *J. Air Pollut. Contr. Assoc.*, 1970, **20**, 303.
19. H. Ogoshi, H. Sugimoto and Z. Yoshida, *Bull. Chem. Soc. Japan*, 1978, **51**, 2369.
20. E. Wiehelm and R. Battino, *Chem. Rev.*, 1973, **73**, 1.
21. H. Kast and A. Schmidt, *Gas-Wasserfach*, 1927, **70**, 821.
22. American Public Health Association, Inc., *Methods of Air Sampling and Analysis*, 2nd Ed., p. 345, Washington, D.C., 1977.
23. J. C. Lambert and R. E. Wiens, *Anal. Chem.*, 1974, **46**, 929.
24. D. A. Levaggi and M. Feldstein, *Am. Ind. Hyg. Assoc. J.*, 1964, **25**, 64.
25. Z. Burianec and J. Burianová, *Collection Czech. Chem. Commun.*, 1963, **28**, 2895.
26. G. Cinhandu and V. Rusu, *Rev. Chim. (Bucharest)*, 1965, **16**, 601.
27. American Industrial Hygiene Association, *Am. Ind. Hyg. Assoc. J.*, 1972, **33**, 353.

MOLECULAR ABSORPTION SPECTROMETRY (MAS) BY ELECTROTHERMAL EVAPORATION IN A GRAPHITE FURNACE—IX

DETERMINATION OF TRACES OF BROMIDE BY MAS OF AlBr AFTER LIQUID-LIQUID EXTRACTION OF BROMIDE WITH TRIPHENYL TIN HYDROXIDE

K. DITTRICH

Department of Chemistry, Karl-Marx University Leipzig, 7010 Leipzig, D.D.R.

B. YA. SPIVAKOV, V. M. SHKINEV and G. A. VOROBEVA

Vernadsky Institute of Geochemistry and Analytical Chemistry, Academy of Sciences, Moscow V-334,
U.S.S.R.

(Received 8 April 1983. Revised 28 June 1983. Accepted 10 August 1983)

Summary—The determination of traces of bromide by molecular absorption spectrometry (MAS) of AlBr (with electrothermal volatilization) is described. It is possible to determine 25 ng of bromide. Many problems are caused by various matrices, so an extraction method for separation (and also preconcentration) was developed. The combination of bromide extraction with triphenyltin hydroxide, stripping with 0.025M barium hydroxide and determination of the extracted bromide by MAS of AlBr (after addition of aluminium ions) gives a very sensitive and selective method for determination of traces of bromide in micro or macro samples, in the presence of large amounts of other species, including chloride and iodide.

Determination of traces of bromide, especially in samples of complex composition, is a difficult practical problem.¹ Sensitive determination of bromide is possible by applying molecular absorption spectrometry (MAS) to thermally stable diatomic bromide-containing molecules,²⁻⁴ such as GaBr, InBr,^{3,5} TlBr,³ AlBr⁴ generated by volatilization in a graphite furnace. The technique is similar to atomic-absorption spectrometry by electrothermal atomization. A disadvantage of MAS as an analytical method is the significant interference effect of the matrix on the molecular absorption signals and the background. It is expedient, therefore, to combine MAS of Br-containing molecules with a suitable method of separation of bromide ions from other components.

Because solutions are used as samples in MAS it is convenient to combine MAS with liquid-liquid extraction separation,⁶ which also offers possibilities for enhancement of the sensitivity by preconcentration.

The extractants commonly used for anions, such as organic oxygen compounds and high molecular-weight amines, are not effective enough for bromide extraction.^{7,8} Bankovsky *et al.* have shown that heptane solutions of amymercury(II) salts quantitatively extract bromide over a wide acidity range, from pH 9 to 15M sulphuric acid,⁹ but this high extraction power makes stripping difficult, and the reagent also extracts chloride and iodide. Bock *et al.*,^{10,11} and

Schweitzer and McCarthy¹² have studied the extraction of halide ions with triphenyltin hydroxide (TPTH) and triphenyl-lead hydroxide into benzene, chloroform and methyl isobutyl ketone (MIBK). It has been shown that these reagents extract bromide quantitatively over the pH range 1-4; extraction from more acidic solutions has not been examined, nor has the possibility of preconcentration of bromide ion and its separation from large amounts of metal cations and other anions.

In this work we have studied the determination of bromide by MAS of AlBr, without and with solvent extraction of bromide by TPTH and stripping with aqueous barium hydroxide solution.

EXPERIMENTAL

Instruments

The molecular absorption was measured with a Jarrell Ash type 811 two-channel double-beam AA-spectrometer and a Beckman graphite furnace, type 1268. The light source was a hydrogen hollow-cathode lamp run at 35 mA. The measurement was made at 278.9 nm. For background-correction the two-line method was used, with a non-specific wavelength of 281 nm.

The distribution of bromide between the organic and aqueous phase was estimated radiometrically with ⁸²Br. The radiochemical purity of the ⁸²Br was tested by means of a Nokia Ge(Li)-detector and an 800-channel analyser (LP 4840) as well as from the half-life measurements. The radioactivity of the organic and aqueous phase was measured on a Tesla Liberec NRG 603 automatic gamma spectrometer.

Table 1. Results of extraction of bromide ions by TPTH solution

C_{Br}, M	5.6×10^{-8}	1×10^{-4}	1.1×10^{-3}	1×10^{-2}	2×10^{-1}
Recovery, %	99.7	99.8	99.3	55.6	5.4

Reagents

TPTH solutions were prepared by equilibration of 0.03M triphenyltin chloride solution in a suitable diluent (*e.g.*, *o*-xylene) with several portions of aqueous 0.1M sodium hydroxide (in 1:1 organic to aqueous phase ratio) until chloride was no longer detectable in the stripping solution. The organic phase was washed free from hydroxide with water and then filtered. Unless otherwise noted, the concentration of TPTH in the diluent was 0.03M, and the concentration of bromide in the aqueous solutions used in the extraction study was $5-10 \times 10^{-7}M$.

Other stock reagent solutions used were of aluminium nitrate (Al^{3+} 10 mg/ml), sodium hydroxide (0.1M); barium hydroxide (0.05M), sodium bromide (Br^- 1 mg/ml), sodium chloride, iodide, sulphate and monohydrogen phosphate (anion 10 mg/ml), metal nitrates [metal (K^+ , Mg^{2+} , Ga^{3+} , In^{3+} , Co^{2+} , Ni^{2+} , Cu^{2+} , Zn^{2+}) 10 mg/ml].

Procedures

Measurement of absorption spectra. The molecular absorption was measured between 290 and 275 nm, point by point at 0.1-nm intervals in the 277–280 nm region (means of five values) and at 1-nm intervals elsewhere.

Analytical investigations without extraction. Aliquots (10 μ l) of solutions containing bromide, aluminium and barium were injected into the graphite furnace. After drying and ashing, the solid was evaporated to give the so-called evaporation phase (the equivalent atomization phase in atomic-absorption spectrometry) and the molecular absorption of AlBr was measured.

Analytical determinations with extraction. Stoppered glass test-tubes or separatory funnels were used in studying the distribution of the elements between the phases. The extraction was done with various phase-volume ratios. For $V_o = V_{aq}$, the volume of each phase was 3 ml. The extraction studies were done at room temperature, and the phases were shaken together for 3 min (it was found in preliminary work that the equilibrium was attained in less than 3 min for all the systems studied). An aliquot of each phase was used for the radioactivity measurements, from which the recovery factors ($R\%$) were estimated. For the stripping 0.05M barium hydroxide was used. After separation of the stripping solution an appropriate volume of aluminium solution was added and the solution was injected into the graphite furnace.

RESULTS AND DISCUSSION

Investigation of the extraction

The extraction of bromide by 0.03M TPTH in *o*-xylene and MIBK from nitric acid and sulphuric acid medium with a 1:1 phase-volume ratio was examined. The recovery factors with use of *o*-xylene were greater than 99.5% over the nitric acid concentration range 0.01–5M. With MIBK the R values were lower, and *o*-xylene was used as the diluent in all subsequent experiments. Bromide was also quantitatively extracted from 0.01–2M sulphuric acid ($R = 99.3\%$), but at sulphuric acid concentrations higher than 0.1M precipitates formed in the organic phase. No precipitate formed in the extraction from nitrate media. The recovery factors were not lower

than 99.7% for bromide extraction from 0.3M sodium, potassium, lithium, lead, cobalt and nickel nitrate solutions in 0.3M nitric acid at $V_o:V_{aq} = 1$, with practically no extraction of the cations.

The results (see Table 1) for the extraction of bromide from 0.01M nitric acid as a function of bromide concentration in the initial aqueous solution (C_{Br}) show that extraction by 0.03M TPTH in *o*-xylene was quantitative for $C_{Br} < 1 \times 10^{-3}M$. The possibility of preconcentration of bromide by extraction with different $V_o:V_{aq}$ ratios is shown in Table 2. It is also seen that TPTH allowed simultaneous separation of bromide from large amounts of metal cations and concentration before subsequent determination.

Table 2. Recovery values in the extraction of bromide ions by 0.03M TPTH in *o*-xylene

Aqueous phase	$V_o:V_{aq}$	Recovery R , %
0.01M HNO_3	1:1	99.6
	1:5	97.9
	1:10	96.3
0.01M HNO_3 , 0.3M KNO_3	1:5	99.4
	1:10	98.5
0.01M HNO_3 , 0.3M $Ni(NO_3)_2$	1:5	99.4
	1:10	98.1

Br^- concentration 10^{-4} – $10^{-5}M$.

Table 3. Recovery values for the extraction of bromide ions by 0.03M TPTH in *o*-xylene from HNO_3 in the presence of foreign anions

Foreign anion	Concentration of foreign anion, M	Recovery, %		
		0.01M* HNO_3	0.1M† HNO_3	1.0M† HNO_3
F^-	10^{-4}	99.2		
Cl^-	10^{-3}	99.8	99.7	99.9
	3×10^{-3}		99.7	98.5
	10^{-2}	96.5	72	74.6
	10^{-1}	19.3		
I^-	10^{-3}	99.7	99.7	99.9
	3×10^{-3}		99.6	99.5
	10^{-2}	99.2	19.0	18.8
	10^{-1}	4.0		
PO_4^{3-}	10^{-3}	99.8		
	10^{-2}	61.5	99.0	99.5
	3×10^{-2}		98.7	99.1
	10^{-1}	2.3	83.7	99.9
SO_4^{2-}	10^{-3}	99.9		
	10^{-2}	99.9	99.0	99.6
	3×10^{-2}		99.9	98.5
	10^{-1}	99.7	99.9	—
	1.0	99.7		

* $V_o:V_{aq} = 1:1$.

† $V_o:V_{aq} = 1:5$.

Table 4. Recovery values in the stripping of bromide ions from the organic extracts (in 0.03M TPTH/*o*-xylene)

Stripping agent	Concentration, M	Recovery, %	
		$V_o = V_{aq}$	$V_o = 2V_{aq}$
NaOH	10^{-3}	—	0.4
	10^{-2}	99.9	98.0
	10^{-1}	99.9	—
Ba(OH) ₂	10^{-3}	—	0.2
	10^{-2}	99.9	99.9
	10^{-1}	99.9	99.9

In contrast to metal cations, anions which are extracted by organotin extraction agents^{10,12,12} can interfere with the extraction of bromide, as shown in Table 3.

The decrease in extraction of bromide with increasing concentration is due to competition for the reagent. A precipitate of TPT fluoride forms in the organic phase at fluoride concentrations higher than $10^{-4}M$ in the aqueous phase, which is why the extraction at higher fluoride concentrations was not examined. It should be noted that in contrast to the sulphuric acid system, no precipitate formed at high sodium sulphate concentrations in the aqueous phase. It is also noteworthy that phosphate depressed the extraction of bromide from 0.1M nitric acid, but not from more acidic solutions. Therefore, the extraction of phosphate and iodide (which strongly affects the extraction of bromide) from 0.01 and 1M nitric acid was studied at anion concentrations (C_{An}) of $1 \times 10^{-3}M$, with ³²P and ¹³¹I as radioactive tracers.

It was found that more than 99% of the iodide was extracted in both cases, but the recovery factor for the phosphate decreased from 93.4% (0.01M HNO₃) to 1.5% (1M HNO₃). This explains the quantitative extraction of bromide at high phosphate concentrations from 1M nitric acid. Protonation of the phosphate results in formation of phosphoric acid, which is not extracted by TPTH and does not suppress the extraction of bromide.

The stripping of bromide into aqueous sodium or barium hydroxide solution was studied (Table 4). Both hydroxides proved effective stripping agents, so the extracts could be directly analysed by MAS. Additional preconcentration could be achieved in the stripping step.

Investigation of molecular absorption of AlBr (without extraction)

The absorption spectrum was investigated by use of solutions with the composition Al³⁺ 1 μg, Ba²⁺ 30 μg, Br⁻ 0.5 μg in 10 μl sample volume. The spectrum was measured between 290 and 275 nm, and is shown in Fig. 1. The maximum of the AlBr absorption band was between 278.9 and 279.1 nm, in agreement with the literature,¹⁴ which gives λ_{max} as 278.9 nm for the C-band system ($X^1\Sigma^+ - AII$; v'/v'' : 0/0 278.9 nm; 1/1 279.1 nm).

Because the band was narrow, it was possible to correct the background by difference measurement with the two-line method (279.1/281 nm).

Optimization of thermal conditions

In a general account of optimization of metal bromide molecule formation^{2,15} it was stated that the choice of temperature for the drying, ashing and evaporation is very important, to avoid losses of bromide ions in the first two steps and to obtain simultaneous evaporation of the metal and bromine species in the third step.

We therefore investigated the influence of the temperature of the ashing and evaporation steps and found that the ashing temperature should not be higher than 900°. The best evaporation temperature was the maximum temperature of the graphite furnace (about 3300°) (see Fig. 2), in spite of the fact that the dissociation energy of the AlBr molecule is not very high (4.5 eV),¹⁴ and this molecule may dissociate at high temperature. The reason for use of this high temperature is the poor and late evaporation of the aluminium species.

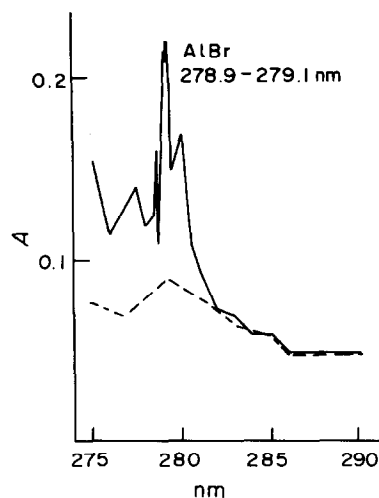


Fig. 1. Molecular absorption spectra of the AlBr molecule (measurement point by point). (—): Al³⁺ 1 μg, Ba²⁺ 27 μg, Br⁻ 0.5 μg in 10 μl; (---): Al³⁺ 1 μg, Ba²⁺ 27 μg in 10 μl.

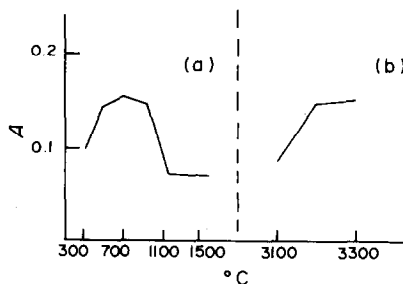


Fig. 2. Dependence of AlBr MA on the temperature of ashing (a) and evaporation (b): (a) evaporation temperature 3300°; (b) ashing temperature 800°.

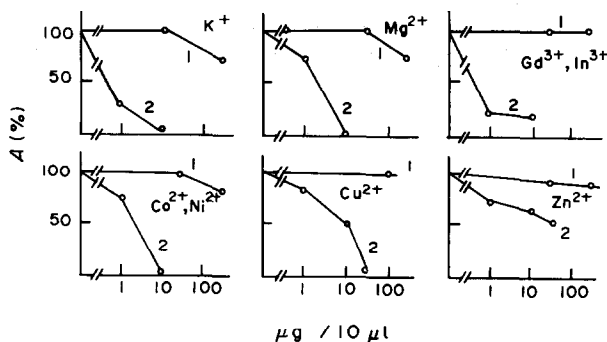


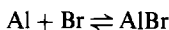
Fig. 3. Dependence of AlBr MA on the presence of other cations (as nitrates): 1, with preliminary extraction of Br^- from $0.1M$ HNO_3 by $0.03M$ TPTH in *o*-xylene; 2, without extraction.

Optimization of the chemical conditions

The addition of barium hydroxide solution up to a concentration of $0.025M$ to give a pH of 10–12 influenced the height of the AlBr signal by decreasing the loss of bromide by volatilization as hydrogen bromide (see also Dittrich and Meister¹⁵). After drying, the solid residue contained barium, bromide, hydroxide and nitrate, all of which are thermally stable. Losses of bromide as HBr by thermal hydrolysis in the ashing phase were avoided.

At the high temperature of the ashing step the substances formed reacted with the graphite of the tube. Hence the rate of volatilization of the bromide-containing particles was reduced. Because aluminium is difficult to vaporize, it evaporates late in the evaporation step, so the decreased rate of vaporization of bromine species was very useful for ensuring simultaneous evaporation of both species. Thus one prerequisite for the formation of a high AlBr concentration in the gas phase was fulfilled.

Next we investigated the influence of the aluminium and barium hydroxide concentrations on the molecular absorption of AlBr. The molecular absorption signal for AlBr increased with increased concentrations of both substances. At high aluminium concentrations the equilibrium



is shifted to the right, and high barium hydroxide concentrations minimize loss of bromide ions. Very high concentrations of these substances are not so efficient, however, because both substances form stable carbides with the carbon of the graphite tube. Evaporation of the very involatile carbides and of the stable double oxides formed enhances the background signal during the evaporation step. The optimal concentrations are $1 \mu\text{g}$ of aluminium and $30 \mu\text{g}$ of barium in $10 \mu\text{l}$ of sample.

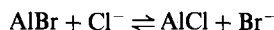
Influence of other cations

In Fig. 3 the very strong influence of certain cations is shown. They decrease the AlBr molecular absorption signals for various reasons. The effect of potas-

sium is due to formation of thermally stable KBr in the gas phase and formation of the easily volatilized KBr as a solid residue in the graphite cuvette, which prevents simultaneous evaporation of bromine and aluminium species. In the case of Mg^{2+} , Ga^{3+} , In^{3+} , Co^{2+} , Ni^{2+} and Zn^{2+} ions, which form only unstable diatomic molecules with bromine, decrease in the AlBr molecular absorption signals is caused by losses of bromide as HBr by thermal hydrolysis in the drying and ashing steps.

Influence of other anions

In Fig. 4 the influence of certain anions is shown. Chloride and iodide also form diatomic molecules with aluminium in the gas phase. Because the dissociation energy of AlCl (5.1 eV) is higher than that of AlBr (4.5 eV) and AlI (3.8 eV) the presence of chloride shifts the equilibrium



to the right and the concentration of AlBr molecules in the gas phase is decreased.

Measurements in the presence of an excess of sulphate are impossible because the insoluble barium sulphate formed affects volatilization of the bromine species. Phosphate at higher concentrations also

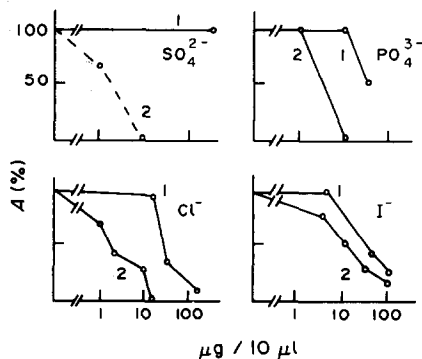


Fig. 4. Dependence of AlBr MA on the presence of other anions (as sodium salts): 1, with preliminary extraction of Br^- from $0.1M$ HNO_3 by $0.03M$ TPTH in *o*-xylene; 2, without extraction.

Table 5. Results of bromide determination of AlBr MA with and without preliminary extraction of bromide (linear range 25–500 ng)

Sample volume, μl	Absolute reciprocal sensitivity ng for 0.01 A	Relative reciprocal sensitivity	
		ppm	M
Without extraction			
10	25	2.5	3.1×10^{-5}
40	25	0.31	7.5×10^{-6}
With extraction			
10*	25	0.5	6.2×10^{-6}
40*	25	0.125	1.6×10^{-6}
10†	25	0.25	3.1×10^{-6}
40†	25	0.031	7.5×10^{-7}

*Initial sample 10 ml, preconcentration factor 5:1.

†Initial sample 20 ml, preconcentration factor 10:1.

forms insoluble salts [e.g., $\text{Ba}_3(\text{PO}_4)_2$] and affects the formation of barium bromide residues. At low phosphate concentration the signals are lowered because of volatilization of hydrogen bromide by the much less volatile phosphoric acid.

Because of these effects of cations and anions, MAS is not convenient for direct analysis of complex samples. We therefore decided to combine it with a prior separation of the bromide.

Analytical results

Pure solutions. First we established the dependence of the AlBr signal on the bromide concentration under the optimal analytical conditions (see above). A linear calibration graph was obtained. The analytical data are given in Table 5. The blank value of 0.025 absorbance units cannot be compensated for. The reciprocal sensitivity is 25 ng of bromide for an absorbance of 0.01, which means that it is possible to determine 2.5 ppm of bromide in 10 μl of aqueous solution ($3.1 \times 10^{-5}M$). To a first approximation this reciprocal sensitivity is comparable to the detection limit. It is possible to improve the concentration detection limit by using a greater sample volume. The absolute amounts of aluminium and barium used should be the same as for the 10- μl sample. We found the same absolute detection limit (25 ng) for a sample volume of 40 μl , which gives a concentration detection limit of 0.3 ppm (or $0.75 \times 10^{-6}M$). The statistical detection limit gives an absorbance of about 0.01. Extraction was used in conjunction with the AlBr determination by shaking a 10 or 20 ml

sample (in 0.1M nitric acid) with 4 ml of 0.03M TPTH solution in *o*-xylene. After separation, a known volume of the organic phase (e.g., 3.0 or 3.5 ml) was pipetted and stripped with half its volume of 0.025M barium hydroxide. After separation, 1 ml of the aqueous solution was pipetted, 0.01 ml of 10-mg/ml aluminium solution was added, and the AlBr molecular absorption was measured. The results are shown in Table 5. Comparison of the results with and without extraction show that it is possible to improve the relative reciprocal sensitivity of the bromide determination by about one order of magnitude by extraction. This sensitivity is adequate for trace determinations and compares well with that of other methods (e.g., the ISE method).

Solutions containing other anions. The effect of other anions is shown in Fig. 4. Chloride and iodide strongly depress the AlBr signals, whether extraction is used or not. Without extraction it is possible to determine traces of bromide in the presence of a 100-fold amount of iodide and 10-fold amount of chloride. Extraction gives an improvement, especially for chloride, which is extracted less efficiently than bromide. With extraction 25 ng of bromide can be determined in presence of a 500-fold amount of chloride and 200-fold amount of iodide. These results are very good in comparison with those for other methods.

The direct determination of bromide in presence of sulphate is impossible, because the sulphate forms insoluble barium sulphate with the barium added. If 0.01M nitric acid medium is used, sulphate is not extracted by the organic TPTH solution, so the sulphate interference is avoided. Bromide determination in presence of more than 1000-fold amount of sulphate is possible.

Bromide can be directly determined in presence of phosphate in up to 40-fold ratio. Extraction from 1.0M nitric acid, from which phosphoric acid is not extracted, gives a larger tolerance for phosphate.

Solution containing other cations. Figure 3 shows the strong influence of many cations on the AlBr signal. Separation of the bromide from these cations

Table 6. Results of bromide determination by AlBr MA with extraction in presence of other salts

Salt	Detection limit, ppm	Salt	Detection limit, ppm
KNO_3	2	$\text{Ni}(\text{NO}_3)_2$	1.3
$\text{Mg}(\text{NO}_3)_2$	1.5	$\text{Co}(\text{NO}_3)_2$	1.3
$\text{Ga}(\text{NO}_3)_3$	2.5	$\text{Cu}(\text{NO}_3)_2$	1.5
$\text{In}(\text{NO}_3)_3$	2.1	$\text{Zn}(\text{NO}_3)_2$	1.7

can improve the detection limit by a factor of up to 1000.

By using the best conditions and a sample concentration of about 0.1–0.3M, it is possible to determine bromide traces in some metal nitrates in the ppm range. The results are shown in Table 6.

In conclusion, we can say that the combination of extraction with the selective determination by means of AlBr molecular absorption is a useful new technique for the determination of traces of bromide.

REFERENCES

1. N. G. Polyansky, *Analytical Chemistry of Bromine* (in Russian), Nauka, Moscow, 1980.
2. K. Dittrich, *Prog. Anal. Atom. Spectrosc.*, 1980, **3**, 209.
3. K. Dittrich and S. Schneider, *Anal. Chim. Acta*, 1980, **115**, 189.
4. K. Tsunoda, K. Fujiwara and K. Fuwa, *Anal. Chem.*, 1978, **50**, 861.
5. K. Dittrich, *Anal. Chim. Acta*, 1978, **97**, 59.
6. Yu. A. Zolotov and N. M. Kuz'min, *Preconcentration of Microelements* (in Russian), Khimiya, Moscow, 1982.
7. Z. I. Nikolotova and N. A. Kartasheva, *Liquid-Liquid Extraction by Neutral Organic Compounds* (in Russian), Atomizdat, Moscow, 1976.
8. E. A. Mezhov, *Liquid-Liquid Extraction by Amines and Amine and Quaternary Ammonium Salts* (in Russian), Atomizdat, Moscow, 1977.
9. Yu. A. Bankovsky, O. E. Veveris, Ya. A. Ashaks, A. P. Pelne and R. S. Mizere, *XIth Mendeleev Meeting on Pure and Applied Chemistry: Summaries of Papers and Communications*, No. 5, p. 18. Nauka, Moscow, 1975.
10. R. Bock, H. T. Niederauer and K. Behrends, *Z. Anal. Chem.*, 1962, **190**, 33.
11. R. Bock and H. Deister, *ibid.*, 1967, **230**, 321.
12. G. K. Schweitzer and S. W. McCarthy, *J. Inorg. Nucl. Chem.*, 1965, **27**, 191.
13. B. Ya. Spivakov, V. M. Shkinev and Yu. A. Zolotov, *International Solvent Extraction Conference, Liege 1980, Summaries of Papers*, Vol. 2, Paper No. 80-85.
14. B. Rosen, *Spectroscopic Data Relative to Diatomic Molecules, International Tables of Selected Constants*, Vol. 17, Pergamon Press, Oxford, 1970.
15. K. Dittrich and P. Meister, *Anal. Chim. Acta*, 1980, **121**, 205.

DETERMINATION OF LOW LEVELS OF BROMIDE IN FRESH WATER AFTER CHROMATOGRAPHIC ENRICHMENT

ULLA LUNDSTRÖM, ÅKE OLIN and FOLKE NYDAHL

Department of Analytical Chemistry, University of Uppsala, P.O.B. 531, S-751 21 Uppsala, Sweden

(Received 24 May 1983. Accepted 30 July 1983)

Summary—A method has been developed for the determination of bromide in fresh water. The analyte is enriched on the anion-exchanger Dowex 1 × 8, which exhibits a considerably greater affinity for bromide than for the major anions in fresh water. Sodium perchlorate is used as eluent and an enrichment factor of ~100 can be achieved. The eluted bromide is oxidized with peroxodisulphate to bromate, which is determined iodometrically by a previously published spectrophotometric method. The enrichment in the presence of the major components of fresh water has been studied. Only bicarbonate has been found to interfere, but this interference can be avoided by acidifying the sample with hydrochloric acid. The recovery from synthetic fresh water with ionic concentrations corresponding to 0.005 equivalent/l. and spiked with bromide was 100% at bromide concentrations larger than 50 nM (4 µg/l.) and about 90% at 10 nM. The detection limit is 1.5 nM and the limit of determination 5 nM for 1-litre samples.

The mean content of bromide in fresh water has been estimated to be about 10 µg/l.¹ With the exception of neutron-activation analysis, there seems to be no method available for the accurate determination of bromide at this concentration level. Recently two investigations have been reported on the determination of bromide in fresh water by ion chromatography.^{2,3} With a sample volume of about 5 ml and a bromide-selective electrode as detector, bromide concentrations around 30–50 µg/l. were determined. The precision was reported to be 2–4% at the 50-µg/l. level. The accuracy is difficult to assess but is probably not better than 10% error. A number of colorimetric methods⁴ are available for the determination of bromide. They are based on oxidation of bromide to bromine, which is then reacted with an added dye; the ensuing change in absorbance is used for determining the bromide. These methods require a bromide concentration exceeding about 100 µg/l. and the accuracy may be affected by organic material as well as inorganic constituents in the sample. The Phenol Red method has recently been automated by segmented-flow analysis.⁵ Chloride interferes in this method and must be corrected for. The detection limit is 10 µg/l.

Thus it seems necessary to employ some method of enrichment before the final determination. In the method reported here, bromide is chromatographically enriched on the chloride form of Dowex 1 × 8, which has considerably higher affinity for bromide than for the major anions of fresh water. After elution with the strongly displacing perchlorate ion, the bromide is spectrophotometrically determined (by production of an equivalent amount of iodine), according to a previously published method,⁶ which has a sensitivity of 2.25 absorbance units per

µmole of bromide (this means that the bromide content of about 350 ml of fresh water of "average" composition should be accumulated in order to obtain an absorbance of 0.1).

EXPERIMENTAL

Apparatus

The ion-exchanger tube was made with a cylindrical funnel at the top, ~70 mm long and wide enough to accommodate the mouth of an inverted 1-litre standard flask. The tube itself was 200 mm long and 8 mm in bore, and was drawn out to a tip with a 1-mm bore tip. Though the resin bed, enclosed between Pyrex wool plugs, was only 40 mm long (bed volume 2 ml) the column length stated was necessary for obtaining a convenient flow-rate under gravity.

Water samples were filtered through a 0.45-µm filter (HAWP 04700) in a Millipore filtration system. The filtration step did not influence the blank. The peroxodisulphate oxidation and the spectrophotometric finish were performed with the previously described equipment.⁶

Chemicals

All solutions were prepared from Merck analytical reagents unless otherwise stated.

Sodium chloride was purified as described earlier.⁶ Hydrochloric acid was freed from iodine and bromine as follows. Add 0.1 g of sodium nitrite to 600 ml of hydrochloric acid (1 + 1), heat to boiling and boil for 10 min. Add 0.5 ml of 30% hydrogen peroxide and boil for another 10 min. Distil the acid and recover the middle 400-ml portion. The purified hydrochloric acid stock solution is ~6.4M and is used in all preparations containing this acid.

Ion-exchange resin. Dowex 1 × 8, (100–200 mesh), pract, Serva Feinbiochemica. Fines are removed by decantation. In order to obtain reproducible flow-rates the decantation procedure must be standardized. With the exchange column and bed height used in this work the following procedure is used. Slurry about 30 g of resin in a tall-form 250-ml beaker filled with water and allow to settle for 5 min. Decant the suspended particles and repeat the procedure until the supernatant liquid is virtually free from particles. The resin

Table 1. Determination of K_{Cl}^{Br} for three Dowex 1 ion-exchange resins of various degree of cross-linking; batch experiments with initial concentration of chloride 5 mM; X_{Br-} is the mole fraction of bromide in the column

Initial $[Br^-]$, mM	Dowex 1					
	× 4		× 8		× 10	
	K_{Cl}^{Br}	X_{Br-}	K_{Cl}^{Br}	X_{Br-}	K_{Cl}^{Br}	X_{Br-}
0.05	2.87	0.00250	3.81	0.00283	1.67	0.00302
0.15	2.82	0.00748	3.46	0.00839	1.45	0.00878
0.45	2.70	0.0222	3.42	0.025	—	—
1.35	2.86	0.0657	3.70	0.0742	1.32	0.0734
4.05	2.64	0.183	3.61	0.210	1.29	0.194

can be further purified after the columns have been made as described in the general procedure below.

Determination of the ion-exchange constant, K_{Cl}^{Br}

The resin in chloride form was conditioned over calcium chloride hexahydrate and its saturated solution before use. The water content of the conditioned resin was about 13%. For each experiment 1 g of resin was shaken in an Erlenmeyer flask for 18 hr with 200 ml of a solution containing chloride and bromide. The resin and the equilibrated solution were then transferred to a column and allowed to drain thoroughly before being eluted with sodium perchlorate. Bromide was determined after oxidation, by titration with thiosulphate.⁶ The capacity of the resin was determined by Mohr titration after elution of chloride with 1M sodium nitrate.

General procedure

The following procedure can be used for fresh water not containing abnormal amounts of dissolved salts and organic matter.

Column preparation. Prepare a 2-ml bed of the resin (chloride form) between two plugs of glass-wool. Treat fresh resin with 40 ml of 1M sodium hydroxide and rinse with water until neutral. Run one regeneration step as described below, before use with a sample.

Sample preparation

Add 2 drops of 0.05% Methyl Orange solution per litre of sample and acidify just to the red colour with 1M hydrochloric acid. Filter the sample if necessary, discarding the first 50 ml of filtrate. Take a sample of known volume, not exceeding 1 litre, in a standard flask.

Enrichment

Place the flask, mouth down, in the funnel of the column. The flow-rate will be about 100 ml/hr, and the equipment can be left unattended, for instance overnight, since the last portion of the sample is retained by capillary forces and hence the bed will not run dry. Elute with three 3-ml portions of 2M sodium perchlorate into a 50-ml Jena Duran bottle and proceed with the analysis as described earlier.⁶

Regeneration

Rinse the column with water and pass through it, in order, 200 ml of 2M sulphuric acid, 15 ml of 1M sodium bicarbonate and 10 ml of 0.6M hydrochloric acid, rinsing with water between each. Eliminate voids formed by the evolution of carbon dioxide, by momentarily applying gentle suction to the tip of the column. Finally, rinse with water until the effluent is neutral.

RESULTS AND DISCUSSION

The enrichment step

The success of the enrichment will depend on the net retention volume V'_R , of the column for bromide. V'_R is given by the retention equation

$$V'_R = V_R - V_M = DV_i$$

where V_R is the total retention volume, V_m is the volume of the mobile phase in the resin bed and V_i is the total volume of the bed. In order to limit the volume eluted the bed volume is restricted to about 2 ml. The distribution ratio, D , of bromide between the bed and the mobile phase depends on the equilibrium constant of the ion-exchange process and the composition of the sample. The main cationic components of fresh water will not affect this distribution and, with the possible exception of Hg(II), trace metals should not cause interference, because of their low concentrations and the high ratio of chloride to bromide. Hence only the influence of the three main anions in fresh water (chloride, sulphate and bicarbonate) was studied.

Influence of chloride. The equilibrium constant for the exchange reaction $R^+Cl^- + Br^- \rightleftharpoons R^+Br^- + Cl^-$,

$$K_{Cl}^{Br} = \frac{[Br^-]_R [Cl^-]}{[Cl^-]_R [Br^-]}$$

has been determined from batch experiments at several bromide loadings on resins of various degree of cross-linking. The results are presented in Table 1. Since the value of K_{Cl}^{Br} is most favourable for Dowex 1 × 8, this resin was selected. The value of the constant (3.5) found in this investigation is somewhat higher than that previously reported (2.8).⁷ The volume capacity of the resin is 1.6 meq per ml of bed volume, which gives $V'_R = 5.6 V_i/[Cl^-]$ at low bromide loadings. For a 1000-ml sample and a bed volume of 2 ml the permissible chloride concentration would then be about 0.01M. This figure was corroborated by experiments in which 1000-ml samples that were 0.25 μM in bromide and had various chloride concentrations were analysed according to the general procedure. The recovery was (100 ± 1)% for $[Cl^-] \leq 0.01M$, as can be seen in Table 2. No difference in recovery was observed between fresh

Table 2. Test of the general procedure in the presence of chloride: 1000 ml of solution 0.25 μM in Br^- and of the stated concentration of NaCl was enriched on fresh and on regenerated resin beds

$[NaCl]$, M	Recovery of bromide, %	
	Fresh resin	Regenerated resin
0.0005	100	100
0.005	101	100
0.01	98	100
0.05	27	26

Table 3. Test of the general procedure in the presence of sulphate: 1000 ml or 200 ml samples, 0.25 μ M or 8.33 μ M in Br⁻ and with the stated concentrations of Na₂SO₄, were enriched

[Na ₂ SO ₄], mM	Recovery of bromide, %		
	1000 ml of 0.25 μ M Br ⁻	1000 ml of 8.33 μ M Br ⁻	200 ml of 8.33 μ M Br ⁻
0.25	100		100
0.5		99	
2.0		98	
2.5	67		100
5.0	53	72	
10			100
25	27		100
50			95

and regenerated resin beds. In this and the other measurements bromide standards were used for the calibration curve in the spectrophotometric finish.

Influence of sulphate. The influence of sulphate ions on the recovery of bromide was studied by analysis of solutions containing bromide and sulphate at various concentration levels. From the results presented in Table 3 we may conclude that quantitative recovery of bromide is obtained for a 1000-ml sample containing up to 2 mmole of sulphate; the average sulphate concentration in fresh water is about 0.25 mM.¹

Influence of bicarbonate. Bicarbonate is the main anionic component in fresh water. On passage of a large volume of sample through the column, the ion-exchanger will be largely converted into its bicarbonate form. The eluate from the column will therefore contain about 3 mmoles of HCO₃⁻. After its titration to about pH 4 before the addition of the peroxodisulphate solution, the eluate will contain a substantial amount of dissolved carbon dioxide, which will be expelled during the oxidation step. It was found that the expulsion of the gas caused low recoveries of bromide. Most likely some bromine, formed as an intermediate in the oxidation, is carried away with the carbon dioxide. This interference can be avoided by acidifying the sample before the enrichment step, as outlined in the general procedure. Alternatively the titrated eluate can be heated to expel the carbon dioxide before the oxidation step.

The enrichment step was further tested on synthetic fresh water of the relative ionic composition suggested by Rodhe⁸ as "standard composition", see Table 4. Chemicals used were specially prepared free from bromide. The blank obtained was the same as for distilled water. The results were very satisfactory,

Table 4. Test of the general procedure with solutions of "standard composition": 1000 ml of 0.005N "standard composition" containing the stated amounts of bromide was enriched; 0.005N "standard composition" contains (meq/l): Ca²⁺ 3.175, Mg²⁺ 0.870, Na⁺ 0.785, K⁺ 0.170, Cl⁻ 0.5, SO₄²⁻ 0.785, HCO₃⁻ 3.715

Bromide added, μ mole	Recovery, % \pm RDS ($n = 3$)
0.01	89 \pm 10
0.05	101 \pm 1
0.25	99.7 \pm 0.2

especially considering the fact that 0.01 μ mole of bromide corresponds to an absorbance of only 0.023.

The elution step

Quantitative elution within a volume suitable for the succeeding steps in the analytical procedure could only be obtained with perchlorate ions. Three 3-ml portions of 2M sodium perchlorate proved adequate for a 2-ml resin bed.

The enrichment factor (the ratio of the concentrations in the eluate and sample) is \sim 100 for a 1-litre sample. The eluate is diluted in the course of analysis however, so the final enrichment factor is \sim 30.

The regeneration step

The regeneration sequence utilizes the high affinity of the exchanger for bisulphate ($K_{Cl}^{HSO_4} = 4.1$) but low affinity for sulphate ($K_{Cl}^{SO_4} = 0.1$).⁷ The perchlorate ions are first eluted with 2M sulphuric acid and the resin is then converted from the sulphate-form into the bicarbonate-form with sodium bicarbonate solution. Finally treatment with a small excess of hydrochloric acid restores the column to the chloride-form. Use of hydroxide instead of bicarbonate (in order to avoid evolution of carbon dioxide) cannot be recommended, since its repeated use tends to cause clogging of the plugs of glass wool used to keep the resin in place. Only a small decrease in capacity has been found after repeated regeneration of the ion-exchanger.

The blank

Significant amounts of bromide always seem to accompany chloride even in analytical-reagent grade chemicals and, therefore, the commercial ion-exchange resin in chloride form will give a rather high blank if not purified. Washing the resin with the specially prepared bromine-free hydrochloric acid reduced the blank considerably but entirely satisfactory results were only obtained if the resin had first been treated with 1M sodium hydroxide. The use of quite large amounts of bromine-free hydrochloric acid is, however, avoided by replacing it by use of the regeneration sequence with sodium hydroxide, sulphuric acid and sodium bicarbonate. The ordinary reagent grade of these chemicals is sufficiently free from bromide, and only 6 mmoles of hydrogen chloride are used for converting the resin into the chloride form.

Although the blank may vary somewhat with the batch of ion-exchanger, the following results are typical. Ten determinations in each of which 1000 ml of distilled water were taken through the analytical procedure yielded a blank of 5.6 ± 0.5 nmoles. The corresponding figures from the peroxodisulphate oxidation of 10 ml of distilled water and the spectrophotometric finish were 2.8 ± 0.5 nmoles. From the standard deviation of the bromide blank a limit of detection (3σ) of 1.5 nM and a limit of determination (10σ) of 5.0 nM can be calculated, corresponding to 0.12 and 0.40 μ g/l., respectively.

Table 5. Determination of the bromide concentration in some lake waters and in waste water (corrected for iodide)

Origin of sample	Sample volume, <i>ml</i>	Bromide, μM
Edasjön, Uppland	1000	0.252
depth 0.3 m	500	0.262
Valloxen, Uppland	896	0.482
depth 0.3 m	500	0.475
Åresjön, Jämtland	1000	0.050
depth 0.3 m		
Incoming waste water	100	3.27
(to the waste water	100	3.25
plant in Uppsala)		
Outgoing waste water	100	3.25
(from the waste water	100	3.25
plant in Uppsala)		

Iodide is taken up quantitatively during the enrichment step but is only partially eluted. A correction for the presence of iodine is made in the spectrophotometric finish.⁶ Work is now in progress to adapt the procedure for a simultaneous determination of iodide.

Applications

The method has been applied to waters from three Swedish lakes and two waste water samples (Table 5). Edasjön and Valloxen are situated in the south of Sweden. Edasjön is a small lake, the first in a lake system, with a drainage area dominated by forests. Valloxen is a large lake, receiving its water from cultivated soils and wooded grounds. Åresjön is one of the first lakes in a large system in a mountain area; the water is poor in nutrients. The waste water samples were taken from the waste water plant at Uppsala. The incoming water was rich in suspended material.

Albeit limited in number, the results indicate that the bromide concentration in fresh waters varies considerably. This subject will be further investigated. It is also interesting to note the substantial increase of the concentration of bromide in waste water, above the natural level. As expected, no

reduction in the bromide content of the water occurs during passage through the waste water plant.

Humic acids present in the sample are, at least partly, taken up by the resin, as evidenced by the dark resin layer formed at the top of the resin bed. Some of the organic substance may be eluted but should be destroyed during the peroxodisulphate oxidation. The regeneration does not remove the humic acids completely but so far no negative effects have been observed from the sorbed material.

Without any special arrangements a single analyst can analyse 10 samples per day. Hence the present method cannot compete with the ion-chromatographic technique with respect to speed of analysis. For waters with bromide concentrations greater than 10–20 $\mu\text{g/l.}$, the ion-chromatographic technique is likely to become the method of choice, particularly in monitoring programmes. For the determination of bromide concentrations lower than 10 $\mu\text{g/l.}$ the present method should be a valuable asset. Its high accuracy should also make it suitable as a reference method for more instrument-oriented procedures.

REFERENCES

1. D. A. Livingstone, *Data of Geochemistry*, 6th Ed., Geological Survey Professional Paper 440-G, United States Government Printing Office, Washington, 1963.
2. H. Akaiwa, H. Kawamoto and M. Osumi, *Talanta*, 1982, **29**, 689.
3. J. Slanina, F. P. Bakker, P. A. C. Jongejan, L. van Lamoen and J. J. Möls, *Anal. Chim. Acta*, 1981, **130**, 1.
4. D. F. Boltz and J. A. Howell, *Colorimetric Determination of Nonmetals*, 2nd Ed., Wiley, New York, 1978.
5. C. L. Basel, J. D. Defreese and D. O. Whittemore, *Anal. Chem.*, 1982, **54**, 2090.
6. U. Lundström, *Talanta*, 1982, **29**, 291.
7. J. Inczédy, in *Analytical Chemistry: Essays in Memory of Anders Ringbom*, E. Wänninen (ed.), p. 357. Pergamon Press, Oxford, 1977.
8. W. Rodhe, *Verhandlungen der Internationalen Vereinigung für theoretische und angewandte Limnologie*, 1949, **X**, 377.

SIMPLIFIED DETERMINATION OF POLYCYCLIC AROMATIC HYDROCARBONS

MICHAEL J. AVERY, JOHN J. RICHARD and GREGOR A. JUNK
Ames Laboratory-USDOE, Iowa State University, Ames, IA 50011, U.S.A.

(Received 20 April 1982. Accepted 27 July 1983)

Summary—Accurate quantitative analysis for selected polycyclic aromatic hydrocarbons present on urban dust can be obtained by using a simple procedure consisting of sonic-probe extraction with cyclohexane; clean-up with Florisil®-XAD-4®, and measurement by high-resolution gas chromatography with flame-ionization detection (HRGC/FID). The analysis can be further simplified by eliminating the clean-up step if HRGC/electron-impact mass-spectrometry (MS) is available. Both the FID and MS methods give results consistent with those obtained by standard procedures. The direct HRGC/MS procedure, combined with chemical ionization, can also be applied to the determination of polycyclic organic materials present in solvent-refined coal, shale oil and crude oil.

Polycyclic aromatic hydrocarbons (PAHs) are generated from a variety of sources^{1,2} and are often associated with urban dust particles. This dust is a composite of particulate matter from sources such as automobile exhaust, wind erosion, road dust and stationary fires. Consequently, extracts of urban dust are usually complex mixtures containing organic compounds such as PAHs, heterocyclics, aliphatic hydrocarbons, aldehydes, ketones, acids and bases. Accurate measurement of individual compounds in these complex mixtures usually requires time-consuming procedures. For example, the determination of PAHs associated with urban dust involves extraction, isolation into a separate fraction, separation into individual compounds, and measurement.³⁻⁵ Procedures for removing the PAHs from urban dusts are soxhlet extraction,⁶⁻⁸ sonic-bath treatment,^{9,10} and sonic-probe treatment¹¹⁻¹³ with various solvents and solvent mixtures. Removal by sublimation has also been reported.^{14,15} Isolation of a PAH-rich fraction from the solvent extracts has included solvent partitioning¹⁶⁻¹⁸ followed by column chromatography on various absorbents¹⁹⁻²¹ or preparative high-pressure liquid chromatography (HPLC).^{22,23} After pretreatment of the extract, the PAHs are separated and measured by high-resolution gas chromatography with flame-ionization detection (HRGC/FID)²⁴ and by analytical HPLC.²⁵ These multiple steps are time-consuming and tedious. Thus a rapid and simple method of screening urban dust samples for the presence of selected PAHs is desirable.

We describe in this report a straightforward procedure based, in part, on the extraction of dust samples and other particles by use of a sonic probe and cyclohexane. The extract is either cleaned by column chromatography and analysed by HRGC/FID or analysed directly by HRGC/mass-

spectrometry (MS). The direct HRGC/MS analyses of polycyclic organic compounds in other complex mixtures such as alternative energy fuels is also described.

EXPERIMENTAL

Samples

Urban dust samples and standard reference material SRM 1649 were obtained from the National Bureau of Standards (NBS). Fly-ash from a coal-burning power plant was collected from the hopper of the electrostatic precipitator. Flue tar was obtained by scraping the inside of the chimney of an airtight wood-burning stove. Alternative energy fuels were obtained from the NBS during participation in an analytical characterization programme sponsored by the Department of Energy.

Extraction

An Artek-Sonic Dismembrator (Artek System Corporation, Farmingdale, NY) equipped with a 3/4-in. probe and operated at 240 W was used to extract 0.25-g samples with 30 ml of solvent. The sonic treatment time was 10 min. The solution was then filtered and extraction was repeated twice with fresh solvent. The three extracts were combined and reduced to 1 ml.

Clean-up

The extract was transferred to a 0.5-cm bore glass column containing 1 g of Florisil®, and then eluted with 15 ml of benzene. The eluate was concentrated to 0.5 ml and transferred to a 1.4-cm bore glass column containing 9 g of 80-100 mesh XAD-4® wetted with ethanol. The XAD-4 column was washed successively with 25 ml of ethanol and 25 ml of pentane, the effluents being discarded. The PAHs were then eluted with 25 ml of benzene, and this eluate was subsequently reduced to 1 ml. This XAD-4 clean-up is a modification of the procedure reported by Spitzer.²⁶

Equipment

The HRGC analyses were performed on a Carlo Erba Fractovap equipped with an FID. The HRGC/MS analyses were performed on a Finnigan 4000 GC/MS operated in the multiple-ion-monitoring mode, with either electron-impact or chemical ionization. All solvent reductions were performed with a rotary evaporator.

HRGC analyses

The components in the extracts were separated on 30-m DB-5 fused silica capillary columns, with hydrogen or helium as carrier gas, on-column or splitless injection, and a temperature programme of 6°/min from 60° to 320° after an initial hold of 2 min. With this programme the analysis time is less than 50 min. External standards were used.

RESULTS AND DISCUSSION*Validation of methodology*

The NBS has issued certified values for the concentrations of five PAHs in SRM 1649, a time-integrated, homogenized sample of Washington DC urban dust. The results of our analyses of this SRM are compared to these NBS certified values in Table 1. The average difference between values is 8%. Comparable reproducibilities were obtained by the two methods. These results are used as validation of the simple and rapid methodology for the determination of selected PAHs in samples as complex as urban dust.

Extraction tests

Tests were conducted to determine the best solvent, the most convenient method of removing residual particles from the extracts, and the optimum number of extractions.

Cyclohexane and dichloromethane (DCM) were both effective in removing the PAHs from the urban dust particles. The DCM extract, however, could not be successfully cleaned-up with the Florisil and XAD-4 columns. This observation reflects the superior efficiency of DCM over cyclohexane in removing organic substances from urban dust.¹⁴ For PAH determination, however, cyclohexane is superior because it discriminates against many of the interfering polar substances while retaining efficiency for removing the neutral PAHs.

After each sonic extraction, the particles must be separated from the extract. Conventional centrifugation was judged to be unsatisfactory because the fine particles generated during the sonic treatment could not be removed from the solution. Ultracentrifugation did remove these particles but this approach is too complicated for a routine procedure. Filtration of the extract through medium-porosity

Table 1. Comparison of the analysis of Washington urban dust SRM 1649.

Compound	Concentration, $\mu\text{g/g}$	
	NBS certified value	This study
Fluoranthene	7.1 ± 0.5	7.6 ± 0.5
Benz(a)anthracene	2.6 ± 0.3	2.9 ± 0.4
Benz(a)pyrene	2.9 ± 0.5	2.7 ± 0.6
Indeno(1,2,3-cd)pyrene	3.3 ± 0.5	3.1 ± 0.6
Benz(ghi)perylene	4.5 ± 1.1	5.0 ± 1.1

Table 2. Relative efficiencies for recovery of PAHs in successive sonic extractions of urban dust

Compound	Fraction in extract, %		
	1	2	3
Phenanthrene	73	27	0
Fluoranthene	80	20	0
Pyrene	79	21	0
Benz(a)anthracene	83	17	0
Chrysene	75	25	0
Benz(a)pyrene	63	37	0
Benz(e)pyrene	68	32	0
Indeno(1,2,3-cd)pyrene	71	29	0
Benz(ghi)perylene	58	34	8

sintered glass was successful and, at the concentrations of interest, no PAHs were lost.

The number of sonic extractions necessary to remove the PAHs was determined by extracting an urban dust sample three times and analysing each extract separately. The results, shown in table 2, indicate that all the PAHs except benz(ghi)perylene are removed in two extractions. This sonic extraction procedure is effective for PAHs present on urban dust at the $\mu\text{g/g}$ level. It is unlikely, however, that this technique can be extended to the ng/g level. Work done at this laboratory²⁷ and others¹³ indicates that less than 30% of several representative PAHs present at the ng/g level are extracted by sonic treatment.

Clean-up

The simple two-step clean-up of the cyclohexane extract with Florisil and XAD-4 yields a fraction rich in PAHs that can be analysed by HRGC/FID. The Florisil removes polar materials and the XAD-4 completes the clean-up by removing any aliphatic hydrocarbons and semipolar materials from the extract. This clean-up is simple and fast, the only disadvantage being the loss of perylene on the Florisil.

The effectiveness of this clean-up procedure is illustrated in Fig. 1 where the HRGC/FID chromatograms of the original and the cleaned-up extracts are shown. Chromatogram A of the original extract is much more complex than chromatogram B from the cleaned-up extract. The original has a large number of interfering peaks at or near the retention times of the five PAHs indicated by the dotted lines between the chromatograms. Many of these interfering components are aliphatic hydrocarbons, which show up as intense discrete peaks. Other interferences appear as a wide unresolved hump. The discrete hydrocarbon interference peaks are not present in chromatogram B of the cleaned-up extract, which is rich in PAHs. Obviously, the PAHs can be determined by HRGC/FID from chromatograms such as B but cannot be measured from chromatograms such as A. A final note about the comparison of these two chromatograms is that the baseline drift, due to column bleed, becomes maximal between components 4 and 5 in chromatogram B, whereas in chromatogram A this drift overlaps the hump from

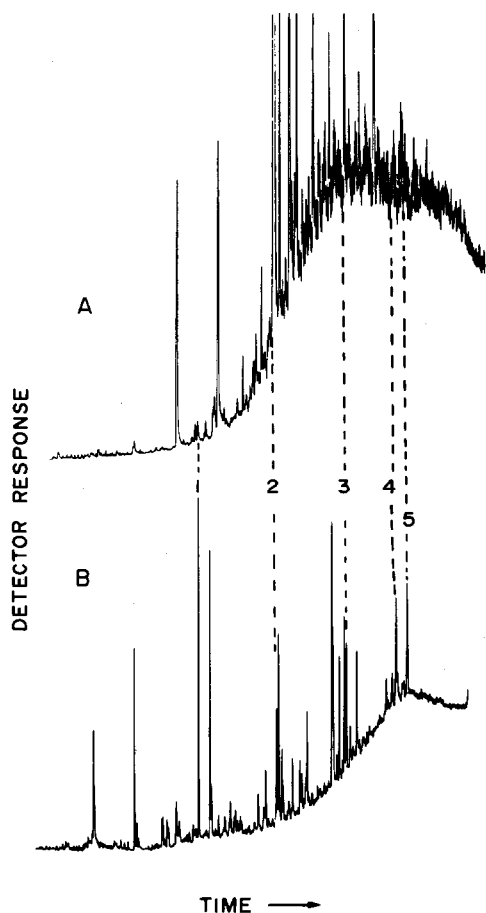


Fig. 1. HRGC/FID chromatograms of (A) original and (B) cleaned-up cyclohexane extracts from sonic-probe extraction of Washington urban dust. Peaks: 1 = fluoranthene; 2 = benz(*a*)anthracene; 3 = benz(*a*)pyrene; 4 = indeno(*1,2,3-cd*)pyrene; 5 = benz(*ghi*)perylene.

the unresolved components between components 3 and 4.

Losses occur whenever solutions containing small

Table 3. Recoveries of PAHs subjected to Florisil-XAD-4 clean-up

Compound	Recovery*, %
Phenanthrene	48
Fluoranthene	71
Pyrene	79
Benz(<i>a</i>)anthracene	80
Chrysene	64
Benz(<i>a</i>)pyrene	70
Benz(<i>e</i>)pyrene	91
Perylene	0
Indeno(<i>1,2,3-cd</i>)pyrene	84
Dibenz(<i>ah</i>)anthracene	84
Benz(<i>ghi</i>)perylene	86

*Relative reproducibility is $\pm 10\%$ (triplicate determinations).

amounts of components in a complex mixture are cleaned-up by some form of column chromatography. The probable loss of selected PAHs was investigated for the Florisil-XAD-4 clean-up employed in this investigation. Standard solutions were prepared and the recovery of individual PAHs was determined. The results are listed in Table 3 where the recoveries, except for perylene, ranged from 48% for phenanthrene to 91% for benz(*e*)pyrene. In all analyses corrections were made for these losses in the clean-up step.

Applications

The simplified procedure was applied to other PAHs in SRM 1649 and to PAHs on particles from other sources. The results of these analyses are listed in Table 4. Quantitative values for five additional PAHs in SRM 1649 are given in columns 2 and 3. The PAH content of St Louis urban dust was also measured and the values are given in column 4. For comparison, the NBS uncertified values for this same dust are listed in column 5. The PAHs measured in a sample of fly-ash from a coal-fired power plant and flue tar from a wood-burning stove are shown in columns 6 and 7. The low values for fly-ash and the high values for flue tar illustrate the effect of firing conditions on the PAH content of the emissions.

Table 4. HRGC/FID determination of PAHs in cleaned-up extracts from various particle samples

Compound	Concentration, $\mu\text{g/g}$					
	Washington urban dust SRM 1649		St Louis urban dust		Fly-ash*	Flue tar†
	This study	NBS value	This study	NBS uncertified		
Phenanthrene	3.3	4.5	4.5	NR§	ND‡	70
Fluoranthene	7.6	7.1¶	7.1	7.9	0.3	143
Pyrene	5.8	7.2	5.9	7.4	0.7	178
Benz(<i>a</i>)anthracene	2.9	2.6¶	2.6	2.8	ND	170
Chrysene	4.3	3.7	6.9	6.6	ND	225
Benz(<i>a</i>)pyrene	2.7	2.9¶	2.4	2.6	0.07	115
Benz(<i>e</i>)pyrene	3.3	3.3	3.6	NR	ND	75
Indeno(<i>1,2,3-cd</i>)pyrene	3.1	3.3¶	3.6	4.8	ND	91
Benz(<i>ghi</i>)perylene	5.0	4.5¶	5.6	5.5	ND	74
Dibenz(<i>ah</i>)anthracene	0.4	0.4	ND	NR	ND	ND

*Electrostatic precipitator ash from a coal-fired power plant.

†Taken from the chimney of an airtight wood burning stove.

§NR = Not reported.

‡ND = Not detected at detection limit of 0.05.

¶Certified values, see also Table 1.

Table 5. Direct HRGC/MS determination of selected PAHs in sonic-probe extracts of SRM 1649, with electron-impact (EI) and chemical ionization (CI)

Compound	Concentration, $\mu\text{g/g}$		
	Cyclohexane	Dichloromethane	
		EI	EI
Benz(<i>a</i>)anthracene	2.5	5.2	2.7
Benz(<i>a</i>)pyrene	2.9	7.0	2.3
Benz(<i>e</i>)pyrene	3.6	8.1	3.3
Indeno(1,2,3- <i>cd</i>)pyrene	3.9	12.7	3.4

Under the efficient burning conditions of the power plant, very low amounts of PAHs are formed, while the inefficient combustion in an airtight wood-burning stove leads to the formation of high amounts of PAHs.

Direct analysis

If GC/MS instrumentation is available, the analytical procedure for PAHs can be made even simpler. The increased selectivity of the mass spectrometer operated in the multiple-ion-monitoring mode enables the analyst to omit the Florisil-XAD-4 clean-up. Direct HRGC/MS analysis, using electron-impact ionization (EI), of a cyclohexane sonic-probe extract of SRM 1649 was performed and the results for four PAHs are listed in column 2 of Table 5. The values are within 15% of the results reported in Table 4, obtained by use of a clean-up procedure and HRGC/FID. If a more polar solvent, such as DCM, is used for the extraction, HRGC/MS with electron-impact ionization is not satisfactory. Use of this procedure gave the high values shown in column 3. This occurs because EI is not capable of discriminating against the large number of interfering components extracted by DCM. These interferences must be removed by an extensive clean-up procedure or by resorting to a higher level of instrumental sophistication such as chemical ionization (CI). For example, isobutane CI yields a simpler mass spectrum, thus reducing the possibility of interferences. When HRGC/CIMS was applied to the DCM extract the data listed in column 4, which agree with those in column 2, were obtained.

The direct HRGC/CIMS procedure, with isobutane as the reagent gas, has also been applied to

analysis for polycyclic organic materials (POMs) in other complex mixtures. Samples of solvent-refined coal, shale oil and crude oil were diluted 100-fold with hexane and analysed directly for selected POMs. The results of these analyses are listed in Table 6. The concentrations of the first six listed POMs agree with the results obtained by other laboratories²⁸ as part of an NBS programme sponsored by the Department of Energy. The results for 1- and 2-methylnaphthalene agree with those obtained by rotationally cooled fluorescence spectroscopy.²⁹ The direct HRGC/CIMS analyses are simpler and less time-consuming than the multi-step procedures normally employed for the determination of selected components in these kinds of complex samples.

CONCLUSION

The simplified procedures used to determine twelve PAHs and three POMs on urban dusts and in process streams can certainly be extended to determine other organic compounds. In each case, the additional compounds need only be tested and the procedure finely tuned to obtain quantitative results.

The simple Florisil-XAD-4 chromatography is not applicable to class separation of all the components present in complex mixtures. The reasons for this conclusion are the known irreversible adsorption of some components on the Florisil and the insufficient documentation of the class-separating capability of the XAD-4.

Acknowledgements—Ames Laboratory is operated for the U.S. Department of Energy by Iowa State University under Contract No. W-7405-Eng-82. This research was supported by the Office of Health and Environmental Research, Office of Energy Research. The authors wish to acknowledge the administrative assistance of Dr. V. A. Fassel.

REFERENCES

1. R. Laflamme and R. Hites, *Geochim. Cosmochim. Acta*, 1978, **42**, 289.
2. M. Guerin, in *Polycyclic Hydrocarbons and Cancer*, H. Gelboin and P. Ts'o (eds.), Vol. 1, p. 3. Academic Press, New York, 1978.
3. E. Sawicki, *CRC Crit. Rev. Anal. Chem.*, 1970, **1**, 275.

Table 6. Analyses for polycyclic organic materials present in complex samples, by direct HRGC/CIMS

Compound	Concentration, $\mu\text{g/g}$		
	Solvent-refined coal	Shale oil	Crude oil
Pyrene	200	161	11
Benz(<i>a</i>)pyrene	250	14	1
Benz(<i>e</i>)pyrene	250	*	0.5
Dibenzthiophene	1064	*	41
Acridine	158	*	13
Carbazole	1913	*	6
1-Methylnaphthalene	*	*	0.6
2-Methylnaphthalene	*	*	0.3

*Not determined.

4. A. Martin and M. Blumer, *Polycyclic Aromatic Hydrocarbons: Occurrence and Analysis—A Partial Bibliography*, Woods Hole Oceanographic Institute, Woods Hole, MA, Rept. WHO1-75-22, 1975.
5. K. Bartle, M. Lee and S. Wise, *Chem. Soc. Rev.*, 1981, **10**, 113.
6. M. Lao, *Anal. Chem.*, 1973, **45**, 908.
7. R. Pierce and M. Katz, *ibid.*, 1975, **47**, 1743.
8. T. Stanley, J. Meeker and M. Morgan, *Environ. Sci. Technol.*, 1967, **1**, 927.
9. R. Clement and F. Karasek, *J. Chromatog.*, 1982, **234**, 395.
10. D. Swanson and J. Walling, *Chromatog. Newslett.*, 1981, **9**, No. 2, 25.
11. E. Sawicki, *Health Lab. Sci.*, 1975, **12**, 407.
12. J. Muller and E. Robbock, *Talanta*, 1980, **27**, 673.
13. W. Griest, L. Yeatts, Jr. and J. Caton, *Anal. Chem.*, 1980, **52**, 199.
14. U. Stenborg and T. Alsborg, *ibid.*, 1981, **53**, 2067.
15. J. Monkman, *Pure Appl. Chem.*, 1970, **24**, 731.
16. D. Hoffman and E. Wynder, *Anal. Chem.*, 1960, **32**, 295.
17. J. Howard and E. Haenni, *J. Assoc. Off. Agric. Chem.*, 1963, **46**, 933.
18. G. Grimmer and H. Böhnke, *J. Assoc. Off. Anal. Chem.*, 1975, **58**, 725.
19. A. Rosen and F. Middleton, *Anal. Chem.*, 1975, **27**, 790.
20. W. Giger and M. Blumer, *ibid.*, 1974, **46**, 1663.
21. L. Snyder and B. Buell, *ibid.*, 1968, **40**, 1295.
22. E. Lankmayr and K. Müller, *J. Chromatog.*, 1979, **170**, 139.
23. A. Krstulovic, P. Rosie and P. Brown, *Anal. Chem.*, 1976, **48**, 1383.
24. M. Lee, K. Bartle and M. Novotny, *ibid.*, 1975, **47**, 540.
25. S. Wise, W. Bonnett and W. May, in *Polynuclear Aromatic Hydrocarbons: and Biological Effects*; A. Bjørseth and A. Dennis (eds.), p. 791. Battelle Press, Columbus, OH, 1980.
26. T. Spitzer, *J. Chromatog.*, 1982, **237**, 273.
27. R. Vick, Private communication.
28. H. Hertz, H. Hilpert, L. May, W. Wise, S. Brown, J. Chelser and F. Guether, *Measurements of Organic Pollutants in Water and Wastewater*, ASTM STP686, C. Van Hall (ed.), p. 291. American Society for Testing and Materials, 1979.
29. J. Hayes and G. Small, *Anal. Chem.*, 1982, **54**, 1202.

DETECTION LIMITS AND SURFACE INTERACTIONS IN QUANTITATIVE NEGATIVE CHEMICAL-IONIZATION MASS SPECTROMETRY

ULTRATRACE DETERMINATION OF METALS AND ORGANIC COMPOUNDS BY MEANS OF THEIR COMPLEXES

I. K. GREGOR and M. GUILHAUS

School of Chemistry, The University of New South Wales, Kensington, N.S.W., Australia

(Received 6 May 1983. Accepted 25 July 1983)

Summary—Details are given of a selective negative-ion mass-spectrometric method appropriate for the ultratrace determination of metals and organic compounds by means of their complexes. Direct introduction of the sample into the ion-source, attachment of low-energy electrons, and selected-ion monitoring are described, and comparative data are given relating to surface effects at the tips of insertion-probes on detection limits. Detection limits for chromium and cobalt, determined as their tris(2,2,6,6-tetramethylheptane-3,5-dione) chelates, were respectively 1.0 and 0.16 pg, and that for nickel [as its bis(*N,N*-diethyldithiocarbamate) complex] was 1.0 pg. Detection limits of 2.0 and 1.0 ng are attainable for malathion and ethion by measurement of the nickel(II) complexes of their *O,O'*-dialkyldithiophosphate hydrolysis products.

We have already drawn attention to some of the advantages and the potential afforded by the method of negative-ion mass spectrometry for the determination of organometallic compounds.¹ Since then there have been significant developments in the use of electron-attachment as a "soft" ionization technique under so-called negative chemical-ionization (NCI) conditions.²⁻⁷ For molecules possessing positive electron-affinity, attachment of low-energy electrons can result in the formation of long-lived negative molecular ions capable of being detected and selectively monitored for quantitative purposes.⁷⁻¹⁰ Electronic and structural criteria for gas-phase electron capture by organometallic substrates, as well as the function of various gases as electron-energy moderators in such reactions, have recently been more precisely defined.¹¹⁻¹⁸ Moreover, there have been considerable advances made in methods for quantitative introduction of solid samples of low volatility or thermal lability into mass-spectrometer ionization sources.¹⁹⁻²² Previous mass-spectrometric determinations of metals (as various metal chelates) have been based largely on either electron-impact (EI) or positive-ion chemical ionization.²³⁻²⁷ Under these conditions very low instrumental background contributions are essential if the analytes are to be detected at ultratrace levels. However, because the normal mass-spectrometer background species are relatively immune to electron attachment, such ion-current contributions are usually minimal under NCI conditions.^{6,28,29} Introduction of gas-chromatography fractions and attachment of electrons under NCI ion-source conditions has been reported for certain classes of metal chelates.^{30,31} In general, this method

has several drawbacks, including the non-quantitative introduction of sample into the ion-source, the thermal lability of various metal chelates, and interaction of the chelates with active sites and surfaces prior to entry into the ionization chamber.³²

In this paper we present details and results of a selective method for ultratrace determination of metal chelates introduced directly into the ion-source under standardized electron-capture NCI conditions. The utility of the technique is demonstrated for the biologically significant metals chromium, cobalt and nickel, and by its extension to analysis for malathion and ethion by formation and determination of the nickel derivatives of their (RO)₂PS₂⁻ hydrolysis products. The analytes tested are listed in Table 1.

EXPERIMENTAL

Instrumentation

Negative-ion mass spectra were obtained and quantitative measurements made on a VG MM-16F single-focusing mass spectrometer fitted with a combined EI/CI source, under conditions described previously^{11-14,18} or specified below (Tables 2-4). Methane (Matheson UHP, 99.97% pure) was used as the electron-energy moderator under measured and controlled ion-source pressure (MKS Baratron system, type 170/315BHS-10) and temperature conditions to achieve optimum sensitivity for molecular-ion signals at the collector.¹⁸ Detection-limit measurements were made by performing repetitive 0.1-sec integrating scans of a selected ion (usually the molecular ion). Thus the signal derived from the collector by the d.c. amplifier and a sample-and-hold circuit could be recorded during the complete evaporation of a quantity of sample within the ion-source, usually within about 30 sec. The signal recorded was Gaussian in shape and corresponded to an evaporation profile.³³ Samples were introduced quantitatively into the ion-source either in fused silica cups (in some cases silanated and sometimes also coated

with SE-30) or on dished Vespel[®] rods positioned in tapered Vespel[®] probe tips which ensured a tight seal in, and electrical insulation from, the ion-source block.^{21,22} The desorption chemical ionization (DCI) method of sample introduction was also used;¹⁹ this involved rapid evaporation of sample within the methane plasma from a platinum wire, heated by the passage of a ramp-programmed current supplied by a VG type MR609 source-heater/emitter-current control unit. Details of our DCI filament, Vespel[®] probe tip and the application of this technique to metal chelates have already been reported.¹⁴

Procedures

Analyte solutions of known concentration were delivered by microsyringe in precise volumes of 1–3 μ l to the solid insertion-probe cups, Vespel[®] rod or DCI filament wire, and the solvent was evaporated in the vacuum lock for the solid insertion-probe. In this way, small accurately known amounts of samples deposited on fused silica, silanated or SE-30 coated silica,²² Vespel[®] or platinum, were introduced quantitatively into the ionization-source methane plasma by the "in-beam" method.¹⁹ Details of typical plasma temperatures and sample heating-rate data have already been given.¹⁴ The evaporation profile data acquired during the evaporation and ionization of the sample were used to determine the total monitored-ion charge produced by a given mass of sample introduced into the ion source (C/ μ g).³³

Materials and reagents

The derivatives analysed were prepared and purified by established methods, and their purity was checked by positive-ion and negative-ion mass spectrometry.^{34–37} Solutions of the analytes were prepared by dilution of stock solutions of accurately known concentration, made with n-hexane, chloroform or methanol, as appropriate.

Glassware was cleaned by procedures similar to those already described.³⁸

RESULTS AND DISCUSSION

Ultratrace metal determination by chelation and NCI mass spectrometry

As speciation of metals in the environment is highly important, analytical methods are needed that not only have high sensitivity, but can also indicate the metal oxidation state and co-ordination number.^{39–41} An analytical procedure based on a "soft" ionization method is well suited for this purpose. Both proton-transfer CI and NCI give less fragmentation of quasimolecular, $[M + 1]^+$, and molecular ions, $[M]^-$, than electron-impact ionization does. However, many metal chelates can be regarded as Lewis acids with the metal functioning as the active

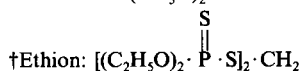
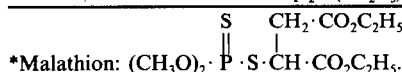
Lewis acid site⁴² and inhibiting proton attachment. Negative ionization, involving attachment of low-energy electrons in metal orbitals of suitable energy, can be seen as a more favourable ionization process, particularly as many metal chelates have been observed to undergo electron-attachment reactions leading to the formation of stable long-lived negative molecular ions.^{11–15,30–31} Though it is known that fluorinated metal chelates may yield between 10 and 5000 times more negative-ion current when present as $[M]^-$ than positive-ion current when present as $[M + 1]^+$, no systematic comparison has been made of the sensitivity given by the three most common methods of ionization modes (EI, CI and NCI).^{30,31} Table 1 lists the metal derivatives which we have determined quantitatively by direct sample introduction, electron-capture NCI, and mass spectrometry. The biologically significant metals, chromium and cobalt, in their tervalent states, were determined in the form of their tris(2,2,6,6-tetramethylheptane-3,5-dione) chelates, $M(\text{dpm})_3$, which give long-lived molecular anions on electron attachment.⁴³ Nickel is best determined as its bis-(*N,N*-diethyldithiocarbamate) complex, $\text{Ni}(\text{Et}_2\text{dtc})_2$.¹⁴

Ultratrace analysis by metal complexation and NCI mass spectrometry

Formation of complexes of metals and various organic analytes, coupled with solvent extraction and spectrophotometric analysis, is a commonplace procedure. The potential specificity and sensitivity afforded by negative chemical-ionization mass spectrometry has not so far been utilized in this way, and one of our aims was to evaluate the combination of metal derivative formation and NCI mass spectrometry. Ethion is commonly determined spectrophotometrically by hydrolysis and subsequent formation of the bis(*O,O'*-diethyldithiophosphate)copper(II) complex, with a practical limit of detection of *ca.* 25 μ g of analyte.^{37,44} A similar method is used for malathion, the corresponding *O,O'*-dimethyldithiophosphate complex being formed. These spectrophotometric methods are not specific for the individual *O,O'*-dialkyldithiophosphate ligands and thus cannot be specific for the parent pesticides.³⁷ Negative-ion mass spectra have

Table 1. List of analytes and their derivatives

Analyte	Derivative
Chromium(III)	$\text{Cr}[(\text{CH}_3)_3\text{C} \cdot \text{CO} \cdot \text{CH} \cdot \text{CO} \cdot \text{C}(\text{CH}_3)_3]_3$; $\text{Cr}(\text{dpm})_3$
Cobalt(III)	$\text{Co}[(\text{CH}_3)_3\text{C} \cdot \text{CO} \cdot \text{CH} \cdot \text{CO} \cdot \text{C}(\text{CH}_3)_3]_3$; $\text{Co}(\text{dpm})_3$
Nickel(II)	$\text{Ni}[\text{S}_2 \cdot \text{CN} \cdot (\text{C}_2\text{H}_5)_2]_2$; $\text{Ni}(\text{Et}_2\text{dtc})_2$
Malathion*	$\text{Ni}[\text{S}_2 \cdot \text{P}(\text{OCH}_3)_2]_2$; $\text{Ni}(\text{Me}_2\text{dtp})_2^\S$
Ethion†	$\text{Ni}[\text{S}_2 \cdot \text{P}(\text{OC}_2\text{H}_5)_2]_2$; $\text{Ni}(\text{Et}_2\text{dtp})_2^\S$



§Derivatives of the hydrolysis product.

Table 2. Effects of sample-surface interactions on evaporation profiles

Surface	Charge, C*	Precision (RSD), %	Profile shape
Vespel [®]	5.5×10^{-10}	8	Symmetrical
Silaned silica/SE-30	2.0×10^{-10}	8	Symmetrical
Untreated fused silica	4.0×10^{-11}	20	Regular with tailing
Heated platinum wire†	4×10^{-12}	60	Irregular

*Charge obtained as negative molecular ions from a sample of bis(*N,N*-diethylthiocarbamate)nickel(II) containing 1 ng of nickel.

†Desorption chemical ionization.

been obtained for many organophosphorus pesticides^{28,45} as well as for metal chelates formed from analogous *O-O'*-dialkyldithiophosphate ligands,¹⁵ those for the former being characterized by a degree of fragmentation which is excessive for precise selective-ion monitoring, whereas those for the latter display little fragmentation under the optimum ion-source conditions. With such metal derivatives the specificity afforded by negative-ionization mass spectrometry can be used to identify (and determine) unequivocally the metal chelate, the chelating ligand and hence the original pesticide. In this work, the metal complexes Ni(Me₂dtp)₂ and Ni(Et₂dtp)₂ were selected as models for determination of malathion and ethion because for these compounds, under controlled conditions, ca. 90% of the total ion-current is carried by [M]⁻ (the ion selected for monitoring).⁴⁶ These two metal complexes are known to be Lewis acids,^{47,48} and this property serves to make their cross-sections for electron capture larger than those of the corresponding parent organic analytes.

Surface effects and their influence on the sensitivity

When the amount of sample introduced on the solid insertion-probe approaches that required to form a monolayer on the surface used (typically 0.1 nmole), the sensitivity can be severely affected by interaction between the surface and the sample.^{22,49} Significant improvements in sensitivity as well as less decomposition of thermally labile compounds have been reported to result from the use of inert surfaces for direct sample introduction.^{21,22} Such methods involve silaning glass surfaces (and sometimes then coating the surface with the non-polar gas-chromatography stationary phase SE-30). Vespel[®] has been used to an increasing degree as a chemically inert surface for direct introduction of thermally labile compounds.²¹ The DCI method, whereby samples are desorbed within the ion-source from heated wires, has also been used for compounds that are thermally labile or difficult to volatilize.^{19,49} However, no systematic evaluation of these surfaces has been made for metal chelate analysis.

To assess the suitability of the surfaces chosen in this work for ultratrace analysis, the average charge carried by negative molecular ions resulting from replicate introduction of 1 ng of nickel [as Ni(Et₂dtp)₂] on the various surfaces was measured.

This derivative was chosen because it has vacant co-ordination sites which could interact with active sites on the various surfaces. The results are summarized in Table 2, and show that the most suitable surface for this chelate is provided by Vespel[®]. The SE-30 coated surface is also effective, but is known to have an upper temperature limitation.²² A considerable loss of sensitivity and precision, as well as tailing of the evaporation profiles, was apparent in the results for uncoated silica surfaces. The low sensitivity and poor reproducibility given by the platinum DCI filament wires is consistent with previously reported results obtained with organic analytes at the ng level.^{19,50}

Detection limits

Detection limits were determined for the analytes listed in Table 1, by introducing into the ion-source successively smaller amounts of their derivatives, on a dished Vespel[®] rod. The detection limit was taken to be the smallest amount of analyte giving an evaporation profile distinguishable from that obtained when only pure solvent was delivered to the rod. The results are given in Table 3 and the calibration graphs are given in Fig. 1.

A major limitation to the realization of lower detection limits is the intensity of the background spectrum. Although the negative-ion background is of lower intensity than that for positive ions, it is significant when the gain of the detection circuitry is very high. The abundance of background ions in the VG mass spectrometer used in this work decreases at $m/z > 300$ and therefore the degree of background

Table 3. Detection limits determined by [M]⁻ monitoring under NCI conditions

Analyte†	[M] ⁻ , <i>m/z</i>	Source temperature,§ °C	Detection limit, <i>pg</i>
Chromium(III)	601	170	1.0
Cobalt(III)	608	170	0.2
Nickel(II)	354	240	1.0
Malathion	372	160	2000
Ethion	428	160	1000

*Methane as electron-energy moderating gas (0.10 mmHg), primary electron energy 50 eV, emission current 1.00 mA (total), accelerating voltage 4.0 kV, repeller voltage 0 V.

†Analyte derivatives introduced on a Vespel[®] rod into the ionization chamber.

§Plasma temperatures were approximately 90% of the source temperature.

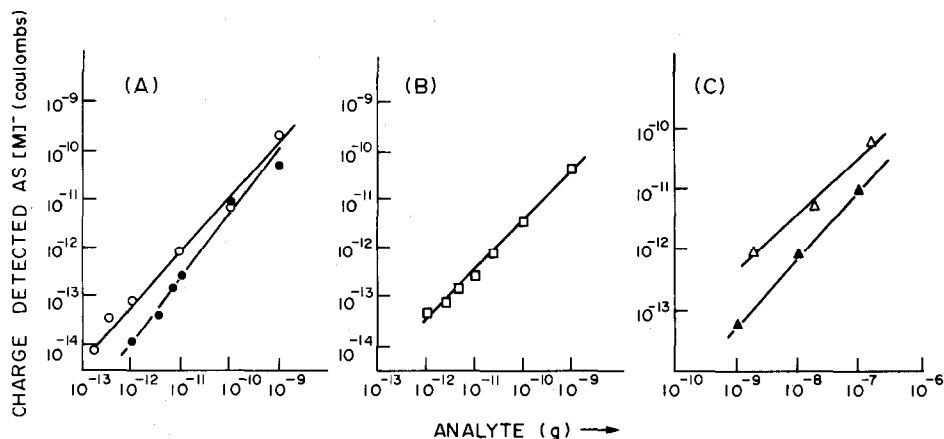


Fig. 1. Calibration graphs. A: Co(III) (○) and Cr(III) (●) as their $M[dpm]_3$ derivatives. B: Ni(II) (□) as $Ni[S_2CN \cdot Et]_2$. C: Malathion (△) and ethion (▲) as the $Ni[(RO)_2PS]_2$ derivatives; each point represents the mean charge detected for triplicate sample introductions, for which the worst r.s.d. was 20%.

interference in the detection of very low levels of analytes is decreased when the derivatives have high masses. It is therefore advantageous to use metal chelates with molecular weights >400 . Background interference becomes apparent when the probe is inserted. When the probe makes contact with and seals the ionization chamber, the pressure in the chamber rises from about 0.01 to 0.10 mmHg (with methane as the electron-energy moderating gas) and this is accompanied by a rise in sensitivity, resulting from the corresponding increase in the thermal-electron concentration in the ionization chamber. If the gain of the detection system is high, then the rise in sensitivity is apparent as a rise in the background ion-current to a plateau representing equilibration of conditions within the ionization chamber. This is illustrated in Fig. 2 which reproduces the evaporation profile obtained on delivery of $1 \mu l$ of pure solvent (blank) to the Vespel[®] rod, with the mass spectrometer tuned to $m/z = 601$. Also shown are profiles for duplicate introduction of 3.3 and 1.0 pg of chromium [as the $Cr(dpm)_3$ chelate] in the same volume of solvent. In these evaporation profiles the current due to the analyte is superimposed on the rising background signal. The drop in ion-current at the end of the evaporation profile corresponds to the withdrawal of the probe. The detection limit of 1.0 pg obtained here for chromium is two orders of mag-

nitude better than that reported for a similar technique.³⁰ The use (in that work) of untreated glass capillaries for sample insertion could have contributed significantly to lowering the sensitivity. Further development of our technique, to minimize rising background signals and thereby produce an improvement in detection limits, could involve either temperature-programming of the probe tip²¹ or the use of polyimide-coated DCI filament wires to eliminate direct interaction between the sample and the wire.⁵¹

At higher resolution some reduction of background interference can be accomplished at the expense of sensitivity.³³ A single-focusing magnetic-sector mass spectrometer with a maximum resolution of 2000 can accomplish this to a limited extent, and only in the low m/z range. In these experiments, a resolution of 1800 (10% valley definition) was used for all measurements except those for the $Ni(Me_2dtp)_2$, $Ni(Et_2dtp)_2$ and $Co(dpm)_3$ derivatives, for which a resolution of 400 was used. Use of the higher resolution reduced the overall sensitivity by 90% and necessitated more frequent tuning of the mass spectrometer to the top of the narrower peaks.

In some cases the detection limit was governed by carry-over of small traces of the sample derivative in the mass-spectrometer probe inlet-lock, with atten-

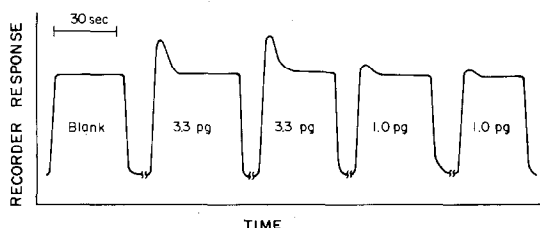


Fig. 2. Recorder responses for the introduction of ultra-trace amounts of Cr(III) as $Cr[dpm]_3$.

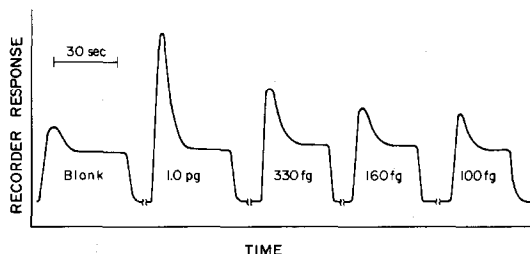


Fig. 3. Recorder responses for the introduction of sub-picogram amounts of Co(III) as $Co[dpm]_3$.

Table 4. Relative sensitivity of the EI, CI and NCI modes.

Analyte*	Relative sensitivity,† C/ng		
	CI‡	EI‡	NCI
Chromium(III)	1	6	350
Cobalt(III)	1	7	750
Nickel(II)	1	63	3 × 10 ⁴
Malathion	1	84	124
Ethion	1	109	71

*Analyte derivatives as in Table 1.

†Instrumental conditions adjusted to optimize sensitivity in each mode.

‡Reagent gas methane (0.05 mmHg) primary electron energy 200 eV, total emission current 0.500 mA, accelerating voltage 4.00 kV, repeller voltage 0 V.

‡Primary electron energy 70 eV, trap current 0.050 mA, accelerating voltage 4.00 kV, repeller voltage 0 V.

||Total electron emission current 0.500 mA, all other instrumental conditions as given in Table 3.

dant superimposition on the background signal for the blank. This is illustrated in Fig. 3 for cobalt at the sub-picogram level, and is a potentially limiting factor for significantly volatile analytes at these ultra-trace levels. Nevertheless the extremely low detection limits obtained here for cobalt illustrate the high sensitivity of the NCI/direct sample-introduction technique.

The detection limits for the nickel(II) derivatives of the ethion and malathion hydrolysis products were higher than those for the other analytes in this work, yet they still represent a significant improvement (by a factor of about 1000) on those attainable by the standard spectrophotometric method.^{37,44} Our method offers a sensitive procedure for a series of similar organophosphorus⁴⁵ pesticides capable of similarly forming metal derivatives. Further refinement of this approach, coupled with use of ion-counting methods for negative-ion detection, should result in still lower detection limits.

Comparative sensitivity of the EI, CI and NCI modes

Comparative measurements were made by separate introduction of 100 ng of each derivative under optimum conditions for each ionization mode. The total charge detected from molecular or quasimolecular ions was measured and the relative sensitivities determined (Table 4). The NCI mode was found to offer the greatest sensitivity for all the analytes tested, except Ni(Et₂dtp)₂. The sensitivity is better than that obtained by the CI mode, by factors in the range 100–1000, and this is consistent with predictions from a kinetic model for positive and negative chemical-ionization.⁵² The high enhancement for the nickel chelate may be a reflection of a very low tendency for the complex to undergo a proton-attachment reaction, which is consistent with the known chemistry for such a square planar complex with a transition metal as the Lewis acid centre.⁴²

It is noteworthy that the relative sensitivities determined for the EI mode are all higher than the corresponding positive-ion CI sensitivities. This is

probably due, at least in part, to the larger ion-source exit-slit area used.

Acknowledgement—Support of this work by the Australian Research Grants Scheme is gratefully acknowledged.

REFERENCES

- D. R. Dakternieks, I. W. Fraser, J. L. Garnett and I. K. Gregor, *Talanta*, 1976, **23**, 701.
- K. R. Jennings, *Specialist Periodical Reports, Vol. 4, Mass Spectrometry*, R. A. W. Johnstone, Senior Reporter, p. 203. The Chemical Society, London, 1977.
- D. F. Hunt and F. W. Crow, *Anal. Chem.*, 1978, **50**, 1781.
- Idem*, *U.S. Natl. Bur. Stds. Spec. Publ.*, 1978, **519**, 601.
- J. G. Dillard, *Biomedical Applications of Mass Spectrometry, First Suppl. Vol.*, G. R. Waller and O. C. Dermer (eds.), p. 927. Wiley-Interscience, New York, 1980.
- R. C. Dougherty, *Anal. Chem.*, 1981, **53**, 625A.
- H. Budzikiewicz, *Angew. Chem. Intern. Ed. Engl.*, 1981, **20**, 624.
- J. H. Bowie and B. D. Williams, in *MTP International Review Science, Physical Chemistry, Series 2, Vol. 5. Mass Spectrometry*, A. Maccoll (ed.), p. 89. Butterworths, London, 1975.
- L. G. Christophorou, *Adv. Electron. Electron Phys.*, 1978, **46**, 55.
- Idem*, *Environ. Health Perspect.*, 1980, **36**, 3.
- J. L. Garnett, I. K. Gregor, M. Guilhaus and D. R. Dakternieks, *Inorg. Chim. Acta*, 1980, **44**, L121.
- D. R. Dakternieks, I. W. Fraser, J. L. Garnett and I. K. Gregor, *Org. Mass Spectrom.*, 1980, **15**, 556.
- P. L. Beaumont, J. L. Garnett and I. K. Gregor, *Inorg. Chim. Acta*, 1980, **45**, L99.
- I. K. Gregor and M. Guilhaus, *Org. Mass Spectrom.*, 1982, **17**, 575.
- N. B. H. Henis, K. L. Busch and M. M. Bursey, *Inorg. Chim. Acta*, 1981, **53**, L31.
- J. E. Szulejko, I. Howe, J. H. Beynon and U. P. Schlunegger, *Org. Mass Spectrom.*, 1980, **15**, 263.
- P. M. George and J. L. Beauchamp, *J. Chem. Phys.*, 1982, **76**, 2959.
- I. K. Gregor and M. Guilhaus, *Abstr. Papers, 30th Ann. Conf. Am. Soc. Mass Spectrom. Allied Topics*, Honolulu, 1982, 141.
- A. P. Bruins, *Anal. Chem.*, 1980, **52**, 605.
- U. Rapp, G. Dielmann, D. E. Games, J. L. Gower and E. Lewis, *Adv. Mass Spectrom.*, 1980, **8**, 1660.
- R. J. Cotter, *Anal. Chem.*, 1980, **52**, 1589A.
- J. P. Thenot, J. Nowlin, D. I. Carroll, F. E. Montgomery and E. C. Horning, *ibid.*, 1979, **51**, 1101.
- A. E. Jenkins and J. R. Majer, *Talanta*, 1967, **14**, 777.
- M. G. Alcock, R. Belcher, J. R. Majer and R. Perry, *Anal. Chem.*, 1970, **42**, 776.
- J. R. Majer and A. A. Boulton, *Methods Biochem. Anal.*, 1973, **21**, 467.
- J. R. Majer, *Talanta*, 1972, **19**, 589.
- T. H. Risby, P. C. Jurs, F. W. Lampe and A. L. Yergy, *Anal. Chem.*, 1974, **46**, 726.
- R. C. Dougherty and E. A. Hett, *Environ. Sci. Res.*, 1978, **12**, 339.
- R. C. Dougherty, *Biomed. Mass Spectrom.*, 1981, **8**, 283.
- S. Prescott, J. E. Campana and T. H. Risby, *Anal. Chem.*, 1977, **49**, 1501.
- T. H. Risby, *Environ. Health Perspect.*, 1980, **36**, 39.
- T. H. Risby, L. R. Field, F. J. Yang and S. P. Cram, *Anal. Chem.*, 1982, **54**, 410R.
- B. J. Millard, *Quantitative Mass Spectrometry*, p. 100. Heyden, London, 1978.
- G. S. Hammond, D. C. Nonhebel and C. S. Wu, *Inorg. Chem.*, 1973, **2**, 73.

35. G. D. Thorn and R. A. Ludwig, *The Dithiocarbamates and Related Compounds*, Elsevier, New York, 1962.
36. L. Malatesta and R. Pizzotti, *Chim. Ind. Milan*, 1945, **27**, 6.
37. J. R. Wasson, G. M. Woltermann and H. J. Stoklosa, *Fortschr. Chem. Forsch.*, 1973, **35**, 65.
38. B. A. Davis, K. S. Hui and A. A. Boulton, *Advances in Mass Spectrometry in Biochemistry and Medicine*, Vol. II, p. 405. Spectrum Publications, London, 1976.
39. J. J. Dulka and T. H. Risby, *Anal. Chem.*, 1976, **48**, 640A.
40. G. B. Morgan and E. W. Bretthauer, *ibid.*, 1977, **49**, 1210A.
41. T. H. Risby, *Natl. Bur. Stand. U.S. Spec. Publ.*, 1981, **618**, 120.
42. D. P. Graddon, *Coord. Chem. Rev.*, 1969, **4**, 1.
43. J. L. Garnett, I. K. Gregor and M. Guilhaus, *Org. Mass Spectrom.*, 1978, **13**, 59.
44. J. R. Graham, *Analytical Methods for Pesticides, Plant Growth Regulators and Food Additives*, G. Zweig (ed.), Vol. II, p. 223. Academic Press, New York, 1964.
45. H.-J. Stan and G. Kellner, *Biomed. Mass Spectrom.*, 1982, **9**, 483.
46. P. L. Beaumont and I. K. Gregor, unpublished results.
47. D. R. Dakternieks and D. P. Graddon, *Aust. J. Chem.*, 1971, **24**, 2509.
48. S. E. Livingstone and A. E. Mihkelson, *Inorg. Chem.*, 1970, **9**, 2545.
49. K. S. Webb, B. J. Wood and R. Davis, *Adv. Mass Spectrom.*, 1980, **8B**, 1921.
50. A. P. Bruins, *Biomed. Mass Spectrom.*, 1981, **8**, 31.
51. V. N. Reinhold and S. A. Carr, *Anal. Chem.*, 1982, **54**, 499.
52. M. W. Siegel in *Practical Spectroscopy, Vol. 3, Mass Spectrometry, Part B*, C. Merritt, Jr. and C. N. McEwen (eds.), p. 297. Dekker, New York, 1980.

DETERMINATION OF TRACES OF OSMIUM BY THE CATALYSED HYDROGEN PEROXIDE-CYANOCUPRATE(I) REACTION

I. N. C. LING and G. SVEHLA

Department of Analytical Chemistry, The Queen's University of Belfast, Belfast, N. Ireland

(Received 1 October 1982. Revised 27 October 1982. Accepted 23 June 1983)

Summary—The reaction between hydrogen peroxide and a mixture of cyanocuprate(I) species at pH 11.2 is selectively catalysed by traces of osmium. With potentiometric or amperometric monitoring, osmium concentrations up to 1 ng/ml can be determined, with a lowest determinable concentration of 0.03 ng/ml. In the presence of luminol a Landolt-type reaction proceeds and visual or instrumental monitoring of the chemiluminescence can be used. A large number of other cations can be tolerated. The kinetics, mechanism, rate constants and Arrhenius parameters have been investigated.

Many methods for the determination of osmium are based on its catalysis of various oxidation reactions.¹⁻³¹ In the literature searches connected with our studies of catalytic methods we came across the report³² that the reaction between hydrogen peroxide and cyanide, in the presence of copper and luminol, can be used as a chemiluminescent clock reaction. Detailed study of the reaction reveals that it is sensitively and selectively catalysed by traces of osmium. In the absence of the luminol (which serves only as an "indicator" in the clock reaction), the reaction can be monitored by potentiometry and amperometry, but with luminol present chemiluminescent monitoring is also possible.

EXPERIMENTAL

Reagents

Analytical grade reagents were used whenever possible. A 1000- μ g/ml standard osmium solution was made from commercially available osmium tetroxide, kept in the dark, standardized gravimetrically,³³ and further diluted as required. To avoid adsorption losses, standards of concentration below 100 ng/ml were made immediately before use.

Solution A. Dissolve 0.0395 g of potassium cyanide, 0.0543 g of cupric sulphate pentahydrate, 71.6 g of potassium dihydrogen phosphate and 32.0 g of sodium hydroxide in water, and dilute to 1 litre.

Solution B. Standardize a 3% hydrogen peroxide solution by iodimetric titration³⁴ and dilute the required volume to 1 litre to obtain a $1.176 \times 10^{-2} M$ solution.

Apparatus

All kinetic measurements were made at $20 \pm 0.2^\circ$, unless otherwise stated, in Metrohm-type jacketed vessels fitted with Metrohm electrode heads; magnetic stirring was used.

Potentiometric monitoring was done with platinum and saturated calomel electrodes, connected to a Radiometer model 26 pH-meter, the mV signal from which was recorded.

Amperometric monitoring was done with a rotating platinum electrode (400-800 rpm) and saturated calomel electrode, at zero applied potential difference with no IR compensation. A longer electrode than normal was con-

structed for use with the Metrohm electrode head. The current was recorded at a chart speed of 2 cm/min.

Chemiluminescence was observed visually in a dark-room, the reaction time being measured with a stopwatch.

Procedure

Prepare reagent solutions A and B freshly (they do not keep for more than 24 hr). Bring these and the neutralized sample solution to $20 \pm 0.2^\circ$ in a water-bath.

Potentiometric monitoring. Set up the apparatus and to the reaction vessel add 10 ml of the neutral sample solution (containing up to 10 ng of osmium) and 10 ml of solution A. Start stirring and recording. Once the signal becomes steady, add 10 ml of solution B. Continue recording until a sharp maximum is observed (Fig. 1). Repeat, using standards and (for the blank) pure water instead of sample. From the recorded curve determine the reaction time t_L (t_L^0 for the blank). The corresponding distances on the chart can be used. Calculate the t_L^0/t_L values. Plot the values for the standards against osmium concentration; the calibration graph is linear.

Amperometric monitoring. Set up the apparatus with sample and solution A in the reaction vessel as above. Set the applied potential at zero and record the diffusion current as a function of time, at a sensitivity of 25-50 μA full-scale deflection. When the current is steady add solution B as above and continue recording until the "end-point" is reached (Fig. 2). Evaluate as above.

Monitoring by chemiluminescence. Dissolve 1.24 g of luminol and 0.4 g of sodium hydroxide in about 100 ml of water, dilute to 1 litre, and add 20 ml of this solution (which is stable for several months) to solution A before this is diluted to 1 litre. Mix the sample and solutions A and B in the dark,

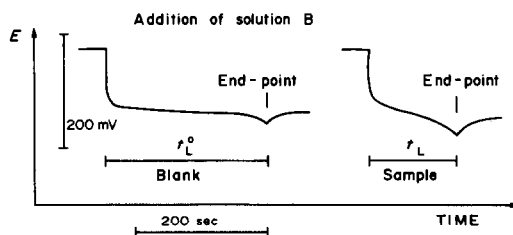


Fig. 1. Potentiometric traces.

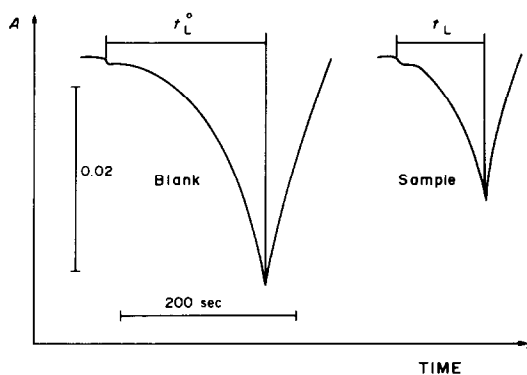


Fig. 2. Amperometric traces.

starting a stopwatch when solution B is added; stop the watch when a faint chemiluminescence appears. Alternatively a photoelectric instrument can be used as detector.

RESULTS AND DISCUSSION

Optimization

If we make the concentrations of hydrogen peroxide and potassium cyanide 100 times those for solutions A and B (and adjust the concentration of copper accordingly to obtain a suitable reaction time), the catalytic action of osmium practically disappears, and only in the presence of 100 ppm osmium does the catalytic action become noticeable. It is worth noting that under such conditions cobalt is the most sensitive catalyst, and can be determined in the range 10–100 ppm. A lengthy optimization procedure resulted in the choice of concentrations used for reagents A and B. It may well be true that even lower reagent concentrations would allow the sensitivity to be extended further, but the end-points on recorded potentiometric and amperometric traces become less sharp under such circumstances.

The sensitivity is maximal at pH 10.8–12.3, and for chemiluminescence monitoring the pH should be at least 11. If the pH is too high, however, some of the phosphate (used both as buffer and masking agent) may precipitate. We recommend using pH 11.2.

The role of the masking agent is to eliminate interferences from other (mainly metallic) ions, which would otherwise catalyse the reaction either on their own, or in combination with osmium. Of the obvious agents we tried tartrate, citrate, fluoride, phosphate and EDTA both on their own and in combination. Phosphate was found not only to act as a masking agent, but also to give remarkable enhancement of the catalytic effect of osmium (it also somewhat enhanced the effect of certain other elements, including Cu, Ag, Ru, Mo, W, U, Zn, Al, Ni, Cd and Co). Replacing phosphate by fluoride made the reaction rather insensitive to osmium, and cobalt was the most efficient catalyst. Tartrate, citrate or EDTA will prevent production of the chemiluminescence, but will not affect the potentiometric or amperometric monitoring.

The temperature affects the reaction times but not the sensitivity. The electrometric end-points are sharper at lower temperatures; 20° is recommended as optimal.

Results obtained with (simultaneous) amperometric and potentiometric monitoring are shown in Table 1. Results obtained by visual monitoring of chemiluminescence are less sensitive ($c_{\min} = 0.05$ ng/ml) and precise.

Interferences

The interference of 37 ions was studied by measuring the reaction time for 0.05-ng/ml osmium in the presence of increasing amounts of interferent, and calculating the inverse of its ratio to the reaction time with no interferent present. A ratio between 0.95 and 1.05 was taken as indicating no interference. The results are listed in Table 2. Ratios less than 0.95 can be taken as resulting from reaction of the interferent with hydrogen peroxide, making the reaction time longer. Full details are given in a thesis.³⁷

It can be seen that the tolerance limits are 0.005 $\mu\text{g/ml}$ for Ni and Mn, 0.05 $\mu\text{g/ml}$ for Cu, 0.5 ppm for Mo, W, Al, Cr, Ru, Au, Ag and Rh, 5 $\mu\text{g/ml}$ for Co, V, Pd, Hg, Ce and Fe(III), 50 $\mu\text{g/ml}$ for Ti, Zn, Fe(II), U, Pt, Re, Pb, Ba, Cd, La, Ir, Sb and Sn, and 500 ppm for Sr, Ca, Mg, Y, Zr and Se. Na and K did not interfere at even higher concentrations. Some tolerance levels may be slightly higher than those listed above, and may be obtained by interpolation in Table 2.

Kinetic study

Whenever a new catalytic method is introduced, it

Table 1. Results obtained for calibration*

$c_{\text{Os}}, \text{ng/ml}$	t_L, sec	t^0/t_L	$\pm \Delta c, \text{ng/ml}^\dagger$
0.0	234.4	1.00	0.021
0.2	173.4	1.35	0.018
0.5	128.1	1.83	0.016
0.6	115.6	2.03	0.016
0.8	100.0	2.34	0.017
1.0	87.5	2.68	0.020

*Equation of the calibration line (with tolerance limits at 0.95 significance level):

$$\frac{t^0}{t_L} = a + bC_{\text{Os}} = (1.006 \pm 0.01) + (1.67 \pm 0.02) C_{\text{Os}}$$

where C_{Os} is in ng/ml.

Coefficient of correlation: $r = 0.9998$.

Lowest determinable concentration of osmium:³⁵

$$c_{\min} = \frac{\tau(s_a + \bar{c}s_b)}{b + s_b} = 0.03 \text{ ng/ml}$$

where s_a, s_b are the standard deviations of the intercept (0.0098) and slope (0.016) respectively, $\pm \tau$ are the limits of integration of the Student distribution function (here $\tau = 2.78$ for $f = 4$ and $P = 0.95$), and \bar{c} is the average of the concentration values (0.52 ng/ml).

†Based on the formula³⁶

$$\Delta c = \frac{\tau s_0}{b} \sqrt{\frac{1}{m} + \frac{1}{n} + \frac{(t_L^0 - \bar{t}_L^0)^2}{b^2 t_L^2 \left[\sum c^2 - \frac{(\sum c)^2}{m} \right]}}$$

where s_0 is the standard deviation of points about the line (0.013), $m = 6$, $n = 3$ (i.e., 3 replicate determinations for each sample).

Table 2. Interference study

[Interferent], Interferent	ng/ml	Ratio t_L (no interferent)/(t_L (interferent present))							
		500	50	5	0.5	0.05	5×10^{-3}	5×10^{-4}	5×10^{-5}
Ni(II)	*	10.20	8.50	1.71	1.10	1.01	1.00	1.00	1.00
Cu(II)	*	*	9.13	1.57	1.06	0.99	1.00	1.00	1.00
Co(II)	*	*	1.51	1.01	1.00	1.00	1.00	1.00	1.00
Mo(VI)	21.86	4.37	1.39	1.02	0.99	1.00	1.00	1.00	1.00
W(VI)	17.00	3.33	1.25	1.03	1.00	1.00	1.00	1.00	1.00
Cr(III)	*	5.10	1.24	1.05	1.01	1.00	1.00	1.00	1.00
Al(III)	3.19	1.47	1.20	1.04	1.00	1.00	1.00	1.00	1.00
Ru(III)	*	5.07	1.20	1.03	1.00	1.00	1.00	1.00	1.00
Au(III)	*	4.33	1.16	1.03	0.99	1.00	1.00	1.00	1.00
Ag(I)	*	2.50	1.16	1.02	0.99	1.00	1.00	1.00	1.00
V(V)	6.40	1.52	1.02	0.98	1.00	1.00	1.00	1.00	1.00
Pd(II)	4.94	1.26	1.03	1.01	1.00	1.00	1.00	1.00	1.00
Ti(III)	1.53	1.04	1.01	1.00	1.00	1.00	1.00	1.00	1.00
Hg(II)	*	1.63	1.02	1.01	1.00	1.00	1.00	1.00	1.00
Zn(II)	1.85	1.03	1.01	1.00	1.00	1.00	1.00	1.00	1.00
Fe(II)	1.22	0.96	0.99	1.00	1.00	1.00	1.00	1.00	1.00
U(VI)	1.14	1.04	0.98	1.00	1.00	1.00	1.00	1.00	1.00
Pt(IV)	1.06	1.00	1.01	1.00	1.00	1.00	1.00	1.00	1.00
Pb(II)	1.20	0.99	1.02	1.00	1.00	1.00	1.00	1.00	1.00
Sr(II)	1.02	1.00	0.99	1.00	1.00	1.00	1.00	1.00	1.00
Re(VII)	—	0.98	0.99	1.00	1.00	1.00	1.00	1.00	1.00
Ca(II)	0.99	1.01	1.00	1.00	1.00	1.00	1.00	1.00	1.00
Mg(III)	0.99	1.00	1.00	1.00	1.00	1.00	1.00	1.00	1.00
Y(III)	0.97	1.01	1.00	1.00	1.00	1.00	1.00	1.00	1.00
Zr(IV)	0.95	1.02	0.99	1.00	1.00	1.00	1.00	1.00	1.00
Se(VI)	0.95	0.98	1.00	1.00	1.00	1.00	1.00	1.00	1.00
Ba(II)	0.93	0.98	1.01	1.00	1.00	1.00	1.00	1.00	1.00
Cd(II)	0.94	0.98	1.02	1.00	1.00	1.00	1.00	1.00	1.00
La(III)	0.93	0.97	1.01	1.00	1.00	1.00	1.00	1.00	1.00
Ir(III)	0.69	0.96	1.01	1.00	1.00	1.00	1.00	1.00	1.00
Sb(III)	0.69	1.01	0.99	1.00	1.00	1.00	1.00	1.00	1.00
Ce(III)	0.74	0.93	0.97	1.00	1.00	1.00	1.00	1.00	1.00
Sn(II)	0.68	1.04	1.01	0.99	1.00	1.00	1.00	1.00	1.00
Sn(IV)	0.66	1.04	0.98	1.01	1.00	1.00	1.00	1.00	1.00
Fe(III)	0.84	0.83	0.96	0.99	1.00	1.00	1.00	1.00	1.00
Rh(III)	0.23	0.29	0.84	0.96	1.01	1.00	1.00	1.00	1.00
Mn(II)	†	†	0.76	0.87	0.93	0.97	1.00	1.00	1.00

*Immediate reaction.

†Very slow reaction.

is important to examine the kinetics and mechanism to find those parameters which influence the rates of the individual reactions and the sensitivity of the determination. A working hypothesis for the mechanism reduces the number of experiments needed.

The purpose of the kinetic study was to find a mechanism for both the uncatalysed and catalysed reactions, consistent with the kinetics, explain the shape of the calibration curve, and determine the Arrhenius parameters.

When formulating our working hypothesis for the mechanism and kinetics of the uncatalysed reaction, we made use of numerous reports in the literature,³⁸⁻⁴⁴ even though some of these regarded the oxidation of luminol as an essential step in the process. The information available on the hydrogen peroxide-cyanide reaction (in the absence of copper)⁴⁵⁻⁴⁹ also contained useful guidelines. As for the mechanism of the reaction in the presence of osmium, the earlier papers^{27,50-53} all suggested that the catalytic action of osmium is based on an Os(VI)/Os(VIII) cycle.

It must be emphasized that the mechanisms described below are simplified in many ways. Even in the absence of osmium the reaction system will contain hydroperoxide (HOO^-), hydroxide, hydro-

gen, cyanate, copper(I) and at least two different cyanocuprate(I) ions. Several of these may be involved in the rate-determining step. The simplified mechanism proposed below is based on the following experimental facts.³⁷

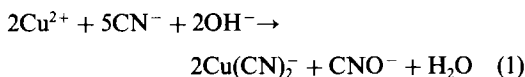
1. Though hydrogen peroxide reacts with cyanide in the absence of copper, this reaction is so much slower than the one proceeding in the presence of copper, that its rate can be excluded from the rate equations. For the bimolecular reaction between hydrogen peroxide and cyanide, Masson⁴⁹ found the value $1 \times 10^{-3} \text{ l. mole}^{-1} \text{ sec}^{-1}$ for the second-order rate constant. It is possible to postulate a mechanism for this reaction that involves two simultaneous processes³⁷ and to calculate the appropriate rate constant. The figure for the uncatalysed rate constant obtained in this way is equal (within 2%) to the figure quoted below.

2. It has been possible to establish³⁷ that the uncatalysed reaction is first order with respect to hydrogen peroxide and second order with respect to copper. Also, the catalysed reaction was found to be first order with respect to osmium.

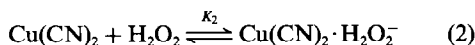
3. The rate depends on pH and shows a definite maximum at pH 11.3 (Fig. 3). As this pH is close to $\text{p}K_{a1}$ for hydrogen peroxide⁵⁴ we may speculate as to

which species (H_2O_2 , HOO^- or even the adduct $[\text{H}_2\text{O}_2 \cdot \text{HOO}^-]$) is involved in the reaction. However, the hydrogen-ion concentration could not be varied in a wide enough range for sound experimental results to be obtained. Thus, we omitted hydrogen and hydroperoxide ions from all the mechanisms, and simply based them on molecular hydrogen peroxide. In any case, in the analytical procedure we recommended the use of a pH 11.3 buffer and the nature of the peroxide species is unimportant from the practical point of view.

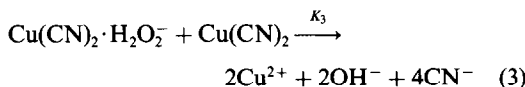
The uncatalysed reaction. In the absence of osmium, the predominant cyanocuprate(I) species in the solution is $\text{Cu}(\text{CN})_2^-$, produced by the overall reaction



This dicyanocuprate(I) ion then forms an adduct with hydrogen peroxide:



which then reacts with another dicyanocuprate(I) ion:



Reaction (3) is rate-determining. Note that by adding reactions (1)–(3) we can express the overall process simply as



That is, in the process, hydrogen peroxide and cyanide ions are consumed. The rate of disappearance of hydrogen peroxide (the "uncatalysed" rate) can be expressed as

$$-\left(\frac{d\{\text{H}_2\text{O}_2\}}{dt}\right)_{\text{un}} = k_3 \{[\text{Cu}(\text{CN})_2 \cdot \text{H}_2\text{O}_2^-]\} \{[\text{Cu}(\text{CN})_2^-]\} \quad (5)$$

where the braces $\{ \}$ stand for instantaneous (actual) concentrations. Applying the law of mass action to

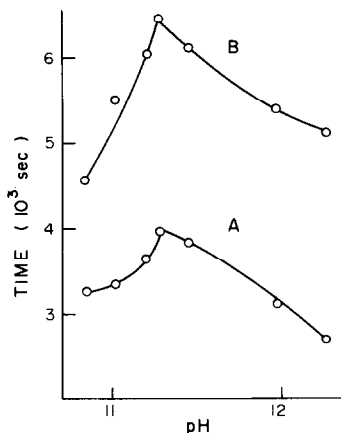


Fig. 3. Variation of the reciprocal reaction time with pH in the absence (A) and presence (B) of osmium.

reaction (2) we have

$$K_2 = \frac{\{[\text{Cu}(\text{CN})_2 \cdot \text{H}_2\text{O}_2^-]\}}{\{[\text{Cu}(\text{CN})_2^-]\} \{[\text{H}_2\text{O}_2]\}} \quad (6)$$

The following mass-balance equation can be written for copper:

$$c_{\text{Cu}} = \{\text{Cu}^{2+}\} + \{\text{Cu}^+\} + \{\text{Cu}(\text{CN})_2^-\} + \{[\text{Cu}(\text{CN})_2 \cdot \text{H}_2\text{O}_2^-]\} \approx \{\text{Cu}(\text{CN})_2^-\} \quad (7)$$

Here c_{Cu} is the "analytical" or "total" concentration of copper, which remains constant during each experiment. As long as free cyanide is present, the approximation expressed by equation (7) is valid. By combining equations (5)–(7), we can express the reaction rate as

$$-\left(\frac{d\{\text{H}_2\text{O}_2\}}{dt}\right)_{\text{un}} = k_{\text{un}} c_{\text{Cu}}^2 \{\text{H}_2\text{O}_2\} \quad (8)$$

where $k_{\text{un}} (= k_3 K_2)$ is the uncatalysed rate constant. Expression (8) now represents a pseudo first-order rate equation, which can be integrated with the boundary conditions that at the beginning of the reaction (time zero) the concentration of hydrogen peroxide is its initial value $\{\text{H}_2\text{O}_2\}_0$, while at the end-point (time = t_L^0), when practically all the free cyanide is used up, its concentration decreases to

Table 3. Kinetic study of the uncatalysed reaction

No.	$\{\text{H}_2\text{O}_2\}_0$, 10^{-3}M	$\{\text{CN}^-\}_0$, 10^{-4}M	c_{Cu} , 10^{-3}M	t_L^0 , sec	k_{un} , $10^3 l^2 \cdot \text{mole}^{-2} \cdot \text{sec}^{-1}$
1	1.76	2.02	7.25	645.3	3.54
2	2.34	2.02	7.25	462.5	3.69
3	2.90	2.02	7.25	364.1	3.79
4	3.51	2.02	7.25	312.5	3.64
5	4.10	2.02	7.25	262.5	3.71
6	5.21	2.02	7.25	190.0	4.03
7	2.70	2.02	7.25	390.6	3.79
8	2.70	2.17	7.25	529.7	4.73
9	2.70	2.31	7.25	746.8	4.74
10	2.70	2.60	7.25	2278.1	2.47
11	3.10	1.98	6.40	890.6	3.38
12	3.10	2.00	6.82	531.3	3.87
13	3.10	2.02	7.25	340.6	3.79
14	3.10	2.04	7.68	254.7	2.67
15	5.90	2.02	7.25	187.5	3.59

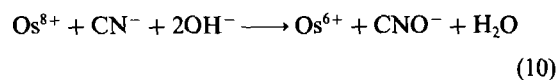
$\{H_2O_2\}_0 - \{CN^-\} - \frac{5}{2}c_{Cu}$. Integration yields the following expression for the uncatalysed rate constant:

$$k_{un} = \frac{1}{c_{Cu}^2 t_L^0} \ln \left(\frac{\{H_2O_2\}_0}{\{H_2O_2\}_0 - \{CN^-\}_0 + \frac{5}{2}c_{Cu}} \right) \quad (9)$$

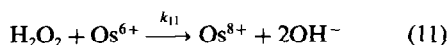
By varying the initial concentrations of hydrogen peroxide, cyanide and copper (within limits imposed by practicality) and measuring the t_L^0 reaction times, values for k_{un} were calculated and are shown in Table 3. The value of k_{un} remains constant for a wide range of reaction times, thus verifying the mechanism. An average value of $k_{un} = (3.70 \pm 0.33) \times 10^3 \text{ l}^2 \cdot \text{mole}^{-2} \cdot \text{sec}^{-1}$ is obtained for this third-order rate constant. The 95% confidence limits are given ($\pm 0.33 \times 10^3$).

The catalysed reaction. In the following reaction scheme the actual ionic forms of osmium(VI) and (VIII) are not identified, but simply denoted as Os^{6+} and Os^{8+} .

When osmium tetroxide is added to the mixture, it will oxidize cyanide in a fast reaction. The overall process follows the stoichiometry



When hydrogen peroxide is added, re-oxidation of the osmium takes place:



Step (11) is rate-determining. Though slow, it is faster than step (3), hence the catalytic effect of osmium. Note that the sum of steps (10) and (11) again equals the net reaction (4). Thus, both copper and osmium are acting as catalysts.

The rate of the catalysed reaction can be expressed from (11) as

$$-\left(\frac{d\{H_2O_2\}}{dt}\right)_{cat} = k_{11} \{H_2O_2\} \{Os^{6+}\} \quad (12)$$

The concentration of the osmium(VI) is unknown, but because reaction (10) is much faster than (11), it can be regarded as equal or at least proportional to the analytical concentration of osmium

$$\{Os^{6+}\} = \alpha c_{Os} \quad (13)$$

where α is an unknown constant. Combining equations (12) and (13) gives

$$-\left(\frac{d\{H_2O_2\}}{dt}\right)_{cat} = k_{cat} c_{Os} \{H_2O_2\} \quad (14)$$

where $k_{cat} (= k_{11}\alpha)$ is a second-order rate constant. Since c_{Os} is constant for a given experiment, again a pseudo first-order rate expression results, which is easier to handle mathematically.

The overall rate. Unlike the uncatalysed reaction, the catalysed process cannot be examined experimentally on its own, as under the conditions of the analytical procedure both reactions always proceed

simultaneously. Hence the overall rate has to be expressed, by adding equations (8) and (14), as

$$-\frac{d\{H_2O_2\}}{dt} = [k_{un} c_{Cu}^2 + k_{cat} c_{Os}] \{H_2O_2\} \quad (15)$$

This differential rate equation can be integrated with the boundary conditions described earlier. Denoting the Landolt-reaction time by t_L , we can express the rate constant k_{cat} as

$$k_{cat} = \frac{1}{c_{Os}} \left[\frac{1}{t_L} \ln \left(\frac{\{H_2O_2\}_0}{\{H_2O_2\}_0 - \{CN^-\}_0 + \frac{5}{2}c_{Cu}} \right) - k_{un} c_{Cu}^2 \right] \quad (16)$$

We tested this equation experimentally by varying the initial concentration of hydrogen peroxide, and the analytical concentration of osmium (within as wide ranges as possible), measuring the reaction times and calculating the k_{cat} value with equation (16). It was not possible to vary either the cyanide or the copper concentrations enough to support our mechanism, as their variation (just as in the case of the uncatalysed reaction, cf. Table 4) caused rather drastic changes in the reaction times. Their levels were kept at those recommended for the analytical procedure. As Table 4 indicates, however, the value of k_{cat} remains fairly constant (even though the errors in the k_{un} rate coefficient are included and magnified in the expression). Thus, for the concentration range covered, we can accept the proposed mechanism and kinetics. The mean of the k_{cat} values is $(11.27 \pm 1.22) \times 10^6 \text{ l} \cdot \text{mole}^{-1} \cdot \text{sec}^{-1}$ (95% confidence limits).

The calibration curve

By combining equations (9) and (16) we can express the ratio t_L^0/t_L , used when constructing the calibration curve, as

$$\frac{t_L^0}{t_L} = 1 + \frac{k_{cat} c_{Os}}{k_{un} c_{Cu}^2} \quad (17)$$

Thus when t_L^0/t_L is plotted against c_{Os} , a straight line is expected, with an intercept of 1.00. The experimental calibration lines (cf. Table 2) agree with these predictions, showing again that the proposed mechanism and kinetics are basically correct.

Table 4. Kinetic study of the catalysed reaction*

No.	$\{H_2O_2\}_0$, $10^{-3} M$	c_{Os} , $10^{-13} M$	t_L , sec	$10^6 k_{cat}$, $l \cdot \text{mole}^{-1} \cdot \text{sec}^{-1}$
1	1.76	8.76	448.4	8.20
2	2.34	8.76	317.2	9.99
3	2.90	8.76	240.6	12.07
4	3.51	8.76	207.8	10.51
5	4.10	8.76	178.1	10.49
6	5.27	8.76	137.5	10.72
7	5.90	8.76	119.7	11.60
8	5.90	10.51	105.5	13.47
9	5.90	14.02	93.5	13.19
10	5.90	17.52	80.1	14.18
11	5.90	3.50	157.8	5.58

* $c_{Cu} = 7.250 \times 10^{-5} M$, $\{CN^-\}_0 = 2.022 \times 10^{-4} M$.

Table 5. Effect of temperature on reaction time*

Temperature, °C	$t_{L,T}^0$, sec	$t_{L,T}$, sec	$F(T)_{un}$	$F(T)_{cat}$	$10^3 k'_{T,un} \cdot \text{mole}^{-2} \cdot \text{sec}^{-1}$
14.0	278.1	220.3	-179.81	-110.72	2.40
16.7	234.2	190.6	-178.46	-110.95	2.89
20.1	187.5	157.8	-176.71	-111.12	3.63
23.5	148.4	128.9	-174.86	-110.60	4.54
26.7	120.3	107.0	-173.21	-110.28	5.57
29.7	100.0	90.6	-171.75	-110.58	6.73

* $\{H_2O_2\}_0 = 5.9 \times 10^{-3} M$, $\{CN^-\}_0 = 2.022 \times 10^{-4} M$, $c_{Cu} = 7.25 \times 10^{-5} M$, $c_{Os} = 3.50 \times 10^{-13} M$.

Temperature effects. Reaction rates vary strongly with temperature. The temperature dependence of a rate constant k_T can be expressed by the modified Wynne-Jones-Eyring⁵⁵ equation:

$$k_T = \frac{kT}{h} \exp\left(\frac{\Delta S^\ddagger}{R}\right) \exp\left(-\frac{\Delta H^\ddagger}{RT}\right) \quad (18)$$

where k_T is the rate constant at absolute temperature T , k is the Boltzmann constant, h is Planck's constant, R the gas constant, ΔS^\ddagger the entropy of activation and ΔH^\ddagger the enthalpy of activation (the so-called Arrhenius parameters). To investigate the reactions of interest, equations (18) and (9) can be combined to define a temperature function $F(T)_{un}$ for the uncatalysed reaction:

$$\begin{aligned} F(T)_{un} &= \Delta S_{un}^\ddagger - \frac{\Delta H_{un}^\ddagger}{T} \\ &= R \ln\left(\frac{h}{kT c_{Cu}^2 t_{L,T}^0}\right) \\ &\quad \times \ln\left(\frac{\{H_2O_2\}_0}{\{H_2O_2\}_0 - \{CN^-\}_0 + \frac{5}{2} c_{Cu}}\right) \quad (19) \end{aligned}$$

while for the catalysed reaction, combination of (18) with (16) gives

$$\begin{aligned} F(T)_{cat} &= \Delta S_{cat}^\ddagger - \frac{\Delta H_{cat}^\ddagger}{T} \\ &= R \ln \frac{h}{kT c_{Os}} \\ &\quad \times \left[\frac{1}{t_{L,T}} \ln\left(\frac{\{H_2O_2\}_0}{\{H_2O_2\}_0 - \{CN^-\}_0 + \frac{5}{2} c_{Cu}}\right) \right. \\ &\quad \left. - k'_{T,un} c_{Cu}^2 \right] \quad (20) \end{aligned}$$

In these equations $t_{L,T}^0$ and $t_{L,T}$ represent the Landolt-reaction times at absolute temperature T for the uncatalysed and catalysed processes, respectively, while $k'_{T,un}$ is the uncatalysed rate constant at temperature T , as calculated from equation (18). Plotting the $F(T)$ values against the reciprocals of the absolute temperatures gives straight lines ("modified" Arrhenius plots) with intercepts equal to the entropies of activation, and slopes giving the enthalpies of activation.

To determine these parameters experiments were done at different temperatures, in the absence and presence of osmium. Initial concentrations of all the

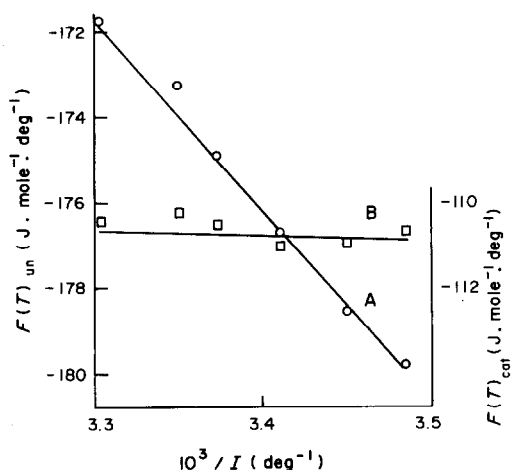


Fig. 4. Modified Arrhenius plots for the (A) uncatalysed and (B) catalysed reactions.

reactants were kept constant. The results are shown in Table 5 and Fig. 4.

Linear regression analysis provided the following values for the Arrhenius parameters (95% confidence limits):

$$\Delta S_{un}^\ddagger = -23.1 \pm 3.8 \text{ J. mole}^{-1} \cdot \text{K}^{-1}$$

$$\Delta S_{cat}^\ddagger = -102 \pm 16 \text{ J. mole}^{-1} \cdot \text{K}^{-1}$$

$$\Delta H_{un}^\ddagger = 45.0 \pm 1.1 \text{ kJ/mole}$$

$$\Delta H_{cat}^\ddagger = 2.5 \pm 4.8 \text{ kJ/mole}$$

It is noteworthy that the enthalpy of activation of the catalysed reaction is exceptionally low (the Arrhenius plot is almost horizontal), which is in fact a manifestation of the high catalytic activity of osmium and accounts for the high sensitivity of the method. The error (4.8 kJ/mole) of ΔH_{cat}^\ddagger is no greater than would normally be expected from such measurements, in which the errors of the uncatalysed parameters are also accumulated [cf. equation (20)].

Acknowledgements—I. N. C. Ling would like to express thanks for minor grants received from Queen's University, Belfast, and from the British Council.

REFERENCES

1. J. Bognár and S. Sárosi, *Magy. Kém. Foly.*, 1961, **67**, 193.
2. J. Bognár and L. Sipos, *Mikrochim. Acta*, 1963, 1066.

3. N. M. Lukovskaya and A. V. Terletskaia, *Ukr. Khim. Zh.*, 1974, **40**, 1193.
4. A. T. Pilipenko and A. V. Terletskaia, *Zh. Analit. Khim.*, 1972, **27**, 1570.
5. A. P. Filippov, V. M. Zyatkovskii and K. B. Yatsimirskii, *ibid.*, 1970, **25**, 1769.
6. T. Shiokawa, *Sci. Rep. Res. Inst. Tohoku Univ. Ser. A*, 1950, **2**, 293.
7. G. A. Konishevskaya, V. F. Romanov and K. B. Yatsimirskii, *Zh. Analit. Khim.*, 1973, **28**, 1154.
8. A. P. Filippov, G. A. Konishevskaya, V. F. Romanov and K. B. Yatsimirskii, *ibid.*, 1974, **29**, 2266.
9. J. Bognár and S. Sárosi, *Magy. Kem. Foly.*, 1961, **67**, 193.
10. I. I. Alekseeva, N. K. Ignatova, A. P. Rysev and K. B. Yatsimirskii, *Zh. Analit. Khim.*, 1972, **27**, 1566.
11. J. Bognár and S. Sárosi, *Magy. Kem. Foly.*, 1961, **67**, 198. See also *Acta Chim. Acad. Sci. Hung.*, 1961, **29**, 395.
12. K. B. Yatsimirskii, *Izv. Vyssh. Uchebn. Zaved. Khim. i Khim. Tekhnol.*, 1961, **4**, 315.
13. K. B. Yatsimirskii and N. V. Parkhomenko, *Zh. Analit. Khim.* 1963, **18**, 229.
14. T. Shiokawa, *Sci. Rep. Res. Inst. Tohoku Univ. Ser. A*, 1950, **2**, 287, 290.
15. J. Bognár, O. Jellinek and S. Sárosi, *Mikrochim. Acta*, 1965, 708.
16. J. Bognár and O. Jellinek, *ibid.*, 1964, 317.
17. J. Bognár and S. Sárosi, *Magy. Kem. Foly.*, 1962, **68**, 53.
18. I. I. Alekseeva, N. K. Ignatova, A. P. Rysev and K. B. Yatsimirskii, *Zh. Analit. Khim.*, 1974, **29**, 335.
19. I. I. Alekseeva, I. B. Smirnova and K. B. Yatsimirskii, *ibid.*, 1970, **25**, 539.
20. A. E. Burgess and J. M. Ottaway, *Talanta*, 1975, **22**, 401.
21. I. I. Alekseeva, N. K. Ignatova, R. P. Rysev and K. B. Yatsimirskii, *Zavodsk. Lab.*, 1972, **38**, 919.
22. I. I. Alekseeva, A. D. Gromova, A. P. Rysev, N. A. Khvorostukhina and K. B. Yatsimirskii, *Zh. Analit. Khim.*, 1974, **29**, 1017.
23. H. L. Pardue and R. L. Habig, *Anal. Chim. Acta*, 1966, **35**, 383.
24. P. A. Rodriguez and H. L. Pardue, *Anal. Chem.*, 1969, **41**, 1376.
25. T. Shiokawa, *Nippon Kagaku Zasshi*, 1949, **70**, 353.
26. V. P. Khvostova, V. I. Shlenskaya and G. I. Kadyrova, *Zh. Analit. Khim.*, 1973, **28**, 328.
27. H. Müller and M. Otto, *Z. Chem.*, 1974, **14**, 159.
28. *Idem*, *Mikrochim. Acta*, 1975 **I**, 519.
29. V. S. Khain, A. A. Volkov and E. V. Fomina, *Zh. Analit. Khim.*, 1976, **31**, 1500.
30. H. Matusieqicz and Z. Kurzawa, *Chem. Anal. Warsaw*, 1976, **21**, 1035.
31. A. T. Pilipenko, L. V. Markova and T. S. Maksimenk, *Zh. Analit. Khim.*, 1973, **28**, 1544.
32. E. H. White, *J. Chem. Educ.*, 1957, **34**, 275.
33. L. Erdey, *Gravimetric Analysis*, Part 2, p. 265. Pergamon Press, Oxford, 1965.
34. I. M. Kolthoff, R. Belcher, V. A. Stenger and G. Matsuyama, *Volumetric Analysis*, Vol. III, p. 282. Interscience, New York, 1957.
35. K. Doerffel, *Statistik in der Analytischen Chemie*, p. 177. VEB Deutscher Verlag für Grundstoffindustrie, Leipzig, 1966.
36. *Idem*, *op. cit.*, p. 173.
37. I. N. C. Ling, *Ph.D. Thesis*, Queen's University, Belfast, 1981.
38. A. J. Steigmann, *J. Soc. Chem. Ind.*, 1942, **61**, 36.
39. S. Musha, *Nippon Kagaku Zasshi*, 1958, **79**, 647.
40. S. Musha, M. Ito, Y. Yamamoto and Y. Inamori, *ibid.*, 1959, **80**, 1285.
41. F. H. Constable and V. Amirhayan, *Istanbul Univ. Fen. Fak. Mecm.*, 1959, **24C**, 217; *Chem. Abstr.*, 1961, **55**, 10017g.
42. A. K. Babko and N. M. Lukovskaya, *Ukr. Khim. Zh.*, 1962, **28**, 861.
43. K. Weber and M. Krajčinić, *Ber.*, 1942, **75B**, 2051.
44. A. T. Pilipenko, G. V. Angelova and I. E. Kalinichenko, *Compt. Rend. Acad. Bulg. Sci.*, 1973, **26**, 1359.
45. Attfield, *J. Soc.*, 1863, **16**, 94.
46. B. Radziszewski, *Ber.*, 1885, **18**, 355.
47. C. J. Martin and R. A. O'Brien, *Proc. Soc. Chem. Ind. (Victoria)*, 1901, **1**, 119.
48. O. Masson, *J. Chem. Soc.*, 1907, **91**, 1449.
49. I. R. Wilson, in *Reactions of Negative Inorganic Ions*, Vol. 6, *Comprehensive Chemical Kinetics*, C. H. Bamford and C. F. H. Tipper (eds.) p. 288. Elsevier, Amsterdam, 1972.
50. R. D. Sauerbrunn and E. B. Sandell, *Mikrochim. Acta*, 1953, 22.
51. R. L. Habig, H. L. Pardue and J. B. Worthington, *Anal. Chem.*, 1967, **39**, 600.
52. G. S. Desmukh and M. G. Bapat, *Z. Anal. Chem.*, 1957, **156**, 105.
53. N. Y. Sidgwick, *Chemical Elements and their Compounds*, p. 1457. Oxford University Press, Oxford, 1950.
54. F. A. Cotton and G. Wilkinson, *Advanced Inorganic Chemistry*, 4th Ed., p. 496. Wiley, New York, 1980.
55. W. F. K. Wynne-Jones and H. Eyring, *J. Chem. Phys.*, 1935, **3**, 492.

ELEKTROCHEMISCHE UNTERSUCHUNG VON BIS(DIPHENYLDITHIOPHOSPHIN) DISULFID

ANGEL SCHISCHKOV, SHIVKO DENTSCHEV und CHRISTINA MALAKOVA
Lehrstuhl für analytische Chemie an der Paissij Chilendarski-Universität-Plovdiv,
VRB-4000 Plovdiv, Bulgarien

(Eingegangen am 11. Februar 1983. Angenommen am 16. Juni 1983)

Zusammenfassung—Die elektrochemischen Untersuchungen von bis(Diphenyldithiophosphin) Disulfid (RSSR), und Diphenylquecksilberdithiophosphinat [(RS)₂Hg], erfolgten in Äthanol-Lithiumperchlorat und Äthanol-Schwefelsäure Medium durch die Methoden der klassischen Polarographie, und Elektrolyse bei kontrollierbarem Potential und eine rotierende Scheibenelektrode. Die Ergebnisse weisen darauf hin, daß RSSR nicht direkt auf einer Quecksilbertropfelektrode reduziert, sondern erst adsorbiert wird. Anschließend unterliegt es einer schnellen chemischen Reaktion unter Bildung von elektroaktivem (RS)₂Hg. Die Elektrolyse bei kontrollierbarem Potential bestätigt, daß (RS)₂Hg eine Zweielektronenreduktion eingeht, bei der als Hauptprodukt Diphenyldithiophosphinsäure (RSH) gebildet wird, während die Oxydation von RSH zur Erhaltung von (RS)₂Hg führt. Obwohl das chemische und das Adsorptionsgleichgewicht bei der Reduktion von RSSR und (RS)₂Hg sehr kompliziert ist, ist die coulometrische Generierung von RSH nicht schwer und erlaubt den Einsatz von RSSR als coulometrisches Reagens.

Die Wechselwirkung der Dithiophosphinsäuren mit den Ionen einer großen Anzahl von Metallen ist eingehend untersucht.¹ Als analytische Reagenzien haben sie zur Extraktionstrennung der Elemente vorwiegend mit spektrophotometrischer Registrierung Anwendung gefunden.^{2,3} Ein Teil der Dithiophosphinatkomplexe absorbieren kein Licht im sichtbaren Spektralbereich, was ihren extraktionsphotometrischen Nachweis beträchtlich erschwert. In dieser Hinsicht erweisen sich die unterschiedlichen elektrochemischen Methoden, insbesondere Polarographie und Coulometrie, die ziemlich häufig bei der Untersuchung der verschiedenen Klassen organischer schwefelhaltiger Reagenzien zum Einsatz kommen,^{4,5} als sehr wertvoll.

Mit Hilfe der klassischen Polarographie, der Elektrolyse bei kontrollierbarem Potential und einer rotierenden Scheibenplatinelektrode wurde das Verhalten von RSSR hinsichtlich dessen Anwendung als coulometrisches Reagens untersucht.

EXPERIMENTELLER TEIL

Geräte

Polarographen OH-103 und OH-105 (Radelkis, Ungarn), Potentiostat P-5848 (UdSSR), rotierende Scheibenplatinelektrode,⁶ und Spektrophotometer Specord UV-VIS (DDR). Die Charakteristik der Kapillare in Äthanol-0,2M Lithiumperchlorat war $m = 3,51$ mg/sec; $t = 1,95$ sec.

Alle elektrochemischen Untersuchungen erfolgten bei $20 \pm 1^\circ$. Sauerstoff wurde mittels Durchleitung reines Argons aus der Lösung entfernt. Als Vergleichselektrode diente eine gesättigte Kalomelektrode.

Reagenzien

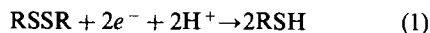
Äthanol, p.a., Schwefelsäure, p.a., Lithiumperchlorat, p.a., (Merck), und destilliertes Wasser. Es wurden Lösungen

von genau bestimmten Mengen an $1 \times 10^{-3}M$ RSSR⁷ und $0,4 \times 10^{-3}M$ (RS)₂Hg verwendet.

ERGEBNISSE UND DISKUSSION

Elektrochemische Untersuchungen in Äthanol-0,2M LiClO₄ Medium

Polarographie von RSSR und (RS)₂Hg auf Quecksilbertropfelektrode. Auf dem Polarogramm sind zwei Reduktionswellen zu sehen (Abb. 1): $E_{1/2}$ der ersten Welle liegt bei $-0,45$ V, $E_{1/2}$ der zweiten dagegen bei $-0,8$ V. Die Diffusionsströme beider Wellen verändern sich linear mit Zunahme der RSSR-Konzentration. Die Reduktion des Disulfids erfolgt nach der Gleichung



Die Gleichung der polarographischen Welle

$$E_{de} = E' + 0,029 \log \left(\frac{i_d - i}{i^2} \right) \quad (2)$$

zeigt daß E eine lineare Funktion von $\log (i_d - i)/i^2$ mit einer Steigung von $0,029$ V ist. Dies bestätigten auch die experimentellen Ergebnisse für Konzentrationen von 1×10^{-5} bis $1 \times 10^{-4}M$ RSSR, nach denen die oben erwähnte Abhängigkeit als eine Gerade mit einer Neigung von $0,030$ – $0,033$ V erscheint. Trägt man i_d gegen $H^{\frac{1}{2}}$ auf, erhält man eine durch den Ursprung laufende Gerade (H = Höhe des Quecksilberniveaus). Diese Angaben weisen darauf hin, daß der elektrochemische Prozeß durch die Diffusion begrenzt wird.

Erhöht sich die Konzentration um das Zehnfache, so verschiebt sich $E_{1/2}$ der ersten Welle nach den

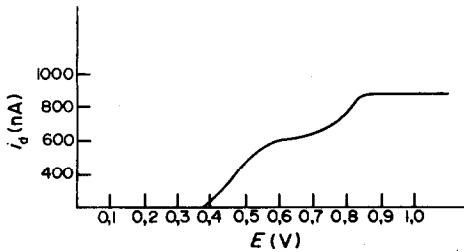
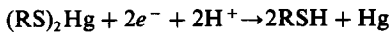


Abb. 1. Klassisches Polarogramm von $1 \times 10^{-4} M$ RSSR in Äthanol- $0,2 M$ LiClO_4 .

negativeren Potentialen unter Nichtbeachtung der linearen Abhängigkeit $E_{1/2} = E - 0,029 \log i_d/2$. Die in Äthanol in Abwesenheit und dann in Gegenwart von RSSR aufgenommenen elektrokapillaren Kurven zeigen eine Depression, die auf einen Adsorptionsprozeß zurückzuführen ist (Abb. 2).

Diese Angaben sprechen für einen komplizierten Prozeß bei der Reduktion von RSSR und Gleichung (1) gibt lediglich unvollständig die Natur der elektrochemischen Wechselwirkungen wieder.

Die für $1 \times 10^{-4} M$ RSSR und $1 \times 10^{-4} M$ $(\text{RS})_2\text{Hg}$ erhaltenen Polarogramme weisen identische Wellen auf, wobei $E_{1/2}$ von $(\text{RS})_2\text{Hg}$ um etwa $0,05 V$ nach den positiveren Potentialen als $E_{1/2}$ von RSSR verschoben wird. $(\text{RS})_2\text{Hg}$ geht folgende elektrochemische Reaktion ein:



Die Gleichung der polarographischen Welle ist mit Gleichung (2) identisch. Ein Gemisch von RSSR und $(\text{RS})_2\text{Hg}$ ergab eine verzerrte Zwischenwelle, wobei die lineare Abhängigkeit des Potentials E_{de} von $\log(i_d - i)/i^2$ im Unterschied zu RSSR nicht befolgt wird, was auf einen komplizierten Prozeß hindeutet.

Polarographie von RSSR und $(\text{RS})_2\text{Hg}$ auf rotierender Scheibenplatinelektrode. Wird RSSR auf einer Quecksilbertropfelektrode direkt reduziert, ohne einer chemischen Reaktion zu unterliegen, so sollte es ebenfalls auf einer rotierenden Scheibenplatinelektrode mit annähernd gleichen Potentialen reduziert werden. Die Polarogramme beider Verbindungen wurden auf einer zweimal mit heißer,

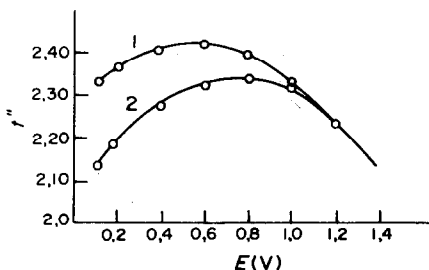


Abb. 2. Elektrokapillarkurve von $1 \times 10^{-3} M$ RSSR in Äthanol- $0,2 M$ LiClO_4 ; 1. in Abwesenheit von RSSR; 2. in Gegenwart von RSSR.

konzentrierter Salpetersäure behandelten und nacheinander mit destilliertem Wasser und Äthanol gewaschenen Platinelektrode erhalten. Die untere Grenze bei einer Kathodenpolarisation in Äthanol- $0,2 M$ Lithiumperchlorat liegt bei $-1,05 V$ gegen die gesättigte Kalomelektrode. Für RSSR-Lösungen wurde in den Grenzen $0,05-1,05 V$ kein Kathodenpolarogramm erhalten. Für $(\text{RS})_2\text{Hg}$ -Lösungen erschien eine Einzelwelle mit $E_{1/2}$ bei $-0,45 V$. Bei einer zweiten Elektrolysierung der schon einmal benutzten RSSR-Lösung ohne Entfernung des Quecksilberfilms auf der Platinelektrode wurde eine Kathodenwelle mit $E_{1/2}$ ähnlich wie für $(\text{RS})_2\text{Hg}$ erhalten. Wird die Elektrode nach dem Hg-Dithiophosphinatpolarogramm mit heißer, konzentrierter Salpetersäure, dest. Wasser und Äthanol gereinigt, so ergibt RSSR keine Kathodenwelle.

Die Ergebnisse zeigen, daß RSSR vor der Elektroreduktion eine chemische Reaktion mit Quecksilber eingehen muß. Auf reiner rotierender Scheibenplatinelektrode wird praktisch keine Kathodenwelle von RSSR beobachtet.

Die lineare Abhängigkeit des Stroms i_d von H^+ und der RSSR-Konzentration beweist, daß diese Reaktion mit großer Geschwindigkeit verläuft.

Elektrolyse von RSSR bei kontrollierbarem Potential. Zur Untersuchung der Elektrolyse bei kontrollierbarem Potential wurden Lösungen von $1 \times 10^{-3} M$ RSSR in Äthanol- $0,2 M$ Lithiumperchlorat eingesetzt. Das Volumen der elektrolysierten Lösung betrug 50 ml und das des Quecksilbers 20 ml . Das Potential wurde bei $-1,00 V$, der Hauptwelle von RSSR auf der Tropfelektrode, konstant eingehalten. Um den Strom bei der Elektrolyse zu kontrollieren, wurde eine keinen elektroaktiven Stoff enthaltende Lösung untersucht. Dabei war kein Stromfluß zu beobachten.

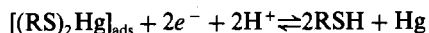
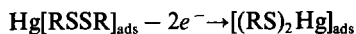
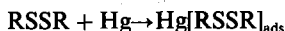
Nach Zugabe der RSSR-Lösung bei offener Kette ließ sich auf der Quecksilberkathode ein weißlicher Niederschlag erkennen. Sein UV-Spektrum zeigt ein Absorptionsmaximum $\lambda_{\text{max}} = 260 \text{ nm}$ und unterscheidet sich dadurch von RSSR mit $\lambda_{\text{max}} = 220 \text{ nm}$. Die Analyse der erhaltenen IR-Spektren weist auf die Anwesenheit von $(\text{RS})_2\text{Hg}$ mit Schmp. $= 274 \pm 1^\circ$ hin. Die mit dem präparativ gewonnenen $(\text{RS})_2\text{Hg}$ verglichenen Angaben stimmen völlig überein.

Um die Elektrolyseprodukte qualitativ zu bestimmen, wurden nach einer $0,2\%$ igen Abnahme der Stromstärke 20 ml der elektrolysierten Lösung entnommen und portionsweise zu je 10 ml zu Ni^{2+} und Co^{2+} Ionen enthaltenden Lösungen getropft. Die erhaltenen Sedimente wurden mit Dichloräthan innerhalb von drei Minuten extrahiert. Gleich darauf wurden ihre Absorptionsspektren aufgenommen (Abb. 3). Sie zeigen eine völlige Übereinstimmung mit den von Larionov u.a. erzielten Ergebnissen.⁸

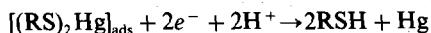
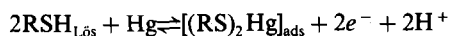
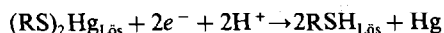
Die Zahl der am Reduktionsprozeß beteiligten Elektronen wurde für zwei Bestimmungen ermittelt $n = 2,02 \pm 0,06$.⁹

Das Erhalten von $(RS)_2Hg$ ist ein Beweis dafür, daß RSSR nicht direkt auf der Quecksilbertropfelektrode reduziert wird, sondern erst in eine zur Bildung von $(RS)_2Hg$ führende chemische Reaktion tritt, das als die elektroaktive Komponente erscheint.

Zusammenfassend läßt sich folgern, daß RSH das Endprodukt der Elektrolyse ist. Die wahrscheinlichen Beziehungen von RSSR auf der Quecksilbertropfelektrode sind nach dem folgenden Schema wiederzugeben:



Die wahrscheinlichen Beziehungen von $(RS)_2Hg$ auf der Quecksilbertropfelektrode sind schematisch folgenderweise zu veranschaulichen:



Elektrochemische Untersuchungen in Äthanol-1M Schwefelsäure

Die polarographischen Kurven für unterschiedliche Konzentrationen sind auf Abb. 4 zu sehen.

Wenn man die polarographischen Wellen bedingt in einzelne Potentialzonen einteilt, so erkennt man bei niedrigeren Konzentrationen nur einen störenden Prozeß, bei höheren Konzentrationen dagegen drei solcher Prozesse. Zur Ermittlung ihrer Natur wurden Elektrokapillarkurven in Äthanol-1M Schwefelsäure Medium aufgenommen (Abb. 5). Die hier ebenfalls zu beobachtende Depression deutet auf das Vorhandensein eines sich auf dem Quecksilbertropfen adsorbierenden Stoffes hin. Bei höheren RSSR-Konzentrationen nimmt die Adsorption zu und die verzögerte Stromzunahme läßt auf die Bildung eines, die elektrochemische Reaktion hemmenden, unlöslichen Films von Molekülen des Depolarisators auf der Quecksilberoberfläche schließen.

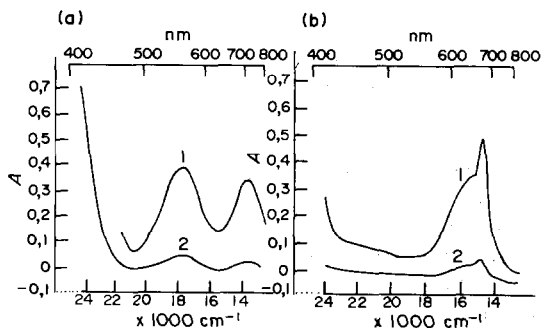


Abb. 3. Absorptionsspektren in Dichloräthan, $b = 1$ cm, von (a) 1. $(RS)_2Ni$; 2. $Ni^{2+} + RSSR$ nach Elektrolyse; (b) 1. $(RS)_2Co$; 2. $Co^{2+} + RSSR$ nach Elektrolyse.

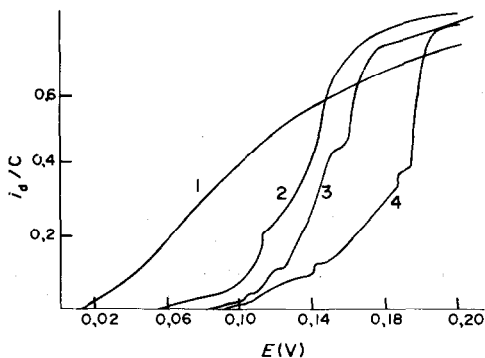


Abb. 4. Klassische Polarogramme von RSSR in Äthanol-1M H_2SO_4 Medium. 1. $0,5 \times 10^{-4}M$; 2. $1 \times 10^{-4}M$; 3. $1,5 \times 10^{-4}M$; 4. $0,3 \times 10^{-3}M$.

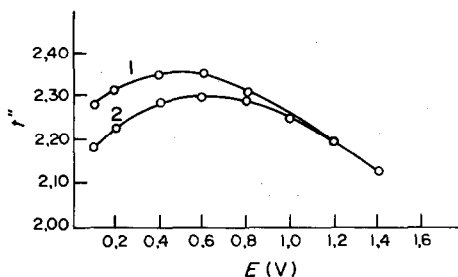


Abb. 5. Elektrokapillarkurven von $1 \times 10^{-3}M$ RSSR in Äthanol-1M H_2SO_4 Medium; 1. in Abwesenheit von RSSR; 2. in Gegenwart von RSSR.

Die schnelle Stromzunahme bei den negativeren Potentialen läßt sich wahrscheinlich auf die Reduktion dieses Films zurückführen, indem RSSR schnell mit Hg reagiert unter Bildung eines unlöslichen Films aus $(RS)_2Hg$, der jedoch bei Kathodenpotentialen, negativer als 0,12 V, reduziert wird.

Es ergibt sich für die erste Welle eine nichtlineare Abhängigkeit der Stufenhöhe von der Konzentration, die auf einen Adsorptionsprozeß hinweist. Der Strom dieser Welle ist ziemlich unabhängig von H^2 , was einen kinetischen Prozeß voraussetzt. Die auf dem Plateau der polarographischen Kurven gemessenen Ströme sind H^2 proportional und befinden sich in linearer Abhängigkeit von der RSSR-Konzentration, welches für eine Einschränkung des elektrochemischen Prozesses durch die Diffusion spricht. Die qualitative Analyse der Produkte der Elektrolyse bei kontrollierbarem Potential zeigt ebenfalls, daß RSH ein Endprodukt ist.

Wenn man von dem Verlauf komplizierter chemischer und elektrochemischer Prozesse absieht, so lassen die experimentellen Ergebnisse erkennen, daß auch die coulometrische Generierung von RSH in Äthanol-1M Schwefelsäure Medium leicht erfolgt.

LITERATUR

1. W. Kuchen und H. Hertel, *Angew. Chem.*, 1969, **81**, 127.
 2. L. K. Kabanova, S. V. Usova und P. M. Solozhenkin, *Izv. AN Trudzh. SSR*, 1971, No. 1, 39.

3. L. K. Kabanova, P. M. Solozhenkin und S. V. Usova, *Dokl. AN Tadzh SSR*, 1972, **15**, No. 1, 27.
4. G. K. Budnikov und N. A. Ulachovic, *Uspekhi Khim.*, 1980, **49**, 147.
5. N. A. Esershaya, *Zh. Analit. Khim.*, 1981, **30**, 2025.
6. R. N. Adams, *Electrochemistry at Solid Electrodes*, p. 286. Dekker, New York, 1969.
7. W. A. Higgins, P. W. Vogel und W. G. Craig, *J. Am. Chem. Soc.*, 1955, **77**, 1864.
8. S. V. Larionov und E. I. Arschikova, *Izv. SO AN SSSR*, 1969, **4**, 80.
9. T. A. Kryukova, S. I. Sinyakova und T. V. Arefeva, *Polyarograficheskii analiz*, p. 104. Goskhimizdat, Moscow, 1959.

Summary—The electrochemical behaviour of bis(diphenyldithiophosphine)disulphide (RSSR) and mercuric diphenyldithiophosphinate [(RS)₂Hg] in ethanol–lithium perchlorate and ethanol–sulphuric acid media was studied by the methods of classical polarography, and electrolysis at controlled-potential and at a rotating disc platinum electrode. The data obtained show that RSSR is not reduced directly on the dropping mercury electrode but is adsorbed. It then undergoes a rapid chemical reaction causing the formation of (RS)₂Hg, which is electroactive. The electrolysis at controlled potential proves that (RS)₂Hg undergoes a two-electron reduction, giving diphenyldithiophosphinic acid (RSH) as a main product, whereas the oxidation of RSH leads to the production of (RS)₂Hg. Regardless of the fact that the chemical and adsorption equilibria during reduction of RSSR and (RS)₂Hg are complex, the coulometric generation of RSH is not difficult to achieve, and permits the use of RSSR as a coulometric reagent.

SHORT COMMUNICATIONS

DETERMINATION OF TOTAL TIN IN GEOLOGICAL MATERIALS BY ELECTROTHERMAL ATOMIC-ABSORPTION SPECTROPHOTOMETRY USING A TUNGSTEN-IMPREGNATED GRAPHITE FURNACE

LIYI ZHOU,* T. T. CHAO† and A. L. MEIER

U.S. Geological Survey, Box 25046, Federal Center, Denver, CO 80225, U.S.A.

(Received 23 June 1983. Accepted 16 August 1983)

Summary—An electrothermal atomic-absorption spectrophotometric method is described for the determination of total tin in geological materials, with use of a tungsten-impregnated graphite furnace. The sample is decomposed by fusion with lithium metaborate and the melt is dissolved in 10% hydrochloric acid. Tin is then extracted into trioctylphosphine oxide–methyl isobutyl ketone prior to atomization. Impregnation of the furnace with a sodium tungstate solution increases the sensitivity of the determination and improves the precision of the results. The limits of determination are 0.5–20 ppm of tin in the sample. Higher tin values can be determined by dilution of the extract. Replicate analyses of eighteen geological reference samples with diverse matrices gave relative standard deviations ranging from 2.0 to 10.8% with an average of 4.6%. Average tin values for reference samples were in general agreement with, but more precise than, those reported by others. Apparent recoveries of tin added to various samples ranged from 95 to 111% with an average of 102%.

Tin occurs in geological materials either as a constituent of the silicate lattice,^{1,3} or in the form of cassiterite.^{1,2} Knowledge of the relative distribution of tin in the two forms is important in studies related to the geochemistry of tin and in geochemical prospecting for tin.^{1,3}

Whereas cassiterite in geological samples can be converted into tin(IV) iodide and volatilized by heating with ammonium iodide,^{2,4-7} total tin can only be released by fusion with an alkaline flux such as lithium metaborate.⁸⁻¹⁰ The tin released may be determined by atomic-absorption spectrophotometry, as tin hydride⁷⁻¹⁰ or through aspiration of an organic tin extract into a nitrous oxide–acetylene flame,^{4,5} or by ICP atomic emission spectroscopy following hydride generation.⁶ The difference between the total tin determined by fusion with lithium metaborate and the cassiterite tin would give an approximate value for the tin held in the lattice of silicates.

The proposed method involves fusion of the sample with lithium metaborate to release the total tin, which is extracted with trioctylphosphine

oxide–methyl isobutyl ketone (TOPO–MIBK), by the procedure of Burke.¹¹ The tin in the organic extract is atomized in a tungsten-impregnated graphite furnace. The sensitivity, precision, and accuracy of the method are desirable features for the determination of tin in geological samples of diverse chemical composition.

EXPERIMENTAL

Apparatus

An Instrumentation Laboratory (IL) Model 951 atomic-absorption spectrophotometer was used for this study.† The spectrophotometer was equipped with the following accessories: controlled-temperature furnace atomizer (IL 555 CTF), auto-sampling device (IL 254 FASTAC), background corrector, and tin hollow-cathode lamp.

Settings for the spectrophotometer were: lamp current 10 mA; wavelength 286.3 nm; band-width, 0.5 nm; integration time, 8 sec; read-out mode, peak height; photo-multiplier voltage (HV), adjusted by the HV control until the log intensity meter reads between 0.2 and 0.8 V.

Settings for the controlled-temperature furnace atomizer were: purge gas, nitrogen at 6.9 l./min; auto operation mode; temperature-feedback on; auto-clean off; atomization programme as follows:

	Drying		Charring		Atomizing	
Step	1	2	3	4	5	6
Temp., °C	0	150	750	1000	2500	2500
Time, × 5 sec	0	1	4	4	0	2

*Geochemist, on leave from the Institute of Geophysical and Geochemical Prospecting, Beijing, China.

†To whom correspondence should be addressed.

‡Use of brand names in this paper is for descriptive purposes only and does not constitute endorsement by the U.S. Geological Survey.

Settings for the auto-sampling device were: "door calibration", 150°; sample deposit time, 2 sec; delay time, 5 sec. The FASTAC sample-delivery system aspirates the sample through a pneumatic nebulizer and converts it into an aerosol in the graphite furnace.

Impregnated graphite tubes. The impregnation of pyrolytic graphite tubes was done following the general guidelines of Fritzsche *et al.*¹² The tubes were soaked overnight in a 7.8% solution of sodium tungstate dihydrate and dried at 120° in an electric oven for 4 hr. Before use, each impregnated tube was conditioned by application of the atomization programme five times.

Reagents

Ascorbic acid. Medium fine crystals (30–80 mesh).

TOPO (trioctylphosphine oxide)–MIBK (methyl isobutyl ketone). Dissolve 4.0 g of TOPO in 100 ml of MIBK.

Lithium metaborate. Anhydrous powder (G. Frederick Smith Chemical Company).

Stock and standard solutions. Prepare the 1000- μ g/ml stock tin solution by dissolving 0.5000 g of reagent-grade tin metal in 250 ml of 50% v/v hydrochloric acid and diluting to 500 ml with water. Prepare the 1- μ g/ml standard tin solution in 10% v/v hydrochloric acid by serial dilution of the stock tin solution. The dilute standard tin solution is stable for at least 6 months in a Pyrex glass bottle.

Organic tin standard solutions in TOPO–MIBK (Sn 0, 0.025, 0.050, 0.075, 0.100, 0.200, 0.300, 0.400 and 0.500 μ g/ml). Using Eppendorf micropipettes, transfer 0, 0.25, 0.50, 0.75, 1.00, 2.00, 3.00, 4.00 and 5.00 of the 1 μ g/ml standard tin solution to individual 25 \times 200 mm screw-cap tubes and make up to a total volume of 40 ml with 10% v/v hydrochloric acid. Scoop 0.75 g of ascorbic acid into each tube and use a vortex mixer to dissolve the solid. Add exactly 10 ml of the TOPO–MIBK solution to each tube, shake for 1 min, and centrifuge the capped tubes to separate the organic phase. Transfer the organic tin extracts to 16 \times 150 mm test-tubes and cap them to prevent evaporation. The tin in the extract is stable for at least 1 week if kept in a refrigerator.

Procedure

Weigh 0.750 g of lithium metaborate and 0.250 g of <100-mesh soil, rock or stream-sediment sample into a 10-ml platinum crucible. Mix the flux and sample by means of a thin glass rod, and fuse the mixture in a muffle furnace at 1000° for 1 hr. After cooling, place the crucible in a 50-ml beaker and put a small magnetic stirring bar in the crucible. Add 30 ml of 10% v/v hydrochloric acid to immerse the crucible. Heat the beaker at 50–60° on a hot-plate (fitted with a magnetic stirrer motor) for about 30 min to dissolve the contents of the crucible completely. Transfer the solution to a 25 \times 200 mm screw-cap tube and wash the beaker and crucible with 10 ml of 10% v/v hydrochloric acid. Add 0.75 g of ascorbic acid and extract the tin with 10 ml of TOPO–MIBK as in the preparation of the organic tin standard solutions.

Determine the absorbance values for the tin in the organic extracts of the standards and samples, using the graphite

furnace/atomic-absorption spectrophotometer system. Correct the results for the blank and for the tin present as a contaminant in the lithium metaborate (as described under "sample decomposition" below).

RESULTS AND DISCUSSION

Sample decomposition

Fusion with lithium metaborate as a flux has been shown to decompose geological materials, bringing both lattice-bound tin and cassiterite tin into solution for the determination of total tin in the sample.^{8–10} The lithium metaborate used in this study was analysed by the proposed procedure for possible contamination by tin, and found to contain 0.74 ± 0.017 ppm Sn (ten replicates). It follows that a correction must be applied for tin in the flux used. There are two ways of doing this: (a) running a complete blank (including the fusion) for each batch of samples, taking care to use virtually identical weights of flux for all tests, or (b) determining a reagent blank (excluding the flux), analysing the lithium borate for tin (and correcting for the reagent blank), and correcting the results for the samples by subtraction of both the reagent blank and the tin contained in the flux (which must be weighed accurately for each sample). The result is then calculated by means of the formula

$$\text{ppm Sn} =$$

$$\frac{[(\text{tin in extract } (\mu\text{g/ml}) - \text{tin in fluxless blank } (\mu\text{g/ml})) \times \text{MIBK volume (ml)}] - \text{tin in flux } (\mu\text{g})}{\text{sample weight (g)}}$$

sample weight (g)

Sensitivity

The characteristic mass (weight of analyte giving 1% absorption) of the method described above has been found to be 7.0 μ g. With a 0.250-g sample, the range of tin concentrations that can be determined is 1.00–20.0 ppm in the sample. If the volume of TOPO–MIBK used for extraction is reduced to 5 ml, the lowest tin concentration that can be accurately determined is 0.50 ppm, which is considered to be below the crustal abundance.¹³

The calibration graph for tin is linear up to 0.200 μ g/ml, corresponding to an absorbance of 0.689 (Table 1), above which curvature occurs. When the concentration of tin in the sample exceeds 20.0 ppm,

Table 1. Effect of tungsten-impregnation on absorbance readings of tin in standard solutions

Standard, μ g/ml	W-impregnated		Untreated	
	Absorbance	R.S.D.,* %	Absorbance	R.S.D.,* %
0.025	0.098	0.8	0.046	6.5
0.050	0.193	1.1	0.108	10.1
0.075	0.277	1.6	0.143	5.1
0.100	0.363	2.3	0.200	9.1
0.200	0.689	2.3	0.417	8.9

*Calculated from three injections.

Table 2. Replicate determinations ($n = 5$) of tin in various U.S. Geological Survey reference samples

Sample	This work		Reported values,		
	Mean, ppm	R.S.D., %	ppm		
Rock reference samples					
BHVO-1, basalt	1.74 ± 0.08	4.6	1.90 ± 0.12 (6.3) ^{*17}	1.8 ¹⁰	2.15 ¹⁸
MAG-1, marine mud	1.90 ± 0.07	3.7	2.98 ± 0.19 (6.4)	3.2	5.0
QLO-1, quartz latite	2.34 ± 0.22	9.4	2.14 ± 0.17 (7.9)	2.4	2.3-4.2
RGM-1, rhyolite	3.65 ± 0.12	3.3	3.78 ± 0.29 (7.7)	4.4	3.9
SCo-1, Cody shale	3.22 ± 0.07	2.2	3.02 ± 0.18 (6.0)	3.9	4.1
SDC-1, mica shist	2.83 ± 0.09	3.2	2.68 ± 0.16 (6.0)	3.2	3.0
SGR-1, oil shale	2.31 ± 0.07	3.0	1.38 ± 0.18 (13.0)	—	1.58
STM-1, nepheline syenite	9.02 ± 0.22	2.4	6.70 ± 0.34 (5.1)	6.7	10 ± 3
Geochemical exploration reference samples					
GXR-1, jasperoid	52.4 ± 1.93	3.7			
GXR-2, soil	1.98 ± 0.06	3.0			
GXR-3, Fe-Mn deposit	0.94 ± 0.07	7.4			
GXR-4, Cu mill head	4.79 ± 0.25	5.2			
GXR-5, soil	2.84 ± 0.09	3.2			
GXR-6, soil	0.86 ± 0.06	7.0			
Glass reference standards					
GSB, glass standard	0.74 ± 0.08	10.8		0.6 ¹⁶	
GSC, glass standard	3.62 ± 0.15	4.1		5	
GSD, glass standard	62.2 ± 1.27	2.0		43	
GSE, glass standard	433 ± 21.9	5.1		440	

*R.S.D. (%) in parentheses.

the sample extract should be diluted with MIBK so that the absorbance is within the linear range of the calibration graph, preferably around 0.500, to reduce experimental error.

Effect of tungsten-impregnation on the performance of the graphite tube

Impregnation of the graphite tube with sodium tungstate solution nearly doubles the absorbance readings for tin standards (Table 1) thereby enhancing the sensitivity, and also improves the precision of the absorbance readings (Table 1). The tungsten-impregnated graphite tube can be used for at least 500 firings.

Interferences

The chelation and extraction of tin from the sample solution with TOPO-MIBK is adapted from

Table 3. Recovery of known amounts of tin added to various reference samples (averages of duplicate analysis of 0.250-g samples)

Sample	Present, μg	Added, μg	Found, μg	Recovery, %
RGM-1	0.93	1.00	1.92	100
	0.93	2.00	2.89	99
SDC-1	0.70	1.00	1.74	102
	0.70	2.00	2.85	106
	0.70	3.00	3.69	100
	0.70	5.00	5.95	104
GXR-5	0.70	1.00	1.89	111
	0.70	2.00	2.73	101
	0.70	3.00	3.74	101
	0.70	5.00	5.83	102
GSB	0.18	0.20	0.41	107
	0.18	0.40	0.55	95

the procedure of Burke¹¹ for the determination of tin in aluminium, iron and nickel-base alloys. The same extraction has been used for determining tin in geological materials⁵ and in mineralized rocks and ores.⁴ Welsch and Chao⁵ found no interferences from 1000 μg of Cu, Pb, Zn, Mn, Hg, Mo, V, and the equivalent of 20% Fe in a 1-g sample in the flame atomic-absorption determination of tin. It is inferred that interferences in the graphite-tube atomic-absorption determination of tin would be minimal. This is supported by the data of Tables 2 and 3 showing the general agreement of the tin values found for the reference samples with those reported by others, and the very good recoveries of tin added to various samples of diverse chemical composition.

Results for geological reference samples

The proposed method was applied to three sets of U.S. Geological Survey reference samples: (1) eight rock standards,¹⁴ (2) six geochemical exploration reference samples,¹⁵ and (3) four glass reference standards.¹⁶ The average tin values obtained for the eight USGS reference rocks are in most cases in general agreement with, but more precise than, the values reported by Terashima,¹⁷ as shown in Table 2.

Replicate analyses of eighteen reference samples with various matrices gave relative standard deviations ranging from 2.0 to 10.8%, with an average of 4.6% (Table 2). Recoveries of tin added to various samples ranged from 95 to 111% with an average of 102% (Table 3).

Thus, the proposed method can be applied to the determination of total tin in a wide range of geological materials of diverse chemical composition.

REFERENCES

1. L. H. Ahrens and W. R. Liebenberg, *Am. Mineral.*, 1970, **35**, 571.
2. J. Agterdenbos and J. Vlogtman, *Talanta*, 1972, **19**, 1295.
3. A. M. R. Neiva, *Min. Mag.*, 1976, **40**, 453.
4. J. D. Mensik and H. J. Seidemann, Jr., *At. Absorp. Newsl.*, 1974, **13**, 8.
5. E. P. Welsch and T. T. Chao, *Anal. Chim. Acta*, 1976, **82**, 337.
6. B. Pahlavanpour, M. Thompson and S. J. Walton, *J. Geochem. Explor.*, 1979, **12**, 45.
7. D. Gladwell, M. Thompson and S. J. Wood, *J. Geochem. Explor.*, 1981, **16**, 41.
8. A. Hall, *Chem. Geol.*, 1980, **30**, 135.
9. K. S. Subramanian, *Talanta*, 1980, **21**, 469.
10. C. Y. Chan and M. W. A. Baig, *Anal. Chim. Acta*, 1982, **136**, 413.
11. K. E. Burke, *Analyst*, 1972, **97**, 19.
12. H. Fritzsche, W. Wegscheider, G. Knapp and H. M. Ortner, *Talanta*, 1979, **26**, 219.
13. Tan Lee and Chi-lung Yao, *Intern. Geol. Rev.*, 1970, **12**, 778.
14. F. J. Flanagan, *U.S. Geol. Survey Prof. Paper*, 840, 1976.
15. G. H. Allcott and H. W. Lakin, *Geochemical Exploration 1974*, p. 659. Elsevier, Amsterdam, 1975.
16. A. T. Myers, R. G. Havens, J. J. Connor, H. M. Conklin and H. J. Rose, *U.S. Geol. Survey Prof. Paper*, 1013, 1976.
17. S. Terashima, *Geostd. Newsl.*, 1982, **6**, 77.
18. E. S. Gladney and W. G. Goode, *ibid.*, 1981, **5**, 31.

SPECTROPHOTOMETRIC DETERMINATION OF TRANEXAMIC ACID WITH CHLORANIL

ABDEL-AZIZ M. WAHBI, ESSAM A. LOTFI and HASSAN Y. ABOUL-EINEI
College of Pharmacy, King Saud University, Pharmaceutical Chemistry Department, Riyadh,
Saudi Arabia

(Received 22 April 1983. Accepted 23 June 1983)

Summary—Tranexamic acid is reacted with aqueous alcoholic chloranil, buffered at pH 9, to give a complex with maximum absorption at 346 nm and with an apparent molar absorptivity of 15.7×10^3 l.mole⁻¹.cm⁻¹. A_{\max} is linearly related to concentration over the range 2–10 µg/ml. When applied to tablets labelled as containing 500 mg each, the mean found was 496 ± 4 mg. The results were comparable with those of the traditional formol titration method for amino-acids.

Tranexamic acid (*trans*-4-aminomethylcyclohexane-carboxylic acid) is a synthetic ω -amino-acid with useful antifibrinolytic properties.¹ An electron-capture gas chromatographic method has been reported for its determination in biological fluids.² In view of the fact that tranexamic acid does not possess characteristic absorption in the ultraviolet region, it was felt useful to develop a spectrophotometric method for its determination. Chloranil (tetrachloroquinone) has been reported to form condensation products with primary and secondary arylamines, amino-acids, phenols and naphthalene.^{3,4} The reaction of some amino-acids with chloranil in aqueous ethanol buffered at certain pH values has been described as $n \rightarrow \pi$ charge-transfer complex formation.⁵ Lin and Cheng⁶ studied the ultraviolet and infrared absorption characteristics, compositions, formation constants and pH dependence of the amino-acid-chloranil complexes. Several amino-acids⁷ and a wide range of pharmaceutical amines^{8,9} have been determined with chloranil buffered at pH 9. On the same basis, chloranil is now used for determination of tranexamic acid.

EXPERIMENTAL

Instrument

A Varian DMS 90 double-beam spectrophotometer with 1-cm quartz cuvettes was used.

Reagents

Chloranil solution. A saturated solution in ethanol.

Buffer solution, pH 9. A 0.05M solution of sodium tetraborate.

Tranexamic acid solution. A 0.010% solution in distilled water.

General procedure

Pipette 1–5 ml portions of standard tranexamic acid solution into 50-ml standard flasks. Add exactly 10 ml of chloranil solution and 2 ml of 0.05M buffer solution to each. Mix and dilute to volume with water. Prepare a reagent blank. Let all the solutions stand for 40 min at room temperature (20°), then measure the absorbance in 1-cm cells at 346 nm during the next 10 min. Treat samples in the

same way. Because of the short time interval available for the measurement, it is best to prepare the test solutions in small batches and at suitable time intervals.

Procedure for tablets

Weigh and powder five tablets. Weigh accurately a quantity of the powder equivalent to about 100 mg of tranexamic acid into a 100-ml standard flask, add 80 ml of water and shake the flask for 30 min. Make up to volume with distilled water and mix. Pipette 10 ml into a 100-ml standard flask and dilute to volume with distilled water, then apply the general procedure to 4 ml of this solution. Calculate the amount of tranexamic acid from the calibration curve or from an equivalent linear equation.

RESULTS AND DISCUSSION

Chloranil in aqueous alcoholic solution buffered at pH 9 reacts with tranexamic acid to form a complex with maximum absorption at 346 nm. Under the experimental conditions described, the absorbance (A) in 1-cm cells is a linear function of the concentration (c , µg/ml), over the range 2–10 µg/ml, the equation being $A = 0.007 + 0.101c$. The apparent molar absorptivity was found to be 15.7×10^3 l.mole⁻¹.cm⁻¹. The standard deviation is 0.07 µg/ml at the 6-µg/ml level, so the error of prediction from the regression line (95% confidence limits) is 0.22 µg/ml.

The reaction time, the volume of chloranil solution, the volume of pH-9 buffer and the final dilution were selected as a compromise between optimum sensitivity, stability and minimum blank reading. Thus, the yellow colour of chloranil in ethanol slowly changes to violet when the solution is added to the pH-9 buffer. The absorbance of the blank solution, measured at 346 nm against water, is about 0.46, so a double-beam spectrophotometer is preferable, for precise results to be obtained. The absorbance of the reaction product at 346 nm increases slowly over a period of 40 min and then remains stable for 10 min, during which the absorbance must be measured (Fig. 1).

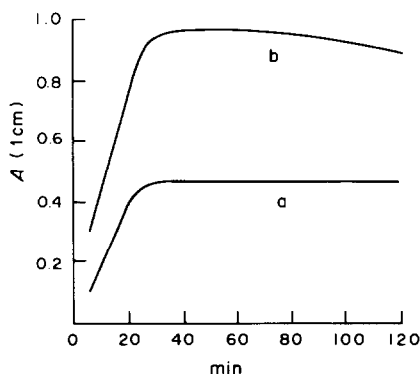


Fig. 1. Rate of colour development and stability of colour.

The mechanism of the reaction between chloranil and amino-acids is still not known with certainty; it is generally supposed to be charge-transfer complex formation, but the lengthy reaction time does not support this. The amino-acid-chloranil reacting ratio has been found to be 1:1 or 1:2 according to the number of amino groups in the amino-acid.⁶

The method has been applied to the determination of tranexamic acid in commercial tablets, the results being compared with those obtained by the traditional formol titration method for amino-acids, which involves the addition of neutral formaldehyde solution to aqueous tranexamic acid solution, followed by titration with 0.1M sodium hydroxide. Table 1 shows that the mean values found were $99.1 \pm 0.7\%$ of the nominal content by the spectrophotometric method and $99.2 \pm 1.0\%$ by the titrimetric method. The results are in good agreement with each other.

The proposed method is suitable for the determination of tranexamic acid in μg quantities, but

Table 1. Determination of tranexamic acid in tablets* by the chloranil and formol titration methods

Found, %	
Spectrophotometry	Titration
99.9	98.9
98.7	98.5
98.6	98.5
99.4	99.2
99.6	99.2
98.2	101.2
Mean \pm s.d.	99.1 ± 0.7 99.2 ± 1.0

*Nominal content 500 mg.

there is positive interference from other amino-acids and water-soluble compounds containing a primary or secondary amino group.

Acknowledgement—The authors would like to thank AB KABI, Kabi Blood Products Division, S-112 87 Stockholm, Sweden, for providing an authentic sample of tranexamic acid, and the tablets analysed.

REFERENCES

1. L. Anderson, I. M. Nilsson, J.-E. Nihlen, U. Hedner, B. Granstrand and B. Melander, *Scand. J. Haematol.*, 1965, **2**, 230.
2. J. Vessman and S. Stromberg, *Anal. Chem.*, 1977, **49**, 369.
3. F. Feigl, *Spot Tests in Organic Analysis*, 7th Ed., pp. 249, 407. Elsevier, Amsterdam, 1966.
4. F. Feigl, V. Gentil and C. Stark-Mayer, *Mikrochim. Acta*, 1957, 350.
5. J. B. Birks and M. A. Slifkin, *Nature*, 1963, **197**, 42.
6. B. Y. Lin and K. L. Cheng, *Anal. Chim. Acta*, 1980, **120**, 335.
7. F. Al-Sulimany and A. Townsend, *ibid.*, 1973, **66**, 195.
8. T. S. Al-Ghabsha, S. A. Rahim and A. Townshend, *ibid.*, 1976, **85**, 189.
9. M. A. Korany and A. M. Wahbi, *Analyst*, 1979, **104**, 146.

ESTIMATION OF CHLORIDE IN OXIDIZING MEDIA BY MEANS OF ION-SELECTIVE ELECTRODES

G. SUBRAMANIAN, NAVIN CHANDRA and G. PRABHAKARA RAO
Central Electrochemical Research Institute, Karaikudi-623006, India

(Received 16 June 1982. Revised 1 August 1983. Accepted 17 August 1983)

Summary—Chloride concentrations down to the ppm level in a large excess of chlorate or perchlorate can be quantitatively estimated by use of chloride ion-selective electrodes (ISEs). Similarly traces of chloride in chromic acid solutions can be estimated with a heterogeneous silicone-rubber based chloride ISE. However, homogeneous chloride ISEs pose a problem for practical applications, because their response in chromic acid solutions changes with time owing to chemical attack on the membrane surface. In permanganate solutions, both homogeneous and heterogeneous type electrodes can be used for monitoring chloride ions. The Orion electrode, however, was found to show a slightly super-Nernstian response in such solutions. The presence of $10^{-3}M$ iron(III) had no adverse effect on the performance of these electrodes in permanganate solutions.

It is generally accepted that the response of ion-sensitive electrodes (ISEs) is not influenced by oxidizing agents in solution. In the case of chloride ISEs both the homogeneous and heterogeneous type are claimed to be free from interference by Cu^{2+} , Fe^{3+} and MnO_4^- ions.^{1,2} However, according to a recent report by Bixler *et al.*,³ Fe^{3+} interferes seriously with the performance of homogeneous chloride ISEs in highly acidic solutions. They also observed that the response of these ISEs is unaffected under similar conditions if the iron is present as Fe^{2+} . Since a number of practical applications of Cl^- ISEs may involve monitoring chloride in the presence of a large excess of oxidizing agent (*e.g.*, in chromic acid anodizing baths and electrolytic cell liquors containing chlorate and/or perchlorate) it seemed worth studying the performance of the chloride ISEs in such oxidizing media.

EXPERIMENTAL

Three different ISEs were examined, *viz.* the Radelkis silicone-rubber based heterogeneous-membrane type electrode (Model OP-C1-7111), the homogeneous-membrane electrode developed at CECRI, and the Orion electrode (Model 94-17 A). The CECRI electrode was based on a homogeneous membrane made of our $Ag_2S/AgCl$ composite.⁴ The active surface of the electrodes was polished with Orion 94-82 polishing paper. For conditioning, the electrodes were dipped in $10^{-2}M$ potassium chloride for 1 hr. After thorough washing the electrodes were immersed in conductivity water for 12 hr. When not in use, the electrode surface was kept immersed in conductivity water.

An Orion Research Microprocessor 901 Ion Analyzer readable to ± 0.1 mV was used. The reproducibility of potentials recorded was ± 0.5 mV, corresponding to $\pm 2\%$ error in the estimation of chloride. A double-junction 1M potassium chloride calomel electrode was used as reference electrode, with the appropriate background solutions in the outer compartment. All the experiments were done at $25 \pm 0.5^\circ$.

All the chemicals used were of analytical or general reagent grade. Stock solutions were prepared in conductivity water and diluted to the desired concentration.

Chromic acid solutions were prepared from Baker chromium trioxide (analysed low-sodium MOS electronic grade).

To estimate the accuracy of the determination in chlorate and perchlorate backgrounds, two methods, *viz.* the calibration-graph and standard-addition methods, were used. The calibration graphs were obtained for 10–1000 ppm chloride in the required background by the “litre beaker” method.⁵ The potentials of the electrode in test solutions containing 50, 100 and 500 ppm chloride in appropriate chlorate or perchlorate media were then measured and the corresponding chloride concentrations read from the standard graph. In the standard-addition method, the change in potential (ΔE) of 100 ml of test solution on addition of a known amount of chloride (as a standard solution) was measured and the chloride concentration in the test solution was calculated by use of the equation⁶

$$C_x = C_s V_s / [V_x + V_s] 10^{\Delta E/S} - V_x$$

where C_x and C_s are the concentrations and V_x and V_s the volumes of the test solution and the standard solution, and S is the slope of the standardization graph.

Studies on the effect of chlorate and perchlorate backgrounds were done in neutral medium, which is of interest in real sample analysis, and extended to acid medium in view of the enhanced oxidizing power of these oxidants in such media. Perchloric acid and nitric acid were used to adjust the pH of the sodium perchlorate and potassium chlorate solutions, respectively.

RESULTS AND DISCUSSION

Chlorate and perchlorate baths

In the production of chlorate by electrolytic oxidation of chloride solutions, monitoring of the chloride concentration at various stages of the electrolysis is essential. During the electrolysis the chloride content of the cell liquors may vary from about 3×10^5 to 10^3 ppm (300–1 g/l.) and the maximum sodium chlorate concentration (at the end of electrolysis) may be about 400–500 g/l.^{7,8} Since chloride in the range 1.8 – 3.55×10^4 ppm can be monitored by chloride ISEs, so a tenfold dilution of the sample will always bring its chloride concentration into the detection range of the ISEs. The response of the ISEs was

measured for the range 10–10⁴ ppm chloride in 42.5-g/l. potassium chlorate background (which also served as ionic strength adjuster). All three electrodes gave Nernstian response, showing that chlorate has no adverse effect.

Similarly in the production of sodium perchlorate the sodium chloride concentration in the cell liquor may also vary from about 3 × 10⁵ to 10³ ppm, depending on the stage of electrolysis, and the maximum sodium perchlorate content may be 500–600 g/l.⁹ A tenfold dilution to keep the chloride concentration in the detection range of the ISEs will bring the concentration of sodium perchlorate to about 50–60 g/l., so this chloride range was tested in 50-g/l. sodium perchlorate background (which again gives almost constant ionic strength). All the three electrodes again gave Nernstian response, showing that perchlorate does not interfere.

These experiments were repeated with lower concentrations of the background salt (15 and 30 g/l.) and also studied at pH 1. The electrode performances remained the same in all cases.

The error of the determination was then evaluated for these systems by the methods used for the response to pure chloride solutions and the results are given in Table 1. The error is again about 2%. For comparison, chloride in neutral solutions containing chlorate and perchlorate was determined by conventional titration with silver nitrate, with potassium chromate as indicator. The results were invariably higher than the ISE results by about 5%.

Chromic acid medium

Analysis of chromic acid solutions is another example of chloride monitoring in an oxidizing media. Levels of chloride above a certain critical value are reported to have adverse effects on the performance of these solutions as anodizing baths. In the present study, the response of the chloride ISEs was measured for typical chromic acid anodizing baths¹⁰ containing 50 and 100 g of chromic acid per litre. To investigate the effect of sulphuric acid another composition (250 g/l. CrO₃ and 2.5 g/l. H₂SO₄) was also studied. In the 50-g/l. chromic acid bath the Radelkis heterogeneous electrode exhibited Nernstian response over the 10–1000 ppm chloride range, and sub-Nernstian response at lower levels, in conformity with its performance in the absence of oxidizing agent (Fig. 1). For the Orion and CECRI ISEs, however, the potential of the electrodes was found to vary with time. Visual observation of the electrode surface after exposure to the chromic acid solutions showed slight etching of the surface of the Orion electrode, whereas the CECRI electrode was covered with a thin film which could be easily wiped off with paper, and no etching of the surface was observed. Since these surface effects were thought to be the cause of drift in the electrode potential, it was felt that the electrodes would give Nernstian response if the measurement were made quickly enough for no

Table 1. Determination of Cl⁻ in chlorate and perchlorate media

[Cl ⁻] taken µg/ml	In 15-g/l. NaClO ₄ background			In 30-g/l. NaClO ₄ background			In 50-g/l. NaClO ₄ (pH 1.0) background					
	Calibration		Standard addition	Calibration		Standard addition	Calibration		Standard addition			
	Cl ⁻ found, µg/ml	Error, %	Cl ⁻ found, µg/ml	Error, %	Cl ⁻ found, µg/ml	Error, %	Cl ⁻ found, µg/ml	Error, %	Cl ⁻ found, µg/ml	Error, %		
50	51.0	+2.0	50.5	+1.0	49.0	-2.0	50.8	+1.6	51.0	+2.0	51.3	+2.6
100	98.5	-1.5	98.8	-1.2	100.0	Nil	98.8	-1.2	100.5	+0.5	101.2	+1.2
500	505	+1.0	498	-0.4	505	+1.0	515	+3.0	500	Nil	503	+0.6
	In 15-g/l. KClO ₄ background			In 30-g/l. KClO ₄ background			In 42.5-g/l. KClO ₄ (pH 1.0) background					
50	50.0	Nil	50.1	+0.1	49.0	+2.0	50.8	+1.6	50.5	+1.0	52.0	+4.0
100	98.0	-2.0	98.0	-2.0	100.0	Nil	100.1	+0.2	99.0	-1.0	99.7	-0.3
500	495	-1.0	503	+0.5	500	Nil	508	+1.6	515	+3.0	516	+3.2

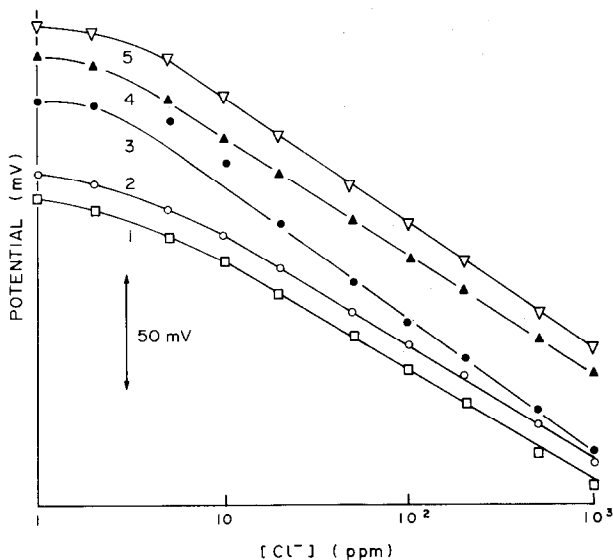


Fig. 1. Response of chloride ISEs in chromic acid solutions. 1—Radelkis ISE, 2—CECRI ISE, 3—Orion ISE, in 50-g/l. chromic acid background; 4 and 5—Radelkis ISE in 100-g/l. chromic acid and 250-g/l. chromic acid/2.5 g/l. sulphuric acid respectively. The total experimental time for obtaining calibration plots 2 and 3 was 5 min (*cf.* text).

significant etching or film formation to take place. To confirm this, experiments were done in which the whole range of chloride concentration was covered within 5 min. The response of the Orion and CECRI electrodes in these experiments is also included in Fig. 1. Both electrodes showed Nernstian behaviour. Hence the homogeneous membrane electrodes which show a time-dependent response in the presence of chromic acid can be used only if the time of immersion of the electrodes can be kept short. Since the homogeneous-membrane ISEs were adversely affected by chromic acid, only the Radelkis heterogeneous membrane ISE was studied at the higher chromic acid concentrations. The electrode showed Nernstian behaviour (Fig. 1), confirming that it is not affected by chromic acid.

Permanganate medium

The effect of permanganate was also included in the study. The chloride range 5×10^{-5} – $10^{-2} M$ in 0.02M permanganate background electrolyte was examined. The electrode responses are shown in Fig. 2. The Orion electrode gave a response that was slightly super-Nernstian (68 mV/pCl), whereas the other two gave Nernstian response. The presence of iron is known to catalyse the oxidation of chloride by permanganate in acid medium. Hence the response of the electrodes to chloride in 0.02M permanganate

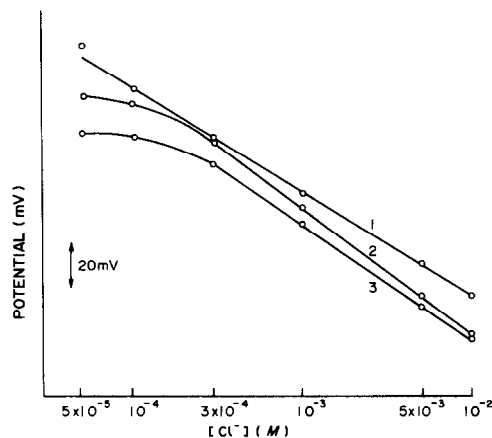


Fig. 2. Response of chloride ISEs in 0.02M potassium permanganate background. 1—CECRI ISE, 2—Orion ISE, 3—Radelkis ISE.

was also studied in the presence of $10^{-3} M Fe^{3+}$. No adverse effect was observed over a period of 15 min.

Acknowledgements—The authors thank Dr. K. S. Rajagopalan, Director, for permission to publish this paper and Dr. V. K. Venkatesan, Scientist, for his interest in the work.

REFERENCES

1. *Instruction Manual—Halide Electrodes*, p. 23. Orion Research Inc., Massachusetts, U.S.A. 1977.
2. *Ion Selective Electrodes*, p. 31. Radelkis Electrochemical Instruments, Budapest, Hungary.
3. J. W. Dixler and R. Nee, *Anal. Chim. Acta*, 1979, **99**, 225.
4. J. W. Ross, in *Ion Selective Electrodes*, R. A. Durst (ed.), pp. 77–78. N.B.S. Special Publication No. 314, 1969.
5. *Orion Newsletter*, 1970, 11, No. 9/10, 42.
6. *Instruction Manual Model 901 Microprocessor Ionalyzer*, p. 4. Orion Research Inc., 1979.
7. H. V. K. Udupa, S. Sampath, K. C. Narasimham, M. Nagalingam, N. Thiagarajan, G. Subramanian, S. Natarajan, P. Subbiah, R. Palanisamy, S. John Peter, S. Pushpavanam and M. Sadagopalan, *Indian J. Tech.*, 1971, **9**, 257.
8. H. V. K. Udupa, S. Sampath, K. C. Narasimham, M. Nagalingam, N. Thiagarajan, G. Subramanian, P. Subbiah, R. Palanisamy, S. John Peter, S. Pushpavanam and M. Sadagopalan, *J. Appl. Chem. Biotechnol.*, 1974, **24**, 43.
9. H. V. K. Udupa, K. C. Narasimham, M. Nagalingam, N. Thiagarajan, G. Subramanian, R. Palanisamy, S. Pushpavanam, M. Sadagopalan and V. Gopalakrishnan, *J. Appl. Electrochem.*, 1971, **1**, 207.
10. *Canning Handbook on Electroplating*, 21st Ed., p. 711. Canning, Birmingham, 1970.

DETERMINATION OF WATER IN ETHANOL AND ACETONE BY DIRECT INJECTION ENTHALPIMETRY BASED ON THE HEAT OF DILUTION

WALACE A. DE OLIVEIRA and CELIO PASQUINI

Instituto de Química, Universidade Estadual de Campinas, C.P. 6154, Campinas, São Paulo, Brazil

(Received 12 January 1983. Revised 28 June 1983. Accepted 30 July 1983)

Summary—Two analytical procedures based on the magnitude of the heat of dilution and direct injection enthalpimetry have been developed for determination of water in ethanol and acetone. The results obtained by means of the heat of dilution were compared with the values given by pycnometry, and gave a relative difference in the range 0.2–3%. The precision depends on the slope of the calibration curve, which varies with the procedure and the concentration of the sample.

Use of the heat of dilution for analytical purposes is not new and was first proposed over 60 years ago.¹ However, only a few applications¹⁻⁴ have been found in the literature. The enthalpy change due to dilution is very large for many compounds. The magnitude of the heat evolved or absorbed depends on the interactions between solute and solvent and is a function of the initial solute concentration. Thus, the temperature changes on dilution can be related to the solute/solvent ratio in a given sample. With the modern capability for measuring very small changes in temperature, the enthalpimetric signal due to dilution can give a precise analysis.

Ethanol and acetone are widely used in the laboratory and industry. Ethanol is employed as a fuel (as hydrated ethanol) and in fuel mixtures (as anhydrous ethanol). The water content is an important factor in the quality control of both ethanol and acetone. The Karl Fischer titration, normally used for water determination, has some disadvantages: active carbonyl groups, such as those present in ketones, cause formation of water by reaction with the alcohol present in the reagent, free SO₂ forms a yellow SO₂I⁻ species which makes visual recognition of the endpoint rather difficult, and the reagent contains toxic substances that are unpleasant to work with.

The objective of the present work was to develop and evaluate analytical methods based on measurement of the heat of dilution. Procedures for the determination of water in ethanol and acetone have been developed.

EXPERIMENTAL

The determinations were performed by direct injection enthalpimetry (DIE) with an apparatus similar to that previously described.⁵ It consists of a 100-ml Dewar flask which contains the thermistor probe (2200 Ω, Thermometrics Inc.), a glass pipette tied to a plastic syringe, and a magnetic stirring bar. The thermistor is connected to a

Wheatstone bridge (Leeds & Northrup, catalogue number 4760), the output voltage from which is fed to a strip-chart recorder. The bridge sensitivity was 6.7 mV/deg. The pipette used delivered 1.30 ml, but any volume between 1 and 2 ml can be used, provided it is kept the same for all samples and standards.

Two procedures were used. In procedure I the Dewar flask was charged with 50.0 ml of distilled water, and the pipette was loaded with sample and immersed in the water in the Dewar flask; after temperature equilibrium had been attained (which was almost instantaneously), the sample was injected into the water and the temperature change due to the heat of dilution was recorded. In procedure II the Dewar flask was charged with 50.0 ml of sample and distilled water (1.30 ml) was added from the pipette after temperature equilibration.

All determinations based on the heat of dilution were accomplished by using calibration graphs obtained with solutions standardized by pycnometry. Comparative determinations were performed with a 30-ml pycnometer according to well-accepted procedures.⁶ Reagent-grade chemicals were used throughout.

RESULTS AND DISCUSSION

The results for five replicates of ethanol and acetone, with various water contents, measured by both procedures, showed that the temperature change on dilution could be measured with a mean standard deviation of 0.002° for ethanol and 0.004° for acetone.

Typical calibration curves for procedure I are shown in Fig. 1. The heat of dilution is exothermic for the two compounds. The curves show similar behaviour, with the slopes increasing in dilute solutions and tending to decrease with high content of solute. In the range of concentration 50–70% and 20–60% of water for ethanol and acetone, respectively, there is a linear relationship, with a correlation coefficient of 0.9999. Figure 2 shows the behaviour of the heat of dilution as a function of the percentage of water in the sample, for procedure II.

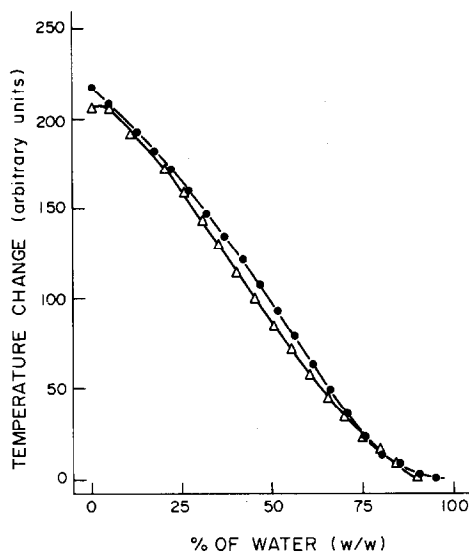


Fig. 1. Calibration curve for determination of water in ethanol (●) and acetone (△) with procedure I. One arbitrary unit is equal to 0.003°C for ethanol and 0.006°C for acetone.

For ethanol, exothermic signals are obtained, which decrease as the amount of water is increased, probably indicating that the total number of hydrogen bonds in the mixture is diminishing. For acetone, the enthalpimetric signal is endothermic for samples with low concentrations of water, but becomes exothermic when the samples contain more than about 5.5% of

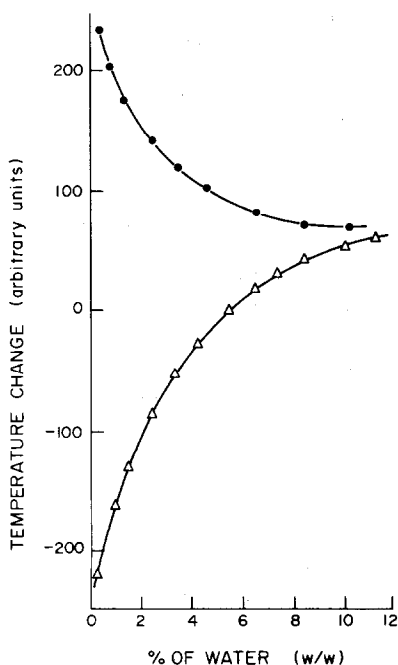


Fig. 2. Calibration curve for water determination in ethanol (●) and acetone (△) with procedure II. One arbitrary unit is equal to 0.003°C for ethanol and 0.006°C for acetone.

water. The endothermic portion of the curve probably indicates that the energy absorbed in the disruption of the water structure is not compensated for by hydrogen-bond formation in the mixture.

As seen from Figs. 1 and 2, the useful composition range for acetone application is 10–90% water for procedure I and 0–10% for procedure II, whereas for ethanol it is 5–80% water by procedure I and 0–5% by procedure II, so the two procedures are complementary.

The precision depends on the sample concentration and the procedure employed. Procedure I, in the linear range, gives a sensitivity of 0.019° and 0.009° per 1% of water for acetone and ethanol respectively. Within the precision of the thermometric measurement, the water content can be obtained with a mean standard deviation of 0.2%. Procedure II is the more attractive way for determination of small amounts of water, owing to the large sensitivity at levels lower than 1%. At this concentration, a sensitivity of about 0.240° and 0.440° per 1% of water was found for ethanol and acetone, respectively. This allows the determination of water with a mean standard deviation of 0.008 and 0.009%.

Because of the non-specific character of the heat of dilution, the enthalpimetric signal may be affected by the presence of other solutes in the sample. In order to assess such contributions to the enthalpimetric signal, the heat of dilution of ethanol was measured before and after the addition of various compounds usually present in fuel or commercial ethanol. The results are given in Table 1. It was observed that the magnitude of interference varies with the compound added to the sample and probably reflects the interactions with the binary system water–ethanol. Table 1 shows that the interference may be relevant if the compound is present in significant percentage. However, in actual samples the percentage of impurities is usually very low⁷ and the influence of interferents on the enthalpimetric signal can be considered to be within the experimental error.

The effect of the ambient temperature on the enthalpimetric signal was studied by repeating the analysis of four samples of ethanol, by procedures I and II, at several temperatures in the range 20–30°. It was found that the magnitude of the signal decreases as the ambient and solution temperatures are

Table 1. Effect of various compounds usually present in commercial and fuel ethanol, on the analytical signal

Compound	Relative analytical signal,* %	
	Procedure I†	Procedure II‡
Ethyl acetate	102.1	100.3
Acetaldehyde	100.0	100.3
Acetic acid	100.7	97.7
Amyl alcohol	101.7	97.6
Benzene	103.1‡	95.0

*With 1.0% of potential interferent present.

†Content of water in sample: 60.2%.

‡Saturated solution at 25°C.

§Content of water in sample: 0.70%.

Table 2. Results for the determination of water in ethanol

Sample	Procedure	Mass of water in 100 g of sample, g		Relative error, %
		Pycnometry	Heat of dilution	
E ₁	I	57.5	57.4	-0.2
E ₂	I	49.6	49.8	+0.4
E ₃	I	54.3	54.0	-0.6
E ₄	I	16.9	16.7	-0.9
E ₅	II	7.60	7.8	+2.6
E ₆	II	5.47	5.50	+0.5
E ₇	II	4.66	4.60	-1.3
E ₈	II	3.26	3.28	+0.6
E ₉	II	2.00	2.03	+1.5
E ₁₀	II	0.83	0.82	-1.2

Table 3. Comparative results for the determination of water in acetone

Sample	Procedure	Mass of water in 100 g of sample, g		Relative error, %
		Pycnometry	Heat of dilution	
A ₁	I	57.2	57.1	-0.2
A ₂	I	44.7	44.6	-0.2
A ₃	I	39.4	39.6	+0.5
A ₄	I	21.6	21.8	+1.1
A ₅	II	4.29	4.22	-1.6
A ₆	II	3.68	3.60	-2.2
A ₇	II	1.37	1.38	+0.7
A ₈	II	1.00	1.03	+3.0

increased. Nevertheless, the effect is smaller than the uncertainty of measurement, for variations of these temperatures within $\pm 2^\circ$.

The accuracy of procedures I and II was checked against pycnometry with synthetic samples. The mean results of three determinations are given in Tables 2 and 3. As can be observed, good correlation was found.

CONCLUSION

The heat of dilution method described in this report is very simple and requires no reagents but the species to be determined (water, in this case). The time needed for one determination is about 3 min and the precision, accuracy and sensitivity are sufficient for water determination in fuel ethanol and commercial acetone and ethanol products. Water solutions of these two substances can be considered as two-component systems, due to the low level of im-

purities, and interference effects are therefore negligible. The Karl Fischer method is more sensitive, but has the disadvantages listed in the introduction. The characteristics of the method indicate potential applications to other substances besides those mentioned in this report.

REFERENCES

1. H. D. Richmond and J. E. Merreywether, *Analyst*, 1917, **42**, 273.
2. F. Hagedorn and G. Peuschel, *ibid.*, 1975, **100**, 810.
3. V. Tep and S. Brun, *Ann. Nutr. Alim.*, 1978, **32**, 899.
4. P. Dupont, *ibid.*, 1978, **32**, 905.
5. W. A. de Oliveira and A. A. Rodella, *Talanta*, 1979, **26**, 965.
6. J. K. Taylor, *Density and Specific Gravity*, in *Encyclopedia of Industrial Chemical Analysis*, F. D. Snell and C. L. Hilton, (eds.), Vol. 1, pp. 546-560. Interscience, New York, 1966.
7. National Council of Oil—Brazil, *Resolução* No. 8/79, Ministério das Minas e Energia, Brasília, 6 March 1979.

DETERMINATION OF CYANIDE BY A HIGHLY SENSITIVE INDIRECT SPECTROPHOTOMETRIC METHOD

M. BLANCO* and S. MASPOCH

Departamento de Química Analítica, Facultad de Ciencias, Universidad Autónoma de Barcelona,
Bellaterra (Barcelona), Spain

(Received 21 March 1983. Accepted 24 June 1983)

Summary—Complexation of Pd^{2+} with cyanide inhibits the extraction of the palladium complex of 5-phenylazo-8-aminoquinoline. This effect is used for the indirect spectrophotometric determination of cyanide at the μg level. Cyanide in industrial waste water and in sea-water is determined after distillation as HCN from the sample and collection in sodium hydroxide solution.

The best known methods for the spectrophotometric determination of cyanide are based on the formation of cyanogen bromide or chloride, which can react with pyridine to yield glutacetaldehyde, which is then condensed with benzidine,¹ pyrazolone² or barbituric acid,^{3,4} producing coloured polymethine dyes. These methods have good sensitivity, their main limitations being the instability of the colour and the need for strict experimental conditions if good reproducibility is to be obtained. Various indirect methods have been developed more recently, based on discharge of the colour of metal complexes by removal of the metal as cyanide complexes. Among these, the most sensitive are those based on the Ag phen-BPR⁵ and Ni-5BrPADAP⁶ complexes. Palladium(II) reacts with 5-phenylazo-8-aminoquinoline (PAQ), producing a green precipitate which is extractable into methyl isobutyl ketone,⁷ the sensitivity being about midway between those of the Ag-phen-BPR and Ni-5BrPADAP systems. This paper reports that the suppression of the reaction of PAQ with Pd(II) can be used to determine the concentration of cyanide.

EXPERIMENTAL

Reagents

Standard potassium cyanide solution ($\sim 0.5 \text{ mg/ml}$). Prepared weekly from 1.30 g of potassium cyanide and 2 g of sodium hydroxide, dissolved and diluted to 1 litre, and standardized potentiometrically by titration with 0.03M silver nitrate; working solutions ($\sim 5 \mu\text{g/ml}$) prepared daily by appropriate dilution.

Standard palladium(II) chloride solution. Prepared from PdCl_2 and 2M hydrochloric acid, to be approximately 0.1% Pd in 0.2M hydrochloric acid, and standardized with dimethylglyoxime.⁸ Diluted to give a 10- $\mu\text{g/ml}$ Pd working solution in 0.1M hydrochloric acid.

PAQ solution, 0.12% in ethanol.

Procedure

Transfer 25 ml of sample, containing less than 4 μg of cyanide, to a 75-ml glass-stoppered centrifuge tube. Acidify

slightly with 2M hydrochloric acid, add 1 ml of 10- $\mu\text{g/ml}$ palladium solution and adjust (if necessary) to pH 2.0-2.5. After 1 hr add 1 ml of 2M formic acid and then 2M sodium hydroxide dropwise until the pH is 3.0, then immediately add 1 ml of PAQ solution, mix, and after 3-5 min add 2M sodium hydroxide until the pH is 11.5-12.0. Dilute to approximately 50 ml, add 10 ml of methyl isobutyl ketone (MIBK), shake the stoppered tube vigorously for 1-2 min, centrifuge, and measure the absorbance of the organic phase at 620 nm against an MIBK blank.

Separation of cyanide by distillation

Use the distillation procedure recommended by APHA.⁴ Dilute 250 ml of the sample, free from oxidizing agents and sulphide, to approximately 500 ml, add 50 ml of sulphuric acid (1 + 1) and 20 ml of 50% magnesium chloride hexahydrate solution, and boil for 2 hr, collecting the vapour in 50 ml of 0.1M sodium hydroxide by suction. Dilute the alkaline solution to 100 ml and analyse a suitable fraction by the procedure above.

RESULTS AND DISCUSSION

The absorption spectra of the PAQ, Pd-PAQ and Pd-PAQ-cyanide systems are shown in Fig. 1. In the presence of cyanide the shape of the Pd-PAQ spectrum remains, but the absorbance is reduced, showing that formation of the Pd-PAQ complex is suppressed. A plot of the absorbance against the cyanide:palladium molar ratio (Fig. 2) indicates that the suppression is due to formation of the $\text{Pd}(\text{CN})_2$ complex (and higher complexes when $[\text{CN}^-]/[\text{Pd}^{2+}] > 2$).

Effect of pH

The reaction between palladium and PAQ takes place in a narrow pH range (2.7-3.3).⁷ The choice of pH range for the palladium-cyanide reaction is restricted by two facts. It was observed that if the palladium(II) solution is kept at $\text{pH} \geq 3.0$ for relatively long periods of time (1 hr or more) before addition of PAQ, the absorbance is lower than it should be, and is less reproducible, possibly because of formation of palladium hydroxo-complexes. On the other hand, if the pH is around 1.5 the anion

*To whom correspondence should be addressed.

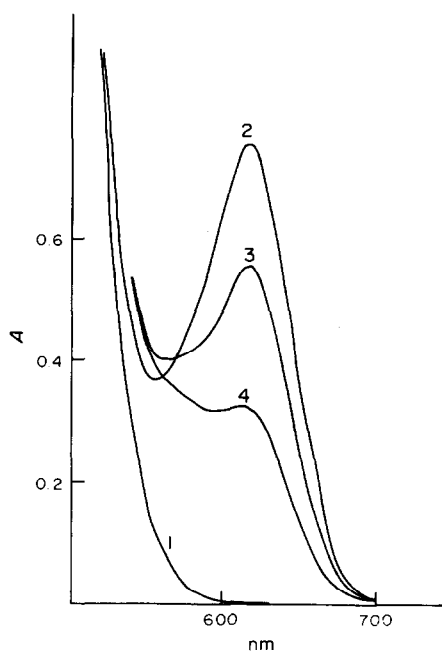


Fig. 1. Absorption spectra of MIBK phase. 1, PAQ; 2, PAQ + 10.1 μg of Pd^{2+} ; 3, PAQ + 10.1 μg of Pd^{2+} + 1.01 μg of CN^- ; 4, PAQ + 10.1 μg of Pd^{2+} + 2.35 μg of CN^- . All spectra recorded against an MIBK blank.

concentration from the acid used (Cl^- , NO_3^- or SO_4^{2-}) is at the tolerance limit. For these reasons a pH range of 2.0–2.5 is recommended. Once this reaction is completed the solution is adjusted to pH 3.0, the PAQ solution is immediately added and the concentration of the Pd–PAQ complex determined.

Kinetics of the palladium–cyanide reaction

In Fig. 3, absorbance is plotted against the time elapsed from the addition of palladium to the cyanide

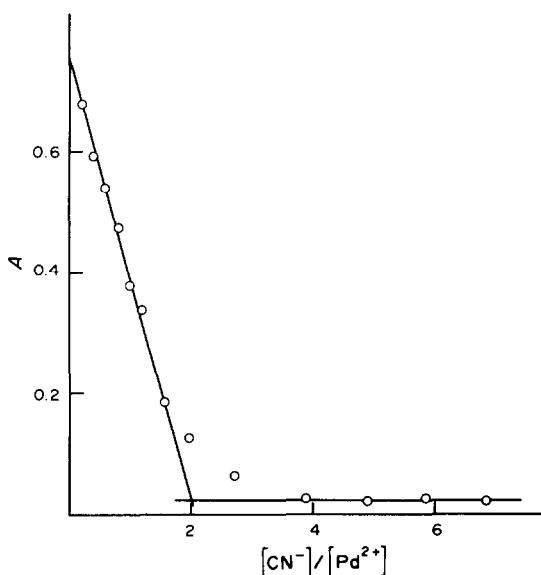


Fig. 2. Effect of cyanide on the extraction of Pd^{2+} –PAQ complex; 10.1 μg Pd^{2+} .

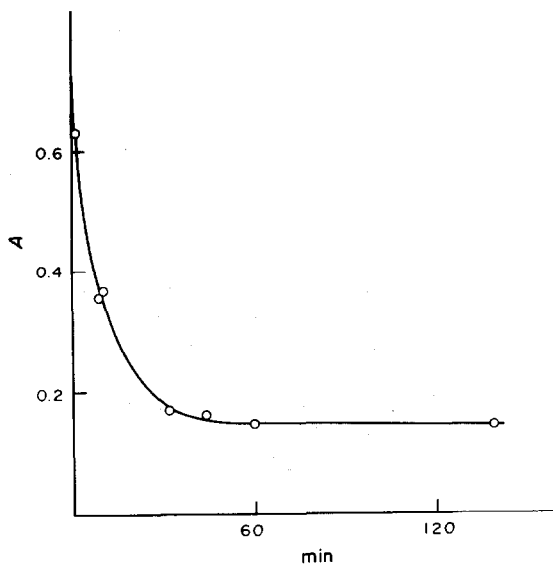


Fig. 3. Pd^{2+} – CN^- reaction kinetics. pH = 2–2.5, 10.1 μg of Pd^{2+} + 3.83 μg of CN^- .

sample at pH 2.0–2.5, to addition of the PAQ. It is observed that the inhibition reaction is complete in about 50 min. Thus, for analytical purposes, the PAQ reaction must not be applied earlier than 60–90 min after addition of the palladium to the cyanide solution.

Effect of foreign ions

The distillation procedure eliminates most of the interferences,⁴ except that of sulphide, which has to be removed beforehand by precipitation with cadmium. A detailed study of the effect of foreign ions on the Pd–PAQ system has already been reported.⁷ The effect of the presence of some of the more frequently encountered metal ions that can form cyanide complexes was therefore studied, by addition of 10 μg of the metal ion and 5 ml of 0.01M EDTA to 25 ml of a solution containing 2.4 μg of cyanide. Table 1 shows that only Co(II) and Hg(II) interfere at this level. The effect of anions on the direct determination was also studied, and it was found that 0.3 mg of SCN^- and I^- , 9 mg of PO_4^{3-} and SO_4^{2-} ,

Table 1. Effect of foreign ions*

Cation	CN^- found, † μg	Recovery, %
Mg(II)	2.41	100.4
Ca(II)	2.47	102.9
Mn(II)	2.33	97.0
Fe(III)	2.40	100.0
Fe(II)	2.35	97.9
Co(II)	2.21	91.9
Ni(II)	2.40	100.0
Cu(II)	2.47	102.9
Zn(II)	2.42	100.8
Cd(II)	2.41	100.4
Hg(II)	2.05	85.4
Al(III)	2.43	101.2

*10 μg added

†2.40 μg of CN^- added. Mean of two determinations

Table 2. Determination of cyanide

	CN ⁻ added, μg/ml	CN ⁻ found, μg/ml	No. of determinations	Recovery, %
Distilled water	0.097	0.097 ± 0.008	4	95-102
Sea-water		0.025 ± 0.007	5	
	0.095	0.126 ± 0.009	5	101-111
Waste water		2.35 ± 0.22	7	
	2.37	4.82 ± 0.47	5	94-116

50 mg of Cl⁻ and 100 mg of NO₃⁻ can be tolerated (these are approximately the maximum permissible amounts for these anions). Sulphide interferes at any level.

The calibration must be done with a recently prepared cyanide solution since the degradation products of cyanide stored in alkaline medium interfere.

Determination of cyanide in waste water and sea-water

The method was tested by analysing an artificial sample containing approximately 0.1 ppm of cyanide and was applied to the analysis of waste water from a water-purification tank in a plastic-products factory and from sea-water near the underwater sewage exit of the same factory. In both cases the presence of oxidizing agents and sulphide ion was tested for first. Only sulphide was found, in the waste water. It was eliminated by adding 10 ml of 0.1% cadmium solution to 2 litres of sample, leaving for 24 hr, then filtering. The cyanide was determined after distillative separation.

The results are shown in Table 2, where the recovery percentage shows the extreme values found. The uncertainty of the results is expressed at the 95% confidence level.

Sensitivity

The absorbance is linearly related to amount of cyanide up to 4 μg, and its relative standard deviation, for seven analyses of a sample containing 2.42 μg of cyanide, was found to be 3.4%. The detection limit of 0.005 μg/ml compares favourably with that of previous methods (*e.g.*, 0.01 μg/ml for barbituric acid, 0.02 μg/ml for pyrazolone, 0.02 μg/ml for Ni5-BrPADAP and 0.04 μg/ml for Ag-phen-BPR).

REFERENCES

1. H. G. Higson and L. S. Bark, *Analyst*, 1964, **89**, 338.
2. J. Epstein, *Anal. Chem.*, 1947, **19**, 272.
3. E. Asmus and H. Garschagen, *Z. Anal. Chem.*, 1954, **138**, 414.
4. *Standard Methods for the Examination of Water and Waste Waters*, 15th Ed., 317. American Public Health Association, American Water Works Association and Water Pollution Control Federation, 1980.
5. R. M. Dagnall, M. T. El-Ghamry and T. S. West, *Talanta*, 1968, **15**, 107.
6. W. Fu-Sheng, L. Yu-Qin, Y. Fang and S. Nai-Kui, *ibid.*, 1981, **28**, 694.
7. M. Blanco and S. Maspoch, *Mikrochim. Acta*, in the press.
8. A. I. Vogel, *A Text-Book of Quantitative Inorganic Analysis*, 3rd Ed., p. 512. Longmans, London, 1961.

ANNOTATION

COMPARISON OF SILVER RESULTS FOR CANADIAN REFERENCE ORES AND CONCENTRATES AND ZINC-PROCESSING PRODUCTS BY ACID DECOMPOSITION, TRIBENZYLAMINE/CHLOROFORM EXTRACTION AND FIRE-ASSAY COMBINED WITH ATOMIC-ABSORPTION SPECTROPHOTOMETRY

ELSIE M. DONALDSON, E. MARK and MAUREEN E. LEAVER

Mineral Sciences Laboratories, Canada Centre for Mineral and Energy Technology, Department of
Energy, Mines and Resources, Ottawa, Canada

(Received 1 June 1983. Accepted 25 July 1983)

Summary—The results obtained for silver in Canadian reference ores and concentrates and in zinc-processing products by three atomic-absorption spectrophotometric methods are compared. "Wet chemical" methods based on the decomposition of the sample with mixed acids yield more accurate results than those based on fire-assay collection techniques. A direct acid-decomposition method involving the determination of silver in a 20% v/v hydrochloric acid-1% v/v diethylenetriamine medium is recommended for the determination of $\sim 10 \mu\text{g/g}$ or higher levels of silver. A method based on chloroform extraction of the tribenzylamine-silver bromide ion-association complex from 0.08M potassium bromide-2M sulphuric acid is recommended for samples containing $< 10 \mu\text{g}$ of silver per g.

Recently, as part of a current CANMET project involving a study of the behaviour of silver in conventional hydrometallurgical processes designed to recover metallic zinc from zinc ores and concentrates, one of the authors developed a simple, sensitive and reliable atomic-absorption spectrophotometric method for the determination of $\sim 0.1 \mu\text{g/g}$ or more of silver in ores and concentrates and $\sim 0.001 \mu\text{g/ml}$ or more in zinc-process solutions.¹ In this method, the sample is decomposed with acids and silver is separated from the matrix elements by chloroform extraction of the tribenzylamine (TBA)-silver bromide ion-association complex from 0.08M potassium bromide-2M sulphuric acid. Silver is stripped from the chloroform phase with 9M hydrobromic acid and ultimately determined by atomic-absorption spectrophotometry (AAS) in a 10% v/v hydrochloric acid-1% v/v diethylenetriamine medium. Because subsequent work showed that relatively large amounts of iron, zinc, lead, nickel and copper do not cause significant error in the determination of silver under these conditions, it was considered probable that, after decomposition with suitable acids, most ores, concentrates and zinc-processing products containing moderate amounts of silver could be analysed directly and relatively rapidly in a dilute hydrochloric acid-diethylenetriamine medium without prior separation of silver. Such a method would also be a useful

alternative to the fire-assay/AAS lead collection method currently used in the CANMET chemical laboratory,^{2,3} and could be used as a comparison (or umpire) method. However, during attempts to evaluate this method by applying it to iron-leach residues and roaster and other zinc-processing products, the results obtained were not always in good agreement with previous results obtained by the fire-assay/AAS method. Ultimately, it was found that these materials were of questionable homogeneity. Consequently, various diverse Canadian Certified Reference Materials Project (CCRMP) reference ores and concentrates, which have been certified for silver and which are of proven homogeneity, were used to evaluate the method. The results obtained for these materials by the recommended acid-decomposition/AAS method are compared with those obtained previously at CANMET during the respective inter-laboratory certification programmes by the fire-assay/AAS method mentioned above and by a similar method based on the collection of silver with molten tin.⁴ The results are also compared with those obtained by the TBA-extraction method¹ and the fire-assay methods (including classical and AAS methods) and acid-decomposition/AAS results obtained during the certification programmes.

EXPERIMENTAL

Apparatus

A Varian-Techtron model AA6 spectrophotometer, equipped with a 10-cm laminar-flow air-acetylene burner

and a silver hollow-cathode lamp, was used under the following conditions.

Wavelength: 328.1 nm
 Lamp current: 3 mA
 Spectral band-pass: 0.20 nm
 Height of light-path above burner: 4 mm
 Acetylene flowmeter reading: 2.0 (~1.5 l./min)
 Air flowmeter reading: 6.5 (~11.5 l./min)
 Flame: strongly oxidizing
 Aspiration rate: 8 ml/min

Reagents

Standard silver solution, 100 µg/ml. Dissolve 0.1000 g of pure silver foil in ~25 ml of 25% v/v nitric acid, add ~10 ml of 50% v/v sulphuric acid and evaporate the solution to fumes of sulphur trioxide. Dissolve the salts in ~100 ml of 50% v/v hydrochloric acid and transfer the solution to a 1-litre standard flask containing ~350 ml each of concentrated hydrochloric acid and water. Allow the solution to cool to room temperature, then dilute to volume with water. This solution is stable for at least 2 months. Prepare a 10-µg/ml solution by diluting 10 ml of this stock solution and 36 ml of concentrated hydrochloric acid to 100 ml with water. Prepare this diluted solution fresh as required.

Diethylenetriamine. A 10% v/v solution in water.

Bromine. A 20% v/v solution in carbon tetrachloride.

Hydrochloric acid, 25% v/v. Store in a plastic squeeze-type wash-bottle.

Hydrochloric acid, 50% v/v.

Nitric acid, 50% v/v.

Sulphuric acid, 50% v/v.

Recommended acid-decomposition method

Calibration solutions. Add 10 ml of 10% diethylenetriamine solution to each of eleven 100-ml standard flasks (Note 1); then, from a burette, add to the first five flasks 2, 4, 6, 8 and 10 ml of 10-µg/ml standard silver solution. To the next five flasks, add 1.5, 2, 2.5, 3 and 4 ml of 100-µg/ml standard silver solution. The last flask contains the zero calibration solution. Add sufficient concentrated hydrochloric acid to each flask for the final solution to be 20% v/v hydrochloric acid, then dilute each solution to volume with water (Note 2).

Procedure. Transfer up to 0.25 g (Notes 1 and 3) of powdered sample, containing up to ~700 µg of silver (Note 4), to a 150-ml beaker. Cover, and add 5 ml of 20% bromine solution in carbon tetrachloride (Note 5) and 10 ml of 50% nitric acid. Mix and allow the solution to stand for ~15 min, then heat gently to remove the bromine and carbon tetrachloride. Add 5 ml each of concentrated hydrochloric and perchloric acids and 5 ml of 50% sulphuric acid and heat until fumes of perchloric acid are evolved. Continue to heat the solution for ~10 min (Note 6), then allow to cool to room temperature. Remove the cover, wash down the sides of the beaker with water (Note 7) and carefully evaporate the solution to dryness. Depending on the expected silver content, add sufficient 50% hydrochloric acid for 20 ml to be present for each 50 ml of final solution (Note 8) and heat gently to dissolve the salts. Cool, then filter the solution (Whatman No. 1 or No. 40 paper) into a standard flask of appropriate size (50–200 ml) containing sufficient 10% diethylenetriamine solution for 5 ml to be present for each 50 ml of final solution (Note 8). Wash the beaker twice with 3–5-ml portions of 25% hydrochloric acid, followed by water, then wash the paper in a similar manner. Discard the paper and dilute the solution to volume with water.

Measure the absorbance at 328.1 nm when the sample solution is aspirated into a strongly oxidizing air-acetylene flame (Notes 9 and 10). Calculate the silver content (in µg) from the absorbances for the sample and for calibration solutions that bracket the sample concentration.

Notes

1. All glassware should be washed with ~25% ammonia solution followed by water.

2. The solutions in the first series (*i.e.*, up to 1 µg of silver per ml) are stable for at least 2 weeks. Those in the second series should be prepared fresh every day because the absorbance obtained slowly decreases with age of the solution.

3. To avoid possible viscosity or interference effects from matrix elements, the use of more than 0.25 g of sample for a final volume of 50 ml is not recommended. Up to 0.5 g of sample can be taken if the final volume is to be 100 or 200 ml. However, this is not recommended if the sample contains appreciable silica, unless the silica is removed by volatilization with hydrofluoric acid. In that case, use a Teflon beaker for the decomposition step and add ~5 ml of concentrated hydrofluoric acid before the solution is evaporated to fumes of perchloric acid. After cooling the solution, add ~15 ml of water and wash down the sides of the beaker with 50% hydrochloric acid from a plastic squeeze-type wash-bottle. Transfer the solution to a 250-ml Pyrex beaker, evaporate to dryness and proceed as described.

4. If lead is present, the amount of sample taken should be such that the lead concentration of the final solution will not exceed ~2500 µg/ml, because otherwise lead chloride may precipitate in the solution either before or after the filtration step. This can cause low results for silver because of adsorption on the precipitate.

5. Bromine is added to oxidize sulphur and sulphides to sulphate.

6. Continued heating of the solution results in the dehydration of any silica present.

7. If appreciable antimony is present, add 5 or 10 ml of concentrated hydrobromic acid at this stage.

8. For final sample solution volumes of 50, 100 and 200 ml, add 20, 40 and 80 ml of 50% hydrochloric acid, respectively. The solution should not be diluted with water at this point because silver chloride may precipitate. The volumes of 10% diethylenetriamine solution to be added are 5, 10 and 20 ml, respectively.

9. About 3–10-fold scale expansion is recommended for the determination of ≤1 µg of silver per ml. Sample solutions containing more than 1 µg/ml should be analysed on the day that they are prepared (Note 2).

10. If dilution of the sample solution is necessary, sufficient 50% hydrochloric acid and 10% diethylenetriamine solution must be added to the aliquot taken for the concentrations of acid and amine in the diluted solution to be the same as in the calibration solutions. For a two-fold dilution, transfer a 25-ml aliquot of the solution to a 50-ml standard flask, add 2.5 ml of the amine solution and 10 ml of 50% hydrochloric acid and dilute the resulting solution to volume with water. For a four-fold dilution, transfer a 25-ml aliquot to a 100-ml standard flask and add 7.5 ml of amine solution and 30 ml of the acid solution.

RESULTS AND DISCUSSION

Preliminary investigation of the direct acid-decomposition/AAS method

Most investigators have found that the determination of silver by AAS is relatively free from interelement effects.⁵⁻⁸ Probably the greatest source of error in all AAS methods for silver is that caused by contamination of the final sample solution with chloride. In nitric or sulphuric acid media, this results in the precipitation of silver chloride, which is adsorbed on the walls of glass containers.⁶ Ammonia,⁸

potassium cyanide,⁹ mercury(II) nitrate^{6,10} and $\geq 25\%$ hydrochloric acid⁷ have been used to dissolve silver chloride and to keep silver in solution for its determination by AAS. However, diethylenetriamine (DTA),¹¹ which is used in conjunction with hydrochloric and nitric acids in the tribenzylamine (TBA) extraction/AAS and fire-assay/AAS methods^{2,3} developed at CANMET, is also effective, convenient to use and considerably less hazardous than potassium cyanide. An acidic DTA medium is also more advantageous than an ammonia medium because iron, aluminium and various other elements form precipitates in ammoniacal media. In the presence of DTA, less hydrochloric acid can be employed, which helps to reduce burner corrosion. Although a 10% hydrochloric acid-1% DTA medium is used in the TBA-extraction method,¹ preliminary work showed that about a 20% hydrochloric acid-1% DTA medium is required for the direct determination of silver in ores and concentrates to keep moderate amounts of lead in solution. Under these conditions, up to at least 7 mg of iron(III), 4 mg of zinc, 2.5 mg each of lead and nickel and 1.5 mg of copper(II) per ml will not cause significant error in the determination of silver in a strongly oxidizing air-acetylene flame. Higher concentrations of lead can cause low results because of the precipitation of lead chloride, which occludes or adsorbs silver.

Tests showed that, after decomposition of the sample as described in the recommended method and the ultimate dissolution of the salts by heating with 50% hydrochloric acid, the solution should be allowed to cool to room temperature before the addition of DTA solution. Low results will be obtained if the DTA solution is added before the heating step. It was also found that some jarosites and iron-leach residues contained black material which was insoluble in a mixture of hydrochloric, nitric and sulphuric acids and which contained microgram quantities of silver. These samples could be effectively decomposed by treatment with this acid mixture, followed by refluxing of the solution with perchloric acid. This also dehydrates any silica present.

Application of the acid-decomposition method to CCRMP reference ores and concentrates and to jarosite residues

Table 1 shows that the results obtained for seven CCRMP reference ores and concentrates¹²⁻¹⁹ of complex composition by the recommended acid-decomposition method are in reasonably good agreement with the mean values obtained by the TBA-extraction method¹ and, except for PTM-1,¹⁵ with the certified values. Except for PTM-1, previously analysed by an earlier CANMET fire-assay/AAS tin-collection method,⁴ and for MP-1 and MP-1a, the results agree well with those obtained at CANMET by the current fire-assay/AAS lead-collection method^{2,3} during the respective interlaboratory certification programmes. The results obtained for several jarosite residues are

also in reasonably good agreement with those obtained at CANMET by the current fire-assay method. For the tests with the jarosite residues all the subsamples were taken within 2 days to eliminate possible error resulting from the absorption of moisture. All the results shown for the recommended acid-decomposition method are for individual subsamples. Each result is the mean of 6 AAS measurements, and the relative standard deviations found under these conditions at about the 0.2, 2 and 3 $\mu\text{g/ml}$ silver levels were ~ 1.1 , 0.7 and 0.6%, respectively. This is in good agreement with the precision of AAS measurements for silver reported by other investigators.^{8,9}

The results obtained for PTM-1 by both the TBA-extraction and acid-decomposition methods are in excellent agreement with those obtained at the National Institute of Metallurgy (NIM) in South Africa²⁰ by "wet-chemical" AAS methods involving leaching of the sample with nitric acid. In that work, silver was determined either directly with compensation in the calibration solutions for viscosity and matrix effects, or after extraction into toluene containing iso-octyl thioglycollate. The mean values obtained at NIM were 73.8 $\mu\text{g/g}$ for 11 results ranging from 69 to 77 $\mu\text{g/g}$ and 74.4 $\mu\text{g/g}$ for 10 results ranging from 73.2 to 75.6 $\mu\text{g/g}$, respectively. The low results obtained for PTM-1 by the tin-collection method⁴ could be due to incomplete co-precipitation of silver with tin powder after the dissolution of the tin button with concentrated hydrochloric acid.²⁰ From the results of early work carried out at CANMET to evaluate the classical fire-assay/lead-collection method for silver,²¹ it is considered probable that slag losses are largely responsible for the low results obtained for MP-1 and MP-1a by the CANMET fire-assay/AAS lead-collection method. Faye and Inman²¹ showed that for materials rich in copper and/or nickel sulphides, or those that produce viscous slags, $\sim 2\%$ or more of the silver present can be lost to the slag. Up to $\sim 0.5\%$ can also be retained by the crucible during fusion. These investigators and others²²⁻²⁵ also showed that, depending on the temperature used, a considerable amount of silver (up to 2% or more²¹) can be lost during the cupellation step in classical fire-assay procedures. However, the CANMET fire-assay/AAS lead-collection method is not subject to this error because it does not involve a cupellation step. Table 2, which shows the mean results (including outliers) obtained for silver in the CCRMP reference materials during the respective interlaboratory certification programmes by both classical fire-assay and fire-assay/AAS methods and by direct acid-decomposition/AAS methods, shows that PTM-1 was certified on the basis of fire-assay results alone. Consequently, from the results obtained by the TBA-extraction and recommended acid-decomposition methods and those obtained at NIM, it is considered highly probable that the certified value for PTM-1 is too low and that it should be $\sim 75 \mu\text{g/g}$ of silver.

Table 1. Determination of silver in CCRMP reference ores and concentrates and jarosite residues by the recommended acid-decomposition method

Sample	Nominal composition, %	Ag found, $\mu\text{g/g}$			
		Certified value and 95% confidence limits, Ag, $\mu\text{g/g}$	Fire-assay/AAS method*	TBA-extraction/AAS method†	Recommended acid-decomposition method
CCU-1 Copper concentrate	24.7 Cu, 3.2 Zn, 30.8 Fe, 35.6 S, 2.6 SiO ₂	139 (136-142)	142.1 (141-144)	140.2	141.6, 140.4
CPB-1 Lead concentrate	64.7 Pb, 4.4 Zn, 8.4 Fe, 17.8 S, 0.7 SiO ₂ , 0.4 Sb	626 (620-632)	620 (604-631)	623.0	630.6, 626.5
CZN-1 Zinc concentrate	44.7 Zn, 7.5 Pb, 10.9 Fe, 30.2 S, 1.0 SiO ₂	93 (90-95)	93.0 (89-96)	94.7	94.3, 95.4
PTM-1 Noble metal-bearing nickel-copper matte	30.2 Cu, 44.8 Ni, 1.6 Fe, 21.6 S	66 (59-73)	68.6 (67.6-70.7)	75.0	74.8, 76.0
KC-1 Zinc-lead-tin-silver ore	20.1 Zn, 6.9 Pb, 16.1 Fe, 28.1 S, 11.1 Si, 0.7 Sn, 0.8 Al, 0.3 Ca	1120 (1110-1130)	1110 (1101-1118)	1117	1116, 1129
MP-1 Zinc-tin-copper-lead ore	15.9 Zn, 1.9 Pb, 5.7 Fe, 11.8 S, 19.4 Si, 3.6 Al, 3.4 Ca, 2.1 Cu, 0.8 As, 2.4 Sn	57.9 (55.7-60.1)	54.7 (52.5-56.2)	59.3	61.4, 59.6, 60.6
MP-1a Zinc-tin-copper-lead ore	19.0 Zn, 4.3 Pb, 6.2 Fe, 5.2 Al, 12.8 S, 19.4 Si, 1.4 Cu, 2.1 Ca, 1.3 Sn, 0.8 As	69.7 (67.9-71.4)	66.4 (64.1-67.9)	67.5	70.9, 69.6
DA-6801 Jarosite residue	58.3 Pb, 0.4 Zn, 0.5 Cu, 0.5 Fe, 14.1 S	—	1100, 1125	—	1138, 1144
DA-6806 Jarosite residue	0.6 Zn, 0.2 Pb, 31.3 Fe, 3.6 Na, 13.3 S	—	54.5, 54.4	—	55.9, 55.6, 54.8

*The results shown for the CCRMP reference materials are the means of 10 values, varying over the ranges shown in parentheses, obtained at CANMET during the respective interlaboratory certification programmes.^{12-16,18,19} Except for PTM-1 (tin-collection method⁴), all the results shown were obtained by the CANMET lead-collection method.^{2,3}

†Mean of 2 or 3 values.¹

Table 2. Correlation of silver results for CCRMP reference ores and concentrates with the analytical method employed

Laboratory	Analytical method and mean Ag value, µg/g*																	
	MP-1 (1972)		PTM-1 (1973)		PTC-1 (1973)		KC-1 (1974)		CCU-1 (1979)		CPB-1 (1979)		CZM-1 (1979)		SU-1a (1980)		MP-1a (1982)	
	FA	AD-AAS	FA	AD-AAS	FA	AD-AAS	FA	AD-AAS	FA	AD-AAS	FA	AD-AAS	FA	AD-AAS	FA	AD-AAS	FA	AD-AAS
1	59.5	66.6	68.6±§	66.0±§	1110±§	1102±§	142±§	139	136-142	626	620-632	93	90-95	4.3	4.1-4.6	69.7	67.9-71.4	
2	58.5†	65.0†	65.0†	6.0†	1133	1140	121	118	118	630	610	94	94	5.3	5.3	67.2	69.4	
3	56.2	57.4	50.8†	5.1†	1146#	1120	1099	134	134	610	643	84†	95	6.0	6.0	68.5	68.5	
4		60.1	67.1	5.8	1127	1160	145			614	614	90	99	3.8	3.8	71.5	71.5	
5		63.4	65.9†	7.0†		1102	144			633†	620±§	97	97	6.3	6.3	68.6	68.6	
6		61.9	71.5†	5.9†		1218	141			629	629	94	94	4.3	4.3	74.6	74.6	
7	58.6				1128	1164#	1161	137	137	624	624	96	96	3.3	3.3	65.7	65.7	
8	53.3	62.3			1162†	1154	131†			627	627	96	96	5.5	5.5	73.2	73.2	
9		56.1				1159				624	624	97	97	4.1	4.1	71.6	71.6	
10		64.8								630	630	89	89			62.7	62.7	
11		59.0			1120	1186				630	630	92	92	4.3±§	4.3±§	65.8±§	65.8±§	
12	54.5±§				1163#	1170	1062			650	650	102	102	4.7†	4.7†	68.3	68.3	
13	54.8±§				1170	1134				629	629	82	82	4.3†	4.3†	67.0±§	67.0±§	
14	56.6				1134	1125				613	613	93	93	4.8†	4.8†			
15					1125	1174#				620	620	90†	90†					
16					1117	1107				602†	602†	93	93					
17										622	622							
18																		
19																		
20																		
21																		
Mean	56.1	61.3	64.8	6.0	1133†	1139	139.3	138.2	138.2	622.6	627.6	92.3	93.0	4.7	4.6	66.9	69.8	

*Numbers in parentheses beside symbols for the reference materials refer to the year they were certified. The figures given below are the certified values and 95% confidence limits. FA and AD refer to fire-assay and acid-decomposition methods, respectively. The laboratory numbers shown bear no relation to those given in the certification documents.

†Original certified value.

‡Silver ultimately determined by AAS.

§Result obtained at CANMET during the interlaboratory certification programme.

Result corrected for cupellation and slag losses.

† Corrected values (#) omitted in calculation of the overall mean value.

Table 3. Comparison of the mean results obtained for CCRMP materials by the recommended acid-decomposition/AAS method with the mean fire-assay (FA) and acid-decomposition (AD) results obtained during the certification programmes

Sample	Ag found, $\mu\text{g/g}$		
	Mean CCRMP FA value	Mean CCRMP AD/AAS value	Mean value by the recommended AD/AAS method*
CCU-1	139.3	138.2	141.0
CPB-1	622.6	627.6	628.6
CZN-1	92.3	93.0	94.9
KC-1	1133	1139	1123
MP-1	56.1	61.3	60.5
MP-1a	66.9	69.8	70.2

*Calculated from values given in Tables 1 and 4.

Comparison of results obtained by the recommended acid-decomposition method with those obtained by fire-assay and acid-decomposition/AAS methods during the CCRMP certification programmes

Table 3 shows that the mean values obtained for the CCRMP materials listed in Table 1 (excluding PTM-1) by the recommended acid-decomposition method are all in excellent agreement with the overall mean acid-decomposition/AAS values (Table 2) calculated from the results obtained during the certification programmes. Except for MP-1¹⁸ and MP-1a,¹⁹ the results are also in reasonably good agreement with the overall mean CCRMP fire-assay results obtained by both classical and AAS methods. The overall mean CCRMP fire-assay and acid-decomposition results (Table 3) are also in good agreement, except for MP-1 and MP-1a. Most of the acid-decomposition methods used in these certification programmes involved the AAS determination of silver in $\geq 25\%$ hydrochloric acid media to avoid error resulting from the precipitation of silver chloride.

In Table 2 the low mean fire-assay value for MP-1a is probably due to the fact that only 4 sets of results were reported compared with 12 sets by acid-decomposition/AAS methods. The low mean fire-assay value for MP-1, as suggested in the certification document,¹⁸ is probably caused by cupellation and slag losses.²¹ As mentioned previously, both types of loss can occur in classical fire-assay methods, but in fire-assay/AAS methods the major loss of silver is to the slag. When the original certified value for MP-1 was calculated, the fire-assay results shown in Table 2 were all corrected by 3% to compensate for these losses, even though some of the methods used involved AAS finishes. Since their certification both MP-1 and KC-1 have undergone oxidation of their sulphide minerals, with subsequent changes in composition. Consequently, in 1978, the certified values were recalculated with correction factors based on the changes in the zinc contents of these ores.¹⁷ That is the reason for the difference between the certified values shown for these ores in Tables 1 and 2. To obtain true overall mean values, all the outliers omitted in the calculation of the CCRMP certified values have been included in

Table 2 and used in the calculations of the overall mean fire-assay and acid-decomposition values. However, in the case of KC-1, classical fire-assay results that were corrected for silver losses by the participating laboratory were not included in the calculations because most of these results were high. For these reasons and because results by methods other than fire-assay and acid-decomposition/AAS methods were not included, some of the overall mean values shown in Table 2 (*viz.* for PTM-1 and PTC-1²⁶) are not the same as the certified values.

Precision for silver in ores by the recommended acid-decomposition method

Table 4 shows that the precision of the results for silver by the recommended acid-decomposition/AAS method at about the 70–100 $\mu\text{g/g}$ level is reasonably good, considering the small amount of sample taken (0.2–0.25 g) in these tests. The relative standard deviation obtained for MP-1a is comparable with the mean value obtained for the two series of results by the CANMET fire-assay/AAS method, but better than that obtained by the TBA-extraction method. The mean relative standard deviation for KC-1 is slightly higher than, but still compares favourably with, the values obtained by the fire-assay and extraction methods. As shown in Table 4 and mentioned previously,¹ the precision of the fire-assay/AAS method would be expected to be slightly better than that of the recommended acid-decomposition and TBA-extraction methods because of the much larger samples usually taken, *i.e.*, $\sim 15\text{--}30$ g.

CONCLUSIONS

From Table 2 it is apparent that direct AAS methods involving an acid attack of the sample are being used increasingly for the determination of silver in ores and related materials.²⁷ However, it is also apparent from the variations in the results obtained for SU-1a by direct acid-decomposition/AAS methods that such methods are not the best for the analysis of samples containing very small amounts of silver, because of the low concentration in the final solution. This was why neither SU-1a²⁸ nor PTC-1²⁶

Table 4. Precision of results for determination of silver in ores

Sample and method	Ag found, $\mu\text{g/g}$	Mean, $\mu\text{g/g}$	Standard deviation, $\mu\text{g/g}$	Relative standard deviation, %
Acid-decomposition/AAS				
MP-1a	70.9, 69.6, 70.8, 70.1, 69.4	70.2	0.68	1.0
KC-1a	1116, 1129, 1128, 1131, 1139 1108, 1132, 1097, 1119, 1129*	1129 1117	8.26 14.61	0.7 1.3
Fire-assay/AAS†				
MP-1a	64.1, 67.0, 66.3, 64.3, 67.1 66.9, 66.5, 67.9, 67.3, 66.5	65.8 67.0	1.46 0.59	2.2 0.9
KC-1	1108, 1114, 1113, 1117, 1111 1106, 1104, 1103, 1118, 1101	1113 1106	3.36 6.73	0.3 0.6
TBA-extraction/AAS				
MP-1a	66.7, 67.0, 66.7, 69.6, 65.0, 69.8	67.5	1.87	2.8
KC-1	1109, 1115, 1111, 1118, 1128, 1119	1117	6.77	0.6

*Silica removed by volatilization with HF (Note 3).

†Results obtained at CANMET during the interlaboratory certification programmes.

was analysed by the recommended acid-decomposition method. The results obtained for SU-1a (Table 2) by fire-assay methods involving AAS finishes show better precision than those obtained by direct acid-decomposition/AAS methods. Furthermore, even though losses can occur, the fire-assay methods are probably more accurate for samples of low silver content than direct acid-decomposition methods because of the much larger subsamples usually taken. However, as reported recently, indirect acid-decomposition/AAS methods, such as extraction methods that involve preconcentration of silver, also yield precise and probably the most accurate results for small amounts of silver.^{29,30} In recent years, many such methods have been reported.³¹ Donaldson¹ obtained a mean value of 5.9 $\mu\text{g/g}$ (3 determinations) with a standard deviation (SD) of 0.4 $\mu\text{g/g}$ for PTC-1 by the TBA-extraction method. This is in excellent agreement with the mean fire-assay/AAS value (Table 2) of 6.0 $\mu\text{g/g}$ (SD = 0.2 $\mu\text{g/g}$ for 10 determinations) obtained at CANMET by the tin-collection method⁴ during the certification programme. It also agrees with the overall mean fire-assay value and with the certified value calculated from 5 sets of fire-assay results mostly obtained by using AAS finishes. The precision of the results obtained for silver in SU-1a by the TBA-extraction method is also comparable with that obtained at CANMET by the fire-assay/AAS lead-collection method. Mean values of 4.6 (6 determinations) and 4.3 $\mu\text{g/g}$ (10 determinations) with standard deviations of 0.3 and 0.2 $\mu\text{g/g}$, respectively, were obtained. It is noteworthy that the mean value obtained for SU-1a by the extraction method is in excellent agreement with both the overall mean fire-assay and acid-decomposition/AAS results shown in Table 2, but is slightly higher than the certified value. The mean value also agrees with the overall mean value of 4.7 $\mu\text{g/g}$ obtained for the 17 sets of silver results reported during the certification programme.²⁸ However, because of the low silver content of SU-1a and the relatively wide variation in the results obtained during the programme, particularly by direct acid-decomposition methods, it was concluded that that value was not the most suitable estimate of the silver

content. Consequently, the certified value was based on the 10 sets of results in which the individual mean values lay within two standard deviations of the overall mean of the five best fire-assay results. In the calculation of the certified value, five of the results obtained by acid-decomposition methods and the first of the fire-assay results shown in Table 2 were treated as outliers. The true silver content of SU-1a is probably closer to 4.6 $\mu\text{g/g}$ than to the certified value of 4.3. However, the difference is probably not too significant at this level.

This investigation has shown that for most ores and related materials of acceptable homogeneity, the recommended acid-decomposition/AAS method yields results that are more accurate than those obtained by classical fire-assay methods and probably often more accurate than those obtained by fire-assay/AAS methods. This is because of the losses of silver that can occur in these methods, particularly to the slag during the fusion process and during some of the subsequent procedural steps.²¹⁻²⁵ Because of these losses, and depending on the amount of silver present, materials that produce viscous slags or have high copper and/or nickel sulphide contents are probably best analysed by direct acid-decomposition/AAS or extraction/AAS methods. Other investigators have also found that these methods yield more accurate results than those based on fire-assay techniques.^{7,8,32} The acid-decomposition method used in this work is recommended for the analysis of samples containing $\sim 10 \mu\text{g/g}$ or more of silver. Both the TBA-extraction/AAS and the CANMET fire-assay/AAS methods are recommended for samples containing $< 10 \mu\text{g/g}$ of silver. However, at this level, if only a small amount of sample is available, the extraction method is preferable because the final solution can be concentrated to 5 or 10 ml. In the fire-assay method, silver is usually determined in a volume of 100 ml or more after dissolution of the lead button with dilute nitric acid. The detection limits of both the extraction and fire-assay methods can be improved by using an electrothermal atomization technique.³¹ Although the recommended acid-decomposition method is extremely simple and relatively rapid, the fire-assay method is probably quicker

when large batches of sample are to be analysed. A minor disadvantage of the method is that calibration solutions containing more than $\sim 1 \mu\text{g}$ of silver per ml must be prepared fresh every day. To obtain accurate results, it is emphasized that all glassware should be washed with $\sim 25\%$ ammonia solution, followed by distilled water, just before use.

Acknowledgement—The authors thank P. E. Moloughney for performing the fire-assay/AAS analyses of the jarosite residues. Most of the CANMET fire-assay/AAS results for the CCRMP reference ores and concentrates were also obtained by Mr. Moloughney during the interlaboratory certification programmes.

REFERENCES

1. E. M. Donaldson, *Talanta*, 1982, **29**, 1069.
2. P. E. Moloughney, *ibid.*, 1977, **24**, 135.
3. *Idem*, *ibid.*, 1980, **27**, 365.
4. P. E. Moloughney and J. A. Graham, *ibid.*, 1971, **18**, 475.
5. R. Belcher, R. M. Dagnall and T. S. West, *ibid.*, 1964, **11**, 1257.
6. I. Rubeška, Z. Šulcek and B. Moldan, *Anal. Chim. Acta*, 1967, **37**, 27.
7. R. C. Mallett, *Miner. Sci. Eng.*, 1970, **2**, 28 (and references therein).
8. G. Walton, *Analyst*, 1973, **98**, 335.
9. S. Kallman and E. W. Hobart, *Talanta*, 1970, **17**, 845.
10. N. L. Fishkova, E. P. Zdorova and N. N. Popova, *Zh. Analit. Khim.*, 1975, **30**, 806.
11. M. C. Greaves, *Nature*, 1963, **199**, 552.
12. G. H. Faye, W. S. Bowman and R. Sutarno, *CANMET Report 79-16*, Canada Centre for Mineral and Energy Technology, Department of Energy, Mines and Resources, Ottawa, Canada, 1979.
13. *Idem*, *ibid.*, 79-15, 1979.
14. *Idem*, *ibid.*, 79-14, 1979.
15. R. C. McAdam, R. Sutarno and P. E. Moloughney, *Technical Bulletin TB 182*, Mines Branch, Department of Energy, Mines and Resources, Ottawa, Canada, 1973.
16. G. H. Faye, W. S. Bowman and R. Sutarno, *ibid.*, TB 193, 1974.
17. G. H. Faye and W. S. Bowman, *CANMET Report 78-2*, 1978 (see also reference 12).
18. G. H. Faye, *Technical Bulletin TB 155*, 1972 (see also reference 15).
19. H. Steger and W. S. Bowman, *CANMET Report 82-14E*, 1982 (see also reference 12).
20. R. V. D. Robèrt, E. van Wyk and K. Dixon, *Natl. Inst. Metallurgy, Johannesburg, Rept.*, No. 1580, 1973.
21. G. H. Faye and W. R. Inman, *Anal. Chem.*, 1959, **31**, 1072.
22. R. V. D. Robèrt and E. van Wyk, *Natl. Inst. Metallurgy, Johannesburg, Technical Memorandum Project, No. 1672*, 1972.
23. Y. Nakamura and K. Fukami, *Bunseki Kagaku*, 1957, **6**, 687, *Chem. Abstr.*, 1958, **52**, 15331a.
24. K. Yaguchi and J. Kaneko, *ibid.*, 1972, **21**, 711; *Chem. Abstr.*, 1972, **77**, 134570j.
25. *Idem*, *ibid.*, 1972, **21**, 601; *Chem. Abstr.*, 1972, **77**, 134571k.
26. R. C. McAdam, R. Sutarno and P. E. Moloughney, *Technical Bulletin TB 176*, 1973 (see also reference 15).
27. H. F. Steger and G. H. Faye, *Talanta*, 1980, **27**, 327.
28. H. F. Steger and W. S. Bowman, *CANMET Report 80-9E*, 1980 (see also reference 12).
29. H. Jedrzejewska, M. Kozlicka and M. Malusecka, *Chem. Anal. (Warsaw)*, 1980, **25**, 809.
30. M. Kozlicka, M. Malusecka, H. Jedrzejewska, M. Kubica and M. Romanska, *Erzmetall*, 1980, **33**, 282; *Chem. Abstr.*, 1980, **93**, 189759p.
31. I. G. Yudelevich and E. A. Startseva, *Ind. Lab.*, 1981, **47**, 792 (and references therein).
32. I. Ya. Korotaeva, E. G. Emets and A. G. Fadeev, *ibid.*, 1981, **47**, 805.

EIN NEUES GRAPHISCHES AUSWERTEVERFAHREN ZUR ERMITTLUNG STÖCHIOMETRISCHER FAKTOREN GELÖSTER KOMPLEXE

TH. PRANGE, U. LECHNER-KNOBLAUCH und F. UMLAND
Anorganisch-chemisches Institut der Universität Münster, Corrensstraße 36,
D-4400 Münster/Westf., BRD

(Eingegangen am 18. Januar 1983. Revidiert am 1. September 1983. Angenommen am 9. September 1983)

Zusammenfassung—Es wird eine computerunterstützte Auswertemethode zur Ermittlung von Komplexzusammensetzungen vorgestellt. Die Methode ist frei von jeglichen Voraussetzungen oder Vereinfachungen und eignet sich daher sowohl für starke als auch für schwache Komplexe. Unterschiedliche Komplexzusammensetzungen in Abhängigkeit vom Konzentrationsverhältnis Metall zu Ligand können in einem einzigen Diagramm identifiziert werden. Nicht stöchiometrische Verbindungen werden von stöchiometrisch zusammengesetzten unterschieden.

Nahezu gleichzeitig mit der Einführung der Photometrie als Analysenmethode begannen Versuche, aus den erhaltenen Daten Rückschlüsse auf Komplexzusammensetzungen zu ziehen. Zu den bekanntesten und geläufigsten Methoden zählen diejenigen von Job,¹ Yoe und Jones,² die Geradenmethode nach Asmus³ und die logarithmische Methode nach Bent und French.⁴

Gemeinsam ist allen vier Methoden eine Einschränkung hinsichtlich der Art der Komplexdissoziation: so sind die beiden erstgenannten nur auf starke, die letzten nur auf schwache Komplexe anwendbar. Der Benutzer dieser Methoden muß daher vor der Ermittlung der Komplexzusammensetzung zumindest annähernd das Dissoziationsverhalten des interessierenden Komplexes kennen.

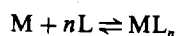
In der Regel läßt sich nach diesen Methoden *nur* eine Komplexzusammensetzung ermitteln, obschon die stufenweise Dissoziation von Komplexen bekannt ist. Von den innerhalb eines Systems Metall:Ligand möglichen Komplexzusammensetzungen wird die scheinbar stabilste erfaßt.

Dieser Nachteil äußert sich besonders drastisch bei den stark dissoziierenden Komplexen, deren Zusammensetzung nur bei Ligandenüberschuß bestimmbar ist. Über den manchmal recht interessanten Bereich des äquimolaren Verhältnisses von Metall zu Ligand oder den Metallüberschußbereich lassen sich keine Aussagen machen.

Obwohl es eine Verbesserung der Bent/French-Methode gibt, die keine Vereinfachungen mehr vornimmt,^{5,6} so fehlt doch ein umfassender theoretischer Ansatz, der die beschriebenen Probleme zu lösen vermag. Eine solche Möglichkeit soll im folgenden geschildert werden.

THEORIE

Für eine Komplexbildung nach



mit $[M] = (m - k)$, $[L] = (l - nk)$ wobei m = Ausgangskonzentration Metall, l = Ausgangskonzentration Ligand, k = Komplexkonzentration, lautet das Massenwirkungsgesetz:

$$\frac{(m - k)(l - nk)^n}{k} = C. \quad (1)$$

Im Falle sehr schwach dissozierender Komplexe kann man in erster Näherung annehmen, daß bis zur vollständigen Komplexbildung die Gleichgewichtskonzentration der in steigendem Maße zugegebenen Komponente annähernd gleich Null ist. Die daraus resultierende Proportionalität zwischen Komplexkonzentration und zugegebener Komponente bildet die Grundlagen des Yoe/Jones- und des Job-Verfahrens.

Mit zunehmender Komplexdissoziation gelten diese einfachen Zusammenhänge jedoch nicht mehr. Ziel einer jeden graphischen Auswertemethode für schwache Komplexe ist es nun, durch geeignete Umformung und zulässige Vereinfachung von Gleichung (1) aus den bekannten Größen m bzw. l und der Meßgröße $E \sim k$ die Stöchiometrie n zu ermitteln. Schwierigkeiten bereitet dabei offensichtlich die Umformung des komplexen Gliedes $(l - nk)^n$. Häufig wird daher die Vereinfachung gemacht, den Subtrahenden nk zu vernachlässigen, was bei hohem Ligandenüberschuß auch durchaus zulässig erscheint. Formt man dann die derart vereinfachte Gleichung (1) um, so erhält man die bekannte Proportionalität $1/l^n \sim 1/k$, die der Näherungsmethode nach Asmus zugrundeliegt. Eine bessere Annäherung an das exakte Ergebnis von n ist nur möglich unter Berücksichtigung des vollständigen Gliedes $(l - nk)^n$, das zur Rechenerleichterung in eine Reihe entwickelt werden sollte.

Es ergibt sich für $1 \leq n \leq 3$:

$$(l - nk)^n = l^n - n^2 l^{(n-1)} k + (2)n^2 l^{(n-2)} k^2 - (3)n^3 k^3 \quad (2)$$

mit $(b) = a!/b!(a-b)!$ Für $n = 1$ sind die beiden letzten, für $n = 2$ das letzte Glied gleich Null.

Setzt man zur Auswertung seiner Meßdaten Gleichung (2) in Gleichung (1) ein, multipliziert zunächst die Klammern aus und dann jedes Glied mit dem Faktor $l^{(n-1)}/k$, und ordnet anschließend alle k enthaltenden Glieder auf die linke Seite, so erhält man Gleichung (3):

$$ml/k + n^2k + (2^n)n^2k(m-k)/l + (3^n)n^3k^2l^{(1-n)}(k-m) = n^2m + (C + l^n)l^{(1-n)}. \quad (3)$$

Es resultiert eine Geradengleichung der Form $y = ax + b$ mit $a = n^2$, $x = m$, $b = (C + l^n)l^{(1-n)}$, der Ausdruck für y umfaßt allerdings die gesamte linke Gleichungsseite und wird sinnvollerweise mit Hilfe einer Rechenanlage bestimmt. Trägt man für $n = 1, 2, 3$ den jeweils linken Gleichungsteil gegen die variable Metallkonzentration auf, so erhält man drei Kurvenzüge. Man vergleicht die Steigungen der Kurvenzüge mit den theoretisch zu erwartenden Steigungen n^2 . Stimmt—gegebenenfalls nur in einem bestimmten Konzentrationsbereich—die Steigung einer Kurve mit der theoretischen überein, so besitzt der Komplex in diesem Bereich die Stöchiometrie ML_n .

Setzt man in Gleichung (3) die Werte von $n = 1, 2$ und 3 ein, erhält man drei Einzelgleichungen, die sich durch Umformen noch etwas vereinfachen lassen:

$$n = 1 \Rightarrow ml/k + k = m + l + C \quad (4a)$$

$$n = 2 \Rightarrow ml^2/k + 4mk + 4lk - 4k^2 = 4lm + l^2 + C \quad (4b)$$

$$n = 3 \Rightarrow ml^3/k + 27mlk - 27mk^2 + 9l^2k - 27lk^2 + 27k^3 = 9l^2m + l^3 + C. \quad (4c)$$

Der Vorteil von Gleichungen (4a–4c) gegenüber Gleichung (3) liegt in der besseren Übersichtlichkeit der gegeneinander aufgetragenen Werte; man muß allerdings dabei in Kauf nehmen, daß die erhaltenen Steigungen noch eine Potenz von l als Faktor enthalten. Welche der Gleichungen, (3) oder (4a–4c), man zur Auswertung benutzt, ist auf Grund der mathematischen Äquivalenz gleichgültig.

Bei Benutzung einer Rechenanlage ist es in jedem Fall zu empfehlen, die Werte der linken Gleichungsseite (n) nicht nur berechnen, sondern mit Hilfe eines Plot-Programmes die drei Kurvenzüge und die theoretisch zu erwartende Steigung ausdrücken zu lassen. Der Arbeitsaufwand dieser Methode reduziert sich dadurch auf das Eingeben von Meßwerten und Konzentrationen in den Rechner und Vergleich von experimenteller und theoretischer Steigung des ausgedruckten Diagrammes.

Ein willkürlich gewähltes Beispiel mit typischen Kurvenzügen zur Veranschaulichung der Auswertemethode zeigt Abb. 1. In diesem Beispiel liegt im

Bereich $m:l = 0-0.13$ ein 1:3-, im Bereich 0.29–0.42 ein 1:2- und im Bereich >0.51 ein 1:1-Komplex vor. Dazwischen liegen jeweils die Bereiche der Komplexumformierung (zwei Komplexe nebeneinander), in denen die theoretisch geforderten Steigungen nicht mit den experimentell gefundenen übereinstimmen können.

Nichtstöchiometrische Verbindungen können dagegen leicht identifiziert werden. Im Übergangsbereich stöchiometrischer Verbindungen ändert sich die experimentelle Steigung derart, daß sie von einem n -Wert weg auf einen anderen hin zustrebt; bei nichtstöchiometrischen Verbindungen dagegen entfernen sich mit zu- oder abnehmendem Metallgehalt alle experimentellen Steigungen *zunehmend* von allen theoretischen, und eine Übereinstimmung aller drei experimentellen mit den theoretischen Steigungen kann im gleichen Konzentrationsbereich auftreten.

Abbildung 2 zeigt als Beispiel dafür die unstöchiometrische Adsorptionsverbindung zwischen Mg und Titangelb, ausgewertet nach obigem Verfahren.

Die Vorteile der beschriebenen Auswertemethode sollen abschließend durch Vergleich mit den üblichen Verfahren aufgezeigt werden. Komplexiert man beispielsweise Co^{2+} mit 4-[Pyridyl-(2)-azo]-resorcin (PAR) bei pH 7.0 (Phosphatpuffer) und überträgt die gemessenen Extinktionen nach der Methode von Yoe und Jones in ein Diagramm, so ergibt sich der Kurvenzug von Abb. 3.

Der Informationsgehalt dieses Diagrammes ist gering. Da der gebildete Komplex anscheinend deutlich dissoziiert, liegen nur die ersten 5 Meßpunkte auf der Extrapolationsgeraden. Die daraus ermittelte Komplexstöchiometrie von 1:3 ist auf Grund mangelhafter Übereinstimmung sehr unsicher.

Wegen der scheinbar nicht zu vernachlässigenden Komplexdissoziation und zur Kontrolle der Ergebnisse empfiehlt sich eine weitere Auswertung nach einer Methode, die für stark dissoziierende

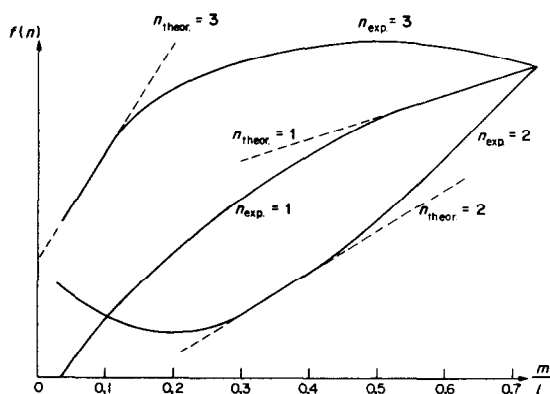


Abb. 1. Ermittlung der verschiedenen Komplexzusammensetzungen in Lösung: $f(n)$ = linke Seite der Gleichungen (4a–4c).

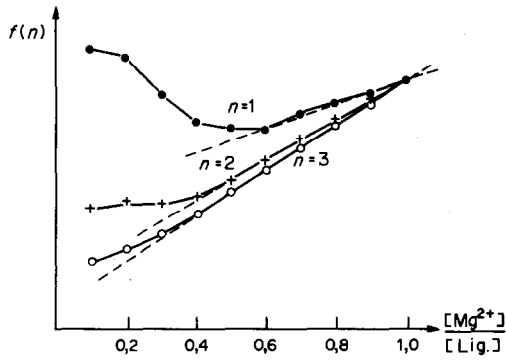


Abb. 2. Graphische Auswertung der unstöchiometrischen Adsorptionsverbindung Mg/Titangelb nach Gleichungen (4a-4c).

Komplexe geeignet ist. Abbildung 4 zeigt die Auswertung der Meßergebnisse nach der Asmus-Methode. Da bei unseren Messungen nicht die Reagenz-, sondern die Metallionenkonzentration variiert wurde, gibt der reziproke Wert von n Aufschluß über die Komplexstöchiometrie.

Aus den gegenläufig gekrümmten Kurvenzügen für $n = 1$ und $n = \frac{1}{3}$ geht hervor, daß die tatsächliche Komplexzusammensetzung dazwischenliegen sollte. Die demnach zu erwartende Stöchiometrie von $M:L = 1:2$ wird aber nur in einem kleinen Konzentrationsbereich durch die Geradenform für $n = \frac{1}{2}$ bestätigt, oberhalb und unterhalb dieses Bereiches ist die $n = \frac{1}{2}$ -Kurve ebenfalls gekrümmt. Die Form der Krümmung deutet dabei auf einen Komplex hin, dessen Zusammensetzung zwischen ML und ML_2 liegt. Andererseits läßt sich der obere Teil des Kurvenzuges (niedrige Metallkonzentrationen) für $n = \frac{1}{3}$ ebenso gut durch eine Gerade wiedergeben wie für $n = \frac{1}{2}$; die Abweichungen bei steigender Metallkonzentration werden allerdings bei $n = \frac{1}{3}$ größer als bei $n = \frac{1}{2}$.

Sollte man aus diesem Diagramm eine Komplexstöchiometrie ermitteln, müßte man trotz der nur mäßigen Übereinstimmung und hauptsächlich gestützt auf die gegenläufig gekrümmten Kurvenzüge für $n = 1$ und $n = \frac{1}{3}$ auf einen 1:2-Komplex schließen.

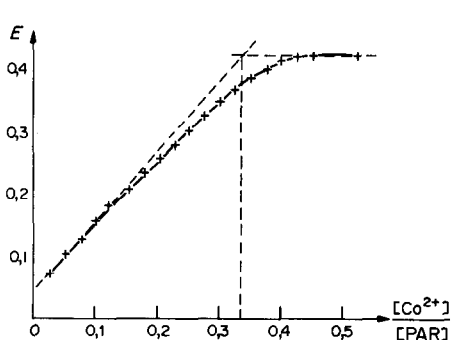


Abb. 3. Kobalt/PAR-Komplex, Auswertung nach Yoe-Jones.

Die Unstimmigkeiten und Ungenauigkeiten lassen das Ergebnis jedoch keinesfalls als gesichert erscheinen.

Somit unterscheiden sich die Ergebnisse aus der Yoe und Jones- bzw. der Asmus-Auswertung; eine Entscheidung über die Komplexstöchiometrie ist nicht möglich.

Weitergehende Aufschlüsse vermittelt dagegen Abb. 5, die die Auswertung nach der hier beschriebenen Methode zeigt. Innerhalb des Konzentrationsbereiches ≤ 0.12 -fach molare Kobaltmenge (die erstens 5 Meßpunkte) liegt ein 1:3-Komplex vor, der sich in genau diesem Bereich auch nach der Methode von Yoe und Jones nachweisen läßt (vgl. Abb. 3). Mit steigender Kobaltmenge ergeben sich Abweichungen vom theoretischen Verhalten eines 1:3-Komplexes. Die theoretische Steigung eines 1:2-Komplexes berührt die experimentelle Kurve nur als Tangente, und lediglich die letzten beiden Meßpunkte (> 0.4 -fach molare Kobaltmenge) stehen in Übereinstimmung mit dem theoretisch zu erwartenden 1:1-Komplex.

Als Resultat dieser Auswertung ergibt sich, daß bei hohem Ligandenüberschuß ein 1:3-Komplex gebildet

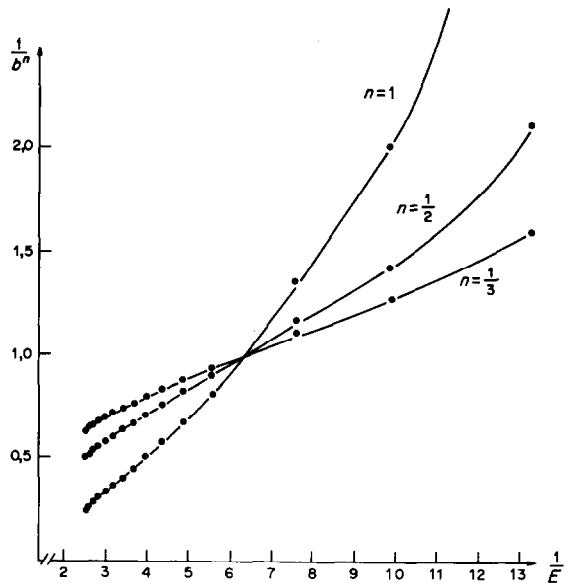


Abb. 4. Kobalt/PAR-Komplex, Auswertung nach Asmus.

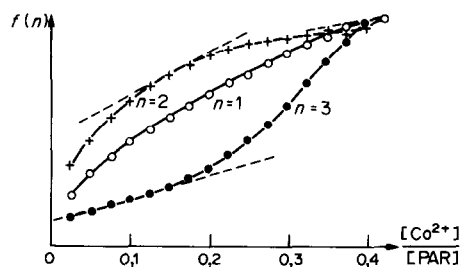


Abb. 5. Kobalt/PAT-Komplex, Auswertung nach Gleichungen (4a-4c).

wird, der bei weiterer Metallzugabe zerfällt. Ein eventuell existierender 1:2-Komplex kann nicht sehr stabil sein, da er in keinem größeren Konzentrationsbereich rein vorliegt. Amwahrscheinlichsten ist der über einen weiten Konzentrationsbereich ausgedehnte Zerfall in einen 1:1-Komplex, der mit abnehmender Ligandkonzentration zunehmend Oberhand gewinnt. Man kann aber einen mehrkernigen M_pL_q -Komplex nicht ausschließen. (Zur Ermittlung der Stöchiometrie solcher Komplexe mit den beiden Unbekannten p und q ist die Meßung einer weiteren Größe, zum Beispiel $[L]$, erforderlich; ein Verfahren dazu wurde ausgearbeitet⁷ und wird in Kürze publiziert.⁸)

Das Ergebnis dieser Auswertung läßt sich mit den Resultaten der Yoe/Jones- und der Asmus-Methode vergleichen. Der stabilste Komplex innerhalb des Systems Co/PAR ist der 1:3-Komplex. Dieser wird zwar von der für stabile Komplexe geeigneten Yoe/Jones-Methode erkannt, sollte der Auswertung nach jedoch instabil sein. Komplexumformierungen lassen sich nach Yoe und Jones nicht erkennen.

Die Asmus-Methode legt die Existenz eines 1:2-Komplexes nahe, doch ist die Aussage nicht gesichert. Erklären läßt sich das falsche Ergebnis durch den großen Konzentrationsbereich, in dem weder 1:3- noch 1:1-Komplexe rein vorliegen. Deren Mischung läßt sich in der Asmus-Darstellung am besten durch einen 1:2-Komplex wiedergeben.

Die Vorteile der beschriebenen Methode liegen in folgenden Punkten.

Es sind—im Gegensatz zu den bisherigen Verfahren keine Vorabinformationen über die Stabilität der untersuchten Komplexe erforderlich.

Die Komplexbildung läßt sich mit *einer* Versuchsreihe und *einer* Auswertemethode über einen sehr großen Bereich Metall:Ligand untersuchen.

Die Methode erlaubt Aussagen über sukzessive Komplexbildungsgleichgewichte.

Aus dem Ordinatenabschnitt der bestangepaßten Geraden läßt sich die Gleichgewichtskonstante C für die jeweilige Komplexbildungsreaktion abschätzen.

Danksagung—Wir danken den Herren H. Pinstock und N. Buschmann für die Erstellung der Rechnerprogramme und für mathematische Diskussionen.

LITERATUR

1. P. Job, *Ann. Chem. Phys.*, 1928, **9**, 113.
2. J. H. Yoe, und A. L. Jones, *Ind. Eng. Chem., Anal. Ed.*, 1944, **16**, 111.
3. E. Asmus, U. Hinz, K. Ohls und W. Richly, *Z. Anal. Chem.*, 1960, **178**, 104.
4. H. E. Bent und C. L. French, *J. Am. Chem. Soc.*, 1941, **63**, 568.
5. F. Umland und K. U. Meckenstock, *Z. Anal. Chem.*, 1959, **165**, 161.
6. *Idem, ibid.*, 1960, **177**, 244.
7. N. Buschmann, *Dissertation*, Münster, in Vorbereitung.
8. B. Bonefeld, *Dissertation*, Münster, in Vorbereitung.

Summary—A computerized plotting method for the determination of the stoichiometry of complexes is introduced. The method has no assumptions or simplifications, and is applicable to both strong and weak complexes. Different stoichiometries, as a function of the metal to ligand concentration-ratio, can be identified in a single diagram. Furthermore, non-stoichiometric complexes can be recognized.

DIFFERENZSPEKTROSKOPISCHE UND PULSPOLAROGRAPHISCHE UNTERSUCHUNGEN ZUR ZUSAMMENSETZUNG DER KUPFER-ALIZARIN S-KOMPLEXE

TH. PRANGE, H. D. SOMMER und F. UMLAND

Anorganisch-chemisches Institut der Universität Münster, Corrensstraße 36,
D-4400 Münster/Westf., BRD

(Eingegangen am 21. März 1983. Angenommen am 8. September 1983)

Zusammenfassung—Aus differenzspektroskopischen, konduktometrischen und pulspolarographischen Daten ließ sich nachweisen, daß drei Cu-Alizarin S-Komplexe mit den Zusammensetzungen 1:2, 1:1 und 2:1 existieren. Die kupferreiche 2:1-Verbindung läßt sich aus wäßriger Lösung fällen. In dem daraus entstehenden 1:1-Komplex in Dimethylformamid Wasser-Mischungen ist das Kupferion in *peri*-Stellung gebunden.

Trotz der schon seit über 100 Jahren bekannten und auch analytisch genutzten Alizarin-Metall-Farbstoffe herrscht noch weitgehende Unklarheit über ihre Stöchiometrie und Ort der Bindung des Metalls in *ortho*- oder *peri*-Stellung. Wir konnten kürzlich zeigen, daß aus pulspolarographischen Daten¹ Rückschlüsse gezogen werden können: zum Beispiel ist in den voltammetrisch nachweisbaren 1:1-Komplexen Aluminium in *ortho*- und Beryllium in *peri*-Stellung an Alizarin S gebunden. In anderen Fällen gibt es noch Unsicherheiten, auch bezüglich der Zusammensetzung.²⁻⁴

Babko und Nazarchuk⁴ fanden nach der Methode von Job bei pH 4.7 in allen Konzentrationsbereichen Cu:Alizarin S nur 1:1-Komplexe, während Yasukouchi und Yashinobu⁵ auf Grund amperometrischer Titrations Komplexzusammensetzungen Cu:Alizarin S = 1:1 und 1:2 angaben. In der vorliegenden Arbeit wurden zur Untersuchung der Kupfer-Alizarin S-Komplexe verschiedene Methoden kombiniert.

EXPERIMENTELLER TEIL

Geräte

Differenzspektren wurden mit dem registrierenden Spektrophotometer Zeiss DMR 21 bei einer Registriereschwindigkeit von 30 min/Trommeldrehung und einem Wellenlängenvorschub von 1 nm/mm aufgenommen. Als Küvetten dienten spezialgefertigte Tandemküvetten⁶ aus Quarzglas der Firma Hellma mit Schichtdicken von jeweils 0.438 cm pro Kammer.

Die pulspolarographischen Untersuchungen wurden mit dem PRG 5 der Firma Tacussel durchgeführt. Als Bezugs elektrode wurde eine Silber/Silberchlorid-Elektrode benutzt.

Die konduktometrischen Daten wurden mit dem Konduktoskop E 365 B der Firma Metrohm unter Verwendung der Leitfähigkeitsmeßzelle EA 608 erhalten.

Reagenzien

Alizarin S Lösung, $10^{-4}M$.

Puffer. Essigsäure/Acetat-puffer 0.1M, pH 4.7.

Als Lösungsmittel bei den differenzspektroskopischen Untersuchungen diente Wasser. Die Polarogramme wurden in Dimethylformamid/Wasser-Mischungen aufgenommen, und bei den konduktometrischen Daten wurde ein 1:1 Ethanol/Wasser-Gemisch benutzt.

ERGEBNISSE UND DISKUSSION

Spektroskopische Messungen

Da sich die Spektren von freiem Ligand und Komplex stark überlappen (Abb. 1), bot sich als empfindliche photometrische Methode die Differenzspektroskopie an.⁶ Bei dieser Meßmethode werden in Meß- und Vergleichsstrahl eines registrierenden Photometers zwei Küvetten mit halbhoher Scheidewand, sogenannte "Tandemküvetten", benutzt, deren eine Hälfte jeweils mit der Lösung des Metallsalzes, und deren andere mit der Lösung des Liganden gefüllt wird. Mißt man beide Küvetten gegeneinander, so muß eine gerade Basislinie resultieren. Nach Durchmischen des Küvetteninhalts im Meßstrahl setzt die Komplexbildung ein, und das Differenzspektrum wird registrierbar (Abb. 2). Dieses ist nicht streng identisch mit der Differenz der Einzelspektren gegen Wasser gemessen (Abb. 1). Es läßt sich aber zeigen,⁶ daß sowohl die positiven als auch die negativen Extinktionswerte der Komplexkonzentration proportional sind und daß differenzspektroskopische Daten sich deshalb vorbehaltlos zur Ermittlung von Komplex stöchiometrien verwenden lassen.

Es wurden Differenzspektren mit konstanter ($10^{-4}M$) Alizarin S und variabler Cu^{2+} -Konzentration ($0.1-8 \times 10^{-4}M$) aufgenommen und aus der absoluten Summe der Differenzextinktionen bei 519 nm und 417 nm mit Hilfe des vor kurzem beschriebenen Auswertverfahrens⁷ die Komplexstöchiometrien dieses Systems ermittelt. Abbildung 3 zeigt das erhaltene Computerdiagramm. Die theoretischen Steigungen sind gestrichelt eingezeichnet.

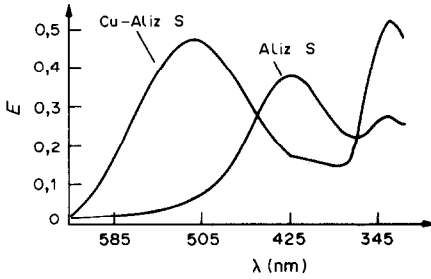


Abb. 1. Spektren von $10^{-4}M$ Cu-Aliz S-Komplex (1:1) bei Kupferüberschuß ($5 \times 10^{-4}M$) und $10^{-4}M$ Aliz S in Wasser gegen Wasser gemessen.

Der Deckungsbereich mit den experimentellen Kurven gibt ungefähr den Existenzbereich der Komplexe an: der 1:1 Cu-Alizarin S-Komplex liegt in Wasser erst bei mehr als zweifachem Metallüberschuß vollständig vor. Bei kleineren Molverhältnissen steht er im Gleichgewicht mit 1:2-Komplexen, die unterhalb Cu:Alizarin S = 0.9:1 dominieren. 1:3-Komplexe konnten nicht nachgewiesen werden.

Konduktometrische Messungen

Weitere Aussagen über Komplexbildung und -umlagerung sind möglich, wenn man die Protonenfreisetzung bei steigender Metallkonzentration und konstanter Ligandenkonzentration in ungepufferter Lösung konduktometrisch verfolgt (Abb. 4).

Die Leitfähigkeitskurve zeigt einen steilen Anstieg bis zum ca. zweifachen Kupferüberschuß, dann ein flaches Übergangsgebiet bis zum ca. fünffachen Kupferüberschuß, gefolgt von einem erneuten, weniger steilen Anstieg. Ab dem ca. achtfachen Kupferüberschuß begann der Komplex auszufallen.

Im flachen Übergangsgebiet werden keine Protonen freigesetzt, da die Steigungen der Leitfähigkeitskurve (Abb. 4a) in diesem Bereich und in einer reinen Kupferlösung (Abb. 4b) gleich sind. Der Anstieg der Leitfähigkeitskurve vor dem Übergangsgebiet läßt sich mit den spektroskopischen Aussagen korrelieren und gestattet die Aufstellung der Reaktionsschemata [Gleichungen (1) und (2)].

Die eingesetzten Ladungen sagen über die tatsächliche Ladung des Komplexes nichts aus. Es

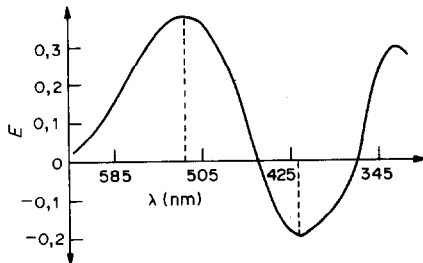


Abb. 2. Differenzspektrum des Cu/Aliz S-Systems in Wasser (Ausgangskonzentrationen $10^{-4}M$ Aliz S und $6 \times 10^{-4}M$ Cu^{2+}).

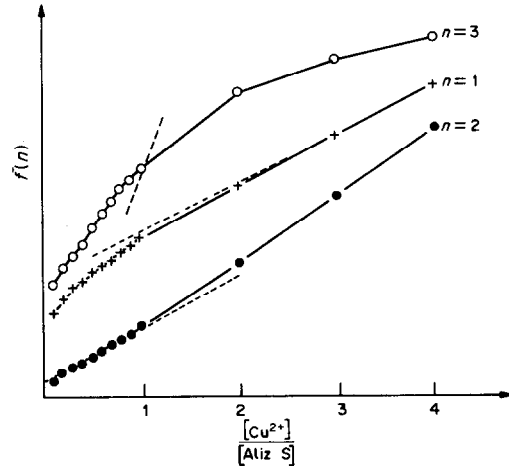


Abb. 3. Ermittlung der Komplexzusammensetzungen im System Kupfer/Aliz S; $f(n)$ = linke Seite der Gleichungen (4a-4c) der vorangehenden Veröffentlichung.⁷

wurde aber durch Fällung mit Kationentensiden nachgewiesen, daß die 1:2- und 1:1-Cu-Alizarin S-Komplexe negativ geladen sind. Sie können aber— wie auch Yasukouchi⁵ für Alizarinkomplexe beschrieb—noch weitere gebundene Anionen enthalten, die hier unberücksichtigt bleiben. Der nach Gleichung (3) ausfallende Komplex ist im ganzen ungeladen.

Zu Beginn der Komplexbildung entsteht bei Ligandüberschuß der 1:2-Komplex (vgl. Abb. 3). Dadurch müssen je Komplexmolekül zwei Protonen frei werden (H_2L = Alizarin S):



Bei mehr als 0.9-fach molarer Kupfermenge entsteht aus dem 1:2-Komplex zunehmend der 1:1-Komplex, der ab der zweifach molaren Kupfermenge rein vorliegt (vgl. Abb. 3).

In diesem Schritt müssen nach Abb. 4 zwei weitere Protonen frei werden. Wir formulieren deshalb den (1:1)-Komplex als Kupferhydroxo-Alizarin-Komplex:

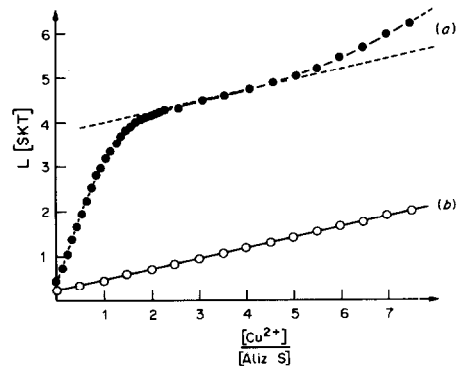
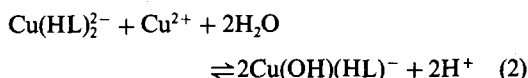
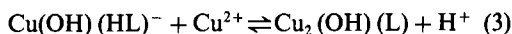


Abb. 4. Leitfähigkeitskurven in Wasser/Ethanol (1:1): (a) einer Aliz S-Lösung in Abhängigkeit von der zugesetzten Cu^{2+} -Menge; (b) einer Aliz S-freien Cu^{2+} -Lösung, bei der die zugesetzte Cu^{2+} -Menge in gleichen Schritten wie bei (a) erhöht wurde.



Der bei *ca.* achtfachem Kupferüberschuß ausfallende Komplex wurde isoliert und analysiert. Er hat die Zusammensetzung Cu:Alizarin S = 2:1. Man kann ihn präparativ am besten aus acetatgepufferter Lösung (pH 4-5) durch Fällung mit der *ca.* zehnfach molaren Kupfermenge herstellen. Unter Berücksichtigung des konduktometrischen Befundes (Abb. 4) müssen bei der Bildung dieses Komplexes noch weitere Protonen frei werden. Es kann sich also nicht um eine einfache Salzbildung mit der Sulfonatgruppe handeln. Wir nehmen deshalb an, daß ein weiteres Cu^{2+} chelatartig gebunden wird. Man kann also schreiben:



wobei bis Beginn der Fällung bei achtfachem Kupferüberschuß nur *ca.* 50% umgesetzt werden. Bei vollständigem Umsatz muß die doppelte Menge Protonen freigesetzt werden als nach Abb. 4 angezeigt wird.

Wenn es sich bei der mit Kupferüberschuß ausgefallenen Verbindung um ein definiertes zweikerniges Chelat handeln sollte, müßten die beiden Cu-Ionen verschieden—eines in *ortho*-, das andere in *peri*-Stellung—an Alizarin S gebunden sein. Es taucht die Frage auf, welche Stellung in den 1:2- und 1:1-Komplexen zuerst besetzt wird.

Polarographische Messungen

Für rein wäßrige Lösungen ließ sich diese Frage pulspolarographisch lösen (s.u.), allerdings nur bei sehr kleinen Kupferkonzentrationen im Bereich des $\text{Cu}(\text{HL})_2$ -Komplexes. Bei Erhöhung der Kupferkonzentration treten zusätzliche positive Peaks durch Adsorption von Kolloidteilchen auf, die eine Auswertung unmöglich machen. Wir gingen deshalb von dem durch Fällung isolierten 2:1-Komplex aus.

Versuche ergaben, daß sich die ausgefallenen Partikel in Dimethylformamid (DMF) recht gut lösen. Diese Lösungen wurden pulspolarographisch untersucht. Die Polarogramme der Komplexlösungen in reinem DMF waren jedoch schlecht interpretierbar, deshalb wurde vorzugsweise in DMF/Wasser-Mischungen gearbeitet.

Man erhält ein Spektrum von drei Peaks (Abb. 5a), die wie folgt zuzuordnen sind: der positivere Peak (I) entspricht dem Cu^{2+} -aqua-Ion, der mittlere Peak (II) dem an Alizarin S gebundenen Kupfer, der negativere Peak (III) ist der Reduktionspeak des komplexgebundenen Alizarin S.

Aus der annähernd gleichen Höhe der Peaks folgt, daß der Komplex in 1:1 DMF/Wasser-Mischungen vollständig in die 1:1-Verbindung und freies Kupfer dissoziiert.

Aus Mischungsreihen darf—wegen der schlechten Auswertbarkeit der Polarogramme in reinem DMF mit Vorbehalt—geschlossen werden, daß in DMF-

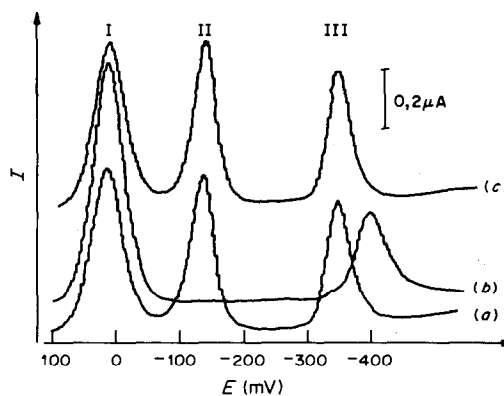


Abb. 5. Pulsarogramme: (a) Lösung des Cu_2 :Aliz S-Komplexes in DMF/Wasser (1:1); (b) wie (a), nach Zusatz von Al^{3+} ; (c) wie (a), nach Zusatz von Be^{2+} .

reichen Lösungen die Dissoziation unvollständig ist und Wasser die Dissoziation sehr stark begünstigt.

Eine weitere Möglichkeit, quantitativ zwischen freiem und gebundenem Kupfer zu unterscheiden, ergibt sich, indem man der Lösung Al^{3+} zusetzt (Abb. 5b). Dieses wird im Komplex gegen Cu^{2+} ausgetauscht, da der Al-Alizarin S-Komplex wesentlich stabiler ist als der Cu-Alizarin S-Komplex. Der Cu-Alizarin S-Peak (II) verschwindet, der Cu-Peak (I) steigt auf das Doppelte. Damit konnte gezeigt werden, daß in Lösung ein 1:1-Komplex vorliegt.

Gegen Be^{2+} läßt sich das gebundene Cu^{2+} nicht austauschen (Abb. 5c). Die Stabilität des 1:1 Cu-Alizarin S-Komplexes liegt also zwischen der des Be-Alizarin S- und des Al-Alizarin S-Komplexes.

Aus der Lage des Peak (III) kann man nun auf die Stellung des noch gebundenen Kupfers rückschließen. Wie bereits früher ausgeführt,¹ verschiebt sich der Reduktionspeak des Alizarin S kaum bei einer komplexen Bindung eines Metallions, wie Al^{3+} , an die beiden phenolischen OH-Gruppen in *ortho*-Stellung. Eine deutliche positive Verschiebung beobachtet man dagegen bei Bindung der Ionen, wie Be^{2+} , in *peri*-Stellung, wobei das polarographisch aktive, chinoid System stärker beansprucht wird. Der Reduktionspeak (III) des Cu-Alizarin S-Komplexes liegt nun beim gleichen Potential wie der entsprechende Be-Alizarin S-Peak und ist gegenüber dem Al-Alizarin S-Peak deutlich positiv verschoben. Das bedeutet, daß sich das in DMF-Lösung gebundene Kupfer in *peri*-Stellung des Alizarin S befindet.

Einen entsprechenden Befund erhält man für sehr verdünnte rein wäßrige Lösungen im Bereich des 1:2-Komplexes.

Zusammenfassend ergibt sich also: bei Zugabe von Cu^{2+} zu einer $10^{-4}M$ Alizarin S-Lösung bildet sich zunächst ein 1:2 Komplex mit *peri*-ständig gebundenem Kupfer, der ab etwa dem Verhältnis Cu:Alizarin S = 0.9:1 zunehmend in einen 1:1-Komplex übergeht. Die Bildung des 1:1 Komplexes ist etwa bei der Kupferkonzentration $2 \times 10^{-4}M$ abgeschlossen. Bei weiter steigender Kupferkonzentration bildet sich

etwa von $5 \times 10^{-4} M$ Cu^{2+} an unter Protonenfreisetzung ein weiterer Komplex, der zunächst in einer Wasser/Äthanol-Mischung in Lösung bleibt. Bei etwa achtfachem Kupferüberschuß ($8 \times 10^{-4} M$) beginnt ein 2:1-Komplex auszufallen. Dieser dissoziiert in 1:1 Wasser/DMF-Mischung vollständig in Cu^{2+} und einen 1:1-Komplex, in dem das Cu^{2+} ebenfalls *peri*-ständig gebunden ist. Es ist anzunehmen, daß das bei hoher Kupferkonzentration zusätzlich eintretende Kupfer *ortho*-ständig gebunden wird.

LITERATUR

1. H. D. Sommer und F. Umland, *Z. Anal. Chem.*, 1977, **285**, 359.
2. J. Dorta-Schaepi, H. Hürzeler und W. D. Treadwell, *Helv. Chim. Acta*, 1951, **34**, 797.
3. S. P. Sangao, *J. Prakt. Chem.*, 1965, **27**, 113.
4. A. K. Babko und T. N. Nazarchuk, *Raboty po khimii rastvorov i kompleksnykh soed.*, 1959, **2**, 199.
5. K. Yasukouchi und J. Yashinobu, *Nippon Kagaku Zasshi*, 1967, **88**, 1229.
6. Th. Prange, U. Lechner-Knoblauch und F. Umland, *Z. Anal. Chem.*, 1981, **306**, 201.
7. *Idem*, *Talanta*, 1984, **31**, 97.

Summary—From differential spectrophotometric, conductometric and pulse polarographic data, three copper-Alizarin S complexes (with compositions 1:2, 1:1 and 2:1) can be identified. The copper-rich 2:1-compound can be precipitated from aqueous solution. In dimethylformamide/water solutions the copper in the 1:1-complex is bound in the *peri*-position.

MODIFIED NORMAL PULSE POLAROGRAPHY OF ALKALI-METAL IONS IN ACID SOLUTION

MINORU HARA and NOBORU NOMURA

Faculty of Education, Toyama University, 3190 Gofuku, Toyama-shi, Toyama 930, Japan

(Received 15 March 1983. Revised 26 August 1983. Accepted 5 September 1983)

Summary—Well-defined polarograms of five alkali-metal ions in 0.01M hydrochloric acid were obtained by means of modified normal pulse polarography. The method uses the procedure of anodic stripping chronoamperometry during the life-time of a drop from a dropping mercury electrode, namely preparation of electrode, accumulating step and anodic stripping step of a metal. The instantaneous polarographic currents were sampled only once per mercury drop after the fall of each pulse. The wave heights for alkali-metal ions by the present method are free from the interference caused by 0.01M hydrochloric acid. The present method is applicable to monitoring of alkali-metal ions in fluid acid streams.

Normal pulse polarography (NPP) and differential pulse polarography (DPP) have been used for the determination of many metal ions, but have scarcely been applied to the determination of alkali-metal ions. D.C. polarography and A.C. polarography of alkali-metal ions have been performed, with tetra-alkylammonium hydroxides as supporting electrolyte,^{1,2} but it is difficult to determine alkali-metal ions in acid solutions by means of D.C. polarography, because the large hydrogen wave interferes in the measurement of the wave heights. Moreover, at low pH the dislodgement of the mercury drops from the dropping mercury electrode (DME) is disturbed by the adhesion of hydrogen bubbles on the electrode surface.

Ishibashi *et al.* investigated the A.C. polarographic behaviour of alkali and alkaline-earth metal ions and reported that the peak heights for a fixed concentration of sodium were constant at pH ≥ 4 but decreased with the pH at lower pH-values.

In a previous paper,⁴ we reported on modified normal pulse polarography (MNPP) in which the current is sampled after the fall of each pulse. A well-defined polarogram for barium in 0.01M hydrochloric acid and 0.1M tetramethylammonium bromide was obtained by means of MNPP, and no hydrogen-ion waves were observed. The timing sequence in modified normal pulse polarography is shown in Fig. 1. The drop-interval of the DME is controlled by a mechanical knocker and the measurement of current is synchronized with dislodgement of the mercury drop. Pulses of short duration, T_2 , and increasingly negative potential are added to the fixed initial potential, E_1 , to give a regularly increasing potential E_2 . The pulses are applied to the DME when the pulse delay time, T_1 , has elapsed after growth of a new drop. The polarographic current is sampled and held after a delay time of T_3 from the fall of the pulse, when the charging current has decayed to an insignificant

value. The amalgamated metals deposited during the pulse duration T_2 are oxidized and the dissolution current is measured. The mercury drop then falls off and a new cycle begins.

In this study, the behaviour of the five principal alkali-metal ions in MNPP was investigated with a view to their determination at lower pH. The effects of initial potential, pulse duration and pH of the sample solution, on the polarograms, are discussed.

EXPERIMENTAL

Apparatus

The modified normal pulse polarograph used was the one reported previously.⁴ The homemade polarograph consisted of a pulse generator, potentiostat, sample-hold circuit and timing circuit, which were constructed from LF356 JFET-input operational amplifiers (National Semiconductor), μ PC252 MOSFET-input operational amplifiers (Nihon Electric), 3SK38A MOSFET switches (Toshiba Electric) and NE555 timer ICs (Signetics). The current-time curves were measured with a Kawasaki Electronica TM-1410 transient memory in combination with a Hitachi 056 pen recorder. A saturated calomel electrode with Vycor glass-plug double junctions was used as a reference electrode in order to avoid contamination of the sample solutions with potassium. The mercury column of the DME was divided

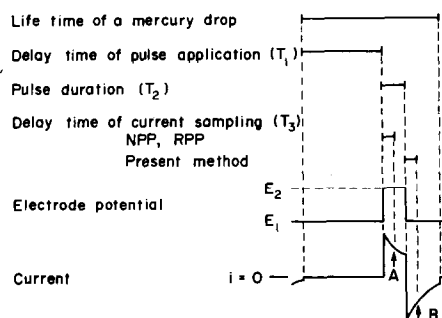


Fig. 1. The timing chart of the modified normal pulse polarograph. The arrow A indicates the sampled value in NPP, and the arrow B shows that in the present method.

into two parts by an air layer just above the capillary, so as to suppress the noise resulting from the A.C. source.⁴ The lead-wire from the DME to the polarograph was attached to the lower part of the column. The flow-rate of the DME was fixed at 0.630 mg/sec.

Reagents

A standard lithium solution was made from lithium chloride prepared from lithium carbonate and hydrochloric acid. Standard solutions of the other alkali-metal ions were prepared by dissolving their chlorides. Reagent-grade tetramethylammonium bromide was employed as supporting electrolyte without further purification. All chemicals used in this experiment were reagent grade. The sample solutions were deaerated by passage of nitrogen through them for 15 min, and nitrogen was flushed over the solutions during measurements.

RESULTS AND DISCUSSION

Polarograms

Three kinds of pulse polarograms for lithium in $1 \times 10^{-3}M$ hydrochloric acid are shown in Fig. 2. The normal pulse polarogram (1) has a large reduction wave for hydrogen ion at $-1.71V$ and a small reduction wave for lithium ion at $-2.35V$. The reduction wave of hydrogen ion in the reverse pulse polarogram (2) is smaller than that of the normal pulse polarogram. The small wave which appears at $-2.1V$ seems to be due to alkali-metal ions in the tetramethylammonium bromide. In reverse pulse polarography of this solution, E_1 should be set at $-2.50V$ or a more negative potential, where the reduction of lithium ion is diffusion-controlled,⁵ but was set at $-2.40V$ in order to avoid the irregular dislodgement of mercury drops. Curve 3 shows a modified normal pulse (MNP) polarogram, which has no hydrogen waves in it. Curve 3 is identical with the polarogram of lithium ion in a neutral solution. Therefore, the present method is suitable for the polarography of species which are reduced together with hydrogen ion in acid solutions.

Effect of initial potential

As shown in Fig. 2, there are no hydrogen waves in the MNP polarogram if E_1 is appropriately chosen.

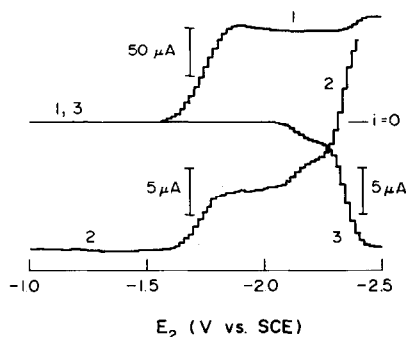


Fig. 2. Three kinds of pulse polarogram for lithium chloride in hydrochloric acid: $0.1M$ Me_4NBr , $1 \times 10^{-3}M$ HCl , $4.26 \times 10^{-4}M$ $LiCl$. $T_1 = 1.111$ sec, $T_2 = 117.6$ msec, $T_3 = 2.3$ msec. E_1 : (1) and (3) $-1.00V$, (2) $-2.40V$. (1) NPP, (2) RPP, (3) present method.

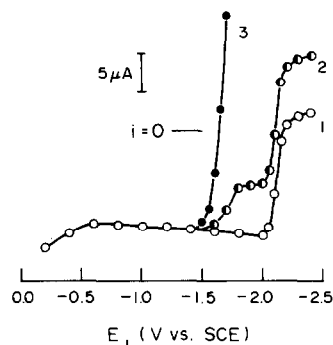


Fig. 3. Effect of E_1 on the oxidation current of sodium: $0.1M$ Me_4NBr (HCl), $4.02 \times 10^{-4}M$ $NaCl$. $T_1 = 1.111$ sec, $T_2 = 117.6$ msec, $T_3 = 2.3$ msec. $E_2 = -2.40V$. pH: (1) 5.6, (2) 2.9, (3) 1.8.

The effect of E_1 on MNP polarograms of sodium chloride at different pH values was therefore studied. The result is shown in Fig. 3. The pulse potential E_2 was fixed at $-2.40V$ and E_1 was varied. The current was measured 2.3 msec after the fall of the pulse. Curves analogous to reverse pulse polarograms were obtained. At pH 2.9, the currents for the E_1 potential range from -1.5 to $-2.0V$ are the sums of the oxidation current of sodium and the reduction current of the hydrogen ion. When E_1 is set at a more positive potential than $-1.4V$, the currents do not contain the hydrogen-ion component, irrespective of pH. An E_1 of $-1.00V$ was therefore chosen.

Effect of pulse duration

When the pulse potential is set in the range for the diffusion-current plateau of the alkali-metal ions, the alkali metals are accumulated in each mercury drop during pulse duration T_2 . Figure 4 shows the effect of pulse duration on the oxidation current of the amalgamated sodium (neutral solution). The currents increase with pulse duration T_2 , but the relation is not simple.^{5,6} The currents may be affected by growth of the mercury drop and the complicated concentration gradient of sodium in the mercury drop. Similar behaviour (at a glassy carbon electrode) was reported for the reverse differential normal pulse voltammetry of iron(II).⁷ In neutral solution, the anodic half-wave

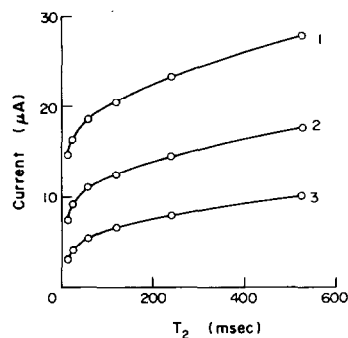


Fig. 4. Effects of the pulse duration and delay time of current sampling on the oxidation current of sodium: $0.1M$ Me_4NBr , $4.02 \times 10^{-4}M$ $NaCl$. $E_1 = -1.00V$, $E_2 = -2.30V$. $T_1 = 1.111$ sec, T_3 (msec): (1) 1.1, (2) 2.3, (3) 5.7.

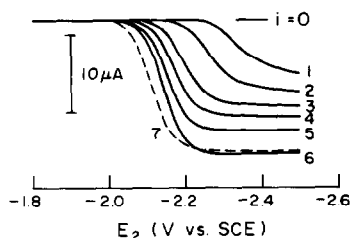


Fig. 5. Effect of pulse duration on the polarogram of sodium chloride in hydrochloric acid: $0.1M$ Me_4NBr , $0.01M$ HCl , $4.02 \times 10^{-4}M$ $NaCl$. $E_1 = -1.00$ V, $T_1 = 1.111$ sec, $T_3 = 2.3$ msec. T_2 (msec): (1) 12, (2) 23, (3) 57, (4) 118, (5) 240, (6) 524. Curve 7, $T_2 = 524$ msec (HCl absent).

potentials of sodium were constant, regardless of the pulse duration.

The effect of pulse duration on oxidation current in acid solution is shown in Fig. 5. The wave height decreases and the half-wave potential shifts to more negative potential with decrease in the pulse duration. When the pulse durations are 12, 23, 57, 118, 240 and 524 msec, the half-wave potentials are -2.34 , -2.26 , -2.20 , -2.17 , -2.16 and -2.15 V *vs.* SCE, respectively. The dashed line shows the polarogram of sodium chloride in a neutral solution, in which the pulse duration is 524 msec and the half-wave potential is -2.11 V *vs.* SCE. In neutral solution the half-wave potential for sodium is independent of the pulse duration. To investigate the cause of the shift of half-wave potentials (Fig. 5), the reduction current *vs.* time curves of hydrogen ion during the pulse period were measured and the results are shown in Fig. 6. The same results as those shown in Fig. 6 were obtained for a solution which did not contain sodium ions. The plateaus on the initial parts of these curves indicate that the reduction of hydrogen ion at the DME is not diffusion-controlled in the plateau range. When the current is very large, the iR -drop between the DME and the tip of the reference electrode cannot be neglected and the real potential drop across the DME-solution interface is smaller than the applied potential. This effect is more significant at the

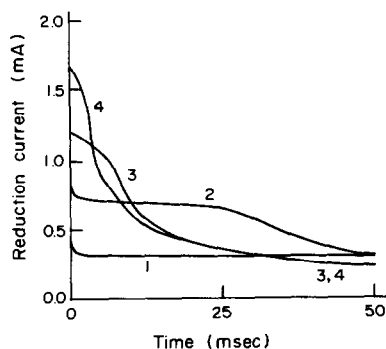


Fig. 6. Current-time curves for reduction of hydrogen ion during pulse periods: $0.1M$ Me_4NBr , $0.01M$ HCl , $4.02 \times 10^{-4}M$ $NaCl$. $T_1 = 1.111$ sec, $T_2 = 117.6$ msec. $E_1 = -1.00$ V, E_2 : (1) -1.80 V, (2) -2.00 V, (3) -2.20 V, (4) -2.40 V.

Table 1. Effect of pH on half-wave potentials and wave heights of alkali-metal ions: $0.1M$ $Me_4NBr(HCl)$, $E_1 = -1.0$ V, $T_1 = 1.111$ sec, $T_2 = 117.6$ msec, $T_3 = 2.3$ msec

Salt	pH	$E_{1/2}$, V <i>vs.</i> SCE	Wave-height, μA
4.26×10^{-4} LiCl	5.6	-2.33	10.4
	2.9	-2.33	10.1
	1.8	-2.39	10.7
4.02×10^{-4} NaCl	5.6	-2.10	10.6
	2.9	-2.11	10.6
	2.4	-2.13	10.5
	1.8	$-2.17(-2.14^*)$	11.0
4.04×10^{-4} KCl	5.6	-2.13	12.7
	2.9	-2.14	12.7
	1.8	-2.19	13.8
4.11×10^{-4} RbCl	5.6	-2.13	13.9
	2.9	-2.13	14.0
	1.8	-2.19	14.8
4.03×10^{-4} CsCl	5.6	-2.10	13.7
	2.9	-2.11	13.8
	1.8	-2.17	14.3

* $0.2M$ Me_4NBr .

beginning of the pulse. Therefore, the shorter the pulse duration, T_2 , the more negative the potential at which the reduction of the sodium ion occurs. Hence the shift of the half-wave potential with decrease of pulse duration may result from insufficient conductivity of the solution, and the large reduction current of the hydrogen ions. Positive feed-back compensation is necessary to eliminate the iR -drop between the DME and the reference electrode.⁸

Effect of pH

As can be seen in Fig. 5, the half-wave potential of sodium (for a fixed pulse duration) becomes more negative as the acidity is increased, but the wave shape does not change remarkably. Table 1 shows the wave heights and the half-wave potentials of alkali-metal ions at various pH values. The current values shown in Table 1 are corrected for the blank value. The wave heights of sodium at these pH values are almost constant, but the half-wave potential becomes more negative with decrease of pH. No sodium waves are observed at pH 0.8. The disappearance of the wave may result from insufficient output from the potentiostat and/or the uncompensated resistance in the cell. The half-wave potential of sodium changes by 0.07 V in $0.1M$ supporting electrolyte between pH 5.6 and pH 1.8, and by 0.04 V in $0.2M$ tetramethylammonium bromide for the same pH range. The current *vs.* time curves for $0.01M$ hydrochloric acid in $0.2M$ tetramethylammonium bromide and reduction during the pulse period had higher and narrower plateaus than the corresponding curves in Fig. 6. This indicates that the shifts of the half-wave potentials are due to insufficient conductivity of the sample solutions. The half-wave potentials and the wave heights for the other alkali metals are also listed in Table 1. The half-wave potentials obtained by the present method for the alkali metals in neutral solu-

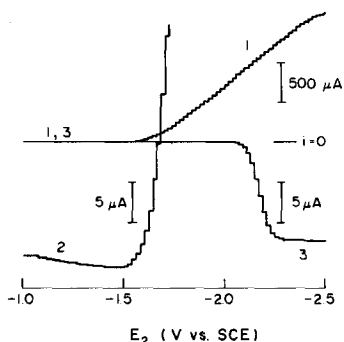


Fig. 7. Three kinds of pulse polarogram for sodium chloride in hydrochloric acid: $0.1M$ Me_4NBr , $0.01M$ HCl , $4.02 \times 10^{-4}M$ NaCl . $T_1 = 1.111$ sec, $T_2 = 117.6$ msec, $T_3 = 2.3$ msec. E_1 : (1) -1.00 V, (2) -2.40 V, (3) -1.00 V. (1) NPP, (2) RPP, (3) present method.

tions were in fair agreement with those for D.C. polarography.

Figure 7 shows three kinds of pulse polarograms of a $4.02 \times 10^{-4}M$ sodium chloride/ $0.01M$ hydrochloric acid/ $0.1M$ tetramethylammonium bromide solution. Only a hydrogen wave was observed in the normal pulse polarogram (1). In the reverse pulse polarogram (2), the current in the potential region more positive than -1.5 V was proportional to the concentration of sodium chloride, but the limiting current was not reproducible. The fluctuation of the limiting current resulted because adhesion of hydrogen bubbles on the DME caused irregular dislodgement of the mercury drops. A well-defined polarogram (3) was obtained by the present method, and the limiting current was reproducible. In the present method, the short period of reduction of hydrogen ions served to dislodge the mercury drops regularly. Therefore, the polarograms for the five alkali-metal ions in $0.01M$ hydrochloric acid medium were well defined.

Calibration curve

The height of the anodic wave resulting from the dissolution of sodium was proportional to the concentration of sodium chloride, even in $0.01M$ hydrochloric acid medium. The calibration curve for sodium ion, obtained under the same conditions as those for curve 3 in Fig. 7 has good linearity at the $10^{-4}M$ level but does not pass through the origin, because of impurities in the tetramethylammonium bromide. The concentration of these impurities in $0.1M$ tetramethylammonium bromide was $6.3 \times 10^{-5}M$ calculated on the assumption that sodium was the only alkali-metal impurity. The relative standard deviation of the wave height for $4.02 \times 10^{-4}M$ sodium chloride in $0.01M$ hydrochloric acid was 1.0% (six replicates).

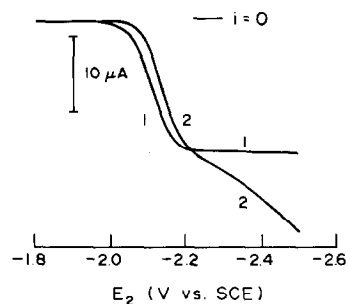


Fig. 8. Modified normal pulse polarograms of sodium nitrate: $0.1M$ Me_4NBr , $4.07 \times 10^{-4}M$ NaNO_3 . $E_1 = -1.00$ V. $T_1 = 1.111$ sec, $T_2 = 524$ msec, $T_3 = 2.3$ msec. HCl : (1) absent, (2) $0.01M$.

Effect of anions

Figure 8 shows the polarograms of $4.07 \times 10^{-4}M$ sodium nitrate in $0.1M$ tetramethylammonium bromide. The polarogram of sodium nitrate in neutral solution was the same as that of sodium chloride. In acid solution, however, the polarographic wave of sodium nitrate not only shifted toward more negative potential but also had a sloping limiting current plateau. Though the reason for this is not clear, the presence of nitrate will cause a positive error in the determination of alkali metal ions in acid solutions.

The polarogram of sodium chloride in $5 \times 10^{-3}M$ sulphuric acid was identical with that in $0.01M$ hydrochloric acid. With appropriate selection of E_1 in the present method, in a similar manner as in reverse pulse amperometry,⁹ there is no faradaic contribution to the analytical signal from either the dissolution of mercury or the reduction of dissolved oxygen in $0.05M$ tetramethylammonium sulphate. Therefore the present method should be useful for the monitoring of alkali-metal ions in acid streams containing dissolved oxygen.

REFERENCES

1. A. Babrowski and Z. Kowalski, *Chem. Anal. Warsaw*, 1976, **21**, 925; *Anal. Abstr.*, 1977, **32**, 3B32.
2. *Idem*, *ibid.*, 1976, **21**, 1137; *Anal. Abstr.*, 1977, **32**, 5B21.
3. N. Ishibashi, H. Kohara and T. Haraguchi, *Bunseki Kagaku*, 1965, **14**, 62.
4. M. Hara and N. Nomura, *ibid.*, 1983, **32**, E185.
5. J. Osteryoung and E. Kirowa-Eisner, *Anal. Chem.*, 1980, **52**, 62.
6. K. B. Oldham and E. P. Parry, *ibid.*, 1970, **42**, 229.
7. T. R. Brumleve, R. A. Osteryoung and J. Osteryoung, *ibid.*, 1982, **54**, 782.
8. D. D. Macdonald, *Transient Techniques in Electrochemistry*, p. 33. Plenum Press, New York, 1977.
9. P. Maitoza and D. C. Johnson, *Anal. Chim. Acta*, 1980, **118**, 233.

SPECTROPHOTOMETRIC DETERMINATION OF Mn(II) WITH 1-(2-QUINOLYLAZO)-2,4,5- TRIHYDROXYBENZENE AND MICRODETERMINATION OF Mn IN FOODSTUFFS

ISHWAR SINGH and MRS. POONAM

Department of Chemistry, Maharshi Dayanand University, Rohtak 124001, India

(Received 23 February 1983. Revised 23 August 1983. Accepted 5 September 1983)

Summary—A method is described for the spectrophotometric determination of manganese in foodstuffs by means of its complex with 1-(2-quinolylazo)-2,4,5-trihydroxybenzene, formed in alkaline medium. The molar absorptivity of the complex is 4.6×10^4 l. mole⁻¹. cm⁻¹.

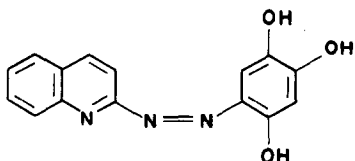
Most widely used methods for the determination of manganese are based on the oxidation of manganese(II) to manganese(VII),¹⁻³ but because of the low sensitivity these methods are not considered useful for trace analysis. Among other reagents for manganese, the heterocyclic azo-dyes PAN⁴⁻⁶ and PAR⁶⁻¹⁰ give high sensitivity but nickel interferes when PAN is used, and iron, cobalt and nickel interfere in determinations with PAR. Moreover, in both cases the manganese is determined by difference, by destruction of the manganese complex. In the work presented here, we have tried to overcome these difficulties by using a newly synthesized heterocyclic azo-dye, 1-(2-quinolylazo)-2,4,5-trihydroxybenzene (QATB).

EXPERIMENTAL

Reagents

Synthesis of QATB. Stoichiometric amounts of 2-hydrazinoquinoline¹¹ (1.59 g, 0.01 mole, dissolved in the minimum amount of dilute hydrochloric acid) and 2,5-dihydroxy-1,4-benzoquinone¹² (1.4 g, 0.01 mole, in ethanol) were refluxed together for 30 min. The solution was cooled and made ammoniacal. Excess of ammonia was boiled off and the solution was allowed to stand overnight. The dark red precipitate obtained was recrystallized from ethanol and dried over phosphorus pentoxide. The purity of the compound was checked by thin-layer chromatography and elemental analysis (found: C 64.2%, H 3.8%, N 15.1%; C₁₅H₁₁N₃O₃ requires C 64.05%, H 3.91%, N 14.95%). A 0.002M reagent solution was prepared by dissolving 0.562 g in 1 litre of ethanol. Reagent solutions were discarded when a week old.

Manganese(II) solution. Stock 0.01M manganese(II) solution prepared by dissolving an appropriate amount of



1-(2-Quinolylazo)-2,4,5-trihydroxybenzene (QATB)

analytical grade manganese(II) chloride tetrahydrate in water, standardized complexometrically with EDTA,¹³ and further diluted as required for working standards.

Ascorbic acid solution. A fresh 1% solution prepared and kept in an amber-coloured bottle.

Potassium cyanide solution, 1%.

Determination of manganese(II)

To a suitable portion of sample (between 1 and 3 ml) containing 1-14 µg of manganese(II) add 0.5 ml of 1% ascorbic acid solution and 1 ml of 0.002M QATB. Add 2.0 ml of 1M sodium hydroxide solution and dilute to volume in a 10-ml standard flask with ethanol, to give a final 50% v/v ethanol concentration. Measure the absorbance at 560 nm against a reagent blank prepared under identical conditions.

RESULTS AND DISCUSSION

Effect of reductant

Addition of an ethanolic solution of QATB to a very dilute solution of manganese(II), in a medium containing not less than 40% v/v ethanol (otherwise a precipitate was obtained), resulted in a dark red solution in alkaline medium, but erratic results were obtained and the colour intensity of the complex decreased on standing. This effect could have been caused by partial aerial oxidation of the manganese(II) to manganese(III) in alkaline medium.^{14,15} Oelschläger¹⁶ and Stary¹⁷ proposed that this effect could be prevented by addition of a reducing agent, viz. hydroxylamine hydrochloride. We tried various reducing agents (hydroxylamine hydrochloride, ascorbic acid, hydrazine hydrate etc.) and observed that addition of 0.2-1.0 ml of 1% ascorbic acid solution yielded consistent and reproducible results.

Spectral characteristics, and effect of pH, etc.

A series of 50% v/v ethanol solutions containing manganese(II) ($2 \times 10^{-5}M$), ascorbic acid (0.1%) and QATB ($2 \times 10^{-4}M$) at different pH values was pre-

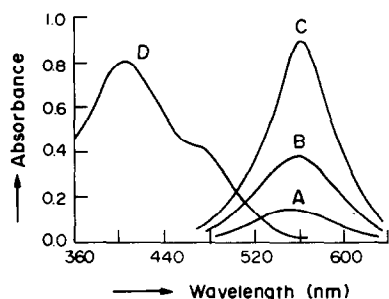


Fig. 1

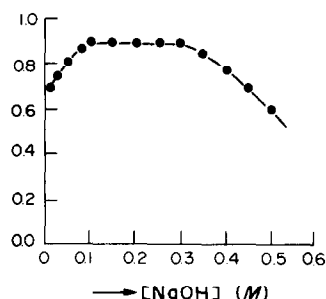


Fig. 2

pared. The spectra were recorded, with a reagent blank as reference. At pH above 9.0 the complex had maximum absorbance at 560 nm (Fig. 1). The complex had maximum absorbance at high alkalinity, and investigation of the effect of sodium hydroxide concentration showed that constant and maximum absorbance was exhibited in 0.1–0.3M sodium hydroxide medium (Fig. 2).

Absorbance data for a series of solutions [$2 \times 10^{-5}M$ manganese(II), 0.1% ascorbic acid, 0.2M sodium hydroxide, 50% v/v ethanol, and varying amounts of reagent] showed that at least an 8:1 molar ratio of QATB to Mn(II) is required to ensure full complexation.

Beer's law is obeyed up to 1.7 $\mu\text{g/ml}$ manganese in the solution measured, and the optimum concentration range for accurate determination (as determined by a Ringbom plot) is 0.1–1.4 $\mu\text{g/ml}$. The composition of the complex is shown by Job's method to be 1:3 (metal:ligand).

The molar absorptivity is $4.6 \times 10^4 \text{ l. mole}^{-1} \text{ cm}^{-1}$. Table 1 gives a comparison of the sensitivities of various reagents for the determination of manganese(II). The mean absorbance found for $10^{-5}M$ manganese(II) was 0.460 (1-cm cell, 8 replicates) with a standard deviation of 0.005.

Effect of diverse ions

In the determination of manganese(II) at the

1.1- $\mu\text{g/ml}$ level in the final solution, sulphate, sulphite, citrate, tartrate, borate, phosphate, alkaline-earth metal ions, lanthanides, aluminium(III), indium(III), antimony(III), bismuth(III), chromium(III), platinum metal species [except palladium(II)], and thorium(IV) did not interfere at all. Certain metal ions were precipitated at the pH used, and the precipitates were removed by centrifugation; these ions did not cause interference, and examination of the precipitates for manganese revealed no loss by co-precipitation. For other ions, the tolerance limits defined as the concentration ($\mu\text{g/ml}$ in the final solution) causing a deviation of less than $\pm 2\%$ in the absorbance, were: bromide, thiocyanate, cyanide, EDTA, 400; sulphide 200; fluoride, iodide 100; oxalate 60; thiosulphate 50; molybdenum(VI), tungsten(VI) 40; uranium(VI), vanadium(V), cadmium(II), mercury(II) 20. Zinc(II) 2, iron(III) 20, and iron(II), cobalt(II), nickel(II), copper(II), palladium(II) 10, were masked by 1% potassium cyanide solution, and zinc(II) 10, was masked by 200 ppm EDTA solution. Potassium cyanide also inhibits the colour formed by lead(II) with QATB.

APPLICATIONS

In recent years considerable attention has been paid to the role of trace elements in human health and

Table 1. Comparison of sensitivities of various spectrophotometric reagents for manganese(II)

Reagent or reaction	Molar absorptivity (λ, nm) $\text{l. mole}^{-1} \text{ cm}^{-1}$	Reference
Oxidation to permanganate	2×10^3 (522)	19
Thenoyltrifluoroacetone	3.0×10^3 (440)	20
	2.5×10^3 (450)	
8-Aminoquinoline	1.8×10^3 (550)	21
8-Hydroxyquinoline	1.1×10^3 (580)	22
Formaldoxime	1.12×10^4 (455)	19
1-(2-Pyridylazo)-2-naphthol/ CHCl_3	4.8×10^4 (562)	5
1-(2-Pyridylazo)-2-naphthol/ C_6H_6	4.7×10^4 (568)	
4-(2-Pyridylazo)resorcinol/ CHCl_3	4×10^4 (550)	9
2-(2-Pyridylazo)- <i>p</i> -cresol/ CHCl_3	1.8×10^4 (560)	23
<i>N,N</i> -Dimethyl- <i>p</i> -(2-pyridylazo)aniline	3.27×10^4 (540)	24
1-(2-Quinolylazo)-2,4,5-trihydroxybenzene	4.6×10^4 (560)	This method

Table 2. Results for determination of manganese(II) in foodstuffs

Food sample	No. of analyses	Sample ashed, g	Aliquot taken, ml	Mn(II) found, μg	Mn(II) added, μg	Total Mn(II) recovered, μg	Range of recovery, %	Average Mn(II) content, $\mu\text{g/g}$
Tea leaves	6	2.0	0.5	3.24, 2.94, 3.08, 3.40, 3.38, 3.45	2.2	5.36, 5.20, 5.19, 5.53, 5.62, 5.67	97.0–102.0	81
Coffee powder	6	2.0	0.5	1.54, 1.76, 1.54, 2.04, 1.92, 1.56	2.2	3.80, 4.00, 3.78, 4.17, 4.08, 3.82	96.6–103.9	43
Wheat flour	6	5.0	1.0	1.34, 1.46, 1.38, 1.42, 1.46, 1.44	2.2	3.50, 3.62, 3.60, 3.68, 3.72, 3.70	97.0–104.2	7.1
Gram	4	5.0	1.0	2.70, 2.58, 2.62, 2.53	2.2	4.85, 4.75, 4.80, 4.79	98.1–102.4	13.0
Rice	4	5.0	1.0	1.27, 1.34, 1.30, 1.22	5.5	6.83, 6.85, 6.75, 6.70	96.2–104.7	6.4
Potato chips	4	5.0	1.0	1.28, 1.16, 1.14, 1.14	5.5	6.74, 6.63, 6.70, 6.64	96.9–105.2	5.9
Cabbage	4	5.0	1.0	2.63, 2.52, 2.43, 2.57	2.2	4.82, 4.76, 4.68, 4.80	99.6–102.0	12.8
Apple	4	10.0	1.0	1.15, 1.35, 1.20, 1.10	5.5	6.68, 6.80, 6.65, 6.53	95.8–103.0	2.9
Banana	4	5.0	1.0	1.20, 1.35, 1.12, 1.20	5.5	6.72, 6.85, 6.66, 6.69	99.2–103.6	6.1
Tomato	4	5.0	1.0	2.10, 1.85, 1.82, 1.95	2.2	4.26, 4.12, 4.08, 4.12	98.1–103.8	9.7

disease. Public health problems have been correlated with trace element imbalances¹⁸ in the human system and thus analysis of foodstuffs is of great importance. We have analysed some foodstuffs for trace amounts of manganese by use of QATB, and the results are given in Table 2.

Analysis of tea leaves and coffee powder

Dry-ash 2 g of material at 450° and digest the ash with 2 ml of a 3:1 v/v mixture of nitric and perchloric acids. Heat gently almost to dryness, repeat again with 2 ml of acid mixture and dilute to volume in a 25-ml standard flask with water. Set aside overnight and then filter, add to a suitable aliquot (up to 1.0 ml of solution) 0.5 ml of 1% ascorbic acid solution and 0.5 ml of 1% potassium cyanide solution. Add 1.0 ml of 0.002M QATB and 2–3 ml of 1M sodium hydroxide, and finally dilute to 10 ml (standard flask) with water and ethanol to give a final 50% v/v ethanol concentration. Measure the absorbance at 560 nm against a reagent blank.

Analysis of foodstuffs

Add to the sample a 5% ethanolic solution of magnesium acetate tetrahydrate, evaporate to dryness and then heat at ~900° until the ash is white. Cool and add ~5 ml of a 1:1 mixture of nitric and perchloric acids. Heat gently almost to dryness, add 3–4 ml of water, filter, and wash the residue 3 or 4 times with hot water. Combine the filtrate and washings and make up to volume in a 25-ml standard flask. Determine the manganese content as already described.

Results obtained for the determination of man-

ganese in various foodstuffs are summarized in Table 2.

The recovery was tested by adding a known amount of manganese to the sample solutions and applying the recommended procedure, and found to be between 94 and 105% in all cases.

Acknowledgements—One of the authors (Mrs. P) is thankful to the Council of Scientific and Industrial Research, New Delhi, India for financial assistance.

REFERENCES

1. Z. Marczenko, *Spectrophotometric Determination of Elements*, Horwood, Chichester, 1976.
2. E. B. Sandell, *Colorimetric Determination of Traces of Metals*, 3rd Ed., Interscience, New York, 1959.
3. F. D. Snell, *Photometric and Fluorometric Methods of Analysis, Metals*, Part I, Wiley, New York, 1978.
4. S. Shibata, Y. Niimi and T. Matsumae, *Nagoya Kogyo Gijutsu Shikensho Hokoku*, 1962, **11**, 275.
5. E. M. Donaldson and W. R. Inman, *Talanta*, 1966, **13**, 489.
6. S. Shibata in H. A. Flashchka and A. J. Barnard, Jr. (eds.), *Chelates in Analytical Chemistry*, Vol. 4, Dekker, New York, 1972.
7. S. Ahrland and R. G. Herman, *Anal. Chem.*, 1975, **47**, 2422.
8. S. G. Nagarkar and M. C. Eshwar, *Chem. Era*, 1975, **11**, 1.
9. W. Berger and H. Elvers, *Z. Anal. Chem.*, 1959, **171**, 185.
10. S. Shibata, *Anal. Chim. Acta*, 1960, **23**, 367; 1961, **25**, 348.
11. W. H. Perkin and R. Robinson, *J. Chem. Soc.*, 1913, **103**, 1078.
12. R. G. Jones and H. A. Shonle, *J. Am. Chem. Soc.*, 1945, **67**, 1034.

13. A. I. Vogel, *A Text Book of Quantitative Inorganic Analysis*, 3rd Ed., p. 434. Longmans, London, 1973.
14. W. G. Scribner, *Anal. Chem.*, 1960, **32**, 966.
15. N. Tanaka, Y. Kikuchi and Y. Sato, *Talanta*, 1964, **11**, 221.
16. W. Oelschläger, *Z. Anal. Chem.*, 1955, **146**, 339.
17. J. Starý, *Anal. Chim. Acta*, 1963, **28**, 132.
18. E. J. Underwood, *Trace Elements in Human and Animal Nutrition*, 3rd Ed., p. 178. Academic Press, New York, 1971.
19. E. B. Sandell and H. Onishi, *Photometric Determination of Traces of Metals, General Aspects*, 4th Ed., Part I, pp. 246, 385. Wiley, New York, 1978.
20. H. Onishi and Y. Toita, *Talanta*, 1964, **11**, 1357.
21. V. K. Gustin and T. R. Sweet, *Anal. Chem.*, 1964, **36**, 1674.
22. K. Motojima, H. Hashitani and T. Imahashi, *ibid.*, 1962, **34**, 571.
23. G. Nakagawa and H. Wada, *Nippon Kagaku Zasshi*, 1962, **83**, 1098.
24. I. M. Klotz and W. C. Loh Ming, *J. Am. Chem. Soc.*, 1953, **75**, 4159.
25. L. C. Thomas and G. J. Chamberlin, *Colorimetric Chemical Analytical Methods*, 9th Ed., Tintometer, Salisbury, 1980.

SPECTROPHOTOMETRIC ANALYSIS OF SIMULTANEOUS PROTOLYSIS EQUILIBRIA*

JÜRGEN POLSTER

Lehrstuhl für Allgemeine Chemie und Biochemie der Technischen Universität München, D-8050
 Freising-Weihenstephan, BRD

(Received 23 February 1983. Revised 11 August 1983. Accepted 29 August 1983)

Summary—Simultaneous protolysis equilibria $(\text{BH} + \text{H}_2\text{O} \xrightleftharpoons{K_1} \text{B}^- + \text{H}_3\text{O}^+; \text{CH} + \text{H}_2\text{O} \xrightleftharpoons{K_2} \text{C}^- + \text{H}_3\text{O}^+)$ can be spectrophotometrically analysed easily by means of absorbance diagrams. The dissociation constants K_1 and K_2 can be determined directly from distinct points on the absorbance diagram by correlation with a photometric titration plot of absorbance *vs.* pH. Furthermore, from the absorbance diagram the ratio K_2/K_1 can be evaluated from the ratio of corresponding sides, and pH-measurement is not necessary. The titration systems of a mixture of 2-nitroso-1-naphthol-4-sulphonic acid with *p*-nitrophenol, and a mixture of *p*-nitrophenol with *o*-nitrophenol have been analysed by these methods, and are described as examples.

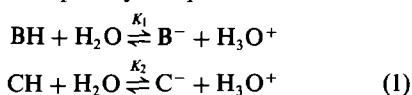
Two basic questions of this and earlier works¹⁻⁵ are (1) what information can be obtained in titration systems from spectrophotometric data alone, and (2) how can this information be correlated with the pH data, to determine equilibrium constants?

As shown below, the quotient of the dissociation constants for two protolysis systems in the same solution can be evaluated from spectrophotometric data alone, by means of absorbance diagrams. Thus an unknown dissociation constant can be obtained from that of a standard substance without any pH measurements. This is useful for systems in which pH measurement presents problems, for example in organic or strongly acidic solutions.⁶

Furthermore, the dissociation constants themselves can be easily evaluated by means of tangents and lines in the absorbance diagram, in combination with a plot of absorbance *vs.* pH. Two systems, consisting of 2-nitroso-1-naphthol-4-sulphonic acid/*p*-nitrophenol and *p*-nitrophenol/*o*-nitrophenol, are used here to illustrate the use of the methods.

The equations required for the analysis can be derived simply by use of a concentration diagram, which can be transformed into the absorbance diagram by linear transformation.

For the pair of protolysis equilibria



taking place in the same solution, the mixed dissociation constants are defined as^{1,2}

$$K_1 = \frac{h[\text{b}]}{[\text{bh}]} \quad \text{and} \quad K_2 = \frac{h[\text{c}]}{[\text{ch}]} \quad (2)$$

where h is the hydrogen-ion activity ($h = a_{\text{H}_3\text{O}^+} = 10^{-\text{pH}}$), and $[\text{b}]$, $[\text{bh}]$, $[\text{c}]$ and $[\text{ch}]$ are the molar concentrations of B, BH, C and CH respectively. From this and the additional stoichiometric conditions

$$b_0 = [\text{b}] + [\text{bh}]; \quad c_0 = [\text{c}] + [\text{ch}] \quad (3)$$

(where b_0 and c_0 are the total molar concentrations of the protolytes) and the definition

$$\kappa = \frac{K_2}{K_1} \quad (4)$$

we obtain the equations

$$[\text{b}] = \frac{b_0 K_1}{h + K_1}; \quad [\text{c}] = \frac{c_0 K_2}{h + K_2} \quad (5)$$

and

$$[\text{b}] = \frac{b_0[\text{c}]}{c_0 \kappa + [\text{c}](1 - \kappa)} \quad (6)$$

A plot of $[\text{b}]$ *vs.* $[\text{c}]$ (as functions of pH) is a conic section (hyperbola) which is dependent on κ (provided $\kappa \neq 1$). Figure 1 presents the curves for $\kappa = 0.316$ and $\kappa = 3.16$. The curves pass through the points $\text{B}_1(0,0)$ and $\text{B}_3(b_0, c_0)$. The side B_1B_3 is an axis of symmetry for the curves κ and $1/\kappa$.

The distinction $\kappa > 1$ and $\kappa < 1$ is arbitrary. It depends on which protolysis system $[\text{BH} \rightleftharpoons \text{B}^- (\text{H}^+)]$ or $[\text{CH} \rightleftharpoons \text{C}^- (\text{H}^+)]$ is the stronger [see equation (1)]. For reasons of graphical representation both cases are shown in Fig. 1.

The tangent vectors to the curves at these two points are B_1B_2 and B_3B_2 or alternatively $\text{B}_1\text{B}'_2$ and $\text{B}_3\text{B}'_2$. At the origin $\text{B}_1(0,0)$, all of B is in the form BH and all of C in the form CH. The two points (0,0) and

*This paper is dedicated to Professor H. Mauser for his 65th birthday.

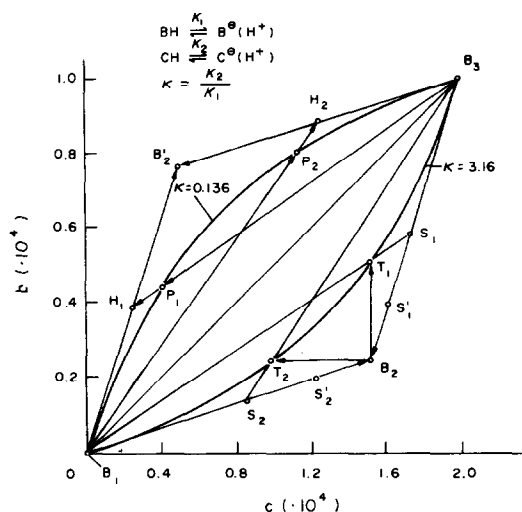


Fig. 1. Concentration diagram of b vs. c for the system $\text{BH} \xrightleftharpoons{K_1} \text{B}^- (\text{H}^-)$; $\text{CH} \xrightleftharpoons{K_2} \text{C}^- (\text{H}^+)$. The triangles $(0,0)$, $(b_0,0)$, (b_0,c_0) and $(0,0)$, $(0,c_0)$, (b_0,c_0) and their interior represent physically admissible points of the system. Outside these areas at least one of the concentrations is negative. P_1 , P_2 , T_1 and T_2 are distinct points of the conic section. The distinction $\kappa > 1$ and $\kappa < 1$ is arbitrary; for reasons of graphical representation the triangles $B_1B_2B_3$ and $B_1B'_2B_3$ are both constructed.

(b_0, c_0) simply represent limiting conditions of the pH:

very low pH: $[b] = [c] = 0$; $[bh] = b_0$ and $[ch] = c_0$
 very high pH: $[b] = b_0$, $[c] = c_0$; $[bh] = [ch] = 0$

The points shown in Fig. 1 have the following properties (P_1 , P_2 , T_1 and T_2 are points of the conic section):

- H_1 and H_2 are the mid-points of sides $B_1B'_2$ and B'_2B_3 (or alternatively B_1B_2 and B_2B_3);
- the vectors B_3P_1 and B_1P_2 have the same direction as B_3H_1 and B_1H_2 ;
- the vectors B_2T_1 and B_2T_2 lie parallel to the axes;
- S_1 and S_2 are the points of intersection of sides B_2B_3 and B_1T_1 or alternatively B_1B_2 and B_3T_2 [analogously S'_1 for B_2B_3 and B_1T_2 (not shown) and S'_2 for B_1B_2 and B_3T_1 (not shown)].

The values pK_1 , pK_2 and κ can be calculated easily from particular points of the curve. The pH values corresponding to T_1 and T_2 give directly the two pK values:

$$\text{pH}(T_1) = pK_1; \quad \text{pH}(T_2) = pK_2 \quad (7)$$

For the pH values corresponding to P_1 and P_2 the following equations apply:

$$\text{pH}(P_1) = pK_1; \quad \text{pH}(P_2) = pK_{II} \quad (8)$$

where

$$K_I = K_1 + K_2; \quad K_{II} = \frac{K_1 K_2}{K_1 + K_2} \quad (9)$$

Thus pK_1 and pK_2 can be determined directly from the pH values corresponding to T_1 and T_2 , or P_1 and P_2 , but only in the case of equations (7) is it possible to assign the dissociation constants to the individual equilibria. Thus in Fig. 1 T_2 lies nearer to B_1 than T_1 does. Therefore the pK value of $\text{CH} \rightleftharpoons \text{C}^- (\text{H}^+)$ is smaller than that of $\text{BH} \rightleftharpoons \text{B}^- (\text{H}^-)$.

The ratio of corresponding sides can be referred to κ . For example (see Fig. 1):

$$\frac{B_2S'_2}{B_1S'_2} = \frac{B_2S'_1}{B_3S'_1} = \frac{1}{1 + \kappa} \quad (10)$$

and

$$\frac{B_2S_2}{B_1S_2} = \frac{B_2S_1}{B_3S_1} = \frac{\kappa}{1 + \kappa} \quad (11)$$

The measurements required are the absorbance values (A_i) obtained at various pH values. If $\epsilon_{\lambda_i, \text{BH}}$ designates the molar absorptivity of BH at wavelength λ_i , etc., the absorbance is given by the Lambert-Beer law:

$$A_{\lambda_i} = \epsilon_{\lambda_i, \text{BH}}[\text{bh}] + \epsilon_{\lambda_i, \text{B}}[\text{b}] + \epsilon_{\lambda_i, \text{CH}}[\text{ch}] + \epsilon_{\lambda_i, \text{C}}[\text{c}] \quad (12)$$

(for unit path-length).

This equation is assumed to be valid for all wavelengths. Thus the two independent variables, $[\text{b}]$ and $[\text{c}]$, can be transformed into the absorbances (A_{λ_1} , A_{λ_2}) by a linear transformation including translation. A plot of A_{λ_1} vs. A_{λ_2} is called the absorbance (A) diagram¹. The equations (7)–(11) are also represented in the A diagram. The triangle $B_1B_2B_3$ (or alternatively $B_1B'_2B_3$) in Fig. 1 leads to the linearly distorted triangle $B_1B_2B_3$ in the A diagram.

EXPERIMENTAL

Reagents

p-Nitrophenol (Merck and Fluka), *o*-nitrophenol (Merck, recrystallized from water¹), 2-nitroso-1-naphthol-4-sulphonic acid (Fluka), potassium chloride (Merck), sodium hydroxide and hydrochloric acid standard solutions ("Titrisol", "Fixanal" ampoules), standard buffer solutions (Riedel-de Haen and Merck).

Procedure

The system oNP/pNP was investigated as described earlier,¹ with the same apparatus. The system 2-nitroso-1-naphthol-4-sulphonic acid/pNP was studied spectrophotometrically with a Perkin-Elmer model 555 spectrophotometer. The pH measurements were made (under nitrogen) with a Beckman model 3560 digital pH-meter. The titrations were performed with a Radiometer ABU 12 auto burette (maximal titration volume 2.5 ml).

RESULTS AND DISCUSSION

Determination of pK_1 and pK_2

In Fig. 2 the spectra of 2-nitroso-1-naphthol-4-sulphonic acid and *p*-nitrophenol at various acidities are shown. For construction of the A diagram the absorbances measured at two wavelengths (for the same set of pH values) are plotted against each other. The most suitable wavelengths are those where large absorbance differences occur. The

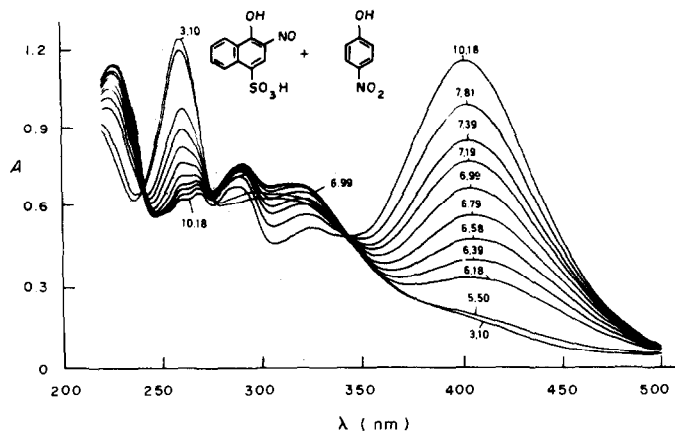


Fig. 2. Titration spectra of 2-nitroso-1-naphthol-4-sulphonic acid and *p*-nitrophenol (with 0.05M KCl as background electrolyte, at 25.0°). The numbers given designate the pH values.

measured points lie on a curve (see Fig. 3). A pH value can be assigned to each point, from a plot of A_λ vs. pH.

In Fig. 3 the points B_1 and B_3 are obtained at low (<3) and high (>10) pH values. The tangents constructed at these points intersect at B_2 . For the determination of pK values the bisecting lines B_3H_1 and B_1H_2 are constructed. They intersect the curve at P_1 and P_2 , for which the pH values are pK_1 and pK_2 . Finally, by use of equations (9) the pK values are obtained: $pK_1 = 6.23$ and $pK_2 = 7.15$.

Without additional information, however, it is not possible to assign the pK values to the individual substances.

The pK values can also be evaluated by using equation (7). In Fig. 3 the sides BHB^- and CHC^- indicate the lines for the separately measured protolysis equilibria of 2-nitroso-1-naphthol-4-sulphonic acid (pK_1) and *p*-nitrophenol (pK_2). Their parallels through B_2 intersect the conic section at T_2 and T_1 . The pH values corresponding to T_2 and T_1 lead to the pK values: $pK_1 = 6.30$ and $pK_2 = 7.20$.

Spectrophotometric analysis³ of the two equilibria separately gives the values $pK_1 = 6.34$ and $pK_2 = 7.18$ (0.05M potassium chloride medium; temperature 25°).

Determination of κ

The ratio of the dissociation constants can easily be determined by means of A diagrams. All the components may absorb, and no pH measurement is necessary. However, the determination of κ is critical for $\kappa \sim 1$, and the method fails at $\kappa = 1$. As a critical test, the *p*-nitrophenol/*o*-nitrophenol system is examined here, because the two pK values are similar.¹

Figure 4 shows the diagram for A_{368} vs. A_{225} , in which the curve is only slight. The titration points for the separately measured *p*-nitrophenol system lie on the straight line BHB^- . The parallel through B_2 intersects the conic section at T_2 . By analogy T_1 can

be constructed from the data for the separately measured *o*-nitrophenol system (only B_2T_1 is shown in Fig. 4). Because T_2 lies nearer to B_1 than does T_1 the pK value of *p*-nitrophenol is smaller than that of *o*-nitrophenol.

By use of T_2 the lines B_1T_2 and B_3T_2 can be constructed. Their intersections with the tangents B_2B_3 and B_1B_2 then give S'_1 and S_2 . Evaluation by means of equations (10) and (11) leads to the value 1.26 for κ . Because *p*-nitrophenol (*p*NP) is more acidic than *o*-nitrophenol (*o*NP), the final result is

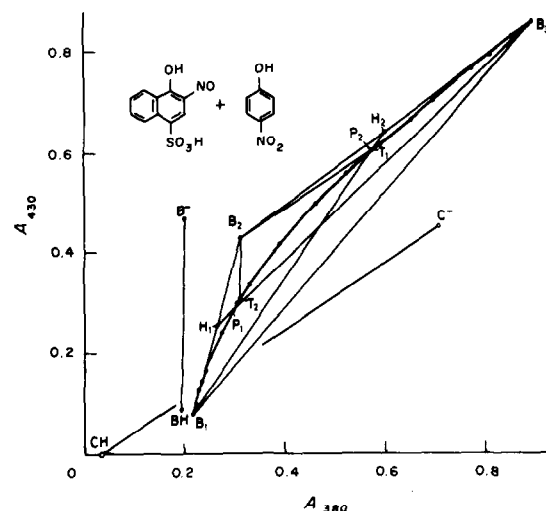


Fig. 3. Absorbance diagram A_{430} vs. A_{380} obtained from Fig. 2. For the construction of B_2 the tangents at B_1 and B_3 were determined by means of the polynomial $A_1 = a_1 + a_2A_2 + a_3A_2^2$. The coefficients a_1 , a_2 and a_3 were obtained by regression analysis from seven measured points. The points of the separately measured protolysis equilibria of 2-nitroso-1-naphthol-4-sulphonic acid and *p*-nitrophenol lie on the sides BHB^- and CHC^- . The parallels to these lines through B_2 lead to T_2 and T_1 . Because T_2 lies nearer to B_1 than does T_1 , 2-nitroso-1-naphthol-4-sulphonic acid is the stronger acid.

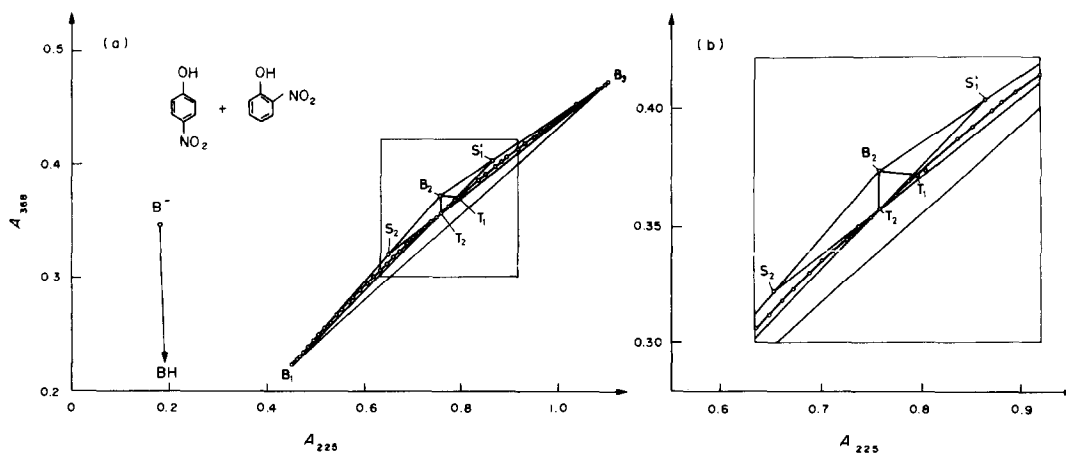


Fig. 4. (a) Absorbance diagram A_{368} vs. A_{225} for pNP and oNP (at 25.0°). For the construction of B_2 the tangents at B_1 and B_3 were determined by means of the polynomial $A_1 = a_1 + a_2 A_2 + a_3 A_2^2$. The coefficients a_1 , a_2 and a_3 were obtained by regression analysis from nine measured points. The titration points of the separately measured pNP system lie on the straight line BHB^- . Its parallel through B_2 leads to T_2 . By analogy the separately measured system oNP leads to T_1 . pNP is more acidic than oNP because T_2 lies nearer to B_1 than does T_1 (i.e., $K_{pNP}/K_{oNP} > 1$). (b) An enlargement ($\times 2$) of the central part of (a).

$\kappa = K_{pNP}/K_{oNP} \approx 1.26$. The mean value found earlier¹ for κ was 1.25.

Conclusions

These model systems demonstrate that the values pK_1 , pK_2 and κ for two protolysis equilibria in the same solution can be determined simply and exactly by the method described. More complicated systems may also be studied. Thus similar problems in biological systems, for example distinct dissociable groups (tyrosine) in a macromolecule (protein), can be studied spectrophotometrically. Nor is the method limited to spectrophotometric data. Any physical measurements, e.g., NMR, circular dichroism, may be evaluated if the measured signal is linearly dependent on the concentrations of the components.

Acknowledgements—The author is indebted to Mrs. Heuser and Mrs. Konstanczak for technical assistance.

REFERENCES

1. R. Blume, H. Lachmann, H. Mauser and F. Schneider, *Z. Naturforsch.*, 1974, **29b**, 500.
2. R. Blume, H. Lachmann and J. Polster, *ibid.*, 1975, **30b**, 263.
3. R. Blume and J. Polster, *ibid.*, 1974, **29b**, 734.
4. J. Polster, *Z. Anal. Chem.*, 1975, **276**, 353; *Z. Phys. Chem. (Frankfurt)*, 1975, **97**, 113; 1977, **104**, 49; *GIT*, 1982, 421, 581, 690; *Inaugural Dissertation*, Tübingen, 1980.
5. F. Göbber and J. Polster, *Anal. Chem.*, 1976, **48**, 1546.
6. L. P. Hammett and A. J. Deyrup, *J. Am. Chem. Soc.*, 1932, **54**, 2721, 4239.

A PROGRAMMABLE POSITIONING STEPPER-MOTOR CONTROLLER WITH A MULTIBUS/IEEE 796 COMPATIBLE INTERFACE

P. PAPOFF and D. RICCI

Istituto di Chimica Analitica Strumentale del C.N.R., c/o Istituto di Chimica Analitica dell'Università di Pisa,
Via Risorgimento, 35, 56100 Pisa, Italy

(Received 17 May 1983. Accepted 17 August 1983)

Summary—A programmable positioning stepper-motor controller, based on the Multibus/IEEE 796 standard interface, has been assembled by use of some intelligent and programmable integrated circuits. This controller, organized as a bus-slave unit, has been planned for local management of up to four stepper motors working simultaneously. The number of steps, the direction of rotation and the step-rate for the positioning of each motor are issued by the bus master microcomputer to the controller which handles all the required operations. Once each positioning has been performed, the controller informs the master by generating a proper bus-vectored interrupt. Displacements in up to 64,000 steps may be programmed with step-rates ranging from 0.1 to 6550 steps/sec. This device, for which only low-cost, high-performance components are required, can be successfully used in a wide range of applications and can be easily extended to control more than four stepper motors.

The increasing use of microprocessors in instrumentation control has given rise to a more efficient exploitation of stepper motors whenever precise and accurate mechanical positioning of instrumental parts is required.

Drive circuits for stepper motors can be easily implemented, in particular with specific integrated circuits.^{1,2} Their control by microcomputer is usually accomplished by direct management of two signals, one to select the direction of rotation and the other to make the motor advance one step for each pulse generated.³

This kind of approach has two main limitations: (1) degradation of the potentiality of the microcomputer, which has to spend time in performing trivial operations such as counting the steps and handling the time interval between them; (2) difficulties may arise in real-time control of the motors when several are required to work simultaneously.

These limitations can be overcome by using an intelligent device able to perform locally all the operations for stepper-motor positioning according to microcomputer instructions. Some devices of this kind are available on the market,⁴ but they may result in redundancy and be relatively expensive in some applications. This paper describes a programmable device, implemented with low-cost components, which handles the displacements and velocities of four stepper motors. Moreover the device is implemented as a general-purpose Multibus-compatible unit, that can be connected to any microcomputer system based on the Multibus, which is a widely used IEEE standard interface.

The Multibus is a communications device for

microcomputer systems. It connects the printed circuit boards of the system over several parallel lines by using a defined mechanical structure as support. It was originally developed by Intel and then became an IEEE standard (IEEE-796). It supports two independent address spaces: one for the memory, using 20-bit addressing; the other for input/output devices, using 16-bit addressing; the data transfer is bidirectional and asynchronous, with 8- or 16-bit data-word size. In addition eight multilevel interrupt lines are available. The units working with the Multibus are either masters or slaves; the master unit can control the bus, whereas the slave unit cannot control the bus but, upon decoding its own address, acts on the command signals from the bus master.^{5,6}

EXPERIMENTAL

Stepping-motor controller architecture

Figure 1 shows the block diagram of the stepping-motor controller, which is a slave Multibus unit based on some very sophisticated and intelligent programmable support integrated circuits. These consist of three programmable interval-timers 8253 (PIT), one programmable peripheral interface 8255 (PPI) and one programmable interrupt-controller 8259 (PIC). These integrated circuits are connected to the Multibus with their address decoder and proper bidirectional bus drivers.⁷⁻¹⁰

The 8253 PIT consists of three independent 16-bit pre-settable down-counters working in six different modes; the mode and the counting number for each counter are software-programmable. Two counters are used for each stepping motor, one (P_i) for the step-rate control, the other (Q_i) for the step-number control.

The 8255 PPI manages three 8-line groups (A, B and C) each of which may be software-programmed as an input or output port. This integrated circuit is used for the management of the control lines in the system, such as the direction selection for each stepping motor.

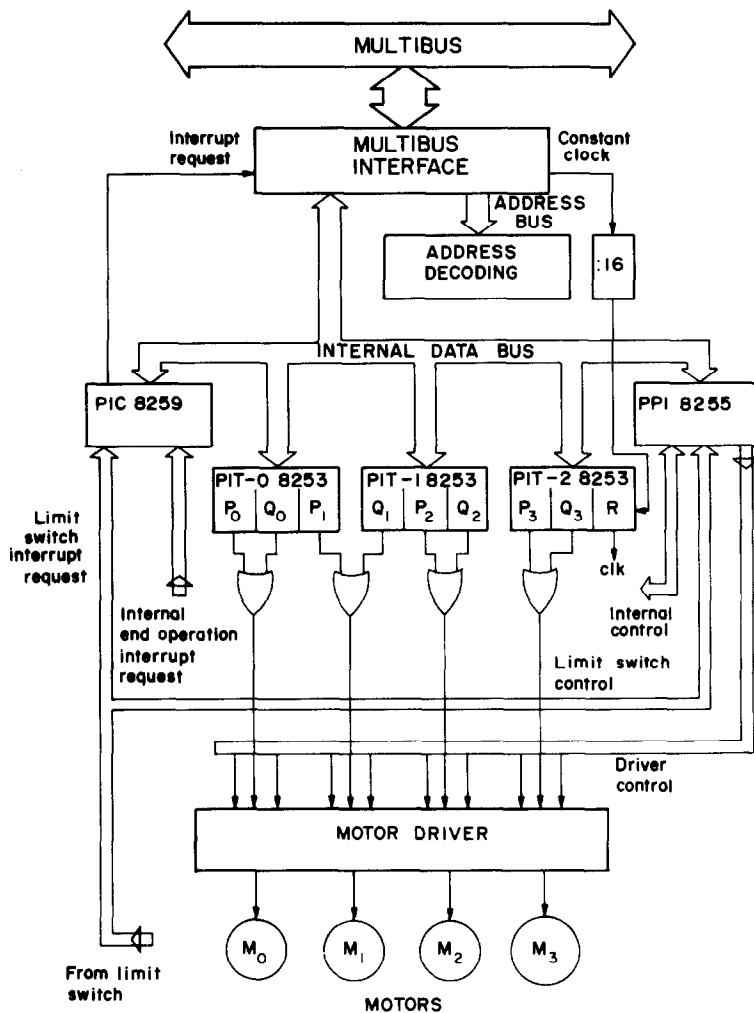


Fig. 1. Controller block diagram.

The 8259 PIC is a device for management of the interrupt logic in microcomputer systems. It handles eight levels of interrupt with priority resolution and addresses the specific service routines according to its programmed working mode. The 8259 PIC is used to inform the master when one (or more) stepping-motors have ended an operation, so as to allow synchronization between software and mechanical operations.

Functional description

Figure 2 shows a schematic diagram for control of one stepping motor (i). One counter (P_i) of a PIT is programmed as a square-wave generator; it receives a clock signal at the input, with period $t_0 = 152 \mu\text{sec}$ (internal clock) and gives a square wave at the output, with period $T = Nt_0$, where N is a 16-bit binary integer number software-loaded on the counter. [The internal clock is obtained by dividing by 1408 the output from the 9.22-MHz constant-clock of the Multibus; for this purpose a PIT counter (R) is used]. Another counter (Q_i) is programmed as a one-shot generator, receiving the square wave ($T = Nt_0$) at the input. A one-shot pulse, with duration $D = MT$, is generated at the output of Q_i every time a rising edge is sent to the counter trigger; M is a 16-bit binary integer number software-loaded on the counter.

The outputs of each counter are connected to the inputs of an OR gate, the output of which is a burst of M pulses with a period Nt_0 , as shown in the timing diagram of Fig. 2. This burst of pulses is sent to the step-line of the drive

circuit of the motor, so that it performs M steps at a rate of $1/Nt_0$ steps/sec. M can range from 1 to 65,535, and $1/Nt_0$ from 0.1 to 6550 steps/sec, since M and N are both 16-bit integer binary numbers, and $T_0 = 152 \mu\text{sec}$.

The 8255 PPI is programmed to work with its ports A and C as latched output and port B as input. Its output lines manage (for each motor):

(a) the "cw/ccw" control of the motor drive, to select the rotation direction: cw/ccw = 0 for clockwise rotation; cw/ccw = 1 for counterclockwise rotation;

(b) the "trigger" of the counter Q_i to enable the stepping motor to start the programmed operation at the rising edge;

(c) the "off" control of the motor drive; when this line is in the high logic level the motor current is set at zero, and the motor is left without holding-torque.

The 8255 input lines are used to test, for each motor, the status of:

(a) the "busy" line, *i.e.*, the output of counter Q_i ; when the line is in the low logic level the motor is busy performing some operation;

(b) the "zero" line which is connected to the motor limit switch to define the "zero" position for absolute positioning.

The "busy" and "zero" lines of each motor are also connected to the inputs of the 8259 PIC. When the PIC is warned by these lines that one or more motors have performed a positioning or have reached their "zero" position, the PIC causes a vectored interrupt to be sent to

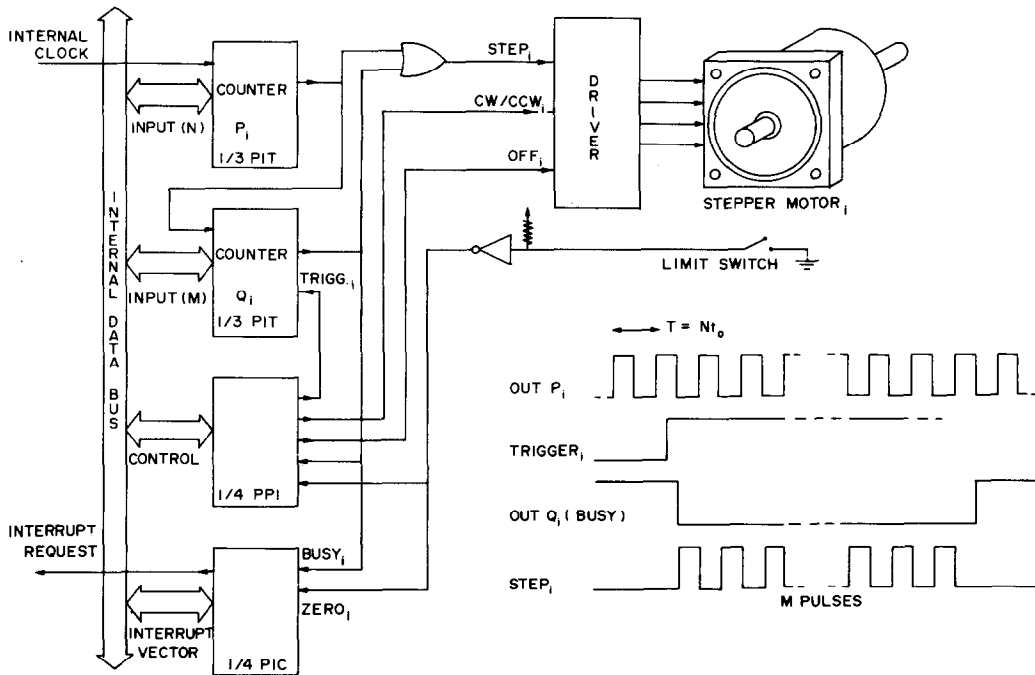


Fig. 2. Motor (i) control schematic diagram.

the master and gives it the restart address of the proper service routine locally resolving the interrupt priority.

Programming of the controller

Controller programming is accomplished by the master microcomputer through the input/output operations issued to the specific addresses assigned to the programmable chips: 8253 PIT, 8255 PPI and 8259 PIC. These addresses are reported in Table 1.

Figures 3a and 3b show the flow-chart of output operations for initialization of the programmable chips. These are programmed to work according to the function required in stepper-motor control. Initialization is necessary only after the powering up or reset of the system. The 8255 PPI is programmed first, then the three 8253 PITs and finally the 8259 PIC of the controller. Since the 8259 PIC of the controller works interactively with the 8259 PIC of the master microcomputer the latter is concordantly programmed.

Figure 4 shows the flow-chart of the input/output operations on the programmable chips to make motor (i) perform *M* steps at the rate of $1/Nt_0$ steps/sec. The 16-bit digital numbers *N* and *M* are sent to counters P₁ and Q₁ respectively, after the "busy₁" line has been tested with an input from port B. The direction of motor operation is selected by setting the proper control line "cw/ccw₁" and the start enabled by "trigger₁", by means of two outputs to port C. Once the motor has been started the master is free to move on to another operation. The end of the motor operation is signalled by the local 8259 PIC.

REMARKS

The programmable controller described can be successfully used in automatic control of chemical instrumentation, whenever stepper motors are required. The device was used at our laboratory in a computer-controlled spectrometer, combined with an inductively-coupled plasma source, designed for au-

tomatic sequential determinations.^{11,12} In the spectrometer the controller handles:

- (a) two stepper motors for the wavelength indexing in an echelle monochromator (where one motor controls the grating, the other the prism);
- (b) a stepper-motor controlled rotatable mirror for the selection of the proper observation zone within the plasma-plume;

Table 1. Controller I/O address assignments

Device	Hexadecimal I/O address	Function
PPI 8255	× ECE	Control
	× EC8	Port A
	× ECA	Port B
	× ECC	Port C
PIT 0 8253	× ED6	Control
	× ED0	Counter P ₀
	× ED2	Counter Q ₀
	× ED4	Counter P ₁
PIT 1 8253	× EDE	Control
	× ED8	Counter Q ₁
	× EDA	Counter P ₂
	× EDC	Counter Q ₂
PIT 2 8253	× EE6	Control
	× EE0	Counter P ₃
	× EE2	Counter Q ₃
	× EE4	Counter R
PIC 8259	× EF0 or	Control 0
	× EF2	
	× EF4 or	Control 1
	× EF6	

× = Insignificant.

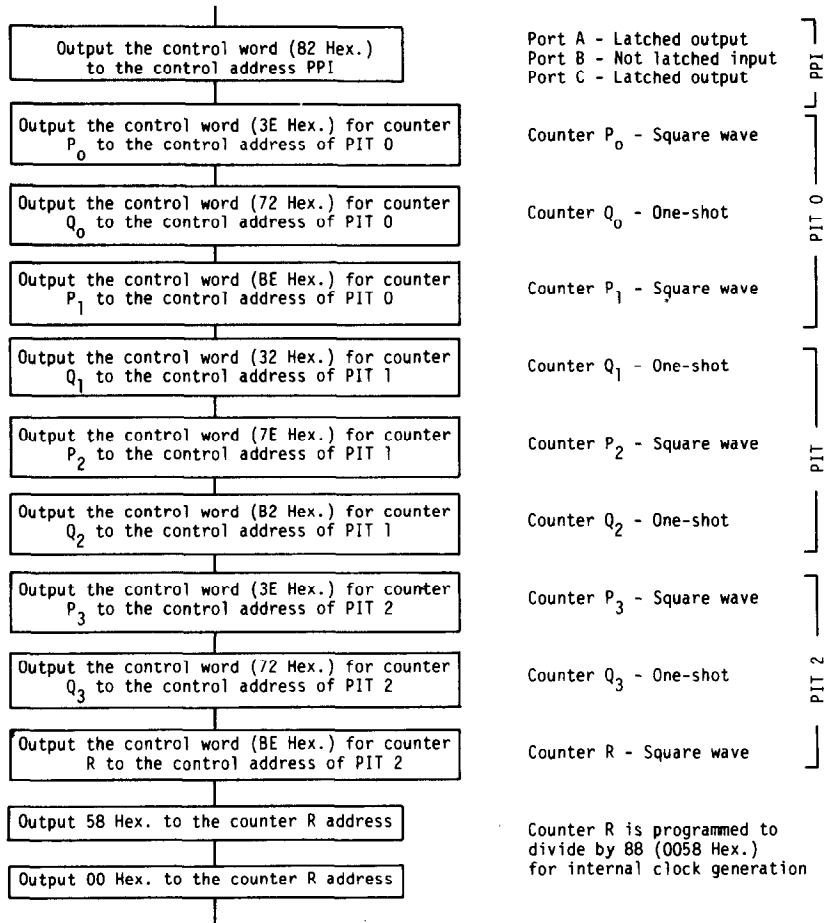


Fig. 3a. PPI and PITs initialization flow-chart.

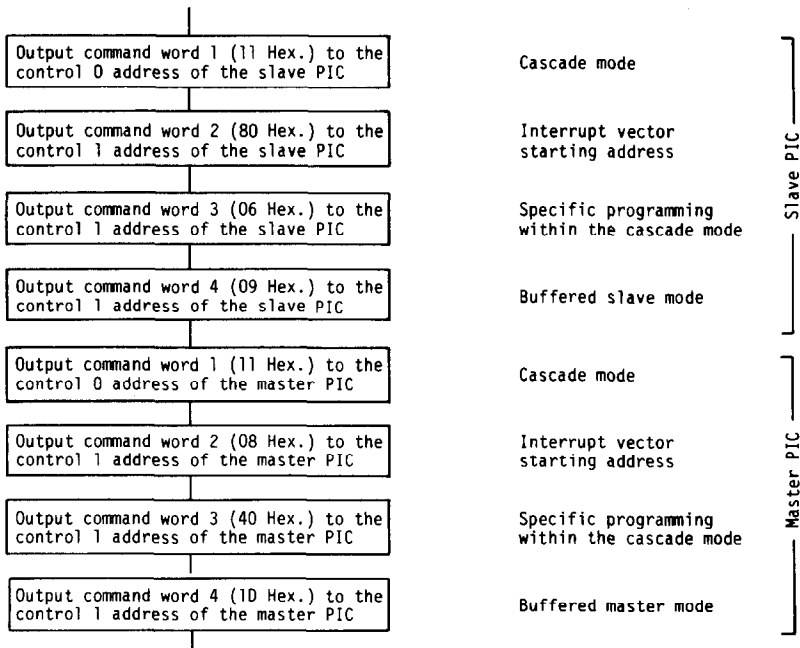


Fig. 3b. Slave PIC and master PIC initialization flow-chart.

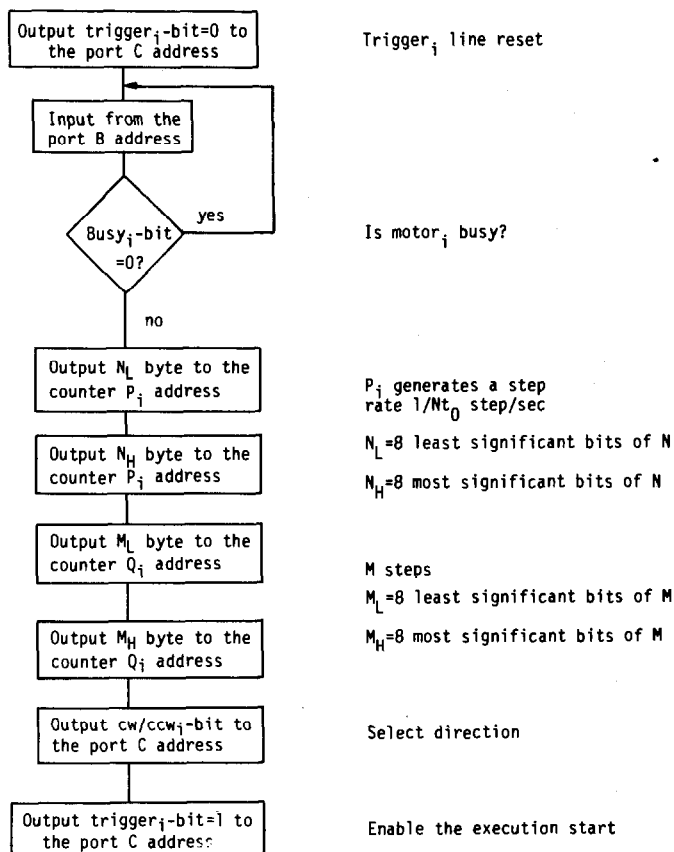


Fig. 4. *M* steps programming flow chart.

Table 2. Intel 86-12A features

1. Multibus-compatible
2. Based on the 16-bit 5-MHz Intel 8086 microprocessor
3. 32 K RAM + 16 K PROM on board
4. 1 serial I/O port EIA standard RS232-C with software-programmable baud rate
5. 3 parallel I/O ports of 8 lines each
6. 8 multilevel interrupt lines

Table 3. Motor driver features

1. For four-phase motors, unipolar mode
2. Up to 500 mA/phase
3. Opto-insulated and TTL-compatible inputs
4. Clockwise/counterclockwise control
5. Power down-function for de-energizing of all motor phases

(c) a stepper-motor peristaltic pump for control of sample flow-rates in the plasma nebulizer.

A Single Board Computer "Intel 86-12A", based on Multibus (its primary features are reported in Table 2), was used as bus master for the controller and the data-acquisition system. The aim was to implement the instrument control along with data acquisition, storage and reduction.

The primary features of the drive circuit for the motors are reported in Table 3.

In the controller, the software routines for the system management were implemented by use of Assembly 86 language, there being one for the con-

troller initialization, one for automatic search of the motor limit switch, and another for the relative positioning. These programs require only a minimum amount of instructions, and can be written by any user, even with little programming experience, owing to the "friendly" programmability of the intelligent circuits used. Details, circuit diagrams and programs are available on request.

Acknowledgements—This work was supported by C.N.R. (Rome). One of the authors (P.P.) gratefully acknowledges the financial support of Min. P.I. (40%).

REFERENCES

1. L. Sherman, *EDN*, 18 August, 1982, 95.
2. D. F. Marino and J. D. Ingle, Jr., *Talanta*, 1982, **29**, 223.
3. M. Bernstein, *Micro, The 6502-6809 Journal*, February 1982, No. 45, 95.
4. T. Ormond, *EDN*, 16 July, 1982, 262.
5. P. Snigier, *Digital Design*, 1982, **12**, No. 10, 52.
6. *Intel Multibus Specification*, Intel Corporation, 3065 Bowers Avenue, Santa Clara, CA 95051.
7. Microprocessors in Analytical Chemistry, *Talanta*, 1981, **28**, No. 7B.
8. *Intel Peripheral Design Handbook, 1980*, Intel Corporation, 3065 Bowers Avenue, Santa Clara, CA 95051.
9. *Intel Application Note*, AP-28A 1979 (in reference 8).
10. *Intel Application Note*, AP-59 1979 (in reference 8).
11. M. A. Floyd, V. A. Fassel, R. K. Winge, J. M. Katzenberger and A. P. D'Silva, *Anal. Chem.*, 1980, **52**, 431.
12. D. L. Anderson, A. R. Foster and M. L. Parsons, *ibid.*, 1981, **53**, 770.

COULOMETRIC TITRATION BY MEANS OF A CONTROLLED-POTENTIAL-PULSED-CURRENT POTENTIOMETRIC TECHNIQUE—I

METAL IONS BY ELECTRO-DEPOSITION

THEOLOGOS ANDRONIDIS and ANNA MARIA GHE

Istituto Chimico G. Ciamician dell'Università, Scuola di Specializzazione in Chimica Analitica,
via Selmi 2, 40126 Bologna, Italy

CESARE PAGURA and SERGIO VALCHER*

Istituto di Polarografia ed Electrochimica Preparativa del C.N.R., Corso Stati Uniti 4, 35100 Padova, Italy

(Received 23 March 1983. Accepted 16 August 1983)

Summary—A new method for electrochemical titrations is proposed, based on the redox transformation of the test species by means of a controlled-potential pulsed current, followed by measurement of the potential in the intervals between the current pulses: the end-point is found by means of Sørensen's linearization technique. Investigations on various metal ions (Ag^+ , Cu^{2+} , Cd^{2+} , Pb^{2+}) have shown that the accuracy and sensitivity, which depend on the nature of the species titrated, are comparable with those of other titration techniques. The method permits analytical separations and determinations of metal ions in mixtures. No particularly elaborate instrumentation is required and the apparatus described is simple to use, reliable and inexpensive.

Controlled-potential coulometry is usually used for analytical separations of metal ions and other electro-active species when the more popular constant-current and pulsed-current coulometry^{1,2} cannot be applied because of their lack of selectivity.

For the controlled-potential technique, the electrolysis current is the parameter generally used to determine the end-point, but this approach may sometimes not be accurate enough, particularly at low concentrations, where the background current becomes significant. A means of direct monitoring of the transformed species may then improve the performance.

Potentiometry is one such means and gives sensitive end-point detection provided equilibrium is obtained rapidly at the indicator electrode. Since this is usually not the case under constant-current electrolysis conditions, potentiometric end-point detection is more effective if the current is switched off while the potential is being measured.

A controlled-potential pulsed-current technique has therefore been devised, which is based on repetitive cycles of the following stages.

(1) Passage of a current pulse at a working-electrode potential controlled at a value suitable for redox transformation of the single species to be determined. The electrolysis current is integrated

until a preset charge has been passed and is then instantaneously reduced to zero.

(2) Measurement of the indicator-electrode potential (at zero current) once its value is steady.

The set of potentials is then processed in order to get a linear function with respect to the charge passed, and from this the titration end-point can be extrapolated.

Besides accuracy, the main advantage of the method is the possibility of evaluating the equivalence point without completing the electrolysis.

EXPERIMENTAL

Apparatus

The apparatus outlined in Fig. 1 has been used for the separation and determination of metal ions according to the principle described above.

The printer and potentiometer are commercial units (Laben 6061 and Orion 701 A, respectively), and the potentiostatic-coulometry unit is specially designed and constructed for use in the method.

The potentiostat (a) provides current at controlled potential. The charge passed in a single pulse is controlled by means of the current-to-voltage converter (b) and the integrator (c), the pulse being terminated by a suitable logical network as soon as the charge passed reaches the value preset on the comparator (d).

The potentiostat-galvanostat (a) and current-to-voltage converter (b) are operationally closely linked.

In the potentiostatic configuration [(i) in Fig. 2] the use of the high-current operational amplifier (No. 1) is quite conventional^{3,4} whereas in the current-to-voltage converter the high-current operational amplifier (No. 2) is used as a

*Author for correspondence.

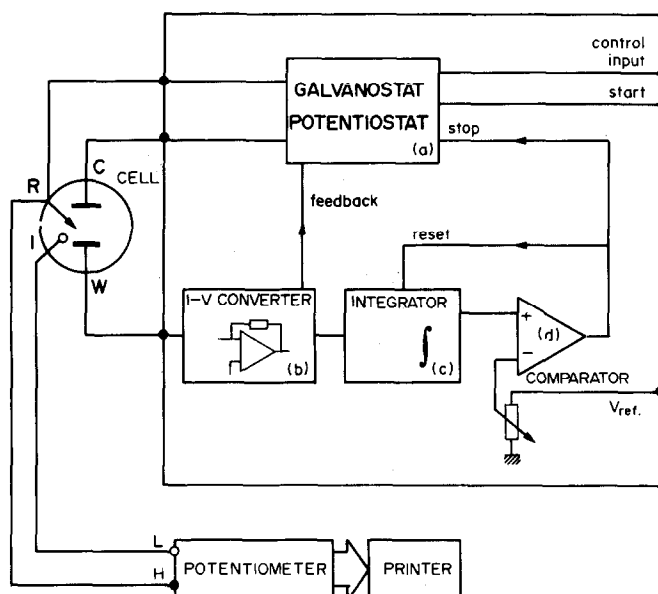


Fig. 1

voltage follower, in conjunction with a second operational amplifier. Diagram (ii) in Fig. 2 clarifies the reasons for this doubling, by showing the logic diagram for current interruption under potentiostatic conditions: instead of the current being switched off, it is instantaneously reduced to zero by activation of a negative feedback loop from the current-to-voltage converter to the potentiostat. This is done to avoid the disadvantages associated with the switching of relatively high currents.

To prevent an unsuitable choice of current range from invalidating the coulometric data, a current limiter has been incorporated which operates by taking control of the working-electrode potential when the output of the current-to-voltage converter reaches the highest allowed value (about 11 V). The high-current operational amplifiers HCA.1 and HCA.2 are made by coupling current boosters (limited at 100 mA) to LH0042 and LM308 operational amplifiers respectively.

The integrator (c), comparator (d) and stop–reset/start logic network, which is suitable for manual operation, is shown in Fig. 3. A flip-flop (1/2 SN7401) is used to switch the system between the potentiostatic and zero-current configurations and to reset the integrator.

Titration

As can be seen in Fig. 1, the electrolysis and the potential measurements can, if desired, be performed at different electrodes. Nevertheless this configuration has been employed only for special cases, it being generally sufficient to use a single electrode as both working and indicator electrode. The electrode potential is transmitted from the digital

output of the potentiometer to a printer (at 10-sec intervals) and is taken as constant if it does not vary by more than 0.1 mV during a time-period chosen in accordance with the behaviour of the electrochemical system.⁵ The charge to be passed in the pulse is preset by means of the current-range and time-constant selectors (according to the concentrations used and the area of the working electrode) so that about 20–30 data points are obtained for titration of a single species.

Cell and electrodes

The cell is equipped with a magnetic stirrer, and a nitrogen inlet for deaeration of the test solution. The counter-electrode (generally made of platinum) is separated from the titration cell by a porous glass disk and is housed in a compartment containing the same background electrolyte as the test solution. The saturated calomel reference electrode is similarly connected.

The working electrode has a surface area of about 1 cm² and is made of various materials, as indicated below.

Solutions

Titration were done (at 25°) on 20-ml samples, containing the species to be tested, and a background electrolyte chosen to give the best current yield and speed of response of the indicator electrode.

The solutions employed are listed in Table 1; they were generally acidic to prevent hydrolysis but care was taken to avoid concentrations at which hydrogen discharge would occur.

Table 1. Composition of the supporting electrolytes for the determination of single ions or ion mixtures

Type	Reagents and concentrations	pH
A	CH ₃ COONa 10 ⁻¹ M + CH ₃ COOH ~ 5 × 10 ⁻³ M	5.8
B	H ₂ SO ₄ 2.5 × 10 ⁻³ M	2.4
C	KCl 10 ⁻¹ M + HNO ₃ 2.5 × 10 ⁻³ M	3.5
D	KCl 10 ⁻¹ M + CH ₃ COOH ~ 5 × 10 ⁻³ M	5
E	CH ₃ COONa 10 ⁻¹ M + CH ₃ COOH 7.5 × 10 ⁻² M	5
F	H ₂ SO ₄ 2.5 × 10 ⁻³ M + (NH ₄) ₂ SO ₄ 2.5 × 10 ⁻⁴ M	2.8

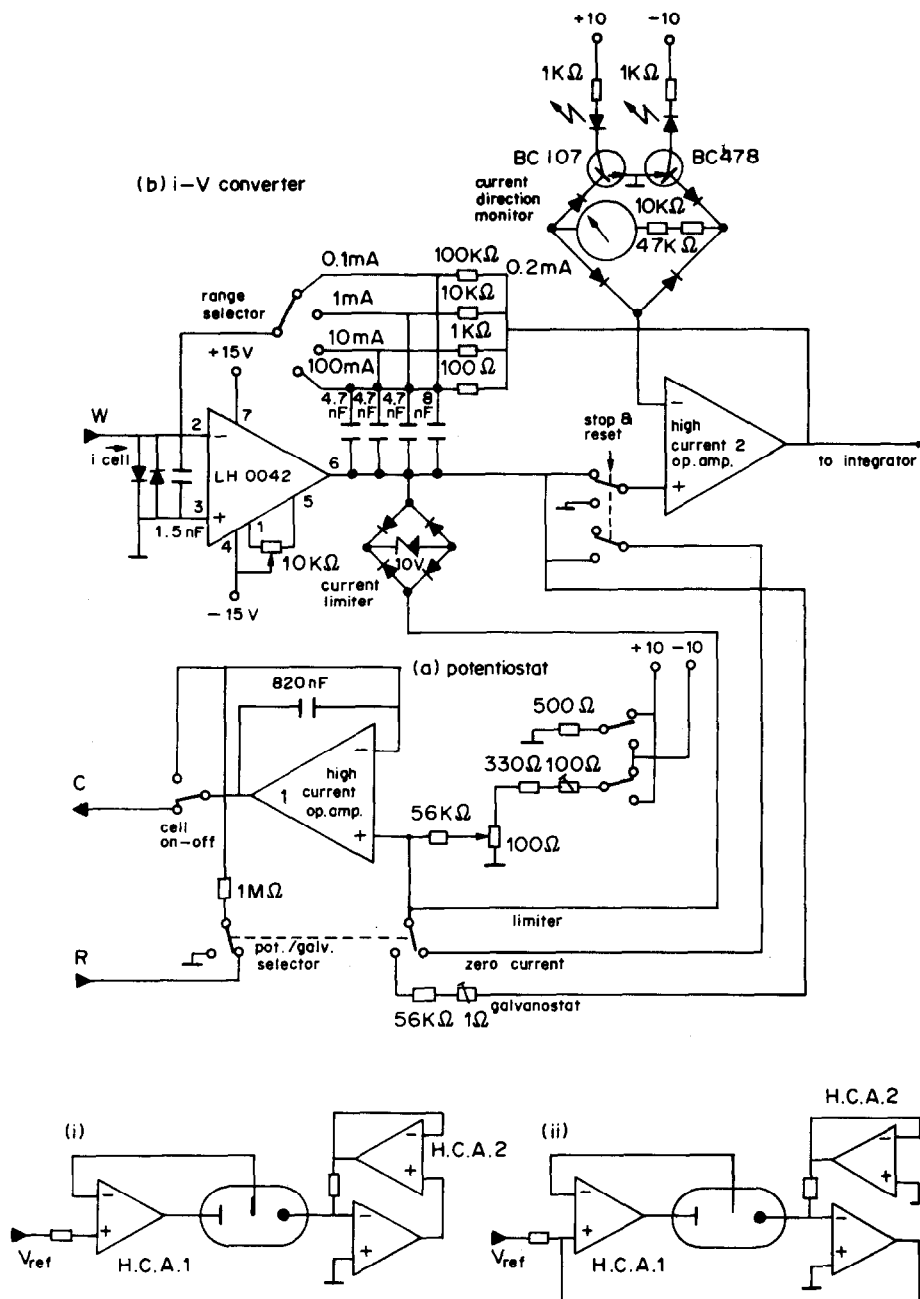


Fig. 2

End-point determination

A linearization technique is used so that the end-point can be deduced from the potentiometric data without completion of the electrolysis reaction.

Sørensen's⁶ method was used instead of Gran's,⁷ as the latter makes corrections for dilution, which does not occur in our method.

Since deviations from linearity may be encountered both for the initial points (because of the state of the indicator electrode surface) and for those near to the end-point (at low concentrations), the straight lines for extrapolation to the equivalence-point are obtained by using only the most linear subset of the experimental data.

This subset is extracted by numerical analysis as described elsewhere⁸ and is referred to here as the highest linearity segment. For a complete set of c data points, it contains $(c + 8)/4$ consecutive points. This segment, comprising the

points $P(n) \dots P(n+m)$, is selected on the basis of the variance minimum given by the three intercepts (on the charge axis) of the segments: (a) $P(n-1) \dots P(n-1+m)$; (b) $P(n) \dots P(n+m)$ and (c) $P(n+1) \dots P(n+1+m)$.

The selected subset is then used for linear regression analysis, which leads to the best straight line, the correlation coefficient, and the 90% confidence limits.

RESULTS AND DISCUSSION

The proposed technique was developed for the determination of ions by electro-deposition, both in systems containing a single species, and in mixture of several metal ion; in other words, for an electrolytic precipitation titration.

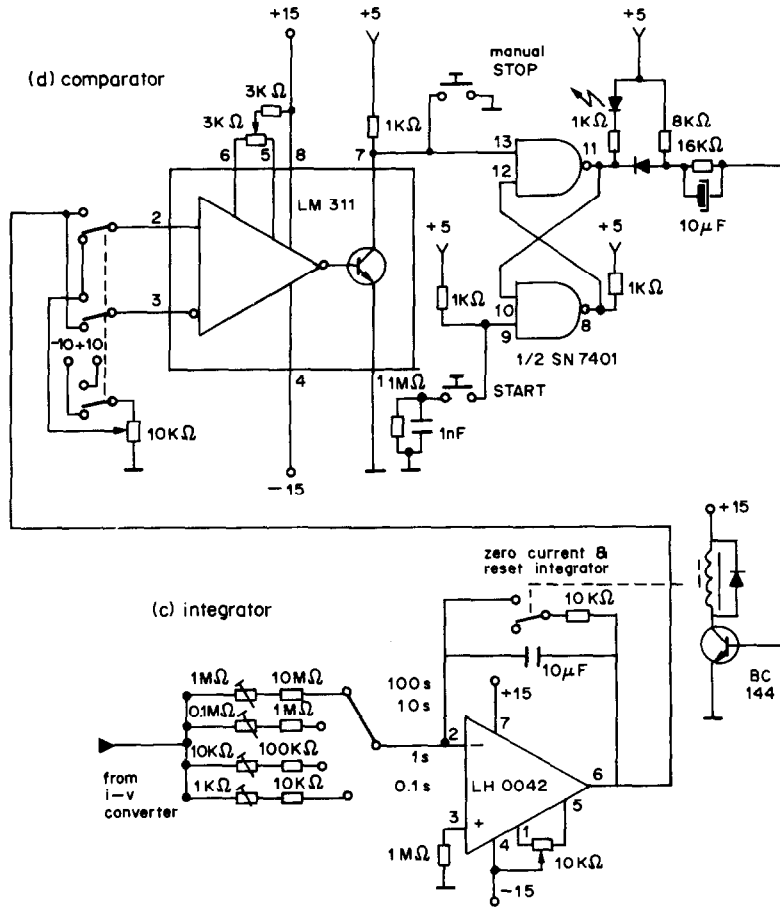


Fig. 3

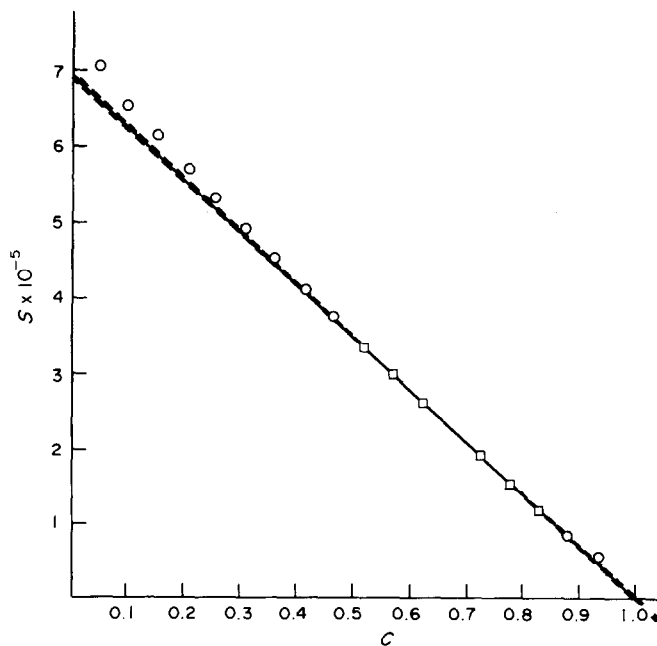


Fig. 4

An example of the diagrams used for the determination of the equivalence point is shown in Fig. 4, where a titration of $5 \times 10^{-4}M$ silver is shown.

In the plot, the Sørensen function S (defined as $S = 10^{nE/0.059}$, n being the number of electrons involved in the reaction, and E the measured electrode potential) is plotted as a function of charge consumed (expressed as $C = Q/nFm$, where m is the number of moles of silver deposited). The points denoted by \square pertain to the highest linearity segment, selected as indicated. In the same figure the linear-regression straight line is shown together with the corresponding 90% confidence hyperbolas, the intercepts of which with the charge axis are the confidence limits for location of the end-point.

Typical results of determinations of single ionic species at various concentrations are shown in Table 2. It is apparent that with all the species tested a comparison between the present technique and conventional controlled-potential coulometry is in favour of the former since lower concentrations of the ions can be determined.² This is especially true for silver and cadmium, which can be determined with acceptable error levels down to concentrations of $5 \times 10^{-5}M$ and $2.5 \times 10^{-5}M$ respectively. Of course the accuracy decreases with decreasing concentration, so the uncertainty range, as given by the confidence limits, broadens.

To improve this situation, titrations were done with a four-electrode configuration (see for instance experiment 5) and gave much better results for silver, both in terms of relative error and of confidence limits. Another possible source of deviation is manifested in titration 8 (of lead) which gave the highest relative errors for high concentrations. This can be related to the fact that lead, at high current densities, produces dendritic deposits, which make it difficult for the potential of the working-indicator electrode to equilibrate rapidly. The formation of dendritic lead is enhanced if silver electrodes are used, because their smoothness is initially poorer than that of platinum. However, the accuracy obtained is similar to that of other potentiometric titrations based on the Gran linearization method.⁹

The technique proposed is particularly interesting for separate determination of ions in mixtures. Various concentration ratios have been explored in this connection.

Table 3 shows typical results obtained for a number of determinations of silver and copper present in the same solution.

The relative error in the determination of silver, the first ion titrated, is very similar, in most instances, to that obtained when silver is the only ion present. The second species to be determined deserves more attention. The overall error for a pair of ions is less than or equal to the sum of the relative errors for the various ions. When the amount of copper is calculated from the difference between the total charge passed and the theoretically "known" amount of

Table 2. Typical results of controlled-potential pulsed-current potentiometric titrations of single species

Run	Ion	Molarity in cell	Counter-ion	Solution composition	Electrode	Electrolysis potential, mV vs. SCE	Coulombs required				Correlation coefficient	Error, %
							Expected	Found	90% Confidence limits	90% Confidence limits		
1	Ag ⁺	5×10^{-3}	NO ₃ ⁻	A	Ag	+150	9.65	9.50	9.45	9.56	1.000	1.5
2	Ag ⁺	5×10^{-3}	NO ₃ ⁻	B	Ag	+150	9.65	9.60	9.58	9.61	1.000	-0.5
3	Ag ⁺	5×10^{-4}	NO ₃ ⁻	B	Ag	+150	9.65×10^{-1}	9.64×10^{-1}	9.60×10^{-1}	9.67×10^{-1}	1.000	-0.1
4	Ag ⁺	5×10^{-5}	NO ₃ ⁻	B	Ag	+150	9.65×10^{-2}	9.2×10^{-2}	8.89×10^{-2}	9.54×10^{-2}	0.998	-4.7
5*	Ag ⁺	5×10^{-5}	NO ₃ ⁻	B	Ag	+150	9.65×10^{-2}	9.73×10^{-2}	9.59×10^{-2}	9.89×10^{-2}	0.998	+0.9
6	Cu ²⁺	2.5×10^{-3}	SO ₄ ²⁻	B	Ag	-250	9.65	9.47	9.39	9.56	1.000	-1.8
7	Cu ²⁺	2.5×10^{-4}	SO ₄ ²⁻	B	Ag	-250	9.65×10^{-1}	9.72×10^{-1}	9.47×10^{-1}	10.0×10^{-1}	0.998	+0.7
8	Pb ²⁺	2.5×10^{-2}	NO ₃ ⁻	A	Ag	-800	96.5	98.5	97.2	99	0.998	+2.1
9	Pb ²⁺	5×10^{-3}	NO ₃ ⁻	A	Pt	-800	19.3	19.08	19.03	19.13	1.000	-1.1
10	Pb ²⁺	2.5×10^{-3}	NO ₃ ⁻	C	Pt	-800	9.65	9.77	9.66	9.87	1.000	+1.2
11	Cd ²⁺	2.5×10^{-3}	CH ₃ COO ⁻	D	Pt	-1100	9.65	9.59	9.50	9.69	1.000	-0.6
12	Cd ²⁺	2.5×10^{-5}	CH ₃ COO ⁻	D	Pt	-1100	9.65×10^{-2}	9.72×10^{-2}	9.14×10^{-2}	10.47×10^{-2}	0.996	+0.8

*Four-electrode measurement system.

Table 3. Titrations of mixtures of Ag⁺ and Cu²⁺ (silver electrode)

Run	Molarity		Respective counter-ions		Solution composition	Electrolysis potential, mV vs. SCE		Coulombs for Ag ⁺		Error, % Ag ⁺
	Ag ⁺	Cu ²⁺				Ag ⁺	Cu ²⁺	Expected	Found	
13	5 × 10 ⁻³	2.5 × 10 ⁻³	NO ₃ ⁻	SO ₄ ²⁻	B	+150	-250	9.65	9.65	0.0
14	5 × 10 ⁻³	2.5 × 10 ⁻³	NO ₃ ⁻	SO ₄ ²⁻	B	+150	-220	9.65	9.5	-1.5
15	5 × 10 ⁻³	2.5 × 10 ⁻³	NO ₃ ⁻	CH ₃ COO ⁻	E	+150	-220	9.65	9.5	-1.5
16	5 × 10 ⁻²	2.5 × 10 ⁻²	NO ₃ ⁻	SO ₄ ²⁻	F	+150	-220	96.5	99	+2.5
17	5 × 10 ⁻³	2.5 × 10 ⁻³	NO ₃ ⁻	SO ₄ ²⁻	F	+150	-220	9.65	9.5	-1.5
18	2.5 × 10 ⁻³	1.25 × 10 ⁻³	NO ₃ ⁻	SO ₄ ²⁻	F	+150	-220	4.825	4.65	-3.5
19	1 × 10 ⁻³	5 × 10 ⁻⁴	NO ₃ ⁻	SO ₄ ²⁻	F	+150	-220	1.93	1.88	-2.6
20	5 × 10 ⁻⁴	2.5 × 10 ⁻⁴	NO ₃ ⁻	SO ₄ ²⁻	F	+150	-220	0.965	0.92	-4.2
21	5 × 10 ⁻⁵	2.5 × 10 ⁻⁵	NO ₃ ⁻	SO ₄ ²⁻	F	+150	-220	9.65 × 10 ⁻²	9.65 × 10 ⁻²	0.0
22	5 × 10 ⁻⁵	2.5 × 10 ⁻³	NO ₃ ⁻	SO ₄ ²⁻	F	+150	-220	9.65 × 10 ⁻²	9.6 × 10 ⁻²	-0.5
23	5 × 10 ⁻³	2.5 × 10 ⁻⁴	NO ₃ ⁻	SO ₄ ²⁻	F	+150	-220	9.65	9.65	0.0
24	5 × 10 ⁻²	2.5 × 10 ⁻⁴	NO ₃ ⁻	SO ₄ ²⁻	F	+150	-220	96.5	94.7	-1.9

Coulombs for Cu²⁺

Run	Expected	Found		Error, % Cu ²⁺		Coulombs for Ag ⁺ + Cu ²⁺		Error, % Ag ⁺ + Cu ²⁺
		I (from Ag found)	II (from Ag taken)	I	II	Expected	Found	
13	9.65	9.9	9.9	+2.6	+2.6	19.3	19.55	+1.3
14	9.65	9.8	9.65	+1.5	0.0	19.3	19.3	0.0
15	9.65	9.8	9.65	+1.5	0.0	19.3	19.3	0.0
16	96.5	93.5	96	-3.1	-0.51	193	192.5	-0.2
17	9.65	9.7	9.55	+0.5	-1	19.3	19.2	-0.5
18	4.825	5	4.825	+3.6	0.0	9.65	9.65	0.0
19	1.93	1.98	1.93	+2.6	0.0	3.86	3.86	0.0
20	0.965	0.97	0.925	+0.5	-4	1.93	1.81	-2
21	9.65 × 10 ⁻²	—	—	—	—	—	—	—
22	9.65	9.50	—	-1.5	—	9.75	9.60	-1.5
23	0.965	0.91	—	-5.2	—	10.61	10.56	-0.5
24	0.965	1.01	—	+5.2	—	97.46	95.71	-1.8

silver, the error is less than when it is calculated on the basis of the charge passed between the two end-points.

This points to the absence of a specific interference between the two ions and indicates that the only additional source of error is the uncertainty affecting the determination of the first ion to be titrated.

Similar considerations can be applied to determinations of ions in other binary mixtures, such as silver and lead (Table 4), for which the figures obtained are quite satisfactory.

The relative proportions of the two components do not greatly affect the results (Tables 3 and 4).

Figure 5 shows that successive determination of more than two metals is a possibility; in particular the system Ag⁺-Cu²⁺-Pb²⁺ has been tested (experimental conditions: three-electrode system; Ag working electrode; solution E; electrolysis potentials respectively +150, -200, -800 mV vs. SCE). The relative errors in the various determinations were of the same order of magnitude as those found when the same ions were determined separately.

CONCLUSIONS

During the present investigation a controlled-potential pulsed-current coulometric method has been developed. The technique, based on the potentiometric determination of the equivalence point by

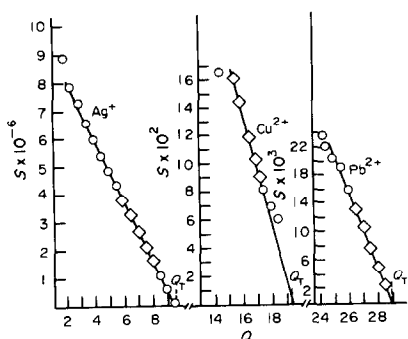


Fig. 5

Table 4. Titrations of mixtures of silver nitrate and lead nitrate (solution A; potential vs. SCE + 150 V for Ag^+ , -800 V for Pb^{2+})

Run	Molarity		Electrode	Coulombs for Ag^+			Error, % Ag^+	Found		Error, % Pb^{2+}		Coulombs for $\text{Ag}^+ + \text{Pb}^{2+}$		Error, % $\text{Ag}^+ + \text{Pb}^{2+}$
	Ag^+	Pb^{2+}		Expected	Found	II (from Ag taken)		I	II	Expected	Found			
				Ag found										
25	5×10^{-3}	2.5×10^{-3}	Ag	9.65	9.6	9.9	-0.5	9.65	9.85	+2.6	+2	19.3	19.5	+1
26	5×10^{-4}	2.5×10^{-3}	Ag	0.965	0.940	9.86	-2.6	9.65	9.835	+2.2	+1.9	10.615	10.800	+1.7
27	2.5×10^{-4}	2.5×10^{-3}	Ag	0.482	0.47	9.63	-2.5	9.65	9.62	-0.2	-0.3	10.132	10.100	-0.3
28	5×10^{-4}	2.5×10^{-2}	Ag	0.965	0.965	94.53	0.0	96.5	94.53	-2	-2	97.46	95.5	-2
29	2.5×10^{-4}	2.5×10^{-2}	Ag	0.482	0.470	96.53	-2.5	96.5	96.52	0.0	0.0	96.98	97	0.0
30	5×10^{-3}	2.5×10^{-3}	Pt	9.65	9.4	9.6	-2.6	9.65	9.35	-0.5	-3.1	19.3	19	-1.5

means of Sørensen's linearization procedure permits reasonably short run times as it does not require the titration to be taken to completion.

The use of a linearization function permits easy statistical analysis and therefore provides a test of the accuracy of the determination. The procedure offers the advantage over constant-current coulometric titrations that it can be used for analytical separations of mixtures of metal ions which can be electro-deposited. The sensitivity and the accuracy compare favourably with those of other titration techniques.

It should be noted that the end-point can also be predetermined in conventional controlled-potential electrolysis (by using plots of $\log i$ vs. time), but there are instrumental complications regarding the stirring conditions, which must be rigorously controlled; furthermore this variation of the method does not have general applicability. In contrast, the proposed technique calls for less sophisticated instrumentation and, because of the short integration times for each current pulse, makes less severe demands on the integrator performance.

REFERENCES

1. J. J. Lingane, *Electroanalytical Chemistry*, 2nd Ed., p. 484. Interscience, New York, 1958.
2. D. D. DeFord, in *Treatise on Analytical Chemistry*, I. M. Kolthoff, P. J. Elving and E. B. Sandell (eds.), Part I, Vol. 4. p. 2475. Interscience, New York, 1963.
3. R. Kalvoda, *Operational Amplifiers in Chemical Instrumentation*, p. 126. Horwood, Chichester, 1975.
4. R. R. Schroeder and I. Shain, *J. Phys. Chem.*, 1969, **73**, 197.
5. B. A. Servell, *J. Electroanal. Chem.*, 1967, **13**, 181.
6. P. Sørensen, *Kem. Maanedstbl.*, 1951, **32**, 73.
7. G. Gran, *Analyst*, 1952, **77**, 661.
8. S. Valcher, C. Pagura, S. Coin and A. M. Ghe, *Chem. Biomed. Environ. Instrum.*, 1982-83, **12**, 327.
9. S. L. Burden and D. E. Euler, *Anal. Chem.*, 1975, **47**, 793.

SHORT COMMUNICATIONS

FLOW ENTHALPIMETRIC DETERMINATION OF GLUCOSE, BASED ON OXIDATION BY 1,4-BENZOQUINONE AND USE OF AN IMMOBILIZED GLUCOSE OXIDASE COLUMN

NOBUTOSHI KIBA, TOSIMITSU TOMIYASU* and MOTOHISA FURUSAWA

Department of Chemistry, Faculty of Engineering, Yamanashi University, Takeda-4, Kofu-shi 400, Japan

(Received 14 June 1983. Accepted 17 August 1983)

Summary—A flow enthalpimetric method for the determination of glucose is presented. The method is based on the reaction of glucose with 1,4-benzoquinone in the presence of immobilized glucose oxidase. D-Glucose concentrations ranging from 0.02 to 75mM can be determined. The method is applicable to the determination of glucose in soft drinks, wines, beers, jams and serum.

Enthalpimetric flow systems using immobilized enzyme reactors have been developed for the determination of glucose. Glucose oxidase (EC 1.1.3.4)¹⁻⁶ and hexokinase^{6,7} were the enzymes immobilized in the reactors. Co-immobilization of glucose oxidase and catalase^{8,9} resulted in an increase in sensitivity and an extension of the linear range of the calibration curve. Glucose oxidase is highly specific for glucose. However, the enzyme can react very rapidly with a variety of acceptors. Oxygen, which is the natural enzyme acceptor, can be replaced by benzoquinone.¹⁰ Williams *et al.*¹¹ and Gorton *et al.*¹² proposed the use of benzoquinone as the enzyme acceptor in an electrochemical assay of glucose. This paper describes the adaption of the reaction to a flow enthalpimetric system for determination of glucose. The method has a wide linear concentration range (0.02–75mM) which would not be possible with oxygen as acceptor in the co-immobilized enzyme system.

EXPERIMENTAL

Reagents

Glucose oxidase (from amagasakiense, 110 units/mg, Nagase Seikagaku Co., Tokyo, Japan) (70 mg) was immobilized on 1 g of the aminoaryl derivative of controlled-pore glass beads (120–200 mesh, pore diameter 55 nm, Electro-Nucleonics, Fairfield, U.S.A.) by diazotization.¹³ A 0.1M buffer solution (KH₂PO₄/Na₂HPO₄, pH 6.0) was used. 1,4-Benzoquinone (Tokyo Kasei, Tokyo, Japan) was recrystallized twice from cyclohexane and dried in a vacuum for 3 hr. The quinone was further purified with a high-speed zone refiner.¹⁴ The activity of the immobilized enzyme was reduced by adhesion of some black compounds present in the crude benzoquinone. Up to 6 g could be purified in a

day. The quinone solution was prepared in the buffer. The stock solution of D-glucose (Merck) (1.0M) was also prepared in the buffer. The solution was allowed to come to anomeric equilibrium (β -D-glucose 63.5%)¹⁵ at room temperature. Calibration standards were made by dilution of the stock glucose solution with the buffered quinone solution.

Apparatus

The enthalpimeter (Japan Electron Optics Laboratory, Tokyo, Japan), piston pump and loop injector used were those employed previously.^{16,17} The detection column (bed 0.8 cm diameter, 3.5 cm length) was packed with the immobilized enzyme (1 g).

Procedure

The quinone solution (45mM) was pumped at a flow-rate of 4.0 ml/min. The sample (1.0 ml) was diluted to 10 ml with 50mM quinone solution in the pH 6.0 buffer, and 2.0 ml of this solution were introduced into the flow-stream by means of the loop injector. The height of the temperature peak was measured as the maximum deflection from the base-line.

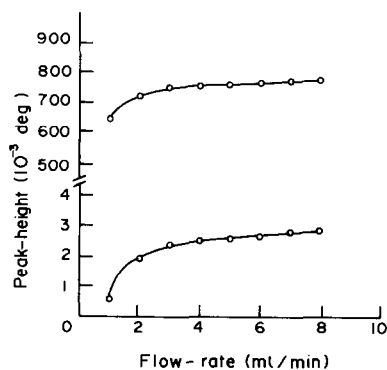


Fig. 1. Dependence of peak-height on flow-rate. A, $6.02 \times 10^{-2}M$ D-glucose; B, $2.00 \times 10^{-4}M$ D-glucose. Sample volume 2.0 ml, 45mM benzoquinone solution (pH 6.0), column temperature 30°.

*Present address: Atsugi Factory, Nippon Valqua Industries Ltd., Atsugi-shi 243, Japan.

Table 1. Determination of glucose

[D-glucose], mM	ΔT , 10^{-3} deg.	C.V.,* % ($n = 5$)
0.0200	0.250	0.8
0.0301	0.375	0.8
0.200	2.50	0.6
0.602	7.50	0.5
2.00	25.0	0.3
6.02	75.5	0.3
20.0	250	0.1
60.2	760	0.1
70.2	878	0.1
75.4	944	0.1

*Coefficient of variation.

Four calibration curves were prepared, covering the D-glucose concentration ranges of 0–0.1, 0.1–1.0, 1.0–10 and 10–75mM.

RESULTS AND DISCUSSION

Peak-height as a function of flow-rate was studied over the range 1.0–8.0 ml/min. As shown in Fig. 1, the reaction was complete at all flow-rates tested, since the peak-height increased linearly with flow-rates above a certain value (3 ml/min). At these higher flow-rates, the rapid passage through the reaction column narrows the peak-width. The apparent fall-off in response at flow-rates below 3 ml/min is due to heat loss from the column.¹⁸ The influence of pH of the buffer on the peak-height and the stability of the quinone solution was studied. Two kinds of buffer solution, acetate buffer (0.1M, pH 4.0–6.0) and phosphate buffer (0.1M, pH 5.5–8.0), were used. The peak-height was independent of pH in the range 4.0–7.0. The type of buffer did not influence the peak-height (at pH 5.5 and 6.0). At pH 8, the quinone solution turned rapidly from yellow to black and a black precipitate separated out within 6 hr. The peak-height was almost independent of sample volume, provided this was larger than 2.0 ml. The linearity of the calibration curve was not influenced by the presence of dissolved oxygen in the quinone solution. Because of vaporization of quinone from the solution, the quinone solution was only stable at concentrations below 50mM. A flow-rate of 4.0 ml/min, a sample volume of 2.0 ml, a phosphate buffer of pH 6.0 and a quinone concentration of 45mM were therefore chosen.

Under these conditions a linear relationship was obtained between peak-height and D-glucose concentration in the range 0.02–75mM. The rate of analysis was 40 samples per hr. The immobilized glucose oxidase served for at least 3000 samples. Table 1 summarizes the results obtained with solutions of known concentration.

The method was applied to the determination of glucose in soft drinks, wines, beers, jams and serum. A 1-ml sample of beverage was boiled for 3 min in a 10-ml evaporation tube, then transferred to a 10-ml standard flask and made up to volume with 50mM

Table 2. Determination of glucose in some samples

Sample	D-glucose, g/100 ml	C.V., % ($n = 6$)	Certificate value, g/100 ml
Soft-drink 1	4.37	0.44	4.3
Soft-drink 2	4.34	0.68	4.3
White wine 1	0.222	1.0	0.2
White wine 2	1.29	0.41	1.2
Red wine 1	0.0536	1.7	0.05
Red wine 2	0.0869	1.5	0.07
Beer 1	0.0259	1.6	0.03
Beer 2	0.0358	1.6	0.03
Strawberry jam	10.8*	0.1	10*
Apricot jam	9.81*	0.1	10*
Serum	0.0984	1.2	0.094–111

*g/100 g.

quinone solution in pH-6.0 buffer. Red wine was filtered through 5 g of Bio-gel P-300 (50–100 mesh) to remove colouring matter before analysis. Jam (1.0 g) was dissolved in hot water, followed by dilution to 50 ml with the buffer. Any insoluble material was filtered off and a 1.0-ml portion of the filtrate was diluted to 10 ml with the quinone solution. For the determination of glucose in serum (Boehringer Mannheim, Precinorm S), a precolumn (0.8 cm bore, 3.5 cm length, CPG beads, 200–400 mesh) was placed in the line between the injector and the enthalpimenter to remove adducts of benzoquinone and proteins in the serum. The results (Table 2) were in agreement with the certified values.

REFERENCES

1. K. Mosbach, B. Danielsson, A. Borgerund and M. Scott, *Biochim. Biophys. Acta*, 1975, **403**, 256.
2. B. Mattiasson, B. Danielsson and K. Mosbach, *Anal. Lett.*, 1976, **9**, 217.
3. *Idem, ibid.*, 1976, **9**, 867.
4. B. Mattiasson, *FEBS Lett.*, 1977, **77**, 107.
5. B. Mattiasson and C. Borrebaeck, *ibid.*, 1978, **85**, 119.
6. J. C. Weaver, C. L. Cooney, S. P. Fulton, P. Schuler and S. R. Tannenbaum, *Biochim. Biophys. Acta*, 1976, **452**, 285.
7. L. D. Bowers and P. W. Carr, *Clin. Chem.*, 1976, **22**, 1427.
8. B. Danielsson, K. Gadd, B. Mattiasson and K. Mosbach, *Clin. Chim. Acta*, 1977, **81**, 163.
9. H. L. Schmidt, G. Krisam and G. Grenner, *Biochim. Biophys. Acta*, 1976, **429**, 283.
10. M. Dixon, *ibid.*, 1971, **226**, 269.
11. D. L. Williams, A. R. Doig, Jr. and A. Korosi, *Anal. Chem.*, 1970, **42**, 118.
12. L. Gorton and K. M. Bhatti, *Anal. Chim. Acta*, 1979, **105**, 43.
13. M. K. Weibel and H. J. Bright, *Biochem. J.*, 1971, **124**, 801.
14. M. Furusawa and M. Tachibana, *Bull. Chem. Soc. Japan*, 1981, **54**, 2968.
15. J. Okuda and I. Miwa, *Anal. Biochem.*, 1971, **39**, 387.
16. N. Kiba, Y. Ishida and M. Furusawa, *Talanta*, 1983, **30**, 187.
17. N. Kiba, K. Shimizu and M. Furusawa, *ibid.*, 1983, **30**, 969.
18. R. S. Schifreen, D. A. Hanna, L. D. Bowers and P. W. Carr, *Anal. Chem.*, 1977, **49**, 1929.

DETERMINATION OF INDIUM AND THALLIUM BY HYDRIDE GENERATION AND ATOMIC-ABSORPTION SPECTROMETRY

DU YAN,* ZHANG YAN, GUANG-SHEN CHENG and AN-MO LI
Department of Chemistry, Peking University, Peking, People's Republic of China

(Received 23 May 1983. Accepted 29 August 1983)

Summary—Hydride generation coupled with atomic-absorption spectrometry was applied to the determination of indium and thallium. The hydrides were generated in 1M HCl (In) and 1–1.5M HCl or HNO₃ (Tl) with 1% NaBH₄ solution, and were flushed with argon into an electrically heated silica tube. The characteristic mass for indium and thallium were 0.13 and 0.12 μg, respectively.

Since 1972, when Braman *et al.*¹ first used sodium borohydride to generate arsine and stibine, hydride generation coupled with atomic-absorption spectrometry (HGAAS) has been widely used for the determination of trace elements in Groups IV, V and VI of the Periodic Table, such as Ge, Sn, Pb, As, Sb, Bi, Se and Te.^{2–6} In 1982 Busheina and Headridge⁷ extended the method to other elements and found that indium could be determined by atomic-absorption spectrometry with hydride generation from aqueous solution. These authors found that not all of the indium(III) is converted into its hydride, a black precipitate (presumed to be metallic indium) being produced on addition of sodium borohydride. The method of determination had poor sensitivity and its characteristic mass was 0.3 μg. We have repeated these experiments and found that the black precipitate produced is probably not metallic indium but a complex of indium hydride, because on addition of water it decomposes with the evolution of a gas which gives absorption signals for indium. Thallium hydride can also be generated by addition of sodium borohydride solution, but the sensitivity of the hydride-generation AAS method is very low (characteristic mass 2.9 μg). However, when other hydride-forming elements such as As, Pb, Te and In are also present, they facilitate thallium hydride formation and the characteristic mass is lowered to 0.12 μg.

EXPERIMENTAL

Apparatus

The hydride generator and quartz tube atomizer have been described previously;⁸ instrumental parameters are summarized below.

Reagents

Standard indium solution. Dissolve 0.1000 g of indium metal (99.99% pure) in the minimum volume of 6M hydrochloric acid, add 2 drops of 30% hydrogen peroxide with gentle heating, and dilute to 100 ml with 1M hydrochloric acid.

Standard thallium solution. Dissolve sufficient pure thallium acetate in 100 ml of demineralized water to give a solution containing 1 mg of Tl per ml.

Sodium borohydride solution. Use 1% solution for indium and a 1% solution containing 0.15% of sodium hydroxide for thallium.

Procedure

Indium. Pipette the sample solution (100 μl) into the reaction vessel and place this in a hot water-bath (60 ± 5°). Attach the reaction vessel to the apparatus and purge with argon for 1 min at a flow-rate of 0.87 l./min. Inject 1 ml of 1% sodium borohydride solution (a black turbidity is produced). Record the absorbance at an atomization temperature of 1080 ± 20°. As soon as the recorder pen returns to the base-line inject 1–1.5 ml of water. Repeat until no further signals are observed. Calculate the total absorbance from a summation of the peak heights (Fig. 1).

Thallium. Pipette 200 μl of standard thallium solution into the hydride generator and place this in an ice-bath. Attach the generator to the apparatus and purge with argon for 1 min at a flow-rate of 0.44 l./min. Inject 2 ml of sodium borohydride solution. Record the absorption signal at an atomization temperature of 980 ± 20°.

RESULTS AND DISCUSSION

Indium

The rate of formation of indium hydride is rather

*Author for correspondence.

Instrumental parameters

Element	AA spectrometer	Wavelength, nm	Band-width, nm	Purge gas
In	Peking Geological Instrument Factory GGX-1	303.9	0.2	argon
Tl	Perkin-Elmer 403	276.8	0.7	argon

Table 1. Effect of HCl concentration on peak absorbance of indium (20 μg)

HCl concentration, M	0.5	1.0	2.0	5.0
Absorbance for 1st signal	0.304	0.230	0.130	0.036
Total absorbance	0.414	0.410	0.383	0.036

Table 2. Influence of lead, arsenic, tellurium and indium on the absorbance of thallium (50 μg)

Species added	—	In ³⁺	Pb ²⁺	As ³⁺	Te ⁴⁺
Absorbance	0.166	0.252	0.353	0.344	0.611

Table 3. Effect of tellurium on thallium hydride formation

Te added, μg	0	1	2	5	25	50
Absorbance due to Tl						
Tl 5 μg	0.018	0.134	0.197	0.145	0.094	0.055
Tl 50 μg	0.166	—	—	0.658	0.490	0.340

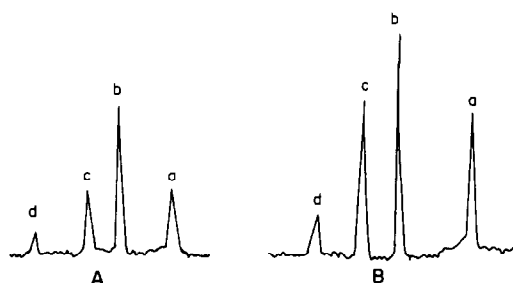


Fig. 1. Recorder traces obtained with A, 4 μg , B, 8 μg of indium in 100 μl of 1M HCl. a, absorption signal after injection of NaBH₄ solution. b, c, d, absorption signals after injection of water.

low and temperature has a great influence on it. At $60 \pm 5^\circ$ the absorbance is about twice that at room temperature. The acid concentration influences not only the production of indium hydride but also its complex formation. When the acid concentration is high (5M) no black precipitate is formed after injection of sodium borohydride solution, and no further signal is produced after injection of water (Table 1). The total absorbance is constant when the acid concentration is in the range 0.5–2.0M, but the first absorption signal increases with decrease in acidity. A concentration of 1M hydrochloric acid was selected. If the sample volume is increased, the absorbance is decreased (100 μl , $A = 0.470$; 200 μl , $A = 0.350$; 300 μl , $A = 0.040$); the optimum volume is 100 μl , as found by Busheina and Headridge.⁷ Attempts were made to use a freezing-out technique (liquid-nitrogen cold trap and helium as purge gas) to collect all the indium hydride and obtain a single absorption signal. The experiment failed because the indium hydride was very unstable. The weight of indium giving 1% absorption is 0.13 μg . The reproducibility (RSD) of the method, based on 10 determinations, is 8.5% (6 μg of indium).

Thallium

There are no previous reports dealing with the

hydride-generation AAS determination of thallium. The present work shows that thallium hydride can be generated in hydrochloric acid or nitric acid (1–1.5M). The optimum volume range is 100–400 μl . Thallium hydride is very unstable and the absorbance obtained on generation at 0° was twice that obtained at room temperature.

Addition of elements which readily form hydrides, such as arsenic and tellurium, produced enhancement effects (Table 2).

It can be seen that tellurium has the greatest effect. Addition of 2 μg of tellurium increased the absorbance due to 5 μg of thallium by a factor of more than 10 (Table 3). The quantity of tellurium to be added depends on the amount of thallium to be determined. If an excessive amount of tellurium(IV) is added, a large quantity of elemental tellurium is produced during the reduction reaction, and the absorbance due to thallium drops.

From these results it is suggested that the addition of hydride-forming elements accelerating the formation of thallium hydride causes the production of complex hydrides. The problems involved in the determination of indium and thallium by hydride-generation AAS in the presence of foreign ions due to the formation of such complex hydrides require further investigation.

REFERENCES

1. R. S. Braman, L. L. Justen and C. C. Foreback, *Anal. Chem.*, 1972, **44**, 2195.
2. K. C. Thompson and D. R. Thomerson, *Analyst*, 1974, **99**, 595.
3. P. N. Vijan and G. R. Wood, *ibid.*, 1976, **101**, 966.
4. D. D. Siemer and P. Koteel, *Anal. Chem.*, 1977, **49**, 1096.
5. R. G. Godden and D. R. Thomerson, *Analyst*, 1980, **105**, 1137.
6. M. O. Andreae and P. N. Froelich, Jr., *Anal. Chem.*, 1981, **53**, 287.
7. I. S. Busheina and J. B. Headridge, *Talanta*, 1982, **29**, 519.
8. An-mo Li and Du Yan, *At. Spectrosc.*, 1981, **1**, 13.

ELECTRO-DEPOSITION OF Cu AND Ag FROM SOLUTIONS OF PPM CONCENTRATION, FOLLOWED BY INDUCTIVELY-COUPLED PLASMA SPECTROMETRY

ROMAN E. SIODA*

Department of Chemistry, The University of Georgia, Athens, GA 30602, U.S.A.

(Received 27 April 1983. Revised 19 August 1983. Accepted 5 September 1983)

Summary—An examination has been made of the kinetics of electro-deposition of copper and silver from acid solution, with special reference to the rate of chemical dissolution of the deposited metal.

Inductively-coupled plasma atomic-emission spectrometry (ICP-AES) is the most sensitive analytical technique for simultaneous determination of several metals in solution at $\mu\text{g/ml}$ and ng/ml concentrations.^{1,2} It also has the advantage that it is very specific, and to a high degree free from interferences. It therefore seems ideal for studies of the mechanism and rates of electro-deposition of metals from such solutions. No such study has been made so far.

Electro-deposition of metals has been studied extensively in the past.³ Two main ranges of metal ion concentration have been used in these studies: (1) millimolar or higher, and (2) below micromolar. In the first case, the amount of deposit and hence the rate of electro-deposition could be determined gravimetrically. In the second case, radiotracers were generally used.⁴ The intermediate concentration range, between micromolar and millimolar, has been studied least. The modern instrumental methods of analysis such as atomic-absorption spectrometry, fluorescence spectrometry, neutron-activation, and especially ICP-AES now make it feasible to study this range, but such investigations are still rare, and the understanding of the kinetic laws of electro-deposition is still based on the early studies using gravimetric or radiotracer analytical techniques.

The aim of the work described in this paper was to use ICP-AES to study the kinetics of the simultaneous electro-deposition of copper and silver from millimolar solutions of their salts.

EXPERIMENTAL

The electro-deposition was conducted on a platinum foil cathode with a surface area of 22 cm^2 . The anode was a straight platinum wire. The electrolysis was done in a covered beaker containing 150 ml of test solution, stirred by a magnetic stirrer. Galvanostatic electrolysis was used, with a current of 0.4 A from a rectifier. The applied voltage was

10–15 V. The compositions of the test solutions are presented in Table 1. Four of the solutions contained sodium sulphate (0.1M) as supporting electrolyte. All reagents used were of analytical purity (Baker Analyzed). At the start of the electrolysis the solution was at room temperature (25°), and during the electrolysis the temperature of the solution increased to 36–38°.

The solutions were analysed with an Applied Research Laboratories ICP-QA 137 ICP spectrometer, as previously described.⁵⁻⁷

RESULTS

As shown in Table 1 the first two experiments were conducted with solutions containing several heavy-metal salts; in the next three experiments only copper and silver salts were present besides the supporting electrolyte. Figures 1 and 2 present the kinetics of the copper and silver electro-deposition. Analysis of the plots shows the kinetics to be first-order or more complex, depending on the composition of the solutions. The highest rate of deposition of copper observed was from a solution containing sulphuric acid (Tables 1 and 2, experiment 4). The presence of nitric acid visibly slows down the rate of electro-deposition (experiment 5) of both copper and silver, but in this experiment copper was deposited slower at the beginning and towards the end of the electrolysis (Fig. 1). The mid increase in the rate of electro-deposition is most probably due to the increase of pH during the electrolysis, from reduction of the nitric acid to ammonia. After 4.5 hr of electrolysis the pH in experiment 5 had increased to 9.6 from the initial value of 2.2, and the solution contained ammonia.

Experiment 6 was different from the others in that the solution did not initially contain heavy metal cations, and a copper foil with surface area 12.5 cm^2 was used as the cathode. After 5 hr of electrolysis at a current of 0.4 A (solution composition as for experiment 5, but without added AgNO_3 and CuSO_4)

*Present address: Institute of Industrial Chemistry, ul. Rydygiera 8, Warsaw, 01-793 Poland.

Table 1. The solutions electrolysed

Experiment	Initial solution composition
1	0.36M NaNO ₃ ; 6.3mM Cd(NO ₃) ₂ ; 9.3mM Co(NO ₃) ₂ ; 7.2mM Cr(NO ₃) ₃ ; 6.4mM Cu(NO ₃) ₂ ; 5.2mM Fe(NO ₃) ₃ ; 11.7mM Pb(NO ₃) ₂ ; 17.9mM Zn(NO ₃) ₂ ; solution acidified to pH = 2.2 with nitric acid.
2	2.0mM AgNO ₃ ; 1.8mM Hg(NO ₃) ₂ ; 5.0mM Mn(NO ₃) ₂ ; 1.8mM Ni(NO ₃) ₂ ; solution acidified to pH = 1.4 with nitric acid.
3	0.10M Na ₂ SO ₄ ; 0.25mM AgNO ₃ ; 0.93mM CuSO ₄ .
4	0.10M Na ₂ SO ₄ ; 0.27mM AgNO ₃ ; 1.00mM CuSO ₄ ; solution acidified to pH = 2.0 with sulphuric acid.
5	0.10M Na ₂ SO ₄ ; 0.27mM AgNO ₃ ; 1.00mM CuSO ₄ ; solution acidified to pH = 2.2 with nitric acid.
6	0.10M Na ₂ SO ₄ ; solution acidified to pH = 3.2 with nitric acid; electrode pure copper foil.

copper was detected in the solution at a concentration of 1.75 μ M (110 ng/ml), well above the limit of detection (40 ng/ml) for copper, with the Babington-type nebulizer used.

The rate of chemical dissolution of copper foil was also directly measured, under the conditions of experiment 6 but without an applied external potential, by determining the decrease in weight of the copper foil with time. The values of the rate obtained from two such determinations (for times of 60 and 90 min) were 0.8×10^{-9} and 1.4×10^{-9} mole. cm⁻². sec⁻¹.

DISCUSSION

Anderson and Sioda recently discussed the mechanism of electro-deposition from solutions of low

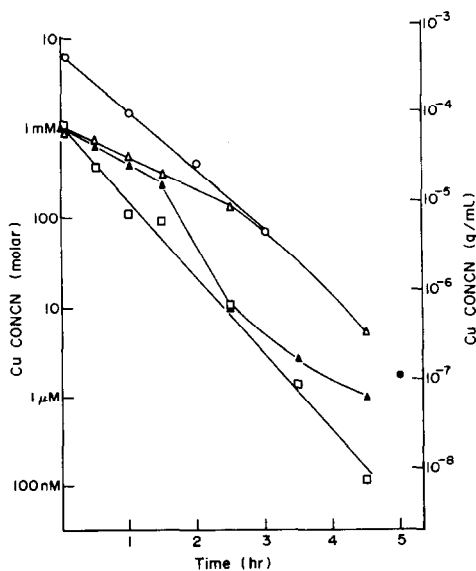


Fig. 1. Semilogarithmic plot of concentration vs. time for copper electro-deposition. The initial compositions of the solutions are shown in Table 1, and the symbols for experiments are: \circ —1; \triangle —3; \square —4; \blacktriangle —5; \bullet —6.

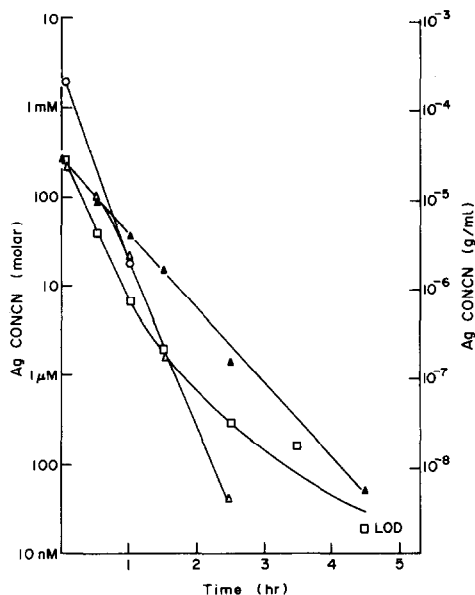


Fig. 2. Semilogarithmic plot of concentration vs. time for silver electro-deposition. The initial compositions of the solutions are shown in Table 1, and the symbols for experiments are: \circ —2; \triangle —3; \square —4; \blacktriangle —5. The lowest concentration point corresponds to the limit of detection (LOD).

concentrations of heavy metal cations.⁸ By use of the hypothesis of Joliot,⁹ the rate equation of the electro-deposition was shown to result from two simultaneous processes of deposition and dissolution. When these two rates become equal an equilibrium concentration of the metal cation in solution is reached. Some of the present results seem to indicate approach to such equilibrium concentrations, namely those from experiment 5 for copper, and experiment 4 for silver. The result of experiment 6 for copper confirms this mechanism, since despite the cathodic current protection of the copper cathode, some of the copper foil dissolved during the electrolysis. The measured concentration of copper in solution after 5 hr of electrolysis may be close to an equilibrium concentration.

Table 2. The measured rate constants of electro-deposition of copper and silver*

Experiment	Rate constants†, 10 ⁻³ cm/sec	
	Copper	Silver
1	2.62 ± 0.14	—
2	—	8.3
3	1.50 ± 0.09	7.71 ± 0.70
4	3.68 ± 0.16	6.88 ± 0.14
5	1.70 ± 0.05	3.34 ± 0.09

*The first-order rate constants are calculated from the slopes of the straight-line segments of the curves in Figs. 1 and 2, obtained by the least-squares method. The slopes corresponding to the semilogarithmic plots have been divided by 3600 sec/hr and the electrode surface area (cm²) and multiplied by the solution volume (ml) and ln 10 (= 2.303).

†Mean and standard deviation.

An equation was recently derived for the equilibrium concentration of metal ion in solution after prolonged electrolysis, when an excess of deposit is present on the electrode surface.¹⁰ Such a case is exemplified by an electrode composed of the metal which is being deposited. The equilibrium concentration, c_{∞} , according to the hypothetical model, is

$$c_{\infty} = k_2/k_1 \quad (1)$$

where k_1 is the rate constant of deposition (in cm/sec), and k_2 is the rate of dissolution (in mole.cm⁻².sec⁻¹). Substituting into equation (1) the measured values of the equilibrium copper concentration (1.75 μM from experiment 6) and the rate constant of deposition, (1.7 × 10⁻³ cm/sec from experiment 5) gives the rate of copper dissolution as 3.0 × 10⁻⁹ mole.cm⁻².sec⁻¹ for the conditions used, including the presence of nitric acid.

The similarity of the values found for k_2 from equation (1), 3.0 × 10⁻⁹ mole.cm⁻².sec⁻¹, and by direct measurement of the dissolution rate, 1.1 × 10⁻⁹ mole.cm⁻².sec⁻¹, may be considered to support the mathematical model leading to equation (1).

The numerical discrepancy between the two values may result, to some extent, from the exclusion of the roughness factor of the deposit in the calculation of k_1 from the measurements in the deposition experiments. The deposits formed were microcrystalline and fluffy, and their true areas probably much higher than the geometrical area of the electrode. As k_1 calculated from the measurements is inversely proportional to the electrode surface area, any increase

in the true electrode surface area caused by the roughness of the deposit should decrease k_1 and, according to equation (1), also decrease the calculated k_2 . Thus, the two separately measured values of the dissolution rate may actually be closer.

It is believed that similar studies to these will be helpful in elucidation of the mechanism and kinetics of electro-deposition of metals from solutions of low concentrations. Such investigations are of special value for the application of electro-deposition as a preconcentration and separation technique for trace and ultratrace analysis.

Acknowledgements—The author is grateful to Charles H. Anderson and Terrance L. Floyd from the U.S. EPA Environmental Research Laboratory in Athens, Georgia, for the ICP-AES analytical determinations.

REFERENCES

1. V. A. Fassel and R. N. Kniseley, *Anal. Chem.*, 1974, **46**, 1110A.
2. R. M. Barnes, *TrAC*, 1981, **1**, 51.
3. N. Tanaka, in *Treatise on Analytical Chemistry*, Part I, Vol. 4, I. M. Kolthoff and P. J. Elving (eds.), pp. 2417ff. Interscience, New York, 1963.
4. M. Haissinsky, *Nuclear Chemistry and Its Applications*, Chapter 20. Addison-Wesley, New York, 1964.
5. C. E. Taylor and T. L. Floyd, *Appl. Spectrosc.*, 1980, **34**, 472.
6. *Idem*, *ibid.*, 1981, **35**, 408.
7. G. R. Henderson and T. L. Floyd, *ibid.*, submitted for publication.
8. J. L. Anderson and R. E. Sioda, *Talanta*, 1983, **30**, 627.
9. F. Joliot, *J. Chim. Phys.*, 1930, **27**, 119.
10. R. E. Sioda, *Anal. Lett.*, 1983, **16**, 739.

DETERMINATION OF HEROIN BY MEANS OF THE PITCH OF INDUCED CHOLESTERIC MESOPHASES

GIOVANNA BERTOCCHI

Istituto di Chimica Farmaceutica e Tossicologica, Facoltà di Farmacia, Università di Bologna, Italy

GIOVANNI GOTTARELLI

Istituto di Scienze Chimiche, Facoltà di Farmacia, Università di Bologna, Italy

ROMANO PRATI

Istituto di Chimica Organica, Facoltà di Chimica Industriale, Università di Bologna, Italy

(Received 12 May 1983. Revised 29 June 1983. Accepted 24 August 1983)

Summary—A method is described for the determination of chromatographic fractions of heroin and strychnine in the μg and sub- μg range by measurement of the pitch and handedness of their induced cholesteric mesophases in MBBA and Phase IV, respectively.

When a chiral "guest" substance is dissolved in a nematic liquid crystal, its molecular chirality is transferred to the bulk of the solvent, which becomes organized into a macrostructural cholesteric helix.¹⁻³ A cholesteric structure is characterized by its handedness and pitch.

Equal amounts of enantiomeric "guests" of equal optical purity induce helical structures with identical pitch and opposite handedness.² Different substances show different abilities to twist a nematic phase. The twisting power of a chiral dopant (β_M) can be defined as^{4,5}

$$\beta_M = 1/pcr$$

where p is the pitch (μm), c is the mole fraction and r the enantiomeric purity of the dopant. For very dilute solutions the concentration can be expressed as the mass ratio of solute to solvent. The parameter β (μm^{-1}), together with the sign + or - for the P-helix or M-helix, characterizes the chiral solute in a similar way to the specific optical rotation. However, the physical origin of the two quantities is entirely different; optical rotation depends on the interaction of light with molecules, while the twisting power originates from interactions between molecules of solute and solvent.⁶ In principle, the quantity β can give information in the same area as that given by the optical rotation, but of different quality owing to the difference in its origin. In particular, the passage from molecular to macrostructural chirality amplifies the molecular dissymmetry. This can be used to characterize molecules with very low optical rotation, such as compounds made chiral by isotopic substitution,⁷ and to detect small amounts of chiral organic substances.⁸

In the present communication, we report deter-

mination of heroin and strychnine from the pitch of induced cholesteric mesophases.

EXPERIMENTAL

The pitch was determined by means of the Grandjean-Cano method, based on the observation of the discontinuity lines appearing when a cholesteric liquid crystal is inserted into a cell of variable thickness.⁹⁻¹¹ A drop of the cholesteric solution (ca. 2.5 mg) was placed between a planoconvex lens and a glass plate, both rubbed previously with tissue paper, the rubbing direction of the lens and plate being kept parallel.¹¹ The preparation was observed with a polarizing microscope and showed both the Grandjean-Cano disclinations (concentric circles, Fig. 1) and the coloured rings which are connected with the variation of the rotatory power with sample thickness.^{12,13} The separation of disclination lines gives the pitch value¹¹ p as

$$\frac{r^2}{R} = (n - \frac{1}{2}) |p| \quad (n = 1, 2, 3)$$

where R is the radius of curvature of the lens and r is the radius of the Grandjean-Cano circles.

Rotation of the analyser displaces the coloured rings, owing to the rotatory power. In particular, if a clockwise rotation of the analyser displaces the circles towards increasing thickness of the sample, the rotatory power is right-handed, and so is the cholesteric helix (if the wavelength of the light used is shorter than the wavelength of the selective reflection band).¹³

The measurements were done with a Zeiss polarizing microscope and "Galileo" planoconvex lenses of radii from 20 to 40 mm.

In order to obtain the disclinations more easily, both the lens and the glass plate were treated with *N*-methylaminopropyl-triethoxysilane (MAP, Dow-Corning).¹⁴ Pitch measurements were made at 18-20°. Temperature effects on the pitch values were negligible.

The liquid crystals used as solvent were MBBA (*p*-methoxybenzylidene-*p'*-*n*-butylaniline) from Riedel de Haen, and PCH [mixture of *trans*-4-alkyl (4-cyanophenyl) cyclohexanes] (nematic phase 1083) and Phase IV (mixture



Fig. 1. Grandjean-Cano disclinations in a sample of heroin dissolved in MBBA.

of azoxy compounds) from Merck. The solutions used for calibration were obtained from a standard solution of GLC-purity heroin in chloroform. Before addition of the liquid crystal, the sample was completely freed from chloroform. Once the liquid crystal was added, the solution was mechanically shaken and heated several times, to above the clearing point. A similar procedure was used for strychnine.

GLC measurements were made on a Varian Aerograph 1400, with SP 2100 glass columns and a flame-ionization detector.

TLC separation of illicit heroin was done on a silica gel plate (5×20 cm) with chloroform-methanol (9:1 v/v) as eluent. The spot corresponding to heroin was extracted with anhydrous chloroform and the solution evaporated to dryness; MBBA was then added and the resulting cholesteric mesophase measured directly.

RESULTS AND DISCUSSION

The twisting power of heroin is positive in both the liquid crystals studied, MBBA and PCH, and the average value of β in MBBA is $+22.0 \pm 0.5 \mu\text{m}^{-1}$.

Plots of $1/p$ as a function of the concentration of the dopant are given in Fig. 2. The concentration was expressed in mg of heroin/5 mg of solvent, as 5 mg of cholesteric mesophase are more than sufficient for two determinations. In MBBA the plot is linear over the concentration range from 1.4×10^{-2} down to 7.75×10^{-4} mg/5 mg, the latter value representing the lowest concentration at which reproducible values

of the pitch were obtained. At concentrations higher than 1.4×10^{-2} mg/5 mg the value of β decreases, probably because of the limited solubility of heroin. In PCH the plot is linear between 4.0×10^{-2} and 9.4×10^{-3} mg/5 mg the significance of these values being the same as for MBBA.

The calibration curve obtained for strychnine in Phase IV is also linear from 2.5×10^{-2} down to

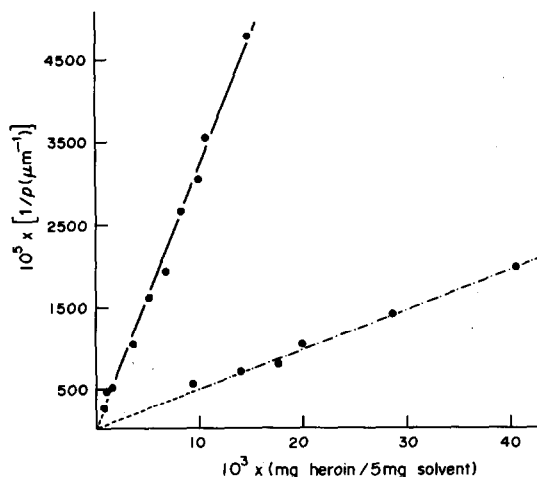


Fig. 2. Plots of inverse of the pitch ($1/p$) vs. concentration of heroin in MBBA (—) and PCH (---).

3×10^{-3} mg/5 mg; the twisting power is $+ 8.0 \pm 0.3 \mu\text{m}^{-1}$.

In MBBA the minimum amount of heroin detectable is $0.38 \mu\text{g}$, *i.e.*, at the level of gas chromatographic determination, and the + sign of the cholesteric mesophase represents a further identification factor.

The technique was checked on a sample of illicit heroin after a TLC analytical separation, the quantity of heroin being determined by the liquid crystal technique. The purity obtained was in good agreement with that determined by GLC.

The general method reported earlier⁸ is based on the determination of the pitch of induced cholesteric mesophases by an infrared optical rotatory dispersion technique. The present method offers the advantage of variable path-length, so that a wide range of pitch is accommodated, and requires only an inexpensive commercial microscope available in all laboratories. Coupled with standard analytical TLC it could be of practical use when more sophisticated and expensive procedures are not available.

Acknowledgements—We thank the Ministero della Pubblica Istruzione for financial support, Professors B. F. Bonini, G.

Maccagnani and A. M. Marinangeli for discussion, and Mr. A. Benassi for technical assistance.

REFERENCES

1. G. Friedel, *Ann. Phys. (Paris)*, 1922, **18**, 273.
2. H. Stegemeyer and K. J. Mainush, *Naturwiss.*, 1971, **58**, 599.
3. G. Gottarelli, P. Mariani, G. P. Spada, B. Samori, A. Forni, G. Solladié and M. Hilbert, *Tetrahedron*, 1983, **39**, 1337.
4. E. H. Korte, B. Schrader and S. Bualek, *J. Chem. Res., (Synop.)*, 1978, 236.
5. J. M. Ruxer, G. Solladié and S. Candau, *Mol. Cryst. Liq. Cryst. (Letters)*, 1978, **41**, 109.
6. G. Gottarelli, B. Samori, C. Stremmenos and G. Torre, *Tetrahedron*, 1981, **37**, 395.
7. G. Gottarelli, B. Samori, C. Fuganti and C. Grasselli, *J. Am. Chem. Soc.*, 1981, **103**, 471.
8. E. H. Korte, *Appl. Spectrosc.*, 1978, **32**, 568.
9. F. Grandjean, *Compt. Rend.*, 1921, 172.
10. R. Cano, *Bull. Soc. Fr. Mineral. Cristallog.*, 1968, **91**, 20.
11. G. Heppke and F. Oestreicher, *Z. Naturforsch.*, 1977, **32a**, 899.
12. J. P. Berthault, J. Billard and J. Jacques, *Compt. Rend.*, 1977, **284C**, 155.
13. J. P. Berthault, *Thèse de Doctorat*, Paris, 1977.
14. F. J. Kahn, *Appl. Phys. Lett.*, 1973, **22**, 8.

INDIRECT DETERMINATION OF CYANIDE IN WATER BY ATOMIC-ABSORPTION SPECTROPHOTOMETRY

XU BO-XING, XU TONG-MING and FANG YU-ZHI

Department of Chemistry, East China Normal University, 3663 Chung Shan Road (N.), Shanghai,
People's Republic of China

(Received 21 February 1983. Revised 1 July 1983. Accepted 23 August 1983)

Summary—An indirect method for determination of trace cyanide in water by atomic-absorption spectrophotometry is described. Cyanide forms a stable complex anion with Pd in alkaline solution. This complex anion can form an ion-association complex with tetra-alkylammonium ions which can be extracted into n-butyl alcohol with an efficiency higher than 90%. The extract can be analysed directly for palladium (and hence indirectly for cyanide) by flame atomic-absorption spectrophotometry. The detection limit for cyanide by this method is 0.1 $\mu\text{g/ml}$ in the n-butyl alcohol extract. Beer's law is obeyed for 0.13–9 μg of CN^- per ml of n-butyl alcohol. Several foreign ions do not interfere.

The determination of cyanide in water is important in monitoring water quality. The methods usually used for determination of trace cyanide in water include colorimetry,¹⁻⁶ potentiometry with ion-selective electrodes,^{7,8} etc. The standard method is colorimetry, but it involves pre-separation and use of a carcinogenic reagent (benzidine).

Considerable effort has been devoted to development of rapid and simple methods for determination of cyanide in water. Indirect determination of cyanide in water by atomic-absorption spectrophotometry (AAS) was developed several years ago.^{9,10} Danchik proposed two methods, one involving formation and extraction of the cyanide ion-association complex with tris(1,10-phenanthroline) iron(II) and the other the formation and removal of a precipitate of silver cyanide. In the first method iron is determined in the extract, and in the second the excess of silver is measured.

In this paper a rapid and simple AAS method for determination of cyanide in water is proposed, based on the following principle. In alkaline solution, cyanide and palladium form a stable tetracyano-palladate(II) complex with *m*-phenoxyphenylmethyltriethylammonium ions, extractable into n-butyl alcohol. n-Butyl alcohol has a low background absorbance in an air-acetylene flame, so palladium in the extract can be determined directly and accurately by flame AAS. The amount of Pd is related to the concentration of cyanide in the water sample. Various foreign ions do not interfere.

The method is highly sensitive and convenient, and can be used for routine determination of cyanide in water.

EXPERIMENTAL

Reagents

Palladium chloride stock solution (Pd 1 mg/ml). Prepared

by dissolving palladium chloride in concentrated hydrochloric acid, almost neutralizing with sodium hydroxide and diluting to the requisite volume. Dilute 100-fold with demineralized water to give a 10 $\mu\text{g/ml}$ working palladium solution.

Stock cyanide solution (100 $\mu\text{g/ml}$). Dissolve 0.125 g of potassium cyanide in water and dilute to volume in a 500-ml standard flask. Dilute 1 ml of this stock solution and 2 drops of 1M sodium hydroxide to volume in a 100-ml standard flask with demineralized water to obtain the working standard (1 $\mu\text{g/ml}$).

Buffer solution. Adjust 500 ml of 1M ammonium chloride with concentrated ammonia solution to pH 9.5 (pH-meter control).

General procedure

To a 60-ml separatory funnel add the following solutions in the order given: 1 ml of 10- $\mu\text{g/ml}$ Pd²⁺ solution, 3 ml of water sample containing <9 μg of cyanide (for the blank solution used 3 ml of demineralized water), 1 ml of pH-9.5 ammonia-ammonium chloride buffer, 0.1 ml of 40% aqueous solution of *m*-phenoxyphenylmethyltriethylammonium chloride and 1 ml of n-butyl alcohol. The total volume of the aqueous solution is about 5 ml. Shake the funnel for 1 min, then let it stand for several minutes. Separate the water phase and aspirate the organic phase into the air-acetylene flame, under the following conditions:

Wavelength:	2476 Å
Pd lamp current:	15 mA
Band-pass:	3.3 Å
Air:	6.5 l./min
Acetylene:	1.2 l./min

RESULTS AND DISCUSSION

Composition of the complex anion

It is known that in alkaline solution the complex anions Pd(CN)₄²⁻ and Pd₂(CN)₆²⁻ may be formed.¹¹ To find the molar ratio of CN⁻ to Pd²⁺ in the complex formed under the experimental conditions, the general procedure was applied to a series of solutions with fixed cyanide concentration and in-

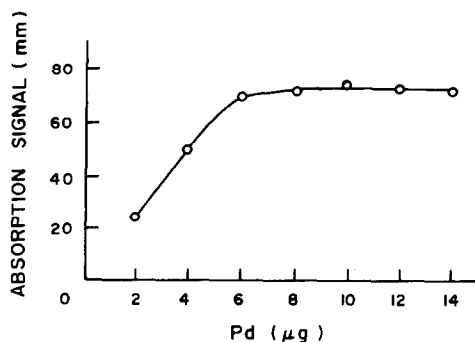


Fig. 1. Mole ratio between CN^- and Pd^{2+} in the CN-Pd complex ($5.0 \mu\text{g}$ of CN^- taken).

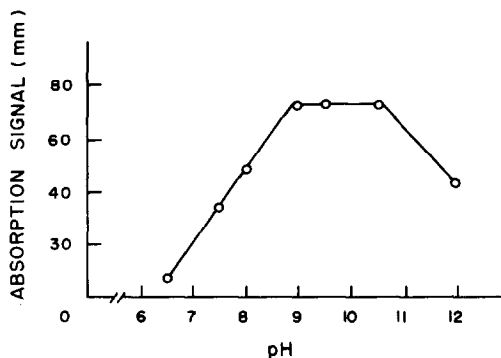


Fig. 2. Effect of pH.

creasing palladium concentration. Figure 1 shows that the mole ratio was nearly 3.8, in reasonable agreement with the expected value of 4. Therefore the species extracted is presumably:



Effect of pH

The pH of the solution strongly affects the formation and extraction of the ion-association complex. Figure 2 shows that the degree of extraction is constant and maximal over the pH range 9.0–10.5.

Effect of amount of counter-ion

Increasing the concentration of *m*-phenoxyphenylmethyltriethylammonium chloride in the aqueous phase increases the absorbance of both the sample and the blank solution, but the net absorbance of the sample remains constant when the volume of 40% counter-ion reagent solution added is 0.06–0.20 ml, so a volume of 0.1 ml is recommended (Fig. 3).

Calibration graph, detection limit and precision

The calibration graph was linear from 0.13 to 9 μg of cyanide per ml of organic phase, and the detection

limit 0.10 μg of cyanide in the organic phase. The relative standard deviation for 10 determinations of 2.5 μg of cyanide was 2%.

Recovery and efficiency of extraction

Apparent recoveries of 90–110% were obtained for the determination of cyanide in five water samples spiked with 3 and 5 μg of cyanide (Table 1). Four analyses of a solution of known cyanide concentration indicated that the extraction efficiency was >90%.

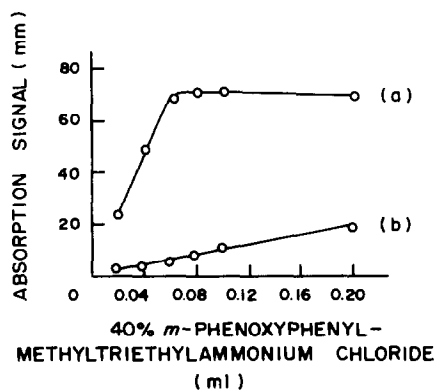


Fig. 3. Effect of amount of counter-ion reagent. (a) Standard solution; (b) blank solution.

Table 1. Recovery of cyanide (5 determinations)

Sample	Sample CN^- taken, ml	CN^- added, μg	CN^- found, μg	Recovery, %
Industrial waste water (1)	3	0	0.43	
		1.5	1.80	91
		3.0	3.25	94
Industrial waste water (2)	1	0	9.20	
		3.0	12.5	110
		5.0	14.0	96
Industrial waste water (3)	0.5	0	0.31	
		5.0	4.80	90
		10.0	9.90	96
Huang Pu river water	3	0	0.33	
		3.0	3.45	104
		5.0	5.84	110
Laboratory waste water	3	0	0.69	
		3.0	3.90	107
		5.0	5.85	103

Table 2. Effect of foreign ions on determination of 2.5 μg of cyanide

Foreign ion	Added, μg	CN ⁻ found, μg	Error, %
Ca ²⁺	100	2.60	+4
Mg ²⁺	100	2.53	+1
Al ³⁺	50	2.53	+1
Zn ²⁺	100	2.41	-4
Cd ²⁺	100	2.59	+4
Mn ²⁺	100	2.50	—
Cu ²⁺	10*	2.56	+2
Cu ²⁺	5	2.45	-2
Cr ³⁺	50	2.61	+4
Fe ³⁺	50	2.53	+1
Au ³⁺	10	2.60	+4
Pb ²⁺	50	2.04	-18
Pb ²⁺	20	2.53	+1
Hg ²⁺	5	1.71	-32
Hg ²⁺	2.5	2.53	+1
Ag ⁺	5	2.28	-9
Ag ⁺	2.5	2.47	-1
Ni ²⁺	10*	2.46	-2
Ni ²⁺	5	0.65	-74
Ni ²⁺	2.5	2.45	-2
NO ₃ ⁻	500	2.50	—
NO ₂ ⁻	100	2.35	-6
SO ₄ ²⁻	1000	2.50	—
PO ₄ ³⁻	500	2.53	+1
Borate	100	2.45	-2
CO ₃ ²⁻	100	2.43	-3
I ⁻	1000	2.44	-2
Br ⁻	500	2.37	-5
S ²⁻	50	2.53	-1
Oxalate	50	2.51	+1
Acetate	100	2.40	-4
Tartrate	100	2.60	+4
Citrate	100	2.50	—
Ascorbic acid	100	2.40	-4
EDTA	100	2.59	+4
Aniline	100	2.40	-4
Phenol	100	2.50	—
Nitrobenzene	100	2.50	—

*After addition of 100 μg of EDTA.

Effect of foreign ions

The effect of various ions was examined (Table 2).

Table 3. Results for determination of CN⁻ in water

Sample	Found*, $\mu\text{g/ml}$	R.S.D., %
Industrial waste water (before treatment)	0.63	13
Industrial waste water (after treatment)	0.18	17
Huang Pu river water	0.11	19
Laboratory waste water	0.21	17

*Mean of 6 determinations.

The interference of Cu²⁺ and Ni²⁺, which also form cyanide complexes, can be reduced by addition of EDTA.

Determination of cyanide in water samples

Various water samples were analysed by the proposed method. The results are shown in Table 3.

Acknowledgement—We are very grateful to Professor Hu Chao-Sheng for his enthusiastic help in finishing this work.

REFERENCES

1. L. S. Bark and H. G. Higson, *Analyst*, 1963, **88**, 751.
2. W. N. Aldridge, *ibid.*, 1944, **69**, 262.
3. J. Epstein, *Anal. Chem.*, 1947, **19**, 272.
4. E. Asmus and H. Garschagen, *Z. Anal. Chem.*, 1953, **138**, 414.
5. K. Ishii, T. Iwamoto and K. Yamanishi, *Bunseki Kagaku*, 1973, **22**, 448.
6. A. Watanabe, I. Ito and A. Hirakoba, *ibid.*, 1977, **26**, 505.
7. J. Vesely, D. Weiss and K. Štulík, *Analysis With Ion-Selective Electrodes*, Horwood, Chichester, 1978.
8. M. S. Frant, J. W. Ross, Jr. and J. H. Riseman, *Anal. Chem.*, 1972, **44**, 2227.
9. G. F. Kirkbright and H. N. Johnson, *Talanta*, 1973, **20**, 442.
10. R. S. Danchik and D. F. Boltz, *Anal. Chim. Acta*, 1970, **49**, 567.
11. J. C. Bailar, H. J. Emeléus, R. Nyholm and A. F. Trotman-Dickenson, *Comprehensive Inorganic Chemistry*, Vol. 3, p. 1284. Pergamon Press, Oxford, 1973.

DOSAGE DE DERIVES DE L'ACIDE PHENYLPROPIONIQUE A ACTIVITE PHARMACOLOGIQUE PAR TITRAGE COULOMETRIQUE

G. KANOUE, E. NIVAUD,* B. PAULET et P. BOUCLY

Laboratoire de Chimie Analytique et d'Electrochimie Organiques, Centre d'études pharmaceutiques,
Université de Paris-Sud, rue J. B. Clément, 92290 Chatenay-Malabry, France

(Reçu le 8 juillet 1983. Accepté le 10 août 1983)

Résumé—L'électrolyse à intensité constante dans un milieu eau-éthanol permet de générer à la cathode les bases fortes éthylate et hydroxyle. Les dérivés de l'acide phényl-2 propionique se réduisant uniquement par attaque du proton carboxylique peuvent être dosés par coulométrie avec indication potentiométrique ou conductimétrique de la fin d'électrolyse.

En milieu neutre dans l'éthanol, les dérivés de l'acide phényl-2 propionique: Ibuprofène, Naproxène, Pirprofène et Acide protizinique (Tableau 1) sont réductibles à une électrode de mercure ou à une électrode de platine, en une seule étape, monoélectronique.

En milieu basique, l'intensité limite des courants de diffusion diminue proportionnellement à la quantité de base forte ajoutée; elle disparaît lorsqu'un équivalent de base est introduit. La réduction de la fonction carboxylique conduit à la formation de l'anion correspondant avec départ d'un hydrogène radicalaire.¹

Nous proposons dans ce mémoire un dosage par coulométrie à intensité imposée avec détection conductimétrique ou potentiométrique du point équivalent après génération de bases fortes *in situ*, dans un mélange éthanol-eau (4:1 v/v).

catrice et, soit une électrode de verre reliée à un millivoltmètre, soit une cellule conductimétrique reliée à un résistivimètre. Dans le compartiment anodique plonge une électrode de platine auxiliaire.

Un millivoltmètre Metrohm E 516 et une électrode de verre combinée à une électrode au calomel sont utilisés pour la détection potentiométrique.

Un conductimètre Tacussel type CD 7 N et une cellule conductimétrique sont utilisés pour la détection conductimétrique.

Les variations de potentiel ou de conductance sont enregistrées sur un graphisplot Sefram type GRVA 5.

Les mesures sont réalisées sur des quantités voisines de 50 mg dissoutes dans 50 ml de solvant contenant du perchlorate de lithium à la concentration 0,1M. Les solutions sont privées d'oxygène par barbotage d'un courant d'azote pendant 10 min. La quantité d'électricité nécessaire à la transformation totale d'une prise d'essai *p* (mg) de substance, de poids moléculaire *M*, étant égale au produit du temps *t* (sec) par l'intensité *A* (mA), la quantité obtenue (%) est donnée par $100 AtM/96487p$.

PARTIE EXPERIMENTALE

Réactifs

Solvants. L'eau bidistillée, utilisée dans la proportion de 20% v/v, permet d'obtenir la réduction du solvant à des potentiels moins négatifs, éliminant l'éventualité d'une réduction de l'électrolyte support. L'éthanol est distillé sur magnésium selon la méthode de Lund et Bjerrum.² Sa neutralité à la phénolphthaléine est vérifiée.

Electrolyte indifférent. Le perchlorate de lithium pour analyses est purifié par recristallisation dans l'éthanol.

Produits étudiés. Ibuprofène, Naproxène, Pirprofène et Acide protizinique sont desséchés sous vide partiel à 25-30° en présence d'anhydride phosphorique.

Appareillage et conditions opératoires (Fig. 1)

L'électrolyse à intensité imposée de 50 mA, est effectuée à l'aide d'un chronoampérostas Tacussel type CEAMD 6, dans 2 compartiments séparés par un pont d'agar-agar afin d'éviter la réaction des protons due à l'oxydation de l'eau à l'anode. Dans le compartiment cathodique contenant la solution à doser plongent une électrode de platine indi-

Tableau 1

Ibuprofène	
Naproxène	
Pirprofène	
Acide protizinique	

*Auteur pour correspondance.

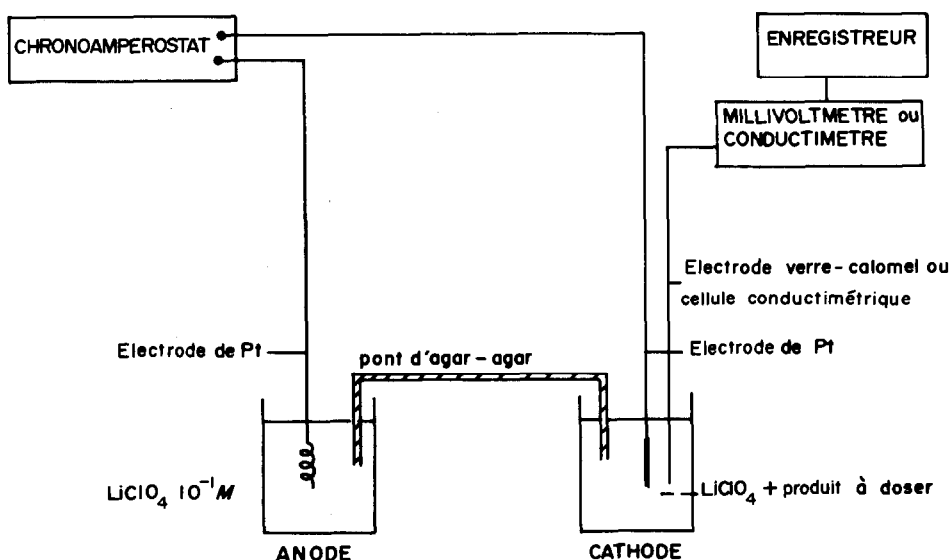


Fig. 1. Schéma de montage.

PRINCIPE

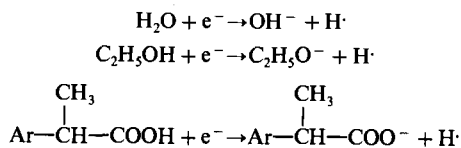
La méthode coulométrique mise en oeuvre consiste à imposer dans un circuit d'électrolyse dont les compartiments anodique et cathodique sont séparés, une intensité maintenue constante à l'aide d'un montage intensitostatique. Lorsque le bilan de toutes les réactions chimiques ou électrochimiques possibles aboutit à la transformation d'un seul composé, il existe selon la loi de Faraday, la relation:

$$Q = mnF/M$$

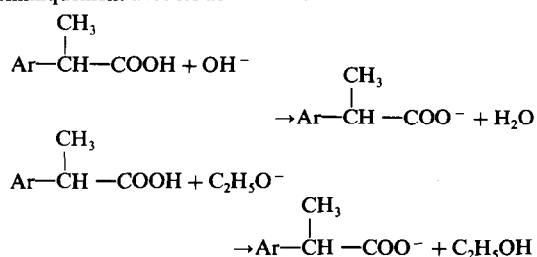
où m = masse d'un produit de poids moléculaire M , n = nombre d'électrons échangés par molécule, F = faraday.

Pour pouvoir utiliser cette relation à des fins analytiques quantitatives il est obligatoire de mesurer avec précision, en fonction du courant imposé, le temps nécessaire pour atteindre le terme de la réaction.

Les différentes réactions électrochimiques susceptibles d'intervenir à une électrode de platine correspondent à la réduction des molécules d'eau, des molécules d'éthanol et des molécules d'acides phénylpropioniques:



La réduction électrochimique des molécules d'eau et d'éthanol aboutit dans ce mélange de solvant à la formation de bases fortes, ions hydroxyle et éthylate, que réagissent chimiquement avec les acides en solution selon les réactions:



Le bilan global réactions chimiques et électrochimiques fait ressortir la consommation d'un faraday par molécule transformée, la totalité du courant étant utilisée à cette fin.

Détection du point équivalent

Deux méthodes sont proposées afin de détecter le temps nécessaire pour atteindre le point équivalent: une méthode conductimétrique et une méthode potentiométrique.

Détection conductimétrique. La technique consiste à mesurer l'impédance de la solution entre deux plaques de platine entre lesquelles est imposé un courant alternatif de fréquence convenablement choisie. Par étalonnage, l'impédance est reliée à la conductance de la solution; la conductance (Λ) est elle-même reliée à la concentration selon la relation:

$$\Lambda = K \sum l_i z_i c_i$$

où K = constante de cellule, l_i = conductivité équivalente de l'ion i en solution, z_i = charge de l'ion i , et c_i = concentration de l'ion i .

Au cours du titrage, avant le point d'équivalence, il y a formation d'ions phénylpropionate, et après le point équivalent formation d'ions hydroxyle et éthylate. La conductivité équivalente limite des ions hydroxyle étant nettement supérieure à celle des autres ions, la pente de la droite $\Lambda = f(t)$ est considérablement modifiée. La courbe représentée (Fig. 2) présente une nette cassure au point équivalent.

Détection potentiométrique. Le point équivalent peut être également détecté en suivant l'évolution du pH de la solution au cours du titrage. Dans le compartiment cathodique de la cellule d'électrolyse la différence de potentiel entre une électrode de verre et une électrode de référence au calomel est mesurée. Avant le point équivalent, le système tampon acide phénylpropionique-phénylpropionate impose le pH, après ce point les bases fortes électrogénérées, éthylate et hydroxyle sont à l'origine d'une brusque variation de pH.

RESULTATS ET DISCUSSION

Pour les quatre dérivés, les résultats présentés (Tableau 2) correspondent à une détection potentiométrique. Afin de déterminer la précision de la

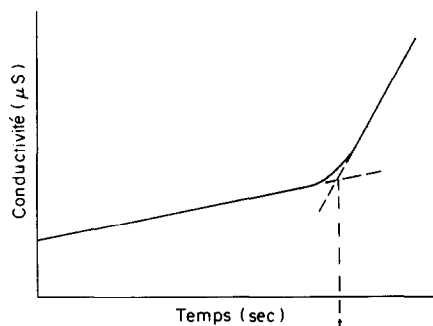


Fig. 2. Courbe conductimétrique de l'Ibuprofène.

méthode nous avons réalisé cinq mesures par échantillon. Les moyennes, les écart-types et la dispersion des résultats expérimentaux sont rassemblés (Tableau 3).

La détection conductimétrique est appliquée à l'Ibuprofène (Tableau 4); la comparaison des moyennes montre que les résultats ne sont pas significativement différents.

La méthode développée ici peut être appliquée à tous les dérivés possédant un hydrogène acide dont la réduction électrochimique conduit uniquement à la forme anionique; elle ne s'applique pas aux dérivés de l'acide phénylpropionique qui, possédant une fonction cétone (Kétoprofène) conduisent à la forme alcool par fixation de deux électrons.³ Ce dernier composé peut être dosé en voltampérométrie classique.⁴

Tableau 2. Résultats obtenus pour le Pirprofène, l'Acide protizinique et le Naproxène, avec une détection potentiométrique

Echantillon	Prise d'essai, mg	Temps, sec	Résultats, %
Pirprofène	94,01	720,6	100,0
	52,48	403,6	100,3
	49,85	381,9	99,9
	71,05	544,4	99,9
	70,56	539,2	99,7
Acide protizinique	62,85	380,3	98,9
	85,90	523,8	99,7
	58,61	357,6	99,7
	62,47	380,6	99,6
	84,65	516,0	99,6
Naproxène	46,60	390,3	99,9
	67,94	569,9	100,1
	42,61	357,6	100,1
	53,73	448,0	99,5
	44,45	372,0	99,2

Tableau 3. Moyenne, écart type et limite de confiance

	Moyenne, %	Ecart type, %	Dispersion, %
Pirprofène*	99,95	0,20	0,30
Acide protizinique*	99,48	0,30	0,41
Naproxène*	99,76	0,37	0,47
Ibuprofène*	99,86	0,187	0,23
Ibuprofène†	99,88	0,365	0,50

*Potentiométrie.

†Conductimétrie.

Tableau 4. Résultats obtenus pour l'Ibuprofène par détection potentiométrique et conductimétrie

Détection	Prise d'essai, mg	Temps, sec	Résultats, %
Potentiométrie	89,50	837,5	100,0
	89,27	833,1	99,7
	91,86	860,9	100,2
	55,86	521,2	99,7
	58,49	545,6	99,7
Conductimétrie	51	474,2	99,4
	51	479,0	100,4
	51	476,6	99,9
	51	478,0	100,2
	51	475,3	99,6

Conclusion

L'électrolyse à intensité constante permet de générer *in situ* le réactif titrant; il en résulte un gain de temps et une reproductibilité qui confèrent à cette méthode des possibilités d'automatisation.

Ces avantages la désignent par conséquent comme une méthode de choix dans le contrôle analytique de certaines matières premières pharmaceutiques. Appliquée aux dérivés de l'acide phénylpropionique ne possédant pas de fonction carbonyle elle donne, quelle que soit la détection, une dispersion des résultats inférieure à 0,5%.

LITTÉRATURE

1. G. Kanoute, *Thèse de Doctorat*, Chatenay-Malabry, 1982.
2. H. Lund et J. Bjerrum, *Ber.*, 1931, **64B**, 210.
3. G. Kanoute, E. Nivaud, P. Boucly et M. Guernet, *Bull. Soc. Chim. France*, sous presse.
4. P. Populaire, B. Terlain, S. Pascal, B. Decouvelaere, G. Lebreton, A. Renard et J. P. Thomas, *Ann. Pharm. Franc.*, 1973, **31**, 679.

Summary—Generation of ethoxide and hydroxide ions in aqueous ethanolic medium by controlled-current electrolysis is suggested for coulometric titration of 2-phenylpropionic acid derivatives. The electroreduction of the carboxylic hydrogen atom leads to the anion by elimination of a hydrogen radical. Potentiometric or conductimetric methods can be used for detection of the end-point.

DETERMINATION BY HPLC OF TRIFLUOROACETATE LEVELS IN PLASMA AND URINE OF PATIENTS ANAESTHETIZED WITH HALOTHANE

M. IMBENOTTE, A. BRICE, F. ERB* and J. M. HAGUENOER

(with the technical assistance of M. C. JACQUEMONT and P. COLEIN)

Laboratoires de Toxicologie, Hydrologie et Hygiène, Faculté de Pharmacie, Rue du Professeur Laguesse,
59045 Lille, France

(Received 11 May 1983. Accepted 3 August 1983)

Summary—A new method is described for determination of trifluoroacetic acid (TFA) in biological fluids. Optimum extraction is achieved by addition of 18-crown-6 ether and acidification of the sample. The 4-bromomethyl-7-methoxycoumarin derivatives of the carboxylic acid are prepared and a sample is subjected to HPLC. A linear analytical curve of peak area against TFA concentrations ranging between 0.2 and 20 $\mu\text{g/ml}$ is obtained, and the minimum detectable concentration is estimated to be 0.1 $\mu\text{g/ml}$.

Halothane (2-bromo-2-chloro-1,1,1-trifluoroethane) is an important volatile anaesthetic currently used at concentrations ranging from 0.5 to 3% v/v. The previous publications on the determination of one of its metabolites, trifluoroacetic acid (TFA), deal with gas chromatographic methods.¹⁻⁴ We attempted direct measurement of TFA levels in biological samples by the head-space method, because of the high volatility of TFA, but without success. The usual methods of derivative formation to lower the volatility, and hence reduce losses, were then applied. The main problem is the high solubility of TFA in aqueous media, which makes its extraction from biological fluids difficult. Most of the derivatives used cannot be made in aqueous media and therefore attempts were made to dehydrate biological samples by lyophilization or drying with sodium sulphate, followed by derivative formation by esterification or reaction with alkylating agents. Methylation with methanol-boron trifluoride mixture and methyl sulphate, followed by esterification with trichloroethanol (TCE) was tried, by analogy with the determination of trichloroacetic acid.⁵ However, even with use of the head-space method, no peak was observed which could be assigned to the ester. Attempts were made to prepare this ester from pure TFA, its anhydride and TCE, but it could not be detected with sufficient sensitivity by gas chromatography. Alkylation with pentafluorobenzyl bromide and tetrabutylammonium hydrogen sulphate in methylene chloride⁶ was also unsuccessful. Gas chromatographic methods were therefore abandoned and it was decided to apply HPLC to the determination of TFA in biological samples.

The purpose of this study was to determine TFA

in the plasma and urine of patients anaesthetized with halothane, by HPLC of the 4-bromomethyl-7-methoxycoumarin derivative.

EXPERIMENTAL

Apparatus

The chromatography system consisted of a Varian model 5000 equipped with a Vari-chrom ultraviolet detector set at 320 nm, and a Varian Fluorichrom fluorescence detector. A 330 I excitation filter and a 3-74 emission filter with a wavelength cut-off at 385 nm were selected because of the fluorescence characteristics of the 4-bromomethyl-7-methoxycoumarin ester of TFA. The column (300 mm \times 6 mm bore) was packed with RP 18 phase (10 μm).

Reagents

The HPLC solvents were Merck methanol and ultrapure water. Fluka 4-bromomethyl-7-methoxycoumarin, "Pestipur" acetone and Merck 18-crown-6 ether were used.

Chromatographic conditions

The mobile phase was a 60:40 v/v mixture of methanol and water, used at a flow-rate of 1 ml/min under isocratic conditions. The solvents were filtered and degassed before use. The temperature was 20° and the pressure 80 bar. The volume injected was 50 μl and the detector sensitivities were set at 0.05 absorbance units for ultraviolet detection and 10 units for fluorescence detection, for full-scale deflection.

RESULTS AND DISCUSSION

The 4-bromomethyl-7-methoxycoumarin ester of TFA was prepared according to the general procedure of Düniges⁷ and its retention time (4.1 min) determined.

In order to extract the maximum amount of trifluoroacetate from the plasma and urine of patients anaesthetized with halothane, 250 μl of a 0.007M solution of 18-crown-6 ether in acetonitrile are added to the sample (0.5 ml). The proteins are precipitated but the trifluoroacetate is expected to remain in solution, as an ion-pair with the crown-ether com-

*Author to whom correspondence is to be addressed

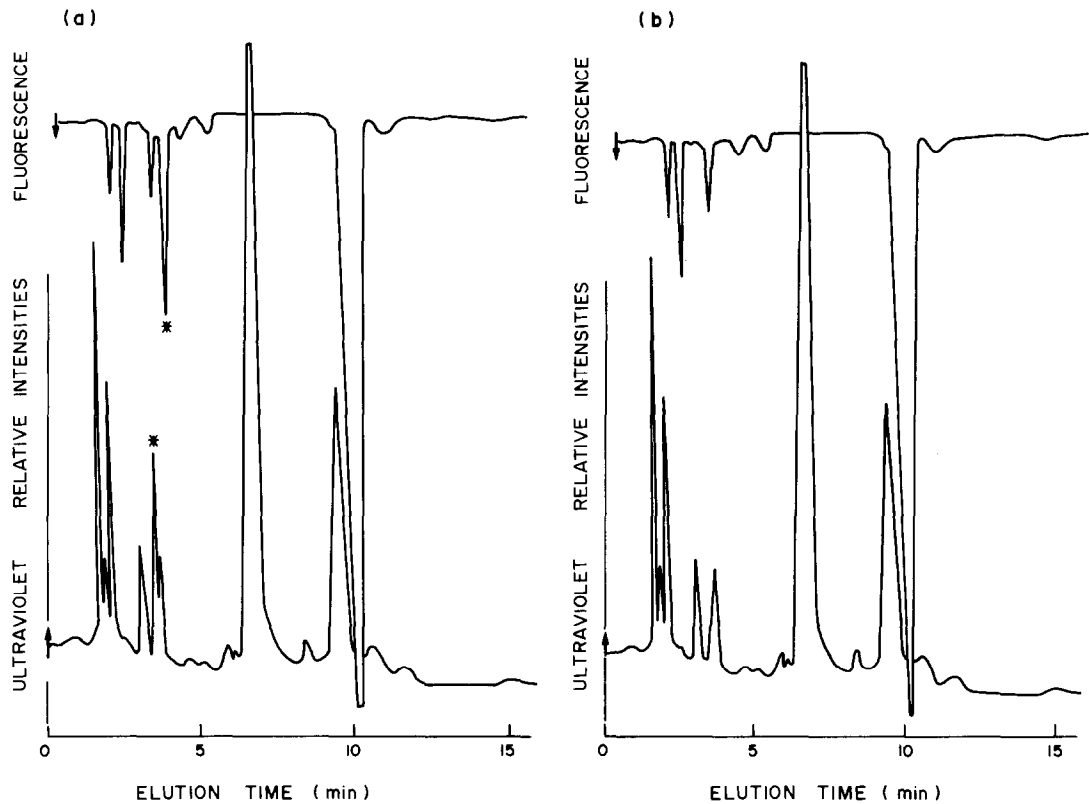


Fig. 1. a, Chromatogram of plasma containing TFA*; b, chromatogram of plasma blank. Both with ultraviolet and fluorescence detection.

plexes of the sodium and potassium ions present. Acidification with 100 μ l of 5M hydrochloric acid then leads to formation of undissociated trifluoroacetic acid. Addition of 10 ml of dry acetone results in a single liquid phase which can be recovered by centrifugation (10 min at 2000 rpm) and contains only the molecular form $\text{CF}_3\text{CO}_2\text{H}$ (because of solvation phenomena and the low dielectric constant). The general procedure for making the 4-bromomethyl-7-methoxycoumarin derivative of a carboxylic acid is then applied (treatment with 500 μ l of a 0.004M acetone solution of the reagent and 2 mg of potassium carbonate for 30 min in a tube protected from light by being wrapped in aluminium foil). The resulting solution is evaporated, the residue dissolved in the solvent system and a sample chromatographed. A representative chromatogram is shown in Fig. 1a. In order to check that no interference is caused by other components of the plasma and urine, a blank test is performed with samples obtained just before the anaesthesia. A typical chromatogram is shown in Fig. 1b.

The optimal conditions for ultraviolet and fluorescence detection are achieved with the solvent system methanol-water (60:40 v/v). There is no interference and the elution times are 4.1 min for the coumarin ester and about 10 min for the

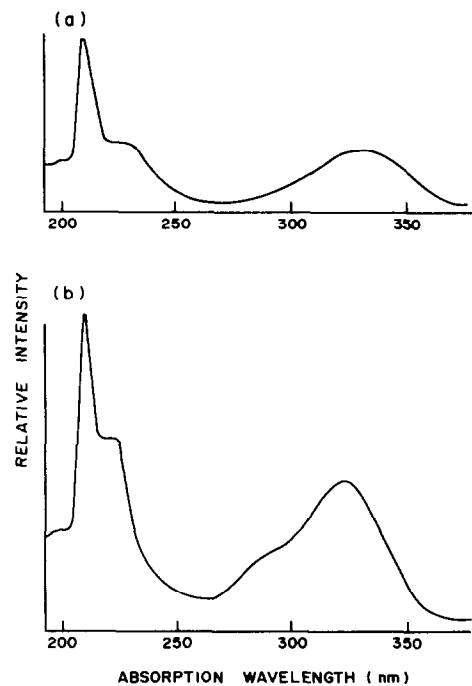


Fig. 2. Ultraviolet absorption spectra in methanol, of a, 4-bromomethyl-7-methoxycoumarin; b, its trifluoroacetate ester.

reaction by-products. The ultraviolet absorption spectra of methanolic solutions of 4-bromomethyl-7-methoxycoumarin and its trifluoroacetate ester are shown in Fig. 2. The wavelength used for ultraviolet detection (320 nm) is that at which the absorbance due to the coumarin ester is maximal in the solvent system used.

The area under the chromatographic peak is a linear function of the TFA concentration over the range 0.2–20 $\mu\text{g/ml}$. The precision is good, as shown by the regression coefficient of 0.997. Moreover the slope ($4.17 \text{ mm}^2 \cdot \text{ml} \cdot \mu\text{g}^{-1}$) shows the sensitivity is good, the minimum detectable concentration being 0.1 $\mu\text{g/ml}$. The reproducibility is also good. This method is therefore appropriate for the determination of the pharmacokinetic parameters of halothane.

Acknowledgements—The authors wish to thank M.-C. Jacquemont and P. Colein for technical assistance.

REFERENCES

1. E. N. Cohen, J. R. Trudell, H. N. Edmunds and E. Watson, *Anesthesiology*, 1975, **43**, 392.
2. D. Karashima, A. Shigematsu, T. Furukawa, T. Nagayoshi and I. Matsumoto, *J. Chromatog.*, 1977, **130**, 77.
3. R. M. Maiorino, A. J. Gandolfi and I. G. Sipes, *J. Anal. Toxicol.*, 1980, **4**, 250.
4. J. B. Bentley, R. W. Vaughan, A. J. Gandolfi and K. C. Cork, *Anesthesiology*, 1982, **57**, 94.
5. L. Witte, H. Nau and J. H. Fuhrhop, *J. Chromatog.*, 1977, **143**, 329.
6. O. Gylledhaal and H. Ehrsson, *ibid.*, 1975, **107**, 327.
7. W. Düniges, *Anal. Chem.*, 1977, **49**, 442.

APPLICATION OF MATRIX-MODIFICATION IN DETERMINATION OF THALLIUM IN WASTE WATER BY GRAPHITE-FURNACE ATOMIC-ABSORPTION SPECTROMETRY

SHAN XIAO-QUAN*, NI ZHE-MING and ZHANG LI

Institute of Environmental Chemistry, Academia Sinica, P.O. Box 934, Beijing, People's Republic of China

(Received 8 April 1983. Accepted 20 June 1983)

Summary—A method has been developed for the determination of thallium in waste water at the ng/ml level by graphite-furnace atomic-absorption spectrometry. If microgram amounts of palladium or platinum are used as a matrix modifier, the ashing temperature for thallium can be raised to 1000°, and the interference of halides and mineral acids is greatly reduced. The relative standard deviation found was 2% (9 replicate determinations) at the 8-ng/ml thallium level, and the detection limit 1 ng/ml.

Severe interference effects are encountered in the determination of thallium by graphite-furnace atomic-absorption spectrometry in the presence of halide, because the atomization temperature for thallium is lower than that required to remove halide in the ashing step, so large concentrations of halide are present in the vapour phase during the atomization step, and produce interference. Fuller¹ found that the absorbance for a 0.5- μ g/ml thallium solution in a Perkin-Elmer HGA-70 was seriously suppressed by 0.01% v/v levels of hydrochloric acid and perchloric acid but there was negligible interference by a mixture of nitric acid and sulphuric acid. He also reported that as little as 0.2 μ g of sodium chloride completely suppressed the thallium absorbance and that the presence of sulphuric acid could reduce this interference.

Many efforts have been made to reduce or eliminate the interference effects in thallium determination. Manning *et al.* used a tungsten wire² and the L'vov platform³ at constant temperature for the determination of thallium in the presence of halide. With the platform, no interference was found with concentrations of less than 0.01% MgCl₂ and 0.05% NaCl, whereas much smaller amounts of halide interfered with atomization at the graphite tube wall. Kujirai *et al.*⁴ described a method for the determination of thallium in nickel and cobalt alloys. It was found that tartaric acid and sulphuric acid permitted a higher ashing temperature of 600°. They therefore dissolved the alloys with hydrofluoric acid, sulphuric acid and hydrogen peroxide and used matrix-matched standards. However, the determination of thallium in complex matrices is still a difficult task, and it seems that a separation or preconcentration procedure is indispensable. The solvent extraction of thallium with diethyl-dithiocarbamate,⁵ Brilliant Green,⁶ and hydrogen bromide⁷ has been reported and applied for the separation of thallium in geological samples. There

are also a few reports on the separation and preconcentration of thallium by a volatilization technique⁸ or by adsorption on an activated carbon filter after complexation of the thallium with *O,O*-diethyl dithiophosphate.⁹

The present study describes the application of palladium or platinum in microgram amounts as a matrix-modifier for the direct determination of thallium at ng/ml levels in waste water. In the presence of palladium or platinum the ashing temperature for thallium can be raised to 1000° to decompose halides and thus minimize the interference effects and allow the direct determination of thallium, down to 1-ng/ml.

EXPERIMENTAL

Apparatus

A Perkin-Elmer model 4000 atomic-absorption spectrometer fitted with a model HGA-400 graphite furnace and a Hitachi model 056 chart-recorder was used for the measurement of thallium absorbance at the 276.8-nm resonance line under "argon stop" conditions. A thallium hollow-cathode lamp was used, operated at 10 mA. The band-width was set at 0.7 nm. A deuterium background corrector was employed throughout. A 20- μ l Eppendorf pipette with disposable polypropylene tips was used to introduce sample solution into the graphite tube.

Reagents

Standard thallium solution, 1000 μ g/ml, was prepared by dissolving 0.1147 g of thallium carbonate (analytical-reagent grade) in 10 ml of nitric acid (1 + 1) and diluting to volume in a 100-ml standard flask with demineralized water. Working thallium standards were prepared from this stock solution by serial dilution with demineralized water. The palladium and platinum solutions were prepared from palladium chloride and platinum chloride (analytical-reagent grade).

Procedure

All waste water samples were stored in polyethylene bottles and refrigerated at 4°. Equal volumes (20 μ l) of waste water and 150- μ g/ml aqueous palladium solution were introduced into the graphite furnace. The temperature program was drying at 110° for 30 sec, ashing at 1000° for

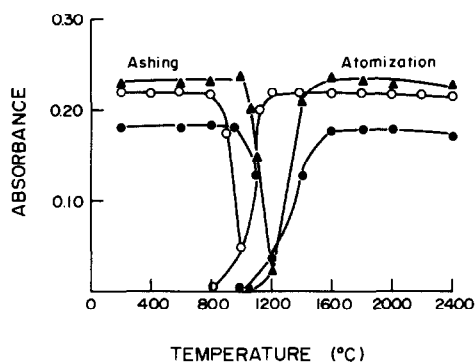


Fig. 1. Effect of ashing and atomization temperature on the absorbance of thallium in the presence or absence of matrix modifiers. Left-hand branches: ashing temperature varied, atomization temperature optimal. Right-hand branches: atomization temperature varied, ashing temperature optimal. (○) 1.0 ng of Tl in 0.01M HNO₃, (●) 1.0 ng of Tl + 3 µg of Pt, (▲) 1.0 ng of Tl + 3 µg of Pd.

30 sec, atomizing at 1800° for 5 sec and cleaning at 2600° for 5 sec. The internal argon flow was interrupted during atomization. The concentration of thallium was determined in the waste water by the standard addition method. Waste water samples containing higher amounts of thallium were

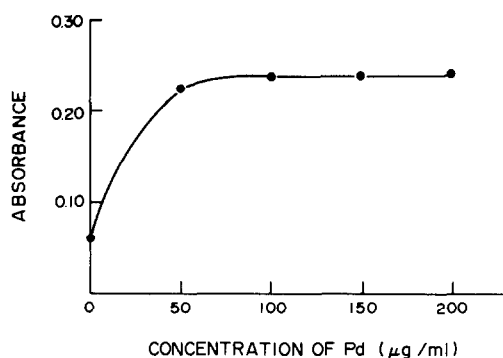


Fig. 2. Dependence of thallium absorbances on palladium concentrations: 1.0 ng of Tl + 20 µl of palladium solution.

diluted further with demineralized water. A wet digestion procedure was used for some samples containing higher levels of organic compounds which interfere with the determination of thallium, even with matrix modification. In this, 20 ml of waste water, in a 50-ml beaker, were evaporated to small volume by heating on a hot-plate, then treated with 0.5 ml of concentrated nitric acid and reheated until the yellow colour disappeared, then cooled to room temperature and diluted with 0.01M nitric acid before thallium was determined by the recommended procedure.

Table 1. Comparison of interference effects in determination of 1 ng of Tl in the presence and absence of 4 µg of Pd

Compound added	Concentration of added compound*	Relative absorbance of thallium	
		Without Pd	With Pd
NaCl	0.002	0.85	
	0.005	0.73	
	0.01	0.63	
	0.5		1.10
	1.0		1.10
	2.0		1.00
MgCl ₂	4.0		1.05
	0.005	0.97	
	0.02	0.33	
	0.2		0.98
CaCl ₂	0.8		0.94
	1.0		0.90
	0.005	0.68	
	0.05	0.61	
KI	1.0		0.96
	2.0		0.95
	3.0		0.84
	0.001	0.85	
Na ₂ SO ₄	0.001	0.35	
	0.2		0.95
	0.5		0.90
	1.0		0.88
HCl	0.003	0.88	
	0.15	0.33	0.96
	0.4		0.90
HClO ₄	0.5		0.84
	0.001	0.66	1.00
	0.01	0.50	0.98
HNO ₃	0.05		0.88
	0.001	0.70	
	0.01	0.14	1.01
HNO ₃	0.05		0.71
	2.0	1.00	0.96
	4.0	1.09	0.98
	8.0	0.76	1.00

*Salts in mg/ml, acids in % v/v (referred to concentrated acid).

Table 2. Recovery of thallium from waste water samples

Sample	Tl concentration, ng/ml	Tl added, ng/ml	Total Tl found, ng/ml	Recovery, %
1	1.4	0	1.4	
		2.0	3.5	105
		4.0	5.5	105
		6.0	7.4	100
		8.0	9.1	96
2	8.5	0	8.5	
		5.0	13.1	92
		10	18.1	96
		15	24.0	103
		20	27.7	96
		30	38.2	99

RESULTS AND DISCUSSION

Stabilizing effects of palladium and platinum

Thallium is one of the relatively volatile elements, so a certain loss may occur during the preatomization steps, and the loss during ashing will increase with temperature and time. A search for suitable matrix modifiers was made and it was found that in the presence of palladium or platinum, the critical ashing temperature for thallium can be raised to 1000°. The results are schematically shown in Fig. 1. Palladium not only raises the critical ashing temperature more than platinum does, but also increases the sensitivity for thallium, and was therefore used in the remainder of this study.

The stabilizing effect of palladium depends on its concentration (Fig. 2). Because palladium can also stabilize mercury,¹⁰ tellurium,¹¹ lead¹² and arsenic,¹³ some competing reactions may occur if these elements are also present in the heated graphite tube, and a certain amount of palladium will be consumed in stabilizing these elements, so a volume of 20 μ l of 150- μ g/ml aqueous palladium solution was used for sample analysis (but any concentration in the range 100–200 μ g/ml will do).

Effect of halides and recovery of thallium

The interference of halides in the thallium determination was studied with and without palladium present. The absorbance data were referred to the values obtained for a pure solution, and are summarized in Table 1. No interference was observed for the determination of thallium (at the 50-ng/ml level) from concentrations of 4 mg/ml for NaCl, 1 mg/ml for MgCl₂ or KI, 2 mg/ml for CaCl₂, 0.4 mg/ml for

Na₂SO₄, and 0.05% v/v HCl, 0.01% v/v HClO₄ and 8% v/v HNO₃ when palladium was used as matrix modifier, but the tolerance level was much lower in the absence of palladium. In contrast to the suppression effect of sodium chloride reported in the literature, a certain enhancement was observed if palladium was used as matrix modifier.

If waste water was introduced into the heated graphite furnace without matrix modification no thallium could be detected, even with a standard thallium solution also directly injected. However, direct determination of thallium in waste water is practicable and recovery quantitative if palladium is added. As can be seen from Table 2, the recovery was found to be 92–105%.

Determination of thallium in waste water

Although no serious interferences were observed and quantitative recovery was obtained when matrix modification was used, the standard-addition method is recommended for the analysis of waste water samples to prevent unpredictable interferences arising from the extreme complexity of industrial effluents.

The relative standard deviation was found to be 2% for 9 replicate determinations for a waste water with a thallium concentration of 8 ng/ml. The detection limit was found to be 1 ng/ml (three times the standard deviation for the blank) if a volume of 20 μ l was injected.

REFERENCES

1. C. W. Fuller, *Anal. Chim. Acta*, 1976, **81**, 199.
2. D. C. Manning, W. Slavin and S. Myers, *Anal. Chem.*, 1979, **51**, 2375.
3. W. Slavin and D. C. Manning, *Spectrochim. Acta*, 1980, **35B**, 701.
4. O. Kujirai, T. Kobayashi and E. Sudo, *Z. Anal. Chem.*, 1979, **297**, 398.
5. R. Keil, *ibid.*, 1981, **309**, 181.
6. N. T. Voskresenkaya, N. F. Pchelintseva and T. I. Tsekhonya, *Zh. Analit. Khim.*, 1981, **36**, 667.
7. C. M. Elson and C. A. R. Albuquerque, *Anal. Chim. Acta*, 1982, **134**, 393.
8. H. Heinrichs, *Z. Anal. Chem.*, 1979, **294**, 345.
9. H. Berndt, J. Messerschmidt, F. Alt and D. Sommer, *Z. Anal. Chem.*, 1981, **306**, 385.
10. Shan Xiao-quan and Ni Zhe-ming, *Hua Hsueh Hsueh Pao*, 1978, **37**, 261; *Chem. Abstr.*, 1980, **92**, 220474x.
11. *Idem*, *Acta. Sci. Circum.* 1981, **1**, 74; *Chem. Abstr.*, 1981, **95**, 225335z.
12. *Idem*, *Can. J. Spectrosc.*, 1982, **27**, 75.
13. Shan Xiao-quan, Ni Zhe-ming and Zhang Li, *Anal. Chim. Acta*, 1983, **151**, 179.

ANALYTICAL DATA

PALLADIUM COMPLEXES WITH TRIETHYLENETETRAMINEHEXA-ACETIC ACID

ALDO NAPOLI

Dipartimento di Chimica, Università "La Sapienza", 00100 Roma, Italy

(Received 8 August 1983. Accepted 28 September 1983)

Summary—The formation of complexes between palladium(II) and triethylenetetraminehexa-acetic acid (TTHA, H_6L) was studied by measuring the hydrogen-ion concentration with a glass electrode; 1:1 and 2:1 metal to ligand complexes with different degrees of protonation were observed and the corresponding equilibrium constants evaluated.

Triethylenetetraminehexa-acetic acid (TTHA, abbreviated as H_6L) is an aminopolycarboxylic acid extensively employed for analytical purposes. It has been used for complexometric titrations utilizing metalochromic indicators¹ or ion-selective electrodes,^{2,3} in the spectrophotometric⁴⁻⁶ and spectrofluorimetric⁷ determination of some metal ions, and in amperometric titrations.⁸⁻¹¹

This complexing agent has ten donor atoms, and therefore easily forms polynuclear species with several metal ions. Also, the metal complexes can be protonated at low pH to form polyprotonated species.

Metal complexes with TTHA have been studied extensively, but no information has been reported on the palladium complex. Therefore, a potentiometric investigation was made at 25° (0.50M sodium perchlorate medium), to identify the various complex species formed in aqueous solution and evaluate the stability constants.

EXPERIMENTAL

The TTHA was obtained from Sigma Chemicals and used as received. The purity was checked by potentiometric titration with sodium hydroxide. The equivalent weight was determined by titration of the ligand in the presence of excess of copper(II) as described by Bohigian and Martell.¹²

Palladium perchlorate was prepared from palladium chloride (Carlo Erba), by addition of the stoichiometric amount of silver perchlorate.

The ionic strength was adjusted to 0.50M with sodium perchlorate.

Potentiometric measurements were made at $25.0 \pm 0.1^\circ$ with glass and reference electrodes immersed in the test solution. The reference electrode was similar to that described by Forsling *et al.*¹³

Ag, AgCl | NaCl, 0.01M; NaClO₄, 0.49M | NaClO₄, 0.50M

The Ag/AgCl electrode was prepared according to Brown¹⁴ and the glass electrode was a Radiometer type G202B, calibrated in concentration units.

In a medium of constant ionic strength, activities can be replaced by concentrations,¹⁵ so the potential of the cell can be expressed, in mV, as:

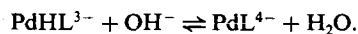
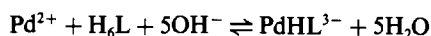
$$E = E^\circ + 59.16 \log [H^+] + E_j$$

where E_j is the junction potential ($-100[H^+]$ mV under our experimental conditions) and E° is a constant determined (in the absence of the ligand) before and after each set of measurements. During the potentiometric titrations a stream of purified nitrogen was used to mix the solutions and to remove carbon dioxide.

RESULTS

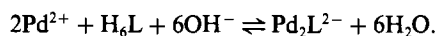
Potentiometric titrations, with sodium hydroxide, of the ligand alone and when mixed with palladium in molar ratios 1:1 and 1:2 are shown in Fig. 1.

For an equimolar mixture of Pd(II) and TTHA, two inflection points are evident, corresponding to 5 and 6 equivalents of sodium hydroxide respectively. These correspond to the reactions:



In addition, beyond the formation of the mono-protonated species, in the first buffer region (up to 5 equivalents of base per mole of ligand), poly-protonated complexes, PdH_4L , may also be formed.

For the 2:1 Pd:L mixture a marked lowering of the $-\log[H^+]$ values is observed and only one inflection point is seen; this corresponds to the equation:



Again, protonated complexes can be formed in acidic medium.

The stability constant for the 1:1 complex and that for the 1:2 complex were initially calculated from the titration data for the mixture of corresponding molar composition. As pointed out by Harju,¹⁶ however, binuclear complexes may be present even in equi-

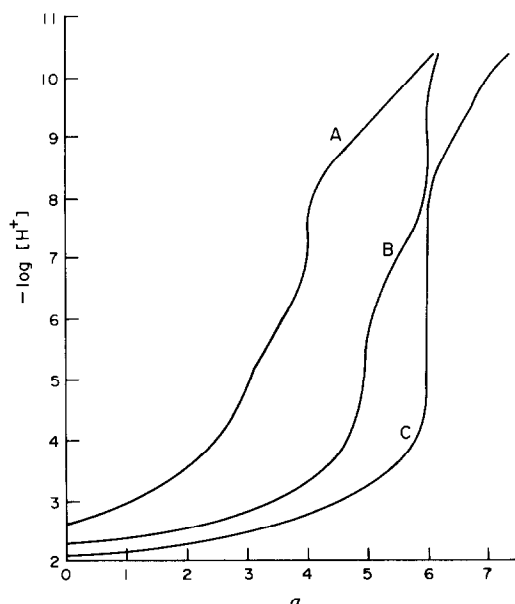


Fig. 1. Potentiometric titration curves of TTHA alone (curve A) and in the presence of palladium perchlorate in molar ratio of 1:1 (curve B) and 1:2 (curve C). $C_L = 2 \times 10^{-3} M$; a = moles of sodium hydroxide added per mole of ligand.

molar solutions, so the values thus calculated are likely to be incorrect.

Therefore, from the analysis of the single curves, approximate values for the formation constants were derived, and successively refined by considering the simultaneous presence of all the species found. The approximate values were obtained by the procedure of Bohigian and Martell¹² by using the protonation constants of the ligand determined in the same experimental conditions:¹⁷

$$\log K_1 = 9.73 \quad \log K_2 = 8.76 \quad \log K_3 = 5.92$$

$$\log K_4 = 3.94 \quad \log K_5 = 2.75 \quad \log K_6 = 2.30.$$

The first values for the formation constants of the complexes were used to calculate titration curves, which were compared with the experimental curves. The value

$$(\Delta a)^2 = (a_{\text{calc}} - a_{\text{exp}})^2$$

was computed for each experimental point (a represents the degree of neutralization) and the values of the constants were varied until the sum of $(\Delta a)^2$ was minimized.

The concentrations of the various species in solution were calculated by the computer program DISDI,¹⁸ and the value of a_{exp} was obtained from the

Table 1. Equilibrium constants for the palladium(II)-TTHA complexes

Equilibrium	log K
$\text{Pd}^{2+} + \text{L}^{6-} \rightleftharpoons \text{PdL}^{4-}$	18.73
$\text{PdL}^{4-} + \text{H}^+ \rightleftharpoons \text{PdHL}^{3-}$	6.92
$\text{PdHL}^{3-} + \text{H}^+ \rightleftharpoons \text{PdH}_2\text{L}^{2-}$	2.90
$\text{PdH}_2\text{L}^{2-} + \text{H}^+ \rightleftharpoons \text{PdH}_3\text{L}^-$	2.50
$\text{PdH}_3\text{L}^- + \text{H}^+ \rightleftharpoons \text{PdH}_4\text{L}$	2.45
$2\text{Pd}^{2+} + \text{L}^{6-} \rightleftharpoons \text{Pd}_2\text{L}^{2-}$	27.50
$\text{Pd}_2\text{L}^{2-} + \text{H}^+ \rightleftharpoons \text{Pd}_2\text{HL}^-$	3.20
$\text{Pd}_2\text{HL}^- + \text{H}^+ \rightleftharpoons \text{Pd}_2\text{H}_2\text{L}$	2.0*

Probable errors in log K units: ± 0.05 (* ± 0.1).

relationship:

$$a_{\text{exp}} = (6C_L - [\text{H}^+] + [\text{OH}^-] - \sum i[\text{H}_i\text{L}^{(6-i)}] - \sum i[\text{PdH}_i\text{L}^{(4-i)}] - \sum i[\text{Pd}_2\text{H}_i\text{L}^{(2-i)}])/C_L$$

where C_L represents the analytical concentration of the ligand and $[\text{OH}^-] = K_w/[\text{H}^+]$ ($\text{p}K_w = 13.73$ under our experimental conditions¹⁹).

Also a value of σ was calculated:

$$\sigma = \sqrt{(\Delta a)^2/(n_e - n_k)}$$

where n_e is the number of experimental points and n_k the number of constants. From the σ value ($= 0.11$ in our case) the deviation between experimental and calculated points can be evaluated.

The equilibrium constants found are collected in Table 1.

REFERENCES

- R. Přebil and V. Veselý, *Talanta*, 1962, **9**, 939.
- E. A. Moya and K. L. Cheng, *Anal. Chem.*, 1970, **42**, 1669.
- A. Napoli, *Ann. Chim. (Roma)*, 1978, **68**, 443.
- F. Bermejo Martinez and A. Longarela Pena, *Acta Cient. Compostelana*, 1971, **8**, 85.
- Idem, ibid.*, 1971, **8**, 119.
- D. S. Kuncheva, P. P. Nenova and B. P. Karadakov, *Dokl. Bolg. Akad. Nauk*, 1979, **32**, 651.
- T. Taketatsu and A. Sato, *Anal. Chim. Acta*, 1978, **98**, 397.
- V. Stará and M. Kopanica, *Chem. Listy*, 1974, **68**, 525.
- P. L. Cignini and A. Napoli, *Ann. Chim. (Roma)*, 1977, **67**, 135.
- S. Rubel and M. Mojciechowski, *Anal. Chim. Acta*, 1979, **109**, 67.
- Idem, ibid.*, 1980, **115**, 69.
- T. A. Bohigian and A. E. Martell, *J. Am. Chem. Soc.*, 1967, **89**, 832.
- V. Forling, S. Hietanen and L. G. Sillén, *Acta Chem. Scand.*, 1952, **6**, 901.
- A. S. Brown, *J. Am. Chem. Soc.*, 1934, **56**, 646.
- G. Biedermann and L. G. Sillén, *Ark. Kemi*, 1953, **5**, 425.
- L. Harju, *Anal. Chim. Acta*, 1970, **50**, 475.
- A. Napoli, *Gazz. Chim. Ital.*, 1976, **106**, 597.
- R. Maggiore, S. Musumeci and S. Sammartano, *Talanta*, 1976, **23**, 42.
- G. Lagerstrom, *Acta Chem. Scand.*, 1959, **13**, 722.

ANNOTATIONS

POLAROGRAPHIC STUDY OF SIMPLE AND MIXED-LIGAND COMPLEX FORMATION

P. H. TEDESCO and J. MARTINEZ

Facultad de Ciencias Exactas de la Universidad Nacional de La Plata, 1900—La Plata, Argentina

(Received 20 December 1982. Revised 9 May 1983. Accepted 9 September 1983)

Summary—Theoretical, experimental and statistical aspects of the polarographic method applied to simple and mixed-ligand complex formation have been studied. Some misunderstandings and erroneous interpretations have been clarified according to experimental results obtained with several systems. A criterion for establishing the number of complex species present in a simple system is proposed. For the first time the polarographic method has been applied to a mixed-ligand complex system where fourteen species co-exist.

There are numerous applications of the polarographic method for the study of complex formation. Simple complex formation is studied principally by the DeFord and Hume method¹ and the Ringbom and Erickson method² (which extends the treatment to the study of complexes irreversibly reduced at the dropping mercury electrode). Mixed-ligand complex formation was first studied by Schaap and McMasters³ and pursued by others.⁴⁻⁷ Nevertheless, several points remain obscure and others require definitive correction, because misunderstandings and erroneous interpretations have been made.

In this paper we deal with the experimental, theoretical and statistical aspects of the polarographic method, based on results obtained with the simple systems copper-acetate, copper-propionate, cadmium-acetate, cadmium-propionate,^{8,9} cadmium-formate, cadmium-iodide and cadmium-bromide, and with the mixed-ligand system cadmium-bromide-iodide.

EXPERIMENTAL

Polarograms were obtained with a manual Sargent polarograph model III and a precision Leeds & Northrup potentiometer at a temperature of $25 \pm 0.1^\circ$, controlled by a Lauda thermostat. Solutions at pH 5.0 with metal-ion concentration of $10^{-3}M$ and increasing ligand concentrations up to $1.5M$ were used in an H-type cell. The system cadmium-bromide-iodide was studied in a cell consisting of a tube, containing the dropping mercury electrode (DME) and the sample solution, connected to the reference SCE through a porous ceramic plug covered by two drops of agar gel, as indicated in Fig. 1. In the SCE sodium chloride was used instead of potassium chloride to prevent precipitation in the perchlorate medium. This cell worked quite well for many days, which was confirmed by the fact that the reference electrode maintained its potential within 0.2 mV (before any change was noticed the agar gel was renewed

and the SCE potential checked). All measurements were made at ionic strength 2.0 (sodium perchlorate). The half-wave potentials were reproducible within 0.8 mV.

RESULTS AND DISCUSSION

Formation of simple complexes

The DeFord and Hume treatment of formation of simple complexes¹ allows calculation of overall stability constants through the relationships:

$$F_0 = \text{antilog} \left(\frac{0.435 nF}{RT} \Delta E_{1/2} + \log \frac{I_s}{I_c} \right) \\ = 1 + \beta_1[X] + \beta_2[X]^2 + \dots$$

$$F_1 = \frac{F_0 - 1}{[X]} = \beta_1 + \beta_2[X] + \beta_3[X]^2 + \dots$$

$$F_N = \frac{F_{N-1} - \beta_{N-1}}{[X]} = \beta_N + \beta_{N+1}[X]$$

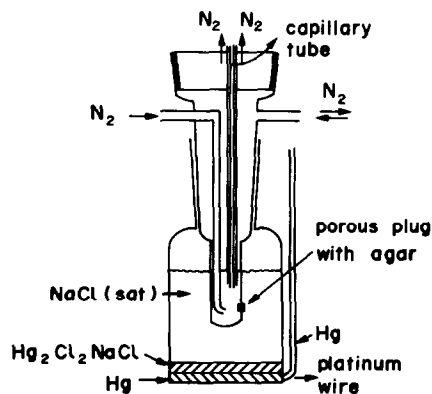


Fig. 1. Polarographic cell.

Table 1. Values of stability constants of several systems, obtained by the polarographic method and calculated for two models with different numbers of constants

System	Calculation	Model 1				Model 2			
		β_1	β_2	β_3	β_4	β_1	β_2	β_3	β_4
1. Cd-formate	Graph. Num.	9.8 11.5 ± 0.5	15 9.8 ± 2.1	50 55.7 ± 1.7	15 15	9.8 9.0 ± 0.2	15 31.5 ± 1.8	15 12.3 ± 3.3	20 22.3 ± 1.7
2. Cd-acetate	Graph. Num.	17 20.1 ± 0.4	95 87.5 ± 4.9	494 401 ± 6.7	125 192 ± 32	17 18.2 ± 0.4	142 130 ± 7	125 192 ± 32	420 326 ± 50
3. Cd-propionate	Graph. Num.	20 20.7 ± 0.2	102 98 ± 2	210 214 ± 4	81 -20.3 ± 35	20 20.9 ± 0.3	112 95 ± 5	152 229 ± 26	81 -20.3 ± 35
4. Cd-formate*	Graph. Num.	11 11.0 ± 0.5	17 16 ± 2.4	55 57 ± 2	25 5.1 ± 5.3	11 10.6 ± 0.8	30 20.9 ± 5	16 47 ± 10	25 5.1 ± 5.3
5. Cd-acetate*	Graph. Num.	20 22.5 ± 1.6	78 71 ± 8	214 176 ± 8	67 87 ± 12	20 16.1 ± 1.3	104 141 ± 11	107 19 ± 23	67 87 ± 12
6. Cd-propionate*	Graph. Num.	30 39 ± 2	96 71 ± 16	262 287 ± 15	95 185 ± 16	30 27 ± 2	129 215 ± 14	139 44 ± 30	95 185 ± 16
7. Cd-bromide	Graph. Num.	53 ± 5 218 ± 59	impossible, as shown in Fig. 4 -142 ± 52	139 ± 84 impossible, as shown in Fig. 6	850 872 ± 105	42 40.4 ± 2.4	123 143 ± 40	372 326 ± 133	850 872 ± 105
8. Cd-iodide	Graph. Num.	46.9 55	597 563 ± 22	$(3 \pm 0.045) \times 10^6$ $(3 \pm 0.045) \times 10^3$	$(7.16 \pm 0.06) \times 10^5$ $(7.16 \pm 0.06) \times 10^5$	82 84 ± 22	1140 952 ± 167	3.7×10^5 $(37 \pm 2.6) \times 10^3$	7.17×10^5 $(7.16 \pm 0.06) \times 10^5$
9. Cu-acetate	Graph. Num.	47 ± 4 55	850 841 ± 21	impossible	impossible	impossible	impossible	impossible	impossible
10. Cu propionate	Graph. Num.	55 ± 3	841 ± 21	impossible	impossible	55 ± 3	734 ± 34	22 ± 10	22 ± 10

*Constants calculated from experimental results published by Pijjac *et al.*¹¹

where $[X]$ is the free ligand concentration, n , F , R and T have the same meaning as in the Nernst equation, $\Delta E_{1/2}$ is the difference in the half-wave potential when $[X] = 0$ and when $[X] \neq 0$, I_s and I_c are the corresponding diffusion current constants and the β values are the stoichiometric overall stability constants at constant ionic strength. The stability constants can be calculated graphically by plotting the F_N functions vs. ligand concentration or numerically by a least-squares treatment. We have used the weighted $1/F_0^2$ method proposed by Momoki.¹⁰

The question of the number of species present in the solution cannot be answered independently by the graphical or the numerical methods. Piljac *et al.*¹¹ have proposed calculating the constants numerically, with a previous graphical derivation of the number of complexes in solution. Nevertheless it has to be pointed out that this derivation is not always unequivocal, especially when three or more species are present. As we have stated before,⁹ F_2 (in the case of three or more complexes) frequently shows uncertain values at low ligand concentrations, because it results from the quotient $[(F_0 - 1/[X]) - \beta_1]/[X]$ and the plotting of the curve is not always precise. This can be seen in Fig. 2 for the cadmium-formate system: if the points at low ligand concentrations are dismissed, F_2 can be considered a straight line; otherwise a curve can be plotted, with no constant slope, and in that case the function F_3 is nearly a straight line and a set of four constants is calculated. For the cadmium-acetate and cadmium-propionate systems the same situation occurs and three or four constants can be derived graphically.⁹

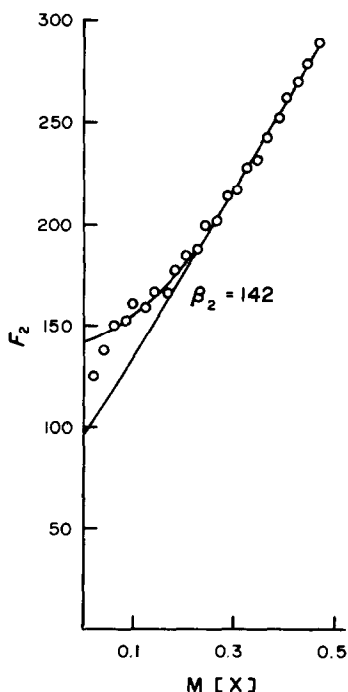


Fig. 2. F_2 as a function of ligand concentration for the cadmium formate system.

Piljac has proposed that the calculated stability constants have to meet the following conditions: (a) all must be positive, (b) the standard error of any constant must be lower than the constant itself, (c) β_1 obtained by the graphical method must agree with the numerically obtained constant, within the standard error of this method. We think that these conditions are necessary but not sufficient and that the definitive criterion is that the correct set of stability constants is that for which reasonable agreement for *all* the constants is obtained by both methods. Table 1 gives results obtained under the same conditions (ionic strength 2.0, perchlorate medium) for several systems. Calculations are made by the graphical and the numerical Momoki method. It can be seen that the Piljac conditions are generally but not always applicable.

It is possible to predict, according to Filipović *et al.*¹² three complexes for systems 3, 4 and 5 and two complexes for system 9, but for systems 1, 2, 6 and 10, two sets, with different numbers of constants, can equally well be predicted. In these cases, the agreement between the values of the constants obtained by the two methods suggests three complexes for systems 1, 2 and 6 and two complexes for system 10. This criterion is supported by the fact that when the graphical method offers no doubt about the number of complexes, the numerical method gives values of the constants in very good agreement with the graphical method.

Figures 3-6 illustrate the graphical treatment of the simple systems cadmium-bromide and cadmium-iodide. It can be seen that four complexes are formed in each case, that F_2 cannot be taken as a straight line, and that the plot of F_3 vs. $[X]$ is an unequivocal straight line. Table 1 shows the excellent agreement between the stability constants obtained by the methods of calculation.

Three conclusions seem in order regarding the calculation of stability constants of simple systems from polarographic data. First, all the systems we

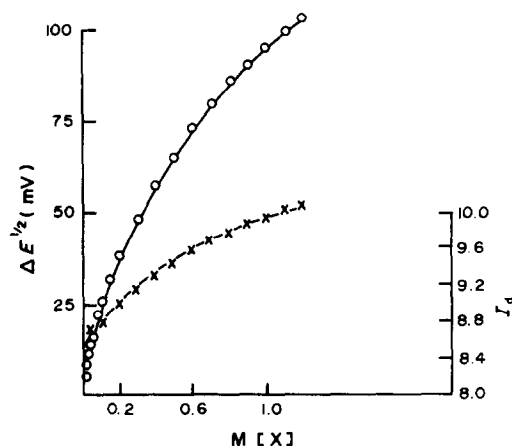


Fig. 3. Plots of ΔE (O) and I_d (X) vs. ligand concentration for cadmium-bromide system.

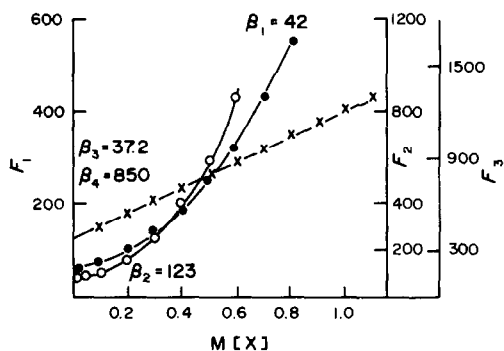


Fig. 4. Plots of F_1 (○), F_2 (●) and F_3 (×) vs. ligand concentration for cadmium-bromide system.

have studied show that the experimental half-wave potential shifts $\Delta E_{1/2}$ and the function F_0 have to be plotted vs. the ligand concentration, and values taken from the resulting smooth curve; the numerical or graphical processing of the crude polarographic data can give quite uncertain results. Secondly, the possible uncertainty of the F_N values is a consequence of the nature of the system, of the polarographic method and of the mathematical treatment, and this frequently makes useless any effort to improve the reproducibility of ΔE values to better than 0.8 mV. Thirdly, a complete graphical treatment followed by the numerical calculation seems advisable in any case, to be sure about the number of complex species and to obtain the statistical errors.

For the cadmium-bromide and cadmium-iodide systems it has been claimed¹³⁻¹⁵ that adsorption of anions by the DME would produce "additional complexation" and the apparent stability constants obtained would be considerably higher than those from other methods. Our results for these systems agree satisfactorily with others indicated in the literature¹⁶ and obtained by other methods (or even are lower), so we think that under our experimental

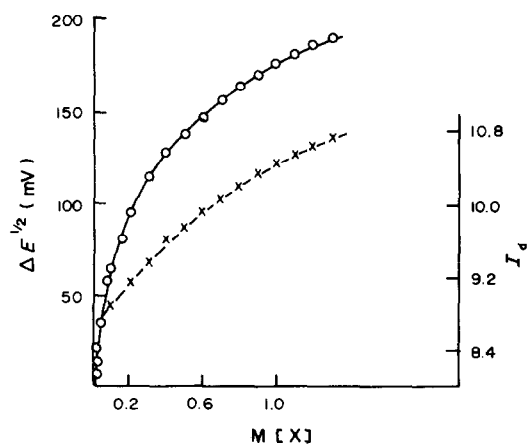


Fig. 5. Plots of ΔE (○) and I_d (×) vs. ligand concentration for cadmium-iodide system.

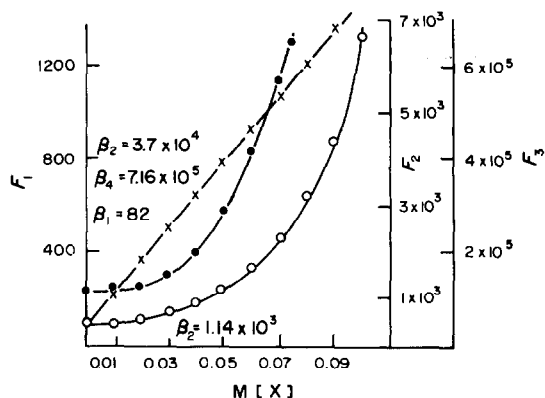


Fig. 6. Plots of F_1 (○), F_2 (●) and F_3 (×) vs. ligand concentration for cadmium-iodide system.

conditions anion adsorption—if it exists—does not produce any noticeable additional complexation and hence any noticeable change in the stability constants.

Formation of mixed-ligand complexes

Schaap and McMasters pointed out³ that in a system in which two or more ligands are present, mixed-ligand complexes should be formed in preference to simple complexes whenever $\beta_{M_{X_i}[X]^i} \sim \beta_{M_{Y_j}[Y]^j}$. We can say that even purely statistical considerations confirm this assertion.

What is more important in consideration of formation of mixed-ligand complexes is to emphasize that generally there is no polarographic signal to show it. The common interpretation⁴⁻⁶ that a further shift of the half-wave potential on the addition of a second ligand to a simple system is a proof of mixed-ligand complex formation is not necessarily correct. It merely indicates additional complexing, which may be with either the original ligand or the

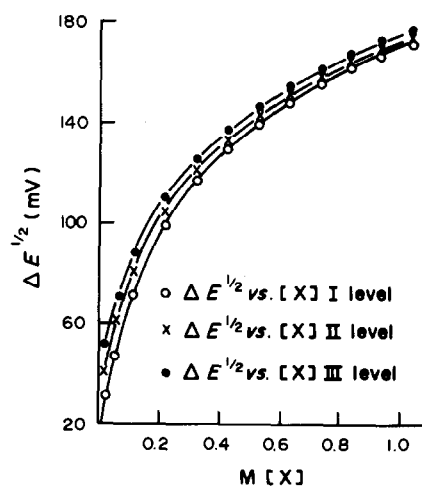


Fig. 7. Plots of ΔE vs. iodide concentration at three bromide concentrations for the mixed-ligand system.

additional ligand. The only case in which the shift in half-wave potential is a proof of formation of mixed-ligand complexes is that in which, at a given concentration of both ligands, the negative shift of the half-wave potential is larger than the shift obtained for either of the simple systems at the same metal and total ligand concentrations, but this is not the common case.

The formation of mixed-ligand complexes is unequivocally indicated by agreement of the experimental results with the equations:

$$F_{00}(X, Y) = \text{antilog} \left(\frac{0.434 nF}{RT} \Delta E_{1/2} + \log \frac{I_s}{I_c} \right) \\ = A + B[X] + C[X]^2 + D[X]^3 + E[X]^4$$

where

$$A = \beta_{00} + \beta_{01}[Y] + \beta_{02}[Y]^2 \\ + \beta_{03}[Y]^3 + \beta_{04}[Y]^4 \\ B = \beta_{10} + \beta_{11}[Y] + \beta_{12}[Y]^2 + \beta_{13}[Y]^3 \\ C = \beta_{20} + \beta_{21}[Y] + \beta_{22}[Y]^2 \\ D = \beta_{30} + \beta_{31}[Y] \\ E = \beta_{40}$$

the β_{ij} values being the overall stability constants of the system (for simple complexes i or $j = 0$).

This treatment represents an extension of the Schaap and McMasters method³ for mixed-ligand complexes to the case in which in the single systems a maximum of four ligands attached to the central ion, as we have seen for cadmium-bromide and cadmium-iodide. This is the first time the Schaap and McMasters treatment has been applied to a system where fourteen complexes co-exist.

The values of all the stability constants in the equations above can be obtained if the half-wave potentials and diffusion currents of at least three

series of solutions are measured, each series at a constant concentration of Y (bromide in our case) and increasing concentrations of X (iodide), as indicated in Fig. 7 for $\Delta E_{1/2}$. The stability constants of the simple systems have already been determined. The constants B , C and D can be obtained from a least-squares treatment of the functions:

$$F_{10} = \frac{F_{00} - A}{[X]} = B + C[X] + D[X]^2 + E[X]^3 \\ F_{20} = \frac{F_{10} - B}{[X]} = C + D[X] + E[X]^2 \\ F_{30} = \frac{F_{20} - C}{[X]} = D + E[X]$$

or an extrapolation to zero ligand concentration of the graphical plot of the corresponding functions, as in Figs. 8-10. A can be obtained in the same way from F_{00} or from the stability constants of the cadmium-bromide system; F is the highest constant of the cadmium-iodide system. As can be seen in Figs. 8-10 and Table 2, A and E obtained graphically or numerically agree satisfactorily with the values obtained from the simple systems.

Graphical and numerical values of B , C and D in each series show excellent agreement, which is a proof of the applicability of the method.

In Table 3 experimental values of the stability constants obtained by graphical and numerical calculation are shown together with maximum deviations calculated from the standard deviations of the constants A , B , C , D and E obtained by least-squares calculation; statistical constants are also shown.

Statistical calculations. The logarithm of the N th root of β_N for a simple complex— $\log \beta_N^{1/N}$ —may be taken as a measure of the free enthalpy change per ligand, due to replacement of the bound water in the aquo complex. Bjerrum¹⁷ used this value as a measure of the tendency of a ligand to form a complex.

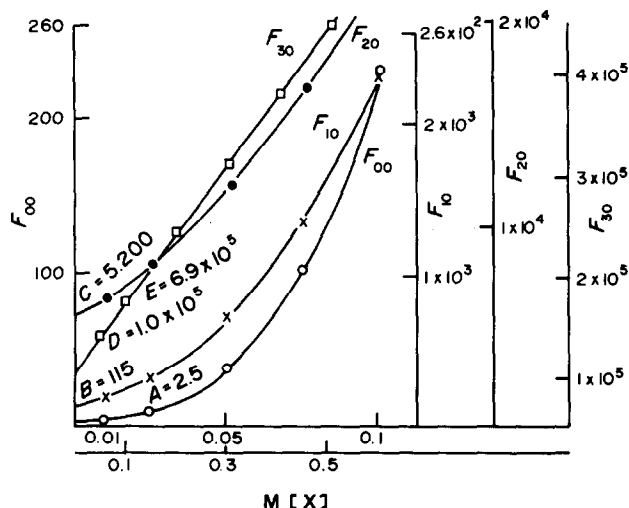


Fig. 8. Plots of F_{00} (○), F_{10} (×), F_{20} (●) and F_{30} (□) vs. iodide concentration at [bromide] = 0.05M for the mixed-ligand system.

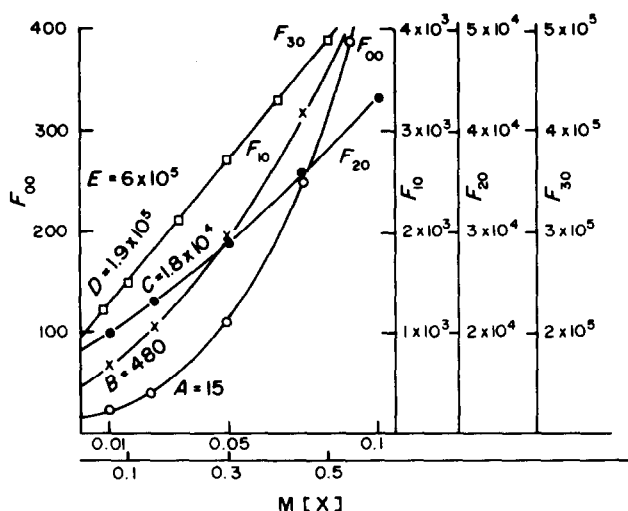


Fig. 9. F_{00} (○), F_{10} (×), F_{20} (●) and F_{30} (□) vs. iodide concentration at [bromide] = 0.2M for the mixed-ligand system.

Assuming that in a system there are two ligands A and B (at the same concentration), each of which is capable of forming four complexes with the central ion, the probability that four successive ligands of the same kind (e.g., A) will be attached to the central ion M is $(1/2)^4 = 1/16$. The same probability holds for MB_4 . The other fourteen combinations are divided among MB_3A , MB_2A_2 and MBA_3 . According to this, the stability constants for these complexes would be predicted to be

$$\beta_{31} = 4.66\beta_{40}^{3/4}\beta_{04}^{1/4}$$

$$\beta_{22} = 4.66\beta_{40}^{2/4}\beta_{04}^{2/4}$$

$$\beta_{13} = 4.66\beta_{40}^{1/4}\beta_{04}^{3/4}$$

In the case of the complexes MAB , MA_2B and MAB_2 the statistical factors favouring mixed-ligand

complex formation are two for the first and three for the second and third. The term $\beta_N^{1/N}$ contains a gross statistical factor of $4/2$ for MAB and $4/3$ for MA_2B and MAB_2 , because there are two and three ligands, respectively, available to occupy four sites around the central ion. Then the ligand factors will be $(2/4)^{1/N}$ and $(3/4)^{1/N}$. In summary, the statistical stability constants for these complexes would be:

$$\beta_{11} = 2\left(\frac{2}{4}\beta_{20} \cdot \frac{2}{4}\beta_{02}\right)^{1/2}$$

$$\beta_{21} = 3\left(\frac{3}{4}\beta_{30}\right)^{2/3}\left(\frac{2}{4}\beta_{03}\right)^{1/3}$$

$$\beta_{12} = 3\left(\frac{2}{4}\beta_{30}\right)^{1/3}\left(\frac{2}{4}\beta_{03}\right)^{2/3}$$

The statistical values according to these calculations are given in Table 3. Attention is drawn to the good agreement between the statistical and experi-

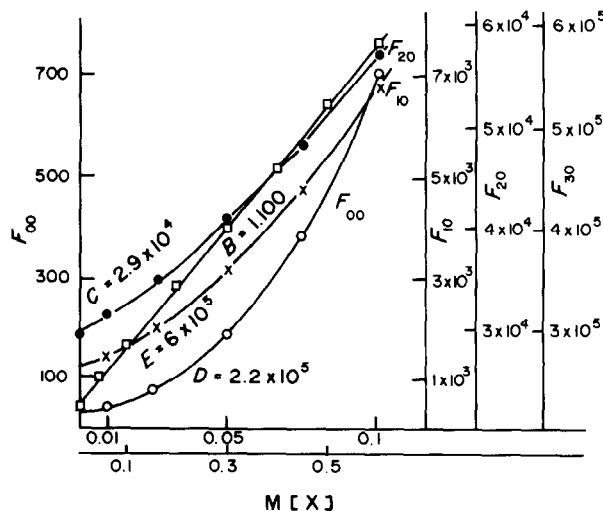


Fig. 10. F_{00} (○), F_{10} (×), F_{20} (●) and F_{30} (□) vs. iodide concentration at [bromide] = 0.3M for the mixed-ligand system.

Table 2. Values of the constants A , B , C , D and E at three levels of bromide concentration (I, 0.05M; II, 0.2M; III, 0.3M)

	Graphical	Numerical
A_I	2.5 ± 0.2	2.2 ± 0.2
A_{II}	15 ± 1	13.5 ± 0.8
A_{III}	25 ± 1	24.3 ± 0.4
B_I	115 ± 10	117.9 ± 1.1
B_{II}	480 ± 50	479 ± 0.8
B_{III}	1100 ± 100	1098 ± 0.6
C_I	$(52 \pm 10) \times 10^2$	$(50.18 \pm 0.06) \times 10^2$
C_{II}	$(180 \pm 10) \times 10^2$	$(180 \pm 0.03) \times 10^2$
C_{III}	$(290 \pm 10) \times 10^2$	$(29.03 \pm 0.02) \times 10^2$
D_I	$(100 \pm 1) \times 10^3$	$(101.5 \pm 0.7) \times 10^3$
D_{II}	$(190 \pm 1) \times 10^3$	$(190.0 \pm 0.2) \times 10^3$
D_{III}	$(220 \pm 1) \times 10^3$	$(219.9 \pm 0.2) \times 10^3$
E_I	$(690 \pm 10) \times 10^3$	$(688.0 \pm 1.2) \times 10^3$
E_{II}	$(600 \pm 10) \times 10^3$	$(599.9 \pm 0.3) \times 10^3$
E_{III}	$(600 \pm 10) \times 10^3$	$(600.1 \pm 0.2) \times 10^3$

Table 3. Graphical, numerical and statistical values of the stability constants of the mixed-ligand complexes in the cadmium-bromide-iodide system

	Experimental		Statistical
	Graphical	Numerical	
β_{11}	423	459 ± 94	382
β_{12}	3.7×10^3	$(3.2 \pm 0.6) \times 10^3$	3.9×10^3
β_{13}	20.7×10^3	$(21.6 \pm 1.1) \times 10^3$	21.3×10^3
β_{11}	67.7×10^3	$(68.6 \pm 1.7) \times 10^3$	18.0×10^3
β_{11}	85.7×10^3	$(83.3 \pm 3.4) \times 10^3$	115.0×10^3
β_{31}	590×10^3	$(607 \pm 9) \times 10^3$	619.8×10^3

mental values, with only the (unexplained) exception of β_{21} .

It has been claimed that the experimental stability constants of mixed-ligand complexes are higher than the statistically calculated constants,^{3,6,7} for electrostatic or steric reasons. According to the results of this work we think that no such effect should be

expected when the ligand characteristics are similar. As Table 3 indicates, the experimental values are not generally higher than the statistical values for the systems examined.

Acknowledgements—Thanks are due to the Consejo Nacional de Investigaciones Científicas y Técnicas de la República Argentina and to the Comisión de Investigaciones Científicas de la Provincia de Buenos Aires for financial support.

REFERENCES

1. D. DeFord and D. N. Hume, *J. Am. Chem. Soc.*, 1951, **73**, 5321.
2. A. Ringbom and L. E. Ericksson, *Acta Chem. Scand.*, 1951, **7**, 1105.
3. W. B. Schaap and D. L. McMasters, *J. Am. Chem. Soc.*, 1961, **83**, 4699.
4. S. C. Khurana and G. Gupta, *J. Inorg. Nucl. Chem.*, 1973, **35**, 209.
5. S. C. Khurana, D. N. Chatuvedi and J. N. Gaur, *ibid.*, 1973, **35**, 1645.
6. S. C. Baghel, K. K. Choudhary and J. N. Gaur, *ibid.*, 1975, **37**, 2513.
7. D. G. Dhuley, D. V. Jahagudar and D. N. Khanokhar, *ibid.*, 1975, **37**, 2135.
8. P. H. Tedesco and J. Martínez, *An. Asoc. Quim. Arg.*, 1978, **66**, 159.
9. *Idem*, *J. Inorg. Nucl. Chem.*, 1980, **42**, 95.
10. K. Momoki, H. Sato and H. Ogawa, *Anal. Chem.*, 1967, **39**, 1072.
11. I. Piljac, B. Gravarić and I. Filipović, *J. Electroanal. Chem. Interf. Electrochem.*, 1973, **42**, 433.
12. I. Filipović, T. Matusmović, B. Mayer, I. Piljac, B. Bach-Dragutinović and A. Bujak, *Croat. Chim. Acta*, 1970, **42**, 541.
13. A. M. Bond and G. Hefter, *J. Electroanal. Chem. Interf. Electrochem.*, 1971, **31**, 477.
14. *Idem*, *ibid.*, 1973, **42**, 1.
15. *Idem*, *ibid.*, 1976, **68**, 203.
16. A. E. Martell and L. C. Sillén, *Stability Constants of Metal-Ion Complexes*, The Chemical Society, London, 1971.
17. J. Bjerrum, *Chem. Rev.*, 1950, **46**, 381.

SOME REMARKS ON THE INFORMATION POWER AND SELECTIVITY OF ANALYTICAL PROCESSES

J. INCZÉDY

Institute of Analytical Chemistry, University of Veszprém, Veszprém, Hungary

(Received 7 March 1983, Revised 1 September 1983. Accepted 8 September 1983)

Summary—The consistency of the equation given by Shannon for the transfer of maximum amount of information in one channel, and the equation deduced by Kaiser for the expression of the information power of analytical methods is shown. The fundamental difference between the maximum amount of information obtainable by an instrument and that by an analytical procedure is reported. In the second case the selectivity of the analytical procedure also has to be taken into consideration.

In the early fundamental work of Shannon,¹ an equation was deduced for the transfer of the maximum average amount of information through a channel, the input being a continuous signal-time function $x(t)$, of duration T and sampled at constant intervals with a sampling frequency of $f_s = 2f_{\max}$, where f_{\max} is the maximum-frequency component of the signal function (carrying useful information). This equation is

$$H_{x(t)} = n_t \log_2 \left[\frac{P_S + P_N}{P_N} \right]^{1/2} \\ = f_{\max} T \log_2 \left[\frac{P_S + P_N}{P_N} \right] \text{ bits} \quad (1)$$

where n_t is the number of sample points (and so is equal to $2f_{\max}T$), P_S is the signal power, P_N is the noise power.

This equation is one of the most important in the theory of telecommunication, because it gives quantitative relations between frequency band-width, time, signal-to-noise ratio and amount of information, the last being expressed in bits. Using a longer time interval and narrower band-width allows the same amount of information to be transferred as with a larger band-width but shorter time interval. To increase the amount of information transferred in unit time, either the frequency band-width or the signal-to-noise ratio has to be increased.

The channel capacity c (expressed in bits) is defined as the maximum average amount of information transferred in unit time.

$$c = \frac{H_{x(t)}}{T} = f_{\max} \log_2 \left[\frac{P_S}{P_N + 1} \right] \text{ bits.} \quad (2)$$

If we wish to transpose equation (1) from the time domain into the frequency domain, *i.e.*, we wish to find the analogous expression in the frequency domain into the frequency domain, *i.e.* we wish to find the analogous expression in the frequency domain, the following points need consideration.

The $x(t)$ signal-time function corresponds to its Fourier transform in the frequency domain. Because

the duration of the signal transfer is finite and the sampling gives discrete data, the transformation can be carried out by the s.c. discrete Fourier transform (which is an estimation of the Fourier transform), which will contain $n_t/2$ terms and $n_t/2$ amplitudes. Using a formulation very similar to equation (1), but defined in the frequency domain, we obtain

$$H_{x(f)} = \frac{n_t}{2} \log_2 \left[\frac{X_i}{\delta X_i} \right] \text{ bits} \quad (3)$$

where X_i stands for the i th amplitude of the spectrum

$$X_i = \sqrt{A_i^2 + B_i^2} \quad (4)$$

A_i denoting the real and B_i the imaginary part of the transform; δX_i denotes the smallest distinguishable difference between two values of the amplitudes. This difference depends on the quality of the channel, *i.e.*, on the noise level. If we use this formula for description of the amount of information obtainable from an instrument then δX depends on the noise of the instrument. Equations (1) and (3) are similar. The square root of the power ratio in equation (1) corresponds to the ratio $X_i/\delta X_i$ in equation (3), with the difference that in the latter case—by convention—the signal and noise are not summed in the numerator, and δX is not the root mean square of the noise, but a value proportional to the noise (*viz.* $2ks$ where k is the value of student's t for the significance level chosen, s is the standard deviation of the noise, and the factor 2 allows for deviation in either direction).

Taking the resolution $R(f)$ as

$$R(f) = \frac{f}{\delta f}, \quad (5)$$

considering that $\delta f = 1/T$, and setting the limits of the frequency band between $f = 0$ and f_{\max} as f_1 and f_2 , then the number of distinguishable amplitudes in the frequency domain will be

$$n_t = \int_{f_1}^{f_2} \frac{R(f)}{f} df \quad (6)$$

and n_f will be less than $n_f/2$ (except when the bandwidth is from $f = 0$ to f_{\max}).

Since the ratio $X/\delta X$ usually depends on the frequency, the mean value of the ratio can be obtained by integration over the frequency range f_1 – f_2 . Thus, the mean value of the $X/\delta X$ ratio, expressed as the average number of distinguishable steps, \bar{N} , is:

$$\bar{N} = \frac{1}{n_f} \int_{f_1}^{f_2} \frac{X}{\delta X} df. \quad (7)$$

By substitution from equations (5)–(7), equation (3) becomes:

$$H_{X(f_1-f_2)} = \int_{f_1}^{f_2} R(f) \frac{df}{f} \log_2 \bar{N}. \quad (8)$$

This equation was first introduced by Kaiser² for expressing the information power of spectroscopy. By generalization—using the z co-ordinate instead of frequency—the equation can be used for any two-dimensional instrumental analytical method. In this general formula the intensity of the amplitude, *i.e.*, the signal we use, is simply x . Thus,

$$H_{x(z_1-z_2)} = \int_{z_1}^{z_2} R(z) \frac{dz}{z} \log_2 \bar{N} \quad (9)$$

Kaiser's ingenious concept corresponds to the general aspects of the telecommunication theory. However, in connection with the use of equation (9) two very important points must be considered.

The first is that it has to be distinguished very clearly whether we speak of the *amount* of information (not the information *power*, because time is not included) obtainable by an instrument, or by an analytical procedure. Equation (9) is valid for both. If we use it for instruments, then the resolution of the instrument $R = z/\delta z$ and $N = x/\delta x$ have to be taken into consideration, and if we use it for an analytical procedure, then the resolution of the procedure, which is the resolution of the components to be determined, (*i.e.*, the selectivity), $R = z/\Delta z$ and $N = c/\Delta c$ has to be used. Thus the R and N values differ considerably, depending on whether the instrument or the analytical procedure is concerned. For expressing N for the instrument we use the signal intensity x , but to express it for the procedure we use the concentration c .

For example, let us consider a spectrophotometer. It has quite a large resolution in the wavelength range 200–800 nm, because $\delta z = 1$ nm can be distinguished. The resolution depends on the dispersion unit and the slit setting used, *i.e.*, on the technical parts of the instrument. The value of δx again depends on the noise of the instrument. It can be approximated by taking four times the root mean square of the noise power. If, however, we wish to express the amount of information obtainable by an analytical procedure, then for R we have to take the resolution of the components, or the resolution of the corresponding wave bands Δz , and the least discernible concentration difference distinguished by the analytical pro-

cedure, Δc , which is connected with the standard deviations of the determinations. The Δz value is usually 50–100 nm. The standard deviations of the determinations include not only the precision of the instrument, but also all the other statistical errors which arise from sampling, preliminary treatment of the sample, the evaluation of the result, calibration errors, *etc.* Thus, $\Delta z \gg \delta z$ and $\Delta c \gg \delta c$.

It is interesting to note that the resolution of a procedure usually does not depend on the resolution of the instrument used for detection, because in most cases $\Delta z \gg \delta z$. This is also the case in chromatography, where the resolution of the detector is fairly high, but the resolution of the procedure depends on the column parameters (selectivity factor, plate number of the column). The detection system becomes the limiting factor of the selectivity of the procedure only when Δz is less than δz , or they are comparable in magnitude.

The smaller the value of Δz for a procedure, the greater is the selectivity, and the greater the number of components with similar behaviour which can be determined by the same procedure in the presence of each other, assuming that their distribution in the direction of co-ordinate z is optimal or favourable. With increasing selectivity, *i.e.*, decreasing Δz value, the maximum amount of information obtained by the procedure will increase. This fully corresponds to the points made in our previous paper³ on the quantitative expression of the selectivity of analytical procedures.

The second important point is that when we use equation (9) for calculation of the amount of information, then in some cases Δz or δz can be considered constant over the range z_1 – z_2 investigated. This is the case, for example, with spectrophotometers or spectrophotometric determinations. In some other cases, however, the ratio $z/\Delta z$ can be taken as constant, *e.g.*, when we want to calculate the amount of information obtainable by a column chromatographic method. When an isocratic elution procedure is used in liquid chromatography the plate number of the column (N) can be assumed constant in the range investigated, since

$$\sqrt{N} = \frac{t_r}{w} = \frac{z}{\Delta z} \quad (10)$$

where t_r and w are the retention time and peak width, respectively.

For a one-dimensional analytical procedure, *e.g.*, determination of iron by titration, or by spectrophotometry in the absence of other components which can be determined similarly, equation (9) reduces to

$$H = \log_2 N = \log_2 \frac{c}{\Delta c} \quad (11)$$

EXAMPLES

(1) The working range of a spectrophotometer is

200–800 nm and its resolution is 1 nm. Hence $z_1 = 200$; $z_2 = 800$; $\delta z = 1$. The precision of determination of the transmittance is *ca.* $\pm 0.5\%$ (*i.e.*, $\delta x = 1.0$). The absorption band-width of a molecule is, in general, 60 nm. The confidence interval for the spectrophotometric determination is *ca.* $\pm 5\%$. What is the maximum amount of information obtainable with the spectrophotometer (maximum number of distinguishable signal values), and what is the maximum amount of information when the spectrophotometer is used as an analytical tool for the determination of the concentration of different molecules?

In both cases equation (9) is used. For the instrument:

$$\int_{200}^{800} \frac{z}{1} \frac{1}{z} dz = \left[z \right]_{200}^{800} = 600$$

$$H_{\text{instr}}^{\text{max}} = 600 \log_2 \frac{100}{1.0} = 3986 \text{ bits.}$$

For the analytical procedure

$$\int_{200}^{800} \frac{z}{60} \frac{1}{z} dz = \frac{1}{60} \left[z \right]_{200}^{800} = 10$$

$$H_{\text{proc}}^{\text{max}} = 10 \log_2 \frac{100}{10} = 33.2 \text{ bits.}$$

This is the maximum amount of information which can be obtained by the analytical procedure if optimal conditions are ensured, *i.e.*, the components are present in equal amounts, the spectra show a uniform distribution, the resolution is optimum, *etc.* Six components can be determined in the presence of each other.

If the spectrophotometer is used for the determination of a single component, then the information obtained is:

$$H_{\text{proc}}^1 = \log_2 10 = 3.32 \text{ bits.}$$

The relative redundancy is

$$100 \left(\frac{33.2 - 3.32}{33.2} \right) = 90\%.$$

(2) An ion-exchange column is used for the separation of cations, with hydrochloric acid as eluent.

The mean plate number of the column for the elution of simple univalent ions under the given conditions (temperature, flow-rate, column length, *etc.*) is 16. The dead-time of the column is 2 min. The detection is based on conductivity measurements. The amounts of the ions present are determined from the recorded peak areas, with an error of $\pm 1\%$. What is the maximum information obtainable by the chromatographic system, if the chromatographic procedure takes (a) 10 and (b) 20 min?

The calculation is done by using equations (10) and (9). First, the value of the resolution is calculated:

$$\sqrt{16} = \frac{t_r}{w} = \frac{z}{\Delta z} = 4.$$

When the elution takes 10 min, since the dead-time is 2 min, the detection is confined to an effluent volume corresponding to the last 8 min of flow, so:

$$4 \int_2^{10} \frac{1}{z} dz = 4 \ln \frac{10}{2} = 6.4$$

$$H_{10}^{\text{max}} = 6.4 \log_2 \frac{100}{2} = 36 \text{ bits.}$$

For the 20-min procedure:

$$4 \int_2^{20} \frac{1}{z} dz = 4 \ln \frac{20}{2} = 9.2$$

$$H_{20}^{\text{max}} = 9.2 \log_2 \frac{100}{2} = 52 \text{ bits.}$$

Thus, the maximum amount of information obtainable by the chromatographic system is 36.1 bits for a 10-min run. In the luckiest case six different ions can be determined. If the 20-min run is chosen, then the total amount of information is remarkably less than twice that obtainable in the 10-min run, since the peak-widths are increasing linearly with time, and only two (or possibly three) further components can be determined by use of the additional 10 min of running time.

REFERENCES

1. C. E. Shannon, *Bell System Tech. J.*, 1948, **27**, 379, 623; *Proc. I.R.E.*, 1949, **37**, 10.
2. H. Kaiser, *Anal. Chem.*, 1970, **42**, No. 2, 24A.
3. J. Inczédy, *Talanta*, 1982, **29**, 595.

ION-PAIR EXTRACTIONS WITH 12-CROWN-4 AND ITS ANALOGUES

G. E. PACEY and Y. P. WU

Miami University, Department of Chemistry, Oxford, OH 45056, U.S.A.

(Received 20 October 1982. Revised 28 August 1983. Accepted 14 October 1983)

Summary—The complexing abilities of 12-crown-4 and its analogues have been investigated by using ion-pair extractions. A relationship exists between the type of substitution on the 12-crown-4 and the complexing ability and selectivity. Additionally, the selectivities vary according to the reagent concentrations. The compound 12-crown-4 can be used to complex sodium selectively in the presence of other alkali-metal ions. A method for determining serum sodium-ion concentrations has been developed.

Potassium and sodium have been determined by flame emission spectrophotometry, potentiometry with ion-selective electrodes, and atomic absorption. Recently, the crown ether and cryptand types of reagent have been used to complex alkali-metal ions selectively. Crown ethers and cryptands can be used in intermolecular ion-pair extractions^{1,2} or synthetically modified to make chromogenic crown ethers³⁻⁷ which can be used in intramolecular ion-pair extractions for the determination of alkali metals. Unfortunately, the determination of sodium by ion-pair extraction has only been accomplished by using the expensive compound called cryptand 211, with picrate as the counter-ion and toluene as the solvent.²

Recent studies on the ion-pair extraction behaviour of 12-crown-4 and benzo-12-crown-4 with picrate as the counter-ion and dichloromethane as the solvent have disclosed another choice of crown ether for the determination of sodium by ion-pair extraction. In addition, several analogues of 12-crown-4 have been studied. This paper reports the ion-pair data for 12-crown-4 and its analogues for various solvents, anions and reagent concentrations. A method for the determination of serum sodium with 12-crown-4 is presented.

investigation were added, and the mixture was mechanically shaken at a constant rate for 10 min at room temperature (*ca.* 24°). After phase separation the concentration of the picrate-crown ether ion-pair complex in the organic phase was determined spectrophotometrically at the appropriate wavelength (Table 1) and compared with the original aqueous concentration of picrate.

Extraction constants were determined by mixing equal volumes of 0.1–10⁻⁴*M* alkali-metal chloride and 10⁻⁴*M* picric acid in a 100-ml round-bottomed flask, and diluting to 10 ml with water, extracting with 10 ml of 10⁻⁴*M* crown ether solution in the solvent under investigation, and analysing the extracts as already described.

Partition coefficients were determined by the Frensdorff method¹ by equilibration of equal volumes of water and the solution of crown ether in organic solvent, followed by spectrophotometric determination of the amount of crown ether extracted into the aqueous phase. The determination was done by addition of picric acid and potassium hydroxide to the aqueous phase and extraction of the crown ether/potassium/picrate complex into dichloromethane. The concentration found in this way for the aqueous phase was subtracted from the initial total concentration of crown ether to deduce the concentration left in the organic phase. The partition coefficients were determined at several crown ether concentrations between 0.01 and 0.1*M* in the organic phase.

The recommended procedure for serum sodium-ion determination is to take 1 ml of serum sample in a 10-ml centrifuge tube and add 4 ml of 1.5% aqueous tri-

EXPERIMENTAL

Reagents

The reagents were 12-crown-4 (Aldrich) and 12-crown-4 analogues⁸ (shown in Fig. 1), spectrophotometric grade solvents (Aldrich) and at least 99.5% pure alkali-metal chlorides (Alfa). The picric acid was titrated potentiometrically to determine its purity. All water was prepared with a Barnstead "Nanopure" system.

Extraction procedures

For all procedures using alkali-metal chlorides the pH of the solution was 3.2, but 11.7 when the hydroxides were used.

The degree of extraction was determined by transferring standard alkali-metal chloride and picric acid solutions into a 100-ml round-bottomed flask and diluting to 10 ml with water to give final concentrations of alkali-metal ion and picric acid of 0.1*M* and 10⁻⁴*M* respectively. Then 10 ml of a crown ether solution (10⁻⁴–10⁻²*M*) in the solvent under

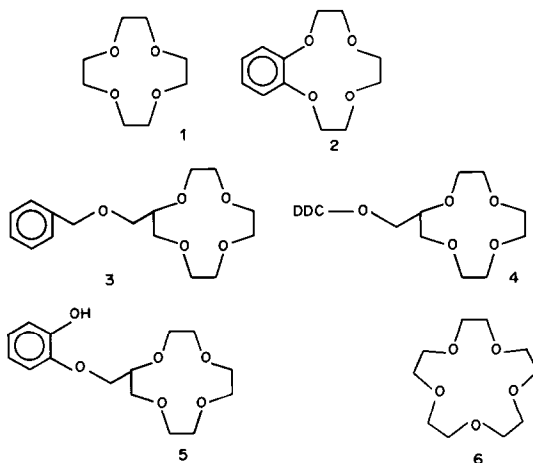


Fig. 1. Crown ethers used: DDC = dodecyl group.

Table 1. Spectral data for picrate-crown ether ion-pair complex in various solvents

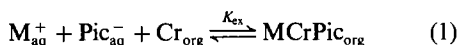
Solvent	λ_{\max} , nm		Complex ϵ_{\max} , $l. \text{mole}^{-1}. \text{cm}^{-1}$
	Picric acid	Complex	
CH ₂ Cl ₂	350	375	1.8×10^4
CH ₃ Cl	—	360	7.3×10^3
CCl ₃ CH ₃	—	380	7.7×10^3

The value of λ_{\max} for the complex is practically independent of which crown ether is used.

chloroacetic acid solution. After thorough mixing (for approximately 5 min), centrifugation of the protein precipitate, and decantation, 1 ml of the solution is transferred into a 250-ml standard flask and diluted to volume with water. In the rest of the procedure the reagent volumes must be dispensed as reproducibly as possible, as slight variations in the reagent concentrations can adversely affect the results. Five ml of the diluted sample are placed in a 100-ml round-bottomed flask with 10 ml of $7 \times 10^{-4}M$ crown ether solution in dichloromethane and 5 ml of $7 \times 10^{-4}M$ picric acid, and the flask is mechanically shaken for 10 min at constant temperature. The absorbance of the organic phase is measured and evaluated with a calibration graph.

RESULTS

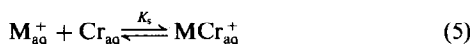
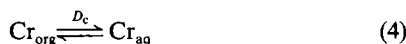
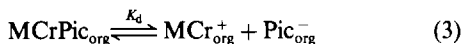
The extraction equilibrium for alkali-metal ion (M^+), picrate ion (Pic^-) and crown ether (Cr) is represented by the equation



where MCrPic denotes the ion-pair in the organic phase. Therefore, the extraction constant is given by¹

$$K_{\text{ex}} = \frac{[\text{MCrPic}]_{\text{org}}}{[M^+]_{\text{aq}} [\text{Pic}^-]_{\text{aq}} [\text{Cr}]_{\text{org}}} \quad (2)$$

Four other equilibria must be kept in mind in order to account for the distribution of all components; the dissociation of MCrPic_(org) [equation (3)], the distribution of the crown ether [equation (4)], the complexation of the metal with the crown ether in the aqueous phase [equation (5)] and the distribution of undissociated picric acid [equation (6)]. If the organic phase is polar, at low concentrations the ion-pair will partially dissociate according to equation (3). Evaluation of the K_d value proved this dissociation to be negligible.



The partition coefficients shown in Table 2 indicate that the best solvent to use is dichloromethane; 12-crown-4 is not appreciably soluble in any other solvent tested. Additionally, the partition coefficients suggest that practically no crown ether will be lost to

the aqueous phase by partition during the extraction. Resazurin (previously used for ion-pair studies with cryptands) exhibited little extraction as a crown ether ion-pair complex, and could not be used.

No detectable extraction was found in the absence of either picrate or crown ether when alkali-metal hydroxides were used, so the concentrations of hydroxide ion and uncomplexed alkali-metal picrate in the organic phase can be taken as negligible under these conditions. However, a certain amount of the picric acid was extracted when alkali-metal chlorides were used and the extraction was done at pH 3.2. This is in agreement with the findings of Gustavii and Schill,¹¹ who reported a value of $10^{2.04}$ for the distribution coefficient of picric acid between water and dichloromethane [$K = [\text{HPic}]_{\text{org}} / ([\text{HPic}]_{\text{aq}} + [\text{Pic}^-]_{\text{aq}})$]. The same authors reported that the apparent dissociation constant of picric acid at 0.1M ionic strength is $10^{-0.33}$, which implies that at pH 3.2 about 13% of the free picrate would be extracted as picric acid. The molar absorptivities ($l. \text{mole}^{-1}. \text{cm}^{-1}$ at 375 nm) in dichloromethane are about 2×10^3 for picric acid and 1.8×10^4 for picrate in an ion-association complex, so the picric acid extracted would give a signal equivalent to that for a crown ether/alkali metal/picrate concentration equal to about 1.5% of the free picrate concentration in the aqueous phase (if equal volumes are used). As the free picrate concentration will depend on the alkali-metal ion concentration, this source of error will also be dependent on the alkali-metal concentration, but will be automatically compensated for in the calibration, provided that the pH and the volume of picrate added are kept practically constant for samples and standards. Under those conditions a blank should not be necessary for a particular batch of reagents and the accompanying calibration graph.

Table 3 indicates several interesting points. First, 12-crown-4, when used with dichloromethane and picrate, is a selective reagent for sodium. With equal concentrations of crown ether and picrate, lithium is extracted more efficiently than potassium, but the reverse is the case at higher crown ether concentrations. This is not surprising since potassium preferentially forms a 2:1 crown ether:metal complex.¹²

Table 2. Partition coefficients (D_c) of 12-crown-4 and benzo-12-crown-4 between various solvents and water ($D_c = [\text{Cr}]_{\text{aq}} / [\text{Cr}]_{\text{org}}$)

Solvents	Crown ether	D_c
Dichloromethane	12-C-4	3.1×10^{-3}
	B-12-C-4	7.4×10^{-4}
Chloroform	12-C-4	NE
	B-12-C-4	6.9×10^{-3}
1,1,1-Trichloroethane	12-C-4	NE
	B-12-C-4	1.6×10^{-3}
Toluene	12-C-4	NE
	B-12-C-4	NE

NE = no extraction.

The degree of extraction is increased when the alkali-metal hydroxides are used instead of the chloride.

We believe this is due to the shift in picric acid dissociation, caused by the change in pH, since the effective picrate concentration will be increased (see preceding paragraph).

Benzo-12-crown-4 does not extract lithium at all in the presence of picrate. For other alkali-metal ions, benzo-12-crown-4, picrate and various solvents, the degree of extraction depends on the solvent used, increasing in the order toluene \ll 1,1,1-trichloroethane $<$ chloroform $<$ dichloromethane. This order is not a function of dielectric constants, since these are in the order chloroform (4.8) $<$ 1,1,1-trichloroethane (7.1) $<$ dichloromethane (9.1).

Compounds 3 and 4 are interesting in comparison to 12-crown-4 and benzo-12-crown-4 in terms of extraction ability. Compound 4 is much more selective than compound 3 for sodium. Molecular models suggest that this may be due to the rigid benzene ring acting as a cap to the cavity. This should increase the stability of the potassium, rubidium and caesium complexes. The dodecyl group would not form a good cap, so only ions that fit well into the cavity would be extracted efficiently. This explanation seems acceptable since the degree of extraction for sodium is essentially the same for both compounds, whereas that for the larger cations varies markedly. Compound 4 behaves similarly to 12-crown-4 but compound 3 has extraction behaviour in between that of benzo-12-crown-4 and of 12-crown-4.

Compound 5 behaves more like benzo-12-crown-4. Deprotonation of the phenolic group enhances the extraction, probably because the charged group will

act as an additional stabilizing factor when positioned over the cyclic crown ring. Interestingly, the difference between compounds 3 and 5 was the extra methylene group in compound 3 and the phenol group in compound 5. If we assume that the protonated phenolic group has little effect on the extraction process, then the addition of the methylene group has a significant impact on the extraction system, possibly because of the extra flexibility of the side-chain.

It appears from all the data that a change in extraction selectivity can be accomplished by varying the ratio of crown ether to counter-ion. With potassium, rubidium and caesium capable of forming 2:1 and 3:2 crown ether to metal complexes, any increase in the crown ether concentration improves the degree of extraction of these ions. If the crown ether concentration is more than ten times that of picrate, the selectivity of the crown ethers will change in favour of the larger alkali-metal ions. The selectivity for the smaller ions is increased by lower (preferably equal) concentrations of crown ether and picrate, but there is some loss of overall extraction efficiency.

Table 4 gives the extraction constants for the crown ether/alkali metal/picrate complexes. The data in Tables 3 and 4 indicate that the ion-pair system with dichloromethane as the solvent and picrate as the counter-ion transforms 12-crown-4 into a selective complexing agent for sodium, in the presence of other alkali metals. The data also indicate that only high concentrations of lithium would interfere seriously. On the other hand, benzo-12-crown-4 exhibits no selectivity other than its exclusion of lithium in the extraction process. The data in Table 4 confirm the

Table 3. Picrate extracted (%) for certain solvent, crown ether and alkali metal systems ([alkali metal] = 0.1M)

Crown ether	Method	Li ⁺	Na ⁺	K ⁺	Rb ⁺	Cs ⁺	Solvent
1	A,C	0.46	2.69	NE	NE	NE	CH ₂ Cl ₂
1	A,D	0.36	1.99	0.08	NE	NE	CH ₂ Cl ₂
1	B,B*	1.7	19.9	5.3	3.5	2.6	CH ₂ Cl ₂
1	B,C	—	28.9	5.8	1.7	0.6	CH ₂ Cl ₂
1	B,D	—	33.45	7.5	1.9	1.1	CH ₂ Cl ₂
2	A,C	—	3.3	7.0	8.9	8.7	CH ₂ Cl ₂
2	A,C	—	0.33	3.1	4.9	7.0	CHCl ₃
2	A,C	—	0.17	2.5	3.4	4.4	TCE
3	B,D*	2.6	15.2	14.1	13.0	12.6	CH ₂ Cl ₂
4	B,D*	1.8	15.4	4.2	3.1	2.6	CH ₂ Cl ₂
5	A,C	—	—	—	—	—	—
	Protonated	—	2.3	8.5	8.9	8.0	CH ₂ Cl ₂
	A,C	—	—	—	—	—	—
	Deprotonated	—	4.1	14.3	15.5	14.3	CH ₂ Cl ₂
6	A,C	2.4	35.6	57.7	38.5	17.6	CH ₂ Cl ₂
6	A,D	NE	18.2	99.9	59.8	32.0	CH ₂ Cl ₂

NE = No extraction.

TCE = 1,1,1-trichloroethane.

Method A = 10⁻⁴M picrate and crown ether.

B = 10⁻⁴M picrate and 10⁻²M crown ether.

C = alkali-metal chloride.

D = alkali-metal hydroxide.

*Data from Miyazaki *et al.*¹⁰

Table 4. Logarithmic extraction constants for crown ether picrate ion-pair extraction of alkali-metals

System	Li ⁺	Na ⁺	K ⁺	Rb ⁺	Cs ⁺
CH ₂ Cl ₂ /12-C-4	1.49 ± 0.14	3.04 ± 0.04	NE	NE	NE
CH ₂ Cl ₂ /B-12-C-4	NE	3.05 ± 0.04	4.01 ± 0.04	4.41 ± 0.06	4.46 ± 0.11
Benzene/12-C-4	-1.62	-1.44	-1.82	-2.10	-2.18 ⁹
Benzene/15-C-5	-1.10	1.51	0.19	-0.25	-0.49 ⁹
CHCl ₃ /B-12-C-4	NE	NE	2.40 ± 0.18	2.90 ± 0.08	3.04 ± 0.07
CCl ₃ CH ₃ /B-12-C-4	NE	NE	3.18 ± 0.03	3.09 ± 0.01	3.01 ± 0.15

Table 5. Serum sodium level determination

Sample	Sodium found, meq/l.	
	This method	Hospital value (flame photometry)
1	147	145
2	136	135
3	136	136
4	142	140

selectivities (especially that of 12-crown-4 for sodium). The data for ion-pair extraction with picrate and benzene show that our system is considerably better and more selective.

In an attempt to find a "real" application for this extraction system, 12-crown-4, picrate and dichloromethane were used to determine sodium in blood serum. A calibration curve was prepared with standard sodium chloride solutions. It was linear over the sodium range 5–150 ppm Na⁺ ($2.1\text{--}65 \times 10^{-4}M$). The least-squares equation for the calibration curve had a small intercept on the ordinate and the correlation coefficient was 0.9983. The dilution needed to bring the sample solution sodium concentration into the linear range was considerably less than that for

the previous cryptand ion-pair method. The results in Table 5 show the concentrations obtained by this method and the value given to us by the hospital where the samples were taken. The agreement is excellent, with no indication of interference from potassium.

REFERENCES

1. H. K. Frensdorff, *J. Am. Chem. Soc.*, 1971, **93**, 600.
2. M. Takagi, H. Nakamura, Y. Sanui and K. Ueno, *Anal. Chim. Acta*, 1981, **126**, 185.
3. H. Sumiyoshi, K. Nakahara and K. Ueno, *Talanta*, 1977, **24**, 1763.
4. N. Nakamura, M. Takagi and K. Ueno, *Anal. Chem.*, 1980, **52**, 1668.
5. G. Pacey, B. Bubnis and Y. Wu, *Analyst*, 1981, **106**, 636.
6. G. Pacey and B. Bubnis, *Anal. Lett.*, 1980, **13**, 1085.
7. B. Bubnis, J. Steger, Y. Wu, L. Meyer and G. Pacey, *Anal. Chim. Acta*, 1982, **139**, 307.
8. G. Pacey, Y. Wu and B. Bubnis, *Syn. Comm.*, 1981, **11**, 323.
9. Y. Takeda, *Bull. Chem. Soc. Japan*, 1980, **53**, 7393.
10. T. Miyazaki, S. Yamagida, A. Itoh and M. Okahara, *ibid.*, 1982, **55**, 2005.
11. K. Gustavii and G. Schill, *Acta Pharm. Suec.*, 1966, **3**, 241.
12. G. A. Melson, *Coordination Chemistry of Macrocyclic Compounds*, Plenum Press, New York, 1979.

SPECTROPHOTOMETRIC STUDIES OF THE REACTIONS OF PENTACYANOFERRATE(II) COMPLEXES WITH THREE N-HETEROCYCLIC ALDOXIMES

NICOLETTA BURGER and VINKA KARAS-GAŠPAREC

Department of Chemistry and Biochemistry, Faculty of Medicine, University of Zagreb, 41000 Zagreb, Šalata 3, Yugoslavia

(Received 13 April 1982. Revised 11 September 1983. Accepted 14 October 1983)

Summary—The colour reactions of three oximes with ammine- and nitrosyl-pentacyanoferrate(II) ions have been studied. The optimum reaction conditions, spectral characteristics and molar compositions have been found and some instability constants determined. The reactions can be used for the detection and determination of small amounts of the oximes examined.

The aquopentacyanoferrate(II) ion (AqP) reacts with different aliphatic and aromatic oximes to form intensely coloured water-soluble complexes,¹ and so do amminepentacyanoferrate(II)² and nitrosylpentacyanoferrate(II)³ ions (abbreviated here as AmP and NP). These reactions have been applied for the detection and determination of small quantities of certain oximes,⁴⁻⁸ and probably take place through a common intermediate, the aquopentacyanoferrate(II) ion, which forms in aqueous solutions of amminepentacyanoferrate(II)^{9,10} and alkaline solutions of nitrosylpentacyanoferrate(II).¹¹

The nature of the reaction product depends very much on the chemical nature of the reacting oxime. In this paper the reactions of AmP and NP with pyridine-2-aldoxime (PA-2), 1-methylpyridinium-2-aldoxime methyl sulphate (PAM-2 CH₃SO₄) and 1-dodecylpyridinium-2-aldoxime chloride (PAD-2 Cl) are described. Because the last two of these oximes, PAM-2 and PAD-2, are antidotes to poisoning with organophosphorus compounds,¹² these investigations also had a practical importance.

EXPERIMENTAL

Reagents

All reagents used were of analytical-reagent grade. Redistilled water was used throughout. Britton and Robinson buffers¹³ were prepared by mixing 100 ml of phosphoric, boric and acetic acid mixture (all 0.04M) with different volumes of 0.20M sodium hydroxide.

Aqueous solutions of Na₃[Fe(CN)₅NH₃]-3H₂O (Touzart-Matignon) were prepared 10–15 min before use. The aqueous Na₂[Fe(CN)₅NO]-2H₂O (Kemika) solutions remained stable for several days if kept in the dark.

The oximes were from different sources, PA-2 and PAM-2 CH₃SO₄ from Fluka and Specia and PAM-2 Cl from Bosnalijek. PAD-2 Cl and PAD-2 I were synthesized.¹² Their solutions were prepared in water (pure ethanol in the case of PAD-2).

Constant ionic strengths of 0.05 and 0.1 were obtained by addition of sodium chloride solutions of appropriate concentrations.

Preparation of samples for measurements

A. To 2 ml of Britton and Robinson buffer of appropriate pH add the oxime, sodium chloride, AmP and enough water to give a volume of 5 ml.

B. To an alkaline NP solution which has stood for 10 min in the dark, add the oxime, sodium chloride and water to give a total volume of 5 ml.

For PAD-2 Cl use 50% ethanol–water medium, leave all solutions in the dark at room temperature to reach equilibrium. Measure the absorbance at the appropriate wavelength of maximum absorption (λ_{max}) against a reagent blank or water.

Determination of oximes

To 2 ml of Britton and Robinson buffer of pH 6.06 (or pH 7.90 for PAM-2 CH₃SO₄) add 2.5 ml of the oxime solution (containing 50–500 μ g of PAM-2 CH₃SO₄, 100–800 μ g of PAD-2 Cl or 50–100 μ g of PA-2) and 0.5 ml of 0.01M AmP (0.04M AmP in the case of PAM-2 CH₃SO₄). Mix well and measure the absorbance at λ_{max} against a reagent blank after equilibrium is reached. Find the amount of oxime by reference to a calibration graph or equation.

Isolation and characterization of the AmP–PAD-2 and AmP–PAM-2 products

Because of the low solubility of PAD-2 Cl and its AmP complex in water the reaction can be used to isolate the latter by precipitation. The oxime (0.0654 g) was dissolved in 2 ml of ethanol and 0.0132 g of AmP was dissolved in 1 ml of water. The solutions were mixed and after 1–2 hr the precipitate was filtered off, washed first with 78% ethanol, then with water, and dried first in the dark in air, then in a desiccator over sodium hydroxide and finally in a vacuum desiccator over phosphorus pentoxide. Qualitative analysis showed that the compound did not contain sodium. Iron was determined complexometrically as Fe³⁺ after decomposition of the compound with *aqua regia*, and C, H and N were determined by elemental analysis. Analysis: C 63.3%, H 8.8%, N 14.6% and Fe 6.9%; C₄₀H₆₂N₈O₂Fe·H₂O requires C 63.14%, H 8.48%, N 14.73% and Fe 7.34%. The product is a dark powder, sparingly soluble in ethanol and insoluble in benzene, acetone, carbon tetrachloride and ether. The same preparation method may be used with 1-dodecylpyridinium-2-aldoxime iodide. The infrared spectra were recorded (KBr pellets). The bands observed were ν_{CN} at 2106 and 2048 cm⁻¹ and ν_{NO} at 1018 cm⁻¹.

The product of the reaction between AmP and PAM-2 Cl was isolated by evaporation of a mixture in which the oxime

was in ninefold molar excess over the AmP (PAM-2 Cl was used instead of PAM-2 CH_3SO_4 because we had more of it). One ml of water containing 0.0621 g of the oxime and 5 ml of water containing 0.0130 g of AmP were mixed and left for 4–5 hr in the dark, then evaporated to dryness *in vacuo*. The residual solid was transferred onto a Schleicher & Schüll white band filter paper and washed with about 50 ml of ethanol until the washings no longer contained oxime (as shown by evaporation). It was dried in the dark in air and later in desiccators over anhydrous calcium chloride and phosphorus pentoxide. Elemental analysis gave C 40.1%, H 4.6%, N 20.1%, Fe 10.7%, Na 4.9%; sodium hydrogen dioximatotetracyanoferrate(II) pentahydrate requires C 39.57%, H 4.98%, N 20.51%, Fe 10.22%, Na 4.21%. The analysis is not satisfactory proof of composition, but the product was difficult to obtain and dry reproducibly. The compound was very soluble in water, and its spectrum had λ_{max} at 525 nm. The colour faded rapidly on addition of hydrogen peroxide but not on addition of ascorbic acid, suggesting that all the iron was present as iron(II). Its infrared spectrum had a broad absorption band at about 3400 cm^{-1} , confirming the presence of water, ν_{CN} at 2110, 2068, 2048 and 2024 cm^{-1} and ν_{NO} at 1012 cm^{-1} . It is not known whether the proton is involved in the complex anion or not.

RESULTS AND DISCUSSION

The products are formed very slowly and the kinetics depend on many factors, primarily on pH and ionic strength. NP forms coloured complexes even in very alkaline media, if its alkaline solution is kept in the dark for 10 min before addition of the oxime. The effects of pH on the AmP reactions are presented in Fig. 1 and some characteristics of the complexes are given in Table 1. It is found that increasing the ionic strength decreases the absorbance.

The composition of the complexes was determined by the method of continuous variations^{14,15} and by the slope-ratio method;¹⁶ the instability constants were calculated from the Job plots and by the methods of Buděšinský¹⁷ and of Frank and Oswalt.¹⁸

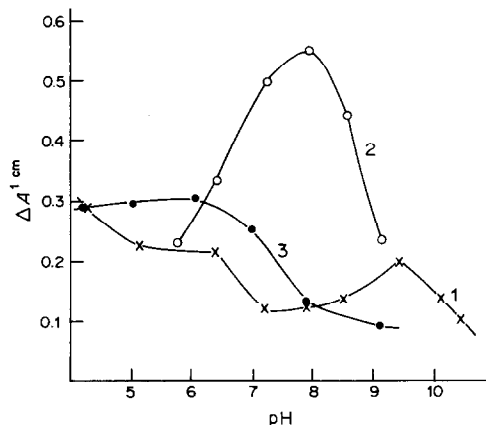


Fig. 1. Effect of pH on the complex formation. 1— $[\text{PA-2}] = [\text{AmP}] = 4 \times 10^{-4}\text{ M}$; 2— $[\text{PAM-2 CH}_3\text{SO}_4] = [\text{AmP}] = 5 \times 10^{-4}\text{ M}$; 3— $[\text{PAD-2 Cl}] = [\text{AmP}] = 5 \times 10^{-4}\text{ M}$. Absorbances measured against water at λ_{max} .

As is evident from Table 1, PA-2 reacts with AmP very slowly indeed. The reactions take 4 days to reach completion, and the composition of the orange product obtained at $\text{pH} \sim 6$ is 1:2 oxime:pentacyanide (Table 2). With NP it reacts even more slowly; at $\text{pH} < 11$ it forms a rose complex with $\lambda_{\text{max}} = 520\text{ nm}$, and at $\text{pH} > 11$ a compound with $\lambda_{\text{max}} = 480\text{ nm}$ and lower absorptivity. The reaction takes about 15 days to reach completion, during which the initial broad spectrum is narrowed and shifted, the direction and magnitude of the shift being a function of the pH (Fig. 2). The pH decreases from the initial value.

With NP, PAM-2 CH_3SO_4 forms a 1:1 complex, which was investigated earlier.³ In the reaction with AmP it seems to react in two different ways. In acid and neutral media it forms a 1:1 complex in about 24 hr whereas in strongly alkaline medium a 2:1 (oxime:pentacyanide) complex is formed within 4 hr.

Table 1. Spectral characteristics and stability of the complexes produced in the reaction of AmP ($I = 0.05$) and NP ($I = 0.1$) with the examined oximes.

Compound	Reagent	λ_{max} , nm	Optimum pH region	Stability of the complex solutions, hr	Reaction time, hr
PA-2	AmP	470	5–6		96
	NP	480	~ 11	24	360
	NP	520	~ 10		360
PAM-2 CH_3SO_4	AmP	520–530	8	1	8–12
	NP	540	11.7		4–8
PAD-2 Cl	AmP	570–580	5.5–6.5	2	2
	NP	570–580	> 11	0.01–0.02	0.25

Table 2. Spectral characteristics, compositions and instability constants of the complexes with AmP ($I = 0.05$) determined by different methods (22°C)

Complex	pH	Composition	Instability constants, pK			ϵ , $l.\text{mole}^{-1}.\text{cm}^{-1}$
			Job plot ^{14,15}	Buděšinský ¹⁷	Frank-Oswalt ¹⁸	
PA-2–AmP	6	1:2	6.93			
	6	1:1		2.82	2.72 ± 0.10	3700
PAM-2 CH_3SO_4 –AmP	8	$\sim 1:1$		3.29	3.12 ± 0.09	3800
	11.7	2:1				

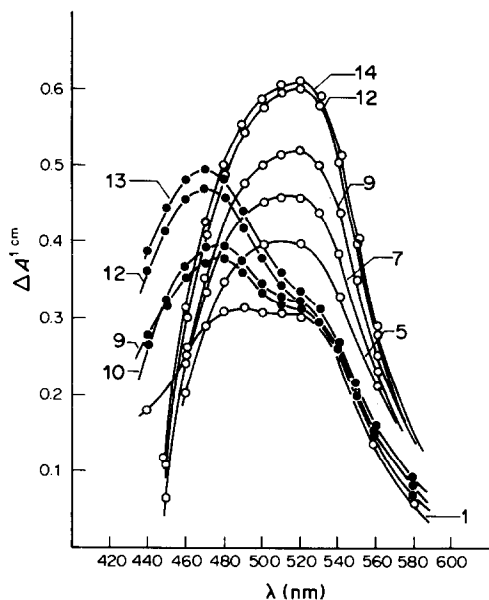


Fig. 2. Dependence of the PA-2-NP reaction on the base concentration. [PA-2] = [NP] = $4 \times 10^{-3}M$. The spectra are labelled with the number of days elapsed at the time of measurement. ○—○ $[OH^-] = 0.02M$. The pH on the 15th day was 9.95. ●—● $[OH^-] = 0.04M$. The pH at the end of the reaction was 11.61.

In a slightly alkaline medium a mixture of the two forms is probably present but the 1:1 complex predominates (Fig. 3). The spectra of the complexes differ (Fig. 4). The molar compositions, absorption coefficients and instability constants of the complexes are given in Table 2.

PAD-2 Cl forms a 2:1 complex with both reagents, in 50% v/v ethanol-water solution. The ethanol lowers the absorbance, and if present in higher concentration shifts the position of λ_{max} .

All our investigations of the reactions of aliphatic and *N*-heterocyclic aldoximes of the mono- and bis-pyridinium type with aquo-, ammine- and nitrosyl-pentacyanoferrate(II) ions¹⁻⁸ show that all three reagents give the same product with a particular oxime.

PA-2 probably forms the same complex with AmP and NP but the complex formed in the latter case at $pH < 11$ exhibits a colour change, probably as a result of dissociation of the oxime hydrogen atom. This conforms with another report²⁰ on the effect of pH on the complex of PA-2 and iron(II). PAD-2 Cl also forms the same complex with AmP and NP. The reaction of PAM-2 with AmP has not yet been completely elucidated.

Applications

The colour reactions described may be used for the detection and determination of small quantities of the oximes.

The recommended qualitative method consists of observing the colour obtained by mixing the oxime with the pentacyanide reagent and the appropriate

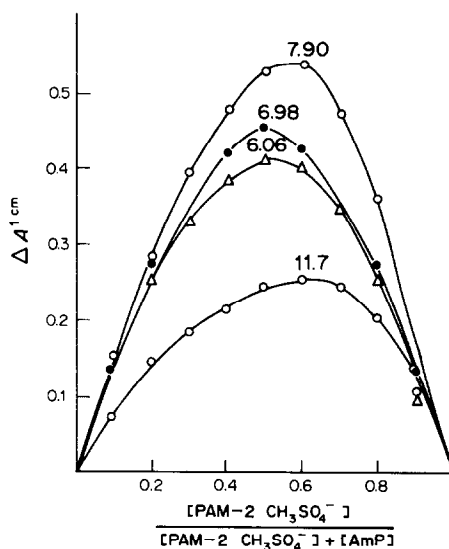


Fig. 3. Job curves at different pH. Total concentrations $10^{-3}M$ except for the solutions at pH 11.7, for which the concentration was $2 \times 10^{-3}M$.

buffer or base. As already described,¹⁹ 2-3 μg of PA-2 and PAM-2 CH_3SO_4 or 15 μg of PAD-2 Cl can be detected in this way. For quantitative analysis the reactants are mixed under the optimum conditions and the absorbance at λ_{max} is measured after equilibrium is reached. It is possible to determine 50-500 μg of PAM-2 CH_3SO_4 , 100-800 μg of PAD-2 Cl or 50-100 μg of PA-2 in 5 ml of reaction mixture by means of a calibration graph. It is also possible to run a standard in parallel with the sample and calculate the amount of oxime in the sample by simple proportion from the absorbances and weight of standard. In this way it is possible to avoid the long delay needed to reach equilibrium (Table 3). The reactions may be used successfully for determination of small quantities of the oximes in tablets and injections. Nitro-

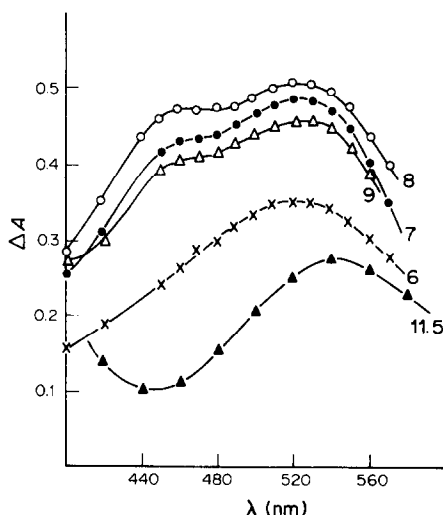


Fig. 4. Absorption spectra at different pH. [PAM-2 CH_3SO_4] = [AmP] = $5 \times 10^{-4}M$ except for pH 11.5, for which the concentrations were $1 \times 10^{-3}M$.

Table 3. Precision of the determinations

Oxime	Taken, μg	ΔA	Found,* μg	Standard deviation, μg	Rel. std. devn., %	No. of detns.
PA-2	61	0.393	61	2	3	5
	76	0.463	77; 71†	3; 1.7	4; 2.4	5; 13
	91	0.531	92	4	4	5
	50	0.080	50	2	4	7
PAM-2 CH_3SO_4	150	0.245	143	5	3	7
	250	0.428	246	16	6	7
	327	0.131	330	2	1	6
PAD-2 Cl	490	0.202	509	10	2	6
	654	0.250	628	11	2	6

*Calculated by means of calibration equations.

†Calculated by simple proportion, from absorbances measured at different times (8, 12, 24 hr) after the mixing of the reactants.

prusside can be used similarly, but the reactions are less sensitive.

Species forming precipitates or complexes with the pentacyanoferrate(II) under the conditions used will interfere, e.g., Cu^{2+} , Hg^{2+} , Au^{3+} , some pyridine derivatives,^{4,21} alkyl and aryl hydrazines and hydroxylamines.²²

REFERENCES

- V. Karas-Gašparec and K. Weber, *Z. Phys. Chem. (Leipzig)*, 1968, **237**, 235.
- V. Hankonyi, V. Ondrušek, V. Karas-Gašparec and Z. Binenfeld, *ibid.*, 1972, **251**, 280.
- V. Hankonyi, N. Burger and V. Karas-Gašparec, *ibid.*, 1975, **256**, 87.
- V. Hankonyi, V. Ondrušek and V. Karas-Gašparec, *Acta Pharm. Jugosl.*, 1972, **22**, 7.
- Z. Smerić and V. Karas-Gašparec, *Arhiv za Farmaciju*, 1976, **5/6**, 453.
- Z. Smerić, V. Hankonyi and V. Karas-Gašparec, *Acta Pharm. Jugosl.*, 1977, **27**, 97.
- N. Burger and V. Karas-Gašparec, *Talanta*, 1977, **24**, 704.
- Idem, ibid.*, 1981, **28**, 323.
- A. D. James, R. S. Murray and W. C. E. Higginson, *J. Chem. Soc. Dalton Trans.*, 1974, 1273.
- Z. Bradić, M. Pribanić and S. Ašperger, *ibid.*, 1975, 353.
- J. H. Swinehart and P. A. Rock, *Inorg. Chem.*, 1966, **5**, 573.
- I. G. Wilson, *Biochim. Biophys. Acta*, 1958, **27**, 196.
- H. M. Rauen, *Biochemisches Taschenbuch*, pp. 651, 654. Springer, Berlin, 1956.
- P. Job, *Ann. Chim. (Paris)*, 1928, **9**, 113.
- W. C. Vosburgh and G. R. Cooper, *J. Am. Chem. Soc.*, 1941, **63**, 437.
- J. H. Yoe and A. L. Jones, *Ind. Eng. Chem., Anal. Ed.*, 1944, **16**, 111.
- B. W. Buděšínský, *Z. Anal. Chem.*, 1972, **258**, 186.
- R. S. Frank and R. L. Oswald, *J. Am. Chem. Soc.*, 1947, **69**, 1321.
- Z. Smerić, N. Burger, V. Hankonyi and V. Karas-Gašparec, *Acta Pharm. Jugosl.*, 1981, **31**, 99.
- G. H. Hanania and D. H. Irvine, *J. Chem. Soc.*, 1962, 2745.
- T. A. Larue, *Anal. Chim. Acta*, 1968, **40**, 473.
- F. Feigl, *Spot Tests in Organic Analysis*, 7th Ed., Elsevier, Amsterdam, 1966.

RAPID ASSAYS BASED ON IMMOBILIZED BIOLUMINESCENT ENZYMES AND PHOTOGRAPHIC DETECTION OF LIGHT-EMISSION

K. GREEN and L. J. KRICKA*

Department of Clinical Chemistry, University of Birmingham, Birmingham B15 2TH, England

G. H. G. THORPE and T. P. WHITEHEAD

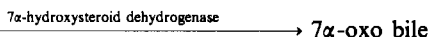
Department of Clinical Chemistry, Wolfson Research Laboratories, Queen Elizabeth Medical Centre,
Birmingham B15 2TH, England

(Received 20 June 1983. Accepted 13 October 1983)

Summary—Sensitive assays have been developed for adenosine 5'-triphosphate, the reduced form of nicotinamide adenine dinucleotide, cholesteryl glycine and alcohol, with immobilized and co-immobilized preparations of bacterial and firefly luciferase as reagents. With high-speed (ASA 20000) instant photographic film as detector, picomole amounts of the various analytes can be detected rapidly. The simplicity and convenience of the analytical combination of co-immobilized bioluminescent enzymes and photographic film for the detection of light make this an ideal technique for rapid screening tests.

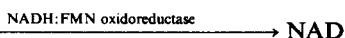
Immobilized and co-immobilized bioluminescent enzymes, such as bacterial luciferase and firefly luciferase can be used as reagents for very rapid and sensitive assays.¹⁻⁶ For example, primary bile acids can be measured in femtomole amounts, according to the reaction sequence shown in equations (1)–(3), by means of bacterial luciferase, NADH:FMN oxidoreductase and 7 α -hydroxysteroid dehydrogenase co-immobilized onto Sepharose particles.³

NAD + primary bile acid (cholesteryl glycine)



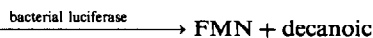
acid + NADH (1)

NADH + FMN



+ FMNH₂ (2)

FMNH₂ + decanal + O₂



acid + CO₂ + light (3)

Light-emission from such reactions is usually measured by means of a photomultiplier tube or a photodiode. It is also possible, however, to detect and measure light-emission from luminescent reactions by using photographic film, although in the past this has been mainly confined to chemiluminescent assays for metal ions.⁷ We have recently described an assay for glucose based on filter pads impregnated with glucose

oxidase and peroxidase, a chemiluminescent indicator reaction involving luminol, and instant photographic film.⁸ The advantages of this approach to analysis are that it is rapid, a permanent record of the results is obtained, and the detection system is simple and requires no power source. The object of this study was to investigate the feasibility of producing analytical systems based on bioluminescent enzymes co-immobilized onto an insoluble microparticulate solid support (Sepharose), and use of instant photographic film.

EXPERIMENTAL

Reagents

Luciferin, dithiothreitol (DTT), decanal, *N*-tris(hydroxymethyl)methyl-2-aminoethanesulphonic acid (TES), cyanogen bromide, and glycylglycine were purchased from Sigma London Chemical Co. Sodium pyrophosphate was obtained from BDH Chemicals Ltd. The glycine conjugate of cholic acid was synthesized as described previously.⁹

Nucleotides

Adenosine 5'-triphosphate (ATP), flavin mononucleotide (FMN) and the reduced form of nicotinamide adenine dinucleotide (NADH) were supplied by Sigma. Nicotinamide adenine dinucleotide (NAD) was purchased from Boehringer Mannheim Corporation.

Enzymes

Firefly luciferase, 7 α -hydroxysteroid dehydrogenase, and alcohol dehydrogenase immobilized onto agarose beads were obtained from Sigma. "NADH monitoring reagent" (a mixture of bacterial luciferase and NADH:FMN oxidoreductase) was purchased from LKB. Bacterial luciferase and NAD(P)H:FMN oxidoreductase were supplied by Boehringer Mannheim Corporation.

Solid supports

Sepharose 4B and cyanogen bromide-activated Sepharose 4B were obtained from Pharmacia Fine Chemicals.

*Author to whom reprint requests should be addressed.

Immobilized enzymes

Various enzymes or mixtures of enzymes were immobilized according to the procedure described by Ford and DeLuca¹ onto CNBr-activated Sepharose 4B (1 g) or onto Sepharose 4B (1 g) which had been freshly activated by treatment with cyanogen bromide according to the method of March *et al.*¹⁰ They were firefly luciferase (10 mg); bacterial luciferase (5 mg) and NAD(P)H:FMN oxidoreductase (10 U); bacterial luciferase and NADH:FMN oxidoreductase (one vial of LKB Monitoring Reagent); bacterial luciferase, NADH:FMN oxidoreductase (one vial of LKB Monitoring Reagent) and 7 α -hydroxysteroid dehydrogenase (3.5 mg). Immobilized enzymes were stored at 0–4° as a suspension (100 g/l.) in phosphate buffer (0.1M, pH 7.0) containing DTT (2mM) and sodium azide (3mM).

The efficiency of the immobilization procedure was assessed by determination of the protein concentration (from the absorbance at 280 nm) in the coupling mixture before and after addition of the activated Sepharose and from the minimum amount of analyte detectable by use of the immobilized enzyme(s).

Enzymes were immobilized on both freshly activated and preactivated cyanogen bromide-Sepharose in order to compare their relative performance. The advantage of using the preactivated Sepharose was that it avoided the local use of cyanogen bromide, which is toxic.

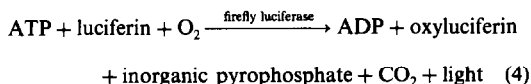
Measurement of light-emission

Photomultiplier tube. A luminometer designed and built in the laboratory, and based on a side-window photomultiplier tube (EMI type 9781A, 94 μ A/lumen) and having facilities for automatic injection of reagents into reaction cuvettes, was used to measure the light-emission.¹¹

Photographic film. Polaroid Land film type 612 (ASA 20000) was used in conjunction with a mask containing 6 plastic tubes (44 \times 11 mm diameter) as described previously.⁸ Exposure times of up to 2 min were used. Photographic results were assessed visually.

Assays

ATP. The principle of the assay is shown in equation (4):



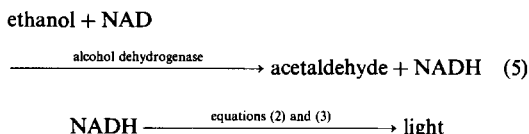
A series of ATP standards was prepared by serially diluting an aqueous stock solution (2mM) in glycylglycine buffer (25mM, pH 7.8). Stock assay mixture comprised 8 ml of glycylglycine buffer (25mM, pH 7.8), 1.0 ml of magnesium chloride solution (0.1M, pH 7.8), and 0.8 ml of aqueous luciferin solution (1mM). A 10- μ l sample of an ATP standard and 10 μ l of a suspension of immobilized firefly luciferase were placed in a 10 \times 10 \times 45 mm cell and the reaction was initiated by injecting 1.0 ml of assay mixture. Peak light-emission was recorded.

NADH. The principle of the assay is shown in equations (2) and (3). A series of NADH standards was prepared by serially diluting an aqueous stock standard (2mM) with distilled water. A decanal-water emulsion was prepared by shaking 5 ml of decanal with 10 ml of distilled water. This was prepared daily and stored at 0–4°. Stock assay mixture comprised 100 μ l of decanal emulsion, 200 μ l of aqueous FMN solution (0.15mM) and 10 ml of phosphate buffer (0.1M, pH 7.0). A 10- μ l sample of an NADH standard, and 10–50 μ l of co-immobilized bacterial luciferase and NAD(P)H:FMN oxidoreductase were placed in a cell and the reaction was initiated by injection of 1.0 ml of assay mixture. Peak light-emission was recorded.

Cholyl glycine. The principle of the assay is shown in equations (1)–(3). A series of cholyl glycine standards was prepared by serial dilution of a stock standard (0.1mM)

with distilled water. A 10- μ l sample of a standard and 10–50 μ l of a suspension of co-immobilized bacterial luciferase, NAD(P)H:FMN oxidoreductase, and 7 α -hydroxysteroid dehydrogenase were placed in a cell and the reaction was initiated by injecting 1.0 ml of an assay mixture prepared by mixing 1 ml of aqueous NAD solution (200mM), 200 μ l of aqueous FMN solution (0.15mM), 100 μ l of decanal emulsion and 10 ml of TES buffer (0.05M, pH 7.0). Peak light-emission was measured.

Ethanol. The principle of the assay is shown in equation (5).



A series of alcohol standards was prepared by serial dilution of an aqueous stock standard (0.1mM) in distilled water. A 10- μ l sample of an alcohol standard, 25 μ l of a suspension of alcohol dehydrogenase immobilized onto agarose [0.1 g/ml in TES buffer (0.05M, pH 7.0)], 10 μ l of a suspension of co-immobilized bacterial luciferase and NADH:FMN oxidoreductase and 10 μ l of aqueous NAD solution (20mM) were mixed together in a cuvette and incubated at room temperature for 2 min. This incubation time was increased to 5 min when plasma or whole blood was used. The bioluminescent reaction was initiated by injecting 1 ml of an assay mixture comprising 100 μ l of decanal emulsion, 200 μ l of aqueous FMN solution (0.15mM) and 10 ml of TES buffer (0.05M, pH 7.0). Peak light-emission was recorded.

In assays using photographic film to detect light-emission the volume of assay mixture added to initiate the bioluminescent reaction was reduced to 400 μ l in order to keep the level of glowing reaction mixture below the top of the mask and thus eliminate exposure of other areas of the film.

Accelerated thermal stability study

A suspension of the immobilized enzymes (1 ml) was incubated at 50° in a water-bath. Samples were removed at various times and the remaining enzyme or coupled enzyme activity was measured by using a 10- μ l sample of the appropriate standard with the highest concentration.

RESULTS AND DISCUSSION

The efficiencies of the coupling of the enzymes to the activated Sepharose, the lower limits of detection of the various substrates and the linear ranges of detection (Table 1) were similar to those previously reported.^{1,3,4,12} Freshly prepared CNBr-activated Sepharose produced a more active immobilized enzyme preparation, as judged by the detection limit for the particular analyte, than the commercially available material. This was not due to a difference in the capacity of the activated Sepharoses, since the efficiency of coupling, determined by loss of protein from the enzyme coupling mixtures, was 5–10% lower for the freshly activated Sepharose. The difference may arise from the surface concentration of reactive groups being higher on freshly activated than on preactivated Sepharose, which would lead to multiple attachments between the Sepharose surface and enzyme molecules and hence less protein denaturation and loss of enzyme activity.

Table 1. Linear ranges and detection limits for bioluminescent analysis, obtained by use of a photomultiplier tube or photographic film to detect light emission

Immobilized enzymes	Coupling efficiency, %	Analyte	Photomultiplier tube detection limit,* <i>pmole</i>			Photographic film detection limit,† <i>pmole</i>
			A	B	Linear range	
Firefly luciferase	86-96	ATP	0.02	0.2	0.02-20000	2
Bacterial luciferase, NAD(P)H:FMN oxidoreductase	85-95	NADH	2	20	2-2000	200
Bacterial luciferase, NAD(P)H:FMN oxidoreductase, 7 α -hydroxysteroid dehydrogenase	80-95	cholyl glycine	50	50	50-5000	50
Bacterial luciferase and NAD(P)H:FMN oxidoreductase-alcohol dehydrogenase	85-95	ethanol	1	—	1-1000	1

*Detection limit: amount of analyte giving twice background light-emission; A, freshly activated; B, preactivated cyanogen bromide Sepharose.

†The amount of analyte giving a photographic response (assessed visually) greater than that given by the blanks.

The thermal stability of the various immobilized enzyme preparations was greater on preactivated Sepharose (Fig. 1); it must be remembered that the initial enzyme activity of these preparations was much lower (by a factor of about 10) than that of those prepared from freshly activated Sepharose.

The lower limits of detection obtained for the various analytes by using instant photographic film are summarized in Table 1. A film with a speed of 20000 ASA was used, as this was the fastest and therefore the most sensitive instant film available. Generally, the detection limits were inferior (by a factor of 100) to those obtaining by using a photomultiplier tube as the detector, but nevertheless they were much lower than those for conventional assays. Detection limits obtained by using the two types of detector are not strictly comparable, as with the photomultiplier tube a peak light-emission was measured whereas with the photographic film the degree of exposure is a measure of the total light emitted. A feature of the light-emission from reactions involving immobilized bioluminescent enzymes is that they produce a steady glow rather than a flash of light (Fig. 2). This feature makes it possible to initiate the reaction before placing the cell in front or on top of the detection system. Exposure times of up to 2 min were used and an example of an ATP assay exposed for 30 sec is presented in Fig. 3. The imprecision of the assay and the insufficient exposure latitude limits the discrimination between different amounts of ATP and thus no attempt was made to determine the real threshold, which lies between 2 and 20 *pmole*. Thus in its present form this type of assay is best used as a "threshold" or "screening" test, *e.g.*, the detection of the presence of >20 *pmole* of ATP in a specimen. Biological specimens were also analysed. Ethanol present in either whole blood or plasma could be detected photographically in a 10- μ l sample, down to levels of 20 mg/100 ml (4.3mM). The presence of proteins and cells reduced the light-emission but the

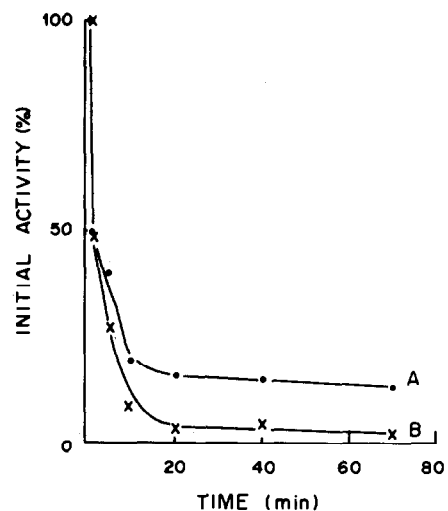


Fig. 1. Thermal stability study (50°) of bacterial luciferase, NADH:FMN oxidoreductase and 7 α -hydroxysteroid dehydrogenase co-immobilized onto (A) preactivated, and (B) freshly activated cyanogen bromide Sepharose 4B. Activity of the coupled enzymes was assessed by using cholyl glycine.

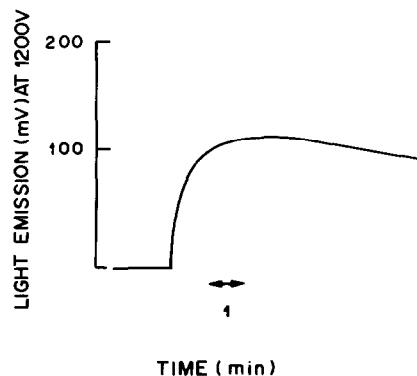


Fig. 2. Time course of light-emission from the reaction of 2000 *pmole* of NADH with co-immobilized bacterial luciferase and NADH:FMN oxidoreductase.

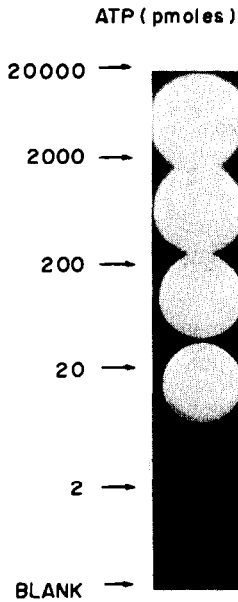


Fig. 3. Photographic determination of various amounts of ATP by using immobilized firefly luciferase (exposure time, 30 sec).

photographic system was still sufficiently sensitive to make it a usable method for screening for alcohol in blood.

CONCLUSIONS

Luminescent assays based on immobilized and co-immobilized bioluminescent enzymes and photographic detection of light-emission by means of "in-

stant" film are both rapid and sensitive. This type of assay is widely applicable since it is possible to base the determination of a range of NAD- and ADP-dependent enzymes and their substrates on the bioluminescent firefly or bacterial luciferase reactions. A limitation of the photographic detection system is the restricted exposure latitude of currently available instant film, which limits this to a threshold-type test, but in the authors' opinion this is far outweighed by the simplicity of the detection system.

Acknowledgement—The financial support of the Department of Health and Social Security is gratefully acknowledged.

REFERENCES

1. J. Ford and M. DeLuca, *Anal. Biochem.*, 1981, **110**, 43.
2. E. Jablonski and M. DeLuca, *Clin. Chem.*, 1979, **25**, 1622.
3. A. Roda, L. J. Kricka, M. DeLuca and A. F. Hofmann, *J. Lipid Res.*, 1982, **23**, 1354.
4. G. Wienhausen and M. DeLuca, *Anal. Biochem.*, 1982, **127**, 380.
5. B. F. Erlanger, M. F. Isambert and A. M. Michelson, *Biochem. Biophys. Res. Commun.*, 1970, **40**, 70.
6. K. Kurkijarvi, R. Raunio and T. Korpela, *Anal. Biochem.*, 1982, **125**, 415.
7. U. Isacsson and G. Wettermark, *Anal. Chim. Acta*, 1974, **68**, 339.
8. T. J. N. Carter, T. P. Whitehead and L. J. Kricka, *Talanta*, 1982, **29**, 529.
9. L. Lack, F. O. Dorrity, T. Walker and G. D. Singletary, *J. Lipid Res.*, 1973, **14**, 367.
10. S. C. March, I. Porath and P. Cautrecasas, *Anal. Biochem.*, 1974, **60**, 149.
11. R. A. Bunce, T. J. N. Carter, L. J. Kricka and T. P. Whitehead, *Brit. Pat. Appl.*, 2,025,609A, 1978.
12. G. K. Wienhausen, L. J. Kricka, J. E. Hinkley and M. DeLuca, *Appl. Biochem. Biotechnol.*, 1982, **7**, 463.

STUDY OF HIGH-VOLTAGE BREAKDOWN AND MATERIAL CONSUMPTION IN SPARK-SOURCE MASS SPECTROMETRY AND THEIR SIGNIFICANCE IN ANALYTICAL APPLICATIONS

J. VAN PUYMBROECK, J. VERLINDEN, K. SWENTERS and R. GIJBELS

Department of Chemistry, University of Antwerp (U.I.A.), Universiteitsplein 1, B-2610 Wilrijk, Belgium

(Received 16 February 1983. Revised 7 July 1983. Accepted 6 October 1983)

Summary—The breakdown voltage has been found to be dependent on the gap width between the electrodes and on the melting point of the sample elements in spark-source mass-spectrometry (SSMS). The number of discharges per pulse train and the time required to reach the first discharge depend only on the chosen breakdown voltage. The spark gap is proportional to the "radius" of the volume sampled (for a given element) and this radius is linearly related to the reciprocal of the melting point of the elements (23 different elements, metals or semiconductors), when fixed spark-parameters are used. The effect of electrode temperature on material consumption can be qualitatively explained by a fictive increase or decrease in melting point of the element. Knowledge of the relations between the different spark and instrumental parameters and the volume or weight of sample consumed can be applied to the study of the homogeneity of samples, to in-depth analysis by SSMS and to the analysis of microsamples.

It is necessary to know the amount of material consumed during spark-source mass-spectrometric analysis and to know the influence of different spark parameters on the weight loss of the electrodes, in order to arrive at an adequate understanding of the erosion by the spark and at a better evaluation of the effect of sample heterogeneity, and before attempting the analysis of thin solid films and microvolumes.

Derzhiev *et al.*¹ have recently discussed the use of spark-source mass-spectrometry (SSMS) for the analysis of thin solid films. SSMS may have some advantages over other surface-analysis techniques (AES, RBS, SIMS, ESCA) when the microvolume has to be checked for nearly all elements of the periodic table simultaneously, the roughness of the sample surface prevents the application of other techniques, and better than semi-quantitative results are required though no suitable standards are available. Since it is possible¹ to keep the spark penetration depth below 0.1 μm , SSMS can be used for surface analysis and depth profiling and is more promising than sputtering techniques when layers of $> 5 \mu\text{m}$ thickness are to be analysed.

EXPERIMENTAL

Measurements were performed with a double-focusing spark-source mass-spectrometer (JMS-01 BM-2, JEOL, Tokyo), equipped with an automatic spark-control system (MS-AS-01, JEOL).

As a measure of the breakdown voltage (U_{br}), the selected "anode voltage" was multiplied by the chosen spark level of the automatic spark controller (100% electrodes not sparking; 0% short circuit). The effective gap voltage is approximately 15 times this "breakdown voltage".

The spark gap was determined by measuring the distance between the electrodes at which stable sparking at a given U_{br} changed to short-circuit. The time required to reach the

first breakdown of each pulse train and the number of breakdowns per pulse train were determined by analysing the oscillograms of the voltage between the electrodes, stored in a fast-memory oscilloscope.

The weight loss of the electrodes sparked in an "as constant as possible" configuration in the ion-source was determined by weighing them before and after collection of a 100-nC charge. The time needed to collect this charge was also measured for each sample.

The influence of the width of the main slit on the times required to collect a charge of 1 nC was also investigated, with the position of the electrodes kept rigidly constant.

Three kinds of electrode geometry were used: graphite powder pressed in the form of cylinders (diameter 2 mm); for diamond, Al, Si, Ti, V, Fe, Co, Ni, Cu, Zn, Ge, Zr, Mo, In, Sn, Sb, W, Au and Pb: rods (cross section $2 \times 2 \text{ mm}$); for Rh, Ag, Ta and Re: thin plates (0.1 mm thickness $\times 2 \text{ mm}$ width). Most of the elements were more than 99% pure. In addition, rods ($2 \times 2 \text{ mm}$) of the following alloys were studied: CuBe (ca. 10 atom% Be), AlZn (25, 50 and 75 atom% Zn). The spark parameters were (unless otherwise stated): U_{br} 3.2 kV (80% spark level), repetition frequency 3 kHz, pulse width 20 μsec . The slit settings were constant: main slit $20 \pm 5 \mu\text{m}$, α - and β -slits 0.7 mm.

RESULTS AND DISCUSSION

For Al, Zr, Mo and Au the gap width (g) was measured as a function of U_{br} , and gave the relationship

$$U_{br} = ag^{0.61} \quad (1)$$

The relative standard deviation (rsd) of the exponent of g was 8% and the value of 0.61 is in excellent agreement with that obtained by Slivkov² and by Germain and Rohrbach,³ namely 0.625. The dependence of the gap width on the breakdown voltage is illustrated in Fig. 1 for some elements (our relative gap-width unit corresponds to about 7 μm). The

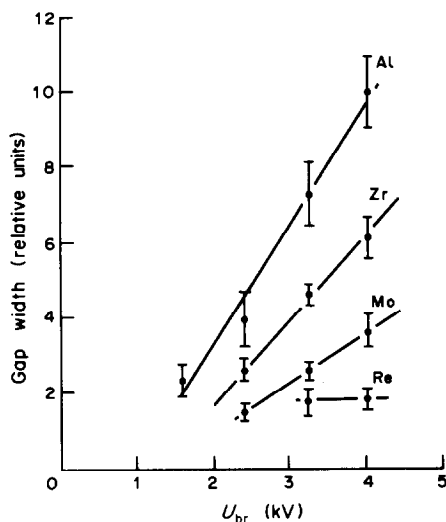


Fig. 1. Dependence of spark-gap width (relative units) on breakdown voltage for Al, Zr, Mo and Re.

relationship is practically linear in the range 10–100 μm .

From Fig. 1 it is clear that the gap width, at a given breakdown voltage, depends on the metal sparked, as has been reported by Ito *et al.*⁴ Therefore, the gap widths measured at constant values of U_{br} were correlated with different physical parameters of the metals. The best correlation was found between g and the melting points (T_m , K) of the elements and the following equation could be derived:

$$g = bU_{br}^{1.6}/T_m \quad (2)$$

The rsd of b was 19% (8 data points, for the elements Al, Ti, Cu, Zr, Mo, Rh, Re and Au). In Fig. 2 the relation between the gap width and the reciprocal of the melting point is shown for these 8 elements at a breakdown voltage of 3.2 kV. Similar relationships were also observed between g and T_m for breakdown voltages of 2.4 and 4.0 kV.

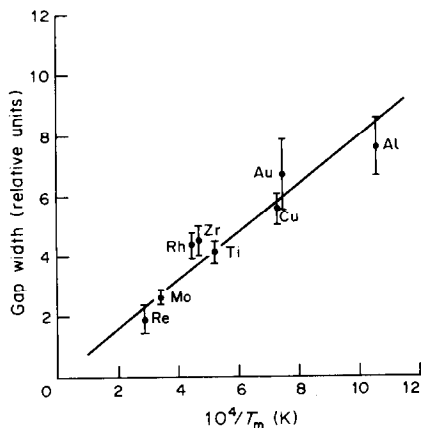


Fig. 2. Relationship between gap width (1 relative unit is about 7 μm) and melting point for 8 metals measured at constant spark parameters (U_{br} 3.2 kV, repetition frequency 3 kHz, pulse width 20 μsec).

Davies and Biondi⁵ measured the influence of initial anode and cathode temperatures on the breakdown voltage. Breakdown was seen to be completely independent of the local cathode-emitter temperature, but in all cases took place when the local temperature in the heated spot of the plane copper anode reached a critical value of 1100 ± 150 K. This temperature is about 250 K lower than the melting point of copper. Observations from arc melting measurements showed that surface melting already occurs at 200–300 K below the melting point of the metal.⁶ These observations suggest that a relation between g and $(T_m - 250)$ would be more appropriate.

The energy liberated per spark pulse (E) is assumed¹ to be proportional to U_{br}^2 ; in order to correlate this energy with the volume of electrode material sampled per pulse or with the number of atoms consumed per pulse, it is necessary to know the number n_p of pulses (discharges) per pulse train, as a function of U_{br} . Therefore, the oscillograms for Au, obtained at different U_{br} -values, were analysed, the repetition frequency and the pulse width being kept constant (3 kHz and 20 μsec respectively). In Fig. 3 the results of such measurements are shown. The following relationship is valid in the region from 1 to 5 kV:

$$n_p = c/U_{br} \quad (3)$$

For the 5 measurements the rsd of c was 10%. The same constant c was also obtained for Mo, indicating that c is an instrumental parameter.

The time necessary to reach (from the onset of the RF-voltage) the first breakdown of a pulse train (t_{br}) was also measured. For gold electrodes, a linear relationship between t_{br} and U_{br} was obtained:

$$t_{br} = d + eU_{br} \quad (4)$$

A correlation coefficient of 1.00 for 6 pairs of values of t_{br} and U_{br} was obtained. Again, Mo yielded results identical with those for Au. In Fig. 4 the relation between t_{br} and U_{br} is illustrated.

The weight loss of Al, Cu, CuBe and Au electrodes was measured as a function of U_{br} , with the repetition frequency and pulse width kept constant (3 kHz, 20

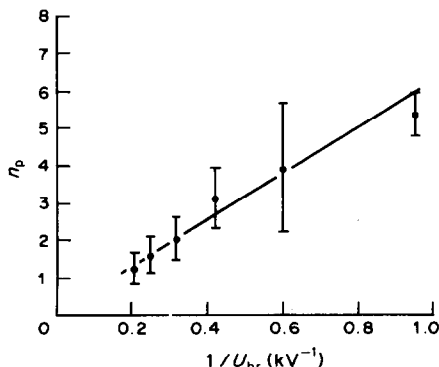


Fig. 3. Number of discharges per pulse train as a function of breakdown voltage, measured for Au electrodes.

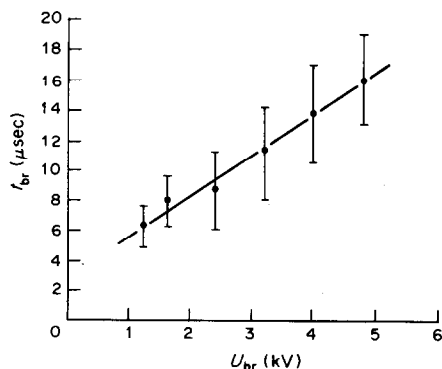


Fig. 4. Time taken to reach the first discharge (after the onset of the radio frequency voltage) as a function of breakdown voltage, measured for Au electrodes.

μsec). The gap width and the number of pulses per pulse train for these experimental conditions were calculated by using equations (2) and (3). Hence, from the time needed to collect a charge of 100 nC, the volume of Al, Cu, CuBe or Au sampled per pulse can be calculated. These results are listed in Table 1a. As stated above, the energy of each pulse was assumed to be proportional to U_{br}^2 and was correlated with the volume loss per pulse. The data were fitted to the equation

$$E = f(\mu\text{m}^3/\text{pulse})^h \quad (5)$$

The values of f , h and the correlation coefficients for the different metals investigated are listed in Table 1b. A mean value of 0.40 (standard deviation 0.07) was obtained for h . It should be noted that this equation only describes the relation between the energy per pulse and the volume effectively lost per pulse. The fraction of material originally vaporized but condensing later on the electrode surfaces could not be taken into account in the experimental approach. In this context it should be noted that variation of the angle between two identically shaped copper electrodes from 0° to 120° did not result in a measurable difference in volume consumed per pulse, indicating that the effect of condensation is not important for weight-loss studies. Combination of equations (1) and (5) then leads to

$$g = k(\mu\text{m}^3/\text{pulse})^{0.33} = kr \quad (6)$$

i.e., there seems to exist a direct proportionality relationship between the gap width g (in μm) and the "radius" r (in μm) of the sampled volume per pulse. The standard deviation of the exponent 0.33 in equation (6) was 0.07.

The weight loss of different metals, for collection of a charge of 100 nC, was measured, at constant spark parameters (U_{br} , repetition frequency, pulse width) and slit settings. The results of these measurements are given in Table 2. A log-log plot of the volume or number of atoms consumed per pulse train (pulse) *vs.* various physical parameters resulted in straight line

relationships. The best correlation was found with the melting point. In Fig. 5 a log-log plot of the number of atoms consumed per pulse train *vs.* the melting point is given. None of the points deviates from the straight line by a factor greater than 2.

However, we know from equation (2) that there exists a relationship between g and $1/T_m$ and from equation (6) that g and r are correlated, hence we can try to relate r to $1/T_m$:

$$r = l/T_m \quad (7)$$

For the 22 elements investigated (other than carbon), an *rsd* of 21% was obtained for l , and a correlation coefficient of 0.96 between r and $1/T_m$. This is very satisfactory and no better correlation coefficients were obtained between r and other physical parameters: 0.68 *vs.* reciprocal of the boiling point, 0.55 *vs.* heat of melting, 0.67 *vs.* heat of vaporization, 0.75 *vs.* heat of sublimation, 0.43 *vs.* vapour pressure at 1600 K. This relationship (r *vs.* reciprocal of the melting point) is illustrated in Fig. 6 and the results are summarized in Table 2.

It is very surprising that the material consumption is independent of the vapour pressure of the elements. For example, Sn and Zn differ by a factor of 10^{12} in vapour pressure at their melting point, but the material consumption seems to be solely dependent on their melting point, judging from the agreement with equation (7) (Table 2). This probably means that there is no direct or initial evaporation of material from the solid electrodes. The elements, sparked as filaments, systematically yielded too high values for l (Table 2), the average difference being +36% from the mean value of l calculated for the other 21 elements. This, we think, is due to poor heat dissi-

Table 1a. Volume of material consumed per pulse at various breakdown voltages

U _{br} , kV	Volume consumed, μm ³ /pulse			
	Al	Cu	CuBe	Au
4.3				405
4.2	206			
4.0		40.2	50.5	
3.7				220
3.6		27.3	33.9	
3.5	143			
3.2	87	17.1	15.6	58
2.8	45	9.2	8.3	
2.7				17
2.4		3.7	3.1	
2.1	18.6	1.5		3.2
1.4	2.6			
1.1				0.15

Table 1b. Factors from equation (5)

Factor	Al	Cu	CuBe	Au
f	1.17	3.47	3.72	2.51
h	0.487	0.404	0.362	0.338
r^*	0.994	0.993	0.998	0.992

*Correlation coefficient.

Table 2. Material consumption in the analysis of elemental metals and semi-conductors

Electrode material	Weight loss, mg/100 nC (2 electrodes)	Volume consumed, $\mu\text{m}^3/\text{pulse train}$	Sparking behaviour†
C (graphite)	2.8	360	S
C (diamond)	0.4	13	S
Al	7.9	337	S
Si	4.9	39	B
Ti	1.6	41	S
V	1.1	33	S
Fe	2.1	30	S
Co	3.1	21	S
Ni	1.9	33	S
Cu	9.0	79	S
Zn	64.1	849	B
Ge	8.4	376	S
Zr	3.2	74	S
Mo	4.7	20	S
Rh	4.3	36	S
Ag	16.6	335	S
In	100.3	1368	B
Sn	84.5	2038	B
Sb	36.2	563	B
Ta	5.1	25	S
W	1.3	7	S
Re	6.0	23	S
Au	17.1	137	S
Pb	102.5	864	B

*Spark parameters: U_{br} 3.2 kV, repetition frequency 3 kHz, pulse width: 20 μsec .

†S = stable, B = bad.

pation and thermal contact to the bulk. The very large positive deviation observed for graphite powder may point to a different mechanism of sampling of material by the spark. Probably, for metals, the surface needs to be melted in order to form a "drop"

which leaves the surface and evaporates on its way to the cathode (Davies and Biondi model³); for graphite powder, the material may be torn off as a solid particle (Cranberg model⁷).

Three observations may be made.

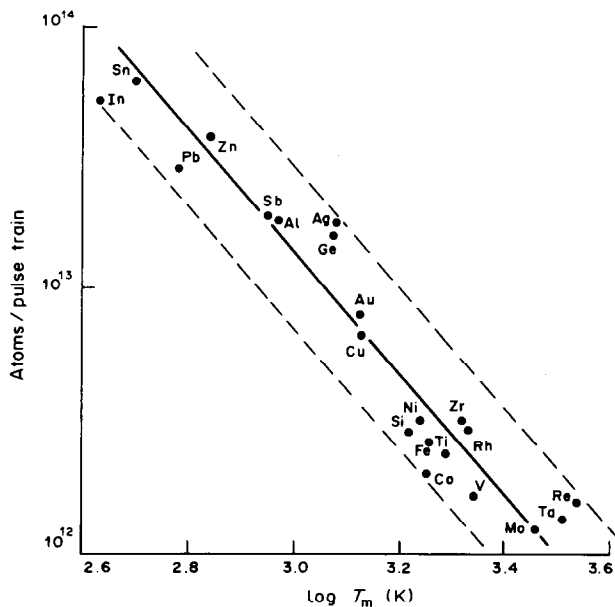


Fig. 5. Number of atoms consumed per pulse train *vs.* melting point at fixed spark parameters (U_{br} 3.2 kV, repetition frequency 3 kHz, pulse width 20 μsec).

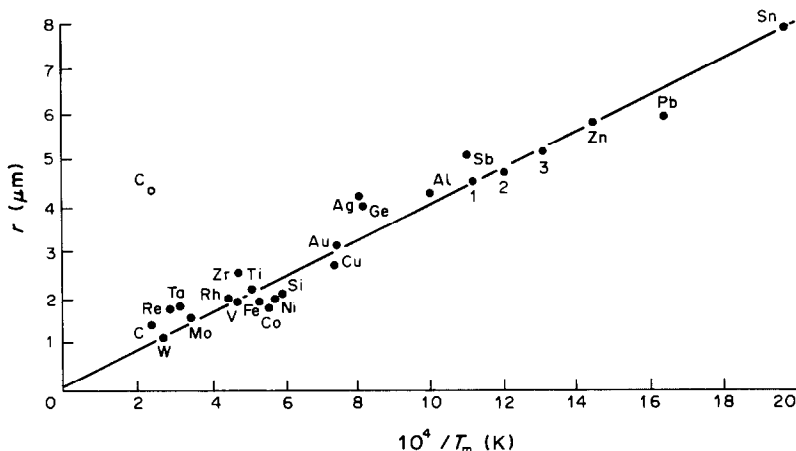


Fig. 6. Radius of sampled volume vs. $10^4/T_m$ (K) for different elements at fixed spark parameters (U_{br} 3.2 kV, repetition frequency 3 kHz, pulse width 20 μ sec); 1, 2 and 3 refer to Al alloys containing 25, 50 and 75 atom% Zn, respectively; \circ = graphite.

1. It is possible to spark graphite electrodes at moderately low U_{br} values, compared with those used for elements having nearly the same melting point.

2. Photomicrographs of the sparked area (metallographic microscope, scanning electron microscope) show, for *all* metallic samples, very strong evidence for a molten surface, whereas this can *not* be concluded for sparked graphite electrode surfaces (Fig. 7).

3. For carbon in the form of diamond the sampled volume is in much better agreement with equation (7) (Fig. 6). It is to be expected from the phase diagram of carbon that the surface of a diamond electrode will become graphitized during sparking but probably the resulting graphite layers will be more coherent than in an electrode of compressed graphite powder. In any case, the experimental data for diamond are in much better agreement than the graphite data with those for other elements.

Besides studying the material consumption for pure metal matrices, we also investigated the weight loss during sparking of AlZn alloys, containing 25, 50 and 75 atom% Zn. The values of r obtained after sparking under the standard experimental conditions obeyed the relationship given in equation (7). This is also illustrated in Fig. 6.

The effect of electrode temperature on material consumption was also investigated. The weight loss of 7 metals, sparked under the experimental conditions described, was measured, the electrode holders being cooled with liquid nitrogen. Assuming that the melting point of the elements studied here is virtually increased by this cooling, then we can calculate [using equation (7)] the radius and consequently the volume sampled for the different metals with and without cooling. The best agreement between experimental and calculated volume ratios (Table 3) was obtained assuming a virtual increase of melting point (with cooling) of 125 K. This is in good agreement with an

experimentally measured temperature difference between cooled and uncooled aluminium electrodes of 113 K (measured 210 sec after sparking), reported by Van Hove⁸.

For practical purposes it is necessary to know the weight loss per unit charge (expressed in nC), collected at the coulometer, for the given experimental conditions. The most important experimental parameters determining the time per nanocoulomb collected at fixed spark parameters, are the position of the electrodes with respect to each other and to the accelerating and main slits, the main slit-width and the α - and β -slit-widths. By measuring the time needed to collect 1 nC, as a function of the main slit-width (keeping all other spark parameters constant), we can calculate (using the data of Table 1a) the number of ions collected per number of atoms atomized (n_i/n_a). This approach was repeated at various breakdown voltages and the results are summarized in Tables 4a and 4b. It can be seen that the efficiency (n_i/n_a) increases with decreasing U_{br} (but analysis time increases) and with increasing main slit-width (but mass-resolution decreases). The optimum choice of experimental conditions depends on the particular analytical problem.

APPLICATIONS

Sample inhomogeneity

The error in the determination of an element in a sample depends on the analytical error, the weight of the sample analysed and the nature and history of the sample. This has been dealt with by Ingamells and Switzer,⁹ who derived the equation

$$R = 100\sqrt{K_s/w} \quad (8)$$

where R = relative standard deviation (%) for the determination of one component ("error-free" ana-

(a)

10 μm

(b)

100 μm

Fig. 7. Scanning electron micrographs of sparked areas. (a) Rhenium; (b) graphite.

Table 3. Effect of cooling on material consumption

Element	$R^*(\text{exp})$	$R^*(\text{calc})$
In	2.0	2.2
Sn	1.9	1.9
Zn	1.6	1.6
Ge	1.3	1.5
Au	1.1	1.3
Cu	1.2	1.3
Mo	1.3	1.1

* R = ratio of volumes consumed without and with cooling.

lytical method), K_s = sampling constant and w = weight of analytical subsample.

It is obvious from Tables 4a and 4b that if there is sufficient sample material available, it is best to spark at high U_{br} values and narrow slit settings: this gives a compromise between speed of analysis, resolution requirements and material consumed, in order to reduce the effects of sample inhomogeneities [equation (8)].

For the analysis of complex matrices by SSMS, photoplate detection is imperative and consequently a number of exposures must be made for different total collected charges, and hence different weights of sample consumed. For determination of the elemental concentrations, the results from the different exposures are used, each having its own subsample weight and inherent R . This is not commonly taken into account in SSMS analyses. If, on the other hand, one element has the same sampling constant in two different matrices, the relative standard deviation of

Table 4a. Time per nanocoulomb collected, as a function of main slit-width for various breakdown voltages*

U_{br}, kV	Time for collection of 1 nC, sec					
	20†	40†	60†	100†	150†	200†
1.4	77	49	43	35	28	25
2.1	44	32	20	15	12	11
2.8	29	22	17	11	9	9
3.5	23	13	10	7	6	6
4.2	20	11	8	6	6	6

*Fixed parameters: α - and β -slit-widths 0.7 mm, pulse width 20 μsec , repetition frequency 3 kHz, sample Al.

†Main slit-width, μm .

Table 4b. Variation of n_i/n_a with main slit-width for various breakdown voltages*

U_{br}, kV	$10^8 \times (\text{ratio of ions collected to atoms evaporated}), (n_i/n_a)$					
	20†	40†	60†	100†	150†	200†
1.4	2.3	3.6	4.1	5.1	6.3	7.1
2.1	0.76	1.0	1.7	2.2	2.8	3.1
2.8	0.71	0.92	1.2	1.9	2.3	2.6
3.5	0.35	0.62	0.81	1.2	1.3	1.3
4.2	0.34	0.62	0.85	1.1	1.1	1.2

*Fixed parameters: α - and β -slit-widths 0.7 mm, pulse width 20 μsec , repetition frequency 3 kHz, sample Al.

†Main slit-width, μm .

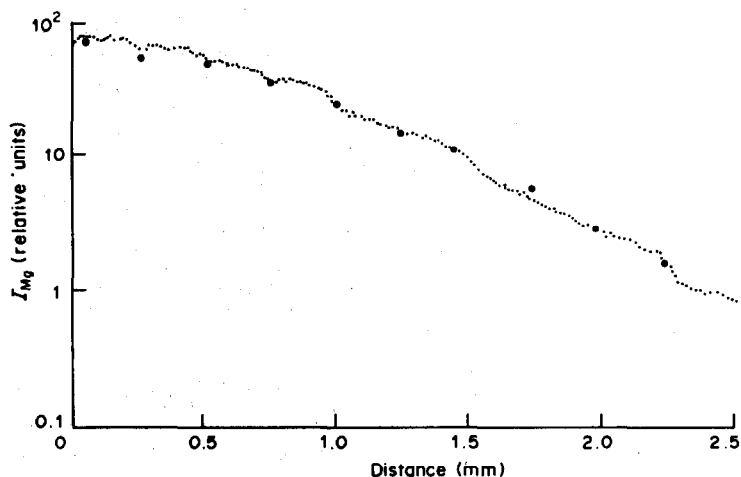


Fig. 8. Concentration profiles measured in Al-AlMg diffusion couples (●SSMS in-depth, ●SIMS laterally).

its determination may depend critically on the weight of the subsample in both matrices.

Depth profile analysis

From our results, it is possible to estimate the depth eroded, in the case of two identical electrodes:

$$d = \frac{VFt}{2A} = \frac{10^{12} W}{\rho A} \quad (9)$$

where d = depth eroded (μm), V = volume consumed per pulse train under the given experimental conditions ($\mu\text{m}^3/\text{pulse train}$), F = repetition frequency (Hz), 2 = factor taking into account that only one electrode is considered, t = erosion time (sec), A = area over which the electrode is sparked (μm^2), W = weight loss of the material (one electrode) and ρ = density of metal studied (g/cm^3).

We have observed that the weight loss per pulse train is independent of the repetition frequency. The effect of the pulse width was not investigated (all our measurements were made with a pulse width of 20 μsec). It is also important to note that in our spark-source mass spectrometer both electrodes gave the same weight loss. By using equation (9) and the results reported in Table 1a, we can select erosion rates ranging from a few nm/sec, or less, up to some $\mu\text{m}/\text{sec}$, depending on the specific problem and sample to be studied. This is a very wide dynamic range, which very few analytical techniques offer. It should, however, be noted that the minimum effective erosion depth is limited by the depth obtained with a single discharge¹ and the problem of depth resolution is not taken into account.

As an application we have measured the depth distribution profile of magnesium in aluminium, obtained by annealing an Al-AlMg diffusion couple at 462° for 525 hr. The magnesium profile in this particular sample is well known from lateral SIMS measurements¹⁰ and extends over more than 2 mm.

For SSMS depth profiling, pure aluminium was used as a counter-electrode. The diffusion couple and the pure aluminium electrode were machined, and bars of 10 mm length, 1.0 mm thickness and 2.3 mm width were obtained. The erosion rate of both electrodes was estimated from the results in Table 1a. The volume loss per pulse was the same for both the Al and AlMg (3 atom% Mg) electrodes, within experimental error. The depth analysis was performed by using electrical detection in the magnetic peak-switching mode. The experimental parameters se-

Table 5. Analysis of doped graphite samples by SSMS*

Element	Amount found, ppm	
	Normal	Micro
K	2.0×10^4	4.2×10^4
Ca	2.5×10^4	1.2×10^4
Ti	0.25	0.16
V	0.20	0.31
Cr	0.21	0.36
Mn	6.8	2.1
Fe	85†	85†
Cu	1.0	0.81
Zn	2.1	4.4
Ga	3.4	1.6
Ge	8.3	13
As	4.4	2.9
Rb	69	63
Sr	620	260
Mo	4.5	3.9
Cd	0.89	≤ 1.2
Sb	0.49	≤ 0.69
Cs	130	130
Ba	32	78
W	23	17

*Spark parameters: normal, U_{br} 2.8 kV, repetition frequency 3 kHz, pulse width 20 μsec ; micro, U_{br} 1.6 kV, repetition frequency 1 kHz, pulse width 20 μsec .

†Internal standard element (determined by instrumental neutron-activation analysis).

lected were U_{br} 3.8 kV, repetition frequency 3 kHz, pulse width 20 μ sec, accelerating voltage 29 kV, main slit-width 100 μ m, α - and β -slit-widths 2 mm, collector slit-width 500 μ m. The collector current of the $^{24}\text{Mg}^+$ isotope was integrated until a charge of 10^{-11} C was collected at the total ion-beam monitor. The time per measurement point was about 10 sec.

By weighing the sample electrode before and after analysis it was possible to convert time into depth. The result of our measurements is shown in Fig. 8 and is compared with the previously obtained profile from lateral SIMS analysis. Fair agreement is obtained, the diffusion coefficient from our SSMS analysis being 7.6×10^{-10} cm²/sec, whereas with SIMS a value of 8.6×10^{-10} cm²/sec was found.

One difficulty associated with our measurements was that the counter-electrode had to be polished after some time of sparking, in order to maintain flat surfaces. This may become unnecessary if more refractory counter-probes are used.

Analysis of "microsamples"

With the help of the results reported above, the minimum volume or weight of a sample needed for analysis can be calculated and the appropriate spark parameters selected (low U_{br} values, slit settings as wide as possible). We were able to analyse 5-mg samples of graphite electrodes doped down to the sub-ppm level.¹¹ The results and spark parameters of

a comparative study ("normal" *vs.* "micro") are summarized in Table 5.

Acknowledgements—This work was partially supported by the Interministerial Commission for Science Policy of Belgium through research grant 80-85/10. K.S. is indebted to the "Instituut tot Aanmoediging van het Wetenschappelijk Onderzoek in Nijverheid en Landbouw (IWONL)" for financial support. The diamond electrodes were kindly donated by "de Belder Diamonds n.v.", Antwerp, through Mr. M. van den Abeelen, High Council for Diamond, Antwerp.

REFERENCES

1. V. I. Derzhiev, G. I. Ramendik, V. Liebich and H. Mai, *Intern. J. Mass Spectrom. Ion Phys.*, 1980, **32**, 345.
2. I. N. Slivkov, *Electric Insulation and Discharge in a Vacuum*, Atomizdat, Moscow, 1972.
3. G. Germain and F. Rohrbach, *Proc. Intern. Conf. Ionization Phenomena in Gases*, 6th, Paris, Vol. 2, p. 111. North-Holland, Amsterdam, 1964.
4. M. Ito, S. Sako and K. Yanagihana, *Anal. Chim. Acta*, 1980, **120**, 217.
5. D. K. Davies and M. A. Biondi, *J. Appl. Phys.*, 1968, **39**, 2979.
6. P. C. Rossin, in *Vacuum Metallurgy*, R. F. Bunshah, (ed.), p. 82. Reinhold, New York, 1958.
7. L. Cranberg, *J. Appl. Phys.*, 1952, **23**, 518.
8. E. Van Hoye, R. Gijbels and F. Adams, *Intern. J. Mass Spectrom. Ion Phys.*, 1979, **30**, 75.
9. C. O. Ingamells and P. Switzer, *Talanta*, 1973, **20**, 547.
10. J. Verlinden and R. Gijbels, *Adv. Mass Spectrom.*, 1980, **8**, 485.
11. K. Swenters, *Licentiaatsthesis*, Antwerp, 1982.

CHEMICAL ANALYSIS OF URANIUM AND TITANIUM NIOBOTANTALATE METAMICT MINERALS BY ION-EXCHANGE CHROMATOGRAPHY AND SPECTROPHOTOMETRIC PROCEDURES

A. MAZZUCOTELLI

Istituto di Chimica Generale, Università di Genova, Italy

R. VANNUCCI

Istituto di Mineralogia e Petrografia, Università di Urbino, Italy

S. VANNUCCI

C.N.R., Centro Studi Mineralogia e Geochimica dei Sedimenti, Firenze, Italy

and

E. PASSAGLIA

Istituto di Mineralogia, Università di Ferrara, Italy

(Received 10 March 1982. Revised 13 September 1983. Accepted 1 October 1983)

Summary—An ion-exchange separation followed by spectrophotometric determinations is applied to some metamict minerals. These minerals, containing very high amounts of elements which present some problems to the analyst, such as uranium, titanium, niobium and rare-earth elements, are fused with potassium bisulphate, and the cooled melts dissolved in sulphuric acid. The solutions are passed through a series of three ion-exchange columns to separate those mineral-forming elements for which the colorimetric procedures suffer interference from the elements listed above. The procedure has been tested with a synthetic solution and with solutions of the minerals.

The term "metamict" means "after-mixed", implying either the rearrangement of the original structure to a new amorphous structure, or denoting an unusual non-crystalline condition for certain minerals of complex composition containing uranium and/or thorium, which in the course of time have passed from a truly crystalline state to an amorphous state.^{1,2} Generally metamict minerals are chemically complex.³ They characteristically show large-scale heterovalent isomorphism in both the cationic and anionic parts of their structures. Metamict minerals occur as oxides, phosphates and silicates. Most are multiple oxides containing niobium, tantalum and/or titanium. Owing to their particular properties, the identification of metamict minerals is difficult, and various physical and chemical methods have been tried, but many of them have limited efficiency.⁴ On account of the complexity of the chemical composition of these minerals, complete chemical analyses are difficult and may be lengthy. Ti, Nb, U, Ta, Th, Zr and rare-earth elements (REE) are the major elements present.^{5,6} Unfortunately these elements are the least sensitive for determination by atomic-absorption spectrophotometry, which is one of the most powerful and selective techniques in inorganic analytical chemistry. The best analytical methods for these elements in terms of sensitivity and accuracy are spectrophotometric: titanium with tiron,^{7,8} niobium

and tantalum with PAR,⁹ zirconium, thorium, uranium and lanthanides plus yttrium with Arsenazo III.¹⁰⁻¹³ Unfortunately there is mutual interference between these elements when these procedures are used. Moreover, because of the scarcity of these minerals, the analysis is ideally done on a single portion of sample. Hence two problems must be solved in reaching a complete chemical identification of these minerals: first, the complete dissolution of the sample, and second, the elimination of the interferences.

Sample dissolution

Acid decomposition is unable to dissolve the oxides of all the refractory elements present in metamict minerals such as betafites. When it is used, it is usually necessary to collect the insoluble residue, ignite it and fuse it with sodium carbonate or another suitable flux.¹⁴ However, this may introduce into the solution a large amount of foreign ions which will interfere in the subsequent separation and determination procedures.

Hitchen and Zechanowitsch¹⁵ have used several procedures for the decomposition of low-grade uranium ores, including potassium pyrosulphate fusion followed by leaching with dilute sulphuric acid, which Bock¹⁶ considers the most powerful method for dissolving refractory and rare-earth oxides. We have

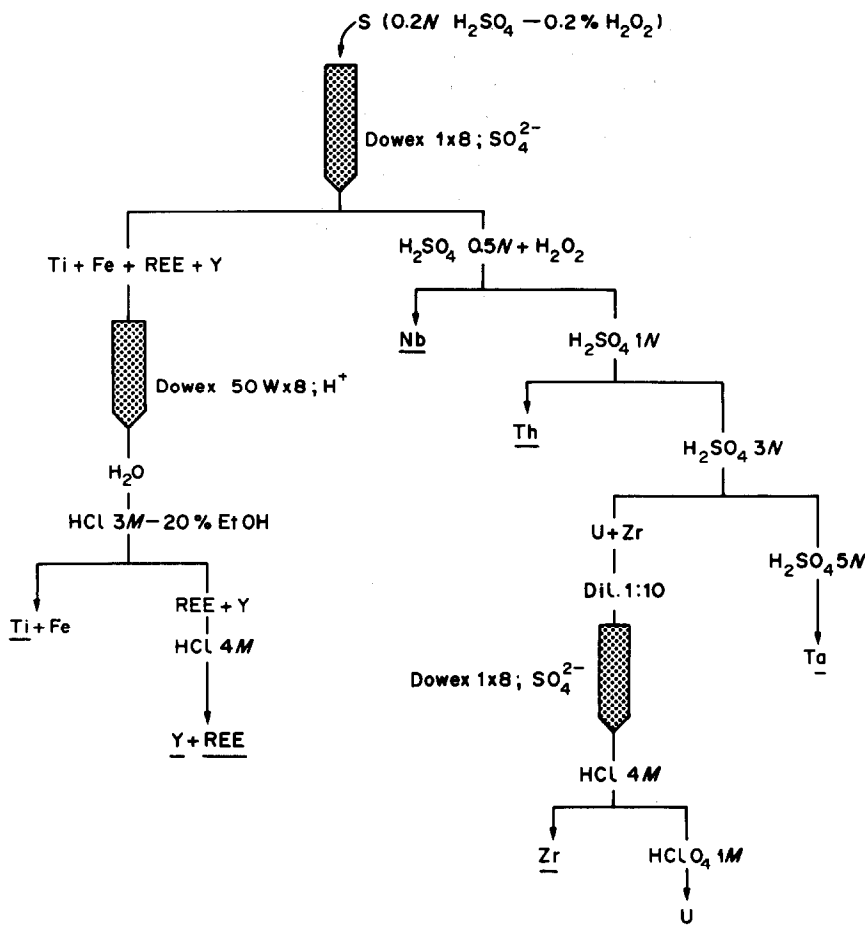


Fig. 1. Scheme of separation procedure.

chosen to use this last method partly because of its power, and partly because it gives a convenient solution matrix for the subsequent separation.

Ion-exchange separations

Several authors^{14,15,17-24} have studied separation methods for complex mixtures of REE, zirconium, hafnium, thorium and scandium, based on solvent-extraction with tri-n-butyl phosphate or liquid anion-exchangers in malonate media. However, these procedures generally relate only to pure solutions of these metals or present some difficulties in extraction of one or more of these elements when they are all present in the sample.

Ion-exchange seem to be the most powerful technique for complete separation of these elements in a single sample.

Because of the decomposition procedure chosen we examined only the separation procedures using sulphuric acid media, and some other schemes²⁵⁻²⁷ for the isolation of refractory or rare-earth elements in rocks and minerals were not considered. Kiriyaama and Kuroda²⁸ have described an ion-exchange separation of zirconium, thorium and uranium in silicate rocks, followed by determination with Arsenazo III.

The sample, dissolved in sulphuric acid, was passed through an anion-exchange column, and Th, Zr and U were successively eluted with sulphuric, hydrochloric and perchloric acids. In this procedure Ti, REE and (presumably) Y, and the silicate matrix are not retained; no mention was made of the behaviour of niobium and tantalum (which are main constituents of betafite minerals).

Strelow and Bothma²⁹ described an anion-exchange separation on a strongly basic resin for elements in sulphuric acid medium and gave the anion-exchange equilibrium coefficients for 52 elements. The coefficients for elements with strong hydrolytic tendencies, such as tantalum and niobium, were determined for media containing hydrogen peroxide. Elution curves were given for the systems Y(III)-Th(IV)-U(VI)-Mo(VI) and Th(IV)-Hf(IV)-Zr(IV)-Mo(VI) to demonstrate the potential of the system.

The chromatographic behaviour of species such as Ti(IV), Fe(II), Fe(III), REE(III) and Y(III) may be inferred from the separations described in a previous paper.³⁰ The separation procedure reported earlier for use in the determination of barium in silicates allows complete separation of the major and minor elements

(such as titanium and iron), present in a common silicate rock, from a group of trace elements, including yttrium and rare-earth elements (plus strontium and barium). The entire separation is done on a cation-exchanger and allows accurate determination of titanium (in presence of large amounts of iron) and of the REE plus yttrium. The yttrium can be separated from the individual REE if desired,³¹ but this can be omitted to simplify the procedure.

Separation procedure

The proposed separation scheme (shown in Fig. 1), is based on the three procedures²⁸⁻³⁰ mentioned above.

The sample solution (in 0.2*N* sulphuric acid) is mixed with hydrogen peroxide to make the separation of elements such as niobium and tantalum easier.^{9,29} The solution is passed through a column of Dowex anion-exchanger: titanium, REE, yttrium and the major elements of the silicate matrix are not retained, and are collected on a Dowex cation-exchange column to separate REE and yttrium from the other matrix elements.³⁰

The elements retained on the anion-exchanger are successively eluted with various sulphuric acid media: niobium with 0.5*N* acid plus hydrogen peroxide, thorium with 1*N* acid, uranium and zirconium with 3*N* acid and tantalum with 5*N* acid. Uranium and zirconium are separated on another anion-exchange column by successive elution with hydrochloric acid and perchloric acid.²⁸ These elements are then all determined spectrophotometrically.

EXPERIMENTAL

Reagents

Triethanolamine buffer. Mix 15 g of triethanolamine and 3.3 ml of concentrated nitric acid and dilute to 200 ml with water.

"Niobium buffer". Dissolve 40 g of ammonium acetate and 2.5 ml of glacial acetic acid with water and dilute to 500 ml.

"Titanium buffer". Dissolve 136 g of sodium acetate trihydrate in 1000 ml of water and add 390 ml of glacial acetic acid.

Procedure

Weigh accurately 1 g of finely powdered sample into a platinum crucible. Add about 3 g of potassium bisulphate and mix it with the sample. Insert the crucible in a suitably sized hole in an asbestos board (to avoid overheating of the walls) and heat it with a Bunsen burner until a clear melt is obtained. Allow the crucible to cool, add 3 ml of concentrated sulphuric acid and warm until a clear solution is obtained. Cool, transfer this solution and 1 ml of 100-volume hydrogen peroxide into a 500-ml standard flask and dilute to volume with water.

Pass half this solution at a flow-rate of 3.5 ± 0.05 ml/min through a borosilicate glass tube (15 mm bore) filled with an 18-cm long column of Dowex 1 \times 8 resin (200-400 mesh, sulphate form), and wash the column with 0.2*N* sulphuric acid/0.2% hydrogen peroxide solution, collecting the effluent in a Teflon beaker and then passing it through a column of Dowex 50W \times 8, as described earlier.³⁰

Elute titanium and other matrix elements (*i.e.*, iron, sodium, potassium, calcium and magnesium) from the Dowex 50W \times 8 with 250 ml of 3*M* hydrochloric acid

containing 20% v/v ethanol, and determine the titanium by the spectrophotometric iron procedure.^{7,8} Elute yttrium plus REE with 4*M* hydrochloric acid and determine the whole group by the Arsenazo III procedure.^{13,37}

Elute the elements from the anion-exchange column successively, niobium with 100 ml of 0.5*N* sulphuric acid/0.2% hydrogen peroxide solution, then thorium with 150 ml of 1.0*N* sulphuric acid, uranium plus zirconium with 200 ml of 3.0*N* sulphuric acid and finally tantalum with 100 ml of 5*N* sulphuric acid. Determine niobium with PAR,^{9,32} thorium with Arsenazo III,^{13,31} and tantalum with PAR.⁹ Separate uranium and zirconium by passing their solution through another Dowex 1 \times 8 column and eluting zirconium with 100 ml of 4*M* hydrochloric acid, and then uranium with 100 ml of 1*M* perchloric acid. Determine both with Arsenazo III.^{10,12}

RESULTS AND DISCUSSION

The scheme was tested with synthetic sample solutions made from pure salts, with the elements in the concentration ratios expected for natural samples. The results obtained are summarized in Table 1.

Table 1. Results of analysis of a standard solution with composition similar to "betafite" samples, by the ion-exchange procedure (6 replicates)

Element	Taken, mg	Found, mg	Standard deviation, mg	Mean recovery, %
Si	2.00	1.90	0.03	95.0
Ca	1.00	1.00	0.01	100.0
Mg	1.00	1.00	0.01	100.0
Fe	100.00	98.60	0.10	98.6
Mn	1.00	1.00	0.01	100.0
Pb	1.00	1.00	0.01	100.0
U	300.00	290.10	0.60	96.7
Th	5.00	5.10	0.30	102.0
Ti	200.00	190.00	0.70	95.0
Nb	300.00	294.70	0.80	98.2
Ta	5.00	4.00	0.40	80.0
Ce	5.00	5.00	0.70	100.0
Zr	1.00	0.94	0.20	94.0
Al	5.00	5.00	0.10	100.0

Table 2. Chemical composition (%) of betafite samples

	B1	B2	B3
SiO ₂	1.80	0.25	0.20
CaO	0.004	0.01	0.05
MgO	0.02	0.10	0.10
Fe ₂ O ₃	10.40	1.72	1.36
MnO	0.06	0.50	0.10
PbO	0.82	0.80	1.20
UO ₂	25.20	27.10	25.80
ThO ₂	0.80	1.00	1.50
TiO ₂	16.00	20.80	18.10
Nb ₂ O ₅	27.50	32.00	35.00
Ta ₂ O ₅	0.80	1.20	2.00
REE*	1.80	2.20	2.00
ZrO ₂	0.30	0.60	0.80
Al ₂ O ₃	4.20	0.12	0.38
L.O.I.†	10.20	12.00	11.30
Total	99.9	100.0	99.9

*Expressed as Ce₂O₃.

†Loss on ignition.

Three betafite samples were then analysed: B1 from the Ambatofotsy–Soavinandriana pegmatite of Madagascar, B2 from the Antsirabe–Vinaninkarena pegmatite and B3 from the pegmatite of Tongafeno Mountain (southern part of Betafo, Madagascar).

The results (Table 2) show good agreement with the literature data.

The minor elements, such as Si, Ca, Mg, Fe, Mn, Pb and Al, were determined by the classical procedure and AAS. They are not important for betafite characterization, and were determined only in order to complete the analysis of the samples studied.

The proposed method is useful for the chemical analysis of minerals (such as betafites) which are of great scientific and economic importance but present severe problems when analysed by purely instrumental techniques.

Acknowledgement—The authors are indebted to Professor G. Carobbi (Commissione Musei ed Esplorazioni Scientifiche, Accademia dei Lincei, Roma, Italy) for organization of the exploration and his encouragement to perform the work.

REFERENCES

1. R. S. Mitchell, *Mineral. Rec.*, 1973, **4**, 177.
2. *Idem, ibid.*, 1973, **5**, 214.
3. G. B. Barsanov, *Aspects of Theoretical Mineralogy in the U.S.S.R.*, pp. 331–345. Macmillan, New York, 1964.
4. J. Lima de Faria, *Identification of Metamict Minerals by X-Ray Powder Photographs*, Junta de Investigacoes do Ultramar, Estudos, Ensaios e Documentos, No. 112. Lisbon, 1964.
5. W. E. Ford, *Dana's Textbook of Mineralogy*, Wiley, London, 1922.
6. H. C. Wedepohl, *Handbook of Geochemistry*, Springer, Berlin, 1978.
7. R. Basso and A. Mazzucotelli, *Per. Mineral.*, 1975, **44**, 3.
8. P. Jeffrey, *Chemical Methods of Rock Analysis*, Pergamon Press, Oxford, 1970.
9. I. M. Gibalo, *Analytical Chemistry of Niobium and Tantalum*, Israel Program for Scientific Translation, Jerusalem, 1968.
10. S. V. Elinson and K. I. Petrov, *Analytical Chemistry of Zirconium and Hafnium*, Ann Arbor, London, 1969.
11. H. Hamaguchi, A. Ohuchi, T. Shimizu, N. Onuma and R. Kuroda, *Anal. Chem.*, 1964, **36**, 2304.
12. P. N. Palei, *Analytical Chemistry of Uranium*, Ann Arbor, London, 1970.
13. D. I. Ryabchikov and V. A. Ryabukhin, *Analytical Chemistry of Yttrium and the Lanthanide Elements*, Ann Arbor, London, 1970.
14. G. Culkin and J. P. Riley, *Anal. Chim. Acta*, 1965, **32**, 197.
15. A. Hitchen and G. Zechanowitsch, *Talanta*, 1980, **27**, 383.
16. R. Bock, *A Handbook of Decomposition Methods in Analytical Chemistry*, International Textbook Co., London, 1979.
17. M. B. Dalvi and S. M. Khopkar, *Talanta*, 1978, **25**, 599.
18. *Idem, ibid.*, 1979, **26**, 892.
19. M. B. Sawant and S. M. Khopkar, *ibid.*, 1980, **27**, 209.
20. *Idem, ibid.*, 1980, **27**, 451.
21. F. W. E. Strelow, *Anal. Chem.*, 1960, **32**, 1185.
22. *Idem, J. South Afr. Chem. Inst.*, 1961, **14**, 51.
23. J. Korkisch, *Modern Methods for the Separation of Rarer Metal Ions*, Pergamon Press, Oxford, 1969.
24. J. Korkisch and G. Arrhenius, *Anal. Chem.*, 1964, **36**, 851.
25. J. S. Fritz and R. G. Greene, *ibid.*, 1964, **36**, 1095.
26. J. Korkisch and H. Hubner, *Talanta*, 1976, **23**, 283.
27. I. Roelandts, G. Duyckaerts and A. O. Brunfelt, *Anal. Chim. Acta*, 1974, **73**, 141.
28. T. Kiriyaama and R. Kuroda, *ibid.*, 1974, **71**, 375.
29. F. W. E. Strelow and C. J. C. Bothma, *ibid.*, 1967, **39**, 595.
30. R. Frache and A. Mazzucotelli, *Talanta*, 1976, **23**, 389.
31. A. Mazzucotelli, R. Frache, A. Dadone, F. Baffi and P. Cescon, *Anal. Chim. Acta*, 1978, **99**, 365.
32. A. Mazzucotelli, R. Frache, A. Dadone and F. Baffi, *Analyst*, 1977, **102**, 825.

EXTRACTION OF RUTHENIUM THIOCYANATE AND ITS SEPARATION FROM RHODIUM BY POLYURETHANE FOAM

SARGON J. AL-BAZI and ARTHUR CHOW

Department of Chemistry, University of Manitoba, Winnipeg, Manitoba,
Canada R3T 2N2

(Received 24 May 1983. Accepted 30 September 1983)

Summary—Conditions for the formation and extraction of the thiocyanate complex of ruthenium are reported. Distribution coefficients of more than 10^4 and a capacity of about 0.24 mole per kg of foam were obtained. The effect of the chloride salts of various univalent cations on the extraction of $\text{Ru}(\text{SCN})_6^{3-}$ indicated that the efficiency of ruthenium extraction depends on how well the cation fits into the polyether segment of the polyurethane foam, which agrees with the "cation-chelation" mechanism. The separation of ruthenium and rhodium indicated that more than 95% of the rhodium remained in the aqueous phase and about 95% of the ruthenium was retained by the polyurethane foam and could be easily recovered.

The oxidation of ruthenium to the volatile tetroxide, followed by distillation, has been widely used for its separation from other platinum metals (except osmium).¹ For preconcentration of the metal, the tetroxide can be extracted into carbon tetrachloride,²⁻⁴ chloroform² or mepasine.⁵ The chloro-complex can be extracted by means of various organophosphorus compounds⁶ and amines.⁷⁻¹⁰ The thiocyanate complexes are also extractable.¹¹⁻¹⁵

The separation of rhodium and ruthenium is of interest to radiochemists since rhodium is a daughter of ruthenium by beta decay. It is usually done by extraction of ruthenium tetroxide into carbon tetrachloride.¹⁶⁻¹⁸

The purpose of the present work was to study the extraction of the thiocyanate complex of ruthenium by means of polyether-based polyurethane foam, and the separation of ruthenium from rhodium.

EXPERIMENTAL

Apparatus and reagents

A Varian 634 spectrophotometer and a Fisher Accumet model 520 pH-meter were used.

Ruthenium trichloride [$\text{RuCl}_3 \cdot 3\text{H}_2\text{O}$] and sodium hexachlororhodate(III) [$\text{Na}_3\text{RhCl}_6 \cdot 12\text{H}_2\text{O}$] were supplied by Johnson-Matthey Chemicals Ltd. All other chemicals were of analytical grade. Polyether-type polyurethane foam (No. 1338 M) was obtained from G. N. Jackson Ltd, Winnipeg, Manitoba, and washed by the procedure previously reported.¹⁹

A $2.5 \times 10^{-3} M$ stock solution of ruthenium(III) was prepared by dissolving the chloride in 0.1M hydrochloric acid. A 3.0M stock solution of potassium thiocyanate was prepared in doubly distilled demineralized water.

Extraction procedure

A known volume of the stock ruthenium chloride solution and the desired amount of thiocyanate were mixed, diluted to about 60 ml, adjusted to pH 2.5 ± 0.1 and transferred quantitatively to a 100-ml standard flask. The solution was heated at 90° for a measured time, cooled to room temperature in ice-water and finally diluted to volume. Then

99 ± 1 mg of the foam was repeatedly squeezed in 95 ml of this solution for a minimum of 10 hr as described previously.¹⁹

The percentage extraction (%E) was calculated by measuring the metal concentration before and after extraction. The distribution coefficient (D , l./kg) was calculated from the concentration ratio of metal in the foam to metal left in solution.

RESULTS AND DISCUSSION

First we established the conditions for maximum formation of the ruthenium-thiocyanate complex in aqueous medium. A fixed amount of ruthenium ($5.35 \mu\text{mole}$) and appropriate amounts of the other reagents were diluted to about 30 ml, adjusted to pH 2.5 ± 0.1 , heated at 90° for the desired time, then immediately cooled in ice-water to room temperature. The violet-blue solution was then diluted to 50 ml and its absorbance at 590 nm, which has been assigned to the $\text{Ru}(\text{SCN})_6^{3-}$ complex,²⁰⁻²² was measured.

Varying the heating time for solutions containing 30 mmole of thiocyanate (Fig. 1) indicated that heat-

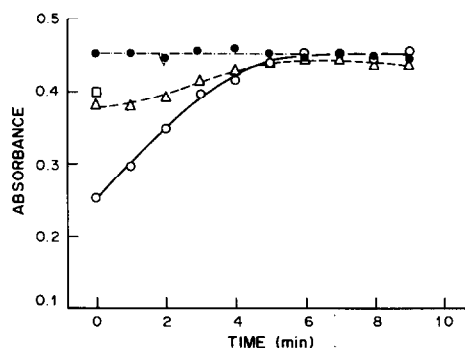


Fig. 1. Influence of time of heating on the formation of ruthenium-thiocyanate complex. Time after solution preparation: (○) immediately, (△) 1 day, (□) 2 days, (●) 9 days.

ing for 6 min is enough for maximum formation of the complex. With shorter heating times, complex formation was incomplete, and subsequent reaction at room temperature very slow, up to 9 days being required to reach an equilibrium value. This experiment also showed that the $\text{Ru}(\text{SCN})_6^{3-}$ complex formed was stable for up to 9 days. In the presence of 100 mmole of lithium chloride in the reaction mixture, the absorbance at 590 nm was 0.353 with no heating, rising with heating time to a maximum of 0.476 after 6 min of heating and then decreasing to 0.445 after 9 min of heating. Since heating the solution for 6 min at 90° in presence or absence of lithium chloride is enough for the maximum formation of $\text{Ru}(\text{SCN})_6^{3-}$, this was used as the optimum time for further studies.

The effect of increasing the amount of lithium chloride present, on the formation of the complex in solutions containing 30 mmole of thiocyanate and heated for 6 min, was to increase the absorbance from 0.451 with no lithium chloride added to 0.478 with 100 mmole or more added. The presence of sufficient neutral salt is not only important in the formation of the $\text{Ru}(\text{SCN})_6^{3-}$ complex, but was also recommended by Shlenskaya and Piskunov²³ for obtaining constant and reproducible values of the absorbance in studies on the reaction of Ru(IV) with thiocyanate.

Varying the hydrochloric acid concentration in solutions containing 15 mmole of thiocyanate caused a decrease in absorbance from 0.397 for 0.1M hydrochloric acid medium to 0.303 for 0.5M and 0.125 for 1M acid (measured after filtration of the brownish cloudy solution). This decolorization of the solution has been attributed to decomposition of the ruthenium–thiocyanate complex¹⁵ and to reduction²² of $\text{Ru}(\text{SCN})_6^{3-}$ to $\text{Ru}(\text{SCN})_6^{4-}$. The reduction process was confirmed in our study by the fact that addition of hydrazine hydrate to the violet-blue solution of the ruthenium–thiocyanate complex turned it yellow (the same change in colour in molten thiocyanate medium was observed by De Haas²²). Addition of hydrogen peroxide to the yellow solution turned it back to violet-blue.

Since ruthenium has a high tendency to hydrolyse,²⁴⁻²⁷ the stability of the ruthenium–thiocyanate complex was studied in solutions containing 30 mmole of thiocyanate and adjusted to different pH values with lithium hydroxide after preparation of the complex. The absorbance decreased from 0.453 at pH 2.5 to 0.398 at pH 5.5 and to 0.320 at pH 8.3. The solutions were therefore adjusted to pH 2.5 ± 0.1 in the extraction studies.

Extraction of ruthenium(III)

Under the optimum conditions for formation of the ruthenium–thiocyanate complex, a study was made of the effect of various parameters on the distribution of the complex between the polyurethane foam and the aqueous phase. The addition of hydrochloric acid after the heating of solutions that were

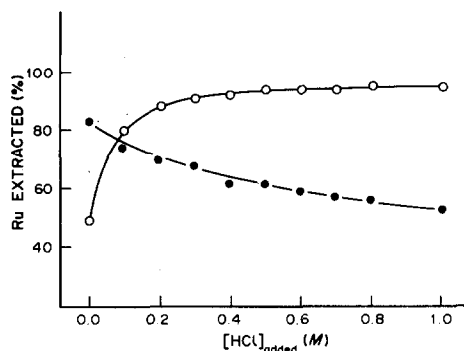


Fig. 2. Effect of hydrochloric acid (added after heating the solution) on ruthenium extraction. Thiocyanate concentration: (○) 0.1M, (●) 0.4M.

initially 0.4M in thiocyanate and 2M in lithium chloride (Fig. 2) caused a slow decrease from 83% extraction ($\log D = 3.67$) with no hydrochloric acid added to 53% extraction ($\log D = 3.04$) at 1M acid concentration. The absorbance of these solutions at 590 nm indicated that $\text{Ru}(\text{SCN})_6^{3-}$ was stable at hydrochloric acid concentrations up to 0.7M but was partly decomposed (by 8%) in 1.0M hydrochloric acid. The absorption spectra did not show bands at 284 and 342 nm, which indicates that 5-amino-1,2,4-dithiazole-3-thione was not formed in the solution.²⁸ Therefore the observed decline in degree of extraction with increase in acid concentration up to 0.7M is probably due to the formation and subsequent extraction of thiocyanic acid. When the experiment was repeated with 0.1M thiocyanate and no lithium chloride present, the extraction (Fig. 2) increased sharply from 49% ($\log D = 2.96$) with no hydrochloric acid added, to 80% ($\log D = 3.59$) at 0.1M acid concentration and then more slowly to 95% ($\log D = 4.28$) at 1.0M acid concentration. The absorbance of these solutions at 590 nm increased only by 4% with increasing acid concentration from zero to 1.0M. Therefore hydrochloric acid mainly influences the distribution of the $\text{Ru}(\text{SCN})_6^{3-}$ complex between the foam and the liquid phase.

A comparison of the two curves in Fig. 2 shows that the effect of hydrochloric acid on the extraction of ruthenium is highly dependent on the thiocyanate concentration of the solution. Therefore at the optimum thiocyanate concentration for formation of the $\text{Ru}(\text{SCN})_6^{3-}$ complex, it is more efficient to perform the extraction at low acidity, and this can only be successful if the complex is extractable through the "cation–chelation" mechanism.^{29,30} Addition of potassium chloride after the heating of ruthenium solutions (at pH 2.5 ± 0.1 ; 0.4M initial thiocyanate and 2M lithium chloride) increased the extraction from 82% ($\log D = 3.63$) with no potassium chloride added, to 96% ($\log D = 4.37$) at 1.0M potassium chloride. The absorbance at 590 nm was independent of potassium chloride concentration. Therefore, the

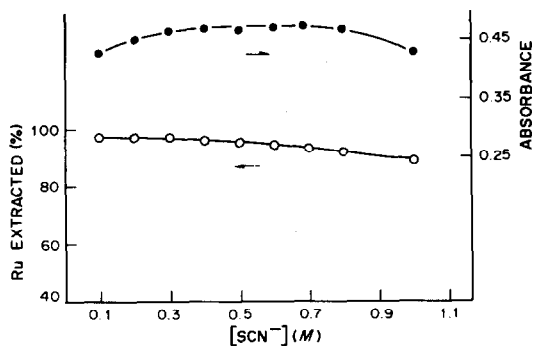


Fig. 3. Effect of initial thiocyanate concentration on the formation and the extraction of ruthenium-thiocyanate complex: (●) formation, (○) extraction.

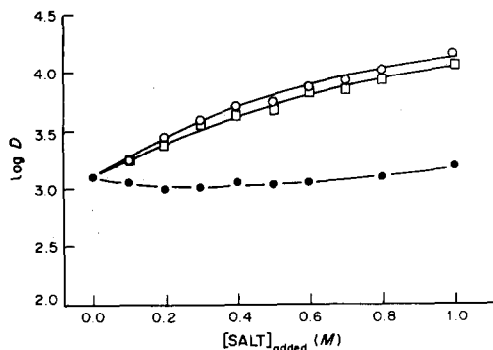


Fig. 4. Effect of salt concentration on the distribution of ruthenium-thiocyanate complex: (○) NH_4Cl , (□) KCl , (●) LiCl .

effect of potassium chloride is mainly on the distribution of $\text{Ru}(\text{SCN})_6^{3-}$.

The dependence of ruthenium extraction on the thiocyanate concentration in solutions at $\text{pH } 2.5 \pm 0.1$ that were $2M$ in lithium chloride (added before heating) and $1M$ in potassium chloride (added after cooling to room temperature) is shown in Fig. 3. At zero thiocyanate concentration, less than 0.5% of the metal was extracted and the absorption spectrum showed absorbances at 386 and 460 nm, which have been related to a mixture of $[\text{RuCl}_m(\text{H}_2\text{O})_{6-m}]^{3-m}$ ions ($m = 0-6$) by Shukla.³¹ The results also indicate that 97% ($\log D = 4.56$) of the ruthenium was extracted from a solution initially $0.1M$ in thiocyanate, but only 89% ($\log D = 3.92$) from $1.0M$ thiocyanate medium. The absorbance at 590 nm (Fig. 3) increased by 9% when the thiocyanate concentration was increased from 0.1 to $0.4M$, then remained constant up to $0.8M$ thiocyanate and decreased again by 9% at $1M$ thiocyanate. The decrease in absorbance at high thiocyanate concentrations is mainly due to reduction by thiocyanate.^{22,23} Therefore, the decrease in the extraction of ruthenium may be due to interference by thiocyanate, as shown for palladium,³³ and/or to the formation of less extractable species.

The effect of changing the ruthenium concentration on its extraction from solutions that were $0.8M$ in initial thiocyanate, and $2M$ in lithium chloride (added before heating) and $1M$ in potassium chloride (added after cooling), indicated that the amount of metal on the foam was almost linearly proportional to the amount left in solution, up to $8 \times 10^{-5}M$ initial ruthenium, and then started to level off with increasing initial ruthenium concentration, reaching a maximum value at $3 \times 10^{-4}M$ ruthenium. At higher concentrations, the amount of ruthenium on the foam remained constant, indicating that 0.24 mole/kg [24.3 g/kg] is the capacity of the polyether-type polyurethane foam for the extraction of ruthenium under the given conditions.

A qualitative study on the recovery of ruthenium from the foam showed that acetone can be used for this with high efficiency.

To confirm that the ruthenium is extracted by the "cation-chelation" mechanism, the effect of various chlorides was investigated and the results (Fig. 4) showed that though even $1M$ lithium chloride had only little effect on the extraction of ruthenium, on the other hand the extraction from solutions containing potassium or ammonium chloride increased linearly with salt concentration up to $0.4M$ and then more gradually at higher concentrations. A significant increase in the extraction of $\text{Ru}(\text{SCN})_6^{3-}$ was also observed from thiocyanate solutions that were $1M$ in sodium chloride. The absorbance values at 590 nm were almost equal, suggesting that the effect of the salt is mainly on the distribution of the $\text{Ru}(\text{SCN})_6^{3-}$ complex between the foam and the aqueous phase.

When the distribution coefficient for the 0.1 , 0.5 and $1.0M$ salt solutions (only $1.0M$ for sodium chloride) are plotted as a function of cation size (Fig. 5), the efficiency of extraction is seen to increase with increasing ionic radius. Since these results are similar to those obtained for the extraction of the $\text{Pd}(\text{SCN})_4^{2-}$ complex^{19,33} and the $\text{Pt}(\text{SCN})_4^{2-}$ com-

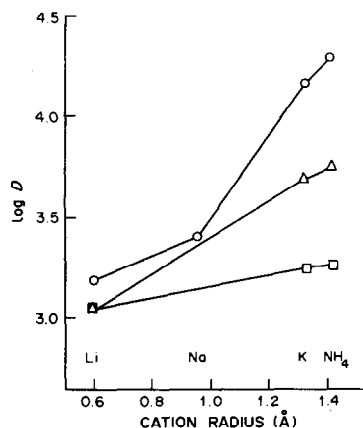


Fig. 5. Effect of the size of various univalent cations on the distribution of ruthenium-thiocyanate complex. Salt concentration: (□) $0.1M$, (△) $0.5M$, (○) $1M$.

plex,³⁴ it can be concluded that the "cation-chelation" mechanism is also the major mode of $\text{Ru}(\text{SCN})_6^{3-}$ extraction into polyurethane foam.

Separation of ruthenium and rhodium

Several differences in the formation as well as the distribution of the thiocyanate complexes of ruthenium and rhodium were observed. For example, 6 min of heating at 90° was found enough for maximum formation of the $\text{Ru}(\text{SCN})_6^{3-}$ complex, whereas heating for 30 min was required³⁵ for $\text{Rh}(\text{SCN})_6^{3-}$. A minimum of 2M hydrochloric acid was required for the extraction of rhodium,³⁶ but a pH of about 2.5 was sufficient for the extraction of ruthenium. Furthermore, the rhodium extraction increased with increasing hydration number of the cation present³⁵ whereas the ruthenium extraction decreased. On this basis, the optimum conditions for the separation of these two metals were determined.

The minimum heating time for maximum formation of $\text{Ru}(\text{SCN})_6^{3-}$ in the presence of ammonium chloride was found by heating about 30 ml of solution (at pH 2.5 ± 0.1 and containing 5.35 μmole of ruthenium, 30 mmole of thiocyanate and 8.03 g of ammonium chloride) at 90° for 4, 5 or 6 min, immediately cooling in ice-water to room temperature, diluting to 50 ml, and measuring the absorbance at 590 nm. Absorbances of 0.452, 0.456 and 0.459 were obtained at 4, 5 and 6 min, respectively. Therefore, a 5-min heating of the solution before extraction was chosen in the separation of ruthenium and rhodium.

Since the efficiency of the separation depends on the differences in the amounts of $\text{Ru}(\text{SCN})_6^{3-}$ and $\text{Rh}(\text{SCN})_6^{3-}$ complexes formed, the time elapsed between preparation of the ruthenium complex and its extraction may be critical. To determine the optimum time, a solution (about 60 ml) at pH 2.5 ± 0.1 , containing 10.7 μmole of ruthenium, 60 mmole of thiocyanate and 16.05 g of ammonium chloride was heated at 90° for 5 min, cooled in ice-water to room temperature, and diluted to 100 ml. A foam cube weighing 0.3 g was then equilibrated with 95 ml of this solution for a selected period of time and the degree of extraction determined. The degree of extraction was found to rise sharply with extraction time to 93% for 19 min then more slowly to 97% for 1 hr, remaining practically constant for longer times. Therefore, 1 hr was chosen as the optimum period of extraction.

Table 1. Effect of rhodium concentration on the extraction of ruthenium by polyurethane foam

[Ru(III)], M	[Rh(III)], M	Ruthenium, %E
1×10^{-4}	0.0	95
1×10^{-4}	1×10^{-4}	95
1×10^{-4}	2×10^{-4}	95
1×10^{-4}	3×10^{-4}	93

The effect of different concentrations of rhodium on the extraction of ruthenium under the optimum conditions was investigated. The results in Table 1 indicate that rhodium in up to threefold molar ratio to ruthenium has almost no effect on the extraction. An atomic-absorption study showed that less than 5% of the rhodium was extracted under these conditions.

CONCLUSIONS

The relatively high distribution coefficients indicate that polyether-type polyurethane foam is highly efficient for the extraction of hexathiocyanatoruthenate(III), compared to many organic solvents.^{3,6,8} Furthermore, the ability of the foam to extract ruthenium at low acidity (pH = 2.5 ± 0.1) minimizes the tendency of thiocyanate to decompose³⁷ and to trimerize.²⁸ The low acidity also reduces interference by thiocyanic acid and the trimerization product, 5-amino-1,2,4-dithiazole-3-thione, which are produced in solutions having high thiocyanate and acid concentrations.^{19,33-36}

The separation of rhodium and ruthenium by polyurethane foam is a useful alternative to the commonly used methods¹⁶⁻¹⁸ in which ruthenium is oxidized to the tetroxide. Small losses of the metal can be caused by volatilization of RuO_4 from the organic solvent⁴ and by reduction of the tetroxide by the extractant.^{4,17} The use of polyurethane foam in the separation of ruthenium and rhodium is also important because no reasonable ion-exchange methods have been reported, on account of the labile character of the chloro-complexes of these two metals toward aquation.

Acknowledgement—This work was supported by the Natural Science and Engineering Research Council of Canada.

REFERENCES

1. F. E. Beamish, *Talanta*, 1960, **5**, 1.
2. R. D. Sauerbrunn and E. B. Sandell, *Anal. Chim. Acta*, 1953, **9**, 86.
3. F. S. Martin, *J. Chem. Soc.*, 1954, 2564.
4. J. W. T. Meadows and G. M. Matlack, *Anal. Chem.*, 1962, **34**, 89.
5. W. Smulek, *Radiochem. Radioanal. Lett.*, 1969, **2**, 265.
6. H. Meier, D. Bosche, E. Zimmerhackl, W. Albrecht, W. Hecker, P. Menge, A. Ruckdeschel, E. Under and G. Zeitler, *Mikrochim. Acta*, 1969, 1083.
7. *Idem, ibid.*, 1969, 1107.
8. Y. Oka and T. Kato, *Nippon Kagaku Zasshi*, 1965, **86**, 1153; *Chem. Abstr.*, 1966, **64**, 8983b.
9. K. A. Bol'shakov, N. M. Sinitsyn, V. V. Borisov, V. I. Efanov and N. A. Pantyukhina, *Uchen. Zap. Mosk. Inst. Tonkoi Khim. Technol.*, 1970, **1**, 35; *Anal. Abstr.*, 1972, **23**, 310.
10. K. A. Bol'shakov, N. M. Sinitsyn, T. M. Buslaeva and A. P. Ivchenko, *Dokl. Akad. Nauk SSR*, 1980, **251**, 1406; *Anal. Abstr.*, 1981, **40**, 1B167.
11. J. H. W. Forsythe, R. J. Magee and C. L. Wilson, *Talanta*, 1960, **3**, 324.
12. W. L. Belew, G. R. Wilson and L. T. Corbon, *Anal. Chem.*, 1961, **33**, 886.

13. Y. Oka and T. Kato, *Nippon Kagaku Zasshi*, 1963, **84**, 249; *Chem. Abstr.*, 1964, **60**, 3542e.
14. *Idem, ibid.*, 1966, **87**, 580; *Chem. Abstr.*, 1966, **65**, 8088d.
15. Z. Marczenko and M. Balcerzak, *Anal. Chim. Acta*, 1979, **109**, 123.
16. D. F. C. Morris and M. A. Khan, *Radiochim. Acta*, 1966, **6**, 110.
17. C. E. Epperson, R. R. Landolt and W. V. Kessler, *Anal. Chem.*, 1976, **48**, 979.
18. J. H. Chiu, R. R. Landolt and W. V. Kessler, *ibid.*, 1978, **50**, 670.
19. S. J. Al-Bazi and A. Chow, *Talanta*, 1982, **29**, 507.
20. H. H. Schmidtke, *J. Inorg. Nucl. Chem.*, 1966, **28**, 1735.
21. H. H. Schmidtke and D. Garthoff, *Helv. Chim. Acta*, 1967, **50**, 1631.
22. K. S. De Haas, *J. Inorg. Nucl. Chem.*, 1973, **35**, 3231.
23. V. I. Shlenskaya and E. M. Piskunov, *Vestn. Mosk. Univ., Ser. II, Khim.*, 1963, **18**, 35; *Chem. Abstr.*, 1963, **59**, 2385g.
24. P. Wehner and J. C. Hindman, *J. Phys. Chem.*, 1952, **56**, 10.
25. V. I. Paramonova and E. F. Latyshev, *Radiokhimiya*, 1959, **1**, 458.
26. F. Pantani, *J. Less-Common Met.*, 1962, **4**, 116.
27. A. Ohyochi, E. Ohyoshi, M. Senoo and M. Shinagawa, *J. Nucl. Sci. Technol.*, 1966, **3**, 237.
28. W. H. Hall and I. R. Wilson, *Aust. J. Chem.*, 1969, **22**, 513.
29. R. F. Hamon, A. S. Khan and A. Chow, *Talanta*, 1982, **29**, 313.
30. A. S. Khan, *Ph.D. Thesis*, Univ. of Manitoba, 1982.
31. S. K. Shukla, *J. Chromatog.*, 1962, **8**, 96.
32. D. M. Stanbury, W. K. Wilmarth, S. Khalaf, H. N. Po and J. E. Byrd, *Inorg. Chem.*, 1980, **19**, 2715.
33. S. J. Al-Bazi and A. Chow, *Talanta*, 1983, **30**, 487.
34. *Idem, Anal. Chem.*, 1983, **55**, 1094.
35. S. J. Al-Bazi, *Ph.D. Thesis*, Univ. of Manitoba, 1983.
36. S. J. Al-Bazi and A. Chow, *Anal. Chem.*, 1981, **53**, 1073.
37. T. I. Crowell and M. G. Hankins, *J. Phys. Chem.*, 1969, **73**, 1380.

STUDIES ON THE LANTHANUM ARSENATE ION-EXCHANGER: PREPARATION, PHYSICO-CHEMICAL PROPERTIES AND APPLICATIONS

ASHIS K. MUKHERJEE* and SUCHITRA K. MANDAL
 Department of Chemistry, Presidency College, Calcutta 700073, India

(Received 13 September 1982. Revised 14 September 1983. Accepted 30 September 1983)

Summary—The cation-exchange behaviour of lanthanum arsenate has been studied. This paper reports the preparation and physicochemical properties of the exchanger. Its analytical utility is compared with that of other arsenate exchangers. Some practical analytical applications are described.

The analytical applications of synthetic ion-exchangers^{1,2} have received considerable attention owing to their high degree of selectivity for certain elements,³ and resistance to nuclear radiation. Of the various inorganic ion-exchangers that have been studied, those based on lanthanum are probably the least investigated. The literature reports deal with the arsenates of Zr, Ti, Cr, Sn, Th, Ce, Fe, Nb and Ta; we now add lanthanum arsenate to the list.

EXPERIMENTAL

Reagents

All reagents and chemicals were of analytical grade. Doubly distilled water was used throughout.

Preparation and composition of the exchanger

The exchanger was synthesized in two ways. In the first, 0.1M lanthanum nitrate solution in 0.1M nitric acid was mixed dropwise in various proportions with 0.1M disodium hydrogen arsenate solution, and the precipitate was digested. In the other, 0.1M lanthanum nitrate solution in 0.1M nitric acid was added in different proportions to 0.1M sodium arsenate solution in presence of excess of hydrogen peroxide, and the precipitate was digested on a water-bath. The products were allowed to stand with the mother liquor for 24 hr, then filtered off, washed, and dried first in air, and finally over anhydrous calcium chloride in a vacuum desiccator. They were converted into the H⁺-form with 1M nitric acid and dried as before.

The powdered product (0.5 g) was dissolved in 25 ml of concentrated nitric acid, and the mixture was evaporated to small volume on a water-bath to expel oxides of nitrogen, and diluted to 100 ml with water. The lanthanum was precipitated as oxalate and ignited at 800° to the oxide,⁴ which was weighed. For the arsenate estimation, 0.5 g of exchanger was dissolved in 25 ml of concentrated hydrochloric acid, and arsenate was determined iodometrically in 4M hydrochloric acid medium. A separate 0.5-g sample was heated at 800° for 1 hr, and the La:H₂O ratio calculated from the weight loss, according to Alberti *et al.*⁵ Details of the syntheses and composition are given in Table 1.

Characteristics

Chemical stability (Table 2). The solubility was determined by shaking 0.5 g of exchanger with 100 ml of solvent for 15 hr, then determining lanthanum in the solution spectrophotometrically⁴ at 550 nm with sodium alizarin sulphonate in acetate buffer, and arsenate at 840 nm by the Molybdenum Blue method.

Potentiometric titration (Fig. 1). A 0.5 g sample was shaken with 100 ml of 2M sodium (or potassium) chloride for 16 hr and the mixture was titrated potentiometrically with standard alkali.

Ion-exchange capacity. One-g portions of specimen B-4 (H⁺-form) were shaken with 100 ml of various metal ion solutions for 2 days with intermittent shaking, and the liberated hydrogen ions were titrated; the exchange capacities are given in Table 3.

The effect of the salt concentration and the time of equilibration on the apparent exchange capacity of lanthanum arsenate are shown in Figs. 2 and 3, respectively. The exchange capacity was also determined for samples of the exchanger that had been heated to different temperatures and compared with that for similarly treated ferric arsenate⁶ and tantalum arsenate⁷ (Fig. 4).

*To whom correspondence should be addressed.

Table 1. Details of synthesis and composition of lanthanum arsenate

Batch	Reactants	Volume ratio La/As, v/v	Stirring time, hr	Temp., °C	pH of mother liquor	Composition, La:As:H ₂ O	Ion-exchange capacity for Na ⁺ , meq/g
B-1	0.1M lanthanum nitrate in 0.1M nitric acid + 0.1M disodium hydrogen arsenate	1:2	4	27 ± 2	1.8	1:1.18:1.17	0.67
B-2		1:2	16	80 ± 5	1.6	1:1.2:1.86	0.72
B-3		3:5	16	80 ± 5	1.6	1:1.03:1	0.19
B-4		1:4	12	80 ± 5	1.65	1:1.4:2.98	0.87
B-5	0.1M lanthanum nitrate in 0.1M nitric acid + 0.1M sodium arsenite + hydrogen peroxide (excess)	1:2	16	80 ± 5	1.85	1:1.12:1.19	0.53
B-6		1:4	16	80 ± 5	1.83	1:1.19:1.16	0.66

Table 2. The solubility of lanthanum arsenate exchanger in different solvents (mg of element dissolved in 100 ml at 25°)

Solvent	B-1		B-2		B-3		B-4		B-5		B-6		B-4 heated at 200°		B-4 heated at 300°	
	La	As	La	As	La	As	La	As	La	As	La	As	La	As	La	As
HCl 0.1M	13.8	7.4	4.9	2.6	10.5	5.7	2.0	1.0	9.8	4.9	6.6	3.4	0.9	0.5	0.4	0.2
HNO ₃ , 0.1M	17.6	9.4	6.1	3.0	11.6	6.2	2.5	1.3	11.1	5.3	7.7	3.7	0.9	0.4	0.4	0.2
H ₂ SO ₄ , 0.1N	11.2	6.0	4.2	2.3	8.8	4.7	1.9	1.0	9.8	5.3	4.8	2.5	0.6	0.3	0.3	0.1
NH ₄ NO ₃ (5%) in 0.1M HNO ₃	19.0	10.0	6.2	3.2	12.1	6.7	2.6	1.3	12.7	5.6	8.9	4.1	1.0	0.4	0.4	0.3

All batches were practically completely insoluble in doubly distilled water, 2M NaOH, 5% NH₄NO₃ solution, 2N oxalic acid and acetylacetone.

Break-through capacity (Table 4). This was determined in the usual way with a column of 5 g of 100–200 mesh exchanger B-4 (H⁺-form) and 0.01M solutions of the metal ions.

Distribution coefficients. The K_D values were determined with preparation B-4, 0.5 g of exchanger being equilibrated with 100 ml of $\sim 10^{-3}M$ test solution by intermittent shaking during two days. After equilibration, the aqueous phase was analysed, colorimetrically^{8,9} for metal ions giving high K_D values and complexometrically^{8,10} for the others. The results are given in Table 5.

Ion-exchange separations. Some binary mixtures of cations were separated on a column of 5 g of 100–200 mesh exchanger (B-4) with eluents chosen on the basis of the distribution coefficient. Hg(II) was separated from Pb(II), Mn(II), Cd(II), Cu(II) and Ce(III); Zn(II) from Pb(II) and Mn(II); Ni(II) from Pb(II), Mn(II), Cd(II) and Ce(III); Co(II) from Pb(II) and Mn(II); Mg(II) from Cd(II), Mn(II) and Pb(II), all with $\pm 1\%$ error. Certain ions in solutions obtained from copper–nickel alloy, ferromanganese and stainless steel were also separated, but there was difficulty in separating Fe(III) from Cu(II) or Cr(III), since their K_D values are similar. It is necessary first to separate these pairs of ions from others with 0.5M ammonium nitrate as eluent and then to separate the components of the pair by ion-exchange in phosphoric acid medium; the iron(III) phosphate complex is sorbed and the chromium or copper comes out in the effluent. Iron can then be eluted with 0.05M hydrochloric acid.

The copper–nickel alloy (0.5 g) was dissolved in hot 6M hydrochloric acid, a few drops of concentrated nitric acid were added, then the mixture was boiled to remove oxides of nitrogen, cooled and diluted to 250 ml. Ferromanganese (0.5 g) was dissolved in a mixture of concentrated hydrochloric acid (20 ml) and nitric acid (5 ml), then the solution was evaporated almost to dryness, cooled and diluted to 250 ml. Stainless steel (0.5 g) was dissolved in hot 6M hydro-

chloric acid, then iron(II) was oxidized with 20 drops of concentrated nitric acid. The solution was evaporated to small volume, cooled and diluted to 250 ml with water. Appropriate fractions were analysed and the results are given in Table 6.

RESULTS AND DISCUSSION

Having high exchange capacities and inertness towards dilute acids, specimens B-2 and B-4 were the most suitable as exchangers. The solubility in acids decreases considerably if the exchanger is heated to 200–300° before use. Table 1 shows that the exchanger is non-stoichiometric, presumably because of partial polymerization or protonation of the arsenate.

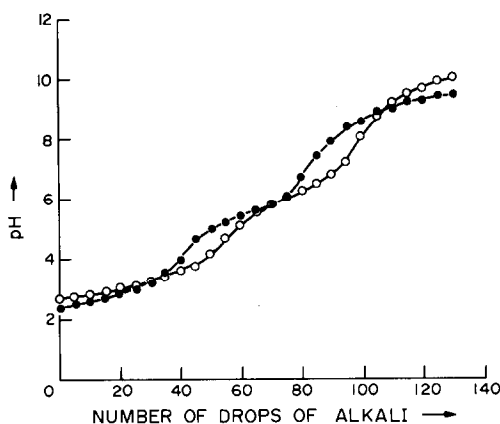


Fig. 1. Potentiometric titration curves. ○, KCl; ●, NaCl. 1 drop = 0.05 ml of 0.1M NaOH.

Table 3. Cation exchange capacities of lanthanum arsenate (B-4) for different metal ions

Metal ions	Concn., M	Exchange capacity, meq/g	Ionic radii (non-hydrated), Å°
Li ⁺	2	0.61	0.68
Na ⁺	2	0.866	0.97
NH ₄ ⁺	2	0.95	—
K ⁺	2	1.06	1.33
Cs ⁺	2	1.17	1.67
Mg ²⁺	0.1	0.31	0.66
Ni ²⁺	0.1	0.34	0.69
Co ²⁺	0.1	0.34	0.72
Cu ²⁺	0.1	0.39	0.72
Mn ²⁺	0.1	0.45	0.80
Pb ²⁺	0.1	0.52	1.20
Zn ²⁺	0.1	0.35	0.74
Cd ²⁺	0.1	0.416	0.97

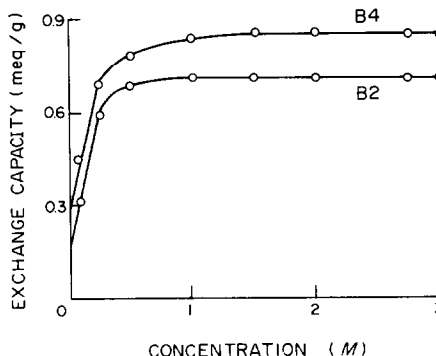
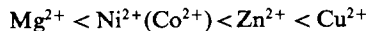


Fig. 2. Concentration equilibrium curve for sodium.

Table 4. Breakthrough capacity of lanthanum arsenate (B-4)

Ion	System	Breakthrough capacity, meq/5g
Ni ²⁺	Water	1.14
Co ²⁺	Water	1.36
Zn ²⁺	Water	1.44
Cu ²⁺	Water	1.76
Cu ²⁺	pH 2 (nitric acid)	1.06

The potentiometric titration (Fig. 1) characterizes the exchanger as having two types of proton-binding sites, resembling crystalline zirconium arsenate in this respect.¹ The breaks in the potentiometric curves suggest that in the equilibration with sodium or potassium chloride solution only the "strong acid" protons are exchanged, and that these give the endpoint break at about pH 4.2; the "weak acid" protons are only exchanged on further titration, by a "push-pull" mechanism of ion-exchange and neutralization. Hence the ion-exchange capacity rises with increasing pH of the solution. The following affinity sequences have been found for univalent and bivalent cation series, with the lanthanum arsenate ion-exchanger.



The sequence for univalent ions resembles that for ion-exchangers of cross-linked type. The exchange capacity (especially for univalent ions) under similar conditions is directly related (Table 3) to the radii of the non-hydrated ions in a homovalent series. This suggests that the hydrated ions of smaller radii are strongly sorbed, since the radii of the hydrated ions tend to decrease with atomic number and the coulombic interaction would increase. However, this is

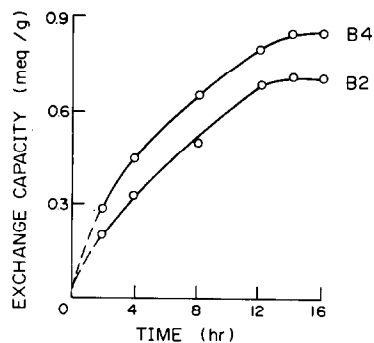


Fig. 3. Time equilibrium curve.

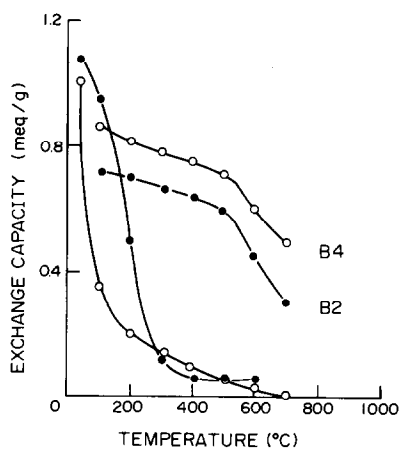


Fig. 4. Effect of heat treatment of exchanger on the exchange capacity. ●, Tantalum arsenate; ○, ferric arsenate.

less evident for the bivalent cations, where not only the ionic size is important, but the electronic structure and polarizing power of the metal ions, together with the solubility products of the metal arsenates, also play a part. Similar irregularities (for which the solubility product factor seems to play a dominating role) have been observed for stannic arsenate.¹

Table 5. Distribution coefficients (K_D) between lanthanum arsenate (B-4) and various systems (T.A. = total absorption)

Metal ion	Water	0.1M NH ₄ NO ₃	0.5M NH ₄ NO ₃	0.1M NH ₄ NO ₃	0.1M NH ₄ NO ₃ in 0.01M NHO ₃	HNO ₃ (pH 2)
Pb(II)	1.3 × 10 ³	9.5 × 10 ²	8.4 × 10 ²	7.4 × 10 ²	6.7 × 10 ²	6.9 × 10 ²
Cd(II)	281	160	127	92	69	89
Cu(II)	257	145	102	68	53	77
Mn(II)	1.0 × 10 ³	8.3 × 10 ²	7.0 × 10 ²	6.4 × 10 ²	4.9 × 10 ²	5.5 × 10 ²
Zn(II)	45	19.2	9.6	4.6	4.6	4.8
Ca(II)	85	51	31	19	11.6	17.1
Ba(II)	25	3.7	3.7	3.7	0.1	0.1
Ni(II)	16.3	0.0	0.0	0.0	0.0	0.0
Co(II)	33	11.1	2.3	2.3	1.1	1.1
Mg(II)	12.9	0.0	0.0	0.0	0.0	0.0
Hg(II)	15.3	3.6	0.0	0.0	0.0	0.0
Bi(III)	T.A.	T.A.	3.4 × 10 ³	2.0 × 10 ³	6.8 × 10 ²	9.2 × 10 ²
Ce(III)	T.A.	T.A.	9.4 × 10 ³	9.4 × 10 ²	5.1 × 10 ²	7.1 × 10 ²
Fe(III)	208	—	91	—	—	71
Cr(III)	195	—	89	—	—	70
Th(IV)	T.A.	T.A.	5.1 × 10 ³	2.6 × 10 ³	8.5 × 10 ²	1.0 × 10 ³

Table 6. Separations of metal ions from alloys on a lanthanum arsenate (B-4) column

Sample	Metal determined	Eluent* and volume, ml		Amount taken, mg	Amount recovered, mg	Error, %
Copper-nickel alloy (B.C.S. No. 180/2)	Ni	D.D.W.	55	6.36	6.36	0.0
	Cu	A	95 ^a	14.3	14.2	-0.6
	Fe	A	25 ^b	0.143	0.145	+1.4
	Mn	B	35	0.160	0.162	+1.3
Ferromanganese (B.C.S. No. 208/2)	Fe	0.5M NH ₄ NO ₃	55	1.95	1.98	+1.5
	Mn	B	120	10.8	10.7	-1.0
Stainless steel (B.A.S. No. 69a)	Ni	D.D.W.	30	0.91	0.91	-0.05
	Cr	A	45 ^a	2.38	2.41	+1.3
	Fe	A	90 ^b	8.90	8.80	-1.2
Stainless steel (Indian Standard Institution No. 302)	Ni	D.D.W.	30	1.03	1.03	0.0
	Cr	A	45 ^a	2.07	2.09	+1.1
	Fe	A	80 ^b	8.01	7.90	-1.4
	Mn	B	35	0.232	0.228	-1.7

*D.D.W. = Doubly distilled water. B = 1M NaNO₃ in 0.01M HNO₃. A = Cu(II) and Fe(III) or Cr(III) and Fe(III) eluted simultaneously with 0.5M NH₄NO₃, leaving Mn(II) on the column. Then 0.1-3 ml of 1N H₃PO₄, depending on the concentration of iron, was added to the mixture of Cu(II)-Fe(III) or Cr(III)-Fe(III) and this was passed through the second resin bed where Cu(II) or Cr(III) was not retained, and the iron sorbed was eluted with 0.05M HCl.

^aPhosphoric acid solution was used as final eluent for Cu(II) and Cr(III); ^b0.05M HCl was used as final eluent for iron.

Thermal treatment has less effect on the exchange capacity of this material than on many similar materials such as ferric arsenate⁶ or tantalum arsenate,⁷ and lanthanum arsenate resembles stannic arsenate¹¹ in this respect.

The concentration of salt solution and the equilibration time affect the exchange capacity. Constant exchange capacity was obtained with 1.5M sodium chloride (Fig. 2) after equilibration for 14 hr (Fig. 3).

Acknowledgements—The authors are grateful to Dr. S. K. Sanyal, Assistant Professor of Chemistry, Presidency College, Calcutta for providing laboratory facilities, and for going through the manuscript. The authors also take pleasure in acknowledging the valuable suggestions received from Dr. R. A. Chalmers, University of Aberdeen, Scotland, in matters of revision of the paper.

REFERENCES

1. V. Vesely and V. Pekárek, *Talanta*, 1972, **19**, 219.
2. V. Pekárek and V. Vesely, *ibid.*, 1972, **19**, 1245.
3. M. Abe, *Bunseki Kagaku*, 1974, **23**, 1245, 1561.
4. R. C. Vickery, *Analytical Chemistry of the Rare Earths*, Vol. 3, Pergamon Press, Oxford, 1961.
5. G. Alberti, U. Costantino and L. Zsinka, *J. Inorg. Nucl. Chem.*, 1973, **34**, 3549.
6. J. P. Rawat and J. P. Singh, *Can. J. Chem.*, 1976, **54**, 2534.
7. J. P. Rawat and S. Q. Muftaba, *ibid.*, 1975, **53**, 2586.
8. A. I. Vogel, *A Text Book of Quantitative Inorganic Analysis*, 4th Ed., Longmans, London, 1978.
9. E. B. Sandell, *Colorimetric Determination of Traces of Metals*, 2nd Ed., Interscience, New York, 1944.
10. F. J. Welcher, *The Analytical Uses of Ethylenediaminetetra-acetic Acid*, Van Nostrand, New York, 1965.
11. M. Qureshi, R. Kumar and H. S. Rathore, *J. Chem. Soc. (A)*, 1970, 1986.

GEL SPECIATION STUDIES—I

THE INTRINSIC DISSOCIATION CONSTANT OF WEAKLY ACIDIC CATION-EXCHANGE GELS

YVES MERLE* and JACOB A. MARINSKY

Department of Chemistry, State University of New York at Buffalo, Buffalo, NY 14214, U.S.A.

(Received 25 April 1983. Accepted 29 September 1983)

Summary—The acid-dissociation properties of three weakly acidic cation-exchange gels, CM-Sephadex C-50-120, Biogel CM-2 and CM-Biogel A, have been studied. Each of the gels was equilibrated in sodium polystyrene sulphonate (NaPSS) solutions at three different concentration levels (0.1, 0.01 and 0.001*M*). The volume of the gels was measured as a function of α (their degree of neutralization), and C_p (the NaPSS concentration); pH and pNa were also measured at each α -value. Intrinsic pK values of 3.25 and 4.55 have been found for CM-Sephadex C-50-120 and Biogel CM-2 respectively.

In the investigation of gel-phase equilibria such as the dissociation of a weakly acidic group that is repeated in a regular way throughout the gel structure, and/or the complexation of metal ions by this acidic group, a Donnan potential term must be calculated to permit estimate of non-ideality at the site of reaction. For this purpose it is necessary to know the gel-phase concentration of the potential-determining counter-ion (Na^+) as well as the solution pH and pNa at every experimental point¹ since

$$pC_{\text{H}}^{\text{g}} = \text{pH}_{(\text{s})} - \text{pNa}_{(\text{s})} + pC_{\text{Na}}^{\text{g}} \quad (1)$$

where

$$pC_{\text{H}}^{\text{g}} - \log \frac{\alpha}{1-\alpha} = pK_{(\text{HA})}^{\text{app}} \quad (2)$$

and

$$pK_{(\text{HA})}^{\text{app}} - pK_{(\text{HA})}^{\text{int}} = -0.434 \frac{e\psi_{(\text{s})}}{kT} + \log \gamma_{\text{H}^+}^{\text{g}} \quad (3)$$

In equation (1) the subscript (s) and the superscript g refer to the solution and gel phases respectively, with C_{H}^{g} and C_{Na}^{g} representing the molar concentration of H^+ and Na^+ in the gel. In equation (2), α refers to the fraction of gel acidic groups that is dissociated and $pK_{(\text{HA})}^{\text{app}}$ corresponds to the apparent pK of the acid unit (HA) which is repeated in the polymer. Finally, in equation (3) the superscript int designates the intrinsic pK of the repeating HA unit, $\psi_{(\text{s})}$ refers to the potential at the surface of the charged gel matrix and $\gamma_{\text{H}^+}^{\text{g}}$ is the molar activity coefficient correction for long-range Debye-type ion-interaction forces acting on the H^+ ion in the gel phase.

To permit the accurate assessment of C_{Na}^{g} in these studies for computation of pC_{H}^{g} , it is desirable to

avoid imbibement by the gel of the sodium salt employed to adjust the ionic strength of the aqueous phase. With highly cross-linked resins, almost complete exclusion of salt is observed when the ionic strength of the aqueous medium is low.² However, with two of the three different gels used in this experimental programme this is not the case. The CM-Sephadex C-50-120 gel is very flexible, swelling remarkably and increasingly as the ionic strength is lowered and as the degree of neutralization is increased,^{1,3} whereas the CM Biogel A is rigid with a very open structure. In either case imbibement at even low ionic strength is considerable. In order to avoid this complication, sodium polystyrene sulphonate (NaPSS) was employed as the ionic medium,³ diffusion into the gel phase being resisted by a sieve effect, the size and charge of the macromolecule causing resistance to its entry.

With invasion of sodium ion avoided in this way, it was possible to evaluate C_{Na}^{g} directly,^{1,4} as follows. Since electroneutrality must be preserved in the gel phase, the Na^+ -ion content of the gel ($\text{Na}_{(\text{g})}^+$) can be equated directly with the quantity (meq) of acid dissociated, (A^-) , or αv , on controlled addition of standard base:

$$(\text{A}^-)_{\text{g}} = \alpha v = bV_{\text{b}} + hV_{\text{s}} = \text{Na}_{(\text{g})}^+ \quad (4)$$

where v is the degree of polymerization, b and h correspond to the molarity of base and acid, respectively, and V_{b} and V_{s} represent the volume of base added and the volume of the aqueous phase after addition of the base. Measurement of the gel volume, V_{g} , then permits evaluation of C_{Na}^{g} :

$$C_{\text{Na}}^{\text{g}} = \frac{\alpha v}{V_{\text{g}}} \quad (5)$$

The neutralization by sodium hydroxide of the cation-exchange gel in equilibrium with a solution of

*Present address: Laboratoire de Chimie Macromoléculaire—ERA 471, Faculté des Sciences de Rouen, F-76130 Mont Saint Aignan, France.

the sodium salt of a strongly acidic polyelectrolyte can be expressed by the equation:^{1,3}

$$\begin{aligned} \text{pH}_{(s)} - \text{pNa}_{(s)} + \log V'_g \\ = \text{p}K'_{(HA)} + \log y_{Na}^{\ddagger} + \log \frac{\alpha^2}{1-\alpha} = S \end{aligned} \quad (6)$$

where V'_g is the specific volume of the gel (in ml/meq).

A plot of S vs. $\log \alpha^2/(1-\alpha)$ generally yields a straight line for the range $0.2 < \alpha < 0.8$. By analogy with the Kern-modified Henderson-Hasselbalch expression, equation (6) can be rewritten as

$$\begin{aligned} S = \text{pH}_{(s)} - \text{pNa}_{(s)} + \log V'_g \\ = \text{p}K' + n \log \frac{\alpha^2}{1-\alpha} \end{aligned} \quad (7)$$

where n is the slope of the straight line that results and $\text{p}K'$ is equal to the value of S at $\alpha = 0.618$ [corresponding to $\log \alpha^2/(1-\alpha) = 0$].

For certain gels, such as CM-Sephadex C-50-120, the value of n is approximately 1,³ and the sum, $\text{p}K' + \log y_{Na}^{\ddagger}$, is constant over certain intervals of α in the presence of sodium salts of strongly acidic polyelectrolytes.

By including y_{Na}^{\ddagger} and other terms such as y_{A-} , the activity coefficient of the acidic unit of the gel, and y_{Na}^h and $y_{H^+}^h$, the solvation contributions for both the H^+ and Na^+ ions in the $\text{p}K'$ term, as done by Slota and Marinsky,¹ the $\text{p}K'$ value can be obtained by means of the relationship:

$$\text{p}K'_{(HA)} = \text{pH}_{(s)} - \text{pNa}_{(s)} + \log V'_g - \log \frac{\alpha^2}{1-\alpha} \quad (8)$$

The research described in the next section was embarked upon to show that with the computation of the Donnan potential term in these two-phase systems, the thermodynamic properties of gels could be uniquely and meaningfully characterized. Until the research of Slota and Marinsky¹ such characterization of gels was based only on the solution-phase measurements: as a consequence the results obtained were a function of the ionic strength employed in a particular study and bore little relationship to the absolute parameters sought.

With the attainment of this goal, the second phase of this study, *i.e.*, the meaningful analysis of multivalent-cation complexation-reactions with the acidic group of the gels selected for study, facilitated by proper assignment of Donnan potential terms, would be ready for entry.

EXPERIMENTAL

Distilled, demineralized water was used in all operations.

Preparation of NaPSS

Sodium polystyrene sulphonate with an average molecular weight of 5×10^5 (Lot ST475-4-87B) was kindly supplied by the Dow Chemical Company of Midland, Michigan. In its preparation for use it was first converted into the H^+ form by passage through a Dowex 50 W $\times 8$ cation-exchange resin column in the H^+ form. Low molecular-

weight impurities were then removed over a one-week interval by dialysis through a cellulose acetate membrane into distilled, demineralized water, which was periodically replaced. The resultant dilute solution of HPSS was then reconcentrated at ambient temperature by continuous removal of water vapour by the action of a fan on the membrane surface. The solution of HPSS so obtained was neutralized to pH 7 with 1M sodium hydroxide. It was then used as the source material for the NaPSS medium employed in a particular series of experiments, its dilution depending on the concentration level chosen for these experiments.

Preparation of gels

The three gels, CM-Sephadex C-50-120 supplied by the Pharmacia Company, and Biogel CM-2 and CM Biogel A supplied by the Bio-Rad Company, were cycled in the Na^+ and H^+ -ion forms by use of 0.5M sodium hydroxide and 0.5M hydrochloric acid. The H^+ forms of the gels were then washed with demineralized, distilled water to remove all traces of the free acid.

Gel volume and density determinations

Gel volumes were determined by the following procedure. First, the ion-exchange capacity per gram of swollen gel was measured by adding an excess of sodium hydroxide to the weighed sample and back-titrating with standard hydrochloric acid. The gel, washed free from simple electrolyte, was then transferred quantitatively to a NaPSS solution at the desired concentration, and allowed to equilibrate for 48 hr. The volume and density of the gel, removed quantitatively from the NaPSS solution by filtration, were measured with n-heptane in a pycnometer. The volume and density of the gel in the H^+ -form were measured similarly. Volume estimates at degrees of dissociation ranging between these two extremes were obtained by measuring the settled gel volumes in a graduated cylinder and subtracting the interstitial volumes from these gross values. Plots of these volume data for the three gels are presented in Fig. 1. The density data are listed in Table 1.

Measurement of pH and pNa of solutions

The pH and pNa of the equilibrated solutions were measured concurrently with Corning Glass electrodes (No. 47621000 for Na) and a Radiometer model 4 pH-meter. The Na-specific electrode was calibrated with standard sodium chloride solutions, and the glass pH electrode with standard reference buffers. All pH and pNa measurements were made in media saturated with nitrogen.

When the pH of the solution was too low, pNa could not be measured directly because of the selective uptake of H^+ -ions by the Na^+ -ion electrode. It was necessary in these instances to employ an isotope dilution technique to measure the Na^+ -ion concentration in solution. The radioactivity of ^{22}Na was measured for this purpose. The single-ion activity coefficient assigned to Na^+ in NaPSS by two different research groups^{6,9} was then used to convert these Na^+ concentrations into Na^+ activities.

For a particular set of experiments a controlled quantity of the ^{22}Na radioisotope was added to NaPSS at the appropriate concentration level. A 15-ml aliquot of this solution was then combined with a known amount (0.1-1.0 meq) of the water-swollen gel in its H^+ -form. After three days of equilibration in the vial container the pH, pNa and radioactivity of the solution were measured. The radioactivity was measured with a Tricarb Packard No. 3375 beta-counter.

In a particular experimental series a controlled quantity of standard sodium hydroxide solution was added by microburette to dissociate the gel further after completion of the measurements of solution radioactivity, pH and pNa at the preceding gel dissociation value. The effect of dilution of the NaPSS by addition of the sodium hydroxide was taken into account.

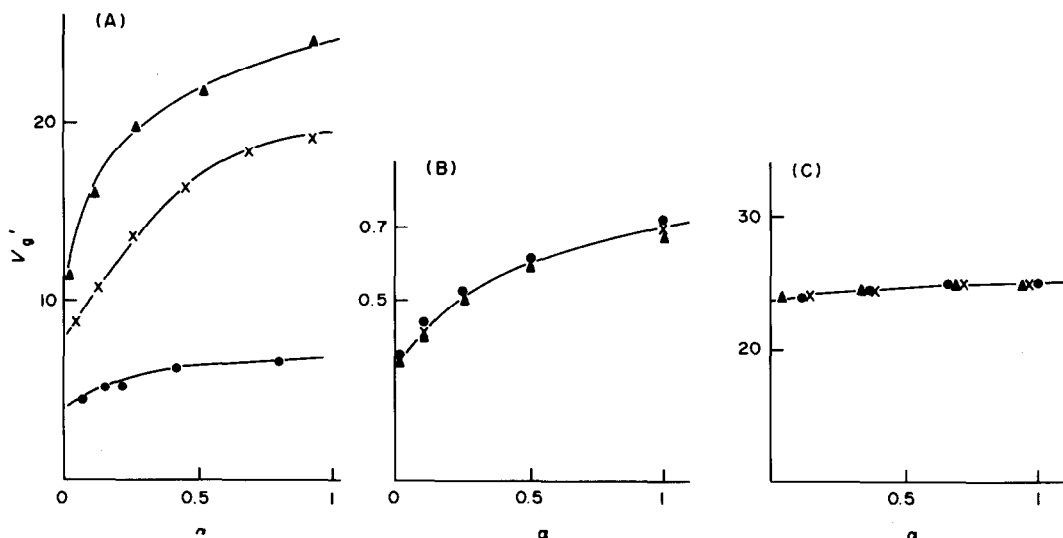


Fig. 1. Variation of the specific volume V_g' (in ml/meq) as a function of the degree of ionization, α , at different concentrations, C_p , of sodium polystyrene sulphonate (NaPSS); $C_p = 0.1M$ (●); $0.01M$ (×), $0.001M$ (▲). (A) CM-Sephadex C-50-120; (B) Biogel CM-2; (C) Biogel A.

RESULTS

Exchange capacity and swelling of gels

The three gels were studied in solutions of NaPSS at three different concentrations (0.10, 0.010 and 0.001M).

The CM-Sephadex C-50-120 gel has a high exchange-capacity (4.8 meq/g of dry gel). Its extent of swelling, which is considerable, depends on the initial NaPSS concentration (C_p) and the degree of ionization (Fig. 1A). The capacity of the swollen gel is as low as 0.031 meq/ml at $\alpha = 1$ in 0.001M NaPSS. The density of the gel is slightly higher than that of the solution (Table 1) except when $C_p = 0.10M$ and $\alpha = 1$. In this case the gel floats and its volume has to be measured with a pycnometer.

The Biogel CM-2 also exhibits a high exchange-capacity (5.3 meq/g of dry resin), but it swells much less than the CM-Sephadex C-50-120 gel, the extent of swelling depending only on the degree of ionization. The dependence of the swelling on the NaPSS concentration is insignificant (Fig. 1B). The capacity of the swollen gel remains high (1.39 meq/ml at $\alpha = 1$) because of its moderate flexibility, and its density is always higher than that of the solution (Table 1).

The CM-Biogel A has a low exchange-capacity (1 meq/g of dry resin) and because of the rigid, open

structure its volume is practically independent of the degree of ionization and of the NaPSS concentration (Fig. 1C). The exchange capacity is 0.04 meq/ml at $\alpha = 1$. The density is always slightly higher than that of the solution (Table 1).

Neutralization of gels

The neutralization properties of the CM-Sephadex C-50-120 gel are strongly affected by the NaPSS concentration of the solution. This result is illustrated in Fig. 2, which presents the neutralization curves obtained at three different NaPSS concentrations (0.1, 0.01 and 0.001M). These data produce three straight-line plots of S vs. $\log \alpha^2/(1-\alpha)$ (Fig. 3). Their slopes are greater than 1 for $C_p = 0.001$ and $0.01M$ and not very different from 1 for $C_p = 0.1M$ (Table 2). The variation of the sum $pK^{app} + \log \gamma_{Na}^{\pm}$ with α at $C_p = 0.01$ and $0.001M$ indicated by these results is to be expected. The sensitivity of the gel volume to changes in α and C_p leads to sizeable variability in polymer concentrations. Just as with linear polyelectrolytes, e.g., polymethacrylic acid, polymer dilution results in less effective screening of the polymer surface charge and greater increase in the value of pK^{app} with increasing degrees of dissociation.⁷ At $C_p = 0.1M$, however, the volume of the gel is reduced and the effect of α on the gel volume

Table 1. Densities (g/ml) of the different gels at the beginning, $\bar{\alpha} = 0$, and the end, $\bar{\alpha} = 1$, of neutralization at different concentrations, C_p , of sodium polystyrene sulphonate (NaPSS), and the density of the NaPSS solutions (density of water at 25°C = 0.99707 g/ml)

	$C_p = 0.1$		$C_p = 0.01$		$C_p = 0.001$	
	$\bar{\alpha} = 0$	$\bar{\alpha} = 1$	$\bar{\alpha} = 0$	$\bar{\alpha} = 1$	$\bar{\alpha} = 0$	$\bar{\alpha} = 1$
CM-Sephadex C-50-120	1.012	1.011	1.003	1.004	1.001	0.998
Biogel CM-2	1.107	1.120	1.099	1.102	1.083	1.090
CM-Biogel A	1.013	1.013	1.013	1.013	1.013	1.013
NaPSS		1.0117		0.9985		0.9972

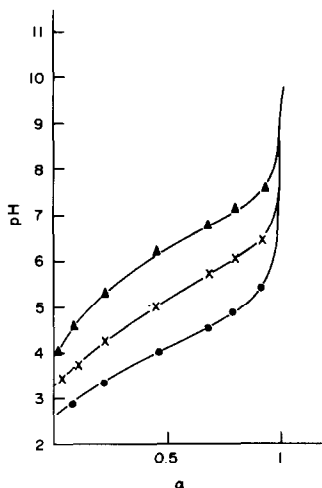


Fig. 2. Neutralization curves for CM-Sephadex C-50-120 as a function of the degree of ionization, α , at different concentrations, C_p , of NaPSS; symbols as in Fig. 1.

is not nearly as large as before. The net effect is a buffered effective surface-charge which results in constancy of the $pK^{app} + \log \gamma_{Na}^{\delta}$ term.

In an earlier study of French supplied CM-Sephadex C-50-120 gel³ less swelling was observed under comparable experimental conditions. The slope of the straight-line plot of S vs. $\log \alpha^2/(1-\alpha)$ was unity, as it is for the most concentrated NaPSS system ($C_p = 0.1M$) in the present investigation. It is probable that the gel used in the earlier study was slightly more cross-linked than the gel employed in this one.

The neutralization curves obtained with Biogel CM-2 are presented in Fig. 4. The solution-phase pH under comparable experimental conditions is always more than one unit higher than that in the CM-Sephadex C-50-120 gel study, which indicates the

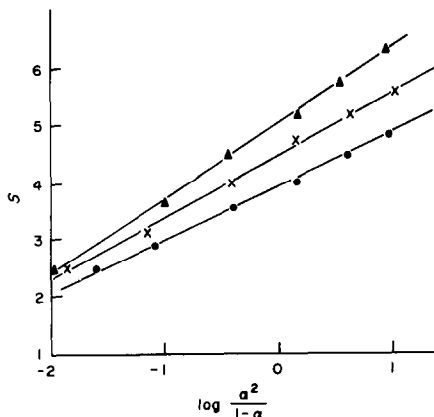


Fig. 3. Variation of S [= $(pH - pNa + \log V_p)$] as a function of $\log [\alpha^2/(1-\alpha)]$ for CM-Sephadex C-50-120; symbols as in Fig. 1.

Table 2. Values of n [equation (7)] for the three gels at different molar concentrations of NaPSS, C_p

Gel	n			
	C_p	0.1	0.01	0.001
CM-Sephadex C50-120	0.96	1.12	1.34	
Biogel CM-2	1.25	1.25	1.25	
CM-Biogel A	0.57	0.94	1.23	

higher concentration of the repeating functional unit in Biogel CM-2.

All the experimental points obtained for Biogel CM-2 with the three different NaPSS solutions fall on a single straight line when S is plotted vs. $\log \alpha^2/(1-\alpha)$ (Fig. 5). This is to be expected when the swelling properties of a gel are independent of C_p , as is the case here, and when there is no penetration of the gel phase by the ionic solution medium (NaPSS). The slope of the straight line, n , is 1.25 (Table 2), showing that the apparent pK of the repeating gel functional unit increases with the degree of ionization, as it does with the CM-Sephadex C-50-120 gel at the two lower NaPSS concentrations.

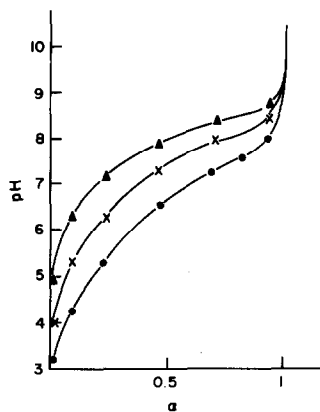


Fig. 4. Neutralization curves of Biogel CM-2 as a function of the degree of ionization α ; symbols as in Fig. 1.

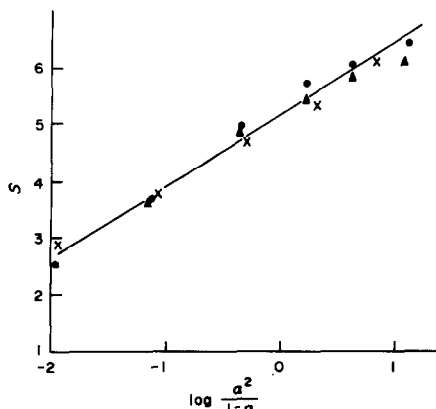


Fig. 5. Variation of S [= $(pH - pNa + \log V_p)$] as a function of $\log [\alpha^2/(1-\alpha)]$ for Biogel CM-2; symbols as in Fig. 1.

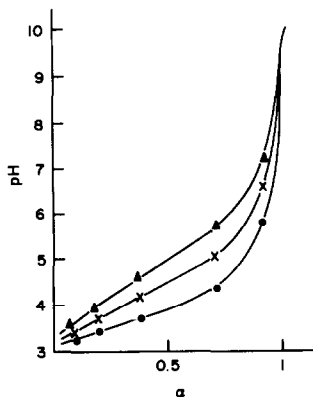


Fig. 6. Neutralization curves for Biogel A as a function of the degree of ionization, α ; symbols as in Fig. 1.

The neutralization curves obtained with the CM-Biogel A are presented in Fig. 6. In this case the solution-phase pH is much lower than that in the CM-Sephadex C-50-120 gel study under comparable experimental conditions. The influence of NaPSS concentration is lower, however. Plots of S vs. $\log \alpha^2/(1-\alpha)$ for the data obtained produce three straight lines, one for each concentration level of the NaPSS employed (Fig. 7). Unlike the result obtained with the CM-Sephadex C-50-120 gel the largest value of S and the lowest slope are obtained with NaPSS at a concentration of $0.1M$ (Table 2). This discordant result is due to the fact that there is diffusion of the NaPSS into the gel. That the rigid, open structure of this gel permits entry of the NaPSS is not too surprising. The macroporous structure is achieved by cross-linking the basic functional unit with a rigid spacer molecule.

Such entry of the NaPSS by diffusion can be sizeable because of the low concentration of functional units and the very weak Donnan exclusion factor which results from this. Equation (6) is no longer applicable since a correction must be made for the effect of NaPSS imbibement on the value of pC_{Na}^{δ} .

Apparent pK values

Equation (8) was employed to evaluate $pK_{(HA)}^{app}$ as a

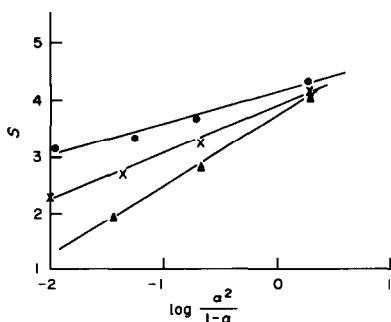


Fig. 7. Variation of $S [= (pH - pNa + \log V_0)]$ as a function of $\log [\alpha^2/(1-\alpha)]$ for Biogel A; symbols as in Fig. 1.

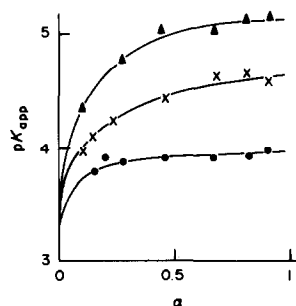


Fig. 8. Apparent pK of CM-Sephadex C-50-120: a plot of pK_{app} vs. degree of ionization, α ; the pK_{app} is calculated by means of equation (8); symbols as in Fig. 1.

function of α for both the CM-Sephadex C-50-120 and the Biogel CM-2 gels at the three different NaPSS concentrations. The results are graphically presented in Figs. 8 and 9. It is evident from Fig. 8 that the apparent pK of the CM-Sephadex C-50-120 gel is strongly influenced by its swelling properties and by the degree of dissociation. Extrapolation of the curves in Fig. 8 to $\alpha = 0$ provides an estimate of the Sphadex $pK_{(HA)}^{int}$; as $\alpha \rightarrow 0$, $\psi_{(a)} \rightarrow 0$, and $pK_{(HA)}^{app} \rightarrow pK_{(HA)}^{int}$. The extrapolation may not be too accurate, but the convergence of the extrapolated lines drawn to merge at a value in the region of 3.3-3.5 at $\alpha = 0$ is consistent with the $pK_{(HA)}^{int}$ value of 3.25 obtained earlier for the CM-Sephadex C-50-120 gel and its polyelectrolyte analogue, carboxymethyl-dextran.⁸

Swelling of the Biogel CM-2 was found to be independent of the ionic strength of the aqueous medium so $pK_{(HA)}^{app}$ should vary only as a function of α . In Fig. 9 the increasingly large scatter in the $pK_{(HA)}^{app}$ values at α values above about 0.7 must therefore be due to other factors. In the α -range from 0.7 to 1.0 the measured pH was equal to or greater than 7 in the study of this system, and inadvertent introduction of CO_2 from the atmosphere is most probably responsible for the observed scatter. At $\alpha < 0.5$ the reproducibility of $pK_{(HA)}^{app}$ is much better and extrapolation to $\alpha = 0$ is straightforward, yielding a $pK_{(HA)}^{int}$ value of about 4.6.

Conclusion

The first objective of this research has been success-

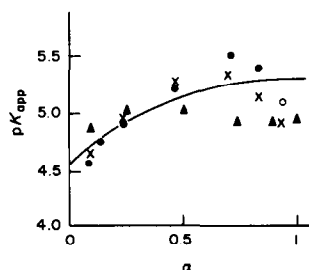


Fig. 9. Apparent pK of Biogel CM-2: a plot of pK_{app} calculated by means of equation (8); symbols as in Fig. 1.

fully achieved through the correct assignment of Donnan potential terms. We have been able to determine for each experimental situation the concentration of hydrogen ion at the site of its reaction with the repeating conjugate-base unit (carboxylate ion) of the gel. Extrapolation to $\alpha = 0$ of a plot of the apparent pK obtained for each gel by this approach [equation (8)], *vs.* α , has led to resolution of the intrinsic pK characterizing the dissociation of the repeating acidic ligand unit in two of the three gels for which the Donnan term was calculable.

It has been of special interest to show how the behaviour of the highly flexible CM-Sephadex C-50-120 gel seems exactly like that of a linear polyelectrolyte if the apparent pK measurement is based on the gel-phase pH. As the gel phase becomes more dilute (*i.e.*, as the NaPSS concentration is decreased) the apparent pK of the acidic group of the gel increases more rapidly with increasing α , from a common intercept on the ordinate at $\alpha = 0$ (intrinsic pK), just as it does for a linear polyelectrolyte, because screening of the charge at the macromolecule

surface by counter-ions is decreased in both cases by dilution of the polymer.

Finally, with this demonstration of the utility and validity of our approach to the thermodynamically sound analysis of equilibria in gels through appropriate assessment of the Donnan potential terms encountered, the second phase of the research, the evaluation of metal-ion complex-formation constants in these gels, is ready for entry.

REFERENCES

1. P. Slota and J. A. Marinsky, in *Ions in Polymers*, A. Eisenberg (ed.), p. 311. American Chemical Society, Washington, 1980.
2. I. Michaeli and A. Kinrot, *Israel J. Chem.*, 1973, **11**, 271.
3. Y. Merle, *J. Polym. S. Polym. Phys. Ed.*, 1976, **14**, 1317.
4. *Idem*, *Europ. Polym. J.*, 1972, **8**, 1265.
5. D. Kozak, J. Kristian and D. Dolar, *Z. Phys. Chem. (Frankfurt)*, 1971, **76**, 85.
6. P. Chu, A. Sarkar and J. A. Marinsky, *J. Phys. Chem.*, 1972, **76**, 1881.
7. A. Katchalsky, *Pure Appl. Chem.*, 1971, **26**, 327.
8. K. Gekko and H. Noguchi, *Biopolymers*, 1975, **14**, 2555.

SHORT COMMUNICATIONS

SPECTROPHOTOMETRIC DETERMINATION OF OSMIUM WITH 1-PHENYL-4,4,6-TRIMETHYL-(1H,4H)-2-PYRIMIDINETHIOL AND EXTRACTION INTO MOLTEN NAPHTHALENE

A. WASEY, R. K. BANSAL and B. K. PURI

Department of Chemistry, Indian Institute of Technology, Hauz Khas, New Delhi 110016, India

A. L. J. RAO

Department of Chemistry, Punjabi University, Patiala, India

(Received 13 January 1983. Revised 9 July 1983. Accepted 1 October 1983)

Summary—Conditions have been developed for the spectrophotometric determination of osmium with 1-phenyl-4,4,6-trimethyl-(1H,4H)-2-pyrimidinethiol after extraction of the complex into molten naphthalene. Beer's law holds for the concentration range of 4–77 μg of osmium in 10 ml of the final solution. The molar absorptivity is $1.33 \times 10^4 \text{ l. mole}^{-1} \cdot \text{cm}^{-1}$. The reagent is highly selective for osmium.

Several pyrimidinethiols have been synthesized and used successfully as analytical reagents.^{1,2} Osmium forms an extractable complex with 1-phenyl-4,4,6-trimethyl-(1H,4H)-2-pyrimidinethiol (PTPT) but only on heating for some time, so the usual liquid-liquid extraction methods are tedious. The present communication describes the extraction of osmium with PTPT into molten naphthalene and its spectrophotometric determination after dissolution of the solidified extract in dimethylformamide (DMF). This technique is especially useful for the extraction of complexes which are formed only at higher temperatures^{3,4} or have low solubility at room temperature.

EXPERIMENTAL

Reagents

Doubly distilled water and analytical-reagent grade acids and salts were used unless otherwise stated. A solution of osmium tetroxide was prepared in 0.2M sodium hydroxide and standardized.

1-Phenyl-4,4,6-trimethyl-(1H,4H)-2-pyrimidinethiol was prepared and purified according to the method given by Mathes *et al.*^{5,6} and a 0.001M solution was prepared in DMF.

Procedure

Take in a beaker a volume of sample containing 3.8–76.8 μg of osmium and add 2 ml of PTPT solution. Add perchloric acid to give an acid concentration of 1.0–3.5M. Transfer the solution to a round-bottomed stoppered flask, warm it to about 60° on a water-bath and add 2 g of naphthalene. Raise the temperature to about 90° to melt the naphthalene and stir the mixture for about 15 min on a combined magnetic stirrer and hot-plate. Cool the solution, filter off the solidified naphthalene, dry it on a filter paper,

dissolve it in DMF and make it up to 10 ml in a standard flask with DMF. Dry this solution with 2 g of anhydrous sodium sulphate and measure the absorbance in a 1-cm cell at 520 nm against a reagent blank. Prepare calibration graph under similar conditions.

RESULTS AND DISCUSSION

Absorption spectrum

The absorption spectrum of the osmium-PTPT complex in naphthalene-DMF medium, measured against water or a reagent blank, has its absorption maximum at 520–530 nm, where the reagent does not absorb at all.

Experimental conditions

Effect of acidity. Osmium is quantitatively extracted over the perchloric acid range 1.0–3.5M. Extraction is incomplete at higher and lower acidity.

Reagent concentrations. The absorbance is constant and maximal with 0.8–4.5 ml of 0.001M PTPT solution, and 1.3–3.5 g of naphthalene. Extraction is incomplete with less than 1.3 g of naphthalene; with more than above 3.5 g it is difficult to dissolve the naphthalene in the 10 ml of solvent used.

Effect of aqueous phase volume. The absorbance is unaffected if the aqueous phase volume does not exceed 60 ml. With larger volumes the extraction is not quantitative.

Stirring time. At 85–90° complete extraction takes a minimum of 10 min (Fig. 1).

Calibration graph. Under the optimum conditions described, the calibration graph (measurement at 520 nm) is linear over the osmium concentration range of

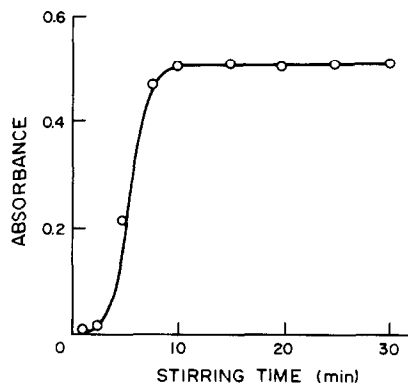


Fig. 1. Effect of stirring time. Os 38.0 μg , PTPT ($1 \times 10^{-3}M$) 2.0 ml, hydrochloric acid 2.0M, naphthalene 2.0 g, wavelength 520 nm.

3.8–76.0 μg in 10 ml of DMF. The molar absorptivity is $1.33 \times 10^4 \text{ l. mole}^{-1} \text{ cm}^{-1}$. The mean absorbance found in ten replicate determinations of 38 μg of osmium was 0.505, with a standard deviation of 0.0025.

Interferences

It was found that 5.0 mg of Cl^- , SO_4^{2-} , I^- , F^- , NO_3^- , PO_4^{3-} , and tartrate, 4.0 mg of citrate, 3.0 mg of SCN^- , 500 μg of Mn(II), Ni(II), Fe(III), Pb(II), Co(II), Th(IV), Mo(VI), W(VI), V(V), Sb(III), As(III), Pt(IV), Ru(III) and Rh(III), and 100 μg of EDTA^{2-} , when added to a test solution containing 38 μg of Os caused less than 2% error. Ir(III) and Pd(II) interfere, and must be removed by prior extraction. Copper (500 μg) does not interfere if the extraction is done at pH 10.

Table 1. Determination of osmium in synthetic mixtures

Composition of synthetic mixture, %	Osmium taken, μg	Osmium found, μg
Ir 50.0, Os 40.0 Pd 10.0	40.0	40.0 39.5 39.8
Pd 5.0, Ir 76.0 Os 14.0, Pt 5.0	28.0	28.2 27.5 27.6
Pd 7.0, Ir 70.0 Os 8.0, Fe 5.0 Ni 5.0, Pt 5.0	16.0	16.0 15.8 15.9

Determination of osmium in various synthetic mixtures

Various synthetic mixtures containing osmium were prepared in 100-ml standard flasks (Table 1), and each was analysed in triplicate for osmium according to the general procedure. The results are summarized in Table 3.

Acknowledgement—One of the authors (A.W.) is grateful to the CSIR, New Delhi, India for the award of a fellowship.

REFERENCES

1. A. K. Singh, M. Katyal, A. M. Bhati and N. K. Ralhan, *Talanta*, 1976, **23**, 337.
2. A. K. Singh, R. P. Singh and M. Katyal, *J. Indian Chem. Soc.*, 1976, **53**, 650.
3. H. Bode, *Z. Anal. Chem.*, 1955, **144**, 165.
4. B. K. Puri and M. Gautham, *Mikrochim. Acta*, 1979 I, 515.
5. R. A. Mathes, F. D. Stewart and F. Swedish, Jr., *J. Am. Chem. Soc.*, 1948, **70**, 1452.
6. R. A. Mathes, *ibid.*, 1953, **75**, 1747.

PULSE POLAROGRAPHY OF NITROSATED GPC FRACTIONS OF HUMIC ACIDS

MARIA TERESA LIPPOLIS, VITTORIO CONCIALINI and GIUSEPPE CHIAVARI
Istituto Chimico G. Ciamician, Università di Bologna, Via Selmi 2, Bologna 40126, Italy

(Received 30 August 1983. Accepted 28 September 1983)

Summary—A pulse polarographic method for the analysis of humic acids fractionated by gel permeation chromatography is described. It is concluded that the pulse polarography of the nitroso-derivatives, already reported as an analytical method for the determination of humic acids, really gives responses due to the presence of iron in the samples. Atomic-absorption measurements confirm this conclusion quite unambiguously.

Humic acids are extremely complex polymeric substances, which have been the subject of extensive research because of their importance in environmental chemistry.¹⁻⁴ Their composition varies according to the origin and nature of the water or soil in which they are found and methods for characterizing them are highly desirable. A variety of techniques have been used for this purpose, such as X-ray scattering,⁵ gel chromatography, viscosity measurement, dialysis and ultrafiltration,^{6,7} chemical analysis⁸ and polarographic determination of the nitroso derivatives.⁹

We have very recently investigated the gel filtration of humic acids, using an electrochemical detector and comparing its performance with that of the usual ultraviolet detector.¹⁰ The present work is a continuation of the investigation, with the aim of comparing the pulse polarography of the nitroso-derivatives of the various fractions obtained in the gel filtration, with the responses given by the electrochemical detector. To clarify a discrepancy observed between the two methods, atomic-absorption measurements were also made.

EXPERIMENTAL

Reagents

Commercial samples of humic acid were purchased from Aldrich and Fluka. The other chemical products were of analytical grade (C. Erba RPE) and used without further purification. The gel filtration columns were made with Ultrogel (LKB) having exclusion limits of 1000-15000. A 0.05M solution of sodium pyrophosphate was used as eluent, at a flow-rate of ca. 0.5 ml/min.

Apparatus

The electrochemical detector was a Metrohm model 656 with a three-electrode detection cell (model EA 1096/2). The working electrode was a carbon-paste electrode, the counter-electrode a glassy-carbon electrode and the reference electrode an Ag/AgCl system.

Atomic-absorption measurements were done with a Perkin-Elmer model 372 instrument.

The gel filtration column was 25 × 1.6 cm, packed according to the maker's instructions and used with an LKB 2112

Redirac fraction collector. Molecular weight calibration of the column is reported elsewhere.¹⁰

The pulse polarograph was a Southern Analytical model A 3100.

Procedure

The nitrosation procedure was essentially the same as that reported by Ederle *et al.*⁹ Each fraction (ca. 3.5 ml) was acidified to pH 4.5 with 1M acetate buffer, 1 ml of 10% sodium nitrite solution was added and the mixture was left at 50-60° for 20 min. After cooling, the solution was diluted to volume in a 25-ml standard flask with water and transferred to a conventional three-electrode polarographic cell, with a platinum counter-electrode and a saturated calomel electrode as reference. After deaeration with pure argon for 10 min, the solution was polarographed with a pulse amplitude of 50 mV and a sweep-rate of 133 mV/min. The peak height (at $E_{\text{peak}} = -0.63$ V vs. SCE) was measured and corrected with respect to that found for a blank solution treated similarly.

RESULTS AND DISCUSSION

Figures 1 and 2 summarize the elution curves obtained by the three techniques, for the gel filtration of the two commercial samples.

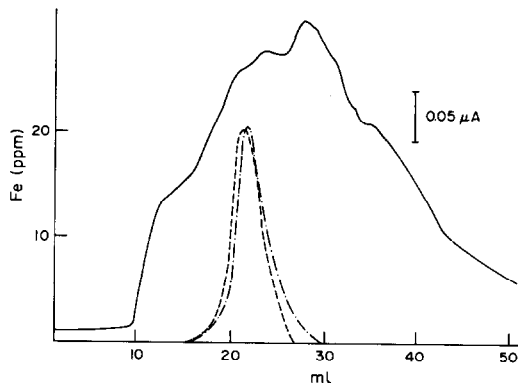


Fig. 1. Elution curves of Fluka humic acid. Sample volume: 0.5 ml of 0.5% solution in 0.05M $\text{Na}_4\text{P}_2\text{O}_7$: — electrochemical detector response (sensitivity 0.5 μA full-scale deflection); --- ppm of iron from pulse polarographic measurements of the nitrosated fractions; —·— ppm of iron from atomic-absorption measurements.

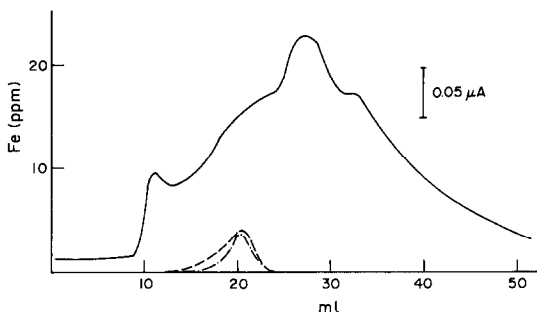


Fig. 2. Elution curves of Aldrich humic acid. Conditions and symbols as for Fig. 1.

The curves obtained by use of the electrochemical detector and by pulse polarography of the nitrosated fractions differ noticeably in shape and in the position of the maximum.

In the earlier communication¹⁰ it was pointed out that the response of the electrochemical detector is mainly due to the oxidation of phenolic and amino groups present in the humic acids. The comparison therefore suggests that the pulse polarographic response is not attributable to nitrosated phenolic compounds.

It is known that the humic acids contain variable amounts of several metals such as Al, Fe, Cu, etc., so we have made atomic-absorption (AA) measurements on the chromatographic fractions, to try to elucidate the discrepancy.

The elution curves obtained by AA by determination of iron, show excellent agreement with those obtained by pulse polarography, so it seems reasonable to attribute the polarographic response to the reduction of some nitroso-complex of iron.

This assumption has been confirmed by nitrosation of solutions containing known quantities of Fe(III),

followed by polarography: these solutions gave a reduction peak at -0.63 V vs. SCE, confirming the attribution to reduction of an iron complex. The peak can be used to evaluate the concentration of iron, as shown in Figs. 1 and 2.

Conclusions

From the results reported we can conclude that though phenolic and amino groups are certainly present in the humic acids, they are not all easily converted into nitroso derivatives, so the nitrosation technique⁹ may give unreliable results.

However, since under our chromatographic conditions the iron is practically concentrated in one or two fractions, the nitrosation technique, coupled with pulse polarography, can be used for the determination of iron traces in natural humic acids.

REFERENCES

1. M. M. Kononova, *Soil Organic Matter*, 2nd Ed., pp. 183-228. Pergamon Press, Oxford, 1966.
2. M. Schnitzer and S. U. Khan, *Humic Substances in the Environment*, pp. 281-302. Dekker, New York, 1966.
3. E. T. Gjessing, *Physical and Chemical Characteristics of Aquatic Humus*, pp. 56-73. Ann Arbor Science, Ann Arbor, 1976.
4. G. T. Felback, in *Soil Biochemistry*, A. D. McLaren and J. Skujins (eds.), Vol. 2, pp. 36-59. Dekker, New York, 1971.
5. R. L. Wershaw, S. L. Heller and D. J. Pinckney, *Adv. X-Ray Anal.*, 1970, 13, 609.
6. J. H. Reuter, *Geol. Soc. America, Abstracts*, 9 (1977).
7. M. Schnitzer and S. I. M. Skinner, *Isotopes and Radiation in Soil Organic Matter Studies*, p. 41. International Atomic Energy Agency, Vienna, 1968.
8. S. A. Visser, *J. Environ. Sci. Health*, 1982, A17, 767.
9. S. H. Ederle, C. Hoesle and C. Krückeberg, IRCh, KFK-1969 UF Kernforschungszentrum Karlsruhe, 1974.
10. G. Chiavari, V. Concialini, M. T. Lippolis and F. Scarponi, *J. Chromatog.*, in press.

THALLIMETRIC OXIDATIONS—IV

ESTIMATION OF MALONIC ACID

S. R. SAGI, K. APPA RAO and M. S. PRASADA RAO

Inorganic Chemistry Laboratories, Andhra University, Waltair 530003, India

(Received 22 June 1983. Accepted 1 October 1983)

Summary—Malonic acid is quantitatively oxidized to carbon dioxide and water when refluxed for 120 min in sulphuric acid medium (concentration $\geq 1.5M$) with at least four times as much thallium(III) as that stoichiometrically required for complete oxidation. The thallium(I) formed is estimated bromatometrically in the presence of 1.5–2M hydrochloric acid, with Methyl Orange as indicator. The indicator correction is negligible. The relative mean deviation is 0.2%. Possible side-reactions and their suppression are discussed.

Most reactions used for the determination of malonic acid do not proceed quantitatively to give the ultimate oxidation products of carbon dioxide and water, and stop either at the formic acid stage¹⁻³ or some non-stoichiometric intermediate stage.^{4,5} For example, in the methods described by Masayoshi *et al.*⁴ and Willard and Young⁵ the consumptions of oxidant are 4.34 and 6.66 equivalents respectively per equivalent of reductant. Jaiswal and Yadava⁶ have described a method for determination of malonic acid by oxidation with excess of ditelluratocuprate(III) to carbon dioxide and titration of the unconsumed oxidant with arsenic(III), but the oxidant used is not quite stable. Sharma and Mehrotra⁷ have described a two-stage procedure in which the malonic acid is first refluxed with excess of cerium(IV) in 1M sulphuric acid for 15 min and then in 12M sulphuric acid for 90 min. This stepwise procedure was said to oxidize the malonic acid first to formic acid and then to carbon dioxide and water. For the second stage concentrated sulphuric acid is added through the condenser by pipette so that no formic acid is lost during the addition. Later, the same authors⁸ reported that pure cerium(IV) sulphate cannot oxidize formic acid to carbon dioxide and water in the second stage, and attributed the complete oxidation reported earlier to the presence of Cr(III) as impurity in the cerium(IV) sulphate used. The drawbacks of their method are (i) it requires 12M sulphuric acid for complete oxidation, which restricts the volume of malonic acid and cerium(IV) solutions that can be used, (ii) the high sulphuric acid concentration used in the oxidation poses difficulties in the estimation of unconsumed cerium(IV), (iii) the addition of concentrated sulphuric acid for the second stage is cumbersome. We have investigated the reaction between thallium(III) and malonic acid and established the conditions for a convenient direct determination of malonic acid by quantitative oxidation to carbon dioxide and water.

EXPERIMENTAL

Reagents

Thallium(III) hydroxide was prepared as reported earlier⁹ and dissolved in a suitable amount of sulphuric acid. The thallium content was estimated iodometrically¹⁰ and verified by other methods.^{9,11}

An aqueous malonic acid solution was prepared and standardized by the procedure of Sharma and Mehrotra.⁷

All the other reagents used were of analytical-reagent grade.

Recommended procedure

To an aliquot containing 0.01–0.10 mmole of malonic acid add 45 ml of 2.5M sulphuric acid and 1.6 mmole of thallium(III) and dilute the mixture to 75 ml. Reflux for 120 min. Add 15 ml of concentrated hydrochloric acid, 0.1 ml of 0.1% Methyl Orange solution, maintain at 60° and titrate the thallium(I) with 0.00829M (1.392 g/l.) potassium bromate until the indicator is destroyed. From the amount of thallium(I) formed, calculate the amount of malonic acid. Malonic acid (mmole) = $0.75 \times$ molarity of $KBrO_3 \times$ volume (ml) of $KBrO_3$.

RESULTS AND DISCUSSION

The reaction between thallium(III) and malonic acid when these are refluxed in sulphuric acid medium was monitored by potassium bromate titration of the thallium(I) formed. At sulphuric acid concentrations $\geq 2M$ the decolorization of Methyl Orange (as indicator) is slow, so Brilliant Ponceaux 5 R was used instead. At lower acidity either indicator can be used. Unreacted malonic acid does not interfere in the titration of thallium(I) at concentrations up to $1.6 \times 10^{-3}M$, but causes positive errors for higher concentrations.

The effect of the concentration of thallium(III) and acid on the oxidation of malonic acid was investigated, and typical results are given in Tables 1 and 2. From these the following conclusions can be drawn.

(a) Refluxing for about 120 min in 1.5M sulphuric acid medium with four times the amount of thal-

Table 1. Effect of thallium(III) concentration on the rate of oxidation of 0.05 mmole of malonic acid in 75 ml of 1.5M sulphuric acid

Amount of thallium(III), <i>mmole</i>	Percentage oxidized							
	5*	20*	30*	60*	75*	90*	120*	180*
0.1	20.0	40.0	48.0	48.3	49.0	49.0	49.0	49.0
0.2	22.0	51.0	64.0	72.0	77.0	82.0	85.0	85.0
0.3	33.0	63.0	76.0	87.5	88.0	90.0	91.0	91.0
0.4	46.0	80.0	89.0	96.5	97.0	97.3	97.8	97.8
0.6	51.0	95.0	96.0	98.0	98.5	98.8	99.3	99.5
0.8	70.0	96.0	97.0	99.0	99.3	99.5	100.0	100.0
1.0	81.0	97.0	98.0	99.0	99.3	99.5	100.0	100.0
1.2	92.0	98.0	98.0	99.0	99.3	99.5	100.0	100.0
1.6	92.0	98.0	98.5	99.0	99.3	99.5	100.0	100.0

*Reflux time, *min.*

Table 2. Effect of sulphuric acid concentration on the rate of oxidation of 0.05 mmole of malonic acid by 0.8 mmole of thallium(III) in 75 ml of solution

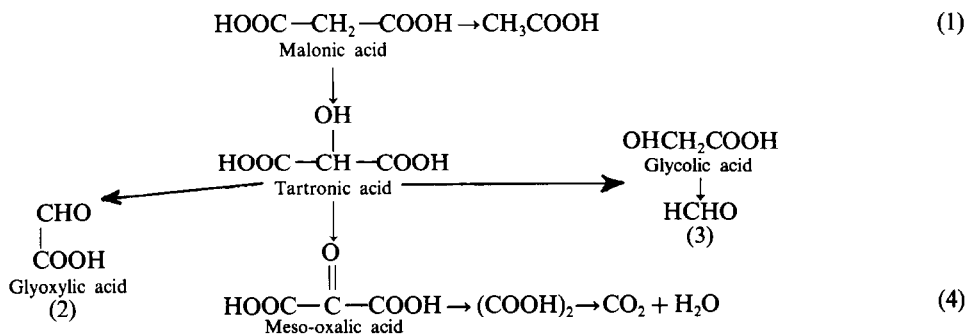
[Sulphuric acid], <i>M</i>	Percentage oxidized						
	30*	45*	60*	75*	90*	120*	180*
0.5	96.8	98.0	98.5	99.0	99.0	99.0	99.0
1.0	97.0	98.5	99.0	99.3	99.5	99.8	99.8
1.5	97.0	98.5	99.0	99.3	99.5	100.0	100.0
2.0	97.0	98.5	99.0	99.3	99.5	100.0	100.0
2.5	97.0	98.5	99.0	99.3	99.5	100.0	100.0

*Reflux time, *min.*

thallium(III) required for complete oxidation of malonic acid, gives complete oxidation to carbon dioxide and water.

(b) At lower sulphuric acid concentration and/or with a smaller excess of thallium(III), negative errors are obtained even with longer reflux times.

It is clear that under the conditions stated in (b) above, side-reactions occur which result in incomplete oxidation. The probable routes of oxidation of malonic acid are:



Studies on the oxidation of glyoxylic acid, glycolic acid and acetic acid under the conditions for com-

plete oxidation of malonic acid showed that acetic acid resists oxidation, glyoxylic acid requires more than 120 min for complete oxidation and glycolic acid undergoes only partial oxidation. Hence the oxidation probably does not take place by routes (1), (2) or (3). On the other hand, tartronic, meso-oxalic and oxalic acid all require less time for complete

*The chromotropic acid and pyrogallol carboxylic acid tests¹² were used but thallium(III) was found to interfere. Hence, the thallium(III) was first reduced to thallium(I) by heating⁹ in the presence of excess of oxalate. Thallium(I) and oxalate do not interfere in these spot-tests.

oxidation than that needed for complete oxidation of malonic acid. Furthermore, the presence of glyoxylic acid or formaldehyde could not be detected in the solution under the conditions [stated under (a) above] for quantitative oxidation of malonic acid. Under the conditions in (b), both glyoxylic acid and formaldehyde can be detected.* Hence the course of complete oxidation of malonic acid by thallium(III)

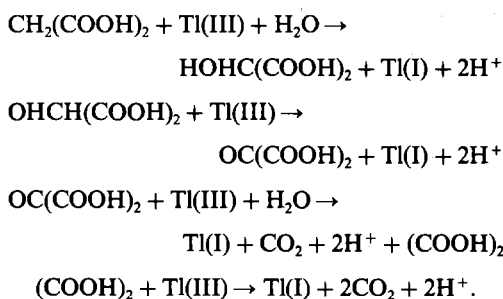
Table 3. Effect of thallium(III) concentration on the extent of oxidation of 0.05 mmole of malonic acid in 75 ml of 1.5M sulphuric acid [x mmole of thallium(III) added, reflux for 120 min, then $(0.8 - x)$ mmole of thallium(III) added and reflux continued for a further 120 min]

x , mmole	Percentage oxidation with x mmole of thallium(III)	Total percentage oxidation with x and $(0.8 - x)$ mmole of thallium(III)
0.00	—	62.5
0.05	23.0	81.0
0.10	48.8	86.0
0.15	65.5	88.5
0.20	85.3	91.0
0.30	90.5	95.8
0.40	97.8	98.0
0.80	100.0	100.0

Table 4. Effect of reflux time on the oxidation of 0.05 mmole of malonic acid in 75 ml of 1.5M sulphuric acid in the presence of different amounts of thallium(III) [x mmole of thallium(III) added, refluxing for t min, then $(0.8 - x)$ mmole of thallium(III) added and reflux continued for 120 min]

x , mmole	Percentage oxidation			
	$t = 30$	$t = 60$	$t = 90$	$t = 120$
0.05	89.0	87.0	85.0	81.0
0.10	92.0	89.0	87.0	86.0
0.20	95.5	93.5	92.3	91.0
0.30	97.3	96.8	96.0	95.8
0.40	98.8	98.5	98.0	98.0
0.80	100.0	100.0	100.0	100.0

is probably by route (4) and may be written as



Separate studies were made on the oxidation of malonic acid with less than the necessary amount of thallium(III) in 1.5M sulphuric acid medium, with refluxing for different initial periods, and followed by refluxing for a further 120 min after addition of enough thallium(III) to bring the reaction mixture to the conditions required for complete oxidation. The results are given in Tables 3 and 4 and show that:

(a) as the thallium(III) concentration initially ad-

Table 5. Estimation of malonic acid

Malonic acid, mmole	
Taken	Found
0.0100	0.0100
0.0188	0.0188
0.0200	0.0200
0.0495	0.0495
0.0500	0.0499
0.0600	0.0603
0.0800	0.0803
0.1000	0.0996

ded is decreased (Table 3), the percentage of malonic acid oxidation is also decreased;

(b) as the time of initial refluxing increases (Table 4), the percentage of malonic acid oxidation is decreased.

These observations show that in the presence of less than 1.5M sulphuric acid and/or less than four times the stoichiometric amount of Tl(III), malonic acid undergoes side-reactions (probably giving rise to acetic acid, glycolic acid or glyoxylic acid) and oxidation is incomplete.

Interferences

Acetic, propionic, succinic, glutaric, adipic and pimelic acids do not interfere. Oxalic, formic, lactic, malic, tartaric and citric acids interfere because they also react with thallium(III) under the conditions used.

Typical results for determination of malonic acid are given in Table 5.

REFERENCES

- G. F. Smith and F. R. Duke, *Ind. Eng. Chem., Anal. Ed.*, 1943, **15**, 120.
- G. G. Rao, I. Subrahmanyam and B. M. Rao, *Talanta*, 1972, **19**, 1083.
- A. Berka, M. Korinková and J. Barek, *Microchem. J.*, 1975, **20**, 353.
- M. Ishibashi, T. Shigematsu and S. Shibata, *Bunseki Kagaku*, 1959, **8**, 380.
- H. H. Willard and P. Young, *J. Am. Chem. Soc.*, 1930, **52**, 132.
- P. K. Jaiswal and K. L. Yadava, *J. Indian Chem. Soc.*, 1974, **51**, 750.
- N. N. Sharma and R. C. Mehrotra, *Anal. Chim. Acta*, 1954, **11**, 417.
- Idem, ibid.*, 1955, **13**, 419.
- S. R. Sagi and K. V. Ramana, *Talanta*, 1969, **16**, 1217.
- J. Proszk, *Z. Anal. Chem.*, 1928, **73**, 401.
- S. R. Sagi and M. S. Prasada Rao, *Talanta*, 1979, **26**, 52.
- F. Feigl, *Spot Tests*, Vol. II, *Organic Applications*, 4th Ed., pp. 241, 253. Elsevier, Amsterdam, 1954.

DETERMINATION OF BISMUTH(III) BY DIRECT POTENTIOMETRY AND POTENTIOMETRIC TITRATION, WITH AN ELECTRODE SENSITIVE TO Bi^{3+}

WALENTY SZCZEPANIAK and MARIA REN

Department of Instrumental Analysis, Faculty of Chemistry, A. Mickiewicz University, Poznań, Poland

(Received 13 May 1983. Accepted 1 October 1983)

Summary—A liquid-state ion-exchange electrode containing the chelate bismuth(III) complex with 5-mercapto-3-(naphthyl-2)-1,3,4-thiadiazole-2-thione in tetrachloroethane is applied to the determination of bismuth(III) by direct potentiometry and potentiometric titration. The influence of various interfering cations is discussed. In the presence of potassium cyanide as masking agent, Ni(II), Co(II), Cu(II), Ag(I) and Hg(II) do not interfere in the potentiometric EDTA titration. Satisfactory results have been obtained for the determination of bismuth(III) in Wood's metal and two pharmaceuticals.

In a previous paper¹ we described a liquid-state membrane electrode sensitive to bismuth(III) cations. The slope of the calibration graph was 18.7 mV/ $p a_{\text{Bi}^{3+}}$ in the $p a_{\text{Bi}^{3+}}$ range 6.5–9.5. The potential of the electrode was established within about 10 sec for 10^{-4} – $10^{-2} M$ Bi(III) solutions and 3 min for 10^{-6} – $10^{-5} M$ Bi(III). The potentials obtained were constant over a 20-day working period. The electrode was characterized by good selectivity coefficients for bivalent cations, and also for Al^{3+} , Fe^{3+} and Th^{4+} ($K_{\text{Bi}^{3+}/M^{2+}} < 10^{-5}$). Cations found to interfere were Ag^+ , Hg^{2+} and Cu^{2+} .

The potentiometric methods proposed below broaden the known possibilities for the determination of bismuth(III).

EXPERIMENTAL

Reagents and apparatus

All reagents used were of analytical-reagent grade. The water used was doubly distilled in a quartz still.

A 0.2M ammonium acetate and 0.7M acetic acid buffer was used throughout unless otherwise stated.

E.m.f. measurements were made with an Elpo pH-meter type N-512, connected to a Zeiss recorder (type G₁B₁) and a Meratronik V 530 digital voltmeter. This system allowed the e.m.f. to be read to ± 0.1 mV. The ion-selective electrode was of liquid-membrane type, based on a $5 \times 10^{-3} M$ solution of the bismuth complex of 5-mercapto-3-(naphthyl-2)-1,3,4-thiadiazole-2-thione(bismuthiol III) in 1,1',2,2'-tetrachloroethane. The construction of the working electrode and measuring cell were as described previously.¹ Measurements were made on the final sample solutions prepared as described below.

Preparation of samples

Wood's metal. A 1-g sample was dissolved in concentrated nitric acid in a heated quartz flask. Metastannic acid was filtered off and washed and the filtrate diluted to volume with water in a 25-ml standard flask. A 1-ml aliquot was diluted to volume with ammonium acetate buffer in a 100-ml standard flask.

Pharmaceutical No. 1. A 2-g sample of the powder was dissolved in hot concentrated nitric acid and the solution

diluted to volume with water in a 100-ml standard flask. A 10-ml aliquot was taken and diluted to volume in a 100-ml standard flask with ammonium acetate buffer.

Pharmaceutical No. 2. A weighed tablet was dissolved in hot concentrated nitric acid in a quartz flask. The solution was filtered and made up to volume in a 100-ml standard flask with water. A 10-ml aliquot was further diluted to 100 ml (standard flask) with ammonium acetate buffer.

RESULTS AND DISCUSSION

As shown in the previous paper¹ the electrode can be used for the determination of Bi(III) in the range $pC_{\text{Bi(III)}} = 2-5$. The linearity of the calibration graph is not affected by Ca(II), Mg(II), Zn(II), Ni(II), Co(II), Mn(II), Cd(II) and Fe(III) in concentrations up to 0.01M. The effect of Cu(II) and Pb(II) is illustrated in Fig. 1.

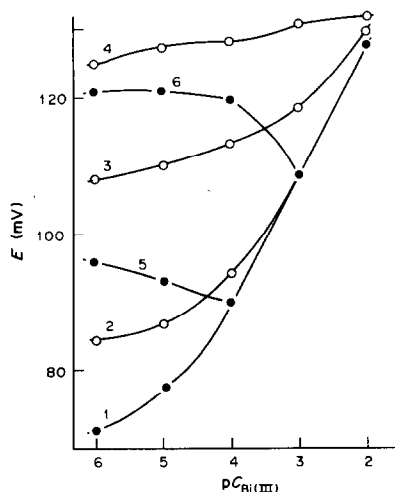


Fig. 1. Calibration curves of the electrode in Bi(III) solutions in the presence of interfering ions; all calibration curves start at $pC_{\text{Bi}} = 2.1$, Bi or Bi + Ni(II), Zn(II) or Fe(III) ($10^{-2} M$); 2, Bi + Cu(II) ($10^{-4} M$); 3, Bi + Cu(II) ($10^{-3} M$); 4, Bi + Cu(II) ($10^{-2} M$); 5, Bi + Pb(II) ($10^{-3} M$); 6, Bi + Pb(II) ($10^{-2} M$).

The application of the method is restricted to the bismuth concentration range 10^{-3} – $10^{-2}M$ in the presence of $10^{-2}M$ Pb(II) and $10^{-4}M$ Cu(II). The effect of lead is especially severe at bismuth concentrations below $10^{-3}M$, and it is therefore necessary to know the approximate molar Pb/Bi ratio in the sample; if this exceeds 10, the determination by potentiometry is impossible. The determination of Bi(III) by direct potentiometry is impossible when the concentration of Cu(II) is greater than $10^{-4}M$. In the presence of a large excess of Cu(II), Pb(II), Hg(II) and Ag(I), the bismuth(III) in its Bismuthiol III complex in the membrane is replaced by the interfering ion, making the electrode sensitive to that ion. A statistical analysis of the results of bismuth determination in the presence of some interfering ions, by the standardization-graph and standard-additions methods, is shown in Table 1. The presence of interfering ions reduces both the accuracy and precision of Bi(III) determination by direct potentiometry. An advantage of this method, however, is that Bi(III) can be determined in the presence of Pb(II) and Cd(II) whereas these ions make the potentiometric titration of bismuth impossible.

The electrode operates successfully as the indicator electrode in potentiometric titrations of Bi(III) with EDTA. Good titration curves are obtained for titration of 5×10^{-5} – $10^{-2}M$ bismuth, but the shape of the titration curves is affected by the presence of certain other cations. Ca(II), Mg(II), Mn(II), Al(III) and Fe(III) ions at concentrations up to $10^{-3}M$ do not interfere with the course of titration of $10^{-3}M$ bismuth (Fig. 2), but Co(II), Ni(II), Cu(II), Zn(II), Ag(I) and Hg(II) causes significant changes in the shape of the titration curves because of their effect on the electrode potential. Despite the good selectivity coefficients for Ni(II), Co(II) and Zn(II), the influence of these ions is apparent at the low concentrations of Bi(III) in the vicinity of the end-point (e.g., Figs 3).

In the presence of Cu(II) ions, it is the sum of Bi(III) and Cu(II) which is titrated, unless the copper is masked, e.g., with cyanide. When Ag(I) and Hg(II) are present, the changes in the shapes of the titration curves are so extensive that Bi(III) can only be determined if the silver and mercury are masked.

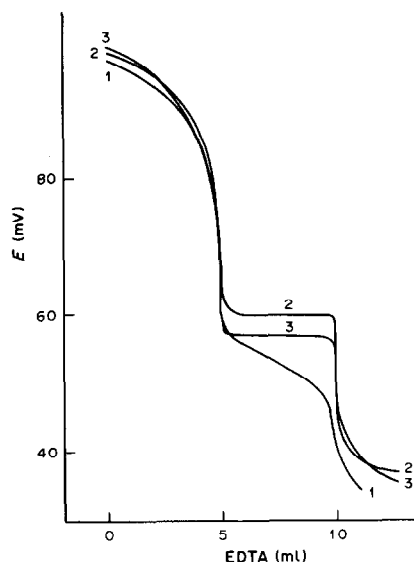


Fig. 2. Potentiometric titration curves for Bi(III) $10^{-3}M$ with EDTA in the presence of interfering ions. 1. Mn(II) or Mg(II), or Ca(II) ($10^{-3}M$), 2. Fe(III) ($10^{-3}M$), 3. Al(III) ($10^{-3}M$), pH = 6.

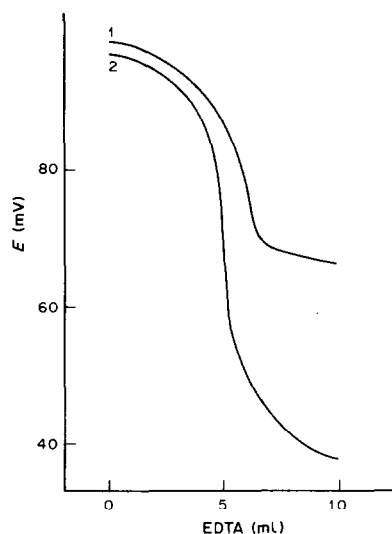


Fig. 3. Potentiometric titration curves for Bi(III) $10^{-3}M$ with EDTA in the presence of Ni(II) ($10^{-3}M$) pH = 6, 1. without masking, 2. in the presence of CN^- .

Table 1. A statistical evaluation of the results of Bi(III) determinations in the presence of interfering ions (concentration $10^{-3}M$) by the standardization graph method (1) and the method of standard additions (2); Bi(III) present = 8.36 mg, $n = 10$

Interfering ion	Average result of determination, mg		Standard deviation, mg		Relative standard deviation, %		Error, %	
	1	2	1	2	1	2	1	2
Pb(II)	8.36	8.33	0.09	0.16	1.1	2.0	0	-0.4
Zn(II)	8.32	8.32	0.27	0.29	3.3	3.5	-0.5	-0.5
Cd(II)	8.28	8.32	0.24	0.13	2.9	1.6	-1.0	-0.5
Fe(III)	8.46	8.28	0.30	0.27	3.6	3.3	+1.2	-1.0
	8.51	8.32	0.30	0.22	3.6	2.7	+1.8	-0.5

Table 2. A statistical evaluation of Bi(III) determination by potentiometric titration with EDTA in the presence of interfering ions and in pure solutions; Bi(III) content 10.45 mg, $n = 10$; for each titration a freshly-mounted electrode was used

Solution analysed	Average result, mg	Standard deviation, mg	Relative standard deviation, %	Error, %
Bi(III)*	10.39	0.04	0.4	-0.6
Bi(III)	10.56	0.09	0.9	+1.0
Bi(III) + $10^{-3}M$ Fe(III)	10.47	0.09	0.9	+0.2
Bi(III) + $10^{-3}M$ Hg(II) (masked with CN^{-})	10.43	0.05	0.5	-0.2

*The same electrode was used for all titrations.

Table 3. Determination of Bi(III) in various samples (5 replicates)

Sample	Method*	Mean \pm confidence interval (95%), g	Relative standard deviation, %
Wood's metal	A	0.440 ± 0.011	0.5
	B	0.439 ± 0.017	0.7
Bismuth nitrate pharmaceutical	C	0.3804 ± 0.0013	0.2
	D	0.381 ± 0.013	2.5
Bismuth aluminate pharmaceutical	B	0.381 ± 0.007	0.9
	C	0.1317 ± 0.0011	0.6
	D	0.132 ± 0.005	2.3
	B	0.132 ± 0.003	1.3

A = standardization graph method. B = EDTA titration (Pyrocatechol Violet). C = EDTA titration (potentiometric). D = standard additions method.

Cyanide can be used for this purpose, and also for masking copper, nickel and cobalt.

Zinc(II) can be satisfactorily masked with 1,4,8,11-tetra-azacyclotetradecane- N,N',N'',N''' -tetramethylphosphonic acid (TATMF).²

The determination of Bi(III) by potentiometric titration both in pure solution and in the presence of $10^{-3}M$ Fe(III) and Hg(II) masked with cyanide has been statistically evaluated (Table 2). The accuracy and precision are not reduced by the presence of interfering ions, and the low values of the standard deviation show that this is a precise method of determining Bi(III).

To test the usefulness of the electrode in the analysis of natural samples, Bi(III) in Wood's metal and two pharmaceuticals was determined. Because of the presence of Cd(II) and Pb(II), the bismuth in

Wood's metal was determined by direct potentiometry (standardization-graph method). Bismuth(III) in the two pharmaceuticals (bismuth nitrate and bismuth aluminate) was determined by potentiometric titration and by the standard-additions method. For comparison, an independent determination was done by EDTA titration, with Pyrocatechol Violet as indicator. The results are presented in Table 3. The results of the determinations by the present method are consistent with those obtained by complexometric titration and show a greater precision.

REFERENCES

1. W. Szczepaniak and M. Ren, *Talanta*, 1983, **30**, 945.
2. W. Szczepaniak and K. Kuczyński, Unpublished work.

LIQUID-LIQUID EXTRACTION OF ZINC(II) AS ITS ETHYL XANTHATE*

A. K. CHAKRAVARTI,† S. MUKHERJEE, H. K. SAHA and T. CHAKRABARTY
Max-Planck-Institut für Biophysik, Kennedy-Allee 70, 6000 Frankfurt 70, West Germany

(Received 11 March 1983. Revised 9 June 1983. Accepted 30 September 1983)

Summary—A method for quantitative extraction of zinc with potassium ethyl xanthate into carbon tetrachloride is described. The optimum conditions are: pH 5–6 and Zn(II) to reagent ~1:8 mole ratio. The effects of other ions on the extraction of Zn^{2+} have been investigated, and its separation from As^{3+} , Pb^{2+} , Cu^{2+} and Fe^{3+} is described. The possibility of repeated use of the solvent (still loaded with xanthate after the zinc has been stripped) for further extractions (after addition of a little extra xanthate) has been explored. Various stripping agents have been examined, and the optimum conditions found.

Extraction of their alkyl xanthate complexes is useful for the separation of certain metal ions,¹⁻⁸ and the solvent extraction of ethyl xanthate complexes has been reviewed by Donaldson.⁹ Zinc(II) forms an extractable ethyl xanthate complex, and this paper describes improved conditions for extraction of the complex, the effect of diverse ions on the extraction, stripping of the zinc from the extract, separation of zinc from interfering ions, and the possible use of the extraction system in counter-current processes.

EXPERIMENTAL

Reagents

Potassium ethyl xanthate was either prepared^{10,11} or purchased (>99% pure, Fluka), and used as a 1% solution in water. All other chemicals used were of CP or analytical-reagent grade. The water used was always demineralized and doubly distilled.

General procedure

Zinc solution (0.08M, 1.0 ml), 9 ml of water and a drop of acetic acid (1:1) were placed in a 100-ml separatory funnel, 10 ml of 1% xanthate solution were added, and the mixture was shaken with 20 ml of carbon tetrachloride for 1–2 min (at about 2 strokes per sec). The organic layer was separated, and the aqueous layer extracted with a further 5 ml of carbon tetrachloride. The combined extracts were used for subsequent studies. The zinc in the organic phase was determined after evaporation of the carbon tetrachloride in the presence of 20 ml of water. In the stripping experiments the organic extract was shaken with an equal volume of stripping solution for 3–4 min (at about 2 strokes per sec), and the zinc concentration in the aqueous phase was determined complexometrically by EDTA titration at pH ~6 (hexamine buffer) with a mixed indicator consisting of Xylenol Orange (0.5% solution, 3 drops) and Methylene Blue (0.1%, 1 drop).

RESULTS AND DISCUSSION

The results are discussed on the basis of single extractions unless otherwise mentioned.

*Part of this work was done in the microanalytical laboratory, Science College, Calcutta 9, India.

†To whom all correspondence should be addressed.

Complete extraction of Zn-xanthate complex and iterative use of the extractant

The stable Zn-xanthate complex (1:2)⁹ is completely extracted at pH 5–6 (Fig. 1). It has been found that if the aqueous zinc solution is adjusted to pH 3–4 (with acetic acid) before addition of the xanthate, the necessary pH value is reached after the xanthate addition. The complex is 97–98% extracted into carbon tetrachloride (1:1 phase-volume ratio) when a 300% excess of xanthate is present. Extraction into chloroform is less complete (~90%)^{12,13} under these conditions. Furthermore, if the carbon tetrachloride extract is stripped with 0.1M hydrochloric acid, the stripped solvent can be used for extraction of another zinc solution, and because the solvent contains the xanthate liberated in the stripping, less xanthate needs to be added to the zinc solution. Thus tests showed that after extraction of 5 mg of zinc (80 μ mole) in the presence of 100 mg of potassium ethyl xanthate, and stripping, the carbon tetrachloride could be used for at least five more similar extractions if 25 mg of xanthate (2.5 ml of 1%

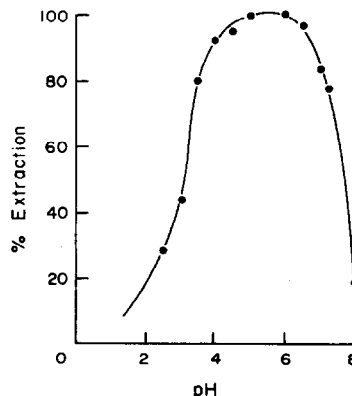


Fig. 1. Effect of pH on extraction of zinc.

Table 1. The effect of various ions on the zinc extraction

Ion	Amount, mg	Apparent extraction,* %
Cu ²⁺	5	Negative interference
Co ²⁺	5	Positive interference
Fe ³⁺	5	Positive interference
Hg ²⁺	10	92.6
UO ₂ ²⁺	20	95.3
Cr ³⁺	5	96.5
Cd ²⁺	10	Positive interference
As(III)	10	96.5
F ⁻	10	91.8
VO ₃ ⁻	10	70.5
SO ₄ ²⁻	10	97.7
H ₂ PO ₄ ⁻	10	95.3
Tartrate	10	96.5
Citrate	10	68.1
EDTA ²⁻	10	64.3

*As found by stripping and EDTA titration.

solution) were added to each fresh zinc solution taken for extraction. This offers economy in the use of xanthate, and has potential applications in counter-current extraction or recycling systems.

Interferences

The effect of various ions on a single extraction of 4 mg of zinc under the conditions of the general procedure was examined. The results are shown in Table 1. It can be seen that Cu²⁺, Co²⁺, Fe³⁺, Hg²⁺, Cd²⁺, F⁻, VO₃⁻, citrate³⁻ and EDTA²⁻ always interfere. It is known^{14,15} that trace amounts of Cu²⁺ and Fe³⁺ form stable xanthate complexes over a wide range of pH (3–11). The copper xanthate is practically insoluble in carbon tetrachloride, but appears to adsorb some zinc xanthate, since the recovery of zinc increases with repeated extraction. Again, a very stable Zn–EDTA complex (conditional stability constant at pH 5 is ~10¹⁰) is formed at the pH at which the zinc xanthate complex is formed. Vanadate probably oxidizes some xanthate. Positive interferences are

due to co-extraction (and subsequent co-titration) of the metal xanthates.

Separation of Zn²⁺ from the interfering ions

From Pb²⁺, Co²⁺ and As(III). Zn²⁺ can be separated from mixtures with Pb²⁺, Co²⁺ and As(III) by extracting Zn²⁺, Pb²⁺ and Co²⁺ with xanthate and carbon tetrachloride at pH ~6, which separates them from As(III), then shaking the organic layer with twice its volume of 1.3M NH₄Cl/7.5M NH₃ buffer (pH ~10) for 5 min, which strips only Zn²⁺.

From Cd²⁺. Zinc is quantitatively separated from cadmium by extraction of a mixture of the two with xanthate at pH ~6 into chloroform (two 20 ml portions) and then stripping of the zinc with two portions of 0.87M NH₄Cl/0.05M NH₃ buffer (pH ~8), each equal in volume to the organic phase, by shaking the mixture for 3 min. Higher concentrations of the buffer components strip some cadmium as well.

From Cu²⁺. The separation can be accomplished in two ways. (a) Thiourea is added before the xanthate, then the mixture is shaken with an equal volume of 6:1 v/v carbon tetrachloride–pyridine mixture (~5 ml of pyridine) for each 2 mg of Cu²⁺. The brown organic layer (which turns light yellow on standing) is separated from the aqueous phase and shaken with an equal volume of 0.3–0.5M hydrochloric acid, which strips only the zinc. (b) The zinc is extracted by the general procedure, and the organic phase is separated from the insoluble yellow copper xanthate present in the aqueous layer.

As already mentioned, large quantities of copper hinder the zinc xanthate extraction. However, repeated extraction with either fresh carbon tetrachloride or organic extract that has been stripped of zinc with 0.1M hydrochloric acid, will separate the rest of the zinc almost completely. A typical set of results is given in Table 2.

Table 2. Separation of Zn²⁺ from Cu²⁺–Zn²⁺ mixture and iterative use of the extractant

Cu ²⁺ soln.* added, ml	Xanthate soln. added, ml	CCl ₄ used, ml	Zn ²⁺ extracted,† %	Total Zn ²⁺ extracted, %
1.0	15.0	1st ~ 25.0	95.7	99.7
		↓ 2nd ~ 25.0	4.0	
2.5	20.0	1st ~ 30.0	83.0	99.5
		↓ 2nd ~ 30.0	14.0	
		↓ 3rd ~ 30.0	2.5	
5.0	30.0	1st ~ 40.0	71.0	98.6
		↓ 2nd ~ 40.0	22.0	
		↓ 3rd ~ 40.0	5.6	

*Cu²⁺ 2 mg/ml.

†Referred to the 5 mg of zinc taken; extract stripped before reuse.

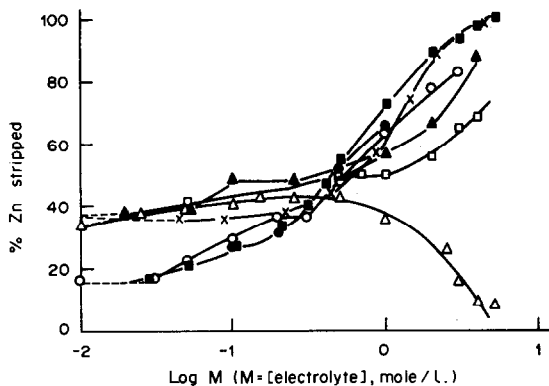


Fig. 2. Stripping of zinc from organic phase to aqueous phase with electrolyte solutions and buffer solutions. Molar concentrations used: (\blacktriangle) NH_4Cl , 0.02–4.0; (\blacksquare) NH_4Ac , 0.02–5.0; (\square) KCl , 0.05–4.0; (\circ) NaAc , 0.01–3.0; (\triangle) NaClO_4 , 0.01–5.0; (\times) $\text{NH}_4\text{Cl}/\text{NH}_3$ buffer (pH \sim 7), 0.217/0.0013–4.35/0.025; (\bullet) NaAc/HAc buffer (pH \sim 6), 0.1/0.1–1.0/1.0.

Carbon tetrachloride, when used in this way, became faint yellow in colour but did not lose much extracting capacity for zinc. In an experiment with extraction of 5 mg of zinc in presence of 5 mg of copper, with two 30-ml portions of carbon tetrachloride, the first extract removed 85% of the zinc, and the second 10%. Addition of further xanthate before the second extraction did not appreciably improve the yield.

From Fe^{3+} . Quantitative separation of 5 mg of Zn^{2+} from 50 mg of Fe^{3+} can be achieved by adding ascorbic acid and then raising the pH to \sim 4 with sodium acetate before adding the xanthate (at least twice the amount needed for the zinc alone), followed by extraction as usual.

Stripping of zinc

Various solutions were tested for stripping the zinc, ranging from 2M hydrochloric acid to pH 10 buffer (1.3M $\text{NH}_4\text{Cl}/7.5\text{M}$ NH_3), and including solutions of potassium iodide, bromide, chloride and nitrate, sodium acetate and perchlorate, ammonium chloride, acetate, nitrate and sulphate, of various concentrations, and two other buffer solutions.

Stripping is almost complete with 0.01M or higher concentrations of hydrochloric acid; with equal vol-

umes of extract and pure water it is \sim 34.5% complete. $\text{NH}_4\text{Cl}/\text{NH}_3$ buffer (pH \geq 7) also strips zinc almost completely. The effect of the other stripping agents is shown in Fig. 2. Only 5.0M ammonium acetate and the most concentrated pH \sim 7 buffer proved really effective.

Ion-exchange tests showed that zinc was present as a cationic species when stripped with sodium acetate or low concentrations of potassium or ammonium chloride, but as anionic complexes when stripped with higher concentrations of the chlorides. The greater efficiency of ammonium acetate as a stripping agent may be due to formation of zinc ammine complexes.

Acknowledgements—One of the authors (A.K.C.) expresses his grateful thanks to Professor R. Schlögl, Director and Head of the Department of Physical Chemistry, Max-Planck-Institut für Biophysik, Frankfurt, for his keen interest and constructive criticisms in the work. He is also grateful to Professor S. K. Gupta, Head of the Department of Chemistry, DDM College, Calcutta 74, Dr. G. Wiedner, W. L. Gore & Co GmbH, München, and Dr. L. G. M. Gordon, University of Otago, New Zealand for their interest and encouragement. Lastly he expresses his thankfulness to Mrs. Z. Bojadzjev for her assistance in the experiments.

REFERENCES

1. A. K. De, *Sepr. Sci.*, 1968, **3**, 103.
2. S. E. Livingstone, *Quart. Rev.*, 1965, **19**, 386.
3. R. Eisenberg, *Progr. Inorg. Chem.*, 1970, **12**, 295.
4. D. Coucouvanis, *ibid.*, 1970, **11**, 233.
5. R. J. Magee, *Rev. Anal. Chem.*, 1973, **1**, 335.
6. G. H. Morrison and H. Freiser, *Solvent Extraction in Analytical Chemistry*, p. 182. Wiley, New York, 1957.
7. J. Starý, *The Solvent Extraction of Metal Chelates*, p. 169. Macmillan, New York, 1964.
8. A. K. De, S. M. Khopkar and R. A. Chalmers, *Solvent Extraction of Metals*, p. 149. Van Nostrand-Reinhold, New York, 1970.
9. E. M. Donaldson, *Talanta*, 1976, **23**, 417.
10. A. I. Vogel, *A Text-book of Practical Organic Chemistry*, 3rd Ed., p. 449. Longmans, London, 1968.
11. T. Chakrabarty and A. K. De, *Z. Anal. Chem.*, 1968, **242**, 152.
12. A. T. Pilipenko and N. V. Ulko, *Zh. Analit. Khim.*, 1955, **10**, 299.
13. K. Hayashi, Y. Sasaki and H. Nojima, *Bunseki Kagaku*, 1970, **19**, 325; *Chem. Abstr.*, 1970, **73**, 21020d.
14. I. M. Korenman and A. I. Anfilov, *J. Appl. Chem. (U.S.S.R.)*, 1940, **13**, 1262 (French); *Chem. Abstr.*, 1941, **35**, 2087^a.
15. A. L. J. Rao and S. Singh, *Z. Anal. Chem.*, 1971, **257**, 133; *J. Indian Chem. Soc.*, 1974, **51**, 503.

INVESTIGATION OF THE USE OF THERMOMETRIC TITRIMETRY FOR THE DETERMINATION OF ACIDIC SUBSTANCES IN WINE

O. E. S. GODINHO, J. A. COELHO, A. P. CHAGAS and L. M. ALEIXO

Instituto de Química, Universidade Estadual de Campinas, C.P. 6154, 13100 Campinas, SP, Brasil

(Received 24 June 1983. Accepted 29 September 1983)

Summary—The use of thermometric titrimetry in the determination of acidic substances in red wine is described. The titration curve obtained in the thermometric titration of red wine with strong base presents two inflections. The stoichiometry corresponding to the first inflection presents good agreement with the so-called "total acidity" of wine, and is proposed for its determination. The second inflection is related to the content of phenolic substances in red wine.

The use of thermometric titrimetry in the determination of inorganic acids, carboxylic acids and phenols has been extensively studied.^{1,2} It is well known that this technique can be used for the alkalimetric titration of even very weak acids.¹ Moreover, being a linear method, thermometric titrimetry may be more suitable than potentiometric titrimetry for end-point detection of components of a mixture of weak acids.³

It is also well known that various acids and phenolic substances are important components of wine, and it appeared to us to be of interest to investigate the application of thermometric acid-base titrimetry to this material, especially in view of the simplicity and low cost of the apparatus, and the ease of automation of the technique.

We first compared the results of conventional thermometric titrimetry with the "total acidity" and the phenolic-substance content of red wine. The values of "total acidity" used for comparison were obtained by potentiometric titration to pH 8.2.⁴ The content of phenolic substances was obtained by permanganate titration according to the procedure of Ribereau-Gayon and Maurie,⁵ modified by Ribereau-Gayon and Peynaud.⁶

EXPERIMENTAL

Procedure for thermometric titration

A 50-ml sample of wine was placed in a 100-ml Dewar flask and titrated with 1.0M sodium hydroxide delivered at a constant rate of 0.4 ml/min from a syringe burette (Syringe pump 351, Sage Instruments). The detection and recording system has already been described.⁷ The first end-point was easy to detect and was given by the intersection of the extrapolations of the linear portions of the first and second parts of the curve (Fig. 1). The second end-point was determined in the same manner, as the intersection of the corresponding extrapolations of the second and third parts of the curve. However, in some cases the third part tended to be continuously rounded, and it was necessary to draw a tangent to it, in a standardized manner. A preliminary estimate of the second end-point is made by visual selection

of point G as the point of deviation of the titration curve from line AB, and drawing a tangent at point F', (located so that the projected distances D' and E' are equal). The intersection locates the "trial" end-point. The tangent can then be redrawn at F, which is located so that projected distances D and E are equal, and the new intersection gives the end-point, B. However, small variations in the length of E do not significantly affect the position of the second end-point.

Procedure for potentiometric titration

A 10-ml sample of wine was pipetted into a 250-ml Erlenmeyer flask, 100 ml of distilled water were added and the solution was titrated with 0.1M sodium hydroxide, the end-point being located at pH 8.2. A Metrohm EA109 glass electrode and EA104 saturated calomel electrode, and an Orion Model 701 pH-meter were used for the pH measurements. The electrodes were calibrated with NBS pH 6.86 buffer before starting the titration.

RESULTS AND DISCUSSION

A typical curve for the thermometric titration of red wine with sodium hydroxide solution is shown in Fig. 1. There is a very distinct break at point A and a second but less distinct one at point B. The stoichiometry corresponding to titration volume C was compared with the so-called "total acidity" obtained by potentiometric titration to pH 8.2,⁴ and that for titration volume D was compared with the content of phenolic substances. If phenol was added to the wine, there was an increase in D, whereas C was unaffected, which supports the attribution of D to titration of phenolic components.

Data for total acidity of wine

The "total acidity" obtained potentiometrically is compared with the stoichiometry corresponding to C, in Table 1. A plot of the potentiometric results, y , vs. the thermometric results, x , gave a straight line described by the equation $y = 0.945x + 0.0045$ (correlation coefficient 0.9884). In view of this we think that the thermometric titration may be proposed for determination of the "total acidity" of wine.

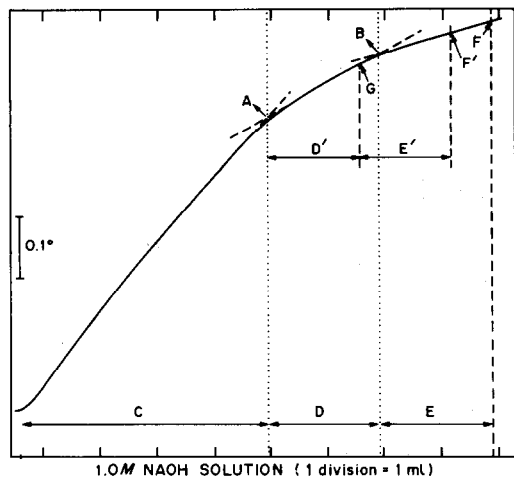


Fig. 1. Curve corresponding to the titration of 50 ml of red wine with 1.0M sodium hydroxide by conventional thermometric titrimetry. A—First equivalence point. B—Second equivalence point. C—Titrant volume corresponding to "total acidity". D—Titrant volume corresponding to phenolic substances. (For D', E, E', F, F', G, see text).

Data for content of phenolic substances in red wine

In Fig. 2 the thermometric titration curves of tartaric acid, gallic acid and a mixture of these acids are shown. The curve for tartaric acid, in which only the carboxylic acid group is titratable, has only one break point. On the other hand, gallic acid, which contains one carboxylic acid and three phenolic groups per molecule, gives two breaks on the curve. The first must correspond to titration of the carboxylic acid group and the second to titration of the phenolic groups. However, the reaction stoichi-

Table 1. Values obtained for "total acidity" of red wine by potentiometric and conventional thermometric titrimetry

Sample number	Total acidity, eq/l.		Difference, %
	Potentiometric	Thermometric	
1	0.1040	0.1058	+1.7
2	0.0910	0.0918	+0.9
3	0.0650	0.0662	+2.0
4	0.0890	0.0905	+1.7
5	0.0830	0.0821	+1.1
6	0.0950	0.0966	-1.7
7	0.0768	0.0757	-1.4
8	0.0795	0.0765	-3.7
9	0.0963	0.0935	-2.9
10	0.0918	0.0893	-2.7
11	0.1145	0.1162	+1.4
12	0.0700	0.0711	+1.5
13	0.0875	0.0850	-2.8
14	0.0835	0.0797	-4.5
15	0.0930	0.0920	-1.1
16	0.0795	0.0901	+0.8

Samples number 1, 4, 5, 6, 7, 8, 9, 10 and 11, Brazilian dry red wine; 12, Chilean dry red wine; 2, 3 and 13, Brazilian sweet red wine; 14 and 15, Brazilian green wine; 16, Portuguese green wine.

ometry for the phenolic groups is lower than expected. This may be due to a very high pK_a for one of the phenolic groups or to hydrogen-bond formation. It is also seen that the addition of gallic acid to tartaric acid results in the appearance of a second break on the titration curve. Addition of phenol to the tartaric acid solution has the same effect.

The titration curve for red wine, shown in Fig. 1, resembles that of the mixture of tartaric and gallic acids or of tartaric acid and phenol. Further, the addition of phenol to the wine results in an increase in the consumption of base in the second part of the titration, and if the red wine is first treated with charcoal there is a large decrease in base-

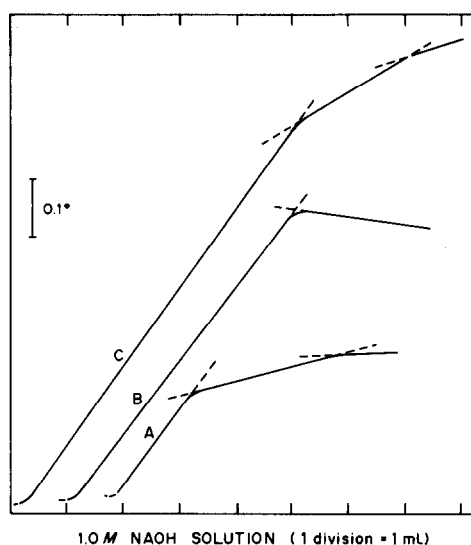


Fig. 2. Curves corresponding to the titration of tartaric and gallic acids with 1.0M sodium hydroxide by conventional thermometric titrimetry. A—50 ml of 0.030M gallic acid; B—40 ml of 0.050M tartaric acid; C—mixture of 40.0 ml of 0.050M tartaric acid and 35.0 ml of 0.03M gallic acid.

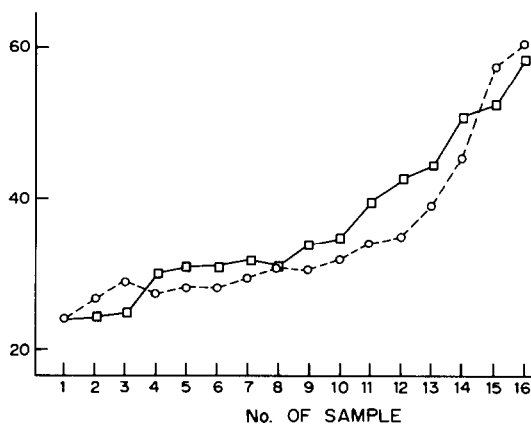


Fig. 3. Relation between the results for content of phenolic substances in red wine by thermometric titrimetry (O) and by permanganate titration (□). Samples number 1, 4, 5, 6, 7, 8, 9, 10 and 11, Brazilian dry red wine; 2, 3 and 13, Brazilian sweet red wine; 12, Chilean dry red wine; 14 and 15, Brazilian green wine; Portuguese green wine.

consumption in the second part. These facts all lead us to conclude that the phenolic groups in the phenolic substances of wine are titrated after the carboxylic acid groups, to give the second part of the curve. However, in view of the results for gallic acid we suppose that the phenolic groups may not be totally titrated.

The second break in the curve is usually very rounded, which is why a standardized procedure is used for locating the second end-point.

The results based on the determination of the end-point as described above are presented in Fig. 3, along with the results obtained by permanganate titration. The results are presented in terms of the number of equivalents of permanganate or sodium hydroxide consumed in titration of 1 litre of the wine.

Acknowledgements—We are grateful to Dr. Takuo Hashizume from ITAL (Instituto de Tecnologia de Alimentos)

for helpful discussion in the course of this work. We are also indebted to "CNPq—Conselho Nacional de Desenvolvimento Científico e Tecnológico" for a fellowship to one of us (J.A.C.).

REFERENCES

1. J. Jordan and W. A. Dunbaugh, Jr., *Anal. Chem.*, 1959, **31**, 210.
2. G. A. Vaughan, *Thermometric and Enthalpimetric Titrimetry*, Van Nostrand-Reinhold, London, 1973.
3. N. D. Jespersen and J. Jordan, *Anal. Lett.*, 1970, **3**, 323.
4. *AOAC Official Methods of Analysis*, 12th Ed., Association of Official Analytical Chemists, Washington, D.C., 1975.
5. J. Ribereau-Gayon and A. Maurié, *Bull. Intern. Vin.*, 1942, **15**, No. 150, 60.
6. J. Ribereau-Gayon and E. Peynaud, *Analisi e Controllo dei Vini*, Edizione Agricola, Bologna, 1966.
7. A. P. Chagas, O. E. S. Godinho and J. M. L. Costa, *Talanta*, 1974, **24**, 593.

DETERMINATION OF CADMIUM(II) AT A GOLD ELECTRODE IN THE PRESENCE OF SELENIUM(IV) BY ANODIC-STRIPPING VOLTAMMETRY WITH ENHANCEMENT BY IODIDE ION

CUI CHUNGUO

Institute of Environmental Chemistry, Academia Sinica, P.O. Box 934, Beijing, People's Republic of China

(Received 6 May 1983. Revised 2 September 1983. Accepted 10 September 1983)

Summary—Anodic-stripping voltammetry (ASV) has been used in the derivative mode for the determination of cadmium, with a gold electrode in sulphuric acid medium containing selenium(IV). The peak height for cadmium is enhanced by the presence of iodide. The sensitivity for cadmium is very high, with a peak in the stripping voltamperogram at -0.27 V (*vs.* Ag/AgCl). The peak height for cadmium is not affected by over a 100-fold level of lead in the presence of selenium(IV). The dependence of peak height on the cadmium concentration is linear in the range 0.05–10 ng/ml.

Heavy-metal species such as copper(II), lead(II) and cadmium(II) are present at above normal levels in natural water in some areas. Cadmium is thought to be brought into the environment mainly by human agency. In the seas and rivers of some industrial areas cadmium concentrations may be a hundred or more times those in unpolluted regions. This creates a need for the determination of cadmium at various levels. This paper presents a method in which cadmium is determined by ASV.

Solid electrodes, the hanging mercury drop electrode and mercury-film electrodes on various solid supports such as carbon paste, graphite and glassy carbon have all been used in anodic-stripping voltammetry. We used a gold electrode in our study because (a) it is easily treated, (b) it is unnecessary to remove oxygen, (c) since the hydrogen overpotential on gold is higher than that on platinum, and gold does not form an oxide film at potentials less positive than $+1.0$ V in mineral acids, it is especially well suited to the determination of metals having a potential more positive than that of mercury.

Gold or gold-film electrodes have previously been used in the determination of copper(II),¹ arsenic(III),² bismuth(III),³ selenium(IV),⁴ mercury(II),⁵ nickel(II),⁶ germanium(IV)⁷ and lead(II).⁸ The work reported here demonstrates the use of a gold electrode for the determination of cadmium in sulphuric acid-iodide medium by derivative anodic-stripping voltammetry.

EXPERIMENTAL

Instruments and apparatus

A model JP-1A oscillopolarograph (Chengdu Electronic Equipment Factory, China) was used in the first-derivative mode, and a 79-1 voltammetric analyser (Jinan Fourth Radio Factory, China) was used in the second-derivative mode. A three-electrode system was used, and

current-potential curves were recorded with an X-Y recorder. Solutions were stirred during the deposition step, with a general-purpose magnetic stirrer.

A gold-disc electrode with a diameter of 2 mm was employed as the working electrode. The surface of the gold electrode was first rubbed with emery paper and then polished with alumina paste to a mirror-like finish. A platinum-coil auxiliary electrode and an Ag/AgCl reference electrode were used, the latter being connected to the sample solution by a saturated potassium chloride salt bridge. The body of the auxiliary electrode and the reference electrode were assembled individually in quartz tubes fitted with porous quartz plugs.

Reagents

The sulphuric acid employed was of super-pure grade. The tetraethylammonium iodide and potassium iodide were of analytical grade. The concentrated ammonia solution was of general-reagent grade. Distilled water from a quartz still was used throughout. Stock solutions (1 mg/ml) of cadmium were prepared by dissolving weighed quantities of the high-purity (99.99%) metal in nitric acid (1 + 1) and diluting to volume with distilled water. Working standards containing up to 1 μ g/ml were prepared daily by diluting the stock solutions with distilled water.

Procedure

The sample solution was introduced into the electrolysis cell and stirred with an electromagnetic stirrer at a constant rate. Cadmium was then deposited at a selected potential for a definite time, after which stirring was stopped and the solution was allowed to rest for 15 sec, during which time the deposition potential was adjusted to the initial value for the scan. The potential was scanned at 100 or 250 mV/sec and the stripping curve recorded. The concentration of cadmium was evaluated by the standard-addition method. After each determination, the potential was swept from $+1.0$ to $+1.8$ V for 1–2 min, to eliminate any trace substances on the electrode.

RESULTS AND DISCUSSION

Choice of base solution

Acidic media have often been used in conjunction with gold electrodes in anodic-stripping analysis, but

when we tried sulphuric acid media no stripping peaks were observed for cadmium (Fig. 1). When tetraethylammonium iodide was added to the sulphuric acid media, however, a stripping peak for cadmium appeared in the voltamperogram (Fig. 1) with a peak potential of -0.27 V and very high sensitivity. This mixed electrolyte was therefore chosen for the determination of cadmium by ASV.

When potassium iodide was used instead of tetraethylammonium iodide the same anodic stripping peak for cadmium was obtained. Thus it may be concluded that the stripping peak of cadmium can be attributed to the effect of the iodide ion.

Choice of concentrations in the base electrolyte

The peak for cadmium was not affected by changes in sulphuric acid concentration over the range $0.0002\text{--}1.44\text{ N}$ when 50 ppm of Et_4NI were present. It can be noted from Fig. 2 that the stripping peak height for cadmium was constant for Et_4NI concentrations ranging from 25 to 200 ppm at a sulphuric acid concentration of 0.36 N , but its repeatability was poorer for Et_4NI concentrations above 150 ppm , owing to oxidation of the iodide on the surface of the gold electrode. Therefore $0.0002\text{--}1.44\text{ N}$ sulphuric acid with 50 ppm Et_4NI was chosen as the base electrolyte. When the cadmium content is very small,

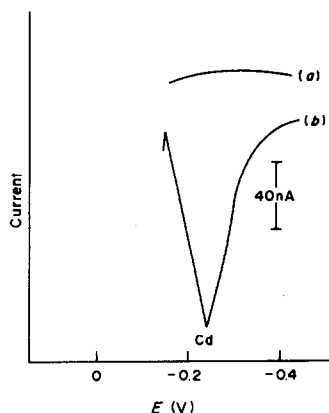


Fig. 1. Anodic-stripping voltammetric curves of cadmium. $\text{Cd(II)} = 20\text{ ng/ml}$, (a) $0.36\text{ N H}_2\text{SO}_4$ (b) $0.36\text{ N H}_2\text{SO}_4\text{--}50\text{ ppm Et}_4\text{NI}$, ($E_{\text{dep}} = 0.4\text{ V}$, $T_{\text{dep}} = 1\text{ min}$).

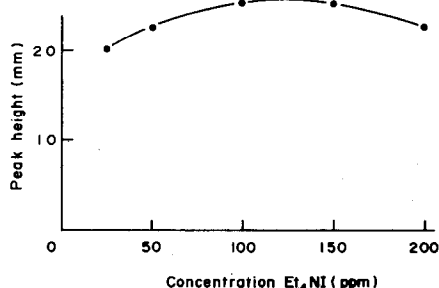


Fig. 2. Dependence of anodic-stripping peak height on Et_4NI concentration. $\text{Cd(II)} = 5\text{ ng/ml}$, ($\text{H}_2\text{SO}_4 = 0.36\text{ N}$, $E_{\text{dep}} = -0.4\text{ V}$, $t_{\text{dep}} = 1\text{ min}$).

the sulphuric acid concentration must not be too high (pH should be $2\text{--}4$) so as to avoid hydrogen evolution on the surface of the gold electrode.

Influence of deposition potential

The stripping current was measured after deposition for a definite time at various potentials. The results obtained are shown in Fig. 3. It can be seen that the peak height is independent of deposition potential in the range from -0.4 to -0.7 V , and diminished at more positive values. More negative potentials are unsuitable because hydrogen evolution on the surface of the electrode would influence the repeatability of the determinations. Therefore, deposition potentials ranging from -0.4 to -0.7 V were chosen as the optimum for the anodic-stripping determination of cadmium.

Influence of deposition time

A solution containing 5 ng of cadmium(II) per ml was used for testing the dependence of the peak height on deposition time. The results obtained are shown in Fig. 4. It can be seen that the peak height is linearly proportional to deposition time but the proportionality constant changes at a deposition time of about 3 min .

Interferences

It was observed that when the concentration of cadmium was as low as 2 ng/ml the following concentration levels of metal ions did not interfere: 100-fold calcium, copper, iron(III), cobalt, nickel, titanium(IV), arsenic(III), molybdenum(VI), chromium(III), manganese(II), zinc and selenium(IV); 30-fold bismuth; 20-fold silver, tin(IV) and mercury; 10-fold antimony(III), indium and lead. It should be

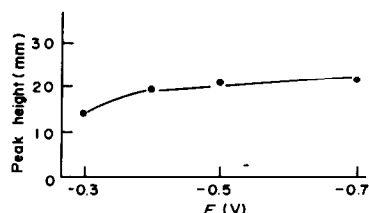


Fig. 3. Dependence of anodic-stripping peak height on the deposition potential in $0.36\text{ N H}_2\text{SO}_4\text{--}50\text{ ppm Et}_4\text{NI}$ medium. $\text{Cd(II)} = 1\text{ ng/ml}$, ($t_{\text{dep}} = 1\text{ min}$).

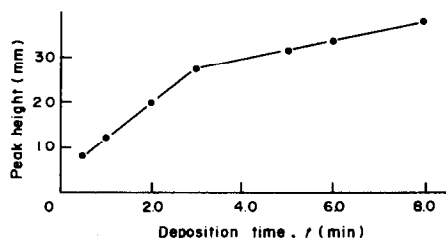


Fig. 4. Dependence of anodic-stripping peak heights on deposition time in $0.36\text{ N H}_2\text{SO}_4\text{--}50\text{ ppm Et}_4\text{NI}$ medium. $\text{Cd(II)} = 5\text{ ng/ml}$, ($E_{\text{dep}} = -0.6\text{ V}$).

noted that selenium has an interesting influence on the cadmium peak. A 100-ng/ml concentration of selenium(IV) diminishes the stripping peak for lead at the 2-ng/ml level and a peak potential of -0.14 V, but a 200-ng/ml level of selenium(IV) does not interfere with the stripping peak for cadmium; even a 300-ng/ml concentration of selenium only reduces the cadmium peak height by 25%. Therefore lead interference with the cadmium peak can be reduced by adding a suitable amount of selenium(IV) to the test solution. For example, the cadmium in tap water can only be determined correctly after addition of a suitable amount of selenium(IV) to the sample solution (Fig. 5). The appropriate amount of selenium(IV) to add can be found from Fig. 6. The peak height for cadmium is not affected by over 100 times as much lead in the presence of selenium(IV) when anodic-stripping voltammetry is used in the second-derivative mode. For such determinations it is therefore preferable to add 60 ng of selenium per ml to all sample and standard solutions.

Calibration

Calibration curves for cadmium under the conditions described are linear over the concentration range 0.05–10 ng/ml. It has been found that calibration curves based on the peak-heights measured in

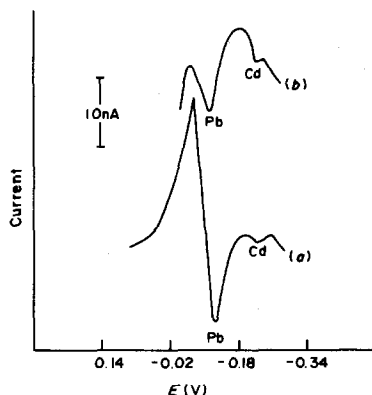


Fig. 5. Anodic-stripping voltammetric curves of cadmium in tap water. (a) Tap water, (b) tap water + 50 ng/ml Se(IV).

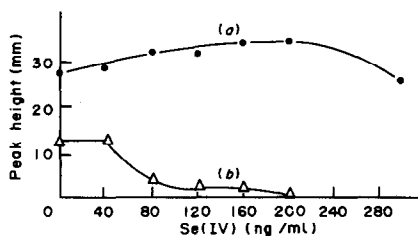


Fig. 6. Influence of selenium(IV) on peak heights of cadmium and lead. (a) Cd(II) = 2 ng/ml, (b) Pb(II) = 2 ng/ml, ($E_{\text{dep}} = -0.6$ V, $t_{\text{dep}} = 1$ min).

Table 1. Recovery tests

Sample	Cd(II) added, ng/ml	Cd(II) found, ng/ml	Recovery, %
Tap water	0.50	0.52	104
River water	1.0	1.1	110
Waste water	2.5	2.3	92

Table 2. Results for cadmium determination in some water samples

Sample	Cd(II) content, ng/ml
Tap water	0.12 ± 0.01 (3)*
River water	0.48 ± 0.03 (3)
Waste water	1.1 ± 0.1 (3)

*Average \pm standard derivation (number of determination).

the first, second and third sweeps after one deposition are linear, both in the absence and in the presence of selenium, though the peaks became progressively smaller in later scans. Interestingly, the peak for lead becomes rapidly smaller in repeated scans, the effect being much more pronounced than it is for cadmium. Thus it is possible to determine small amounts of cadmium in the presence of much larger amounts of lead by measuring the height of the stripping peak in the second or third scan.

Recovery and application

A 10-ml sample of water, which had been acidified before use, was introduced into the electrolysis cell, the pH adjusted to 2–4 with 5% ammonia solution or 0.9N sulphuric acid, then 0.05 ml of 10-mg/ml Et_4NI solution and 0.06 ml of 10- $\mu\text{g/ml}$ selenium(IV) solution were added. Deposition was performed for a set time, with stirring, then after a 15-sec pause the voltamperogram was recorded. Calibration was done by the standard-addition method. The recoveries were 92–110% (Table 1). The analytical results obtained are listed in Table 2. With this method it is possible to determine cadmium in domestic tap water and in some natural waters.

REFERENCES

1. Cui Chunguo, *Huanjing Kexue Congkan*, 1980, 1, 56.
2. G. Forsberg, J. W. O'Laughlin, R. G. Megargle and S. R. Koertyonn, *Anal. Chem.*, 1975, 47, 1586.
3. Cui Chunguo, *Huanjing Kexue*, 1982, 4, 13.
4. T. W. Hamilton and J. Ellis, *Anal. Chim. Acta*, 1979, 110, 87.
5. L. Sipos, J. Golimowski, P. Valenta and H. W. Nürnberg, *Z. Anal. Chem.*, 1979, 298, 1.
6. M. M. Nicholson, *Anal. Chem.*, 1960, 32, 1058.
7. Deng Jiaqi, Zhang Quingyuan, and Wang Zhaizhong, *Huaxue Xuebao*, 1982, 2, 151.
8. Cui Chunguo and Zhang Yulann, *Huanjing Huaxue*, 1982, 5, 392.

ANALYSIS OF EQUILIBRIUM IN HEME MODEL SYSTEMS, BY A SUCCESSIVE LINEAR REGRESSION METHOD

LUIZ A. MORINO and HENRIQUE E. TOMA

Instituto de Química, Universidade de São Paulo, C.P. 20780, São Paulo, SP, Brasil

(Received 19 August 1983. Accepted 5 September 1983)

Summary—A method for determination of equilibrium constants in heme model systems is proposed, based on successive linear regression applied to spectrophotometric titrations. The method is illustrated for bis(dimethylglyoximate) iron(II) complexes with pyridine and 4-cyanopyridine ligands.

In this work we describe a convenient approach for dealing with successive equilibria, based on a simple computational method adapted for spectrophotometric titrations. As a matter of interest, we have chosen typical iron(II)-glyoximate complexes, because of their importance as models for the heme group.^{1,2} These complexes are usually stabilized in the presence of axial bases, such as N₂H₄, py and imidazole, forming Fe(Hdmg)₂(base)₂ adducts. Mixed complexes of the type Fe(Hdmg)₂XY are also known, especially with contrasting X and Y ligands, such as N₂H₄ and CO. When the bases are chemically similar, the mixed complexes are formed in equilibrium with the pure species. Their characterization requires a detailed analysis of the equilibrium reactions involved in the system.

EXPERIMENTAL

Reagents

Iron(II) acetate was prepared by reacting iron powder (Carlo Erba) with glacial acetic acid (Merck) under argon. Pyridine (Carlo Erba), 4-cyanopyridine (Aldrich), dimethylglyoxime (Carlo Erba) and chloroform (Merck) were used as supplied.

Fe(Hdmg)₂(CNpy)₂ and Fe(Hdmg)₂(py)₂ were synthesized from iron(II) acetate and the corresponding ligands, by the method of Pang and Stynes.³ C₁₈H₂₄N₆O₄Fe requires C 48.66%, N 18.92%, H 5.90%; analysis gave C 48.6%, N 19.1%, H 5.4%. C₂₀H₂₂N₈O₄Fe requires C 48.60%, N 22.67%, H 4.49%; analysis gave C 48.4%, N 22.8%, H 4.5%.

Measurements

The electronic spectra of the complexes were recorded on a Cary 17 spectrophotometer fitted with constant-temperature cell compartments. The titration cell consisted of a conventional rectangular cuvette directly attached to a 10-ml cylindrical reservoir. The complexes and reagents were transferred under an argon atmosphere by syringe techniques. The measurements were made in duplicate, after 10–15 min, to ensure complete equilibration of the system.

Calculations

The procedure employed for the evaluation of equilibrium constants is described in the next section. The data used for computational analysis were selected from the experimental plots of measured molar absorptivities *vs.* ligand concentration. The calculations were done on a Burroughs B6900 computer.

RESULTS AND DISCUSSION

The measured absorptivity of a system involving a series of successive equilibria, equation (1), can be expressed by equation (2).



$$\epsilon_i = \frac{\epsilon_0 + \epsilon_1\beta_1X + \epsilon_2\beta_2X^2 + \dots + \epsilon_n\beta_nX^n}{1 + \beta_1X + \beta_2X^2 + \dots + \beta_nX^n} \quad (2)$$

In equation (2) the subscript zero refers to the starting complex, and $X = [B]/[A]$. It is assumed that the ligands A^{*} and B do not absorb at the wavelengths employed for the measurements. When A is the solvent, the concentration of B should replace X in equation (2).

There are several methods^{4,5} dealing with the evaluation of the equilibrium constants and molar absorptivities from equation (2). An extensive review has already been made by McBryde⁶ and will be omitted from this paper. One of the problems associated with the methods available is the error introduced by using successive extrapolations. To overcome this problem, we have modified equation (2) in the following way:

$$H_i = \frac{(\epsilon_i - \epsilon_0) - \sum_{j=1}^{n-2} (\epsilon_j - \epsilon_i)\beta_jX^j}{(\epsilon_n - \epsilon_i)X^{n-1}} = \frac{(\epsilon_{n-1} - \epsilon_i)}{(\epsilon_n - \epsilon_i)}\beta_{n-1} + \beta_nX \quad (3)$$

In equation (3), $j = 1, 2, \dots, n-2$, and the other terms have the conventional meaning. Starting with previously known ϵ_0 , ϵ_n , ϵ_j and β_j parameters, it is possible to evaluate ϵ_{n-1} , β_{n-1} and β_n by linear regression analysis. As a matter of fact the linear dependence between H_i and X in equation (3) provides a means of finding ϵ_{n-1} . By assuming an initial value of ϵ_{n-1} and varying it successively in a series of linear regression analyses, we can find the point of maximum correlation. This point leads to the opti-

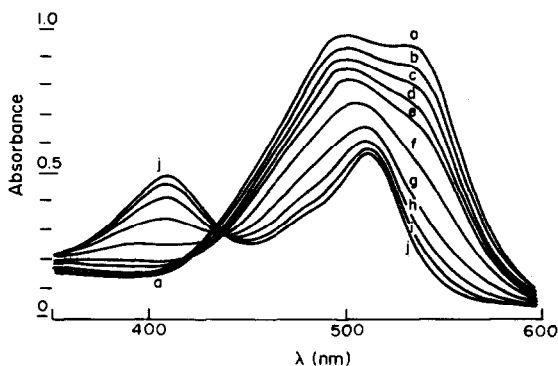
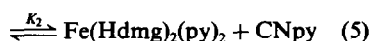
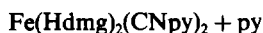


Fig. 1. Spectrophotometric titration of $\text{Fe}(\text{Hdmg})_2(\text{CNpy})_2$ ($6.32 \times 10^{-5} M$) (spectrum a) with pyridine (0.150–143.0 mM) (spectra b–j), in the presence of 4-cyanopyridine (8.36 mM), in chloroform solution, at 25° , argon atmosphere.

imum parameters, minimizing simultaneously the errors for β_{n-1} and β_n . The computational work is quite simple, and can be performed even with small pocket computers.

Using this method, we have investigated the equilibrium reactions of the *trans*-bis(4-cyanopyridine)bis(dimethylglyoximate)iron(II) complex, in the presence of pyridine, in chloroform solutions:



Typical spectral changes observed for this system are shown in Fig. 1. A large excess of 4-cyanopyridine and pyridine relative to the iron(II) complex was used to make the free ligand concentrations practically identical to the total concentrations.

The variation of the correlation coefficient, and of the standard deviations of β_1 and β_2 , as a function of ϵ_1 , is shown in Fig. 2. The best correlation was found at $\epsilon_1 = 5.4 \times 10^3 \text{ l. mole}^{-1} \cdot \text{cm}^{-1}$, coinciding

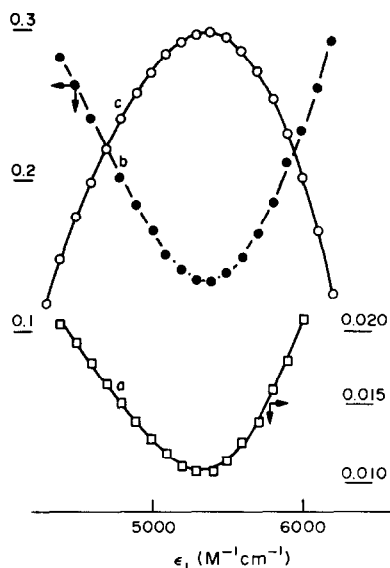


Fig. 2. Variation of the standard deviation of (a) β_2 , (b) β_1 and (c) the correlation coefficient as a function of ϵ_1 (535 nm), based on equation (3).

with the minimum on the standard deviation curves for β_1 and β_2 . The optimum parameters are collected in Table 1.

When a computer is not available, ϵ_{n-1} , β_{n-1} and β_n can be calculated by a graphical procedure. By plotting the left-hand side of equation (3) against X , we obtain from the intercept:

$$\lim_{X \rightarrow 0} H_i = \frac{(\epsilon_{n-1} - \epsilon_0)\beta_{n-1}}{\epsilon_n - \epsilon_0} = I \quad (6)$$

Combining equations (6) and (3) gives

$$\frac{H_i}{X} - \frac{I(\epsilon_n - \epsilon_0)}{(\epsilon_n - \epsilon_i)X} = \beta_n + \beta_{n-1} \frac{(\epsilon_0 - \epsilon_i)}{(\epsilon_n - \epsilon_i)X} \quad (7)$$

The equilibrium constants β_n and β_{n-1} are obtained from the linear plots of the left-hand side of equation (7) against $(\epsilon_0 - \epsilon_i)/(\epsilon_n - \epsilon_i)X$. Substitution of β_{n-1} into equation (6) leads to ϵ_{n-1} . The results calculated in this way for the dimethylglyoximate complexes can also be seen in Table 1. There is a reasonable

Table 1. Equilibrium constants of substitution in $\text{Fe}(\text{Hdmg})_2(\text{CNpy})_2$ by pyridine*

Method	$K_1 (\pm \delta)$	$K_2 (\pm \delta)$	ϵ_1, \S $10^3 \text{ l. mole}^{-1} \cdot \text{cm}^{-1}$
Iterative†	7.32 (0.01)	0.36 (0.02)	5.40
Graphical‡	7.4 (0.3)	0.4 (0.2)	5.7
Yatsimirskii¶	8 (3)	0.2 (0.3)	6.4

*In CHCl_3 , at 25° , argon atmosphere.

†Based on equation (3), including refinement cycles for free ligand concentration.

‡Based on equation (7).

§Molar absorptivity of the mixed complex at 535 nm; $\epsilon_0 = 1.47 \times 10^4$ and $\epsilon_2 = 3.53 \times 10^3 \text{ l. mole}^{-1} \cdot \text{cm}^{-1}$.

¶Method described in reference 8.

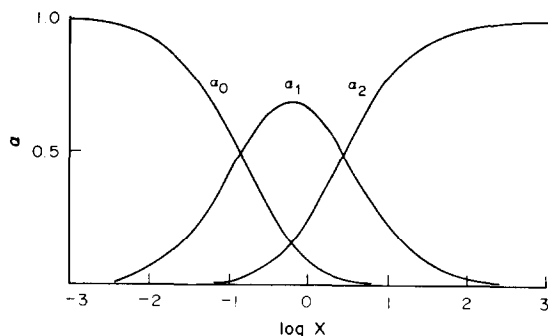


Fig. 3. Distribution coefficients for the $\text{Fe}(\text{Hdmg})_2(\text{CNpy})_2$, $\text{Fe}(\text{Hdmg})_2(\text{CNpy})(\text{py})$ and $\text{Fe}(\text{Hdmg})_2(\text{py})_2$ complexes, vs. $\log [\text{py}]/[\text{CNpy}] (=X)$.

agreement with the optimum values based on the computational analysis.

Equation (7) is also suitable for linear regression. Starting with an estimate of I , the point of maximum correlation can be easily determined, yielding the optimized equilibrium constants.

The distribution plots for the dimethylglyoximate complexes are shown in Fig. 3. The fact that K_1 is 20 times K_2 indicates a strong *trans* influence (in addition to the statistical effect), preferentially stabilizing the mixed $(\text{CNpy})\text{Fe}(\text{Hdmg})_2(\text{py})$ complex. It is consistent with the observed tendency for the heme group to bind contrasting axial ligands, such as imidazole and CO, or imidazole and thioether residues of amino-acids (e.g.,⁵ in cytochrome-c).

As shown in Table 1, the method gives accurate results. It is ideal for a system with two successive equilibria, as for the complexes investigated here. In a system with three equilibria, K_1 and ϵ_1 should be previously determined, by working, for instance, with a large excess of the metal ion relative to the ligands. Like other methods based on equation (2), the actual free ligand concentrations are now known. Refinement cycles, starting with the total concentrations, might be necessary, until self-consistency is achieved.

Acknowledgement—A fellowship from FAPESP is gratefully acknowledged.

REFERENCES

1. B. A. Jillot and R. J. P. Williams, *J. Chem. Soc.*, 1958, 462.
2. L. Vaska and T. Yamaji, *J. Am. Chem. Soc.*, 1971, **93**, 6673.
3. I. W. Pang and D. V. Stynes, *Inorg. Chem.*, 1977, **16**, 590.
4. F. J. C. Rossotti and H. S. Rossotti, *The Determination of Stability Constants*, McGraw-Hill, New York, 1961.
5. M. T. Beck, *Chemistry of Complex Equilibria*, Van Nostrand-Reinhold, London, 1970.
6. W. A. E. McBryde, *Talanta*, 1974, **31**, 979.
7. R. E. Dickerson and R. Timkovich, *The Enzymes*, P. Boyer (ed.), Vol. XI, Chap. 7, p. 397. Academic Press, New York, 1975.
8. K. B. Yatsimirskii, *Zh. Neorgan. Khim.*, 1956, **1**, 2306.

ANALYTICAL DATA

EFFECT OF pH ON CHROMIUM(VI) SPECIES IN SOLUTION

R. K. TANDON,* P. T. CRISP and J. ELLIS

Department of Chemistry, University of Wollongong, Wollongong, N.S.W. 2500, Australia

R. S. BAKER

Cell Biology Laboratory, Commonwealth Institute of Health, University of Sydney,
 N.S.W. 2006, Australia

(Received 14 October 1983. Accepted 28 October 1983)

Summary—Published values of equilibrium constants were used to calculate the percentage of each chromium(VI) species (CrO_4^{2-} , $\text{Cr}_2\text{O}_7^{2-}$, HCrO_4^- and H_2CrO_4) present in aqueous solution at total chromium(VI) concentrations of 10^{-2} – $10^{-6}M$ in the pH range 1–8.

The analytical chemistry of chromium(VI) has been described extensively in the literature¹⁻³ but no tabulation of the abundance of chromium(VI) species at different pH values and metal concentrations has been published apart from a brief account of the $\text{HCrO}_4^-/\text{CrO}_4^{2-}$ equilibrium. Such data are essential for studies of environmental chromium speciation. Chromium(VI) may be present in aqueous solution as chromate (CrO_4^{2-}), dichromate ($\text{Cr}_2\text{O}_7^{2-}$), hydrogen chromate (HCrO_4^-), dihydrogen chromate (chromic acid, H_2CrO_4), hydrogen dichromate (HCr_2O_7^-), trichromate ($\text{Cr}_3\text{O}_{10}^{2-}$) and tetrachromate ($\text{Cr}_4\text{O}_{13}^{2-}$). The last three ions have been detected only in solutions of $\text{pH} < 0$ or at chromium(VI) concentrations greater than $1M$.²⁻⁴ Polyanions containing > 4 chromium atoms are not known, and probably do not exist, on account of chromium–oxygen multiple bonding.⁴ Three pH regions may be distinguished for chromium(VI) species: (i) $\text{pH} \leq 0$, where H_2CrO_4 is a significant species, (ii) $\text{pH} = 2$ – 6 , where HCrO_4^- and $\text{Cr}_2\text{O}_7^{2-}$ occur together, and (iii) $\text{pH} > 6$, where CrO_4^{2-} predominates.

The published values of the chromium(VI) equilibrium constants used in the calculations in this paper are given in Table 1. Contributions from

HCr_2O_7^- , $\text{Cr}_3\text{O}_{10}^{2-}$ and $\text{Cr}_4\text{O}_{13}^{2-}$ are negligible at $\text{pH} > 1$ and at chromium(VI) concentrations $\leq 10^{-2}M$. The concentration of H_2CrO_4 (x) in a solution of pH p and total chromium(VI) concentration C was obtained by solving the quadratic equation

$$x + \frac{k_1x}{p} + \frac{k_1k_2x}{p^2} + \frac{k_3k_1^2x^2}{p^2} - C = 0$$

The concentrations of the other chromium(VI) species were obtained from

$$\begin{aligned} [\text{HCrO}_4^-] &= k_1x/p \\ [\text{CrO}_4^{2-}] &= k_1k_2x/p^2 \\ [\text{Cr}_2\text{O}_7^{2-}] &= k_3k_1^2x^2/p^2 \end{aligned}$$

The equations were solved on a Univac 1100 computer by using a Fortran program (available on request from the authors).

RESULTS AND DISCUSSION

Results obtained by using $k_3 = 98$ are given in Table 2. This value of k_3 was determined at an ionic strength (μ) of unity.⁷ If a value of $k_3 = 35.5$ ($\mu = 0$) is used, the dichromate concentrations are approximately half those given in Table 2 and the concentrations of the other species are correspondingly greater. The results in Table 2 are consistent with

*Author for correspondence.

Table 1. Published values of equilibrium constants

Equilibrium	Ionic strength, M	Equilibrium constant (at 25°C)	Reference
$\text{H}_2\text{CrO}_4 \rightleftharpoons \text{H}^+ + \text{HCrO}_4^-$	~0.16	$k_1 = 0.18$	4-6
$\text{HCrO}_4^- \rightleftharpoons \text{H}^+ + \text{CrO}_4^{2-}$	0.33-0.63	$k_2 = 3.2 \times 10^{-7}$	6
$2\text{HCrO}_4^- \rightleftharpoons \text{Cr}_2\text{O}_7^{2-} + \text{H}_2\text{O}$	< 0.022	$k_3 = 33.3$	8
	1	$k_3 = 98$	7
	0	$k_3 = 35.5$	7

Table 2. Calculated abundances of chromium(VI) species in aqueous solution at pH 1-8 and total chromium(VI) concentrations (C) in the range 10^{-2} - 10^{-6} M.

pH	C, M	Abundance, %			
		CrO ₄ ²⁻	Cr ₂ O ₇ ²⁻	HCrO ₄ ⁻	H ₂ CrO ₄
1	10 ⁻²	0.0	23.6	49.1	27.3
	10 ⁻³	0.0	3.7	61.9	34.4
	10 ⁻⁴	0.0	0.4	64.0	35.6
	10 ⁻⁵	0.0	0.0	64.3	35.7
	10 ⁻⁶	0.0	0.0	64.3	35.7
2	10 ⁻²	0.0	36.0	60.6	3.4
	10 ⁻³	0.0	7.5	87.6	4.8
	10 ⁻⁴	0.0	1.0	94.0	5.0
	10 ⁻⁵	0.0	0.0	95.0	5.0
	10 ⁻⁶	0.0	0.0	95.0	5.0
3	10 ⁻²	0.0	37.7	62.0	0.3
	10 ⁻³	0.0	8.2	91.3	0.5
	10 ⁻⁴	0.0	1.0	98.5	0.5
	10 ⁻⁵	0.0	0.1	99.3	0.6
	10 ⁻⁶	0.0	0.0	99.4	0.6
4	10 ⁻²	0.2	37.7	62.1	0.0
	10 ⁻³	0.3	8.2	91.5	0.0
	10 ⁻⁴	0.3	1.0	98.7	0.0
	10 ⁻⁵	0.3	0.4	99.3	0.0
	10 ⁻⁶	0.3	0.1	99.6	0.0
5	10 ⁻²	2.0	36.7	61.3	0.0
	10 ⁻³	2.9	7.8	89.3	0.0
	10 ⁻⁴	3.0	1.0	96.0	0.0
	10 ⁻⁵	3.1	0.1	96.8	0.0
	10 ⁻⁶	3.1	0.0	96.9	0.0
6	10 ⁻²	17.3	28.6	54.1	0.0
	10 ⁻³	23.0	5.0	72.0	0.0
	10 ⁻⁴	24.0	0.7	75.3	0.0
	10 ⁻⁵	24.2	0.1	75.7	0.0
	10 ⁻⁶	24.2	0.0	75.8	0.0
7	10 ⁻²	72.4	5.0	22.6	0.0
	10 ⁻³	75.8	0.6	23.6	0.0
	10 ⁻⁴	76.2	0.0	23.8	0.0
	10 ⁻⁵	76.2	0.0	23.8	0.0
	10 ⁻⁶	76.2	0.0	23.8	0.0
8	10 ⁻²	96.9	0.1	3.0	0.0
	10 ⁻³	97.0	0.0	3.0	0.0
	10 ⁻⁴	97.0	0.0	3.0	0.0
	10 ⁻⁵	97.0	0.0	3.0	0.0
	10 ⁻⁶	97.0	0.0	3.0	0.0

qualitative and quantitative descriptions of the chromium(VI) system by other authors^{1-4,9} and indicate that at neutral pH the principal species in solution are CrO₄²⁻ (80%) and HCrO₄⁻ (20%).

Acknowledgements—The authors wish to thank Dr. E. von Nagy-Felsobuki for assistance in writing the Fortran program and gratefully acknowledge the information provided by Dr. E. C. Martin, now retired and formerly of the Department of Chemistry, University of New South Wales, Sydney. The work was part of a metal mutagenicity testing project funded by the Australian Welding Research Association, under Contract 90.

REFERENCES

1. M. S. Cresser and R. Hargitt, *Talanta*, 1976, **23**, 153.
2. J. J. Lingane, *Analytical Chemistry of Selected Metallic Elements*, Reinhold, New York, 1966.
3. J. K. Beattie and G. P. Haight, Jr., *Prog. Inorg. Chem.*, 1972, **17**, 93.
4. F. A. Cotton and G. Wilkinson, *Advanced Inorganic Chemistry*, pp. 841-842. Wiley, New York, 1972.
5. H. Freiser and Q. Fernando, *Ionic Equilibria in Analytical Chemistry*, pp. 296-297. Wiley, New York, 1966.
6. J. D. Neuss and W. Rieman, *J. Am. Chem. Soc.*, 1934, **56**, 2238.
7. J. Y. Tong and E. L. King, *ibid.*, 1953, **75**, 6180.
8. W. G. Davies and J. E. Prue, *Trans. Faraday Soc.*, 1955, **51**, 1045.
9. I. M. Kolthoff, E. B. Sandell, E. J. Meehan and S. Bruckenstein, *Quantitative Chemical Analysis*, 4th Ed., pp. 1053-1054. Macmillan, London, 1969.

ANNOTATION

SEPARATION ET IDENTIFICATION DES PRODUITS D'HYDROLYSE DE LA TETRYZOLINE

A. NICOLAS et M. MIRJOLET

Laboratoire de Chimie Analytique et Bromatologie, Faculté des Sciences Pharmaceutiques et Biologiques,
5 rue Albert Lebrun, 54001 Nancy, B.P. 403, France

J. M. ZIEGLER

Service Commun de Spectrométrie de Masse de l'Université de Nancy I, 54001 Nancy, France

(Reçu le 15 février 1983. Révisé le 4 juillet 1983. Accepté le 9 septembre 1983)

Résumé—On propose un schéma de dégradation de la tétryzoline [(tétrahydro-1,2,3,4 naphthyl-1)-2 Δ_2 -imidazoline] après avoir soumis cette molécule à des réactions d'hydrolyse en milieu alcalin et acide. Les composés intermédiaires ont été isolés, purifiés et identifiés par les techniques modernes d'analyse. L'utilisation de la spectrométrie de masse a permis d'établir leur structure. Après ouverture du cycle imidazoline en milieu alcalin, l'hydrolyse acide conduit à la perte de la chaîne latérale précédemment obtenue et à l'obtention d'acide tétrahydro-1,2,3,4 naphthoïque-1 et d'éthylènediamine.

La tétryzoline, [(tétrahydro-1,2,3,4 naphthyl-1)-2 Δ_2 -imidazoline], est une molécule à propriétés vasoconstrictrices entrant dans la composition de plusieurs spécialités pharmaceutiques et dont le schéma de dégradation n'a pas été décrit à ce jour. Cependant, d'autres imidazolines ont fait l'objet d'études de stabilité: naphazoline,¹⁻³ indanazoline,⁴ tolazoline.⁵ Dans tous les cas, la première étape de dégradation conduit à une amide substituée, qui est ultérieurement hydrolysée en acide aromatique et en éthylènediamine. La tétryzoline n'étant pas fondamentalement différente de ces imidazolines par sa structure chimique (Fig. 1), son schéma de dégradation doit être voisin. Nous nous proposons de le vérifier en isolant les produits intermédiaires et en déterminant leur structure par les techniques spectroscopiques habituelles.

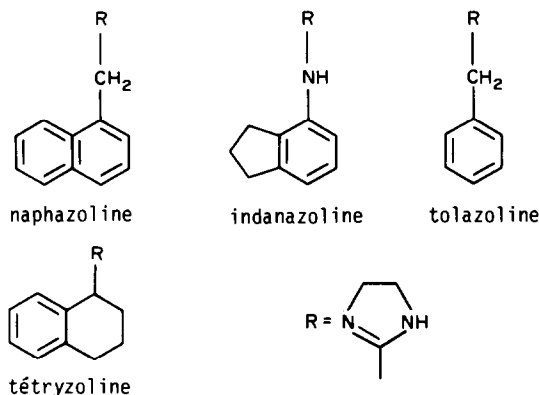


Fig. 1. Structure chimique des imidazolines.

PARTIE EXPERIMENTALE

Méthodes

Chromatographie en couche mince. Elle est réalisée sur des plaques de silice type 60 F 254 (Merck). Le solvant est un mélange ammoniacque 25%-eau-éthanol (5:15:80 v/v). La révélation est effectuée soit par le rayonnement ultra-violet à 254 nm, soit par pulvérisation d'une solution de ninhydrine à 1% dans de l'éthanol.

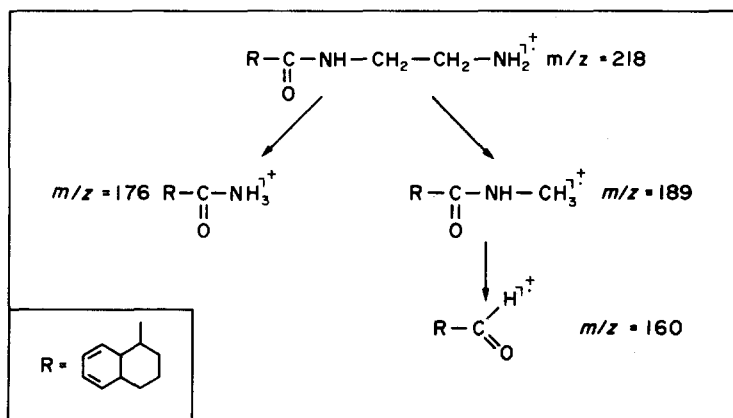
Chromatographie en phase gazeuse. L'appareil utilisé est de marque Girdel série 30. La colonne de verre est remplie de phase OV₁ 3% sur Chromosorb Q (100-120 mesh). Le détecteur est à ionisation de flamme. Les conditions de température sont fixées à 180° pour le four, 240° pour l'injecteur et le détecteur. Le débit d'azote est de 25 ml/min.

Spectroscopie infra-rouge. Les spectres sont réalisés avec un appareil Beckman type Acculab IV. Les composés sont analysés à la concentration de 1% sous forme de pastilles de bromure de potassium.

Spectrométrie de masse. Les spectres de masse sont obtenus par introduction directe sur un appareil LKB 2091 avec les conditions opératoires suivantes: énergie d'ionisation par impact électronique 70 eV; potentiel d'accélération 3,5 kV; température de la source 280°; courant "trap" 50 μ A.

Obtention du produit d'hydrolyse alcaline de la tétryzoline. Le chlorhydrate de tétryzoline (1,18 g, 5 mmole) est chauffé à reflux et à l'ébullition sous agitation magnétique pendant 1 hr en présence de 50 ml de soude 1N. Après refroidissement, le produit est extrait successivement par deux fois 20 ml de chloroforme. Les phases organiques sont séchées par du sulfate de sodium anhydre, filtrées et évaporées sous pression réduite. Le produit (P₁) est blanc, visqueux et cristallise progressivement (Tf = 81-82°).

Obtention du produit d'hydrolyse acide du composé P₁. Composé P₁ (0,5 g) est chauffé à reflux en présence de 25 ml d'acide chlorhydrique 2M pendant 20 hr. Après refroidissement et alcalinisation par de la lessive de soude, le milieu est extrait par deux fois 20 ml de chloroforme afin d'éliminer les composés neutres et basiques éventuellement présents. Après acidification de la phase aqueuse par l'acide

Fig. 2. Schéma de fragmentation du composé P₁.

chlorhydrique concentré, les composés sont extraits par deux fois 20 ml de chloroforme. Les phases organiques sont réunies, séchées par du sulfate de sodium anhydre, filtrées et évaporées sous pression réduite. Le résidu cristallise sous forme de cristaux blancs (P₂) de point de fusion voisin de 79–81°.

RESULTATS ET DISCUSSION

Analyses chromatographiques

Le composé P₁ présente les caractéristiques d'un produit pur aussi bien en chromatographie en couche mince ($R_f = 0,61$) qu'en chromatographie en phase

gazeuse ($t_r = 3$ min). Dans chacune de ces analyses, on ne retrouve pas la tétryzoline ($R_f = 0,33$ et $t_r = 2$ min). De plus, le composé P₁ est révétable par la ninhydrine, ce qui indique la présence d'un groupement amine primaire.

Le composé P₂ est obtenu à partir de P₁ par hydrolyse acide. Le temps de réaction a été déterminé en suivant la disparition de P₁ par chromatographie en phase gazeuse. En chromatographie en couche mince, le composé P₂ présente un R_f de 0,71. Il est révétable uniquement par le rayonnement ultra-violet.

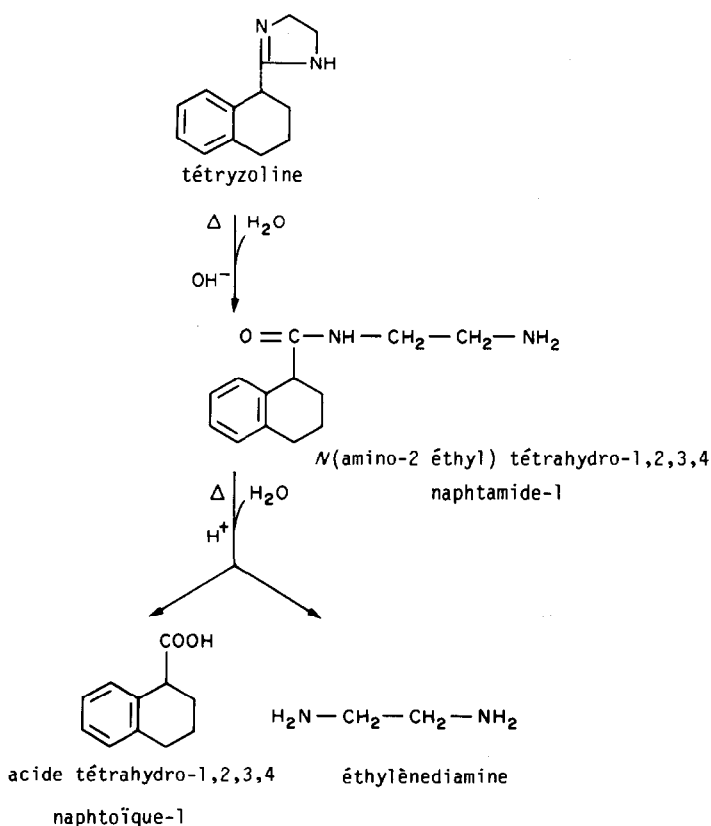


Fig. 3. Schéma de dégradation de la tétryzoline.

Analyses par spectrométrie infra-rouge

Le spectre infra-rouge du composé P₁ présente les bandes caractéristiques d'un groupement amide: bande CO à 1640 cm⁻¹ et bandes NH à 3280 cm⁻¹ et 1540 cm⁻¹. Par contre, le spectre du composé P₂ présente uniquement les bandes caractéristiques d'un groupement carboxyle à 1680 cm⁻¹ et 2930–3100 cm⁻¹.

Analyses par spectrométrie de masse

L'emploi d'un spectromètre de masse à secteur magnétique met en évidence un certain nombre d'ions dits "métastables". Ce type d'ions permet de suivre directement l'ordre de certaines fragmentations grâce à la relation $m^* = m_2^2/m_1$ dans laquelle m^* est la position en u.m.a. de l'ion métastable, m_1 celle de l'ion père et m_2 celle de l'ion fils. L'étude analytique de Porter et Baldas sur les imidazolines nous donne également de précieuses indications.⁶

Spectre de masse de la tétryzoline. Il présente un pic moléculaire qui est aussi pic de base à $m/z = 200$. L'ion à $m/z = 185$ résulte très certainement de la perte d'un groupement (CH₂ + H)* d'un noyau imidazoline tandis que l'ion à $m/z = 171$ provient de l'ion moléculaire par perte du fragment CH₂ = NH (ion métastable à $m/z = 147$). L'ion à $m/z = 131$ résulte de la perte du cycle imidazoline et le pic à $m/z = 91$ (ion tropylium) est le résultat de la rupture du cycle tétrahydronaphtalénique.

Spectre de masse du composé P₁. Il présente un pic moléculaire à $m/z = 218$. Le fragment à $m/z = 189$ provient de l'ion moléculaire par perte d'un fragment CH₂ = NH (ion métastable à $m/z = 164$). De même le pic à $m/z = 176$ a pour précurseur le pic à $m/z = 218$ par perte d'un fragment de masse 42 (ion métastable à $m/z = 141$). Le pic à $m/z = 189$ est lui-même précurseur de l'ion à $m/z = 160$ (ion métastable à $m/z = 135,5$). Le pic de base à $m/z = 131$ correspond à la perte de la totalité de la chaîne latérale. Ces observations permettent de considérer le composé P₁ comme résultant de l'addition d'une molécule d'eau après ouverture du cycle imidazoline pour donner l'amide correspondante. Le schéma de fragmentation proposé est représenté à Fig. 2.

Spectre de masse du composé P₂. Le pic moléculaire est situé à $m/z = 176$ et correspond à l'acide tétrahydro-1,2,3,4 naphthoïque-1. Le pic de base à $m/z = 131$ résulte de la perte du groupement carboxylique pour obtenir comme précédemment le noyau tétrahydronaphtalénique.

Proposition d'un schéma de dégradation

Considérant les résultats des analyses spectrales pratiquées, les composés P₁ et P₂ peuvent être dénommés respectivement la N (amino-2 éthyl) tétrahydro-1,2,3,4 naphthamide-1 et l'acide tétrahydro-1,2,3,4 naphthoïque-1. Le schéma de dégradation logique proposé est représenté à Fig. 3.

CONCLUSION

Plusieurs imidazolines ont fait l'objet d'études concernant leur mode de dégradation.¹⁻⁵ Cependant, la structure des composés n'avait pas été clairement établie et il s'agissait surtout de la teneur en imidazoline soit par colorimétrie,³ soit par chromatographie liquide haute pression.⁴ Seul, Schwartz *et al.*² ont séparé les produits acides et basiques résultant de l'hydrolyse. Ils ont déterminé leur composition centésimale et ont étudié leur spectre d'absorption dans l'ultra-violet.

L'étude que nous avons menée sur la tétryzoline apporte les éléments d'analyse structurale nécessaires à caractériser sans ambiguïté les produits formés. Elle montre également que l'originalité structurale de la tétryzoline—absence de pont entre les noyaux tétrahydronaphtalénique et imidazoline—ne conduit pas à un schéma particulier de dégradation.

LITTÉRATURE

1. K. Miescher, A. Marxer et E. Urech, *Helv. Chim. Acta*, 1951, **34**, 1.
2. M. A. Schwartz, R. Kuramoto et L. Malspeis, *J. Am. Pharm. Assoc. Sci. Ed.*, 1956, **45**, 814.
3. M. J. Stern, L. D. King et A. D. Marcus, *ibid.*, 1959, **47**, 641.
4. H. J. Dechow, K. Lammerhirt, C. H. Pich et M. Schikarski, *Arzneim. Forsch.*, 1980, **30**, 1738.
5. D. Kottke, *Zentralbl. Pharm.*, 1978, **117**, 918.
6. Q. N. Porter et J. Baldas, *Mass Spectrometry of Heterocyclic Compounds*, Wiley-Interscience, New York, 1971.

Summary—The products of hydrolysis of tetrahydrozoline [2-(1,2,3,4-tetrahydro-1-naphthyl)-2-imidazoline] have been isolated by thin-layer chromatography and identified by ultraviolet and infrared spectroscopic analysis. Their structure has been well established by use of mass spectrometry and a degradation scheme advanced. Alkaline hydrolysis opens the imidazoline ring to give an amide compound which undergoes further hydrolysis, in acid solution, to 1,2,3,4-tetrahydronaphthoic acid and ethylenediamine.

LETTER TO THE EDITOR

THE SPECTROPHOTOMETRIC EVALUATION OF ACIDITY CONSTANTS:
 THE DOUBLE INCOMPLETE COLOUR CHANGE

SIR,

On the basis of the indirect colorimetric methods described by Sacconi,¹ Ingman² formulated various equations applicable in cases in which the molar absorptivity of one or both of the limiting forms of an acceptor-donor system, e.g., \mathcal{E}_{HR} and \mathcal{E}_R of an acid-base conjugate pair HR/R, is unknown. There is a point in this paper which deserves attention.

Linear equations in four terms and three unknowns³ can be used to evaluate the pK_a of a monoprotic acid:

$$\frac{[H]_i A_i}{K_a} - \frac{[H]_i \mathcal{E}_{HR}}{K_a} - \mathcal{E}_R = A_i$$

in which A_i is the absorbance of a solution containing a mixture of HR and R, and charges are omitted for simplicity. The results for any three solutions give, after an appropriate arrangement:

$$K_a = \frac{[H]_3 (A_3 - A_2) ([H]_1 - [H]_2) + [H]_1 (A_1 - A_2) ([H]_2 - [H]_3)}{(A_3 - A_2) ([H]_2 - [H]_1) + (A_1 - A_2) ([H]_3 - [H]_2)}$$

By dividing numerator and denominator of this equation by $[H]_1 (A_1 - A_2)$ and writing, as in Ingman's paper, $(A_3 - A_2)/(A_1 - A_2) = r''$, $[H]_1/[H]_2 = q_I$ and $[H]_3/[H]_2 = q_{II}$, we get:

$$K_a = \frac{q_{II} r'' (q_I - 1) + q_I (1 - q_{II})}{r'' (1 - q_I) + (q_{II} - 1)} [H]_2 \quad (1)$$

which is equivalent to the expression established by Ingman for the case that Sacconi called the double incomplete colour change.¹ An expression equivalent to (1) was deduced by Romain and Colleter.⁴ It means that the only restriction to be imposed on the absorbance and pH values selected for the evaluation of pK_a is that they differ enough to be accurately distinguishable. Likewise, for \mathcal{E}_{HR} and \mathcal{E}_R we obtain:

$$\mathcal{E}_{HR} = \frac{A_3 (q_{II} - 1) + A_1 r'' (1 - q_I)}{r'' (1 - q_I) + (q_{II} - 1)} \quad (2)$$

$$\mathcal{E}_R = \frac{q_{II} r'' (A_1 - A_2 q_I) + q_I (A_2 q_{II} - A_3)}{q_{II} r'' (1 - q_I) + q_I (q_{II} - 1)} \quad (3)$$

Equations (2) - (3) have not been reported so far by other workers. A program (input data pH_1 , A_1 , pH_2 , A_2 , pH_3 , A_3 ; output data, K_a , pK_a , ϵ_{HR} , ϵ_R ; 6 labels, 193 steps) for use with a Texas TI 58/59 pocket calculator and based on equations (1) - (3) has been devised and is available upon request to the authors.

REFERENCES

1. L. Sacconi, J. Phys. Coll. Chem., 1950, 54, 829.
2. F. Ingman, Talanta, 1973, 20, 993.
3. D.H. Rossenblatt, J. Phys. Chem., 1954, 58, 40.
4. P. Romain and J.C. Colleter, Compt. Rend., 1958, 247, 1456.

14 November 1983

A.G. ASUERO and M.J. NAVAS

Department of Bromatology, Toxicology
and Applied Chemical Analysis,
Faculty of Pharmacy,
The University of Seville,
Spain

D. ROSALES

Department of Analytical Chemistry,
Faculty of Chemistry,
The University of Seville,
Spain

SOLVENT EXTRACTION-SPECTROPHOTOMETRIC DETERMINATION OF PHOSPHATE WITH MOLYBDATE AND MALACHITE GREEN IN RIVER WATER AND SEA-WATER

SHOJI MOTOMIZU, TOSHIAKI WAKIMOTO and KYOJI TÔEI

Department of Chemistry, Faculty of Science, Okayama University, Tsushima-naka, Okayama-shi, Japan

(Received 23 June 1983. Revised 19 September 1983. Accepted 22 November 1983)

Summary—Molybdophosphate, formed between orthophosphate and molybdate in sulphuric acid solution, is extracted into a mixture of toluene and 4-methylpentan-2-one (1:3 v/v) with Malachite Green as counter-ion. A single extraction with equal phase volumes gives an apparent molar absorptivity for phosphate of 2.3×10^5 l.mole⁻¹.cm⁻¹ at 630 nm; the absorbance of the reagent blank is 0.03. With an organic to aqueous phase-volume ratio of 1:10, the molar absorptivity is 2.5×10^5 l.mole⁻¹.cm⁻¹ and the absorbance of the reagent blank 0.08. By the proposed method, ng/ml levels of phosphorus can be determined, and the detection limit is about 0.1 ng/ml. The standard deviation and relative standard deviation for the determination of phosphorus in tap water (4.3 ng/ml) are 0.05 ng/ml and 1.1%, respectively. The method can also be applied to the determination of phosphorus in river water and sea-water.

Most spectrophotometric methods for phosphate are based on the formation of a heteropoly acid with molybdate. The heteropoly acid formed can be extracted into an organic phase, as an ion-pair with a bulky cation such as a quaternary ammonium ion or cationic dye. Several studies on the solvent extraction of molybdophosphate with cationic dyes have already been reported.¹⁻⁶ The main advantage of cationic dyes over that of quaternary ammonium salts is their greater light-absorbing ability. We have already used Ethyl Violet as counter-ion for molybdophosphate.⁶ The spectrophotometric determination of phosphate by solvent extraction of molybdophosphate with Ethyl Violet is more sensitive than those previously reported¹⁻⁵ and less troublesome: a single extraction is adequate. However, in the determination of phosphorus at ng/ml levels in waters it has certain disadvantages. First, the absorbance of the reagent blank becomes too large for the concentration effect achieved by the solvent extraction to be of much use: for example, when 20 ml of sample solution and 5 ml of organic solvent were used, the absorbance of the reagent blank was 0.14. Secondly, the shaking time needed was long and the colour of the extract faded gradually if the shaking lasted more than 30 min. In the course of attempts to improve on this method, we noticed that Malachite Green gave a stable dark yellow species in 1.5*M* sulphuric acid (probably a protonated one), whereas Ethyl Violet became colourless within 30 min even in only 0.5*M* sulphuric acid.

Malachite Green has been used as the chromophore for the determination of phosphate in serum, plasma and urine⁷⁻¹⁵ and in water.¹⁶ Altman *et al.*¹⁷

reported the mechanism of the colorimetric reaction between molybdophosphate and Malachite Green. This dye has also been used in a flotation separation of molybdophosphate.¹⁸ However, it has been seldom used as the counter-ion for the extractive spectrophotometry of phosphate, because an ion-pair formed between Malachite Green and molybdophosphate has been considered less extractable than that formed by Safranin T or Crystal Violet.

In this work, we attempt to improve the extractability of the ion-pair formed between Malachite Green and molybdophosphate. Though the molar absorptivity obtained is about 10% less than that for the Ethyl Violet system, the method has several advantages: (1) the absorbance of the reagent blank is very small, and 20-fold concentration of phosphate by solvent extraction is possible, (2) the reagent solution, which consists of Malachite Green, molybdate and 1.5*M* sulphuric acid is stable at least for a month, (3) the method is less troublesome and shaking for 5 min is enough to complete the extraction, and (4) colour fading in the organic phase does not occur during shaking and standing.

EXPERIMENTAL

Apparatus

The absorptiometric measurements were made on a Hitachi EPS recording spectrophotometer and a Hitachi-Perkin-Elmer Model 139 spectrophotometer in glass cells of 10-mm path length. An Iwaki Model V-S Type KM shaker was used to shake the separatory funnel and the stoppered test-tubes.

Reagents

Cationic dyes. Triphenylmethane dyes [pararosaniline, Crystal Violet, Ethyl Violet, Malachite Green (chloride and

oxalate), Brilliant Green, Hoffman's Violet, New Fuchsin and Methyl Violet] and Methylene Blue were examined. These dyes were commercially available and used (without further purification) as solutions in distilled water.

Standard phosphate solution. Potassium dihydrogen phosphate was dried at reduced pressure (about 5 mmHg) and 60° to constant weight; 0.2722 g of the dried compound was dissolved in distilled water and diluted to give 1 litre of $2 \times 10^{-3}M$ solution. For calibration purposes, this solution was accurately diluted with distilled water before use.

Extracting solvent. Ketones, alcohols, esters, benzene and toluene were examined.

Reagent solution. Dissolve 86 g of ammonium heptamolybdate tetrahydrate in about 900 ml of distilled water, add 86 ml of concentrated sulphuric acid, dissolve 0.23 g of Malachite Green (oxalate) and 20 g of tartaric acid in the mixture, and dilute to 1 litre with distilled water. About 1 hr after mixing, filter the solution through a 0.45- μ m membrane filter.

All reagents used were of analytical-reagent grade.

Procedure

Transfer 10 ml of the sample solution, containing up to 0.7 μ g of phosphorus as orthophosphate, into a 25-ml test-tube. Add 1 ml each of 4.5M sulphuric acid and the reagent solution and mix. Shake the solution with 5 ml of a 1:3 v/v mixture of toluene and 4-methylpentan-2-one (MIBK) for 5 min. After phase separation, measure the absorbance of the organic phase at 630 nm against a reagent blank, in 1-cm cells.

RESULTS AND DISCUSSION

Selection of the cationic dye and extracting solvent

The colour changes and ionization of triphenylmethane dyes are very complex. Adams and Rosenstein¹⁹ studied the behaviour of Crystal Violet at various pH values. The mechanism of colour change was explained by considering three kinds of coloured quinonoid ions, four kinds of colourless benzenoid ions and colourless carbinol and its protonated ions. Goldacre and Phillips,²⁰ and Cigén,²¹ have also studied the ionization behaviour of Crystal Violet. They found that in acidic medium it is easily transformed into a protonated but colourless carbinol. Ethyl Violet may behave similarly to Crystal Violet and transform into its carbinol.

We have examined the colour fading of cationic dyes in acidic medium. Of the nine dyes listed under *Reagents*, above, Malachite Green, pararosaniline, New Fuchsin, Hoffman's Violet and Methylene Blue were dark yellow, pale yellow, red, violet and blue in 0.5M sulphuric acid, respectively, and the others were colourless within about 60 min from preparation of the solution. When Hoffman's Violet, Methyl Violet and Methylene Blue were used as the counter-ion for molybdophosphate, a coloured precipitate occurred at the interface and the ion-pair was scarcely extracted at all into a 1:3 v/v mixture of toluene and 4-methylpentan-2-one. Pararosaniline and New Fuchsin also failed as reagents for extraction of the molybdophosphate. The oxalate of Malachite Green was preferable to the chloride, because it gave a more stable aqueous solution and was purer than the

chloride. Recrystallization did not significantly improve the purity (~90%).

Table 1 shows the results for the efficiency of the extracting solvent, with Malachite Green as the counter-ion. A 1:2 v/v mixture of benzene and 4-methylpentan-2-one is best in terms of molar absorptivity and reagent blank absorbance. However, we prefer a 1:3 v/v mixture of toluene and the ketone, because of the lower toxicity of toluene.

Effect of acidity and reagent concentration

To 10 ml of sample solution containing 0.364 μ g of phosphorus, sulphuric acid, molybdate and Malachite Green solutions were added in that order. The solution was diluted to 12 ml, and shaken with 5 ml of an extracting solvent for 5 min.

Sulphuric acid concentration. When the acid concentration was varied from 0.3 to 1.0M, the absorbance for phosphorus samples measured against the reagent blank was maximal and constant for the acidity range 0.42–0.67M. The absorbance of the reagent blank decreased gradually with increase in sulphuric acid concentration, but was almost constant in the acid range of 0.5–0.83M. A sulphuric acid concentration of about 0.5M was therefore selected as optimal.

Malachite Green concentration. The dye concentration was varied from 2×10^{-5} to $2 \times 10^{-4}M$. The absorbance for phosphorus (measured against the reagent blank) was maximal and constant with a dyestuff concentration between 2.5×10^{-5} and $8.5 \times 10^{-5}M$. The absorbance of the reagent blank increased gradually as the dye concentration was increased. A dye concentration of $4 \times 10^{-5}M$ was therefore chosen.

Molybdate concentration. When the molybdate concentration was varied from 1×10^{-2} to $7.5 \times 10^{-2}M$, the absorbance for phosphorus, measured against the reagent blank was maximal and constant for [molybdate] = 1.5 – $4.5 \times 10^{-2}M$. The absorbance of the reagent blank increased gradually as the molybdate concentration was increased. A molybdate concentration of $4 \times 10^{-2}M$ was chosen.

Contamination from reagents. When sulphuric acid, molybdate and Malachite Green solutions were added in that order to the sample solution, the reagent blank was larger than that obtained by adding the mixed reagent solution, and differed according to the source of the ammonium molybdate. Table 2 shows the absorbances obtained by varying the concentration of molybdate. The small absorbance of about 0.02 obtained without the addition of molybdate may be attributed to some degradation products of Malachite Green. The difference between the absorbances of solutions with and without molybdate is probably due to phosphate contained in the molybdate. From the slope of plots of absorbance *vs.* molybdate concentration, the phosphate content of the ammonium molybdate was calculated and found to range from 6×10^{-5} to $8 \times 10^{-5}\%$. On the other hand, the absorbances obtained by using the mixed

Table 1. Comparison of solvents for extraction of the Malachite Green molybdophosphate ion-pair*

Extracting solvent	Absorbance of reagent blank	Molar absorptivity, $10^4 \text{ l. mole}^{-1} \text{ cm}^{-1}$
Benzene + MIBK		
1 + 1		flotation†
1 + 2	0.046	26
1 + 3	0.077	23
1 + 4	0.089	20
Toluene + MIBK		
1 + 2	0.048	20
1 + 3	0.058	23
1 + 4	0.084	23
Cyclohexane + MIBK		
1 + 3	0.050	16
1 + 4	0.064	21
1 + 5	0.073	21
Isobutyl acetate + MIBK		
1 + 1	0.032	12
1 + 2	0.070	15
1 + 3	0.091	15
MIBK(4-methylpentan-2-one)	0.116	10
Dipropyl ketone	0.122	14
Di-isobutyl ketone		flotation†
Cyclohexane	} very large	
Isoamyl alcohol		
Ethyl acetate		
Isobutyl acetate		

*Malachite Green oxalate; wavelength 630 nm; phosphorus 0–0.8 μg in 10 ml of sample; extracting solvent volume 5 ml.

†Hardly extracted, but floated at interface.

Table 2. Comparison of ammonium molybdate from different suppliers (A–E)

Ammonium molybdate, mg	Absorbance*				
	A	B	C	D	E
0	0.021	0.018	0.020	0.019	0.022
35.4 (0.02M)	0.054	0.059	0.066	0.057	0.055
53.1 (0.03M)	0.071	0.077	0.081	0.076	0.069
70.8 (0.04M)	0.083	0.089	0.103	0.088	0.086
70.8†	0.043	0.044	0.045	0.049	0.046
Phosphorus content, § 10 ⁻⁶ %	6.0	6.9	8.0	6.7	6.2

*Aqueous phase 10 ml (0.5M sulphuric acid); organic phase 5 ml; measured against solvent, at 630 nm.

†Molybdate and Malachite Green were dissolved in dilute sulphuric acid and the solution was filtered through a 0.45- μm membrane before use.

§As phosphate in ammonium molybdate.

Table 3. Effect of volume of sample solution

Sample solution taken, ml	Sulphuric acid added, ml	Reagent solution added, ml	Absorbance of reagent blank	Absorbance units for 1-ng/ml phosphorus	Molar absorptivity,* $10^5 \text{ l. mole}^{-1} \text{ cm}^{-1}$
5	0.5	0.5	0.034	0.007	2.30
10	1.0	1.0	0.044	0.015	2.26
25	2.5	2.5	0.062	0.038	2.31
50	5.0	5.0	0.078	0.080	2.48
100†	10.0	10.0	0.122	0.124	2.69

Extracting solvent 5 ml of a 1:3 mixture of toluene and 4-methylpentan-2-one.

Phosphorus 0–0.8 μg .

*Organic phase volume was assumed to be 5 ml.

†7 ml of extracting solvent were used.

Table 4. Effect of other ions

Ion	Added as	Concentration, M		Absorbance*
None				0.549
Na ⁺ , Cl ⁻	NaCl	0.3		0.545
K ⁺	KCl	1 × 10 ⁻²		0.548
SO ₄ ²⁻	Na ₂ SO ₄	1 × 10 ⁻²		0.552
Ca ²⁺	CaCl ₂	1 × 10 ⁻²		0.551
Mg ²⁺	MgCl ₂	1 × 10 ⁻²		0.548
HCO ₃ ⁻	NaHCO ₃	1 × 10 ⁻²		0.556
Al ³⁺	KAl(SO ₄) ₂	1 × 10 ⁻³		0.550
Fe ³⁺	FeNH ₄ (SO ₄) ₂	1 × 10 ⁻³		0.551
NH ₄ ⁺	NH ₄ Cl	1 × 10 ⁻³		0.557
NO ₃ ⁻	NaNO ₃	1 × 10 ⁻³		0.548
Cr ³⁺	CrCl ₃	1 × 10 ⁻³		0.549
Mn ²⁺	MnCl ₂	1 × 10 ⁻³		0.549
Co ²⁺	CoCl ₂	1 × 10 ⁻³		0.549
Cd ²⁺	CdCl ₂	1 × 10 ⁻³		0.552
Ni ²⁺	NiCl ₂	1 × 10 ⁻³		0.549
Cu ²⁺	CuCl ₂	1 × 10 ⁻³		0.553
Zn ²⁺	ZnCl ₂	1 × 10 ⁻³		0.546
Br ⁻	NaBr	1 × 10 ⁻³		0.546
B(III)	Na ₂ B ₄ O ₇	1 × 10 ⁻³		0.552
SiO ₃ ²⁻	Na ₂ SiO ₃	5 × 10 ^{-4†}		0.553
VO ₃ ⁻	NH ₄ VO ₃	1 × 10 ⁻⁵		0.556
WO ₄ ²⁻	(NH ₄) ₁₀ W ₁₂ O ₄₁	1 × 10 ⁻⁵		0.554
I ⁻	NaI	1 × 10 ⁻⁵		0.550
Laurylsulphate	Na salt	5 × 10 ^{-6†}		0.549
Laurylbenzenesulphonate	Na salt	5 × 10 ^{-6†}		0.547
ClO ₄ ⁻	NaClO ₄	1 × 10 ^{-6†}		0.557
Ti ⁴⁺	TiCl ₄	1 × 10 ⁻⁶		0.551

*Sample solution 10 ml; organic phase 5 ml; phosphorus 0.366 μg; measured against reagent blank.

†Tolerance limit.

reagent solution were almost all the same. This is because the ion-pair formed between molybdophosphate and Malachite Green is only slightly soluble in water and filtration of the reagent solution 1 hr after its preparation removes about two-thirds of the molybdophosphate.

On the basis of these results, the mixed reagent solution was used throughout further work.

Shaking and standing time. Figure 1 shows that 3 min of shaking is adequate. Compared with the Ethyl Violet method the proposed method has the advantages that (1) the shaking time is shorter, (2) there is

Table 5. Conversion of phosphorus in phosphorus-containing compounds into orthophosphate

Compounds, μg/10 ml	Methods*	Absorbance					
		Heating time (min) at 95°					
		0	15	30	60	90	120
Na ₂ HPO ₄ , 1.81	I	0.017	0.026	0.030			
	II	0.003	0.540	0.557	0.605	0.643	0.643
NaPH ₂ O ₇ , 1.56	I	0.020		0.047			
	II	0.006	0.581	0.606	0.652	0.660	0.666
(C ₂ H ₃ O) ₂ POH, 2.02	I	0.012		0.039			
	II	0.009	0.529	0.618	0.631	0.650	0.653
(C ₆ H ₅ O) ₃ P, 4.62	I	0.027		0.050			
	II	0.015	0.501	0.550	0.611	0.655	0.661
C ₁₀ H ₁₄ N ₅ O ₇ P·H ₂ O, † 5.51	I	0.022		0.057			
	II	0.014	0.537	0.610	0.616	0.657	0.659
C ₆ H ₄ NNa ₂ O ₆ P·6H ₂ O, § 5.64	I	0.044		0.078			
	II	0.031	0.585	0.623	0.692	0.713	0.718

The sample solution (10 ml), in a 25-ml stoppered test-tube, was heated in a water-bath.

*I: 1 ml of 4.5M sulphuric acid was added to the sample solution; II: 1 ml of 4.5M sulphuric acid and 0.1 ml of 40% ammonium peroxydisulphate solution were added.

†5-Adenylic acid.

§Disodium *p*-nitrophenylphosphate.

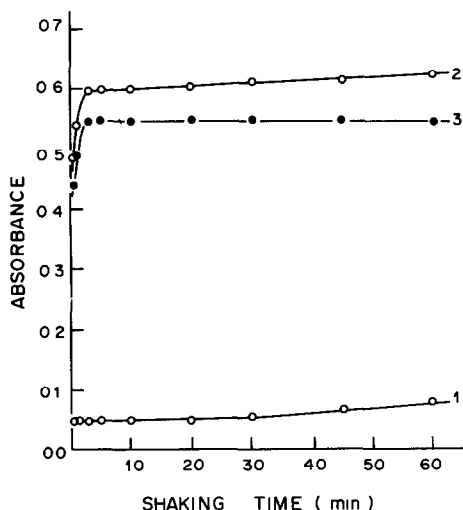


Fig. 1. Effect of shaking time: (curve 1) reagent blank (reference, extracting solvent); (curve 2) phosphorus, 0.364 μg (reference, extracting solvent); (curve 3) phosphorus 0.364 μg (reference, reagent blank); aqueous phase, 12 ml; organic phase, 5 ml.

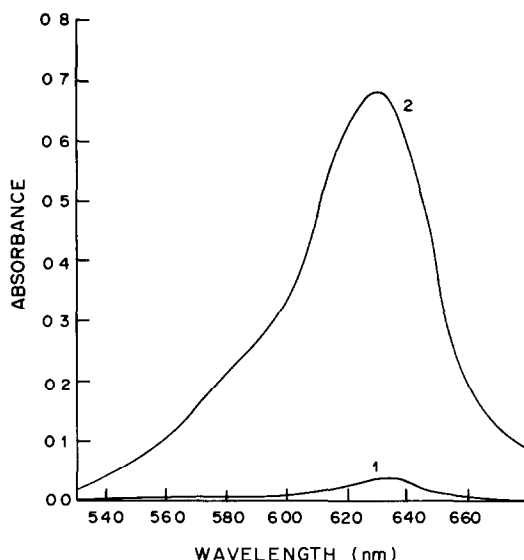


Fig. 2. Absorption spectra in the organic phase: (curve 1) reagent blank (reference, extracting solvent); (curve 2) phosphorus, 0.428 μg (reference, extracting solvent); aqueous phase, 12 ml; organic phase, 5 ml.

no colour fading during 60 min of shaking and (3) the absorbance of the reagent blank is constant during 30 min of shaking. Complete phase separation after the shaking takes about 1 min, and the absorbance of the organic phase remains constant for at least one day.

Absorption spectra and calibration graph

The absorption spectra of the ion-pair and the reagent blank are shown in Fig. 2. Linear calibration graphs are obtained even when the aqueous phase volume is increased to 100 ml (and 7 ml of extracting solvent are used). The results obtained by varying the volume of sample solution are shown in Table 3,

which shows that when 50 ml of sample solution are used, 0.1 ng/ml of phosphorus can be detected.

Effect of other ions

This was examined by using 10 ml of sample solution and the results are shown in Table 4. Most cations and anions commonly found in natural waters do not interfere, but arsenic(V) causes large positive errors: arsenic(V) at a concentration of 10 ng/ml produces an absorbance of 0.070 but can be masked with tartaric acid (added in the reagent

Table 6. Determination of phosphorus in river and sea-water, and recovery test

Sample	Phosphorus found,* ng/ml	Recovery test					
		Sample taken, ml	P in sample, ng	P added, ng	P found, ng	Recovery, %	
Asahi River	A	6.0	8	48	248	299	101
	B	17.9	8	143	248	387	99
Yoshii River	A	17.5	8	140	248	392	101
	B	16.4	8	131	248	390	103
	C	27.0	8	216	248	459	99
	D	39.4	5	197	248	446	100
Seashore of Seto Inland Sea							
Kojima	46.0	5	230	248	477	100	
Shibukawa	17.4	8	139	248	391	101	
Tamano	15.3	8	122	248	381	103	
Ushimado	12.8	8	102	248	351	100	
Nishiwaki	20.9	8	167	248	419	101	

The samples were adjusted to about pH 3 with dilute sulphuric acid after sampling, and filtered through a membrane filter (0.45 μm). An appropriate amount of sample was transferred to a 25-ml test-tube, 1 ml of 4.5M sulphuric acid was added, and the mixture was heated at 95° for 30 min. The sea-water samples were diluted to 25 ml with distilled water. A 10-ml sample was used, except for Yoshii River sample D and the Kojima sea-water for which 5-ml samples were used. In the recovery tests, the river water was diluted to 10 ml with distilled water after the addition of 248 ng of phosphorus (as phosphate), and the sea-water was diluted to 25 ml with distilled water after the addition of phosphorus.

*The values are the means of 3 determinations.

solution). When arsenic(V) was present at concentrations of 50 ng/ml, it was masked with 0.1 ml of $10^{-4}M$ sodium thiosulphate added after the sulphuric acid (see *Procedure*).

For a 25-ml sample, almost all the foreign ions tested, when present at the concentrations listed in Table 4, produced an absorbance of less than 0.005.

With 50 ml of sample solution, the effect of several ions commonly found in fresh water was examined. The following ions produced an absorbance of less than 0.005: Mg^{2+} ($10^{-2}M$), Ca^{2+} ($10^{-2}M$), SO_4^{2-} ($10^{-2}M$), Na^+ ($10^{-3}M$), K^+ ($10^{-3}M$), Fe^{3+} ($10^{-3}M$), Al^{3+} ($10^{-3}M$), NH_4^+ ($10^{-3}M$), Cl^- ($10^{-3}M$), HCO_3^- ($10^{-3}M$), SiO_3^{2-} ($5 \times 10^{-4}M$) and NO_3^- ($5 \times 10^{-4}M$). These concentrations refer to the sample itself; the effect of the sulphate and ammonium ions present in the reagent solution is compensated for by the reagent blank.

Determination of phosphorus in waters

Phosphorus occurs in natural water as orthophosphate, condensed phosphate and organically-bound phosphorus, all of which may be present in soluble forms and in suspension. By the method proposed in this work, only orthophosphate can be directly determined. Condensed phosphate, however, can be completely hydrolysed to orthophosphate by acidifying the solution with sulphuric acid ($0.4M$) and heating for 30 min at above 90° .^{6,16} In Table 5, the efficiency of conversion of phosphorus compounds into orthophosphate is shown. Under the conditions used for hydrolysis of condensed phosphate, these compounds were scarcely decomposed, but in the presence of ammonium peroxodisulphate were completely converted into orthophosphate by heating for more than 90 min. When 0.1 ml of 40% peroxodisulphate solution was used, the absorbance of the reagent blank became a little larger: 0.080. In further experiments on determination of phosphorus in natural waters, the decomposition treatment with peroxodisulphate was omitted, because it did not increase the amount of phosphate found. Table 6

shows the results for determination of phosphorus in waters. Less than 15 ml of sea-water was taken as sample, and was diluted to 25 ml with distilled water, because of its high chloride content ($\sim 0.5M$).

Recovery tests were done by adding known amounts of phosphate. The results are also shown in Table 6. The recovery of phosphorus was good: 99–103%. The relative standard deviation for phosphorus was 0.6% for 21.0 ng/ml in sea-water (12 replicates) and 1.1% for 4.28 ng/ml in tap water (10 replicates).

REFERENCES

1. L. Ducret and M. Drouillas, *Anal. Chim. Acta.*, 1959, **21**, 86.
2. F. P. Sudakov, V. I. Klitina and T. Ya. Dan'shova, *Zh. Analit. Khim.*, 1966, **21**, 1333.
3. A. K. Babko, Yu. F. Shkaravskii and V. I. Kulik, *ibid.*, 1966, **21**, 196.
4. T. Matsuo, J. Shida and W. Kurihara, *Anal. Chim. Acta*, 1977, **91**, 385.
5. G. S. Kirkbright, R. Narayanaswamy and T. S. West, *Anal. Chem.*, 1971, **43**, 1434.
6. S. Motomizu, T. Wakimoto and K. Tôei, *Anal. Chim. Acta*, 1982, **138**, 329.
7. K. Itaya and M. Ui, *Clin. Chim. Acta*, 1966, **14**, 361.
8. I. Štěpánová, *ibid.*, 1967, **16**, 330.
9. A. J. Bastiaanse and C. A. M. Meijers, *Z. Klin. Chem. Klin. Biochem.*, 1968, **6**, 48.
10. *Idem*, *ibid.*, 1968, **6**, 109.
11. W. Hohenwallner and E. Wimmer, *Clin. Chim. Acta*, 1973, **45**, 169.
12. A. Kallner, *ibid.*, 1975, **59**, 35.
13. C. L. Penney, *Anal. Biochem.*, 1976, **75**, 201.
14. B. Anner and M. Moosmayer, *ibid.*, 1975, **65**, 305.
15. D. J. Stewart, *ibid.*, 1974, **62**, 349.
16. S. Motomizu, T. Wakimoto and K. Tôei, *Analyst*, 1983, **108**, 361.
17. H. J. Altmann, E. Fürstenau, A. Gielewski and L. Scholz, *Z. Anal. Chem.*, 1971, **256**, 274.
18. A. K. Babko, Yu. F. Shkaravskii and E. M. Ivashkovich, *Ukr. Khim. Zh.*, 1969, **35**, 961.
19. E. Q. Adams and L. Rosenstein, *J. Am. Chem. Soc.*, 1914, **36**, 1452.
20. R. J. Goldacre and J. N. Phillips, *J. Chem. Soc.*, 1949, 1724.
21. R. Cigén, *Acta Chem. Scand.*, 1958, **12**, 1456.

INFLUENCE AND ROLE OF METAL IONS IN ENZYMATIC CATALYSIS WITH E.C. 1.2.3.2. XANTHINE OXIDASE*

APPLICATION TO TRACE ANALYSIS

ANNA MARIA GHE,† CLAUDIO STEFANELLI and DANIELA CARATI

Istituto Chimico "G. Ciamician" dell'Università, Scuola di Specializzazione in Chimica Analitica,
 Via Selmi 2, 40126 Bologna, Italia

(Received 13 July 1983. Revised 3 October 1983. Accepted 21 November 1983)

Summary—The effect of metal ions on the reductive half-reaction of xanthine oxidase (XOD) in the catalytic conversion of xanthine into uric acid has been studied spectrophotometrically in Tris-HCl buffer at pH 7.4, $37 \pm 0.1^\circ$ and ionic strength 0.04M. Some metal ions display inhibitor properties, the sequence of inhibiting efficiency being $\text{Ag(I)} > \text{Hg(II)} > \text{Cu(II)} > \text{Cr(VI)} > \text{V(V)} > \text{Au(III)} > \text{Tl(I)}$ and for these the I_{50} values were determined. Only Tl(I), V(V) and Cu(II) showed reversible inhibition and therefore for these the mechanisms were assessed [competitive for V(V) and Tl(I); uncompetitive for Cu(II)]. The conditional inhibition constants (K_i) were also determined. The effect of EDTA for protection of the enzyme against metal inhibition, and for its reactivation after inhibition, was also investigated. Utilization of the linear relationship between relative enzyme activity and inhibitor concentration allowed sensitive and selective (though not specific) determination of Ag(I) and Hg(II) (10^{-9} – $10^{-8}M$), and of Cu(II) and Cr(VI) (10^{-7} – $10^{-6}M$), the maximum relative error being $\pm 4\%$. For a few metal ions, e.g., Ag(I) and Cr(VI), in the presence of EDTA, a certain specificity is observed.

The study of the effect of traces of metal ions on enzymatic activity has attracted considerable interest in recent years, particularly in the use of enzymes for the analysis of substrates and inhibitors,¹⁻⁶ and in the modification of biological systems.⁷⁻⁹ The concentration limit for determination depends on the stability of the complex formed [(enzyme-inhibitor) or (enzyme-activator) or possibly (enzyme-substrate)-inhibitor].¹⁰ The method is not always specific, but is both sensitive and selective. These characteristics can be improved, in the case of prosthetic metal determination of metal-enzymes, by means of apoform reactivation, e.g., by removal of the metal by complexation.¹¹

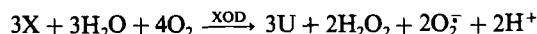
The accuracy of the analytical determination of trace elements, and the study of the role of metallic ions in a given metabolic cycle, are not, however, the sole goals of these studies, since the acquisition of structural data on the active sites or the nature of the metal-enzyme bond, and on the formation and decomposition mechanism of metal complexes is also a worthwhile objective.¹²

In the present work we have studied the enzymatic catalysis of xanthine oxidase (XOD). This enzyme (average molecular weight¹³ $\sim 2.8 \times 10^5$) is composed of two subunits, generally considered identical,¹⁴ each containing three prosthetic groups: (a) one Mo atom

at the active site for oxidation of xanthine, (b) an FAD (flavinadenine dinucleotide) molecule at the active site for reduction of oxygen and (c) two iron/sulphur systems (I and II), non-equivalent,¹⁵ which probably act as electron-reservoirs during the catalytic cycle, so that electron transfer takes place according to the sequence:¹³



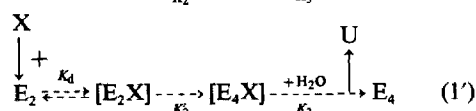
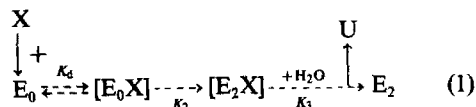
The enzyme oxidizes xanthine to uric acid, molecular oxygen acting as the electron acceptor and being reduced to hydrogen peroxide and the superoxide radical (O_2^-), within an overall reaction which, on the basis of the behaviour of milk xanthine oxidase,¹⁶⁻¹⁸ can be shown schematically as



where X stands for xanthine and U for uric acid.

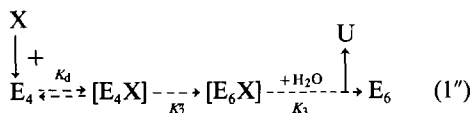
This overall reaction can be subdivided into two half-reactions, the enzyme reductive step leading to the formation of uric acid¹⁶ and the enzyme oxidative half-reaction^{17,18} leading to the formation of H_2O_2 and O_2^- .

The first half-reaction can be envisaged as follows:



*Work done with the financial support of the Ministero della Pubblica Istruzione (Italy), for research of national interest, 11835.

†Author to whom correspondence should be addressed.



where E = enzyme (XOD). The subscript accompanying E stands for the number of electrons responsible for reduction of the enzyme (E_0 = fully oxidized XOD; E_6 = fully reduced enzyme, the 6 electrons being supplied in pairs by X). K_d is the dissociation constant of the enzyme-substrate complex; K_2 , K_3 , etc. are the rate constants of the respective reactions.

In our work we have concentrated our attention on this half-reaction, with reference to the way it is affected by the presence of metallic ions. Other authors who have examined this problem, either directly or indirectly, include Bergel,¹⁹ Guilbault,²⁰ Kela^{21,22} and Ramadoss.²³

EXPERIMENTAL

Apparatus

The enzyme reaction was monitored spectrophotometrically by means of a double-beam Perkin-Elmer grating spectrometer (Model 554), with a microcomputer-driven recorder and a water-circulation thermostat, Iulabo R5-6A. The pH readings were taken with an Orion Model 701 A pH-meter at $37 \pm 0.1^\circ$. Conductivity measurements were obtained by means of an Analytical Control Model 101 Conductimeter.

Reagents

All reagents and solutions were prepared with doubly distilled demineralized water (conductance = 1×10^{-6} mho at 25°) and stored in the dark in polyethylene containers to avoid any cation-exchange in the solution.²⁴ Glassware was washed according to Thiers,²⁵ stored in 6% v/v nitric acid²⁶ and washed with doubly distilled demineralized water before use.

Buffer. Tris-buffer [tris(hydroxymethyl)aminomethane], 0.05M, prepared²⁷ with "Trizma base" and "Trizma HCl" (Sigma Chemical Co.), pH 7.40 at 37° , was used throughout.

Enzyme. Grade I buttermilk xanthine oxidase suspension in 2.3M ammonium sulphate containing 0.02% sodium salicylate (Sigma Chemical Co.), nominal specific activity 0.76 U/mg of protein at 25° , essentially uricase-free, was used and kept refrigerated at 4° . The working solution was prepared daily (to avoid loss of enzyme activity) by dissolving 10 μ l in 1 ml of Tris-buffer at pH 7.4 (concentration = 370 μ g/ml, $\sim 1.3 \times 10^{-6}$ M; specific activity = 1.4 U/mg of protein, at 37° and pH 7.4). The solution was kept refrigerated at 4° and proved stable over a 6-hr period.

Substrate. The 1×10^{-3} M xanthine stock solution was prepared by dissolving the necessary quantity of purine base (U.S. Biochemical Corp., Cleveland, Ohio) in 0.5 ml of 2M potassium hydroxide and diluting to 200 ml with Tris-buffer. The solution was kept at 4° and protected from light.

Cation and anion solutions. The 3×10^{-2} M stock solutions of the various metal ions were prepared by dissolving in water suitable quantities of the Merck analysis-grade reagents (chlorides and sulphates of most ions; nitrate for Ag^+ ; ammonium and sodium salts for the anions); the concentration of solutions was checked complexometrically²⁸ or by AAS. Before use, solutions of the desired concentration were obtained by dilution with Tris-buffer (pH 7.4).

Analytical procedure

The XOD-catalysed enzymatic oxidation of xanthine to uric acid was monitored spectrophotometrically in Tris-buffer (pH 7.4) at an ionic strength of 0.04M and at $37 \pm 0.1^\circ$, by measuring the uric acid absorption at 291 nm. The experiments were done under pseudo zero-order conditions, *i.e.*, with a large excess of substrate. The kinetic behaviour was studied by means of the initial rate method,²⁹ during the first 10 min of the reaction.

The effect of inhibitors was measured under the following standard conditions; into a quartz cell, with an optical path of 10 mm, the following solutions were placed in the order given: 0.18 ml of 1×10^{-3} M xanthine (this gave a final concentration of 6×10^{-3} M); 1.30 ml of Tris-buffer; 1.50 ml of cation or anion solution of suitable concentration in Tris-buffer. The mixture was brought to $37 \pm 0.1^\circ$ and 20 μ l of 1.3×10^{-6} M enzyme solution (to give $\sim 8.9 \times 10^{-9}$ M final concentration, equivalent to 2.5 μ g of protein per ml) were added. The total solution volume in the cell was 3 ml in all experiments. Absorbance readings were taken against a blank containing no enzyme. A similar procedure was followed for monitoring the reaction rate in the absence of inhibitors. Plots of absorbance *vs.* time were used to determine the initial reaction rate (v_0), expressed as $\Delta A_{291}/\text{min}$.

In order to minimize errors due to loss of activity of the enzyme during successive determinations, the relative activity was used:

$$\alpha = \frac{v_0}{v_0} = \frac{(\text{initial reaction rate in presence of inhibitor})}{(\text{initial reaction rate in absence of inhibitor})}$$

RESULTS AND DISCUSSION

The optimum standard operating conditions described were chosen on the basis of a few preliminary investigations aimed at determining (a) the optimum substrate concentration with respect to assessment of metal effect on the reaction of interest; (b) the effect of pH on the initial rate of the XOD-catalysed reaction, it having been previously established that, under standard conditions, there was a linear relationship between v_0 and XOD concentration.

The dependence of v_0 on substrate concentration is shown in Fig. 1. It appears that over the concentration range 4×10^{-5} – 1×10^{-4} M, v_0 is independent of substrate concentration (pseudo zero-order conditions), and no inhibition by excess of substrate is

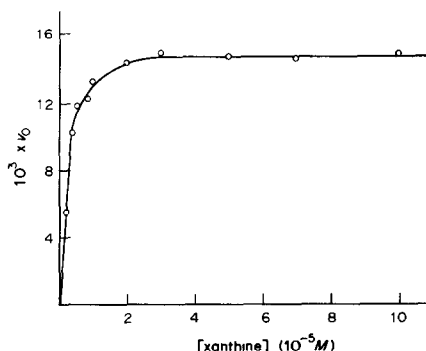


Fig. 1. Substrate-concentration dependence of initial reaction rate v_0 for XOD-catalysed xanthine to uric acid conversion.

observed.³⁰ On the basis of this behaviour the standard xanthine concentration was established, namely $6 \times 10^{-5} M$.

As illustrated in Fig. 2, v_0 is practically constant in the vicinity of pH 7.4 ± 0.1 . This is therefore the optimum operating pH because it is also close to physiological values. (The study was done over the pH range 6.7–8.7, the usual pH range available at 37° with this buffer.)

At the chosen pH, the Michaelis constant K_m for xanthine was determined at different enzyme concentrations, according to the method of Lineweaver and Burk,³¹ and found to be $5.77 \pm 0.17 \times 10^{-6} M$, in good agreement with literature values^{32,33} obtained under similar conditions.

The effect of a number of ions at low concentration on the XOD-catalysed xanthine \rightarrow uric acid conversion was examined without considering the form in which they were present in solution under typical experimental conditions.³⁴ A few showed no measurable effect when present in the concentration range 1×10^{-7} – $1 \times 10^{-4} M$, viz. Li(I), Ca(II), Ba(II), Mg(II), Cd(II), Zn(II), Fe(II), Fe(III), Cr(III), Al(III), Se(IV), Mo(VI) and W(VI).

Another series, composed of Co(II), Pb(II), V(III) and V(IV), was not stable in the buffer utilized. Finally, a third series, comprising Tl(I), Ag(I), Cu(II), Hg(II), Au(III), V(V) and Cr(VI), showed inhibiting effects to varying degrees.

The inhibition strength of these species, expressed as I_{50} [the overall metal concentration producing 50% inhibition ($\alpha = 0.5$)], is shown in Table 1, and Fig. 3 shows how α and $I\%$ [$= (1 - \alpha)\%$], vary with metal ion concentration. It is apparent that strong inhibition is brought about by Ag(I) and Hg(II), which have a considerable effect even at concentrations similar to the enzyme concentration, and at 2×10^{-7} and $1.3 \times 10^{-6} M$ concentrations, respectively, produce almost complete and irreversible deactivation (Table 2). The order of decreasing inhibiting power of the other five ions in this group is $Cu(II) > Cr(VI) > V(V) > Au(III) > Tl(I)$.

The behaviour of Ag(I) and Hg(II) can be explained in terms of their high affinity toward a thiol group in the enzyme,³⁵ although the role of the thiol itself is still not clear.³⁶ The much lower inhibiting power of Cu(II) can be reasonably ascribed to the formation of an $Me(Tris)^{2+}$ complex, which appears to be very stable.³⁴

The reactivation of the enzyme (type R experiments) and the protection of the enzyme against inhibitor (type P experiments) were also examined for all inhibitors. Type R measurements were obtained by incubating the enzyme for 1 min in the presence of the inhibitor (with formation of the enzyme-inhibitor [EI] complex), then treating it with a strong metal-complexing agent (EDTA) to free the enzyme and restore its activity.

Type P data (protection data) were obtained by treating the inhibitor with the complexing agent to

Table 1. Effect of various metals on XOD-catalysed xanthine oxidation to uric acid

Metal	$I_{50}, *M$
Tl(I)	9.9×10^{-4}
Au(III)	6.2×10^{-4}
V(V)	1.9×10^{-4}
Cr(VI)	7.5×10^{-5}
Cu(II)	5.6×10^{-5}
Hg(II)	4.2×10^{-7}
Ag(I)	7.7×10^{-8}

*Inhibitor concentration necessary to produce 50% inhibition ($\alpha = 0.5$).

form the complex [EDTA-I], which if stable enough will prevent formation of complex [EI] when the enzyme is added, leaving the enzyme free to exert catalytic activity.

For both R and P measurements and for the blank (without EDTA), the substrate was then added to the reaction mixture to initiate the catalysed reaction.

Inhibition by Cr(VI) could not be studied in this way since it does not form an EDTA complex under the experimental conditions.³⁷ Alizarin Red S [which should complex Cr(VI) at pH 3–8],³⁸ did not work either.

The results obtained for enzyme reactivation (R) and protection (P) are reported in terms of relative activity (α_R and α_P , respectively) in Table 2.

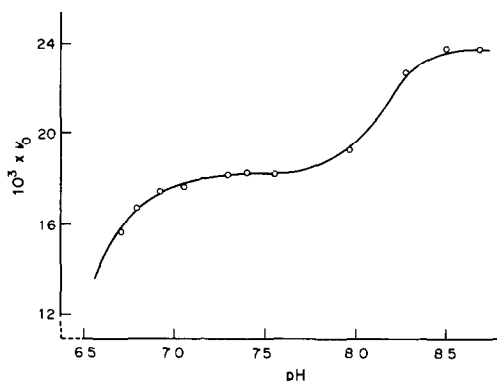


Fig. 2. pH-dependence of initial reaction rate v_0 , for XOD-catalysed xanthine to uric acid conversion.

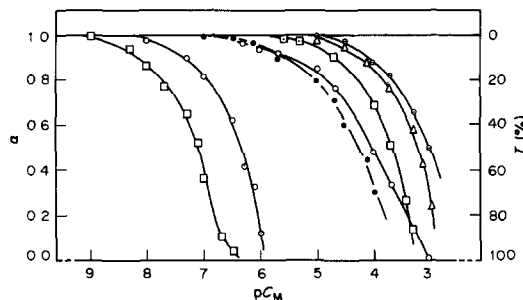


Fig. 3. Metal-concentration dependence of inhibition for various metals; α (relative activity) and $I\%$ [percentage inhibition $= (1 - \alpha)\%$] are both plotted. \square Ag(I); \circ Hg(II); \bullet Cu(II); \circ Cr(VI); \square V(V); \triangle Au(III); \ominus Tl(I).

Table 2. Effect of EDTA on reactivation (R) of the inhibited enzyme and on its protection (P) against inhibition*

Inhibitor	Blank		Reactivation (R)		Protection (P)	
	(no EDTA present)	$\alpha_B = \frac{v_0}{v_0}$	$I + E \xrightleftharpoons[EDTA]{EDTA} [I-EDTA] + E$	$\alpha_R = \frac{v_{0R}}{v_0}$	$I + EDTA \xrightarrow{+E} [I-EDTA] + E$	$\alpha_P = \frac{v_{0P}}{v_0}$
None	—	1	—	1	—	1
Tl(I)	1×10^{-3}	0.49	—	0.94	—	0.98
Au(III)	5×10^{-4}	0.39	—	0.60	—	0.95
V(V)	5×10^{-4}	0.15	—	0.88	—	0.86
Cu(II)	5×10^{-4}	0.00	—	0.75	—	1
Hg(II)	1×10^{-6}	0.15	—	0.16	—	0.95
Ag(I)†	1×10^{-6}	0.00	—	0.00	—	0.00

*Cell concentration: enzyme = 25 μ g/ml; xanthine = 6×10^{-5} M; EDTA = 1×10^{-3} M.

α_B = relative activity of the inhibiting reaction in the absence of EDTA (blank).

α_R = relative activity of the inhibition reversibility reaction due to EDTA.

α_P = relative activity of protection against inhibition reaction in the presence of EDTA.

†Experiments carried out in Tris-HNO₃, pH 7.4; AgNO₃ solution.

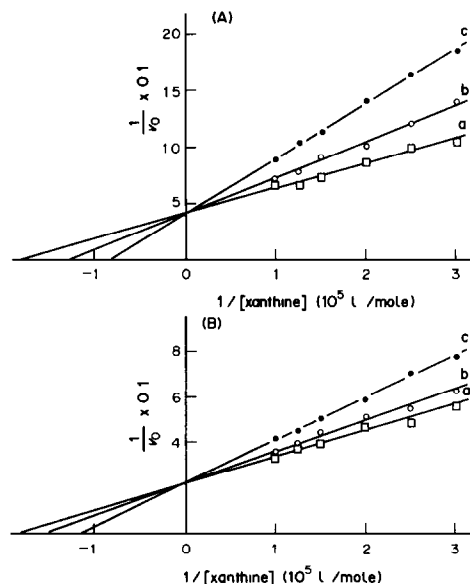


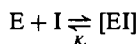
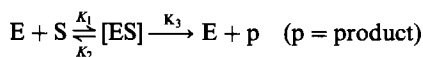
Fig. 4. A, Inhibition mechanism for Tl(I) (competitive); (a) [Tl] = 0; (b) [Tl] = 1×10^{-4} M; (c) [Tl] = 3×10^{-4} M. B, Inhibition mechanism for V(V) (competitive); (a) [V] = 0; (b) [V] = 3×10^{-5} M; (c) [V] = 1×10^{-4} M.

It can be seen that there is very efficient enzyme reactivation (hence reaction reversibility) for Tl(I), V(V) and Cu(II), but none for Au(III), Hg(II) and Ag(I). On the other hand, enzyme protection by EDTA is about 100% in all cases studied, except for Ag(I) which forms only a weak EDTA complex.

For the reversible inhibitors [Tl(I), V(V) and Cu(II)] it proved possible to determine the inhibition mechanism and the conditional inhibition constant K_i , given either by the dissociation constant of complex [EI] (in the case of a competitive linear mechanism) or by the dissociation constant of the enzyme-substrate-inhibitor complex [ESI] (the dissociation reaction being [ESI] = [ES] + I), in the case of uncompetitive inhibition.

Methods described in the literature³⁹ were applied, utilizing double reciprocal plots with lines fitted by the least-squares procedure. The results obtained are shown in Table 3, where pK_i values for the various inhibitors are collected, and in Figs. 4 and 5.

Tl(I) and V(V) show a similar inhibition mechanism (linear competitive)⁴⁰ characterized by the inhibitor (I) competing with the substrate (S) in binding to the enzyme (E):



The inhibitor complex [EI] does not undergo any further reaction such as formation of a ternary complex [EIS] between enzyme, inhibitor and substrate.

For this type of inhibition the rate equation, expressed in the reciprocal form suitable for the

Table 3. Inhibition mechanism and values of the conditional inhibition constant K_i for reversible inhibitors in XOD-catalysed xanthine to uric acid conversion

Inhibitor	Inhibiting mechanism*	K_i , M	pK_i
Tl(I)	Linear competitive	$2.20 \pm 0.09 \times 10^{-4}$	3.65 ± 0.02
V(V)	Linear competitive	$1.70 \pm 0.02 \times 10^{-4}$	3.77 ± 0.01
Cu(II)	Linear uncompetitive	$2.49 \pm 0.25 \times 10^{-5}$	4.60 ± 0.05

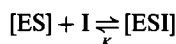
*pH 7.4; $\mu = 0.04M$ (Tris buffer); $T = 37 \pm 0.1^\circ$; $K_m = 5.77 \pm 0.17 \times 10^{-6}M$; $pK_m = 5.24 \pm 0.01$.

double reciprocal plots, is

$$\frac{1}{v_0} = \frac{1}{v_{\max}} \left[1 + \frac{K_m}{[S]} \left(1 + \frac{[I]}{K_i} \right) \right]$$

where v_0 = initial rate, v_{\max} = maximum rate, $[S]$ and $[I]$ are the concentrations of substrate and inhibitor, respectively, K_m is the Michaelis constant and K_i the conditional inhibition constant.

Cu(II), on the other hand (Fig. 5A), gives inhibition of the linear non-competitive type,⁴⁰ according to the scheme



which is described by the initial-rate law

$$\frac{1}{v_0} = \frac{1}{v_{\max}} \left[\left(1 + \frac{[I]}{K_i} \right) + \frac{K_m}{[S]} \right]$$

This mechanism has been confirmed (Fig. 5B) by construction of a Hanes⁴¹ plot, of $[S]/v_0$ vs. $[S]$ at different inhibitor concentrations. Thus inhibition by Cu(II) involves the formation of the ternary complex $[ESI]$, which prevents the formation of uric acid.³⁹

The behaviour of V(V), in agreement with a recent suggestion of Ramadoss,²³ can be envisaged as a competitive interaction of the metal at the active site of oxidation of xanthine (in particular interaction with Mo), which prevents the substrate from interacting at this site. The behaviour of Tl(I) can be similarly explained, although the identification of Mo as the interaction site is less certain.

The linear relationship between α and the inhibitor concentration over ranges typical of each metal allows some analytical determinations down to the nanogram region. The determination is selective but not specific, since different metals can act simultaneously as inhibitors. Modifications such as change of buffer, or masking of interferents by complexation, may give more specificity, however.

Calibration curves for Ag(I), Hg(II), Cu(II), Cr(VI), V(V), Au(III) and Tl(I) are shown in Fig. 6; Table 4 shows the detection limits, analytical concentration ranges, and relative standard deviations. The method is most useful for silver and mercury, which have detection limits of about 1×10^{-9} and $1 \times 10^{-8} M$, respectively, which is much better than the value $2.5 \times 10^{-7} M$ obtained by other authors²⁰ for the same reaction but a different method. The XOD-method for silver has a lower detection limit than those using alcohol dehydrogenase,⁴² urease,⁴³ invertase,⁴⁴ or glucose oxidase⁴⁵, whereas the limit of detection for mercury is much the same as that obtained by Townshend and Vaughan with alcohol dehydrogenase.⁴² Thus of the enzymes studied for subnanogram levels of silver and mercury,^{4,42-46} XOD and alcohol dehydrogenase are the most effective.

XOD is also promising for determination of Cu(II) and Cr(VI), the detection limit being about $10^{-7} M$, but other techniques are to be preferred for V(V), Au(III) and Tl(I), for which the XOD performance is not as good.

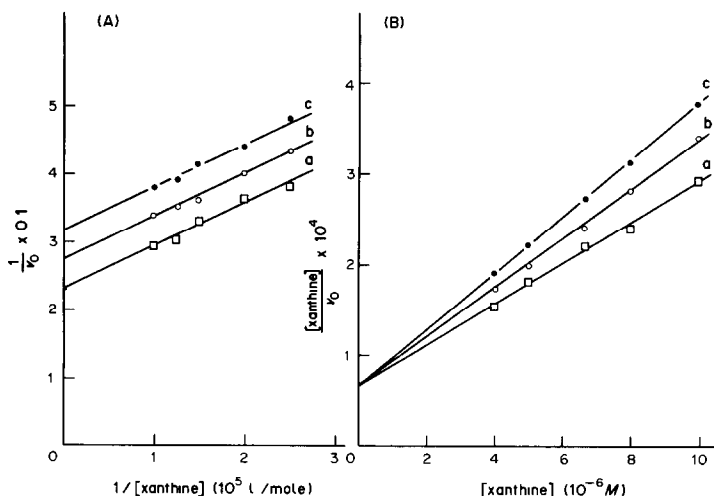


Fig. 5. Inhibition mechanism for Cu(II) (uncompetitive); A, double reciprocal plots, B, Hanes plot: (a) $[Cu] = 0$; (b) $[Cu] = 5 \times 10^{-6}M$; (c) $[Cu] = 1 \times 10^{-5}M$.

Table 4. Detection limits and concentration ranges for inhibitor determination in XOD-catalysed xanthine to uric acid conversion

Inhibitor	Detection limits,* ng/ml	Concentration range, M
Ag(I)	0.11	1×10^{-9} – 1×10^{-7}
Hg(II)	2	1×10^{-8} – 5×10^{-7}
Cu(II)	6.3	1×10^{-7} – 5×10^{-6}
Cr(VI)	16	3×10^{-7} – 1×10^{-5}
V(V)	2×10^2	4×10^{-6} – 1×10^{-5}
Au(III)	2×10^3	1×10^{-5} – 1×10^{-4}
Tl(I)	6×10^3	3×10^{-5} – 1×10^{-4}

*Minimum inhibitor cell concentration to produce a detectable decrease in α ($\Delta\alpha$). Standard conditions.

For the four best applications the relative standard deviation ranges from 1 to 10%, the average being about 2.5%, and the relative error of the mean of 5 determinations does not exceed $\pm 4\%$ (see Table 5).

The lack of specificity can be partially circumvented as already explained. In particular a degree of specificity for Ag(I) and Cr(VI) can be achieved by use of EDTA. Cr(VI) cannot be complexed under the experimental conditions,³⁷ and Ag(I) has very strong affinity for the enzyme and very little for EDTA. This can be explained as follows. The conditional inhibition constant K_i is the inverse of the stability constant of the [EI] or [ESI] complexes, and pK_i can be directly compared with $\log K'_{MY}$ [the logarithm of the conditional stability constant of the EDTA (Y) complex of the inhibitor metal (M)]. At pH 7.4, the $\log K'_{MY}$ values are 4.2 for Ag(I), 3.5 for Tl(I), 15.6 for Cu(II), 10.4 for Hg(II), 15.1 for V(V); Cr(VI) cannot be complexed under the conditions used,³⁷ and Au(III) is reduced to the metal by EDTA.⁴⁷

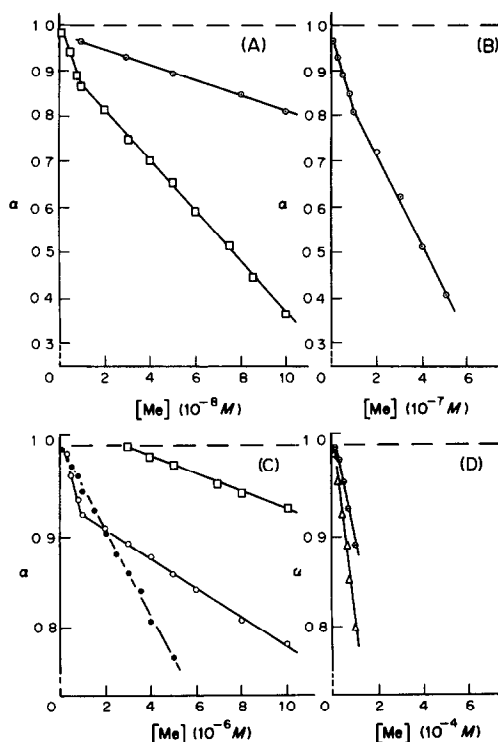


Fig. 6. Enzymatic determination of metal ions. Variation of α with inhibitor concentration. A, \square Ag(I); \circ Hg(II); B, \circ Hg(II); C, \bullet Cu(II); \circ Cr(VI); \square V(V); D, \triangle Au(III); \circ Tl(I).

Whereas pK_i is very high for Ag(I), it is only about 3.6 for Tl(I), which is comparable with the $\log K'_{TY}$ value, and this means that the ratio of [TIE] to [TIY] would be about the same as the concentration ratio of XOD to EDTA, and that excess of EDTA could

Table 5. Quantitative enzymatic determination of metallic inhibitors based on the XOD-catalysed xanthine to uric acid conversion

Inhibitor	Theoretical cell concentration, M	Cell concentration found*		Relative error, %
		\pm standard deviation, M	rsd, %	
Ag(I)	2×10^{-9}	$2.08 \pm 0.10 \times 10^{-9}$	5	+4
	7×10^{-9}	$7.15 \pm 0.12 \times 10^{-9}$	1.7	+2.1
	1×10^{-8}	$0.96 \pm 0.09 \times 10^{-8}$	10	-4
	2.5×10^{-8}	$2.52 \pm 0.06 \times 10^{-8}$	2.4	+0.8
Hg(II)	4.7×10^{-8}	$4.66 \pm 0.06 \times 10^{-8}$	1.4	-0.8
	2×10^{-8}	$2.06 \pm 0.10 \times 10^{-8}$	5	+3
	7×10^{-8}	$7.14 \pm 0.11 \times 10^{-8}$	1.6	+2
	1.3×10^{-7}	$1.28 \pm 0.07 \times 10^{-7}$	6	-1.5
Cu(II)	2×10^{-7}	$1.98 \pm 0.05 \times 10^{-7}$	2.5	-1
	3.7×10^{-7}	$3.8 \pm 0.04 \times 10^{-7}$	1	+2.7
	3×10^{-7}	$3.08 \pm 0.15 \times 10^{-7}$	5	+2.7
	7×10^{-7}	$7.10 \pm 0.08 \times 10^{-7}$	1	+1.4
Cr(VI)	1.4×10^{-6}	$1.35 \pm 0.11 \times 10^{-6}$	8	-3.6
	2.5×10^{-6}	$2.45 \pm 0.05 \times 10^{-6}$	2	-2
	4×10^{-6}	$4.10 \pm 0.04 \times 10^{-6}$	1	+2.5
	4×10^{-7}	$4.12 \pm 0.06 \times 10^{-7}$	1.5	+3
Cr(VI)	7×10^{-7}	$7.08 \pm 0.07 \times 10^{-7}$	1	+1.1
	1.3×10^{-6}	$1.25 \pm 0.10 \times 10^{-6}$	8	-3.8
	3.5×10^{-6}	$3.55 \pm 0.08 \times 10^{-6}$	2	+1.4
	6.6×10^{-6}	$6.40 \pm 0.10 \times 10^{-6}$	1.6	-1.5

*Average value from 5 determinations.

effectively mask the Tl(I), whereas Ag(I) will not be masked. The Cu(II) and V(V) complexes with EDTA are much stronger than the XOD complexes, so these species are masked by EDTA. Hg(II) presents an interesting case. As a result of formation of hydroxo-complexes of mercury(II), $\log K'_{\text{Hg}}$ is comparatively low (10.4 at pH 7.4), but Hg(II) has high affinity for the enzyme thiol groups. It is of interest that the mercury(II) can be masked by a large excess of EDTA added *before* the enzyme, but the enzyme activity cannot be restored if the EDTA is added after the (EI) complex has already been formed.

Obviously the strongest inhibitors, Ag(I) and Hg(II), can be separately determined at low concentrations (1×10^{-9} – 1×10^{-7} M) in the presence of the weaker inhibitors when these are present at concentrations below the detection limits ($\sim 1 \times 10^{-7}$ M, Table 4).

In the case of XOD, where two active sites with different functions are present, a certain specificity in the determination of inhibitors might be achieved if they react differently with the two sites.

This possibility is currently being explored by studying the metal–enzyme interaction through the XOD-catalysed NADH–NAD⁺ oxidation, since it is known that in this reaction the substrate NADH interacts with the active site of flavin.¹³

REFERENCES

- G. G. Guilbault, *Anal. Chem.*, 1966, **38**, 527R; 1968, **40**, 459R; 1970, **42**, 334R.
- M. M. Fishman and H. F. Schiff, *ibid.*, 1972, **44**, 543R; 1974, **46**, 367R; 1976, **48**, 326R.
- M. M. Fishman, *ibid.*, 1978, **50**, 261R; 1980, **52**, 185R.
- A. Vanni and P. Amico, *Ann. Chim. Roma*, 1976, **66**, 719; 1977, **67**, 29.
- G. G. Guilbault, *Handbook of Enzymatic Methods of Analysis*, pp. 405–424, Dekker, New York, 1976.
- M. Yozo and N. Toru, *Agric. Biol. Chem.*, 1982, **46**, 807.
- G. L. Eichhorn, *Inorganic Biochemistry*, Elsevier, New York, 1973.
- H. Sigel (ed.), *Metal Ions in Biological Systems*, Dekker, New York, 1973–1979.
- P. Amico and A. Vanni, *Ann. Chim. Roma*, 1978, **68**, 175.
- A. Townshend and A. Vaughan, *Talanta*, 1970, **17**, 289.
- A. Vanni, E. Roletto and V. Zelano, *Ann. Chim. Roma*, 1982, **72**, 375.
- M. M. Jones, *Ligand Reactivity and Catalysis*, Academic Press, New York, 1968.
- R. C. Bray, in *The Enzymes*, P. D. Boyer (ed.), Vol. 12, pp. 299–419, Academic Press, New York, 1975.
- W. F. Cleere, C. O'Reagan and M. P. Coughlam, *Biochem. J.*, 1974, **143**, 465.
- D. Edmonson, D. Ballon, A. Van Heuvelen, G. Palmer and V. Massey, *J. Biol. Chem.*, 1973, **248**, 6135.
- J. S. Olson, D. P. Ballon, G. Palmer and V. Massey, *ibid.*, 1974, **249**, 4363.
- R. Hille and V. Massey, *ibid.*, 1981, **256**, 9090.
- A. G. Porras, J. S. Olson and G. Palmer, *ibid.*, 1981, **256**, 9096.
- F. Bergel and R. C. Bray, *Symp. Biochem. Soc.*, 1958, **15**, 64.
- G. G. Guilbault, D. N. Kramer and P. L. Cannon, Jr., *Anal. Chem.*, 1964, **36**, 606.
- V. Kela and R. Vijayvargiya, *Biochem. J.*, 1980, **193**, 799.
- Idem*, *Curr. Sci. India*, 1980, **49**, 392.
- C. S. Ramadoss, *Z. Naturforsch.*, 1980, **35C**, 702.
- A. W. Struempfer, *Anal. Chem.*, 1973, **45**, 2251.
- R. E. Thiers, in *Trace Analysis*, J. H. Yoe and H. J. Koch (eds.), p. 637, Wiley, New York, 1957.
- K. M. Bone and W. D. Hibbert, *Anal. Chim. Acta*, 1979, **107**, 219.
- Sigma Technical Bulletin*, No. 106B, November 1979.
- H. A. Flaschka, *EDTA Titrations*, Pergamon Press, Oxford, 1959.
- H. B. Mark and G. A. Rechnitz, *Kinetics in Analytical Chemistry*, p. 27, Interscience, New York, 1968.
- J. Fridovich and P. Handler, *J. Biol. Chem.*, 1958, **233**, 1581.
- H. Lineweaver and D. Burk, *J. Am. Chem. Soc.*, 1934, **56**, 658.
- M. G. Battelli, E. Lorenzoni and F. Stürpe, *Biochem. J.*, 1973, **131**, 191.
- H. Iwata, I. Yamamoto and E. Goda, *Biochem. Pharmacol.*, 1973, **22**, 1845.
- B. E. Fischer, U. K. Häring, R. Tribolet and H. Sigel, *Eur. J. Biochem.*, 1979, **94**, 523.
- V. Massey, P. E. Brumby, H. Komai and G. Palmer, *J. Biol. Chem.*, 1969, **244**, 1682.
- V. Massey, in *Iron-Sulfur Proteins*, W. Lovenberg (ed.), Vol. I, p. 301, Academic Press, New York, 1973.
- R. M. Smith and A. E. Martell, *Critical Stability Constants*, Vol. 1, p. 204, Plenum Press, New York, 1974.
- S. P. Sangal, *Chim. Anal. Paris*, 1964, **46**, 492.
- S. A. Todhunter, in *Methods in Enzymology*, Vol. 63, p. 383, Academic Press, New York, 1979.
- H. J. Fromm, *ibid.*, p. 468.
- G. N. Wilkinson, *Biochem. J.*, 1961, **80**, 324.
- A. Townshend and A. Vaughan, *Talanta*, 1970, **17**, 299.
- E. C. Toren and F. J. Burger, *Microchim. Acta*, 1968, 1049.
- D. Mealor and A. Townshend, *Talanta*, 1968, **15**, 747, 1371.
- E. C. Toren and F. J. Burger, *Microchim. Acta*, 1968, 538.
- G. G. Guilbault and D. N. Kramer, *Anal. Biochem.*, 1967, **18**, 313.
- W. A. Hynes, L. K. Yanovski and J. E. Ransford, *Mikrochem. Ver. Mikrochim. Acta*, 1950, **35**, 160.

SPECTROPHOTOMETRIC DETERMINATION OF TRACE AMOUNTS OF BERYLLIUM IN SILICATE MATERIALS

ALFRED SAUERER and GEORG TROLL*

Institut für Mineralogie und Petrographie der Universität, Theresienstrasse 41, D-8000 München 2, BRD

(Received 27 July 1983. Accepted 16 November 1983)

Summary—Although photometric determination of beryllium is generally quite satisfactory in trace analysis, application to geochemical samples is restricted because of the numerous interfering ions. Introduction of an extraction procedure eliminates the interference of Al and Fe, which occur in high concentrations in most silicate rocks, and enables beryllium to be determined with Eriochrome Cyanine R. Use of the method for analysis of six international geochemical reference samples containing between 1 and 30 ppm beryllium has given satisfactory results (relative standard deviation from 1.6 to 7.8%).

Although a great number of photometric methods for determining beryllium have been proposed, very few are suitable for determining traces of beryllium in rocks and minerals. For this analysis the technique used must meet several criteria.

1. The limit of detection should be near $0.5 \mu\text{g}$ (preferably $0.1 \mu\text{g}$) of beryllium.
2. Aluminium and iron contents up to 10^5 times that of beryllium must not interfere.
3. The results must be reproducible.
4. The standard deviation should be within the limits usual for trace analysis.

A survey of the literature shows that only a few of the published procedures for the photometric determination of beryllium in silicate materials fulfil these requirements.

To work out an analytical technique for determining beryllium in geochemical samples, we chose Eriochrome Cyanine R from the numerous substances which form chelates with beryllium (Beryllon, Fast Sulphon Black, Eriochrome Cyanine R, Quinalizarin, Aluminon, etc.). The complex has a molar absorptivity of $1.5 \times 10^4 \text{ l. mole}^{-1} \text{ cm}^{-1}$ at 512 nm, the wavelength of the absorption maximum, so the method should have relatively high sensitivity. Hill¹ obtained good results by using Eriochrome Cyanine R, and his work was made the basis of our initial investigations. Hill had found that Al, Fe, Ti and P interfered, and used EDTA for masking. The extent to which these ions interfere in Hill's procedure was therefore investigated. It was found that while the measurements were only slightly influenced by phosphate and permanganate, aluminium and iron(III) interfered considerably in the determination of beryllium despite the addition of EDTA as masking agent (see Table 1). The negative absorbances for solutions

containing aluminium are presumably due to precipitation of the dyestuff (the absorbance is measured against a reagent blank). Since aluminium and iron are abundant in rocks and soils their influence on the beryllium determination was examined carefully. Figures 1 and 2 show the individual effects and Fig. 3 shows their combined influence. The graphs show that the determination is highly sensitive to the iron and aluminium concentrations above a certain level, and that there is a variable degree of compensation when both elements are present, depending on their concentration ratio. Such effects tend to conceal the true magnitude of the individual interferences. The experiments performed indicate that when Hill's method is used, the simultaneous presence of 2 mg each of iron and aluminium will cause significant interference in determination of $2.5 \mu\text{g}$ of beryllium. Hence for an "average" granite (13% Al_2O_3 , 1.5% Fe_2O_3 , 3 ppm Be), Hill's method in its original form would not be suitable for determination of beryllium.

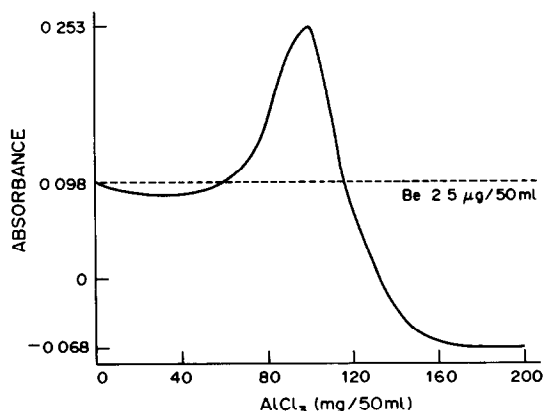


Fig. 1. Interference with the beryllium-Eriochrome Cyanine complex by Al^{3+} , as a function of AlCl_3 concentration, in presence of EDTA ($\lambda = 512 \text{ nm}$).

*Author for correspondence.

Table 1. Effect of various ions on absorbance (at 512 nm) of Be solutions

Present	Absorbance
2.5 μg Be	0.096
5.0 μg Be	0.180
7.5 μg Be	0.248
2.5 μg Be + 200 mg FeCl_3	0.203
2.5 μg Be + 400 mg AlCl_3	-0.181
2.5 μg Be + 200 mg FeCl_3 + 400 mg AlCl_3	-0.127
2.5 μg Be + 4 mg H_3PO_4	0.100
2.5 μg Be + 16 mg KMnO_4	0.094

We have therefore combined the photometric determination of beryllium by the Eriochrome Cyanine R method with prior extraction of the beryllium to separate it from the interfering substances. We have modified the extraction procedure given by Adam *et al.*,² who used acetylacetone and chloroform for the purpose and masked interfering ions such as aluminium and iron with EDTA.

EXPERIMENTAL

Apparatus

A Perkin-Elmer 552 double-beam grating spectrophotometer equipped with thermostatically controlled cells (Haake, FRG), and a Metrohm E532 pH-meter were used. The extractions were done in Pyrex funnels cleaned with 3M hydrochloric acid and thrice rinsed with distilled water. As far as possible polyethylene apparatus was used.

Reagents

A 5% solution of Merck analytical grade acetylacetone in distilled water was prepared. The Eriochrome Cyanine R

solution was prepared by dissolving 500 mg of the Merck reagent in 125 ml of distilled water along with 12 g of sodium chloride, 12 g of ammonium nitrate and 1 ml of concentrated nitric acid, adding 50 ml of ethanol, and diluting to volume with water in a 500-ml standard flask. Chloroform stabilized with ethanol (Merck) was used. Aqueous 5% disodium EDTA and sodium acetate solutions were prepared. All chemicals were of analytical grade. Standard 50- $\mu\text{g}/\text{ml}$ beryllium solution was prepared by dissolving 983 mg of $\text{BeSO}_4 \cdot 4\text{H}_2\text{O}$ in 25 ml of 5M hydrochloric acid and diluting accurately to 1000 ml with water, and further diluted as required (several drops of 5M hydrochloric acid being added whenever dilutions were made).

Extraction procedure

A known volume (40 ml is suitable) of the acid sample solution (containing 1–10 μg of Be) is pipetted into a 100-ml separatory funnel, mixed with 5 ml of EDTA solution, and adjusted to pH 6.9–7.0 with dilute ammonia solution ($\sim 3M$). Then 5 ml of the acetylacetone solution are added, and the pH is readjusted to 7.0. The mixture is shaken with 10 ml of chloroform for 2 min. The organic phase is collected in a second separatory funnel. A further 0.1 ml of acetylacetone solution and 10 ml of chloroform are added to the aqueous phase and the mixture is shaken for 2 min, and the organic phase is added to the first. The combined organic phases are shaken for 2 min with 15 ml of 5M hydrochloric acid and the aqueous phase is collected. The stripping step is repeated. The two hydrochloric acid phases are combined and evaporated on a hot-plate to about 0.25 ml and then diluted to about 5 ml with water.

Photometric determination

The concentrated aqueous phase is adjusted to pH 2–3 with 2.5M sodium hydroxide, and 2 ml each of the EDTA, sodium acetate and Eriochrome Cyanine R solutions are added. Sodium hydroxide solution is then added until the colour of the solution changes from yellow to reddish violet (the pH then lies between 10.5 and 11.5). The solution is diluted to 20 ml, the pH is adjusted with hydrochloric acid to exactly 9.8, and the solution is transferred to a 25-ml

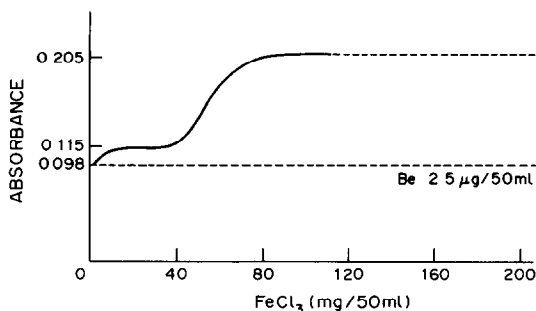


Fig. 2. Interference with the beryllium-Eriochrome Cyanine complex by Fe^{3+} , as a function of FeCl_3 concentration, in presence of EDTA ($\lambda = 512$ nm).

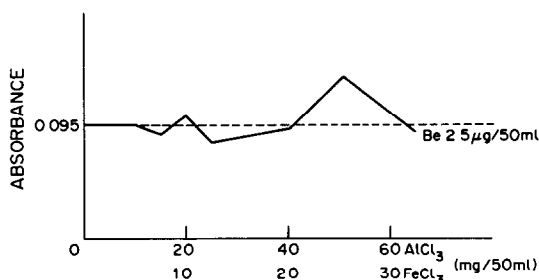


Fig. 3. Interference with the beryllium-Eriochrome Cyanine complex by the simultaneous presence of Al^{3+} and Fe^{3+} and EDTA ($\lambda = 512$ nm).

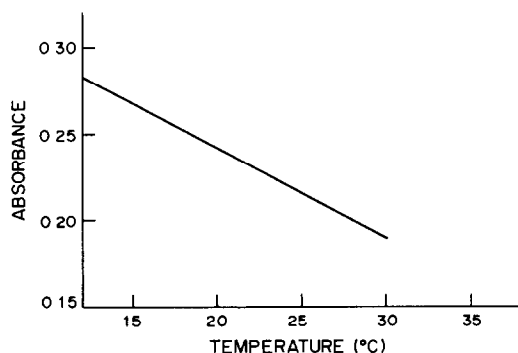


Fig. 4. Absorbance of the beryllium-Eriochrome Cyanine complex as a function of temperature ($\lambda = 512$ nm).

Table 2. Beryllium concentrations in six international reference samples

Reference sample	Reported values (ppm)	Mean (ppm)	Analytical method*	Reference		
SY-2	22.8; 24.1; 22.9; 19.4	22.3	HYJ	this work		
	16		OVS	4		
	20		OVS	10		
	20		OOO	4		
	14		OOO	4		
	29		OVS	4		
	29		OVS	4		
	22		BVS	4		
	24		HOA	4		
	28		OVS	4		
	27		OCJ	4		
	NIM-G		6.0; 5.9; 5.8	5.9	HYJ	this work
			10†		OOO	7
7.6		OVS	10			
7.47		FCJ	9			
NIM-L	25.7; 22.7; 24.4; 24.2;	24.3	HYJ	this work		
	20†		OOO	7		
	25.8		FCJ	9		
QLO-1	1.7; 1.6; 1.5; 2.0	1.7	HYJ	this work		
	1.83		HYA	5		
	1.65		FCJ	3		
	2.02; 2.09; 2.43; 2.16; 2.10; 2.01		OOS	6		
STM-1	9.8; 10.3	10.0	HYJ	this work		
	8.75		HYA	5		
	9.02		FCJ	3		
	11.2; 11.7; 12.6; 11.8; 11.5; 12.3		OOS	6		
SDC-1	1.9; 2.1	2.0	HYJ	this work		
	2.52		HYA	5		
	2.57		FCJ	3		
	3.95; 3.74; 3.68; 3.52; 3.60; 3.82		OOS	6		

*Code^a for the analytical methods used.

(i) <i>Sample pretreatment</i>	(ii) <i>Separations</i>	(iii) <i>Final measurement</i>
B pelletization	C chromatography, ion-exchange	A atomic-absorption
F fusion, sintering	V bulk volatilization	J absorptiometric, fluorimetric
H acid decomposition	Y solvent extraction	S spectrographic
O none used or not specified	O none used or not specified	O not specified

†“Magnitudes” according to Flanagan⁷.

standard flask and diluted to the mark with water. After 45 min for colour development the absorbance is measured at 512 nm against a blank solution prepared by applying the photometric procedure to 1.0 ml of 3M hydrochloric acid.

Because of the formation and stability of the complex and hence the absorbance are strongly temperature-dependent (Fig. 4), all measurements must be done at the same temperature. Although measurement at lower temperatures would increase the sensitivity, for reasons of speed it is desirable to use temperatures close to room temperature.

Calibration graph

For construction of the calibration graph, different amounts of standard solution are pipetted and treated by the procedures of extraction and analysis described above. The calibration graph is linear in the range up to 0.25 µg/ml in the final solution. A decrease of pH from 9.8 to 9.7 diminishes the absorbance by about 9%.

RESULTS AND DISCUSSION

The beryllium concentrations of six international geochemical reference samples were determined; for every determination a separate digestion was performed (routine digestion with 15 ml of concentrated hydrofluoric acid and 2 ml of concentrated sulphuric

acid for 0.5–1.5 g of sample). The results of the determinations (Table 2) demonstrate an accuracy and precision satisfactory for most geochemical problems and for analysis of a wide variety of matrices containing beryllium at concentrations down to 1.5 ppm. For routine analysis of large numbers of samples, the various steps of the procedure should be systematized, e.g., by using two sets of separatory funnels set up in two ranks, one above the other, and by using an automatic shaker for the extractions. In this way the analysis time and possible external contamination can be reduced.

Acknowledgement—The authors are gratefully indebted to Dr. B. R. Willeford, Jr., Bucknell University, Lewisburg, Pennsylvania, for his kind and helpful comments.

Note added in proof

During the period this article was in press, Watkins and Thompson published a paper on “Determination of beryllium and zirconium in 45 geochemical reference samples by inductively coupled plasma emission spectrometry” (*Geostand. Newslett.*, 1983, 7, 273) and reported beryllium data on the reference samples SY-2, NIM-G and NIM-L.

REFERENCES

1. U. T. Hill, *Anal. Chem.*, 1958, **30**, 521.
2. J. A. Adam, E. Booth and J. D. H. Strickland, *Anal. Chim. Acta*, 1952, **6**, 462.
3. V. Macháček, I. Rubeška, V. Sixta and Z. Šulcek, *U.S. Geol. Survey Prof. Paper*, 1976, **840**, 73.
4. S. Abbey, A. H. Gillieson and G. Perrault, *SY-2, SY-3 and MRG-1. A Report on the Collaborative Analysis of Three Canadian Rock Samples for Use as Certified Reference Materials*, pp. 1-32. Canada Centre for Mineral and Energy Technology, Ottawa, 1975.
5. E. Y. Campbell and F. O. Simon, *Talanta*, 1978, **25**, 251.
6. F. G. Walthall, A. F. Dorrzapf, Jr. and F. J. Flanagan, *U.S. Geol. Survey Prof. Paper*, 1976, **840**, 99.
7. F. J. Flanagan, *Geochim. Cosmochim. Acta*, 1973, **37**, 1189.
8. J. F. Steinbach and H. Freiser, *Anal. Chem.*, 1953, **25**, 881.
9. F. W. E. Strelow, R. G. Böhmer and C. H. S. W. Weinert, *ibid.*, 1976, **48**, 1550.
10. P. K. Hofmeyr, *Chem. Geol.*, 1972, **9**, 23.

FLUORIMETRIC KINETIC STUDIES AND SUB- μ M DETERMINATION OF ALUMINIUM WITH 2-HYDROXY-1-NAPHTHALDEHYDE *p*-METHOXYBENZOYLHYDRAZONE

P. C. IOANNOU and P. A. SISKOS*

Laboratory of Analytical Chemistry, University of Athens, 104 Solonos Street,
Athens 10680, Greece

(Received 31 January 1983. Revised 21 June 1983. Accepted 12 November 1983)

Summary—A fluorimetric study has been made of the kinetics of the reaction of 2-hydroxy-1-naphthaldehyde *p*-methoxybenzoylhydrazone with aluminium, and a rate equation and a possible kinetic scheme are proposed. Experimental conditions are defined under which 0.020–10.0 μ M aluminium can be determined with an average error of 3.7% and a coefficient of variation of about 4.6%.

Hydrazones (characterized by the grouping C=N—N, and related to Schiff's bases), have been used as photometric and fluorimetric analytical reagents for the determination of metals.¹ The formation of a highly fluorescent chelate through the combination of a metal ion and an organic ligand has often proved to be a sensitive and specific method for the determination of metals, particularly those which are difficult to measure by atomic-absorption spectroscopy.²

Fluorescent complexes of aluminium have received a great deal of attention. Some scores of papers give analytical methods for a wide variety of samples.³ Fluorimetric applications of hydrazones for the determination of aluminium, on the other hand, are few in number, the main reasons being the slow reactions and the lack of kinetic and mechanistic studies.

2-Hydroxy-1-naphthaldehyde *p*-methoxybenzoylhydrazone (HNAMBH) has been used recently for fluorimetric determinations of aluminium, scandium and thorium,⁴⁻⁶ though the procedure for the determination of aluminium has some limitations.⁷ Kinetic methods of analysis offer greater speed and specificity.

In this study we have combined the merits of kinetic methods and spectrofluorimetry to study the kinetics of the reaction between HNAMBH and aluminium ions and, on the basis of optimized experimental conditions, have developed a kinetic fluorimetric method for the determination of aluminium in aqueous solution. A rate equation and a possible kinetic scheme are proposed for the reaction. The method developed is simple, rapid, very sensitive and more selective than non-kinetic methods. Microamounts of aluminium in the range 0.020–10.0 nmole in the spectrofluorimeter cell have been determined

with a relative standard deviation of 4.6% and measurement times of about 60 sec.

EXPERIMENTAL

Apparatus

A Perkin-Elmer model 512 double-beam fluorescence spectrophotometer with a 150-W xenon lamp was used. For all measurements standard rectangular cells of 1.000-cm path-length, made of fluorescence-free fused silica, were used. The cell compartment was modified and a magnetic stirrer was mounted under the sample cell holder. A constant temperature of $25.0 \pm 0.1^\circ$ in the sample cell was maintained by using a thermostatic water-bath. The fluorescence intensity vs. time curves were recorded on a Sargent-Welch XKR potentiometric recorder.

The following instrumental settings were used for measurements: ratio mode; dynode voltage 750 V; excitation wavelength 420 nm with a band-width of 20 nm; emission wavelength 475 nm with a band-width of 20 nm.

Reagents

All solutions were prepared in demineralized distilled water from reagent-grade materials, unless otherwise stated.

2-Hydroxy-1-naphthaldehyde p-methoxybenzoylhydrazone (HNAMBH), solution, 10^{-3} M, in acetone. The synthesis of the reagent has been previously described.⁴ The stock solution is stable for several months.

Standard aluminium solution, 1000 ppm (37mM). This solution was prepared by dissolved an ampoule of Merck "Titrisol" aluminium standard solution (1.000 ± 0.002 g of Al) in 1 litre of 0.1M hydrochloric acid. Working solutions were prepared by appropriate dilution with water.

Stock 0.1M glycine/0.1M sodium chloride buffer, pH 3.50. Prepared by dissolving 7.51 g of glycine and 5.85 g of sodium chloride in 700 ml of water, adjusting to pH 3.50 with 0.1M hydrochloric acid and diluting with water to 1 litre.

Working buffer solution, pH 4.80. Prepared by mixing 300 ml of the stock glycine buffer with 600 ml of acetone, adjusting the pH to 4.80 with hydrochloric acid and diluting with water to 1 litre.

Procedure

Transfer 2.00 ml of buffer solution and 1.00 ml of sample or standard aluminium solution into the cuvette and start the stirrer. Cover the cell and record the fluorescence

*Author for correspondence.

intensity until it is steady. Inject, through a plastic septum in the cover, 100 μl of the reagent solution and record the changing fluorescence intensity for 2–3 min. Construct a kinetic calibration curve by plotting initial reaction rate (slope method) vs. aluminium concentration.

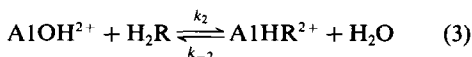
RESULTS AND DISCUSSION

Kinetic studies of the HNAMBH–Al system

Choice of buffer solution. It is known that aluminium ions form a 1:1 complex with HNAMBH in weakly acidic solution and that the maximum fluorescence intensity of the complex (λ_{ex} 420 nm and λ_{em} 475 nm) is obtained in the pH range 3.50–4.50 (40% acetone solution), depending on the aluminium concentration.⁷ In that study it was noticed that acetate buffer solutions were not suitable, because acetate forms complexes with aluminium ions. Likewise, citrate buffers gave no measurable fluorescence. Glycine buffers, on the other hand, were found suitable, since the same maximum fluorescence intensity was observed as for solutions with the same pH but adjusted only with hydrochloric acid. Hence glycine buffer was chosen for the kinetic studies of this reaction.

Figure 1 shows the effect of pH on the initial reaction rate for different aluminium concentrations. The maximum reaction rate was observed at pH 4.7–5.1, a range which is not so broad as that when measurements are made under equilibrium conditions, and means that the optimal pH range does not depend largely on aluminium concentration.⁷ This situation makes the kinetic conditions more favourable for analytical application. A pH of 4.8 was chosen for the kinetic studies and the analytical method.

Determination of the equilibrium constants. The formation of complexes between aluminium ions and HNAMBH(H_2R) in weakly acidic solution can be expressed by the equations:



where reaction (2) is known to be fast.

H_2R has two dissociation constants and in the pH range 3.00–5.50 the predominant species is H_2R .⁵ The equilibrium constant of reaction (1)

$$K_1 = \frac{k_1}{k_{-1}} = \frac{[\text{AlHR}^{2+}][\text{H}^+]}{[\text{Al}^{3+}][\text{H}_2\text{R}]} \quad (4)$$

was calculated by using the first ionization constant of H_2R ,⁵

$$K_{\text{H}_2\text{R}} = \frac{[\text{H}^+][\text{HR}^-]}{[\text{H}_2\text{R}]} = 1.1 \times 10^{-9} \quad (5)$$

and the instability constant of the complex, K_{inst} .⁷

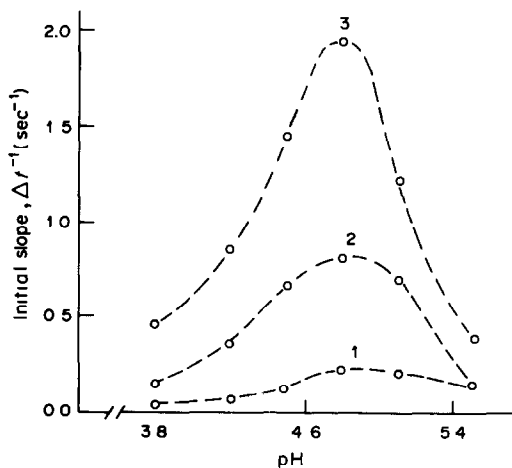


Fig. 1. Effect of pH on the initial slope. $[\text{HNAMBH}] = 32 \mu\text{M}$, $[\text{Al}]$, μM : (1) 1.6; (2) 4.8; (3) 6.4; other conditions as in procedure.

$$K_{\text{inst}} = \frac{[\text{Al}^{3+}][\text{HR}^-]}{[\text{AlHR}^{2+}]} = 1.6 \times 10^{-6} \quad (6)$$

Combining equations (4)–(6) we get

$$K_1 = \frac{K_{\text{H}_2\text{R}}}{K_{\text{inst}}} = 7.0 \times 10^{-4} \quad (7)$$

so this reaction is not significant.

The equilibrium constant for reaction (3) at pH 4.8 is given by

$$K_2 = \frac{k_2}{k_{-2}} = \frac{[\text{AlHR}^{2+}]}{[\text{AlOH}^{2+}][\text{H}_2\text{R}]} \quad (8)$$

and was calculated by combining the aluminium hydrolysis constant⁹

$$K_h = \frac{[\text{AlOH}^{2+}][\text{H}^+]}{[\text{Al}^{3+}]} = 6.2 \times 10^{-6} \quad (9)$$

with $K_{\text{H}_2\text{R}}$ and K_{inst} to yield

$$K_2 = \frac{K_{\text{H}_2\text{R}}}{K_{\text{inst}} K_h} = 1.14 \times 10^2 \quad (10)$$

Thus reaction (3) will predominate at the optimum pH.

Determination of reaction order and rate constants. If the formation of the complex is monitored fluorimetrically, the following general reaction-rate equation can be written:

$$\text{Rate} = \frac{d[\text{AlHR}^{2+}]}{dt} = k[\text{Al}]^a [\text{H}_2\text{R}]^b [\text{H}^+]^c \quad (11)$$

where $[\text{Al}]$ stands for the total initial concentration of aluminium.

By keeping the concentrations of two of the three reagents constant and in large excess and varying the concentration of the third, pseudo first-order conditions were achieved with respect to each reagent in turn.

Figure 2 shows the first-order plots for the reaction of three different concentrations of aluminium with an excess of HNAMBH at optimum pH. The mean calculated pseudo first-order rate constant, k_{obs} , was $(1.83 \pm 0.11) \times 10^{-3} \text{ sec}^{-1}$ (mean of 3 experimental results), which means that under these conditions the initial slope, $\Delta F/\Delta t$, where F is the fluorescence intensity, is directly proportional to the aluminium concentration. From recorded kinetic curves for runs with different concentrations of aluminium, a mean value for a of 1.13 ± 0.09 (3 determinations) was found.

By using the infinite time method for pseudo first-order conditions, k_{obs} can be determined from the recorded reaction traces by plotting $\ln [F - F_t]$ vs. time, where F and F_t are the fluorescence intensities at equilibrium and time t respectively. In this way, a series of k_{obs} values was obtained for different HNAMBH concentrations (Table 1). The reaction order (b) with respect to [HNAMBH] can be obtained by plotting $\ln k_{\text{obs}}$ vs. $\ln [\text{HNAMBH}]$. By regression analysis a value of 0.96 was obtained for b , indicating that the reaction is first-order with respect to the organic reagent.

Table 2 shows kinetic results for the determination of reaction order with respect to pH. The pH range studied covers values above and below the optimum pH range. By regression analysis a value of -1.15 (4 results) was obtained for c , indicating a first-order reaction with respect to pH in the range 3.8–4.8.

The experimental kinetic results can be explained by taking into consideration the hydrolysis of aluminium, and that the complex is formed according to reaction (3), for which the following rate equation can be written:

$$\frac{d[\text{AlHR}^{2+}]}{dt} = k_2[\text{AlOH}^{2+}][\text{H}_2\text{R}] - k_{-2}[\text{AlHR}^{2+}] \quad (12)$$

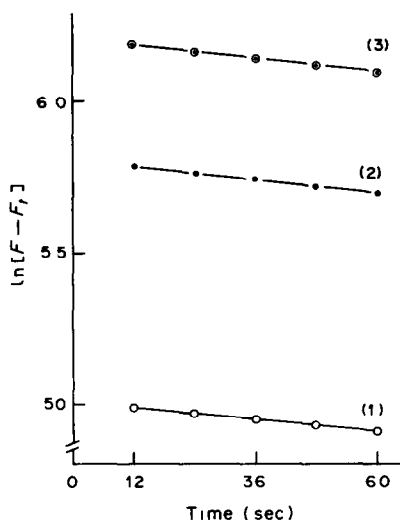


Fig. 2. First-order plots. [HNAMBH] = $20 \mu M$, [Al], μM : (1) 0.50; (2) 1.00; (3) 1.50. Other conditions as in procedure.

Table 1. Kinetic results for the determination of reaction order with respect to [HNAMBH]

k_{obs} , $\text{sec}^{-1} \times 10^4$	$-\ln [\text{HNAMBH}]$	$-\ln k_{\text{obs}}$
6.80	11.869	7.368
12.0	11.226	6.725
18.0	10.820	6.320
22.0	10.557	6.113

Regression equation $y = 4.08 + 0.96x$; ($n = 4$, $r = 0.999$).
[Al] = $0.50 \mu M$, optimum pH 4.80 in 40% acetone,
 $T = 25^\circ$, ionic strength $0.02 M$ NaCl.

or, taking into consideration equation (9):

$$\frac{d[\text{AlHR}^{2+}]}{dt} = k_2 \frac{K_h}{[\text{H}^+]} [\text{Al}^{3+}][\text{H}_2\text{R}] - k_{-2}[\text{AlHR}^{2+}] \quad (13)$$

At low pH ($\text{pH} < \text{p}K_h$) the reaction rate depends inversely on $[\text{H}^+]$, [see equation (13) and Fig. 1], because as $[\text{H}^+]$ is decreased $[\text{AlOH}^{2+}]$ is increased.

In the optimum pH range, where $[\text{H}^+] \sim K_h$, the reaction rate is independent of pH. If $[\text{H}_2\text{R}]$ is in constant excess, so that

$$k'_2 = k_2[\text{H}_2\text{R}] \quad (14)$$

equation (13) can be rewritten as

$$\frac{d[\text{AlHR}^{2+}]}{dt} = k'_2[\text{Al}^{3+}] - k_{-2}[\text{AlHR}^{2+}]. \quad (15)$$

By using the infinite time method, the pseudo first-order constant

$$k_{\text{obs}} = k'_2 + k_{-2} \quad (16)$$

can be determined (see Fig. 2). From equations (8) and (16) k_2 and k_{-2} can be calculated:

$$k_2 = \frac{K_2 k_{\text{obs}}}{1 + K_2} \quad (17)$$

$$k_{-2} = \frac{k_{\text{obs}}}{1 + K_2} \quad (18)$$

giving $k_2 = 90.9 \pm 5.7 \text{ l. mole}^{-1} \cdot \text{sec}^{-1}$ and $k_{-2} = 0.80 \pm 0.05 \text{ sec}^{-1}$ (3 observations).

For $\text{pH} > 5.20$, the observed decrease in reaction rate is due to further hydrolysis of aluminium ions

Table 2. Kinetic results for the determination of reaction order with respect to pH

k_{obs} , $\text{sec}^{-1} \times 10^4$	$-\log [\text{H}^+]$	$-\log k_{\text{obs}}$
13.1	3.80	2.883
31.9	4.20	2.496
61.9	4.50	2.208
75.3	4.80	2.123
63.8	5.10	2.195
13.1	5.45	2.883

Regression equation $y = 7.52 - 1.15x$ [$n = 4$; $r = 0.950$ (the first four points)]. [Al $^{3+}$] = $4.8 \mu M$, [HNAMBH] = $33 \mu M$, $T = 25^\circ$, ionic strength = $0.02 M$ NaCl, 40% acetone.

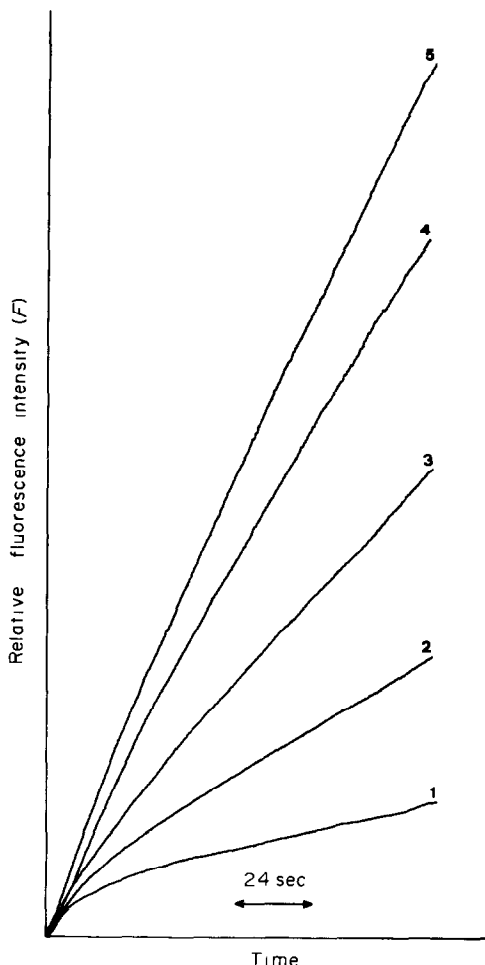


Fig. 3. Typical recorded kinetic curves. [Al], μM : (1) 0.20; (2) 0.40; (3) 0.60; (4) 0.80 and (5) 1.00. Other conditions as in procedure.

and probably a new chromogenic complex is formed, of the type $\text{Al}(\text{HNAMBH})_2$.⁷

Effect of ionic strength. The rate of the reaction is independent of ionic strength over the range 0.05–0.30M sodium perchlorate in the optimum pH range. This provides evidence that one of the reacting species should be uncharged, namely H_2R .

Effect of temperature. The reaction rate has a mean temperature coefficient of about $14 \pm 3\%$ /deg over the range 27–41.5°. From an Arrhenius plot the activation energy was found to be 19 kcal/mole and the pre-exponential factor 5.4×10^{10} . The large activation energy and hence the large temperature variation, is both disadvantageous, because strict temperature control is needed, and advantageous in analytical applications, because the sensitivity of the reaction could be increased by increasing the temperature.

Analytical applications

The initial reaction rate under pseudo first-order experimental conditions is linear with respect

Table 3. Analytical results for aqueous aluminium solutions

Initial slope, $\text{sec}^{-1} \times 10^2$	[Aluminium], μM		Relative error, %
	Taken	Found*	
Range A			
5.0	0.020	0.019	-5.0
14	0.040	0.038	-5.0
26	0.060	0.065	8.3
35	0.080	0.082	2.5
41	0.100	0.096	-4.0
			Mean 5.0
Range B			
16	0.20	0.22	10.0
43	0.40	0.38	-5.0
76	0.60	0.57	-5.0
121	0.80	0.83	3.7
151	1.00	1.00	0
			Mean 4.7
Range C			
39	2.00	2.05	2.5
79	4.00	3.95	-1.3
121	6.00	5.97	-0.5
164	8.00	7.99	-0.1
207	10.00	10.03	0.3
			Mean 0.9

*Mean of 2 runs.

Regression equations:

Range A $y = -0.037 + 4.71x$, ($n = 5$, $r = 0.994$).

Range B $y = -0.225 + 1.74x$, ($n = 5$, $r = 0.996$).

Range C $y = -0.040 + 0.21x$, ($n = 5$, $r = 0.999$).

to aluminium concentration in the range 0.020–0.100 μM (range A), 0.20–1.00 μM (range B) and 2.0–10.0 μM (range C). Figure 3 shows typical recorded kinetic curves. Results for the determination of aluminium in pure aqueous solution are given in Table 3. They indicate that aluminium in the range 0.020–10 μM (0.54–270 ng/ml) can be determined with a mean relative error of about 3.7%. The

Table 4. Effect of foreign ions on aluminium determination at a concentration of 1.0 μM (27 ng/ml)

Foreign ion	Added as	Tolerance molar ratio [Ion]/[Al]
Group A		
Sc(III)	Sc_2O_3^*	6.7
Ga(III)	$\text{Ga}(\text{NO}_3)_3 \cdot 8\text{H}_2\text{O}$	6.7
Group B		
Fe(II)	$(\text{NH}_4)_2\text{Fe}(\text{SO}_4)_2 \cdot 6\text{H}_2\text{O}$	0.6
Fe(III)	$\text{Fe}(\text{NO}_3)_3 \cdot 9\text{H}_2\text{O}$	0.6
Y(III)	Y_2O_3^*	0.6
Cu(II)	$\text{CuCl}_2 \cdot 2\text{H}_2\text{O}$	1.0
U(VI)	$\text{UO}_2(\text{NO}_3)_2 \cdot 6\text{H}_2\text{O}$	1.0
Co(II)	$\text{Co}(\text{ClO}_4)_2 \cdot 6\text{H}_2\text{O}$	3.3
Ni(II)	$\text{NiSO}_4 \cdot 6\text{H}_2\text{O}$	10.0
Th(IV)	$\text{Th}(\text{ClO}_4)_4 \cdot \text{H}_2\text{O}$	33.0
Sr(II)	$\text{Sr}(\text{NO}_3)_2$	67.0

Group A: these ions in the stated ratio caused an error of about +5%.

Group B: these ions in the stated ratio caused an error of about -5%.

*The oxides were dissolved in concentrated hydrochloric acid.

linearity of the method covers the range 0.020–10.0 μM . The sensitivity of the method can be increased by increasing the temperature.

Five replicate determinations at each of the 0.020, 0.20 and 2.0 μM aluminium levels had relative standard deviations of 5.4, 4.4 and 4.0% respectively.

Interferences

Table 4 summarizes the effects of interfering ions. Scandium and gallium cause positive errors, whereas the other ions investigated cause negative errors. It seems that all the ions examined form complexes with the reagent, but the tolerance levels for some ions are lower in the kinetic method than in the equilibrium method.⁶ Scandium reacts 300 times faster with HNAMBH than aluminium does. The possibility of developing a differential simultaneous kinetic method for the determination of scandium and aluminium in aqueous mixtures and real samples is being examined.

Acknowledgements—This paper is dedicated to the memory of the late Professor Konstantin P. Stolyarov, State University of Leningrad. P. C. Ioannou is grateful to Dr. Nikolai

N. Grigoriev, State University of Leningrad, for introducing her to the interesting field of fluorescence spectrophotometry.

REFERENCES

1. R. B. Singh, P. Jain and R. P. Singh, *Talanta*, 1982, **29**, 77.
2. *Fluorescence Applications*, Perkin-Elmer Ltd, Buckinghamshire, England.
3. *Fluorimetry Reviews*, Turner Associates, Palo Alto, California, 1967.
4. A. V. Dolgorev, N. N. Pavlova and V. A. Ershova, *Zavodsk. Lab.*, 1973, **39**, 658; *Anal. Abstr.*, 1974, **26**, 777.
5. A. V. Dolgorev, N. S. Sivak, T. I. Pal'nikova and L. M. Gurevich, *J. Anal. Chem. U.S.S.R.*, 1979, **34**, 83.
6. A. V. Dolgorev, Yu. A. Serikov and V. L. Zolotavin, *ibid.*, 1978, **33**, 1809.
7. P. C. Ioannou, I. O. Kushumova, N. N. Grigoriev and K. P. Stolyarov, *Probl. Sovrem Anal. Chem. (U.S.S.R.)*, 1981, **3**, 79.
8. K. P. Stolyarov, N. N. Grigoriev, P. C. Ioannou, D. B. Gladiliovitsh, N. V. Grishenko, B. M. Kondrationok, *ibid.*, 1981, **3**, 73.
9. F. Secco and M. Venturini, *Inorg. Chem.*, 1975, **14**, 1978.

ANALYTICAL CHARACTERIZATION OF CuInS_2 SEMICONDUCTOR MATERIAL

C. F. HUNG, P. Y. CHEN, L. Y. WENG, H. L. HUANG
and M. H. YANG*

National Tsing Hua University, Hsinchu, Taiwan 300, People's Republic of China

(Received 10 September 1982. Revised 3 November 1983. Accepted 12 November 1983)

Summary—Systematic analytical procedures have been developed for determination of the stoichiometry of CuInS_2 and estimation of trace elements, including dopants and impurities, in the material. Samples of CuInS_2 are digested in an oxidizing acid to ensure completely transformation into Cu^{2+} , In^{3+} and SO_4^{2-} ions. The stoichiometry determination is made sequentially by controlled potential electro-deposition of copper, followed by its EDTA titration, titrimetric determination of indium and gravimetric determination of sulphate, in a single sample solution. The relative errors for the determination of Cu and In are found to be -0.08% and $+0.11\%$ respectively, fulfilling the requirement for accurate stoichiometry assessment; that for S is -0.66% , which though rather high is still acceptable. For the determination of trace elements in CuInS_2 , multistage combined procedures are employed. Cu in the sample solution is removed by electro-deposition and In by extraction of HInBr_4 with isopropyl ether, then most of the trace elements are finally determined by atomic-absorption spectrometry, and the rest by neutron-activation analysis. All the steps involved in the procedures have been optimized by using radioisotopes as tracers. By the procedures developed, a wide range of trace elements in CuInS_2 , down to submicrogram level, can be determined.

Copper indium sulphide (CuInS_2) is an important ternary semiconductor material.¹ As with other semiconductors, determination of the stoichiometry of this compound is important to avoid crystal defects.² Equally important is the absence, or control at the nanogram level, of certain trace elements which can seriously affect the electrical, optical and other physical properties.³

The analytical approaches chosen by us were largely dictated by the limited amount of sample available, consisting of single crystals or thin films of CuInS_2 . By necessity, the methods therefore had to be suitable for the determination of all three elements in the same sample portion. We chose the following approach. After dissolution of the sample in concentrated nitric acid under pressure, copper is removed by electro-deposition, then dissolved in nitric acid and titrated with EDTA at pH 2.3–2.5. The electrolyte from the copper determination is treated with hydrochloric acid to expel nitric acid, then indium is titrated with EDTA under the same conditions as for copper. After titration of the indium, sulphate is precipitated and finally weighed as barium sulphate.

The trace elements are mainly determined by flame atomic-absorption spectrometry (AAS), and some by neutron-activation analysis (NAA) after sequential removal of copper either electrolytically or by precipitation with thioacetamide, and indium by extraction with isopropyl ether from 5M hydrobromic acid or 6M hydrochloric acid medium. We used radiotracer techniques to check and optimize the recovery of the

trace elements concerned throughout the separation procedure.

EXPERIMENTAL

Reagents and radiotracers

Reagent grade chemicals were used throughout. Stock analyte solutions (0.1%) were prepared, and diluted to give the other standard solutions used. The water used throughout the stoichiometry analysis was prepared by single distillation followed by passage through a demineralizer. For the trace analysis, the water was further distilled in a two-stage quartz distillation apparatus (Berghof, West Germany) and the acids (nitric and hydrochloric) in a sub-boiling quartz distillation apparatus (Becher, West Germany).

The radiotracer solutions (^{65}Zn , ^{64}Cu , ^{56}Mn , etc.) were obtained by irradiating appropriate salts in the Swimming Pool Reactor of the National Tsing Hua University (1 MW power, flux 10^{12} n.cm⁻².sec⁻¹), followed by dissolution and adjustment to a suitable medium composition. The radiotracer ^{210}Pb was purchased from the Radiochemical Centre, Amersham, England.

Apparatus

A Berghof pressure digestion system, with a 10-ml PTFE liner, was used for decomposition of the CuInS_2 samples.

Two radioactivity counting systems were used: one was a multichannel γ -ray spectrophotometer comprising a 4096-channel pulse-height analyser coupled with a Hewlett-Packard 2116 C Basic Computer, and a 43-cm³ Ge(Li) detector (ORTEC). The other was a NaI(Tl) γ -scintillation counter (ORTEC). The choice of system depended on whether one nuclide was to be determined or several, and on the counting efficiency required.

Atomic-absorption spectrometry was done with an Instrumentation Laboratory 257 unit with a flame furnace.

A Hilger and Watts spectrometer, digital Model H 1620/H 1621, was also used.

*To whom correspondence should be addressed.

The controlled potential electro-deposition system consisted of a 30-ml lucite electrolysis cell (with two platinum electrodes, each of 6.3 cm² area, and one calomel reference electrode), a potentiostat and d.c. power supply, and a magnetic stirrer.

Procedures

CuInS₂ stoichiometry. A portion of powder or crystal samples weighing 50–100 mg is heated for 2 hr at 100° in a PTFE-lined pressure bomb with 5 ml of concentrated nitric acid. The solution is evaporated to expel the excess of acid and diluted to 20 ml. Copper is then electroplated on a platinum electrode for 100 min at –0.5 V *vs.* SCE. The copper deposited is dissolved with 2 ml of concentrated nitric acid, and after dilution with water to 20 ml, the solution is adjusted to pH 2.3–2.5 with ammonia solution and the copper is titrated with 0.01M EDTA with PAN as indicator.

The copper-free electrolyte is heated with three successive 5-ml portions of concentrated hydrochloric acid to expel the nitric acid, the pH is adjusted to 2.3–2.5 with ammonia solution and the indium is titrated with 0.01M EDTA, with Cu-PAN as indicator.

After titration of the indium, the sulphate is precipitated with barium chloride solution. The barium sulphate is filtered off, washed, ignited at 950° for 5 hr, cooled and weighed.⁴

Determination of trace elements in CuInS₂. Another sample portion (50–100 mg) is dissolved in nitric acid and copper removed electrolytically as above. The electrolyte is evaporated to dryness, and 3 ml of 5M hydrobromic acid are added, followed by extraction of the indium with two portions of di-isopropyl ether (total volume 5 ml). The organic phase is discarded. The aqueous phase is evaporated to dryness and taken up in 0.1M nitric acid. Cd, Co, Sb, Ca, Mg, Ni, Mn, Pb and Zn are determined in this solution by flame AAS, and P is determined by conversion into Molybdenum Blue, and spectrophotometry at 840 nm. The sensitivity of the Cd, Co, Mn, Ni, Pb and Zn determinations can be increased by extracting these elements at pH 4.5 with 5 ml of 0.1% ammonium pyrrolidine dithiocarbamate (APDC) solution into 5 ml of chloroform and determination by neutron-activation analysis (NAA). Elements such as Ag and Hg which are co-deposited with Cu are dissolved off the electrode with 2 ml of 6M nitric acid, and then subjected to neutron irradiation. The irradiated sample is set aside for 1 week to allow the decay of ⁶⁴Cu, and finally measured by gamma-spectrometry.

In an alternative procedure, some trace elements (Ga, Tl and Fe) are directly extracted from 6M hydrochloric acid medium with di-isopropyl ether after evaporation of the copper-free electrolyte to dryness. AAS is used to determine the elements thus isolated.

DISCUSSION

CuInS₂ has the chalcopyrite structure and a high melting point.⁵ It is only sparingly soluble in hydrofluoric, hydrochloric or nitric acid but is readily decomposed by heating with nitric acid under pressure, about 5 ml being sufficient for 100 mg of CuInS₂. Hydrochloric acid cannot be used because part of the sulphur would be lost as hydrogen sulphide. Nitric acid has the advantage that it oxidizes the sulphur in the sample to sulphate, which can then be precipitated as barium sulphate. Nitric acid also provides the proper medium for electro-deposition of the copper and oxidation of trace elements such as Fe, Sb and Tl to their higher oxidation states.

Stoichiometry of CuInS₂

Determination of copper. Electro-deposition was finally chosen for the separation of copper because of its high selectivity. Preliminary tests were made, to verify that this procedure is applicable to the limited sample weights available for analysis. From the current *vs.* cathode-potential curve it was found that a cathode-potential maintained at about –0.5 V *vs.* SCE., was optimal for the deposition. The amount of copper remaining in the electrolyte was determined by extraction with diethyldithiocarbamate into chloroform and spectrophotometric measurement at 435 nm.⁶ It was established that 100 min of electrolysis time is ample to reduce the copper content to below 30 µg.

Determination of indium. The solution left after the electrolysis is well suited for the determination of indium by titration with EDTA. We have found that a direct EDTA titration of indium in the presence of copper is not feasible. Such a method, applied in alkaline medium, with potassium cyanide as masking agent, has been described,⁷ but we always obtained low results (from –3 to –5% error) when we applied this procedure to CuInS₂. In our opinion this is possibly due to partial interaction of In(III) with excess of cyanide, and this method is suitable only when copper is present as a minor constituent of the sample.

Determination of sulphur. The determination of sulphur in the solution remaining after the titration of indium, while not as precise as that of copper and indium, is adequate and is being used by us in routine analysis.

An alternative based on the evolution of hydrogen sulphide is under investigation, and the initial results look encouraging.

Results for determination of copper, indium and sulphur in simulated samples by the scheme outlined above are given in Table 1. They show good precision and accuracy for copper and indium. The

Table 1. Accuracy and precision tests for the determination of Cu, In and S in a simulated sample solution

Element (amount)	Found, mg	Error, mg	Mean relative error, %	Relative std. devn., %
Cu (26.20 mg)	26.18	–0.02	–0.1	0.1
	26.22	+0.02		
	26.18	–0.02		
	26.15	–0.05		
	26.17	–0.03		
In (47.37 mg)	47.42	+0.05	+0.1	0.2
	47.31	–0.06		
	47.15	+0.08		
	47.50	+0.13		
	47.44	+0.07		
S (26.45 mg)	26.25	–0.20	–0.7	0.9
	26.16	–0.29		
	26.23	–0.22		
	26.42	–0.03		

Table 2. Typical analytical results of stoichiometry for CuInS₂ samples from different synthetic batches

Sample	Measured amount, mg			Atomic proportions		
	Cu	In	S	Cu	In	S
1	25.67	46.73	28.04	1.000	1.007	2.17
2	26.18	48.34	26.30	1.000	1.022	2.00
3	25.86	48.22	26.40	1.000	1.032	2.03
4	26.17	48.22	25.80	1.000	1.019	1.96

somewhat greater errors observed in the sulphur results can be largely attributed to the limited quantity of sample available for analysis and to an effect of the In-EDTA complex on quantitative precipitation of barium sulphate. When the proposed procedure was applied to actual samples of CuInS₂, the results reported in Table 2 were obtained.

The correlation of stoichiometry with physical properties will be discussed sometime in the future.

Determination of trace elements in CuInS₂

In the determination of trace elements in metal samples, the detectability and accuracy obtainable by direct instrumental techniques will in most cases be seriously affected by matrix effects. To determine the trace elements in CuInS₂ sensitively and accurately, special efforts must be made to develop and optimize the analytical procedures, involving first the elimination of copper and indium, and then determination of the isolated trace elements by instrumental methods. The efficiency of isolation of the trace elements was mainly estimated by using radioisotopes as tracers.

Removal of copper. Since the proposed procedure involves the electro-deposition of copper, it was necessary to determine the extent, if any, of co-

deposition of trace elements expected to occur in CuInS₂. This information is provided in Table 3. As would be expected, silver and mercury are quantitatively deposited with the copper. Gold was not considered in this study because it remains insoluble when a sample of CuInS₂ is dissolved in nitric acid. An alternative method for removal of copper, by precipitation with thioacetamide in hydrochloric acid medium,⁸ was also investigated. Table 4 shows the retention of various elements in solution when CuS is precipitated with thioacetamide at 90°.

Comparison of the two copper-removal techniques indicates that the CuS precipitation is simpler and less time-consuming but gives poorer decontamination of copper and greater chance of introduction of impurities. We therefore prefer the electro-deposition method. It must be realized, however, that some elements such as Ag, Hg, and probably Pd are co-deposited with copper and hence cannot be determined by this procedure without modification (see Table 3).

Removal of indium. Indium must be removed before the final determination of trace elements. We prefer the ion-association extraction of indium with di-isopropyl ether from 5M hydrobromic acid to extraction of indium chelate complexes^{9,10} (which are all pH-dependent).

In addition to In(III), Tl(III) is also quantitatively extracted with di-isopropyl ether, while As(III), Ga(III), Fe(III), Sn(IV) and Sb(V) are partially extracted.¹¹ Table 5 gives the results of tests to establish

Table 3. Retention of various elements in the electrolytic solution after controlled cathode-potential electro-deposition of Cu ($E_c = -0.5$ V vs. SCE)

Element	Taken, μ g	Retention in electrolytic solution, %
Zn(II)	10,000	99
	100	100
	5.5	99
Pb(II)	20	85
	100	99
Cr(VI)	50	100
	5	98
Cd(II)	600	100
	50	99
Ga(III)	0.5	98
	1000	98
Co(II)	50	96
	0.5	98
Ni(II)	50	98
	0.5	98
Mn(II)	50	98
	50	98
Sb(V)	6	3
	120	2
Ag(I)	20	100
	30	99
Mo(VI)		
P(V)		

Table 4. Retention of elements in solution after precipitation of CuS with thioacetamide

Element	Content, μ g	Retention in solution, %	
		3M HCl	5M HCl
Co(II)	50	95	95
	5	95	95
Cr(VI)	50	98	98
	600	93	94
Ga(III)	50	94	95
	93	99	99
Mn(II)	9.3	99	99
	0.93	97	98
Pb(II)	20	96	95
	50	97	92
Ni(II)	50	96	96
	60	96	97

Amounts of elements in 30 ml of HCl solution: $\text{Cu}^{2+} = 26.2$ mg, $\text{In}^{3+} = 43.7$ mg and $\text{SO}_4^{2-} = 79.4$ mg.

Table 5. Retention of trace elements in 5M HBr after solvent extraction with di-isopropyl ether

Element	Content, μg	Retention in HBr, %
Zn(II)	20	99
	9	95
Co(II)	6	99
Cd(II)	5	99
Mn(II)	5	99
Ni(II)	50	99
As(V)	5	31
Pb(II)	4	98
Sb(V)	5	98
Mo(VI)	10	49
Ga(III)	10	71
Fe(III)	100	1
Tl(III)	10	1
In(III)	10,000	0.2

Volume ratio: Aqueous phase 15 ml/organic phase 5 ml.

the degree of the retention of trace elements in the aqueous phase after extraction with di-isopropyl ether. About 99.8% of the indium is extracted. More than one extraction may be required to reduce the indium in the aqueous phase to a level suitable for AAS determination of the Ca, Cd, Co, Mg, Mn, Ni, Pb and Zn. P is determined spectrophotometrically after conversion into Molybdenum Blue. If the final measurement of the trace element is to be based on neutron activation, species such as Na^+ , Br^- and SO_4^{2-} which form interfering nuclides (^{24}Na , ^{82}Br and ^{32}P) must also be removed. This can be achieved by APDC-chloroform extraction, thus allowing the determination of a group of trace elements such as Co, Cd, Mn, Ni and Zn. The data in Table 5 also indicate that important trace elements, such as Ga, Tl, Fe and Mo, are either partially or completely extracted into di-isopropyl ether. Also of interest is the extraction of some trace elements into di-isopropyl ether from 6M hydrochloric acid, with indium left in the aqueous phase.^{12,13} Tests done with the help of tracers have indicated that Ga, Tl and Fe are extracted with yields ranging from 86 to 98%, but Mo is extracted poorly.

By use of both these extraction procedures, from hydrobromic and hydrochloric acid media, a wide range of elements can be determined. The two schemes do not cover Ag and Hg, which are co-deposited with Cu, but these elements can be deter-

mined by neutron activation. After irradiation, the sample is allowed to stand until the ^{64}Cu (half-life 12.7 hr) has completely decayed. The trace elements of interest can then be determined by measuring the characteristic gamma peaks of the nuclides with half-lives greater than that of ^{64}Cu . The suggested extraction procedure is not suited for the determination of As, Mo and possibly some other elements not covered by this investigation.

In the multistage procedures outlined above, the blank values for Ag, Sb, Co and Zn are in the range 1–10 ng/g while those for Hg, Cd, Mn, Pb and Ni are of the order of 10–100 ng/g. Sources of the blanks are presumably impurities in the reagents, the apparatus, and the laboratory surfaces and air, all of which should be meticulously controlled. The limit of detection of the elements listed is estimated to be in the range of 10–100 ng/g, based on the criterion $X_s = X_b + 3\sigma_b$ where X_s and X_b are the values of the sample signal and the mean blank signal respectively, and σ_b is the standard deviation of the mean blank value.¹⁴

Table 6 gives typical results obtained for trace elements in the form of impurities and dopants in actual samples of CuInS_2 . The limit of detection and the relative standard deviation for triplicate analysis of each element are indicated. The reliability of the analytical data have been checked for some elements (Co, Cd, Zn and P) by the method of standard additions.

Acknowledgement—This work was supported by a grant from the National Science Council of the Republic of China (NSC 70-0204-M007-03).

REFERENCES

1. J. L. Shay and J. H. Wernick, *Ternary Chalcopyrite Semiconductors, Growth, Electronic Properties and Application*. Pergamon Press, New York, 1976.
2. P. F. Kane and G. B. Larradbee, *Characterization of Semiconductor Materials*. McGraw-Hill, New York, 1970.
3. R. A. Laudise, *Analytical Chemistry: Key to Progress on National Problems*, NBS Special Publication 351, p. 19. US Department of Commerce, National Bureau of Standards, Washington, 1972.
4. I. M. Kolthoff and E. B. Sandell *Textbook of Quantitative Inorganic Analysis*, 3rd Ed., p. 331. Macmillan, New York, 1952.

Table 6. Analytical results for the determination of trace and dopant elements in CuInS_2

Sample*	Impurity elements, $\mu\text{g/g}$								
	Ag	Pb	Co	Cd	Hg	Ni	Sb	P†	Zn†
1	0.9	< 0.1	0.34	0.3	< 0.1	0.5	0.36	1.1	4.4
2	0.8	< 0.1	0.26	< 0.1	< 0.1	< 0.1	0.6	2200	4500
DL§	0.05	0.1	0.02	0.1	0.1	0.1	0.02	0.2	0.02
RSD,§ %	5	—	8	12	—	18	15	3	5

*Samples 1 and 2 are respectively synthesized-charge and CVT (chemical vapour transport) crystals.

†P and Zn in sample 2 are intentionally added dopant elements.

§DL and RSD are respectively the detection limit and relative standard deviation of triplicate analysis for each element.

5. H. M. Kasper, *Solid State Chemistry, Proceedings of the 5th Materials Research Symposium, July 1972*, p. 671. NBS Special Publication No. 364.
6. E. B. Sandell, *Colorimetric Determination of Traces of Metals*, 3rd Ed. Interscience, New York, 1959.
7. K. Ueno, *Chelatometric Titration*, 10th Ed. Nanko-To, Tokyo, 1964.
8. E. Jackwerth and P. G. Willmer, *Z. Anal. Chem.*, 1976, **279**, 23.
9. R. Bock, H. Kusche and E. Bock, *ibid.*, 1953, **138**, 167.
10. H. M. Irving and F. J. C. Rossotti, *Analyst*, 1952, **77**, 801.
11. O. G. Koch and G. A. Koch-Dedic, *Handbuch der Spurenanalyse*, Vol. 1, p. 265. Springer-Verlag, Berlin 1974.
12. F. C. Edwards and A. F. Voigt, *Anal. Chem.*, 1949, **21**, 1204.
13. N. H. Nachtrieb and R. E. Fryxell, *J. Am. Chem. Soc.*, 1949, **71**, 4035.
14. G. Tölg, *Talanta*, 1972, **19**, 1489.

EXTRACTIVE-SPECTROPHOTOMETRIC DETERMINATION OF MOLYBDENUM WITH 4-UNSUBSTITUTED-5-PYRAZOLONES

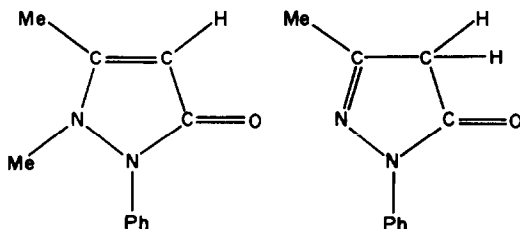
A. AHMAD, F. IK. NWABUE* and G. E. EZEIFE
Department of Chemistry, University of Nigeria, Nsukka, Nigeria

(Received 19 September 1983. Accepted 2 November 1983)

Summary—A fairly sensitive and selective method for rapid determination of tracer amounts of molybdenum(V) as mixed-ligand complexes with thiocyanate and 4-unsubstituted-5-pyrazolones is described. The red complexes are extractable into chloroform from 1–5*M* hydrochloric or perchloric acid or 1–3*M* sulphuric acid media. The molar absorptivities are in the range $1.72\text{--}2.15 \times 10^4 \text{ l. mole}^{-1} \text{ cm}^{-1}$ at 455 nm (λ_{max}). The method has been applied to the estimation of molybdenum in various synthetic and alloy-steel samples. In presence of excess of the reagent, Cu(II), Co(II), Mn(II), Fe(II), Fe(III), Al(III), Cr(III), Cr(VI), Ti(III), Ti(IV), Zr(IV), Hf(IV), V(III), V(IV), V(V), Nb(V), Ta(V), W(VI) and U(VI) do not interfere.

Since Braun's work¹ in 1863 on the use of thiocyanate for the determination of molybdenum, a considerable literature has appeared on the subject. Much of it concerns improved methods of reducing Mo(VI) to Mo(V)^{2–10} prior to determination, as well as formation of mixed-ligand complexes of molybdenum with thiocyanate and O-, N- or S-containing complexants^{11–17} to enhance sensitivity and selectivity. Spectrophotometric methods based on the use of these systems suffer from various difficulties, including the poor availability and low purity of many of the complexants.

In our search for various analytical uses of 5-pyrazolones we have found 2,3-dimethyl-1-phenylpyrazol-5-one (HDMPP), **A**, commonly known as antipyrine, and 3-methyl-1-phenylpyrazol-5-one (HMPP), **B**, most promising as simple and selective reagents for the determination of trace amounts of molybdenum in presence of thiocyanate. The reagents are easy to prepare pure and are commercially available, and the method is fairly sensitive and rapid.



A, HDMPP

B, HMPP

EXPERIMENTAL

Reagents

All reagents and solvents used were of analytical grade. All aqueous solutions were prepared with distilled and demineralized water.

Standard molybdenum(VI) solution. Prepared by dissolving 0.1840 g of ammonium heptamolybdate tetrahydrate in water and standardized by the oxine method.¹⁸ The working solution was prepared by appropriate dilution.

HDMPP and HMPP solutions. Prepared as 1% solutions in chloroform.

Ammonium thiocyanate and ascorbic acid solutions. Freshly prepared as 20% and 10% solutions respectively.

Procedure

To about 3 ml of solution containing 1–90 μg of Mo(VI) add 2 ml each of the ammonium thiocyanate and ascorbic acid solutions and of 10*M* hydrochloric or sulphuric acid. Dilute to 10 ml with distilled water and shake with 10 ml of either HDMPP or HMPP solution for 2 min. Separate the organic layer, dry it for 2 min over anhydrous sodium sulphate (1 g) and measure its absorbance at 455 nm against a reagent blank.

Procedure for steel analysis

Dissolve 0.1 g of steel sample in a few ml of *aqua regia* and evaporate the solution to dryness. Heat the residue with 3 ml of concentrated sulphuric acid until fuming; repeat this step twice and then heat to fumes with 3 ml of concentrated perchloric acid. Cool and take up the salts in 10 ml of 1*M* hydrochloric acid. Add 1 g of ammonium oxalate to mask any interference from V(V), U(VI) and W(VI) and make up accurately to 100 ml with distilled water. Determine molybdenum in a suitable aliquot, as already described.

RESULTS AND DISCUSSION

Spectral characteristics

The absorption spectra of the metal chelates, ligands and the Mo–SCN complex extracted into chloroform from 1*M* hydrochloric acid are shown in

*Author to whom correspondence should be addressed.

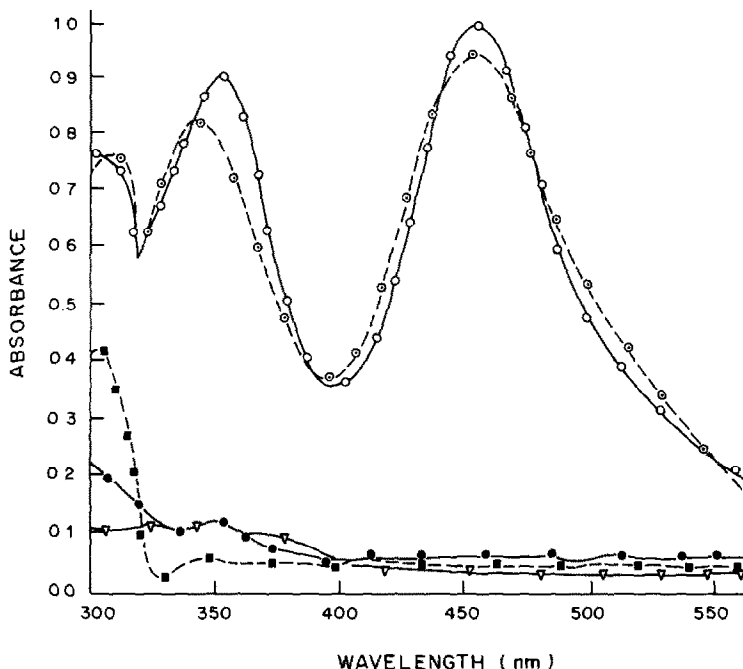


Fig. 1. Absorption spectra. $[HCl]$ 2M; $[SCN]$ 4%; [ascorbic acid] 2%; (○—○—○) Mo-SCN-DMPP complex; (○—○—○) Mo-SCN-MPP complex; (●—●—●) Mo-SCN-complex; (■—■—■) 1% HMPP; (▽—▽—▽) 1% HDMPP.

Fig. 1. The spectra of the chelates are similar, with maxima at 455 nm and about 350 nm. The absorption at 455 nm is the higher and is therefore used for the determination. The reagents and the Mo-SCN complex have negligible absorption at this wavelength.

Choice of solvent and reducing agent

Chloroform, carbon tetrachloride, benzene, toluene and methyl isobutyl ketone (MIBK) were tried as solvents. The reagents are readily soluble in chloroform and MIBK but dissolve with difficulty in the rest. MIBK, however, developed an undesirable colour by reaction with thiocyanate, and this interfered with the determination. Chloroform showed high extractibility and its solution gave the highest absorbance for the metal chelates; hence it was chosen as solvent. Ascorbic acid has been shown^{10,17} to have advantages as a reducing agent in molybdenum determinations involving thiocyanate. The effect of variation in the amount of ascorbic acid was examined by using the recommended procedure with the acid concentration varied in the range 1–10% with 4 μ g of molybdenum. Maximum colour development and extraction were observed over the concentration range 1.5–2.7%. Outside this range the absorbance decreased considerably. A concentration of 2.0% was chosen as the final ascorbic acid concentration in the solution to be extracted.

Effect of other variables

The effect of variation in the HMPP and HDMPP concentration was examined in the range 0.1–10%.

Complete extraction was obtained with concentrations above 1%, without variation in absorbance. Hence 1% was selected as a convenient concentration. The effect of variation in thiocyanate concentration was examined similarly and it was found that the range 3.4–5.0% was necessary for complete recovery of molybdenum. A total thiocyanate concentration of 4.0% in the solution to be extracted was chosen.

The acidity of the aqueous phase was systematically varied with hydrochloric, sulphuric and perchloric acids. The optimum acidity ranges for HDMPP were 1–5M hydrochloric or perchloric acid, and 1–3M sulphuric acid, and for HMPP 1–3.5M hydrochloric or sulphuric acid, and 1–2M perchloric acid. Within these ranges the same values of λ_{max} and molar absorptivity were obtained. Acid concentrations above these ranges decreased the extraction efficiency because of increased miscibility of chloroform with the aqueous phase, and below these ranges colour development was either slow or incomplete. Hence 2M hydrochloric or sulphuric acid was preferred for ease of manipulation and increased selectivity. Nitric acid gave no colour development but fumes of nitric oxide were evolved, probably owing to its redox reaction with ascorbic acid.

Preliminary tests indicated that a shaking time of 2 min was sufficient for quantitative extraction of molybdenum. Variations in temperature from 18 to 40° and in volume of the aqueous phase from 5 to 40 ml had no effect on the absorbance and extraction efficiency. Stability of the colour was studied at room

Table 1. Effect of diverse ions on the determination of 4 ppm of Mo(VI) with thiocyanate and HDMPP

Ion added	Tolerance limit,* mg/ml	Ion added	Tolerance limit,* mg/ml
Pb(II)	5	Hf(IV)	3
Mn(II)	5	V(IV)	1
Ni(II)	1	V(V)	2†
Fe(II)	2.5	Nb(V)	2
Cu(II)	5	Ta(V)	2.5
Zn(II)	5	Cr(VI)	2†
Co(II)	2	W(VI)	2†
V(III)	2†	U(VI)	2†
Cr(III)	2	EDTA	8
Fe(III)	2.5	F ⁻	3
Al(III)	5	Cl ⁻	6
La(III)	5	NO ₃ ⁻	1
Bi(III)	1.5	ClO ₄ ⁻	6
Ti(IV)	1	PO ₄ ³⁻	4
Th(IV)	3	SO ₄ ²⁻	7
Zr(IV)	4	C ₂ O ₄ ²⁻	6

*Average of 5 determinations, <1% error.

†In presence of 1% ammonium oxalate.

temperature (about 25°). Maximum absorbance was obtained within 1 min after extraction and remained constant for at least 3 days. The order of addition of the reagents was not critical.

Calibration range, sensitivity and precision

The calibration graph is linear over the range 0.1–9 ppm of Mo with an optimal working range of 0.3–6 ppm (Ringbom plot). At 455 nm, the molar absorptivities of the metal–DMPP–SCN and metal–MPP–SCN chelates in chloroform are 2.15×10^4 and 1.72×10^4 l.mole⁻¹.cm⁻¹. The relative standard deviation (twelve determinations of 4 ppm Mo) is 0.9% with both reagents.

Effect of diverse ions

The effect of some ions, particularly those associated with molybdenum ores and alloy steels, in the determination of 4 ppm of molybdenum by the recommended procedure, was examined. Chloride, bromide, sulphate, phosphate, chlorate, oxalate and

alkali metals in up to 5000-fold amount, alkaline-earth metals and fluoride up to 3000-fold amount, and nitrate up to 1000-fold amount (relative to molybdenum) do not interfere. The tolerance limits for other ions are given in Table 1.

Composition of the complex

Job's method and the mole-ratio method indicated a mole ratio of 1:2:1 for Mo:thiocyanate:HDMPP or HMPP. The species extracted are probably MoO(SCN)₂(DMPP) and MoO(SCN)₂(MPP), in which the deprotonated ketonic form of the pyrazolone (as a carbanion) co-ordinates to the metal through the 5-keto oxygen atom and the carbon atom at the 4-position, which has previously lost an active hydrogen atom. Thus a carbon–metal bond is formed, conferring increased stability on the 4-membered chelate ring, as expected of such organometallic compounds. This is probably why the colour is stable for many days.

Applications

The recommended procedure was tested with synthetic solutions and two British Chemical Standard steels. Results for analysis of the alloy steels were 0.15–0.16% for BCS 325 (certified value 0.16%) and 0.22–0.24% for BCS 320 (certified value 0.22%). The relative standard deviations for six replicates were 0.8% and 1.1% respectively. Results of analysis of the synthetic solutions are given in Table 2.

REFERENCES

1. C. D. Braun, *Z. Anal. Chem.*, 1863, **2**, 36.
2. A. T. Dick and J. B. Bingley, *Nature*, 1964, **158**, 516.
3. F. N. Ward, *Anal. Chem.*, 1951, **23**, 788.
4. C. E. Crouthamel and C. E. Johnson, *ibid.*, 1954, **26**, 1284.
5. C. H. Williams, *J. Sci. Food Agric.*, 1955, **6**, 104.
6. R. P. Hope, *Anal. Chem.*, 1957, **29**, 1053.
7. A. M. Wilson and O. K. McFarland, *ibid.*, 1964, **36**, 2488.
8. *Determination of Molybdenum*, British Standards Handbook No. 19, British Standards Institution, London, 1970.

Table 2. Determination of molybdenum in various synthetic matrices

Contents per ml	Mo found,* µg/ml	Relative standard deviation, %
5 µg Mo(VI) + 2 mg Fe(III) + 2 mg Cr(III) + 2 mg W(VI) + 2 mg U(VI) + 5 mg Zn(II)	4.97	1.2
3.5 µg Mo(VI) + 2 mg V(V) + 2 mg W(VI) + 2 mg Cr(III) + 4 mg PO ₄ ³⁻ + 2 mg Hf(IV)	3.51	0.8
6 µg Mo(VI) + 2 mg V(V) + 2 mg Nb(V) + 4 mg Zr(IV) + 1 mg Ti(IV)	6.01	1.1
4 µg Mo(VI) + 1 mg Ni(II) + 5 mg Mn(II) + 5 mg Zn(II) + 2 mg Co(II) + 2.5 mg Fe(III)	3.96	1.0

*Average of 8 determinations.

9. E. G. Lillie and L. P. Greenland, *Anal. Chim. Acta*, 1974, **69**, 313.
10. A. G. Fogg, J. L. Kumar and D. T. Burns, *Analyst*, 1975, **100**, 311.
11. M. M. Khosla and S. P. Rao, *Anal. Chim. Acta*, 1971, **57**, 323.
12. C. Różycki and J. Kamińska, *Chem. Anal. (Warsaw)*, 1972, **17**, 1209.
13. V. Yatirajam and J. Ram, *Mikrochim. Acta*, 1974, 671.
14. B. Tamhina, M. J. Herak and V. Jagodić, *Anal. Chim. Acta*, 1975, **76**, 417.
15. B. Tamhina and M. J. Herak, *Mikrochim. Acta*, 1976 **I**, 553.
16. M. Mitra and B. K. Mitra, *Talanta*, 1977, **24**, 698.
17. K. S. Patel and R. K. Mishra, *ibid.*, 1982, **29**, 791.
18. A. I. Vogel, *A Textbook of Quantitative Inorganic Analysis*, 3rd Ed., p. 508. Longmans, London, 1961.

ANION-EXCHANGE RESIN MODIFIED WITH BISMUTHIOL-II, AS A NEW FUNCTIONAL RESIN FOR THE SELECTIVE COLLECTION OF SELENIUM(IV)

MORIO NAKAYAMA

Department of Industrial Chemistry, Kumamoto University, 2-39-1 Kurokami, Kumamoto 860, Japan

KAZUO ITOH

Environmental Pollution Research Institute, City of Nagoya, Minami-ku, Nagoya 457, Japan

MASAHIKO CHIKUMA

Chest Disease Research Institute, Kyoto University, Sakyo-ku, Kyoto 606, Japan

HIROMU SAKURAI

Faculty of Pharmaceutical Sciences, Tokushima University, Shomachi, Tokushima 770, Japan

HISASHI TANAKA

Faculty of Pharmaceutical Sciences, Kyoto University, Sakyo-ku, Kyoto 606, Japan

(Received 15 June 1983. Revised 17 September 1983. Accepted 28 October 1983)

Summary—A functional resin for the collection of selenium(IV) has been prepared simply by the conversion of a common ion-exchange resin with bismuthiol-II which has three functional properties, namely the capabilities of selective reaction with selenium(IV), ion-exchange reaction with ion-exchange resin and strong physical sorption to the ion-exchange resin matrix. The binding ratio of selenium(IV) to bismuthiol-II on the resin was confirmed to be 1:4. The reaction was represented as follows: $4RSH + H_2SeO_3 \rightarrow R-S-Se-S-R + R-S-S-R + 3H_2O$. Highly selective sorption of selenium(IV) was achieved, based on the formation of stable selenotrisulphide on the resin. Selenium(IV) sorbed on bismuthiol-II resin was eluted effectively with 8–13M nitric acid or some thiols, such as cysteine and penicillamine. In the cases of thiols, the elution of selenium was found to be also based on the formation of selenotrisulphide, and the bismuthiol-II resin was regenerated. Satisfactory results were obtained when this resin was applied to the determination of selenium(IV) in river, estuarine or sea water samples.

The development of a simple method for the selective collection of trace amounts of selenium in environmental and biological material has been attempted by the use of a common ion-exchange resin loaded with a reagent which has three important analytical properties: selective reaction with selenium(IV), an ion-exchange reaction with the resin, and strong physical adsorption on the resin. We have found that selenium(IV) can be collected on an anion-exchange resin loaded with azothiopyrine disulphonic acid,¹ but the method is not satisfactory for low selenium levels. The selenium is collected by means of its reaction with the thiol group of azothiopyrine disulphonic acid to form a selenotrisulphide. We have now found that bismuthiol-II (Fig. 1) also forms a stable selenotrisulphide and can be used for making a functional resin for selective collection of selenium(IV), even at trace levels. This bismuthiol-II resin is suitable for analysis of environmental samples.

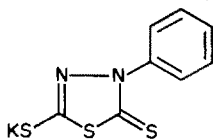


Fig. 1. Bismuthiol-II.

EXPERIMENTAL

Apparatus

Absorption spectra in the ultraviolet and visible regions were measured with a Hitachi 330 spectrophotometer. A Shimadzu RF-500 spectrofluorophotometer was used for the fluorometric determination of selenium(IV) with 2,3-diaminonaphthalene (DAN). Metal ions were determined by atomic-absorption spectrometry with a Shimadzu AA-630-01 atomic-absorption spectrophotometer.

Reagents

Amberlite IRA-400 (8% divinylbenzene) in the chloride form, 100–200 mesh, was used as the anion-exchange resin. The exchange capacity of the resin was found to be 3.2 meq per g of air-dried resin. Bismuthiol-II and DL-penicillamine were obtained from Dojindo Laboratories and Sigma Chemicals Co., respectively. All other reagents used were of analytical grade quality.

Preparation of bismuthiol-II resin

The anion-exchange resin was added to an aqueous solution of bismuthiol-II and the mixture was shaken at 30° for 60 min. The resin loaded with bismuthiol-II was filtered off, washed with water and methanol, and dried, stored in a refrigerator, and vacuum-dried before use. The amount of bismuthiol-II in the supernatant solution was found by absorbance measurement at 335 nm, for determination of the exchange capacity.

Determination of amount of chloride ion released in ion-exchange reaction

One g of the anion-exchange resin was shaken for 12 hr with 50 ml of solution containing bismuthiol-II (0.1, 0.2, 0.4 and 1.0 mmole). Twenty-five ml of the solution were titrated with standard silver nitrate solution for determination of chloride.

Determination of bismuthiol-II released by sodium chloride

A 50-mg portion of resin, loaded with various amounts of bismuthiol-II (0.2, 0.4 and 1.0 mmole/g), was shaken for 24 hr with 5 ml of sodium chloride solution (0.1, 0.5 and 1.0M) in a test-tube. The amount of bismuthiol-II released was determined by measurement of the absorbance at 335 nm and pH 5.

Binding-capacity for selenium(IV)

Resin, 50 mg, loaded with various amounts of bismuthiol-II (0.2, 0.4, 0.6 and 1.0 mmole/g) was shaken with an excess of selenium(IV). The hydrochloric acid concentration of this sample solution was adjusted by addition of 5M hydrochloric acid, before it was shaken with the resin. The amount of selenium(IV) left in the solution was determined fluorometrically. The resin with 0.2-mmole/g bismuthiol-II loading was used to determine the binding ratio of selenium(IV) to bismuthiol-II by the molar ratio method.

Collection of selenium(IV) and the effect of metal ions at various pH values

Bismuthiol-II resin (0.2 mmole/g, 100 mg) was shaken for 5 hr with 50 ml of 2-mg/l. solutions of copper(II), manganese(II), chromium(VI), iron(III), zinc(II) and selenium(IV), adjusted to the desired pH with acetate buffer and hydrochloric acid. The ionic strength was maintained at 0.5 by addition of 5M sodium chloride. The resin was then filtered off on a fritted-glass funnel, and an appropriate volume of the filtrate was taken for the determination of selenium(IV) and metal ions by fluorometry and atomic-absorption spectrometry, respectively.

Sorption isotherm

Bismuthiol-II resin (0.2 mmole/g, 100 mg) was shaken with 50 ml of 0.3M hydrochloric acid containing known amounts of selenium(IV), for 5 hr at 30°. After equilibration, an aliquot of the solution was analysed for selenium(IV) by fluorometry.

Elution of selenium(IV) sorbed on bismuthiol-II resin

Method I. Bismuthiol-II resin (0.2 mmole/g, 200 mg) was shaken with 50 ml of 0.3M hydrochloric acid containing 100 µg of selenium(IV), for 5 hr at 30°. The resin, which completely sorbed the selenium(IV), was packed in a glass tube (7 mm bore). Selenium was eluted with 20 ml of 6–13M nitric acid. An aliquot of eluate was analysed for selenium(IV) by fluorometry after adjustment to pH 1 with ammonia solution.

Method II. Bismuthiol-II resin (0.2 mmole/g, 100 or 200 mg) was shaken with 50 ml of 0.3M hydrochloric acid containing 100 or 500 µg of selenium(IV), for 5 hr at 30°. The resin (which completely sorbed the selenium) was packed in a glass tube (7 mm bore). The eluent under test, 20 ml, was passed through the column at a flow-rate of 1.0 ml/min, and the column was washed with 50 ml of distilled demineralized water. Then 20 ml of 10M nitric acid were passed through the column, and the amount of selenium(IV) eluted was determined. The recovery shown in Table 2 was derived by subtracting the amount of selenium eluted with nitric acid from that sorbed on the resin.

Absorption spectrum of the solution after elution of selenium with penicillamine

Selenium(IV), 0.01 mmole, was sorbed completely on 500 mg of 0.2-mmole/g bismuthiol-II resin, and the resin was

filtered off and air-dried, then shaken with 40 ml of 0.01M penicillamine solution at pH 5. After 3 hr, the absorption spectrum of the solution was measured.

Collection of selenium(IV) by column operation

The column (1.0 cm bore) was packed with 0.2-mole/g bismuthiol-II resin to a height of 5.0 cm and washed with 100 ml of distilled demineralized water, then 10-mg/l. selenium(IV) solution in 0.3M hydrochloric acid was passed through the column at a flow-rate of 1.0 ml/min. The amount of selenium(IV) in the effluent was determined by fluorometry. The resin was washed with 50 ml of distilled demineralized water, then eluted with 0.1M penicillamine at pH 5 (flow-rate 1.0 ml/min) and washed with 50 ml of distilled demineralized water. After this elution cycle, 10-mg/l. selenium(IV) solution in 0.3M hydrochloric acid was again passed through the column to reuse the bismuthiol-II resin.

Collection of trace amount of selenium(IV)

After addition of 1.0 and 0.1–1.0 µg of selenium(IV) to 500 ml of 0.4M sodium chloride and 1 litre of pure water respectively, the solutions were treated as in the column operation just described. The selenium eluted with 0.1M penicillamine was determined fluorometrically after digestion with perchloric acid–nitric acid or nitric acid–hydrochloric acid–hydrogen peroxide mixture.

Application of bismuthiol-II resin to the collection of trace amounts of selenium(IV) from environmental water samples

The water samples were filtered (Whatman GF/C, 4.7 cm) immediately after they were taken. Concentrated hydrochloric acid was added to the fresh sample to make the acid concentration 0.5M and this solution was applied to a 1-cm bore column packed with the resin, which was loaded with 0.2 or 0.4 mmole of bismuthiol-II per g, to give a resin bed 5.0 or 10.0 cm in height. Selenium collected on the column was eluted with 20 ml of 0.1M penicillamine or 0.05M cysteine (0.1M in hydrochloric acid) at a flow-rate of 1.0 ml/min. Selenium in the eluate was determined by fluorometry after acid digestion.

RESULTS AND DISCUSSION

Conversion of the anion-exchange resin into bismuthiol-II resin

The anion-exchange resin could be converted into bismuthiol-II resin simply by mixing it with an aqueous solution of bismuthiol-II. The exchange-capacity for bismuthiol-II was found to be 3.1 mmole per g of resin, which is comparable with that for chloride, 3.2 mmole/g. The time required for loading of the resin was dependent on the amount of reagent to be immobilized. Loading of 50% of saturation took 30 min. The 0.2-mmole/g bismuthiol-II resin, which required only 5 min for preparation, was mainly used. When bismuthiol-II was reacted with the anion-exchange resin in the chloride form, the ratio of chloride released to bismuthiol-II sorbed was about 1, indicating that bismuthiol-II is bound to the resin by an ion-exchange mechanism.

Bismuthiol-II was found to be retained on the resin, even when the resin was exposed to 0.1, 0.5 and 1.0M sodium chloride, as shown in Table 1, particularly at low loading. The strong immobilization of bismuthiol-II on the resin must therefore be due to some physical interaction besides simple ion-

Table 1. Bismuthiol-II released with sodium chloride

Eluent	Bismuthiol-II released, %		
	0.2 mmole/g of resin	0.4 mmole/g of resin	1.0 mmole/g of resin
0.1M NaCl	0.26	0.32	0.54
0.5M NaCl	0.68	0.77	1.50
1.0M NaCl	0.83	1.09	2.18

Batch operation: bismuthiol-II resin 50 mg; eluent 5 ml; shaking time 24 hr.

exchange. Some chelating agents, such as dithi-zonesulphonic acid,² azothiopyrinesulphonic acid³ and some formazansulphonic acids⁴ have been found to be bound to anion-exchange resin through their sulphonic acid group, and also strongly sorbed on the resin by some physical interaction. The use of these reagents is more advantageous than that of 8-hydroxyquinoline-5-sulphonic acid, which leaks considerably to the solution in the presence of chloride ion, on account of weaker physical sorption.^{5,6} In bismuthiol-II, which does not have a sulphonic acid or carboxylic acid group, but is strongly sorbed on the ion-exchange resin, the thiolate anion is considered to act as the ion-exchange group, but after immobilization of the reagent on the resin by physical interaction, the thiol group is able to react with selenium(IV) in acid medium. The terfunctional property of bismuthiol-II is thus explained.

Collection of selenium(IV) with bismuthiol-II resin

The binding-capacity of bismuthiol-II resin for selenium(IV) in 0.5M hydrochloric acid is shown in Fig. 2. The time required for 50% uptake of selenium(IV) was less than 20 min. After the sorption of selenium(IV) had reached equilibrium, no turbidity due to release of elemental selenium was observed in the supernatant liquid, and the colour of the resin changed from light brown to pale yellow. The binding-capacity for selenium(IV) increased linearly with increase of the amount of bismuthiol-II on the resin. The reacting ratio of selenium(IV) to bismuthiol-II was found to be approximately 1:4

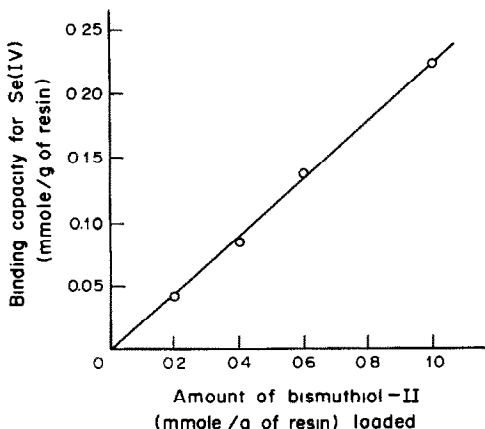


Fig. 2. Binding-capacity of bismuthiol-II resin for selenium(IV).

under the conditions used, as shown in Fig. 3, which corresponds to the ratio in the reaction of selenium(IV) with bismuthiol-II in solution.⁶

The collection of selenium(IV) was complete at pH below 2, as shown in Fig. 4. Selenite is not sorbed on the resin itself under these conditions, so the sorption on the bismuthiol-II resin can be attributed to formation of selenotrisulphide according to equation (1). The optimum pH range for the collection of selenium(IV) agreed with that for the complete extraction of the selenium-bismuthiol-II complex into chloroform.⁷ The reactions of selenium(IV) with some thiols have been expressed as equation (1), although the assumed reaction product (selenotrisulphide) has not been fully characterized, and

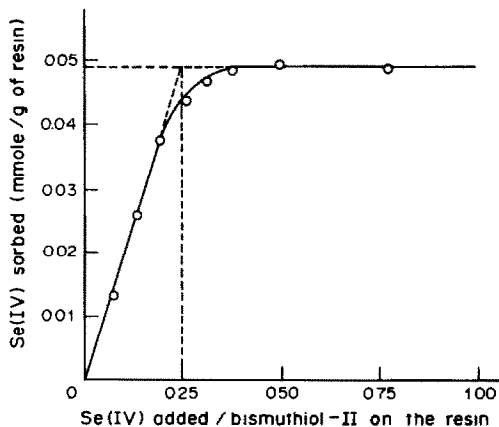


Fig. 3. Binding ratio of selenium(IV) to bismuthiol-II loaded on the resin; bismuthiol-II 0.2 mmole/g of resin.

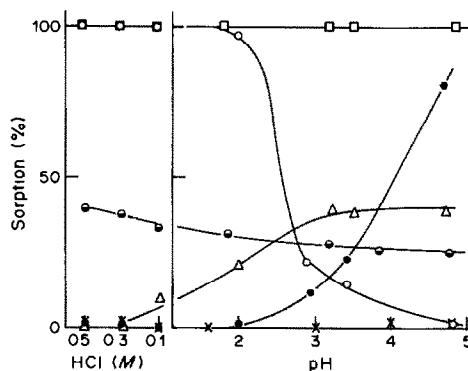
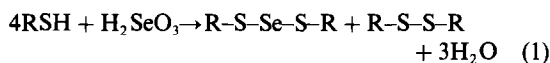


Fig. 4. Collection of selenium(IV) and metal ions. ○ selenium(IV); ● iron(III); ◐ zinc(II); ◑ copper(II); △ chromium(VI); × manganese(II).

in most cases is referred to as unstable.⁸



R = free form of bismuthiol-II

The collection of copper(II), manganese(II), chromium(VI), iron(III), zinc(II) and selenium(IV) by bismuthiol-II resin at various pH values is shown in Fig. 4.

At pH below 2, the collection of selenium(IV) is complete, whereas that of the metal ions is low, except for copper(II). The collection of selenium(IV) from strongly acid medium indicates the high selectivity of this reaction.

Sorption isotherms for selenium(IV) in 0.3M hydrochloric acid with and without 0.5M sodium chloride were almost identical, and the maximum uptake was practically independent of the selenium concentration from 0.001 to about 2 mg/l. Thus the bismuthiol-II resin should be effective for collection of selenium(IV) at very low concentration even from strongly saline samples such as estuarine water and sea-water. Selenium(VI), another important form of selenium, did not react with bismuthiol-II resin under the experimental conditions of this study.

Elution of selenium

There are two possibilities for the elution:

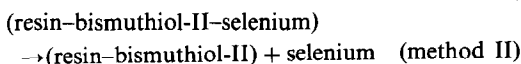
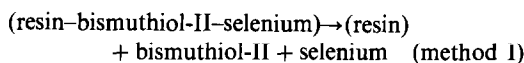


Table 2. Elution of selenium from bismuthiol-II resin by method II

Eluent	Recovery, %
0.01M KMnO ₄	0.0
0.1M KMnO ₄	3.3
0.1M I ₂	0.0
0.1M KIO ₃	0.0
3% H ₂ O ₂	3.6
0.1M NaBH ₄	87.1
0.1M Ascorbic acid	0.0
0.1M Na ₂ S ₂ O ₃	15.3
0.1M SnCl ₂ in 0.1M H ₂ SO ₄	35.7
0.1M thiourea	19.6
0.1M thiourea in 0.1M HCl	8.8
0.5M thiourea	27.3
1.0M thiourea	32.7
0.05M cysteine	98.4
0.01M cysteine	86.5
0.1M cysteine in 0.1M HCl	94.6
0.1M cysteine at pH 4	95.1
0.1M cysteine at pH 7	75.1
0.2M cysteine	79.4
0.05M penicillamine	88.4
0.1M penicillamine	98.2
0.2M penicillamine	98.1

Bismuthiol-II resin 100 mg (0.2 mmole/g of resin); selenium sorbed 100 μg.

where the species in parentheses are in the solid state. Selenium sorbed on bismuthiol-II resin was about 93% eluted with 8–13M nitric acid by method I. The eluate, which contains selenium(IV), can be analysed directly by fluorometry after adjustment to pH 1 with ammonia solution. The high recovery indicates that the collection of selenium(IV) was essentially quantitative. The recovery of selenium(IV) decreased by only about 4% if the selenium(IV) was left on the resin for 23 days before elution, indicating that if selenotrisulphide is formed from bismuthiol-II on the resin, it is unusually stable, and that the resin is valuable for use in field work.

Various reagents were tried as eluents (Table 2). Cysteine and penicillamine were found to be best. Sodium borohydride also gives high recovery, but is not suitable because it forms bubbles in the column.

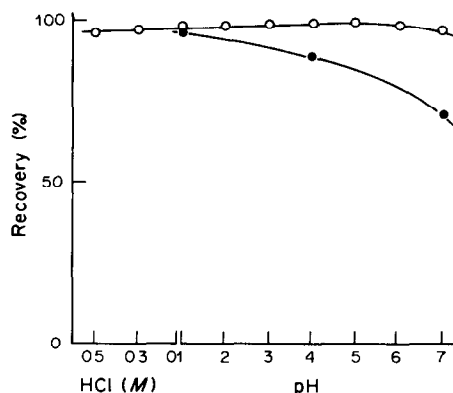


Fig. 5. Elution of selenium from bismuthiol-II resin with penicillamine and cysteine (method II). Bismuthiol-II resin 200 mg (0.2 mmole/g). Selenium sorbed 500 μg. Eluting agent: —○— 0.1M penicillamine, —●— 0.05M cysteine.

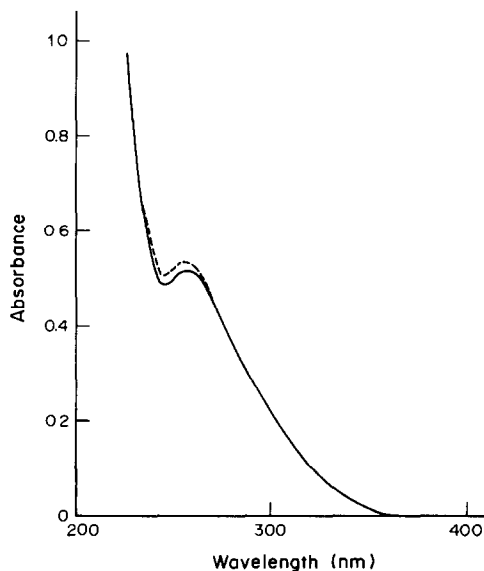


Fig. 6. Absorption spectrum of the solution after elution of selenium with penicillamine. — After elution of 0.01 mmole of selenium from bismuthiol-II resin with 40 ml of 0.01M penicillamine at pH 5; ---- solution of 0.01 mmole of selenium in 40 ml of 0.01M penicillamine at pH 5, concentration of selenium $2.5 \times 10^{-4} M$.

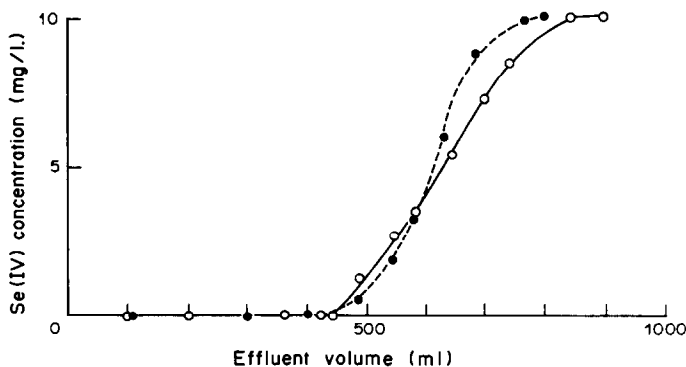


Fig. 7. Break-through curves for selenium(IV). Bismuthiol-II resin: (I) —○— 0.2 mmole/g, (II) ···●··· regenerated with 0.1M penicillamine at pH 5. Resin column 10 × 50 mm. Concentration of selenium(IV) in the sample solution 10 mg/l., in 0.3M hydrochloric acid. Flow-rate 40 ml/hr.

As shown in Fig. 5, penicillamine can be used over a wider pH range than cysteine. When cysteine was used, a slight red turbidity appeared if the eluate was allowed to stand for a week, but this did not occur with penicillamine, so the selenotrisulphide formed with penicillamine is presumably more stable than that formed with cysteine. When 0.01 mmole of selenium was eluted with 0.01M penicillamine at pH 5 by batch operation, the absorption spectrum of the eluate (Fig. 6) was almost identical with that of a solution of 0.01 mmole of selenium in 0.01M penicillamine at pH 5. The reaction-ratio of penicillamine to selenium(IV) at pH 5 was found to be 4:1 by the molar-ratio method and absorbance monitoring at 260 nm. This result indicates that selenium(IV) reacts with penicillamine in the same way as with bismuthiol-II [equation (1)]. This conclusion is supported by the results of a ^{77}Se nuclear magnetic resonance study, which will be reported elsewhere.

The recovery of selenium(IV) and the regeneration of bismuthiol-II resin were investigated by column operation. The break-through curve is shown in Fig. 7. When the bismuthiol-II resin was repeatedly

used and recovered, similar break-through curves were obtained and the concentration of selenium in the effluent up to the break-through point was found to be constantly below 1 $\mu\text{g/l}$.

Application of bismuthiol-II resin to the collection of selenium(IV) from environmental water samples

Bismuthiol-II resin exhibits advantageous features in the selective collection and elution of selenium(IV). The recovery of selenium(IV) from 0.4M sodium chloride is consistently about 95% irrespective of eluent flow-rate from 1.0 to 7.5 ml/min. The recovery from distilled water is also about 95% over the range from 0.1 to 1.0 $\mu\text{g/l}$. The collection of selenium from river, estuarine and sea water by bismuthiol-II resin was examined. Table 3 shows typical results and a comparison result for one sample, by co-precipitation with tellurium.⁹ We have studied extensively the amount and chemical form of selenium in the water of the coast of Nagoya City, which is one of the leading industrial areas in Japan. The results will be reported in detail elsewhere. The values ob-

Table 3. Determination of selenium(IV) in environmental water samples

Sample	Se(IV), $\mu\text{g/l}$.
Ise Bay (Nagoya Harbor), Nagoya, Aichi August, 1983	0.060
Ise Bay (Nogoya Harbor), Nagoya, Aichi August, 1983	0.061*
Ise Bay (Nogoya Harbor), Nagoya, Aichi December, 1982	0.063
Shirakawa River, Kokai, Kumamoto October, 1982	0.075
Shirakawa River, Kokai, Kumamoto March, 1983	0.099
Amakusa Basin, Matsushima, Kumamoto November, 1982	0.016

*Value obtained by co-precipitation with tellurium.⁹

tained were comparable with those obtained by the tellurium co-precipitation method for samples from other places.⁹

In conclusion, this method for collection of selenium(IV) is advantageous in its selectivity and simplicity, and the stability of the reaction product on the resin. It is also useful for preconcentration prior to fluorometric determination (the currently most widely used method for the determination of selenium).

Acknowledgement—Financial support from the Ministry of Education, Science and Culture of Japan (Grant-in-Aid No. 587017) is gratefully acknowledged.

REFERENCES

1. M. Nakayama, M. Chikuma, H. Tanaka and T. Tanaka, *Talanta* 1983, **30**, 455.
2. H. Tanaka, M. Chikuma, A. Harada, T. Ueda and S. Yube, *ibid.*, 1976, **23**, 489.
3. M. Nakayama, M. Chikuma, H. Tanaka and T. Tanaka, *ibid.*, 1982, **29**, 503.
4. M. Grote, P. Wigge and A. Kettrup, *Z. Anal. Chem.*, 1982, **310**, 369.
5. M. Chikuma, M. Nakayama, T. Itoh, H. Tanaka and K. Itoh, *Talanta*, 1980, **27**, 807.
6. K. S. Lee, W. Lee and D. W. Lee, *Anal. Chem.*, 1978, **50**, 255.
7. H. Yoshida, M. Taga and S. Hikime, *Bunseki Kagaku*, 1965, **14**, 1109.
8. H. E. Ganther, *Biochemistry*, 1968, **7**, 2898.
9. K. Hiraki, O. Yoshii, H. Hirayama, Y. Nishikawa and T. Shigematsu, *Bunseki Kagaku*, 1973, **22**, 712.

BINARY DATA ACQUISITION FROM INSTRUMENTATION WITH BCD-CODED OUTPUT: A HARDWARE CONVERTER AND AN EXAMPLE OF THE RELATIVE SOFTWARE CONTROL

L. LAMPUGNANI, D. GUIDARINI and N. FANELLI

Istituto di Chimica Analitica Strumentale del C.N.R., Via Risorgimento 35, 56100 Pisa, Italia

(Received 13 July 1983. Accepted 10 October 1983)

Summary—Simple hardware for conversion from BCD into binary code is described. The device is of low cost, performs a 16-bit conversion in a maximum time of 400 nsec, and is able to output the converted number to either an 8-bit or a 16-bit data bus. An example of the software necessary to perform data acquisition from a digital voltmeter by using this converter is also presented.

Electronic instruments such as pH-meters, automatic burettes, voltmeters and automatic balances, which have wide utilization in a chemical laboratory, are usually able to supply two kinds of output: one is the digital display that can be read by the user for manual data collection, the other is a digital output whereby the data are coded in an electrical signal train so that they can be utilized for high-speed automatic data collection.

The latter kind of output provides the user with a more efficient utilization of such instruments, once they have been interfaced with a logic processor spanning from a simple microprocessor for data-logging to a multiuser-multitask minicomputer for complete instrumentation control.¹

For reasons of design simplicity and standardization the most common code used for the digital output from electronic instruments is the one known as BCD (Binary Coded Decimal),² which uses four bits for each digit of the decimal number of interest, despite the two significant inconveniences that this code presents.

First, the BCD code is not compact, and requires appreciably more bits than the corresponding binary representation. The saving made by use of binary coding increases with the number of digits, but we shall limit the discussion to 5-digit numbers, since larger numbers are unlikely to occur in instrumental analysis.

Secondly, when a number transmitted from the instrumentation must be handled by the computer, it is necessary to translate the BCD datum into a binary datum, since computers operate with binary arithmetic. This could be done by using a software routine called into use each time a datum is stored, but a routine of this kind, which depends on the logical processor used, would be different for each specific circumstance and might be difficult for an experimenter to write and would certainly be inefficient in the use of computer time and resources.

To overcome both difficulties, we propose a hardware code-converter interface that is simple to build and to use, and is based on a low cost IC, the SN74184,³ that could fill a gap existing at present in the commercial market.

An example is also given of the software necessary to control a device of this kind in order to carry out data-acquisition from a digital voltmeter.

HARDWARE

Figure 1 shows a diagram of the circuit and the power supply. The 1-k Ω resistors on the output pins are used to pull the open collector output to TTL level.

The algorithm used for the conversion³ can be outlined as follows. Save the last bit of the input word as the least significant bit of the converted word; divide the bits left into four-bit decades; examine each of these decades and subtract 3 from those containing a binary number larger than 7; save the new last bit of the resultant word as the next least significant bit and continue the process until the last decade left contains a binary number smaller than 8; save these bits as the three most significant bits of the converted word.

Considering that each SN74184 is only able to handle six bits at a time, to implement the algorithm it is necessary to cascade a number of these chips in a combination of series and parallel connections (obviously dictated by the initial number to be converted).

As already said, numbers with more than five digits are not taken into consideration, but a further limitation to numbers between 0 and 65535 will be made, because these can be represented by 16-bit binary numbers. Hence nineteen SN74184 circuits are necessary.

The 16-bit binary numbers can be transferred in two ways, depending on the I/O port available on the processor.

With fairly inexpensive personal computers the I/O port for parallel communications is usually able to accept only eight data lines, but with more sophisticated (and more expensive) computers the I/O port capability easily increases up to sixteen or more bits.

To cope with both possibilities, the sixteen bits forming the converted word can be multiplexed on an 8-bit or a 16-bit bus by using two SN74298s.⁴

The SN74298s are in fact able to control the transfer of eight input lines to four output lines by using two logical signals. When the word select (WS) line is kept low the first four bits are transferred to the output at the negative edge

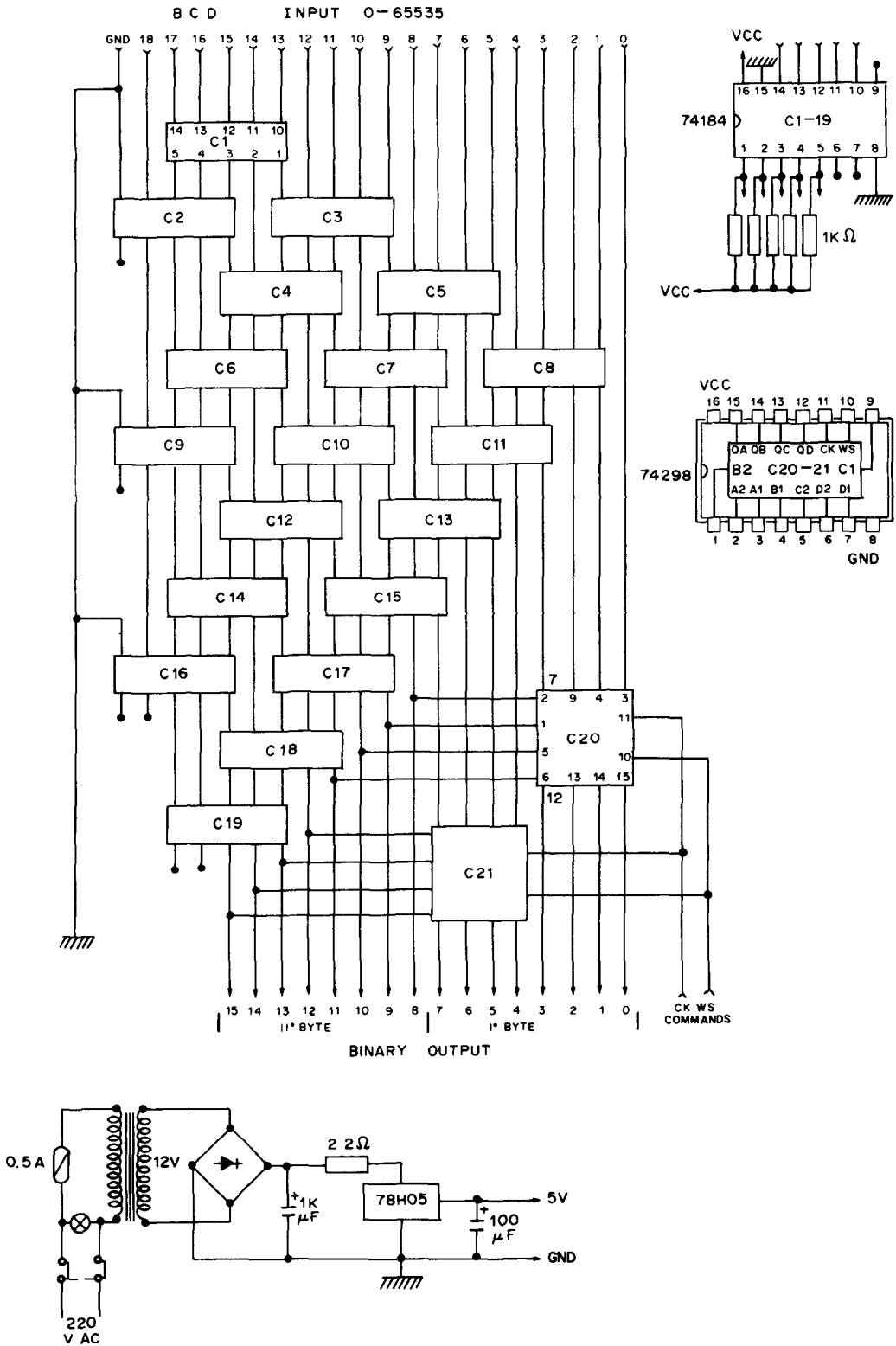


Fig. 1. Schematic diagram of circuit and power supply for the BCD-binary converter.

of the clock line (CK); when the WS is kept high the second four bits are again transferred at the negative-going transition of CK while the output remains latched at the levels entered with the last negative transition of CK.

Figure 2 shows the two protocols to be used in the case of a 2-byte transfer or of a complete word transfer. The different timing takes into account the delay introduced by each circuit.

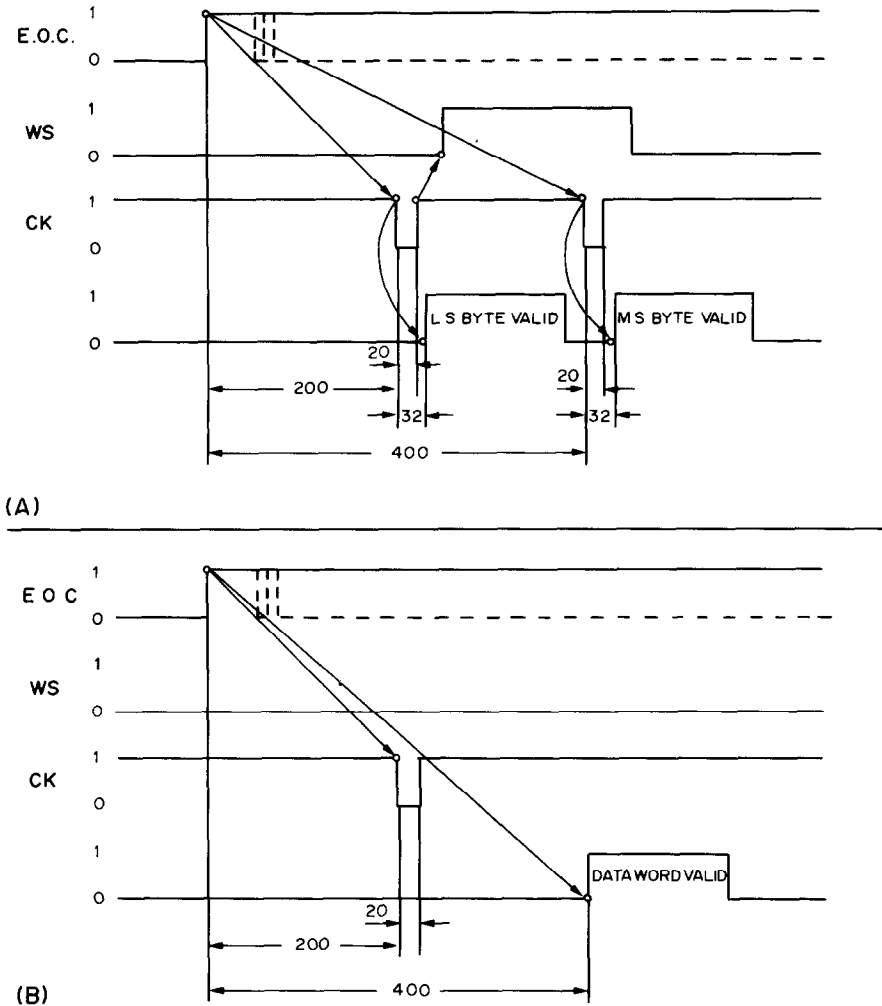


Fig. 2. Transfer time diagrams for (A) 8-bit transfer, (B) 16-bit transfer. Time intervals between events are in nsec and represent the minimum required for reliable operation.

The maximum delay introduced by each SN74184 is 40 nsec; for the eight least significant bits the total delay can be as high as 200 nsec, owing to the five levels of conversion involved for these bits. After 200 nsec, the first CK transition can be applied, the WS being at low level.

As the propagation delay for the SN74298 is 32 nsec, after 232 nsec the least significant byte of the converted number is ready to be loaded.

The most significant byte is correctly converted after 400 nsec (ten levels involved) and is then ready to be loaded after a total of at most 432 nsec from the beginning of the BCD-binary conversion.

Since the microcomputers now on the market can acknowledge an external event in about 1 μ sec, the operation performed by this kind of BCD-binary converter is completely transparent to the software program which manages the data acquisition.

Thus the logic of the program will be simpler and the data will be gathered more rapidly, at a rate depending only on the speed at which the instrumentation can supply the data.

SOFTWARE

We shall now describe an example of a rather complex utilization of this converter, from which simpler applications can easily be derived.

To gather data from a calorimetric apparatus used in our

laboratory, a Solartron A203 digital voltmeter with $4\frac{1}{2}$ digits of resolution (± 19999) was interfaced to an HP 21MX computer.

The data had to be sampled from four different sources by means of an analogue multiplexer, in temporal sequences specified by the characteristics of the kind of experiment performed.

For this purpose a main program written in HP FORTRAN manages the procedures, each time specifying the channel to be sampled, the number of samples to be drawn, the time between each sample, the data storage area, and the kind of bus to be used for the data transfer, in this case always a 16-bit bus.

Each time a data acquisition has to be made, control is transferred to an Assembler subroutine (ACQ1) by a CALL SUBROUTINE statement. Once this task has been done control is returned to the main program, which processes the data gathered or performs another data acquisition. Figure 3 shows the flow chart for the routine ACQ1. This routine initializes the counters for the number of samples and the number of clock intervals between samplings, programs the clock interval length at 1 msec, selects the multiplexer channel for the analogue signal of interest, enables the routines to handle the interrupts and finally sends the start conversion command to the voltmeter ACD and the start command to the clock.

At this point it checks whether the required number of samples has been accumulated. If so, it disables the clock

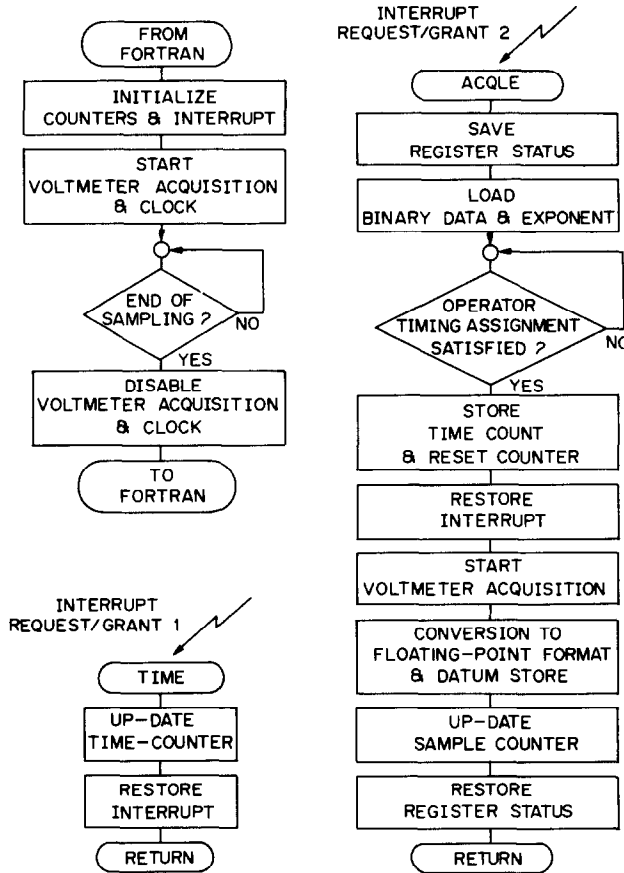


Fig. 3. Flow-chart diagram of the external Assembler routine ACQ1 for data acquisition from FORTRAN main program.

and the DVM converter in order to return to the MAIN program; otherwise, the "check" becomes a loop which stands waiting for the interrupt signals coming from the clock (time-tick marks) and from the ADC (DVM end of conversion) each being handled by the opportune service routine, the TIME routine and the ACQLE routine respectively.

Whenever the time routine is invoked, it increments in a counter the number of clock-tick marks and re-enables the clock interrupt control to its "ready" condition for the next interrupt.

The ACQLE routine, activated by the ADC interrupts, loads the voltmeter output (as a BCD-to-binary converted number), a sign bit and a 3-bit scale number. It then checks whether the time so far elapsed, *i.e.*, the time between the start and the end of the conversion, is less than the stated interval between two samplings. If so, it continues looping until enough time has passed. When the time reaches the value fixed by the operator, or if the time employed by the ADC conversion has been longer than the interval fixed between two samplings, the routine stores the time-counter value. This is necessary to check whether the DVM conversion has taken more time than the interval-between-sampling specified, for instance if a change of scale were to be performed by the DVM. Then it sets the time-counter at zero, starts a new DVM conversion, and proceeds to convert the binary loaded datum to a floating-point format and store it ready to be used for the following data treatments. It then increments the counter for the number of samples

and returns to the ACQ1 point where it was when the interrupt occurred.

It should be noted that the last operations described for the ACQLE, in particular the conversion from the fixed to the floating point with $97 \mu\text{sec}$ as maximum execution time, can be performed during the time required by the DVM for a conversion, without creating any recursivity in the normal program flow, if this conversion time is at least $\sim 150 \mu\text{sec}$.

The ACQ1 routine managed data acquisition at the maximum speed for the DVM used, *i.e.*, 10 points per second, but it could work with a faster DVM up to a speed of 7000 points per second.

The listings for the routines ACQ1, ACQLE and TIME in HP Assembler are available from the authors upon request.

Acknowledgement—The authors wish to thank Professor Paolo Papoff for his encouragement and helpful discussions throughout this work.

REFERENCES

1. *Microprocessors in Analytical Chemistry, Talanta*, 1981, **28**, No. 7B (special issue).
2. T. C. Bartee, *Digital Computer Fundamentals*, pp. 57–60. McGraw-Hill, New York, 1981.
3. *The TTL Data Book*, pp. 7-290, 7-295. Texas Instruments, 1980.
4. *Ibid.*, pp. 7-432, 7-436.

STUDY OF 1,4-DIHYDROXYANTHRAQUINONE AS AN ACID-BASE INDICATOR IN ISOPROPYL ALCOHOL MEDIUM

EVALUATION OF COLOUR-CHANGE LIMITS THROUGH COMPLEMENTARY CHROMATICITY PARAMETERS

J. BARBOSA, J. SANCHEZ and E. BOSCH

Department of Analytical Chemistry, University of Barcelona, Barcelona, Spain

(Received 16 March 1983. Revised 30 May 1983. Accepted 10 October 1983)

Summary—The use of 1,4-dihydroxyanthraquinone as an acid-base indicator in isopropyl alcohol medium is proposed. The acid dissociation constants of the indicator in isopropyl alcohol solution are $pK_{a1} = 12.95 \pm 0.03$ and $pK_{a2} = 15.96 \pm 0.07$. The sharpness of the indicator transition is described by means of complementary chromaticity parameters. The indicator is used for determination of weak organic acids, with errors of less than 1%.

At present, there is considerable interest in a search for non-aqueous solvents convenient for the titration of weak acids, because such acids show serious conjugation problems in slightly acidic solvents such as acetonitrile, sulpholane and nitromethane.

It is known that several hydroxyanthraquinones¹⁻³ are suitable as neutralization indicators in aqueous solutions. It was considered useful to study one of them, 1,4-dihydroxyanthraquinone (quinizarin) as an acid-base indicator in isopropyl alcohol medium, because, in water, it gives a clear colour change at high pH, and because isopropyl alcohol is a solvent that has good solvation properties, a relatively large dielectric constant ($\epsilon = 19.9$) and weak acidic and basic characteristics ($K_{HS} = 10^{-22.0}$)⁴⁻⁶ and is hence a good solvent for titration of weak organic acids.⁷⁻⁹

The work involved the spectrophotometric study of quinizarin in isopropyl alcohol, the determination of its ultraviolet-visible spectra in different media, and spectrophotometric determination of its dissociation constants and colour-change intervals, together with the study of its analytical applications.

The colours of the limiting forms of the indicator transition are described in terms of the complementary chromaticity system proposed by Reilly *et al.*^{10,11} The dissociation constants are recalculated from the complementary chromaticity parameters and comments are made on the quality of the colour change.

EXPERIMENTAL

Apparatus

A Beckman Acta M-VII spectrophotometer and a Radiometer pH-meter with glass and calomel electrodes were used. The calomel electrode was filled with a saturated solution of potassium chloride in methanol, and a salt bridge containing a saturated solution of tetramethylammonium chloride in isopropyl alcohol was used.

Reagents

1,4-Dihydroxyanthraquinone (Merck) solution, 4.37 × 10⁻⁴M.

Isopropyl alcohol (Koch-Light, analytical grade, 0.1% H₂O).

Tetrabutylammonium hydroxide (TBAH) (Merck). A 0.1M solution in isopropyl alcohol/methanol (4:1 v/v).

Buffer solutions in isopropyl alcohol. Prepared according to Aleksandrov *et al.*¹² from mixtures of 0.01M veronal and 0.01M potassium hydroxide.

Determination of standard potential

The glass electrode was calibrated as described by Kolthoff *et al.*¹³ with mixtures of picric acid and tetrabutylammonium picrate, taking into account the incomplete dissociation of the acid ($K = 1.84 \times 10^{-4}$) and the salt ($K = 1.1 \times 10^{-3}$) in isopropyl alcohol in the concentration range used ($\sim 10^{-3}$ M). The value obtained for the standard potential was -502 ± 4 mV (*vs.* S.C.E. in methanol, as indicated above). It was shown that the liquid-junction potential of the system is significant only in strongly acid (pH < 4) or strongly basic (pH > 18) solutions and therefore it can be considered negligible in this work.

Procedure

The acid dissociation constants of quinizarin were determined spectrophotometrically by standard procedures, as described by Albert and Serjeant.¹⁴ In the calculation, the formation of ion-pairs was not taken into account according to the considerations of Petrov *et al.*,¹² because of the low concentrations (10^{-3} M) of the solutions employed.

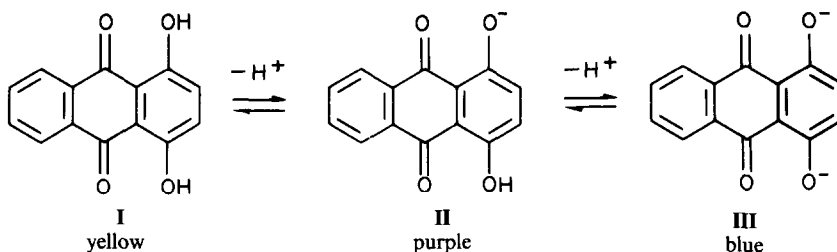
The pH range of the colour change and its sharpness were evaluated by titrations of benzoic acid and veronal with 0.1M TBAH in isopropyl alcohol/methanol medium, monitored simultaneously by potentiometry and continuous measurement of the absorbance at 610, 550 and 480 nm (the wavelengths of maximum absorption of the indicator). The titration solution was continuously circulated through the titration vessel and the spectrophotometer cuvette by a peristaltic pump.

The complementary chromaticity co-ordinates were determined by the weighted ordinate method, with absorbance readings between 380 and 700 nm, at 10-nm intervals. The evaluation was based on the CIE table of coefficients for standard illuminant C.¹⁵ Diluted solutions (1/25 and 1/10)

of the quinizarin stock solution were used, and the determinations were made at intervals of approximately 0.2 pH units over the colour-change pH range. The dissociation constants of quinizarin were calculated from the complementary chromaticity co-ordinates.^{11,16}

RESULTS AND DISCUSSION

Figure 1 shows the ultraviolet-visible absorption spectra of quinizarin in isopropyl alcohol at various pH values. The three forms I, II and III show different colours:



The dissociation constants obtained by the standard spectrophotometric method¹⁴ are reported in Table 1. Because of the high value of pK_2 , the pure doubly dissociated form (III) is not reached during a titration, so the colour change observed corresponds to conversion of quinizarin from its molecular form (I) (yellow) into a mixture of the singly dissociated (II) and doubly dissociated (III) forms (blue purple).

The visual colour-change interval in isopropyl alcohol lies between pH 12.5 and 14.3. The photometric colour-change interval (the interval of maximum slope in the absorbance-pH curve) is 12.4–14.6. The agreement between the potentiometric, spectrophotometric and visual end-points was tested in a series of titrations, and the reversibility of the indicator was confirmed in the same way.

Colour-change evaluation

The indicator colours are described by their complementary chromaticity co-ordinates, calculated by the weighted ordinate method, and by the "colour concentration", J , which is the only concentration-dependent term. The values are given in Table 2.

The plot of these values in the complementary chromaticity diagram (Fig. 2) shows two linear segments that correspond to conversion of form (I) into (II), and of (II) into (III) respectively. The colour

point corresponding to the singly charged form (II), which never exists alone because of the closeness of the two pK values, can be found on the complementary chromaticity diagram from the intersection of the two linear segments. This colour point is used for evaluation of the pK values from the chromaticity parameters.

The quality of the colour change at the end-point depends on the distance between the colour points for before and after the transition. However, the actual locations of the points in the diagram are also very important. It can be seen from Fig. 2 that the colour

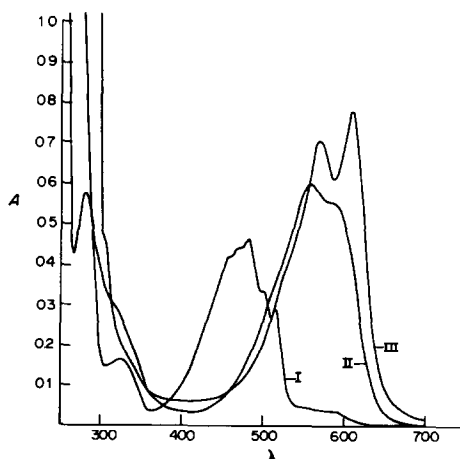


Fig. 1. Absorption spectra of quinizarin. (I) Molecular form, (II) singly charged form, (III) doubly charged form.

Table 1. Values of the dissociation constants of quinizarin, obtained by the standard method

$E(mV)$	A	pK	
255	0.155	12.94	
256	0.160	12.93	
263	0.175	12.98	
264	0.187	12.93	
268	0.198	12.94	
270	0.209	12.92	
274	0.218	12.94	
278	0.227	12.96	
282	0.237	12.97	
285	0.245	12.98	
286	0.247	12.98	
298	0.278	12.98	
303	0.289	12.97	
309	0.305	12.92	
424	0.385	16.03	
432	0.419	15.99	
433	0.420	16.00	$A_{II} = 0.274$
435	0.433	15.97	$A_{III} = 0.630$
437	0.448	15.93	$\lambda = 550 \text{ nm}$
439	0.457	15.92	Mean $pK_1 = 12.95 \pm 0.03$
441	0.458	15.95	
447	0.490	15.89	
			$A_{II} = 0.274$
			$A_{III} = 0.630$
			$\lambda = 610 \text{ nm}$
			Mean $pK_2 = 15.96 \pm 0.07$

Table 2. Complementary chromaticity co-ordinates and colour concentration at various pH values

pH	Q	Q_y	J
9.50	0.133	0.138	0.111
10.44	0.135	0.145	0.112
11.45	0.140	0.157	0.112
11.97	0.159	0.187	0.115
12.42	0.199	0.251	0.122
12.80	0.253	0.339	0.132
13.58	0.335	0.470	0.150
15.05	0.370	0.509	0.161
15.40	0.380	0.504	0.165
15.53	0.385	0.503	0.167
15.88	0.409	0.495	0.179
16.02	0.419	0.492	0.185
16.11	0.424	0.490	0.188
16.28	0.433	0.485	0.195
16.40	0.438	0.482	0.199
16.49	0.440	0.479	0.202
16.77	0.447	0.473	0.215

	Q_x	Q_y	J
molecular form (I)	0.133	0.139	0.111
singly charged form (II)	0.360	0.514	0.155
doubly charged form (III)	0.447	0.473	0.215

The J values refer to 10-mm path-length and a quinizarin concentration of $1.748 \times 10^{-5}M$.

points for forms (I) and (III) can be joined by a segment that passes through the grey point. This means that the indicator transition takes place between complementary colours, a characteristic of the best visual indicator transitions. Also since both colour points are near the periphery of the chromaticity diagram, the colours are bright, again characteristic of a good visual end-point.

For the determination of the dissociation constants, the expression

$$pK = pH + \log \left[\frac{J_a (Q_{r,b} - Q_{r,m})}{J_b (Q_{r,m} - Q_{r,a})} \right]$$

was used, where the subscripts a, b and m refer to the acid, basic and intermediate forms of the indicator, Q_r symbolizes the complementary chromaticity co-ordinates (Q_x , Q_y or Q_z) and J is the colour concentration. The advantage of the method is that it allows use of the colour-point co-ordinates of the singly charged form, which appears only in a very restricted pH range. Q_x and Q_y can be determined from the chromaticity diagram and the J value at this point can be found from the intersection of the straight lines on the graph of $Q_y J$ vs. $Q_x J^{11}$ corresponding to the successive transitions.

The pK results obtained from the chromaticity co-ordinates agree with those found by using the standard method,¹⁴ as can be seen from Tables 1 and 3.

Finally, various acidic organic substances were titrated in isopropyl alcohol medium in order to evaluate the usefulness of quinizarin as a neutralization indicator. Some are of pharmacological interest, such as aromatic acids, aliphatic acids, aromatic heterocyclics, amino-acids and phenols. Amounts between 15 and 50 mg were taken and 5–10 determinations for each substance were made. The relative error was less than 1% in all cases. Table 4 shows the results obtained and the standard deviations (s).

Acknowledgement—The authors thank Professor E. Casasas for his helpful suggestions.

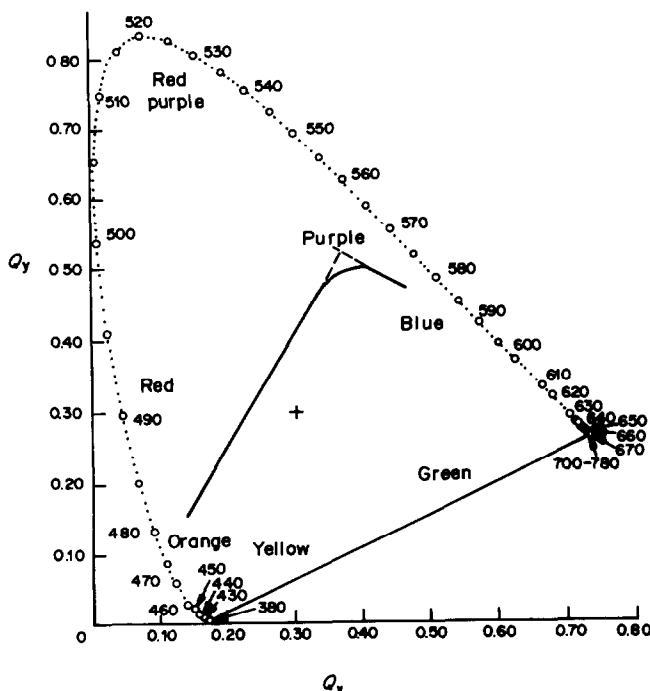


Fig. 2. Colour points in the complementary chromaticity diagram.

Table 3. Values of the dissociation constants of quinizarin from the complementary chromaticity parameters (*A*, quinizarin $1.748 \times 10^{-5}M$; *B*, quinizarin concentration $4.371 \times 10^{-5}M$)

pH	$Q_r = Q_x$	pK_1 $Q_r = Q_y$	pH	$Q_r = Q_x$	pK_2 $Q_r = Q_y$
<i>A</i>					
11.45	13.09	12.87	15.40	16.07	16.04
11.97	13.00	12.94	15.53	16.07	16.04
12.42	12.95	12.93	15.88	15.91	16.09
12.80	12.89	12.88	16.02	15.84	16.10
13.58	12.82	12.85	16.11	15.81	16.11
			16.28	15.71	16.04
$pK_1 =$	12.95 ± 0.14	12.89 ± 0.05	$pK_2 =$	15.90 ± 0.20	16.07 ± 0.04
<i>B</i>					
11.47	13.06	12.89	15.51		16.02
12.09	12.98	12.94	15.65		16.04
12.42	12.96	12.93	15.91		15.99
12.57	12.97	12.95	16.09		15.93
12.75	12.93	12.91	16.17		15.93
13.04	12.90	12.89	16.37		15.91
$pK_1 =$	12.97 ± 0.10	12.92 ± 0.03	$pK_2 =$		15.97 ± 0.06

Table 4. Titration of acids in isopropyl alcohol with 0.1M TBAH in isopropyl alcohol/methanol

	Acid	Error, mg	Relative error, %
<i>Aromatic acids</i>	Benzoic	0.0028	0.6
	<i>o</i> -Nitrobenzoic	0.0010	0.2
	Salicylic	0.0037	0.5
<i>Aliphatic acids</i>	Ascorbic	0.0020	0.3
	Chloroacetic	0.0015	0.2
	Palmitic	0.0022	0.4
	Tartaric	0.0027	0.4
	Trifluoroacetic	0.0006	0.3
<i>Aminoacids</i>	Anthranilic	0.0028	0.7
	<i>N</i> -Methylantranilic	0.0038	0.5
<i>Aromatic heterocycles</i>	5,5-Diethylbarbituric	0.0014	0.3
	Nicotinic	0.0025	0.3
	Thiamylal	0.0032	0.7
<i>Phenols</i>	2,4-Dinitrophenol	0.0038	0.5
	2,4,6-Trichlorophenol	0.0007	0.2

REFERENCES

- L. S. Malowan, *Chemist-Analyst*, 1955, **44**, 75.
- J. S. Fritz and J. J. Ford, *Anal. Chem.*, 1953, **25**, 1640.
- J. Barbosa and M. Blanco, *Quim. Anal.*, 1976, **30**, 203.
- M. K. Chantooni and I. M. Kolthoff, *Anal. Chem.*, 1979, **51**, 133.
- L. N. Bykova and S. I. Petrov, *Zh. Analit. Khim.*, 1972, **27**, 1076.
- J. S. Fritz, *Acid-Base Titrations in Non-Aqueous Solutions*, Allyn & Bacon, Boston, 1973.
- L. E. I. Hummelstedt and D. N. Hume, *Anal. Chem.*, 1960, **32**, 1792.
- M. Logowska and M. Machtruger, *Bull. Soc. Chim. France*, 1968, **12**, 5084.
- G. A. Harlow and G. E. A. Wyld, *Anal. Chem.*, 1958, **30**, 73.
- C. N. Reilley, H. A. Flaschka, S. Laurent and B. Laurent, *ibid.*, 1960, **32**, 1218.
- C. N. Reilley and E. M. Smith, *ibid.*, 1960, **32**, 1233.
- S. M. Petrov and G. B. Bogolyuk, *Izv. Vysch. Uchebn. Zaned, Khim. Khim. Tekhnol.*, 1979, **22**, 1205.
- I. M. Kolthoff and M. K. Chantooni, *J. Phys. Chem.*, 1978, **82**, 994.
- A. Albert and E. P. Serjeant, *The Determination of Ionization Constants*, Chapman & Hall, London, 1962.
- D. B. Judd, in M. G. Mellon, *Analytical Absorption Spectroscopy*, p. 515, Wiley, New York, 1953.
- H. Flaschka, *Talanta*, 1961, **8**, 342.

SHORT COMMUNICATIONS

TITRIMETRIC DETERMINATION OF PHENOL RESORCINOL AND PHLOROGLUCINOL

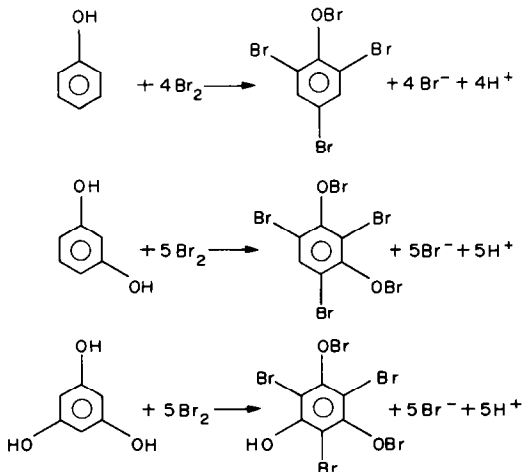
D. AMIN and W. A. BASHIR

Department of Chemistry, College of Science, University of Mosul, Mosul, Iraq

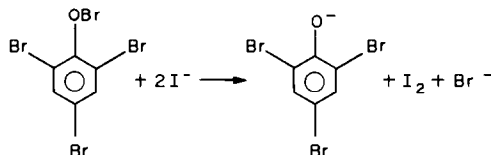
(Received 2 August 1983. Accepted 7 November 1983)

Summary—A new and sensitive titrimetric method with an amplification procedure has been worked out for the determination of 10–1000 μg of phenol, resorcinol or phloroglucinol. The method is based on reaction of the phenols with an excess of bromine to form bromosubstituted aryl hypobromites. After removal of excess of bromine with formic acid, the hypobromites are treated with iodide to liberate an equivalent amount of iodine, which is extracted into chloroform, then reduced to iodide and determined by the Leipter procedure with 6-fold amplification. The coefficient of variation does not exceed 0.4% for amounts of determinand >100 μg , but increases to 1.5% at the 10- μg level.

Phenol can readily be brominated to tribromophenol,¹ and with an excess of bromine the substitution goes further to tribromophenyl hypobromite, which, however, is decomposed by iodide to give tribromophenol and a corresponding amount of iodine. Titrimetric methods for determination of resorcinol have principally been based on iodometry.²⁻⁴ The bromate-bromide mixture used for determination of resorcinol¹ gives tribromo substitution. However, some of these methods are not sensitive, and others are tedious. Phloroglucinol has also been determined by treatment with excess of bromate-bromide mixture and iodometric determination of the surplus,⁵ or by oxidation with excess of ceric sulphate and back-titration with iron(II).⁶ We have developed a new, simple, rapid and sensitive titrimetric method with an amplification procedure for the determination of phenol, resorcinol and phloroglucinol, based on the reaction of these compounds with excess of bromine to form tribromoaryl hypobromites:



The tribromoaryl hypobromites react with iodide to give the corresponding substituted tribromophenol and iodine, e.g.,



The iodine liberated is extracted with chloroform and reduced to iodide, then determined by iodometric titration of the iodate formed by the Leipter procedure.⁷

EXPERIMENTAL

Reagents

All chemicals used were of analytical grade. Standard solutions (1 mg/ml) of phenol, resorcinol and phloroglucinol were prepared with distilled water. Less concentrated solutions were prepared by dilution. Sodium thiosulphate solutions, 0.01 and 0.001N, were prepared and standardized against potassium iodate solutions of similar normality. Concentrated formic acid, bromine water (saturated), sodium sulphite solution (1%), and potassium iodide solution (5%) were also prepared.

Procedure

Place the sample solution, containing 10–1000 μg of phenol, resorcinol, or phloroglucinol, in a 50-ml separating funnel and dilute to 10 ml with distilled water. Add 1–2 ml of bromine water, stopper the flask and shake it for 2 min. Destroy excess of bromine by shaking with 1 ml of formic acid for 1 min. Add 1 ml of 5% potassium iodide solution, shake for 1–2 min, then extract the liberated iodine with three 10-ml portions of chloroform. Collect the extracts in another funnel and reduce the iodine to iodide by shaking with 10 ml of water containing 1 ml of 1% sodium sulphite solution. Transfer the aqueous layer, containing iodide, into a 50-ml conical flask, add 2 ml of bromine water, shake for 3 min, and add 2 ml of formic acid to remove excess of bromine. Add about 0.5 g of potassium iodide and titrate

Table 1. Accuracy and precision

Compound	Amount taken, μg	Recovery,* %	R.S.D.,* %
Phenol	10	98.2	1.5
	100	99.6	0.3
	1000	99.9	0.2
Resorcinol	10	98.4	1.1
	100	99.5	0.2
	1000	100.0	0.1
Phloroglucinol	10	98.0	1.4
	100	99.2	0.4
	1000	99.0	0.3

*Mean of 5 determinations.

the liberated iodine with 0.01*N* thiosulphate in the usual way, using starch as indicator. For low concentrations (less than 50 μg of determinand) use 0.001*N* thiosulphate. Run a blank determination. 1 ml of 0.01*N* thiosulphate \equiv 0.078 mg of phenol or 0.046 mg of resorcinol or 0.068 mg of phloroglucinol.

RESULTS AND DISCUSSION

Preliminary studies confirmed that phenol, resorcinol and phloroglucinol readily undergo bromination to give the tribromo derivatives, and with a large excess of bromine, the substitution goes further to form the tribromophenyl hypobromite. Both OH groups in resorcinol undergo substitution, but in

phloroglucinol only two of the three OH groups undergo substitution. This may be due to the introduction of two hypobromite groups decreasing the acidity of the third OH group sufficiently for it not to be converted into a hypobromite group. It was found that the bromination is fast, and complete within 1–2 min. Reduction of the tribromophenyl hypobromite to the tribromophenol can be achieved with 0.5–1.0 ml of 5% potassium iodide solution. A larger excess of iodide hinders the extraction of iodine with chloroform (by tri-iodide formation); complete liberation of the iodine requires 1–2 min.

The working procedure finally developed has been applied successfully to the determination of quantities of phenol, resorcinol or phloroglucinol as low as 10 μg . Table 1 shows the accuracy and precision of the method.

REFERENCES

1. I. M. Kolthoff and R. Belcher, *Volumetric Analysis*, Vol. III, pp. 537 and 542. Interscience, New York, 1957.
2. H. H. Willard and A. L. Wooten, *Anal. Chem.*, 1950, **22**, 585.
3. *Idem, ibid.*, 1950, **22**, 670.
4. J. Mlodecka, *Chem. Anal. (Warsaw)*, 1965, **10**, 431.
5. W. Bielenberg, H. Goldhalm and A. Zoff, *Oel u. Kohle*, 1941, **37**, 496.
6. T. Takahashi, K. Kimoto and S. Minami, *J. Chem. Soc. Japan, Ind. Chem. Sect.*, 1953, **56**, 491.
7. T. Leipert, *Mikrochemie, Pregl Festschrift*, 1929, 266.

IMPROVEMENT OF END-POINT DETECTION IN THE NON-AQUEOUS TITRATION OF SULPHACETAMIDE SODIUM

SOBHI A. SOLIMAN, SAIED BELAL and MONA BEDIAR

College of Medicine & Allied Sciences, King Abdulaziz University, Jeddah, Saudi Arabia

(Received 30 March 1983. Revised 27 September 1983. Accepted 1 November 1983)

Summary—The sluggish end-point in the non-aqueous titration of sulphacetamide sodium in glacial acetic acid can be improved by addition of acetic anhydride to the titration medium, and selective determination of sulphacetamide sodium in presence of phenylephrine hydrochloride in eye drops then becomes possible. A mixture of sulphacetamide sodium and the antihistamine drug phenyltoloxamine dihydrogen citrate can also be analysed.

Titration of sulphonamide derivatives with standard perchloric acid in glacial acetic acid medium has been found to give low recoveries and a sluggish indicator colour-change.¹ One way of circumventing such a difficulty is the use of back-titration.² Addition of certain aprotic solvents, e.g., benzene, chloroform or carbon tetrachloride, to the glacial acetic acid medium in the back-titration has been found to improve the end-point detection,³ but the procedure is time-consuming and tedious shaking is required during the titration.

Addition of acetic anhydride to the glacial acetic acid medium has long been known^{4,5} to improve end-point detection in the non-aqueous titration of salts of weak acids. We have used this approach to improve the end-point detection in non-aqueous titrimetric determination of sulphacetamide sodium, alone or in admixture with allied drugs.

EXPERIMENTAL

Apparatus

Titrimeter (Pye model 79) equipped with a combination electrode (Pye catalogue No. 401 E07) magnetic stirrer and 10-ml microburette.

Reagents

Perchloric acid (0.1M) in glacial acetic acid, 0.02% solution of Gentian Violet in glacial acetic acid, 0.5% solution of C.I. Solvent Blue 19 indicator (Oracet Blue B indicator, Ciba) in glacial acetic acid, 0.2% Quinaldine Red indicator in a mixture of 90 ml of acetic anhydride and 10 ml of methanol, and a 5% solution of mercuric acetate in glacial acetic acid.

Determination of sulphacetamide sodium

An accurately weighed amount (300–900 mg) of sulphacetamide sodium or the residue left after evaporating a known volume of ophthalmic solution containing 100–200 mg of the drug was dissolved in 5 ml of glacial acetic acid and 25 ml of acetic anhydride in a 100-ml beaker. The sample was dissolved by gentle heating, the solution

was cooled and 1 or 2 drops of Gentian Violet, Solvent Blue 19, or Quinaldine Red indicator solution were added. The solution was titrated potentiometrically with 0.1M perchloric acid in glacial acetic acid, and the indicator colour-changes coinciding with the potentiometric end-points were noted: the changes were to blue, rose red, and colourless for Gentian Violet, Solvent Blue 19 and Quinaldine Red respectively.

Determination in presence of phenylephrine hydrochloride

Accurately weighed amounts of sulphacetamide sodium (250 mg) and phenylephrine hydrochloride (50 mg) were dissolved in 5 ml of glacial acetic acid and 25 ml of acetic anhydride; 5 ml of mercuric acetate solution were added and the solution was titrated as described above.

Analysis of mixtures of sulphacetamide sodium and phenyltoloxamine dihydrogen citrate

Determination of total base. Accurately weighed amounts of sulphacetamide sodium (100.0 mg) and phenyltoloxamine dihydrogen citrate (100.0 mg) were dissolved in the glacial acetic acid–acetic anhydride mixture, and titrated without addition of mercuric acetate (*A* ml of 0.1M titrant required).

Determination of sulphacetamide. Accurately weighed amounts of sulphacetamide sodium (100.0 mg) and phenyltoloxamine dihydrogen citrate (100.0 mg) were dissolved in 5 ml of concentrated hydrochloric acid, and the sulphacetamide sodium content was determined by titration with 0.1M sodium nitrite solution according to the B.P. method⁶ (*B* ml). Then (*A* – *B* ml) represents the volume of 0.1M perchloric acid equivalent to the phenyltoloxamine dihydrogen citrate.

RESULTS AND DISCUSSION

The curve for potentiometric titration of sulphacetamide in glacial acetic acid with perchloric acid gives an ill-defined break (Fig. 1, curve D) that is difficult to use for locating the exact end-point. The colour change of Gentian Violet in this titration is also sluggish. This is to be expected, because of the low basicity of the sulphacetamide molecule.

Figure 1 shows the potentiometric titration curves of sulphacetamide sodium in different solvent systems. The titration of the drug in acetic anhydride–

Table 1. Determination of sulphacetamide sodium in various dosage forms

Form	Mean recovery \pm SD, %		
	Proposed method		
	Potentiometric detection	Visual detection	B.P. 1973 method
Pure	100.1 \pm 1.3 (10)*	100.6 \pm 1.3 (9)*	100.7 \pm 0.5 (4)*
Ophthalmic solutions†	101.2 \pm 0.9 (6)*	100.9 \pm 0.8 (7)*	103.3 \pm 0.5 (5)*
In the presence of phenylephrine hydrochloride	—	100.1 \pm 0.9 (5)*	
In the presence of phenyltoloxamine dihydrogen citrate	—	100.5 \pm 0.8 (5)*	

*Number of experiments.

†Sulphacetamide sodium eye-drops, Alexandria Co. for Pharmaceuticals and Chemical Industries.

glacial acetic acid mixture yields an excellent curve (A) with a sharper inflexion than that obtained with either of the other solvents tried (curves B and C). In the acetic anhydride-glacial acetic acid solvent system the visual end-point was also sharp. Results of the titration of sulphacetamide sodium by the proposed procedure are listed in Table 1 and compare favourably with those obtained by the B.P. method. The visual end-points coincided with the potentiometric end-points.

Application of the proposed method to the determination of sulphacetamide sodium in commercial ophthalmic solutions containing 10% w/v of the drug gave results that were equivalent to the results of the B.P. nitrite method in accuracy and precision (Table 1).

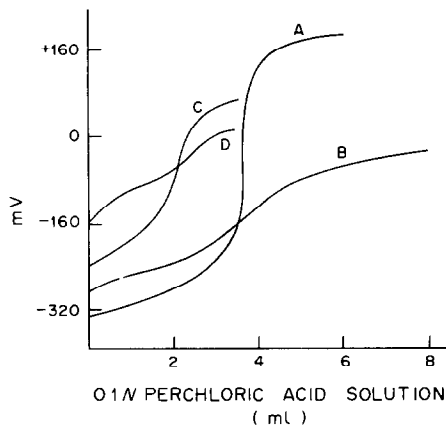


Fig. 1. Potentiometric titration curves for sulphacetamide sodium in different solvent systems: A, acetic anhydride-glacial acetic acid; B, dioxan; C, glacial acetic acid; D, sulphacetamide in glacial acetic acid.

In ophthalmic solutions sulphacetamide sodium may be compounded with phenylephrine hydrochloride (added as an adrenergic drug). The sulphacetamide sodium in such mixtures can be determined by taking advantage of acetylation of the secondary amine group of the phenylephrine by acetic anhydride. Complete acetylation of this group can be clearly demonstrated by the absence of an inflexion point on the potentiometric curve for titration of the acetylation product. The proposed procedure gives quantitative and reproducible recoveries for sulphacetamide sodium, without interference from phenylephrine hydrochloride (Table 1).

Sulphacetamide sodium is also frequently encountered in ophthalmic solutions containing phenyltoloxamine dihydrogen citrate as an antihistamine. The latter component contains a tertiary nitrogen atom and therefore application of the proposed method to mixtures of the two compounds gives an end-point corresponding to the total amount of the two drugs. Sulphacetamide sodium can then be selectively determined by the B.P. nitrite method and the phenyltoloxamine dihydrogen citrate calculated by difference. Table 1 shows that acceptable results are obtained.

REFERENCES

1. Y. Jajika and M. Aikawa, *J. Pharm. Soc. Japan*, 1954, **74**, 1125.
2. J. A. Gautier and F. Pellerin, *Ann. Pharm. Franc.*, 1952, **10**, 401.
3. J. Meulenhoff, *Pharm. Weekblad*, 1958, **93**, 262.
4. J. S. Fritz and M. O. Fulda, *Anal. Chem.*, 1954, **25**, 1837.
5. C. A. Streuli, *ibid.*, 1958, **27**, 997.
6. *The British Pharmacopoeia* 1973, pp. 445-449. The Pharmaceutical Press, London, 1973.

TITRIMETRIC DETERMINATION OF SOME PHENOTHIAZINE DERIVATIVES, WITH FERRICYANIDE

A. S. ISSA and M. S. MAHROUS

Department of Pharmaceutical Chemistry, Faculty of Pharmacy, University of Alexandria,
 Alexandria, Egypt

(Received 21 April 1983. Revised 19 October 1983. Accepted 28 October 1983)

Summary—Six phenothiazine drugs (chlorpromazine hydrochloride, promethazine hydrochloride, promazine hydrochloride, perphenazine, acetophenazine maleate and trifluoperazine hydrochloride) have been determined by titration with potassium ferricyanide in phosphoric acid medium with Methylene Blue as a screening indicator. The results were in agreement with those obtained by the official methods.

Various methods have been used for estimation of phenothiazines. Potassium bromate and ceric sulphate have been used for their oxidative titration.¹ Methods based on the protonated nitrogen atom of the molecules include non-aqueous titration,² two-phase titration,³⁻⁵ precipitation with tetraphenylborate⁶⁻⁸ or ammonium reineckate,⁹ and titration

with the picrates of lead, copper, cadmium and zinc.¹⁰ Potassium iodobismuthate,¹¹ hexathiocyanatochromate(III),¹² tetracyanozincate¹³ and iodine monochloride¹⁴ have also been used for the estimation of phenothiazine derivatives.

Oxidizing agents used for the colorimetric determination of phenothiazine derivatives include ferric

Table 1. Results obtained by the potassium ferricyanide and the B.P. 1980 methods

Compound	Potassium ferricyanide		B.P. 1980	
	Taken, mg	Recovery,* %	Taken, mg	Recovery, %
Chlorpromazine.HCl (Neurazine) ^M				
Powder	5-20	100.4 ± 0.5	50.0	99.6 ± 1.3
Ampoules (25 mg/ml)	10	103.3 ± 0.3	0.5	104.1 ± 1.5
Tablets (25 mg/tablet)	10	98.1 ± 0.5	0.5	97.3 ± 0.5
Promethazine.HCl (Promantine) ^M				
Powder	5-20	100.0 ± 0.4	50.0	98.7 ± 0.7
Ampoules	10	102.5 ± 0.9	0.5	104.2 ± 0.9
Laboratory-prepared tablets†	10	99.5 ± 0.5	0.5	98.3 ± 1.0
Promazine.HCl (Sparine) ^W				
Powder	5-20	100.2 ± 0.2	50.0	101.0 ± 0.4
Vials (50 mg/ml)	10	101.7 ± 0.8	0.5	103.0 ± 0.3
Perphenazine (Trilafon) ^{Sc}				
Powder	5-20	100.3 ± 0.4	50.0	99.2 ± 1.1
Tablets (8 mg/tablet)	10	102.2 ± 0.8	0.5	102.2 ± 0.9
Trifluoperazine.2HCl (Stelazine) ^K				
Powder	5-20	100.5 ± 0.4	50.0	101.0 ± 0.8
Tablets (5 mg/tablet)	10	102.7 ± 0.6	0.5	105.1 ± 0.8
Acetophenazine maleate ^{Sc}				
Powder	5-20	100.0 ± 0.5	50.0	98.3 ± 0.3
Laboratory-prepared tablets†	10	99.6 ± 1.2	50.0	98.4 ± 0.6

M = Misr; K = Kahira; Sc = Schering; W = Wyeth.

*Mean and standard deviation (6 results), calculated on nominal content in sample.

†Tablet prepared with lactose, starch, talc, magnesium stearate in proportions 90:7:2.7:0.3.

chloride,¹⁵ hydrogen peroxide,¹⁶ *p*-benzoquinone¹⁷ and chloramine-T.¹⁸ Other reagents used include *cis*-aconitic anhydride¹⁹ and Nitrazine Yellow.²⁰

Gas chromatography has also been used for the determination of phenothiazine derivatives.²¹⁻²⁶

EXPERIMENTAL

Reagents

Potassium ferricyanide, 0.01M.

Orthophosphoric acid, 85% w/v.

Methylene Blue solution, 0.1%.

General procedure

A solution of 5–20 mg of the drug in 10 ml of alcohol is treated with 50 ml of phosphoric acid and 5 drops of Methylene Blue solution. The mixture is titrated with 0.01M potassium ferricyanide to a full blue colour.

Procedure for tablets

Twenty tablets are weighed and powdered. A quantity of the powder containing about 100 mg of the drug is transferred to a 100-ml standard flask, 50 ml of alcohol are added and the mixture is shaken for 20 min, then diluted to the mark with ethanol and filtered. An aliquot of the filtrate (containing about 10 mg of the drug) is analysed as in the general procedure.

For injections and liquid preparations

An amount of sample containing about 100 mg of the drug is measured accurately into a 100-ml standard flask and made up to volume with ethanol. An aliquot containing about 10 mg of the drug is analysed as in the general procedure.

RESULTS AND DISCUSSION

Phosphoric acid was found to be the best medium for the oxidation reaction. When sulphuric or hydrochloric acid was used it was very difficult or impossible to detect the end-point. In phosphoric acid medium (70–85% v/v phosphoric acid) the end-point is shown by disappearance of the red colour of the phenothiazine. The addition of Methylene Blue sharpens the end-point, since under the reaction conditions used, the potassium ferricyanide oxidizes only the phenothiazine, first to a red intermediate with loss of one electron and then to a colourless product with loss of a second electron.¹ Hence the end-point is shown by the change to the full blue colour of the Methylene Blue.

The common tablet fillers such as lactose, talc, starch and magnesium stearate do not interfere, as

shown in recovery tests by the standard addition method, the recovery ranging from 99.4 to 101.0% for 5–20 mg of added drug.

All results obtained agreed reasonably well with those obtained by using the B.P. 1980 methods (Table 1). The procedure can be recommended for routine analysis of phenothiazine drugs.

REFERENCES

1. G. Dusinsky and O. Liskova, *Chem. Zvesti*, 1958, **12**, 213.
2. J. Milne, *J. Pharm. Assoc.*, 1959, **48**, 117.
3. J. Blažek and M. Travnicková, *Cesk. Farm.*, 1975, **24**, 100.
4. S. Rolski and Z. Zakrzewki, *Farm. Pol.*, 1969, **25**, 621.
5. F. Albert, H. Aftalion and R. Simionovici, *Rev. Chim. (Bucharest)*, 1968, **19**, 283.
6. Gh. Morait, V. Turculeate and Gh. Ciogolea, *Farmacia (Bucharest)*, 1970, **18**, 267.
7. J. Dobrecky and B. E. Gonzalez, *Rev. Asoc. Bioquim. Argent.*, 1969, **34**, 168.
8. S. Prinzzanti and V. Dal Piaz, *Boll. Chim. Farm.*, 1972, **111**, 512.
9. A. Olech, *Acta Pol. Pharm.*, 1972, **29**, 57.
10. M. Gajewska, *Chem. Anal. (Warsaw)*, 1973, **18**, 651.
11. H. Basinska and M. Tarasiewicz, *Acta Pol. Pharm.*, 1969, **26**, 343.
12. A. Olech, *ibid.*, 1973, **30**, 505.
13. B. Dembinski and K. Novakowski, *Farm. Pol.*, 1974, **30**, 423.
14. Y. A. Beltagy, A. S. Issa and M. S. Mahrous, *Talanta*, 1978, **25**, 349.
15. M. K. Youssef and I. A. Attia, *Indian J. Pharm.*, 1975, **37**, 121.
16. H. Basinska, H. Puzanowska-Tarasiewicz and M. Tarasiewicz, *Chem. Anal. (Warsaw)*, 1970, **15**, 405.
17. J. Mounier and B. Viassat, *Ann. Pharm. Franc.*, 1968, **26**, 429.
18. A. S. Issa, Y. A. Beltagy and M. S. Mahrous, *Talanta*, 1978, **25**, 710.
19. Y. A. Beltagy, A. S. Issa and M. S. Mahrous, *J. Pharm. Sci., Egypt*, 1978, **19**, 107.
20. *Idem*, *ibid.*, 1977, **18**, 221.
21. E. Donald, C. F. R. Johnson and H. P. Burchfield, *Biochem. Pharmacol.*, 1965, **14**, 1453.
22. P. Kraph-Sorensen, N. E. Larsen, H. C. Eggert and J. Naestoft, *Acta Psychiat. Scand. Suppl.*, 1972, **15**, 246.
23. F. Michael, W. David and H. David, *Clin. Chem.*, 1978, **24**, 41.
24. S. Cooper, J. M. Albert, R. Dugal, M. Bertrand and R. Elie, *Arzneim.-Forsch.*, 1979, **29**, 158.
25. T. M. Astanina, S. V. Merinova, T. P. Kazakova and M. I. Shmar'yan, *Farmatsiya (Moscow)*, 1979, **28**, 26.
26. B. N. David and G. J. John, *Clin. Chem.*, 1979, **25**, 1211.

SPECTROPHOTOMETRIC DETERMINATION OF PHENOTHIAZINES, TETRACYCLINES AND CHLORAMPHENICOL WITH SODIUM COBALTINITRIDE

M. S. MAHROUS and M. M. ABDEL-KHALEK

Department of Pharmaceutical Chemistry, Faculty of Pharmacy, University of Alexandria,
Alexandria, Egypt

(Received 18 July 1983. Accepted 13 October 1983)

Summary—A spectrophotometric method for determining some phenothiazines, some tetracyclines and chloramphenicol is described. Chlorpromazine hydrochloride, promazine hydrochloride, promethazine hydrochloride, perphenazine and fluphenazine hydrochloride are reacted with sodium cobaltinitrite in phosphoric acid. The red colour developed is measured at 530, 513, 515, 530 and 500 nm, respectively. Tetracycline hydrochloride, oxytetracycline hydrochloride, chlortetracycline hydrochloride, doxycycline hyclate and demeclocycline hydrochloride are reacted with the reagent in aqueous acetic acid. The yellow colour produced is measured at 256, 294, 262, 243 and 246 nm, respectively. Chloramphenicol is determined similarly to the tetracyclines after hydrolysis with 40% sodium hydroxide solution and the colour is measured at 240 nm. The proposed method has been successfully applied to the determination of these drugs in various pharmaceutical preparations.

In the British Pharmacopoeia method,¹ phenothiazine derivatives are determined by titration in non-aqueous media. Phenothiazines have been determined spectrophotometrically, after oxidation with various oxidizing agents.^{2,3} The nitration products of phenothiazines can also be measured spectrophotometrically after ether extraction from alkaline medium.⁴ Phenothiazines have been assayed by various titrimetric techniques, e.g., photometric titration at 420 nm with ferric sulphate,⁵ direct titration with arylsulphonic acids,⁶ two-phase titration with Bromophenol Blue⁷ or sodium lauryl sulphate.⁸ Polarographic,⁹ gas-chromatographic^{10,11} and thin-layer chromatographic¹² methods have also been reported.

Several methods have been described for the determination of tetracyclines. These include fluorimetric,^{13,14} chromatographic^{15,16} and titrimetric¹⁷ methods.

Chloramphenicol has been determined spectrophotometrically in acetone-dimethylformamide medium with tetraethylammonium hydroxide.¹⁸ Reduction of the nitro group allows diazotization and coupling with various reagents.^{19,20} Other methods include polarography,²¹ non-aqueous titration with perchloric acid in glacial acetic acid,²² and oxidation of its hydrolysis product with sodium periodate²³ or potassium dichromate.²⁴ Sodium cobaltinitrite has been proved to be a valuable reagent for the detection and determination of several phenolic compounds and drugs.²⁵⁻²⁹ This paper describes its use for the spectrophotometric determination of some phenothiazines, some tetracyclines, and chloramphenicol.

EXPERIMENTAL

All chemicals and reagents used were of analytical-reagent or pharmaceutical grade. Distilled water was used throughout.

General procedure for phenothiazines

An ethanol solution containing from 0.2 to 1.0 mg of the drug was transferred to a test-tube and evaporated to dryness on a boiling water-bath. The residue was treated with 1 ml of 0.2% sodium cobaltinitrite solution and 5 ml of phosphoric acid. The mixture was shaken well and then heated in a boiling water-bath for 15 min. The mixture was then transferred into a 25-ml standard flask and diluted to the mark with phosphoric acid. The absorbance was measured at the selected wavelength (Table 1) for the drug, against a corresponding reagent blank.

For tablets. Twenty tablets were weighed and powdered. An accurately weighed portion of the mixed powder, equivalent to about 25 mg of the drug, was shaken with ethanol in a 50-ml standard flask for 20 min. The solution was diluted to the mark with ethanol, mixed well and then filtered through a dry filter-paper into a dry flask, and 1 ml of this solution was analysed as described above for phenothiazines.

For injections. A quantity of sample equivalent to about 50 mg of the drug was transferred into a 100-ml standard flask and diluted to the mark with ethanol. A 1-ml aliquot was analysed by the general procedure.

General procedure for tetracyclines

A solution containing from 0.5 to 1.5 mg of the drug in 2 ml of water was transferred into a test-tube, mixed with 2 ml of glacial acetic acid and 2 ml of 5% sodium cobaltinitrite solution. The mixture was heated in a boiling water-bath for 15 min, cooled, transferred into a 50-ml standard flask and diluted to the mark with water. The absorbance was measured at the selected wavelength (Table 1).

For capsules and tablets. A quantity of the mixed contents of 20 capsules or tablets, equivalent to about 25 mg of the drug, was transferred into a 50-ml standard flask and

Table 1. λ_{\max} , concentration ranges, regression equations and correlation coefficients for sodium cobaltinitrite colour reaction with different compounds

Compound	λ_{\max} , nm	Conc. range (C), mg/ml	Regression equation	Correlation coefficient
Chlorpromazine. HCl	530	0.008–0.04	$A = 0.001 + 30.85C$	0.9999
Promazine. HCl	513	0.008–0.04	$A = 0.004 + 33.50C$	0.9999
Promethazine. HCl	515	0.008–0.04	$A = 0.005 + 26.53C$	0.9999
Perphenazine	530	0.008–0.04	$A = 0.005 + 27.40C$	0.9999
Fluphenazine. HCl	500	0.008–0.04	$A = 0.001 + 19.48C$	0.9999
Tetracycline. HCl	256	0.01–0.03	$A = 0.002 + 33.86C$	0.9999
Oxytetracycline. HCl	294	0.01–0.03	$A = 0.003 + 32.66C$	0.9999
Chlortetracycline. HCl	262	0.01–0.03	$A = 0.000 + 30.34C$	0.9998
Doxycycline hyclate	243	0.01–0.03	$A = 0.006 + 47.70C$	0.9999
Demeclocycline. HCl	246	0.01–0.03	$A = 0.012 + 36.14C$	0.9993
Chloramphenicol	240	0.01–0.03	$A = 0.000 + 43.98C$	0.9999

shaken with 25 ml of water for 20 min. The solution was diluted to the mark with water and then filtered. A 2-ml portion of the filtrate was assayed by the general procedure.

General procedure for chloramphenicol

A quantity of chloramphenicol powder containing 50 mg of the drug was transferred into a test-tube, followed by 10 ml of 40% sodium hydroxide solution. The solution was boiled for 30 min, cooled, transferred into a 50-ml measuring flask and then made up to the mark with glacial acetic acid, with cooling before final adjustment. Serial dilutions containing from 0.5 to 1.5 mg of the drug were analysed by the general procedure for tetracyclines.

For capsules and injections. An accurately weighed portion of the mixed contents of capsules or injections was assayed as just described.

RESULTS AND DISCUSSION

Sodium cobaltinitrite oxidizes chlorpromazine hydrochloride, promazine hydrochloride, promethazine hydrochloride, perphenazine and fluphenazine hydrochloride in acidic solutions to give a red colour. The colour is attributed to formation of a radical cation. This conclusion is supported by the finding that the wavelength of the absorption maximum found experimentally corresponded to that reported in the literature for the free radicals formed by oxidation of phenothiazines.³⁰⁻³² The effect of variation in the concentration of sodium cobaltinitrite

Table 2. Determination of phenothiazines, tetracyclines and chloramphenicol by the sodium cobaltinitrite procedure and the official method

Compound	Recovery* \pm s.d., %	
	Proposed method	Official method (ref.)
Chlorpromazine. HCl powder	100.4 \pm 0.3	99.6 \pm 1.3 (1)
Neurazine tablets (Misr)	97.0 \pm 1.0	97.3 \pm 0.5 (1)
Neurazine injections (Misr)	103.4 \pm 0.7	104.1 \pm 1.5 (1)
Promazine. HCl powder	100.3 \pm 0.3	101.0 \pm 0.4 (1)
Promazine. HCl tablets§	99.5 \pm 0.4	101.5 \pm 0.5 (1)
Sparine injections (Wyeth)	103.0 \pm 1.1	103.0 \pm 0.3 (1)
Promethazine. HCl powder	100.2 \pm 0.3	98.7 \pm 0.7 (1)
Promethazine. HCl tablets§	99.4 \pm 0.4	98.3 \pm 1.0 (1)
Promantine injections (Misr)	102.1 \pm 0.8	104.2 \pm 0.9 (1)
Perphenazine powder	99.6 \pm 0.4	99.2 \pm 1.0 (1)
Trilafon tablets (Schering)	101.4 \pm 0.9	102.2 \pm 0.9 (1)
Fluphenazine. HCl powder	100.3 \pm 0.5	98.2 \pm 0.4 (1)
Fluphenazine. HCl tablets§	99.2 \pm 0.6	98.8 \pm 0.5 (1)
Tetracycline. HCl powder	100.1 \pm 0.5	100.1 \pm 0.7 (34)
Tetracycline capsules (Adwic)	101.5 \pm 0.6	101.7 \pm 0.6 (34)
Micycline capsules (Misr)	98.6 \pm 0.6	97.5 \pm 0.5 (34)
Oxytetracycline. HCl powder	100.9 \pm 0.7	99.9 \pm 0.4 (34)
Oxytetrin capsules (Memphis)	102.0 \pm 0.9	101.3 \pm 0.5 (34)
Chlortetracycline. HCl powder	100.8 \pm 0.3	—
Chlortetracycline. HCl tablets§	99.3 \pm 1.0	—
Doxycycline hyclate powder	100.3 \pm 0.3	—
Vibramycin capsules (Pfizer)	98.3 \pm 0.8	—
Demeclocycline. HCl powder	100.1 \pm 0.2	99.9 \pm 1.0 (34)
Demeclocycline. HCl tablets§	99.3 \pm 0.5	99.0 \pm 0.3 (34)
Chloramphenicol powder	100.4 \pm 0.3	99.8 \pm 0.6 (34)
Veracetine capsules (Nile)	96.5 \pm 1.0	97.6 \pm 0.9 (34)
Cidocetine injections (Cid)	102.2 \pm 1.0	102.4 \pm 0.8 (34)

*Average of 6 determinations.

§Laboratory-prepared tablets containing the drug, lactose, talc, starch and magnesium stearate.

used was studied and it was found that maximum absorbance was obtained with 1 ml or more of 0.2% sodium cobaltinitrite solution. Phosphoric acid was used as the medium for the reaction; if hydrochloric or acetic acid was used as the medium the colour developed was found to be unstable. Evaporation of the ethanol is essential, since the coloured products are unstable in the presence of ethanol.

Tetracyclines react with sodium cobaltinitrite in aqueous acetic acid to give a yellow colour which is stable for at least 4 hr.

Chloramphenicol is hydrolysed by heating with sodium hydroxide to give *p*-nitrophenol.³³ Treatment of the hydrolysis product with sodium cobaltinitrite in aqueous acetic acid gives a stable yellow colour, with an absorption maximum of the same wavelength as that observed when *p*-nitrophenol is reacted with the reagent under the same conditions.

Sodium cobaltinitrite in aqueous acetic acid has been used for the identification of phenols having free positions *ortho* to the OH-group.²⁵ Feigl²⁵ suggested that an *o*-nitroso derivative was formed which in its tautomeric oxime form yielded a yellow to brown chelate with cobalt(I). The reaction of *p*-cresol with sodium cobaltinitrite was studied by Smith and Garst,²⁶ who found that atomic-absorption analysis of the yellow product did not reveal the presence of cobalt. They identified the product as 2-nitro-*p*-cresol. Accordingly, they categorized sodium cobaltinitrite as acting in acid medium as a nitrating agent rather than a nitrosating agent. A reaction mechanism has been suggested involving the formation of nitro derivatives during the oxidation of tetracyclines of hydrolysed chloramphenicol with sodium cobaltinitrite.²⁹

Beer's law is valid over the concentration ranges presented in Table 1. The regression equations in Table 1 were calculated from the standard calibration curve of each drug. The unknown drug concentration in different pharmaceutical formulations can be calculated from their corresponding regression equations.

The proposed method was applied to the determination of phenothiazines, tetracyclines and chloramphenicol in various pharmaceutical preparations. The excipients present did not interfere. The results of the assays of tablets, capsules and injections presented in Table 2 compare favourable with those obtained by the official method.^{1,34}

REFERENCES

1. *British Pharmacopoeia* 1980, HM Stationery Office, London, 1980.
2. H. Basinska, H. Puzanowska-Tarasiewicz and M. Tarasiewicz, *Chem. Anal. (Warsaw)*, 1970, **15**, 405.
3. J. Meunier and B. Viossat, *Ann. Pharm. Franc.*, 1968, **26**, 25.
4. A. H. Charles, *Clin. Chem.*, 1961, **7**, 130.
5. S. P. Agarwal and M. I. Blake, *J. Pharm. Sci.*, 1969, **58**, 1011.
6. S. Rolski and Z. Zakrzewski, *Farm. Pol.*, 1969, **25**, 621.
7. K. Kigasawa, H. Shimizu and M. Ibuki, *Yakugaku Zasshi*, 1972, **92**, 1009.
8. I. Simonyi and S. K. Zukovics, *Acta Pharm. Hung.*, 1975, **45**, 250.
9. V. A. Gorishnii, K. N. Ryzhkov and G. N. Kilyakova, *Farmatsiya (Moscow)*, 1978, **27**, 86.
10. T. M. Astanina, S. V. Merinova, T. P. Kazakova and M. I. Shmar'yan, *ibid.*, 1979, **28**, 26.
11. S. Cooper, J. M. Albert, R. Dugal, M. Bertrand and R. Elie, *Arzneim. Forsch.*, 1979, **29**, 158.
12. J. Breiter, R. Helger, E. Intershick and H. Wuest, *J. Clin. Chem. Clin. Biochem.*, 1978, **16**, 127.
13. H. Poiger and C. Schlatter, *Analyst*, 1976, **101**, 808.
14. A. Regosz and A. Swiryo, *Farm. Pol.*, 1978, **34**, 17.
15. E. Ragazzi and G. Veronese, *J. Chromatog.*, 1977, **134**, 223.
16. K. Tsuji and J. H. Robertson, *J. Pharm. Sci.*, 1976, **65**, 400.
17. I. Haroun and F. Khattab, *Indian J. Pharm.*, 1978, **40**, 12.
18. F. M. Freeman, *Analyst*, 1956, **81**, 299.
19. C. Baloescu, S. Creanga and M. Tudor, *Farmacia Buc.*, 1966, **14**, 1.
20. A. F. Solodava, *Farmatsiya (Moscow)*, 1967, **16**, 45.
21. G. B. Hess, *Anal. Chem.*, 1950, **22**, 649.
22. J. Mitchell and G. E. Ashly, *J. Am. Chem. Soc.*, 1945, **67**, 161.
23. U. Chandra and P. N. Pandey, *Labdev.*, 1967, **5**, 333.
24. R. Puga, *Rev. Farm. (Buenos Aires)*, 1951, **93**, 290.
25. F. Feigl, *Spot Tests in Organic Analysis*, 7th Ed., Elsevier, Amsterdam, 1966.
26. R. V. Smith and M. J. Garst, *Anal. Chim. Acta*, 1973, **65**, 69.
27. M. A. Korany, M. Abdel-Salam and A. M. Wahbi, *Analyst*, 1977, **102**, 683.
28. M. A. Korany, N. Abdel-Salam and M. Abdel-Salam, *J. Assoc. Off. Anal. Chem.*, 1978, **61**, 169.
29. A. M. Wahbi, H. Abdine, M. A. Korany and M. Abdel-Hay, *ibid.*, 1978, **61**, 1113.
30. H. Auterhoff and J. Kuehn, *Arch. Pharm. (Weinheim)*, 1973, **306**, 241.
31. J. Meunier, B. Viossat, P. Leterreir and P. Douzou, *Ann. Pharm. Franc.*, 1967, **25**, 683.
32. P. G. Ramappa, H. Sanke Gowda and A. N. Nayak, *Analyst*, 1980, **105**, 663.
33. W. Doell, *Arzneim. Forsch.*, 1955, **5**, 97.
34. *U.S. Pharmacopoeia* 1980, 20th Revision, Mack, Easton, 1980.

ADSORPTION OF BISMUTH ON HYDROUS LEAD DIOXIDE FROM BISMUTH-EDTA SOLUTION

SHINICHI ITO

Kyoto Institute of Public Health and Environment, Kyoto, Japan

TOSHIO MATSUDA and TOYOSHI NAGAI

Department of Chemistry, Ritsumeikan University, Kyoto, Japan

(Received 14 June 1983. Revised 23 September 1983. Accepted 22 November 1983)

Summary—The adsorption of bismuth(III) on hydrous lead dioxide (HLD) from solutions of the bismuth-(II)-EDTA complex was studied by differential pulse polarography. It was found that HLD collected bismuth quantitatively from bismuth-EDTA solution over the pH range from 1 to 12, with shaking for 1 hr, even at bismuth-EDTA concentrations as low as 10^{-8} – $10^{-7}M$. In addition, the reaction of HLD with EDTA was investigated in order to consider the participation of EDTA with respect to the adsorption behaviour of bismuth. It can be assumed that the adsorption of bismuth on HLD from bismuth-EDTA solution is correlated to the adsorptive property of HLD and to the surface redox process between HLD and EDTA.

The hydroxides or hydrous oxides of various metals have been studied as co-precipitation¹ or ion-exchange²⁻⁴ reagents for separation or concentration of trace inorganic ions. Lead dioxide, though sparingly soluble, has not previously been studied for these purposes.

Recently, the redox reactions of hydrous lead dioxide (HLD), freshly prepared by the hydrolysis of lead tetra-acetate, with sodium oxalate,⁵ chromium(III)^{6,7} and EDTA⁸ have been reported from our laboratory. In another paper,⁹ an investigation of the individual adsorption of bismuth(III) and copper(II) on HLD was reported. HLD was found to be a superior adsorbent for bismuth in acidic medium, and used in the determination of trace amounts of bismuth in a copper metal standard (about $10^{-50}\%$) by differential pulse polarography.

In the present work, the adsorption of bismuth on HLD from solutions of bismuth-EDTA is studied. In addition, the reaction of HLD with EDTA is investigated in connection with the role played by EDTA in this adsorption system.

EXPERIMENTAL

Reagents and apparatus

A 0.01M bismuth-EDTA standard solution was prepared by mixing bismuth nitrate of reagent grade with Dotite disodium EDTA in 1:1 molar ratio. This stock solution was accurately diluted as required. A 0.05M lead tetra-acetate solution in glacial acetic acid was standardized by potentiometric titration with sodium oxalate.¹⁰ A 0.01M EDTA stock solution was prepared from the Dotite reagent.

A Princeton Applied Research Model 174A polarograph and a Watanabe Model WX-451 X-Y recorder were used. The lead dioxide suspensions were shaken by means of a Yamato Water Bath Incubator, Model BT-31.

Procedure

HLD was prepared by adding 10 ml of 0.05M lead tetra-acetate solution dropwise to 100 ml of distilled water, and then centrifuging to remove the acetic acid produced. The HLD was washed twice with 100-ml portions of distilled water (separated by centrifugation). About 0.12–0.14 g of HLD (taken as $PbO_2 \cdot 2H_2O$) was used for each adsorption test.

A 200-ml Erlenmeyer flask fitted with a rubber stopper was used as the reaction vessel. HLD, a known amount of bismuth-EDTA solution, an appropriate buffer solution and 10 ml of 1M potassium nitrate were added to the flask and the mixture was diluted to 100 ml with distilled water. The pH of the suspension was adjusted with 0.02M HNO_3 - CH_3COOH , CH_3COOH - CH_3COONa , HNO_3 - $Na_2B_4O_7$ and $Na_2B_4O_7$ - $NaOH$ buffers. The suspension was shaken for 1 hr, at 30°. The HLD was then filtered off with a membrane filter (Toyo Kagaku, Type TM-2, pore size 0.45 μm). The differential pulse polarogram of bismuth in the filtrate was recorded, the supporting electrolyte¹¹ consisting of 2 ml of 1.5M sodium citrate, 20 ml of 0.2M EDTA and 2.5 ml of 1M potassium nitrate, diluted to 50 ml. The amount of bismuth adsorbed was determined by measurements of the bismuth concentration before and after adsorption.

For direct determination of the adsorbed bismuth, the HLD was dissolved with sodium oxalate, supporting electrolyte was added, the pH was adjusted to 5.0–5.5, and the bismuth in the solution was determined by differential pulse polarography.

For determination of the dissolved lead(II) in the suspension, the filtrate (obtained as already described) was acidified to 0.2M in nitric acid, and then analysed for lead by differential pulse polarography.

The reaction of HLD with EDTA was studied by adjusting the pH of a suspension containing HLD and an appropriate amount of EDTA, and shaking the mixture for 1 hr at 30°. An appropriate amount of the filtered liquid phase was adjusted to pH 4.7 and the lead(II) in it was removed by controlled-potential electrolysis with a mercury pool cathode. The anodic wave of EDTA was then measured by normal pulse polarography.

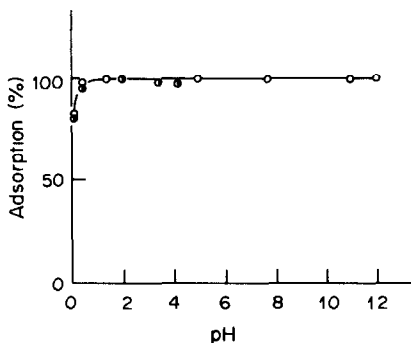


Fig. 1. Effect of pH on the adsorption of bismuth from $2 \times 10^{-5} M$ bismuth-EDTA solution and $2 \times 10^{-5} M$ bismuth(III) solution on hydrous lead dioxide (HLD). HLD 0.14 g; solution volume 100 ml; shaking time 1 hr; temperature 30° : \circ bismuth-EDTA; \bullet bismuth(III).

RESULTS AND DISCUSSION

Effect of pH

The effect of pH on the adsorption of bismuth on HLD from $2 \times 10^{-5} M$ bismuth-EDTA solution is shown in Fig. 1. There is almost 100% adsorption over the pH range from 1 to 12. Similar values were obtained for $3 \times 10^{-4} M$ bismuth-EDTA solution.

The effects of shaking time and temperature on the adsorption were also investigated. The adsorption equilibrium was reached within 1 hr, and the adsorption values were practically constant over the temperature range from 30 to 70° .

Effect of bismuth-EDTA concentration

The relation between concentration of bismuth-EDTA and amount of bismuth adsorbed on HLD is shown in Fig. 2. At each pH tested, there was almost 100% adsorption when the concentration of bismuth-EDTA was less than $4 \times 10^{-4} M$. The adsorption capacity at each pH (except 10) was almost equal to that for adsorption from a simple bismuth(III) solution.⁹ A log-log plot of equilibrium concentration of bismuth-EDTA *vs.* amount of bismuth adsorbed per mole of HLD was linear.

Adsorption at trace concentrations

The effectiveness of adsorptive collection of trace amounts of bismuth(III), present as the

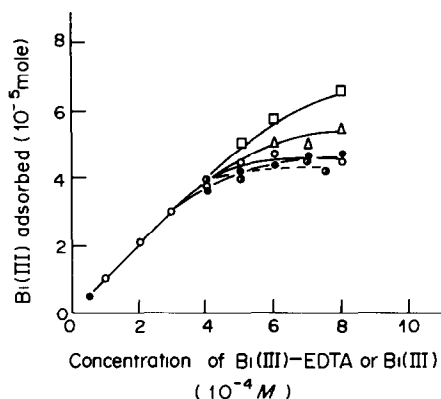


Fig. 2. Relation between the concentration of bismuth-EDTA or bismuth(III) added and the amount of bismuth adsorbed on HLD. HLD 0.14 g; solution volume 100 ml; shaking time 1 hr; temperature 30° . Bismuth-EDTA: \bullet pH 1.8, \circ pH 3.9, \triangle pH 7.3, \square pH 10.0. Bismuth(III): \bullet pH 1.8.

bismuth-EDTA complex, was investigated. HLD, a known amount of bismuth-EDTA solution, 50 ml of $1 M$ potassium nitrate and an appropriate buffer solution were added to a 1000-ml Erlenmeyer flask and the mixture was diluted to 500 ml with distilled water. The suspension (bismuth-EDTA concentration from 1×10^{-6} to $5 \times 10^{-8} M$) was shaken for 1 hr at 30° . The bismuth adsorbed on the HLD was determined directly by the procedure given above. The results obtained for pH 2.5 and 10 are shown in Table 1. The recovery of bismuth was almost 100% at each pH value.

Lead(II) dissolved during the adsorption

The amount of lead(II) dissolved was much higher for adsorption of bismuth from bismuth-EDTA solution than for adsorption from the simple bismuth(III) solution examined previously.⁹ The results obtained at pH 2, 4, 7 and 10 are shown in Fig. 3. The amount of lead(II) increased at each pH with increase in the amount of bismuth-EDTA present, but tended to reach a limiting value. From the slopes of the straight lines up to the plateau, the molar ratio of lead(II) dissolved to bismuth-EDTA taken was found to be about 4 at pH 2, 3 at pH 4 and 0.7 at

Table 1. Recovery of bismuth from the solution of bismuth-EDTA

pH	Initial concentration of bismuth-EDTA, M	Amount of bismuth, μg		Average recovery, %
		Taken,	Found*	
2.5	9.91×10^{-7}	104	101 ± 2	97
2.5	1.98×10^{-7}	20.7	19.7 ± 0.5	95
2.5	0.99×10^{-7}	10.4	10.6 ± 0.8	102
2.5	0.50×10^{-7}	5.2	5.3 ± 0.2	102
10.1	10.01×10^{-7}	105	102 ± 2	97
10.1	2.00×10^{-7}	20.9	21.2 ± 0.4	101
10.1	1.00×10^{-7}	10.5	10.1 ± 0.8	96
10.1	0.50×10^{-7}	5.2	5.4 ± 0.6	104

*Average and deviation are based on two or three replicates.

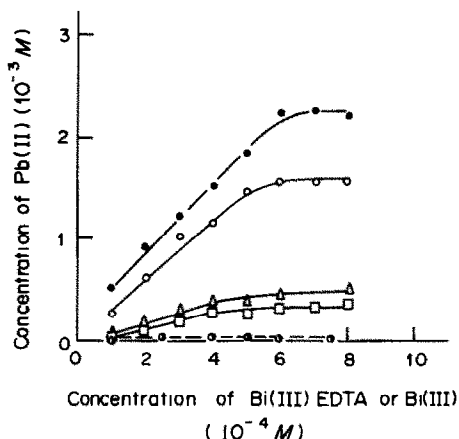


Fig. 3. Relation between the concentration of bismuth-EDTA or bismuth(III) added and the concentration of lead(II) dissolved into the supernatant liquid. HLD 0.14 g; solution volume 100 ml; shaking time 1 hr; temperature 30°. Bismuth-EDTA: ● pH 1.8, ○ pH 3.9, △ pH 7.3, □ pH 10.0. Bismuth(III): ○ pH 1.8.

pH 10. These results suggest that the oxidation of EDTA by HLD proceeds at the interface during the adsorption process.

Reaction of EDTA with HLD

The effect of pH on the decrease in EDTA concentration was investigated, with $2 \times 10^{-4} M$ EDTA. A typical set of results is shown in Fig. 4. About 100% decrease at pH 5 and $23 \pm 3\%$ at pH 10 were observed. Similar results were obtained when the shaking time was increased to 3 hr.

The amount of lead(II) dissolved was also measured (Fig. 5). The molar ratio of lead(II) dissolved to EDTA added was about 3 at pH 5 and about 0.6

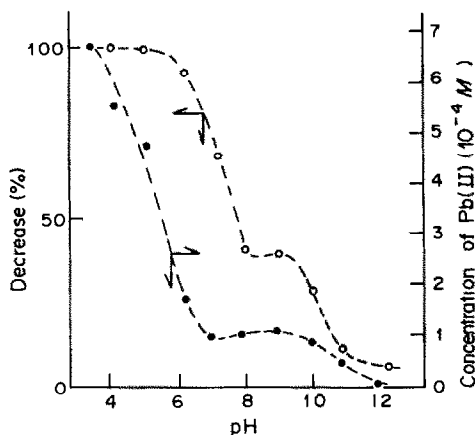


Fig. 4. Per cent decrease of initial EDTA or the concentration of lead(II) dissolved as a function of pH. EDTA $1.6 \times 10^{-4} M$; HLD 0.14 g; shaking time 1 hr, temperature 30°

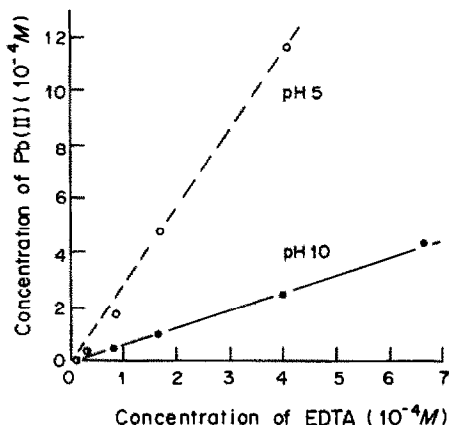


Fig. 5. Relation between the initial concentration of EDTA and the concentration of lead(II) dissolved. HLD 0.14 g; solution volume 100 ml; shaking time 1 hr; temperature 30°.

at pH 10, in agreement with the results for adsorption of bismuth from bismuth(III)-EDTA solution.

From these results, it is evident that the oxidation reaction of EDTA with HLD proceeds over the pH range from 1 to 12. Though the mechanism has not been fully elucidated, it seems probable that the bismuth-EDTA complex is primarily adsorbed on the HLD and oxidized on the surface, the bismuth ion being retained on the HLD, as a compound such as the hydroxide.

Conclusions

The adsorptive property of hydrous lead dioxide prepared *in situ* by the hydrolysis of lead tetra-acetate has been investigated, with reference to the adsorption of bismuth from bismuth-EDTA solution. The results show that HLD collects bismuth quantitatively over the pH range from 1 to 12, and that bismuth can be collected quantitatively 10^{-8} - $10^{-7} M$ bismuth-EDTA solution in this way.

Acknowledgement—This work was partially supported by a Grant-in-Aid for Special Project Research from the Ministry of Education, Science and Culture.

REFERENCES

1. N. Shigematsu, *Bunseki Kagaku*, 1973, **22**, 618.
2. M. Abe, *ibid.*, 1974, **23**, 1254.
3. K. Terada, *Bunseki*, 1980, 47.
4. V. Vesely and V. Pekárek, *Talanta*, 1972, **19**, 219, 1254.
5. S. Ito, T. Matsuda and T. Nagai, *Bunseki Kagaku*, 1977, **26**, 687.
6. T. Nagai, T. Matsuda and Y. Kouji, *ibid.*, 1978, **27**, 749.
7. *Idem*, *ibid.*, 1980, **29**, 115.
8. S. Ito, T. Matsuda and T. Nagai, *Talanta*, 1980, **27**, 25.
9. *Idem*, *Bunseki Kagaku*, 1980, **29**, 655.
10. T. Nagai, T. Matsuda and N. Sugii, *ibid.*, 1971, **20**, 1412.
11. M. Ishibashi, T. Nagai, T. Fujinaga and W. Funasaka, *ibid.*, 1959, **8**, 107.

FURTHER APPLICATION OF THE DIAZOTIZATION-COUPPLING SPECTROPHOTOMETRIC TECHNIQUE TO THE DETERMINATION OF AROMATIC AMINES WITH 8-AMINO-1-HYDROXYNAPHTHALENE-3,6-DISULPHONIC ACID AND *N*-(1-NAPHTHYL)-ETHYLENEDIAMINE AS COUPLING AGENTS

GEORGE NORWITZ and PETER N. KELIHER*

Chemistry Department, Villanova University, Villanova, PA 19085, U.S.A.

(Received 22 August 1983. Accepted 26 October 1983)

Summary—Twenty-two aromatic amines are determined by the diazotization-coupling spectrophotometric technique, using 8-amino-1-hydroxynaphthalene-3,6-disulphonic acid (H-acid) and *N*-(1-naphthyl)ethylenediamine (N-na) as coupling agents. The following are determined by both methods: 2- and 4-ethylaniline, 4-aminobenzonitrile, 3- and 4-aminoacetophenone, 4-aminobenzophenone, 4-iodoaniline, 2,5-dichloroaniline, 4-aminohippuric acid, 2-aminobenzyl alcohol, 3-aminobenzamide, sulphathiazole, 2-, 3- and 4-methoxyaniline and 2,4-, 3,4- and 3,5-dimethylaniline. It is possible to determine 2,3- and 2,5-dimethylaniline only by the H-acid method, but 2,6-dimethylaniline cannot be determined by either method. 2-Aminobenzamide can only be determined by the N-na method. In the application of the H-acid method to the methoxyanilines and dimethylanilines, the colour is developed by adding a large excess of sodium bicarbonate and H-acid. In the application of the N-na method to the ethylanilines, methoxyanilines and 2,4-, 3,4- and 3,5-dimethylanilines, the colour is developed by addition of a large excess of N-na reagent and allowing the solution to stand overnight.

We recently proposed methods for the determination of aromatic amines by the diazotization-coupling spectrophotometric technique, using 8-amino-1-hydroxynaphthalene-3,6-disulphonic acid (H-acid) and *N*-(1-naphthyl)ethylenediamine (also called *N*-(1-naphthalenyl)-1,2-ethanediamine or N-na) as coupling agents.¹ Subsequently, aminophenols, phenylenediamines, dinitroanilines, trichloroanilines and tetrachloroaniline were determined by using N-na and special techniques.² In the present work, 22 more aromatic amines of importance in industry and pharmacology are determined by the H-acid and N-na coupling methods.

EXPERIMENTAL

Apparatus and reagents

A Bausch and Lomb model 70 spectrophotometer (1-cm cell) and a Cary model 219 recording spectrophotometer (1-cm cell) were used.

All chemicals were of reagent grade except where indicated. The aromatic amines were obtained from the Eastman Kodak Co. or Aldrich Chemical Co. and purified by recrystallization or distillation if necessary.

H-acid reagent (0.75%). Purify technical grade H-acid monosodium salt as follows. Dissolve 20 g of the salt in about 200 ml of boiling water. Cool in ice, filter off the precipitate on a Whatman No. 41 paper by suction and wash it four times with cold water and three times with acetone. Let stand in air for 1–2 hr to volatilize acetone. Make-up a 0.75% solution in water fresh every 3 days and store in a brown bottle.

*Author to whom correspondence should be addressed.

N-na reagent (0.75%, in water). Prepare fresh every 3 days and store in a brown bottle.

Standard aromatic amine solution A (2.50 mg/ml). Dissolve 0.2500 g of the aromatic amine (except 2-aminobenzamide) in methanol and dilute to volume in a 100-ml standard flask with methanol. Dissolve 2-aminobenzamide in a mixture of methanol and 5 ml of concentrated hydrochloric acid and dilute to 100 ml with methanol.

Standard aromatic amine solution B (25 µg/ml). Prepare fresh daily by diluting a 5-ml aliquot of standard aromatic amine solution A to volume in a 500-ml standard flask with water.

Procedures

The following are determined by both methods: 2- and 4-ethylaniline, 4-aminobenzonitrile, 3- and 4-aminoacetophenone, 4-aminobenzophenone, 4-iodoaniline, 2,5-dichloroaniline, 4-aminohippuric acid, 2-aminobenzyl alcohol, 3-aminobenzamide, sulphathiazole, 2-, 3- and 4-methoxyaniline and 2,4-, 3,4- and 3,5-dimethylaniline. 2,4- and 2,5-dimethylaniline can be determined only by the H-acid method and 2,6-dimethylaniline cannot be determined by either method. 2-Aminobenzamide can be determined only by the N-na method.

H-acid method. For all the aromatic amines to which the H-acid method is applicable (except the methoxyanilines and dimethylanilines) proceed as follows. Prepare a calibration curve by transferring portions of standard aromatic amine solution B to 100-ml standard flasks. The volumes should be chosen in accordance with the sensitivities indicated in Table 1, to cover the absorbance range up to 0.6. Dilute to about 75 ml with water, add 2.0 ml of 0.3*M* hydrochloric acid and 2.0 ml of 1% sodium nitrite solution, swirl and allow to stand for 5 min. Add 2.0 ml of 3% sulphamic acid solution, swirl, wash down the neck of the

flask and allow to stand for 10 min. Add 10 ml of 6% sodium bicarbonate solution, swirl, add 2.0 ml of H-acid reagent, swirl again, dilute to the mark, mix, and store in the dark for 15–45 min. Measure the absorbance against water at the wavelength indicated in Table 1. Deduct the blank and plot absorbance against mg of the aromatic amine per 100 ml. For the determination of the methoxyanilines and dimethylanilines, proceed as above but use 1.0 ml of 0.3*N* hydrochloric acid, 5 g of sodium bicarbonate, 5.0 ml of H-acid reagent, and store in the dark for 60–90 min. For the analysis of samples, transfer an appropriate aliquot to a 100-ml standard flask and proceed as for the calibration curve.

N-na method. For all the aromatic amines to which the N-na method is applicable (except the methoxyanilines and dimethylanilines) proceed as follows. Prepare a calibration

curve by transferring portions of standard aromatic amine solution B to 50-ml standard flasks, the volumes being chosen (Table 1) to cover the absorbance range up to 0.6. dilute to 30–35 ml with water, add 3.0 ml of 1*M* hydrochloric acid and 1.0 ml of 1% sodium nitrite solution, swirl and allow to stand for 5 min. Add 1.0 ml of 3% sulphamic acid solution, swirl, wash down the neck of the flask and allow to stand for 10 min. Add the amount of N-na reagent indicated in Table 1, dilute to the mark and mix. Measure the absorbance against water at the wavelength and time indicated in Table 1. Deduct the blank and plot absorbance against mg of aromatic amine per 50 ml. For the determination of 2,3-, 3,4- and 3,5-dimethylaniline, proceed as above but use 2.0 ml of 1*M* hydrochloric acid. For the methoxyanilines use 2.5 ml of N-na reagent and 90 min standing for 3-methoxyaniline, and 10 ml of reagent and

Table 1. Spectrophotometric determination of aromatic amines by the H-acid and N-na methods

Aromatic amine	H-acid			N-na					
	Colour	λ_{\max} , nm	Absorbance*	Reagent, ml	Colour	λ_{\max} , nm	Time for development	Absorbance†	
2-Ethylaniline	cherry red	532	0.25	10.0	purplish red	548	16–24 hr	0.14	
4-Ethylaniline	cherry red	530	0.62	10.0	reddish purple	569	16–24 hr	0.51	
4-Aminobenzonitrile	cherry red	529	0.51	1.0	purplish red	543	10 min	0.39	
3-Aminoacetophenone	cherry red	524	0.40	1.0	purplish red	545	10 min	0.32	
4-Aminoacetophenone	cherry red	532	0.68	1.0	purplish red	551	10 min	0.51	
4-Aminobenzophenone	cherry red	537	0.46	1.0	reddish purple	550	10 min	0.36	
4-Iodoaniline	cherry red	534	0.40	1.0	purplish red	557	10 min	0.27	
2,5-Dichloroaniline	cherry red	531	0.42	1.0	purplish red	536	10 min	0.28	
4-Aminohippuric acid	cherry red	530	0.43	1.0	purplish red	549	10 min	0.34	
2-Aminobenzyl alcohol	cherry red	536	0.52	2.5	reddish purple	551	90 min	0.27	
2-Aminobenzamide (anthranilimide)	Not recommended*			2.5	reddish purple	553	90 min	0.25	
3-Aminobenzamide	cherry red	527	0.49	1.0	reddish purple	547	10 min	0.42	
Sulphathiazole (4-amino- <i>N</i> -2-thiazolylbenzene-sulphanilimide)	cherry red	531	0.33	2.5	reddish purple	546	30 min	0.27	
2-Methoxyaniline (<i>o</i> -anisidine)	purplish red	540	0.58	10.0	violet	574	16–24 hr	0.44	
3-Methoxyaniline (<i>m</i> -anisidine)	cherry red	525	0.61	2.5	reddish purple	555	90 min	0.43	
4-Methoxyaniline (<i>p</i> -anisidine)	purplish red	541	0.32	10.0	violet	580	16–24 hr	0.22	
2,3-Dimethylaniline	cherry red	534	0.22		Not recommended§				
2,4-Dimethylaniline	cherry red	538	0.42	10.0	reddish violet	560	16–24 hr	0.18	
2,5-Dimethylaniline	cherry red	536	0.22		Not recommended§				
2,6-Dimethylaniline	Not recommended§				Not recommended§				
3,4-Dimethylaniline	cherry red	538	0.63	10.0	reddish violet	567	16–24 hr	0.40	
3,5-Dimethylaniline	cherry red	530	0.42	10.0	reddish violet	561	16–24 hr	0.22	

*For 2 $\mu\text{g/ml}$.

†For 1 $\mu\text{g/ml}$.

§The absorbance for the indicated concentration was less than 0.05.

overnight standing for the other two. For analysis of samples transfer an appropriate aliquot to a 50-ml standard flask and proceed as for the calibration curve.

RESULTS AND DISCUSSION

Preparation of the stock amine solutions

The stock amine solutions (except 2-amino-benzamide) are prepared with methanol as solvent, but ethanol is equally satisfactory for all the amines tested in this and the previous papers. For the stock solution of 2-aminobenzamide, 5 ml of concentrated hydrochloric acid must be added.

Colours obtained

Many of the H-acid dyes of the aromatic amines tested in this paper are light-sensitive so the solutions should be stored in the dark after addition of the H-acid. The N-na dyes are not light-sensitive. The spectral characteristics of the dyes are shown in Table 1. Beer's law is obeyed for all the systems tested.

Dimethylanilines (xylidines)

For determination of the dimethylanilines by the H-acid method, it is necessary to use only 1.0 ml of 0.3M hydrochloric acid for the diazotization (instead of 2.0 ml) and 5 g of sodium bicarbonate to give a pH of 7.7 (instead of 10 ml of 6% sodium bicarbonate solution to give a pH of 7.2). It is also necessary to use 5 ml of H-acid reagent (instead of 2 ml) and allow the solution to stand for 60–90 min for the development of the colour (instead of 15–45 min). The sodium bicarbonate takes 2–3 min to dissolve, but this does not matter, since even a 1 hr interval between addition of the sodium bicarbonate and the H-acid does not affect the result.

For the determination of 2,4-, 3,4- and 3,5-dimethylaniline by the N-na method, it is advisable to use 2.0 ml of 1M hydrochloric acid for the diazotization-coupling (instead of 3.0 ml); it is also necessary to use a large excess of N-na reagent (10 ml) and allow the solution to stand overnight for colour development. Little or no colour was produced when the N-na method was applied to 2,3-, 2,5- and 2,6-dimethylaniline and no improvement could be achieved by alteration of the acidity, nitrite concentration and time of diazotization, or by adding a catalyst (sodium bromide) and cooling in ice during the diazotization, using ammonium sulphamate or urea (instead of sulphamic acid) to destroy the excess of nitrite, and heating during the coupling.

The only previous investigator to study the application of the N-na method to the determination of dimethylanilines was Daniel,³ who treated 1 ml of sample solution with 1 ml of 2M hydrochloric acid and 1 ml of 0.25% sodium nitrite solution, and after 15 min added 1 ml of 2.5% ammonium sulphamate

solution. He then allowed the mixture to stand for 1 min, added 1 ml of 1% N-na reagent and diluted to volume in a 10-ml standard flask. Alternatively, after adding the ammonium sulphamate, he added 1 ml of 3M sodium acetate and 1 ml of the N-na reagent and diluted to 10 ml. We concur with Daniel that little or no colour is produced by 2,3-, 2,5- and 2,6-dimethylaniline in the N-na method. However, we obtained greater colour development than Daniel for 2,4- and 2,6-dimethylaniline and our values for λ_{\max} differed significantly from his.

Methoxyanilines

The same H-acid procedure is recommended for methoxyanilines as that for dimethylanilines and the N-na procedure recommended for methoxyanilines is that previously described for aminophenols.²

Ease of coupling

Electron-withdrawing groups in the aromatic nucleus tend to facilitate coupling by increasing the positive charge on the diazonium ion. Consequently, aromatic amines which contain CN, COCH₃, COC₆H₅, I, Cl and CONHCH₂CH₂COOH groups (all strong electron-withdrawing groups) require only 1 ml of N-na reagent and colour development is complete in 10 min (Table 1). Aromatic amines containing less strong electron-withdrawing groups, or strong electron-donating groups (C₂H₅, OCH₃ or two CH₃ groups) require more N-na reagent and a longer time for development of the colour. For the H-acid method, the effect of strong electron-donating groups (OCH₃ and two CH₃ groups) is such that a larger excess of H-acid reagent and a longer standing time are required for development of the colour. It is not known why the H-acid method is applicable to 3-aminobenzamide but not to 2-aminobenzamide and why the colour for the N-na method develops more readily with 3-aminobenzamide (in 10 min with 1 ml of reagent) than with 2-aminobenzamide (in 90 min with 2.5 ml of reagent). A possible explanation is that 2-aminobenzamide is more basic than 3-aminobenzamide and this may affect the coupling. This difference in basicity is the reason for addition of hydrochloric acid in preparation of the stock 2-aminobenzamide solution.

The accuracy (average relative error about 5%) and precision of the methods is about the same as that obtained previously in the determination of aromatic amines by the H-acid and N-na methods.^{1,2}

REFERENCES

1. G. Norwitz and P. N. Keliher, *Anal. Chem.*, 1982, **54**, 807.
2. *Idem, ibid.*, 1983, **55**, 1226.
3. J. W. Daniel, *Analyt.*, 1962, **86**, 640.

ANALYTICAL APPLICATIONS OF LIQUID-LIQUID PHASE EQUILIBRIA: ANALYSIS OF BINARY MIXTURES OF CHEMICALLY SIMILAR COMPONENTS

S. K. SURI* and MOHINDER PAL

Chemistry Department, Indian Institute of Technology, New Delhi 110016, India

(Received 9 August 1983. Accepted 20 October 1983)

Summary—A new, simple and rapid method based on the principle of liquid-liquid phase equilibria has been developed for the analysis of binary mixtures of chemically similar organic compounds. The method does not require elaborate instrumentation and can be used to analyse mixtures of members of homologous series. The application of the method has been illustrated by analysing binary mixtures of n-hexane and n-octane; the maximum uncertainty in this analysis is ~2%.

Analysis of binary and ternary mixtures of organic compounds by phase titration¹⁻⁵ is based on the appearance of a second phase in a homogeneous liquid mixture, giving a turbidimetric end-point. In this communication we describe a method, based on liquid-liquid phase equilibria, for the analysis of binary mixtures made up of chemically similar organic compounds. Many of these mixtures cannot be analysed by procedures based on chemical reactions because these are usually slow or incomplete, and various interfering consecutive reactions may occur when the system is allowed to proceed to equilibrium. The proposed method is illustrated by its application to the analysis of mixtures of n-hexane and n-octane.

THEORY

The phase diagram for a ternary system containing one pair of mutually immiscible or only partially miscible components A and B and a consolute component C is shown in Fig. 1. If a further substance A' is chemically similar to A, it will have similar solubility behaviour towards pure B and C. However, the effect of the consolute component on the miscibility of A' and B will be different from that on the miscibility of A and B, and therefore the binodal curve for the system A'-B-C (dashed line in Fig. 1) will be different from that for A-B-C.⁶

For a pseudo-ternary system composed of (A + A'), B and C, the binodal curve will lie somewhere between the binodal curves for the systems A-B-C and A'-B-C and its locus will depend upon the relative amounts of A and A' in the mixture.

A ternary mixture A-B-C having the composition represented by the point O in Fig. 1 will split into two

different phases represented by points L and M (where LM is the tie line). The relative amounts of the two phases are given by the lever rule, *i.e.*,

$$\frac{\text{Amount of phase of composition L}}{\text{Amount of phase of composition M}} = \frac{OM}{OL}$$

The corresponding ternary mixture A'-B-C defined by point O will similarly separate into two phases having the compositions represented by the points L' and M', the relative amounts being given by the ratio OM'/OL'. It is, therefore, evident that on gradual replacement of A by A' (*i.e.*, increasing the ratio A'/A), in the pseudo-ternary mixture (A + A')-B-C, the relative amounts of the two phases will move from OM/OL to OM'/OL'. A calibration curve can, therefore, be obtained for the relative amounts of the two phases in the pseudo-ternary mixture (A + A')-B-C as a function of %A/(%A + %A'). From a knowledge of the binodal curves for the ternary mixtures A-B-C and A'-B-C

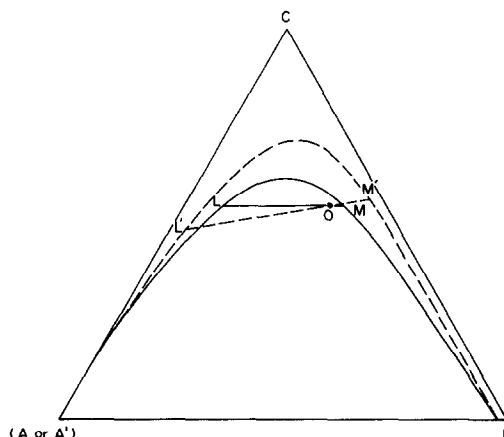


Fig. 1. Phase diagram and relative amounts of two equilibrium phases corresponding to the ternary composition at point O for the systems A-B-C (—) and A'-B-C (---).

*To whom correspondence should be addressed.

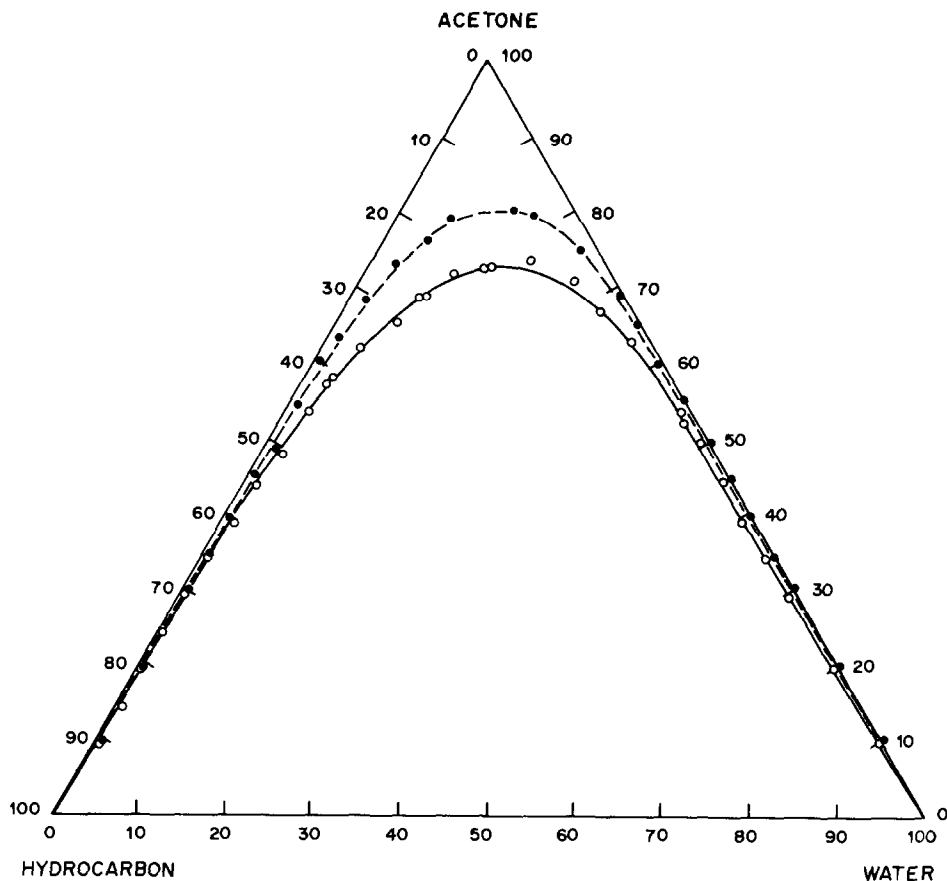


Fig. 2. Binodal curves for the ternary systems n-hexane-acetone-water (○) and n-octane-acetone-water (●) at $25 \pm 0.05^\circ$.

a position of point O can be computed that will give a large difference between the ratios OM/OL and OM'/OL' . One possible route to obtain optimum precision is to keep OM fairly small, so that the difference $(OM' - OM)$ is much larger than the difference $(OL' - OL)$. The method holds good even when the tie lines for the ternary mixtures $A-B-C$ and $A'-B-C$ are not parallel. The effect of the difference in the slope of the tie lines is taken into account in the calibration curve.

EXPERIMENTAL

Materials

Analytical-reagent grade samples of n-hexane and n-octane were purified by drying over sodium metal, followed by fractional distillation.⁷ Laboratory-reagent grade acetone was refluxed over potassium permanganate, distilled and stored over anhydrous potassium carbonate. The solvents were fractionally distilled immediately before use. Distilled water was used throughout.

Determination of binodal curves for the ternary mixtures $A-B-C$ and $A'-B-C$

The binodal curves for the hydrocarbon-acetone-water mixtures were obtained by titrating a set of binary mixtures of hydrocarbon and acetone with water and another set of binary mixtures of water and acetone with hydrocarbon, to a turbidimetric end-point.⁸ Details of the apparatus and experimental technique have been given earlier.⁹

The binodal curves for the two sets of ternary mixtures, n-hexane-acetone-water and n-octane-acetone-water at $25 \pm 0.05^\circ$ are shown in Fig. 2. It can be observed that though the miscibilities of n-hexane and n-octane with water are of the same order of magnitude, the addition of acetone yields fairly distinct solubility curves, and this differentiating effect of the consolute allows the new method to be used for the analysis of binary mixtures of the two hydrocarbons.

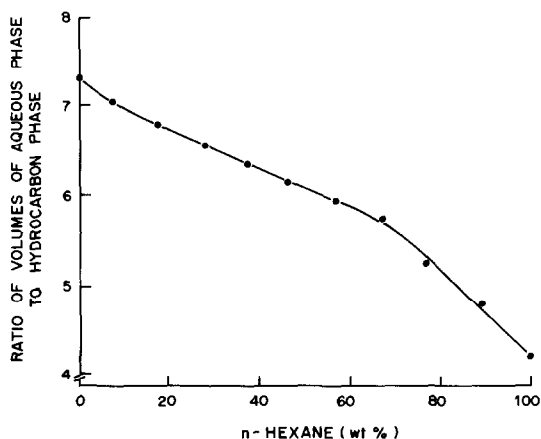


Fig. 3. Calibration curve for the analysis of mixtures of n-hexane and n-octane at $25 \pm 0.05^\circ$.

Table 1. Comparison of results for synthetic mixtures

Wt.% n-hexane		<i>n</i>	Relative standard deviation %
Present	Found*		
9.72	7.6	3	—
18.67	17.3	5	10
33.52	32.4	2	—
44.63	45.8	8	2.7
55.08	56.4	2	—
66.34	66.7	2	—
75.87	76.8	5	1.4
83.40	83.9	2	—
91.32	90.4	2	—

*Average value of *n* determinations.

The apparatus used for determining the amount of two immiscible phases in equilibrium is a 50-ml stoppered measuring cylinder (made from a burette) with an outer jacket for the circulation of water from a thermostatic reservoir.

Calibration curves

To obtain the calibration curve, a set of binary mixtures of n-hexane and n-octane covering the entire w/w composition range was prepared. Seven ml of the hydrocarbon mixture, 37 ml of acetone and 6 ml of distilled water were added to the specially designed measuring cylinder described above and the mixture was shaken intermittently until thermal equilibrium at $25 \pm 0.05^\circ$ was obtained. The volumes of the two phases in equilibrium were measured and a calibration curve (Fig. 3) of the ratio of the volumes of the two phases against the composition of the binary mixture was drawn.

A set of synthetic mixtures containing both n-hexane and n-octane, having the same volume ratios of acetone, water and total hydrocarbon as those used to obtain the calibration curve, but with different amounts of n-hexane and n-octane in the hydrocarbon component, was prepared and

subjected to analysis. The volumes of the two phases in equilibrium were measured and the composition of the hydrocarbon mixture read from the calibration curve.

RESULTS AND DISCUSSION

The results obtained for the synthetic mixtures were compared with the actual values (Table 1) and on the whole, the agreement was good. The maximum absolute difference found was $\sim 1\%$ for solutions rich in n-hexane and $\sim 2.2\%$ for solutions rich in n-octane. An examination of the calibration curve reveals that the method will yield more precise results for binary mixtures rich in n-hexane.

Although we have illustrated the method by using water and acetone as the components B and C respectively, there are many alternative choices for these components. Their suitability, however, will depend on the nature of the calibration curve obtained, since this governs the precision of the method.

REFERENCES

1. D. W. Rogers, D. L. Thomson and I. D. Chawla, *Talanta*, 1966, **13**, 1389.
2. S. K. Suri, K. Prasad, J. C. Ahluwalia and D. W. Rogers, *ibid.*, 1981, **28**, 281.
3. S. K. Suri, *ibid.*, 1974, **21**, 604.
4. *Idem*, *ibid.*, 1972, **19**, 804.
5. D. A. Dunnery and G. R. Atwood, *ibid.*, 1968, **15**, 855.
6. A. W. Francis, *Liquid-Liquid Equilibrium*, Interscience, New York, 1963.
7. J. A. Riddick and W. B. Bunger (eds.), *Techniques of Organic Chemistry*, Vol. II, *Organic Solvents*, Wiley-Interscience, New York, 1970.
8. S. K. Suri, A. P. Rao and V. Ramakrishna, *Indian J. Chem.*, 1966, **4**, 194.
9. S. K. Suri, *Talanta*, 1970, **17**, 577.

RAPID PHOTOMETRIC DETERMINATION OF PHOSPHORUS IN IRON ORES AND RELATED MATERIALS AS PHOSPHOMOLYBDENUM-BLUE

OM P. BHARGAVA and MICHAEL GMITRO
Stelco Inc., P.O. Box 2030, Hamilton, Ontario, Canada

(Received 3 August 1983. Accepted 14 October 1983)

Summary—A rapid, simple and accurate method for determining phosphorus photometrically in iron ores and related materials, obviating the use of perchloric acid, is described. The sample is fused with sodium peroxide in a zirconium crucible and the melt dissolved in hydrochloric acid. The molybdenum-blue complex is developed by the addition of ammonium molybdate and hydrazine sulphate and the absorbance is measured at 725 nm. The range of the method is from 0.005 to 1.0% P. A batch of 6 samples can be analysed in about 2 hr.

The molybdate/magnesia method¹ has been the traditional referee procedure for determining phosphorus gravimetrically as magnesium pyrophosphate in minerals and iron ores. The method is quite tedious and cumbersome, and suffers interference from titanium. Both the ASTM method² and the British Standard method³ require digestion of the sample in nitric-hydrochloric-perchloric acid mixture, and treatment of the insoluble matter, including removal of silica, subsequent fusion of the remaining residue, dissolution of the product, and subsequent formation of the phosphovanadomolybdate complex; this complex is then extracted either with isobutyl alcohol or MIBK (methyl isobutyl ketone), prior to photometric measurement. The phosphovanadomolybdate methods are quite tedious and lengthy. An equally accurate but more cost-effective approach is preferred. In general, considerable time and effort are needed for complete dissolution of the sample. We have already reported a technique for rapid dissolution of materials encountered in the steel industry, including iron ores.⁴ A procedure for determining phosphorus photometrically was also described. The sample was fused with sodium peroxide and sodium carbonate in a vitreous carbon crucible and the melt dissolved in perchloric acid, the medium used for developing the final molybdenum blue colour for photometric measurements. It is well known that the perchloric acid concentration is quite critical and the usual practice of adding bismuth compounds was found unsuccessful in our other investigations. Further, the use of perchloric acid in the laboratory is becoming rarer, particularly in North America, owing to its hazardous nature and the strict safety control required.

Recently our laboratory was required to determine phosphorus in an unknown sample (refractory in nature), of concern in occupational hygiene. As usual, the sample was fused with sodium peroxide,

but the melt could not be dissolved in perchloric acid. It readily dissolved in hydrochloric acid, however, and an attempt to develop the phosphomolybdenum blue in hydrochloric acid medium by addition of molybdate and hydrazine, followed by reduction with sodium sulphite, was successful. However, when this method was applied to phosphorus in iron ores it was found that the concentration of hydrochloric acid in the solution was important and needed investigation. An attempt was also made to replace the expensive vitreous carbon crucible by a zirconium crucible.

EXPERIMENTAL

Reagents

Only reagents that need special preparation are mentioned here. Others are given in the procedure. Pure distilled water is used throughout.

Ammonium molybdate solution, 20 g/l. To 500 ml of water, add cautiously and slowly 300 ml of sulphuric acid and cool. Add 20 g of ammonium heptamolybdate tetrahydrate $[(\text{NH}_4)_6\text{Mo}_7\text{O}_{24} \cdot 4 \text{H}_2\text{O}]$. Stir to dissolve and dilute to 1 litre with water.

Fusion blank. Dissolve 4 g of sodium peroxide in 40 ml of water. Add 30 ml of concentrated hydrochloric acid. Boil for 2 min. Cool and dilute to volume in a 100-ml standard flask.

Hydrazine sulphate solution, 1.5 g/l.

Molybdate-hydrazine sulphate solution. Add 50 ml of the ammonium molybdate solution to 100 ml of water, followed by 20 ml of the hydrazine sulphate solution, and dilute to 200 ml.

Sodium sulphite solution, 100 g/l. Prepared with anhydrous sodium sulphite.

Standard phosphorus solution. Dry anhydrous disodium phosphate (Na_2HPO_4) at 105°, cool it in a desiccator, then dissolve 0.2292 g of it in 200 ml of water. Dilute to volume in a 1-litre standard flask, and mix. This is the standard 'A' 50- $\mu\text{g}/\text{ml}$ phosphorus solution. Transfer 10.00 ml of this solution into a 50-ml standard flask, dilute to the mark with water and mix. This solution 'B' is the 10- $\mu\text{g}/\text{ml}$ standard phosphorus solution for calibration. *Note.* Except for the first and last, the reagents should be prepared fresh as needed.

Table 1

P content, %	Weight of sample, g	Sample aliquot, ml	Fusion blank, ml
0.005-0.15	0.3	10.00	none
0.15-0.50	0.1	10.00	none
0.50-1.0	0.1	5.00	5.00

Procedure

Transfer the amount of test sample (weighed to ± 0.1 mg) specified in Table 1 into a 50-ml zirconium crucible. Add 2 g of sodium peroxide and mix with a dry stainless-steel spatula. Fuse over a burner, swirling the crucible until the melt is cherry red and clear. Remove from the heat and swirl until the melt solidifies on the wall of the crucible. Place the crucible in a dry 250-ml beaker and cool. Cover the beaker with a watch-glass and add about 10 ml of water to the crucible. When the reaction has ceased transfer the crucible contents into the beaker and wash the cover and crucible with water. Add 15 ml of concentrated hydrochloric to the crucible and thence into the beaker. Rinse the crucible with water and add the rinsings to the beaker. Boil for 2 min, cool, transfer the contents into a 50-ml standard flask. Dilute to volume with water and mix. Transfer an appropriate aliquot of the test solution and the fusion blank (Table 1) into the same 150-ml beaker. Add 15 ml of sodium sulphate solution, mix and bring to the boil. Add 20 ml of molybdate-hydrazine sulphate solution. Bring to the boil then heat for 10 min in a boiling water-bath. Cool. Transfer to a 50-ml standard flask and dilute to the mark with water and mix. Within the next 2 hr measure the absorbance of the solution and of the calibration standards at 725 nm with water as the reference. Subtract the blank (see below) to obtain the net absorbance, and read off the weight of phosphorus from the calibration graph.

$$\% \text{ P} = \frac{\mu\text{g of phosphorus}}{\text{sample weight (g)} \times \text{sample aliquot (ml)}}$$

Calibration standards

Into a series of five 150-ml beakers transfer 10.00-ml portions of fusion blank solution and then 0, 0.50 and 2.50 ml of 'B' and 1.00 and 2.00 ml of standard 'A' phosphorus solution, corresponding to 0, 5, 25, 50 and 100 μg of phosphorus respectively. To each beaker add 15 ml of sodium sulphite solution, and continue from this point as described above for the test solution. Plot the net absorbance [obtained by subtracting the blank (0- μg P) absorbance] against μg of phosphorus in the coloured solution.

RESULTS AND DISCUSSION*Effect of hydrochloric acid concentration*

As mentioned earlier, the hydrochloric acid concentration is important. Varying the volume of concentrated hydrochloric acid added to the fusion melts

Table 3. Effect of arsenic on phosphorus determination

Iron ore	P		
	(certificate value), %	As added, %	P found, %
NBS 690	0.011	—	0.009
NBS 690	0.011	0.05	0.015
NBS 693	0.056	—	0.056
NBS 693	0.056	0.10	0.064

obtained from synthetic mixtures and from NBS 692 iron sample (0.04% P), gave the results shown in Table 2.

Table 2 demonstrates that the 15 ml of hydrochloric acid used in the procedure is optimal, giving excellent precision for the synthetic solutions as well as for the reference standard iron ore sample.

Effect of zirconium

In our earlier study⁴ it was suspected that zirconium would interfere, as zirconium phosphate is reported to be insoluble; hence the fusion with sodium peroxide was done in a vitreous carbon crucible. However, further investigation showed that fusion in a zirconium crucible gave the same results as those obtained by using a vitreous carbon crucible. The expensive (\$70 each) vitreous carbon crucibles, which are also rapidly consumable (18 fusions at the most) can therefore advantageously be replaced by the relatively less expensive zirconium crucibles, which are suitable for several hundred fusions with sodium peroxide. Since zirconium does not interfere, titanium should not either, and it was later found that up to 6.4% of TiO_2 had no effect.

Effect of arsenic and silicon

Normally the arsenic content of iron ores and concentrates is 0.01% or less, but its possible interference was investigated with a much higher level. Two standard reference iron ores (NBS 690 and NBS 693) were analysed with and without addition of arsenic. The results are given in Table 3, and demonstrate that arsenic causes a positive error, approximately 0.01% of phosphorus per 0.1% of arsenic present. Thus the interference of 0.01% of arsenic is equivalent to only 0.001% of phosphorus, which lies well within the acceptable experimental deviation.

Table 2. Effect of amount of hydrochloric acid on absorbance at 725 nm

HCl, ml	P, μg	Absorbance					
		0	5	25	50	100	24*
11		0.018	—	0.208	0.408	0.789	0.289
13		0.002	—	—	0.400	—	0.203
15		0.001†	0.042†	0.203†	0.401†	0.802†	0.193†
18		0.001	—	0.204	0.400	—	0.192
20		0.002	—	—	0.402	—	0.173

*NBS 692 (0.04% P), corresponding to 24 μg of phosphorus.

†Absorbance is an average of 4 independent replicates, with $s = 0.0005$.

Table 4. Composition of iron ores and concentrates (%)

Iron ore	Fe	SiO ₂	Al ₂ O ₃	TiO ₂	CaO	MgO	S	P	MnO
BCS 302	35.5	20.0	7.24	0.36	3.3	1.07	0.12	0.71	—
Japan 850-1	66.83	2.6	0.55	0.09	0.39	0.77	0.017	0.017	0.04
Japan 830-1	60.63	2.3	0.12	6.37	0.70	2.17	0.006	0.125	0.66
Japan 800-1	62.92	2.6	2.01	0.09	0.05	0.25	0.075	0.042	0.22
BCS 377	52.5	8.6	3.40	0.19	10.8	1.1	0.083	0.31	0.65
NBS 690	66.83	3.73	0.20	0.022	0.21	0.18	0.002	0.011	0.24
NBS 692	59.58	10.18	1.46	0.043	0.026	0.035	0.005	0.039	0.46
BCS 303	36	17	7	0.3	20	2	0.2	0.54	1.29
Minette	32	9	4	0.2	16	2	0.1	0.66	0.26
BCS 378	61.8	5.2	0.80	0.12	6.6	0.2	0.031	0.037	0.17
NBS 693	65.11	3.87	1.02	0.035	0.016	0.013	0.005	0.056	0.91

Table 5. Comparison of results

Standard reference material	Phosphorus, %	
	Certificate value	Found
BCS 302	0.71	0.69
BCS 303	0.54	0.53
BCS 378	0.037	0.039
Japan 800-1	0.042	0.043
Japan 850-1	0.017	0.018
BCS 377	0.31	0.31
MINETTE	0.66	0.63

Table 6. Precision and accuracy test

Standard reference material	Phosphorus, %		
	Certificate value	Found	
		Day 1	Day 2
Japan 830-1	0.125	0.125, 0.125	0.125, 0.126
NBS 690	0.011	0.009, 0.009	0.009, 0.009
NBS 692	0.039	0.040, 0.040	0.040, 0.040
NBS 693	0.056	0.056, 0.056	0.056, 0.056

Silicon is also a possible (though improbable) source of interference, but up to 20% of SiO₂ was found to have no effect.

Finally the procedure was tested on a number of standard reference iron ores and concentrates encompassing a large variation both in matrix as well as phosphorus content. Table 4 lists the composition of the iron ores analysed and the comparative results are shown in Table 5. There is excellent agreement with the certificate values. The standard deviation was found to be less than 0.001% phosphorus (Table 6).

The method has potential for further application for rapid determination of total phosphorus in effluents, sediments *etc.*, without the use of perchloric acid.

Acknowledgement—Grateful appreciation is expressed to Stelco Inc. for permission to publish this contribution.

REFERENCES

1. G. E. F. Lundell, J. I. Hoffman and H. A. Bright, *Chemical Analysis of Iron & Steel*, Wiley, New York, 1931.
2. *1982 Annual Book of ASTM Standards*, Part 12, American Society for Testing Materials, Philadelphia.
3. British Standards Institution, *BS 4158: Part 2: 1970*.
4. O. P. Bhargava and M. Gmitro, *Talanta*, 1980, **27**, 263.

DETERMINATION OF ARSENIC BY POLYURETHANE FOAM EXTRACTION AND X-RAY FLUORESCENCE

A. S. KHAN and A. CHOW*

Department of Chemistry, University of Manitoba, Winnipeg, Manitoba, Canada

(Received 3 August 1983. Accepted 13 October 1983)

Summary—A method based on extraction with polyurethane foam and determination by X-ray fluorescence has been developed for the determination of arsenic. Arsenic concentrations as low as 36 $\mu\text{g/ml}$ can be detected in 100 ml of aqueous solution.

The extensive use of arsenic in agriculture, medicine and industry, along with awareness of its carcinogenic effects,¹ has created a need to develop new methods and improve existing methods of arsenic determination at trace levels. Arsenic has been determined by various techniques, including gas chromatography,² ion-exchange chromatography,³ activation analysis,⁴ atomic-absorption spectrophotometry (AAS),^{5,6} and polarography,⁷ and the spectrophotometric method based on formation of a reduced arsenomolybdate complex is one of the recommended methods for trace levels.⁸ Formation and extraction of arsenomolybdate is the basis of an indirect atomic-absorption spectrophotometric method.^{9,10} The generation of arsine by reduction with sodium tetrahydroborate is often used prior to an atomic-absorption determination.⁶

Although AAS has become the most popular technique for arsenic determination,⁶ X-ray fluorescence (XRF) has also been used. Owing to the low sensitivity, however, a preconcentration step is necessary for the XRF analysis of water samples. In one procedure arsenic is extracted with ammonium pyrrolidine dithiocarbamate into chloroform, followed by evaporation of the organic layer on a filter paper for the determination of arsenic by XRF,¹¹ and in another the arsenic is co-precipitated with dibenzylidithiocarbamate and collected on a membrane filter for XRF analysis.¹² The use of molybdenum sulphide as co-precipitant has also been reported.¹³

It has recently been shown that extraction by polyurethane foam can be used successfully in conjunction with XRF spectrometry for the determination of trace elements.¹⁴⁻¹⁶ This paper describes extension of this technique to determination of arsenic at trace levels. The method involves the formation of arsenomolybdate, its extraction by polyether-based polyurethane foam, and direct determination on the foam by XRF.

EXPERIMENTAL

Apparatus

A Varian 634 UV-visible spectrophotometer was used to determine the arsenomolybdate complex in solution. A Fisher Accumet model 520 pH-meter was used when adjusting the acidity. The foam extractions were done with a multiple automatic squeezer and the arsenic on the polyurethane foam was determined with an energy-dispersive X-ray fluorescence system as described previously.¹⁴

Reagents

An appropriate amount of arsenic oxide (As_2O_3) was dissolved in a minimum volume of 1.0M sodium hydroxide, and the solution was acidified with dilute hydrochloric acid before dilution to the required volume. A 0.05M sodium molybdate solution and a solution containing 0.25 g of iodine and 0.4 g of potassium iodide per 100 ml were prepared in water.

All chemicals were reagent grade, and the solutions were prepared with doubly distilled, demineralized water and stored in polyethylene bottles. A polyether-based polyurethane foam sheet was obtained locally and cut into circular plugs (~ 2 cm in diameter, ~ 1.5 cm in height and weighing 0.125 ± 0.005 g), with sharpened tubular bits. The foam plugs were washed as previously described.¹⁷

Procedure

An aliquot of solution containing not more than 0.35 mg of arsenic was transferred to a 100-ml standard flask and 1 ml of the iodine solution was added to oxidize As(III) to As(V) [because As(III) does not form arsenomolybdate] followed by 20 ml of sodium molybdate solution. Water was then added to give a volume of nearly 90 ml and the pH was adjusted to 1.5. After 10 min the solution was made up to volume with water. The arsenomolybdate was extracted into the polyurethane foam plug by squeezing the plug in the solution in an extraction cell for 1 hr, at constant temperature. The foam plug was then removed from the solution, washed with 0.01M hydrochloric acid and then water, and dried by squeezing between paper towels. The area of the arsenic K_α peak was obtained by placing the foam plug on Mylar film stretched across the X-ray source and detector, accumulating the spectrum for 100 sec and integrating the arsenic peak area over a fixed range of channel numbers.

RESULTS AND DISCUSSION

In the preliminary studies arsenomolybdate was extracted from aqueous solution under conditions

*Author for correspondence.

similar to those described by Simon and Boltz¹⁸ except that polyether foam was used in place of the organic solvent. Spectrophotometric determination of arsenic in the aqueous sample before and after equilibration with the foam plug showed that the extraction was quantitative. A study in which foam plugs were squeezed for various times from 10 min to 3 hr showed that equilibrium was reached in 30 min of squeezing. In all further studies the squeezing was done for 1 hr to ensure establishment of equilibrium.

Optimum conditions for the determination were established by study of the effects of variables.

The absorbance at 385 nm for a solution $2 \times 10^{-5} M$ in As(V) and $2.5 \times 10^{-3} M$ in MoO_4^{2-} was found to be maximal between pH 1.3 and 2.0; a similar pH for the formation of arsenomolybdate was observed by Boltz and co-workers^{9,18} whereas Yamamoto *et al.*¹⁰ reported that the formation is quantitative between pH 0.5 and 6.0. To establish the optimum pH-range of extraction a series of 100-ml solutions which were $2 \times 10^{-5} M$ in As(V) and $2.5 \times 10^{-3} M$ in MoO_4^{2-} and at different pH values were equilibrated with foam plugs. The results are shown in Fig. 1, along with the results of two other experiments using higher initial molybdate concentrations (0.005 and 0.01M). It is clear that the optimum pH-range for extraction varies with the initial molybdate concentration. However, as can be seen for molybdate concentrations ranging from 2.5×10^{-3} to $1 \times 10^{-2} M$, the extraction of arsenomolybdate by polyether foam is optimal between pH 1.0 and 1.9. A pH of 1.5 was selected for further studies; the extraction of arsenomolybdate into various organic solvents has been reported to be optimal at different pH values.^{9,19,20} This difference is due to the fact that the pH range for extraction of heteropolymolybdates depends on the nature of the organic solvent.

The effect of initial molybdate concentration was also studied by equilibrating a series of 100-ml solutions, $2 \times 10^{-5} M$ in As(V), at pH 1.5 ± 0.1 and con-

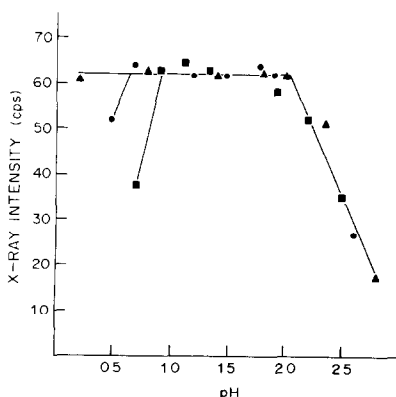


Fig. 1. Effect of acidity on the extraction of arsenomolybdate. $[MoO_4^{2-}]$: (■) 0.0025M; (●) 0.005M; (▲) 0.01M.

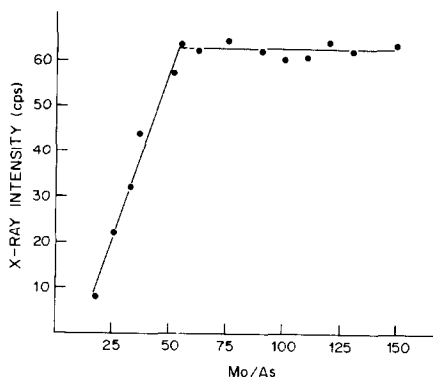


Fig. 2. Influence of initial molybdate: arsenic ratio on the extraction of arsenomolybdate.

taining various amounts of sodium molybdate, with foam plugs. Figure 2 indicates that no detectable amount of arsenic was extracted with less than a 15-fold ratio of molybdate to arsenic (V), but the extraction increased with molybdate concentration, becoming maximal and constant with a 55-fold or higher ratio of molybdate to arsenic. Although a very large excess of molybdate is usually recommended for the solvent extraction of heteropolymolybdates,²¹ the polyurethane foam-extraction of phosphomolybdate has been found to be quantitative even with only a 25-fold ratio of molybdate to phosphorus.²²

To determine the concentration range for linear X-ray response, a series of 100-ml solutions containing 50–500 μg of arsenic was extracted. The results were linear up to 350 μg of arsenic and the deviation for larger quantities was most likely due to saturation of the foam. The detection limit, calculated as three times the standard deviation of the background, was 5.7 $\mu g/100$ ml (*i.e.*, 57 ng/ml). The detection limit can be improved by using smaller foam plugs or larger volumes of sample solution. The results of one such study with small foam plugs showed a linear response up to 100 μg of arsenic and indicated a detection limit of 36 ng/ml under these conditions. It should be noted that the E.P.A. allowable limit for arsenic in drinking water is 50 ng/ml.²³ More sensitive XRF equipment should reduce the detection limit to 1–5 ng/ml for this procedure. To estimate the precision,

Table 1. Precision of the method

Trial	Arsenic, $\mu g/ml$	
	2.50	0.50
1	2.40	0.54
2	2.51	0.51
3	2.52	0.48
4	2.46	0.49
5	2.64	0.56
mean	2.51	0.52
s	0.09	0.034
RSD, %	3.6	6.6

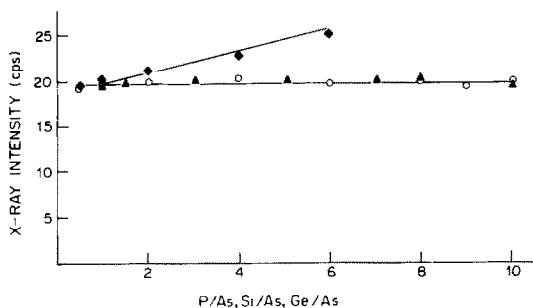


Fig. 3. Effect of interferent:arsenic molar ratio on the determination of arsenic ($0.5 \mu\text{g/ml}$). ▲ Phosphate; ○ silicate; ◆ germanate.

five 100-ml solutions containing 250 or $50 \mu\text{g}$ of arsenic were analysed. The means found were 251 and $52 \mu\text{g}$, the standard deviations being 9 and $3.4 \mu\text{g}$ respectively, indicating good precision; as expected, the precision is better at the higher concentration.

Since it was observed earlier that polyurethane foam is also very effective for the extraction of phosphomolybdate, silicomolybdate and germanomolybdate,²⁴ the effect of these heteropoly anions was studied. The criterion for non-interference was a change of less than 10% in the X-ray intensity for a given arsenic level when the test solution contained the potential interferent. Figure 3 shows the observed X-ray intensities of the arsenic K_{α} radiation for various P/As, Si/As and Ge/As ratios at a fixed arsenic concentration ($0.5 \mu\text{g/ml}$). It is clear that up to 10-fold molar ratios of phosphate and silicate to arsenate do not interfere, whereas the germanate causes 10% interference even when present in concentrations only twice that of the arsenic. The positive deviation caused by the presence of germanate is due to the poor resolution of the XRF unit used, and should be eliminated by using a unit with higher resolution. In the presence of sufficient molybdate and acid in the aqueous phase, the amount of heteropoly interferent that can be tolerated is limited by the size of the foam plug that can be effectively analysed by the instrument used.

X-ray fluorescence in conjunction with the use of polyurethane foam for the preconcentration of

arsenic as arsenomolybdate provides a simple method of arsenic determination. Although the method is less sensitive than some, the ease of operation, the low cost and the simultaneous multielemental capability of the XRF technique compensate for this.

Acknowledgements—This work was financially supported by the Natural Sciences and Engineering Research Council of Canada and by the Research Board of the University of Manitoba.

REFERENCES

1. J. M. Harrington, J. P. Middaugh, D. L. Morse and J. Housworth, *Am. J. Epidem.*, 1978, **108**, 377.
2. Y. Talmi and V. Norvell, *Anal. Chem.*, 1975, **47**, 1510.
3. G. Baglino, G. Grassini and L. Ossicini, *J. Chromatog.*, 1964, **14**, 238.
4. B. J. Ray and D. L. Johnson, *Anal. Chim. Acta*, 1972, **62**, 196.
5. M. Fishman and R. Spencer, *Anal. Chem.*, 1977, **49**, 1589.
6. R. R. Brooks, D. E. Ryan and H. Zhang, *Anal. Chim. Acta*, 1981, **131**, 1.
7. D. J. Meyer and J. Osteryoung, *Anal. Chem.*, 1973, **45**, 267.
8. Z. Marczenko, *Spectrophotometric Determination of Elements*, p. 132. Ellis Horwood, Chichester, England 1976.
9. R. S. Danchik and D. F. Boltz, *Anal. Lett.*, 1968, **1**, 901.
10. Y. Yamamoto, T. Kumamaru, Y. Hayashi, M. Kanke and A. Matsui, *Talanta*, 1972, **19**, 1633.
11. F. J. Marcie, *Environ. Sci. Technol.*, 1967, **1**, 164.
12. H. R. Lindner, H. D. Seltner and B. Schreiber, *Anal. Chem.*, 1978, **50**, 896.
13. T. M. Reymont and R. J. Dubois, *Anal. Chim. Acta*, 1971, **56**, 1.
14. A. Chow, G. T. Yamashita and R. F. Hamon, *Talanta*, 1981, **28**, 437.
15. A. S. Khan and A. Chow, *Anal. Lett.*, 1983, **16**, 265.
16. A. Chow and S. L. Ginsberg, *Talanta*, 1983, **30**, 620.
17. A. S. Khan, W. G. Baldwin and A. Chow, *Can. J. Chem.*, 1981, **59**, 1490.
18. S. J. Simon and D. F. Boltz, *Anal. Chem.*, 1975, **47**, 1758.
19. T. V. Ramakrishna, J. W. Robinson and P. W. West, *Anal. Chim. Acta*, 1969, **45**, 43.
20. P. Pakalns, *ibid.*, 1969, **47**, 225.
21. D. F. Boltz and M. G. Mellon, *Anal. Chem.*, 1948, **20**, 749.
22. A. S. Khan and A. Chow, *Talanta*, 1983, **30**, 173.
23. *U.S. Environmental Protection Agency Water Quality Criteria (1973)*, EPA R 73-033, EPA, Washington, D.C., 1973.
24. A. S. Khan, *Ph.D. Thesis*, University of Manitoba, 1982.

OPEN WET ASHING OF SOME TYPES OF BIOLOGICAL MATERIALS FOR THE DETERMINATION OF MERCURY AND OTHER TOXIC ELEMENTS

H. F. HAAS and V. KRIVAN

Sektion Analytik und Höchstreinigung, Universität Ulm, Oberer Eselsberg N-26,
D-7900 Ulm/Donau, F.R.G.

(Received 8 August 1983. Accepted 10 October 1983)

Summary—An open wet decomposition procedure for trace element analysis of biological material has been worked out. It is based on the utilization of nitric acid, hydrochloric acid and hydrogen peroxide and is well suited for the determination of As, Bi, Cd, Cr, Hg, Pb, Sb, Se and Tl. For these elements the recoveries were examined by the radiotracer technique, with lichens, pine needles, grass and human hair as representative biological samples. In addition to the conventional labelling technique, use was also made of *in situ* labelling. In all cases, recoveries between 93 and 100% were achieved, which are adequate for quantitative trace element analysis.

Most of the powerful determination methods for trace element analysis of biological and environmental material require decomposition of the sample. Because of the danger of losses, biological samples for the determination of toxic elements, especially of mercury, have usually been decomposed in closed systems,¹⁻³ or in open systems coupled with means of trapping the volatile elements.³⁻⁵ In many instances, simple, open decomposition procedures would be of advantage. One wet decomposition method⁶ provides quantitative recoveries of mercury, but the resulting chloric acid medium is often not suitable for the procedures used for the determination.

In an earlier study of the pre-atomization losses of mercury in graphite tube atomic-absorption spectrometry,⁷ it was proved that losses from hydrochloric acid/hydrogen peroxide and nitric acid/hydrochloric acid/hydrogen peroxide mixtures at temperatures up to 220–250° are undetectable. On the basis of the stabilization effect of these media, a simple wet decomposition procedure for the determination of mercury and a number of other elements in biological materials has been developed and is described in the present paper.

EXPERIMENTAL

Chemicals and apparatus

The concentrated nitric acid and hydrochloric acid used were of "suprapur" grade and the 30% hydrogen peroxide was of "pro analysi" grade (Merck). The radiotracers ⁵¹Cr, ⁷⁵Se, ⁷⁶As, ¹²⁴Sb and ²⁰³Hg were prepared by neutron-activation, in the FRG-2 reactor, Forschungszentrum, Geesthacht (thermal neutron flux = 10¹⁴ n.cm⁻².sec⁻¹), of the residues from evaporation of solutions of suitable compounds of the elements in "suprasil" quartz ampoules (Heraeus). The specific activities (μCi/μg) at the end of irradiation were 0.5 for ⁵¹Cr, 0.06 for ⁷⁵Se, 52 for ⁷⁶As, 30 for ¹²⁴Sb and 0.4 for ²⁰³Hg. After irradiation, the ampoules were opened and the following solutions prepared: a hydro-

chloric acid solution of ⁵¹Cr, ⁷⁶As and ¹²⁴Sb; a water solution of ⁷⁵Se; a nitric acid solution of ²⁰³Hg. The radiotracer ¹⁰⁹Cd was supplied by NEN Chemicals GmbH, Dreieich, F.R.G., as a hydrochloric acid solution with a specific activity of 354 μCi/μg.

The radiotracers ²⁰²Tl, ²⁰³Pb and ²⁰⁶Bi were prepared by irradiation of HgO, Tl and Pb targets with protons at 22, 20 and 25 MeV, the nuclear reactions being ²⁰²Hg(p, n)²⁰²Tl, ²⁰³Tl(p, n)²⁰³Pb and ²⁰⁶Pb(p, n)²⁰⁶Bi, respectively. The irradiations were performed at the isochronous cyclotron at the Nuclear Research Centre, Karlsruhe. Solvent extraction was used for the separation of ²⁰³Pb from the thallium matrix and of ²⁰⁶Bi from the lead matrix; ²⁰²Tl was isolated from the mercury matrix by ion-exchange.

The radioactive purity of the radiotracers was checked by γ-ray spectrometry, and in no case could any impurity be determined. In the radiotracer experiments, a single-channel analyser (Berthold, Wildbad, F.R.G.) with a well-type NaI(Tl)-detector and a high-resolution γ-ray spectrometer consisting of an Ortec Ge(Li)-detector and a Canberra multichannel analyser were used for counting.

The *in situ* labelling of lichens, hair, grass and pine needles was achieved by their irradiation at the nuclear reactor with the neutron flux given above.

Decomposition procedure

A sample weighing about 0.2 g is placed in a 25-ml Erlenmeyer flask and heated with 3 ml of concentrated nitric acid and 0.15 ml of concentrated hydrochloric acid at 120° for 5–10 min. During the heating, 0.1–0.2 ml of 30% hydrogen peroxide is added dropwise. After the major part of the organic matter has dissolved, 1.5 ml of concentrated hydrochloric acid is added and the temperature is increased to 180°. During the evaporation, 0.1–0.2 ml of 30% hydrogen peroxide is again added dropwise. The evaporation is stopped when the residual solution has a volume of about 0.5 ml (there must be no evaporation to dryness!), and this is then taken up with 3 ml of concentrated hydrochloric acid. This solution is evaporated again, with dropwise addition of 0.1–0.2 ml of 30% hydrogen peroxide, until about 0.5 ml remains. The residue is then taken up with 6M hydrochloric acid, but other concentrations can also be used.

For larger amounts of sample the reagent volumes must be correspondingly increased. Sample amounts up to 0.5 g were examined. In the radiochemical neutron-activation

Table 1. Recoveries in the decomposition of lichens, obtained by conventional and *in situ* labelling

Element/ radioisotope	Yield, %	
	Conventional labelling	<i>In situ</i> labelling
As/ ⁷⁶ As	97.7 ± 1.0* 99.1 ± 0.6†	97.6 ± 0.9§
Bi/ ²⁰⁶ Bi	98.8 ± 3.0*	
Cd/ ¹⁰⁹ Cd	92.6 ± 1.4* 93.0 ± 2.8†	
Cd/ ¹¹⁵ Cd		95.5 ± 0.6§
Co/ ⁶⁰ Co		100.4 ± 2.0‡
Cr/ ⁵¹ Cr	100.4 ± 2.2†	94.7 ± 0.5‡
Cs/ ¹³⁴ Cs		93.7 ± 2.3‡
Fe/ ⁵⁹ Fe		97.0 ± 0.4‡
Hg/ ²⁰³ Hg	93.0 ± 2.3* 94.4 ± 1.0†	93.3 ± 0.5§
Pb/ ²⁰³ Pb	99.6 ± 0.2*	
Sb/ ¹²⁴ Sb	98.6 ± 4.3* 99.7 ± 1.3†	98.6 ± 3.9‡
Sc/ ⁴⁶ Sc		95.0 ± 2.7‡
Se/ ⁷⁵ Se	95.1 ± 3.1* 94.1 ± 1.8†	95.3 ± 1.6§
Tl/ ²⁰² Tl	100.0 ± 1.0†	
Zn/ ⁶⁵ Zn		99.0 ± 1.4‡

*Carrier-free radiotracer used.

†Radiotracer contained 100 µg of carrier.

§Pretreatment of the samples with dilute solutions of Se(IV), As(V), Cd(II) and Hg(II) before the irradiation.

‡*In situ* labelling of the original material without pretreatment.

analysis, the irradiated sample is decomposed in the opened quartz ampoule and six times greater reagent volumes are used, after addition of carrier.

Tracer experiments

The yields for the elements As, Bi, Cd, Cr, Hg, Pb, Sb, Se and Tl were checked by the radiotracer technique in the following ways. First, the decomposition was performed on inactive lichen material to which the appropriate radiotracer (carrier-free and with 100 µg of carrier) was added. After decomposition, the resulting hydrochloric acid solution was centrifuged at 3000 rpm for 10 min, and a 5-ml portion was measured either with the single-channel analyser (if labelled with a single radioisotope) or with the γ -ray spectrometer (if labelled with several radioisotopes simultaneously).

In the second mode of labelling, the wet ashing was done on neutron-irradiated lichens, hair, grass and pine needles. In the case of lichens, grass and pine needles, before activation the homogenized material was treated with dilute solutions of Se(IV), As(V), Cd(II) and Hg(II) and then dried under an infrared lamp. After the irradiation, the ashing procedure was applied and the yields of the different elements were determined by measuring the resulting solutions as above.

RESULTS AND DISCUSSION

The proposed decomposition procedure was investigated, grass, pine needles, lichens and human hair being used as representative biological materials. For the determination of the recoveries, the radiotracer technique proved to be best.

In addition to conventional labelling by addition of a small portion of a radiotracer solution to the test

material before the decomposition, *in situ* labelling by irradiation of the biological materials with reactor neutrons before the decomposition was also used. Because the content of As, Se, Cd and Hg in lichens, grass and pine needles was at the detection limits of the activation γ -ray spectrometry technique or below, in a series of experiments the content of these elements was increased by a pre-irradiation treatment of the original material with dilute solutions of the corresponding ions of the elements. The amounts of carrier taken up by a sample portion of 150 mg were approximately 1 µg for As, 10 µg for Se and Hg, and 60 µg for Cd.

The results obtained are summarized in Tables 1 and 2, and are the mean values of at least three separate determinations (the corresponding mean deviations are also given). They show that, in all the experimental modes, the recoveries and their deviations meet the requirements for quantitative trace element analysis. Some important aspects are discussed in more detail below.

In the case of lichens, pine needles and grass, a very slight residue remained after the centrifugation, but it contained no detectable amount of any of the elements in question. In addition, the radiotracer experiments proved that there was no detectable adsorption of the test elements on the vessel walls. Complete decomposition of hair samples was achieved, and direct visual observation indicated similar behaviour for wood, blood and bovine liver, but these materials were not examined by the radiotracer technique.

Comparison of the results obtained by the conventional labelling method for carrier-free radiotracers and radiotracers containing 100 µg of carrier showed that varying the amount of the elements did not cause deviations greater than the mean deviations of the yields.

Since the chemical form of the radiotracers at the beginning of the decomposition was different for the two labelling modes, and probably also in the various matrices after the *in situ* labelling, the results pro-

Table 2. Recoveries obtained in the decomposition of hair, grass and pine needle samples, with use of *in situ* labelling

Element/ radioisotope	Yield, %		
	Hair*	Grass†	Pine Needles‡
As/ ⁷⁶ As	—	96.1 ± 1.2	96.0 ± 1.8
Cd/ ¹¹⁵ Cd	—	95.7 ± 2.6	94.5 ± 3.4
Co/ ⁶⁰ Co	101.0 ± 1.2		
Cr/ ⁵¹ Cr	94.1 ± 1.3		
Fe/ ⁵⁹ Fe	100.2 ± 0.8		
Hg/ ²⁰³ Hg	93.5 ± 1.6	94.6 ± 1.6	94.2 ± 2.8
Sb/ ¹²⁴ Sb	96.7 ± 4.5		
Se/ ⁷⁵ Se	92.3 ± 3.9	95.8 ± 2.1	94.3 ± 3.0
Zn/ ⁶⁵ Zn	98.7 ± 0.5		

**In situ* labelling of the original material without pretreatment.

†Pretreatment of the samples with dilute solutions of Se(IV), As(V), Cd(II) and Hg(II) before the irradiation.

vided some information about the effect of the chemical state of the elements on their recoveries. The results given in Tables 1 and 2 indicate that the chemical form does not affect the recovery of arsenic, cadmium, mercury, antimony and selenium, where the mean yields for the two modes of labelling the lichens (Table 1) and for the *in situ* labelling of hair, grass, and pine needles (Table 2) agree well each with other. In the case of chromium, there is excellent agreement between the results from *in situ* labelling of lichens ($94.7 \pm 0.5\%$) and hair ($94.1 \pm 1.3\%$), but significantly higher recovery ($100.4 \pm 2.2\%$) was obtained if the chromium tracer containing $100 \mu\text{g}$ of carrier was added as Cr(III) in dilute hydrochloric acid to lichens. The *in situ* labelling could not be applied for thallium, lead and bismuth, since no suitable indicator radionuclides were produced from these elements by neutron activation.

The recovery results for mercury are in good accordance with the results obtained in a study of pre-atomization losses in graphite tube atomic-absorption spectrometry, in which quantitative recoveries were obtained with the decomposition systems hydrochloric acid/hydrogen peroxide and hydrochloric acid/nitric acid/hydrogen peroxide at pretreatment temperatures up to above 200° . They show that this open decomposition procedure is also well suited for decomposition of biological materials for the determination of mercury, which must normally be performed in closed systems.

In the decomposition of some materials such as metals, considerable losses of arsenic have been observed in spite of the presence of an oxidizing medium.^{8,9} The high recoveries for arsenic in this work (96.0–99.1%) show that the oxidation power of the nitric acid/hydrochloric acid/hydrogen peroxide medium used in the procedure is sufficient to convert the arsenic of the biological materials into the stable quinquevalent form.

Losses of antimony by formation of difficultly soluble compounds and/or adsorption on the vessel walls have been reported for some decomposition systems,¹⁰ but we did not observe any when using the present procedure.

Recovery data for Co, Cs, Fe, Sc and Zn obtained

by the *in situ* labelling technique for lichens and hair are also given in Tables 1 and 2.

It is worth mentioning that the hydrochloric acid solution obtained is, in general, well suited for the further separation, preconcentration and determination step. However, the procedure is suitable for the decomposition of only certain types of biological materials, such as plants. For example, it cannot be used for the decomposition of fats. Further, the yields of the elements in the resulting solutions are given with regard to the total amounts but not to their chemical forms. Only for mercury in the decomposition of lichens was the degree of mineralization in the sample solution checked by ion-exchange, and the separation yields indicated that all the mercury was present in the solution as Hg^{2+} . Because of the somewhat higher reagent volumes used in the present open technique the reagent blanks are expected to be higher than those for the closed decomposition systems. Therefore, all three reagents used should be of highest purity (e.g., the acids obtained by sub-boiling distillation¹¹ and the hydrogen peroxide by low-temperature vacuum sublimation¹²) and the decomposition should be carried out at a clean-bench, when extremely low contents are to be determined.

REFERENCES

1. L. Kotz, G. Kaiser, P. Tschöpel and G. Tölg, *Z. Anal. Chem.*, 1972, **260**, 207.
2. L. Kotz, G. Henze, G. Kaiser, S. Pahlke, M. Veber and G. Tölg, *Talanta*, 1979, **26**, 681.
3. W. Zmijewska, *J. Radioanal. Chem.*, 1977, **35**, 389.
4. G. Knapp, S. E. Raptis, G. Kaiser, G. Tölg, P. Schrammel and B. Schreiber, *Z. Anal. Chem.*, 1981, **308**, 97.
5. H. B. Han, G. Kaiser and G. Tölg, *Anal. Chim. Acta*, 1982, **134**, 3.
6. G. Knapp, B. Sadjadi and H. Spitz, *Z. Anal. Chem.*, 1975, **274**, 275.
7. L. Lendero and V. Krivan, *ibid.*, 1982, **54**, 579.
8. R. Caletka and V. Krivan, *Z. Anal. Chem.*, 1982, **313**, 125.
9. *Idem*, *Anal. Chim. Acta*, 1982, **143**, 269.
10. S. Bajo and U. Suter, *Anal. Chem.*, 1982, **54**, 49.
11. E. C. Kuehner, R. Alveres, P. J. Paulsen and T. J. Murphy, *ibid.*, 1972, **44**, 2050.
12. J. W. Mitchell, *ibid.*, 1978, **50**, 194.

ANNOTATION

VERIFICATION OF CERTIFIED SULPHUR VALUES IN STEEL REFERENCE MATERIALS BY ISOTOPE-DILUTION MASS SPECTROMETRY, AND CHARACTERIZATION OF SULPHUR PRESENT ON THE SOLID SAMPLES

KAZUO WATANABE

Analytical Chemistry Laboratory, Japan Atomic Energy Research Institute, Tokai-mura,
Ibaraki-ken, Japan

(Received 27 May 1983. Revised 9 July 1983. Accepted 22 November 1983)

Summary—Sulphur in a number of steel reference materials has been determined by isotope-dilution mass spectrometry, utilizing both open-beaker and sealed-tube dissolution techniques. It is confirmed that the sulphur present in most samples can be completely converted into sulphate by the conventional open-beaker dissolution technique. The results on reference materials are in good agreement with the certified values for BCS samples and the recent or revised certified values for JSS and NBS samples. It is found that the sulphur concentration in the vicinity of the surface of the sample chips is higher than the average and that a significant amount of elemental sulphur is present on most chip samples. The ratio of elemental sulphur to average sulphur content tends to vary in proportion to the manganese content when this is less than 1%.

Sulphur in steels, even at trace levels, has a deleterious influence on their mechanical properties so a rapid and accurate determination of sulphur is indispensable for production control in steel-making. Instrumental techniques are commonly used for the purpose. As the accuracy depends largely upon the standards used for calibration of the instruments, certified reference materials (CRMs) play an extremely important role in the analyses. The barium sulphate gravimetric method, despite its lack of sensitivity, has long been used for evaluation of the sulphur content in CRMs. For its accurate determination by this method, all the sulphur must be converted into sulphate and recovered as barium sulphate. An isotope-dilution mass spectrometric (IDMS) method has been developed for the accurate and precise determination of sulphur in heat-resisting alloys and steels,¹ but here again all the sulphur must be converted into sulphate. It must also be mixed thoroughly with the spike (enriched ³⁴S) since the spike used is in the form of sulphate because the rate of isotopic equilibration between different chemical forms is normally too slow for other forms to be used for the determination: it takes more than several days to attain isotopic equilibration between sulphate and sulphide, even at 300° and 1000 bars.²

Recently, Paulsen *et al.* have developed an isotope-dilution spark-source mass spectrometric procedure (ID-SSMS) for the accurate determination of sulphur in iron-base alloys,³ they used a sealed-tube dissolution technique to prevent volatilization losses and to effect isotopic equilibration. They found that there was a significant loss of sulphur during open-beaker

dissolution for particular low-alloy steels.⁴ We have also employed the sealed-tube dissolution procedure for several low-alloy steel Standard Reference Materials (SRMs) from the National Bureau of Standards (NBS)⁵ and confirmed that use of the open-beaker dissolution for SRMs 362 and 364 yields low sulphur results. We found that part of the sulphur present in these samples was lost as sulphur dioxide during the dissolution, and suggested that when the sealed-tube dissolution technique is used, any sulphur dioxide evolved in the closed vessel is absorbed and oxidized to sulphate by the acid mixture at high temperature and pressure.

It is important to know whether the use of the open-beaker dissolution technique always yields low results, because the gravimetric method currently in use is based on open-beaker dissolution. We have applied both the sealed-tube and the open-beaker dissolution techniques to a number of steel reference materials from British Chemical Standards (BCS), Japanese Standards of Iron and Steel (JSS) and NBS, including the samples which we reported on earlier.⁶ All the results obtained by the use of both dissolution techniques agree well with each other except for NBS SRMs 362 and 364.

The cause of our earlier low results for reference materials in comparison with the certified values⁶ has now been traced to our treatment of the samples before analysis: the sample chips were rinsed with water, ethanol and acetone, and then dried at 80°. We have now found that a significant amount of elemental sulphur, which can easily be removed by the rinsing, is present on the surface of most steel chip

samples, and have investigated the origin of this elemental sulphur.

EXPERIMENTAL

Reagents

Analytical-reagent grade chemicals were used.

Spike solution. Fifteen mg of 94% enriched ^{34}S isotope (Oak Ridge National Laboratory) was dissolved in a mixture of 2 ml of concentrated nitric acid, 1 ml of concentrated hydrochloric acid and 0.1 ml of bromine. One ml of 10% potassium hydroxide solution was then added and the solution evaporated to dryness. The residue was dissolved and diluted to volume with water in a 100-ml standard flask, and standardized by IDMS with a standard potassium sulphate solution (of natural isotopic composition) prepared by weight.

Reducing solution. Hydriodic acid (500 ml, 57% w/v), hypophosphorous acid (245 ml, 50% w/v) and hydrochloric acid (813 ml, 36% w/v) were mixed.⁷ Any sulphur compounds present in the mixture were removed by refluxing in a stream (80 ml/min) of pure nitrogen (99.999% pure) for 1 hr before use.

Apparatus

Isotopic analysis of sulphur was performed with a CEC 21-103C mass spectrometer equipped with a Cary 401 vibrating reed electrometer and a recorder.

Spectrophotometric determination of elemental sulphur was done with a Hitachi model 200 double-beam spectrophotometer.

Procedures

Determination of sulphur by IDMS. The analytical procedure used in this study is slightly different from the one used in previous work.^{1,6} The amount of acids used for the sample dissolution is decreased; the spike solution is added before the sample dissolution; the combustion procedure for conversion of silver sulphide into sulphur dioxide is simplified.

Sample dissolution in an open beaker. To 0.5–1.5 g of sample in a 200-ml beaker, a weighed aliquot of the spike solution, 0.3 ml of bromine, 4 ml of concentrated nitric acid and 2 ml of concentrated hydrochloric acid were added. After the sample had been left for about 30 min at room temperature, 0.2 ml of bromine and 2 ml of concentrated hydrochloric acid were added. Then the sample was heated on a hot-plate at 80° till the sample had completely dissolved. If dissolution was incomplete, several drops of hydrofluoric acid were added. The solution was evaporated to dryness on a hot-plate at 200°. Nitrogen oxides were removed by repeated evaporation with 4-ml portions of concentrated hydrochloric acid. The residue was finally dissolved in 4 ml of concentrated hydrochloric acid.

Sample dissolution in a borosilicate-glass sealed tube. The procedure is described in detail elsewhere⁵ and is similar to the one used by Burke *et al.*⁴ so is described here only briefly.

A weighed aliquot of the spike solution was added to 0.5 g of sample in a glass tube (15 mm outside diameter, 2 mm wall thickness and 30 cm long) sealed at one end. The tube was placed in a slush of solid carbon dioxide and ethanol to freeze the contents. Seven ml of concentrated nitric acid and 3 ml of concentrated hydrochloric acid were added and the tube was sealed in an oxygen-gas flame and placed in a stainless-steel shell with about 20 g of solid carbon dioxide. The shell was heated in an oven at 180–200° overnight. After cooling, the tube was placed in the slush to freeze the sample solution.

The tube was then moved into liquid nitrogen, scored and opened. After gradual thawing at room temperature, the solution was transferred to a 200-ml beaker. Nitrogen oxides were removed as described above.

Reduction of sulphate. Twenty-five ml of the reducing mixture were transferred to a 300-ml round-bottomed flask

fitted with a reflux condenser, and boiled for 1 hr while a stream of pure nitrogen at a flow-rate of 80 ml/min was passed through the system. After the solution had cooled, the spiked sample solution was added to the flask and the mixture was again refluxed for 1 hr, with passage of nitrogen. The hydrogen sulphide evolved was carried by the nitrogen stream through water and then absorbed in a mixture of 2 ml of 0.1M cadmium acetate and 40 ml of water. Cadmium sulphide was finally converted into silver sulphide by addition of 3 ml of 0.1M silver nitrate. After coagulation by heating, the silver sulphide was filtered off on a tightly packed quartz-wool plug inserted in a quartz tube (15 mm outside diameter and 5 cm long, drawn out at one end). The precipitate was washed with water, ethanol and then acetone. A tuft of quartz wool was inserted into the wider end of the tube and the precipitate was dried in an oven at 120°.

Combustion of silver sulphide. The quartz tube was inserted into a second quartz tube (18 mm outside diameter and 15 cm long) sealed at one end. The outer tube was then attached to a vacuum line by means of a vacuum-tight Cajon union (Cajon Co., Solon, Ohio). The tube was flamed under a pressure of about 3×10^{-4} Pa for 10 min to remove any volatile compounds, then oxygen was introduced into the tube to give a pressure of about 3×10^4 Pa. The precipitate was heated with a four-burner oxygen torch to about 1000° until the black silver sulphide could no longer be seen; this took about 1 min. The sulphur dioxide evolved was collected in a U-tube cooled with liquid nitrogen, more volatile products being pumped off. The sulphur dioxide was then cryogenically transferred to a sampling bottle for subsequent mass spectrometric analysis.

Determination of elemental sulphur on sample chips. This procedure is a modification of the one used by Koren⁸ for the determination of elemental sulphur in ore.

Five ml of chloroform were pipetted into a 20-ml standard flask which contained 3–5 g of sample chips. The sample was subjected to ultrasonic radiation for 1 min. The absorbance of the solution was then measured at 265 nm.

RESULTS AND DISCUSSION

Sulphur in 23 steel reference materials from BCS, JSS and NBS was determined by IDMS, with both the open-beaker and sealed-tube dissolution techniques, and the results were then compared. No significant discrepancy between the results obtained by the two dissolution techniques was observed for most samples, with the notable exception of the low-alloy steel NBS SRMs 362 and 364: the results obtained for these by the open-beaker dissolution were significantly low. The results are shown in Table 1, the "open-beaker" results are included in calculation of the averages except for NBS SRMs 362 and 364. It seems that sulphur in most steel samples can be completely converted into sulphate by the conventional open-beaker dissolution technique; however, it might be desirable to check whether there is a loss of sulphur during the dissolution, by using a completely reliable technique such as the sealed-tube dissolution when sulphur in a new sample has to be determined.

The IDMS results are generally in good agreement with the recent or revised certified values for JSS and NBS, and in excellent agreement for BCS samples irrespective of the year of certification. Our previous suggestion⁶ that there was systematic bias in the methods of standardization of BCS, JSS and

Table 1. Determination of sulphur in steel reference materials and elemental sulphur on the samples

Sample	Certified values		Average IDMS values, $\mu\text{g/g}^\dagger$		Elemental sulphur, $\mu\text{g/g}$	Mn content, (certified value, %)
	Year	%	(as received)	(rinsed)		
NBS						
32e, Ni-Cr steel	1957	0.021	204	180	18	0.798
33d, Ni-Mo steel	1955	0.010	94.2	90.0	3	0.537
72f, Cr-Mo steel	1957	0.024	219	206	17	0.545
133a, Cr-Mo steel	1956	0.329	3300	2720	594	1.03
361, low-alloy steel	1970	0.017*	144	132	14	0.66
362, low-alloy steel	1970	0.038	359	358§	0	1.04
363, low-alloy steel	1970	0.009*	67.5	64.4	2	1.50
364, low-alloy steel	1971	0.029*	251	246§	3	0.25
365, electrolytic iron	1970	0.006*	n.d.	56.1	0	0.0056
BCS						
211/1, 13% Cr rustless steel	1958	0.032	316	310	0	0.32
219/4, Ni-Cr-Mo steel	1977	0.027	267	257	5	0.81
232/2, carbon steel	1970	0.126	1250	1200	57	1.18
241/2, 9.9% W high-speed steel	1968	0.025	234	216	11	0.27
402, low-alloy steel	1971	0.023	245	236	8	0.19
403, low-alloy steel	1971	0.036	363	350	6	1.69
455, mild steel	1974	0.061	620	618	0	0.09
495, 13% Mn steel	1972	0.014	138	125	6	13.6
JSS						
152-4, alloy steel	1971	0.022	195	189	7	0.42
242-5, carbon steel	1973	0.031	303	281	4	0.72
508-2, Ni-Cr steel	1968	0.017	157	151	4	0.49
150-7, low-alloy steel	1979	0.034	328	n.d.	3	0.11
151-7, low-alloy steel	1979	0.017	164	n.d.	13	1.48
152-7, low-alloy steel	1979	0.043	425	n.d.	30	0.42
150-6, low-alloy steel¶	1979	0.035	348	—	—	0.11
151-6, low-alloy steel¶	1979	0.017	166	—	—	1.48
152-6, low-alloy steel¶	1979	0.043	440	—	—	0.42

n.d. = not determined.

*Most recent certified values⁴ are 0.015% for SRM 361, 0.0068% for SRM 363, 0.025% for SRM 364 and 0.0056% for SRM 365.

†Average for two or more determinations; relative standard deviation better than 1%.

§The results obtained by the open-beaker dissolution are 301 $\mu\text{g/g}$ for SRM 362 and 213 $\mu\text{g/g}$ for SRM 364.

¶Disk samples for spectroscopic analysis.

NBS is now seen to arise from our rinsing of the samples.

In an attempt to explain the discrepancy between our earlier IDMS results and theirs, Burke *et al.* suggested⁴ that there was a possibility of loss of sulphur during dissolution before the addition and equilibration of the ³⁴S spike, if the spike was added *after* the sample dissolution. However, it is sulphate sulphur that is determined by the IDMS, since the spike used is in the form of sulphate, and if there were losses of sulphur as volatile compounds during the open-beaker dissolution, it would be impossible to determine them by IDMS even if the spike was added *before* the sample dissolution. We have observed no significant difference between the results obtained, whether the spike was added before and/or after the dissolution, for both the open-beaker and the sealed-tube dissolution techniques. Addition of the spike before sample dissolution may be preferable to prevent loss of sulphate in the sample solution by spillage before the isotopic equilibration.

In attempts to trace the cause of the discrepancy between the two sets of IDMS results, we found that a significant amount of elemental sulphur was present on the surface of most sample chips, and that this was easily removed by rinsing with ethanol and acetone.

Figure 1 shows absorption spectra for elemental sulphur dissolved in chloroform and for chloroform in which chip samples had been soaked for about 1 hr. These spectra strongly indicate the presence of elemental sulphur on the steel surface, and show that it can be determined spectrophotometrically after extraction into chloroform.

In the 5th column in Table 1, the results obtained by IDMS for the rinsed samples are shown. The difference between the two sets of IDMS results for each sample (as received and rinsed) is in good agreement with the spectrophotometric result for elemental sulphur.

To examine the origin of the elemental sulphur on the chip samples, we prepared sample chips from low-alloy steel disks (JSS spectroscopic standards) with a shaper. Spectrophotometric examination of these sample chips soon after they had been prepared showed no elemental sulphur on their surface, but five months after the preparation, elemental sulphur was observed; during that time the sample chips had been stored in a weighing bottle in a desiccator.

To obtain the depth distribution of sulphur in the prepared sample chips, they were dissolved stepwise with a mixture of concentrated nitric and hydrochloric acids and bromine under ultrasonic radiation

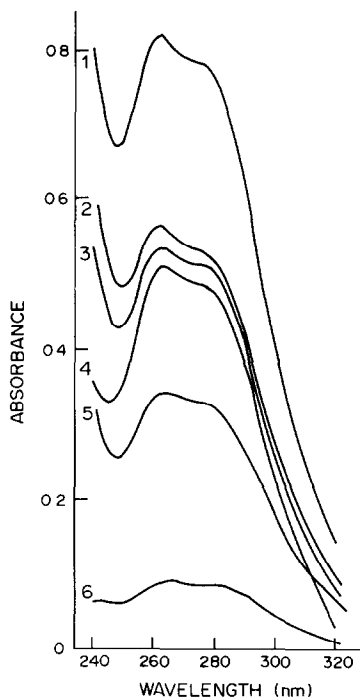


Fig. 1. Absorption spectra of elemental sulphur in chloroform and the chloroform extract of some steel reference materials: 1, elemental sulphur (30 $\mu\text{g}/\text{ml}$); 2, BCS 241/2 (4.9 g); 3, NBS SRM 32e (2.9 g); 4, JSS 242-5 (5.5 g); 5, NBS SRM 364 (5.5 g) 6, elemental sulphur (4 $\mu\text{g}/\text{ml}$). Recorder ensitivity factor: 1, $\times 1$; 2, $\times 2$; 3, $\times 2$; 4, $\times 5$; 5, $\times 5$; 6, $\times 1$.

and the sulphur in each fraction dissolved was determined by IDMS; the results are shown in Fig. 2. The concentration of sulphur near the sample surface is very high, but decreases rapidly with depth, becoming considerably lower than the average content. We also examined the distribution of sulphur in some of the standard chip samples in the same manner, and obtained similar results: the sulphur concentration in the vicinity of the surface is extremely high. It seems that sulphur in steels tends to migrate to the surface during the preparation of chips by cutting.

Most of the sulphur in steels is known to be present in the form of iron sulphide and manganese sulphide.⁹ It is therefore assumed that the metal sulphides migrate to the surface and are gradually

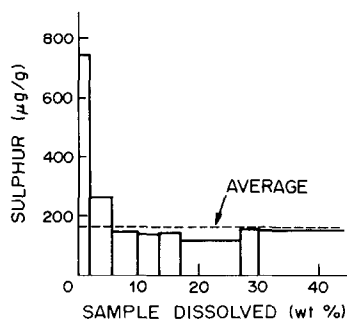


Fig. 2. Depth distribution of sulphur in the prepared sample chips: low-alloy steel JSS 151-6 (S 166 $\mu\text{g}/\text{g}$).

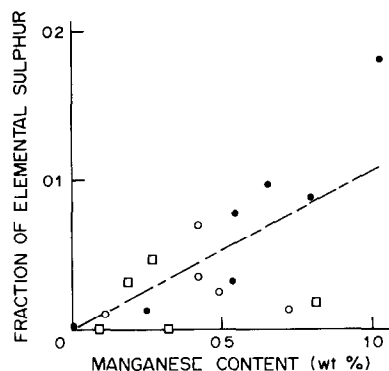
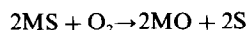


Fig. 3. Relationship between elemental sulphur on the chip samples and manganese content (less than 1%). \square BCS samples; \circ JSS samples; \bullet NBS SRMs.

oxidized by atmospheric oxygen to elemental sulphur:



The free-energy changes of this reaction are $\Delta G = -36.9$ kcal/mole for manganese sulphide and $\Delta G = -35.4$ kcal/mole for iron sulphide,¹⁰ so it can take place spontaneously. In Fig. 3 the ratio of the elemental sulphur to average sulphur content for each sample is plotted against the manganese content. The elemental sulphur on the surface tends to vary in proportion to the manganese content if this is less than 1% (correlation coefficient 0.69); this suggests an intimate connection between sulphur and manganese. Although the amount of the elemental sulphur may depend largely upon the surface area of the sample, we did not examine this factor in the study reported here, because the steel reference materials are relatively of uniform size. Similar results have been found by Yasuda¹¹ in work on standards for X-ray fluorescence spectrometry, who found that the X-ray signal for sulphur increased with increasing manganese content. He attributed this to differences in size and shape of the MnS particles, but it may equally be due to the migration effect reported here.

Acknowledgements—The author is grateful to Mr S. Tamura and colleagues for valuable advice. Acknowledgement is also made to Dr T. Komori for helpful discussions.

REFERENCES

1. K. Watanabe, *Anal. Chim. Acta*, 1975, **80**, 117.
2. H. Sakai and F. W. Dickson, *Earth Planet. Sci. Lett.*, 1978, **39**, 151.
3. P. J. Paulsen, R. W. Burke, E. J. Maienthal and G. M. Lambert, *New Analytical Techniques for Trace Constituents of Metallic and Metal-Bearing Ores*, A. Jarier-Son (ed.), p. 113, ASTM Spec. Technical Publ. 747, 1980.
4. R. W. Burke, P. J. Paulsen, E. J. Maienthal and G. M. Lambert, *Talanta*, 1982, **29**, 809.
5. K. Watanabe, *Bunseki Kagaku*, 1981, **30**, T103.
6. *Idem*, *Talanta*, 1979, **26**, 251.
7. H. G. Thode, J. Monster and H. B. Dunford, *Geochim. Cosmochim. Acta*, 1961, **25**, 159.
8. J. G. Koren, *Appl. Spectrosc.*, 1969, **23**, 275.
9. T. Ishii and M. Ihida, *Tetsu to Hagane*, 1971, **57**, 86.
10. R. C. Weast, *CRC Handbook of Chemistry and Physics*, 54th Ed., CRC Press, Columbus, OH 1973-1974.
11. H. Yasuda, *Tetsu to Hagane*, 1982, **68**, 65.

COULOMETRIC TITRATION BY A CONTROLLED-POTENTIAL PULSED-CHARGE POTENTIOMETRIC TECHNIQUE—II*

ACID-BASE, PRECIPITATION AND HOMOGENEOUS REDOX SYSTEMS

THEOLOGOS ANDRONIDIS, ANNA MARIA GHE† and SERGIO VALCHER

Istituto Chimico "G. Ciamician" dell'Università, Scuola di Specializzazione in Chimica Analitica, Via Selmi 2, 40126 Bologna, Italia

(Received 4 July 1983. Revised 9 December 1983. Accepted 19 December 1983)

Summary—An unconventional coulometric method, based on electrolysis at controlled potential by means of discrete charge-pulses, with end-point detection obtained by mathematical linearization of potentiometric data, has been applied to various systems. The results appear very satisfactory: very weak acids can be determined with high accuracy; in the case of precipitation reactions the selectivity is high enough to allow titration of the components of halide mixtures; for homogeneous redox systems some problems caused by irreversibility at the indicator electrode are overcome.

An improved method for coulometric titrations, devised to provide selectivity in the separation and determination of metals that can be electro-deposited, was proposed in Part I of this series.¹

The method is based on electrochemical titration reactions performed at controlled potential by means of discrete charge-pulses, the end-point being located by means of a mathematical linearization of the potentiometric data, which is analogous to Sørensen's method² for conventional titrations.

Since the proposed technique, like other conventional and unconventional coulometric methods,^{3,4} appears to be suitable for application to a wider field, other types of titration have been examined and the results obtained with acid-base systems, precipitation reactions and a particular type of homogeneous redox reaction are reported here.

EXPERIMENTAL

Titration were done with the potentiostatic system already described;¹ it was generally used in a "three-electrode" configuration, and connected to a potentiometer equipped with a printer. For acidimetric determinations, however, a "four-electrode" configuration was used, with a glass electrode for potentiometric detection, and an Ag/AgCl electrode as reference electrode, both for electrolytic and potentiometric conditions (see Fig. 1).

All measurements were made at 25° on 10–20 ml samples. Analytical grade reagents were used. The background electrolytes were chosen so that 100% current efficiency and fast equilibration of the indicator electrode were obtained. For the determinations of acids, potassium chloride was used in large excess (100-fold ratio to the test species) and a mixture of potassium sulphate and sulphuric acid at pH 1–2 for redox systems. For halide determinations potassium nitrate was employed, to prevent co-precipitation effects,⁵ the pH

being adjusted with ammonia and acetic acid to values suitable for the different species titrated.

Other experimental conditions and details of the potentiometric data treatment were given in previous papers.^{1,6}

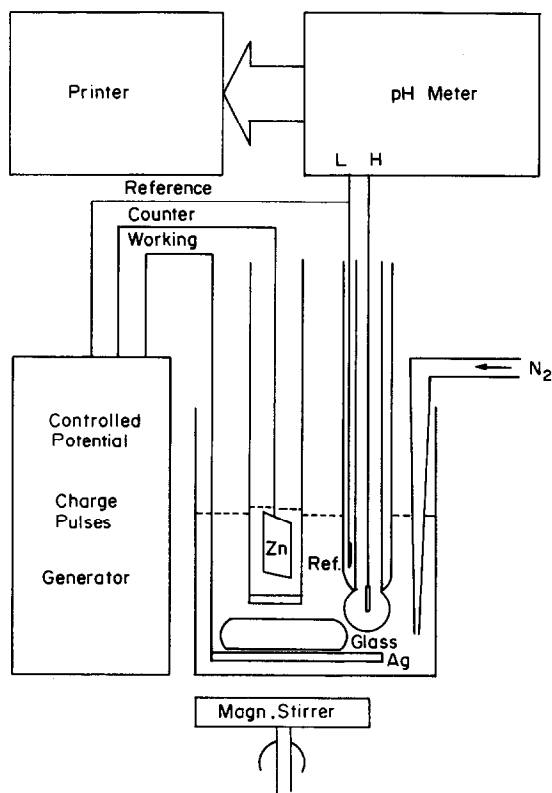


Fig. 1. Apparatus for controlled-potential pulsed-charge coulometric titrations with potentiometric equivalence point determination: block scheme for acidimetric determinations with "four-electrode configuration" (glass indicator electrode).

*Part I—*Talanta*, 1984, 31, 123.

†Author for correspondence.

Table 1. Acidimetric titrations

Acid*	Concentration in cell, M	Coulombs required			90% Confidence limits	Correlation coefficient	Error, %
		Theoretical	Found				
HCl	1×10^{-4}	9.65×10^{-2}	9.7×10^{-2}		$9.72-9.69 \times 10^{-2}$	1.000	+0.6
Phenol	1×10^{-2}	9.65	9.73		9.75-9.70	1.000	+0.8
H ₂ PO ₄ ⁻	$1 \times 10^{-2\dagger}$	9.25†	9.32		9.33-9.31	1.000	+0.8

Working electrode Pt; electrolysis potential 1900 mV vs. Ag/AgCl (Cl⁻ 3M); total sample volume 10 ml.

*The functions $10^{E/0.059}$ and $Q10^{E/0.059}$ were utilized to linearize the potentiometric data obtained with strong and weak acids respectively.

†Evaluation based on a previous H₃PO₄ determination by the same technique.

RESULTS AND DISCUSSION

Acid-base systems

Strong and weak acids were titrated by cathodic reduction of hydrogen ions. The end-point was determined by extrapolation of the potentiometric data, linearized as a function of charge (Q) by means of the equations

$$S = 10^{E/0.059} \quad (1)$$

$$S' = Q10^{E/0.059} \quad (2)$$

for strong and weak acids respectively (E = potential). Typical results are shown in Table 1.

The accuracy and precision are quite satisfactory even for acids as weak as phenol. The sensitivity is limited by the linearization method, which does not take into account the autoprotolysis of water, which is not negligible for concentration regions lower than those examined here.

Precipitation reactions

Chloride, bromide and iodide were determined by precipitating them with silver ions coulometrically generated at a silver anode, the potential of which was monitored. The data were then linearized by means of function (1).

The pH must be selectively adjusted to get the best results for the various halides. We found the most suitable ranges to be: pH 9-10 for iodide; pH 7-9 for bromide, and pH ~ 5 for chloride.

The results obtained in the determinations of single halides are shown in Table 2, along with the experimental conditions, including pH.

It was observed that the time required by the electrode to reach equilibrium in the absence of current was not significantly affected by the thickness of the silver halide layer, which may be quite large for high sample concentrations.

The possibility of determining two halides in a mixture was also examined, and typical results are shown in Table 3.

In all cases tested the precision was slightly poorer than that for solutions containing only one halide. The overall error for the sum of the tested species was generally small, but it appears that there is some kind of mutual interference. This fact cannot be explained in terms of co-precipitation, however, since both negative and positive errors are found in the determination of the first ion.

As shown in Fig. 2, quite good results are obtainable for determination of all three halides in a mixture.

Homogeneous redox systems

Among the various redox couples examined, Fe³⁺/Fe²⁺ and Ce⁴⁺/Ce³⁺ deserve attention in view of the peculiarity of the method used (see below) to obtain a correct analytical determination of the oxidized forms.

Attempts at titrations by reduction at a platinum electrode (with a platinum indicator-electrode) were unsuccessful because these redox-couple electrode systems do not behave according to the Nernst equation.

To overcome this difficulty the possibility of utilizing a different redox system for indirect determination of Fe³⁺ and Ce⁴⁺ was considered.

Table 2. Silver halide precipitation: single-ion determinations

Halide	Concentration in cell, M	Electrolysis potential, mV vs. SCE	pH	Coulombs required		90% Confidence limits	Correlation coefficient	Error %
				Theoretical	Found			
I ⁻	5×10^{-3}	-60	9.32	9.65	9.52	9.54-9.50	1.000	-1.3
	5×10^{-5}	-50	9.72	9.65×10^{-2}	9.90×10^{-2}	$9.99-9.80 \times 10^{-2}$	1.000	+2.6
Br ⁻	5×10^{-3}	+80	9.18	9.65	9.73	9.78-9.69	1.000	+0.8
	5×10^{-5}	+250	6.97	9.65×10^{-2}	9.75×10^{-2}	$9.92-9.58 \times 10^{-2}$	1.000	+1
	5×10^{-6}	+200	6.96	9.65×10^{-3}	9.42×10^{-3}	$10.25-8.81 \times 10^{-3}$	0.993	-2.4
Cl ⁻	5×10^{-3}	+300	4.65	9.65	9.62	9.65-9.59	1.000	-0.3
	5×10^{-3}	+300	5.10	9.65	9.67	9.73-9.61	1.000	+0.2
	5×10^{-4}	+300	4.73	0.965	0.990	0.996-0.985	1.000	+2.6

Working electrode Ag; total sample volume 20 ml.

Table 3. Silver halide precipitation: binary mixture analysis (Ag working electrode)

	I*		II†		III*		IV*	
	I ⁻	Cl ⁻	I ⁻	Cl ⁻	Br ⁻	Cl ⁻	I ⁻	Br ⁻
Electrolysis potl. <i>mV</i> vs SCE	-80	+350	-70	+350	+60	+350	-80	+100
pH	9.1	~ 5	9.7	~ 5	9.0	~ 5	9.05	9.05
Coulombs, theory	9.65	9.65	0.965	0.965	9.65	9.65	9.65	9.65
Coulombs, sum of ions, theory	19.30		1.930		19.30		19.30	
Coulombs, found	9.65	9.49§ 9.51‡	0.930	0.986§ 0.951‡	9.83	9.67§ 9.84‡	9.43	9.41§ 9.19‡
Error, %	0.0	-1.7§ -1.7‡	-3.6	+2.2§ -1.5‡	+1.9	+0.2§ +2.0‡	-2.3	-2.5§ -4.8‡
Error, sum of ions, %	-0.8		-0.7		+1.0		-2.4	

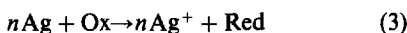
*Each component $5 \times 10^{-3}M$ in cell solution (20 ml).

†Each component $5 \times 10^{-4}M$ in cell solution (20 ml).

§Data referred to value *found* for first species.

‡Data referred to *theoretical* charge required for first species.

If a silver working-indicator electrode is used, once the reaction



has taken place, it might be expected from the relative values of the standard potentials that the Ox form initially present could be determined indirectly by titration¹ of the silver ions produced. Such a titration might be expected to be slow, reaction (3) being incomplete if electrolysis is started immediately after the electrode and the test solution come into contact, since a heterogeneous reaction system is involved. In practice, however, titrations done under different

time schedules show that the results are not dependent on the time elapsed before the electrolysis is started. In all cases the amount of Ag^+ found is equivalent to that of Ox initially present.

These facts can be rationalized by considering the dynamics of equilibration of the indicator electrode under these experimental conditions.

Reaction (3) will proceed during the potentiometric phases, throughout the titration, without current at the indicator electrode, mass transport being the limiting factor.

By use of Nernst's approximate concept of the diffusion layer, the flows (at the electrode) of the

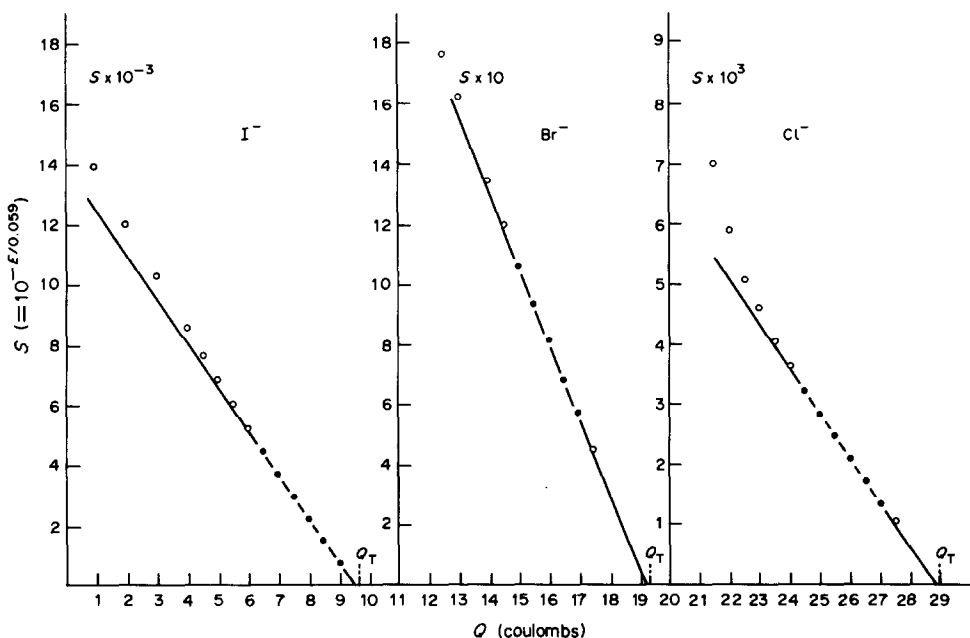


Fig. 2. Titration plot of $S (= 10^{-E/0.059})$ vs. Q (coulombs) for iodide, bromide and chloride, simultaneously present at equal concentration ($5 \times 10^{-3}M$) in a mixture: Q_T = theoretical equivalence point; Ag working electrode; sample volume 20 ml; electrolysis potentials (*mV* vs. SCE) -80, -50, +350 respectively for iodide, bromide and chloride. Titration of Br^- and I^- at pH 9, of Cl^- at pH 5.

Table 4. Homogeneous redox systems

Redox system	Concentration in cell,* M	pH	Coulombs required			Correlation coefficient	Error,%
			Theoretical	Found	90% Confidence limits		
Fe ³⁺ /Fe ²⁺	1.67 × 10 ⁻³	1.3	3.21 ₇	3.19 ₀	3.19 ₃ -3.18 ₇	1.000	-0.8
	1.67 × 10 ⁻⁴	1.3	0.321 ₇	0.321 ₄	0.325 ₅ -0.317 ₅	0.999	-0.1
	1.67 × 10 ⁻⁵	2.0	3.21 ₇ × 10 ⁻²	3.16 ₄ × 10 ⁻²	3.21 ₀ -3.12 ₁ × 10 ⁻²	0.999	-1.6
Ce ⁴⁺ /Ce ³⁺	5 × 10 ⁻³	1.3	9.65	9.65	9.66-9.64	1.000	0.0

Working electrode Ag; total sample solution 20 ml; electrolysis potential +150 mV *vs.* SCE.

*Values referred to the oxidized species (initial concentration of reduced species = 0).

species implicated in reaction (3) may be written as

$$D_{\text{Ox}} \left(\frac{[\text{Ox}]_{\infty} - [\text{Ox}]_0}{\delta_{\text{Ox}}} \right) = D_{\text{Red}} \left(\frac{[\text{Red}]_0 - [\text{Red}]_{\infty}}{\delta_{\text{Red}}} \right) \\ = D_{\text{Ag}^+} \left(\frac{[\text{Ag}^+]_0 - [\text{Ag}^+]_{\infty}}{\delta_{\text{Ag}^+}} \right) \quad (4)$$

where D is the diffusion coefficient, δ the diffusion-layer thickness (which may be considered proportional to D^{γ} , with $0 < \gamma < 1$ in a stirred solution) and subscripts 0 and ∞ indicate the electrode surface and the bulk of the solution, respectively. If reaction (3) is shifted completely towards the right (that is $[\text{Ox}]_0 \sim 0$), we obtain

$$[\text{Ag}^+]_0 = n \left(\frac{D_{\text{Ox}}}{D_{\text{Ag}^+}} \right)^{1-\gamma} [\text{Ox}]_{\infty} + [\text{Ag}^+]_{\infty} \quad (5)$$

From the charge Q previously exchanged and the partial transformation due to reaction (3), the concentration of Ox in the bulk of the solution at any instant is given by

$$[\text{Ox}]_{\infty} = C_{\text{Ox}}^* - \frac{[\text{Ag}^+]_{\infty}}{n} - \frac{Q}{nFV} \quad (6)$$

where C_{Ox}^* is the initial Ox concentration, F is the Faraday constant and V is the volume of solution.

If $D_{\text{Ox}} \sim D_{\text{Ag}^+}$, from (5) and (6) we obtain

$$[\text{Ag}^+]_0 = nC_{\text{Ox}}^* - \frac{Q}{FV} \quad (7)$$

which indicates that, just as in the case of Ag⁺ titration, the concentration of the silver ion at the electrode is only a function of the degree of electrolysis, and not of the chemical reaction.

Furthermore the electrode potential measured in the potentiometric phase will depend on the equilibrium



which will lead to an equation of the type

$$S = 10^{E/0.059} = K(nC_{\text{Ox}}^* VF - Q) \quad (8)$$

if equation (7) for $[\text{Ag}^+]_0$ is substituted into the Nernst equation.

It should be noticed that for a truly homogeneous redox system, linearization should be done by means of a function of type (2).

Typical results obtained in the titration of Ce⁴⁺ and Fe³⁺ with a silver electrode (in a three-electrode configuration), by linearization of the potentiometric data according to equation (8), are reported in Table 4 and show the fairly good accuracy, precision and sensitivity of the procedure proposed. In particular, the narrow range of the confidence limits and the values of the correlation coefficients confirm that linearization according to equation (8) is valid, and that the behaviour of the silver electrode has been correctly interpreted.

These facts show the possibility of overcoming irreversibility problems in reductions by making use of a type-1 electrode with a standard potential more negative than that of the redox couple under examination. It should be pointed out, however, that in the case of the titration of Fe³⁺, the equilibrium constant of reaction (3) is small (~ 0.33 , as calculated from the standard potentials); nevertheless the reaction can be considered sufficiently shifted towards the right for the observed behaviour, provided the iron concentration is much smaller than 0.33M. This type of indirect titration offers clear advantages with respect to other indirect procedures.

REFERENCES

1. T. Andronidis, A. M. Ghe, C. Pagura and S. Valcher, *Talanta*, 1984, **31**, 123.
2. P. Sørensen, *Kem. Maanedst.*, 1951, **32**, 73.
3. J. J. Lingane, *Electroanalytical Chemistry*, 2nd Ed., p. 484. Interscience, New York, 1958.
4. J. E. Harrar, in *Electroanalytical Chemistry*, Vol. VIII, A. J. Bard (ed.), p. 1. Dekker, New York, 1975.
5. J. J. Lingane and L. A. Small, *Anal. Chem.*, 1949, **21**, 1119.
6. S. Valcher, C. Pagura, S. Coin and A. M. Ghe, *Chem. Biomed. Environ. Instrum.*, 1982-83, **12**, 327.

DIFFERENTIAL PULSE POLAROGRAPHIC DETERMINATION OF NITRATE IN ENVIRONMENTAL MATERIALS

HIROTOSHI HEMMI

Graduate School of Environmental Science, Hokkaido University, Sapporo 060, Japan

KIYOSHI HASEBE,* KUNIO OHZEKI and TOMIHITO KAMBARA†

Department of Chemistry, Faculty of Science, Hokkaido University, Sapporo 060, Japan

(Received 12 August 1983. Accepted 19 December 1983)

Summary—Nitrate can be determined with reliable accuracy and sensitivity by differential pulse polarography utilizing the catalytic reaction between nitrate and uranyl ion in the presence of potassium sulphate. The differential pulse polarographic peak-height is proportional to nitrate concentration from 1 to 50 μM . The calculated detection limit for nitrate is $8 \times 10^{-7} \text{ M}$ in pure aqueous solution. The method has been applied to determination of nitrate in fresh snow, and river waters and animal feeds.

Because of the importance of the role of nitrite and/or nitrate as a precursor in the formation of *N*-nitrosamines, which can be formed in water and sewage, at least *in vitro*,¹⁻³ it is essential that a sensitive and accurate method be available for the determination of these ions. Many methods have been reported for the determination of nitrate, principally involving colorimetry. These methods have been summarized.⁴ They all have limited sensitivity and dynamic range, and frequently depend on unstable colours and long reaction times. Methods based on use of an ion-selective electrode are very simple, but the results vary because of interference from co-existing ions, and because of effects dependent on the previous history of the electrode.⁵⁻⁸ Determinations of nitrite and of nitrate by polarography have been reported. Chang *et al.*⁹ have studied the differential pulse polarographic determination of nitrite, based on nitrosation of diphenylamine in the presence of sodium thiocyanate as catalyst. This method is most sensitive and has been extended to include determination of nitrate subsequent to that of nitrite. Kato *et al.*¹⁰ reported a polarographic determination of nitrite and nitrate by use of the catalytic wave of the 1,2-diaminocyclohexanetetra-acetate (DCTA) complex of vanadium (IV). However, as the determination of nitrate in the mixture was affected by nitrite, a calibration curve for nitrate in the presence of a known amount of nitrite was obtained by using 1–10mM V(IV)–DCTA, and nitrate in the mixture could then be determined. The d.c. polarographic determination of nitrate in the presence of

uranyl ion in acid solution has been described by Kolthoff *et al.*¹¹ and by Keilin and Otvos.¹² The simultaneous reduction of uranyl ion catalyses the reduction of nitrate in dilute hydrochloric acid medium. The first uranium wave results from the reduction of uranium(VI) to the quinquevalent state, and the second corresponds to reduction of uranium(V) to the tervalent state. The catalytic nitrate wave occurs at the same potential as the second uranium wave. The catalytic mechanism has not been clarified and is complicated: uranium(III) formed at the electrode surface might be the actual nitrate-reducing agent.

In this paper, we have re-examined the catalytic reaction between nitrate and uranyl ion by differential pulse polarography (DPP). The present work aimed at establishing the most suitable and effective conditions for the determination of nitrate in actual environmental samples, with satisfactory sensitivity, precision and simplicity.

EXPERIMENTAL

Reagents

All chemicals used were of analytical reagent grade and were dissolved in demineralized and distilled water. A standard 0.02M uranyl solution was prepared by dissolving 4.2408 g of uranyl acetate [$\text{UO}_2(\text{CH}_3\text{COO})_2 \cdot 2\text{H}_2\text{O}$] in 60 ml of 6M hydrochloric acid, and making up accurately to 500 ml with water; it was kept in a polyethylene bottle. Dilute solutions of nitrate were prepared from a stock $1.00 \times 10^{-2} \text{ M}$ potassium nitrate solution, by appropriate quantitative dilution or direct pipetting into samples. Purified nitrogen was used for deaerating solutions, and keeping them oxygen-free.

Apparatus

Polarographic data were obtained with a Model P-1000 Voltammetric Analyser with a mechanical drop knocker (Yanagimoto Mfg. Co., Japan), and recorded on a

*To whom correspondence should be addressed.

†Present address: Hakodate Technical College, Tokura-cho 226, Hakodate 042, Japan.

Watanabe X-Y recorder, Model WX-4401. The dropping mercury electrode (DME) used had the following characteristics: mercury flow-rate $m = 0.9647$ mg/sec in water (open circuit), and natural drop-time $t_d = 8.50$ sec in $0.1M$ hydrochloric acid containing potassium sulphate and $10^{-4}M$ uranyl acetate, at a mercury head $h = 70.0$ cm. An SCE was used as reference, and a platinum wire as the counter-electrode. Except for temperature-dependence studies, the polarographic solutions were kept at constant temperature ($25 \pm 0.5^\circ$) in a thermostatic bath.

Analytical procedures

Animal feeds. Weigh accurately about 0.5 g of powdered sample, previously dried in the oven at 75° for 90 min, and transfer it into a stoppered flask or bottle with about 120 ml of water. Shake the mixture for 30 min, then filter with a No. 5A filter paper (Toyo Roshi Co.), and wash the filter paper with a small amount of water. Filter the extract and washings through a $0.65\text{-}\mu\text{m}$ membrane filter, and dilute accurately to 200 ml with water. The yield in a single extraction is about 98% and a second extraction makes the yield completely quantitative. Pipette a suitable volume of the extract into the supporting electrolyte solution, and deaerate for about 10 min. Measure the catalytic nitrate reduction wave in the DP mode in the potential range from -0.75 to -1.1 V *vs.* SCE, and then calibrate by the standard addition procedure, or use an appropriate calibration graph. Under typical optimized working conditions, the corresponding linear regression equation and the coefficient of correlation, r , are $C = 18.08 i_p - 25.22$ and $r = 0.999$, the units being μM for C and μA for i_p .

River waters and snow. Just before analysis, thaw the frozen samples of river water or snow, stored in the refrigerator, and filter through a $0.45\text{-}\mu\text{m}$ pore-size membrane filter. Add an appropriate volume of the filtrate to the supporting electrolyte and use without further treatment, because there are unlikely to be any interfering substances present. Complete the determination as described for animal feeds.

RESULTS AND DISCUSSION

Effect of pH on the catalytic reduction

The reduction of uranyl ion in acid solution by d.c. polarography gives two waves, the first resulting from the reduction of U(VI) to U(V) and the second, which is almost twice as large as the first, corresponding to a further 2-electron reduction to the tervalent state.

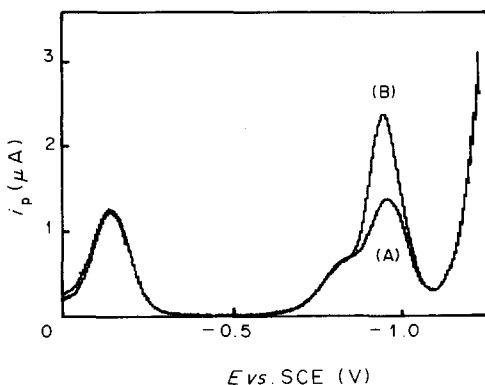


Fig. 1. Differential pulse polarograms of uranyl ion with and without nitrate present. Conditions: $[\text{UO}_2(\text{CH}_3\text{COO})_2] = 100\mu\text{M}$; $[\text{K}_2\text{SO}_4] = 5\text{mM}$; pH 1.0 (HCl); pulse amplitude, -100 mV; scan-rate, 1 mV/sec; pulse interval, 6 sec. (A): $[\text{KNO}_3] = 0\mu\text{M}$. (B): $[\text{KNO}_3] = 20\mu\text{M}$.

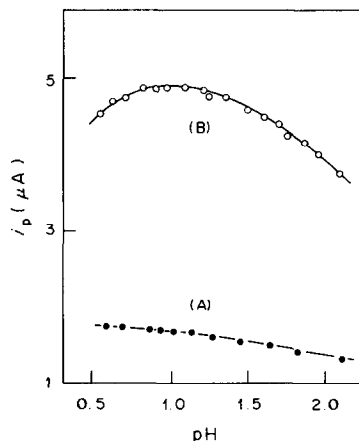


Fig. 2. Effect of pH on the DP peak current. Conditions: $[\text{UO}_2^{2+}] = 100\mu\text{M}$; $[\text{KCl}] = 0.1M$; pH adjusted with HCl. (A): $[\text{KNO}_3] = 0\mu\text{M}$. (B): $[\text{KNO}_3] = 100\mu\text{M}$. Other conditions are the same as for Fig. 1.

If nitrate is present in the polarographic solution, the catalytic nitrate wave occurs at the same potential as the second uranium wave, as shown by the typical DP polarograms in Fig. 1. However, the height of the second peak is almost the same as that of the first, though it is accompanied by a DPP prewave. The pH-dependence of the height of the catalytic nitrate peak is shown in Fig. 2. Over the pH range from 0.7 to 1.4, the electrode chemical reaction for the uranium-nitrate system, and hence the catalytic peak, is found to be relatively unaffected by the polarographic measurement time. An optimum pH of 1.0 was chosen for further study in order to characterize the electrode process and for the development of an analytical procedure. Above pH 1.5, the second peak of uranium(V) decreases gradually with increasing pH, and the catalytic peak current also decreases because of the decrease of effective concentration of uranium(V) in the electrical double-layer or possibly because of a change in the rate of reaction. The slope of the usual log plot for the first d.c. wave is 60 mV, corresponding to reversible reduction with $n = 1$. The peak half-width, $W_{1/2}$, at a pulse amplitude of -100 mV is 128 mV, almost equal to the theoretical value of 125 mV for $n = 1$. The log plot for the second wave, however, gives a straight line with slope of 78 mV, so the reduction of uranium(V) to uranium(III) does not proceed reversibly. The half-width of the second peak is the same as that for the first peak, which is 23% larger than the theoretical value of 102 mV for $n = 2$. The second d.c. wave is almost twice as high as the first wave, which would be expected for twice the charge transfer. However, the two peaks in DPP are almost the same in width, because though the first step is reversible, the second is not.

Effect of uranyl ion concentration

If we use larger amounts of uranyl ion as the activator, the wave at -0.93 V *vs.* SCE becomes correspondingly greater. The minimum uranyl ion

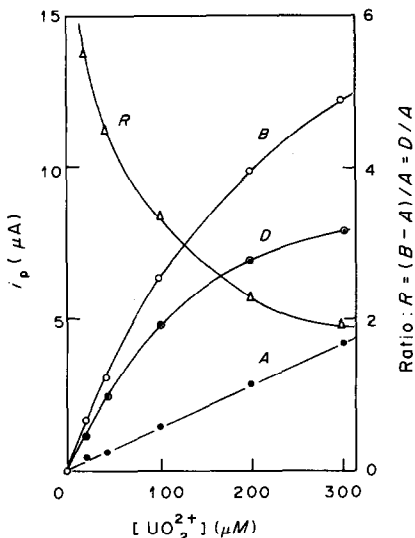


Fig. 3. Effect of uranyl ion concentration on the nitrate reduction peak current. Conditions the same as for Fig. 1 except for uranyl ion concentration.

concentration is that required to maintain linearity between the current and the nitrate concentration. The nitrate limiting current is measured as the difference between the total current at -0.93 V vs. SCE and the limiting current for the uranyl ion, as determined in a blank experiment. The ratio, R , of the nitrate current, D , to the limiting current for the uranyl ion, A , is plotted in Fig. 3 as a function of the uranyl ion concentration: the lower this concentration, the greater the ratio, R . However, we have found a bigger spread of results when low concentrations of uranyl ion are used, and therefore conclude that the uranyl ion concentration is best kept at $100\mu\text{M}$.

Effect of chloride and sulphate concentration

The influence of several salts on the peak-height was next studied. The nitrate catalytic reduction wave gradually decreased with increasing chloride concentration above $0.1M$, but at chloride concentrations below $0.1M$, the peak-height remained unchanged. Figure 4 shows the effect of sulphate concentration on the nitrate reduction current. The catalytic peak current reaches a maximum at sulphate concentrations higher than $5mM$. Thus, the current when the chloride concentration is below $0.1M$ and the sulphate is about $5mM$ is about 1.4 times that when no sulphate is present. If we consider the interaction of uranyl ion and nitrate in the presence of chloride in terms of some specific effects of anions in solution and in the electrical double-layer, we can see similarities to the behaviour of Methylene Blue and leuco Methylene Blue in the presence of certain anions.^{13,14} Chloride is known to be specifically adsorbed on the mercury electrode.^{13,14} The addition of sulphate causes an increase in the catalytic current, suggesting that sulphate displaces chloride from the adsorbed

layer and then itself contributes to the interaction between uranyl ion and nitrate.

Effect of standing time and temperature

Solutions containing potassium nitrate at $50\mu\text{M}$ concentration (3.1 ppm) were allowed to stand in the laboratory at room temperature for a month. On analysis the peak height and wave form were found to be unchanged, with a relative standard deviation of 0.5% ($n = 150$) over the period. The temperature-dependence of the catalytic peak was also studied in the range between 5 and 35° . The relative temperature coefficient of the peak-height was 2.8%/deg at 20° because of the catalytic mechanism, but that of the second peak of the uranyl ion was only 1.3%/deg, which is typical of a diffusion-controlled electro-reduction.

Effect of instrumental parameters

In the case of hydrogen evolution catalysed by tellurium(IV), the slower the scan-rate, the greater the peak current and the higher the sensitivity.¹⁵ In this work, the catalytic nitrate reduction peak-current was almost independent of scan-rate from 0.5 to 1 mV/sec. We chose 6 sec as drop-time because the peak-height gradually increased with drop-time. It was also found advantageous to use a large modulation amplitude, e.g., $\Delta E = -100$ mV for these micro determinations.¹⁶

Interferences

The effects of several common ions on the determination was examined, and tolerances for them are given in Table 1. Nitrite and phosphoric acid interfere seriously and should be absent if accurate results are to be obtained. The tolerance for some interferents

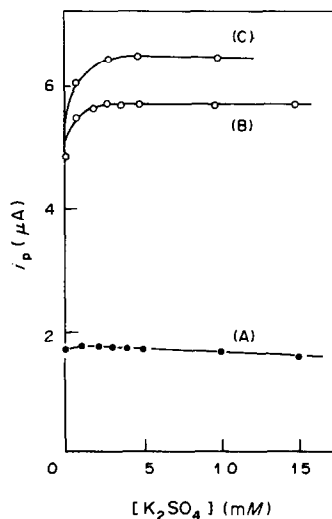


Fig. 4. Effect of sulphate concentration on the DP peak height. Conditions: pH 1.0 (HCl); other conditions the same as for Fig. 2 except for K_2SO_4 concentration and curve (C). (C): without KCl.

Table 1. Permissible concentrations of foreign ions in the determination of 10 μM NO_3^- (to give < 5% error)

Species	Added as	Concentration, M
Na^+	NaCl	0.1
K^+	KCl	0.1
NH_4^+	NH_4Cl	0.1
Mg^{2+}	MgCl_2	10^{-2}
Ca^{2+}	$\text{Ca}(\text{CH}_3\text{COO})_2$	5×10^{-3}
Mn^{2+}	MnCl_2	10^{-2}
Cl^-	NaCl	0.1
H_2CO_3	Na_2CO_3	0.1
H_2PO_4^-	K_2HPO_4	10^{-6}
SiO_2	SiO_2 (carbonate fusion)	0.1
NO_2^-	KNO_2	6×10^{-6}

Polarographic solution $1 \times 10^{-5}\text{M}$ KNO_3 + 10^{-4}M $\text{UO}_2(\text{OAc})_2$ + 5mM K_2SO_4 adjusted to pH 1.0 with HCl. Modulation amplitude -100 mV ; scan-rate 1 mV/sec ; pulse interval 6 sec.

such as heavy metal ions can be improved by addition of masking reagents (*e.g.*, EDTA). The strongest interference is given by phosphoric acid, which is significant even when the acid is present at the same concentration as nitrate, since it forms a stable uranyl salt.

Comparison with another method

To verify the validity of the DPP technique, river water samples were analysed by high-pressure liquid chromatography (HPLC) with a Zorbax Sil ion-association silica-gel column. The agreement between the two sets of results (Table 2) suggests that the DPP method can be used with a fair degree of confidence. Further results for river waters and for snow are shown in Table 3. The river water samples were also tested for nitrite, but no nitrite peak was observed on the HPLC chromatograms. It was concluded that the nitrite content did not exceed $1.5\mu\text{M}$ (the detection limit of the HPLC method).

Sample storage and nitrate extraction

All dried plant and silage samples were ground to pass through a 0.5-mm sieve, then stored in sealed

Table 2. The comparison of the DPP and HPLC methods

Sample No.	Nitrate found, μM	
	DPP method	HPLC method
1	61.7	63.8
2	65.1	64.6
3	61.4	60.8
4	61.4	63.7
5	62.2	64.4
6	62.6	67.3
Mean	62.4	64.1
R.S.D.(%)	2.25	3.25

River water sampled at Hachikenbashi Bridge in Sapporo on 18 February 1983. HPLC conditions: Shimadzu Model LC-3A HPLC with Zorbax Sil (4.6 mm bore, 25 cm length) with Shimadzu SPD-2A UV detector at 220 nm; 10^{-3}M $\text{NH}_4\text{H}_2\text{PO}_4$ and 10^{-4}M tetrabutylammonium bromide as mobile phase at 1 ml/min. Injection volume 10 μl .

Table 3. Determination of nitrate in river water and snow gathered at several points of the River Hassamugawa

Sampling point	Nitrate found, μM	R.S.D., %
Heiwanotaki (upstream) (water)	6.23	2.43($n = 3$)
Yamanotobashi (middle stream) (water)	21.5	3.56($n = 3$)
Hachikenbashi (downstream) (water)	54.7	0.80($n = 3$)
Heiwanotaki (upstream) (snow)	6.27	3.50($n = 3$)
Hachikenbashi (downstream) (snow)	12.0	5.12($n = 2$)

Polarographic conditions as in Table 1. Sampling date 11 February 1983.

Table 4. Nitrate in animal feeds, determined by the DPP method

Dried plant sample	Nitrate content, * mg/g
Alfalfa silage	0.935
Perennial Buckwheat petiole	5.70
Indian corn silage	5.76
Orchard grass	13.5
Barley silage	16.4
Perko petiole	27.1
Sunflower petiole	69.1

*Means of duplicate determinations, rounded to three significant figures.

containers at room temperature. According to Milham *et al.*,⁵ water samples stored under atmospheric conditions often show spectacular changes in nitrate content. Therefore, these samples must be analysed as soon as possible, or be frozen to suppress microbial action.

The efficiency of nitrate extraction under various conditions was studied and the extracted nitrate was determined by HPLC. The results of the extraction of nitrate from animal feeds was independent of the phase-volume ratio, and duration of shaking from 10 to 60 min (at 100 strokes/min). Nitrate was extracted quantitatively by all variations of sample treatment. The results obtained by the procedures described are given in Tables 3 and 4. The nitrate concentrations in the upstream river samples show little variation, but increase downstream because of microbial action and run-off from agricultural land that has been treated with fertilizers. The nitrate contents of the plants show a wide variation, which is probably due to breeding and environment rather than the kind of plant.

Acknowledgements—We are grateful to Mr. K. Ataku, Department of Dairy Science, the College of Dairying, Ebetsu-shi, Hokkaido, for a gift of several type of animal feeds, and to Mr. A. Yamaguchi for doing the HPLC work.

REFERENCES

1. A. Ayanaba and M. Alexander, *J. Environ. Qual.*, 1974, **3**, 83.
2. A. L. Mills and M. Alexander, *ibid.*, 1976, **5**, 437.
3. M. M. Nikaido, D. Dean-Raymond, A. J. Francis and M. Alexander, *Water Res.*, 1977, **11**, 1085.
4. S. Hirano (ed.), *Muki Ohyoh Hishoku Bunseki*, Vol. 3, p. 426. Kyoritsu Shuppan, Tokyo, 1974.
5. P. J. Milham, A. S. Awad, R. E. Paull and J. H. Bull, *Analyst*, 1970, **95**, 751.
6. K. Ataku, N. Narasaki, N. Yoshida and T. Asahi, *J. Coll. Dairying*, 1979, **8**, 61.
7. K. Suzuki, H. Ishiwada, T. Shirai and S. Yanagisawa, *Bunseki Kagaku*, 1980, **29**, 816.
8. H. Hara, S. Okazaki and T. Fujinaga, *ibid.*, 1981, **30**, 86.
9. Shaw-kong Chang, R. Kozeniauskas and G. W. Harrington, *Anal. Chem.*, 1977, **49**, 2272.
10. N. Kato, K. Yoshikiyo, K. Nakano and K. Tanaka, *Bunseki Kagaku*, 1983, **32**, 139.
11. I. M. Kolthoff, W. E. Harris and G. Matsuyama, *J. Am. Chem. Soc.*, 1944, **66**, 1782.
12. B. Keilin and J. W. Otvos, *ibid.*, 1946, **68**, 2665.
13. V. Svetličić, J. Tomaić, V. Žutić and J. Chevalet, *J. Electroanal. Chem.*, 1983, **146**, 71.
14. K. Hasebe and T. Kambara, *Rev. Polarog. (Japan)*, 1973, **19**, 44.
15. K. Hasebe, *Bull. Chem. Soc. Japan*, 1979, **52**, 1056.
16. J. Osteryoung and K. Hasebe, *Rev. Polarog. (Japan)*, 1976, **22**, 1.

KINETIC-SPECTROPHOTOMETRIC DETERMINATION OF Cu(II) AND PYRIDINE BY USE OF THE AERIAL OXIDATION OF DIMEDONE BISGUANYLHYDRAZONE

F. SALINAS LÓPEZ, J. J. BERZAS NEVADO and A. ESPINOSA MANSILLA

Department of Analytical Chemistry, Faculty of Sciences, University of Extremadura, Badajoz, Spain

(Received 29 March 1983. Revised 17 November 1983. Accepted 17 December 1983)

Summary—The synthesis and analytical properties of dimedone bisguanylhydrazone (DIBG) are described for the first time. DIBG is oxidized by aerial oxygen and the reaction is catalysed by copper(II). The catalytic effect of copper(II) is increased by the presence of pyridine. Kinetic methods are described for determining trace amounts of copper(II) and pyridine. The reaction is followed spectrophotometrically by measuring the rate of change of absorbance at 550 nm. The calibration graphs are linear in the range 0.6–9.5 μg for copper(II) and 0.2–8.8 mg for pyridine. The methods have been applied to the determination of copper in galena and of pyridine in piperidine and isoamyl alcohol. The kinetic parameters of the reaction have been determined.

Schiff's bases, including oximes, hydrazones, thiosemicarbazones, etc., are interesting as analytical reagents as they form complexes with transition metals, and also because their oxidation may be catalysed by metal ions, in particular by copper(II).¹ However, guanylhydrazones have not been very much studied as analytical reagents.

We have initiated the study of these Schiff's bases with pyridine-2-aldehyde guanylhydrazone (PAG)² which forms yellow complexes with copper, cobalt, palladium, nickel and iron(II). In this paper, the synthesis and analytical properties of dimedone bisguanylhydrazone (DIBG) are described for the first time. DIBG undergoes aerial oxidation at $\text{pH} \approx 7$, catalysed by copper(II), producing a red-violet colour suitable for a spectrophotometric kinetic determination of trace amounts of copper, in which the rate of change of absorbance at 550 nm is measured. The rate of the catalysed reaction increases in the presence of pyridine, which can therefore also be determined by this approach. The action of pyridine as an activator in catalysis by copper(II) has been discussed by Bontchev³ and has been used for analytical purposes.⁴

EXPERIMENTAL

Apparatus

A Zeiss DMR 11 spectrophotometer equipped with constant-temperature cell-holders and 1.0-cm glass or quartz cells.

Solutions

All reagents should be of analytical-reagent grade.

Dimedone bisguanylhydrazone reagent solution, 0.1%

Copper(II) solution. Prepare by dissolving copper oxide in nitric acid and diluting with water, and standardize.

Buffer solution, pH 7.9. Dissolve 12.11 g of tris-(hydroxymethyl)aminomethane (Tris) in 42 ml of 1M perchloric acid and dilute with water to 1 litre.

Buffer-fluoride solution, pH 7.9. Dissolve 12.11 g of tris-(hydroxymethyl)aminomethane (Tris) and 83.98 g of sodium fluoride, and enough 1M perchloric acid to give pH 7.9, and dilute with water to 1 litre.

Aqueous pyridine solutions.

Synthesis of dimedone bisguanylhydrazone (DIBG)

Dissolve 2.15 g of aminoguanidine bicarbonate in 10 ml of water and neutralize with hydrochloric acid. Add the mixture to 1.10 g of dimedone in 40 ml of ethanol, then add 3 ml of concentrated hydrochloric acid, reflux for 2 hr and cool. Filter off the white product and wash it with ethanol-water (4:1 v/v). Yield 60%, m.p. 273°. Found: 31.6% C, 6.1% H, 30.3% N, 28.2% Cl. Calculated for $\text{C}_{10}\text{H}_{17}\text{N}_8 \cdot 3\text{HCl} \cdot \text{H}_2\text{O}$: 31.87% C, 5.84% H, 29.74% N, 28.15% Cl.

Determination of copper

To a solution containing between 0.6 and 9.5 μg of copper, in a 25-ml standard flask, add 1 ml of pH-7.9 buffer, 3 ml of 2.5M pyridine, and 1 ml of DIBG solution and dilute to volume with water. Mix well, then transfer a portion to a 1.0-cm cell at $25 \pm 0.1^\circ$ and follow the reaction by recording the absorbance (vs. a reagent blank) at 550 nm as a function of time, beginning the measurements 1 min after preparation of the sample. Calculate the reaction rate from the slope of the absorbance-time curve.

Determination of copper in galena

Weigh out about 0.2 g of dried sample and dissolve it in a few ml of nitric acid. Add about 10 ml of water and some sodium sulphate to precipitate lead sulphate. Centrifuge the solution to separate the precipitate and transfer the solution to a 25-ml standard flask. Add the washings, then make up to the mark with water. Transfer an aliquot to another 25-ml standard flask, neutralize with sodium hydroxide to the pale pink colour of phenolphthalein as indicator, then add 1 ml of pH-7.9 buffer-fluoride solution, 3 ml of 2.5M pyridine and 1 ml of DIBG solution, dilute to volume with water and complete the determination as above.

Determination of pyridine

To an aqueous solution containing 0.2–8.8 mg of pyridine, in a 25-ml standard flask, add 1 ml of pH 7.9 buffer solution, 2 ml of DIBG solution, 5 ml of $3.2 \times 10^{-4}\text{M}$

copper(II) and dilute to volume with water. Transfer an aliquot of the reaction mixture to a 1.0-cm cell at $25 \pm 0.1^\circ$ and make the kinetic measurements as for copper determination.

Determination of pyridine in piperidine

To 1 ml of a 2M neutralized aqueous solution of piperidine, in a 25-ml standard flask, apply the procedure specified for pyridine determination: 0.3% of pyridine in piperidine can be determined.

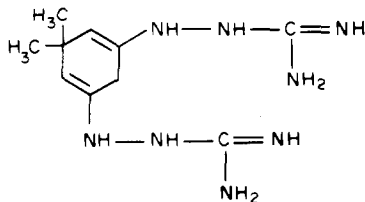
Determination of pyridine in isoamyl alcohol

Shake 2 ml of the alcohol with 80 ml of water in a 100-ml standard flask till a single phase is obtained. Dilute to the mark with water, mix well, then transfer 10 ml of this solution to a 25-ml standard flask and follow the procedure for pyridine determination: 0.3% of pyridine in isoamyl alcohol can be determined.

RESULTS

Analytical properties of the reagent

DIBG is very soluble in water, dimethylsulphoxide (DMSO) and dimethylformamide (DMF) and sparingly soluble in ethanol, at room temperature. The infrared spectrum (KBr disc) shows bands assignable to the stretching vibrations of -NH- and -NH_2 (3100 and 3400 cm^{-1}), and to the guanidinium group (1610 and 1670 cm^{-1}). The ultraviolet absorption spectrum for DIBG in water shows a maximum at 294 nm. The NMR spectrum indicates the most likely structure to be



The dissociation constant for an aqueous solution of $2.6 \times 10^{-5} \text{ M}$ DIBG was determined by the Stenström and Goldsmith method⁵ at ionic strength 0.1, temperature 20° , and different pH values from 0.5 to 8.0. Solutions of $\text{pH} > 8$ are unstable and the spectrophotometric measurements are no longer reproducible. The average result obtained was $\text{p}K = 3.7 \pm 0.2$.

Reactions with inorganic ions

The reactions of DIBG with 40 inorganic ions, up to a concentration of 1 g/l., at various pH values, were tested. The most interesting reactions took place in neutral medium with copper(II) and platinum (IV), a red-violet colour being produced.

Permanganate, dichromate, persulphate, periodate and ferricyanide react with DIBG, giving the same red-violet colour. Mercury(II) gives a violet precipitate which is insoluble in organic solvents (*e.g.*, ethanol, DMF, DMSO).

Spectrophotometric study of the copper(II)-DIBG system

In the preliminary studies of this reaction, we

observed that the sensitivity towards copper(II) was concentration-dependent, and that with more dilute solution the colour was slower to appear. Because the colour obtained with oxidizing species was the same as that produced with copper, we concluded that an oxidation was taking place, with oxidation by aerial oxygen dissolved in the solution, and that the reaction was catalysed by copper ions.

We also found that DIBG in neutral aqueous solutions was slowly oxidized by a stream of air, but was stable under an atmosphere of nitrogen even when small amounts of copper were present. Only when higher concentrations of copper were present was the red-violet colour then observed.

The catalytic behaviour has been used in a new kinetic-spectrophotometric method for determining trace amounts of copper.

Catalytic effect of copper(II)

The catalytic action of copper(II) is favoured in neutral medium by the presence of a few mmoles of pyridine. The absorption spectrum of the complex, and its variation with time are shown in Fig. 1, from which the reaction rate can be calculated.

Effect of reaction variables

The oxidation of DIBG is influenced by the reagent and copper(II) concentrations, pH, buffer composition, pyridine concentration and temperature. All these variables have been investigated, by the tangent method. The fixed time or fixed absorbance methods cannot be applied because the red-violet colour is not sufficiently stable.

The effect of temperature on the reaction rate ($dA/dt = \tan \alpha$) was studied in the range $10-43^\circ$ with solutions containing 200 ng of Cu(II), 5 ml of 0.01%

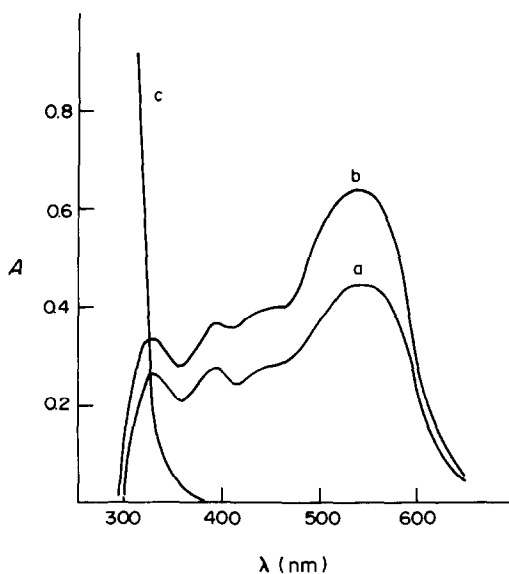


Fig. 1. Variation of absorption spectra of DIBG in presence of Cu(II). (a) DIBG-Cu(II) at 11 min; (b) DIBG-Cu(II) at 15 min; (c) DIBG.

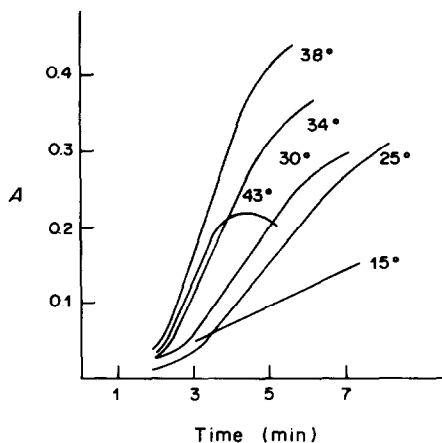


Fig. 2. Absorbance vs. time curves as a function of temperature.

DIBG solution, 5 ml of 1M pyridine and 5 ml of pH 7.5 buffer solution. The absorbance–time curves (Fig. 2) show the temperature dependence. The plots of $\log \tan \alpha$ vs. $1/T$ are linear between 286 and 303 K. A temperature of 298 K was chosen for subsequent studies. It would be preferable to bring all solutions employed to this temperature before mixing them.

The pH-dependence of the system was studied by use of mixtures of tris(hydroxymethyl)aminomethane (Tris) and perchloric acid. Hydrochloric acid was also tried, but chloride decreases the reaction rate, whereas perchlorate does not.

Two solutions, one of Tris and the other of pro-

tonated Tris (TrisH^+), obtained by mixing equimolar solutions of Tris and perchloric acid, were prepared, and with these, two series of samples were made: in one the concentration of Tris was kept constant, and in the other the concentration of TrisH^+ was kept constant.

Taking into account that the other reagent concentrations remain constant, the following relationships should be valid:

$$\log(\tan \alpha / [\text{TrisH}^+]^n) = K - x \text{ pH} \quad (1)$$

$$\log(\tan \alpha / [\text{Tris}]^m) = K' - x \text{ pH} \quad (2)$$

The absorbance vs. time curves for $[\text{Tris}] = \text{constant}$ and $[\text{TrisH}^+] = \text{constant}$ are shown in Fig. 3. By plotting equations (1) and (2), for different m and n values, polygonal graphs were obtained, the slopes of which coincided only for $m = -1$ and $n = 0$. From these graphs (Fig. 4), the following x values were obtained:

$$x = -2 \text{ (pH} < 7.4\text{); } x = -1 \text{ (7.4} < \text{pH} < 8.0)$$

and

$$x = 1 \text{ (8.0} < \text{pH} < 8.4).$$

For $\text{pH} > 8.4$ the solutions are unstable.

The effect of DIBG concentration on the reaction rate was studied in the range from $0.21 \times 10^{-4}M$ to $2.63 \times 10^{-4}M$. A logarithmic plot showed that the reaction rate was independent of the DIBG concentration in the range $0.74\text{--}2.50 \times 10^{-4}M$. For lower

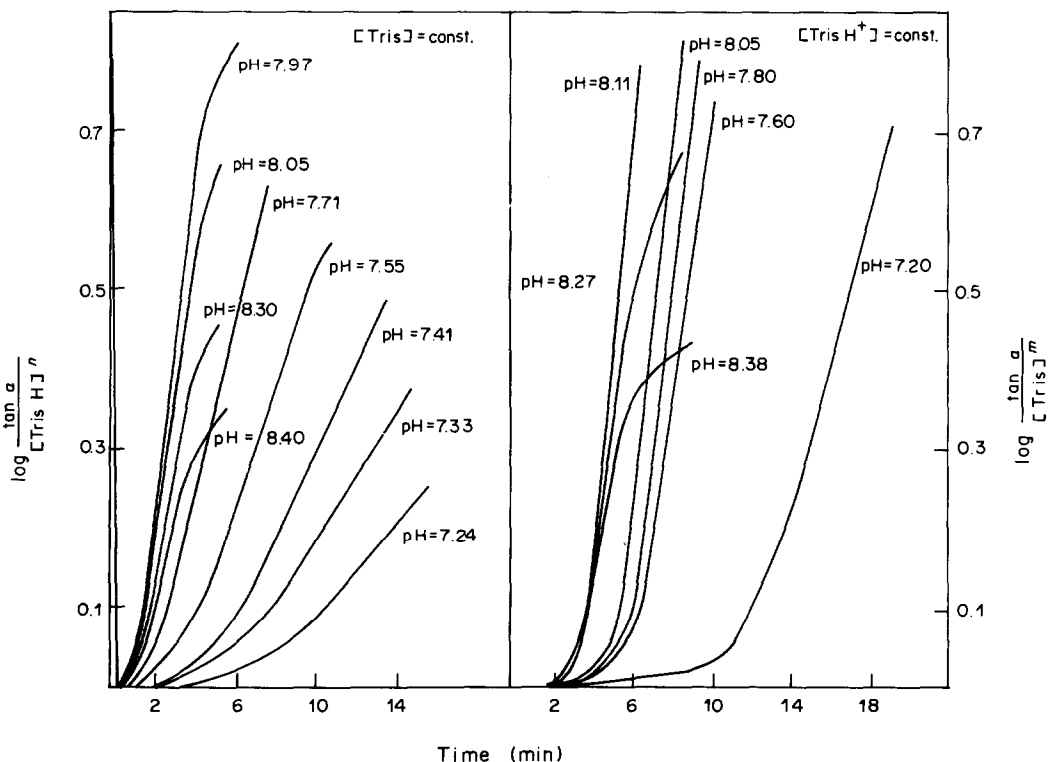


Fig. 3. Absorbance vs. time curves for $[\text{Tris}] = \text{constant}$ and $[\text{TrisH}^+] = \text{constant}$ at different pH values.

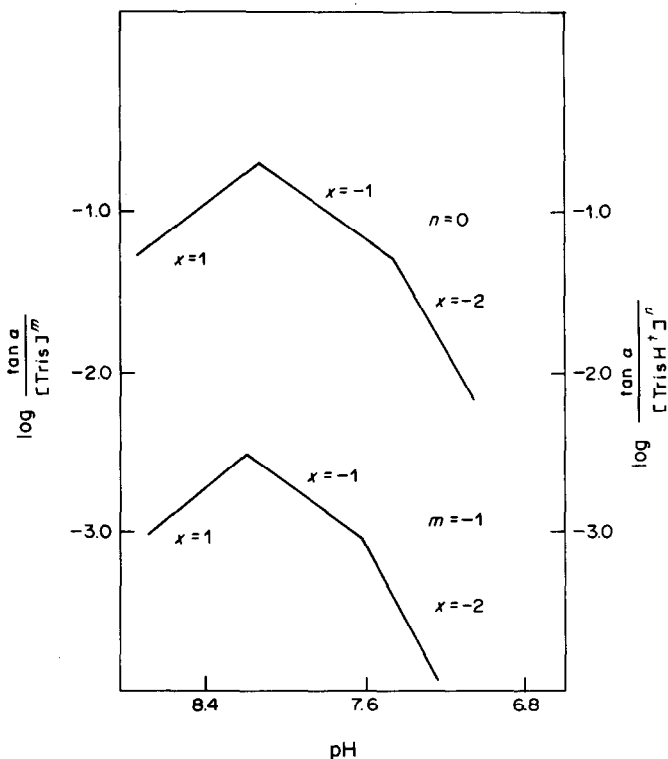


Fig. 4. Determination of pH reaction order for protons at different pH values.

DIBG concentrations an order of $2/3$ was found, and for higher DIBG concentrations an order of $-2/3$ (Fig. 5). A $1 \times 10^{-4} M$ DIBG concentration was chosen for subsequent studies; this concentration was obtained by use of 1 ml of 0.1% DIBG solution per 25 ml of final solution.

Pyridine increases the reaction rate. This effect was studied for solutions containing 150 ng/ml copper(II) and different pyridine concentrations. A logarithmic plot showed that the reaction rate depended linearly on the pyridine concentration in the range 0.05–0.4M. The partial order for pyridine in the rate equation is 1. Smaller amounts of pyridine can be used when the copper(II) solutions for analysis are more concentrated, but a 0.3M pyridine concentration was chosen for further work, obtained by use of 3 ml of 2.5M pyridine per 25 ml of final solution.

Rate equation and calibration graphs

The absorbance *vs.* time curves for solutions con-

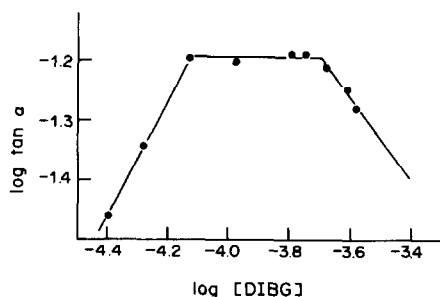


Fig. 5. Influence of DIBG concentration on rate of reaction.

taining different amounts of Cu(II) were recorded, measured against similar solutions containing no Cu(II). On the basis of the kinetic investigation, the following equation is suggested for the copper(II)-catalysed oxidation of DIBG at pH 7.9 in the concentration range $0.74\text{--}2.50 \times 10^{-4} M$.

$$d(\text{DIBG})_{\text{ox}}/dt = K \frac{[\text{pyridine}][\text{Cu(II)}]}{[\text{H}^+][\text{Tris}]} \quad (3)$$

The tangent method was applied to the absorbance *vs.* time curves. The calibration graph is linear over

Table 1. Influence of foreign ions on the kinetic determination of Cu(II) (200 ng/ml) by the tangent method

Tolerated ratio to Cu, w/w	Ions
$> 10^4$	Nitrate, iodate, bromate, perchlorate, sulphate, Na^+ , K^+ , Ca^{2+} , Ba^{2+} , Sr^{2+} , Mg^{2+}
10^4	Chloride
2.5×10^3	Fluoride
250	Oxalate, citrate, tartrate
100	Li^+ , Be^{2+} , persulphate
50	Ni^{2+} , Al^{3+} , Zn^{2+} , Cd^{2+} , As(V) , Pb^{2+} , Fe^{3+} , Zr(IV)^*
20	Pd(II) , Co^{2+} , Mn^{2+} , Mo(VI) , In^{3+} , Hg(II) , Ag^+
10	Mn(VII) , Cr^{3+} , Th^{4+}
5	Periodate, Bi^{3+} , Pt(IV) , Cr(VI)
1	W(VI) and V(V)
0.2	Ferrocyanide, ferricyanide, EDTA
0.1	Cyanide

*Fluoride added (10 mg).

Table 2. Determination of copper(II) in galena

Sample	Cu(II) found, ppm	
	Atomic absorption	Catalytic method*
a	124	120
b	110	110
c	22	26
d	812	844
e	159	167

*Mean value for three samples.

the Cu(II) concentration range 25–380 ng/ml. The relative error (95% confidence level) is 0.9% for 200 ng/ml.

Interferences

The influence of foreign ions was examined by the tangent method. The results are summarized in Table 1. Cyanide, EDTA, ferrocyanide and ferricyanide interfere seriously by decolorizing the solution. The interferences from Fe(III), Zr and Be are caused by precipitation of the corresponding hydroxides, but can be eliminated by the addition of fluoride.

Application to the estimation of copper in galena

The interference study shows that the method can

be used for determining copper in some natural samples. We have applied the method to galena and compared the results with those obtained by atomic-absorption spectrometry. Five different galenas were tested. The results are shown in Table 2.

Determination of pyridine

Equation (3) shows that pyridine can also be determined by the kinetic-spectrophotometric method. To increase the sensitivity of this determination, higher copper(II) concentrations are used.

We had verified previously that 200 ppm of pyridine will increase the reaction rate for copper concentrations up to 24 ppm. For higher copper(II) concentrations equation (3) is not valid. A 20-ppm copper level was chosen for the determination of pyridine, and a DIBG concentration of $2 \times 10^{-4}M$. Under these conditions, equation (3) remains unchanged.

The absorbance *vs.* time curves for solutions containing different amounts of pyridine were recorded, with measurement against similar solutions containing no pyridine.

The calibration graph (tangent method) is linear over the pyridine range 8–350 $\mu\text{g/ml}$, becoming convex at higher concentrations. The relative error (95% confidence level) is $\pm 2\%$ for 150 $\mu\text{g/ml}$.

Table 3. Influence of diverse, organic compounds on the kinetic determination of pyridine by the tangent method

Substance	Concentration ratio, substance/pyridine, w/w	Pyridine, mM		
		Taken	Found	Error, %
2-Chloropyridine	3	1.98	1.97	-0.5
	6	1.98	1.98	0
4-Dimethylaminopyridine	1	1.98	2.05	+3.4
	3	1.98	2.10	+6.1
	6	1.98	2.05	+3.4
Urea	3	1.98	1.98	0
	6	1.98	2.00	+0.9
Quinine	1	1.98	2.00	+0.9
	3	1.98	1.98	0
	6	1.98	1.98	0
Piperidine	6	1.98	1.98	0
	70	2.48	2.39	-3.6
	300	2.48	2.27	-8.2
	300	0.248	0.237	-4.4
Isoamyl alcohol	50	1.73	1.70	-2.1
	300	0.248	0.259	-4.4

Table 4. Determination of pyridine in piperidine and isoamyl alcohol

Pyridine in piperidine			Pyridine in isoamyl alcohol		
Taken, %	Found*, %	Error, %	Taken, %	Found*, %	Error, %
0.14	0.13	-7.1	0.15	0.14	-7.1
0.28	0.27	-3.6	0.30	0.31	+3.4
0.57	0.58	+2.2	0.60	0.62	+3.3
1.40	1.33	-1.7	1.49	1.45	-2.6
1.95	1.91	-2.0	2.07	2.03	-1.9
2.77	2.68	-3.1	2.93	2.97	+1.4
			3.50	3.53	+0.8
			4.34	4.25	-2.1

*Mean value for three samples.

The influence of various organic compounds on the reaction rate was tested. The results are summarized in Table 3. From the study of piperidine, we concluded that the concentration of piperidine should not be greater than 0.16M since higher concentrations produce an interference, independent of the pyridine concentration. On the other hand, the permissible volume of isoamyl alcohol is limited solely by its solubility in water.

We have therefore applied the method to determination of pyridine in piperidine and isoamyl alcohol. The results are summarized in Table 4. A 0.3%

level of pyridine in piperidine or isoamyl alcohol can be determined with 4% error.

REFERENCES

1. F. Toribio, *Ch. D. Thesis*, University of Córdoba, 1979, Spain.
2. M. Román, J. J. Berzas Nevado and A. Espinosa, *Talanta*, 1981, **28**, 134.
3. P. R. Bontchev, *ibid.*, 1972, **19**, 675.
4. S. Gantcheva and P. R. Bontchev, *ibid.*, 1980, **27**, 893.
5. W. Stenström and N. Goldsmith, *J. Phys. Chem.*, 1926, **30**, 1683.

SAMPLING AND ANALYSING MIXTURES OF SULPHATE, SULPHITE, THIOSULPHATE AND POLYTHIONATE

CARL O. MOSES*, D. KIRK NORDSTROM† and AARON L. MILLS

University of Virginia, Department of Environmental Sciences, Clark Hall, Charlottesville, VA 22903,
U.S.A.

(Received 15 July 1983. Accepted 11 December 1983)

Summary—Interpreting the redox chemistry of sulphur in aqueous systems requires the analysis of mixtures of various sulphony anions. Previous methods have been too involved to permit high sample throughput if good quality control is to be maintained. Methods based on ion chromatography have been developed for the direct determination of SO_4^{2-} , SO_3^{2-} , $\text{S}_2\text{O}_3^{2-}$ and SCN^- . The determination of thiocyanate permits the indirect determination of polythionates by treatment with cyanide. Formate, acetate, F^- , Cl^- , CO_3^{2-} and PO_4^{3-} do not interfere, but NO_2^- and NO_3^- interfere with determination of SO_3^{2-} . The sample preservation treatment includes addition of formaldehyde, cation-exchange and cold storage, to retard oxidation of $\text{S}_2\text{O}_3^{2-}$ and SO_3^{2-} , and inhibits the rearrangement of $\text{SO}_3^{2-}/\text{S}_2\text{O}_3^{2-}/\text{S}_n\text{O}_6^{2-}$ mixtures caused by bimolecular nucleophilic displacement (S_n2) reactions. Treated samples may be stored for up to 6 weeks with only minor loss of thiosulphate.

The analysis of mixtures of sulphony anions in aqueous solution is a valuable and necessary tool for investigating the chemistry of sulphur-rich wastewater effluents such as mining and milling wastes,¹ oil-shale retort wastes,² paper pulp wastes,³ and acid mine drainage.⁴ Hydrogeochemical processes also involve mixtures of dissolved sulphur species in various oxidation states, *e.g.*, redox processes in sulphur-rich groundwaters⁵ and geothermal waters,⁶ pyrite oxidation in alkaline waters,⁷ and sulphur oxidation in soils.⁸ The present work was aimed at determining concentrations of stable and metastable sulphony anions, *viz.*, sulphate, sulphite, thiosulphate and the polythionates (sulphane disulphonates, $\text{S}_n\text{O}_6^{2-}$, $n = 4-6$).

Numerous methods are available for analysing solutions of the single species sulphite, thiosulphate, sulphate, and polythionate.⁹⁻¹³ The analysis of solutions that contain mixtures of these species is difficult, owing to similarities in the reactions with the reagents used (*e.g.*, sulphite and thiosulphate with iodine) or because reactions between the sulphony species alter the solution composition. Previous methods of analysing mixtures have relied on complicated schemes for determining the ions partly collectively and partly individually; in some cases, one of the species must be determined by difference. Table 1 compares several schemes by which mixtures of sulphony anions have been analysed. Their principal limitations are (a)

failure to account for all four sulphony species dealt with in this study, (b) low sample throughput owing to the time that each aliquot requires for analysis, (c) complex manipulations that introduce the risk of contamination or other error, and (d) failure to stabilize the mixtures properly at the time of sampling. The method developed in the work described here is rapid and reliable, has no complicated manipulations, and includes provision for stabilizing samples for storage. It requires only two aliquots of each sample (total of 7 ml) for the direct determination of sulphite, thiosulphate and sulphate, the indirect determination of total $\text{S}_n\text{O}_6^{2-}$ ($n = 4-6$) and the average value of n .

Summary of aqueous sulphony anion chemistry

There are two general types of reaction that metastable sulphony anions readily undergo: redox and bimolecular nucleophilic displacement (S_n2) reactions. In solutions that contain molecular oxygen or other oxidants, these species tend to be oxidized to sulphate. Attainment of stable equilibrium in the aqueous systems may be slow and the metastable species also tend to interact and disproportionate. The result of these reactions is over-recovery of sulphate and under-recovery of the other species, as well as the change in composition of complex mixtures. A survey of the reactions which can alter the sample composition is therefore a necessary part of analytical method development. Sulphite oxidation is mediated by free radicals, catalysed by redox-sensitive transition metal ions [*e.g.*, Fe(III) and Cu(II)], and is fastest when the pH is below 7 and

*To whom reprint requests should be addressed.

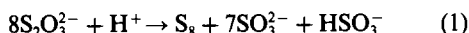
†Present address: U.S. Geological Survey, 345 Middlefield Road, Menlo Park, CA 94025, U.S.A.

Table 1. Methods for analysing mixtures of sulphyoxy anions

Sulphyoxy anions	Methods	References
$S_2O_3^{2-}$, $S_nO_6^{2-}$	Cyanolysis and spectrophotometry for Fe(III)-SCN ⁻	14, 8, 15
SO_3^{2-} , $S_2O_3^{2-}$, $S_nO_6^{2-}$	Ultraviolet spectroscopy	16, 17, 18
SO_3^{2-} and $S_2O_3^{2-}$	Iodometric titration	-19
$S_nO_6^{2-}$	Cyanolysis with spectrophotometry for Fe(III)-SCN ⁻	-20
SO_3^{2-}	Thermometric titration with dichromate	
SO_4^{2-}	Direct injection enthalpimetry	-21
SO_4^{2-}	Atomic-absorption spectrophotometry of excess of Ba ²⁺ after precipitation of BaSO ₄	
Total other S species	Oxidation with H ₂ O ₂ and determination as SO ₄ ²⁻	22, 23
SO_3^{2-} , SO_4^{2-}	Ion-chromatography	
$S_2O_3^{2-}$ + $S_nO_6^{2-}$	Acidimetric titration	1
SO_3^{2-} , $S_2O_3^{2-}$, SO_4^{2-}	Ion-chromatography	24
$S_2O_3^{2-}$	HgCl ₂ titration in presence of formaldehyde to mask sulphite, using Hg ²⁺ electrode	-5, 25, 26
$S_2O_3^{2-}$ + SO_3^{2-}	Same, without formaldehyde, sulphite by difference	
SO_4^{2-}	BaCl ₂ titration, using Ba ²⁺ electrode	-27
SO_3^{2-}	Iodometric titration	
$S_2O_3^{2-}$	Iodometric titration (sulphite masked by formaldehyde) and cyanolysis with spectrophotometry for Fe(III)-SCN ⁻	
$S_nO_6^{2-}$	Cyanolysis with spectrophotometry for Fe(III)-SCN ⁻	-This study
SO_4^{2-}	EDTA titration of excess of Ba ²⁺ after precipitation of BaSO ₄	
SO_3^{2-} , $S_2O_3^{2-}$ and SO_4^{2-}	Ion-chromatography	-This study
$S_nO_6^{2-}$	Cyanolysis with ion-chromatographic determination of SCN ⁻ and S ₂ O ₃ ²⁻	

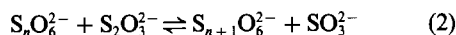
bisulphite (HSO₃⁻) predominates over sulphite.²⁸⁻³² Oxidation of thiosulphate (to tetrathionate and thence to sulphate) is also mediated by radicals and catalysed by oxidants such as I₂, Fe(III), and Cu(II).³³

Although thiosulphate is not oxidized very rapidly in the absence of transition metal ions, it is prone to acid decomposition at pH < 5 to sulphite and elemental sulphur. The mechanism of this reaction leads to a complex mixture of species and involves a chain of S_N2 reactions as shown in Fig. 1.^{34,35} If the chain terminates with ring closure (Fig. 1B), the overall stoichiometry is



The mechanism in Fig. 1C provides other terminations that lead to polysulphides [very unstable in the presence of S(IV)] and polythionates, as well as fragmentary elemental sulphur chains.

An aqueous mixture of sulphite, thiosulphate and polythionate is known as Wackenroeder's solution. The metastable equilibrium



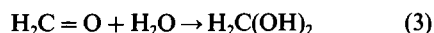
governs the interactions of these species.³⁶⁻⁴¹ This equilibrium involves S_N2 reactions like the one illustrated in Fig. 1D. Sulphite is a stronger nucleophile than thiosulphate, so pH > 7 favours polythionate chain-shortening, whereas bisulphite formation, at pH < 7, removes sulphite from reaction (2) and favours chain-lengthening. Since reaction (2) is a metastable equilibrium, and thiosulphate and sulphite are so easily removed from the system, the behaviour of Wackenroeder's solution is difficult to predict by applying thermodynamic relationships or to measure

experimentally. Although the qualitative behaviour of metastable sulphyoxy species has been extensively reviewed,^{12,38,42} much work remains in the development of quantitative models.

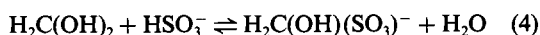
Reaction quenching

For analytical results to represent accurately the solution composition at the time of sampling, the redox and S_N2 reactions outlined above must be quenched. Ideally, the samples should be analysed immediately after sampling. In practice, this is rarely possible, so the sample composition must be stabilized for storage.

Formaldehyde has proved to be a particularly useful inhibitor of sulphite oxidation. Its most familiar form, an aqueous solution of dihydroxymethane, is produced by the rapid hydration of gaseous formaldehyde upon dissolution in water:⁴³



Dihydroxymethane and bisulphite form an addition product, hydroxymethanesulphonate, which is resistant to oxidation:⁴⁴



Reaction (4) is reversed at high pH, so the addition product is a convenient means of fixing sulphite as long as the sample pH can be kept below 7 until the time of analysis.^{11,23-25} This is particularly convenient for ion-chromatography (IC) methods because there is usually no obstacle to keeping the sample pH below 7, and the IC eluent pH is > 11, causing the reversal of reaction (4). Furthermore, hydroxymethanesulphonate can be crystallized as a sodium salt,

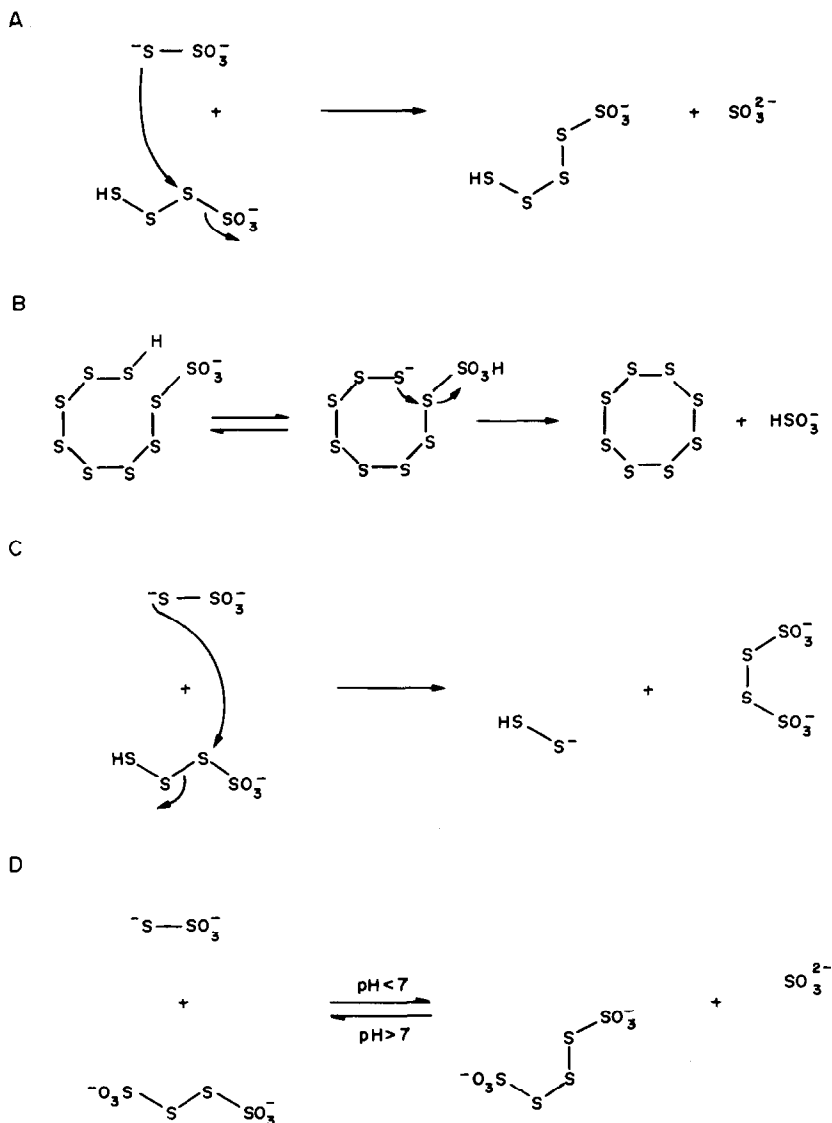


Fig. 1. Mechanisms of S_N2 reactions in mixtures of sulphy species:

A. Nucleophilic attack of thiosulphate on trisulphane monosulphonate, yielding tetrasulphane monosulphonate and sulphite.

B. Ring closure of octasulphane monosulphonate, yielding solid sulphur and bisulphite.

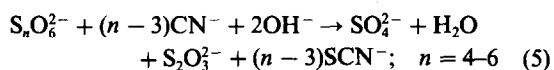
C. Alternative direction of attack of thiosulphate on trisulphane monosulphonate, yielding disulphide and tetrathionate.

D. Rearrangement of Wackenroeder's solution, a mixture of sulphite, thiosulphate, and polythionates.

$\text{NaSO}_3\text{H}_2\text{COH}$, a stable primary standard for sulphite.²³

Thiosulphate is not as sensitive to air oxidation as sulphite, and the anhydrous sodium salt is suitable as a primary standard. Thiosulphate is, however, easily oxidized in solution by transition metal ions, so this reaction must be quenched. Thiosulphate is most stable at near-neutral pH so its storage at pH 6 is compatible with the storage of hydroxymethanesulphonate. The sulphur in polythionates is oxidized indirectly, by oxidation of the thiosulphate or sulphite produced from them by reaction (2). To prevent this or an alteration of polythionate chain

length by means of reaction (2) the polythionates can be reacted with cyanide, a strong nucleophile.⁴⁶⁻⁴⁸



Reaction (5) is very rapid at room temperature for pentathionate and hexathionate, and requires 1.5 min for tetrathionate.⁴⁷ Trithionate, $\text{S}_3\text{O}_6^{2-}$, can also be cyanolysed, but several hours or heating in a boiling water-bath and an extra determination are required.^{14,47} Trithionate was not dealt with in the present work, but the analytical procedure could be modified to include it. Thiosulphate reacts with cy-

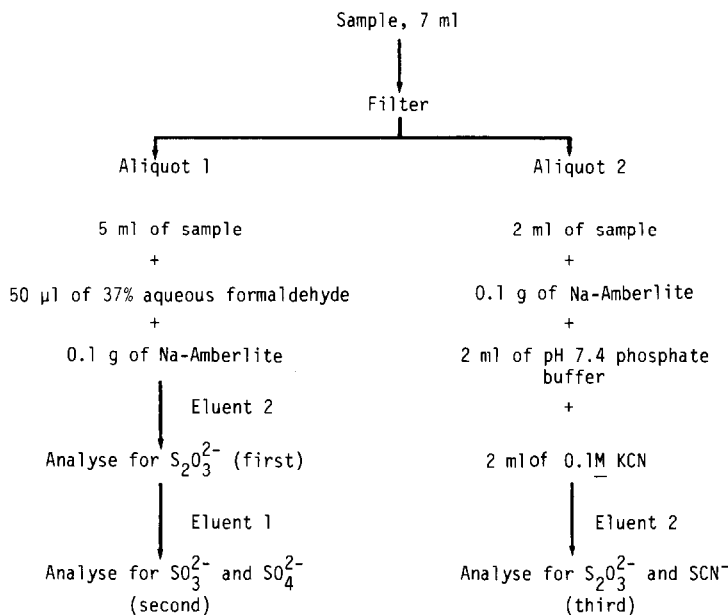


Fig. 2. Sample splitting and treatment. Aliquot 1 was used for direct analysis for thiosulphate, sulphite and sulphate; aliquot 2 was used for indirect analysis of cyanolysed polythionates.

anide in the presence of transition metal ions, such as Fe(III) or Cu(II). This reaction would interfere with the direct determination of thiosulphate, resulting in under-recovery. In our method, a sodium-saturated cation-exchange resin was added to the samples to reduce transition metal concentrations and, thereby, to reduce thiosulphate oxidation and cyanolysis.

An advantage of cyanolysis over any direct technique for determination of polythionates is that primary standards are available for thiosulphate and thiocyanate. Only sodium tetrathionate can be obtained commercially, and then not in high purity, and the synthesis of high-purity polythionate salts is tedious. Furthermore, decomposition of polythionate salts during storage is inevitable. Previous studies of cyanolysis have substantiated the 1:1 ratio of recovered thiosulphate to original polythionate, shown in reaction (5),^{14,19,48} so it was not considered necessary to have a pure polythionate salt available for the present work. An advantage of ion-chromatographic analysis over spectrophotometric determination of cyanolysis products is that it can determine thiosulphate and thiocyanate simultaneously. This allows the determination of the average polythionic composition from equation (6), which can be derived from the stoichiometry of reaction (5):

$$\bar{n} = ([\text{SCN}^-]/[\text{S}_2\text{O}_6^{2-}]) + 3 \quad (6)$$

EXPERIMENTAL*

Sample treatment

Samples from laboratory experiments were filtered through 0.45- μm pore-size Gelman or Millipore mem-

branes, and field samples were filtered through 0.1- μm pore-size filters to exclude sulphur-oxidizing bacteria. The filters were leached with at least 500 ml of distilled water in the laboratory or 500 ml of sample water for field work before the samples were collected. After filtration, samples were immediately split into two aliquots and stabilized, and were analysed within 10 days, as shown in Fig. 2. Between collection and analysis the samples were stored at 2–5°.

Reagents

Phosphate buffer (pH 7.4). Prepared by titrating 0.5M potassium dihydrogen phosphate with 2.0M sodium phosphate to pH 7.4.

Potassium cyanide solution, 0.1M.

Eluent 1. A 0.75mM sodium carbonate + 0.75mM *p*-cyanophenol solution adjusted to pH 11.4 with 2.0M sodium hydroxide.

Eluent 2. A 3.0mM sodium carbonate + 0.75mM *p*-cyanophenol solution adjusted to pH 11.8 with 2.0M sodium hydroxide.

Combined $\text{S}_2\text{O}_3^{2-}/\text{SCN}^-$ standards. Prepared with pH-7.4 phosphate buffer in the same dilution as in aliquot 2 (Fig. 2, *i.e.*, 1:2 buffer:standard solution). All standard salts were stored in a desiccator and protected from strong light. Stock solutions were discarded after calibration standards had been prepared from them. New calibration standards were mixed not less frequently than every 4 weeks and reproducibility records were kept to detect deterioration. Solutions were also prepared from Na_2SO_3 and $\text{Na}_2\text{S}_4\text{O}_6$ and mixed to simulate the collection of unstable samples. The tetrathionate solutions had to be filtered through 0.45- μm membranes to remove the elemental sulphur formed by decomposition during storage.

Preparation of Na-Amberlite. Amberlite CG-120 cation-exchange resin, sodium-form (chromatographic grade, Mallinckrodt), 100–200 mesh, was washed well with demineralized water, charged with sodium ions by soaking for 24 hr in 1.0M sodium chloride, rinsed with demineralized water until the conductivity of the effluent equalled that of the demineralized water, and allowed to dry thoroughly. The exchange capacity of each batch must be experimentally determined (see Results).

CAUTION. Cyanide and thiocyanate salts and solutions

*The use of brand names in this report is for identification purposes only and does not imply endorsement by the U.S. Geological Survey.

are toxic and should be handled with care. Formalin is toxic and a suspected carcinogen. Cyanolysis and formalin treatment should be done in well-ventilated areas. *p*-Cyanophenol is an irritant, and though its toxic status is unclear it should be handled with care.

IC methods

The output of a Dionex Model 14 Ion Chromatograph was recorded on a Honeywell dual-pen 1000-mV strip-chart recorder. Results were quantified by measuring peak height and normalizing with respect to conductivity units ($\mu\text{S}/\text{cm}$). Integrating the peak area does not give better precision than measuring the peak height does.

Two sets of operating conditions were used.

A. For aliquot 1, SO_3^{2-} and SO_4^{2-}

Eluent 1: 0.75mM Na_2CO_3 /0.75mM *p*-cyanophenol/pH 11.4
 Flow-rate: 40% (3.1 ml/min)
 System pressure: 80–280 psig
 Precolumn: none
 Separator column: 4 × 140 mm L-20 anion separator (Dionex No. 30364) trimmed to 72 mm length
 Suppressor column: 6 × 250 mm anion suppressor (Dionex No. 30064)
 Suppressor regenerant: 1.0N H_2SO_4
 Injection loop volume: 100 μl
 Conductivity (full-scale): 300 $\mu\text{S}/\text{cm}$ (strip-chart, full-scale: 15–150 $\mu\text{S}/\text{cm}$)

B. For aliquot 1, $\text{S}_2\text{O}_3^{2-}$ and for aliquot 2, $\text{S}_2\text{O}_3^{2-}$ and SCN^- : as for A above, except:

Eluent 2: 3.0mM Na_2CO_3 /0.75mM *p*-cyanophenol/pH 11.8
 Separator column: 4 × 140 mm L-20 anion separator (Dionex No. 30364), trimmed to 95 mm length.

Calculations

Concentrations were calculated from the slopes of the calibration curves. For the determination of $\text{S}_n\text{O}_6^{2-}$ in aliquot 2 the following calculations were needed.

(1) Calculate $\text{S}_n\text{O}_6^{2-}$:

$$[\text{S}_n\text{O}_6] = [\text{S}_2\text{O}_3^{2-}] \text{ in aliquot 2} - [\text{S}_2\text{O}_3^{2-}] \text{ in aliquot 1}$$

(2) Calculate \bar{n} :

$$\bar{n} = ([\text{SCN}^-]/[\text{S}_n\text{O}_6^{2-}]) + 3.$$

Determination of method detection limit (MDL)

The MDL was experimentally determined by the following procedure.⁴⁹

1. A useful estimate of detection limit was obtained by converting the minimum readable recorder deflection (2 chart units in 1000 with our recorder) to an equivalent concentration by use of a previously-obtained calibration graph for the constituent in question.

2. Seven aliquots of a standard of concentration 3–5 times the estimated MDL were handled and analysed according to the procedure given above, and the standard deviation, S_c , was calculated.

3. The S_c value was multiplied by the Student-*t* value (one-tailed test) for 6 degrees of freedom (d.f.) at the 99% confidence level ($p = 0.01$) to obtain the MDL ($\text{MDL} = 4.317 S_c$).

4. The upper and lower 95% confidence limits (95% UCL and 95% LCL) for the MDL were calculated from the χ^2 distribution:

$$\frac{\text{LCL}}{\sqrt{\chi_{(p=0.025)}^2/\text{d.f.}}} < \text{MDL} < \frac{\text{UCL}}{\sqrt{\chi_{(p=0.975)}^2/\text{d.f.}}};$$

for d.f. = 6, this reduces to LCL = 0.64 MDL; UCL = 2.20 MDL.

RESULTS AND DISCUSSION

Calibration and sensitivity

Figure 3 shows typical chromatograms obtained by this method. Table 2 summarizes the data on sensitivity, MDL, and retention times.

The linear correlation coefficient for calibration of each species was excellent for such a wide range of concentration (in each case, $r > 0.999$, significant at $\ll 1\%$ level), but there was $> 9\%$ variability in method sensitivity (defined as ratio of response to concentration) for sulphite and sulphate over this range. There were no trends, however, so, rather than attributing the variability to a gain or loss of conductimetric sensitivity with increasing concentration, we regard it as due to inefficiency of the weak eluent that was used for these species. Calibration over a narrower range (for example, by bracketing standards around a group of samples of similar concentration), gave much-improved precision. For example, the sulphate sensitivity in the range 100–200 μM , had a

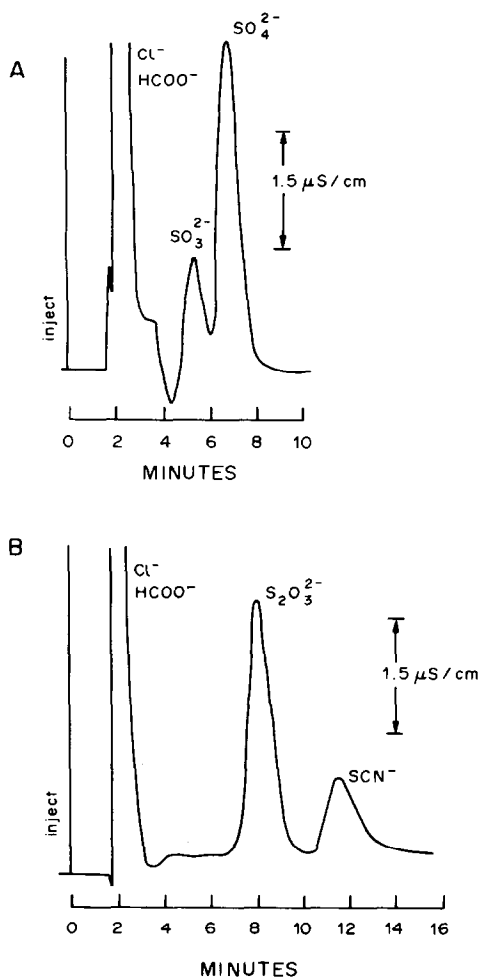


Fig. 3. Chromatograms obtained by injecting standards mixed in 0.01M NaCl and treated with 37% aqueous formaldehyde (1:100); specific conductance is shown in $\mu\text{S}/\text{cm}$. A, 100 μM sulphite and sulphate; B, 100 μM thio-sulphate and thiocyanate.

Table 2. Performance data for IC analyses for SO_3^{2-} , SO_4^{2-} , $\text{S}_2\text{O}_3^{2-}$ and SCN^- (calibration range = 0–1000 μM)

Species	Eluent*	Retention time†, min	Sensitivity§, $\mu\text{S}/\text{cm}/\mu\text{M}$	Estimated MDL‡, μM	Experimental MDL¶
					(95% UCL; 95% LCL), μM
SO_3^{2-}	1	6.0	0.0127 ($\pm 9.6\%$)	2.36	5.44 (11.0; 3.48)
SO_4^{2-}	1	8.0	0.0360 ($\pm 9.2\%$)	0.83	4.58 (10.1; 2.93)
$\text{S}_2\text{O}_3^{2-}$	2	8.0	0.0321 ($\pm 4.3\%$)	0.93	5.33 (11.7; 3.41)
SCN^-	2	11.4	0.0094 ($\pm 3.3\%$)	3.19	4.14 (9.11; 2.65)

*Eluent 1 = 0.75mM Na_2CO_3 /0.75mM *p*-cyanophenol/pH 11.4;

Eluent 2 = 3.0mM Na_2CO_3 /0.75mM *p*-cyanophenol/pH 11.8.

†Typical retention time for 100 μM standard in 0.01M NaCl.

§Sensitivity = (conductimetric response/concentration), ($\pm \text{RSD}\%$) ($N = 6$), measured across the calibration range.

‡Estimated by calculating concentration equivalent to 2/1000 of full-scale deflection (the limit of chart readability) for 300 $\mu\text{S}/\text{cm}$ full-scale conductance and 50 mV full-scale voltage.

¶Determined by method of Ref. 49; $N = 7$; defined matrix: 0.01M NaCl, 1% 37% formaldehyde solution, single-species standard about 3 times the concentration of estimated MDL; UCL, LCL = upper and lower confidence limits.

relative standard deviation (RSD) of 0.9% ($N = 5$). If the origin was included (*i.e.*, calibration from 0 to 200 μM), the linear regression slope differed from the mean sensitivity by <0.2%. In contrast, the sensitivity for thiosulphate and thiocyanate, which were eluted with a stronger eluent, showed little variability over the range from 10 to 1000 μM . The sensitivity differed from the linear regression slope by <0.9% for thiosulphate and <2.1% for thiocyanate.

Cyanolysis calibration (see Table 3) based on a sodium tetrathionate salt of approximately 83% purity also showed very good linearity over the 0–1000 μM range ($r > 0.999$, significant at <<1% level). Figure 4 shows a chromatogram of thiosulphate and thiocyanate in the presence of the phosphate buffer. Injections of standard solutions and a blank, prepared in the buffer, were required for the accurate and precise interpolation of the baseline under the thiosulphate and thiocyanate peaks.

Separation and interferences

The L-20 separator columns were essential for rapid analysis, but the two L-20 columns used in this work had very different performance characteristics. This indicates the need to evaluate the column per-

formance at an early stage in development or setting up of the method. Of these two columns, one was "too fast" for sulphite and sulphate, even with very weak eluents. With a strong eluent, however, it separated thiosulphate and thiocyanate into well-

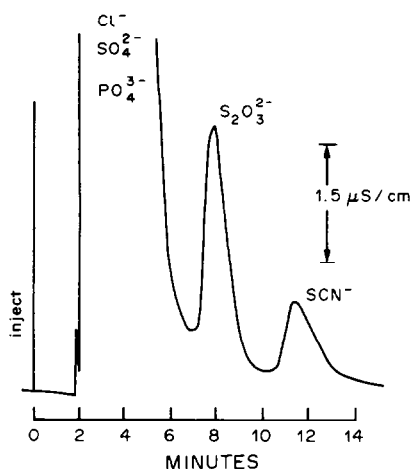


Fig. 4. Chromatogram obtained by injecting a cyanolysed approximately 100 μM $\text{S}_4\text{O}_6^{2-}$ standard in 0.01M NaCl and phosphate buffer; the standard was treated in the same way as aliquot 2 sample.

Table 3. Cyanolysis calibration

$\text{S}_4\text{O}_6^{2-}$ *, μM	$\text{S}_2\text{O}_3^{2-}/\text{S}_4\text{O}_6^{2-}$ †	$\text{S}_4\text{O}_6^{2-}$ recovery§, %	$\text{SCN}^-/\text{S}_2\text{O}_3^{2-}$ ‡
10	0.842	101.5	1.200
50	0.822	99.0	1.124
100	0.823	99.2	1.086
500	0.922	111.1	0.989
1000	0.927	111.7	0.981
mean	0.867	104.5	1.076
r.s.d. ($N = 5$)	6.1%	6.1	8.6%

*These concentrations assume that the $\text{Na}_2\text{S}_4\text{O}_6$ was pure.

†Estimated recovery of $\text{S}_4\text{O}_6^{2-}$, if the $\text{Na}_2\text{S}_4\text{O}_6$ were pure. If extrapolated to infinite dilution, these data suggest 83% purity and an increase in $\text{S}_2\text{O}_3^{2-}$ recovery of about 1.1%/100 μM $\text{S}_4\text{O}_6^{2-}$ (these conclusions are significant at <5% level, $N = 5$).

§Based on 83% purity.

‡This ratio gives \bar{n} in $\text{S}_n\text{O}_6^{2-}$ ($n = \text{ratio} + 3$). Extrapolating to infinite dilution suggests $\bar{n} = 4.139$ and a decrease in ratio of about 1.9%/100 μM $\text{S}_n\text{O}_6^{2-}$ (these conclusions are significant at <5% level, $N = 5$).

resolved, rapidly eluted peaks. The other column was "too slow" for thiosulphate or thiocyanate, except with very strong eluents, and these rapidly expended the suppressor column; this column worked very well for sulphite and sulphate. These columns have plastic bodies and were carefully trimmed in length to optimize retention time and resolution.

Figure 3 shows that chloride (100mM) and formate (100 μ M) did not interfere in sulphite and sulphate determination. Carbonate could not be detected except at high concentrations (>3mM); even at higher levels it did not interfere, because it was eluted in about 4 min. Eluent 1 eluted acetate (1mM) in about 3 min. Nitrite and nitrate when present at >10 μ M concentration interfered with sulphite determination. Figure 4 shows that phosphate up to 0.16M did not interfere in thiosulphate or thiocyanate determinations, though baseline extrapolation is needed at high concentrations. Phosphate interfered with determination of sulphate in aliquot 1 if the eluent pH was not adjusted properly; a pH that was too low caused the elution of HPO₄²⁻ at about the same time as sulphate. Raising the pH allowed longer retention of the phosphate and complete resolution of sulphate and phosphate, because of dissociation of HPO₄²⁻ to PO₄³⁻ in the eluent stream. The pK_a for this dissociation is 12.3, but the pH did not have to be raised to this value to resolve sulphate and phosphate. In fact, pH 12.3 (20mM OH⁻) gave an eluent that was much too strong for determination of sulphite and sulphate. In the case of eluent 2, adjustment to pH 11.8 was required for the rapid elution of thiosulphate and good resolution of thiosulphate and thiocyanate.

Quenching sulphite and thiosulphate oxidation

The efficacy of a 1% v/v addition of formaldehyde as a fixative for sulphate is demonstrated in Fig. 5. The samples were stored in closed plastic bottles. Even though refrigeration slowed the oxidation of sulphate, it was neither a substitute for, nor a helpful adjunct to, formalin treatment.

To determine whether Na-Amberlite is an effective agent for removing iron from samples, 0.1 g of Na-Amberlite was added to each of five 5-ml aliquots of

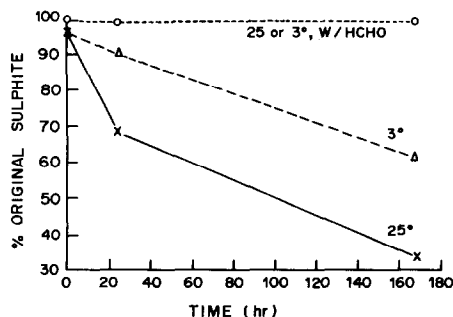


Fig. 5. Efficacy of 1:100 v/v addition of 37% aqueous formaldehyde solution as a sulphite fixative. 100% = approximately 100 μ M SO₃²⁻; 25°C denotes storage at room temperature; 3°C denotes refrigerated storage.

a 1mM solution of Fe(III) (FeCl₃ · 6H₂O) and, after 24 hr the iron concentration was determined by the Ferrozine method.⁵⁰ The Fe(III) concentration was decreased to 18.1 μ M (r.s.d. 20%) or about 1.8% of the original concentration. This single-point measurement suggests a cation-exchange capacity of about 147 μ eq/g. This decrease in iron concentration enabled 100 μ M thiosulphate/1mM Fe(III) medium (if treated with 1% of formalin and 0.1 g of Na-Amberlite) to be kept for 1 week with a thiosulphate loss of only about 12.5 μ M (r.s.d. 8.4%, N = 5). Refrigeration (at 2–5°) extended this storage period to about 6 weeks, with a similar loss. Addition of formalin alone to the thiosulphate/iron system allowed a loss of almost 100% over 1 week and no treatment at all allowed a loss of almost 95% in only 4 hr.

To determine the potential for sulphate interference resulting from the use of Na-Amberlite, 0.1 g of Na-Amberlite was added to each of five 5-ml aliquots of demineralized water. After 24 hr, the average sulphate concentration was 18.1 μ M (r.s.d. 2.2%). This concentration is equivalent to 90.5 nmoles of sulphate in the 5 ml of solution. The excellent reproducibility of this sulphate concentration, regardless of time elapsed between addition of Na-Amberlite and analysis (4–30 hr), suggests that this interference was governed by a rapidly attained stable equilibrium. This conclusion is further supported by the fact that addition of 0.1-g portions of Na-Amberlite to 5-ml aliquots of standards covering the 10–1000 μ M range caused less than 1% change in the slope of the calibration graph, and the amount of sulphate added by the Na-Amberlite decreased with increasing standard concentration. Thus, the process by which Na-Amberlite adds sulphate to samples seems to be controlled by equilibrium with the sulphate in solution. For each batch of analyses, determination of the effect of the Na-Amberlite addition on blanks and on standards with sulphate concentration less than 100 μ M is recommended.

Analysis of mixtures

The sodium tetrathionate that was used for investigating cyanolysis contained sulphate and sulphite as decomposition products, and therefore solutions made from this salt were really mixtures. Analyses of this mixture over the 0–1000 μ M range revealed behaviour that was qualitatively consistent with that discussed in the introduction to this paper. The average ratio of recovered thiosulphate to that expected (assuming 100% pure tetrathionate, see Table 3) suggests that this salt was only about 87% pure in terms of tetrathionate. There was, however, a weak trend toward increased recovery at higher tetrathionate concentrations, and extrapolation of this trend to infinite dilution of the salt gave an estimate of 83% purity. The average ratio of thiocyanate to thiosulphate indicated \bar{n} = 4.08, but the extrapolation suggested \bar{n} = 4.14.

We prefer the extrapolated estimates of purity and \bar{n} to the average values, because the latter were biased by solution chemistry in the calibration standards. The pH of these salt solutions was >7 and, as reaction (2) shows, such a mixture should tend toward chain-shortening; this process would be accelerated at higher concentrations. Chain-shortening before cyanolysis would cause a decrease in thiocyanate recovery and, therefore, in $\text{SCN}^-/\text{S}_2\text{O}_3^{2-}$ ratio. Although the tetrathionate salt contained no detectable thiosulphate impurity, reaction (2) in reverse would yield some thiosulphate, and this could account for the observed increase in thiosulphate recovery at higher concentrations. Similarly, Urban⁴⁸ observed a decrease in thiocyanate recovery over 4 days in a solution of hexathionate; he attributed this behaviour to chain-shortening as the solution aged.⁴⁸ We have observed concentrated solutions ($500\text{--}5000\mu\text{M}$) of tetrathionate to precipitate sulphur on standing (equivalent to chain-shortening accompanied by decomposition of the resultant thiosulphate). For example, 1 litre of a $5000\mu\text{M}$ solution lost 40.7 mg of elemental sulphur ($159\mu\text{moles of S}_8$) on standing for 2 weeks at room temperature.

Although mixtures of polythionates cannot be expected to remain constant in composition, samples that have been cyanolysed can be expected to maintain a constant ratio of $\text{SCN}^-/\text{S}_2\text{O}_3^{2-}$, subject to the constraints on thiosulphate stability. This ratio showed some variability for a cyanolysed $100\mu\text{M}$ tetrathionate standard over 2 weeks (1.086, r.s.d. 9.2%, $N = 5$), but there was no trend towards decreasing or increasing ratio during this period.

To demonstrate the analysis of mixtures of all four sulphony anions by this method, three mixtures of SO_3^{2-} , SO_4^{2-} , $\text{S}_2\text{O}_3^{2-}$ and $\text{S}_n\text{O}_6^{2-}$ were prepared. The pH of each was adjusted to ~ 6 , appropriate for storage of hydroxymethanesulphonate and thiosulphate. Replicate analyses were performed by the procedure given, and the results are presented in Table 4.

If these results are taken to represent typical performance of this method for analysing mixtures, we can make the following observations. Sulphite values

were within 6% of those expected, but the "true" recovery is probably slightly less because some of the sulphite was an artefact produced in the rearrangement of the uncyanolysed polythionate in aliquot 1. We attribute the under-recovery of thiosulphate to the same process, namely chain-lengthening of the polythionate through reaction (2) at $\text{pH} < 7$ (see Fig. 1D). The observed increase in thiocyanate/polythionate ratios also suggests that chain-lengthening took place in aliquot 2 before cyanide was added, in which case the polythionate concentrations should not change; Table 4 shows the polythionate recoveries are all close to 100%. Sulphate over-recovery was most likely due to the oxidation of sulphite that took place before the formalin addition (the sulphate expected was that from contamination of the sulphite and polythionate salts). Finally, the over-recovery of total sulphur was due to the great increase in \bar{n} over that expected from the cyanolysis calibration in high pH solutions. The expected value was biased low for a mixture at pH 6. The discrepancy between total sulphur expected and found was less than the discrepancy between \bar{n} expected and found, because of the under-recovery of thiosulphate.

CONCLUSIONS

An IC method has been developed for the direct determination of sulphite, sulphate and thiosulphate in one formalin-treated sample aliquot, by use of two eluents in succession and the same column. Polythionate concentration and composition are determined indirectly in a second aliquot by IC analysis for thiosulphate and thiocyanate produced by cyanolysis. Other sample treatments include filtration, addition of a cation-exchange resin, and storage at $2\text{--}5^\circ$. This combination of treatments permits samples to be stored for up to 6 weeks with only slight loss of thiosulphate.

Development of the IC method involved consideration of column length and resin material, eluent strength and pH, and the sampling and storage

Table 4. Analyses of mixtures of SO_3^{2-} , SO_4^{2-} , $\text{S}_2\text{O}_3^{2-}$ and $\text{S}_n\text{O}_6^{2-}$

	Mixture A			Mixture B			Mixture C		
	Expected, μM	Found, μM	r.s.d.*, %	Expected, μM	Found, μM	r.s.d.*, %	Expected, μM	Found, μM	r.s.d.*, %
SO_3^{2-}	36	34.8	1.4	7.2	6.82	7.7	72	75.5	1.0
SO_4^{2-}	250	261	8.2	244	240	6.6	250	266	7.8
$\text{S}_2\text{O}_3^{2-}$	25	20.9	2.0	50	42.5	1.0	10	8.45	5.3
$\text{S}_n\text{O}_6^{2-}$	20.8	20.4	7.5	83.0	81.5	1.1	41.5	38.5	3.9
Total S	422†	438§	5.2	695†	729§	2.8	514†	547§	4.5
	<i>Ratios</i>								
SCN^-	1.139‡	1.960	5.7	1.139‡	1.875	1.5	1.139‡	1.901	1.9
$\text{S}_n\text{O}_6^{2-}$									

* $N = 4$.

†Total S expected was determined in the same way as total S found (see §), except \bar{n} assumed to be 4.14, according to the cyanolysis calibration.

§Total S found = $\bar{n} [\text{S}_n\text{O}_6^{2-}] + 2[\text{S}_2\text{O}_3^{2-}] + [\text{SO}_3^{2-}] + [\text{SO}_4^{2-}]$, where $\bar{n} = (\text{SCN}^-/\text{S}_n\text{O}_6^{2-}) + 3$.

‡The expected ratio was based on the values extrapolated to infinite dilution from the cyanolysis calibrations.

treatments. An important factor not considered, however, was injection-loop volume. With all other factors kept constant, increase in the loop volume would be expected to increase the sensitivity and decrease the MDL.

In analysis of mixtures, the method has produced results which substantiate the qualitatively known pH-dependent behaviour of mixtures of sulphoxy anions. The method should provide the means to develop a more quantitative understanding of the pH- and time-dependent changes in such complex mixtures, particularly the Wackenroeder equilibrium represented by reaction (2).

Acknowledgements—This work was supported by National Science Foundation grant EAR-7911144; the Ion Chromatograph was obtained through the support of the U.S. Department of Energy grant DE-FG05-79EV10209. We also wish to acknowledge helpful discussions with William Keene and Art Fitchett. Review of the manuscript by Jerry Leenheer and Yousif Kharaka was greatly appreciated. An earlier version of this report was presented at the 24th Rocky Mountain Conference, Denver, Colorado, August, 1982.

REFERENCES

1. R. Makhija and A. Hitchen, *Talanta*, 1978, **25**, 79.
2. H. A. Stuber, J. A. Leenheer and D. S. Farrier, *J. Environ. Sci. Health*, 1978, **A13**, 663.
3. S. P. Bhatia, in *Sulfur in the Environment, Part 1: The Atmospheric Cycle*, J. O. Nriagu (ed.), pp. 51–83. Wiley, New York, 1978.
4. D. K. Nordstrom, in *Acid Sulfate Weathering*, J. A. Kittrick, D. F. Fanning and L. R. Hossner (eds.), pp. 37–56. Soil Science Society, Madison, 1982.
5. J. Boulegue, J. P. Ciabrin, C. Fouillac, G. Michard and G. Ouzounian, *Chem. Geol.*, 1979, **25**, 19.
6. A. L. Day and E. T. Allen, *The Volcanic Activity and Hot Springs of Lassen Peak*, Carnegie Institution of Washington, No. 360, 1925.
7. M. B. Goldhaber, *Am. J. Sci.*, 1983, **283**, 193.
8. Y. M. Nor and M. A. Tabatabai, *Soil Sci.*, 1976, **122**, 171.
9. E. Blasius, G. Horn, A. Knochel, J. Munch and H. Wagner, in *Inorganic Sulphur Chemistry*, G. Nickless (ed.), pp. 199–240. Elsevier, Amsterdam, 1968.
10. L. C. Haff, in *The Analytical Chemistry of Sulfur and its Compounds, Part I*, J. H. Karcher (ed.), pp. 183–284.
11. L. Szekeres, *Talanta*, 1974, **21**, 1.
12. A. Hitchen and C. W. Smith, *A Review of Analytical Methods for the Determination of Polythionates, Thio-sulphate, Sulphite, and Sulphide in Mining Effluents*, CANMET, Energy, Mines, and Resources Canada, MRP/MSL 76-208, 1976.
13. W. J. Williams, *Handbook of Anion Determination*, Butterworths, London, 1979.
14. D. P. Kelly, L. A. Chambers and P. A. Trudinger, *Anal. Chem.*, 1969, **41**, 898.
15. T. Mizoguchi and T. Okabe, *Bull. Chem. Soc. Japan*, 1975, **48**, 1799.
16. T. E. Eriksen and S. O. Engman, *Acta Chem. Scand.*, 1972, **26**, 3333.
17. T. E. Eriksen and J. Lind, *ibid.*, 1972, **26**, 3325.
18. T. E. Eriksen, J. Lind and S. O. Engman, *ibid.*, 1972, **26**, 3337.
19. T. Koh and K. Taniguchi, *Anal. Chem.*, 1973, **45**, 2018.
20. L. D. Hansen, L. Whiting, D. J. Eatough, T. E. Jensen and R. M. Izatt, *ibid.*, 1976, **48**, 634.
21. H. F. Steger and L. E. Desjardins, *Talanta*, 1979, **24**, 675.
22. T. S. Stevens, V. T. Turkelson and W. R. Albe, *Anal. Chem.*, 1977, **49**, 1176.
23. L. D. Hansen, B. E. Richter, D. K. Rollins, J. D. Lamb and D. J. Eatough, *ibid.*, 1979, **51**, 633.
24. L. J. Holcombe, E. E. Ellsworth, B. F. Jones and F. B. Meserole, *The Quantitative Determination of Sulphite, Sulphate, and Thiosulphate Using the Ion Chromatograph*, 2nd National Symp. IC Anal. Environ. Pollutants, Raleigh, North Carolina, 1978.
25. J. Boulegue, J. L. Lord III and T. M. Church, *Geochim. Cosmochim. Acta*, 1982, **46**, 453.
26. J. Boulegue and G. Popoff, *J. Fr. Hydrologie*, 1979, **10**, 83.
27. E. Rolia and F. Barbeau, *Talanta*, 1980, **27**, 596.
28. E. Abel, *Monatsh. Chem.*, 1951, **82**, 815.
29. L. Schroeter, *J. Pharm. Sci.*, 1961, **50**, 891.
30. E. Hayon, A. Treinin and J. Wilf, *J. Am. Chem. Soc.*, 1972, **94**, 47.
31. O. J. Zeck, Jr. and D. W. Carlyle, *Inorg. Chem.*, 1974, **13**, 34.
32. J. Freiberg, *Atmos. Environ.*, 1975, **9**, 661.
33. R. C. Brasted, *Comprehensive Inorganic Chemistry*, Vol. 8, Van Nostrand, New York 1953.
34. R. E. Davis, *J. Am. Chem. Soc.*, 1958, **80**, 3565.
35. B. Meyer, L. Peter and K. Spitzer, *Inorg. Chem.*, 1977, **16**, 27.
36. M. Schmidt, *Z. Anorg. Allg. Chem.*, 1957, **289**, 158.
37. A. Fava and S. Bresadola, *J. Am. Chem. Soc.*, 1955, **77**, 5792.
38. O. Foss, *Acta Chem. Scand.*, 1958, **12**, 959.
39. E. Blasius and W. Burmeister, *Z. Anal. Chem.*, 1959, **168**, 1.
40. O. Foss, *Acta Chem. Scand.*, 1961, **15**, 1610.
41. O. Foss and I. Kringlebotn, *ibid.*, 1961, **15**, 1608.
42. W. M. Dowson and W. F. Jones, *Mikrochim. Acta*, 1974, 339.
43. J. D. Roberts and M. C. Caserio, *Basic Principles of Organic Chemistry*, Benjamin, New York, 1964.
44. R. T. Morrison and R. N. Boyd, *Organic Chemistry*, 3rd Ed., Allyn & Bacon, Boston, 1973.
45. P. K. Dasgupta, K. DeCesare, J. C. Ullrey, *Anal. Chem.*, 1980, **52**, 1912.
46. P. J. Urban, *Z. Anal. Chem.*, 1961, **179**, 415.
47. *Idem*, *ibid.*, 1961, **179**, 422.
48. *Idem*, *ibid.*, 1961, **180**, 110.
49. J. A. Glaser, D. L. Foerst, G. D. McKee, S. A. Quave, and W. L. Budde, *Environ. Sci. Technol.*, 1981, **15**, 1426.
50. L. L. Stookey, *Anal. Chem.*, 1970, **42**, 779.

MOLECULAR ABSORPTION SPECTROMETRY BY ELECTROTHERMAL EVAPORATION IN THE GRAPHITE FURNACE—X

DETERMINATION OF CHLORIDE TRACES BY AlCl_3 IN GRAPHITE CUVETTES AFTER LIQUID-LIQUID EXTRACTION OF CHLORIDE WITH TRIPHENYL TIN HYDROXIDE

K. DITTRICH

Department of Chemistry, Karl-Marx-Universität Leipzig, 7010 Leipzig, G.D.R.

B. YA. SPIVAKOV, V. M. SHKINEV and G. A. VOROB'eva

Institute of Geochemistry and Analytical Chemistry, Academy of Sciences of U.S.S.R., Moscow V-334,
U.S.S.R.

(Received 8 August 1983. Revised 9 October 1983. Accepted 11 December 1983)

Summary—The determination of traces of chloride by means of the molecular absorption of AlCl_3 in graphite cuvettes is described. An extraction method for separation and preconcentration of the chloride has been developed, to avoid matrix effects. Extraction was done with 0.03M triphenyltin hydroxide in *o*-xylene, and stripping with 0.025M barium hydroxide. The method is sensitive and specific for chloride. The detection limit is about 1.5 ng of chloride, and the chloride content of 20 ml of $10^{-7}M$ solution can be determined. The determination is possible in presence of excess of bromide and iodide.

As indicated in our previous paper on bromide determination,¹ the determination of traces of chloride is an important and difficult practical problem. Sensitive determination is possible by use of ion-selective electrodes, but the accuracy, especially in presence of bromide, is not good. As we have shown,² sensitive and selective determination of chloride ions is possible by means of the molecular absorption spectrometry (MAS) of diatomic chloride-containing molecules (e.g. AlCl_3 , GaCl_3 , InCl_3), generated by evaporation in a graphite furnace. Fuwa and co-workers have also worked in this field.^{3,4} In recent years this method has been extended to the alkaline-earth metal chlorides.^{5,6}

An important disadvantage of MAS with electrothermal vaporization is the significant interference from the matrix, which affects both the MA signals and the background.

It was shown in our previous paper¹ that liquid-liquid extraction, e.g., with triphenyltin hydroxide (TPTH) followed by back-extraction into an aqueous solution of sodium or barium hydroxide, makes it possible to improve the sensitivity and accuracy of determination by MAS. This is achieved by means of the preconcentration by extraction and back-extraction and the simultaneous separation of metal cations and some anions which interfere with the subsequent absorption measurements.

Bock *et al.*,^{7,8} and Schweitzer and McCarthy⁹ have shown that TPTH solutions in methyl isobutyl ketone (MIBK) or benzene can extract chloride ions at pH 1.6-4.4. In the present work we have studied the

extraction of chloride by TPTH from more acidic solutions, for the purpose of preconcentration of chloride and its separation from large amounts of metal cations and also from some anions which can be extracted by organotin compounds.⁷⁻¹⁰ *o*-Xylene, which gives higher distribution coefficients than MIBK and benzene for halide ions, was used as diluent. The data obtained were used to develop a method of determining chloride in aqueous solution by MAS.

EXPERIMENTAL

Apparatus

The molecular absorption was measured with a Jarrell Ash double-channel double-beam AA spectrometer, type 811, fitted with a Beckman graphite furnace, type 1268. The light-source was a hydrogen hollow-cathode lamp run at 35 mA. The molecular absorption of AlCl_3 was measured at 261.4 nm. For background correction the two-line method was used, the non-specific wavelength being 260 nm.

The distribution of chloride between the organic and aqueous phase was estimated radiometrically with ^{36}Cl . The radiochemical purity of the ^{36}Cl was tested by means of a Ge(Li) detector and Nokia 800-channel analyser P4840) as well as from half-life measurements. The radioactivity of the organic and aqueous phases was measured with Tesla Liberec NRG 603 automatic gamma spectrometer.

Reagents

TPTH solutions were prepared by equilibration of 0.03M triphenyltin chloride (or bromide) solution in *o*-xylene with several portions of 0.1M aqueous sodium hydroxide (phase-volume ratio 1:1) until no further chloride was found in the aqueous phase. The organic phase was washed free from the hydroxide with water and then filtered. The concentration of TPTH in the diluent was 0.03M and the concentration of

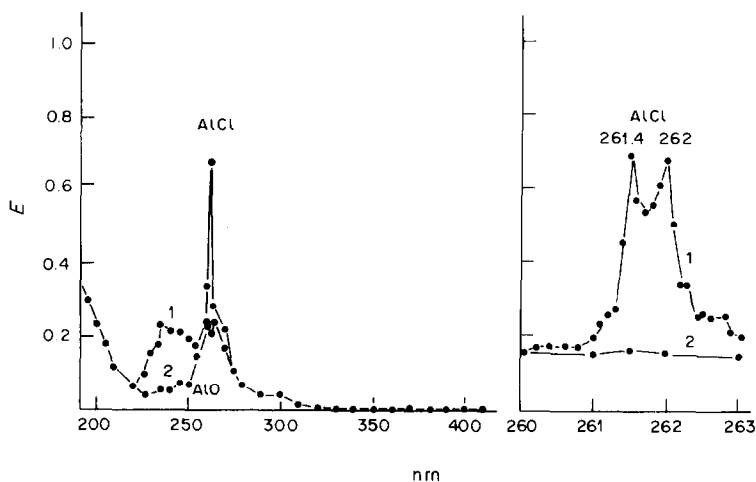


Fig. 1. Molecular absorption spectra of the AlCl molecule (measurement point by point): curve 1, 1 μg Al^{3+} ; 27 μg Ba^{2+} 0.2 μg $\text{Cu}^{-}/10 \mu\text{l}$; curve 2, 1 μg Al^{2+} ; 27 μg $\text{Ba}^{2+}/10 \mu\text{l}$.

chloride in the initial aqueous solution, unless otherwise noted, was 10^{-6} – 10^{-4} M, for the extraction studies. The following aqueous stock solutions were used: Al^{3+} 10 mg/ml [$\text{Al}(\text{NO}_3)_3$]; NaOH 0.1M; $\text{Ba}(\text{OH})_2$ 0.05M; Cl^{-} 1 mg/ml (NaCl); X 10 mg/ml (X = Br^{-} , I^{-} , SO_4^{2-} , as Na^{+} salts); M 10 mg/ml (M = K^{+} , Mg^{2+} , Ga^{3+} , Co^{2+} , Ca^{2+} , Ni^{2+} , Zn^{2+} , as nitrates).

Procedures

Absorption spectra. The molecular absorption of AlCl was measured between 200 and 400 nm, point by point. Figure 1 shows part of the spectrum.

Analytical investigations without extraction. Microvolumes (10 μl) of solutions containing Cl^{-} , Al^{3+} and Ba^{2+} ions were placed in the graphite furnace. After drying and ashing, the substances were evaporated in the so-called evaporation phase, (equivalent to the atomization phase in AAS), and the AlCl MA signal was measured.

Analytical determinations with extraction. Stopped glass test-tubes or separatory funnels were used for distribution of chloride between the two phases. The extraction was done with different V_o/V_{aq} ratios. When $V_o = V_{\text{aq}}$, the volume of each phase was 3 ml. The extraction studies were done at room temperature, and the phases were shaken for 3 min (it was established beforehand that equilibrium was attained in less than 3 min in all the systems studied). An aliquot of each phase was taken for the radioactivity measurement, from which the recovery factors ($R\%$) were estimated.

For the back-extraction 0.05M barium hydroxide was used. After separation of the stripping solution, an appropriate microvolume of aluminium solution was added and an aliquot was placed directly in the graphite furnace.

RESULTS AND DISCUSSION

Investigation of the extraction

The data in Table 1 for the extraction of chloride from 0.01M nitric acid with $V_o/V_{\text{aq}} = 1$, as a function

of chloride concentration in the initial aqueous solution ($C_{\text{Cl}^{-}}$) show that high recovery values are achieved if $C_{\text{Cl}^{-}} < 10^{-2}$ M. Increasing the nitric acid concentration in the aqueous phase up to 5M does not affect the extraction with $V_o/V_{\text{aq}} = 1$. Even with $V_o/V_{\text{aq}} = 0.1$, the recovery of chloride is practically quantitative (Table 2). Large amounts of metal cations such as Ni^{2+} or K^{+} (Table 2) and other non-ferrous, alkali-metal and alkaline-earth metal ions do not suppress the extraction of chloride. The metal cations themselves are practically not extracted by TPTH. Other halide ions and some oxo-anions extracted by organotin reagents⁷⁻⁹ can affect the recovery of chloride, by competition for the reagent. The extraction of chloride from 0.1 and 1M nitric acid in the presence of ammonium or sodium bromide, iodide, sulphate and phosphate at $V_o/V_{\text{aq}} = 0.2$ was examined. Bromide and chloride do not influence the recovery of chloride if their concentrations in the aqueous solution are below 3×10^{-3} M. Phosphate does not suppress the extraction from 1M nitric acid, but for extraction from 0.1M nitric acid 10^{-2} M phosphate lowers the recovery for chloride to 90%. Sulphate does not interfere with the extraction from 0.1 or 1M nitric acid even at concentrations as high as 0.1M.

The back-extraction of chloride by sodium and barium hydroxide solutions was studied (Table 3). Both hydroxides strip the chloride quantitatively from the TPTH extracts, which allows the MAS analysis to be done with the most convenient media.^{1,2} It should be noted that additional preconcentration of chloride is possible during the back-extraction.

Table 1. Results of extraction of chloride ions by TPTH solution

$C_{\text{Cl}^{-}}$, M	7×10^{-5}	1.7×10^{-4}	1×10^{-3}	1×10^{-2}	2×10^{-1}
Recovery, %	99.6	99.0	98.7	97.0	2.9

Table 2. The recovery factors in the extraction of chloride by 0.03M TPTH in *o*-xylene

Aqueous phase	$V_o:V_{aq}$	Recovery %
0.01M HNO ₃	1:1	99.6
	1:5	98.5
	1:10	97.8
1M HNO ₃	1:1	99.8
	1:10	97.3
5M HNO ₃	1:1	99.6
0.01M HNO ₃ , 0.3M KNO ₃	1:5	98.2
	1:10	97.6
0.01M HNO ₃ , 0.3M Ni(NO ₃) ₂	1:5	98.0
	1:10	96.6

Table 3. The recovery factors in the back-extraction of chloride from 0.03M TPTH in *o*-xylene extracts

Back-extracting agent	Concentration, M	Recovery, %		
		1:1*	2:1*	5:1*
NaOH	1×10^{-2}	99.8	99.5	—
	1×10^{-1}	99.8	99.9	99.7
Ba(OH) ₂	1×10^{-2}	99.9	99.9	—
	1×10^{-1}	99.9	99.9	99.9

* $V_o:V_{aq}$ *Molecular absorption of AlCl (without extraction)*

MA spectra. As we have already shown^{2,11} and in Fig. 1, for the AlCl molecule we found a narrow absorption band between 261.4 and 262.0 nm with a maximum at 261.4 nm. This is in agreement with the literature,¹² which gives the maximum for the A-band system ($X^1\Sigma^+ \rightarrow A^1\pi$) as being at 261.4 nm [$V'/V'' = 0/0$ (Q)]. Because we found a narrow band, it was possible to correct the background by difference measurements with the two-line method (261.4/260.0 nm).

In principle it is also possible to use the molecular absorption of CaCl,² InCl² and MgCl⁷ for the determination of chloride, but because the AlCl system gives the highest sensitivity, we investigated this system together with extraction.

Optimization of thermal conditions. The temperature of the drying, ashing and evaporation steps has a great influence on the AlCl MA-signal.^{2,11} It is important to avoid losses of chloride ions in the first two steps and to obtain simultaneous evaporation of aluminium and Cl⁻ in the third step. The best evaporation temperature is the maximum temperature of the furnace. In the second phase we can use temperatures up to 1000° without losses of chloride.

Optimization of chemical conditions for determination. The addition of 0.05M barium hydroxide up to a concentration of 0.025M influenced the height of the AlCl MA-signals by decreasing the volatilization of free chloride species (see also references 2 and 11). In the drying phase Ba-Cl species are formed, as solid residues. These substances are thermally stable and losses of chloride as HCl by thermal hydrolysis in the ashing phase are avoided. At high ashing temperatures the solid residues react with the graphite of the tube, forming carbides containing Ba and Cl. Therefore the evaporation rate of the chloride decreases and there is simultaneous evaporation of Ba, Cl and Al. In accordance with the dissociation energies^{2,11,12} AlCl molecules are formed in the plasma.

Analytical results of chloride determination by AlCl MA

Pure solutions with and without extraction. First we established the dependence of the AlCl MA-signal on the chloride concentration, under the optimal conditions 1 µg of Al³⁺ and 30 µg of Ba²⁺ per 10 µl. The results are shown in Table 4. The blank absorbance of 0.03 cannot be compensated for. The reciprocal sensitivity is 1.5 ng of Cl⁻ for 0.01 absorbance, which means that it is possible to determine 1.5 ng of chloride in 10 µl of aqueous analyte solution (i.e. 4×10^{-6} M solution). The reciprocal sensitivity is comparable with the 3s detection limit for measurements in graphite furnaces. It is possible to improve the detection limit by using a larger sample

Table 4. Results of the chloride determination by AlCl MA with and without preliminary extraction of chloride

Sample volume and injection volume	Absolute reciprocal sensitivity, ng for $A = 0.01$	Relative reciprocal sensitivity		Linear working range, ng
		ppm	M	
Without extraction				
10 µl	1.5	0.15	4×10^{-6}	1.5-50
40 µl	1.5	0.038	10^{-6}	1.5-50
With extraction				
10 ml*				
10 µl	1.5	0.03	8×10^{-7}	1.5-50
40 µl	1.5	0.00075	2×10^{-7}	1.5-50
20 ml†				
10 µl	1.5	0.015	4×10^{-7}	1.5-50
40 µl	1.5	0.0038	10^{-7}	1.5-50

*Preconcentration 5-fold.

†Preconcentration 10-fold.

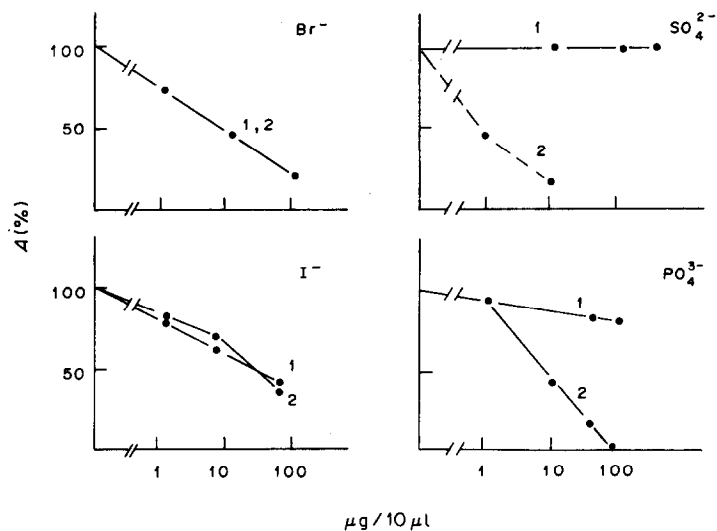


Fig. 2. Dependence of the AlCl MA on the presence of other anions: 1, with preliminary extraction of the Cl^- ion from $0.1M$ HNO_3 by $0.03M$ TPTH in *o*-xylene; 2, without extraction.

volume. Extraction was combined with the AlCl determination in the following way. A 10- or 20-ml sample ($0.1M$ nitric acid medium) was extracted with 4 ml of $0.03M$ TPTH solution in *o*-xylene. Exactly 3 or 3.5 ml of the organic solution were separated and mixed with exactly 1.5 or 1.75 ml ($V_o/V_{\text{aq}} = 2$) of $0.025M$ aqueous barium hydroxide solution and shaken to strip the chloride. After separation of the phases $10 \mu\text{l}$ of aluminium stock solution were added to 1 ml of the aqueous phase and the AlCl MA-signal was measured. The results are also shown in Table 4. By comparison of the results obtained with and without extraction, we see that it is possible to improve the reciprocal sensitivity by about an order of magnitude. This sensitivity is also very good in comparison to that of ion-selective electrodes.

Effects of other anions, with and without extraction.
The influence of other anions is shown in Fig. 2. Halides strongly depress the signal both with and without extraction. Nevertheless, it is possible to determine traces of chloride in presence of more than 1000-fold w/w ratio of iodide and bromide ions. The direct determination of chloride in presence of sulphate is impossible because the sulphate forms insoluble barium sulphate with the barium in the stripping solution. If $0.01M$ nitric acid medium is used, sulphate is not extracted by organic TPTH solutions, and the interference of sulphate in the chloride determination is then avoided. Chloride can be determined in the presence of more than 10000 times as much as sulphate. The direct determination of chloride is possible in presence of up to 50-fold

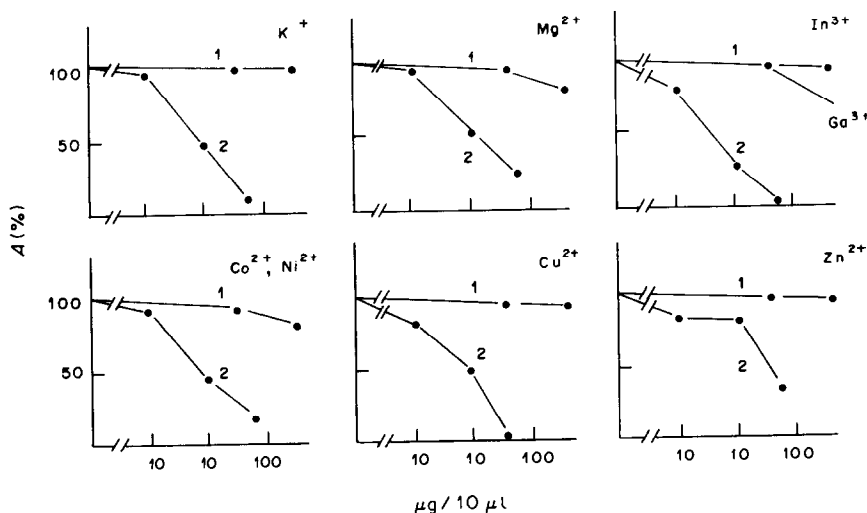


Fig. 3. Dependence of the AlCl MA on the presence of some cations: 1, with preliminary extraction of the Cl^- ion from HNO_3 by $0.03M$ TPTH in *o*-xylene; 2, without extraction.

Table 5. Results of the chloride determination by AlCl MA with extraction in presence of other salts

Salt	Detection limit, ppm	Salt	Detection limit, ppm
KNO ₃	0.1	Ni(NO ₃) ₂	0.08
Mg(NO ₃) ₂	0.08	Co(NO ₃) ₂	0.08
In(NO ₃) ₃	0.1	Cu(NO ₃) ₂	0.08
Ga(NO ₃) ₃	0.15	Zn(NO ₃) ₂	0.08

w/w ratio of phosphate, which can be improved to 10000-fold ratio by extraction from 1.0M nitric acid medium (from which phosphate is not extracted, because of protonation to H₃PO₄).

Effects of other cations, with and without extraction. As shown previously and in Fig. 3, although many cations have an adverse effect on the direct determination of chloride by the AlCl MA method, use of the extraction step improves the tolerance units for these cations by factors of 1000 and more.

By using the optimum preconcentration and conditions and maximum sample concentrations of about 0.1–0.3M, it is possible to determine traces of chloride in certain metal nitrates at below the ppm level. Some results are shown in Table 5. We can conclude from these results that the combination of TPTH

extraction and selective determination by AlCl MA is a useful new trace technique for the determination of chloride.

REFERENCES

1. K. Dittrich, B. Ya. Spivakov, V. M. Shkinev and G. A. Vorob'eva, *Talanta*, 1984, **1**, 39.
2. K. Dittrich and P. Meister, *Anal. Chim. Acta*, 1980, **121**, 205.
3. E. Yoshimura, Y. Tanaka, K. Tsunoda, S. Toda, K. Fuwa, *Bunseki Kagaku*, 1977, **26**, 646.
4. K. Tsunoda, K. Fujiwara and K. Fuwa, *Anal. Chem.*, 1978, **50**, 861.
5. K. Dittrich and B. Vorberg, *Anal. Chim. Acta*, 1982, **140**, 237.
6. K. Tsunoda, K. Chiba, H. Haraguchi, C. L. Chakrabarti and K. Fuwa, *Can. J. Spectrosc.*, 1982, **27**, 94.
7. R. Bock, H. T. Niederauer and K. Behrends, *Z. Anal. Chem.*, 1962, **190**, 33.
8. R. Bock and H. Deister, *ibid.*, 1967, **230**, 321.
9. C. K. Schweitzer and S. W. McCarthy, *J. Inorg. Nucl. Chem.*, 1965, **27**, 191.
10. B. Ya. Spivakov, V. M. Shkinev and Yu. A. Zolotov, *International Solvent Extraction Conference Liège, 1980, Summaries of Papers*, Vol. 2, p. 180.
11. K. Dittrich, *Anal. Chim. Acta*, 1979, **111**, 123.
12. B. Rosen (ed.) *International Tables of Selected Constants*, Vol. 17, *Spectroscopic Data Relative to Diatomic Molecules*, Pergamon Press, Oxford, 1970.

A COMPARATIVE STUDY OF FLAME ATOMIC-ABSORPTION METHODS FOR DETERMINATION OF ZINC IN SERUM AND BLOOD PLASMA

M. J. SORIANO and M. DE LA GUARDIA*

Departamento de Química Analítica, Facultad de Ciencias Químicas, Universidad de Valencia, Valencia, España

(Received 26 April 1983. Revised 1 December 1983. Accepted 7 December 1983)

Summary—Seven selected methods for determination of zinc in blood plasma by flame atomic-absorption spectroscopy have been compared. Analytical characteristics such as sensitivity, detection limit, precision, analytical recovery, accuracy and physical interferences were studied. Two of the seven methods are recommended as the most suitable for the purpose.

Zinc is an essential nutrient and is contained at relatively stable levels in the biological fluids and tissues of healthy subjects. However, several diseases (diabetes, myocardial infarction, liver disorders, atherosclerosis, etc.) cause disturbances in zinc metabolism, resulting in an increase or a decrease in the zinc concentration in serum and blood plasma.¹⁻⁷ The determination of zinc in these biological fluids is therefore not only interesting, but necessary for proper diagnosis of such diseases.

Zinc has been determined in serum and blood plasma by a variety of techniques, including neutron activation, fluorimetry, colorimetry, atomic-fluorescence, atomic-absorption and plasma atomic-emission spectroscopy. Of these, flame atomic-absorption spectroscopy (FAAS) is the most widely used for routine analysis because it is precise, simple, sensitive and is relatively free from interferences. Table 1 summarizes the methods described in the literature for the determination of zinc in serum and blood plasma by FAAS.

The methods have been classed into four different groups according to the treatment of the samples and the standards.

(1) Methods involving deproteination.

(2) Methods based on sample dilution with demineralized water, and addition of some reagents to aqueous standards to obtain similar physical characteristics for the diluted samples and the standards.

(3) Methods based on sample dilution with demineralized water and use of aqueous standards (without additional reagents).

(4) Methods involving liquid-liquid extraction of a zinc complex and analysis by FAAS.

Procedures in the first three groups are simpler than those in the fourth because they avoid the solvent-extraction step. So, from the methods pro-

posed in the literature we have selected seven: two involving sample deproteination¹³⁻²⁹ and five involving sample dilution with demineralized water.^{9,10,21,28,30,31} In two of these five methods, standards containing glycerol were prepared,^{28,30,31} and in the other three,^{9,10,21} aqueous solutions without any additional reagent were used as standards. We have evaluated the seven selected methods in terms of accuracy, precision, detection limit, sensitivity and analytical recovery.

We have also studied the effects of physical interferences by taking into account changes in aspiration rate of samples and standards. Matrix interferences were studied by comparing the results from calibration curves with those obtained by the standard-addition method.

We have followed the published procedures in all cases except for that given by Fuwa *et al.*,⁹ where we employed an air/acetylene flame and a conventional burner instead of the flame and instrumentation used by the authors.

Some of the methods selected were proposed only for determination of zinc in blood serum. However, in other publications the methods are said to be applicable to the determination of zinc in blood plasma. Since there is not too much difference between serum and blood plasma from the analytical point of view, we have applied all seven methods to analysis of both materials.

EXPERIMENTAL

Instrumentation

A Perkin-Elmer model 460 double-beam atomic-absorption spectrophotometer was used with a zinc hollow-cathode lamp and a conventional air/acetylene burner.

Reagents

A 1000-ppm zinc standard solution ("DILUT IT", J. T. Baker Chemical Co.) was used as a zinc stock solution. Trichloroacetic acid, glycerol and potassium and sodium

*Author for correspondence.

Table 1. Methods for the determination of zinc in serum and blood plasma by FAAS

Elements determined	Procedure	Reference	Elements determined	Procedure	Reference
Zn	Deproteination with conc. HCl	8	Zn	Dilution 1:19 with demineralized water	20
Zn	Dilution 1:9 with demineralized water	9	Zn	Dilution 1:4 with demineralized water	21
Fe, Cu, Zn	Dilution 1:1 with demineralized water	10	Cu, Zn	Standards and samples diluted 1:4 with 10% v/v propan-1-ol	22
Zn	Lyophilization, addition of 2M HCl, heating at 60° for 5 min, and deproteination with 10% TCA	11	Zn	Dilution 1:1 with 2% v/v "Acationox"; standards diluted with 2% v/v "Acationox"	23
Cu, Zn	Dilution 1:1 with demineralized water; standards contain 3% bovine albumin	12	Fe, Zn	Extraction into amyl alcohol	24
Cu, Zn	Deproteination with 10% TCA; dilution 1:1; heating at 90° for 15 min	13	Zn	Dilution 1:9 with demineralized water; standards prepared in water, physiological saline, synthetic serum or dilute HNO ₃	25
Zn	Deproteination with TCA	14	Cu, Fe, Zn	Deproteination with TCA or dilution 1:7 with demineralized water	26
Zn	Dilution 1:4 with demineralized water	15	Zn	Dilution 1:4 with demineralized water	27
Cu, Zn	Dilution 1:9 with 1% HCl	16	Zn	Dilution 1:4 with demineralized water; standards prepared in 5% glycerol	28
Zn	Dilution 1:1 with demineralized water; standards contain 3% dextran	17	Zn	Deproteination with 5% TCA; dilution 1:3	29
Zn	Dilution 1:19 with 0.1M HCl; standards diluted with 0.1M HCl and a "salt solution"	18	Cd, Cr, Zn	Dilution 1:1 with demineralized water; standards contain 20% glycerol and 0.5% NaCl	30
Cu, Zn	Dilution 1:9 with 6% n-butanol; standards diluted with 6% n-butanol and 0.88% NaCl	19	Zn	Dilution 1:4 with demineralized water; standards prepared in 5% glycerol	31

chloride were also used to prepare working standards. A certified serum (CATION-CAL TM-DADE) was used to check the accuracy of the seven selected methods.

General procedure

To avoid any contamination of samples and standards, both glassware and plastic ware were soaked in 50% nitric acid for at least 24 hr, and were then rinsed several times with demineralized water.

Blood plasma samples were kept in tightly stoppered polypropylene vials, frozen at -33°.

Before the zinc determination was started, instrumental settings such as wavelength, slit-width, and lamp current were optimized. Gas-flow settings for air and acetylene, and the burner height, were set to give the greatest sensitivity for each of the seven methods.

The sensitivity was established from the slope of the analytical curve³² and by means of the zinc concentration required to give 1% absorption (*i.e.*, the characteristic concentration).

The detection limit (X_L) was established from the slope of the analytical curve and the standard deviation of the absorbance readings for a blank solution and calculated from the equation:

$$X_L = \bar{X}_{bl} + K S_{bl}$$

where \bar{X}_{bl} is the mean and S_{bl} the standard deviation of the blank readings, and K the numerical factor corresponding to the selected confidence level (we used $K = 3$). The detection limit values were also calculated, taking into account the sample dilution.

To establish the precision of the methods, we did twelve independent analyses of a blood plasma sample on the same day, and calculated the standard deviation and relative standard deviation.

The accuracy of the methods was checked in all cases by doing five independent analyses of the certified serum sample by each method, then comparing the mean of the results with the certified value. The accuracy was expressed in terms of the deviation between the values.

To detect any physical interferences due to differences in the physical properties of the samples and standards, the aspiration flow-rates were measured and compared.

Matrix effects on the accuracy of the methods were examined by means of the results for determination of zinc in a blood plasma sample. The recovery was calculated from the difference in the amount of zinc found in the original sample and in samples spiked with a known amount of zinc. Matrix effects were further studied by comparison of the results obtained by the calibration graph and standard-addition methods.

RESULTS AND DISCUSSION

All concentrations are given in ppm and all absorbance readings in absorbance units.

The use of the same instrumental conditions for all the methods could cause disadvantages in some cases, so we first determined the best instrumental settings for each method (Table 2).

We found little difference between the optimal atomization conditions for purely aqueous standards and standards containing low concentrations of trichloroacetic acid (TCA) or glycerol. Generally, the utilization of standards containing these reagents presupposes the use of a flame richer in acetylene than one employed for the analysis of purely aqueous solutions.

Sensitivity

All in one day, working with the optimized instrumental settings for each, we measured the absorbances of the standards, took the mean of the readings for each, and established the analytical curve by a regression least-squares fit.

The sensitivities, estimated from the slopes of the analytical curves, were 0.35 for the methods involving purely aqueous zinc standards, 0.40 for methods involving standards containing 5 and 10% of TCA or 5% of glycerol. For the method using standards containing 20% of glycerol, the value was 0.30 (14% less). The corresponding characteristic concen-

Table 2. Instrumental settings (lamp current 15 mA, bandwidth 0.7 nm, wavelength 213.8 nm, damping 2 sec)

Reference	Gas flow-rates, l./min		Observation height above burner, cm
	Air	Acetylene	
29	17.5	4.7	2.00
13	21.6	4.7	2.25
28, 31	17.5	4.7	2.00
30	19.5	5.4	2.00
9	19.5	4.7	2.00
21	19.5	4.7	2.00
10	19.5	4.7	2.00

Table 3. Performance characteristics of the seven selected methods

Reference	Sensitivity, ppm ⁻¹	Detection limit, ppm			Precision (n = 12)		Accuracy (n = 5), ppm	Recovery %	$\frac{\theta_{\text{sample}}}{\theta_{\text{std}}}$
		Diluted sample	Original sample	C.C.,* ppm	S.D., ppm	RSD, %			
29	0.40	0.016	0.064	0.011	0.03	4.3	105	1.00	
13	0.40	0.015	0.030	0.011	0.06	7.1	108	1.0 ₄	
28, 31	0.40	0.016	0.080	0.012	0.05	5.6	107	1.0 ₁	
30	0.30	0.019	0.038	0.014	0.05	5.6	116	1.2 ₅	
9	0.35	0.009	0.090	0.013	0.06	6.7	103	1.0 ₃	
21	0.35	0.009	0.045	0.013	0.07	7.8	101	1.0 ₅	
10	0.35	0.009	0.018	0.013	0.03	3.3	85	0.90	

*C.C. = characteristic concentration.

†θ = aspiration rate.

trations were 0.013 ppm for aqueous solutions, 0.011 ppm for the TCA standards, 0.012 ppm for the 5% glycerol standards and 0.014 ppm for the 20% glycerol standards.

Detection limits

While there is no great difference in the sensitivities of the selected methods, there is a significant difference in the limits of detection, which range from 0.018 ppm of zinc in serum or plasma by the Sprague and Slavin method¹⁰ involving simply a 1:1 dilution of the sample, to 0.090 ppm by the method of Fuwa *et al.*,⁹ which uses 1:9 dilution and aqueous standards (Table 3).

Precision

The precision was expressed as the standard deviation and relative standard deviation, which were calculated from the results obtained by carrying out several independent analyses. These values usually vary, depending on both the number of indepen-

dently performed analyses and the nature of the sample.

We analysed twelve independent aliquots of normal human plasma (zinc content 700–1000 ng/ml), to compare the selected methods with respect to precision, and the results obtained (shown in Table 3) were all similar. These results indicated that the differences in sample treatment required for each method did not affect the precision. However, day-to-day instrumental and gas-flow fluctuations do influence the precision.

Accuracy

The accuracy of the selected methods was established by comparing the results obtained for zinc in a certified serum sample, by application of each method, with the certified value.

The results obtained for the method proposed by Arpadyan and Kachov³⁰ show a mean error of +10.3%, in agreement with the high recovery found (116%) and the higher aspiration rate measured for

Table 4. Comparison of the seven methods, using simple

Reference	Direct method		Standard-addition method		Zinc concentration (<i>n</i> = 5), ppm	
	Analytical curve	$S_{y/k}$	Analytical curves	$S_{y/k}$	Direct method	Std. addn. method
29	$X = 0.202C + 0.009$	4.57×10^{-3}	$X = 0.223_5C + 0.045$ $X = 0.216_5C + 0.045$ $X = 0.216_5C + 0.046$ $X = 0.211_5C + 0.047$ $X = 0.218C + 0.047$	2.27×10^{-3} 3.02×10^{-3} 3.63×10^{-3} 5.30×10^{-3} 4.65×10^{-3}	0.67	0.7
13	$X = 0.246_5C + 0.007$	3.88×10^{-3}	$X = 0.233C + 0.123$ $X = 0.257C + 0.123$ $X = 0.237C + 0.132$ $X = 0.240_5C + 0.132$ $X = 0.236_5C + 0.131$	1.09×10^{-2} 1.50×10^{-2} 8.87×10^{-3} 1.27×10^{-2} 9.33×10^{-3}	1.04	1.0
28, 31	$X = 0.227C + 0.003$	8.76×10^{-4}	$X = 0.222_5C + 0.031$ $X = 0.224_5C + 0.032$ $X = 0.223C + 0.033$ $X = 0.223_5C + 0.034$ $X = 0.225C + 0.035_5$	2.60×10^{-3} 2.31×10^{-3} 2.02×10^{-3} 1.46×10^{-3} 7.07×10^{-3}	0.7	0.7
30	$X = 0.157C + 0.007$	4.13×10^{-3}	$X = 0.187_5C + 0.077_5$ $X = 0.187C + 0.080$ $X = 0.191C + 0.079$ $X = 0.186C + 0.081$ $X = 0.198_5C + 0.075$	8.66×10^{-4} 2.85×10^{-3} 1.55×10^{-3} 2.63×10^{-3} 5.21×10^{-3}	0.93	0.8
9	$X = 0.217_5C + 0.002$	2.02×10^{-3}	$X = 0.204C + 0.021$ $X = 0.204C + 0.017$ $X = 0.202_5C + 0.018_5$ $X = 0.206C + 0.017$ $X = 0.201C + 0.020$	3.70×10^{-3} 2.63×10^{-3} 8.70×10^{-4} 2.32×10^{-3} 9.50×10^{-4}	0.7	0.8
21	$X = 0.191C + 0.002$	1.40×10^{-3}	$X = 0.182_5C + 0.032$ $X = 0.185_5C + 0.030$ $X = 0.173_5C + 0.033$ $X = 0.180_5C + 0.033$ $X = 0.185C + 0.031$	2.60×10^{-3} 1.53×10^{-3} 1.07×10^{-3} 1.83×10^{-3} 1.73×10^{-3}	0.78	0.8
10	$X = 0.212_5C + 0.001$	2.63×10^{-3}	$X = 0.204C + 0.082$ $X = 0.200C + 0.082$ $X = 0.213C + 0.077$ $X = 0.187_5C + 0.086_5$ $X = 0.188_5C + 0.086$	4.94×10^{-3} 5.20×10^{-3} 5.50×10^{-3} 2.40×10^{-3} 3.50×10^{-3}	0.72	0.8

*Direct and standard-addition methods.

†Values refused for a 95% statistical confidence level.

the diluted samples compared with that for the standards.

For the method proposed by Sprague and Slavin,¹⁰ we found a low recovery (85%) and a mean error of -13.8%. In this case the aspiration rate of the standards is higher than that of the diluted samples.

Because of these errors, we think that these two methods cannot be recommended for the determination of zinc in serum or plasma. Moreover, we later confirmed the inadequacy of these two methods by comparing the calibration graphs obtained by application of the direct method and the standard-addition method: they were not parallel.

The method proposed by Pekarek *et al.*,²¹ showed -6.9% mean error but the recovery was good. We also found very similar aspiration rates for the diluted samples and standards.

For the other selected methods, the accuracy found was good.

Interferences

We did not find any influence from other ions on the atomization of zinc. However, albumin and other matrix components cause a viscosity increase. Hence the most important interference in zinc determination in serum and blood plasma is caused by physical properties of the solutions. There is a significant difference between the aspiration rates for samples and standards for methods involving a 1:1 sample dilution with demineralized water. When aqueous standards containing 20% of glycerol were used, sample aspiration rates were higher than those of standards, but when aqueous standards were used, sample aspiration rates were lower than those of standards. For both these methods, we observed that the results were in agreement with the recoveries found for plasma samples and for a certified serum sample.

calibration (direct) or standard-addition procedures

Precision ($n = 5$)		Comparison of the results obtained by both methods, Fisher's T	Comparison of the curves (standard addition method)		Comparison of two curves	
Direct method	Std. addn. method		Hartley's F (homogeneity) $S_{y/x}$	Snedecor's F (coincidence of the curves)	Snedecor's F (homogeneity) $S_{y/x}$	Student's t (equality of slopes)
SD = 0.02 RSD = 3%	SD = 0.05 RSD = 7%	0.476	5.45	0.209†	2.09	-1.472
SD = 0.02 RSD = 1.9%	SD = 0.06 RSD = 6%	0.476	2.05	0.349	0.157	0.489
SD = 0.07 RSD = 10%	SD = 0.07 RSD = 10%	0.000	23.45	0.589	0.136	0.449
SD = 0.02 RSD = 2.2%	SD = 0.04 RSD = 5%	2.063	36.19	0.664	2.207	-8.950†
SD = 0.05, RSD = 7.8%	SD = 0.1 RSD = 12.5%	0.719	18.08	0.741	0.839	0.819
SD = 0.02 RSD = 2.6%	SD = 0.05 RSD = 6.3%	0.317	5.90	1.283	0.527	1.790
SD = 0.01 RSD = 1.4%	SD = 0.09 RSD = 11.3	0.775	5.25	0.651	0.412	2.809†
		$T_{\text{tab.}} = 2.306$ $P = 0.95$ $n = 5; N = 8$	$F_{\text{tab.}} = 50.7$ $k = 5; n = 4;$ $v = n - 1 = 3$	$F_{\text{tab.}} = 0.232$ $F_{\text{tab.}} = 3.85$ $k = 5; n = 4; v = 2$	$F_{\text{tab.}} = 3.95$ $F_{\text{tab.}} = 0.070$ $v = 3; v = 18$	$T_{\text{tab.}} \pm 2.080$ $v = 21$

For other selected methods, we found very similar aspiration rates for samples and standards.

We also studied the influence of the sample matrix on the zinc atomization process, by comparing the direct and the standard-addition methods. The results obtained are shown in Table 4.

Using the optimal instrumental settings for each method, we analysed the same sample five times by the direct method (according to the recommended procedure) and five times by the standard-addition method, all on the same day.

The variance homogeneity for the five analytical curves obtained by the standard addition method was checked by the Hartley test.³³ We also checked the parallelism of these analytical curves by a global test.³³ From these five analytical curves another analytical curve was calculated, and this was compared with the analytical curve obtained by the direct method.

For five methods, we checked both types of analytical curve for variance homogeneity by Snedecor's test and for parallelism by Student's *t*-test.³³

For two methods, those of Arpadyan and Kachov³⁰ and a Sprague and Slavin¹⁰ we found that the analytical curves were not parallel, and hence think these methods are not adequate for determining zinc in serum and blood plasma.

Finally, we compared by Fisher's test³⁴ the results for five analyses performed by the direct method with those for five analyses by the standard-addition method, and found they were comparable.

All statistical tests were applied for the 95% probability level.

CONCLUSIONS

We have found that five of the seven flame atomic-absorption methods tested were adequate for zinc determination in serum and blood plasma.

All the methods are comparable with respect to sensitivity but the addition of 5% or 10% of glycerol to aqueous standards of zinc gives a sensitivity higher than that with aqueous standards, whereas addition of 20% of glycerol gives a lower sensitivity. The less the sample dilution, the better the detection limit.

The precision obtained is similar for all the methods and depends more on the characteristics of the analysed samples and daily variation in the experimental conditions, than on the manipulation required for each method. All the methods have good accuracy, except two, both of which involved 1:1 sample dilution, one using aqueous standards and the other using standards containing 20% of glycerol.

Methods involving simple sample dilution are quicker than those requiring a deproteination step.

The most exact and precise methods are those proposed by Smith *et al.*^{28,31} and Fuwa *et al.*⁹ The first

is more sensitive than the second, but requires the use of standards containing 5% of glycerol.

Acknowledgement—We wish to thank Dr Luis Aparisi for his help and encouragement throughout the work.

REFERENCES

1. B. Fernandez, J. De Quiros, C. Iniguez Lobeto and J. Carreres Quevedo, *Rev. Clin. Espan.*, 1978, **151**, 87.
2. J. Lekaris and A. Kalofoutis, *Clin. Chem.*, 1980, **26**, 1660.
3. A. S. Prasad, *Am. J. Clin. Nutr.*, 1970, **23**, 581.
4. J. A. Halsted, B. Hackley, C. Rudzki and J. C. Smith, *Gastroenterology*, 1971, **54**, 1098.
5. R. I. Henkin, in *Newer Aspects of Copper and Zinc Metabolism*, W. Mertz and W. E. Cornatzer (eds.), Dekker, New York, 1971.
6. A. M. Kahn, H. W. Helwig, A. G. Redeker and T. B. Raynods, *Am. J. Clin. Pathol.*, 1971, **44**, 426.
7. H. J. Holtmeier, M. Kuhn and K. Rummel, *Zink—ein lebenswichtiges Mineral*, Wissenschaftliche Verlag, Stuttgart, 1976.
8. N. Honegger, *Ärztz. Lab.*, 1963, **2**, 41.
9. K. Fuwa, P. Pulido, R. McKay and B. L. Vallee, *Anal. Chem.*, 1964, **36**, 2407.
10. S. Sprague and W. Slavin, *Atom. Absorp. Newsl.*, 1965, **4**, 228.
11. A. S. Prasad, D. Oberleas and J. A. Halsted, *J. Lab. Clin. Med.*, 1965, **66**, 508.
12. M. M. Parker, F. L. Humoller and D. J. Mahler, *Clin. Chem.*, 1967, **13**, 40.
13. A. D. Olson and W. B. Hamlin, *Atom. Absorp. Newsl.*, 1968, **7**, 69.
14. K. Oiwa, T. Kimura, H. Makino and M. Okuda, *Bunseki Kagaku*, 1968, **17**, 810.
15. H. Matsumoto, K. Tsunematsu and T. Shiraishi, *ibid.*, 1968, **17**, 703.
16. M. L. Girard, *Clin. Chim. Acta*, 1968, **20**, 243.
17. B. M. Hackley, J. C. Smith and J. A. Halsted, *Clin. Chem.*, 1968, **14**, 1.
18. J. B. Dawson and B. E. Walker, *Clin. Chim. Acta*, 1969, **26**, 465.
19. S. Meret and R. I. Henkin, *Clin. Chem.*, 1971, **17**, 369.
20. N. Arroyo and M. C. Coca, *Med. y Seg. Trabajo*, 1971, **75**, 15.
21. R. S. Pekarek, W. R. Beisel, P. J. Bartelloni and K. A. Bostian, *Am. J. Clin. Pathol.*, 1972, **57**, 506.
22. R. T. Peaston, *Med. Lab. Technol.*, 1973, **30**, 249.
23. M. Arroyo and E. Palenque, *Revista Clinica Esp.*, 1974, **133**, 211.
24. K. T. Lee and E. Jacob, *Mikrochim. Acta*, 1974 **I**, 65.
25. B. Moncilovic, B. Belonje and B. G. Shah, *Clin. Chem.*, 1975, **21**, 588.
26. T. I. Mzhel'skaya, *Lab. Delo*, 1976, **4**, 229.
27. M. D. Stevens, W. F. Mackenzie V. D., *Biochem. Med.*, 1977, **18**, 158.
28. G. P. Butrimovitz and W. C. Purdy, *Anal. Chim. Acta*, 1977, **94**, 63.
29. J. R. Kelson and R. J. Shamberger, *Clin. Chem.*, 1978, **24**, 240.
30. S. Arpadyan and I. Kachov, *Zentralbl. Pharm. Pharmakoter. Laboratoriums-diagn.*, 1978, **117**, 237.
31. J. C. Smith, G. P. Butrimovitz and W. C. Purdy, *Clin. Chem.*, 1979, **25**, 1487.
32. IUPAC, *Compendium of Analytical Nomenclature*, Pergamon Press, Oxford, 1978.
33. Commissariat de l'Energie Atomique, *Statistique appliquée à l'Exploitation de Mesures*, Masson, Paris, 1978.
34. Y. Lacroix, *Analyse Chimique: Interpretation des Resultats par le Calcul Statistique*, Masson, Paris, 1973.

SEPARATION AND CONCENTRATION OF MOLYBDENUM(VI) AND TUNGSTEN(VI) WITH CHELATING ION-EXCHANGE RESINS CONTAINING SULPHUR LIGANDS

CHUEN-YING LIU* and PENG-JOUNG SUN

Department of Chemistry, National Taiwan University, Taipei, Taiwan

(Received 29 April 1983. Revised 24 November 1983. Accepted 7 December 1983)

Summary—Three chelating ion-exchange resins based on macroreticular polyacrylonitrile-divinylbenzene copolymers with thioglycolic acid and cysteine as functional groups have been tested for separation of molybdenum(VI) and tungsten(VI). On a short column of the thioglycolic acid resin, molybdenum(VI) and tungsten(VI) can be selectively sorbed from pH-4.3 acetate buffer and eluted with 2*M* hydrochloric acid and a mixture of 0.1*M* sodium hydroxide and 0.1*M* sodium chloride, respectively, with quantitative recovery even at very low concentrations. Simulated sea-water samples have been analysed.

The synthesis and characterization of chelating ion-exchange resins containing thioglycolic acid and cysteine as functional groups, and their analytical applications to noble metals, have been described.^{1,2} As part of a systematic survey of the behaviour of metal ions with these resins, the chromatography of molybdenum(VI) and tungsten(VI) species has now been studied.

EXPERIMENTAL

Instrumentation

A Radiometer pH-meter was used with saturated calomel (Type K 401) and glass (Type G 202 B) electrodes, and calibrated with Beckman standard buffers of pH 4.00 and 7.00. A Hitachi model 624 digital spectrophotometer connected to a Hitachi model QD₁₅ recorder was used, with 10-mm quartz cells.

Reagents

Previously published procedures were used to synthesize the macroreticular polyacrylonitrile—divinylbenzene copolymers.^{1,2} The nitrile groups were hydrolysed to carboxylic acid groups. The carboxylic acid resin (200 g) was mixed with 600 g of molten 1,6-hexanediol (m.p. 41°) or 500 g of ethylene glycol, and 40 ml of concentrated sulphuric acid (as catalyst), and kept at 70° for 30 hr for the first esterification. Then a mixture of 150 g of this product with 460 g of thioglycolic acid and 40 ml of concentrated sulphuric acid was reacted at 70° for 30 hr for the second esterification. The 1,6-hexanediol or ethylene glycol served both as linking agent and reaction medium, the products being Resins I and II respectively.¹ The carboxylic acid resin was similarly treated with 1,6-hexanediol and L-cysteine in a two-step esterification to give Resin III.² The final product was collected by filtration under suction and washed sequentially with water, concentrated hydrochloric acid, water and acetone.

Spectrophotometric determination of molybdenum(VI) and tungsten(VI)

The procedures used were essentially those reported by Sandell.³ Maximum colour development and stability were obtained with ascorbic acid as reducing agent for the determination of molybdenum(VI). The sensitivity was increased by extraction of the molybdenum(V) and tungsten(V) thiocyanate complexes into *n*-butyl acetate.

Sorption by the batch method

Exactly 0.3 g of dry polymer was pre-equilibrated with 20 ml of 1*M* sodium perchlorate–0.5*M* sodium acetate mixture, the pH being periodically adjusted to the required value with perchloric acid or sodium hydroxide until it had remained constant for 6 hr. The solution was removed by filtration. The metal ion solution (10 ml, 0.062*M*) was then added to 10 ml of 2*M* sodium perchlorate and 10 ml of 1*M* sodium acetate, and the pH adjusted to the required value. The prepared metal ion solution, diluted to 50 ml, was added to the pre-equilibrated polymer and stirred for 18 hr. The pH was then checked for constancy, and the resin was filtered off and washed with the appropriate acetate buffer. The filtrate and washings were combined and analysed for molybdenum(VI) or tungsten(VI).

The distribution coefficient for molybdenum(VI), as a function of hydrochloric acid concentration, was also determined by a batch equilibrium method; 25 ml of a mixture containing various amounts of acid and 0.4 mmole of metal ion were stirred with 0.2 g of air-dried resin for 18 hr at 25°. The resin was filtered off and washed, and the molybdenum(VI) in the filtrate was determined.

Equilibration rates

From the capacity studies, the total capacity of each resin for molybdenum(VI) and tungsten(VI) at the optimal pH was known. Twice the quantity of molybdenum(VI) or tungsten(VI) corresponding to saturation of 0.3 g of resin at pH 4.3 was diluted in the appropriate buffer to give 0.03*M* metal ion concentration. Then 0.3 g of the air-dried resin was introduced into this solution and equilibrated. Samples of solution were removed at intervals and their metal ion content was determined.

*Author for correspondence.

Separation of molybdenum(VI) and tungsten(VI)

Resin I was packed into a glass tube (10×0.6 cm) and conditioned with 20 ml of 1M acetate buffer (pH 4.3). After conditioning, 9.3 μ moles each of molybdenum(VI) and tungsten(VI) were loaded on to the column, and molybdenum(VI) was eluted with 2M hydrochloric acid at 0.5 ml/min. Tungsten(VI) was retained on the column and then eluted with 0.1M sodium hydroxide-0.1M sodium chloride mixture at the same flow-rate.

Concentration of trace metals

Portions (500 ml) of water containing various amounts of molybdenum(VI) or tungsten(VI) were adjusted to pH 4.3 and passed at 0.5 ml/min through a preconditioned 7.0×0.6 cm resin column, and the molybdenum(VI) and tungsten(VI) eluted as above and determined. Recovery of 9.70 μ g of molybdenum(VI) and 0.01 μ g of tungsten(VI) from 1 litre of simulated sea-water⁴ was similarly determined.

RESULTS AND DISCUSSION

The pH-dependence of the sorption behaviour of Resins I-III towards molybdenum(VI) and tungsten(VI) was tested by the batch equilibrium method. Table 1 shows the distribution coefficients obtained. Resins I and II, which contained the same functional groups but different linking agents, behaved similarly. The length of the linking agent slightly influenced the capacity. The similarity of the distribution coefficients for molybdenum(VI) and tungsten(VI) at pH 2-7 prevents simple separation of the metals in this pH range. The distribution coefficients for molybdenum(VI) between hydrochloric acid and Resins I-III are shown in Table 2. Tungsten(VI) precipitated from the acid solution, so could not be studied. Molybdenum(VI) or tungsten(VI) at pH 4.3 was used to assess the kinetics of sorption, 50% of the

Table 2. Distribution coefficients of molybdenum(VI) on the three resins in hydrochloric acid

Resin	Concentration of HCl, M							
	0.1	0.5	1	2	4	5	6	7
I	75	25	16	1	27	43	38	30
II	56	19	12	2	31	49	36	29
III	64	82	72	62	42	42	41	40

available sites of Resin I being occupied by molybdenum(VI) and tungsten(VI) in 12 min and 21 min, respectively. From the results of the batch equilibrium study, the possibility of separating molybdenum(VI) and tungsten(VI) by using a Resin I column was obvious. The molybdenum(VI) and tungsten(VI) sorbed can be easily stripped quantitatively from the resin column in succession by 2M hydrochloric acid and 0.1M sodium hydroxide-0.1M sodium chloride mixture, respectively. Figure 1 shows such a separation.

The effect of foreign ions on the recovery of molybdenum(VI) and tungsten(VI) with Resin I was studied. The results are reported in Table 3. Since the sulphur content of Resin I was 1.56 mmole/g, the silver(I) capacity was 1.52 mmole/g, the mercury(II) capacity was 0.80 mmole/g, the molybdenum(VI) capacity was 0.75 mmole/g, and the tungsten(VI) capacity was 0.35 mmole/g, silver(I) and mercury(II) interfered severely, even if the mole ratio to molybdenum or tungsten was reduced to 1, whereas copper(II), zinc(II) and tin(IV) did not interfere at this concentration ratio. The resin exhibited no affinity for the alkali and alkaline-earth metals studied. Small quantities of the resin can therefore be used to concentrate trace metals from samples with a high electrolyte content, such as sea-water and biological

Table 1. Distribution coefficients for molybdenum(VI) and tungsten(VI) on the three resins

pH	Resin I		Resin II	Resin III	
	Mo	W	Mo	Mo	W
1.60				166	
2.20			11		
2.25	11				
2.28					47
3.40	65		49	18	47
3.70		25			
3.80	71		94	17	
4.10	73		100	18	
4.28		35			
4.30	71		97	26	55
4.40			90		
4.80	60	35	60	11	
4.86					51
4.95		36			
5.15	53		40	4	
5.25			26		
5.95	11				
6.05					26
6.12	26				
6.58		37			
7.10			26		
7.30				11	

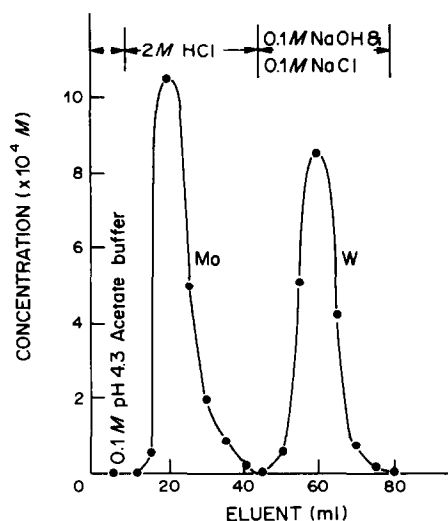


Fig. 1. Separation of molybdenum(VI) and tungsten(VI) with Resin I: (Column 10.0×0.6 cm bore, flow-rate 0.5 ml/min; 9.3 μ mole of each metal absorbed).

Table 3. Effects of foreign ions on the recovery of molybdenum(VI) and tungsten(VI) (35 μg each) respectively, with Resin I

Foreign metal	Amount added, mg	Molybdenum found, μg	Tungsten found, μg
Ag ⁺	0.04	6.0	5.1
K ⁺	5	35.0	35.0
Na ⁺	5	35.0	35.0
Ca ²⁺	2	35.0	35.0
Co ²⁺	1	35.0	37.3
Cu ²⁺	0.02	33.6	33.0
Hg ²⁺	0.07	17.4	15.1
Mg ²⁺	1	35.0	35.1
Mn ²⁺	1	35.0	34.9
Ni ²⁺	1	35.0	38.1
Pb ²⁺	0.07	33.1	30.1
Zn ²⁺	0.02	24.9	35.0
Al ³⁺	1	34.9	34.9
Fe ³⁺ *	10	35.0	36.1
Sn ⁴⁺	0.04	34.9	33.0
U(VI)	1	34.8	35.0
W(VI)†	1	35.0	

* In the presence of 5 drops of 10% ascorbic acid solution.

† In the presence of 5 drops of 10% sodium tartrate solution.

Table 5. Preconcentration and determination of molybdenum(VI) and tungsten(VI) in simulated sea-water*

Metal ion	Amount added, μg	Amount found, μg	Recovery of total metal, %
Mo(VI)†	0.0	9.4	97
	10.2	19.9	100
W(VI)§	10.3	11.1	98
	10.3	11.1	98

* Metal content in original sample: Mo = 9.70 $\mu\text{g/l}$, W = 0.10 $\mu\text{g/l}$.

† Sample 1 litre.

§ Sample 10 litres.

fluids, since the resin would not become saturated by the alkali or alkaline-earth metals present.

Very low concentrations of molybdenum(VI) and tungsten(VI) in pure water and simulated sea-water can be concentrated with Resin I before their determination. Tables 4 and 5 show the recoveries.

Table 4. Recovery of metal ions from very dilute solution with Resin I

Metal ion	Amount added* μmole	Eluent	Amount found, μmole	Recovery, %
Mo(VI)	0.37	2M HCl	0.37	100
Mo(VI)	0.104	2M HCl	0.100	96
W(VI)	0.37	0.1M NaOH-0.1M NaCl	0.37	100
W(VI)	0.37	0.5M NaOH-0.5M NaCl	0.37	100
W(VI)	0.025	0.1M NaOH-0.1M NaCl	0.021	84

* In 500 ml of pH-4.3 0.1M acetate buffer.

Table 6. Colour imparted to the solution by the three resins with excess of molybdenum ions

pH or acidity	Colour		
	Resin I	Resin II	Resin III
7M HCl	green	green	pale yellow
6M HCl	green	green	pale yellow
5M HCl	brown	brown	pale yellow
3M HCl	brown	brown	pale yellow
2M HCl	yellow-brown	yellow-brown	pale yellow
1M HCl	yellow-brown	yellow-brown	pale yellow
0.5M HCl	yellow-brown	yellow-brown	pale yellow
0.1M HCl	blue	blue	blue
pH 1.60	—	—	blue
pH 2.20	—	blue	—
pH 2.25	blue	—	—
pH 3.80	—	—	colourless
pH 4.00	green	—	—
pH 4.10	—	green	—
pH 4.30	—	—	colourless
pH 4.40	—	green	—
pH 4.80	yellow-green	—	—
pH 5.15	—	—	colourless
pH 5.25	—	pale green	—
pH 5.95	yellow-green	—	—
pH 6.12	colourless	—	—
pH 7.10	—	colourless	—
pH 7.30	—	—	colourless

Molybdenum(VI) can be reduced to molybdenum(V) in 2*M* hydrochloric acid and to molybdenum(III) at higher acid concentrations.⁵ The colours imparted to the solution by the chelating ion-exchange resins in presence of molybdenum(VI) species are listed in Table 6. The colours, taken in conjunction with those of chemical forms of molybdenum(V) at various concentrations of hydrochloric acid,⁵ suggest that molybdenum(VI) is reduced by the resins, *e.g.* to molybdenum(V) in 0.5*M* hydrochloric acid. Because of this reductive behaviour of the resin, the possibility of using the Mo–thioglycollic acid and Mo–cysteine resin systems for catalysing hydrogenation reactions is obvious. Investigation of the

catalytic behaviour of these systems in the nitrogenase reaction as model are in progress.

Acknowledgement—This work was supported by a grant from the National Science Council of the Republic of China, to which many thanks are due.

REFERENCES

1. C. Y. Liu and P. J. Sun, *J. Chinese Chem. Soc.*, 1981, **28**, 75.
2. *Idem*, *Anal. Chim. Acta*, 1981, **132**, 187.
3. E. B. Sandell, *Colorimetric Determination of Traces of Metals*, 3rd Ed., Interscience, New York, 1959.
4. L. G. Danielsson, B. Magnusson and S. Westerlund, *Anal. Chim. Acta*, 1978, **98**, 47.
5. G. Charlot, *Qualitative Inorganic Analysis*, Methuen, London, 1963.

APPLICATIONS OF LIGAND-EXCHANGE—III

PREPARATION AND PROPERTIES OF PHENOL-FORMALDEHYDE-BASED RESIN IN THE IRON(III) FORM

B. M. PETRONIO, A. LAGANÀ and G. D. ANDREA
Department of Chemistry, University of Rome, Rome, Italy

(Received 14 June 1983. Revised 15 September 1983. Accepted 7 December 1983)

Summary—A number of resins containing ethylenediamine acetic acid groups have been prepared, and these intermediates (resin-EDTA) converted into the iron(III) form. The capacities of these exchangers in the formation of iron(III)-phenol complexes have been studied and compared with those of the Chelex-iron(III) resin. The character of the exchanger matrix is very important in connection with the retention of phenols and with the elution order. The modified Amberlite CG 4B in the iron(III) form can be used for the quantitative separation of phenolic compounds, a separation that is not possible with the Chelex-iron(III) resin.

As reported in a previous work¹ we have performed the chromatographic separation of a number of phenolic compounds (phenol, 2-nitrophenol, 2,4-dichlorophenol, pentachlorophenol) on a chelating ion-exchanger containing iminodiacetic acid groups, in the presence of iron(III) as complex-generating metal ion, with sodium hydroxide solution as mobile phase.

From the distribution coefficients of the phenols between the resin phase and the eluent it is possible to predict the course of the separation and the optimum conditions. In some cases quantitative separation of the compounds is not possible, because the difference between the separation factors is too small.

Since the nature of the exchanger matrix is an important factor in the strength of binding of a particular ligand and therefore the elution order for compounds of the same class,² an important aspect of research into the resolution of mixtures compounds capable of producing complexes is the preparation of resins having different matrices but the same functional groups.

On this basis we propose the preparation of stationary phases with different matrices and containing iminodiacetic acid groups and have examined their capacities in the formation of iron(III)-phenol complexes and the matrix effect on the elution order.

EXPERIMENTAL

Reagents

Standard solutions (1 mg/ml) of phenol, 3,4-dichlorophenol, 2,4-dichlorophenol, 4-chlorophenol, 2-chlorophenol, 2,4,6-trichlorophenol, 2,3,4,6-tetrachlorophenol and pentachlorophenol were prepared by dissolving weighed amounts of the pure compounds in acetone. Portions of these solutions were then diluted with distilled water to give the test solutions. All chemicals were analytical grade.

Iron(III) solution was prepared by dissolving the reagent grade chloride in water.

Ethylenediaminetetra-acetic acid solution was prepared by dissolving the reagent grade disodium salt in water.

Preparation of the iron(III) resins

An intermediately basic anion-exchange resin of the cross-linked acrylic copolymer type (Amberlite IRA 68, Carlo Erba) and a weakly basic anion-exchanger of the phenol-formaldehyde copolymer type (Amberlite CG 4B, Carlo Erba) were used; this second resin also contains phenolic groups. The resins (100–200 mesh) were stirred for 10 hr with 1M EDTA, then the solution was decanted and the sorbent washed with water until the washings were EDTA-free. These intermediates (resin-EDTA) were converted into the iron(III) form by mechanical shaking for 3 hr with 100 ml of 1M iron(III)chloride. After filtration the resin obtained was washed with distilled water until the effluent was free from iron(III). In a second set of experiments the Amberlite CG 4B resin, a weakly acidic chelating resin of polystyrene type (Chelex 100, Bio-Rad) and a weakly acidic resin of acrylic type (Bio-Rex 70, Bio-Rad) were used. The resins were converted into the iron(III) form in the same way as the EDTA-modified resins.

Retention of phenolic compounds

The prepared resins [4 g, iron(III) form] were packed into 10-mm bore glass tubes. A solution containing 20 µg each of phenol, 2,4-dichlorophenol, 3,4-dichlorophenol, 2-chlorophenol, and 4-chlorophenol in water (100 ml) was passed through the resin column at a flow-rate of 2 ml/min. The column was washed with 10 ml of water and the amount phenolic compounds remaining in the effluent was determined by gas chromatography. The effluent and an equal volume of test sample were both acidified and extracted with methylene dichloride, dried with granular anhydrous sodium sulphate and, after addition of a known amount of 2,4-xilene as an internal standard, were concentrated to a volume of approximately 0.3 ml and analysed.

The same procedure was used with a water solution containing 20 µg each of 2,4,6-trichlorophenol, 2,3,4,6-tetrachlorophenol and pentachlorophenol, and chromatographic columns packed with Chelex-iron(III), Amberlite CG 4B-EDTA-iron(III) and Amberlite CG 4B-iron(III); internal standard, heptadecanoic acid.

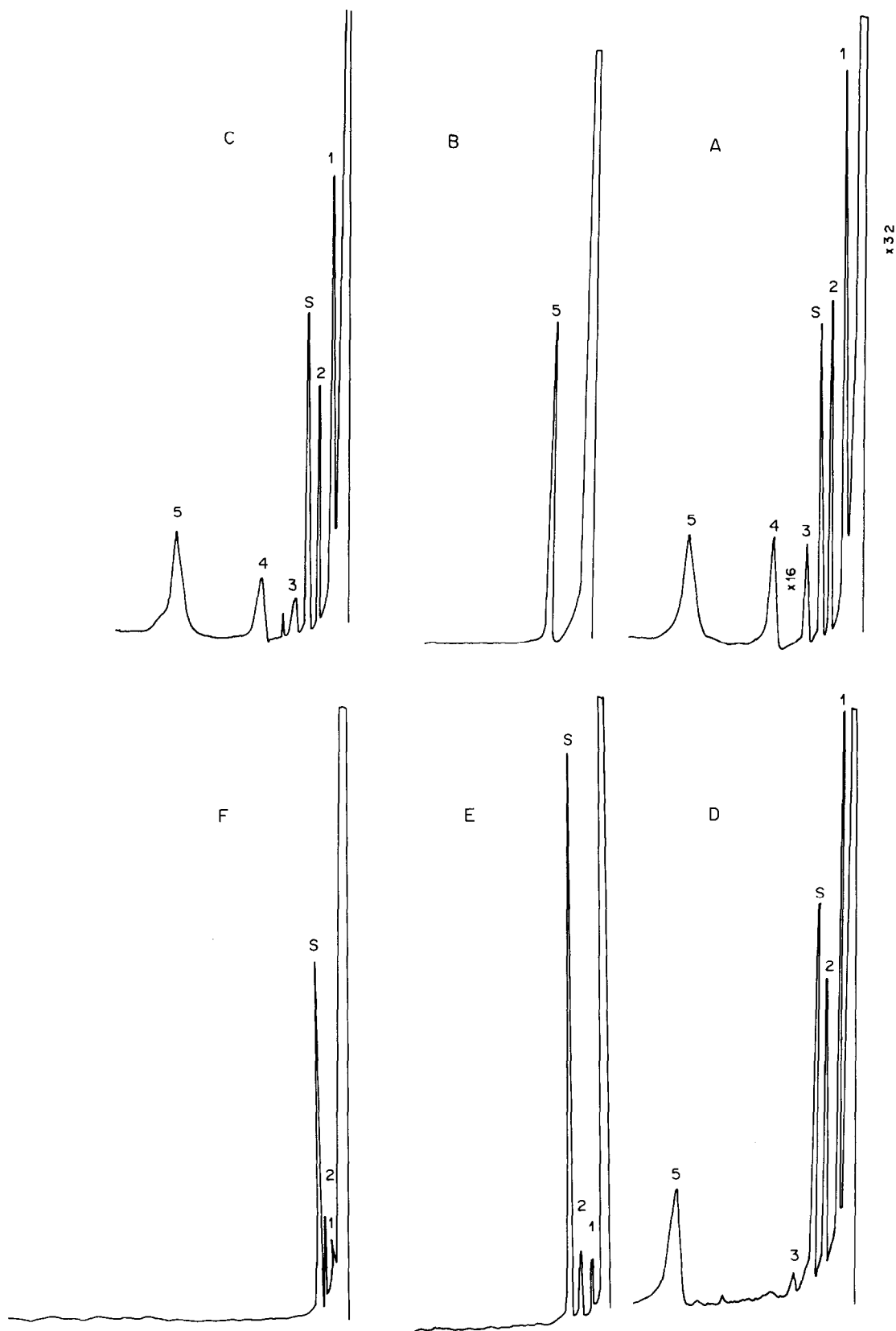


Fig. 1. Retention of phenolic compounds on different resins in the iron(III) form. 1 = Phenol; 2 = 2-chlorophenol; S = internal standard; 3 = 2,4-dichlorophenol, 4 = 4-chlorophenol, 5 = 3,4-dichlorophenol; A = standard solution, B = Chelex-iron(III), C = Bio-Rex 70-iron(III), D = IRA 68-EDTA-iron(III), E = CG 4B-EDTA-iron(III), F = CG 4B-iron(III).

The conditions for the gas chromatography were as follows³

Column: glass (190 × 0.2 cm) loaded with 0.2% w/w FFAP on glass microbeads (80–100 mesh).

Carrier gas: Nitrogen saturated with formic acid; flow-rate 5 ml/min.

Injector temperature: 185 or 230°.

Volume injected: 0.5 μ l.

Column temperature: 165 or 210°.

Effect of pH on the distribution coefficients

To a glass bottle containing 3 g of resin in the iron(III) form, 100 ml of water containing 0.5 μ mole of a phenol were added. The mixture was shaken at room temperature for a given time (20 min), the aqueous phase was decanted and the resin was washed with water. The amount of phenol remaining in the filtrate was determined by means of its absorbance at 283 nm (2,3-dichlorophenol), 275 nm (3,4-dichlorophenol), 270 nm (phenol), 265 nm (2,3,4,6-tetrachlorophenol), 250 nm (pentachlorophenol), measured with a Perkin-Elmer 320 spectrophotometer and 1.0-cm cells.

The resin was then shaken with 100 ml of sodium hydroxide solution and when this mixture had reached equilibrium, the resin was filtered off on glass-wool and the concentration of the phenol in the aqueous phase was determined spectrophotometrically as before. The pH of the aqueous phase was also measured.

The distribution coefficient K_d was calculated from:

$$K_d = \frac{\text{mg of phenol in resin-iron(III) phase/g of dry resin}}{\text{mg of phenol in solution phase/ml of solution}}$$

Separation of phenols

The Amberlite CG 4B-EDTA-iron(III) resin (2 g) was packed into a 10-mm bore glass tube, and 500 ml of a water solution containing 50 μ g each of phenol, 2,3,4,6-tetrachlorophenol and pentachlorophenol were passed through the column at a flow-rate of 2 ml/min. The phenols retained on the column were eluted with 200 ml of a $3.2 \times 10^{-3} M$ sodium hydroxide (pH 11.5). The phenols separated by this stepwise elution were determined spectrophotometrically in successive 10-ml fractions of eluate.

RESULTS AND DISCUSSION

The results for retention of the phenolic compounds on the different resins in the iron(III) form are shown in Fig. 1. The anionic resin of acrylic type in the EDTA-iron(III) form (Fig. 1D) was not able to retain all the phenolic compounds tested: only 2,4-dichlorophenol and 4-chlorophenol were totally bound, phenol and 2-chlorophenol were partially retained and 3,4-dichlorophenol was not retained at all. On the other hand, the Amberlite CG 4B-EDTA-iron(III) showed high affinity for phenols (Fig. 1E, Fig. 2B) as did Amberlite CG 4B-iron(III) resin (Fig. 1F, Fig. 2B) and the results obtained were comparable to those for the Chelex-iron(III) resin (Fig. 1B, Fig. 2B).

Particularly interesting is the behaviour of Amberlite CG 4B in the iron(III) form and in the EDTA-iron(III) form during the elution with sodium hydroxide. There is no elution of phenols from Amberlite iron(III) with 200 ml of $3.2 \times 10^{-3} M$ sodium hydroxide, but complete elution from the resin in the EDTA-iron(III) form. The difference between the behaviour of same resin in the two forms

can be attributed to the difference in the anionic functional groups, chloride in the first case, and EDTA-iron(III) in the second. The iron(III) present in the Amberlite-EDTA-iron(III) resin is bound either to EDTA or to phenolic ions, whereas in the Amberlite-iron(III) resin it is bound only to phenolic ions and the anionic groups (chloride) are free. On introduction of relatively high concentrations of hydroxide ions the chloride ions are desorbed, and displacement of the phenols by ligand-exchange chromatography is not possible even with 200 ml of $3.2 \times 10^{-3} M$ sodium hydroxide. This is demonstrated by the difference in the pH of the eluent before (11.5) and after (4) passage through the chromatographic column, and by the absence of phenolic compounds but presence of chloride ions in the eluate.

The phenols were also not retained on the acrylic-type cation-exchanger in the iron(III) form (Fig. 1C).

The effect of pH on the distribution coefficients was examined, and Fig. 3 compares the results obtained

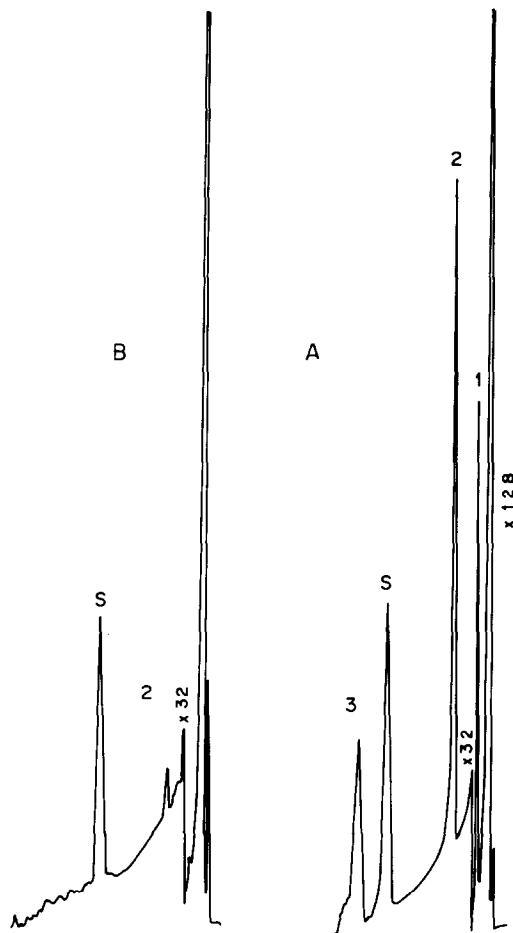


Fig. 2. Retention of phenolic compounds on different resins in the iron(III) form. 1 = 2,4,6-Trichlorophenol, 2 = 2,3,4,6-tetrachlorophenol, S = internal standard, 3 = pentachlorophenol.

A = Standard solution.

B = Chelex-iron(III), CG 4B-EDTA-iron(III), CG 4B-iron(III).

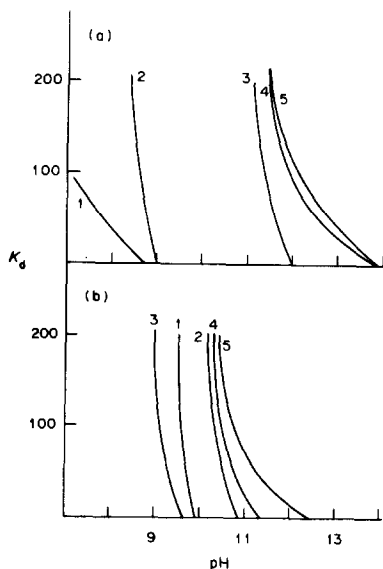


Fig. 3. Effect of pH (NaOH concentration) on the distribution coefficients of phenols: 1 = phenol, 2 = 3,4-dichlorophenol, 3 = 2,4-dichlorophenol, 4 = 2,3,4,6-tetrachlorophenol, 5 = pentachlorophenol. (a) Chelex-iron(III); (b) CG 4B-EDTA-iron(III).

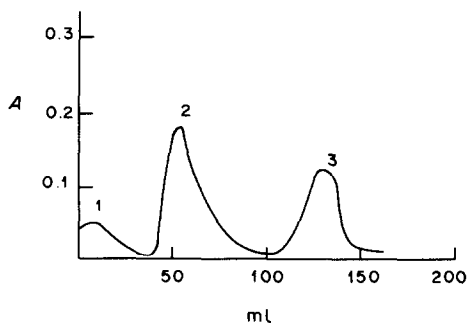


Fig. 4. Elution curve of a mixture of phenol (1), 2,3,4,6-tetrachlorophenol (2), and pentachlorophenol (3): eluent $3.2 \times 10^{-3} M$ NaOH.

with Amberlite CG 4B-EDTA-iron(III) and iron(III)-Chelex resin. The K_d values for the phenols examined with both sorbents decrease with increasing pH but the separation factors calculated from the K_d values are not the same for the two exchangers. The elution order differs for the two resins; the sequence for iron(III)-Chelex is phenol > 3,4-dichlorophenol > 2,4-dichlorophenol > 2,3,4,6-tetrachlorophenol = pentachlorophenol and for Amberlite-EDTA-iron(III) it is 2,4-dichlorophenol > phenol > 3,4-dichlorophenol > 2,3,4,6-tetrachlorophenol > pentachlorophenol.

From these distribution coefficients it is possible to predict the course of the separation. For example, the small separation factor for tetrachlorophenol and pentachlorophenol on the Chelex-iron(III) resin indicates that ligand-exchange separation with sodium hydroxide is not possible. On the other hand, the values obtained for the Amberlite system are also not very large but it is possible to achieve the separation with 200 ml of $3.2 \times 10^{-3} M$ sodium hydroxide at pH 11.5 (Fig. 3B, Fig. 4). In contrast, 3,4-dichlorophenol can be separated from 2,3,4,6-tetrachlorophenol on Chelex resin.

Conclusions

It is possible to retain phenolic compounds on an exchanger by a chromatographic process that involves iron(III) bound to the stationary phase, but the character of the exchanger matrix is very important. On an acrylic-type matrix the retention of phenols is poor, whereas it is very good on a styrene-divinylbenzene copolymer or on a phenol-formaldehyde copolymer. With the proper matrix the resin in the iron(III) form may be used for the analytical separation of phenolic compounds.

REFERENCES

1. B. M. Petronio, E. De Caris and L. Iannuzzi, *Talanta*, 1982, **29**, 691.
2. K. Shimomura, L. Dickson and H. F. Walton, *Anal. Chim. Acta* 1967, **37**, 102.
3. L. Zoccolillo and M. Ronchetti, *J. Chromatog.*, 1982, **245**, 321.

THE SURFACTANT-SENSITIZED ANALYTICAL REACTION OF NIOBIUM WITH 8-HYDROXYQUINOLINE-5-SULPHONIC ACID

J. I. GARCIA ALONSO, M. E. DIAZ GARCIA and A. SANZ MEDEL*

Department of Analytical Chemistry, Faculty of Chemistry, University of Oviedo, Oviedo, Spain

(Received 17 May 1983. Revised 14 June 1983. Accepted 7 December 1983)

Summary—Cationic surfactants, such as cetylpyridinium bromide (CPB), sensitize the colour reaction of Nb(V) with 8-hydroxyquinoline-5-sulphonic acid (H_2L). The formation of a ternary complex of stoichiometry 1:3:3 (Nb-L-CPB) is responsible for the observed enhancement in absorptivity and the quenching in the fluorescence of the Nb-L chelate, when a surfactant is present. The ternary complex exhibits maximum absorption at 383 nm ($\epsilon = 1.46 \pm 0.01 \times 10^4 \text{ l. mole}^{-1} \text{ cm}^{-1}$) at pH 5.7, and Beer's law is obeyed up to $6 \mu\text{g/ml}$ Nb concentration. Conditional formation constants of the niobium chelate in the presence and absence of CPB have been determined. On the basis of a detailed spectrophotometric and fluorimetric study the nature of the chromophoric reagent-surfactant interaction and the peculiar features of the sensitization by CPB are discussed.

The enhancement (sensitization) of the colour reactions of metal ions with chelating dyes by the presence of surfactants (usually of the cationic type) provides an inexpensive alternative to atomic spectroscopy methods, for meeting the present demands for determination of ever lower concentrations of elements. The coloured complexes formed in micellar media are characterized by high molar absorptivities (often greater than $10^5 \text{ l. mole}^{-1} \text{ cm}^{-1}$) and high stability over a wide pH range, and usually by a large bathochromic shift caused by addition of surfactants to the binary complex formed in water.^{1,2} Moreover, some fluorescent binary chelates may dramatically increase their quantum yield in micellar media, thus providing exceptionally sensitive fluorimetric methods.³

A deep knowledge of the fundamental aspects of these "surfactant sensitized" reactions should be invaluable in the understanding and design of new analytical methods. Unfortunately, however, very little attention has been paid so far to the study of the mechanism and nature of such micellar effects.

In the course of our search for new methods of Nb(V) determination^{4,5} we have studied several 8-hydroxyquinoline derivatives^{5,6} which form coloured and fluorescent chelates with niobium. The 7-sulphonic and 5-sulphonic acids of 8-hydroxyquinoline, and 7-iodo-8-hydroxyquinoline-5-sulphonic acid (ferron) should provide surfactant-sensitized reactions with Nb(V) because all of them are strong acids readily yielding a negatively charged group (sulphonate) to interact with the positive head of cationic surfactants. We have found that the 7-sulphonic acid does not give a positive reaction with Nb(V), but the other two reagents do. However, in fluorimetric work

there is the possibility of "heavy atom" effects with ferron (due to the iodine in this reagent), so we decided to study 8-hydroxyquinoline-5-sulphonic acid (H_2L).

In this paper we report a detailed spectrophotometric and fluorimetric study of its reaction with Nb(V), sensitized by cetylpyridinium bromide (CPB). The analytical characteristics of the colour reaction are given and the nature of the interactions of the reagent with surfactant and of the binary chelate with surfactant is discussed.

EXPERIMENTAL

Reagents

Nb(V) stock solution ($200 \mu\text{g/ml}$; $2.14 \times 10^{-3} \text{ M}$). Prepared as described elsewhere.⁴ Standard Nb(V) solutions were prepared fresh, by appropriate dilution of the stock solution with 2% tartaric acid solution.

CPB solution, 0.2%; $4.7 \times 10^{-3} \text{ M}$. Prepared by dissolving the surfactant in water by warming. The surfactant concentration was determined by titration with tetraphenylborate.⁷

H_2L solution; $2.14 \times 10^{-3} \text{ M}$. Made by dissolving 0.5180 g of the reagent in 1000 ml of water, and standardized by titration with sodium hydroxide.

Buffer solution (pH 5.7). Acetic acid (1M) adjusted to pH 5.7 with 1M sodium acetate (pH-meter control).

All reagents were of analytical-reagent grade and were used as received. Distilled demineralized water was used throughout.

Apparatus

Absorption measurements and spectra were obtained with a Perkin-Elmer model 124 spectrophotometer with automatic recording; 1.00-cm quartz cells were used. Uncorrected fluorescence spectra were recorded and measurements made on a Perkin-Elmer MPF-44 spectrofluorimeter, with a high-pressure xenon tube and standard 1.00-cm quartz cells. A WTW pH-meter, model 391, calibrated against Radiometer buffers, was used for pH determinations. The conductivity measurements were made with a Beckman RC-18A bridge, at 25°. A conventional stalagmometer was used for surface-tension measurements.

*Author for correspondence.

General procedure

Pipette standard Nb(V) solutions (containing up to 60 μg of the metal) into a series of 10-ml standard flasks. To each flask, add in the order shown and mixing after each addition: 3 ml of H_2L solution, 3 ml of acetate buffer solution and 1 ml of CPB solution. Mix thoroughly and dilute to the mark with water. Allow 5 min for development of the colour, then measure the absorbance at 383 nm, and/or the fluorescence intensity ($\lambda_{\text{em}} = 500$ nm and $\lambda_{\text{ex}} = 355$ nm). For both types of measurement run a parallel reagent blank, without Nb(V).

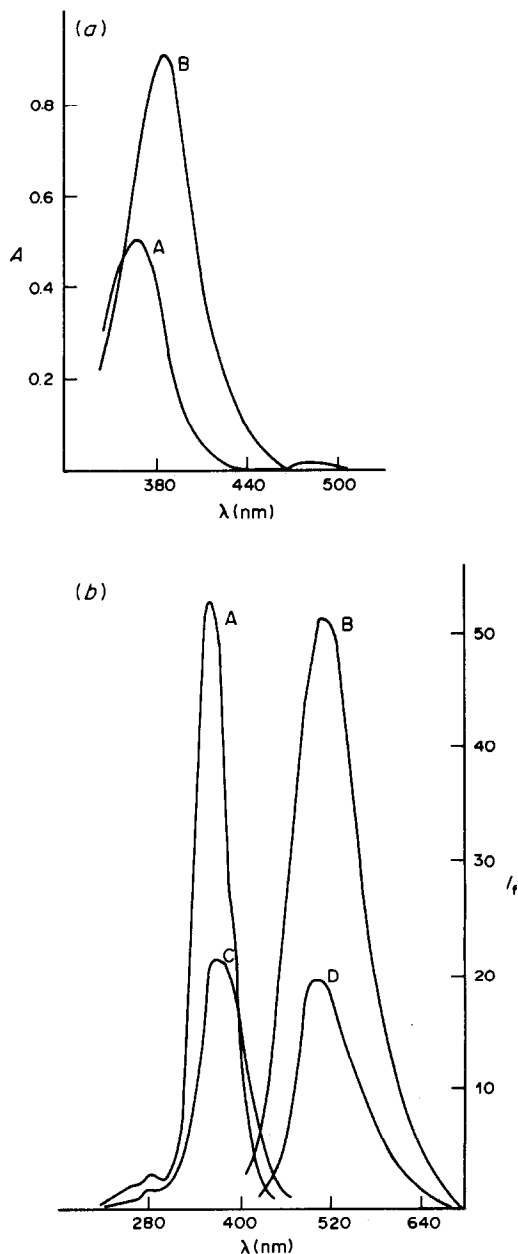


Fig. 1. (a) Absorption spectra of the binary (A) and ternary (B) complexes. (b) Excitation and fluorescence spectra of the binary (A and B) and ternary (C and D) complexes: pH = 5.7, $[\text{Nb}] = 6.42 \times 10^{-5} \text{M}$, $[\text{L}] = 8.56 \times 10^{-4} \text{M}$, $[\text{CPB}] = 7.05 \times 10^{-4} \text{M}$.

RESULTS AND DISCUSSION

Spectral characteristics

Figure 1 shows the absorption spectra (1a) and the uncorrected excitation and fluorescence spectra (1b) for the binary and ternary systems. The addition of surfactant leads to a bathochromic shift of 18 nm in the absorption maximum of the binary complex (365 nm), accompanied by a hyperchromic effect. In contrast, the fluorescence is considerably quenched by the surfactant.

Trimethylcetylammmonium bromide gave analogous results, but non-micelle-forming voluminous cations (*N,N'*-diphenylguanidinium and tetraethylammmonium) or the non-ionic surfactant Triton X-100, did not produce any change in the absorption and emission maximum wavelengths or in the absorptivity of the binary complex.

The Nb(V)-L complex is sensitized by cationic surfactants, but enhancement is observed only in the absorptometric mode. Therefore, optimum working conditions were studied for a spectrophotometric determination of the metal in micellar CPB media.

Effect of experimental conditions on colour development

The influence of pH on the absorbance of the ternary system and the corresponding blank is shown in Fig. 2. The optimum pH range for formation of the sensitized complex is 5–6. We selected a pH of 5.7 because the blank absorbance is minimal at this pH.

The absorbance of the ternary complex Nb(V)-L-CPB depends slightly on the order of addition of the reagents, the best order being cation, H_2L , buffer, CPB. Under the experimental conditions of the general procedure, full colour development takes less than 5 min, and the absorbance does not change for at least two days. Increasing the ionic strength from 0.1 to 0.5M with the buffer solution has no noticeable effect.

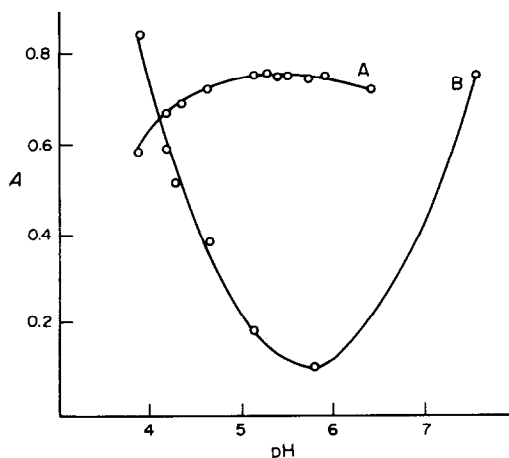


Fig. 2. Influence of pH on complex formation. (A) Ternary complex against reagent blank. (B) reagent blank against water. $[\text{Nb}] = 5.35 \times 10^{-5} \text{M}$, $[\text{L}] = 8.56 \times 10^{-4} \text{M}$, $[\text{CPB}] = 7.05 \times 10^{-4} \text{M}$, $\lambda = 383$ nm.

Maximal and constant absorbance was obtained with H_2L concentration at least 10 times that of $Nb(V)$, in the presence of excess of CPB. With a 10-fold ratio of H_2L to $Nb(V)$, maximal reproducible absorbances are obtained when the CPB concentration ratio to $Nb(V)$ is at least 6. Even very high surfactant: $Nb(V)$ concentration ratios did not decrease the absorbance, in contrast to many other micellar systems.⁸

Beer's law, sensitivity and precision

The calibration graph showed that the complex obeys Beer's law up to 6 $\mu g/ml$ of $Nb(V)$. The apparent molar absorptivity was calculated to be 1.46 (± 0.01) $\times 10^4$ l. mole⁻¹. cm⁻¹ at 383 nm. The relative standard deviation, evaluated from ten independent determinations of 5 ppm of $Nb(V)$, was 0.8%.

Interference studies

The influence of those metals which can be associated with niobium in natural or manufactured niobium materials is shown in Table 1. As can be seen, the selectivity is poor (owing to the relatively high pH of the determination), although the addition of EDTA as masking agent clearly improves the situation.

Among the anions tested (fluoride, citrate, oxalate, EDTA and phosphate), only phosphate prevented the formation of the ternary complex, and did so even at very low concentrations. EDTA can be tolerated up to 0.016M concentration.

Table 1. Tolerance for interfering ions (Nb 3 ppm)

Ion	Ratio to Nb (w/w)*	Absorbance	Ratio to Nb (w/w)†	Absorbance
None	—	0.455	—	0.455
Al(III)	1	1.245	1	0.487
Ba(II)	10	0.450	10	0.445
Bi(III)	10	1.410	50	0.448
Ca(II)	100	0.487	100	0.455
Cd(II)	1	0.705	100	0.463
Co(III)	1	1.027	1	0.458
Cr(III)	1	—	1	0.455
Cu(II)	1	0.802	1	0.452
Fe(III)	1	0.780	1	0.468
Hg(II)	1	0.566	100	0.463
Mg(II)	10	0.470	100	0.461
Mn(II)	10	1.030	20	0.462
Mo(VI)	1	—	1	1.040
Ni(II)	1	0.920	10	0.458
Pb(II)	10	0.872	100	0.452
Sn(IV)	1	0.570	1	0.477
Sr(II)	100	0.452	100	0.451
Ta(V)	1	0.524	1	0.491
Ti(IV)	1	0.920	1	0.560
U(VI)	1	0.485	1	0.506
V(V)	1	1.020	1	0.857
W(VI)	1	0.471	1	0.471
Zn(II)	1	0.940	100	0.457
Zr(IV)	1	0.855	1	0.523

*Minimum ratio tested = 1:1.

†In presence of 0.016M EDTA.

MECHANISMS OF THE SURFACTANT ACTION

Chromophoric reagent—surfactant interaction

The marked spectral changes observed on adding the cationic surfactant CPB to H_2L solutions (Fig. 3) clearly demonstrate a chemical interaction. Increasing the amount of CPB gradually shifts the characteristic two-peak spectrum of H_2L at pH = 3.2 towards a single absorption maximum at around 310–315 nm (typical of the free reagent spectrum at pH 6).

According to the values of $pK_{a1} = 3.8$ and $pK_{a2} = 8.4$, determined by us from spectrophoto-

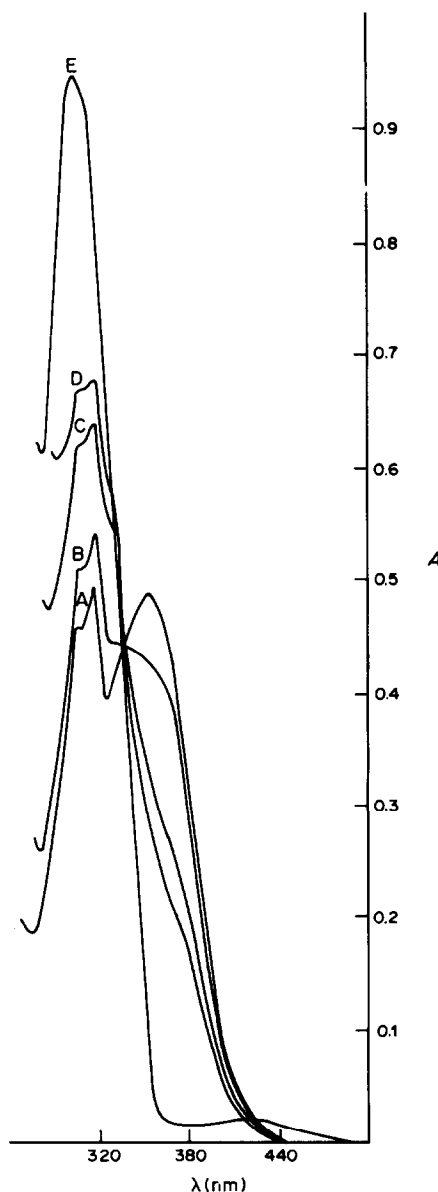
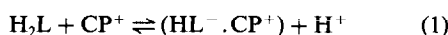


Fig. 3. Absorption spectra of L at pH = 3.2 (curves A–D) and at pH = 6 (curve E) for varying CPB concentrations. (L) = $2.14 \times 10^{-4}M$; [CPB] = 0 (A, E); $4.7 \times 10^{-4}M$ (B); $1.41 \times 10^{-3}M$ (C), $2.35 \times 10^{-3}M$ (D).

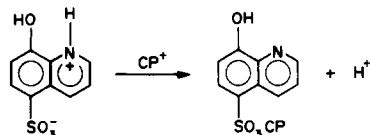
metric data (and in good agreement with those reported in the literature⁹), at pH 3.2 most of the reagent will be present as H_2L whereas at pH 6 virtually all will be in the form HL^- . Therefore, it seems clear that the surfactant promotes dissociation of the chromophoric reagent and the chemical interaction can be formulated as:



That is to say, an equilibrium is established between the undissociated form H_2L and an ion-association complex of HL^- with the surfactant (as indicated by the isosbestic point at around 335 nm, the same wavelength as for the corresponding H_2L/HL^- acid-base pair). The existence of this equilibrium is confirmed by conductivity experiments of the type used in the determination of critical micelle concentrations (cmc) of surfactants: the conductivity of surfactant solutions plotted as a function of CPB concentration shows a clear break at $6.39 \times 10^{-4} M$ (Fig. 4, curve A: cmc value). Analogous experiments in the presence of $8.56 \times 10^{-4} M$ H_2L show much higher conductivities for corresponding surfactant concentrations (Fig. 4, curve B). This enhancement must be due to the release of protons, according to equilibrium (1), and the chromophore-surfactant association seems to be relatively weak, as suggested by the gradual change in the slope of the "titration curve" (Fig. 4, curve C).

The chromophore-surfactant interaction may be due to electrostatic attraction between the sulphonate group of the reagent and the cationic head group of the surfactant, resulting in soluble ion-association complexes, even at concentrations below the cmc of

the CPB. This "neutralization" of the sulphonate group would promote the splitting off of the proton from the nitrogen atom of the quinolinium zwitterion:



It is worth noting that at pH ≥ 8.5 addition of CPB does not appear to promote deprotonation of the $-OH$ group. On the contrary, it has been observed that in this pH-range the absorption spectrum of the chromophore gradually flattens with increasing surfactant concentration until it coincides with the spectrum of the ion-association complex.

Goto *et al.*¹⁰ reported a similar tendency of the hydroxyl group of ferron to remain undissociated in micellar media.

Critical micelle concentrations of CPB solutions

To clarify the role of micelles in sensitized reactions it is important to know the surfactant concentration at which they form (the cmc).

The cmc of CPB in pure water, as determined by us, was $6.39 \times 10^{-4} M$ and $6.86 \times 10^{-4} M$ by conductivity and surface tension measurements respectively (in good agreement with published data¹¹). The presence of $8.56 \times 10^{-4} M$ H_2L decreased the cmc to $3.76 \times 10^{-4} M$ (surface tension measurements).

Decrease in the cmc in the presence of dyes seems to be due to formation of mixed micelles of dye ions and surfactant at well below the cmc. In these cases, it is said that the dye induces micelle formation¹² and the "spectral change dye method" for determining surfactant cmc values gives values much lower than those obtained by conductivity and surface tension measurements (without dye). The spectral change method seems to reveal only the first appearance of such mixed aggregates.

In fact, our results on the cmc of CPB, with eosin as the dye,⁴ indicate the formation of such mixed dye/surfactant micelles, as the first spectral change (cmc) is observed at $6.55 \times 10^{-6} M$ surfactant concentration, well below the usual cmc of CPB (for homomolecule formation).

Nature of the ternary complex

The molar ratio of Nb(V) to chromophore in the binary complex, determined by Job's method, is 1:3. The composition of the ternary complex was investigated by the continuous-variations and molar-ratio methods, initially with a large excess of CPB. A molar ratio of Nb(V) to chromophore of 1:3 was found for the ternary system by Job's method (Fig. 5) and by the molar-ratio method (by varying the concentration of metal). No definitive conclusion can be reached by varying the concentration of chromophore in the molar-ratio method because the exact

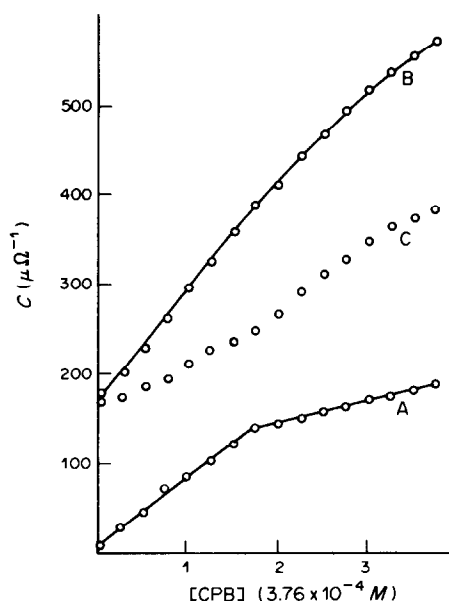


Fig. 4. Variation of the conductivity with CPB concentration in water (A) and in presence of $8.56 \times 10^{-4} M$ L (B). Curve C, difference (B - A).

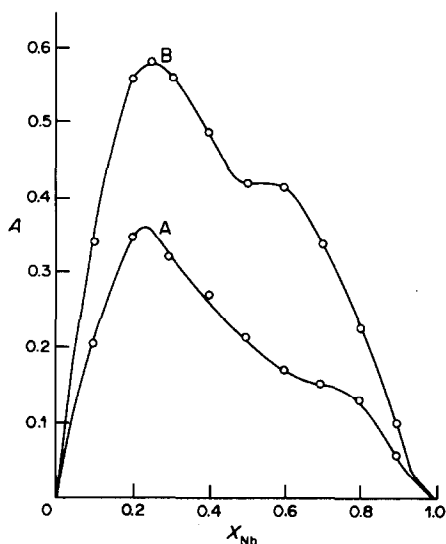


Fig. 5. Continuous variations method for Nb/L ratio. Total concentration = $1.28 \times 10^{-4} M$ (A) and $2.14 \times 10^{-4} M$ (B); $[CPB] = 7.05 \times 10^{-4} M$; $\lambda = 383 \text{ nm}$; $\text{pH} = 5.7$.

break in the plot depends on the Nb(V) concentration used. Figure 6 shows the effect of CPB concentration on the absorbance of solutions containing constant amounts of Nb(V) and chromophore. Maximum colour development is reached at an Nb(V):CPB ratio close to 1:4, but the exact ratio depends on the Nb(V) concentration. These facts can be explained as due to reaction (1) acting as a side-reaction between the chromophore and CPB.

Additional information on the composition of the ternary complex was provided by the continuous-variation method applied to isomolar solutions of surfactant and previously formed 1:3 binary complex. A binary complex/CPB molar ratio of 1:3 was found. Thus, it can be concluded that the ternary complex has a metal-chromophore-CPB molecular ratio of 1:3:3.

To gain additional insight into the surfactant sensitization mechanism, changes in the fluorescence intensity of the Nb(V)-H₂L complex on addition of CPB were studied. The results, illustrated in Fig. 7, indicate that a constant degree of quenching appears at the same surfactant concentrations (below the cmc) as those for complete sensitization of absorbance (compare Figs 6 and 7). As bromide itself did not significantly diminish the fluorescence of the complex, the quenching observed has to be attributed to the phenomenon responsible for the enhanced absorption: the chemical interaction between CP⁺ and the NbOL₃³⁻ complex. In other words, the fluorescence quenching arises from formation of the ternary species NbOL₃(CP)₃ which seems to be much less fluorescent than the NbOL₃³⁻ complex (alkylpyridinium compounds are known to quench the fluorescence of aromatic compounds).¹³

Comparative stability constants

As a quantitative estimate of the effect of CPB on the Nb(V)-H₂L reaction, the conditional stability constants (at pH 5.7) of the binary and ternary complexes were evaluated.

The constant, for the $\beta'_{1,3,0}$ binary complex NbOL₃³⁻ was found from the experimental data for absorbance as a function of ligand concentration. The corresponding constant $\beta'_{1,3,3}$ for the ternary complex NbOL₃(CP)₃ was similarly calculated from the data for constant metal and surfactant concentrations, and from the isomolar Job's method data.

The values obtained are $\beta'_{1,3,0} = 2.5 \times 10^{10}$ and $\beta'_{1,3,3} = 1.4 \times 10^{14}$. The corresponding molar absorptivity coefficients, extrapolated to complete formation of the complexes are: $\epsilon_{1,3,0} = 1.00 \times 10^4$ and $\epsilon_{1,3,3} = 1.46 \times 10^4 \text{ l. mole}^{-1} \cdot \text{cm}^{-1}$.

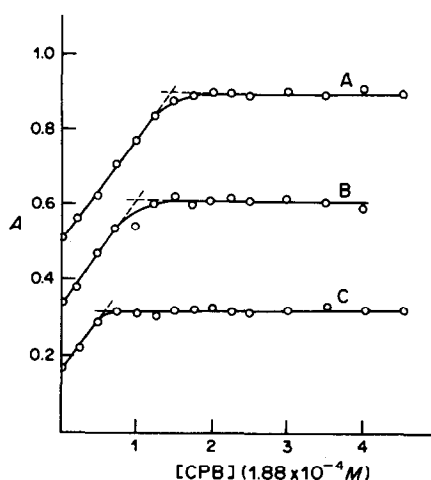


Fig. 6. Influence of CPB concentration on complex absorbance at pH = 5.7. $[L] = 8.56 \times 10^{-4} M$; $[Nb] = 6.42 \times 10^{-5} M$ (A); $4.28 \times 10^{-5} M$ (B); $2.14 \times 10^{-5} M$ (C). $\lambda = 383 \text{ nm}$.

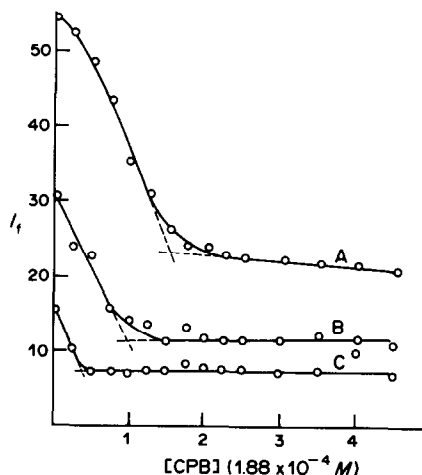


Fig. 7. Influence of CPB concentration on relative fluorescence of the complex at pH = 5.7. $[L] = 8.56 \times 10^{-4} M$; $[Nb] = 6.42 \times 10^{-5} M$ (A); $4.28 \times 10^{-5} M$ (B); $2.14 \times 10^{-5} M$ (C). $\lambda_{\text{ex}} = 355 \text{ nm}$; $\lambda_{\text{em}} = 500 \text{ nm}$.

CONCLUSIONS

Cationic surfactants sensitize the reaction of Nb(V) with 8-hydroxyquinoline-5-sulphonic acid, typical features of surfactant-sensitized reactions^{1,2} being observed, *viz.* bathochromic shift and absorptivity enhancement on addition of CPB (surfactant interaction favours the charge-transfer transition responsible for absorption). Non-detergent cationic counter-ions do not alter the binary-complex spectral characteristics. Moreover, the assumed ternary complex is more stable than the binary complex and forms at pH values at which the binary complex is hardly formed.

The reaction mechanism with CPB, however, is quite peculiar because: (a) below the surfactant cmc no precipitation or turbidity is observed, in contrast with most cases,^{8,14} (b) it is not necessary to reach the "normal" cmc critical micelle concentration of the surfactant to get maximum sensitization; (c) a fixed 1:3 ratio of metal chelate to surfactant is observed. It is clear that if sensitization by surfactant were due to a simple inclusion of the complex into the micelles⁸ it would be essential to ensure homomicelle formation (*i.e.*, [CPB] > cmc) and a fixed stoichiometry would be meaningless.

Summing up our results, a possible mechanism for the reaction could be that the positive head group of the surfactant interacts with the binary NbOL₃³⁻ complex, through the negatively charged sulphonate groups of L²⁻, building up the ion-association ternary complex NbOL₃(CP)₃. The surfactant in that complex does not behave as a simple counter-ion, however. In fact, it appears that the resulting species

is a true ternary complex, but behaves like a soluble mixed micelle of low aggregation number.¹⁵ In such mixed micelles the niobium complex would be isolated from the bulk aqueous solution by the hydrophobic long chains of the surfactant, twisting towards the hydrophobic complex. In this way a hydrophobic environment, similar to that found in a typical micelle, would be created around the chromophore. This new environment and the electrostatic interactions, acting together, would account for the absorbance and fluorescence changes observed.

REFERENCES

1. R. K. Chernova, *Zh. Analit. Khim.*, 1977, **32**, 1477.
2. V. N. Tikhonov, *ibid.*, 1977, **32**, 1435.
3. W. L. Hinze, *Solution Chemistry of Surfactants*, Vol. 1, K. L. Mittal (ed.), p. 104. Plenum Press, New York, 1979.
4. A. Sanz Medel, C. Cámara Rica and J. A. Pérez-Bustamante, *Anal. Chem.*, 1980, **52**, 1035.
5. A. Sanz Medel and M. E. Diaz García, *Analyst*, 1981, **106**, 1268.
6. M. M. Bonilla Simón and A. Sanz Medel, *Anal. Quim.*, 1978, **74**, 595.
7. J. T. Cross, *Analyst*, 1965, **90**, 315.
8. E. Blanco González, M. E. Diaz García and A. Sanz Medel, *Microchem. J.*, in press.
9. R. G. W. Hollingshead, *Oxine and its Derivatives*, Vol. 3. Butterworths, London, 1956.
10. K. Goto, S. Taguchi, K. Miyabe and K. Hariyama, *Talanta*, 1982, **29**, 569.
11. G. A. Davies, *J. Am. Chem. Soc.*, 1972, **94**, 5089.
12. P. Mukerjee and K. J. Mysels, *ibid.*, 1955, **77**, 2937.
13. R. A. Hanna, D. R. Rosseinsky and T. P. White, *J. Chem. Soc. Faraday Trans. 2*, 1974, **70**, 1522.
14. Z. Marzenko and M. Jarosz, *Analyst*, 1982, **107**, 1431.
15. R. L. Reeves, *J. Am. Chem. Soc.*, 1975, **97**, 6019.

TWIN-SPRAY FLAME ATOMIC-ABSORPTION SPECTROMETRIC DETERMINATION OF ANTIMONY, BISMUTH AND MERCURY IN GEOCHEMICAL SAMPLES

YU XIAN-AN, DONG GAO-XIANG and LI CHUN-XUE

Shenyang Institute of Geology and Mineral Resources, Shenyang, Liaoning, People's Republic of China

(Received 24 June 1983. Revised 7 November 1983. Accepted 7 December 1983)

Summary—A new flame atomic-absorption method for determination of antimony, bismuth and mercury, called the twin-spray method, has been established. The operating conditions and potential interferences have been investigated in detail. Under the optimized conditions the sensitivities obtained are 20, 30 and 70 times higher for antimony, bismuth and mercury respectively, than those of conventional AAS. The method can be used to determine as little as 0.00n% of antimony, 0.000n% of bismuth and 0.0n% of mercury in geochemical samples. The procedures are very simple and easy and need no extra apparatus for hydride generation.

Flame atomic-absorption spectrophotometry is well established for determination of antimony and bismuth, but the sensitivity is poor. Because the sensitivity for mercury is also low, up till now flame atomic-absorption spectrometric determination of mercury has not found wide practical application. However, a new method called twin-spray flame atomic-absorption spectrometry has been established,¹ based on the simultaneous aspiration of a solution containing the element to be determined (e.g., Sb, Bi, Hg) and of a solution of potassium borohydride, into an air-acetylene flame. The antimony or bismuth hydride or the elemental mercury generated during the continuous mixing and nebulization of sample solution and reducing reagent solution is carried with the mixed spray into the flame, where the hydride (or metal) is atomized. The aim of the present work was to study the determination of antimony, bismuth and mercury by the twin-spray technique and apply the method to analysis of geochemical samples having various matrix compositions, such as rocks, sediments, copper ores, iron ores and pyrites. As little as 0.00n% of antimony, 0.000n% of bismuth and 0.0n% of mercury can be determined simply and easily in this way.

EXPERIMENTAL

Apparatus

A model WFD-Y₂ atomic-absorption spectrometer with a model WF-3 digital read-out system, made by the Second Optical Instrument Factory in Beijing, was used.

A schematic diagram of the twin-spray apparatus is shown in Fig. 1. It is very simple, and easy to make. Three stainless-steel capillaries, A, B, C, are fixed in a piece of plastic (e.g., polyacrylamide) to form a Y-piece. The capillary C is connected to the entry-port of the AAS instrument. A plastic capillary (E) is connected to A and carries a syringe needle (F) at its other end; F dips into the potassium borohydride solution; a second capillary (E) connected to B

dips into the sample solution. The ratio of the flow-rates through A and B is 1:4.

Reagents

Standard working solutions (antimony and bismuth 20 µg/ml; mercury 100 µg/ml) were prepared by diluting stock solutions with water.

The potassium borohydride solution contained one pellet of potassium hydroxide per 200 ml.

Determination of antimony in ores and pyrites

Weigh 0.1 g of powdered sample into a 50-ml beaker and add 15 ml of concentrated nitric acid, 5 drops of concentrated sulphuric acid and 1 ml of 70% perchloric acid. Cover the beaker with a watch-glass, heat to dissolve the sample, then evaporate the solution to fumes of perchloric acid. Cool, add 10 ml of hydrochloric acid (1 + 1), warm gently and transfer the solution and residue into a 50-ml standard flask. Add 5 ml of 25% thiourea-5% ascorbic acid-0.5% potassium iodide solution. Dilute to the mark with water and mix thoroughly.

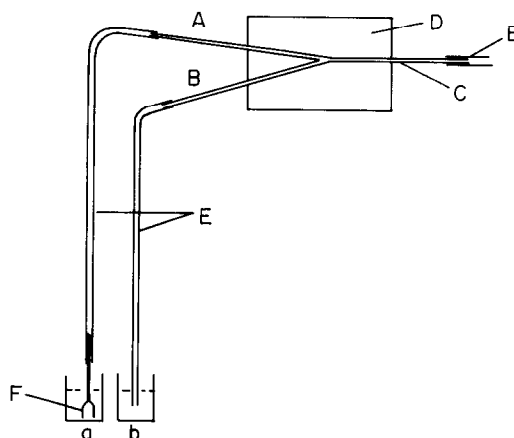


Fig. 1. Schematic diagram of twin-spray apparatus, A, B and C are stainless-steel capillaries (length 20 mm, bore 0.6 mm); D is a piece of polyacrylamide plastic (20 × 10 × 5 mm); E is plastic capillary tubing (bore 0.9 mm); F is a No. 7 syringe needle (length 32 mm, bore 0.2 mm); a is the solution of potassium borohydride and b is the test solution.

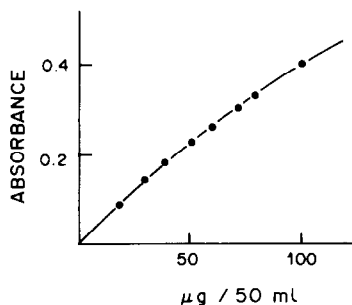


Fig. 2. The calibration graph for antimony.

For the determination the 0.2% potassium borohydride solution is drawn up through A and the sample (or 10% hydrochloric acid for zero adjustment) through B. A typical calibration graph is shown in Fig. 2.

Determination of bismuth in water sediments

Weigh 0.5 g of powdered sample into a 100-ml beaker and add 15 ml of concentrated hydrochloric acid and 5 ml of concentrated nitric acid. Cover the beaker with a watch-glass, boil to dissolve the sample, then evaporate the solution nearly to dryness. Add 10 ml of nitric acid (1 + 1) and heat to dissolve the salts. Transfer the resulting solution and residue into a 50-ml standard flask, dilute the solution to the mark with water and mix thoroughly. Set it aside until the solution becomes clear. Make the measurements as for antimony, but use 0.3% potassium borohydride solution. A typical calibration graph for bismuth is shown in Fig. 3.

Determination of bismuth in copper ores (>2% of copper)

Decompose a 0.5-g sample as for sediments, then evaporate the solution nearly to dryness. Add 10 ml of water and 1 ml of hydrochloric acid (1 + 1) and heat to dissolve the salts. Add 1 ml of 2.5% lanthanum nitrate solution followed by 20 ml of ammonia solution (1 + 1). Check that precipitation is complete. Filter off the precipitate, wash it three times with 20% ammonia solution, then redissolve it in 20 ml of nitric acid (1 + 1) heated just to boiling. Collect the solution in the original beaker and transfer it into a 50-ml standard flask, dilute to the mark with water and mix. Complete the determination of bismuth as before.

Determination of bismuth in pyrites containing gold (>50 g/ton)

Decompose a 0.5-g sample as for sediments, and evaporate the solution to about 2 ml. Add 10 ml of water, warm, and pour the solution into a funnel having a 6-cm stem containing a chromatographic column (shown in Fig. 4, and prepared as follows). Treat 5 g of PTFE with 10 ml of 15% tributyl phosphate solution in ether, let the ether evaporate, then soak the material in dilute hydrochloric acid and pack

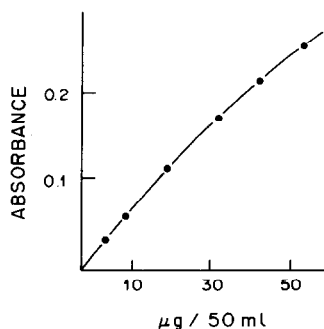


Fig. 3. The calibration graph for bismuth.

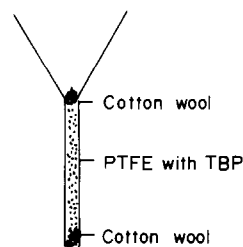


Fig. 4. Chromatographic column funnel.

it in the funnel stem between cotton-wool plugs, to give a flow-rate of 1–2 ml/min. Condition the column for use by washing it first with an acid mixture consisting of 15 ml of concentrated hydrochloric acid and 5 ml of concentrated nitric acid diluted to 100 ml with water, and then once with 10 ml of 1M hydrochloric acid, collecting the sample solution and washings in a 100-ml beaker. Evaporate the solution nearly to dryness. Add 10 ml of nitric acid (1 + 1) and measure as for sediments.

Determination of mercury in ores

Weigh a 0.1-g sample into a 100-ml beaker. Add 5 ml each of concentrated hydrochloric acid and nitric acid, cover the beaker with a watch-glass, boil gently for 5 min, then remove the watch-glass and continue heating gently for 10–15 min. After cooling, transfer the solution into a 50-ml standard flask, dilute it to volume with water and mix. For the determination use 0.05% potassium borohydride solution and “10% mixed acid” (see Table 1) solution to adjust the zero point. The calibration graph is linear up to 500 μg of mercury in the final 50 ml of solution.

RESULTS AND DISCUSSION

Optimization of operating conditions

The effects of acetylene flow-rate, observation height, and concentrations of potassium borohydride and acids, on determination of antimony, bismuth and mercury were studied systematically. The effect of potassium borohydride concentration is shown in Fig. 5. It was found that the response signals were practically constant at hydrochloric acid, nitric acid or sulphuric acid concentrations between 5 and 20%

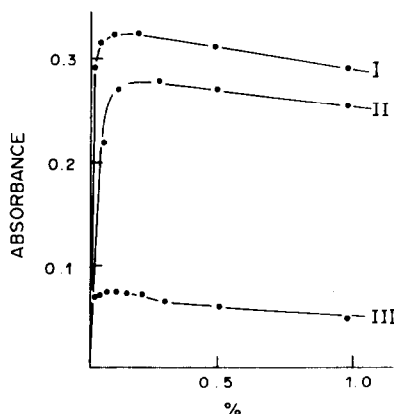


Fig. 5. Effect of concentration of potassium borohydride on determination of (I) 2 ppm of antimony, (II) 1 ppm of bismuth and (III) 2 ppm of mercury.

Table 1. Optimal operating conditions for the twin-spray method

Element	Antimony	Bismuth	Mercury
Wavelength, nm	217.6	223.0	253.0
Lamp current, mA	12	9	9
Acetylene flow-rate, l./min	1.3	0.9	1
Air flow-rate, l./min	4.0	4.0	4.0
Slit-width, mm	0.1	0.2	0.2
Concentration of acid	10% HCl	10% HNO ₃	10% 1:1 v/v HCl and HNO ₃ mixture*
Concentration of potassium borohydride, %	0.2	0.3	0.05

*“10% mixed acid”.

Table 2. Comparison of characteristic concentrations ($\mu\text{g/ml}$ for 1% absorption)

Element	Twin-spray method	Conventional AAS
Antimony	0.022	0.5
Bismuth	0.02	0.68
Mercury	0.13	10

Table 3. Recovery of bismuth after prior separation of interferences

Separation of gold by extraction chromatography [250 μg of Au(III)]		Separation of copper by co-precipitation [50 mg of Cu(II)]	
Bi(III), μg		Bi(III), μg	
Added	Found	Added	Found
5.0	4.9, 5.0	5.0	5.0, 5.0
10.0	10.0, 9.8	10.0	10.0, 10.2

for antimony, at concentrations of hydrochloric acid and nitric acid between 5 and 20% for bismuth and at concentrations of hydrochloric acid and nitric acid between 5 and 20% (in 1:1 v/v mixture) for mercury. An acid concentration of 10% (as listed in Table 1) was chosen as the best compromise. To vary the ratio of flow-rate through A and B, syringe needles of different bore were employed. When a No. 7 needle (0.2 mm bore, 32 mm long) was used, the absorption signal was maximal, so this needle was selected to control the flow-rate through A. The ratio of flow-rates through A and B was then about 1:4.

Sensitivity of twin-spray methods

It was found (Fig. 5) that the simultaneous mixing and nebulization of the two solutions caused the atomic-absorption signal to increase sharply only if

the concentration of potassium borohydride was very low. The characteristic concentrations under the optimized conditions are shown in Table 2. They are improved by factors of about 20 for antimony, 30 for bismuth and 70 for mercury, by use of the very simple twin-spray apparatus.

Effect of other cations

The effects of different cations on the determination of antimony, bismuth and mercury were investigated.

There was no interference in determination of antimony (2 $\mu\text{g/ml}$) at the following levels of other cations: 5 mg of Co(II), Cd, Ni, Cu(II), Zn, Pb, Ca, Mg, Mn(II), Ti(IV), Al; 1 mg of As(III), Bi; 0.5 mg of Sn(IV); 0.1 mg of Se(IV), Te(IV), Ag, Hg(II). The interference of 100 mg of Fe(III) and 100 μg of Au(III) (which decrease the antimony signal) could be minimized by using thiourea and ascorbic acid as masking agents.

In determination of bismuth (0.4 $\mu\text{g/ml}$) the tolerances for other elements were: 50 mg of Fe(III); 25 mg of As(III); 10 mg of Cu(II), Pb, Zn; 5 mg of Co(II), Cd; 1 mg of Sn(IV); 0.25 mg of Ag; 0.1 mg of Hg(II); 30 μg of Se(IV), Te(IV); 20 μg of Au(III). Larger amounts of iron slightly increased the bismuth absorbance, and larger amounts of copper, gold, selenium and tellurium seriously suppressed the response. Copper can be removed by co-precipitation with lanthanum hydroxide,² and gold by extraction chromatography with TBP.³ However, the concentrations of selenium and tellurium are unlikely to exceed 50 ppm in normal geochemical work. The effect of a large amount of iron can be compensated for by adding about the same amount to the calibration solutions. For example, for a 0.5-g sample of

Table 4. Comparison of results of determination

	Rock A Sb	Rock B Sb	GSD* 2 Bi	GSD* 6 Bi	Copper ore 4C Bi	Mercury ore A Hg	Mercury ore B Hg
Mean value, %	0.007	0.017	0.00022	0.00052	0.00038	0.060	0.229
Recommended value, %	0.005	0.022	0.00016	0.00050	0.00039	0.058	0.223

*Sediment sample.

pyrite, 250 mg of Fe(III) needs to be added to each of the standard solutions.

The following amounts of various elements had no significant effect on determination of mercury (4 $\mu\text{g/ml}$): 25 mg of Fe(III), Cu(II), Ca, Mg; 10 mg of Pb, Zn, Cd, Al, Ti(IV), Mn(II), As(III), Sn(IV), La; 5 mg of Co(II), Ni; 2.5 mg of Sb(III); 0.2 mg of Bi; 0.1 mg of Se(IV), Ag; 10 μg of Te(IV), Au(III). Generally speaking, there is no need to separate mercury from cations commonly accompanying it, if the sample weighs not more than 0.1 g, because the gold and tellurium concentrations very rarely exceed 100 $\mu\text{g/g}$ in normal rocks.

Applications

The method has been used to determine traces of antimony and bismuth and low levels of mercury in geochemical samples and some standard samples. The values obtained are compared with the certified values for standard reference samples, in Table 4.

Determination of antimony and bismuth in pyrites was also tested, by the method of standard-additions. The amounts of antimony and bismuth added to samples before decomposition were recovered quantitatively.

CONCLUSIONS

The operating conditions for "twin-spray" atomic-absorption spectrometric determination of antimony, bismuth and mercury have been established. Many

elements commonly accompanying these metals show no significant interference. The effects of large amounts of iron and gold on the determination of antimony may be minimized by adding thiourea and ascorbic acid as masking reagents. The main interferences from copper and gold in determination of bismuth can be overcome by prior separation of copper by co-precipitation² and separation of gold by extraction chromatography with the TBP-PTFE-HCl system.³ Under the optimized operating conditions the sensitivities of the twin-spray method are 20, 30 and 70 times higher for antimony, bismuth and mercury respectively, than those of conventional AAS methods. Trace amounts of antimony and bismuth and low amounts of mercury in various geochemical samples can be satisfactorily determined. The relative standard deviations are 2% for mercury, and 5–10% for antimony and bismuth. The procedures are very simple and easy, and a special feature is that they need no additional apparatus for hydride generation.

Acknowledgement—The authors wish to thank Professor Shu-Chuan Liang and Professor Jin Yu-gui for valuable advice and generous help.

REFERENCES

1. Dong Gao-xiang, *Yan Kuang Ce Shi*, 1982, **4**, 68.
2. M. Thompson, B. Pahlavanpour, S. J. Walton and G. F. Kirkbright, *Analyst*, 1978, **103**, 705.
3. Yu Xian-en and Li Su-fen, *Fen Hsi Hsu Hsueh*, 1981, **4**, 432.

DETERMINATION OF CADMIUM BY DIFFERENTIAL PULSE ANODIC-STRIPPING VOLTAMMETRY AFTER SALTING-OUT EXTRACTION INTO ACETONITRILE

YUKIO NAGAOSA and TOSHIHIRO YAMADA

Faculty of Engineering, Fukui University, 3-9-1 Bunkyo, Fukui 910, Japan

(Received 26 October 1983. Accepted 6 December 1983)

Summary—A selective and specific method is presented for anodic-stripping voltammetric determination of cadmium after extraction with 0.1M tetrabutylammonium iodide solution in acetonitrile from aqueous ammonium sulphate solutions. The detection limit of this method is 0.2 ng/ml (in the acetonitrile extract). Interference from matrices or large amounts of elements reduced at more positive potentials can be eliminated by prior extraction. The method has been applied to trace analysis for cadmium in zinc, lead and indium metals, and some inorganic salts.

Although numerous voltammetric methods have been developed for the determination of cadmium in various samples,¹⁻⁴ anodic-stripping voltammetry (a.s.v.) in the differential pulse mode is widely utilized because of its low detection limits (of the order of 0.1 ng/ml) and its relative freedom from matrix effects.⁵⁻¹⁰ Our preliminary experiments showed that serious interferences were caused by the presence of lead, indium, nickel or zinc in the conventional a.s.v. determination of cadmium. Like polarography, the a.s.v. method applied in aqueous medium suffers from interferences by large amounts of matrix elements or cations reduced at more positive potentials than the analyte. In such cases a preliminary separation is usually necessary to isolate the analyte (in this work, cadmium) from interfering elements prior to the a.s.v. determination, particularly in the analysis of complicated matrices.

Fujinaga and Nagaosa have overcome the problem of poor selectivity by utilizing a salting-out extraction followed by polarography in acetonitrile as solvent.¹¹ Exploitation of differential pulse polarography after such an extraction, however, often seems inadequate for trace analysis of real samples.

The aim of the present work was to demonstrate the capability of the proposed, a.s.v. method following extraction into acetonitrile, for the determination of cadmium in aqueous solutions containing interfering elements. The cadmium is extracted as its iodide complex from an aqueous ammonium sulphate solution into a salted-out acetonitrile phase containing tetrabutylammonium iodide (TBAI) (0.1M), then determined by direct differential pulse a.s.v. measurement on the non-aqueous phase. It has been shown that this method can be applied to the determination of cadmium in zinc, lead, aluminium and inorganic salts with good results. This a.s.v.

method would have potential for application to a wide range of trace analyses for metals, particularly in steels, alloys and environmental samples.

EXPERIMENTAL

Apparatus

All voltammetric measurements were made with a Princeton Applied Research (PAR) Model 174A polarographic analyser with a Model 303 static mercury-drop electrode assembly. A Riken Denshi Model F-3EP X-Y recorder was used to obtain current-potential curves in the cyclic and a.s.v. experiments. The three-electrode system consisted of a hanging mercury-drop electrode as the working electrode, a silver-silver chloride reference electrode and a platinum-wire auxiliary electrode. The a.s.v. analyses were performed with a Fuso Model 915 controller, at the following settings: deposition potential, -0.95 V; deposition time, 180 sec; rest period, 30 sec; modulation amplitude, 25 mV; scan-rate, 5 mV/sec; drop-size, medium.

Reagents

Acetonitrile, ammonium sulphate and TBAI were as described previously.¹¹ The other reagents used were of guaranteed reagent grade from Wako Pure Chemicals Co., Ltd. The 50% ammonium sulphate solution used as aqueous phase was stripped of any cadmium in the salt used, by extraction with three 10-ml portions of 0.1M TBAI in acetonitrile. Standard cadmium nitrate solution (1 µg/ml) was diluted as required, to give the working solutions. The high-purity water used throughout was produced by a Millipore Milli-Q system.

Procedure

An aliquot of the sample solution (not exceeding 5 ml) was taken in a 50-ml stoppered centrifuge-tube, and 20 ml of 50% ammonium sulphate solution and 20 mg of ascorbic acid were added, and the volume was made up to 25 ml with water. Ten ml of 0.1M TBAI solution in acetonitrile were added and the two phases shaken vigorously to extract the tetraiodocadmiate-TBA ion-pair. Exactly 8.0 ml of the acetonitrile phase were transferred into an electrolytic cell. After deaeration of the acetonitrile solution with nitrogen (saturated with acetonitrile) for 5 min, the a.s.v. determination of cadmium was performed at 25°, with continued passage of the nitrogen over the solution surface.

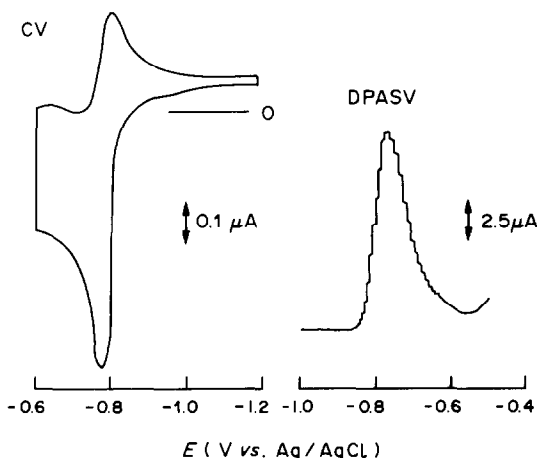


Fig. 1. Typical voltamperograms obtained for cadmium in acetonitrile extract. Cyclic voltammetry (CV): 1.0 $\mu\text{g/ml}$ Cd(II); scan-rate 20 mV/sec. Differential pulse anodic-stripping voltammetry: 0.1 $\mu\text{g/ml}$ Cd(II); experimental conditions as described in the text.

Sample dissolution

About 1 g of a metal sample, in a 100-ml beaker, was dissolved in 10 ml of concentrated nitric acid by heating at *ca.* 50°, and this was followed by evaporation almost to dryness. After cooling, the residue was dissolved in 10 ml of 2M nitric acid and diluted to volume in a 100-ml standard flask with water. Inorganic salt samples were dissolved in moderately concentrated hydrochloric acid and diluted to standard volume.

RESULTS AND DISCUSSION

Voltamperograms

The degree of extraction of cadmium with TBAI into a salted-out acetonitrile phase was sufficiently high (99.5% in a single extraction) for the purpose of this study.¹¹ The amount of cadmium present in commercially available ammonium sulphate was large enough to be detectable by our extraction-a.s.v. procedure under the chosen conditions. The ammonium sulphate solution was therefore purified by extraction with 0.1M TBAI solution in acetonitrile.

Figure 1 shows a cyclic voltammogram and a differential pulse a.s.v. curve for the cadmium complex extracted into the acetonitrile phase. The difference between the two peak potentials on the cyclic voltammogram, 30 mV, indicates a quasi-reversible electrode reaction with two-electron transfer. The anodic wave, which is about three times as high as the corresponding cathodic wave, is more suitable for analytical use. It is probable that the presence of iodide from the TBAI facilitates stripping of the deposited cadmium into the acetonitrile solution. A differential pulse a.s.v. peak was obtained at -0.78 V *vs.* Ag/AgCl and was ten times as sensitive as that obtained in 0.1M hydrochloric acid medium. Selectivity as well as sensitivity is shown to be improved by the acetonitrile extraction method using the salting-out technique.

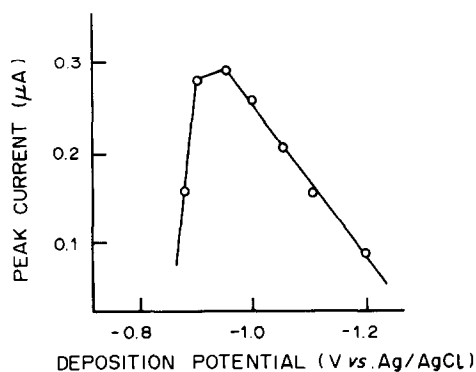


Fig. 2. Effect of deposition potential on peak current. Cd(II) 8.0 ng/ml; deposition time 3 min.

Effect of experimental conditions on a.s.v. peak heights

It is clear from the data shown in Fig. 2 that the cadmium peak height is approximately constant only for the narrow range of deposition potentials from -0.90 to -0.95 V *vs.* Ag/AgCl. Outside this range, the peak height decreases sharply. This result can be understood from the fact that the tetraiodocadmiate complex gives a minimum d.c. wave at potentials between -1.1 and -1.5 V; in this potential range, the cadmium complex anion undergoes coulombic repulsion by the negatively charged mercury. A deposition potential of -0.95 V was used for the determination of cadmium.

As shown in Fig. 3, the cadmium peak height increases linearly with increasing deposition time up to 8 min, beyond which the increase is more gradual. A deposition time of 3 min was used in this study, though longer deposition times are recommended for ultratrace analysis if necessary.

The cadmium peak height was found to increase by a factor of about 3 as the scan-rate was decreased from 10 to 1 mV/sec. With decreasing scan-rate, the peak potential shifted to more positive values and the peak width became narrower. The serious effect of scan-rate on peak height may be due to the irreversible electrode reaction of the cadmium complex in the acetonitrile extract. A scan-rate of 5 mV/sec

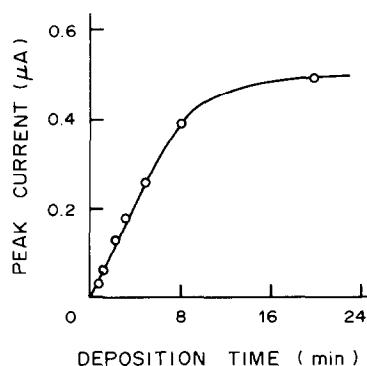


Fig. 3. Effect of deposition time on peak current. Cd(II) 4.0 ng/ml; deposition potential -0.95 V.

was therefore chosen as optimal for the determination of cadmium.

Sensitivity and reproducibility

Calibration graphs for cadmium under the chosen conditions showed good linearity up to a concentration of 50 ng/ml in the acetonitrile extract. Higher concentrations of cadmium can be determined directly by differential pulse polarography of the extract. A relative standard deviation of *ca.* 5% was found for 5 replicate determinations at the 1-ng/ml level and *ca.* 10% at the 0.4-ng/ml level (10 replicates). The cadmium peak height obtained in the blank test was 8 nA, corresponding to 0.2 ng/ml Cd: this may be due to cadmium in the mercury and reagents used. A detection limit of 0.2 ng/ml was estimated, on the basis of the detection limit being twice the standard deviation of the blank signal.

Standard-additions method

The cadmium in indium metal (99.99% purity) was determined by the standard-additions method, with aqueous cadmium solution added to the acetonitrile extract. The cadmium content thus found, 0.10 ppm, was in good agreement with the value (0.12 ± 0.02 ppm) obtained from the calibration graph. Application of the standard-additions method in this way was found to be satisfactory: the cadmium-TBAI complex is formed in the acetonitrile phase.

Interferences

The effect of foreign ions on the a.s.v. determination of 4.0-ng/ml cadmium was studied under the established conditions. Table 1 gives the results. A 10^4 -fold w/w ratio (to cadmium) of iron(III), bismuth, cobalt(II), chromium(VI), antimony(III), manganese(II), tin(II), aluminium, nickel and silver (as their nitrates or sulphates) was tolerated, along with 200 mg of chloride and 40 mg of nitrate. The tolerance limit for these ions is expected to be much higher than the amount usually present in the test samples. Copper(II), which is reduced and co-extracted as the iodide complexes of copper(I), tends to reduce the peak height of cadmium, but a concen-

Table 1. Effect of diverse ions on the determination of 40 ng of cadmium(II)

Added	Amount, μg	Cd found, ng	Error %
Cu(II)	200	38.3	-4.3
	400	—	—
Fe(III)	400	39.7	-0.7
	400 + NaF	42.9	+7.2
Bi(III)	400	39.7	-0.8
Co(II)	400	38.6	-3.4
Cr(VI)	400	38.2	-4.6
Sb(III)	2000	41.4	+3.5
Mn(II)	400	41.6	+4.0
Sn(II)	400	38.8	-3.1
Al(III)	400	41.9	+4.7
Ni(II)	400	42.0	+5.0
Ag(I)	400	42.8	+7.0
Cl ⁻	200 mg	37.8	-5.6
NO ₃ ⁻	40 mg	40.1	+0.2

Table 2. Effects of Pb, In and Zn on the determination of Cd

Added	Amount, mg	Cd added, ng	Total Cd found, ng
Pb(II)	40	40	40.5
	400	40	46.6
	400	0	5.7
In(III)	4	40	51.4
	50	40	190
	200	40	646
	200	0	597
Zn(II)	4	40	40.5
	40	40	50.5
	200	40	80.5
	200	0	41.9

Pb and Zn were added as nitrates, and In was added as sulphate.

tration as high as 20 $\mu\text{g}/\text{ml}$ can be tolerated under the conditions used.

Table 2 indicates the degree of interference by lead, indium and zinc. The presence of cadmium in the metal salts tested was confirmed by the standard-additions method. Zinc, as matrix element, exhibits an a.s.v. peak at -0.90 V, being partially extracted as its iodide complex into the acetonitrile phase, but

Table 3. Analytical results for cadmium in various samples

Sample	Found, ppm	Certified, ppm
NBS 94c (Zinc Base Alloy)	26 ± 2	20
NBS 683 (High Purity Zn)	0.98 ± 0.10	1.1
Zn(NO ₃) ₂ · 6H ₂ O	0.0460 ± 0.0004	
Indium (99.99%)	0.12 ± 0.02	max. 4
In ₂ (SO ₄) ₃ · 9H ₂ O	1.01 ± 0.03	
Lead (99.999%)	0.25 ± 0.03	max. 1
Pb(NO ₃) ₂	0.0089 ± 0.0001	
NaCl	0.0249 ± 0.0016	max. 0.01
(NH ₄) ₂ SO ₄	0.0015 ± 0.0002	max. 0.01
KNO ₃	0.0193 ± 0.0014	

fortunately does not interfere, since the peak is well separated from that for cadmium. Salts such as sodium chloride, ammonium sulphate and potassium nitrate were also analysed for cadmium (Table 3), about 1 g of sample being used.

Applications

The samples selected for study were zinc, indium, lead and their salts, because these metals often interfere in the determination of cadmium by the conventional a.s.v. method. Table 3 summarizes the results obtained. Those for the NBS zinc samples agree satisfactorily with the certified values. As in the case of the analysis of lead and indium, the method seems applicable to other samples with good selectivity. We hope that some problems in the a.s.v. or polarographic method have been resolved by the

preliminary separation in the solvent extraction step; it is, however, a somewhat tedious procedure.

REFERENCES

1. I. M. Kolthoff and J. J. Lingane, *Polarography*, 2nd Ed., Interscience, New York, 1952.
2. L. Meites, *Polarographic Techniques*, 2nd Ed., Interscience, New York, 1967.
3. E. Barendrecht, *Electroanalytical Chemistry*, Vol. 2, pp. 53-109. Dekker, New York, 1967.
4. W. R. Heineman and P. T. Kissinger, *Anal. Chem.*, 1980, **52**, 138R.
5. M. D. Ryan and G. S. Wilson, *ibid.*, 1982, **54**, 20R.
6. Kh. Z. Brainina, *Stripping Voltammetry in Chemical Analysis*, Wiley, New York, 1974.
7. K. Štulík and K. Mařík, *Talanta*, 1976, **23**, 131.
8. M. Oehme and W. Lund, *Z. Anal. Chem.*, 1979, **298**, 260.
9. J. Golimowski, P. Valenta, M. Stoepler and H. W. Nürnberg, *Talanta*, 1979, **26**, 649.
10. T. M. Florence, *Anal. Chim. Acta*, 1982, **141**, 73.
11. T. Fujinaga and Y. Nagaosa, *Bull. Chem. Soc. Japan*, 1980, **53**, 416.

THIN-LAYER ION-SELECTIVE ELECTRODE DETECTION OF ANTICARDIOLIPIN ANTIBODIES IN SYPHILIS SEROLOGY

YOSHIO UMEZAWA*

Department of Chemistry, Faculty of Science, The University of Tokyo, Hongo, Tokyo 113, Japan

SUSUMU SOFUE and YOSHIKI TAKAMOTO

Iatron Laboratories, Inc., 1-11-4 Higashi-kanda, Chiyodaku, Tokyo 101, Japan

(Received 13 July 1983. Accepted 25 November 1983)

Summary—A method for a serological diagnosis of syphilis is presented, in which a thin-layer ion-selective electrode is used for monitoring the complement-mediated immune lysis of antigen-sensitized phospholipid liposomes in microlitre sample volumes. The liposomes are loaded with tetrapentylammonium ions (TPA^+) which are then released from the liposomes by the immuno reaction and are monitored by a TPA^+ ion-selective electrode. This is a direct but much amplified measure of the syphilitic antibodies to be assayed. The principles and evaluation of the method are given. The results have been compared and correlated with those of a conventional method.

The most important factors in potentiometric immunoassay are the achievement of two critical requirements: (1) high selectivity without interference from other proteins, and (2) use of as small a sample volume as possible. Recently, we have developed a novel method for fulfilling these requirements. It uses a thin-layer ion-selective electrode (ISE)¹ to monitor the complement-mediated immune lysis of antigen-sensitized phospholipid liposomes² in microlitre volumes of solution. The liposomes are loaded with a concentrated solution of water-soluble membrane-impermeable molecules or ions as a marker. The marker retained within the liposomes will not cause a response in the corresponding ISE. Complement-mediated lysis of the liposomes releases the marker ions to a dilute solution, where the relevant ISE can respond sufficiently rapidly, under the conditions used, for the rate of response to be a valid measure of the rate at which the marker is released from the liposomes.

In the present paper, the proposed method is applied to the serological diagnosis of syphilis.

PRINCIPLE

Membrane immunochemistry

Liposomes prepared from a mixture of the pure lipids, cholesterol, lecithin and cardiolipin, are able to bind antibodies active against the spirochaete causing the disease (*Treponema pallidum*).³ In the presence of complement, an immunological lysis of the membrane takes place (Fig. 1). This membrane lysis can be monitored by first trapping marker ions or mole-

cules inside the liposomes and then using an appropriate ISE or species-selective electrode, to follow their release, which is a direct but much amplified measure of the antibodies to be assayed. In the present study, the tetrapentylammonium ion (TPA^+) was chosen as marker, and a TPA^+ ion-selective electrode was used. This ion was chosen as marker because it is large enough for its background leakage to be negligible during an experiment and because its selectivity coefficients towards Na^+ and K^+ are 5.0×10^{-6} and 6.2×10^{-6} respectively, so interference by Na^+ and K^+ in sera will be negligible.

Thin-layer potentiometry

A μl -sample solution is held as a thin-layer in a narrow space between the flat bottom of the ISE sensor and a plate-shaped silver/silver halide reference electrode (Fig. 2). With this arrangement the necessary sample volume can be reduced by three or four orders of magnitude (to the μl level) from that for ordinary ISE measurements (1–10 ml level) without miniaturizing the ISE itself. This assembly makes potentiometric measurements of immunological systems practicable.

EXPERIMENTAL

The multilamellar liposomes were prepared from chloroform solutions of dipalmitoyl phosphatidylcholine (DPPC, Sigma), cardiolipin (CL, Sigma), cholesterol (CH, Nakarai Co.) and stearylamine (SA, Sigma) in molar ratio 2:0.02:1.5:0.21. After evaporation of the chloroform, the dried lipids were swollen in aqueous 0.15M TPA^+ solution (pH 7.4). Untrapped marker ions were removed by centrifugation (17400 g) for 10 min each time, at 0°, with five portions of modified veronal saline (VBS) (3.12mM barbital, 1.82mM barbital sodium salt, 0.15mM CaCl_2 , 0.5mM MgCl_2 , 0.147M NaCl). The liposomes were prepared according to Kinsky *et al.*⁴ A plate-shaped Ag/AgCl reference

*Author for correspondence.

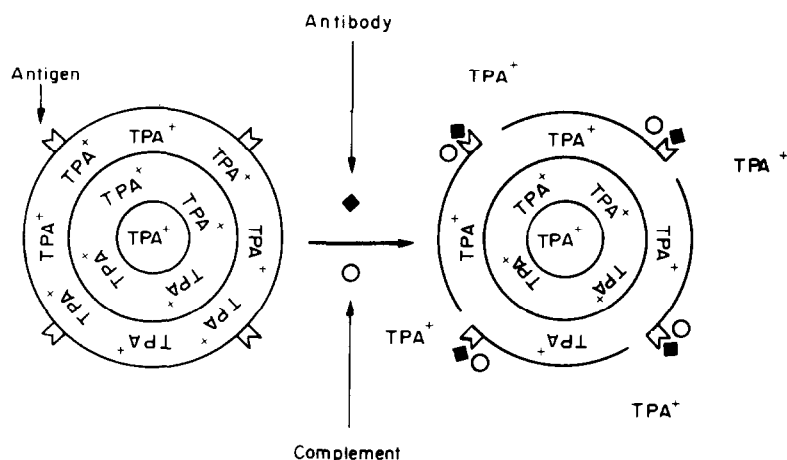


Fig. 1. Immune lysis of sensitized liposomes by antibody and complement, and resulting leakage of marker ion, TPA⁺ (tetrapentylammonium ion).

electrode was made by anodic oxidation of a silver plate (4×7 cm, 2 mm thick) in 0.1M potassium chloride at +0.5 V *vs.* SCE for 5 min. A TPA⁺ ISE was made with PVC and dioctyl phthalate, in the body of an Orion Model 95 electrode. The electrode response was Nernstian over the TPA⁺ range from 1 to 10^{-6} M. Seropositive and normal human sera were provided by the Japan Red Cross Blood Centre (Tokyo). The titre value for the seropositive sera used was determined to be 1:512 by a standard semi-quantitative method, SST (Serodiagnosis of Syphilis Test, Iatron Co. Tokyo). The SST method is based on careful observation by the naked eye of the extent of precipitates composed of antigen-antibody complexes and fine carbon powder. The reagents used for the SST method are the same lipids as those for the constituents of liposomes mentioned above, except for the stearylamine (which was added to increase the trapping efficiency of liposomes for positively charged marker ions). All human sera used were treated at 56° for 30 min before testing, in order to eliminate the complement activity from the human serum itself. The complement used was from guinea pig serum, which was stored at -80°. The titre value for this was found to be 267 CH50/ml by a simplified Mayer method.⁵

A typical procedure was as follows. To a 50- μ l or other (suitable) liposome aliquot were added an equal volume of Wassermann-seropositive serum and an equal volume of fresh guinea pig serum (source of complement). After 30 min incubation at 25°, typically 20–50 μ l of the mixture was placed on the Ag/AgCl reference electrode and the ISE body (in an upright position) was lowered onto the sample droplet. Thus, the sample solution was kept in a thin layer between the flat bottom of the ISE and the reference electrode, for e.m.f. measurement. The e.m.f. were measured on a millivolt meter (Model HM-5bs, TOA Electric Co.,

Tokyo) at 21° after a wait of 3 min for equilibrium to be attained.

It is known that the phase-transition temperature for liposomes differs according to the kinds of phospholipids used. Thus, it seems important to choose an appropriate temperature for incubation. We selected an incubation temperature of 25° for the immune lysis reaction, as a trade-off between the greater possibility of background release of marker ions at higher temperatures and the optimum temperature of around 37° for the immunoreaction. Indeed, the release of marker ions was 11, 14 and 85% greater at 30°, 37° and 55° respectively, than at 25°. It should be noted, however, that this release of TPA⁺ ions refers to incubation, in which rather vigorous stirring under warm conditions is general. In contrast, in the static conditions of the thin-layer ISE measurement in the present case, such background release of marker ions was quite negligible during the course of the experiment.

RESULTS AND DISCUSSION

Maximum potential change and optimum complement level

The crucial point for obtaining maximum potential change was found to be minimization of the anti-complement reaction induced by unidentified constituents in human sera. To do this, the haptenic antigen-sensitized liposome was first complexed with the corresponding antibody (Wasserman antibody), and any unwanted components in the sera were separated from the system. The procedure was to bind the antigen-sensitized liposome sufficiently with the anti-serum by heating at 37° for 30 min, and then wash it adequately with VBS by centrifugation, with two changes of VBS. It was assumed that after this, most of the active haptenic antigen sites on the surface of the liposome membrane were occupied by corresponding antibodies. The haptenic antigen-sensitized liposomes thus made were then reacted with various concentrations of guinea-pig serum (complement source) so that the effect of complement concentration was accurately measured. The results are shown in Fig. 3, where ΔE is the difference between E_c (the e.m.f. reading when the active complement

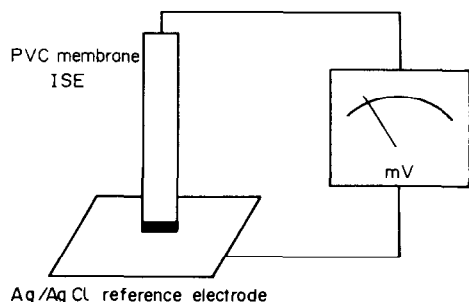


Fig. 2. Thin-layer potentiometry for microlitre samples.

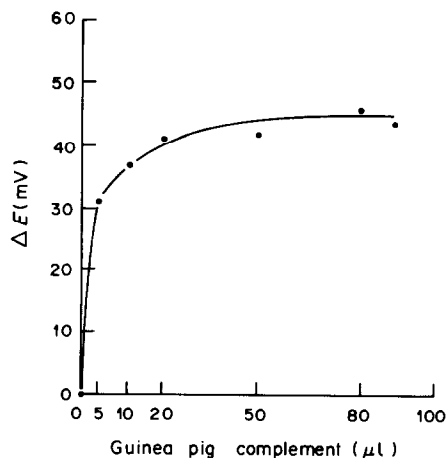


Fig. 3. Effect of complement concentration on TPA⁺ release from the antigen-antibody sensitized liposomes (200 μl) (see text). G.P.C.—guinea-pig serum as complement source (100 μl). $\Delta E = E_c - E'_c$.

was used) and E'_c [the e.m.f. when the inactive complement (heat-treated at 56° for 30 min) was used but under otherwise identical conditions]. The advantage of using ΔE is that the background correction is accurate, because the total protein concentration is the same for the sample (with active complement) and the blank solution (with deactivated complement) even if the level of complement has to be changed. As seen in Fig. 3, the maximum change in potential thus obtained as about 45 mV, at rather high complement levels.

Dependence on antibody concentration

The ISE potential was measured as a function of dilution (concentration) of seropositive human sera (titre 1:512) (Fig. 4). Blank values were again obtained by use of an identical concentration of deactivated complement but under otherwise identical conditions, as in the preceding section. Also, the same

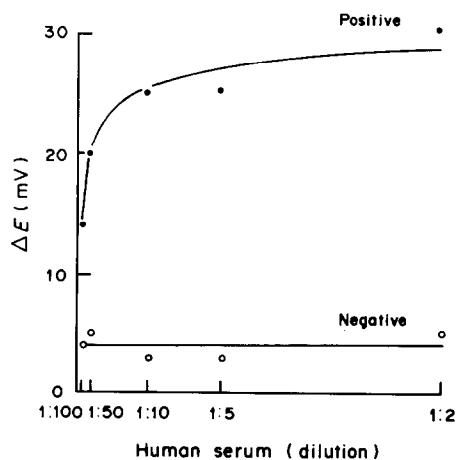


Fig. 4. Effect of seropositive serum (titre 1:512) dilution (concentration) on TPA⁺ release from liposomes. G.P.C. 1:3 dilution.

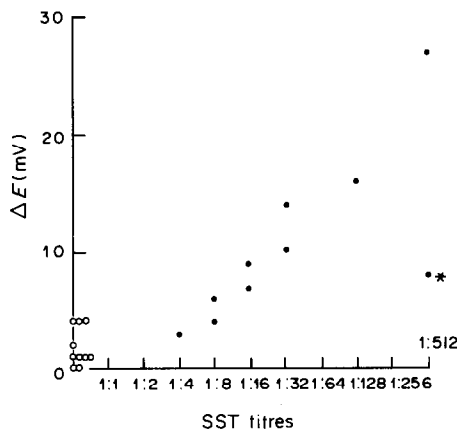


Fig. 5. Correlation between the present method and a conventional (SST) method for the diagnosis of syphilis. Twenty different human sera (both from normal persons and patients) were collected from the Japan Red Cross Blood Centre, Tokyo. ● Positive serum (1:5 dilution); ○ negative serum (1:5 dilution); G.P.C. 1:3 dilution.

experiments were performed, for comparison, with normal human sera, which of course show no potential changes with dilution. However, it was found that even with use of normal human sera, ΔE values of 4–5 mV were observed, in contrast to expectation. The reason for this is not clear at the moment, but probably some components of unknown nature in the guinea-pig serum (complement source) rather than of normal human serum may cause lysis of liposomes to a certain extent, because normal human sera at varied levels gave similar ΔE values. Also, the fact that the relation between ΔE and normal sera concentration becomes parallel to the abscissa suggests that the influence of serum concentration on the potential change of the Ag/AgCl reference electrode is negligible, even though the latter is in direct contact with the sample solutions. It should also be pointed out here that although the Ag/AgCl electrode is by itself a chloride ion-selective electrode, unwanted shifts of the reference potential due to possible variations of chloride ion activity from one sample to another was strictly eliminated by use of saline buffers. As shown in Fig. 4, the potentials with positive sera change with dilution, levelling off at $\Delta E = 30$ mV. The maximum potential change obtained in this case is somewhat smaller than that in Fig. 3. This may be due to inhibition of the lysis reaction, caused by an anti-complement component in human sera, the influence of which was carefully eliminated experimentally in the case of Fig. 3.

Correlation with a standard method

In an attempt to judge the present method for assaying anticardiolipin antibodies, a series of different seropositive syphilitic sera was examined both by the standard procedure (a standard semi-quantitative method, SST, see experimental section) and the present method. The results, which are correlated in Fig. 5, are mainly in good agreement.

With normal sera in which antibody activity is negative, ΔE is only 0–3 mV, whereas positive sera give an appreciable increase in ΔE with increasing titre values. It should be noted, however, that one point (marked with an asterisk) in Fig. 5 does not fit this correlation. The exact reason for this is not clear, but it may be attributed to some basic differences between the two methods; for instance, it is known that depending on the extent of syphilitic disease, corresponding antibodies in the sera change in composition from IgM-rich to IgG-rich.^{6,7} It is also reported that in the complement-fixation reaction, IgM antibody can be detected more sensitively than IgG. In the ISE method, the leakage of marker ions is observed through the complement-mediated immune lysis of liposomes, whereas in the SST method the quantity of the antigen-antibody complex is directly measured. Also, it should be noted that the potential change for less sero-positive sera (titre values between 1:1 and 1:4) is smaller than expected from the value in Fig. 4, where a 100-fold dilution of a seropositive serum (titre, 1:512) gives a ΔE value of 14 mV. The crucial difference in these two cases is the extent of dilution of human sera; more dilution gives higher potential change, although the final titre values are the same. This is caused by an anti-

complement reaction induced by unknown components in human sera. For preventing this anomaly, the procedure mentioned in the first section of the discussion is recommended. However, a simple 8-fold dilution of human samples rather than 2–4-fold is a more convenient trade-off. Greater sensitivity would be expected if single lamellar liposomes were used.

Acknowledgement—The authors express their sincere gratitude to Professor S. Fujiwara for his encouragement and support in this study.

REFERENCES

1. Y. Umezawa and S. Fujiwara, *Nippon Kagaku Kaishi*, 1980, 1477, and references therein.
2. Y. Umezawa, K. Shiba, T. Watanabe, S. Ogawa and S. Fujiwara, in *Ion-Selective Electrodes*, 3, E. Pungor (ed.), p. 349 and references therein. Elsevier and Akadémiai Kiadó, Amsterdam and Budapest, 1981.
3. E. Rosenquist and A. I. Vistnes, *J. Immunol. Methods*, 1977, 15, 147.
4. S. C. Kinsky, J. Haxby, C. B. Kinsky, R. A. Deamel, L. L. M. van Deenen, *Biochem. Biophys. Acta*, 1968, 152, 174.
5. S. Inai, *Nippon Rinsho*, 1968, 26, 384.
6. W. M. Lesinska and A. Jakubowski, *Brit. J. Vener. Dis.*, 1970, 46, 380.
7. H. Maruta and N. Minami, *Rinsho Meneki*, 1973, 5, 149.

APPLICATION OF THE DEFORD AND HUME METHOD MODIFIED FOR QUASI-REVERSIBLE AND IRREVERSIBLE PROCESSES TO THE CHELATES OF Bi(III) WITH AZOMETHINE DERIVATIVES OF 2-BENZOYLPYRIDINE

M. A. GOMEZ-NIETO,* J. L. CRUZ SOTO,† M. D. LUQUE DE CASTRO* and M. VALCARCEL*

*Department of Analytical Chemistry and †Department of Mathematics, Faculty of Sciences, University of Córdoba, Spain

(Received 29 November 1982. Revised 18 April 1983. Accepted 15 November 1983)

Summary—The polarographic behaviour of the bismuth complexes of the oxime, hydrazone and thiosemicarbazone of 2-benzoylpyridine has been studied by differential pulse polarography. The DeFord and Hume method, modified for use with quasi-reversible and irreversible processes, has been applied for the calculation of the formation constants of these chelates, which exhibit different degrees of reversibility in their electroreduction.

We have studied the electroreduction of the azomethine derivatives of 2-benzoylpyridine at the dropping mercury electrode, by d.c. polarography and differential pulse polarography.¹⁻³ We have also developed a modification to the DeFord and Hume method that is applicable to quasi-reversible and irreversible systems, and have written three computer programs for calculation of complex-formation constants from the results obtained by the method.⁴

In the present work we first made a photometric study of three of these reagents with 37 metal ions to detect which combinations gave complexes (Table 1), then a polarographic study to find which complexes gave reduction waves that were in the polarographically useful region and not overlapped by the ligand reduction wave (Table 2). In this way we identified the systems suitable for study by DPP.

A preliminary literature survey brought out the following points.

(1) The ligands used in earlier studies have almost all been not reducible at the working potential. The others had a reduction potential more cathodic than that of the complex; otherwise the measurements necessary for calculation of the stability constants had to be made on the diffusion plateau for the ligand, with the consequent disadvantages of ligand adsorption on the electrode surface and the impossibility of obtaining constants other than that for the first complex, without determination of the free metal concentration.

(2) The ligands were small, to minimize adsorption on the electrode, since adsorption effects on the value of the constants obtained are not clearly defined.^{5,6}

(3) The ligands had to be fairly soluble since the investigations were based on the effect of the ligand

concentration on the reduction potential of the complex.

(4) The choice of cations was limited to those giving reversible reduction.

(5) Only three bismuth complexes had been studied: those with EDTA,⁷ 5-methoxymethylquinoline⁸ and nitrilotriacetic acid.⁹

(6) DPP was very little used for this type of study.¹⁰⁻¹²

In view of these features, the present research represents an important departure from previous practice.

EXPERIMENTAL

Apparatus

A Metrohm E-505 polarograph and E-506 recorder system, with Ag/AgCl electrodes as reference and auxiliary electrodes, in conjunction with conventional dropping mercury and hanging drop electrodes. A Perkin-Elmer 575 spectrophotometer with 1.0-cm glass cells and an electronic thermostat. A Beckman 3500 pH-meter with combined calomel-glass electrode.

Reagents

Ethanolic solutions of 2-benzoylpyridine oxime (BPO) (0.05M) and 2-benzoylpyridine hydrazone (BPH) (0.1M) and a dimethylformamide solution of 2-benzoylpyridine thiosemicarbazone (BPT) (0.05M). Aqueous solutions (1.0M) of sodium perchlorate, potassium nitrate, potassium chlorate, potassium chloride and tetramethylammonium bromide were used as supporting electrolytes.

Britton and Robinson buffers (pH 1-12). Gelatine solution (1%).

Aqueous standardized Bi(III) solution (1000 ppm). More dilute solutions were prepared as required. All solvents were of analytical grade.

Study of experimental variables

Unless otherwise specified, the working conditions were as follows.

Table 1. Reactions of the azomethine derivatives of 2-benzoylpyridine

Cation	BPO			BPT			BPH		
	A	M	B	A	M	B	A	M	B
Be(II)	3	1	3	3	1	3	3	2	3
Fe(II)	3	1	1	1	4	4	1	1	1
Co(II)	1	1	1	1	1	1	2	1	1
Ni(II)	3	1	1	1	1	1	1	1	1
Pd(II)	1	1	1	1	1	1	2	1	1
Cu(II)	1	1	1	1	1	1	1	1	1
Zn(II)	3	3	3	3	3	1	3	1	1
Cd(II)	3	3	3	3	3	4	3	3	3
Hg(II)	3	3	3	3	2	4	3	1	3
Mn(II)	3	1	3	3	2	1	3	3	3
Sn(II)	3	1	3	3	1	3	2	3	3
Pb(II)	3	4	3	3	3	3	3	3	3
Mo(VI)	3	1	3	3	1	3	3	1	1
W(VI)	3	3	3	3	3	3	3	2	3
U(VI)	3	3	1	3	3	3	3	2	3
Cr(VI)	2	2	2	3	2	2	1	2	2
Ag(I)	3	3	3	3	4	4	3	3	3
Tl(I)	3	3	3	3	3	3	3	3	3
Os(VIII)	3	2	2	1	1	1	3	2	1
Fe(III)	3	1	3	1	1	1	2	1	1
Bi(III)	3	1	3	3	1	3	3	1	3
Sb(III)	3	1	3	3	1	3	3	3	3
As(III)	3	1	3	3	1	3	3	3	3
Cr(III)	3	3	3	3	3	3	3	2	3
La(III)	3	3	3	3	2	3	3	3	3
Al(III)	3	3	3	3	3	3	3	3	3
Au(III)	1	1	1	3	3	4	1	1	1
In(III)	3	3	3	3	1	1	3	3	3
Ti(IV)	1	1	1	1	1	1	1	1	1
Zr(IV)	2	1	1	3	1	1	3	1	1
Hf(IV)	1	1	1	3	1	1	3	1	1
Pt(IV)	3	2	3	3	1	1	3	2	2
Ce(IV)	3	1	3	3	2	3	2	2	2
Se(IV)	3	3	3	3	3	3	3	3	3
Th(IV)	3	3	3	3	1	3	3	3	3
V(V)	3	3	3	3	2	3	3	3	3
As(V)	3	3	3	3	1	3	3	3	3

Degree of reaction

pH

1. Positive

A 2.0

2. Slightly positive

M 4.8

3. Negative

B 10.1

4. Precipitate formation

General conditions

Initial potential 0.2 V

Scan-rate 5 mV/sec

Drop-time 0.6 sec

Rate of mercury flow 0.8083 mg/sec

Pulse amplitude 50 mV

Temperature 25°

Height of mercury column 50 cm

Special conditions

	Bi-BPO	Bi-BPH	Bi-BPT
Organic solvent, %	1.6	2.0	2.0
[Bi(III)], <i>M</i>	3.0×10^{-5}	2.0×10^{-5}	2.0×10^{-5}
[Ligand], <i>M</i>	1.6×10^{-3}	1.0×10^{-3}	8.0×10^{-4}

RESULTS AND DISCUSSION

Influence of type and concentration of supporting electrolyte

NaClO₄, KClO₃, KNO₃, KCl and Br(CH₃)₄N solutions covering the concentration range

0.05–0.70*M* were used. The KCl solution gives more reversible processes (smaller peak-width) for the Bi–BPH and Bi–BPT systems. For Bi–BPO, KNO₃ was used as supporting electrolyte because, although the peak-width is slightly greater than when KCl is used, the peak is less overlapped by that for mercury oxidation and by the first reduction peak of the oxime. Since the fundamental parameters of DPP are not altered when the supporting electrolyte concentration is varied in the interval studied, a concentration of 0.5*M* was used for all further experiments, so that the electrode process remained the same throughout, and the migration current was constant.

Effect of surfactants

The reagents were examined in the concentration range 0.004–0.040%, and found to modify the reversibility of the processes, shifting the peak potential to more negative values and exponentially increasing the peak-width, *W*, with increasing concentration of surfactant.

Effect of pH

The influence of pH in the range 1.9–12.0 on the fundamental parameters of the DPP technique is very different for each system, as shown in Table 3 and Fig. 1. We can offer no explanation for the fluctuations in *W* with pH, but they have been repeatedly observed. The effect seems too large to be explainable in terms of localized irreversible chemical changes occurring during the pH adjustment. The pH values chosen for subsequent experiments are also shown in Table 3. The number of protons exchanged per mole of complex was calculated on the assumption that the systems are mononuclear.

Influence of temperature

The interval 20–50° was examined for all three systems. Figure 2 shows the change in peak-current, *I*_p, and peak-width, *W*, as a function of temperature (*T*). Table 3 gives the equations of the straight lines *I*_p = *f*(*T*), the temperature coefficients, and the temperatures used for further experiments (chosen so that deviations would have minimum influence on the fundamental parameters and so that the reversibility of the processes would be maximal). At temperatures above 35° the Bi–BPT system shows anomalous behaviour, probably as a result of adsorption of the complex on the electrode surface. We have observed similar behaviour for the Co–BPT system.¹⁴

Organic solvent

The solvents used to increase the ligand solubility were ethanol (Bi–BPO and Bi–BPH systems) and dimethylformamide, DMF, (Bi–BPT system). Figure 3 shows there was a decrease in *I*_p and an increase in *W* when the proportion of organic solvent in the test solution was increased.

Table 2. Polarographic behaviour of the metal chelates of azomethine derivatives of 2-benzoylpyridine

SPECIES	Peak potential, V									CHARACTERISTICS
	0	0.2	0.4	0.6	0.8	1.0	1.2	1.4	1.6 (V)	
As (III)						—				2,4
Bi (III)	—									1
Co (II)							—			2,3
Cr (III)								—		2,3
Cu (II)	—									2,4
Fe (II)								—		2
Fe (III)										5
Hf (IV)										5
In (III)					—					1
Mo (VI)				—						4
Ni (II)						—				2,3
Os (VIII)										5
Pd (II)										5
Pb (II)				—						2
Sb (III)		—								1
Sn (II)			—							2
Ti (IV)										5
Zn (II)							—			2,3
Zr (IV)										5

- *1. Well-defined peaks.
- 2. Ill-defined peaks.
- 3. Processes influenced by adsorption.
- 4. Overlapped peaks.
- 5. No processes.

Height of mercury column (h)

The variation of $\ln I_p$ with $\ln h$ was linear, but the slopes were between 0.7 and 0.85 (Table 4). Since the life-time of the mercury drop is constant in pulse

polarography, a change in mercury head affects only the rate of mercury flow.

Drop-time, pulse amplitude and scan-rate

These parameters were studied to establish the working conditions for maximal reversibility of the electrode processes.

In all cases I_p increases and E_p becomes more positive when the drop-time t_d is increased, for all values of pulse amplitude (ΔE) and scan-rate (V), though the effect is higher for the Bi-BPO system; $\ln I_p$ is a linear function of $\ln t_d$ for all the systems (Table 4). For the Bi-BPO and Bi-BPT systems, the slopes of the straight lines increase with the pulse amplitude, indicating diffusion-controlled processes. For the Bi-BPT system, the slopes at high pulse-amplitudes are greater than 2/3 because of adsorption effects under these working conditions. For the Bi-BPH system the slopes go through a maximum. The W values decrease with increasing t_d (ΔE and V kept constant), which indicates greater reversibility of these processes when the drop life-time is increased. The W value that corresponds to a reversible three-electron process is not attained for any working conditions, although for the Bi-BPT system W is very close to this theoretical value when the pulse amplitude is small. The plot of E_p vs. $\ln t_d$ is nearly linear

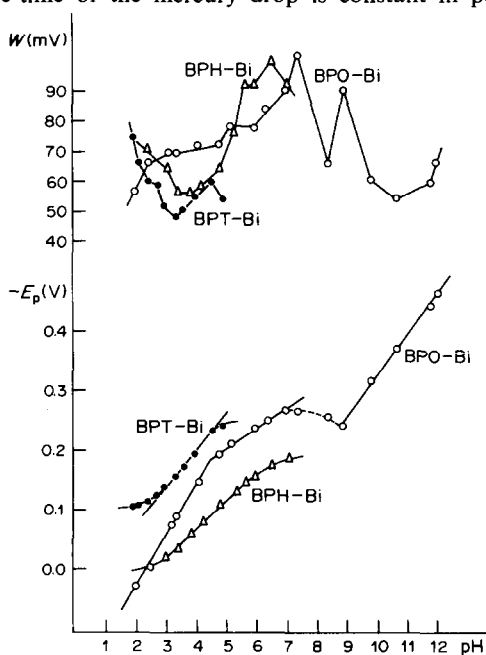


Fig. 1. Variation of W and E_p with pH.

Table 3. Study of the experimental variables for the Bi-azomethine systems

Parameter	System	Equation	Working conditions	
E_p, V	BPO-Bi =	$0.193_3 - 0.0832 \text{ pH}$	pH-range 1.90-4.71	} pH = 3.45 pH = 4.00 pH = 3.36
	BPO-Bi =	$-0.040_2 - 0.0329 \text{ pH}$	pH-range 4.71-6.99	
	BPO-Bi =	$0.370_3 - 0.0690 \text{ pH}$	pH-range 8.90-12.02	
	BPH-Bi =	$0.109_2 - 0.0449 \text{ pH}$	pH-range 3.01-5.91	
	BPT-Bi =	$0.020_3 - 0.0546 \text{ pH}$	pH-range 1.88-4.90	
$I_p, \mu A$	BPO-Bi =	$0.0999 + 0.0021 T^*$	$\beta^{0t} = 1.5\%$	$T = 30.0^\circ$
	BPH-Bi =	$0.0658 + 0.0024 T^*$	$\beta^{0t} = 2.1\%$	$T = 22.0^\circ$
	BPT-Bi =	$0.2181 + 0.0024 T^*$	$\beta^{0t} = 0.9\%$	$T = 25.0^\circ$

* T = temperature, $^\circ C$.† β^0 = temperature coefficient.

for the Bi-BPO system, but not for the others, which shows a higher degree of reversibility for these two systems.

Increasing ΔE , with t_d and V kept constant, results in increase in I_p and a shift of E_p to more negative

values, and a plot of I_p vs. $(\sigma - 1)/(\sigma + 1)$ [where $\sigma = \exp(2nF/RT\Delta E)$] for the Bi-BPT system is linear, corroborating the reversibility of the electrode process,¹⁵ but the plots for the other two systems are non-linear (Fig. 4).

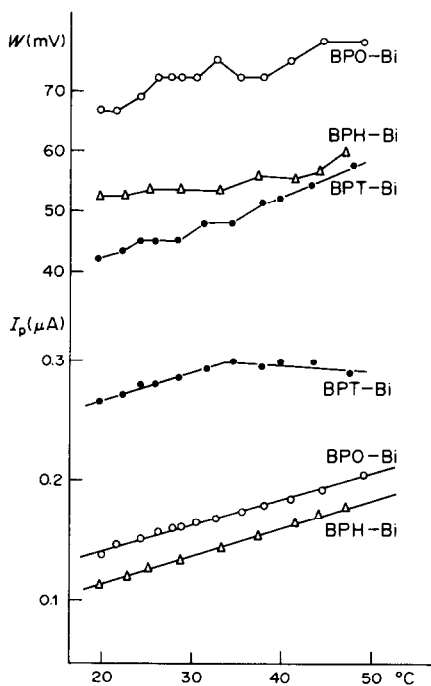
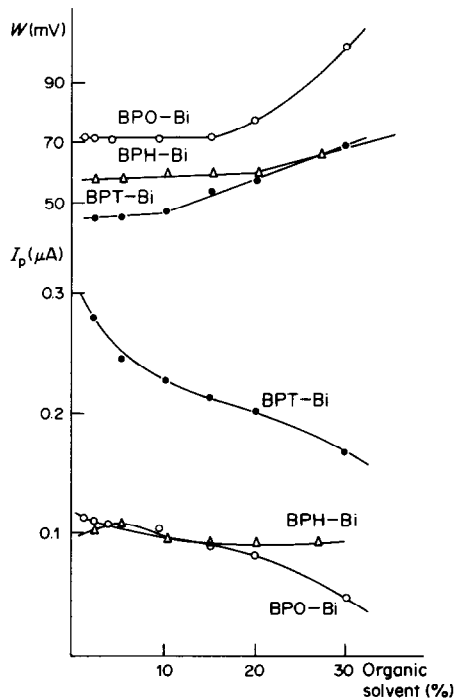
Fig. 2. Influence of temperature on W and I_p .

Fig. 3. Influence of the concentration of organic solvent.

Table 4. Study of the instrumental variables for the Bi-azomethine systems

	Equation	Correlation, r^2	Pulse, mV
BPO-Bi	$\ln I_p = -5.2300 + 0.7984 \ln h$	0.9943	-50
BPH-Bi	$\ln I_p = -4.9287 + 0.7063 \ln h$	0.9973	-50
BPT-Bi	$\ln I_p = -4.7652 + 0.8480 \ln h$	0.9982	-50
BPO-Bi	$\ln I_p = 3.5191 + 0.3751 \ln t$	0.9822	-10
	$\ln I_p = -2.4660 + 0.5214 \ln t$	0.9888	-25
	$\ln I_p = -2.1867 + 0.5764 \ln t$	0.9950	-35
	$\ln I_p = -1.7999 + 0.6269 \ln t$	0.9978	-50
BPH-Bi	$\ln I_p = -3.2150 + 0.5999 \ln t$	0.9853	-10
	$\ln I_p = -2.4103 + 0.6930 \ln t$	0.9930	-25
	$\ln I_p = -2.1653 + 0.6047 \ln t$	0.9958	-35
	$\ln I_p = -1.9426 + 0.5920 \ln t$	0.9927	-50
BPT-Bi	$\ln I_p = -2.4092 + 0.6582 \ln t$	0.9893	-10
	$\ln I_p = -1.4691 + 0.8456 \ln t$	0.9967	-25
	$\ln I_p = -1.1552 + 0.9022 \ln t$	0.9991	-35
	$\ln I_p = -0.8340 + 0.9870 \ln t$	0.9991	-50

* I_p in μA , h in cm, t in sec.

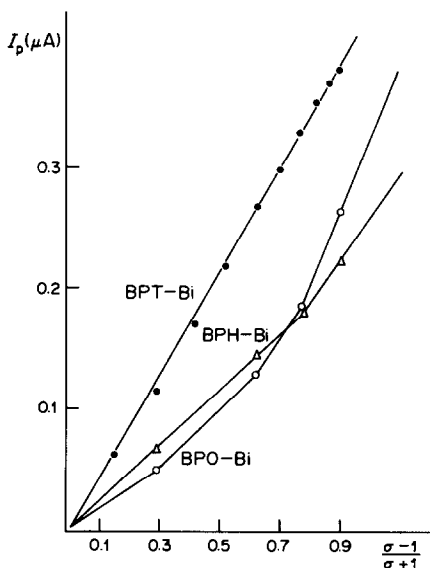


Fig. 4. Reversibility of the electrochemical processes for the Bi-azomethine systems.

If the potential scan-rate is decreased, with ΔE and t_d kept constant, E_p shifts to less negative values, I_p increases and W decreases.

Metal ion concentration and stoichiometry

The range of concentration for this study was limited by the solubility of the ligands and by the acidic character of Bi(III), which promotes its precipitation as hydroxide when it is not complexed. The ligand concentration was kept constant and the cation concentration varied as follows.

System	[Ligand], $10^{-4}M$	[Bi(III)], $10^{-5}M$
Bi-BPO	1.0	2.0-20.0
Bi-BPH	1.0	1.5-20.0
Bi-BPT	1.0	1.9-48.0

E_p and W are practically independent of the cation concentration in the Bi-BPO and Bi-BPH systems, but not in the Bi-BPT system. Plots of I_p against [ligand]/[Bi(III)] ratio, Fig. 5, allow the deduction of the stoichiometry of the complexes formed under these conditions.

For the Bi-BPO and Bi-BPH systems the ligand-bismuth ratio is 1.5, which could correspond to a 3:2 stoichiometry, but the existence of such a complex is unlikely, in view of the scant tendency of bismuth to form polynuclear complexes, and the restrictive conditions for the existence of these systems. It is much more probable that this ratio is due to the formation of two complexes (1:1 and 2:1) that predominate in the concentration range used for the study.

The plot for the Bi-BPT system clearly indicates a 2:1 complex.

Effect of ligand concentration and calculation of stability constants

Table 5 gives the data for this study. The low

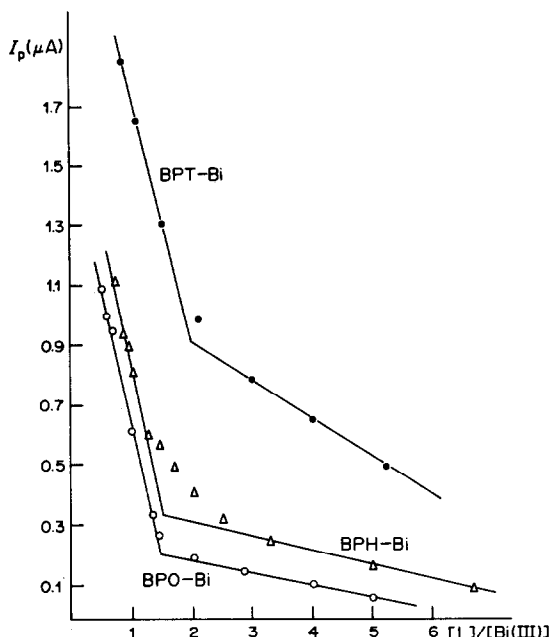


Fig. 5. Stoichiometries of the Bi-azomethine systems.

solubility of the ligands permits their concentration to be varied over only a very narrow range, so the change in reduction potential is small; it is also a function of the stability constant of the complex and this explains why the BPH system gives the smallest shift although it is the most soluble of the reagents, and the least soluble (BPT) gives the biggest shift.

The bismuth concentration was fixed at $2.0 \times 10^{-5}M$, the drop-time at 1.2 sec, pulse amplitude at 25 mV and the scan-rate potential at 2.5 mV/sec. The other conditions were as follows.

	Bi-BPO	Bi-BPH	Bi-BPT
pH	3.45	4.00	3.36
Temperature, °C	30.0	22.0	25.0
Organic solvent, %	5	6	3

The data in Table 5 were treated in the following way. The peak-potential values were obtained by means of the program F0(I)⁴ which applies the weighted least-squares method to the equation of the Tomes lines for a.c. polarography and DPP.¹³ By means of this program the intensity and potential measurements for each peak are weighted by a factor, ω_i , given by:

$$\omega_i = \frac{4I_p I_i^2 (I_p - I_i)}{I_p^2 + I_i^2}$$

where I_p is the peak current and I_i the current at the i th potential. The currents were directly measured on the polarograms. The program also calculated the number of electrons involved in the electrode process and the values of the F0 term in the DeFord and Hume equation and of the corresponding term F1 in

Table 5. Influence of the ligand concentration on the Bi-azomethine systems

System	[Ligand], mM	I_p , mA	$-E_p$, mV	F0	$n\alpha$	F1
BPO-Bi	0.0	90.0	96.9	1.00	1.47	1.00
	0.4	87.0	101.4	1.73	1.38	1.52
	0.8	76.0	108.9	4.70	1.29	2.88
	1.2	74.0	112.6	7.38	1.30	3.51
	1.6	78.0	113.6	7.85	1.26	3.64
	2.0	77.0	117.0	11.76	1.27	4.31
	2.4	72.0	118.1	14.26	1.23	5.03
	2.8	68.5	120.5	19.75	1.19	6.09
	3.2	72.5	122.5	23.48	1.21	6.22
	4.4	64.7	129.3	57.4	1.10	9.98
4.8	66.5	130.8	66.4	1.15	10.17	
BPH-Bi	0.0	133.5	82.9	1.000	2.65	1.000
	2.0	183.8	86.3	1.085	2.63	1.048
	2.6	183.8	86.4	1.098	2.60	1.079
	3.2	181.5	86.5	1.125	2.61	1.097
	3.8	186.5	86.9	1.147	2.59	1.126
	4.4	179.9	86.7	1.162	2.62	1.123
	5.0	179.0	87.2	1.239	2.61	1.195
	6.0	183.8	88.0	1.326	2.64	1.243
BPT-Bi	0.0	168.0	158.1	1.00	2.46	1.00
	0.16	258.0	168.1	2.09	3.00	1.42
	0.32	267.0	174.2	4.12	2.77	2.85
	0.48	170.0	189.3	37.76	1.92	15.05
	0.64	132.0	202.8	235.2	1.93	53.7
	0.80	125.0	293.4	266.4	1.95	60.6
	0.96	118.0	211.6	735.0	2.13	152.6
	1.12	113.0	218.8	1780.0	2.27	364.1

our modification of the DeFord and Hume method for use with quasi-reversible and irreversible systems.⁴

$$F0 = \exp\left[\frac{nF}{RT}\Delta E_{1/2}\right] + \ln \frac{I_{dM}}{I_{dC}} = \sum_{j=0}^N \beta_{ML_j} C_L^j$$

$$= 1 + \beta_1 C_L + \beta_2 C_L^2 + \dots + \beta_N C_L^N \quad (1)$$

$$F1 = \frac{I_{pM}^{(n\alpha)_j/(n\alpha)_0}}{I_{pC}} \exp\left[\frac{(E_{pM} - E_{pC})(n\alpha)_j F}{RT}\right]$$

$$= \sum_{j=0}^N \beta_{ML_j} C_L^j = 1 + \beta_1 C_L + \beta_2 C_L^2 + \dots + \beta_N C_L^N \quad (2)$$

As can be observed in Table 5, the F0 values are higher than the F1 values, because the theoretical value of 3 for the number of electrons involved (considered in F0) is never attained by the product $n\alpha$. On the other hand the variation of F0 with ligand concentration is higher than that for F1, which means in practice that the coefficients of the C_L polynomial (stability constants of the complexes) are smaller than those calculated when the theoretical number of electrons is considered; moreover, the constants that correspond to lower stoichiometries have a greater weight (which is shown graphically by smaller slopes for the curves).

Three computer methods were used for solving equations (1) and (2) for determination of the formation constants. They are described here only briefly, since a detailed description has been given elsewhere.⁴

The programs GIP(II) (Gauss iteration program) and F0W (F0 weighted) are based on application of the method of weighted least-squares to equations (1)

and (2). GIP linearizes the equations by approximate and initially estimative values of the constants; these values are called $\delta\beta_j$ and are refined by an iterative method until a preselected convergence criterion is satisfied. F0W directly linearizes equations (1) and (2) by minimizing the errors through weighting the F0 and F1 values by the factor ω_i , given by:

$$\omega_i = 1/[F0(i)]^2$$

where $[F0(i)]^2$ is the value obtained for the first member of the DeFord and Hume equation (or our equation), from the i th experiment.

The third program, MSE (minimal sum of errors) is based on a numerical approximation method which gives the values of the stability constants which minimize the difference between the experimental and theoretical values of F0 and F1.

The results are given in Table 6 and the following comments may be made.

Bi-BPO system

Similar values for the stability constants are obtained by all three programs. When the theoretical number of electrons is considered [equation(1)], only one formation constant is obtained, corresponding to 1:2 cation-ligand stoichiometry. Application of our proposed modification to the DeFord and Hume method gives significant values of β_1 , as well as of β_2 , which is in agreement with the stoichiometry shown in Fig. 5 (1:1.5), and with the molar fraction of the 1:1 and 1:2 complexes, obtained for each ligand concentration by the MSE program.

Table 6. Formation constants for the Bi-azomethine systems

System	Program	β_1	β_2
BPO-Bi	GIP II F0W M.S.W.	0	<i>Original method</i> (27.4 ± 0.8) × 10 ⁵
		0	(26.6 ± 1.30) × 10 ⁵
		0	(28.7 ± 0.1) × 10 ⁵
	GIP II F0W M.S.E.	(15.4 ± 1.7) × 10 ²	<i>Modified method</i> (83.0 ± 44.4) × 10 ³
		(16.2 ± 1.7) × 10 ²	(59.8 ± 45.3) × 10 ³
		(16.8 ± 0.1) × 10 ²	(49.8 ± 0.1) × 10 ³
BPH-Bi	GIP II F0W M.S.E.	20.4 ± 16.2	<i>Original method</i> (49.2 ± 33.8) × 10 ²
		21.0 ± 6.2	(47.7 ± 13.0) × 10 ²
		24.0 ± 1.0	(47.6 ± 0.1) × 10 ²
	GIP II F0W M.S.E.	16.4 ± 8.5	<i>Modified method</i> (37.7 ± 17.7) × 10 ²
		16.5 ± 5.1	(37.4 ± 10.8) × 10 ²
		18.0 ± 1.0	(37.5 ± 0.1) × 10 ²
BPT-Bi	GIP II F0W M.S.E.	0	<i>Original method</i> (9.2 ± 1.80) × 10 ⁸
		0	(4.1 ± 0.30 × 10 ⁸
		0	(8.67 ± 0.01) × 10 ⁸
	GIP II F0W M.S.E.	0	<i>Modified method</i> (2.0 ± 0.3) × 10 ⁸
		0	(1.3 ± 0.1) × 10 ⁸
		0	(1.79 ± 0.01) × 10 ⁸

A value of zero was obtained throughout for β_3 .

Bi-BPH system

Both the DeFord and Hume method and ours give significant values of β_1 and β_2 , in total agreement with the stoichiometry found and the molar fraction values calculated by using the MSE program. The constants are lower than those for Bi-BPO system, and the uncertainty in the values is therefore higher.

Bi-BPT system

Both methods gave only one significant value, for the constant corresponding to 1:2 cation-ligand stoichiometry. The relative errors are of the order of 10%, which is reasonable in view of the characteristics of the system.

CONCLUSIONS

The study of the effect of the cation concentration is important, since it provides information about the types of complex formed; the number and degree of the possible constants are necessary input data for the programs.

In none of the systems is a stoichiometry greater than 1:2 observed. In the absence of the ligand the Bi(III) begins to form hydroxo-complexes at a pH close to zero; hence the E_{pM} values are not the same for the three systems, since each is examined at a different pH.

The three systems studied show a variable degree of reversibility as a function of the ligand concentration; that is why the DeFord and Hume method

is not really suitable, as is demonstrated by its failure to detect some of the complexes that are experimentally shown to be present (in the study of the effect of cation concentration). These complexes are detected, however, by use of our modification.

The MSE program gives smallest uncertainty in the constants, and is the one recommended.

REFERENCES

1. M. A. Gómez-Nieto, M. D. Luque de Castro and M. Valcárcel, *Electrochim. Acta*, 1982, **27**, 435.
2. *Idem, ibid.*, 1983, **28**, 325.
3. *Idem, ibid.*, 1983, **28**, 1725.
4. M. A. Gómez-Nieto, M. D. Luque de Castro and M. Valcárcel, *Anal. Chim. Acta*, 1984, **156**, 77.
5. I. Cernatescu, A. Popescu, M. Craciom and N. Iorga, *Studii Cerc. Sti. Inst. Chim. Iasi*, 1958, **9**, 1.
6. D. D. DeFord and D. N. Hume, *J. Am. Chem. Soc.*, 1951, **73**, 5321.
7. V. G. Sochevano and G. A. Volkova, *Neorgan. Khim.*, 1969, **14**, 118.
8. E. G. Chikryzova and Sh. E. Vassershtein, *Zh. Analit. Khim.*, 1971, **26**, 1479.
9. N. Alenkova and T. Nedelcheva, *J. Electroanal. Chem.*, 1980, **108**, 239.
10. T. Jochsberger, A. Cutie and J. Mills, *J. Pharm. Sci.*, 1979, **68**, 1061.
11. B. Pokorny, *Makrotest. Sb. Prednasek. Celostatni Konf.*, 1978, **5**, 239.
12. H. Bilinski, R. Huston and W. Stumm, *Anal. Chim. Acta*, 1976, **84**, 157.
13. A. M. Bond, *Modern Polarographic Methods in Analytical Chemistry*, p. 301. Dekker, New York, 1980.
14. M. A. Gómez-Nieto, unpublished results.
15. E. P. Parry and R. A. Osteryoung, *Anal. Chem.*, 1965, **37**, 1634.

BACKGROUND-CURRENT SUBTRACTION IN VOLTAMMETRIC DETECTION FOR FLOW-INJECTION ANALYSIS

JOSEPH WANG* and HOWARD D. DEWALD

Department of Chemistry, New Mexico State University, Las Cruces, NM 88003, U.S.A.

(Received 30 June 1983. Revised 21 November 1983. Accepted 7 December 1983)

Summary—A new approach for background-current subtraction for flow-injection systems using potential-scanning voltammetric detection is described. The method is based on recording voltamperograms while the sample and carrier solutions flow through the cell, and taking the difference as the net response for the sample. Background currents due to hydrogen evolution, oxygen reduction, solvent oxidation or surface processes are thus compensated, and detection limits at submicromolar levels can be obtained. The compensation for oxygen reduction current means that samples do not need to be deaerated. The method has been evaluated for reproducibility, concentration dependence, detection limit, etc. A flow-cell with a stationary disk electrode, a 200- μ l sample volume, and rapid differential pulse scanning are used. At a flow-rate of 0.3 ml/min about 15 samples can be assayed per hour. Chlorpromazine, phenol, acetaminophen, norepinephrine, lead, cadmium, bismuth and zinc were used as test species.

Flow-injection analysis (FIA) is a versatile and fast method of automated analysis, based on the injection of reproducible sample volumes into a continuously flowing carrier stream.^{1,2} The use of electrochemical transducers as detectors in FIA is growing rapidly.³ Most electrochemical transducers utilize constant-potential amperometric detection, mainly because of its inherent sensitivity. The increasing demand for improved selectivity and multi-component determinations in flow-injection systems has resulted in the incorporation of dynamic voltammetric detection based on rapid potential scanning.^{4,5} A voltamperogram recorded during passage of the sample plug through the detector gives instantaneous electro-analytical data. Thus, the resolution of voltammetry adds selectivity to flow-injection systems, the peak potentials serving for identification. However, there is a loss in sensitivity as a result of background currents associated with the potential scan.

This paper reports a subtractive approach for background-current correction in FIA with voltammetric detection. Subtractive techniques, based on subtracting the blank voltamperogram from the sample response, have been applied in anodic-stripping voltammetry^{6,7} and conventional a.c. polarography.⁸ The flow manifold of FIA systems can easily be exploited to obtain a subtractive response. By subtraction of the voltamperogram for the carrier stream from that for the sample plug, a net signal for the analyte can be obtained, free from background effects (provided that the background electrolyte content of the sample matches that of the carrier). Two systems can be used: (1) placing two "identical" working

electrodes before and after the injection port, and subtracting the carrier response from that of the sample plug; (2) using a single working electrode, and recording the "background" and "sample" voltamperograms while the carrier and sample plugs, respectively, flow through the cell. The second option seems the more promising, since it eliminates problems associated with matching two electrodes and the need for an additional polarograph. The characteristics and applications of this procedure are described below.

EXPERIMENTAL

Apparatus

The flow-injection system consisted of carrier and sample reservoirs (400-ml Nalgene beakers), a Model RP-SY FMI reciprocating piston pump (Fluid Metering, Inc.), a Rheodyne Model 7010 injection valve with a 200- μ l sample loop, and the electrochemical detector. All connections were made with 0.5-mm bore Teflon tubing and fittings (Pierce Chemical Co.). The tubing connecting the valve to the detector was 8 cm long.

The electrochemical detector has already been described.⁵ A solution flow channel was drilled through the plexiglas body. Various 3-mm diameter disk working electrodes were employed, including mercury-coated glassy carbon, bare glassy carbon and carbon paste. The Ag/AgCl reference electrode (Model RE-1, Bioanalytical Systems) joined the working-electrode compartment close to the face of the working electrode.⁵ The carbon-rod auxiliary electrode dipped into the solution in the outlet channel. All measurements were made with a Sargent-Welch Model 4001 polarograph.

Reagents

Millimolar stock solutions of phenol, acetaminophen and norepinephrine were made up fresh each day. Standard bismuth and zinc solutions were stored in polyethylene containers. Supporting electrolytes were 0.05M phosphate buffer and 0.1M potassium nitrate. Other chemicals and reagents used have already been described.^{9,10}

*Author for correspondence.

Procedure

The carrier solution was pumped continuously at constant rate (usually in the range 0.2–0.4 ml/min). After gravity filling of the injection loop with sample, the valve was turned into the injection position. Rapid (1–2 V/min) differential pulse scans were initiated 15–40 and 120–150 sec after the injection, to record the “sample” and “background” voltamperograms, respectively. The optimum times for initiating the potential scans depend upon the experimental conditions and the species measured, as will be described later. For measurements in the cathodic region, the glassy-carbon electrode was coated with a mercury film by passing $5 \times 10^{-5} M$ mercury(II) in the carrier solution through the detector at a rate of 0.2 ml/min for 20 min, with a potential of -0.8 V imposed on the working electrode; a gravity flow was used in these cathodic experiments. The subtractive voltamperograms were obtained by using a time-sharing computer as described previously.¹⁰

RESULTS AND DISCUSSION

Though the differential pulse waveform effectively corrects for the non-faradaic charging current, various faradaic background currents remain and limit the detection power. The subtractive mode corrects for these background currents, and was first tested with single-species systems. Figure 1 shows FIA voltamperograms for various species, recorded in the conventional way and also after background-current subtraction. The species were chosen to illustrate compensation of background currents from different sources: zinc (hydrogen evolution and reduction of oxygen); chlorpromazine and phenol (oxidation of

water and redox reactions of the carbon surface functional groups); bismuth (reduction of oxygen). Well-shaped and easily measured peaks, with relatively flat base-lines, are obtained in the subtractive mode. Correction for oxygen reduction (curves C and D) is of special interest because removal of oxygen from small volumes of injected solutions requires a relatively cumbersome procedure,¹¹ and is not effective if the flow analyser is constructed from Teflon tubing, which is readily permeated by oxygen. All the data reported in this paper were obtained with samples that had not been deaerated.

For effective background-subtraction, however, careful matching of the electrolyte content and pH of the sample and carrier solutions is essential. For example, for background currents that are pH-dependent (e.g., hydrogen evolution, oxygen reduction) solutions of different pH would yield incompletely corrected base-lines. Partial matching of the sample and carrier solutions (especially when real samples are concerned) can be done by diluting the sample with the carrier (supporting electrolyte) solution, or by adding to the carrier some of the sample macro constituents; if matching is essential but incomplete, the base-line will not be flat.

Because of the dispersion process in FIA systems, careful and reproducible timing is required for recording the two voltamperograms, so that the appropriate solution is in the detector. For this, exact knowledge of the concentration profile of the sample

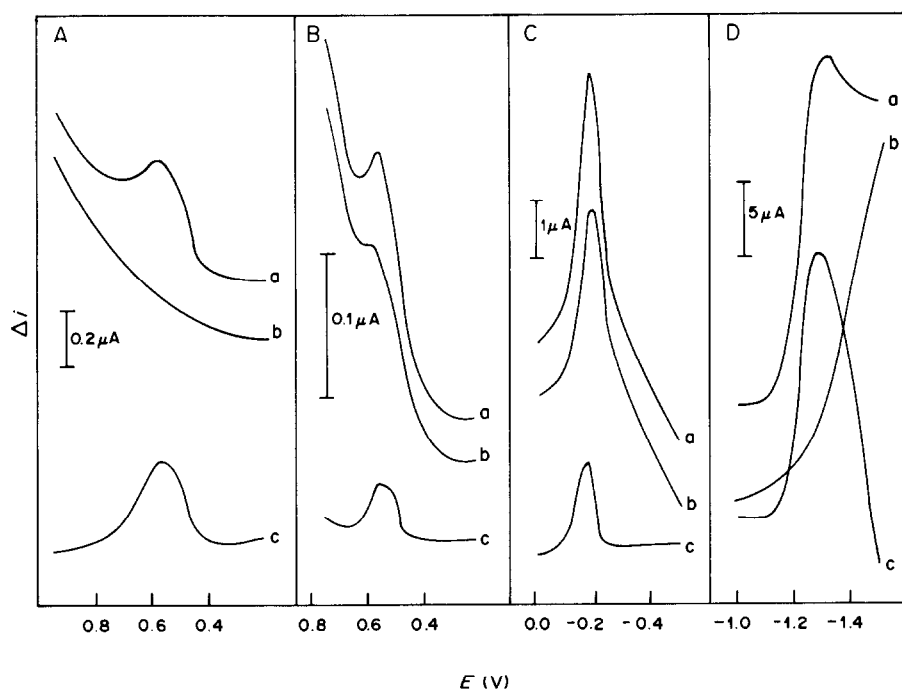


Fig. 1. FIA/differential pulse measurements of $5 \times 10^{-5} M$ phenol (A), $5.2 \times 10^{-5} M$ chlorpromazine (B), $3.6 \times 10^{-5} M$ bismuth (C), and $1 \times 10^{-4} M$ zinc (D). (a) “Analytical” (sample) curve; (b) “background” (carrier) curve; (c) the subtractive response, (a) – (b). Differential pulse scan-rate, 2 (A, B, D) and 1 (C) V/min; amplitude, 50 mV; repetition time, 0.5 sec. Carrier and supporting electrolyte, 0.05M phosphate buffer (A, B), 0.1M KNO_3 (C, D). Electrodes, carbon paste (A, B), mercury-coated glassy carbon (C, D). Flow-rate, 0.3 (A, B, C) and 0.5 (D) ml/min.

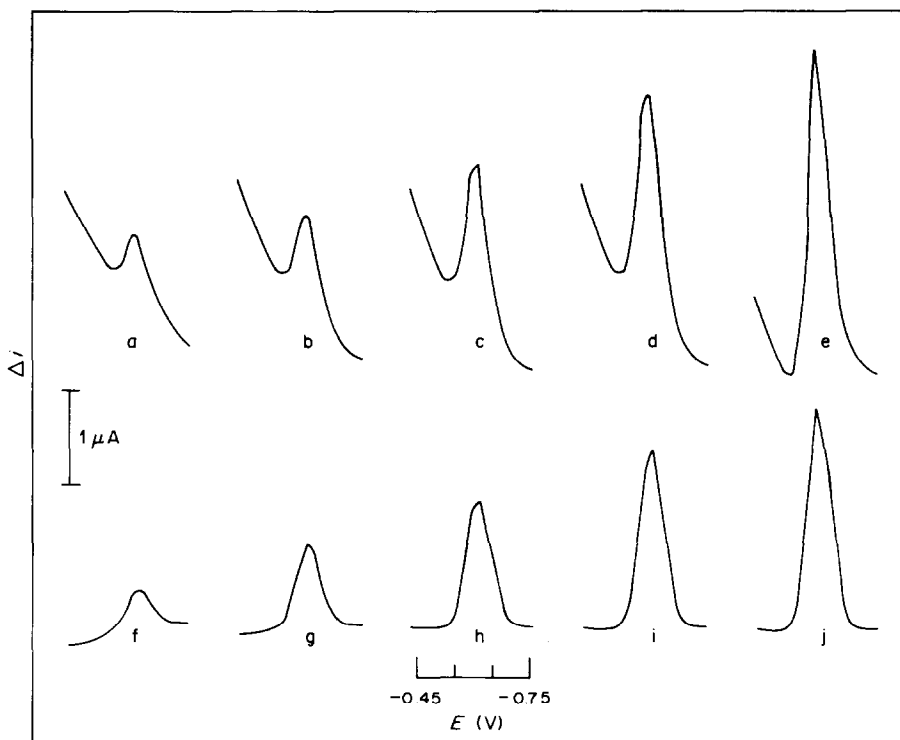


Fig. 2. Comparison of voltammetric (a-e) and subtractive voltammetric (f-j) response obtained after injections of lead solutions of increasing concentrations: (a, f) $5.0 \times 10^{-6}M$, (b, g) $1.0 \times 10^{-5}M$, (c, h) $1.5 \times 10^{-5}M$, (d, i) $2.0 \times 10^{-5}M$, and (e, j) $2.5 \times 10^{-5}M$. Carrier and supporting electrolyte, $0.1M KNO_3$. Electrode, mercury-coated glassy carbon. Differential pulse ramp and flow-rate as for Fig. 1C.

zone is required; this is usually obtained by preliminary measurement of the current-time profile or by initiating the potential scan at different times after sample injection. To allow scanning of a 1.0-V potential region during passage of the peak concentration sample zone (60–100% of the concentration maximum) through the detector, a flow-rate of 0.2 ml/min and a scan-rate of 2 V/min were used.⁵ Obviously, when mixtures of species with different redox potentials are analysed, some species are measured before and some after their concentration peak has passed the detector. To minimize carry-over, the “background” voltamperogram must not be initiated earlier than 120 sec after sample injection. For analytes that interact (by adsorption or extraction) with the electrode surface, *e.g.*, chlorpromazine [Fig. 1(B)], longer delay times are required to ensure removal of these surface species. As a compromise between sensitivity and speed, a delay time of 150 sec has been used for such species, resulting in a partial loss of the analytical signal (as the peak for residual chlorpromazine, shown in the “background” response, is subtracted from that of the “analytical” one). The influence of the experimental variables affecting the voltammetric scan and the dispersion of the sample plug has been discussed elsewhere in detail.⁵

Figure 2 compares voltamperograms recorded in the conventional and subtractive modes for lead solutions of increasing concentration. The con-

ventional current peaks are affected by the background current, associated mainly with oxygen reduction, whereas well-defined peaks and a horizontal base-line are obtained in the subtractive mode. The peak currents in the subtractive mode are proportional to the lead concentration (least-squares analysis yields a slope of $0.12 \mu A \cdot l \cdot \mu mole^{-1}$ (correlation coefficient 0.9997, intercept $-0.16 \mu A$). Similar calibration experiments for cadmium, zinc and dopamine (concentration ranges 10–50, 100–200 and 50–125 μM , respectively) also yielded linear plots. From the signal-to-background characteristics of the response [Fig. 2(f)] the detection limit for lead would be near $5 \times 10^{-7}M$ (corresponding to 20 ng in the volume injected).

The precision of the method was estimated by repeated injection of $2.5 \times 10^{-5}M$ lead (conditions as in Fig. 2). The mean peak current was $2.78 \mu A$, range 2.77 – $2.80 \mu A$, relative standard deviation 0.4% (7 replicates).

Figure 3c illustrates application of the method to analysis of mixtures. The bismuth, lead, cadmium and zinc mixture (micromolar concentrations) yields well-defined and separated peaks, over a relatively flat base-line. Comparison with the conventional voltamperogram (curve a) shows the superiority of the subtractive mode, especially for zinc and bismuth. Similar improvement was obtained for a mixture of oxidizable species: $5 \times 10^{-5}M$ norepinephrine, ace-

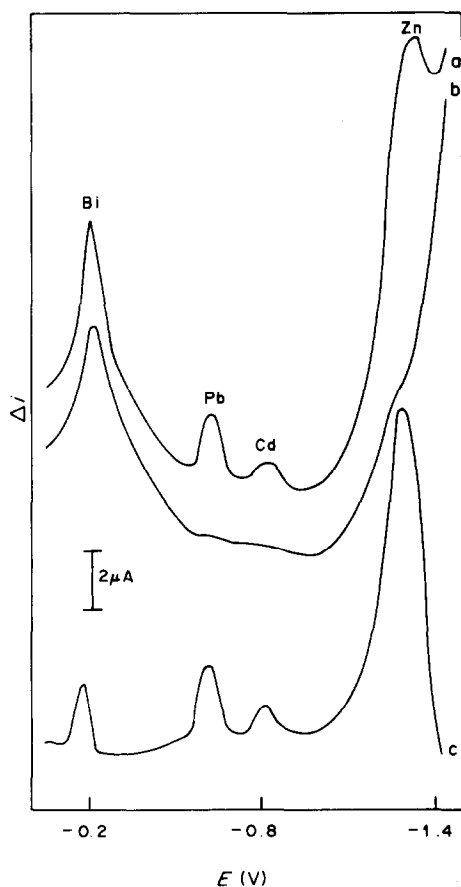


Fig. 3. Response for the injection of a sample mixture ($2 \times 10^{-5}M$ bismuth, lead and cadmium and $5 \times 10^{-5}M$ zinc). (a) "Analytical" curve; (b) "background" curve; (c) the subtractive response, (a) - (b). Differential pulse ramp, flow-rate, working electrode, and supporting electrolyte as for Fig. 1C; scan-rate 2 V/min.

taminophen and chlorpromazine. Depending on the peak potentials and peak half-widths of the sample components, up to 6 species can be measured in one injection.

These results confirm the utility of the approach. The method is applicable to other dynamic FIA detection modes, e.g., scanning spectroscopy. The approach may also be used with segmented flow systems. Because of the time required to record the voltamperograms, the method has a slower injection rate (about 15 samples per hour) than FIA with amperometric detection, but this is offset by the multi-component detection capability. Higher injection rates could be achieved by using faster potential pulse techniques, e.g., rapid square-wave voltammetry,¹² and by recording the "background" voltamperogram at given time intervals (e.g., every 30 min) rather than after each injection (or at the beginning of a series of injections). As in all FIA studies, highly reproducible timing is essential. An extension of this methodology toward subtractive anodic stripping voltammetry, with depositions during the passage of the sample and carrier solutions through the detector, has been accomplished recently in our laboratory.¹³

Acknowledgement—This work was supported by a grant from the U.S. Department of the Interior, through the New Mexico Water Resources Research Institute.

REFERENCES

1. D. Betteridge, *Anal. Chem.*, 1978, **50**, 832A.
2. J. Růžička and E. H. Hansen, *Anal. Chim. Acta*, 1978, **99**, 37.
3. E. Pungor, Z. Fehér, G. Nagy, K. Tóth, G. Horvai and M. Gratzl, *ibid.*, 1979, **109**, 1.
4. J. Janata and J. Růžička, *Anal. Chim. Acta*, 1982, **139**, 105.
5. J. Wang and H. D. Dewald, *ibid.*, 1983, **153**, 325.
6. W. Kemula, *Pure Appl. Chem.*, 1967, **15**, 283.
7. J. Wang and M. Ariel, *J. Electroanal. Chem.*, 1977, **85**, 289.
8. K. J. Martin and I. Shain, *Anal. Chem.*, 1958, **30**, 1808.
9. J. Wang, H. D. Dewald and B. Grecnc, *Anal. Chim. Acta*, 1983, **146**, 45.
10. J. Wang and B. A. Freiha, *Talanta*, 1983, **30**, 837.
11. J. Y. Lewis, J. P. Zodda, E. Deutch and W. R. Heineman, *Anal. Chem.*, 1983, **55**, 708.
12. J. Wang, E. Ouziel, C. Yarnitzky and M. Ariel, *Anal. Chim. Acta*, 1978, **102**, 99.
13. J. Wang and H. D. Dewald, *Anal. Chem.*, 1984, **56**, 156.

SHORT COMMUNICATIONS

DETERMINATION OF ULTRA TRACE CONCENTRATIONS OF NITRITE IN POLLUTED WATERS AND SOIL

ABHA CHAUBE, ANIL K. BAVEJA and V. K. GUPTA*

Department of Chemistry, Ravishankar University, Raipur (M.P.), 492010 India

(Received 11 March 1983. Revised 31 October 1983. Accepted 17 December 1983)

Summary—The nitrite is used to diazotize *o*-nitroaniline and the *o*-nitrophenyldiazonium chloride formed is coupled with *N*-(1-naphthyl)ethylenediamine dihydrochloride. The red-violet dye (absorption maxima at 545 nm) is stable and extractable into isoamyl alcohol. Beer's law is obeyed in the range 0.1–0.6 ppm nitrite in the original sample if the aqueous system is measured, and 0.025–0.15 ppm in the sample if extraction is used. The molar absorptivity is $6.04 \times 10^4 \text{ l. mole}^{-1} \cdot \text{cm}^{-1}$.

Industrial effluents and the nitrogen cycle add to contamination of the environment with nitrite. Nitrite is undesirable in water owing to its toxicity.^{1,2} The maximum permissible in potable water is fixed by the U.S. Public Health Service at 0.06 ppm.³

Most spectrophotometric methods for determination of nitrite in water and waste water are based on the Griess–Ilosvay reaction^{4,5} and some include use of solvent extraction to enhance the sensitivity.^{6,7} Here we introduce *o*-nitroaniline as the substrate for diazotization. The *o*-nitrophenyldiazonium chloride formed is coupled with *N*-(1-naphthyl)ethylenediamine dihydrochloride in acid medium to give a red-violet dye (absorption maxima at 545 nm), extractable into isoamyl alcohol. The molar absorptivity is $6.04 \times 10^4 \text{ l. mole}^{-1} \cdot \text{cm}^{-1}$. The method is more sensitive than some recently reported methods.^{8–11}

EXPERIMENTAL

Reagents

All reagents used were of analytical-reagent grade.

Standard 1000 µg/ml nitrite solution. Prepared in de-aerated doubly distilled water from reagent dried for 4 hr at 110°, and standardized;¹² a small amount of chloroform was added as stabilizer. A 1-µg/ml working standard was prepared by dilution with de-aerated, doubly distilled water.

***o*-Nitroaniline solution, 0.001M.** Prepared in 20% aqueous ethanol from a twice recrystallized commercial reagent.

***N*-(1-Naphthyl)ethylenediamine dihydrochloride solution, 0.1%.**

Solutions of foreign ions were prepared according to West.¹³

Procedure

To a known volume of water sample (containing 2.5–15 µg of nitrite) in a 25-ml standard flask, add 1 ml of *o*-nitroaniline solution and adjust to 1M hydrochloric acid concentration. Shake the flask occasionally during the next 2 min to ensure complete diazotization. Add any masking agent needed and 2 ml of NEDA solution, and make up to the mark with 5M hydrochloric acid. Measure the absorbance at 545 nm against distilled water after 5 min. Prepare

a calibration graph for 2.5–15 µg of nitrite in a similar manner.

Solvent extraction

Place a known volume of sample (up to 100 ml, containing 2.5–15 µg of nitrite) in a 250-ml separatory funnel and form the red-violet dye as described above, except that the final acidity is adjusted to 2.5M hydrochloric acid. Extract the dye with two 10-ml portions of isoamyl alcohol, dry the combined extracts with anhydrous sodium sulphate and dilute to volume in a 25-ml standard flask with the solvent. Measure the absorbance at 545 nm against a reagent blank similarly treated. Prepare a calibration graph by treating standards in a similar manner.

RESULTS AND DISCUSSION

The absorption spectrum of the red-violet dye shows maximum absorption at 545 nm. Under the recommended conditions the dye is stable for up to 20 hr, and the absorbance varies by not more than 2% over a period of up to 30 hr.

Reaction conditions

The effect of acidity on the diazotization was studied. A hydrochloric acid concentration of at least 1M was found necessary for complete diazotization; a 1–6M acidity range gave constant absorbance. Constant absorbance values were obtained for diazotization reaction times from 1 to 90 min, and the minimum time for the coupling reaction was found to be 2 min.

The effects of varying the molar ratio of *o*-nitroaniline (ONA) and NEDA to nitrite were examined. For ONA and nitrite, the absorbance was constant for ONA:NO₂⁻ molar ratios ≥1:1. Similarly maximum absorbance was obtained with NEDA:NO₂⁻ ratios ≥10:1.

Analytical characteristics

The colour system was found to obey Beer's law in the range 2.5–15 µg of nitrite per 25 ml of initial aqueous sample for the direct procedure, and 2.5–15 µg per 100 ml of sample when the extraction procedure was used. The molar absorptivity was found

*Senior author, to whom correspondence should be addressed.

Table 1. Effect of diverse species on determination of 0.1 ppm of nitrite (100 ml of solution, extraction method)

Tolerance limit, ppm	Species
800	SO ₄ ²⁻ , NO ₃ ⁻ , PO ₄ ³⁻ , HCO ₃ ⁻ , SiO ₃ ²⁻
150	Mg ²⁺ , Ca ²⁺ , Sr ²⁺ , Ba ²⁺ , Zr ⁴⁺ , Co ²⁺ , Zn ²⁺ , Cd ²⁺ , Hg ²⁺ , Pb ²⁺
100	Li ⁺ , Be ²⁺ , Cr ³⁺ , Mo(VI), W(VI), Ni ²⁺ , Sb ³⁺ , Bi ³⁺ *, Se(IV), Te(IV), F ⁻ , Br ⁻
50	Fe ³⁺ *
40	I ⁻ †, aniline, HCHO, phenol
10	SO ₃ ²⁻ ‡, SO ₂ §
2	Cu ²⁺

*Masked with 1 ml of 10% sodium potassium tartrate solution.

†Masked with 1 ml of 10% tetrachloromercurate solution.

§Masked with H₂O₂.

to be 6.04×10^4 l. mole⁻¹. cm⁻¹ for both systems. The reproducibility was studied by replicate analysis of a standard nitrite solution over a period of 7 days. The relative standard deviation was found to be 1.1% and 1.5% for the direct and extraction procedures respectively.

Effect of foreign species

Since the method was developed mainly for the analysis of water samples, the effects of foreign species at the levels commonly present in tap water, river water and tank water were studied. The tolerance limits shown in Table 1 are the concentrations of foreign species that cause $\leq 2\%$ error in the determination of 0.1 ppm of nitrite by the extraction method (100-ml samples). Cu(II), Fe(II) and SO₂ interfere but the interference of up to 100 ppm of SO₂ can be eliminated by oxidizing it to sulphate with hydrogen peroxide. Bismuth and Fe(III) require masking with tartrate.

Solvent extraction

The limit of detection can be lowered by employing solvent extraction. Of the solvents tested, isoamyl alcohol was found the best. The molar absorptivity was lower when higher alcohols such as hexanol and octanol were used, and the dye was unstable in chloroform. Extraction was incomplete with benzene, dichlorobenzene or carbon tetrachloride. By use of a large sample (100 ml) and extraction of the dye into isoamyl alcohol, very low concentrations of nitrite (0.025 μ g/ml) can be determined.

Application to polluted waters and soil

Samples were collected in wide-mouthed plastic vessels at different points upstream and downstream from the source of industrial effluents. Samples of potable water were collected from different tanks. Mercuric chloride (4 mg per 100 ml of sample) was used for preservation and samples were frozen at 0° within 1 hr of sampling. Samples were filtered through a Whatman No. 41 paper before analysis.

Soil samples of manured garden soil, farmland soil and roadside soil were taken. Each sample was broken up into lumps, and a 5-g portion dried at 55° in an oven for 12–16 hr. The heating stops further changes.¹⁴ The dried sample was ground, passed through a 2-mm mesh sieve and transferred to a Whatman No. 50 filter paper on a Buchner funnel. Sufficient water (containing 1 or 2 drops of concentrated sulphuric acid) was poured on to soak the soil completely. After a few minutes gentle suction was applied and the soil was washed with doubly distilled water until about 250 ml of filtrate had been collected. The filtrate was made up to a standard volume and aliquots were analysed.

Two sets of experiments were performed to check the validity of the method. In the first set, the volume of test solution was varied and the absorbance was plotted *vs.* volume taken. For all the samples linear plots were obtained, which could be extrapolated to the same point as that obtained for demineralized water; this indicates that the determination was quantitative. In the second set, recovery of nitrite was checked by adding various amounts of nitrite to a

Table 2. Tap water analysis (means of five analyses, 10-ml samples)

Nitrite added, μ g/25 ml	Present method		Standard method	
	Nitrite found, μ g/25 ml	Recovery, %	Nitrite found, μ g/25 ml	Recovery, %
2.5	2.50	100.00	2.51	100.4
5.0	4.95	98.8	5.00	100.0
7.5	7.49	99.9	7.45	99.3
10.0	10.00	100.0	10.00	100.0
12.5	12.45	99.6	12.51	100.1
15.0	15.00	100.00	15.00	100.0

Table 3. Tank water analysis by the standard addition method (means of five analyses, 10-ml samples)

Sample	Nitrite found, $\mu\text{g}/25\text{ ml}$	
	Present method	Standard method
1	0.22	0.21
2	0.12	0.12
3	0.00	0.00
4	0.13	0.14
5	0.18	0.18
6	0.20	0.20
7	0.00	0.00

Table 4. River water analysis*

Nitrite found, ppm	
Present method†	Standard method‡
0.24	0.23
0.37	0.38
0.65	0.65
0.71	0.71
0.36	0.35
0.78	0.78
0.52	0.52
0.79	0.80
0.82	0.81
0.72	0.72
0.66	0.64
0.98	0.97

*Kharoon river water was sampled: the first six samples are from upstream and the second six from downstream of the source of effluent.

†A 5-ml sample was diluted to 100 ml prior to the determination, as the samples contained a high concentration of nitrite. Extraction procedure was used.

‡A 10-ml sample was used for each determination.

fixed volume of test solution. Recoveries were between 98.7 and 100%. The results are given in Tables 2 and 3.

Comparison with standard method³

The values obtained for the water and soil samples by the standard method and the proposed method were compared (Tables 4 and 5). The coefficients of correlation of the two methods were found to be 0.986 and 0.99 for 12 samples from the river Kharoon and the soil samples respectively. The results of the two methods were almost identical, so the accuracy of the method is satisfactory.

Conclusion

The proposed method is about 30% more sensitive than the standard method. The rapid colour development, excellent reproducibility, and freedom from

Table 5. Soil analysis* (means of five analyses)

Nitrite found, %	
Present method	Standard method
0.192	0.191
0.161	0.162
0.116	0.115
0.115	0.113
0.108	0.109
0.016	0.017
0.054	0.052
0.018	0.018
0.007	0.006
0.015	0.015

*The first five samples were freshly manured garden soil, the next three farmland soil near a fertilizer plant, and the last two roadside soil.

pH-effects and interference by a large group of foreign ions are advantages of the method. The extraction method is advantageous because it lowers the detection limit by the concentration effect. A further improvement might be obtained by using a longer path-length cell.

Acknowledgements—The authors are grateful to the Head of the Department of Chemistry for providing laboratory facilities. A.C. and A.K.B. thank the University Grants Commission, New Delhi and C.S.I.R., New Delhi for providing fellowships.

REFERENCES

1. F. A. Patty, *Industrial Hygiene and Toxicology*, Vol. II, p. 917. Interscience, New York, 1963.
2. E. J. Calabrese, *Pollutants and High-Risk Groups*, pp. 99, 187. Wiley-Interscience, New York, 1978.
3. American Public Health Association and Water Pollution Control Federation, *Standard Methods For The Examination of Water and Waste Water*, 14th Ed. p. 434. American Public Health Association, New York, 1975.
4. C. A. Steruli and P. R. Averell, *The Analytical Chemistry of Nitrogen and Its Compounds*, Part I p. 121. Wiley-Interscience, New York, 1970.
5. A. K. Babko and A. T. Pilipenko, *Photometric Analysis—Methods of Determining Non-metals*, p. 35. Mir, Moscow, 1976.
6. H. D. Zeller, *Analyst*, 1955, **80**, 632.
7. A. Foris and T. R. Sweet, *Anal. Chem.*, 1965, **37**, 701.
8. W. A. Bashir and S. Flamerz, *Talanta*, 1981, **28**, 697.
9. S. Flamerz and W. A. Bashir, *Analyst*, 1981, **106**, 243.
10. A. K. Baveja and V. K. Gupta, *ibid.*, 1981, **106**, 955.
11. K. R. Paul and V. K. Gupta, *Environ. Intern.*, 1981, **5**, 153.
12. I. M. Kolthoff, V. A. Stenger, R. Belcher and G. Matsuyama, *Volumetric Analysis*, Vol. III, pp. 69–70. Interscience, New York, 1957.
13. P. W. West, *J. Chem. Educ.*, 1941, **18**, 528.
14. S. L. Chopra and J. S. Kanwar, *Analytical Agricultural Chemistry*, Kalyani, New Delhi, 1976.

A SENSITIVE SPECTROPHOTOMETRIC METHOD FOR THE DETERMINATION OF METHYL ALCOHOL IN AIR AND WATER

PRATIMA VERMA and V. K. GUPTA*

Department of Chemistry, Ravishankar University, Raipur 492010, India

(Received 30 March 1983. Revised 24 November 1983. Accepted 17 December 1983)

Summary—A sensitive spectrophotometric method for the indirect determination of methyl alcohol in air and water is described. The methyl alcohol is oxidized to formaldehyde which is then determined in acidic medium with *p*-aminoazobenzene and sulphur dioxide. Beer's law is obeyed in the range 100–600 μg of methyl alcohol in 25 ml of final solution and the wavelength of maximum absorption is 505 nm. The lower limit of determination is 5 $\mu\text{g}/\text{ml}$ in the sample. Several common organic co-pollutants do not interfere. The method can be used for determination of methyl alcohol in blood.

Methanol is used extensively as an industrial solvent, particularly in the lacquer industry, and as a starting material for chemical syntheses. Ingestion of large amounts can cause blindness, intoxication and death.¹ The threshold limit value (TLV) for methanol in air is 200 ppm.²

A survey of the literature reveals only a few methods for the direct determination of methanol. Most of them are not specific, and involve reaction of the –OH functional group.³ Various methods used for the determination of formaldehyde have been modified for the determination of methanol.^{4–10} Jephcott⁴ used acidic potassium permanganate to oxidize methanol to formaldehyde and added oxalic acid to remove the excess of oxidant before finally developing a colour with Schiff's reagent. Bhatt and Gupta⁵ also oxidized methanol with acidic potassium permanganate but removed the excess by reaction with hydrogen peroxide, then used the colour reaction with oxalyldihydrazide (ODH) and copper(II) in acetate buffered medium. Boss,⁶ and Rayner and Jephcott,⁷ used chromotropic acid and Schiff's reagent for the estimation of formaldehyde. Barns and Speicher⁸ determined formaldehyde by Schryver's method with phenylhydrazine. Edwin⁹ used chromotropic acid for the determination of oxidized methanol.

In the present communication a new combination is described for the indirect spectrophotometric determination of methanol. The methanol is again oxidized with acidic potassium permanganate⁶ and the formaldehyde formed is determined with the *p*-aminoazobenzene and sulphur dioxide reagent system,¹¹ which was originally used for the estimation of sulphur dioxide.¹² The pink dye formed in acidic medium exhibits maximum absorption at 505 nm.

EXPERIMENTAL

Apparatus

A Carl Zeiss Spekol and an ECIL spectrophotometer model GS-865 with 10-mm matched silica cells were used for all spectral measurements. Midget impingers of 35-ml capacity were used for air sampling. Calibrated rotameters (PIMCO) were used for measuring flow-rates.

Reagents

Standard methanol solution. Dilute 0.5 g of analytical grade methanol to 100 ml with demineralized water and further dilute 4 ml of this solution to 100 ml to obtain a working standard solution containing 200 μg of methanol per ml.

Oxidizing solution. Dissolve 3 g of potassium permanganate in 20 ml of distilled water plus 15 ml of concentrated phosphoric acid and dilute to 100 ml.

Sulphite solution. Prepare a 3% solution of analytical grade anhydrous sodium sulphite in distilled water.

***p*-Aminoazobenzene.** Prepare a 0.02% solution in 25% aqueous ethanol, with recrystallized reagent.

Absorption solution. Dilute 1 ml of oxidizing solution to 5 ml with doubly distilled water.

Phosphoric acid, 50% v/v. Dilute 50 ml of concentrated phosphoric acid to 100 ml with water.

Procedure

Water samples. Transfer a measured volume of sample (x ml, not exceeding 5 ml), containing 100–600 μg of methanol, to a 25-ml standard flask, add 1 ml of oxidizing solution and $(x-5)/15$ ml of 50% v/v phosphoric acid, mix and let stand for 10 min. Then remove the excess of potassium permanganate by adding sodium sulphite solution dropwise. Add 1 ml of *p*-aminoazobenzene solution. After 20 min add 1 ml of concentrated hydrochloric acid and make up to the mark with distilled water. Measure the absorbance and also that of a reagent blank, at 505 nm, against distilled water. Prepare a calibration graph in a similar manner.

Air samples. Connect two midget impingers, containing 5 ml of absorption solution, in series. Draw the air sample through the absorption solution at a rate of 500 ml/min for 20 min. After sampling, develop the colour with *p*-aminoazobenzene as described for water samples. Between 96 and 100% of the methanol is absorbed in the first impinger.

*To whom correspondence should be sent.

Table 1. Interferences in the determination of methanol (300 μg in water)

Tolerance limits*, mg
Acetaldehyde (0.62), benzaldehyde (12.5), aniline (1.25), toluene (20), benzene (37), urea (25), phenol (12.5), formic acid (2.5), acetic acid (3.7), ethanol (25), ethylamine (2.5), ammonia (0.62), nitrobenzene (12.5), nitrogen dioxide (1.1), isobutyl methyl ketone (2.5), acetone (25), hydrogen sulphide (6.2), ethoxyethanol (1.2), methoxymethanol (1.0)

*The weight of foreign species in the solution measured, which will cause not more than $\pm 2\%$ error.

RESULTS AND DISCUSSION

The oxidation mixture consists of potassium permanganate and phosphoric acid, the latter being used because it inhibits colour production by other aldehydes.¹⁰ The excess of potassium permanganate is reduced with sodium sulphite solution, which also serves as a source of sulphur dioxide for the colour reaction,¹² which makes it preferable to other reducing agents.¹³ An excess of sodium sulphite has no effect on the absorbance.

The acidity of the solution for oxidizing the methanol is maintained with phosphoric acid; an acid concentration of at least 0.5M is necessary for complete oxidation and no change in the measured absorbance is observed over the range 0.5–1.5M phosphoric acid. After oxidation, the acidity during colour development is increased by addition of hydrochloric acid, it was observed that maximum absorbance was obtained in the range 0.4–1.2M hydrochloric acid.

The effect of time and temperature on the colour development was studied: maximum colour was obtained after 30 min, and remained stable for 2 hr in the temperature range from 15 to 40°.

Beer's law, reproducibility and sensitivity

The absorption maximum of the pink dye is at 505 nm. The colour system was found to obey Beer's law over the concentration range 100–600 μg of methanol per 25 ml of final solution. The reproducibility of the method was checked by replicate analysis of a solution containing 300 μg of methanol, over a period of 7 days. The results showed that the method is fairly reproducible, with a relative standard

Table 2. Recovery of methanol from blood (sample size 0.5 ml)

Methanol added, μg	Methanol found*, μg	Standard dev., μg	Recovery %
100	83	0.7	83
200	170	0.8	85
300	262	0.4	87
400	340	0.7	85
500	422	0.7	85

*Means of 5 replicate analyses.

Table 3. Comparison with other methods

Method	Reference	Lower limit of determination, ppm	Reaction time	Colour stability	Sample	Medium	Limit of determination for formaldehyde, ppm	Reference
Schiff's reagent	4	100	3 hr	30 min	Air, 60 ft ³	HCl	0.10	7
Schryver's method	3	75	—	15 min	—	HCl	1.00	8
ODH method	5	60	55 min	150 min	Water, 9–10 litres	Acetate buffer (pH 5.8–7)	0.60	14
Chromotropic acid method	15	4	—	24 hr	—	H ₂ SO ₄	1.00	9
p-Aminoazobenzene method (present method)	—	4	30 min	120 min	Water, 10 litres	H ₃ PO ₄ (0.5–1.5M) HCl (0.4–1.2M)	0.08	11

deviation of 1.7%. The method is fairly sensitive for methanol.

Effect of foreign species

Other organic compounds which yield formaldehyde on oxidation interfere with this and most other methods. Ethanol, the major co-pollutant, does not interfere. Hydrocarbons, aldehydes, phenol, various organic pollutants, several metal ions, esters such as ethyl acetate and diethyl malonate do not interfere. Diethyl oxalate causes negative errors. Glycol and glycerol, which on oxidation both yield formaldehyde, cause positive errors. Results are given in Table 1. The interference of nitrite can be removed by adding 1 ml of 3% sulphamic acid solution and sulphide can be removed from air sample by passing the air through a tube containing lead acetate solution. Sulphur dioxide does not interfere with this method.

Determination in air

A modification of Wilson's procedure^{14,15} was used to simulate air samples containing methanol: purified air was passed through an evaporation chamber preheated to 60–70°, and known amounts of methanol were added gradually dropwise with the help of a microburette and evaporated from the chamber, the air stream sample being sampled as described, with two 35-ml impingers connected in series to an air-sampling train fitted with a rotameter and vacuum pump.

Determination of methanol in blood

The method can be applied for the detection and estimation of methanol in biological fluids: it is separated from biological materials by distillation,^{16,17} and absorbed in a solution of acidic potassium permanganate, then the resulting formaldehyde is determined by reaction with *p*-aminoazobenzene as described. The method was tested with known amounts of methanol added to blood samples which had been shown to be free from methanol. The recovery is shown in Table 2, which suggests that

there is some loss of methanol during distillation. This has been reported before.^{16,17}

Comparison with other methods

The present method compares favourably with the Schiff's reagent method,^{4,7} Schryver's method,^{3,8} ODH method^{5,15} and the chromotropic acid method,^{9,13} in all of which methanol is estimated after its conversion into formaldehyde. The data summarized in Table 3 show that the present method is far more sensitive. It is simple and can be used satisfactorily for industrial hygiene work. The method is free from common organic interferences.

Acknowledgements—The authors are thankful to the Head, Department of Chemistry, Ravishankar University, Raipur, for providing laboratory facilities. One of them (PV) is thankful to Ravishankar University, Raipur for the award of a fellowship.

REFERENCES

1. F. A. Patty, *Industrial Hygiene and Toxicology*, Vol. II, 2nd Ed., p. 1409. Interscience, New York, 1962.
2. W. Leithe, *The Analysis of Air Pollutants*, p. 274. Ann Arbor Science Publishers, Ann Arbor, 1971.
3. W. E. Ruch, *Quantitative Analysis of Gaseous Pollutants*, pp. 146–149. Ann Arbor Science Publishers, Ann Arbor, 1975.
4. C. M. Jephcott, *Analyst*, 1935, **60**, 588.
5. A. Bhatt and V. K. Gupta, *Indian J. Environ. Health*, 1980, **22**, 203.
6. R. N. Boss, *Anal. Chem.*, 1948, **20**, 964.
7. A. G. Rayner and C. M. Jephcott, *ibid.*, 1961, **33**, 627.
8. E. C. Barns and H. W. Speicher, *J. Ind. Hyg. Toxicol.*, 1942, **23**, 10.
9. F. Z. Edvin, *Z. Anal. Chem.*, 1937, **110**, 22.
10. M. B. Jacobs, *The Analytical Chemistry of Industrial Poisons, Hazards and Solvents*, 2nd Ed., p. 616. Interscience, New York, 1949.
11. P. Verma and V. K. Gupta, *Talanta*, 1983, **30**, 443.
12. S. K. Kniseley and L. J. Throop, *Anal. Chem.*, 1966, **38**, 1270.
13. M. Feldstein and N. C. Klendshoj, *ibid.*, 1954, **26**, 932.
14. K. N. Wilson, *ibid.*, 1958, **30**, 1127.
15. J. Nair and V. K. Gupta, *Talanta*, 1979, **26**, 962.
16. A. O. Gettler, *J. Biol. Chem.*, 1920, **42**, 311.
17. F. D. Snell and C. T. Snell, *Colorimetric Methods of Analysis*, Vol. IIIA, p. 34, Van Nostrand, Princeton, 1961.

SIMULTANEOUS DETERMINATION OF ACETAMINOPHEN AND DEXTROPROPOXYPHENE NAPSYLATE IN PHARMACEUTICAL PREPARATIONS BY REVERSE PHASE HPLC

S. SA'SA' and A. RASHID
Yarmouk University, Irbid, Jordan

I. JALAL

Al-Hikma Pharmaceuticals, P.O. Box 182400, Amman, Jordan

(Received 14 September 1983. Accepted 24 November 1983)

Summary—The method reported provides a fast, sensitive, accurate and reproducible reverse-phase HPLC assay for acetaminophen and dextropropoxyphene simultaneously. The total elution time is <5 min. The method is stability-indicating since it can also determine *p*-aminophenol, a degradation product of acetaminophen, in a concentration as low as 0.005% of the acetaminophen concentration.

Acetaminophen (AAP, paracetamol, *p*-hydroxyacetanilide) is a widely used non-prescription analgesic. Dextropropoxyphene napsylate (DPN) is a widely prescribed analgesic for mild to moderate pain, either alone or in combination with acetaminophen or aspirin. AAP has been determined in dosage forms by various methods such as gas chromatography (GC),¹ reverse-phase HPLC with detection at 254 nm,²⁻⁵ and HPLC with electrochemical detection.⁶ Recently, a normal phase HPLC method⁷ has been used.

AAP in biological fluids has been determined by GC⁸ and HPLC.⁹⁻¹⁴ The current USP method for the determination of AAP in dosage forms is too lengthy, since it requires separation by silica gel column chromatography, followed by detection at 249 nm.

DPN has been determined in biological fluids by GC.¹⁵⁻¹⁹ In pharmaceutical preparations, propoxyphene hydrochloride has been determined by extraction followed by normal phase HPLC.²⁰ The degree of contamination of propoxyphene by its carbinol diastereomers has been detected by HPLC.²¹

The present USP assay for AAP and DPN²² involves extraction followed by GC with helium as carrier gas for the determination of compounds related to DPN, GC with nitrogen as carrier gas for the determination of DPN, and separation followed by derivative formation and GC with helium as carrier gas for the determination of AAP. This method, though specific, is time-consuming.

The method described in this paper provides a fast, sensitive and reliable reverse-phase HPLC assay for AAP and DPN simultaneously. The method is stability-indicating since it can determine *p*-aminophenol (PAP), a degradation product of AAP, at a concentration as low as 0.005% of that of the AAP.

EXPERIMENTAL

Materials

Reagent-grade potassium dihydrogen phosphate, ammonium formate and disodium hydrogen phosphate were obtained from BDH, England. *p*-Aminophenol (reagent grade) was obtained from Riedel-de-Haen, Hanover. HPLC grade methanol (Fluka) and distilled, demineralized water were used. Standards of AAP (Graesser Salicylates, Deeside, England) and DPN (Siegfried, Basle, Switzerland) were used as received.

Apparatus

The Varian 5000 LC HPLC system, equipped with a Valco Instruments manual loop injector, was connected to a Varian UV-50 variable-wavelength detector and a Varian 9176 chart-recorder. A Varian Micropak MCH-10 reverse-phase octadecylsilane column was used.

Chromatographic conditions

The mobile phase was prepared by dissolving 1.361 g of potassium dihydrogen phosphate and 1 g of ammonium formate in 700 ml of water and 300 ml of methanol. The solution was adjusted to pH 6 with a saturated solution of disodium hydrogen phosphate. The mobile phase was always filtered through a Gelman 0.45- μ m membrane and degassed under reduced pressure before use. The flow-rate was 2 ml/min and the pressure about 2200 psig. The detector sensitivity was 0.5 absorbance units full-scale for AAP and DPN, and 0.02 for PAP. The chart-speed was 0.5 cm/min.

Standards

A two-component standard solution (AAP 325 μ g/ml and DPN 100 μ g/ml) was prepared in methanol. For the determination of PAP a 1.625 μ g/ml standard solution was prepared in methanol. The solutions were filtered through a 0.45 μ m membrane before use.

Sample preparation

For the assay, 20 capsules were emptied and the contents weighed. The average content of a capsule was weighed out and dissolved in 100 ml of methanol. The solution was filtered (0.45- μ m membrane) and 5 ml of the filtrate were diluted to 50 ml with methanol. For the PAP assay, the average content of a capsule was weighed out and dissolved in 10 ml of methanol and the solution filtered (0.45- μ m membrane).

Table 1. Recovery studies for AAP, DPN and PAP

Standard	Recovery,* %
AAP	99.8 ± 0.9
DPN	99.6 ± 1.1
PAP	97.0 ± 2.0

*Mean ± RSD for 8 samples.

Table 2. Recovery studies for *p*-aminophenol

PAP,* %	% Recovery†
1.0	102.0 ± 2.0
0.46	100.9 ± 2.6
0.092	98.9 ± 6.5
0.005	99.6 ± 2.4

*Relative to AAP.

†Mean ± RSD for 6 samples.

Table 3. Precision studies

Day*	A		B		C		D	
	AAP	DPN	AAP	DPN	AAP	DPN	AAP	DPN
1	101.7 ± 1.9	99.2 ± 1.6	97.6 ± 1.2	97.8 ± 1.5	100.3 ± 1.6	100.7 ± 1.1	101.5 ± 2.2	101.6 ± 1.3
2	98.7 ± 2.3	101.6 ± 4.5	98.1 ± 1.7	98.4 ± 2.1	99.2 ± 1.4	100.4 ± 0.5	101.9 ± 1.9	100.6 ± 0.5
3	100.3 ± 1.5	98.7 ± 2.0	101.5 ± 2.7	99.6 ± 0.0	99.8 ± 2.0	97.9 ± 1.4	100.1 ± 1.5	97.6 ± 0.9
4	98.9 ± 0.8	100.0 ± 1.1	102.6 ± 1.1	99.6 ± 1.8	100.2 ± 1.5	100.2 ± 1.9	100.9 ± 1.4	98.5 ± 2.4
\bar{X}	100.0 ± 2.0	100.0 ± 2.7	100.0 ± 2.7	98.8 ± 1.8	99.9 ± 1.5	99.8 ± 1.6	101.1 ± 1.4	99.6 ± 2.1

*Mean ± RSD for 5 readings; \bar{X} = mean ± RSD for 20 readings. A and B are two different samples of Dolostop (a pharmaceutical preparation containing 325 mg of AAP and 50 mg of DPN per capsule). C and D are two different samples of Dolostop Forte (a pharmaceutical preparation containing 325 mg of AAP and 100 mg of DPN per capsule).

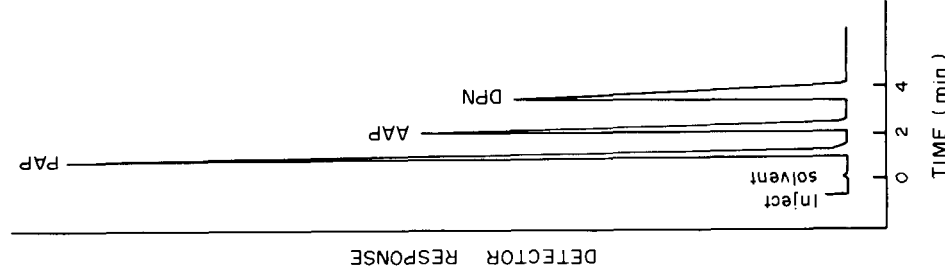


Fig. 1. Separation obtained with a synthetic mixture containing 2.5 μ g (10- μ l injection) each of PAP, AAP and DPN. Eluting solvent, pH 6.0 phosphate buffer-30% methanol; flow-rate 2.0 ml/min; 1.0 absorbance unit full-scale; ambient temperature; λ = 229 nm.

Assay

Equal volumes (10 μ l) of standard and sample preparations were injected and chromatographed under the conditions described above. The sample concentrations were calculated by simple proportion from the peak heights for the sample and standard. The amounts injected were always within the range giving linear response.

RESULTS AND DISCUSSION

To determine the linearity of the detector response, calibration standards of AAP, DPN and PAP were

Table 4. Stability studies*

Period elapsed, days	Product A†		Product B	
	AAP	DPN	AAP	DPN
1	100.5 ± 0.7	100.5 ± 0.6	100.5 ± 0.5	100.8 ± 0.4
7	99.2 ± 1.2	100.0 ± 1.1	100.6 ± 0.4	99.0 ± 0.3

*Nominal content ± RSD for 6 samples.

†A. Dolostop capsules, B. Dolostop Forte capsules.

Table 5. Accuracy studies*

Method	AAP	DPN
HPLC	99.6 ± 1.6	100.6 ± 0.9
Modified BP 80	99.1 ± 1.1	100.3 ± 1.2

*Nominal content ± RSD for 6 samples of Dolostop Forte.

prepared and quantities ranging from 0.2 to 5 µg of compound were injected. A plot of peak height vs. amount injected was linear up to 5 µg for AAP and PAP and 1 µg for DPN, with correlation coefficients of 0.9954, 0.9957 and 0.9968 respectively.

To determine the accuracy, each standard was spiked with a placebo and subjected to HPLC analysis at least 6 times. In all cases, satisfactory recoveries and reproducibility of peak heights were obtained (Table 1). No interference due to the placebo formulation was detected in the chromatograms produced. Furthermore the sensitivity of the method is illustrated by the high recovery of very low concentrations of PAP relative to AAP (Table 2).

It is well known that acetaminophen degrades to yield *p*-aminophenol. The specificity of the analytical method is illustrated by the complete separation of AAP, DPN and PAP in less than 5 min (Fig. 1).

The detection limit was determined by diluting the standard solutions with methanol and injecting 1 µl of each solution into the column. The detection limits were found to be 2.8, 2.4 and 2.0 ng for AAP, DPN and PAP, respectively.

The reproducibility of the HPLC procedure was determined by analysing day-to-day results. The results of the analysis on commercial products presented in Table 3 show excellent reproducibility with no statistical difference at the 5% level.

A stability study was performed on commercially available products, by placing samples in tubes in a humid atmosphere at 80°. A sample was taken daily and assayed. The data presented in Table 4 reveal no significant loss in activity throughout the study.

The accuracy of the method was further supported by the closeness of the results to the nominal content and to those obtained by the following modified BP 80 procedure performed in another laboratory. DPN was extracted into chloroform from aqueous alkali, which retained AAP. DPN was then determined by non-aqueous titration as in BP 80 for DPN capsules.²³ The aqueous alkaline layer was used to determine AAP spectrophotometrically as in BP 80 for

paracetamol (AAP) tablets.²⁴ Results obtained are listed in Table 5.

The principal objective of this study was to develop an HPLC method involving minimum sample manipulation, maximum resolution and minimum elution time. This was achieved, with a run time of 5 min. The method is reliable, accurate, specific, fast and stability-indicating.

Acknowledgements—The financial support provided by Yarmouk University is gratefully acknowledged. The authors would also like to thank Al-Hikma Pharmaceuticals, Amman, Jordan, for providing the raw materials and standards.

REFERENCES

1. L. L. Alber, M. W. Overton and D. E. Smith, *J. Assoc. Off. Anal. Chem.*, 1971, **54**, 620.
2. P. P. Ascione and G. P. Chrekian, *J. Pharm. Sci.*, 1975, **64**, 1029.
3. D. Rosenbaum, *Anal. Chem.*, 1974, **46**, 2226.
4. F. J. Sena, J. J. Piechocki and K. L. Li, *J. Pharm. Sci.*, 1979, **68**, 1465.
5. V. Das Gupta, *ibid.*, 1980, **69**, 110.
6. R. M. Riggen, A. L. Schmidt and P. T. Kissinger, *ibid.*, 1975, **64**, 680.
7. J. W. Munson and E. J. Kubiak, *Anal. Lett.*, 1980, **13**, 705.
8. W. A. Dechtiaruk, G. F. Johnson and H. M. Solomon, *Clin. Chem.*, 1979, **22**, 879.
9. C. G. Fletterick, T. H. Grove and D. C. Hohnadel, *ibid.*, 1979, **25**, 409.
10. J. H. Knox and J. Jurand, *J. Chromatog.*, 1977, **442**, 651.
11. G. R. Gotelli, P. M. Kabra and L. J. Marton, *Clin. Chem.*, 1977, **23**, 957.
12. R. A. Horvitz and P. I. Jetlow, *ibid.*, 1977, **23**, 1596.
13. D. Blair and B. H. Rumack, *ibid.*, 1977, **23**, 745.
14. K. S. Pang, A. M. Taburet, J. A. Hinson and J. R. Gillette, *J. Chromatog.*, 1979, **174**, 165.
15. W. R. Maynard, R. B. Bruce and G. G. Fox, *Anal. Lett.*, 1973, **6**, 1005.
16. J. F. Nash, I. F. Bennett, R. J. Bopp, M. K. Brunson and H. R. Sullivan, *J. Pharm. Sci.*, 1975, **64**, 429.
17. K. Verebely and C. E. Inturrisi, *J. Chromatog.*, 1973, **75**, 195.
18. R. L. Wolen and C. M. Gruber, *Anal. Chem.*, 1968, **40**, 1243.
19. M. Cleemann, *J. Chromatog.*, 1977, **132**, 287.
20. R. K. Gilpin, J. A. Koppi and C. A. Janicki, *ibid.*, 1975, **107**, 115.
21. R. W. Souter, *ibid.*, 1977, **134**, 187.
22. *USP XX*, Mack Publishing Co., Easton, Pa 18042.
23. *British Pharmacopoeia 1980*, Vol. II. p. 528. HMSO, London.
24. *Ibid.*, Vol. II, p. 799.

EXTRACTION OF CATECHOL VIOLET, CHROME AZUROL S AND ERIOCHROME CYANINE R WITH CHLOROFORM SOLUTIONS OF LIQUID ANION-EXCHANGERS

S. PRZESZLAKOWSKI and H. WYDRA

Department of Inorganic and Analytical Chemistry, Medical School, 20-081 Lublin, Poland

(Received 17 February 1983. Revised 7 December 1983. Accepted 19 January 1984)

Summary—The extraction of Catechol Violet, Chrome Azurol S and Eriochrome Cyanine R with chloroform solutions of tri-*n*-octylamine (TOA), TOA hydrochloride and Aliquat 336 has been investigated. From the extraction isotherms, absorption spectra of the organic phases and dependence of the extraction coefficients on extractant concentration, it was found that the singly-charged anions HL^- are extracted preferentially, but acidic groups other than sulphonate can also form ion-pairs with alkylammonium cations at higher pH values of the aqueous phase, and at high acidity these dyes can be extracted other than by an anion-exchange reaction. The three dyes (especially Eriochrome Cyanine R and Chrome Azurol S) were strongly extracted with the liquid anion-exchanger used and Aliquat 336 was a better extractant than TOA or TOA hydrochloride. The absorption spectra for the organic phases containing Chrome Azurol S and Eriochrome Cyanine R depended on the extractant used.

Many sensitive spectrophotometric methods for metals are based on the formation of ion-association complexes composed of anionic complexes and large organic cations. In addition to methods based on ternary complexes involving chelating agents and cationic surfactants, methods utilizing the extraction of anionic metal-sulphonated chelating agent complexes by solutions of liquid anion-exchangers in organic solvents often give better sensitivity and selectivity than the conventional spectrophotometric methods.¹ Although excess of sulphonated chelating agent can also be extracted by a liquid anion-exchanger, only a few such cases (nitroso-R salt,² ferron^{2,3} and some sulphonated formazans⁴) have been investigated. It therefore seems important to study such systems in order to improve the design of extraction-spectrophotometric methods for metals, and of selective metal-sorbents consisting of chelating anion/alkylammonium cation combinations.^{5,6}

Sulphonated triphenylmethane dyes are important reagents for spectrophotometric determination of metals, and as metallochromic indicators.⁷ The ternary complexes formed from metal ion, sulphonated triphenylmethane dye and organic cationic surfactant in aqueous solution have been utilized in several very sensitive spectrophotometric methods for metals.^{8,9} Tertiary amines and quaternary ammonium salts have been used similarly. Thus a very sensitive method for determination of tin is based on extraction of the anionic tin(IV)-Catechol Violet complex with diphenylguanidine in butanol.¹⁰ Molybdenum has been determined with Catechol Violet directly in the organic phase after extraction from sulphuric acid with tri-*n*-octylamine in toluene.¹¹ Shijo¹² developed a very sensitive method for iron ($\epsilon = 1.73 \times 10^5$

$l \cdot mole^{-1} \cdot cm^{-1}$) based on extraction of the iron-(III)-Eriochrome Cyanine R complex by tridodecyl-ethylamine bromide in xylene.

Our earlier results obtained chromatographically (paper extraction chromatography and the "moist paper" technique)¹³ suggested that Catechol Violet, and especially Chrome Azurol S and Eriochrome Cyanine R, can be effectively extracted from aqueous acidic solutions with ternary amines and quaternary alkylammonium salts in benzene or chloroform; however, the rather strong adsorption of these reagents on cellulose makes it difficult to interpret the chromatographic data quantitatively. Therefore the corresponding water/chloroform extraction systems were investigated in the present work.

EXPERIMENTAL

All experiments were done at room temperature ($21 \pm 2^\circ$).

Reagents

Pure tri-*n*-octylamine (TOA) was purified by vacuum distillation, the fraction boiling at $192-198^\circ$ (11-12 mmHg) being collected. TOA hydrochloride was made by shaking a 0.1M solution of the free amine in chloroform with an equal volume of 0.2M hydrochloric acid; after separation, the organic phase was washed twice with doubly distilled water and filtered through a cellulose filter. More dilute TOA or TOA hydrochloride solutions were prepared by dilution with freshly distilled chloroform.

Aliquat 336 (93.3% w/w quaternary alkylammonium chloride) was freed from iron by shaking its 0.1M chloroform solution with an equal volume of 0.01M hydrochloric acid, then the organic phase was washed five times with an equal volume of doubly distilled water; finally the organic phase was filtered through a cellulose filter. More dilute solutions were prepared by dilution with freshly distilled chloroform.

The chloroform solutions of Aliquat 336 and TOA hydrochloride were standardized by potentiometric titration (after

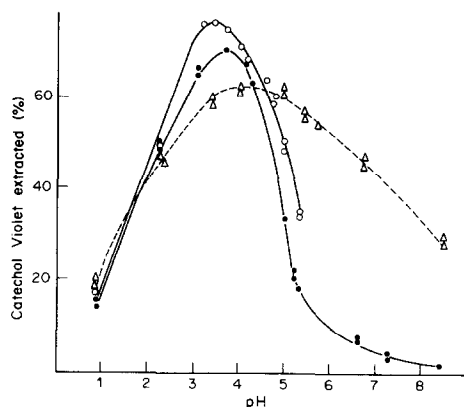


Fig. 1. Effect of pH on the extraction of Catechol Violet ($5 \times 10^{-4}M$). Extractants: $10^{-3}M$ TOA (●---●), $10^{-3}M$ TOA hydrochloride (○---○) in chloroform, $2 \times 10^{-4}M$ Aliquat 336 (△---△) in chloroform.

evaporation of chloroform) with $0.01M$ silver nitrate in ethanol-water (70:30 v/v).

All other reagents were of analytical grade.

Procedure

Catechol Violet (CV), Chrome Azurol S (CAS) and Eriochrome Cyanine R (ECR) were extracted by shaking together for 10 min equal volumes (usually 5 or 10 ml) of the aqueous reagent (previously adjusted to an appropriate pH with $0.1M$ hydrochloric acid or $0.1M$ sodium hydroxide) and chloroform or a chloroform solution of TOA, TOA hydrochloride or Aliquat 336, in cylindrical separating funnels. The lower (organic) phase was then filtered through a cellulose filter to remove the remaining aqueous solution and the aqueous phase was centrifuged. The reagents were determined spectrophotometrically in the aqueous phase by use of calibration graphs obtained for aqueous solutions of appropriate pH, at the wavelength of the absorption maximum. Since the absorbance of the aqueous CV solution was not stable at $pH > 7$, and the absorption maximum of the organic phase changed with time, alkaline aqueous solutions of CV, after extraction, were adjusted to $pH 3.8-3.9$ with dilute hydrochloric acid; CV was then determined at 445 nm from a calibration graph obtained analogously. Also, the aqueous phase after extraction of CAS was always adjusted to $pH 1$ with hydrochloric acid and the absorbance measured at 465 nm .

RESULTS AND DISCUSSION

Preliminary experiments with equal concentrations of the triphenylmethane dyes in acidic aqueous solutions and a constant concentration of TOA, TOA hydrochloride or Aliquat 336 in the organic phase indicated very rapid extraction—shaking for 15 sec was sufficient for equilibrium to be reached. Since all the three dyes contain a sulphonate group and phenolic groups, and CAS and ECR also have two carboxylate groups, it was expected that pH would have a strong influence on the extraction.

It was found that CV is not extracted with pure chloroform at the pH values studied, and ECR is only partially extracted (extraction coefficients ~ 0.1) at $pH 1$, whereas CAS is feebly extracted from acidic or neutral solutions. However, all three are quite well

extracted from acidic aqueous solutions with chloroform solutions of the liquid anion-exchangers, if the concentration of the latter is sufficient to neutralize the charge of the sulphonate group of the reagent. The degree of extraction of ECR and CAS decreases with increasing equilibrium pH of the aqueous phase, whereas for CV the extraction is maximal at $3.4-4.9$, depending on the extractant used (Figs. 1-3). TOA and TOA hydrochloride behave similarly, and the extraction is very low at $pH > 8$ (the TOA hydrochloride is then converted into the free amine). Aliquat 336 is a better extractant and is the only one of the three that extracts the dyes from alkaline solution. This seems to confirm that anion-exchange is the major mechanism in the extraction process.

The extraction isotherms (Figs. 4-6) confirm that Aliquat 336 has the best extraction properties. Eriochrome Cyanine R was practically quantitatively extracted with $10^{-3}M$ chloroform solutions of the liquid anion-exchangers used, when its concentration in the initial aqueous solution was below about $10^{-3}M$. Aliquat 336 and TOA hydrochloride in chloroform (except for extraction of Chrome Azurol S with TOA hydrochloride) will extract more of the dyestuffs than corresponds to a 1:1 complex. For example, the mole ratio of dyestuff to Aliquat 336 can attain the value 1.2 for Chrome Azurol S, 1.3 for Catechol Violet and 5.9 for Eriochrome Cyanine R. The extraction isotherm for Chrome Azurol S seems to indicate that when the pH of the aqueous phase is 4.6, only the sulphonate group of the reagent is bound with the alkylammonium cation in the ion-pair, although the anions H_3L^- and H_2L^{2-} should be present in the aqueous solution (the carboxyl group

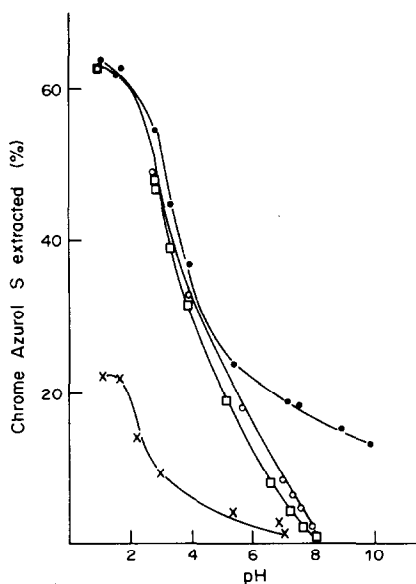


Fig. 2. Effect of pH on the extraction of Chrome Azurol S ($5 \times 10^{-4}M$). Extractants: $10^{-4}M$ chloroform solutions of TOA (○---○), TOA hydrochloride (□---□), Aliquat 336 (●---●); or chloroform (×---×).

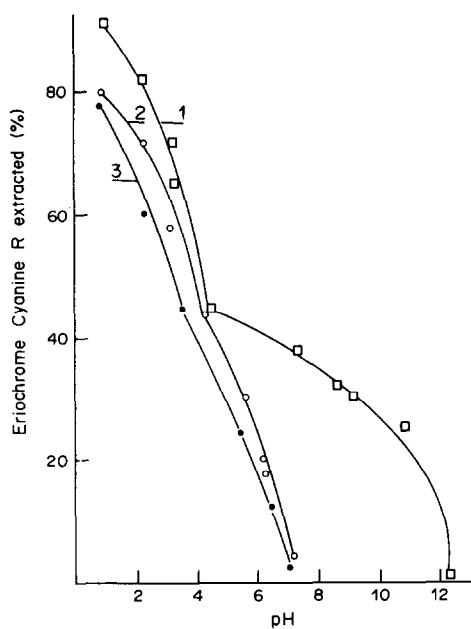


Fig. 3. Effect of pH on the extraction of Eriochrome Cyanine R ($5 \times 10^{-3} M$). Extractants: $10^{-3} M$ chloroform solutions of TOA (●---●), TOA hydrochloride (○---○) or Aliquat 336 (□---□).

would be partially dissociated).¹⁴ Although chloroform does not extract Catechol Violet or Eriochrome Cyanine R (at $\text{pH} > 1$), the presence of the ion-pair consisting of the dyestuff anion and an alkylammonium cation should change the physical properties of the chloroform and some of the dyestuff might then be extracted by a mechanism other than simple anion-exchange. The extraction of a "superstoichiometric" amount of Eriochrome Cyanine R from aqueous solution at $\text{pH} 1$ can be explained if the "neutral" (zwitterion) species H_4L present along with the H_3L^- anions in the aqueous solution is also extracted.¹⁵ Chrome Azurol S is also almost quantitatively extracted from aqueous solution at $\text{pH} 1$ when the concentration of Aliquat 336 in the organic phase is half the concentration of the reagent in the aqueous solution before extraction (see Table 1). Further association of carboxylate dyestuffs in the organic phase cannot be excluded (especially when acidic aqueous media are used) and the extraction of such aggregates could also lead to the apparent superstoichiometric extraction of the dyestuff.

The high degree of extraction of Chrome Azurol S and Eriochrome Cyanine R from aqueous acidic solutions just discussed prevents investigation of the extraction mechanism by slope analysis. For Cate-

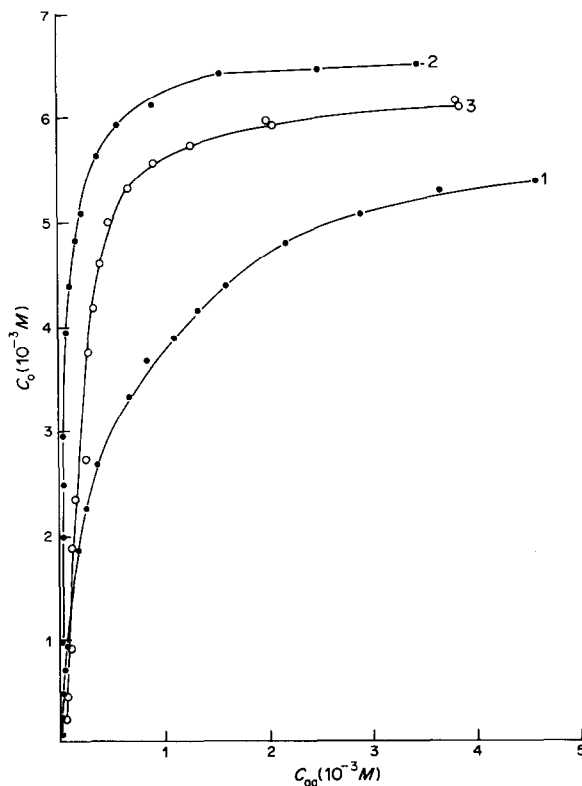


Fig. 4. Extraction isotherms for Catechol Violet ($\text{pH} \sim 3$). Extractants: $5 \times 10^{-3} M$ chloroform solutions of TOA (curve 1), TOA hydrochloride (curve 3) or Aliquat 336 (curve 2). C_o and C_a are the equilibrium concentrations in the organic and aqueous phases respectively.

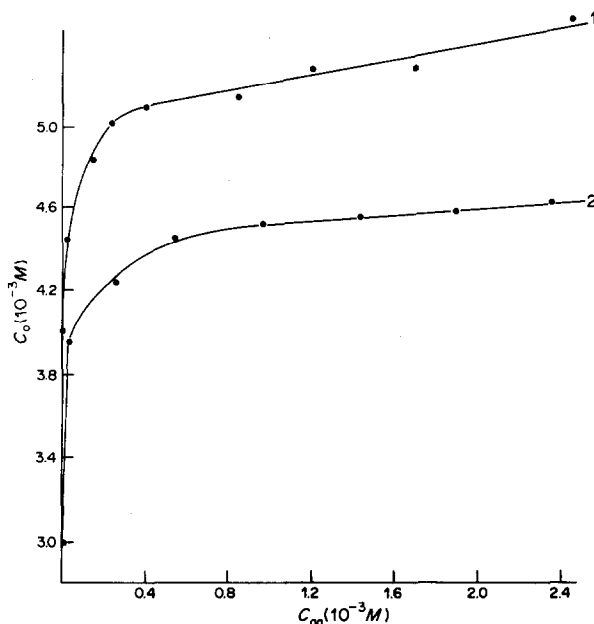
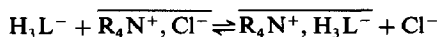


Fig. 5. Extraction isotherms for Chrome Azurol S (pH 4.7). Extractant: $5 \times 10^{-3} M$ chloroform solutions of Aliquat 336 (curve 1) or TOA hydrochloride (curve 2). C_o and C_a are defined as for Fig. 4.

chol Violet a slope of 1.0 was found at pH 2.23 for $\log D$ vs. $\log [\text{Aliquat 336}]$; this suggests that only the sulphonate group binds to the alkylammonium cation, as expected for a simple anion-exchange reaction (at pH 2.2 the anion H_3L^- should be predominant in the aqueous solution¹⁶):



Woodward and Freiser¹⁷ suggested that in strongly alkaline media not only the sulphonate groups but also the phenolate groups of sulphonated azo-dyes can bind to alkylammonium cations. The experimental results for the extraction of Chrome Azurol S from aqueous solutions at pH 11.1 (Fig. 7) seem to confirm this. The slope of 3.8 suggests that along with the sulphonate group, two carboxylate groups and, partially, the phenolate group of the reagent are neutralized with alkylammonium cations and the ion-association complex $(\text{R}_4\text{N}^+)_4 \cdot \text{L}^-$ is formed in the organic phase.

If sulphonated triphenylmethane dyes are extracted by anion-exchange reactions, chloride ions should be transferred into the aqueous phase when the extraction is done with alkylammonium chlorides. Therefore, chloride was determined in the aqueous and organic phases after extraction of Catechol Violet, Chrome Azurol S and Eriochrome Cyanine R with chloroform solutions of Aliquat 336 or TOA hydrochloride. The results obtained are collected in Table 2.

It should be noted that the ratio of the chloride concentrations in the organic and aqueous phase increased when an excess of the dyestuff (relative to the alkylammonium salt) was used. For instance,

chloride was transferred into the aqueous phase quantitatively after extraction of an $8 \times 10^{-3} M$ aqueous solution of Eriochrome Cyanine R with a $10^{-3} M$

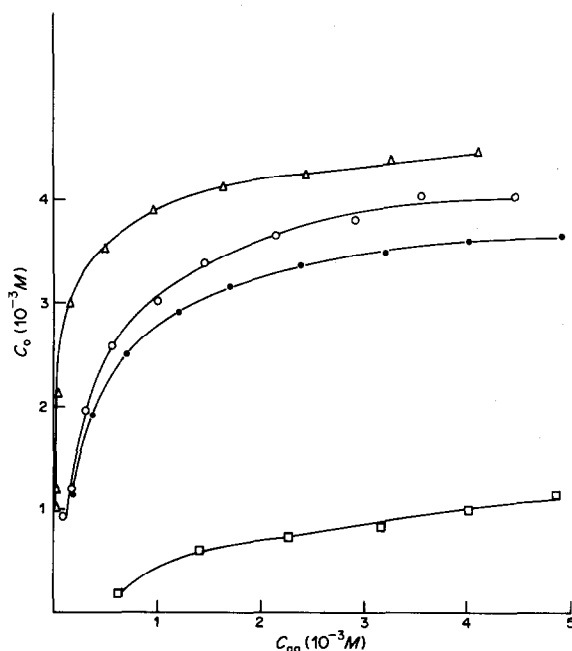


Fig. 6. Extraction isotherms for Eriochrome Cyanine R (pH 1.0). Extractants: chloroform (\square --- \square) or $10^{-3} M$ chloroform solutions of TOA (\bullet --- \bullet), TOA hydrochloride (\circ --- \circ) or Aliquat 336 (Δ --- Δ). For the upper three curves the C_o values correspond to the difference between the total concentration of Eriochrome Cyanine R in the organic phase containing amine, and the concentration when the dyestuff is extracted with chloroform alone; C_a is the equilibrium concentration in the aqueous phase.

Table 1. Dependence of the extraction coefficient (D) and percentage of Chrome Azurol S extracted (initial concentration of the reagent $5 \times 10^{-3}M$) on the concentration of Aliquat 336

[Aliquat 336], $10^{-3}M$	pH 4.65*		pH 0.97*	
	D	Extracted, %	D	Extracted, %
0.1	0.02	1.8	0.37	27.0
0.2			0.46	31.4
0.5	0.09	8.2	0.86	46.0
0.75	0.18	15.1	1.4	58.4
1.0	0.28	21.6	1.86	65.0
1.5			4.81	82.8
2.0	0.72	42.0	40.6	97.6
2.5	1.17	54.0	250	99.6
3.0	1.78	64.0	> 1000	100
3.5	2.47	71.2		
4.0	4.32	81.2		
4.5	8.43	89.4		
5.0	124	99.2		
6.0	300	99.7		
6.5	500	99.9		
7.0	830	99.9		

*pH of the aqueous phase.

solution of Aliquat 336 or TOA hydrochloride in chloroform. This confirms that anion-exchange is occurring in the extraction process. However, for equal initial concentrations of the dyestuff in the aqueous solution and the extracting agent in the organic phase (see Table 2), the extraction coefficients were always higher than the final $[Cl^-]_{aq}/[Cl^-]_o$ ratios (especially for Eriochrome Cyanine R). This confirms the observation that some of the dyestuff can be extracted by a mechanism other than anion-exchange.

The colours of the organic phases containing the sulphonated triphenylmethane dyes and alkylammonium cations were sometimes different from the colours of the aqueous solutions of the dyestuffs at the same pH values.

Absorption spectra for organic solutions containing Catechol Violet and an excess of alkylammonium salt (necessary to ensure quantitative extraction) are shown in Figs. 8 and 9. The organic phases were yellow when the extraction was done from sufficiently acidic solutions and a single absorbance maximum at 440 nm was found for Catechol Violet extracted with TOA or TOA hydrochloride from aqueous solutions in the equilibrium pH range 0.9–3.9. It should be added that the absorbance depends on the pH of the aqueous solution and attains maximal and constant values when the equilibrium pH range is 2.8–3.7, over which the yellow anion H_3L^- is predominant in the aqueous solution.¹⁶ The shapes of the spectra for Catechol Violet extracted with Aliquat 336 depend on the equilibrium pH value of the aqueous phase (Fig. 9) and a single absorbance maximum at 445 nm was found only on extraction from distinctly acidic solutions of the reagent (pH 0.9–2.0). At an equilibrium pH of 3.8, a second maximum appears at 620 nm (the organic phase is then green). The absorbance at 445 nm decreases and the absorbance at 620 nm

increases with increasing pH of the aqueous phase and attains a maximum (at 620 nm) at pH 7.35; at pH 8.3 the maximum at 445 nm disappears and a third maximum at 360 nm appears (curve 6 in Fig. 9). The lack of isosbestic points is probably due to inadequate purity of the dyestuff.

The absorbance of Catechol Violet in the organic phase was stable only when TOA hydrochloride was used as extracting agent; then no changes in absorbance were found even after 24 hr. The absorbance of Catechol Violet extracted with Aliquat 336 was stable only at an equilibrium pH of 5.6; when extraction was done from more acidic or more alkaline solutions, the absorbance at 445 nm increased very slightly and the absorbance at 620 nm distinctly decreased in 24 hr.

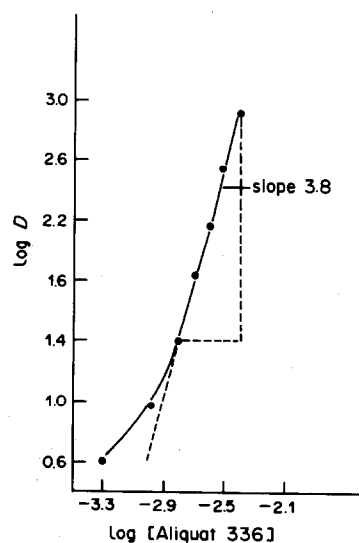


Fig 7. Log-log plot of the extraction coefficients (D) for Chrome Azurol S ($5 \times 10^{-3}M$, pH 11.1) vs. concentration of free Aliquat 336 in chloroform.

Table 2. The ratio of the chloride concentration in the aqueous and organic phases after extraction of Catechol Violet, Chrome Azurol S and Eriochrome Cyanine R with chloroform solutions of Aliquat 336 and TOA hydrochloride: the initial concentrations of the dyestuff in the aqueous solution and of the alkylammonium salt in the organic phase were $5 \times 10^{-3}M$ for Catechol Violet and Chrome Azurol S and $10^{-3}M$ for Eriochrome Cyanine R

	pH	Aliquat 336		TOA.HCl	
		$\frac{[Cl^-]_{aq}}{[Cl^-]_o}$	<i>D</i>	$\frac{[Cl^-]_{aq}}{[Cl^-]_o}$	<i>D</i>
Catechol Violet	2.3	5.25	15.1	1.1	4.6
Chrome Azurol S	4.6	9.0	32	6.1	8.2
Eriochrome Cyanine R	3.0	2.85	> 250	2.57	> 250

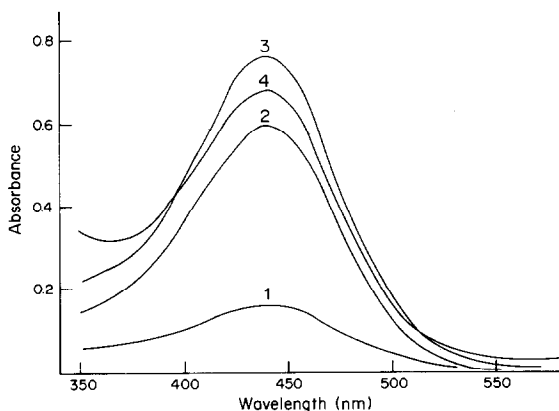


Fig. 8. Absorption spectra for organic phases after extraction of Catechol Violet ($5 \times 10^{-5}M$) with a $5 \times 10^{-3}M$ chloroform solution of TOA hydrochloride. Equilibrium pH values of the aqueous phases: 0.9—curve 1; 1.9—curve 2; 2.8 or 3.65—curve 3; 3.85—curve 4.

The absorption spectra for organic solutions of Catechol Violet seem to indicate that various anions of the dyestuff can be transferred into the organic phase; their charge is neutralized by alkylammonium cations. Extraction of Catechol Violet from distinctly acidic aqueous solutions leads to formation of a yellow ion-pair $R_4N^+ \cdot H_3L^-$. When the pH increases, the anions H_2L^{2-} are formed in the aqueous solution (the absorbance maximum for this anion is at 590 nm)¹⁶ and these can probably also be extracted as an ion-association complex with two alkylammonium cations.

Absorption spectra for Chrome Azurol S extracted with TOA hydrochloride and Aliquat 336 in chloroform differ significantly (Fig. 10). The organic phases are pink (λ_{max} 510 nm, $\epsilon = 1.38 \times 10^4$ l. mole⁻¹. cm⁻¹) after extraction of the dyestuff from acidic aqueous solutions with TOA hydrochloride in chloroform. The organic phase containing Chrome Azurol S and

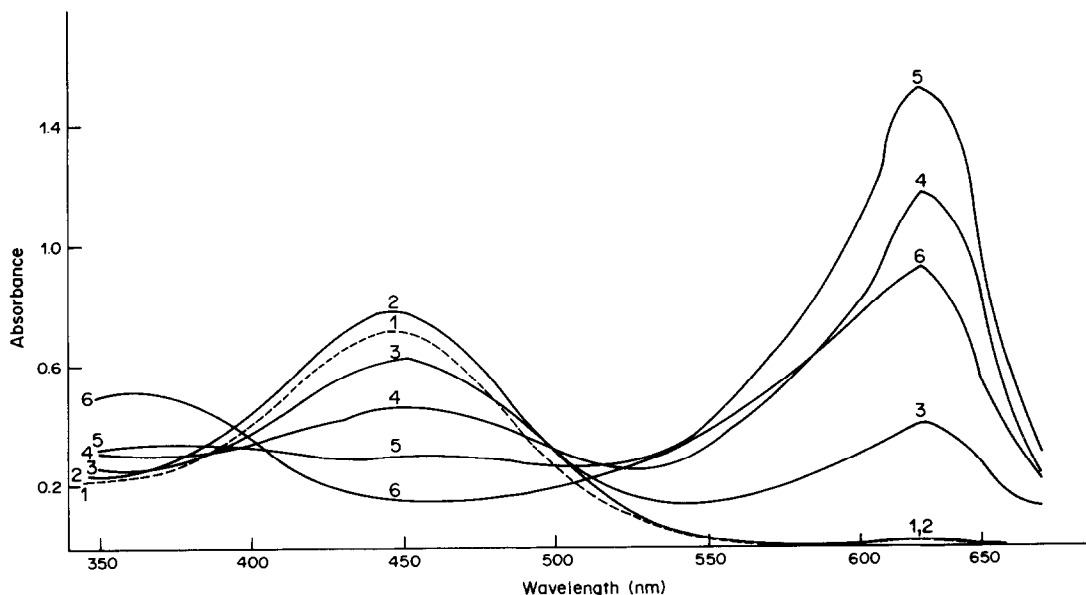


Fig. 9. Absorption spectra for organic phases after extraction of Catechol Violet ($5 \times 10^{-5}M$) with a $5 \times 10^{-3}M$ chloroform solution of Aliquat 336. Equilibrium pH values of the aqueous phases: 0.87—curve 1; 1.93—curve 2; 3.84—curve 3; 5.6—curve 4; 7.35—curve 5; 8.3—curve 6.

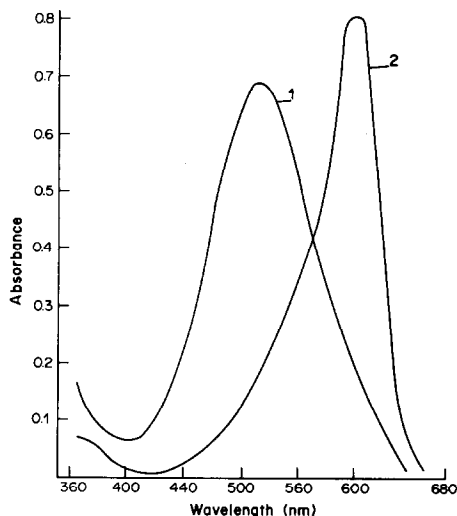


Fig. 10. Absorption spectra for organic phases after extraction of Chrome Azurol S ($5 \times 10^{-5}M$) with a $5 \times 10^{-4}M$ chloroform solution of TOA hydrochloride ($pH_{\text{equil}} 3.4$ —curve 1) or Aliquat 336 ($pH_{\text{equil}} 3.6$ —curve 2).

the equivalent amount or an excess of Aliquat 336 is violet for the pH range 3.6–7.4. The organic phase obtained on extraction of the dyestuff from a strongly alkaline medium (pH 12.65) with a chloroform solution of Aliquat 336 is initially yellow; after separation the yellow colour changes to violet, irrespective of the concentration ratio of Aliquat 336 to dyestuff in the range from 1:2 to 10:1. The colour of the organic phase changes immediately on removal of water from it by addition of anhydrous sodium sulphate or filtration through a cellulose filter. In the equilibrium pH range 3.6–7.4, the absorbance of the organic phase at 600 nm is constant ($\epsilon = 1.6 \times 10^4$ l. mole $^{-1}$. cm $^{-1}$) and the absorbances obtained at 1:1 and 10:1 mole ratios of Aliquat 336 to Chrome Azurol S are practically the same. The absorbance of the organic phases remains unchanged for at least 24 hr. These results seem to suggest that only the ion-pair $R_4N^+ \cdot H_3L^-$ is formed on extraction of the dyestuff from acidic and moderately alkaline solutions; however, the high stability of the absorbance of the organic phases obtained by extraction of Chrome Azurol S from acidic aqueous solutions is rather surprising, because it is well known that the orange H_3L^- (λ_{max} 480 nm) and red H_2L^{2-} (λ_{max} 510 nm) are not stable in aqueous solution, unlike the yellow HL^{3-} and violet L^{4-} .¹⁴ It is also difficult to explain the marked differences in λ_{max} between organic phases containing Chrome Azurol S bound with TOA and those with it bound with Aliquat 336, at almost identical equilibrium pH values of the aqueous phase.

The absorption spectra for organic phases containing Eriochrome Cyanine R bound with TOA or Aliquat 336 (Fig. 11) are somewhat similar to the corresponding spectra for Chrome Azurol S. The absorbance of the organic solutions of Eriochrome

Cyanine R was not stable and was constant only when measured within 0.5–1 hr of extraction; subsequently it increased with time, especially when the extractant was Aliquat 336 in chloroform. The absorbance values for the lilac organic phases depend also on the pH of the aqueous phase. The absorbance for Eriochrome Cyanine R extracted with TOA hydrochloride or Aliquat 336 reached a maximum at an equilibrium pH of 2.1 (H_3L^- is then predominant in the aqueous solution¹⁵). The absorbance maximum was at 510 nm ($\epsilon = 6.8 \times 10^3$ l. mole $^{-1}$. cm $^{-1}$) for the dyestuff extracted with TOA hydrochloride and at 570 nm ($\epsilon = 8.2 \times 10^3$) for Eriochrome Cyanine R extracted with Aliquat 336. The organic phase was initially yellow when Eriochrome Cyanine R was extracted with Aliquat 336 from aqueous solution at pH 12.5; after 30 min the colour changed to red-violet ($\epsilon_{570} = 5.3 \times 10^3$) and the absorbance of the organic phase then remained unchanged for at least 9 hr.

The differences between the absorption spectra for Eriochrome Cyanine R and Chrome Azurol S (and also the differing stabilities of the absorbance of the organic phase) extracted with TOA hydrochloride and Aliquat 336 seem to be important when an extractant for extraction–spectrophotometric determination of metals is to be chosen, since an excess of reagent is always used in the determination and the reagent is then extracted together with the anionic metal complex.

The extraction data confirm the earlier supposition based on chromatographic data¹³ that Eriochrome Cyanine R and Chrome Azurol S are more strongly extracted than Catechol Violet with liquid anion-exchangers; however, all three dyestuffs can be ex-

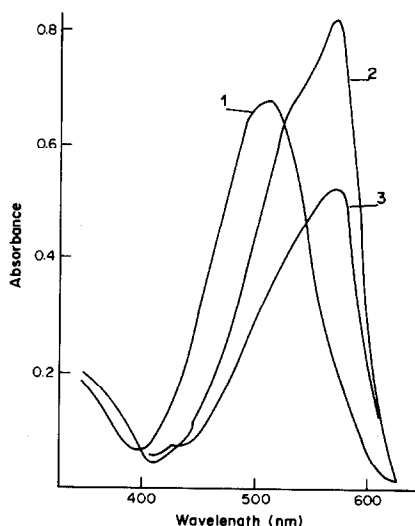


Fig. 11. Absorption spectra for organic phases after extraction of Eriochrome Cyanine R ($10^{-4}M$) with a $10^{-3}M$ chloroform solution of TOA hydrochloride ($pH_{\text{equil}} 2.05$ —curve 1) or Aliquat 336 ($pH_{\text{equil}} 2.05$ —curve 2 or 11.5—curve 3). The absorbance was measured 30 min after separation of the phases.

tracted quantitatively with just a small excess of TOA hydrochloride or Aliquat 336. The high degree of extraction of the reagents (especially with Aliquat 336) suggests that ion-pairs composed of a sulfonated triphenylmethane dye and a hydrophobic alkylammonium cation could find application in the preparation of selective sorbents for some metal ions.⁵

Acknowledgements—This work was supported by the Institute of Chemistry of the Maria Curie-Skłodowska University in Lublin (Grant No. MR.I.14.B1.29). Thanks are due to Professor Dr. Edward Soczewiński for his interest in this work.

REFERENCES

1. Z. Marczenko, *Spectrophotometric Determination of Elements*, Horwood, Chichester, 1976.
2. S. Przeszlakowski, R. Kocjan and E. Habrat, *Chem. Anal. (Warsaw)*, 1982, **27**, 73.
3. S. Przeszlakowski and E. Habrat, *Analyst*, 1982, **107**, 1320.
4. M. Grote and A. Ketttrup, *Formazan-Loaded Liquid and Solid Anion Exchangers*, Abstracts of 3rd Intern. Conf., Physicochemical Methods for Water and Wastewater Treatment, Lublin, 1981, p. 1.
5. S. Przeszlakowski, E. Soczewiński, R. Kocjan, J. Gawecki and Z. Michno, *Pol. Patent*, P 219 538, 9 November 1979.
6. S. Przeszlakowski and R. Kocjan, *Chromatographia*, 1982, **15**, 717; 1983, **17**, 266.
7. E. Bishop (ed.) *Indicators*, Pergamon Press, Oxford, 1972.
8. Z. Marczenko, *Chem. Anal. (Warsaw)*, 1979, **24**, 551.
9. *Idem*, *C.R.C. Crit. Rev. Anal. Chem.*, 1981, **10**, 195.
10. N. L. Shestidesyatnaya, L. I. Kotelyanskaya and M. I. Yanik, *Zh. Analit. Khim.*, 1976, **31**, 67.
11. A. A. Ponomareeva and N. A. Agrinska, *Zavodsk. Lab.*, 1972, **38**, 790.
12. Y. Shijo, *Bull. Chem. Soc. Japan*, 1975, **48**, 2793; *Chem. Abstr.*, 1976, **84**, 53537f.
13. S. Przeszlakowski and H. Wydra, *Chromatographia*, 1981, **14**, 685.
14. M. Malát, *Anal. Chim. Acta*, 1961, **25**, 289.
15. O. Ryba, J. Cifka, M. Malát and V. Suk, *Collection Czech. Chem. Commun.*, 1956, **21**, 349.
16. A. J. Hegedüs, *Mikrochim. Acta*, 1963, 831.
17. C. Woodward and H. Freiser, *Talanta*, 1973, **20**, 417.

LINEAR TITRATION PLOTS FOR THE ANALYSIS OF MIXTURES OF THREE WEAK ACIDS OR BASES

DEREK MIDGLEY

Central Electricity Generating Board, Central Electricity Research Laboratories, Kelvin Avenue,
Leatherhead, Surrey, England

COLIN MCCALLUM

University of Edinburgh, Edinburgh Regional Computing Centre, The King's Buildings, Mayfield Road,
Edinburgh, Scotland

(Received 14 November 1983. Accepted 13 January 1984)

Summary—Linearly related functions have been derived which enable mixtures of three weak acids or bases in solution to be analysed by means of pH-titration data. This theory has been tested with data from the titration of a variety of mixtures of acids. The data required for the functions are pH, volume of titrant, the equilibrium constants relevant to the mixture, and an independently determined equivalence volume. This may be the equivalence volume for one of the components of the mixture or the sum of the equivalence volumes for any two or all three of the components. It is immaterial how this equivalence volume is obtained, but it is usually possible to obtain the total equivalence volume from data in another part of the same titration curve (when a large excess of titrant has been added).

A linear titration plot is a means of transforming titration data so that the information contained within a set of data can be extracted more easily than is the case for the conventional S-shaped titration curve of pH or e.m.f. plotted against volume of titrant added. The aim is always to derive two functions that are linearly related and can be calculated from the titration data and known constants. When one function is plotted against the other, the equivalence volumes of titrant for the components in the sample are obtained from the intercept and gradient of the resultant straight line.

Linear titration plots have the advantage of being in a form that provides an obvious visual warning that the interpretation of the results may be suspect: curvature in the plot indicates either that the sample contains substances different from (or additional to) those expected, or that the experimental technique is in error. Linear titration plots have been derived that are capable of allowing for the finite solubility of a precipitate,¹ polyfunctionality of an acid or base,² partial neutralization of an acid or base,³ and mixtures of two polyfunctional weak acids.⁴

In contrast to the conventional S-curve, linear titration plots require an accurate and precise determination of pH and a certain amount of calculation in preparing the functions for plotting. In most cases the functions can be calculated with a "scientific" calculator although for the most rigorous and general treatment a computer would be necessary.

It is implicit in the linearity of the plots that only two unknowns can be determined simultaneously. For analysing mixtures of three components by linear titration plot, therefore, one concentration, or the sum of any two or all three concentrations, must first

be found independently. In many cases a selected portion of the titration data can be made to yield the required concentration and the rest of the data then used to calculate the remaining concentrations.

Midgley⁵ analysed a mixture of nitric acid, acetic acid and ammonium ion by applying a plot⁴ for two-component analysis, first in the pH range 3.5-4.9 to give the concentrations of nitric and acetic acids, and then in the range pH 8.5-9.7 to give the ammonium ion concentration and the combined concentration of nitric and acetic acids.

This paper treats the problem more generally and develops linear titration plot functions for ternary mixtures of either acids or bases. The new functions can resolve two of the unknown concentrations simultaneously, given an independently determined quantity which may be the concentration of the third component or the sum of all three or of any two concentrations. The theory is developed for all these possibilities. In most cases the independently determined quantity can be obtained from data taken from the same titration, and one experiment, therefore, serves for the determination of all three unknown concentrations.

THEORY

Notation

Both acids and bases are represented by the general formulae H_aX_p , H_bY_q and H_cZR_r . X, Y and Z represent the unprotonated radicals to which a , b and c protons respectively are attached. P, Q and R are univalent ions of charge j_P , j_Q and j_R respectively, present in the numbers p , q and r necessary to maintain electrical neutrality. The numbers p , q and r depend on the number of negative charges, n_X , n_Y

and n_z on the unprotonated radicals and the number of protons attached. Note that the number of association steps, k_x , k_y or k_z , for each radical is not identical with the proton number a , b or c respectively, but is characteristic of the radical itself. This notation applies to acids, salts and bases, as shown by the following examples: acetic acid, $n_x = k_x = a = 1$, $p = 0$; sodium acetate $n_x = k_x = p = 1$, $a = 0$; ammonia $n_x = a = p = 0$, $k_x = 1$.

Three weak acids

Consider the titration of V_0 ml of a mixture of three acids, $H_a X P_p$, $H_b Y Q_q$ and $H_c Z R_r$, with a strong base of normality C_B . For each acid there exists a series of overall association constants:

$$\begin{aligned} K_{X_i} &= \{H_i X\} / \{X\} \{H\}^i \\ &= [H_i X] F_{X_i} / [X] f_X \{H\}^i; \quad i = 1 \rightarrow k_X \\ K_{Y_i} &= \{H_i Y\} / \{Y\} \{H\}^i \\ &= [H_i Y] F_{Y_i} / [Y] f_Y \{H\}^i; \quad i = 1 \rightarrow k_Y \\ K_{Z_i} &= \{H_i Z\} / \{Z\} \{H\}^i \\ &= [H_i Z] F_{Z_i} / [Z] f_Z \{H\}^i; \quad i = 1 \rightarrow k_Z \end{aligned}$$

In the equations above, $\{ \}$ denotes an activity and $[\]$ a concentration; f_X , f_Y and f_Z are the activity coefficients of the fully deprotonated forms X^{n_x-} , Y^{n_y-} and Z^{n_z-} respectively and F_{X_i} , F_{Y_i} and F_{Z_i} are the activity coefficients of the i th protonated form of each ion. With this notation, a strong acid is automatically covered by the theory since it is regarded as a weak acid with $K_x = 0$. Discrimination between strong acids is not possible. We can now derive the functions from the mass- and charge-balance equations for each data point (V , pH), where V is the volume of titrant added.

Mass balances

$$\begin{aligned} \text{Total X, } T_X &= [X] + [HX] + \dots [H_i X] \\ &\quad + \dots [H_{k_X} X] \\ &= [X](1 + \beta_X) \\ &= C_B V_X / a (V_0 + V) \end{aligned}$$

$$\begin{aligned} \text{Total Y, } T_Y &= [Y] + [HY] + \dots [H_i Y] \\ &\quad + \dots [H_{k_Y} Y] \\ &= [Y](1 + \beta_Y) \\ &= C_B V_Y / b (V_0 + V) \end{aligned}$$

$$\begin{aligned} \text{Total Z, } T_Z &= [Z] + [HZ] + \dots [H_i Z] \\ &\quad + \dots [H_{k_Z} Z] \\ &= [Z](1 + \beta_Z) \\ &= C_B V_Z / c (V_0 + V) \end{aligned}$$

In the equations above, V_X , V_Y and V_Z are the volumes of titrant equivalent to each acid and β_X , β_Y ,

β_Z are given by

$$\beta_X = \sum_{i=1}^{k_X} K_{X_i} \{H\}^i f_X / F_{X_i}$$

$$\beta_Y = \sum_{i=1}^{k_Y} K_{Y_i} \{H\}^i f_Y / F_{Y_i}$$

and

$$\beta_Z = \sum_{i=1}^{k_Z} K_{Z_i} \{H\}^i f_Z / F_{Z_i}$$

Total titrant

$$T_B = C_B V / (V_0 + V)$$

$$j_P [P] = (n_x - a) T_X$$

$$j_Q [Q] = (n_y - b) T_Y$$

$$j_R [R] = (n_z - c) T_Z$$

Charge balance

$$\begin{aligned} i_P [P] + i_Q [Q] + i_R [R] + [H] + T_B - [\text{OH}] \\ &= n_X [X] + (n_X - 1) [HX] + \dots \\ &\quad (n_X - i) [H_i X] + \dots (n_X - k_X) [H_{k_X} X] + \\ &\quad n_Y [Y] + (n_Y - 1) [HY] + \dots \\ &\quad (n_Y - i) [H_i Y] + \dots (n_Y - k_Y) [H_{k_Y} Y] + \\ &\quad n_Z [Z] + (n_Z - 1) [HZ] + \dots \\ &\quad (n_Z - i) [H_i Z] + \dots (n_Z - k_Z) [H_{k_Z} Z] \end{aligned}$$

Substituting for [P], [Q] and [R] on the left and collecting terms on the right, we obtain

$$\begin{aligned} (n_X - a) T_X + (n_Y - b) T_Y + (n_Z - c) T_Z \\ + T_B + [H] - [\text{OH}] \\ = n_X T_X - \alpha_X [X] + n_Y T_Y - \alpha_Y [Y] \\ + n_Z T_Z - \alpha_Z [Z] \end{aligned} \quad (1)$$

where

$$\alpha_X = \sum_{i=1}^{k_X} i K_{X_i} \{H\}^i f_X / F_{X_i}$$

$$\alpha_Y = \sum_{i=1}^{k_Y} i K_{Y_i} \{H\}^i f_Y / F_{Y_i}$$

and

$$\alpha_Z = \sum_{i=1}^{k_Z} i K_{Z_i} \{H\}^i f_Z / F_{Z_i}$$

Rearranging (1) gives

$$\begin{aligned} T_B + [H] - [\text{OH}] &= a T_X + b T_Y + c T_Z - \alpha_X [X] \\ &\quad - \alpha_Y [Y] - \alpha_Z [Z] \\ &= T_X \left(a - \frac{\alpha_X}{1 + \beta_X} \right) \\ &\quad + T_Y \left(b - \frac{\alpha_Y}{1 + \beta_Y} \right) \\ &\quad + T_Z \left(c - \frac{\alpha_Z}{1 + \beta_Z} \right) \end{aligned}$$

Substituting for T_x , T_y , T_z and T_b from the mass-balance equations gives

$$\begin{aligned} \frac{C_B V}{V_0 + V} + [H] - [OH] &= \frac{C_B V_x}{a(V_0 + V)} \left(a - \frac{\alpha_x}{1 + \beta_x} \right) \\ &+ \frac{C_B V_y}{b(V_0 + V)} \left(b - \frac{\alpha_y}{1 + \beta_y} \right) \\ &+ \frac{C_B V_z}{c(V_0 + V)} \left(c - \frac{\alpha_z}{1 + \beta_z} \right) \end{aligned}$$

Hence

$$\begin{aligned} \frac{(V_0 + V)([H] - [OH])}{C_B} + V &= \frac{V_x}{a} (a - \theta_x) \\ &+ \frac{V_y}{b} (b - \theta_y) + \frac{V_z}{c} (c - \theta_z) \quad (2) \end{aligned}$$

where

$$\theta_x = \frac{\alpha_x}{(1 + \beta_x)}, \quad \theta_y = \frac{\alpha_y}{(1 + \beta_y)}, \quad \theta_z = \frac{\alpha_z}{(1 + \beta_z)}.$$

Since $\text{pH} = -\log \{H\}$, and the autoprotolysis constant for water is $K_w = \{H\} \{OH\}$, we obtain

$$\begin{aligned} [H] &= \{H\}/f_H = 10^{-\text{pH}}/f_H \quad \text{and} \\ [OH] &= \{OH\}/f_H = \frac{K_w}{10^{-\text{pH}} f_H}, \end{aligned}$$

where f_H is the univalent-ion activity coefficient.

Rewriting equation (2), we obtain

$$\begin{aligned} \frac{(V_0 + V)(\{H\} - K_w/\{H\})}{f_H C_B} + V &= \frac{V_x}{a} (a - \theta_x) \\ &+ \frac{V_y}{b} (b - \theta_y) + \frac{V_z}{c} (c - \theta_z) \quad (3) \end{aligned}$$

In equation (3) the left-hand side and the functions θ_x , θ_y and θ_z can all be calculated from measured variables and known constants, and a , b and c are known, leaving the unknown equivalence volumes V_x , V_y and V_z . Since a linear titration plot can resolve only two unknowns, we need a further piece of information, which will usually be obtainable from a different treatment of the same titration data or may come from the use of another analytical technique. This extra information may be any one of

$$V_x, V_y, V_z, V_{xy} = V_x + V_y, V_{xz} = V_x + V_z,$$

$$V_{yz} = V_y + V_z \quad \text{and} \quad V_E = V_x + V_y + V_z.$$

One equivalence volume known

Suppose one of the equivalence volumes, say V_z , is known, then rearranging equation (3) gives the calculable function U_0 :

$$\begin{aligned} U_0 &= \frac{(V_0 + V)(\{H\} - K_w/\{H\}) + V f_H C_B}{f_H C_B (a - \theta_x)} \\ &- \frac{V_z (c - \theta_z)}{c (a - \theta_x)} \\ &= \frac{V_x}{a} + \frac{V_y}{b} U_A \end{aligned}$$

where $U_A = (b - \theta_y)/(a - \theta_x)$. Plotting U_0 against U_A enables V_x and V_y to be calculated from the intercept and slope respectively.

Exactly analogous functions (U_0 , U_A) will be obtained if V_x or V_y is known.

Sum of two equivalence volumes known

Suppose $V_{yz} = V_y + V_z$ is known, then rearranging equation (3) gives a calculable function U_0

$$\begin{aligned} U_0 &= \frac{(V_0 + V)(\{H\} - K_w/\{H\}) + V f_H C_B}{f_H C_B (a - \theta_x)} \\ &- \frac{V_{yz} (c - \theta_z)}{c (a - \theta_x)} \\ &= \frac{V_x}{a} + \frac{V_y}{b} U_A \end{aligned}$$

where

$$U_A = \left(\frac{b}{c} \theta_z - \theta_y \right) / (a - \theta_x).$$

Plotting U_0 against U_A enables V_x and V_y to be calculated from the intercept and slope respectively. Analogous functions (U_0 , U_A) will be obtained if V_{xy} or V_{xz} is known.

Total equivalence volume known

If V_E is known, rearranging equation (3) gives a calculable function U_0

$$\begin{aligned} U_0 &= \frac{(V_0 + V)(\{H\} - K_w/\{H\}) + V f_H C_B}{f_H C_B \left(\frac{a}{c} \theta_z - \theta_x \right)} \\ &- \frac{V_E (c - \theta_z)}{\frac{a}{c} \theta_z - \theta_x} \\ &= \frac{V_x}{a} + \frac{V_y}{b} U_A \end{aligned}$$

where

$$U_A = \left(\frac{b}{c} \theta_z - \theta_y \right) / \left(\frac{a}{c} \theta_z - \theta_x \right).$$

Plotting U_0 against U_A enables V_x and V_y to be calculated from the intercept and slope respectively.

Choice of plot

The choice between the plots derived above depends on which equivalence volume can be determined independently, but that leaves several variations for each type of plot, depending on nomination of the acids as X, Y and Z.

With perfectly accurate data, the nomination of acids would not matter, but with real pH values and

association constants some choices are more convenient than others. Of the functions θ_X , θ_Y and θ_Z above, θ_X occurs the most frequently. If one of the acids is a strong acid it is convenient to nominate it as acid X, since this makes $\theta_X = 0.0$ and saves calculation.

The weakest of the three acids, *i.e.*, that with the largest association constants, should not normally be chosen as acid Y, since the large constants exaggerate the effect of any errors, especially at the extremes of the plot. With a graphical solution the outlying points are easily seen and can be ignored but with a computed solution the selection of points becomes more difficult.

It is also found that for graphical solution, nominating the acids as X, Y and Z in order of increasing association constants gives the set of values for U_0 and U_A that can most conveniently be handled, since the numbers tend to be neither very large (as when the weakest acid is Y) nor very small (as when the weakest is X) and negative numbers are avoided.

Since the general theory involves activity coefficients, the problem can only be solved iteratively if the ionic strength is kept constant. In dilute solution ($< 10^{-4}M$) it is, however, usually valid to assume that activity coefficients can be set to unity, which makes iteration unnecessary. Experimental verification is given below.

Three weak bases

The derivation and notation are almost identical with that for three weak acids, except that C_B is now the concentration of the acidic titrant. One of the bases may be a strong base, *e.g.*, an alkali metal hydroxide, but no discrimination is possible between different strong bases.

Instead of equation (3) for three weak acids, we obtain from the mass- and charge-balance equations

$$\begin{aligned} & \frac{(V_0 + V)(\{H\} - K_w/\{H\}) - V}{f_H C_B} - V \\ &= \frac{V_X}{(k_X - a)}(a - \theta_X) + \frac{V_Y}{(k_Y - b)}(b - \theta_Y) \\ &+ \frac{V_Z}{(k_Z - c)}(c - \theta_Z) \end{aligned} \quad (4)$$

To obtain any two of the equivalence volumes we need to know from some other source one of the following:

$$\begin{aligned} & V_X, \quad V_Y, \quad V_Z \\ & V_{XY} = V_X + V_Y, \\ & V_{YZ} = V_Y + V_Z, \\ & V_{XZ} = V_X + V_Z, \\ & V_E = V_X + V_Y + V_Z. \end{aligned}$$

One equivalence volume known

If V_Z is known, we obtain a calculable function U_0

$$\begin{aligned} U_0 &= \frac{(V_0 + V)(\{H\} - K_w/\{H\}) - Vf_H C_B}{f_H C_B(a - \theta_X)} \\ &\quad - \frac{V_Z(c - \theta_Z)}{(k_Z - c)(a - \theta_X)} \\ &= \frac{V_X}{k_X - a} + \frac{V_Y}{k_Y - b} U_A \end{aligned}$$

where

$$U_A = (b - \theta_Y)/(a - \theta_X).$$

A plot of U_0 against U_A enables V_X and V_Y to be determined from the intercept and slope respectively. Analogous functions result if V_X or V_Y is known.

Sum of two equivalence volumes known

If V_{YZ} is known, we obtain by rearrangement of equation (4) a calculable function U_0 :

$$\begin{aligned} U_0 &= \frac{(V_0 + V)(\{H\} - K_w/\{H\}) - Vf_H C_B}{f_H C_B(a - \theta_X)} \\ &\quad - \frac{V_{YZ}(c - \theta_Z)}{(k_Z - c)(a - \theta_Y)} \\ &= \frac{V_X}{(k_X - a)} + \frac{V_Y}{(k_Y - b)} U_A \end{aligned}$$

where

$$U_A = \left(\frac{b}{c} \theta_Z - \theta_Y \right) / (a - \theta_X),$$

A plot of U_0 against U_A allows V_X and V_Y to be determined from the intercept and slope respectively. Analogous functions result if V_{XY} or V_{XZ} is known.

Total equivalence volume known

If V_E is known, we obtain by rearrangement of equation (4) a calculable function U_0 :

$$\begin{aligned} U_0 &= \frac{(V_0 + V)(\{H\} - K_w/\{H\}) - Vf_H C_B}{f_H C_B \left(\frac{a}{c} \theta_Z - \theta_X \right)} \\ &\quad - \frac{V_E(c - \theta_Z)}{\left(\frac{a}{c} \theta_Z - \theta_X \right)} \\ &= V_X + V_Y U_A \end{aligned}$$

where

$$U_A = \frac{\frac{a}{c} \theta_Z - \theta_Y}{\frac{a}{c} \theta_Z - \theta_X},$$

A plot of U_0 against U_A allows V_X and V_Y to be determined from the intercept and slope respectively.

Special case of strong bases

With a strong base as X, say, in the general derivation, we would have $[X] = [\text{OH}]$, but $[\text{OH}]$ already occurs because of the autoprotolysis of water and no meaningful value can be given to K_{X_1} and hence α_X , β_X and θ_X .

Carrying out the derivations for this special case gives sets of functions (U_0 , U_A) corresponding to those for the general case. Assuming that the strong base is X, these special functions are obtained from the general ones shown above by assigning θ_X a value of 1 (with $a = 0$, $k_X = 1$, $K_X = 0.0$).

Choice of plot

As with weak acids, the plots can take various forms, depending on the assignment of the bases as X, Y or Z. Similar considerations as those for acid mixtures apply; the strongest base (largest acid association constant) should be X, the next strongest, Y and the weakest, Z. Completely dissociated hydroxides such as sodium hydroxide are entered as X with $K_X = 0.0$ and $\theta_X = 1$.

EXPERIMENTAL

Apparatus

Measurements were made with a Radiometer PHM64 digital pH-meter, with Radiometer G2040C and K4040 glass and calomel electrodes respectively. The sample solution was contained in a water-jacketed glass titration cell (Radiometer V535) and the titrant was added from a Radiometer ABU.13 piston burette.

Reagents

Stock solutions of 1M nitric and acetic acids were prepared from concentrated volumetric solutions (B.D.H.). Stock solutions of 0.1M ammonium chloride, 0.01M benzoic acid, 0.1M tris(hydroxymethyl)methylamine and 0.1M sodium acetate were prepared from analytical-grade chemicals. More dilute stock solutions, which were used to make up the titrated mixtures, were prepared by dilution of the stock solutions.

Standard sodium hydroxide solution was prepared by dilution of saturated sodium hydroxide solution, which was dispensed under a nitrogen blanket into a container of deaerated demineralized water. This dilute solution was standardized potentiometrically against nitric acid.

Titration procedure

Different mixtures of acids or bases for titration were prepared by pipetting appropriate volumes of their standard solutions into the titration vessel and adding demineralized water to give an accurately known total volume of about 20 ml. Water (at 25°) was circulated through the water-jacket surrounding the titration vessel.

The solution was stirred mechanically by the Radiometer TTA60 titration assembly. Nitrogen was passed over the surface of the solutions throughout the titration in order to prevent the absorption of atmospheric carbon dioxide during the alkaline phase of the titration.

The titrant solution was added from a piston burette equipped with a digital counter. The volume added and the corresponding e.m.f. were noted when a steady trace was observed on a chart recorder connected to the pH-meter. Titrations with acid were continued until the pH was less than 4, those with base until the pH was greater than 9.5.

The glass electrode was calibrated before each titration by reference to standard NBS buffer solutions (pH 4.008 and 9.180 at 25°).

Calculations

Calculations were done with the aid of an IBM 370 computer and a FORTRAN program TREBLE. This program can first calculate the total equivalence volume by using Gran's method⁶ and then automatically apply this result to the calculation of the functions U_0 and U_A required for resolving the mixture into its components. Literature values of equilibrium constants were used.⁷

PROPERTIES OF THE LINEAR TITRATION PLOTS

The effect of systematic errors in pH and the association constants was investigated with computer-generated data for a hypothetical titration of 100-ml portions of solution containing equal concentrations of either three monobasic acids ($K_X = 0.0$, $K_Y = 10^5$, $K_Z = 10^9$ or $K_Y = 0.0$, $K_Y = 10^4$, $K_Z = 10^6$) or three monoacidic bases ($K_X = 0.0$, $K_Y = 10^9$, $K_Z = 10^5$). Base X was sodium hydroxide and the titrant was 1.0N strong base or acid as appropriate.

In all the examples below, V_E is the independently determined equivalence volume, but the functions are such that similar causes would produce similar deviations from the theoretical plots if V_Z or V_{YZ} were known.

Effect of an error in the association constants

Figure 1 shows plots for the titration of a hypothetical acid solution with $K_X = 0.0$, $K_Y = 10^5$, $K_Z = 10^9$. Use of an overestimate of K_Y produces deviations above the theoretical line over most of the plot and the effect of errors in K_Z is seen only as U_A tends to its limiting value ($b/a = 1$) in this example). This is best seen in the inset. An overestimate of K_Z produces positive deviations and an underestimate results in

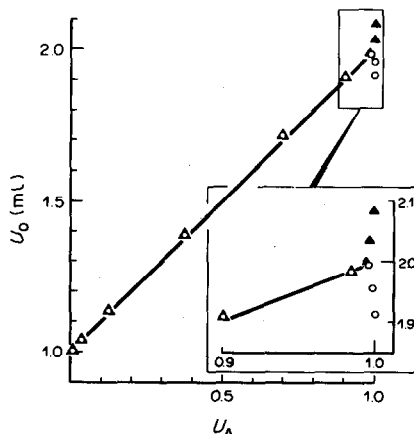


Fig. 1. Effect of errors in the association constants on the plot for the titration of three acids ($V_0 = 100$ ml, $K_X = 0.0$, $K_Y = 10^5$, $K_Z = 10^9$, $T_X = T_Y = T_Z = 10^{-2}N$). — theoretical line; \circ — $K_Y = 1.1 \times 10^5$, $K_Z = 0.9 \times 10^9$; \blacktriangle — $K_Y = 1.1 \times 10^5$, $K_Z = 1.1 \times 10^9$. \blacktriangle and \circ —coincidence of \blacktriangle and \circ .

negative deviations. The effect of an underestimate of K_Y is not shown, but the points are almost symmetrically displaced to the opposite side of the theoretical line, from the positions shown in Fig. 1, except where the effect of errors in K_Z predominates (the points then remain as shown in the inset).

The titration of a hypothetical basic solution produces plots that differ little from those in Fig. 1, except that overestimates of K_Y or K_Z produce negative deviations from the theoretical line and underestimates produce positive deviations, *i.e.*, deviations are in the opposite direction from those for acidic solutions.

Effect of an error in pH

Figure 2 shows the plot for the titration of an acidic solution ($K_X = 0.0$, $K_Y = 10^5$, $K_Z = 10^9$) when the pH values used are in error by $+0.05$ (V_E known). As U_A tends to a constant value (unity in this case), the deviations from the theoretical line become large but these points are easily discerned and would be ignored in a graphical solution of the plot. Low pH values produce deviations above the theoretical line and the effect of an error of -0.05 pH units would be virtually a mirror image of that shown.

In the titration of bases, the deviations produced by an error in pH are opposite to those for the titration of acids. An error of -0.05 pH units in titration of a mixture of bases ($K_X = 0.0$, $K_Y = 10^9$, $K_Z = 10^5$, each base $0.01N$) would give a plot virtually indistinguishable from that shown in Fig. 2 for an error of $+0.05$ pH units in the hypothetical titration of acids.

Figure 2 shows that although a systematic error of 0.05 pH units produces considerable deviations from the theoretical line as U_A tends to its limiting value, deviant points can be easily identified and the plot remains useful over 95% of its range. Titrating an acidic solution when the pH has a negative bias results in an overestimate of the strongest acid (X) and an underestimate of the weakest acid (Z). Titrating an alkaline solution when the pH has a negative bias results in an underestimate of the strongest base (X) and an overestimate of the (Z) weakest base. The effect on the intermediate (Y) acid or base is unpredictable, since a real titration produces only a limited number of data points, which cannot be guaranteed to be symmetrically distributed within the range $0 < U_A < b/a$. Depending on this distribution, the intermediate acid or base may be either over- or underestimated.

A positive bias in pH produces errors opposite and almost equal to those described above. Random errors in pH result in scattered plots and hence less precisely known but unbiased concentrations.

The errors produced by as large a bias in pH as 0.05 units are still fairly small, *e.g.*, for the results shown in Fig. 2, a least-squares fit of the points in the range $0 < U_A < 0.997$ gave errors of -1.6% , $+0.6\%$ and $+1.0\%$ for acids X ($K_X = 0$), Y ($K_Y = 10^5$) and Z

($K_Z = 10^9$) respectively. With stronger acids the errors are larger, *e.g.*, the results in Fig. 2 for X ($K_X = 0$), Y ($K_Y = 10^4$) and Z ($K_Z = 10^6$) gave errors of -2.3% , -0.5% and $+2.8\%$ when fitted by least-squares over the range $0 < U_A < 0.97$; the bigger deviations in this case are more clearly seen as U_A tends towards unity.

Effect of an error in V_E

Since an independently determined equivalence volume is required in all the plots, an error in this volume will influence the ordinates of the plots. Figure 3 shows the effect of an underestimate of the total equivalence volume on the plot for a mixture of three acids ($K_X = 0.0$, $K_Y = 10^5$, $K_Z = 10^9$). The effect of the error in V_E is seen only as U_A approaches its maximum possible value (*i.e.*, $U_A > 0.99$), the plot then deviating above the theoretical line. For an overestimate of V_E , the deviation would be below the line. In practice there would be no difficulty in using a plot such as that in Fig. 3 to determine V_X and V_Y accurately, but the error in V_E would be transmitted to V_Z . This problem is worse when $V_X + V_Y \gg V_Z$.

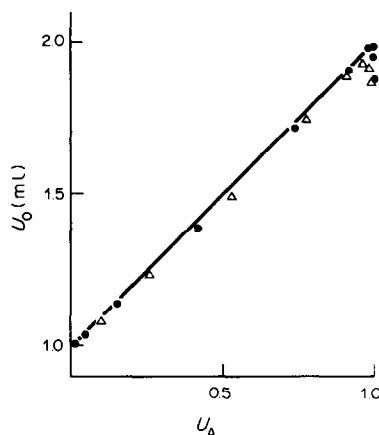


Fig. 2. Effect of an error of $+0.05$ in pH on plots for the titration of three acids ($T_X = T_Y = T_Z = 10^{-2}N$). ●— $V_0 = 100$ ml, $K_X = 0.0$, $K_Y = 10^5$, $K_Z = 10^9$; △— $V_0 = 100$ ml, $K_X = 0.0$, $K_Y = 10^4$, $K_Z = 10^6$; — theoretical line for both plots.

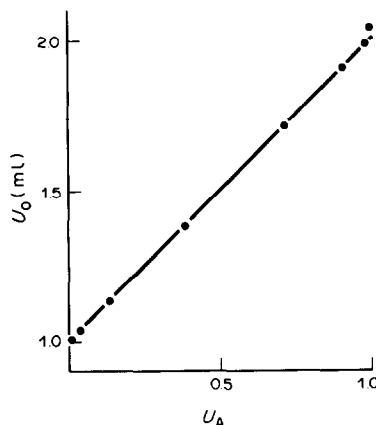


Fig. 3. Effect of an error in V_E . $V_0 = 100$ ml, $K_X = 0.0$, $K_Y = 10^5$, $K_Z = 10^9$, $T_X = T_Y = T_Z = 10^{-2}N$ acid. — theoretical line ($V_E = 3.0$ ml) ●—calculated with $V_E = 2.5$ ml.

RESULTS

Acidic solutions

Table 1 shows that moderately concentrated mixtures of three acids (each $1-5 \times 10^{-3}N$) with widely spaced association constants can be analysed with errors of 1-2% for two of the components and 1-10% for the third (Runs 1.1 and 1.2). When two of the acids have similar association constants, e.g., acetic and benzoic acids, the analysis tends to be less accurate (Run 1.3), although even with three similar acids (Run 1.4) the error for one component can be less than 10%.

In more dilute mixtures (each acid $10^{-5}-10^{-4}N$) the results were less accurate, since the errors for acids with widely spaced association constants (Runs

2.1-2.3 of Table 2) could exceed 10% and resolution of acetic and benzoic acids (Runs 2.4 and 2.5) was poor.

Effect of neglecting activity coefficients

Since the time required for calculation is much reduced if activity coefficients can be neglected, linear titration plots for Runs 1.1 and 2.1 were calculated with and without activity-coefficient corrections. The results and a selection of data points from these runs are shown in Table 3. At the lower ionic strength ($\sim 10^{-4}$) of Run 2.1, activity coefficients have a negligible effect on the co-ordinates (U_A, U_0). Least-squares fitting of the results gives equivalence volumes that differ by less than 2% from the values with activity corrections, but it is doubtful whether the

Table 1. Analysis of moderately concentrated mixtures of acids

Run	Composition (meq/l.)				Concentrations found, meq/l.				pH range
	X	Y	Z	Total	X	Y	Z	Total	
1.1	nitric (5)	acetic (1)	ammonium (1)	(7)	5.04 5.05	1.01 0.99	1.01 1.02	7.06 7.06	4.0-5.2 4.1-8.3
1.2	nitric (4)	acetic (1)	HTris ⁺ (1)	(6)	3.97	1.11	1.01	6.10	3.9-7.4
1.3	nitric (5)	benzoic (1)	acetic (1)	(7)	5.13	1.20	0.78	7.11	3.2-4.7
1.4	monochloroacetic (1.82)	benzoic (1.82)	acetic (1.82)	(5.46)	1.86	1.89	1.70	*	3.0-4.0

*Theoretical total equivalence volume supplied to the program

Table 2. Analysis of dilute acid mixtures

Run	Composition (μ eq/l.)				Concentrations found, μ eq/l.				pH range
	X	Y	Z	Total	X	Y	Z	Total	
2.1	HNO ₃ (50)	HOAc (15)	NH ₄ ⁺ (50)	(115)	45.9	17.2	51.8	*	5.0-6.4
2.2	HNO ₃ (100)	HOAc (60)	NH ₄ ⁺ (20)	(180)	102.9 75.1	64.2 91.8	12.9 3.8	* 170.7	4.1-6.0 4.4-6.0
2.3	HNO ₃ (50)	HOAc (60)	NH ₄ ⁺ (50)	(160)	42.8	67.8	49.4	*	4.4-6.5
2.4	HNO ₃ (50)	HOBz (60)	HOAc (50)	(160)	43.2	65.6	55.7	164	4.0-5.1
2.5	HNO ₃ (50)	HOAc (100)	HOBz (60)	(210)	50.9	46.5	112.5	210	4.0-4.6

*Theoretical total equivalence volume supplied to the program.

Table 3. Effect of neglecting activity coefficients

<i>V</i> , ml	pH	Activity coefficients used		Activity coefficients = 1.0	
		10 <i>U</i> _A	<i>U</i> ₀	10 <i>U</i> _A	<i>U</i> ₀
Run 1.1*					
1.050	4.047	1.751	1.071	1.636	1.069
1.111	4.538	3.965	1.118	3.769	1.117
1.146	4.803	5.480	1.149	5.272	1.149
1.200	5.307	7.949	1.201	7.806	1.201
		<i>V</i> _X = 1.035		1.036	
		<i>V</i> _Y = 0.209		0.213	
		<i>V</i> _Z = 0.206		0.201	
Run 2.1†					
0.326	5.010	6.450	0.395	6.423	0.394
0.360	5.189	7.330	0.406	7.306	0.405
0.396	5.493	8.469	0.419	8.453	0.418
0.434	6.420	9.790	0.436	9.787	0.436
		<i>V</i> _X = 0.318		0.316	
		<i>V</i> _Y = 0.119		0.121	
		<i>V</i> _Z = 0.359		0.359	

**V*₀ = 20 ml, *C*_B = 0.0965*N*.

†*V*₀ = 25 ml, *C*_B = 0.00361*N*.

co-ordinates could be plotted precisely enough for this difference to be discernible in a graphical evaluation of the equivalence volumes.

At the higher ionic strength ($\sim 7 \times 10^{-3}$) of Run 1.1, the effect on the co-ordinates is more noticeable, especially for U_A , but the difference in the equivalence volumes is at most 2.5%.

Determination of the total equivalence volume

All the results in Tables 1 and 2 were obtained with plots that used V_E as the independently determined equivalence volume. V_E was determined by Gran's method,⁶ with pH data from the extremes of the titration curves. With solutions containing no ammonium ions, V_E could be determined accurately from data at pH > 9, but when ammonium ions were present, data in the pH range 10.2–11.0 were needed for accurate results. In the runs in Table 2 it was not possible to add enough titrant to reach such high pH values and V_E was underestimated by 30% when calculated from data at pH below 9.5, so the expected value of V_E was used for the calculations. The inability to reach the required pH was peculiar to these runs and is not a general problem.

Alkaline solutions

Results for mixtures of sodium hydroxide, ammonia and sodium acetate showed low (70–80%) recoveries of sodium hydroxide, although the errors in the other components were smaller. It was decided that with the apparatus used, protection against contamination with carbon dioxide was inadequate and that acidification of the solutions, followed by back-titration, was more practical.

DISCUSSION

Linear titration plots have been used to analyse mixtures of three acids, a titration problem for which a solution has not been reported, even with use of such theoretically powerful methods as multi-parametric curve-fitting.⁸ Moreover, the method has been applied at concentrations below $10^{-4}N$. The method requires that one of the equivalence volumes (or the sum of two or three of them) can be determined independently. If this is possible the resultant plot is little more complicated than that for a mixture of two acids and the co-ordinates can easily be calculated with the aid of a programmable calculator if activity coefficients are either kept constant or, in dilute solution, neglected. As with all linear titration plots, the method can cope with polyfunctional acids or bases and is independent of the existence of points of inflexion in the conventional titration curve of pH against volume added.

Acknowledgement—This work was done, in part, at the Central Electricity Research Laboratories and is published with the permission of the Central Electricity Generating Board.

REFERENCES

1. C. McCallum and D. Midgley, *Anal. Chim. Acta*, 1973, **65**, 155.
2. D. Midgley and C. McCallum, *Talanta*, 1976, **23**, 320.
3. *Idem*, *Z. Anal. Chem.*, 1978, **290**, 230.
4. C. McCallum and D. Midgley, *Anal. Chem.*, 1976, **48**, 1232.
5. D. Midgley, *CERL Report No. TPRD/L/2452/R83*, Leatherhead, 1983.
6. G. Gran, *Analyst*, 1952, **77**, 661.
7. R. A. Robinson and R. H. Stokes, *Electrolyte Solutions*, 2nd Ed. revised, p. 517. Butterworths, London, 1965.
8. L. Meites, *CRC Crit. Rev. Anal. Chem.*, 1979, **8**, 1.

ETUDE POLAROGRAPHIQUE DU NIOBIUM DANS LES MELANGES EAU-FLUORURE D'HYDROGENE EN PRESENCE D'IONS TETRAALKYLAMMONIUM

HUGUES MENARD et REJEAN BEAUDOIN

Département de chimie, Faculté des sciences, Université de Sherbrooke, Sherbrooke, Québec, Canada

(Reçu le 28 juin 1983. Révisé le 11 novembre 1983. Accepté le 13 janvier 1984)

Résumé—On a étudié la réduction polarographique du niobium sous forme du complexe NbF_6^- dans les mélanges eau-fluorure d'hydrogène jusqu'à 50% p/p. L'addition d'ions tétraalkylammonium dans ce mélange permet le déplacement du potentiel de réduction de l'hydrogène et le dosage du niobium par polarographie impulsionnelle différentielle à une limite de détection inférieure à 1 ppm. En présence d'ions tétraalkylammonium, on observe une hausse importante du courant de réduction du niobium aux concentrations en HF où le complexe non réductible NbOF_3^- est prépondérant.

Il est connu qu'en polarographie le potentiel de dégagement d'hydrogène se déplace dans le sens positif lorsqu'on augmente la concentration en acide de l'électrolyte de support, ce qui peut devenir gênant pour l'analyse d'un ion métallique dont le potentiel de demi-vague est assez négatif. La réduction du niobium¹ s'effectue à un potentiel proche de la réduction de l'hydrogène, ce qui limite le seuil de détection. Il est clair que tout déplacement négatif du potentiel du dégagement de l'hydrogène qui n'affecterait pas le potentiel de demi-vague du niobium améliorerait la limite de détection.

Dans le but de déplacer le potentiel du mur de réduction de l'hydrogène et d'étendre le domaine utile dans les mélanges eau-fluorure d'hydrogène de l'ordre de 50%, nous avons ajouté des hydroxydes de tétraalkylammonium. La concentration du HF étant de 24M, le pH de la solution est inchangé par l'addition d'une faible quantité d'hydroxyde.

Gierst *et al.*² ont déjà effectué une étude du comportement des ions tétraalkylammonium à l'interphase mercure-solution. Les travaux ont démontré que (1) ces ions sont spécifiquement adsorbés, (2) l'adsorption est principalement localisée dans le domaine de charges négatives; (3) l'adsorbabilité croît avec la longueur de la chaîne carbonée, c'est-à-dire avec le caractère hydrophobe de l'ion; (4) la cinétique de l'adsorption aux faibles concentrations peut être contrôlée par le transfert massique vers la surface.

PARTIE EXPERIMENTALE

Les produits utilisés sont du KF certifié de Fisher, Me_4NOH et Et_4NOH reagent de B.D.H., Pr_4NOH reagent de Eastman et Bu_4NOH reagent de Baker, Nb_2O_5 99,9% de Alfa Product, et HF J. T. Baker 49,1%.

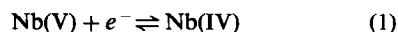
La cellule polarographique est constituée d'un béccher en polyméthylpentane d'une capacité de 50 ml surmonté d'un couvercle de Teflon qui sert à maintenir les électrodes. L'électrode de référence au calomel saturé est munie d'une double jonction séparée de la solution par une gaine de Teflon et un disque de polyéthylène poreux. L'électrode

auxiliaire est un fil de platine. L'électrode de travail est un capillaire polarographique Sargent-Welch S-2417 recouvert de polyéthylène³ et dont la période de chute est contrôlée par un dispositif électronique réalisé dans nos ateliers. Tous les potentiels se réfèrent à l'électrode de calomel saturé. L'analyseur polarographique PAR est le modèle 364 (ou 174); la table traçante est une Techneurop, Sefram T.G.M. 101.

Les solutions de niobium sont préparées de la façon suivante: le Nb_2O_5 est dissous dans du HF puis la solution est évaporée, le résidu est ensuite redissous dans HF 49,1%. La solution-mère est diluée avec de l'eau déminéralisée ou du HF pour obtenir la concentration en acide et en niobium désirée. La solution de tétraalkylammonium est ajoutée immédiatement avant la mesure.

RESULTATS ET DISCUSSIONS

En milieu fluorure d'hydrogène 50%, le niobium sous forme de complexe NbF_6^- se réduit de façon réversible à un potentiel de $-0,880$ V vs. E.C.S. [équation (1)].¹



On peut donc prévoir que le potentiel de réduction ne sera pas déplacé par addition d'espèces adsorbées à l'électrode, mais que la valeur du courant de diffusion sera susceptible de varier. Le courant de réduction mesuré varie dès qu'il y a présence d'une faible concentration d'ions tétraalkylammonium. La vague de réduction de l'hydrogène est déplacée cathodiquement, permettant une meilleure définition de l'onde du niobium.

L'augmentation graduelle de la concentration en ions tétraméthylammonium (Me_4N^+) provoque un accroissement de la hauteur de la vague de réduction du niobium, en polarographie impulsionnelle différentielle (P.I.D.) et un déplacement du mur de réduction de l'hydrogène vers des potentiels plus négatifs.

La figure 1 montre les polarogrammes P.I.D. obtenus pour plusieurs concentrations de Me_4N^+ .

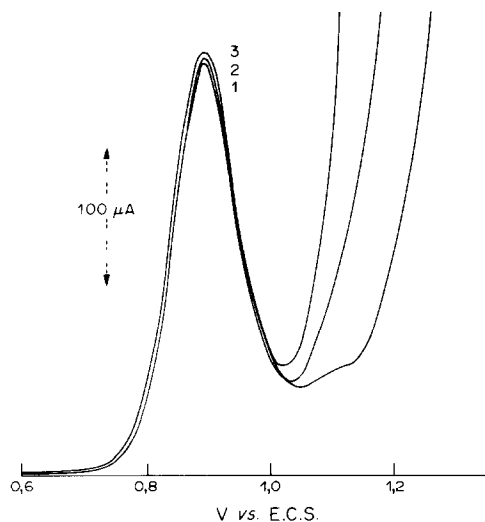


Fig. 1. Polarogrammes (P.I.D.) d'une solution de niobium $2,25 \times 10^{-3} M$ dans: (1) HF 49,1%, (2) HF 49,1% + Me_4NOH $0,012 M$; (3) HF 49,1% + Me_4NOH $0,17 M$.

L'augmentation du pic de réduction est rapide jusqu'à $0,25 M$ et le déplacement du mur de réduction de l'hydrogène suit une progression semblable.

Ce gain de courant de pic est attribué à la soustraction du courant résiduel constitué principalement par la réduction de l'hydrogène. Bond et Grabaric⁴ ont mis au point un système de traitement mathématique pour soustraire le courant résiduel en polarographie impulsionnelle différentielle. L'approche consiste à calculer, à l'aide d'un ordinateur, l'équation de la courbe du courant résiduel et soustraire sa valeur du pic de réduction de l'espèce électroactive. Dans notre cas, l'addition de l'ion tétraalkylammonium déplace le mur de réduction de l'hydrogène et diminue le courant résiduel sous la vague de réduction du niobium.

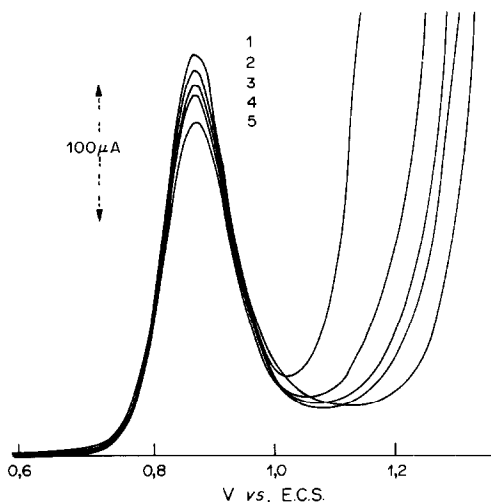


Fig. 2. Polarogrammes (P.I.D.) d'une solution de niobium $2,25 \times 10^{-3} M$ dans: (1) HF 49,1%; (2) HF 49,1% + Et_4NOH $0,69 \times 10^{-2} M$; (3) HF 49,1% + Et_4NOH $1,39 \times 10^{-2} M$; (4) HF 49,1% + Et_4NOH $2,08 \times 10^{-2} M$; (5) HF 49,1% + Et_4NOH $3,43 \times 10^{-2} M$.

Par ailleurs, le déplacement du mur de réduction de l'hydrogène suit la même progression que la hauteur de la vague de réduction du niobium. Nous sommes donc dans un cas où le déplacement du mur de réduction de l'hydrogène peut être attribué à un effet ψ_{δ^*} , (le potentiel au plan externe d'Helmholtz modifié par l'espèce adsorbée), alors que le taux de recouvrement de l'électrode est faible.²

Dans le cas de l'ion tétraéthylammonium (Et_4N^+) la vague du niobium diminue, puis se stabilise. La figure 2 montre la diminution rapide du pic en P.I.D. pour des concentrations allant jusqu'à $3,5 \times 10^{-2} M$ Et_4N^+ . Le déplacement du mur de réduction de l'hydrogène est le plus important de tous ceux mesurés dans la série des quatre ions tétraalkylammonium étudiés.

L'explication de ces résultats est liée à l'importance du recouvrement de l'électrode pour cette concentration. Nous avons une diminution du courant jusqu'à ce que le recouvrement soit maximal, après quoi la vitesse de réduction demeure constante. Nous pouvons donner une explication semblable pour le déplacement du mur de réduction de l'hydrogène lorsque le recouvrement de l'électrode est maximum, le potentiel ψ_{δ^*} de l'électrode devient constant et le potentiel observé pour la réduction de l'hydrogène ne se déplace plus. Le déplacement est plus important que dans les autres cas, parce que le retard est à la fois dû à l'effet ψ_{δ^*} et au recouvrement de l'électrode.²

L'ion tétrapropylammonium (Pr_4N^+) agit de la même façon que le Et_4N^+ . La figure 3 montre que la hauteur du pic en P.I.D. diminue rapidement jusqu'à la concentration de $3,5 \times 10^{-4} M$ pour ensuite se stabiliser à une valeur très faible. Le déplacement du mur d'hydrogène présente une tendance analogue. On explique ce comportement par le fait que cet ion est beaucoup plus volumineux que le précédent dans la série alkyl et qu'il recouvre beaucoup plus l'électrode.

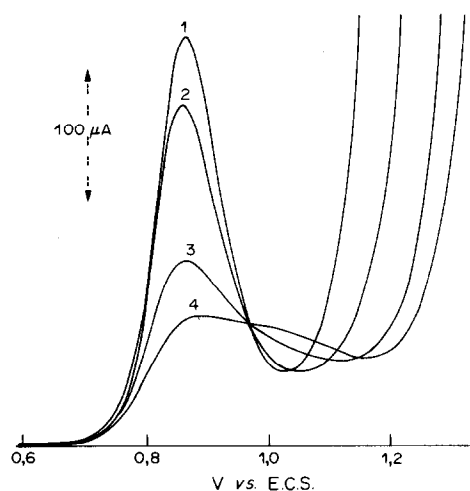


Fig. 3. Polarogrammes (P.I.D.) d'une solution de niobium $2,25 \times 10^{-3} M$ dans: (1) HF 49,1%; (2) HF 49,1% + Pr_4NOH $1,18 \times 10^{-4} M$; (3) HF 49,1% + Pr_4NOH $3,35 \times 10^{-4} M$; (4) HF 49,1% + Pr_4NOH $9,41 \times 10^{-4} M$.

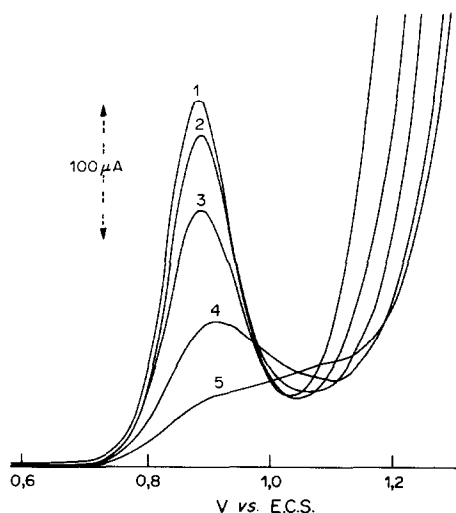


Fig. 4. Polarogrammes (P.I.D.) d'une solution de niobium $2,25 \times 10^{-3} M$ dans: (1) HF 49,1%; (2) HF 49,1% + Bu_4NOH $1,44 \times 10^{-3} M$; (3) HF 49,1% + Bu_4NOH $4,16 \times 10^{-3} M$; (4) HF 49,1% + Bu_4NOH $6,68 \times 10^{-3} M$; (5) HF 49,1% + Bu_4NOH $7,87 \times 10^{-3} M$.

L'ion tétrabutylammonium (Bu_4N^+) agit de manière beaucoup plus importante comme le montre la figure 4. Le pic en P.I.D. diminue rapidement pour disparaître complètement à une concentration de $9 \times 10^{-5} M$. Il n'y a pas de stabilisation de la hauteur du pic comme dans les autres cas car sa disparition survient avant que le recouvrement soit maximal. Ceci est démontré par le fait que le mur de réduction de l'hydrogène se déplace encore régulièrement dans la région de concentration en tétrabutylammonium où le pic du niobium disparaît.

Nous avons quantifié l'effet des ions Me_4N^+ et Et_4N^+ sur le pic P.I.D. de réduction du niobium à plusieurs concentrations de HF en calculant la résolution du pic. On calcule la résolution en mesurant la hauteur du pic (H_{pic}) divisée par la largeur (l) à 10% de la hauteur et par la valeur du courant résiduel ($H_{rés.}$) après le pic:

$$\text{résolution} = \frac{H_{pic}}{lH_{rés.}} \quad (2)$$

Dans HF commercial 50%, la présence de ces ions permet d'augmenter de 30% la résolution du pic de réduction du niobium. Un excès de ceux-ci provoque l'effet contraire en diminuant sensiblement le courant de réduction.

La concentration en HF a un effet important sur la hauteur du pic de réduction du niobium à cause de l'équilibre entre le complexe réductible NbF_6^- et le complexe non réductible $NbOF_5^{2-}$,^{1,5,6}



Les espèces $HNbF_6$ et H_2NbOF_5 sont des espèces ionisables fortement solvatées.

Les courbes (a) des figures 5 et 6 montrent l'effet de la concentration en HF sur la résolution du pic obtenu en absence d'ions tétraalkylammonium. La

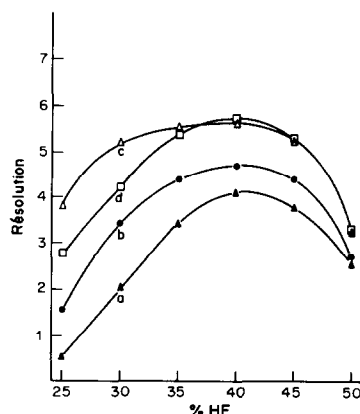


Fig. 5. Résolution des polarogrammes P.I.D. du niobium en fonction de la concentration en HF et en présence de Me_4N^+ : (a) $0 M$; (b) $0,05 M$; (c) $0,20 M$; (d) $0,32 M$.

résolution est maximale pour une concentration en HF de 40%. Dans cette région, le mur de réduction de l'hydrogène est assez loin du pic de réduction du niobium pour permettre une bonne résolution et l'équilibre entre les espèces NbF_6^- et $NbOF_5^{2-}$ favorise encore l'espèce réductible.

La résolution pour des concentrations en HF plus faibles que 40% est meilleure que pour HF 50% mais la hauteur du pic est diminuée par l'équilibre entre les deux complexes du niobium. Dans HF 40% et en présence de $0,015 M Et_4N^+$, on peut doser 1 ppm comme le montrent les polarogrammes de la figure 7.

L'addition des ions Me_4N^+ et Et_4N^+ améliore beaucoup plus la résolution lorsque la concentration en HF diminue. Les figures 5 et 6 montrent que la résolution du pic dans la région de 25 à 35% en HF devient suffisamment élevée pour permettre le dosage du niobium. Cependant, la résolution n'est pas modifiée par le déplacement du mur d'hydrogène mais par une augmentation du courant de réduction comme le montrent les figures 8 et 9. Le dosage du niobium dans ces solutions est rendu difficile à cause de l'équilibre entre les deux complexes qui peut être modifié par les espèces en solution.

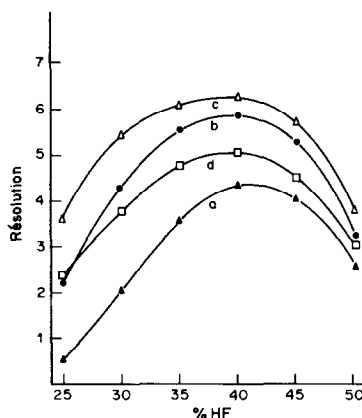


Fig. 6. Résolution des polarogrammes P.I.D. du niobium en fonction de la concentration en HF et en présence de Et_4N^+ : (a) $0 M$; (b) $0,025 M$; (c) $0,10 M$; (d) $0,30 M$.

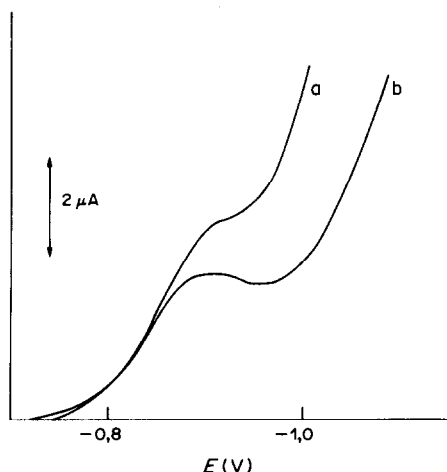


Fig. 7. Polarogrammes P.I.D. du niobium, 1 ppm: (a) HF 40%; (b) HF 40%, Et_4N^+ 0,015M.

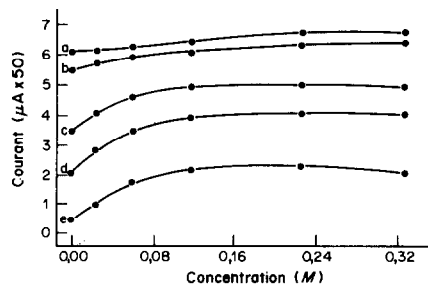


Fig. 8. Hausse du courant de réduction du niobium en présence de Me_4N^+ pour des solutions de HF: (a) 49,1%; (b) 39,3%; (c) 29,5%; (d) 25,5%; (e) 19,6%.

L'ion Et_4N^+ donne des résultats plus intéressants que le Me_4N^+ parce que la quantité nécessaire est plus faible (0,01M par rapport à 0,1M) et le déplacement du mur de réduction de l'hydrogène est le plus important dans la série des ions tétra-alkylammonium.

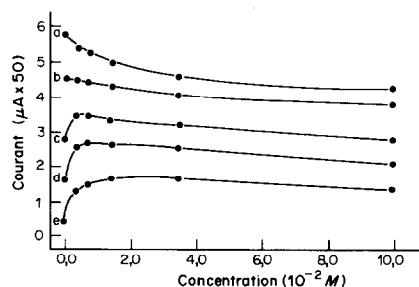


Fig. 9. Hausse du courant de réduction du niobium en présence de Et_4N^+ pour des solutions de HF: (a) 49,3%; (b) 39,3%; (c) 29,5%; (d) 25,5%; (e) 19,6%.

Conclusions

Les ions Me_4N^+ et Et_4N^+ déplacent le mur de réduction de l'hydrogène et affectent peu le pic en P.I.D. de réduction du niobium. Les ions Pr_4N^+ et Bu_4N^+ provoquent la disparition de la vague du niobium. La résolution du pic en P.I.D. peut être améliorée de 30% dans HF commercial à 50%. Pour des concentrations en HF plus faibles, la résolution est accrue par une augmentation du courant de réduction. L'ion Et_4N^+ donne le plus grand déplacement de mur de réduction de l'hydrogène et donne accès à une limite de détection inférieure à 1 ppm de Nb(V) dans HF 40%.

Remerciements—Les auteurs sont reconnaissants des octrois de recherche du Conseil de recherches en sciences naturelles et en génie du Canada et du Ministère de l'Éducation du Québec qui ont rendu ce travail possible.

LITTÉRATURE

1. H. Ménard et R. Beaudoin, *Can. J. Chem.*, 1983, **61**, 2699.
2. L. Gierst, J. Tondeur et E. Nicolas, *J. Electroanal. Chem.*, 1965, **10**, 307.
3. H. Ménard et F. Leblond-Routhier, *Anal. Chem.*, 1978, **50**, 687.
4. A. M. Bond et B. S. Grabaric, *ibid.*, 1979, **51**, 337.
5. N. S. Nikolaev et Yu. A. Buslaev, *Russ. J. Inorg. Chem.*, 1959, **4**, 84.
6. O. L. Keller, *Inorg. Chem.*, 1963, **2**, 783.

DIFFUSION COEFFICIENTS AND COMPLEX EQUILIBRIA IN SOLUTION—IV. EXPERIMENTAL DETERMINATION AND MANIPULATION OF DIFFUSION DATA

D. R. CROW

Department of Physical Sciences, The Polytechnic, Wolverhampton, England

(Received 4 November 1983. Accepted 13 January 1984)

Summary—An experimental method for effectively measuring the change of diffusion current of a metal ion in the presence of increasing concentration of a complexing ligand is described and applied to five metal–ligand systems. The method has been applied to cases of reversible and irreversible electrochemical behaviour and is shown to provide reliable formation-curve data. The systems selected have formation constants which range over some ten orders of magnitude and in most cases the values obtained agree satisfactorily with those reported in the literature. In one case equilibrium data have been calculated for the first time.

There are a number of practical problems associated with manipulation and measurement in the examination of a large number of solutions containing a given metal ion, supporting electrolyte and complexing agent. If a great many data points are needed for use in subsequent calculations, the many solutions required can prove very costly in the case of some ligands and must always prove costly in terms of time. Further, the parameters measured may depend in a particularly sensitive way upon the concentration of metal ion; this is noticeable in the case of diffusion currents. It can prove to be an extremely difficult matter to ensure that precisely the same analytical concentration of metal ion is present in each separate solution.

Dilution techniques have been used, but in differing ways. Aggarwal *et al.*¹ “titrated” a solution containing metal ion, supporting electrolyte and the maximum amount of ligand with a solution containing the same concentration of supporting electrolyte and metal ion as the “titrand”. In this case, however, half-wave potentials were of prime concern. Lane *et al.*² used a similar method for complexes of thiourea and substituted thioureas. Again, these authors’ main aim was the determination of half-wave potentials, although they reported current variations which subsequent analysis appears to support as entirely reliable. Crow and Fonseca³ have even applied a similar dilution method in cases where an indicator ion is used to supply information regarding the complexation of a further metal ion.

It is noticeable that the diffusion-current data reported by authors who have worked with individually prepared solutions often vary in an erratic manner with increase in ligand concentration. This is undoubtedly due not only to the difficulty in reproducing in a large number of solutions an identical

(and usually very low) concentration of metal ion, but also to the difficulty of exactly restoring electrode parameters after replacement of working solutions. The fewer the disturbances introduced during the whole process of measuring either currents or potentials as a function of ligand concentration, the more satisfactory are the resulting data likely to be. Any method which starts with, and maintains during its application, a single sample of metal ion while additions of ligand are made in stages (as with titrations based on pH-measurements) offers attractive advantages.

An extremely simple and economical technique based upon this principle, and intended for measurements of polarographic diffusion currents, has been successfully applied to a large number of complexation systems, with equilibrium data which cover many orders of magnitude. It amounts to a titration technique; the “titrand” consists of a solution containing the metal ion in question (normally at a concentration of $10^{-3}M$) together with a suitable non-complexing supporting electrolyte (normally $0.1M$). The “titrant” consists of a solution containing exactly the same concentration of the supporting electrolyte and as high a concentration of the required ligand as is consistent with its solubility and the expected stability and extent of co-ordination with the metal ion.

EXPERIMENTAL

A very carefully measured volume (usually 50 ml) of “titrand” was placed in a *dry* polarographic cell. The various electrodes were dried before insertion into the solution, which was deoxygenated by passage of a gentle stream of oxygen-free nitrogen for 20 min. Care was taken over the drying, in order to avoid any dilution by means other than addition of “titrant”. The temperature of the solution was maintained at $25 \pm 0.1^\circ$ by means of a water

jacket fed from a bath by a thermostatically controlled circulator (Grant Instruments Type SU5). After the solution had stood for 2 min with nitrogen passing *gently* over the surface, a polarogram was run on a Princeton Applied Research Model 174A Polarographic Analyzer. The settings controlling current range, start potential, scan-rate, damping, drop-time, *etc.* were adjusted as appropriate and thereafter were kept unchanged during the remaining measurements.

Small increments of "titrant" were then added and between additions careful deoxygenation (for 3 min, which also ensured restoration of temperature equilibrium) was followed by standing for 2 min with nitrogen passing over the surface and then a polarogram was run. Each dilution and deoxygenation phase was reproduced as exactly as possible. The essential features of the technique are as follows.

(i) Wave heights decrease during the addition of "titrant" due to (a) dilution and (b) complexation of the metal ion with the ligand component of the "titrant".

(ii) The supporting electrolyte concentration remains constant so that, for neutral ligands, the ionic strength remains constant.

(iii) Observed diffusion currents, i_{obs} , (measured at a constant potential throughout the range of ligand concentration used) may be corrected for the dilution effect by means of the "amperometric" relationship involving the initial (V) and incremental (v) volumes, *viz.*

$$i_{\text{corr}} = i_{\text{obs}} \left(\frac{V+v}{V} \right)$$

(iv) The concentration of ligand ($[X]$) in each effective working solution produced after each addition of "titrant" may be estimated from the relation:

$$[X] = C \left(\frac{v}{V+v} \right)$$

where C is the concentration of ligand in the titrant solution.

RESULTS AND DISCUSSION

Cadmium-thiourea

Figure 1 shows the values of diffusion current, obtained from experimental data, plotted against the calculated values of thiourea concentration. Although there is scatter of the points, as expected, the large number of points allows a more reliable curve

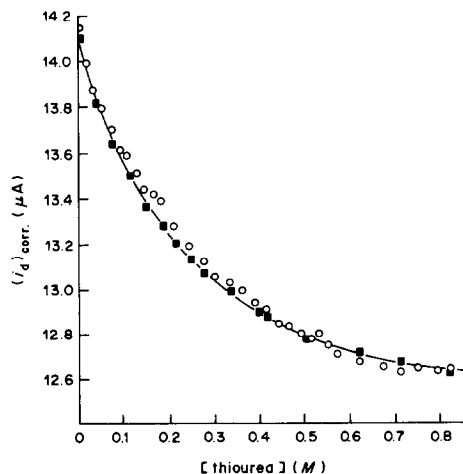


Fig. 1. Corrected diffusion current values plotted against calculated values of ligand concentration for the system cadmium-thiourea.

to be drawn through them. For subsequent analysis—either from the pseudo-formation curve or from the functions $(\bar{D} - D_{MX_j})$ —interpolated values of i_d at convenient values of free ligand concentration were used. Values of the diffusion coefficients for the various complex species were calculated by the methods described earlier⁴ and the methods of graphical analysis were applied. The values $\beta_1 = 20 \pm 2$; $\beta_2 = 142 \pm 30$; $\beta_3 = (4.5 \pm 1.0) \times 10^2$; $\beta_4 = (1.2 \pm 0.2) \times 10^3$ compare very favourably with the previously reported data.

Cadmium-urea

Although the shift in half-wave potential of the cadmium ion induced by a 2M urea concentration was only about 0.01 V (and so made estimation of formation constants, and even perhaps the assumption of complexation, dubious) the change in diffusion current was quite substantial; Δi_d was about 2 μ A, approximately 15% of the value for the simple metal ion (Fig. 2). "Titration" with 2M urea/0.1M potassium nitrate solution yielded the data shown in Fig. 3.

At first sight this polarographic behaviour is very unusual; the almost negligible change in half-wave potential suggests that the extent of complexing between cadmium ion and urea is negligible, whereas the relatively large change in diffusion current would suggest that significant association between the two species had occurred. It is possible that the reduction in current could have arisen from causes other than complexation, such as adsorption of the ligand at the electrode surface so that the environment within which the aquo ion underwent reduction was changed. If this or some other such effect was operative, it would *not* be expected that a realistic analysis for equilibrium data would be possible. In practice, however, very clearly defined data emerged. In any case, urea complexes are not unknown and there have been investigations made of the distinguishing features of those containing oxygen- or nitrogen-bonded urea.⁵

The graph of calculated $\log F'_0$ data *vs.* $\log [\text{urea}]$ shows a limiting slope of 1.9 in the region corresponding to the maximum amount of urea (Fig. 4). At this stage there is no indication whatever of the extent of co-ordination, but since the limiting slope should approximate to N/k (N being the maximum co-ordination developed and k being defined by $k \log F'_0 = \log F_0$) it is clear that k can have the values 1.05, 1.58 or 2.11, corresponding to $N = 2, 3$ or 4. Somewhat surprisingly, graphical analysis (by the methods described previously) was only successful for $k \sim 2.11$ and the following preliminary set of equilibrium data was obtained: $\beta_1 = 7.0$; $\beta_2 = 18$; $\beta_3 = 30$; $\beta_4 = 144$. Subsequent analysis in terms of $(\bar{D} - D_{MX_j})$ functions yielded the values $\beta_1 = 7.0$; $\beta_2 = 23$; $\beta_3 = 44$; $\beta_4 = 88$. The two sets of data agree satisfactorily enough and show the common characteristic noticed earlier, *viz.* that analysis by means of the pseudo

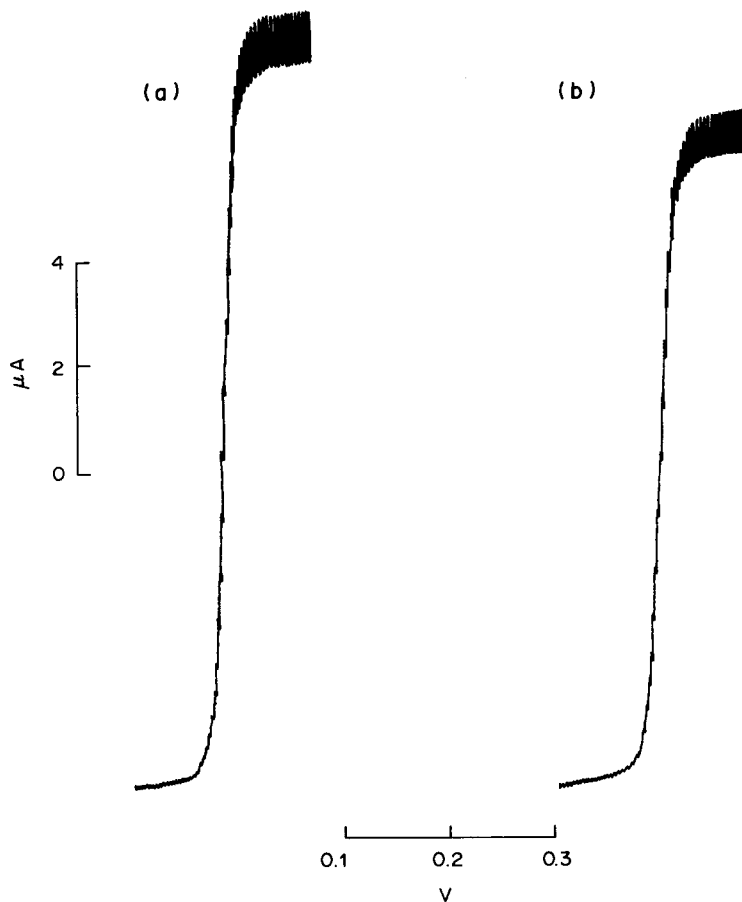


Fig. 2. Polarograms (d.c.) of $10^{-3}M$ Cd^{2+} in $0.1M$ KNO_3 in the absence (a) and presence (b) of $2.0M$ urea. Both waves start at $-0.4V$ vs. SCE.

formation-curve tends to produce an overestimate in the value for the highest complex.

Cadmium-imidazole

For this system reliable formation-constant data from a number of sources are reported in the literature. The values are so high that when cadmium ions are present the difference between total and free imidazole concentration is by no means negligible unless the total cadmium concentration is very small indeed relative to that of the ligand. The overall changes in diffusion current are small⁶ and, because of the higher stability of the complexes, are maximal at fairly low ligand concentrations. These features were seen as providing a particular challenge to both the methods of calculation and the experimental technique for obtaining the small changes in current.

A preliminary range of Δi_d vs. [imidazole] data was obtained by means of manually plotted polarograms on individually prepared solutions containing $5 \times 10^{-4}M$ cadmium, $0.1M$ potassium nitrate and imidazole varying up to a maximum of $0.04M$. Although co-ordination with $0.04M$ imidazole was incomplete ($\bar{n} \sim 2.5$), the results could be analysed to

obtain equilibrium data corresponding to four complexes.

Selected F_0 and derived data are given in Table 1. Values for the first three formation constants are of the same order as reported previously, although that for β_4 is more than an order of magnitude higher than expected. This is undoubtedly due to two causes, (i) the general tendency for calculation by means of the pseudo formation-curve to produce a high result for the highest complex, (ii) the manipulation of data obtained for ligand concentrations corresponding to the lower complexes in order to generate equilibrium data for complexes of higher co-ordination.

Since only a very low cadmium concentration was used in the investigations above, the difference between total and free ligand concentration is not very great except at the lowest values of the latter. However, when using the "titration" technique it was desirable to have large diffusion currents and accordingly a metal ion concentration of $2 \times 10^{-3}M$ was used. This fairly high value caused a significant difference between the total and free imidazole concentrations and provided a useful means of testing the methods adopted for correction of the experi-

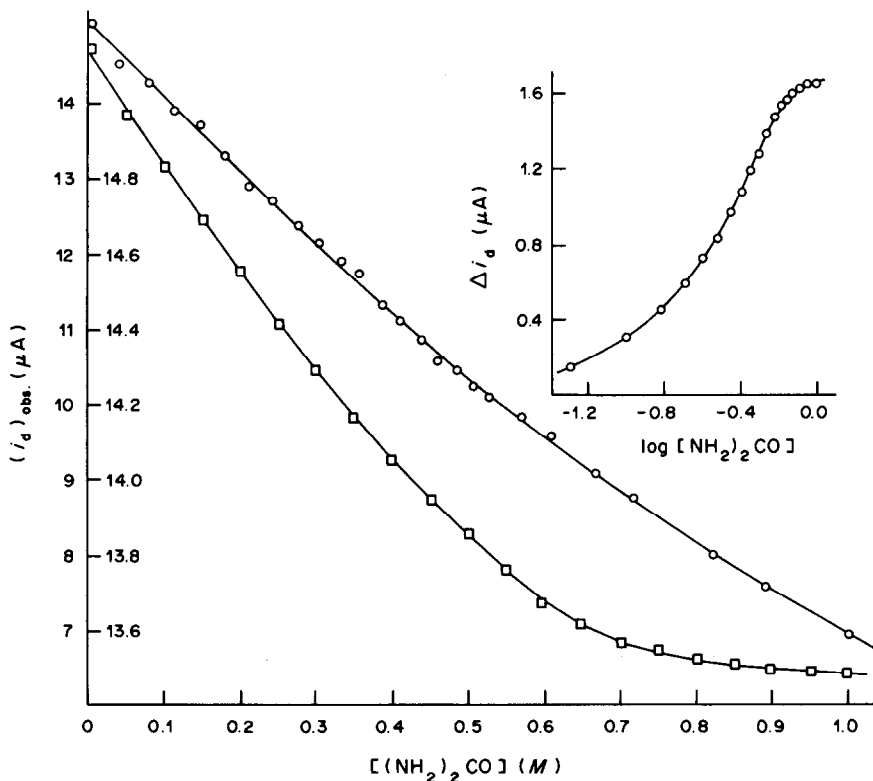


Fig. 3. Graphs of observed (○) and corrected (□) diffusion currents vs. calculated ligand concentration for the system cadmium-thiourea. Inset shows the derived pseudo-formation curve.

mental data. Further, correction of the observed currents to allow for any variation in residual current at the potential at which values of Δi_d were determined, was of less significance. In fact, the base-lines were virtually horizontal for the experimental polarograms at the sensitivity settings required. A plot of corrected diffusion current vs. imidazole concentration is shown in Fig. 5. Although the scatter of points increases at the highest concentrations, this is offset by the large number of data points obtainable, giving enhanced confidence in the final curve drawn.

A plot of directly observed Δi_d values vs. \bar{n} values estimated from literature values of the stability con-

stants, though approximately linear, does not pass through the origin. This is to be expected since the free imidazole concentrations for which the \bar{n} values were calculated did not correspond to the actual free ligand concentrations at which the Δi_d values were obtained. In the case of a system for which the equilibrium data are quite unknown, it is necessary to have a reliable means of deducing the free concentration of complexing agent. The results which follow show how this can be done.

Integration of the pseudo-formation curve, drawn simply as a plot of Δi_d vs. total analytical concentration of imidazole, provides F_0 data according to

Table 1. Selected values of F_0 and derived functions estimated from the pseudo-formation curve for the cadmium-imidazole system at 25°: $[\text{Cd}^{2+}] = 5 \times 10^{-4} M$, $[\text{KNO}_3] = 0.1 M$

[Imidazole], <i>M</i>	F_0	F_1	F_2	F_3	F_4
0.000	1.00	—	—	—	—
0.002	3.00	1.00×10^3	1.50×10^5	—	—
0.005	9.42	1.68×10^3	1.97×10^5	1.34×10^7	—
0.008	21.9	2.62×10^3	2.40×10^5	1.37×10^7	—
0.010	36.0	3.50×10^3	2.80×10^5	1.50×10^7	9.0×10^8
0.015	105.1	6.94×10^3	4.16×10^5	1.91×10^7	8.7×10^8
0.020	251.6	12.53×10^3	5.92×10^5	2.31×10^7	8.5×10^8
0.025	539	21.52×10^3	8.33×10^5	2.81×10^7	8.8×10^8
0.030	1016	33.8×10^3	11.04×10^5	3.25×10^7	8.8×10^8
0.04	2990	74.7×10^3	18.51×10^5	4.30×10^7	9.2×10^8

$$\beta_1 \sim 7.0 \times 10^2; \beta_2 \sim 1.3 \times 10^5; \beta_3 \sim 6.0 \times 10^8; \beta_4 \sim 8.8 \times 10^8.$$

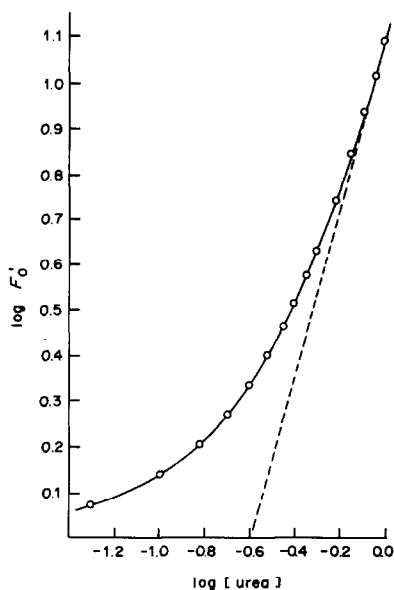


Fig. 4. Determination of k in the relation $k \log F'_0 = \log F_0$ from plot of $\log F'_0$ vs. $\log [\text{urea}]$. Limiting slope $\sim 1.9 \sim n_{\text{max}}/k$, whence $k \sim 2.1$ if $n_{\text{max}} = 4$.

the method described.⁶ Although this procedure uses erroneous values of free ligand concentration, the F_0 data obtained may be used to generate provisional values of formation constants for four complexes. Some selected data obtained by this treatment are presented in Table 2.

It is clear that the values of the apparent overall constants are considerably lower than the reported values. However, the various derived curves show very little scatter and some confidence may be placed in the conditional data obtained by these means. This confidence is augmented by recalculation of the data in terms of $(\bar{D} - D_{\text{MX}_i})$ functions. From the clearly defined limiting value of Δi_d shown by the pseudo-formation curve it was possible to infer an approximate value of $4.92 \times 10^{-6} \text{ cm}^2/\text{sec}$ for the diffusion coefficient of the MX_4 species and hence to interpolate values for all intermediate complexes. The graphical analysis was extremely satisfactory for this

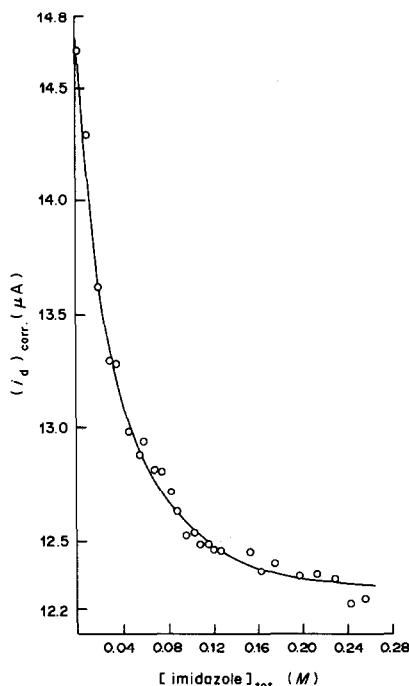


Fig. 5. Corrected values of diffusion current, $(i_d)_{\text{corr.}}$, plotted against ligand concentration for the cadmium-imidazole system. Subsequent calculations were based upon current readings, at convenient values of $[\text{imidazole}]$, read from the line drawn through the 26 experimental points.

case (Fig. 6); selected tabulated data are given in Table 3. The constancy of the ratio $G_4/(\bar{D} - D_{\text{MX}_4})$ is quite remarkable.

Assuming that the highest value of Δi_d corresponds approximately to $\bar{n} = 4$, estimates of \bar{n} were made at the analytical concentrations of ligand used. These were then used to assess the approximate concentration of imidazole bound to Cd^{2+} . Use of the free imidazole concentration thus calculated caused a significant change in the shape of the pseudo-formation curve (Fig. 7).

Integration of this new curve provided refined F_0 data, the functions derived from which showed little

Table 2. Selected values of provisional F_0 and derived data estimated from the pseudo-formation curve for the cadmium-imidazole system at 25°: $[\text{Cd}^{2+}] = 2 \times 10^{-3} M$, $[\text{KNO}_3] = 0.1 M$

[Imidazole], M	F_0	F_1	F_2	F_3	F_4
0.01	2.15	115	—	—	—
0.03	10.2	307	6.57×10^3	—	—
0.05	34.6	672	1.12×10^4	1.19×10^5	—
0.07	90.1	1273	1.66×10^4	1.62×10^5	1.52×10^6
0.10	273.0	2720	2.61×10^4	2.21×10^5	1.53×10^6
0.12	513.0	4.27×10^3	3.46×10^4	2.45×10^5	1.58×10^6
0.16	1351	8.44×10^3	5.21×10^4	2.92×10^5	1.48×10^6
0.20	3.18×10^3	15.9×10^3	7.89×10^4	3.68×10^5	1.56×10^6
0.26	8.68×10^3	33.4×10^3	12.8×10^4	4.72×10^5	1.60×10^6

$$\beta'_1 = 110; \beta'_2 = 5.3 \times 10^3; \beta'_3 = 5.5 \times 10^4; \beta'_4 = 1.55 \times 10^6.$$

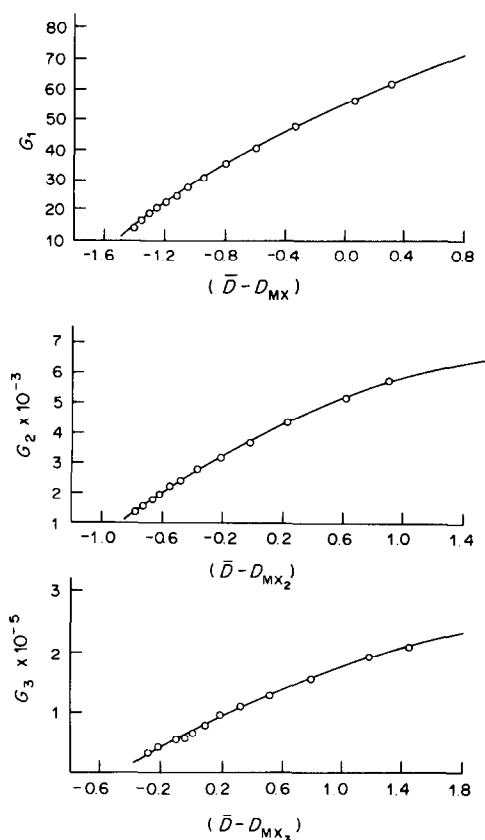


Fig. 6. G_j vs. $(\bar{D} - D_{MX_j})$ plots for the cadmium-imidazole system. Data estimated at ligand concentrations uncorrected for ligand bound to metal ion, so β_j data are only provisional.

scatter, and in their turn yielded a new set of formation constants. These partially corrected values were used to calculate more refined \bar{n} data and a final correction to the formation curve. The four sets of data obtained are collected with some literature values in Table 4; the agreement between the latter and those obtained by the successive refinement described is entirely satisfactory.

Nickel-imidazole

The titration technique described above was used again. Particular care was required in this case since

the characteristic initial positive shift of half-wave potential induced by the complexation of nickel was clearly seen. A selection of polarograms obtained for one titration is shown in Fig. 8. No attempt was made to remove the large maximum which featured prominently on polarograms obtained from solutions containing ligand. The diffusion current was observed at a constant potential (-1.3 V vs. SCE) for all solutions. Great care was required to ensure that the titration/deoxygenation routine was repeated in as nearly identical a manner as possible at each addition of "titrant". The change in current, even allowing for that due to the dilution effect, was small, so that the final corrected values for Δi_d were very small indeed.

The combined effects of very high values for formation constants, very small observed changes in current, the large difference between $[Im]_{total}$ and $[Im]_{free}$ and the inherent complications present in many systems involving nickel complexes probably represent the ultimate test of both the experimental techniques and the principles of calculation employed. Equilibrium data obtained under such constraints are unlikely to be of the standard realized in the other systems reported. However, the following values were obtained: $\beta_1 \sim 1.5 \times 10^3$; $\beta_2 \sim 6 \times 10^5$; $\beta_3 \sim 1.3 \times 10^8$; $\beta_4 \sim 2 \times 10^9$; $\beta_5 \sim 1 \times 10^{10}$; $\beta_6 \sim 5.5 \times 10^{11}$. These are of the same order of magnitude as those reported by Li *et al.*⁹ and by Sklenskaya *et al.*¹⁰

Cadmium-thiocyanate

Although the titration technique described above is rather more difficult to apply realistically to complexes with charged ligands, it was considered appropriate at least to *attempt* to apply it to the very first system treated by the DeFord and Hume method. In nitrate media the values of the overall formation constants do not increase regularly with n , and it was required to establish whether the variations in diffusion current would reflect this. Despite the fact that the solutions produced by the titration procedure showed a considerable range of ionic strengths, the values estimated for the first three overall formation constants followed very closely the irregular trend reported by Hume *et al.*¹¹ The value of β_4 was obscured at lower thiocyanate concentrations by the uncertainty in the values of the higher derived functions; at higher ligand concentrations the effects of

Table 3. Selected derived values of G_j and of complementary $(\bar{D} - D_{MX_j})$ functions for identification and characterization of complexes in the Cd^{2+} -imidazole system (G and D values have units of 10^{-6} cm²/sec)

$[Im], M$	\bar{D}	G_1	$(\bar{D} - D_{MX_1})$	G_2	$(\bar{D} - D_{MX_2})$	G_3	$(\bar{D} - D_{MX_3})$	G_4	$(\bar{D} - D_{MX_4})$	$G_4/(\bar{D} - D_{MX_4})$
0.00	7.20		0.611		1.193		1.748		2.276	
0.01	6.63	57.0	0.042	5.23×10^3	0.624	1.94×10^5	1.179	3.57×10^6	1.707	2.09×10^6
0.04	5.78	35.5	-0.810	3.14×10^3	-0.228	1.08×10^5	0.327	1.62×10^6	0.855	1.89×10^6
0.08	5.39	22.7	-1.202	1.95×10^3	-0.620	0.653×10^5	-0.065	0.93×10^6	0.463	2.01×10^6
0.12	5.23	16.5	-1.363	1.40×10^3	-0.781	0.460×10^5	-0.226	0.64×10^6	0.302	2.12×10^6
0.20	5.10	10.5	-1.490	880	-0.908	0.284×10^5	-0.353	0.38×10^6	0.175	2.17×10^6
0.24	5.08	8.8	-1.514	734	-0.926	0.234×10^5	-0.371	0.31×10^6	0.157	1.97×10^6

$$\beta'_1 = 110; \beta'_2 = 5.28 \times 10^3; \beta'_3 = 1.34 \times 10^5; \beta'_4 = 2.04 \times 10^6.$$

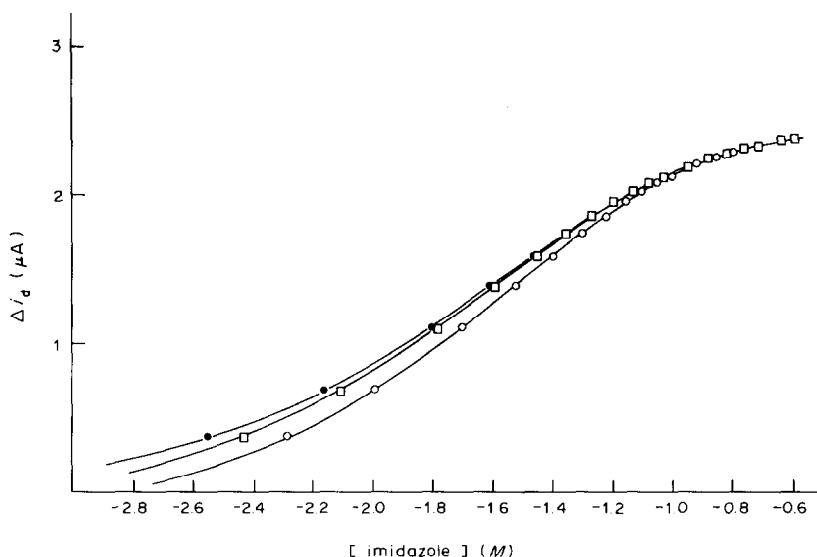


Fig. 7. Pseudo-formation curves with progressive correction for the difference between total and free ligand concentration for the system cadmium-imidazole: (i) no correction (○); (ii) with primary correction based on assessment of ligand bound to metal ion from approximate values of \bar{n} estimated from Δi_d (□); (iii) final correction based on calculation of approximate values of \bar{n} from provisional formation-constant data derived from curve (ii). (●).

increasing ionic strength become very significant. This is clearly seen in a comparison of the graphs of F_0 values vs. $[\text{SCN}^-]$ obtained by Hume *et al.* and from the observed currents obtained in the present study (Fig. 9). Evidently, below a thiocyanate concentration of $0.65M$, the effect of ionic strength on the values of F_0 and the derived functions is negligible: above this value the effect becomes increasingly marked.

Hume *et al.*¹¹ made no attempt to determine values of F_4 for thiocyanate concentrations below $0.7M$; it is, however, interesting to see that the present analysis, at $[\text{SCN}^-] = 0.6$ and $0.65M$ (just before the region where the effects of increasing ionic strength become significant), gives values of F_4 of 62 and 61.5 respectively. These values are very close to the value of 60 for β_4 determined and reported earlier.

Table 4. Apparent and refined equilibrium data for the cadmium-imidazole system

	β_1	β_2	β_3	β_4
(a)	1.10×10^2	5.3×10^3	5.5×10^4	1.55×10^6
(b)	1.10×10^2	5.3×10^3	1.34×10^5	2.04×10^6
(c)	6.0×10^2	5.5×10^4	1.0×10^6	3.3×10^7
(d)	6.3×10^2	8.0×10^4	2.2×10^6	3.6×10^7
(e)	6.3×10^2	7.94×10^4	2.82×10^6	3.80×10^7
(f)	—	11.8×10^4	2.88×10^6	3.02×10^7

(a) Apparent, uncorrected data, obtained from pseudo-formation curve.

(b) Apparent, uncorrected data, obtained from diffusion coefficients.

(c) Apparent data, after preliminary refinement.

(d) Final data, after further correction.

(e) Data of Tanford and Wagner,⁷ for $I = 0.15$.

(f) Data of Li, White and Doody,⁸ for $I = 0.15$.

It is well known that in a perchlorate supporting medium the formation constants have quite different values. The diffusion current data reported for the cadmium-thiocyanate system by Senise and de Almeida Neves,¹² for $2M$ sodium perchlorate medium, yielded a pseudo-formation curve which could be used to generate two alternative sets of formation data, viz. $\beta_1 = 23$; $\beta_2 = 75$; $\beta_3 = 80$; $\beta_4 = 450$ or $\beta_1 = 23$; $\beta_2 = 75$; $\beta_3 = 0$; $\beta_4 = 570$.

These authors obtained the following values from the potential data: $\beta_1 = 25$; $\beta_2 = 75$; $\beta_3 = 85$; $\beta_4 = 240$.

Conclusions

The titration method described has proved to be successful for systems involving uncharged ligands. Variations in diffusion current estimated from observed values are reliable and have even been used with very fair success in the case of an ionic ligand, with no corrections made for the effects of increasing ionic strength.

Unlike earlier dilution methods, the one described here does not maintain a constant concentration of metal ion. In terms of the observed current signal this offers a practical advantage for systems such as those involving imidazole or other molecules inducing only very small changes in the diffusion coefficients of metal ions. In terms of the possible non-ideality of the solutions obtained and interference of the titration process with metal-ligand equilibria, the technique might still be shown to involve undesirable complications in some instances. The main advantages are those to be gained by use of the large number of working solutions which are obtainable. This feature is already revealing subtleties in the shapes of Δi_d vs. ligand concentration curves, which have previously

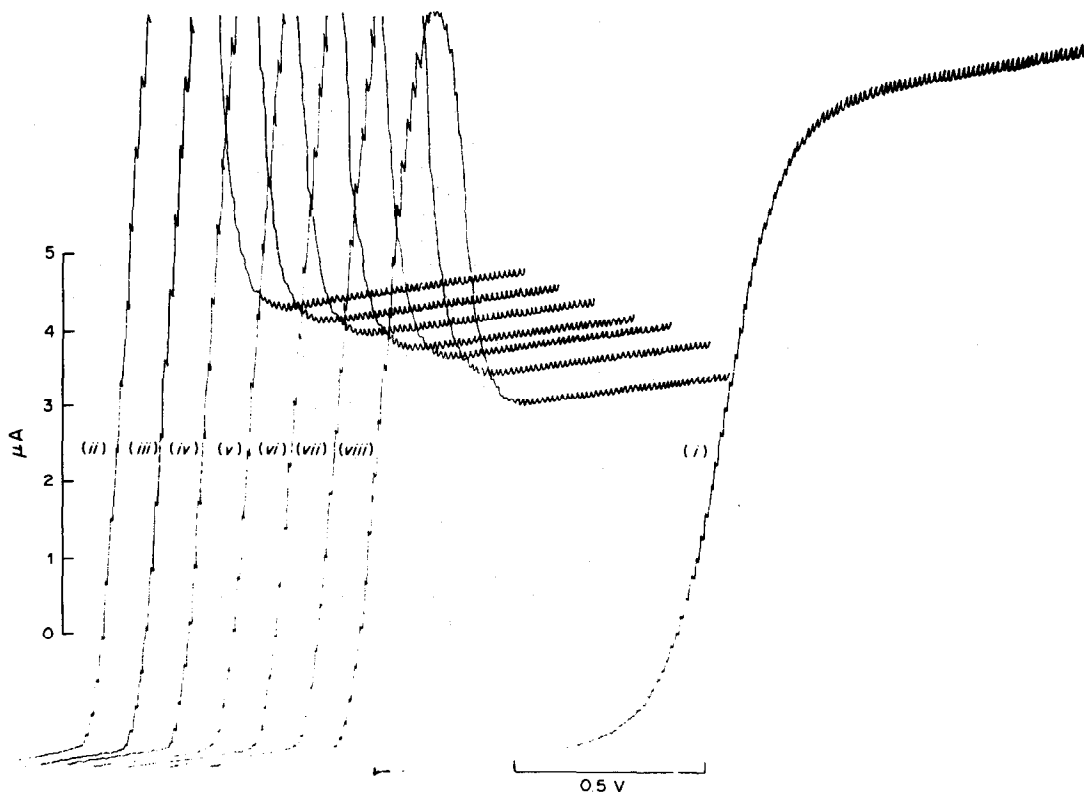


Fig. 8. A selection of experimental polarograms from one dilution run for the nickel-imidazole system. (i) Polarogram (d.c.) of $5 \times 10^{-4} M$ Ni^{2+} in $0.1 M$ KNO_3 . Wave starts from -0.1 V vs. SCE, $E_{1/2} \sim 1.110$ V. Remaining waves derive from a starting potential of -0.4 V vs. SCE. (ii) $[Im]_{total} = 0.109 M$; $E_{1/2} \sim 0.925$ V. (iii) $[Im]_{total} = 0.121 M$; $E_{1/2} \sim 0.930$ V. (iv) $[Im]_{total} = 0.132 M$; $E_{1/2} \sim 0.935$ V. (v) $[Im]_{total} = 0.143 M$; $E_{1/2} \sim 0.945$ V. (vi) $[Im]_{total} = 0.153 M$; $E_{1/2} \sim 0.949$ V. (vii) $[Im]_{total} = 0.162 M$; $E_{1/2} \sim 0.955$ V. (viii) $[Im]_{total} = 0.188 M$; $E_{1/2} \sim 0.970$ V.

been obscured by the considerable scatter of a small number of data points. Indeed, it is due to the larger number of such points, coupled with the newer methods of calculation (which are able to make more reliable use of data for lower ligand concentrations than has been the case with more traditional methods), that the problems associated with varying ionic strength are reduced.

The current changes are markedly sensitive to variations in metal-ligand interaction, as is shown by the efficiency with which irregular sequences of overall formation constants may be dealt with. It is doubtless true that the observed differences between the values of the formation constants of cadmium complexes of thiocyanate in nitrate and in perchlorate media, arise to some extent from interference in the former case from interaction between Cd^{2+} and NO_3^- ions, as has been investigated quantitatively.¹³ However, there could well be a further complication. Unusual sequences of formation data appear to be a fairly common feature of systems involving sulphur-containing ligands; the irregularities seem to be more pronounced when the measurements involve mercury electrodes.

Equilibrium data deriving from measurements of potential reflect the nature of the complex species and

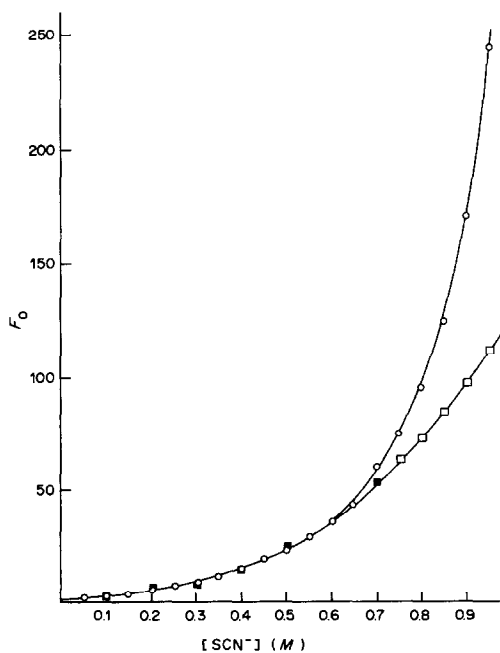


Fig. 9. Comparison of F_0 values of different origin: \circ —calculated from pseudo-formation curve; \blacksquare —values reported by Hume *et al.*;¹¹ \square —values interpolated from experimental data of Hume *et al.*¹¹

their behaviour *at the electrode surface*. Under the necessary conditions of reversibility, complexes either react rapidly and directly with the electrode, or they dissociate and the resulting aquo-ions react with the electrode (both processes rapid). If complications should arise on account of interaction of either the ligand or the complexes with the mercury of the electrode, the potentials and the data derived from them reflect such interactions as well as those of metal ion and ligand in the bulk solution. That such interactions are possible is shown by the effects on the anodic dissolution curve of mercury in the presence of sulphur-containing ligands such as thiocyanate, thiosulphate,¹⁴ thiourea *etc.*; effects of this sort are even evident in the presence of urea.¹⁵ Analysis by means of diffusion coefficients under these conditions should give different values for formation constants from those estimated from potentials. Diffusion coefficients reflect the nature of various species in bulk solution—a nature which is presumably retained at least until their entry into the diffuse double-layer.

REFERENCES

1. P. K. Aggarwal, W. R. W. Bradman and D. R. Crow, *J. Polarog. Soc.*, 1968, **XIV**, 93.
2. T. J. Lane, J. W. Thompson and J. A. Ryan, *J. Am. Chem. Soc.*, 1959, **81**, 3569.
3. D. R. Crow and D. Fonseca, *J. Inorg. Nucl. Chem.*, 1980, **42**, 1595.
4. D. R. Crow, *Talanta*, 1983, **30**, 659.
5. R. B. Penland, S. Mizushima, C. Curran and J. V. Quagliano, *J. Am. Chem. Soc.*, 1957, **79**, 1575.
6. D. R. Crow, *Talanta*, 1982, **29**, 739.
7. C. Tanford and M. L. Wagner, *J. Am. Chem. Soc.*, 1953, **75**, 434.
8. N. C. Li, J. M. White and E. Doody, *ibid.*, 1954, **76**, 6219.
9. N. C. Li, T. L. Chu, C. T. Fujii and J. M. White, *ibid.*, 1955, **77**, 859.
10. E. V. Sklenskaya and M. Kh. Karapet'yants, *Russ. J. Inorg. Chem.*, 1966, **11**, 1102.
11. D. N. Hume, D. D. DeFord and G. C. B. Cave, *J. Am. Chem. Soc.*, 1951, **73**, 5323.
12. P. Senise and E. F. de Almeida Neves, *ibid.*, 1961, **83**, 4146.
13. C. E. Vanderzee and H. J. Dawson, *ibid.*, 1953, **75**, 5659.
14. I. M. Kolthoff and C. S. Miller, *ibid.*, 1941, **63**, 1405.
15. D. R. Crow, unpublished results.

POLYURETHANE FOAM FOR THE EXTRACTION OF RHODIUM AND ITS SEPARATION FROM IRIDIUM

S. J. AL-BAZI and A. CHOW

Department of Chemistry, University of Manitoba, Winnipeg, Manitoba, Canada

(Received 28 November 1983. Accepted 22 December 1983)

Summary—The rate of reaction of rhodium with thiocyanate at 90° in the presence of lithium chloride or sufficient hydrochloric acid and the subsequent extraction of the metal from hydrochloric acid medium by polyether-type polyurethane foam was investigated. The effect of the chloride salts of different cations decreased in the order $\text{Li}^+ > \text{Na}^+ > \text{K}^+$ indicating that $\text{Rh}(\text{SCN})_6^{3-}$ is extracted through a simple solvent-extraction mechanism rather than the "cation-chelation" mechanism. The separation of rhodium and iridium was also examined and the results indicated that in the presence of 5-fold excess of iridium, an average of $95 \pm 2\%$ iridium remained in the aqueous phase while an average of $93 \pm 2\%$ rhodium was retained by the foam.

Many difficulties arise in the solvent extraction of rhodium, owing to its characteristic feature of forming inert complexes with many ligands, including chloride. Thus the use of a catalyst¹⁻⁴ and/or heating the aqueous phase before extraction⁵⁻¹⁰ has been required except when the extraction took place by an ion-association mechanism.

Solvent extraction has been widely used to separate rhodium and iridium. The greater lability of rhodium in the formation of chelates or solvent complexes has played an important role in their separation.^{1,11-15}

The purpose of the present work was to study the kinetic behaviour of the reaction of rhodium with thiocyanate, and the subsequent extraction of the metal by polyether-type polyurethane foam. The study also included the mechanism of distribution of the rhodium-thiocyanate complex between foam and aqueous phase, and a method for the separation of rhodium and iridium.

EXPERIMENTAL

Apparatus and reagents

Rhodium was determined with a Perkin-Elmer model 306 atomic-absorption spectrometer. A Baird-Atomic model 530A single-channel gamma-ray spectrometer fitted with a Harshaw well-type NaI(Tl) crystal was used for iridium-192 measurements. Spectrophotometric measurements were made with a Varian model 634S spectrophotometer.

Polyether-type polyurethane foam (No. 1338 M) was obtained from G. N. Jackson Ltd., Winnipeg, Manitoba, and washed by the procedure previously reported.¹⁶

Stock solutions of $4.9 \times 10^{-3} M$ rhodium(III) (freshly prepared for each experiment to minimize the hydrolysis of RhCl_6^{3-} to $[\text{RhCl}_{6-x}(\text{H}_2\text{O})_x]^{3-x}$ ($x = 1-6$) ions¹⁷⁻¹⁹) and $2.6 \times 10^{-3} M$ iridium were made from $\text{Na}_3\text{RhCl}_6 \cdot 12\text{H}_2\text{O}$ and $\text{Na}_2\text{IrCl}_6 \cdot 6\text{H}_2\text{O}$ (Johnson-Matthey Ltd.) in 0.1M hydrochloric acid. ¹⁹²Ir was obtained as $(\text{NH}_4)_2\text{IrCl}_6$ in 3M hydrochloric acid from Amersham-Searle Ltd., Ontario. A 5.0M solution of potassium thiocyanate was prepared in doubly distilled demineralized water.

Extraction procedure

A known volume of the stock solution of rhodium or iridium and the desired amounts of the other reagents were

placed in a 100-ml standard flask and diluted to about 60 ml. Sufficient ¹⁹²Ir tracer was added to the iridium samples to yield a count-rate of at least 150 cps for 10 ml of sample in a 15-mm internal diameter test-tube. The solution was heated at 90° for a measured time, cooled to room temperature and finally diluted to volume. The extraction of 95 ml of this solution with 50 ± 1 mg of foam for a minimum of 10 hr and the calculations of percentage extraction (%E) and distribution coefficient (D , l./kg) were performed as described previously.¹⁶

RESULTS AND DISCUSSION

When rhodium chloride solutions containing sufficient thiocyanate were heated, two different complexes were formed, depending on the acidity of the solution.¹⁶ $\text{Rh}(\text{SCN})_6^{3-}$ was formed at low acidity, whereas a different complex was produced at high acidity. The latter was not characterized and will be denoted as RhY. These complexes have been reported to be highly extractable by polyether-type polyurethane foam.¹⁶ The rates of formation and subsequent extraction of these complexes by the foam were investigated.

The formation and extraction of $\text{Rh}(\text{SCN})_6^{3-}$

Varying the heating time for solutions at pH 2.4 ± 0.1 showed (Fig. 1) an increase in the extraction from 4% ($\log D = 1.78$) without heating to 80% ($\log D = 3.77$) at 2 hr and 92% ($\log D = 4.22$) after 5 hr of heating. The absorbance at 288 nm, which corresponds to the $\text{Rh}(\text{SCN})_6^{3-}$ complex,²⁰ increased with heating time and was found to be proportional to the amount of rhodium extracted.

When the effect of heating time was investigated with different concentrations of lithium chloride, both the formation of the complex (Fig. 2) and its subsequent extraction (Fig. 3) increased with increasing salt concentration and heating time. The degree of extraction of rhodium [94% ($\log D = 4.46$) and 95% ($\log D = 4.54$)] from 2M lithium chloride

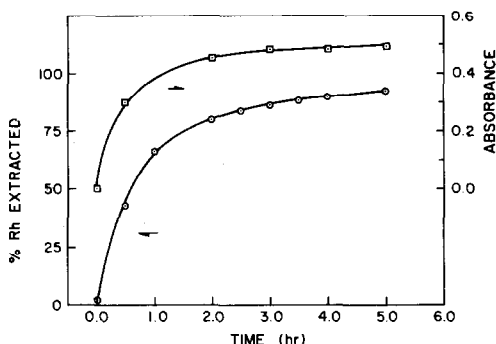
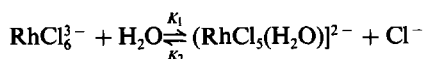


Fig. 1. Effect of heating time on the formation and extraction of rhodium-thiocyanate complex. (□) Formation; conditions: 60-ml solutions at pH 2.4 ± 0.1 containing $24.5 \mu\text{moles}$ of Rh(III) and 0.6 mmoles of KSCN, heated at 90° . (○) Extraction; conditions: $97 \pm 2 \text{ mg}$ of foam; 145 ml of solution $2M$ in HCl added after heating.

medium with heating for 30 and 60 min, respectively indicated that the rate of formation of $\text{Rh}(\text{SCN})_6^{3-}$ is increased by the presence of lithium chloride in the solution.

We have reported¹⁶ that the labile character of rhodium toward complexation with thiocyanate increases with decreasing number of water molecules in the initial $[\text{RhCl}_{6-x}(\text{H}_2\text{O})_x]^{x-3}$ complex. Furthermore, the kinetics of the aquation of RhCl_6^{3-} and of replacement of the water in $[\text{RhCl}_5(\text{H}_2\text{O})]^{2-}$, i.e.,



have been described by the rate law:²¹

$$-d[\text{RhCl}_6^{3-}]/dt = K_1[\text{RhCl}_6^{3-}] - K_2[\text{RhCl}_5(\text{H}_2\text{O})^{2-}][\text{Cl}^-]$$

($K_1 = 0.11 \text{ min}^{-1}$ and $K_2 = 0.013 \text{ min}^{-1} \cdot 1 \text{ mole}^{-1}$ at 25°).

Thus, in the presence of lithium chloride, the decrease in time of heating required for the formation of $\text{Rh}(\text{SCN})_6^{3-}$ is due to the decrease in the rate of

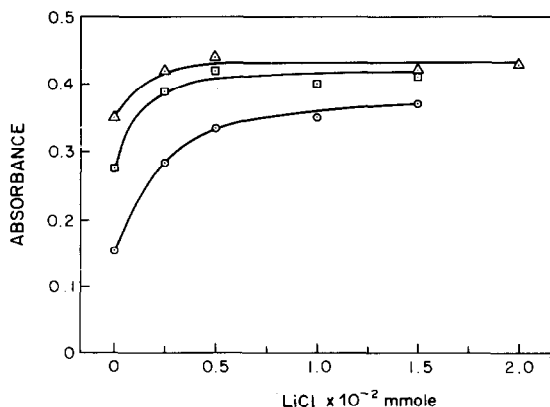


Fig. 2. Influence of lithium chloride concentration on the formation of rhodium-thiocyanate complex; conditions: 60-ml solutions at pH 2.5 ± 0.1 containing $16.3 \mu\text{moles}$ of Rh(III), 0.4 mmoles of KSCN, different volumes of $10M$ LiCl and heated at 90° for (○) 10 min, (□) 30 min (Δ) 60 min.

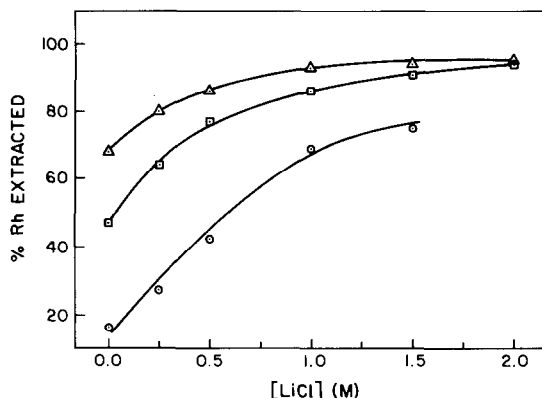


Fig. 3. Effect of lithium chloride, added before heating of solutions for different times, on the extraction of rhodium; conditions: $50 \pm 1 \text{ mg}$ of foam; 95 ml of solutions of $1.6 \times 10^{-4}M$ Rh(III), $4 \times 10^{-3}M$ KSCN, made $2M$ in HCl after heating at 90° for (○) 10 min, (□) 30 min, (Δ) 60 min.

aquation of RhCl_6^{3-} to $[\text{RhCl}_{6-x}(\text{H}_2\text{O})_x]^{x-3}$, caused by heating the solution. Similar observations have been made for the formation of the $\text{Ru}(\text{SCN})_6^{3-}$ complex,²² which is also labile towards aquation.

The formation and extraction of the RhY complex

Since formation of the RhY complex depends on the concentration of thiocyanate and hydrochloric acid as well as on the heating schedule, two experiments were performed to establish the minimum heating time required before its extraction. Varying the thiocyanate concentration with different heating times indicated (Fig. 4) that the degree of extraction increases both with increasing thiocyanate concentration (though this must be less than $2 \times 10^{-2}M$, to minimize thiocyanic acid interference) and with heating time, reaching a maximum at 95% ($\log D = 4.54$) for a solution initially $1.6 \times 10^{-2}M$ in thiocyanate and heated for 60 min.

Replotting of these results as percentage extracted vs. initial thiocyanate concentration, for solutions

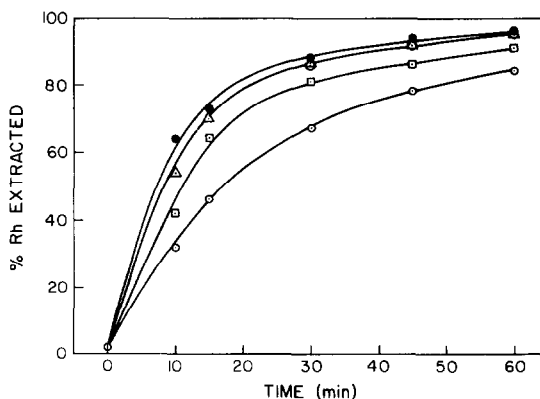


Fig. 4. Effect of heating time of solutions containing different concentrations of thiocyanate on the extraction of rhodium when some of the acid was added before heating; conditions: $49 \pm 1 \text{ mg}$ of foam; 95 ml of $1.6 \times 10^{-4}M$ Rh(III), total HCl $2M$ (30 mmoles of HCl added before heating); KSCN: (●) $1.6 \times 10^{-2}M$; (Δ) $8 \times 10^{-3}M$; (□) $4 \times 10^{-3}M$; (○) $2 \times 10^{-3}M$.

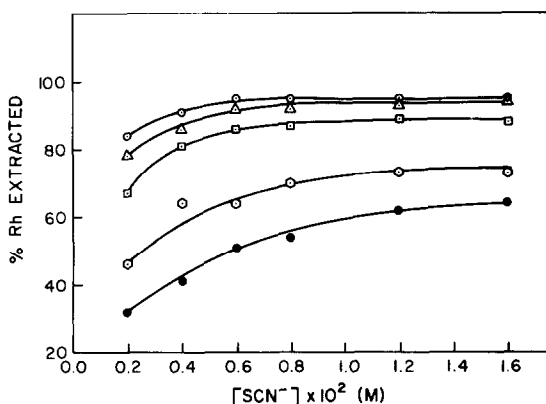


Fig. 5. Effect of thiocyanate on the extraction of rhodium from solutions heated for different times and containing some hydrochloric acid added before heating; conditions: 49 ± 1 mg of foam; 95 ml of $1.6 \times 10^{-4} M$ Rh(III), total HCl 2M (30 mmoles of HCl added before heating); heating time: (●) 10 min; (○) 15 min; (□) 30 min; (△) 45 min; (○) 60 min.

heated for different times (Fig. 5), makes it clear that for solutions with an initial thiocyanate concentration $> 6 \times 10^{-3} M$ and heated for more than 30 min, the extraction of rhodium is almost independent of thiocyanate concentration. The ultraviolet spectra indicated that the absorbance band at 288 nm and the band at 246 nm (which corresponds to RhY) increased with increasing amounts of thiocyanate and heating time. Furthermore, at high thiocyanate concentrations and longer heating times, the absorbance at 288 nm decreased while that at 246 nm continued to increase with larger thiocyanate concentrations and longer heating; this can be attributed to the conversion of $Rh(SCN)_6^{3-}$ into RhY.

The contribution of hydrochloric acid in reducing the necessary heating time was studied at the optimum thiocyanate concentration. The results (Fig. 6) indicated that the extraction of rhodium increased

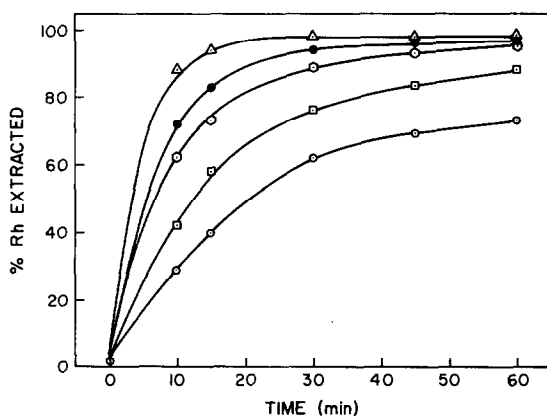


Fig. 6. Extraction of rhodium as a function of time of heating solutions containing different concentrations of hydrochloric acid initially added before heating; conditions: 49 ± 1 mg of foam; 95 ml of $1.6 \times 10^{-4} M$ Rh(III), $1.2 \times 10^{-2} M$ in KSCN, total HCl 2M [HCl added before heating: (○) 0.1 mmoles; (□) 10 mmoles; (●) 30 mmoles; (△) 160 mmoles HCl].

with longer heating times and with larger amounts of hydrochloric acid added before heating the solution. The ultraviolet spectra showed that for solutions of low acidity the absorbance at both 288 nm [$Rh(SCN)_6^{3-}$ complex] and 246 nm [RhY complex] increased with increasing heating time, whereas for highly acidic solutions the absorbance at 288 nm decreased while that at 246 nm still increased. In addition, when solutions which initially contained as little as 80 mmoles of hydrochloric acid per 60 ml were heated for more than 30 min, another absorption peak, at 306 nm (also due to RhY) was observed and both absorbances for RhY increased with heating time up to 60 min. The maximum absorbance at both 306 and 246 nm was observed for solutions with initially 160 mmoles of hydrochloric acid per 60 ml, when these were heated for a minimum of 30 min.

Since high thiocyanate and acid concentrations produced hydrogen sulphide in solution, the increase in the rate of formation of the RhY complex might be due to the reduction of Rh(III) to Rh(II), which acts as a soft acid²³ and hence will have a high affinity toward the soft base thiocyanate. The reduction of Rh(III) to Rh(II) has also been proposed by Ryan⁵ to explain the increase in the rate reaction of rhodium with 2-mercapto-4,5-dimethylthiazole when a hydrochloric acid solution of trivalent rhodium is boiled with excess of reagent.

Mechanism of the extraction of Rh(III)-thiocyanate complex

The possibility of a "cation-chelation" mechanism^{24,25} as a mode for the extraction of $Rh(SCN)_6^{3-}$ by the foam was investigated. With $4 \times 10^{-3} M$ thiocyanate solutions at pH 2.5 ± 0.1 , the effect of different concentrations of sodium or potassium chloride added after heating for 4 hr was studied. The extraction increased from 38% ($\log D = 3.07$) with no salt to 47% ($\log D = 3.22$) at 0.5M sodium chloride and then remained constant. For solutions containing potassium chloride, the extraction increased to 52% ($\log D = 3.32$) at 0.4M salt concentration and then decreased to 41% ($\log D = 3.12$) for 2M salt.

In a second experiment, solutions at pH 2.5 ± 0.1 were heated for 4 hr before addition of different chloride salts and adjustment of the hydrochloric acid concentration. The results (Fig. 7) indicated that for all the acid concentrations, the extraction of rhodium decreased according to the salt cation added, in the order $Li^+ > Na^+ > K^+$, which is the order of decreasing hydration number of these cations.

In the ultraviolet spectra of the solutions in both these experiments the absorption band at 288 nm had the same shape and intensity, indicating that the influence of the solution conditions was on the distribution of $Rh(SCN)_6^{3-}$ between foam and aqueous phase rather than on the formation of the complex.

No appreciable increase in the extraction of $Rh(SCN)_6^{3-}$ was observed with increased concentrations of sodium or even potassium ions. Further-

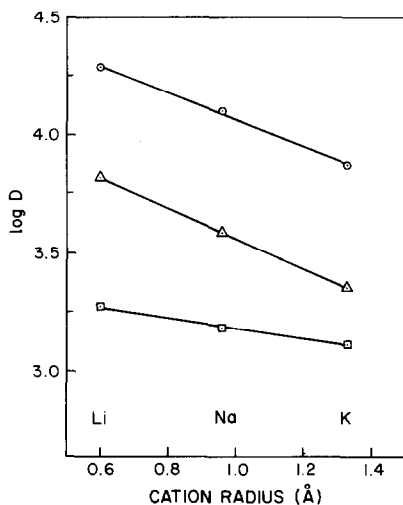


Fig. 7. Effect of the size of the alkali metal on the distribution of rhodium-thiocyanate complex between foam and aqueous solutions containing different concentrations of hydrochloric acid added after heating; conditions: 50 ± 1 mg of foam; 95 ml of $1.6 \times 10^{-4}M$ Rh(III), $4 \times 10^{-3}M$ in KSCN, 2M in salt; [HCl]: (□) $3 \times 10^{-3}M$; (△) 0.5M; (○) 1M.

more, the results in Fig. 7 did not show the increase in extraction in the order $Li^+ < Na^+ < K^+$ that has been observed for the thiocyanate complexes of palladium,^{26,27} platinum,²⁸ ruthenium and osmium,²² which are extracted through the "cation-chelation" mechanism. Consequently, it is concluded that there is not a significant contribution from the "cation-chelation" mechanism^{24,25} in the extraction of the rhodium complex(es) by polyether foam.

A minimum hydrochloric acid concentration of 2M was required for the extraction of rhodium by the foam,¹⁶ which is significantly greater than the 0.5M acid required for the $Pd(SCN)_4^{2-}$ complex²⁶ and the Pt(II)-thiocyanate complex.²⁸ However, this effect of acid concentration is in agreement with that reported for rhodium extraction from thiocyanate solutions by many organic solvents,^{7,9} and because $H_3Rh(SCN)_6$ can be formed at high acid concentrations,⁷ the distribution of $Rh(SCN)_6^{3-}$ between the foam and aqueous phase may be regarded as a simple solvent extraction, probably of $H_3Rh(SCN)_6$. This mechanism has been suggested by several workers^{29,30} for the extraction of some metals by polyurethane foam and explains the increasing extraction of rhodium with increasing hydration number of the salt cation added (*i.e.*, there was a simple salting-out mechanism).

Separation of rhodium and iridium

To determine the degree of extraction of iridium as a function of the amount of lithium chloride added before heating, solutions at $pH\ 2.5 \pm 0.1$ containing 8.66 μ moles of iridium, 3.0 mmoles of thiocyanate and different volumes, up to 40 ml, of 10M lithium chloride in approximately 60 ml total volume were

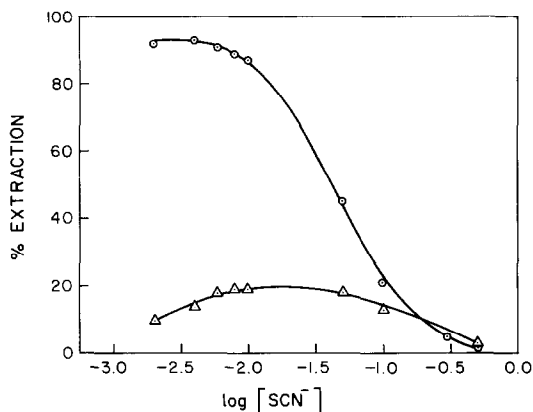


Fig. 8. Effect of thiocyanate on the extraction of rhodium and iridium from solutions containing acid added after heating; conditions: 49 ± 1 mg of foam; 95 ml of 2M HCl, 1M in LiCl; (○) $1.6 \times 10^{-4}M$ Rh(III); (△) $8 \times 10^{-5}M$ Ir(IV).

heated at 90° for 1 hr, then cooled to room temperature, made 2M in hydrochloric acid and finally diluted to 100 ml. A foam cube weighing 50 ± 1 mg was then equilibrated with 90 ml of final solution for 15 hr. The results indicated that the extraction decreased from 11.3% ($\log D = 2.36$) with no lithium chloride to 4.5% ($\log D = 1.94$) at 4M salt concentration. This decrease in extraction is most likely due to the decrease in the amount of iridium-thiocyanate complex formed, which is analogous to results obtained for osmium²² and may be attributed to competition between thiocyanate and chloride ions for iridium.

The effect of thiocyanate on the extraction of iridium and rhodium was investigated, with 100 mmoles of lithium chloride added before heating for 1 hr. The results (Fig. 8) showed low extraction of iridium over the thiocyanate range studied, whereas a high extraction of rhodium was obtained at low thiocyanate concentrations.

An average extraction of $5.0 \pm 1.2\%$ ($\log D = 1.67 \pm 0.12$) for iridium and $94 \pm 1\%$ ($\log D = 4.18 \pm 0.06$) for rhodium was obtained, independently of pH, when solutions containing 0.20 mmole of thiocyanate, 200 mmoles of lithium chloride and 8.66 μ moles of iridium or 16.3 μ moles of rhodium were adjusted to various pH values from 1.7 to 6.0 with hydrochloric acid or lithium hydroxide before heating for 30 min. Furthermore, when the amount of lithium chloride was increased to 400 mmoles, an average of $4.0 \pm 0.6\%$ ($\log D = 1.58 \pm 0.08$) iridium was extracted. When the experiments were repeated with rhodium, the extraction increased from 90% ($\log D = 3.94$) at 1.5M lithium chloride to a maximum of 95% ($\log D = 4.20$) at 3M, then decreased to 91% ($\log D = 3.98$) at 4M lithium chloride.

The extraction of iridium showed a slight increase when a series of solutions at $pH\ 2.5 \pm 0.1$ containing 0.20 mmole of thiocyanate and 300 mmoles of lithium chloride were adjusted to hydrochloric acid concen-

Table 1. Separation of rhodium and iridium from thiocyanate solutions by polyurethane foam

[Rh(III)], M	[Ir(IV)], M	Rhodium,		Iridium,	
		%E	Log D	%E	Log D
1.5×10^{-4}	tracer only*	94	4.17	6.2	1.78
1.5×10^{-4}	1.3×10^{-4}	94	4.16	6.2	1.77
1.5×10^{-4}	2.6×10^{-4}	95	4.22	5.8	1.75
1.5×10^{-4}	5.2×10^{-4}	93	4.11	3.2	1.47
1.5×10^{-4}	7.8×10^{-4}	90	3.92	3.5	1.51

*Less than $1 \times 10^{-12}M$.

trations up to 3M after 30 min of heating. Only 3.0% (log $D = 1.45$) of iridium was extracted from 1M acid solutions and this increased to 4.5% (log $D = 1.62$) for 1.5M acid and then remained independent of acidity at higher acid concentration. Under the same conditions, the extraction of rhodium increased from 85% (log $D = 3.72$) at 1M initial acid to 93% (log $D = 4.11$) at 2M and stayed almost constant at higher concentrations.

The separation of the two metals was studied under the best conditions for the extraction of rhodium and almost the worst for iridium. Solutions containing up to 78 μ moles of iridium at pH 2.5 ± 0.1 with 14.7 μ moles of rhodium, 0.20 mmole of thiocyanate and 300 mmoles of lithium chloride in about 60 ml were heated at 90° for 30 min, then cooled to room temperature; 200 mmoles of hydrochloric acid were added and the solutions diluted to 100 ml. A foam cube weighing 100 ± 1 mg was then equilibrated for 15 hr with 90 ml of a solution thus prepared. The results (Table 1) indicate that up to a 5-fold molar ratio of iridium to rhodium has little or no effect on the extraction of rhodium. These results indicate that rhodium and iridium can be separated with reasonable success, considering the difficulty of their separation, and in comparison with other techniques.

Conclusions

The presence of lithium chloride or hydrochloric acid accelerates the reaction of rhodium with thiocyanate to form an extractable species. Furthermore, while the effect of lithium chloride is to facilitate the formation of the rhodium thiocyanate complexes it inhibits that of the iridium complexes and therefore makes the separation more efficient and quantitative.

Acknowledgement—This work was supported by the Natural Science and Engineering Research Council of Canada.

REFERENCES

1. A. Diamantatos, *Anal. Chim. Acta*, 1973, **66**, 147.
2. G. A. Vorob'eva, Yu. A. Zolotov, L. A. Izosenkova, A. V. Karyakin, L. I. Pavlenko, O. M. Petrukhin, I. V. Seryakova L. V. Simonova and V. N. Shevchenko, *J. Anal. Chem. USSR*, 1974, **29**, 425.
3. Yu. A. Zolotov, O. M. Petrukhin, V. N. Shevchenko, V. V. Dumina and E. G. Rukhadze, *Anal. Chim. Acta*, 1978, **100**, 613.
4. M. Mojski, *Talanta*, 1980, **27**, 7.
5. D. E. Ryan, *Analyst*, 1950, **75**, 557.
6. R. Rigamonti and S. Marchetti, *Atti Accad. Sci. Torino, Class. Sci. Fis. Mat. Nat.*, 1959, **94**, 25.
7. J. H. W. Forsythe, R. J. Magee and C. L. Wilson, *Talanta*, 1960, **3**, 330.
8. E. W. Berg and E. Y. Lau, *Anal. Chim. Acta*, 1962, **27**, 248.
9. M. Di Casa and R. Stella, *Radiochem. Radioanal. Lett.*, 1972, **10**, 331.
10. D. J. Nicolas, *Natl. Inst. Metall., Repub. S. Afr.*, Project No. 01374, 5 December 1974.
11. E. W. Berg and W. L. Senn, *Anal. Chem.*, 1955, **27**, 1255.
12. D. E. Ryan, *Can. J. Chem.*, 1961, **39**, 2389.
13. G. G. Tertipis and F. E. Beamish, *Anal. Chem.*, 1962, **34**, 623.
14. A. Diamantatos, *Anal. Chim. Acta*, 1973, **67**, 317.
15. A. Diamantatos and A. A. Verbeek, *ibid.*, 1977, **91**, 287.
16. S. J. Al-Bazi and A. Chow, *Anal. Chem.*, 1981, **53**, 1073.
17. C. K. Jørgensen, *Acta Chem. Scand.*, 1956, **10**, 500.
18. W. C. Wolsey, C. A. Reynolds and J. Kleinberg, *Inorg. Chem.*, 1963, **2**, 463.
19. C. Pohlandt and H. Hegetschweiler, *Natl. Inst. Metall. Repub. S. Afr.* Project No. 03276, 30 January 1978.
20. H. H. Schmidtke, *Z. Phys. Chem. (Frankfurt)*, 1964, **40**, 96.
21. W. Robb and G. M. Harris, *J. Am. Chem. Soc.*, 1965, **87**, 4472.
22. S. J. Al-Bazi, *Ph.D. Thesis*, University of Manitoba, 1983.
23. R. G. Pearson, *J. Chem. Educ.*, 1968, **45**, 581; 1968, **45**, 643.
24. R. F. Hamon, A. S. Khan and A. Chow, *Talanta*, 1982, **29**, 313.
25. A. S. Khan, *Ph.D. Thesis*, University of Manitoba, 1982.
26. S. J. Al-Bazi and A. Chow, *Talanta*, 1982, **29**, 507.
27. *Idem*, *ibid.*, 1983, **30**, 487.
28. *Idem*, *Anal. Chem.*, 1983, **55**, 1094.
29. H. J. M. Bowen, *J. Chem. Soc.*, 1970, 1082.
30. J. J. Oren, K. M. Gough and H. D. Gesser, *Can. J. Chem.*, 1979, **57**, 2032.

PHOTOMETRIC AND FLUORIMETRIC KINETIC DETERMINATION OF MANGANESE BY MEANS OF THE OXIDATION OF SODIUM 4,8-DIAMINO-1,5-DIHYDROXYANTHRAQUINONE-2,6-DISULPHONATE

A. NAVAS and F. SANCHEZ ROJAS

Department of Analytical Chemistry, Faculty of Sciences, University of Málaga, Spain

(Received 16 February 1983. Revised 7 January 1984. Accepted 12 January 1984)

Summary—Three kinetic methods for the determination of manganese, two of them by photometric monitoring and another by fluorimetric monitoring, based on the oxidation of sodium 4,8-diamino-1,5-dihydroxyanthraquinone-2,6-disulphonate are described. A critical comparative evaluation of both monitoring techniques and their effect on the analytical figures of merit of the methods has been made. Manganese contents between 6.5 and 21.7 ng/ml can be determined with relative standard deviation of $\pm 3.7\%$. Under appropriate working conditions, the fluorimetric method can be satisfactorily applied to the determination of manganese in environmental samples of tap water and workroom metallic fumes.

Although the general advantages and limitations of kinetic methods of analysis have been discussed,¹⁻⁸ study of the influence of the reaction monitoring technique on the analytical characteristics of kinetic methods is very interesting in evaluation of the analytical figures of merit of two kinetic methods based on the same chemical reaction.

Molecular absorption spectrophotometry and spectrofluorimetry are both widely used as monitoring techniques in kinetic methods of analysis.⁹ Usually the intrinsically higher sensitivity of fluorimetry is offset by the low degree of completeness of reaction when initial-rate kinetic measurements are used, and the overall sensitivity depends on both the monitoring technique and the mode of calculation.

This paper reports the spectrophotometric kinetic determination of manganese by means of the oxidation of sodium 4,8-diamino-1,5-dihydroxyanthraquinone-2,6-disulphonate (DADHADS) in acidic medium. The reaction is characterized by the appearance of a pink oxidized product ($\lambda_{\text{max}} \sim 500$ and 540 nm) and disappearance of the blue colour of DADHADS ($\lambda_{\text{max}} \sim 570$ nm).

The oxidized product presents a pink fluorescence ($\lambda_{\text{max}} \sim 580$ nm) when excited at 525 nm, and this may be used for fluorimetric monitoring and kinetic determination of traces of manganese.

In the present work, the method has been applied to determination of manganese in fumes in industrial work places. Welding operations generate fumes containing very small solid particles, a high percentage of which are in the respirable size-range, and produce the risk of poisoning, given the known toxicity of manganese.¹⁰⁻¹³ The threshold limit value (TLV) for environmental manganese¹⁴ is 1 mg/m³, so adequate

control of the manganese concentration in the environment is needed for worker protection in workshops.

EXPERIMENTAL

Reagents

DADHADS stock solution, 0.01%. The solution is stable for at least 1 month.

Standard manganese(II) solution, 50.0 µg/ml. Prepared by dissolving manganese sulphate monohydrate in 0.1M hydrochloric acid, and standardized by EDTA titration.

All chemicals used were of analytical-grade, and demineralized distilled water was used throughout. The dilute solutions were prepared immediately before use, and all reagents and analyte solutions were brought to the same temperature in a thermostatically controlled water-bath.

Apparatus

A Perkin-Elmer MPF-43A spectrofluorimeter equipped with a 150-W xenon lamp, 1 × 1 cm quartz cells and a Hamamatsu R-777 photomultiplier was used, and no spectral corrections were made. A Shimadzu UV-240 Graphicord spectrophotometer was used. The analytical signals were recorded with a chart-recorder.

Procedure

Pipette 10 ml of DADHADS solution ($1 \times 10^{-4}M$ for photometric measurement or $1.05 \times 10^{-3}M$ for fluorimetric measurement), and an aliquot (1–10 ml) of sample (pH 3–10) containing 3–11 µg of manganese (photometric procedure) or 0.16–0.54 µg of manganese (fluorimetric procedure) into a dry 25-ml standard flask. Add 2 ml of 0.2M sodium hydroxide and mix. Make up to volume with 0.5M hydrochloric acid and monitor the absorbance at 518 nm or 606 nm, or the fluorescence intensity ($\lambda_{\text{exc}} = 525$ nm, $\lambda_{\text{em}} = 585$ nm), starting 60 sec after the addition of hydrochloric acid.

Collection and treatment of samples

Fume samples were collected in workshop environments according to the NIOSH Manual,¹⁵ in 37-mm three-body cassettes with mixed cellulose-ester membrane filters (0.8 µm cellulose-ester membrane filters (0.8 µm pore size,

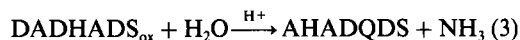
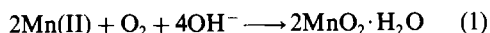
MSA). Battery-powered personal sampling pumps (MSA, model G) were used at flow-rates of 1.5 l./min. Each filter was treated with 10 ml of concentrated nitric acid; the acid was evaporated to dryness by heating on a hot-plate in a clean-air fume-cupboard and the residue dissolved in 5 ml of 10% v/v nitric acid. The clear solution was quantitatively transferred to a 50-ml standard flask and diluted to volume with demineralized water. An aliquot of this solution was then subjected to the kinetic procedure.

Tap water samples were collected in Málaga and stored in polyethylene bottles, which had been previously washed with 20 ml of saturated potassium permanganate solution, emptied, left for 10 min, then repeatedly washed with the inner surface in contact with concentrated sulphuric acid (10 ml). The bottles were then repeatedly filled with the tap water, before a sample was retained. Tap water samples were concentrated tenfold by evaporation before analysis if the standard-addition method was not used.

RESULTS AND DISCUSSION

It has been found that in strongly acidic media DADHADS undergoes very slow reaction with the oxygen dissolved in water, and this is catalysed by certain cations,^{16,17} or by the action of oxidants such as cerium(IV).¹⁸ The DADHADS-Mn(II) reaction does not occur in either alkaline or acidic media, but, if a solution containing both reagents in an alkaline medium is acidified with hydrochloric acid, the oxidation process takes place.

This suggests that a Winkler-type mechanism is the most likely route of the oxidative reaction of DADHADS with manganese, as follows:



in which the hydrolysis product (AHADQDS) is a fluorescent diquinone-type compound.¹⁶ It is consistent with this hypothesis, that the reaction goes only after acidification of an alkaline solution.

This transformation is rather slow and permits the photometric and fluorimetric monitoring of the kinetic curves. Figure 1 shows the absorption (*b*) and excitation and emission (*a*) spectra of DADHADS and its oxidation product, from which it can be seen that DADHADS does not fluoresce and is blue in colour ($\lambda_{\text{max}} = 606 \text{ nm}$), and the pink ($\lambda_{\text{max}} = 518 \text{ nm}$) oxidation product is a fluorescent compound that shows an excitation maximum at 525 nm and emission maximum at 585 nm.

Effect of the reaction variables

The effect of the concentration of each reagent on the initial rate and on the standard deviation of the initial rate was studied, for the optimization of variables. The optimum concentration of a species was taken as the concentration at which the relative standard deviation of the initial rate measurement was minimal, the remaining variables being fixed. The optimum concentration will be that for which the reaction order of the species is zero or as close to it as possible, since small fluctuations in concentration will not affect the initial rate of a zero-order reaction.

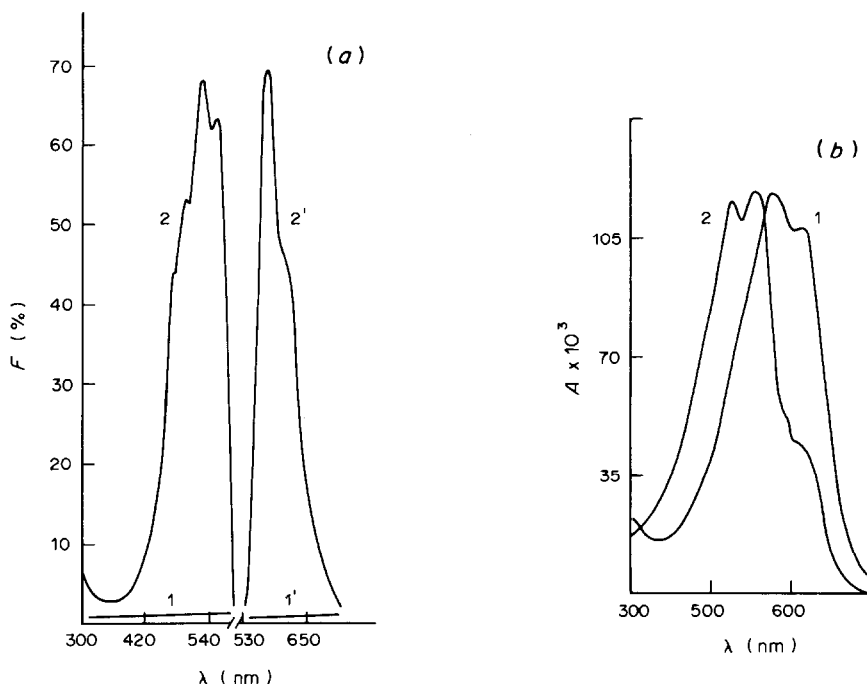


Fig. 1. (*a*) Uncorrected excitation and emission spectra of DADHADS (1, 1') and its oxidation product (2, 2'). [NaOH] 0.016M; [DADHADS] $8 \times 10^{-6}M$; $[\text{Mn}^{2+}] 7.3 \times 10^{-4}M$; [HCl] 0.4M. (*b*) Absorption spectra of DADHADS (1) and its oxidation product (2). [NaOH] 0.016M; [DADHADS] $8.4 \times 10^{-6}M$; $[\text{Mn}^{2+}] 8.3 \times 10^{-4}M$; [HCl] 0.16M.

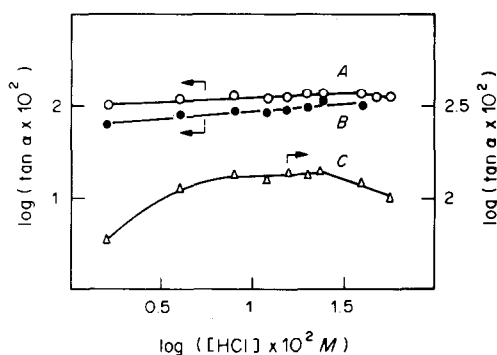


Fig. 2. Effect of the acidity of the initial reaction rate: *A* ($\lambda = 518$ nm) and *B* ($\lambda = 606$ nm), photometric method; [DADHADS] $1.6 \times 10^{-5} M$; $[Mn^{2+}] 1.9 \times 10^{-5} M$; [NaOH] $0.016 M$. *C*, fluorimetric method; [DADHADS] $8 \times 10^{-6} M$; $[Mn^{2+}] 1.9 \times 10^{-5} M$; [NaOH] $0.016 M$.

Since manganese and sodium hydroxide must be present before the reaction is started by the addition of hydrochloric acid, the effects were studied of sodium hydroxide concentration and standing time before acidification on the initial reaction rate. The results obtained show that these variables are not critical, since the reaction is zero-order with respect to [NaOH] over the range studied (0.004 – $0.12 M$) and standing times up to 30 min do not affect the initial reaction rate. For further work, a sodium hydroxide concentration of $0.016 M$ (2 ml of $0.2 M$ alkali per 25 ml) was selected as it ensures an alkaline medium for moderately acidic samples ($pH > 3$) and provides reproducible results.

The effect of [HCl] on the initial reaction rate is shown in Fig. 2. The log-log plot indicates an ample range of concentrations in which the reaction rate is zero-order with respect to this variable. A hydrochloric acid concentration between 0.04 and $0.4 M$ ensures reproducible results, which implies 2–20 ml of $0.5 M$ acid per 25 ml of final solution.

The influence of [DADHADS] on the initial rate (photometric monitoring) is shown in Fig. 3; the initial rate increases steadily with [DADHADS]. The

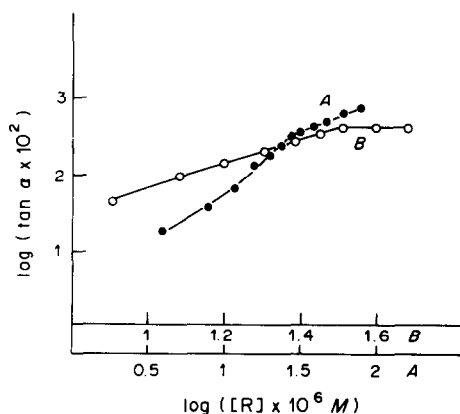


Fig. 3. Influence of the reagent concentration on the initial rate (photometric method). *A*, $\lambda 606$ nm; *B*, $\lambda 518$ nm. $[Mn^{2+}] 1.9 \times 10^{-5} M$; [NaOH] $0.016 M$; [HCl] $0.16 M$.

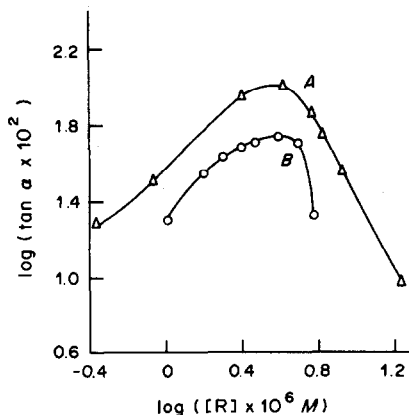


Fig. 4. Influence of the reagent concentration on the initial rate (fluorimetric method). *A*, $[Mn^{2+}] 4.7 \times 10^{-7} M$; *B*, $[Mn^{2+}] 2.4 \times 10^{-7} M$. [NaOH] $0.016 M$; [HCl] $0.16 M$.

relative standard deviation in the initial rate was 2–3% (measurement at 606 nm) for [DADHADS] between $2.8 \times 10^{-5} M$ and $8 \times 10^{-5} M$. Since the rates were lower at lower [DADHADS], and the standard deviation of the initial rate began to be significant, the precision decreased at lower [DADHADS].

The log-log plot for measurement at 518 nm shows zero-order reaction order with respect to DADHADS over the concentration range 3.2 – $4.8 \times 10^{-5} M$, so [DADHADS] = $4 \times 10^{-5} M$ was selected for further photometric work.

Figure 4 shows the influence of [DADHADS] on the initial rate measured fluorimetrically. Curves for two concentrations of manganese are shown. For both, the initial rate is zero-order with respect to [DADHADS] in the range 2 – $4.5 \times 10^{-6} M$. For [DADHADS] $> 4.5 \times 10^{-6} M$, the initial reaction rate falls as a consequence of pre- and post-filter effects, as the absorption spectrum of DADHADS and the excitation and emission spectra of the reaction product overlap (Fig. 1). This effect increases with [DADHADS], as seen in Fig. 4, curve B, in which the reagent excess is higher. From these results [DADHADS] = $4.2 \times 10^{-6} M$ has been selected as optimal for fluorimetric measurements.

Analytical parameters

Under optimal conditions, the log-log calibration graph is linear for manganese(II) concentrations ranging from 6.5 to 21.7 ng/ml for the fluorimetric procedure, and from 0.22 to 0.54 $\mu g/ml$ ($\lambda = 518$ nm, oxidized product monitored) or from 0.13 to 0.44 $\mu g/ml$ ($\lambda = 606$ nm, reagent monitored) for the photometric procedures. Further details of the analytical methods are summarized in Table 1.

It should be noted that, in spite of the higher sensitivity, the fluorimetric method is more precise than the photometric methods. The reasons for the poorer accuracy and precision of the photometric methods can be related to the spectral overlap at both monitoring wavelengths. As can be seen in Fig. 1, at

Table 1. Analytical parameters of the kinetic methods for the determination of manganese

Method	Analytical response	Wavelength, nm	Range, ng/ml	Taken, ng/ml	Found (\bar{x}), ng/ml	n	S, ng/ml	RSD, %	G, %
1	Photometric	518	220-540	330	329	10	30	9.1	6.4
2	Photometric	606	130-440	170	164	10	10	8.0	6.2
3	Fluorimetric	525/585	6.5-21.7	15.2	15.6	10	0.6	3.7	2.6

\bar{x} = mean value; n = number of determinations; S = standard deviation; RSD = relative standard deviation; G = relative error ($100 tS/\bar{x}n^{1/2}$), 95% confidence.

Table 2. Effects of various ions on the determination of manganese by the kinetic methods

Photometric monitoring ($\lambda = 518$ nm)		Fluorimetric monitoring	
Tolerance ratio*	Foreign ion or species	Tolerance ratio†	Foreign ion or species
60	UO ₂ ²⁺ , F ⁻	10000	UO ₂ ²⁺ , Zn ²⁺
30	Ca ²⁺ , SO ₄ ²⁻ , NO ₃ ⁻	6000	Ca ²⁺ , F ⁻
15	tartrate, citrate, EDTA	2500	Pb ²⁺ , Cd ²⁺ , Al ³⁺ , SO ₄ ²⁻ , NO ₃ ⁻
5	Zn ²⁺ , Cd ²⁺ , Pb ²⁺ , Al ³⁺ , Ti ⁴⁺ , Mo(VI), IO ₃ ⁻ , C ₂ O ₄ ²⁻	1500	Pd ²⁺ , C ₂ O ₄ ²⁻
1	Ni ²⁺ , Co ²⁺ , Fe ²⁺ , Fe ³⁺ , Au ³⁺ , I ⁻	1000	tartrate, citrate, EDTA
0.1	Hg ²⁺ , Ce ⁴⁺ , BrO ₃ ⁻	20	Ni ²⁺ , Fe ²⁺ , Au ³⁺ , I ⁻ , IO ₃ ⁻ , BrO ₃ ⁻
<0.1	Cu ²⁺ , Pd ²⁺ , V(V), Cr ³⁺	7	Fe ³⁺ , Ti ⁴⁺ , Mo(VI)
		1	Hg ²⁺ , V(V)
			Co ²⁺ , Cu ²⁺ , Cr ³⁺ , Ce ⁴⁺

*Manganese concentration 0.33 μ g/ml.

†Manganese concentration 15 ng/ml.

518 and 606 nm, both DADHADS and the oxidized product absorb.

Selectivity study

The effect of various ions on the determination of manganese(II) at the 0.33- μ g/ml level (photometric monitoring of the oxidized product at 518 nm) and at the 0.015- μ g/ml level (fluorimetric method) was investigated. The criterion for interference was a variation in the initial rate of more than $\pm 6.4\%$ (photometric monitoring) or $\pm 3\%$ (fluorimetric monitoring), from the value expected for manganese alone. The results are given in Table 2.

Interferences in these methods arise from four main chemical sources: (1) oxidizing substances act-

ing on DADHADS [Ce(IV), BrO₃⁻, Hg(II)]; (2) catalysts of the oxidation process [V(V), Au(III), Fe(III), Cr(III)]; (3) species causing a decrease in the DADHADS concentration by complexation reactions, [Cu, Co, Pd];¹⁹ (4) substances reducing manganese(III), [I⁻, Fe(II)]. Spectral interferences should be minimal in the fluorimetric method owing to the inherent selectivity of fluorimetry. For the fluorimetric method, the interference of cobalt up to a C_{Co}/C_{Mn} ratio of 25 can be eliminated by addition of 1 ml of $1.9 \times 10^{-3}M$ tartrate or up to $C_{Co}/C_{Mn} = 50$ with 1 ml of $1.25 \times 10^{-3}M$ citrate. Cu(II) up to a ratio of $C_{Cu}/C_{Mn} = 25$ can be masked by addition of 1 ml of $1.25 \times 10^{-3}M$ citrate, and of Cr(III) up to $C_{Cr}/C_{Mn} = 10$ by addition of 1 ml of $8.9 \times 10^{-3}M$ fluoride.

Applications

To test the reliability of the proposed fluorimetric method, it was applied to the determination of manganese in environmental samples and tap water.

The results of analysis of four different environmental samples, a synthetic mixture and tap water are presented in Table 3. The standard-addition graphs were analysed by regression procedures to obtain the intercepts. The results obtained indicate the existence of a more pronounced matrix effect in the environmental samples and demonstrate the reliability of the fluorimetric method for the determination of manganese in these samples.

Table 3. Determination of manganese in four environmental samples of metallic fumes, a tap water and a synthetic mixture

Sample	Mn present,* ng/ml	Mn found,† ng/ml
1	15.0	14.1
2	15.0	16.2
3	16.0	14.8
4	15.0	14.1
Tap water	1.23§	1.27
S.M.‡	15.2	14.8

*By atomic-absorption spectrometry.

†Mean values based on analysis of three aliquots.

§Standard-addition method.

‡Synthetic mixture, composition (ng/ml): Mn, 15.2; Cr, 1.0; Cu, 4.0; Pb, 7.0; Fe, 200.0.

Acknowledgement—The authors are grateful to A. Arbaizar for sampling facilities and for the A.A.S. analysis.

REFERENCES

1. K. B. Yatsimirskii, *Kinetic Methods of Analysis*, Pergamon Press, Oxford, 1966.
2. G. Svehla, *Selected Annual Revs. Anal. Sci.*, 1971, **1**, 235.
3. H. A. Mottola, *CRC Crit. Rev. Anal. Chem.*, 1975, **5**, 229.
4. H. B. Mark, Jr., *Talanta*, 1972, **19**, 717.
5. R. L. Wilson and J. D. Ingle, Jr., *Anal. Chem.*, 1977, **49**, 1060.
6. P. W. Carr, *ibid.*, 1978, **50**, 1602.
7. J. D. Ingle, Jr. and S. R. Crouch, *Anal. Chem.*, 1973, **45**, 333.
8. J. D. Ingle, Jr. and M. A. Ryan, in *Modern Fluorescence Spectroscopy*, E. L. Wehry (ed.), Vol. 3, pp. 95–142. Plenum Press, New York, 1981.
9. H. A. Mottola and H. B. Mark, Jr., *Anal. Chem.*, 1982, **54**, 62R.
10. B. Kesic and V. Hausler, *Arch. Ind. Hyg. Occupational Med.*, 1954, **10**, 336.
11. F. A. Patty, *Industrial Hygiene and Toxicology*, Vol. 2, Interscience, New York, 1963.
12. E. Browning, *Toxicity of Industrial Metals*, Butterworths, London, 1961.
13. J. J. Dulka and T. H. Risby, *Anal. Chem.*, 1976, **48**, 640A.
14. National Institute of Safety and Hygiene, *Toxic Substance List*, Cincinnati, Ohio, 1982.
15. *Idem*, *Manual of Sampling Data Sheets*, Cincinnati, Ohio, 1976.
16. F. Garcia Sanchez, A. Navas, M. Santiago and F. Grases, *Talanta*, 1981, **28**, 835.
17. A. Navas and F. Sanchez Rojas, *Quim. Anal.*, 1983, **II(2)**, 112.
18. A. Navas, F. Sanchez Rojas and F. Garcia Sanchez, *Mikrochim. Acta*, 1982, **I**, 175.
19. A. Navas and F. Garcia Sanchez, *Anal. Quim.*, 1979, **75**, 506.

IMPROVED TRIBENZYLAMINE-SILVER BROMIDE EXTRACTION/ATOMIC-ABSORPTION SPECTROPHOTOMETRIC METHOD FOR THE DETERMINATION OF SILVER IN ORES, RELATED MATERIALS AND ZINC PROCESS SOLUTIONS

ELSIE M. DONALDSON

Mineral Sciences Laboratories, Canada Centre for Mineral and Energy Technology, Department of
Energy, Mines and Resources, Ottawa, Canada

(Received 3 October 1983. Accepted 19 December 1983)

Summary—An improved tribenzylamine extraction/atomic-absorption method for the determination of silver in ores, related materials and zinc process solutions is described. The method, which involves the separation of silver by a single methyl isobutyl ketone extraction of the tribenzylamine-silver bromide ion-association complex from ~ 0.5 – $2M$ sulphuric acid– $0.14M$ potassium bromide, is simpler and more rapid than a previous method based on a triple chloroform extraction of the complex. Silver is stripped with $12M$ hydrochloric acid containing 1% thiourea as a complexing agent. Thiourea is destroyed with nitric and perchloric acids and silver is ultimately determined by atomic-absorption spectrophotometry in an air-acetylene flame, at 328.1 nm, in a 10% v/v hydrochloric acid–1% v/v diethylenetriamine medium. Cadmium and bismuth are partly co-extracted but do not interfere. Results obtained by this method are compared with those obtained previously by the tribenzylamine/chloroform extraction method and with those obtained by a direct acid-decomposition/atomic-absorption method.

The objective of a current CANMET project, which involves a study of the behaviour, form and distribution of silver in conventional zinc hydrometallurgical processes (designed to recover metallic zinc from zinc ores and concentrates), is to increase the recovery of this valuable by-product in Canadian zinc plants. Recently, as part of this project, a solvent extraction/atomic-absorption spectrophotometric (AAS) method for the determination of ~ 0.1 $\mu\text{g/g}$ or more of silver in ores and concentrates and ~ 0.001 $\mu\text{g/ml}$ or more in zinc process solutions was developed.¹ In this method, silver is separated from the matrix elements by a triple chloroform extraction of the tribenzylamine (TBA)-silver bromide ion-association complex from $\sim 2M$ sulphuric acid– $0.08M$ potassium bromide. It is subsequently stripped from the chloroform phase with $9M$ hydrobromic acid and ultimately determined by AAS in a 10% v/v hydrochloric acid–1% v/v diethylenetriamine medium. However, in more recent work it was found that this method was not applicable to some industrial zinc process solutions of very high salt content, because of the severe emulsification encountered during the extraction step. Consequently, a similar method based on the use of TBA in conjunction with a solvent of much lower specific gravity (< 1) than chloroform was sought.

The proposed method involves the separation of silver by a single extraction of the TBA-silver bromide complex into methyl isobutyl ketone (MIBK)

from ~ 0.5 – $2M$ sulphuric acid– $0.14M$ potassium bromide. Silver is then stripped with $12M$ hydrochloric acid containing thiourea. Results obtained for ores and concentrates are compared with those obtained by the TBA/chloroform extraction method and with those obtained recently by a direct acid-decomposition/AAS method.²

EXPERIMENTAL

Apparatus

A Varian-Techtron model AA6 spectrophotometer was used under the conditions described previously.^{1,2}

Reagents

Standard silver solution, 100 $\mu\text{g/ml}$. Prepare the solution as described previously¹ but add ~ 10 ml of 50% v/v sulphuric acid instead of 1 ml and evaporate the solution to fumes of sulphur trioxide. Cool the solution, dissolve the salts by heating gently with ~ 100 ml of concentrated hydrochloric acid, then dilute the solution to volume with water in a 1-litre standard flask containing ~ 300 ml of concentrated hydrochloric acid.

Potassium bromide, 20% solution.

Potassium chloride, 0.2% solution.

Tribenzylamine. A 0.5% solution in MIBK.

Hydrochloric acid-thiourea solution. A 1% solution of thiourea in concentrated hydrochloric acid.

Phenolphthalein. A 0.2% solution in ethanol.

Chloroform. Analytical reagent-grade.

Procedures

Calibration solutions. Prepare as described previously.¹ (Notes 1 and 2).

Ores and related materials. Decompose up to 1 g of powdered sample, containing up to ~ 100 μg of silver and not more than 10 mg of calcium and ~ 400 mg of lead, as described previously,¹ but add 15 ml of 50% sulphuric acid,

10 ml of concentrated hydrochloric acid and 5 ml of concentrated perchloric acid (Note 3) after the bromine-nitric acid treatment. After the removal of silica and antimony, if necessary, by volatilization as the fluoride and bromide, respectively, evaporate the solution to fumes of perchloric acid, then cover the beaker and continue to heat for ~15 min. Remove the cover, wash down the sides of the beaker with water and evaporate the solution to ~3 or 4 ml. Cool, add 10 ml each of water and 50% sulphuric acid, heat to dissolve the salts, then, if necessary, filter the solution (Whatman 11-cm No. 40 paper) into a 125-ml separatory funnel marked at 50 ml. Wash the beaker and the paper and residue with 25% ammonia solution as described previously¹ (Note 4), using 3- or 4-ml portions each time, then wash the paper with ~3 ml of 5% sulphuric acid. Discard the paper, dilute the solution to ~50 ml with water and mix thoroughly.

Add 5 ml each of methanol (Note 5) and 20% potassium bromide solution and 50 ml of 0.5% tribenzylamine solution to the resulting solution, stopper the funnel and shake it for 2 min. Allow several min for the layers to separate (Note 6), then drain off and discard the lower (aqueous) phase. Wash the MIBK phase by shaking it gently for ~20 sec with 5 ml of water. Discard the wash solution. Add 15 ml each of chloroform and concentrated hydrochloric acid containing 1% of thiourea, stopper tightly and, using a wrist-action shaker, shake for 5 min. Allow the layers to separate, then drain the lower (aqueous) layer into a 150-ml beaker and wash the stem of the funnel with water. Wash the MIBK-chloroform phase twice by shaking it for ~1 min and then for ~30 sec with 5-ml portions of hydrochloric acid-thiourea solution and add the washings to the beaker. Wash the stem of the funnel with water each time. Add 1 ml of 0.2% potassium chloride solution, cover the beaker, add 5 ml of concentrated nitric acid and heat the solution to destroy thiourea (Note 7). Evaporate the solution to ~20 ml, then add 5 ml of concentrated nitric acid and 3 ml of concentrated perchloric acid and evaporate the solution to fumes of perchloric acid. Continue to heat the solution for ~10 min to destroy organic material, then remove the cover and, without baking, evaporate the solution to dryness. Depending on the expected silver content, proceed with the additions of concentrated hydrochloric acid (Note 8) and 10% diethylenetriamine solution and the subsequent determination of silver as described previously (Note 9).¹

Zinc process solutions. Transfer up to 25 ml of solution, containing up to ~100 μg of silver, to a 125-ml separatory funnel marked at 50 ml (Note 10) and add 3 ml of 50% sulphuric acid (Note 11). Dilute the solution to the mark with water, add 5 ml each of methanol and 20% potassium bromide solution, then proceed with the extraction (Note 6) of silver as described above. Wash the MIBK phase twice with 5-ml portions of water, then strip and determine silver as described.

Notes

1. All glassware should be washed with ~25% ammonia solution, followed by water.

2. The solutions in the first series (*i.e.*, up to 1 μg of silver per ml) are stable for at least 2 weeks. Those in the second series should be prepared fresh every day because their absorbance slowly decreases on standing.²

3. The use of perchloric acid is recommended because recent work² with some zinc-processing products such as jarosites and iron-leach residues showed that a small amount of silver may remain in the residue after the sample is decomposed with nitric and sulphuric acids alone as described previously.¹ Hydrochloric acid is also recommended to help to decompose iron oxides in these materials.² The subsequent addition of hydrofluoric acid may not be necessary if the sample contains little or no silica. In this case, a pyrex beaker can be used for the decomposition.

4. To wash the residue effectively, any that adheres to the

sides of the paper should be gently loosened with a glass rod. The total volume of ammonia solution used should not exceed ~25 ml.

5. Methanol helps to prevent emulsification.

6. If emulsification occurs or the layers do not separate quickly enough, add 5 ml more of methanol and shake the solution gently for ~5 sec.

7. Destruction of thiourea with nitric acid results in the formation of globules of liquid (probably carbon disulphide) which is volatilized during the subsequent evaporation of the solution. Because of the foul odour produced, an efficient fume-hood should be used for this step.

8. Usually the salts dissolve most readily if the solution is heated gently after the addition of concentrated hydrochloric acid and about an equal volume of water. Subsequently the solution should be cooled to room temperature before the addition of diethylenetriamine solution. Not too much water should be added, because silver may precipitate as the chloride if the hydrochloric acid concentration is less than ~25% v/v.

9. Sample solutions containing more than ~1 μg of silver per ml should be analysed the day they are prepared (Note 2).

10. If the solution is basic, add 1 drop of 0.2% phenolphthalein solution, neutralize with 50% sulphuric acid, then add 3 ml in excess and proceed as described.

11. In the case of ores and concentrates silver is extracted from ~1.5–2M sulphuric acid. However, the addition of less 50% sulphuric acid is recommended for zinc process solutions because some solutions can contain up to ~150 g of sulphuric acid per litre.

RESULTS AND DISCUSSION

Separation of silver by tribenzylamine/MIBK extraction

In the TBA/chloroform extraction method described previously,¹ three extractions are required for the complete separation of up to ~500 μg of silver as the bromide-TBA ion-association complex from large amounts of iron, zinc and other elements. Because zinc process solutions do not usually contain a large amount of silver, a simpler and more rapid extraction procedure was sought in which up to ~100 μg of silver could be completely extracted as the TBA-silver bromide complex in a single extraction into a solvent of specific gravity < 1. Non-polar solvents such as toluene, heptane and xylene were found to be unsuitable as diluents for TBA because it forms a white addition compound with bromide which is relatively insoluble in these solvents.³ Although this compound can be kept in solution by adding sufficient methanol before the extraction step, tests with heptane and toluene containing 0.5% TBA showed that, at the 100- μg level, silver is not completely extracted in one extraction with an equal volume of these solvents under approximately the conditions of acidity and potassium bromide concentration used previously.¹ Xylene was not tested because of its noxious nature.

Because MIBK is a good diluent and extractant for metal halide-amine systems,⁴ tests were done to determine whether MIBK containing TBA would be an effective extractant for silver from bromide media. These tests, in which silver was added in the form of a dilute sulphuric acid solution, showed that up to at

least 100 μg of silver can be quantitatively extracted in one extraction from ~ 0.1 – $4.5M$ sulphuric acid that is at least $0.04M$ in potassium bromide by shaking for 2 min with an equal volume of MIBK containing $\sim 0.5\%$ TBA. Higher concentrations of TBA than this ($\sim 0.017M$) cannot be used because of the precipitation of the insoluble bromide addition compound during the extraction step. At higher concentrations of sulphuric acid, the extraction of silver is incomplete. Because concentrated hydrobromic acid, previously used for stripping silver from the chloroform extract,¹ is miscible with MIBK, concentrated ammonia solution was used in these tests and the excess was removed by boiling before the AAS determination of silver. However, an acidic stripping solution was sought because bismuth, which is co-extracted, forms an insoluble hydrous oxide in ammoniacal solutions. Concentrated hydrochloric acid containing thiourea as a complexing agent for silver was found to be effective if chloroform was added to the organic phase to increase its density and aid in phase separation. However, in subsequent tests with pure silver solutions and with synthetic zinc process solutions of high sodium content (composition given in Table 1), low and erratic results were obtained for silver when the final solutions were treated with nitric and perchloric acids to destroy thiourea and TBA and then evaporated to dryness. In these tests the extracts were washed twice with 5-ml portions of water to remove mechanically entrained sodium and/or potassium. Ultimately, it was found that evaporation of the solutions to dryness in the presence of perchloric (or sulphuric) acid results in the formation of a refractory silver compound, presumably an oxide, which does not dissolve completely when the residue is heated with 50% hydrochloric acid. This error can readily be eliminated by adding ~ 1 mg of potassium (as ~ 2 mg of the chloride) to the solution before it is evaporated to dryness. Although the hydrobromic acid strip solutions obtained previously¹ were treated in a similar manner, negative errors were not observed, probably because the chloroform extracts were not washed to remove entrained ions and/or because chloroform may retain more of the aqueous phase containing potassium and other ions than MIBK does.

Complete recovery of silver (100 μg) was obtained when the procedural steps described above were applied to synthetic zinc process solutions that were ~ 0.5 – $2M$ in sulphuric acid and $\sim 0.08M$ in potassium bromide. However, low results were obtained for some industrial zinc process solutions, particularly thickener overflows of very high salt content, to which the same amount of silver was added. It was found that with these solutions more potassium bromide was required during the extraction step. Complete recovery of the added silver was obtained when the bromide concentration was increased to $\sim 0.14M$. Under these conditions, and when silver is extracted in the range of sulphuric acid concentration

mentioned above, very little zinc and iron are co-extracted.

Effect of diverse ions

As found previously,¹ bismuth and cadmium are partly co-extracted as bromide ion-association complexes into MIBK containing TBA, under the conditions used for the extraction of silver. At the 25- and 200-mg levels, respectively, these elements will not interfere with the extraction of silver, and the amounts co-extracted will not affect its determination by AAS even if a 10-ml final volume is used. Little or no molybdenum(VI) is co-extracted at the 200-mg level. However, at this level, a white insoluble compound forms when the solution is shaken with MIBK containing TBA. This compound, which is probably an addition compound of TBA and molybdic acid, can be readily dissolved by adding sufficient methanol to the solution.

Up to at least 2 g of zinc, 500 mg of copper(II) and iron(III), 400 mg of lead, 200 mg of magnesium and the same quantities of all the other ions mentioned previously,¹ including chloride, will not interfere in the determination of silver by the proposed method. Interference from antimony(V) is avoided as described previously. Co-extraction of any chromium(VI),⁵ present in solutions derived from ores and concentrates and resulting from the evaporation of the solution to fumes of perchloric acid, can be avoided by reducing it to chromium(III) with hydrogen peroxide. Several drops of 30% w/v peroxide solution should be added to the solution obtained after dissolution of the salts in dilute sulphuric acid, and the solution should then be boiled vigorously or evaporated to fumes of sulphur trioxide to destroy the excess of hydrogen peroxide before the filtration and extraction steps. Because some of the industrial zinc process solutions investigated contained a large amount of sodium, washing the MIBK extract several times with 5-ml portions of water is recommended to reduce the amount of mechanically entrained sodium in the final solution. This also reduces the amount of entrained iron and other ions. At the 50- μg silver level, the loss of silver to the wash solution under these conditions does not exceed ~ 0.2 μg . The magnitude of this loss depends on the amount of salts stripped into the wash solution. No loss of silver occurs if the extract does not contain entrained ions.

Tests with MP-1 (composition given in Table 3), in which low (~ 5 – 8 $\mu\text{g/g}$) and erratic results were obtained when 1-g subsamples were taken, indicated that calcium sulphate retains silver and that, unlike the case with lead sulphate, this occluded silver cannot be completely removed by washing the precipitate with 25% ammonia solution. This was verified with pure silver solutions containing calcium. This interference was not apparent in the earlier work,¹ probably because the sample solution was diluted much more before the filtration step than in the

Table 1. Recovery of silver from synthetic zinc process solutions

Solution taken*	Total	
	Ag present, μg	Ag found, μg
25-ml aliquots of 0.5M sulphuric acid	2.4 ₂	2.4 ₃
containing 150 g of ZnSO ₄ , 30 g of Fe ₂ (SO ₄) ₃ ,	5.4 ₂	5.6 ₁
10 g of MnSO ₄ , 20 g of MgSO ₄ , 5 g of CdSO ₄ and	10.4	10.5
80 g of Na ₂ SO ₄ per litre	50.4	50.1
	100.4	100.4

*Triplicate determinations of silver (present in the ZnSO₄) in 25-ml aliquots of the solution (without added silver) gave 0.4₃, 0.4₁ and 0.4₃ μg . The sulphuric acid concentration of the test solutions was adjusted to 2M before extraction.

preent method and, under these conditions, calcium sulphate is more soluble. Consequently, less would be present in the residue and less silver would be occluded. These findings show that calcium can be a source of error in the TBA/chloroform extraction method.¹ In the proposed method, up to 10 mg of calcium can be present in the sample without producing appreciable error in the result.

Applications

Tables 1 and 2 show that the results obtained by the proposed method for a series of synthetic zinc process solutions in which the added silver was varied from 2 to 100 μg , and for industrial solutions to which 5 and 100 μg were added, agree favourably with the calculated amount present. In these tests, silver was added as a solution in dilute sulphuric acid. Table 3 shows that the results obtained for seven diverse Canadian Certified Reference Materials Project (CCRMP) certified reference ores and concentrates are in excellent agreement with those obtained recently by a direct acid-decomposition/AAS method² and, except for MP-1 and MP-1a, with those obtained by the TBA/chloroform extraction method.¹ From the findings regarding the occlusion of silver by calcium sulphate, it is considered highly probable that this is the reason for the slightly low results

obtained for MP-1 and MP-1a by the TBA/chloroform extraction method. Except for PTM-1 and MP-1, the results are also in good agreement with the certified values. Those obtained for SU-1a and PTM-1 support recent conclusions² that the certified values for these ores are too low and that they should be ~ 4.6 and ~ 75 $\mu\text{g/g}$, respectively. Similarly, the results obtained for MP-1, in conjunction with those obtained previously² by a direct acid-decomposition method and those obtained by similar methods during the interlaboratory certification programme, suggest that the certified value for this ore should also be slightly higher, *viz.* ~ 59 – 62 $\mu\text{g/g}$. The results shown in Tables 1–3 are the means of five AAS measurements. All the results shown in Tables 2 and 3 are for individual subsamples.

The precision for silver at about the 4–100 $\mu\text{g/g}$ levels was determined by analysing five subsamples each of SU-1a, MP-1a and CZN-1. The results obtained (standard deviations of 0.14, 1.53 and 0.38 $\mu\text{g/g}$, respectively) showed that the proposed method yields slightly more precise results than the TBA/chloroform extraction method. It is also quicker and simpler because only one extraction is required and both the extraction and stripping steps are performed in the same separatory funnel. The

Table 2. Recovery of silver from industrial zinc process solutions

Solution*	Ag found, μg	Total Ag present after addition of Ag, $\mu\text{g}\dagger$	Total Ag found, μg
First stage solution	0.3 ₇ , 0.4 ₆	5.4 ₂	5.4 ₅
		100.4	101.1
Second stage solution	0.2 ₇ , 0.3 ₅	5.3 ₁	5.1 ₇
		100.3	100.2
Sodium arsenate solution	0.3 ₀ , 0.3 ₀	5.3 ₀	5.2 ₄
		100.3	99.5
No. 1 Thickener overflow	1.3 ₂ , 1.1 ₈	6.2 ₅	6.0 ₉
		101.3	102.3
No. 3 Thickener overflow	1.1 ₂ , 1.1 ₄	6.1 ₃	6.1 ₁
		101.1	102.0
No. 4 Thickener overflow	1.5 ₈ , 1.6 ₂	6.6 ₀	6.5 ₄
		101.6	101.4
Spent-to-residue leach	0.8 ₅ , 0.7 ₇	5.8 ₁	5.7 ₈
		100.8	101.2
Sodium carbonate solution to jarosite	0.3 ₁ , 0.3 ₂	5.3 ₂	5.5 ₁
		100.3	100.1

*25-ml aliquots taken.

†Values include mean value for silver present in 25 ml of solution plus silver added *viz.* 5 or 100 μg .

Table 3. Determination of silver in CCRMP reference ores and concentrates

Sample	Nominal composition, %	Certified value and 95% confidence limits, Ag, µg/g	TBA/chloroform extraction/AAS*	Ag found, µg/g		Proposed method†
				decomposition/AAS†	Acid- decomposition/AAS†	
CCU-1 Copper concentrate	24.7 Cu, 3.2 Zn, 30.8 Fe, 35.6 S, 2.6 SiO ₂	139 ± 3	140.2	141.0	140.5, 143.5	
CZN-1 Zinc concentrate	44.7 Zn, 7.5 Pb, 10.9 Fe, 30.2 S, 1.0 SiO ₂	93 ± 2	94.7	94.9	94.3, 94.1	
SU-1a Nickel-copper- cobalt ore	~20 Fe, ~10 S, ~38 SiO ₂ , 1.3 Ni, 1.2 Cu, 5.0 Al	4.3 ± 0.3	4.6	—	4.7, 4.8	
PTC-1 Noble metal-bearing sulphide concentrate	5.2 Cu, 9.4 Ni, 26.9 Fe, 23.5 S	5.8 ± 0.4	5.9	—	6.0, 5.9	
PTM-1 Noble metal-bearing nickel-copper matte	30.2 Cu, 44.8 Ni, 1.6 Fe, 21.6 S	66 ± 7	75.0	75.4	75.0, 74.3	
MP-1 Zinc-tin-copper- lead ore	15.9 Zn, 1.9 Pb, 5.7 Fe, 11.8 S, 19.4 Si, 3.6 Al, 3.4 Ca, 2.1 Cu, 0.8 As, 2.4 Sn	57.9 ± 2.2	59.3	60.5	60.1, 60.7, 60.8	
MP-1a Zinc-tin-copper- lead ore	19.0 Zn, 4.3 Pb, 6.2 Fe, 12.8 S, 19.4 Si, 5.2 Al, 1.4 Cu, 2.1 Ca, 1.3 Sn, 0.8 As	69.7 ± 2.2	67.5	70.2	71.3, 69.4	

*Mean values obtained previously.¹†Mean values obtained previously.²

‡Except for MP-1 (0.3 g) and MP-1a and CCU-1 (0.5 g), the remainder of the results shown were obtained with 1-g subsamples.

silver bromide-TBA complex is considerably more soluble in MIBK than in chloroform, and up to 500 μg of silver can be extracted essentially quantitatively (99.5%) in one extraction.

Although the possibility of determining silver directly in the extract by AAS was mentioned in the earlier work,¹ this was not investigated at the time because it was considered that aqueous calibration solutions are easier to prepare and more convenient to use for routine work. In the present work, tests made with synthetic zinc process solutions (composition given in Table 1) to determine whether this approach would be more feasible for solutions of low silver content yielded poor precision and low results. Probably, this negative error was caused by the greater viscosity of the extracts⁴ derived from the synthetic solutions, from which cadmium was co-extracted, compared with calibration extracts prepared by extracting known amounts of silver under the same conditions but in the absence of matrix elements.

The proposed method is suitable for silver in ores and related materials at levels as low as $\sim 0.1 \mu\text{g/g}$ and in zinc process solutions down to the $\sim 0.004 \mu\text{g/ml}$ level. It is emphasized that reliable results can only be obtained if a small amount of potassium is added to the final solution before it is evaporated to dryness in the presence of perchloric acid. Care should also be taken that the subsample used does not contain more than 10 mg of calcium. If TBA is not available, tri-n-octylamine can probably be used instead under essentially the same conditions.⁴

REFERENCES

1. E. M. Donaldson, *Talanta*, 1982, **29**, 1069.
2. E. M. Donaldson, E. Mark and M. Leaver, *ibid.*, 1984, **31**, 89.
3. G. H. Morrison and H. Freiser, *Solvent Extraction in Analytical Chemistry*, p. 150. Wiley, New York, 1957.
4. B. Ya. Spivakov, V. I. Lebedev, V. M. Shkinev, N. P. Krivenkova, T. S. Plotnikova, I. P. Kharlamov and Yu. A. Zolotov, *Zh. Analit. Khim.*, 1976, **31**, 757.
5. E. M. Donaldson, *Talanta*, 1980, **27**, 779.

SOLVENT EXTRACTION-ELECTROTHERMAL ATOMIC-ABSORPTION ANALYSIS

A. B. VOLYNSKY, B. YA. SPIVAKOV and YU. A. ZOLOTOV
V.I. Vernadsky Institute of Geochemistry and Analytical Chemistry,
Academy of Sciences of the U.S.S.R., Moscow, U.S.S.R.

(Received 29 September 1983. Accepted 19 December 1983)

Summary—The review discusses the problems of rational combination of solvent-extraction separation and preconcentration of trace elements with their determination by electrothermal atomic-absorption spectrometry.

Atomic-absorption spectrometry (AAS) is currently one of the most widely used techniques in analytical chemistry. The high selectivity and sensitivity of this technique in many cases enable direct analysis of samples. However, when the elements to be determined are present in very small amounts in materials of complex composition, preconcentration is necessary. Liquid-liquid extraction is a very versatile and convenient method of obtaining both separation and preconcentration.

The reason for the wide use of extraction in combination with flame AAS is the improvement in sensitivity arising partly from the increased element concentration but partly because nebulization of organic solvents can produce a more finely-dispersed aerosol.¹ With electrothermal atomization (ETA), however, the use of organic extracts instead of aqueous solutions does not, as a rule, enhance the atomic-absorption signal. Nevertheless, the tendency nowadays is an increasing use of hybrid methods based on combinations of element extraction and ETA, thanks mostly to the higher sensitivity of the determination method itself.

It has been suggested² that in the analysis of extracts ETA should have a number of advantages over flame atomization. Those authors believed that the absence of a nebulizer would permit viscous extracts to be analysed and that the complete removal of organic solvents from the electrothermal atomizer by drying would eliminate the non-specific light absorption during the atomization step, as well as the effect of solvent on the AA-signal amplitude. It has also been suggested that non-flammable chlorine-containing solvents can then be included in the range of extractants suitable for use in atomic-absorption analysis.¹

Later investigations have shown, however, that the nature of the organic solvent has a strong effect on the AA-signal amplitude. Soaking of the extract into the graphite or its spread over the atomizer surface, the volatility of certain extracted compounds at elevated temperatures, and other factors may also

hinder the combination of extraction with ETA-AAS. The literature data concerning the behaviour of organic extracts in ETA are largely contradictory. One of the reasons for this is the considerable sensitivity of the extracts (compared to aqueous solutions) to atomizer parameters (geometry and material),³ shield-gas composition and the method used for recording the AA-signal.

It should be noted that some of the AAS techniques involving extraction of the determinand elements from the matrix have become obsolete, since they were originally adapted to the first ETA models which were not as perfect as the modern ones. Improved ETA characteristics also considerably improve the sensitivity of extract analysis.⁴

To date there has been only one review published which deals with certain aspects of the effect of the nature of the extracted complex on elemental analysis by ETA-AAS.⁵ The effect of the nature of the organic solvent on the AA-signal amplitude in ETA has been studied in work devoted specifically to the analysis of petroleum products by ETA-AAS.⁶

In this paper we consider the most important aspects of the analysis of organic extracts by ETA-AAS.

EFFECT OF ORGANIC SOLVENT

Extract sampling and behaviour on the atomizer surface

Analysis by ETA is accompanied by a number of effects that are common to all organic extracts and are due to their good wetting ability with respect to graphite, plastics and metals.

The wetting of plastic micropipette tips with the extracts results in a sampling error of as much as 7% (compared to 1.5% with aqueous solutions).⁷ The amount of extract remaining in the tip may depend largely on the reactant concentration and be as high as 30% of the total amount added.⁸ Extract-sampling reproducibility may be improved if the micropipette tip is made to touch the atomizer surface. This can

be done by enlarging the sampling orifice,⁹ using a bent tip¹⁰ or a graphite platform. An alternative is to wash the tip with acetone or chloroform and add the washings as well.¹¹

The reliability of extract analysis may be improved by automatic sampling. For instance, the Perkin-Elmer AS-1 autosampler ensures a sampling reproducibility of better than 1%.¹² The capillary of the autosampler can be treated with an organofluorine compound which will decrease wetting of the capillary by the organic extract and thereby improve the sampling reproducibility.¹³

When automatic sampling is used, the recommended practice is to use organic solvents that are denser than water; to prevent evaporation, the extracts may then be covered with a supernatant layer of water¹⁴ or the aqueous phase.¹² For solvents less dense than water it is recommended to alternate the sample extracts in the autosampler with extracts containing reference amounts of the determinand elements, which allows corrections to be made for concentration variations due to solvent evaporation.¹⁵

The good wetting of graphite by organic solvents promotes its penetration by the extracts. Partial penetration, observed even in analysis of aqueous solutions^{16,17} may give rise to signals of complicated shape. To prevent this undesirable effect, organic extracts¹⁸ and petroleum products¹⁷ can be added to the electrothermal atomizer heated to the "drying" temperature, and this will also prevent sample from spreading over the atomizer surface.¹⁹

In some cases, however, the spread of extracts over the atomizer surface may somewhat improve the sensitivity. It has been shown^{20,21} that by starting the temperature control programme 2.5 min after addition of the extract to the ETA (HGA-2000) and using temperatures below the solvent (methyl isobutyl ketone; MIBK) boiling point for slow drying, a better spread of the extract may be achieved. In this way the signals of Ni, Co and Cd extracted as their pyrrolidine dithiocarbamates (PDTC) are enhanced by a factor of 1.2–2.

As a rule, however, the spreading of extracts on the atomizer surface hampers analysis, distorts the AA-signals, renders the analytical curve non-linear²² and decreases the sensitivity.²³ Owing to the tendency of extracts to spread, their analysis is affected to a greater extent than that of aqueous solutions by the presence of a temperature gradient along the heated graphite tube (GT).^{24,25}

It appears to have been sample-spreading that was responsible for the considerably poorer precision reported for analysis of extracts (than for analysis of aqueous solutions)^{26–28} (in this work the first commercial ETA models, the HGA-70 and HGA-2000, were mostly used). It was found possible to improve the precision considerably by using a "grooved" GT allowing localization of the sample in the central part of the tube.²⁶ For example, the relative standard deviation for 0.1- $\mu\text{g/ml}$ copper in MIBK extracts was

2% for the "grooved" GT (HGA-70) but 10% for the standard GT.²⁷ It has also been proposed to use a graphite boat or a tantalum cup for localizing the sample in the central part of the electrothermal atomizer^{7,29} or to restrict the volume of solvent fed into the ETA.^{30,31}

Normally, the use of a GT with a coating to prevent the penetration but not the spreading of the extract does not allow a high precision to be obtained. For example, covering a GT with tantalum foil to improve the sensitivity of barium determination³² resulted in an increase of the relative standard deviation from 3% for aqueous solutions to 8% for MIBK extracts of barium thenoyltrifluoroacetate, and this was attributed primarily to the spreading of the extract over the atomizer (HGA-70) surface. Similar effects have been observed for a GT with a pyrolytic coating.³³ For example, the relative standard deviation in the determination of lead and cadmium extracted as diethyldithiocarbamates (DDTC) into carbon tetrachloride is 14%, compared to 3% when a porous graphite tube is used.³⁴

Hence, the suggestion that the deterioration of the precision of extract analysis by ETA-AAS is due to soaking into the graphite³⁵ and that it may be prevented by using a pyrographite-coated GT (reference 1, p. 30), is not necessarily correct. That the pyro-coated GT can successfully be used for analysis of extracts has been attributed primarily to localization of the sample at the centre of the atomizer.³⁶

Attempts have been made to establish a correlation between the precision of the analysis of extracts and the physical properties of the analysis solution (surface tension, viscosity, density).^{37,38} For example, Young and Baldwin,³⁹ for the determination of cobalt by AAS after extraction of the PDTC complex, tried several solvents (benzene, chloroform, carbon tetrachloride, MIBK, ethyl acetate) and selected the last because it had the lowest surface tension. However, the advantages offered by solvents selected on the basis of the surface tension criterion have not been discussed in this work.

By use of modern ETA apparatus having a small geometrical size and furrows for sample localization, it has been possible to reduce considerably the adverse effect of sample spreading. Thus with the HGA-70 the relationships between the absorbance and extract volume fed into the atomizer are linear up to a sample volume of 10 μl ,³¹ and for the HGA-74 up to 50 μl .⁴⁰ The precision of extract analysis with modern ETA equipment is largely determined by sampling precision,¹² the chemical composition of the solvent and the extracted complex,⁴¹ and may be as good as that of AAS analysis of aqueous solutions.⁴²

Chemical and spectral interferences

Recently more and more evidence has been gathered that confirms the strong effect of the nature of the organic solvent on ETA analysis. With a few exceptions the mechanism of the effect is not yet

clear, so generalized recommendations for use of one or another solvent in ETA methods have been rare and contradictory. For instance, Dornemann and Kleist⁴³ hold MIBK to be an unsuitable solvent for ETA-AAS, whereas Fuller²⁴ recommends the use of xylene and MIBK as solvents for organometallic compounds, and Elson and Albuquerque⁴⁴ regard MIBK as having good compatibility with ETA.

Determination of elements in the presence of halogen-containing solvents may involve considerable difficulties. Even in one of the first works on extract analysis by ETA² it was reported that the use of chloroform and carbon tetrachloride was apparently responsible for the poor sensitivity of determination of a number of elements and made the charring step necessary. The adverse effect of halogen-containing solvents on the determination of Pb,³¹ Cd,⁴ Ge,⁴⁵ Co,⁴⁶ Fe,⁴⁷ Ga and In,⁴⁸⁻⁵² Cd, Fe, Ag, Ni and Co,³ Be⁵³ and Sn⁵⁴ has also been shown experimentally.

The depressive influence of solvents such as chloroform, di(2-chloroethyl) ether (DCEE) or carbon tetrachloride may be quite considerable. This can be seen from determination characteristics of gallium and indium oxinates in MIBK and chloroform medium, and of their halide complexes in MIBK and DCEE.⁵² The suppression and distortion of the AA-signals in the presence of halogen-containing solvents⁴⁷ are usually attributed to formation of the thermally stable and volatile halides which are partially carried away from the electrothermal analyser, undissociated. The formation of halides is promoted by the existence of halogen compounds with graphite of the type $C_n^+X^- \cdot 3X_2$ that are stable at temperatures of up to 2000°.⁵⁵ It should be noted, however, that AA-signal suppression in the presence of carbon tetrachloride has also been observed when a tungsten atomizer was used.⁴⁵

Volland *et al.*³ assume that the depressive effect of halogen-containing solvents on AA-signals may be due to the formation of volatile organometallic compounds such as CF_3ZnI . Using radioactive isotopes, they have shown for Fe and Co that the presence of chloroform lowers the temperature at which these elements begin to be lost, the loss being proportional to the duration of the charring step.

In some cases the depressive effect of chlorine-containing solvents can be eliminated by introducing ascorbic acid into the ETA, especially when a furnace-platform atomizer is used.⁵² Table 1 gives the signals obtained in the analysis of gallium and indium extracts in an HGA-74 atomizer in which graphite disks, 4 mm in diameter, 1.25 mm thick and having a 1-mm deep groove, were used as the platform. For chloroform extracts, the combination of a platform and ascorbic acid greatly enhances the signal (76-fold for indium acetylacetonate).⁵² Attempts to eliminate the depressive influence of chloroform on the AA-signals of Cd and Fe by feeding mineral acids and hydrogen peroxide into the graphite-tube furnace³ were unsuccessful.

Determination of tin in the presence of chlorine-containing solvents ($CHCl_3$, CCl_4) is accompanied by the appearance of a maximum on the signal *vs.* charring-temperature curve (the charring curve).⁵⁴ The sensitivity may be improved if the charring step is continued for a period of 40–60 sec, but in view of the maximum, control is necessary to maintain the charring temperature (T_{char}) at the optimum level. If a 5% aqueous ascorbic acid solution is added to the atomizer (HGA-76B) before the analysis a plateau is obtained on the charring curve; the charring step may be shortened to 10 sec and the sensitivity for tin improved.

In analysis of carbon tetrachloride extracts containing cobalt-DDTC the AA-signal is not only strongly suppressed but also shifted to a temperature 300° higher.⁴⁶ These authors believe that this shift can, in part, be attributed to modification of the properties of graphite by the chlorine that is formed on decomposition of carbon tetrachloride. For example, the penetrability of graphite increases, enhancing the diffusion of cobalt compounds into its bulk. These effects disappear when a tantalum boat, which precludes interaction between carbon tetrachloride and the graphite, is used. The degree of interference can also be reduced by adding water together with the chlorine-containing solvents, to the graphite atomizer.^{46,47} On heating, the water reacts with the graphite to form hydrogen, which combines with the chlorine to give hydrogen chloride, which is carried away from the GT during the charring treatment. Hydrogen can

Table 1. Effect of ascorbic acid (asc) on the AA-signal for indium and gallium (0.1 and 0.08 $\mu\text{g/ml}$, respectively) in extracts and aqueous solutions; atomization from the GT wall (A_w) and disk (A_d)

Solution or extract	In			Ga		
	A_w	A_d	A_d , asc	A_w	A_d	A_d , asc
0.1M HNO ₃	0.101	0.177	0.127	0.154	0.209	0.276
0.1M HCl	0.026	0.072	0.212	0.064	0.105	0.264
0.1M HBr	0.022	0.085	0.205	0.057	0.094	0.213
Chloride complex in MIBK	0.032	0.130	0.221	0.061	0.138	0.271
Chloride complex in DCEE	—	—	—	0.012	0.109	0.224
Bromide complex in MIBK	0.025	0.072	0.126	0.045	0.130	—
Oxinate in MIBK	0.075	0.094	0.107	0.070	0.132	0.247
Oxinate in CHCl ₃	0.008	0.021	0.310	0.006	0.071	0.228

also be formed in ETA through thermal decomposition of hydrocarbons.⁴⁶ To eliminate chlorine interference in determination of lead, Frech and Cedergren⁵⁶ added hydrogen to the shield gas.

However, in the case of certain elements, *viz.* copper,^{38,57} gold and palladium⁵⁸ and selenium,⁵⁹ chlorine-containing solvents tend to increase the AA-signal. Absence of any depressive effect of chloroform and carbon tetrachloride on the signals of Fe, Cd, Cu, Ni, V, Pb has been recorded.^{31,38}

Solvents of other types generally have less effect than the halogen-containing compounds on ETA-AAS determinations, but the effects do not, as a rule, lend themselves to any reasonable explanation.³ It is not yet clear why for the chloride and bromide complexes of indium and gallium the sensitivity follows the order MIBK > butyl acetate (BAC) ≥ amyl acetate (AAC), whereas for indium iodide it is BAC = AAC > MIBK.^{49,50} It has been found⁵³ that the signals obtained for beryllium in organic solvents decrease in the order aromatic hydrocarbons > esters = alcohols ≥ MIBK > chlorine-containing hydrocarbons; the order is practically the same for the *N*-cinnamoyl-*N*-phenylhydroxylamine and acetylacetone complexes.

We have found⁵⁴ that in analysis of extracts containing tin oxinate in chloroform, tin losses occur at $T_{\text{char}} > 500^\circ$, and for extracts in *o*-xylene at $T_{\text{char}} > 800^\circ$. Also, the dependence of the AA-signal on the ETA heating rate during charring is considerably decreased when *o*-xylene is used. Kamada *et al.*⁵⁹ believe that selenium diethyldithiocarbamate can be sublimed along with MIBK during charring. To improve the sensitivity for selenium they proposed use of carbon tetrachloride as the organic solvent.

In recent years, more and more attention has been given to investigation of non-specific light-absorption caused at the atomization stage by residues of an organic solvent.^{49,50,58,60} Until recently it was common to believe that no such problem existed at all, since the organic solvents used for extraction usually have relatively low boiling points and hence should be completely removed from the electrothermal atomizer during drying of the extract. Nevertheless, investigations of the relationship between non-specific light-absorption and wavelength in the region of 200–350 nm for a number of organic solvents have shown⁶¹ that even after charring (at 800° for 30 sec) the non-specific absorption occurring during the atomization step may not be always compensated by the deuterium background-corrector. The non-specific absorption was particularly intense in the presence of cyclohexane. However, cyclohexane does not cause non-specific light absorption at wavelengths shorter than 200 nm in ETA.⁶²

The extent of non-specific absorption in the presence of organic solvent residues may also depend on the material the atomizer is made from. We have found that with a GT coated with a layer of pyrolytic graphite, a non-specific absorption is observed in the

presence of *o*-xylene at the tin resonance-line wavelength (224.6 nm), which could not be compensated for by the deuterium background corrector ($T_{\text{char}} = 800^\circ$, for 40 sec). On the other hand, no difficulties of this kind arise in analysis of *o*-xylene tin extracts when a porous graphite tube is used.

EFFECT OF THE NATURE OF THE EXTRACTED COMPLEX

Volatility and thermal stability of compounds in ETA

It is well known that many chelates, halides and some other metal compounds can be sublimed undecomposed (*e.g.*, Sokolov⁶³). Aggett and West,² who were apparently the first to observe the effect of organic reagents on sensitivity, assumed that it was due to the incomplete atomization of chelates which underwent sublimation. They hypothesized that interferences of this kind would result in particular difficulties in analysis of extracts by use of ETA systems. This opinion is currently advocated by Sturgeon *et al.*⁶⁴ Pelosi and Attolini⁴⁸ preferred cupferron as an extracting reagent for gallium because its chelates are non-volatile.

There have been only a few cases, however, where this effect has been experimentally observed. Keil⁶⁵ believes that the partial sublimation of chelates during the charring step is responsible for the low sensitivity and poor precision of thallium determination in MIBK extracts of its DDTC complex. Kamada *et al.*⁵⁹ who observed that the sensitivity for selenium was higher for the diethyldithiocarbamate than the pyrrolidine dithiocarbamate (solvent MIBK), assumed that the latter complex has a higher volatility. According to our results,⁵⁴ certain tin chelates (the diethyldithiocarbamate and oxinate) can undergo sublimation when their extracts are analysed with the HGA-76B. This both lowers the sensitivity and tends to decrease the maximum T_{char} from the 800° permissible for aqueous solutions and extracts containing chloride complexes and non-volatile tin chelates (cupferronate, *N*-benzoyl-*N*-phenylhydroxylamine) to 500° for the oxinate and 700° for the diethyldithiocarbamate (solvent chloroform).

It is really difficult to analyse extracts in which the elements to be determined are present as iodide complexes. For example, Clark and Viets⁶⁶ found that of 18 elements (including In, Sn, Pb, As, Sb, Bi, Se) extracted as iodide-complexes by means of amine solutions in MIBK, only Pt and Pd could be determined by direct ETA analysis. In view of the high volatility of metal iodides, it has been recommended to use stripping when working with this kind of extraction system.^{66,67} Aruscavage,⁹ however, was able to analyse directly a toluene solution of the As, Se and Sb iodide complexes by using nickel nitrate as a matrix modifier for the determination of As and Se. The iodide system (with amyl or butyl acetate as extractant) has been recommended⁵⁰ for the extrac-

tion and AAS determination (HGA-74) of indium, since the sensitivity is higher and the extraction is quantitative over a broader acid concentration range for the iodide complexes than for the chloride and bromide systems. There are reports of the possibility of direct determination of Sn,⁶⁸ Pb,⁶⁹ Bi,^{70,71} and Se⁷² in iodide extracts.

Data about the volatility of compounds of other classes have been published. It has been shown⁷³ that the drying temperature should not be higher than 40° for isoamyl alcohol extracts of the platinum–tin(II) chloride complex. Startseva *et al.*⁷⁴ believed that it was high volatility which prevented direct determination of molybdenum in phosphomolybdic acid (MPA) extracted into a 1:3 mixture of *n*-butanol and carbon tetrachloride; they were compelled to strip the molybdenum. On the other hand, Tyson and Stewart⁷⁵ could directly analyse an MPA extract by use of the A3700 atomizer (graphite rod); perhaps the analysis was facilitated because they used a different solvent (isobutyl acetate).

To improve the sensitivity of tin determination by means of its volatile chelates we used slow heating during the charring step, to cause thermal decomposition of the complexes.⁵⁴ For example, when we changed the heating rate from 600°/sec to 8°/sec (heating-rate selector of the HGA-76B changed from zero to the 2 × 30 setting), the magnitude of the AA-signal of tin (oxinate in chloroform) increased 2.8 times ($T_{\text{char}} = 900^\circ$). Considerable improvement in sensitivity was also achieved by adding ascorbic acid. In the analysis of aqueous solutions of tin or of MIBK extracts containing its chloride complexes or non-volatile chelates the addition of aqueous ascorbic acid to the GT enhanced the signal by as little as 20–30%, whereas in the case of volatile chelates (oxinate, diethyldithiocarbamate) the signal was enhanced 2.0–2.8 times.⁵⁴ The sensitivity for tin may be further improved by using a tungsten carbide-coated GT and a graphite platform.

Cases have been reported in which chelate volatility did not have any significant effect on extract analysis with ETA. It has been shown⁷⁶ that the sensitivities and charring curve shapes obtained for analysis (with the HGA-74) of extracts containing different cobalt chelates do not differ much. On the other hand, a correlation has been observed between the cobalt chelate volatility and the magnitude of the AA-signal when a tantalum boat is used for flame atomization. According to Borggaard *et al.*,¹³ cobalt diethyldithiocarbamate (solvent xylene) is not sublimed during the charring step, over a temperature range of 175–1100°, although according to thermal data this chelate should sublime at 267°.

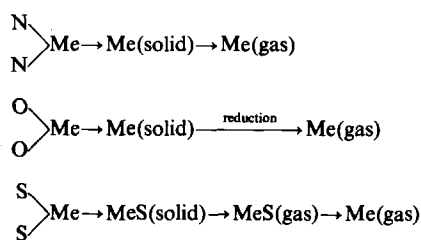
By extraction of its dithizonate into chloroform Halász *et al.*⁷⁷ were able to make mercury much less volatile than it is in the form of inorganic compounds. Extraction in this case not only separated the determinand from the matrix but also prevented its loss during the drying step.

Also important in ETA–AAS are the thermal stability and volatility of the molecules formed in thermal destruction of the compounds containing the analyte elements. The lower permissible T_{char} and sensitivity for lead and cadmium determination when extracts of the PDTC complexes were used instead of aqueous solutions was attributed³¹ to the formation of the volatile sulphides CdS and PbS by thermal decomposition of the chelates in the inert atmosphere used (argon). If an oxidizing atmosphere is used during the charring step, the less volatile oxides and oxysulphides are formed, and the lead signals for extracts and aqueous solutions are similar. The low sensitivity of tin determination in DDTC extracts and in the presence of a number of sulphur-containing substances (sulphuric acid, cysteine) is also attributed to the formation of the thermally stable and volatile monosulphide.⁷⁸

Halide ions tend to interfere with the determination of gallium and indium in aqueous solutions and extracts containing halide complexes of these elements.^{49,50} With a view to finding the reasons for such effects, the absorption spectra of the GaO, GaX, InO, InX (X = Cl, Br) molecules formed in the graphite atomizer during the charring and atomization of halide aqueous solutions and MIBK based extracts, were recorded.⁵¹ It has been shown that the higher the halide ion concentration in the analysis solution the greater is the ratio MeX/MeO (Me = In, Ga). Since the dissociation energy of MeO is lower than that of MeX, the formation of the monohalides is liable to decrease the sensitivity. The reduction of the gallium signal in the order oxinate > dichloro-oxinate > dibromo-oxinate (extraction with 0.02M reagent solutions in *o*-xylene) is also apparently due to the formation of the monohalides. The signal for the dichloro-oxinate is also lower than that for the oxinate (solvent toluene) for beryllium.⁵³

Dependence of the atomization mechanism on the nature of the donor atom

The composition of the extractable complex may have a strong effect on the atomization mechanism. Hulanicki *et al.*⁷ have investigated the mechanisms of atomization of copper and nickel, using a broad range of reagents. For chelates containing the same donor atoms the log *A* vs. 1/*T* relationships have practically the same slopes. On these grounds the following atomization mechanisms were proposed for complexes with nitrogen, oxygen and sulphur as donor atoms:



The AA-signal magnitude has also been compared with the bond type in the complex by Komárek *et al.*⁷⁶

The number as well as the nature of the atoms that directly react with the metal in the chelate is important. Atomization of cobalt from an hydrochloric acid solution and from a solution of cobalt-DDTC in MIBK follows, apparently, the same mechanism.⁴⁶ However, if an aqueous solution of cobalt is analysed with a graphite tube which has been impregnated with carbon disulphide, the atomization activation energy is increased by an amount about equal to the heat of formation of cobalt sulphide. The effect of the sulphur-containing reagent concentration on arsenic determination in a molybdenum microtube has been reported.⁷⁹ Signals of different shape were obtained for two chelates containing As-S bonds (diethyldithiocarbamate and thionalide complexes). The authors attributed this to the different solubilities of the reagents in organic solvents: the readily soluble thionalide creates an excess of sulphur in the ETA, and this tends to change the atomization mechanism.

When lead was determined in aqueous solutions and organic extracts (with ETA as a molybdenum microtube) it was found that for naphthenate, oxinate and diethyldithiocarbamate the AA-signal was maximal at a lower atomization temperature than for inorganic compounds of lead.⁸⁰ In this case the sensitivity for the oxinate and DDTC was better than for chloride or nitrate solutions of lead. The authors assumed that decomposition of these chelates produced free metal rather than its oxide.

Ishizaki and Ueno⁸¹ advanced a hypothesis that the size of the chelate had a strong effect on ETA analysis of extracts. The larger the molecular volume of the organic reagent used, the less the chelate will soak into the graphite, and therefore the higher the AAS sensitivity. However, in later work^{53,82} this hypothesis was not verified experimentally.

Non-specific light absorption

Incomplete removal of organic materials during the charring step may cause considerable difficulties in the ETA analysis of extracts. Charring conditions have been found for extracts of different nature, under which there is no non-specific light-absorption at the analytical lines of gallium (287.4 nm) and indium (303.9 nm) during the atomization step,^{49,50} but when such poorly volatile extractants as tributyl phosphate (TBP) and trioctylamine were used, an extra (initial) charring cycle (500° for 45–90 sec) was necessary to remove the bulk of the extractant. Nevertheless, the temperatures for the second charring cycle had to be 1400° and 1050°, respectively.

There is evidence that whatever its original form in the solution (TBP included) phosphorus cannot be carried away from the ETA at a temperature <800°. Fishkova *et al.*⁶² were unable to detect selenium after its extraction as 4,5-benzopiazselenol into TBP, even though the deuterium corrector was

used. Probably, the reason was that even at relatively high atomization temperatures much of the phosphorus is transferred into the gas phase in the form of species (P₂, PO, PO₂, *etc.*)⁸⁴ which result in a structured background. The sensitivity of ETA-AAS determination of elements in TBP-based extracts is usually significantly poorer than that in aqueous solution.^{49,50,85} Therefore, the use of organophosphorus compounds for the extraction of elements of high and medium volatility that are to be determined by the ETAA technique is attended by apparent hindrances.

A structured background which hampers analysis also appears in the determination of arsenic in dialkyltin dinitrate extracts.⁸⁶ Matrix modification with nickel nitrate allows T_{char} to be increased to 800°; at this temperature all the organic components of the extracts are totally decomposed, but significant amounts of tin remain in the graphite tube, and also hamper the AA analysis. The non-specific absorption at the analytical line of arsenic (193.7 nm) may be reduced to a level that can be compensated for by the deuterium background-corrector only by using a graphite platform and modification of the sample with nickel nitrate.

Saturated solutions of ammonium pyrrolidine dithiocarbamate and hexamethyleneammonium hexamethylenedithiocarbamate in MIBK cause an insignificant background absorption in ETA-AAS over the wavelength range 200–300 nm.⁶¹ However, during storage of PDTC solutions, products are formed that give rise to non-specific light-absorption that cannot be fully counterbalanced by the deuterium corrector. Therefore, only fresh PDTC solutions should be used for extraction/atomic-absorption analysis. Non-specific absorption by organic reactants may also increase with aging of the graphite tube.⁵⁸

COMPARISON OF SENSITIVITIES FOR AQUEOUS SOLUTIONS AND ORGANIC EXTRACTS

Fuller²⁴ (p. 48) states that during extract analysis by ETA most complexes decompose into stable inorganic compounds in the charring step, which ensures about the same sensitivity as in analysis of aqueous solutions. He determined Fe, Ni, Co and Cu in extracts containing the DDTC complexes of these elements or their complexes with 4,7-diphenyl-1,10-phenanthroline (solvent MIBK), using aqueous standard solutions (HGA-70, grooved graphite tube).^{87,88} Calibration with aqueous solution standards, which possess some advantages over extracts (longer shelf-life, ease of preparation), has also been used in others.^{2,10,11,89,90}

Several papers have reported that ETA-AAS sensitivity is better for extracts than for aqueous solutions.^{41,80,91–96} Most of these investigations used a metal tube (molybdenum or tungsten) for the ETA;

perhaps in these cases the better sensitivity was due to the construction of the atomizer structure, and was not in fact higher for all the extracts investigated.

Bratzel *et al.*⁹¹ obtained interesting results when they determined gold and silver in geological and metallurgical samples (with a CRA-61). The analyte elements were first extracted into MIBK as their chloride and thiophosphoric acid tri-iso-octyl ester complexes respectively. It was found that the characteristic gold concentration (*i.e.*, the concentration giving 1% absorption) is three times as large for aqueous solutions as for extracts; for silver the characteristic concentrations were the same. Exposure of the atomizer to a diffusion hydrogen flame did not affect the sensitivity for silver in aqueous solutions, whereas in the case of extracts the characteristic concentration decreased by as much as three orders of magnitude. The authors assumed that under these conditions direct atomization of silver occurred as its complex burned.

Very often the literature contains contradictory data about sensitivity of analysis of extracts by ETA-AAS. For determination of tin in aqueous, water-ethanol and heptane solutions with an HGA-2100, Trachman *et al.*⁹⁷ obtained almost the same sensitivity with all the solutions investigated, whereas Varnes and Gaylor⁹⁸ found AA-signals for aqueous and water-alcohol solutions were about the same, but half the size for 3% acetic acid media and only a sixth as large for heptane solutions.

All in all, the problem of the relative sensitivities for analysis of aqueous solutions and organic extracts by ETA has not yet been thoroughly studied. Comparison of our results with others allows us to conclude that in most cases the sensitivity is somewhat poorer for organic extracts than for aqueous solutions, and that this is due to various combinations of the causes we have already discussed, *viz.* spreading of the extract on the ETA surface, volatility of the extracted compound, effects of the nature of solvent and organic reagent, *etc.*

SOME OTHER FEATURES OF EXTRACT ANALYSIS

In a number of cases it is very difficult to differentiate between the effects of organic solvent, of the form of the element in the extract, of the atomizer material and geometry, and other factors, on the ETA analysis of extracts. We will now consider the combined effects of these factors.

The products of incomplete combustion of the organic matrix may strongly affect the ETA analysis. Margulis *et al.*⁹⁹ attempted to determine platinum and palladium in the third phase formed in the hexadiantipyrylmethane-chloroform (benzene) system with the hope of increasing the preconcentration factor by 1–2 orders of magnitude. They diluted the viscous third phase with ethanol and applied it to the GT. However, after evaporation of the solvent an

organic residue remained in the GT which was hard to decompose and therefore hampered the AA analysis. For more complete destruction of the organic matrix during determination of ruthenium in extracts, Dornemann and Kleist¹⁰⁰ blew air through the HGA-500 used, during the charring step.

The same authors assume that in ETA, MIBK shows a tendency towards polymerization and coking, which affects the atomization reproducibility, especially in the case of highly volatile elements;⁴³ they propose use of a 7:3 v/v di-isopropyl ketone/xylene mixture (instead of MIBK), which is completely evaporated when the electrothermal atomizer is heated. The lower sensitivity for vanadium when extracts of certain of its chelate and thiocyanate complexes are subjected to charring in a tungsten atomizer has been attributed to the formation of vanadium carbide through reaction of the element with the organic matrix residue.⁹⁵

There is evidence concerning a positive effect of the carbon that is formed on decomposition of the extract in the atomization process. Thus it has been suggested⁷⁶ that in analysis of cobalt extracts CoO is more effectively reduced to the metal in this way, and for this reason the sensitivity is higher for determination of cobalt in extracts than in an aqueous solution of cobalt acetate.

Data concerning the effect of organic extracts on the lifetime of the graphite tube are scarce and contradictory.^{61,101,102}

ADDITIONAL TREATMENT OF EXTRACTS

When the extraction system used is insufficiently selective, the co-extracted components may give rise to considerable non-specific light-absorption¹⁰³ or suppress the analytical signal,³⁷ for equal interferent concentrations these effects may be larger for extracts than for aqueous solutions.¹⁰⁴ Also, the preconcentration achieved by extraction may fall short of meeting detection limit requirements.^{105,106} Therefore, various treatments are resorted to in extraction/atomic-absorption analysis, apart from optimization of the AAS conditions, use of more powerful and selective extraction systems,¹⁰⁷ or the analyte-addition technique.²⁶

Modification of matrix

This approach has become rather commonly used owing to the small labour requirement and the possibility of using the same modifiers as those used in analysis of aqueous solutions. The use of transition metal compounds for increasing T_{char} and improving the sensitivity of determination of selenium, arsenic and antimony^{9,72,86,108–111} is a typical example. For example, the analysis element (selenium) and the modifying element (copper) are extracted simultaneously as the DDTC and PDTC complexes.^{112,113}

After extraction of the platinum group elements (Me) with a solution of 1,1-hexamethylene-3-phenylthiourea (HMPTU) in chloroform, the presence of a copper/HMPTU complex (Me:Cu = 1:200) in the extract eliminates the considerable mutual effects of the platinum metals themselves.¹¹⁴

To concentrate bismuth for determination in water and urine samples, it can be extracted as the iodide complex into MIBK.⁷¹ By using palladium chloride solution as a modifier it is possible to raise the charring temperature to 1000° and substantially improve the sensitivity of bismuth determination in the extract. It was mentioned that there should be physical contact between the analyte and the solution of the modifier element (100 μ l of aqueous palladium chloride were added to 20 μ l of the extract).

Selenium losses during charring following the extraction of its compound with 1,2-diamino-4-nitrobenzene into chloroform were prevented by using a GT coated with zirconium carbide.⁹⁶

Apart from transition element compounds, organic and inorganic acids, chelating agents, *etc.* may be used as matrix modifiers. We have discussed above the effect of ascorbic acid on aqueous solutions and extracts containing In, Ga and Sn.^{52,54} When analysing extracts and aqueous solutions of Pb, Bi, As, Sb with a metallic electrothermal analyser, Ohta and Suzuki^{70,79,94,115} were able to eliminate the interference from the matrix and improve the determination sensitivity, by adding a solution of thiourea.

A sulphuric acid solution was added to the electrothermal atomizer to prevent thallium losses during the charring step, in its determination in aqueous solutions and in toluene extracts containing the ion-association complex of $TlCl_4^-$ and Brilliant Green.⁹⁰ Keil⁶⁵ could determine thallium in extracts containing its DDTC complex in MIBK only after addition of 0.5 ml of 2M nitric acid and 3.5 ml of ethanol to 1 ml of extract. Extract modification has also been used by others.^{72,113,116}

Back-extraction

Such multi-purpose measures as back-extraction of determinand^{74,117} and washing extracts free from interferents^{9,75,99} are often used to improve the quality of the extraction/atomic-absorption determination of elements in ETA-AAS. Back-extraction allows the use of extraction systems that contain the analyte element as a volatile compound,¹¹⁸ use of aqueous standards for calibration, further preconcentration of the element to be determined,^{28,119} and can considerably increase the shelf-life of test solutions.⁶⁴ Fitchett *et al.*¹²⁰ succeeded in separating organic and inorganic arsenic compounds at the back-extraction stage. Various modifiers are used in analysis of back-extracts, to improve the determination sensitivity and eliminate interferences.¹²¹⁻¹²⁴ The drawbacks of methods relying on back-extraction of the analyte elements include more complicated procedures and higher blank corrections.

Increase in preconcentration factor

To obtain a higher concentration of the determinand, such techniques as extract evaporation,^{106,107,125-127} back-extract evaporation,¹²⁸ and a series of successive "extraction-stripping" cycles^{53,129} are used; the preconcentration factor may then be as high as 10⁴.¹⁰⁶

Combined separation methods

Combination of solvent extraction with other separation and concentration methods or combination of two different extraction systems has been used for increasing the selectivity of separation of the elements to be determined. For example, the main interferents (Fe, Cu, *etc.*) have been removed by extraction as cupferronates and the elements to be determined subsequently extracted (nickel as its hexamethylenedithiocarbamate with a mixture of diisopropyl ketone and xylene,¹³⁰ tellurium as its chloride complex,²⁸ and manganese as its cupferronate into MIBK¹³¹).

For its determination in biological samples, selenium has been separated from the matrix with Amberlite IR-120 cation-exchanger and subsequently extraction as selenium dithizonate into carbon tetrachloride, permitted the element to be concentrated.¹¹⁰ Extraction of the platinum elements with a solution of *n*-octylaniline in chloroform has been used for additional concentration after a fire assay with nickel sulphide as the collector.²⁵

Co-precipitation with bismuth and ferric hydroxides was used for separation of chromium in different oxidation states,¹³² before determination of the chromium by ETA the macroelements were separated by extraction of their chloride complexes with a 5% solution of tri-iso-octylamine in *p*-xylene. Combined separation methods based on precipitation (co-precipitation) and solvent extraction have also been described.^{21,133}

CONCLUSION

The combination of liquid-liquid extraction and ETA-AAS is a rather effective and versatile hybrid technique for trace analysis. The difficulties arising in its practical applications are due primarily not to any limitations of the principle of the method but to its being insufficiently developed. The choice of the extraction system with regard to its particular behaviour under the conditions used in ETA, and application of such techniques as modification, atomization from a graphite platform, and variation of the ETA heating rate at all analysis stages, permit the determinations to be carried out with good sensitivity, accuracy and precision.

Acknowledgements—The authors are grateful to Dr. I. Khavezov (Institute of General and Inorganic Chemistry, Bulgarian Academy of Sciences, Sofia, Bulgaria) for discussion of this paper and his valuable advice.

REFERENCES

1. M. S. Cresser, *Solvent Extraction in Flame Spectroscopic Analysis*, Butterworths, London, 1978.
2. J. Aggett and T. S. West, *Anal. Chim. Acta*, 1971, **57**, 15.
3. G. Volland, G. Kölblin, P. Tschöpel and G. Tölg, *Z. Anal. Chem.*, 1977, **284**, 1.
4. K.-R. Sperling, *ibid.*, 1982, **310**, 254.
5. J. Komárek and L. Sommer, *Talanta*, 1982, **29**, 159.
6. V. Sychra, I. Lang and Šebor, *Prog. Anal. Atom. Spectrosc.*, 1981, **4**, 341.
7. R. Karwowska, E. Bulska, K. A. Barakat and A. Hulanicki, *Chem. Anal. (Warsaw)*, 1980, **25**, 1043.
8. E. N. Gil'bert, N. V. Korneva, Zh. O. Badmaeva and I. G. Yudelevich, *Zavodsk. Lab.*, 1979, **45**, 714.
9. P. Aruscavage, *J. Res. U.S. Geol. Surv.*, 1977, **5**, 405.
10. R. A. Barfoot and J. G. Pritchard, *Analyst*, 1980, **105**, 551.
11. N. A. Borshch, Yu. A. Zolotov, L. N. Kolonina, O. M. Petrukhin, V. N. Shevchenko and O. A. Shiryayeva, *Zh. Analit. Khim.*, 1980, **35**, 2369.
12. K.-R. Sperling, *Z. Anal. Chem.*, 1979, **299**, 103.
13. O. K. Borggaard, H. E. M. Christensen, Th. K. Nielsen and M. Willems, *Analyst*, 1982, **107**, 1479.
14. M. Tominaga and Y. Umezaki, *Bunseki Kagaku*, 1979, **28**, 495.
15. B. Pedersen, M. Willems and S. S. Jørgensen, *Analyst*, 1980, **105**, 119.
16. B. V. L'vov, *Atomic Absorption Spectrometric Analysis*, p. 281. Nauka, Moscow, 1966.
17. K. G. Brodie and J. P. Matoušek, *Anal. Chem.*, 1971, **43**, 1557.
18. T. T. Chao, R. F. Sanzalone and A. E. Hubert, *Anal. Chim. Acta*, 1978, **96**, 251.
19. C. W. Fuller, *Atom. Absorpt. Newslett.*, 1973, **12**, 40.
20. M. J. Dudas, *ibid.*, 1974, **13**, 67.
21. *Idem*, *ibid.*, 1974, **13**, 109.
22. T. Inui, N. Fudagawa and A. Kawase, *Z. Anal. Chem.*, 1979, **299**, 190.
23. F. J. Szydlowski and F. R. Vianzon, *Atom. Spectrosc.*, 1980, **1**, 39.
24. C. W. Fuller, *Electrothermal Atomization for Atomic Absorption Spectrometry*, p. 48. Chemical Society, London, 1977.
25. J. Haines, R. V. D. Robert and T. W. Steele, *Report N M34, Mintek*, 1982.
26. R. D. Beaty, *Atom. Absorpt. Newslett.*, 1974, **13**, 38.
27. F. J. Fernandez, *ibid.*, 1972, **11**, 123.
28. G. P. Sighinolfi, M. A. Santos and G. Martinelli, *Talanta*, 1979, **26**, 143.
29. G. D. Renshaw, C. A. Pounds and E. F. Pearson, *Atom. Absorpt. Newslett.*, 1973, **12**, 55.
30. D. A. Segar, *Papers 3rd Intern. Congr. Atom. Absorpt. Atom. Fluoresc. Spectrom.*, Paris, 1971, **2**, 523.
31. S. Gomišček, Z. Lengar, J. Černetič and V. Hudnic, *Anal. Chim. Acta*, 1974, **73**, 97.
32. G. D. Renshaw, *Atom. Absorpt. Newslett.*, 1973, **12**, 158.
33. S. S. Chao and E. E. Pickett, *Anal. Chem.*, 1980, **52**, 335.
34. K. Yasuda, S. Toda, C. Igarashi and S. Tamura, *ibid.*, 1979, **51**, 161.
35. D. C. Manning and F. Fernandez, *Atom. Absorpt. Newslett.*, 1970, **9**, 65.
36. K. Kazuo, *Bunseki Kagaku*, 1980, **29**, T90.
37. D. Clark, R. M. Dagnall and T. S. West, *Anal. Chim. Acta*, 1973, **63**, 11.
38. G. Hall, M. P. Bratzel and C. L. Chakrabarti, *Talanta*, 1973, **20**, 755.
39. C. M. Young and J. M. Baldwin, *Microchem. J.*, 1977, **22**, 489.
40. I. Rubeška, J. Korečková and D. Weiss, *Atom. Absorpt. Newslett.*, 1977, **16**, 1.
41. K. Ohta and M. Suzuki, *Anal. Chim. Acta*, 1975, **77**, 288.
42. M. M. Barbooti and F. Jasim, *Talanta*, 1982, **29**, 107.
43. A. Dornemann and H. Kleist, *Analyst*, 1979, **104**, 1030.
44. C. M. Elson and C. A. R. Albuquerque, *Anal. Chim. Acta*, 1982, **134**, 393.
45. K. Ohta and M. Suzuki, *ibid.*, 1979, **104**, 293.
46. A. Hulanicki, R. Karwowska and J. Sowinski, *Talanta*, 1981, **28**, 455.
47. R. Karwowska, E. Bulska and A. Hulanicki, *ibid.*, 1980, **27**, 397.
48. C. Pelosi and G. Attolini, *Anal. Chim. Acta*, 1976, **84**, 179.
49. L. N. Sukhoveeva, B. Ya. Spivakov, A. V. Karyakin and Yu. A. Zolotov, *Zh. Analit. Khim.*, 1979, **34**, 693.
50. B. Ya. Spivakov, L. N. Sukhoveeva, K. Dittrich, A. V. Karyakin and Yu. A. Zolotov, *ibid.*, 1979, **34**, 1947.
51. K. Dittrich, S. Schneider, B. Ya. Spivakov, L. N. Sukhoveeva and Yu. A. Zolotov, *Spectrochim. Acta*, 1979, **34B**, 257.
52. L. N. Sukhoveeva, G. G. Butrimenko and B. Ya. Spivakov, *Zh. Analit. Khim.*, 1980, **35**, 649.
53. A. T. Pilipenko and A. I. Samchuk, *ibid.*, 1982, **37**, 614.
54. A. B. Volynskii, E. M. Sedykh, B. Ya. Spivakov and Yu. A. Zolotov, *Zh. Analit. Khim.*, 1983, **38**, 435.
55. G. Hennig, *J. Chem. Phys.*, 1952, **20**, 1443.
56. W. Frech and A. Cedergren, *Anal. Chim. Acta*, 1976, **82**, 83.
57. A. Janssen, H. Melchior and D. Scholz, *Z. Anal. Chem.*, 1977, **283**, 1.
58. T. M. Korda, L. V. Zelentsova and I. G. Yudelevich, *Zh. Analit. Khim.*, 1981, **36**, 86.
59. T. Kamada, T. Shiraiishi and Y. Yamamoto, *Talanta*, 1978, **25**, 15.
60. B. Magnusson and S. Westerlund, *Anal. Chim. Acta*, 1981, **131**, 63.
61. M. Betz, S. Güger and F. Fuchs, *Z. Anal. Chem.*, 1980, **303**, 4.
62. N. L. Fishkova, I. I. Nazarenko, V. A. Vilenkin and Z. A. Petrakova, *Zh. Analit. Khim.*, 1981, **36**, 115.
63. D. N. Sokolov, *Gas Chromatography of Volatile Complexes of Metals*, Nauka, Moscow, 1981.
64. R. S. Sturgeon, S. S. Berman, A. Desaulniers and D. S. Russell, *Talanta*, 1980, **27**, 85.
65. D. Keil, *Z. Anal. Chem.*, 1981, **309**, 181.
66. J. R. Clark and J. G. Viets, *Anal. Chem.*, 1981, **53**, 61.
67. T. S. Plotnikova, N. P. Krivenkova and B. Ya. Spivakov, *Zavodsk. Lab.*, 1979, **45**, 881.
68. H. L. Boiteau and C. Metayer, *Analisis*, 1978, **6**, 350.
69. J. K. Kapur and T. S. West, *Anal. Chim. Acta*, 1974, **73**, 180.
70. K. Ohta and M. Suzuki, *ibid.*, 1978, **96**, 77.
71. Jin Long-zhu and Ni Zhe-ming, *Can. J. Spectrosc.*, 1981, **26**, 219.
72. P. M. Grohse, J. F. McGaughey and D. E. Wagoner, *Abstr. Papers, 31st Pittsburgh Conf. Anal. Chem. and Appl. Spectrosc.*, Atlantic City, 1980, No. 774.
73. N. L. Fishkova and V. A. Vilenkin, *Zh. Analit. Khim.*, 1978, **33**, 897.
74. E. A. Startseva, N. M. Popova, V. P. Khrapai and I. G. Yudelevich, *Izv. Sib. Otd. AN SSSR, Ser. Khim. Nauk*, 1979, **14**, No. 6, 139.
75. J. F. Tyson and G. D. Stewart, *Anal. Proc.*, 1981, **18**, 184.
76. J. Komárek, D. Kolčava and L. Sommer, *Collection Czech. Chem. Commun.*, 1980, **45**, 3313.
77. A. Halász, K. Polyák and E. Gegus, *Mikrochim. Acta*, 1981 **II**, 229.
78. P. Hocquelliet and N. Labeyrie, *Analisis*, 1975, **3**, 505.
79. K. Ohta and M. Suzuki, *Talanta*, 1978, **25**, 160.
80. *Idem*, *Anal. Chim. Acta*, 1976, **83**, 381.
81. M. Ishizaki and S. Ueno, *Talanta*, 1979, **26**, 523.

82. H. Monien and R. Stangel, *Z. Anal. Chem.*, 1982, **311**, 209.
83. I. Havezov, E. Russeva and N. Jordanov, *ibid.*, 1979, **296**, 125.
84. J.-Å. Persson and W. Frech, *Anal. Chim. Acta*, 1980, **119**, 75.
85. M. Yanagisawa and T. Takeuchi, *ibid.*, 1973, **64**, 381.
86. V. M. Shkinev, I. Khavezov, B. Ya. Spivakov, S. Mareva, E. Ruseva, Yu. A. Zolotov and N. Iordanov, *Zh. Analit. Khim.*, 1981, **36**, 896.
87. C. W. Fuller and J. Whitehead, *Anal. Chim. Acta*, 1974, **68**, 407.
88. C. W. Fuller, *Atom. Absorpt. Newslett.*, 1975, **14**, 73.
89. P. Battistoni, P. Bruni, L. Cardellini, G. Fava and G. Gobbi, *Talanta*, 1980, **27**, 623.
90. N. T. Voskresenskaya, N. F. Pchelintseva and T. I. Tsekhonya, *Zh. Analit. Khim.*, 1981, **36**, 667.
91. M. P. Bratzel, C. L. Chakrabarti, R. E. Sturgeon, M. W. McIntyre and H. Agemian, *Anal. Chem.*, 1972, **44**, 372.
92. Y. Yamamoto, T. Kumamaru, T. Kamada and T. Tanaka, *Eisei Kagaku*, 1975, **21**, 71.
93. K. Ohta and M. Suzuki, *Anal. Chim. Acta*, 1976, **85**, 83.
94. *Idem*, *Z. Anal. Chem.*, 1979, **298**, 140.
95. *Idem*, *Anal. Chim. Acta*, 1979, **108**, 69.
96. Shan Xiao-quan, Jin Long-zhu and Ni Zhe-ming, *Atom. Spectrosc.*, 1982, **3**, 41.
97. H. L. Trachman, A. J. Tyberg and P. D. Branigan, *Anal. Chem.*, 1977, **49**, 1090.
98. A. W. Varnes and V. F. Gaylor, *Anal. Chim. Acta*, 1978, **101**, 393.
99. V. B. Margulis, B. I. Petrov and T. N. Vinetskaya, *Zavodsk. Lab.*, 1981, **47**, 17.
100. A. Dornemann and H. Kleist, *Z. Anal. Chem.*, 1982, **313**, 319.
101. B. M. Patel, P. M. Bhatt, N. Gupta, M. M. Pawar and B. D. Joshi, *Anal. Chim. Acta*, 1979, **104**, 113.
102. M. M. Barbooti and F. Jasim, *Talanta*, 1981, **28**, 359.
103. E. N. Gilbert, N. V. Androsova and Zh. O. Badmaeva, *Zh. Analit. Khim.*, 1979, **34**, 1150.
104. G. L. Everett, T. S. West and R. W. Williams, *Anal. Chim. Acta*, 1974, **70**, 291.
105. G. P. Klinkhammer, *Anal. Chem.*, 1980, **52**, 117.
106. R. B. Brooks, A. K. Chatterjee and D. E. Ryan, *Chem. Geol.*, 1981, **33**, 163.
107. L. Hagemann, L. Torma and B. E. Ginther, *J. Assoc. Off. Anal. Chem.*, 1975, **58**, 990.
108. F. J. Szydlowski, *Atom. Absorpt. Newslett.*, 1977, **16**, 60.
109. P. Hocquellet, *Analisis*, 1978, **6**, 426.
110. M. Ishizaki, *Talanta*, 1978, **25**, 167.
111. Sun Han-wen, Shan Xiao-quan and Ni Zhe-ming, *ibid.*, 1982, **29**, 589.
112. T. Kamada and Y. Yamamoto, *ibid.*, 1980, **27**, 473.
113. K. Ohta and M. Suzuki, *Z. Anal. Chem.*, 1980, **302**, 177.
114. E. A. Startseva, N. M. Popova, V. P. Khrapai and I. G. Yudelevich, *Izv. Sib. Otd. AN SSSR, Ser. Khim. Nauk*, 1980, **12**, No. 5, 94.
115. K. Ohta and M. Suzuki, *Talanta*, 1979, **26**, 207.
116. G. A. Vall, M. V. Usol'tseva, I. G. Yudelevich, I. V. Seryakova and Yu. A. Zolotov, *Zh. Analit. Khim.*, 1976, **31**, 27.
117. K. Cammann and J. T. Andersson, *Z. Anal. Chem.*, 1982, **310**, 45.
118. J. R. Clark and J. G. Viets, *Anal. Chem.*, 1981, **53**, 65.
119. Tsu Kai Jan and D. R. Young, *ibid.*, 1978, **50**, 1250.
120. A. W. Fitchett, E. H. Daughtrey and P. Mushak, *Anal. Chim. Acta*, 1975, **79**, 93.
121. M. Bengtsson, L.-G. Danielsson and B. Magnusson, *Anal. Lett.*, 1979, **12**, 1367.
122. K. Ohta and M. Suzuki, *Anal. Chim. Acta*, 1979, **107**, 245.
123. R. W. Dabeka, *Anal. Chem.*, 1979, **51**, 902.
124. F. Puttemans and D. L. Massart, *Anal. Chim. Acta*, 1982, **141**, 225.
125. R. Woodriff, B. R. Culver, D. Shrader and A. B. Super, *Anal. Chem.*, 1973, **45**, 230.
126. A. I. Ryabinin and E. A. Lazareva, *Zh. Analit. Khim.*, 1978, **33**, 298.
127. T. Shimizu, Y. Kawamata, Y. Kimura, Y. Shijo and K. Sakai, *Bunseki Kagaku*, 1982, **31**, 299.
128. K. W. Bruland, R. P. Franks, G. A. Knauer and J. H. Martin, *Anal. Chim. Acta*, 1979, **105**, 233.
129. H. Yoshimitsu, F. Kazuko, S. Hajime and K. Kan, *Anal. Chem.*, 1979, **51**, 651.
130. A. Dornemann and H. Kleist, *Z. Anal. Chem.*, 1980, **300**, 197.
131. G. B. Belling and G. B. Jones, *Anal. Chim. Acta*, 1975, **80**, 279.
132. E. Nakayama, T. Kuwamoto, H. Tokoro and T. Fujinaga, *ibid.*, 1981, **131**, 247.
133. C. J. Eskell and M. E. Pick, *ibid.*, 1980, **117**, 275.

DETERMINATION OF URANIUM IN WET PHOSPHORIC ACID

HELENA GÓRĘCKA and HENRYK GÓRĘCKI

Institute of Inorganic Technology and Mineral Fertilizers, Technical University of Wrocław, Poland

(Received 15 June 1983. Revised 18 November 1983. Accepted 17 December 1983)

Summary—A method for quantitative determination of uranium in wet phosphoric acid containing 0.001–0.02% of uranium has been developed. After reduction with Fe or $\text{FeSO}_4 \cdot \text{H}_2\text{O}$, uranium(IV) is extracted with a kerosene solution of an equimolar mixture of mono- and dinonylphenylphosphoric acids. The uranium is stripped with an oxidizing medium consisting of 10M H_3PO_4 containing NaClO_3 . The uranium stripped is determined spectrophotometrically with Arsenazo III.

Phosphate minerals contain 0.001–0.020% of uranium. In the decomposition of these minerals with sulphuric acid (widely used in most of the wet production methods) about 80% of the uranium contained in the minerals is dissolved. The rest remains in the phosphogypsum wastes. Many methods for uranium recovery in the wet phosphoric acid industry have already been developed and applied on the commercial scale, mainly in the USA, Canada, France and Japan.¹⁻⁴

The need for process control as well as determination of material balance requires a sensitive and accurate analysis for uranium in phosphoric acid.

Determination of uranium in the presence of different mineral impurities is a difficult analytical problem, especially as the uranium content being determined is much smaller than the content of impurities coming from the different minerals present and from the solutions used for their decomposition. Many analytical methods for uranium, making use of various laboratory and instrumental techniques, have already been published, but so far, none of them is universal enough to be directly applied to determination of uranium in wet phosphoric acid, phosphogypsum and phosphate rocks. Most of them refer to determination of uranium in specific materials, e.g., sulphuric acid,⁵ aluminium nitrate solutions,⁶ protective materials used in nuclear power-plants,⁷ Portland cement,⁸ sea-bottoms,⁹ rocks and minerals,¹⁰⁻¹⁵ uranium ores,¹⁶ soils,¹⁷ sea-water^{9,18} and natural water.¹⁹

Methods for determination of uranium in phosphate rocks²⁰ and aqueous solutions obtained by their decomposition with mineral acids²¹ are also known. The methods are often based on solvent extraction²² with reagents such as tributyl phosphate^{23,24} or trialkylamines.²⁵

Many methods for uranium determination can be used in the presence of thorium,^{6,9,11} iron, copper, thorium, molybdenum, vanadium and chromium,²⁶ or thorium and zirconium.^{13,27}

The highest sensitivity is provided by the methods developed by Korkisch,^{12,14} based on use of Arsenazo III, but they have the disadvantage that most heavy metals, fluorine compounds and phosphate (the main component of wet phosphoric acid) cause errors. Although procedures for diminishing these effects have been suggested,²⁸ their direct application still yields unsatisfactory results.

Thus the fundamental problem is to separate uranium from wet phosphoric acid with an extraction system characterized by a high distribution coefficient and good phase separation, together with an effective method of stripping with a medium in which uranium can be determined by a sensitive colorimetric method. Kerosene solutions of mono- and dinonylphenylphosphoric acids (NPPA)²⁹ seem suitable for this purpose.

EXPERIMENTAL

Preparation of the liquid ion-exchanger NPPA

The phosphorylation was performed in a four-necked 2-litre flask equipped with a stirrer, thermometer and bubbler for the nitrogen supply. The contents of the flask were heated with a 375-W infrared lamp. Three moles of non-phenol (375 g) were placed in the flask and constantly stirred while 1.1 mole of phosphorus pentoxide (156.9 g) was introduced in small portions at such a rate that the temperature in the flask did not exceed 70°. The mixture was then heated for 5 hr at 95–105° under a nitrogen atmosphere. After cooling, the product was a dark, brown-orange liquid, and was diluted with extraction grade kerosene (Polish standard 68/C-96040). The solution of NPPA is resistant to orthophosphoric acid and acidic hydrolysis at temperatures up to 90°, and characterized by low solubility in water (which minimizes loss during the extraction). This liquid ion-exchanger effectively extracts U(IV) from strongly acidic solution and does not form kerosene-insoluble salts or complexes.

Uranium extraction

Add 2 g of $\text{FeSO}_4 \cdot \text{H}_2\text{O}$ to 50 ml of "wet" phosphoric acid containing 20–30% of P_2O_5 (3.3–5.3M H_3PO_4). Shake this solution with 10 ml of 0.16M NPPA solution in kerosene at 25–35° for 1 hr. After phase separation strip the kerosene phase by shaking it with three 25-ml portions of 10M

phosphoric acid containing 0.2% of sodium chlorate, at 55°, for 30 min in each extraction. Combine the extracts and analyse them for uranium as below.

Spectrophotometric determination of uranium

The Korkisch method^{12,14} is used, modified to allow for presence of phosphoric acid in the samples.

Dilute 5 ml of the combined stripping solutions to volume with distilled water in a 100-ml standard flask. Transfer 2.5 ml of this solution (containing 2–20 μg of uranium) into a 50-ml conical flask and add 7.5 ml of concentrated hydrochloric acid (bringing the solution to 9M HCl concentration). Add 0.3 g of oxalic acid to eliminate the effect of iron and then 1.1 g of zinc powder to reduce uranium(VI) to uranium(IV). After adding the zinc, carefully plug the conical flask and mix the contents until the zinc has completely dissolved. Then add 1 ml of 0.1% aqueous solution of Arsenazo III. Measure the absorbance at 665 nm after 15 min. Optimum results are obtained for 2–10 μg of uranium.

RESULTS AND DISCUSSION

The extraction of uranium was performed in a thermostatic shaker unit (UNIPAN type 357) at temperature T_e , with phase-volume ratio (aqueous to organic) f_e , for a time t_e . The uranium was extracted from phosphoric acid, concentration $C_{\text{P}_2\text{O}_5}$, to which $\text{FeSO}_4 \cdot \text{H}_2\text{O}$ had been added. The back-extraction was done in n steps (each with shaking for 30 min) at 55°, with phase-volume ratio (aqueous to organic) f_r , 10M phosphoric acid containing 0.2% sodium chlorate being used as the stripping agent.

All experiments were done three times and the points shown in the figures are the arithmetic means. The results presented are equilibria data, and indepen-

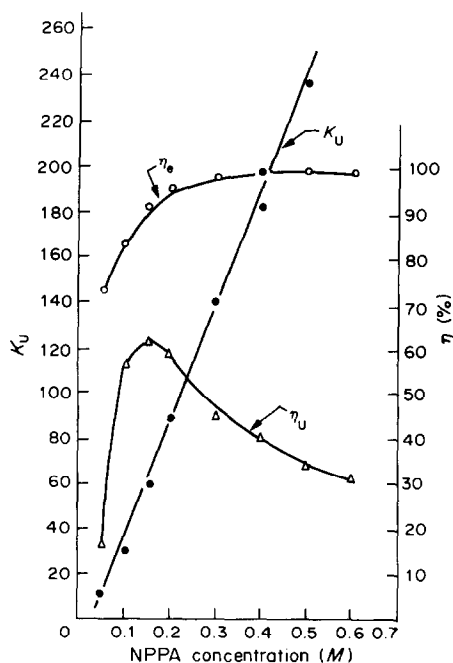


Fig. 1. The effect of NPPA concentration on the distribution coefficient K_U , uranium extraction η_e (%) and uranium recovery η_u (%) from a solution of phosphoric acid containing 28% P_2O_5 (4.9M H_3PO_4) and 0.026% U(IV). $T_e = 21^\circ$, $n_e = 1$ and $f_e = 5.0$.

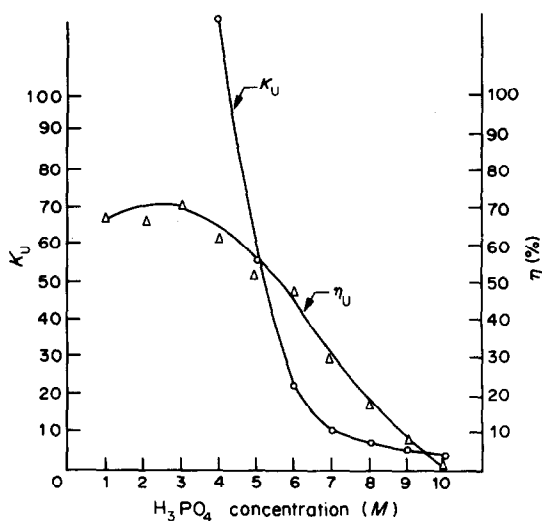


Fig. 2. The effect of phosphoric acid concentration on the distribution coefficient K_U and uranium recovery η_u (%) when using 0.16M solution of NPPA.

dent of the duration of the equilibrium. Experiment showed extraction equilibrium was reached in 10 min.

Figure 1 presents the effect of the NPPA concentration in the organic phase on the distribution coefficient K_U , the degree of extraction η_e (%) and the degree of uranium recovery η_u (%) in the extraction and stripping processes. In this case a single 30-min back-extraction was used, with $f_r = 5.0$. It is seen that the NPPA concentration should be kept in the range 0.1–0.2M. Higher concentrations of NPPA make it difficult to strip the uranium from the organic phase, but do not appreciably increase the initial extraction efficiency.

The effect of phosphoric acid concentration on the uranium recovery η_u , and on K_U , is shown in Fig. 2. The extraction was done in a single step at 40° with $f_e = 5.0$ and 0.2% Fe(II) in the aqueous phase. Stripping was also done in a single step (30 min shaking) with $f_r = 5.0$. It is seen that the stripping is most effective when the concentration of phosphoric acid in the aqueous phase is at least 7M.

It should be noted, however, that the values of η_u and K_U also depend markedly on the Fe(II) concentration and the temperature, though these factors do not significantly affect the shape of the graph of dependence on acidity.

Figure 3 shows the effect of Fe(II) concentration on the extraction (η_e) and stripping (η_r) by triple back-extraction with $f_r = 2.5$. It shows that in the presence of 0.15% Fe(II) in the phosphoric acid solution, over 80% uranium extraction is possible. Higher concentrations of Fe(II) give a higher degree of extraction but would require higher concentrations of sodium chlorate in the aqueous phase for the back-extraction. From the dependence of K_U on temperature (Fig. 4) it is evident that the extraction is best done in the temperature range 25–30°. For the stripping, the presence of not less than 0.2% of

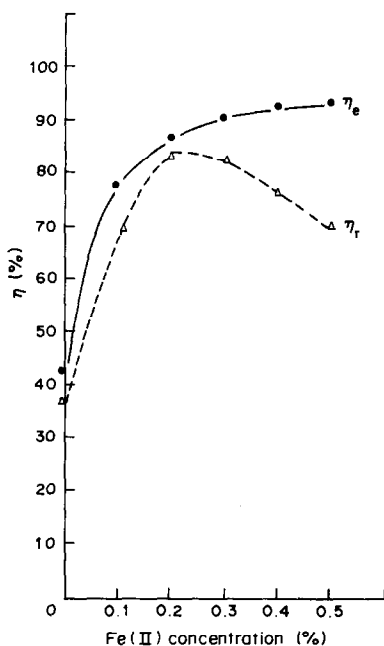


Fig. 3. The dependence of extraction yield η_e (%) and degree of back-extraction η_r (%) on concentration of Fe(II) introduced as ferrous sulphate. Uranium extracted from phosphoric acid solution containing 28% P_2O_5 (4.9M H_3PO_4) and 0.012% U. $T = 20^\circ$, $f = 5.0$, $\tau = 1$ hr and $n = 1$.

sodium chloride in the acid used is indispensable, but higher concentrations do not increase the stripping yield. The stripping was found to work best within the temperature range 45–60°.

In the analysis of acids containing a higher amount of organic compounds (e.g., black acid from Florida or Morocco) 1–2% of activated charcoal should be added and the analysis performed after the charcoal has been filtered off on paper. Tests have shown that 90–95% of the impurities contained in wet phosphoric acid are not stripped along with the uranium.

To determine the tolerance limits for potentially interfering species, various amounts were added to a stripping solution containing 4 μ g of uranium per ml, and the uranium was determined. The results listed in Table 1 indicate that only iron(II) has a serious effect.

From these results it follows that the direct determination of uranium in wet phosphoric acid

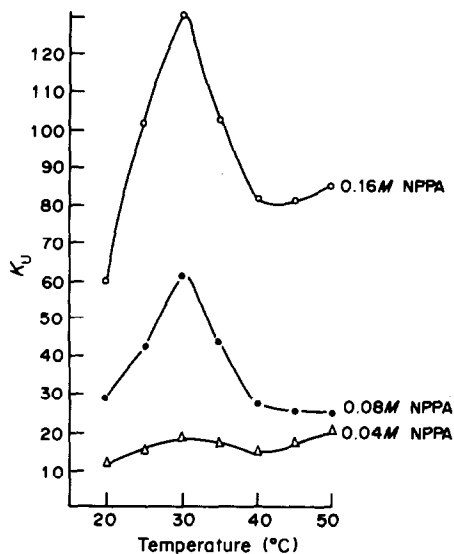


Fig. 4. The dependence of the distribution coefficient K_d on temperature for NPPA concentrations of 0.04, 0.08 and 0.13M. $C_{P_2O_5} = 28\%$, $f = 5.0$, $\tau = 1$ hr and $Fe(II) = 0.3\%$.

and phosphogypsum with an error below 5% is impossible.

A major problem in the analysis is the effect of phosphoric acid on the absorbance of the Arsenazo III–uranium(IV) complex since the w/w ratio of P_2O_5 to U in the sample is between 6×10^4 and 5×10^5 . Figure 5 shows the effect of increasing phosphoric acid content on the absorbance for 5, 10 and 15 μ g of uranium. Figure 5 shows that the amount of phosphoric acid used must be closely controlled and should be as identical as possible for all samples and standards.

CONCLUSIONS

The method presented seems attractive for determination of uranium in crude wet phosphoric acids. The calibration can be done by applying the entire procedure to known amounts of uranium in phosphoric acid of concentration not exceeding 30% P_2O_5 (5.3M H_3PO_4). An alternative which completely eliminates the effect of mineral impurities is based on determination of the calibration graph for the particular kind of wet phosphoric acid being analysed.

Table 1. The effect of foreign ions on the determination of 10 μ g of uranium in the presence of 92 mg of P_2O_5 (127 mg of H_3PO_4) and 0.625 mg of $NaClO_3$

Quantity of foreign ions, μ g	Uranium found, μ g							
	SO_4^{2-}	F^-	SiF_6^{2-}	Ca^{2+}	Fe^{2+}	Al^{3+}	K^+	Na^+
0	10.6	10.0	10.0	10.0	10.0	10.0	10.0	10.0
10	9.9	10.1	10.2	10.1	10.0	10.1	10.0	10.1
100	10.1	10.1	10.3	10.1	10.0	10.3	10.2	10.2
250	9.9	10.1	10.6	10.0	9.2	10.2	9.9	10.5
500	9.8	10.0	10.3	10.1	9.1	9.9	10.2	9.9
1000	9.8	10.4	10.4	10.4	8.3	10.2	10.3	10.2
5000	9.7	10.2	10.4	10.5	6.6	10.2	10.4	10.0

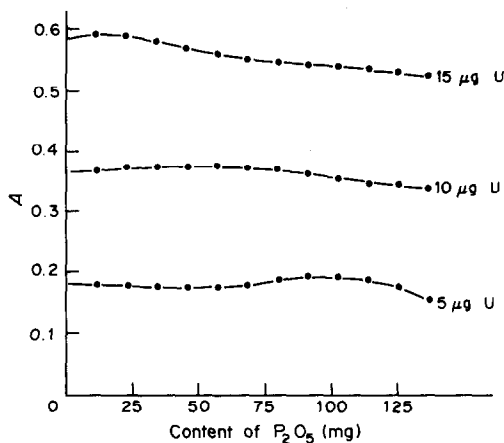


Fig. 5. The dependence of absorbance A on phosphoric acid content in samples containing 5, 10 and 15 μg of uranium.

It involves preliminary extraction of the uranium contained in the test-acid, with a kerosene solution of NPPA, followed by addition of standard amounts of uranium to portions of the "cleaned up" acid, and determination by the entire procedure. The relative standard deviation found for 15 independent measurements of 0.01% U was 2.8%. The limit for detection for uranium is 10 $\mu\text{g/g}$ in wet phosphoric acid. Fifty samples of wet phosphoric acid containing from 0.0004 to 0.0098% U were analysed by the method described and by X-ray fluorescence. The results obtained by the X-ray fluorescence method were lower by an average of about 5%.

The method can also be used for determination of uranium in the waste phosphogypsum and for monitoring the distribution of uranium in the decomposition of phosphate raw materials with sulphuric acid.

REFERENCES

1. P. Kouloheris, *Chem. Age (India)*, 1980, **31**, 1.
2. *Phosph. Potass.*, 1980, **108**, 20.
3. *Ibid.*, 1981, **111**, 31.
4. H. Górecki and H. Górecka, *Przem. Chem.*, 1981, **60**, 373.
5. E. A. Kanevski, G. R. Pavlovskaya and V. B. Rengevich, *Radiokhimiya*, 1978, **20**, 189.
6. T. V. Ramakrishna and R. S. S. Murthy, *Bull. Chem. Soc. Japan*, 1980, **53**, 2376.
7. B. W. Moran, *Nucl. Technol.*, 1979, **46**, 98.
8. S. K. Chakarvarti and K. K. Nagpaul, *World Cement Technol.*, 1979, **4**, 97.
9. P. Szefer and S. Ostrowski, *Studia i Materiały Oceanologiczne No. 25, Chemia Morza*, 1978, **3**, 250.
10. R. Coppens, P. Richard and S. Bashir, *Nucl. Instr. Meth.*, 1977, **147**, 87.
11. P. Sulovsky, *Radiochem. Radioanal. Lett.*, 1979, **38**, 325.
12. J. Korkisch and D. Dimitriadis, *Talanta*, 1973, **20**, 1199.
13. T. Kiriyaama and R. Kuroda, *Anal. Chim. Acta*, 1974, **71**, 375.
14. J. Korkisch and H. Hübner, *Talanta*, 1976, **23**, 283.
15. F. W. E. Strelow and T. N. Van der Walt, *S. Afr. J. Chem.*, 1979, **32**, 169.
16. T. M. Florence and Y. J. Farrar, *Anal. Chem.*, 1970, **42**(2), 271.
17. T. Hashimoto, K. Taniguchi, H. Sugiyama and T. Sotobayashi, *J. Radioanal. Chem.*, 1979, **52**, 132.
18. P. G. Barbano and L. Rigali, *Anal. Chim. Acta*, 1978, **96**, 199.
19. P. Minkkinen, *Finn. Chem. Lett.*, 1977, Nos. 4-5, 134.
20. R. Levin and S. Ronen, *Nucl. Res. Cent.*, 1977, 433.
21. F. T. Bunus, *Talanta*, 1977, **24**, 117.
22. P. Pakalns, *Anal. Chim. Acta*, 1972, **62**, 207.
23. A. Sobkowska, *Radiochem. Radioanal. Lett.*, 1978, **33**, 381.
24. I. Obrenović-Paligorić, I. J. Gal and V. Vajgand, *Anal. Chim. Acta*, 1968, **40**, 534.
25. S. J. Lyle and M. Tamizi, *ibid.*, 1979, **108**, 347.
26. S. K. Mandal, *Talanta*, 1979, **26**, 133.
27. S. B. Savvin, *ibid.*, 1961, **8**, 673.
28. F. W. E. Strelow and T. N. Van der Walt, *ibid.*, 1979, **26**, 537.
29. H. Górecki and H. Górecka, *Pol. Pat. Appl.*, P-237 275, 1982.

SHORT COMMUNICATIONS

DISCRETE MICROSAMPLE INJECTION INTO A GASEOUS CARRIER

ABDULRAHMAN S. ATTIYAT

Chemistry Department, Yarmouk University, Irbid, Jordan

and

GARY D. CHRISTIAN

Department of Chemistry, University of Washington, Seattle, WA 98195, U.S.A.

(Received 7 September 1983. Revised 15 December 1983. Accepted 13 January 1984)

Summary—Discrete injection (DI) of μl -volume liquid samples into a continuous flow of air as carrier is demonstrated. Atomic-absorption (AA) detection is used. Calibration graphs for zinc, obtained by using the DI-AA-air carrier method have a slope 1.8 times that of graphs obtained by the flow-injection analysis (FIA)-AA-air carrier method. The DI-AA-air carrier signals are higher and sharper than the FIA-AA-water carrier signals, and even exceed the AA steady-state signals for the same zinc solutions, owing to improved nebulization/atomization. The air-carrier method is more rapid than the liquid-carrier method. Measurement rates of 600/hr are possible. The signals show precision comparable to that attainable with water as carrier. The method is particularly useful for flame or plasma detectors and is potentially useful with different gases or vapours as carriers, and for gas-liquid reactions in FIA.

Flow-injection analysis (FIA) is a technique in which the sample is introduced, in the form of a liquid plug, into a flowing liquid stream.¹ This liquid stream either serves merely to carry the sample to the detector, or includes a reagent or a mixture of reagents to produce a detectable product from the sample and transport it to the detector.² The FIA signal depends on the reaction time and the dispersion of the sample. The longer the reaction time, the more the amount of product, but increased reaction time also increases the dispersion and dilution of the sample.^{1,3} Consequently, the optimum conditions for flow-rate and length of the mixing (dispersion) coil, will be a compromise between longer reaction time and lower dispersion. It would sometimes be of great advantage to the analyst to be able to limit the dispersion and also increase the reaction time. The use of gaseous reagents and carriers would enable the analyst to achieve this goal because a liquid sample transported by a gaseous carrier has very limited dispersion. Gardner and Malczyk⁴ recently described discrete injection of liquid samples in an AutoAnalyzer flow system with colorimetric detection, to allow the use of smaller samples. We describe here the discrete injection (DI) of liquid samples into a continuous flow of air as carrier stream for atomic-absorption (AA) detection and compare the results with those obtained by using water as carrier stream.

EXPERIMENTAL

Reagents

Zinc stock solution (Fisher certified atomic-absorption standard, 1000 ppm) was used to prepare 1, 2, 4, 5 and 10 ppm zinc standards. Demineralized water was used throughout for solution preparation and as liquid carrier.

Apparatus

A Perkin-Elmer model 403 atomic-absorption spectrophotometer with a strip-chart recorder was used for the AA measurements. A Rheodyne loop injection-valve was used for sample introduction. Teflon tubing of 0.5 mm bore was used in the DI-AA flow system and for sampling loops, and for connecting the sample injector to the capillary of the AA spectrophotometer. No pump was used in the AA system; the negative pressure of the nebulizer provided the necessary flow. Plastic syringes (1 and 3 ml) were used for filling sampling loops. The operating conditions for DI-AA are listed in Table 1.

Generation of the signals

The FIA signals obtained with the liquid-carrier system were generated by pumping distilled demineralized water into the detector system, and injecting the sample solution into the carrier stream by means of the injection port. Zinc standards were injected for FIA-AA.

Table 1. Experimental conditions for the FIA- and DI-AA system

Atomic-absorption settings:	
Wavelength	213.8 nm
Lamp current	15 mA
Slit-width	0.1 mm
Flame	Air-acetylene
Gas flow	Air 8 l./min Acetylene 1./min
Burner	Premix nebulizer-burner
Observation height	8 mm above burner
Recorder output	10 mV
Injection system:	
Liquid carrier	Water
Gaseous carrier	Air
Flow-rate of liquid carrier	2.5 ml/min
Length of dispersion coil	15 cm
Bore of dispersion coil	0.5 mm
Bore of pumping tube	0.5 mm
Volume of sample loop	100 μl

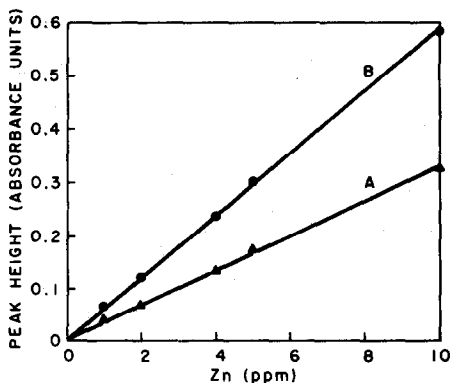


Fig. 1. Calibration graphs for the determination of zinc by FIA-AA-liquid carrier (A) and DI-AA-gas carrier (B).

DI signals obtained with the gaseous carrier system were generated in the same way, but with air pumped through the carrier system at the same rate as for the liquid carrier.

RESULTS AND DISCUSSION

Figure 1 depicts the calibration plot for the determination of zinc by FIA-AA with liquid carrier (A) and by DI-AA with gaseous carrier (B), for 100- μ l injections. The slope of B is 1.8 times that of A. The precision was similar for both methods, 2.1% relative standard deviation for the measurements with liquid carrier and 2.7% for those with gaseous carrier. Figure 2 shows the DI-AA signals with air as carrier

for the repeated injection of the five zinc standards used in constructing the calibration curves. Care must be taken to remove traces of the previous sample from the injector tubing connecting the injection port to the sample loop, or carry-over will cause a slight error in the signal for the next sample if the two samples differ appreciably in concentration (e.g., see the first peak in each batch in Fig. 2). This precaution is common when liquid carriers are used.

Figure 3 shows the FIA-AA signal with liquid carrier (B), the DI-AA signal with gaseous carrier (C) and the steady-state AA signal (A), all for a 5-ppm zinc solution. The signal with air as the carrier stream is significantly higher than that with water as carrier and somewhat higher than the steady-state signal. Also, the DI-air carrier peaks are sharper than the FIA-liquid carrier peaks, the widths at half height being 3 and 6 sec respectively. The reason for the DI-air carrier peaks being higher and narrower is believed to be enhanced vaporization/atomization of the sample, combined with diminished dispersion.

Effect of sample volume

Figure 4 shows the dependence of the AA signal (with air as carrier stream) on the sample volume. The signal increases rapidly with sample volume up to 100 μ l, then starts to level off. This means that if the amount of sample is limited, the sample volume can be reduced from 200 to 100 μ l without significant sacrifice in sensitivity. When water was used as

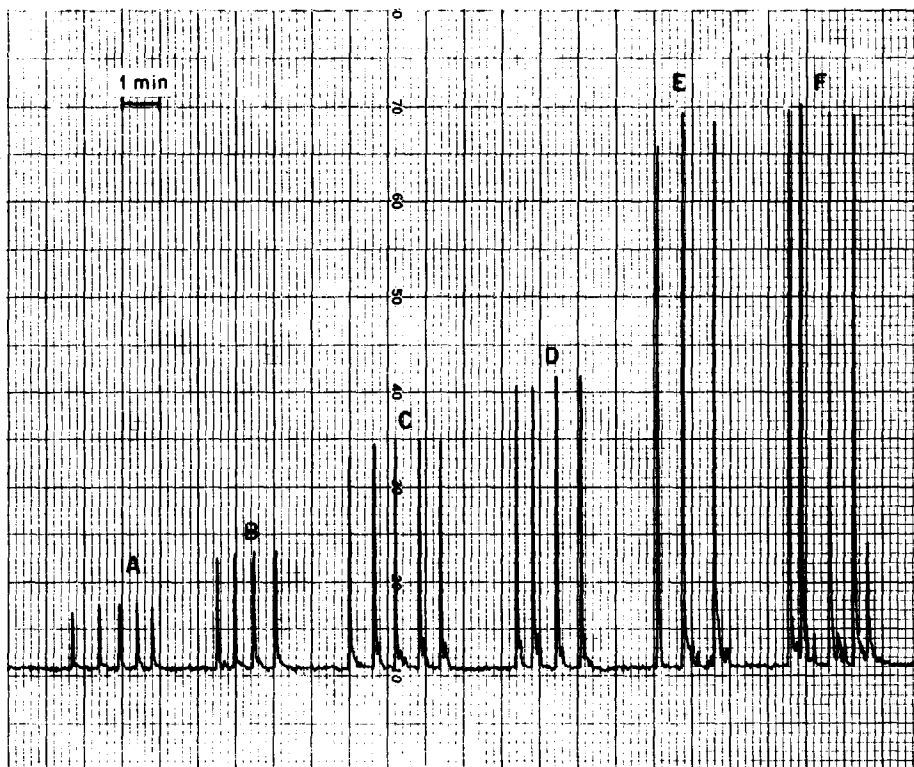


Fig. 2. DI-AA-air carrier peaks for five zinc standards, 1 ppm (A), 2 ppm (B), 4 ppm (C), 5 ppm (D) and 10 ppm (E and F).

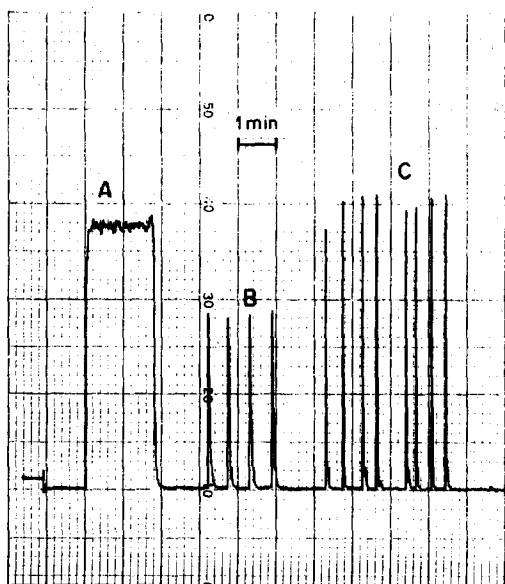


Fig. 3. Atomic-absorption signals for a 5-ppm zinc solution. (A) Steady state signal, (B) FIA-AA-liquid carrier signals, and (C) DI-AA-air carrier signals.

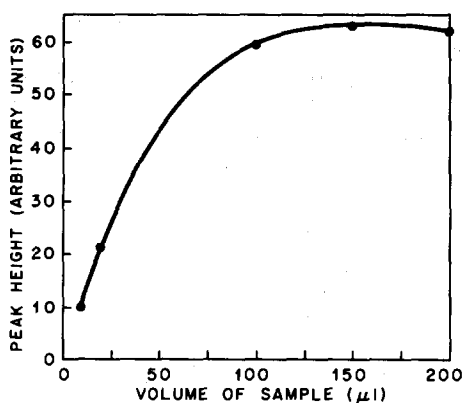


Fig. 4. The dependence of DI-AA-air carrier signals on the volume of sample injected.

carrier, the signal was still increasing with sample volume even at volumes $> 200 \mu\text{l}$.

Effect of the length of the dispersion coil

Figure 5 depicts the dependence of the AA peak height, with air as carrier, on the length of the

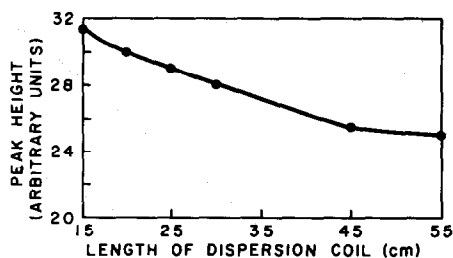


Fig. 5. The dependence of the DI-AA-air carrier signals on the length of the dispersion coil.

dispersion coil. The decrease in signal is significant but relatively small. The total decrease was about 20%, compared with a decrease of about 70% with water carrier, for the range of lengths shown. This will be of great benefit when the carrier gas also acts as a chemical reagent in gas-liquid reactions in FIA.

Analysis time

The DI-AA-air carrier peak emerges within 3 sec after the injection (compared to 4 sec with water as carrier). The average peak width at the base-line is about 6 sec. In principle, this permits up to 600 measurements per hour, and readily gives 350 per hour.

The DI-AA-gas carrier method is more sensitive and rapid than the liquid carrier method. It has good reproducibility and many potential applications. It is particularly well suited for flame or plasma detectors. The gas carrier technique has potential for application with different gases or vapours as carriers and for utilization of gas-liquid reactions in flow-injection analysis.

Acknowledgement—The financial assistance of Yarmouk University to A.S.A. for this research is gratefully acknowledged.

REFERENCES

1. J. Růžicka and E. H. Hansen, *Flow Injection Analysis*, Wiley, New York, 1981.
2. B. Rocks and C. Riley, *Clin. Chem.*, 1982, **28**, 409.
3. J. Růžicka, *Phil. Trans. R. Soc. Lond.*, 1982, **A305**, 645.
4. W. S. Gardner and J. M. Malczyk, *Anal. Chem.*, 1983, **55**, 1645.

DETECTION AND DETERMINATION OF PHENYLHYDRAZINE

N. KRISHNA MURTY,* V. JAGANNADHA RAO and N. V. SRINIVASA RAO
Department of Engineering Chemistry, Andhra University, Waltair, India

(Received 8 August 1983. Revised 17 December 1983. Accepted 13 January 1984)

Summary—Cacotheline has been employed successfully as a new qualitative and quantitative reagent for phenylhydrazine. The spot-test is performed at pH 4.5–5.5 with a limit of detection of 0.5 $\mu\text{g/ml}$ in the sample solution. The method can be extended to the colorimetric estimation and photometric titration of phenylhydrazine with cacotheline. Beer's law is obeyed over the range 0.1–2 mg.

Among the few reagents proposed for the detection of phenylhydrazine may be mentioned 2,6-dichloro-*p*-benzoquinone-4-chloramine,¹ pyridine-2-aldehyde,² Devarda's alloy and Raney alloy,³ and silver nitrate in presence of sodium hydroxide.⁴ Some of these methods are indirect, or involve the use of rare chemicals and heating. A direct and simple method is now proposed for the detection of phenylhydrazine with cacotheline, a nitro-derivative of brucine, as reagent. Few methods have been proposed for the spectrophotometric estimation of phenylhydrazine,^{5–7} so the new spot-test is extended to the colorimetric estimation and photometric titration of phenylhydrazine.

EXPERIMENTAL

Reagents

Cacotheline solution is prepared and standardized as described earlier.⁸ Phenylhydrazine solution is prepared and standardized⁹ with potassium iodate (carbon tetrachloride end-point detection).

Procedures

Detection of phenylhydrazine. Mix 1 ml of 0.2M sodium acetate and 1 ml of 0.2M acetic acid in a test-tube, and add 1 ml of cacotheline solution and 1 ml of test solution. An immediate pink colour, stable for more than 30 min, indicates the presence of phenylhydrazine. The limit of detection is 0.5 μg in the 1 ml of sample.

Alternatively place 0.05 ml of 0.2M sodium acetate and 0.05 ml of 0.2M acetic acid in a cavity on a spot-plate, add 0.05 ml of cacotheline solution and 0.05 ml of test solution and mix with a glass rod. An immediate pink colour, stable for more than 30 min, indicates the presence of phenylhydrazine. The limit of detection is 0.25 μg in the 0.05 ml of test solution.

Colorimetric estimation. In a 50-ml standard flask place 10 ml of 0.2M sodium acetate and 10 ml of 0.2M acetic acid, and add 5 ml of cacotheline solution. Add a suitable known volume of test solution or phenylhydrazine standard solution and dilute to the mark with water. Measure the intensity of the pink colour with a photoelectric colorimeter fitted with a green filter, or measure the absorbance at 530 nm. Prepare a calibration graph.

Photometric titration. Mix 2 ml of 0.2M sodium acetate and 2 ml of 0.2M acetic acid in a suitable titration cell, and add 2 ml of test solution containing 0.5–2 mg of phenylhydrazine. Pass carbon dioxide through the mixture for

about 10 min, then titrate with cacotheline solution, added in portions of 0.1–0.2 ml. Stop the passage of carbon dioxide before measurement. Apply a volume correction when plotting the titration curves.

RESULTS AND DISCUSSION

Preliminary tests showed the optimal acidity to be in the range pH 4.5–5.5. The absorption spectrum of the product obtained by reduction of cacotheline with phenylhydrazine under these conditions has a maximum at 530 nm. The stoichiometry of the reaction is 1:1, each component undergoing a 2-electron reaction and the course of the reaction is the same whether the cacotheline or phenylhydrazine is added first. The apparent molar absorptivity of the reduced cacotheline is $3.3 \times 10^3 \text{ l. mole}^{-1} \text{ cm}^{-1}$. Beer's law is obeyed over the range 0.1–2 mg of phenylhydrazine.

Hydrazine, hydroxylamine, 2,4-dinitrophenylhydrazine, phenylhydrazine-4-sulphonic acid hemihydrate, *o*-phenylhydroxylamine hydrochloride, semicarbazide hydrochloride, isonicotinic acid hydrazide, chloralhydrazine, benzoylhydrazine, salicyloylhydrazine and nicotonylhydrazine, have no effect on the determination of phenylhydrazine. Various species such as Sb(V), Sb(III), V(V), V(IV), Mo(VI), W(VI), chloride, bromide, acetate and citrate do not interfere, but U(IV), Sn(II), Ti(III) and Mo(V) interfere when present at any concentration.

The relative error was found to be 1% or less for the colorimetric determinations, and 0.5% or less for the photometric titration.

REFERENCES

1. F. Feigl and E. Jungreis, *Talanta*, 1958, **1**, 367.
2. F. Feigl and L. Ben-Dor, *ibid.*, 1963, **10**, 1111.
3. F. Feigl, *Anal. Chem.*, 1961, **33**, 1118.
4. L. Légrádi, *Mikrochim. Acta*, 1969, 472.
5. E. Montignie, *Bull. Soc. Chim. France*, 1930, **47**, 128.
6. B. C. Bose and R. Vijayvargiya, *Indian J. Pharm.*, 1966, **28**, 329.
7. J. P. Ravat and P. Bhattacharjee, *Mikrochim. Acta*, 1976 **II**, 619.
8. G. G. Rao, N. K. Murty and V. N. Rao, *Talanta*, 1965, **12**, 243.
9. C. O. Miller and N. H. Furman, *J. Am. Chem. Soc.*, 1937, **59**, 161.

*Author for correspondence.

ION-CHROMATOGRAPHIC DETERMINATION OF CHLORIDE AND FLUORIDE IN ELECTROLYTE FROM THE HALOGEN TIN-PLATING PROCESS

W. KORTH and J. ELLIS

Department of Chemistry, University of Wollongong, P.O. Box 1144, Wollongong, N.S.W. 2500, Australia

(Received 5 December 1983. Accepted 13 January 1984)

Summary—A simple and rapid procedure is proposed for the determination of chloride and free fluoride in tin electroplating fluid. Suppressor-column ion-chromatography is used after oxidation of hexafluorostannate(II) to hexafluorostannate(IV) with hydrogen peroxide. Concurrent determination of tin(II) and total tin then allows calculation of the concentrations of fluoride, hexafluorostannate(II) and hexafluorostannate(IV).

In common with many large tin-plate plants, the electroplating line at Australian Iron and Steel (Port Kembla) uses a fluoride electrolyte consisting predominantly of sodium chloride and sodium hexafluorostannate(II). In addition, small amounts of ferrocyanide (to scavenge heavy metals) and other compounds such as organic brightening agents are present. Typical concentrations are given in Table 1.

During use, the electrolyte concentrations of tin(II) and free fluoride are depleted progressively by the oxidation of tin(II) to tin(IV), which is converted into the electrochemically inactive hexafluorostannate(IV). Periodic additions of tin(II) and fluoride are therefore required to maintain the specified concentration ranges for these ions. In particular, a free fluoride/tin(II) ratio of at least 6:1 is required. This necessitates regular monitoring of the electrolyte for tin(II), tin(IV), fluoride and chloride. At present, both chloride and fluoride are determined by titrimetric analysis.^{1,2} This paper describes a simple ion-chromatographic procedure which is faster and more precise than the titrimetric methods and which could be adapted to automated process control.

EXPERIMENTAL

Apparatus

The ion-chromatography system consisted of a solvent-delivery pump (6000A, Waters, U.S.A.), a pneumatic high-pressure injection valve (7000, Rheodyne, U.S.A.) fitted with a 10- μ l loop, an anion separator column and cation-exchange suppressor column (Dionex, U.S.A.), a conductivity meter (P/N9505, Phillips, U.S.) and a chart recorder (EB5247-15, Houston Instruments, U.S.A.). A flow-rate of 3.0 ml/min was employed, with the detector at 10 μ S/cm full-scale deflection, recorder at 0.1 V full-scale deflection and a chart-speed of 0.25 cm/min.

Procedure

Filter a sample of electrolyte (Whatman 541) and pipette 5.00 ml of the filtrate into a 500-ml standard flask containing 10 ml of aqueous hydrogen peroxide (30% w/v). Dilute to volume, inject 10 μ l into the Dionex anion separator

column and elute with sodium carbonate (3.0mM)/sodium bicarbonate (2.4mM) solution. Convert peak areas into concentrations by use of calibration graphs obtained by injecting a solution of sodium chloride and sodium fluoride. Determine tin(II) and total tin by titrimetry.³

DISCUSSION

Fluoride is present in the electrolyte in three forms: free fluoride, hexafluorostannate(II) and hexafluorostannate(IV). Hexafluorostannate(II) is labile and hexafluorostannate(IV) is inert. Ion-chromatography will thus detect the free fluoride and also the fluoride dissociated from the tin(II) complex. Dissociation of the SnF_6^{4-} ion is forced to completion by the binding of the released tin(II) by the resin of the suppressor column, which must consequently be regenerated more frequently. With a single-column (electronic suppression) system, the tin(II) interferes more, since heavy-metal ions poison the column. Accordingly, attempts were made to prevent this interference, including precipitation of tin with sulphide, or sodium hydroxide or ammonia; use of a cation-exchange resin or a chelating ion-exchange resin; and complexation with EDTA. All these methods were successful, but either were too lengthy to be practical or caused subsequent interferences.

Therefore, the hexafluorostannate(II) was oxidized to kinetically inert hexafluorostannate(IV). The free fluoride ($[\text{F}^-]$) was then readily detected (along with chloride). The dual-column system gave a constant baseline between chromatographic peaks and a faster

Table 1. Composition of electrolyte (pH 4.0)

Species	Concentration, g/l.
Sn(II)	12.0
Sn(IV)	5.5
F ⁻	28.0
Cl ⁻	38.0
Fe(CN) ₆ ⁴⁻	1.0

Table 2. Comparison of ion-chromatography and titrimetric analysis for Cl⁻ and F⁻

Sample	Cl ⁻ ,* g/l.	F ⁻ ,* g/l.		Sn(II), g/l.	Sn(IV), g/l.
		a	b		
1	42.7 (42.5)	13.5	26.0 (25.7)	9.0	4.0
2	42.2 (41.5)	13.3	25.8 (25.7)	8.5	4.5
3	38.3 (39.0)	15.7	32.5 (33.7)	11.0	6.5
4	38.7 (39.5)	14.3	30.6 (31.3)	11.0	6.0
5	43.0 (42.5)	14.2	27.6 (28.1)	9.5	4.5
6	38.0 (37.0)	17.6	32.5 (31.8)	11.0	4.5

*Titrimetric values given in parentheses.

a = free fluoride after oxidation of tin; b = total fluoride.

separation than the single-column system, and was used in all subsequent work. The concurrent titrimetric determination of tin(II) and total tin³ allowed the total fluoride concentration to be calculated from

$$[\text{F}^-]_{\text{total}} = [\text{F}^-] + 0.960[\text{Sn}]_{\text{total}}$$

where all concentrations are expressed in units of g/l.

Hexafluorostannate(II) was calculated from:

$$[\text{SnF}_6^{4-}] = ([\text{F}^-]_{\text{total}} - [\text{F}^-]) \times 2.04 \times \frac{[\text{Sn(II)}]}{[\text{Sn(IV)}]}$$

Table 2 compares mean ($n = 3$) values for fluoride and chloride concentrations determined by titrimetry with those determined by hydrogen peroxide oxidation/ion-chromatography (a) before and (b) after oxidation of tin(II). Actual electrolyte samples were used in each case, over the concentration ranges (g/l.) 8.5–11.0 [tin(II)], 4.5–6.5 [tin(IV)], 25.8–32.5 [F⁻] and 38.0–43.0 [Cl⁻].

The ion-chromatographic analysis gave complete resolution of the chromatographic peaks and linear calibration graphs for chloride and fluoride over the concentration ranges 0–350 and 0–250 mg/l. respectively. The precision was determined by replicate analysis of a solution containing 283 mg/l. of chloride and 189 mg/l. of fluoride; relative standard deviations were 0.5% ($n = 10$) and 0.8% ($n = 10$) respectively. Because of the poor precision of the titrimetric analysis for fluoride (± 2 g/l. for [F⁻] ~ 28 g/l.), the

accuracy of the ion-chromatographic procedure was checked by using a synthetic electrolyte prepared by dissolving NaCl, NaF and SnCl₂·2H₂O in water and oxidizing the tin with hydrogen peroxide. The mean chloride concentration found was 472 mg/l. (470 mg/l. taken) and fluoride concentration 239 mg/l. (237 mg/l.).

CONCLUSION

The ion-chromatography procedure provides simultaneous measurement of fluoride and chloride with a precision that for chloride is comparable with titrimetry, and for fluoride is much better. Sample pretreatment is minimal and the analysis time (< 5 min) is much shorter than that for the titrimetric method (> 30 min). Because of its minimal requirements for sample handling and addition of reagents, it should be readily adaptable for automated on-line analysis and process control.

Acknowledgement—We thank Mr. T. Yeoman, Australian Iron & Steel, Port Kembla, for the use of the ion-chromatograph and the provision of electrolyte samples.

REFERENCES

1. A. I. Vogel, *A Text-book of Quantitative Inorganic Analysis*, 3rd Ed., p. 274. Longmans, London, 1961.
2. D. G. Foulke and F. E. Crane, Jr., *Electroplaters' Process Control Handbook*, p. 221. Reinhold, New York, 1963.
3. *Idem*, *op. cit.*, p. 219.

SELECTIVE COMPLEXOMETRIC DETERMINATION OF TIN, WITH MERCAPTANS AS RELEASING AGENTS

K. N. RAOOT and SARALA RAOOT

Defence Metallurgical Research Laboratory, Kanchanbagh, Hyderabad-500258, India

(Received 9 November 1983. Accepted 12 January 1984)

Summary—A method is proposed for selective complexometric determination of tin, mercaptans being used as releasing agents. To a solution containing tin and other cations, excess of EDTA is added and the surplus is back-titrated at pH 5–6 with lead nitrate (Xylenol Orange as indicator). Thioglycollic acid or mercaptopropionic acid is then added to decompose the tin–EDTA complex and the liberated EDTA is titrated with lead nitrate. The interference of various cations has been studied and the method has been employed for the estimation of tin in a variety of alloys.

Gravimetric methods for tin are normally subject to errors caused by adsorption, co-precipitation or occlusion of other elements present and require more or less elaborate separations or purification of the final oxide.¹ The titrimetric determinations based on oxidation to the quadrivalent state by means of a standard solution of iodate or other suitable oxidant are definitely superior, but complete reduction of tin to the bivalent state and subsequent prevention of aerial oxidation to tin(IV) are mandatory,^{1,2} and demand special care and apparatus

EDTA³⁻⁵ forms strong complexes with both tin(II) and tin(IV) and thus complexometric methods for tin are expected to be free from problems of oxidation or reduction. EDTA methods, in general, are also more convenient and rapid. Surprisingly, the number of complexometric methods for tin is comparatively small^{5,6} and those capable of determining tin in the presence of other cations with the help of selective masking agents, are still fewer in number. Oxalate,^{7,8} fluoride,^{8,9} and lactic acid¹⁰ appear to be the only reagents used for selective decomposition of the tin–EDTA complex.

Tartaric acid¹¹ has been used for masking tin during the EDTA titration of other cations. We recently reported the use of tartaric acid and citric acid as selective releasing agents for tin.¹² During earlier work¹³ in which thioglycollic acid and mercaptopropionic acid were used for the decomposition of the copper(II)–EDTA complex, serious interference was caused by tin. A detailed investigation was therefore undertaken to examine the usefulness or otherwise of these mercaptans for the quantitative release of EDTA from its tin complex. The results are presented in this paper.

EXPERIMENTAL

Reagents

Tin(II) chloride solution. Prepared by dissolving 1.92 g of stannous chloride in 20 ml of concentrated hydrochloric acid and making up to 1 litre, and standardized.

Tin(IV) chloride solution. Prepared by dissolving 1.00 g of pure tin metal in 150 ml of hydrochloric acid (1 + 1) and diluting to 1 litre with 1M hydrochloric acid, and standardized.

EDTA solution, 0.01M.

Lead nitrate solution, 0.01M.

Xylenol Orange indicator. A 0.1% aqueous solution.

Thioglycollic acid and mercaptopropionic acid, 20% solutions in water.

Glycerol, 50% aqueous solution.

Hexamine buffer. A 30% aqueous solution.

Solutions of various metal ions (concentration 1 mg/ml) were prepared from suitable salts. All chemicals were of analytical-reagent grade.

Estimation of tin in presence of other cations

To a solution containing 5–50 mg of tin(II) or tin(IV) and various amounts of foreign ions, add excess of 0.01M EDTA and dilute to 70–80 ml with distilled water [when tin(IV) is present add 10 ml of 20% glycerol solution]. Adjust to pH 5–6 with hexamine solution. Add a few drops of Xylenol Orange indicator and back-titrate the excess of EDTA with 0.01M lead nitrate to the sharp colour change from yellow to red. Add 5–25 ml of 20% solution of thioglycollic acid or mercaptopropionic acid. Heat the solution to boiling and boil for 4–5 min, cool and titrate the liberated EDTA with 0.01M lead nitrate.

Determination of tin in alloys

Dissolve 0.2–0.5 g of sample in 10–20 ml concentrated hydrochloric acid and 2–4 ml of concentrated nitric acid and dilute to 100 ml in a standard flask. Take a suitable aliquot containing 5–50 mg of tin in a 250-ml conical flask, and determine tin as described above.

RESULTS AND DISCUSSION

Both tin(II) and tin(IV) are known to form strong complexes with EDTA, but tin(IV) is reported to hydrolyse in alkaline or even neutral medium in presence of EDTA.³⁻⁶ This fact has been used for the separation of tin from other metal ions.¹⁴⁻¹⁶ In the EDTA methods for tin(IV), the metal is mostly estimated^{8,17,18} at lower pH such as 2, and in those few cases where back-titration is done at pH 5–6, a caution is invariably given that the pH should be adjusted to 2 and then slowly and homogeneously be brought to 5 by small additions of the buffer.^{4,10,19} To

overcome this limitation Ottendorfer²⁰ suggested the addition of potassium chloride, which causes an initial shift in pH and also prevents dissociation of the tin(IV)-EDTA complex. We have found that glycerol is more effective than potassium chloride, since it is capable of keeping tin(IV) in solution even up to pH 10, whereas with potassium chloride a slight turbidity appears at about pH 6. Addition of 5 ml of 50% glycerol solution was found to be adequate for 10 mg of tin. Glycerol has also been used for masking iron(III) and chromium(III) in EDTA titration of some bivalent cations²¹ and tin(IV)²² respectively.

Various dissolution procedures have been suggested for the alloys of tin^{1,2,23} and the choice mainly depends on the oxidation state of tin required by method of analysis. Earlier chelatometric methods also appear to have such requirements, some being for tin(II)²⁴⁻²⁶ and others for tin(IV).¹⁷⁻¹⁹ In the most common dissolution procedures, employing mineral acids, nitric acid and atmospheric oxygen tend to oxidize the tin,¹ whereas the associated metals such as zinc, lead, *etc.* in the alloys exert a reducing effect on it.^{1,27} It is therefore most likely that the solution thus obtained will contain a mixture of tin(II) and tin(IV). The mercaptans used in the present investigation are equally effective for bivalent and quadrivalent tin and hence the present method is superior to the earlier ones using oxalate,^{7,8} fluoride^{8,9} and lactic acid¹⁰ as releasing agents, which are reported to be useful only for tin(IV). It was observed during the preliminary experiments that 5 ml of 20% thioglycollic or mercaptopropionic acid will release the EDTA combined with 10 mg of tin, on heating at 100° for 4-5 min. A larger volume has no adverse effect, but a smaller amount will require the boiling period to be longer.

A number of cations have been examined for their possible interference in the present titration and it has been found that large amounts of lead, zinc, nickel, cobalt(II), cadmium, iron(III), aluminium, indium, arsenic(V), antimony(V), vanadium(IV), zirconium and rare-earths do not interfere. However, when aluminium is present, to ensure its complete complexation with EDTA it is necessary to boil the solution for 2-3 min after addition of the excess of EDTA and adjustment to pH 3. Copper(II)-EDTA is also quantitatively decomposed by the mercaptans used¹³ and hence copper will interfere, but this can easily be obviated by masking the copper with thiourea,²⁸ so larger samples can be used for alloys containing smaller percentages of tin. Manganese(II), owing to the low stability of its EDTA complex under the experimental conditions, caused difficulty in the end-point detection, particularly when more than 5 mg of it was present. Bismuth(III) interfered seriously. An interesting feature of the present method is that it remains unaffected by large amounts of titanium(IV), which seriously interferes with all the masking or releasing agents used earlier.⁷⁻¹¹ The method can thus be used for the estimation of tin in titanium alloys. The results for tin in alloys are presented in Table 2.

Table 1. Determination of tin in presence of foreign ions

Foreign ion, mg	Taken	Sn ²⁺ , mg			Sn ⁴⁺ , mg		
		Found		Found		MPA	
		with TGA	with MPA	with TGA	with MPA		
Cu ²⁺	80.60*	4.80	4.81	4.81	4.01	4.01	4.04
	5.06*	36.00	36.00	35.90	35.00	34.96	34.90
Ni ²⁺	60.20	7.20	7.21	7.18	6.00	5.99	5.97
	12.40	38.40	38.34	38.46	35.00	35.08	35.02
Pb ²⁺	56.75	13.20	13.24	13.29	10.00	9.97	10.03
	5.68	42.00	41.90	42.08	40.00	39.88	39.88
Zn ²⁺	26.00	18.04	18.04	17.92	15.00	15.05	14.96
	6.00	24.00	23.98	24.04	22.00	21.96	22.08
Co ²⁺	28.80	7.20	7.18	7.15	6.00	5.97	6.05
	5.80	36.00	36.03	36.14	30.00	30.09	29.97
Cd ²⁺	60.40	13.20	13.18	13.24	18.00	17.93	17.98
	6.08	21.60	21.60	21.54	10.00	10.00	10.03
Mn ²⁺	4.90	18.00	17.92	18.10	15.00	15.13	15.08
	2.65	7.20	7.15	7.21	6.00	5.94	6.05
Fe ³⁺	25.00	4.80	4.78	4.81	4.00	4.01	4.01
	5.00	24.00	23.92	24.10	22.00	21.96	22.02
Al ³⁺	20.50†	15.00	15.02	14.96	18.00	18.10	17.98
	4.10†	36.00	35.97	36.09	35.00	34.96	35.08
In ³⁺	50.50	13.20	13.24	13.24	15.00	15.05	15.02
	6.10	38.40	38.28	38.46	40.00	39.88	40.06
Sm ³⁺	35.00	4.80	4.78	4.84	10.00	10.03	9.97
	7.00	21.60	21.72	21.66	30.00	29.91	29.97
La ³⁺	28.00	24.00	23.92	24.04	22.00	22.14	21.96
	7.50	42.00	42.08	41.96	40.00	40.12	39.94
Ce ³⁺	32.10	15.00	15.08	14.96	12.00	12.05	11.93
	6.40	26.40	26.53	26.41	35.00	34.96	34.96
As ³⁺	15.60	18.00	17.98	17.98	18.00	17.93	17.98
	4.68	38.40	38.56	38.40	22.00	22.02	21.96
Sb ³⁺	20.40	21.60	21.66	21.49	12.00	11.93	11.93
	10.20	15.00	15.02	14.96	35.00	35.02	35.14
V ⁴⁺	15.80	13.20	13.29	13.29	15.00	15.02	15.08
	7.90	36.00	35.90	36.09	35.00	34.90	35.08
Zr ⁴⁺	25.60	4.80	4.78	4.78	4.00	4.04	3.98
	5.30	26.40	26.59	26.47	30.00	29.91	30.09
Ti ⁴⁺	80.60	4.80	4.78	4.84	6.00	5.97	6.05
	20.20	42.00	41.90	42.14	40.00	40.12	39.88

*Copper masked with thiourea.

†Excess of EDTA added, pH adjusted to 3, solution boiled for 3 min.

TGA = thioglycollic acid.

MPA = mercaptopropionic acid.

Table 2. Determination of tin in alloys

Alloy	Tin, %		Relative error %
	Present	Found	
Leaded bronze	9.35	9.30*	-0.5
BCS No. 364		9.42†	+0.8
Leaded gun-metal	7.27	7.24*	-0.4
BCS No. 183/4		7.30†	+0.4
Ounce metal 9	4.56	4.60*	+0.9
NBS No. 124D		4.54†	-0.4
Lead-base white metal	5.07	5.10*	+0.6
BCS No. 177/2		5.04†	-0.6
Tin-base white metal	82.20	82.0*	-0.2
BCS No. 178/2		82.4†	+0.3
Tin-base white metal	88.57	88.3*	-0.3
NBS No. 54D		88.7†	+0.2
Solder	39.30	39.4*	+0.3
NBS No. 127b		39.1†	-0.5
Titanium-base alloy	2.47	2.46*	-0.4
NBS No. 176		2.50†	+1.2

*With thioglycollic acid.

†With mercaptopropionic acid.

It is seen that the maximum relative error, 1.2%, is for an alloy containing only 2.5% tin. For alloys with higher percentages of tin, the relative errors were much smaller. A suite of three alloy samples can conveniently be analysed in 1 hr. It can thus be concluded that the method is simple, selective, accurate and fairly rapid.

Acknowledgement—Our grateful thanks are due to Dr. P. Rama Rao, Director, DMRL, for permission to publish this paper.

REFERENCES

1. I. M. Kolthoff, P. J. Elving and E. B. Sandell, *Treatise on Analytical Chemistry*, p. 327. Interscience, New York, 1961.
2. K. Kodama, *Quantitative Inorganic Analysis*, p. 203. Interscience, New York, 1963.
3. R. Přibil, *Analytical Applications of EDTA and Related Compounds*, p. 236. Pergamon Press, Oxford, 1972.
4. J. Kragten, *Talanta*, 1975, **22**, 505.
5. T. S. West, *Complexometry with EDTA and Related Reagents*, p. 209. BDH, Poole, 1969.
6. G. Schwarzenbach and H. Flaschka, *Complexometric Titrations*, 2nd Ed., p. 292. Methuen, London, 1969.
7. J. Kinunnen and B. Wennerstrand, *Chemist-Analyst*, 1957, **46**, 34.
8. *Idem*, *ibid.*, 1957, **46**, 92.
9. M. Goldstein and G. Kober, *Z. Anal. Chem.*, 1976, **279**, 287.
10. Y. C. Chen, C. V. Hsiao and C. G. Faug, *Acta Chim. Sinica*, 1964, **30**, 330.
11. I. M. Yurist and O. I. Korotkova, *Zavodsk. Lab.*, 1962, **28**, 660.
12. Sarala Raoot and K. N. Raoot, *Indian J. Technol.*, In the press.
13. Sarala Raoot, K. N. Raoot and N. R. Desikan, *ibid.*, 1983, **21**, 39.
14. R. Přibil, *Collection Czech. Chem. Commun.*, 1951, **16**, 542.
15. B. Bieber and Z. Večera, *Slevarenstvi*, 1957, **4**, 48.
16. G. Lanfranco and F. Cerrato, *Anal. Chim. Acta*, 1967, **39**, 47.
17. I. M. Yurist, *Zavodsk. Lab.*, 1965, **31**, 267.
18. J. Jankovský, *Chem. Listy*, 1957, **51**, 313.
19. J. Kragten, *Analyst*, 1974, **99**, 43.
20. L. J. Ottendorfer, *Chemist-Analyst*, 1958, **47**, 96.
21. F. Krieza, *Croat. Chem. Acta*, 1967, **19**, 47.
22. F. Krieza and V. N. Vuetic, *ibid.*, 1970, **42**, 75.
23. S. Sriveeraraghavan and N. Parthasarathy, *Metal Finish*, 1971, **69**, 105.
24. J. Dubsky, *Collection Czech. Chem. Commun.*, 1959, **24**, 4045.
25. I. A. Crişan and V. Bolos, *Rev. Chim. Bucharest*, 1967, **18**, 307.
26. A. Janitsch, *Z. Anal. Chem.*, 1982, **311**, 520.
27. H. Nehamakin, *Chemist-Analyst*, 1960, **49**, 20.
28. O. B. Budevsky and L. Simova, *Talanta*, 1962, **9**, 769.

APPLICATION OF ANION-EXCHANGE TECHNIQUES TO THE DETERMINATION OF TRACES OF MOLYBDENUM IN SEA-WATER

TETSUYA KIRIYAMA

Laboratory for Chemistry, Faculty of Education, Kagoshima University, Kagoshima, Japan
and

ROKURO KURODA

Laboratory for Analytical Chemistry, Faculty of Engineering, University of Chiba, Chiba, Japan

(Received 9 November 1983. Accepted 14 December 1983)

Summary—A combined ion-exchange spectrophotometric method has been developed for the determination of molybdenum in sea-water. Molybdenum is sorbed strongly on Amberlite CG 400 (Cl^-) at pH 3 from sea-water containing ascorbic acid and is easily eluted with 6M nitric acid. Molybdenum in the effluent can be determined spectrophotometrically with potassium thiocyanate and stannous chloride. The combined method allows selective and sensitive determination of traces of molybdenum in sea-water. The precision of the method is 2% at a molybdenum level of $\sim 10 \mu\text{g/l}$.

Because of the low abundance of molybdenum in natural waters, preliminary isolation methods have usually been employed in its determination. Coprecipitation¹⁻³ and solvent extraction⁴⁻⁶ separations are most often used for this purpose. The other preconcentration methods available for molybdenum include co-crystallization,⁷ sorption on chitosan and modified cellulose,⁸ cation-exchange sorption on Zeo-Karb 225¹ and Chelex 100,^{9,10} concentration on Sephadex G-25¹¹ and (as the pyrrolidine dithiocarbamate complex) on charcoal.¹²

Kuroda and Kawabuchi have concentrated molybdenum by anion-exchange from sea-water containing acid and thiocyanate¹³ or hydrogen peroxide^{13,14} and determined it spectrophotometrically. Korkisch *et al.*¹⁵ have concentrated molybdenum from natural waters on Dowex 1-X8 in the presence of thiocyanate and ascorbic acid. A sodium citrate and ascorbic acid system¹⁶ has also been worked out for the concentration of molybdenum on Dowex 1-X8 (citrate form) as a citrate complex from tap and mineral waters.

In this work it has been found that molybdenum can be concentrated from sea-water simply on the strongly basic anion-exchange resin to which only ascorbic acid has been added. The anion-exchange concentration, coupled with the thiocyanate-stannous chloride method, allows sub-ppm levels of molybdenum to be determined successfully.

EXPERIMENTAL

Reagents

A stock solution (10 mg/ml) of molybdenum (as sodium molybdate dihydrate) was prepared with demineralized

water and standardized chelatometrically. One g of ferrous ammonium sulphate and 0.5 ml of concentrated sulphuric acid were dissolved in demineralized water and the mixture was diluted to 100 ml with water.

The strongly basic anion-exchange resin Amberlite CG 400 in the chloride form (100-200 mesh) was used. A slurry of 5 g of the resin in water was poured into a conventional ion-exchange tube (2.5 cm diameter) to make a bed 2.3 cm long.

A Hitachi Model 101 spectrophotometer with 1-cm glass cells was used.

Determination of distribution coefficients

The distribution coefficients of molybdenum(VI) were determined by the batch equilibrium method. Weighed portions of air-dried resin (1.0 g each) were mixed with 1.00 ml of molybdenum solution [0.110 mmole of Mo(VI)] and 40.0 ml of buffer solution containing ascorbic acid at various concentrations. The buffer solutions used were 0.1M potassium chloride-0.1M hydrochloric acid for pH 2, and 0.1M sodium acetate-0.1M acetic acid for pH 3-6. The mixtures were shaken for 20 hr and the distribution coefficients determined as described earlier.¹⁷

Procedures

Ion-exchange concentration. Filter the water sample through a membrane filter (0.45- μm , Millipore). Take a 500-ml portion of the filtrate, add 0.9 g of ascorbic acid and adjust the pH to 3.0 ± 0.1 . Pass the mixture through the ion-exchange column at a flow-rate of 5 ml/min. Wash the column with 250 ml of 0.01M ascorbic acid (pH 3). Strip the molybdenum by elution with 70 ml of 6M nitric acid.

Spectrophotometric determination. Evaporate the effluent to dryness. Add 2 ml of concentrated nitric acid and again evaporate to dryness. Take up the residue with 2 ml of hydrochloric acid and a small amount of water. Transfer the solution to a separatory funnel, add 1 ml of 1% ferrous ammonium sulphate solution and 3 ml of 10% potassium thiocyanate solution. Swirl, add 2 ml of 10% stannous chloride solution in 1M hydrochloric acid and immediately extract with 5.0 ml of di-isopropyl ether, shaking for 30 sec. Measure the absorbance of the organic layer at 460 nm against a reference blank.

Table 1. Distribution coefficients of molybdenum on Amberlite CG 400 (Cl⁻ form) in ascorbic acid and 0.5M sodium chloride

pH	Distribution coefficient			
	1.0M*	0.10M*	0.010M*	0.0010M*
Ascorbic acid alone				
2.1	3.4×10^3	7.1×10^3	7.7×10^3	6.2×10^3
2.9	9.8×10^3	$>10^4$	$>10^4$	$>10^4$
4.0	2.7×10^3	$>10^4$	$>10^4$	$>10^4$
5.0	1.2×10^3	$>10^4$	$>10^4$	$>10^4$
Sodium chloride present				
2.2	8.4×10^2	2.4×10^3	2.8×10^3	3.2×10^3
3.2	1.4×10^3	5.0×10^3	6.6×10^3	7.2×10^3
4.0	3.6×10^2	4.2×10^3	5.0×10^3	4.4×10^3
5.0	1.2×10^2	1.2×10^3	1.1×10^3	4.9×10^2
5.9	44	98	30	11

*Ascorbic acid concentration.

RESULTS AND DISCUSSION

The distribution coefficients of molybdenum on Amberlite CG 400 in the chloride form are listed in Table 1 as a function of ascorbic acid concentration in the pH range 2–5. Molybdenum sorbs very strongly from dilute ascorbic acid solutions ($\leq 0.1M$) over the pH range 3–5, the coefficient reaching $> 10^4$ under these conditions. The distribution coefficients of molybdenum in the presence of 0.5M sodium chloride are also shown in Table 1 for the pH range 2–6, as a function of ascorbic acid concentration. Generally the coefficients are lower in sodium chloride–ascorbic acid media than those in

ascorbic acid alone, in the pH range 2–5. However, the coefficients in the mixed media are sufficiently high to allow traces of molybdenum to be concentrated from large volumes of brine.

Korkisch and Krivanec¹⁶ claim that the ready displacement of ascorbate ion by the anions contained in natural water is one of the disadvantages of ascorbic acid when employed alone for concentrating molybdenum and vanadium from water samples by anion-exchange. However, the distribution coefficient of molybdenum is sufficiently high to allow its strong retention on Amberlite CG 400 even when the resin is in the chloride form (Table 1).

Table 2. Determination of molybdenum in saline water (0.5M NaCl) and sea-water

Sample*	Sample Volume, l.	Mo added, μg	Mo found, μg	Original content $\mu\text{g/l.}$
Saline water	1.0	0	0.12, 0.05	av. 0.09
	1.0	8.48	8.42, 8.25	av. 8.37 ± 0.15 †
			8.18, 8.56	
8.42				
Sea-water A	0.5	0	4.27, 4.51	8.54, 9.02
	1.0	0	4.39	8.78
			8.90	8.90
			4.24	8.98
			8.48	8.64
av. 8.81 ± 0.19				
Sea-water B	0.5	0	4.85, 4.70	9.70, 9.40
	1.0	0	4.85	9.70
			9.48	9.48
			4.24	9.56
			8.48	9.44
av. 9.55 ± 0.13				
Sea-water C	0.5	0	4.11, 4.08	8.22, 8.16
	1.0	0	4.29	8.58
			8.54	8.54
			4.24	8.40
			8.48	8.44
av. 8.39 ± 0.17				

*Sea-water A: collected at Kamoike Harbour, Kagoshima Bay, Japan, on 23 June 1983, Salinity 33.48‰.

Sea-water B: collected on the shore at Kushikino, East China Sea, on 30 June 1983, Salinity 34.03‰.

Sea-water C: collected at Yamagawa Harbour, Kagoshima Bay, Japan, on 6 July 1983, Salinity 31.55‰.

†Average recovery of total present after addition of Mo.

Chakravorty and Khopkar¹⁸ attempted to separate uranium(VI) from thorium, zirconium, titanium and other elements, including molybdenum, in ascorbate media (pH 4.5). In their procedure, uranium was eluted with 1M hydrochloric acid followed by molybdenum with dilute ammonia (1 + 7) containing 3% ammonium persulphate. We attempted to remove the molybdenum by elution with 4M perchloric acid, but recoveries were often about 25% lower than expected, owing to volatilization of some molybdenum during the strong fuming with perchloric acid.¹⁹ A gentle, careful evaporation did not yield serious loss of molybdenum. However, we found that molybdenum can be easily stripped from the column by elution with 70 ml of 6M nitric acid in accordance with the anion-exchange sorption characteristics of molybdenum in nitric acid media.²⁰

The high distribution coefficients of molybdenum in ascorbate media and its strong sorption in the presence of high concentrations of sodium chloride indicate that molybdenum should be sorbed on the resin from large volumes of natural water samples. To evaluate the feasibility of using the ascorbate system as the concentration method, a brine simulating sea-water (0.5M sodium chloride) spiked with a known amount of molybdenum was analysed by the present procedure and the results are given in Table 2. As can be seen, the recoveries for the 8 μ g of molybdenum added to 500 or 1000 ml samples are satisfactory.

The sorption of an ascorbate complex and subsequent elution with 6M nitric acid is not specific for molybdenum. Some information is available on the sorption of several other metals on anion-exchange resins in ascorbate media.^{18,21} In this study those elements which interfere with the determination of molybdenum by the thiocyanate-stannous chloride method and are at least as abundant in sea-water as molybdenum have been chosen and their interferences examined. The results suggest that titanium (130 μ g), vanadium(IV) (200 μ g), vanadium(V) (170 μ g), iron(III) (1000 μ g), nickel (480 μ g), copper(II) (130 μ g), zinc (300 μ g), arsenic(III) (290 μ g), tin(IV) (260 μ g), lead (60 μ g) and uranium(VI) (440 μ g), in the amounts shown in brackets, do not interfere with the determination of 8 μ g of molyb-

denum (error within $\pm 3.8\%$). These quantities are more than 50 times those present in 1 litre of sea-water. Even if they behave the same as molybdenum in the anion-exchange concentration and elution steps, these metal ions do not interfere with the determination of molybdenum in a 1 litre sea-water sample.

The results of repeated determinations of molybdenum in three sea-water samples are given in Table 2. The accuracy of the method was tested by adding molybdenum and determining overall recoveries. The recoveries and precision (r.s.d. 1.4–2.2%) of the method are satisfactory.

REFERENCES

1. K. M. Chan and J. P. Riley, *Anal. Chim. Acta*, 1966, **36**, 220.
2. N. Ohta, M. Fujita and K. Tomura, *Bunseki Kagaku*, 1979, **28**, 277.
3. V. G. Prabhu, L. R. Zarapkar and M. S. Das, *Mikrochim. Acta*, 1980 **II**, 67.
4. L. R. P. Butler and P. M. Matthews, *Anal. Chim. Acta*, 1966, **36**, 319.
5. Y. K. Chau and K. Lum-Shue-Chan, *ibid.*, 1969, **48**, 205.
6. Y. Akama, T. Nakai and F. Kawamura, *Nippon Kaisui Gakkai-shi*, 1979, **33**, 180.
7. A. I. Kulathilake and A. Chatt, *Anal. Chem.*, 1980, **52**, 828.
8. R. A. A. Muzzarelli and R. Rocchetti, *Anal. Chim. Acta*, 1973, **64**, 371.
9. J. P. Riley and D. Taylor, *ibid.*, 1968, **41**, 175.
10. W. H. Ficklin, *Anal. Lett.*, 1982, **15**, 865.
11. K. Yoshimura, S. Hiraoka and T. Tarutani, *Anal. Chim. Acta*, 1982, **142**, 101.
12. H. A. v.d. Sloot, G. D. Wals and H. A. Das, *ibid.*, 1977, **90**, 193.
13. K. Kawabuchi and R. Kuroda, *ibid.*, 1969, **46**, 23.
14. R. Kuroda and T. Tarui, *Z. Anal. Chem.*, 1974, **269**, 22.
15. J. Korkisch, L. Gödl and H. Gross, *Talanta*, 1975, **22**, 669.
16. J. Korkisch and H. Krivanec, *Anal. Chim. Acta*, 1976, **83**, 111.
17. T. Kiriyaama and R. Kuroda, *Talanta*, 1983, **30**, 261.
18. M. Chakravorty and S. M. Khopkar, *Chromatographia*, 1977, **10**, 372.
19. E. B. Sandell, *Colorimetric Determination of Traces of Metals*, 3rd Ed., p. 72. Interscience, New York, 1959.
20. J. P. Faris and R. F. Buchanan, *Anal. Chem.*, 1964, **36**, 1157.
21. M. Chakravorty and S. M. Khopkar, *Chromatographia*, 1977, **10**, 100.

ANALYTICAL DATA

DISSOCIATION CONSTANTS, NEUTRALIZATION ENTHALPIES AND REACTIONS OF 3-STYRYL-2-MERCAPTOPROPENOIC AND 3-(1-NAPHTHYL)-2-MERCAPTOPROPENOIC ACIDS

A. IZQUIERDO, E. BOSCH and J. L. BELTRAN

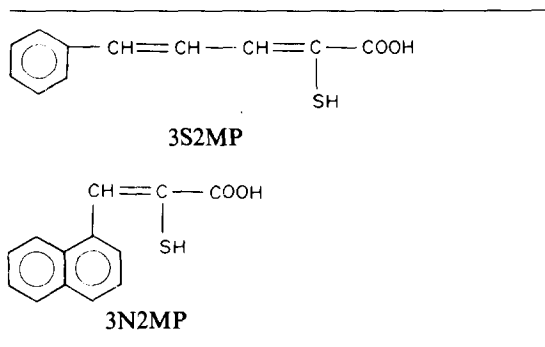
Department of Analytical Chemistry, University of Barcelona, Barcelona, Spain

(Received 17 May 1983. Accepted 17 November 1983)

Summary—Dissociation constants (pK_{a1} and pK_{a2} in water-ethanol medium for 3-styryl-2-mercaptopropenoic and 3-(1-naphthyl)-2-mercaptopropenoic acid have been determined potentiometrically, and pK_{a2} for both in aqueous medium, spectrophotometrically. Neutralization enthalpies in water-ethanol medium have been determined by thermometric titration. The reactions with metal ions have been studied, and the main reactions are described. The most sensitive reactions are with titanium(IV) ($pD = 7.00$) and nickel(II) ($pD = 6.50$).

Studies of some 3-aryl-2-mercaptopropenoic acids have been reported in previous papers, in which the aryl groups (Ar) were phenyl,¹ 2-furyl,² 2-pyrrolyl, 2-thienyl and 2-hydroxyphenyl.³

These compounds react with many metal ions. The conjugated double bond between the carboxyl and aryl groups makes the complexes more stable than those formed from reagents without this double bond. In the present work 3-styryl-2-mercaptopropenoic acid (3S2MP) and 3-(1-naphthyl)-2-mercaptopropenoic acid (3N2MP) have been studied to find the effects of extending the unsaturated chain and enlarging the 3-aryl group.



Potentiometric and thermometric titrations with alkali were used to determine the two acid groups (-SH and -COOH). The enthalpies of neutralization were determined by thermometric titration.

EXPERIMENTAL

Apparatus

Crison Digilab 517 and Radiometer PHM 84 pH-meters were used with a Radiometer G 202 B glass electrode,

Metrohm EA 120 combined glass electrode, an Ag/AgCl reference electrode,⁴ and a Wilhelm-type salt bridge.⁵ The spectrophotometer was a Beckman Acta M-VII and the thermometric titration assembly was that described in the previous work.⁶

Solutions

All solutions were deaerated with nitrogen before use, and all reagents were of analytical grade. The buffers for the spectrophotometry (0.01M ionic strength) were prepared according to Perrin.⁷ The ionic medium (NaClO_4) was prepared by a literature method.⁸

Carbonate-free sodium hydroxide solution was standardized against potassium hydrogen phthalate, and protected from atmospheric carbon dioxide.

Perchloric acid, stock solutions, 0.05-0.1M were standardized against sodium carbonate. The Gran method⁹ was used for both sets of standardizations.

Ethanolic solutions of the mercapto acids (0.1-1%) were prepared with deaerated ethanol.

Mercapto acids

These were synthesized as described by Campaigne and Cline,¹⁰ by condensation of cinnamaldehyde or 1-naphthaldehyde with rhodanine, subsequent hydrolysis in alkaline medium, and acidification with mineral acid. Recrystallization from benzene or toluene under nitrogen yielded products with m.p. 159° (3S2MP) and 178° (3N2MP). The purity was tested by thin-layer chromatography, and determined by potentiometric and thermometric titrations with sodium hydroxide in aqueous ethanol (purity > 99.5%).

For 3S2MP analysis gave C 63.9%, H 4.8%, S 15.4%; $\text{C}_{11}\text{H}_{10}\text{O}_2\text{S}$ requires C 64.05%, H 4.89%, S 15.51%. For 3N2MP analysis gave C 64.7%, H 4.3%, S 13.7%; $\text{C}_{13}\text{H}_{10}\text{O}_2\text{S}$ requires C 64.60%, H 4.38%, S 13.90%.

The solubilities (g per 100 ml of solution at 25°) were determined by the Wittenberger technique,¹² and were (3S2MP given first): water (0.05, 0.07); ethanol (1.20, 5.45); isoamyl alcohol (1.42, 1.90); acetone (3.70, 6.30); methyl isobutyl ketone (1.38, 3.91); chloroform (3.19, 2.98); diethyl ether (1.80, 3.97); toluene (1.16, 0.75); benzene (0.90, 0.95); hexane (0.01, 0.02). The ultraviolet-visible spectra were in accordance with the literature.¹⁰ The infrared spectra (KBr

Table 1. pK_a values in water-ethanol medium at $25 \pm 0.1^\circ$

	$I = 0.2M$		$I = 1.0M$	
	pK_{a1}	pK_{a2}	pK_{a1}	pK_{a2}
3S2MP	4.34 ± 0.02	8.91 ± 0.04	4.30 ± 0.02	8.43 ± 0.04
3N2MP	4.18 ± 0.01	9.80 ± 0.02	4.07 ± 0.02	9.32 ± 0.02

discs) had characteristic bands (cm^{-1}) at 1275 (C-O), 1410 (O-H), 1660 (C=O) and 2560 (S-H) for 3S2MP, and 1255 (C-O), 1330 (O-H), 1645 (C=O) and 2600 (S-H) for 3N2PP.

Procedures

Acidity constants. The dissociation equilibria were studied at $25 \pm 0.1^\circ$ by titration¹³ in 50% v/v water-ethanol with sodium hydroxide, because the compounds are poorly soluble in water, at two ionic strengths (0.2 and 1.0M) with sodium perchlorate as ionic medium. Before and during the titration pure nitrogen¹⁴ was passed through the solution to remove dissolved oxygen.

The pK_{a2} value was also determined spectrophotometrically¹⁵ with $5 \times 10^{-3}M$ mercapto acid in aqueous medium containing 1% ethanol and at 0.01M ionic strength. Great care was taken to avoid oxidation, but some did occur. Therefore, absorbance measurements at the analytical wavelengths were made immediately after preparation of the solutions.

Thermometric titrations and heats of neutralization. The mercapto acids were titrated thermometrically with sodium hydroxide in water-ethanol medium at 0.2M ionic strength (sodium perchlorate), and the heats of neutralization were determined. The procedure has already been described.⁶

The enthalpies of neutralization were determined from the heat capacity of the cell (Q), measured by means of a reaction of known enthalpy [neutralization of hydrochloric acid with sodium hydroxide ($\Delta H = -13.35$ kcal/mole at 25°),¹⁶ which in 50% v/v water-ethanol has the same value⁶]. The temperature increments were measured by the Barthel method.¹⁷ The heat capacity of the cell was found by means of the equation for an adiabatic system.

$$n \Delta H + Q \Delta T = 0$$

where n moles of HCl are titrated, ΔH is the enthalpy change of the reaction (cal/mole) and ΔT the temperature change. The value of Q was found to be 37.0 ± 0.1 cal/deg

under the conditions used. From this value the heats of neutralization of the mercapto acids can be determined from the temperature increase in their titration.

Reactions with metal ions. These were investigated by the Benedetti-Pichler technique¹⁸ for the whole pH range, with a 1% ethanolic solution of the reagent and 1-g/l. solutions of the metal ions.

RESULTS AND DISCUSSION

Dissociation equilibria

The pK_a values in water-ethanol medium were determined from the overall protonation constants β_1 and β_2 , calculated by the linearization method of Irving and Rossotti.¹⁹ The experimental data were treated by the least-squares program MINIPOT.²⁰

Table 1 shows the pK_a values for the two acids, and Figs. 1 and 2 show the theoretical formation curves (\bar{n} vs. $\log h$) and the experimental points for the titrations done at 1.0M ionic strength.

The pK_{a2} values were also determined spectrophotometrically because the experimental conditions (aqueous medium with 1% ethanol, low concentration and ionic strength) are such that the experimental pK_a values are close to the thermodynamic values and can be compared with those for other 3-aryl-2-mercaptopropenoic acids. Figures 3 and 4 show the spectra of 3S2MP and 3N2MP solutions at various pH values. The wavelengths of the absorption maxima were used as analytical wavelengths. Table 2 shows the results obtained.

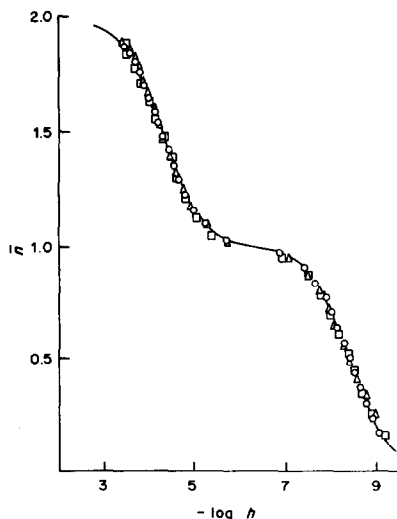


Fig. 1. Formation curve for 3S2MP (solid line = theoretical curve). Δ , $[3S2MP] = 1.752 \times 10^{-3}M$; \circ , $[3S2MP] = 1.997 \times 10^{-3}M$; \square , $[3S2MP] = 2.899 \times 10^{-3}M$.

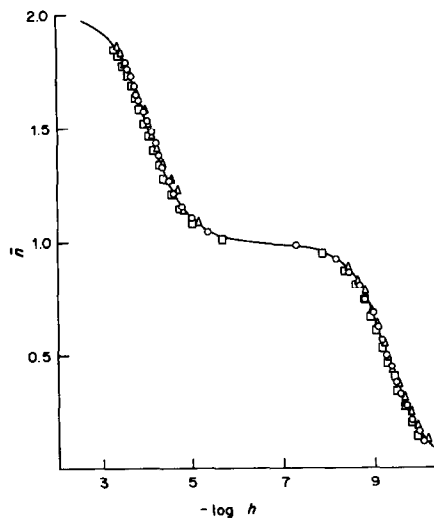


Fig. 2. Formation curve for 3N2MP. \circ , $[3N2MP] = 1.297 \times 10^{-3}M$; Δ , $[3N2MP] = 3.361 \times 10^{-3}M$; \square , $[3N2MP] = 2.418 \times 10^{-3}M$.

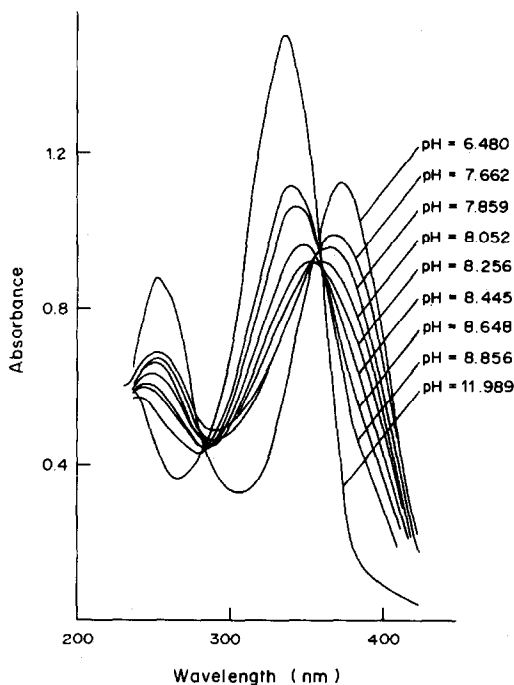


Fig. 3. Spectra for the determination of pK_{a2} of 3S2MP. For this compound, some oxidation has occurred during the recording of each spectrum and this accounts for the poor isosbestic points.

Reactions with metal ions

The reactions are similar to those of other 3-aryl-2-mercaptopropenoic acids.^{2,3} Precipitates

Table 2. pK_{a2} values in aqueous medium at 22 ± 0.5 and $I = 0.01M$

	3S2MP	3N2MP
Analytical wavelengths, nm	372 336	355 313
pK_{a2}	7.96 ± 0.03	8.73 ± 0.02

were formed with many cations that form insoluble sulphides, and some colour reactions were obtained with transition metals. The complexes formed were readily extracted with polar organic solvents (isoamyl alcohol, MIBK, diethyl ether).

Notable reactions are the red colour with Ti(IV) ($pD = 7$ by extraction, *i.e.*, dilution limit is $\sim 0.1 \mu\text{g/ml}$) in acetic acid-acetate medium (this reaction does not occur with saturated aryl mercaptoacids). Another interesting reaction is that of Ni(II) in alkaline medium ($pD = 6.5$) because the few interfering ions are easily removed. Table 3 lists the most sensitive reactions. The sensitivity of reactions is expressed in terms of pD [*i.e.*, $-\log(\text{dilution limit})$].

Thermometric titrations

The titration curves for both mercapto acids display two equivalence points, corresponding to the successive neutralization of the carboxylic and thiol groups. From the shapes of the curves it is concluded that both mercapto acids can be determined by thermometric titration. The titration error was found to be less than 1%.

Table 3. Most sensitive reactions

Metal ion	3S2MP			3N2MP		
	Medium	Without extraction	With extraction	Medium	Without extraction	With extraction
Cu^{2+}	HOAc	y(5.8)		HOAc	y-gr(6.0)	y-gr(6.3)A,B
	NaOH		y(6.7)A,B	NaOAc	y-gr(6.0)	y-gr(6.3)A,B
Pd^{2+}	HCl, HOAc	r(6.3)		HCl, HOAc	r-y(6.3)	r-y(6.5)A,B
	NaOAc	r(6.4)	r(6.5)C	NaOAc	r-y(6.0)	r-y(6.5)A,B
	NH_3 , NaOH	r(6.0)				
Mo^{6+}	HCl	r(6.4)	r(7.1)C	HCl, HOAc	y-or(6.3)	y-or(6.5)A,B
	HOAc, NaOAc	r(6.3)		NaOAc	y-or(6.2)	y-or(6.2)A
Fe^{2+}	NaOAc	gr(6.4)	gr(6.5)A	NaOAc	gr-bl(6.7)	gr-bl(6.7)A
	NH_3	gr(6.3)		NH_3	gr(6.6)	gr(6.6)A
Co^{2+}	NaOAc	y-gr(6.3)		NaOAc	y-gr(6.3)	y(6.8)A,B
	NH_3	y-gr(6.2)		NH_3	y-gr(5.7)	y(6.3)A,B
Ni^{2+}	NaOH	y-gr(6.2)	y(6.7)A	NaOH	y-gr(6.3)	y(6.9)A,B
	NaOAc	y(6.4)		NaOAc	y-gr(6.7)	y-gr(6.8)A
	NH_3	y(6.0)		NH_3	y-gr(6.5)	
V^{5+}	NaOH	y(6.0)	y(6.5)A	NaOH	y-gr(6.5)	y(6.5)A
Ti^{4+}	NaOAc	y-gr(6.0)	y(6.4)A			
W^{6+}	NaOAc	r(6.5)	r(7.1)A,A+C	NaOAc	r(6.6)	r(6.9)A,(7.0)C
Ti^{3+}	HCl, HOAc	y(6.1)				
	HCl, HOAc	y(6.1)				

Solvents

A = isoamyl alcohol
B = MIBK
C = diethyl ether

Colours

y = yellow r = red
y-gr = yellow-green
gr-bl = green-blue
y-or = yellow-orange

Table 4. Neutralization enthalpies (kcal/mole) at 22 ± 0.5 and $I = 0.2$

	-COOH group	-SH group	Total neutralization
3S2MP	-10.56 ± 0.07	-7.49 ± 0.10	-18.05 ± 0.20
3N2MP	-10.60 ± 0.11	-5.38 ± 0.12	-15.98 ± 0.20

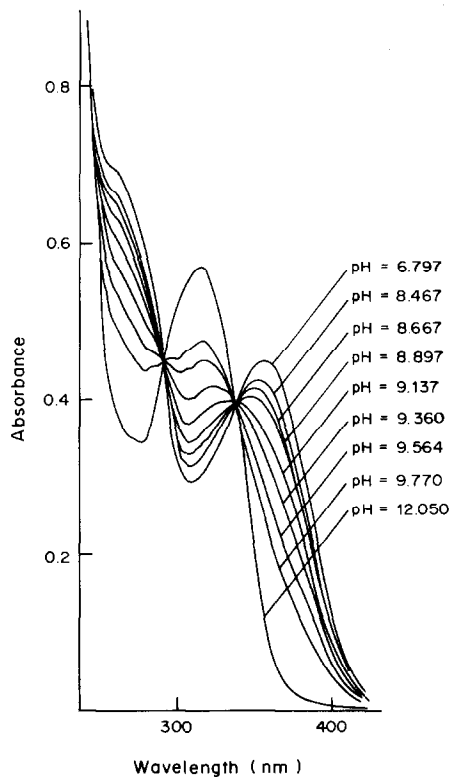
Fig. 4. Spectra for the determination of pK_{a_2} of 3N2MP.

Table 4 lists the ΔH values, calculated as shown above. The ΔH values for the carboxylic group are very similar (*cf.* the pK_{a_1} values), whereas the ΔH

value for the thiol group is higher for 3S2MP than for 3N2MP, in agreement with the pK_{a_2} values.

REFERENCES

1. A. Izquierdo and N. Garriga, unpublished work.
2. A. Izquierdo and J. Calmet, *Quim. Anal.*, 1974, **28**, 148.
3. A. Izquierdo and M. Giné, *An. Quim.*, 1978, **74**, 53.
4. A. S. Brown, *J. Am. Chem. Soc.*, 1934, **56**, 646.
5. W. Forsling, S. Hietaneo and L. G. Sillén, *Acta Chem. Scand.*, 1952, **6**, 601.
6. A. Izquierdo and J. Carrasco, *Talanta*, 1981, **28**, 341.
7. D. D. Perrin and B. Dempsey, *Buffers for pH and Metal Ion Control*, Chapman & Hall, London, 1974.
8. *Some Laboratory Methods*, The Royal Institute of Technology, Stockholm, 1959.
9. G. Gran, *Analyst*, 1952, **77**, 661.
10. E. Campaigne and R. E. Cline, *J. Org. Chem.*, 1956, **21**, 32.
11. A. Izquierdo and L. Garcia, *An. Quim.*, 1983, **79B**, 254.
12. W. Wittenberger, *Chemische Laboratoriumstechnik*, 6th Ed., Springer, Vienna, 1963.
13. F. J. C. Rossotti and H. S. Rossotti, *The Determination of Stability Constants*, pp. 22, 53. McGraw-Hill, New York, 1961.
14. L. Meites, *Polarographic Techniques*, 2nd Ed., p. 89. Wiley, New York, 1965.
15. A. Albert and E. P. Serjeant, *The Determination of Ionization Constants*, Chapman & Hall, London, 1971.
16. J. Barthel, F. Becker and N. G. Schmahl, *Z. Phys. Chem.*, 1961, **29**, 58.
17. J. Barthel, *Thermometric Titrations*, Wiley, New York, 1975.
18. A. Benedetti-Pichler, *Microtechnique of Inorganic Analysis*, Wiley, New York, 1950.
19. H. Irving and H. S. Rossotti, *J. Chem. Soc.*, 1953, 3397.
20. F. Gaizer and A. Puskás, *Talanta*, 1981, **28**, 565.

A CONTRIBUTION TO THE USE OF THORIN AS AN ANALYTICAL REAGENT: SPECTROPHOTOMETRIC STUDY OF ITS COMPLEXATION WITH BARIUM AND APPLICATION TO SULPHATE DETERMINATION IN ATMOSPHERIC PARTICULATES*

P. BRUNO, M. CASELLI, A. TRAINI and A. ZUFFIANÒ
Dipartimento di Chimica, Università di Bari, 70126 Bari, Italia

(Received 11 April 1983. Revised 16 January 1984. Accepted 9 February 1984)

Summary—The complexation of Ba^{2+} by Thorin in the pH range 2–9 in aqueous ethanol medium has been investigated. The dissociation constants of Thorin in the ethanolic medium have been determined spectrophotometrically and the distribution of the protonated species has been used to explain the behaviour of the apparent complexation constant. On the basis of the apparent constants found, and mass-balances, the effect of sulphate on the absorbance has been calculated, and the best conditions for determination of sulphate have been established. Cation and anion interferences have been studied and means of overcoming them are proposed. The method developed has been applied to sulphate determination in atmospheric particulates. As little as $1 \mu g$ of sulphate can be measured.

Since its introduction by Kuznetsov,¹ 1-(*o*-arsenophenylazo)-2-naphthol-3,6-disulphonic acid (Thorin) has found wide application in analytical chemistry. It forms complexes with practically all metals. Thorium,² lithium,³ bismuth,⁴ lanthanides⁵ and beryllium⁶ have been detected by reaction with Thorin. The complexes with uranium(VI),⁷ and magnesium, calcium and strontium⁸ have been studied and the reagent has been recommended as an indicator in the titrimetric determination of sulphate^{9,10} and for the determination of sulphur dioxide,¹¹ sulphur trioxide¹² and sulphuric acid.¹³

Although an extensive investigation on the effect of pH and alcohol concentration has been reported by Haartz,¹⁴ the titration method is not the most suitable for small quantities of sulphate, and concentrations below $10^{-4} M$ give erroneous results.

A colorimetric Thorin method for sulphate has been proposed by Persson¹⁵ and reviewed by Bertolaccini,¹⁶ but the optimum pH and barium concentration were not thoroughly considered in either paper.

Here we present a study on the complexation of barium by Thorin at pH 2.0–9.0 in 60% v/v ethanol medium (54% w/w). The dissociation constants of Thorin in this solvent have been determined spectrophotometrically and the results used to interpret the behaviour of the apparent complexation constant. The effect of sulphate on the absorbance has been calculated and the optimum conditions for sulphate determination predicted.

The method thus designed has been applied to determination of sulphate in real samples of atmospheric particulates. Quantities of sulphate as small as $1 \mu g$ can be determined.

EXPERIMENTAL

Apparatus

A Perkin-Elmer 555 spectrophotometer and an Orion 901 Ionanalyzer were used. The glass electrode was standardized with acetic acid/sodium acetate and ammonium perchlorate/ammonia buffers prepared in 60% v/v ethanol medium. The pK_a values for acetic acid (5.97) and ammonium ion (8.55) in aqueous ethanol were calculated by the relationships:¹⁷

$$\Delta pK_a(HA) = \log f_{H^+} + m_- y_-$$

$$\Delta pK_a(BH^+) = \log f_{H^+} + m_0 y_0$$

Values for $\log f_{H^+}$, m_- , y_- , m_0 , y_0 are reported in (or can be easily calculated from) the literature.¹⁷⁻¹⁹ Once standardized in this way, the electrode reproduced within 0.02 units the pH values calculated by these equations for acetic acid/sodium acetate, ammonium/ammonia and formic acid solutions.

The dissociation and complexation constants were measured at 25°, but no temperature control was used for analytical determinations.

Airborne particulates were sampled with Millipore 0.45- μm filters in a Tecora Ecol CTE electronic atmospheric sampler.

Reagents

The Thorin (RPE, C. Erba) was recrystallized from water. A standard stock solution was prepared and checked by titration.²⁰ All other reagents were of analytical grade.

RESULTS

pK_a of Thorin in aqueous ethanol

The absorbances of Thorin in aqueous ethanol were measured at 520 (Fig. 1A) and 430 nm as a

*This work was supported by C.N.R. (Rome), Contract No. 82.01065.83

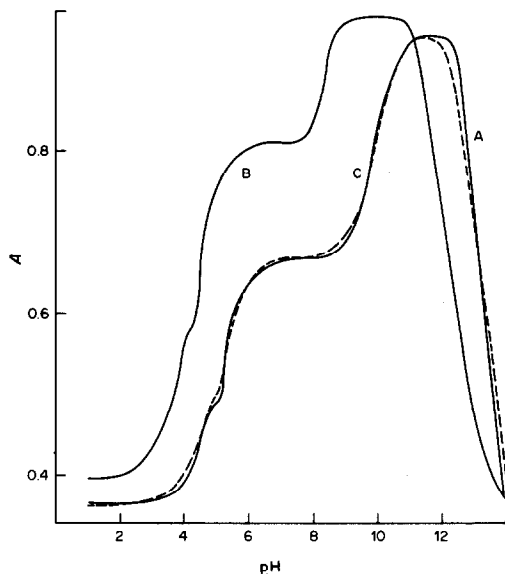


Fig. 1. Absorbance of $6.45 \times 10^{-5} M$ Thorin *vs.* pH. (A) Experimental curve at variable ionic strength; (B) at $\mu = 0.1 M$ (NaClO_4); (C) Curve calculated from data reported in Table 1.

function of pH, and also (Fig. 1B) with the ionic strength kept constant at 0.1 with sodium perchlorate. For Fig. 1A the sodium concentration was the minimum compatible with the pH values; for $\text{pH} < 11$ it was $< 5 \times 10^{-4} M$. The pH-shift on increase of the sodium concentration is too large to be ascribable to an ionic strength effect, and clearly shows complexation of sodium by Thorin. This effect will be described and evaluated later, but for the moment we can say that sodium has no substantial influence on the absorbance if its concentration is $< 10^{-4} M$. The $\text{p}K_a$ values for the various protonated Thorin species were obtained from curve A in Fig. 1 and are reported in Table 1 together with the molar absorptivities of the conjugate bases, and other results. The first proton is completely dissociated even at the lowest pH. The real value of $\text{p}K_5$ is probably higher than 13.3 because at this pH level the sodium concentration is high enough to produce a shift towards lower pH. The value reported in Table 1 is

merely indicative. However, if $\text{p}K_5$ is ≥ 13.3 it does not influence the distribution of the protonated species at $\text{pH} < 11$. The averages of the $\text{p}K_a$ values in aqueous solution^{20,21} give a meaningful linear correlation ($r = 0.9965$) with the $\text{p}K_a$ values in the mixed solution:

$$\text{p}K_{\text{EtOH}(54\%)} = 1.52 + 1.02 \text{p}K_{\text{H}_2\text{O}} \quad (1)$$

This is rather surprising because the extent of ionization of a given acid in two different media is determined by (a) the basicity of the solvent and (b) the dielectric constant. Water is 400 times as basic as ethanol,²² irrespective of the acid ionized, but (b) depends on the electrostatic energy involved in the charge separation. According to Wynne-Jones²³ the electrostatic contribution to $\Delta\text{p}K$ between two media can be expressed by

$$\Delta\text{p}K_{\text{el}} = \frac{e^2}{4.6KTr} \left(\frac{D_2 - D_1}{D_1 D_2} \right) \left(1 - \frac{2z_B + 1}{R} \right) \quad (2)$$

where r is the radius of H_3O^+ , $R = r_{\text{AH}}/r_{\text{H}_3\text{O}^+}$, z_B the charge on the conjugate base of the acid AH , and D_1 and D_2 are the dielectric constants of the two media. Therefore $\Delta\text{p}K_{\text{el}}$ should increase with increasing z_B and $\Delta\text{p}K$ should increase for successive dissociations of a polyprotic acid. However, if R is large enough, the second term in parentheses in equation (2) can be neglected, and in that case, for Thorin the sum of $\Delta\text{p}K_{\text{el}}$ and of the basicity effect (assumed roughly proportional to the mole fraction of ethanol) is very close (1.33) to the intercept of equation (1).

Figure 2 is a distribution diagram for the protonated species of Thorin (α_i) as a function of pH. In this calculation the $\text{p}K_5$ determined at 520 nm is used, since the first inflexion is poorly defined in the measurements made at 430 nm. From the α_i and ϵ_i values reported in Table 2, the absorbance *vs.* pH curve can be recalculated (dashed line, C, in Fig. 1).

Determination of the Ba^{2+} -Thorin apparent complexation constants

When a barium salt is added to an aqueous ethanol solution of Thorin the absorbances near 520 and 430 nm increase and decrease respectively. Between these

Table 1

Equilibrium	$\text{p}K_{\text{EtOH}/\text{H}_2\text{O}}$		$\text{p}K_{\text{H}_2\text{O}}^*$	$\text{p}K_{\text{H}_2\text{O}}^\dagger$	$\Delta\text{p}K^\S$	$\epsilon'_{(520\text{nm})}$ $l. \text{mole}^{-1}. \text{cm}^{-1}$
	$\lambda = 520 \text{ nm}$	$\lambda = 430 \text{ nm}$				
$\text{H}_5\text{T} \xrightleftharpoons{k_1} \text{H}^+ + \text{H}_4\text{T}^-$	Strongly acid		Strongly acid	Strongly acid		5.66×10^3
$\text{H}_4\text{T}^- \xrightleftharpoons{k_2} \text{H}^+ + \text{H}_3\text{T}^{2-}$	4.20	4.40	—	2.37	1.83	6.93×10^3
$\text{H}_3\text{T}^{2-} \xrightleftharpoons{k_3} \text{H}^+ + \text{H}_2\text{T}^{3-}$	5.40	5.40	3.70	4.35	1.70–1.05	1.05×10^4
$\text{H}_2\text{T}^{3-} \xrightleftharpoons{k_4} \text{H}^+ + \text{HT}^{4-}$	10.05	10.00	8.30	8.26	1.75	1.50×10^4
$\text{HT}^{4-} \xrightleftharpoons{k_5} \text{H}^+ + \text{T}^{5-}$	13.25	13.35	11.80	11.18	1.45–2.07	4.96×10^3

*Reference 20; measured at 290 and 345 nm.

†Reference 21.

§Between aqueous ethanol and aqueous medium.

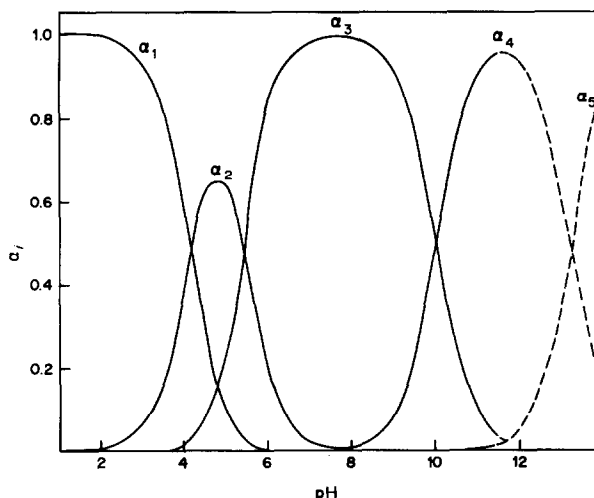


Fig. 2. Fractions of the ionized forms of Thorin.

wavelengths there is an isosbestic point (Fig. 3), behaviour typical of a metal-ligand complex.

Figure 4 plots the absorbances for $6.45 \times 10^{-5} M$ Thorin mixed with various concentrations of barium (C_{Ba}) for different values of pH obtained by addition of $HClO_4$, CH_3COOH/CH_3COONa , NH_4ClO_4/NH_4OH , according to the pH required. When cations were added in the buffers, their concentration was kept below $10^{-3} M$. As shown later, this concentration does not produce detectable error in the equilibrium constant, provided that $C_{Ba} > 4 \times 10^{-5} M$ is used for the calculations and the absorbances at a given pH in absence of barium (A_0) are taken from curve A in Fig. 1. Figure 4 shows that for $pH > 7$ the plots are linear for low C_{Ba} and give constant absorbance at high C_{Ba} . The extrapolated linear portions intersect at a C_{Ba} value practically equal to the Thorin concentration, indicating a 1:1 complex with a relatively high formation constant. At lower pH the plots become more rounded and do not reach a constant absorbance. For $C_{Ba} > 4 \times 10^{-4} M$, and after a period of time depending on the pH, a red precipitate appears, which is found by atomic-absorption analysis to contain 20.6% barium, in good agreement with a 1:1 complex. The infrared spectrum shows changes

from that of Thorin, in the ranges 1230–1120 and 1080–1025 cm^{-1} , corresponding to the SO-stretching of RSO_3^- groups.²⁴

The curves in Fig. 4 have been analysed to obtain K_{app} , according to the relationship

$$K_{app} = \frac{(A - A_0)(A_\infty - A_0)}{(A_\infty - A) \{C_{Ba}(A_\infty - A_0) - C_T(A - A_0)\}} \quad (3)$$

where A_∞ is the limiting absorbance, A the absorbance corresponding to C_{Ba} , and C_T is the analytical Thorin concentration. Equation (3) is readily obtained by taking into account the complex and free ligand absorbances and the mass balance. As will be shown in the discussion, equation (3) is still valid even if several 1:1 complexes with different ionic forms of a polyprotic acid are formed simultaneously, but in this case K_{app} is a function of α_i and K_i . When the absorbance reaches no limiting value in the range of possible barium concentrations, equation (3) can be put into the form:²⁵

$$F(A) = \frac{[Ba^{2+}] C_T}{A - A_0} = \frac{1}{K_{app}(\epsilon_{app} - \epsilon_0)} + \frac{[Ba^{2+}]}{(\epsilon_{app} - \epsilon_0)} \quad (4)$$

where $\epsilon_{app} = A_\infty/C_T$. As $[Ba^{2+}]$ is unknown, in prin-

Table 2

pH	$\log K_{app}$	ϵ_{app}^* $10^4 l. mole^{-1}. cm^{-1}$	$-\log \alpha_2$	$-\log \alpha_3$	$-\log \alpha_4$	$-\log \alpha_5$
2.08	2.75	1.50	2.12	5.43	13.40	24.56
2.47	3.32	1.51	1.72	4.61	12.16	22.91
3.00	3.64	1.53	1.23	3.63	10.68	20.93
3.60	4.21	1.53	0.70	2.50	8.95	18.60
4.15	4.56	1.56	0.34	1.60	7.49	16.59
4.65	4.76	1.63	0.19	0.94	6.34	14.94
5.25	5.09	1.75	0.25	0.41	5.20	13.20
6.10	5.26	1.84	0.78	0.08	4.03	11.18
7.00	5.32	1.86	1.62	0.01	3.06	9.31
7.50	5.48	1.86	2.10	0.00	2.56	8.30
8.25	5.80	1.88	2.86	0.01	1.82	6.81
9.10	6.23	1.91	3.70	0.04	1.04	5.22

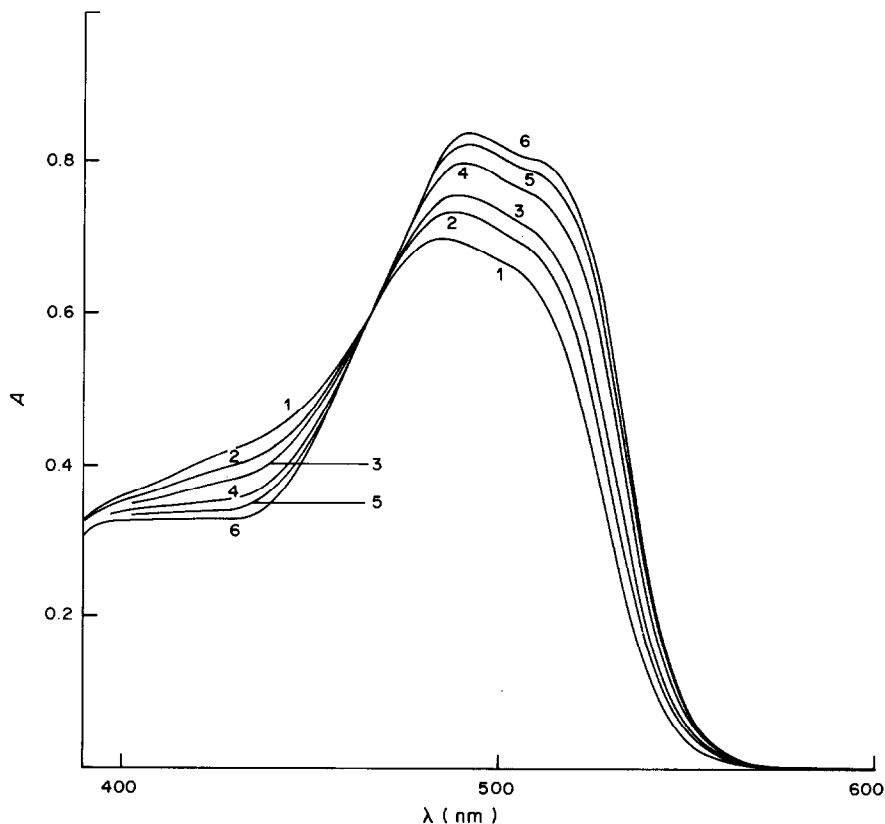


Fig. 3. Spectrum of Thorin in the presence of Ba^{2+} . $C_T = 6.45 \times 10^{-5} M$; pH = 5.7; (1) Thorin; (2-6) increasing concentration of Ba^{2+} .

ciple an iterative convergence process can be used, starting from the analytical barium concentration.

Examples of the linear plots obtained for $F(A)$ vs. $[\text{Ba}^{2+}]$ are shown in Fig. 5. The K_{app} and ϵ_{app} values are collected in Table 2, together with the α_i values

corresponding to a given pH. The K_{app} values were found to be reproducible within $\pm 10\%$ for the lower pH levels and within 50% for pH > 7. At pH = 9.1 the fraction of uncomplexed barium is only about 10% when $C_{\text{Ba}} = C_T$ and the error in K_{app} can then be

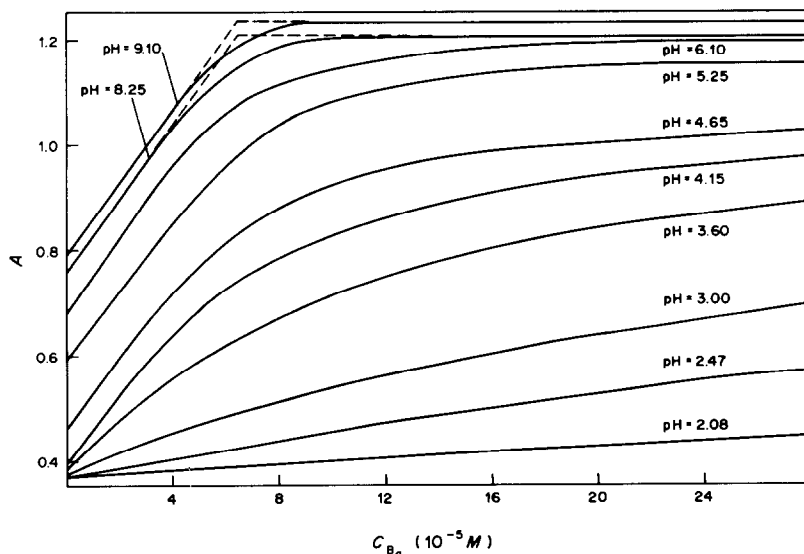


Fig. 4. Absorbance vs. C_{Ba} at $\lambda = 520 \text{ nm}$; pH reported on each curve; $C_T = 6.45 \times 10^{-5} M$.

greater. The K_{app} reported in Table 2 for this pH must be considered as only indicative; an error of 100% is possible. For pH > 9, K_{app} becomes too high to be obtained by spectrophotometric methods.

DISCUSSION

True Ba-Thorin complexation constant determination

The behaviour of K_{app} in Table 2 is such that it cannot be explained by assuming complexation by only one of the ionized forms of Thorin (since K_{app} should then be proportional to one of the sets of α_i values). Both α_2 and α_3 present a maximum (at pH 4.6 and 7.7 respectively); α_4 has monotonic behaviour in the pH range considered, but does not show any proportionality to K_{app} . However, if we suppose that barium forms 1:1 complexes with more than one form of Thorin we shall have:

$$A = \sum_{i=0}^{i=5} (\epsilon_i^T [T_i] + \epsilon_i^C [BaT_i]) \quad (5)$$

where

$$[T_i] = [H_{5-i}T^{i-}] = \alpha_i C_{NC} = \alpha_i (C_T - \Sigma[BaT_i]) \quad (6)$$

$$[BaT_i] = K_i [Ba^{2+}] [T_i] \quad (7)$$

C_{NC} is the concentration of non-complexed Thorin and ϵ_i^T and ϵ_i^C are the molar absorptivities of T_i and BaT_i respectively. From (6) and (7), we have

$$C_{NC} = \frac{C_T}{1 + [Ba^{2+}] \Sigma \alpha_i K_i} \quad (8)$$

From (7) and (8) we can rewrite (5) as

$$A = \frac{C_T (\Sigma \alpha_i \epsilon_i^T + [Ba^{2+}] \Sigma \epsilon_i^C \alpha_i K_i)}{1 + [Ba^{2+}] \Sigma \alpha_i K_i} \quad (9)$$

Putting $\Sigma \alpha_i K_i = K_{app}$ and $\Sigma \epsilon_i^C \alpha_i K_i / \Sigma \alpha_i K_i = \epsilon_{app}$, we

can write (9) in the form

$$A - A_0 = \frac{C_T [Ba^{2+}] (\epsilon_{app} - \epsilon_0) K_{app}}{1 + [Ba^{2+}] K_{app}} \quad (10)$$

where $A_0 = C_T \epsilon_0 = C_T \Sigma \alpha_i \epsilon_i^C$. Equation (10) is the same as (4). Alternatively, since

$$\Sigma [BaT_i] = C_T - C_{NC} = \frac{C_T K_{app} [Ba^{2+}]}{1 + K_{app} [Ba^{2+}]} \quad (11)$$

equation (10) can be written as

$$\begin{aligned} A - A_0 &= (\epsilon_{app} - \epsilon_0) \Sigma [BaT_i] \\ &= (A_\infty - A_0) \frac{\Sigma [BaT_i]}{C_T} \end{aligned} \quad (12)$$

or

$$\begin{aligned} \frac{A - A_0}{A_\infty - A} &= \frac{\Sigma [BaT_i]}{C_{NC}} = K_{app} [Ba^{2+}] \\ &= K_{app} (C_{Ba} - \Sigma [BaT_i]) \end{aligned} \quad (13)$$

If $\Sigma [BaT_i]$ from (12) is substituted in (13), solving for K_{app} gives equation (3).

The K_i value can be obtained from $\Sigma \alpha_i K_i = K_{app}$ by iteration if there are ranges where a single complex strongly predominates. In this case a straight line with a slope very close to unity will be obtained for a log-log plot of K_{app} against the right α_i . This happens for pH 2.0-4.2 if $\log \alpha_2$ is taken as abscissa. Further, in this pH range the relatively low solubility and the infrared spectrum are in agreement with formation of the neutral salt H_3BaT .

Once a first approximation is obtained for K_2 , it is possible to obtain first approximations for K_3 and K_4 by plotting $\log (K_{app} - \alpha_2 K_2)$ vs. $\log \alpha_3$ in the range pH 5-7 and $\log (K_{app} - \alpha_2 K_2 - \alpha_3 K_3)$ in the range pH 7-9. The values can then be refined by iteration. Figure 6 shows the final straight lines for

$$\log \left(K_{app} - \sum_{j \neq i} \alpha_j K_j \right) \text{ vs. } \log \alpha_i.$$

Final values for K_i are: $K_2 = 6.9 \times 10^4$, $K_3 = 2.0 \times 10^5$ and $K_4 = 1.0 \times 10^7$. The slope for the K_4 plot is 0.8 and this can be attributed to the low precision for K_{app} at the highest pH.

In Fig. 7 experimental values for $\log K_{app}$ (circles) are compared with those calculated from $\Sigma \alpha_i K_i = K_{app}$ (continuous line).

Effect of complexation by buffer cation

Univalent ions are complexed by Thorin though less strongly than bivalent ions. To evaluate their effect, the apparent complexation constants were measured at various pH levels for Na^+ and NH_4^+ (Table 3). It is rather surprising that even for univalent ions equation (3) gives a constant value of K_{app} for a 1:1 ($T_i M^+$) complex but not a 1:2 complex. However, a plot of absorbances vs. $[M^+]$, at pH 8.0, gives a plateau and then an absorbance increase when the cation concentration exceeds $10^{-2} M$.

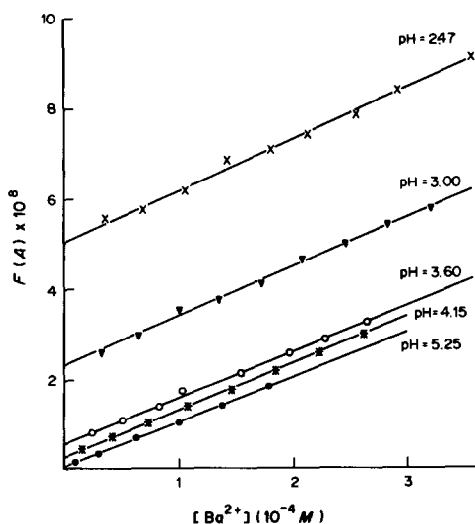


Fig. 5. $F(A)$ (see text) vs. $[Ba^{2+}]$ for different values of pH.

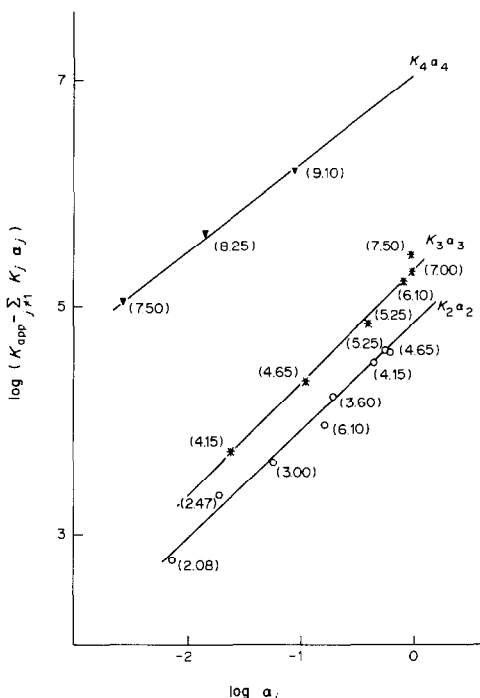


Fig. 6. Final iteration for

$$\log \left(K_{app} - \sum_{j=1}^n K_j \alpha_j \right) \text{ vs. } \log \alpha_i.$$

Numbers in parentheses are the corresponding pH values.

In presence of both barium and a univalent ion, equation (10) becomes

$$A - A_0 = \frac{C_T \{ [Ba^{2+}] K_{app}^{Ba} (\epsilon_{app}^{Ba} - \epsilon_0) + [M^+] (\epsilon_{app}^M - \epsilon_0) K_{app}^M \}}{1 + [Ba^{2+}] K_{app}^{Ba} + [M^+] K_{app}^M} \quad (14)$$

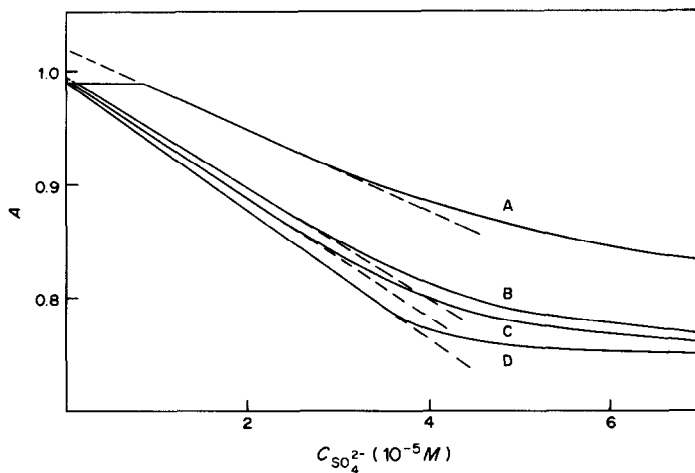


Fig. 8. Absorbance of a Ba-Thorin solution during a precipitation by SO_4^{2-} , calculated for different values of K_s . $C_T = 6.45 \times 10^{-5} M$; $C_{Ba} = 4.0 \times 10^{-5} M$; $C_{Na} = 4.0 \times 10^{-3} M$; $K_{app}^{Ba} = 4.6 \times 10^5$; $K_{app}^{Na} = 330$; $\epsilon_0 = 1.02 \times 10^4$; $\epsilon_1 = 1.86 \times 10^4$; $\epsilon_{Na} = 1.27 \times 10^4 \text{ l. mole}^{-1} \cdot \text{cm}^{-1}$; (A) $K_s = 5 \times 10^{-11}$; (B) $K_s = 9 \times 10^{-12}$; (C) $K_s = 5 \times 10^{-12}$; (D) $K_s = 1 \times 10^{-12}$.

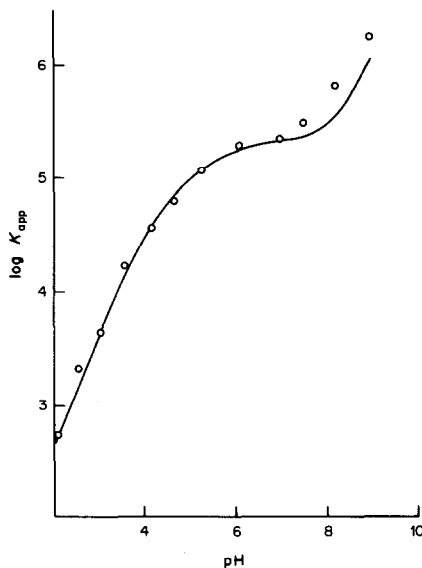


Fig. 7. Experimental $\log K_{app}$ (circles) vs. pH compared with the values calculated by equation (9) (continuous line).

Of course the M^+ effect is negligible if $K_{app}^{Ba} [Ba^{2+}] \gg K_{app}^M [M^+]$. To evaluate the influence of M^+ , theoretical absorbances were calculated from equation (14), taking into account the mass balances for the chemical species. Numerical values introduced into equation (14) were: $K_{app}^{Ba} = 6.0 \times 10^4$, $K_{app}^{Na} = 70$, $C_{Na} = 4.0 \times 10^{-3} M$, $C_T = 6.45 \times 10^{-5} M$, $\epsilon_{Ba} = 1.67 \times 10^4$, $\epsilon_{Na} = 1.25 \times 10^4$, $\epsilon_T = 7.13 \times 10^3 \text{ l. mole}^{-1} \cdot \text{cm}^{-1}$. These data correspond to $\text{pH} = 4.6$, where the ratio K_{Ba}/K_{Na} is the most unfavourable. The calculated absorbances, when introduced into equation (3) (used without correction for the presence of Na^+) gave $K_{app}^{Ba} = 6.1 \times 10^6$, for Ba concentrations $> 4.0 \times 10^{-5} M$.

Effect of sulphate on Ba-Thorin complex

When sulphate is added to a solution containing Thorin and a barium salt, buffered at a given pH, in such a quantity that the solubility product for barium sulphate is exceeded, the concentrations are ruled by the relationships:

$$C_T = \Sigma[\text{BaT}_i] + \Sigma[\text{MT}_i] + \Sigma[\text{T}_i];$$

$$[\text{SO}_4^{2-}] = C_{\text{SO}_4} - C_{\text{Ba}} + \Sigma[\text{BaT}_i] + [\text{Ba}^{2+}];$$

$$C_M = \Sigma[\text{MT}_i] + [\text{M}^+];$$

$$K_{\text{app}}^{\text{Ba}} = \frac{\Sigma[\text{BaT}_i]}{[\text{Ba}^{2+}]\Sigma[\text{T}_i]};$$

$$K_{\text{app}}^{\text{M}} = \frac{\Sigma[\text{MT}_i]}{[\text{M}^+]\Sigma[\text{T}_i]};$$

$$K_s = [\text{Ba}^{2+}][\text{SO}_4^{2-}]$$

Figure 8 shows the calculated absorbance *vs.* analytical concentration of sulphate when the initial total barium concentration is $4.0 \times 10^{-5}M$. Curves are calculated for pH 8.0 and different values of the solubility product. The pH is supposedly buffered by $\text{NH}_4^+/\text{NH}_3$, assuming $[\text{NH}_4^+] = 4.0 \times 10^{-3}M$. Values of $K_{\text{app}}^{\text{Ba}}$ and $K_{\text{app}}^{\text{Na}}$ are taken from Fig. 7 and Table 3. The absorbance is a linear function of C_{SO_4} practically up to the equivalence point if the solubility product is $K_s < 2.0 \times 10^{-12}$.

Figure 9 shows the calculated differences ($A_i - A$) plotted *vs.* C_{SO_4} where A_i is the absorbance of the barium-Thorin solution in absence of sulphate. The curves can be obtained experimentally if the barium-Thorin solution is positioned in the spectrophotometer sample compartment and the barium-Thorin-sulphate mixture in the reference compart-

Table 3

pH	Ion	K_{app}	$10^3 \epsilon_{\text{app}} \cdot \text{l. mole}^{-1} \cdot \text{cm}^{-1}$
2.5	Na^+	~ 2	12.5
4.8	Na^+	70	13.0
8.0	Na^+	400	13.4
8.0	NH_4^+	330	12.7

ment. Different pH levels and initial concentrations of barium are considered in Fig. 9. A value of 1.0×10^{-12} was used for K_s , on the basis of the better fit between the experimental and calculated curves. The curves for low pH are linear for a wide range of initial Ba concentration, but the sensitivity is low. The curves for pH 5 present the best sensitivity. They are linear up to $C_{\text{SO}_4} = 2.5 \times 10^{-5}M$ if $C_{\text{Ba}} = 4.0 \times 10^{-5}M$ and present no linearity at all if $C_{\text{Ba}} = 8.0 \times 10^{-5}M$. The curves for pH 8 have slightly lower sensitivity but better linearity than those at pH 5.

ANALYTICAL APPLICATIONS

Calibration plots and foreign ion effects

The equations reported above allow some prediction of the best conditions for analytical use of Thorin. For instance, calculation of the curves for titration of sulphate with barium (Fig. 10) shows that the error rapidly increases as the sulphate concentration decreases. The limiting sulphate concentration for acceptable error is $1.0 \times 10^{-4}M$. In effect the relative error decreases with decrease of Thorin concentration, but a limit is set by the ability to discriminate the colour change visually. Moreover,

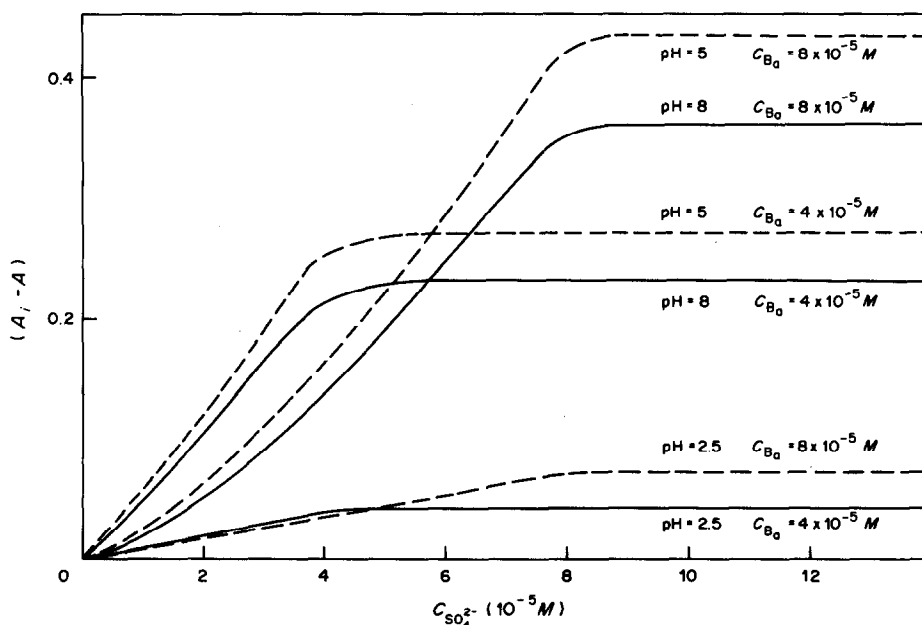


Fig. 9. Decrease in Ba-Thorin absorbance on addition of SO_4^{2-} ions, for different pH values and Ba^{2+} concentrations.

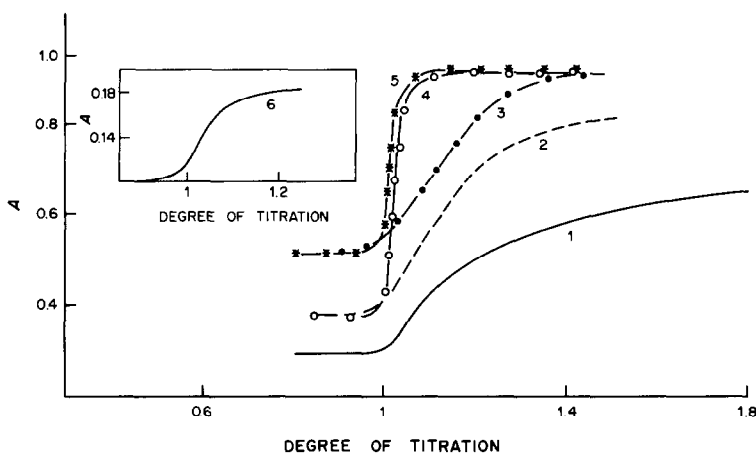


Fig. 10. Calculated curves for titration of sulphate by Ba^{2+} with Thorin as indicator (based on the values of K_{app} and ϵ reported in the text). (1-5) $C_T = 5 \times 10^{-3} M$; (6) $C_T = 1 \times 10^{-3} M$; (1) $\text{pH} = 2.5$ and $C_{\text{SO}_4} = 2 \times 10^{-3} M$; (2) $\text{pH} = 5.0$ and $C_{\text{SO}_4} = 2 \times 10^{-4} M$; (3) $\text{pH} = 8.0$ and $C_{\text{SO}_4} = 2 \times 10^{-4} M$; (4) $\text{pH} = 5.0$ and $C_{\text{SO}_4} = 2 \times 10^{-3} M$; (5) $\text{pH} = 8.0$ and $C_{\text{SO}_4} = 2 \times 10^{-3} M$; (6) $\text{pH} = 8.0$ and $C_{\text{SO}_4} = 2 \times 10^{-4} M$.

Table 4. Parameters for $A = a + bC$ (C = sulphate concentration, $\mu\text{g/ml}$); r = correlation coefficient

pH	a	b , $\text{ml}/\mu\text{g}$	r	l.r.,* $\mu\text{g/ml}$	d.l.,† $\mu\text{g/ml}$
5.0	-2.24×10^{-3}	0.0778	0.9990	0-3	0.15
8.0	-2.19×10^{-3}	0.0538	0.9985	0-3.5	0.28

*Linearity range.

†Detection limit, at $p = 0.01$.

titrations at $\text{pH} < 3$ involve a great excess of titrant, as shown experimentally for propyl alcohol medium.¹⁴ Some of these difficulties can be overcome by a spectrophotometric determination. Table 4 gives the relevant parameters for calibration plots at 520 nm, for pH 5 and 8. The sensitivity is slightly better at pH 5, but the choice of pH effectively depends on the interferences. To verify, this the effect of cations and anions was studied. Cations were added as the perchlorate salts, since this anion has a negligible effect on the absorbance. Univalent cations give negative errors and can be tolerated at up to ten times the sulphate concentration. The tolerance limits for bivalent cations are much lower, so their preliminary removal by ion-exchange is practically essential.

The effect of the anions most frequently present in atmospheric particulates is reported in Fig. 11. The error due to phosphate is the most serious. If present, phosphate must be removed, for instance with magnesium carbonate. Other anions generally give positive errors. Should the quantity of nitrate or chloride be large, a separation of sulphate on a weakly basic anion-exchanger, with a dilute carbonate solution as eluent, is advisable, but this is a time-consuming operation. Hence, a larger margin of error may be tolerated as the price of a more rapid analysis. Alternatively, the error in the sulphate determination can be minimized if the same amount of interfering anions is added to the Ba-Thorin reference solution. Under these conditions a level of nitrate up to fifty

times that of the sulphate gives a negligible error. This procedure is not always possible, however, *e.g.*, for phosphate, and demands a previous analysis for interfering anions. In some cases, however, *e.g.*, for atmospheric particulates, such analyses are more or

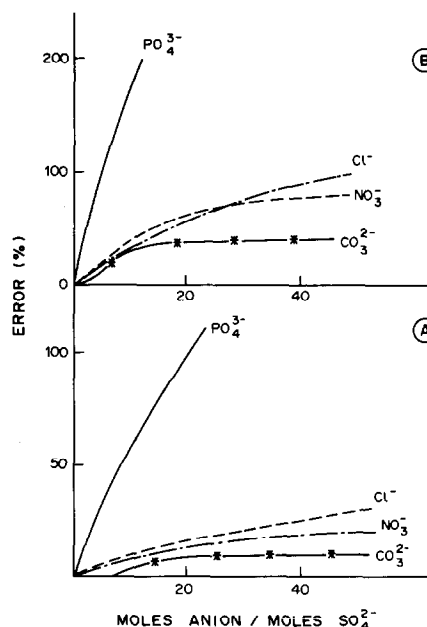


Fig. 11. Anion interference in the sulphate determination: $C_{\text{SO}_4} = 1 \times 10^{-5} M$; (A) $\text{pH} = 5.0$; (B) $\text{pH} = 8.0$.

Table 5

Volume sampled, m^3	Total particulates, $\mu g/m^3$	SO_4^{2-} , $\mu g/m^3$	NO_3^- , $\mu g/m^3$	Cl^- , $\mu g/m^3$	PO_4^{3-} , $\mu g/m^3$
17.1	85.6	4.1	52.0	2.1	—
15.5	60.7	6.3	43.3	2.9	0.2
17.3	107.3	4.9	73.9	1.5	—
17.3	62.6	3.8	31.9	1.7	0.15
		4.2*			
19.9	104.3	3.3	54.1	2.5	0.18

*Without compensation for interfering anions.

less routine. Interference of anions is generally higher at pH 8 than at pH 5, so this pH is chosen for atmospheric particulate analysis.

Analysis of atmospheric particulates

Since the sulphate fraction in atmospheric particulates essentially consists of soluble sulphates,^{26,27} the filter was leached with 10 ml of boiling water. Then 2 ml of the extract were passed through a cation-exchange column (10 cm \times 0.7 cm i.d., packed with a Dowex 50W-X8, 100/200 mesh, hydrogen-form exchange resin); the effluent and \sim 3 ml of rinsing water were collected in a 25-ml standard flask; 15 ml of ethanol, 500 μ l of 0.2M sodium acetate, 3 ml of 0.2M acetic acid, 400 μ l of 0.2% Thorin solution and 100 μ l of 1.0×10^{-2} M barium perchlorate were added, the volume was adjusted to the mark and the absorbance was read in a 500- μ l microcell against a corresponding Ba-Thorin solution after 10 min.

Sulphate was determined by standard addition of 5.0×10^{-3} M sulphate (0.2–1 μ l). Results of five analyses are reported in Table 5. The results for the chloride analysis (turbidimetric method), nitrate (Saltzman method²⁸ after reduction with zinc) and phosphate (molybdenum blue method²⁹) are also presented in Table 5. Since the phosphate/sulphate ratio was lower than 0.1 and the maximum quantity of nitrate was such that 10% maximum error could be estimated (see Fig. 11) no anion-exchanger was used, but the nitrate effect was compensated for as described above.

CONCLUSIONS

The absorbance of the barium-Thorin complexes in presence of sulphate allows the determination of small amounts of sulphate. Attention to the effect of pH and buffer composition on the complexation allows choice of the best conditions for the analysis. For analysis of atmospheric particulates the best results are obtained at pH 5. The detection limit is about 0.15 μ g/ml and quantities as low as 1 μ g of sulphate can easily be detected.

This method can be used for the determination of other anions (for instance phosphate) giving insoluble barium salts.

Acknowledgements—The authors are very grateful to Dr. R. A. Chalmers for his thorough revision of the text and for his useful suggestions.

REFERENCES

- V. I. Kuznetsov, *J. Gen. Chem. (U.S.S.R.)*, 1944, **14**, 914.
- P. F. Thomason, M. A. Perry and W. M. Byerly, *Anal. Chem.*, 1949, **21**, 1239.
- A. V. Nikolaev and A. A. Sorokina, *Dokl. Akad. Nauk S.S.S.R.*, 1951, **77**, 427.
- K. N. Bagdasarov, P. N. Kovalenko and A. A. Rabtsun, *Fiz.-Khim. Metody Analiza i Kontrolya Proizv. Sb.*, 1961, 115.
- A. K. Dey, S. N. Sinha, S. P. Sangal and K. N. Munshi, *U.S. Dept. of Commerce, Clearing-house Sci. Tech. Inform.*, AD 627221, 1965, 151.
- D. I. Eristavi, V. D. Eristavi and Sh. A. Kekeliya, *Tr. Gruz. Politekh. Inst.*, 1968, **5**, 56.
- S. P. Sangal and A. K. Dey, *J. Prakt. Chem.*, 1963, **20**, 219.
- K. Kina and K. Toei, *Bull. Chem. Soc. Japan*, 1971, **44**, 2416.
- J. S. Fritz and M. Q. Freeland, *Anal. Chem.*, 1954, **26**, 1593.
- J. S. Fritz and S. S. Yamamura, *ibid.*, 1955, **27**, 1461.
- U. S. Dept. of Labor, OSHA, *Sulfur Dioxide, Occupational Exposure, Fed. Reg.*, 1975, **40**, 54520.
- M. Katz (ed.), *Methods of Air Sampling and Analysis*, 2nd Ed., p. 737. American Public Health Association, Washington, D.C., 1977.
- Criteria for a Recommended Standard... Occupational Exposure to Sulfuric Acid*, p. 74. DHEW Pub. (NIOSH), 1974.
- J. C. Haartz, P. M. Eller and R. W. Hornung, *Anal. Chem.*, 1979, **51**, 2293.
- G. A. Persson, *Air Water Pollut.*, 1966, **10**, 845.
- M. A. Bertolaccini, *Inquinamento*, 1978, **11**, 49.
- B. Gutbezahl and E. Grunwald, *J. Am. Chem. Soc.*, 1953, **75**, 565.
- E. Grunwald and B. J. Berkowitz, *ibid.*, 1951, **73**, 4939.
- B. Gutbezahl and E. Grunwald, *ibid.*, 1953, **75**, 559.
- D. W. Margerum, C. H. Byrd, S. A. Reed and C. V. Banks, *Anal. Chem.*, 1953, **25**, 1219.
- M. K. Akhmedli and F. B. Imamverdieva, *Azerb. Khim. Zh.*, 1966, **3**, 122.
- I. M. Kolthoff, *J. Phys. Chem.*, 1931, **35**, 2732.
- W. F. K. Wynne-Jones, *Proc. Roy. Soc.*, 1933, **A140**, 440.
- A. D. Cross and A. R. Jones, *An Introduction to Practical IR Spectroscopy*, p. 95. Butterworths, London, 1969.
- P. Bruno, M. Caselli and M. Della Monica, *Inorg. Chim. Acta*, 1974, **10**, 121.
- T. Novakov, in *Analysis of Airborne Particles by Physical Methods*, H. Malissa (ed.), p. 191. CRC Press, West Palm Beach, 1978.
- R. L. Dod and T. Novakov, paper presented at the ACS Symposium on Industrial Applications of Surface Analysis, New York, 24–25 August 1981.
- B. E. Saltzman, *Anal. Chem.*, 1954, **26**, 1949.
- G. R. Bartlett, *J. Biol. Chem.*, 1959, **234**, 466.

CHROMATOGRAPHIC ANALYSIS OF PHOSPHOLIPID AND CHOLESTEROL OXIDATION

ULRICH J. KRULL, MICHAEL THOMPSON and ANITA ARYA

Chemical Sensors Group, Department of Chemistry, University of Toronto, 80 St. George Street,
Toronto, Ontario, Canada

(Received 29 November 1983. Accepted 3 February 1984)

Summary—Capillary thin layer and gas chromatographic methods for analysis of the extent of oxidation in phosphatidyl choline/cholesterol samples are described. Examples of systems suitable for qualitative and quantitative analysis, based on use of unmodified samples or of their derivatives, are illustrated. A method for concurrent quantitative determination of phospholipid and sterol without prepreparation is introduced and is based on extension of a previous lipid trans-methylation technique.

The analysis of the various classes of lipids, including the sterol group, has been the subject of intensive study for the last thirty years. Separation and determination are often difficult, owing to the chemical similarity of the large number of species present in most natural samples, and the amphipathic (asymmetrically polar) and often zwitterionic nature of these molecules. Numerous methods have been developed for separation of lipids into well defined groups, followed by use of more specialized techniques and methods for identification within a particular class.

Qualitative analysis can be accomplished through use of derivative formation coupled with techniques such as thin-layer chromatography (TLC) on plates treated with silver nitrate or reverse-phase TLC gas chromatography, and reverse-phase high-pressure liquid chromatography.¹ Identification generally involves acyl chain determinations since particular lipid classes are defined in terms of their polar head-groups. Formation of derivatives by means of head-group cleavage followed by acetylation or silylation,² or by trans-esterification³ at the ester linkages connecting fatty acid moieties to the head-group region encompasses the most prevalent methods of sample preparation. Many products, including cholesterol derivatives (of which there are more than 50 because of autoxidation⁴), free fatty acids and esters, can be readily chromatographed on TLC plates and can be detected by use of specific spray reagents and compared with known standards.⁵ Lipids which contain unsaturated acyl chains are also susceptible to autoxidation through an autocatalytic process.⁶⁻¹⁰ The reactivity of such species is partially determined by the number of double bonds in a chain. For example, a linoleic hydrocarbon is twentyfold more reactive than an oleic chain, and susceptibility to oxidation increases at least twofold for each additional double bond.⁶ One method of determining the extent of acyl chain oxidation for chains with two or more double bonds is based on the fact that autoxidation produces

compounds with conjugated systems which can be determined by ultraviolet spectrophotometry.¹¹ A more general quantitative method involves the use of gas chromatographic techniques for separation of lipid acyl chain methyl esters, which are the derivatives of choice in such analyses.¹

Gas chromatographic analysis of lipid and sterol derivatives has been performed, for the most part, on packed column systems, although capillary columns, particularly those constructed from glass, have been used with considerable success.¹² Lipid derivatives in common use for gas chromatography include those obtained by boron trifluoride-methanol treatment,¹³ and acid¹⁴ and base³ catalysed trans-esterifications. Difficulties encountered with the first two methods include dependence of the reaction on sample size, and undesirable side-reactions.¹⁵ The base-catalysed reactions are rapid, clean and efficient and are suitable for sample sizes as small as 1 mg.

Gas chromatographic analysis of cholesterol and its oxidation products is commonplace, though proper resolution of such compounds usually necessitates prepreparation from other lipid materials in the sample matrix.^{1,4} A typical approach involves preparative TLC followed by sample isolation, formation of the silyl or acetyl derivatives and dissolution in a volatile organic solvent.

This paper reports procedures for routine evaluation of the extent and nature of oxidation in lipid/sterol samples, a critical factor in lipid membrane technology. Concurrent quantitative analyses for lipid and sterol are performed by high-efficiency capillary gas chromatography without prepreparation. In addition, rapid TLC methods for quality control are described.

EXPERIMENTAL

Reagents

The lipid employed exclusively in this work was phosphatidyl choline derived from eggs (Avanti Biochemicals

Table 1. Thin-layer chromatographic solvent systems for separation of cholesterol and lipid oxidation products

Method	Number of plate irrigations	Solvents	Solvent ratios, v/v	Detection system	Purpose
1	1	CHCl ₃ /MeOH/H ₂ O	4/1/0.1	Acidic phosphomolybdate spray, 150° char (where applicable for reference standard)	Separation of lipid and cholesterol for subsequent capillary chromatographic analysis
2	1	CHCl ₃ /MeOH/H ₂ O	3/1/0.1	As above	Analysis of lipid oxidation
3	2	Ethyl acetate/heptane	1/1	UV characterization followed by cerium/H ₂ SO ₄ char at 150°	Analysis of cholesterol oxidation
4	2	Ethyl acetate/heptane	1/2	As above	As above
5	1	Ethyl acetate/heptane	7/1	As above	As above
6	1	Benzene/ethyl acetate	3/2	As above	As above
7	2	Hexane/diethyl ether	92/8	Cerium/H ₂ SO ₄ char at 150°	Separation of lipid acyl chain methylates with 0-2 ethylenic residues
8	2	Hexane/diethyl ether	40/60	As above	As above, for separation of chains with 3-6 ethylenic residues

Inc., Birmingham, AL). Reagent-grade cholesterol (Research Plus Inc., Bayonne, NJ) was used as the primary sterol from which oxidized products were evolved.

Trans-methylation was performed with 0.5M sodium methoxide freshly prepared by reaction of sodium metal with methanol. Silylation was accomplished with Tri-Sil-Z (Pierce Chemical Company, Rockford, ILL). All other solvents were of reagent grade and were kept anhydrous.

Apparatus

Thin-layer Chromatography. Two types of glass-based chromatographic plate were employed for separation of cholesterol and lipid oxidation products. These were Anasil GF-250 (Analabs, North Haven, CT) and Sil G-25 HR (Macheray-Nagel, Duren, Germany), both 250- μ m silica gel, and Sil G-25 UV254, a 250- μ m silica gel hardened with gypsum and treated with a fluorescent agent with excitation maximum at 254 nm (Macheray-Nagel). The thickness of the plate coatings was chosen to optimize analytical separation while maintaining sufficient loading for subsequent extraction. The Anasil plates employed for lipid analysis required further preparation for methylate separation, which was based on resolution of lipid acyl chains having varying degrees of unsaturation. The procedure consisted of saturating the plates with 0.1M silver nitrate solution in 1:1 v/v methanol/water mixture. The solvent was removed with a warm air stream, then the plates were immediately baked at 110° for 20 min. This provided sufficient activation for methylate separation if the plates were used immediately after the baking.

Capillary gas chromatography. A conventional packed-column Varian Aerograph 2740-10 gas chromatograph (Varian Associates, Walnut Creek, CA) was modified for capillary gas chromatographic investigation of lipid oxidation. A glass-lined splitter assembly (Inlet Splitter System; Chromalytic Technology P/L), including a septum-purge and a buffer-volume to reduce gas viscosity effects, replaced the conventional inlet. The stainless-steel glass-lined inlet tubing and nickel outlet tubing were of 0.25 mm internal diameter and included a T-junction for make-up gas at the end of the column to reduce dead-volume effects. All tubing connectors were chosen to minimize dead-volume effects. The detector was based on a sensitive flame-ionization electrometer assembly, with hydrogen/air fuel mixture and helium as carrier and make-up gas. A separate gas-flow controller (Pressure Control System, Chromalytic Technology) was used because of the low volumes of gas required. The column employed was a 30 m \times 0.25 mm ID Durabond fused-silica column with DB-1 (equivalent to SE-30) 0.25- μ m coating and a practical efficiency of $N_{eff} = 10^5$ (J + W Scientific, Inc., Rancho Cordova, CA). Data analysis was performed with a Hewlett-Packard model 3390A reporting integrator.

Procedures

Thin-layer chromatographic techniques. Several solvent systems were employed for various separations of cholesterol and lipid oxidation products in decane solutions. These are summarized in terms of function and detection system in Table 1. Irrigation was performed in closed glass chambers which were initially purged with nitrogen. The solvent front was allowed to advance 12 cm, after which the detection system was applied or, after momentary warm-air drying, the plates were re-irrigated to increase separation and resolution before detection. Detection by means of charring consisted of evenly spraying the plates with a 1:1 v/v mixture of concentrated sulphuric acid and saturated aqueous ceric ammonium sulphate solution and heating to 150° for 10 min to produce a uniform black-brown char.

Routine TLC methods were employed for separation of phospholipid from sterols for standard gas chromatographic analysis. Table 1 gives some suitable systems

for the pre-separation. Sterol products on the silica gel were manually removed from the TLC plates by scratching, then extracted with chloroform; the solutions were concentrated by evaporation and finally analysed by gas chromatography.

Derivative formation. The sterol products isolated in the TLC procedure could be chromatographed directly or first be modified by silylation to limit problems caused by thermal decomposition. A few mg of sterol product were placed in a dry Teflon-lined septum vial and 20 μ l of Tri-Sil-Z (trimethylsilylimidazole in dry pyridine, 1.5 meq/ml) were added. After the mixture had been heated in a water-bath at 60° for 30 min (during which the vial was capped under a nitrogen blanket) the excess of pyridine was removed in dry conditions under nitrogen to concentrate the sample before gas chromatography of the silyl ethers.

Phospholipid modification for TLC and gas chromatographic analysis consisted of trans-methylation to produce methyl esters of the lipid acyl chains. Numerous methods of doing this have been described, but the best method for complete concentration-independent conversion of small samples employs a base-catalysed reaction.³ The following method is a modification of a standard methylation procedure. The lipid sample (1–10 mg) was reacted for 15 min at 22° with a mixture of 1 ml of freshly prepared 0.5M sodium methoxide (in methanol) and 1 ml of dry benzene. The product was extracted with 3 ml of diethyl ether, which was then washed with two 3-ml portions of 1M aqueous sodium chloride. The diethyl ether/benzene extract was then dried over anhydrous sodium sulphate, concentrated with a stream of nitrogen and submitted to gas chromatography.

RESULTS AND DISCUSSION

Thin-layer chromatography

Thin-layer chromatography is the simplest and most versatile method suitable for general separation of the major oxidation products of both lipid and cholesterol. The results obtained for lipid/sterol mixtures by use of the preferred separation systems listed in Table 1 are summarized in Table 2. It must be emphasized that no universal method for complete separation exists and choice of method is determined by the resolving ability for a desired component. For unmodified samples a maximum of 3 lipid products and 15 sterols can be routinely separated.

The autoxidation of cholesterol involves initiation and propagation processes that act to produce reactive intermediates such as hydroperoxides and cholest-5-en-3-one,⁴ which react to form the other commonly observed products. The sterols separated have been tentatively identified by use of standards and of various literature sources describing similar product mixtures and chromatographic systems.^{5,16} Retention indices relative to cholesterol provide reproducible data suitable for identification of products, but confidence in the identification can be greatly increased by use of spray reagents or fluorescence methods selective for functional groups.^{5,16}

Phospholipid analysis by TLC is a much more difficult task, since the molecules are amphipathic and also contain ionized groups in the head-group zone. Standard procedures can separate classes of

Table 2. Retention factors obtained by various TLC methods

Method (Table 1)	R_f for most significant resolvable compounds	Tentative identity ^{5,20}
2	0.79 ± 0.03	Oxidized cholesterol
	0.70	Cholesterol
	0.59	Oxidized cholesterol
	0.39	Phosphatidyl choline
	0.26	Lyso-PC
	0.13	Oxidized PC
	0.93	
	0.86	
	0.82	
	0.78	Cholesta-3,5-dien-7-one
3	0.74	Cholesterol
	0.71	
	0.65	
	0.62	
	0.57	
	0.53	25-Hydroxycholesterol
	0.50	7-Ketocholesterol
	0.36	7 α and 7 β -Hydroxycholesterol
	0.28	3 β ,5-Dihydroxy-5 α -cholestan-6-one
	0.07	Cholestane-3 β ,5 α ,6 β -triol
6	0.98	Cholesta-3,5-diene and 3,5-dien-7-one
	0.77	Cholesta-4-en-3-one
	0.67	Cholesterol
	0.51	5,6-Epoxycholestan-3 β -ol
	0.42	7-Hydroperoxide and 7-ketocholesterol
	0.23	7 α -Hydroxycholesterol
	0.19	7 β -Hydroxycholesterol
0.05	Cholestane-3 β ,6 α ,5 β -triol	

phospholipids only poorly, and determination of structural unsaturation is generally not possible. A number of enzymatic methods have been employed to cleave the charged groups from phosphatidyl cholines and ethanolamines, resulting in mixtures which can be separated by conventional TLC systems;² however, identification of acyl chain unsaturation remains difficult. Such work can be readily performed after treatment of the phospholipid to form methyl esters of the acyl chains. Base-catalysed trans-methylation provides a clean, efficient one-step process which is apparently not concentration-dependent and does not cause isomerization at the double bonds.¹³ Specially prepared TLC plates are required for analysis of the unsaturated methyl esters, since separation must be largely based on the subtle differences between similar long-chain hydrocarbons. Plates treated with silver nitrate provide active silver sites for binding with the π -orbital electrons of ethylenic or acetylenic bonds. The sample migration rate on the plate is almost entirely determined by the number of available unsaturation sites, since retention increases with π -orbital complexation. Plates are conventionally prepared by mixing solid silver nitrate (5–10% w/w) with the silica gel G/water slurry employed for plate-coating. The simplified method of plate preparation employed in this work also achieved reproducible results but was extremely sensitive to plate activation by the baking process.¹⁷

Table 3 presents typical data obtained with these TLC plates and illustrates the value of changing the solvent ratio for separation of unsaturated acyl chains. All the TLC methods described here are generally only suitable for qualitative analysis, though quantitative work by means of a scanning densitometer is possible.

Capillary gas chromatography

Gas chromatographic analysis optimizes qualitative results and simplifies determination since the concentrations of similar materials can readily be

Table 3. Retention factors for TLC separation of lipid acyl chain methylates

Method (Table 1)	R_f	Identity
7	0.92	Saturated methylate
	0.77	Monoenate
	0.46	Dienate
	0.08	—
8	0.02	—
	0.95	—
	0.62	Trienate
	0.31	Tetraenate
	0.15	Pentaenate
	0.03	Hexaenate

*TLC plates pretreated with silver nitrate solution as described in text.

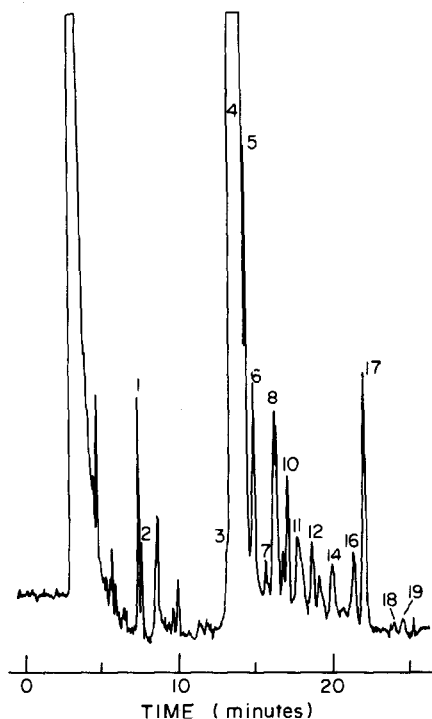


Fig. 1. Capillary gas chromatogram of cholesterol and autoxidation products after sterol silylation. The column was a 30 m \times 0.5 mm G SCOT/B system coated with OV101. Separation under isothermal conditions with a column temperature of 280°C and an injection temperature of 300°C.

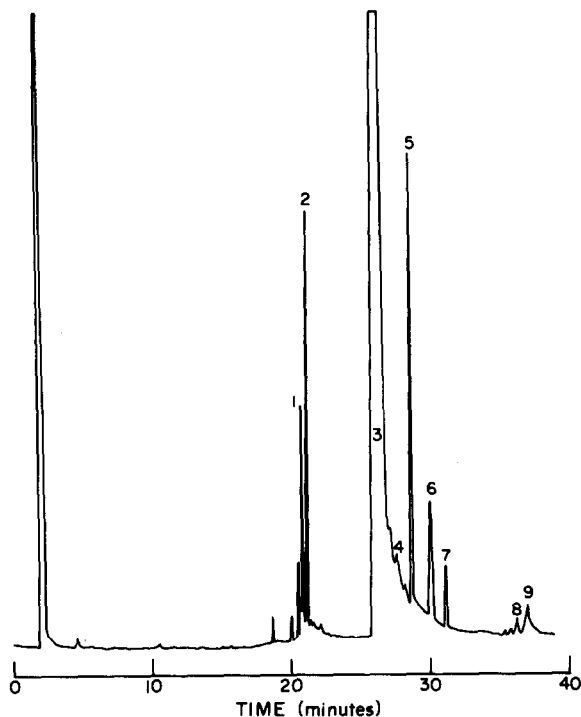


Fig. 2. Capillary gas chromatogram of unmodified cholesterol and autoxidation products. The column was a 30 m \times 0.25 mm fused silica system permanently coated with DB-1 (equivalent to SE-30). The injection temperature was 325°C, and temperature programming was started on injection, from 200°C to 280°C at 4°C/min. The initial attenuation factor was 16, reduced to 2 after 8 min, and 1 after 12 min.

found by normalization of the peak areas. The problems encountered in the separation of closely related materials are alleviated by use of high-efficiency capillary columns. The inherent sensitivity of flame-ionization detection is sufficient to measure nanogram quantities of the lipid materials investigated.

Sterol analysis is conventionally performed by TLC separation of the sterols from other lipids, followed by extraction and derivative formation before gas chromatographic analysis. Derivatives such as the silylated products employed in this work give chromatograms like that in Fig. 1. The sterol derivatives are well separated and thermal decomposition is minimized.¹⁸ Sterol samples, in a volatile solvent, can be directly injected into the chromatograph without prior conversion into derivatives, though the common cholesterol autoxidation products often decompose at the temperatures required to vaporize them. With constant injector and column temperature, a reproducible chromatogram of native and pyrolysed sterol products is obtained, as shown in Fig. 2. Identification of some of the major products has been attempted by analysis of sterol products pre-separated by TLC and also through use of commercially available standards. The tentative identifications are listed in Table 4. Comparison of Figs. 1 and 2 indicates that silylation is best for optimal sterol resolution, but

both methods produce chromatograms which are suitable for quantitative analysis when the chromatographic conditions are carefully controlled and reproduced, and the pyrolysis peaks are linked to the appropriate parent compound. Control of the chromatographic conditions is particularly important for the pyrolysis chromatogram, which under good con-

Table 4. Identification of cholesterol oxidation products separated by capillary gas chromatography as shown in Figs. 1 and 2

Product number		Tentative identity
Figure 1	Figure 2	
3	1	7 α -Hydroxycholesterol
—	2	5,6-Epoxycholestan-3 β -ol
4	3	Cholesterol
—	4	Cholesta-3,5-diene
5	5	Cholesta-3,5-dien-7-one
—	6	5 α -Cholestane-3 α ,5,6 β -triol
10	7	5,6-Epoxycholestan-3 β -ol
—	8	5 α -Cholestan-3 α ,5,6 β -triol
17	9	7-Ketocholesterol

Known decompositions:

7-ketocholesterol \rightarrow cholesta-3,5-dien-7-one.

7 α -hydroxycholesterol \rightarrow decomposition envelope adjacent to products 1 and 2 in Fig. 2.

ditions produces quantitative results with a variability of 5–10%. A major technical problem in measurement of peak areas occurs when an electronic integrator is not available, since many of the sterols are present in extremely low concentrations relative to the parent cholesterol. To record all these species concurrently and quantitatively, a two-channel recorder with one channel attenuated by a factor of 10 is sufficient for determination of cholesterol and other oxidized sterol products.

Sterol analysis of lipid/sterol mixtures is conventionally accomplished by the techniques above, preceded by TLC separation. Phospholipid acyl chain analysis is also routinely performed by gas chromatography after trans-methylation, but usually is performed only on samples separated from the sterol. This work has established that concurrent phospholipid/sterol analysis can be performed quantitatively by gas chromatography when the trans-methylation procedure is employed. The reaction procedure for methylating the acyl chains gives complete conversion into the required product in the presence of the sterol. One difficulty in the procedure arises from the extraction steps required to isolate the methylate and remove free fatty acids. The solvent systems employed are suitable for the extraction of unwanted fatty acids and also sterols. The extraction step removes most of the sterol present, so variable attenuation of the chromatographic signal is required, because of the small sample quantities routinely used. Sufficiently large signals are readily

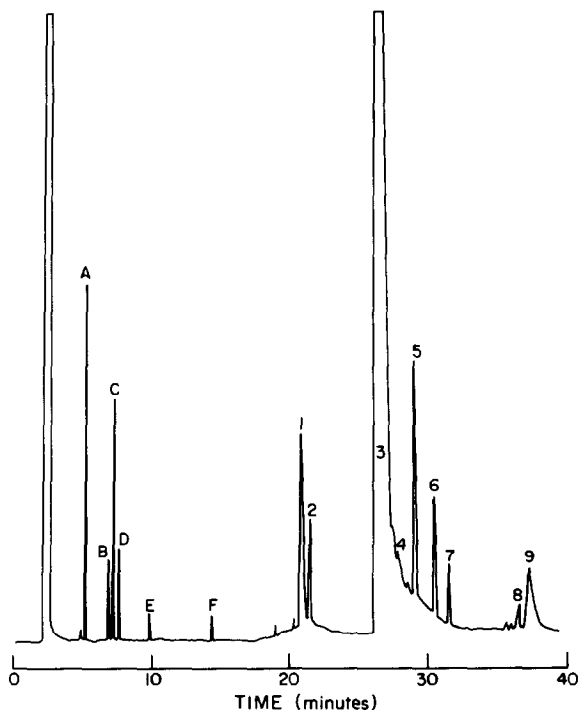


Fig. 3. Capillary gas chromatogram of a mixture of phosphatidyl choline, cholesterol and autoxidation products after methylation. Column and conditions as for Fig. 2.

Table 5. Identification of lipid acyl chain methylates separated by capillary gas chromatography, as shown in Fig. 3

Product	Retention factor relative to cholesterol	Identification (alkene position)
A	1.00	16:0
B	1.33	18:2
C	1.37	18:1
D	1.46	18:0
E	1.85	20:4
F	2.70	22:6

achieved for the methylation products, but the maximum sensitivity of the flame-ionization detector is required for detection of the minute amounts of sterol. A typical chromatogram is shown in Fig. 3, and is similar to that shown in Fig. 2 for analysis of the unmodified sample obtained by initial TLC extraction. The methyl esters identified in Table 5 are much more volatile than the sterols, so temperature programming is valuable for increased efficiency. The operating conditions shown for Fig. 3 are readily and reproducibly achieved.

One critical area of concern is the accuracy of the combined phospholipid/sterol analysis compared to that of the conventional methods requiring TLC pre-separation. Extensive study of *in-situ* oxidation has established that the best results are obtained only with carefully controlled oxygen-free separations and reactions. TLC separations for rigorously quantitative lipid or sterol determinations are performed in developing tanks which are nitrogen-purged and with solvents that are degassed and contain about 0.05% BHT.¹⁹ Our results indicate that such protective measures are generally unnecessary if relative errors of 5–10% can be tolerated. Similar protective measures have been employed in the trans-methylation procedure and have proven successful in eliminating oxidation, though the BHT does tend to complicate the gas chromatographic analysis since it has a retention value close to that of the C22:6 methyl ester. The capability for performing complete trans-methylation at room temperature should also be noted, since it is of considerable advantage in view of the lability of the compounds of interest.

Even though identical total quantitative evaluation of the parent cholesterol is obtained, one area in the chromatograms shown in Figs. 2 and 3 does differ significantly. It involves the multiplet of oxidized-sterol signals which appear before the cholesterol peak and are produced by the 7-diol and epoxy species, and also some pyrolysis decomposition products. Since the peak distributions and areas for the two methods of analysis differ even when controlled conditions which prevent oxidation are used, the effect must be due to differences between the gas-phase pyrolysis patterns or between the extraction procedures. The invariability of results with change in the solvents used for extraction indicates that the effect is not related to a difference in selective solu-

bility in the extraction steps. Table 4 gives the relative retention indices of the compounds responsible for the envelope of peaks. One of these oxidized sterol products is the reactive epoxy compound, which is expected to be sensitive to variations in procedure. Further analysis (by use of clean standards) of all the chromatogram peaks associated with the epoxy compound itself, indicates that the methylation procedure tends to induce conversion of the epoxy compound into products which are chromatographically identical to the 7-diol compound and its associated decomposition envelope. Proper determination of each of these individual species would be difficult, and the results are best expressed as sums of the combined 7-diol and epoxy signals, when the unmodified sterols are analysed by gas chromatography. Since the region located before the cholesterol signal is not usually well defined with respect to identifiable compounds and is associated with the pyrolysis products, the differences between the results of the two techniques are not critical provided they are reproducible and the remaining well-defined portions of the chromatograms are not significantly affected.

Rapid and quantitative analysis of concurrent lipid/sterol chemistry is vitally important in the understanding of the physical properties of bilayer lipid membranes (BLM), which are formed from mixtures of these compounds. Significant changes in BLM electrochemistry occur as oxidation progresses, reflecting changes in chemical and electrical-potential energy barriers in the membrane. Applications of the techniques described in this work will allow assessment of the influence of oxidization products and will be presented in a future article.

Acknowledgements—We thank the Natural Sciences and Engineering Research Council of Canada and the Air Resources Branch of the Ministry of the Environment, Province of Ontario, for support of this work. In addition,

we are indebted to L. I. Bendell-Young and L. Hanley for technical assistance.

REFERENCES

1. W. W. Christie, *Lipid Analysis*, Pergamon Press, Oxford, 1982.
2. A. Kuksis, in *Analysis of Lipids and Lipoprotein*, E. G. Perkins (ed.), p. 36. Am. Oil Chem. Soc., Champaign, Ill., 1975.
3. N. Pelick and V. Mahadevan, in *Analysis of Lipids and Lipoprotein*, E. G. Perkins (ed.), p. 27. Am. Oil Chem. Soc., Champaign, Ill., 1975.
4. L. L. Smith, *Cholesterol Autoxidation*, Plenum Press, New York, 1981.
5. L. L. Smith, W. S. Matthews, J. C. Price, R. C. Bachmann and B. Reynolds, *J. Chromatog.*, 1967, **27**, 187.
6. R. T. Holman, *Progr. Chem. Fats Lipids*, 1966, **9**, 3.
7. W. O. Lundberg and P. Jarvi, *ibid.*, 1971, **9**, 377.
8. D. Swern, in *Autoxidation and Antioxidants*, W. O. Lundberg (ed.), Vol. 1, p. 1. Wiley-Interscience, New York, 1966.
9. N. A. Porter, L. S. Lehman, B. A. Weber and K. J. Smith, *J. Am. Chem. Soc.*, 1981, **103**, 6447.
10. H. Weenen and N. A. Porter, *ibid.*, 1982, **104**, 5216.
11. R. A. Klein and P. Kemp, in *Methods in Membrane Biology*, E. D. Korn (ed.), Vol. 8, p. 51. Plenum Press, New York, 1977.
12. R. P. W. Scott, *Trends Anal. Chem.*, 1983, **2**, 1.
13. L. D. Metcalfe and A. A. Schmitz, *Anal. Chem.*, 1961, **33**, 363.
14. M. E. Mason and G. R. Waller, *ibid.*, 1964, **36**, 583.
15. H. L. Solomon, W. D. Hubbard, A. R. Prosser and A. J. Sheppard, *J. Am. Oil Chem. Soc.*, 1974, **51**, 424.
16. J. E. Van Lier and L. L. Smith, *Anal. Biochem.*, 1968, **24**, 419.
17. O. Renkonen, in *Progress in Thin-Layer Chromatography and Related Methods*, A. Niederwieser and G. Pataki (eds.), Vol. 2, p. 143. Ann Arbor Science, Michigan, 1971.
18. V. Korhani, J. Bascoul and A. Crastes de Paulet, *J. Chromatog.*, 1981, **211**, 392.
19. T. S. Neudocffer and C. H. Lea, *ibid.*, 1966, **21**, 138.
20. M. Kimura, Y. Jin and T. Sawaya, *Chem. Pharm. Bull.*, 1979, **27**, 710.

SELENIUM IN HUMAN URINE DETERMINATION, SPECIATION AND CONCENTRATION LEVELS

H. J. ROBBERECHT* and H. A. DEELSTRA

Department of Pharmaceutical Sciences, University of Antwerp (UIA), Universiteitsplein, 1, 2610 Wilrijk, Belgium

(Received 17 June 1983. Revised 24 November 1983. Accepted 3 February 1984)

Summary—Procedures for determination of selenium in urine samples are reviewed. Basic problems encountered in sampling and sample-treatment are discussed. Concentration levels and speciation of the element are summarized.

Since the discovery that selenium is an essential element¹ and plays a role in glutathione peroxidase activity² there has been increased interest in this element. Earlier it was its toxicity that was of interest³⁻⁵ and this must still be remembered.⁶⁻¹⁰ Current interest in the element stems mainly from the following four observations.

First, selenium has been reported to inhibit carcinogenesis by chemical agents such as aminoazo compounds, polycyclic aromatic hydrocarbons, nitrosamines, *etc.*,^{7,11-22} and this has been extensively reviewed.²³⁻²⁹ Variations in dietary selenium intake have been suggested as an explanation for differences in the incidence of cancers in various human populations.³⁰⁻³²

Secondly, selenium may play an important role in the prevention of cardiovascular diseases and myocardial infarction: selenium is reported to be important in experimentally induced heart diseases in animals;³³⁻³⁵ inverse epidemiological relationships have been observed between human heart disease and environmental or blood selenium,³⁶⁻⁴¹ Keshan disease,⁴²⁻⁴⁶ a cardiomyopathy that affects children in certain areas of the People's Republic of China, is reported as virtually eliminated in the population groups at risk, after a large-scale intervention with selenium supplements.

A third effect of selenium in different organisms is its reported antagonistic action towards various toxic metals,⁴⁷ such as arsenic,⁴⁸ cadmium,⁴⁹⁻⁵⁶ copper,⁵⁷ lead,^{58,59} inorganic mercury⁶⁰⁻⁷³ or methylmercury compounds,⁷⁴⁻⁸¹ silver,⁷¹ tellurium,⁵⁸ tin⁵⁸ and zinc.⁷² Magos and Webb have published an excellent review⁵⁴ on this topic.

Finally, for several conditions in patients receiving parenteral alimentation, selenium deficiency has been claimed to have played a role,⁸²⁻⁹² and alcoholic

cardiomyopathy to be aggravated or accelerated by the concomitant occurrence of selenium deficiency.⁹³

These literature data indicate that there is a range of selenium intake that is consistent with health, and outside this range deficiency or toxicity effects can occur. Since it is the element with the narrowest difference between the two levels, reliable methods are needed to check the selenium status of man and to monitor the occupational exposure to this element by measuring its concentration in body fluids. Serum, plasma or whole blood are usually taken as samples for measurement, although several authors⁸³ claim the glutathione peroxidase activity as being the best parameter.

For trace element levels in man, blood and hair are normally taken as indicator samples,⁹⁴ but for selenium hair has to be omitted since selenium is added to certain shampoos as an antidandruff agent and may be adsorbed on the hair, which would vitiate the analysis.⁹⁵⁻⁹⁷ In cases of intoxication or to provide information on the balance between intake and output, the selenium level in the urine is taken as an indicator, since the kidney is an important feature in body homeostasis.⁹⁸ Moreover, urine specimens are readily available and easy to sample.

In this paper the sampling, sample treatment, determination procedures and concentration levels of selenium in urine are reviewed and the scarce data on selenium species in urine are discussed.

SAMPLING AND STORAGE

As with most analyses for urine components, the selenium determination must be done on the urine collected during a 24-hr period. One reason for this is that many constituents exhibit diurnal variation, with variable peak excretions as a result of variation in drinking patterns.

At the beginning of the collection period (usually when the patient awakens) the bladder should be emptied, that specimen being discarded, and the time noted. All urine specimens passed during the next 24

*Present address: Provinciale Hoger Technisch Instituut voor Scheikunde, Kronenburgstraat, 47, B-2000 Antwerp, Belgium.

hr are collected in an appropriate container. Usually precleaned polyethylene or polypropylene bottles are used, to prevent contamination or adsorption losses. At the end of the collection period the bladder is emptied, this specimen being added to those already collected. Transfer of the urine from the body into the vessel can introduce contamination from clothes and skin, but for selenium this may be not as critical as for other elements.⁹⁹ Determination of total creatinine excretion in the 24-hr period may be used as a guide to the adequacy of the collection. This is particularly useful if several 24-hr urine specimens are collected from the same person, since the 24-hr creatinine excretion, largely a function of muscle mass, is relatively constant from day to day. Since the data are often expressed in $\mu\text{g}/24\text{ hr}$ the total volume of urine must be measured to allow comparison of selenium contents or daily excretions when various units are used. As a preservative, to prevent bacterial growth and especially to minimize adsorption losses, concentrated hydrochloric acid,^{100,101} boric acid, nitric acid,^{102,103} benzoate⁴⁴ or toluene^{104,105} can be added. The bottles must be stored in the refrigerator when not actually in use during the collection, and the samples must be frozen if the analysis cannot be done immediately. Greger and Marcus¹⁰⁶ found that the concentration of selenium in fresh urine samples and in the same samples after 6 months storage in the freezer was similar.

Cornelis *et al.*⁹⁹ have proved that selenium can be enriched in urine sediments, so the bottles must be shaken very vigorously after thawing, to homogenize the suspension before the sample treatment is begun. The precipitate occurring after extended standing of the sample or after thawing, contains about 15% of the total selenium in the urine, according to Fodor and Barnes.¹⁰⁷

SAMPLE TREATMENT

All manipulations should be performed in specially designed hoods in dust-free rooms (clean-rooms) to minimize introduction of contamination. All vessels *etc.* used should be cleaned by extensive washing with a succession of reagents and finally with doubly distilled water; all reagents and solvents must be of ultrapure quality.

Treatment of the urine samples depends on the method of analysis. Except for neutron-activation analysis, where simple lyophilization of a few ml of urine can be applied,⁹⁹ the whole sample must be brought into solution and all the selenium converted into the quadrivalent state. Wet oxidation is of particular interest for this purpose, most commonly with nitric acid-sulphuric acid,^{102,105} nitric acid-hydrogen peroxide,¹⁰⁸ nitric acid-perchloric acid,¹⁰⁹⁻¹¹¹ or a suitable combination thereof.¹¹² Satisfactory use of these mixtures depends on satisfying two potentially troublesome demands: complete conversion of the native forms of selenium into selenite

or selenate, and prevention of significant loss of selenium during the oxidation.

Several investigators have shown that loss of selenium in open wet oxidation systems can be prevented if charring of samples is avoided,^{109,112,113} but this may be difficult when sulphuric acid is a component of the mixture. Sometimes mercuric oxide is added to prevent volatilization losses.^{114,115} Unless both requirements are met, accurate analysis for urine selenium cannot be obtained. For instance, some investigators have found that part of the urinary selenium resists acid digestion.¹¹⁰⁻¹¹⁶ Janghorbani *et al.*¹¹⁷ have recently shown that complete oxidation of rat urine requires use of nitric acid-perchloric acid and that other mixtures such as nitric acid-hydrogen peroxide or nitric acid-sulphuric acid are not suitable. This is due, at least in part, to the presence of the trimethylselenium ion (TMSe^+) in the urine,¹¹⁸⁻¹²¹ which resists oxidation¹¹⁰ except with nitric acid-perchloric acid. The other forms of selenium in the urine, as far as been ascertained, do not appear to require perchloric acid for their oxidation.

Janghorbani *et al.*¹¹⁷ extensively studied the kinetics and reproducibility of the TMSe^+ conversion, and finally recommended adding 5 ml of concentrated hydrochloric acid and 20 ml of concentrated nitric acid to 25 ml of sample and boiling for about 20 min (air condenser) until colourless. Since in most determination procedures selenium(IV) is the mandatory form, complete conversion of selenate into selenite is necessary. This is mostly achieved by boiling the wet-ashed sample in 6M hydrochloric acid for a suitable length of time.^{110,112,117,118} A similar digestion procedure with gradual heating up to 210° has been shown to give less than 10% loss of metabolically incorporated selenium in rat urine.¹¹¹

DETERMINATION PROCEDURES

Spectrophotometry

This was probably the technique most often used in the past, but is not always sensitive enough for the determination of selenium in trace amounts and is prone to several interferences. Only in two older publications is this technique mentioned for the determination of selenium in urine. Roquebert and Truhaut¹¹⁹ dry-ashed urine in the presence of nitric acid and magnesium nitrate but found serious losses of the element, whereas Lott *et al.*,¹²⁰ starting with a 10-ml urine sample and mineralization with nitric, perchloric and sulphuric acids, and forming the selenium-diaminonaphthalene complex, found no native selenium present; added selenium, however, was completely recovered.

Spectrophotometric methods based on catalytic reactions are generally much more sensitive than those based on stoichiometric reactions. Most catalytic methods involve oxidation-reduction reactions in which the catalyst, usually a multivalent ion, changes its oxidation state.

Feigl and West¹²¹ proposed a very sensitive qualitative test for selenium, based on its catalysis of the reduction of Methylene Blue by sodium sulphide, and regarded the catalyst as being elemental selenium. West and Ramakrishna¹²² later used selenite for calibration. De Moor¹²³ clearly demonstrated that the decolorization strongly depends on the chemical form of the selenium, and since not all the chemical forms of selenium metabolites are known and hence are not available for calibration, this method cannot be recommended for urine analysis.

Fluorimetry

3,3'-Diaminobenzidine (DAB) is used as a sensitive fluorimetric reagent for selenium, since the piaz-selenol formed with selenium(IV) shows strong fluorescence. 2,3-Diaminonaphthalene (DAN) is even more frequently used for the same purpose, since it gives greater sensitivity and better extractability into organic solvents from acidic media. Although the fluorimetric method is sensitive, it is lengthy and pH-dependent, and the reagent solutions must generally be prepared daily. Strong oxidizing or reducing agents must be absent, and the addition of masking agents¹²⁴ or EDTA¹²⁵ is necessary. Nevertheless the method is frequently used for selenium determination in many materials, including urine. All the procedures include a digestion step, followed by a reduction to bring all selenium into the quadrivalent form, a complexation and extraction step, and finally the spectrophotometric measurement with excitation at 360 nm and emission measured at 520 nm. Watkinson's method¹⁰⁹ for analysis of biological material is often used for urine samples.

Nitric-perchloric acid mixture is mostly used for the digestion step, DAN as the fluorimetric reagent, and cyclohexane for the extraction. Reduction with hydrochloric acid under defined conditions is used to bring all the selenium into the selenite form. If the Schöniger flask combustion is used, no reduction step is necessary, as proved by Tausky *et al.*¹²⁶ Chen *et al.*¹²⁷ omitted the reduction step in their single-tube process for selenium determination, but hence risked obtaining low results for hair, serum and urine samples.

All the methods require only a small amount of sample (0.4–4 ml) and the precision is mostly better than 7%. The detection limit can be as low as 0.4 ng/ml.¹²⁵

Atomic-absorption spectrometry methods (AAS)

The use of AAS has increased during the last two decades and now covers a large fraction of selenium determinations. Robberecht and Van Grieken¹²⁸ have recently reviewed AAS determinations of selenium in water samples, and Verlinden *et al.*¹²⁹ have reviewed the AAS-procedure for determination of selenium in various materials, including biological samples.

Flame AAS (FAAS). This technique in its conventional form is not sensitive enough for direct

determination of selenium in urine samples. Background absorption at 196 nm, interfering cations and anions, and severe scattering in the 180–220 nm region by inorganic salts, which are highly concentrated in urine, make digestion and separation of selenium from the urine matrix necessary.

Urine samples are wet-ashed, either with a mixture of nitric, perchloric and sulphuric acids¹¹⁴ or a nitric-perchloric acid mixture.^{130,131} Generation of hydrogen selenide by reduction with sodium tetrahydroborate in acid medium is used in nearly all methods for the separation of selenium from the matrix. Previous conversion of all selenium into selenite is then necessary, and usually obtained by boiling with hydrochloric acid.

Electrothermal AAS (ETAAS). This technique is especially suitable for direct analysis because of its high sensitivity (detection limit 90 pg of selenium), but it is not simple, nor free from interferences or volatilization losses. Pyrolytic coating of the graphite furnace or addition of various metal salts, such as those of nickel,^{114,132–135} molybdenum¹³² or silver¹³² has been shown to diminish the chemical interferences in urine analysis, allow use of higher temperatures without losses of selenium, and result in a significantly enhanced sensitivity. A heated silica cell^{9,136–138} can be used instead of a graphite furnace^{133–135} for the atomization.

After acid decomposition of the sample, selenium can be preconcentrated by the generation of hydrogen selenide, complexation with aromatic *o*-diamines and extraction into toluene¹³³ or complexation with dithizone and extraction into carbon tetrachloride.^{134,135} Boiling with hydrochloric acid^{133,136,137} or hydroxylamine hydrochloride^{134,135,138} is necessary to reduce selenate to selenite, which is essential for the following complexation or hydride-generation step.

Procedures for speciation of selenium in urine are scarce. The only procedure for trimethylselenium ion (TMSe⁺), "free state selenium-ion" (presumably selenite + selenate) and total selenium in human urine, is the graphite-furnace AAS method of Oyamada and Ishizaki,^{134,135} based on a procedure established by Ishizaki.¹³⁹ The TMSe⁺ was separated on a Dowex 50 W-8X ion-exchange column. Nickel nitrate was used as matrix modifier in the ETAAS analysis, and the detection limit for TMSe⁺ was 1 µg/l.

Atomic-emission spectroscopy. The use of an inductively-coupled plasma (ICP) as an excitation source in optical atomic-emission spectroscopy (AES) for single and multielement inorganic trace analysis is becoming widespread. The recent availability of commercial instruments has stimulated its use for the determination of metals and metalloids in diverse environmental materials, ranging from airborne particulates and fly-ash to industrial effluents and waste waters. The capabilities and limitations of ICP-AES in water pollution analysis have been re-

viewed by Barnes.¹⁴⁰ Robbins and Caruso¹⁴¹ have summarized the development of hydride-generation methods for atomic spectroscopic analysis, including ICP-AES, and Thompson *et al.*¹⁴² have described the possibility of simultaneous determination of trace concentrations of arsenic, antimony, bismuth, selenium and tellurium in aqueous solutions, by hydride-generation and ICP-AES. Unfortunately, the technique has a number of disadvantages. One of the most serious (in urine analysis) is that the power of detection for hydride-forming elements is insufficient for direct determination of ultratrace concentrations of these metals in many biological materials, even under optimized conditions. For the determination of such trace elements in urine by ICP-AES, Barnes and Genna¹⁴³ used preconcentration with a poly-(dithiocarbamate) chelating resin. Fodor and Barnes¹⁰⁷ reported the use of complexation of Se, As, Fe, Bi, Sb and Sn by poly(dithiocarbamate) resin in the determination of these elements with a combined hydride-ICP-AES technique and application of this approach for distinguishing the oxidation states of Se and Te in urine. The detection limit, based on the integrated peak-area for a 10-ml sample with a tenfold resin preconcentration was as low as 0.04 $\mu\text{g/l.}$, and recovery at the $\mu\text{g/l.}$ level ranged from 80 to 108% for both selenate and selenite.

X-Ray emission analysis

As with most other techniques, it is impossible to determine selenium directly by X-ray emission methods at the concentration levels in urine samples: the detection limits are around 200 $\mu\text{g/l.}$, for elements such as selenium,¹⁴⁴ with secondary target energy-dispersive X-ray fluorescence analysis or X-ray emission spectrometry (XES).

A single evaporation enrichment step is not very helpful: even under optimized conditions, spotting on a cellulose filter paper and drying results in a detection limit of 30 $\mu\text{g/l.}$ and the risk of selenium losses is severe.¹⁴⁵ For highly saline samples, such as urine and brine, heterogeneity problems make accurate analysis improbable.

Clearly, there is a need for chemical preconcentration techniques to boost the sensitivity of X-ray emission analysis sufficiently for application to urine. Vos *et al.*¹⁴⁶ tried using chelating DEN-filters^{147,148} for multi-element analysis of urine, but abandoned this approach because nitrogen compounds in the urine interfered in the complexation step. They therefore adapted and extended the method proposed by Nielson and Kalkwarf,¹⁴⁹ but did not obtain quantitative recovery.

Several authors¹⁵⁰⁻¹⁵² have adapted the small-sample X-ray fluorescence system of Alfrey *et al.*,¹⁵³ in which the sample is lyophilized, oven-dried and ashed at 450°, after which 250 μg of the ash are used for target preparation. Alfrey *et al.*¹⁵³ did not give any values for selenium, but Tsongas and Ferguson¹⁵⁰ claimed to determine selenium down to the 1 $\mu\text{g/l.}$

level. Holynska and Lipinska-Kalita¹⁵⁴ used an acid decomposition followed by selective reduction of selenium compounds with a mixture of stannous chloride and hydroxylamine and co-precipitation with tellurium, and finally XES determination.¹⁵⁶ With a 250-ml sample they were able to detect selenium at the $\mu\text{g/l.}$ level. However, if the solution is too acid the precipitation with tellurium can be incomplete,¹⁵⁴ so there is a risk of low results. A similar preconcentration procedure based on reduction of selenite by ascorbic acid was proposed by Robberecht and Van Grieken;¹⁵⁶ activated carbon was used as a strong adsorbent and collector for the elemental selenium. Their destruction procedure, using nitric and perchloric acid and gradual heating to 210°, was tested on different biological tissues in which selenium was metabolically incorporated.¹¹¹ For urine samples the average recovery was 95% and under optimal conditions with a 20-ml urine sample a limit of detection of 1 $\mu\text{g/l.}$ could be obtained.¹⁵⁶

Neutron-activation analysis (NAA)

Because of its high sensitivity (1–10 ng of Se) and the simple pretreatment of the sample, this technique is widely used for determination of selenium, especially in biological materials. Thermal neutrons are most often used for the activation, giving radioactive selenium isotopes by (n, γ) reactions. Hence, ^{77m}Se and ⁷⁵Se are predominantly utilized in activation analysis of biological material. ^{77m}Se, which gives the highest sensitivity thanks to its very short half-life (17.5 sec), is used only in instrumental neutron-activation analysis (INAA). Although this technique is well established for biological tissues,¹⁵⁷ hair,¹⁵⁸ serum and semen,¹⁵⁸ it does not seem to have been applied to urine, probably because there would be a relatively large Compton background from ³⁸Cl and ²⁴Na. Pre-irradiation dialysis against demineralized water might partly solve this problem¹⁵⁹ but could cause losses of selenium, though these were not noted after dialysis of serum samples.

⁷⁵Se is used more often because its long half-life (120.4 days) allows chemical separation, but long activation and cooling times are required. The sample material is usually irradiated in a nuclear reactor for at least one day with a flux of 10^{13} – 10^{15} n. cm⁻². sec⁻¹. The activity of the irradiated samples is measured with a high-resolution Ge(Li) γ -ray detector coupled to a multi-channel analyser or sometimes with an NaI(Tl) detector.

Multi-element analysis has been done after non-destructive analysis of 20-ml urine samples, enclosed in quartz vials,¹⁶⁰⁻¹⁶² or after lyophilization of 10-ml aliquots.⁹⁹ Extensive separation schemes, based on ion-exchange procedures, have been developed by Wester *et al.*¹⁶³ for multi-element analysis of smaller urine aliquots and applied in several balance studies.¹⁶⁴⁻¹⁶⁶ After irradiation and cooling, the sample is decomposed with sulphuric acid and hydrogen peroxide, followed by HBr distillation and acid precip-

itation for the selenium determination. Recoveries of 80% are obtained.¹⁶⁴

Another selective procedure for selenium in urine, sensitive down to 0.6 µg/l., was presented by Weingarten *et al.*,¹⁶⁷ but it included some critical and potentially error-producing preconcentration steps, such as evaporation of the urine, addition of sulphuric acid and evaporation to dryness (danger of charring), and reduction by ascorbic acid (which is only effective if all the selenium is present in the quadrivalent form) and the maximum recovery was only 81%, which fell to 50% if a digestion time of 45 min was used.

Janghorbani *et al.*^{108,168} have used stable isotopes for the study of selenium metabolism in healthy adults. The conversion of urinary selenium into selenium(IV) by wet oxidation with different acid mixtures was checked and proved to be satisfactory only with a nitric-perchloric acid mixture and subsequent reduction with hydrochloric acid.¹¹⁷ Ammonium pyrrolidine dithiocarbamate has been used for precipitation of Se(IV).¹⁶⁹ The chemical yield was not quantitative and ⁷⁵Se tracer of high specific activity had to be used for correlation. In this way an analytical method was developed for the study of selenium metabolism in healthy adults, by use of the stable isotope ⁷⁴SeO₃²⁻.¹⁰⁸

Gas-liquid chromatography (GLC)

Determination of selenium in urine by GLC is based on formation of a volatile piaszelenol by reaction of selenium(IV) with an aromatic diamine. Piazselenols can readily be extracted from water and injected into a gas chromatograph, and are usually detected with an electron-capture detector, which gives the highest sensitivity and selectivity for such compounds.

Young and Christian¹⁰³ digested 10 ml of urine with a mixture of nitric, sulphuric and perchloric acids, with molybdate as catalyst, and used DAN as complexing agent without a prior reduction step, and then extraction into hexane. Down to 0.5 ng of selenium could be determined. A low value was found for the only urine sample analysed, probably owing to the omission of a reduction step.

Poole *et al.*¹⁷⁰ used a similar detection technique after sample decomposition with a mixture of nitric acid and magnesium nitrate. 5-Nitropiazselenol was formed after conversion of all selenium into selenite by boiling with hydrochloric acid. The complex was extracted into toluene.

Cappon and Smith¹⁷¹ produced a scheme of analysis for specific forms of selenium in biological materials, including human urine. The method was based on selective reaction of selenium(IV) with 4-nitro-*o*-phenylenediamine to form the 5-nitropiazselenol, which was extracted into benzene and measured by GLC (with electron-capture detection). For organoselenium plus selenium(IV) the sample was digested with concentrated nitric acid. Total

selenium was determined by applying the same digestion procedure and boiling the resulting solution with hydrochloric acid. The difference between the last two values obtained represented the selenium(VI) content. The selenium recovery ranged from 75 to 90% and was assessed by using a ⁷⁵Se-labelled tracer (Na₂SeO₃) for a liquid scintillation spectrometric assay. The method permitted detection of selenium down to 1 µg/l., with a mean deviation of 2.3%. The limitations of this method will be discussed in the section on speciation, below.

Reamer and Veillon¹⁷² have shown that selenium in biological materials can be determined by stable isotope dilution and GLC-mass spectrometry. Urine samples were digested with nitric acid, phosphoric acid and hydrogen peroxide, then 5-nitropiazselenol was formed and extracted into toluene for gas-chromatography-mass spectrometric analysis after spiking of the samples with enriched ⁸²Se. The isotopic ratio of ⁸⁰Se to ⁸²Se was measured by dual ion monitoring and made it possible to determine selenium at the µg/l. level. Human urine samples, spiked with ⁷⁵Se, showed a recovery of 86%.

Electrochemical methods

Faulkner *et al.*¹⁰² tried polarography over a concentration range of 0.5–14 mg/l., which is far too high to be useful for urine analysis. The same applies to the complicated procedure developed by Patriarche¹⁷³ which used a coulometric back-titration and had a detection limit of 100 µg/l.

Titrimetric method

Glover¹¹⁵ digested 300 ml of urine with a sulphuric-nitric acid mixture, plus mercuric oxide to prevent escape of volatile selenium compounds. Distillation with hydrobromic acid-bromine solution separated the selenium as the tetrabromide, which was reduced with sulphur dioxide to the elemental form; this was filtered off, dissolved and converted into selenite, and determined by titration with iodine and thiosulphate. The method was judged accurate down to a selenium level of 20 µg/l. of selenium.

CHEMICAL SPECIES OF SELENIUM IN URINE

Knowledge of the different selenium species present in urine is important, because it can give definite indications about the biochemical conversion of the element and the detoxification mechanisms, and also about the selenium status.¹⁷⁴ Nearly all information on selenium species in urine refers to rats and mice; studies on selenium metabolites in human urine are very scarce and prone to several inconsistencies.

Excretion in the breath¹⁷⁵⁻¹⁸³ and urine^{174,177,180,184-190} and through the gastrointestinal tract¹⁸⁸ has been found to account for most of the elimination of toxic doses of selenium compounds. Trimethylselenium

ion (TMSe^+), a detoxification metabolite of selenium, that is excreted in the urine, was first isolated and identified in rat urine.¹⁸⁴⁻¹⁸⁶ It was found to be only about a tenth as toxic as inorganic and other organic selenium species.¹⁹¹ It was also found that TMSe^+ itself is inactive and easily and almost completely excreted in the urine when fed to selenium-deficient animals.¹⁹² The stability of this metabolite is further demonstrated by the fact that it is not converted into selenite by boiling with a mixture of concentrated nitric acid and hydrogen peroxide. Since TMSe^+ is excreted in urine at both high and low levels of selenium, it is suggested¹⁸⁵ to be a normal metabolite of selenium.

Nahapetian *et al.*¹⁷⁴ have presented a study on urinary selenium metabolites of ^{75}Se -labelled selenite, selenomethionine and selenocystine fed to rats at both low and high dose levels. The purpose was to assess the significance of TMSe^+ in relation to the normal homeostasis of body selenium metabolism. TMSe^+ was the major urinary selenium metabolite (57-69% of urinary ^{75}Se and 16-25% of the oral ^{75}Se dose) at high levels, and a minor metabolite (10% of urinary ^{75}Se ; 3-4% of oral dose) at low, for all three compounds tested. These authors hypothesized that when the intake is at requirement level, trace or no TMSe^+ is excreted in the urine, but it becomes a major excretory metabolite when the intake exceeds requirement level, probably serving as a means of detoxification. They were not able to characterize the non- TMSe^+ metabolites. Free selenite was not detected, although selenite bound to sulphur-containing amino-acid,^{193,194} and selenate,^{188,185} could not be excluded.

Burk¹¹⁶ has reported some findings on the major urinary metabolites of selenium in man. Urine from a young man who had a testicular tumour and was given ^{75}Se -labelled selenite, was analysed by two-dimensional paper chromatography with phenol/water (73:27 w/w) and butanol/acetic acid/water (4:1:1 v/v) as solvent systems. The R_f -values of the TMSe^+ ion agreed with those of a major ^{75}Se spot for the urine sample, and the R_f -values for the other main urinary spot were similar to those for the "U-2" compound present in rat urine.¹⁸⁶ The TMSe^+ ion and the U-2 component accounted for 14-21% and 19-34% of the urinary radioactivity, respectively, and the percentages of selenium in these two fractions appeared to increase over a 10-hr interval. These results strongly suggest that the major selenium metabolites are similar for rat and man. Palmer and Olson¹⁸⁷ have reported that other excretory forms of selenium were found in poultry, so other species cannot be ruled out for man.

The type of animal tested is obviously important, but the chemical form of selenium used in the metabolic experiments can also be of major significance, as will be discussed (in a complementary review¹⁹⁶). For human urine samples, all but three^{107,137,174} of the literature reports deal only with the total selenium

content. Cappon and Smith¹⁷¹ reported a scheme for the determination of organoselenium and selenite, total selenium and selenate, but it was prone to some failures, mainly because the nitric acid oxidation of the organic material could disturb the equilibrium of the naturally existing species. Selenium species found after the acid treatment are not necessarily present in the same form before the treatment. These investigators also checked their procedure by tracer work with only one selenium species, $\text{Na}_2^{75}\text{SeO}_3$.

No details of the organoselenium forms were presented. Oyamada and Ishizaki¹³⁴ were able to give more valid data for the different selenium metabolites. No "free state" selenium (oxidation state not specified) was detected in human urine, collected before luncheon, whereas TMSe^+ constituted 10-47% of the total selenium content. Fodor and Barnes¹⁰⁷ have been able to separate selenate and selenite from urine samples by using different pH-values for complexation by a poly(dithiocarbamate) resin. For the urine of 11 healthy persons the selenite content (8.6 $\mu\text{g/l.}$) was on average about three times the selenate concentration (3.1 $\mu\text{g/l.}$). About 15% of the total selenium occurred in the precipitate resulting after extended standing of the sample or after thawing of the frozen urine. For patients receiving total parenteral nutrition both selenite and selenate concentrations were below the 0.1- $\mu\text{g/l.}$ limit of detection. Hence, in this case all the selenium apparently occurred exclusively in the sample precipitate. Two criticisms can be made of the speciation procedure: no information concerning organoselenium compounds was obtained, and the addition of 50 ml of concentrated hydrochloric acid per litre of urine, could have resulted in a definite redistribution of the original species equilibrium.

CONCENTRATION LEVELS

Literature values for the concentration level of total selenium in urine samples taken from healthy persons are listed in Table 1, along with method of analysis, number of persons tested and other specific characteristics, when mentioned in the studies. Most of the concentrations are simply expressed as $\mu\text{g/l.}$, but as the selenium concentration is a function of the volume excreted, and subject to climate, fluid intake and transpiration, it is felt that a more reliable basis for comparison may be given by the total urinary selenium excreted in 24 hr. Hojo¹⁹⁸ considers it advantageous to express the concentration in μg of Se per g of creatinine excreted, claiming this unit is less susceptible to variation in conditions, and on this basis used individual urine samples instead of 24-hr samples in the estimation of urinary selenium levels. Relative selenium concentrations are not especially useful for comparison, and readers are probably best advised to consult the original articles and assess their validity themselves. The selenium content reported for urine samples varies widely (Table 1) but the

mean amounts of selenium in 24-hr samples are generally below the 30- μg level, except where there is exposure to high environmental selenium levels, which is probably the most important cause of an enhanced urinary excretion level. Likewise, the suggested¹⁴² maximum allowable concentration of 100 $\mu\text{g}/\text{l}$. is generally not exceeded.

No significant sex-related differences in selenium excretion have been found by some authors,^{99,125,134,137} but others^{151,204,205} have found definitely lower excretion figures for females than for males, whether the concentration is expressed as $\mu\text{g}/\text{l}$. or $\mu\text{g}/24$ hr.

Although no extended studies have been made on selenium excretion as a function of age, preliminary results for Belgium indicate that the urinary concentration level is lower for older people than young adults,¹³⁷ perhaps because of lower intakes and/or increased diuresis.

Selenium figures for urine samples from populations exposed to industrial selenium or an environment with a highly seleniferous soil were published more than forty years ago,²⁰⁹⁻²¹¹ but the techniques of analysis were certainly not sensitive enough, and hence these data have to be treated with reserve.

Table 2 summarizes some selenium concentration levels for urine from patients with pathological conditions, together with comparison values for healthy volunteers, some of whom were exposed to various occupational hazards.

The selenium content shows much the same pattern for both the patients and the healthy volunteers, and although Hojo¹⁹⁹ reported that cancer and epilepsy patients showed significantly lower selenium levels than those for any other group examined, the results quoted in Table 2 seem to indicate a skew distribution. Factory workers exposed to heavy metals were found to have significantly higher urinary selenium levels than other groups. This may partly be due to enhanced intake of selenium, which occurs in substantial quantity in sulphide minerals, and partly because ingested minerals accelerate excretion of body selenium as the metal selenides (possibly without interaction with body fluids).

Chlorthalidone treatment of hypertensive patients in Sweden^{168,169} was found not to alter the urinary selenium excretion. Nine alcoholic subjects were reported to show a lower mean daily urinary excretion of selenium compared to normal subjects.²⁰⁶ Urinary selenium excretion appeared to increase during hospital treatment and cessation of alcohol consumption, which might, of course, simply be a consequence of change in intake levels.

Significant selenium depletion has been reported to occur in burn patients and to persist until at least one month after injury, as monitored by urinary selenium excretion,²⁰⁸ but again the distribution seems skewed.

In this type of study there is always the question of whether a lower or higher selenium excretion is a cause or a consequence of a pathological condition. Several diseases may seem to be aggravated or allevi-

ated by changes in selenium status, as has been claimed for alcoholic cardiomyopathy,⁹³ but selenium is not necessarily the causative agent and care must be taken to avoid spurious correlations. It is interesting, for example, that in an extensive study of a seleniferous zone,¹⁰¹ it was reported that mean selenium levels of 636 μg per g of creatinine did not pose severe health hazards for the children who formed the sample populations.

The relation between selenium intake, the chemical form of the element and the daily excretion and selenium levels in urine will be discussed in more detail in the further review¹⁹⁶ already mentioned, which includes more details on the medical aspects and clinical implications.

CONCLUSION

Fluorimetric analysis is the most commonly applied technique for selenium determination in urine samples, but whatever technique is used, except non-destructive neutron-activation analysis, the procedure used for decomposition of the samples has to be checked carefully to prevent volatilization losses and to obtain complete destruction of TMSe^+ , a major selenium metabolite in urine.

Information concerning the speciation of selenium in urine is scarce and contradictory, and often subject to several inconsistencies. Literature data on selenium levels in urine, which must be checked carefully with regard to the units used for expression of results, reveal that the maximum allowable concentration level of 100 $\mu\text{g}/\text{l}$. is seldom exceeded. The normal selenium values for urine are below 30 $\mu\text{g}/\text{l}$. Only in some cases of intoxication or exposure to high environmental selenium levels are enhanced urinary excretion values obtained. Changes in urinary selenium levels in pathological conditions have been reported, but whether such changes are associated with the cause of the pathological condition is open to question.

The daily excretion level is the best indication of selenium content in urine, but several other parameters must be taken into account in assessing selenium status in man.

Much of the information in the literature is based on analysis of very limited numbers of samples, and information is not always given about the reproducibility and accuracy attained in the research. Possible skewness in distributions may pass without comment (which is regrettably all too often the case in work of this nature) and significance is sometimes attached to results for as few as two samples. Much more work, with bigger sample populations, seems needed before definitive conclusions can be drawn.

Acknowledgements—Harry Robberecht thanks the Belgian Ministry of Health (Division of Food Inspection) for financial support. R. Van Grieken (Department of Chemistry) reviewed the XES part of this work.

Table 1. Concentration levels ($\mu\text{g}/\text{l}$) of selenium in urine samples, taken from n healthy persons

Country	n	Range	Concentration level mean value (\pm SD)	Sample source	Method	Ref.
Belgium	69	3-79	31 ± 61	young adults	HGAAS	137
	40	5-33	13 ± 6	old people	HGAAS	137
	1	—	20	—	ETAAS	133
	1	15-25	—	woman (various times)	NAA	99
	1	(20-27)* 25-184 (37-184)*	38 (90)*	man (various times)	NAA	99
Canada	30	29-198	96 ± 47	men	F	197
France	92	2.6-47	12 ± 8	adults (14-17 yr)	F	125
Germany (W)	18	12-60 (9-23)†	23.5 (16 ± 4.6)†	—	HGAAS	138
Gr. Britain	5	2-11	5 ± 2	men	GCECD	170
Israel	5	—	25	adults	NAA	167
Italy	10	(2.3-14)*	6.2*	daily intake: 17 $\mu\text{g}/\text{day}$ 20 $\mu\text{g}/\text{day}$ 24 $\mu\text{g}/\text{day}$ 31 $\mu\text{g}/\text{day}$	NAA	162
	10	(7.2-75)*	14*		NAA	162
	10	(6.7-42)*	12*		NAA	162
	10	(15.2-30)*	22*		NAA	162
	3	35-61	47 ± 20		adults	F
Japan	8	(33-36)† 19-248 (26-240)†	(35 ± 11)† 99 ± 28 (95 ± 12)†	(single-void samples)	F	198
	21	20-113 (27-128)†	58 ± 26 (60 ± 25)†	adults (single-void samples)	F	199
	5	20-140	—	women	ETAAS	134
	5	27-114	—	men	—	134
	15	—	64	fishermen	GCECD	171
Korea	15	—	64	fishermen	GCECD	171
New Guinea	100	0.9-13.6 (1.1 ± 13.9)*	—	—	—	200
New Zealand	3	—	6.5	—	F	201
	13	(6-20)*	—	young women (unrestricted diet)	F	202
	7	(7-19)*	—	(constant diet)	—	202
	13	(10-20)*	—	(fish + kidney diet)	—	202
	39	—	21 ± 9 (17 ± 10)*	boys (5-15 years) —South Otago	F	104
Scotland	31	—	30 ± 8 (24 ± 12)* (24 ± 8.5)**	—North Canterbury	—	104
	16	—	—	—	—	87
	11	4.8-24	13.5 ± 8	—	ICP-AES	107
	1	—	7	—	GCECD	103
	1	—	19	—	ETAAS	136
U.S.A.	27	—	44 ± 18 (69 ± 25)*	Colorado (non-exposed) women	XRF	151
	22	—	71 ± 44 (96 ± 35)*	men	—	151
	21	—	81 ± 31 (144 ± 57)*	Colorado (seleniferous water) women	XRF	151
	17	—	131 ± 51 (174 ± 52)*	men	—	151
	16	15-94	49	—	F	203
	66	—	(28.7 ± 8.3)†	children (5-18 years)	F	127
	21	20-114	52 ± 27	South Dakota	F	204
	5	—	36.3 ± 1.9	Ohio (women)	F	205
	6	—	52.9 ± 3.9	(men)	F	205
	—	—	(54 ± 4)*	—	F	206
	28	14-338	79 ± 48	New Mexico (seleniferous water source)	HGAAS	131
	35	22-203	79 ± 39	New Mexico (seleniferous water source)	HGAAS	130
	—	—	37	Oregon (low caries area)	—	207
	—	—	75	(high caries area)	—	207
	87	10-231 (13-265)*	76 115*	Colorado	XRF	150
191	—	(79 ± 49)*	intake: 213 ± 11 $\mu\text{g}/\text{day}$	—	208	

Country	n	Range	Concentration level mean value (\pm SD)	Sample source	Method	Ref.
Venezuela	1055	—	152 (207) [†] 3900	children (5–16 years) highest individual level	F F	100 100
	111	—	224 [†]	children (Caracas)	F	101
	50	—	636 [†]	(seleniferous area)	F	101

* μ g/24 hr.[†] μ g/g of creatinine.

ETAAS: electrothermal atomic-absorption spectrometry.

F: fluorimetry.

GCECD: gas chromatography with electron-capture detection.

HGAAS: hydride-generation atomic-absorption spectrometry.

ICP-AES: inductively coupled plasma atomic-emission spectroscopy.

NAA: neutron-activation analysis.

XRF: X-ray fluorescence spectrometry.

Table 2. Concentration levels (μ g/l.) of selenium in urine samples in pathological and normal conditions

Country	n	Concentration		Sample source	Method	Ref.	
		range	mean value \pm SD				
Japan	23	10–66 (13–66) [†]	26 \pm 14 (34 \pm 15) [†]	cancer patients	F	199	
	21	10–75 (19–77) [†]	36 \pm 16 (45 \pm 18) [†]	epilepsy patients	F	199	
	2	29–60 (98–100) [†]	45 \pm 22 (99 \pm 1)	hypertension	F	199	
	22	15–170 (19–266) [†]	69 \pm 49 (92 \pm 68) [†]	Mn-exposed workers	F	199	
	14	56–198 (40–283) [†]	107 \pm 45 (146 \pm 86) [†]	Cr-exposed workers	F	199	
	5	93–219 (126–365) [†]	166 \pm 57 (198 \pm 98) [†]	Cd-exposed workers	F	199	
	1	—	288 172**	Hg-exposed worker	F	199	
	3	35–61 (33–36) [†]	47 \pm 20 (35 \pm 11) [†]	healthy adults	F	198	
	8	19–248 (26–240) [†]	99 \pm 28 (95 \pm 12) [†]	healthy adults	F	198	
	21	20–113 (27–128) [†]	58 \pm 26 (60 \pm 25) [†]	healthy controls	F	199	
	Scotland	20	—	(18 \pm 12) [†]	coeliac disease	—	87
		17	—	(26 \pm 14) [†]	ulcerative colitis	—	87
		18	—	(26 \pm 14) [†]	Crohn's disease	—	87
16		—	(24 \pm 8.5) [†]	reference population	—	87	
Sweden	16	(3–55)*	(30 \pm 14)*	hypertensive patients	—	—	
	16	(18–69)*	(36 \pm 14)*	—before chlorthalidone treatment	NAA	165	
	6	—	(32 \pm 11)*	—after treatment	NAA	165	
	6	—	(38 \pm 12)*	hypertensive patients —before chlorthalidone treatment	NAA	168	
—	—	—	—after 6 months treatment	NAA	168		
USA	1	—	450	amyotrophic lateral sclerosis	—	8	
	17	—	(16 \pm 29)*	burn patients	—	208	
	191	—	(79 \pm 49)*	matched controls	—	208	
	9	—	(30 \pm 11)*	alcoholic subjects (47 \pm 3 years)	F	206	
	—	—	(54 \pm 4)	controls	F	206	

* μ g/24 hr.[†] μ g/g creatinine.

F: fluorimetry.

NAA: neutron-activation analysis.

REFERENCES

1. K. Schwarz and C. M. Foltz, *J. Am. Chem. Soc.*, 1957, **79**, 3292.
2. J. Rotruck, A. Pope, H. Ganther, A. Swanson, D. Hafeman and W. Hoekstra, *Science*, 1973, **179**, 588.
3. I. Rosenfeld and O. A. Beath, in *Selenium*, p. 441. Academic Press, New York, 1964.
4. C. H. Diskin, C. L. Tomasso, J. C. Alper, M. I. Glaser and S. E. Fliegel, *Arch. Intern. Med.*, 1979, **139**, 824.
5. C. Wilber, *Clin. Toxicol.*, 1980, **17**, 171.
6. L. Fishbein in *Toxicology of Trace Elements*, R. A. Goyer and M. A. Mehlman (eds.), p. 191. Wiley, New York, 1977.
7. A. C. Griffin, *Adv. Cancer Res.*, 1979, **29**, 419.
8. A. W. Kilness and E. H. Hochberg, *J. Am. Med. Assoc.*, 1977, **237**, 2843.
9. I. D. Civil and M. J. McDonald, *N.Z. Med. J.*, 1978, **87**, 354.
10. A. Schecter, W. Shanske, A. Stenzler, H. Quintilian and H. Steinberg, *Chest*, 1980, **77**, 554.
11. C. C. Clayton and C. A. Bauman, *Cancer Res.*, 1949, **9**, 575.
12. R. Shamberger, *J. Natl. Cancer Inst.*, 1970, **44**, 931.
13. J. Harr, J. Exon, P. Weswig and P. Whanger, *Clin. Toxicol.*, 1973, **6**, 487.
14. M. M. Jacobs, B. Jansson and A. C. Griffin, *Cancer Lett.*, 1977, **2**, 133.
15. A. C. Griffin and M. M. Jacobs, *ibid.*, 1977, **3**, 177.
16. A. H. Daoud and A. C. Griffin, *ibid.*, 1980, **9**, 299.
17. C. Ip and M. M. Ip, *Carcinogenesis*, 1981, **2**, 915.
18. C. Ip, *Cancer Res.*, 1981, **41**, 2683.
19. C. Ip and D. J. Sinha, *Carcinogenesis*, 1981, **2**, 435.
20. D. Medina and F. Shepherd, *ibid.*, 1981, **2**, 451.
21. M. Schillaci, S. E. Martin and V. A. Milner, *Mutation Research*, 1982, **101**, 31.
22. P. R. Harbach and J. A. Swenberg, *Carcinogenesis*, 1982, **2**, 575.
23. J. R. Shapiro, *Ann. N.Y. Acad. Sci.*, 1972, **192**, 215.
24. G. N. Schrauzer, *Bioinorg. Chem.*, 1976, **5**, 275.
25. A. C. Griffin, *J. Cancer Res. Clin. Oncol.*, 1980, **98**.
26. G. F. Nordberg and O. Andersen, *Environ. Health Perspect.*, 1981, **40**, 65.
27. G. Kazantzis, *ibid.*, 1981, **40**, 143.
28. K. W. Jennette, *ibid.*, 1981, **40**, 233.
29. A. C. Griffin in *Molecular Interrelations of Nutrition and Cancer*, M. S. Arnott, J. Van Eys and Y. M. Wang (eds.), p. 401. Raven Press, New York, 1982.
30. G. N. Schrauzer, D. White and C. Schneider, *Bioinorg. Chem.*, 1977, **7**, 35.
31. G. N. Schrauzer, *Adv. Exp. Biol. Med.*, 1977, **91**, 323.
32. *Idem*, *Am. J. Clin. Nutr.*, 1980, **33**, 1892.
33. C. A. Grant, *Acta Vet. Scand.*, 1961, **2**, 1.
34. J. F. Van Fleet, V. J. Ferrans and G. R. Ruth, *Lab. Invest.*, 1977, **37**, 188.
35. G. D. Cawley and R. Bradley, *Vet. Rec.*, 1978, **103**, 239.
36. R. J. Shamberger, in *Trace Substances in Environmental Health*, D. D. Hemphill (ed.), Vol. XI, p. 15. University of Missouri, Columbia, 1975.
37. R. J. Shamberger, M. S. Gunsch, C. E. Willis and L. J. McCormack, in *Trace Substances in Environmental Health*, D. D. Hemphill (ed.), Vol. XII, p. 48. University of Missouri, Columbia, 1978.
38. R. J. Shamberger, C. E. Willis, L. J. McCormack, in *Trace Substances in Environmental Health*, D. D. Hemphill (ed.), Vol. XIII, p. 59. University of Missouri, Columbia, 1979.
39. *Idem*, *Fed. Proc.*, 1979, **38**, 391.
40. R. J. Shamberger, *J. Environ. Path. Toxicol.*, 1980, **4**, 305.
41. J. T. Salonen, G. Alfthan, J. Pikkarainen, J. K. Huttunen and P. Puska, *Lancet*, 1982 (2), 175.
42. Keshan Disease Research Group, *Chinese Med. J.*, 1979, **92**, 471.
43. *Idem*, *Nutr. Rev.*, 1980, **38**, 278.
44. X. Chen, G. Yang, J. Chen, X. Chen, Z. Wen and G. Ge, *Biol. Trace Elem. Res.*, 1980, **2**, 91.
45. B. Cheng, S. Ju, S. Yue, R. He and S. Sheng, *Acta Pedologica Sinica*, 1980, **17**, 55.
46. Editorial, *Lancet*, 1979 (2), 889.
47. C. H. Hill, *Fed. Proc.*, 1975, **34**, 2096.
48. G. N. Schrauzer, D. A. White, J. McGinness, C. J. Schneider and L. Bell, *Bioinorg. Chem.*, 1978, **9**, 245.
49. R. W. Chen, P. D. Whanger and P. H. Weswig, *ibid.*, 1975, **4**, 125.
50. J. R. Prohaska, M. Mowafy and H. E. Ganther, *Chem. Biol. Interactions*, 1977, **18**, 253.
51. T. A. Gasiewicz and J. C. Smith, *Environ. Health Perspect.*, 1978, **25**, 133.
52. P. D. Whanger, *ibid.*, 1979, **28**, 115.
53. P. D. Whanger, J. W. Ridlington and C. L. Holcomb, *Ann. N.Y. Acad. Sci.*, 1980, **355**, 333.
54. L. Magos and M. Webb, *CRC Crit. Rev. Toxicol.*, 1980, **8**, 1.
55. J. L. Early and R. C. Schnell, *Toxicol. Appl. Pharmacol.*, 1981, **58**, 57.
56. S. L. V. Van Puymbroeck, W. J. J. Stips and O. L. J. Vanderborgt, *Arch. Environ. Contam. Toxicol.*, 1982, **11**, 103.
57. J. J. Dougherty and W. G. Hoekstra, *Proc. Soc. Exp. Biol. Med.*, 1982, **169**, 201.
58. S. C. Rastogi, J. Clausen and K. C. Srivastava, *Toxicology*, 1976, **6**, 377.
59. G. O. Howell and C. H. Hill, *Environ. Health Perspect.*, 1978, **25**, 147.
60. J. H. Koeman, W. H. M. Peeters, C. H. M. Koudstaal-Hol, P. S. Tsjioe and J. J. M. De Goeij, *Nature*, 1973, **245**, 383.
61. R. W. Chen, P. D. Whanger and S. C. Fang, *Pharmacol. Res. Commun.*, 1974, **6**, 571.
62. N. J. Mackay, M. N. Kazalos, R. J. Williams and M. I. Leedow, *Mar. Pollut. Bull.*, 1975, **6**, 57.
63. J. H. Koeman, W. S. M. Van de Ven, J. J. M. De Goeij, P. S. Tsjioe and J. L. Van Haaften, *Sci. Total Environ.*, 1975, **3**, 279.
64. M. M. El-Begearmi, M. L. Sunde and H. E. Ganther, *Poultry Sci.*, 1977, **56**, 313.
65. R. Martoja and D. Viale, *Compt. Rend.*, 1977, **285D**, 109.
66. H. C. Freeman, G. Shum and J. F. Uthe, *J. Environ. Sci. Health*, 1978, **113**, 235.
67. T. G. Smith and F. A. J. Armstrong, *Arctic*, 1978, **31**, 75.
68. T. Kari and P. Kauranen, *Bull. Environ. Contam. Toxicol.*, 1978, **19**, 273.
69. L. J. Kling and J. H. Soares, *Poultry Sci.*, 1978, **56**, 1286.
70. M. Berlin, *Environ. Health Perspect.*, 1978, **25**, 67.
71. H. E. Ganther, *Ann. N.Y. Acad. Sci.*, 1980, **355**, 212.
72. J. C. Hansen and P. Kristensen, *Arch. Toxicol.*, 1980, **46**, 273.
73. C. Lucu and M. Skreblin, *Marine Environ. Res.*, 1981, **5**, 265.
74. H. E. Ganther, C. Goudie, M. L. Sunde, M. J. Kopecky, P. Wagner, O. Sang-Hwan and W. G. Hoekstra, *Science*, 1972, **175**, 1122.
75. R. W. Chen, V. L. Lacy and P. D. Whanger, *Res. Commun. Chem. Pathol. Pharmacol.*, 1975, **12**, 297.
76. G. Ohi, S. Nishigaki, H. Seki, Y. Tamura, T. Maki, H. Maeda, S. Ochiai, H. Yamada, Y. Shihamura and H. Yagyu, *Toxicol. Appl. Pharmacol.*, 1975, **32**, 527.
77. K. Sumino, R. Yamamoto and S. Kitamura, *Nature*, 1977, **268**, 73.
78. M. A. Friedman, L. R. Eaton and W. H. Carter, *Bull. Environ. Contam. Toxicol.*, 1978, **19**, 436.

79. S. Skerfving, *Environ. Health Perspect.*, 1978, **25**, 57.
80. H. E. Ganther, *ibid.*, 1978, **25**, 71.
81. M. Hayashi, H. Kito and T. Masukawa, *J. Toxicol. Sci.*, 1980, **5**, 282.
82. D. A. Hankins, M. C. Riella, B. H. Scribner and A. L. Babb, *Surgery*, 1976, **79**, 674.
83. A. M. Van Rij, C. D. Thomson, J. M. McKenzie and M. F. Robinson, *Am. J. Clin. Nutr.*, 1979, **32**, 2076.
84. G. S. Fell, A. Shenkin, A. Main and R. Russell, *Proc. Nutr. Soc.*, 1980, **39**, 36A.
85. S. Amin, S. Y. Chen, P. J. Collipp, M. Castro-Magana, V. T. Maddaiah and S. W. Klein, *Nutr. Metab.*, 1980, **24**, 311.
86. P. J. Collipp and S. Y. Chen, *N. Engl. J. Med.*, 1981, **304**, 1304.
87. G. S. Fell, P. Stromberg, A. Main, R. Spooner, R. Campbell, R. Russell, A. Brown and R. Ottaway, *Proc. Nutr. Soc.*, 1981, **40**, 76A.
88. H. W. Lane, S. Dudrick and W. C. Warren, *Proc. Soc. Exp. Biol. Med.*, 1981, **167**, 383.
89. R. A. Johnson, S. S. Baker, J. T. Fallon, E. P. Maynard, J. N. Ruskin, Z. Wen, K. Ge and A. J. Cohen, *N. Engl. J. Med.*, 1981, **304**, 1210.
90. V. R. Young, *ibid.*, 1981, **304**, 1228.
91. W. W. King, L. Michel, W. C. Wood, R. A. Malt, S. S. Baker and H. J. Cohen, *ibid.*, 1981, **304**, 1305.
92. R. M. Mathias and A. A. Jackson, *Lancet*, 1982, (1), 1312.
93. L. S. Goldman and N. E. Kantrowitz, *N. Engl. J. Med.*, 1981, **305**, 701.
94. M. Laker, *Lancet*, 1982 (2), 260.
95. T. Johannesson, G. Lunde and E. Steinnes, *Acta Pharmacol. Toxicol.*, 1981, **48**, 185.
96. T. S. Davies, *Lancet*, 1982 (2), 935.
97. I. H. Qureshi, M. S. Chaudhary and S. Ahmad, *J. Radioanal. Chem.*, 1982, **68**, 209.
98. R. F. Burk, *Wld. Rev. Nutr. Diet.*, 1978, **30**, 88.
99. R. Cornelis, A. Speecke and J. Hoste, *Anal. Chim. Acta*, 1975, **78**, 317.
100. M. C. Mondragón and W. G. Jaffé, *Arch. Latinoam. Nutr.*, 1971, **21**, 185.
101. W. G. Jaffé, M. Ruphael D., M. C. Mondragón and M. A. Cuevas, *ibid.*, 1972, **22**, 595.
102. A. G. Faulkner, E. C. Knoblock and W. C. Purdy, *Clin. Chem.*, 1961, **7**, 22.
103. J. W. Young and G. D. Christian, *Anal. Chim. Acta*, 1973, **65**, 127.
104. P. B. Cadell and F. B. Cousins, *Nature*, 1960, **185**, 163.
105. G. D. Christian, E. C. Knoblock and W. C. Purdy, *J. Assoc. Off. Anal. Chem.*, 1965, **48**, 877.
106. J. L. Greger and R. E. Marcus, *Ann. Nutr. Metabol.*, 1981, **25**, 97.
107. P. Fodor and R. M. Barnes, *Spectrochim. Acta*, 1983, **38B**, 229.
108. M. Janghorbani, B. T. G. Ting and V. R. Young, *Am. J. Clin. Nutr.*, 1981, **34**, 2816.
109. J. H. Watkinson, *Anal. Chem.*, 1966, **38**, 92.
110. O. E. Olson, I. S. Palmer and E. E. Cary, *J. Assoc. Off. Anal. Chem.*, 1975, **58**, 117.
111. H. J. Robberecht, R. E. Van Grieken, P. A. Van Den Bosch, H. A. Deelstra and D. A. Vanden Berghe, *Talanta*, 1982, **29**, 1025.
112. J. Nève, M. Hanocq and L. Molle, *Mikrochim. Acta*, 1980 **I**, 259.
113. A. B. Grant, *N.Z.J. Sci.*, 1963, **6**, 577.
114. T. J. Kneip, R. S. Ajemian, J. N. Driscoll, F. I. Grunder, L. Kornreich, J. W. Loveland, J. L. Moyers and R. J. Thompson, *Health Lab. Sci.*, 1977, **14**, 53.
115. J. R. Glover, *Ann. Occup. Hyg.*, 1967, **10**, 3.
116. R. F. Burk, in *Trace Elements in Human Health and Disease*, Vol. II, *Essential and Toxic Elements*, A. S. Prasad and D. Oberlas (eds.), p. 105. Academic Press, New York, 1976.
117. M. Janghorbani, B. T. G. Ting, A. Nahapetian and V. R. Young, *Anal. Chem.*, 1982, **54**, 1188.
118. R. Bye, *Talanta*, 1984, **30**, 993.
119. J. P. Roquebert and R. Truhaut, *Bull. Soc. Pharm. Bordeaux*, 1962, **101**, 143.
120. P. F. Lott, P. Cukor, G. Moriber and J. Solga, *Anal. Chem.*, 1963, **35**, 1159.
121. F. Feigl and P. W. West, *ibid.*, 1947, **19**, 351.
122. P. W. West and T. V. Ramakrishna, *ibid.*, 1968, **40**, 966.
123. J. De Moor, *MS Thesis*, University of Antwerp, Wilrijk, Belgium, 1980.
124. M. Tanaka and I. Kawashima, *Talanta*, 1965, **12**, 211.
125. A. Geahchan and P. Chambon, *Clin. Chem.*, 1980, **26**, 1272.
126. H. H. Taussky, A. Washington, E. Zubillaga and A. T. Milhorat, *Microchem. J.*, 1966, **10**, 470.
127. S. Y. Chen, P. J. Collipp, L. H. Boasi, D. S. Isenschmid, R. J. Verolla, G. A. San Roman and J. K. Yeh, *Ann. Nutr. Metabol.*, 1982, **26**, 186.
128. H. J. Robberecht and R. E. Van Grieken, *Talanta*, 1982, **29**, 823.
129. M. Verlinden, H. Deelstra and E. Adriaenssens, *ibid.*, 1981, **28**, 637.
130. J. L. Valentine, H. K. Kang and G. H. Spivey, *Environ. Res.*, 1978, **17**, 347.
131. J. L. Valentine, H. K. Kang, P. M. Dang and M. Schluchter, *J. Toxicol. Environ. Health*, 1980, **6**, 731.
132. K. H. Schaller and H. Schweiger, *Beckmans Rep.*, 1978, **1**, 15.
133. J. Nève, M. Hanocq and L. Molle, *J. Pharm. Belg.*, 1980, **35**, 345.
134. N. Oyamada and M. Ishizaki, *Abstracts from 9th Intern. Conf. on Atomic Spectroscopy and XXII Coll. Spectroscopium Intern.*, 4-8 September 1981, Tokyo, Japan, p. 501.
135. N. Oyamada, *Japan. J. Ind. Health*, 1982, **24**, 320.
136. D. H. Cox and A. E. Bibb, *J. Assoc. Off. Anal. Chem.*, 1981, **64**, 265.
137. M. Verlinden, *Ph.D. Thesis*, Wilrijk, Belgium, 1981.
138. P. Schierling, C. Oefele and K. H. Schaller, *Arztl. Lab.*, 1982, **28**, 21.
139. M. Ishizaki, *Talanta*, 1978, **25**, 167.
140. R. M. Barnes, *Toxicol. Environ. Chem. Rev.*, 1978, **2**, 187.
141. W. B. Robbins and J. A. Caruso, *Anal. Chem.*, 1979, **51**, 889A.
142. M. Thompson, B. Pahlavanpour, S. J. Walton and G. F. Kirkbright, *Anal. Chem.*, 1978, **50**, 568.
143. R. M. Barnes and J. S. Genna, *Anal. Chem.*, 1979, **51**, 1065.
144. R. Van Grieken, K. Bresseleers, J. Smits, B. Vanderborgh and M. Vanderstappen, *Adv. X-Ray Anal.*, 1976, **19**, 435.
145. J. Smits and R. Van Grieken, *Anal. Chim. Acta*, 1977, **88**, 97.
146. L. Vos, H. Robberecht, P. Van Dyck and R. Van Grieken, *ibid.*, 1981, **130**, 167.
147. J. A. Smits and R. E. Van Grieken, *Anal. Chem.*, 1980, **52**, 1479.
148. *Idem*, *Int. J. Environ. Anal. Chem.*, 1981, **9**, 61.
149. K. K. Nielson and D. R. Kalkwarf, in *Electron Microscopy and X-Ray Applications to Environmental and Occupational Health Analysis*, P. A. Russell and A. E. Hutchings (eds.), p. 31. Ann Arbor Science, Ann Arbor, 1978.
150. T. A. Tsongas and S. W. Ferguson, in *Trace Substances in Environmental Health*, D. D. Hemphill (ed.), Vol. XI, p. 30. University of Missouri, Columbia, 1977.
151. *Idem*, in *Trace Element Metabolism in Man and Animals* (Tema 3), M. Kirchgessner (ed.), p. 320. Freising-Weihestephan, West Germany, 1978.

152. W. Snodgrass, B. H. Rumack and J. Sullivan, *Clin. Toxicol.*, 1981, **18**, 211.
153. A. C. Alfrey, L. C. Nunnelley, H. Rudolph and W. P. Smythe, *Adv. X-Ray Anal.*, 1976, **19**, 497.
154. B. Holyńska and K. Lipinska-Kalita, *Radiochem. Radioanal. Lett.*, 1977, **30**, 241.
155. B. Holyńska and A. Markowicz, *ibid.*, 1977, **31**, 165.
156. H. Robberecht and R. Van Grieken, *Anal. Chim. Acta*, 1983, **147**, 113.
157. D. M. McKnown and J. S. Morris, *J. Radioanal. Chem.*, 1978, **43**, 411.
158. J. S. Morris, M. F. Smith, R. E. Morrow, E. D. Heimann, J. C. Hancock and T. Gall, *ibid.*, 1982, **69**, 473.
159. D. M. McKnown and J. S. Morris, in *Trace Substances in Environmental Health*, D. D. Hemphill (ed.), Vol. XI, p. 338. University of Missouri, Columbia, 1977.
160. G. F. Clementi and G. G. Mastinu, *J. Radioanal. Chem.*, 1974, **20**, 707.
161. L. C. Rossi and G. F. Clementi, *Arch. Environ. Health*, 1976, **31**, 160.
162. G. F. Clementi, L. C. Rossi and G. P. Santaroni, *J. Radioanal. Chem.*, 1977, **37**, 549.
163. P. O. Wester, D. Brune and K. Samsahl, *Int. J. Appl. Radiat. Isotopes.*, 1964, **15**, 59.
164. D. Brune, K. Samsahl and P. O. Wester, *Clin. Chim. Acta*, 1966, **13**, 285.
165. P. O. Wester, *Acta Med. Scand.*, 1973, **194**, 505.
166. *Idem, ibid.*, 1974, **196**, 489.
167. R. Weingarten, Y. Shamai and T. Schlesinger, *Int. J. Appl. Radiat. Isotopes.*, 1979, **30**, 585.
168. M. Janghorbani, M. J. Christensen, A. Nahapetian and V. R. Young, *Am. J. Clin. Nutr.*, 1982, **35**, 647.
169. J. Starý, *The Solvent Extraction of Metal Chelates*, Pergamon Press, Oxford, 1974.
170. C. F. Poole, N. J. Evans and D. G. Wibberley, *J. Chromatog.*, 1977, **136**, 73.
171. C. J. Caddon and J. C. Smith, *J. Anal. Toxicol.*, 1978, **2**, 114.
172. D. C. Reamer and C. Veillon, *Anal. Chem.*, 1982, **53**, 2166.
173. G. J. Patriarche, *Anal. Lett.*, 1972, **5**, 45.
174. A. T. Nahapetian, M. Janghorbani and V. R. Young, *Fed. Proc.*, 1982, **41**, 529; *J. Nutr.*, 1983, **113**, 401.
175. F. Hofmeister, *Arch. Exp. Pathol. Pharmacol.*, 1894, **33**, 198.
176. J. Schultz and H. B. Lewis, *J. Biol. Chem.*, 1940, **133**, 199.
177. K. P. McConnell, *ibid.*, 1942, **145**, 55.
178. H. E. Ganther and C. A. Baumann, *J. Nutr.*, 1962, **77**, 210.
179. H. E. Ganther, O. A. Levander and C. A. Baumann, *ibid.*, 1966, **88**, 55.
180. L. L. Hopkins, Jr., A. L. Pope and C. A. Baumann, *ibid.* 1966, **88**, 61.
181. T. Hirooka and J. T. Galambos, *Biochem. Biophys. Acta*, 1966, **130**, 313.
182. J. Sternberg, J. Brodeur, A. Imbach and A. Mercier, *Int. J. Appl. Radiat. Isotopes.*, 1968, **19**, 669.
183. S. Jiang, H. Robberecht and D. A. Vanden Berghe, *Experientia*, 1983, **39**, 293.
184. J. L. Byard, *Arch. Biochem. Biophys.*, 1969, **130**, 556.
185. I. S. Palmer, R. P. Gunsalus, A. W. Halverson and O. E. Olson, *Biochim. Biophys. Acta*, 1969, **177**, 336.
186. *Idem, ibid.*, 1970, **208**, 260.
187. I. S. Palmer and O. E. Olson, *Fed. Proc.*, 1976, **35**, 578.
188. K. P. McConnell, *J. Biol. Chem.*, 1941, **141**, 427.
189. H. E. Ganther and G. A. Baumann, *J. Nutr.*, 1962, **77**, 408.
190. A. W. Halverson, P. L. Guss and O. E. Olson, *ibid.*, 1962, **77**, 408.
191. B. D. Obermayer, I. S. Palmer, O. E. Olson and A. W. Halverson, *Toxicol. Appl. Pharmacol.*, 1971, **20**, 135.
192. D. T. Tsay, A. W. Halverson and I. S. Palmer, *Nutr. Rep. Int.*, 1970, **2**, 203.
193. K. Schwarz and E. Sweeney, *Fed. Proc.*, 1964, **23**, 421.
194. L. M. Cummins and J. L. Martin, *Biochemistry*, 1967, **3**, 3162.
195. B. B. Westfall and M. I. Smith, *J. Pharmacol. Exp. Therap.*, 1941, **72**, 245.
196. H. Robberecht and H. Deelstra, *Clin. Chim. Acta*, 1984, **136**, 107.
197. L. Lalonde, Y. Jean, K. D. Roberts, A. Chapdelaine and G. Bleau, *Clin. Chem.*, 1982, **28**, 172.
198. Y. Hojo, *Bull. Environ. Contam. Toxicol.*, 1981, **27**, 213.
199. *Idem, ibid.*, 1981, **26**, 466.
200. B. L. Adkins, D. E. Barmes and R. G. Schamschula, *Bull. Wld. Health Org.*, 1974, **50**, 495.
201. C. Thomson, *N.Z. Med. J.*, 1974, **80**, 163.
202. N. M. Griffiths, *Proc. Univ. Otago Med. Sch.*, 1973, **51**, 8.
203. D. M. Hadjimarkos, C. A. Storvick and L. F. Remmert, *J. Pediat.*, 1952, **40**, 451.
204. M. Howe, *Arch. Environ. Health.*, 1979, **34**, 444.
205. D. L. Palmquist, A. L. Moxon and A. H. Cantor, *Fed. Proc.*, 1979, **38**, 391.
206. S. K. Dutta, P. Miller, L. Greenberg and O. A. Levander, *Am. J. Clin. Nutr.*, 1982, **35**, 845.
207. D. M. Hadjimarkos, C. A. Storvick and L. F. Remmert, *J. Pediat.*, 1952, **40**, 451.
208. D. Hunt, H. Lane, D. Beesinger, K. Gallagher, B. J. Rowlands and D. Johnston, *Fed. Proc.*, 1983, **42**, 927.
209. J. H. Sterner and V. J. Lidfeldt, *J. Pharmacol. Exp. Ther.*, 1941, **73**, 205.
210. M. I. Smith, K. W. Franke and B. B. Westfall, *Publ. Hlth. Rep. (Wash.)*, 1936, **51**, 1496.
211. M. I. Smith and B. B. Westfall, *ibid.*, 1937, **52**, 1375.

COMPARISON OF THE SUB- AND SUPER-EQUIVALENCE AND SUBSTOICHIOMETRIC METHODS OF ISOTOPE DILUTION ANALYSIS FOR THE DETERMINATION OF A TRACE AMOUNT OF ANTIMONY

H. YOSHIOKA and T. KAMBARA

Radiochemistry Research Laboratory, Faculty of Science, Shizuoka University, 836 Ōya, Shizuoka 422,
Japan

(Received 21 April 1983. Revised 23 November 1983. Accepted 3 February 1984)

Summary—The sub- and super-equivalence methods of isotope dilution analysis (SSE-IDA) have been compared with substoichiometric isotope dilution analysis (Subst-IDA) for the determination of a trace amount of antimony by means of a redox reaction. For this comparison, the difference between the amount separated and the theoretical value was determined under various conditions. Under conditions in which the substoichiometric reaction and separation gave unsatisfactory results, accurate determination could still be performed by SSE-IDA. The reason for this is discussed.

Since substoichiometry¹⁻³ was introduced into isotope dilution analysis (IDA), various modifications of this method (Subst-IDA)⁴⁻⁶ have been developed because of its accuracy, sensitivity and relative freedom from interference. Trace amounts of antimony in a metal have been determined by use of an oxidation-reduction reaction in substoichiometric activation analysis (Redox Subst-NAA⁷ and Redox Subst-IDA⁸).

Subst-IDA requires that the amounts of reagent reacted and product separated must always be constant. Ideally, more than 99% of the reagent should be converted into product, but even if the reagent does not react quite so quantitatively, the method can still be used provided that the amount separated is constant (such cases are not common).

The "sub- and super-equivalence" method of isotope dilution analysis (SSE-IDA) was therefore proposed by Klas *et al.*,⁹ and is applicable under conditions other than those listed above. Various types of SSE-IDA^{9,10} have been thought out, and theoretical studies¹¹ and applications to the determination of Co, vitamin B₁₂, Se, Tl, Fe and Zn¹² have been reported. We too have examined this method, applying Redox SSE-IDA for the determination of a trace amount of antimony.¹³

However, no detailed analysis has been made of why (in contrast to Subst-IDA) SSE-IDA makes accurate determination possible when the basic conditions are not strictly fulfilled. We have therefore examined the degree of reaction under various conditions and the effect of departure from the required conditions, and have determined antimony in the presence of an interfering species [As(III)].

PRINCIPLE OF THE METHOD

The principle of SSE-IDA¹⁰ is explained below in parallel with the experimental procedure.

Two series of solutions are necessary. In the first, each solution contains the same amount of sample (x) and the same amount of radioactive isotope (A). In the second, each solution contains k times the amount of sample and radioisotope used in the first series. It is not essential to use replicate analysis for the second series, but doing so will give a more reliable average value.

The solutions in the first series are isotopically diluted by the addition of regularly increasing amounts of carrier (iy , where $i = 1, 2, \dots$), so that their specific activities become $A/(x + iy)$. No carrier is added to the solutions in the second series, so their specific activities are all A/x .

All solutions of both series are brought to the same volume and acid concentration by addition of the solvent and an appropriate amount of acid. Next, the same substoichiometric amount of the reagent which is to react with the analyte is added to all the solutions in both series.

After completion of the reaction, the products are isolated and the radioactivities (a_x, a_{x+iy}, a_{kx}) of the isolated products (masses m_x, m_{x+iy}, m_{kx}) are measured.

As the total activity of the analyte is not changed by the separation, the specific activity in the first series is defined by

$$A/(x + iy) = a_{x+iy}/m_{x+iy} \quad (1)$$

Similarly, for the second series

$$A/x = a_{kx}/m_{kx} \quad (2)$$

Hence

$$a_{kx}/a_{x+iy} = iy m_{kx}/x m_{x+iy} + m_{kx}/m_{x+iy} \quad (3)$$

As the extent of chemical reaction is dependent on the concentrations of the reactants, the degree of reaction of a fixed substoichiometric amount of re-

agent will depend on the concentration of the element to be determined. However, for a solution with the same total analyte concentration in both series, the degree of reaction and separation should also be the same, so in principle a solution could be prepared in the first series with j increments of carrier such that

$$m_{x+jy} = m_{kx} \quad (4)$$

Under these conditions

$$a_{kx}/a_{x+jy} = k \quad (5)$$

From equations (3)–(5), we obtain

$$x = jy/(k - 1) \quad (6)$$

The quantity x is then obtained graphically as shown in Fig. 4, by plotting a_{kx}/a_{x+jy} against jy and finding the abscissa value (jy) corresponding to $a_{kx}/a_{x+jy} = k$ for any value of k , and applying equation (6).

If $m_{x+jy} = m_{kx}$, which is the condition required for conventional substoichiometry, equation (7) can be derived:

$$a_{kx}/a_{x+jy} = iy/x + 1 \quad (7)$$

This is one limiting case of SSE-IDA.

EXPERIMENTAL

Reagents

¹²⁵Sb(III) tracer solution.^{14,15} ¹²⁵Sb (100–300 μg, ca. 1 μCi/100 μl in 6M hydrochloric acid) was mixed with 10 ml of concentrated hydrochloric acid and refluxed for 30 min in order to reduce the antimony. This ¹²⁵Sb(III) tracer solution in 6M hydrochloric acid was always prepared just before use, for labelling the sample solution.

Synthetic sample solution. The solution of inactive Sb(III) to be determined was labelled with the ¹²⁵Sb(III) tracer solution and was used as the labelled synthetic sample solution [Sb(III) + ¹²⁵Sb(III), ca. 10 μg/ml in 6M hydrochloric acid]. It was stored in a brown bottle and kept in the dark to avoid self- and photo-oxidation¹⁵ of the ¹²⁵Sb(III).

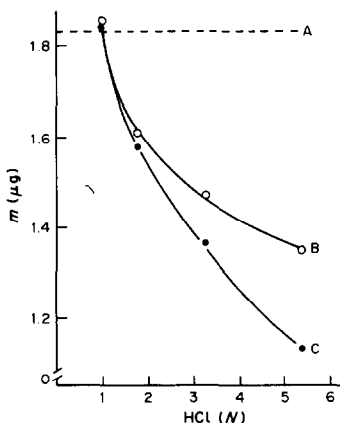


Fig. 1. Effect of $[HCl]_{ox}$ on the amount of Sb(V) separated. A, Theoretical line; B, Sb(III) $8 \times 10^{-2} \mu\text{eq}$; C, Sb(III) + As(III) $8 \times 10^{-2} \mu\text{eq} + 4 \times 10^{-1} \mu\text{eq}$. Vol_{ox} 8.5, 4.5, 2.5 and 1.5 ml for $[HCl]_{ox}$ 1, 2, 3 and 5N respectively. $\text{K}_2\text{Cr}_2\text{O}_7$ $3 \times 10^{-2} \mu\text{eq}$, $[HCl]_{ex} = 0.8N$, $\text{Vol}_{ex} = 10.5$ ml. $[HCl]_{ox}$ Vol_{ox} are the acid concentration and total volume respectively after the addition of $\text{K}_2\text{Cr}_2\text{O}_7$; $[HCl]_{ex}$ and Vol_{ex} are the acid concentration and total volume for the extraction stage.

This solution was stable for at least a week, without change in the oxidation state of the antimony.

Sb(III) carrier solution. Prepared by dissolving reagent grade Sb_2O_3 (99.999% pure) in 6M hydrochloric acid, and standardized by bromate titration.

Oxidant. Commercially available 0.1N potassium dichromate, suitably diluted.

Separation reagent. A 0.05M solution of *N*-benzoyl-*N*-phenylhydroxylamine (BPA) in chloroform was used for separation of Sb(III) from Sb(V).¹⁶

Activity measurements

The activity of ¹²⁵Sb was measured with a scintillation counter, NaI(Tl), well-type, to eliminate interference by the activity of the daughter nuclide ^{125m}Te ($t_{1/2} = 58$ days; 35 and 110 keV).

Procedure

1st series. Aliquots (0.1 ml) of the synthetic sample solution [Sb(III) + ¹²⁵Sb(III), 24.1 μg/ml in 6M hydrochloric acid], were placed in seven brown test-tubes equipped with ground-in stoppers, and 0, 0.1, ..., 0.6 ml of carrier solution [non-radioactive Sb(III) solution, 24.1 μg/ml in 6M hydrochloric acid] were added. Then 1.1, 1.0, ..., 0.5 ml of 6M hydrochloric acid were added so that all the solutions had the same volume and acidity.

2nd series. Pairs of 0.2, 0.3, 0.4, 0.5 and 0.6 ml portions (i.e., $k = 2, 3, 4, 5, 6$) of the synthetic sample solution were placed in test-tubes of the type used for the first series.

All the solutions in both series were adjusted to the same volume and acid concentration by addition of 2.0 ml of 1.8M hydrochloric acid.

Oxidation and separation. Exactly 0.1 ml of $0.6 \times 10^{-4}N$ potassium dichromate was added to each tube, to give a total volume of 3.3 ml and acidity of 3.27M. The solutions were mixed and then stood for 15–30 min to complete the oxidation. The acid concentration was then reduced to 1.0M by addition of 8.0 ml of 0.001M hydrochloric acid, and the unreacted antimony was extracted with 3.0 ml of 0.05M BPA solution in chloroform.

The radioactivity of the antimony(V) in each aqueous phase was then measured.

RESULTS AND DISCUSSION

As stated in the introduction, the amounts of reagent and product separated must be strictly controlled in Subst-IDA, so the concentration ranges of the reagents, interfering elements and the species to be determined are narrow, and large errors are caused by any deviation from the permitted range. In contrast, these limitations do not apply to SSE-IDA. We therefore examined the effect of the concentrations of the interfering element As(III), of hydrochloric acid and the reactant Sb(III) in order to define a set of the conditions under which Subst-IDA would not be practicable, but SSE-IDA would. Determination of the amount of product (m) is usually difficult, but it was possible here because we used a synthetic sample; m was calculated by means of the equation for Subst-IDA, since the radioactivities before separation (A) and after separation (a), the quantity of Sb(III) to be determined (x) and that of non-radioactive carrier (iy) added to x , had already been measured.

Effect of acidity

The relationship between the amount of Sb(V) produced and the acid concentration was examined

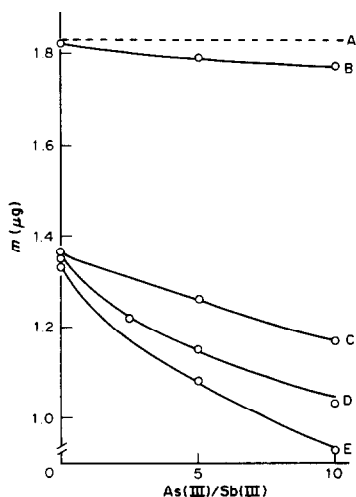


Fig. 2. Effect of the molar ratio, As(III)/Sb(III), on the amount of Sb(V) separated.

A, Theoretical line.

	Sb(III) μeq	[HCl] _{ox} M	Vol _{ox} ml	[HCl] _{ex} M	Vol _{ex} ml
B	4×10^{-2}	1.0	8.5	0.8	10.5
C	12×10^{-2}	5.4	1.5	0.8	10.5
D	8×10^{-2}	5.4	2.0	0.9	11.8
E	4×10^{-2}	5.4	1.5	0.8	10.5

$K_2Cr_2O_7$ 3×10^{-2} μeq.

under the conditions shown in Fig. 1, by use of the procedure above.

The curves in Fig. 1 show that the amount separated decreases with increasing C_{HCl} and the difference from the expected value becomes remarkable. This suggests that some of the dichromate may react with the hydrochloric acid or that the equilibrium constant of the redox reaction between Sb(III) and $K_2Cr_2O_7$ becomes smaller with increasing acidity. In either case, the amount of Sb(III) oxidized would decrease.

The values near $C_{HCl} = 1M$ are almost equal to the theoretical in each case, but the decrease in oxidation at higher acidities is larger when arsenic(III) is also present. It is concluded that the dichromate reaction with 3–5 μg of antimony(III) is quantitative when done at around $C_{HCl} = 1M$, in agreement with previous results,⁸ and the interference of arsenic(III) is negligible at this acidity, but conspicuous at $C_{HCl} > 2M$, suggesting that arsenic(III) is also oxidized.

Although the effect of C_{HCl} on the oxidation of Sb(III) can be very large, it can be made practically constant if the hydrochloric acid concentration is kept the same for all the solutions tested, as shown before.¹³

Effect of $C_{As(III)}$

The effect of $C_{As(III)}$ on the oxidation of Sb(III) was examined under the conditions indicated in Fig. 2.

In 1M hydrochloric acid medium, As(III) does not interfere in the oxidation of Sb(III) over the range

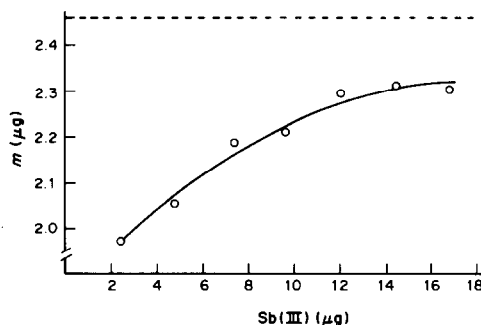


Fig. 3. Effect of amount of Sb(III) on amount of Sb(V) separated.

$K_2Cr_2O_7$ 4×10^{-2} μeq; $[HCl]_{ox} = 3.3M$; $Vol_{ox} = 4.4$ ml; $[HCl]_{ex} = 0.7M$; $Vol_{ex} = 19.4$ ml.

tested. However, at high acid concentration, As(III) takes part in the oxidation and its effect becomes larger with increasing $C_{As(III)}$ at constant $C_{Sb(III)}$ and C_{HCl} . On the other hand, if $C_{As(III)}/C_{Sb(III)}$ and C_{HCl} are kept constant, its effect becomes smaller with increasing $C_{Sb(III)}$.

Effect of $C_{Sb(III)}$

Under the conditions shown in Fig. 3, the amount of Sb(V) separated increases with increasing $C_{Sb(III)}$ at constant $C_{As(III)}$ and C_{HCl} . This follows from the results shown in Fig. 2, and confirms that As(III) interferes by competing with Sb(III) for oxidation with $K_2Cr_2O_7$.

Determination by SSE-IDA under conditions unsuitable for Subst-IDA

To illustrate the usefulness of SSE-IDA, it was tested under conditions unsuitable for the use of conventional Subst-IDA.

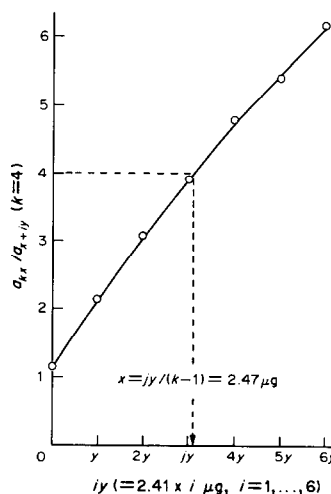


Fig. 4. An example of the determination of Sb(III) in the presence of an interfering element [As(III)] by Redox SSE-IDA: 0.2 ml of $[Sb(III) + ^{125}Sb(III)]$ 12.04 μg (total) + As(III) 7.49 μg/ml solution in 6M HCl was taken. $K_2Cr_2O_7$; 6×10^{-2} μeq; $[HCl]_{ox} = 3.3M$; $Vol_{ox} = 3.3$ ml; $[HCl]_{ex} = 0.9M$; $Vol_{ex} = 11.3$ ml.

Table 1. Results of determination of 2.41 μg of antimony(III) by Redox SSE-IDA (conditions as for Fig. 4)

k	Found, μg	Error, %
2	2.32	-3.7
3	2.40	-0.4
4	2.47	2.5
5	2.44	1.2
6	2.47	2.5

An example of the graphical method for calculating the result is shown in Fig. 4, and the values obtained by use of various k -values are shown in Table 1. Table 2 shows the values calculated by means of various equations¹⁷ for Subst-IDA, from the data obtained for each aliquot in the first series in this experiment, on the assumption that the amounts of Sb(V) separated are equal to the theoretical quantities. As expected, a large error is introduced in the Subst-IDA results, whereas SSE-IDA permits accurate determination within the expected error limit.

The amounts separated were measured in order to confirm the reason given for the difference between the two sets of results. The amounts, m_i , separated under the conditions for Fig. 4, were calculated on the basis of the radioactivities (Table 3) by use of equation (1) in Table 2. These values are plotted in Fig. 5 against the total amount of Sb(III) in each aliquot in both series. The curves shows that m_{x+iy} increases with increasing $x + iy$ and kx as in Fig. 3, and that the strict conditions for Subst-IDA are no longer fulfilled. At the same concentrations in both series, $x + 1y = 2x, \dots, x + 5y = 6x$, however, the amounts separated are equal over the whole range. This result accords with the principle of SSE-IDA and ensures the accurate determination under conditions not suitable for Subst-IDA.

Table 3. Radioactivities of the Sb(V) isolated from each aliquot ($A = 14690$ cpm; conditions as for Fig. 4)

Amount of Sb(III) $x + iy, \mu\text{g}$	Activities of separated Sb(V)	
	1st series a_{x+iy}, cpm	2nd series a_{kx}, cpm
$x = 2.41$	$a_x = 9291$	
$x + y = 4.82$	$a_{x+y} = 5011$	$a_{2x} = 10227$
$x + 2y = 7.23$	$a_{x+2y} = 3489$	$a_{3x} = 10508$
$x + 3y = 9.64$	$a_{x+3y} = 2726$	$a_{4x} = 10672$
$x + 4y = 12.05$	$a_{x+4y} = 2284$	$a_{5x} = 11337$
$x + 5y = 14.46$	$a_{x+5y} = 1968$	$a_{6x} = 11632$
$x + 6y = 16.87$	$a_{x+6y} = 1736$	

SSE-IDA obviously has many advantages over Subst-IDA and is a promising method for determination of trace amounts of metals in various substances. We are now planning to determine metals in living bodies by this method.

Acknowledgement—This work was supported by a Grant-in-Aid for Scientific Research (No. 57540327) from the Ministry of Education, Science and Culture.

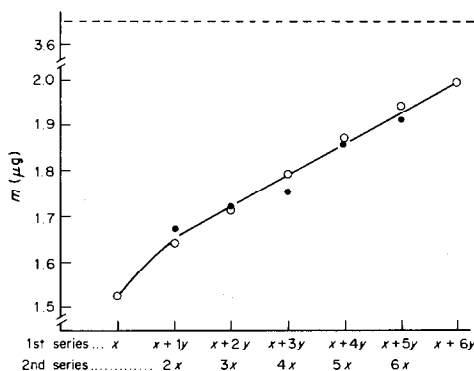


Fig. 5. Relationship between the amount of Sb(V) separated, m , and the total amount of Sb(III) in each aliquot in both series. Sb(III) taken (x) = 2.41 μg ; $iy = 2.41 \times i \mu\text{g}$, $i = 1, 2, \dots, 6$. The conditions are the same as for Fig. 4.

Table 2. Results of determination of 2.41 μg of antimony(III) by Redox Subst-IDA (conditions as for Fig. 4)

Equation Subst-IDA	Found, μg	Error, %	Data used† (see Table 3)
I	8.29	244	$a_{x+y}, A = 14690$ cpm, $m_{\text{theory}} \ddagger = 3.65 \mu\text{g}$
II	2.82	17	a_{x+y}, a_x
III	2.89	20	a_{x+y}, a_{x+2y}, a_x
IV	2.81	17	a_{x+3y}, a_{x+3y}
V	3.13	30	$a_{x+y}, a_{x+2y}, a_{x+3y}, a_x$

*The following equations of Subst-IDA were used.

Reverse Substoichiometric Isotope Dilution Method

I One-point method $x = (m_{x+y}) (A/a_{x+y}) - y$

II Two-point method¹⁸ $x = y a_{x+y} / (a_x - a_{x+y})$

III Graph method¹ $a_x/a_{x+iy} = (1/x)iy + 1$

Reverse Substoichiometric Isotope Double Dilution Method

IV Two-point method¹⁹ $x = (y_2 a_{x+2y} - y a_{x+y}) / (a_{x+y} - a_{x+2y})$

V Graph method²⁰ $iy = (m_{x+iy}) (A/a_{x+y}) - x$

†Only the values giving the best result for antimony found were used from Table 3.

‡ m_{theory} = weight of Sb equivalent to dichromate added.

REFERENCES

1. N. Suzuki, *Proc. 2nd Conf. Radioisotopes (Japan) 1958*, 151.
2. I. E. Zimakov and G. S. Rozhavsii, *Tr. Komis. po Analit. Khim.*, 1958, **9**, 231.
3. J. Růžička and J. Stary, *Talanta*, 1961, **8**, 228.
4. *Idem*, *Substoichiometry in Radiochemical Analysis*, Pergamon Press, Oxford, 1968.
5. K. Kudo and N. Suzuki, *J. Radioanal. Chem.*, 1975, **26**, 327.
6. *Idem*, *ibid.*, 1980, **59**, 605.
7. T. Kambara, J. Suzuki, H. Yoshioka and T. Nakamura, *Radioisotopes*, 1980, **29**, 590.
8. T. Kambara, J. Suzuki, H. Yoshioka and Y. Ugai, *J. Radioanal. Chem.*, 1980, **59**, 315.
9. J. Klas, J. Tölgyessy and E. H. Klehr, *Radiochem. Radioanal. Lett.*, 1974, **18**, 83.
10. J. Klas, J. Tölgyessy and J. Lesný, *ibid.*, 1977, **31**, 171.
11. J. Klas, *ibid.*, 1981, **47**, 355.
12. J. Lesny, J. Tölgyessy, O. Rohon, J. Stefanec, J. Klas and M. P. Chacharkar, *ibid.*, 1980, **42**, 9.
13. T. Kambara and H. Yoshioka, *Chem. Lett.*, 1978, 1225.
14. K. H. Jones and M. Kahn, *J. Inorg. Nucl. Chem.*, 1965, **27**, 497.
15. T. Kambara, K. Hasegawa, H. Yoshioka, Y. Kamiya, T. Kotani and K. Tabei, *J. Radioanal. Chem.*, 1977, **36**, 87.
16. S. J. Lyle and A. D. Shendrikar, *Anal. Chim. Acta*, 1973, **36**, 286.
17. T. Shigematsu and K. Kudo, *Nippon Kagaku Zasshi.*, 1981, 103.
18. N. Suzuki and K. Kudo, *Anal. Chim. Acta*, 1965, **32**, 456.
19. J. R. De Voe, *NBS Technical Note 248*, p. 111. NBS, Washington, D. C., 1966.
20. K. Kambara, J. Suzuki, H. Yoshioka and T. Nakamura, *Chem. Lett.*, 1975, 927.

EXTRACTIVE FLUORIMETRIC DETERMINATION OF ULTRATRACES OF LEAD WITH 18-CROWN-6 AND EOSIN

A. SANZ-MEDEL, D. BLANCO GOMIS, E. FUENTE and S. ARRIBAS JIMENO

Departamento de Química Analítica, Facultad de Química, Universidad de Oviedo, Oviedo, España

(Received 7 June 1983. Revised 20 December 1983. Accepted 1 February 1984)

Summary—A highly sensitive and selective spectrofluorimetric procedure for the determination of lead in the range 0.003–0.5 ppm, based on solvent extraction of the ion-pair formed between the eosinate anion and the cationic complex of Pb^{2+} with 18-crown-6, has been developed. The relative standard deviation is 3.7% at the 0.1 ppm level. The metal:ligand:counter-ion molecular ratio in the ion-pair extracted is 1:1:1, but aggregation of the complex may occur in the organic phase. The system proposed is exceptionally selective for extraction of lead in the presence of other cations frequently associated with it. The proposed method has been tested in the determination of lead in tap water. The results show good agreement with those found by the more common extractive atomic-absorption method using ammonium tetramethylenedithiocarbamate.

Reports have been published on the complexation of bivalent cations with synthetic macrocyclic polyethers, showing that lead(II) forms markedly stable complexes with some 18-crown-6 polyethers.^{1,2} Moreover, such cationic lead complexes exhibit a high degree of extractability into several organic solvents, with picrate as counter-ion.^{3,4} The solvent extraction of the ion-pair formed by these crown ether complexes and a suitable highly fluorescent organic anion could form the basis for a sensitive fluorimetric determination of lead.

We have already reported the impressive sensitivity and selectivity that can be achieved by using this principle in the fluorimetric determination of potassium with 18-crown-6 and eosin.⁵ Alkali metal ions can be similarly determined spectrophotometrically by use of a highly coloured counter-ion.^{6,7} A spectrophotometric determination of this type, using the cryptand 2.2.2, has recently been published for lead.⁸ As far as we know, however, no fluorimetric determination of lead has yet been based on macrocyclic compounds. In our work on extraction and determination of potassium with 18-crown-6 we found that all the colorimetric methods for potassium that we tested⁶ were analytically less satisfactory (poorer sensitivity and selectivity) than our fluorimetric one.⁵ We also found a strong positive interference from lead^{5,6} in agreement with the high values of the reported stability of the binary complex of 18-crown-6 with lead, and its extractability as an ion-pair. Subsequent investigation showed that with eosinate as counter-ion, the lead/18-crown-6 complex is extractable from alkaline media, whereas the alkali metal complexes are extracted only from slightly acidic solution.⁵ As other cations frequently associated with lead form only very weak 18-crown-6 complexes, if any, the method should be highly selective for lead.

We have therefore undertaken a detailed investigation on the extraction of Pb(II) with 18-crown-6 and eosin into different organic solvents. As a result a new fluorimetric determination of lead, with high sensitivity and selectivity, is proposed. The method has been tested for the determination of lead in tap water.

EXPERIMENTAL

Apparatus

Fluorescence intensity measurements were made on a Perkin-Elmer MPF-44A spectrofluorimeter; 2-nm bandwidths were used in both the excitation and emission systems.

Reagents

All reagents were of analytical grade and redistilled and demineralized water was used.

18-Crown-6 stock solution. An aqueous stock solution ($3.6 \times 10^{-3} M$) of the crown ether was diluted as required, every day, before use. The 18-crown-6 used was prepared by the Pedersen method⁹ with the second step of the synthesis modified as recommended by Gokel and Cram.¹⁰ The product was purified either by recrystallization from petroleum ether or by the Gokel *et al.* method¹¹ of complexation with acetonitrile. The latter purification technique proved to be the more efficient for eliminating metal traces in the final product. The fluorimetric blanks obtained with the 18-crown-6 thus purified were considerably lower than those observed for the commercial 18-crown-6 reagent tested.

Pb(II) stock solution (1000 ppm). Prepared by dissolving 1.598 g of lead nitrate in water, and diluting to 1 litre, and standardized gravimetrically by precipitation of lead sulphate. All standard lead solutions were freshly prepared by dilution of this stock solution.

Eosin solution $5.4 \times 10^{-3} M$. A solution of the disodium salt (as received from Merck), prepared daily to avoid possible dimerization of the dye.

Buffer solution (pH 8.5). Prepared by dissolving 38.14 g of sodium tetraborate 10-hydrate in about 800 ml of redistilled and demineralized water, adjusting to the required pH with 1M hydrochloric acid and diluting to 1 litre with water.

Dichloromethane. Merck "Uvasol" grade for fluorimetry.

General procedure

Transfer into 50-ml separating funnels known volumes of standard lead solution (containing from 0.025 to 2.5 μg of lead). To each funnel add 0.5 ml of the 18-crown-6 stock solution, 1 ml of buffer solution, 0.5 ml of eosin solution, and dilute to 5 ml with redistilled and demineralized water (final pH 8.5 ± 0.1). After mixing, add 5 ml of dichloromethane (previously equilibrated with lead-free buffered aqueous phase) and extract the complex by shaking for 2–5 min. Allow the phases to separate and measure the fluorescence intensity, I_F , of the organic phase at 549 nm (excitation wavelength 537 nm).

Run a reagent blank in the same way and subtract its fluorescence from that of the sample. The plot of the corrected fluorescence against amount of lead should be a straight line passing through the origin.

Procedure for lead determination in tap water

Pipette 2 ml of the sample into a 50-ml separating funnel, add the 18-crown-6 solution and other reagents and continue as described for the general procedure. If the water sample was acidified for conservation, add enough tetramethylammonium hydroxide solution to neutralize most of the acidity before adding the buffer.

RESULTS AND DISCUSSION

Choice of organic solvent

Toluene, chlorobenzene, isobutyl methyl ketone, 1,2-dichloroethane, dichloromethane, chloroform and carbon tetrachloride were tested as solvents in the extraction. The fluorescence intensities, corrected for the corresponding blank, for 0.7 μg of lead were in the order: dichloromethane > 1,2-dichloroethane > chloroform > isobutyl methyl ketone > chlorobenzene. No fluorescence was observed when toluene or carbon tetrachloride was used. Therefore, dichloromethane was selected as the organic solvent.

Absorption and emission spectra

Figure 1 shows the excitation and emission spectra of the blank and the complex extracted into dichloromethane from an aqueous medium of pH 8.5. These spectra are uncorrected for variations in the emission characteristics of the xenon lamp and the response characteristics of the photomultiplier. The complete excitation spectrum exhibits two maxima: the more intense one (at 537 nm) is shown in Fig. 1; the other maximum (at 318 nm) is not shown. The emission maximum appears at 549 nm. The blank spectra observed exhibit the same shape and characteristics, indicating unwanted extraction of eosin. To obtain the largest difference in fluorescence emission between the complex and the blank when extraction is done at pH 8.5, the excitation wavelength of 537 nm is used, with 2-nm spectral band-pass for both excitation and emission, to minimize possible first-order scatter.

Effect of pH

The influence of pH on the extraction was evaluated by measuring the fluorescence intensity due to 0.2 ppm of lead in the test solution, and that of the corresponding blanks, over the pH range from 4 to 11 (adjusted by addition of acetic acid, lithium carbonate, lithium hydroxide or tetramethylammonium hydroxide).

Maximum fluorescence is obtained for extraction at pH 8.5 ± 0.1 , as shown in Fig. 2. Lead is extracted at a much higher pH than are alkali metals with this system (as shown in Fig. 2, and in our earlier work,⁵ potassium extraction is optimal at pH 5.9). Atomic-absorption analysis of the two phases shows that in

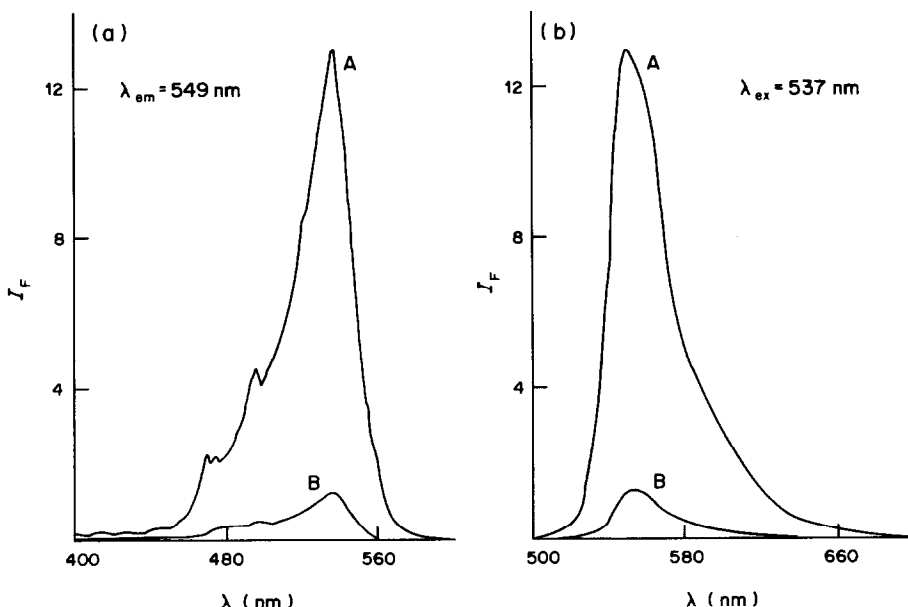


Fig. 1. Excitation (a) and emission (b) spectra of blank (B) and ion-association lead complex (A); I_F in arbitrary units.

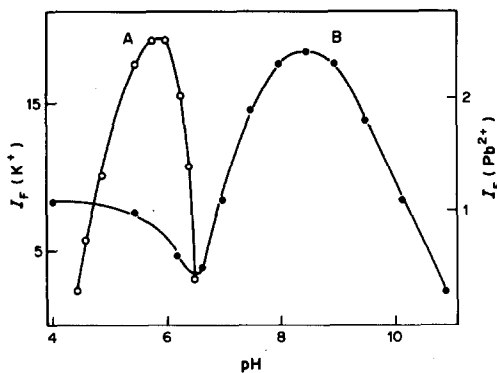


Fig. 2. Variation of fluorescence intensity with pH. (A) Potassium ion-association complex (4 ppm K); (B) lead ion-association complex (0.2 ppm Pb); I_f in arbitrary units.

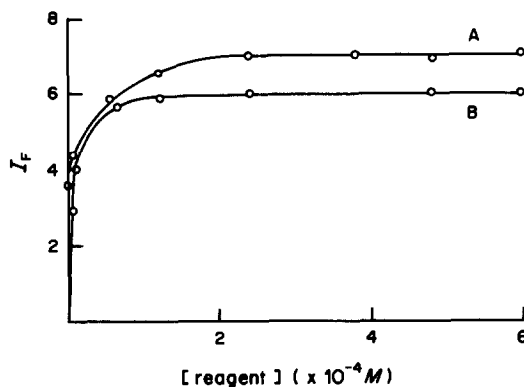


Fig. 3. Variation of fluorescence intensity as a function of reagent concentration: (A) molar concentration of 18-crown-6; (B) molar concentration of eosin; I_f in arbitrary units.

the extraction at pH 8.5, all the potassium remains in the aqueous phase. This is in accordance with formation of the doubly charged eosinate anion at $\text{pH} > 5-6$.¹²

Reagent concentrations

The influence of the crown ether and eosin concentrations on the fluorescence signal of the extracted ion-pair was studied with a fixed amount of lead (1 μg) and a single extraction step. The results are plotted in Fig. 3, which shows that the signal becomes constant at a total 18-crown-6 concentration of $2.0 \times 10^{-4} M$ (for a fixed eosin concentration of $3.0 \times 10^{-3} M$), and constant maximum fluorescence intensity is observed at eosin concentrations higher than $1.4 \times 10^{-4} M$ (with a fixed 18-crown-6 concentration of $3.6 \times 10^{-4} M$).

Rate of extraction and stability of the extract

A plot of corrected I_f vs. shaking-time shows that the degree of extraction is constant and reproducible after 1 min of shaking. The green fluorescence produced in the dichloromethane layer remains constant for at least 4 hr. The order of addition of the reagents

is unimportant, provided that the crown ether is added before the pH adjustment. Separation of the phases is rather slow, however, as the organic layer appears quite cloudy (especially if the room temperature is low) and, without centrifugation, it takes about 30 min to become clear and ready for fluorescence measurements.

The experiments were usually done at $20 \pm 1^\circ$, but no significant influence of the temperature on the fluorescence was noted over the range $20 \pm 5^\circ$.

Precision and recovery

The efficiency of the extraction, under the conditions of the general procedure, was found by determining the lead extracted from five independent samples and blanks. ICP emission photometry was used for the analysis and the recovery of lead in a single extraction was found to be $92.6 \pm 2.6\%$.

The recommended procedure was applied to the repetitive determination of 0.7 μg of lead during a period of several days. Ten determinations produced a relative standard deviation of 3.7%.

Selectivity

We have studied the effect of several metal ions, selected from those capable of forming stable complexes with 18-crown-6 (*i.e.*, alkali and alkaline-earth metals) and those most commonly associated with lead (*i.e.*, Hg, Zn, Cd, *etc.*) and disturbance of many of the colorimetric/fluorimetric methods for its determination.

Except for sodium, the maximum amounts tested for the alkali and alkaline-earth ions were 1000-fold molar ratio to lead. For the rest of the potential interferences a 100-fold molar ratio was initially tested. Ions which were found to interfere at these levels were then tested at lower concentrations. An ion was considered to interfere when it changed the fluorescence intensity for 0.7 μg of lead by more than twice the relative standard deviation (*i.e.*, by more than $\pm 8\%$).

The results are shown in Table 1. As can be seen, for alkali and alkaline-earth metal cations the observed degree of interference is in agreement with the values of the stability constants of the corresponding LM^{n+} complexes in aqueous solution.^{1,13} Only Sr^{2+} and Ba^{2+} constitute an exception to the general trend: as shown in Table 1 the effect of both metals on the lead determination is virtually the same despite the fact that the stability constants reported ($\log K_f^{\text{LSr}} = 2.72$, $\log K_f^{\text{LBa}} = 3.87$) indicate that the strontium complex is much the weaker.¹ This result is in agreement with our previous findings⁵ for extraction at $\text{pH} 5.9 \pm 0.1$, and with Takeda and Kato's observations for picrate as counter-ion:³ knowledge of the stability constant of the LM^{n+} complex is not enough for prediction, even qualitative, of the degree of extraction (interference) of metal M, because the extractability of the corresponding ion-pair complex $LM^{n+}A^{n-}$ sometimes becomes the dominant factor.

Table 1. Effect of foreign ions (M) on the determination of 0.7 μg of lead

Cation	M:Pb (molar ratio)	Apparent recovery, %
Li ⁺	1000	103.7
Na ⁺	1000	102.1
K ⁺	200	101.4
Cs ⁺	100	104.7
NH ₄ ⁺	100	96.3
Tl ⁺	100	104.4
Ag ⁺	100	101.1
Mg ²⁺	1000	102.6
Ca ²⁺	500	103.7
Sr ²⁺	50	108.0
Ba ²⁺	50	107.3
Ni ²⁺	100	97.3
Cu ²⁺	100	100.4
Zn ²⁺	100	106.6
Cd ²⁺	100	96.7
Hg ²⁺	100	108.0
Co ²⁺	100	98.1
Mn ²⁺	100	98.5
Fe ³⁺	5	97.0
Al ³⁺	100	98.4
Cr ³⁺	50	94.1
Bi ³⁺	50	97.4

Curiously enough, Fe³⁺, which is not known to form complexes with 18-crown-6, can be tolerated at only a relatively low level. Increasing iron concentration [even of Fe(II)] inhibits the extraction of lead. This effect is attributed to the relatively high working pH, which results in the precipitation of iron hydroxide, the adsorption characteristics of which would hinder the formation and extraction of the lead complex [relatively high levels of Cr(III) and Bi(III) also tend to hinder the extraction, probably for a similar reason]. Several masking agents were tested as a means of keeping the iron in solution, fluoride being the most effective [a 25-fold molar ratio of iron to lead can be tolerated in the presence of 1.1M N(CH₃)₄F]. In any case, for samples with a high content of iron the best choice is to extract the Fe(III) first, at pH 1.5 with a 1:1 mixture of acetylacetone and chloroform, and finally wash the aqueous layer with chloroform.¹⁴ Analysis for lead in the remaining aqueous layer by the recommended procedure has demonstrated that iron in up to 400-fold molar ratio to lead can be eliminated in this way.

An inspection of Table 1 indicates that most of the elements likely to be found associated with lead in drinking water do not interfere. The proposed extraction would also be very useful for determination of lead in biological materials. In fact, the ubiquitous element sodium in amounts up to 2×10^5 times that of the lead present had no noticeable effect on the lead determination.

The effect of the common anions fluoride, chloride, nitrate and sulphate was negligible, even for amounts higher than 5×10^4 times that of the lead.

Except for the indirect influence of iron, the method proposed is highly selective for lead.

Stoichiometry of the extracted complex

Job's method, with fluorescence measurements, was used to establish the stoichiometry of the lead complex extracted in the presence of eosin. The results obtained with excess of eosin present are shown in Fig. 4, and indicate a 1:1 lead-crown ether molar ratio. These results agree with those previously obtained by Takeda and Kato³ with picrate as counter-ion.

The molar ratio of lead to eosin in the ion-pair was initially determined by the "equilibrium-shift" and Job methods (Figs 4 and 5). Both methods indicate a 1:2 lead-eosin molar ratio, although the Job method also indicates the possible presence of a 1:1 complex. From the dissociation constants of eosin¹² and the pH used (8.5), only a neutral complex (1:1)

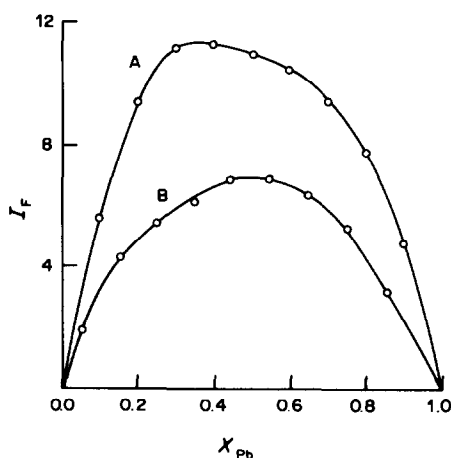


Fig. 4. Composition of the ion-association complex by Job's method. (A) Pb/eosin; $C_L = 3.6 \times 10^{-3}M$; $C_{Pb} + C_{eosin} = 6.76 \times 10^{-6}M$; (B) Pb/L; $C_{eosin} = 5.4 \times 10^{-3}M$; $C_{Pb} + C_L = 6.76 \times 10^{-6}M$; I_F in arbitrary units.

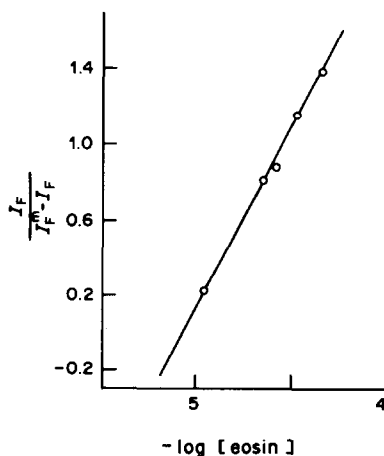


Fig. 5. Equilibrium-shift method for the Pb/eosin relationship. $C_{Pb} = 1.35 \times 10^{-6}M$; $C_L = 7.2 \times 10^{-4}M$. I_F = fluorescence intensity of a given mixture, I_F^0 = saturation fluorescence intensity with excess of reagent (I_F in arbitrary units).

Table 2. Actual concentrations of lead and eosin in the organic phase in the extraction of 200 ppm of lead

$[\text{Pb}]_{\text{org}}, 10^{-4}\text{M}$	$[\text{Eosin}^{2-}]_{\text{org}}, 10^{-4}\text{M}$	$[\text{Eosin}^{2-}]_{\text{org}}/[\text{Pb}]_{\text{org}}$
6.64	7.59	1.14
5.40	6.05	1.12
4.18	4.80	1.14
3.38	3.81	1.13
2.62	3.02	1.15
2.07	2.37	1.15
1.68	1.89	1.12
1.34	1.50	1.12
1.10	1.20	1.09

lead:crown:eosin) should be extracted. Therefore, to clear up this point, we made measurements of the distribution ratio of lead and eosin between the organic and aqueous phase at pH 8.5. The lead concentrations in both phases were measured by atomic-absorption and ICP emission for two series of experiments, one with 200 ppm and the other with 50 ppm of lead. Equilibrium eosin concentrations in each case were determined by spectrophotometry at 516 nm. The results obtained are summarized in Fig. 6 and Table 2. Figure 6 shows clearly the existence of two different situations: apparently a 1:1:1 complex is extracted at low eosin concentrations, but a 1:1:2 complex forms at higher eosin concentrations. However, determination of the total concentrations of lead and eosin actually present in the organic phase for every experiment (Table 2) demonstrated that in all cases the actual molar ratio of lead to eosin was 1:1 (allowance has to be made, from reagent blanks, for extraction of eosin itself, which accounts for the values obtained being slightly higher than 1.0).

The species extracted has a metal:ligand:counterion molecular ratio of 1:1:1. The observed change in slope of the $\log D$ vs. $\log[\text{eosin}]$ plots at higher eosin concentrations can be attributed to aggregation processes in the organic phase (*cf.* Sekine and Hasegawa,¹⁵ and Müller and Diamond¹⁶).

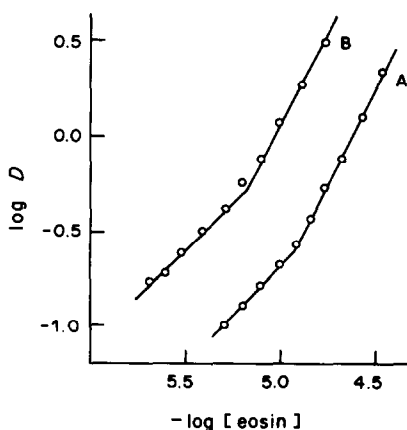


Fig. 6. Dependence of the lead distribution ratio on the eosin concentration in the aqueous phase. (A) $C_{\text{Pb}} = 9.66 \times 10^{-4}\text{M}$, $C_{\text{L}} = 9.66 \times 10^{-2}\text{M}$, $C_{\text{eosin}} = 10^{-4}$ – 10^{-3}M ; (B) $C_{\text{Pb}} = 2.42 \times 10^{-4}\text{M}$, $C_{\text{L}} = 2.00 \times 10^{-1}\text{M}$, $C_{\text{eosin}} = 3.15 \times 10^{-3}$ – $2.50 \times 10^{-4}\text{M}$; I_{F} in arbitrary units.

Table 3. Lead determination in tap water

Sample	Extraction-flame method, $\mu\text{g/l.}$	Proposed method, $\mu\text{g/l.}$
1 (Oviedo)	20 ± 0.9	21 ± 0.9
2 (Oviedo)	23 ± 0.7	26 ± 0.7
3 (Aviles)	25 ± 1.4	28 ± 0.9
4 (Aviles)	24 ± 0.3	26 ± 2.3
5 (Gijón)	19 ± 1.0	19 ± 0.9
6 (Meres)	25 ± 0.3	23 ± 1.0
7 (La Manjoya)	11 ± 0.7	13 ± 1.0
8 (Sama)	23 ± 1.1	26 ± 0.7
9 (Salinas)	20 ± 0.7	24 ± 1.2
10 (Soto del Barco)	33 ± 0.7	31 ± 1.0

Determination of lead in tap water

Lead was determined in tap water from the Asturias district. The proposed method was tested, without any preconcentration step, and the results compared with those obtained by the extractive atomic-absorption method using a ten-fold preconcentration with ammonium tetramethylenedithiocarbamate.¹⁷

The results obtained are summarized in Table 3. It can be concluded that similar accuracy and precision are obtained by both methods. The fluorimetric method proposed here, however, is more sensitive and would allow the use of much smaller sample volumes.

Acknowledgement—The assistance of J. R. García Alvarez with the crown synthesis work and preliminary experiments is gratefully acknowledged.

REFERENCES

- R. M. Izatt, R. E. Terry, B. L. Haymore, L. D. Hansen, N. K. Dalley, A. G. Avondet and J. J. Christensen, *J. Am. Chem. Soc.*, 1976, **98**, 7620.
- J. J. Christensen, D. J. Eatough and R. M. Izatt, *Chem. Rev.*, 1974, **74**, 351.
- Y. Takeda and H. Kato, *Bull. Chem. Soc. Japan*, 1979, **52**, 1027.
- T. Sekine, K. Shioda and Y. Hasegawa, *J. Inorg. Nucl. Chem.*, 1979, **41**, 571.
- A. Sanz-Medel, D. Blanco Gomis and J. R. García Alvarez, *Talanta*, 1981, **28**, 425.
- P. Arias Abrodo, D. Blanco Gomis and A. Sanz-Medel, *Microchem. J.*, in press.
- M. Takagi, H. Nakamura, Y. Sanui and K. Ueno, *Anal. Chim. Acta*, 1981, **126**, 185.
- V. Szczepaniak and B. Juskowiak, *ibid.*, 1982, **140**, 261.
- C. J. Pedersen, *J. Am. Chem. Soc.*, 1967, **89**, 7017.
- G. W. Gokel and D. J. Cram, *Org. Syn.*, 1973, **53**, 1978.
- G. W. Gokel, D. J. Cram, C. L. Liotta, H. P. Harris and F. L. Cook, *ibid.*, 1977, **57**, 30.
- N. O. Mchedlov-Petrosyan, L. B. Adamovich and L. E. Nikishina, *Zh. Analit. Khim.*, 1980, **35**, 1495.
- J. D. Lamb, R. M. Izatt, C. S. Swain and J. J. Christensen, *J. Am. Chem. Soc.*, 1980, **102**, 475.
- J. P. McKaveney and H. Freiser, *Anal. Chem.*, 1957, **29**, 290.
- T. Sekine and Y. Hasegawa, *Solvent Extraction Chemistry*, p. 222. Dekker, New York, 1977.
- W. Müller and R. M. Diamond, *J. Phys. Chem.* 1966, **70**, 3469.
- R. P. Mitcham, *Analyt.*, 1980, **105**, 43.

EXCHANGE EQUILIBRIA BETWEEN BICARBONATE, CARBONATE, CHLORIDE AND BROMIDE ON DOWEX 1 × 8

ULLA LUNDSTRÖM and ÅKE OLIN

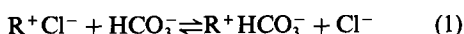
Department of Analytical Chemistry, University of Uppsala, P.O.B. 531, S-751 21 Uppsala, Sweden

(Received 8 November 1983. Accepted 24 January 1984)

Summary—The exchange reaction $2R^+HCO_3^- + CO_3^{2-} \rightleftharpoons R_2^+CO_3^{2-} + 2HCO_3^-$ has been studied on Dowex 1 × 8 in the presence of bicarbonate solution in equilibrium with atmospheric carbon dioxide (open system). The experiments showed, as theory predicts, that the composition of the resin phase is independent of the concentration of the bicarbonate solution. The mole fraction of carbonate at equilibrium is about 0.4 and the equilibrium constant is 0.15M at 20°. With this value of the constant, the composition of the ion-exchanger for various bicarbonate concentrations has been calculated for a closed system. At $[HCO_3^-] < 0.01M$ a substantial part of the resin is in the carbonate form, whereas for $[HCO_3^-] > 0.05M$ the resin is present almost exclusively in bicarbonate form. The exchange constants of bromide at trace level have been determined for the bicarbonate and mixed carbonate forms of the ion-exchanger. The exchange constant $K_{Cl}^{HCO_3}$ has been determined over the whole composition range and the results can be represented by $K_{Cl}^{HCO_3} = 0.428 - 0.063x_{Cl} - 0.115x_{Cl}^2$, where x_{Cl} is the mole fraction of chloride in the resin. The constants are used to discuss the conditions for the chromatographic enrichment of bromide from fresh water.

A method for the determination of bromide has recently been presented,¹ based on oxidation of bromide to bromate by peroxodisulphate, followed by reaction of the bromate with excess of iodide in the absence of air, and spectrophotometric measurement of the iodine liberated. The sensitivity of the method is 2.25 absorbance units (AU) per μ mole of bromide, or, in terms of the bromide concentration of the original sample, 0.0225 AU.l. μ mole⁻¹. For determination of low levels of bromide an enrichment of the ion is therefore necessary. In the analytical procedure developed for the determination of trace amounts of bromide in fresh water, this was accomplished by chromatographic enrichment of Dowex 1 × 8 in chloride form.² The uptake of bromide in the presence of the main constituents of fresh water was studied and the results of the investigations with chloride and sulphate were reported.² The direct influence of the normally predominant anion, bicarbonate, on the enrichment was eliminated in the analytical procedure by acidifying the sample. The ion-exchange equilibria involving the bicarbonate ion have now been investigated and are reported here.

The equilibrium constant of the reaction



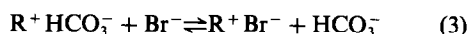
has been determined by both the batch³ and the column⁴ technique. The practical constant defined by

$$K_{Cl}^{HCO_3} = \frac{[HCO_3^-]_R [Cl^-]}{[Cl^-]_R [HCO_3^-]} \quad (2)$$

is about 0.3–0.5, depending on the composition of the resin phase (subscript R denotes concentrations in

this phase). In similar measurements with bromide instead of chloride, we found that when a solution containing bicarbonate and bromide was passed through a column containing Dowex 1 × 8 in chloride form, there was a considerable drop in pH in the first portions of the effluent. It was therefore suspected that the ion-exchanger was partly converted into the carbonate form even though the carbonate activity is small in bicarbonate solutions. Apparently this possibility has not been considered before, and our investigation showed that a considerable part of the ion-exchanger was present in the carbonate form.

These findings could be of importance for the accuracy of previously determined values of $K_{Cl}^{HCO_3}$. Therefore, this constant was redetermined under conditions where no carbonate was present in the resin phase. Under the same conditions, the constant for the reaction



was determined at high bicarbonate loadings on the resin. This constant is of importance for the uptake of bromide from fresh water of high alkalinity.

EXPERIMENTAL

The experiments were done at 20°.

Chemicals

All solutions were prepared by dissolving Merck analytical-grade reagents in demineralized distilled water. The ion-exchange resin, Dowex 1 × 8 (100–200 mesh, pract., Serva Feinbiochemica), was treated before use, as already described.²

Apparatus

In the experiments where the column technique was used for equilibration, the ion-exchange tube already described² was employed. The batch equilibrations were performed in 250-ml glass-stoppered Erlenmeyer flasks, which were continuously shaken for 24 hr. The potentiometric titrations for the determination of carbonate and chloride were performed with the Metrohm Titroprocessor, E636, equipped with a Dosimat burette, E635.

Analysis

The resin phase was eluted with 2M sodium perchlorate. The eluate and the solution in equilibrium with the resin were analysed by the following methods. Bromide was determined as previously described,² chloride by a potentiometric titration with standard silver nitrate, carbonate by a potentiometric titration with standard acid to the bicarbonate end-point, and total carbonate by titration with standard acid in the usual way. Prior to elution the resin was thoroughly drained. The residual liquid causes an error of at most 1% in the composition found for the resin.

Determination of $K_{2\text{HCO}_3}^{\text{CO}_3}$

The column technique, with 2 ml of resin, originally in chloride form, was utilized. Air was passed through sodium bicarbonate solutions of known concentrations until a constant pH was reached, before they were passed through the column. The air was presaturated with water vapour by passing it through wash-bottles containing bicarbonate solution of the same concentration as the test solution. The attainment of equilibrium in the column was established by measurement of the pH of the inflowing and outflowing solutions. The resin was then analysed for carbonate and total carbonate.

Determination of $K_{\text{HCO}_3}^{\text{Br}}$ and $K_{\text{CO}_3}^{2\text{Br}}$

The same procedure was used as for the determination of $K_{2\text{HCO}_3}^{\text{CO}_3}$. The solution passed through the column also contained bromide at a concentration of $1 \times 10^{-5}M$. The resin was analysed for bromide, carbonate and total carbonate.

Determination of $K_{\text{HCO}_3}^{\text{Br}}$

The batch technique was used, 200 ml of a solution containing known varied amounts of bromide and bicarbonate being shaken with 2 ml of the resin in bicarbonate form. All solutions were saturated with carbon dioxide (at 1 atm pressure) and the equilibration took place in a CO_2 atmosphere. The bicarbonate form of the resin was prepared by treating the resin (in chloride form) first with 100 ml of 0.2M bicarbonate solution, and then with 20 ml of a solution having the bicarbonate concentration used in the equilibration experiment. The resin was analysed for bicarbonate and bromide.

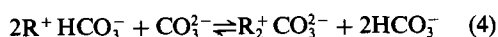
Determination of $K_{\text{Cl}}^{\text{HCO}_3}$

Essentially the same technique was used as for the determination of $K_{\text{HCO}_3}^{\text{Br}}$. For $x_{\text{Cl}} < 0.5$ the resin was initially in the bicarbonate form and for $x_{\text{Cl}} > 0.5$ in the chloride form. The resin and the equilibrium solution were both assayed for chloride and bicarbonate.

CALCULATIONS AND RESULTS

The HCO_3^- - CO_3^{2-} exchange

The equilibrium constant of the reaction



is given by

$$K_{2\text{HCO}_3}^{\text{CO}_3} = \frac{\{\text{CO}_3\}_{\text{R}} \{\text{HCO}_3\}^2}{\{\text{HCO}_3\}_{\text{R}}^2 \{\text{CO}_3\}} \quad (5)$$

Brackets are used to denote activities, charges have been left out, and subscript R denotes the resin phase. In the following, mole fractions will be used instead of activities in the resin phase. The practical equilibrium constant written with the use of mole fractions will be denoted by K_{R} . It is not a true constant. The carbonate species also take part in the acid-base equilibria

$$K_1 = \frac{\{\text{H}\} \{\text{HCO}_3\}}{\{\text{H}_2\text{CO}_3\}} \quad (6)$$

$$K_2 = \frac{\{\text{H}\} \{\text{CO}_3\}}{\{\text{HCO}_3\}} \quad (7)$$

By combining equations (5)–(7) we obtain

$$K_{\text{R}} K_2 = \frac{x_{\text{CO}_3}}{x_{\text{HCO}_3}^2} \{\text{HCO}_3\} \{\text{H}\} \quad (8)$$

and

$$\frac{K_{\text{R}} K_2}{K_1} = \frac{x_{\text{CO}_3}}{x_{\text{HCO}_3}^2} \{\text{H}_2\text{CO}_3\} \quad (9)$$

In the first experiments bicarbonate solutions were passed through the ion-exchange column with the resin initially in the chloride form. The approach towards equilibrium was followed by measurement of the pH of the inflowing and outflowing solutions. The pH-values varied erratically, however, and constant values could not be reached. This can be understood by considering the autoprotolysis of the bicarbonate ion, $2\text{HCO}_3^- \rightleftharpoons \text{CO}_3^{2-} + \text{H}_2\text{CO}_3$, in conjunction with equation (9). A solution of bicarbonate will generally be over- or under-saturated with respect to the partial pressure of carbon dioxide in air. Hence the concentration of carbonic acid in the test solution will vary and the exchange equilibrium will shift continuously.

As a consequence of the experience gained from the first series of measurements, air presaturated with water vapour was passed through the bicarbonate solution until a constant pH was reached. The equilibrium $\text{CO}_2(\text{g}) + \text{H}_2\text{O} \rightleftharpoons \text{H}_2\text{CO}_3$ ensures a well-defined and constant carbonic acid activity in the test solution (provided there is no large variation in the CO_2 concentration in the ambient air). From equation (9) it follows that the composition of the ion-exchange resin should be constant and independent of the concentration of the bicarbonate solutions. This was verified by our results for the three concentrations used (Table 1).

The value of K_{R} was calculated from equation (9), $\{\text{H}_2\text{CO}_3\} = 1.28 \times 10^{-5}M$, $K_1 = 4.16 \times 10^{-7}M$, and $K_2 = 4.20 \times 10^{-11}M$.⁵ It was also obtained from equation (8) with $\{\text{HCO}_3^-\}$ calculated from

$$\{\text{HCO}_3^-\} = \frac{y_1 C}{1 + 2y_1 K_2 / y_2 \{\text{H}\}} \quad (10)$$

where C is the total concentration of sodium bicarbonate in the test solution, and y_1 and y_2 are the activity coefficients of the bicarbonate and carbonate

Table 1. Determination of the exchange constant, K_R , of the reaction $2R^+HCO_3^- + CO_3^{2-} \rightleftharpoons R_2^+CO_3^{2-} + 2HCO_3^-$ on Dowex 1 \times 8 at 20°C; open system in equilibrium with aerial carbon dioxide; x_{CO_3} is the mole fraction of carbonate in the resin

[HCO ₃] <i>M</i>	pH	<i>x</i> _{CO₃}	<i>K_R</i> , mole/l.	
			Equation (8)	Equation (9)
0.003	8.69	0.402	0.145	0.143
0.005	8.90	0.407	0.143	0.147
0.010	9.09	0.390	0.159	0.133

Mean values: x_{CO_3} 0.399 \pm 0.018; K_R 0.146 \pm 0.014 mole/l.

ions, calculated in the usual way. The results are presented in Table 1. Both methods of calculation yield concordant values of K_R . The mean values of x_{CO_3} and \bar{K}_R are 0.399 \pm 0.018 and 0.146 \pm 0.014 *M*, respectively (16 determinations). The somewhat low precision reflects the difficulty of obtaining true equilibrium in the system and of determining carbonate in the presence of bicarbonate by a conventional titration. Our measurements demonstrate that in an open system a considerable part of the ion-exchanger is in the carbonate form. Reckoned in equivalents, the carbonate form will constitute about 60% of the exchange capacity.

No measurements have been performed on a closed system *i.e.*, a system where no exchange of carbon dioxide with the atmosphere takes place. In practical enrichment work, the conditions are expected to be somewhere in between those of a closed and an open system. Therefore theoretical calculations of the composition of the resin phase have been made for a closed system. In these calculations, $K_R = 0.146M$ and activities for the species in the aqueous phase were used. The results are presented in Fig. 1. They show that a considerable part of the ion-exchanger can be expected to be present in the carbonate form at low bicarbonate concentrations. This fraction rapidly diminishes with increasing bicarbonate concen-

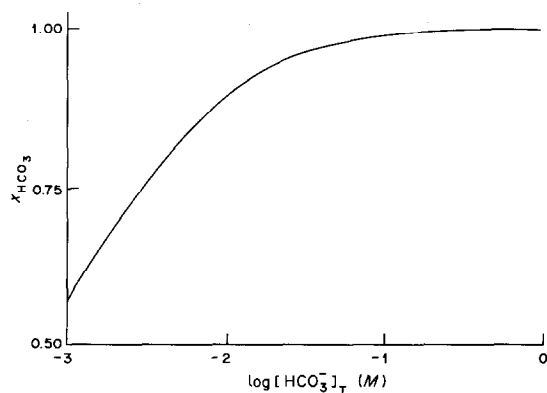


Fig. 1. The calculated mole fraction of bicarbonate, x_{HCO_3} , in Dowex 1 \times 8 as a function of the total bicarbonate concentration in the external solution, for a closed system. Equilibrium constants given in the text were used.

tration and for $[HCO_3^-] > 0.05M$ the ion-exchanger is almost entirely in the bicarbonate form. Since the normal bicarbonate concentration in fresh water is below 0.005*M*, our findings suggest that equilibria involving also the carbonate form of the ion-exchanger will be of importance in the chromatographic enrichment of trace anions from such water.

The $HCO_3^- - CO_3^{2-} - Br^-$ exchange

The equilibrium constant of reaction (1) is about 0.4. In a fresh water of standard composition⁶ the ratio $[HCO_3^-]/[Cl^-]$ is about 7.5. Hence the ratio x_{HCO_3}/x_{Cl} would be about 3 at equilibrium. From the results of the previous section we infer that an even larger part of the ion-exchanger will be present in carbonate forms than indicated by this figure. Thus equilibria between carbonate, bicarbonate and bromide will be of importance for the enrichment of bromide from fresh waters.² The pertinent equilibrium constants are defined by

$$K_{HCO_3}^{Br} = \frac{x_{Br} \{HCO_3\}}{x_{HCO_3} \{Br\}} \quad (11)$$

$$K_{CO_3}^{2Br} = x_{Br}^2 \{CO_3\} / x_{CO_3} \{Br\}^2 \quad (12)$$

we also have

$$K_R = (K_{HCO_3}^{Br})^2 / (K_{CO_3}^{2Br}) \quad (13)$$

$K_{HCO_3}^{Br}$ was determined for an open system in equilibrium with the partial pressure of carbon dioxide in air. Solutions with varying total concentrations of bicarbonate between 0.003 and 0.02*M* in equilibrium with air and containing bromide at $1 \times 10^{-5}M$ concentration were passed through ion-exchange columns until equilibrium was reached. From the analysis of the resins and the known compositions of the equilibrium solutions, $K_{HCO_3}^{Br}$ was found to be 14.4 ± 0.8 ($n = 12$). This constant refers to a resin with $x_{CO_3} \approx 0.4$. The mole fraction of bromide is very small. From equation (13) $K_{CO_3}^{2Br}$ is calculated to be $(1.42 \pm 0.16) \times 10^3$ l./mole.

$K_{HCO_3}^{Br}$ was also determined in batch experiments for a resin with $x_{HCO_3} = 1$, in the presence of an atmosphere of pure carbon dioxide. This ensures that no carbonate will be present in the resin phase. The value of $K_{HCO_3}^{Br}$ was found to be 10.1 ± 0.2 , ($n = 5$).

The $HCO_3^- - Cl^-$ exchange

In previous determinations^{3,4} of $K_{Cl}^{HCO_3}$ the possible formation of carbonate in the resin phase was not considered. The constant was therefore redetermined under conditions (see experimental) that precluded the formation of carbonate as counter-ion in the resin. The value of $K_{Cl}^{HCO_3}$ was found to increase steadily from 0.25 at $x_{Cl} = 1$, to 0.43 at $x_{Cl} = 0$. The same trend was observed by Fekete and Inczedy,⁴ who report 0.33 ($x_{Cl} = 1$) and 0.52 ($x_{Cl} = 0$). Their value of $\log K_{Cl}^{HCO_3}$ was linearly dependent on x_{Cl} . Our

data do not fit this relationship. The equation

$$K_{\text{Cl}}^{\text{HCO}_3} = 0.428 - 0.063x_{\text{Cl}} - 0.115x_{\text{Cl}}^2 \quad (14)$$

can be used to find $K_{\text{Cl}}^{\text{HCO}_3}$ at intermediate x_{Cl} .

The numerical values of the constant obtained in the two investigations agree quite well, which indicates that the extent of carbonate formation was small in the column experiments.⁴ This agrees with our calculations for a closed system (Fig. 1), since the bicarbonate concentrations in the external solution were in the range 0.1–0.015M.

For an ion-exchanger in equilibrium with a solution containing bicarbonate and chloride, the following expression for the adjusted retention volume, V'_R , can be derived for the ion A^{z-} at trace levels:

$$V'_R = \frac{E}{1 + x_{\text{CO}_2}} \left(\frac{x_{\text{CO}_2}}{[\text{HCO}_3^-]} \right)^z K_{\text{HCO}_3}^A \quad (15)$$

where E is the total exchange capacity of the resin bed in meq. For bromide in fresh water of standard composition, the values of V'_R are estimated from our

constants to be 4.2 litres for an open system and 5.8 litres for a closed system. These values pertain to a 2-ml resin bed with a capacity of 3.2 meq. The larger value for the closed system is due to the increased concentration of carbonic acid, which leads to a smaller value of x_{CO_2} and a larger value of x_{HCO_3} as compared to the open system. If the formation of the carbonate form of the ion-exchanger is neglected, V'_R becomes 6.5 litres. For an open system the carbonate formation thus reduces V'_R by about 35%.

REFERENCES

1. U. Lundström, *Talanta*, 1982, **29**, 291.
2. U. Lundström, Å. Olin and F. Nydahl, *ibid.*, 1983, **30**,
3. R. M. Wheaton and W. C. Bauman, *Ind. Eng. Chem.*, 1951, **43**, 1088.
4. E. Fekete and J. Inczedy, *Acta Chim. Acad. Sci. Hung.*, 1975, **84**, 121.
5. W. Stumm and J. J. Morgan, *Aquatic Chemistry*, 2nd Ed., Wiley, New York, 1981.
6. W. Rodhe, *Verhandl. Intern. Verein. Theor. Angew. Limnologie*, 1949, **X**, 377.

SPECTROPHOTOMETRIC STUDIES ON ION-PAIR EXTRACTION EQUILIBRIA OF THE IRON(II) and IRON(III) COMPLEXES WITH 4-(2-PYRIDYLAZO)RESORCINOL

HITOSHI HOSHINO and TAKAO YOTSUYANAGI

Department of Applied Chemistry, Tohoku University, Aoba, Aramaki, Sendai, 980 Japan

(Received 8 March 1983. Revised 8 December 1983. Accepted 16 January 1984)

Summary—The ion-pair extraction equilibria of the iron(II) and iron(III) chelates of 4-(2-pyridylazo)resorcinol (PAR, H₂L) are described. The anionic chelates were extracted into chloroform with benzyldimethyltetradecylammonium chloride (QCl) as counter-ion. The extraction constants were estimated to be $K_{ex}^{Fe(II)} = [Q\{Fe^{II}(HL)L\}]_o/[Q^+]\{Fe^{II}(HL)L\}^- = 10^{8.59 \pm 0.11}$, $K_{ex}^{Fe(III)} = [Q_2\{Fe^{III}L_2\}]_o/[Q^+]\{Fe^{III}L_2\}^- = 10^{12.17 \pm 0.10}$ and $K_{ex}^{Fe(III)} = [Q\{Fe^{III}L_2\}]_o/[Q^+]\{Fe^{III}L_2\}^- = 10^{6.78 \pm 0.15}$ at $I = 0.10$ and 20° , where $[]_o$ is concentration in the chloroform phase. Aggregation of $Q\{Fe^{III}L_2\}$ in chloroform was observed and the dimerization constant ($K_d = [Q_2\{Fe^{III}L_2\}]_o/[Q\{Fe^{III}L_2\}]_o^2$) was evaluated as $\log K_d = 4.3 \pm 0.3$ at 20° . The neutral chelates of $\{Fe^{II}(HL)_2\}$ and $\{Fe^{III}(HL)L\}$, and the ion-pair of the cationic chelate, $\{Fe^{III}(HL)_2\}ClO_4$, were also extracted into chloroform or nitrobenzene. The relationship between the forms and extraction properties of the iron(II) and iron(III) PAR chelates are discussed in connection with those of the nickel(II) and cobalt(III) complexes. Correlation between the extraction equilibrium data and the elution behaviour of some PAR chelates in ion-pair reversed-phase partition chromatography is also discussed.

Spectrophotometric determination of iron(II) and iron(III) with 4-(2-pyridylazo)resorcinol (PAR, H₂L) has been proposed,¹⁻⁵ but data on the structures and acid properties of these chelates do not seem to be consistent. For example, Nonova *et al.* reported the formation equilibria of $\{Fe^{II}(HL)L\}^-$ and $\{Fe^{III}(HL)L\}$, but paid no attention to any other iron-PAR complexes in solution.⁴ Russeva *et al.*⁵ reported the formation of Fe(III)-PAR complexes, but did not describe that of the 1:2 Fe:PAR complexes which are predominant under analytical conditions, *i.e.*, in the presence of PAR in large excess.

In our studies on extraction of the PAR chelates of some transition metal ions, as ion-pairs with quaternary ammonium cations,⁶⁻¹⁰ we noticed that the extraction behaviour varied markedly, according to the nature of the central metal ion.^{9,10} Equilibrium studies on these extraction systems should yield important information about the sometimes puzzling nature of PAR chelates, as well as understanding of the basis for these extractive colorimetric determinations.⁶⁻¹³ Such equilibrium data may also serve for prediction of the order of elution of PAR chelates in ion-pair reversed-phase partition chromatography.¹⁴

In this paper, the extraction equilibria of the PAR complexes of iron(II) and iron(III) with benzyldimethyltetradecylammonium chloride (BDTACl, QCl) are reported and interpreted.

EXPERIMENTAL

Apparatus

A Hitachi model 124 double-beam recording spectrophotometer with 1-cm glass cells, and a Hitachi-Horiba M-5 pH-meter were used.

Reagents

Aqueous stock solutions of iron(II) and iron(III) ammonium sulphate were made from guaranteed reagent grade salts, with a few drops of concentrated sulphuric acid added to prevent hydrolysis. The solutions of PAR and QCl were prepared as previously reported.⁹ Chloroform and nitrobenzene were purified by distillation and saturated with water before use. All other reagents used were of analytical grade.

Procedure

The extraction procedure has already been described.⁹ To prevent aerial oxidation of iron(II) during the extraction, a small amount of L-ascorbic acid (enough to give a concentration of about $10^{-4}M$) was added. The metal-PAR ratio was found to be 1:2 by the molar-ratio method, for both Fe(II) and Fe(III). An ionic strength of 0.10 was maintained with sodium sulphate unless otherwise stated. The formation constants, $\beta_2 = \{[FeL_2]/[Fe][L^2]^{-2}\}$, for both chelates, are so large, $10^{31.4}$ and $10^{34.2}$ for Fe(II) and Fe(III) respectively,^{15,16} that hydrolysis of the PAR chelates in neutral and slightly alkaline solutions was negligible if excess of PAR was present and the absorbance was measured within 2 hr. The formation of sulphate, chloride and ascorbate complexes can also be neglected under the conditions used. All studies were made at 20° .

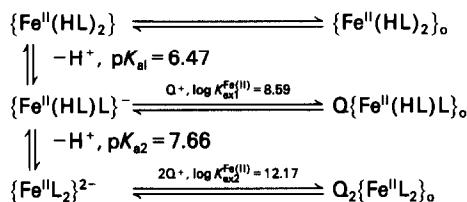
RESULTS

The extraction equilibrium scheme is shown in Fig. 1. In the discussion below, the complexes present in the aqueous phase will be indicated by use of braces ($\{\}$), as in the summary.

Extraction of Fe(II)-PAR chelates

The absorbance-pH curve (Fig. 2, curve A) for aqueous solution shows two distinct changes over the pH range 2-10 and the spectral change at higher pH

Fe(II)



Fe(III)

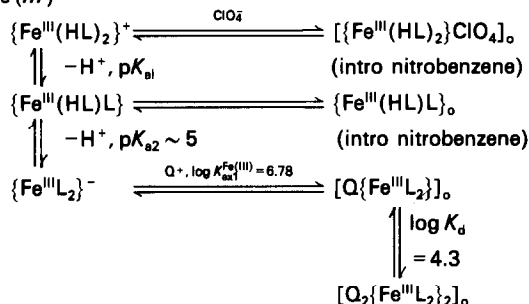


Fig. 1. Equilibrium scheme for extraction of iron(II) and iron(III) PAR chelates into chloroform.

agrees well with that found in a previous investigation.⁴ The Fe(II)–PAR species in acidic solution is expected to be the neutral $\{\text{Fe}^{\text{II}}(\text{HL})_2\}$, because at pH 3–5 the red chelate is partly extracted into chloroform even in the absence of Q^+ .

The absorbance spectra (Fig. 3) and the absorbance–pH curves (Fig. 2, curves B and C) show that at least two kinds of PAR chelate are involved in the extraction process. The Job plots indicate that the species extracted at pH 8.0 is $\text{Q}\{\text{Fe}^{\text{II}}(\text{HL})\text{L}\}$. The species extracted from more alkaline solution is expected to be $\text{Q}_2\{\text{Fe}^{\text{II}}\text{L}_2\}$. The absorbance–pH curve when a slight excess of Q^+ is present has maximal absorbance at about pH 7 (curve B), whereas with a large excess of Q^+ the absorbance is highest at pH 9–10 (curve C). This suggests that $\text{Q}_2\{\text{Fe}^{\text{II}}\text{L}_2\}$ is less

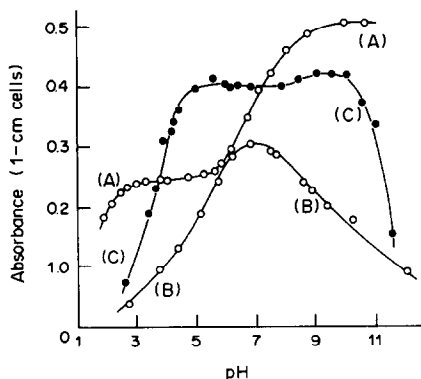


Fig. 2. Absorbance–pH curves for the iron(II)–PAR–QCl system. (A) Absorbance in aqueous solution, $C_{\text{Fe}} = 9.99 \times 10^{-6} \text{M}$, $C_{\text{L}} = 2.05 \times 10^{-5} \text{M}$, $I = 0.10$ ($\text{H,Na}\text{ClO}_4$), at 495 nm. (B) Absorbance in chloroform, $C_{\text{Fe}} = 1.00 \times 10^{-5} \text{M}$, $C_{\text{L}} = 2.00 \times 10^{-5} \text{M}$, $C_{\text{Q}} = 2.14 \times 10^{-5} \text{M}$, $I = 0.10$ (Na_2SO_4), at 505 nm. (C) Absorbance in chloroform, concentrations and conditions the same as for Fig. 3, at 505 nm.

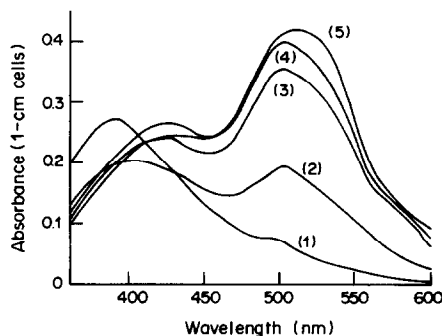
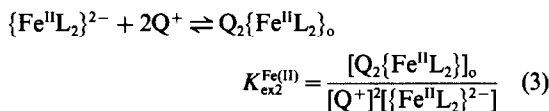
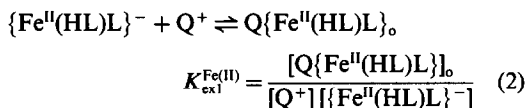
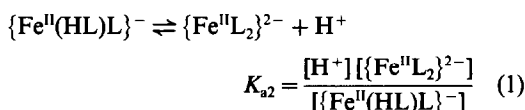


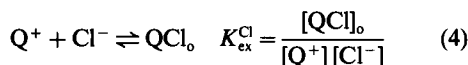
Fig. 3. Absorption spectra of the extracted species in chloroform for the iron(II)–PAR–QCl system in the pH range 2.36–9.05. pH: (1) 2.36, (2) 3.38, (3) 4.41, (4) 6.10, (5) 9.05. $C_{\text{Fe}} = 9.99 \times 10^{-6} \text{M}$, $C_{\text{L}} = 2.05 \times 10^{-5} \text{M}$, $C_{\text{Q}} = 5.35 \times 10^{-4} \text{M}$, $I = 0.10$ (Na_2SO_4).

extractable than $\text{Q}\{\text{Fe}^{\text{II}}(\text{HL})\text{L}\}$. The molar absorptivities (ϵ) of $\text{Q}\{\text{Fe}^{\text{II}}(\text{HL})\text{L}\}$ and $\text{Q}_2\{\text{Fe}^{\text{II}}\text{L}_2\}$ in chloroform were found to be $4.00 \times 10^4 \text{l. mole}^{-1} \cdot \text{cm}^{-1}$ at 500 nm and 4.50×10^4 at 510 nm, respectively.

A quantitative description of the extraction equilibria of the Fe(II)–PAR chelates with Q^+ at pH 7–10 requires consideration of the reactions:



as well as the distribution of the ion-pairs of QCl and QHL,⁹



where the subscript o indicates the species in the organic phase.

The chelate formation constant in the aqueous phase is large ($\log \beta_2 = 31.4$),¹⁵ so formation of the iron(II) chelate should be almost quantitative at pH 7–9 in the presence of a small excess of PAR. Evaluation of the relevant equilibrium constants provides a check on the validity of the assumptions made above.

From equations (1)–(3), the following expression is obtained:

$$\frac{K_{\text{ex2}}^{\text{Fe(II)}} K_{a2}}{K_{\text{ex1}}^{\text{Fe(II)}}} = \frac{[\text{H}^+][\text{Q}_2\{\text{Fe}^{\text{II}}\text{L}_2\}_o]}{[\text{Q}^+][\text{Q}\{\text{Fe}^{\text{II}}(\text{HL})\text{L}\}_o]} \quad (6)$$

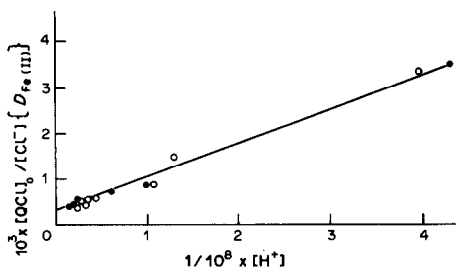
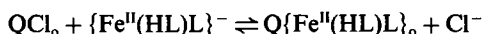


Fig. 4. Plots of equation (9). (●) $C_{Fe} = 1.99 \times 10^{-5} M$, $C_L = 4.01 \times 10^{-5} M$, $C_Q = 5.35 \times 10^{-5} M$; (○) $C_{Fe} = 9.93 \times 10^{-6} M$, $C_L = 4.01 \times 10^{-5} M$, $C_Q = 1.07 \times 10^{-4} M$. C_{borate} or $C_{phosphate} = 2.5 \times 10^{-3} M$, $I = 0.10$ (NaCl).

The values of the constants in equation (6) cannot be determined simultaneously. Hence the values of K_{a2} and $K_{ex1}^{Fe(II)}$ were estimated in 0.10M sodium chloride medium, where the extraction of $Q_2\{Fe^{II}L_2\}$ can be neglected since its extractability relative to that of the chloride ion-pair is expected to be sufficiently low (see Appendix I).

The ion-exchange extraction is expressed by



$$K = \frac{[Q\{Fe^{II}(HL)L\}]_o [Cl^-]}{[QCl]_o [\{Fe^{II}(HL)L\}^-]} = \frac{K_{ex1}^{Fe(II)}}{K_{ex}^{Cl}} \quad (7)$$

and the distribution ratio of iron(II), $D_{Fe(II)}$, is given by

$$D_{Fe(II)} = \frac{[Q\{Fe^{II}(HL)L\}]_o}{[\{Fe^{II}(HL)L\}^-] + [\{Fe^{II}L_2\}^{2-}]} \quad (8)$$

where the concentrations of the ion-pair and the neutral chelate $\{Fe^{II}(HL)_2\}$ in the aqueous phase are neglected. From equations (1), (7) and (8), and the material-balance equation for Q^+ , we obtain

$$\frac{[QCl]_o}{D_{Fe(II)} [Cl^-]} = \frac{1}{K} + \frac{K_{a2}}{K[H^+]} \quad (9)$$

where $[QCl]_o = C_Q - [QHL]_o - [Q\{Fe^{II}(HL)L\}]_o$, C_Q being the total concentration of Q^+ . The data plotted in Fig. 4 are taken over the pH range 7.4–9.0. From the slope and intercept, the values of the constants in equation (9) were found to be $K_{a2} = 10^{-7.66 \pm 0.10}$ and

$K = 10^{3.48 \pm 0.08}$ at $I = 0.10$ (NaCl). Thus, $K_{ex1}^{Fe(II)} = K K_{ex}^{Cl} = 10^{8.59 \pm 0.11}$.

Under conditions in which both the chelate and HL^- are quantitatively extracted [$C_Q > 2 \times 10^{-4} M$ is required at $I = 0.10$ (Na_2SO_4)], the change in absorbance, A , over the pH range 7–10 (Fig. 3, curve C) can be used to evaluate $K_{ex2}^{Fe(II)}$ by means of equation (6):

$$K_{ex2}^{Fe(II)} = \frac{K_{ex1}^{Fe(II)} [H^+]}{K_{a2} [Q^+]} \left(\frac{A - A_1}{A_2 - A} \right) \quad (10)$$

where A_1 and A_2 are the constant absorbances at $pH < 7.5$ and > 9.5 , respectively. From equation (11), the value of $[Q^+]$ can be calculated:

$$K_{ex}^{Cl} [Q^+]^2 + \{1 + K_{ex}^{Cl} \alpha\} [Q^+] - (C_Q - \alpha) = 0 \quad (11)$$

where $\alpha = C_L - C_{Fe}[(A_2 - A)/(A_2 - A_1)]$, C_L and C_{Fe} being the total concentrations of PAR and $Fe(II)$, respectively. Derivation of equation (11) is given in Appendix II. The results of the calculations are shown in Table 1 and lead to $K_{ex2}^{Fe(II)} = 10^{12.17 \pm 0.10}$ at $I = 0.10$ (Na_2SO_4).

At total concentrations of $Q\{Fe^{II}(HL)L\}$ and $Q_2\{Fe^{II}L_2\}$ in chloroform up to $2 \times 10^{-3} M$, the results gave no evidence for dimer formation.

Extraction of Fe(III)-PAR chelates

The absorption spectra of the species extracted in the $Fe(III)$ -PAR- QCl system at various pH values are shown in Fig. 5. In the presence of a large excess of Q^+ , the extracted species has an absorption maximum at 495 nm ($\epsilon = 6.03 \times 10^4 l. mole^{-1}. cm^{-1}$) with a distinct shoulder at 540 nm, and maximum and constant absorbance is obtained over the pH range 4–9 (Fig. 6, curve B). For comparison, the absorbance-pH curve in aqueous solutions is given as curve A in Fig. 6.

Two other kinds of iron(III)-PAR chelates are extractable into nitrobenzene, *viz.* the cationic $\{Fe^{III}(HL)_2\}^+$, with perchlorate as counter-ion ($\lambda_{max} = 535$ nm, Fig. 6, curve C), and the neutral $\{Fe^{III}(HL)L\}$ ($\lambda_{max} = 496$ nm, curve D).

The form of the ion-pair with Q^+ in chloroform was confirmed by continuous-variation plots at pH 8.2 to be $Q\{Fe^{III}L_2\}$.

Table 1. Equilibrium extraction data for $[Fe^{II}L_2]^{2-}$ with QCl into chloroform [$I = 0.10$ (Na_2SO_4) in $2.5 \times 10^{-3} M$ borate buffer]

C_{Fe}, M	1.26×10^{-5}	1.51×10^{-5}	1.26×10^{-5}	1.51×10^{-5}			
C_L, M	3.04×10^{-5}	4.05×10^{-5}	4.05×10^{-5}	4.05×10^{-5}			
C_Q, M	5.12×10^{-4}	5.12×10^{-4}	2.56×10^{-4}	2.56×10^{-4}			
pH	$\log K_{ex2}^{Fe(II)}$	pH	$\log K_{ex2}^{Fe(II)}$	pH	$\log K_{ex2}^{Fe(II)}$	pH	$\log K_{ex2}^{Fe(II)}$
7.02	12.11	7.98	12.45	6.97	12.18	6.97	12.10
7.30	12.45	8.30	12.33	7.45	12.40	7.31	12.40
7.59	12.41	8.58	12.17	7.82	12.03	7.79	12.23
7.91	12.44	8.72	12.30	8.07	11.92	8.15	12.25
8.22	12.39	9.18	12.08	8.34	11.85	8.50	12.20
8.51	12.39	9.75	12.18	8.65	11.75	8.77	12.11
8.80	12.23			9.00	11.82	9.00	12.25
				9.33	11.76	9.62	12.03
				9.78	12.00		

$\log K_{ex2}^{Fe(II)} = 12.17 \pm 0.10$ (average value of 30 experiments).

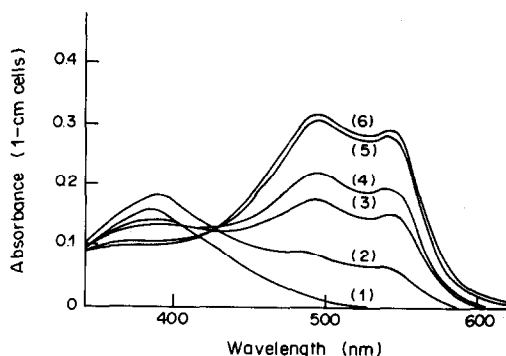
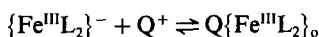


Fig. 5. Absorption spectra of the extracted species in chloroform for the iron(III)-PAR-QCl system in the pH range 1.95–6.08. pH: (1) 1.95, (2) 2.60, (3) 2.89, (4) 3.21, (5) 4.22, (6) 6.08. $C_{Fe} = 5.05 \times 10^{-6}M$, $C_L = 1.22 \times 10^{-5}M$, $C_Q = 4.83 \times 10^{-4}M$, $I = 0.10$ (Na_2SO_4).

The distribution ratio of the $Q^+\{Fe^{III}L_2\}^-$ ion-pair into chloroform significantly increased with total concentration of the chelate, owing to the extensive aggregation of the ion-pair in chloroform. The extraction constant of the $\{Fe^{III}L_2\}^-$ chelate was obtained from the extraction data at concentrations of the chelate lower than $6 \times 10^{-6}M$, where the contribution of dimerization (or higher aggregation) was found to be negligible. The extraction constant of the ion-pair is given by



$$K_{ex}^{Fe(III)} = \frac{[Q\{Fe^{III}L_2\}_o]}{[Q^+][\{Fe^{III}L_2\}^-]} \quad (12)$$

The extraction curve with nitrobenzene (Fig. 6, curve D) indicates that the pK_{a2} value of the chelate [equation (13)] is smaller than 5.5.



Thus, the predominant Fe(III)-PAR species con-

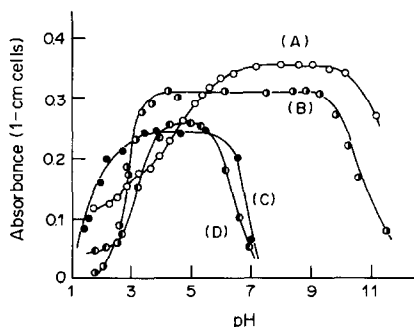


Fig. 6. Absorbance-pH curves of the iron(III)-PAR chelates in the several extraction systems. (A) Absorbance in aqueous solution at 495 nm. $C_{Fe} = 5.70 \times 10^{-6}M$, $C_L = 1.60 \times 10^{-5}M$, $I = 0.10$ [$(H,Na)ClO_4$]. (B) Absorbance in chloroform at 495 nm. Concentrations and conditions are the same as for Fig. 5. (C) Absorbance in nitrobenzene at 535 nm. With $0.1M$ $NaClO_4$, $C_{Fe} = 1.01 \times 10^{-5}M$, $C_L = 2.10 \times 10^{-5}M$. (D) Absorbance in nitrobenzene at 495 nm. C_{Fe} and C_L are the same as for (C).

cerned in the extraction at pH 8.2 is $\{Fe^{III}L_2\}^-$. Since the aqueous concentrations of free ferric ion and the ion-pair, $Q\{Fe^{III}L_2\}$ can be neglected, the distribution ratio of Fe(III), $D_{Fe(III)}$ is given by

$$D_{Fe(III)} = \frac{[Q\{Fe^{III}L_2\}]_o}{[\{Fe^{III}L_2\}^-]} \quad (14)$$

Substitution of (14) in (12) gives the extraction constant

$$K_{ex}^{Fe(III)} = \frac{D_{Fe(III)}}{[Q^+]} \quad (15)$$

and $[Q^+]$ can be obtained from the material-balance equations (see Appendix II):

$$K_{ex}^{Cl}[Q^+]^2 + \{1 + K_{ex}^{Cl}\alpha\}[Q^+] - (C_Q - \alpha) = 0 \quad (16)$$

where $\alpha = [QHL]_o + [Q\{Fe^{III}L_2\}]_o$. The concentrations of $[QHL]_o$ and $[Q\{Fe^{III}L_2\}]_o$ were determined by solving the simultaneous equations for the absorbances measured at 400 and 495 nm.

The logarithmic plot of equation (15) gave a straight line with a slope of unity, and the value of $K_{ex}^{Fe(III)}$ was evaluated by least-squares calculation: $K_{ex}^{Fe(III)} = 10^{6.78 \pm 0.15}$ at $I = 0.10$ (Na_2SO_4).

When dimer formation takes place, the distribution ratio of the Fe(III) at pH 8.2 is described by

$$D_{Fe(III)} = \frac{[Q\{Fe^{III}L_2\}]_o + 2[Q_2\{Fe^{III}L_2\}]_o}{[\{Fe^{III}L_2\}^-]} \quad (17)$$

The dimerization constant is defined as

$$K_d = \frac{[Q_2\{Fe^{III}L_2\}]_o}{[Q\{Fe^{III}L_2\}]_o^2} \quad (18)$$

From equations (12), (17) and (18), we obtain

$$\frac{D_{Fe(III)}}{[Q^+]} = K_{ex}^{Fe(III)} + 2K_d(K_{ex}^{Fe(III)})^2[\{Fe^{III}L_2\}^-][Q^+] \quad (19)$$

The concentration of free Q^+ was calculated from equation (16), with $\alpha = [QHL]_o + [Q\{Fe^{III}L_2\}]_o + 2[Q_2\{Fe^{III}L_2\}]_o$. Since the data were scattered to some extent, as shown in Fig. 7, the value of K_d could be determined only with poorer precision, as $10^{4.3 \pm 0.3}$ from the linear plot of equation (19) by least-squares calculation in which the $K_{ex}^{Fe(III)}$ value obtained from equation (15) was put on the corresponding position of the ordinate in Fig. 7.

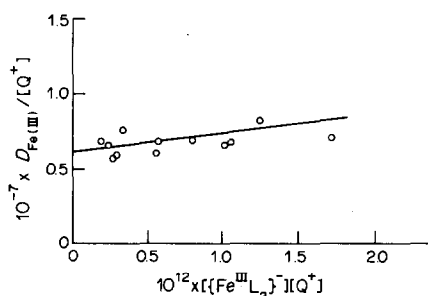


Fig. 7. Plots of equation (19).

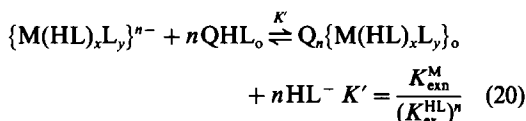
Table 2. Equilibrium constants and ϵ values (CHCl₃ medium) for some PAR chelates ($I = 0.10$; 20°C)

Anion	$\log K_{\text{ex}}$	$\log K_d$	$\text{p}K_{a1}$	$\text{p}K_{a2}$	$\epsilon, 10^4 \text{ l. mole}^{-1} \cdot \text{cm}^{-1}$
[Fe ^{III} L ₂] ⁻	6.78	4.3	—	~5	6.03 (495 nm)
[Co ^{III} L ₂] ⁻ (a)	6.37	4.04	3.64	4.41	6.41 (520 nm)
[V ^{VO} ₂ L] ⁻ (b)	6.54	—	4.40	—	3.35 (560 nm)
[Fe ^{II} (HL)L] ⁻	8.59	—	—	—	4.00 (500 nm)
[Fe ^{II} L ₂] ²⁻	12.17	—	6.47 ^(c)	7.66	4.50 (510 nm)
[Ni ^{II} L ₂] ²⁻ (d)	11.16	—	6.2 ^(e)	7.1 ^(e)	8.08 (500 nm)
HL ⁻ (d)	7.31	—	5.43 ^{(b)(e)}	12.13 ^{(b)(f)}	3.11 (400 nm)
Cl ⁻ (d)	5.11	—	—	—	—
ClO ₄ ⁻ (d)	7.40	—	—	—	—

(a) Ref. 10, (b) ref. 17, (c) ref. 15, (d) ref. 9, (e) dissociation of 1-hydroxy group, (f) dissociation of 3-hydroxy group.

DISCUSSION

The equilibrium constants obtained in this work are listed in Table 2 with those for some other metal-PAR chelates. The relative order of the ion-pair extraction constants can be established as {Fe^{II}(HL)L}⁻ > HL⁻ > {Fe^{III}L₂}⁻ > {Fe^{II}L₂}²⁻ by considering the exchange equilibrium



This order seems to be reasonable for {Fe^{II}(HL)L}⁻ > HL⁻ > {Fe^{II}L₂}²⁻ with respect to the size and charge-type effects,^{18,19} but the position of {Fe^{III}L₂}⁻ is unusual on the basis of these criteria. Furthermore, no evidence for dimerization was observed in the {Fe^{II}L₂}²⁻-Q⁺ and {Ni^{II}L₂}²⁻-Q⁺ systems, though it was in the {Fe^{III}L₂}⁻-Q⁺ system ($\log K_d = 4.3$). Very similar behaviour to that of {Fe^{III}L₂}⁻ was also found for the {Co^{III}L₂}⁻-Q⁺ system [$\log K_{\text{ex}}^{\text{Co(III)}} = 6.37$ and $\log K_d = 4.04$].¹⁰ The closeness of the values K_{ex} and K_d for Fe(III) and Co(III) should be attributed to the similarity in the nature of the ion-pairs. The situation may be similar for the PAR chelates of {M^{II}L₂}²⁻ [M = Fe(II) and Ni(II)], since their extraction constants are $\log K_{\text{ex}}^{\text{Fe(II)}} = 12.17$ and $\log K_{\text{ex}}^{\text{Ni(II)}} = 11.16$. From comparison of the extractability of the different types of PAR chelates, it is concluded that the 1-hydroxy groups (*para* to the azo group) in the chelates play an important role in the extraction process, both in ion-pair formation and in solvation of the ion-pairs.

As shown in the discussion above, detailed data for the ion-pair extraction equilibria provide useful information about the forms of some analytically important metal chelates in solution, as well as the quantitative basis for understanding the extractive colorimetric determination of metal ions with PAR and the separation of some PAR chelates by ion-pair reversed-phase partition chromatography.¹⁴ For example, there is a linear correlation (Fig. 9) between the extraction constants of the PAR chelates and their capacity factors (k') calculated from the chromatogram shown in Fig. 8.

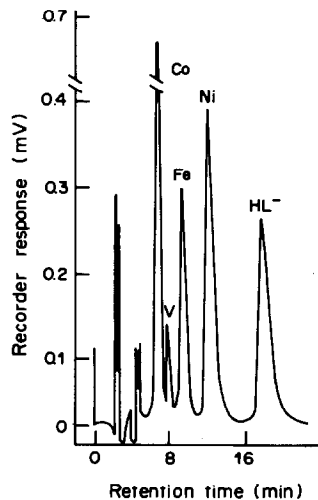


Fig. 8. Separation of PAR chelates by ion-pair reversed-phase partition chromatography. $C_M = 2 \times 10^{-6} M$, $C_L = 8.0 \times 10^{-3} M$, pH 7.5 ($5 \times 10^{-3} M$ sodium acetate), 0.100 ml injected. Column, Yanapak ODS-T column (Yanagimoto Mfg., 4 mm bore, 250 mm length); mobile phase 47 w/w% aqueous methanol containing tetrabutylammonium bromide (0.01 mole/kg), sodium acetate (0.04 mole/kg) and EDTA (10^{-4} mole/kg); flow-rate 1.0 ml/min. Detection at 500 nm, 1 mV = 0.04 absorbance.

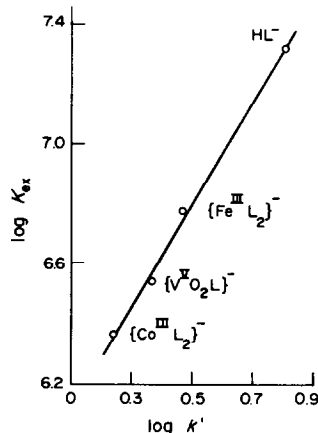


Fig. 9. Relationship between $\log K_{\text{ex}}$ and $\log k'$ for singly negatively-charged PAR chelates. The capacity factor, k' , is given by $k' = (t_r - t_0)/t_0$, where t_0 and t_r are the retention times of a non-retarded component (solvent front) and of the separated species, respectively.

APPENDIX I

Extractability of $\{Fe^{II}L_2\}^{2-}$ chelate from 0.1M sodium chloride solution

Equation (3) is combined with equation (4), and with use of the values in Table 2, the following relation is derived:

$$\frac{K_{ex}^{Fe^{II}}}{(K_{ex}^{Cl})^2} = \frac{[Q_2\{Fe^{II}L_2\}]_0 [Cl^-]^2}{[QCl]_0^2 [\{Fe^{II}L_2\}^{2-}]} = 10^{1.95} \quad (A-1)$$

Under the conditions $[Cl^-] = 0.10M$ and $[QCl]_0 = 5 \times 10^{-4}M$ (approximately similar to those for Fig. 4), the value of $[Q_2\{Fe^{II}L_2\}]_0 / [\{Fe^{II}L_2\}^{2-}]$ is estimated to be $10^{-2.65}$, so only 0.2% of the $\{Fe^{II}L_2\}^{2-}$ can be extracted.

Equation (6) is multiplied by the reciprocal of equation (4):

$$\frac{[Cl^-][H^+][Q_2\{Fe^{II}L_2\}]_0}{[QCl]_0[Q\{Fe^{II}(HL)L\}]_0} = 10^{-9.19} \quad (A-2)$$

Under the conditions above for $[Cl^-]$ and $[QCl]_0$, even at the highest pH in Fig. 4, pH 9.0, the ratio $[Q_2\{Fe^{II}L_2\}]_0 / [Q\{Fe^{II}(HL)L\}]_0$ is estimated to be only $10^{-2.49}$.

APPENDIX II

Derivation of equations (11) and (16)

Here α is the sum of the concentration terms which can be spectrophotometrically determined in the material-balance equation for Q^+ ion.

For equation (11) four mass-balance equations are needed:

$$C_Q = [Q^+] + [QCl]_0 + \alpha \quad (A-3)$$

where

$$\alpha = [QHL]_0 + [Q\{Fe^{II}(HL)L\}]_0 + 2[Q_2\{Fe^{II}L_2\}]_0 \quad (A-4)$$

$$C_{Cl} = C_Q = [Cl^-] + [QCl]_0 \quad (A-5)$$

$$C_{Fe} = [Q\{Fe^{II}(HL)L\}]_0 + [Q_2\{Fe^{II}L_2\}]_0 \quad (A-6)$$

$$C_L = [QHL]_0 + 2C_{Fe} \quad (A-7)$$

where the aqueous concentrations of ferrous ion, its chelates, HL⁻ and their ion-pairs with Q^+ ion are neglected. By use of equation (4), equation (A-3) is rewritten as

$$C_Q = [Q^+] (1 + K_{ex}^{Cl}[Cl^-]) + \alpha \quad (A-8)$$

From equations (A-3) and (A-5):

$$[Cl^-] = [Q^+] + \alpha \quad (A-9)$$

If equation (A-9) is substituted in (A-8), a quadratic equation with respect to $[Q^+]$ is obtained:

$$K_{ex}^{Cl}[Q^+]^2 + (1 + K_{ex}^{Cl}\alpha)[Q^+] - (C_Q - \alpha) = 0 \quad (A-10)$$

From equations (A-4), (A-6) and (A-7), the following equation is obtained:

$$\alpha = C_L - [Q\{Fe^{II}(HL)L\}]_0 \quad (A-11)$$

The absorbances A_1 , A_2 and A can be written as

$$A_1 = \epsilon_1 C_{Fe}$$

$$A_2 = \epsilon_2 C_{Fe}$$

$$A = \epsilon_1 [Q\{Fe^{II}(HL)L\}]_0 + \epsilon_2 [Q_2\{Fe^{II}L_2\}]_0 \quad (A-12)$$

where ϵ_1 and ϵ_2 are the molar absorptivities of the ion-pairs, $Q\{Fe^{II}(HL)L\}$ and $Q_2\{Fe^{II}L_2\}$, respectively, in chloroform. With use of equations (A-11) and (A-6), rearrangement of equation (A-12) gives

$$[Q\{Fe^{II}(HL)L\}]_0 = \left(\frac{A_2 - A}{A_2 - A_1} \right) C_{Fe}$$

which is substituted into equation (A-10) to give the final equation for α as

$$\alpha = C_L - C_{Fe} \left(\frac{A_2 - A}{A_2 - A_1} \right) \quad (A-13)$$

Equation (16) is readily derived in a similar manner, by using the material-balance equation

$$C_Q = [Q^+] + [QCl]_0 + [QHL]_0 + [Q\{Fe^{III}L_2\}]_0 \quad (A-14)$$

Here, α is defined as $\alpha = [QHL]_0 + [Q\{Fe^{III}L_2\}]_0$, where $[QHL]_0$ and $[Q\{Fe^{III}L_2\}]_0$ are directly determined by measuring the absorbance at 400 nm (for $[QHL]_0$) and 495 nm (for $[Q\{Fe^{III}L_2\}]_0$). The term $2[Q_2\{Fe^{III}L_2\}]_0$ is added to equation (A-14) when dimer formation takes place.

REFERENCES

1. T. Takeuchi and Y. Shijo, *Bunseki Kagaku*, 1965, **14**, 930.
2. T. Yotsuyanagi, K. Goto and M. Nagayama, *ibid.*, 1969, **18**, 184.
3. T. Yotsuyanagi, R. Yamashita and K. Aomura, *Anal. Chem.*, 1972, **44**, 1091.
4. D. Nonova and B. Evtimova, *J. Inorg. Nucl. Chem.*, 1973, **35**, 3581.
5. E. Russeva, V. Kuban and L. Sommer, *Collection Czech. Chem. Commun.*, 1979, **44**, 374.
6. T. Yotsuyanagi, Y. Takeda, R. Yamashita and K. Aomura, *Anal. Chim. Acta*, 1973, **67**, 297.
7. R. Yamashita, T. Yotsuyanagi and K. Aomura, *Bunseki Kagaku*, 1971, **20**, 1282.
8. T. Yotsuyanagi, R. Yamashita, H. Hoshino, K. Aomura, H. Satoh and N. Masuda, *Anal. Chim. Acta*, 1976, **82**, 431.
9. H. Hoshino, T. Yotsuyanagi and K. Aomura, *ibid.*, 1976, **83**, 317.
10. T. Yotsuyanagi and H. Hoshino, *Bunseki*, 1976, 743.
11. Lj. Maric, M. Siroki and M. J. Herak, *J. Inorg. Nucl. Chem.*, 1975, **37**, 2309.
12. D. Nonova and K. Stoyanov, *Anal. Chim. Acta*, 1982, **138**, 321.
13. D. Nonova and S. Pavlova, *ibid.*, 1981, **123**, 289.
14. H. Hoshino, T. Yotsuyanagi and K. Aomura, *Bunseki Kagaku*, 1978, **27**, 315.
15. H. Hoshino, unpublished results.
16. K. Momoki, J. Sekino, H. Satoh and N. Yamaguchi, *Anal. Chem.*, 1969, **41**, 1286.
17. M. Tajika, H. Hoshino, T. Yotsuyanagi and K. Aomura, *Nippon Kagaku Kaishi*, 1979, 85.
18. H. Kohara and N. Ishibashi, *Bunseki Kagaku*, 1971, **20**, 65.
19. H. M. N. H. Irving and A. D. Damodaran, *Anal. Chim. Acta*, 1971, **53**, 267.

URANYL COMPLEXES OF n-ALKANEDIAMINOTETRA-ACETIC ACIDS

M. L. SIMÕES GONÇALVES,* A. M. ALMEIDA MOTA and J. J. R. FRAÚSTO DA SILVA

Centro de Química Estrutural, Instituto Superior Técnico, 1096 Lisboa Codex, Portugal

(Received 13 July 1983. Revised 24 November 1983. Accepted 16 January 1984)

Summary—The uranyl complexes of n-propanediaminetetra-acetic acid, n-butanediaminetetra-acetic acid and n-hexanediaminetetra-acetic acid have been studied by potentiometry, with computer evaluation of the titration data by the MINQUAD program. Stability constants of the 1:1 and 2:1 metal:ligand chelates have been determined as well as the respective hydrolysis and polymerization constants at 25° in 0.10M and 1.00M KNO₃. The influence of the length of the alkane chain of the ligands on the complexes formed is discussed.

In a previous paper¹ we reported the results of a potentiometric study of the complexes formed by the uranyl ion UO₂²⁺ with EDTA. Using graphical plots,² we concluded that both mononuclear and binuclear complexes are formed, which are subsequently hydrolysed to give the corresponding hydroxo species and more complex products resulting from successive condensations. Hence, for 1:1 molar ratio mixtures of UO₂²⁺ and EDTA the composition of the solutions was interpreted in terms of the formation of MHL, MHLOH, MLOH and (MHLOH)₂ complexes, where M stands for UO₂²⁺; in 2:1 molar ratio mixtures of UO₂²⁺ and EDTA, the results were better interpreted in terms of a "core + links" mechanism³ where the complexes formed corresponded to the general formula M₂L[M₂(OH)₂L]_{n-1}·2H₂O, with $n_{\min} = 1$ and $n_{\max} \rightarrow \infty$, although the species corresponding to high values of n are unlikely.

This study has now been extended to other n-alkanediaminotetra-acetic acids, corresponding to the general formula



where $n = 3, 4$ and 6 , i.e., n-propanediaminetetra-acetic acid (PDTA), n-butanediaminetetra-acetic acid (BDTA) and n-hexanediaminetetra-acetic acid (HDTA), thus affording the possibility of examining the influence of the length of the hydrocarbon chain of the ligands on the type and stability of the various complexes formed.

In these cases, the fitting of the experimental results to the theoretical curves by graphical procedures is not satisfactory, contrary to what happens with the UO₂²⁺-EDTA system. We have therefore used a computational method, namely the MINQUAD program,^{4,5} which selects the set of products that gives best correspondence to the experimental results on the basis of the statistical criteria chosen (as discussed later in the results and discussion section) and calculates the formation constants. For comparison, we have re-examined the UO₂²⁺-EDTA system with this program.

EXPERIMENTAL

Reagents

PDTA and BDTA were prepared by condensation of n-propanediamine and n-butanediamine with monochloroacetic acid, following the current procedures.⁶ The products were recrystallized from aqueous ethanol.

HDTA and uranyl nitrate were commercial products of analytical grade (Fluka) and used without further purification. The concentration of the stock UO₂²⁺ solutions was confirmed by gravimetric analysis. The potassium hydroxide solutions used as titrants were prepared under nitrogen from Merck "titrisol" vials, with CO₂-free demineralized water. The concentration of these solutions and the absence of carbonate was checked regularly by potentiometric titration with standard hydrochloric acid.

Potentiometric measurements

A Corning-Eel 112 digital potentiometer was used with Corning electrodes (pH triple-purpose, Ag/AgCl internal and calomel reference electrodes, both No. 476022). The readings of potential were converted into log [H⁺] values according to the expression $E = K + \alpha \log [H^+]$. The experimental value of α determined at 25.0° was 59.2 ± 0.1 mV, in good agreement with the theoretical value of 59.15 (the drift of the liquid-junction potential during the measurements in the pH-range of the titrations was found to be negligible and was not considered in the expression used). The cell constant K was calculated from a previous titration of hydrochloric acid in the appropriate medium with potassium hydroxide, by Gran's method.⁷ The calibration was repeated before and after each series of titrations, at regular intervals during the day.

The ionic product of water in 0.10M and 1.00M potassium nitrate media was determined from these titrations; the values obtained at 25.0° were 1.68×10^{-14} and 1.86×10^{-14} respectively, in good agreement with those reported previously.⁸

Method

A range of ligand and metal concentrations between 5×10^{-4} and 4×10^{-3} M was used, to allow the study of polymeric species. At concentrations below 5×10^{-4} M no polymeric species are formed and at concentrations above 4×10^{-3} M the polymeric species precipitate as soon as they are formed.

In all cases the ionic strength of the medium was kept constant at 1.00M with potassium nitrate.

Some titrations were also performed with concentrations of ligand and metal below 10^{-3} M but the ionic strength at 0.10M (KNO₃). These were aimed particularly at the study of the simple MHL and M₂L complexes.

The titrations were performed in a double-walled titration-cell at a temperature controlled at $25.0 \pm 0.1^\circ$ by circulating water from a thermostat. The titrant was added from a 10.00 ± 0.01 ml Brand burette provided with soda-lime guard-tubes.

After each addition of base, the equilibrium potential was reached within 30–120 sec.

RESULTS AND DISCUSSION

The potentiometric curves of the n-alkanediaminetetra-acetic acid in the presence of uranyl ion (1:1 and 1:2 molar ratios) are analogous for all the ligands and the titration curves of BDTA are presented as an example (Fig. 1); the onset of precipitation of the hydroxo complexes occurs at a lower degree of neutralization as the hydrocarbon chain of the ligand increases.

Referring to this figure, it can be seen that curve (b), corresponding to the titration of a 1:1 molar mixture of UO_2^{2+} and the ligand, has an inflection at $a = 3$, which suggests the formation of a protonated complex MHL, where M represents UO_2^{2+} and L the deprotonated ligand. This is the only inflection point, in contrast to the corresponding situation for EDTA, where a second inflection point is apparent at $a = 5$.¹

Curve (c), corresponding to the titration of 2:1 molar mixtures of UO_2^{2+} and the ligand, has an inflection point at $a = 4$, indicating the formation of an M_2L complex. Both MHL and M_2L are subsequently hydrolysed, but since the inflections of the curves are not well defined, the hydrolysed species are already present before $a = 3$ or $a = 4$ in curves (b) and (c), as can be seen from the curves showing the distribution of the different species (Fig. 2).

The set of species to be considered, apart from MHL and M_2L , is not obvious, since the number of possibilities is large. The initial choice for an unknown system must be based on chemical grounds but, in the present case, the task is made simpler since a considerable amount of information is already available from the study of the UO_2^{2+} -EDTA system.¹

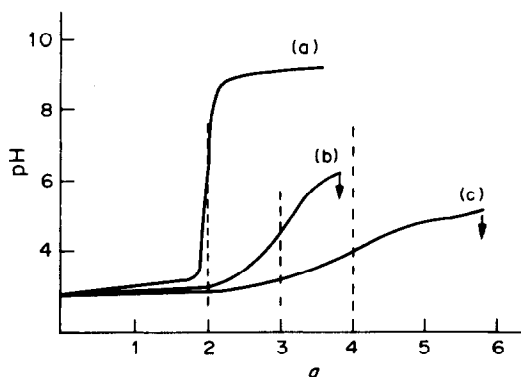


Fig. 1. Titration curves of BDTA (a) and BDTA + uranyl ion in the ratio 1:1 (b) and 1:2 (c), at 25° and ionic strength $0.1M$ KNO_3 , $C_{\text{BDTA}} = 10^{-3}M$; a = moles of base per mole of acid (degree of neutralization); ↓ indicates the precipitation of hydroxo complexes.

The formation constants of the complexes were obtained by a least-squares refinement process using the MINQUAD program. This program also calculates the standard deviations of the constants and an agreement factor R defined as:⁹

$$R = \left[U / \sum_{i=1}^m (C_{M_i}^2 + C_{L_i}^2 + C_{H_i}^2) \right]^{1/2}$$

where U is the sum of squared residuals for all the mass-balance equations:⁴

$$U = \sum_{i=1}^m [(C_M - C'_M)_i^2 + (C_L - C'_L)_i^2 + (C_H - C'_H)_i^2]$$

m represents the number of experimental points and the values C_M , C_L , C_H are the experimental values for the total concentration of metal, ligand and hydrogen ion; C'_M , C'_L and C'_H represent the same concentrations calculated from the mass-balance equations.

The best set of species is selected by analysing the values of the statistical outputs of the program.

A certain chemically probable set of species is unusually acceptable if the agreement factor R is less than 0.004, which is the permitted deviation from a calculated R , based on the experimental errors.¹⁰ The relative deviation of the formation constants should be less than 10%, although when many species are present values up to 25% may still be acceptable.

The formation constants of the species are defined as

$$\beta_{p,q,r} = \frac{[\text{M}_p\text{L}_q\text{H}_b(\text{OH})_a]}{[\text{M}]^p[\text{L}]^q[\text{H}]^r}$$

where $r = b - a$, and correspond to the reactions



Solvation of the species is not considered, for the sake of simplicity. Each species is defined by three numbers— p , q , r —which represent the number of metal ions, ligand ions and the sum of the hydrogen(+) and hydroxide(−) ions in the complex.

The ionization constants of the ligands (Table 1), the ionic product of water and the hydrolysis constants of the uranyl ion at $\mu = 0.1M$ and $1.0M$ (KNO_3)^{11,12} (Table 2) were included as fixed values in the data to be dealt with by the program.

The best sets of results for the various systems at ionic strength $1.00M$ (KNO_3) are presented in Table 3 together with the calculated standard deviations of the constants ($\log \beta$) and the values of the R factor. The results for EDTA presented in Table 4 have been redetermined by using the MINQUAD program, for comparison.

For all the systems, the value of the R parameter decreases significantly when the polymeric species due to hydrolysis of the complexes are considered. This supports the postulation of existence of these species in solution.

The results obtained for ionic strength $0.10M$ are not so conclusive, although there is a slight decrease

Table 1. Stability constants of the proton complexes of the ligands introduced as fixed constants in the MINIQUAD program [(A) 25°, 0.1M KNO₃; (B) 25°, 1.0M KNO₃]

	Ligand	β_{011}	β_{012}	β_{013}	β_{014}
(B)	EDTA	8.59×10^9	1.45×10^{16}	5.50×10^{18}	5.61×10^{20}
(A)	PDTA	1.78×10^{10}	1.12×10^{18}	4.79×10^{20}	6.31×10^{22}
(B)		1.07×10^{10}	6.76×10^{17}	2.29×10^{20}	1.82×10^{22}
(A)	BDTA	2.84×10^{10}	2.70×10^{19}	1.39×10^{22}	8.5×10^{23}
(B)		1.73×10^{10}	2.14×10^{19}	5.75×10^{22}	—
(A)	HDTA	3.72×10^{10}	1.71×10^{20}	9.79×10^{22}	—
(B)		2.24×10^{10}	8.13×10^{19}	2.95×10^{22}	—

Table 2. Hydrolysis constants of uranyl ion and ionic product of water introduced as fixed constants in the MINIQUAD program [(A) 25°, 0.1M KNO₃ (ref. 11); (B) 25°, 1.0M KNO₃ (ref. 12)]

	β_{10-1}	β_{20-2}	β_{30-4}	β_{30-5}	β_{40-7}	K_W
(A)	3.16×10^{-6}	1.26×10^{-6}	4.90×10^{-13}	3.47×10^{-17}	1.74×10^{-23}	1.68×10^{-14}
(B)	—	1.1×10^{-6}	1.62×10^{-6}	6.17×10^{-17}	—	1.86×10^{-14}

Table 3. Stability constants of UO₂²⁺ + L complexes for the best model obtained with the MINIQUAD program, with their standard deviations (25°; 1.00M KNO₃)

Ligand	log β_{111}	log β_{210}	log β_{21-1}	log β_{220}	log β_{42-2}	log β_{42-4}	log β_{63-4}	R
PDTA	18.14 ± 0.08	17.25 ± 0.02	12.40 ± 0.03	28.47 ± 0.03	27.47 ± 0.1	17.91 ± 0.03	—	0.0029
	18.11 ± 0.09	17.37 ± 0.03	12.48 ± 0.02	28.41 ± 0.03	—	18.01 ± 0.03	38.52 ± 0.1	0.0026
BDTA	19.26 ± 0.02	18.40 ± 0.02	13.45 ± 0.02	30.33 ± 0.1	29.83 ± 0.06	20.19 ± 0.03	—	0.0017
	19.15 ± 0.009	18.37 ± 0.02	13.44 ± 0.02	—	29.72 ± 0.06	20.10 ± 0.03	—	0.0018
HDTA	19.48 ± 0.09	18.77 ± 0.08	13.1 ± 0.2	30.98 ± 0.2	30.9 ± 0.2	19.8 ± 0.2	—	0.0032
	19.16 ± 0.07	18.71 ± 0.07	—	—	30.7 ± 0.1	19.6 ± 0.1	—	0.0035

Table 4. Stability constants of UO₂²⁺ + EDTA complexes, obtained by (I) graphical methods, (II) MINIQUAD program (25°; 1.00M KNO₃)

	log β_{111}	log β_{110}	log β_{11-1}	log β_{210}	log β_{21-1}	log β_{220}	log β_{42-2}	log β_{42-4}	log β_{63-4}
I	17.55	10.88	4.58	17.77	—	24.59	25.10	—	33.96
II	16.28 ± 0.04	—	—	16.14 ± 0.02	11.33 ± 0.03	25.04 ± 0.1	—	15.34 ± 0.04	34.3 ± 0.1

of R with the addition of the polymeric species to the set considered. Since in this case we did not change, at least significantly, the total metal and ligand concentrations (the supporting electrolyte would hardly keep the ionic strength constant) not enough data were obtained to allow distinction between monomers and the corresponding dimers. Nevertheless the best set of species found for ionic strength 1.00M has been accepted by the program (except for the dimer 42-2), and the formation constants of the species are consistent (Table 5).

From the plots of the percentages of the ligand and metal in each species, as a function of pH, for the 1:1 and 2:1 metal/ligand molar ratio mixtures, which are similar for all the ligands, it can be seen that the species MHL and M₂L, with general formula

Table 5. Stability constants of UO₂²⁺ + L complexes for the same species as those obtained at ionic strength 1.00M KNO₃, with their standard deviations (25°; 0.1M KNO₃)

Ligand	log β_{111}	log β_{210}	log β_{21-1}	log β_{220}	log β_{42-2}	log β_{42-4}	log β_{63-4}	R
PDTA	18.80 ± 0.02	18.66 ± 0.01	14.05 ± 0.02	30.2 ± 0.1	Rejected	20.64 ± 0.07	Rejected	0.0040
BDTA	19.61 ± 0.007	19.06 ± 0.007	13.83 ± 0.04	31.04 ± 0.05	Rejected	19.76 ± 0.02	—	0.0025
HDTA	20.22 ± 0.003	19.43 ± 0.004	14.23 ± 0.01	31.89 ± 0.05	Rejected	20.18 ± 0.02	—	0.0010

and



are present in solution up to about pH 6, being dominant between pH 3.00 and 5.00 (Fig. 2 for PDTA and HDTA ligands). At pH above 4 the hydrolysed species of these complexes begin to form. The M₂LOH (21-1) species, with one water molecule hydrolysed, is the first complex to be formed; its importance decreases from EDTA to HDTA, whereas the concentration of the dimer 42-2, with two bridging hydroxyl groups, increases.

For EDTA the equilibrium seems to favour the higher complex 63-4 of the "core + links" mechanism, instead of 42-2 for which the formation constant has a large error. For PDTA there are some doubts as to the existence of the second or third species of the series, i.e., 42-2, or 63-4, the co-

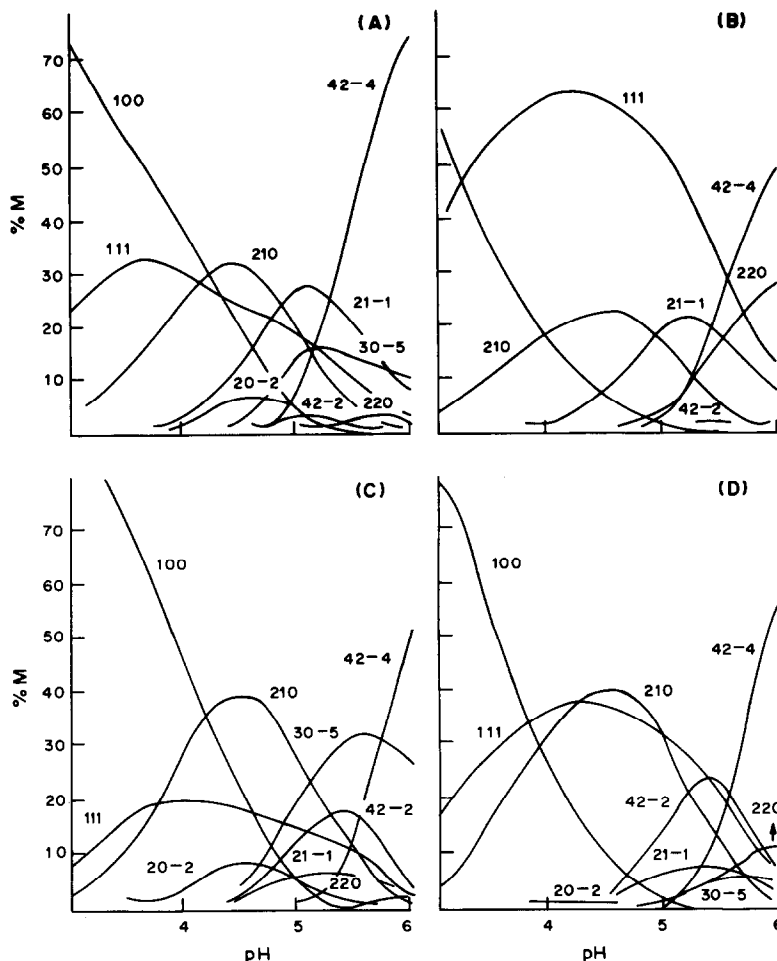


Fig. 2. Fraction of total metal, present in each complex, as a function of pH, for the systems: A, 2:1 UO_2^{2+} /PDTA; B, 1:1 UO_2^{2+} /PDTA; C, 2:1 UO_2^{2+} /HDTA; D, 1:1 UO_2^{2+} /HDTA.

existence of both being rejected by the program. The reason for the discrepancy cannot be ascertained; we believe that the tendency to form 63-4 decreases along the series and may be significant only for EDTA.

The species 42-4 is an intermediate between 42-2 and 63-4; on the basis of the behaviour of UO_2^{2+} aminocarboxylate complexes in solution¹³ it is likely to be formed by two M_2L molecules bound by two hydroxyl groups and with one hydrolysed water molecule co-ordinated to each UO_2^{2+} group. This species becomes clearly dominant at pH above 5 for all the systems.

For the same reason, the dimer 220 probably corresponds to two MHL molecules bound by two hydroxyl groups rather than to M_2L_2 , but the potentiometric data are not sufficiently conclusive to indicate the real structure. This species (more significant at the 1:1 metal/ligand ratio) is detectable for the EDTA and PDTA systems but for the BDTA and HDTA its existence in solution is doubtful.

The hydrolysis of the uranyl ion becomes more important in the systems involving ligands with longer $-\text{CH}_2-$ chains. The products of hydrolysis of

UO_2^{2+} together with the H_2L^{2-} and 42-4 species are the reason for the less satisfactory fit of the experimental points to the theoretical curves established assuming only the "core + links" mechanism. As Fig. 3 shows, their importance increases from the EDTA to the HDTA system, and their fraction of the total metal concentration passes through a minimum between pH 4 and 5.

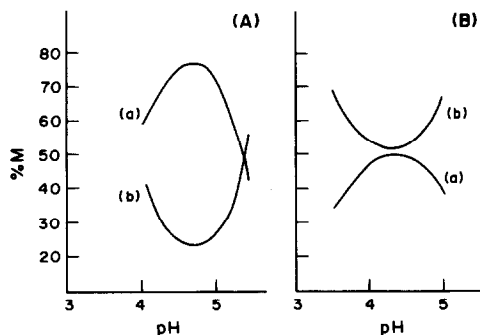


Fig. 3. Distribution curves (as functions of pH) for the systems A, 2:1 UO_2^{2+} /EDTA and B, 2:1 UO_2^{2+} /HDTA for (a) fraction of total metal present in all "core + links" species; (b) fraction of total metal present in the other species.

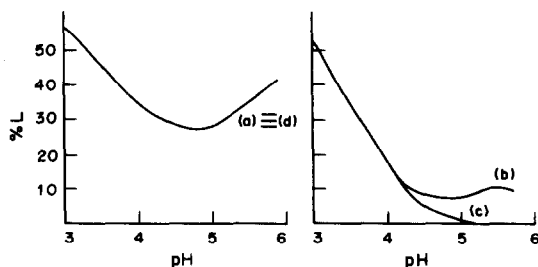


Fig. 4. Fraction of free H_2L , as a function of pH, for BDTA in the presence of uranyl ion in molar ratio of M:L 1:1 (a) and 2:1 (b). Curves (c) and (d) are the corresponding curves [to (b) and (a) respectively] after subtraction of hydrolysed uranyl ion species.

A curious result is obtained when the mass balance of species is considered in terms of L. The distribution curves of H_2L species as a function of pH have an analogous shape for all the ligands, with a minimum between pH 4.0 and 5.0, this being clearer for the 1:1 metal/ligand ratio (Fig. 4a, b). This behaviour is not the usual, since these curves generally increase to a maximum value and then decrease until they practically disappear owing to the competitive formation of other species. For the 2:1 metal/ligand ratio the increase of H_2L species after the minimum may be due mainly to the hydrolysis of uranyl ion, which increases the concentration of H^+ and displaces the equilibrium $H + MHL \rightleftharpoons H_2L + M$ to the right. This hypothesis has been confirmed by comparison of the H_2L distribution curves with the hypothetical ones obtained from a model without the hydrolysed species $M_2(OH)_2$, $M_3(OH)_3$ and $M_4(OH)_4$ (Fig. 4c). For the 1:1 metal/ligand ratio the minimum can be explained in terms of the increasing concentration of the 2:1 M:L species, which gives more free ligand available in the form of H_2L species. The hydrolysis of the uranyl ion does not affect the distribution curves within experimental error (Fig. 4d).

From the results in Table 4 it can be seen that the two sets of species—one obtained by graphical methods and the other by using the MINQUAD program for the EDTA + UO_2 system—are similar, although the formation constants for the well-defined species

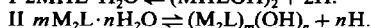
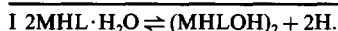
common to both methods differ by up to 1.5 log units ($\log M_{MHL}$ and $\log \beta_{M_2L}$). The set obtained with the computer program also considers the species 21-1 (monomer of 42-2) and 42-4 that do not belong to the "core + links" mechanism. On the other hand it does not consider the dimer 42-2 or the monomers 11-1 and 110 (monomer of 220) postulated in the graphical methods (since graphical methods used for the study of 1:1 mixtures do not include the 2:1 species, the 11-1 complex had to be introduced to fit the experimental points and the theoretical curves in the high pH range). It is worth noting that the 2:1 metal ligand species have a strong weight even when 1:1 mixtures are considered, as can be seen in Figs. 2 and 3. These seem to be the reasons why our present values for the EDTA system differ from those presented in our previous paper.¹ It must also be pointed out that in the present work more experimental data were used. In fact, when computer calculation is used, the entire titration curve is considered, whereas with graphical plots different parts of the curve are used for calculating the stability constants of the hydrolysed species and of the MHL or M_2L species.

A similar set of species obtained with the MINIQUAD program is reported for EDTA at ionic strength 0.10M by other authors¹⁴ but the dimers 42-4 and 220 are replaced by their monomers 21-2 and 110 since in the experimental conditions used no polymeric species due to hydrolysis were found.

From these results we can conclude that all the systems can be interpreted in terms of the same set of species: 111, 210, 21-1, 220, 42-2 and 42-4, where only 210 and 42-2 belong to the "core + links" series of general formula $M_2L[M_2L(OH)_2]_{n-1} \cdot 2H_2O$. As remarked before, for EDTA the 63-4 species of this mechanism may still exist, whereas 42-2 is doubtful. For PDTA, the existence of 63-4 is less likely and for the other systems this species was not accepted by the computer program. This seems to mean that species of the "core + links" series for $n > 1$ become progressively less probable the longer the chain of the ligand. The same happens with the dimer 220, which is also favoured by ligands with shorter chains, namely EDTA and PDTA. This effect is expected

Table 6. Hydrolysis constants of the UO_2L complexes, defined in terms of the species 210 or 111 [(A) 25°, 0.1M KNO_3 ; (B) 25°, 1.0M KNO_3]

Ligand	$-\log K_{220}^{111}$	$-\log K_{12-1}^{210}$	$-\log K_{42-2}^{210}$	$-\log K_{42-4}^{210}$	$-\log K_{63-4}^{210}$
(B) EDTA	7.52	4.81	—	16.94	14.12
PDTA	7.83	4.89	—	16.73	13.61
BDTA	8.22	4.95	6.97	17.61	—
HDTA	7.98	5.65	6.68	17.73	—
(A) PDTA	7.39	4.61	—	16.75	—
BDTA	8.18	5.26	—	18.35	—
HDTA	8.55	5.20	—	16.68	—
Reaction type	I	II $m = n = 1$	II $m = n = 2$	II $m = 2$ $n = 4$	II $m = 3$ $n = 4$



because a longer chain length corresponds to an increased basicity of the ligands (nitrogen donors) and the resulting electron density in the uranyl ion is higher; the ionization of the water molecule bonded to the central atom becomes more difficult and so does hydrolysis. The same reason explains the decrease of the hydrolysis constants (defined in terms of M_2L or MHL) with increase in the chain-length of the ligands, *i.e.*, with the basicity of their nitrogen atoms, as measured by pK_{HL} values (Table 6).

A final comment on these and similar results may be in order: although various sets of species may, in certain cases, be statistically possible, the comparison of a series of analogous systems can be of help to decide on the most probable set, particularly if and when they conform to chemical thinking.

Acknowledgement—A. M. Almeida Mota thanks Dr. P. Gans, of Leeds University, for his assistance in the use of the MINQUAD program and the interpretation of its results.

REFERENCES

1. J. J. R. Fraústo da Silva and M. L. Sadler Simões, *Talanta*, 1968, **15**, 609.
2. H. Rossotti and F. Rossotti, *The Determination of Stability Constants*, McGraw-Hill, New York, 1961.
3. L. G. Sillén, *Acta Chem. Scand.*, 1954, **8**, 299, 318, 1607.
4. A. Sabatini, A. Vacca and P. Gans, *Talanta*, 1974, **21**, 53.
5. P. Gans, A. Sabatini and A. Vacca, *Inorg. Chim. Acta* 1976, **18**, 237.
6. A. Schwarzenbach and Ackerman, *Helv. Chim. Acta*, 1948, **31**, 1029.
7. G. Gran, *Analyst*, 1952, **77**, 661.
8. R. M. Smith and A. E. Martell, *Critical Stability Constants*, Vol. 4, Plenum Press, New York, 1976.
9. A. Sabatini, A. Vacca and M. A. Gristina, *Coord. Chem. Rev.*, 1972, **8**, 45.
10. A. Sabatini and A. Vacca, *ibid.*, 1975, **16**, 161.
11. R. N. Sylva and M. R. Davidson, *J. Chem. Soc. Dalton*, 1979, 465.
12. S. Ahrland, *Acta Chem. Scand.*, 1951, **5**, 199.
13. J. J. R. Fraústo da Silva and M. L. S. Simões, *J. Inorg. Nucl. Chem.*, 1970, **32**, 1313.
14. P. A. Overvoll and W. Lund, *Anal. Chim. Acta*, 1982, **143**, 153.

ORGANIZATION AND EVALUATION OF INTERLABORATORY COMPARISON STUDIES AMONG SOUTHERN AFRICAN WATER ANALYSIS LABORATORIES

R. SMITH

National Institute for Water Research, Council for Scientific and Industrial Research, P.O. Box 395,
Pretoria 0001, South Africa

(Received 3 August 1983. Revised 24 November 1983. Accepted 15 January 1984)

Summary—Interlaboratory comparison studies provide a useful “external” supplement to the various “internal” quality-control procedures which must be employed in the water-analysis laboratory in order to maintain a high degree of reliability in the production of analytical results. Such studies have been made regularly for many years by various overseas organizations, and were introduced in South Africa in 1976. Since that time 16 studies have been made, involving more than 40 laboratories. In this paper the various factors involved in the successful organization of interlaboratory comparison studies are discussed, and details are given of the sample-preparation, analysis-instruction and result-reporting procedures used in the southern African studies. Techniques used for the statistical evaluation of the analytical results submitted are described and discussed, for example, methods for the rejection of outliers, measures of accuracy and precision, determination of total error, tests of significance, Greenberg’s assessment technique, Madden’s ranking technique and Youden’s graphical technique. A brief review is given of the studies made to date, along with specific findings and recommendations arising from them. The need for a recognized updated set of standard methods for use by water and wastewater analysis laboratories in southern Africa is highlighted.

The main function of a laboratory engaged in water and wastewater analysis is the provision of data which indicate the concentrations and characteristics of constituents in water samples submitted to that laboratory. These data are often employed as the basis for important decisions concerning, for example, process control of water and wastewater treatment or the assessment of the value and progress of research investigations. It is essential, therefore, to ensure the reliability of all analytical results produced. In order to achieve a high degree of reliability, effective quality-control procedures must be applied, for example, the use of appropriate sampling and sample-preservation techniques and recognized standard methods of analysis, frequent calibration of apparatus, and the application of a regular system of data verification.

An extremely useful “external” supplement to these “internal” quality-control procedures is the use of interlaboratory comparison (“calibration” or “collaborative” or “round-robin”) studies, in which identical reference samples are distributed to all participating laboratories for analysis for designated constituents, and submission of the results for statistical evaluation and comparison (the concentrations of the constituents of the samples are known only to the originator of the study).

Interlaboratory comparison studies can be of considerable benefit to the laboratories taking part. As well as providing the means by which each laboratory

can compare its ability with that of other laboratories in the production of acceptable results, the information gained can also enable the participants to assess the reliability of their particular analytical methods and to initiate improvements or alterations where necessary. Certain studies can also provide a mechanism for evaluating the reliability of specific analytical procedures.

Comparison studies involving laboratories engaged in water and wastewater analysis have been made regularly for many years by various overseas organizations, for example, the U.S. Environmental Protection Agency, the Canada Centre for Inland Waters, the U.K. Water Research Centre and the National Swedish Environment Protection Board. Similar studies for southern African water-analysis laboratories, however, were not established until 1976, when the National Institute for Water Research introduced a series of six studies, in which 16 invited laboratories participated (Table 1).¹⁻⁷

On completion of this programme in 1978, it was decided to continue the studies on a larger scale, to include any laboratory engaged in water or wastewater analysis in South Africa, Namibia, or Zimbabwe, and interested in taking part. A second series, consisting of ten studies, involving 46 laboratories from industry, government and statutory organizations, and various municipalities, was commenced in 1979 and completed in 1982 (Table 2).⁸⁻¹⁸

This paper describes the organization of the vari-

Table 1. Programme of studies (1976-78)

Study No.	Title	Determinands	No. of participants
76/A,B	Introductory study	Chemical oxygen demand, total organic carbon, Kjeldahl, ammonia, nitrate and nitrite nitrogen, total and orthophosphate, chloride, sulphate, fluoride, silicon, total alkalinity, pH, electrical conductivity, sodium, potassium, calcium, magnesium, cadmium, chromium, cobalt, copper, iron, lead, manganese, nickel, strontium, zinc, arsenic, mercury	15
77/A	COD, pH and electrical conductivity analysis	Chemical oxygen demand, pH, electrical conductivity	18
77/B	Nutrient analysis	Kjeldahl, ammonia, nitrate and nitrite nitrogen, total and orthophosphate	16
77/C	Mineral analysis	Sodium, potassium, calcium, magnesium, chloride, sulphate, fluoride, total alkalinity	16
78/A	Trace metal analysis	(1) Mercury, cadmium, chromium, cobalt, copper, iron, lead, manganese, nickel (2) Zinc, aluminium, arsenic, selenium, beryllium, lithium, strontium, vanadium, barium, silver	14
78/B	Boron, silicon, MBAS, cyanide, phenol, sulphide, BOD, colour and turbidity analyses	Boron, silicon, Methylene Blue active substances, cyanide, phenol, sulphide, biochemical oxygen demand, colour, turbidity	14

ous studies and the statistical evaluation of the results obtained, and summarizes the findings and recommendations arising from these studies.

ORGANIZATION OF THE STUDIES

For an interlaboratory comparison study to produce meaningful results, a number of important

factors must be taken into consideration with regard to the organization of the study.

(1) To be able to evaluate satisfactorily the methods and data and prepare comprehensive written reports on the results, the originator (or co-ordinator) of the study should be well-qualified and experienced in analytical chemistry, especially in water analysis, and

Table 2. Programme of studies (1979-1982)

Study No.	Title	Determinands	No. of participants
79/A	Analysis of a surface water and a sewage effluent	pH, electrical conductivity, colour, turbidity, chemical oxygen demand, Methylene Blue active substances, Kjeldahl, ammonia, nitrate and nitrite nitrogen, total phosphorus, orthophosphate, chloride, sulphate, fluoride, total alkalinity, total filterable residue, silica, boron, cyanide, phenols, calcium, magnesium, potassium, sodium, copper, iron, manganese, zinc, aluminium, mercury	44
79/B	Evaluation of the comparative reliability of the COD determination	Chemical oxygen demand	37
80/A	Analysis of major cations and anions	Calcium, magnesium, potassium, sodium, chloride, sulphate, total alkalinity	47
80/B	Determination of trace metals	Cadmium, chromium, copper, iron, lead, manganese, zinc, arsenic, selenium, mercury	28
80/C	Determination of trace metals in sewage sludge	Aluminium, cadmium, chromium, copper, iron, lead, manganese, nickel, zinc	20
81/A	Nitrogen and phosphorus analysis	Kjeldahl, ammonia, nitrate and nitrite nitrogen, total phosphorus, orthophosphate	45
81/B	Determination of physical properties	pH, electrical conductivity, total residue, colour, turbidity	42
81/C	Determination of chlorinated hydrocarbon pesticides in water	Aldrin, dieldrin, DDD, DDE, DDT, heptachlor, chlordane	7
82/A	Determination of boron, silica, fluoride, MBAS, phenols, cyanide and sulphide	Boron, silica, fluoride, Methylene Blue active substances, phenols, cyanide, sulphide	31
82/B	Analysis of a drinking-water and a mine drainage effluent	pH, electrical conductivity, colour, turbidity, chemical oxygen demand, Kjeldahl, ammonia, nitrate and nitrite nitrogen, total phosphorus, orthophosphate, chloride, sulphate, fluoride, total alkalinity, total filterable residue, silica, calcium, magnesium, potassium, sodium, copper, iron, manganese, zinc, aluminium	40

have a reasonable knowledge of the application of statistics.

(2) The objective of the study should be clearly stated and understood. Clear, concise, unambiguous instructions for performing the study must be issued, along with a suitable form for the recording and return of the required data.

(3) Careful selection, preparation, preservation and packaging of the samples is essential.

(4) Complete co-operation of the participating laboratories in adhering exactly to the instructions supplied must be enlisted.

Samples

More or less similar sample preparation procedures were employed for all the studies involving the analysis of synthetic water samples. These samples were generally prepared by dissolving the calculated amounts of analytical-reagent grade chemicals (or standard metal solutions) in known volumes of demineralized distilled water containing, where applicable, the necessary preservative.¹⁹ In the case of natural water samples, only the required preservative was added. Suitable aliquots of each sample were sent to each participating laboratory.

The samples were contained in either 250-ml or 500-ml polythene bottles, which, prior to addition of the sample solutions, had been treated, along with their plastic caps, as follows.

(1) Soaking for a minimum of 24 hr in a 100-ml/l. Decon cleaning solution, followed by rinsing with demineralized distilled water.

(2) Soaking for a minimum of 24 hr in a 100-ml/l. nitric or hydrochloric acid solution (depending on the constituents in the sample), followed by rinsing with demineralized distilled water.

(3) Rinsing with sample solution.

Instructions

Each laboratory was supplied with a table detailing the constituents to be determined, along with the concentration range of each constituent in the sample. For all studies to date, the participants were allowed complete freedom of choice as to the analytical procedure to be employed. It was also requested that references to or brief details of the method used should be recorded along with the results in the data sheets provided.

A period of one month was generally allowed for analysis of the sample and submission of the results. Complete anonymity was maintained by allocating to each laboratory, at the beginning of each programme of studies, a code number, which was known only to that laboratory and the co-ordinator of the study.

STATISTICAL EVALUATION OF THE RESULTS

On completion of each study, all the results submitted were first examined for the presence of "outliers",

i.e., results which deviate to such a degree from the other results in the same set that they are considered irreconcilable with the other data. Rejection of outliers is often necessary in the evaluation of interlaboratory comparison studies, but considerable care must be exercised, as the treatment of outliers is a somewhat controversial subject. Literature on their detection and rejection is relatively extensive, and includes a wide variety of suggested techniques, for example Dixon's Q -test,^{20,21} Cochran's maximum variance test,²⁰ Grubb's test,²¹ Student's t -test,²¹ coefficient of variance test,²¹ and coefficient of skewness test.²¹

For simplicity and because it is recommended in a standard text on water analysis, the ASTM procedure for outlier rejection²² was selected for application in these studies. In this method, a suspected outlier is tested by calculating its " T value". If the T value is greater than that recorded in a table of critical values for T , the outlier may be rejected:

$$T_n = \frac{(x_n - \bar{x})}{s}$$

where $T_n = T$ for the observation being tested, x_n = individual value being tested, \bar{x} = arithmetic mean of all values in the level containing x_n , s = estimated standard deviation of the set of results.

After the removal of outliers, the mean value of each set of results was then calculated, followed by the determination of simple measures of accuracy (mean error and relative mean error) and precision (standard deviation and coefficient of variation). For certain studies, the 95% confidence limits were also calculated. At this stage, an interim report, showing details of the results and statistical evaluations, was sent to all participants. An example of such a report, taken from study No. 77/B,³ is shown in Table 3.

In almost all the studies involving the analysis of synthetic water samples, two sets of similar samples were sent to each participating laboratory, the sets containing the same constituents but in slightly different concentrations. This was to allow for use of Youden's graphical technique of statistical evaluation.²³ In this technique, a graph is prepared of the results for each constituent determined by each laboratory, the results from one sample being plotted on the x -axis and those from the other on the y -axis. The two scales must be subdivided in the same units. Thus for each laboratory's pair of results, one point is produced, and is indicated by the code number of that laboratory. A horizontal line is then drawn through the mean of the values reported for the first sample and a vertical line through the mean of the values reported for the second sample. These two lines divide the graph into four quadrants (Fig. 1).

Graphical representation of the data in this manner allows interpretation to indicate the overall performance of a laboratory, as well as the types of error

Table 3. Study No. 77/B—summary and statistical evaluation of the results

Determinand	Laboratory number																	True value, mg/l.	Mean value, mg/l.	Mean error, mg/l.	Relative mean error, %	Standard deviation, mg/l.	Coefficient of variation, %	No. of outliers
	1	2	4	5	6	7	8	9	10	11	12	13	14	15	16	17								
Kjeldahl nitrogen	1	26.0	25.5	27.9	—	28.3	24.3	—	23.6	26.2	28.0	29.7	26.2	25.7	31.7	—	—	28.0	26.9	1.1	3.8	2.3	8.5	0
Ammonia	1	16.3	16.0	17.4	—	16.7	15.2	—	15.6	16.4	18.0	19.6	16.2	16.8	22.1	—	—	17.5	16.8	0.7	3.9	1.2	7.2	0
Nitrogen	2	9.7	10.5	10.0	—	11.1	10.2	9.9	7.4	9.5	10.2	10.9	9.0	9.7	11.2	—	—	10.0	10.1	0.1	0.1	1.1	11.2	0
Nitrate	1	12.1	14.5	9.8	—	15.2	12.4	12.2	12.5	12.0	12.4	13.8	10.8	12.6	12.1	12.9	10.5	12.8	12.4	0.4	3.4	1.4	11.0	0
Nitrogen	2	7.4	9.7	7.1	7.6	9.5	7.9	8.4	9.0	7.5	7.8	8.1	7.1	7.9	7.9	7.1	7.0	8.0	7.9	0.1	1.2	0.8	10.5	0
Nitrite	1	2.1	2.2	2.0	2.2	2.0	2.2	1.8	2.0	1.5	1.7	2.1	2.1	1.6	2.0	1.8	1.5	2.0	1.9	0.1	5.0	0.2	12.6	0
Nitrogen	2	1.3	1.5	1.2	1.4	1.4	1.4	1.1	1.4	0.7	1.1	1.3	1.4	1.0	1.1	1.4	1.0	1.2	1.2	0	0	0.2	17.5	0
Total	1	9.5	12.2	9.6	—	9.8	9.1	—	8.7	—	—	—	9.7	8.0	—	—	—	9.6	9.6	0	0	1.2	12.8	0
phosphorus	2	5.2	7.4	6.0	—	6.3	6.3	—	5.6	—	—	—	6.2	4.8	—	—	—	6.0	6.0	0	0	0.8	13.3	0
Ortho-	1	8.4	12.2*	8.0	8.4	8.5	8.7	7.8	7.7	—	8.7	6.9	7.9	8.2	7.6	4.2*	7.0	8.0	8.0	0	0	0.8	7.3	2
phosphate	2	5.2	7.4*	5.0	5.1	5.2	5.1	4.9	4.6	—	5.4	4.5	5.1	5.0	4.7	2.7*	4.0	5.0	4.9	0.1	2.0	0.4	7.6	2

*Outlier.

which may account for poor performance by a particular laboratory. For example (Fig. 1), points lying close to the intersection of the horizontal and vertical lines represent a high degree of accuracy (laboratories 1 and 2), whereas distant points represent poor accuracy (laboratories 3 and 4). Points lying close to one line but far from the other demonstrate inconsistent performance (laboratories 5 and 6). Information on a participating laboratory's precision may also be obtained from the graph. If all participants achieved perfect precision (*i.e.*, no determinate error), but each had its own constant absolute bias, then all the paired points would fall in a 45° line passing through the origin (laboratories 1, 4, 7 and 8). Therefore, the distance of each laboratory's point from this 45° line is indicative of the measure of that laboratory's precision. Still further interpretation is possible for points lying far from the intersection of the horizontal and vertical lines. In theory, due to random or chance factors affecting the results, an equal number of points should fall into each of the four quadrants. In practice, however, this rarely occurs; most graphs of this nature show the majority of points falling in the upper right or lower left quadrants, suggesting that systematic errors consistently produce high or low results. Each quadrant identifies different effects which influence a laboratory's results. In general, results in the upper right or lower left quadrants are indicative of the presence of systematic errors, for example poor instrument calibration, inaccurate standards and/or faulty technique. Results in the upper left or lower right quadrants are inconsistently affected, and may be due to human errors such as those caused by mistakes in the calculation, recording, or reporting of results.²⁴ An actual example of a Youden graph, taken from study No. 77/C,⁴ is shown in Fig. 2.

The results were then statistically assessed according to the method of Greenberg *et al.*,²⁴ viz. (i) results falling between the mean and ± 1 standard deviation are acceptable; (ii) results falling between ± 1 and ± 2 standard deviations are acceptable but questionable; (iii) results outside the limits of ± 2 standard deviations are unacceptable.

An example of such an assessment, taken from study No. 77/B,³ is shown in Table 4.

Finally, the values obtained from the assessment of the results according to Greenberg's method were processed further by means of Madden's "ranking" technique employed by the Oklahoma Water Resources Board in their laboratory certification programme.²⁵ Each laboratory was allocated five points for every result within ± 1 standard deviation of the mean, two points for every result between ± 1 and ± 2 standard deviations, and no points for any result falling outside ± 2 standard deviations. The total number of points gained was then divided by the total number of analyses done, to give a quotient. The maximum quotient possible is 5.0. The laboratories were then ranked in order of the quotient

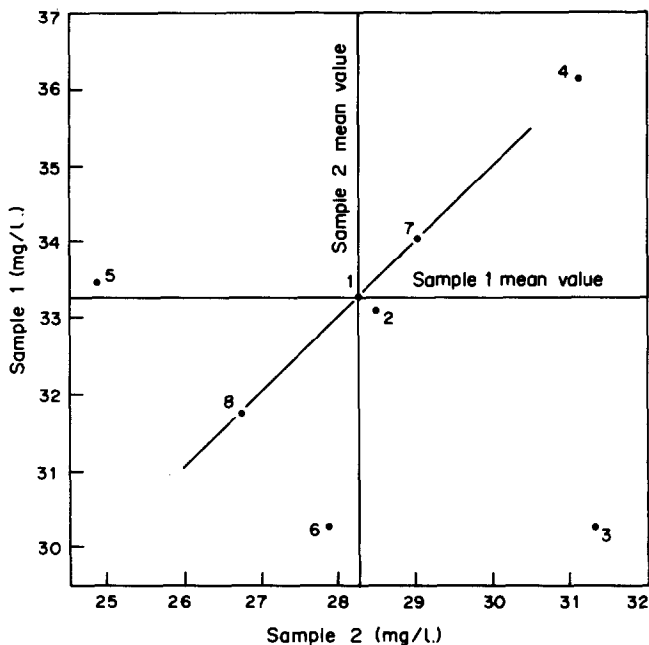


Fig. 1. Example of Youden's graphical technique for result evaluation.²³

obtained. An example of a ranked assessment, again taken from study 77/B,³ is shown in Table 5.

In the Oklahoma laboratory certification programme, if all the determinands available are analysed for by a particular laboratory, and that laboratory obtains a quotient of greater than 2.5, it is certified "A" for unrestricted analysis. If a laboratory analyses for all the available determinands and obtains a quotient of between 2.0 and 2.5 it is certified "R" for restricted analysis. If not all the determinands available are analysed for, and the laboratory obtains a quotient of greater than 2.0, is

also certified "R". If a laboratory obtains a quotient of less than 2.0, it is not given certification, and is regarded as being unable to submit to the Board "data relating to the discharge of industrial water and to natural water quality".²⁵

Quotients obtained by the 16 laboratories participating in the first programme of studies ranged from 2.9 to 4.7, with a mean of 4.0. In the second programme of studies the quotients obtained by the 46 participants ranged from 2.7 to 4.5 with a mean of 3.8. In both studies, therefore, all the laboratories would have qualified for certification in terms of the

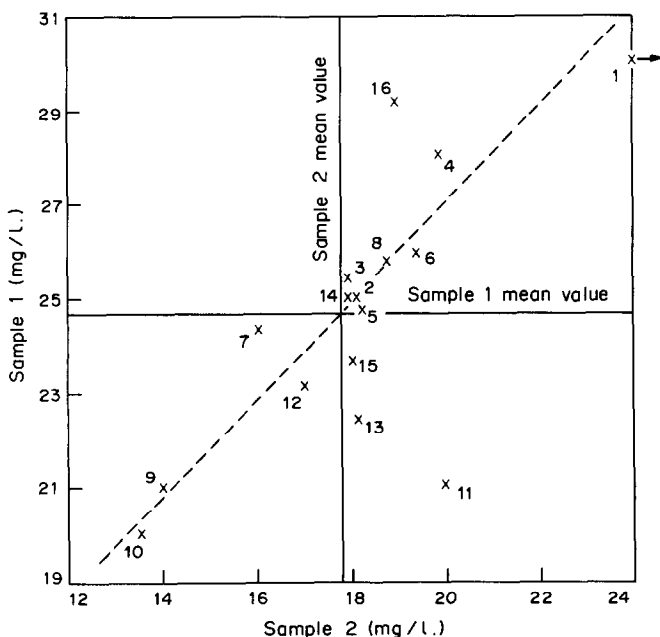


Fig. 2. Youden graph: magnesium results (Study 77/C).

Table 4. Study No. 77/B: statistical assessment of results according to method of Greenberg²⁴

Lab. No.	Kjeldahl N			Ammonia N			Nitrate N			Nitrite N			Total P			Ortho P			Totals		
	a	b	c	a	b	c	a	b	c	a	b	c	a	b	c	a	b	c	a	b	c
1	2	—	—	2	—	—	2	—	—	2	—	—	2	—	—	2	—	—	12	—	—
2	2	—	—	2	—	—	—	1	1	—	2	—	—	1	1	—	—	2	4	4	4
4	2	—	—	2	—	—	1	1	—	2	—	—	2	—	—	2	—	—	11	1	—
5	—	—	—	—	—	—	2	—	—	1	1	—	—	—	—	2	—	—	5	1	—
6	2	—	—	2	—	—	—	2	—	2	—	—	2	—	—	2	—	—	10	2	—
7	—	2	—	2	—	—	2	—	—	1	1	—	2	—	—	1	1	—	8	4	—
8	—	—	—	2	—	—	2	—	—	2	—	—	—	—	2	—	—	8	—	—	
9	1	1	—	—	2	1	1	—	2	—	—	2	—	—	2	—	—	8	2	2	
10	2	—	—	2	—	—	2	—	—	—	1	1	—	—	—	—	—	6	1	1	
11	2	—	—	2	—	—	2	—	—	2	—	—	—	—	—	2	—	8	2	—	
12	—	1	1	2	—	—	2	—	—	2	—	—	—	—	1	1	—	7	2	1	
13	2	—	—	2	—	—	1	1	—	2	—	—	2	—	—	2	—	11	1	—	
14	2	—	—	2	—	—	2	—	—	1	1	—	2	—	—	2	—	9	3	—	
15	—	—	2	2	—	—	2	—	—	2	—	—	—	—	2	—	—	8	—	2	
16	—	—	—	—	—	—	2	—	—	2	—	—	—	—	—	2	—	4	—	2	
Totals	17	4	3	24	0	2	23	6	1	23	6	1	12	3	1	20	4	4	119	23	12

a = Results between mean and ±1 standard deviation.
 b = Results between ±1 and ±2 standard deviations.
 c = Results outside ± standard deviations.

Oklahoma Water Resources Board certification programme.

Other methods exist for ranking interlaboratory comparison-study results, for example, those of Thompson,²⁶ Youden,²⁶ and the National Environmental Research Centre,²⁶ but they are generally rather more complicated than the technique employed in these studies.

Where applicable, precision data obtained in the various studies were compared with those from similar overseas studies (mainly in the U.S.A. and Canada). In general, the comparison was favourable. However, in order to establish arbitrarily whether reasonable precision has been obtained in a particular study, use may be made of an equation derived from a study by Horwitz of the results obtained in

over 150 independent interlaboratory comparison studies.²⁷ The equation relates interlaboratory coefficients of variation with concentration, as follows:

$$CV(\%) = 2^{(1 - 0.5 \log c)}$$

Where CV = coefficient of variation, c = concentration expressed in kg/l.

To be acceptable, the coefficient of variation obtained in the study for a particular concentration should approximate to or be less than the value obtained from the general curve based on this equation (Fig. 3).

In some studies, it was possible to apply "tests of significance" to the results; for example, in cases where two or more methods of analysis were

Table 5. Study No. 77/B: ranked assessment of results according to method of Madden²⁵

Position	Lab. No.	a	b	c	No. of points	No. of analyses	Quotient
1	1	12	0	0	60	12	5.00
1	8	8	0	0	40	8	5.00
3	4	11	1	0	57	12	4.75
3	13	11	1	0	57	12	4.75
5	6	10	2	0	54	12	4.50
5	5	5	1	0	27	6	4.50
7	11	8	2	0	44	10	4.40
8	14	9	3	0	51	12	4.25
9	7	8	4	0	48	12	4.00
9	15	8	0	2	40	10	4.00
9	10	6	1	1	32	8	4.00
12	12	7	2	1	39	10	3.90
13	9	8	2	2	44	12	3.67
14	16	4	0	2	20	6	3.33
15	2	4	4	4	28	12	2.33
Totals		119	23	12	641	154	Average = 4.16

a, b, and c as in Table 4.

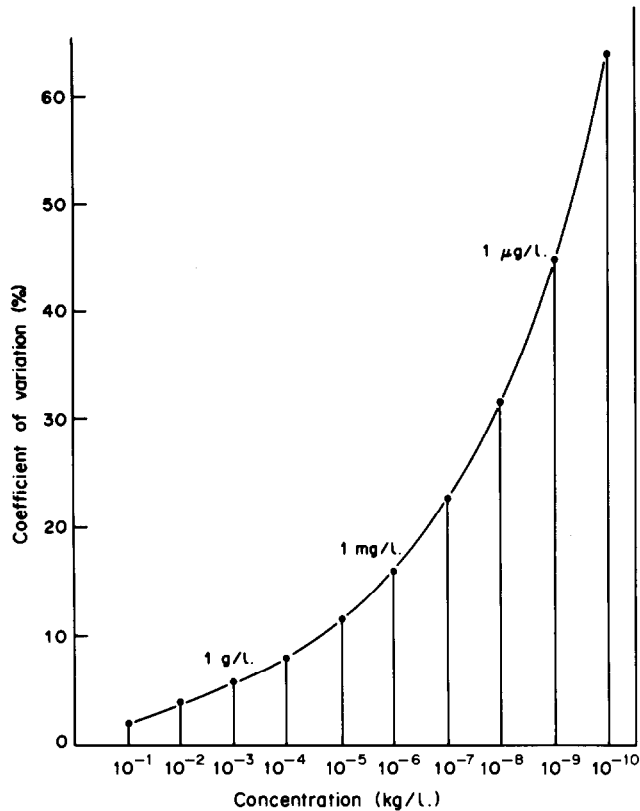


Fig. 3. General curve relating interlaboratory coefficients of variation with concentration.²⁷

sufficiently employed to allow comparison of their accuracy by means of the *t*-test (which determines the significance of differences between the means of two sets of results), and of their precision by means of the *F*-test (which determines the significance of differences between the standard deviations of two sets of results).²⁸

Mention should also be made of one other statistical evaluation technique. In certain studies, particularly those in which the reliability of particular analytical methods is being investigated, an evaluation which combines both the precision and the accuracy in an estimate of a "total error" can be used to judge the acceptability of a method:

$$\text{Total error (\%)} = \frac{(\bar{x} - T) + 2s}{T} \times 100$$

where \bar{x} = arithmetic mean of the results, T = true value, s = estimated standard deviation of the set of results. Methods where the calculated value of the total error is less than 25% are rated as "excellent"; those where the value is greater than 25% but less than 50% are rated "acceptable"; and those where the value exceeds 50% are rated "unacceptable".²⁹

SPECIFIC FINDINGS AND RECOMMENDATIONS

The information on analytical methods gained from the various studies has allowed a fairly comprehensive picture to be built up of the state of water

analysis in southern Africa. It became evident early in the series that many of the laboratories involved in the studies were employing, for many determinands, a wide variety of both standard^{19,22,30} and non-standard methods, as well as outdated standard procedures. The preparation of an updated recognized set of standard methods for the analysis of waters and wastewaters was therefore recommended, and this task has been undertaken by the National Institute for Water Research. In the interim, a list of recommended methods of water analysis, based on those given in the latest editions of *Standard Methods for the Examination of Water and Wastewater*¹⁹ and *Methods for Chemical Analysis of Water and Wastes*³⁰ was drawn up and issued to the participating laboratories, along with a list of recommended sampling and sample-preservation procedures, also given in the same texts.¹⁸ Also included in the list were the recommended SI units and the form in which the concentrations of the various determinands should be reported. The adoption of approved standard methods of analysis, units of concentration, and sample-collection and preservation procedures can significantly improve the reliability and comparability of the results obtained by water-analysis laboratories in southern Africa.

Specific findings and recommendations made during the studies included the following.

- (1) Several laboratories initially submitted results

expressed as "trace", "not detectable", "nil", or "0". Such results are of little value. "Trace" and "not detectable" are practically meaningless unless accompanied by further explanation. Results should not be reported as "nil" or "0", but rather as less than the detection limit of the method used, for example, $< 25 \mu\text{g/l.}$, $< 0.01 \text{ mg/l.}$ ^{8,17}

(2) A wide variety of digestion procedures was used for total Kjeldahl nitrogen and total phosphate determinations, which could result in varying degrees of effectiveness in the digestion process, particularly where significant quantities of organic nitrogen and organic phosphorus compounds were present.^{3,8,13,17}

(3) An examination of total alkalinity results showed that significantly higher values were obtained by laboratories using the indicator titration method than were obtained by laboratories using either the potentiometric titration or automated colorimetric techniques. In the case of laboratories employing the indicator titration method, the most accurate and precise results were obtained by those using the mixed Bromocresol Green/Methyl Red indicator. The high positive bias found could be attributed to the results submitted by laboratories using Methyl Orange as indicator.¹⁰

(4) A few laboratories determined some of the trace metals, as well as boron and silica, by means of inductively-coupled plasma optical-emission spectroscopy. The excellent results obtained are indicative of the value of this new, but as yet relatively expensive, technique for trace element determination.^{12,16,17}

(5) The recommended interference suppressants should be used in the flame atomic-absorption determination of many of the major and trace metals routinely determined in water and wastewater, in particular calcium, magnesium, chromium, iron and manganese.^{4,5,10,11,19,30,31}

(6) The use of similar interference suppressants was also recommended for the determination of metals in sewage sludge, as well as the use of background correction for metals such as cadmium, lead and nickel.¹²

(7) For purposes of standardization and comparison, all electrical conductivity determinations should be done at the standard temperature of 25° ,^{19,30} or, alternatively, the appropriate correction factor should be applied.^{2,8}

(8) Results of turbidity determinations should be reported only in nephelometric turbidity units (NTU) as recommended in the latest standard texts.^{6,8,19,30}

(9) It was observed that several laboratories were still employing manoxol OT as the standard reference material in the determination of Methylene Blue active substances (MBAS). The use of linear alkylate sulphonate (LAS) as the only standard reference material was recommended, as specified in *Standard Methods*,¹⁹ since the detergent industry changed over in 1965 from the use of alkylbenzenesulphonate (ABS) to the more biodegradable LAS.^{6,16,19}

CONCLUSIONS

It is hoped that these programmes of inter-laboratory comparison studies have been of assistance to the participating laboratories in assessing the effectiveness of their analytical procedures and the comparative reliability of the results obtained, and that the foregoing findings and recommendations will make a significant contribution to the achievement of a greater degree of standardization in methodology among water analysis laboratories in southern Africa.

Similar comparison studies, in which any water or wastewater analysis laboratory in southern Africa is welcome to participate, will continue to be conducted at regular intervals. Future studies will also be concerned, *inter alia*, with method comparison and evaluation.

Interlaboratory comparison studies such as those described in this paper can easily be adapted for use by any group of laboratories engaged in the analysis of a given type of material, for example food, pharmaceuticals, toiletries and detergents, soils, minerals, iron and steel, coal, and oil.

Acknowledgements—The assistance and co-operation of the staff of the following laboratories, who regularly participated in the studies, is gratefully acknowledged. Laboratory and Technical Services Branch, City Health Department, Johannesburg; Municipality of Pretoria; Municipality of Cape Town; Municipality of Durban; Municipality of Port Elizabeth; Municipality of Kempton Park; Municipality of Germiston; Municipality of Springs; Municipality of Vereeniging; Municipality of Witbank; Municipality of Rustenburg; Municipality of Pietersburg; Municipality of Pinetown; Municipality of Bloemfontein; Municipality of Bulawayo; Municipality of Harare; Municipality of Windhoek; McLachlan and Lazar (Pty) Ltd., Johannesburg; Anglo-American Corporation of South Africa Ltd., Research Laboratory, Crown Mines; AECI Ltd., Modderfontein; AECI Ltd., Somerset West; AECI Ltd., (Fluid Services), Sasolburg; JCI, Central Laboratory, Knights; JCI, P.F. Retief Laboratory, Bleskop; Iscor, Analytical Laboratory, Pretoria; Escom, Research & Development Laboratory, Johannesburg; Fedmis (Pty) Ltd., Milnerton; Chemical Services (Pty) Ltd., Chloorkop; Blinkpan Koolmyne Bpk., Koorfontein Laboratory, Blinkpan; National Institute for Water Research, Water Quality Division, Pretoria; National Institute for Water Research, Cape Regional Laboratory, Bellville; National Institute for Water Research, Natal Regional Laboratory, Durban; National Institute for Water Research, SWA Regional Laboratory, Windhoek; National Institute for Water Research, Technological Applications Division, Pretoria; National Institute for Water Research, Technological Applications Division, Isipingo, KwaZulu; National Institute for Water Research, Technological Applications Division, Zwelitsha, Ciskei; National Institute for Water Research, Technological Applications Division, Seshego, Lebowa; Health Chemical Services, Department of Health and Social Welfare, Pretoria; Hydrological Research Institute, Department of Environment Affairs, Pretoria; South African Bureau of Standards, Water Division, Pretoria; Rand Water Board, Vereeniging; Divisional Council of the Cape, Cape Town; South African Railways, Pretoria; Lowveld Fisheries Research Station, Marble Hall; Government Analyst's Laboratory, Harare; Directorate of Water Affairs, Windhoek.

This paper is published with the approval of the Chief Director of the National Institute for Water Research.

REFERENCES

1. R. Smith, *Water S.A.*, 1977, 3, 66.
2. *Idem, ibid.*, 1978, 4, 4.
3. *Idem, ibid.*, 1978, 4, 161.
4. *Idem, ibid.*, 1979, 5, 61.
5. *Idem, ibid.*, 1979, 5, 128.
6. *Idem, ibid.*, 1980, 6, 31.
7. *Idem, ibid.*, 1980, 6, 37.
8. *Idem, NIWR Interlaboratory Comparison Study No. 79/A: Analysis of a Surface Water and a Sewage Effluent.* CSIR Research Report 367, Pretoria, 1979.
9. *Idem, NIWR Interlaboratory Comparison Study No. 79/B: Evaluation of the Comparative Reliability of the COD Determination.* CSIR Research Report 368, Pretoria, 1979.
10. *Idem, NIWR Interlaboratory Comparison Study No. 80/A: Analysis of Major Cations and Anions.* CSIR Research Report 379, Pretoria, 1980.
11. *Idem, NIWR Interlaboratory Comparison Study No. 80/B: Determination of Trace Metals.* CSIR Research Report 394, Pretoria, 1981.
12. *Idem, NIWR Interlaboratory Comparison Study No. 80/C: Determination of Trace Metals in Sewage Sludge.* CSIR Research Report 395, Pretoria, 1981.
13. *Idem, NIWR Interlaboratory Comparison Study No. 81/A: Nitrogen and Phosphorus Analysis.* CSIR Research Report 398, Pretoria, 1981.
14. *Idem, NIWR Interlaboratory Comparison Study No. 81/B: Determination of Physical Properties.* CSIR Research Report 571, Pretoria, 1982.
15. R. Smith and A. J. Hassett, *NIWR Interlaboratory Comparison Study No. 81/C: Determination of Chlorinated Hydrocarbon Pesticides in Water.* CSIR Research Report 572, Pretoria, 1982.
16. R. Smith, *NWIR Interlaboratory Comparison Study No. 82/A: Determination of Boron, Silica, Fluoride, MBAS, Phenols, Cyanide and Sulphide.* CSIR Research Report 575, Pretoria, 1982.
17. *Idem, NIWR Interlaboratory Comparison Study No. 82/B: Analysis of a Drinking-Water and Mine Drainage Effluent.* CSIR Research Report 577, Pretoria, 1983.
18. *Idem, NIWR Interlaboratory Comparison Studies Nos. 79/A-82/B: Conclusions.* CSIR Research Report 578, Pretoria, 1983.
19. *Standard Methods for the Examination of Water and Wastewater*, 15th Ed., American Public Health Association, Washington, D.C., 1980.
20. ISO 5725. *Precision of Test Methods—Determination of Repeatability and Reproducibility of Inter-Laboratory Tests*, 1st Ed., International Organization for Standardization, Switzerland, 1981.
21. R. Dybczynski, *Anal. Chim. Acta*, 1980, 117, 53.
22. American Society for Testing and Materials. *Annual Book of ASTM Standards, Part 31—Water*. Philadelphia, Pennsylvania, 1979.
23. W. J. Youden, *Anal. Chem.*, 1960, 32, No. 13, 23A.
24. A. E. Greenberg, N. Moskowitz, B. R. Tamplin and J. Thomas, *J. Am. Wat. Wks. Assoc.*, 1969, 61, 599.
25. M. P. Madden, *Wat. Sewage Wks.*, 1978, February, 70.
26. A. C. Green and R. Naegle, *EPA-600/4-77-031: Development of a System for Conducting Interlaboratory Tests for Water Quality and Effluent Measurements*. U.S. Environmental Protection Agency, Cincinnati, Ohio, 1977.
27. W. Horwitz, *Anal. Chem.*, 1982, 54, 67A.
28. R. J. Lishka and E. F. McFarren, *Water Physics No. 1: Report Number 39*, pp. 144-146. U.S. Environmental Protection Agency, Cincinnati, Ohio, 1971.
29. E. F. McFarren, R. J. Lishka and J. H. Parker, *Anal. Chem.*, 1970, 42, 358.
30. U.S. Environmental Protection Agency, *Methods for Chemical Analysis of Waters and Wastes*. Cincinnati, Ohio, 1979.
31. R. Smith, E. M. Bezuidenhout and A. M. Van Heerden, *Wat. Res.*, 1983, 17, 1483.

SHORT COMMUNICATIONS

EXTRACTION-SPECTROPHOTOMETRIC DETERMINATION OF SMALL AMOUNTS OF BORON IN COPPER METAL AND COPPER-BASE ALLOYS WITH METHYLENE BLUE

ZDENĚK ČÍŽEK and VLASTA ŠTUDLAROVÁ

Central Research Institute, Škoda Co., 316 00 Plzeň, Czechoslovakia

(Received 7 November 1983. Accepted 19 January 1984)

Summary—A sensitive and rapid spectrophotometric method for the determination of small amounts of boron in copper metal and some copper alloys is described. The method is based on the extraction of a BF_4^- -Methylene Blue complex into dichloroethane after decomposition of the sample with hydrogen peroxide and sulphuric acid. The optimum reaction conditions and the influence of alloying elements have been investigated. Boron contents in the range 0.00–0.1% can be determined with a relative error ranging from about 9 to 2%.

Boron is not usually determined in pure copper and copper-base alloys, mainly because it is generally present only as an impurity, though in special cases it may be added to improve some property of the metal, e.g., grain refinement. Hence little attention has been paid to development of methods for the determination. Spectrographic methods are most commonly used for the purpose; the fluorimetric determination based on the boron–2,4-dihydroxybenzophenone complex in sulphuric acid medium¹ and the spectrophotometric method based on the boron–curcumin complex² can also be used.

Here we propose use of the well-known tetrafluoroborate–Methylene Blue method,^{3–11} which has been applied to boron determination in various types of inorganic materials, e.g., steels,^{4,8,9,10,12–17} aluminium,^{18,19} nickel alloys,²⁰ and sediments and rocks.²¹

For the sample decomposition we use hydrogen peroxide and sulphuric acid.^{22,23}

EXPERIMENTAL

Apparatus

Teflon separating funnels (100 ml) were used for extraction.

Reagents

All reagents used were of analytical grade.

Sulphuric acid. Concentrated, and a 2.5M solution.

Hydrogen peroxide, 30%.

Hydrofluoric acid, 5% v/v solution.

Methylene Blue. A 0.002M solution, in water.

1,2-Dichloroethane. Purification by double distillation is recommended.

Standard boron solution, 0.100 mg/ml. Dissolve 0.572 g of boric acid in water and make up to 1000 ml. Before use, dilute to 10 µg/ml.

General procedure

Transfer 0.100 g of sample into a silica (or boron-free glass) tube (about 20 cm long and 1.5 cm internal diameter).

For copper metal samples add 1 ml of 30% hydrogen peroxide and then 0.7 ml of concentrated sulphuric acid. Mix well and let the sample dissolve without application of heat. When the dissolution is complete (ca. 1 min) add 10 ml of water. For alloys containing iron (e.g., brass, bronze) use 1 ml of 30% hydrogen peroxide followed by 2 ml of 2.5M sulphuric acid and warm gently in a water-bath; when the sample has dissolved, add 3 ml of 2.5M sulphuric acid and 5 ml of water. For all samples, next mix thoroughly and heat the tube in a water-bath (90–95°) for about 10 min. After cooling, transfer the contents of the tube into a 100-ml Teflon separating funnel, rinsing the tube with 5 ml of water. Add 5 ml of 5% hydrofluoric acid and mix again. Leave to stand at room temperature for 1 hr. Then add 5 ml of 0.002M Methylene Blue and 25 ml of dichloroethane and shake the funnel vigorously for 1 min. Allow several minutes for the layers to separate, then drain the organic layer into a dry 25-ml beaker. Immediately transfer a 5-ml aliquot into a dry 25-ml standard flask and dilute to the mark with dichloroethane. Mix the contents and measure the absorbance at 660 nm in 5-mm or 1-cm cells against a blank prepared in the same way with boron-free high-purity copper.

Calibration graph

Weigh six 0.100 g portions of boron-free high-purity copper into silica tubes and dissolve them as described in the general procedure. Add 0, 1, 2, 3, 4, 5 ml of the standard 10-µg/ml boron solution and dilute each solution to 10 ml with water. Mix well, heat the tubes in a water-bath (90–95°) for about 10 min, and complete by the procedure described above.

RESULTS AND DISCUSSION

Sample decomposition

Nitrate and chloride interfere particularly strongly in the BF_4^- -Methylene Blue method, mainly by increasing the blank. Therefore decomposition with hydrogen peroxide and sulphuric acid was examined. It was found that the sample dissolved very rapidly if the sulphuric acid was added after the hydrogen

Table 1. Analytical results for synthetically prepared standards

Sample	Boron added, $\mu\text{g/g}$	Boron found, $\mu\text{g/g}$	Relative standard deviation,* %
Pure copper (99.995%)	—	≤ 2	—
	10	9.8	8.6
	250	251	2.8
	500	504	2.4
Copper metal (99%)	—	≤ 2	—
	10	10.4	9.1
	250	246	2.3
ČKD 312† (Sn 0.84%, Sb 0.23%, As 0.023%)	—	≤ 2	—
	20	21	7.6
	250	245	3.1
ČKD 292† (Sn 12.84%, Pb 0.54%, Ni 1.18%)	—	≤ 2	—
	20	21	8.1
	250	243	2.4
	500	493	2.3

*For 5 determinations.

†ČKD = Czechoslovakian standard bronzes.

peroxide to a sample in the form of fine chips. The use of dilute acid for decomposition of copper alloys containing iron is to prevent the fast catalytic decomposition of the hydrogen peroxide. Both decomposition methods are rapid and quantitative and give the proper acidity for the extraction. So far as we can tell, decomposition of any borides is also complete. For accurate determination, the decomposition should be done in silica, boron-free glass, or plastic ware (polyethylene, polypropylene, Teflon). Any residual hydrogen peroxide after heating in the water-bath does not interfere in the formation of the BF_4^- -Methylene Blue complex.

Optimization of the reaction conditions

The extraction of the BF_4^- -Methylene Blue complex into dichloroethane has been studied in detail by a number of authors, so only certain aspects were investigated, *viz.* the formation of tetrafluoroborate in the presence of a large amount of copper(II), and optimization of the conditions for the boron determination.

It is known that the rate of formation of BF_4^- is slow, and the conversion of borate into BF_4^- is therefore the slowest part of the analytical procedure. The reaction can be accelerated by adding iron(III), which has a catalytic effect. However, it was found that in the presence of a large amount of copper(II) the conversion takes only 15 min, and if iron(III) is also present, it does not further increase the reaction rate. If the solution containing fluoride is left for more than 20 hr there is slight loss of boron (4% after 24 hr) by volatilization of boron trifluoride.

The reaction medium (type of acid used, acidity and the concentration of fluoride) has a significant influence on the formation of the BF_4^- complex, and on the extraction of the BF_4^- -Methylene Blue complex, and also on the blank value. The influence of the sulphuric and hydrofluoric acid concentrations and

the volume ratio of the aqueous and organic phases (R) was investigated by factorial experiment. The importance of the three factors decreases in the order $R > c_{\text{HF}} > c_{\text{H}_2\text{SO}_4}$. An increase in R or $c_{\text{H}_2\text{SO}_4}$ ($> 0.5M$) decreases the extraction efficiency; increasing c_{HF} increases the blank value. On the basis of the factorial experimentation, the optimum conditions are those given in the general procedure ($R = 1:1$, $0.5M$ sulphuric acid and 5 ml of 5% hydrofluoric acid used for the conversion). Under these conditions, the sensitivity is twice that for many other methods, the blank value is small and the results have good reproducibility.

Zinc, tin, aluminium, lead, antimony and arsenic do not interfere at concentrations (w/w in the sample) of 30, 15, 10, 4, 1 and 0.1%, respectively. If the tin content is greater than 1%, the metastannic acid precipitate should be filtered off after the sample decomposition; any loss of boron is negligible.

The calibration graph constructed by the method given is not linear and this must be taken into consideration in calculating the boron content if other aliquot volumes of sample solution are chosen.

Accuracy and precision

As standard samples of copper metal with certified boron content are not available, the method was validated by analysing synthetically prepared standard and real samples of copper alloys containing small amounts of boron.

The accuracy and precision established by spiking various types of copper metals and copper-base alloys with known amount of boron after the sample decomposition are summarized in Table 1. Similar precision was found by repeated determination of boron in real samples of copper alloys containing boron (special welding electrodes). The relative standard deviations were 2.3, 4.3 and 9.2% for 0.038,

0.006 and 0.0009% of boron, respectively. The detection limit (defined as three times the standard deviation of the blank) is 0.0002% B.

REFERENCES

1. P. V. Kristalev and M. N. Chelnokova, *Zh. Analit. Khim.*, 1974, **29**, 1650.
2. P. Pakalns, *Analyst*, 1969, **94**, 1130.
3. L. Ducret, *Anal. Chim. Acta*, 1957, **17**, 213.
4. L. Pasztor, J. D. Bode and Q. Fernando, *Anal. Chem.*, 1960, **32**, 277.
5. L. Pasztor and J. D. Bode, *Anal. Chim. Acta*, 1961, **24**, 467.
6. O. B. Skaar, *ibid.*, 1963, **28**, 200.
7. A. Strizovic and J. A. Caldwell, *Analyst*, 1967, **92**, 200.
8. O. Kammori, I. Taguchi and I. Ishiguro, *Bunseki Kagaku*, 1966, **15**, 1316.
9. D. Blazejak-Ditges, *Z. Anal. Chem.*, 1969, **247**, 20.
10. F. Vernon and J. M. Williams, *Anal. Chim. Acta*, 1970, **51**, 533.
11. E. Grallath, P. Tschöpel, G. Kolblin, U. Stix and G. Tölg, *Z. Anal. Chem.*, 1980, **302**, 40.
12. Yu. G. Eremin and P. N. Romanov, *Zavodsk. Lab.*, 1963, **29**, 420.
13. Y. Endo and T. Kurata, *Bunseki Kagaku*, 1965, **14**, 742.
14. K. F. Lüdemann, R. Zimmermann and H. Wemme, *Neue Huetten*, 1966, **11**, 755.
15. J. Mrozinski, *Chem. Anal. (Warsaw)*, 1967, **12**, 93.
16. O. P. Bhargava and W. G. Hines, *Talanta*, 1970, **17**, 61.
17. J. Pietrosz and J. Czyz, *Hutnicke Listy*, 1979, **34**, 658.
18. A. G. Coedo and J. L. J. Seco, *Revta. Metal*, 1968, **4**, 447.
19. R. R. Elton-Bott, *Anal. Chim. Acta*, 1976, **86**, 281.
20. V. I. Klitina and V. F. Bakurova, *Ref. Zh. Khim.*, 1971, 19GD, Abstr., Nr. 23G 182.
21. R. E. Stanton, J. Alison and A. J. McDonald, *Analyst*, 1966, **91**, 775.
22. J. Brinn, *Chemist-Analyst*, 1960, **49**, 117.
23. W. T. Elwell and I. R. Scholes, *Analysis of Copper and its Alloys*, Pergamon Press, Oxford, 1967.

DETERMINATION OF HEXACELSIAN BY INFRARED SPECTROSCOPY

M. CARMEN GUILLEM VILLAR* and CLAUDIO GUILLEM MONZONÍS

Department of Inorganic Chemistry, Faculty of Chemistry, University of Valencia, Valencia, Spain

(Received 30 June 1983. Accepted January 1984)

Summary—Hexacelsian has been determined by infrared spectroscopy with KBr discs and $K_4Fe(CN)_6$ as internal standard. A KBr particle size of $<40\ \mu\text{m}$ gave better homogenization of the sample-KBr mixture than a particle size in the $40\text{--}70\ \mu\text{m}$ range. For determinations of hexacelsian in synthetic samples containing amorphous phase or celsian, calibration curves were constructed. A least-squares fit yielded correlation coefficients of 0.998 and 0.997.

Hexacelsian, the hexagonal modification of barium feldspar ($BaAl_2Si_2O_8$), is thermodynamically stable between 1590 and 1760° , but persists as a metastable phase up to 1590° .¹ On heating of an equimolar mixture of kaolin and barium carbonate^{1,2} the first product of the reaction is an amorphous phase formed between 650 and 950° ; from this amorphous phase hexacelsian crystallizes at about 1000° and finally, at $>1200^\circ$, celsian begins to be formed. Celsian is the monoclinic modification of barium feldspar, stable up to 1590° .

Hexacelsian has a sheet-like structure³ consisting of SiO_4 and AlO_4 tetrahedra which form a double sheet parallel to the (0001) plane, with hexagonal symmetry. Barium atoms occupy positions between such double sheets, with a co-ordination number of 12, holding the sheets together. Hexacelsian has a perfect cleavage parallel to the (0001) plane, where the double sheets with residual negative charges (due to replacement of Si by Al) are matched by Ba^{2+} ions. Accordingly, it shows a high tendency towards a preferred orientation when examined by X-ray diffraction. For this reason, the X-ray diffraction technique cannot be applied to the determination of hexacelsian. In this work, a method for determining hexacelsian by infrared spectroscopy is described.

EXPERIMENTAL

Standards of the phases found in a sample containing hexacelsian obtained by synthesis were prepared, *i.e.*, the pure amorphous, hexacelsian and celsian phases. These pure phases were obtained from a standard equimolar mixture of kaolin and barium carbonate. The following raw materials were used: barium carbonate, analytical-reagent grade; kaolin, particle size $<2\ \mu\text{m}$ (from Lage, Spain), with the following chemical composition (in %): SiO_2 , 45.7; Al_2O_3 , 38.3; Fe_2O_3 , 0.2; CaO , 0.2; MgO , 0.1; Na_2O , 0.1; K_2O , 0.1; weight loss at 1100° , 14.5.

The pure amorphous phase, hexacelsian and celsian were prepared by heating this mixture for 24 hr at 800 , 1020 and 1350° , respectively.

In order to select the key band for determination of hexacelsian, infrared spectra of the three pure phases were obtained (Figs. 1-3). The strong band at about $1220\ \text{cm}^{-1}$ produced by hexacelsian suffers minimum interference from other bands and was therefore selected for hexacelsian determination.

The potassium bromide disc method⁴⁻⁸ was employed. The use of an internal standard eliminates the need for determination of sample thickness and makes preparation of the calibration graph easier. The strong, sharp band of potassium ferrocyanide at about $2100\ \text{cm}^{-1}$ was used for this purpose.

Sample treatment

Sample particle size has a marked effect on absorbance in infrared spectrometry.^{9,10} To standardize the particle size distribution, the samples were ground by hand for 5 min in a porcelain mortar and then sieved with a $40\text{-}\mu\text{m}$ mesh sieve. Then about 10 mg of the fraction passing the sieve was placed in a small agate mortar, 5 drops of absolute ethanol were added, and the mixture was ground until just dry. This wet grinding was repeated twice more.

Sample and internal standard concentration

To minimize the relative error the absorbance should be in the range 0.2-0.8. Tests were made with different proportions of standard hexacelsian to potassium bromide to find the minimum and maximum proportions corresponding to this absorbance range. The same was done with the potassium ferrocyanide. The amount of KBr used for making a disc was also varied between 50 and 100 mg.

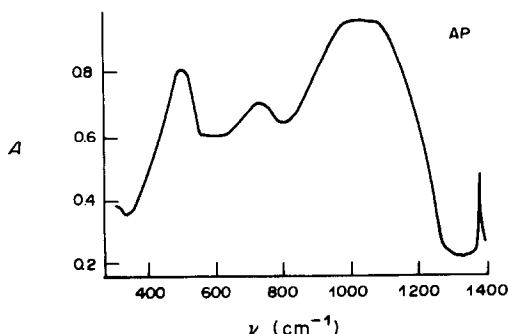


Fig. 1. Infrared spectrum of amorphous phase.

*To whom all correspondence should be addressed at:
Departamento de Química Inorgánica, Facultad de
Ciencias Químicas, Dr. Moliner, 50, Burjasot, Valencia,
Spain.

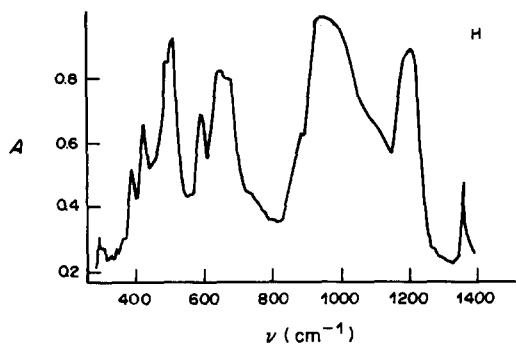


Fig. 2. Infrared spectrum of hexacelsian.

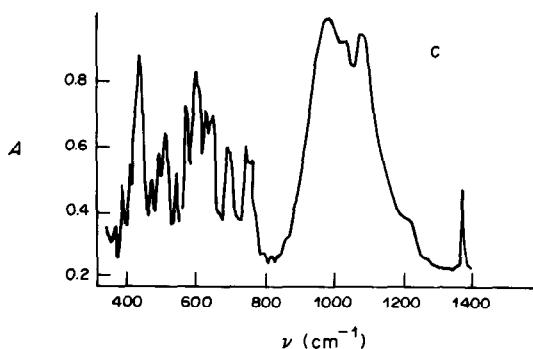


Fig. 3. Infrared spectrum of celsian.

Use of a mixture of 2 mg of sample and 0.6 mg of potassium ferrocyanide per 100 mg of potassium bromide, and of about 50 mg of mixture per disc was found to be the most suitable combination, because it gives an absorbance in the optimum range, and mixing is easy.

Analytical grade potassium bromide and potassium ferrocyanide were used. The latter was ground in the same way as the samples and then dried at 100°.

Previous experiments showed that a difference between particle sizes of matrix and sample affected the absorbance values measured. On the basis of these results, a potassium bromide fraction having particle size $< 40 \mu\text{m}$ was used, and was heated at 450° for the time required to remove all residual water. This was monitored by means of the infrared spectrum and it was found that heating for 10 hr was sufficient for the water content to become negligible. The mixture was thoroughly homogenized with absolute ethanol in a planetary type ball mill for 1 hr.

Preparation of discs

About 100 mg of sample-matrix mixture was homogenized in a small agate mortar for 30 min. About 50 mg of this mixture was pressed into a disc 13 mm in diameter. The force on the plunger was 9.5 tons, maintained for 2 min. Two discs were prepared and two values of absorbance measured, the difference indicating the degree of homogenization.

Operating conditions

Measurements were made with a Pye Unicam IR-SP 2000 double-beam spectrophotometer in the range 1000–1400 cm^{-1} for hexacelsian and 1800–2400 cm^{-1} for the internal standard. Spectra were recorded with a linear absorbance scale, so a reproducible zero setting was achieved and the absorbance could be measured directly on the spectrum. Normal slit-width, a scanning speed of 95 $\text{cm}^{-1}/\text{min}$ and a time constant of 10 sec were selected.

The absorbance was measured from the band maximum to a base-line drawn tangentially to the spectrometer tracing, at 1215 cm^{-1} for hexacelsian and 2060 cm^{-1} for the internal standard.

Calibration graphs

Samples containing hexacelsian can also contain either amorphous phase or celsian. Calibration graphs for both types were obtained by use of standard mixtures of the pure phases: amorphous phase-hexacelsian and celsian-hexacelsian. About 100-mg quantities of standards containing 10, 20, 30, 40, 50, 60, 70, 80 and 90% of hexacelsian were prepared. They were mixed by grinding in a small agate mortar, first in the dry form for 30 min and then (three times) to dryness after addition of 0.5 ml of absolute ethanol.

By the procedure described above, two discs of each calibration sample were prepared. On the corresponding infrared spectra, the absorbances at the wavenumber for the hexacelsian maximum, A_H , and that for the ferrocyanide standard, A_S , were measured. The ratio, A_H/A_S , for each disc, and the average ratio for each sample, $\overline{A_H/A_S}$, were calculated. The two calibration curves were constructed by plotting $(\overline{A_H/A_S})$ vs. concentration of hexacelsian (H) expressed as mg of H per 100 mg of KBr. The linearity of both plots shows that the Beer-Lambert law is obeyed. Least-squares analysis yielded correlation coefficients of 0.998 for samples containing amorphous phase and 0.997 for those containing celsian.

Points corresponding to samples containing low percentages of hexacelsian are not used because the broad intense absorption band, either of amorphous phase or of celsian, near the analytical band, interferes by its effect on the base-line on the low wavenumber side. The highest interference is observed in samples containing hexacelsian and amorphous phase, because the band of the amorphous phase overlaps the analytical band to a greater extent than the band of celsian does.

RESULTS AND DISCUSSION

The method of quantitative analysis described in this paper has been applied to samples obtained by heating equimolar mixtures of kaolin and barium carbonate at temperatures from 900 to 1200° for 6 hr,¹¹ and also to the kinetic study of hexacelsian formation and the hexacelsian \rightarrow celsian phase transition.¹²

In the analysis of samples, A_H and A_S were measured and the A_H/A_S ratio was calculated for each disc. The least-squares fitting of the $\overline{A_H/A_S}$ values and mg of H per 100 mg of KBr for the calibration standards was made by a computational program that also handled the measured A_H/A_S values for the test samples (obtained in the same measurement session) to output the mg of H per 100 mg of KBr ratios for the samples. The mg of sample per 100 mg of KBr ratio was known from the quantities used in preparing the discs. The ratio of the hexacelsian content of the unknown samples (mg of H/100 mg of KBr) to the weighed amount of these samples (mg of sample/100 mg of KBr) gave the hexacelsian/sample weight ratio. This proportion, compared with the theoretical value calculated from the reaction equation, assuming a maximum yield of 100%, gave the degree of conversion. For each sample, the average of

the values for the two discs was taken. This allowed the rate of formation of hexacelsian from the amorphous phase to be found, and also the extent of conversion of hexacelsian into celsian, when the samples analysed had been heated in the temperature range in which this transition took place.

To study the reproducibility, twelve pellets of an equimolar mixture of kaolin and barium carbonate were heated, all at the same time, at 1000° for 6 hr. From ten of them the corresponding individual sample-matrix mixtures were prepared. From each of the other two, eight sample-matrix mixtures were prepared. The standard deviations obtained in the analyses were 1.6% hexacelsian for the 10 separate samples identically synthesized, 1.3% hexacelsian for the 8 mixtures of one sample, and 1.4% for the 8 mixtures of the other sample. The standard deviations were also calculated for the duplicate discs obtained from each sample-matrix mixture. The average value for these standard deviations was 0.8% hexacelsian.

CONCLUSIONS

A particle size of <40 μm should be used, because it gives better homogenization than the 40–70 μm size range recommended earlier. The results obtained show the importance of using, for the calibration samples, a matrix as similar as possible to that present in the samples to be analysed, because of the partial overlap of the spectral bands of matrix and analyte.

The method has the advantages of small sample size, easy handling and reproducibility of sample preparation. It provides a method of analysis for those cases, such as hexacelsian, where the X-ray

diffraction technique cannot be applied. Although the method has been described for the specific case of samples obtained by synthesis and which can therefore contain amorphous phase or celsian, the method can be applied to any sample containing hexacelsian. Furthermore, the lower limits to the determination of hexacelsian in the presence of amorphous phase (>30%) or of celsian (>15%) are reduced where these two phases are not present. In order to apply the method to other samples the effect of the matrix must be taken into account, and if the hexacelsian content is <10% then the sample size must be increased above the 2 mg per 100 mg of KBr recommended here.

REFERENCES

1. M. C. Guillem Villar, C. Guillem and V. Lambies, *Bol. Soc. Esp. Ceram. Vidrio*, 1982, **21**, 239.
2. M. C. Guillem Villar, C. Guillem and J. Alarcón, *Trans. Br. Ceram. Soc.*, 1983, **82**, 69.
3. B. Yoshiki and K. Matsumoto, *J. Am. Ceram. Soc.*, 1951, **34**, 283.
4. C. N. R. Rao, *Chemical Applications of Infrared Spectroscopy*, pp. 62, 533, 585. Academic Press, New York, 1963.
5. M. Avram and Gh. D. Mateescu, *Spectroscopie Infrarouge*, pp. 159, 174. Dunod, Paris, 1970.
6. A. L. Smith, *Applied Infrared Spectroscopy: Fundamentals, Techniques and Analytical Problem-Solving*, p. 77. Wiley, New York, 1979.
7. J. J. Kirkland, *Anal. Chem.*, 1955, **27**, 1537.
8. *Idem, ibid.*, 1957, **29**, 1127.
9. W. M. Tuddenham and R. J. P. Lyon, *ibid.*, 1960, **32**, 1630.
10. V. C. Farmer and J. D. Russell, *Spectrochim. Acta*, 1966, **22**, 389.
11. M. C. Guillem Villar, C. Guillem and P. Escribano, *Trans. Br. Ceram. Soc.*, 1983, **82**, 197.
12. M. C. Guillem Villar, *Doctoral Thesis*, University of Valencia, Spain, 1982.

UREA AS THE BASIC COMPONENT IN PYRIDINE-FREE KARL FISCHER REAGENT

M. Bos

Department of Chemical Technology, Technical University Twente, P.O. Box 217, 7500 AE Enschede,
The Netherlands

(Received 6 December 1983. Accepted 18 January 1984)

Summary—A solution of urea, sulphur dioxide and sodium salicylate in methanol is proposed as the solvent in the Karl Fischer titration, with a separate iodine solution as titrant. Comparison of the performance of this solvent with that of some commercial reagents shows that it has distinct advantages for use with amine samples.

Since the elucidation of the reaction mechanism of the Karl Fischer titration by Verhoef and Barendrecht,^{1,2} a number of compounds have been proposed to replace the pyridine in the classical reagent, viz. sodium acetate,³ diethanolamine⁴ and imidazole.⁵ These components serve, as the pyridine did, to buffer the titration medium at a pH-value that ensures a convenient overall titration rate and a stable end-point. Other criteria that determine the usefulness of the reagents are the long-term stability of the solution and the number of classes of compound for which the water determination can be done without problems.

The goal of the investigation described here was the preparation of a new reagent that—just like the original pyridine-containing reagent—would have its buffering action in a more acidic range than that of the reagents mentioned above.

EXPERIMENTAL

Reagents

The following substances were used as received: urea (puriss. p.a.), triethanolamine (puriss. p.a.) and imidazole (purum) from Fluka, sodium salicylate (zur Analyse) from Merck, triethylamine (puriss.) from Koch-Light, salicylic

acid from ACF, sulphur dioxide from Matheson, and the sodium salt of benzenesulphonic acid from Janssen. The methanol used to prepare the Karl Fischer solvents was reagent grade from Baker, and dried with 3A molecular sieve (Union Carbide) for 24 hr before use. The lithium chloride (Merck, Suprapur) was dried for 24 hr at 150°.

The commercial Karl Fischer solvents used were Karl Fischer Lösung A (Merck, Pyridin Schwefeldioxid Lösung), Karl Fischer Lösungsmittel Pyridinfrei (Merck) and Hydranal solvent (Riedel-de Haën).

Apparatus

The titrations were done with Radiometer Karl Fischer titration equipment consisting of the Karl Fischer titration assembly TT-A1-KF, titrator TTT11b and mV/pH-meter PHM28. The pH of the titration medium was measured with a Knick pH-meter, type PH60, and an Ingold combined glass/reference electrode, type 405, of which the reference electrode compartment was filled with a saturated solution of lithium chloride in methanol. The electrode was calibrated with methanolic solutions of salicylic acid and sodium salicylate as described by Bos and Lengton.⁶

Procedure

The titration procedure is based on the separate titrant/solvent-reagent system and was performed as follows. The titration vessel was filled with 20 ml of the reagent under study (SO₂/base/methanol) and pretitrated with the iodine/methanol titrant to a preset end-point (300 mV) with

Table 1. The amount of water that can be titrated in 20 ml of reagent, and the resulting pH-change

Reagent	pH-change	Water capacity, mg
Karl Fischer (Verhoef)	5.0-2.1	55
Hydranal (Riedel-de Haën)	5.6-2.6	130
Karl Fischer Lösung A (Merck)	4.2-1.2	250
1M Imidazole/ 0.5M SO ₂ /MeOH	6.7-4.7	100
1.5M Urea/1.5M SO ₂ / 0.5M Na salicylate/MeOH	1.6-0.9	140
0.5M Urea/0.5M Na benzenesulphonic acid/ 1M SO ₂ /MeOH	2.1-0.9	90
0.5M Triethylamine/ 0.5M triethanolamine/ 1M SO ₂ /MeOH	9.0-7.0	110

Table 2. Long-term stability of Karl Fischer solvent with composition 1.5M urea/0.5M Na salicylate/1.5M SO₂/MeOH

Storage time, weeks	Water content of 20 ml of solvent, mg
—	4.63
1	4.64
2	4.63
3	4.65
4	4.70
5	4.82
6	4.91
7	5.03
8	5.25
9	5.39

Table 3. Titration speed and pH-change for the titration of 100 mg of water in 20 ml of urea/Na salicylate/SO₂/methanol reagent

[Urea], M	[Salicylate], M	[SO ₂], M	pH-change	Titration time, min
1.0	0.5	1.0	1.8–0.9	10.0
1.2	0.5	1.0	1.7–1.0	8.5
1.4	0.5	1.0	1.7–1.0	7.0
1.6	0.5	1.0	1.8–1.0	6.0
1.8	0.5	1.0	1.9–1.0	5.5
2.0	0.5	1.0	1.9–1.0	5.0
1.4	0.5	1.5	1.6–1.3	7.5
1.6	0.5	1.75	1.6–1.3	5.0
1.8	0.5	2.0	1.7–1.3	4.0
2.0	0.5	2.25	1.7–1.3	3.8

Table 4. Comparison of 1.5M urea/0.5M Na salicylate/1.5M SO₂/MeOH with commercial Karl Fischer solvents

Sample	H ₂ O found, % remarks		
	Hydranal	KF Lösungsmittel pyridinfrei (Merck)	Urea/Na salicylate/SO ₂ /MeOH
Na tartrate.2H ₂ O 2aq.	15.65 precipitate when >250 mg sample added	15.64	15.64
acetone	no results, owing to ketal formation	no results, owing to ketal formation	no results, owing to ketal formation
methyl acetate	0.0597	0.060	0.0585
ethanol	0.0718	0.0720	0.0719
acetic acid	0.0593 dragging end-point with increasing number of samples	0.0643 dragging end-point with increasing number of samples	0.0665 dragging end-point with increasing number of samples
chloroform	0.00989 large variations in results	0.0100 no problems	0.0107 no problems
diethyl ether	0.0424 accurate results after 3 samples	0.0441 first determination inaccurate	0.0474 first determination inaccurate
dimethylformamide	0.0343 solvents turns dark	0.0359 solvent turns dark	0.0346 slight darkening
petroleum ether	no results, owing to precipitation	no results, owing to precipitation	0.00903 precipitation only after 4 g of sample added
n-butylamine	no results strongly dragging end-point	2.30 dragging end-point	2.29 stable end-point
n-dibutylamine	0.619 inaccurate, dragging end-point	0.462 first determination inaccurate, somewhat dragging end-point	0.451 no problems
tributylamine	0.166 inaccurate, dragging end-point	0.115 dragging end-point	0.105 no problems
quinoline	0.160	0.151	0.148
benzylamine	1.30 inaccurate, dragging end-point	1.20 no problems	1.21 no problems

the bipotentiometric detection system, operated with a fixed current in the range 2–3 μ A. The value of 300 mV should persist for at least 20 sec. After this pretitration the water-containing sample was introduced into the titration vessel and the titrator was started again.

The short-term stability of the reagent was checked by measuring the iodine titrant consumption after the stop criterion of the titration was met, by continuing the titration in the "no stop mode". The iodine/methanol reagent was standardized against weighed samples of pure water. The long-term stability of the reagent was checked by periodically measuring the amount of iodine titrant consumed in the pretitrations.

RESULTS

Table 1 shows the amount of water that can be titrated in 20 ml of solvents of various compositions, together with the change in pH that accompanies the process.

A solvent with the composition 1M urea/1M SO₂/methanol gave inaccurate results because the reaction proceeded very slowly, and was not studied any further.

As can be seen, the urea/sodium salicylate/SO₂/methanol mixture is the most acidic of the reagents tested and the only one that shows overlap in pH-range on the acidic side with the classical pyridine/SO₂/methanol reagent as manufactured by Merck. The amount of water that can be titrated in 20 ml of this reagent compares favourably with that for the commercial products not containing pyridine.

The urea/sodium salicylate/SO₂/methanol mixture was investigated somewhat further with regard to its stability on storage (Table 2) and with regard to the influence of the concentrations of its constituents on the speed of the titration (Table 3).

Table 2 shows that the stability on storage is rather good. No significant increase in the water content of the reagent was observed during the first 4 weeks of storage at room temperature, and only a minor increase after that period.

From Table 3 it can be seen that an increase in the concentrations of urea and sulphur dioxide considerably speeds up the titration of 100 mg of water. At concentrations of urea and sulphur dioxide above 1.5M the gain in titration speed levels off. This composition seemed a good compromise between reagent cost and titration speed and was compared with two commercial products in the consecutive titration of a number of actual samples of different chemical classes (Table 4). All titrations were performed with 20 ml of reagent as solvent. The sample size varied between 1 and 4 g, depending on the water content. For the entries marked "no problems" in Table 4, the reproducibility was better than $\pm 1\%$.

In general the results obtained with the urea-containing reagent are comparable with those obtained with the commercial reagents. However, for the amine samples there is a significant difference; these can only be titrated successfully in the urea-containing reagent. It is likely that this is due to the more acidic nature of this reagent. The effect of varying the sodium salicylate concentration was not examined, since the 0.5M concentration initially used seemed suitable enough.

Acknowledgements—The author wishes to acknowledge the co-operation and financial support of J. T. Baker Chemicals B.V. in this investigation and expresses his thanks to R. Groot Rouwen and W. Lengton for performing the experimental work.

REFERENCES

1. J. C. Verhoef and E. Barendrecht, *J. Electroanal. Chem.*, 1976, **71**, 305.
2. *Idem, ibid.*, 1977, **75**, 705.
3. J. C. Verhoef, *Mechanism and Reaction Rate of the Karl Fischer Titration Reaction*, Dissertation, University of Amsterdam, 1977.
4. E. Scholtz, *Z. Anal. Chem.*, 1981, **309**, 30.
5. *Idem, ibid.*, 1982, **312**, 462.
6. M. Bos and W. Lengton, *Anal. Chim. Acta*, 1973, **76**, 149.

DETERMINATION OF TRACE WATER IN ORGANIC SOLVENTS BY A SPECTROFLUORIMETRIC METHOD

CI YUNXIANG and JIA XIN

Department of Chemistry, Peking University, Beijing, People's Republic of China

(Received 7 September 1983. Accepted 6 December 1983)

Summary—A new method for the spectrofluorimetric determination of water in organic solvents has been developed. It is based on formation of the exciplex of pyridoxal with water. The procedure is sensitive, reproducible and useful for the determination of trace water in cyclohexane, petroleum ether, benzene, carbon tetrachloride, diethyl ether, tetrahydrofuran, dioxan, *etc.* The solubility of water in benzene at various temperatures has been determined.

Many methods have been developed for determination of water in organic solvents. The early methods¹⁻⁴ suffered from certain limitations and lack of precision and accuracy. The modern methods, such as the isotope-dilution method,⁵⁻⁷ the infrared difference-spectroscopy method⁸ and chromatography,^{9,10} have greatly increased the accuracy, and the results obtained by different methods have become more and more consistent. These methods involve some quite complicated procedures, however, which limits their application. The widely used Karl Fischer method has certain shortcomings in trace analysis. In order to extend the work in this area, a new spectrofluorimetric method has been developed for the determination of trace water in organic solvents, and is presented here. It is based on the formation of an exciplex¹¹ between pyridoxal and water. The method is characterized by its simplicity, sensitivity and accuracy. Representative solvents examined include cyclohexane, petroleum ether, benzene, carbon tetrachloride, diethyl ether, tetrahydrofuran, dioxan, ethanol and methanol. The solubility of water in benzene at various temperatures has been determined.

EXPERIMENTAL

Reagents

The organic solvents used were preliminarily treated by addition of a molecular sieve, shaking for 3 hr in a vibrator and standing for about 2 weeks. The pyridoxal (PL) solution ($5 \times 10^{-3}M$) was prepared by dissolving pyridoxal hydrochloride in methanol. A standard solution of water was prepared by adding redistilled water to the dried solvent

with a miniature injector. All reagents were of analytical grade.

Procedure

To 4.75 ml of organic solvent containing water add 0.25 ml of pyridoxal solution in methanol, and mix thoroughly. Let stand for 30 min at room temperature, then measure in a 1-cm quartz cell with a suitable spectrofluorimeter.

RESULTS AND DISCUSSION

Excitation and emission spectra

Pyridoxal has an excitation maximum at about 305 ± 5 nm and an emission maximum at 330 nm. When trace water is present in the solvent, a new maximum may appear at 385 ± 5 nm in the emission spectrum and show a small bathochromic shift with increase in the solvent polarity, except for dioxan and diethyl ether (Table 1).

Figure 1 shows the excitation and emission spectra for tetrahydrofuran (THF) medium. The new emission band at 385 nm was considerably enhanced by increase in the amount of water, and the fluorescence intensity of pyridoxal at 330 nm was decreased.

In the case of carbon tetrachloride, however, no new emission band appeared when water was introduced and only the decrease in fluorescence intensity at 330 nm was observed.

It appears that the new emission band results from the interaction of pyridoxal and water, presumably to form an exciplex, $[PL \cdot H_2O]^*$.

Table 1. Maximum emission wavelength in PL-H₂O-solvent systems

Solvent*	1	2	3	4	5	6	7	8
Dielectric constant (20°)	2.023	2.284	—	7.58	2.209	4.34	24.30	32.63
λ_{max} , nm	380	380	385	385	390	390	390	390

*1, cyclohexane; 2, benzene; 3, petroleum ether; 4, tetrahydrofuran; 5, dioxan; 6, diethyl ether; 7, ethanol; 8, methanol.

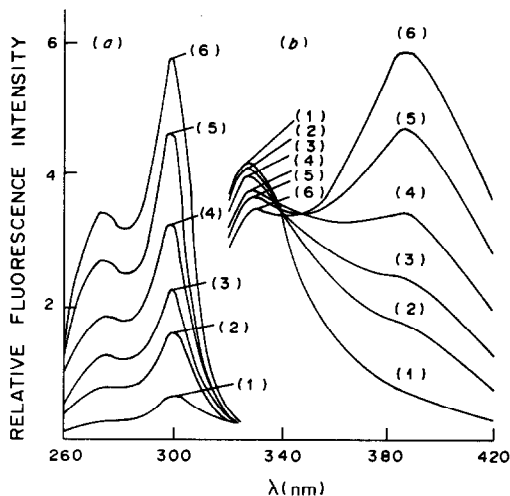


Fig. 1. Excitation (a) and emission (b) spectra of PL-H₂O-THF. Water concentration, % v/v: (1) 0; (2)–(6) 0.05%–1.00%; C_{PL} : $2.5 \times 10^{-4}M$.

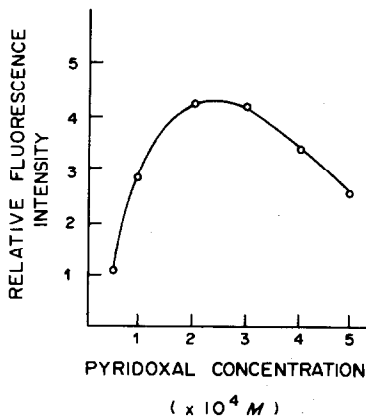


Fig. 2. Effect of pyridoxal concentration.

Effect of pyridoxal concentration

The pyridoxal concentration affects the fluorescence intensity. Figure 2 shows that for maximum fluorescence intensity a pyridoxal concentration of 2.0 – $3.0 \times 10^{-4}M$ is optimal.

Pyridoxal has very low solubility in non-polar organic solvents, and it is necessary to add a small amount of methanol or ethanol to ensure dissolution of the pyridoxal added. Nevertheless, the amount of methanol should not be too large, or it will decrease the sensitivity for the determination of water.

Table 2. Relative fluorescence intensity (RFI,%) of response of PL-H₂O-solvent

Solvent*	1	2	3	4	5	6	7	8
RFI, %	100	98	73	26	18	10	5	1

*1, cyclohexane; 2, petroleum ether; 3, benzene; 4, diethyl ether; 5, tetrahydrofuran; 6, dioxan; 7, ethanol; 8, methanol.

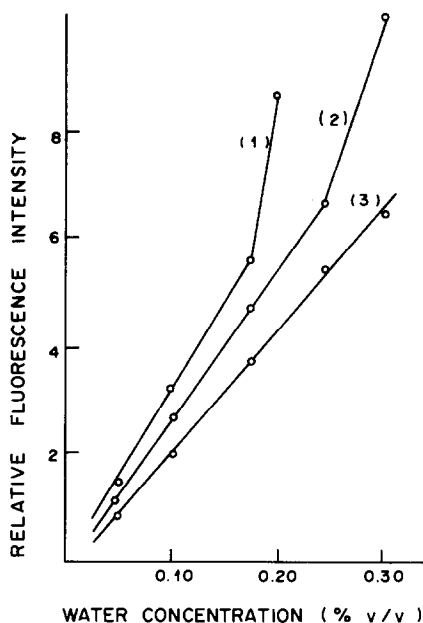


Fig. 3. Effect of pyridoxal concentration in benzene, C_{PL} : (1) $2.5 \times 10^{-4}M$; (2) $3.5 \times 10^{-4}M$; (3) $4.5 \times 10^{-4}M$.

Equilibration time

It takes only 30 min from the addition of pyridoxal for the fluorescence spectra to become stable, and there is then no change in excitation and emission spectra or fluorescence intensity for at least 24 hr, at room temperature.

Calibration graph

The calibration graphs based on the fluorescence at 385 ± 5 nm are linear, but the sensitivity (slope) depends on the solvent, and decreases in the order:

cyclohexane > petroleum ether > benzene
> diethyl ether > tetrahydrofuran
> dioxan > ethanol > methanol

When the pyridoxal concentration is $2.5 \times 10^{-4}M$, the relative sensitivities are given in Table 2.

It can be seen from Table 2 that the sensitivity in aliphatic hydrocarbons is much higher than that in

Table 3. The solubility of water in benzene (ppm, w/w)

$T, ^\circ C$	20	25	30	35	40	45
(1)	608	723	859	1011	1164	—
(2)	600	745	847	951	—	—
(3)	637	739	859	1021	1178	1334*
(4)	616	727	871	1043	1252	—
(5)	607	719	847	1003	1131	1342
n	4	4	4	5	4	5
RSD, %	± 2	± 3	± 2	± 1	± 4	± 4

(1) AgClO₄ method; (2) isotope-dilution method; (3) infrared difference-spectroscopy method; (4) gas chromatography method; (5) present method; n = number of determinations.

*This value was measured at 43.78° .

benzene, ether and alcohols, which is in keeping with the order of solubility of water in these solvents. In other words, the higher the solubility of water, the lower the fluorescence sensitivity. For instance, the lowest limit of determination of water is 10 ppm (v/v) in cyclohexane, 20 ppm in benzene, 500 ppm in methanol and so on.

The linearity was examined up to water concentrations (% v/v) of 0.06, 0.04, 0.15, 0.20, 1.0, 1.0, 2.0, 2.0 respectively for the eight solvents listed in Table 2. In the case of carbon tetrachloride, the decrease in fluorescence intensity of pyridoxal at 330 nm may be used to determine the water content.

The pyridoxal concentration affects the range of linearity: the larger the concentration of pyridoxal, the wider the linear range for water (Fig. 3).

Determination of solubility of water in benzene

As an application of this method, the solubility of

water in benzene at various temperatures was determined. Table 3 shows the results and the values reported in the literature.⁹

REFERENCES

1. C. W. Clifford, *Ind. Eng. Chem.*, 1921, **13**, 631.
2. E. Hill, *J. Am. Chem. Soc.*, 1923, **45**, 1143.
3. C. K. Rosenbaum and J. H. Walton, *ibid.*, 1930, **52**, 3568.
4. L. A. K. Staveley, J. H. E. Jeffers and J. A. E. Moy, *Trans. Faraday Soc.*, 1943, **39**, 5.
5. G. G. Joris and H. S. Taylor, *J. Chem. Phys.*, 1948, **16**, 45.
6. J. R. Jones and C. B. Monk, *J. Chem. Soc.*, 1963, 2633.
7. J. W. Roddy and C. F. Coleman, *Talanta*, 1968, **15**, 1281.
8. D. C. Moule and W. M. Thurston, *Can. J. Chem.*, 1966, **44**, 1361.
9. Wang Weitong and Wu Xinjie, *Fenxi Hauxue*, 1980, **1**, 80.
10. Wu Xinjie, *ibid.*, 1982, **5**, 288.
11. R. Foster, *Molecular Association*, Vol. 2, Chap. 5. Academic Press, London, 1979.

ANALYTICAL DATA

THE pK_a VALUES OF THE CONJUGATE ACID OF IMIDAZOLE IN WATER-ETHANOL MIXTURES

JANUSZ OSZCZAPOWICZ* and MAŁGORZATA CZURYŁOWSKA
Department of Chemistry, University of Warsaw, Poland

(Received 11 October 1983. Accepted 19 January 1984)

Summary—The pK_a values of protonated imidazole in 10 different water-ethanol mixtures were determined at 25° by potentiometric titration in a cell without liquid junction (glass and silver-silver bromide electrodes). The pK_a values can be used in a standardization procedure that allows determination of pK_a values for protonated organic nitrogen bases in aqueous ethanol.

For determination of the pK_a values of the conjugate acids of organic bases in non-aqueous solvents, either appropriate buffers of known pH or standard compounds with known pK_a values in the solvents are necessary. In the second case the pK_a values can be calculated from the expression¹

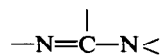
$$pK_{a_i} = pH_{x_i} + pK_{a_s} - pH_{x_s}$$

where pK_{a_i} and pK_{a_s} are the pK_a values of the sample (*i*) and standard (*s*) and pH_{x_i} is the pH reading at the degree of titration $x = C_{HA}V_{HA}/C_0V_0$ (where C_0 is the initial concentration of the sample, V_0 the initial volume of titrand, and C_{HA} and V_{HA} are the concentration and volume of added titrant) for the sample (pH_{x_i}) and standard (pH_{x_s}) respectively.

For many organic bases the pK_a values of the conjugate acids in various water-ethanol solutions can be found in the literature, but unfortunately there is much inconsistency in the data. To study the influence of various solvents on the sensitivity of the basicity of organic bases to substitution effects, all the data must be related to a single standard. The pK_a values for this standard in the solvents concerned should be determined under the same conditions and, if possible, in one laboratory. Such a procedure should ensure self-consistent results, because systematic errors ought to be the same for all the solutions.

In the course of our study on the influence of substitution on basicity of amidines and related compounds,²⁻⁶ imidazole was chosen as a convenient standard. It is commercially available, can be easily purified by recrystallization and is stable enough to be stored. It is very convenient as a standard for determination of the basicity of such compounds as amidines, guanidines and heterocyclic compounds

containing the



group, because the protonation of imidazole also occurs on the imino-nitrogen atom of this group, and therefore any unpredictable effects due to change of solvation in different solvents are comparable and the resulting errors minimized.

EXPERIMENTAL

Reagents

Water-ethanol mixtures were prepared by mixing appropriate weights of analytical grade azeotropic rectified spirit, fractionally distilled before use, with water that had been twice distilled in quartz apparatus. The sodium carbonate, sodium bromide, perchloric acid (60%) and imidazole used were of analytical grade.

Procedure

All pH values were measured with a Radiometer PHM 64, with a constant temperature cell without liquid junction, equipped with a glass electrode (GE) and silver-silver bromide electrode:

GE || 0.1M (imidazole + HClO₄ + NaBr);

water-ethanol || Ag-AgBr

The 50-ml samples contained about 0.5 mmole of imidazole in 0.1M sodium bromide. Silver-silver bromide electrodes were prepared by immersion of a cleaned 0.1-mm diameter silver wire for 30 min in aqueous ferric bromide solution, rinsing, drying in air and then aging for at least two days in aqueous potassium bromide solution.

The titrant was prepared by dilution of 1.1 ml of 60% perchloric acid with 98.9 ml of 0.1M sodium bromide in the water-ethanol mixture to be used for the determination; it was standardized by potentiometric titration of sodium carbonate in water.

RESULTS AND DISCUSSION

To obtain reliable results some precautions were taken. To prepare water-ethanol mixtures, redistilled rectified spirit was used, because it does not contain

*Author for correspondence.

Table 1. Experimental data for titration of imidazole in 95.6% ethanol

V , <i>ml</i>	E , <i>mV</i>	E_a^{o*} , <i>mV</i>	pK_a^\dagger
1.5	-257.3		5.965
1.8	-265.3		5.947
2.0	-270.1		5.940
2.2	-274.8		5.932
2.4	-279.0		5.931
2.6	-283.1		5.930
2.8	-287.1		5.929
3.0	-291.3		5.929
3.5	-302.5		5.933
4.0	-315.0		5.959
8.0		-633.5	
8.2		-633.5	
8.4		-631.8	
8.8		-632.1	
9.0		-632.8	
9.5		-629.0	
10.0		-629.4	

*Mean value 632.1 ± 1.1 mV.†Mean value 5.94 ± 0.01 .

the impurities which may remain from preparation of so-called "absolute alcohol". Also, its azeotropic composition (95.6% ethanol, w/w) is known and constant.

A newly prepared Ag-AgBr electrode always behaves as a cathode with respect to older ones that have been aged in a bromide solution.^{7,8} Its potential changes considerably during the initial 20–30 hr and equilibrium is sometimes reached only after two days. For that reason the Ag-AgBr electrode was kept for at least 48 hr in 0.01M aqueous potassium bromide before use.

The pK_a value of the conjugate acid of imidazole was determined by the direct method given by Zikolov *et al.*^{9,10} for aqueous solutions. The shapes of the titration curves indicate that his method can be used for water-ethanol solutions as well.

The pK_a values were calculated from the equation⁷

$$pK_a^c = \frac{E - E^o}{59.16} + \log \left(\frac{x}{1-x} \right)$$

where E is the e.m.f. of the cell, E^o is E for $[H^+] = 1$; x is the degree of titration and 59.16 is the value of $2.303RT/nF$ at 25°.

For calculations only the E values for x within the range 0.3–0.8 were taken, because only in this range was the titration curve approximately linear. The E^o value was determined by measuring the cell e.m.f. after the equivalence point, according to the equation⁷

$$E = E^o + 59.16 \log [C_2H_5OH_2^+]$$

The constancy of the E^o value determined in each titration indicated that perchloric acid is fully dissociated in the conditions used, and thus this equation is valid.

In the direct method of pK_a determination, the ionic strength must be kept constant, so the titrations

Table 2. The pK_a values of imidazole in water-ethanol mixtures

Ethanol, % w/w	pK_a
99.8*	6.30 ± 0.04
95.6	5.94 ± 0.01
80.0	5.73 ± 0.01
70.0	5.80 ± 0.01
60.0	5.76 ± 0.01
50.0	5.63 ± 0.02
40.0	6.18 ± 0.01
30.0	6.64 ± 0.01
20.0	6.82 ± 0.01
10.0	6.80 ± 0.02
0	6.92 ± 0.02

*Commercial "absolute alcohol."

are usually done in the presence of an inert and completely ionizable salt (KCl) at a concentration at least an order of magnitude greater than that of the titrant. Alkali metal chlorides have low solubilities in ethanolic solutions, so are unsuitable. Therefore, sodium bromide had to be used to maintain the ionic strength, and this in turn required use of the Ag-AgBr electrode.

Accuracy

The error in potential measurements should not exceed 0.05 mV, so the corresponding error in the pK_a values should be less than 0.05. Errors caused by the ionic-strength changes occurring during the titration are much smaller than this and can be neglected. The errors in the mean values given in Tables 1 and 2 refer to a confidence level of 95%.

Changes in pK_a values with solvent composition

The value of pK_a depends on the nature, acidity, dielectric constant and solvation ability of the solvent. In water-ethanol mixtures these properties change with composition, thus the difference between pK_a values measured in water and in 95.6% ethanol is 0.98. For imidazole, the pK_a values pass through a minimum.

REFERENCES

- G. Charlot and B. Trémillon, *Les réactions chimiques dans les solvants et les sels fondus*, pp. 40, 316. Gauthier-Villars, Paris, 1963.
- J. Oszczapowicz, R. Orliński and E. Hejchman, *Polish J. Chem.*, 1979, **53**, 1259.
- J. Oszczapowicz and R. Orliński, *ibid.*, 1980, **54**, 1901.
- J. Oszczapowicz and E. Raczynska, *ibid.*, 1981, **55**, 1583.
- J. Oszczapowicz and J. Osek, *ibid.*, 1982, **56**, 93.
- J. Oszczapowicz and E. Raczynska, *ibid.*, in press.
- R. E. Smith and J. K. Taylor, *J. Res. Natl. Bur. Stds.*, 1938, **20**, 837.
- Idem*, *Roczniki Chem.*, 1938, **18**, 762.
- P. Zikolov, T. Zikolov and O. Budevsky, *Talanta*, 1975, **22**, 511.
- Idem*, *ibid.*, *Talanta*, 1975, **23**, 587.

ANNOTATION

ANALYSIS OF SEDIMENTS FOR HEAVY METALS BY A RAPID ELECTROTHERMAL ATOMIC-ABSORPTION PROCEDURE

M. J. T. CARRONDO, F. REBOREDO, R. M. B. GANHO and J. F. S. OLIVEIRA

Departamento de Ciências do Ambiente, Faculdade de Ciências e Tecnologia, Universidade Nova de Lisboa, 2825 Monte da Caparica, Portugal

(Received 11 April 1983. Revised 21 November 1983. Accepted 18 January 1984)

Summary—A rapid electrothermal atomic-absorption spectrophotometric procedure with homogenization as the only pretreatment is compared with two wet pretreatment methods followed by flame atomic-absorption, in a statistically designed experiment. Samples from the top 5 cm of sediments at three different points of the Tejo estuary were used for the tests. The results show that the electrothermal procedure performed as well as whichever was the better of the flame methods for the determination of cadmium and nickel, irrespective of the sand content of the samples; although not statistically significant, there was apparently a decrease in recovery for chromium, copper and lead by the electrothermal method as the sand content of the sample increased. For zinc the electrothermal method gave results statistically different from those of the flame procedures when the sand content was high but not when the organic content of the sample was high. Because of the limited degree of replication (5 variates) the relative differences between the average values obtained by the three methods were significant only if they exceeded 15%. The electrothermal method has the advantage of substantially greater speed.

Before the determination of the total heavy metal content of a sample, it is normally necessary to bring the metals into solution, exceptions being the use of neutron-activation analysis, X-ray fluorescence spectroscopy and, in some situations, electrothermal atomic-absorption spectrophotometry (AAS).^{1,2} For environmental samples AAS is the method of choice for the majority of heavy metal determinations.³

The procedures available for bringing the heavy metals into solution depend on the matrix and are generally grouped into three classes: fusion with molten salts, dry ashing followed by acid dissolution, and wet digestion with acids (individually or in mixtures).^{1,4} These are all potentially applicable to sediment analysis. Fusion methods greatly increase the salt content and contamination, thus making it difficult to use atomic-absorption methods. Dry ashing might cause loss of metals by volatilization, e.g., cadmium and lead, and does not always yield complete recovery of metals.^{4,5} Various acids are utilized for wet digestion, namely nitric, sulphuric, perchloric, hydrochloric and hydrofluoric; even though the use of automated digestion techniques and digestion bombs has improved the method, losses due to volatilization, retention or loss of insoluble species in the digestion vessel or poor recovery from the matrix might occur.^{1,6,7}

These pretreatments are time-consuming. If the sample is amenable to homogenization, electrothermal atomic-absorption procedures may be util-

ized without pretreatment.^{5,8} Various types of interference arise in electrothermal atomic-absorption⁹ but it is generally accepted that this method can be used for matrices that are mainly organic in nature.^{9,10} An increase in inorganic salt content makes the method less reliable, especially for the more volatile elements cadmium, lead and zinc.^{10,11}

This paper evaluates the applicability of a procedure previously reported for sewage and sewage sludge analysis,^{5,8,11} based on ultrasonic homogenization followed by electrothermal atomization for total heavy-metal analysis of sediments. Consequently the statistical design was the same as that of this earlier work; it became apparent later that the limited degree of replication made statistical differentiation rather insensitive, a relative difference of at least 15% being required for statistical significance. The samples used were taken from three different points in the Tejo estuary (Fig. 1), as part of a survey sponsored by U.N.D.P. and U.N.E.S.C.O.

EXPERIMENTAL

Instrumentation

A Perkin-Elmer model 503 atomic-absorption spectrophotometer fitted with a deuterium background-corrector was utilized for all determinations. A single-slot air-acetylene burner and an HGA72 graphite atomizer were used for flame and electrothermal analyses respectively. The operating conditions were slightly modified from those recommended by the manufacturer and have been reported elsewhere.^{5,8}

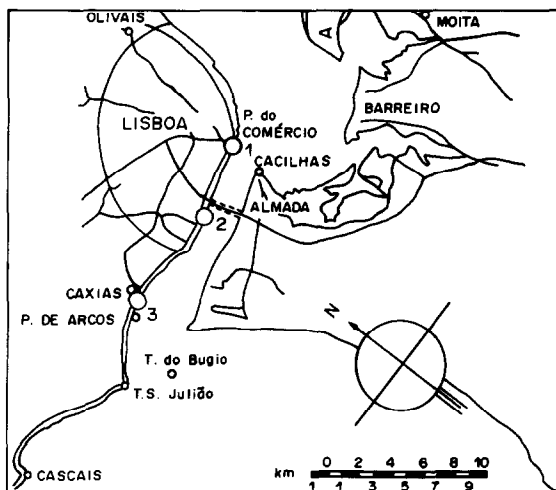


Fig. 1. Location of the sampling points.

Reagents

Pro analysi grade reagents (Merck) were used for the treatment of the samples to minimize blank values. Standards were prepared by serial dilution of commercially available stock solutions (Fisher).

Homogenization

Samples to be analysed by electrothermal analysis were diluted and acidified to contain 1% (v/v) nitric acid and homogenized with an Ultra Turrax T 45 N in a similar way to that previously described.^{5,8,11} Results obtained by direct comparison with aqueous standards and by the standard-addition method were found to be in good agreement.

Nitric-sulphuric acid digestion

Digestions were done in a similar way to that described previously^{8,11} but 100-ml borosilicate beakers were used instead of 500-ml flasks. For each g of wet sediment 20 ml of concentrated nitric acid and 5 ml of concentrated sulphuric acid were used.

Nitric-perchloric acid digestion

Digestions were done in a similar way to that previously described,⁷ again with 100-ml borosilicate beakers. For each g of sediment 20 ml of concentrated nitric acid and 5 ml of 60% perchloric acid were used.

Other analytical parameters

The solids content was determined according to reference 12 and the geological analysis was done by the methods given by Maxwell.¹³

RESULTS AND DISCUSSION

Samples taken from the top 5 cm of the sediment were obtained from three points in the estuary; a rough characterization of the samples is presented in Table 1; sample 1 can be seen to have a rather high organic content but no sand. The sand fraction increased as the samples were taken from nearer the ocean and beaches, the organic and clay silt fractions decreasing correspondingly.

Each sample was divided into three groups of five subsamples. Two of the groups of five samples were used for digestion with the acid mixtures and analysis by flame atomic-absorption. The samples in the other

group were individually homogenized and analysed by electrothermal atomic-absorption, Eppendorf micropipettes being used for injection of 20 or 50 μ l aliquots. Two blanks were also run for each pretreatment. In all cases analysis was by direct comparison with acidic standards.

The results were treated statistically; the mean values, within-group relative standard deviation and the results of an analysis of variance by the *F*-test¹⁴ are reported in Table 2. Tukey's procedure¹⁴ was used to identify which means were statistically different at the 0.05 significance level. Metal recoveries obtained by the different procedures, calculated on the assumption that the higher flame result corresponded to complete recovery, are also compared in Table 2. It was not possible to make a statistically significant discrimination between means, however, unless the relative difference was at least 15%.

From the comparisons presented in Table 2, no statistically significant difference exists between the best digestion-flame procedure and the homogenization-electrothermal procedure for the determination of chromium, copper and nickel. Nevertheless there is an apparent decrease in recovery by the homogenization method with decrease in organic content and increase in sand present: this effect is more pronounced for copper and, to a lesser extent, chromium in sample 3, recoveries lower than 90% having been obtained. The low recoveries obtained for chromium by the perchloric acid digestion procedure might be due to the volatilization of chromyl chloride.^{1,13}

As the more serious matrix interference effects reported in the literature for the electrothermal technique are usually associated with cadmium, lead and zinc,^{9,10} the results obtained for chromium, copper and nickel were to be expected. More surprisingly, the results in Table 2 indicate that the homogenization procedure compares well with the better of the flame methods for determination of cadmium and lead. For lead the recovery appears to fall with the increase in inorganic content, but not for cadmium. The apparent absence of interferences may be entirely fortuitous or may result from a match between enhancement and suppression effects. Alternatively, synergic effects may have occurred, similar to those reported for lead and cadmium in fertilizer samples.¹⁵ The most marked matrix influence takes place in the determination of zinc, a recovery of less than 70% having been obtained for the high sand-content sample 3, which is consistent with previous studies.^{10,16}

Table 1. Characterization of the samples

Sample	Solids		Solid fraction		
	Total, g/kg	Volatile, % of total solids	Organic %	Clayey, silty, %	Sand, %
1	555	7.3	8.3	91.7	—
2	532	6.2	5.4	63.4	31.2
3	824	1.3	0.8	2.7	96.5

Table 2. Comparison of metal concentrations by the three methods

Metal	Sample	Pretreatment	F-test*	Mean conc., † mg/kg	C.I., § mg/kg	R.S.D., %	Recovery, ‡ %
Cadmium	1	H ₂ SO ₄ -HNO ₃	0.01	0.84A	±0.11	10.7	—
		HClO ₄ -HNO ₃		0.60B	±0.15	20.7	71.4
		Homogen.		0.80A	±0.09	8.8	95.2
	2	H ₂ SO ₄ -HNO ₃	0.01	0.85A	±0.16	15.3	—
		HClO ₄ -HNO ₃		0.50B	±0.11	18.4	57.6
		Homogen.		0.83A	±0.10	9.9	97.6
	3	H ₂ SO ₄ -HNO ₃	0.01	0.35A	±0.05	11.4	—
		HClO ₄ -HNO ₃		0.16B	±0.05	25.0	46.2
		Homogen.		0.33A	±0.07	18.2	94.3
Chromium	1	H ₂ SO ₄ -HNO ₃	0.01	40.7A	±3.0	5.9	—
		HClO ₄ -HNO ₃		25.4B	±4.2	13.4	62.4
		Homogen.		39.7A	±3.4	6.8	97.5
	2	H ₂ SO ₄ -HNO ₃	0.01	28.9A	±2.9	8.0	—
		HClO ₄ -HNO ₃		17.4B	±3.2	14.9	60.2
		Homogen.		27.3A	±2.5	7.3	94.5
	3	H ₂ SO ₄ -HNO ₃	0.01	26.5A	±2.6	7.9	—
		HClO ₄ -HNO ₃		11.5B	±2.6	18.6	43.4
		Homogen.		23.5A	±4.6	15.7	88.7
Copper	1	H ₂ SO ₄ -HNO ₃	0.05	63.7A	±6.0	7.5	87.4
		HClO ₄ -HNO ₃		72.9B	±4.0	4.4	—
		Homogen.		70.6AB	±9.1	10.3	96.8
	2	H ₂ SO ₄ -HNO ₃	N.S.	38.2A	±5.3	11.3	86.8
		HClO ₄ -HNO ₃		44.0A	±5.8	10.7	—
		Homogen.		41.5A	±3.4	6.5	94.3
	3	H ₂ SO ₄ -HNO ₃	N.S.	8.6A	±1.4	13.3	87.8
		HClO ₄ -HNO ₃		9.8A	±1.6	13.3	—
		Homogen.		8.4A	±0.9	8.4	85.7
Nickel	1	H ₂ SO ₄ -HNO ₃	N.S.	15.6A	±3.2	16.7	97.5
		HClO ₄ -HNO ₃		16.0A	±3.1	15.6	—
		Homogen.		15.4A	±1.2	6.8	96.3
	2	H ₂ SO ₄ -HNO ₃	N.S.	33.0A	±5.6	13.6	97.1
		HClO ₄ -HNO ₃		34.0A	±2.7	6.5	—
		Homogen.		33.6A	±3.2	7.7	98.9
	3	H ₂ SO ₄ -HNO ₃	N.S.	25.4A	±1.6	5.1	89.1
		HClO ₄ -HNO ₃		28.5A	±4.1	11.6	—
		Homogen.		27.0A	±3.4	10.0	94.7
Lead	1	H ₂ SO ₄ -HNO ₃	0.01	125A	±9.2	5.9	50.5
		HClO ₄ -HNO ₃		248B	±29	9.3	—
		Homogen.		239B	±15	5.0	96.3
	2	H ₂ SO ₄ -HNO ₃	0.01	94A	±12	10.6	41.1
		HClO ₄ -HNO ₃		228B	±33	11.5	—
		Homogen.		209B	±21	8.1	91.4
	3	H ₂ SO ₄ -HNO ₃	0.05	8.7A	±1.5	13.8	66.9
		HClO ₄ -HNO ₃		13.0B	±2.7	16.9	—
		Homogen.		11.4B	±3.0	20.7	87.7
Zinc	1	H ₂ SO ₄ -HNO ₃	0.01	413A	±58	11.2	78.8
		HClO ₄ -HNO ₃		524B	±25	3.8	—
		Homogen.		510B	±68	10.8	97.3
	2	H ₂ SO ₄ -HNO ₃	0.01	296A	±35	9.6	75.0
		HClO ₄ -HNO ₃		394B	±64	13.0	—
		Homogen.		366B	±27	5.9	92.9
	3	H ₂ SO ₄ -HNO ₃	0.01	113A	±15	11.0	83.6
		HClO ₄ -HNO ₃		135B	±25	14.9	—
		Homogen.		92C	±17	14.8	68.3

*N.S. = not significant at the 0.05 significance level.

†Means not followed by a common letter are significantly different at the 0.05 significance level.

§95% confidence interval.

‡Assuming the result of the better flame method corresponds to complete recovery.

Undoubtedly, the use of the deuterium background-corrector is invaluable for this type of analysis, particularly for the volatile elements lead, cadmium and zinc. The low recovery obtained for lead by the sulphuric acid digestion procedure can be accounted

for by the low solubility of the sulphate. The incomplete recovery of zinc by the sulphuric acid method and of cadmium by the perchloric acid method is less easy to explain; the latter has been reported previously.⁷

Reported values for the precision of the rapid method applied to sewage sludge samples⁵ and sewages and sewage effluents⁸ averaged 8 and 6%, respectively, whereas in these sediment samples, admittedly harder to homogenize, the average is closer to 10% for the procedure as a whole.

Comparing the absolute metal concentrations in the Tagus sediments with those reported for other estuaries,^{17,18} it is apparent that sample 3 is relatively uncontaminated whereas samples 1 and 2 present concentrations ranging from two (for cadmium) to five (for lead) times those reported for unpolluted rivers.

CONCLUSION

The rapid electrothermal procedure described here can be used advantageously for routine analysis for total heavy metals in sediments associated with contamination by currents and matrices with reasonably high organic content. As the amount of sand in the sample increases, this procedure yields lower results for zinc. Recoveries for copper, chromium and lead might drop to about 90% for samples containing almost only sand. The time saved is considerable, because homogenization takes only 5 min as opposed to the 3–6 hr required for a digestion. This more than compensates for the additional time (2–3 min) required for the electrothermal analysis.

Acknowledgements—The authors are thankful for authorization to work in the laboratories of Instituto Hidrográfico, Complexo Interdisciplinar I and Faculdade de Ciências de Lisboa.

REFERENCES

1. N. W. Hanson (ed.), *Recommended Methods of Analysis*, 2nd Ed., The Society for Analytical Chemistry, London, 1974.
2. E. I. Hamilton, *Sci. Total Environ.*, 1976, **5**, 1.
3. J. J. Dulka and T. H. Risby, *Anal. Chem.*, 1976, **48**, 640A.
4. T. T. Gorsuch, *The Destruction of Organic Matter*, Pergamon Press, Oxford, 1970.
5. M. J. T. Carrondo, R. Perry and J. N. Lester, *Anal. Chim. Acta*, 1979, **106**, 309.
6. H. Agemian and A. S. Y. Chau, *ibid.*, 1975, **80**, 61.
7. *Idem*, *Analyst*, 1976, **101**, 761.
8. M. J. T. Carrondo, R. Perry and J. N. Lester, *Sci. Total Environ.*, 1979, **12**, 1.
9. C. W. Fuller, *Electrothermal Atomization for Atomic Absorption Spectrometry*, Chemical Society, London, 1977.
10. R. B. Cruz and J. C. van Loon, *Anal. Chim. Acta*, 1974, **72**, 231.
11. M. J. T. Carrondo, R. Perry and J. N. Lester, *Analyst*, 1979, **104**, 937.
12. *Standard Methods for the Examination of Water and Wastewater*, 14th Ed., American Public Health Association, Washington, D.C. 1976.
13. J. A. Maxwell, *Rock and Mineral Analysis*, Interscience, New York, 1968.
14. A. H. Bowker and G. J. Lieberman, *Engineering Statistics*, Prentice Hall, New Jersey, 1972.
15. T. C. Woodis Jr., G. B. Hunter and F. J. Johnson, *Anal. Chim. Acta*, 1977, **90**, 127.
16. D. A. Lord, J. W. McLaren and R. C. Wheeler, *Anal. Chem.*, 1977, **49**, 257.
17. R. E. Jones, *Technical Rep. TR 73*, Water Research Centre, U.K. 1978.
18. U. Forstner and W. Salomons, *Environ. Technol. Lett.*, 1980, **1**, 494.

A VERSATILE LOW-COST LABORATORY COMPUTER NETWORK

R. L. A. SING and ERIC D. SALIN*

Department of Chemistry, McGill University, Montreal, Quebec, Canada

(Received 3 February 1984. Accepted 23 February 1984)

Summary—An inexpensive but powerful computer network particularly suited to the research laboratory is discussed. The primary advantages of the system are low cost, flexibility, freedom of choice of manufacturer, and convenience of upgrading. The principal limitations are speed of data transfer and the requirement for a certain level of skill during setting up. The system operates with both the CP/M and MP/M operating systems, but the principles of operation are generally applicable.

Laboratory automation has many advantages for both the research and the production laboratory. In general, laboratory automation can provide higher sample throughput with an attendant reduction in cost per sample. The digitized data can be stored and later retrieved and processed by application programs or data-base management systems, for production of reports.

In the research laboratory, automation not only allows the rapid collection of large amounts of data but encourages use of intensive statistical and graphical evaluation, which might otherwise be too laborious. Research work often makes unusual demands on the acquisition hardware and software. Versatility, flexibility and low cost may be far more important in the research laboratory than in the production laboratory.

We have found that an excellent solution to these requirements is a laboratory computer network. Networks in the laboratory have been discussed in general by Dessy¹ and specifically by Levy and Terpstra.² We will present here a discussion of a very effective and inexpensive laboratory computer network which is particularly well suited to the research laboratory and its unpredictable future needs.

NETWORK DESIGN

There are several features of computer networks which are particularly important in a research laboratory involved in the development of instrumentation, though these attributes may be considered to be universal. The "dedicated microcomputer" network has been discussed previously³ and appears to meet these needs far more efficiently than any other. The most important network attributes are listed below and will be discussed in order to allow readers to evaluate their importance for their own laboratories.

The laboratory computer-network should:

- (1) have a powerful, fast "dedicated" computer;
- (2) use low-cost hardware and software;
- (3) offer flexible expansion;
- (4) produce graphics;
- (5) have long-term data-storage in real time;
- (6) possess multiple high-level language capabilities;
- (7) use simple operating procedures;
- (8) not be entirely dependent on the products of a particular manufacturer.

In a "local computer" or "dedicated computer" network, microcomputers act as dedicated I/O (input/output) modules and provide local processing of data so that only information requiring storage or sophisticated processing is sent to a central laboratory computer. The dedicated computer's functions are relatively limited: local I/O operations, collection of data as fast as required, primitive processing and transmission of the processed data. The central laboratory computer (hereafter called simply the laboratory computer) provides storage, powerful processing capability and extensive I/O capability (*e.g.*, printers and plotters). Our particular network configuration provides the advantages of (1) remote operation, (2) autonomous local I/O, (3) local control and processing and (4) a certain degree of modularity if several of the dedicated processors are of the same type. Serial communication techniques allow convenient transmission over distances up to several kilometres, and by use of telephone lines communication can be made over almost unlimited distances. Local processing of the data may be desirable for several reasons: (1) local output, particularly hardcopy, can be used for operational monitoring, or back-up in case of network failure, and (2) the transmission of only the vital information will minimize the network traffic (high traffic might slow down the laboratory computer and cause loss of

*Author to whom correspondence should be addressed.

information. Conventional serial transmission techniques are not always satisfactory if data-rates are high. With a conventional 9600 baud (bits/sec) transmission rate, the system may be limited to the transfer of approximately 100 data values per second.³ This will certainly not be satisfactory for some experiments, though adequate for most. There are at least two solutions to this problem. If the distances between the dedicated and the central laboratory computers are short, then parallel transmission techniques may be used. If the data set is not too large, a more convenient solution may simply be expansion of the memory of the dedicated computer to allow the set to be stored until the end of the acquisition period (delayed transmission).

Another limitation to a network of this type can be the limited software capabilities of some of the microcomputers most appropriate for the dedicated function. It might, for example, be much more convenient to use compiler BASIC for acquisition and processing, since it can be two orders of magnitude faster than interpreter BASIC and is far more convenient and efficient in many aspects than assembler-level coding, particularly when used by laboratory personnel. Arguments can be made for other compiler languages, since they have their own particular advantages, but they almost inevitably require a disk-based system, which will increase the cost. Generally then, when using the term "powerful" in connection with a dedicated computer, we are referring to a high-level language capability, usually an interpreter language such as BASIC or a compiler-interpreter language.⁵ Other factors, such as ease of physical interfacing, might initially appear to be important, but almost all major processor manufacturers include powerful timer-counter, parallel and serial interface integrated circuits in their equipment, and many of the single-board computers can either be acquired with these or easily expanded.

The cost of a small single-board computer suitable for the dedicated function is usually quite low, but that of a suitable laboratory computer can be quite high and usually represents over 80% of the total network cost when the price of the software is included in the total price. Generally the 8-bit computer systems are significantly cheaper than 16-bit systems, and because of their popularity and high-volume sales, a great variety of powerful low-cost software is available. The apparent advantage of 16-bit systems is their ability to address directly large blocks of memory. This should enable them to run larger programs faster as well as being more efficient for multi-user operating systems.

Graphics may not be important in all laboratories, but humans are excellent pattern recognizers and work far more efficiently with graphical than with tabular data. The power of graphical information has been recognized by many manufacturers, who now have gone beyond simple graphical display to an intelligent use of colour so as to transmit more

information to an operator. Some graphics systems use sections of computer memory, while others have their own memory for image storage. Image generation can take up quite a lot of computation time. For example, a 500×500 pixel display consists of 2.5×10^5 pixels, each of which must be set, often with additional intensity or colour information. Intelligent independent graphics systems or subsystems can minimize laboratory computer slow-down by doing these computations themselves, often with specialized software.

If the laboratory computer is to be truly useful to the researchers in the laboratory, then it must do more than store the data. It must be able to process and output those data at a time convenient to the researcher. This is one of the distinct advantages of operating the laboratory computer with a multi-user capability. Data can be acquired from an experiment while other researchers are processing their data from other experiments. If the number of simultaneous users is relatively small, then an 8-bit computer can satisfactorily handle the task provided there is sufficient mass-storage. If intensive disk usage is required then a fast disk system may be essential, but most computational work tends to be processor-intensive, and fast storage, though always convenient, may not be essential.

Because scientists may come from a wide variety of backgrounds and possess different programming skills, it is important to be able to offer a selection of software which will allow each user to achieve maximum efficiency with minimum of frustration. BASIC (Beginners All-Purpose Symbolic Instruction Code) is ideal for simple calculations and can easily be learned independently. Certain software manufacturers (*e.g.*, Microsoft) have made available compiler versions which can run significantly faster than the interpreter forms. Pascal has a wide variety of data and programming structures which make it an extremely flexible and powerful language for computation as well as other purposes. It is a highly structured language, which makes it popular as a professional tool because the rigid structuring makes the written code easy to follow, and it is easy for new programmers to take over programming responsibilities. A great deal of powerful software is available for 16- and 8-bit computers. In general, the 8-bit software is less expensive and can often be purchased from a maker other than that of the hardware or the software operating system.

It quickly becomes apparent that the laboratory computer is the system which is most likely to be overloaded and consequently need upgrading. The dedicated computer is normally purchased with a given experiment or apparatus in mind, and as long as this does not change considerably, there is no need to change the dedicated computer. On the other hand, the load on the laboratory computer will increase with time. Additional dedicated computers will be added, and researchers will increase their

demands on the laboratory system as they become increasingly competent in its use. The laboratory staff will often come to use the laboratory computer for a great deal of what might be called "administrative" work, such as data-base management, and report-writing with the use of word processors and computer "spread sheets" like VisiCalc. The word processor will often be extremely popular because it can be used as a text editor for programming as well as in its more traditional role. Some word processors are highly disk-intensive, owing to the use of menus and search requirements. This creates an additional load on the laboratory computer. For these reasons, the laboratory computer is more likely than the dedicated computers to be outgrown. Because of the investment of researchers' time in learning and developing software, it is imperative that the software run by the laboratory computer should be highly portable. It is obviously most satisfactory if the software can be transferred to a more powerful computer and run completely without modification.

Perhaps the most difficult problem to overcome is that of the networking software. The most desirable dedicated computer may not be made by the same firm as the most suitable laboratory computer, or investments may already have been made in one or the other of these. Our solution to this is quite simple. We have installed on our laboratory computer a modern multi-user operating system which we run entirely without modification. Each of our dedicated computers is physically connected to the laboratory computer by a standard RS-232C protocol and appears to it to be a user terminal. The only operating-system modifications that we make are very simple and are limited to the dedicated computer, which is unlikely to be outgrown by the particular experiment for which it was purchased. An arrangement of this type allows us to replace the laboratory computer with a more powerful unit without any modifications to the dedicated computers as long as the laboratory computer operating system remains the same. We have achieved a certain degree of independence from the manufacturer by using an operating system which is used by many manufacturers on a wide variety of computers. From analysis of the trade journals, it appears that the operating system will be utilized into the foreseeable future.

NETWORK SPECIFICS

Hardware

Our laboratory computer is an S-100 bus-based computer (IEEE-696 standard)² which at present operates with 256 kbytes of R/W memory and two 8-in. flexible disk drives for mass storage. A more complete configuration listing is provided in Table 1. The graphics are provided by the MicroAngelo, an intelligent 512 × 480 pixel video subsystem which relieves the main processor of the heavy burden of graphics generation. The MicroAngelo has its own Z-80 processor with 32 kbytes of R/W memory for image storage and an instruction set in ROM on a single S-100 board. We have developed our own software to transfer the screen image directly to an Epson MX-80 printer with Grafrax Plus. Commercial versions of this type

of software are available. The image transfer takes 3 min, but we have found that the printer has the advantage that it can be left unattended while multiple text or graphics print-outs are made, whereas most of the cheaper plotters require manual sheet-feeding.

The dedicated computer selected is the Rockwell AIM-65 single-board computer. Table 2 lists the features of the AIM, the most important for network use being the on-board printer, the use of BASIC, and the very well documented monitor (operating system). The printer is important because it allows the AIM to be used autonomously and to get hardcopy output data if the laboratory computer breaks down. BASIC allows convenient processing of the data before passing them on to the laboratory computer, and the source-code listing for the monitor allows slight modifications to the monitor for convenient operation within the network. All the software can be contained in the Read-Write (also called R/W or RAM) memory, but if the system is RESET the operator has to reinitialize certain pointers. The monitor ROM can readily be modified so that the AIM loads the program and starts the task automatically as soon as it is switched on.

The minimal configuration AIM is equipped with a 20-mA current-loop serial communication line. This interface is implemented primarily through software using a 6522 Versatile Interface Adapter (VIA) rather than with an integrated circuit specifically designed for serial communication, such as a 6551 ACIA (Asynchronous Communication Interface Adapter). Though adequate for operation with a terminal, this system is not adequate for network operation, because of the low speed at which transactions take place. The 20-mA loop system simply does not respond quickly enough, and characters are lost during the simple transmission procedure that we insist upon. For this reason we expanded the AIM with a 6551 ACIA, an integrated circuit specifically designed for serial communications, and some EPROM memory to contain the networking software. By using the 6551 ACIA, we are able to communicate at 9600 baud. We have found it convenient to build our own combined board which includes a 6522 VIA, a 6551 ACIA, and memory sockets which can be used for RAM (6116), ROM (2316) or EPROM (2716). Once again, the excellent documentation of the AIM make this a relatively straightforward task. The increased memory capacity allows more data to be stored before transmission to the laboratory computer and consequently minimizes the load on the latter. The circuit diagram for the interface is available from the authors, but serial communication expansion ports, memory and additional parallel I/O can be purchased commercially from a number of vendors, some of whom are listed in Table 3.

Software

We have adopted for our laboratory computer what appears to be the most common operating system, CP/M, with the expectation that MP/M, the multi-user version, will become equally as popular. CP/M and MP/M are both produced by Digital Research, which seems to nullify our claim to be tied to one manufacturer, but there are over 100 manufacturers of different computers which run CP/M, and many of these can run MP/M. They range from the oldest 8080 CPU-based systems through the popular 8088-8086 Intel family to the very powerful 68000 series. The use of this operating system then frees us from dependence on any particular manufacturer of computers or family of logic devices, or manufacturer of integrated circuits. This will allow us in the future to expand or replace the laboratory computer with a more modern system without having to discard either our own high-level language application programs which run on the laboratory computer, or our dedicated computers and their communication techniques.

The CP/M and MP/M operating systems used on the laboratory computer are run without modification. Instead,

Table 1. Laboratory computer specifications

Bus	S-100 (IEEE 696 standard) 20-slot mainframe	Cromemco Inc., 280 Bernardo Ave., Mountain View, CA 94043
CPU	SBC-200-Z80 CPU -serial port -parallel port -phantom ROM	SD Systems, P.O. Box 28810, Dallas, TX 75228
Memory	Expandoram III with 256 kbytes of dynamic RAM	SD Systems
Storage	Dual 8-in. single-sided double- density disk drives (801 R) Versafloppy II disk controller	Shuggart, 475 Oakmead Parkway, Sunnyvale, CA 94086 SD Systems
I/O	TUART—2 serial ports -2 parallel ports	Cromemco
Graphics	MicroAngelo 512 × 480 pixel graphics subsystem On board—Z80 CPU -32 kbytes ROM -32 kbytes RAM	Scion Corporation, 12310 Pincrest Road, Reston, VA 22091
Printer	Epson MX-80 with Grafrax Plus (bit graphics capability)	Epson America Inc., 3415 Kashiwa Street, Torrance, CA 90505
Software	CP/M (MP/M) operating system MBASIC interpreter BASIC BASIC 80 Compiler PASCAL MT+ WORDSTAR SUPERFILE	Digital Research, P.O. Box 579, Pacific Grove, CA 93950 Microsoft, 10800NE Eighth, Suite 819, Bellevue, WA 98004 Microsoft Digital Research MicroPro, 1299 4th Street, San Rafael, CA 94901 FYI, Inc., P.O. Box 10998 615, Austin, TX 78766

Table 2. Rockwell AIM-65 features

Hardware:	6502 CPU 4 kbytes RAM 20 kbytes ROM (see software) 20-character display 20-column thermal printer 2-bit programmable parallel ports with handshake (6522 VIA) 20-mA serial interface
Software:	Monitor Editor BASIC interpreter Assembler
Documentation:	AIM 65 User's Guide R6500 Programming Manual R6500 Hardware Manual BASIC Language Reference Manual AIM 65 Monitor Program Listing Rockwell R6500 Microcomputer System Application Notes "INTERACTIVE", Rockwell International Newsletter "THE TARGET—an AIM65 newsletter", c/o Donald Clem, RR # 2, Spencerville, OHIO 45887

Table 3. AIM 65 expansion interface vendors

This is a partial listing of the major vendors of expansion interfaces for the AIM 65.

Rockwell International 3310 Miraloma Avenue P.O. Box 3669 Anaheim, CA 92803	Expansion mother boards Memory boards (RAM, ROM, EPROM) Parallel ports Serial ports (RS 232C) Floppy disk controllers CRT controllers IEEE 488 interfaces Modems
Forethought Products 87070 Dukhobar Road Eugene, OR 97402	Expansion mother boards Memory boards (RAM, ROM, EPROM) STD bus interfaces Video expansion Floppy disk controllers Parallel ports Timer/counter boards Serial interface (RS 232C)
Seawell Marketing Inc. P.O. Box 17170 Seattle, WA 98107	Expansion mother boards Memory boards (RAM, ROM, EPROM) Parallel ports Floppy disk controllers EPROM programmers Proto boards Power supplies

the AIMS are provided with software to make them comply with the requirements of CP/M and MP/M.

Networking software had to be developed only for the AIM. The excellent documentation of the AIM monitor made this task quite straightforward. A program of only 350 bytes was required to allow a number of operating modes for the AIM within the network (listings of the software are available from the authors). The network software provides the AIM with the ability to communicate to the laboratory computer one character at a time or to transfer program and data files to the disks of the laboratory computer. The latter task is accomplished by having the AIM emulate a user and transfer the data as characters to the disk by using the CP/M Peripheral Interchange Program (PIP). Most operating systems have a Peripheral Interchange Program (PIP in CP/M or MP/M, PIP for DEC RT-11, COPY for MS DOS) and these operate in much the same manner. Therefore, our implementation of the laboratory network could easily be adapted to other laboratory computers.

The AIM software allows the RS 232C network interface to be used either as an auxiliary input/output device or as the main input/output device (enabling direct external control of the AIM). There are routines which perform file transfers by using the PIP with either monitor (operator) control or BASIC program control. The latter is used to transfer data files to the laboratory computer. In order to make the software as general-purpose as possible, the handshake strategy adopted was the echo and XON/XOFF protocol; that is, each character transferred on the network interface must be echoed by the receiver and the latter can halt and resume the transmission by using the XON/XOFF (terminal on/off) protocol. This handshake strategy is supported by most of the Peripheral Interchange Programs of the various operating systems when interacting with a console.

NETWORK OPERATING MODES

Figure 1 shows the many system configurations obtainable, with the same hardware in each case. These configurations are completely interchangeable with a minimum of effort, quite often by simply

choosing the single- or multi-user version of the operating system. Figures 1c and 1d illustrate the two modes of operation of the network as we have arranged it. The first (Fig. 1c) can be called the "slave" network operating mode while the second (Fig. 1d) can be called the "co-user" mode. With the 256-kbyte memory of our laboratory computer, the operating system allows up to 5 independent users (terminals or AIMS) or tasks on the system at any given time.

In the "co-user" mode of operation (Fig. 1d), the laboratory computer runs MP/M, the multi-user operating system, and each of the dedicated computers acts as a user at the same level as a user at a terminal. The AIMS have the capability of initiating any process on the laboratory computer that a terminal user can. Generally, an operator at the experimental site will load and execute a program on the AIM, which will perform the experiment and then, using the file-transfer routines of the network software, will transfer the data as a file to the laboratory computer disks through use of the PIP. The AIM can execute a continually running program which will perform the experiment on a series of samples and send the sample data files to the laboratory computer without operator intervention. The program on the AIM could, in fact, execute an application program for a data-base management system, interact with it, and thereby ensure transfer of the processed sample data directly into the laboratory data-base. The AIMS printer can be used to obtain hard copy for verification and back-up in case of network malfunction.

In the "slave" mode of operation (Fig. 1c), the dedicated computers are put under direct control of

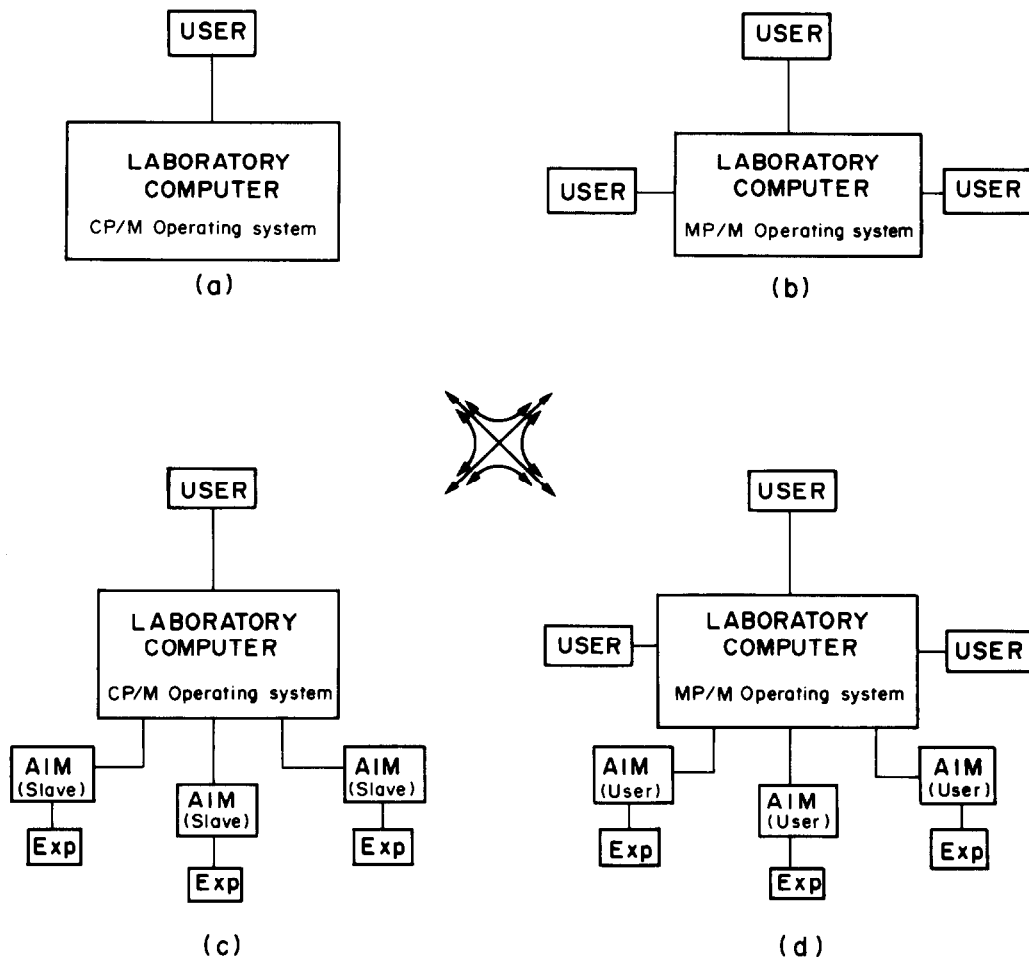


Fig. 1.

the laboratory computer and a single user. This is done by entering AIM BASIC and then selecting the RS 232C interface to the laboratory as the main input/output device. Generally, this mode requires that the laboratory computer be running the CP/M operating system (single user), though MP/M could be tolerated under certain circumstances. The single user could be at a terminal or could equally be one of the dedicated computers in its user-emulating role. The program being executed on the laboratory computer is responsible for sending commands and programs to the AIMs and receiving their output. This mode of operation of the network is that which allows the highest possible rate of data acquisition, since the laboratory computer is dedicated to the execution of a single process.

The laboratory computer program can, in this mode, synchronize the activities of a number of dedicated computers. For example, if one AIM were controlling a stepper motor attached to a spectrometer drive and another interfaced to a data-acquisition system, the laboratory computer would send to the drive-controlling AIM the wavelengths needed to locate the line of interest, but would receive

information from the data-acquisition AIM in order to position the drive exactly at the position corresponding to the spectral line. An additional feature of the CP/M operation is that it uses only a quarter of the 256 kbytes available on the laboratory computer. The remaining 192 kbytes can be used for disk emulation so that data can be stored at significantly higher rates than on flexible or rigid disks. Memory-disk emulation (RAM disk) products are commercially available for many systems.

The languages and programs that we have found useful for running under CP/M or MP/M are listed in Table 1. We generally avoid writing at the assembler level on the laboratory system, because of the lack of portability. BASIC has proved to be especially valuable, owing to its ease of use. Programs are developed by using the interpreter and then compiled if they are slow and need to be used often. Pascal is used for more complex programs, on account of its highly structured nature. Our particular implementation of Pascal supports the use of a 9511 arithmetic processor to increase the speed of computation and decrease the program size, but we have not yet felt the need to instal it.

CONCLUSIONS

An inexpensive laboratory computer network which is not dependent on any particular hardware supplier has been developed, and requires a relatively low level of expertise. Proper selection of components and operating procedures allows the laboratory computer to be used for unrelated processing during the data-acquisition process. Though the network does not provide the high transfer rates available with the proprietary networks, the simplicity of operation does allow a high degree of flexibility and control, which is very advantageous in a research laboratory, where the nature of the work may frequently change.

The system can be upgraded by acquisition of hardware and software from a wide variety of sources. Software compatibility when upgrading can be ensured by the use of a popular hardware-independent operating system.

REFERENCES

1. R. E. Dessy, *Anal. Chem.*, 1982, **54**, 1167A.
2. G. C. Levy and D. Terpstra, *Computer Networks in the Chemical Laboratory*, Wiley, New York, 1981.
3. E. D. Salin, *Am. Lab.*, 1982, No. 10, 156.
4. R. L. A. Sing, S. W. McGeorge and E. D. Salin, *Talanta*, 1983, **30**, 805.
5. E. D. Salin, *Am. Lab.*, 1982, No. 5, 132.

CRITICAL STUDY OF THE DETERMINATION OF TIN BY ELECTROTHERMAL ATOMIC-ABSORPTION SPECTROMETRY USING RESONANCE AND NON-RESONANCE LINES

JÁNOS FAZAKAS

Center for Analytical Spectrochemistry, Bd. Mărăști 61, R-71331 Bucharest 32, Rumania

(Received 23 September 1983. Revised 25 January 1984. Accepted 23 February 1984)

Summary—The 235.48 nm non-resonance line of tin gives a sensitivity for AAS determination equal to that given by the most sensitive resonance line. Vaporization from a platform improves some twofold the sensitivities of all lines investigated. The atomization temperature has only slight influence on the relative sensitivities given by the non-resonance tin lines studied. Phosphoric acid shows a rather peculiar interference pattern, low concentrations (0.05%) depressing the signal, but high concentrations (1%) enhancing it. Contrary to expectation, the resonance and non-resonance lines are affected to the same extent by phosphoric acid. Platform-vaporization does not change the interference pattern of phosphoric acid. Calibration can be done by injecting various volumes of a single standard solution onto a platform coated with tantalum carbide. This method yields calibration graphs that are just as linear as those obtained with identical volume of standards of various concentrations. Some suggestions are made for further improvement of the analytical potential of non-resonance lines.

The analytical potential of non-resonance lines in electrothermal atomic-absorption spectrometry has formed the subject of several papers¹⁻⁷ from this laboratory. The non-resonance lines of palladium,¹⁻⁵ lead, indium and thallium,⁶ as well as those of gallium⁷ all show considerable analytical potential. Besides sensitivity, another factor worth mentioning is the better linearity of some calibration graphs when non-resonance rather than resonance lines are used. The present paper continues our previous studies with another element of low volatility, namely tin.

EXPERIMENTAL

Details of the commercially available electrothermal atomizer (radiational feed-back, 2000°/sec heating rate) and spectrometer (time resolution 20 msec) were given in previous papers.^{6,7} Pyrocoated graphite furnaces were used as provided by the manufacturer.

The solid pyrographite platforms used have also been described elsewhere.² The normal platforms were coated with tantalum carbide.⁸ The solid pyrographite could not be coated efficiently with tantalum carbide since it tended to flake off after a few firings. The normal platforms were coated by a single soaking in coating solution followed by repeated injections of it.⁸ The colour of the coated platform was shiny bronze.

Drying and ashing temperatures for wall-vaporization were as recommended by the manufacturer.⁹ For platform-vaporization, drying was done at 200° for 60 sec with a ramp of 5°/sec, and ashing was done as for wall-vaporization, *i.e.*, at 800°. Atomization was always done in the "temperature control" mode (radiational feed-back). Argon was used as purge gas at a flow-rate of *ca.* 2 l./min.

Working solutions were prepared by dilutions of a 1000- μ g/ml stock solution. According to the manufacturer (Merck) the stock solution contains tin(IV) chloride in 1M hydrochloric acid. The calibration was done by injecting various volumes (5, 10, 15 and 20 μ l) of a single standard solution.

A Varian hollow-cathode lamp was used as the primary radiation source and was operated at 10 mA. A spectral bandpass of 0.2 nm was used for all wavelengths. Some characteristics of the transitions studied are given in Table 1.

In order to prevent the continuum radiation of the platform from reaching the detector, a 1-mm aperture was placed after the furnace when high atomization temperatures were used (over 2200°).

RESULTS AND DISCUSSION

Influence of set atomization temperature on signal strength

As seen from Table 1, considerable controversy exists in the literature as to the most sensitive line for

Table 1. Spectral characteristics of some tin lines, and literature values for relative sensitivities

λ , nm	Spectral term energy values, cm^{-1}	gf^{10}	Relative sensitivities			
			Ref. 11	Ref. 12	Ref. 13	Ref. 14
224.61	0-44509	0.20	1	—	1	—
235.48	1692-44145	0.93	1.6	1	2.0	1
284.00	3428-38629	2.5	—	—	—	—
288.33	0-34914	0.65	1.6	1.3	1.5	—

A relative sensitivity of 3 would mean that the line gives a sensitivity that is worse by a factor of 3 than that given by the line with which it is compared.

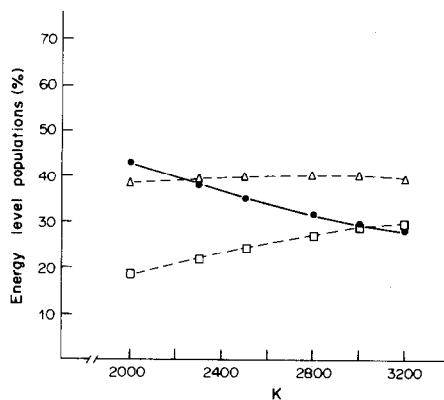


Fig. 1. Variation of the population of energy levels of tin as a function of temperature. The curves drawn are based on the data of Parsons *et al.*¹⁵ ●—●—● 0 cm^{-1} ; Δ — Δ — Δ 1691.8 cm^{-1} ; \square — \square — \square 3427.7 cm^{-1}

the determination of tin. Some of the discrepancies in the literature data are probably due to the use of different flames (air- H_2 , air- C_2H_2 , N_2O - C_2H_2). As a consequence of the different flame temperatures, the population of the excited states and hence the sensitivity of the non-resonance lines will vary.

The influence of temperature on the sensitivity of resonance and non-resonance lines was recognized by Parsons *et al.*¹⁵ as long ago as 1973. Rather unfortunately, not much attention was paid to their highly interesting article. Parsons *et al.*¹⁵ have calculated the population of the excited states for some elements, as well as the relative sensitivities, as a function of temperature. For tin they predicted the 224.61 nm resonance line would be the most sensitive. However, the sensitivity of the 235.48 nm non-resonance line increases with temperature, almost equalling that of the 224.61 nm line at around 2800 K. Parsons *et al.*¹⁵ also calculated the population of various energy levels of tin at different temperatures. Their results are summarized in Fig. 1. It may be seen from this figure that the depletion of the ground-state population with temperature is mostly due to population of the 3428 cm^{-1} level. It is certainly interesting to note that as shown in Fig. 1, at a temperature of 3200 K the ground state ranks only third in atomic population.

With flames it is only possible to vary the temperature of the analytical zone (and hence the population of excited states) by changing the flame stoichiometry or the observation height. However, in most cases it will mean a departure from the optimum atomization conditions. Thus any gain in the relative population of excited states will be more than offset by the decrease in the total number of free atoms available. However, with graphite furnaces it is possible to vary the temperature, without changing the chemistry of the atomic environment, and thus to keep constant the total number of free atoms available in the system.

Table 2 shows the relative sensitivity of various tin lines with wall- and platform-vaporization. It is in

Table 2. Relative sensitivities of some tin lines under various experimental conditions

Wavelength, nm	224.61	235.48	284.00	286.33
Wall 2200°C	2.1	2.2	4.5	2.8
Wall 2800°C	2.0	2.1	4.2	2.8
Platform 2200°C	1.2	1.2	2.2	1.4
Platform 2800°C	1	1	2.3	1.4

The absolute sensitivity for tin (amount giving 0.00436 absorbance or absorbance.sec) at 224.61 and 235.48 nm with platform vaporization at 2800° is ca. 5 pg for peak-height and ca. 8 pg for peak-area measurement. Relative sensitivities are similar for peak height and area. The results from this table represent the average value of several hundred measurements made during ca. 1 year with various graphite tubes and platforms.

order to note here that though the manufacturer recommends⁹ atomization at 2400°, we have found that a sensitivity plateau is already reached at 2200°, and that the relative sensitivity varies very little with atomization temperature. Also there is very little difference in relative sensitivity between wall- and platform-vaporization. This is contrary to our experiments with another element of low volatility (palladium)^{2,3} but in accordance with data for indium,⁶ a rather volatile element with non-resonance lines originating from levels close to those of tin. It was recently proposed¹⁶ that the ratio of the absorption at resonance lines to that at non-resonance lines be used to characterize graphite furnaces and draw conclusions on the temperature of the atom cloud. Since in our case there is little difference in the sensitivity ratios with wall- and platform-vaporization, it is tempting to conclude that the temperature of the atom cloud is not influenced by atomization temperature. This is probably not the case, but for the time being we cannot offer any reasonable explanation for the phenomena observed. One possibility would be that the population of an excited state is not purely thermally controlled but rather is governed by collisions with electrons emitted by the furnace. Thus the actual temperature would have little influence on relative sensitivities even though the electron flux should be dependent on the furnace temperature. More work is needed with other elements before definite conclusions are drawn.

It should be mentioned that many of the other tin lines¹⁰ show analytically useful absorption signals, but are not all discussed here since it would be beyond the scope of the present work to investigate the complete atomic-absorption spectrum of tin.

Before proceeding further we have to mention that the detection limits with the non-resonance lines are much better than those with the resonance lines. This is no doubt at least partly due to the fact that non-resonance lines are emitted more intensely by hollow-cathode lamps (and probably also by EDLs), thus allowing the use of much lower photomultiplier voltages than those needed when resonance lines are used.

The sensitivity of low-volatility elements is known to be impaired by the use of platform-vaporization. We have found this to be also the case for palladium.² It was concluded² that the peak-height sensitivity for palladium is lower with platform- than with wall-vaporization, because of the slower heating rate of the platform. Contrary to our expectations we have found that for tin both peak-height and area are almost doubled by use of platform-vaporization. Since it is known that tin has a strong tendency towards carbide formation we think it likely that the enhancement of both resonance and non-resonance lines may be due to the platform material being more inert than the furnace itself. A similar trend was noted by Manning.¹⁷ Similar sensitivities were obtained by us whether the platform was of solid pyrographite or normal graphite coated with tantalum carbide.

It is certainly interesting to note the rather remarkable sensitivity of the 284.00 nm non-resonance line (Table 2). Though the 284.00 nm line was reportedly used¹⁸ for temperature measurements in the graphite furnace, there is no mention in the literature of any analytical application of it.

The temperature of atomic vapour in electrothermal atomizers

Several attempts¹⁸⁻²¹ have been made to determine the temperature of the atomic vapour in graphite furnaces,^{18,19} on filaments²⁰ and in metal tube atomizers.²¹ Most workers concluded that the temperature of the furnace fill gas (and hence the temperature of atoms) closely follows the wall temperature.

In a system at thermal equilibrium, the resonance and non-resonance line peaks should appear simultaneously. Previous work with palladium³ has shown that a considerable difference exists in the peak characterization times of the resonance and non-resonance lines. This should be taken to mean that the furnaces used were far from reaching thermal equilibrium during the evolution of the atom cloud.

In the work of Manning¹⁷ it was found that with wall-vaporization there is indeed a considerable difference in the peak times of the resonance and non-resonance lines. His results are summarized in Table 3, from which it may also be seen that even with platform-vaporization the difference in peak times still persists, even though much less than that for wall-vaporization. The logical conclusion is that

vaporization conditions are far from isothermal even with the use of a platform, and even one second after the onset of atomization. Even though Manning¹⁷ used an experimental system different from ours, we consider that since the time-resolution of the detection systems and the heating rates of the furnaces are very similar, our data are directly comparable. Unfortunately we had no possibility to monitor the peak shapes with the present experimental arrangement. In an independent work, Ohta and Suzuki²¹ also found different peak shapes for the 224.61 nm resonance and 235.48 nm non-resonance lines. These authors found that the peak for the non-resonance line appears later and at higher temperature than that for the resonance line. However, they found the non-resonance line to be less sensitive than the resonance line under their experimental conditions. It is indeed remarkable that our data and those of Manning and of Ohta and Suzuki are in such close agreement, in spite of the quite different instrumentation used (graphite furnaces of different design by us and Manning and a molybdenum microtube atomizer by Ohta and Suzuki). This proves yet again, that when optimized experimental systems are used (high atomizer heating rates and high time-resolution of the detection system), reproducible, reliable and accurate results may be obtained from different laboratories.

In view of the above we consider that the rather optimistic view of atomic-vapour temperature taken by previous workers is probably due to the inaccuracy of the *gf* values used in their calculations. Thus we believe it worthwhile to make further refinements in the design of furnace atomizers, with a view to increasing the atomic-vapour temperature. The "contour"²² and "curtain"²³ tubes as well as the use of capacitive discharge heating²⁴ with or without platform-vaporization may prove to be at least a temporary panacea for those ardently pursuing isothermality in non-isothermal, pulsed atomizers.

Linearity of calibration curves

In previous papers from this laboratory²⁻⁷ we discussed the reasons for the linearity of the calibration graphs being better for non-resonance than for resonance lines. For tin we have found that the 235.48 nm non-resonance line gives a much more linear calibration than the 224.61 nm resonance line. However, the 286.33 nm resonance line yields just as linear a calibration (up to a peak-height absorbance of *ca.* 1). When speaking of the linearity of calibration curves we consider only the absorbance domain. With the detection system used, there is no instrumental contribution to the non-linearity of calibration curves.

As mentioned earlier, we did the calibration by using various volumes of a single standard. Such a procedure was previously considered as inherently yielding less linear calibration than that from injection of the same volume of solutions of different concentrations, on account of differences in the spreading when different volumes are injected.

Table 3. Peak times for tin (*msec*) under various vaporization conditions¹⁷

	224.6 nm	235.3 nm
Wall 2350°C	200	300
Wall 2500°C	190	270
Platform 2350°C	1020	1060
Platform 2500°C	890	970

Atomization in an HGA-500 with pyrocoated furnaces and solid pyroplatforms.

Recent work in our laboratory²⁵ on the reduction of interferences by use of carbide coatings showed that this is due to better spreading of the sample drop on the carbide coat than on pyrocoated or normal graphite surfaces. Aqueous samples will wet the carbide-coated surfaces, thus covering a larger surface area and hence reducing the risk of formation of macrocrystals of the matrix salts. In the case of carbide-coated platforms, even a 5- μ l sample will cover the whole recess in the platform. The same is true for a 20 μ l sample, so the surface area covered will not be dependent on the sample volume, at least in the range 5–20 μ l. As a result of this, the calibration graphs constructed by use of various volumes of a single standard are just as linear as those constructed by using a constant volume and different solution concentrations. In the case of real samples, the magnitude of the tolerable background may set an upper limit for sample volumes, but for most aqueous samples it will be possible to use the varied volume method for calibration when a carbide-coated platform is used. Though only tantalum carbide was tested in the present work, it is quite likely that other carbide coatings will behave similarly. Tantalum carbide was chosen because it is the only refractory-metal carbide that is not black, and the formation or destruction of the protective carbide layer can be monitored visually.

Interference patterns of phosphoric acid

Our previous results¹⁻⁷ with non-resonance lines of different elements seemed to indicate that interference patterns may be different for resonance and non-resonance lines, as a result of the different appearance times of the two peaks. The non-resonance line would be expected to be more affected than the resonance line by vapour phase dissociation interferences at low atomizer heating-rates. In such cases, because of the early vaporization atoms will escape from the furnace before the gas temperature is high enough to populate excited states. However, with high heating rates (such as used in the present study) the whole mass of analyte plus matrix is vaporized practically instantaneously and the non-resonance line should be less affected than the resonance line by vapour phase dissociation interferences. The non-resonance peak will occur later in time^{3,17,21} (so at a higher atomic-vapour temperature), so the dissociation of molecular compounds should be more complete than at the time of measurement of the resonance line peak.

The influence of phosphoric acid on the AAS of tin has been discussed by at least two groups of workers.^{21,26} Though one group used a graphite-furnace atomizer²¹ and the other a molybdenum microtube,²⁶ both noted considerable enhancement of the tin signal by phosphoric acid. Both also noted earlier appearance of the tin peak, *i.e.*, at lower atomic-vapour temperature.

Our results are shown in Fig. 2. It is seen that while 1% phosphoric acid considerably enhances the tin

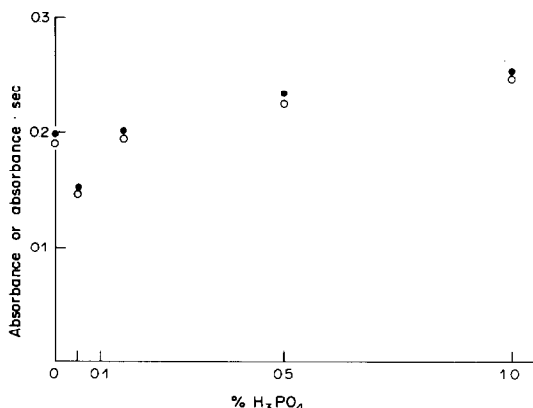


Fig. 2. Influence of phosphoric acid on tin signals. Atomization temperature 2200°C, with vaporization from the wall. Wavelength 286.33 nm. ●—●—● Peak height; ○—○—○ Peak area.

signal, there is signal depression at the 0.05% acid level. Our results illustrate that extreme care should be exercised when postulating positive or negative interferences since concentration of the interferent may have an important effect. Since we do not consider to have elucidated the effect of phosphoric acid on the tin signal, no line is drawn through the data points in Fig. 2.

Since previous workers noted a shift of the tin peak towards lower temperatures we expected the non-resonance line to be more affected than the resonance line. Contrary to our expectations, the 235.48 nm non-resonance line is affected to the same extent as the resonance line. The interference patterns were the same with both wall- and platform-vaporization. Measurement with background correction showed that there was no molecular absorption, so the explanation should be sought elsewhere. The effect described above might have been expected, however, from the constancy of the relative sensitivity of the non-resonance line at different atomization temperatures (Table 2). More work is needed with other elements and various excited levels in order to elucidate these phenomena.

CONCLUSIONS

The non-resonance lines of tin show a considerable analytical potential in electrothermal atomic-absorption spectrometry.

The 235.48 nm non-resonance line has a sensitivity equal to that of the 224.61 resonance line, but gives better linearity of response and better detection limit. Vaporization from a solid pyrographite platform or a normal graphite platform coated with tantalum carbide gives a sensitivity twice that obtained by wall-vaporization. The atomization temperature seems to have little influence on the relative sensitivity of the non-resonance lines. It seems likely that the non-resonance lines originating at energy levels below ca. 4000 cm^{-1} are little affected by atomization tem-

perature, at least in the range normally used in furnace work (2000–3000°).

The interference patterns of phosphoric acid are rather curious and the interaction mechanism is not yet clear. Low acid concentrations (0.05%) depress the signal, but higher concentrations (1%) enhance it.

The calibration for tin (and other elements) may be done by placing various volumes of a single standard on a tantalum carbide coated platform.

In view of earlier work on palladium³ and tin^{17,21} and the present work with tin, it seems necessary to reconsider some literature data on temperature of the atomic vapour in electrothermal atomizers. It is now quite clear that since the resonance and non-resonance peaks have different appearance times, the ratio of the peak absorbances will not necessarily yield the true atomic-vapour temperature, and thus may be misleading.

It certainly seems worthwhile to investigate further the analytical potential of the non-resonance lines of various elements, but the full potential will only be realized in atomizers isothermal in space and time. Unfortunately such atomizers are not yet available commercially. Optimization of sensitivity at the non-resonance lines is not an aim in itself. It should be borne in mind that the best sensitivity for non-resonance lines is achieved when the atomic-vapour temperature is highest. The very same conditions should mean a reduction of interferences at the resonance line. It is also to be expected that the optimum conditions for non-resonance line AAS will also be optimum for electrothermal atomic-emission spectrometry.

Our work on the non-resonance lines is not intended to relegate the use of resonance lines to a minor importance. Their use is here to stay, but we regard the non-resonance lines as being a welcome addition to the analytical arsenal of practising spectroscopists, since they may considerably enlarge the flexibility of the technique.

The first paper to draw attention to the analytical potential of non-resonance lines was by Siemer and Stone²⁷ in 1975. Rather unfortunately, however, that paper soon passed into oblivion. We hope that our series of papers¹⁻⁷ will not suffer the same fate, but will succeed in drawing the attention of our colleagues to this unjustly neglected aspect of atomic-absorption spectrometry. We believe the time has

come to give this step-child of atomic absorption its rightful place.

Acknowledgements—The author is deeply indebted to D. C. Manning for supplying details of his work¹⁷ and for permission to quote it. He also wishes to thank Mr. P. V. Botha for drawing the figures, and to David Tyreman (Pye Unicam Ltd.) for supplying some of the graphite tubes.

REFERENCES

1. J. Fazakas, *Anal. Lett.*, 1981, **14**, 535.
2. *Idem, ibid.*, 1982, **15**, 245.
3. *Idem, Z. Anal. Chem.*, 1982, **312**, 227.
4. *Idem, Spectrosc. Lett.*, 1982, **15**, 21.
5. *Idem, Spectrochim. Acta*, 1982, **37B**, 921.
6. P. V. Botha and J. Fazakas, *Spectrochim. Acta*, 1984, **39B**, 379.
7. *Idem, Anal. Chim. Acta*, in the press.
8. V. Zátka, *Anal. Chem.*, 1978, **50**, 538.
9. T. C. Dymott, *Atomic Absorption with Electrothermal Atomization*, Pye Unicam, Cambridge, 1981.
10. R. Mavrodineanu and H. Boiteux, *Flame Spectroscopy*, Wiley, New York, 1965.
11. *Analytical Methods Manual*, Perkin-Elmer, Norwalk, Conn., 1977.
12. *Hollow Cathode Lamp Data*, Varian Techtron, 1973.
13. P. J. Whiteside and B. A. Milner, *Pye Unicam Atomic Absorption Data Book*, 4th Ed., Pye Unicam, Cambridge, 1981.
14. *Atomic Absorption Methods Manual*, Vol. 2, *Flameless Operations*, Instrumentation Laboratory Inc., Lexington, Massachusetts, 1976.
15. M. L. Parsons, B. W. Smith and P. M. McElfesh, *Appl. Spectrosc.*, 1973, **27**, 471.
16. D. D. Siemer, *ibid.*, 1983, **37**, 73.
17. D. C. Manning, Private communication.
18. R. E. Sturgeon and C. L. Chakrabarti, *Spectrochim. Acta*, 1977, **32B**, 231.
19. W. N. G. T. Van den Broek, L. de Galan, J. P. Matousek and E. J. Czobik, *Anal. Chim. Acta*, 1978, **100**, 121.
20. Y. Iida, M. Yagomisaua, K. Kitagawa and T. Takenchi, *J. Spectrosc. Soc. Japan*, 1975, **24**, 123.
21. M. Suzuki and K. Ohta, *Progr. Anal. Atom. Spectrosc.*, 1983, **6**, 49.
22. D. C. Manning and W. Slavin, *Anal. Chim. Acta*, 1980, **118**, 301.
23. W. Slavin, G. R. Carnick, D. C. Manning and E. Pruszkowska, Paper No. 240 presented at the Pittsburgh Conference on Analytical Chemistry and Applied Spectroscopy, Atlantic City, N.J., March, 1983.
24. C. L. Chakrabarti, H. A. Hamed, C. C. Wan, W. C. Li, P. C. Bertels, D. C. Gregoire and S. Lee, *Anal. Chem.*, 1980, **52**, 167.
25. J. Fazakas, unpublished work.
26. E. J. Czobik and J. P. Matousek, *Talanta*, 1977, **24**, 573.
27. D. D. Siemer and R. W. Stone, *Appl. Spectrosc.*, 1975, **29**, 240.

STUDY OF THE POTENTIAL RESPONSE OF SOLID-STATE CHLORIDE ELECTRODES AT LOW CONCENTRATION RANGES

E. G. HARSÁNYI, K. TÓTH and E. PUNGOR

Institute for General and Analytical Chemistry, Technical University, Budapest, Hungary

YOSHIO UMEZAWA

Department of Chemistry, Faculty of Science, The University of Tokyo, Hongo, Tokyo 113, Japan

SHIZUO FUJIWARA

Department of Chemistry, Faculty of Science, Chiba University, Yayoi, Chiba, Japan

(Received 14 December 1983. Accepted 23 February 1984)

Summary—Ion-selective electrodes based on silver chloride precipitates have been investigated in the low concentration range, by use of a specially designed cell of small volume. Electrode potential measurements and silver determinations in the corresponding solutions by atomic-absorption spectrometry were made. The results prove that the potential response of these ion-selective electrodes in the low concentration ranges is governed by inequality of the ion concentrations in the boundary zone of the test solution contacting the electrode membrane. This is a result of adsorption-desorption processes, a dissolution process followed by recrystallization of the silver chloride at the electrode membrane surface, and photoreduction of silver ions at the electrode surface.

Our earlier studies¹ on ion-selective electrodes based on silver iodide showed that use of a micro-cell with electrode membranes of relatively large surface area allowed information to be obtained for processes taking place at the electrode/solution interface. Deviations from the ideal Nernstian response at concentrations below $10^{-4} M$ were explained by adsorption-desorption processes, which means that the solubility of the precipitate-based membranes is not the only process to be considered in interpreting the behaviour of the electrode at concentrations near the detection limit. Silver iodide has a relatively low solubility product, and it is a question whether the same considerations hold for membranes based on precipitates with higher solubility products, such as silver chloride (for which² K_{sp} is 1.56×10^{-10} at 25°).

Various authors have based theoretical equations on the solubility product, for describing the electrode potential *vs.* activity function of silver chloride based ion-selective electrodes at low concentrations.³⁻⁷ However, the theoretical and practical calibration curves did not match completely (*e.g.*, in the work of Morf^{6,7}) but no detailed explanation for this anomalous behaviour was given. In spite of this, chloride has been determined potentiometrically at the ng/ml level, with good reproducibility, by optimization of the analytical conditions (temperature, *etc.*) for the particular analytical problem.⁸⁻¹¹

The combined potentiometric and atomic-absorption technique described in our previous papers^{1,12} seemed to be appropriate for studying the membrane/solution interface processes in the case of

the silver chloride based membrane electrodes, and to interpret their anomalous behaviour in the lower concentration ranges.

EXPERIMENTAL

Electrodes

(a) A home-made AgCl-based homogenous pressed-pellet electrode. A mixture of 100 ml of 1M potassium chloride, 300 ml of distilled water and 100 ml of 1M nitric acid was potentiometrically titrated to the equivalence point, with 1M silver nitrate, a Radelkis OP-Ag-711 silver ion-selective electrode and OP 820 P Ag/AgCl, KNO₃ double-junction reference electrode being used. Analytical grade reagents were used throughout the work.

(b) A home-made Ag₂S/AgCl electrode, prepared as described earlier.¹³

(c) An Ag/AgCl electrode of the second kind. A properly pretreated silver disc (12 mm diameter) was covered electrolytically with a silver chloride layer.¹⁴ Pellets (diameter 12 mm) were pressed from the precipitates used for electrodes (a) and (b), at a pressure of $10^6 N/cm^2$, and were glued onto glass tubes with "Araldite". The inner electrode was an Ag/AgCl electrode of the second kind, and the inner electrolyte was $10^{-3} M$ potassium chloride.

Cell and measuring device

The same micro-cell and measuring method were used as described in our previous papers.^{1,12} The volume of the cell was 300 μ l and the electrode potentials were measured every minute after immersion of the electrodes, but the readings taken at the tenth minute were accepted as the final value. After the potential measurements the actual silver concentrations of the solutions were determined by atomic-absorption spectrometry (Varian AA6 instrument). All potential measurements were done at $25 \pm 0.5^\circ$.

Conditioning of the electrode membranes

Before potentiometric measurements were made the elec-

trodes were conditioned in most cases in stirred distilled water for 30 min, or in special cases in counter-ion solutions, e.g., in 0.1M potassium chloride before investigation of silver-ion response and in 0.1M silver nitrate before that of chloride-ion response.

Calibration was done over the concentration range 10^{-6} – 10^{-2} M silver nitrate or potassium chloride, in both micro- and macro-cells. The activity values were calculated by means of the Debye-Hückel theory.¹⁵

RESULTS AND DISCUSSION

The calibration graphs for the three kinds of electrode are presented in Fig. 1. The graphs are similar but the E° values differ slightly, which is in agreement with the earlier findings of Marton and Pungor.¹⁶

To follow membrane/solution interface reactions by measuring the activity changes in the test solution, the potentiometric calibrations were repeated with the $\text{Ag}_2\text{S}/\text{AgCl}$ -based electrode in the micro-cell (Fig. 2) after the electrode had been conditioned in distilled water. Similar curves were obtained with the other two types of electrodes.

Figure 2 shows that the calibration graphs for silver and chloride are not mirror images. To compare the experimental and theoretical curves, the latter were calculated on the basis of the existing theories based on the solubility equilibrium ($K_{sp} = 1.5 \times 10^{-10}$ at 25°). With the E° data obtained from extrapolation of the calibration graphs, the theoretical calibration curves supposed to be valid in the region of the lower detection limit were calculated by using the following equation:³

$$E = E^\circ \pm \frac{RT}{F} \ln \left(\frac{a_y + [a_y^2 + 4K_p]^{1/2}}{2} \right) \quad (1)$$

where E is the calculated electrode potential, E° is the standard potential, a , is the activity of the ionic species (Ag^+ or Cl^-), K_p is the solubility product of

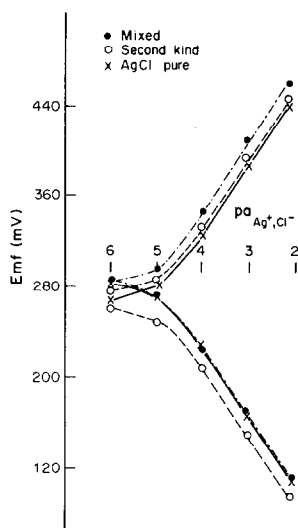


Fig. 1. Calibration graphs for the three types of silver chloride electrodes (25 ml solution volumes).

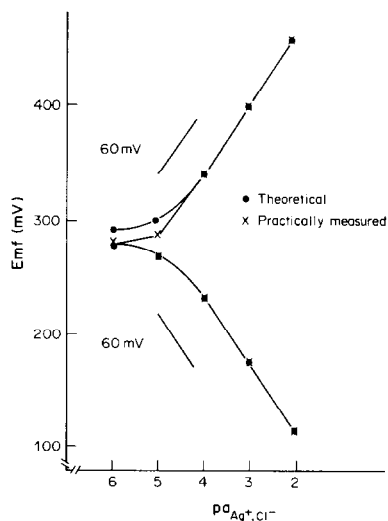


Fig. 2. Calibration graphs for an $\text{Ag}_2\text{S}/\text{AgCl}$ electrode in the micro-cell.

the membrane material and R , T and F have the usual electrochemical meaning. Theoretically the two calibration graphs should be mirror images, but Fig. 2 shows that the theoretical curve for silver-ion response is higher than the experimental one.

To interpret this anomalous behaviour, the following processes were considered: dissolution of the membrane material; adsorption and recrystallization of the membrane surface layer; kinetic processes; photoreduction.

Dissolution of the membrane material

Figure 3 shows the rate of dissolution of silver ions from the surface of the $\text{Ag}_2\text{S}/\text{AgCl}$ -based membrane in the microlitre cell filled with distilled water (similar curves were recorded for the other two types of electrode). The silver concentration was measured both potentiometrically in a microcell and by AAS. The dissolved silver concentrations measured in the tenth minute after the introduction of the electrode into the micro-cell are compared and summarized in Table 1. The silver concentration was found to be about $2\text{--}4 \times 10^{-6}$ M, which is much less than expected

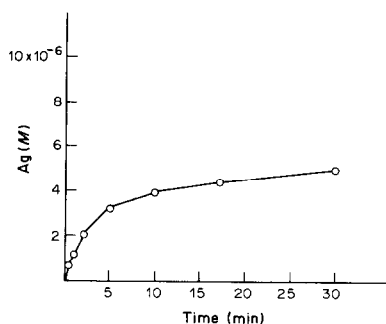


Fig. 3. Silver-ion dissolution as a function of time; measured in a 300- μl cell with an $\text{Ag}_2\text{S}/\text{AgCl}$ membrane in contact with distilled water.

Table 1. The silver and chloride ion concentrations in 300 μ l of distilled water in contact with different types of AgCl-selective electrodes

Type of electrode	[Ag ⁺] measured by AAS, 10 ⁻⁶ M		[Cl ⁻], 10 ⁻⁶ M	
	Average	RSD, %	Calculated by solubility equilibrium from [Ag ⁺] data measured	Measured by Cl ⁻ electrode
AgCl pressed pellet	3.0	5.0	52	50
Ag ₂ S/AgCl pressed pellet	3.85	2.0	40.5	50
Ag/AgCl of the 2nd kind	2.75	7.0	57	40

for equilibrium solubility. If we assume that the solubility equilibrium still holds at the membrane/solution interface, the chloride concentrations calculated from K_{sp} and the silver concentration measured by AAS are about one order of magnitude higher than the silver concentrations (Table 1, second column). The chloride concentrations (determined as described later) are also summarized in Table 1 and indicate that the concentrations of the silver and chloride ions in a solution in contact with silver chloride are not equal.

Adsorption of ions on the membrane surface; recrystallization of the surface layer

The difference between the silver and chloride ion concentrations in distilled water in contact with a silver chloride membrane may be interpreted as due to the different adsorptivity of the two ions on the AgCl pellets. To prove the existence of adsorption the actual silver ion concentrations were measured during calibration with a series of standard silver nitrate or potassium chloride solutions (Table 2). Evidently at low silver concentrations ($\leq 10^{-6}M$) the effect of dissolved silver ions cannot be neglected, but at higher concentrations the decrease in the bulk concentrations, caused by adsorption, seems to be more important. This phenomenon characterized by the decrease in silver ion concentration is supposed to be followed by formation of silver chloride microcrystals on the membrane surface. For the chloride cali-

bration, on the other hand, the AAS values for the silver concentration are around $10^{-6}M$ or less, which is lower than the values calculated on the basis of the solubility equilibrium.

The phenomenon is even more pronounced if we treat an AgCl-based electrode with the counter-ion before the calibration (e.g., conditioning for 30 min in stirred 0.1M chloride before the silver calibration and *vice versa*). The counter-ion treatment is also characterized by the potentiometric behaviour shown in Fig. 4, where the silver and chloride calibration curves cross each other if counter-ion treatment is used. The values given at the points of the curves are the actual silver concentrations measured by AAS. This anomalous deviation of the calibration curves is rectified by replotting the calibration curve with the silver concentrations actually measured by AAS, instead of the nominal values (Fig. 5). It is evident from Fig. 5 that the Nernstian behaviour for silver holds even down to $10^{-6}M$. From these results, it may be concluded that the detection limit is governed by the actual concentration of the relevant ions in the solution boundary phase, which is affected by adsorption and microcrystal formation with counterions; the latter effect always exists, owing to dissolution of the electrode membrane material.

Figure 6 shows electronmicrographs (magnification $\times 540$) of the surface of the Ag₂S/AgCl electrodes; A shows the surface of a polished but non-treated electrode pellet, B the surface of a pellet

Table 2. Silver concentrations measured in the 300- μ l cell by AAS and by potentiometry (with calibration of the AgCl-based electrode in the same cell with AgNO₃ or KCl solutions)

	Nominal sample concentration, M	Measured silver concentration, M	
		AgNO ₃ solution	KCl solution
Without electrode conditioning	0 (distilled water)	2.9×10^{-6}	3.1×10^{-6}
	10^{-6}	4.3×10^{-6}	3.1×10^{-6}
	10^{-5}	8.1×10^{-6}	2.3×10^{-6}
	10^{-4}	8.4×10^{-5}	1.1×10^{-6}
	10^{-3}	9.4×10^{-4}	5.4×10^{-7}
Electrode conditioned with 0.1M counter-ion before calibration	0 (distilled water)	1.8×10^{-6}	4.6×10^{-5}
	10^{-6}	2.8×10^{-6}	8.6×10^{-6}
	10^{-5}	8.3×10^{-6}	3.7×10^{-6}
	10^{-4}	9.2×10^{-5}	1.4×10^{-6}
	10^{-3}	—	7.0×10^{-7}

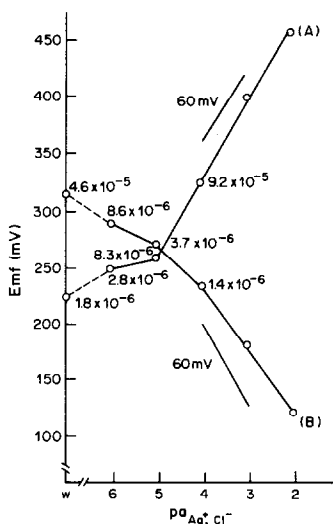


Fig. 4. Calibration graphs for an AgCl electrode after conditioning in counter-ion solutions: (A) treatment with 0.1M KCl; (B) treatment with 0.1M AgNO₃.

treated with 0.1M silver nitrate for 30 min, and C shows the electrode surface after treatment in 0.1M potassium chloride for 30 min. The pictures clearly show the formation of microcrystals at the surface, indicating that a recrystallization process takes place during use of the electrode.

Kinetic processes

These time-dependent membrane/solution interface processes were studied by recording potential *vs.* time curves. If it is supposed that the anion and cation activities in a solution contacting an AgCl membrane are at the same level as a function of time, then the potential measured in the micro-cell should not change with time. This means that *E vs. t* curves with a positive or negative slope are a proof of

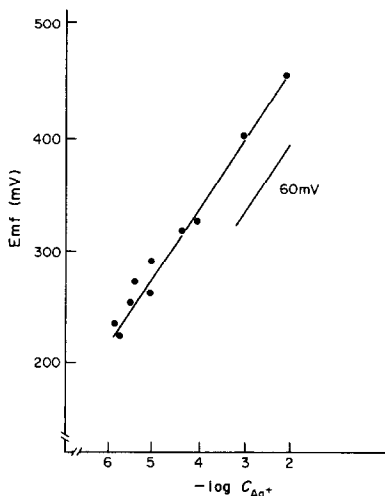


Fig. 5. Emf *vs.* log C_{Ag⁺} in the dissolution range for the AgCl electrode.

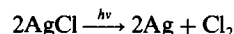
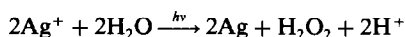
unequal concentration of cation and anion in the boundary zone of the test solution. Typical examples of *E vs. t* curves are shown in Fig. 7. For chloride, the potentials measured in a micro-cell filled with distilled water generally decrease with time (curve c) in contrast to the case for a macro-cell (curve d). In the latter case, the *E vs. t* curve is horizontal, which probably means that the effects of deposition or dissolution of the component ions of the membrane, on the primary ion activities in the boundary zone of the sample solution, are not so pronounced, owing to the steady-state diffusion of the ions dissolved, towards the bulk. *E vs. t* curves with a negative slope suggest that chloride ions are in excess in the solution phase, compared to silver ions. This conclusion is consistent with the results obtained in the work on dissolution of the membrane material. The *E vs. t* curves which exhibited an increase in chloride concentration with time in the microlitre cell were used to determine the chloride ion concentration dissolved from the membrane, as mentioned above.

The measurement of the actual dissolved chloride concentration was attempted in the following way. During 10 min after the immersion of the electrode in distilled water in a micro-cell the ion activities develop according to the solubility equilibrium and the corresponding electrode potential can be measured. The chloride ion concentration at the tenth minute was evaluated by means of a chloride calibration curve recorded in the micro-cell a few seconds ("zero minutes") after immersion of the electrode; it is supposed that at this time the dissolution of the electrode membrane material is insufficient to influence the bulk concentrations. The concentration data obtained by this method are in good correlation with the calculated values (Table 1, third column). This evaluation method was also checked by means of a calibration curve plotted on the basis of macro-cell measurements.

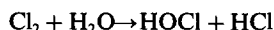
Photoreduction

Ion-adsorption at the membrane surface does not explain satisfactorily the anomaly observed in the low concentration ranges. There must also be another effect, which is more pronounced for the silver response than the chloride response and results in a deviation from the theoretical silver calibration graph in the direction of more negative potential values.

As silver chloride is photosensitive, the photo-effect has also to be considered in interpretation of the anomalous response behaviour. If it is supposed that there is photoreduction of the adsorbed silver on the solid membrane face or of the silver chloride membrane material, to metallic silver, *e.g.*,¹⁷



and



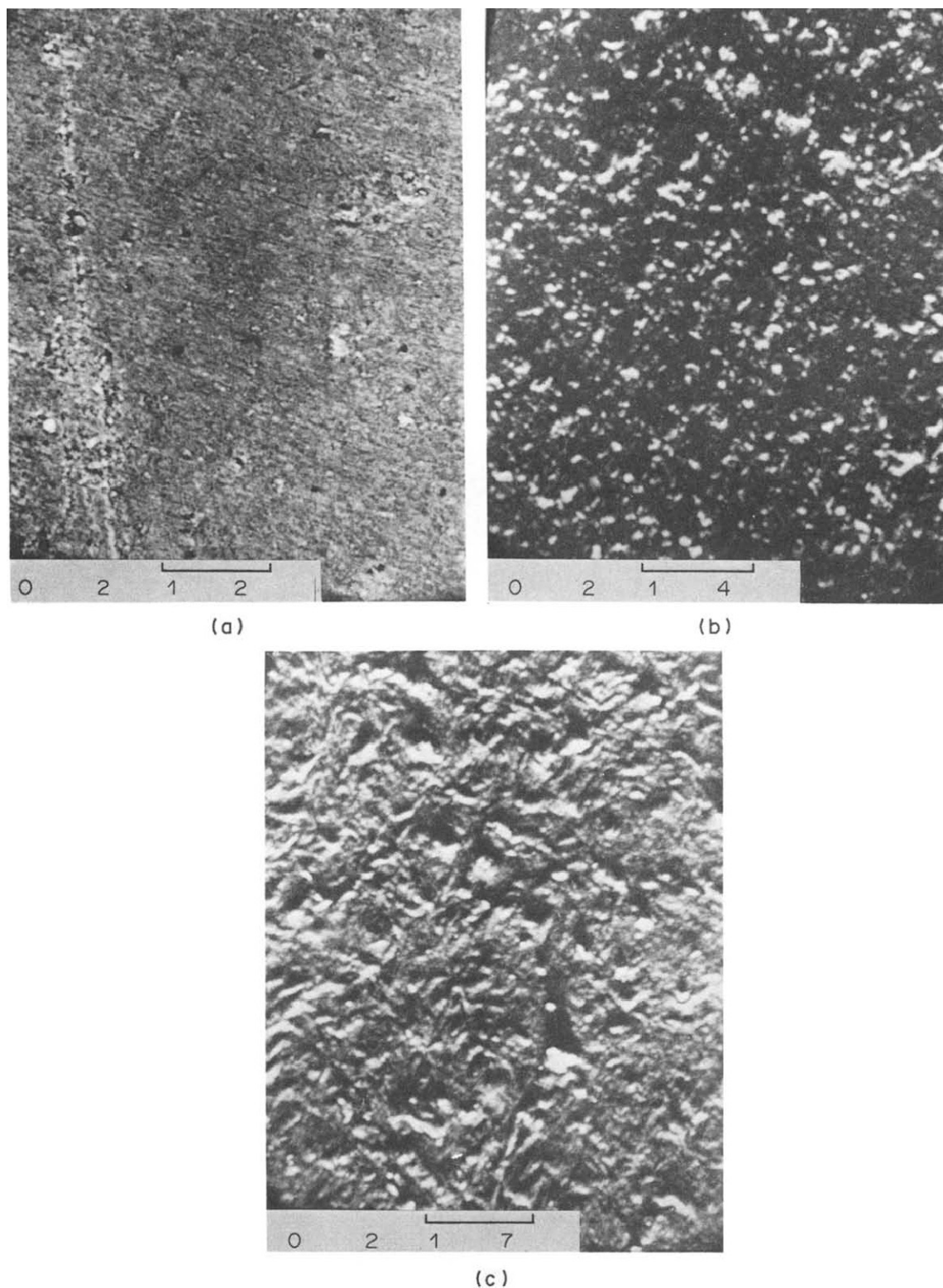


Fig. 6. Electron micrographs of $\text{Ag}_2\text{S}/\text{AgCl}$ membrane surfaces. (a) Polished untreated membrane surface; (b) membrane surface after treatment in $0.1M$ AgNO_3 for 30 min; (c) membrane surface after treatment in $0.1M$ KCl for 30 min. Magnification $\times 540$.

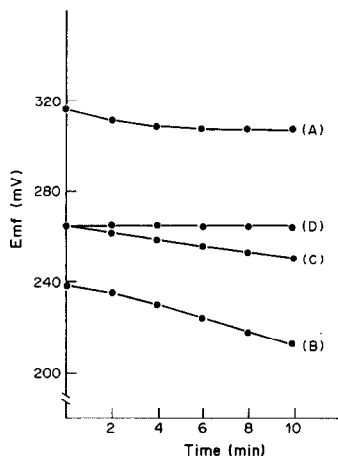


Fig. 7. Emf vs. time functions for an AgCl electrode: (A) after treatment in $0.1M$ $AgNO_3$, measured in $300 \mu l$ of distilled water; (B) after treatment in $0.1M$ KCl , measured in $300 \mu l$ of distilled water; (C) without treatment, measured in $300 \mu l$ of distilled water; (D) without treatment, measured in $25 ml$ of distilled water.

then the silver concentration in the solution phase should decrease. Thus the shift of the *E* vs. *t* curves towards more negative potentials is even more understandable. Some decrease in the silver concentration of the test solutions could also be attributed to the action of light, since the experiments were all done in daylight.

The photoreduction can be made more pronounced by irradiation with ultraviolet light. To prove the effect of photoreduction the following studies were made. A 1-g portion of the $Ag_2S/AgCl$ precipitate used for pressing the membrane pellets was suspended in $20 ml$ of distilled water and stirred for 10 min. The pH and the chloride and silver concentrations of the solution were then measured. The pH was found to be 5.6, $[Cl^-]$ $1.1 \times 10^{-5}M$ and $[Ag^+]$ $2.5 \times 10^{-6}M$.

The suspension, in a quartz beaker, was then irradiated with ultraviolet light for 10 min. After irradiation the pH had decreased to 4.7, and $[Cl^-]$ had increased to $1.5 \times 10^{-4}M$. The silver concentration measured by AAS was $3.6 \times 10^{-6}M$; that determined potentiometrically was $1 \times 10^{-6}M$. The slight difference in silver concentrations observed could be explained by the fact that the AAS data give the total silver concentration, not just the ionic concentration.

Similar experiments done with the micro-cell containing a silver chloride ion-selective membrane elec-

trode in contact with distilled water confirmed these findings.

These experiments explain the data shown in Fig. 7, curve A, and prove that the photoeffect must also be taken into consideration in interpretation of the response of the AgCl-based chloride electrode at low concentrations.

CONCLUSION

From the experimental findings it can be concluded that the potential response of the silver chloride ion-selective electrodes in the low concentration ranges is governed by inequality in the ion concentrations in the boundary zone of the test solution in contact with the electrode membrane. This is a result of adsorption-desorption processes and a dissolution process followed by formation of microcrystals of silver chloride at the electrode membrane surface. The effect of light may also contribute to the anomalous potentiometric behaviour observed. These effects were found for the three different types of AgCl-based ion-selective electrodes tested.

Acknowledgements—The authors thank the Hungarian Academy of Sciences and the Japan Society for Promotion of Sciences for supporting this research work.

REFERENCES

1. E. G. Harsányi, K. Tóth, L. Pólos and E. Pungor, *Anal. Chem.*, 1982, **54**, 1094.
2. *CRC Handbook of Chemistry and Physics*, 62nd Ed., CRC Press, Boca Raton, Florida, 1981–82.
3. E. Pungor and K. Tóth, *Analyst*, 1970, **95**, 625.
4. R. P. Buck, *Anal. Chem.*, 1968, **40**, 1432.
5. F. G. Baucke, *Electrochim. Acta*, 1972, **17**, 851.
6. W. E. Morf, *The Principles of Ion-Selective Electrodes and of Membrane Transport Studies*, in *Analytical Chemistry 2*, Akadémiai Kiadó and Elsevier, 1981.
7. W. E. Morf, G. Kahr and W. Simon, *Anal. Chem.*, 1974, **46**, 1538.
8. V. V. Bardin, *Zavodsk. Lab.*, 1962, **28**, 910.
9. T. M. Florence, *J. Electroanal. Chem.*, 1971, **31**, 77.
10. V. V. Bardin, O. F. Shartukov and V. N. Tolstousov, *Zh. Analit. Khim.*, 1972, **27**, 25.
11. K. Tomlinson and K. Torrance, *Analyst*, 1977, **102**, 1.
12. E. G. Harsányi, K. Tóth and E. Pungor, *Anal. Chim. Acta*, 1983, **152**, 163.
13. E. Pungor, J. Havas, K. Tóth and G. Madarász, *French Patent*, 1,402,343, 1965.
14. *Reference Electrodes, Theory and Practice*, D. J. G. Ives and G. I. Janz (eds.), Academic Press, New York, 1961.
15. R. A. Robinson and R. H. Stokes, *Electrolyte Solutions*, Butterworths, 1968.
16. A. Marton and E. Pungor, *Anal. Chim. Acta*, 1971, **54**, 209.
17. *Gmelins Handbuch der Anorganischen Chemie*, 8. Auflage, Silber. Band B1, Verlag Chemie, Weinheim, 1971.

EXTRACTION OF POTASSIUM *p*-NITROPHENOXIDE WITH MACROCYCLIC CROWN ETHERS AND CRYPTANDS FROM AQUEOUS MEDIUM INTO DIVERSE ORGANIC SOLVENTS: A SYSTEMATIC EVALUATION*

E. BUNCEL and H. S. SHIN

Department of Chemistry, Queen's University, Kingston, Canada

R. A. B. BANNARD and J. G. PURDON

Chemical Defence Section, Defence Research Establishment Ottawa, Shirley Bay, Ottawa, Canada

B. G. COX

Department of Chemistry, University of Stirling, Stirling, Scotland

(Received 13 December 1983. Accepted 23 February 1984)

Summary—A systematic study has been made of the extraction of potassium *p*-nitrophenoxide from aqueous medium into a number of organic solvents that are immiscible or partly miscible with water, in the presence of several macrocyclic crown ether and cryptand complexing agents. The efficiency of extraction varies extremely widely with the nature of the ligand and the solvent. For some solvent systems, DC-18-C-6 is more efficient than [2.2.2] cryptand as an extractant. The extraction values, however, provide only limited insight into the fundamental reasons behind the observed results. Hence equilibria involved have been considered and the results analysed in terms of the equilibrium constants. The microscopic and macroscopic properties of these systems are discussed.

Macrocyclic crown ethers and cryptands have found increasing use in various areas of chemistry through their characteristic ability to bind metal cations.¹⁻⁵ One important usage results from the solubilization of typical inorganic salts in non-polar and polar aprotic organic solvents, enabling reaction of the salts with a variety of organic compounds in homogeneous solution. Concomitantly, the binding of the metal cation by the macrocyclic ligands often leads to greatly enhanced reactivity of the "naked"⁶ anion;† hence such macrocycles can be of special value in studies of nucleophilic reactivity as well as in proton-abstraction processes.⁸

Partition of metal cation complexes of macrocyclic polyethers and cryptands between water and organic solvents has been extensively used as a measure of the complexing capability of the ligands.⁹ Indeed, newly synthesized ligands are generally examined in this manner.¹⁰⁻¹² However, despite the importance of extraction studies, for example in membrane model systems,^{13,14} analytical applications¹⁵ and phase-transfer catalysis,¹⁶ systematic studies have seldom been made.

In the present paper we report the results of a systematic study of the extraction of potassium

p-nitrophenoxide from aqueous medium into a number of organic solvents, with several common macrocyclic ligands as complexing agents. At the simplest, though nonetheless useful, level, the study provides a systematic body of data on the efficiency of the various ligand/solvent systems for extraction of potassium with *p*-nitrophenoxide as counter-ion. One advantage of the latter is the ease of its spectrophotometric measurement. At a deeper level, analysis of the equilibrium constants involved in this system provides insight into the fundamental relationships governing extractions, such as solute-solute and solute-solvent interactions, in the context of the special properties of the macrocyclic ether and cryptand ligands and their interactions with metal cations.

RESULTS

The extraction study was performed with dicyclohexano-18-crown-6 ether (DC-18-C-6), dibenzo-18-crown-6 ether (DB-18-C-6), 18-crown-6 ether (18-C-6), and [2.2.2]cryptand (2,2,2) as the complexing agents. The stability constants (K_s) of the potassium complexes with these ligands in water are known (Table 1). The distribution constants (K_{dc}) of the ligands between the aqueous and organic phases were determined by the method of Frensdorff² and are also given in Table 1.

The degrees of extraction of potassium *p*-nitro-

*Part of this work was presented at the Fifth Symposium on Macrocyclic Compounds, Provo, Utah, 1981.

†Special cases are known, however, in which the macrocyclic ligands have a *retarding* effect on the rate.⁷

Table 1. Distribution constants (K_{dc}) between the aqueous phase and organic solvents for macrocyclic ligands, and stability constants (K_s) in water

Ligand Solvent	K_{dc}			
	DC-18-C-6	DB-18-C-6	18-C-6	(2,2,2)
1 Methylene chloride	2.00×10^3	$> 10^{4**}$	5.00	5.00
2 Anisole	1.74×10^2	$> 10^{4**}$	0.13	0.69
3 Phenetole	1.23×10^2	$> 10^{4**}$	0.33	0.90
4 TFTP†	41.3	2.04×10^2	0.23	0.37
5 1,4-Dioxaspiro-[4,5]decane	1.65×10^2	$> 10^{4**}$	0.24	0.012
6 n-Propyl THPE§	57.0	$> 10^{4**}$	0.11	0.48
7 Isobutyronitrile	53.8	3.11×10^2	0.17	0.53
8 Phenylacetonitrile	9.06	2.52	0.27	0.43
9 Adiponitrile	78.3	$> 10^{4**}$	12.3	0.34
10 2-Methyl-3-hexanone	46.8	2.86×10^2	0.13	0.083
11 Cyclohexanone	22.4	6.30×10^2	0.13	0.25
12 Acetophenone	1.65×10^2	$> 10^{4**}$	0.20	0.36
13 Cyclohexanol	1.70×10^2	$> 10^{4**}$	0.34	1.56
14 2-Phenylethanol	7.75×10^2	$> 10^{4**}$	6.50	0.68
15 tert.-Amyl alcohol	1.23×10^2	1.94×10^2	0.53	1.33
16 Benzyl alcohol	3.06×10^2	$> 10^{4**}$	4.20	1.38
K_s	100‡	45#	115¶	$2.5 \times 10^{5**}$

*Lower limit for K_{dc} by use of the experimental method.²

†2-(Tetrahydrofurfuryloxy)tetrahydropyran.

§n-Propyl tetrahydropyran ether.

‡Reference 17.

#Reference 18.

¶Reference 19.

**Reference 20.

Table 2. Equilibrium constants* and degree of extraction for potassium *p*-nitrophenoxide with complexing agents between aqueous phase and organic solvents

Solvent	Complexing agent	Extraction %	K_{ds}	K'_e	K_e	K_{dcs}	K_a
1 Methylene chloride	—	0	—	—	—	—	—
	DC-18-C-6	88.0	—	1.57×10^2	1.61×10^2	3.24×10^3	—
	DB-18-C-6	9.0	—	3.40	3.50	7.70×10^2	—
	18-C-6 (2,2,2)	34.8 99.9	—	9.40 2.90×10^4	82.8 1.10×10^8	3.60 2.30×10^3	—
2 Anisole	—	0	—	—	—	—	—
	DC-18-C-6	68.2	—	42.4	52.6	91.6	—
	DB-18-C-6	0.36	—	1.06	0.19	42.2	—
	18-C-6 (2,2,2)	0.19 10.1	—	3.40×10^{-2} 2.70	33.5 2.36×10^5	3.79×10^{-2} 0.65	—
3 Phenetole	—	0	—	—	—	—	—
	DC-18-C-6	31.2	—	8.90	13.2	16.2	—
	DB-18-C-6	5.4	—	13.2	13.3	2.97×10^3	—
	18-C-6 (2,2,2)	3.6 8.3	—	0.92 2.33	1.33×10^2 2.86×10^5	0.38 1.04	—
4 TFTP	—	7.5	0.32	—	—	—	—
	DC-18-C-6	16.2	—	1.59×10^2	2.80×10^2	1.16×10^2	8.76×10^2
	DB-18-C-6	6.9	—	1.10×10^2	1.26×10^2	5.77×10^2	3.94×10^2
	18-C-6 (2,2,2)	1.0 2.9	—	15.5 21.6	4.70×10^2 4.22×10^6	0.940 6.25	1.47×10^3 1.32×10^7
5 1,4-Dioxaspiro-[4,5]decane	—	0.9	3.76×10^{-2}	—	—	—	—
	DC-18-C-6	24.1	—	12.0	14.7	24.3	3.91×10^3
	DB-18-C-6	0.7	—	11.3	8.08	1.81×10^3	2.15×10^2
	18-C-6 (2,2,2)	1.1 6.0	—	0.60 3.60	92.2 1.88×10^7	0.20 0.90	2.45×10^2 5.00×10^8
6 n-Propyl THPE	—	0	—	—	—	—	—
	DC-18-C-6	5.0	—	2.63	4.09	2.33	—
	DB-18-C-6	0	—	—	—	—	—
	18-C-6 (2,2,2)	0 4.5	—	— 3.60	— 4.29×10^5	— 0.830	—
7 Isobutyronitrile	—	3.3	0.14	—	—	—	—
	DC-18-C-6	94.7	—	8.92×10^3	1.38×10^4	7.42×10^3	9.86×10^4
	DB-18-C-6	62.8	—	1.55×10^3	1.65×10^3	1.16×10^4	1.19×10^4
	18-C-6 (2,2,2)	20.6 73.4	—	2.05×10^2 2.26×10^3	3.73×10^4 2.75×10^8	55.1 5.84×10^2	2.66×10^5 1.96×10^9

Table 2—cont.

Solvent	Complexing agent	Extraction %	K_{ds}	K'_e	K_e	K_{dcs}	K_a
8 Phenylacetonitrile	—	61.8	6.47				
	DC-18-C-6	80.1		3.01×10^3	3.22×10^4	2.91×10^3	4.98×10^3
	DB-18-C-6	25.8		2.95×10^2	4.73×10^3	2.66×10^2	7.31×10^2
	18-C-6	13.8		1.24×10^2	3.72×10^4	88.7	5.75×10^3
	(2,2,2)	82.7		3.84×10^3	1.54×10^9	2.63×10^3	2.39×10^8
9 Adiponitrile	—	45.7	3.36				
	DC-18-C-6	96.4		1.94×10^4	4.95×10^4	3.87×10^4	1.47×10^4
	DB-18-C-6	90.8		7.48×10^3	1.44×10^4	3.21×10^6	4.29×10^3
	18-C-6	67.1		1.31×10^3	8.43×10^3	8.98×10^2	2.51×10^3
	(2,2,2)	90.9		6.87×10^3	2.43×10^9	3.28×10^3	7.23×10^8
10 2-Methyl-3-hexanone	—	0	—				
	DC-18-C-6	29.5		2.77×10^2	4.38×10^2	2.05×10^2	
	DB-18-C-6	6.6		97.7	1.05×10^2	6.72×10^2	
	18-C-6	2.0		9.8	2.63×10^3	2.56	
	(2,2,2)	6.0		71.7	3.84×10^7	12.8	
11 Cyclohexanone	—	18.6	9.38				
	DC-18-C-6	90.2		5.47×10^4	8.81×10^4	1.98×10^4	9.39×10^3
	DB-18-C-6	22.7		1.29×10^4	1.64×10^4	2.28×10^5	1.75×10^3
	18-C-6	29.8		3.66×10^3	1.54×10^5	1.74×10^2	1.64×10^4
	(2,2,2)	81.2		4.00×10^4	1.24×10^9	1.24×10^3	1.33×10^8
12 Acetophenone	—	5.3	0.22				
	DC-18-C-6	92.6		1.68×10^4	2.07×10^4	3.40×10^4	9.39×10^4
	DB-18-C-6	74.6		2.19×10^3	2.33×10^3	5.20×10^5	1.06×10^4
	18-C-6	32.1		2.41×10^2	3.78×10^4	66.3	1.72×10^5
	(2,2,2)	92.6		6.16×10^3	1.14×10^9	1.63×10^3	5.18×10^9
13 Cyclohexanol	—	41.1	28.0				
	DC-18-C-6	69.6		1.96×10^4	3.51×10^4	5.97×10^4	1.25×10^3
	DB-18-C-6	18.8		8.15×10^3	1.45×10^4	3.25×10^6	5.18×10^2
	18-C-6	39.3		4.37×10^3	1.07×10^5	3.20×10^2	3.84×10^3
	(2,2,2)	89.2		7.70×10^4	5.53×10^8	3.45×10^3	1.97×10^7
14 2-Phenylethanol	—	11.7	5.28				
	DC-18-C-6	82.6		3.34×10^4	3.73×10^4	2.89×10^5	7.06×10^3
	DB-18-C-6	72.7		2.02×10^4	2.31×10^4	5.16×10^6	4.37×10^3
	18-C-6	81.0		3.65×10^4	6.94×10^4	3.92×10^3	1.31×10^4
	(2,2,2)	98.0		3.98×10^5	4.06×10^9	1.11×10^4	7.69×10^8
15 tert.-Amyl alcohol	—	43.8	31.6†				
	DC-18-C-6	49.3		5.81×10^3	1.08×10^4	1.33×10^4	3.42×10^2
	DB-18-C-6†	16.7		2.14×10^3	4.30×10^3	1.87×10^4	1.52×10^3
	18-C-6	17.3		1.38×10^3	2.96×10^3	13.5	93.6
	(2,2,2)	67.4		1.72×10^4	1.52×10^8	8.13×10^2	4.81×10^6
16 Benzyl alcohol	—	18.9	9.4				
	DC-18-C-6	78.4		2.80×10^4	3.55×10^4	1.09×10^5	3.78×10^3
	DB-18-C-6	73.8		2.33×10^4	2.89×10^4	6.48×10^6	3.07×10^3
	18-C-6	84.0		4.42×10^4	1.1×10^5	4.0×10^3	1.17×10^4
	(2,2,2)	93.6		1.45×10^5	7.96×10^8	4.39×10^3	8.47×10^7

*The units are not given—they can be deduced from the relevant equations.

†For tert.-amyl alcohol, the experiments with DB-18-C-6 were done with a different KOH concentration from that used with the other complexing agents (see Table 3), necessitating the measurement of a new K_{ds} value (2.83) under those conditions, for use in the calculation of K'_e , K_e , K_{dcs} and K_a .

phenoxide were determined spectrophotometrically.² In the procedure used, both potassium and ligand were usually present in excess. Results obtained in the absence and presence of ligand are given in Table 2. The former yield the distribution coefficient of the salt, K_{ds} , between the aqueous and organic phases. Other equilibrium constant data, as defined in the next section and calculated according to the method given in the Appendix, are presented in Table 2.

To test the procedure, sample calculations were done for various concentrations of potassium hydroxide and complexing agent; the resulting K_e values showed satisfactory agreement, confirming that the

scheme accommodates variations in the concentrations of potassium hydroxide and complexing agent as well as of the salt.

DISCUSSION

The results show a wide range in the effectiveness of the macrocyclic ligands in extraction of potassium *p*-nitrophenoxide from aqueous medium into organic solvents of various polarities. To explain the observed differences in behaviour, an analysis of various factors which determine the microscopic and macroscopic properties of the systems is presented.

Table 3. Initial concentrations of complexing agent (C), *p*-nitrophenol (ArOH) and potassium hydroxide in the extraction experiments

Solvent	Complexing agent (C)	Extraction, %	[ArOH], M	[KOH], M	[C], M
1 Methylene chloride	DC-18-C-6	88.0	4.65×10^{-2}	0.25	0.263
	DB-18-C-6	9.0	4.82×10^{-2}	0.25	0.123
	18-C-6 (2,2,2)	34.8 99.9	4.65×10^{-2} 4.68×10^{-2}	0.25 0.125	0.26 9.80×10^{-2}
2 Anisole	DC-18-C-6	68.2	4.62×10^{-2}	0.25	0.263
	DB-18-C-6	0.36	4.73×10^{-2}	0.25	1.36×10^{-2}
	18-C-6 (2,2,2)	0.19 10.1	4.73×10^{-2} 4.73×10^{-2}	0.25 0.25	0.197 0.175
3 Phenetole	DC-18-C-6	31.2	4.85×10^{-2}	0.50	0.119
	DB-18-C-6	5.4	4.85×10^{-2}	0.50	1.12×10^{-2}
	18-C-6 (2,2,2)	3.6 8.3	4.85×10^{-2} 4.85×10^{-2}	0.50 0.50	0.100 8.10×10^{-2}
4 TFTP	DC-18-C-6	16.3	5.75×10^{-4}	0.25	5.00×10^{-3}
	DB-18-C-6	6.9	5.75×10^{-4}	0.25	2.70×10^{-3}
	18-C-6 (2,2,2)	1.0 2.9	5.75×10^{-4} 5.75×10^{-4}	0.25 0.25	4.87×10^{-3} 5.45×10^{-3}
5 1,4-Dioxaspiro-[4,5]decane	DC-18-C-6	24.1	4.29×10^{-2}	0.25	0.120
	DB-18-C-6	0.73	4.29×10^{-2}	0.25	6.89×10^{-3}
	18-C-6 (2,2,2)	1.20 6.0	4.29×10^{-2} 4.29×10^{-2}	0.25 0.25	8.17×10^{-2} 7.56×10^{-2}
6 <i>n</i> -Propyl THPE	DC-18-C-6	5.0	4.96×10^{-2}	0.25	8.40×10^{-2}
	DB-18-C-6	—	4.96×10^{-2}	0.25	8.70×10^{-4}
	18-C-6 (2,2,2)	— 4.5	4.73×10^{-2} 4.96×10^{-2}	0.25 0.25	7.70×10^{-2} 5.54×10^{-2}
7 Isobutyronitrile	DC-18-C-6	94.7	6.67×10^{-4}	0.25	8.69×10^{-3}
	DB-18-C-6	62.8	6.67×10^{-4}	0.25	4.78×10^{-3}
	18-C-6 (2,2,2)	20.6 73.4	6.67×10^{-4} 6.67×10^{-4}	0.25 0.25	5.16×10^{-3} 5.36×10^{-3}
8 Phenylacetonitrile	DC-18-C-6	80.1	4.92×10^{-4}	0.25	5.40×10^{-3}
	DB-18-C-6	25.8	4.92×10^{-4}	0.25	4.70×10^{-3}
	18-C-6 (2,2,2)	13.9 82.7	4.92×10^{-4} 4.92×10^{-4}	0.25 0.25	5.20×10^{-3} 5.09×10^{-3}
9 Adiponitrile	DC-18-C-6	96.4	5.08×10^{-4}	0.25	5.85×10^{-3}
	DB-18-C-6	90.8	5.08×10^{-4}	0.25	5.40×10^{-3}
	18-C-6 (2,2,2)	67.4 90.9	5.08×10^{-4} 5.08×10^{-4}	0.25 0.25	6.60×10^{-3} 5.86×10^{-3}
10 2-Methyl-3-hexanone	DC-18-C-6	29.5	5.03×10^{-4}	0.25	6.10×10^{-3}
	DB-18-C-6	6.6	5.03×10^{-4}	0.25	2.82×10^{-3}
	18-C-6 (2,2,2)	2.0 6.0	5.03×10^{-4} 5.03×10^{-4}	0.25 0.25	8.26×10^{-3} 5.00×10^{-3}
11 Cyclohexanone	DC-18-C-6	90.2	4.80×10^{-4}	0.025	6.65×10^{-3}
	DB-18-C-6	22.7	4.80×10^{-4}	0.025	1.00×10^{-3}
	18-C-6 (2,2,2)	29.8 81.2	4.80×10^{-4} 4.80×10^{-4}	0.025 0.025	4.80×10^{-3} 4.72×10^{-3}
12 Acetophenone	DC-18-C-6	92.6	5.12×10^{-4}	0.25	3.43×10^{-3}
	DB-18-C-6	74.6	5.12×10^{-4}	0.25	5.80×10^{-3}
	18-C-6 (2,2,2)	32.1 92.6	5.12×10^{-4} 5.12×10^{-4}	0.25 0.25	8.00×10^{-3} 8.56×10^{-3}
13 Cyclohexanol	DC-18-C-6	69.6	5.26×10^{-4}	0.025	4.92×10^{-3}
	DB-18-C-6	18.8	5.26×10^{-4}	0.025	1.20×10^{-3}
	18-C-6 (2,2,2)	39.6 89.2	5.26×10^{-4} 5.26×10^{-4}	0.025 0.025	6.14×10^{-3} 4.64×10^{-3}
14 2-Phenylethanol	DC-18-C-6	82.6	5.23×10^{-4}	0.025	6.28×10^{-3}
	DB-18-C-6	72.7	5.23×10^{-4}	0.025	5.70×10^{-3}
	18-C-6 (2,2,2)	81.0 98.0	5.23×10^{-4} 5.23×10^{-4}	0.025 0.025	5.10×10^{-3} 5.67×10^{-3}
15 <i>tert.</i> -Amyl alcohol	DC-18-C-6	49.3	4.98×10^{-4}	0.025	6.92×10^{-3}
	DB-18-C-6	16.7	4.70×10^{-4}	0.25	4.00×10^{-4}
	18-C-6 (2,2,2)	17.3 67.4	4.98×10^{-4} 4.98×10^{-4}	0.025 0.025	6.10×10^{-3} 5.08×10^{-3}
16 Benzyl alcohol	DC-18-C-6	78.4	4.78×10^{-4}	0.025	5.54×10^{-3}
	DB-18-C-6	73.8	4.78×10^{-4}	0.025	5.20×10^{-3}
	18-C-6 (2,2,2)	84.0 93.8	4.78×10^{-4} 4.78×10^{-4}	0.025 0.025	5.20×10^{-3} 4.53×10^{-3}

K_{dc} values

An important consideration in these extractions is partition of the ligand itself between the aqueous and organic phases. Earlier studies have shown that ligands such as (2,2,2), 18-C-6 and their analogues strongly prefer the aqueous phase to a purely hydrocarbon solvent such as cyclohexane. The present results, for organic solvents of varying polarity, show that for the cyclohexano- and benzo-ligands there is in all cases a strong preference for the organic phase. With the exception of phenylacetonitrile, where K_{dc} (DC-18-C-6) > K_{dc} (DB-18-C-6), the largest values of K_{dc} are observed for DB-18-C-6, which is clearly in accord with the hydrophobic nature of this ligand. On the other hand, for (2,2,2) and 18-C-6 there is generally a preference for the aqueous phase, which is in accord with the more hydrophilic nature of these ligands.

It should also be noted that in the presence of a complexing salt, the partitioning of the ligand into the aqueous phase will be accentuated. This means that in considering extraction equilibria it is generally not valid to regard the ligand as confined to the organic phase (*vide infra*).

K_{ds} values

The results in Table 2 show that though potassium *p*-nitrophenoxide is not detectably soluble in methylene chloride or the ethereal solvents anisole, phenetole or *n*-propyl THPE (*n*-propyl tetrahydropyran ether), it is somewhat soluble in several of the more polar solvents, especially cyclohexanol, *tert*-amyl alcohol, phenylacetonitrile and adiponitrile. However, quantitative evaluation of this factor is complicated by the fact that some of these organic solvents are miscible to various degrees with water, which might be expected to influence strongly the partitioning of the salt between the two phases. This partitioning, however, must be allowed for in calculation of the various constituent equilibrium constants in the subsequent treatment.

Extraction efficiencies

The results in Table 2 show that the degree of extraction varies widely, depending on the solvent and ligand used. The ethereal solvents *n*-propyl THPE, TFTP [2-(tetrahydrofurfuryloxy)tetrahydropyran] and 1,4-dioxaspiro(4,5)decane are quite poor in this respect, while phenetole and anisole are marginally better. Also, somewhat surprisingly, 2-methyl-3-hexanone is considerably poorer than the other ketones. With these exceptions, it is clear that efficient extraction can be achieved with most of these solvents, especially with DC-18-C-6 and (2,2,2) as the ligands. It is noteworthy that in some cases DC-18-C-6 is in fact more efficient than (2,2,2), which could have important practical implications in view of the large difference in cost of these ligands. It is, however, difficult to make strict comparisons of the extraction

efficiencies from the degrees of extraction since a uniform set of conditions could not be maintained, owing to the widely different efficiencies in the respective systems. Such comparisons are more readily made in discussion of the equilibrium data.

K_e and K'_e values

The equilibrium constant for extraction (as ligand-complexed ion-pairs) of a salt MX that is dissociated in the aqueous phase, is defined by

$$K_e = \frac{[MC^+X^-]_{org}}{[M^+]_{aq}[X^-]_{aq}[C]_{org}} \quad (1)$$

where C is the ligand. However, for many systems discussed in the literature,^{2,5,10} the authors appear to use an apparent equilibrium constant (which we will call K'_e), defined by

$$K'_e = \frac{[MC^+X^-]_{org}}{[M^+]_{aq}[X^-]_{aq}[C]_{org}} \quad (2)$$

in which $[M^+]_{aq}$ and $[C]_{org}$ are the total concentrations of M^+ and C, exclusive of $[MC^+X^-]_{org}$. Thus:

$$[M^+]_{aq} = [M^+]_{tot} - [MC^+X^-]_{org} \quad (3)$$

$$[C]_{org} = [C]_{tot} - [MC^+X^-]_{org} \quad (4)$$

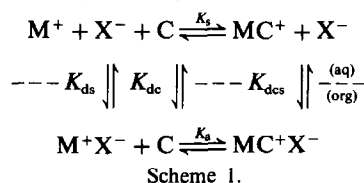
In the definition of K'_e , it is assumed that there is no ligand in the aqueous phase and no uncomplexed salt in the organic phase, and that no polymeric species are formed. Therefore, for solvent/ligand systems in which partitioning of either free or complexed ligand into the aqueous phase is very small, the K'_e values are a valid measure of the extraction equilibria. K'_e values can be calculated for systems where K_{dc} data are not available, and can be useful in an exploratory study. Values of K'_e calculated according to the expressions above are given in Table 2.

For phenetole and *n*-propyl THPE, K'_e is quite small, but is somewhat larger for 1,4-dioxaspiro(4,5)decane and TFTP, being comparable with the value for 2-methyl-3-hexanone. Much larger K'_e values are observed for phenylacetonitrile and adiponitrile, and for *tert*-amyl alcohol and benzyl alcohol.

Our previous considerations show that, particularly in the case of (2,2,2) and 18-C-6, considerable partitioning of the ligand into the aqueous phase occurs and therefore a more rigorous analysis of the equilibria is required.

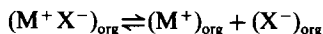
Detailed analysis of equilibria

A pictorial representation of the equilibria involved in this system is given in Scheme 1.

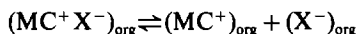


In this scheme, it is assumed that the degrees of dissociation of the uncomplexed ion-pair into free

ions, *i.e.*,



and of dissociation of the complexed ion-pairs into free charged species, *i.e.*,



in the organic phase are both negligible. The assumption that $(M^+X^-)_{org}$ does not dissociate into the free ions is probably valid for rather non-polar organic solvents. It is considered that this and the assumption that $(MC^+X^-)_{org}$ does not dissociate, will not affect the overall conclusions regarding the trends observed (see below).

The equilibrium constants in Scheme 1 are defined as:

K_s : stability constant for complex formation in aqueous phase;

K_{ds} : distribution constant of salt between aqueous and organic phases;

K_{dc} : distribution constant of complexing agent between aqueous and organic phases;

K_{dcs} : distribution constant of complexed salt between aqueous and organic phases;

K_a : equilibrium constant for complexation of salt in organic phase.

The algebraic expressions for the respective equilibrium constants are given in equations (5)–(9). Concentrations are used instead of activities, because of the lack of activity coefficient data. The agreement between the K_c values obtained on variation of the concentrations of the complexing agent, *p*-nitrophenoxide and potassium ions suggests that the procedure and approximations used are valid.

$$K_s = \frac{[MC^+]_{aq}}{[M^+]_{aq}[C]_{aq}} \quad (5)$$

$$K_{ds} = \frac{[M^+X^-]_{org}}{[M^+]_{aq}[X^-]_{aq}} \quad (6)$$

$$K_{dc} = \frac{[C]_{org}}{[C]_{aq}} \quad (7)$$

$$K_{dcs} = \frac{[MC^+X^-]_{org}}{[MC^+]_{aq}[X^-]_{aq}} \quad (8)$$

$$K_a = \frac{[MC^+X^-]_{org}}{[M^+X^-]_{org}[C]_{org}} \quad (9)$$

For purposes of calculation, only four of the constants above are independent and the first three can be determined separately from extraction experiments. In the scheme, seven different species exist in equilibrium. Their concentrations can be determined under equilibrium conditions by evaluation of the stoichiometric relationships (10)–(12):

$$[C]_{tot} = [C]_{aq} + [C]_{org} + [MC^+]_{aq} + [MC^+X^-]_{org} \quad (10)$$

$$[M^+]_{tot} = [M^+]_{aq} + [MC^+]_{aq} + [M^+X^-]_{org} + [MC^+X^-]_{org} \quad (11)$$

$$[X^-]_{tot} = [X^-]_{aq} + [M^+X^-]_{org} + [MC^+X^-]_{org} \quad (12)$$

together with the equilibrium constants K_s , K_{ds} and K_{dc} [equations (5)–(7)] and the measured concentration of $[X^-]_{aq}$. An iterative procedure described in the Appendix was used for derivation of the various quantities which are further discussed below.

Evaluation of results

Comparison of K_c and K'_c values. The values of these two equilibrium constants are expected to agree provided that (i) the partition of the ligand into the aqueous phase is small (K_{dc} large), and (ii) the stability constants (K_s) of the aqueous complexes are small.

The results in Table 2 show that these conditions are mostly met for the DC-18-C-6 and DB-18-C-6 complexes. On the other hand large differences between K_c and K'_c are found for the 18-C-6 complexes and especially for the (2,2,2) complexes (note that the K_c/K'_c ratios vary by up to 10^6). For the latter complexes, this is the result of moderate partitioning of the free ligand into the aqueous solution, in conjunction with very strong complex formation in aqueous solution.

Absolute K_c values. In all cases in Table 2, the highest K_c values are observed for the (2,2,2) complexes, while DB-18-C-6 is in general associated with the lowest K_c values. With the exception of the (2,2,2) systems, methylene chloride and the ethereal solvents are associated with K_c values which are orders of magnitude smaller than those obtained with the other solvents. The overall extraction efficiency, as represented by K_c values, is extremely favourable for the (2,2,2) complexes, for all the solvent/ligand systems studied.

Thus examination of the K_c data has revealed a relative order quite different from that for the experimental degrees of extraction, which suggested that (2,2,2) and DC-18-C-6 are often comparable in extraction efficiency. The reason for the relatively diminished degree of extraction with (2,2,2) is that a significant amount of this ligand is held in the aqueous phase, unlike DC-18-C-6.

K_{dcs} values. A different picture emerges for the extraction of the complexed salt as represented by the K_{dcs} values. Except for the solvents phenylacetonitrile, and methylene chloride, for which K_{dcs} (DC-18-C-6) $>$ K_{dcs} (2,2,2) $>$ K_{dcs} (DB-18-C-6), and amisol $[K_{dcs}$ (DC-18-C-6) $>$ K_{dcs} (DB-18-C-6)], the K_{dcs} values for DB-18-C-6 are the largest. The smallest K_{dcs} values are observed for 18-C-6.

The observation that DB-18-C-6 is associated with large K_{dcs} values can presumably be accounted for by the hydrophobic nature of this ligand and hence also of the complexed cation. However, the much less

hydrophobic nature of 18-C-6 and the fact that interactions between the cation and solvent molecules can still occur in the plane perpendicular to the ligand in the 18-C-6-complexed cation, together result in making this the least efficiently extracted of the various complexed salts.

The case of (2,2,2) is somewhat intermediate. Although this ligand is not hydrophobic, it forms a 3-dimensional cavity containing the complexed cation, which leads to the overall result observed.

Comparison of K_{ds} and K_{dcs} . It is interesting that there appears to be no correlation between the K_{dcs} and K_{ds} values. For example, in terms of K_{dcs} values, methylene chloride is comparable to the other solvents, whereas it is very poor on the basis of the K_{ds} values. This is a reflection of the fact that once the cation is complexed, specific cation-solvent interactions are essentially removed. As K_{dcs} values are governed by the complexation reaction and the K_{ds} values by the specific interactions, any connection between these quantities can only be fortuitous.

K_a values. These give a measure of the complexing ability of the ligand in the organic phase. The experimentally observed order of K_a values in practically all cases is (2,2,2) \gg (18-C-6) $>$ DC-18-C-6 $>$ DB-18-C-6, which is the order for the K_s values in methanol and water.^{21,22} It appears, therefore, that the different microscopic states of the salt, *i.e.*, free ions in water or methanol, and ion-pairs in the organic solvents, do not significantly affect the relative order of the stability constants of the complexes with the different ligands.

EXPERIMENTAL

Materials

The macrocyclic ligands were purchased from BDH, Aldrich, Merck or Parish Chemical Co. and used as received. The organic solvents were purified, dried and distilled. *p*-Nitrophenol was recrystallized from 2% v/v aqueous hydrochloric acid.

Extraction procedure

A standard aqueous solution of potassium *p*-nitrophenoxide was prepared from *p*-nitrophenol and a standard potassium hydroxide solution, the latter being in excess. A standard solution of the ligand in a particular organic solvent was also prepared. Equal volumes (1 ml) of the two solutions were placed in a small glass-stoppered test-tube and after thorough mixing on a Vortex mixer for 1 min, allowed to stand for phase separation to occur; alternatively, separation was effected by centrifugation. The equilibrium concentration of *p*-nitrophenoxide ion in both phases was determined spectrophotometrically after appropriate dilution. The measured value of the *p*-nitrophenoxide concentration in the organic phase agreed satisfactorily with the difference in the concentration in the aqueous solution before and after extraction. A "blank" extraction in the absence of ligand was also performed with each solvent for evaluation of the distribution constant K_{ds} . Only solvents which were partially miscible with water dissolved the potassium salt to a measurable degree. Details of the concentrations of reagents used are given in Table 3. The results are based on duplicate or triplicate determinations, which usually agreed within $\pm 2\%$.

K_{dc} values were measured spectrophotometrically as described by Frensdorff.²

APPENDIX

For the present systems, two cases in which K^+ is in excess relative to the other species involved can be considered for evaluation of the various equilibrium constants.

(1) The solubility of K^+X^- in the organic phase is negligible, *i.e.*, $[K^+X^-]_{org} = 0$.

Then

$$[K^+]_{aq} = [K^+]_{tot} - [KC^+X^-]_{org} \quad (A1)$$

$$[X^-]_{aq} = [X^-]_{tot} - [KC^+X^-]_{org} \quad (A2)$$

From equation (4), $[C]_{org} = [C]_{tot} - [KC^+X^-]_{org}$, and from equation (10) $[C]_{tot} = [C]_{aq} + [C]_{org} + [KC^+]_{aq} + [KC^+X^-]_{org}$, *i.e.*,

$$[C]_{org}' = [C]_{aq} + [C]_{org} + [KC^+]_{aq} \quad (A3)$$

From equation (7), $[C]_{aq} = [C]_{org}/K_{dc}$, and from equation (5), $[KC^+]_{aq} = K_s[K^+]_{aq}[C]_{aq}$; hence

$$[KC^+]_{aq} = K_s[K^+]_{aq}[C]_{org}/K_{dc} \quad (A4)$$

Substitution for $[C]_{aq}$ from equation (7) and $[KC^+]_{aq}$ from equation (A4), converts equation (A3) into

$$[C]_{org} = \frac{[C]_{org}}{1 + 1/K_{dc} + K_s[K^+]_{aq}/K_{dc}} \quad (A5)$$

For the first iteration, $[K^+]_{aq}$ is determined experimentally from equation (A1) and $[C]_{org}$ from equation (4). Substitution of these values into equation (A5) yields the first value of $[C]_{org}$ which with equation (7) gives $[C]_{aq}$ and with equation (A3) gives $[KC^+]_{aq}$. These first estimates permit the use of the more exact expression for $[K^+]_{tot}$, *viz.* equation (11), to calculate a new $[K^+]_{aq}$ since $[K^+X^-]_{org}$ is assumed to be zero. The cycle is repeated, using equations (4), (A5), (7) and (A3) to yield new values for $[K^+]_{aq}$ until the values converge (usually 2 or 3 cycles), giving all the concentrations required for calculation of K_s and K_{dcs} .

(2) The solubility of K^+X^- in the organic phase is significant. In this case, the total amounts of X^- and K^+ in the organic phase are measured, and

$$[X^-]_{org} = [K^+]_{org} = [K^+X^-]_{org} + [KC^+X^-]_{org} \quad (A6)$$

For the first iteration, the approximation $[KC^+]_{aq} = 0$ is employed in equation (11), yielding:

$$[K^+]_{aq} = [K^+]_{tot} - [K^+]_{org} \quad (A7)$$

Substitution of equation (A6) into equation (12) yields a value for $[X^-]_{aq}$:

$$[X^-]_{aq} = [X^-]_{tot} - [X^-]_{org} \quad (A8)$$

These values of $[K^+]_{aq}$ and $[X^-]_{aq}$, when substituted into equation (6), give a value for $[K^+X^-]_{org}$ which with equation (A6) yields a value for $[KC^+X^-]_{org}$:

$$[KC^+X^-]_{org} = [K^+]_{org} - [K^+X^-]_{org} \quad (A9)$$

To finish the cycle, equations (4) and (A5) are invoked, with the current values of $[K^+]_{aq}$ and $[KC^+X^-]_{org}$, to yield $[C]_{org}$ which, when substituted back into equations (7) and (A3) gives a value for $[KC^+]_{aq}$.

For the second cycle, the full expression for K^+ , equation (11), is used: $[K^+]_{aq} = [K^+]_{tot} - [KC^+]_{aq} - [K^+X^-]_{org} - [KC^+X^-]_{org}$, which on substitution from equation (A6), reduces to

$$[K^+]_{aq} = [K^+]_{tot} - [KC^+]_{aq} - [K^+]_{org} \quad (A10)$$

The cycle of equations (A10), (A8), (6), (A6), (4), (A5), (7) and (A3) is repeated until there is convergence of the desired values.

Acknowledgement—This research was supported by Supply and Services Canada, Department of National Defence (Contract No. 2SU79-00255).

REFERENCES

1. C. J. Pedersen, *J. Am. Chem. Soc.*, 1967, **89**, 7017.
2. H. K. Frensdorff, *ibid.*, 1971, **93**, 4684.
3. J. M. Lehn, *Structure and Bonding*, (Berlin), 1973, **16**, 1.
4. J. D. Lamb, R. M. Izatt and J. J. Christensen, in *Chemistry of Macrocyclic Compounds*, G. Melson (ed.), Plenum Press, New York, 1979.
5. F. de Jong and D. N. Reinhoudt, *Adv. Phys. Org. Chem.*, 1980, **17**, 279.
6. C. L. Liotta, E. Grisdale and H. P. Hopkins, Jr., *Tetrahedron Lett.*, 1975, 4205.
7. E. Buncel, E. J. Dunn, R. A. B. Bannard and J. G. Purdon, *J. Chem. Soc., Chem. Commun.*, 1984, 163.
8. E. Buncel and B. C. Menon, *J. Am. Chem. Soc.*, 1977, **99**, 4457.
9. E. Buncel, H. S. Shin, R. A. B. Bannard and J. G. Purdon, *Can. J. Chem.*, in the press.
10. E. P. Kyba, R. C. Helgeson, K. Madan, G. W. Gokel, T. L. Tarnowski, S. S. Moore and D. J. Cram, *J. Am. Chem. Soc.*, 1977, **99**, 2564.
11. J. Jawaid and F. Ingman, *Talanta*, 1978, **25**, 91.
12. D. M. Dishong, C. J. Diamond, M. I. Cinoman and G. W. Gokel, *J. Am. Chem. Soc.*, 1983, **105**, 586.
13. R. M. Izatt, D. V. Dearden, P. R. Brown, J. S. Bradshaw, J. D. Lamb and J. J. Christensen, *ibid.*, 1983, **105**, 1785.
14. T. M. Fyles, V. A. Malik-Diemer, C. A. McGavin and D. M. Whitfield, *Can. J. Chem.*, 1982, **60**, 2259.
15. I. M. Kolthoff, *Anal. Chem. Rev.*, 1979, **51**, 1R.
16. C. M. Starks and C. Liotta, *Phase Transfer Catalysis*, p. 77. Academic Press, New York, 1978.
17. R. M. Izatt, J. H. Rytting, D. P. Nelson, B. L. Haymore and J. J. Christensen, *Science*, 1969, **164**, 443.
18. E. Shchori, N. Nae and J. Jagur-Grodzinski, *J. Chem. Soc. Dalton Trans.*, 1975, 2381.
19. R. M. Izatt, R. E. Terry, B. L. Haymore, L. D. Hansen, N. K. Dalley, A. G. Avondet and J. J. Christensen, *J. Am. Chem. Soc.*, 1976, **98**, 7620.
20. J. M. Lehn and J. P. Sauvage, *Chem. Commun.*, 1971, 440.
21. B. G. Cox, *Ann. Repts. Chem. Soc. London, C*, 1981, 3.
22. M. H. Abraham, A. F. Danil de Namor and R. A. Schulz, *J. Chem. Soc. Faraday Trans. I*, 1980, **76**, 869.

DIFFERENTIAL PULSE POLAROGRAPHIC DETERMINATION OF MOLYBDENUM AFTER SEPARATION BY 8-HYDROXYQUINOLINE EXTRACTION INTO DICHLOROMETHANE

YUKIO NAGAOSA and KATSUNORI KOBAYASHI

Faculty of Engineering, Fukui University, 3-9-1 Bunkyo Fukui 910, Japan

(Received 21 November 1983. Accepted 23 February 1984)

Summary—A polarographic investigation of several metal 8-hydroxyquinolates in dichloromethane medium following solvent extraction has been made. From the data obtained, a selective, specific and sensitive method for the determination of molybdenum at ng/ml levels has been developed involving direct differential pulse polarographic measurement on the dichloromethane extract. In this work, EDTA is used as an effective masking agent to separate molybdenum from other metals. The proposed method has been applied to the determination of molybdenum in a variety of steels and NBS-SRM 1577 bovine liver with good accuracy and precision.

Molybdenum is one of the important elements affecting the physical properties of steels, alloys and high-purity metals, and it is also an essential trace element in biological systems. Therefore, numerous analytical methods have been developed for its determination, e.g., by spectrophotometry,¹ atomic-absorption,²⁻⁴ X-ray fluorescence,⁵ neutron-activation analysis⁵ and various electrochemical methods.⁶⁻⁸ Of these, a polarographic method utilizing a catalytic wave of molybdenum enables the metal to be determined with high sensitivity,⁹⁻¹² as does anodic-stripping voltammetry at mercury and graphite electrodes.¹³

In general, a preliminary separation by solvent extraction provides good selectivity for instrumental methods of analysis that tend to be subject to matrix effects or interferences from concomitant elements. Several extraction-polarographic methods for the determination of molybdenum have been reported, with ethyl acetate or chloroform as solvent for its 8-quinolinol (oxine)^{14,15} or benzohydroxamic acid^{16,17} complexes. Polarographic measurements in such cases were made after the extracts had been diluted with a polar solvent such as ethanol or acetic acid in order to enhance the conductivity of the solution. These methods are highly selective but troublesome as routine analytical procedures. Direct polarographic measurement on organic solvent phases after extraction with methyl isobutyl ketone,¹⁸ acetylacetone¹⁹ or acetonitrile²⁰ improves the simplicity and sensitivity of determination. More recently, we have developed a new extraction-polarographic method using dichloromethane,²¹ which gives a simpler and more sensitive procedure for the determination of nickel.

The present paper describes the differential pulse polarographic determination of molybdenum(VI)

after its separation by extraction of its oxine complex into dichloromethane from aqueous medium. It is demonstrated that this method is acceptably sensitive and very specific, and it has been successfully applied to the determination of molybdenum in steels and NBS-SRM 1577 bovine liver at the ppm level.

EXPERIMENTAL

Apparatus

Direct current (d.c.) and differential pulse (d.p.) polarographic measurements were made with Yanako Model P-8 and P-1100 polarographic analysers respectively, equipped with a Rika Denki Kogyo Model RW-11 X-Y recorder. A silver-silver chloride electrode served as the reference electrode and a platinum wire electrode as the counter-electrode. The dropping-mercury working electrode had the characteristics: $m = 1.9$ mg/sec and $t = 4.00$ sec in dichloromethane at open circuit. A Toa Dempa Model HM-5A pH meter was used to measure the pH of the aqueous phase after extraction

Reagents

Guaranteed-grade reagents were used unless otherwise stated.

Standard molybdenum solution (10.0 μ g/ml). Pure molybdenum trioxide (1.500 g) was dissolved in 50 ml of 2M sodium hydroxide solution, then diluted to 1 litre with water. The standard solution was prepared by diluting 10 ml of the stock solution to 1 litre with water.

Standard metal solutions. Prepared from Wako Pure Chemicals standard solutions (1000 μ g/ml) for use in atomic-absorption spectrometry.

Extraction solution. A 0.1M oxine (Wako Pure Chemicals)/0.1M tetrabutylammonium perchlorate (Tokyo Kasei Chemicals) solution in dichloromethane (Wako Pure Chemicals).

All solutions were prepared with water obtained from a Millipore Milli-Q water system.

Sample treatment

A steel sample weighing 0.1-1.0 g was transferred to a 100-ml beaker, and decomposed with 10 ml each of concentrated hydrochloric acid and 50% nitric acid on a hot

water-bath. After addition of 5 drops of concentrated hydrofluoric acid, the solution was evaporated almost to dryness. The residue was taken up with 10 ml of 2M hydrochloric acid and diluted to volume in a 100-ml standard flask with water. An aliquot of the sample solution was subjected to the polarographic determination of molybdenum as described below.

A biological sample (NBS-SRM 1577) weighing up to 5 g was transferred to a 1-litre beaker and decomposed with 10 ml each of concentrated nitric acid, concentrated sulphuric acid and concentrated perchloric acid with gentle heating (the final temperature should not exceed 170°). The subsequent procedure was the same as that described for the treatment of steel samples.

Procedure

A known volume of the sample solution was transferred to a 100-ml separatory funnel, the pH was adjusted by addition of 2M hydrochloric acid or a buffer solution, and the solution was made up to a total volume of about 50 ml. It was then shaken with 10 ml of a 0.1M oxine-0.1M TBAP mixed solution in dichloromethane for 3 min. An aliquot of the extracted organic layer was transferred into a polarographic cell, and dissolved oxygen was removed by passage of nitrogen saturated with dichloromethane. The nitrogen stream was then directed over the solution surface and the d.c. and d.p. polarograms were recorded at 25° under the following conditions: modulation amplitude, 25 mV; drop-time, 1 sec; scan-rate, 5 mV/sec.

RESULTS AND DISCUSSION

Direct current polarographic behaviour of metal oxinates

Polarographic studies were made for all metal oxinates which could be extracted into dichloromethane from aqueous solution, at the optimum pH values. In the available potential range from 0 to -1.2 V vs. Ag/AgCl electrode, most of the metal ions examined gave d.c. polarograms after extraction into the organic phase containing 0.1M TBAP as supporting electrolyte. Table I lists pH values after extraction, half-wave potentials ($E_{1/2}$), limiting currents, and slopes of the standard potential vs. current log-plot for d.c. polarograms, obtained under the experimental conditions. The data indicate that the Fe(III), Sn(IV), Mn(II) and Mo(VI) complexes all

exhibit well-defined d.c. waves which could be useful for polarographic analysis. However, the polarographic determination of molybdenum(VI) is particularly favourable because the $E_{1/2}$ value differs greatly from those of the other metal complexes and also the limiting current per unit concentration is large compared with the others. From the results shown in Table I it can be estimated that the d.c. diffusion current corresponding to a one-electron reduction was ca. 0.4 μ A for a 10^{-4} M solution (in the dichloromethane extract) for the capillary used. On this basis it is likely that the d.c. waves for Mo(VI) as well as for U(VI) and probably for Bi(III) complexes are catalytic in nature. Therefore, a highly sensitive polarographic determination of molybdenum(VI) is possible.

Linear calibration curves for molybdenum(VI) were obtained over the concentration range from 0.04 to 20 μ g/ml with respect to the dichloromethane extract, at modulation amplitudes of 25 and 50 mV. The extraction technique using EDTA as a masking agent rendered the determination of molybdenum(VI) more specific in the presence of other ions (e.g., Fe, Bi and Cu) in sample solutions.

Effect of pH on the d.c. polarogram of the molybdenum complex

In order to determine the optimum pH-value for the determination of Mo(VI) we examined d.c. polarograms of the molybdenum complex after extraction at various pH-values. The pH was adjusted with hydrochloric acid and sodium hydroxide. A maximum and approximately constant limiting current was obtained over the pH range from 1.0 to 1.5, as shown in Fig. 1. The pH range 1.0-1.5 almost coincides with that for quantitative extraction of the molybdenum(VI) oxine complex from acidic solutions, probably as the form of MoO₂ (oxine).²² For analytical determinations the pH was kept in the range 1.0-1.2. The $E_{1/2}$ value shifted to more negative potentials with increasing pH of the aqueous solution.

Table I. Polarographic data for various metal oxinates

Metal	pH	$E_{1/2}$, V vs. SSE	I_l , μ A*	Slope of the log plot, mV
Cu(II)†	2.70	-0.342	0.97	99
Fe(III)	3.43	-0.425	0.39	50
Pb(II)†	8.51	-0.622	0.81	98
Sn(IV)	2.51	-0.453	0.37	85
		-0.625	0.78	51
Mn(II)	5.82	-0.610	0.66	67
Mo(VI)	3.09	-0.800	7.21	93
Bi(III)†	5.14	-0.431	3.02	61
Cd(II)	11.30	-0.525	0.98	160
Sb(III)†	4.01	-0.704	1.26	62
Pd(II)	2.86	-0.781	0.71	98
U(VI)	7.08	-0.722	2.95	50

*Concn. of metal ion: 10^{-4} M.

†Maximum appears.

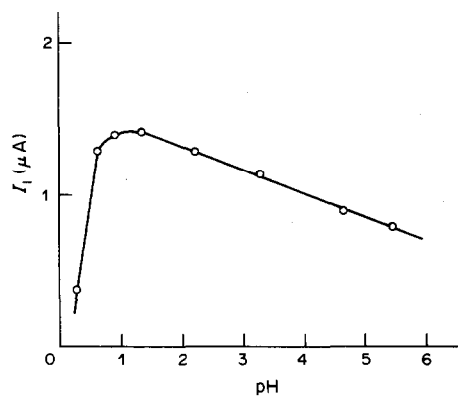


Fig. 1. Effect of pH on the limiting current for the molybdenum(VI)-oxinate complex. Molybdenum(VI) taken: 1.0 $\mu\text{g/ml}$.

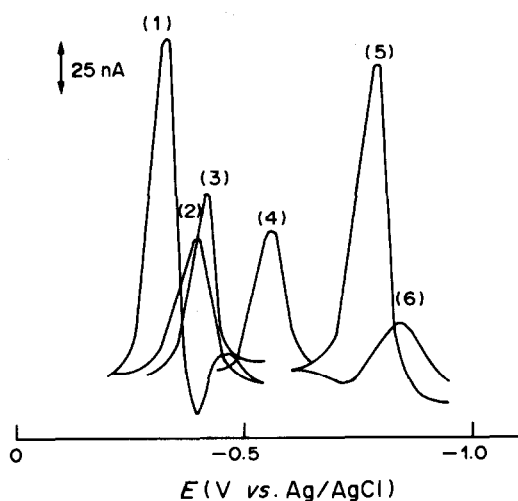


Fig. 2. Differential pulse polarograms of metal oxinates. (1): Cu(II), (2): Fe(III), (3): Bi(III), (4): U(VI), (5): Mo(VI), (6): Pb(II). pH: 4.6 ± 0.1 (10.5 for Pb and 1.2 for Mo). Each metal ion taken: 10 $\mu\text{g/ml}$ (23.8 $\mu\text{g/ml}$ for U). Conditions were modulation amplitude, 25 mV; scan-rate, 5 mV/sec; drop-time, 1 sec.

Differential pulse polarographic determinations of molybdenum(VI)

In order to improve the sensitivity of the direct d.c. polarographic determination of molybdenum, d.p. polarographic studies were undertaken on dichloro-

methane extracts of the oxine complex. Maximum sensitivity was obtained at the same optimum pH-values observed for d.c. polarographic studies. Figure 2 shows the d.p. polarograms obtained for the copper(II), iron(III), bismuth(III), uranium(VI), molybdenum(VI) and lead(II) complexes in a dichloromethane solution containing 0.1M TBAP as supporting electrolyte. As stated previously, the d.p. polarographic determination of molybdenum(VI) was investigated in detail because the response is sensitive and the peak well separated from those for other metals. When a large modulation amplitude and a short drop-time were used for the d.p. polarographic measurement, the peak height became maximal. In the present work, a modulation amplitude of 25 mV and drop-time of 1 sec were chosen as being very suitable for analytical purposes.

Calibration curve for determination of molybdenum(VI)

The peak height increased linearly from 0.01 to 2.0 $\mu\text{g/ml}$ molybdenum concentration in a dichloromethane extract at a modulation amplitude of 25 mV. In five replicate determinations of 1.0- $\mu\text{g/ml}$ molybdenum(VI), the average peak height was (17.5 ± 0.4) nA. If a ca. 10% relative standard deviation is acceptable, the lower limit of molybdenum(VI) determination is 0.005 $\mu\text{g/ml}$ at a modulation amplitude of 50 mV, corresponding to 1 ng/ml molybdenum(VI) in the original aqueous solution.

Interferences

EDTA could be used as the masking agent for selective extraction of the molybdenum(VI)-oxine complex into dichloromethane, since iron(III), copper(II) and bismuth(III) are not extracted in its presence. For example, the interference from 10 mg of iron(III) is eliminated by addition of 2.0 ml of 0.1M EDTA (disodium salt). The data shown in Table 2 indicate that foreign oxo-anions in large amounts may interfere to varying degrees with the d.p. polarographic determination of molybdenum(VI). However, interferences are generally minimal and a rapid reliable method can be developed for most matrices.

Table 2. Effect of diverse anions on the determination of Mo(VI)

Ion	Added, mg	Mo(VI) found, μg	Error, %
None	—	10.00	—
CrO_4^{2-}	0.02	10.12	+1.2
	0.05	9.09	-9.1
VO_3^-	5.0	10.57	+5.7
	10.0	—	—
MnO_4^-	0.01	10.64	+6.4
	0.02	10.91	+9.1
WO_4^{2-}	0.5	10.05	+0.5
	1.0	6.49	-35.1

Masking agent: 2.0 ml of 0.1M EDTA.

Table 3. Analytical results for various samples

Sample	Sample taken, mg	Mo found,* %	Certified value, %
NBS 160b (Stainless steel)	0.2	2.34 ± 0.13	2.38
NBS 163 (Steel)	10†	0.0288 ± 0.001	0.029
NBS 362 (Low-alloy steel)	5	0.069 ± 0.004	0.068
JJS 503-4 (Ni-Cr steel)	10†	0.0127 ± 0.0004	0.013
JJS 505-5 (Ni-Cr-Mo steel)	2	0.219 ± 0.003	0.22
SRM 1577 (Bovine liver)	200	3.39 ± 0.24§	3.4§

*Based on 5 replicate determinations.

†0.1M EDTA: 2.0 ml.

§ppm.

Analytical applications

The present method was applied to the determination of molybdenum in various steels and in bovine liver (SRM-1577). The analytical results are given in Table 3. Extractions were done after addition of 2.0 ml of 0.1M EDTA to the sample solution, and the dichloromethane extract was subjected to direct d.p. polarographic measurements. It is evident that the molybdenum contents of such samples are consistent with the certified values. We conclude that this polarographic method is accurate and specific for the determination of molybdenum in such samples.

Acknowledgement—We thank Professor A. M. Bond of Deakin University for thorough reading of the manuscript and for helpful suggestions.

REFERENCES

1. E. B. Sandell, *Colorimetric Determination of Traces of Metals*, 3rd Ed., p. 640. Interscience, New York, 1959.
2. L. Wish, *Anal. Chem.*, 1962, **34**, 625.
3. C. H. Kim, C. M. Owens and L. E. Smythe, *Talanta*, 1976, **23**, 229.
4. E. M. Donaldson, *ibid.*, 1980, **27**, 79.
5. J. J. Dulka and T. H. Risby, *Anal. Chem.*, 1976, **48**, 640A.
6. G. P. Haight, *ibid.*, 1951, **23**, 1505.
7. P. Jost, P. Lagrange, M. Wolff and J. P. Schwing, *J. Less-Common Metals*, 1974, **36**, 169.
8. V. F. Toropova, V. A. Vekslina and N. G. Chovnik, *Zh. Analit. Khim.*, 1973, **28**, 967.
9. A. T. Vialanda and W. D. Cooke, *Anal. Chem.*, 1964, **36**, 2287.
10. B. Stah and K. Schöne, *Mikrochim. Acta*, 1977 **II**, 565.
11. G. D. Christian, J. L. Vandenblanck and G. J. Patriarcho, *Anal. Chim. Acta*, 1979, **108**, 149.
12. P. Lanza, D. Ferri and P. L. Buldini, *Analyst*, 1952, **24**, 366.
13. K. Ogura and Y. Enaka, *J. Electroanal. Chem.*, 1978, **93**, 213.
14. R. M. Dagnall and S. K. Hasanuddin, *Talanta*, 1968, **15**, 1025.
15. P. Bossermann and D. T. Sawter, *Anal. Chem.*, 1978, **50**, 1300.
16. S. K. Bhowal and F. Umland, *Z. Anal. Chem.*, 1976, **282**, 197.
17. S. K. Bhowal and M. Bhattacharyya, *ibid.*, 1982, **310**, 124.
18. T. Kitagawa and A. Ichimura, *Bunseki Kagaku*, 1975, **24**, 41.
19. T. Fujinaga and H. L. Lee, *Talanta*, 1977, **24**, 395.
20. Y. Nagaosa, *ibid.*, 1979, **26**, 987.
21. Y. Nagaosa and K. Kobayashi, *Anal. Lett.*, to be published.
22. J. Starý, *Anal. Chim. Acta*, 1963, **28**, 132.

SIMULTANEOUS SEPARATION OF COPPER, CADMIUM AND COBALT FROM SEA-WATER BY CO-FLOTATION WITH OCTADECYLAMINE AND FERRIC HYDROXIDE AS COLLECTORS

L. M. CABEZON, M. CABALLERO, R. CELA and J. A. PEREZ-BUSTAMANTE
Department of Analytical Chemistry, Faculty of Sciences, Cadiz, Spain

(Received 20 October 1983. Accepted 23 February 1984)

Summary—A method is proposed for the simultaneous quantitative separation of traces of Cu(II), Cd(II) and Co(II) from sea-water samples by means of the co-flotation (adsorbing colloid flotation) technique with ferric hydroxide as co-precipitant and octadecylamine as collector. The experimental parameters have been studied and optimized. The drawbacks arising from the low solubility of octadecylamine and the corresponding sublates in water have been avoided by use of a 6*M* hydrochloric acid–MIBK–ethanol (1:2:2 v/v) mixture. The results obtained by means of the proposed method have been compared with those given by the usual ammonium pyrrolidine dithiocarbamate/MIBK extraction method.

Considerable attention has been paid in the past few years to flotation methods,¹ especially co-flotation,¹⁻⁸ on account of their promising analytical potential for separation and preconcentration of trace elements, both as anionic or cationic species, in media of low and high salinity. There is special interest in application to the analysis of marine waters.^{2,3,6,9-11}

Most of the papers published so far are centred on the selection of experimental conditions for quantitative flotation of individual species,²⁻⁸ considerably less attention being paid to multielement preconcentration and separation methods.⁹⁻¹³ Also, most of the systems investigated involve use of anionic surfactants as collectors because of their greater solubility in aqueous media, which is advantageous in subsequent dissolution of the sublates for analytical purposes.

Since the flotation yield generally decreases with increasing ionic strength, the use of high molecular-weight amine-type cationic surfactants as well as of chelating surfactants is a convenient alternative in the analysis of sea-water.⁹⁻¹⁴

Results are presented here on a multielement co-flotation investigation on Cu, Cd and Co in sea-water, based on use of octadecylamine as collector and ferric hydroxide as precipitant. The sublates are readily soluble in an acidified mixture of ethanol, water and MIBK, which also increases the sensitivity in the determination of these elements by flame atomic-absorption.

EXPERIMENTAL

Reagents

All reagents used were of analytical grade except the octadecylamine (stearylamine) (Eastman, pract.) and were used without purification. A Cu(II), Cd(II), Co(II) (1000 ppm each) multistandard stock solution was suitably diluted daily for use in standard-additions work and for calibration standards. The calibration standards were matched with the

samples in all respects (solution composition and treatment).

Apparatus

A Pye-Unicam SP9-800 atomic-absorption spectrophotometer was used with an air-acetylene flame under optimized conditions (Table 1) giving a coefficient of variation of 1%.¹⁵

The co-flotation apparatus was the same as described elsewhere.^{16,17}

Procedure for co-flotation

Place 500 ml of the sea-water sample in a 600-ml beaker and add 4 ml of 0.05*M* iron (III) solution. Adjust to pH 9.5–9.9 with concentrated ammonia solution, with continuous stirring to avoid adding ammonia in excess. Transfer the mixture quantitatively into the flotation column and adjust the air flow to 150 ml/min. Add 15 ml of 0.3% octadecylamine solution in ethanol, and 2 min later add a further 5 ml of this solution and 5 ml of 0.3% sodium lauryl sulphate (NaLS) solution. After 5 min switch off the air stream and suck off the mother liquor, first through the side-drain of the column and finally through the sintered-glass plate at the bottom of the column. Dissolve the precipitate with a few 10-ml portions of 6*M* hydrochloric acid–MIBK–ethanol mixture (1:2:2 v/v), collecting the solution in a 50-ml standard flask under suction, and making up to the mark with the solvent mixture. Measure the Cu, Cd and Co in this solution by AAS, using calibration graphs or the standard-additions method.

Under the conditions given, the sensitivity is too low to allow reliable determination (especially of cobalt) at levels below 5 ng/ml. It is then necessary to use a larger volume of samples or an analytical technique with lower detection limits (e.g., graphite-furnace AAS). For 2-litre samples the amounts of the reagents must be increased to 6 ml of iron(III) solution, 25 ml of octadecylamine solution and 10 ml of NaLS solution, and the air-flow increased to 180 ml/min.

RESULTS AND DISCUSSION

Influence of salinity

According to Matsuzaki and Zeitlin,⁹ octadecylamine floats Fe(III) and Th(IV) hydroxides at pH 6–7, Hg(II) sulphide and Mn(IV) oxide at pH 3–9 and Cd(II) sulphide at pH ~9 but will not float

Table 1. Experimental parameters for the determination of Co, Cd and Cu in the sublate solutions by AAS

	Co	Cd	Cu
Acetylene flow*	9-10	9-10	9-12
Observation height, mm	6-7	5-8	6
Band-pass, nm	0.2	0.5	0.5
Integration time, sec	2.0	2.0	2.0
No. of determinations	5	5	5

*Rotameter reading.

Al(III) hydroxide. These results refer to high-salinity solutions (sea-water) and no information was given for low-salinity solutions.

Our first experiments with iron(III) hydroxide as co-precipitant at pH 5-10 showed a clear trend of the flocs to ascend to the surface, with very little tendency to form a stable foam layer, so the flocs re-entered the mother solution. Even so, the co-floatation yields obtained within 45-60 sec were >90% for Cu(II), Cd(II) and Co(II) in the pH range 9-9.5. Also, at pH > 10, obtained by addition of sodium hydroxide, the froth layer was thicker and firmer, indicating that the froth formation and, hence overall yield, depends on the salinity. This is illustrated in Fig. 1, showing the variation of cadmium concentration in a solution subjected to co-floatation with iron(III) hydroxide and octadecylamine, as a function of time. Practically all the cadmium is removed from the solution within the first 45 sec, then re-enters it. Addition of 2.5 g of sodium chloride, followed by 5 ml of octadecylamine solution, gives a quick and sharp increase in the removal of cadmium, without rapid reversal of the process. Thus octadecylamine is especially useful for floatation from high-salinity solutions.

Choice of co-precipitant

Iron(III), aluminium, thorium and lanthanum hydroxides were tried as co-precipitants for removal of Cu(II), Cd(II) and Co(II) (present at the 2- μ g/ml level) from solutions of salinity similar to that of sea-water. The initial results seemed to indicate good floatation yields (over 90% for all three species at pH 9-10, whichever co-precipitating agent was used), the solutions becoming clear very quickly, though the

stability of the froth layers was generally not very satisfactory.

These results were mainly contradictory to those of Matsuzaki and Zeitlin,⁹ who reported that octadecylamine does not bring about the floatation of iron(III), thorium and aluminium hydroxides at pH 9-10. We noticed, however, that though floatation took place readily when Cu(II), Cd(II) and Co(II) were present, in their absence there was practically no floatation of lanthanum and thorium hydroxides and only partial floatation of aluminium hydroxide, whereas iron(III) hydroxide was readily floated.

Experiments on the floatation of Cu(II), Cd(II) and Co(II) hydroxides without a co-precipitant present gave yields of over 60%, even when the metals were present at very low concentration levels (about 0.05 μ g/ml), which strongly suggests that they are co-precipitated on the surface of the aluminium, lanthanum and thorium hydroxide precipitates, and consequently modify the floatation behaviour of these hydroxides; this could explain the apparent difference between Matsuzaki and Zeitlin's results⁹ and ours.

The most suitable of the co-precipitants tested was clearly iron(III) hydroxide, which was therefore investigated further.

Co-floatation with iron(III) hydroxide

Influence of pH. Figure 2 shows the influence of pH on the co-floatation of Cu(II), Cd(II) and Co(II) with iron (III) hydroxide as co-precipitant in 3.5% sodium chloride medium. The pH is particularly critical in the case of Co(II), and the practical pH-range is restricted to 9.5-10. Figure 2 also gives information on the co-floatation yields obtained after 20 min of operation with solutions at pH 10.5 and 11, obtained by addition of sodium hydroxide (filled circles on the graphs). These yields are all higher than those obtained when the pH was adjusted with ammonia (remaining data on the graphs), presumably because formation of the amine complexes will inhibit co-precipitation of the hydroxides. Further, alkalization with sodium hydroxide makes the rate of the floatation separation much slower than that when ammonia is used.

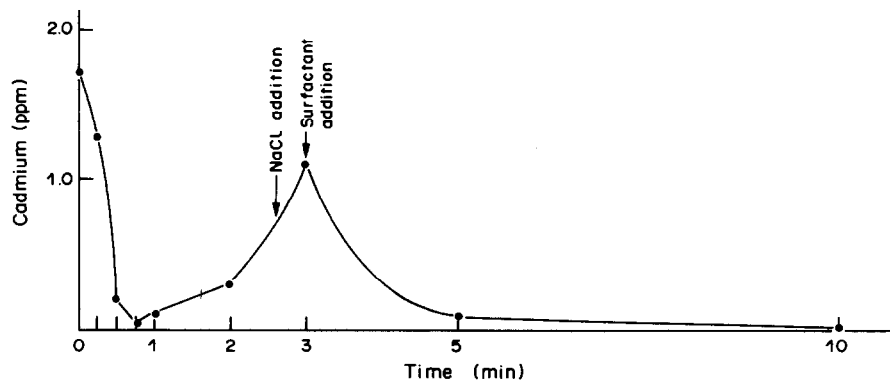


Fig. 1. Influence of salinity on the co-floatation of Cd(II) co-precipitated with iron(III) hydroxide and octadecylamine as collector.

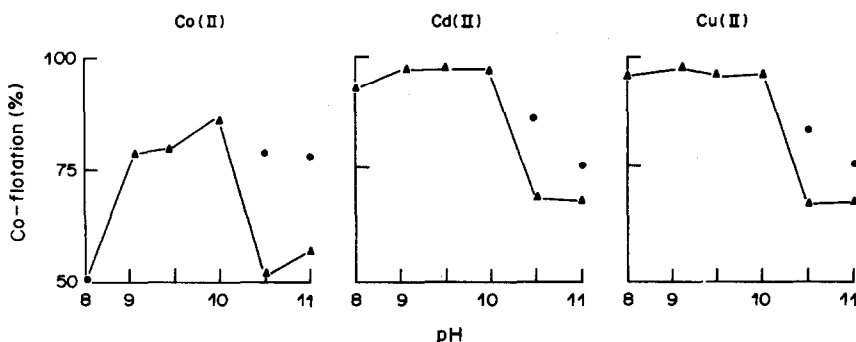


Fig. 2. Influence of the pH on the co-flotation of Cu(II), Cd(II) and Co(II).

Because, in general, the foam layer formed is not very stable, any increase in the time needed for the flotation necessitates periodic additions of surfactant to maintain the consistency of the froth layers. This is a practical inconvenience, so the use of ammonia for alkalization is generally to be preferred. However, as shown below (collector/co-precipitant ratio), though the resulting increase in surfactant concentration increases the process rate, it does not result in better yields, suggesting that the observed differences in flotation kinetics and co-flotation yield are directly related to the type of alkalization reagent and to the surface characteristics of the precipitate, respectively.

It was also observed that octadecylamine does not cause flotation of the magnesium hydroxide precipitated when the sea-water samples are made fairly strongly alkaline. This precipitate does not decrease the co-flotation yields, but in practice diminishes the final recovery of the sublates by plugging the pores of the sintered-glass plate of the column, thereby practically nullifying one of the main advantages of co-flotation over co-precipitation for isolation and preconcentration of trace ions. Addition of 1 ml of concentrated ammonia solution to a 500-ml sea-water sample that has been acidified to pH < 2 for preservation^{18,19} will raise the pH to 9.5-9.8, which guarantees that no magnesium hydroxide will be precipitated.

Influence of the flotation-gas flow-rate. Figures 3 and 4 show that the gas flow-rate does not play a significant role in the process, and it has also been

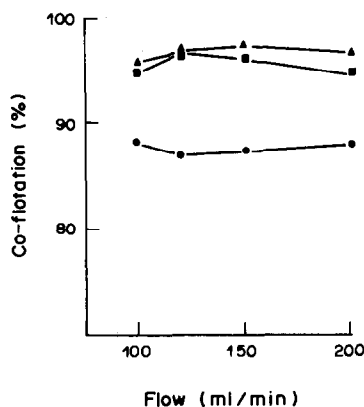


Fig. 3. Influence of the air flow-rate on the co-flotation yield [—●— Co(II); —■— Cu(II); —▲— Cd(II)].

found not to influence appreciably the amount and consistency of the froth layer. A flow-rate of 150 ml/min was systematically established as optimal.

Collector/co-precipitant ratio. The influence of the octadecylamine/iron(III) hydroxide molar concentration ratio (ϕ) on the process yield and kinetics is represented in Figs. 5 and 6, which show that the process yield is practically independent of ϕ but the rate increases with increasing ϕ to become constant at $\phi \geq 2.4$. It should be noted that the ϕ values shown refer to the starting conditions, and any octadecylamine periodically added to improve the stability of the foam layer may give rise to much greater ϕ values if the process is very prolonged.

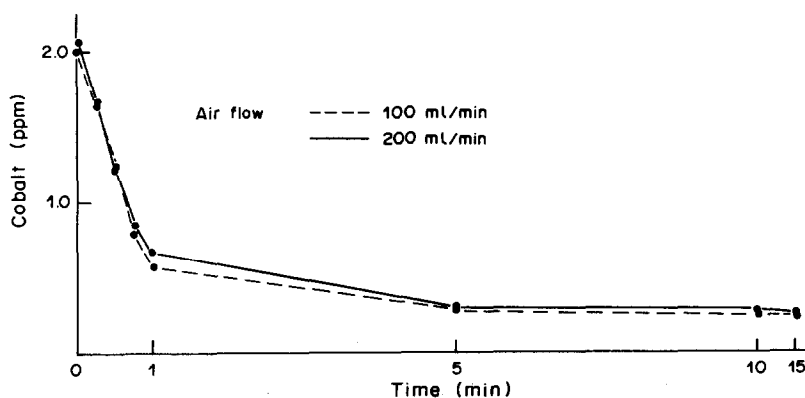


Fig. 4. Influence of the air flow-rate on the Co(II) co-flotation kinetics.

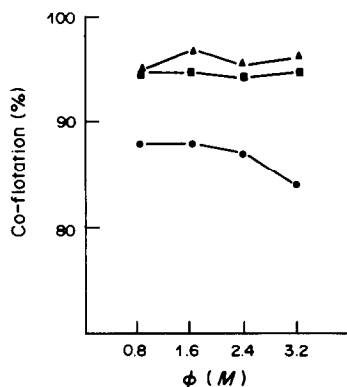


Fig. 5. Influence of the collector/co-precipitant ratio (ϕ) on the co-fotation yield [—●— Co(II); —■— Cu(II); —▲— Cd(II)].

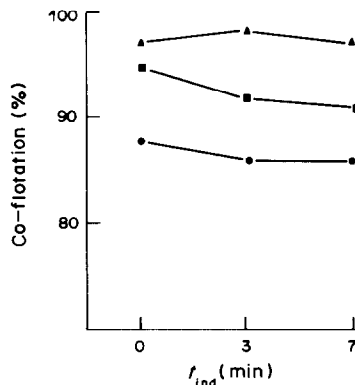


Fig. 7. Influence of the induction time on the co-fotation yield [—●— Co(II); —■— Cu(II); —▲— Cd(II)].

Induction time. Figure 7 shows that the process yield is apparently very little influenced by this parameter despite the fact that the yield tends to decrease with increasing induction time. Figure 8, however, shows a clearly negative effect of the induction time on the kinetics (similar results were obtained for copper and cobalt). Hence zero induction time is optimal, which means that the usual stirring of the precipitate in contact with the surfactant must be omitted, and this is a further advantage of octadecylamine over other surfactants. Further, Fig. 8 clearly shows a decrease in the process yield (down to about 40%) for induction time > 0 , which is compensated for by the periodical additions of octadecylamine for foam stabilization. In fact, the data of Fig. 7, which are related to the yields obtained after 15 min of co-fotation, do not properly depict the influence of the induction time, thus showing the importance of simultaneously testing both the yield and the kinetics to achieve optimization of the co-fotation process.

Use of auxiliary agents for foam formation

As mentioned repeatedly above, the foam layer formed by octadecylamine is not very stable, and the

foam initially formed coalesces after 4–5 min. The periodical addition of the surfactant to maintain the foam gives satisfactory separation yields but increases the surfactant consumption and requires continuous attention by the operator. An occasional consequence of coalescence of the foam layer is adherence of the sublate flocs to the column walls, resulting in lower recovery for analysis. To reduce such effects the addition of small amounts of non-ionic surfactants (Triton X-100, *etc.*) has been proposed,²⁰ but anionic and cationic surfactants can also be used. We have tried the addition of sodium lauryl sulphate (NaLS) and hexadecyltrimethylammonium bromide (HTAB), on the basis of our earlier work,^{13,16} which indicated that under the salinity and pH conditions considered here they do not cause flotation of the iron(III) hydroxide but simply improve the stability of the foam layer. They can be added during the flotation process or along with the main surfactant at the start (making it unnecessary to make further additions of it). The greater consistency thus imparted to the froth layer gives better support to the sublate, and formation of a clean and compact foam layer, thus avoiding the floc re-entry into the mother solution that can occur on coalescence of the foam formed by the principal surfactant.

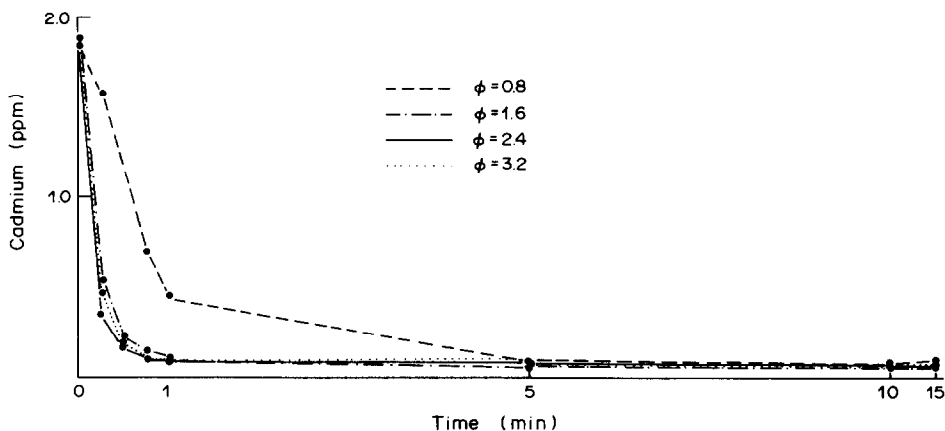


Fig. 6. Influence of the collector/co-precipitant ratio (ϕ) on the co-fotation yield [—●— Co(II); —■— Cu(II); —▲— Cd(II)].

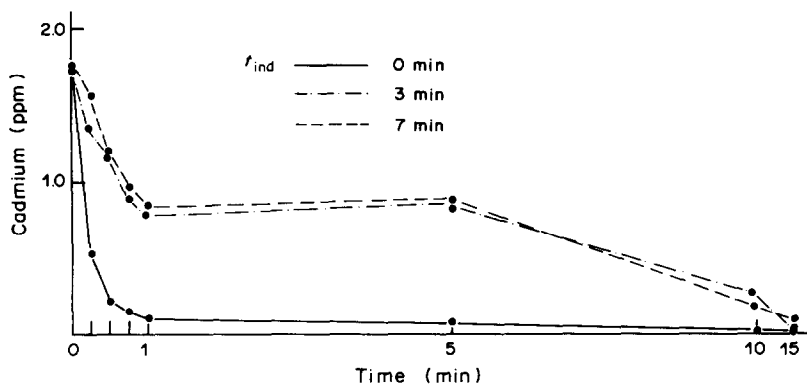


Fig. 8. Influence of the induction time on the co-floitation yield [—●— Co(II); —■— Cu(II); —▲— Cd(II)].

Recovery and dissolution of the sublates

Octadecylamine dissolves in most hot solvents which are suitable for AAS work,²¹ but is insoluble in hot or cold water. The use of hot organic solvents produces practical problems in the recovery of the sublates adhering to the column wall, however, since the solvent rapidly becomes cold on the column wall.

We therefore sought a mixed solvent which would dissolve the sublates in the cold. From the data in Table 2 it can be seen that ethanol-containing binary mixtures are suitable. In principle the MIBK-ethanol mixture would be selected on the basis of the excellent suitability of MIBK for AAS work, but in any case the solvent mixtures have to contain hydrochloric acid to dissolve the sublates.

However, when a 1:2:2 v/v 12M hydrochloric acid-MIBK-ethanol mixture was used in analysis of sea-water samples or synthetic solutions of 3.5‰ salinity, a large insoluble residue was obtained. AAS analysis of the solution phases showed, however, that practically all the Fe(III) collector and the co-precipitated metals were totally dissolved, and the insoluble residue was found to be mostly sodium chloride. The proportion of water in the solvent

Table 3. Comparative results for analysis of a synthetic sea-water sample by the Fe(OH)₃/octadecylamine co-floitation and APDC extraction methods

Species*	Found, † ng/ml	
	APDC/MIBK	Co-floitation
Copper	39 ± 8	40 ± 2
Cadmium	37 ± 5	41 ± 3
Cobalt	38 ± 3	44 ± 2

*Concentration 40 ng/ml.

†Blank values were subtracted in all cases.

mixture was therefore increased in order to dissolve the residue completely, but without bringing about phase separation. A similar ternary mixture containing 6M hydrochloric acid was therefore used for all subsequent work, and this concentration of acid is sufficient²¹ to prevent phase separation. This mixture dissolves the sublata in the cold, and the solution remains stable for about 1 hr, after which small amounts of precipitate may appear. However, the mixture influences the AAS measurements, making it mandatory to optimize the operating conditions. The recommended parameters are given in Table 1; the set conditions increase the sensitivity of the deter-

Table 2. Fe(OH)₃/octadecylamine sublata solubility in different solvents and solvent mixtures (acidified with concentrated hydrochloric acid)

Solvent	Sublata solubility		Phase separation
	Cold	Hot	
Ethanol	—	++	no
MIBK	—	+++	yes
Isoamyl alcohol	—	+++	yes
Acetone	+	+++	no
Ethyl acetate	—	—	
Di-isopropyl ether	—	—	
2-Octanol	+	+++	yes
Amyl alcohol	—	+++	yes
Acetone/ethanol (1:1)	+	+++	no
MIBK/ethanol (1:1)	+++	+++	no
2-Octanol/ethanol (1:1)	+++	+++	no
Amyl alcohol/ethanol (1:1)	+++	+++	no
Isoamyl alcohol/ethanol (1:1)	+	+++	no

— not detectable.

+, + + partial.

+, + + total.

Table 4. Cu(II), Cd(II) and Co(II) recovery from spiked sea-water samples by the co-floitation method ($V = 2000$ ml) and the APDC/MIBK method ($V = 400$ ml)

Method	Element addition, ng/ml	Species, ng/ml					
		Cu(II)		Cd(II)		Co(II)	
		found	rsd,%	found	rsd,%	found	rsd,%
Co-floitation	0.0	2.5	13.3	0.8	6.0	5.8	7.0
	5.0	5.6	9.5	4.3	6.0	11.4	5.6
	10.0	10.1	2.0	8.4	3.4	15.9	4.7
	Mean recovery (%)	83 ± 6		79 ± 4		98 ± 5	
APDC/MIBK	0.0	4.1	29.4	2.8	14.5	3.2	22.0
	5.0	7.0	4.4	7.6	7.2	7.5	2.7
	10.0	13.8	8.2	12.0	4.9	11.7	1.7
	Mean recovery (%)	87 ± 6		94 ± 2		92 ± 2	

minations by a factor of about 3 for the elements investigated.

Analysis of real and synthetic sea-water samples

To compare the performance of the proposed method with that of the common APDC/MIBK preconcentration method, as recommended by Rodier,²² a synthetic sea-water sample²³ was prepared with high-purity reagents, and a 40- μ g/l. concentration of each of the elements investigated. The results are given in Table 3 and show our proposed method is satisfactory.

Table 4 shows results for real sea-water samples, some of which have been spiked with the elements investigated. The recovery and precision are both satisfactory. The results obtained by the APDC/MIBK preconcentration method are also given for comparison. It should be noted that the results obtained for the unspiked samples are not directly comparable, since the samples were taken on different dates, though from the same site.

Acknowledgements—The authors express their thanks to the Comision Asesora de Investigacion Cientifica y Tecnica of the Spanish Ministry of Science and Education for a grant to carry out this work.

REFERENCES

1. R. Lemlich (ed.), *Adsorptive Bubble Separation Techniques*, Academic Press, New York, 1972.
2. Y. S. Kim, and H. Zeitlin, *Sepr. Sci.*, 1971, **6**, 505.
3. *Idem*, *ibid.*, 1972, **7**, 1.
4. G. Leung, Y. S. Kim and H. Zeitlin, *Anal. Chim. Acta*, 1972, **60**, 229.
5. F. Chaine and H. Zeitlin, *Sepr. Sci.*, 1974, **9**, 1.
6. S. Nakashima, *Analyst*, 1978, **103**, 1031, and private communication.
7. J. C. Barnes, J. M. Brown, N. A. K. Mumallah and D. J. Wilson, *Sepr. Sci. Technol.*, 1979, **14**, 177.
8. S. D. Huang and D. J. Wilson, *Sepr. Sci.*, 1976, **11**, 215.
9. C. Matsuzaki and H. Zeitlin, *ibid.*, 1973, **8**, 185.
10. M. Hiraide, Y. Yoshida and A. Mizuike, *Anal. Chim. Acta*, 1976, **81**, 185.
11. M. Hiraide, T. Ito, M. Baba, H. Kawaguchi and A. Mizuike, *Anal. Chem.*, 1980, **52**, 804.
12. E. H. de Carlo, H. Zeitlin and Q. Fernando, *ibid.*, 1981, **53**, 104.
13. L. Cabezon, R. Cela and J. A. Perez-Bustamante, *Afinidad*, 1983, **40**, 144.
14. W. D. Allen, M. M. Jones, W. D. Mitchell and D. J. Wilson, *Sepr. Sci. Technol.*, 1979, **14**, 769.
15. Pye-Unicam SP-9 Series Atomic Absorption Spectrophotometer Users Manual, Pye-Unicam Ltd., Cambridge, England.
16. R. Cela and J. A. Perez-Bustamante, *Afinidad*, 1982, **39**, 124.
17. J. Cervera, R. Cela and J. A. Perez-Bustamante, *Analyst*, 1982, **107**, 1425.
18. K. S. Subramaniam, C. L. Chakrabarti, J. E. Sueiras and I. S. Maines, *Anal. Chem.*, 1978, **50**, 444.
19. R. E. Sturgeon, S. S. Berman, J. A. H. Desautniers, A. P. Mykitluk, J. W. McLaren and D. S. Russell, *ibid.*, 1980, **52**, 1585.
20. E. H. de Carlo, H. Zeitlin and Q. Fernando, *ibid.*, 1982, **54**, 898.
21. M. S. Cresser, *Solvent Extraction in Flame Spectroscopic Analysis*, Butterworths, London, 1978.
22. J. Rodier, *L'analyse de l'eau*, Dunod, Paris, 1978.
23. D. R. Kester, J. W. Duedall, D. N. Connors and R. M. Pytkowicz, *Limnol. Oceanog.*, 1967, **12**, 176.

CHEMILUMINESCENT REACTION OF LUCIGENIN WITH REDUCING SUGARS

ROBERT L. VEAZEY,† HOWARD NEKIMKEN and TIMOTHY A. NIEMAN*

Department of Chemistry, University of Illinois, 1209 W. California St., Urbana, Illinois 61801, U.S.A.

(Received 28 November 1983. Revised 4 January 1984. Accepted 17 February 1984)

Summary—The chemiluminescent reaction, in alkaline solution, of lucigenin with the reducing sugars sorbose, fructose, lactose, glucose, xylose, galactose, arabinose and mannose has been studied. There is a linear relationship (correlation coefficient = 0.996) between the emission intensity and the second-order rate constant for the alkaline oxidation of these sugars. The emission intensity is linearly related to the sugar concentration; at high sugar concentrations (> 5 mM) it is independent of the lucigenin concentration, but at low concentrations (< 0.05 mM) is linearly related to the lucigenin concentration. These facts support the view that the rate-limiting step is the tautomerization of the sugars to the 1,2-enediol form; the enediol then undergoes reaction with lucigenin.

The use of chemiluminescence in solution to determine clinically-important organic species is becoming common. One such reaction is that of lucigenin (*N,N'*-dimethyl-9,9'-biacridinium dinitrate) in aqueous solution. We have reported on the use of lucigenin chemiluminescence for stopped-flow determination of reductants, such as glucose, uric acid, ascorbic acid, creatinine, glucuronic acid and glutathione,¹ for HPLC detection in ascorbic acid determinations² and for determination of the mucopolysaccharide heparin.³

Chemiluminescent reactions of lucigenin with hydrogen peroxide and with reducing agents were first reported by Gleu and Petsch.⁴ Since that time the reaction has received considerable mechanistic study,⁵⁻⁷ but lucigenin probably remains the least understood of all classic organic chemiluminescent agents. Maskiewicz *et al.*⁸ have recently studied the kinetics of several reactions of lucigenin; for reactions with hydrogen peroxide, they concluded that the rate-determining step is the conversion of lucigenin(OOH) to lucigenin(OO⁻); for reactions with hydroxide ion and other nucleophiles, they concluded that the rate-determining steps involve the production of *N*-methylacridone from lucigenin(OH) or lucigenin(OH)₂. We report results which deal with the reaction of lucigenin and reducing sugars, and from these results, the rate-limiting step in the reaction can be identified.

EXPERIMENTAL

Reagents

The concentrations used are those previously shown to yield good signal-to-noise ratios for chemiluminescence detection.¹ All solutions were prepared with demineralized, glass-distilled water. Lucigenin (Aldrich Chemical Co.) was

used without further purification. Potassium hydroxide stock solution was prepared from an "Acculute" solution (Anachemia Chemicals, Ltd.). Sugars were obtained as follows: arabinose and xylose (Sigma), fructose (Pfanstiehl Lab.), galactose (Nutritional Biochemicals), glucose and lactose (Mallinckrodt), mannose (Baker), sorbose (Aldrich).

Apparatus

All measurements were made with a home-made inert stopped-flow instrument, described previously.¹ This consists of three glass-barrelled syringes driven by an air piston. The syringes deliver solution through check valves and a mixer to the observation cell. The solutions come into contact only with surfaces of glass, Teflon, Kel-F and sapphire. The observation cell is a modification of one described previously.⁹ The cell cavity and inlet and exit ports are machined in a Teflon block; this piece is pressure-sealed against a glass window. The cell has a volume of 100 μ l and exposes a 2.0-cm² surface area to the detector. The photomultiplier detector (RCA 1P28) was approximately 4 cm from the cell window; no wavelength discrimination was used. A Pacific Instruments model 126 photometer was used to amplify the photocurrent and give an output signal to a strip-chart recorder.

Procedure

The stopped-flow syringes were filled with the solutions of lucigenin, base and reductant, and delivered three portions of each solution to rinse the mixer and cell thrice, and a fourth portion for the experiment itself. Data collection began with completion of the last delivery, and continued for 75 sec. An auxiliary valve to the flow cell was then opened and a peristaltic pump activated to flush the cell and mixer with approximately 4 ml of nitric acid (1 + 1). This acid rinse was necessary to remove reaction products (such as *N*-methylacridone) which were insoluble in the aqueous alkaline reaction mixture. This measurement routine was then repeated three times, to give a total of four measurements with each sample. Sample solutions were alternated with blank solutions. The analytical signal was the average of four sample measurements minus the average of four blank measurements. All intensities reported are given in arbitrary units and are the maximum intensity observed (relative to the blank) within the 75-sec observation period.

The data-acquisition time was chosen by consideration of the emission intensity *vs.* time curve. The emission intensity reaches approximately 90% of its peak value after 1 min, but continues to increase very slowly, not reaching the peak for 10-15 min. The chosen observation period (75 sec) gives a

*To whom correspondence should be sent.

†Present address: Union Camp R&D, P.O. Box 412, Princeton, NJ 08540, U.S.A.

Table 1. Chemiluminescent emission intensities for the reaction of lucigenin with various reducing sugars*

Sugar	Intensity†		
	1M KOH	0.5M KOH	0.1M KOH
Sorbose	100.0	70.4	16.2
Fructose	94.3	79.1	16.8
Lactose	23.5	20.3	3.80
Glucose	17.0	12.7	1.90
Xylose	16.4	15.2	3.32
Galactose	13.3	12.2	1.82
Arabinose	12.7	10.6	2.14
Mannose	7.44	5.85	0.95

*1mM lucigenin, 0.6mM sugar, base concentration indicated in table, temperature 25°.

†Expressed as a percentage of the intensity observed with sorbose in 1M KOH.

Table 2. Rate data for oxidation of reducing sugars

Sugar	Temperature, °C	k_s , l.mole ⁻¹ .min ⁻¹	k_s/k_g
Sorbose	25	0.597	5.63
Fructose	25	0.593	5.59
Lactose	25	0.131	1.24
Glucose	25	0.106	1.00
Glucose	30	0.236	1.00
Glucose	35	0.575	1.00
Xylose	30	0.178	0.755
Galactose	30	0.134	0.568
Arabinose	30	0.095	0.402
Mannose	35	0.183	0.318

*All k_s values are calculated from data given by Nath and Singh.^{13,14}

reasonable compromise between experiment time and signal intensity. The maximum intensity observed within the 75-sec period is about 93% of the peak intensity.

RESULTS

Table 1 lists the emission intensities observed for the reaction of 0.6mM solutions of each sugar with 1.0mM lucigenin at three different concentrations of potassium hydroxide. The intensities are normalized so that the largest signal (sorbose with 1M alkali) has a value of 100. A wide range of relative emission intensities is observed with these reductants. MacDonald *et al.* have noted a strong correlation between emission intensity and metal-ion reduction potential for lophine chemiluminescence in the presence of trace metal ions.¹⁰ With the lucigenin-sugar system there is apparently no such relationship; regression analysis of emission intensity as a function of reduction potential^{11,12} yields a correlation coefficient of only 0.11.

In order to identify which property of these sugars is important in determining relative intensity, the rates of oxidation for reducing sugars have been studied. Nath and Singh studied the oxidation of sugars by alkaline ferricyanide^{13,14} and from the data they present we have calculated values for the second-order rate constants (k_s) for the oxidation of each sugar (Table 2). To facilitate comparison with our

observations of the chemiluminescent emission intensity (at a single constant temperature of 25°), we have normalized the rate data. Conveniently, rate data are available for glucose at several temperatures. The factor k_s/k_g is the ratio of the rate constant for a given sugar to the rate constant for glucose at the same temperature; this removes the temperature dependence of the rate data provided that the different sugars have nearly identical activation energies for alkaline oxidation. The assumption concerning activation energies is reasonable. Singh and Ghosh¹⁵ have determined the activation energies for alkaline oxidation of arabinose, galactose, glucose and xylose as 29.2, 28.7, 27.0 and 25.8 kcal/mole, respectively, at 30°. For xylose, galactose and arabinose the value of the activation energy can be used to compute k_s at 25° instead of 30°, as in Table 2. The k_s/k_g values for these three sugars are then 0.818, 0.568 and 0.397 at 25°; they agree within 10% of the values at 30° of 0.755, 0.568 and 0.402, given in Table 2. No activation energy value is available for mannose. Judging from the mean value and the spread of the four available activation energies, it can be estimated that the k_s/k_g value for mannose is within 20% of the correct value. The rate of sugar oxidation is not dependent on the difference between the standard potentials for the reductant and the oxidant; the correlation coefficient is only 0.14 for the rate of oxidation as a function of potential difference.

It is noteworthy that there is a good correlation between emission intensity and rate of oxidation. Figure 1 shows a plot of emission intensity (from Table 1) *vs.* k_s/k_g (from Table 2). The emission intensities are for reaction with 1M potassium hydroxide. Similar graphs using the intensities for 0.5M and 0.1M potassium hydroxide show the same trend; the slopes are different because the intensities decrease as the concentration of potassium hydroxide decreases (Table 1). The least-squares correlation coefficients for the 1M, 0.5M and 0.1M potassium hydroxide plots are 0.998, 0.994 and 0.995, respectively. To make sure that this high degree of correlation was not an artifact of our chosen mea-

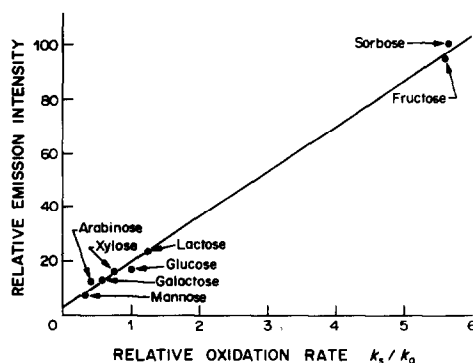


Fig. 1. Relative chemiluminescent emission intensity *vs.* relative oxidation rate for sugars. The solid line is the least-squares line.

surement time of 75 sec, we repeated the experiments with a measurement time of 15 sec. All the intensities were lower, but the plots showed the same trend as that in Fig. 1 and had correlation coefficients larger than 0.99.

We have also examined the dependence of the emission intensity on reagent concentration, with glucose as a representative sugar. The concentrations were varied (one at a time) over the following ranges: lucigenin (0.05–1.00mM), potassium hydroxide (0.05–1.00M) and glucose (0.28–9.71mM). When not varied, the concentrations were held at 1.00mM for lucigenin, 1.00M for potassium hydroxide and generally 6.00mM for glucose. Least-squares analysis of plots of log emission intensity *vs.* log concentration yielded the following values (\pm the standard deviation) for the slopes: OH^- 0.45 ± 0.04 , glucose 0.91 ± 0.02 . The slope for the lucigenin plot depends upon the glucose concentration. At high glucose concentrations ($> 5\text{mM}$) the slope is essentially zero (0.01 ± 0.02 at 6mM). The slope increases as the glucose concentration decreases. The slope was 0.92 ± 0.03 at a glucose concentration of 0.05mM while in the absence of glucose (*i.e.*, for the background reaction between lucigenin and OH^-) the slope was 1.3 ± 0.2 .

It is interesting that the intensity is independent of lucigenin concentration at high glucose concentrations. In reactions of lucigenin with hydrogen peroxide and with OH^- and other nucleophiles, the reaction rate is dependent on the first power of the lucigenin concentration. Our observation that the dependence on lucigenin concentration can vary from zero-order to first-order, depending on experimental conditions, is consistent with other observations. Totter¹⁶ has observed that the emission intensity is independent of the lucigenin concentration for the reaction with fructose and is related to the square root of the lucigenin concentration for the reaction with hydroxylamine. With glucuronic acid, the emission intensity has been reported to be linearly related to the lucigenin concentration.³

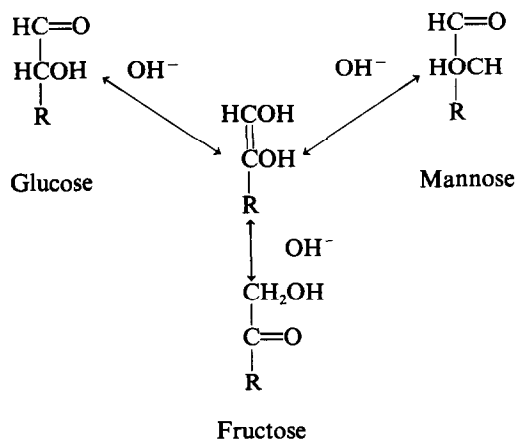
The half-order dependence on OH^- concentration seemed unusual, so we examined the effect of OH^- concentration on the emission intensity in the reaction between hydrogen peroxide and lucigenin. At OH^- concentrations below 0.05M the emission intensity increases as the OH^- concentration increases. However, at above 0.05M OH^- (the region studied with the sugars) the emission intensity decreases with OH^- concentration. Therefore, the half-order dependence is probably a combination of a higher order dependence on the OH^- concentration in the lucigenin–sugar portion of the reaction and a negative order dependence in some later step of the lucigenin chemiluminescence.

DISCUSSION

For a chemiluminescent reaction, one factor controlling the observed emission intensity is the rate-

determining step leading to production of excited states. Therefore observation of changes in emission intensity with changes in experimental conditions can shed light on the nature of that rate-determining step. Totter¹⁶ suggested that the rate-determining step in the reaction between lucigenin and fructose was a slow reaction between fructose and OH^- . This hypothesis was proposed because the emission intensity was independent of the lucigenin concentration and because fructose was oxidized at the same rate (under the same conditions) by lucigenin as by ferricyanide. The results of our study support this hypothesis. In the case of the eight reducing sugars studied, the emitted light intensity is strongly correlated with the rate of alkaline oxidation of the sugar (Fig. 1), independent of the lucigenin concentration (at high sugar concentrations), linearly proportional to the sugar concentration, and proportional to the base concentration to a power of greater than one-half. Studies of the kinetics of the oxidations of reducing sugars by alkaline ferricyanide^{13,14} and by alkaline cupric ion^{15,17} have shown these reactions to be first-order with respect to the reducing sugar and hydroxyl ion and zero-order with respect to the oxidant. The rate-determining step in the chemiluminescent reaction between lucigenin and reducing sugars is thus probably the same as that in the alkaline oxidation of those sugars by ferricyanide or copper(II).

The alkaline oxidation rates of reducing sugars are thought to be dependent on the rate of formation of their 1,2-enediol tautomeric forms in the Lobry de Bruyn–Alberda van Eckenstein rearrangement.^{13,14,18}



The 1,2-enediol is a stronger reducing agent than the parent sugar. Apparently, the sugars (in their aldo or keto forms) are not sufficiently strong reductants to react with lucigenin. Hence the rate-limiting step in the chemiluminescent reaction between lucigenin and reducing sugars is the production of the 1,2-enediol tautomer. This intermediate enediol is oxidized by lucigenin in a subsequent series of faster steps so that the emission intensity (and therefore the overall reaction rate) is independent of the lucigenin concentration.

The results of our study suggest that relative oxidation for other reducing sugars might be conveniently determined by comparison of lucigenin chemiluminescent emission intensities for sugars of known oxidation rate, and the results used in planning the analytical procedures.

Acknowledgement—This work was supported by the National Science Foundation (CHE-78-01614, CHE-81-08816).

REFERENCES

1. R. L. Veazey and T. A. Nieman, *Anal. Chem.*, 1979, **51**, 2092.
2. *Idem*, *J. Chromatog.*, 1980, **200**, 153.
3. R. A. Steen and T. A. Nieman, *Anal. Chim. Acta*, 1983, **155**, 123.
4. K. Gleu and W. Petsch, *Angew. Chem.*, 1935, **48**, 57.
5. F. McCapra, *Q. Rev. Chem. Soc.*, 1966, **20**, 485.
6. *Idem*, in *Progress in Organic Chemistry*, W. Carruthers and J. K. Sutherland (eds.), Vol. 8, pp. 231–77. Wiley, New York, 1973.
7. K.-D. Gundermann, *Top. Curr. Chem.*, 1974, **46**, 61.
8. R. Maskiewicz, D. Sogah and T. C. Bruice, *J. Am. Chem. Soc.*, 1979, **101**, 5347, 5355.
9. S. Stieg and T. A. Nieman, *Anal. Chem.*, 1978, **50**, 401.
10. A. MacDonald, K. W. Chan and T. A. Nieman, *ibid.*, 1979, **51**, 2077.
11. L. Meites and P. Zuman, *Electrochemical Data*, Part I, Vol. A, pp. 242–3. Wiley, New York, 1974.
12. A. J. Bard (ed.) *Encyclopedia of Electrochemistry of the Elements*, Vol. XII, pp. 19–20. Dekker, New York, 1978.
13. N. Nath and M. P. Singh, *Z. Phys. Chem. (Leipzig)*, 1962, **221**, 204; 1963, **224**, 419.
14. *Idem*, *J. Phys. Chem.*, 1965, **69**, 2038.
15. M. P. Singh and S. Ghosh, *Z. Phys. Chem. (Leipzig)*, 1957, **207**, 187; 198.
16. J. R. Totter, *Photochem. Photobiol.*, 1975, **22**, 203.
17. M. P. Singh, B. Krishna and S. Ghosh, *Z. Phys. Chem. (Leipzig)*, 1956, **205**, 285.
18. C. A. L. de Bruyn and W. A. van Eckenstein, *Rec. Trav. Chim.*, 1895, **14**, 195.

STANDARD-ADDITION DETERMINATION OF NITROGEN IN COAL WITH AN AMMONIA-SENSITIVE ELECTRODE*

T. D. RICE, V. SWEENEY, R. SEMITEKOLOS and G. J. RHYDER

New South Wales Department of Mineral Resources, Chemical Laboratory Branch, P.O. Box 76, Lidcombe, 2141, Australia

(Received 8 November 1983. Accepted 17 February 1984)

Summary—After semimicro Kjeldahl digestion of the coal sample with a $K_2SO_4-V_2O_5-Se$ catalyst and sulphuric acid, the digest is cooled, diluted with water, neutralized and then made alkaline with NaOH/EDTA solution. The ammonia thus formed is determined by measuring the potential of a properly conditioned ammonia-sensitive electrode containing an appropriate filling solution; a gravimetric standard-addition technique is used. Known additions of 1–2 μg of N per g to blank solutions enables all measurements of potential to be made in the linear region of the electrode-response curve. The electrode measurement procedure gives blank-corrected recoveries of between 99.0 and 101.0% for synthetic sample solutions. Results obtained for nitrogen in reference coal samples by the electrode procedure have been found to agree well with those obtained by other methods.

Doolan and Belcher¹ have shown that the ammonia-sensitive electrode provides a valid alternative to standard ammonia-distillation procedures for determining nitrogen in coal. The following modifications, described in this paper, have streamlined the procedure of Doolan and Belcher.¹

1. Use of specially designed tubes and a heated aluminium block enables up to 40 Kjeldahl digestions to be performed concurrently.

2. Use of samples ground to pass a 212- μm sieve instead of a 76- μm sieve.

3. Use of 10M NaOH/0.02M EDTA solution instead of 10M NaOH solution minimizes the possibility of the electrode membrane being clogged by precipitate.

4. Exact weighing of the test solution is not necessary—any weight between 230 and 280 g can be used without significant effect on the result.

5. Electrode measurements are done by gravimetric single standard-addition,² after appropriate conditioning of the electrode, instead of by direct comparison with standards (which requires that all measurements be done at the same temperature). The electrode-response slope is assumed to have linear temperature-dependence, and is conveniently obtained by replicate double standard-addition measurements previously done on the same day. The electrode used was chosen because it has a fast response time and a long-lasting, easily replaced membrane.

EXPERIMENTAL

Reagents

Catalyst. As described by Doolan and Belcher,¹ this consists of K_2SO_4 (anhydrous), V_2O_5 and Se finely ground and mixed in 93:5:2 w/w ratio. Bradstreet³ has also recom-

mended this catalyst. *Safety note.* Skin contact with the catalyst must be avoided. The catalyst must be handled with care so that none of it becomes airborne.

Electrode internal filling solution. A 0.01M $(NH_4)_2SO_4/0.50M NaNO_3$ solution plus (for easy visibility in the electrode) 0.002 g of Rhodamine B per 200 ml.

Nitrogen standard solution No. 1 (5000 μg of N per g). Weigh, to the nearest 0.01 g, 56.6–56.7 g of analytical grade ammonium sulphate (of guaranteed or known purity, and previously dried for 2 hr at 105°) by difference into a 1000-ml beaker. Dissolve it in 600 ml of water and transfer quantitatively (using less than 200 ml of water) to a dry 2.5-litre polyethylene bottle previously weighed. Dissolve 158 g of low nitrogen-content sodium sulphate in 1200 ml of water. Transfer to the bottle containing the ammonium sulphate solution, and dilute with water to give a weight of solution 42.40 times the weight of ammonium sulphate taken. Seal the bottle and mix the contents well. Transfer about 180 ml of this solution to a 250-ml polyethylene dispensing bottle.⁴

Nitrogen standard solution No. 2 (500.0 μg of N per g). Weigh about 18 g of standard solution No. 1 (to 10 mg) into a 250-ml polyethylene dispensing bottle. Dilute the solution to exactly 10 times its weight with water.

Other reagents. Concentrated sulphuric acid (low nitrogen content); 0.3M sodium sulphate; 10M NaOH/0.02M EDTA solution, conveniently prepared by diluting 2 volumes of technical grade 60% sodium hydroxide solution with 1 volume of 0.06M EDTA; 2M sulphuric acid; sucrose. Use demineralized water throughout.

Apparatus

Digestion tubes. Borosilicate glass, 26 mm outside diameter, 310 mm long, with a constriction towards the top (Tecator, Sweden; No. 1000-0154). They are conveniently held in a 50-position stainless-steel stand.

Digestion apparatus. A Tecator DS-40 digestion block housed in a fume cupboard. This block can hold 40 tubes at a time; its temperature stability at 380° is $\pm 4^\circ$ and its repeatability of temperature setting is $\pm 3^\circ$.

Polypropylene jars for diluted digests. Capacity 360 ml, with snap-on plastic lids and a line at the 250-ml mark.

Measurement lid. A snap-on lid of the type supplied with the polypropylene jars, drilled with a 19-mm diameter hole for electrode insertion and a 4-mm diameter hole for standard addition.

Ammonia electrode. HNU Model ISE-10-10-00 with

*Presented in part at the Seventh Australian Symposium on Analytical Chemistry, Adelaide, Australia, August 1983.

screw-on cap containing built-in membrane (HNU Systems, Inc., Newton, Massachusetts 02164, U.S.A.)

pH/millivolt meter. Orion Model 811 with Orion Model 91-70-02 temperature-measurement probe and Orion Model 090020 electrode holder.

Electronic top-loading balances. Sartorius 1602 MP6, for weighing subsamples; 1205 MP, for standard additions and preparation of standard solution No. 2, and 3802 MP for preparation of standard solution No. 1. The precision and accuracy should be regularly checked with reference weights.

Stirrer bars. PTFE-coated, length 45 mm.

Sampling

All samples were ground to pass a 212- μm sieve and equilibrated with the laboratory atmosphere before analysis. Moisture determinations, by loss in weight on heating 300-mg samples for 2 hr at 105°, enabled calculation of results on a dry basis.

Procedures

Solution preparation. Weigh a 100-mg sample into a dry digestion tube. In each batch of analyses include 2 control samples and 2 blanks (comprising either 100 mg of sucrose plus catalyst and acid or merely catalyst and acid). Add 2.0 g of catalyst down the inner wall of the tube so that all sample particles are transferred to the bottom of the tube. Add 3 antibumping granules. Swirl to mix, 4.0 ± 0.2 ml of concentrated sulphuric acid, and swirl again. Place the tube (uncovered) in the digester block, already heated to $380 \pm 5^\circ$. Digest for 60 min. Remove the tube and let it cool for 10 min, then add 25 ml of water and carefully swirl it. Pour the solution down a glass stirring rod into a polypropylene jar, rinsing in with three 20-ml portions of water. Add a further 130 ml of water to the jar. With continuous manual stirring, slowly add ~ 11 ml of NaOH/EDTA solution until the solution changes from blue to green (indicating a pH of 3–7). At this pH ammonia cannot be lost from the solution. If the solution turns dark blue or brown, indicating that the pH may be above 7, add 2M sulphuric acid dropwise to restore the green colour.

Add water until the solution reaches the 250-ml mark on the jar, and weighs 230–280 g. Seal the jar and let the contents cool to ambient temperature $\pm 0.5^\circ$ before electrode measurement.

Electrode measurement. The electrode is stored with its cap immersed in a synthetic sample solution consisting of 240 ml of 0.3M sodium sulphate, 1.5 g of nitrogen standard solution No. 2 and 5 ml of NaOH/EDTA solution kept in a polypropylene jar containing a stirrer bar and sealed with a measurement lid.

The standard-addition technique is essentially the same as that recently described for fluoride determination.² The electrode-response slope is determined by double standard-addition measurements on the first 6 solutions of a batch. The average of these slopes is then used for evaluating single standard-addition measurements on the remaining solutions in the batch and obtaining single standard-addition results for the first 6 solutions. Figure 1 shows a flow diagram describing the electrode conditioning and measurement procedure. With the electrode used in our laboratory, the potential reached equilibrium within 40–60 sec and then increased by not more than 0.1 mV in the ensuing 30 sec. This slight upward drift was probably due to slight loss of ammonia from the solution and slight migration of water vapour through the electrode membrane from the sample solution. *Note:* if the sample contains less than about 0.2–0.3% nitrogen, add a known weight M (about 0.5–1.0 g), of nitrogen standard solution No. 2 after the initial insertion of the electrode, to bring the electrode signal into the linear region of the response graph; do the same for the blank measurements (blanks are run by applying the whole procedure without sample present).

Calculations. The iterative procedure for calculating electrode slope by double standard-addition has already been described.² Table 1 gives the formulae for the calculations, which can conveniently be done with a programmed calculator. Details of a Texas Instruments TI-59 program for these calculations are available on request.

Care of electrode. When the electrode is in regular use, replace the internal filling solution every 14 days and store the electrode with its cap immersed in synthetic sample solution as described above. Add a few drops of nitrogen standard solution No. 1 to this storage solution at ~ 7 -day intervals to prevent excessive lowering of its ammonia concentration with time; prepare fresh storage solution after 3 months. If the electrode will not be used for several months, drain the filling solution, rinse the electrode body and cap with water, and store the disassembled unit dry.

Experience in this laboratory indicates that a single membrane and cap can be used for at least six months before needing replacement.

RESULTS AND DISCUSSION

Importance of proper conditioning of electrode

The aim of the electrode conditioning procedure (Fig. 1) is to eliminate memory effects of the type described by Evans and Partridge,⁵ and Umezawa *et al.*⁶ Its reliability has been repeatedly checked by

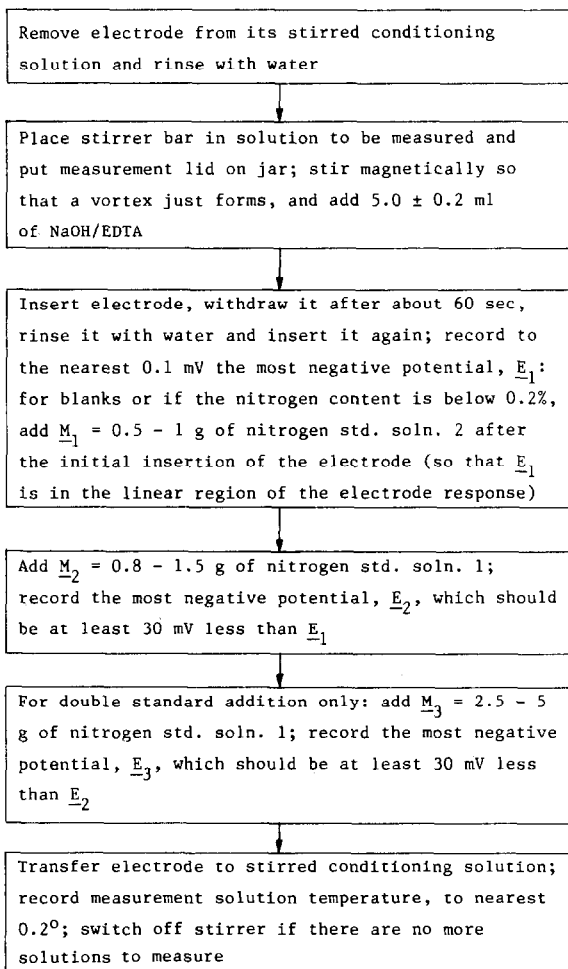


Fig. 1. Flow-sheet for potentiometric measurement of nitrogen content by gravimetric standard addition.

Table 1. Formulae required for calculation with a nominal sample solution mass of 250 g

Quantity	Formula
Solution concentration,	$C_x = \frac{5000M_2/(250 + M_1 + M_2)}{\text{antilog} \{(E_1 - E_2)298/ST\} - \{(250 + M_1)/(250 + M_1 + M_2)\}}$
Electrode response slope at 25°,	$S = \left(\frac{E_2 - E_3}{\log \frac{\{C_x(250 + M_1) + 5000(M_2 + M_3)\}(250 + M_1 + M_2)}{\{C_x(250 + M_1) + 5000M_2\}(250 + M_1 + M_2 + M_3)}} \right) \frac{298}{T}$
N in sample, %	$\frac{\{(250 + M_1)C_x - 500M_1\}10^{-4}/M_s}{\text{blank}}$

Notes. 1. The first formula is the "single standard-addition formula." For the electrode used in this laboratory, S is initially taken to be 57.9 mV per decade at 25°C.

2. The symbols are defined in Fig. 1, with the exception of: (i) T , the absolute temperature of measurement and (ii) M_s , the weight of sample (g).

3. The blank is the mean blank value for the batch, expressed as % N, and calculated from the formula for the nitrogen content, for a nominal 0.1000-g nitrogen-free sample.

analysis of a synthetic sample solution comprising 240–245 ml of 0.3M sodium sulphate and about 3 g of nitrogen standard solution No. 2 (weighed to 2 mg). The blank-corrected nitrogen recovery has always been in the range 99.0–101.0%.

A simpler conditioning procedure consists of placing the electrode in stirred conditioning solution for at least 60 sec and then rinsing it with water, between samples; *i.e.*, the conditioning in the solution to be measured (third step in Fig. 1) is omitted. However, this procedure gives blank-corrected nitrogen recoveries in the range 99.5–104.0% and so is inferior to the full conditioning procedure. This bias towards high results is consistent with the fact that in the full conditioning procedure the E_1 value obtained before removal of the electrode, rinsing with water and re-insertion can be as much as 0.6 mV more negative than the value recorded after the rinsing and re-insertion. The second value is the more reliable.

Variability of the blank

When the simpler conditioning procedure was used, individual blank values for a batch of analyses typically ranged between 0.02 and 0.11% nitrogen in spite of every precaution being taken to avoid contamination of solutions by airborne ammonia. The full conditioning procedure gave lower blanks with much less variation, typically $0.02 \pm 0.01\%$ nitrogen.

Unimportance of exact solution mass

It can readily be shown that replacement of the number 250 (the nominal number of grams of measurement solution) in the formulae in Table 1 by 220 or 280 causes a change of less than 0.1 mV/decade in the calculated response slope (for 25°) and a change in the blank-corrected result not exceeding 0.002% nitrogen.

Single vs. double standard-addition

Many analyses of synthetic sample solutions in our laboratory have shown that single standard-addition, with the response slope taken as the mean of 6 replicate slope values obtained by double standard-

addition on the same day, is at least as reliable as the lengthier double standard-addition. A slope value differing from the mean by 0.5–0.7 mV per decade has occasionally been obtained by double standard-addition measurement of a synthetic sample solution; the single standard-addition recovery in such a case has always been found to be nearer to 100.0% than the double standard-addition recovery was.

Constancy of electrode slope

The means of 12 sets of 6 replicate response slope determinations at 25° during a 6-week period by double standard-addition varied randomly with time between 57.7₁ and 58.0₄ mV per decade. The mean range of the individual sets of 6 slope values was 0.52 mV per decade. The overall mean slope and 99% confidence limit was $57.9_0 \pm 0.1_0$ mV per decade. Rather than assuming from this result that the slope remains constant, it is probably sounder to assume that slight day-to-day variations of slope occur, and that the slope should be determined during each batch of measurements.

For a single standard-addition measurement with $E_1 - E_2 = 20, 30$ and 40 mV, an error of ± 0.10 mV per decade in the response slope can be shown to cause a relative error in the concentration measurement of $\pm 0.25, 0.29$ and 0.34% respectively; an error of ± 0.1 mV in $E_1 - E_2$ will increase these relative errors to $\pm 0.76, 0.63$ and 0.60% respectively.²

Results for reference coal samples

Single 100-mg samples of five reference coals were included in batches of nitrogen analyses done on different days by the procedure described. Table 2 shows that the results agree well with those obtained in other laboratories by other methods.

Sample throughput

An analyst using this procedure can readily determine nitrogen in 18 samples plus 2 control samples and 2 blanks in a 7-hr day.

Table 2. Results for nitrogen in reference coal samples

Reference coal	N, %*	
	Electrode method (this lab.)	Other methods (other labs.)
NBS SRM 1632a	1.28 ₅ ± 0.014 (18)	1.27 ± 0.08 (5)† 1.19 ± 0.08 (5)‡ 1.27 ± 0.02‡
Australian reference coal, ASCRM-001	1.67 ₄ ± 0.019 (14)	1.65 ± 0.04 #
SARM 18	1.91 ₂ ± 0.025 (10)	1.88 ± 0.02‡ 1.92 ± 0.039 (6)¶
SARM 19	1.41 ₈ ± 0.014 (11)	1.40 ± 0.02‡ 1.42 ± 0.008 (6)¶
SARM 20	1.13 ₂ ± 0.026 (11)	1.15 ± 0.02‡ 1.14 ± 0.028 (6)¶

*Mean (on dry basis) ± standard deviation; the number of replicates is given in parentheses.

†By neutron-capture prompt gamma-ray activation analysis.⁷

‡By oxygen-bomb combustion followed by chemiluminescence measurement.⁸

‡Mean ± pooled standard deviation obtained from duplicate analysis of 4 samples by the ISO semimicro Kjeldahl method.⁹ Laboratory: BHP Central Research Laboratories, Shortland 2307, Australia.

#Mean of results from 9 laboratories, 8 of which used standard methods.¹⁰

¶ISO semimicro Kjeldahl method.⁹ Laboratory: Australian Coal Industry Research Laboratories Ltd., North Ryde 2113, Australia.

SARM 18, 19 and 20 are South African coal samples obtained from E. J. Ring, Council for Mineral Technology, Private Bag X3015, Randburg 2125, South Africa.

Conclusion

The procedure described provides a simple and reliable alternative to current standard procedures for determination of nitrogen in coal which involve distillation and titration of ammonia, and should be readily usable for determination of nitrogen in Kjeldahl digests of other materials.

Acknowledgements—Permission to publish this paper was given by the Secretary, Department of Mineral Resources, New South Wales, Australia. The authors thank K. Ferguson and W. Halford for help with some of the experimental work.

REFERENCES

1. K. J. Doolan and C. B. Belcher, *Talanta*, 1978, **25**, 398.
2. T. D. Rice, *Anal. Chim. Acta*, 1983, **151**, 383.
3. R. B. Bradstreet, *The Kjeldahl Method for Organic Nitrogen*, p. 104. Academic Press, New York, 1965.
4. T. D. Rice, *Anal. Chim. Acta*, 1978, **97**, 213.
5. W. H. Evans and B. F. Partridge, *Analyst*, 1974, **99**, 367.
6. Y. Umezawa, I. Tasaki and S. Fujiwara, in *Ion-Selective Electrodes*, 3, E. Pungor (ed.), pp. 359–374. Elsevier, Amsterdam, 1980.
7. M. P. Failey, D. L. Anderson, W. H. Zoller, G. E. Gordon and R. M. Lindstrom, *Anal. Chem.*, 1979, **51**, 2209.
8. R. A. Nadkarni, in *Coal and Coal Products: Analytical Characterisation Techniques*, E. L. Fuller, Jr. (ed.), pp. 147–162. American Chemical Society, Washington, D.C., 1982.
9. *Coal and Coke—Determination of Nitrogen—Semimicro Kjeldahl Method*, ISO Standard 333, 1975.
10. Standards Association of Australia, *SAA Tech. Rept.*, TR2.1-1982, 1982.

A COMPARISON OF CATIONIC POLYMERIZATION AND ESTERIFICATION FOR END-POINT DETECTION IN THE CATALYTIC THERMOMETRIC TITRATION OF ORGANIC BASES

EDWARD J. GREENHOW and PILAR VIÑAS*

Department of Chemistry, Chelsea College, University of London, Manresa Road, London, England

(Received 17 October 1983. Accepted 17 February 1984)

Summary—A systematic comparison has been made of two indicator systems for the non-aqueous catalytic thermometric titration of strong and weak organic bases. The indicator reagents, α -methylstyrene and mixtures of acetic anhydride and hydroxy compounds, are shown to give results (for 14 representative bases) which do not differ significantly in coefficient of variation or titration error. Calibration graphs for all the samples, in the range 0.01–0.1 meq, are linear, with correlation coefficients of 0.995 or better. Aniline, benzylamine, *n*-butylamine, morpholine, pyrrole, L-dopa, α -methyl-L-dopa, DL- α -alanine, DL-leucine and L-cysteine cannot be determined when acetic anhydride is present in the sample solution, but some primary and second amines can. This is explained in terms of rates of acetylation of the amino groups.

Various indicator reagents have been used in the non-aqueous catalytic thermometric titration of organic bases.¹⁻³ Vajgand *et al.*¹ employed a mixture of acetic anhydride and water, the indicator reaction being the exothermic hydration of the anhydride, catalysed by the first excess of the titrant, perchloric acid, when the organic base had been neutralized. Later, Greenhow² showed that very weak bases could be determined if the co-reagent with the acetic anhydride was an alcohol or a phenol instead of water. A completely different type of thermometric indicator is α -methylstyrene, which undergoes exothermic cationic polymerization when the perchloric acid titrant appears in excess in the sample solution.³

In the present work the esterification² and cationic polymerization³ systems are compared for the determination of representative strong and weak primary, secondary and tertiary amines and an amide, thiourea, in terms of precision of replicate titrations, titration error and linearity of calibration graphs relating titrant volume to sample size. In addition, the limitations of the two end-point methods for the determination of primary and secondary amines have been assessed.

Titrations were done on sample solutions in which acetic anhydride had been added to the α -methylstyrene indicator, in order to compare the effect of acetic anhydride on the determination of primary and second amines by both end-point procedures, *i.e.*, cationic polymerization and esterification. Acetic anhydride is known to have a beneficial effect on the sharpness of the end-point inflection when α -methylstyrene is the indicator, if

the sample solution contains trace amounts of water, which normally inhibit or retard the cationic polymerization.

EXPERIMENTAL

Reagents

Hydroquinone, quinhydrone, α -methylstyrene, 4-hydroxy-4-methylpentan-2-one, acetic acid, acetic anhydride, 98–100% formic acid and 71–73% perchloric acid were analytical-reagent grade. Acetic acid and formic acid were dried over a molecular sieve, type 4A, before use.

Amines, amino-acids, catecholamines and thiourea were of laboratory-reagent grade. The 0.1M perchloric acid in acetic acid was prepared by the method of Belcher *et al.*⁴ Solutions were standardized against solutions of analytical-grade potassium hydrogen phthalate in dry acetic acid.

Apparatus

Details of the automatic titration apparatus, in which the titrant is introduced by means of a motor-driven micrometer syringe and the temperature is measured by means of a thermistor and recorded on a potentiometric chart-recorder, are given elsewhere.⁵ The titration vessel was a Dewar beaker (14 ml) and solutions were stirred with a magnetic stirrer.

Procedure

To 0.01–0.1 meq samples of the base dissolved in 3 ml of acetic acid, or in 2.5 ml of acetic acid + 0.5 ml of formic acid in the case of the more difficultly soluble amino-acids and catecholamines, in the Dewar beaker, was added the appropriate amount of indicator solution, either (a), 0.5 ml of α -methylstyrene dissolved in 4 ml of acetic acid or 4 ml of acetic anhydride, as desired, or (b), 4 ml of acetic anhydride + 0.5 ml of 4-hydroxy-4-methylpentan-2-one or 4 meq of hydroquinone or quinhydrone. The titrant was added at a rate of about 0.2 ml/min, and the chart recorder set for 400 mV full-scale deflection. The end-point was measured on the titration graph at the point where the tangent to the main heat rise left the curve at the lower temperature end (see Fig. 1a), as suggested by Vaughan and Swithenbank to allow for the "overlap" of the determinative and indicator reactions in the thermometric titration of very weak acids, with acetone as indicator,⁶ except for titrations

*Present address: Department of Analytical Chemistry, Faculty of Sciences, University of Murcia, Murcia, Spain.

of primary amines in the absence of acetic anhydride (the true titration value then corresponded more closely to the point obtained as shown in Fig. 1f). It appears that when a mixture of acetic anhydride and α -methylstyrene is the indicator reagent, the overlap effect is dominant, but in the absence of acetic anhydride this is not so.

RESULTS AND DISCUSSION

Titration curves obtained for the primary, secondary and tertiary amines with α -methylstyrene, and mixtures of acetic anhydride with 4-hydroxy-4-methylpentan-2-one, hydroquinone and quinhydrone as indicator reagents are shown in Figs. 1-3.

It can be seen in Figs. 1-3 that the end-point inflections are sharp when strong bases, or their hydrochlorides, are titrated, but are more rounded in the titrations of weak bases such as thiourea, pyrrole and caffeine. Figure 3 shows that the sharpness of the end-point inflections is similar, irrespective of the nature of the oxygen grouping(s) of the indicator reagent.

When acetic anhydride was present in the sample solution, some primary amines could not be determined quantitatively; these included *n*-butylamine, benzylamine, aniline and its hydrochloride, representative α -amino-acids (DL- α -alanine, DL-leucine and L-cysteine) and L-dopa and α -methyl-L-dopa. The secondary amines pyrrole and morpholine also could not be determined quantitatively, but it is interesting that diethylamine, pyrrolidine and adrenaline tartrate

could be determined, in the presence of acetic anhydride. The effect of allowing morpholine and diethylamine to remain in contact with acetic anhydride in the sample solution for various periods of time was examined, and it was found that the rate of acetylation of the sample, as measured by the reduction in the titration value as this delay time was increased, was much faster for morpholine than for diethylamine, so that while the latter could be determined quantitatively under normal titration conditions, *i.e.*, titration times of about 5 min, the former could not. As expected, all the tertiary amines can be determined quantitatively in the presence of acetic anhydride.

As noted previously,⁴ the hydrochlorides of several amines and the hydrogen tartrate of adrenaline can be determined by the catalytic thermometric method without addition of mercury(II) acetate to the sample solution, though this is a requirement when visual indicators are used in the non-aqueous titration of amine hydrochlorides with perchloric acid.

Precision and accuracy

In Tables 1 and 2, values for the precision of three replicate determinations of samples that can be titrated quantitatively are shown as the coefficients of variation (CV; relative standard deviation). In addition, the average relative errors (E) are quoted, calculated on the assumption that the samples are 100% pure (which, of course, is not in fact the case).

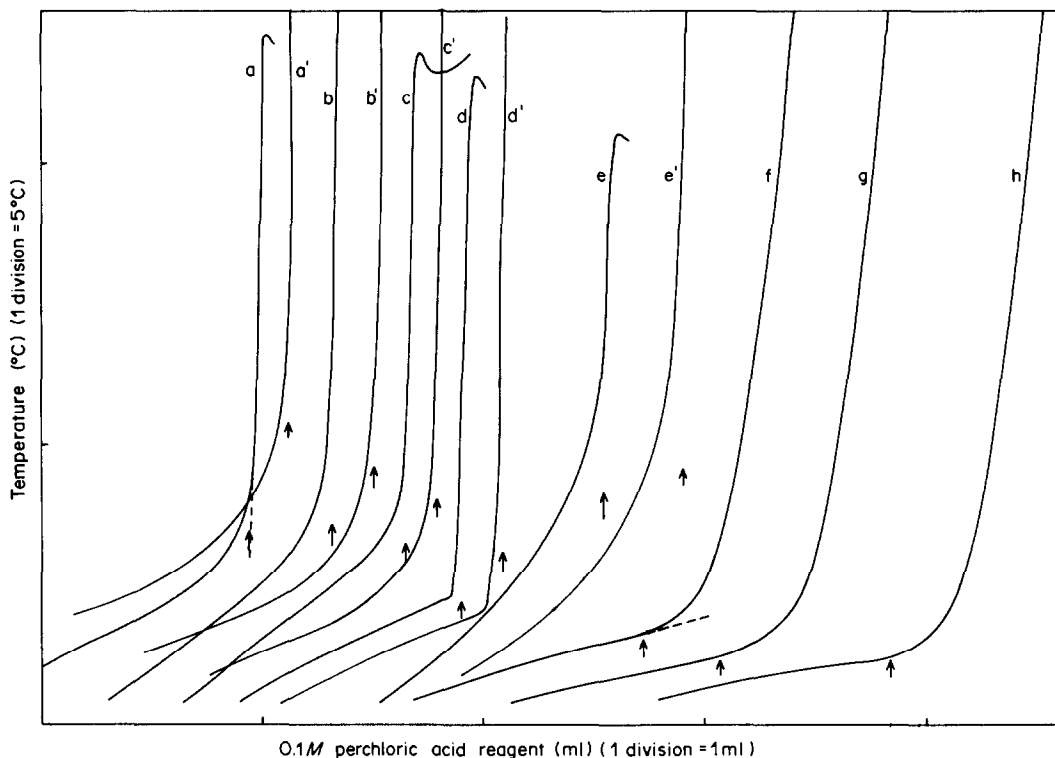


Fig. 1. Catalytic thermometric titration of primary amines with 0.1M perchloric acid. Amine (mg): a/a', dopamine·HCl 18.94; b/b', DL-noradrenaline·HCl 20.91; c/c', ethylamine·HCl 8.21; d/d', tris buffer 12.05; e/e', thiourea 7.87; f, aniline 9.83; g, aniline·HCl 12.98; h, benzylamine 11.14. Indicators: a-h, α -methylstyrene (a-e, with acetic anhydride; f-h, without acetic anhydride); a'-e', acetic anhydride + 4-hydroxy-4-methylpentan-2-one. Arrows indicate end-points.

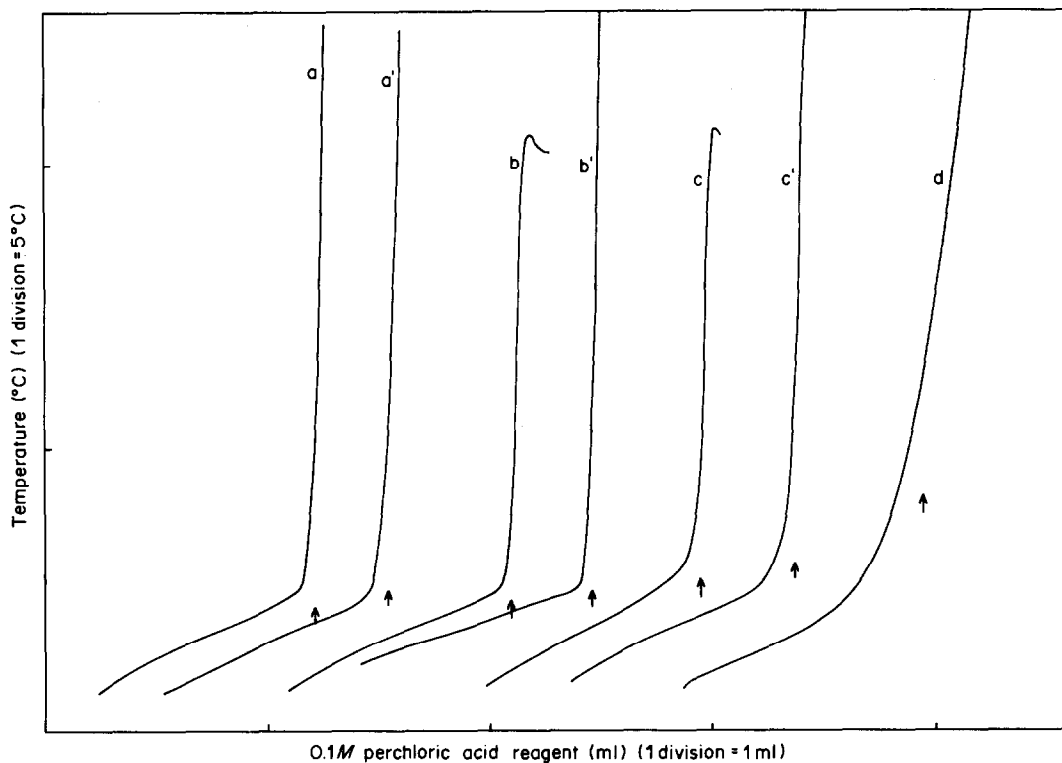


Fig. 2. Catalytic thermometric titration of secondary amines with 0.1M perchloric acid. Amine (mg): a/a', adrenaline tartrate 33.01; b/b', diethylamine 7.29; c/c', pyrrolidine 7.12; d, pyrrole 7.09. Indicators: a-d, α -methylstyrene (a-c, with acetic anhydride; d, without acetic anhydride); a'-c', acetic anhydride + 4-hydroxy-4-methylpentan-2-one. Arrows indicate end-points.

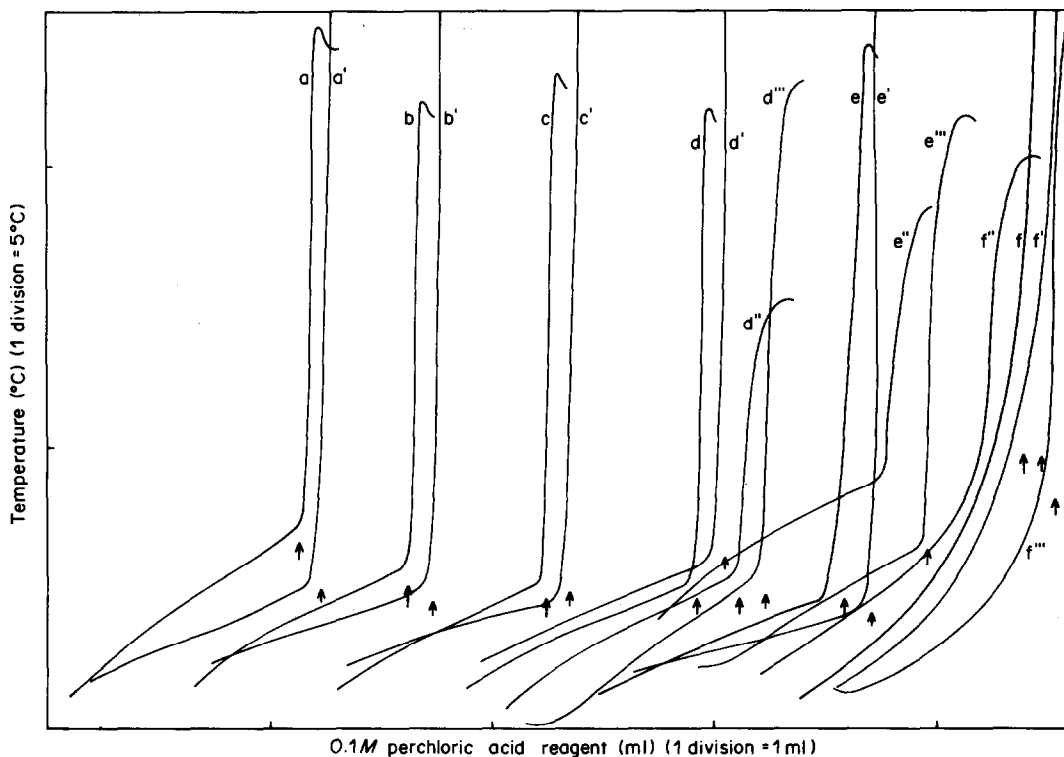


Fig. 3. Catalytic thermometric titration of tertiary amines with 0.1M perchloric acid. Amine (mg): a/a', triethanolamine 15.82; b/b', triethylamine 9.82; c/c', diethylaminoethanol 11.33; d/d'/d'', pyridine 8.56; e/e'/e'', diazepam 29.34; f/f'/f'', caffeine 19.68. Indicators: a-f, α -methylstyrene; a'-f', acetic anhydride + 4-hydroxy-4-methylpentan-2-one; d''-f'', acetic anhydride + quinhydrone; d'''-f''', acetic anhydride + hydroquinone. Arrows indicate end-points.

Table 1. Results for precision and "accuracy" in titrations of amines, with α -methylstyrene and acetic anhydride + 4-hydroxy-4-methylpentan-2-one as indicator reagents

Compound	Sample weight, mg	α -Methylstyrene indicator			Acetic anhydride + 4-hydroxy-4-methylpentan-2-one indicator		
		Mean titre,* meq	CV, %†	E, §%	Mean titre,* meq	CV, %†	E, §%
Dopamine·HCl	18.95	0.0993	0.5	-0.6	0.1003	0.6	+0.4
DL-Noradrenaline·HCl	20.91	0.1010	0.5	-0.7	0.1006	0.6	-1.1
Ethylamine·HCl	8.21	0.1001	0.5	-0.6	0.1007	0.5	-0.04
Tris buffer	12.05	0.0980	0.7	-1.4	0.0987	0.9	-0.8
Thiourea	7.87	0.1042	0.5	+0.8	0.1035	0.7	+0.1
Aniline‡	9.83	0.1050	0.6	-0.5			
Aniline·HCl‡	12.98	0.0997	0.6	-0.4			
Benzylamine‡	11.14	0.1033	0.6	-0.7			
n-Butylamine‡	7.35	0.0998	0.5	-0.7			
α -Methyl-L-dopa‡	23.80	0.0990	0.7	-0.9			
L-Dopa‡	19.49	0.0984	0.6	-0.5			
Adrenaline tartrate	33.04	0.0984	1.0	-0.8	0.0987	0.9	-0.4
Diethylamine	7.29	0.0999	0.5	+0.4	0.1007	0.5	+1.1
Pyrrolidine	7.12	0.1003	0.6	+0.2	0.1000	0.8	-0.2
Pyrrole‡	7.09	0.1051	0.5	-0.6			
Triethanolamine	15.82	0.1060	0.5	-0.02	0.1064	0.6	+0.4
2-Diethylaminoethanol	11.33	0.0970	0.8	+0.36	0.0972	0.5	+0.5
Triethylamine	9.82	0.0977	0.2	+0.7	0.0980	0.7	+1.0
Pyridine	8.56	0.1071	0.4	-0.9	0.1077	0.5	-0.5
Diazepam	29.34	0.1036	0.5	-0.4	0.1037	1.0	+0.5
Caffeine	19.68	0.1007	0.5	-0.6	0.1006	0.5	-0.7

* Three determinations.

† Calculated by using sample standard deviation [$\sqrt{n/(n-1)}$ factor].

‡ E calculated on the assumption that samples are 100% pure.

§ E calculated on the assumption that samples are 100% pure.

‡ Acetic anhydride absent from the α -methylstyrene indicator reagent.

Table 2. Results for precision and "accuracy" in titrations of amines, with quinhydrone and hydroquinone as co-reagents with acetic anhydride in the thermometric indicator

Compound	Sample weight, mg	Quinhydrone			Hydroquinone		
		Mean titre,* meq	CV, %†	E, §%	Mean titre,* meq	CV, %†	E, §%
Diazepam	29.34	0.1028	0.5	-0.4	0.1022	0.9	-1.0
Caffeine	19.68	0.1006	0.6	-0.7	0.1004	0.9	-0.9
Pyridine	8.56	0.1073	0.6	-0.8	0.1066	0.8	-1.5

* See footnotes to Table 1.

Simple comparison tests (F and t) applied to the results show that there is no significant difference, at the 5% probability level, between the CV and mean titration values for individual compounds determined by the two methods, the averages of the CV values for all the compounds, and the variances of the E values for each indicator system. For the results in Table 2, there is again no statistical evidence to show that the average precisions *etc.* differ, or that they differ from those in Table 1.

The results obtained show that in terms of precision and applicability to titration of very weak bases, there is nothing to choose between the two indicator systems considered. However, an important difference is that the α -methylstyrene indicator can be used in the absence of acetic anhydride, provided that the solvents are dried efficiently, *e.g.*, with a molecular sieve. This means that primary and secondary amines that are readily acetylated can be determined quantitatively by use of this polymerization indicator,

whereas they cannot be determined by using the acetic anhydride/esterification indicator system.

Graphs of titration volume *vs.* sample size over the range 0.01–0.1 meq for the bases titrated all showed a good linear correlation (6 points, coefficients better than 0.995).

Acknowledgement—P.V. gratefully acknowledges a Fellowship from the Estaban Romero Foundation (Spain).

REFERENCES

- V. J. Vajgand, T. A. Kiss, F. F. Gaal and I. J. Zsigrai, *Talanta*, 1968, **15**, 699.
- E. J. Greenhow, *Analyst*, 1977, **102**, 584.
- E. J. Greenhow and L. E. Spencer, *ibid.*, 1973, **98**, 81.
- R. Belcher, A. J. Nutten and A. M. G. Macdonald, *Quantitative Inorganic Analysis*, 3rd Ed., Butterworths, London, 1970.
- E. J. Greenhow and L. E. Spencer, *Analyst*, 1973, **98**, 98.
- G. A. Vaughan and J. J. Swithenbank, *ibid.*, 1970, **95**, 890.

DETERMINATION POLAROGRAPHIQUE DE FACTEURS VITAMINIQUES P (RUTINE ET SES DERIVES)

F. FAHRAT, M. KALLEL et A. CAIOLA

Laboratoire de Chimie Analytique, Faculté de Pharmacie de Monastir, Tunisie

D. CANTIN et J. ALARY*

Laboratoire de Chimie Analytique et Bromotologie, Faculté de Pharmacie de Grenoble, France

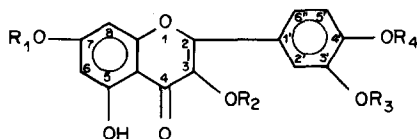
(Reçu le 8 juillet 1983. Révisé le 17 janvier 1984. Accepté le 30 janvier 1984)

Résumé—Plusieurs molécules polyphénoliques appartenant à la classe des flavonols et ayant un intérêt thérapeutique incontestable grâce à leurs propriétés vasculaires ont été étudiées. Elles dérivent toutes du quercétol, qui est un *o*-diphénol. L'oxydation électrochimique de ces molécules a été envisagée en utilisant des électrodes solides tournantes. Le choix du solvant et du pH est discuté. Les résultats obtenus en polarographie à courant continu et à impulsions sont présentés. Une relation a été établie entre la structure et le comportement électrochimique. L'application au contrôle des médicaments est envisagée; la technique représente à la fois un moyen d'identification, un critère de pureté et peut être appliquée sur le plan quantitatif. Il y a en effet une bonne linéarité de réponse de 5×10^{-6} à $10^{-4}M$, ce qui représente une sensibilité largement suffisante pour le dosage dans les formes pharmaceutiques.

Plusieurs molécules polyphénoliques appartenant à la classe des flavonols ont un intérêt thérapeutique incontestable grâce à leurs propriétés vasculaires. Ces molécules sont prescrites en effet dans tous les états pathologiques se traduisant par une fragilité vasculaire, car elles renforcent la résistance des capillaires et diminuent leur perméabilité. Elles sont classées dans la série des molécules à activité vitaminique P. Dans cette série figurent la rutine (flavonol naturel) et ses dérivés hémisynthétiques. Leur structure polyphénolique leur confère une facilité d'oxydation, exploitée d'ailleurs pour leur détermination quantitative par voie chimique.

Nous avons essayé de réaliser une oxydation quantitative de ces flavonols par voie électrochimique dans le but d'une part d'étudier la relation entre structure et comportement électrochimique, et d'autre part, d'appliquer la polarographie de ces molécules à leur contrôle dans les formes pharmaceutiques.

Toutes les molécules étudiées sont des flavonols, dont la structure de base est le quercétol, diversement substitué dans le cas des dérivés:



Si l'hydroxyle en 5 est toujours libre, l'hydroxyle en 3 est lié aux sucres dans les hétérosides et les hydroxyles en 7, 3' et 4' sont éventuellement sous forme d'étheroxydes. Les dérivés étudiés sont présentés dans le Tableau 1.

Plusieurs des dérivés présentés sont des *o*-diphénols qui ont été traités par différents agents oxydants comme le nitrite de sodium ou le molybdate de sodium, produisant en milieu éthanolique des dérivés d'oxydation colorés en rouge.¹ L'acide périodique peut aussi conduire à un titrage potentiométrique.²

Toutes ces molécules présentent également un spectre d'absorption dans l'ultra-violet du fait de leur structure polyinsaturée, de la présence d'un carbonyle et des substitutions phénoliques. L'absorption maximale se situe vers 368 nm pour les génines et vers 342 nm pour les hétérosides.¹

La spectrofluorimétrie a également été mise à profit. Si le substituant en 5 est un hydroxyle phénolique ou un groupement méthoxylé, la molécule possède une fluorescence importante, mais qui manque de spécificité par rapport aux dérivés flavoniques.³

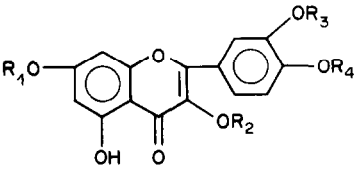
Les méthodes chromatographiques ont été proposées pour l'identification et le dosage de la rutine et de ses dérivés, notamment la chromatographie en phase gazeuse⁴ et la chromatographie en phase liquide sous pression avec détecteur ultra-violet.⁵

Les méthodes électrochimiques ont été peu exploitées dans ce domaine. Une réduction des flavones, chalcones et flavonnes à l'électrode à goutte de mercure a été proposée par Geissman.^{6,7} Davideck propose la détermination polarographique du quercétol après sa transformation en chélate de cobalt.⁸ Enfin Hamilton⁹ étudie la réduction de flavonols préalablement oxydés par voie enzymatique.

La réduction directe du quercétol en milieu acide et en phase hydro-organique a été décrite par Haluk.¹⁰ Le mécanisme réactionnel proposé est le suivant: il y aurait réduction du carbonyle 4, en alcool, accompagnée d'une réduction de l'hydroxyle

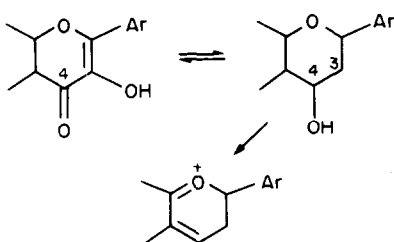
*Auteur pour correspondance.

Tableau 1. Molécules étudiées



	R ₁	R ₂	R ₃	R ₄
Quercétine	H	H	H	H
Rutine	H	Rutinose	H	H
Morpholinoéthylrutine (Ethoxazorutine)	$-\text{CH}_2-\text{CH}_2-\text{N} \begin{array}{c} \diagup \\ \diagdown \end{array} \text{O}$	Rutinose	H	H
Trioxyéthylrutine	$-\text{C}_2\text{H}_4\text{OH}$	Rutinose	$-\text{C}_2\text{H}_4\text{OH}$	$-\text{C}_2\text{H}_4\text{OH}$

en 3. Dans une deuxième étape, une déshydratation intramolécule se produirait.



C'est l'oxydation du quercétol et de ses dérivés qui a retenu notre attention. En effet, considérant la présence d'un noyau diphenolique-1,2 dans la molécule, nous avons pensé à un rapprochement possible avec d'autres catéchols et en particulier les catécholamines étudiées par Cantin.¹¹

Nous avons donc recherché si les facteurs vitaminiques P à étudier étaient oxydables par voie électrochimique grâce à certaines électrodes solides tournantes.

PARTIE EXPERIMENTALE

Solution de fond

Solvant. Son choix a été guidé par les impératifs suivants:

- assurer une bonne solubilité de la totalité des molécules étudiées,
- avoir un domaine d'électroactivité étendu vers les potentiels positifs,
- ne présenter ni un caractère trop acide (hydrolyse des hétérosides), ni un caractère trop basique (oxydation spontanée des molécules),
- présenter une constante diélectrique suffisante (> 30).

C'est le mélange diméthylformamide-eau (1:4 v/v) qui a été retenu. Il répond aux impératifs cités et permet d'obtenir une vague polarographique bien reproductible avec les composés étudiés.

Tampon. Nous avons adopté le tampon phosphate de Sørensen à pH 7 (39,2 ml de KH_2PO_4 0,07M et 60,8 ml de $\text{Na}_2\text{HPO}_4 \cdot 12\text{H}_2\text{O}$ 0,07M) qui permet d'obtenir un courant de diffusion élevé, sans risque d'auto-oxydation (i_d croît légèrement avec le pH) (Tableau 2). Ce tampon joue également le rôle d'électrolyte support.

Appareillage

Polarographe. Polarographe Tacussel type PRG₅ pouvant fonctionner en polarographie classique à courant continu et en polarographie à impulsions d'amplitude constante.

Electrodes. Il s'agit d'un montage classique à trois électrodes.

—Electrodes de travail: plusieurs électrodes solides tournantes ont été comparées:

platine: les phénomènes d'adsorption entraînent des déformations des vagues;

carbone vitreux: les courants de diffusion sont peu importants et les pics mal définis en polarographie impulsionnelle;

électrode à disque de graphite: c'est celle qui s'est avérée la plus satisfaisante; elle est constituée d'un disque de graphite de 3 mm de diamètre (Tacussel type Ed₁); sa vitesse de rotation a été réglée à 2500 tours/min grâce à un amplificateur de type Controvit; cette vitesse de rotation permet d'obtenir un courant de diffusion à la fois intense et reproductible; la surface du graphite est repolie avant chaque détermination au moyen d'un papier abrasif imprégné de solution de fond, puis elle est rincée soigneusement à l'eau.

—Electrode de référence: c'est une électrode au calomel saturé, munie d'une allonge renfermant la solution tampon de Sørensen à pH 7.

—Electrode auxiliaire: il s'agit d'une électrode de platine plongeant directement dans la solution à polarographier.

Conditions de travail

La vitesse de déroulement des potentiels a été fixée à 2 mV/sec. La sensibilité a été choisie de telle sorte que la mesure de la hauteur de vague puisse se faire avec précision. Les valeurs retenues vont de 2,5 à 25 μA pour 25 cm de papier. En polarographie à impulsions, la valeur de l'amplitude de l'impulsion surimposée (ΔE) a été fixée à 100 mV. Pour chaque molécule, les tracés ont été réalisés après 10 min de dégazage. L'exploration est faite de $-0,2$ à $+1,7$ V contre E.C.S. La température est fixée à 25°. Les solutions mères 10^{-4} M de flavonols sont obtenues par dissolution dans le diméthylformamide (DMF), en ajoutant ensuite le tampon phosphate à pH 7 pour respecter la composition du

Tableau 2. Variation de i_d et de $E_{1/2}$ en fonction du pH

pH tampon	pH final	i_d , μA	$E_{1/2}$, V (contre E.C.S.)
5,0	5,1	1,75	0,080
5,5	5,6	1,75	0,080
6,0	6,4	1,9	0,090
6,5	7,1	2,0	0,090
7,0	7,6	2,1	0,090
7,5	7,9	2,1	0,090
8,0	8,3	2,1	0,100

Valeurs obtenues à partir d'une solution de quercétine à 5×10^{-5} M dans le mélange DMF-tampon (1:4 v/v).

Tableau 3. Valeurs obtenues pour le comportement électrochimique

	$E_{1/2}$, V (contre E.C.S.)	i_d , μA	E_p , V (contre E.C.S.)	i_p , μA	$W_{1/2}$, mV
Quercétine	+0,08	2,10*	+0,125	27	110
Rutine	+0,19	1,45	+0,240	5,5	140
Morpholinoéthylrutine	+0,23	0,70	+0,275	2,0	160
Trioxéthylrutine			+1,450	0,41	100

Concentration: $5 \times 10^{-5} M$ en solution tampon Sørensen–DMF (4:1 v/v) à pH 7,6.

*Déviation standard 0,02 μA ($n = 10$).

solvant: DMF–tampon pH 7 (1:4 v/v). Les dilutions ultérieures sont réalisées avec le même solvant. Ces solutions sont conservées à 4° et à l'abri de la lumière. Leur conservation ne doit pas excéder 48 hr.

RESULTATS ET DISCUSSION

Pour chaque molécule étudiée les valeurs de $E_{1/2}$, de E_p , de i_d et $W_{1/2}$ sont présentées dans le Tableau 3. Chaque chiffre représente la moyenne de cinq déterminations. Les valeurs de i_d sont celles obtenues avec une solution $5 \times 10^{-5} M$.

Relation structure–comportement électrochimique

Parmi les molécules étudiées, seule la trioxéthylrutine n'est pas oxydable à un potentiel inférieur à 1 V contre E.C.S., dans les conditions expérimentales adoptées. C'est du reste la molécule la plus substituée puisque seul l'OH en 5 est libre.

Les autres molécules sont oxydables en donnant

une vague bien définie en polarographie classique et un pic en polarographie impulsienne.

Quercétol, rutine et morpholinoéthylrutine possèdent la structure *o*-diphénolique. Ils sont très facilement oxydables au même titre que les catécholamines.¹¹ Ces molécules se distinguent seulement par le nombre d'hydroxyles libres sur le cycle du chromane. La facilité d'oxydation décroît avec ce nombre de fonctions hydroxylées. Le blocage de l'OH-3 par un ose déplace le $E_{1/2}$ de 110 mV et le potentiel de pic de 114 mV vers les potentiels positifs, lorsqu'on passe du quercétol à la rutine. L'influence du blocage de l'OH-7 est moins importante, le déplacement supplémentaire vers les potentiels positifs est alors de 40 mV en D.C. est de 35 mV en polarographie à impulsions (morpholinoéthylrutine).

La valeur du courant de diffusion semble proportionnelle au nombre de fonctions phénoliques libres. Il apparaît donc que la structure catéchol ne soit pas la seule en cause dans le mécanisme réactionnel. Ce

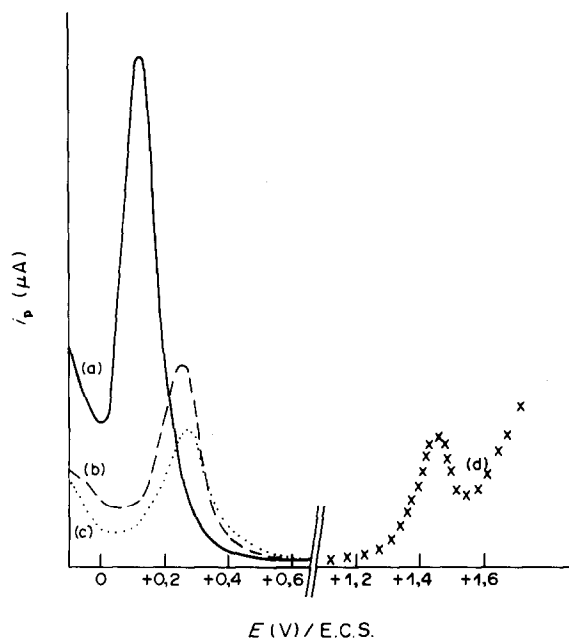


Fig. 1. Polarogrammes de solutions $5 \times 10^{-5} M$ dans le mélange DMF–tampon (1:4 v/v) à pH 7,6 ($\Delta E = 100$ mV). (a) Quercétine: $E_p = +0,125$ V ($S = 2 \mu A/cm$). (b) Rutine: $E_p = +0,240$ V ($S = 1 \mu A/cm$). (c) Morpholinoéthylrutine: $E_p = +0,275$ V ($S = 0,5 \mu A/cm$). (d) Trioxéthylrutine: $E_p = +1,450$ V ($S = 0,2 \mu A/cm$). (S = sensibilité de l'enregistrement).

mécanisme reste donc à démontrer, ce que nous nous proposons de faire dans l'avenir.

Application au contrôle des médicaments

Le comportement électrochimique des molécules étudiées permet d'envisager des applications qualitatives et quantitatives.

Les différences de $E_{1/2}$ permettent dans une certaine mesure d'utiliser ces valeurs comme critère d'identité. Ce sont surtout les E_p qui présentent dans ce cadre un intérêt. Néanmoins, il n'est pas possible de distinguer la rutine de l'éthoxazorutine (Fig. 1).

Les mêmes déterminations peuvent être mises à profit comme critère de pureté. On peut par exemple rechercher la présence de quercétol libre dans la rutine ou les dérivés hémisynthétiques. On peut également envisager d'identifier la rutine (matière première) dans la trioxyéthylrutine.

Sur le plan quantitatif enfin, les courbes d'étalonnage réalisées en D.C. sur toutes les molécules oxydables ont montré la très bonne linéarité de $5 \times 10^{-6} M$ à $10^{-4} M$, ce qui représente une sensibilité très largement suffisante pour le dosage dans les formes pharmaceutiques.

La limite supérieure de $10^{-4} M$ ne peut être dépassée car des phénomènes d'adsorption se produisent alors à l'électrode et déforment les vagues, ce qui semble en relation avec la structure phénolique de ces molécules.

En polarographie à impulsions, si les valeurs de potentiel de pic sont bien reproductibles, par contre les courants de pic sont fluctuants.

C'est la raison pour laquelle dans nos conditions opératoires, la polarographie à impulsions nous semble surtout utile sur le plan qualitatif, d'autant plus

que la valeur des courants de pics enregistrés permet de déceler des traces de produit.

Conclusion

L'oxydation électrochimique des facteurs vitaminiques P étudiés a pu être obtenue grâce à une électrode de graphite. L'intensité du courant de diffusion est importante, ce qui permet d'envisager des applications quantitatives intéressantes dans le cadre du contrôle des médicaments.

Les différences de comportement électrochimique en fonction de la structure peuvent également être mises à profit dans une optique qualitative et pour le contrôle de pureté de ces molécules.

LITTÉRATURE

1. J. Roberts et P. F. T. Vaughan, *Phytochemistry*, 1971, **10**, 2649.
2. M. Guernet, E. Espinassou et M. Hamon, *Ann. Pharm. Franc.*, 1973, **31**, 343.
3. M. F. Shostakovski, N. A. Tyukavikina, A. I. Kirillov, K. I. Lapteva et N. G. Deyatko, *Izv. Sib. Otdel. Akad. Nauk SSSR, Ser. Khim. Nauk*, 1969, **1**, 121.
4. R. A. Andersen et T. H. Vaughan, *J. Chromatog.*, 1970, **52**, 385.
5. G. Charalambous, K. J. Bruckner, W. A. Hardwick et A. Unnebach, *Tech. Q. Master Brew. Assoc. Am.*, 1973, **10**, 74.
6. W. Engelkemeir, T. A. Geissman, W. R. Crowell et S. L. Friess, *J. Am. Chem. Soc.*, 1947, **69**, 155.
7. T. A. Geissman et S. L. Friess, *ibid.*, 1949, **71**, 3893.
8. J. Davidek et Z. Prochažka, *Collection Czech. Chem. Commun.*, 1961, **26**, 2947.
9. J. W. Hamilton et A. L. Tappel, *J. Am. Oil Chem. Soc.*, 1963, **40**, 52.
10. J. P. Haluk et M. Metche, *Chim. Anal. Paris*, 1970, **52**, 1245.
11. D. Cantin, *Thèse Doctorat*, Grenoble, 1976.

Summary—Several flavonols of therapeutic interest on account of their vascular properties have been studied. They were all derived from the *o*-diphenol quercetol. Their electrochemical oxidation at a rotating solid electrode has been examined, and the choice of solvent and pH is discussed. Results obtained by d.c. and pulse polarography are presented. A relation between their structure and electrochemical behaviour has been established. Application to drug analysis is proposed, giving identification, determination and purity assay simultaneously. There is a linear response over the range 5×10^{-6} – $10^{-4} M$, a sufficient range for analysis of pharmaceuticals.

SHORT COMMUNICATIONS

CHEMICAL IONIZATION MASS SPECTROMETRY OF NITROSAMINES

YIN FANG, DING JIAHUA* and LIU SHILIT

Department of Chemistry, China University of Science and Technology, Hefei, China

(Received 30 June 1981. Accepted 24 February 1984)

Summary—The mass spectra of eight nitrosamines have been recorded, with excitation by chemical ionization (CI) and electron impact (EI). Comparison of the intensities of the base peaks under CI and EI conditions gives intensity ratios in the range 1.4–1.9 for low resolution measurements and up to 10 for high resolution measurements, confirming the enhanced sensitivity available in the CI mode.

As a preliminary test for the presence of volatile nitrosamines, the technique of gas chromatography (GC) is usually used. However, for the identification of a specific nitrosamine, it is most commonly combined with mass spectrometry (MS). A number of publications have reported the analysis of nitrosamines by electron-impact mass spectrometry (EIMS)¹ since Collin first described the mass spectra of five nitrosamines.² Later, the technique of chemical-ionization mass spectrometry (CIMS) was developed and the first successful results were reported by Munson and Field in 1966.³ The fragmentation patterns obtained are much simpler than those obtained with conventional EIMS, and conform more closely to the structures of the molecules to be identified. The CIMS spectra are therefore more useful for both qualitative and quantitative analysis.

Gadbois *et al.*⁴ used this technique for the determination of dimethylnitrosamine. They used methane as the reagent gas, and monitored the ion current at $m/z = 75$. Gaffield *et al.*⁵ reported the CIMS spectra for ten nitrosamines, and gave preliminary sensitivity measurements for two of them, nitrosodimethylamine and nitrosodiphenylamine. They used a combination of gas chromatography with CIMS. At the present time there is still a need for more reference chemical-ionization mass spectra of nitrosamines. This paper presents such spectra for eight commercially available pure nitrosamines. A comparison of sensitivities is made for the CI and EI modes of operation with the same mass spectrometer.

EXPERIMENTAL

Apparatus

A JMS-D300 CIMS, coupled to a JMA-2000 computer system was used with methane as reagent gas. It was

operated at a resolution of 500 (10% valley) and a source temperature of 200°, with an ionizing voltage of 200 V and a trap current of 300 μ A. Samples were introduced by means of a direct insertion probe or an adjustable leak valve attached to the gas-liquid inlet.

A gas chromatograph was connected by a solvent-venting valve and a glass jet separator to the mass spectrometer; the glass chromatographic column (2 m \times 1.8 mm bore) was packed with 15% PEG-20M/1% KOH on Chromosorb W AW-DMCS. Helium was used as carrier gas at a flow-rate of 40 ml/min, the column temperature was 120° for *N*-nitrosodimethylamine and 160° for *N*-nitrosopyrrolidine, and the sample inlet and interface temperatures were both 200°.

Sensitivity measurement

The sensitivities in the CI and EI modes of operation were compared by setting the instrument to a resolution of 7000 and using the peak-matching facility. The mass range in the vicinity of the appropriate parent ion (74.0480 or 100.06366) and the quasimolecular ion (75.05583 or 101.07149) were continuously scanned. The output was displayed on the oscilloscope of the peak-matching unit, thus enabling the nitrosamine and reference ion-currents to be alternately monitored every 2 sec. The peak height on the oscilloscope gave the appropriate sensitivity.

RESULTS AND DISCUSSION

A summary of the mass spectra of the nitrosamines, obtained by low-resolution CIMS, is given in Table 1. The abundances of the ions listed are in agreement with those reported by Gaffield *et al.*⁵ Five of the eight nitrosamines have spectra in which the base peak is that for $(M + 1)^+$. The corresponding EI mass spectra include only three in which the base peak is M^+ . The fraction of the total ion-current (σ) carried by the ion responsible for the base peak (expressed as %) for both the CI and EI modes is given in Table 2. It can be seen that this fraction is over 50% for the CI mode and less than 30% for the EI mode for all the nitrosamines except nitrosodiphenylamine. Operation in the CI mode therefore offers increased sensitivity.

Although a rigorous comparison of the sensitivities

*Present address: The Sanitation and Antiepidemic Station of Jilin Province, Changchun, China.

†Present address: Beijing Environmental Protection Research Institute, Beijing, China.

Table 1. Summary of mass spectra of nitrosamines, obtained by CIMS using methane as reagent gas*

Compound	(M+41) ⁺	(M+29) ⁺	(M+1) ⁺	(M-29) ⁺	(M-30) ⁺
Nitrosodimethylamine	1.1	0	100	0	1.6
Nitrosodiethylamine	2.6	3.8	100	0	0.8
Nitrosodi-n-propylamine	3.6	10.0	100	0	0
Nitrosopyrrolidine	2.4	1.2	100	0.7	3.6
Nitrosopiperidine	3.6	5.7	100	0.7	3.0
Nitrosodiphenylamine	0	0	3.4	100	34.1
Nitrosomethylphenylamine	0	0	1.4	37.9	6.3
Nitrosodiethanolamine	0.4	2.7	4.7	8.9	12.8

*All values refer to the intensity relative to the ion with the base peak set equal to 100.

Table 2. Comparison of σ values* for the CI and EI modes of operation

Compound	EI		CI	
	<i>m/z</i>	σ , %	<i>m/z</i>	σ , %
Nitrosodimethylamine	74	29.5	75	87.5
Nitrosodiethylamine	102	23.6	103	82.1
Nitrosodi-n-propylamine	70	20.2	131	65.0
Nitrosopyrrolidine	100	32.5	101	78.8
Nitrosopiperidine	42	17.5	115	75.2
Nitrosodiphenylamine	169	19.8	169	30.8
Nitrosomethylphenylamine	106	28.8	108	58.1
Nitrosodiethanolamine	42	18.9	74	59.2

* σ is the fraction of total ion-current carried by the ion responsible for the base peak, expressed as %.

of CI and EI mass spectrometry cannot be made for any given nitrosamine, it is possible to compare the intensities of the base peaks for the CI and EI modes. The intensity ratio is a measure of the relative sensitivity of the instrument in the two operating modes. The measured intensity ratios are 1.87, 1.44 and 1.90 for nitrosodimethylamine, nitrosodiethylamine and nitrosodiphenylamine, respectively. Thus the sensitivity of CIMS is higher than that of EIMS under low-resolution conditions. The improvement in sensitivity is even more marked under high-resolution conditions (by the peak-matching technique), the intensity ratio rising as high as 10. Therefore high-resolution CIMS with peak-matching is a useful method of detecting specific nitrosamines in complex mixtures.

Acknowledgements—The authors are grateful to the Sanitation and Antiepidemic Station of Jilin Province, Changchun, China, for the use of the JMS-D300 mass spectrometer, and to Mrs. Yang Ying-hua, Mr. Jiang Yinfei and Mr. Su Li-zhong for their assistance.

REFERENCES

1. T. A. Gough, *Analyst*, 1978, **103**, 785.
2. J. Collin, *Bull. Soc. Roy. Sci., Liege*, 1954, **23**, 201.
3. M. S. B. Munson and F. H. Field, *J. Am. Chem. Soc.*, 1966, **88**, 2621.
4. D. F. Gadbois, E. M. Ravesi, R. C. Lundstrom and R. S. Maney, *J. Agr. Food Chem.*, 1975, **23**, 665.
5. W. Gaffield, R. H. Fish, R. L. Holmsteak, J. Poppiti and A. L. Yergey, in *Environmental N-Nitroso Compounds, Analysis and Formation*, E. A. Walker, P. Bogovski and L. Gričiute (eds.), p. 11. International Agency for Research on Cancer (IARC), Scientific Publication No. 14, Lyons, 1975.

GRAVIMETRIC DETERMINATION OF THE ABUNDANCE RATIO OF ZIRCONIUM AND HAFNIUM, BASED ON THE *in situ* THERMAL DECOMPOSITION OF $K_4[(Zr, Hf)(C_2O_4)_4] \cdot 5H_2O$

TOMITARO ISHIMORI*, MASATOMI SAKAMOTO and TADAO WATANABE
Faculty of Engineering, Ehime University, Matsuyama 790, Japan

(Received 19 August 1983. Revised 10 February 1984. Accepted 23 February 1984)

Summary—Careful heating of $K_4[(Zr, Hf)(C_2O_4)_4] \cdot 5H_2O$ results in a two-step thermal decomposition which can be written as: $K_4[(Zr, Hf)(C_2O_4)_4] \cdot 5H_2O \rightarrow K_4[(Zr, Hf)(C_2O_4)_4] \rightarrow \{2K_2CO_3 + (Zr, Hf)O_2\}$. The weight-ratio of the successive decomposition products depends on the abundance ratio of Zr and Hf, and forms the basis for the present method of gravimetric determination.

It is well known that both zirconium and hafnium form potassium tetrakis(oxalato)zirconohafnate at all Zr/Hf ratios.¹ The thermal decomposition of the mixed metal complex salt gives thermogravimetric (TG) curves with two well-defined plateaus in the temperature ranges 170–240° and 450–650°, corresponding to the formation of $K_4[(Zr, Hf)(C_2O_4)_4]$ and $\{2K_2CO_3 + (Zr, Hf)O_2\}$, respectively.

As can be deduced from theory, the percentage weight losses at these two plateaus depend on the relative abundance of Zr and Hf in the complex salt. Therefore, a new method for determining the abundance ratio can be based on analysis of the TG curve.

EXPERIMENTAL

Materials

Reactor-grade zirconium metal containing only 42 ppm of hafnium was received from the Japan Atomic Energy Research Institute, Tokai. Three commercial materials were also utilized: hafnium oxide, 99 mole% purity (Merck, Darmstadt); hafnium oxide, 87 mole%; zirconium oxychloride, 97 mole%.

Preparation of the complex salt

Metallic zirconium or hafnium oxide was chlorinated^{2,3} in order to prepare aqueous solutions of zirconium and hafnium; aqueous solutions of zirconium oxychloride were prepared directly from the reagent.

A series of zirconium–hafnium solutions with the desired abundance ratios was prepared by mixing standard solutions of known composition. Both zirconium and hafnium in these solutions were converted into the complex salt by the conventional procedure.¹ The Zr/Hf ratios in the salts were the same as in the solutions. In the present study, 7 mixtures with different abundance ratios were prepared, and labelled A, B, C... G.

Thermal decomposition and gravimetric measurements

About 5 mg of the complex salt was decomposed by heating it on an electric balance, Cahn Model 2000, under a normal atmosphere, in order to measure the change in

weight. The temperature was raised at a rate of about 0.7°/min.

RESULTS AND DISCUSSION

Figure 1 shows the typical TG curves for samples A and G. In the temperature regions II and IV, both curves give two well-defined plateaus. The TG curves for all 7 samples displayed these plateaus. Experimental checks showed that the plateaus remain in the same position regardless of the rate of temperature change.

Determination of Zr–Hf abundance ratio

The plateaus in the regions II and IV provide more

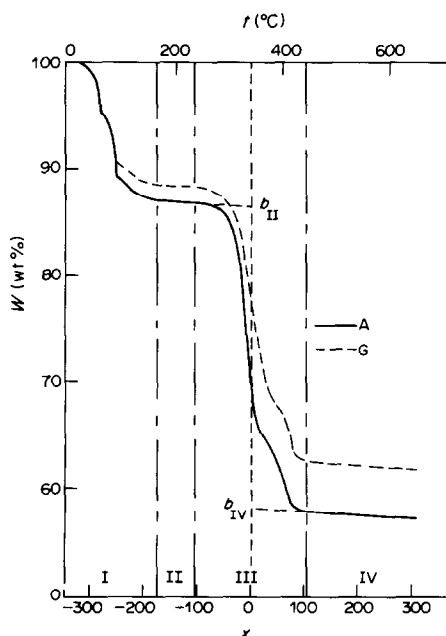


Fig. 1. TG curves for samples A and G.

*Author for correspondence.

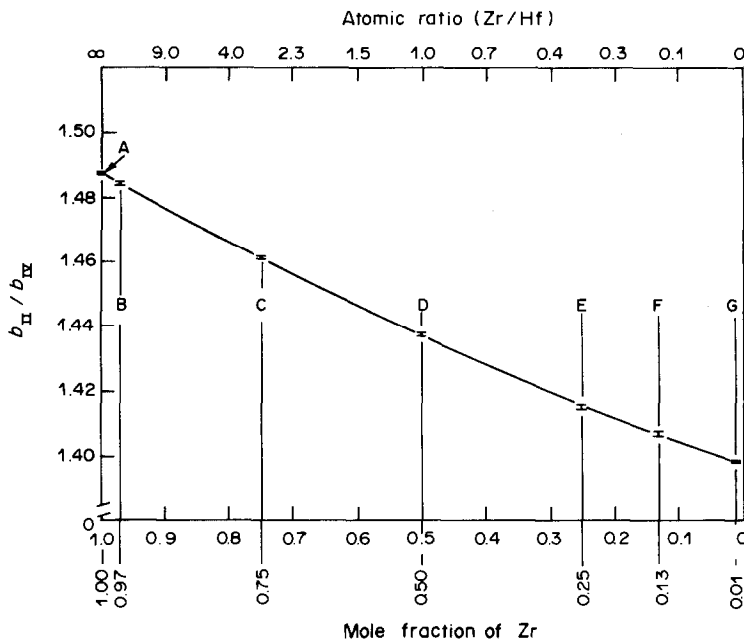


Fig. 2. Plots of b_{II}/b_{IV} vs. the mole fraction of Zr and atomic ratio Zr/Hf. Value of b_{II}/b_{IV} : 1.4870 ± 0.0001 (A); 1.4846 ± 0.0006 (B); 1.4613 ± 0.0005 (C); 1.4380 ± 0.0007 (D); 1.4154 ± 0.0013 (E); 1.4074 ± 0.0009 (F); 1.3987 ± 0.0006 (G).

than 25 data points in each run. Therefore the constants in the following equations can be determined very precisely by least-squares fitting of the data:

$$W_{II} = a_{II}x + b_{II} \quad \text{and} \quad W_{IV} = a_{IV}x + b_{IV}$$

where suffix II or IV stands for the plateau in the temperature region II or IV respectively, W represents $100 \times [\text{observed weight}/\text{initial weight}]$, a is the slope of the plateau region, and x denotes observed temperature minus 345° . The origin of the temperature axis is moved to 345° in order to minimize geometrical errors; this temperature corresponds to the mid-point between the two plateaus.

Although both b_{II} and b_{IV} are found from many observed values, they are related to the initial weight of the sample at room temperature, which is measured just once for each experimental run. In the present work, the ratio b_{II}/b_{IV} is used instead of b_{II} or b_{IV} as the variable related to the relative abundance of Zr and Hf, so that the effect of the geometrical errors on the relationship shown in Fig. 2 will be minimized. The values of b_{II} and b_{IV} have no stoichiometric significance, but are used because they can be accurately calculated from the data, whereas the values corresponding to the completion of the two thermal decomposition steps are somewhat dependent on experimental variables such as heating rate and weight of sample. The method of calculation is purely empirical.

Experimental values of b_{II}/b_{IV} are plotted against mole fraction of Zr. The experimental points fall on a smooth curve and have satisfactorily small standard deviations, showing that this curve can be used for

the determination of the abundance ratio. This relationship can be seen in Fig. 2, in which the abundance ratio is given both as mole fraction of Zr and atomic ratio Zr/Hf. The standard deviations for b_{II}/b_{IV} were obtained by repetition of the thermal decomposition. Geometric consideration of Fig. 2 leads to the conclusion that the standard deviation for the mole fraction of Zr in an "unknown" sample should lie in the range (0.005–0.02).

Recommended procedure

Add 20 ml of concentrated hydrochloric acid and 50 ml of 16% mandelic acid solution to the starting solution, containing not more than 300 mg of Zr + Hf. Dilute the solution to 100 ml with water and digest it at 85° for 20 min. Filter off precipitate on a suitable paper and wash it with hot 5% mandelic acid solution in hydrochloric acid (1 + 50).⁴ This procedure frees the Zr and Hf from practically all kinds of impurities. Ignite the precipitate to $(Zr, Hf)O_2$ in a platinum crucible. Mix the product with 2–3 times its weight of carbon, place the mixture in a porcelain boat and insert this into a silica tube (25 mm internal diameter, 1000 mm long), connected to a product collector. Purge the tube first with nitrogen and then with chlorine. Maintain a slow flow of chlorine through the reaction tube and heat it to 900° . The $(Zr, Hf)Cl_4$ produced deposits in the collector.³

To 20 ml of aqueous solution of 400 mg of the mixed tetrachlorides add 20 ml of an aqueous solution containing 1200 mg of $K_2C_2O_4 \cdot H_2O$ and 400 mg of $H_2C_2O_4 \cdot 2H_2O$, dropwise with stirring. Heat the mixture to boiling, cool it to room temperature, then add 30 ml of ethanol dropwise. Filter off the precipitate, wash it with ethanol and dissolve it with hot water (70°). Cool this solution to room temperature, add ethanol to reprecipitate the mixed oxalate, and wash it first with ethanol, and then with diethyl ether. Mount about 5 mg of the salt on the thermobalance and heat it for TG curve measurement. Calculate b_{II} and b_{IV} by extrapolation of the least-squares best fit for the points on

plateaus II and IV. From b_{II}/b_{IV} and the calibration curve (Fig. 2), read off the mole fraction of Zr or the atomic ratio Zr/Hf.

CONCLUSION

The method is based on the *in situ* thermal decomposition of the mixed complex oxalato salt on the balance, and empirical analysis of the data. Losses of zirconium and hafnium during the decomposition procedure are expected to be negligible. The amounts of sample required are much smaller than those used in other gravimetric methods for Zr/Hf ratio determination.

Acknowledgement—The authors would like to express their hearty thanks to Dr. Kaoru Ueno, Japan Atomic Energy Research Institute, for his sending them reactor-grade zirconium.

REFERENCES

1. *Inorganic Syntheses*, Vol. VIII, pp. 40, 42.
2. V. L. Hansley, H. Greenberg and S. Schott, *U.S. Patent*, 2916351 (1959); *Chem. Abstr.*, 1960, **54**, 7087d.
3. U.S. Atomic Energy Commission, *Brit. Patent*, 971458 (1964); *Chem. Abstr.*, 1965, **62**, 258b.
4. C. A. Kumins, *Anal. Chem.*, 1947, **19**, 376.

SPECTROPHOTOMETRIC DETERMINATION OF ZINC WITH 2-(3,5-DIBROMO-2-PYRIDYLAZO)-5- DIETHYLAMINOPHENOL IN THE PRESENCE OF ANIONIC SURFACTANT

TAN ZHE

Analytical and Testing Institute of Hunan Province, Changsha, People's Republic of China

and

SHUI-SHENG WU*

Changsha Institute of Technology, P.O. Box 410003, 506, Changsha, Hunan, People's Republic of China

(Received 20 December 1982. Revised 24 January 1984. Accepted 23 February 1984)

Summary—A sensitive spectrophotometric method for zinc has been established by reacting zinc with 2-(3,5-dibromo-2-pyridylazo)-5-diethylaminophenol (3,5-diBr-PADAP) in the presence of an anionic surfactant, sodium lauryl sulphate. The molar absorptivity is $1.3 \times 10^5 \text{ l. mole}^{-1} \text{ cm}^{-1}$ at 570 nm. The molar ratio of zinc to 3,5-diBr-PADAP is 1:2. Beer's law is obeyed up to 0.7 ppm of zinc. With pre-separation of zinc by extraction of its thiocyanate complex, the method has been applied to the determination of zinc in waste water.

Silver¹ and uranium² have been determined spectrophotometrically with 2-(3,5-dibromo-2-pyridyl-azo)-5-diethylaminophenol (3,5-diBr-PADAP) in the presence of anionic surfactant. We have now investigated this kind of colour reaction for zinc, and worked out a sensitive spectrophotometric method for determination of zinc with 3,5-diBr-PADAP in the presence of sodium lauryl sulphate (SLS). The practical molar absorptivity is $1.3 \times 10^5 \text{ l. mole}^{-1} \text{ cm}^{-1}$ at pH 7-10 and at 570 nm, making the reaction one of the most sensitive known for zinc. If the zinc is pre-separated by extraction of its thiocyanate complex and stripping, the reaction can be used for the determination of trace amounts of zinc in waste water samples, except when cobalt is present.

EXPERIMENTAL

Reagents

Zinc standard solution, 1 mg/ml. Dissolve 0.1245 g of pure zinc oxide in 10 ml of hydrochloric acid (1 + 1) in a 100-ml standard flask and dilute to volume with water. Dilute the solution as required.

3,5-DiBr-PADAP, 5×10^{-4} M ethanolic solution. Dissolve 0.020 g of 3,5-diBr-PADAP, synthesized by the procedure described previously,¹ in 100 ml of ethanol.

Sodium lauryl sulphate (SLS) solution, 1%.

Ammonium thiocyanate solution, 40%.

Thiourea solution, 10%.

Buffer solution, pH 8.2. Adjust 0.1M sodium borate with hydrochloric acid to pH 8.2, using a pH-meter. Unless otherwise stated, all reagents used were of analytical-reagent grade, and demineralized water was used throughout.

Recommended procedure

Take a known volume (up to 30 ml) of water sample in

a 60-ml separatory funnel. Add 2 ml of hydrochloric acid (1 + 1), 3 ml of thiourea solution and 3 ml of ammonium thiocyanate solution. Dilute to about 40 ml with water, add 10 ml of methyl isobutyl ketone (MIBK), shake the mixture for 6 min, allow the phases to separate, and draw off the aqueous layer. Shake the aqueous phase with another 10 ml of MIBK, combine the extracts and discard the aqueous phase.

Add 10 ml of hydrochloric acid (1 + 1) to the organic phase and shake the mixture for 6 min. Allow the phases to separate, and collect the aqueous layer in a 100-ml standard flask. Repeat with another 10 ml of hydrochloric acid, add the aqueous layer to the standard flask, dilute to volume with water and mix. Pipette a portion containing not more than 7 μg of zinc into a 10-ml standard flask, adjust to about neutrality with ammonia solution (1 + 1), and add, in the following order and with mixing between additions, 2 ml of pH 8.2 buffer, 0.75 ml of 3,5-diBr-PADAP solution and 2 ml of SLS solution. Dilute to volume with water, mix, and let stand at room temperature for 10 min. Measure the absorbance at 570 nm against a reagent blank similarly prepared, with 1-cm cells.

RESULTS AND DISCUSSION

Spectral characteristics

The absorption spectra of 3,5-diBr-PADAP-SLS, 3,5-diBr-PADAP-Zn and 3,5-diBr-PADAP-Zn-SLS mixtures in aqueous solution at various pH-values have been studied. The spectra at pH 8.2 are shown in Fig. 1. Aqueous solutions of 3,5-DiBr-PADAP-SLS at pH from 2 to 11 are all orange-yellow and give an absorption maximum within the range 445-465 nm (curve A). The 3,5-diBr-PADAP-Zn system forms a new product and exhibits an absorption peak at 600 nm (curve B). In the ternary system, 3,5-diBr-PADAP-Zn-SLS, the zinc complex formed exhibits two absorption peaks, at 530 and 570 nm,

*Author for correspondence.

Table 1. Efficiency of prepreparation of 1 mg of zinc from mixtures with other ions

No.	Ions added,* mg	Residual amounts of ions, determined by AAS		Recovery of zinc, %
		In initial aqueous phase, after extraction, mg	In aqueous phase from stripping of organic extract, mg	
1	Ca ²⁺ 5.00, Mg ²⁺ 5.00	Ca 5.12, Mg 5.20	Ca 0.1, Mg 0.06	102
2	Al ³⁺ 1.5	Al 1.43	Al 0.02	100
3	Fe ³⁺ 1.00	Fe 0.1	Fe 0	100
4	Mn ²⁺ 1.00	Mn 1.06	Mn 0.13	100
5	Pb ²⁺ 1.00	Pb 0.74	Pb 0	100
6	Cr(VI) 1.00	Cr 0.96	Cr 0.014	100
7	Ni ²⁺ 1.00	Ni 0.83	Ni 0	100
8	Cd ²⁺ 1.00	Cd 0.72	Cd 0.016	100
9	Cu ²⁺ 0.5	Cu 0.25	Cu 0.24	100
10	V(V) 0.5	V 0.14	V 0.077	102
11	Ag ⁺ 0.5	Ag 0.44	Ag 0.055	98
12	Bi ³⁺ 0.5	Bi 0.4	Bi 0	97
13	Ba ²⁺ 0.5	Ba 0.35	Ba not detected	97
14	Co ³⁺ 0.5	Co 0.14	Co 0.47	122
15	CTMAB 100			95
16	SLS 100			97
17	Ca ²⁺ 5.00, Mg ²⁺ 5.00, Al ³⁺ 1.5, Fe ³⁺ 1.00, Mn ²⁺ 1.00, Pb ²⁺ 1.00, Cr(V) 1.00, Ni ²⁺ 1.00, Cd ²⁺ 1.00, V(V) 0.5, Cu ²⁺ 0.5, Ag ⁺ 0.5, Bi ³⁺ 0.5, Ba ²⁺ 0.5, CTMAB 1.00, SLS 1.00	Ca 4.7, Mg 5.22, Al 1.4, Fe 0.06, Mn 1.08, Pb 0.74, Cr 0.93, Ni 0.83, Cd 1.09, V 0.21, Cu 0.32, Ag 0.43, Bi 0.47, Ba 0.35	Ca 0.1, Mg 0.02, Al 0.3, Fe 0, Mn 0.008, Pb 0, Cr 0.01, Ni 0, Cd 0.003, V 0.09, Cu 0.3, Ag 0.5, Bi 0, Ba 0	103

*Total volume of mixture was 40 ml.

These aqueous phases were diluted to 100 ml before analysis.

By spectrophotometry.

In the presence of thiourea.

and the molar absorptivity is about twice that in the absence of SLS (curve C). The optimal wavelength for measurement of the zinc complex against a reagent blank is 570 nm. The absorbance of the zinc complex in the 3,5-diBr-PADAP-Zn-SLS system is practically constant when the colour is developed in the pH range 7.5-10.

For 7 μg of zinc in 10 ml of solution, the optimum reagent concentrations of the final solution are $3.0-4.0 \times 10^{-5} M$ 3,5-diBr-PADAP and 0.2-0.25% SLS. The reaction of zinc with 3,5-diBr-PADAP in the presence of SLS gives complete colour development at room temperature on standing for 10 min, and the absorbance at 570 nm remains constant for at least 48 hr. The absorbance does not vary with temperature over the range 15-50°.

The calibration graph prepared according to the recommended procedure is linear and passes through the origin, the colour system obeying Beer's law for zinc concentrations up to 0.7 $\mu\text{g}/\text{ml}$ in the solution measured. The practical molar absorptivity at 570 nm is $1.3 \times 10^5 \text{ l. mole}^{-1} \text{ cm}^{-1}$.

Composition of the complex

The nature of the complex was investigated by the continuous-variations and molar-ratio methods at fixed SLS concentration. The molar ratio of zinc to 3,5-diBr-PADAP in the complex was found to be 1:2.

Effect of diverse ions

Because 3,5-diBr-PADAP produces colour reactions with a number of common metal ions, it was necessary to find a suitable method for prepreparation of zinc, if the method were to be usable for determination of zinc in some practical water samples. The method described earlier³ was considered adequate for the purpose. The thiocyanate complex of zinc is extracted from 0.3-2.1M hydrochloric acid into methyl isobutyl ketone, and then zinc is stripped with 6M hydrochloric acid. This separates the zinc from various other metal ions in the sample. The efficiency of the method has been checked by the determination of 1.00 mg of zinc in the presence of a number of other ions, both individually and collectively. The

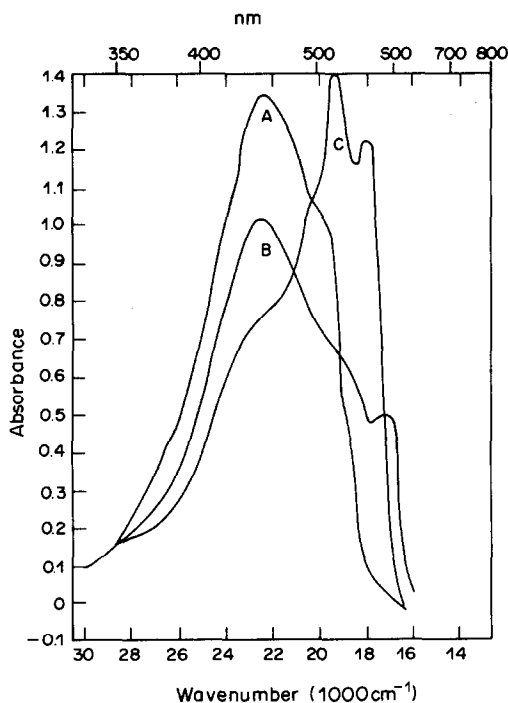


Fig. 1. Absorption spectra. Curve A—3,5-diBr-PADAP ($5 \times 10^{-5}M$)—SLS (0.2%). Curve B—3,5-diBr-PADAP ($5 \times 10^{-5}M$)—Zn (0.5 ppm). Curve C—3,5-diBr-PADAP ($5 \times 10^{-5}M$)—Zn (0.5 ppm)—SLS (0.2%).

recovery of zinc was determined by the recommended procedure, and the distribution of the foreign ions between the residual aqueous phase from the extraction and the stripping solution was determined by atomic-absorption spectrophotometry (AAS). The

Table 2. Comparison of analytical results for zinc

Sample	AAS method, ppm	Proposed method, ppm
1	122.5	120.1
2	3.89	3.87
3	1.90	1.80
4	1.40	1.38
5	0.28	0.27

results are shown in Table 1. The effect of cetyltrimethylammonium bromide (CTMAB) was also examined, in case it affected the action of the SLS in the determination.

Application

The proposed method has been applied to the determination of zinc in industrial waste-water. The analytical results obtained agreed well with those from atomic-absorption spectrophotometry, as shown in Table 2.

Seven replicate portions of a waste-water sample containing zinc were analysed individually by the recommended procedure and gave an average value of 38.8 ppm with a standard deviation of 0.045 ppm.

Acknowledgement—The authors wish to thank Mr. Yin Zhong-chao and Mr. Yi Bu-rong, Analytical and Testing Institute of Hunan Province, Changsha, China for their help.

REFERENCES

1. Shui-Chieh Hung, Chang-Ling Qu and Shui-Sheng Wu, *Talanta*, 1982, **29**, 85.
2. *Idem, ibid.*, 1982, **29**, 629.
3. Tan Zhe, *Chemical Analysis and Physical Testing (in Chinese)*, 1979, **6**, 19.

STUDIES ON EXTRACTION OF THORIUM FROM NITRATE SOLUTIONS WITH QUATERNARY AMMONIUM HALIDES

I. S. EL-YAMANI and E. I. SHABANA

Nuclear Chemistry Department, Nuclear Research Centre, Atomic Energy Authority, Cairo, Egypt

(Received 28 October 1983. Accepted 23 February 1984)

Summary—Thorium can be quantitatively extracted with 0.1M Hyamine 1622 in dichloroethane from 0.25M nitric acid/2M sodium nitrate and stripped from the organic phase with 0.1M sulphuric acid. The equilibration takes 20 min. Thorium can thus be separated from a large number of elements which are usually associated with it in monazite and in fission products of nuclear fuel.

The use of long-chain amines in the solvent extraction of thorium has been summarized and critically reviewed, but this method for its extractive separation is of limited application.^{1,2} It has been pointed out that the extraction efficiency of quaternary ammonium halides is higher than that of amines.³ The efficiency is enhanced when the number of carbon atoms in the quaternary salt is ≥ 24 . Moreover, the introduction of a benzyl group in place of an aliphatic group greatly enhances the extracting ability of the quaternary salt.⁴ Hyamine 1622, which justifies such a generalization, has been used previously for the extraction and separation of zirconium.⁵ The present investigation is part of a programme of systematic studies on liquid-liquid extraction of some nuclear materials; it reports recently obtained data on extraction of thorium from nitrate solutions by Hyamine 1622 in dichloroethane and the separation of the metal from rare-earth elements.

EXPERIMENTAL

Reagents

Hyamine 1622 (Hn), $R_3R'NCl$, (Rohm and Haas), a pure crystalline quaternary ammonium halide of molecular weight 466.1 and bulk density 0.44 g/cm³, was used as received. Other chemicals were of reagent grade.

Isotope solutions

²³⁴Th was milked from uranium through successive extraction from a solution of uranyl nitrate (50 g) in 6M hydrochloric acid (100 ml) with 30% tributyl phosphate in xylene;⁶ ²³⁴Th remained in the aqueous phase. The isotope solution was evaporated nearly to dryness, converted into nitrate form then diluted to a suitable volume. Other tracers were obtained through (n, γ) reactions or by separation of the initial nuclide from the daughter product (⁹³Zr).⁷

Extraction procedure

Equal volumes (5 ml) of aqueous phase containing the tracer [or the tracer-labelled or even the unlabelled species, the latter being aluminium, gallium and uranium(VI)] in nitric acid of appropriate concentration and of the organic phase pre-equilibrated with nitric acid, were shaken mechanically in glass-stoppered tubes for 20 min at room temperature ($20 \pm 3^\circ$). After centrifugation, aliquots of both

phases were placed in glass cups, evaporated to dryness, then counted with an end-window Geiger-Müller counter (for ²³⁴Th). The γ -activities were measured with a scintillation counter and NaI(Tl) crystal. Gallium and aluminium were determined complexometrically by back-titration with zinc, (dithizone as indicator, at pH 2.8 and 4.6 for Ga and Al respectively),^{8,9} and U(VI) was determined spectrophotometrically by the hydrogen peroxide method.¹⁰ Experiments were conducted in duplicate and the distribution ratio (D) was calculated as the ratio of the activities of the tracer (or the metal concentrations) in the organic and aqueous phases. The separation factor (selectivity, S) was computed from $S = D_{Tn}/D_M$, where M is the metal ion concerned.

Analyses of the extracted complexes

The analytical composition of the species extracted was determined experimentally by saturation of an organic phase consisting of 0.01 or 0.1M Hn in dichloroethane, by shaking it for 20 min each time with eight successive aqueous feeds of 0.09M thorium in 5M nitric acid. The concentration of thorium in the saturated organic phase was determined complexometrically (with Xylenol Orange as indicator) after stripping with 0.1M sulphuric acid,¹¹ and the nitrate concentration was determined by reduction in methanolic solution to ammonia, which was then distilled into excess of hydrochloric acid, the surplus of which was determined titrimetrically.¹²

RESULTS AND DISCUSSION

Effect of initial HNO₃ concentration

The extraction of thorium from its aqueous solution, with 0.1M Hn in dichloroethane, was examined at different acidities (0.25–10.0M); results are shown in Fig. 1. Higher D values are obtained at lower acidities ($\leq 5M$), presumably because of formation of anionic complexes, and the lower values given at higher acid concentrations may be attributed to competition between thorium and nitric acid for association with the extractant, and/or formation of less readily extractable complexes. From Fig. 1, it may be inferred that extraction of thorium with Hn is dominated by solvating and ion-exchange reaction mechanisms at lower ($\leq 5M$) and higher acidities

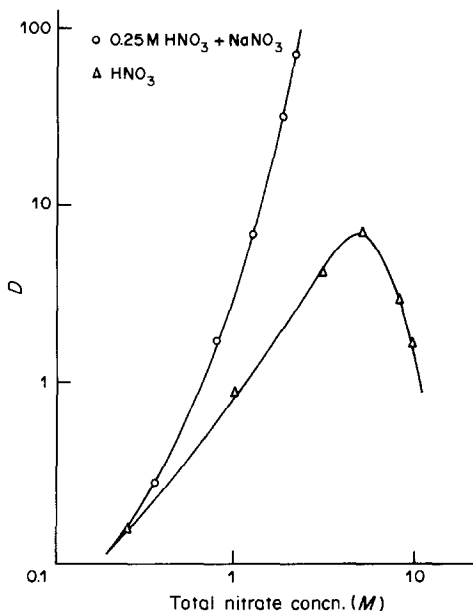


Fig. 1. Extraction of thorium from nitric acid and 0.25M HNO₃/NaNO₃ solutions by 0.1M Hn in dichloroethane.

respectively, a view consistent with the behaviour of the V(IV)-HCl-Aliquat 336 system.¹³

When the nitric acid in the aqueous phase is partly replaced with sodium nitrate (Fig. 1), *D* for the HNO₃/NaNO₃ mixture is found to increase steadily with increase in total nitrate concentration. This indicates that the controlling factor in the extraction behaviour is the total nitrate ion concentration and hence the fall of the *D* curve for purely nitric acid media at higher acidities may be ascribed to the effect of the hydrogen ion. Quantitative extraction was obtained with a 0.25M HNO₃/2M NaNO₃ solution.

Dependence on metal and extractant concentration

The variation of thorium concentration in the organic phase was examined, for extraction with 0.1M Hn in dichloroethane. Maximum loading values of about 0.045 and 0.042M were obtained at 5.3 and 8.6M nitric acid respectively, implying that two quaternary extractant molecules are associated with each metal ion extracted. This is in agreement with the number calculated from a plot of log *D* vs. log [Hn]; the extractant concentration was varied between 0.005 and 0.1M, the acidities used were 3.2, 5.3 and 8.5M, and trace level concentrations of thorium (~10⁻⁶M) were used. *D* increased linearly with rise of Hn concentration up to about 0.05M, above which the slopes of the curves considerably increased. The slopes obtained were consistent and approximated to unity at lower Hn concentration (≤0.05M) and 2 at higher molarities, indicating a first or second power dependence of *D* on Hn concentration, according to the acidity. The slopes are given in Table 1.

If Th(NO₃)₄ is considered to be the neutral species, and Th(NO₃)₅⁻ and Th(NO₃)₆²⁻ the anionic species, Th(NO₃)₆²⁻ existing predominantly,¹⁴ then if the re-

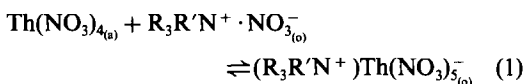
Table 1. Slopes of plots of log *D* vs. log[Hyamine 1622] for extraction of Th(IV) from HNO₃

[HNO ₃], M	[Hn] ≤ 0.05M	[Hn] > 0.05M
3.2	1.2	1.9
5.3	1.3	2.0
8.6	1.2	1.6

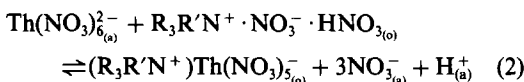
agent species is R₃R'N⁺ · NO₃⁻ at lower acidities and the adduct R₃R'N⁺ · NO₃⁻ · HNO₃ at higher acid concentrations, analogous to Aliquat 336, the extraction mechanism may be expressed as follows.

(a) For [Hn] ≤ 0.05M:

(i) at lower acidities (≤5M)

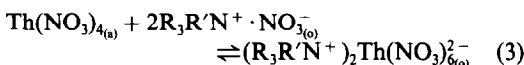


(ii) at higher acidities

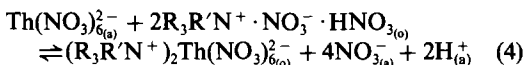


(b) For [Hn] > 0.05M:

(i) at lower acidities (≤5M)



(ii) at higher acidities



in which (a) and (o) represent the aqueous and organic phases respectively.

The stoichiometries proposed for the extracted species are also supported by analyses of the organic extracts. The organic solutions, saturated with thorium, gave a molar ratio of Th:NO₃⁻ of about 1:5 and 1:6 at 0.01 and 0.1M Hn concentration re-

Table 2. Separation factors for various metal ions with respect to Th(IV) extracted into 0.1M Hn in dichloroethane from 0.25M HNO₃/2M NaNO₃

Ion	Concentration, M	S
U(VI)	10 ⁻²	20.6
Pa(V)	C.F.	68.3
Zr(IV)	6 × 10 ⁻²	3.7 × 10 ⁴
Hf(IV)	8 × 10 ⁻⁴	7.3 × 10 ⁴
Fe(III)	10 ⁻⁵	2.5 × 10 ⁴
Al(III)	10 ⁻²	7.3 × 10 ⁴
Ga(III)	10 ⁻²	3.7 × 10 ⁴
In(III)	1.6 × 10 ⁻²	5 × 10 ³
Cr(III)	10 ⁻²	3.7 × 10 ⁴
Ce(III)	C.F.	4 × 10 ³
La(III)	C.F.	6 × 10 ³
Eu(III)	10 ⁻²	1.8 × 10 ³
Y(III)	C.F.	4.5 × 10 ³
Co(II)	10 ⁻²	1.2 × 10 ⁴
Zn(II)	10 ⁻²	3.6 × 10 ⁴
Be(II)	10 ⁻²	7.3 × 10 ⁴

C.F. Carrier-free.

spectively, thus confirming the maximum loading and slope-analysis data, and also justifying postulation of the penta and hexanitrate-complexes as the species extracted.

Extraction time

With optimum extraction conditions (0.25M HNO₃/2M NaNO₃, 0.1M Hn in dichloroethane), the equilibrium period was varied between 1 and 30 min. It was found that the optimum duration was 10 min. However, to ensure complete equilibration, 20 min shaking time was used in further work.

Stripping of thorium

Thorium extracted into the organic phase from 0.25M HNO₃/2M NaNO₃ solution with 0.1M Hn, may be readily stripped with dilute sulphuric or hydrochloric acid. Shaking the extract for 10 min with 0.1M sulphuric acid quantitatively strips the thorium.

Effect of diverse ions

Table 2 shows the separation factors for various metal ions from thorium. The higher extractability of thorium, compared to those of rare earths, Zr(IV), Hf(IV), Be(II) etc., affords a useful approach to separating thorium from rare earths processed from monazite or fission products. U(VI) and Pa(V), however, should be separated or masked before thorium determination. From this study, we suggest the following method for thorium/rare-earth separation and for thorium determination.

An aliquot (0.02M thorium containing not more than 0.5 mg/ml Ce³⁺, La³⁺, Eu³⁺ and Y³⁺ in 0.25M nitric acid/2M sodium nitrate) is shaken mechanically for 20 min with an equal volume of pre-equilibrated 0.1M Hn in dichloroethane at room temperature (~20°). After centrifugation, the two layers are sep-

arated. The aqueous phase is extracted twice more with fresh organic phase. Thorium is then stripped from the combined organic phases by shaking with two portions of 0.1M sulphuric acid (each equal to the organic phase in volume). Thorium in the back-extract is then determined complexometrically with Xylenol Orange as indicator (recovery is 99.0 ± 1.0%). The separation from trivalent Ce, La, Eu and Y is shown by γ -spectrometry to be practically complete.

REFERENCES

1. Y. Marcus and A. S. Kertes, *Ion Exchange and Solvent Extraction of Metal Complexes*, p. 751. Wiley-Interscience, London, 1969.
2. A. K. De, S. M. Khopkar and R. A. Chalmers, *Solvent Extraction of Metals*, pp. 206, 207. Van Nostrand Reinhold, London, 1970.
3. M. L. Good, S. L. Srivastava and F. F. Holland, Jr., *Anal. Chim. Acta*, 1964, **31**, 534.
4. A. M. Wilson, L. Churchill, K. Kiluk and P. Hovsepian, *Anal. Chem.*, 1962, **34**, 203.
5. I. S. El-Yamani, M. Y. Farah and F. A. Abd El-Aleim, *Talanta*, 1978, **25**, 714.
6. T. Ishimori, K. Watanabe and E. Nakamura, *Bull. Chem. Soc. Japan*, 1960, **33**, 636.
7. I. S. El-Yamani, M. Y. Farah and F. A. Abd El-Aleim, *J. Radioanal. Chem.*, 1978, **45**, 125.
8. F. J. Welcher, *The Analytical Uses of Ethylenediaminetetraacetic Acid*, p. 168. Van Nostrand, New York, 1961.
9. G. Charlot, *Les Méthodes de la Chimie Analytique*, pp. 584, 757. Masson, Paris, 1966.
10. F. D. Snell and C. T. Snell, *Colorimetric Methods of Analysis*, 3rd Ed., Vol. II, p. 492. Van Nostrand, London, 1967.
11. J. Körbl and R. Přibil, *Chemist-Analyst*, 1956, **45**, 102.
12. A. I. Vogel, *A Text-book of Quantitative Inorganic Analysis*, 3rd Ed., p. 255. Longmans, London, 1961.
13. T. Sato, S. Ikoma and T. Nakamura, *J. Inorg. Nucl. Chem.*, 1977, **39**, 395.
14. D. J. Carswell and J. J. Lawrance, *ibid.*, 1959, **11**, 69.
15. T. Sato, H. Watanabe and S. Kikuchi, *J. Appl. Chem. Biotechnol.*, 1975, **25**, 63.

STUDIES ON EXTRACTION OF INDIUM BY TRIBUTYL PHOSPHATE FROM THIOCYANATE SOLUTIONS

I. S. EL-YAMANI and E. I. SHABANA

Nuclear Chemistry Department, Nuclear Research Centre, Atomic Energy Authority, Cairo, Egypt

(Received 28 October 1983. Accepted 23 February 1984)

Summary—Indium can be quantitatively separated from a large number of elements which are usually associated with it, by extraction with 15% tributyl phosphate solution in kerosene from hydrochloric acid (pH 1)/0.5M potassium thiocyanate medium and stripping with 6M nitric acid. The equilibration takes 20 min.

The importance of indium and its alloys in nuclear reactors [as indicators, control rods, fuel (*e.g.*, In-Pu alloy) or cladding (Zr-In alloy), *etc.*]^{1,2} is increasing with recent progress in nuclear reactor technology. Attention has been focused, in the last few decades, on the use of tributyl phosphate for analytical and hydrometallurgical aspects of refining nuclear materials. Although tributyl phosphate has been used for extraction of indium from chloride solutions, it has only limited applications.^{3,4} Since the donor power of thiocyanate ions is stronger than that of chloride, it might be assumed that indium thiocyanate would be more readily extracted than the chloride.⁵ The extraction of americium, iron(III) and uranium from thiocyanate solutions with tributyl phosphate has been summarized and critically reviewed.⁶ Similarly, De and Sen utilized the thiocyanate system for the extraction of some transition elements such as cobalt(II), copper(II) and iron(III) with tributyl phosphate.⁷ Other workers have made similar studies for beryllium,⁸ aluminium and gallium.⁵ Most of the work done on the In-SCN-tributyl phosphate system was directed only towards stability constant measurements for indium complexes,^{9,10} and information on extractive separation of indium from thiocyanate medium is lacking. In the present investigation, indium was quantitatively extracted and separated from associated elements with tributyl phosphate from thiocyanate solutions.

EXPERIMENTAL

Reagents

Tri-*n*-butyl phosphate (TBP), was purified as reported elsewhere.¹¹ Odourless kerosene (Misr Petroleum Co.), was used as diluent. ^{114m}In was obtained through the (*n*, γ) reaction. Other chemicals were of reagent grade.

A stock solution of indium was prepared by dissolving 1.84 g of reagent-grade indium metal (99.99% pure) in the minimum amount of hydrochloric acid, and making up to 100 ml with distilled water. The solution was standardized complexometrically.¹²

Recommended procedure

An aliquot (5 ml) of solution containing about 10 mg of indium in hydrochloric acid (pH 1)/0.5M potassium thio-

cyanate medium, is shaken mechanically for 20 min at room temperature ($\sim 20^\circ$) with an equal volume of 15% TBP solution in kerosene. After centrifugation, the two layers are separated. Indium is stripped from the loaded organic phase by shaking for 10 min with two successive 10-ml portions of 6M nitric acid, then determined complexometrically in the aqueous extract at pH 4 with Xylenol Orange as indicator.

RESULTS AND DISCUSSION

Effect of acidity and TBP concentration

The concentration of hydrochloric acid was varied from 0.001 to 1M and that of TBP from 1 to 15% (0.04–0.55M). All experiments were done with a fixed 0.5M concentration of potassium thiocyanate, and the distribution ratio, *D*, was calculated as the ratio of activity in the organic to that in the aqueous phase, measured with a well-type NaI(Tl) γ -scintillation counter. It was observed (Table 1), that the extraction was incomplete with only about 1.5% TBP in any acid range, but quantitative with 10–15% TBP at pH 1–3 (no significant difference occurs over this range), because at this acidity the chloro-complex has no effect on the degree of extraction. At higher acidity, there was a decrease in extraction, presumably due to competitive complexation by the additional chloride. Even with higher TBP concentration, the extraction was not quantitative at acidities higher than 0.5M. It was possible to strip the extracted indium into the aqueous phase by equilibrating twice, for 10 min, with equal volumes of 6M nitric acid.

Effect of thiocyanate concentration

The concentration of thiocyanate was varied from 0.1 to 4M in presence of hydrochloric acid (pH 1); 3% and 5% TBP solutions in kerosene were used. The results showed that when the concentration of potassium thiocyanate was 0.1, 0.5, 1, 2 and 4M, the corresponding degree of extraction was 37.5, 74.4, 54.6, 33.3 and 13.0% with 3% TBP and 86.7, 97.2, 95.7, 84.4 and 83.1% with 5% TBP. Optimum results were obtained at about 0.5M potassium thiocyanate solution.

Table 1. Distribution ratio for 9.2 mg of In^{3+} , as a function of acidity and TBP concentration (0.5M KSCN)

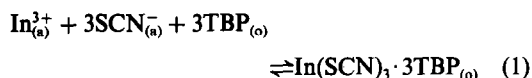
[TBP]	Initial [HCl], M	Distribution ratio, D	Extraction, %
1% (0.04M)	0.001	0.68	40.5
	0.01	0.58	36.7
	0.1	0.40	28.6
	0.5	0.04	3.7
	1.0	0.01	1.0
1.5% (0.06M)	0.001	0.65	39.4
	0.01	0.59	37.1
	0.1	0.39	28.1
	0.5	0.03	3.3
	1.0	0.01	0.6
2% (0.07M)	0.001	4.80	82.8
	0.01	4.20	80.8
	0.1	2.80	73.7
	0.5	0.28	21.9
	1.0	0.03	2.4
3% (0.11M)	0.001	5.00	83.3
	0.01	5.00	83.3
	0.1	2.70	73.0
	0.5	0.26	20.6
	1.0	0.03	2.4
5% (0.18M)	0.001	58.8	98.3
	0.01	50.2	98.1
	0.1	34.2	97.2
	0.5	4.20	80.8
	1.0	0.41	29.1
10% (0.37M)	0.001	398	99.8
	0.01	345	99.7
	0.1	242	99.6
	0.5	31.2	96.9
	1.0	3.10	75.6
15% (0.55M)	0.1	822	99.9
	0.5	88.2	98.9
	1.0	7.5	88.2

Nature of the extracted species

The variation in the concentration of indium in the organic phase as a function of initial aqueous indium concentration was examined with 14.5% TBP in kerosene. Maximum indium loading values of 0.17 and 0.18M were obtained at pH 1 and 2, indicating that the indium thiocyanate is solvated with three TBP molecules. This conclusion is confirmed by the linear dependence of $\log D$ vs. \log [free TBP] at various hydrochloric acid (10^{-4} –1.5M) and potassium thiocyanate (0.1–4M) concentrations, [free TBP] being calculated as $C_{\text{Tot}} - 3C_{\text{In}}$, where C_{Tot} is the total TBP concentration and C_{In} the indium concentration in the organic phase. The slopes of plots of the function (Table 2) were observed to be independent of the acidity and hence only one indium species is extracted over the whole acid range. The results also indicate the predominant formation of a trisolvate at lower thiocyanate concentration ($\leq 2M$) and tetrasolvate at higher concentrations ($> 2M$).

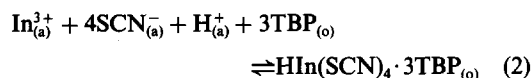
Since $\text{In}(\text{SCN})_3$ is considered to be the major species at lower thiocyanate concentration ($\leq 0.5M$), and $\text{In}(\text{SCN})_4^-$ or $\text{In}(\text{SCN})_5^{2-}$ can exist at higher concentrations,¹⁰ the extraction mechanism may be expressed as follows.

(i) At lower thiocyanate concentration ($\leq 0.5M$):

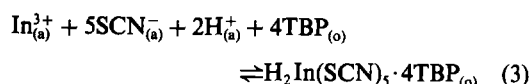


where subscripts (a) and (o) denote the aqueous and organic phases respectively.

(ii) At higher thiocyanate concentration (> 0.5 –2M):



(iii) At $> 2M$ thiocyanate solutions:



Period of extraction

With optimum extraction conditions, the equilibrium period was varied between 1 and 50 min. It was found that the optimum time is 20 min.

Effect of temperature

The extraction of indium from aqueous solutions containing 0.5M potassium thiocyanate, by 14.5% TBP in kerosene, at various temperatures (17–52°), was examined. The extraction decreases markedly with rise of temperature (at 17, 21, 31, 42 and 52°, the distribution ratios were 1600, 1000, 625, 304 and 175 for 0.01M HCl and 240, 142, 73, 28.2 and 13.2 for 0.5M HCl medium). Since lower temperature favours higher D , the extraction process is assumed to be exothermic. Extraction at room temperature ($\sim 20^\circ$) is therefore advised.

Effect of other ions

Several ions were tested for their effect on the extraction of indium. The tolerance limit was calculated as described earlier.¹³ It was observed that alkali and alkaline-earth metal ions, Cd^{2+} , Zn^{2+} , Al^{3+} , Cr^{3+} , La^{3+} , Ce^{3+} , Y^{3+} , Eu^{3+} , Nd^{3+} , NO_3^- , SO_4^{2-} , PO_4^{3-} , tartrate and citrate were tolerated in ratios of at least 100:1 relative to indium. Hg^{2+} and Ga^{3+} were tolerated in 50:1 ratio to indium, and Co^{2+} , Sn^{2+} and Pb^{2+} in 40:1 ratio. UO_2^{2+} , Fe^{3+} , Th^{4+} , VO_3^- , MoO_4^{2-} , F^- and $\text{C}_2\text{O}_4^{2-}$ should be separated or masked before indium determination. Indium usu-

Table 2. Slopes of plots of $\log D$ vs. \log [TBP] at various HCl and KSCN concentrations

[HCl] ^a , M	Slope	[KSCN] [†] , M	Slope
10^{-4}	2.7	0.1	2.7
10^{-3} – 10^{-2}	2.8	0.5	2.9
10^{-1}	2.9	1.0	3.0
0.5	2.9	2.0	2.7
1.0	2.8	4.0	3.6
1.5	2.8		

^a[KSCN] = 0.5M.

[†]At pH 1.

ally occurs associated with tin, aluminium, gallium, lead, zinc and iron in ores. The present method is simple, fairly rapid and selective, with a relative standard deviation of $\pm 0.8\%$. It also has the advantage of using lower concentrations of TBP and thiocyanate and lower pH values, rendering the process economically attractive and satisfactory for analytical as well as industrial purposes.

REFERENCES

1. M. A. Greenfield, R. L. Koontz, A. A. Jarrett and J. K. Taylor, *Nucleonics*, 1957, **15**, March, 57.
2. F. Haessner, G. Petzow and E. Preisler, *Proc. 3rd U.N. Intern. Conf. Peaceful Uses Atomic Energy, New York*, 1965, **9**, 430.
3. A. K. De and A. K. Sen, *Talanta*, 1967, **14**, 629.
4. M. Goliński, *Proc. Intern. Solvent Extraction Conf., Vol. I.*, p. 603, Society of Chemical Industry, London, 1971.
5. A. M. Golub, Fam Wang Ch'a and V. M. Samoilenko, *Russ. J. Inorg. Chem.* 1971, **16**, 282.
6. A. K. De, S. M. Khopkar and R. A. Chalmers, *Solvent Extraction of Metals*, pp. 174, 175, 180. Van Nostrand Reinhold, London, 1970.
7. A. K. De and A. K. Sen, *Sepr. Sci.* 1966, **1**, 641.
8. S. Kalyanaraman and S. M. Khopkar, *Anal. Chem.*, 1975, **47**, 2041.
9. Y. Hasegawa, *Bull. Chem. Soc. Japan*, 1970, **43**, 2665.
10. Y. Hasegawa and T. Sekine, *J. Inorg. Nucl. Chem.*, 1974 **36**, 421.
11. F. A. Saleh, *Z. Anorg. Allgem. Chem.*, 1966, **347**, 205.
12. J. Kinnunen and B. Wennerstrand, *Chemist-Analyst*, 1957, **46**, 92.
13. I. S. El-Yamani and E. N. Abd El-Messieh, *Talanta*, 1978, **25**, 704.

DETERMINATION OF POLY(OXYETHYLENE) NON-IONIC SURFACTANTS BY TWO-PHASE TITRATION

MASAHIRO TSUBOUCHI and YOSHIKO TANAKA

Laboratory of Chemistry, Kochi Medical School, Oko, Nankoku, Kochi 781-51, Japan

(Received 11 January 1984. Accepted 17 February 1984)

Summary—The solvent extraction of non-ionic surfactants with sodium hydroxide and tetraphenylborate has been studied, and a method developed for the determination of non-ionic surfactants by two-phase titration. A hydrophobic indicator system was used. The method is valid only when the concentration of anionic surfactant in the sample solution is lower than $1 \times 10^{-4}M$.

A mixture of anionic and poly(oxyethylene) non-ionic surfactants is widely used is both industrial and domestic detergents. It is known that the non-ionic surfactant can form spirals which can trap metal ions such as potassium^{1,2} and barium.³ The reaction between anions and the complex cation formed by the non-ionic surfactant and the metal ions has been made the basis for gravimetric,⁴ spectrophotometric,^{1,2,5} and titrimetric³ methods for determination of the non-ionic surfactant. However, it is generally difficult to determine total non-ionic surfactants in the presence of anionic surfactants because the metal ion complexes of the non-ionic surfactants form ion-pairs with the anionic surfactants present.

Two-phase titration is one of the most frequently used methods for the determination of ionic surfactants. This paper presents an indirect method for the determination of non-ionic surfactant in the presence of anionic surfactant by two-phase titration.

EXPERIMENTAL

Reagents

The non-ionic surfactants used were Triton X-100, Triton X-405 (Rohm & Haas Company), polyethylene glycol mono-*p*-iso-octylphenyl ether (Wako Pure Chemical Ind., and Nakarai Chemicals Ltd.), polyoxyethylene lauryl alcohol ether, and polyoxyethylene sorbitan monopalmitate (Nakarai Chemicals Ltd.). The number-average degree of polymerization of the surfactants used is 8-12, except for Triton X-405 (for which it is 40). The surfactants, Zephiramine (tetradecyldimethylbenzylammonium chloride), and sodium tetraphenylborate were dried at 80° and dissolved in water. Victoria Blue B (Colour Index 44045, C₃₃H₃₂N₃Cl) was dissolved in ethanol to make a 0.01% solution; it was used as an indicator. A pH-9.0 buffer solution was prepared by adding 6M sodium hydroxide to 0.3M sodium dihydrogen phosphate/0.05M sodium borate solution.

Procedure

To 10 ml of a mixture of a non-ionic and an anionic surfactant (non-ionics, 2-0.2 mg/10 ml; anionics, less than $1 \times 10^{-4}M$) in a separatory funnel, add 2 ml of 6M sodium hydroxide and 5 ml of $2 \times 10^{-3}M$ sodium tetraphenylborate, and shake the solution vigorously with 10 ml of 1,2-dichloroethane. After separation of the layers, run off the extract into a glass tube through a filter paper to remove

droplets of water. Place a 5-ml portion of the extract in a 200-ml Erlenmeyer flask, and add 5 ml of buffer solution and 2 drops of indicator. Titrate the mixture with $2 \times 10^{-4}M$ Zephiramine with vigorous shaking after each addition, until there is a colour change from blue (λ_{\max} 615 nm) to red (λ_{\max} 505 nm) in the organic phase. Titrate a reagent blank prepared in the same way (titre ca. 0.6 ml). One mg of non-ionic surfactant requires ca. 5.1 ml of $2 \times 10^{-4}M$ titrant, irrespective of the anionic surfactant present.

RESULTS AND DISCUSSION

It is reported that a 12-unit ethylene oxide polymer combines with one barium ion regardless of the kind of alkyl or alkylaryl groups in the non-ionic surfactant.³ The non-ionic surfactant can also trap sodium ions in its spirals and be extracted into dichloroethane from 0.2-2M sodium hydroxide, as an ion-pair with tetraphenylborate, but any anionic surfactant in the mixture is not extracted. A blank titration is necessary because tetraphenylborate is slightly extracted even in the absence of non-ionic surfactant. The extracted non-ionic surfactant-sodium-tetraphenylborate complex is decomposed by the Zephiramine used as titrant and the Zephiramine-tetraphenylborate ion-pair is formed in the organic phase. The blue indicator-tetraphenylborate complex in the extracts reacts with excess of titrant to form the free indicator (red) at the end-point. The aqueous phase remains colourless throughout the titration, because of the insolubility of Victoria Blue B in alkaline water. This is a hydrophobic indicator system,⁶ though a dye-transfer method is usually used in two-phase titrations.

The volume of titrant required is proportional to the amount of non-ionic surfactant present in the sample solution, indicating that the non-ionic surfactant is stoichiometrically extracted. The volumes of $2 \times 10^{-4}M$ Zephiramine needed for 1 mg of non-ionic surfactant were found to be: Triton X-100, 5.-5.1 ml (mean of 10 titrations was 5.06 ml, standard deviation 0.04 ml); Triton X-405, 5.1-5.2 ml; poly-

ethylene glycol mono-*p*-iso-octylphenyl ether, 4.8–4.9 ml; polyoxyethylene lauryl alcohol ether, 5.2–5.3 ml; polyoxyethylene sorbitan monopalmitate, 5.1–5.2 ml. The volumes vary slightly with the products and type of surfactant, but it seems that in general the volume needed for the same weight of non-ionic surfactant is almost constant, about 5.1 ml of $2 \times 10^{-4} M$ Zephiramine per mg of non-ionic surfactant. It is reasonable to consider that the hydrophile–lipophile balance values of the surfactants used are similar, making the method usable for a range of surfactants.

If less than 2 ml of $2 \times 10^{-3} M$ tetraphenylborate is added, the titrant volume needed decreases slightly. Variation of the pH between 8.5 and 9.5 does not affect the results. Chloroform cannot be used as the organic solvent, since it does not give a sharp endpoint. If methyl isobutyl ketone is used as the organic solvent, the sodium salts of the anionic surfactants are extracted as well as the non-ionic surfactants.

The following species do not interfere at the $10^{-3} M$ level: K^+ , NH_4^+ , Ca^{2+} , Cl^- , SO_4^{2-} and triethanolamine. However, high concentrations ($> 10^{-2} M$) of potassium and ammonium ions give tetraphenylborate precipitates, causing negative errors. Anionic surfactants ($1 \times 10^{-4} M$) such as dodecylsulphate, dodecylbenzenesulphonate, and bis(2-ethylhexyl)sulphosuccinate do not disturb the determination, but separation of the two layers is poor when the concentration of these anionic surfactants is $\geq 2 \times 10^{-4} M$. The recommended procedure is based on these results.

Application to commercial detergents

The number-average degree of polymerization of the commercial non-ionic surfactants is mainly 8–13.

A commercial detergent for wool was diluted with water, and the anionic surfactant was first titrated as follows. To 10 ml of the sample solution were added 5 ml of buffer solution (pH 9), 2 drops of Victoria Blue B indicator, and 4 ml of 1,2-dichloroethane. The mixture was titrated with $2 \times 10^{-4} M$ Zephiramine with vigorous shaking after each addition, until a colour change from blue to red took place in the organic phase. A blank titration was not necessary. The titrant volume corresponded to the anionic surfactant present, irrespective of the non-ionic surfactant present, this was verified with sodium dodecylsulphate, dodecylbenzenesulphonate, and bis(2-ethylhexyl)sulphosuccinate.

A second aliquot of sample solution was diluted with water to reduce the concentration of anionic surfactant to $1 \times 10^{-4} M$ or less, and the non-ionic surfactant was then determined by the recommended procedure. The result found was 0.25M anionic surfactant and 0.13 g/ml non-ionic surfactant in the detergent. A recovery test was done by adding 0.52 mg of Triton X-100 to the 2500-fold diluted detergent, and 0.50 mg was found.

REFERENCES

1. L. Favretto, B. Stancher and F. Tunis, *Analyst*, 1978, **103**, 955.
2. K. Toei, S. Motomizu and T. Umamo, *Talanta*, 1982, **29**, 103.
3. T. Uno and K. Miyajima, *Chem. Pharm. Bull. (Tokyo)*, 1963, **11**, 80.
4. A. Barber, G. C. T. Chinnick and P. A. Lincoln, *Analyst*, 1956, **81**, 18.
5. N. H. Anderson and J. Girling, *ibid.*, 1982, **107**, 836.
6. M. Tsubouchi, N. Yamasaki, H. Mitsushio and K. Matsuoka, *Talanta*, 1981, **28**, 857.

USE OF AMMONIUM MOLYBDATE IN THE COLORIMETRIC ASSAY OF CEPHALOSPORINS

M. M. ABDEL-KHALEK and M. S. MAHROUS

Department of Pharmaceutical Chemistry, Faculty of Pharmacy, University of Alexandria, Alexandria,
 Egypt

(Received 21 October 1983. Revised 22 December 1983. Accepted 17 February 1984)

Summary—A colorimetric method for the determination of five cephalosporins (cefoxitin sodium, cefotaxime sodium, cephalirin sodium, cephalothin sodium and cephaloridine), based on the blue colour formed by reaction of the cephalosporins with ammonium molybdate, is described. The effects of reagent concentration and reaction conditions are discussed. The proposed method has been applied to the analysis of cephalosporin injections, the results of which are in good agreement with those obtained by the official method of the British Pharmacopoeia.

Cephalosporins have been determined iodometrically after hydrolysis of the β -lactam ring,^{1,2} and titrimetrically with *N*-bromosuccinimide³ or potassium iodate⁴. Cephalosporins have also been determined spectrophotometrically after treatment with hydroxylamine-nickel reagent⁵ and after preliminary acid hydrolysis.⁶ Cephalirin has been assayed spectrophotometrically after degradation under controlled conditions.⁷ An air-segmented continuous-flow spectrophotometric method has been utilized for the determination of cephalosporins.⁸ In addition, the use of high-pressure liquid chromatography,^{9,10} and fluorimetric^{11,12} and polarographic^{13,14} methods of analysis have been reported.

The aim of the present work was to develop a simple and accurate quantitative method for determining cephalosporins, with ammonium molybdate

as reagent. This procedure has been applied to a wide variety of cephalosporins (for structures see Table 1) in pure form and in injections. The reaction product is presumably an isopoly molybdenum blue.

EXPERIMENTAL

Apparatus

A Perkin-Elmer Model 550 S spectrophotometer with matched 1.00-cm quartz cells was used for absorbance measurements.

Reagents

Ammonium molybdate solution, 1.5%.

Sulphuric acid, 0.5M.

Cephalosporin solutions, 0.2 mg/ml, freshly prepared in water. Laboratory reference standards were used for calibration. A sample of cefoxitin was provided by Merck Sharp and Dohme (UK), of cefotaxime by Hoechst Orient Laboratories (Egypt), of cephalirin by Bristol Laboratories

Table 1. Structures of cephalosporins

	R	R'	R''
Cefoxitin		-OCH ₃	-COONH ₂
Cefotaxime		-H	-COOCH ₃
Cephalirin		-H	-COOCH ₃
Cephalothin		-H	-COOCH ₃
Cephaloridine		-H	

Table 2. Optical characteristics, accuracy and precision (10 replicates)

Cephalosporin	λ_{\max} , nm	Molar absorptivity, $l.mole^{-1}.cm^{-1}$	Coefficient of variation, %
Cefoxitin sodium	684–696	7.1×10^3	0.4
Cefotaxime sodium	686–697	5.9×10^3	0.1
Cephapirin sodium	692–708	5.2×10^3	0.2
Cephalothin sodium	684–694	4.8×10^3	0.2
Cephaloridine	684–695	4.3×10^3	0.5

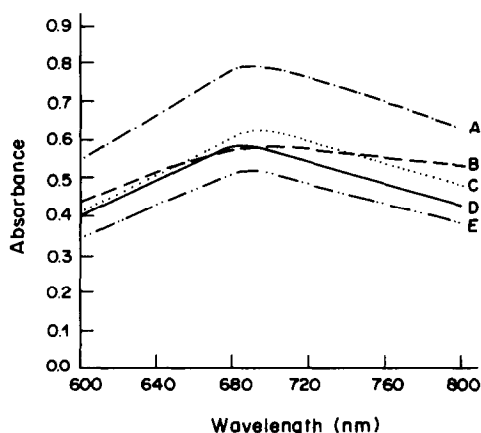


Fig. 1. Absorption spectra of the coloured products from: A, cefoxitin sodium; B, cefotaxime sodium; C, cephapirin sodium; D, cephalothin sodium; and E, cephaloridine. [Cephalosporin] = 50 μ g/ml in each instance.

(U.S.A.) and samples of other cephalosporins by Lilly Research Centre Ltd. (U.S.A.).

All chemicals and reagents used were of analytical-reagent or pharmaceutical grade. Distilled water was used throughout.

General procedure and preparation of calibration graph

Transfer 5 ml of an aqueous solution containing from 0.2 to 1.0 mg of the sample into a test-tube. Add 1 ml of ammonium molybdate solution and 1 ml of 0.5M sulphuric acid. Prepare a corresponding blank solution with 5 ml of water. Mix well and heat the solutions in a boiling water-bath for 30 min. Cool and transfer into a 10-ml standard flask and dilute to volume with water. Measure the absorbance of the blue colour at λ_{\max} for the drug (Table 2). Prepare a calibration graph of absorbance *vs.* concentration of the reference cephalosporin.

For injections. Mix the powder from a vial, and accurately weigh a portion equivalent to about 10 mg of the drug and dissolve it in water. Dilute with water to volume in a 100-ml standard flask. Transfer 5 ml of this solution into a test-tube and complete the assay as described above.

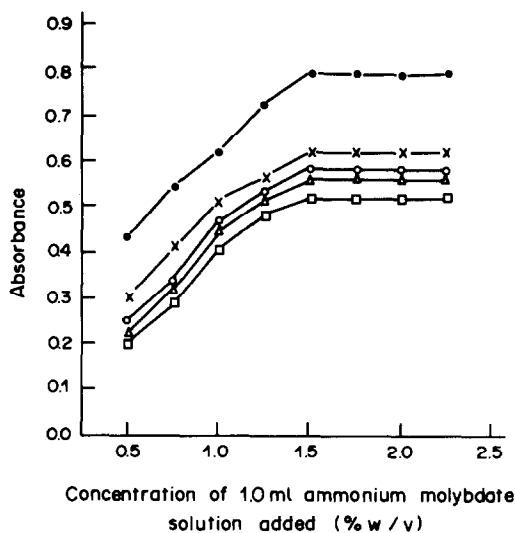


Fig. 2. Effect of ammonium molybdate concentration on the absorbance at λ_{\max} of the coloured products from: ●—● cefoxitin sodium; ×—× cefotaxime sodium; ○—○ cephapirin sodium; △—△ cephalothin sodium; and □—□ cephaloridine. [Cephalosporin] = 50 μ g/ml in each instance.

RESULTS AND DISCUSSION

Absorption spectra

The absorption spectra of the reaction products in the range 600–800 nm are shown in Fig. 1. Cephalosporins and ammonium molybdate all have negligible absorbance at and near the λ_{\max} regions.

Beer's law is obeyed over the concentration range 20–100 μ g/ml. The molar absorptivities are given in Table 2. The coefficient of variation was less than 0.4%.

Choice of analytical conditions

A sulphuric acid concentration of about 0.5M is optimal (Table 3). Use of 1 ml of 1.5–2.5% ammo-

Table 3. Influence of acidity on the absorbance

[H ₂ SO ₄], M	Absorbance at λ_{\max}				
	Cefoxitin sodium	Cefotaxime sodium	Cephapirin sodium	Cephalothin sodium	Cephaloridine
0.00	0.160	0.140	0.130	0.120	0.110
0.25	0.500	0.450	0.380	0.400	0.370
0.50	0.800	0.624	0.586	0.585	0.520
0.75	0.770	0.595	0.566	0.560	0.505
1.00	0.710	0.530	0.516	0.520	0.492
1.25	0.410	0.380	0.367	0.366	0.350
1.50	0.280	0.240	0.215	0.242	0.230
1.75	0.200	0.198	0.190	0.187	0.180
2.00	0.040	0.032	0.027	0.026	0.020

Table 4. Results for determination of cephalosporins in pure form and in injections

Cephalosporin	Found* \pm s.d.,%			
	Proposed method	BP method	$t_{\text{calc.}}$ †	$F_{\text{calc.}}$ ‡
Cefoxitin sodium powder	100.4 \pm 0.4	—	—	—
Mefoxin injection (MSD)	101.3 \pm 0.4	—	—	—
Cefotaxime sodium powder	99.7 \pm 0.1	—	—	—
Claforan injection (Hoechst)	101.6 \pm 0.3	—	—	—
Cephapirin sodium powder	99.8 \pm 0.2	—	—	—
Cephatrexyl injection (Bristol)	100.5 \pm 0.1	—	—	—
Cephalothin sodium powder	99.7 \pm 0.2	99.9 \pm 0.3	1.6	1.5
Keflin injection (Lilly)	101.0 \pm 0.4	101.2 \pm 0.4	1.3	1.2
Cephaloridine powder	100.7 \pm 0.3	100.9 \pm 0.4	1.4	1.6
Keflodin injection (Lilly)	101.1 \pm 0.5	101.3 \pm 0.5	1.1	1.0

*Average of ten determinations, referred to nominal content.

†Critical value 2.1 ($p = 0.05$).

‡Critical value 3.2 ($p = 0.05$).

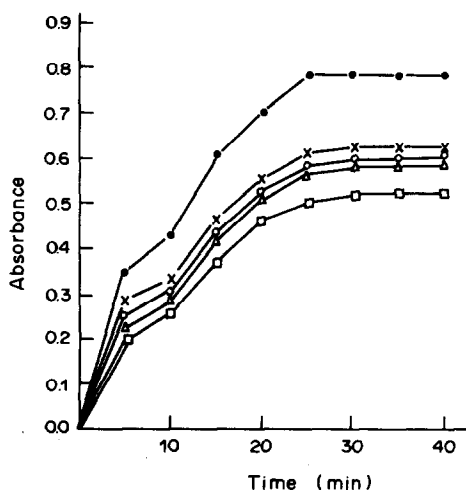


Fig. 3. Effect of heating time on the formation of the coloured product. ●—● cefoxitin sodium; ×—× cefotaxime sodium; ○—○ cephalopirin sodium; △—△ cephalothin sodium; and □—□ cephaloridine. [Cephalosporin] = 50 $\mu\text{g}/\text{ml}$ in each instance.

nium molybdate solution in the total volume of 10 ml gives maximum absorbance (Fig. 2). Figure 3 shows that heating for at least 30 min is essential for full colour development. The absorbance remains constant for about an hour after maximum colour development. The order of addition of reagents is not critical.

Table 4 gives the results obtained by application of the proposed method and the official method 1 to the determination of cephalosporins in pure form and in injections. The results are in good agreement. Statistical comparison by the Student t -test and the variance ratio, F ,¹⁵ shows no significant difference be-

tween the two sets of results. However, the molybdenum blue is simpler and faster than the BP method (but is not stability-indicating).

Interferences

The possibility of interference by other constituents in injections cannot be overlooked. In the determination of cephalosporins in capsules, the excipients usually added, such as starch, lactose and glucose, interfere in the analysis by the proposed method.

REFERENCES

1. *British Pharmacopoeia 1980*, H.M. Stationery Office, London, 1980.
2. S. Okada, K. Hattori and T. Takano, *Bull. Chem. Soc. Japan*, 1965, **38**, 2186.
3. J. F. Alicino, *J. Pharm. Sci.*, 1976, **65**, 300.
4. J. K. Grime and B. Tan, *Anal. Chim. Acta*, 1979, **105**, 369.
5. D. L. Mays, F. K. Bangert, W. C. Cantrell and W. G. Evans, *Anal. Chem.*, 1975, **47**, 2229.
6. P. Papazova, P. R. Bontchev and M. Kacarova, *Talanta*, 1983, **30**, 51.
7. J. E. Bodnar, W. G. Evans and D. L. Mays, *J. Pharm. Sci.*, 1977, **66**, 1108.
8. M. A. Abdalla, A. G. Fogg, J. G. Bader and C. Burgess, *Analyst*, 1983, **108**, 53.
9. J. S. Wold and S. A. Turnispeed, *J. Chromatog.*, 1977, **136**, 170.
10. P. A. Coomber, J. P. Jefferies and J. D. Woodford, *Analyst*, 1982, **107**, 1451.
11. R. Aikawa, M. Nakano and T. Arita, *Chem. Pharm. Bull.*, 1976, **24**, 2350.
12. J. L. Fabregas and J. E. Beneyto, *Analyst*, 1980, **105**, 813.
13. J. A. Squella, L. Nunez-Vergara and E. M. Gonzatez, *J. Assoc. Off. Anal. Chem.*, 1979, **62**, 556.
14. A. G. Fogg and M. J. Martin, *Analyst*, 1981, **106**, 1213.
15. L. Saunders and R. Fleming, *Mathematics and Statistics*, 2nd Ed., pp. 192–197, Pharmaceutical Press, London, 1971.

POLAROGRAPHIC DETERMINATION OF TRACES OF ZIRCONIUM IN ORES BY USE OF COMPLEX-FORMING COMPOUNDS ADSORBABLE AT THE DROPPING MERCURY ELECTRODE

YE HUA-LI

Research Laboratory of Hunan Bureau of Geology, People's Republic of China

HE YOU-HUA

Group Testing Laboratory of Hubei Bureau of Petrochemical Industry, People's Republic of China

(Received 16 November 1982. Revised 5 December 1983. Accepted 17 February 1984)

Summary—A polarographic method is proposed for the determination of trace zirconium down to the $5 \times 10^{-9} M$ level, based on the adsorption of the complex of zirconium with oxalic acid + cupferron + diphenylguanidine at the dropping mercury electrode in sodium acetate-acetic acid solution (pH 5.7). Under optimum conditions the wave-height is proportional to the concentration of zirconium in the range from 0 to 0.4 $\mu\text{g/ml}$. The serious interference from titanium(IV) can be effectively eliminated by solvent extraction with 3% tri-*n*-octylamine from 1*N* sulphuric acid and stripping with 0.1*M* perchloric acid-1*M* hydrochloric acid-2*M* nitric acid mixture. The mechanism giving rise to the wave for the zirconium complex has been investigated. The method has been applied to the determination of trace zirconium in ores and ceramics.

The polarographic determination of zirconium has been little used, especially for analysis of ores. Budnikov *et al.*¹ have examined the polarographic wave of the zirconium-4-(2-pyridylazo)-resorcinol complex at pH 1.8-2.0 in ammonium chloride supporting electrolyte, but the sensitivity was low (the determination limit was 2 $\mu\text{g/ml}$) and the polarographic wave was poor.

More recently Yao Xiu-ren *et al.*² have suggested that the zirconium-cupferron-diphenylguanidine complex can produce a more sensitive oscillopolarographic wave in ammonium chloride supporting electrolyte, but it is difficult to find an optimum linear range for the determination of zirconium. However, this reaction at the dropping mercury electrode is so sensitive that we have tried to find supporting electrolytes that would improve the determination. We have found that a well-defined high-sensitivity peak for the zirconium-cupferron-diphenylguanidine complex can be obtained at a potential of about -1.02 V (*vs.* SCE) in sodium acetate-acetic acid buffer (pH 5.5-6.0), but the peak rapidly disappears. Therefore a stabilizing agent was sought and oxalic acid was found to give the best effect.

The effect of some potentially interfering ions, temperature, time and the height of the mercury column on the peak current has been investigated. The advantages of the proposed method are its simplicity, high sensitivity, good selectivity and reproducibility.

EXPERIMENTAL

Apparatus

A Cheng Dou JP-1A single-sweep polarograph with a three-electrode system [a dropping mercury electrode

(DME) as cathode, an SCE as reference and a platinum electrode as auxiliary] and a Czechoslovak LP-60 d.c. polarograph were used.

Reagents

Unless otherwise mentioned, all reagents used were of analytical reagent grade.

Buffer solution. Sodium acetate (3.5*M*)-acetic acid (0.35*M*), pH 5.7.

Oxalic acid dihydrate solution, 1%.

Cupferron solution, 0.07%. If protected from light, this can be used for up to 15 days.

Diphenylguanidine solution, 0.04%. The base was dissolved with a few drops of 6*M* hydrochloric acid, then diluted with water.

Tri-*n*-octylamine (TNOA) solution, 3% v/v in benzene.

Standard zirconium solution (74 $\mu\text{g/ml}$). A stock solution containing 74 μg of zirconium per ml (ZrO_2 100 $\mu\text{g/ml}$) is prepared by heating 0.1000 g of zirconium oxide in a platinum crucible with 10 drops of concentrated sulphuric acid and 5-7 ml of concentrated hydrofluoric acid until fumes of sulphur trioxide appear, cooling, washing down the crucible wall with a little water, again evaporating to fumes, and repeating this step, then finally dissolving the residue in 2*M* hydrochloric acid and diluting to 1 litre with the same acid. The solution is finally diluted to give a working solution in 0.6*M* hydrochloric acid, containing 1.48 μg of Zr per ml (2 μg of ZrO_2 per ml).

Recommended procedure

Transfer various amounts of zirconium standard solution into 50-ml beakers. Add 0.2 ml of perchloric acid (1 + 1), evaporate to fumes, and cool. Add 15 ml of buffer solution, 3 ml of oxalic acid solution, 1 ml of cupferron solution and 1 ml of diphenylguanidine solution and mix. Measure the height of the oscillopolarographic peak at a potential of -1.02 V *vs.* SCE (Fig. 1).

Determination of zirconium in ores

A 0.1000 or 0.2000 g sample is fused in an alumina crucible with 2-3 g of sodium peroxide at 650-700°, and the cooled melt is leached with about 100 ml of water. Then 20 mg of magnesium oxide (as carrier) are added, followed by

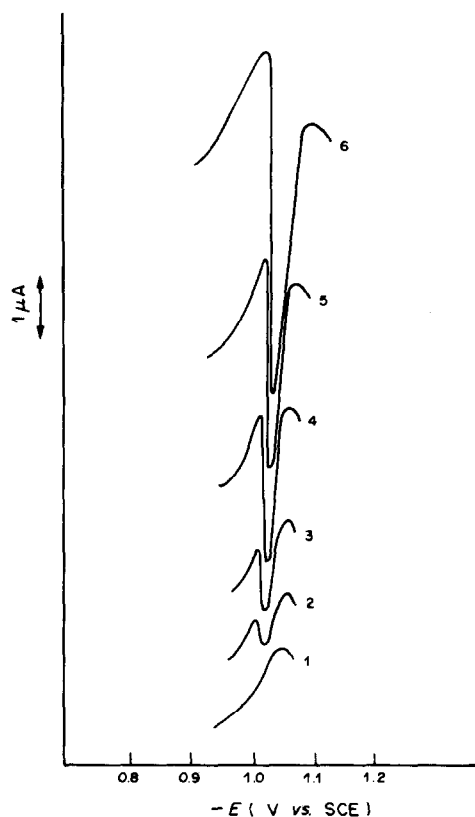


Fig. 1. Oscillographic peak of Zr complex at the dropping mercury electrode. Peak potential about -1.02 V. Scan-rate 0.25 V/sec. Zr concentration, $\mu\text{g/ml}$; 1, 0.0; 2, 0.0185; 3, 0.037; 4, 0.074; 5, 0.111; 6, 0.185.

10 ml of 50% triethanolamine solution, and the solution is boiled. After cooling, the precipitate is filtered off and washed twice with 1% sodium hydroxide solution and then with water. The precipitate is dissolved with hot 1N sulphuric acid, the solution being collected in a 50-ml standard flask and diluted to volume with 1N sulphuric acid. Then a 10-ml aliquot of this solution is transferred into a 60-ml separatory-funnel, and shaken for 1 min with 10 ml of 3% TNOA solution in benzene. The aqueous phase is removed, and the organic phase washed with 3-5 ml of 1N sulphuric acid. Then the organic phase is shaken for 1 min with 10 ml of 0.1M HClO_4 /1M HCl /2M HNO_3 mixture to back-extract the zirconium. After phase separation the aqueous phase is transferred into a 50-ml beaker and evaporated to fumes of perchloric acid. The residue is cooled and the zirconium is determined as described in the recommended procedure.

RESULTS AND DISCUSSION

Choice of supporting electrolyte and reagents

Effect of pH. Figure 2 shows the effect of pH on the peak height. A pH of 5.7 was chosen, since it gives a pH tolerance of about ± 0.2 , and good sensitivity. The concentration for the buffer was selected as the middle of the range that gave maximum peak height (Table 1).

Effect of oxalic acid. The peak was stabilized by the addition of oxalic acid to the mixture. A concentration of 1.2×10^{-2} M was found to be optimal.

Effect of cupferron. The presence of a certain amount of cupferron is very important for prod-

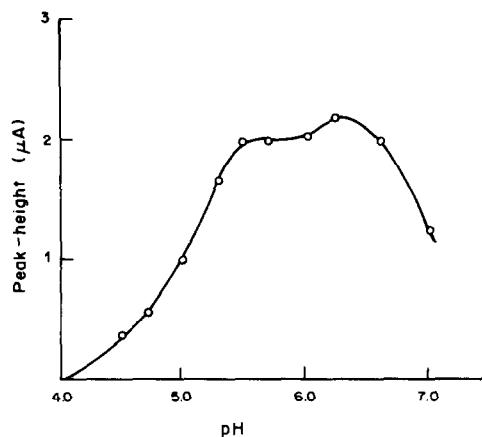


Fig. 2. Effect of pH on the peak-height.

uction of the peak. A concentration of 2.2×10^{-4} M was found to be optimal with regard to sensitivity and stability.

Effect of diphenylguanidine. The presence of the base up to a certain concentration increases the peak height remarkably, but the peak height is essentially constant when the diphenylguanidine concentration is between 8.3×10^{-5} and 2.0×10^{-4} M. A concentration of 1.0×10^{-4} M is selected.

Under the optimum conditions, the calibration graph is linear over the range from 0 to 4 μg of Zr per ml, and the peak heights remain stable for 3 hr.

Interferences and their elimination

The influence of more than 30 ions was investigated. Tolerance limits for some cations in the determination of 4 μg of Zr are given in Table 2. Hydrochloric, sulphuric, perchloric and nitric acids and their anions do not interfere when present in 0.05M concentration (or even more), but more than about 3 mg of phosphoric acid increases the peak-height slightly. Ascorbic acid and triethanolamine do not interfere.

Hafnium gives a polarographic peak, but at the same potential the peak-height is only 10% of that of the zirconium peak, for equal weights of Hf and Zr.

The main interferences are from iron, titanium and fluoride ions, but zirconium can be separated from iron and fluoride by co-precipitation in alkaline solution with magnesium oxide in the presence of triethanolamine, and from titanium by extraction with tri-n-octylamine.

Table 1. Effect of buffer concentration

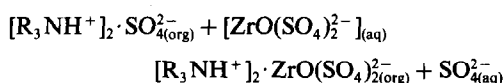
Sodium acetate, M	Acetic acid, M	Peak height, μA
4.0	0.40	2.40
3.5	0.35	2.40
3.0	0.30	2.40
2.5	0.25	2.34
2.0	0.20	1.86
1.5	0.15	1.26
1.0	0.10	1.02
0.5	0.05	0.20

Table 2. Interference of various ions in determination of Zr at the 0.3 $\mu\text{g}/\text{ml}$ level in 20 ml of supporting electrolyte

Ion	Tolerance limit, μg	Ion	Tolerance limit, μg
Ca^{2+}	7000	As(III)	50
Mg^{2+}	5000	Bi^{3+}	50
Al^{3+}	1000	Se(IV)	50
Mn^{2+}	1000	Be^{2+}	50
Ni^{2+}	500	V(IV)	50
Cu^{2+}	300	Ga^{3+}	30
Pb^{2+}	300	In^{3+}	30
Zn^{2+}	300	Ta(V)	30
Sb(III)	100	Lanthanide $^{3+}$	20
Sn(IV)	100	Th^{4+}	20
Co^{2+}	50	Nb(V)	10
Cd^{2+}	50	Te(IV)	10

Zirconium has been extracted with tri-n-octylamine from 11M hydrochloric acid³ and separated by paper chromatography with sulphuric acid as eluent, but the separation from titanium by these methods is not satisfactory.

It has been found that zirconium can be quantitatively extracted from 0.5–1.5N sulphuric acid by tri-n-octylamine (TNOA) and that titanium is not extracted. The mechanism of the extraction is



where $\text{R} = \text{CH}_2(\text{CH}_2)_6\text{CH}_3$. Obviously, the equilibrium is shifted to the left by increase in sulphuric acid concentration, and 1N sulphuric acid is considered optimal for the extraction. Because hydrochloric acid and perchloric acid have a considerable effect on the paper chromatography of zirconium with sulphuric acid as eluent, these acids, separately and in combination, were tested as stripping agents. Nitric acid was also tested, and a combination of 0.1M $\text{HClO}_4/1\text{M HCl}/2\text{M HNO}_3$ was found empirically to give the best back-extraction. By means of this extraction system, 10 mg of Fe(III) and 2 mg of Ti(IV) can be eliminated efficiently. Hafnium accompanies the zirconium quantitatively.

Nature of the zirconium wave

No wave is observed for a solution of oxalic and diphenylguanidine at the peak potential of -1.02 V (*vs.* SCE) in the absence of zirconium and cupferron. On the basis of the following observations it is considered that the four components form a mixed-ligand complex, which is adsorbed on the mercury drop.

(i) The relationship between the height of the mercury column and the peak-height corresponds to the formula for an adsorption current:⁵

$$I_a = kh$$

(ii) The relative temperature coefficient of the peak-height for zirconium is $+4.7\%/^\circ\text{C}$ over the range $0-20^\circ$. This value corresponds to an electrode

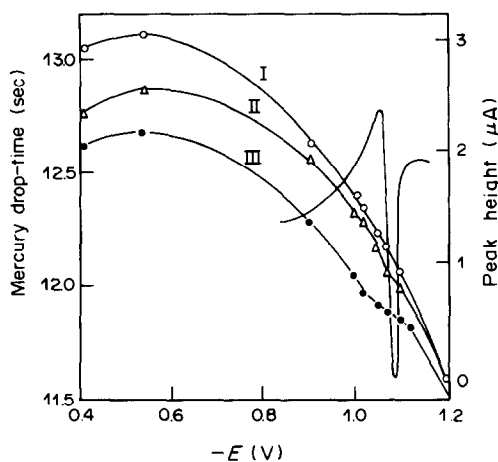


Fig. 3. Electrocapillary curves. Mercury column height 53 cm, temperature 11° , Zr $4.66 \times 10^{-8}\text{ M}$. I, sodium acetate/acetic acid buffer; II, buffer plus cupferron; III, buffer + cupferron + oxalic acid + Zr + diphenylguanidine.

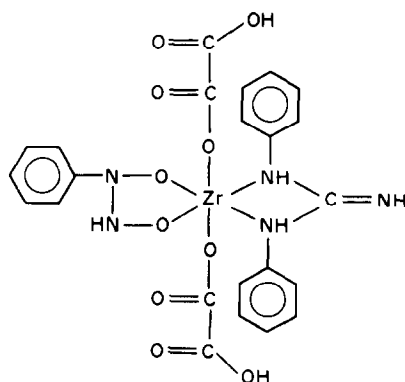
reaction with adsorption, and is clearly larger than that for a diffusion-controlled process. The peak-heights do not change in the range $25-45^\circ$ and a negative temperature coefficient appears at temperatures above 45° .

(iii) The electrocapillary curves shown in Fig. 3 indicate strong adsorption of the zirconium complex at a potential of about -1.02 V , corresponding to the oscillographic peak.

(iv) Adsorption was confirmed by the fact that a log-log plot of current *vs.* time had a slope greater than unity (1.125).

It is concluded that the zirconium peak is due to adsorption of the zirconium complex, with the cupferron component preferentially adsorbed on the surface of the mercury drop.

The composition of the product has been shown to be 1:2:1:1 Zr(IV)-oxalic acid-cupferron-diphenylguanidine, by the isomolar continuous-variations and slope-ratio methods. Ion-exchange tests show that the product is anionic and we conclude that its structure is



Analysis of ores

The results shown in Table 3 are in good agreement with those obtained by the X-ray fluorescence (XRF) method and with the certified values.

Table 3. Ore analyses

Sample	ZrO ₂ , µg/g		
	Present method	XRF method	Certified value
1	315, 309	282	313
2	471, 452	428	462
3	211, 222	193	221
4	178, 185	169	190
5	162, 168	152	170
6	206, 198	204	217

REFERENCES

1. G. K. Budnikov, V. N. Maistrenko and V. F. Toropova, *Zavodsk. Lab.*, 1976, **42**, 512.
2. Yao Xiu-ren, Zhou Jixing and Yin Ming, *Fen Hsi Hua Hsueh*, 1981, **9**, 22.
3. E. Cerrai and C. Testa, *Anal. Chim. Acta*, 1962, **26**, 204.
4. Zhuang Wen De, *Fen Hsi Hua Hsueh*, 1975, **3**, 204.
5. Gao Xiao and Yao Xiu-ren, *The Polarographic Catalyst Wave of the Platinum Family Elements*, pp. 97-105. Chinese Scientific Publishing Co., 1972.

A STUDY OF THE REACTION OF *N*-CHLOROSUCCINIMIDE WITH INDOLES AND ITS ANALYTICAL APPLICATION

IMADUL ISLAM, D. D. MISRA, R. N. P. SINGH and J. P. SHARMA*

Department of Chemistry, University of Allahabad, Allahabad, India

(Received 10 October 1983. Accepted 17 February 1984)

Summary—The reaction of *N*-chlorosuccinimide with indole and few of its derivatives in acid medium has been studied. The purified products have been identified by TLC, elemental analysis and infrared studies, and a reaction mechanism is proposed on the basis of the results. The reaction proceeds smoothly and consistently, and can be used for microdetermination of indole and its derivatives.

The indole ring is found in many naturally occurring compounds, and recently some synthetic indole derivatives have been reported to possess antiparkinsonian activity.¹⁻³ Numerous methods have been proposed for titrimetric determination of indole and its derivatives, mainly based on use of brominating agents such as bromine,⁴ *N*-bromoacetamide,⁵ *N*-bromosuccinimide⁶ and bromine monochloride.⁷ Decomposition of the reagents and loss of bromine during the reaction are the chief disadvantages of these methods.⁸ Spectrophotometric,^{8,9} polarographic,¹⁰ gas-chromatographic¹¹ and fluorimetric¹² methods have also been described. We have found that *N*-chlorosuccinimide, which is much more stable than *N*-bromosuccinimide or *N*-bromoacetamide,¹³ can conveniently be used for determination of indoles.

EXPERIMENTAL

Reagent

N-Chlorosuccinimide solution, 0.02*M*. Dissolve 0.2670 g of *N*-chlorosuccinimide in the minimum amount of warm distilled water. Dilute to 100 ml with cold water and standardize iodometrically.¹⁴

The reaction product was isolated by dissolving 100 mg of indole in about 25 ml of glacial acetic acid, slowly adding 0.1*M* *N*-chlorosuccinimide with constant stirring till a permanent brown colour persisted, letting stand for 4 hr, filtering off the brown product, washing it with water and air-drying it. The dried compound was recrystallized from chloroform to yield shining brown needles (m.p. 197°). Thin-layer chromatography of this compound on silica gel G with chloroform-96% acetic acid (95:5 v/v) showed a single spot. Analysis showed the presence of 2 atoms of chlorine in the product molecule. The infrared spectrum revealed intense absorption bands for C=O (1630 cm⁻¹) and C-Cl (730 cm⁻¹).

The products from indole derivatives gave similar results except for carbazole, for which the product molecule still contained two chlorine atoms but had no C=O absorption band in its infrared spectrum.

General procedure

Take an accurately weighed sample (2-8 mg) in a 100-ml iodine flask (an aliquot of solution containing 2-8 mg of the

indole can also be used). Add 2 ml of glacial acetic acid and 15 ml of 0.02*M* *N*-chlorosuccinimide, stopper the flask and shake it well. Let stand for 25 min at room temperature, then add 5 ml of 5% potassium iodide solution and titrate the liberated iodine with 0.04*M* sodium thiosulphate, using 2% starch as indicator. Run a blank with the same volume of *N*-chlorosuccinimide under identical conditions.

The amount of indole compound (mg) is $MW(B-A)/2n$ where *B* and *A* are the volumes (ml) of thiosulphate (molarity *M*) needed for the blank and sample respectively, and *n* is the molar reacting ratio of *N*-chlorosuccinimide to sample compound (of molecular weight *W*).

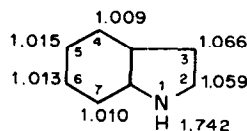
RESULTS AND DISCUSSION

N-Chlorosuccinimide is a mild oxidizing and chlorinating reagent. It has been suggested¹⁵ that the reactive species of *N*-chlorosuccinimide (NCS) is the protonated molecule $NCSH^+$, which gives rise to the electrophilic chloronium ion:



Investigation of the reaction stoichiometry by application of the method to samples of known purity showed that the reacting ratio was three moles of *N*-chlorosuccinimide per mole of indole compound, except for carbazole, for which the ratio was only 2:1.

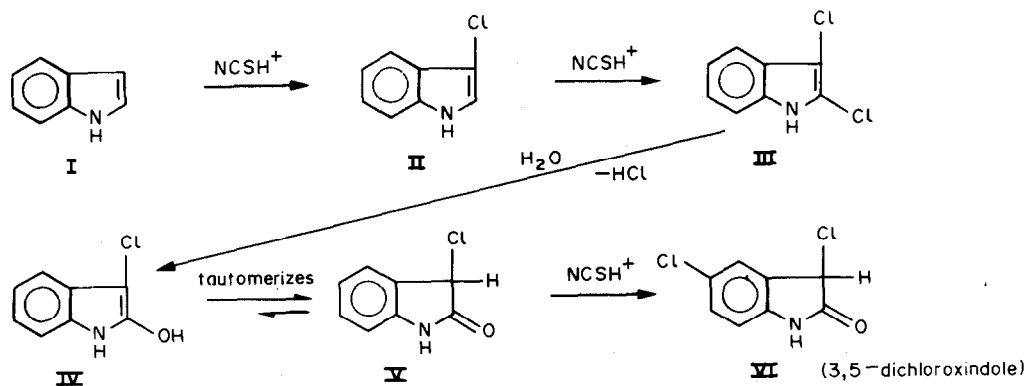
The π -electron densities¹⁶ on the indole nucleus are shown below and indicate that position 3 is the most susceptible to electrophilic attack. If, however, position 3 is already occupied, position 2 is preferentially attacked by electrophiles, and then position 5.



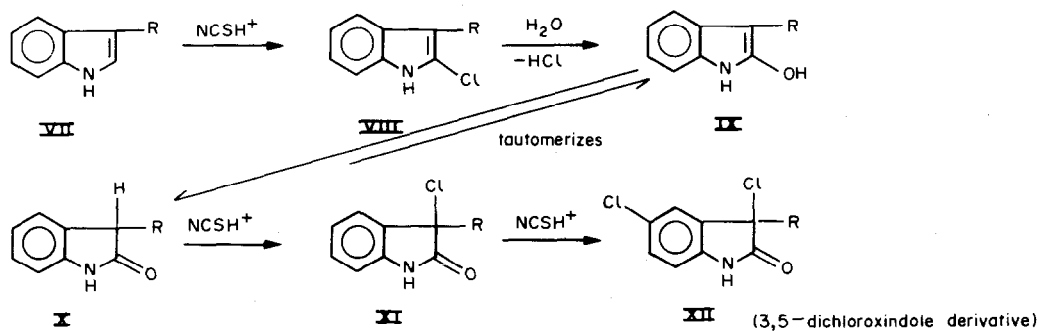
Scheme 1a.

On the basis of the observed stoichiometry, chlorine content of the reaction products, and the infrared spectra, the reaction can be explained as

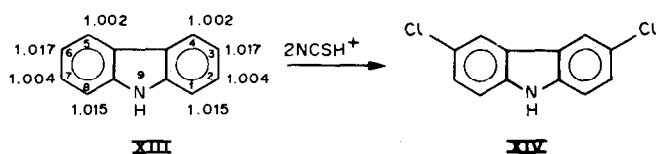
*To whom correspondence should be addressed.



Scheme 1b



Scheme 2



Scheme 3

given in Schemes 1 (for indole) and 2 (for indole 3-derivatives except carbazole).

In the case of indole, electrophilic substitution of chlorine atoms takes place first at position 3, and then at position 2. The chlorine atom at position 2 is the more likely to be hydrolysed, and this is in keeping with the well known activated nucleophilic substitution in aromatic compounds. Intermediate IV tautomerizes to V, which reacts with another protonated *N*-chlorosuccinimide molecule to give the final product 3,5-dichloroindole. Chlorination of position 6 in preference to position 5 is ruled out by the combined electron-withdrawing effect of the $-NH$ and $>C=O$ groups on the benzene ring further lowering the electron density at position 6.

Since position 3 is already occupied in the case of indole 3-derivatives (Scheme 2), the first step is the chlorination of position 2 followed by hydrolysis and tautomerization. Two chlorine atoms are then introduced at positions 3 and 5 by electrophilic attack by the reagent, giving a 3,5-dichloroindole-3-derivative (XII) as the final product.

The electron densities of the carbazole molecule¹⁷ (XIII) indicate that electrophilic substitution would occur preferentially at positions 3 and 6. Since the stoichiometry of the reaction with *N*-chlorosuccinimide is 1:2, the reaction may be formulated as shown in Scheme 3.

The proposed method has been applied to determination of indole and some of its derivatives, and the results are presented in Table 1. The maximum error is $\pm 1.2\%$ and the relative standard deviation 0.8%.

Variation of the acetic acid concentration does not affect the method. The reaction with indole derivatives is not instantaneous, and is only about 50% complete when titrated immediately after addition of the *N*-chlorosuccinimide. The rate of reaction is independent of the concentration of the reagent. The lower determination limit for all the samples tested is about 1 mg; erroneous results are obtained with smaller amounts.

Acknowledgements—We are grateful to the U.G.C. for the award of Junior Research Fellowships to I. Islam and D. D.

Table 1. Microdetermination of indoles

Sample	Amount taken, mg	Recovery range, mg	Mean recovery mg	Error, %	Relative standard deviation, %
Indole	2.034	2.038-2.079	2.059	+1.2	0.8
	4.068	4.070-4.098	4.084	+0.4	0.3
	6.102	6.088-6.139	6.116	+0.2	0.3
	8.136	8.120-8.129	8.135	0.0	0.2
Indole acetic acid	2.012	2.019-2.035	2.026	+0.7	0.3
	4.024	4.011-4.041	4.023	0.0	0.3
	6.036	6.022-6.059	6.036	0.0	0.3
	8.048	8.041-8.086	8.069	+0.2	0.3
Indole propionic acid	2.018	2.020-2.035	2.028	+0.5	0.3
	4.036	4.042-4.056	4.050	+0.3	0.3
	6.054	6.005-6.028	6.015	-0.6	0.1
	8.072	8.021-8.054	8.034	-0.5	0.2
Indole butyric acid	2.020	2.004-2.015	2.012	+0.4	0.3
	4.040	4.026-4.068	4.042	0.0	0.5
	6.060	6.022-6.048	6.037	-0.4	0.2
	8.080	8.020-8.048	8.041	-0.5	0.1
Tryptamine	2.006	2.001-2.019	2.011	+0.2	0.3
	4.012	4.020-4.045	4.031	+0.5	0.3
	6.018	6.020-6.045	6.031	+0.2	0.1
	8.024	8.029-8.049	8.040	+0.2	0.1
Carbazole	2.022	2.039-2.052	2.041	+0.9	0.3
	4.044	4.026-4.040	4.036	-0.2	0.2
	6.066	6.039-6.059	6.048	-0.3	0.1
	8.088	8.059-8.099	8.073	-0.2	0.2

Misra and financial assistance under the faculty improvement programme to R. N. P. Singh. We are also grateful to the Regional Sophisticated Instrument Centre, C.D.R.I., Lucknow, for the infrared spectra.

REFERENCES

1. P. Kumar, C. Nath, K. P. Bhargava and K. Shanker, *Current Sci., India*, 1983, **53**, 795.
2. C. Dumont, J. Guillaume and L. Nedelec, *German Patent 2738646*, 1978.
3. A. Kumar, J. C. Agarwal, C. Nath, S. Gurtu, J. N. Sinha, K. P. Bhargava and K. Shanker, *J. Heterocyclic Chem.*, 1981, **18**, 1269.
4. S. Kazimierz, *Ann. Univ. Mariae Curie-Sklodowska, Lublin-Polonia*, 1957, Sect. A, **10**, No. 31, 25.
5. M. Gopal, G. Srivastava, U. C. Pandey and R. D. Tiwari, *Mikrochim. Acta*, 1977 **II**, 215.
6. J. P. Sharma, V. K. S. Shukla and A. K. Dubey, *Analyst*, 1976, **101**, 867.
7. *Idem*, *Chem. Pharm. Bull.*, 1977, **25**, 1493.
8. P. E. Pilet, *Rev. Gen. Bot.*, 1957, **64**, 106; *Chem. Abstr.*, 1957, **51**, 8897.
9. A. Q. N. Manzer and A. N. Kost, *Pak. J. Sci. Ind. Res.*, 1980, **23**, 245.
10. A. G. Pozdeeva, *Zh. Priklad. Khim.*, 1961, **34**, 1842.
11. Y. Hoshika, *J. Chromatog. Sci.*, 1981, **19**, 444.
12. D. Yamamoto, M. Tsukada and T. Segawa, *Bunseki Kagaku*, 1975, **24**, 663.
13. C. K. Narang and N. K. Mathur, *The Determination of Organic Compounds with NBS and Allied Reagents*, p. 2. Academic Press, New York, 1975.
14. M. Z. Barakat and M. F. Abd El-Wahab, *Anal. Chem.*, 1954, **26**, 1973.
15. M. D. Carr and B. P. England, *Proc. Chem. Soc.*, 1958, 350.
16. R. M. Acheson, *An Introduction to the Chemistry of Heterocyclic Compounds*, 2nd Ed., p. 152. Interscience, New York, 1967.
17. *Idem*, *op. cit.*, p. 167.

PURIFICATION OF XYLENOL ORANGE BY PREPARATIVE PAPER CHROMATOGRAPHY, AND EXAMINATION OF ITS ZIRCONIUM COMPLEX

V. MICHAYLOVA

Department of Analytical Chemistry, University of Sofia, 1126 Sofia, Bulgaria

L. ŠŮCHA✠, and M. SUCHÁNEK

Department of Analytical Chemistry, Institute of Chemical Technology, 16628 Prague 6, Czechoslovakia

(Received 20 October 1982. Revised 15 February 1984. Accepted 2 March 1984)

Summary—Preparative paper chromatography is proposed as a suitable method for purification of Xylenol Orange (XO). The last three dissociation constants of pure XO have been determined with the aid of the program SPEKTFOT, the values found being $pK_9 = 12.34$; $pK_8 = 10.66$; $pK_7 = 6.69$ ($0.1M$ KNO_3 , $20 \pm 0.5^\circ$). The complexation of zirconium with the purified reagent has been studied and the co-existence of ML and M_2L complexes proved by use of the program DALSF EK. The following conditional stability constants of the complexes and their molar absorptivities were computed: $\log \beta_{ML} 4.58$; $\log \beta_{M_2L} 11.59$; $\epsilon_{ML} 2.00 \times 10^4$; $\epsilon_{M_2L} 9.40 \times 10^4$ $l \cdot mole^{-1} \cdot cm^{-1}$ at 550 nm.

The modern tendency to use group reagents in spectrophotometry requires knowledge of their properties, equilibria in solution and complex formation with various ions. There is thus a need for high-purity reagents so that reliable values can be obtained for various constants. Because of the excellent properties of Xylenol Orange (XO) as a group reagent¹ it seemed to be worth while to study its purification and equilibria in solution.

The present study deals with the purification of XO by preparative chromatography. The pure XO obtained was used for studying its equilibria in solution and its complex formation with zirconium.

EXPERIMENTAL

Reagents

Lachema Xylenol Orange was used in the purification procedure. The concentration of XO was determined by spectrophotometric microtitration with $3.00 \times 10^{-3}M$ zinc dipyriddy thiocyanate at 580 nm and pH 6.10 (acetate buffer). The zinc dipyriddy thiocyanate was prepared as described by Buděšínský² and used as a standard. A weighed amount was dissolved in a small volume of $0.1M$ hydrochloric acid and diluted to standard volume.

$ZrOCl_2 \cdot 8H_2O$ (Merck, *p.a.*) was used to prepare $2 \times 10^{-3}M$ zirconium solution in $2M$ perchloric acid, which was stable for a month. It was standardized by addition of excess of EDTA and back-titration with bismuth nitrate (XO as indicator).

Whatman No. 3 chromatographic paper, washed first with alkaline $10^{-3}M$ EDTA to remove metal ions, then many times with demineralized water, was used for the paper chromatography.

All solutions were prepared from reagent-grade substances with demineralized water.

Apparatus

Absorption spectra were obtained with a Zeiss Specord UV-Vis Spectrophotometer. Spectrophotometric mea-

surements were performed with a Zeiss VSU-2P spectrophotometer. A Radelkis OP-201/2 pH-meter with an OP-8071-1/A electrode was used for checking the pH of solutions.

Purification of XO

According to some authors^{3,4} the earlier column and thin-layer chromatography methods for purification of XO^{5-8} are complex and time-consuming procedures which do not lead to good results. Ion-exchange chromatography has been claimed to give better results.³ Our experiments with gel-chromatography⁹ and column chromatography with Whatman CF 11 cellulose powder failed to give satisfactory results, and now we propose preparative paper chromatography as more suitable. The XO was purified in two ways. In one, XO was first separated by extraction from the Semi-Xylenol Orange (SXO) and Cresol Red (CR) present in the commercial sample. In the other, this step was omitted. The system consisting of $0.1M$ hydrochloric acid and *n*-butanol-benzene (1:7 v/v) saturated with $0.1M$ hydrochloric acid, used in 1:1 v/v ratio, was used for the separation of CR from XO and SXO. XO and SXO were then separated by partition between *n*-butanol-benzene (3:1 v/v) and $0.1M$ hydrochloric acid in 1:1 volume ratio.¹⁰ The aqueous hydrochloric acid solution of XO was evaporated under reduced pressure and the XO extracted from the solid residue with absolute ethanol to separate it from the sodium chloride present. The alcohol was evaporated and the purity of the XO was checked by means of paper chromatography.^{5,6,9}

Paper chromatography

Descending development was used, with a 4:1:2 v/v *n*-butanol-acetic acid-water mixture as developing solvent. The mixture was prepared just before use because of the adverse influence of the *n*-butyl acetate formed.¹¹ The chromatographic paper strips (5 × 55 cm) were kept for 4-5 hr in the 20 × 30 × 65 cm chromatographic tank for saturation with the solvent vapours. Then 5, 10 or 20 μl of solution containing 5 μg of sample per μl were spotted by micropipette on the starting line and the strips were returned to the tank and developed for 14-16 hr. They were then taken out and dried at room temperature.

Preparative paper chromatography

This method permits easy separation of up to 0.8 mg of sample, the amount used depending on the initial purity. There is a sufficiently sharp separation, into a yellow spot of XO, followed by two spots of unknown compounds (UC₁ and UC₂) and that of SXO. The mean *R_f* values were 0.23 for XO, 0.28 for UC₁, 0.31 for UC₂ and 0.35 for SXO.

A chromatographic test of the XO isolated by extraction showed the presence of UC₁, UC₂ and small amounts of SXO. This XO was purified chromatographically: about 9 mg of it in acidic form were dissolved in 0.4 ml of 0.1M sodium hydroxide and the solution was uniformly spotted onto six 7 × 25 cm paper strips with a 20-μl micropipette, two spots on each strip, and the strips were developed for 15–20 hr as described above. The strips were taken out and dried in air until the solvent smell was completely removed. The spots of XO obtained were used for preparation of a pure XO solution: they were cut out and eluted with water (~15 ml for each pair of spots); the solution was filtered through a Schleicher & Schüll "white label" filter and its concentration was checked by spectrophotometric titration with ZnPy₂(SCN)₂ at pH 6 and 580 nm, the predominant complex being ZnXO.^{3,6,12} The concentration of pure XO solution was also determined by measuring its absorbance at 435 nm and pH 4–5, ϵ_{XO} being taken as 2.85×10^4 l.mole⁻¹.cm⁻¹.

The purity of XO was also checked by a chromatographic test. Two spots, those of XO and UC₁, were observed. The spot of UC₁ always appeared together with the spot of XO even after the latter had been submitted to chromatography 3 or 4 times. It is probable that UC₁ is a decomposition product, formed on passing the developing solvent through the spot of pure XO.

The following spectrophotometric data were found for the purified XO: $\epsilon_{\text{XO}} = 2.80 \times 10^4$ l.mole⁻¹.cm⁻¹ (430 nm, pH 4–5) and $\epsilon_{\text{Zn}_2\text{XO}} = 6.90 \times 10^4$ l.mole⁻¹.cm⁻¹ (570 nm, pH 5.65), these values being similar to those already reported.³

The Lachema commercial XO was purified directly by the same procedure without preliminary isolation of the reagent by extraction. In this case up to 0.5 mg of sample was treated and a more intense SXO spot was observed. The results were compared with those obtained by extraction followed by chromatography. A similar degree of purification was achieved, as well as the same spectrophotometric data.

These results confirm the suitability of the preparative paper chromatography for purification purposes. The direct purification of commercial XO can be recommended for practical use.

Determination of zirconium

Place enough 2M perchloric acid to give a final total acidity of 0.1–0.5M in a 25-ml standard flask. Add 5.00 ml of $\sim 2 \times 10^{-5}$ M XO and 0.20–2.00 ml of the test solution ($\sim 10^{-4}$ M Zr, freshly prepared), dilute to volume and mix. After 15 min, read the absorbance in a 3-cm cuvette at 550 nm with water as a reference. In a similar way prepare a calibration graph covering the zirconium concentration range 0.16–0.68 μg/ml.

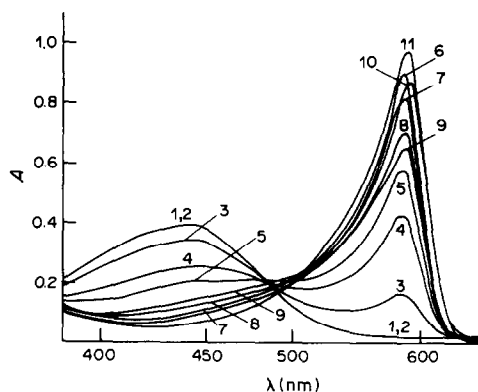


Fig. 1. Absorption spectra of Xylenol Orange at different acidities. $C_{\text{XO}} = 2.72 \times 10^{-6}$ M, $\mu = 0.1$, 5-cm cells, vs. water. pH: 1, 1.70; 2, 4.05; 3, 6.03; 4, 6.84; 5, 7.16; 6, 9.05; 7, 9.98; 8, 10.60; 9, 11.0; 10, 12.40; 11, 13.85.

RESULTS AND DISCUSSION

Solution equilibria of Xylenol Orange

The XO solution was prepared by elution of the chromatographic spots with water. Although this had been shown spectrophotometrically to be stable for several days, a freshly prepared solution was used for the investigations. The absorption spectra of the XO solution showed the presence of different ionic forms of the reagent in acidic and basic media, Fig. 1. The last three dissociation constants of XO were determined by applying the program SPEKTFOT¹³ to the curves for *A vs. pH* [$\mu = 0.1$ M (KNO₃), temperature $20 \pm 0.5^\circ$]. The results given in Table 1 are similar to data already published.^{3,6}

COMPLEX FORMATION OF ZIRCONIUM WITH XYLENOL ORANGE

The reaction of Zr(IV) with XO was studied twenty years ago^{14–16} but more recent investigations with purified reagent have provided more precise data.¹⁷

Our studies confirm that the Zr–XO reaction proceeds in strongly acid medium. The absorption spectra presented in Fig. 2 show that the equilibria are complicated and depend on the concentration ratio of metal ion and reagent. With a significant excess of metal ions present a violet complex ($\lambda_{\text{max}} = 550$ nm) is formed.

Table 1.

Ion	$\lambda_{\text{max}}, \text{nm}$	Molar absorptivity, $10^4 \text{ l.mole}^{-1} \text{ cm}^{-1}$	pK
XO ⁶⁻	582	8.08*	
HXO ⁵⁻	578	5.58*; 5.12†	pK ₁ 12.34
H ₂ XO ⁴⁻	578	7.43*; 6.86†	pK ₂ 10.66
H ₃ XO ³⁻	—	3.00§	pK ₃ 6.69
at pH 1–5	435		

*580 nm; †570 nm; §435 nm.

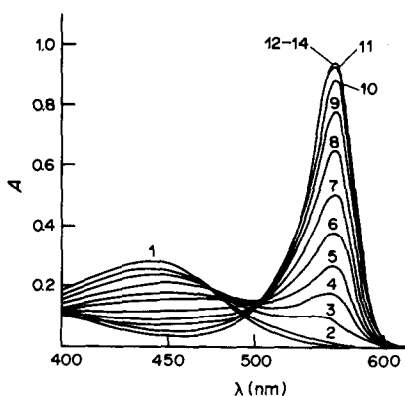


Fig. 2. Absorption spectra for the complexation equilibrium of Zr(IV) with XO. $C_{XO} = 3.28 \times 10^{-6} M$, $0.3 M HClO_4$, 3-cm cells, vs. water. $C_{Zr/XO}$: 1, 0.00; 2, 0.26; 3, 0.52; 4, 0.77; 5, 1.03; 6, 1.29; 7, 1.62; 8, 1.94; 9, 2.26; 10, 2.59; 11, 3.23; 12, 3.87; 13, 5.18; 14, 6.71.

Study of the reaction conditions

To prevent hydrolysis and polymerization of the zirconium a strong acid medium and a low concentration of Zr(IV) were used.¹⁸ The optimal acidity was found to be 0.1–0.5M perchloric acid, the absorbance then being constant.

The time needed for colour development and the stability of the absorbance were determined for different concentrations of the reagents in 0.5M perchloric acid. It was found that the colour developed immediately and was stable for several days in solutions containing excess of metal. With XO in excess the colour developed in 10–15 min after mixing of the reagents and was also stable for several days.

The influence of temperature on the reaction rate and on the polymerization equilibria¹⁷ of zirconium were also studied. For this purpose two solutions, (a) $2.11 \times 10^{-5} M Zr(IV)/1.60 \times 10^{-6} M XO$ and (b) $1.05 \times 10^{-6} M Zr(IV)/2.70 \times 10^{-6} M XO$, both in 0.5M perchloric acid, were investigated.

Aliquots of $2.11 \times 10^{-4} M$ zirconium solution in 2M perchloric acid [prepared daily from $2.11 \times 10^{-3} M Zr(IV)$] and the corresponding quantity of perchloric acid needed were placed in 25-ml standard flasks. The flasks were heated for 20 min in a water-bath (at $\sim 95^\circ$) then taken out and cooled to room temperature. Corresponding aliquots of XO solution ($\sim 10^{-5} M$) were added and the solutions were diluted somewhat, heated once again for 30 min, cooled and diluted to volume with water. The absorbances at 550 nm were measured with water as reference.

For comparison, the absorbances of solutions prepared at room temperature were also measured. The differences between corresponding absorbance values were within the limits of the photometric error. On the basis of these results it was concluded that no polymerization of Zr(IV) occurs under these conditions, and all later experiments were performed at room temperature.

Stability constants

The formation of Zr(IV) complexes with Xylenol Orange was investigated by the mole-ratio method with $1.96 \times 10^{-6} M XO$, $0.422 \times 10^{-5} M Zr(IV)$ and 0.48M perchloric acid. The data were analysed by the program DALSFEEK.¹² The results obtained show the co-existence of two complexes, ML and M_2L . The conditional stability constants of these complexes and their molar absorptivities were found to be: $\log \beta'_{ML} = 4.58$; $\log \beta'_{M_2L} = 11.59$; $\epsilon_{M_1} = 2 \times 10^4$ and $\epsilon_{M_2L} = 9.4 \times 10^4$ l. mole⁻¹. cm⁻¹ at 550 nm.

SPECTROPHOTOMETRIC DETERMINATION OF ZIRCONIUM

Because of the complicated equilibrium between Zr(IV) and XO, Beer's law is valid only at certain wavelengths, e.g., at 530 nm for the zirconium concentration range 0.16–0.58 $\mu g/ml$ ($\epsilon = 2.14 \times 10^4$ l. mole⁻¹. cm⁻¹). It is also valid at wavelengths close to 530 nm. The linear part of the calibration curve for measurement at 530 nm (Zr 0.16–0.68 $\mu g/ml$) might be used for the determination of small amounts of zirconium, since the sensitivity is higher ($\epsilon = 4.14 \times 10^4$ l. mole⁻¹. cm⁻¹) and the absorbance of XO is negligibly small.

The tolerance limits for other ions in determination of 10 μg of zirconium are: U(VI) 5.0 mg, Mo(VI) 0.5 mg, Th 4.0 mg, Ga 0.7 mg, Fe(II) 3.5 mg, PO_4^{3-} 0.8 mg, Fe(III) 50 μg , Sn(II) 50 μg , Bi 10 μg . Aluminium and indium do not interfere but fluoride and oxalate should be absent.

REFERENCES

1. J. Kőrbl, R. Přibil and E. Emr, *Collection Czech. Chem. Commun.*, 1957, **22**, 961.
2. B. Buděšínský, *Chem. Listy*, 1955, **49**, 1726.
3. H. Sato, Y. Yokoyama and K. Momoki, *Anal. Chim. Acta*, 1977, **94**, 217.
4. Analytical Methods Committee, *Analyst*, 1975, **100**, 675.
5. D. C. Olson and D. W. Margerum, *Anal. Chem.*, 1962, **34**, 1299.
6. M. Murakami, T. Yoshino and S. Harasawa, *Talanta*, 1967, **14**, 1293.
7. M. Yamada and M. Fujimoto, *Bull. Chem. Soc. Japan*, 1971, **44**, 294.
8. *Idem, ibid.*, 1976, **49**, 693.
9. R. P. Pantaler and I. V. Pulyaeva, *Zh. Analit. Khim.*, 1977, **32**, 2450.
10. V. Radil, The Institute of Nuclear Fuels, Prague, unpublished data.
11. M. A. H. Hafez, *Ph.D. Thesis*, Pardubice, 1980.
12. F. R. Hartley, C. Burgess and R. Alcock, *Solution Equilibria*, Horwood, Chichester, 1980.
13. M. Suchánek, *Dissertation*, Institute of Chemical Technology, Prague, 1976.
14. K. L. Cheng, *Anal. Chim. Acta*, 1963, **28**, 41.
15. A. K. Babko and V. T. Vasilenko, *Zavodsk. Lab.*, 1961, **27**, 640.
16. B. Buděšínský, *Collection Czech. Chem. Commun.*, 1963, **28**, 1858.
17. H. Sato, Y. Yokoyama and K. Momoki, *Anal. Chim. Acta*, 1978, **99**, 167.
18. J. Kragten, *Atlas of Metal-Ligand Equilibria in Aqueous Solution*, Horwood, Chichester, 1978.

SPECTROPHOTOMETRIC DETERMINATION OF HALOGENATED 8-HYDROXYQUINOLINE DERIVATIVES

F. BELAL*

Department of Analytical Chemistry, Faculty of Pharmacy, University of Mansoura, Mansoura, Egypt

(Received 6 September 1983. Accepted 23 February 1984)

Summary—A spectrophotometric method is proposed for the determination of 8-hydroxyquinoline and three of its iodinated derivatives: 5-chloro-7-iodo-8-hydroxyquinoline (clioquinol), 5,7-di-iodo-8-hydroxyquinoline (iodoquinol) and 8-hydroxy-7-iodo-quinolone-5-sulphonic acid (chinoxal). The suggested method depends on the reaction with 4-aminoantipyrine in the presence of an alkaline oxidizing agent. A red antipyrine dye with an absorption peak at 500 nm is produced in all cases. The reacting ratio has been determined and a reaction mechanism is presented. The proposed method can be applied to the analysis of pharmaceutical preparations containing the compounds studied, and the results obtained compare favourably with those obtained with the standard methods.

The halogenated derivatives of 8-hydroxyquinoline have been widely used as anti-amoebic compounds, both in the treatment of amoebic dysentery and intestinal amoebiasis, and as topical anti-infectives, because of their very low toxicity. Several methods are available in the literature for the determination of the halogenated derivatives of 8-hydroxyquinoline, in the pure state and in pharmaceutical preparations.

The gravimetric and titrimetric methods include precipitation with cadmium iodide in acetone and weighing the cadmium complex formed,¹ or precipitation with mercuric acetate in acetic acid and weighing the mercury complex.² The total halogen content can be determined by fusion with sodium carbonate and titration by the Volhard method, and the iodide by iodate titration.³ Soliman⁴ described an alternative method involving refluxing the compounds with 15% sodium hydroxide solution and zinc powder, followed by titration of the halide(s) with standard iodate solution. These compounds have also been determined by precipitation of the copper complex, and iodometric determination of the copper content.⁵ Fusion with potassium carbonate and titration with *N*-bromosuccinimide has also been reported.⁶ In non-aqueous media, these compounds can be determined by titration with sodium methoxide, in dimethylformamide⁷ or pyridine⁸ as solvent.

Colorimetric methods include reaction with iron(III),⁹ copper sulphate,^{10,11} sodium nitrite¹² and alcoholic potassium hydroxide.¹³

Other techniques used include polarography,¹⁴ X-ray spectrography¹⁵ and gas-liquid chromatography.¹⁶

In this paper, a simple and more direct analytical method that is applicable to the determination of low concentrations of halogenated 8-hydroxyquinoline

derivatives and their formulations is reported; the method has proved successful for determining accurately the compounds either alone or mixed with the ingredients commonly encountered in dosage forms.

EXPERIMENTAL

Reagents

4-Aminoantipyrine, 2% solution in methanol.

Sodium carbonate, 1% solution in water.

Potassium hexacyanoferrate(III), 4% solution in water.

Materials

Pure drug samples were obtained as gifts from various manufacturers, and used without further purification. Pharmaceutical preparations containing the compounds studied were obtained from commercial sources in the Egyptian market.

Sample preparation

Stock 1.0-mg/ml solutions of each of the compounds studied were prepared in appropriate solvents (Table 1).

Calibration graph

Aliquots (1 ml) of standard solutions of the drug, covering the calibration range (Table 1), were transferred to 25-ml standard flasks. Then 1.5 ml of sodium carbonate solution, 0.6 ml of 4-aminoantipyrine solution, and 1 ml of potassium hexacyanoferrate(III) solution were added to each, in that order, and the solutions diluted to volume with water. The absorbances at 500 nm were measured against a reagent blank and plotted against the final solution concentrations.

Assay procedure for dosage forms

Tablets. Twenty tablets were weighed and pulverized, and a quantity of the powder equivalent to 50 mg of the pure drug was accurately weighed and transferred to a 100-ml beaker and dissolved in the appropriate solvent (Table 1) by heating on a water-bath. The solution was filtered into a 100-ml standard flask and diluted to the mark with the same solvent, then analysed by the calibration procedure.

Syrups. A volume of the suspension equivalent to about 150 mg of the active ingredient was accurately measured and centrifuged at 5000 rpm for 30 min. The clear supernatant liquid was discarded and the residue shaken with a 40-ml portion of distilled water until it was completely in suspension. This mixture was centrifuged as before for 30 min

*Present address: 2360 West Broad Street, Apt. # 133, Athens, Georgia 30606, U.S.A.

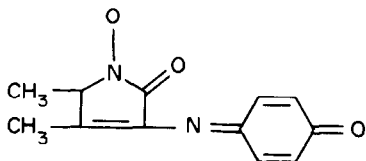
and the clear supernatant liquid discarded. The washing and centrifugation were repeated, with a further 40-ml portion of water. The residue was transferred completely into a 250-ml standard flask with dimethylformamide (DMF) and dissolved by heating on a water-bath. The solution was diluted to volume with DMF, and the determination completed as already described.

Ointments. A composite sample was prepared by mixing the contents of five containers and a sample equivalent to 100 mg of the drug was accurately weighed into a 100-ml beaker, dissolved in 80 ml of a hot mixture of 4:1 DMF-water mixture and heated on a water-bath for 5 min. The solution was cooled in ice for 10 min, allowed to warm to room temperature, diluted to volume in a 100-ml standard flask with the DMF-water mixture, mixed and filtered. The determination was completed as before.

DISCUSSION

8-Hydroxyquinoline and its derivatives are phenolic compounds, and can therefore react with 4-aminoantipyrene in the presence of an alkaline oxidizing agent to form an antipyrene dye;¹⁷ the product has maximum absorption at 500 nm.

It is reported that in this reaction of 4-aminoantipyrene with phenolic compounds, a quinonoid structure of the following type is formed:

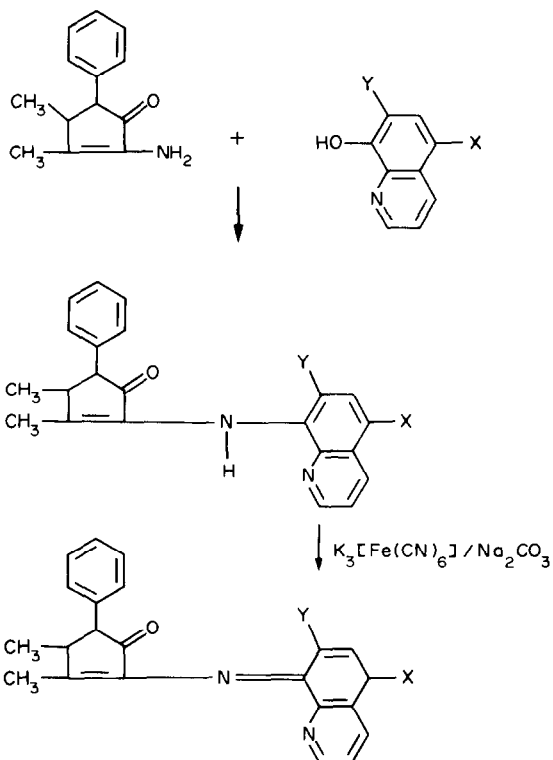


This necessitates the position *para* to the phenol group being either free or substituted with a group that can be expelled during the reaction. In the case of the halogenated 8-hydroxyquinoline derivatives, an iodine atom in the *para* position is difficult to expel under the reaction conditions described. An alternative reaction pathway is suggested in the scheme below (X and Y substituents at positions 5 and 7 respectively), and is substantiated by the fact that 8-hydroxyquinoline (with the *para* position unsubstituted) and the other members of the group have nearly identical molar absorptivities (Table 1), indicating that the chromophore formed is the same in all cases.

To study the reaction further, the reacting ratio of 4-aminoantipyrene and 8-hydroxyquinoline or clioquinol (as an example of a *para*-substituted compound) was studied by the continuous-variation method¹⁸ and found to be 1:1 in both cases.

Table 1 summarizes the data for the reaction between 4-aminoantipyrene and the compounds studied. The time listed in the table is critical. After the specified time, precipitation will occur. The molar absorptivities are the average of 10 separate determinations.

Table 2 shows the analytical results obtained by means of the proposed method and the compendial



ones.¹⁹⁻²¹ There was no significant difference between the results obtained by the two methods.

In Table 3 the results obtained for clioquinol, iodoquinol and chionoform in pharmaceutical preparations are given. Tablet excipients, such as starch, gelatine, talc, soluble saccharine and silica do not interfere. Substances likely to be encountered in clioquinol or iodoquinol suspensions or ointments, such as sulphaguanidine, bismuth subcarbonate, light kaolin, sodium citrate, sucrose, carboxymethylcellulose, liquid extract of belladonna, hydrocortisone or prednisolone, also do not interfere. The recovery of clioquinol from commercial suspensions was determined by adding a known amount of the pure drug to suspensions already analysed for clioquinol. Representative results are given in Table 4. These control experiments were conducted in order to differentiate between experimental error and errors due to the interaction of other constituents of the system, or errors resulting from the bulk production.

The method developed in this investigation has the advantages of being simple and applicable over a convenient range of concentrations to the determination of halogenated 8-hydroxyquinoline derivatives in the pure state or in pharmaceutical formulations. In addition, it requires no special skill. A spectrophotometer is the only instrumentation required, and this is an advantage in developing and underdeveloped countries, where preparations containing halogenated 8-hydroxyquinoline derivatives are most needed.

Table 1. Collective data for the reaction of 4-aminoantipyrine with halogenated derivatives of 8-hydroxyquinoline

Compound	Solvent	Molar absorptivity, $l.mol^{-1}.cm^{-1}$	Range of conc., $\mu g/ml$	Stability time min
8-Hydroxyquinoline	Methanol	1.20×10^4	2-24	15
Clioquinol	DMF	1.22×10^4	2-20	10
Iodoquinol	Hot DMF	1.29×10^4	4-32	5
Chinoform	Hot water	1.23×10^4	2-20	5

Table 2. Determination of halogenated 8-hydroxyquinoline derivatives by the proposed and official methods

Compound	Recovery, %	
	Proposed method	Official or other method
8-Hydroxyquinoline	100.3 (0.4)	99.7 ²² (0.5)
Clioquinol	99.8 (0.5)	99.3 ¹⁹ (0.6)
Iodoquinol	98.9 (0.3)	99.1 ²⁰ (0.4)
Chinoform	99.1 (0.5)	100.4 ²¹ (0.5)

The results are the averages of 10 separate determinations. The figures in brackets are the coefficients of variation.

Table 3. Determination of halogenated 8-hydroxyquinoline derivatives in synthetic and commercial preparations

Preparation	Recovery, %	
	Proposed method	Official method
Enterovioform tablets (200 mg of clioquinol per tablet)	98.3 (0.5)	99.1 (0.5)
Parameb tablets (250 mg of iodoquinol per tablet)	101.3 (0.3)	101.0 (0.5)
Nimarol suspension (3% clioquinol suspension)	104.5 (0.4)	105.0 (0.6)
Vioderm ointment (3% clioquinol ointment)	103.2 (0.4)	102.9 (0.4)
Chinoform tablets (prepared tablets containing 200 mg per tablet)	100.6 (0.4)	100.2 (0.2)

The results are the averages of 6 separate determinations. The figures in brackets are the coefficients of variation.

REFERENCES

1. K. G. Anantanrayanan, N. G. Kudalkar, M. S. Madiwale, H. H. Desai and M. B. Waldwalker, *Indian J. Pharm.*, 1959, **21**, 263.
2. J. Mohoric, *Farm. Vest.*, 1969, **20**, 1; *Anal. Abstr.*, 1970, **19**, 670.

Table 4. Recovery of iodoquinol added to 5 ml of commercial suspensions nominally containing 125 mg of the drug

Added amount of drug, mg	Total recovered, mg	Recovery of added drug, %
0.0	131.2	
100.0	231.0	99.8
0.0	130.5	
200	331.0	100.3

3. S. L. Mukerje and A. P. Dey, *Drug Stand.*, 1959, **27**, 18; *Anal. Abstr.*, 1959, **6**, 4158.
4. S. A. Soliman, *Analyst*, 1975, **100**, 696.
5. E. Vinkler, F. Klivenyi and M. Gati, *Acta Pharm. Hung.*, 1972, **42**, 141; *Anal. Abstr.*, 1972, **23**, 4910.
6. M. Z. Barakat, M. Bassioni and M. El-Wakil, *Analyst*, 1972, **97**, 466.
7. H. H. Kavarana, *Am. J. Pharm.*, 1959, **131**, 1059.
8. J. Renault, J. G. Giraud and M. F. Cartron, *Ann. Pharm. Franc.*, 1965, **23**, 335.
9. J. Cohen and E. Kluchesky, *J. Pharm. Sci.*, 1963, **52**, 693.
10. B. Özsöz, *Türk. İfityen Tecrubi Biyol Dergisi*, 1963, **23**, 113; *Anal. Abstr.*, 1963, **10**, 4888.
11. J. J. Windheuser and D. Y. Chu, *J. Pharm. Sci.*, 1967, **50**, 519.
12. D. J. Vadodaria, B. R. Desai and S. P. Mukherji, *Indian J. Pharm.*, 1965, **27**, 257.
13. S. A. Ismaiel and D. A. Yassa, *Pharmazie*, 1973, **28**, 611.
14. L. W. Brown and E. Krupski, *J. Pharm. Sci.*, 1961, **50**, 49.
15. G. J. Papariello, H. Letterman and W. J. Mader, *Anal. Chem.*, 1962, **34**, 1147.
16. M. P. Gruber, R. W. Klein, M. E. Fox and J. Campisi, *J. Pharm. Sci.*, 1972, **61**, 1147.
17. R. W. Martin, *Anal. Chem.*, 1949, **21**, 1419.
18. P. Job, *Anal. Chim. Paris*, 1928, **9**, 113.
19. *British Pharmacopoeia*, p. 114. The Pharmaceutical Press, London 1973.
20. *United States Pharmacopoeia*, XXth Revision, pp. 413, 546, 547, 699. Mack Publishing, Easton, Pa., 1980.
21. *The Egyptian Pharmacopoeia*, p. 211. English Text, Cairo, 1953.
22. J. A. Joseph and L. Szekeres, *Talanta*, 1976, **23**, 558

LETTER TO THE EDITOR

THE COLOURS OF CO-ORDINATION COMPOUNDS: METHODS OF CLASSIFICATION

Sir,

The colours of compounds and, in particular, metal complexes are an important parameter and should be accurately reported. However, the literature abounds with colour names that are ambiguous, and thus meaningless to other workers. This arises because the names given to the colours of compounds are arbitrarily chosen by individual workers, who assign a name to the colour of an object by comparing it with their colour memory. Most people have a poorly developed colour memory. If an observer has difficulty in recalling colours, it will be even more difficult for him to convey a recalled colour impression to another person.¹

It is possible to describe the colour of solids and liquids accurately and simply by reference to a colour order system, a number of which have been proposed. The most popular is that of Munsell.² An alternative that has the advantages of cheapness and simplicity is the Methuen system.¹ Some interconversions between different systems have been reported.^{1,3,4}

Three parameters are required to describe a particular colour completely:

- (a) hue - that property of visual perception by which different regions of the spectrum are distinguished and named, e.g., red, yellow;
- (b) saturation - the intensity of a hue or its degree of freedom from admixture with white;
- (c) lightness - the variation of visual perception along the continuum between white and black.

In the Munsell system these parameters are referred to as hue, chroma and value respectively

Although colour order systems have been used extensively in fields such as biology, pharmacology and geology, to our knowledge there has been no extension of these methods to co-ordination compounds. We have therefore classified a number of complexes by both the Methuen and Munsell colour systems (see Table). From the Munsell notation a systematic name that unequivocally describes the colour of the complex can be derived by means of the ISCC-NBS* method of designating colour.³

Whenever possible the complexes were assessed in the form in which they were prepared. Only in the case of very intense colours was it necessary to grind the crystals to bring about a reduction in saturation. For complexes having colours with a low degree of lightness [e.g., Cr(pd)₃] grinding also results in a slight change in hue, which in turn may give rise to a change in the colour name.

* Inter Society Colour Council - National Bureau of Standards

Table 1. Colour classification and systematic colour names of some co-ordination compounds

Compound*	Reported colour	Treatment †	Colour notation		Colour name	
			Methuen ¹	Munsell ²	Methuen ¹	ISCC-NBS ³
$[\text{Co}(\text{en})_3]\text{I}_3 \cdot \text{H}_2\text{O}$	deep orange ⁵	P	5A 8	7.5YR 7.5/→15	deep orange	vivid orange yellow
$\text{K}_2\text{Cr}_2\text{O}_7$	red, ⁶ orange red ⁷	P	7A8	1.5YR 6/15	reddish orange	vivid reddish orange
$\text{Na}_2[\text{Fe}(\text{NO})(\text{CN})_5] \cdot 2\text{H}_2\text{O}$	ruby red ⁷	G ₂	7D6	1.5YR 5/5.5	light brown	greyish reddish orange
K_2PtCl_4	red brown ⁶	P	8D8	10R 4/8	reddish brown	dark reddish orange
		G ₂	8C6.5	10R 5/8	brownish red	moderate reddish orange
$\text{Cr}(\text{pd})_3$	red violet ⁸	G ₂	11F7	1R 2/4	violet brown	dark purplish red
		G ₃	11E4	5.5RP 4/3	violet brown	greyish purple
$\text{trans-}[\text{K}[\text{Co}(\text{ox})_2(\text{py})_2] \cdot 3\text{H}_2\text{O}]$	pink ⁹	P	15A4.5	6.5P 7/8	light lilac	light purple
$\text{Co}(\text{py})_2\text{Cl}_2$ α form	violet ¹⁰	P	16A6	5P 5.5/11	reddish violet	strong purple
β form	deep blue	G ₁	20A8	7.5PB 4/17	vivid blue	vivid blue
$\text{Cu}(\text{pd})_2$	light blue ^{6,11}	P	21D5	6PB 4.5/6.5	greyish blue (dull blue)	moderate blue

* en = ethylenediamine; pd = 2,4-pentanedionate (acetylacetonate); py = pyridine.

† p = assessed as prepared or obtained; G₁ = coarse grinding; G₂ = medium grinding; G₃ = fine grinding.

This method of colour classification would be of greatest utility for complexes with very dark colours (i.e., low degree of lightness) and for those of metal ions which form a large number of complexes with similar colours [e.g., Cu(II), Rh(III)].

School of Natural Resources,
University of the South Pacific,
P.O. Box 1168, Suva, Fiji

FRANZ LUDWIG WIMMER and LAURENCE PONCINI

13 February 1984

REFERENCES

1. A. Cornerup and J.H. Wanscher, Methuen Handbook of Colour, 2nd Ed., Methuen, London, 1967.
2. Munsell Book of Colour, Munsell Colour Company, Baltimore, 1942.
3. K.L. Kelly and D.B. Judd, The ISCC-NBS Method of Designating Colours and a Dictionary of Colour Names, Circular 553, National Bureau of Standards, Washington, 1955.
4. For example, see W. Budde, H.E. Kundt and G. Wyszecski, Farbe, 1955, 4, 83; M. Richter, ibid., 1957, 6, 49.
5. J.A. Broomhead, F.P. Dwyer and J.W. Hogarth, Inorg. Synth., 1960, 6, 183.
6. R.C. Weast (ed.), CRC Handbook of Chemistry and Physics, 58th Ed., CRC Press, West Palm Beach, 1977-1978.
7. B.D.H. Chemicals Co., Catalogue, 1981-1982.
8. W.C. Fernelius and J.E. Blanch, Inorg. Synth., 1957, 5, 130.
9. Y. Ida, S. Fujinami and M. Shibata, Bull. Chem. Soc. Japan, 1977, 50, 2665.
10. N.S. Gill, R.S. Nyholm, G.A. Barclay, T.I. Christie and P.J. Pauling, J. Inorg. Nucl. Chem., 1961, 18, 88.
11. M.M. Jones, J. Am. Chem. Soc., 1959, 81, 3188.

OXYDATION VANADIQUE DE LA KHELLINE: APPLICATIONS ANALYTIQUES

J. E. HILA, M. TSITINI-SOULEAU et M. HAMON

Laboratoire de chimie analytique, Faculté de Pharmacie, Chatenay Malabry, Paris XI,
2, rue J. B. Clément, 92290 Chatenay Malabry, France

M. CHASTAGNIER

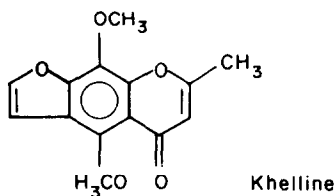
Laboratoire des gaz, Faculté de Pharmacie de Paris V, 4, avenue de l'Observatoire, 75006 Paris, France

(Reçu le 29 novembre 1982. Révisé le 28 février 1984. Accepté le 18 avril 1984)

Résumé—L'oxydation vanadique de dérivés hétérocycliques oxygénés a montré la réactivité de cette structure à l'égard de l'ion vanadate. L'oxydation de la khelline nous a permis d'obtenir une méthode sensible de dosage de ce produit, puisque la consommation de réactif oxydant est de 16 moles par mole de produit. Dans le milieu réactionnel ont été isolées des quantités importantes d'acide furanne dicarboxylique-2,3. Cette méthode d'oxydation est utilisable à des fins préparatives pour obtenir ce produit.

L'étude de l'oxydation vanadique de dérivés hétérocycliques oxygénés tels que le chromanol-4 et la chromanone-4 montre¹ la réactivité de cette structure, mais aussi la stabilité de la chromone formée au cours de la réaction. Des études précédentes ont d'autre part permis de constater que la présence de groupements éther-oxyde de phénol sur un cycle aromatique entraîne une fragilité plus grande de la molécule vis à vis de cet oxydant.²

La khelline, furanochromone naturelle^{3,4} utilisée pour ses propriétés thérapeutiques, présente de tels groupements. Aussi, avons-nous envisagé son oxydation qui est intéressante tant du point de vue fondamental que pour ses éventuelles applications analytiques.



PARTIE EXPERIMENTALE

Réactif

La solution sulfovanadique (0,1M)⁴ présente une concentration finale en acide sulfurique voisine de 0,72M et est étalonnée par titrage avec une solution de sulfate de fer(II) et d'ammonium.

Mode opératoire

Une prise d'essai de 25 mg de khelline soit 96 μ moles, est introduite dans une fiole conique rodée de 100 ml; 30 ml de la solution de pentoxyde de vanadium sont ensuite ajoutés ainsi que 10 ml d'acide sulfurique 2,5M et 10 ml d'acide sulfurique 8M. La fiole est munie d'un réfrigérant à reflux, l'oxydation est réalisée au bain marie bouillant. Au cours de la réaction, le vanadium(V) en excès est dosé par une solution de sulfate de fer(II) et d'ammonium 0,3M avec une indication potentiométrique.

Isolement et dosage de composés au cours de l'oxydation vanadique

Les quantités de dioxyde de carbone libérées au cours de l'oxydation ont été déterminées par la technique de Chaigneau.⁵ L'isolement du formaldéhyde est réalisé par entraînement à la vapeur d'eau dans un appareil de Parmas et Wagner. L'identification et le dosage sont obtenus par formation d'une déhydrolutidine selon la méthode de Hantzsch.⁶

Les acides formique et acétique sont isolés après distillation du milieu réactionnel. Ils ont été identifiés par chromatographie sur couche mince et dosés par chromatographie en phase liquide après réaction avec une nitrocoumarine.^{7,8} Les résultats ont été comparés avec ceux obtenus sur des solutions étalons d'acide formique et d'acide acétique en solution sulfovanadique, réduite préalablement par du sulfate de fer(II) et d'ammonium.

Isolement, identification et dosage de l'acide furanne dicarboxylique-2,3

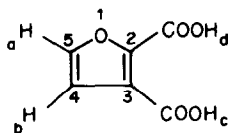
Par extraction étherée du milieu réactionnel, est isolée une substance jaunâtre de caractère acide. Le point de fusion de ce produit est de 228°. Les résultats expérimentaux de l'analyse élémentaire sont conformes aux valeurs calculées pour un acide furanne dicarboxylique: calculé C 46,25%, H 2,56%; trouvé C 46,3%, H 2,7%. Le dosage titrimétrique en milieu aqueux de cet acide par la soude 0,1M permet de déterminer deux pK_A (2,40 et 7,35) concordant avec des travaux antérieurs.⁹

Le spectre de résonance magnétique nucléaire du proton à 60 MHz d'une solution dans le diméthyl sulfoxyde-*d*₆, met en évidence deux protons à 6,9 et 8 ppm (*a* et *b*) sous forme de doublets. Le proton *b* est légèrement plus déblindé que le proton équivalent de l'acide furanne-3 monocarboxylique.¹⁰ Le singulet à 11,1 ppm correspond d'après l'intégration aux deux protons acides (*c* et *d*).

Le spectre de résonance magnétique nucléaire du carbone-13 dans le chloroforme deutérié permet de constater que les carbones 4 et 5 se distinguent des carbones quaternaires, indépendamment des spectres "of resonance", par l'effet Overhauser qui n'est que partiel dans le cas des carbones quaternaires. Les résonances de ces derniers ont des intensités faibles, par rapport à celles des carbonyles. Les attributions proposées sont fondées sur les effets en α et β de la substitution par un oxygène de carbones insaturés.¹¹

L'identification des carbonyles doit tenir compte de l'effet mésomère de l'oxygène furannique. Celui-ci entraîne une résonance à champs relativement élevés comme le montre l'exemple de l'ester méthylique de l'acide furanne carboxylique-2 où l'on observe un déplacement chimique de $\delta = 159$ ppm pour le carbonyle.¹²

En outre, la disubstitution *ortho* crée un effet stérique supplémentaire responsable lui aussi d'un déplacement des résonances vers les champs élevés.



Le spectre infra-rouge du produit isolé est voisin de celui de l'acide furanne carboxylique-3. A 3100 et 3050 cm^{-1} , on peut observer deux bandes dues à la vibration de valence de la liaison carbone-hydrogène du noyau furanne. A 1640 cm^{-1} , on observe une bande double qui peut être attribuée à la fonction carboxyle, cette bande est légèrement déplacée par rapport à celle de l'acide furanne carboxylique-3 qui se trouve à 1670 cm^{-1} .¹³ Ce déplacement vers des nombres d'ondes plus petits est dû probablement à la présence d'un système conjugué de deux carbonyles. La présence du deuxième carboxyle augmente d'ailleurs comme cela est prévisible l'intensité de la bande à 1610 cm^{-1} (bande de la liaison carbone-carbone du cycle furannique).¹⁴

Nous avons étudié le spectre de masse de l'ester diméthylé, obtenu après méthylation au diazométhane¹⁵ et séparation par chromatographie en phase gazeuse.

Le spectre obtenu est voisin de celui de l'ester diméthylé de l'acide furanne dicarboxylique-2,5.¹⁶ Les différences obtenues à la fragmentation peuvent être expliquées par la présence du deuxième carboxyle en 3 au lieu de 5. Les principaux pics observés et leur abondance relative sont indiqués dans le tableau 1.

Le mécanisme envisagé est proposé ci-dessous:

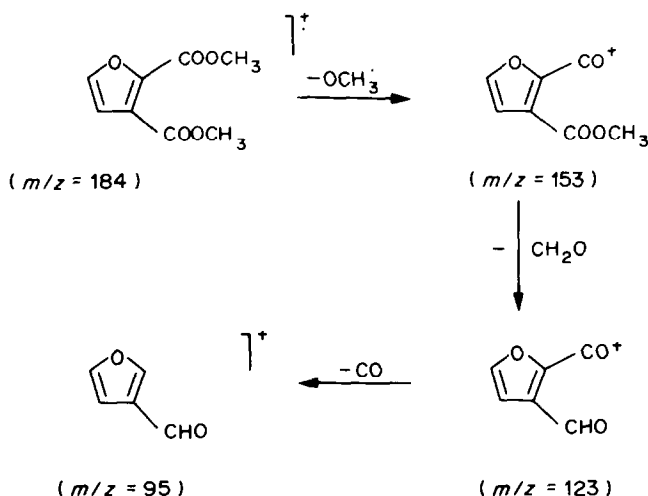


Tableau 1.

m/z	Abondance relative, %
184	11,7
153	100
123	62,7
95	24,8

Identification du méthyl-2 méthoxy-5 formyl-6 hydroxy-7 chromone

Ce produit a été identifié par spectrométrie de masse couplée à la chromatographie en phase gazeuse par comparaison avec la fragmentation d'un échantillon authentique.¹⁷

RESULTATS

Cinétique d'oxydation

Pour différentes concentrations de khelline dans le milieu sulfovanadique, après une heure de réaction au bain marie bouillant, la consommation d'oxydant est proportionnelle à la quantité de khelline soumise à l'oxydation. En effet, pour des concentrations de khelline entre 0,16 et 0,80 mg/ml, nous avons remarqué que la quantité d'oxydant consommé est une fonction linéaire ($r = 0,9987$) de la quantité de produit de départ soumise à l'oxydation.

Une étude statistique sur cinq échantillons à 25 mg de khelline, oxydés dans les mêmes conditions opératoires que celles utilisées pour établir la courbe d'étalonnage, a montré que l'erreur expérimentale maximale par rapport à cette même courbe était égale à 0,1%.

Dans ces conditions opératoires et dans l'intervalle de concentrations en produit de départ cités ci-dessus, la consommation d'oxydant rapportée est de 16 moles à une mole de khelline en milieu sulfurique 2,5M.

Nous avons constaté que l'oxydation est terminée au bout d'une heure comme le montre la cinétique de l'oxydation en fonction du temps représentée ci-dessous (Fig. 1).

Produits d'oxydation

Pour expliquer la quantité d'oxydant consommée et la cinétique de l'oxydation, nous avons isolé et dosé un certain nombre de produits d'oxydation. Le dosage du dioxyde de carbone a montré qu'en milieu sulfurique 2,5M, il y a formation de 3,37 moles de

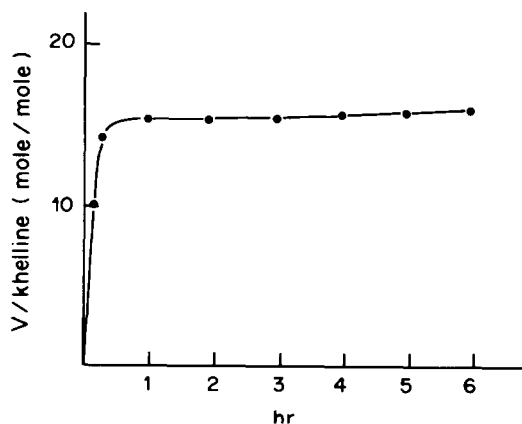


Fig. 1. Oxydation sulfovanadique de la khelline en milieu 2,5M en acide sulfurique (concentration 1,92 μ mole/ml).

dioxyde de carbone par mole de khelline. Le dosage du formaldéhyde produit en milieu sulfurique 2,5M a montré que la concentration de cet aldéhyde passe par un maximum et diminue en fonction du temps (Fig. 2). En ce que concerne les trois acides isolés, une mole de khelline forme 0,68 mole d'acide formique, 0,63 mole d'acide acétique et 0,67 mole d'acide furanne dicarboxylique-2,3 en milieu sulfurique 2,5M.

Proposition d'un mécanisme réactionnel

La formation en milieu sulfurique 2,5M de quantités voisines d'acide furanne dicarboxylique-2,3, d'acide acétique et d'acide formique laisse prévoir que ces trois produits pourraient se former selon un même mécanisme réactionnel qui intéresse les 2/3 (66%) des molécules présentes. Ce mécanisme induit une attaque initiale soit au niveau du noyau pyranique, soit au niveau du noyau benzénique substitué, mais laisse intact le cycle furannique.

L'isolement et l'identification du méthyl-2 méthoxy-5 formyl-6 hydroxy-7 chromone montre l'existence d'un second mécanisme réactionnel, sans pour autant qu'actuellement un dosage de cette molécule ait pu être mis en oeuvre. L'oxydation selon le

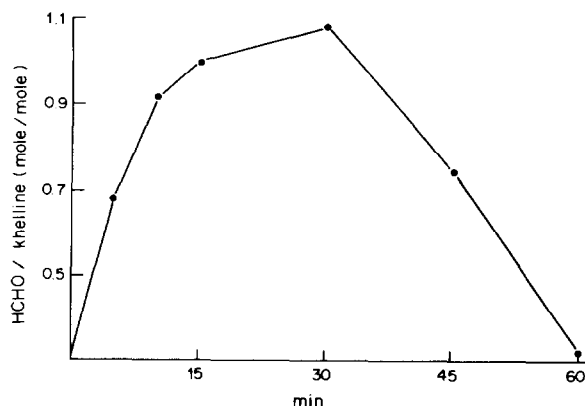
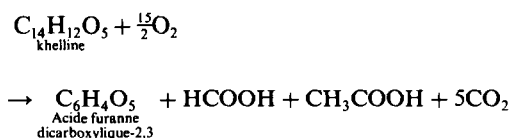


Fig. 2. Cinétique de formation du formaldéhyde en fonction du temps.

premier de ces deux mécanismes peut être schématisée selon l'équation:



Cependant, ceci suppose que les groupements méthoxylés subissent une oxydation totale en dioxyde de carbone. Or, dans les conditions opératoires envisagées lors de cette oxydation, l'hypothèse du passage par un état CH_3 ou CH_3^+ conduisant par réaction avec le solvant à du méthanol est plausible compte tenu du caractère radicalaire de la réaction. Aussi, avons-nous soumis le méthanol à l'oxydation dans les mêmes conditions. Nous avons constaté qu'une mole de méthanol en milieu sulfurique 2,5M ne réduit que 1,67 moles d'ion vanadyle.

Ces valeurs nettement inférieures aux 6 moles nécessaires pour une oxydation totale peuvent, peut être, s'expliquer par la volatilité des molécules considérées. En tout état de cause, ce palier de la quantité d'oxydant consommé ne peut être dépassé quelque soit le temps de la réaction.

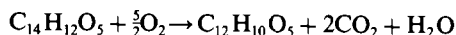
Ainsi pouvons-nous considérer que ce ne sont pas 30 moles d'ion vanadyle, correspondant aux 7,5 moles O_2 , qui sont réduites, mais:

$$30 - 2(6 - 1,7) = 21,4 \text{ moles}$$

Si ce mécanisme intéresse les deux tiers des molécules, la quantité d'oxydant consommée est de:

$$\frac{21,4 \times 2}{3} = 14,3 \text{ moles}$$

Dans le cas où le second mécanisme conduirait essentiellement à la méthoxy-5 formyl-6 hydroxy-7 chromone, l'équation serait:



L'oxydation dans ce cas d'un seul groupement méthoxylé nous conduit par le même raisonnement à envisager la consommation, non pas de 10 moles d'ions vanadyle théoriquement prévues dans le cas de l'oxydation complète du groupement méthoxylé, mais seulement de 5,7 moles. En appliquant le même type de calcul, puisque le tiers des molécules initiales peut être justiciable de ce mécanisme, la consommation serait de $5,7/3 = 1,9$ moles d'ions vanadyle.

La consommation totale serait donc de $14,3 + 1,9 = 16,2$ moles d'oxydant par mole de khelline.

L'hypothèse concernant le second mécanisme est beaucoup plus délicate à émettre et fera l'objet d'un travail ultérieur.

Application au contrôle de médicament

Nous avons dosé la khelline par spectroscopie ultraviolette et par oxydation sulfovanadique dans

Tableau 2. Comparaison des deux méthodes de dosage: 1, dosage sur une solution pure; 2, dosage après dépôt sur une plaque de C.C.M. et extraction

Étalon, mg	Absorbance à 326 nm		Consommation d'oxydant, μeq	
	1	2	1	2
2	0,438	0,400	123	116
3	0,656	0,609	186	178
4	0,871	0,811	244	237
5	1,09	0,998	305	296

une forme pharmaceutique contenant de la khelline et de la prométhazine (Khelline-Prométhazine sirop, Laboratoires Berthier).

Méthode d'extraction et de préparation des échantillons. Les deux produits sont extraits du sirop par le dichlorométhane. L'extrait organique est évaporé à sec à 40° sous pression réduite. Le résidu est repris par un volume de dichlorométhane exactement mesuré. Une fraction de la solution obtenue est déposée sur une plaque de silice GF 254 (0,2 mm) dont le support est en feuille d'aluminium. Le dépôt a été fait grâce au déposeur (Camag 10-74-F), car la résolution des bandes est d'autant meilleure que le dépôt est fin.

Après séparation chromatographique (solvant utilisé: acétate d'éthyle 40, toluène 50, acide formique 10) et séchage, la bande correspondant à la khelline est récupérée par un volume précis de dichlorométhane. Pour avoir des résultats comparatifs, une fraction de l'éluat est utilisée pour le dosage spectrophotométrique et une autre est oxydée par le pentoxyde vanadium. D'autre part, une partie de la plaque chromatographique parcourue par la phase mobile est traitée de la même manière. L'éluat obtenu est utilisé comme "blanc" pour les deux méthodes.

La droite de régression obtenue pour quatre analyses effectuées par spectrophotométrie ultra-violet et oxydation sulfovanadique montre une bonne corrélation entre les deux méthodes ($r = 1$) (Tableau 2).

L'exactitude de la méthode et le rendement de l'extraction ont été déterminés en déposant sur la plaque chromatographique des quantités connues de khelline. Les valeurs obtenues, données dans le Tableau 2, montrent un meilleur résultat pour le dosage oxydimétrique que pour le dosage spectrophotométrique.

Les dosages effectués sur la spécialité mentionnée précédemment ont donné respectivement des valeurs de 33 mg/100 g pour la méthode oxydimétrique et de 32,5 mg/100 g pour la méthode spectrophotométrique pour une valeur théorique indiquée sur le conditionnement de 36 mg/100 g de sirop. Il est possible de conclure que les teneurs déterminées par les deux méthodes sont très voisines et qu'elles correspondent à une valeur acceptable si l'on considère des limites de $\pm 10\%$.

CONCLUSION

En conclusion, l'oxydation de la khelline nous a permis d'obtenir une méthode de dosage de ce produit pouvant être appliquée à de faibles quantités puisque la consommation de réactif oxydant est de 16 moles par mole de produit. La sensibilité de la technique est au moins comparable à celle obtenue par la spectrométrie ultra-violette. L'identification et le dosage des produits réactionnels, nous a conduit à isoler notamment l'acide furanne dicarboxylique-2,3, dont nous avons pu déterminer les différents paramètres spectrométriques.

LITTÉRATURE

1. J. E. Hila, M. Tsamis, J. P. Délécroix et M. Hamon, *Analisis*, 1982, **10**, 220.
2. M. J. Waechter, J. Likforman et M. Hamon, *ibid.*, 1977, **5**, 34.
3. M. Tsamis, M. Chaigneau, M. Hamon et J. Likforman, *ibid.*, 1980, **8**, 428.
4. M. Tsamis, *Thèse de Doctorat Paris-Sud*, 1980-1981.
5. M. Chaigneau, *Bull. Soc. Chim. France*, 1970, 4133.
6. T. Nash, *Biochem. J.*, 1953, **55**, 416.
7. H. Cisse, R. Farinotti et S. Kirkiarcharian, *J. Chromatog.*, 1981, **225**, 509.
8. G. Mahuzier et R. Farinotti, Communication personnelle.
9. O. Shigeru, F. Naomichi et W. Takao, *Bull. Chem. Soc. Japan*, 1965, **38**, 1247.
10. *Sadtler Handbook of Proton N.M.R. Spectra*, No. 2604, Sadtler, Heyden, Philadelphia, 1978.
11. G. C. Levy et G. L. Nelson, *Carbon-13 Nuclear Magnetic Resonance for Organic Chemists*, pp. 62-82. Wiley-Interscience, New York, 1972.
12. L. P. Johnson et W. Jankowsky, *Carbon-13 N.M.R. Spectra*, Wiley-Interscience, New York, 1972.
13. *Sadtler Handbook of Infrared Spectra*, No. 2604, Sadtler, Heyden, Philadelphia, 1978.
14. M. Avram et G. H. D. Matescu, *Spectroscopie Infra Rouge*, p. 306. Dunod, Paris, 1970.
15. I. Kushnir, J. I. Feinberg et J. W. Pensabene, *J. Food Sci.*, 1975, **40**, 427.
16. J. Pettersen et E. Jellum, *Clin. Chim. Acta*, 1972, **41**, 199.
17. S. Ahamsson, F. W. McLafferty et E. Stenhagen, *Registry of Mass Data*, Vol. 2, Wiley-Interscience, New York, 1974.

Summary—In studies of the reactivity of oxygen heterocycles, it has been found that khelline gives a molar reacting ratio of 1:16 with vanadate in 2.5M sulphuric acid, the products being vanadium(IV), 2,3 furan dicarboxylic acid, formic acid, acetic acid and carbon dioxide. This reaction can be used for determination of khelline and also for preparation of 2,3-furan dicarboxylic acid.

STABLE-ISOTOPE RATIO ANALYSIS BASED ON ATOMIC HYPERFINE STRUCTURE AND OPTOGALVANIC SPECTROSCOPY

WILLIAM G. TONG and EDWARD S. YEUNG*

Department of Chemistry and Ames Laboratory, Iowa State University, Ames, Iowa 50011, U.S.A.

(Received 31 January 1984. Accepted 5 April 1984)

Summary—Atomic hyperfine structures were measured for the Cu I transition at 5782 Å by optogalvanic spectroscopy at high resolution, with a cw dye laser. Samples were electro-deposited on the demountable cathode of a home-made hollow-cathode lamp. By spectral deconvolution, the relative isotopic abundances of ⁶³Cu and ⁶⁵Cu could be determined with good accuracy and precision. The technique is applicable to copper concentrations as low as 1.6 ppm.

Reliable and safe application of isotopes as tracers is important in many areas, including biomedical, environmental and geochronological sciences. The presence of trace levels of both essential and non-essential elements can significantly affect biological processes. It is important to study how and where metals are absorbed, distributed and accumulated in various parts of the body. Radioactive isotopes have been most frequently utilized for these studies. However, the application of these techniques in humans is severely limited because of the hazardous nature of the radioactive isotopes. An alternative is measurement of the abundance ratio of stable isotopes, which can be done by a variety of mass spectrometric methods, including GC-MS,^{1,2} thermal ionization MS,³ field ionization MS,⁴ ICP-MS,^{5,6} fast-atom bombardment MS,⁷ electron-impact ionization MS,⁸ and spark-source MS.⁹ The major disadvantage of all mass spectrometric methods is the interference caused by other ions having exactly the same *m/e* value as the analyte. The resolving power of most commercial mass spectrometers is not sufficient to avoid some of these interferences,⁷ and the overall sensitivity decreases if higher resolving powers are used.

In this paper, we report a new approach to stable-isotope ratio analysis, based on atomic hyperfine structure available from the optical absorption profile. This spectroscopic scheme is virtually interference-free because of the highly selective and specific nature of hyperfine structures. Each hyperfine structure has its own unique shape and profile within a narrow range of frequencies (less than 15 GHz or 0.5 cm⁻¹). Thus, a minor constituent in a complex matrix can be studied without extensive sample preparation.

The study of isotope shifts and hyperfine structures of optical transitions in atomic spectra has yielded detailed information about the changes in the radial

moments of the nuclear charge distribution for the isotopes of an element. The high spectral resolution necessary to study hyperfine splittings has been achieved by using a wide variety of spectroscopic tools including etalons,¹⁰⁻¹³ interferometers,¹⁴⁻²⁰ and spectrometers.²¹ Atomic-beam sources^{22,23} have been used to minimize the Doppler broadening of the line-widths. However, it was not until the development of tunable dye lasers that measurements with high spectral resolution and high precision for a large number of elements were possible, for optical transitions ranging from the infrared to the ultraviolet regions. Important laser spectroscopic techniques include Doppler-free²⁴ and non-linear²⁵⁻²⁷ optical methods.

In this work we use a single-frequency tunable cw dye laser as the optical excitation source and a specially designed and constructed demountable cathode discharge as the atomizer and detector. Hyperfine profiles are collected by monitoring the optogalvanic signal²⁸ generated between the two electrodes of the discharge when the laser frequency is scanned across the optical transition range. Optogalvanic spectroscopy has become a powerful technique, with applications in many areas of research including analytical chemistry,^{29,30} wavelength measurements and calibration,^{31,32} and atomic³³ and molecular³⁴ spectroscopy. Since the electrical signal is directly generated from the optical absorption, no optical detection is required. In the low-pressure environment (2-7 mmHg) of the discharge plasma, the Lorentzian line-width broadening is negligible and the spectral resolution is limited only by Doppler broadening. Some Doppler-free optogalvanic techniques have been used^{35,36} to study isotope shifts and hyperfine structures. However, for obtaining isotope ratios, it is not always necessary to use Doppler-free methods to obtain baseline resolution of hyperfine components. All components that are convoluted under the Doppler-limited spectrum can be recovered by matching the experimental and theoretical

*Author for correspondence.

hyperfine profiles by a least-squares criterion. This method is demonstrated here for the determination of ⁶³Cu and ⁶⁵Cu by using the hyperfine structure of the Cu I 5782 Å, ²D_{3/2-2}P_{1/2} transition.

THEORY

Splitting of an optical transition for a single isotope into two or more hyperfine components is due to the interaction of the nuclear magnetic moment with the electronic magnetic field. The number of hyperfine splittings *F* depends on the nuclear angular momentum of the isotope *I*, and the electronic angular momentum *J*:

$$F = (I + J), (I + J) - 1, (I + J) - 2, \dots (I - J) \quad (1)$$

For the Cu I 5782 Å (²D_{3/2-2}P_{1/2}) transition, *J*' = 3/2 and *J* = 1/2, and both ⁶³Cu and ⁶⁵Cu have *I* = 3/2. Therefore, for each isotope, there are two hyperfine splittings (*F* = 2, 1) at the upper level and four hyperfine splittings (*F*' = 3, 2, 1, 0) at the lower level. The selection rule, Δ*F* = ±1, 0, allows six hyperfine transitions *K*_{*F**F*'} as shown in Fig. 1. Consequently, the ⁶³Cu and ⁶⁵Cu isotopes each have a set of six hyperfine components, resulting in a 12-component hyperfine structure.

The relative hyperfine-component strengths of a set of hyperfine lines are well defined, and can be calculated from their direct relation to the excitation or emission rate. Excitation rate is directly proportional to ξ², where ξ can be defined by the expression

$$\xi = \langle \alpha J I M_F | \hat{\epsilon} \cdot \bar{r} | \alpha' J' I F' M_{F'} \rangle \quad (2)$$

for weak fields; $\hat{\epsilon}$ is the polarization vector and \bar{r} is the position vector, *J* and *M_F* are the quantum numbers needed for complete specification of the states for the upper level and α', *J*' and *M_F'* are those for the lower level. It is assumed here that no optical, fine-structure or hyperfine-structure pumping effects exist. For linear polarization along the *z* axis,³⁷

$$\xi_{[F' M_{F'} \rightarrow F M_F]} = \left\langle \alpha J I M_F \left| \left(\frac{4\pi}{3} \right)^{\frac{1}{2}} r T_0^{(1)} \right| \alpha' J' I F' M_{F'} \right\rangle \quad (3)$$

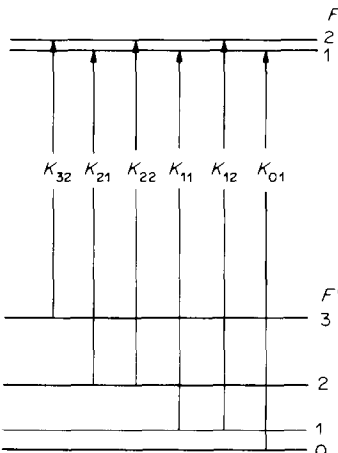


Fig. 1. Hyperfine transitions for the Cu I atomic line at 5782 Å.

where *T*₀⁽¹⁾ is a spherical tensor *T*_q^(k) of rank *k* in *J*-space with *k* = 1 and *q* = 0, and *r* is the distance along the *z* axis. We then use the Wigner–Eckart theorem³⁸ to remove the dependence of matrix elements of *T*₀⁽¹⁾ on the magnetic quantum numbers *M_F* and *M_F'*. The result is

$$\xi = (-1)^{F-M_F} \begin{pmatrix} F & 1 & F' \\ -M_F & 0 & M_{F'} \end{pmatrix} \times \left\langle \alpha J I F \left\| \left(\frac{4\pi}{3} \right)^{\frac{1}{2}} r T_0^{(1)} \right\| \alpha' J' I F' \right\rangle \quad (4)$$

where

$$\begin{pmatrix} F & 1 & F' \\ -M_F & 0 & M_{F'} \end{pmatrix}$$

is a 3-*J* symbol³⁸ and

$$\left\langle \alpha J I F \left\| \left(\frac{4\pi}{3} \right)^{\frac{1}{2}} r T_0^{(1)} \right\| \alpha' J' I F' \right\rangle$$

is a reduced matrix element,

$$\begin{aligned} & \langle \alpha J I F \parallel r T_0^{(1)} \parallel \alpha' J' I F' \rangle \\ &= (-1)^{J+I+F'+1} [(2F+1)(2F'+1)]^{1/2} \\ & \times \begin{Bmatrix} F & 1 & F' \\ J' & I & J \end{Bmatrix} \langle \alpha J \parallel r T_0^{(1)} \parallel \alpha' J' \rangle \end{aligned} \quad (5)$$

where

$$\begin{Bmatrix} F & 1 & F' \\ J' & I & J \end{Bmatrix}$$

is a 6-*J* symbol.³⁸ By combining equations (5), (4) and (2), and summing over *M_F* and *M_F'*, it is apparent that the excitation rate ξ² is directly proportional to the transition strength *K* and

$$\begin{aligned} K_{[F' \rightarrow F]} &= \sum_{M_F} \sum_{M_{F'}} K_{[F' M_{F'} \rightarrow F M_F]} \\ &= (2F+1)(2F'+1) \begin{Bmatrix} F & 1 & F' \\ J' & I & J \end{Bmatrix}^2 \\ & \times \sum_{M_F} \sum_{M_{F'}} \begin{pmatrix} F & 1 & F' \\ -M_F & 0 & M_{F'} \end{pmatrix}^2 \end{aligned} \quad (6)$$

Since the last term in equation (6) becomes unity, the final expression for the relative hyperfine-component strength is

$$K_{F'F} = (2F+1)(2F'+1) \begin{Bmatrix} F & 1 & F' \\ J' & I & J \end{Bmatrix}^2 \quad (7)$$

By means of equation (7), the six hyperfine-component strengths K_{32} , K_{21} , K_{22} , K_{11} , K_{12} and K_{01} of the Cu I 5782 Å line, as shown in Fig. 1, are calculated and the results agree with the experimentally observed data.

To simulate the actual absorption profiles, the magnitudes of the hyperfine shifts must next be found. For the Cu I 5782 Å transition, there are 12 hyperfine-component frequencies $\nu_{0,n=1-12}$, and the hyperfine shift values Δ_n (i.e., $\nu_{0,n+1} - \nu_{0,1}$) have been reported by other workers.³⁹⁻⁴¹ However, these values vary slightly, depending on the measurement method, the electric field and the geometry and dimension of the electrodes used. Since it is essential to obtain these values with high accuracy (within $\pm 0.0005 \text{ cm}^{-1}$), they must be determined for the specific type of discharge plasma used. This is accomplished by least-squares fitting of experimental profiles from a sample with known isotope abundances, by varying each $\nu_{0,n}$ value by 0.001 cm^{-1} at a time until the best matching set of $\nu_{0,n}$ is obtained.

Once all $K_{0,n=1-12}$ and $\nu_{0,n=1-12}$ values have been determined, we can simulate theoretical profiles for various combinations of isotope ratio R , and plasma temperature T , by summing over the individual Doppler-broadened contributions. Ratio R is used to adjust the relative absorption strengths of the two isotopes, $K_{0,n}$ (^{63}Cu) and $K_{0,n}$ (^{65}Cu). Figure 2 shows the two 6-component sets of hyperfine structure simulated for ^{63}Cu and ^{65}Cu , with the natural $^{63}\text{Cu}/^{65}\text{Cu}$ abundance ratio of 2.235 and plasma temperature of 20 K for the lower traces and 1400 K for the upper trace. The isotope ratio of the analyte is calculated by matching the experimental hyperfine structure to these theoretical profiles and picking the set which yields the least squared deviation.

EXPERIMENTAL

A schematic diagram of the experimental arrangement is shown in Fig. 3. An argon ion laser (Control Laser, Orlando, FL, Model 554 A) is used to pump a high-resolution (40 MHz jitter) cw ring dye laser (Spectra Phys-

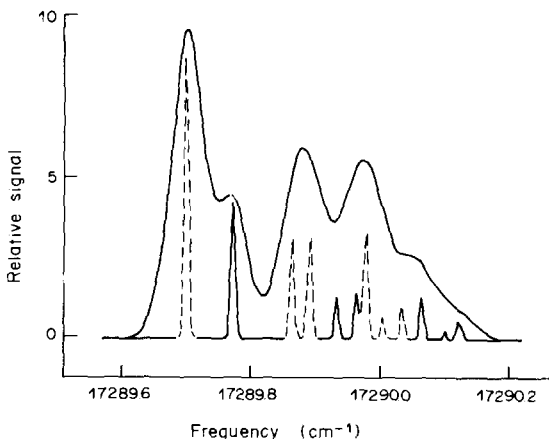


Fig. 2. Doppler-broadened hyperfine structure. Top, 1400 K; bottom 20 K, broken lines for ^{63}Cu and solid lines for ^{65}Cu .

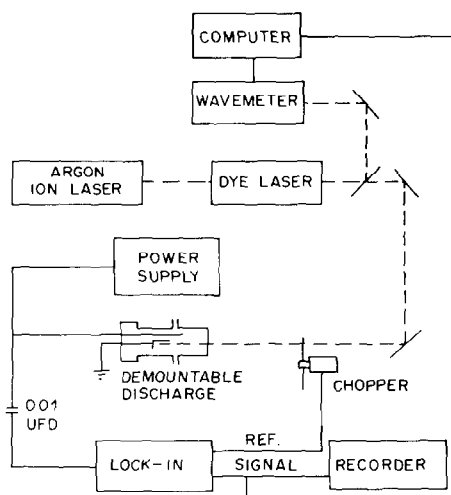


Fig. 3. Experimental arrangement for optogalvanic measurements. Optical paths are shown as broken lines and electrical connections are shown as solid lines.

ics, Mountain View, CA, Model 380 A) which provides tunable single-frequency radiation which can be electronically scanned over 30 GHz. A wavemeter (Burleigh Instruments, Fishers, NY, Model WA-20) accurate to 0.01 cm^{-1} , is used to monitor the laser frequency, and the I/O port of the wavemeter is interfaced to a minicomputer (Digital Equipment Corp., Maynard, MA, PDP 11/10) to collect and store the frequency values. A mechanical chopper (Rofin, Newton Upper Falls, MA, Model 7510) is used to modulate the laser beam at 1 kHz modulation frequency. The dye laser beam is directed into the cathode cavity of the demountable hollow-cathode discharge tube (constructed in our workshops) operated by a constant-current power supply, and the resulting optogalvanic signal is sent to a lock-in amplifier (Princeton Applied Research, Princeton, NJ, Model HR-8) where a 1-sec time constant is used. The output of the lock-in amplifier is connected to a digital voltmeter (Keithley, Cleveland, OH, Model 160 B), and the analogue output of the voltmeter is digitized by the laboratory peripheral system (LPS-11) of the minicomputer. The computer takes simultaneous readings of both the optogalvanic signal and the laser frequency every 0.5 sec, and the real-time spectrum is displayed on a graphics terminal (Visual Technology Inc., Tewksbury, MA, Model 550). The real-time spectrum monitoring is useful for detecting any experimental defects, such as laser mode-hopping, while the experiment is in progress.

A simple demountable cathode discharge tube can be constructed from a 1.5-in. outside diameter (o.d.) 6-in. long Pyrex-to-Kovar joint with a quartz window attached on the glass end and a 3-in. diameter stainless-steel vacuum flange welded on the Kovar end. A 3-in. diameter $\frac{3}{4}$ -in. thick nylon flange is attached to the stainless-steel flange to allow dismantling. Vacuum seal is provided by an O-ring between the flanges. The cathode and anode are mounted on the nylon flange through the central axis of two nylon bolts screwed onto the flange through O-ring seals. A $\frac{1}{8}$ -in. diameter 7-in. long tungsten welding rod (Welders Engineering Research Co., Charlotte, NC, Cleaned Finish) is used as the anode. A screw-mount cathode rod and cathode housing assembly is shown in Fig. 4. A $\frac{1}{8}$ -in. diameter nickel (or copper) rod serving as the cathode is screw-mounted in a 4-mm inner diameter, 8-mm long nickel housing through a 5-40 thread (the high-purity nickel used, containing less than 0.9 ppm copper, was obtained locally from the Ames Laboratory). Pyrex tubing is sealed on the cathode housing for insulation and to confine cathode sputtering inside the cathode cavity. The gap between the cathode and anode is

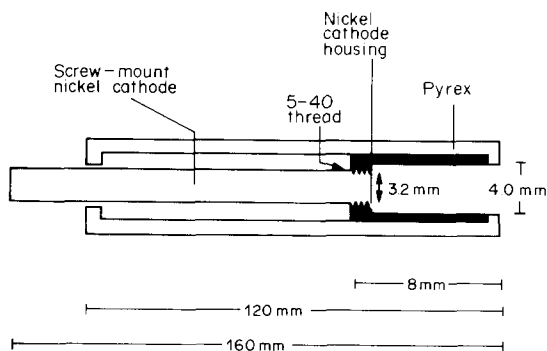


Fig. 4. Demountable hollow cathode.

9 mm. The anode rod is approximately 1 in. longer than the cathode assembly so that the sharp edge of the tip of the anode rod is facing away from the cathode cavity. This reduces the chance of electrical arcing between the electrodes, especially at higher gas pressures and lamp currents. Analyte, at trace level, is deposited onto the $\frac{1}{8}$ -in. diameter end-surface of the cathode tip. Research grade (99.9999%) neon gas (Matheson, East Rutherford, NJ) is used for the discharge gas, and the gas pressure is monitored by a capacitance manometer (0–10 mmHg full scale; MKS Instruments, Burlington, MA, Model 221A). No brass is used in the vacuum line and only a mechanical vacuum pump is used for the vacuum system. The discharge tube can be disassembled and assembled, and the electrodes replaced, within a few seconds. After the vacuum has been broken and the electrodes exposed to the atmosphere, a baking period of 10 min is sufficient to restore a noise-free discharge base-line. Baking is done by simply firing the lamp at normal operating current (30 mA) and then flushing with the discharge gas. A reasonably stable galvanic base-line can be obtained even without any baking, each time the lamp is reassembled after exposure to the atmosphere. The lamp intensity and optogalvanic signal generated are comparable to or better than those for a commercial hollow-cathode lamp (Perkin-Elmer Corp., Norwalk, CT).

All enriched isotopes, ^{63}Cu (99.89%) and ^{65}Cu (99.69%), were purchased from Oak Ridge National Laboratory. Stock solutions were prepared by dissolving the isotopes in 10% nitric acid (containing less than 0.05 ppm Cu). Natural-abundance copper stock solutions were prepared by dissolving electrolytic copper metal powder (Electrolytic Purified, Fisher Scientific Co., Fairlawn, NJ) in 2% nitric acid. Copper is deposited on the cathode tip by controlled-potential electro-deposition with the cathode rod as the working electrode, a platinum wire as the counter-electrode and a saturated calomel electrode as the reference electrode. A controlled potential of -0.35 V vs. SCE is applied to the cathode rod. All the cathode rod surface that is submerged in the solution, except the flat tip, is insulated by Teflon tape so that the electro-deposition is concentrated on the small area of the cathode tip. All electro-depositions are done at pH 2 with potassium nitrate as supporting electrolyte. After deposition, the cathode rod is rinsed with triply distilled demineralized water and air-dried before installation in the demountable lamp.

Human whole blood samples (3-ml portions) obtained from the Ames Laboratory medical department were digested with 20 ml of a 1:1 v/v mixture of 70% perchloric and 70% nitric acids in a miniaturized Bethge apparatus. A reflux time of 30 min was sufficient to obtain a clear solution. For larger amounts of blood, water condensate was removed from the side-arm of the Bethge apparatus in order to raise the perchloric acid concentration and increase the oxidizing power.

The ring dye laser has a fairly good electronic wavelength-scanning mechanism with minimum scan-rate

deviation. However, even slight deviation was unacceptable for our scheme for fitting the hyperfine-component frequencies with $\pm 0.0005\text{ cm}^{-1}$ accuracy. Hence the wavemeter was interfaced to the minicomputer so that signal data could be collected simultaneously with the corresponding frequency values. The I/O port of the wavemeter was connected to the digital I/O port of the LPS-11, and the laser frequency (in BCD code) from the wavemeter converted to base-10 number, as displayed on the wavemeter LEDs. However, the wavemeter frequency-updating rate (every 1.6 sec) was too slow for our data-collection rate (every 0.5 sec). The result was inadequate resolution along the frequency co-ordinate. This problem was solved by using a 5-point data-smoothing routine to smooth the frequency co-ordinate. This was justified because the dye laser itself was stable to 40 MHz, whereas the wavemeter had a resolution of only 300 MHz.

All calculations, including generation of theoretical profiles and least-squares fitting of experimental profiles, were done by using a minicomputer (Digital Equipment Corp., Maynard, MA, PDP 11/45) with a floating-point processor. The computer determined the base-line of the experimental profile. Then an adjusted base-line was determined. Finally, the whole profile was normalized with respect to area. For experimental profiles with noisy background, 5–21 point third-degree polynomial smoothing routines were available to reduce the noise level without substantially degrading the spectral resolution. For fitting at the lowest concentration of 1.6 ppm, only the region from 17289.6 to 17289.8 cm^{-1} (Fig. 2) was used, to avoid excessive contributions from base-line instability.

RESULTS AND DISCUSSION

Abundance analysis

By use of equation (7), the six relative hyperfine-component strengths K_{FF} for both the ^{63}Cu and ^{65}Cu isotopes are calculated to be $K_{32} = 1.0000$, $K_{21} = 0.3571$, $K_{22} = 0.3571$, $K_{11} = 0.3571$, $K_{12} = 0.0715$ and $K_{01} = 0.1429$. Both isotopes yield the same K_{FF} values since they have the same nuclear angular momentum of $I = 3/2$. From these K_{FF} values, the central frequencies, $\nu_{0,n=1-12}$, are calculated from the signals obtained by using a solid copper cathode in our home-made lamp, operated at 30 mA. The ^{63}Cu - ^{65}Cu isotope shift is found to be $0.067 \pm 0.0005\text{ cm}^{-1}$, which compares well with results reported by other workers.^{24,39-41} The reliability of this isotope-ratio measurement scheme depends largely on how accurately the central frequencies of the hyperfine lines can be determined. To double check our calculated $\nu_{0,n}$ values, we used pure ^{63}Cu and ^{65}Cu isotopes respectively for calculations of $\nu_{0,n=1-6}$ (^{63}Cu) and $\nu_{0,n=1-6}$ (^{65}Cu) separately. These $\nu_{0,n=1-12}$ values agree very well with those determined from a natural-abundance Cu sample. Theoretical profiles generated by using these K_{FF} and $\nu_{0,n}$ values are stored in reference tables in the computer for various values of R and T . A base-line-subtracted, area-normalized and frequency-aligned experimental profile is tested for fit with each theoretical profile in the reference tables. Figure 5 illustrates the goodness of spectral fit of our experimental profile with theoretical profile that yields the least sum of squares of the deviations (SSD). The reliability and accuracy of

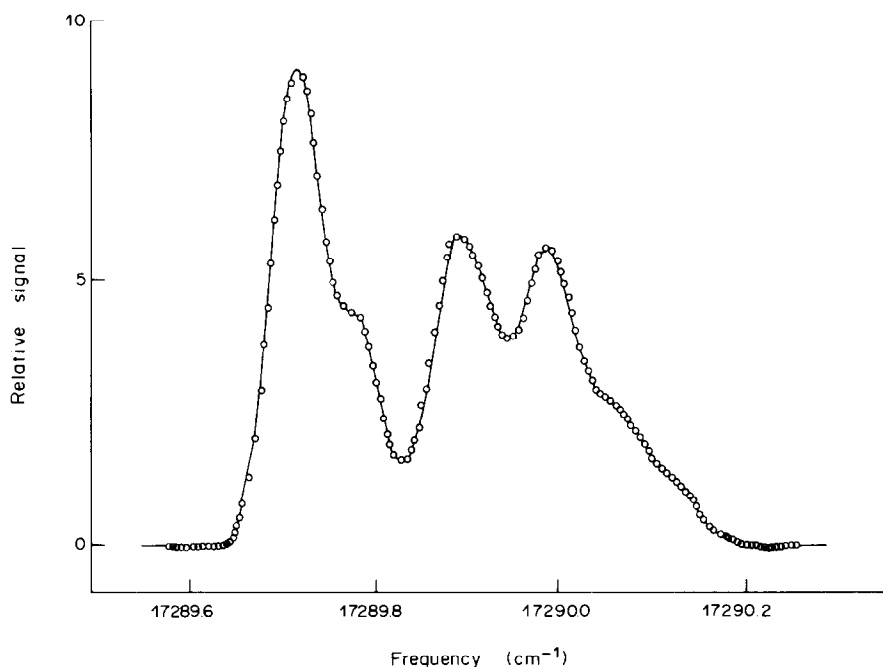


Fig. 5. Fitting of the atomic hyperfine profile. Circles, experimental profile; solid line, theoretical profile.

the ratio calculation depend on the ability of the computer to decide which theoretical profile yields the least SSD. To ensure this, the calculated surface of SSD in the entire range of R and T values should have only a single minimum point, forming a smooth "hole". Figure 6 displays a typical calculated surface of SSD, showing that such a condition is satisfied.

The abundances of ^{63}Cu and ^{65}Cu isotopes are determined by using the demountable cathode lamp with natural-abundance copper and enriched copper isotopes deposited on it. The results are shown in Table 1. The reliability and accuracy of these calculations are tested for some extreme cases, such as calculation for a minor isotope (5% abundance) in the presence of a major isotope (95% abundance). Ratio analysis can be performed successfully in this way for

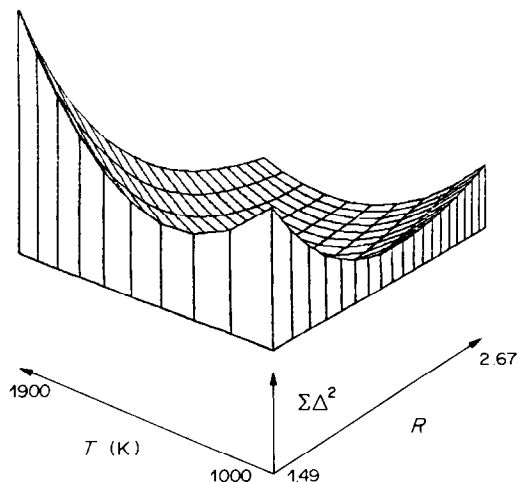


Fig. 6. Calculated surface of the SSD of the fitting.

a copper concentration as low as 1.6 ppm. Table 1 shows that both the accuracy and the precision of the method are in the $\pm 1\%$ range for concentrations at the 50-ppm level or higher. At the 9-ppm concentration level, the precision is about $\pm 2\%$. Below this concentration, the precision is probably not sufficient for practical applications. Although absolute total copper detection is possible at much lower concentration, the accuracy of ratio analysis decreases because of distortion of the hyperfine structure at very weak signal levels. Human blood serum contains 20–50 $\mu\text{g}/\text{ml}$ copper and human urine excretion of copper is 200–500 μg in a 4-hr period. These biological samples provide sufficient amounts of copper for ratio analysis by our scheme. A 3-ml human whole blood sample was analysed, and as expected, the isotopic ratio determined was equal to the natural abundance ratio, since only normal copper is available in diet. This shows that matrix effects are not important in these measurements.

Since most elements have at least one isotope possessing non-zero nuclear angular momentum, unique hyperfine structures for these elements are available for many optical transitions. Thus, the

Table 1. Determination of isotopic abundances

Sample concentration,* ppm	Actual %		Experimental %	
	^{63}Cu	^{65}Cu	^{63}Cu	^{65}Cu
47	69.09	30.91	67.3 ± 1.5	32.7 ± 1.5
9.3	69.09	30.91	69.0 ± 2.2	31.0 ± 2.2
1.6	69.09	30.91	70.1 ± 3.1	29.9 ± 3.1
50	91.0	9.0	91.0 ± 0.3	9.0 ± 0.3
94	95.3	4.7	96.0 ± 1.0	4.0 ± 1.0

*Concentrations refer to sample solution from which copper is deposited onto the nickel cathode.

isotopic-ratio analysis scheme can be applied to all these elements, by using appropriate optical excitation sources. All information necessary to generate theoretical profiles for any element can be readily calculated once the optical transition is known. In fact, copper is probably one of the most difficult cases because of the complexity of the hyperfine structure. For elements with well-resolved isotopic lines, deconvolution is not necessary, and even higher precision can be expected. Application of this scheme is useful not only in biological studies, but also in environmental analysis such as the identification of pollution sources, by use of tracer isotopes. It should also be useful in geochronological studies, including the determination of the source and age of oceanic rock samples, and for isotope dating (e.g., lead-210). It is even applicable for detection of art forgeries by characterization and authentication of paintings, based on the isotopic ratios of an artist's lead pigment.^{42,43}

Stark effect

The hyperfine-component frequencies $\nu_{0,n=1-12}$ for the commercial cathode discharge and the demountable cathode discharge were found to be slightly different, as shown in Table 2. The major contributing factor is the electric field shift, caused by the difference in electric field strengths available for the two discharges. The electric field effect on hyperfine shift was further tested by applying two different electric fields (volts/electrode distance) in the demountable cathode discharge, by modifying the positions of the electrodes. As expected, the higher electric field (348 V/mm) shifted the hyperfine lines toward higher frequencies.

Pressure effects

The pressure effect on hyperfine-component frequencies was also tested for the useful range of gas pressures in the discharge. The discharge can be operated from about 2.5 to 7 mmHg neon pressure without sacrificing the stability or intensity of the optogalvanic signal. Hyperfine structures measured

at different neon pressures (2.6 and 7.1 mmHg) were compared, and no significant difference was observed. Therefore, the discharge can be operated over a reasonably wide range of useful gas pressures, without affecting the hyperfine frequencies.

Conclusions

We have demonstrated a novel method for determining isotopic ratios in complex samples. It benefits from many advantages of optogalvanic spectroscopy. The advantages of using a discharge as the atomizer include narrower Doppler width and negligible Lorentzian broadening, because of the lower temperature and pressure of the plasma, compared to, for example, those of an analytical flame. Because of the high electron-sputtering energy, the discharge provides higher collisional excitation. Although analytical flames provide a more convenient way of analyte introduction, the simple electro-deposition step used for preparing the discharge tube is an effective procedure for concentration of the analyte from very dilute solution. This scheme yields the ratios of all isotopes present, with a single sweep of the laser frequency and within a few seconds of calculation time. This is more efficient than some mass-spectrometric methods where the peak-match unit has to be switched between the exact masses of the isotopes of interest. Also, the instrumentation is less expensive than mass spectrometers with a comparable resolving power. Finally, this scheme is extremely selective and interference-free, because each hyperfine structure has its own unique shape, within a narrow range of frequency. Since both resonance and non-resonance optogalvanic effects can be readily observed, plenty of transition lines are available, from which to choose an excitation wavelength where spectral interference is minimal. If needed, sensitivity and selectivity can be further enhanced by utilizing multiphoton optogalvanic methods.

Acknowledgements—W.G.T. thanks Dr. David A. Lewis for some valuable discussions in the theoretical calculations. The Ames Laboratory is operated by the U.S. Department of Energy by Iowa State University under Contract No. W-7405-eng-82. This work was supported by the Office of Basic Energy Sciences.

Table 2. Electrical field effect in demountable discharge tube

Frequency*	Commercial cathode	Demountable cathode	
		14 V/mm	348 V/mm
$\nu_{0,1}$	17289.724	17289.720	17289.729
$\nu_{0,2}$	17289.791	17289.789	17289.798
$\nu_{0,3}$	17289.882	17289.885	17289.889
$\nu_{0,4}$	17289.915	17289.917	17289.921
$\nu_{0,5}$	17289.959	17289.960	17289.964
$\nu_{0,6}$	17289.995	17289.995	17289.999
$\nu_{0,7}$	17290.000	17289.997	17290.001
$\nu_{0,8}$	17290.029	17290.020	17290.029
$\nu_{0,9}$	17290.057	17290.057	17290.066
$\nu_{0,10}$	17290.082	17290.075	17290.079
$\nu_{0,11}$	17290.116	17290.121	17290.130
$\nu_{0,12}$	17290.143	17290.140	17290.149

*Values in cm^{-1} .

REFERENCES

1. D. L. Hachey, J. C. Blais and P. D. Klein, *Anal. Chem.*, 1980, **52**, 1131.
2. R. Kowantzki, F. Peters, G. H. Reil and G. Haas, *Biomed. Mass. Spectrom.*, 1980, **7**, 540.
3. A. L. Yergey, N. E. Vieira and J. W. Hansen, *Anal. Chem.*, 1980, **52**, 1811.
4. W. D. Lehmann and H. Kessler, *Stable Isotopes*, Elsevier, Amsterdam, 1982.
5. R. S. Houk and J. J. Thompson, *Biomed. Mass Spectrom.*, 1983, **10**, 107.
6. D. J. Douglas, E. S. K. Quan and R. G. Smith, *Spectrochim. Acta*, 1983, **38B**, 39.
7. D. L. Smith, *Anal. Chem.*, 1983, **55**, 2391.

8. W. T. Buckley, S. N. Huckin, J. J. Budac and G. K. Elgendorf, *ibid.*, 1982, **54**, 504.
9. B. R. Harvey, *ibid.*, 1978, **50**, 1866.
10. A. Steudel, *Z. Physik*, 1952, **132**, 429.
11. K. Murakawa, *J. Phys. Soc. Japan*, 1953, **8**, 382.
12. *Idem*, *ibid.*, 1954, **9**, 876.
13. D. N. Stacey, *Proc. Roy. Soc.*, 1964, **280A**, 439.
14. D. J. Schroeder and J. E. Mack, *Phys. Rev.*, 1961, **121**, 1726.
15. R. P. Edwin and W. H. King, *J. Phys. B*, 1969, **2**, 260.
16. G. L. Epstein and S. P. Davis, *Phys. Rev. A*, 1971, **4**, 464.
17. W. H. King, A. Steudel and M. Wilson, *Z. Physik*, 1973, **265**, 207.
18. E. L. Lewis, *Am. J. Phys.*, 1977, **45**, 38.
19. T. E. Manning, C. E. Anderson and W. W. Watson, *Phys. Rev.*, 1950, **78**, 417.
20. G. F. Hately and T. A. Littlefield, *J. Opt. Soc. Am.*, 1958, **48**, 851.
21. F. A. Moscatelli, O. Redi, P. Schonberger, H. H. Stroke and R. L. Wiggins, *ibid.*, 1982, **72**, 918.
22. M. F. Crawford, F. M. Kelly, A. L. Schawlow and W. M. Gray, *Phys. Rev.*, 1949, **76**, 1527.
23. M. Gustafsson, I. Lindgren, J. Lindgren, A. Rosen and H. Rubinsztein, *Phys. Lett.*, 1977, **72B**, 166.
24. D. C. Gerstenberger, E. L. Latush and G. J. Collins, *Opt. Comm.*, 1979, **31**, 28.
25. C. W. P. Palmer, P. E. G. Baird, J. L. Nicol, D. N. Stacey and G. K. Woodgate, *J. Phys. B*, 1982, **15**, 993.
26. R. C. Thompson, A. Hanser, K. Bekk, G. Meisel and D. Frolich, *Z. Physik A*, 1982, **305**, 89.
27. C.-J. Lorenzen and K. Niemax, *J. Phys. B*, 1982, **15**, L139.
28. G. M. Hieftje, J. C. Travis and F. E. Lytle (eds.), *Lasers in Chemical Analysis*, Chapter 5, pp. 93–124. Humana Press, Clifton, NJ, 1981.
29. R. B. Green, R. A. Keller, G. C. Luther, P. K. Schenck and J. C. Travis, *J. Am. Chem. Soc.*, 1976, **98**, 8517.
30. G. C. Turk, J. C. Travis, J. R. DeVoe and T. C. O'Haver, *Anal. Chem.*, 1978, **50**, 817.
31. N. J. Dovichi, D. S. Moore and R. A. Keller, *Appl. Opt.*, 1982, **21**, 1468.
32. G. J. Beenen and E. H. Piepmeier, *Anal. Chem.*, 1981, **53**, 239.
33. E. F. Zalewski, R. A. Keller and R. Engleman, Jr., *J. Chem. Phys.*, 1979, **70**, 1015.
34. C. R. Webster and R. T. Menzies, *ibid.*, 1983, **78**, 2121.
35. D. R. Lyons, A. L. Schawlow and G.-Y. Yan, *Optics Comm.*, 1981, **38**, 35.
36. A. Siegel, J. E. Lawler, B. Couillaud and T. W. Hansch, *Phys. Rev. A*, 1981, **23**, 2457.
37. L. Armstrong, Jr., *Theory of the Hyperfine Structure of Free Atoms*, Chap. 2. Wiley, New York, 1971.
38. M. Weissbluth, *Atoms and Molecules*, p. 159. Academic Press, New York, 1978.
39. R. Ritschl, *Z. Physik*, 1932, **79**, 1.
40. H. Schuler and T. Schmidt, *ibid.*, 1936, **100**, 113.
41. K. Murakawa, *J. Phys. Soc. Japan*, 1956, **11**, 774.
42. B. Keisch and R. C. Callahan, *Archaeometry*, 1976, **18**, 181.
43. S. Fleming, *Physics Today*, 1980, April, 34.

UNTERSUCHUNGEN ZUR ANWENDUNG TERNÄRER KOMPLEXE IN DER PHOTOMETRIE—III

DIE BESTIMMUNG DES TITANIUM(IV) MIT BROMPYROGALLOLROT IN GEGENWART VON NITRILOTRIESSIGSÄURE bzw. ETHYLENEDIAMINTETRAESSIGSÄURE

S. KOCH, G. ACKERMANN und H. MOSLER

Bergakademie Freiberg, Sektion Chemie, Lehrstuhl für Analytische Chemie, 9200 Freiberg,
Deutsche Demokratische Republik

(Eingegangen am 10. Januar 1984. Angenommen am 5. April 1984)

Zusammenfassung—Zur Bewertung ternärer Komplexe in der Photometrie wurden die Modellsysteme (BPR = Brompyrogallolrot) Ti(IV)/BPR (I), Ti(IV)/BPR/EDTE (II) und Ti(IV)/BPR/NTE (III) analytisch charakterisiert. Neben der Ermittlung der Kennzahlen Arbeitsbereich, Extinktionskoeffizient, Standardabweichung, Variationskoeffizient, Eichfunktion, Nachweisgrenze und Erfassungsgrenze erfolgte auch eine Untersuchung der Störung durch 47 Ionen. Es zeigte sich, daß die ternären Systeme—besonders System II—gegenüber dem binären System I eine höhere Selektivität aufweisen.

Zur Bewertung ternärer Komplexe für die photometrische Analyse wurden die Systeme Titanium(IV)/Tiron und Titanium(IV)/Tiron/Aminopolycarbonsäure (APC) umfassend charakterisiert.^{1,2} Die Untersuchungen ergaben, daß für eine Reihe von Störionen das Verfahren selektiver wird, wenn das Titanium als ternärer (Ti/Tiron/APC) und nicht als binärer Komplex (Ti/Tiron) bestimmt wird. Genannte Selektivitätssteigerung ist besonders deutlich bei den Zweitliganden Ethylendiamintetraessigsäure (EDTE) und Nitrilotriessigsäure (NTE), die Empfindlichkeit dieser Reaktionen ist aber gegenüber dem einfachen Tironverfahren geringer. Eine Erhöhung der Empfindlichkeit der Reaktionen dieser ternären Komplextypen mit Tiron ist aus komplexchemischen Gesichtspunkten prinzipiell nicht möglich, so daß man auf einen stark chromophoren Liganden mit Resonanzsystem (Farbstoff) angewiesen ist. Auf Grund der analytisch funktionellen Gruppierung für Titanium(IV)³ ist als chromophorer Ligand Brompyrogallolrot (Dibrompyrogallolsulphophthalein, BPR) geeignet, zumal dieses Reagens mit Titanium(IV)^{4,5} und einer Reihe weiterer Kationen⁶ empfindliche Farbreaktionen gibt. Weiterhin ist die Bildung ternärer Titaniumkomplexe mit BPR in Gegenwart von H₂O₂⁷ sowie NTE⁸ bekannt, so daß folgende Systeme charakterisiert wurden:

System I Ti(IV)/BPR

System II Ti(IV)/BPR/EDTE

System III Ti(IV)/BPR/NTE

System I wurde dabei mit untersucht, um exakte Vergleiche zu den ternären Systemen ziehen zu können.

KOMPLEXBILDUNG IM SYSTEM TITANIUM(IV)/BPR bzw. TITANIUM(IV)/BPR/APC

Titanium(IV) reagiert mit BPR bei pH > 1 zu intensiv violetten Lösungen, welche durch Reaktion mit der *o*-OH-Gruppierung des Farbstoffs entstehen. Die Färbungen bleiben je nach pH auch in Gegenwart von Zweitliganden wie Diethylentriaminpentessigsäure, Ethylendiamintetraessigsäure, Nitrilotriessigsäure, Iminodiessigsäure, Tartrat, Citrat und Oxalat erhalten. Nach Untersuchungen von Suk *et al.*⁴ wird die Reaktion des Titanium(IV) mit BPR analytisch wertvoller, wenn in Gegenwart von Gelatine gearbeitet wird. Die beschriebene Wirkung der Gelatine findet man auch bei anderen Reaktionen von Metallkationen mit Triphenylmethanfarbstoffen, wobei folgende Vorteile bestehen: zeitliche Stabilität der Systeme, bathochrome Verschiebung von $\lambda_{\max}(\text{MeR}_n)$, so daß ein großer Farbkontrast $\Delta\lambda = \lambda_{\max}(\text{MeR}_n) - \lambda_{\max}(\text{R})$ resultiert, hohe Empfindlichkeit der Reaktionen.

Den Gelatineeffekt konnten wir im System Titanium(IV)/BPR auch in Gegenwart von EDTE sowie NTE nachweisen, wobei nur Lösungen mit pH ≤ 3,5 mehrere Stunden stabil sind. Bei allen hier untersuchten Lösungen wurde deshalb zur Stabilisierung Gelatine benutzt. In den Systemen Ti(IV)/BPR/(APC) liegen—wie die Wirkung der Gelatine zeigt—äußerst komplizierte Gleichgewichte in der Lösung vor, so daß ihre komplexchemische Untersuchung deshalb problematisch ist.

Die Charakterisierung der Systeme Titanium(IV)/BPR/APC erfolgte mit Hilfe spektral-photometrischer Methoden. Zum Nachweis ternärer

Komplexe in der Lösung diente die Methode des isobestischen Punktes,⁹ wonach bei

$$E_{\text{iso}}(\text{Ti/BPR/APC}) \neq E_{\text{iso}}(\text{Ti/BPR/BPR})$$

ternäre Komplexe anzunehmen sind. Die Ermittlung der Molarkoeffizienten n für BPR erfolgte nach der Methode der photometrischen Titration mit (C_{Ti} , pH, C_{APC}) = konst. Desweiteren wurde der Koeffizient n nach der Job-Methode für ternäre Komplexe¹⁰ bestimmt. Aus der allgemeinen Job-Gleichung erhält man für $\epsilon_2 = \epsilon_L = 0$:

$$Y = E - \frac{M\epsilon_L V_L d}{V_2}$$

und mögliche Substitutionseffekte können wegen $C_{\text{APC}} \gg C_{\text{Ti}}$ vernachlässigt werden ($\epsilon_2 = \text{Extinktionskoeffizient von } ML_m$; $\epsilon_L = \text{Extinktionskoeffizient von } L$; $Y = \text{von } E \text{ abgeleitete Hilfsfunktion}$; $E = \text{Extinktion}$; $M = \text{Konzentration der Metall-Stammlösung in mole/l}$; $\epsilon_L = \text{Extinktionskoeffizient von } L'$; $V_L = \text{zugesetztes Volumen der Stammlösung } L'$; $d = \text{Schichtdicke in cm}$; $V_2 = \text{Arbeitsvolumen}$).

Zur Beschreibung der einzelnen Gleichgewichte sollen folgende Symbole dienen: H_4R (BPR); H_4Y (EDTE); H_3X (NTE); Ligandenüberschuß p ($p = C_R/C_{\text{Ti}}$); Ligandenüberschuß s ($s = C_{Y(X)}/C_{\text{Ti}}$).

System $Ti(IV)/BPR$

Nach Untersuchungen von Suk *et al.*⁴ liegen bei kleinen Ligandüberschüssen ($p = 4$) in Gegenwart von Gelatine im pH-Bereich 2,2 bis 2,9 Komplexe mit dem Komponentenverhältnis 1:2 bzw. 1:3 vor. Schon die Wellenlängenabhängigkeit des Molarkoeffizienten bei pH 2,2 nach der Methode von Job [$x_{\text{max}} = f(\lambda)$] weist darauf hin, daß kein einheitlicher Reaktionsmechanismus vorliegt. Wie eigene Ergebnisse bei pH 3,5 (photometrische Titration) zeigen, existiert auch unter diesen Bedingungen kein einheitlicher Komplex. Der ermittelte Molarkoeffizient $n(R) = 2,2$ deutet auch Komplexe der Zusammensetzung 1:2 bzw. 1:3 an. Die Funktion $E = f(\text{pH})$ ($C_{\text{Ti}} = 2 \times 10^{-5} M$, $p = 10$) ist im pH-Bereich 2,7 bis 3,5 konstant, so daß bei pH 3,5 eine photometrische Titaniumbestimmung (Verfahren I) möglich ist.

System $Ti(IV)/BPR/EDTE$

Die pH-Kurve ($C_{\text{Ti}} = 2 \times 10^{-5} M$, $p = 10$, $s = 1000$) zeigt im pH-Bereich 3,0 bis 3,8 einen Verlauf $E = f(\text{pH}) = \text{konst.}$ Bei pH 3,5 ($p = 10$, $s = 1000$, $C_{\text{Ti}} = 10^{-5} M$) muß wegen

$$E_{\text{iso}}(\text{T}) > E_{\text{iso}}(\text{B})(\text{R})$$

wo (T) = System (Ti/BPR/APC); (B) = (Ti/BPR); (R) = (BPR) ternäre Komplexbildung angenommen werden. Mit Hilfe der photometrischen Titration ($C_{\text{Ti}} = 2 \times 10^{-5} M$, $s = 1000$, $p = 0-4$) wurde bei pH 3,5 der Molarkoeffizient $n(R) = 2,2$ gefunden. Dieser Wert konnte mit der Job'schen Methode ($C_0 = 10^{-4} M$) bestätigt werden.

Nach den durchgeführten Untersuchungen existiert im System Titanium(IV)/BPR/EDTE in schwach saurer Lösung ein ternärer Komplex in Gegenwart binärer Titanium-BPR-Komplexe. Im pH-Bereich 3,0 bis 3,8 sind die optischen Eigenschaften des Systems nahezu pH-unabhängig, so daß es deshalb zur photometrischen Titaniumbestimmung (Verfahren II) geeignet ist.

System $Ti(IV)/BPR/NTE$

Für die pH-Kurve ($C_{\text{Ti}} = 2 \times 10^{-5} M$, $p = 10$, $s = 1000$) gilt im pH-Bereich 3,1 bis 3,6 $E = f(\text{pH}) = \text{konst.}$ Bei pH 3,5 ($p = 10$, $s = 1000$, $C_{\text{Ti}} = 10^{-5} M$) liegt wegen

$$E_{\text{iso}}(\text{T}) > E_{\text{iso}}(\text{B})(\text{R})$$

ternäre Komplexbildung vor. Die photometrische Titration ($C_{\text{Ti}} = 2 \times 10^{-5} M$, $s = 1000$, $p = 0-4$) ergab bei pH 3,5 einen Molarkoeffizient von $n(R) = 2,5$, welcher auch nach der Methode von Job ($C_0 = 10^{-4} M$) bestätigt wurde.

Auch im System Titanium(IV)/BPR/NTE liegt ein ternärer Komplex im Gleichgewicht mit binären Titanium-BPR-Komplexen vor. Auf Grund der optischen Eigenschaften ist das ternäre System bei pH 3,5 ebenfalls zur photometrischen Titaniumbestimmung (Verfahren III) geeignet.

EXPERIMENTELLER TEIL

Für die photometrischen Messungen dienten die Geräte VSU 2 und Specord UV-VIS des VEB Carl Zeiss Jena. Zur Kontrolle der pH-Werte kamen die Geräte MV 85 (VEB Präcitronek Dresden) sowie TM 5 (Forschungsinstitut Meinsberg) zum Einsatz.

Reagenzien

EDTE, NTE (VEB Berlin-Chemie). BPR (Ferak, 24 Stunden bei 100° getrocknet). Gelatine (DAB 7, VEB Laborchemie Apolda).

Komplexchemische Untersuchungen

Bei der Herstellung der Lösungen wurde nach folgender Variante gearbeitet: Ti, APC, BPR, pH \approx 2, Gelatine (2 ml 1%ig), pH. Die Messungen erfolgten bei 620 nm nach 1 Stunde gegen Wasser bzw. eine Vergleichsprobe (BPR). Zur Herstellung der verwendeten Ti-Stammlösung gingen wir von einer bereits beschriebenen Vorschrift¹¹ aus.

Analytische Untersuchungen

Ti-Stammlösung. Es wurde 1,6681 g TiO_2 mit der 8-fachen Menge $K_2S_2O_7$ aufgeschlossen, die erkaltete Schmelze in 2M Schwefelsäure gelöst und damit auf 1 Liter aufgefüllt (Ti Gehalt: 1 mg/ml). Aus der Stammlösung wird eine Lösung hergestellt, welche 0,1M an Schwefelsäure ist (Ti Gehalt: 5 μ g/ml).

Alkalische EDTE(NTE)-Lösung. Zu einer 0,2M EDTE (NTE)-Lösung gibt man soviel Natriumhydroxid, daß sich beim Hinzufügen von 5 ml dieser Lösung zu 15 ml 0,1M Schwefelsäure ein pH-Wert von etwa 2,5 einstellt.

Forniatpuffer. Es wurde 45 ml 85%ige Ameisensäure sowie 15 g Natriumhydroxid auf 1 Liter aufgefüllt und der pH-Wert auf 3,5 eingestellt. Die so erhaltene Pufferlösung ist etwa 1M.

Stammlösungen der Störelimente. Die verwendeten Störlösungen (5 mg/100 ml) wurden weitgehend nach Koch und Koch-Dedic¹² hergestellt, wobei als Säure 0,2M Schwefelsäure bevorzugt wurde.

Arbeitsvorschriften

Verfahren I. Zur schwefelsauren Probelösung (etwa 0,1M an Schwefelsäure) gibt man soviel 0,1M Schwefelsäure hinzu, daß insgesamt 15 ml Lösung vorliegen. Die Lösung wird mit 10 ml $10^{-3}M$ BPR-Lösung und danach mit 2 ml 1% ige Gelatinelösung versetzt. Mit 1M Natriumhydroxid stellt man den pH-Wert von 3,5 ein, fügt 5 ml Formiatpuffer dazu und füllt mit Wasser auf 50 ml auf. Die Proben werden nach 20 Minuten bei 615 nm in 1-cm Küvetten gegen eine Blindprobe gemessen.

Verfahren II. Zur schwefelsauren Probelösung (etwa 0,1M an Schwefelsäure) gibt man soviel 0,1M Schwefelsäure hinzu, daß insgesamt 15 ml Lösung vorliegen. Die Lösung wird mit 5 ml alkalischer 0,2M EDTE-Lösung, 10 ml $10^{-3}M$ BPR-Lösung und danach mit 2 ml 1%ige Gelatinelösung versetzt. Mit 1M Natriumhydroxid stellt man den pH-Wert von 3,5 ein, fügt 5 ml Formiatpuffer zu und füllt mit Wasser auf 50 ml auf. Die Proben werden nach 30 Minuten bei 610 nm in 1-cm Küvetten gegen eine Blindprobe gemessen.

Verfahren III. Die Proben werden wie bei Verfahren II hergestellt, nur daß an Stelle von EDTE eine alkalische 0,2M NTE-Lösung Verwendung findet. Nach 20 Minuten werden die Proben bei 610 nm ebenfalls gegen eine entsprechende Blindprobe gemessen.

DISKUSSION

Vergleichende Charakterisierung der Verfahren

Zur vergleichenden Charakterisierung der einzelnen Verfahren machte sich eine statistische Kennzeichnung der Systeme I, II und III notwendig, wobei nach den schon beschriebenen Prinzipien¹ vorgegangen wurde. Die Berechnung der scheinbaren Extinktionskoeffizienten sowie der Standardabweichungen (mit $f = 20$ Freiheitsgraden) erfolgte für 25 μg Titanium. Bei der Berechnung der Eichfunktionen mit Hilfe der Regressionsrechnung (mit $f = 8$ Freiheitsgraden und $P = 0,99$) wurde von $y = bx + a$ ausgegangen. In Tabelle 1 sind die erhaltenen Daten zusammengestellt.

Die zur Kennzeichnung der Selektivität ermittelten Grenzverhältnisse g (bis maximal $g = 1000$) für 25 μg Titanium sind in Tabelle 2 enthalten. Das Grenzverhältnis ist nach

$$g = \frac{C_{\text{Störion}}}{C_{\text{Ti}}}$$

definiert und stellt ein Verhältnis dar, bis zu welchem keine Störung vorliegt. Die Ermittlung von g erfolgte wie bereits beschrieben durch lineare Extrapolation¹ unter Berücksichtigung von $3s$ -Schranken für den Grundwert. Durch Untersuchung der Einflüsse von Natriumchlorid, Natriumnitrat sowie Natriumsulfat konnten eventuelle Störungen dieser Salze (Metall-Stammlösungen) ausgeschlossen werden.

Ein Vergleich der ermittelten Kennzahlen von Verfahren I (Ti/BPR), II (Ti/BPR/EDTE) und III (Ti/BPR/NTE) in Tabelle 1 zeigt, daß die Aminopolycarbonsäuren die analytischen Eigenschaften der Systeme beeinflussen. Die Extinktionskoeffizienten bzw. Eichfunktionen weisen auf empfindliche Verfahren hin, wobei die Empfindlichkeit von Verfahren II und III gegenüber Verfahren I etwas größer ist. Der genannte Effekt läßt sich mit der Unterdrückung

Tabelle 1. Statistische Kennzeichnung von Brompyrogallolrot-Verfahren zur photometrischen Titaniumbestimmung

Kennzahl	Verfahren		
	I	II	III
Arbeitsbereich, μg	5-55	4-55	4-55
ϵ' , l. mole ⁻¹ . cm ⁻¹	$(3,50 \pm 0,01) \times 10^4$	$(3,912 \pm 0,005) \times 10^4$	$(3,620 \pm 0,009) \times 10^4$
ϵ'' , ml. μg^{-1} . cm ⁻¹	$0,732 \pm 0,002$	$0,817 \pm 0,001$	$0,756 \pm 0,002$
Standardabweichung, μg	0,4	0,2	0,3
Variationskoeffizient, %	1,54	0,61	1,08
Eichfunktion, $C_T \mu g/ml$	$E = (0,75 \pm 0,04)c - (0,01 \pm 0,03)$	$E = (0,82 \pm 0,01)c - (0,004 \pm 0,006)$	$E = (0,75 \pm 0,04)c + (0,00 \pm 0,02)$
Nachweisgrenze, μg	2,2	1,2	1,0
Erfassungsgrenze, μg	3,0	1,8	1,7

von Hydrolysereaktionen des Titanium(IV) durch die APC erklären, und wegen der höheren Zähnnigkeit der EDTE gegenüber NTE ist die Empfindlichkeitssteigerung bei Verfahren II besonders deutlich. Auf Grund der wenig unterschiedlichen Empfindlichkeiten aller drei Verfahren ergeben sich auch nur unwesentliche Abweichungen in Arbeitsbereich, Nachweisgrenze sowie Erfassungsgrenze.

Wie aus der Analyse der Variationskoeffizienten (F -Test, $\bar{P} = 0,99$, $f = 20$ Freiheitsgrade) folgt, besteht ein signifikanter Unterschied zwischen den Zufallsfehlern der Verfahren I/II bzw. II/III. Besonders auffällig ist der niedrige Variationskoeffizient (0,6%) für Verfahren II, d.h. unkontrollierbare Nebenreaktionen des Titanium(IV) werden besonders wirksam durch EDTE unterdrückt.

Tabelle 2. Störungen bei Brompyrogallolrot-Verfahren zur photometrischen Titaniumbestimmung

Störion	Verbindung	Störion-Lösung	Grenzverhältnis, g		
			Verf. I	Verf. II	Verf. III
Ag(I)	AgNO ₃	0,2M H ₂ SO ₄	50	90	40
Al(III)	AlCl ₃ ·6H ₂ O	0,2M H ₂ SO ₄	0,1	5	1
As(III)	As ₂ O ₃	0,2M H ₂ SO ₄	540	1000	830
Au(III)	AuCl ₃	0,5M HCl	2,8↓	0,2↓	12↓
Ba(II)	BaCl ₂ ·2H ₂ O	0,1M HCl	25	4	4
Be(II)	BeSO ₄ ·4H ₂ O	0,2M H ₂ SO ₄	16	140	100
Bi(III)	Bi(NO ₃) ₃ ·5H ₂ O	1M HNO ₃	0,5	260	9
Ca(II)	CaCl ₂ ·6H ₂ O	0,1M HCl	25↓	1000	1000
Cd(II)	CdCl ₂ ·2H ₂ O	0,2M H ₂ SO ₄	590	1000	1000
Ce(III)	Ce(SO ₄) ₃ ·8H ₂ O	0,2M H ₂ SO ₄	3,4	1000	230
Co(II)	Co(NO ₃) ₂ ·6H ₂ O	0,2M H ₂ SO ₄	20↓	860	240
Cr(III)	Cr ₂ (SO ₄) ₃ ·18H ₂ O	0,2M H ₂ SO ₄	23	90	25
Cs(I)	CsCl	0,2M H ₂ SO ₄	1000	1000	1000
Cu(II)	CuSO ₄ ·5H ₂ O	0,2M H ₂ SO ₄	0,6	55	65
Fe(III)	Fe(NO ₃) ₃ ·9H ₂ O	0,2M H ₂ SO ₄	0,1	26	0,1
Ga(III)	Ga	0,1M HCl	0,2	85	0,3
		0,1M HNO ₃			
Ge(IV)	GeO ₂	Aufschluß mit K ₂ CO ₃	0,2	0,3	0,3
Hg(II)	HgCl ₂	0,2M H ₂ SO ₄	100	1000	1000
In(III)	In	0,1M HCl	0,3	1000	40
		0,1M HNO ₃			
Ir(IV)	Na ₂ IrCl ₆	1M HCl	5↓	0,8↓	7,5↓
K(I)	KCl	0,2M H ₂ SO ₄	1000	1000	1000
La(III)	LaCl ₃ ·7H ₂ O	0,2M H ₂ SO ₄	7	1000	640
Li(I)	Li ₂ SO ₄ ·H ₂ O	0,2M H ₂ SO ₄	1000	1000	1000
Mg(II)	MgSO ₄ ·7H ₂ O	0,2M H ₂ SO ₄	1000	1000	1000
Mn(II)	MnCl ₂ ·4H ₂ O	0,2M H ₂ SO ₄	1,9↓	130↓	13↓
Mo(VI)	Na ₂ MoO ₄ ·2H ₂ O	0,2M H ₂ SO ₄	0,2	0,2	0,2
Na(I)	NaCl	0,2M H ₂ SO ₄	1000	1000	1000
Nb(V)	Nb ₂ O ₅	Aufschluß mit K ₂ CO ₃	0,2	0,3	0,4
Ni(II)	NiSO ₄ ·6H ₂ O	0,2M H ₂ SO ₄	400↓	200	190
Pb(II)	Pb(NO ₃) ₂	0,1M HNO ₃	16	1000	1000
Pd(II)	PdCl ₂	1M HCl	0,4	550↓	23
Pt(IV)	H ₂ PtCl ₆	H ₂ O	11↓	75↓	50↓
Rb(I)	RbCl	0,2M H ₂ SO ₄	1000	1000	1000
Rh(III)	Na ₃ RhCl ₆	H ₂ O	360	780	260
Sb(III)	SbCl ₃	6M HCl	0,4	1,6	0,8
Se(IV)	SeO ₂	0,2M H ₂ SO ₄	1000	1000	1000
Sn(II)	SnCl ₂ ·2H ₂ O	1M HCl	0,5	0,8	0,7
Sr(II)	SrCl ₂ ·6H ₂ O	0,1M HCl	40↓	440	130
Ta(V)	Ta ₂ O ₅	Aufschluß mit K ₂ CO ₃	4,7	1,2	3,5
Te(IV)	Te	4M HCl	2,5	3,2	2,1
		2M HNO ₃			
Th(IV)	Th(NO ₃) ₄	0,2M H ₂ SO ₄	0,5	14	50
Tl(I)	TlNO ₃	0,2M H ₂ SO ₄	1000	1000	1000
U(VI)	UO ₂ (CH ₃ COO) ₂ ·2H ₂ O	0,2M H ₂ SO ₄	0,5	3	0,6
V(V)	NH ₄ VO ₃	1M H ₂ SO ₄	0,1	3,5↓	1,1
W(VI)	Na ₂ WO ₄ ·2H ₂ O	H ₂ O	0,5	0,3	0,3
Zn(II)	ZnSO ₄ ·7H ₂ O	0,2M H ₂ SO ₄	540	1000	1000
Zr(IV)	ZrOCl ₂ ·8H ₂ O	0,2M H ₂ SO ₄	0,3	0,6	1,2

Wenn die Anwesenheit eines Störions zur Erniedrigung der Extinktion führte, wurde dies mit ↓ gekennzeichnet.

Zur Betrachtung der Selektivität können die ermittelten Grenzverhältnisse in Tabelle 2 herangezogen werden. Die angegebenen g -Werte zeigen, daß durch den Einsatz ternärer Systeme für 33 von 47 Ionen die Störungen herabgesetzt sind. Der nach

$$S = \frac{\sum_{i=1}^n g_i}{n} \quad (n \text{ Anzahl der Störionen})$$

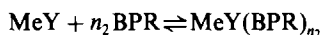
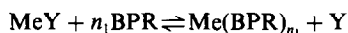
definierte Selektivitätskoeffizient S hat wegen seiner eingeschränkten Aussagekraft zwar nur formale Bedeutung, macht aber die Selektivitätserhöhung bei den Verfahren II und III besonders deutlich. Die Stör-elemente Cs, K, Li, Mg, Na, Rb, Se, Tl gehen dabei nicht mit ein, da in allen drei Systemen praktisch keine Störungen ($g = 1000$) vorliegen.

$$S_I = 72$$

$$S_{II} = 329 \quad (n = 39)$$

$$S_{III} = 204$$

Wie man sieht, existieren deutliche Vorteile bei der Anwendung von EDTE (Verfahren II) gegenüber NTE (Verfahren III). Die Ursache dafür liegt ganz allgemein in der hohen Stabilität von EDTE-Störion-Chelaten sowie der weitgehenden Absättigung von Koordinationsstellen dieser Ionen durch den sechszähligen Liganden, so daß die Bildung von binären bzw. ternären BPR-Chelaten



erschwert ist.

Eine Ausnahme dazu bilden die Ionen der Elemente Au, Cu, Ir, Nb, Ta, Th, Zr, wo die Störungen mit NTE (Verfahren III) geringer sind. Während bei Nb, Ta, Th, Zr auf Grund ihrer hohen Koordinationszahlen ($Z = 8$) die entsprechenden EDTE-Komplexe (1:1) den zweizähligen Ligand BPR unter Bildung ternärer Species noch anlagern können, ist die Koordinationssphäre dieser Kationen bei den NTE-Komplexen (1:2) wegen der Vierzähligkeit von NTE abgesättigt, und es resultiert eine geringere Störung mit NTE gegenüber EDTE. Im Falle von Au und Ir handelt es sich offensichtlich um eine oxydative Zerstörung von BPR, welche möglicherweise durch Stabilisierung von (Au, Ir)-Zwischenstufen in Gegenwart von EDTE begünstigt wird. Bei Cu schließlich besteht ein Vorteil für NTE, weil die Eigenfärbung des Chelates CuX^- weniger intensiv ist als die von CuY^{2-} .

Es konnte bereits mit Hilfe der Selektivitätskoeffizienten gezeigt werden, daß das Verfahren II selektiver als Verfahren III ist. Im weiteren soll deshalb einiges zur Selektivität des Verfahrens II gegenüber Verfahren I (binäres System) herausgestellt werden.

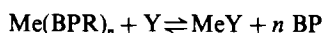
Für folgende Ionen tritt durch EDTE eine starke Verbesserung der Selektivität ($g_{II}/g_I \geq 10$) auf: Al(50),

Bi(520), Ca(40), Ce(290), Co(40), Cu(90), Fe(260), Ga(420), Hg(10), In(3300), La(140), Mn(70), Pb(60), Pd(1400), Sr(10), Th(30), V(40). In Klammern sind dabei die gerundeten Quotienten g_{II}/g_I angegeben. Eine schwache Verbesserung der Selektivität ($10 > g_{II}/g_I > 1$) ist bei den Elementen Ag(2), As(2), Be(9), Cd(2), Cr(4), Ge(2), Nb(2), Pt(7), Rh(2), Sb(4), Sn(2), U(6), Zn(2), Zr(2) zu finden.

Bei folgenden Ionen ist keine Verbesserung ($g_{II}/g_I = 1$) zu beobachten: Cs, K, Li, Mg, Mo, Na, Rb, Se, Te, Tl.

Dagegen konnte eine Verschlechterung der Selektivität ($g_{II}/g_I < 1$) bei den Elementen Au(0,1), Ba(0,2), Ir(0,2), Ni(0,5), Ta(0,3), W(0,6) nachgewiesen werden.

Die in dem System Titanium(IV)/BPR/EDTE gefundene Erhöhung der Selektivität gegenüber dem System Titanium(IV)/BPR für eine große Zahl von Störionen wird naturgemäß von den Stabilitätsverhältnissen Me-EDTE und Me-BPR unter vorliegenden Reaktionsbedingungen bestimmt. In Abhängigkeit dieser Stabilitätsverhältnisse ist die Lage der entsprechenden Gleichgewichte schematisch



$$[\epsilon(\text{Me}(\text{BPR})_n) \gg \epsilon(\text{MeY})]$$

im Zusammenhang mit dem Extinktionskoeffizienten entscheidend für den Grad der Selektivitätserhöhung. Bei den Ionen mit $g_{II}/g_I = 1$ existieren in Lösung keine bzw. nur wenig stabile EDTE-Chelate, eine Verbesserung der Selektivität tritt hier deshalb nicht ein. Die Unterdrückung der Störungen bei Ca^{2+} , Pb^{2+} und Sr^{2+} mit EDTE beruht darauf, daß die im System Ti/BPR auftretenden schwer löslichen Sulfate durch die Aminopolycarbonsäure vollständig bzw. teilweise aufgelöst werden. Wie die Werte $g_{II}/g_I < 1$ zeigen, existieren auch einige wenige Fälle, wo die Anwesenheit von EDTE eine Verschlechterung der Selektivität mit sich bringt. Als Ursachen dafür kommen Redox-Reaktionen (Au, Ir/BPR), Fällungsreaktionen (Ba/SO_4), Eigenabsorption (Ni/Y) sowie Hilfskomplexbildnerwirkung (Ta, W/Y) in Frage.

REFERENCES

1. S. Koch, G. Ackermann und G. Winkler, *Talanta*, 1979, **26**, 821.
2. S. Koch, G. Ackermann und V. Scholze, *ibid.*, 1981, **28**, 915.
3. L. Sommer, *ibid.*, 1962, **9**, 439.
4. V. Suk, I. Němcová und M. Malát, *Collection Czech. Chem. Commun.*, 1965, **30**, 2538.
5. L. I. Ganago und L. A. Zharnovskaya, *Zh. Analit. Khim.*, 1973, **28**, 933.
6. A. Jeničková, V. Suk und M. Malát, *Collection Czech. Chem. Commun.*, 1956, **21**, 1257.
7. E. Lassner und R. Püschel, *Mikrochim. Acta*, 1964, 753.
8. S. Koch, G. Ackermann und V. Kubáň, *Z. Chem.*, 1978, **18**, 191.
9. S. Koch und G. Ackermann, *Chem. Anal. (Warsaw)*, 1983, **28**, 427.
10. *Idem, ibid.*, 1974, **19**, 23.

11. *Idem*, *Z. Anorg. Allg. Chem.*, 1981, **473**, 231. *Spurenanalyse*, Teil 2, S. 1511. Springer Verlag, Berlin.
12. O. G. Koch und G. A. Koch-Dedic, *Handbuch der* 1974.

Summary—As part of a continued investigation of the analytical applications of ternary complexes, the systems Ti(IV)/BPR, (I), Ti(IV)/BPR/EDTA (II), and Ti(IV)/BPR/NTA (III), where BPR = Bromopyrogallol Red, have been investigated and compared in terms of working concentration range, molar absorptivity, standard deviation, coefficient of variation, calibration sensitivity, limit of detection and of determination. A novel way of summarizing the effects of interferences of a large group of ions (some 47 in all) is presented. The results show that the ternary systems, in particular system II, have a better selectivity than the simple binary system I of titanium with Bromopyrogallol Red.

SPECTROPHOTOMETRIC DETERMINATION OF CYANIDE BY UNSEGMENTED FLOW METHODS

A. RIOS, M. D. LUQUE DE CASTRO and M. VALCARCEL

Department of Analytical Chemistry, Faculty of Sciences, University of Córdoba, Córdoba, Spain

(Received 31 December 1983. Accepted 5 April 1984)

Summary—Photometric methods for cyanide determination by normal and reversed FIA techniques and by completely continuous monitoring are proposed. The sampling rates for the first two techniques are 20 and 28/hr, respectively, the r.s.d. being less than 0.8% in both cases. A simulation of cyanide control in industrial waste waters shows the usefulness of the continuous monitoring method.

The toxicity of cyanide has long made necessary its determination in a great variety of samples, and fast methods for continuous or non-continuous monitoring are still needed. The unsegmented flow techniques offer a wide range of possible methodologies. Thus flow-injection analysis in its conventional form (nFIA;¹ injection of sample into a continuous flow of the reagent) allows analysis for cyanide with minimum consumption of the sample solution. In cases such as waste-water analysis, where the reagents constitute the major cost of the determination, reversed FIA (rFIA)² is more suitable. In this the reagents are injected into a continuous flow of the sample to be analysed. When possible variations in sample composition necessitate continuous monitoring, an analysis utilizing completely continuous flow³ (continuous recording of the signal produced after the confluence of very small sample and reagent streams) is ideal.

Of these unsegmented flow techniques, only nFIA has previously been used for determination of cyanide. Pihlar *et al.*⁴ have proposed voltammetric determination of cyanide over a wide range of concentrations (from 0.5 $\mu\text{g/l.}$ to 1 g/l.), but there were many interfering species. In a later paper,⁵ many of the interferences were eliminated by prior distillation of the sample and decomposition of possible cyanide complexes by irradiation with ultraviolet light. The only potentiometric determination of cyanide, by Müller,⁶ used a selective Ag_2S electrode, but interferences were not studied. The determination range was 10^{-6} – 10^{-3} M . The only method involving optical detection is the fluorimetric determination by catalysis of the aerial oxidation of pyridoxal or pyridoxal-5-phosphate. The range of determination is similar with the two reagents (0.1–20.0 $\mu\text{g/ml}$). Interferences were eliminated or their tolerance levels increased by use of a stopped-flow technique.⁷

Since the most common detector in a control laboratory is likely to be a colorimeter or spectrophotometer, we considered that a simple, well-

tested classical reaction would be the most convenient to use. We chose a reaction in which a dye is formed by use of chloramine-T, pyridine and barbituric acid.⁸ Three variants are proposed, for analysis of (a) scarce or valuable samples (use of normal FIA), (b) waste waters (use of reversed FIA), (c) a continuous stream (completely continuous method).

EXPERIMENTAL

Reagents

All reagents were of analytical-reagent grade and solutions were prepared with distilled water.

Pyridine–barbituric acid reagent. Place 15 g of barbituric acid in a 250-ml standard flask and add just enough water to wash the sides of the flask and wet the barbituric acid. Add 75 ml of pyridine and mix. Add 15 ml of concentrated hydrochloric acid, mix and cool to room temperature. Dilute to volume with water and mix.

Chloramine-T solution. Dissolve 1.0 g in 100 ml of water.

Sodium dihydrogen phosphate–sodium hydroxide buffer solution. Dissolve 138 g of $\text{NaH}_2\text{PO}_4 \cdot \text{H}_2\text{O}$ and 2 g of sodium hydroxide in 1 litre of distilled water (total phosphate concentration = 1.0M and pH = 6.3).

Cyanide solution. Aqueous potassium cyanide solution containing 1.000 g of cyanide per litre.

Apparatus

A Pye Unicam SP 6-500 spectrophotometer was used as a detector, connected to a Radiometer REC 80 recorder. The accessory instruments were a Beckman pH-meter and a thermostat. A Gilson Minipuls-2 peristaltic pump, a Hellma 178.10 flow-cell (inner volume 18 μl), a Tecator L 100-1 injection valve and a Tecator TM II "chemifold" were used.

Manifolds

Figure 1 shows the various manifolds used and the optimum values of the variables for each method.

NORMAL FIA

In this method (Fig. 1a) the carrier consists of a mixture of chloramine-T solution and buffer into which the sample is injected. In reactor L_1 , CNCl is formed from chloramine-T; the subsequent confluence of the CNCl bolus with a stream of

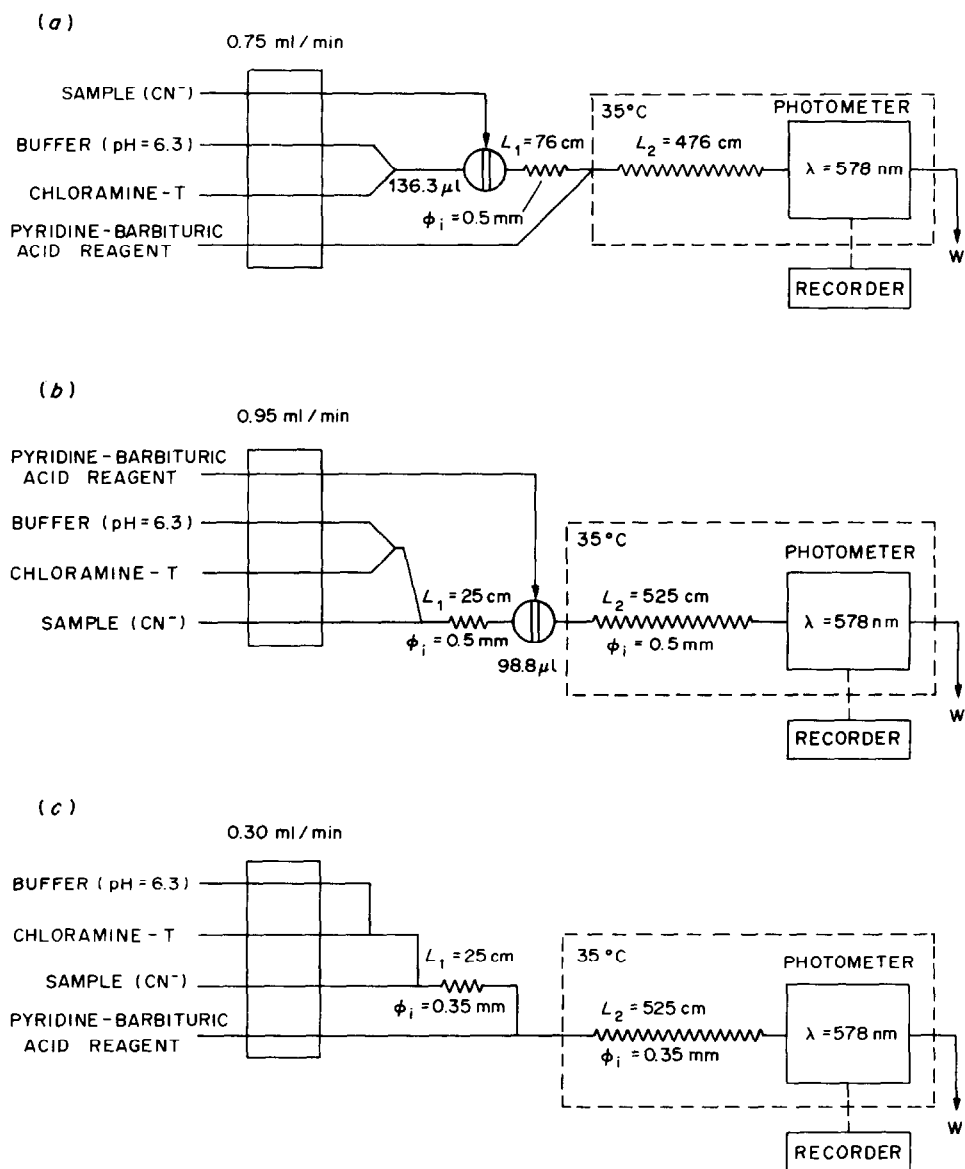


Fig. 1. Manifolds and optimum working conditions for the determination of cyanide by: (a) normal FIA; (b) reversed FIA; (c) completely continuous technique.

pyridine-barbituric acid solution causes the formation in L_2 of the detectable product, which is violet with an absorption maximum at 578 nm.

The FIA variables (flow-rate, length of the reactor sections L_1 and L_2 and volume of the injected sample) were optimized by a modified simplex method.⁹ Later, the influence of the bore of the reactor sections (0.35, 0.50 and 0.70 mm) was studied. There were five initial experiments, then 19 more points in 10 different cycles with 9 reflections, 3 expansions and 3 positive contractions. For each point (in duplicate) the corresponding blank (distilled water) was recorded, because the change in the refractive index¹⁰ between the carrier and the sample caused a small peak which must be subtracted from the sample

signal. The addition of pyridine to the sample solution to equalize the refractive index of the sample and carrier was unsatisfactory. The maximum response (height of the FIA peak) was obtained for the following values of the variables: $q = 0.48$ ml/min; $V_i = 136.3$ μl; $L_1 = 76$ cm; $L_2 = 476$ cm. Some variables had to be limited for operational reasons. Thus, the simplex treatment shows the optimum flow-rate should be about zero, but it must be set at 0.45 ml/min for a reasonably high sampling rate to be obtained (though at the expense of a 10% decrease in the absorbance). The length of reactor L_1 should also be zero, and its minimum value was initially set at 10 cm. Subsequent operations established the practical optimum value as 76 cm.

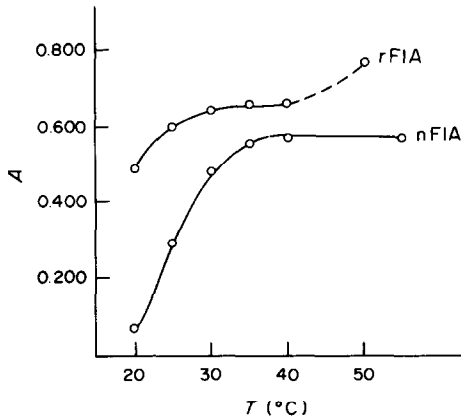


Fig. 2. Effect of temperature in the normal (1 ppm CN^-) and reversed (4 ppm CN^-) techniques.

The optimum values for the FIA variables are logical from the chemical point of view. The flow-rate has to be small because the reaction between CNCl and the pyridine–barbituric acid mixture is slow. For this reason the value of L_2 is also high, although the dispersion requirements limit its value. On the other hand, the length of L_1 is small because CNCl can be hydrolysed to form CNO^- , which does not react to give the coloured compound.

The height of the FIA peak increases with the volume of sample injected, but samples bigger than $136.3 \mu\text{l}$ cause a double peak to appear, because the reaction is incomplete in the central zone of the bolus.

Study of physical and chemical variables

The pH of the carrier and sample solutions was

kept between 6 and 8. More acidic pH values cause loss of cyanide as hydrogen cyanide gas. Values above 8 are not desirable because the reaction between chloramine-T and cyanide is then followed by a fast hydrolysis.

Concentrations of chloramine-T more or less than 1% make the response function decrease slightly. An increase in concentration of the pyridine–barbituric acid mixture improves the response of the system, but at higher concentrations than the one used the barbituric acid does not dissolve completely.

The influence of temperature was studied for the range 20–55° and the results are given in Fig. 2. A sharp rise in the signal is observed between 20 and 40°. A temperature of 35° was chosen as an optimum working temperature; although the signal obtained at 40° is slightly higher, small bubbles are then formed in the reactor.¹¹

Determination of trace levels of cyanide

The absorbance *vs.* concentration calibration graph consists of two distinct segments (Fig. 3a). The equations for these segments are:

$$A = 0.44[\text{CN}^-] - 0.015$$

for $[\text{CN}^-] = 0.1\text{--}0.4 \mu\text{g/ml}$ ($r = 0.992$)

and

$$A = 0.67[\text{CN}^-] - 0.108$$

for $[\text{CN}^-] = 0.4\text{--}1.0 \mu\text{g/ml}$ ($r = 0.998$).

The relative standard deviations calculated from the results for 11 samples of cyanide were 0.8% and 0.5%, respectively. The lower detection limit corresponds to the first segment, although its sensitivity (slope of the straight line) is less than that for the

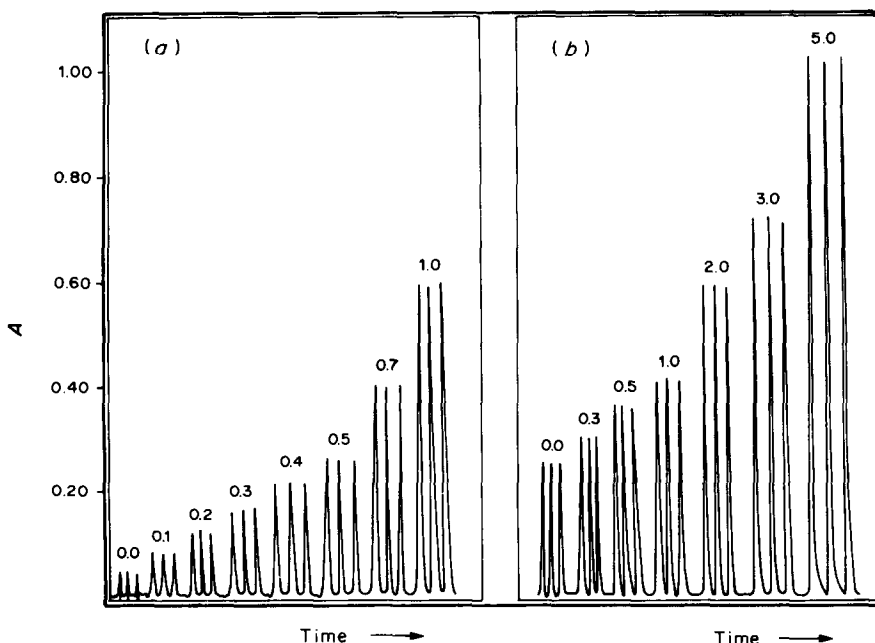


Fig. 3. Calibration runs for determination of cyanide by (a) nFIA and (b) rFIA.

second. The precision in both cases is good. The sampling frequency is about 20/hr.

REVERSED FIA

Here (Fig. 1*b*) the main carrier is the sample solution, mixed before the injection valve with a secondary carrier consisting of a mixture of buffer and chloramine-T. The formation of CNCl occurs in reactor L_1 . Later, this product reacts in L_2 with the pyridine-barbituric acid mixture injected to produce the violet colour.

Study of FIA variables

The flow-rate, lengths of the reactors and injected volume were optimized as before. In this case it is again necessary to subtract from each signal the corresponding blank, and in rFIA the signal produced by the blank is six times the one obtained by normal FIA. This significant increase in the blank signal causes a higher detection limit for cyanide. Addition of pyridine to equalize the refractive indices again does not help. The simplex involved five initial experiments and a total of 18 points in 11 cycles, with 9 reflections, 2 expansions and 2 contractions (one positive and the other negative). The maximum response corresponds to the values: $q = 0.95$ ml/min; $V_1 = 98.9$ μ l; $L_1 = 25$ cm; $L_2 = 525$ cm. Some variables again had to be limited, and the values again can be related to the chemistry. The higher flow-rate used here necessitated a greater length of L_2 to provide the same reaction time. The volume injected (reagent in this case) now has to be smaller to decrease the blank signal. The bore of the reactors has very little influence on the signal, although for a tubing diameter of 0.50 mm the peak is slightly higher.

Study of physical and chemical variables

The influence of the concentration of the reagents is similar to that in nFIA. However the temperature affects the system in different ways, as can be seen in Fig. 2. Between 40 and 50° the signal increases, but this is not analytically useful, because bubbles form along the manifold. The working temperature chosen was therefore again 35°.

Determination of traces of cyanide

The calibration graph is linear for the cyanide range 0.3–5.0 μ g/ml, the equation being

$$A = 0.146[\text{CN}^-] + 0.031 \quad (r = 0.999).$$

Eleven injections of a 2.0 μ g/ml cyanide solution gave a 95% confidence interval of $\pm 0.7\%$. The sampling-rate was 28 samples/hr.

COMPLETELY CONTINUOUS METHOD

The manifold for this (Fig. 1*c*) is similar to that for reversed FIA (Fig. 1*b*), but without an injection

valve. The analyte and reagents flow continuously through the measurement cell and the cyanide concentration is determined without interruption. Thus it is very useful for the control of cyanide in industrial waste waters.

Influence of the variables

Since the manifold is the same as that for rFIA (omitting the injection valve), the same conditions are used, with the advantage now that the blank does not give a signal and only the variation of cyanide concentration with time is recorded.

To reduce consumption of sample and reagent, the flow-rate is restricted to 0.30 ml/min, and the bore of the reactors is 0.35 mm.

Simulation of continuous control of cyanide in waste water

Figure 4*a* shows a calibration run for cyanide in waters. The calibration range is 0.7–4.0 μ g/ml, and the graph is a straight line with the equation:

$$A = 0.30[\text{CN}^-] - 0.19 \quad (r = 0.989).$$

Figure 4*b* shows the results of a simulation of analysis for cyanide in waste waters throughout a working day. The cyanide came from a 2-litre container which initially contained 500 ml of distilled water. Another vessel containing cyanide solution was fixed to this tank. Periodically different volumes of cyanide or distilled water were added to the container in such a way that the cyanide concentration was changed.

COMPARISON OF THE RESULTS

Two sorts of comparison of the results obtained in this work can be made:

- the traditional technique can be compared with the unsegmented-flow techniques;
- the three unsegmented-flow techniques used in this paper can be compared with one another.

The first (a) is summarized in Table 1. The flow techniques have clear advantages over the traditional photometric one (except that the sensitivity and the detection limit are more favourable in the traditional technique).

The second (b) is made in Table 2. The highest sensitivity and lowest detection limit are obtained by nFIA. This finding is at variance with previous observations. Previously the main advantage claimed for rFIA has been higher sensitivity.^{2,12} The relative loss of sensitivity observed in this work may be due to the large increase of the blank signal in the rFIA, which can mask sample peaks at concentrations below 0.3 μ g/ml. An alternative cause is the inability to ensure presence of the excess of reagent necessary for the optimum reaction in rFIA. The detection limit is lower in the FIA methods than in the completely continuous one. nFIA permits determination of cy-

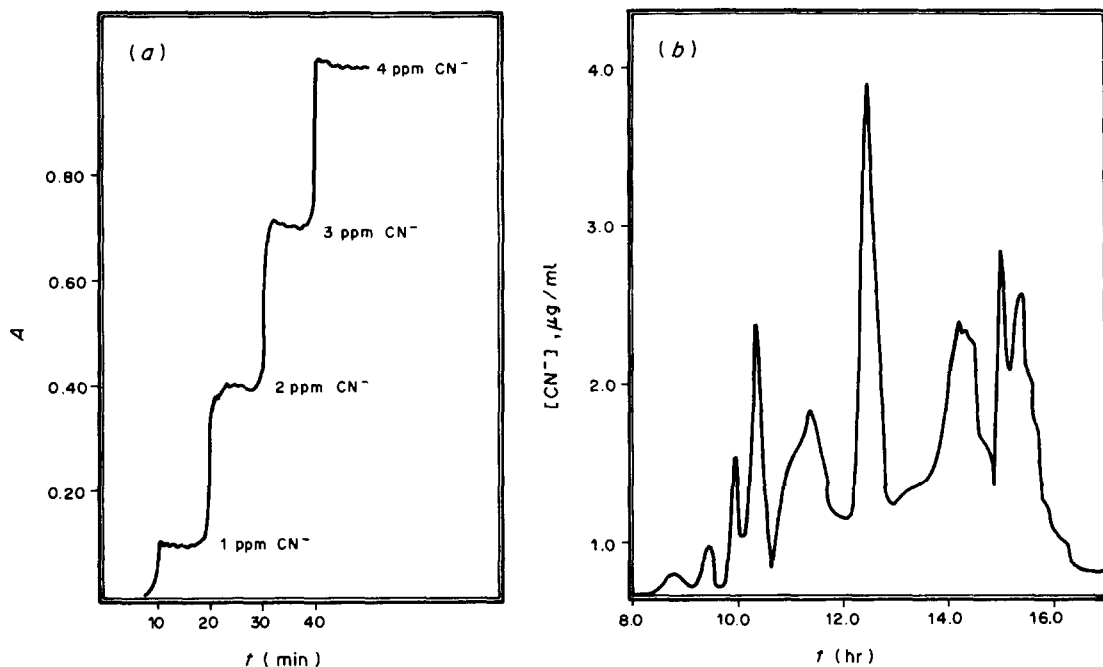


Fig. 4. Completely continuous technique. (a) Calibration run; (b) simulation of continuous monitoring of $[\text{CN}^-]$ in waste waters during a working day.

anide levels as low as $0.1 \mu\text{g/ml}$ (linear range $0.1\text{--}1.0 \mu\text{g/ml}$); on the other hand, rFIA permits determination over a wider range ($0.3\text{--}5.0 \mu\text{g/ml}$)

with a straight line calibration graph. The sampling frequency is a little higher in rFIA. Table 2 suggests applications for the three modifications.

Interferences

As shown in Table 3, the most significant interferences come from species with cyanide groups (thiocyanate, ferrocyanide and ferricyanide are positive interferences) and cations that form complexes with cyanide (silver, copper, cobalt, nickel, *etc.*, which cause negative interference). Bromide and iodide diminish the analytical signal, perhaps because of formation of CNBr and CNI , which do not react with the pyridine-barbituric acid. Fluoride does not interfere. Sulphide and nitrite, which interfere seriously in the conventional method,^{8,13} are tolerated in these flow methods when present in up to tenfold ratio to cyanide.

The interferences are practically the same in the three unsegmented flow methods, although in rFIA they appear to be slightly less severe.

Table 1. Comparison between the unsegmented flow methods for determination of cyanide and the conventional method

Conventional photometric method	Unsegmented flow methods
Lower detection limit Higher sensitivity	Higher analysis rate Easier handling Greater versatility for the required type of analysis Good precision Automated continuous methods are possible Minimum exposure of the analyst to the highly toxic CNCl Diminution of interferences

Table 2. Comparison of the unsegmented flow methods

Method	Typical application	Samples/hr	$[\text{CN}^-]$, $\mu\text{g/ml}$	Slope of calibration line
Normal FIA	Scanty samples	20	0.1–0.4	0.44
Reversed FIA	Waste water analysis	28	0.4–1.0	0.67
Completely continuous	Automated continuous analysis	Continuous	0.3–5.0	0.15
			0.7–4.0	0.30

Table 3. Interferences in determination of cyanide by the unsegmented flow methods*

Tolerance ratio	Added species		
	nFIA	rFIA	Completely continuous
100	F ⁻ , Cl ⁻ , NO ₃ ⁻ , NO ₂ ⁻ , SO ₄ ²⁻ , SO ₃ ²⁻ , S ₂ O ₃ ²⁻ , CO ₃ ²⁻ , CH ₃ COO ⁻ , PO ₄ ³⁻ , ClO ₃ ⁻ , EDTA, Na ⁺ , K ⁺ , NH ₄ ⁺ , Ca ²⁺ , Mg ²⁺ , Cr ³⁺	F ⁻ , Cl ⁻ , NO ₃ ⁻ , NO ₂ ⁻ , SO ₄ ²⁻ , SO ₃ ²⁻ , S ₂ O ₃ ²⁻ , CO ₃ ²⁻ , C ₂ O ₄ ²⁻ , CH ₃ COO ⁻ , PO ₄ ³⁻ , ClO ₃ ⁻ , EDTA, Na ⁺ , K ⁺ , NH ₄ ⁺ , Ca ²⁺ , Mg ²⁺ , Pb ²⁺ , Cr ³⁺	F ⁻ , Cl ⁻ , NO ₃ ⁻ , NO ₂ ⁻ , SO ₄ ²⁻ , SO ₃ ²⁻ , S ₂ O ₃ ²⁻ , CO ₃ ²⁻ , C ₂ O ₄ ²⁻ , CH ₃ COO ⁻ , PO ₄ ³⁻ , ClO ₃ ⁻ , EDTA, Na ⁺ , K ⁺ , NH ₄ ⁺ , Ca ²⁺ , Mg ²⁺ , Cr ³⁺
50	C ₂ O ₄ ²⁻ , S ₂ O ₈ ²⁻ , Zn ²⁺ , Cd ²⁺	S ₂ O ₈ ²⁻ , Zn ²⁺ , Cd ²⁺	S ₂ O ₈ ²⁻ , Zn ²⁺ , Cd ²⁺ , Pb ²⁺
10	S ²⁻ , IO ₄ ⁻ , Pb ²⁺	S ²⁻ , Mn ²⁺	S ²⁻
1	Br ⁻ , I ⁻ , Mn ²⁺	Br ⁻ , I ⁻ , Fe ³⁺	Br ⁻ , Fe ³⁺
<1	Fe(CN) ₆ ⁴⁻ , Fe(CN) ₆ ³⁻ , SCN ⁻ , Cu ²⁺ , Co ²⁺ , Ni ²⁺ , Fe ³⁺ , Hg ²⁺ , Ag ⁺	Fe(CN) ₆ ⁴⁻ , Fe(CN) ₆ ³⁻ , SCN ⁻ , Cu ²⁺ , Co ²⁺ , Ni ²⁺ , Hg ²⁺ , Ag ⁺	Fe(CN) ₆ ⁴⁻ , Fe(CN) ₆ ³⁻ , SCN ⁻ , I ⁻ , IO ₄ ⁻ , Cu ²⁺ , Co ²⁺ , Ni ²⁺ , Hg ²⁺ , Ag ⁺ , Mn ²⁺

*For 2.0 µg/ml of cyanide.

REFERENCES

1. J. Růžicka and E. H. Hansen, *Flow Injection Analysis*, Wiley, New York, 1981.
2. K. S. Johnson and R. L. Petty, *Anal. Chem.*, 1982, **54**, 1185.
3. M. Goto, *TrAC*, 1983, 92.
4. B. Pihlar, L. Kosta and B. Hristovski, *Talanta*, 1979, **26**, 805.
5. *Idem*, *Anal. Chim. Acta*, 1980, **114**, 275.
6. H. Müller, in *Ion-Selective Electrodes 3*, E. Pungor (Ed.), p. 279. Elsevier, Amsterdam, 1981.
7. P. Linares, M. D. Luque de Castro and M. Valcárcel, *Anal. Chim. Acta*, in the press.
8. *Standard Methods for Examination of Water and Waste Waters*, 15th Ed., pp. 312–328. American Public Health Association, Washington, DC, 1980.
9. J. A. Nelder and R. Mead, *Computer J.*, 1965, **78**, 308.
10. G. Ham, *Anal. Proc.*, 1981, **18**, 69.
11. D. Betteridge and B. Fields, *Z. Anal. Chem.*, 1983, **390**, 314.
12. F. Lázaro, M. D. Luque de Castro and M. Valcárcel, *Analyst*, in the press.
13. N. J. Csikai and A. J. Barnard, Jr., *Anal. Chem.*, 1983, **55**, 1677.

AEROSOL COLLECTION AND RF PLASMA VOLATILIZATION ON A TUNGSTEN WIRE ELECTRODE

KEIJO HAAPAKKA* and ROGER STEPHENS†

Trace Analysis Research Centre, Department of Chemistry, Dalhousie University, Halifax, Nova Scotia, Canada

(Received 24 January 1984. Accepted 2 April 1984)

Summary—Electrostatic trapping of desolvated aerosols on a wire electrode is described. A capacitively-coupled radiofrequency discharge is used to vaporize and excite collected material. The apparatus shows a clear and controllable transition between different modes of electrostatic collection. Boron shows unexplained anomalous behaviour.

Electrostatic trapping has been applied to the collection of atmospheric particulates^{1,2} and to the pre-concentration of aqueous solutions.^{3,4} In the latter case the solution is converted into an aerosol, desolvated, and deposited on either a wire or a liquid-filled trough electrode. However neither of these types of electrode is ideal. The former is unsatisfactory because of the difficulty of removing trapped material without also destroying the wire. A liquid collector avoids this problem, but is tedious to set up and must be renewed each time it is used.

The present work examines an alternative method of performing an electrostatic collection and retrieval cycle, which works for a wide range of elements and requires no manipulation of the electrode system between samples. The method uses a wire point as the collector. The high field-gradient associated with the small radius of curvature at the tip of the wire ensures that material is collected with high efficiency and is deposited over a small surface area. Given this geometry, the subsequent removal of deposited material is easily achieved by volatilization with a low-power capacitively-coupled radiofrequency (RF) plasma, which can be made to vaporize the surface coating of the wire while leaving the substrate intact. In the present work the plasma was used both to evaporate the sample and excite it so that the vaporized material could be detected by means of its atomic emission.

EXPERIMENTAL

The device used in the present work is shown in Fig. 1. Dry aerosol entering from B flows around a wire electrode E (the working electrode) which is connected to a suitable high voltage (either positive or negative). Some of the aerosol particles are attracted to the electrode surface and retained. The process is continued until sufficient material has built up on the working electrode to allow its subsequent

detection by atomic emission from a plasma generated directly at the electrode surface. A ground electrode was also used during the collection cycle to collect aerosol particles which might become charged and repelled from the working electrode. The trapping efficiency of a wire collector and the stability of the atomizing plasma both depend on the cell geometry used because of build-up of static charge on insulating surfaces. The cell shown in Fig. 1 was found to be suitable. The body was made of Pyrex glass. The working (E) and ground (F) electrodes were made of 0.5 mm diameter tungsten wire, with lengths of 6 and 2 mm, respectively. A ground plane was provided by wrapping a few turns of copper wire (D) around the body of the cell.

The RF plasma used to volatilize the collected material was generated in argon by a laboratory-built supply which delivered 30 W at 2 MHz. The output was connected to the working electrode and ground plane through an impedance-matching transformer which developed a zero-load secondary voltage of 3 kV. This was sufficient for spontaneous initiation of the plasma, which appeared as a stable, arc-like streamer between the working electrode and the glass of the

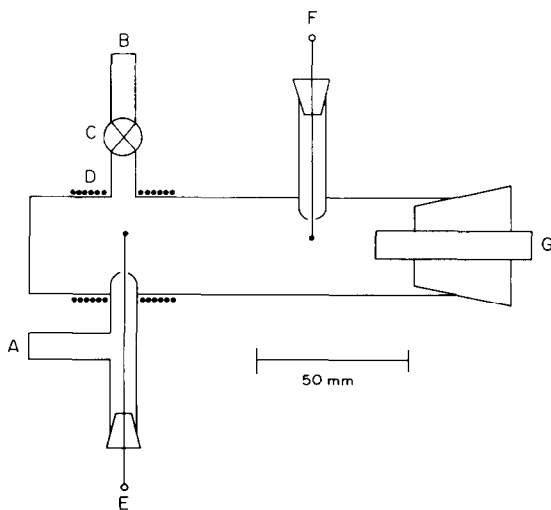


Fig. 1. The collection cell. A, argon inlet; B, sample inlet; D, copper ground wire; E, F, working and ground electrodes; G, gas outlet; the gas inlet stopcock (C) is open during collection and closed during plasma generation.

*Present address: Department of Chemistry, University of Turku, SF 20500 Turku 50, Finland.

†Author to whom correspondence should be addressed.

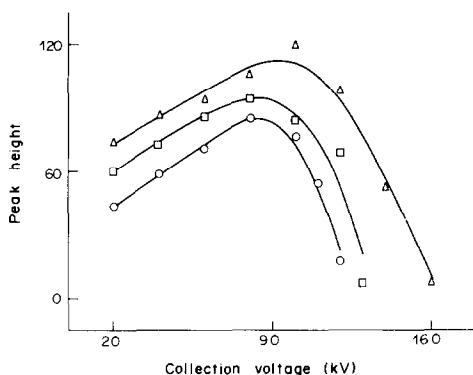


Fig. 2. Effect of collection voltage on the emission intensity of Ag (O), Cd (Δ), B (\square). Starting concentrations were 0.8, 2, 4 $\mu\text{g/ml}$, respectively. Collection volume 20 ml.

cell body. The electrode became red-hot during this process, but its temperature was insufficient to cause thermal volatilization of the majority of compounds examined. It was concluded that sputtering by the plasma was the primary cause of vaporization.

Detection of vaporized material was by atomic emission, measured with a Varian AA5 spectrometer. The optical alignment which gave the best signal-to-noise ratio was that in which the image of the electrode was slightly offset (in either direction), when the monochromator was viewing a section of the plasma immediately adjacent to the electrode surface.

Procedure

The d.c. collection voltage was connected to the working electrode. Sample solutions were aspirated with a pneumatic nebulizer and desolvated as described in earlier work. Air was used as the carrier. After collection was complete the gas supply was switched to argon to purge the cell. The argon flow was reduced, normally to 0.04 l./min with the present cell, and the working electrode switched over to the RF supply to initiate the plasma. A transient atomic-emission signal was observed, with a duration of a few msec. A burn time of 5 or 10 sec normally cleared the electrode even of heavy salt deposits; this is a sufficiently short interval to avoid serious etching of the tungsten surface (even if traces of oxidizing gases are present in the argon supply).

RESULTS

The elements Ag, B and Cd were selected to test the behaviour of the system. The effects of trapping voltage and of argon flow-rate are shown in Figs. 2 and 3.

The results in Fig. 2 show that collection efficiency for all three elements increased to a maximum at about 9 kV. The maximum efficiency was found, by methods described previously,³ to be around 30%. This is a lower efficiency than was achieved with earlier designs because, although a high field-gradient exists around the electrode, its influence extends over only a small volume.

For trapping voltages below 9 kV, transferring the plasma to the ground electrode (F in Fig. 1) gave only a weak emission signal. Washing the inside of the cell also failed to reveal any material deposited on the glass walls. It was concluded that the bulk of the trapped aerosol was retained on the working elec-

trode. These results altered as the collection voltage was increased above 9 kV. Increasing amounts of material were transferred to the walls and to the ground electrode. At the same time a faint corona became visible. Therefore the occurrence of the maximum in Fig. 2 was attributed to a change in the mechanism of collection, from one involving attraction of polarized aerosol particles to the working electrode at low collection voltages, to one in which the aerosol particles became charged in the corona and repelled away from the working electrode.

Boron alone showed erratic behaviour for collection voltages below 9 kV. Borax gave apparently normal emission signals for initial boron concentrations above 0.4 $\mu\text{g/ml}$, but for lower concentrations the response fell abruptly to zero. Addition of 2 $\mu\text{g/ml}$ of sodium chloride corrected this behaviour and all results for boron were obtained in this way. However, boron as boric acid failed to give any response at all, even in the presence of sodium chloride. This sensitivity to the physical and chemical nature of the aerosol is similar to the behaviour of the liquid collector.⁴ It is apparently related to the different properties of the two collection modes and presumably reflects the complex behaviour of boron oxyanions. However, the unusual magnitude of the variations caused by minor changes in the initial solution remains an unexplained curiosity.

The effects of varying the argon flow-rate during the atomization cycle are shown in Fig. 3. The results indicate that the volatilization process is not particularly sensitive to the argon flow, but that the excitation temperature falls as the argon flow increases. However, the argon flow could not be completely stopped or the plasma column itself became unstable.

Results were repeated for ground and working electrodes varying in length from 1 to 10 mm, but no major variations were observed. Other plasma gases were examined but none gave as satisfactory results as argon, possibly because of the low RF power used. Following these preliminary results, the collection voltage and argon flow-rate during plasma generation were fixed at 8 kV and 0.04 l./min.

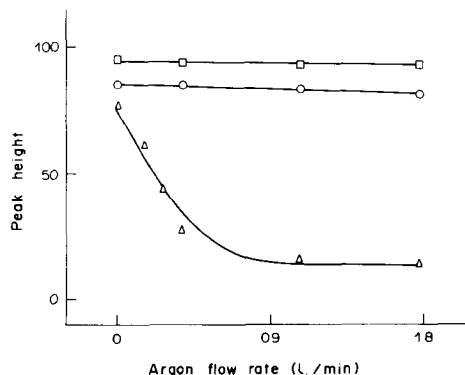


Fig. 3. Effect of argon flow on the emission intensity of Ag (O), Cd (Δ), B (\square). Conditions as in Fig. 2.

Table 1. Behaviour of Ag, B and Cd

Element	Source	Wavelength, nm	Upper limit of linear working curve, $\mu\text{g/ml}$	Precision, %	Detection† limit, $\mu\text{g/ml}$
Ag	Silver nitrate	328.1	0.01	2 (at 0.008 $\mu\text{g/ml}$)	0.0002
B	Borax in 2- $\mu\text{g/ml}$ NaCl	249.7	0.3	10 (at 0.4 $\mu\text{g/ml}$)	0.06
Cd	Cadmium chloride	228.8	0.1	17 (at 0.06 $\mu\text{g/ml}$)	0.004

*Relative standard deviation of 6 successive readings.

†For a signal corresponding to 3 times the relative standard deviation of 6 successive blank readings, 50-ml sample volume.

Table 2. Summary of detection limits

Element	Source	Wavelength, nm	Detection limit*, $\mu\text{g/ml}$
Al	$\text{Al}_2(\text{SO}_4)_3 \cdot 16\text{H}_2\text{O}$	396.2	0.1
Ba	$\text{Ba}(\text{C}_2\text{H}_3\text{O}_2)_2$	553.6	0.01
Ca	$\text{Ca}(\text{NO}_3)_2 \cdot 4\text{H}_2\text{O}$	422.7	0.3
Cr	$\text{CrCl}_3 \cdot 6\text{H}_2\text{O}/\text{HCl}$	359.4	0.9
Co	$\text{Co}(\text{NO}_3)_2/\text{HNO}_3$	240.7	0.1
Cu	CuO/HNO_3	324.7	0.02
Pb	$\text{Pb}(\text{NO}_3)_2/\text{HNO}_3$	405.8	0.08
Mg	MgCl_2/HCl	285.2	0.004
Mn	MnSO_4	403.1	0.08
Hg	HgCl_2	253.7	0.006
Ni	Ni/HNO_3	232.0	0.3
Si	$\text{Na}_2\text{SiO}_3 \cdot 9\text{H}_2\text{O}$	251.6	0.09
Sr	SrCl_2	460.7	0.2
Sn	$\text{SnCl}_2 \cdot 2\text{H}_2\text{O}$	284.0	0.1
V	$\text{V}_2\text{O}_5/1\text{M HCl}$	318.4	0.3
Zn	ZnO/HNO_3	213.8	0.03
Zr	$\text{ZrOCl}_2 \cdot 8\text{H}_2\text{O}/5\text{M HCl}$	360.1	0.8

*For a signal corresponding to 3 times the relative standard deviation of 6 successive blank readings, 50-ml sample volume.

respectively. The analytical behaviour of the three test elements was examined and the detection limits for others were determined. Results are summarized in Tables 1 and 2.

In order to assess the sensitivity of the apparatus to matrix effects, or to the action of added buffering agents, the responses of the three test elements in the

presence of sodium chloride were observed. The results are shown in Fig. 4. Sodium chloride was found to influence the response by increasing the intensity of the (wide-band) background emission. This was particularly marked at short wavelengths as shown by the Cd response in Fig. 4 (total emission at the Cd wavelength). In addition, sodium chloride causes a reduction in collection efficiency, shown by the fall of the curves for Ag and B in Fig. 4 (corrected for wide-band emission by dual-wavelength measurements). The spectroscopic interference appears to be the more serious; the collection process itself tolerates small amounts of sodium chloride reasonably well.

CONCLUSIONS

The behaviour of the present apparatus shows that an aerosol can be collected onto a single pointed wire electrode with useful efficiency. It also shows the ability of a low-power RF plasma to volatilize refractory materials, such as oxygen-containing or hydrated salts of B, Si and Zr, from the surface of the wire.

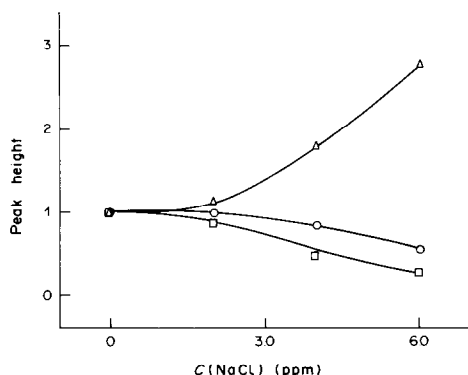


Fig. 4. Effect of NaCl on the emission intensity of Ag (O), Cd (Δ), B (□). Conditions as in Fig. 2.

Considerable sensitivity is lost in the present apparatus through the inefficient delivery of vaporized material to the region of highest temperature in the plasma, and through spreading of the sample over a larger volume than can be observed by the optical system. In principle, the technique is capable of good sensitivity, since the material collected from a large volume of solution can be retained on a surface of small area, and reintroduced into the vapour phase over a time interval of a few msec.

The technique is of use in its present form because it provides a simple method of loading wire probes to any desired level. It also affords a convenient way of examining the transition between different modes of collection (*i.e.*, attraction of particles to the working electrode or coronal charging and repulsion). This transition is observed with any type of electrostatic trap, but its onset is sensitive to design and operation of the trap as well as to the nature of the aerosol. The

present behaviour is unusual in that the transition occurs abruptly, leading to a sudden switch from efficient collection to zero, or *vice versa*, as a result of small changes in operating conditions. Its investigation is of interest partly because of this sensitivity *per se*, and partly because of the necessity to control the transition point for a given type of aerosol.

Acknowledgements—The authors are indebted to the Natural Sciences and Engineering Research Council of Canada for support of this work. One of them (KH) thanks the Killam Trust for the award of a postdoctoral fellowship.

REFERENCES

1. G. Torsi and E. Desimoni, *Anal. Lett.*, 1979, **12**, 1361.
2. G. Torsi, E. Desimoni, F. Palmisano and L. Sabbatini, *Anal. Chem.*, 1981, **53**, 1035.
3. P. A. Michalik and R. Stephens, *Talanta*, 1981, **28**, 37.
4. *Idem, ibid.*, 1981, **28**, 43.

GEL SPECIATION STUDIES-II

AN EXTENSION OF EARLIER STUDIES OF THE PROTONATION EQUILIBRIA OF CROSS-LINKED CARBOXYMETHYLDEXTRAN

SALVADOR ALEGRET

Department of Analytical Chemistry, The Autonomous University of Barcelona, Bellaterra, Spain

MARIA-TERESA ESCALAS

Escola de Mestres "Sant Cugat", The Autonomous University of Barcelona, Bellaterra, Spain

JACOB A. MARINSKY

Department of Chemistry, State University of New York at Buffalo, Buffalo, New York 14214, U.S.A.

(Received 10 January 1984. Accepted 26 March 1984)

Summary—The potentiometric properties of the rigidly cross-linked Sephadex gel CM-25 have been studied. The gel was equilibrated in sodium perchlorate at fixed concentration levels (0.010 and 0.0010M) and with variable concentration levels of NaClO₄ (from 0.0010 to 0.10M). The volume of the gel was measured for every equilibrated sample simultaneously with the solution pH and pNa. The pK computed after correction for a Donnan potential term was found to be independent of α , the degree of neutralization, and ionic strength; its value of 3.35 ± 0.15 was in excellent agreement with the intrinsic pK measured earlier for the flexible CM-50 Sephadex gel and reported for its linear polyelectrolyte analogue, carboxymethyl-dextran. An interesting observation from these studies is the efficient screening of the charged surface by the counter-ions in the presence of a three-dimensional charged network.

It has been shown that in the investigation of gel-phase equilibria, such as the dissociation of a weakly acidic group repeated in a regular way throughout the gel structure, and/or the complexation of metal by this acidic group, a Donnan potential term must be calculated^{1,2} to permit an estimate of non-ideality at the site of the reaction. For this purpose it is necessary to know the gel-phase concentration of the potential-determining counterion (e.g. Na⁺) as well as the solution pH and pNa at every experimental point, since

$$pC_{\text{H}}^g = \text{pH}_{(s)} - \text{pNa}_{(s)} + \text{p}C_{\text{H}}^g \quad (1)$$

where

$$\text{p}C_{\text{H}}^g - \log \frac{\alpha}{(1-\alpha)} = \text{p}K_{(\text{HA})}^{\text{app}} \quad (2)$$

and

$$\text{p}K_{(\text{HA})}^{\text{app}} - \text{p}K_{(\text{HA})}^{\text{int}} = -0.434 \frac{e\psi_{(a)}}{kT} + \log \gamma_{\text{H}^+}^g \quad (3)$$

In equation (1) the subscript s and the superscript g refer to the solution and gel phases, with C_{H}^g and C_{Na}^g representing the molar concentration of H⁺ and Na⁺ in the gel. In equation (2) α refers to the fraction of gel acidic groups that is dissociated and $\text{p}K_{(\text{HA})}^{\text{app}}$ corresponds to the apparent pK of the acid unit (HA) which is repeated in the polymer. Finally, in equation (3) the superscript int designates the intrinsic pK of the repeating HA unit, $\psi_{(a)}$ refers to the potential at the surface of the charged gel matrix, and $\gamma_{\text{H}^+}^g$ is the molar activity-coefficient correction for long-range

Debye-type ion-interaction forces acting on the H⁺ ion in the gel phase.

Since electroneutrality must be preserved in the gel phase, the Na⁺ content of the gel can be equated directly with the quantity (meq) of acid dissociated, (A⁻), or αv , on controlled addition of standard base, by means of equation (4):

$$(A^-)_v = \alpha v = bV_b + hV_s = \text{Na}_{(g)}^+ \quad (4)$$

where b and h are the molarities of the base and acid, respectively, and V_b the volume of base added and V_s the volume of the aqueous phase after the addition of base. Measurement of the gel volume, V_g , then permits evaluation of C_{Na}^g with equation (5):

$$C_{\text{Na}}^g = \frac{v\alpha}{V_g} \quad (5)$$

The neutralization by sodium hydroxide of the cation-exchange gel in equilibrium with a sodium salt of a strongly acidic polyelectrolyte such as sodium polystyrene sulphonate, NaPSS, can be expressed by the equation

$$\begin{aligned} \text{pH}_{(s)} - \text{pNa}_{(s)} + \log V_g^* \\ = \text{p}K_{(\text{HA})}^{\text{app}} + \log \gamma_{\text{Na}}^g + \log \frac{\alpha^2}{(1-\alpha)} = S \end{aligned} \quad (6)$$

where V_g^* is now defined as the specific volume (ml per l meq of the gel).

By inclusion of γ_{Na}^g and other terms such as γ_{A^-} , the activity coefficient of the acidic unit of gel, and γ_{Na}^h and $\gamma_{\text{H}^+}^h$, the solvation contributions of both the H⁺

and Na^+ ions in the pK^{app} term, as done by Slota and Marinsky,¹ the pK^{app} value can be obtained by the relationship:

$$pK_{(\text{HA})_v}^{\text{app}} = \text{pH}_{(s)} - \text{pNa}_{(s)} + \log V_g^* - \log \frac{\alpha^2}{(1-\alpha)} \quad (7)$$

If a simple neutral electrolyte, *e.g.*, sodium perchlorate, is used to control the ionic strength of the aqueous medium, an accurate estimate of the extent of gel invasion by the salt [which is reduced sufficiently by the use of a high molecular-weight polyelectrolyte (NaPSS) to be neglected in equations (5)–(7)], must now be made for correct assessment of $pK_{\text{Na}}^{\text{app}}$ with equation (1). At equilibrium the activity of sodium perchlorate is the same in both phases:

$$a_{\text{NaClO}_4}^{\text{g}} = a_{\text{NaClO}_4}^{\text{s}} \quad (8)$$

so

$$(\gamma_{\text{g}}^{\pm})^2 (C_{\text{Na}}^{\text{g}}) (C_{\text{ClO}_4}^{\text{g}}) = (\gamma_{\text{s}}^{\pm})^2 (C_{\text{Na}}^{\text{s}}) (C_{\text{ClO}_4}^{\text{s}}) \quad (9)$$

where γ^{\pm} represents the mean molar activity coefficient of sodium perchlorate in the separate solution (s) and gel (g) phases. Now

$$C_{\text{Na}}^{\text{g}} = \frac{v\alpha}{V_g} + C_{\text{NaClO}_4}^{\text{g}} \quad (5a)$$

and

$$(\gamma_{\text{g}}^{\pm})^2 \left(\frac{v\alpha}{V_g} + C_{\text{NaClO}_4}^{\text{g}} \right) (C_{\text{NaClO}_4}^{\text{g}}) = (C_{\text{NaClO}_4}^{\text{s}})^2 (\gamma_{\text{s}}^{\pm})^2 \quad (9a)$$

Little error is introduced by equating $(\gamma_{\text{g}}^{\pm})_{\text{g}}$ with $(\gamma_{\text{g}}^{\pm})_{\text{s}}$ in equation (9a) to facilitate evaluation of $C_{\text{NaClO}_4}^{\text{g}}$ from the resultant quadratic equation. The value of C_{Na}^{g} [equation (5a)] so corrected can then be transferred to equations (5)–(7) for a more accurate analysis of the potentiometric data with equation (7a):

$$pK_{(\text{HA})_v}^{\text{app}} = \text{pH}_{(s)} - \text{pNa}_{(s)} - \log \frac{\alpha}{(1-\alpha)} - \log \left(\frac{\alpha}{V_g^*} + C_{\text{NaClO}_4}^{\text{g}} \right) \quad (7a)$$

The research described below was intended to extend an earlier study of the potentiometric behaviour of Sephadex, a weakly cross-linked carboxymethyl dextran. A Sephadex gel (CM-25) more rigid than that used in the earlier studies^{1,2} was employed to increase the effective concentration range of counter-ions in the gel beyond that examined before, so that the effect of counter-ion screening of the charged macromolecular surface, confined to a gel-network geometry, could be observed over an extended counter-ion concentration range.

EXPERIMENTAL

Preparation of the resin

Sephadex CM-25, commercially available from Pharmacia fine chemicals (Sweden), was obtained in the sodium form with a nominal capacity of 4.5 meq/g for the material. It was first placed in water to swell before transfer to a chromatographic column for conversion into the acid form,

by slow passage of large excess of 0.2M perchloric acid through the resin column. Use of more concentrated acid was avoided, to prevent hydrolysis of the glycosidic bonds of the carboxymethyl dextran. After the conversion was, complete doubly distilled water was passed through the column until the pH of effluent and influent were the same. The wet resin was then stored in sealed polyethylene containers.

Batch equilibration procedure

Approximately 1-g samples of wet resin were accurately weighed out and transferred quantitatively to 20-ml screw-capped glass tubes. Controlled volumes of standard sodium hydroxide solution were then added to each sample, under a nitrogen atmosphere, to cover the neutralization range from approximately 5 to 85%. The final volume of the solution varied from 10.0 to 20.0 ml. In one type of experiment the ionic strength was maintained constant in each sample at 0.010 or 0.001 by addition of a volume of 0.020M or 0.002M sodium perchlorate (as appropriate), just equal to the volume of base added in adjusting the degree of neutralization of a particular sample. At the lower α values, 0.010M or 0.001M sodium perchlorate was added to the sample to bring the final volume up to 10.0 ml. In the other type of experiment the ionic strength was allowed to vary.

Each of the samples was equilibrated at ambient temperature ($20 \pm 2^\circ$) for at least 15 hr with continuous agitation provided by a rotating platform. The samples were sealed with parafilm to avoid the absorption of CO_2 during equilibration. At the end of the equilibration period essentially all of the supernatant solution was collected, under a nitrogen atmosphere, for potentiometric pH and pNa measurement.

Gel volume determinations

The surface of the residual solution, defined by a 1–2 mm depth beyond the gel boundary, was first marked by a line drawn on the exterior wall of the tube, tangentially to the solution meniscus (the tube was ~ 10 mm in diameter). Exactly 1.00 ml of a 0.010% aqueous solution of Blue Dextran 2000, a macromolecular dye with an average molecular weight of 2×10^6 (from Pharmacia Fine Chemicals of Sweden) was then added to the resin and the residual solution. After vigorous shaking to ensure complete mixing of the dye with the solution as rapidly as possible, a small aliquot of the solution was withdrawn for spectrophotometric measurement at 620 nm, with a Perkin-Elmer model 554 spectrophotometer. The brief interval ($< 1/2$ min) of agitation before sampling was believed to keep the absorption and/or diffusion of the dye sufficiently low to avoid any disturbance of the volume measurement. To obtain the volume of resin, the volume of solution, accurately accessible from this measurement, was then subtracted from the total volume of resin and solution, determined by weighing the quantity of water needed to fill the tube to the added mark, after the resin and solution had been quantitatively added to the supernatant solution withdrawn earlier for the electrochemical measurement of pH and pNa.

Total resin capacity measurement

The total capacity of each resin sample was determined by back-titration with standard acid of the excess of standard sodium hydroxide solution added to each gel–solution mixture.

Potentiometric measurements

All electrochemical measurements were made (to ± 0.1 mV) with a Crison (Barcelona) digital pH-meter equipped with an Ingold combination (405–M5) electrode (a glass electrode and an Ag/AgCl internal reference electrode) for the pH determinations and a Radiometer sodium ion-selective electrode (G502 Na) joined with a reference calomel electrode (Radiometer K401) for the pNa determinations. During each measurement nitrogen gas was used

to blanket the solution to prevent interference by CO_2 . Before and after each series of measurements the electrodes were calibrated, the glass electrode with standard buffer solutions and the sodium electrode with standard sodium perchlorate solutions. The pH and pNa ranges encountered in the experimental programme were covered in the calibration programme. Since there is interference by H^+ in the electrochemical measurement of the Na^+ , its extent was quantitatively estimated when necessary, by the "separate solution" method.⁴ With this approach a mean potentiometric interference parameter, $K_{\text{Na}(\text{H})}^{\text{pot}}$, equal to 5.0, was found applicable in the modified Nernst equation used to compute pNa:

$$E = E_0 + g \log (a_{\text{Na}} + K_{\text{Na}(\text{H})}^{\text{pot}} a_{\text{H}^+}) \quad (10)$$

where $g = 59.16 \text{ mV/decade}$ at 25° .

Reagents and solutions

All chemicals used were Merck analytical grade products. Solutions were prepared with doubly distilled demineralized water. The sodium perchlorate solution was made by neutralizing pure perchloric acid with pure sodium carbonate.⁵ The $0.100M$ sodium hydroxide was prepared from 50% sodium hydroxide stock solution and standardized against potassium hydrogen phthalate; the $0.100M$ perchloric acid was standardized with tris(hydroxymethyl)aminomethane. The stock sodium perchlorate solution used to prepare the standard solutions for calibration of the sodium ion-selective electrode was standardized gravimetrically by precipitation of sodium zinc uranyl acetate.⁶

RESULTS AND DISCUSSION

The potentiometric data obtained in the first type of experiment (fixed ionic strength) have been used directly in the standard Henderson-Hasselbalch equation

$$\text{pH}_{(\text{s})} - \log \frac{\alpha}{(1-\alpha)} = \text{p}K_{(\text{HA})}^{\text{app}}, \quad (11)$$

to obtain the two separate plots of $\text{p}K_{(\text{HA})}^{\text{app}}$, vs. α presented in Fig. 1. The points of the upper curve correspond to such an analysis of the pH data for the $0.0010M$ sodium perchlorate system, and the middle

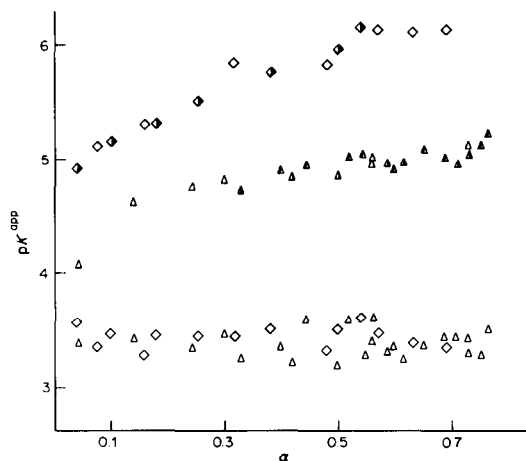


Fig. 1. Plots of apparent $\text{p}K$ vs α : in the two upper curves the \diamond and \blacklozenge ($I = 0.0010M$) and \triangle and \blacktriangle ($I = 0.010M$) points were computed by means of equation (11); the lower curve was obtained by using equation (7a) to incorporate a Donnan potential term for the resolution of $\text{p}K$.

curve is based on data obtained with the $0.010M$ sodium perchlorate system. When these potentiometric data are analysed by using equation (7a), where correction is made for the Donnan-potential term, $\text{pNa}_{(\text{g})} - \text{pNa}_{(\text{s})}$, all of the computed $\text{p}K_{(\text{HA})}^{\text{app}}$ values fall on a single straight line of zero slope. The $\text{p}K$ value of 3.35 ± 0.15 , defined by the best straight line that can be drawn through these points, is in excellent agreement with the intrinsic $\text{p}K$ determined for the linear, uncross-linked carboxymethyl dextran analogue⁷ of the Sephadex gel employed in this study. This result once again provides support for the model proposed and used for analysis of the protonation equilibria in gels.^{1,2}

Potentiometric data obtained from the second type of experiment (variable ionic strength) have also been analysed by means of equation (7a). The data from this phase of the research are listed in Table 1. The

Table 1. A potentiometric study of the protonation equilibria of Sephadex CM-25

v , meq	Base added, meq	$\text{pH}_{(\text{s})}$	$\text{pNa}_{(\text{s})}$	α	$\frac{A^-}{V_g}$	C_{NaClO_4}	$\text{pNa}_{(\text{g})}$	$\text{p}K_{(\text{HA})}^{\text{app}}$
1.359	0	2.230	0.986	0.052	0.063	0.076	0.857	3.362
1.354	0.100	2.758	1.201	0.090	0.069	0.037	0.975	3.537
1.309	0.241	3.469	1.508	0.195	0.152	0.012	0.785	3.361
1.304	0.351	3.865	1.646	0.271	0.211	0.002	0.672	3.321
1.261	0.047	2.480	1.026	0.070	0.197	0.038	0.629	3.306
1.246	0.151	3.020	1.201	0.131	0.239	0.033	0.565	3.206
1.246	0.430	4.210	1.751	0.348	0.207	0.022	0.640	3.372
1.246	0.109	3.470	2.217	0.090	0.065	5.62×10^{-4}	1.183	3.441
1.246	0.142	3.682	2.236	0.116	0.092	3.65×10^{-4}	1.034	3.362
1.301	0.520	5.336	2.808	0.340	0.193	1.3×10^{-5}	0.714	3.530
1.271	0.620	5.597	2.828	0.487	0.261	—	0.583	3.375
1.292	0.707	5.756	2.855	0.549	0.345	—	0.462	3.278
1.384	0.352	4.580	2.366	0.254	0.162	1.14×10^{-4}	0.790	3.472
1.326	0.452	5.069	2.628	0.341	0.208	2.7×10^{-5}	0.682	3.409
1.314	0.553	5.546	2.823	0.421	0.255	—	0.593	3.454
1.339	0.653	5.724	2.865	0.488	0.276	—	0.559	3.439
1.435	0.854	5.966	2.869	0.595	0.265	—	0.577	3.507

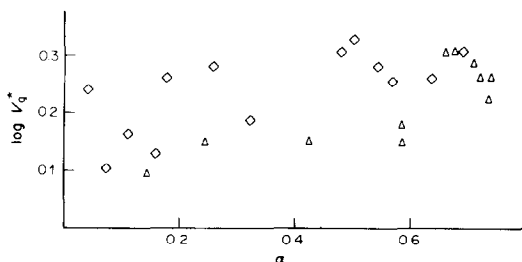


Fig. 2. A representation of gel volume measurements at different degrees of neutralization in 0.0010M NaClO₄ (\diamond) and 0.010M NaClO₄ (Δ) media.

pK values obtained in these experiments corroborate the earlier results; the pK value of 3.35 ± 0.15 is (1) independent of ionic strength and degree of neutralization, and (2) identical with the intrinsic pK already found for the repeating functional unit of the Sephadex. The scatter of ± 0.15 in the pK value is, we believe, attributable to the experimental uncertainty in the value of the gel volume determined in each individual experiment. The V_g^* values measured in the constant ionic-strength experiments are plotted *vs.* α in Fig. 2 to demonstrate this point.

The observation that V_g^* is, within experimental error, independent of the ionic strength of the system, is to be expected; only with this result can the pK *vs.* α curve obtained by using equation (7a) be completely independent of ionic strength. It has already been demonstrated² that with the flexible Sephadex gel (CM-50-125) the $pK_{(HA)}^{app}$, found with equation (7a) is a sensitive function of the solution ionic strength, like the behaviour of a typical polyelectrolyte. In this instance, deviation from ideality arising from the charged surface of the gel matrix is enhanced at each α value by a decrease in the shielding efficiency of the counter-ions in the increasingly expanded gel as the

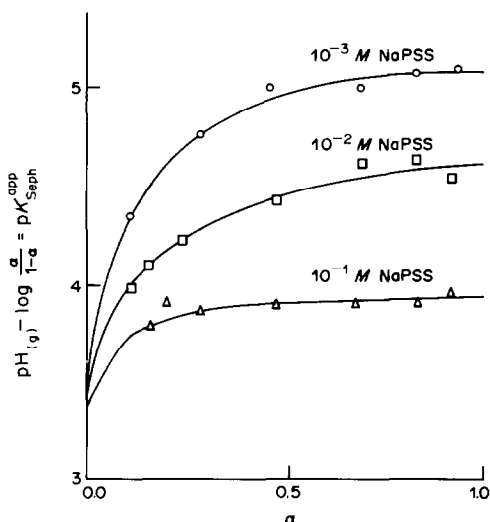


Fig. 3. The potentiometric properties of a flexible Sephadex gel at different water activities.

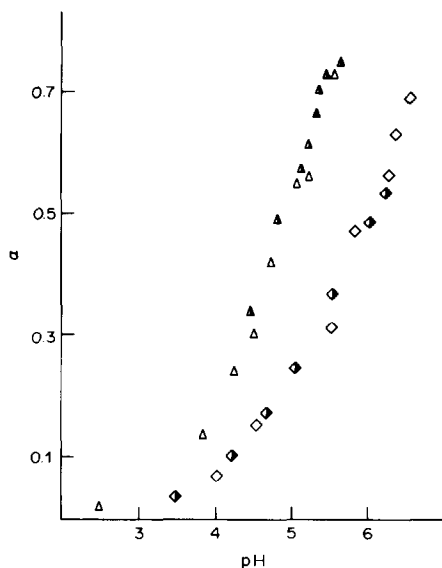


Fig. 4. A plot of α *vs.* pH for a Sephadex gel in 0.0010M (\diamond , \blacklozenge), and 0.010M (Δ , \blacktriangle) NaClO₄ media.

water activity is increased by reducing the ionic strength of the system. This result is pictured in Fig. 3 where $pK_{(HA)}^{app}$, values computed with equation (7a) for the flexible Sephadex CM-50, NaPSS, system studied at three different NaPSS concentrations (0.0010, 0.010, and 0.10M) is plotted *vs.* α . These curves, when compared with the Sephadex CM-25 pK data obtained in this study, show how easily a three-dimensional arrangement of charge is screened by increasing the concentration of the counter-ions.

The rigidity of the Sephadex CM-25 may not seem fully demonstrated, because of the experimental uncertainty of the gel-volume measurements. However,

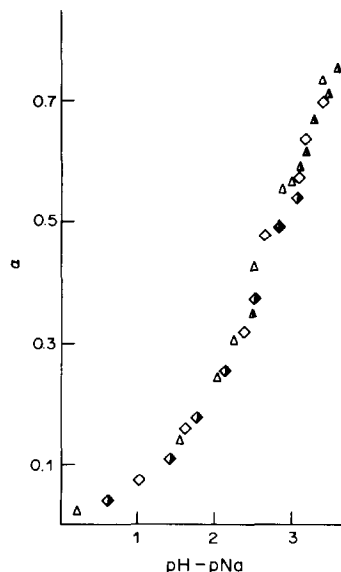


Fig. 5. A plot of α *vs.* $MH_3 - pNa_3$ for a Sephadex gel in 0.0010M (\diamond , \blacklozenge) and 0.010M (Δ , \blacktriangle) NaClO₄ media.

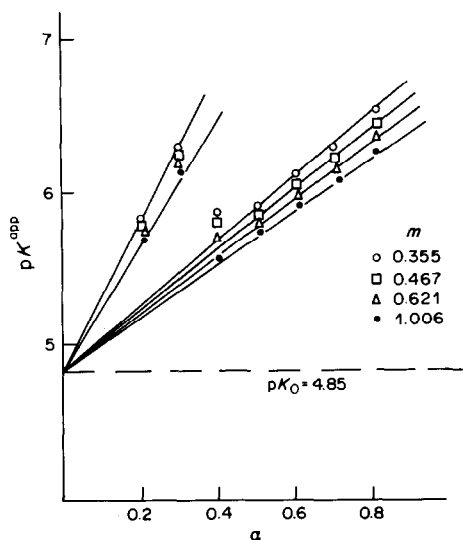


Fig. 6. A plot of pK vs. α for salt-free polymethacrylic acid.

the following argument demonstrates unambiguously that the gel matrix of the Sephadex C-25 is indeed so rigid that a unique gel volume, independent of the water-activity in the external solution phase, is obtained at each α value. With such rigidity of the gel matrix, the concentration of Na^+ in the gel ($p\text{Na}_g^+$) is essentially fixed at each particular α value (neglecting electrolyte invasion). Since $p\text{H}_g - p\text{Na}_g = p\text{H}_s - p\text{Na}_s$, equation (1), a plot of $p\text{H}_s$ vs. α should be dependent on the ionic strength of the system, whereas a plot of $p\text{H}_s - p\text{Na}_s$ vs. α should not. That this is indeed the case with our system can be seen from comparing Figs. 4 and 5.

An important initial objective of this programme was examination of the shielding efficiency of counter-ions in a three-dimensionally charged network. A qualitative estimate of this aspect has been provided by comparing the screening efficiency of

counter-ions in a linear, hydrophobic polyelectrolyte (two-dimensional surface) with screening observations obtained from the CM-50^{1,2} and the CM-25 gel (three-dimensional network). We present in Fig. 6 plots of $pK_{(\text{HA})}^{\text{app}}$, vs. α for four salt-free polymethacrylic acid samples, initially 0.335, 0.467, 0.621 and 1.006*m*, respectively, using equation (11) for the computation.⁸ It is quite apparent from a comparison of these plots with those obtained for Sephadex (Fig. 3) that the drop in efficiency of counter-ion screening of surface potential with concentration is a great deal smaller in the polyelectrolyte system. By the time the counter-ion concentrations reach 0.3–0.4*M* the charged matrix of the Sephadex gel is completely screened. For the polyelectrolyte system the magnitude of the $\exp[-e\psi_{(a)}/kT]$ term is still a factor of about 20.

Acknowledgements—This research was initiated at the Department of Inorganic Chemistry, Royal Institute of Technology, Stockholm, with funds from the Swedish Natural Science Research Council (NFR), which are gratefully acknowledged.

REFERENCES

1. P. Slota and J. A. Marinsky, *Ions in Polymers*, A. Eisenberg (ed.), p.311. American Chem. Soc., Washington, D.C., 1980.
2. Y. Merle and J. A. Marinsky, *Talanta*, 198.
3. Y. Merle, *J. Polym. Sci., Polym. Phys. Ed.*, 1976, **14**, 1317.
4. *Pure Appl. Chem.*, 1976, **48**, 129.
5. *Some Laboratory Methods*, Dept. of Inorganic Chemistry, Royal Institute of Technology, Stockholm, 1959.
6. A. I. Vogel, *A. Text-book of Quantitative Inorganic Analysis*, 3rd Ed., p. 559. Longmans, London, 1961.
7. K. Gekko and H. Noguchi, *Biopolymers*, 1975, **14**, 2555.
8. G. M. Torrence, *Ph. D. Thesis*, State University of New York at Buffalo, 197 .
9. G. M. Torrence, S. Amdur and J. A. Marinsky, *J. Phys. Chem.*, 1971, **75**, 2144.

SHOT-NOISE LIMIT FOR OPTICAL POLARIMETERS

JOUKO J. KANKARE*

Department of Chemistry, University of Turku, SF-20500 Turku 50, Finland

and

ROGER STEPHENS

Trace Analysis Research Centre, Department of Chemistry, Dalhousie University, Halifax, Nova Scotia, Canada

(Received 17 November 1983. Accepted 1 March 1984)

Summary—The methods of Jones's calculus are used to derive expressions for the signal-to-noise ratio in polarimetric measurements. The formulae show that in shot-noise limited systems there is an optimum angle between the polarization planes of the polarizer and analyser and that, once this angle is employed, the signal-to-noise ratio of the system cannot be appreciably improved by improving the quality (*i.e.*, lowering the extinction ratio) of the polarizers used. The main way to improve the signal-to-noise ratio is to use an intense light source, large optical aperture and a long integration time.

There is an increasing need for developing more sensitive methods to measure optical rotation. For example, a large number of naturally occurring compounds, carbohydrates, and a number of amino-acids do not show high absorbance in the ultraviolet region, but do possess optical activity. One advantageous way of employing the latter property might be for detection in HPLC. However, the polarimeters available commercially do not meet the sensitivity requirements for trace analysis. Yeung *et al.*¹ managed to construct a highly sensitive polarimeter, using rather impressive equipment: a 0.5-W argon ion laser as the light-source, a selected pair of prism polarizers, and two Faraday rotators as polarization modulators. According to these authors, the performance of such an instrument depends on the extent to which it can reject light of improper polarization, *i.e.*, on the quality of the polarizers which are used. In this paper we shall consider how this requirement could be eased in certain cases. It is also intended to produce working equations for the relative signal-to-noise ratio of a standard photoelectric polarimeter with a non-ideal polarizer and analyser, and to devise a way to optimize the performance of the device.

THEORY

The mathematical treatment of the theory of optical equipment working with polarized light is most conveniently done by using the Jones matrix formalism (see *e.g.*, reference 2 and references cited therein). According to this, an ideal polarizer with the polarizing plane aligned with the *x*-axis can be represented by a matrix

$$\mathbf{P}_x = \begin{pmatrix} 1 & 0 \\ 0 & 0 \end{pmatrix} \quad (1)$$

and the corresponding "crossed" analyser

$$\mathbf{P}_y = \begin{pmatrix} 0 & 0 \\ 0 & 1 \end{pmatrix} \quad (2)$$

In practice, however, no polarizer is ideal, and a better representation of a polarizer is

$$\mathbf{P}_x = \gamma_x \begin{pmatrix} 1 & 0 \\ 0 & k \end{pmatrix} \quad (3)$$

where γ_x is a scalar attenuating factor and k is a parameter representing the non-ideal polarizing properties of the device. The off-diagonal elements of the matrix \mathbf{P}_x are still assumed to be zero. In fact, any symmetric or Hermitian matrix can be brought into the form (3) by an orthogonal transformation. In the optical train an orthogonal transformation means nothing else but the rotation of the optical element around the optical axis. In the general case the transformation leads to complex values of γ and k .

In practice, the quality of a pair of polarizers is characterized by their extinction ratio ϵ , which is defined as the ratio of the intensity observed when the two polarizers are crossed, to that observed when their transmission axes are parallel.

When the incoming light is unpolarized, the intensity of light (I) transmitted by an optical element A is²

$$I = \frac{1}{2} I_0 \text{Tr}(\mathbf{A}^\dagger \mathbf{A}) \quad (4)$$

where \mathbf{A} is the Jones matrix of A , and I_0 is the intensity of the incident non-polarized light. By applying this first to the crossed polarizers, we obtain

$$\begin{aligned} I_{\perp} &= \frac{1}{2} I_0 \text{Tr}(\mathbf{P}_y^\dagger \mathbf{P}_x \mathbf{P}_x^\dagger \mathbf{P}_y) \\ &= \frac{1}{2} I_0 |\gamma_x|^2 |\gamma_y|^2 (|k_x|^2 + |k_y|^2) \quad (5) \end{aligned}$$

*Author for correspondence.

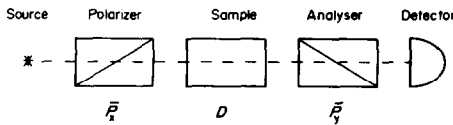


Fig. 1. Schematic diagram of a simple polarimeter.

For the axes parallel, this becomes

$$I_{\parallel} = \frac{1}{2} I_0 \text{Tr}[(\mathbf{P}_x^\dagger)^2 \mathbf{P}_x^2] \\ = \frac{1}{2} I_0 |\gamma_x|^2 |\gamma_y|^2 (1 + |k_x|^2 |k_y|^2) \quad (6)$$

Consequently

$$\epsilon = \frac{I_{\perp}}{I_{\parallel}} = \frac{|k_x|^2 + |k_y|^2}{1 + |k_x|^2 |k_y|^2} \quad (7)$$

With nearly ideal polarizers, k is very small and equation (7) becomes

$$\epsilon \approx |k_x|^2 + |k_y|^2 \quad (8)$$

The polarimeter to be analysed by the Jones calculus is shown schematically in Fig. 1. It is assumed that the co-ordinate axes are defined according to the transmission and extinction axes of \mathbf{P}_y . The transmission axis of \mathbf{P}_x is now assumed to make an "offset angle" θ with the extinction axis (x -axis) of \mathbf{P}_y . The introduction of this offset angle has important consequences for the behaviour of the system. The total matrix \mathbf{S} of the system is now

$$\mathbf{S} = \mathbf{P}_y \mathbf{D} \mathbf{R}_\theta \mathbf{P}_x \mathbf{R}_\theta^\dagger \quad (9)$$

The sample, denoted by matrix \mathbf{D} , is assumed to be circularly dichroic and optically active:²

$$\mathbf{D} = \exp\left[j \frac{\omega b}{c} (\hat{n}_+ + \hat{n}_- - 2)\right] \begin{pmatrix} \cos \chi & -\sin \chi \\ \sin \chi & \cos \chi \end{pmatrix} \quad (10)$$

where ω is the circular frequency of the wave, b is the path-length, c the velocity of light, $j = \sqrt{-1}$, and

$$\hat{n}_+ = n_+ + j \frac{\alpha_+ c}{2\omega}; \quad \hat{n}_- = n_- + j \frac{\alpha_- c}{2\omega} \quad (11)$$

n_+ and n_- being the indices of refraction for right and left circularly polarized light and α_+ and α_- the corresponding Napierian absorption coefficients. The angle χ is the complex angle of rotation

$$\chi = \chi' + j\chi'' = \frac{\omega b}{2c} (\hat{n}_- - \hat{n}_+) \quad (12)$$

The offset angle θ of the polarizer is taken into account by means of the orthogonal transformation matrix \mathbf{R}_θ :

$$\mathbf{R}_\theta = \begin{pmatrix} \cos \theta & -\sin \theta \\ \sin \theta & \cos \theta \end{pmatrix} \quad (13)$$

It is seen that the sample matrix \mathbf{D} also has the form of the orthogonal rotation matrix and therefore may be denoted by

$$\mathbf{D} = \exp\left[j \frac{\omega b}{c} (\hat{n}_+ + \hat{n}_- - 2)\right] \mathbf{R}_\chi \quad (14)$$

Thus \mathbf{R}_θ and \mathbf{R}_χ can be combined as

$$\mathbf{R}_\theta \mathbf{R}_\chi = \mathbf{R}_\chi \mathbf{R}_\theta = \mathbf{R}_{\theta+\chi} \quad (15)$$

The intensity of light transmitted by the system of Fig. 1 is

$$I = \frac{1}{2} \text{Tr}(\mathbf{S}^\dagger \mathbf{S}) I_0 = \frac{1}{2} \exp[-\frac{1}{2} b(\alpha_+ + \alpha_-)] \\ \times \text{Tr}(\mathbf{R}_\theta \mathbf{P}_x^\dagger \mathbf{R}_{\theta+\chi}^\dagger \mathbf{P}_y^\dagger \mathbf{P}_y \mathbf{R}_{\theta+\chi} \mathbf{P}_x \mathbf{R}_\theta) I_0 \\ = \frac{1}{2} \exp[-\frac{1}{2} b(\alpha_+ + \alpha_-)] \\ \times \text{Tr}(\mathbf{P}_x \mathbf{P}_x^\dagger \mathbf{R}_{\theta+\chi}^\dagger \mathbf{P}_y^\dagger \mathbf{P}_y \mathbf{R}_{\theta+\chi}) I_0 \quad (16)$$

Here the orthogonality of \mathbf{R}_θ , commutativity under the trace operation, and equation (15) have been used. After some algebraic manipulation equation (16) can be cast into the form:

$$I = \frac{1}{2} I_0 \exp[-\frac{1}{2} b(\alpha_+ + \alpha_-)] |\gamma_x|^2 |\gamma_y|^2 \\ \times [(|k_x|^2 + |k_y|^2) |\cos(\theta + \chi)|^2 \\ + (1 + |k_x|^2 |k_y|^2) |\sin(\theta + \chi)|^2] \\ = \frac{1}{2} I_0 \exp[-\frac{1}{2} b(\alpha_+ + \alpha_-)] |\gamma_x|^2 |\gamma_y|^2 \\ \times [(|k_x|^2 + |k_y|^2) \cos^2(\theta + \chi') \\ + (1 + |k_x|^2 |k_y|^2) \sin^2(\theta + \chi') \\ + (1 + |k_x|^2)(1 + |k_y|^2) \sinh^2 \chi''] \quad (17)$$

This equation allows the intensity transmitted by the system to be determined. The resultant electronic signal observed at the detector will now be defined as the difference between the results of two measurements, the first taken with the optically active sample in the cuvette and the second with pure solvent, *i.e.*, $\chi = 0$. Assuming that the system noise is dominated by photon noise, the noise σ_1 is proportional to the square root of the light intensity at the detector and inversely proportional to the square root of the integration time:³

$$\sigma_1 = g \left(\frac{I}{t}\right)^{1/2} \quad (18)$$

In the present case the intensity can be presented generally as:

$$I = f(\theta, \chi) I_0 \quad (19)$$

and hence the signal-to-noise ratio becomes:

$$S/N = \frac{(I_0)^{1/2} [f(\theta, \chi) - f(\theta, 0)]}{g [f(\theta, \chi) + f(\theta, 0)]^{1/2}} \quad (20)$$

In order to optimize the detector in terms of the influence of θ on S/N , the constant coefficient in equation (20) is unimportant. Further, we are concerned, in particular, with the signal-to-noise ratio at very small values of χ . Hence it is useful to define a new parameter, the relative signal-to-noise ratio, r :

$$r = \lim_{\chi \rightarrow 0} \frac{1}{\chi} \frac{[f(\theta, \chi) - f(\theta, 0)]}{[f(\theta, \chi) + f(\theta, 0)]^{1/2}} \quad (21)$$

Substitution of equation (17) into (21) gives

$$r = \frac{1}{2} |\gamma_x| |\gamma_y| (1 - |k_x|^2)^{1/2} (1 - |k_y|^2)^{1/2} \times \frac{\sin 2\theta}{(\beta + \sin^2 \theta)^{1/2}} \quad (22)$$

where $\beta = \epsilon / (1 - \epsilon)$. The relative signal-to-noise ratio is now differentiated with respect to θ :

$$\frac{dr}{d\theta} = |\gamma_x| |\gamma_y| (1 - |k_x|^2)^{1/2} (1 - |k_y|^2)^{1/2} \times \frac{2(2\beta + 1) \cos 2\theta - \cos^2 2\theta - 1}{(\beta + \sin^2 \theta)^{3/2}} = 0 \quad (23)$$

which gives

$$\theta_{opt} = \frac{1}{2} \arccos [2\beta + 1 - 2\sqrt{\beta(\beta + 1)}] = \arctan \epsilon^{1/4} \quad (24)$$

The maximum value of r is obtained by substituting (24) into (22):

$$r_{max} = |\gamma_x| |\gamma_y| (1 - |k_x|^2)^{1/2} (1 - |k_y|^2)^{1/2} \sqrt{\cos 2\theta_{opt}} = |\gamma_x| |\gamma_y| (1 - |k_x|^2)^{1/2} (1 - |k_y|^2)^{1/2} \sqrt{\frac{1 - \sqrt{\epsilon}}{1 + \sqrt{\epsilon}}} \quad (25)$$

EXPERIMENTAL

Apparatus

The measurements were made by using the apparatus shown schematically in Fig. 2. The light-source was a sodium hollow-cathode lamp (Varian-Techtron) run at ca. 5 mA. The polarizer and analyser were two identical 2-in. plastic square dichroics (Edmund Scientific Co., N.J.). The length of the sample cuvette was 8.3 cm and the sample was a 2% solution of sucrose, which gave a calculated optical rotation angle of 1.1°. The photomultiplier was a 1P28 with a calibrated gain curve.

Procedure

With the sample cuvette removed, the extinction ratio of the polarizer-analyser pair was measured, giving $\epsilon = 6.5 \times 10^{-4}$. The measurements were started by first crossing the polarizer and analyser, and recording the "blank" signal on a recorder. Then the sample cuvette was inserted into the light-path and the signal recorded again. This procedure was repeated with intermittent rotation of the polarizer. The offset angles θ were calculated from the equation derivable from equation (17):

$$\theta = \arcsin \sqrt{\left(\frac{I_\theta - I_\perp}{I_\parallel}\right) \left(\frac{1}{1 - \epsilon}\right)} \quad (26)$$

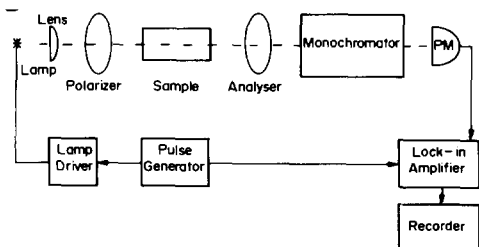


Fig. 2. Block diagram of the polarimeter used in the present work.

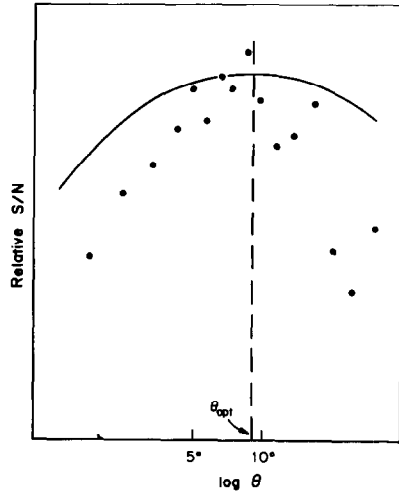


Fig. 3. Relative signal-to-noise ratio as a function of the offset angle of the polarizer. ●: experimental points; —: calculated from equation (22) and scaled to fit the experimental points.

where I_θ is the intensity measured with the offset angle θ , I_\perp with the polarizer and analyser crossed and I_\parallel with the parallel polarization axes. The noise was measured as the average peak-to-peak noise from the recorder tracing during a 10-sec interval.

RESULTS AND DISCUSSION

The values of experimental signal-to-noise ratios plotted against $\log \theta$ are shown in Fig. 3, along with the theoretical relative signal-to-noise ratios calculated from equation (22). The theoretical curve is scaled to optimize the fit with the experimental points. The optimum offset angle θ_{opt} calculated from equation (24) is 9.07° and is marked in Fig. 3. The position of the optimum is very well matched by the experimental points, although the shapes of the observed and calculated curves differ somewhat.

Equation (25) for the maximum value of r shows one of the results of present interest. The upper limit of r which is attainable by any real polarizer and analyser is unity. The inexpensive polarizer sheet used in this work had an extinction ratio of 6.5×10^{-4} which gives $r = 0.975$, assuming that $\gamma_x = \gamma_y = 1$. Naturally there are losses represented by γ_x and γ_y , but equally there are reflection and aperture losses in the case of the much more expensive prism polarizers. Hence the unavoidable conclusion is that there is little point in investing in high-performance polarizers when practically the same signal-to-noise ratio is obtained by using cheap plastic dichroic filters (or even reflection polarizers for work in the ultraviolet). It should be noted that this conclusion is strictly valid for shot-noise limited systems. For instance, in our system the change in the transmitted intensity is recorded as the sample is changed from optically active to inactive. The offset angle of the polarizer is maintained constant. With very small optical activities the changes in the intensity may be buried in the

flicker noise of the source. The signal-to-noise ratio can then be improved by modulating the offset angle, as done by Yeung *et al.*¹ With a high-grade polarizer the optimum modulation amplitude is small, and a non-mechanical and highly stable Faraday rotator can be used for modulation. With polarizers of low quality the optimum modulation amplitude is large, Faraday rotation cannot be used, and corresponding demands are made on the mechanical or optical stability of the system. Thus high stability is the price to be paid for using cheap polarizers.

According to equation (20), the principal way to improve the signal-to-noise ratio is to increase the integration time or the source intensity, either directly or by increasing the optical aperture. The latter option is more easily achieved if prism polarizers are

avoided, since dichroics have a larger area and less need for collimation. If measurement at a single wavelength is sufficient, a laser is an ideal light-source.

Acknowledgements—The authors are indebted to the National Sciences and Engineering Council of Canada and to the Finnish Academy for support of this work.

REFERENCES

1. E. S. Yeung, L. E. Steenhoek, S. D. Woodruff and J. U. Kuos, *Anal. Chem.*, 1980, **52**, 1399.
2. J. J. Kankare and R. Stephens. *Spectrochim. Acta*, 1980, **35B**, 849.
3. H. V. Malmstadt, C. G. Enke and S. R. Crouch, *Electronics and Instrumentation for Scientists*, p. 410. Benjamin/Cummings, Calif., 1981.

VOLTAMMETRIC STUDY OF THE REDOX BEHAVIOUR OF THE Hg(II)/Hg(I)/Hg SYSTEM AT A ROTATING METAL-RING/GLASSY-CARBON DISC ELECTRODE

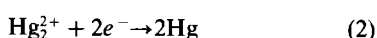
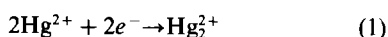
P. KIEKENS, E. TEMMERMAN and F. VERBEEK

Laboratorium voor Analytische Scheikunde, Rijksuniversiteit Gent, Krijgslaan 281, S12, B-9000 Gent, Belgium

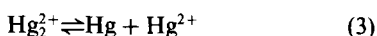
(Received 5 December 1983. Accepted 28 February 1984)

Summary—The reduction of Hg(II) at a glassy-carbon electrode in various electrolytes has been studied by rotating ring-disc voltammetry. Reduction proceeds directly to metallic mercury in a single 2-electron step. However, at the foot of the wave, and only during the first reduction sweep after pretreatment of the electrode surface, a small amount of Hg(I) species is detected at the ring. The appearance of an Hg(I) intermediate is most pronounced in sulphuric acid solution. The reduction of Hg(II) is found to proceed irreversibly and to be of first order. At sufficiently negative potentials the reduction is convective-diffusion controlled. Stripping voltammetric experiments indicate that the dissolution of mercury gives Hg(II) in complexing electrolytes. In non-complexing electrolytes the initially formed Hg(II) reacts with mercury atoms on the electrode surface to give Hg(I). During electro-dissolution, two stripping peaks may be observed as a result of underpotential adsorption of mercury on glassy carbon. The difference in peak potential between the adsorption (mono) layer peak and the bulk mercury peak has been related to the difference in work functions of the deposit (mercury) and substrate (carbon). A rotating glassy-carbon electrode has been used for the anodic stripping determination of mercury. When an appropriate amount of a cation such as cadmium(II) or copper(II) is added to the test solution, mercury down to $2 \times 10^{-9} M$ (0.4 ng/ml) can be determined in acidified thiocyanate electrolyte with a relative standard deviation of about 22%.

Several papers have dealt with the reduction of Hg(II) at graphite electrodes.¹⁻⁶ With a freshly polished electrode only a single reduction wave is obtained. From the standard potentials of the reactions⁷



which are 0.920 and 0.789 V respectively, two individual waves would be expected, and for the disproportionation equilibrium⁸



we have $K = 6.0 \times 10^{-3}$.

As the stepwise reduction of Hg(II) may result in production of the dimeric Hg(I), it seemed to us of interest to use a rotating ring-disc electrode system, which has been proved to be very efficient in detecting electroactive intermediates,^{6,9,10} to find whether this occurs.

Mercury has widespread use in electroanalytical chemistry. In stripping voltammetry, a mercury film on solid electrodes offers great advantages and has been used in a large number of researches. However, the kinetics of electro-dissolution of mercury itself from a solid electrode have received little attention and no unambiguous answer can be found to the problem of the oxidation state of the mercury ions formed in the process. The oxidation may produce

only one of the two states, or both. The present study was undertaken to try to elucidate this problem and to obtain an insight into the kinetics of electro-dissolution of mercury.

Anodic stripping (oxidation) of thin metal films from solid electrodes often shows two or even three dissolution peaks.^{10,12-15} The extra peaks at potentials which are more positive than the normal dissolution peak potential of the bulk metal, are generally due to dissolution of the deposited metal atoms in direct contact with the solid substrate electrode.

If more than one extra dissolution peak is observed in addition to the bulk stripping peak, interaction of the atoms of the first monolayer with different sites on the electrode substrate is thought to occur.¹²

Underpotential adsorption of mercury on glassy carbon has scarcely been studied. According to Dunsch,¹⁶ underpotential monolayer adsorption of mercury on glassy carbon can be observed, provided that the electrode surface is freed from "oxides", which are characteristic for glassy carbon.¹⁶⁻¹⁸

As part of an extended study of the redox reactions of the Hg(II)/Hg(I)/Hg system on glassy carbon, the mercury monolayer adsorption behaviour was also investigated by the rotating ring-disc technique.

Anodic stripping voltammetry (ASV) is a very suitable technique for determining metal ions at extremely low concentrations. The introduction of solid electrodes enables ASV to be used for the

determination of noble metals such as gold, platinum, iridium and mercury. The present work also deals with the determination of microamounts of mercury by ASV after deposition of this element on a rotating glassy-carbon disc electrode. To enhance the sensitivity and reproducibility of the analytical method, a second ion, *e.g.* Cd(II), was added to the test solution.

EXPERIMENTAL

Experiments were performed in 1M sulphuric acid, 0.1M solutions of perchloric acid and nitric acid and 0.1M solutions of sodium sulphate, potassium nitrate, sodium perchlorate and sodium thiocyanate at various pH values. Solutions were prepared from analytical grade reagents (Merck) and water freshly generated by a Milli-Q system (Millipore Inc.). A 0.1M standard Hg(II) solution was prepared from the nitrate. This solution was stabilized by addition of enough concentrated nitric acid to give a final acid concentration of 0.1M.

Home-made ring-disc electrodes with a glassy carbon (GC) (Tokai Electrode Mfg. Co., Tokyo) disc and a gold or platinum ring were used. The dimensions were 0.249 and 0.225 cm for the disc radii, 0.270 and 0.246 cm for the inner ring radii and 0.301 and 0.268 cm for the outer ring radii, the first value referring to the gold system and the second to platinum. This gives a theoretical collection efficiency,¹⁹ N_0 , of 0.25 for the gold-GC electrode and 0.21 for the platinum-GC electrode.

The cell consisted of a Teflon vessel of about 150 ml capacity in which the rotating ring-disc electrode was centrally placed. A platinum auxiliary electrode was placed in a compartment separated from the cell by a fritted glass disc. A saturated calomel electrode (SCE) was connected to the cell by means of a U-tube and a salt bridge, filled with saturated potassium chloride solution and the cell solution respectively. All potentials are referred to the SCE. Experiments were performed at $25.0 \pm 0.1^\circ$.

Electrode rotation was achieved by a Brion-Leroux motor (Biotax, Type I) and the speed controlled by means of a proximity probe (Philips PR 9373) and frequency meter (Philips PM 6601).

Potential control was maintained by means of a GSATP Tacussel sweep generator and a BI-PAD potentiostat. Curves were recorded on a Hewlett-Packard X-YY recorder, Model HP 7046 A.

Standard metallographic procedures were used for polishing the electrode. Final polishing was done with 0.05- μ m alumina on Buehler microcloth to a mirror-like finish. Ultrasonic cleaning served to remove any alumina or other impurities that might adhere to the electrode surface.

The electrochemical pretreatment of the glassy-carbon disc consisted of continuous cycling of the potential between fixed values (in the range from -1.5 to 1 V) in the working electrolyte at a sweep-rate of 0.1 V/sec until a reproducible and very low background current was obtained. The ring was pretreated in the same way. During this pretreatment nitrogen containing <1 ppm of oxygen was passed through the cell solution. After the electrode activation period, a nitrogen atmosphere was maintained above the cell solution.

Experiments at the disc were started from an initial potential positive enough to avoid Hg(II) reduction, the potential being made more negative. The ring potential, E_R , was held at a value sufficiently positive to ensure a convective-diffusion controlled oxidation of any Hg(I) ions leaving the disc electrode.

Stripping experiments at the disc were performed by switching the potential of the disc to the desired deposition potential, E_{dep} . After the deposition, the disc potential was scanned linearly in the anodic direction and the mercury

dissolution curve (disc) and collection curve (ring) were recorded.

RESULTS AND DISCUSSION

Reduction of Hg(II)

Figure 1 shows the voltammetric curves for the reduction of 0.99mM Hg(II) in 1M sulphuric acid at a glassy-carbon disc, and the corresponding ring current at $E_R = 1.4$ V, where the only possible reaction is the oxidation of Hg(I). A substantial oxidation current at the gold ring was observed during the first voltammetric curve recorded with a newly polished and activated electrode. This ring current first increases with decreasing disc potential and then drops to zero. This means that Hg(I) is produced at the disc surface or in the adjacent solution layer in a restricted potential range, at the foot of the reduction wave of Hg(II) at the disc. Subsequent scans obtained without reactivating the electrode surface produced much lower amounts of Hg(I) (Fig. 1).

At potentials more positive than that giving the current maximum for the oxidation of Hg(I) at the ring, $I_{R,M}$, I_R increases proportionally with the disc current I_D and obeys the equation

$$I_R = N_0 I_D \quad (4)$$

This means that the production of Hg(I) probably occurs according to equation (1). Once the current maximum at the ring is reached, the disc current starts rising more steeply and I_R/I_D becomes smaller than N_0 . Finally the ring oxidation current drops to zero.

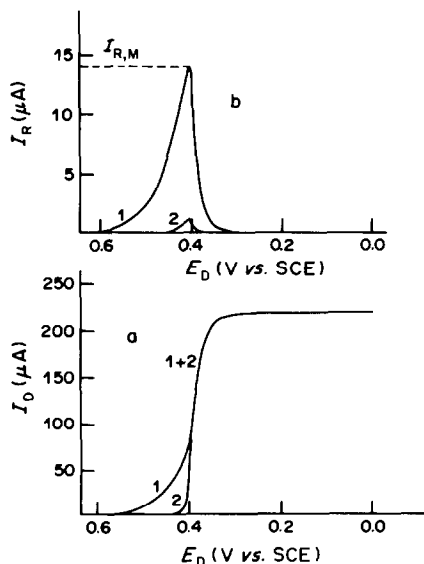


Fig. 1. Current-potential curves for the reduction of 0.99mM Hg(II) in 1M H_2SO_4 at a glassy-carbon disc (a), and corresponding curves for the oxidation of the intermediate Hg_2^{2+} at the gold ring (b), as a function of the disc electrode potential. $E_R = 1.4$ V vs. SCE; $\omega = 157$ rad/sec; $v = 0.01$ V/sec. (1) Obtained during first scan with freshly pretreated electrode; (2) second and subsequent scans.

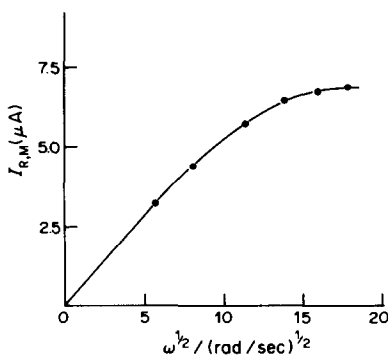
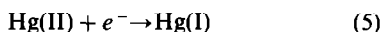


Fig. 2. Plot of the maximum current for the oxidation of Hg_2^{2+} at the ring. $I_{R,M}$ plotted against $\sqrt{\omega}$, for $1M \text{H}_2\text{SO}_4$ medium; $c_{\text{Hg(II)}} = 0.50mM$; $E_R = 1.4 \text{ V vs. SCE}$.

The variation of the current maximum for the oxidation of Hg(I) at the ring, $I_{R,M}$, with the speed of rotation of the electrode, is represented in Fig. 2. The result is typical of a disc-electrode reaction controlled partially by mass transfer and charge transfer at the potential of the ring-current maximum. The subsequent beginning of the direct reduction of Hg(II) to metallic mercury prevents the full development of the first wave into a diffusion-controlled region at still more negative potentials.

From an equation derived by Levich²⁰ for reactions that are controlled by mixed charge-transfer and diffusion kinetics, the standard heterogeneous rate constant for the Hg(II)/Hg(I) couple was calculated to be about 10^{-7} cm/sec . Consequently the reduction of Hg(II) to Hg(I) is highly irreversible. Plots of $\log [I/(I_L - I)]$ vs. potential are linear at potentials more positive than 0.4 V . Assuming a one-electron transfer, the transfer coefficient obtained from the slopes of these plots varies between 0.54 and 0.60 . Here I_L was taken as half of the limiting current for the subsequent reduction of Hg(II) to metallic mercury at more negative potentials. This result is indicative of a first-order reaction in which soluble species are involved, according to the equation



Production of Hg(I) during the reduction of Hg(II) at glassy-carbon has also been observed in $0.1M$ sulphuric acid, $1M$ perchloric acid, $0.1M$ nitric acid and $0.1M$ sodium sulphate ($\text{pH} = 2$) media, but to an extent that is only a tenth or less of that in $1M$ sulphuric acid. The more pronounced wave of Hg(II)/Hg(I) reduction in $1.0M$ sulphuric acid may result from the superior complexing properties of sulphate for mercury.²¹

In sulphuric acid medium, specific adsorption of sulphate ions²² may increase the rate of the Hg(II) reduction so that the Hg(II)/Hg(I) reaction is favoured by anion interaction with the transition state.

Generally, the production of Hg(I) becomes less

when the acidity of the solution decreases and it is possible that the activity of the glassy-carbon towards the Hg(II)/Hg(I) reduction decreases with increasing pH because of a change in the surface state of the glassy-carbon. This material has a redox potential which is pH-dependent^{23,24} owing to the electrode reaction of oxygen adsorbed on the surface or present in solution.

In the case of $0.1M$ sodium sulphate ($\text{pH} = 2.0$), the solubility of the Hg(I) generated is lower than that in $1M$ sulphuric acid.²⁵ This could result in the formation of a precipitate on the electrode surface, and hindrance to detection of Hg(I) at the ring. At potentials more negative than that giving the current maximum at the ring, the direct reduction of Hg(II) to metallic mercury gradually replaces the one-electron transfer and the ring current drops to zero.

Kinetic parameters for the reduction of Hg(II) at disc potentials more negative than the potential at which $I_{R,M}$ occurs at the ring, have been evaluated by the method of Frumkin and Tedoradze.²⁶ Reciprocal currents, $1/I$, recorded at constant potentials in the region preceding the limiting-current plateau, gave linear plots against the reciprocals of the square roots of the rotation rates, $1/\sqrt{\omega}$. These plots were used to derive the kinetic currents, I_k , by extrapolation to $1/\sqrt{\omega} = 0$. These currents were used to calculate the apparent standard heterogeneous rate constant, k_{sh}^a , at E° of the Hg(II)/Hg couple. In $0.1M$ sodium sulphate solution ($\text{pH} = 2.0$) the value of k_{sh}^a obtained in this way was *ca.* 10^{-5} cm/sec with αn ($\alpha =$ cathodic transfer coefficient) equal to 0.55 . Thus the reduction of Hg(II) proceeds irreversibly. The observed dependence of the half-wave potentials on the rate of stirring was also indicative of an irreversible process.

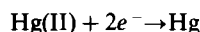
The linear dependence of $1/I$ on $1/\sqrt{\omega}$ points to a first-order reduction. The order of the reaction was also evaluated by the method of Frumkin and Tedoradze.²⁶

Their procedure is demonstrated in Fig. 3 which shows in addition to the limiting currents, I_L , the currents at different potentials along the rising portion of the wave, as a function of ω . The nature of the plot indicates that before the limiting plateau is reached, the electrode reaction is under mixed control.

The order, μ , can be found by using the equation

$$\mu = \frac{\log(AC/BC)}{\log(AC/AB)} \quad (6)$$

The reaction was found to be first-order, since μ varied between 0.80 and 0.92 ($0.1M \text{Na}_2\text{SO}_4$, $\text{pH} = 2$). This confirms the ring-disc results and shows that the reduction to metallic mercury involves only one mercury atom:



It was found that at sufficiently negative potentials the limiting reduction current, I_L , at the disc was proportional to $\sqrt{\omega}$ (with zero intercept) for all

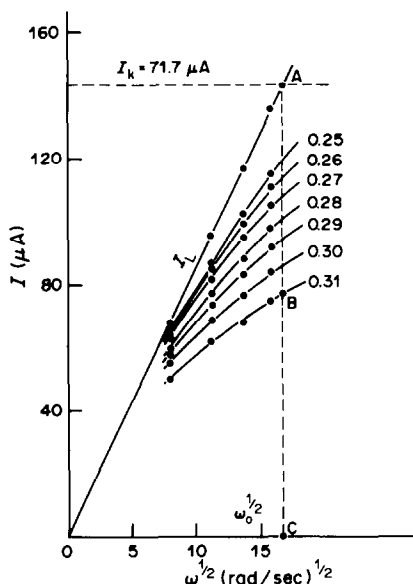


Fig. 3. I vs. $\sqrt{\omega}$ plot for the reduction of 0.50mM Hg(II) at a glassy-carbon disc in 0.1M Na_2SO_4 (pH 2.0). Numbers indicate applied potential, V vs. SCE; I_L is the limiting current; I_k the cathodic kinetic current at 0.31 V obtained after extrapolation of $1/I$ to $\omega = \infty$.

concentrations of Hg(II) . Thus the Levich equation²⁷ for a convective diffusion-limited process was obeyed.

For 0.1M sodium perchlorate and 1M potassium nitrate solutions we examined the influence of a change in pH on the reduction wave of Hg(II) . Both solutions responded in almost the same way. An increase in pH resulted in the appearance of two well-separated waves (Fig. 4); from about pH 3, the

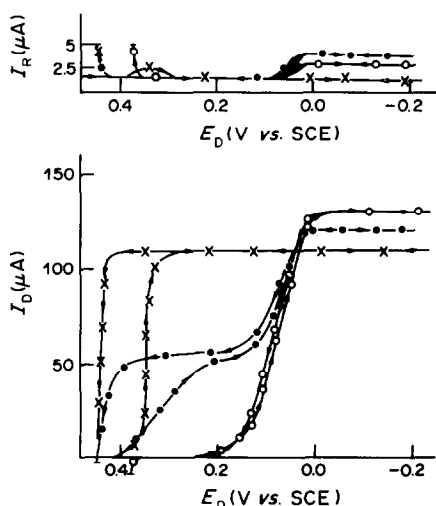


Fig. 4. Current-potential curves obtained with a newly activated electrode for the reduction of 0.50mM Hg(II) at a glassy-carbon disc and corresponding curves for the oxidation of the intermediate, Hg(I) , at the ring in 0.1M NaClO_4 at pH values of 2.0 (\times), 3.9 (\bullet) and 8.9 (\circ) as a function of the disc electrode potential. $E_R = 1.4$ V; $\omega = 188$ rad/sec; $v = 0.01$ V/sec.

original wave started to decrease and a second wave appeared, shifting to more negative potentials with increasing pH. At pH ~ 6 the first wave had almost vanished, while at pH 8–9 only the second wave remained ($E_{1/2} \sim 0.07$ V vs. SCE). When the pH was increased still further, this wave also disappeared.

The ring current indicated that it was only during the second wave that Hg(I) ions left the disc, no Hg(I) being detected during the first wave. With increasing pH, the production of Hg(I) passed through a maximum (at pH = 4–5).

We believe that during the first reduction wave Hg^{2+} ions are reduced, but during the second wave HgOH^+ and/or Hg(OH)_2 are also reduced. The occurrence of these complexes is predicted by a Pourbaix diagram.²⁸ With increasing pH, more Hg(OH)_2 is formed and more Hg(I) ions are produced at the disc and detected at the ring. For example, at pH 2, the ratio of the amounts of free Hg^{2+} ions and Hg(OH)_2 is about 100, while at pH 4, it is about 0.01.²⁸

The decline of the ring current with increasing pH after reaching a maximum can have several causes. The Hg(I) ions formed at the disc may be transformed into polynuclear complexes²⁹ which become more stable with increasing pH. On the other hand solubility limitations are also important, not only for Hg(OH)_2 but also for the Hg(I) complexes.

Oxidation of metallic mercury

A survey of the literature data^{11,30–37} for electro-dissolution of mercury indicates that Hg(II) ions are mainly formed as a reaction product in complexing electrolytes, whereas Hg(I) ions are found in non-complexing electrolytes. Some of these data are summarized in Table 1. There is one exception, however; according to Combet and Dozol,³⁶ electro-dissolution of mercury in perchloric acid and nitric acid media at a glassy-carbon electrode produces only Hg(II) ions.³³

According to Brainina,³⁵ a linear relation is expected between the anodic peak potential, E_p , of the metal-stripping curve and the logarithm of the potential scan-rate, v . Such a relationship was found for mercury in various electrolytes. From the slope,³⁸ the

Table 1. Electro-dissolution products of mercury at various electrodes in diverse electrolytes

Electrode	Electrolyte	Mercury species formed	Reference
Platinum	$\text{KNO}_3, \text{HClO}_4$	Hg(I)	30
Glassy-carbon	H_2SO_4	Hg(I)	11
Platinum	HClO_4	Hg(I)^*	31
Gold	$\text{HNO}_3, \text{H}_2\text{SO}_4$	Hg(I)	32
Platinum	HClO_4	Hg(II)^\dagger	31
Mercury	KSCN	Hg(II)	33
Graphite	KSCN	Hg(II)	34
Graphite	KSCN	Hg(II)	35
Glassy-carbon	$\text{HClO}_4, \text{HNO}_3$	Hg(II)	36
Mercury	NaCN	Hg(II)	37

* $E_d < 0.6$ V.

† $E_d < 0.85$ V.

value of βn (β = anodic transfer coefficient) was found to be 1.44 for 0.1M sodium thiocyanate + 0.01M perchloric acid and 1.74 for 0.1M perchloric acid media. Other values obtained are 1.31 for 1M sulphuric acid and 1.69 for 0.1M acetate buffer (pH 4.66).

These results suggest that ions formed during the electro-oxidation must be Hg^{2+} (irrespective of the electrolyte used) if a reasonable value for β is to be obtained.³⁹

However, ring-disc experiments in perchloric acid and sulphuric acid media have proved the existence of Hg_2^{2+} ions during electro-dissolution. This finding is also in accordance with the experiments by Allen and Johnson.¹¹ The Hg(I) ions produced at the disc may react at a sufficiently positive potential at the ring to give Hg(II), or they may also react at a negative ring potential to give metallic mercury. This is shown in Fig. 5. The ring collection peaks at 1.4 V (oxidation) and -0.2 V (reduction) are almost equal, indicating that the mercury deposited is stripped mainly as Hg(I). This is in contradiction to the results obtained from simple semilogarithmic analysis of the mercury ionization peak at the disc, as mentioned before.

These conflicting experimental results can be explained by assuming the occurrence of a special type of chemical reaction following the mercury electro-dissolution, which we will call "reproportionation". The Hg(II) ions first formed are supposed to react with unoxidized mercury atoms still present on the electrode surface, leading to the formation of Hg(I)

ions. This explanation is acceptable, as the value of the equilibrium constant, K , for the reaction



is 166,⁸ indicating that mercury(I) is the dominant species. These Hg(I) ions reach the surrounding ring electrode where they can be oxidized or reduced.

This proposed reaction mechanism for mercury dissolution also explains why the stripping peak obtained with thiocyanate solutions (or generally with complexing electrolytes) is double the size of the dissolution peaks obtained in perchloric acid medium (or generally with non-complexing electrolytes). In non-complexing electrolytes, half of the mercury deposit may be stripped from the electrode surface in a non-electrochemical way, because of the reproportionation reaction. For a complexing electrolyte, however, our experiments indicate that the Hg(II) ions newly formed at the electrode surface are involved in subsequent chemical reactions, stabilizing the Hg(II) ions as complex ions. Investigations with an electrolyte solution of constant ionic strength containing xM sodium thiocyanate + $(2-x)M$ sodium perchlorate + 0.01M perchloric acid suggest that $\text{Hg}(\text{SCN})_3^-$ is the primary product of mercury electro-dissolution ($0.1 \leq x \leq 2$). The co-ordination number of 3 is derived from the dependence of the anodic peak potential on the thiocyanate concentration.³⁵ The co-ordination number is reported to be 4 for the species present in the bulk of the solution.³⁴⁻⁴⁰ The ability of complexed Hg(II) species to oxidize mercury atoms is less than that of uncomplexed or weakly complexed Hg(II) ions. In complexing electrolytes, the absence of Hg(I) ions is also confirmed by ring-disc experiments. At the ring, only the reduction signal for stripped Hg(II) ions can be obtained at sufficiently negative potentials. It is concluded that the complexing properties and concentration of the electrolyte are important in electro-dissolution of mercury. For example, at low hydrochloric acid concentrations, e.g., 0.01M, an oxidation as well as a reduction peak for Hg(I) ions produced at the disc can be observed at the ring. With increasing chloride concentration, both the dissolution peak at the disc and the reduction peak at the ring grow, while the oxidation peak at the ring diminishes. This means that more Hg(II) ions are produced instead of Hg(I) ions and that reproportionation becomes less important because of the increased formation of Hg(II) chloride complexes. At a hydrochloric acid concentration exceeding 2M, the mercury dissolution peak reaches its maximum value and no oxidation peak at the ring can be observed. This indicates exclusive formation of Hg(II) ions at the disc.

Figure 6 shows the voltammetric curves for the electro-dissolution of mercury at the glassy-carbon disc and simultaneous collection (oxidation) of stripped mercury ions at the platinum ring of the rotating ring-disc electrode in 0.1M potassium

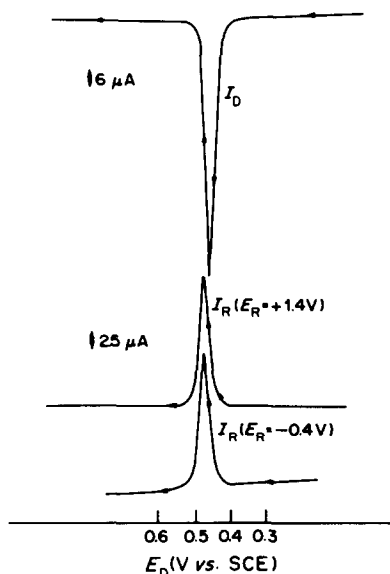


Fig. 5. Current-potential curves for electro-dissolution of mercury at a glassy-carbon disc and simultaneous collection of stripped mercury ions at the platinum ring of a rotating ring-disc electrode in 0.1M HClO_4 . $c_{\text{Hg(II)}} = 5 \mu\text{M}$; deposition time = 1 min; $\omega = 188$ rad/sec; $E_{\text{dep}} = -1.0$ V; $v = 0.1$ V/sec; E_R = ring potential; E_D = disc potential.

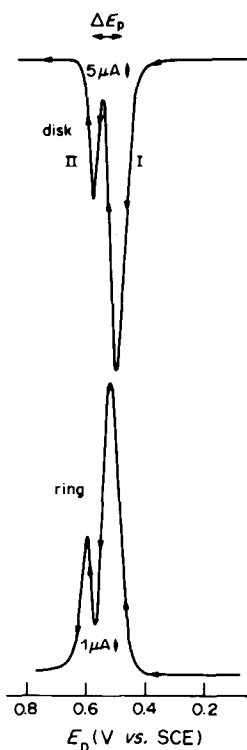


Fig. 6. Current-potential curves for the electrodisolution of mercury at a glassy-carbon disc and simultaneous collection (oxidation) of stripped mercury ions at the platinum ring of a rotating ring-disc electrode in $0.1M$ $KNO_3 + 0.01M$ HNO_3 . $c_{Hg(II)} = 5 \mu M$; deposition time = 6 min; $E_{dep} = -0.5$ V; $E_r = 1.4$ V; $v = 0.05$ V/sec; $\omega = 188$ rad/sec; E_D = disc potential.

nitrate + $0.01M$ perchloric acid. At the disc, a small stripping current peak is obtained at more positive potentials, in addition to the large peak due to the electro-oxidation of the bulk deposit. The smaller peak is assumed to result from the oxidation of a monolayer of mercury atoms which are more tightly bound to the electrode surface. The stripping curve at the disc in Fig. 6 is obtained after 11 min of electrolysis at a deposition potential of -0.5 V. More negative deposition potentials, *e.g.*, -1.0 V, appear to inhibit the formation of a mercury adsorption layer in which the mercury atoms are more firmly bound to the carbon surface. In all cases, it is necessary to keep the electrolysis potential for a sufficient time at a negative value to overcome the poor adhesion of the mercury atoms to the glassy-carbon surface (in agreement with the finding of Morcos).¹⁵

For a close packed monolayer of mercury atoms, a total of $205 \mu C$ per cm^2 of electrode surface is needed for the area under the stripping peak, assuming a mercury atom radius of 0.15 nm,⁴¹ and the exclusive production of $Hg(I)$ ions during stripping. In $0.01M$ potassium nitrate + $0.01M$ nitric acid solution the total charge associated with the adsorption peak (peak II in Fig. 6) may even exceed the

theoretical charge for a monolayer. Simultaneously with the increase of the charge associated with the adsorption peak, there is a decrease in the difference of peak potential, ΔE_p , between the bulk and adsorption layer peaks (Fig. 7).

For a theoretically complete monolayer, *i.e.*, complete coverage of the electrode surface, $\theta = 1$, a value of 73 ± 6 mV for ΔE_p is found experimentally (Fig. 7). The half-width¹³ δ of the monolayer stripping-peak is 41 ± 4 mV. According to Kolb *et al.*,¹³ the underpotential shift (ΔE_p) is related to the difference in work function ($\Delta\Phi$) for the substrate atom (carbon) and monolayer atom (mercury):

$$\Delta E_p = \alpha \Delta \Phi$$

where $\alpha = 0.5$ V/eV. Reasonable values for Φ (C) and Φ (Hg) are 4.6 and 4.5 eV respectively,^{42,43} from which ΔE_p is calculated to be 50 mV. This differs from the experimental value but the discrepancy may be ascribed to the uncertainty of the value to be used for Φ (C). The literature values refer to a well-outgassed polycrystalline material that is not subject to oxygen adsorption.⁴⁴ As glassy-carbon is supposed to be covered with oxide in the experiments performed, a somewhat higher value for Φ (C) should not be excluded,⁴⁵ resulting in larger ΔE_p values. Deviations of ΔE_p might also be due to specific interactions between monolayer and substrate,¹³ a roughening of the electrode surface (pretreatment), a difference in the value of the electrostripping oxidation state γ and charge of the mercury ions,⁴⁶ co-adsorption of anions, or surface imperfections.¹⁴ As mentioned previously,

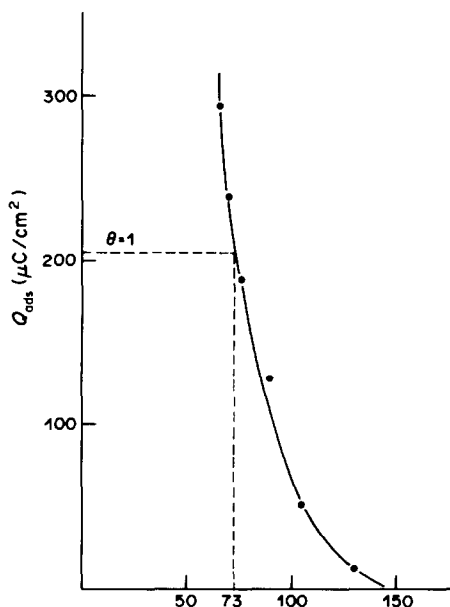


Fig. 7. Charge (Q_{ads}) under the adsorption layer peak *vs.* underpotential shift ΔE_p (see text) at a glassy-carbon disc electrode in $0.1M$ $KNO_3 + 0.01M$ HNO_3 . $c_{Hg(II)} = 10 \mu M$; deposition time variable; other conditions as for Fig. 2; θ = assumed coverage of the glassy-carbon surface with mercury.

the area of the adsorption layer peak (Fig. 6) can correspond to a charge greater than that for a monolayer. Consequently more mercury atoms than can be accommodated in a monolayer may be interacting with the glassy-carbon surface. At the same time ΔE_p decreases to a constant value of about 60 mV (Fig. 7). With increasing deposition time and mercury(II) concentration, ΔE_p remains practically constant at 60 mV. Finally, the bulk stripping peak grows so that it interferes severely with (or even masks) the adsorption peak, and hence no further measurements of that peak are possible. The appearance of the monolayer adsorption peak depends on the deposition potential at which electrolysis takes place and is favoured by a negative deposition potential (which, however, does not produce any significant reduction of hydrogen ions), e.g., -0.5 V for $0.01M$ potassium nitrate + $0.01M$ nitric acid medium.

Simultaneous reduction of hydrogen ions would inhibit the formation of a mercury atom layer with stronger binding between the metal and the electrode material. According to Combet and Dozol,³⁶ the reduction of hydrogen ions might replace the reduction of Hg(II) ions at more active sites on the electrode. These sites act as places at which the tendency of the mercury atoms to form an adsorption layer is more pronounced. This might explain the limited appearance of a mercury adsorption layer as found for $0.1M$ perchloric acid medium, and the absence of any adsorption peak at any deposition potential, for $1M$ perchloric acid medium.

Any other ion deposited at the plating potential of the mercury ions acts in the same way as the hydrogen ions, the adsorption peak completely disappearing with the addition of a sufficient concentration of the interfering ion, e.g., $1\mu M$ Cu(II). In this case, the reduction of Hg(II) may take place on the reduced copper atoms, which may explain the "support effect"^{3,47,48} of ions such as copper and cadmium. Obviously this "support effect" enhances the analytical possibilities of the carbon electrode.^{3,11,47,48}

Determination of mercury

Glassy-carbon is a useful electrode material for mercury determination by stripping analysis. Amalgamation of the electrode substrate by the deposited mercury, which occurs when gold or platinum electrodes are used, is avoided.

Stripping experiments for mercury determination were performed with $0.1M$ perchloric acid and $0.1M$ sodium thiocyanate + $0.01M$ perchloric acid media. These two solutions can be taken as typical of non-complexing and complexing electrolytes respectively. With $0.1M$ perchloric acid it was found that the lowest detectable concentration of mercury was $7 \times 10^{-7}M$. Because of the weak adhesion forces between mercury and glassy-carbon,¹⁵ the reduction and deposition of mercury from dilute solutions is a serious problem.¹⁶ This may be overcome by the addition of a known concentration of other metal

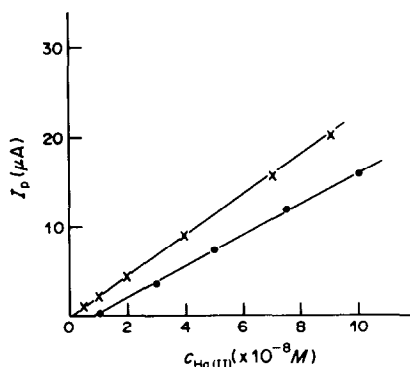


Fig. 8. Dependence of the electrodisolution peak current, I_p , on Hg(II) concentration in $0.1M$ HClO₄ (—●—) and in $1M$ NaSCN + $0.01M$ HClO₄ (—x—). $v = 0.1$ V/sec; $\omega = 188$ rad/sec; (—●—) $E_{\text{dep}} = -1.0$ V; $t_{\text{dep}} = 24$ min; (—x—) $E_{\text{dep}} = -1.5$ V; $t_{\text{dep}} = 16$ min.

ions to the sample solution. These metals are electro-deposited together with the mercury to be determined. Various authors⁴⁹⁻⁵¹ have found that the introduction of these auxiliary elements in sufficient amounts decreases the detection limit of the determination, provided that they are oxidized (stripped) from the electrode surface at potentials more negative than the dissolution potential of the metal to be determined. Therefore metals such as copper, cadmium and lead (electronegative elements) should be used for determination of mercury (an electropositive element).

To detect very small quantities of mercury in $0.1M$ perchloric acid medium, cadmium(II) was added to the cell solution. The effect on the mercury dissolution peak is clearly perceptible with about $10^{-6}M$ Cd(II). Optimal results are obtained in the $1-20\mu M$ cadmium(II) concentration range. The effect of the co-deposition of cadmium allows mercury to be determined at concentrations of $10^{-8}M$ (Fig. 8).

The acidified thiocyanate medium was chosen for stripping experiments because of the excellent results obtained with it previously.^{48,52-54} Anodic stripping voltamperograms for mercury in $0.1M$ sodium thiocyanate + $0.01M$ perchloric acid solution containing Hg(II) ($5-70nM$) and Cd(II) ($1\mu M$) are presented in Fig. 9. A second ion [here Cd(II)] must be added to the cell solution to make the detection of microamounts of Hg(II) possible. Our results also indicate that a very negative deposition potential, e.g., -1.5 V, is necessary to obtain a well-defined oxidation signal. This very negative electrolysis potential inhibits the deposition of copper. It is possible that the formation of a copper hydride is responsible for the difficulties encountered in Hg(II) determination in the presence of Cu(II) ions at such negative deposition potentials. Cadmium(II) is therefore preferred as support ion for mercury deposition on glassy-carbon. Cd(II) is also preferred to Cu(II) for the detection of Hg(II) because the copper electro-

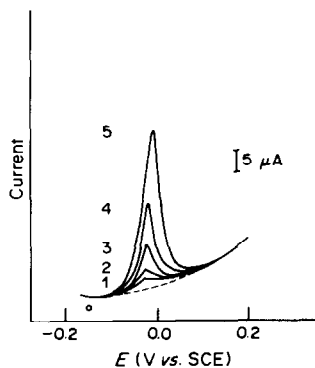


Fig. 9. Current-potential curves for the anodic stripping of mercury at a glassy-carbon disc electrode in $0.1M$ $\text{NaSCN} + 0.01M$ HClO_4 . $E_{\text{dep}} = -1.5$ V; $t_{\text{dep}} = 30$ min; $v = 0.1$ V/sec; $\omega = 188$ rad/sec; $c_{\text{Hg(II)}} = (1) 5$ mM, (2) 10 mM, (3) 20 mM, (4) 40 mM, (5) 70 mM.

dissolution peak at -0.2 V may interfere with the mercury stripping peak at about 0.0 V. This is particularly true for very small Hg(II) concentrations, since the Cu(II) stripping peak resulting from a hundredfold or higher ratio of copper to mercury may partially mask the mercury stripping peak.

The sensitivity for Hg(II) achieved with the stripping voltammetric technique at glassy-carbon by using the support effect is $2 \times 10^{-9}M$ (0.4 ng/ml). A calibration curve is shown in Fig. 8, for a deposition potential of -1.5 V, deposition time of 20 min, rotation of the electrode at 188 rad/sec and anodic sweep rate of 0.1 V/sec, with $1 \mu\text{M}$ Cd(II) also present in the cell solution. At the detection limit the reproducibility of the determination was about 22%.

According to Ulrich and Rügsegger,⁴⁸ the detection limit for mercury at a carbon-paste electrode in $0.1M$ potassium thiocyanate + $0.025M$ hydrochloric acid containing 25 ng/ml copper(II) is about $1.25 \times 10^{-8}M$. The better results obtained in the present work may be due to the use of cadmium as support element for mercury deposition and to the rotation of the electrode during the whole experiment (deposition and stripping).

According to Kendall⁵⁵ 0.5 ppm ($2.5 \times 10^{-9}M$) mercury(II) can be determined in $0.1M$ perchloric acid medium with a glassy-carbon electrode; Allen and Johnson¹¹ found the mercury detection limit to be $5 \times 10^{-10}M$ in $1.0M$ sulphuric acid. They used a glassy-carbon rotating ring-disc electrode with a thin film of gold (two monolayer equivalents) electroplated on the disc electrode.

REFERENCES

- G. Torsi and G. Mamantov, *J. Electroanal. Chem.*, 1971, **32**, 465.
- M. Štulíková, *ibid.*, 1973, **48**, 33.
- Z. Yoshida and S. Kihara, *ibid.*, 1979, **95**, 159.
- R. G. Dhaneshwar and A. V. Kulkarni, *ibid.*, 1979, **99**, 207.
- Idem*, *J. Electrochem. Soc. India*, 1980, **29**, 48.
- P. Kiekens, R. M. H. Verbeeck, H. Donche and E. Temmerman, *J. Electroanal. Chem.*, 1983, **147**, 235.
- W. M. Latimer, *The Oxidation States of the Elements and Their Potentials in Aqueous Solutions*, 2nd Ed., p. 175. Prentice-Hall, Englewood Cliffs, 1956.
- F. A. Cotton and G. Wilkinson, *Advanced Inorganic Chemistry*, 3rd Ed., p. 509. Interscience, New York, 1972.
- L. N. Nekrasov, *Elektrokhimiya*, 1975, **11**, 851.
- Z. Yoshida and S. Kihara, *J. Electroanal. Chem.*, 1978, **86**, 167.
- R. E. Allen and D. C. Johnson, *Talanta*, 1973, **20**, 799.
- B. H. Vassos and H. B. Mark, Jr., *J. Electroanal. Chem.*, 1967, **13**, 1.
- D. M. Kolb, M. Przasnyski and H. Gerischer, *ibid.*, 1974, **54**, 25.
- W. J. Lorenz, H. D. Hermann, N. Wüthrich and F. Hilbert, *J. Electrochem. Soc.*, 1974, **121**, 1167.
- I. Morcos, *J. Electroanal. Chem.*, 1975, **66**, 250.
- L. Dunsch, *Z. Chem.*, 1979, **19**, 77.
- L. Dunsch and R. Naumann, *ibid.*, 1974, **14**, 31.
- F. Hine, M. Yasuda and M. Iwata, *J. Electrochem. Soc.*, 1974, **121**, 749.
- W. J. Albery and M. L. Hitchmann, *Ring-disc Electrodes*, p. 17. Clarendon Press, Oxford, 1971.
- V. G. Levich, *Physicochemical Hydrodynamics*, p. 75. Prentice-Hall, Englewood Cliffs, 1962.
- L. G. Sillén and A. E. Martell, *Stability Constants of Metal-Ion Complexes*, Spec. Publ. No. 17, The Chemical Society, London.
- N. M. Zagudaeva, V. S. Vibinskaya, M. R. Tarasevich and G. V. Shteinberg, *Elektrokhimiya*, 1981, **17**, 467.
- J. Doležal and K. Štulík, *J. Electroanal. Chem.*, 1968, **17**, 87.
- M. Majer, V. Veselý and K. Štulík, *ibid.*, 1973, **45**, 113.
- W. M. Latimer and J. H. Hildebrand, *Reference Book of Inorganic Chemistry*, 3rd Ed., p. 143. Macmillan, New York, 1951.
- A. N. Frumkin and G. A. Tedoradze, *Z. Elektrochem.*, 1958, **62**, 251.
- V. G. Levich, *Physicochemical Hydrodynamics*, p. 69. Prentice Hall, Englewood Cliffs, 1962.
- M. Pourbaix, *Atlas d'Equilibres Electrochimique*, p. 421. Gauthier-Villards, Paris, 1963.
- H. Guiter, *Bull. Soc. Chim. France*, 1947, 272.
- A. M. Hartley, A. G. Hiebert and A. J. Cose, *J. Electroanal. Chem.*, 1968, **17**, 81.
- M. Z. Hassan, D. F. Untereker and S. Bruckenstein, *ibid.*, 1973, **42**, 161.
- T. R. Lindstrom and D. C. Johnson, *Anal. Chem.*, 1981, **53**, 1855.
- A. Eluard and B. Trémillon, *J. Electroanal. Chem.*, 1967, **13**, 208.
- A. I. Kartushinskaya, A. G. Stromberg and N. A. Kolpakova, *Elektrokhimiya*, 1971, **7**, 1243.
- Kh. Z. Brainina and E. Ya. Neiman, *Zh. Analit. Khim.*, 1971, **26**, 875.
- S. Combet and M. Dozol, *Electrochim. Acta*, 1979, **24**, 1283.
- E. Kirova-Eisner, D. Talmor and J. Osteryoung, *Anal. Chem.*, 1981, **53**, 581.
- Kh. Z. Brainina, *Stripping Voltammetry in Chemical Analysis*, Wiley, New York, 1974.
- H. Verplaetse, P. Kiekens, E. Temmerman and F. Verbeeck, *J. Electroanal. Chem.*, 1980, **115**, 235.
- R. W. Murray and D. J. Gross, *Anal. Chem.*, 1966, **38**, 392.
- A. Bondi, *J. Phys. Chem.*, 1964, **68**, 441.
- R. C. West (ed.), *Handbook of Chemistry and Physics*, 61st Ed., p. E-83. CRC Press, Cleveland, 1980-1981.
- S. Trasatti, *J. Electroanal. Chem.*, 1971, **33**, 351.

44. J. C. Rivière in *Solid State Surface Science*, M. Green (ed.), Vol. I, p. 179, Dekker, New York, 1969.
45. A. Eberhagen, *Fortschr. Phys.*, 1960, **8**, 245.
46. J. W. Schultze and D. Dickertmann, *Surface Sci.*, 1976, **54**, 489.
47. E. M. Roizenblat and G. N. Veretina, *Zh. Analit. Khim.*, 1974, **29**, 2376.
48. L. Ulrich and P. Rügsegger, *Z. Anal. Chem.*, 1975, **277**, 349.
49. E. M. Roizenblat and Kh. Z. Brainina, *Elektrokhimiya*, 1969, **5**, 396.
50. L. N. Vasil'eva and T. A. Koroleva, *Zh. Analit. Khim.*, 1971, **26**, 1682.
51. E. M. Roizenblat, T. A. Krapivkina and G. N. Veretina, *Zavodsk. Lab.*, 1974, **40**, 370.
52. S. P. Perone and W. J. Kretlow, *Anal. Chem.*, 1965, **37**, 968.
53. M. Štulíková and F. Vydra, *J. Electroanal. Chem.*, 1973, **42**, 127.
54. L. Luong and F. Vydra, *ibid.*, 1974, **50**, 379.
55. D. R. Kendall, *Anal. Lett.*, 1972, **5**, 867.

EFFECT OF SURFACE-ACTIVE COMPOUNDS ON VOLTAMMETRIC STRIPPING ANALYSIS AT THE MERCURY FILM ELECTRODE

JOSEPH WANG* and DEN-BAI LUO†

Department of Chemistry, New Mexico State University, Las Cruces, NM 88003, U.S.A.

(Received 23 November 1983. Accepted 30 April 1984)

Summary—The effects of various organic compounds on the differential-pulse anodic-stripping voltammetric response at the *in-situ* plated mercury film electrode are explored. These effects vary from metal to metal and from one organic compound to another. The most pronounced effects are observed in measurements of copper. The main effect of the organic compound is to depress the peak current rather than change the peak shape or potential. The differences between the organic interferences observed at the mercury film electrode and those reported at the hanging mercury drop electrode are explained by the different morphology and geometry of the two electrodes. The implications of these interferences for the reliability and feasibility of stripping measurements in natural waters are discussed. Gelatin, camphor, humic acid, starch, agar, sodium dodecyl sulphate and albumin were used as representative organic compounds, and cadmium, lead, and copper as test metal ions.

Stripping analysis and, in particular, differential-pulse anodic-stripping voltammetry (DPASV) have recently received much attention because of their great sensitivity for determination of several metals of environmental and biological significance.¹⁻⁴ As a result of its inherent sensitivity, DPASV is widely used for direct measurements on various environmental samples. Such measurements are subject to interference from organic substances present in the sample, particularly surface-active compounds. The adsorption of organic compounds on the mercury working electrode may affect both the deposition and stripping steps, leading to a decrease or increase in the peak current and a shift in peak potential.⁵ Two comprehensive studies of the possible effects of organic compounds on the response of stripping voltammetry were made by Brezonik *et al.*⁵ and Sagberg and Lund.⁶ Both studies employed the hanging mercury drop electrode and various representative organic compounds.

The aim of the present study was to characterize the effect of model organic compounds on the DPASV response of the mercury film electrode (MFE). The inherent sensitivity, improved resolution, and better mechanical stability of the MFE make it preferable in many practical situations.⁴ Of the various MFEs, the glassy-carbon electrode mercury-plated *in situ* seems to be the electrode of choice.^{7,8} It has been pointed out that organic compounds exhibit different effects on the stripping response obtained at the MFE and hanging mercury drop electrode.⁹ Such differences are to be expected, from consideration of the morphology and geometry of both electrodes. Microscopic examination¹⁰ shows that the MFE consists of tiny mercury droplets, the dimensions and distribution of which depend on the deposition potential. Thus, not all the exposed car-

bon substrate is coated with mercury, and the electroactive surface is a composite of mercury and carbon sites.¹¹ The additional carbon sites of the MFE may result in adsorption characteristics different from those of the homogeneous surface of the hanging mercury drop. The geometry of the two electrodes can also affect their filming by organic compounds. The hanging mercury drop, being deformable, can flex and continuously break and renew the surface.⁹ In addition, the continuously renewed surface of the *in-situ* plated MFE may alter the adsorption process. With the increasing use of the MFE, a detailed knowledge of the changes in its stripping response in the presence of organic compounds occurring in natural waters is required for understanding and minimizing the organic interferences. Thus systematic investigations in this field seem justified.

EXPERIMENTAL

Apparatus and reagents

The electrochemical cell and the reagents have been described previously,¹² except as noted. The working electrode was a thin mercury film deposited on a 0.20-cm diameter glassy-carbon disk. Measurements were made with a Sargent-Welch Model 4001 and EG&G PAR Model 174 polarographic analysers. Solutions (200 ppm) of the organic compounds were prepared daily by dissolving the reagent grade materials at room or elevated temperature. Most samples were prepared in 0.1M acetate buffer (pH 4.6). Various "real" samples, such as Las Cruces tap water and Rio Grande river water, were used. The river water sample was acidified to pH 1.3 with nitric acid, and 10 ml of the acetate buffer were added to 90 ml of the tap water.

Procedure

A 95-ml portion of the supporting electrolyte solution and 5 ml of $1 \times 10^{-3}M$ mercury solution were introduced into the cell. The mixture was deaerated by passage of nitrogen for 5 min, while the working electrode was kept at 0.0 V. The nitrogen delivery tube was then raised above the solution, and a potential of -1.0 V was applied while the

solution was stirred at 550 rpm. After 8 min, the potential was switched to 0.0 V and held there for 2 min. Following this, the electrode was ready for use in an analytical run. Background and sample measurements were made successively, by applying a deposition potential of -1.1 V for 2 min, stopping the stirring, and after 15 sec stripping the metals from the mercury by applying a differential-pulse anodic potential ramp, the scan being stopped at 0.0 V; after 1 min the system was ready for the next cycle. The mercury film was removed at the end of the experiment by wiping with a soft tissue wetted with 1M nitric acid.

RESULTS AND DISCUSSION

The differential-pulse stripping mode was employed throughout most of this study, as it is widely used for ultratrace measurements on sea-water and known to be more susceptible to organic interferences.¹³ Similarly, acetate medium (pH 4.6), commonly used in environmental studies, was employed. Figures 1-4 show the effects of gelatin, humic acid, camphor and starch, respectively, on the stripping response for cadmium, lead and copper. It is obvious that the effect of the organic compounds varied from metal to metal and from one organic compound to another. In all cases, the copper peak was most severely affected. The copper peak-current continued to decrease with increasing concentration of the four organic compounds; at the 15-ppm level of the organic material, the copper peak was depressed by 15-70%.

The addition of gelatin (Fig. 1), a known maximum suppressor in polarography and a representative colloidal protein, only slightly affects the lead peak. Six ppm of gelatin will depress the cadmium peak-current by 40% but further addition (up to 18 ppm) causes no further decrease. A 55% depreciation of the cadmium peak was observed when the hanging mercury drop electrode was used following the addition of 20 ppm gelatin (at pH 3).⁵ A 70% reduction of the copper peak-current is observed at the 18-ppm gelatin level. Humic acid (Fig. 2) depresses the peak-current for all three metals: a slight (20% at the 15-ppm humic acid level) and gradual decrease is observed for the cadmium peak; the lead peak-current decreases sharply (35%) on addition of 3 ppm humic acid, and then

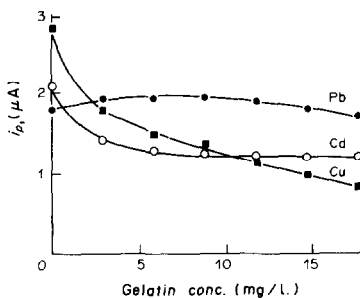


Fig. 1. Effect of gelatin on the determination of Cd, Pb, and Cu by DPASV at the MFE. Conditions: 3 min deposition at -1.1 V with stirring at 550 rpm. Pulse amplitude, 50 mV; scan-rate, 1.0 V/min. $1.1 \times 10^{-7}M$ Cd, $1.0 \times 10^{-7}M$ Pb, $1.5 \times 10^{-7}M$ Cu.

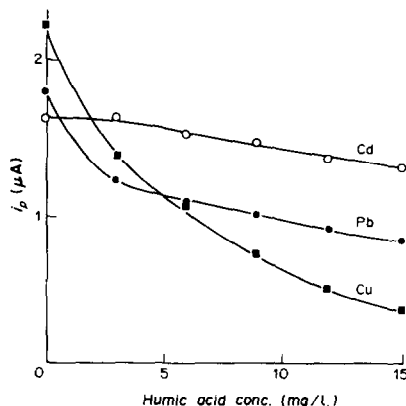


Fig. 2. Effect of humic acid on the determination of Cd, Pb, and Cu by DPASV at the MFE. Conditions as in Fig. 1.

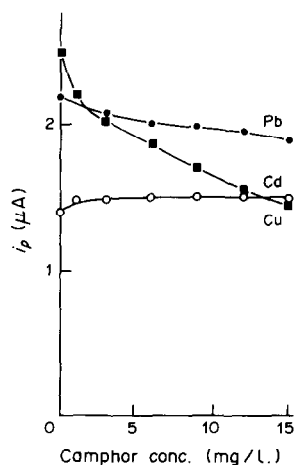


Fig. 3. Effect of camphor on the determination of Cd, Pb, and Cu by DPASV at the MFE. Conditions as in Fig. 1, except that the Cu concentration was $1.4 \times 10^{-7}M$.

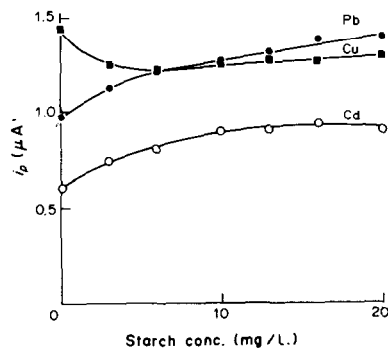


Fig. 4. Effect of starch on the determination of Cd, Pb, and Cu by DPASV at the MFE. Conditions as in Fig. 1, except that the Cu concentration was $1.3 \times 10^{-7}M$.

only slightly with further humic acid; the copper peak progressively decreases (by 85% with 15 ppm humic acid). As humic acid is a natural chelating agent, as well as a surface-active compound, part of the peak depression may be due to complexation of the metal ions. Thus, it is very difficult to distinguish between the effect of complexation and of adsorption, unless

strongly acidic conditions—so that no complexation occurs—are employed (or when the peak current in the presence of surfactants is independent of pH⁶). The situation may be further complicated when the adsorbed organic species participates in the complexation reaction.¹⁴ Because of these combined effects, it is important to re-emphasize the danger inherent in the use of stripping analysis for characterizing metal binding by organic chelating agents. Additional information on the effects of humic acid may be obtained from the shape of the stripping peaks and standard-addition data, as will be described later.

Camphor (Fig. 3) has only a slight effect on the cadmium and lead peak-currents and a pronounced effect (45% depression for 15 ppm camphor) on the copper peak. The addition of starch (Fig. 4), a representative polysaccharide, causes approximately 40% increases in the cadmium and lead peaks, and a 15% decrease in the copper peak. With the hanging mercury drop and pH 3, no change in the cadmium and lead response is observed.⁵

The effect of varying the organic compound concentration in the 0–15 ppm range was also evaluated for agar, sodium dodecyl sulphate and albumin (not shown; conditions as in Fig 1). Addition of 8 ppm of the polysaccharide agar caused 40–60% increases in the three metal peaks, but further addition up to 15 ppm caused no further change. With the hanging mercury drop electrode and pH 3, agar causes no change in the cadmium and copper response.⁵ The addition of 6 ppm of the anionic surfactant sodium dodecyl sulphate did not alter the lead and cadmium peaks, but addition of 10 ppm caused a 75% depression of these peaks. In contrast, the copper peak gradually decreased (up to 40% depression at the 10 ppm sodium dodecyl sulphate level) with successive additions of the surfactant. Significant peak-current depressions (~80% of the copper peak, ~65% of the cadmium and lead peaks) were observed on adding 1 ppm of albumin—another model high molecular-weight organic compound. Further additions of albumin, up to 10 ppm, caused only slight (~5%) further depression in the responses. As in the case of humic acid, part of this depression is attributed to complexation by the albumin binding sites.

For most of the organic compounds discussed (except albumin and sodium dodecyl sulphate) the adsorption phenomenon did not vary with time. Four successive runs at each concentration of the organic compound yielded relatively reproducible stripping-peak currents. This is in contrast to the effect frequently observed for surfactants, that successive voltamperograms, *i.e.*, increased contact time with the solution, show progressive decrease in the peak height, owing to gradual blocking of the electrode surface.¹⁵ The relatively stable response observed in this study may be a feature of the *in-situ* plated MFE, at which a continuously renewed surface is maintained.

Another interesting response characteristic ob-

served in this study was that only minor changes in the stripping-peak shape or potential accompanied the changes in magnitude of the peak current (caused by the organic compounds). Figure 5 shows stripping voltamperograms for cadmium, lead, and copper obtained in the absence (a) and presence (b) of different organic compounds: camphor (A), humic acid (B), and gelatin (C). These compounds do not affect the shape and potential of the lead and

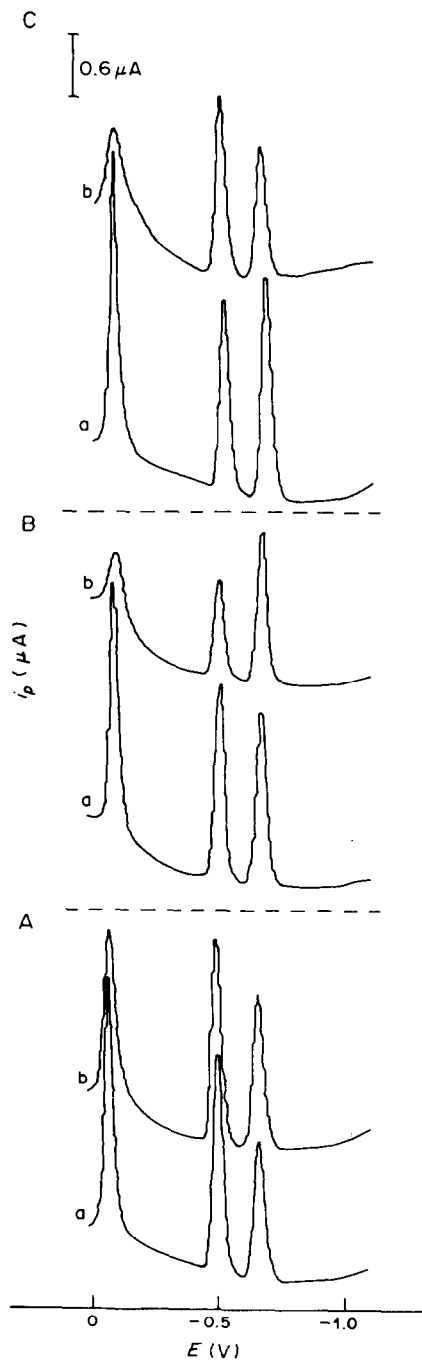


Fig. 5. Stripping voltamperograms for $1 \times 10^{-7} M$ Pb and Cd, and $1.3 \times 10^{-7} M$ Cu, obtained in the absence (a) and presence (b) of 9 ppm camphor (A), humic acid (B), and gelatin (C). Conditions as in Fig. 1.

cadmium peaks. In contrast, significant broadening of the copper peak (width at half-height doubled from 35 to 70 mV) is observed in the case of gelatin and humic acid. In the humic acid experiment, the copper-peak broadening is accompanied by a slight (30 mV) cathodic shift in the potential. Such a shift may be attributed to complexation rather than to sorption. The addition of starch, agar and sodium dodecyl sulphate to $1 \times 10^{-7} M$ cadmium, lead and copper solutions did not change the shape and location of the stripping peaks (not shown; conditions as for Fig. 5). The relatively minor changes in the peak shape and potential indicate that the main effect of surface-active organic compounds at the *in-situ* plated MFE is to hinder the transport of the metals to the surface during the deposition step (and thus to change the magnitude of the peak current). Except for the copper peak, no effect on the reversibility of the stripping reaction was observed. This is especially important, as the differential-pulse stripping response is known to be more sensitive to small changes in the rate of the electrode reaction. The differential-pulse mode is known also to yield organic

adsorption/desorption peaks; such peaks were not observed for the compounds tested in this study. Some of these observations may be features of the *in-situ* plated MFE.

From the analytical point of view, certain organic interferences can be corrected by using the standard-addition procedure. This correction is valid when the interferent changes the slope of the calibration graph (which must be linear), and in effect a calibration specific for the interferent concentration present can be obtained by spiking the sample with aliquots of standard metal solution. For example, Fig. 6A shows that the standard-addition method can compensate for the decrease in the stripping-peak currents caused by the addition of gelatin to a tap water sample: the response after the addition of known amounts of a metal is proportional to the added metal concentration. However, when the fraction of the electrode area covered by the organic compounds progressively increases with time or a slow metal-organic compound combination occurs, the standard-addition method would not correct for the peak depression. For example, non-linear responses were obtained

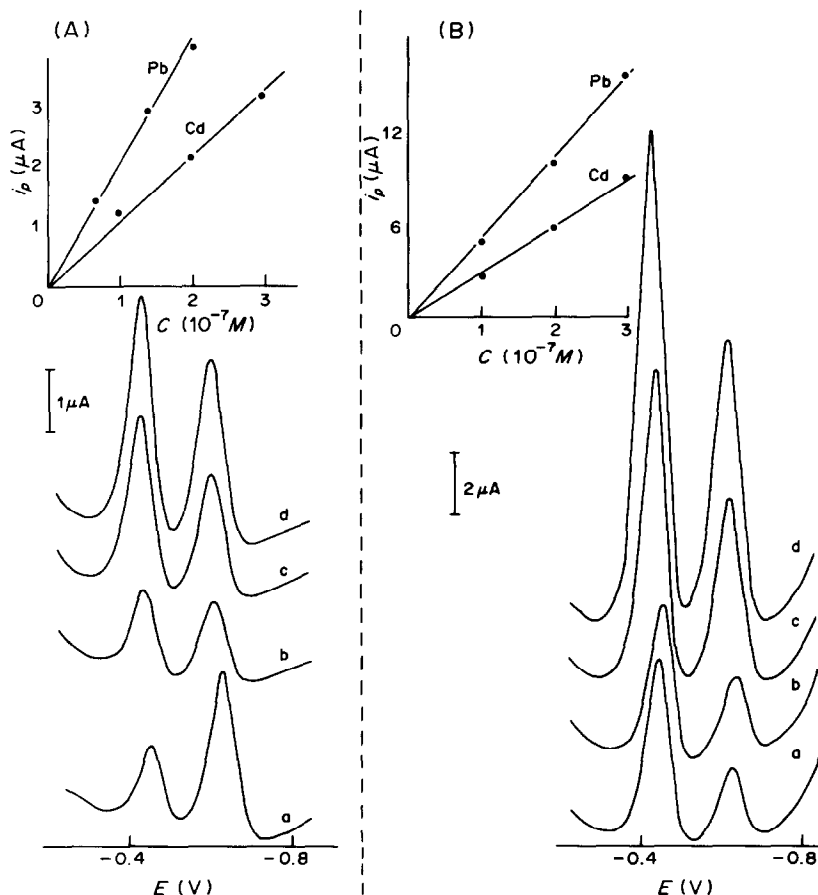


Fig. 6. Differential pulse voltamperograms for (A) tap water and (B) river water samples. (a) Samples spiked with Cd ($1 \times 10^{-7} M$) and Pb ($7 \times 10^{-8} M$) (A), and $1 \times 10^{-7} M$ Cd and Pb (B); (b) same as (a), but after addition of 10 ppm of gelatin (A) or humic acid (B); (c) and (d), same as (b) but after addition of (c) $1 \times 10^{-7} M$ and (d) $2 \times 10^{-7} M$ Pb and Cd. Conditions, 1 (A) or 2 (B) min deposition at $-1.1 V$, with stirring at 550 rpm. Pulse amplitude, 25 mV; scan-rate, 5 mV/sec. Also shown are the resulting calibration plots based on the data for (b)-(d).

following successive additions of aliquots of standard metal solution to samples containing 10 ppm sodium dodecyl sulphate and humic acid (not shown). When metal-organic compound combination is responsible for the non-linearity, lower pH values may be used to prevent the complexation (however, because of the suppressive effect of chloride on copper stripping peaks,¹⁶ hydrochloric acid should not be used for acidifying acetate media). Figure 6B illustrates this approach for a river water sample that had been acidified to pH 1.3 (as in the usual preservation procedures) and then spiked with humic acid, cadmium and lead. The stripping peaks for the solutions containing standard additions of cadmium and lead are proportional in height to the added metal concentrations and though the slope for the lead response is lower than that in the absence of humic acid (*cf.* curves a and b), that for cadmium is not affected by the humic acid. However, for convenience and to avoid erroneous conclusions, especially when analysing organic-rich water samples, *e.g.*, inshore or near-shore waters, waste-water or sewage, it is best to destroy the organic matter beforehand by ultraviolet radiation.⁴

Acknowledgement—Den-bai Luo acknowledges financial support from UNESCO (United Nations Educational, Scientific and Cultural Organization).

REFERENCES

1. T. R. Copeland and K. R. Skogerboe, *Anal. Chem.*, 1974, **46**, 1257A.
2. J. Wang, *Environ. Sci. Technol.*, 1982, **16**, 104A.
3. *Idem*, *J. Electroanal. Chem.*, 1982, **139**, 225.
4. G. E. Batley, *Marine Chem.*, 1983, **12**, 107.
5. P. L. Brezonik, P. A. Brauner and W. Stumm, *Water Res.*, 1976, **10**, 605.
6. P. Sagberg and W. Lund, *Talanta*, 1982, **29**, 457.
7. T. M. Florence, *J. Electroanal. Chem.*, 1970, **27**, 273.
8. W. Lund and M. Salberg, *Anal. Chim. Acta*, 1975, **76**, 131.
9. G. E. Batley and T. M. Florence, *J. Electroanal. Chem.*, 1974, **55**, 23.
10. M. Štulíková, *ibid.*, 1973, **48**, 33.
11. N. Hume and J. N. Carter, *Chem. Anal. (Warsaw)*, 1972, **17**, 747.
12. J. Wang, *Talanta*, 1982, **29**, 125.
13. T. M. Florence, *Anal. Chim. Acta*, 1980, **119**, 217.
14. J. Buffle and F. L. Greter, *J. Electroanal. Chem.*, 1979, **101**, 231.
15. R. G. Clem and A. T. Hodgson, *Anal. Chem.*, 1978, **50**, 102.
16. T. M. Florence and G. E. Batley, *J. Electroanal. Chem.*, 1977, **75**, 791.

INFLUENCE OF VOLATILE HYDRIDE-FORMING ELEMENTS ON ANTIMONY DETERMINATION BY ATOMIC-ABSORPTION SPECTROMETRY WITH HYDRIDE-GENERATION

LAURI H. J. LAJUNEN*, TIMO MERKKINIEMI and HANNU HÄYRYNEN
Department of Chemistry, University of Oulu, SF-90570 Oulu 57, Finland

(Received 14 April 1983. Revised 27 February 1984. Accepted 5 April 1984)

Summary—A study was undertaken to determine the interfering effects of arsenic, bismuth, germanium, lead, selenium, tin and tellurium on trace determination of antimony by atomic-absorption spectrometry with hydride-generation. A 1% NaBH₄ solution was used as reductant and a small amount of oxygen was added to the hydrogen produced, to support the combustion and atomization of SbH₃. The interference from selenium in the determination of antimony is removed if potassium iodide-ascorbic acid solution or copper sulphate is added to the sample solution. The interference of tin and tellurium can also be avoided by adding potassium iodide-ascorbic acid solution. A possible interference mechanism is discussed.

Interferences caused by a number of metal ions are a serious problem in the practical use of the hydride-generation method in the atomic-absorption determination of volatile hydride-forming elements (the most studied are As and Se).¹⁻⁸ The interference studies in the literature fall into two groups: (a) those on elements predominantly in the periodic groups VIII and Ib (especially Cu, Ni, Pd and Pt) and (b) those on the mutual interactions of the elements forming volatile hydrides. Most papers deal with the first type of interference, but relatively little information is available on the second, especially in the determination of antimony.

The aim of the present work was to study this second aspect in the determination of antimony by the hydride-generation atomic-absorption method originally developed by Siemer and Hageman⁹ for selenium determination, and in particular to find methods for removing the interferences. In addition, possible interference mechanisms were considered.

EXPERIMENTAL

Reagents

Distilled and demineralized water was used throughout.

Sodium borohydride solution, 1%. Prepared weekly, and stabilized by addition of one pellet of potassium hydroxide per 100 ml.¹⁰

Standard antimony(III) stock solution (1000 µg/ml). Prepared by diluting a "Titrisol" solution (Merck) containing 1.000 g of antimony (as SbCl₃) to 1 litre with 5% w/v hydrochloric acid.

Standard arsenic(III) stock solution (1000 µg/ml). Prepared by dissolving 1.320 g of As₂O₃ (Merck, analytical grade) in 50 ml of concentrated hydrochloric acid and diluting to 1 litre with water.

Standard selenium(IV) stock solution (1000 µg/ml). Prepared by diluting a "Titrisol" solution (Merck) containing 1.000 g of selenium (as SeO₂) to 1 litre with water.

Standard tin(II) stock solution (1000 µg/ml). Prepared by dissolving 1.000 g of metallic tin in 200 ml of concentrated hydrochloric acid and diluting to 1 litre with water.

Standard lead(II) stock solution (1000 µg/ml). Prepared by dissolving 1.598 g of Pb(NO₃)₂ (Merck, analytical grade) and diluting to 1 litre with water.

Standard bismuth(III) stock solution (1000 µg/ml). Prepared by dissolving 1.115 g of Bi₂O₃ (Merck, analytical grade) in 50 ml of concentrated hydrochloric acid and diluting to 1 litre with water.

Standard tellurium(IV) stock solution (1000 µg/ml). Prepared by dissolving 1.000 g of tellurium in a mixture of 15 ml of concentrated hydrochloric acid and 5 ml of concentrated nitric acid and dilution to 1 litre with water.

Standard germanium(IV) stock solution (1000 µg/ml). Prepared by dissolving 1.441 g of GeO₂ (Merck, analytical grade) in a mixture of 15 ml of concentrated hydrochloric acid and 5 ml of concentrated nitric acid and diluting to 1 litre with water.

Standard potassium iodide stock solution (1M). Prepared by dissolving 16.6 g of potassium iodide (Merck, analytical grade) and 2.0 g of ascorbic acid in 100 ml of water.

Standard copper(II) stock solution (5000 µg/ml). Prepared by dissolving 3.140 g of CuSO₄ (Merck, analytical grade) in 250 ml of water.

Apparatus and method

A Pye Unicam SP 9-800 atomic-absorption spectrometer equipped with an SP 9 computer, hollow-cathode lamps, a conventional deuterium-lamp for background correction, and a hydride generator and atomization unit were used in the determinations.^{9,11} The hydride generator and atomization unit was attached in place of the burner of the spectrometer. Table 1 shows the instrumental parameters of the spectrometer. Deuterium-lamp background correction was used for each measurement.

Table 1. Spectrometer settings used for the Sb absorbance measurements

Wavelength	217.58 nm
Lamp current	10.0 mA
Band-width	0.2 nm
Integration time for peak area	20 sec
Recorder sensitivity	5-20 mV
Chart speed	10 mm/min

*To whom correspondence and requests for reprints should be addressed.

Hydrogen was used as the carrier gas at a flow-rate of 1.1–1.2 l./min to flush the generated hydrides into the atomization tube. A small hydrogen–oxygen flame was ignited inside the quartz tube to support the combustion and atomization of the hydrides. A safe oxygen flow-rate was 50–60 ml/min. The excess of hydrogen was burned at the ends of the quartz tube.

The specimen (volume 4 ml) was added to the hydride-generation cell with an injection syringe, and reductant with a Socorex sampler (volume 5 ml). A load of about 0.5 kg was attached to the piston of the sampler to keep the addition rate constant. The hydride-generation cell was washed with about 10 ml of distilled and demineralized water between successive injections.

The absorbance measurements were begun after the flame had burned for at least 10 min. The peak area was used for measurement, and each sample was analysed 3–5 times. When the excess of hydrogen was burned at the ends of the quartz tube, it caused a small signal. The area of this signal for a blank run with 5M hydrochloric acid was measured and always deducted from the measured antimony signals. The reading cycle was induced manually. The background absorption of the antimony signals was low and symmetrically distributed around the peak, which permitted automatic induction of the reading cycle.

Procedures

Effect of HCl on antimony determination. The effect of the concentration of hydrochloric acid on the antimony atomic-absorption signal was investigated with 20- $\mu\text{g/l.}$ antimony solutions over the hydrochloric acid concentration range 1–12M.

Interference studies. The solutions to be measured (and working standards) were prepared from the standard solutions by dilution with 5M hydrochloric acid. Two series of test solutions were always prepared, with antimony concentrations of (a) 20 and (b) 50 $\mu\text{g/l.}$, and the interfering

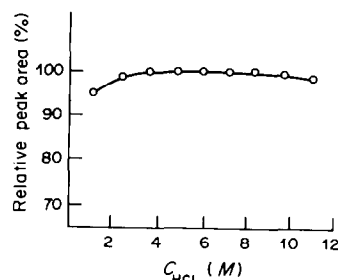


Fig. 1. The effect of HCl on the determination of antimony.

element at 0, 100, 250, 500, 1000, 2000 and 4000 $\mu\text{g/l.}$ concentration.

Masking studies. To the solution containing Sb(III) and the interfering ion, 1 ml of 1M potassium iodide or 5% copper solution was added in the hydride-generation cell just before the addition of the sodium borohydride.

RESULTS AND DISCUSSION

We have recently reported on the performance of the apparatus and procedure.¹¹ The optimum range extended from 1 to 50 $\mu\text{g/l.}$, the calibration curve then being linear. The detection limit was found to be about 0.5 $\mu\text{g/l.}$ (taken as the mean value of the blank signal plus three times its standard deviation) and the slope of the calibration curves (absorbance *vs.* weight of Sb) 4.4 μg^{-1} . The peak-area was found to give greater sensitivity than the peak-height. With peak-area detection the relative standard deviation varied

Table 2. Influence of various interfering elements on the determination of antimony, and the effect of masking agents

Interferent	[Sb] $\mu\text{g/l.}$	Masking agent	Relative intensities of the Sb signals (%) at various interferent concentrations						
			0*	100*	250*	500*	1000*	2000*	4000*
Pb	20	—	100	102	101	102	102	100	101
	50	—	100	99	99	100	100	100	99
Bi	20	—	100	100	99	93	93	89	87
	50	—	100	100	99	97	94	90	88
	20	CuSO ₄	100	100	100	100	98	96	94
	50	CuSO ₄	100	100	100	100	98	97	96
As	20	—	100	99	91	82	77	66	49
	50	—	100	99	92	86	78	67	50
Te	20	—	100	98	90	79	67	61	56
	50	—	100	98	91	80	69	63	57
	20	KI–ascorbic acid	100	99	98	95	93	96	97
	50	KI–ascorbic acid	100	100	99	97	93	95	96
Ge	20	—	100	98	90	76	62	50	40
	50	—	100	98	91	76	62	51	42
Se	20	—	100	99	86	66	54	43	35
	50	—	100	98	87	68	56	46	36
	20	CuSO ₄	100	100	100	100	99	96	92
	50	CuSO ₄	100	100	100	99	101	102	103
	20	KI–ascorbic acid	100	100	101	101	100	100	101
	50	KI–ascorbic acid	100	100	100	101	101	100	101
Sn	20	—	100	91	80	61	11	9	9
	50	—	100	93	87	67	12	8	8
	20	KI–ascorbic acid	100	100	103	99	103	102	101
	50	KI–ascorbic acid	100	103	102	104	103	102	96

*Concentration of interferent ($\mu\text{g/l.}$)

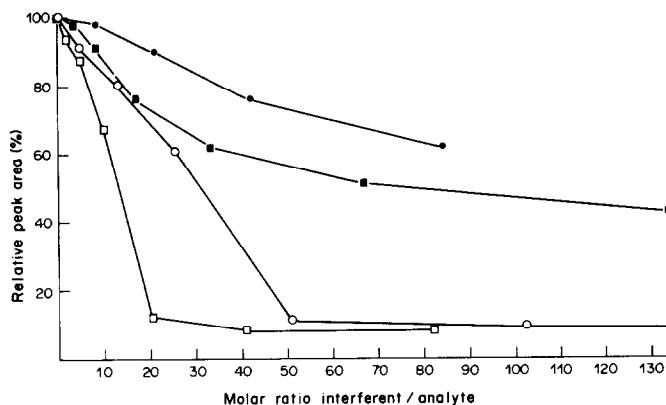


Fig. 2. The effect of Sn on the determination of Sb (○: Sb 20 ng/ml and □: Sb 50 ng/ml), and Ge on the determination of Sb (●: Sb 20 ng/ml and ■: Sb 50 ng/ml).

between 2 and 7%, depending on the antimony content and the nature of the matrix.

Figure 1 shows that the hydrochloric acid concentration has only a small effect on the determination; the optimum is in the range 4–8M and 5M acid medium was therefore selected.

Table 2 shows the influence of the different elements forming volatile hydrides, on the determination of antimony(III). All those studied, except bismuth and lead, strongly interfere by decreasing the absorption signal for Sb, the interference increasing in the order $Pb < Bi < As < Te < Ge < Se < Sn$. Lead has practically no effect at all, and for the others (except Bi) the interfering effect becomes noticeable only when the concentration of the interfering cation is above 100 $\mu\text{g/l}$. The same effect is obtained at two different Sb concentrations (20 and 50 $\mu\text{g/l}$), and the interference seems to be independent of the analyte/interferent ratio and to depend only on the concentration of the interfering element. On the other hand, in consideration of the mechanism, the number of atoms of analyte and interferent must be compared, so the concentrations of analyte and interferent must be translated into molarities. Figure 2 shows, for example, the interference of Sn and Ge at two different Sb concentrations. The shapes of the

curves are similar in both cases but the degree of interference is greater for the greater Sb concentration.

Antimony also influences the determination of the other elements forming volatile hydrides, as illustrated in Fig. 3. Its effect on the determination of Se is considerably less pronounced than that of Se on Sb determination, whereas it has a greater effect on determination of As than As has on determination of Sb.

A possible explanation for the mutual interference is a competitive reaction between the reducing species. NaBH_4 decomposes in acidic solutions to give H_3BO_3 and H_2 , and if most of the reductant is consumed in this way, only a limited amount will be available for the production of hydrides. If there is more than one hydride-forming element in the test solution, the reductant should be consumed predominantly by the element which reacts fastest with it. If this explanation is correct, the most severe signal suppressions can be expected for slowly reacting analyte elements in the presence of interfering elements that react more quickly. Figure 4 superimposes the absorption signals obtained for Sb(III), As(III) and Se(IV) as a function of time elapsed after addition of the reductant. Sb(III) and Se(IV) seem to react

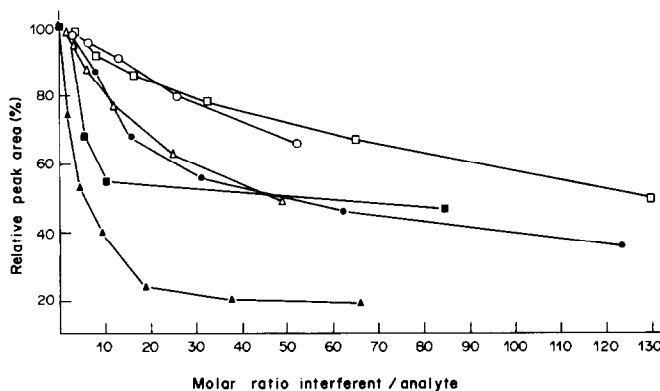


Fig. 3. The effect of Sb on the determination of Se (○), As on the determination of Sb (□), Sb on the determination of As (△), Se on the determination of Sb (●), As on the determination of Se (■), and Se on the determination of As (▲). The concentration of the analyte was 50 ng/ml in each case.

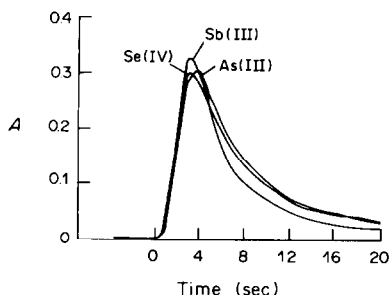


Fig. 4. Superimposed recorder tracings for 5 ng/ml As(III), 5 ng/ml Sb(III), and 10 ng/ml Se(IV) in 5M HCl. Chart-speed 300 mm/min.

at practically the same rate, and As(III) a little more slowly. If the competitive reaction theory is correct, the mutual interferences between Sb and Se should be about the same, and the depressive influence of these faster reacting elements on determination of the slower reacting As should be more pronounced than that of arsenic on their determination. From the results shown in Fig. 3 it seems likely that competition is not the reason for the effect, since the effect of Se on Sb is much greater than that of Sb on Se. Further, a simple calculation shows that the reductant is present in very large excess, so hydride generation should be complete anyway.

Dedina and Rubeska¹² have shown that the atomization of selenium hydride is not caused by thermal decomposition but by free radicals generated in the reaction zone of the diffusion flame. They also used a system with atomization of gaseous hydrides in an extremely fuel-rich hydrogen-oxygen flame burning inside an unheated quartz tube. The probability of formation of free atoms from the hydrides is proportional to the number of collisions with free H atoms and OH radicals. Welz and Melcher⁸ have investigated the decomposition mechanism of selenium and arsenic hydrides in a heated quartz-tube atomizer and concluded that the atomization under these conditions is also due to collisions with free radicals.

If this free-radical mechanism occurs, there might often be conditions in which there is a lack of radicals. Then if the decomposition rate of the various hydrides were the same, the ease of volatilization of the hydrides would be the decisive factor, since the hydrides volatilized first would decrease the number of radicals, so that there would be insufficient radicals to cause the quantitative atomization of hydrides volatilized later. If this explanation is correct, the effect of Se and Sb on the As signal should be stronger than that of As on their signals, and that of Sb on Se similar to that of Se on Sb. Again the Sb/Se system gives anomalous results (Fig. 3). Thus, according to our findings there might also be differences in decomposition rates of the different volatile hydrides and/or interactions between the hydrides in the gas phase. On the other hand, it can be expected that the mutual interference described above will depend on both the molar concentration of the interfering

hydride which consumes radicals, and its molar concentration ratio to the analyte hydride, since the degree of interference caused by a given number of interferent atoms is the greater, the smaller the number of analyte atoms (Fig. 2). However, the degree of interference, as well as the acidity required, also depends on the structure of the apparatus.

When the mutual interference of the volatile hydrides occurs in the gas phase in the atomizer, it is possible to decrease or eliminate this interference by preventing the formation or evaporation of the interfering hydride. As shown in Table 2, the interference caused by selenium, tellurium and tin can be avoided completely by using potassium iodide-ascorbic acid solution as a masking agent and the interference of bismuth as well as selenium can be eliminated by addition of copper(II) sulphate (but not nitrate, since nitrate itself interferes¹³). The masking reagents react with the interfering ions and prevent their evaporation as covalent hydrides. Iodide-ascorbic acid solution reduces Se(IV) to Se, and iodide forms complexes with Sn(II) and Te(IV), but does not prevent the formation and evaporation of SbH₃. According to the theory proposed by Meyer *et al.*,⁶ SeH₄ reacts with Cu(II) by forming an insoluble copper selenide, CuSe, in acid medium, whereas Cu(II) does not prevent the evaporation of SbH₃. Because selenium and tellurium are chemically very similar, it is reasonable to think that the mechanism in the case of Cu(II) and Te(IV) is similar to that for Cu(II) and Se(IV). Arsenic and antimony are also chemically very similar, and it is therefore very difficult to find a masking agent which would prevent the production of AsH₃, but not of SbH₃.

CONCLUSIONS

In the determination of antimony the degree of interference of the elements forming volatile hydrides is significant when the concentrations of the interferent is more than about 100 µg/l. The interference is dependent on the concentration ratio of the analyte and interferent. The interference seems to occur in the gas phase in the atomizer tube, and to be due to collisions with free radicals, as postulated first by Dedina and Rubeska¹² for arsenic and selenium. All the interfering elements studied have a depressive influence on the Sb signal, increasing in the order: Pb < Bi < As < Te < Ge < Se < Sn. The influence of Se, Te and Sn can be avoided by the addition of KI-ascorbic acid solution, and that of Te and Se by the addition of Cu(II) sulphate.

REFERENCES

1. A. E. Smith, *Analyst*, 1975, **100**, 300.
2. D. Pierce and H. R. Brown, *Anal. Chem.*, 1976, **48**, 693.
3. M. Bedard and J. D. Kerbyson, *Can. J. Spectrosc.*, 1976, **21**, 64.
4. F. D. Pierce and H. R. Brown, *Anal. Chem.*, 1972, **49**, 1417.
5. G. F. Kirkbright and M. Taddia, *Anal. Chim. Acta*, 1978, **100**, 145.

6. A. Meyer, Ch. Hofer, G. Tölg, S. Raptis and G. Knapp, *Z. Anal. Chem.*, 1979, **296**, 337.
7. M. Verlinden and H. Deelstra, *ibid.*, 1979, **296**, 253.
8. B. Welz and M. Melcher, *Anal. Chim. Acta*, 1981, **131**, 17.
9. D. D. Siemer and L. Hagemann, *Anal. Lett.*, 1975, **8**, 323.
10. J. R. Knechtel and J. L. Fraser, *Analyst*, 1978, **103**, 104.
11. L. H. J. Lajunen, H. Häyrynen, E. Hakala and E. Yrjänheikki, *University of Oulu, Report Series in Chemistry*, Report No. 7 (1982).
12. J. Dedina and I. Rubeska, *Spectrochim. Acta*, 1980, **35B**, 119.
13. F. J. Fernandez and D. C. Manning, *At. Absorb. Newsl.*, 1971, **10**, 86.

SHORT COMMUNICATIONS

REACTION OF IRON(III) WITH TIRON IN THE PRESENCE OF FERROZINE, AND DETERMINATION OF TIRON

NINUS SIMONZADEH and BRUNO JASELSKIS

Department of Chemistry, Loyola University of Chicago, Chicago, IL 60626, U.S.A.

(Received 24 February 1984. Accepted 16 April 1984)

Summary—Tiron is oxidized by iron(III) in the presence of Ferrozine with an apparent four-electron transfer and aromatic ring opening. The apparent molar absorptivity referred to the Tiron in the reaction corresponds to approximately $1.12 \times 10^5 \text{ l. mole}^{-1} \text{ cm}^{-1}$.

Tiron (1,2-dihydroxybenzene-3,5-disulphonate), forms coloured iron (III) complexes which differ in stoichiometry according to the pH. The colour of these complexes has been used for the determination of small amounts of iron(III).¹ However, in the presence of ligands capable of stabilizing iron(II), iron(III) oxidizes Tiron as well as other catechols. Rapid oxidation of catechols by iron(III) in the presence of 1,10-phenanthroline, with a two-electron transfer, has been reported,² and D- α -tocopherol (vitamin E) has been determined by use of iron(III) in the presence of Ferrozine.³ In the determination of vitamin E it was observed that after a rapid transfer of two electrons, the vitamin E was further oxidized. This has led us to investigate the reaction of Tiron with iron(III) in the presence of Ferrozine, and we have developed a suitable colorimetric method for the determination of small amounts of Tiron.

EXPERIMENTAL

Reagents

All reagents were of analytical grade. Demineralized water was used to make all solutions.

Iron(III) solution. Prepared by dissolving approximately 193 mg of ferric ammonium sulphate, $\text{Fe}(\text{NH}_4)(\text{SO}_4)_2 \cdot 12\text{H}_2\text{O}$ (Baker Analyzed) in 1.0 ml of concentrated sulphuric acid and a sufficient amount of water. The solution was transferred to a 250-ml standard flask and diluted to volume.

Buffer solution, 0.3M, pH 3.4. Prepared by adding sodium hydroxide pellets to 0.3M monochloroacetic acid.

Tiron standard solution. A stock solution was prepared by dissolving exactly 440 mg of disodium-1,2-dihydroxybenzene-3,5-disulphonate monohydrate (G. Frederick Smith Chemical Co.) in 1000 ml of demineralized water. Other catechols tested were recrystallized from n-hexane and used for comparative studies.

Ferozine solution. Prepared by dissolving 171 mg of 3-(2-pyridyl)-5,6-bis(4-phenylsulphonic acid)-1,2,4-triazine disodium salt trihydrate (Aldrich Chemical Co.) in 100 ml of demineralized water and stored in a tinted glass bottle.

Procedure

In all experiments the reagents were added to 50-ml standard flasks in the following order: 20 ml of 0.3M chloroacetate buffer followed by 6.0 ml of 0.003M Ferrozine, a varied amount (50–200 μl) of Tiron standard solution and water to give a volume of about 45 ml. The flasks were then placed in a constant-temperature bath (40°) for approximately 10 min; 3.0 ml of 0.002M iron(III) were added to each flask, the solutions diluted to volume, and timing was started. Tinted glass flasks or flasks covered with aluminium foil were used in order to protect the solutions from sunlight. For kinetic studies, a 3.0-ml sample was withdrawn every 5 min and the absorbance measured at 562 nm against water. Similarly, a blank containing all of the reagents except Tiron was prepared, and its absorbance measured as a function of time. The net absorbance was used for kinetic and analytical purposes. The reaction was studied at different temperatures. At temperatures below 40° the absorbance measurements were made at 10 or 15 min intervals. The data were used to evaluate the pseudo first-order rate constants and the Arrhenius activation energy.

The amount of Tiron in a given sample was determined by measuring the net absorbance of a solution heated for 40 min at 40° or left for 3 hr at room temperature. Other catechols were determined in a similar manner, except that longer reaction times were needed.

RESULTS AND DISCUSSION

The oxidation of Tiron and of other substituted catechols by iron(III) in the presence of Ferrozine at pH 3.4 proceeds in two steps. In the first, Tiron is rapidly oxidized by a two-electron transfer and in the second, which is slower, an additional two electrons are transferred, resulting in the opening of the aromatic ring.

Cleavage of the carbon-carbon bond in catechols by copper(II) in pyridine solutions and in the presence of oxygen has been reported.⁴ This cleavage of catechols proceeds with a four-electron transfer and the formation of *cis,cis*-muconic acids. A similar cleavage of catechols in the presence of iron(III), nitrilotriacetic acid and pyrocatechase as a catalyst

Table I. Absorbance of Iron(II) Ferrozine produced, as a function of Tiron concentration*

Concentration of Tiron, $10^{-6}M$	Absorbance†	Molar absorptivity, $10^5 l. mole^{-1}. cm^{-1}$
1.42	0.159 ± 0.004	1.12
2.12	0.236 ± 0.005	1.11
2.83	0.317 ± 0.007	1.12
5.65	0.598 ± 0.010	1.06

*Reaction at 40° with $1.2 \times 10^{-4}M$ iron(III) and $3.6 \times 10^{-4}M$ Ferrozine.

†Measured after 40 min reaction time and corrected for the blank. The average and range of four determinations are reported.

has been observed.⁵ In the determination of vitamin E the second step was prevented by the addition of bifluoride or orthophosphate.³

At pH values ≥ 5 Tiron forms different coloured complexes with iron(III) and has been used for the determination of small amounts of iron(III).¹ However, in the presence of an excess of iron(III) and ligands which stabilize iron(II), Tiron is oxidized with opening of the aromatic ring. A pH of 3.4 was chosen for the method described here, because at this pH the iron(II)–Ferozine complex is stable, iron(III) does not form a precipitate of hydrous oxide, and the oxidation of Tiron proceeds quite readily.

Examination of the reaction of Tiron with iron(III) in the presence of Ferrozine, as a function of time and temperature shows that the change in absorbance levels off after about 35 min when the reaction is done at 40° , but after about 2.5 hr when the reaction is done at room temperature. Absorbance values for different concentrations of Tiron are summarized in Table I. The apparent molar absorptivity, referred to Tiron, is about $1.12 \times 10^5 l. mole^{-1}. cm^{-1}$, whereas referred to iron(II)–Ferozine it is $2.80 \times 10^4 l. mole^{-1}. cm^{-1}$. The ratio of these molar absorptivities is 4, which is in agreement with the number of electrons transferred in the oxidation process.

The reactivity of catechols with iron(III) is affected not only by substituent groups but also by their

positions, and decreases in the order Tiron > catechol > 4-chlorocatechol > tetrabromocatechol.

The pseudo first-order reaction activation energy calculated from the rate constants for various catechols at different temperatures is in the range of 30–60 kJ/mole, indicating that the opening of the aromatic ring most likely proceeds through a free-radical intermediate. In fact, the reaction is somewhat faster in an atmosphere of nitrogen than in the presence of oxygen. Also, the reaction is affected by sunlight. Hence the blank and sample solutions are protected from direct sunlight by covering the flasks with aluminium foil or using tinted glass flasks. In this manner Tiron can be determined at ppm levels with a relative precision of better than 3%. Substances which can be oxidized by iron(III) must be eliminated before the determination.

REFERENCES

1. J. H. Yoe and A. L. Jones, *Ind. Eng. Chem., Anal. Ed.*, 1944, **16**, 111.
2. M. Kimura, S. Yamabe and T. Minato, *Bull. Chem. Soc. Japan*, 1981, **54**, 1699.
3. W. Adeniyi and B. Jaselskis, *Talanta*, 1980, **27**, 933.
4. M. M. Rogie and T. R. Damien, *J. Am. Chem. Soc.*, 1978, **100**, 17.
5. M. G. Weller and U. Weser, *ibid.*, 1982, **102**, 3752.

TITRIMETRIC DETERMINATION OF VANADIUM(IV) WITH DCTA

RAM PARKASH*, KULDIP SINGH, JITENDRA PAL KAUR
and R. L. SINGHAL

Department of Chemistry, Panjab University, Chandigarh, India

(Received 26 August 1982. Revised 18 February 1984. Accepted 17 April 1984)

Summary—Vanadium(IV) has been determined by DCTA titration conductometrically, spectrophotometrically and visually (with Alizarin Red S, Gallein and Catechol Violet as indicators at pH 4.0, 4.2 and 4.5–4.6 respectively). The interference of nickel, copper, lead, aluminium and thorium can be removed, and the method utilized for the analysis of binary mixtures of vanadium(IV) with nickel, copper or thorium.

Except for an attempt by Mendez and Diez¹ to determine it spectrophotometrically, no work has been reported on the estimation of vanadium(IV) with 1,2-diaminocyclohexanetetra-acetic acid (DCTA). In the investigation described here, vanadium(IV) alone or in the presence of various ions has been determined by direct titration with DCTA, conductometrically, spectrophotometrically and visually, Alizarin Red S, Catechol Violet and Gallein being used as indicators.

EXPERIMENTAL

Procedures

Vanadium(IV) sulphate solution ($5 \times 10^{-3}M$, 0.5–10 ml) was titrated with DCTA solution after addition of 10 drops of 0.5% aqueous Alizarin Red S solution or 2 drops of 0.2% ethanolic Gallein solution or 1 drop of 0.1% aqueous Catechol Violet solution as indicator, at pH 4.0, 4.2 and 4.5–4.6 respectively, to the corresponding sharp colour changes (from orange red to greenish yellow, from light violet through weakly pink to yellow, and from blue to lemon yellow). The pH was adjusted with 0.1M sodium acetate-acetic acid buffer² (5–10 ml) or by addition of water and/or glacial acetic acid, as required.

Copper(II) (10 μ moles) was masked by adding ascorbic acid (~5 ml of 0.1% solution) and potassium cyanide (~10 ml of 1% solution), and Gallein or Catechol Violet was used as indicator. The interference of 10 μ moles of lead was dealt with by adding ~1 ml of 0.5M sulphuric acid; the excess of acid was partly neutralized with ammonia before addition of the buffer for the titration. Potassium fluoride (~1 ml of 0.5% solution) was added to mask 10 μ moles of aluminium or thorium. Potassium cyanide (~2 ml of 1% solution) was added to remove the interference due to 10 μ moles of nickel in titrations employing Gallein or Catechol Violet as indicator (Table 1).

Conductometric titration was done in the usual way, the specific conductance being measured 2–3 min after each addition of DCTA, with at least 5 or 6 readings taken each side of the equivalence point. No buffer was used.

For the spectrophotometric titrations, Catechol Violet solution (2 drops) or Alizarin Red S solution (10 drops) was added to 1–5 ml of vanadium(IV) solution which was then buffered to pH 4.5 or 4.0, respectively, with ~10 ml of 0.1M sodium acetate-acetic acid buffer, and titrated with DCTA solution with measurement of absorbance at 607 nm (Catechol Violet) and 520 nm (Alizarin Red S) (Figs. 1 and 2). The absorbance was corrected for dilution and plotted as a function of the volume of DCTA added (Fig. 3).

The titrations were repeated at least five times at each concentration level.

RESULTS AND DISCUSSION

The study confirms that vanadium(IV) reacts with DCTA stoichiometrically in 1:1 molar ratio as expected. The titrations are quantitative and satisfactory when done at room temperature (25–30°). If DCTA is titrated conductometrically with vanadium(IV), the equivalence point found is not reliable, whereas the reverse titration is satisfactory.

Vanadium(IV) and Alizarin Red S form a stable orange red complex at pH 4.0 (λ_{\max} 485 nm); the corresponding Catechol Violet complex is blue (λ_{\max} 620 nm at pH 4.5) (Figs. 1 and 2). The yellow vanadium(IV)–DCTA complex shows no significant absorbance in these wavelength regions, which can therefore be used in the spectrophotometric titration (Fig. 3). The error in the spectrophotometric titration is less than that in the visual titration, particularly at low concentrations of vanadium(IV). The slight curvature near the equivalence point is customary in spectrophotometric titrations based on use of indicators.

Interferences

The determination is not affected by 100-fold molar ratio of lithium, sodium, potassium, magnesium, strontium, chloride, nitrate, sulphate or acetate to vanadium. The visual titration is not affected by silver, though a precipitate of silver chloride is formed if chloride is present (and this causes inter-

*To whom correspondence should be addressed (present address: Pro-Vice-Chancellor, Kurukshetra University, Kurukshetra, India).

Table I. Visual determination of vanadium(IV) with DCTA in presence of various ions

Ion added, mg	V(IV) taken, mg	V(IV) found, mg†		
		Alizarin Red S	Gallein	Catechol Violet
	0.20	0.20 (5)	0.20 (5)	0.20 (7)
	1.02	1.02 (6)	1.02 (6)	1.03 (8)
	2.04	2.03 (6)	2.04 (5)	2.06 (8)
Ca ²⁺	16.1	2.04	2.03 (10)	2.04 (6)
	32.1	2.04	interferes	interferes
	160.5	2.04	interferes	interferes
Ba ²⁺	11.0	0.41	0.41 (9)	0.41 (7)
	110	2.04	interferes	2.02 (8)
	550	2.04	interferes	interferes
Hg ²⁺	2.8	0.71	0.71 (8)	0.72 (10)
	16.1	2.04	2.02 (8)	2.04 (7)
	88.4	2.04	interferes	interferes
Pb ²⁺	0.8	0.20	0.20* (13)	0.20* (12)
	31.1	1.53	1.54* (12)	1.55* (13)
	78.9	1.94	1.94* (12)	1.96* (14)
Al ³⁺	0.3	0.61	0.61* (10)	0.62* (11)
	3.8	1.43	1.44* (12)	1.43* (12)
	9.2	1.73	1.72* (11)	1.72* (13)
Cr ³⁺	1.0	0.41	0.41 (10)	0.41 (10)
	2.0	1.53	1.54 (11)	1.53 (9)
	5.0	1.83	interferes	interferes
F ⁻	3.8	0.41	0.40 (9)	0.41 (10)
	19.0	2.04	2.02 (9)	2.03 (9)
	76.1	2.04	interferes	2.02 (10)
S ²⁻	1.9	0.61	0.60 (9)	0.60 (8)
	12.8	2.04	interferes	2.05 (10)
	14.1	2.04	interferes	2.04 (8)

*After masking/removing the interfering ion.

†Standard deviation (μ g) in brackets.

ference in the spectrophotometric titration). With Alizarin Red S, Gallein and Catechol Violet as indicators, the corresponding tolerance limits (molar ratio to vanadium) are 10, 100 and 10 for calcium, 10, 20 and 60 for barium, 10, 10 and 1 for mercury(II), 25, 100, and 25 for fluoride, and 5, 10 and 10 for

sulphide. Higher levels of calcium and barium result in formation of precipitates, presumably of sulphate, which interfere in detection of the end-point (surprisingly, there is better tolerance for strontium). Chromium(III) does not interfere if its concentration is less than 0.17 mg/ml. Cobalt, zinc and thorium are

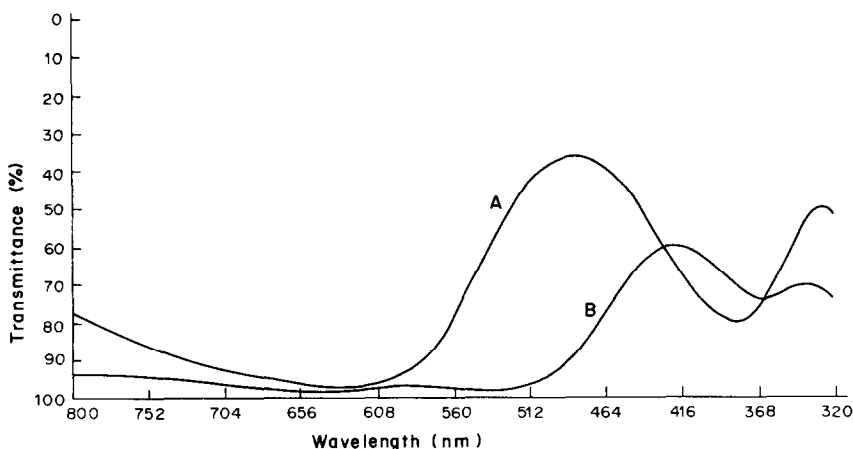


Fig. 1. Absorption spectra of V(IV)-Alizarin Red S complex in absence (A) and presence (B) of excess of DCTA; pH 4.0.

Table 2. Analysis of certain binary mixtures of vanadium(IV)*

Metal ion in mixture (M)	Taken, mg		Found, mg					
			Gallein		Catechol Violet		Alizarin Red S	
	V	M†	V	M†	V	M†	V	M†
Cu ²⁺	0.41	0.32	0.41 (9)	0.32 (8)	0.40 (7)	0.33 (7)	—	—
	1.22	0.95	1.21 (8)	0.95 (10)	1.22 (8)	0.94 (11)	—	—
	1.43	2.54	1.45 (10)	2.53 (7)	1.44 (10)	2.54 (9)	—	—
Th ⁴⁺	0.61	1.16	0.62 (8)	1.16 (10)	0.61 (8)	1.16 (9)	0.61 (7)	1.15 (9)
	1.02	4.64	1.06 (9)	4.64 (8)	1.01 (10)	4.65 (9)	1.04 (8)	4.63 (8)
	2.04	8.12	2.05 (10)	8.16 (11)	2.03 (8)	2.06 (11)	2.02 (10)	8.10 (9)
Ni ²⁺	0.41	0.59	0.40 (8)	0.59 (9)	0.42 (10)	0.59 (9)	—	—
	1.02	0.88	1.02 (8)	0.90 (7)	1.03 (9)	0.89 (10)	—	—
	1.63	1.47	1.65 (7)	1.48 (8)	1.65 (8)	1.46 (9)	—	—

*Standard deviations (μg) in brackets.

†From difference in titration values in presence and absence of masking agent.

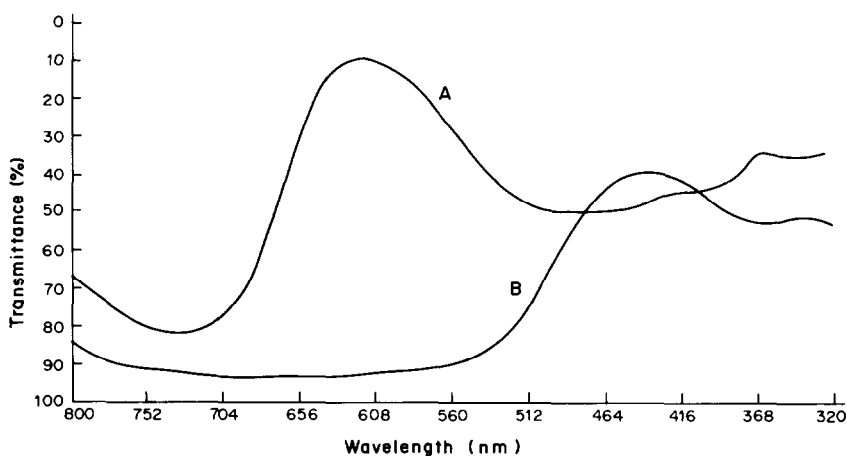


Fig. 2. Absorption spectra of V(IV)-Catechol Violet complex in absence (A) and presence (B) of excess of DCTA; pH 4.5.

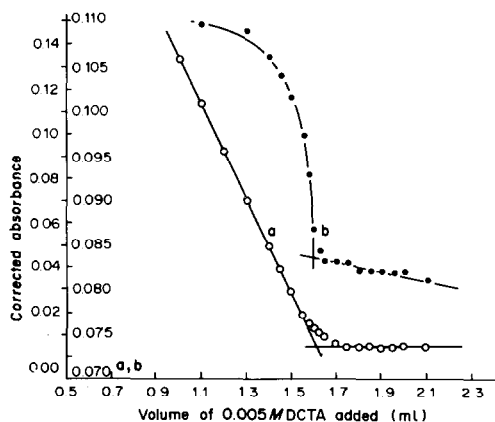


Fig. 3. Photometric titration of 2.00 ml of 0.004M V(IV) with (a) Catechol Violet as indicator (607 nm) and (b) Alizarin Red S as indicator (520 nm).

quantitatively co-titrated. Manganese(II), nickel, copper(II) and cadmium are also quantitatively co-titrated when Gallein or Catechol Violet is used as indicator. Lead and aluminium also interfere.

Lead can be masked by precipitation as sulphate, and aluminium and thorium can be masked with potassium fluoride. Copper(II) is masked by adding ascorbic acid and potassium cyanide solution, and the interference due to nickel is dealt with by adding potassium cyanide solution (but the end-point is not clear if Alizarin Red S is used as the indicator).

Attempts to mask cobalt, manganese(II), zinc and cadmium with common masking agents have not been successful. The application of the titration is therefore rather restricted.

REFERENCES

1. J. H. Mendez and L. P. Diez, *An. Quim.*, 1977, **73**, 83.
2. G. S. Walpole, *J. Chem. Soc.*, 1914, **105**, 2501.

THE POLISHED PRECIPITATE ELECTRODE: A NEW VOLTAMMETRIC METHOD WITH THE SOLID ELECTRODE

TAIIRO FUJINAGA

Nara University of Education, Takabatake, Nara 630, Japan

TAKASHI KIMOTO*

Kimoto Electric Co., Ltd., 3-1, Funahashi-Cho, Tennoji-Ku, Osaka 543 Japan

(Received 6 January 1984. Revised 1 February 1984. Accepted 10 April 1984)

Summary—A new surface-renewal technique at the solid electrode has been developed, based on continuous polishing. Well-defined and reproducible current-voltage curves similar to those obtained in polarography are given by the “polished precipitate electrode” (PPE). The method can be used for the continuous determination of electroactive substances and for the study of electrode reaction mechanisms at the solid-liquid interface.

Voltammetry with solid electrodes should give information about charge-transfer across solid-liquid interfaces, but most conventional solid electrodes are not satisfactory because of surface contamination.

Polarography has no such contamination problems because the electrode surface is continuously renewed. Recently, for the investigation of charge-transfer between two immiscible electrolyte solutions, the electrolyte dropping electrode (EDE), similar to the dropping mercury electrode (DME) in polarography, has been developed.¹⁻⁵

In this paper we describe a new “polished precipitate electrode” (PPE), the surface of which is continuously renewed by polishing with a magnetic stirrer bar coated with silicon carbide. This idea was first used by Hirata *et al.*⁶ in application of a ceramic-type ion-selective electrode for a process-monitoring detector system.

EXPERIMENTAL

Apparatus

Polished precipitate electrode. The assembly of this electrode is shown in Fig. 1 and a more detailed diagram is given in Fig. 2. The polished precipitate electrode is in a flow-cell, the sample flowing in at the base and out from the upper part, at approximately 1 ml/min. The working electrode (silver-silver halide) is at the centre of the electrode body and is 3 mm in diameter and 10 mm long. It is lowered into the ring-type counter-electrode (4 mm inner diameter and 6 mm outer diameter), the gap between the working electrode and counter-electrode being filled with epoxy resin to provide electrical insulation. The outside of the counter-electrode is also coated with epoxy resin. A cylindrical polishing magnetic stirrer bar (6 mm in diameter, 7 mm long) is mounted on top of the combined working and counter-electrode. The surface of the bar is coated with a paste consisting of a 7:3 w/w mixture of 600-mesh silicon carbide powder and epoxy resin. The bar is rotated at 600

rpm by the motor-driven magnet under the electrode, thus continuously polishing the electrode surface.

The sample flows from the working electrode to the counter-electrode because of the action of the stirrer. The electrode surface is thus kept clean and free from any contamination. An Ag/AgCl electrode in 1M potassium chloride solution is used as reference electrode (normal silver electrode: NSE) installed above the stirrer bar.

Preparation of working electrode. Silver sulphide-silver iodide powder (Ag₂SI) was precipitated from solution at room temperature, and used after drying at 60° for several hr: 130 mg of this powder were mixed thoroughly with 50 mg of silver bromide powder and pressed into a cylindrical

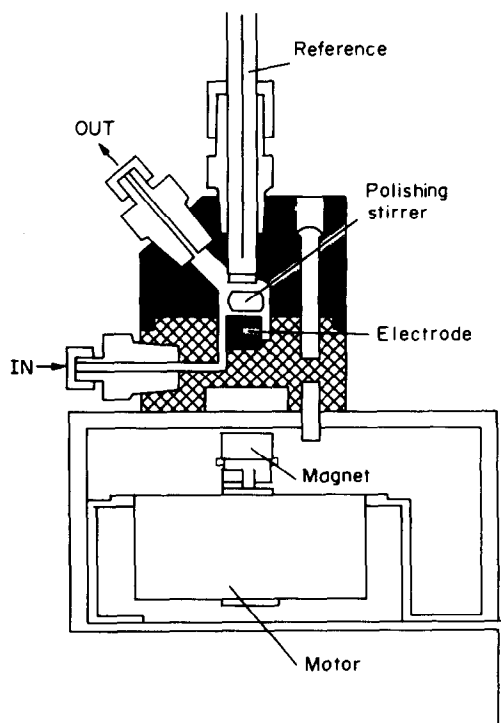


Fig. 1. Schematic diagram of the polished electrode.

*To whom correspondence should be addressed.

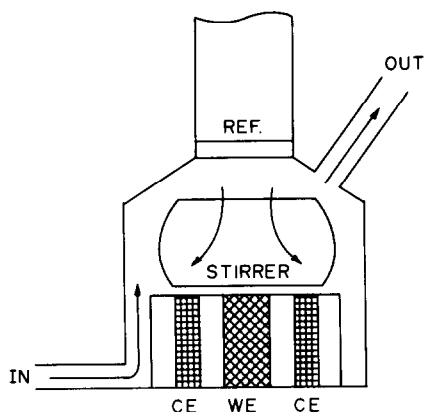


Fig. 2. Detailed diagram of working electrode and counter-electrode.

pellet (3 mm in diameter and 5 mm long). Once the pellet had been formed, 100 mg of silver metal and 100 mg of the Ag_3SI powder ($\text{Ag}/\text{Ag}_3\text{SI}$) were added and the whole compressed again to make a single pellet 3 mm in diameter and 10 mm long. A wire was attached to the surface of the $\text{Ag}/\text{Ag}_3\text{SI}$ pellet with silver paint. When silver metal was used as the working electrode, a silver cylinder 3 mm in diameter and 10 mm long was used instead of the silver halide precipitate pellet.

RESULTS AND DISCUSSION

The result of experiments on continuous renewal of the solid electrode is shown in Fig. 3, the current-voltage curves at room temperature being recorded at a rate of 1 mV/sec.

The curves were obtained with the polished silver-metal electrode (PSE) in the base electrolyte (0.1M potassium nitrate) in the absence (curve 1) and presence (curve 3) of a mixture of chloride, bromide and iodide, each $2 \times 10^{-4}M$. The polished electrode gives well-defined current-voltage curves similar to those obtained in polarography.

Curve 2 was obtained with the unpolished electrode, the surface being engraved in order to prevent polishing by the stirrer. The solution used for curve

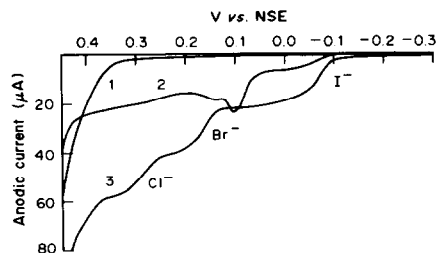


Fig. 3. Current-voltage curves obtained with the polished silver electrode at a scan-rate of 1 mV/sec. Curve 1, polished, base electrolyte 0.1M KNO_3 . Curve 2, unpolished, $2 \times 10^{-4}M$ Cl^- , $2 \times 10^{-4}M$ Br^- and $2 \times 10^{-4}M$ I^- in 0.1M KNO_3 . Curve 3, polished, test solution as for curve 2.

2 was the same as that for curve 3. Comparison of the curves shows that the polished electrode can overcome the contamination problems associated with solid electrodes, making possible quantitative analysis by voltammetry with such electrodes.

At the surface of the polished silver-metal electrode, ionization of the metallic silver and formation of the silver halide take place at the same solid-liquid interface. Therefore, the half-wave potential of each halide ion is shifted to more negative values according to the solubility product of its silver salt.

Figure 4 shows the reproducibility of the diffusion current for various concentrations of iodide in 0.1M potassium nitrate. The potential during this measurement was set at 0.05 V vs. NSE. As the figure shows, the diffusion current is proportional to the concentration of iodide ion. The gradual increases and decreases in diffusion current on changing the test solution are not due to slow response of the electrode but to delay in mixing.

As the recorder was undamped during this measurement, current oscillations due to stirring can be seen. When the stirrer was turned off, the diffusion current fell almost to zero (a in Fig. 4). When stirring was restarted, the current returned immediately to the original level. As can be seen from Fig. 4, the diffusion current is proportional to the concentration of halide in the test solution.

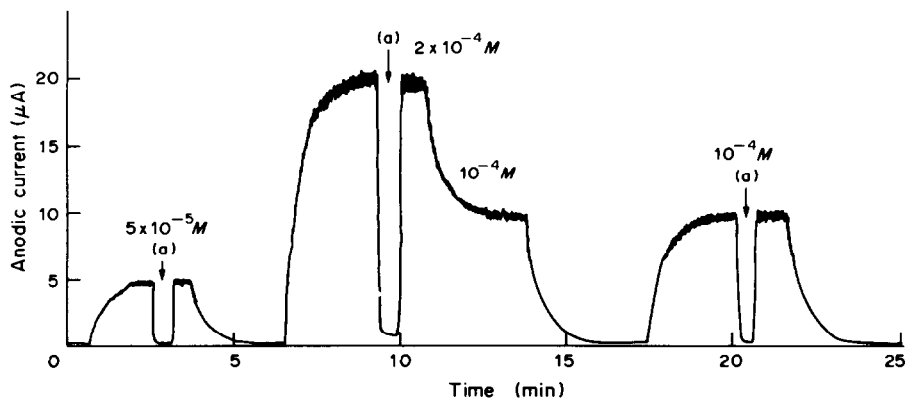


Fig. 4. Reproducibility of the diffusion current measured by the polished silver electrode. Sample flow-rate 1 ml/min; setting potential 0.05 V vs. NSE; test solution $5 \times 10^{-5}M$, $10^{-4}M$ and $2 \times 10^{-4}M$ I^- in 0.1M KNO_3 . (a) indicates the period during which the polishing stirrer is switched off.

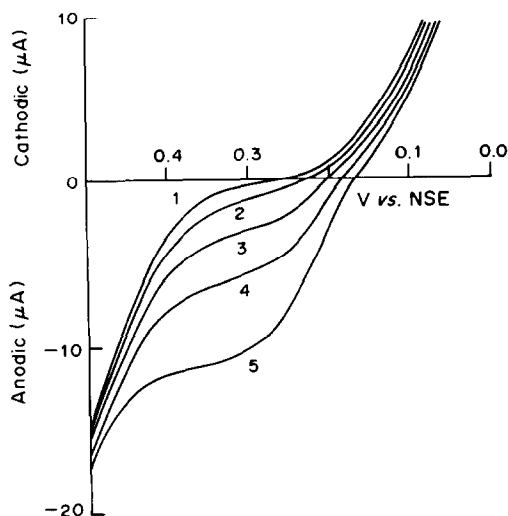
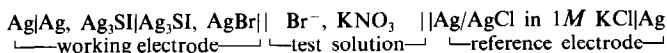


Fig. 5. Current-voltage curves obtained with the silver halide precipitate polished electrode ($\text{AgBr}/\text{Ag}_3\text{SI}$, SH-PPE) at a scan-rate of 1 mV/sec, base electrolyte 0.1M KNO_3 , $[\text{Br}^-]$: 1, nil; 2, 10^{-5}M ; 3, $2.5 \times 10^{-5}\text{M}$; 4, $5 \times 10^{-5}\text{M}$; 5, 10^{-4}M .

Figure 5 shows the current-voltage curves obtained with the silver halide polished precipitate electrode (SH-PPE) having an $\text{AgBr}/\text{Ag}_3\text{SI}$ pellet as the working electrode. The cell can be written as:



The curves in Fig. 5 were recorded for the base electrolyte (0.1M potassium nitrate) in the absence and presence of bromide ion.

In the curves in Fig. 3, no cathodic current is observed from +0.4 to -0.3 V vs. NSE. However, in the curves in Fig. 5, cathodic waves do appear and the zero-current potential for each wave is shifted to more negative values, according to the concentration of bromide ion in the aqueous phase.

CONCLUSION

The polished precipitate electrode has been developed in order to avoid contamination problems on solid electrode surfaces. Voltammetry with this electrode may be used for quantitative analysis and in the investigation of charge-transfer processes at the solid-liquid interface.

REFERENCES

1. J. Koryta, P. Vanysek and M. Brezina, *J. Electroanal. Chem.*, 1976, **67**, 263.
2. Z. Samec, V. Marecek, J. Weber and D. Homolka, *ibid.*, 1979, **99**, 385.
3. T. Fujinaga, *Phil. Trans. Roy. Soc. London*, 1982, **A305**, 631.
4. S. Kihara, Z. Yoshida and T. Fujinaga, *Brunseki Kagaku*, 1982, **31**, E297.
5. *Idem, ibid.*, 1982, **31**, E301.
6. H. Hirata, M. Arai and N. Tonooka, *Nippon Kagaku Kaishi*, 1980, 1475.

POLAROGRAPHIC DETERMINATION OF MALONONITRILE

D. PH. ZOLLINGER, M. BOS, A. M. W. VAN VEEN-BLAAUW and W. E. VAN DER LINDEN
Department of Chemical Technology, Twente University of Technology, P.O. Box 217, 7500 AE
Enschede, The Netherlands

(Received 11 January 1984. Accepted 5 April 1984)

Summary—A procedure is proposed for the determination of malononitrile by differential pulse polarography in methanolic 0.1M tetraethylammonium iodide/0.001M tetramethylammonium hydroxide as the supporting electrolyte. In this medium malononitrile is chemically converted into an electroactive species. With close control of timing of the steps in the procedure the error of the method is $\pm 1.5\%$ in the concentration range 0.0001–0.001M. Acrylonitrile, benzonitrile and succinic acid dinitrile do not interfere.

Malononitrile is an important compound in the technical synthesis of vitamin B1, various herbicides and insecticides, and a number of dyes. The methods described for its determination include gas chromatography,¹ thin-layer chromatography,² titration in non-aqueous solvents³ and a luminescence procedure.⁴ Some of these methods also apply to the assay of the riot-control agent *o*-chlorobenzal malononitrile (CS) by hydrolysis of this compound to chlorobenzaldehyde and malononitrile.^{4,5}

For CS, Tarantino⁶ has described a polarographic method based on the electroreduction of the compound itself or the *o*-chlorobenzaldehyde formed from it by hydrolysis. The other hydrolysis product (malononitrile) was found to be electro-inactive in his study.

We have observed that malononitrile gives rise to a polarographic reduction wave in alkaline methanolic medium. This paper describes a procedure for the polarographic determination of malononitrile based on this.

EXPERIMENTAL

Reagents

Methanol (p.a.), tetraethylammonium iodide (TEAI) (für die Polarographie), tetramethylammonium hydroxide (TMAOH) (0.1M in propan-2-ol/methanol), tetraethylammonium chloride (TEACl) (zur Synthese), lithium chloride (Suprapur), dimethylsulphoxide (zur Synthese) and ethanol (p.a.) were used as received from Merck. The malononitrile (Merck-Schuchardt, zur Synthese) was recrystallized from ethanol until a colourless product was obtained. Succinic acid dinitrile (Fluka, puriss.) and benzonitrile (Riedel de Haen) were used as received. Acrylonitrile, malonic acid and cyanoacetic acid were from Fluka and used as received. The dimer of malononitrile, 2-amino-1,1,3-tricyanopropene, was synthesized according to the procedure given by Carboni *et al.*⁷

Apparatus

A Metrohm E536 polarograph was used. The polarographic cell was kept at $25 \pm 0.1^\circ$ with a Tamson thermostat. Two mercury electrodes were used; their characteristics (open circuit in 0.1M TEAI/MeOH) were $m = 0.795$ mg/sec,

$t = 4.73$ sec for DME # 8 and $m = 0.77$ mg/sec, $t = 4.92$ sec for DME # 5 and a mercury height of 66 cm. The reference electrode was a silver/silver chloride electrode in methanol saturated with TEACl. A platinum wire was used as the auxiliary electrode.

The nitrogen used for deaeration was saturated with methanol to prevent loss of solvent from the sample during removal of dissolved oxygen.

Procedure

The polarographic measurements on calibration standards and samples of malononitrile were performed as follows. A 35-ml portion of the supporting electrolyte (0.1M TEAI/0.001M TMAOH in methanol) was deaerated by passage of nitrogen for 5 min. Then the malononitrile sample or standard was added and nitrogen was passed for 15 min. Then either the sampled d.c. or differential pulse polarogram was recorded over the range from -1.0 to -2.0 V applied potential *vs.* silver/silver chloride (in saturated TEACl/MeOH). The drop-time used was 0.4 sec. In the DPP technique a pulse amplitude of 20 mV was used.

The sampled d.c. polarograms were evaluated by the use of a three-parameter curve-fitting procedure, for the parameters limiting current, half-wave potential and slope of the log plot of current *vs.* potential.⁸

RESULTS AND DISCUSSION

When malononitrile is polarographed in 0.1M TEAI/0.001M TMAOH/MeOH, a reduction wave can be observed if a polarogram is run after the usual deaeration period (see Fig. 1). Its half-wave potential lies at -1.50 V *vs.* silver/silver chloride (in saturated TEACl/MeOH). Drop-time variation shows that this reduction wave is diffusion-controlled (Table 1). The slopes of the log plots indicate irreversibility and most likely a one-electron transfer.

The diffusion current for this reduction decreases if the alkaline solution of the malononitrile is kept for longer than 1 hr (Table 2), presumably because of chemical conversion of the electroactive species. However, in the period 30–60 min after mixing of the malononitrile and the supporting electrolyte, the limiting current remains fairly constant.

The formation and decomposition of the electro-

Table 1. Sampled d.c. polarography of 0.00111M malononitrile in 0.1M TEAI/0.001M TMAOH/MeOH (DME No. 5)

Drop-time, sec	Limiting current, i_d , μA	Half-wave potential, V	Slope of log plot, V/decade	$i_d/t^{1/6}$, $\mu A/sec^{1/6}$
0.6	1.493	-1.519	0.1035	1.63
0.8	1.627	-1.506	0.0893	1.69
1.0	1.655	-1.503	0.0888	1.66
1.4	1.827	-1.497	0.0902	1.69
2.0	1.970	-1.499	0.0955	1.76
3.0	2.098	-1.494	0.0907	1.75

active species is strongly influenced by the concentration of TMAOH in the supporting electrolyte, as can be seen from Table 3. If the polarograms are run about 15 min after mixing of the malononitrile and the supporting electrolyte, the optimum concentration of TMAOH is about 0.001M.

Malononitrile is known to form a dimer, 2-amino-1,1,3-tricyanopropene, in alkaline solutions.⁹ Polarography of this product, synthesized according to the procedure given by Carboni *et al.*⁷ showed a reduction wave at -1.76 V, but not at -1.50 V, so this dimer cannot be the electroactive species.

Malononitrile itself is reported to be electroinactive in 0.1M lithium nitrate/MeOH.⁶ In the media 0.1M NaOH/water, phosphate buffer (pH 7)/water, 0.1M LiCl/0.001M TMAOH/DMSO and 0.1M LiCl/MeOH, malononitrile is also polarographically inactive. The reduction wave at around -1.50 V, however, is present in polarograms of malononitrile in 0.1M LiCl/0.001M TMAOH/MeOH and with a

much smaller limiting current in 0.1M LiCl/0.001M TMAOH/EtOH.

These findings indicate that the base TMAOH and the alcoholic solvent take part in the conversion of the malononitrile into the electroactive species. This was confirmed by ultraviolet spectrometry measurements. Malononitrile shows no ultraviolet absorption in methanol. Addition of $4 \times 10^{-4}M$ TMAOH to $4.5 \times 10^{-4}M$ malononitrile produces an absorption peak with a maximum shifting from 230 nm to 250 nm, with substantial broadening over a period of 30 min. Again this behaviour is different from the behaviour of the dimer, which shows a rather stable absorption peak at 300 nm under these conditions.

Attempts to isolate and identify this electroactive species by UV, MS and NMR spectrometry were

Table 2. Time-dependence of limiting current for 0.000535M malononitrile in 0.1M TEAI/0.001M TMAOH/MeOH

Time of measurement, min	Limiting current, μA
30	1.193
45	1.169
60	1.180
75	1.164
90	1.150
105	1.132
120	1.099
135	1.055
150	1.008
165	1.020
180	0.985
195	0.919
210	0.949
225	0.908

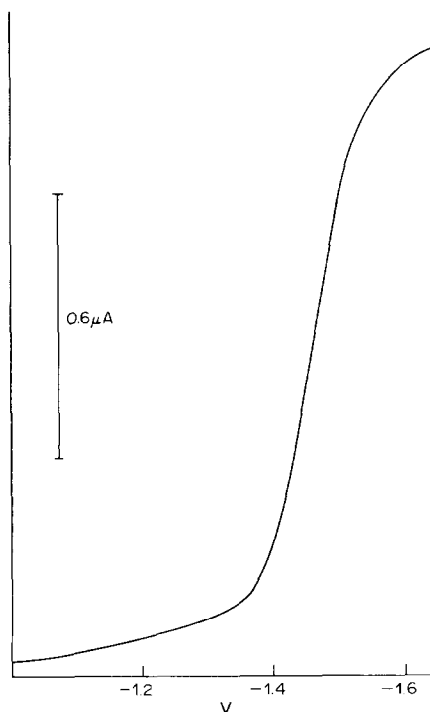
Fig. 1. Direct current polarogram of $5.35 \times 10^{-4}M$ malononitrile in 0.1M TEAI/0.001M TMAOH/MeOH.

Table 3. Influence of TMAOH concentration on limiting current of 0.001M malononitrile in 0.1M TEAI/TMAOH/MeOH

[TMAOH], mM	Limiting current, μA
—	no reduction wave
0.26	0.198
0.52	0.620
1.04	1.232
2.56	1.316
5.00	1.030
9.52	1.033

Table 4. Calibration data for differential pulse polarography of malononitrile in 0.1M TEAI/0.001M TMAOH/MeOH (DME No. 8; DPP amplitude 20 mV; t_{drop} 0.4 sec; measurement after 15 min)

[Malononitrile], $10^{-4}M$	Peak current measured, μA	Peak current cubic spline approximation, μA
0.984	0.570	0.570
1.967	1.056	1.058
2.951	1.529	1.519
3.935	1.914	1.930
4.909	2.294	2.286
5.902	2.613	2.603
6.886	2.910	2.925
7.870	3.248	3.240
8.854	3.426	3.427

(Test sample: $3.84 \times 10^{-4}M$ taken; peak current 1.912 $\mu A \pm 0.4\%$; $3.89 \times 10^{-4}M \pm 0.5\%$ found; relative error 1.3%; 6 replicates).

unsuccessful, most likely because of the instability of the electroactive compound.

Nevertheless, on the basis of the findings mentioned above, it was possible to develop a procedure for the polarographic determination of malononitrile in which the parameters that influence the formation of the electroactive species are closely controlled. This was accomplished by accurate temperature control of the polarographic cell, standardization of the concentration of TMAOH in the supporting electrolyte, and a strict time schedule in the procedure.

The results for measurement of a number of standard and test solutions, prepared by directly weighing

purified malononitrile and dissolving it in methanol, are given in Table 4. The calibration graph is not linear, but the calibration data can be fitted to a cubic spline function with 3 knots equally spaced over the concentration interval measured, and this function used to retrieve the concentration of the test sample. This approach allows automation of the system. The deviation between the amount taken and found was 1.3%, and the standard deviation for 6 replicate samples was 0.5%.

The procedure was tested for interference by the compounds cyanoacetic acid, malonic acid, acrylonitrile, benzonitrile and succinic acid dinitrile. These compounds did not change the reduction wave of the malononitrile at -1.50 V when present at concentrations not exceeding that of the malononitrile.

Acknowledgement—The authors wish to thank Drs. V. W. L. J. Aarts for her helpful suggestions during this work.

REFERENCES

1. H. Binder and E. Stuerzenbecher, *J. Chromatog.*, 1977, **130**, 405.
2. H. G. Eulenhoefer, *ibid.*, 1968, **36**, 198.
3. J. S. Fritz, *Anal. Chem.*, 1952, **34**, 674.
4. U. Fritsche, *Z. Anal. Chem.*, 1980, **302**, 119.
5. S. Sass, T. L. Fisher, M. J. Jascot and J. Herban, *Anal. Chem.*, 1971, **43**, 462.
6. P. A. Tarantino and S. Sass, *J. Electrochem. Soc.*, 1969, **116**, 430.
7. R. A. Carboni, D. D. Coffman and E. G. Howard, *J. Am. Chem. Soc.*, 1958, **80**, 2838.
8. M. Bos, *Anal. Chim. Acta*, 1976, **81**, 21.
9. S. Bloch and G. Toupance, *J. Chim. Phys.*, 1975, **72**, 1157.

ANALYTICAL DATA

THE STABILITY OF METAL COMPLEXES WITH 8-MERCAPTOQUINOLINE AND ALKYL-SUBSTITUTED 8-MERCAPTOQUINOLINES IN DIMETHYLFORMAMIDE

N. A. ULAKHOVICH, H. C. BUDNIKOV, T. S. GORBUNOVA and A. P. STURIS
Faculty of Chemistry, V.I. Ul'yanov-Lenin State University, Lenina 18, Kazan, 420008, USSR

(Received 13 March 1984. Accepted 5 April 1984)

Summary—The stoichiometry and stability constants of 8-mercaptoquinoline and alkyl-8-mercaptoquinoline complexes of Zn(II), Cd(II), Pb(II), Ni(II), Bi(III) and Ag(I) were determined potentiometrically in dimethylformamide. The stability of the 8-mercaptoquinolinates decreases in the order Ag(I) > Bi(III) > Ni(II) > Pb(II) > Cd(II) > Zn(II). Metal 7-methyl-8-mercaptoquinolinates are the most stable. The presence of the alkyl group in the 2-position (which has a steric effect) lowers the strength of metal-ligand bonding.

8-Mercaptoquinoline and alkyl-8-mercaptoquinolines are well known as complexing reagents for heavy metals.¹ These reagents are especially promising when used for combining concentration and separation with a sensitive method of determination. Hence the stability constants of these complexes in non-aqueous solutions should prove of interest. As a rule the extracted species is a non-electrolyte. Therefore, in order to study the stability of the 8-mercaptoquinolinates by potentiometry it is necessary to add some polar solvent to the extract or to use only a polar solution.

This article deals with measurement of the redox potentials of systems containing the ligand (8-mercaptoquinolinolate anion), an oxidized form of the ligand (the disulphide of 8-mercaptoquinoline), and metal ion, at a constant concentration of the disulphide.^{2,3} The conditions for application of the method are that the electrode process is reversible and the metal complexes only with the reduced form of the ligand.

The stability constants of Zn(II), Cd(II), Pb(II), Ni(II), Bi(III) and Ag(I) alkyl-8-mercaptoquinolinates in dimethylformamide have been determined, the alkyl positions in the ligand being 2,4, 6,7 and 2,7.

EXPERIMENTAL

Reagents

The sodium salts of the alkyl-8-mercaptoquinolines and corresponding disulphides were prepared as described in the literature.⁴ The analytical (total) concentrations of the ligand and disulphide were constant in all experiments, and $5 \times 10^{-4}M$ and $2.5 \times 10^{-4}M$ respectively. The metal ion concentrations were varied in the range 1×10^{-4} – $1 \times 10^{-3}M$. Stock solutions of the anhydrous metal perchlorates (twice recrystallized) were prepared from the solids and standardized by EDTA titration.⁵ Lithium perchlorate solution (0.1M) was used as the background

electrolyte. Dimethylformamide (DMF) was used as solvent. The purity of the electrolyte was checked by recording polarograms with a platinum electrode. The base-line for DMF was run as a check on electrochemical purity.

Apparatus and potentiometric measurements

Potentiometric measurements were made with an R363 potentiometer (USSR) at $25 \pm 0.2^\circ$. The indicator electrode was a platinum plate, the reference electrode a saturated calomel electrode. The solutions were deoxygenated, and a slow stream of argon was passed over the solution throughout the experiment. The logarithmic values obtained from a series of measurements differed by not more than ± 0.1 , even in the most unfavourable conditions.

The stability constants were obtained from the experimental data by the method of Schulman *et al.*³ with some slight alterations. Instead of the simultaneous titration of a ligand with a metal and a background electrolyte, the redox electrode potentials in the presence and absence of metal ions were measured to save time. The values of the stability constants were calculated according to Bjerrum, with the formulae

$$-\log[L] = \frac{\Delta E}{0.059} - \log C_L$$
$$\bar{n} = \frac{C_L(1 - 10^{-\Delta E/0.059})}{C_M}$$

where C_L and C_M are the total concentrations of the ligand and metal respectively, ΔE is the difference in the equilibrium potential of the ligand redox-system in the presence and absence of metal ions. In a number of cases, where the values of the stepwise stability constants were rather close, another method of calculating was used to correct the data.⁶

RESULTS AND DISCUSSION

The relations between the average ligand number, \bar{n} , and the corresponding concentration of the free, uncomplexed, ligand are shown in Fig. 1 for some metal-ligand systems. Logarithmic values of the stability constants are given in Table 1, and show that the metal alkylmercaptoquinolinates have high

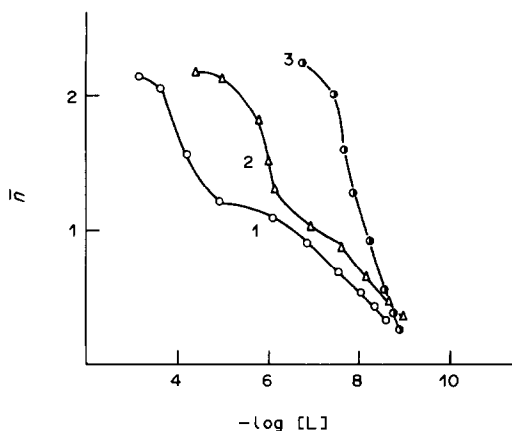


Fig. 1. Formation curves of zinc 8-mercaptoquinolate (1), cadmium 2-methyl-8-mercaptoquinolate (2) and nickel 6-methyl-8-mercaptoquinolate (3).

stability. The chelating power of an alkylmercaptoquinoline is accounted for by the donor heterocyclic nitrogen atom, the sulphur atom conjugated with the quinoline ring, the dative π -bonding of the central atom and finally by the formation of five-membered rings. In the case of Ag(I), Zn(II), Cd(II), Pb(II) and Bi(III) stepwise complex formation takes place. Simultaneous addition of two molecules of the ligand to nickel occurs in accordance with the values of the stepwise constants. When a metal with occupied d -orbitals forms a cationic complex with an alkylmercaptoquinoline, bonding characteristics do not vary apart from a slight decrease in the conjugation of the chelating ring, which makes the metal-sulphur bonding more ionic.

The situation is more complicated for the complexes formed by a metal with empty d -orbitals. It is well known that the stability of complexes depends on the possibility for charge levelling by σ -bonding and π -back-bonding. Like many polyatomic ligands the alkylquinolate ligands can have the special features of σ -donation and π -back-donation, the canonical structures *b*, *c*, *d* providing the greatest contribution (Scheme 1).¹

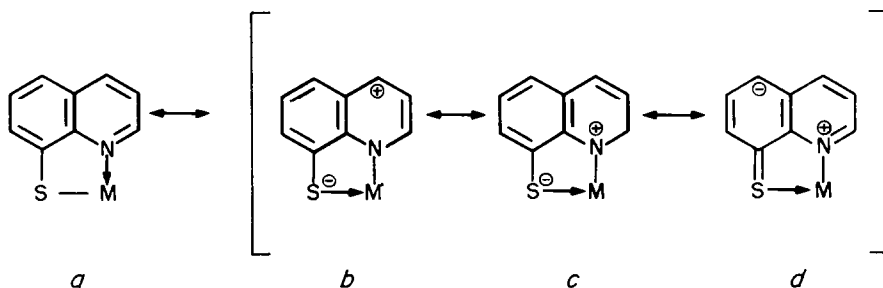
The donor-acceptor interaction $M \leftarrow S$ which more or less increases the stability of the dative $M \rightarrow S$ π -bonding, and the existence of the dative π -bonding formed by the d -electrons of the central atom and the delocalized p -orbitals of the quinoline nucleus, are a

Table 1. Logarithmic values of the stability constants of the alkyl-8-mercaptoquinolate complexes

Metal	R	$\log k_1$	$\log k_2$	$\log \beta_2$
Zn(II)	H	8.1	4.3	12.4
	2-CH ₃	8.5	6.4	14.9
	4-CH ₃	8.3	6.2	14.5
	6-CH ₃	8.3	6.2	14.5
	7-CH ₃	10.8	8.3	19.1
	2,7-(CH ₃) ₂	9.1	6.9	16.0
	2- <i>i</i> -C ₃ H ₇	5.9	5.4	11.3
Cd(II)	H	8.3	4.9	13.2
	2-CH ₃	8.4	6.1	14.5
	4-CH ₃	8.1	6.1	14.2
	6-CH ₃	9.3	7.1	16.4
	7-CH ₃	9.8	6.2	16.0
	2,7-(CH ₃) ₂	9.2	6.9	16.1
	2- <i>i</i> -C ₃ H ₇	5.1	4.6	9.7
Pb(II)	H	8.6	5.5	14.1
	2-CH ₃	8.8	5.3	14.1
	4-CH ₃	8.4	5.1	13.5
	6-CH ₃	9.4	6.9	16.3
	7-CH ₃	10.6	6.7	17.3
	2,7-(CH ₃) ₂	10.0	6.5	16.5
	2- <i>i</i> -C ₃ H ₇	4.5	3.9	8.4
Ni(II)	H	9.5	6.6	16.1
	2-CH ₃	8.1	5.3	13.4
	4-CH ₃	9.7	7.3	17.0
	6-CH ₃	9.2	7.3	16.5
	7-CH ₃	11.3	7.9	19.2
	2,7-(CH ₃) ₂	8.2	6.0	14.2
	2- <i>i</i> -C ₃ H ₇	3.9	3.6	7.5
Ag(I)	H	13.8	4.4	18.2
	2-CH ₃	14.7	4.6	19.3
	4-CH ₃	15.7	5.3	21.0
	6-CH ₃	14.9	5.5	20.4
	7-CH ₃	15.1	5.8	20.9
	2,7-(CH ₃) ₂	14.1	6.7	20.8
	2- <i>i</i> -C ₃ H ₇	8.9	8.5	17.4
Bi(III)	H	12.7	8.3	26.2
	2-CH ₃	12.4	9.2	28.5
	4-CH ₃	13.3	10.8	30.5
	6-CH ₃	13.6	11.4	32.4
	7-CH ₃	13.5	9.8	29.5
	2,7-(CH ₃) ₂	13.7	9.4	30.0
	2- <i>i</i> -C ₃ H ₇	7.2	7.0	20.8

characteristic feature of the meso-ionic structures of the complexes. This strengthening of bonding leads to greater stability of the transition metal chelates, e.g., in the case of nickel.

The introduction of an alkyl group into the



Scheme 1.

8-mercaptoquinoline molecule generally increases the complex stability (Table 1). This is connected with strengthening of the basic properties of the donor nitrogen atom and weakening of the acid properties of the mercapto group. An alkyl group in the 7-position causes further weakening of the acidity of the mercapto group. The reduced acidity strengthens the covalent bonding $M \rightarrow S$, distorts the π - d -conjugation of the sulphur atom with the quinoline ring and finally increases the basicity of the nitrogen atom. The possibility of coplanarity being destroyed in the case of the 7-alkyl ligand, together with the factors mentioned above, brings about the greater stability of the metal 7-alkyl-8-mercaptoquinolinates. A greater influence of the 7-alkyl group appears for the nickel chelates. The increase in basicity of the nitrogen atom results in a greater stabilization of the meso-ionic structure. The greatest stability of the meso-ionic structure and a thus higher stability constant is characteristic of the nickel 4-methyl-8-mercaptoquinolate complex. This is likely to be a result of the hyperconjugation of the methyl group with the quinoline ring and increase in the basicity of the nitrogen atom.

The lower stability of the nickel complex with the 2-alkylmercaptoquinolines is notable in the range of metal complexes studied. This is likely to be a result of the steric effects of an alkyl group in the 2-position, which cause the nickel complex to take the configuration of a distorted tetrahedron, whereas all the other nickel complexes have a square-planar configuration.⁷ The deviation from the square-planar configuration is assumed to decrease the strength of the dative $d_{\pi}-p_{\pi}$ bonding formed by the d -electrons of the central atom and the delocalized p -orbitals of the quinoline nucleus. The alkyl group in the 2-position influences the stability of other metal 8-mercaptoquinolinates in a similar manner, although to a lesser extent (because these metal 8-mercaptoquinolinates do not have a square-planar configuration). Therefore the chelates with 2,7-dimethyl-8-mercaptoquinoline are the most stable. In spite of the steric hindrance the methyl group in the 2-position strengthens the basicity of the nitrogen atom. Furthermore the methyl group in the 7-position helps to strengthen the metal-ligand bonding. Attention should be drawn to the determination of the stability constants of silver alkyl-8-mercaptoquinolinates in DMF containing 2.5% water. The character of the relation between the stability constant and the water content has been clarified for the silver 6-methyl-8-mercaptoquinolate complex. The stability of this complex was found to increase with increase in the DMF content. A plot of $\log k$ vs. the reciprocal of the dielectric constant of the medium is linear (Fig. 2) and extrapolation to 100% DMF (points A_1 and A_2 in Fig. 2) makes it possible to compare the stability constant for the silver complex with those for other

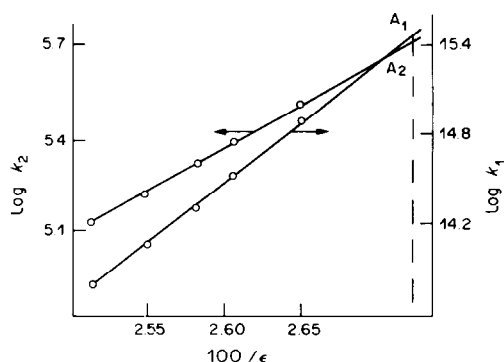


Fig. 2. The relation between stepwise stability constants of silver 6-methyl-8-mercaptoquinolinates and the composition of the medium.

8-mercaptoquinolinates. The values obtained are $\log k_1 = 15.4$; $\log k_2 = 5.7$. To extrapolate the values for the other silver complexes is difficult, because of the low solubilities in DMF. The complexes are also adsorbed on the platinum electrode when there are traces of water in the DMF, and this causes unsatisfactory results.

According to the data obtained, the number of ligands in the complex is usually the same as the oxidation state of the central atom, over a large range of concentrations. The reason for this is considered to be the large size of the 8-mercaptoquinoline molecule and the ease of polarization of sulphur, which transfers charge to the central atom and therefore prevents the appearance of a high co-ordination number. However, in silver 8-mercaptoquinolate two ligands are bonded to the metal, forming the species $[AgL_2]^-$. The possibility of existence of analogous complexes has been reported by Suprunovich and Shevchenko.⁸ The central atom is likely to use the electron-acceptor $5s$ -, $5p$ - and $5d$ -orbitals for bonding the second molecule of 8-mercaptoquinoline. The stability of the complexes decreases in general in the order $Bi(III) > Ag(I) > Ni(II) > Pb(II) \sim Cd(II) \sim Zn(II)$.

REFERENCES

1. Yu. A. Bankovskii, *The Chemistry of the Mercaptoquinoline Chelates and their Derivatives*, Zinatne, Riga, 1978.
2. V. M. Shulman and T. V. Kramareva, *Izv. Akad. Nauk USSR (Siberia Dept.)*, 1961, 55.
3. S. V. Larionov, V. M. Shulman and L. A. Podolskaya, *Zh. Neorgan. Khim.*, 1967, 12, 1253.
4. Yu. A. Bankovskii, D. E. Zaruma, E. A. Luksha and A. P. Sturis, *Izv. Akad. Nauk. Latv. SSR*, 1966, 387.
5. G. Schwarzenbach and H. Flaschka, *Die komplexometrische Titration*, Enke Verlag, Stuttgart, 1965.
6. F. Rossotti and H. Rossotti, *The Determination of Stability Constants and other Equilibrium Constants in Solution*, McGraw-Hill, New York 1961.
7. L. Ya. Pech, Ya. K. Ozols, A. P. Sturis and A. F. Ievinsh, *Izv. Akad. Nauk. Latv. SSR*, 1974, 621.
8. V. I. Suprunovich and Yu. I. Shevchenko, *Koord. Khim.*, 1979, 5, 1167.

DETERMINATION OF THERMODYNAMIC IONIZATION CONSTANTS FOR EIGHT MEDICINAL BENZYLIMIDAZOLINES

J. E. KOUNTOURELLIS*, N. PAPADOPOULOS and A. RAPTOULI
School of Pharmacy, Aristotelian University of Thessaloniki, Greece

(Received 19 March 1984. Accepted 17 April 1984)

Summary—The thermodynamic dissociation constants at 25° for eight medicinal benzylimidazolines have been determined by potentiometric titration.

The common feature of the compounds investigated is that they include in their molecular structure the 2-imidazoline ring. Apart from this, they possess different pharmacological actions:^{1,2} tolazoline and phentolamine are alpha-adrenergic blocking agents. Naphazoline, xylomethazoline, oxymetazoline, cirazoline and tymazoline have marked alpha-adrenergic activity, and antazoline is an antihistamine.

The compounds are the active ingredients of many liquid pharmaceutical preparations such as decongestants, injectable solutions and ointments. Because they undergo rapid base-catalysed hydrolysis³ in aqueous solutions, the development of a stability-indicating assay was initiated.

High-pressure liquid chromatography (HPLC) has been studied as a means of identification and determination of 2-imidazolines and their degradation products.⁴ The proposed method employs a cation- or anion-exchange resin, and a mobile phase buffered at about pH 12. Since the chromatographic conditions have to be varied from compound to compound, we have determined pK_b for the compounds because we believe that accurate values will help in the development of better chromatographic systems.

EXPERIMENTAL

Reagents

The samples supplied by the manufacturers included phentolamine mesylate and the hydrochlorides of tolazoline, naphazoline, xylometazoline, oxymetazoline, cirazoline, tymazoline, and antazoline. The melting points of the compounds agreed with those quoted in the literature. The PMR and ¹³CMR spectra were in agreement with the molecular structures. Water was purified with a Millipore ion-exchange apparatus.

Apparatus

A Radiometer PHM 63 digital pH-meter and a Radiometer GK 2401 B combined glass electrode were used. The electrode was calibrated with a series of buffer solutions.⁵

Determination

In each case, a sample of the salt of the base was dissolved in 50 g of freshly demineralized water to give a solution with a concentration of about $1 \times 10^{-3} M$. The titrations were done under a nitrogen atmosphere in a water-jacketed vessel kept at $25 \pm 0.1^\circ$. The amounts of sodium hydroxide added were determined by weighing. The thermodynamic dis-

*To whom correspondence should be addressed.

Table 1. The pK_b values for the eight 2-imidazolines

Compound	pK_b	Compound	pK_b
Xylometazoline	3.15 ± 0.04	Antazoline	3.77 ± 0.03
Tolazoline	3.41 ± 0.01	Tymazoline	4.42 ± 0.02
Oxymetazoline	3.46 ± 0.02	Cirazoline	4.44 ± 0.02
Naphazoline	3.52 ± 0.02	Phentolamine	4.71 ± 0.01

sociation constants pK_b were calculated from the equations:^{6,7}

$$pK_b = -\log [OH^-] + \log \frac{[BOH]}{[B^+]} - 2 \log \gamma_{\pm}$$

$$pK_w = 14.00$$

$$[B^+] = C_{\text{tot}} + [OH^-] - [Na^+]$$

$$[BOH] = C_{\text{tot}} - [B^+]$$

$$-\log \gamma_{\pm} = 0.512 \sqrt{I} / (1 + 1.6 \sqrt{I}).$$

The symbols have their usual meanings.

RESULTS AND DISCUSSION

Table 1 shows the data obtained for the eight benzylimidazolines. The decrease in basicity from xylometazoline to phentolamine follows the increase of electron-withdrawing ability of the aromatic substituent in the 2-position of the imidazoline (heterocyclic) ring. Different substituents in the aromatic ring do not cause great differences in the pK_b values, since the aromatic and the heterocyclic moieties of the molecule are separated by a bridging methylene group. The basicity of the compounds decreases when a heteroatom is attached to the linking methylene group.

Acknowledgement—The authors would like to thank Prof. P. P. Georgakopoulos for his helpful discussions and suggestions.

REFERENCES

1. Martindale, *The Extra Pharmacopoeia*, 28th Ed., The Pharmaceutical Press, London, 1982.
2. A. G. Gilman, L. S. Goodman and A. Gilman, *The Pharmacological Basis of Therapeutics*, 6th Ed., Macmillan, New York, 1980.
3. D. J. G. Davis, *Proc. APGI Conf. Paris*, 1980, **2**, 217.
4. J. A. Mollica, G. R. Padmanabham and R. Strusz, *Anal. Chem.*, 1973, **45**, 1859.
5. R. G. Bates, *ibid.*, 1968, **40**, No. 6, 28A.
6. A. Albert and E. P. Sergeant, *The Determination of Ionisation Constants*, Chapman & Hall, London, 1971.
7. L. Z. Benet and J. E. Goyan, *J. Pharm. Sci.* 1967, **56**, 665.

HYDROXIDE COMPLEXES OF LANTHANIDES—VII* NEODYMIUM(III) IN PERCHLORATE MEDIUM

J. KRAGTEN and L. G. DECNOP-WEEVER

Laboratorium voor Analytische Chemie der Universiteit van Amsterdam, Nieuwe Achtergracht 166,
 1018 WV, Amsterdam, The Netherlands

(Received 12 March 1984. Accepted 17 April 1984)

Summary—From the precipitation borderline in the $\text{pNd}'\text{-pC}_\text{H}$ diagram the stability constants for the mononuclear and polynuclear species of neodymium hydroxide have been established. The values found were $\log^*\beta_1 = -8.1$, $\log^*\beta_2 = -16.2$, $\log^*\beta_3 = -24.3$, $\log^*\beta_{2,2} = -11.6$ and $\log^*K_{s0} = 19.4$. The data refer to precipitates prepared under CO_2 -free conditions at room temperature ($21.5 \pm 0.5^\circ$) in sodium perchlorate medium with an ionic strength of 1.

The hydrolysis constants of neodymium(III) reported in the literature¹⁻⁵ (Table 1), like those of the other rare earths studied before, show a fair diversity. Moreover the set of constants is not completely known, hence description of the hydrolytic behaviour at $\text{pH} > 7$ is impossible. The diversity can be attributed mainly to the fact that most investigations were done with concentrated solutions over small pH ranges, usually 4.5-7. Under these conditions the average hydroxide co-ordination number remains below 0.01, so determination of all the constants is impossible. Moreover, the affinity of Nd^{3+} ions for carbonate ions has been neglected in all cases.

Burkov *et al.*⁶ postulated the presence of $\text{Nd}_2(\text{OH})_2^{4+}$ and $\text{Nd}(\text{OH})^{2+}$ from the concentration dependence of the hydrolysis curves. If their results, $\log^*\beta_{2,2} = -13.93$ and $\log^*\beta_1 = -9.4$ (perchlorate medium, $I = 3$, 25°), are corrected for the presence of soluble carbonate-neodymium complexes and a lower ionic strength ($I = 1$), $\log^*\beta_{2,2} = -12$ and $\log^*\beta_1 = -8$ can be estimated, but these data are too unreliable to be of any practical value.

Azhipa *et al.*⁵ determined $\log^*K_{s0} = 20.4$ from the precipitation line, but obviously also did not consider the interference of insoluble carbonate. However, the

conclusion that the region of polycomplexation is rather small, with its 1% borderline intersecting the pH-axis near $\text{pH} = 5$, does seem reliable.

Our experiments were designed to cover a wide range of concentration and pH (Fig. 1) and were done in sodium perchlorate medium ($I = 1.0$ at $21.5 \pm 0.5^\circ$) in a nitrogen atmosphere in a glove-box. All manipulations were standardized for reasons discussed before.⁸⁻¹¹ The precipitate was formed by a procedure similar to that for ytterbium.¹¹ At $\text{pC}_\text{H} < 12$ the pC_H value was determined with a pH-meter calibrated in pC_H units;¹⁰ for $\text{pC}_\text{H} > 12$ the pC_H value was established by potentiometric titrations.^{11,12}

RESULTS AND CONCLUSIONS

The borderline of the precipitation region for Nd (Fig. 1) consists of two straight lines connected by a curve from $\text{pC}_\text{H} 8$ to $\text{pC}_\text{H} 9$. From regression analysis a slope of 3.5 ± 0.3 can be deduced for the steep part up to $\text{pNd}' = 4.5$. This suggests that a polynuclear hydroxide complex with charge 4+ is present in solution. Of the series of possible species $\text{Nd}_2(\text{OH})_2^{4+}$, $\text{Nd}_3(\text{OH})_3^{4+}$, etc., only the first is likely.¹³

*Part VI: *Talanta*, 1983, 30, 134.

Table 1.

Reference	$\log^*\beta_1$	$\log^*\beta_{2,2}$	\log^*K_{s0}	Medium	Method
1	-9.0 -7.5			sulphate, 0.001M sulphate, 0.05M, 25°	potentiometric titration
2	-9.57 -8.5			NaClO_4 , $I = 3$, 25° NaClO_4 , $I = 0.3$, 25°	potentiometric titration
3	-7.0			$(\text{H, Li})\text{ClO}_4$, $I = 0.1$, 25°	solvent extraction and radiochemical indication
4	-8.5 ± 0.4			$I = 0.1$, 25°	potentiometric titration
5			20.4	chloride, $I = 0.1$, 25°	oscillographic polarography
6	-9.4 ± 0.4	-13.93		NaClO_4 , $I = 3$, 25°	potentiometric titration
7	-8.0	-13.86	18.6	$I = 0.1$	critical review

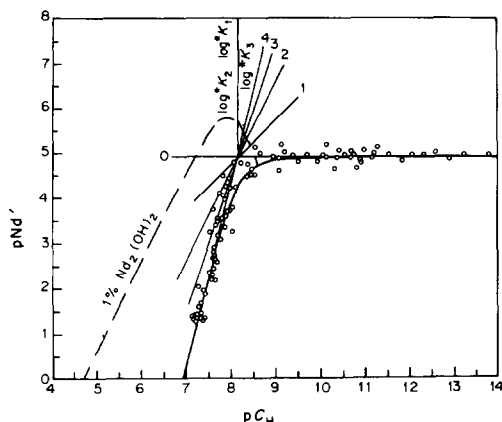


Fig. 1. The solid curve [the borderline of precipitation of $\text{Nd}(\text{OH})_3$] was constructed by the values given in Table 3. The dashed line is the borderline for 1% polycomplexation. The numbers 0, 1, 2, 3 and 4 near the straight lines correspond to the slopes of the straight-line segments [equations (1a)–(1e)] approximating the exact envelope curve. The circles denote the experimental results.

According to the theory⁸⁻¹⁰ in which straight-line segments determine the borderline of precipitation, we can assign equation (1a) (see Table 2) to the steep part, giving as the best fit

$$p\text{Nd}' = 4pC_{\text{H}} - (27.4 \pm 0.05) \quad (2)$$

Hence

$$2 \log^*K_{s0} + \log^*\beta_{2,2} = (27.1 \pm 0.05) \quad (3)$$

Equation (1e) can be assigned to the horizontal part of the borderline. The best fit corresponds to

$$p\text{Nd}' = 4.93 \pm 0.03 \quad (4)$$

from which follows, with equation (1e)

$$\log^*K_{s0} + \log^*\beta_3 = -4.93 \pm 0.03 \quad (5)$$

Because it is found that with the equation

$$[\text{Nd}']_{\text{max}} = 10^{-(4pC_{\text{H}} - 27.4)} + 10^{-4.93} \quad (6)$$

a good fit is obtained for the rather sharp bend connecting the straight-line parts, it can be concluded that the major species in equilibrium with the precipitate are $\text{Nd}_2(\text{OH})_2^{4+}$ and $\text{Nd}(\text{OH})_3$. If one of the ions Nd^{3+} , $\text{Nd}(\text{OH})^{2+}$ or $\text{Nd}(\text{OH})_2^+$ were present, the corresponding equation from the set (1b)–(1d) would contribute to the shape of the envelope curve. The

Table 3.

$\log^*\beta_1 = -8.1$	$\log^*\beta_{2,2} = -11.6$
$\log^*\beta_2 = -16.2$	
$\log^*\beta_3 = -24.3$	$\log^*K_{s0} = 19.4$

alteration in the shape would involve first the bend in the curve, as can be seen by moving the corresponding lines (in Fig. 1) from left to right. It follows that there must be limiting positions for the straight-line segments. As a consequence, p^*K_i ($= \log^*\beta_i - \log^*\beta_{i-1}$) cannot exceed certain values (the line segments intersect at $pC_{\text{H}} = p^*K_i$).

A series of plots was made with p^*K_i values approaching 8.1, the value that corresponds to the pC_{H} value of the intersection point of the line-segments corresponding to equations (2) and (4). It was found that $\log^*K_1 = \log^*K_2 = \log^*K_3 = -8.1$ are upper limits and hence $p^*\beta_1 = 8.1$, $p^*\beta_2 = 16.2$ and $p^*\beta_3 = 24.3$. If we combine these values with equations (5) and (3) we can deduce $\log^*K_{s0} = 19.4$ and $\log^*\beta_{2,2} = -11.6$.

Substitution in equation (1f), which represents the 1%-borderline of the polycomplex region, gives

$$p\text{Nd}'_{1\%} = 2pC_{\text{H}} - 9.3 \quad (7)$$

On this borderline, by definition, 1% of the total Nd is present as polycomplex [here $\text{Nd}_2(\text{OH})_2$], which corresponds in this case to an average hydroxide co-ordination number of 0.01. Lower p^*K_i values cause a shift of this line to lower pC_{H} . Thus, equation (7) represents the 1%-borderline that is furthest to the right.

In earlier work with other rare earths, an additional criterion has been adopted, namely that the region of polycomplexation should be as small as possible. In some cases, we could find support for this assumption from investigations of others. In the case of neodymium we again have support for this assumption from the experimental results of Burkov *et al.*⁶ These authors found 1% co-ordination in a region just inside our polycomplex region, but the experiments were done at higher ionic strength ($I = 3$). Thus, we may conclude that the set of hydrolysis constants reported in Table 3 can be regarded as useful for analytical practice. Neodymium shows no amphoteric character at high pC_{H} values.

It is difficult to discuss the accuracy of the individual constants. If the envelope curve is constructed,

Table 2.

Equation	p	q	Slope ($np - q$)	Equation for the borderline segment
1a	2	2	4	$p\text{Nd}' = 4pC_{\text{H}} - (2 \log^*K_{s0} + \log^*\beta_{2,2} + 0.3)$
1b	1	0	3	$p\text{Nd}' = 3pC_{\text{H}} - \log^*K_{s0}$
1c	1	1	2	$p\text{Nd}' = 2pC_{\text{H}} - \log^*K_{s0} + \log^*\beta_1$
1d	1	2	1	$p\text{Nd}' = pC_{\text{H}} - (\log^*K_{s0} + \log^*\beta_2)$
1e	1	3	0	$p\text{Nd}' = -(\log^*K_{s0} + \log^*\beta_3)$
1f				$p\text{Nd}'_{1\%} = 2pC_{\text{H}} + \log^*\beta_{2,2} + 2.3$

$$*\beta_{q,p} = \frac{[\text{Nd}_p(\text{OH})_q][\text{H}^+]^p}{[\text{Nd}^{3+}]^p} \quad \text{and} \quad *\beta_{q,1} = *\beta_q$$

the position of the actual Nd'_{max} value is uncertain within 0.1 log units, and this offers an estimate for the spread around the line. It holds for both the steep part and the horizontal part, assuming a "fresh precipitate" and CO_2 -free conditions.

Acknowledgements—We are indebted to Mr. Coert van Duijnen and Mr. Geert van der Meij for their valuable contributions to the experimental work.

REFERENCES

1. T. Moeller, *J. Phys. Chem.*, 1946, **50**, 742.
2. U. K. Frolova, V. N. Kumok and V. V. Serebrennikov, *Izv. Vys. Ucheb. Zaved. SSSR, Khim. i. Khim. Tekhnol.*, 1966, **9**, 176.
3. R. Guillaumont, B. Desire and M. Galin, *Radiochem. Radioanal. Letters*, 1971, **8**, 189.
4. R. S. Tobias and A. B. Garrett, *J. Am. Chem. Soc.*, 1958, **80**, 3532.
5. L. T. Azhipa, P. N. Kovalenko and M. M. Evtifeev, *Russ. J. Inorg. Chem.*, 1967, **12**, 601.
6. K. A. Burkov, L. S. Lilich, Nguyen Din Ngo and A. Yu. Smirnov, *ibid.*, 1973, **18**, 797.
7. C. F. Baes, Jr. and R. E. Mesmer, *The Hydrolysis of Cations*, pp. 129–138, 436. Wiley-Interscience, New York, 1976.
8. J. Kragten and L. G. Decnop-Weever, *Talanta*, 1978, **25**, 147.
9. *Idem, ibid.*, 1979, **26**, 1105.
10. *Idem, ibid.*, 1980, **27**, 1047.
11. *Idem, ibid.*, 1982, **29**, 219.
12. *Idem, ibid.*, 1983, **30**, 134.
13. Reference 7, p. 420.

DISSOCIATION CONSTANTS OF SOME ORGANIC ACIDS

Zs. WITTMAN

Hungarian Oil and Gas Research Institute, Veszprém

(Received 29 November 1983. Accepted 23 February 1984)

Summary—Dissociation constants of di(nonylphenyl)dithiophosphoric acid, di(nonylphenyl)phosphoric acid and 9-phenyltetracosansulphuric acid, determined by two methods, are reported.

There are two methods for determination of dissociation constants of organic acids that are poorly soluble or insoluble in water: potentiometric titration in 40 or 50% w/w ethanol in water,^{1,2} and distribution between two phases.³⁻⁵ The constants for some organic phosphoric acids are listed in Table 1.

Higher members of homologous acid series, and alkylphenyldithiophosphoric acids, are insoluble in water, and benzenesulphuric acid derivatives with long alkyl chains only poorly soluble. In this paper, the determination of the dissociation constants of two organic phosphoric acids and a sulphuric acid are described. These acids were synthesized and examined as part of a systematic investigation of industrial acids of this kind.

EXPERIMENTAL

Samples

Di(nonylphenyl)dithiophosphoric acid; found: acid number 1.87 mmole/g, P = 5.8%, S = 12.0%; theory requires P = 5.80%, S = 11.98%. Di(nonylphenyl)phosphoric acid; found: acid number = 1.99 mmole/g, P = 6.2%; theory requires 6.18%. 9-Phenyltetracosansulphuric acid; found: acid number = 2.02 mmole/g, S = 6.5%; theory requires S = 6.47%. All the reagents used were of analytical grade.

Apparatus

The pH measurements were made with a Radelkis pH-meter type OP-204/1, glass electrode OP-07181 and calomel electrode OP-08301.

Procedure

The method was adopted from Handley *et al.*³ The dissociation constants of di(nonylphenyl)dithiophosphoric acid and di(nonylphenyl)phosphoric acid (Table 2) were

Table 2. Dissociation constants (\pm standard deviations) for di(nonylphenyl)dithiophosphoric acid (A) and di(nonylphenyl)phosphoric acid (B) (ionic strength = 1.0M at 25.0°)

Acid	Solvent system	pK
A	CCl ₄ -water	5.40 \pm 0.05
	n-hexane-water	5.38 \pm 0.05
B	CCl ₄ -water	6.30 \pm 0.06
	n-hexane-water	6.26 \pm 0.06

calculated from data obtained from distribution between aqueous sodium chloride solution and carbon tetrachloride or n-hexane.

No evidence was found for the dimerization of the acids in the organic phase, since $\log c_{\text{org}} \text{ vs } \log [H^+][R^-]$ was a straight line with slope equal to one.

The dissociation constant of 9-phenyltetracosansulphuric acid was determined by the method of White.² This potentiometric titration was done in 50% w/w ethanol in water at 25.0° by using the non-thermodynamic cell and buffer solution proposed by White.² A value was calculated for the constant in water, $pK = 3.31 - 1.66 = 1.65$, by applying a correction of $\Delta pK = 5.87 - 4.21 = 1.66$ by analogy with the pK values for benzoic acid measured in water and in 50% w/w ethanol in water. The standard deviation was 0.02.

REFERENCES

1. V. E. Toropova, M. K. Saikina and R. Sh. Aleshov, *J. Gen. Chem., (USSR)*, 1967, **37**, 679.
2. J. R. White, *J. Org. Chem.*, 1950, **72**, 1859.
3. T. H. Handley, R. H. Zucal and J. A. Dean, *Anal. Chem.*, 1963, **35**, 1163.
4. D. Dyrssen, *Acta Chem. Scand.*, 1957, **11**, 1771.
5. Z. A. Sheka and E. I. Sinyarskaya, *Russ. J. Inorg. Chem.*, 1965, **10**, 212.

Table 1. Dissociation constants of organic phosphoric acids

Compounds	pK at 25°	Method	Reference
<i>O,O'</i> -diethyldithiophosphoric acid	2.11 \pm 0.01	Potentiometric titration in 0.8M KNO ₃ , and 40% w/w ethanol in water.	1
<i>O,O'</i> -diethylthiophosphoric acid	1.83 \pm 0.07		
di-n-decylorthophosphoric acid	3.28 \pm 0.08	Potentiometric titration	2
di-n-dodecylorthophosphoric acid	3.40 \pm 0.07	in 50% w/w ethanol in water.	
diethyldithiophosphoric acid	-0.01	Distribution between CCl ₄ and 1M NaCl.	
di-isopropyldithiophosphoric acid	0.00		
di-n-butyldithiophosphoric acid	0.22		3
di-isobutyldithiophosphoric acid	0.10		
di-n-butylphosphoric acid	1.00 \pm 0.01	Distribution between CHCl ₃ or n-hexane and 0.1M and 1M HClO ₄ -NaClO ₄ .	4
<i>O,O'</i> -dibutylphosphoric acid	-0.3	Distribution: conditions unknown.	5

POTENTIOMETRIC INVESTIGATION OF THE STABILITY OF SILVER(I) COMPLEXES OF SOME *N*-METHYL SUBSTITUTED 4-H-DIETHYLENETRIAMINES IN AQUEOUS SOLUTION

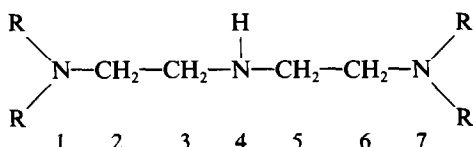
J. YPERMAN, J. MULLENS, J.-P. FRANÇOIS and L. C. VAN POUCKE

Limburgs Universitair Centrum, Departement SBM, Universitaire Campus, B-3610 Diepenbeek, Belgium

(Received 3 October 1983. Accepted 13 March 1984)

Summary—By means of potentiometric pH and pAg measurements, the stability constants and the stoichiometric composition of the silver(I) complexes of some *N*-methyl-substituted 4-H-diethylenetriamines, in aqueous medium of ionic strength 1.3 and at a temperature of 25.00°, have been determined. In addition to mononuclear and polynuclear complexes, together with their protonated forms, some hydroxo complexes are formed. The values of the stability constants are discussed in terms of possible structures.

The formation of complexes between silver(I) and some *N*-methyl-substituted 4-methyldiethylenetriamines has already been studied.¹ This paper describes the investigations of the *N*-methyl-substituted 4-H-diethylenetriamines, namely, diethylenetriamine (PSP); 1-methyldiethylenetriamine (SSP); 1,1-dimethyldiethylenetriamine (TSP) and 1,1,7,7-tetramethyldiethylenetriamine (TST):



where R stands for CH₃ or H. The shorthand notation given in parentheses indicates whether the amino groups, in the sequence end, central, end, are primary (P), secondary (S) or tertiary (T). Complex formation between PSP and silver(I) has been investigated by various workers;²⁻⁵ the species reported include AgL,^{2,4,5} AgLH,^{2,4} Ag₂L,^{2,4} and AgLH₂,⁴ where L is PSP and charges are omitted for simplicity. For imino-bis(methylene-2-pyridine) and silver(I), Rometsch *et al.*⁶ found only the mononuclear species corresponding to AgL and AgL₂.

In contrast to these results, for the analogous ligands, the 4-methyl derivatives,¹ in addition to these complexes, we have found dinuclear and trinuclear complexes, together with protonated and hydroxo complexes. Diethylenetriamine is of analytical interest; for example it has been shown to be the most satisfactory of a number of aliphatic amines for impregnating the silica gel layer in TLC separation of metal ions.⁷

EXPERIMENTAL

Apparatus and reagents

The pH values were obtained by means of a calibration procedure using Gran plots.⁸ The Ag₂S-electrode used gave

Nernstian response. More details are given in previous papers.^{1,9}

Measurements

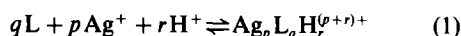
Because a great diversity of complexes is expected, a large concentration range is needed. On the other hand it is desirable that the concentration of free ligand should be calculable without any assumptions about the stoichiometric composition of the complexes formed, *i.e.*, by using the Österberg method¹⁰ (method 1) or the dilution method (method 2).¹¹

Titration curves for PSP and Ag⁺ were measured and treated by using the Österberg method.¹⁰ It was found that a very small change in the pK_A-values causes a very great change in the calculated free ligand concentration. On the other hand, the so-called "dilution method", which was described¹¹ and applied¹ earlier, gives very good results in the calculation of free ligand concentrations, and the experimental data can be treated without any transformation. As the experimental data were finally to be handled by the computer program Miniquad,¹² and knowledge of the free ligand concentration was therefore not needed, a third set of data was added, in which C_L/C_{Ag} and C_{Ag} were changed for each titration curve (method 3).

For the so-called "dilution method", titration curves were recorded for C_L/C_{Ag} = 3, by the procedure used earlier.¹ In the third set of experimental data, the C_L/C_{Ag} ratios studied were 10, 5, 2, 1, 0.5 and 0.25. More details were given earlier.^{1,9}

RESULTS AND DISCUSSION

The general formation reaction of the complex Ag_pL_qH_r is given by equation (1):



The overall concentration stability constant is given by:

$$\beta_{pqr} = \frac{(Ag_p L_q H_r^{(p+r)+})}{(Ag^+)^p (L)^q (H^+)^r} \quad (2)$$

Negative values for *r* imply formation of hydroxo complexes.

From the titration curves, obtained by method 2,

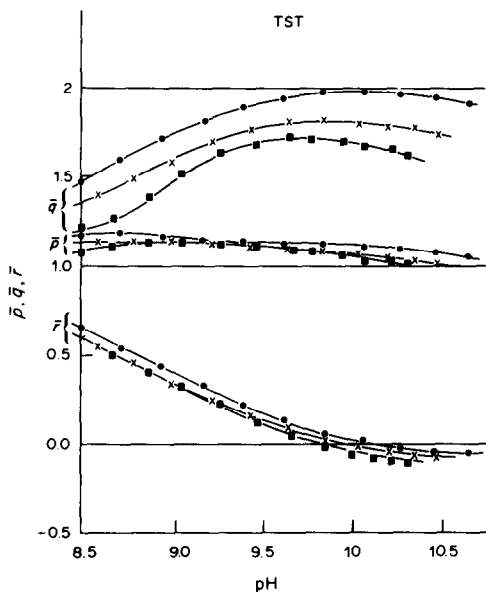


Fig. 1. \bar{p} , \bar{q} and \bar{r} for TST vs. the pH for three different but constant C_L and C_{Ag} values. The "dilution method" is used. C_L , $10^{-3}M$: ● 17.1; × 8.52; ■ 4.26. C_{Ag} , $10^{-3}M$: ● 5.71; × 2.86; ■ 1.43.

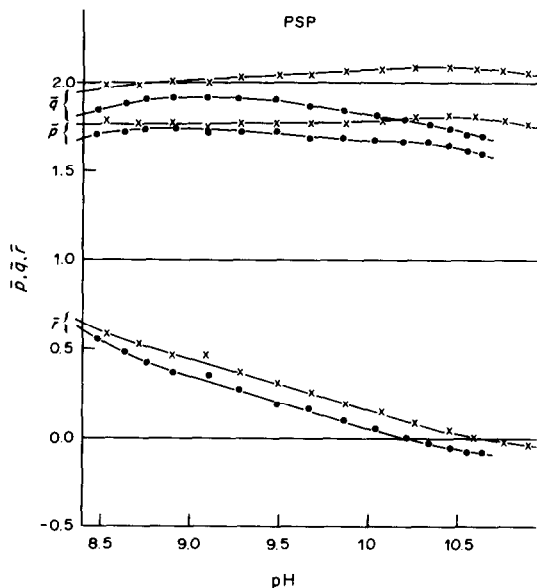


Fig. 2. \bar{p} , \bar{q} and \bar{r} for PSP vs. the pH for two different but constant C_L and C_{Ag} values. The "dilution method" is used. × C_L 0.0120M; C_{Ag} 0.00400M; ● C_L 0.00460M; C_{Ag} 0.00154M.

it is found that there is some weak complex formation before the first equivalence point. In calculating the free ligand concentration, as a first approximation we neglected this complex formation and later found that corrections for it, calculated from the stability constants obtained, were insignificant.

The results obtained by means of this method for TST are shown in Fig. 1, where \bar{p} , \bar{q} and \bar{r} are the mean values found for p , q and r . This figure shows

that mononuclear species are dominant. Because \bar{p} is slightly greater than 1, the polynuclear TST complexes are not negligible. By comparison, the results for PSP (Fig. 2) indicate that polynuclear complex formation is much more pronounced. TSP and SSP give figures similar to that for PSP. The values of \bar{q} are always higher than the corresponding \bar{p} values, and \bar{r} varies between 1.0 and -0.1 .

From these results it can be concluded that for TST

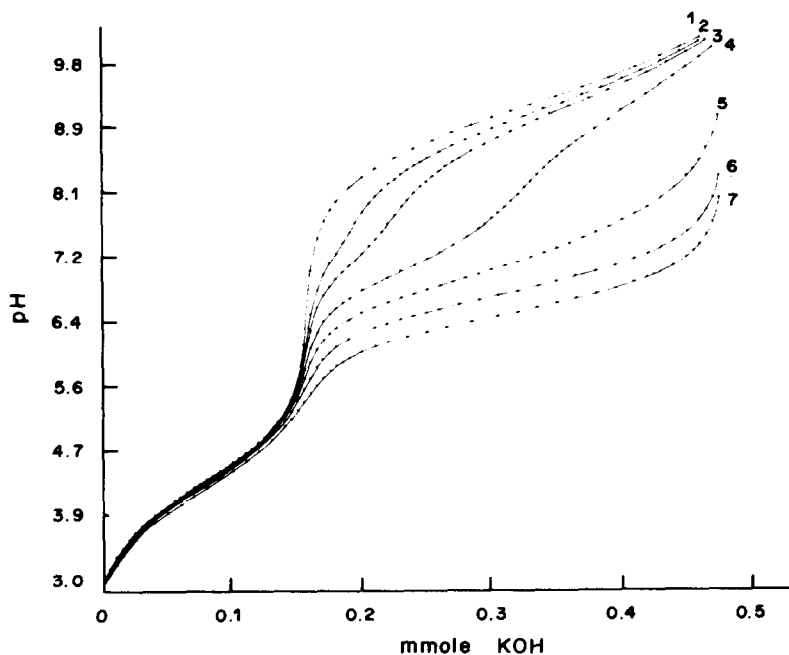


Fig. 3. pH vs. amount of KOH added for PSP with and without Ag^+ . Curve 1: $C_L = 0.1571$ mmole and $C_{Ag} = 0.0$ mmole. Curve 2: $C_L/C_{Ag} \approx 10/1$. Curve 3: $C_L/C_{Ag} \approx 5/1$. Curve 4: $C_L/C_{Ag} \approx 2/1$. Curve 5: $C_L/C_{Ag} \approx 1/1$. Curve 6: $C_L/C_{Ag} \approx 1/2$. Curve 7: $C_L/C_{Ag} \approx 1/4$.

the most probable species formed are AgL, AgLH, AgL₂ and AgL₂H. As there is some indication of the presence of polynuclear complexes, Ag₂L₂ must be taken into account, and hydroxo complexes are also possible.

For TSP, SSP and PSP, the most likely species are Ag₂L₂, and AgL₂, and their corresponding protonated species. The presence of AgL and perhaps AgLH is less probable than in the case of TST, but cannot be excluded.

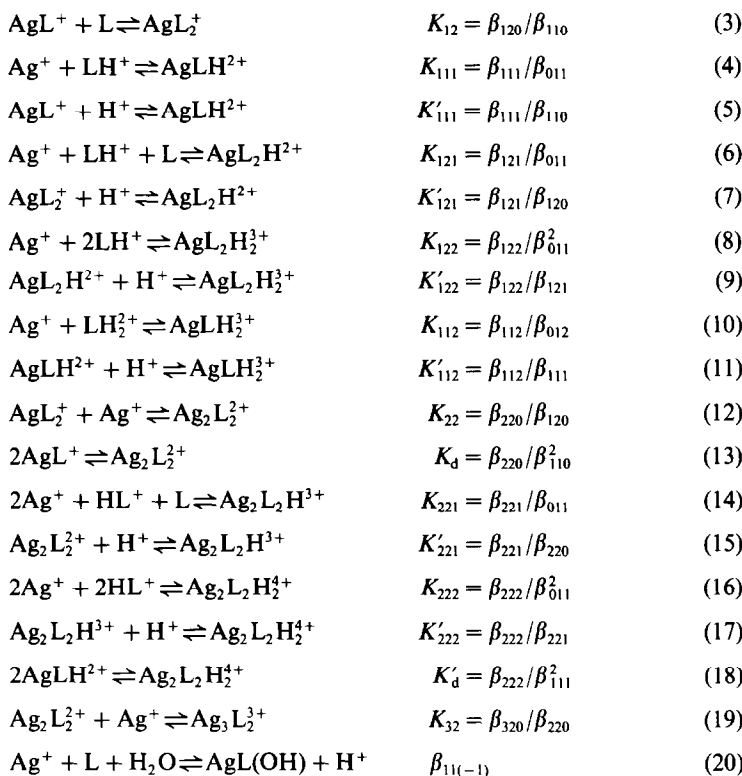
For PSP even the complex Ag₂L₃ can be considered. There are also some indications of the presence of a hydroxo complex.

In Fig. 3, as an example, the experimental data obtained by method 3 for PSP, with and without Ag⁺, are presented, *i.e.*, the measured pH *vs.* the amount of potassium hydroxide added. From this

elimination of complexes in the minimization process are given in our previous article.¹ The final results of these calculations are summarized in Table 1.

For all four ligands the following complexes were found to be formed: AgLH₂, AgLH, AgL₂H₂, AgL₂, Ag₂L₂, Ag₃L₂ and AgL(OH). In the dilution method \bar{p} never exceeds 2 but it must be remembered that C_L/C_{Ag} is fixed at 3. A number of protonated Ag₂L₂ complexes were detected for PSP, SSP and TSP, but not for TST. AgL₂H was not found for TSP. AgL was found only for TST. Several attempts were made to prove or disprove the existence of AgL for SSP, PSP and TSP, but no positive evidence was found. We must conclude that this species is not present for these triamines. The complex Ag₂L₃ was found only for PSP, but only in small amounts.

The further discussion requires definition of the following equilibria and their equilibrium constants.



figure, it can be seen that weak complexation occurs before the first equivalence point. For TST, TSP and SSP the picture is very similar, but the less the degree of *N*-methyl substitution, the greater the difference in pH between the titration curves, *i.e.*, the stronger and probably the more diverse the complexation is before and after the first equivalence point.

Only the experimental data from methods 2 and 3 were treated by the computer program Miniquad, in order to handle all the triamines in the same way, and seek the best model for the stoichiometric compositions and corresponding stability constants. For each system, more than 1000 titration points over a wide concentration range were used. Criteria for

The log *K* and the log *K'* values can thus be calculated from the log β_{par} values in Table 1 and the values of log β_{01r} , the formation constants⁹ of the three protonated forms of L. The log β_{01r} values are given in Table 2. The absence of the species AgL in the case of PSP, SSP and TSP is very striking. It was found earlier,¹³ in a study of complexes of Ag⁺ with ethylenediamine, that the complex AgL was not present at all. A possible reason for this might be the increasingly high stability of the polynuclear complexes formed, especially Ag₂L₂ and even Ag₃L₂, with decrease in the degree of *N*-substitution of the ligand.

In the case of PSP, SSP and TSP, equilibrium (13) is shifted strongly towards the right, because of the

Table 1. The log β_{pqr} values for the complexes formed according to reaction (1) for the four ligands; for AgL(OH), reaction (20) must be considered

Complex	β_{pqr}	PSP	SSP	TSP	TST
AgLH ₂	β_{112}	20.32 (1)	20.56 (1)	19.56 (1)	18.81 (1)
AgLH	β_{111}	13.73 (2)	13.77 (1)	13.18 (1)	12.59 (0)
AgL	β_{110}	—	—	—	4.14 (0)
AgL ₂ H ₂	β_{122}	27.29 (3)	27.33 (2)	25.99 (2)	24.15 (2)
AgL ₂ H	β_{121}	17.78 (4)	17.75 (4)	—	15.81 (1)
AgL ₂	β_{120}	7.90 (3)	7.87 (2)	7.74 (1)	7.24 (0)
Ag ₂ L ₂ H ₂	β_{222}	30.03 (3)	30.04 (2)	28.41 (3)	—
Ag ₂ L ₂ H	β_{221}	22.72 (2)	22.33 (1)	20.86 (2)	—
Ag ₂ L ₂	β_{220}	15.10 (0)	14.41 (0)	13.84 (0)	10.89 (1)
Ag ₃ L ₂	β_{320}	17.94 (0)	16.74 (1)	15.35 (1)	12.35 (1)
AgL(OH)	$\beta_{11(-1)}$	-5.54 (2)	-6.10 (4)	-5.96 (2)	-6.62 (1)
Ag ₂ L ₃	β_{230}	16.39 (4)	—	—	—

The numbers in brackets are the standard deviations and refer to the last significant figure, *i.e.*, (1) means 0.01.

great stability of the Ag₂L₂ complexes, their log β_{202} values being 3 units greater than log β_{202} for the TST complex (Table 1).

The great stability of the Ag₂L₂ complex can only be explained by suggesting that this species has a ring structure. It is found that the smaller the ring size for rings with more than six members, the greater the stability. Therefore a ten-membered ring is proposed for the species Ag₂L₂, besides a ring with sixteen members, especially in the case of PSP. Examination of the magnitudes of the log K_{22} values (Table 2), shows that the formation constants for the PSP, SSP and TSP complexes are twice that of the TST complex. This demonstrates again the great dependence of the stability of the Ag₂L₂ complex on the nature of the ligand.

For PSP, SSP and TSP, the magnitude of these formation constants (log K_{22}) is of the same order as the log β_{120} values. We conclude, therefore, that reaction (12) involves formation of two further Ag-N bonds: in other words, ring closure. The log K_{22} value for TST refers to the formation of only one extra

Ag-N bond. Probably a terminal tertiary N-Ag bridge is formed: because of extra charge repulsions a displacement of the central N-Ag bridge is possible.

As already mentioned, AgL but not Ag₂L₂ was previously reported in the case of PSP as ligand.^{2,4,5} Prue and Schwarzenbach² also reported the complex Ag₂L, but Machtinger *et al.*⁴ mentioned only the possible existence of this species. We made several attempts to demonstrate the presence of this complex, but our computer-preferred model always gave the species Ag₂L₂ and Ag₃L₂ rather than Ag₂L.

It is also striking that the complex AgLH₂ is found for these 4-H-derivatives but not for the 4-methyl derivatives.¹ The log K_{112} values and, to a lesser extent, the log K'_{112} values, show that this complex is not very stable. The nature of the central amino group plays an important role in the structure and possibility of existence of this complex.

The log β_{120} values indicate^{1,14} that AgL₂ must have a linear structure, and the log K_{121} and log K_{122} values show that binding of another proton does not change the proposed linearity. The formation constants are of the same magnitude as the log β_{120} values, though somewhat lower because of the extra positive charge. For TST the log K_{122} value is much smaller, possibly because of competition between Ag⁺ and H⁺, concerning the most likely N-Ag or N-H bond. The log K'_{122} and log K'_{121} values support this.

For PSP, SSP and TSP, the addition of one or two H⁺-ions to Ag₂L₂ results in partial ring opening, as is demonstrated by the smaller log K_{221} and log K_{222} values, in comparison with the log β_{220} values.

The log $\beta_{11(-1)}$ values show a very peculiar sequence, according to the nature of the ligand. This was also found in the study of the 4-methyl derivatives.¹ An explanation for this is a change in the co-ordination number of Ag⁺, as reported by Ohtaki *et al.*^{15,16}

REFERENCES

- J. Yperman, J. Mullens, J.-P. François and L. C. Van Poucke, *Inorg. Chem.*, 1983, **22**, 1361.
- J. E. Prue and G. Schwarzenbach, *Helv. Chim. Acta*, 1950, **33**, 985.

Table 2. The log K and log K' values for the complexes formed according to reactions (3)-(19) for the four triamines

Constant	Ligand				Complex
	PSP	SSP	TSP	TST	
log K_{111}	3.63	3.53	3.27	3.00	AgLH (4)
log K'_{111}	—	—	—	8.45	AgLH (5)
log K_{112}	0.83	0.74	0.53	0.26	AgLH ₂ (10)
log K'_{112}	6.59	6.79	6.38	6.22	AgLH ₂ (11)
log K_{12}	—	—	—	3.10	AgL ₂ (3)
log K_{121}	7.68	7.51	—	6.22	AgL ₂ H (6)
log K'_{121}	9.88	9.88	—	8.57	AgL ₂ H (7)
log K_{122}	7.09	6.85	6.17	4.97	AgL ₂ H ₂ (8)
log K'_{122}	9.51	9.58	—	8.34	AgL ₂ H ₂ (9)
log K_{22}	7.20	6.54	6.10	3.65	Ag ₂ L ₂ (12)
log K_d	—	—	—	2.61	Ag ₂ L ₂ (13)
log K_{221}	12.62	12.09	10.95	—	Ag ₂ L ₂ H (14)
log K'_{221}	7.62	7.92	7.02	—	Ag ₂ L ₂ H (15)
log K_{222}	9.83	9.56	8.59	—	Ag ₂ L ₂ H ₂ (16)
log K'_{222}	7.31	7.71	7.55	—	Ag ₂ L ₂ H ₂ (17)
log K_d	2.57	2.50	1.55	—	Ag ₂ L ₂ H ₂ (18)
log K_{32}	2.84	2.33	1.51	1.46	Ag ₃ L ₂ (19)

3. G. Schwarzenbach, *ibid.*, 1953, **36**, 23.
4. M. Machtinger, M. Sloim-Bombard and B. Trémillon, *Anal. Chim. Acta*, 1979, **107**, 349.
5. A. M. Neduv, A. Ya. Fridman and N. M. Dyatlova, *Soviet J. Coord. Chem.*, 1977, **3**, 125.
6. R. Rometsch, A. Marxer and K. Miescher, *Helv. Chim. Acta*, 1952, **34**, 1611.
7. S. P. Srivastava, V. K. Dua and K. Gupta, *Chromatographia*, 1978, **11**, 539.
8. G. Gran, *Analyst*, 1952, **77**, 661.
9. J. Yperman, J. Mullens, J.-P. François and L. C. Van Poucke, *J. Phys. Chem.*, 1982, **86**, 298.
10. R. Österberg, *Acta Chem. Scand.*, 1960, **14**, 471.
11. L. C. Van Poucke, J. Yperman and J.-P. François, *Inorg. Chem.*, 1980, **19**, 3078.
12. A. Sabatini, A. Vacca and P. Gans, *Talanta*, 1974, **21**, 53.
13. L. C. Van Poucke, *ibid.*, 1976, **23**, 161.
14. R. M. Smith and A. E. Martell, *Critical Stability Constants*, Vol. 2, Plenum Press, New York, 1975.
15. H. Ohtaki and K. Cho, *Bull. Chem. Soc. Japan*, 1977, **50**, 2674.
16. H. Ohtaki and Y. Ito, *J. Coord. Chem.*, 1973, **3**, 131.

ANNOTATIONS

COMMENT ON LASER-EXCITED FLUORESCENCE LINE-NARROWING: AN ANALYTICAL STUDY

J. M. HAYES and G. J. SMALL

Ames Laboratory—USDOE, Iowa State University, Ames, Iowa 50011, U.S.A.

(Received 7 December 1983. Accepted 20 April 1984)

Summary—A recent paper (D. Bolton and J. D. Winefordner, *Talanta*, 1983, 30, 9) on the analytical utility of laser-excited fluorescence line-narrowing is critically assessed.

In a recent paper¹ Bolton and Winefordner (BW) reported on the limit of detection (LOD) for fluorescence line-narrowing spectroscopy (FLNS) of polycyclic aromatic hydrocarbons (PAHs) in a glycerol:ethanol:water glass at 4.2 K. The PAHs studied were anthracene, 2- and 9-methylanthracene, 9,10-dimethylanthracene, perylene and pyrene. The LOD values were compared with those determined for the same compounds by room-temperature fluorescence and low-temperature fluorescence spectrometry. In our opinion the BW paper presents a very misleading assessment of the analytical utility of FLNS. Because of our experience in exploring this question²⁻⁹ we feel compelled to make the following comments.

1. The procedure and apparatus used by BW for FLNS are similar to those employed by us. The liquid-helium bath, sample preparation, sample cool-down procedures and monochromator bandpass (1 Å) are identical. Comparison of the N₂-pumped dye lasers, monochromator apertures and slit-widths utilized by BW and by us indicates there should be approximate parity in sensitivity. Nevertheless, for the compounds listed, BW report LOD values between 100 and 1000 ng/ml. For the same compounds and several others our *standard* FLN spectra were generally obtained with *very high* signal-to-noise ratio (S/N) at 200 ng/ml.^{3,5} Indeed, for perylene (BW LOD = 100 ng/ml), pyrene (BW LOD = 300 ng/ml), and 1-methylpyrene we obtained a detection limit (S/N > 5) of ~0.02 ng/ml.⁵ In the *direct* analysis of a solvent-refined coal II sample, 1-methylpyrene, benzo[*e*]pyrene, benzo[*a*]pyrene, anthracene, perylene and benzo[*k*]fluoranthene were characterized and determined at concentrations ranging between ~2 and 30 ng/ml (in the glass).³ Thus, the rather bleak sensitivity picture for FLNS painted by BW is hardly warranted. As discussed elsewhere,^{3,5} with improvements in the FLNS apparatus used in reference 3, detection limits of 1 pg/ml are readily

achievable for strongly fluorescent PAHs in *pure* solvents.

2. The failure of BW to achieve with FLNS the respectable LOD for PAHs that is routinely obtained in our laboratory may be due, in part, to the different gated-detection electronics and data-handling procedure they utilize. They mention a problem with high background signals but are not specific about it. We have never experienced background interference except at very low concentrations (<1 ng/ml).⁵ Nor has small bubble formation from boiling He posed an insurmountable problem as it did in their work.⁵ However, another problem in the BW studies appears to be their choice of excitation wavelength (λ_{ex}) and emission wavelength (λ_{em}). For example, in the case of anthracene, $\lambda_{ex} = 364.0$ nm (as used by BW) excites vibronic bands at an energy level some 1200 cm⁻¹ above the S₁ origin. At this energy there is considerable overlapping of vibronic bands, so FLN is observed from several isochromats. Although a similar λ_{ex} (363.8 nm) was used in reference 2, that work was done with a non-tunable Ar⁺ laser. A better choice of λ_{ex} is given in references 3 and 5. In that work $\lambda_{ex} = 373.8$ nm was used. This corresponds to excitation into the centre of the first vibronic band, so that only a single isochromat will fluoresce. Consider also the case of 9-methylanthracene. The $\lambda_{ex} = 382.5$ nm chosen by BW is midway between the centres of two overlapping vibronic absorption bands. Thus two bands, separated by the vibronic energy difference, will emit. This emission will be weak because the excitation is into the tail of each band. Furthermore, the most intense zero-phonon line associated with the emissions will be at ~388 nm and ~393 nm, respectively. The λ_{em} value chosen by BW, however, is 390.6 nm, in a "valley" nearly midway between the two zero-phonon lines! Finally, it has been observed in our laboratory that 2-methylanthracene is not amenable to FLN analysis in glycerol, water, ethanol glasses at concentrations greater than 100 ng/ml (BW's LOD

for this species). At these concentrations the emission is broad, owing to aggregation.⁵

3. BW assert that the loss of FLN behaviour when λ_{ex} pumps vibronic levels of the fluorescent state possessing $\geq 1500 \text{ cm}^{-1}$ excess vibrational energy is due to "rapid local site-melting". This explanation is erroneous. The correct explanation^{2,3,10} has to do with the fact that at such high excess vibrational energy several isochromats belonging to different overlapping vibronic absorption bands are pumped.

In conclusion, BW report LOD values for FLNS which are *anomalously* high, do not discuss their results in the light of those from earlier work,^{3,5} and ignore several other attributes of the technique. For example, FLNS possesses high selectivity,³⁻⁹ which was initially the reason why our laboratory pursued and developed it as an analytical technique. Another example is that water-based glasses impart to it a versatility which other solid-state fluorescence methods do not possess. For example, by acidification of the glass the amino-derivatives of PAHs can be studied.⁷⁻⁹ As another example we cite recent work where we have successfully applied FLNS to aromatic carcinogen-DNA adducts and shown that two adducts formed by different metabolic paths for benzo[a]pyrene can be distinguished in a mixture.^{9,11}

Acknowledgement—Ames Laboratory is operated for the U.S. Department of Energy by Iowa State University under contract No. W-7405-Eng-82. This research was supported by the Office of Health and Environmental Research, Office of Energy Research.

REFERENCES

1. J. D. Winefordner and D. Bolton, *Talanta*, 1983, **30**, 9.
2. J. C. Brown, M. C. Edelson and G. J. Small, *Anal. Chem.*, 1978, **50**, 1394.
3. J. C. Brown, J. A. Duncanson, Jr. and G. J. Small, *ibid.*, 1980, **52**, 1711.
4. J. C. Brown, J. M. Hayes, J. A. Warren and G. J. Small, in *Lasers and Chemical Analysis*, G. M. Hieftje and F. E. Lytle (eds.), Humana Press, Clifton, NJ, 1981.
5. J. C. Brown, *Ph.D. Dissertation*, Iowa State University, 1981.
6. J. M. Hayes, I. Chiang, M. J. McGlade, J. A. Warren and G. J. Small, *Proc. SPIE-Int. Soc. Opt. Eng.*, 1981, No. 286, 117.
7. I. Chiang, J. M. Hayes and G. J. Small, *Anal. Chem.*, 1982, **54**, 315.
8. I. Chiang, *M.S. Thesis*, Iowa State University, 1981.
9. M. J. McGlade, *M.S. Thesis*, Iowa State University, 1983.
10. R. I. Personov, in *Spectroscopy and Excitation of Condensed Molecular Systems*, V. M. Agranovich and R. M. Hochstrasser (eds.), Chap. 10. North Holland, New York, 1983.
11. V. Heisig, A. M. Jeffrey, M. J. McGlade and G. J. Small, *Science*, 1984, **223**, 289.

[A reply to this comment will be found on p. 753; Ed.]

TESTING THE ADEQUACY OF EQUILIBRIUM MODELS FOR COMPLEX FORMATION

COMPLEXATION BETWEEN MOLYBDATE AND OXALATE REVISITED

ERIK SYLVEST JOHANSEN and OLE JØNS*

Royal Danish School of Pharmacy, Department of Pharmaceutical Chemistry AD, 2 Universitetsparken,
DK-2100 Copenhagen, Denmark

(Received 11 January 1984. Accepted 31 March 1984)

Summary—In potentiometric studies of metal–ligand equilibria a given model is tested by adjustment of the corresponding stability constants with the purpose of obtaining as good a fit as possible to the experimental data. When judging the goodness-of-fit it is of great importance to be in control of any possible systematic error in concentrations or electrode parameters. The molybdate–oxalate system is used to demonstrate how one crucial parameter influences the evaluations of goodness-of-fit. The system is simple, having only one complex species, $\text{MoO}_3\text{oxal}^{2-}$, with logarithmic stability constant 13.816 in the pH-range 4–7.

For several decades potentiometric methods have been applied to the study of complex-formation in solution. Above all, the glass electrode has proved valuable in the determination of accurate formation constants. Admittedly, experimental conditions must be carefully controlled and even then there remain uncertainties concerning the electrode parameters.

These uncertainties will be transmitted to the next phase of the study: the calculation of formation constants of the equilibrium model under trial, and the evaluation of some measure of goodness-of-fit, often the sum of the square of the differences between observed and calculated values. If the number of complex species formed is unknown the experimental uncertainties will contribute to the problem of when to stop adding species to the model.

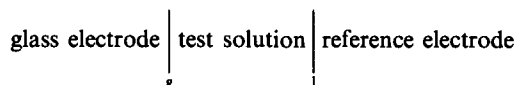
May *et al.*¹ have described these problems at length and proposed some computational methods for the simultaneous determination of protonation constants and glass-electrode parameters. The purpose of this paper is to direct attention to one source of error which in our investigations appeared to be crucial when judging the adequacy of a model.

The complex formation between molybdate(VI) and oxalate will be used to demonstrate how a modified electrode calibration procedure led to significant improvement in the description of the equilibrium system. The molybdenum(VI)–oxalic acid system has been the subject of several investigations. Recently Beltran *et al.*² applied spectroscopy and saline cryoscopy to the problem and concluded that species with Mo/oxalate stoichiometric ratios 1:2 and 2:2 were present. According to

Mikešová and Bartušek,³ using potentiometric titration techniques, a monomeric 1:1 species is present. This was also found by Starý.⁴ Chalmers and Sinclair,⁵ who used spectroscopy and pH measurements, also reported a 1:1 complex, but considered that a dimeric structure was also possible; their work was done with much higher concentrations of molybdate and acid than those used by us, however. It seems that potentiometric titrations combined with comprehensive computerized methods have not yet been applied to the system.

THEORY

The electrochemical cell used in this work is very conventional:



The boundaries, g and l, respectively, indicate the glass membrane and the liquid junction between the test solution and the salt bridge. The measured emf of the cell is given by the equation:

$$E_{\text{cell}} = E^0 + \frac{RT}{F} \ln\{\text{H}^+\} \quad (1)$$

where E^0 is a "constant" including the standard electrode potentials and the liquid-junction potential.

The experimental conditions relevant to this work seem to ensure constancy of the liquid-junction potential. In accordance with others we find the glass electrode to exhibit a Nernstian response over a wide range of concentration. Since we are not interested in the hydrogen-ion activity, the ionic strength of the solution is kept constant, and consequently equation

*Author for correspondence.

(1) can be simplified:

$$E_{\text{cell}} = E_{\text{const}} + s \log[\text{H}^+] \quad (2)$$

where s has the theoretical Nernstian value and $[\text{H}^+]$ represents the concentration of free hydrogen ions. Hence, all constants (including the hydrogen-ion activity coefficient) are collected as E_{const} . Because of small variations in the asymmetry potential, E_{const} has to be determined for each titration. An internal calibration performed in the test solution itself is highly desirable but not always possible. In the present investigation of molybdate-oxalate mixtures, internal calibration is not feasible. The electrode calibration for a titration taking place with pH-values below 7 will be based on measurements on solutions with known concentrations of hydrogen ions in the pH range of about 2.3–2.9. The test solution is completely characterized by the total concentrations of the individual reactants and by the corresponding formation constants. A number of mass-balance equations will correlate these concentrations to the model; for example

$$T_{\text{H}} = [\text{H}^+] + \sum_p \sum_r r \beta_{pr} [\text{L}]^p [\text{H}^+]^r \quad (3)$$

$$T_{\text{L}} = [\text{L}] + \sum_p \sum_r p \beta_{pr} [\text{L}]^p [\text{H}^+]^r \quad (4)$$

The data-processing in the present work sets no theoretical limits to the number of equations necessary to define the model, *i.e.*, the number of complex species. All parameters needed, *viz.* E_{const} , analytical concentrations, and titration volumes, are subject to errors which impose uncertainties on the model testing, by influencing the measure of goodness-of-fit.

In this work T_{H} is singled out as the dependent variable, *i.e.*, it is calculated as a function of all the other parameters and compared with the expected value by a non-linear least-squares method.

EXPERIMENTAL

Reagents

Sodium oxalate and sodium molybdate (both Merck *p.a.*) were titrated with a standardized permanganate solution according to methods described by Vogel.⁶ Standardized nitric acid diluted from Merck *Suprapur* nitric acid was used as the acidic titrant. The ionic strength was kept constant at 0.150 by means of potassium nitrate (Merck *p.a.*). In a few titrations potassium nitrate (Merck, *Suprapur*) was used for comparison.

Apparatus

The emf values were measured as described earlier⁷ but a few changes were made in the equipment. The motor-driven burette used was a Radiometer ABU80, and a Radiometer PHM84 pH-meter was used as an electrometer. The free hydrogen-ion concentration was monitored by means of a glass electrode (Metrohm EA 109), and a calomel electrode (Metrohm EA 494) was used as reference electrode. The cell temperature was kept constant at $25.00 \pm 0.05^\circ$ by means of a water thermostat. The electronic timers⁷ were replaced by a computer, HP9825 B/T, used as a process controller. The motor-driven burette was controlled by a relay actuator, HP59306A. BCD outputs from the pH-meter and the

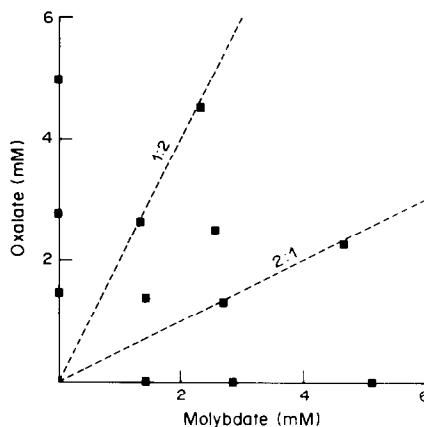


Fig. 1. Concentration diagram showing the concentrations used.

burette were input to the computer by means of a BCD-interface, HP98033A. The process controller ensured that equilibrium was attained before read-out and before the next addition of titrant.

The absolute concentration ranges used are displayed in Fig. 1 for the separately titrated solutions of molybdate and oxalate and for the mixtures. The metal-to-ligand ratio was varied between 1:2 and 2:1 in the mixtures, which were titrated in the pH-range from *ca.* 7 to *ca.* 4. For titration of oxalate and for the calibrating titrations of potassium nitrate the pH-range was extended down to *ca.* 1.8.

Calculations

All calculations were performed on the RC8000/15 at this Institution. The software program TITRER is essentially the same as that outlined earlier.⁷ The non-linear least-squares minimization algorithm has been improved so that even very poor initial guesses can now be effectively handled. The weighting has been slightly adjusted along the lines described by Avdeef;⁸ the weighting factor is calculated from

$$\sigma(\text{ml})^2 = \text{weight}^{-1} = \sigma_b^2 + [\sigma_e d(\text{ml})/dE(\text{mV})]^2$$

In the present work the values $\sigma_b = 0.003$ ml and $\sigma_e = 0.1$ mV, respectively, are used, and the necessary slopes are calculated by means of a cubic spline technique. The weighting has proved reasonable, since simple test systems with known models give variance values close to those expected for a normalized distribution, namely unity.

NUMERICAL EXPERIMENTS

The two protonation constants of oxalic acid were determined, with E_{const} from equation (2), and the results are displayed in Table 1. Simulations of the titrations were then run with synthetic errors added

Table 1. Protonation constants of oxalic acid using different calibration systems; 5 titrations with a total of 52 points

Calibration method	$\log \beta_{11}$	$\log \beta_{12}$	Variance
E_{const} equation (2)	3.825	4.831	3.17
E_{const} equation (6)			
(individual calibrations)	3.744	4.768	0.51
E_{const} equation (6)			
(combined calibrations)	3.748	4.742	0.57

to one primary parameter at a time. These numerical experiments clearly proved the initial concentration of hydrogen ions to be the most sensitive parameter. Indeed, this observation has been made on other systems by other authors and some methods have been proposed for the analysis of titration curves.¹ We have adopted the practice of introducing an additive correction to the initial concentration of hydrogen ions and letting the data-fitting program optimize the corrections as parameters specific to the individual titrations, in the hope that the corrections to the initial hydrogen-ion concentration will be so small compared with the analytical uncertainty that they can be accepted, and the adequacy of the model can be evaluated without bias. When the corrections are too great to be accepted it has been the practice to revise the model or discard the titration. The new procedure described below is of value in making an objective evaluation of the goodness-of-fit.

CALIBRATION OF ELECTRODE

Calibration of the glass electrode is in principle the calculation of E_{const} from measurements of E_{cell} in solutions with known hydrogen-ion concentration

$$E_{\text{const}} = E_{\text{cell}} - s \log[\text{H}^+] \quad (5)$$

Because of experimental uncertainties it is necessary to take the mean value of E_{const} over a pH-range. For some time we have been haunted by too large an error in the initial hydrogen-ion concentration predicted by analysis of titration curves. At the same time it was clear to us that the calibration procedure for the glass electrode was not quite satisfactory, since stable values for E_{const} emerged only from a rather narrow range of low pH-values and, more seriously, the values obtained from higher pH-values were systematically low. The procedures of May *et al.*¹ remedy this adverse situation by simultaneously refining E_{const} and the titrant acid concentration. Following such a procedure, however, we arrived at greater changes in titrand concentration than were acceptable. An obvious cause for this could be the presence of a hydrolytic system in the ionic-strength buffer (0.150M KNO_3) so that the calibration was being performed with a constant bias to the hydrogen-ion concentration

$$E_{\text{const}} = E_{\text{cell}} - s \log([\text{H}^+] + \Delta) \quad (6)$$

where s is assumed to have the theoretical Nernstian value. By performing a non-linear regression analysis on the experimental data (E_{cell} and the analytical $[\text{H}^+]$) we arrived at very well determined values for E_{const} and Δ , and a very satisfying fit to the calibration curve. It turned out, as expected, that Δ had a negative sign corresponding to an alkaline impurity. To find out whether this impurity was real or an artefact, we tested several batches of potassium nitrate, including Merck *Suprapur* quality, and it turned out that Δ was clearly related to batches and

was virtually nil for the *Suprapur* salt. Potassium nitrate of analytical grade showed a hydrogen-ion concentration of -0.07 ± 0.005 mole% whereas the *Suprapur* quality showed -0.005 ± 0.002 mole%. This conclusion is supported by the observation that calibrating with use of varied volumes of salt solutions leads to different (but all in the same direction) deviations from the extrapolated values of E_{const} and that introduction of Δ yields the same correction to the total hydrogen-ion concentration (Fig. 2).

Calibrations performed in this way are in fact quantitative determinations of very small amounts of acid or base in the potassium nitrate. The value of Δ is consequently used to correct the initial concentrations of hydrogen-ion for all titrations of protolytic systems. Thereafter equation (2) is applied for the calculation of $[\text{H}^+]$.

The discrepancy between the extrapolated and computed values of E_{const} should be noted. The final proof of the reality of the alkaline impurity comes from the fact that when titrations of oxalic acid (and some hydroxy acids to be reported) were re-examined, introduction of Δ from the calibrations led unconditionally to better fits. The oxalic acid system especially benefited from the adjustment, since without it the curve fitting would have an unacceptably large variance (far from the ideal value of unity). The calibration procedure now adopted at this laboratory is to make frequent calibrating titrations of potassium nitrate and then to make a combined curve-fitting with all the calibrating titrations in a short series, so as to produce an $[\text{H}^+]$ -correction common to all the titrations, but with individual values for E_{const} . There seems to be no need for recrystallizations of the potassium nitrate. The presence of a slight amount of alkali will not lead to an initially alkaline solution, since the unavoidable presence of carbon dioxide will turn it into a buffer system. The pH of such a solution (without additional strong acid) is ill-defined, but definitely in the acidic part of the pH-scale.

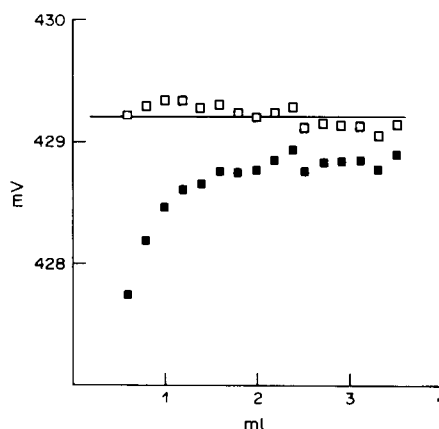


Fig. 2. Calculated values of E_{const} obtained by using equations (2) (■) and (6) (□). Horizontal line indicates the best value of E_{const} with equation (6).

Table 2. Stability constants ($\log \beta_{pqr}$) of complex species $M_pA_rH_r$ (M = molybdate, A = oxalate, H = proton) in $0.15M$ KNO_3 at $25^\circ C$

	Species			Number of titration points/ number of titrations	$\log \beta_{pqr}$ $\pm 3\sigma$	Variance
	p	q	r			
Oxalate	0	1	1	52/5	3.748 ± 0.002	0.57
	0	1	2			
Molybdate	1	0	1	122/15	3.809 ± 0.038	2.42
	7	0	8			
	7	0	9			
Molybdate-oxalate with fixed primary parameters	1	1	2	51/6	13.816 ± 0.003	2.83
	1	1	2		13.816 ± 0.003	
Molybdate and molybdate-oxalate with only oxalate as fixed parameter	1	0	1	173/21	3.805 ± 0.033	2.54
	7	0	8			
	7	0	9			
	7	0	10		61.793 ± 0.032	

A special computer program called ENUL has been written in ALGOL8 for non-linear curve-fitting for a series of calibration titrations.

Table 1 shows how the formation constants depend on the calibrating procedure. The variances are satisfactorily small with the new procedure, as they ought to be for a simple system with a known model.

RESULTS AND DISCUSSION

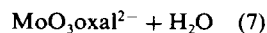
There are a number of papers concerning the problem of deciding whether a species is really present in solution or is only an artefact caused by excessive interpretation of the titration data. Kayali and Berthon⁹ summarize seven investigations on the copper(II)-histidine system. There is consensus agreement on the major species predicted, but for minor species there is little agreement. The selection of species and the calculation of stability constants are the subject of a paper by Vacca *et al.*¹⁰ Their R_{lim} factor has the same significance as our variance. More recently Avdeef⁸ has discussed the proper weighting of potentiometric data with the purpose (amongst others) of obtaining relevant values of the goodness-of-fit for comparison of models. In his experience refinements of pK -values converge at goodness-of-fit values in the range 0.5-1.2.

Our results for the molybdate(VI)-oxalate system are presented in Table 2.

For the molybdate system the set of species previously reported by us was used. The corresponding stability constants are slightly changed because of the new calibration procedure. The variance for this system is a little high compared to that for the simpler oxalate system. It is possible to get a lower variance (1.49) by replacing the $H_2Mo_7O_{24}^{4-}$ species ($p, q, r = 7, 0, 10$) with the H_2MoO_4 species (1, 0, 2), but that model does not work well in connection with oxalate, and furthermore neither species is of much concern in mixtures with oxalate.

As is clearly demonstrated by the data in Table 2, just one complex species ($p, q, r = 1, 1, 2$) will fit the

titrations in a very satisfactory way.



We found no other single species with the same property. The fit is so close that inclusion of more species is not warranted, and testing of the species claimed by Beltran *et al.*² did not lower the variance, the new species simply being rejected by the least-squares program.

The concentration ranges used in this work proved to be amply wide to distinguish between ML and M_2L_2 type complexes. The "best" M_2L_2 complex tested gave a variance which exceeded that for the best ML complex by a factor of 50.

Previously we tested a final model for internal consistency by letting the optimizing program adjust the values for both the ternary complex and the entire molybdate system. If only small changes in formation constants and variance resulted, the model was accepted. As is seen from Table 2, the changes are comfortably small. The stability constant found ($\log \beta_{112} = 13.816$) is in agreement with the value 13.98 found by Mikešová and Bartušek,³ using poten-

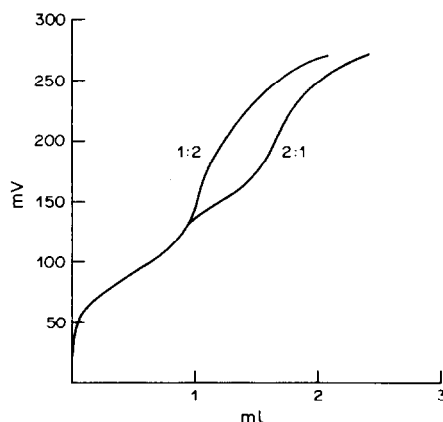


Fig. 3. Titration curves for mixtures of molybdate and oxalate in the ratio 2:1 and 1:2, respectively.

tiometric titrations in potassium nitrate medium, $I = 0.22$.

When performing the test just mentioned it was necessary to include the titrations made on molybdate only, because the molybdate-oxalate complex is so strong that most titrations on mixtures contained so little information on molybdate alone, that the "global" fitting was somewhat uncertain.

An alternative method for confirming the existence of only one molybdate-oxalate complex is to compare titration curves of mixtures of molybdate and oxalate in exactly the ratios 2:1 and 1:2, respectively.

The two curves in Fig. 3 are identical in the first part of the titrations until two equivalents of H^+ have been added. This confirms the equilibrium (7). In the more acidic regions of the titration curves, the excess of molybdate and oxalate, respectively, is titrated.

REFERENCES

1. P. M. May, D. R. Williams, P. W. Linder and R. G. Torrington, *Talanta*, 1982, **29**, 249.
2. A. Beltrán, F. Caturla, A. Cervilla and J. Beltrán, *J. Inorg. Nucl. Chem.*, 1981, **43**, 3277.
3. M. Mikešová and M. Bartušek, *Collection Czech. Chem. Commun.*, 1978, **43**, 1867.
4. J. Starý, *Anal. Chim. Acta*, 1963, **28**, 132.
5. R. A. Chalmers and A. G. Sinclair, *J. Inorg. Nucl. Chem.*, 1967, **29**, 2065.
6. A. I. Vogel, *Textbook of Quantitative Inorganic Analysis*, 4th Ed., (revised by J. Bassett *et al.*), Longmans, London, 1978.
7. E. S. Johansen and O. Jøns, *Acta Chem. Scand.*, 1981, **A35**, 233.
8. A. Avdeef, *Anal. Chim. Acta*, 1983, **148**, 237.
9. A. Kayali and G. Berthon, *Polyhedron*, 1982, **1**, 371.
10. A. Vacca, A. Sabatini and M. A. Gristina, *Coord. Chem. Rev.*, 1972, **8**, 45.

PRELIMINARY COMMUNICATION

A SENSITIVE METHOD FOR THE FLUOROMETRIC DETERMINATION OF LITHIUM WITH A "CROWNED" BENZOTHAZOLYLPHENOL

Kenichiro Nakashima, Shin'ichi Nakatsuji and Shuzo Akiyama*

Faculty of Pharmaceutical Sciences, Nagasaki University, Bunkyo-machi,
Nagasaki 852, Japan

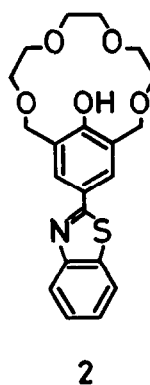
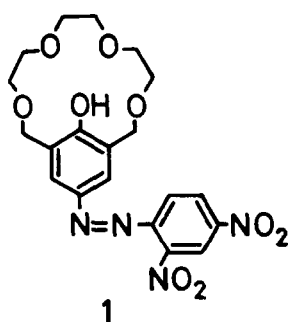
Isamu Tanigawa, Takahiro Kaneda and Soichi Misumi*

The Institute of Scientific and Industrial Research, Osaka University, Mihogaoka,
Ibaraki 567, Japan

(Received 25 June 1984. Accepted 29 June 1984)

Recently, a new method has been proposed,¹ for the spectrophotometric determination of lithium in the concentration range 25-250 ng/ml with a "crowned" dinitrophenylazophenol (CDPA, I). It was the first example of the determination of lithium with a crown ether. The incorporation of a fluorescent moiety in the place of the dinitroazo group of CDPA should much improve the sensitivity in the determination of lithium.²

A new fluorescent "crowned" benzothiazolylphenol (CBTP, II, pale yellow crystals, m.p. 155-156°) has now been synthesized and shows characteristic fluorescence with the alkali and alkaline-earth metal ions.³



This communication reports a highly sensitive fluorometric determination of lithium based on complex formation with CBTP, followed by the measurement of the fluorescence of the phenolate of the complex, obtained by treatment with triethylamine (TEA).

The procedure is as follows. To a 50- μ l portion of LiCl solution in methanol (Li 7.8 μ g/ml) in a 10-ml standard flask, 5.0 ml of 10^{-4} M CBTP in benzene are added and mixed in.

* To whom requests for reprints should be addressed.

After addition of 50 μ l of TEA the mixture is diluted to the mark with benzene and mixed well, then the relative fluorescence intensity (RFI) is measured at 410 nm, with excitation at 375 nm.

Figure 1 shows the excitation spectra for the complex (a) and a reagent blank (c) and the emission spectra of the complex (b) and the reagent blank (d) excited at 375 nm. The excitation maximum for the reagent blank is at 330 nm, and the emission intensity of the reagent blank is negligible compared with that of the complex when an excitation wavelength of 375 nm is used. The emission maximum of the blank is at 382 nm if λ_{ex} is 330 nm.

Before establishment of this procedure the effects of the CBTP, TEA and MeOH concentrations were examined. Figure 2 shows that at least a 10-fold molar excess of reagent is necessary in the final concentration. Maximal RFI of the complex was obtained with final concentrations of 0.5–1.1% v/v TEA and 0.3–0.5% v/v MeOH. The fluorescence developed immediately and its RFI was constant during 120 min or more when the solution was kept in the dark, but decreased by about 84% within 120 min if kept in room lighting.⁵ The cause of this quenching is not known, but is being investigated.

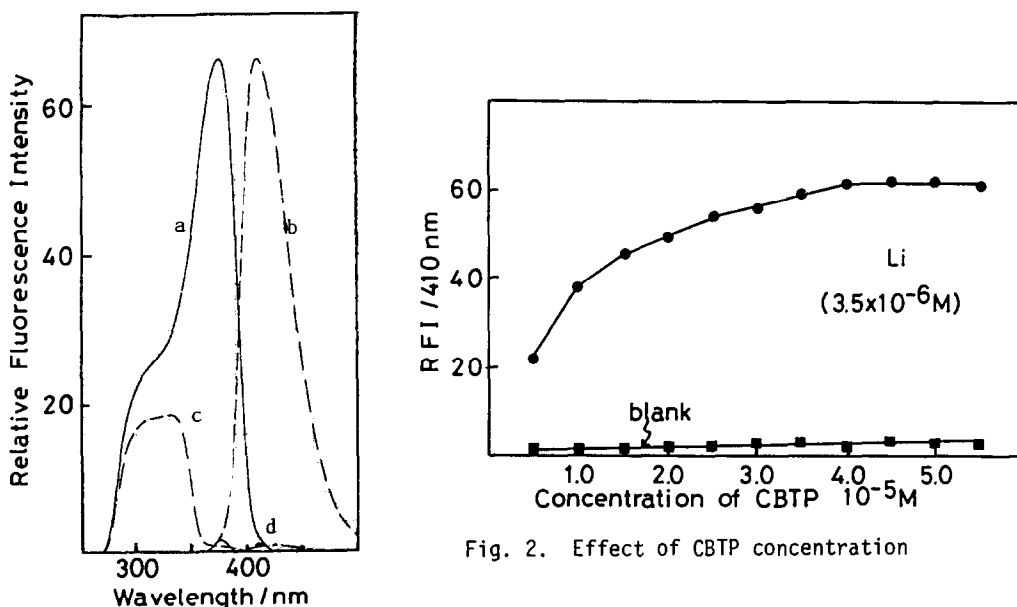


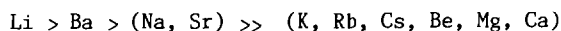
Fig. 2. Effect of CBTP concentration

Fig. 1. Fluorescence spectra

The calibration graph obtained by the standard method passed through the origin and was linear from 0.39 to 39 ng/ml. The coefficient of variation for five replicates at the 24-ng/ml level was 2.2%.

The principal advantages of the method are that it is simple, rapid, and sensitive. The sensitivity is superior to that of the CDPA method¹ and of the method based on the 1,8-dihydroxyanthraquinone complex (50–450 ng/ml).⁴

The RFI of each of the CBTP- M^{n+} complexes (M^{n+} = alkali or alkaline-earth metal ion) obtained by the procedure was measured. The order of decreasing RFI is



In this series the intensity ratios of the Li to Ba, Na, and K complexes were about 2, 4 and 10 respectively. It is interesting to note that the RFI of the Na, Be, Ba, and Sr complexes,

which would interfere in the determination of Li(I), decrease remarkably within 30 min, even in the dark. This behaviour (also not yet explained but under investigation) should be useful for improving the selectivity, and work along this line is in progress.

The authors wish to express their gratitude to the Japan Ministry of Education, Science, and Culture for a Grant-in-Aid for Scientific Research.

REFERENCES

1. K. Nakashima, S. Nakatsuji, S. Akiyama, T. Kaneda and S. Misumi, Chem. Lett., 1982, 1781.
2. For recent crown ether-based fluorometric reagents for metal ions, see H. Nishida, Y. Katayama, H. Katsuki, H. Nakamura, M. Takagi and K. Ueno, ibid., 1982, 1853.
3. I. Tanigawa, K. Tsuamoto, T. Kaneda and S. Misumi, 16th Symposium on Structural Organic Chemistry, Saitama, Japan, 1983, Abstr. No. B-3-47.
4. M.R. Ceba, A. Fernandez-Gutierrez and M.C. Mahedero, Anal. Lett., 1981, 14, 1579.

LETTER TO THE EDITOR

Comment on "LASER-EXCITED FLUORESCENCE LINE-NARROWING: AN ANALYTICAL STUDY"

Sir,

The paper by Bolton and Winefordner (Talanta, 1983, 30, 9) has been commented upon by Hayes and Small (HS).* We agree that J.C. Brown, M.C. Edelson, and G.J. Small (Anal. Chem., 1978, 50, 1394) were among the first to explore the analytical use of fluorescence line narrowing spectroscopy (FLNS), and in fact our study resulted because of that paper. We did not intend to imply that our study was the first analytical one. We wish, however, to respond to the first three points of the HS comment.

1. As far as the poor limits of detection (LODs) are concerned, these are the values we obtained for the experimental conditions listed. We realize the LODs are considerably poorer than the ones obtained by Small et al. (references 3 and 5 in HS's comment).

2. We made numerous attempts over a period of more than a year to improve our detection power but no matter what excitation/emission wavelengths and boxcar detector conditions were used, the LODs remained in the concentration range of approximately 1-1000 ng/ml. It is possible that our high LODs are correlated to an abnormally high background, but this is difficult to rationalize since our studies were done over a long period of time, with several batches of reagents and a variety of experimental arrangements and conditions.

3. The hypothesis of rapid local site-melting causing a loss of FLNS behaviour when λ_{ex} pumps vibronic levels of the fluorescent state possessing $\geq 1500 \text{ cm}^{-1}$ excess vibrational energy was not ours but rather that of the authors of the two papers cited in our manuscript

Despite our analytically limited results for FLNS, we still feel the method has considerable analytical use, primarily because of the fine work by Small, Hayes, and their colleagues at Iowa State University.

Department of Chemistry,
University of Florida,
Gainesville, Florida 32611, U.S.A.

J.D. WINEFORDNER

2 March 1984

*Talanta, 1984, 31, 741.

SOLVENT EXTRACTION OF NOBLE METALS BY FORMAZANS—I

COMPARATIVE STUDY ON THE EXTRACTABILITY OF Pt(IV), Pd(II) AND Ag(I) BY FORMAZANS COMBINED WITH A LIQUID ANION-EXCHANGER

M. GROTE, U. HÜPPE and A. KETTRUP*

Fachbereich Chemie und Chemietechnik, "Angewandte Chemie", Universität-GH Paderborn, Warburger
Straße 100, D-4790 Paderborn, Bundesrepublik Deutschland

(Received 23 September 1983. Revised 2 May 1984. Accepted 10 May 1984)

Summary—The extraction properties of ion-pairs composed of quaternary ammonium cations and a sulphonated formazan were compared with those of an unsulphonated formazan, for various solvent media. In dichloromethane the combined system behaves as a "coloured anion-exchanger", with displacement of the sulphonated formazan, whereas in toluene Pd(II) and Ag(I) are extracted as the metal formazan chelates from aqueous medium. The rates of extraction are remarkably higher than with the simple extractants. Because of the higher stability only the simple chelating extraction systems afford satisfactory separation of Pd(II) from excess of Pt(IV) and of Ag(I) from Cu(II). The extracted metals can be stripped and the extractant regenerated.

The removal and recovery of valuable metals from aqueous solutions by use of ion-exchangers and liquid extracts is a growing need in, for example, the electroplating industry and hydrometallurgy.¹⁻⁶ The extractants used should be highly selective and easy to regenerate. Liquid-liquid extraction systems usually offer a wider range of stripping methods and better preconcentration factors than solid ion-exchangers do. Anionic complexes of the noble metals have been extracted with solid⁷⁻¹⁰ as well as "liquid" ion-exchangers.^{6,11-17} The behaviour of analogous functional groups in the two systems is similar, but the liquid-liquid extraction behaviour can differ markedly from the sorption behaviour. Our investigations on chelating ion-exchangers with high affinity for noble metals have resulted in use of formazan-modified strongly basic polystyrene and silica gel.^{18,19} These sorbents separate silver(I) from an excess of Cu(II) and allow complete removal of the noble metals. This work has now been extended by use of solvent extraction with mixtures of liquid anion-exchangers and sulphonated formazans.

The ion-pairs formed by quaternary ammonium salts with anionic chelate complexes have been extensively used in extraction-spectrophotometric determinations and offer advantages in selectivity and sensitivity over conventional spectrophotometric methods based on metal complexes in aqueous solutions.²⁰⁻²⁵ The chelates can be formed in the aqueous phase and extracted with an organic solution of the ammonium salt, or the metal can be extracted with an organic solution of both the chelating agent and the ammonium salt.

Thus Przeszlakowski and Habrat²⁵ efficiently extracted Fe(III) by means of the ion-association compound formed by its ferron complex and Aliquat 336 in chloroform. This reaction is analogous to the one we have produced by use of the sulphonated formazan F32 (Fig. 1) and a quaternary ammonium salt in various solvents (Table 1).

The properties of the $Q_L F32-T$ and $Q_L F32-D$ systems can be compared with those of the corresponding simple chelating extraction systems with the unsulphonated *o*-chloro-substituted ligand F43 (Fig. 1, Table 1).

EXPERIMENTAL

Reagents

The preparation of the formazans F32 and F43 has already been described.^{18,26} The solvents used were toluene (T) and dichloromethane (D) (the symbol T/D will be used to indicate that either solvent can be used but both are being investigated). A 0.01M $Q_L^+ Cl^-$ solution in T or D was prepared with methyltriocetylammmonium chloride ($Q_L^+ Cl^-$)

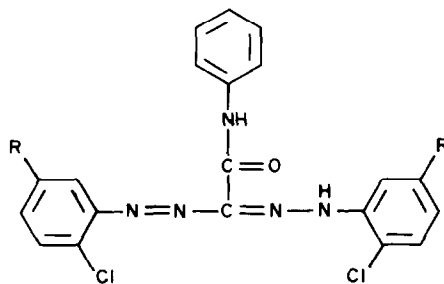


Fig. 1. Structure of formazans used for liquid-liquid extraction (R = H: F43; R = SO₃H: F32).

*Author for correspondence.

Table 1. Composition of the extraction systems

Symbol	Solvent	Chelating agent	Liquid anion-exchanger
Q _L F32-T	Toluene	F32 (sulphonated)	main component: (C ₈ H ₁₇) ₃ N ⁺ CH ₃ Cl ⁻ ; (Q _L ⁺ Cl ⁻)
Q _L F32-D	Dichloromethane		
F43-T	Toluene	F43 (unsulphonated)	—
F43-D	Dichloromethane		

(Merck) and 500 ml of it were shaken with five successive 100-ml portions of 0.1M hydrochloric acid and then with five successive 500-ml portions of water. The tendency to form emulsions could be reduced by adding a small amount (0.2% v/v) of 1-octanol. The same procedure was applied, with 0.1M nitric acid, to obtain the nitrate form Q_L⁺NO₃⁻ of the liquid anion-exchanger.

Q_LF32-T/D

F32 was extracted by shaking 500 ml of Q_L⁺Cl⁻-T/D with 100 ml of 0.2% aqueous formazan solution for 2 min and rejecting the aqueous phase. The process was repeated about ten times with fresh formazan solution until the absorbance of the organic phase at 436 nm became constant. The organic phase was then washed several times with 500-ml portions of water to remove excess of F32, and stored in a brown glass bottle to prevent decomposition by light. The binary systems Q_LF32-T/D in the nitrate form were analogously prepared and were preferred for extraction of silver, to prevent interference by chloride.

Determination of the concentration of F32 in Q_LF32-T/D

Irving's method²⁷ was used. The stock solution of Q_LF32-T/D was diluted 100-fold with toluene or dichloromethane, and 5 ml of the diluted solution were shaken for 1 min with 5 ml of 0.1M sodium perchlorate. The formazan stripped was determined photometrically by dilution of an aliquot of the centrifuged aqueous phase with water and measurement of its absorbance at 436 nm against water. The acid dissociation constants of the formazans were evaluated spectrophotometrically by the method of Pelizzetti.²⁸ Solutions of F43 in dioxan and of F32 in water were diluted with aqueous buffer to give final solutions with concentrations in the range 0.4–1 × 10⁻⁴M. Isosbestic points were observed at 470 nm (F43) and 505 nm (F32).

Determination of distribution ratios

All experiments were performed at ambient temperature (22 ± 2°), by mechanically shaking 5 ml of 0.001M aqueous solutions of the appropriate metal salt (Na₂PtCl₆, Na₂PdCl₄, AgNO₃) containing dilute mineral acid (hydrochloric or nitric) or a buffer (10⁻²M citric acid, 10⁻³M sodium tetraborate) with an equal volume of the extractant solution (~0.004M) in a 50-ml separatory funnel. For work with silver the funnels were covered with aluminium foil, to prevent photodecomposition. After phase separation the aqueous solution was centrifuged and analysed by d.c. plasma atomic-emission spectrometry (see below). The distribution ratio *D* was calculated in the usual way.

A Beckman Spectraspan III d.c. argon-plasma emission spectrometer with a three-electrode plasma jet was used, as described elsewhere.^{29,30} The wavelengths used were based on the manufacturer's recommendations: Pt 265.945 nm (85th order); Pd 340.458 nm (66th order); Ag 338.289 nm (66th order); Cu 324.754 (69th order). The spectral background was compensated for by matrix-matching of samples and standards.

The standard solutions were prepared from commercially available stock solutions (1000 and 500 mg/l., SPEX Industries Inc.). Noble metal salts were donated by Degussa, Hanau. A Perkin-Elmer 554 spectrophotometer and a Bruker WP 250 Fourier-transform spectrometer were used.

Separation of Pd(II) from Pt(IV)

Stock solutions (10⁻²M) of Pd(II) and Pt(IV) were prepared by dissolving Na₂PdCl₄ or Na₂PtCl₆ in 10⁻²M hydrochloric acid. The metal content of each solution was determined by d.c. plasma emission spectrometry before use. Solutions containing various amounts of Pd and Pt were obtained by mixing appropriate aliquots of the stock solutions and diluting with 10⁻²M hydrochloric acid.

Extraction. Twenty ml of a mixture containing ~10 mg/l. Pd and between 10 and 2000 mg/l. Pt were placed in a 100-ml separatory funnel and 20 ml of 4 × 10⁻³M extractant were added. The mixture was shaken for 24 hr, then the phases were separated. The palladium concentration in the aqueous phase was then determined.

Stripping. Ten ml of the organic layer from the extraction system were transferred to a 50-ml separatory funnel and shaken with 10 ml of 5% thiourea solution in 0.1M hydrochloric acid for 48 hr. The amounts of Pd and Pt stripped were measured simultaneously in the separated aqueous phase.

A 5-ml aliquot of the organic phase regenerated by stripping was transferred to a glass beaker and the solvent was carefully evaporated. Then 5 ml of concentrated nitric acid were added and boiled down to 2 ml, then 0.5 ml of 70% perchloric acid was added and the solution evaporated to dryness. The residue was dissolved with 3 ml of aqua regia and the solution evaporated to dryness. The residue was taken up in 5 ml of 6M hydrochloric acid and the solution diluted to 10 ml with water, before measurement by emission spectrometry.

Separation of Ag(I) from Cu(II)

Appropriate aliquots of standard 0.01M silver nitrate and standardized 0.1M copper nitrate were mixed in a 100-ml glass beaker. After dilution of 5 ml of 1M sodium citrate and 5 ml of 0.1M sodium tetraborate the mixture was

Table 2. Dissociation constants and spectrophotometric data of formazans

Formazan	pK _a	λ _{max} , nm	pH 1		pH 13		Solvent
			λ _{max} , nm	ε _{max} , 10 ⁴ l.mole ⁻¹ .cm ⁻¹	λ _{max} , nm	ε _{max} , 10 ⁴ l.mole ⁻¹ .cm ⁻¹	
F43	12.19	435	521	2.64	2.47		water/dioxan (6:4 v/v)
F32	11.48	441	513	1.40	1.87		water

diluted with water to ~40 ml and the pH adjusted to 9.4 by dropwise addition of 1M sodium hydroxide or nitric acid. The solution was diluted to volume in a 50-ml standard flask with water, giving a final concentration of 0.1M citrate and 0.01M borate. The final concentration of Ag(I) was ~10 mg/l., and that of Cu(II) varied from 62 to 6240 mg/l.

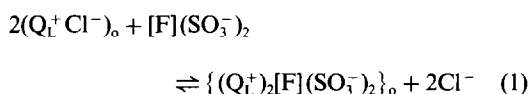
The separation procedures and analytical measurements were similar to those described above. A shaking time of 15 min was sufficient for the extraction of silver with F43-D, and it was stripped by 10 ml of 0.01M nitric acid within 2 min.

Some dichloromethane was present in the nitric acid after the stripping and interfered in the simultaneous determination of Ag and Cu by atomic-emission spectroscopy. It was therefore necessary to evaporate the solution to dryness (on a steam-bath); to prevent losses of silver; 5 ml of concentrated nitric acid were added before the evaporation. The residue was taken up in 5 ml of concentrated nitric acid, 5 ml of water were added, and the final solution was analysed.

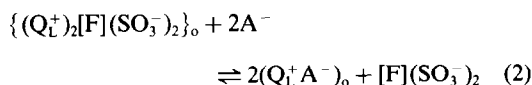
The extractant remaining from the stripping was analysed for copper and silver as already described, the final residue being taken up in 2 ml of concentrated nitric acid and 2 ml of water.

RESULTS AND DISCUSSION

F32 may be extracted by quaternary ammonium cations (Q_L^+) in accordance with the equilibrium:



where [F] represents formazan, and subscript o the organic phase. Determination of F32 in the binary system $Q_L F32-T$ showed that in toluene medium the molar ratio of Q_L^+ to F32 is reproducibly about 2:1 as predicted by equation (1), but in dichloromethane, a solvent of higher polarity, excess of F32 is extracted and the ratio varies from 2:1 to nearly 1:1. $Q_L F32-T$ and $Q_L F32-D$ solutions are fairly stable for a period of weeks in the dark and in daylight (Table 3), whereas aqueous solutions of F32 decompose more rapidly after storage for 100 days in the dark. Some anions (A^-) may interfere in the extraction by displacement of the chelating anion:



To study this displacement (Table 4), equal volumes of $Q_L F32-T$ or $Q_L F32-D$ and aqueous phases con-

Table 4. Displacement of F32 (%) by various anions from binary extraction systems (shaking time 1 min)

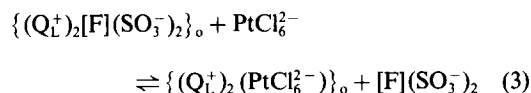
Aqueous solution	$Q_L F32-T$	$Q_L F32-D$
HCl, 7M	3.69	precipitation
3M	0.38	precipitation
1M	0	0.77
0.1M	0	0
HNO ₃ , 1M	4.92	10.3
0.1M	0.77	9.23
0.01M	0	1.38
NaClO ₄ 0.1M	10.31	9.85
NaOH, 1M	4.30	6.46
0.1M	3.92	3.77
0.01M	1.92	0.31
citric acid buffer, pH 7-9	0	0
borate buffer, pH 8-10	0	0

taining various acids or salts were shaken for 1 min. The dichloromethane system ($Q_L F32-D$) was very unstable in contact with mineral acids and alkalis. Thus the $Q_L F32-D$ system has the typical properties of the "coloured liquid anion-exchangers" utilized by Itoh *et al.*³¹ and Irving and co-workers^{27,32} for the spectrophotometric determination of perchlorate. In the toluene system displacement of the chelating agent is more difficult, so the reagent is fairly stable in the presence of dilute hydrochloric acid and alkaline buffers.

Extractability of Pd(II) and Pt(IV)

Palladium and platinum form similar chloro-complexes, which are difficult to separate by normal anion-exchange. Their distribution in the presence of formazans was investigated by shaking together equal volumes of the aqueous metal salt solution and the extractant for at least 1 min. The properties of the $Q_L F32-D$ system differ considerably from those of the $Q_L F32-T$ system.

$Q_L F32-D$ system. This is characterized by displacement reactions, and a shaking time of 1 min is sufficient to replace some of the F32 by $PtCl_6^{2-}$. This exchange reaction is rather inhibited in the presence of citric acid. Analysis showed that F32 and platinum are exchanged in about 1:1 ratio, in accordance with the reaction:



in contrast, $PdCl_4^{2-}$ is virtually unable to displace the formazan in this period of shaking (Table 5). This difference in extractability conforms with the hypothesis that the extraction of anions is favoured by increase in size (the "hole theory").³³ In principle, separation of Pt(IV) from Pd(II) by anion-exchange extraction seems to be possible with the $Q_L F32-D$ system, but the distribution ratios for Pt(IV) are too low for the system to find practical application.

Table 3. Stability of the $Q_L F32-T$ extraction system

Time elapsed, days	Decomposition, %		
	$Q_L F32-T$ light	$Q_L F32-T$ dark	Aqueous solution of F32 (0.01M) dark
4	9	3	4.5
30	18	14	16
100	20	20	32

Table 5. Displacement of F32 by Pt(IV) and Pd(II) complexes from the binary system $Q_L F32-D$ (shaking time 1 min)

Aqueous phase	[F32] in the aqueous phase, mM	
	Pt(IV)	Pd(II)
HCl, 0.01M	0.207	0.016
0.1M	0.463	0.033
1.0M	0.728	0.022
citric acid buffer		
pH 2	0.009	0.016
pH 4	0.020	0.006

$Q_L F32-T$ system. There was much less exchange between this system and platinum and palladium, even after shaking time of 24 hr, than between these metals and $Q_L^+ Cl^-$ in toluene. This behaviour (Fig. 2) is analogous to that of solid anion-exchange resins with and without formazan-loading.¹⁸

Sorption of Pd(II) by the F32-loaded solid resin is fast, and complete up to a metal:ligand ratio of 1:1, but solvent extraction of Pd(II) with the $Q_L F32$ system proceeds very slowly, a reaction time of 24 hr not being sufficient for equilibrium at pH 2 to be reached (Fig. 3), though 96% of the noble metal is extracted.

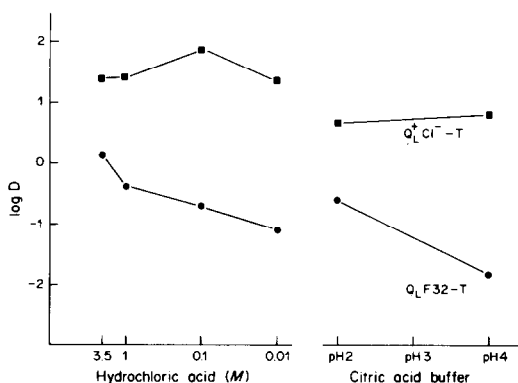


Fig. 2. Extractability of Pt(IV) by the liquid anion-exchanger $Q_L^+ Cl^-$ in comparison with the combined system $Q_L F32$ in toluene (shaking time 1 min).

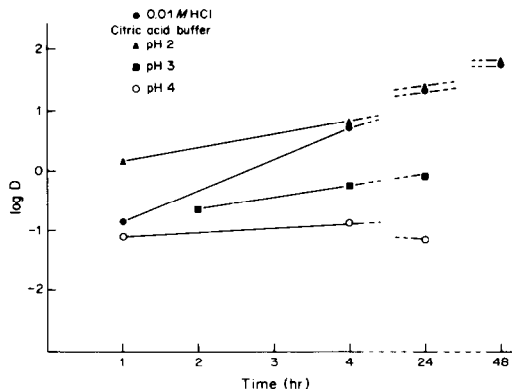


Fig. 3. Extraction of Pd(II) by $Q_L F32-T$, as a function of time.

In this process the colour of the organic phase changes from red to green, indicating the formation of a formazan-Pd(II) chelate. Stripping of this chelate by means of perchlorate enables it to be isolated and characterized. Thin-layer chromatography and infrared and ultraviolet spectroscopy show it to be the 1:2 metal chelate described earlier, called " $Pd-F32$ ".³⁴

The low rate of complexation of palladium in solvent extraction with formazans was also observed by Panzel.³⁵ In general a low rate of complex formation by platinum metals affects their solvent behaviour.²⁴ In view of the difference in the distribution ratios, separation of platinum and palladium by means of the $Q_L F32-T$ system seems possible, the separation factor being ~ 50 for a shaking time of 24 hr and 0.01M hydrochloric acid medium, but the extraction of Pd is incomplete (96%, see above). In citric acid medium buffered at pH 3 the extractability of Pd is reduced by its complexation side-reaction with citric acid. To test this separation, three synthetic solutions, containing 105 μg of Pd and various amounts of Pt, were treated individually with the extractant $Q_L F32-T$. The results, shown in Table 6, reveal that platinum inhibits the complete extraction of palladium. With higher concentrations of Pt ($5 \times 10^{-3} M$) some of the green formazan-Pd(II) chelate was stripped by $PtCl_6^{2-}$. Thus the application of the combined system is impossible for the quantitative separation of Pd from Pt.

Comparison with the simple F43 chelate extraction system

The extraction behaviour of the hydrophobic *o*-chloroformazan F43, dissolved in toluene (F43-T), differs markedly from that of the mixture of liquid anion-exchanger and water-soluble F32 ($Q_L F32-T$). As expected, the distribution ratios of Pt(IV) between F43-T and hydrochloric acid (0.01-1M) or citric acid buffer are very low ($D \sim 0.07$). The extraction of Pd(II) with the simple extractant at room temperature is also less effective ($D = 0.64$, shaking time 24 hr) than that with the combined system (Fig. 4), and is also very slow.

A higher distribution ratio ($D \sim 170$) was found for Pd when the dichloromethane system (F43-D) was used.

Table 6. The effect of varying amounts of Pt(IV) on the extraction of Pd(II) with $Q_L F32-T$ (shaking time 24 hr; [HCl] 0.01M; [F32] = $4 \times 10^{-3} M$, 10 ml of extractant; phase volume ratio 1:1)

Pt present, μg	Pd added, μg	Pd extracted, %
104	105	96.3
202		91.8
1050		63.6*

*The formazan-Pd(II) chelate is partly stripped.

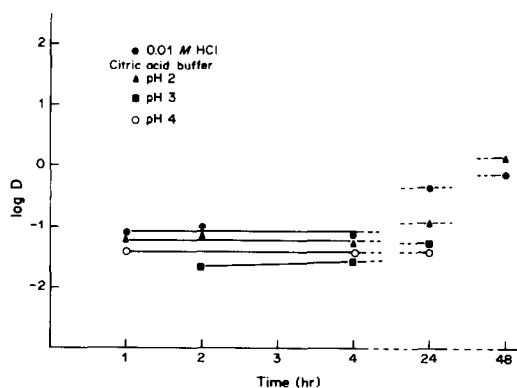


Fig. 4. Extraction of Pd(II) by F43-T, as a function of time.

Separation of Pd(II) from Pt(IV)

In contrast to the Q_1F32-T system, F43-D will give complete separation of small amounts of Pd from excess of Pt provided the w/w ratio of Pt to Pd is not much more than about 20 (see Table 7), but up to almost 200-fold ratio can be tolerated if citric acid is added to give a final concentration of 0.01M (pH 2) in the aqueous phase.

The palladium extracted can be stripped and the extractant regenerated with an acidified solution of thiourea, but the rate of ligand substitution in the stripping step is slower than the rate of extraction. Small amounts of Pt are co-extracted and are also stripped from the organic phase. To investigate the efficiency of the stripping procedure, the regenerated extractants were first evaporated to dryness. The residues were then mineralized with nitric and perchloric acids, taken up in hydrochloric acid solutions and analysed. Not even traces of Pt could be detected and only small amounts of Pd (0.2–0.4 μg per 10 ml of extractant).

Extractability of Ag(I)

We have already reported that spectroscopic data indicate that the model compound Ag-F43 is an N,O-co-ordinated complex. Silver is sorbed from slight alkaline sodium acetate or citrate buffers onto solid supports modified with the chelating formazan,

Table 8. The effect of the concentration of tetraborate on the extraction of Ag(I) with F43-D (shaking time 30 min; $[\text{Ag(I)}] 1 \times 10^{-3}M$, $[\text{F43}] 4 \times 10^{-3}M$)

$[\text{B}_4\text{O}_7^{2-}]$, mM	Ag extracted, %
0.1	21.3
0.5	71.2
1.0	91.1
10.0	97.8

Table 9. Effect of pH on the extraction of Ag(I) from tetraborate solution with F43-D (shaking time 30 min; $[\text{Ag(I)}] = [\text{B}_4\text{O}_7^{2-}] = 1.0mM$)

pH	Ag extracted, %
8.0	49.4
8.5	88.3
9.0	~ 100
9.5	~ 100

but its liquid-liquid extraction from the same media with the combined (Q_1F32-T/D) and simple (F43-T/D) systems is poor ($D = 0.4$). However, the extraction is much more effective from sodium tetraborate medium.

F43-T/D. The effect of tetraborate concentration on the distribution ratio of silver between the aqueous phase and the extractant F43-D at a fixed concentration of F43 is summarized in Table 8.

The enhanced extraction with increase in tetraborate concentration may be due to the increasing alkalinity of the aqueous phase, and this is confirmed by the data in Table 9 for the effect of pH at a fixed concentration of silver and tetraborate.

Depending on the concentration, pH and temperature, various complexes may be formed in the system $\text{Ag}_2\text{O}-\text{B}_2\text{O}_3-\text{H}_2\text{O}$.³⁶ However, a plot of $\log D$ vs. $\log [\text{F43}]$ has a slope of unity, indicating a 1:1 metal-F43 chelate is extracted. This result agrees with the structure assumed for the Ag-F43 compound, prepared by liquid-liquid extraction under similar conditions.³⁴ No evidence was found for additional co-ordination of an inorganic ligand. The extraction

Table 7. Results of separation of Pd(II) from Pt(IV) with F43-D (extraction conditions: $[\text{HCl}] 0.01M$, $[\text{F43}] 4 \times 10^{-3}M$; 24 hr shaking time; stripping with 5% thiourea in 0.1M HCl, 48 hr shaking time; phase volume ratio 1:1; amounts of each metal are calculated for a total phase-volume of 10 ml)

Pd added, μg	Pt present, mg	Pd extracted, μg	Amount of metal stripped, μg	
			Pd	Pt
99.7	0.099	99.5	99.8	25.7
	0.196	99.1	99.7	22.0
	0.992	99.4	98.4	25.0
	1.95	99.3	106	32.4
	9.97	93.5	91.8	36.6
	19.48	79.8 (98.1)*	73.1	27.8

*0.01M citric acid medium.

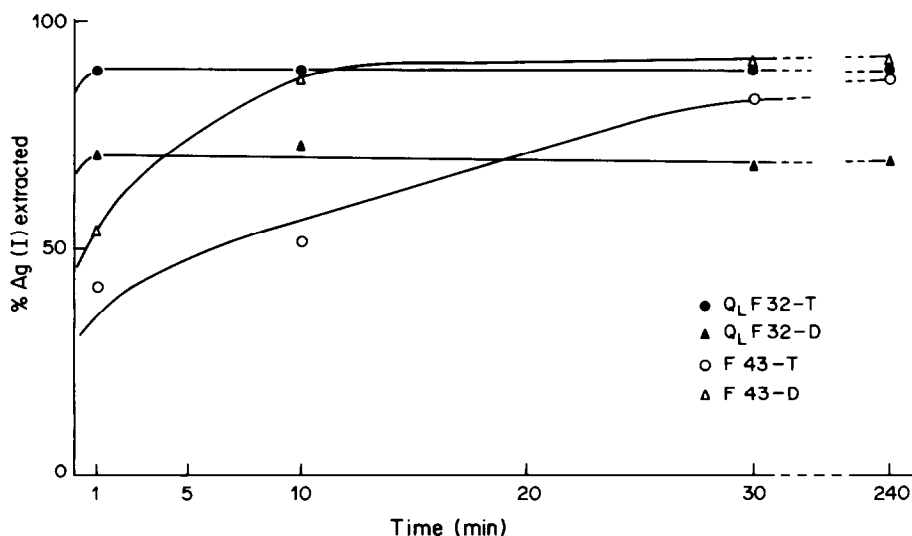


Fig. 5. Extraction of Ag(I) with various extractants, as a function of time.

of silver is much faster than that of palladium, distribution equilibrium with F43-D being established within 30 min (Fig. 5). In toluene medium the rate of co-ordination is slower and the extraction yield lower (Fig. 5).

Q_LF32-T/D. Vigorous shaking of either of these systems with an aqueous solution of silver and sodium tetraborate (each $10^{-3}M$) immediately produces a deep violet colour in the organic phase, indicating very rapid extraction. The distribution is much faster than with the simple extractants (Fig. 5), equilibrium being established within 1 min.

The extractant Q_LF32-D, which is subject to displacement reactions in contact with Pt and Pd solutions, is as stable as Q_LF32-T in the presence of aqueous mixtures of tetraborate and silver. Though the rates of extraction with the two combined systems are the same, the degree of extraction is lower with Q_LF32-D (69%) than with Q_LF32-T (90%) under identical conditions.

Stripping of silver. Except for the Q_LF32-D system, stripping is nearly complete with 0.01M nitric acid in a single extraction in 1 min shaking time (Table 10). Stripping with $10^{-3}M$ nitric acid is less effective.

Separation of Ag(I) from Cu(II)

Silver was extracted from mixtures of silver and copper under conditions similar to those for silver alone. The alkaline aqueous solutions (pH 9.4) contained sodium tetraborate, and sodium citrate to prevent precipitation of copper salts. When the Q_LF32-T system is used, higher concentrations of Cu ($\geq 10^{-2}M$) displace the Ag-F32 chelate, and the extraction yields of Ag are lower than 96%. However, about 100 μg of silver can be successfully separated (99.7%) from large amounts of copper by extraction with F43-D (see Table 11). A shaking time of 15 min is sufficient for quantitative extraction. Silver and traces of co-extracted copper are easily stripped with

0.01M nitric acid (2 min shaking time). Mineralization of the stripped extractants and analysis of the residue for metals show that only 0.1–0.25 μg of Ag and ~ 0 –0.6 μg of Cu remain in 10 ml of the organic phase after the single stripping. The regenerated F43-D system may be used again for extraction, which is promising for the development of cyclic separation processes.

Conclusion

The rate of extraction of Pd(II) and Ag(I) is much higher with the combined extractants (Q_LF32-T/D) than with the simple chelating systems (F43-T/D) but combination of the lipophilic ligand F43 with the

Table 10. Back-extraction of silver with nitric acid (5 ml of Ag-loaded extractant, 5 ml of HNO₃, shaking time 1 min)

Extractant	Ag extracted, μg	Ag back-extracted, %*	
		$10^{-3}M$ HNO ₃	$10^{-2}M$ HNO ₃
Q _L F32-T	405	88.7	100.1
Q _L F32-D	312	76.1	79.9
F43-T	437	77.0	99.7
F43-D	432	95.9	96.5

*Mean of three single strippings.

Table 11. Results of separation of Ag(I) from Cu(II) with F43-D (extraction conditions: [F43] = $4 \times 10^{-3}M$; 0.1M citrate; 0.01M borate; pH 9.4; 15 min shaking time; stripping conditions: 0.01M HNO₃; 2 min shaking time; amounts of each metal are calculated for a total phase-volume of 10 ml; phase volume ratio 1:1)

Ag added, μg	Cu present, mg	Ag extracted, μg	Metal stripped, μg	
			Ag	Cu
103	0.624	103	98	0.6
106	6.24	106	101	3.3
106	62.4	106	109	2.3

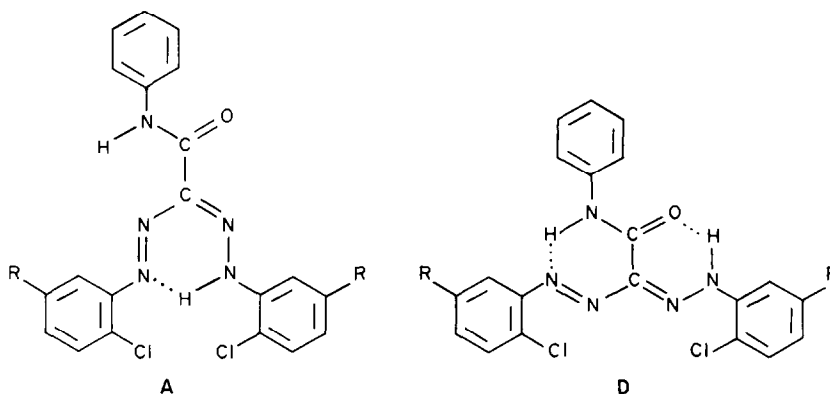


Fig. 6. Structure of isomers of formazans.

quaternary ammonium compound gives no improvement of the extractant rates. The differences found in the extraction behaviour are not yet fully understood. The cationic surfactant makes the extraction mechanism more complicated, and the influence of micelles should be taken into consideration.²³ However, the higher N–H acidity and hydrophilicity of F32 [pK_a (F32) = 11.4; pK_a (F43) = 12.2] may increase the rate of extraction. Furthermore, there may be activation of the sulphonated agent by the surfactant. Similar activating effects are reported in the literature on the formation of mixed-ligand complexes. Savvin *et al.*³⁷ interpreted the enhanced reactivity of triphenylmethane reagents with metal ions and *N*-cetylpyridinium chloride in aqueous solution as a deprotonation process. Improved extractability of lanthanides by use of ion-association complex formation in conjunction with chelation by 8-hydroxyquinoline derivatives was observed by Tochiyama and Freiser.³⁸ It must also be taken into account that in the presence of surfactants and sulphonated chelating agents metal ions could be favourably co-ordinated at the interface of the two phases and not in the aqueous phase.²⁵

The rate of extraction in metal chelate extraction systems can be limited by the rate of reaction between the metal ion and the ligand, as well as by diffusion and transport factors. In the case of the 3-phenylcarbamoylformazans, Pd(II) and Ag(I) are bound by different isomers (Fig. 6).³⁴ Thus the co-ordination of the noble metal ions is accompanied by ligand conversion. An investigation of the Q_L F32 ion-pair by proton n.m.r. spectroscopy (C_6D_6 medium) gave evidence for only the N–H...N and N–H...O bichelated isomer **D**, which is favoured for the co-ordination of Ag(I). In contrast to the extractant F43–T (10% of isomer **A**) and the solid polystyrene loaded with QF32 (30% of **A**)³⁴ no mono-chelated isomer **A** could be detected.

We assume that the different isomer ratios affect the efficiency of the reaction of both the liquid extractants and solid sorbents with palladium and silver. The binary solvent-extraction system Q_L F32–T

extracts silver faster and more completely than the similar formazan-modified polystyrene QF32 and silica gel Si-QF32,^{18,19} but is less effective for extraction of Pd(II).

Unfortunately, the extractant Q_L F32–T is unstable in contact with metal salt solutions of higher concentrations and will find no practical use in separation processes. Only application of the simple chelating system F43–D to synthetic mixtures of Pd/Pt and Ag/Cu gives acceptable results.

Additional studies on the extractability of noble metals and base metals by other substituted formazans are in progress and will be applied to various samples containing noble metals.

Acknowledgements—Financial support from “Fonds der Chemischen Industrie” and “Deutsche Forschungsgemeinschaft” is gratefully acknowledged. The authors wish to thank Degussa, Hanau for donating noble metal salts.

REFERENCES

1. M. Knothe and S. Ziegenbalg, *Z. Chem.*, 1982, **22**, 295.
2. W. H. Waitz, *Plat. Surf. Finish.*, 1982, **69**, 56.
3. J. Krüger, *Z. Metallkd.*, 1983, **74**, 61.
4. R. Kunin, in J. A. Marinsky, *Ion Exchange and Solvent Extraction*, Vol. 4, Chap. 3. Dekker, New York, 1973.
5. S. Ziegenbalg, *Neue Hütte*, 1975, **20**, 181.
6. A. Warshawsky, *Sepr. Purif. Methods*, 1982–83, **11**, 95.
7. E. Blasius and U. Wachtel, *Z. Anal. Chem.*, 1954, **142**, 341.
8. S. S. Berman and W. A. McBryde, *Can. J. Chem.*, 1958, **36**, 835.
9. R. K. Petric and J. W. Morgan, *J. Radioanal. Chem.*, 1982, **74**, 15.
10. M. Knothe, *Z. Anorg. Allg. Chem.*, 1980, **463**, 204.
11. H. Green, *Talanta*, 1973, **20**, 139.
12. H. Irving and A. D. Damodaran, *Anal. Chim. Acta*, 1969, **48**, 267.
13. L. M. Gindin, *High Purity Mater. Sci. Technol., Int. Symp., Proc. 5th*, 1980, **1**, 173.
14. *Idem*, in J. A. Marinsky, *Ion Exchange and Solvent Extraction*, Vol. 8, Chap. 4. Dekker, New York, 1981.
15. S. Przesziakowski and A. Fliieger, *Talanta*, 1981, **28**, 557.
16. M. R. Shivade and V. M. Shinde, *Indian J. Chem.*, 1982, **21A**, 336.

17. A. Warshawsky, *Sepr. Purif. Methods*, 1983, **12**, 1.
18. M. Grote, P. Wigge and A. Kettrup, *Z. Anal. Chem.*, 1982, **310**, 369.
19. M. Grote, A. Schwalk and A. Kettrup, *ibid.*, 1982, **313**, 297.
20. A. R. Cyganov, E. M. Rachman'ko and G. L. Starobinec, *Izv. AN BSSR, Ser. Khim. Nauk*, 1980, **2**, 63.
21. S. Przeszlakowski and H. Wydra, *Chromatographia*, 1982, **15**, 301.
22. C. Woodward and H. Freiser, *Talanta*, 1973, **20**, 417.
23. S. Koch, *Z. Chem.*, 1982, **22**, 317.
24. T. Sekine and Y. Hasegawa, *Solvent Extraction Chemistry*, Chap. 7. Dekker, New York, 1977.
25. S. Przeszlakowski and E. Habrat, *Analyst*, 1982, **107**, 1320.
26. A. Kettrup and M. Grote, *Z. Naturforsch.*, 1976, **31b**, 1689.
27. H. Irving and J. Hapgood, *Anal. Chim. Acta*, 1980, **119**, 207.
28. E. Pelizzetti and C. Verdi, *J. Chem. Soc., Perkin Trans. 2*, 1973, 808.
29. J. Reednick, *Am. Lab.*, **11**, 53.
30. R. J. Decker, *Spectrochim. Acta*, 1980, **35B**, 19.
31. J. I. Itoh, H. Kobayashi and K. Ueno, *Anal. Chim. Acta*, 1979, **105**, 383.
32. W. E. Clifford and H. Irving, *ibid.*, 1964, **31**, 1.
33. H. Irving and A. D. Damodaran, *ibid.*, 1971, **53**, 267.
34. M. Grote, A. Schwalk, U. Hüppe and A. Kettrup, *Z. Anal. Chem.*, 1983, **316**, 247.
35. H. Panzel, *Dissertation*, University of Ulm, 1976.
36. N. Sadeghi, *Ann. Chim. (Paris)*, 1967, **2**, 123.
37. S. B. Savvin, R. K. Chernova and I. V. Lobocheva, *Zh. Analit. Khim.*, 1981, **36**, 1471.
38. O. Tochiyama and H. Freiser, *Anal. Chem.*, 1981, **53**, 874.

THE DETERMINATION OF TRACES OF FORMALDEHYDE

A. D. PICKARD*†

IHD, University of Aston in Birmingham, Birmingham, England

E. R. CLARK

Department of Chemistry, University of Aston in Birmingham, Gosta Green, Birmingham, England

(Received 15 August 1983. Revised 27 March 1984. Accepted 14 May 1984)

Summary—An extensive critical review of the methods utilized to determine trace formaldehyde concentrations is presented. The methods are grouped under the physical techniques employed and are discussed with reference to interfering agents, sensitivity, reagent stability and analysis time. The applicability of the procedures is considered for routine monitoring of occupational and environmental exposure to gaseous formaldehyde.

Formaldehyde has been identified as a combustion product from many sources, including automobile exhausts¹ and cigarette smoke.² It was estimated in a 1972-4 survey in the United States that 1.6 million workers in some 40 industrial categories were exposed to formaldehyde.³ Formaldehyde is an odorous, lachrymatory and physiologically active compound. The present threshold limit value (TLV) is 3 mg/m³ for a 10-min time-weighted average limit (which has now replaced the old "ceiling" limit) for occupational exposure.⁴ The health risks associated with the compound are to be assessed by the Advisory Committee on Toxic Substances with a possible view to establishing a control limit. In the United States the ceiling limit for formaldehyde has been reduced to 1.2 mg/m³ and it has been designated as a suspected carcinogen, class A2.⁵ The toxicity of formaldehyde to man and animals has been the subject of a number of reviews,^{3,6,7} and studies are still in progress. It has been established as a primary irritant and as a mutagen. Animal studies indicate that it is carcinogenic but epidemiological data have not proved this connection in man.

The proposed changes in exposure limits and the need for data for epidemiological studies have led to increased interest in determining exposure patterns. Workers in clinical laboratories, foundries and the building trade are particularly likely to be exposed, and the use of formaldehyde-based resins in foams and other insulating materials now means that a large proportion of the population may come into contact with the compound.

Concern over environmental pollution from and occupational exposure to formaldehyde, has led to the need to develop methods for the determination of formaldehyde in air. Some of these techniques mea-

sure the concentration in air directly, but most require the air to be sampled through an absorbing medium designed to trap formaldehyde selectively prior to analysis. The analytical method used often determines the method of sampling, which can be by solid sorbent, diffusion badge or liquefaction. A discussion of sampling strategies, including the efficiency of collection and the effects of humidity, temperature and interfering agents, could constitute a review in itself. As this review is devoted to the analytical techniques available for determination of formaldehyde only a summary of trapping methods is included here.

Impingers have proved popular and a variety of solutions have been used. The most efficient absorbents are those which give a chemical reaction with formaldehyde. The chemistry of these reactions has been reported⁸ and a summary of the solutions and collection efficiencies is given in Table 1. Solid sorbents have been used as sampling media,⁹ and some have been treated with chemicals to promote a chemical reaction. Chemical treatment, however, limits flow-rates and collection efficiency. A comparison has been made of a reaction in solution and on a solid support.¹⁰ Some reagents and solid supports used are listed in Table 2.

Units

The diversity of units used in the literature results in unnecessary difficulties in comparison of analytical methods. The concentration units used throughout this review refer to the weight of formaldehyde per unit volume.¹¹ Of necessity, however, this has led to assumptions and approximations being made in converting from the units given in some of the original papers. For solvent systems the unit of volume is taken as 1 ml of solvent. For direct analysis of gaseous samples, the unit of volume quoted is taken as 1 m³ of air. Detection limits are quoted in terms of the weight of formaldehyde actually introduced into the instrument.

*Author for correspondence.

†In association with Dutom Meditech, Warwick Street, Birmingham.

Table 1. Solutions used in impingers and their collection efficiencies for formaldehyde (one impinger)

Solution	Collection efficiency, %	Reference
Water	80	12
5mM hydrochloric acid	72	35
5mM hydrochloric acid	85	41
0.05% MBTH aqueous	84	28
5% ammonium acetate	80-95	18
7% ammonium acetate, with a saturated oxalyldihydrazine solution	95-96	30
2,4-DNPH in 2M hydrochloric acid	80-99	10
1.6mM 2,4-DNPH in acetonitrile with a trace of perchloric acid	97.5	66
1% sodium bisulphite	98	19
0.1% chromotropic acid in* conc. sulphuric acid	100	17

*See Ref. 19 regarding the importance of the order of reagent addition.

Table 2. Solid sorbents and reagent coatings for collection of formaldehyde

Reagent	Solid support	Reference	Comments
—	Alumina	9	Sampling period limited to 30 min due to instability of formaldehyde on the sorbent. Immediate desorption required. Desorption efficiency 85%.
—	Molecular sieve 13X	48 79	Quantitative desorption. The sampling period is limited. Water vapour competes for adsorption sites.
2-Benzylaminoethanol	Chromosorb 102	56	Desorption efficiencies vary with batch. Sampling rates are restricted to 50 ml/min.
2,4-DNPH	Glass beads	10	The collection and desorption efficiencies vary widely and are poor under dry conditions.
2,4-DNPH	Amberlite XAD-2	67	Collection efficiency reported comparable to that of a bisulphite impinger
Oxidizing agent	Charcoal	68 69	Instability of the oxidized product on the charcoal has been shown.
J-acid	Silica	—	Results obtained are comparable with collection by a bisulphite impinger and analysis with chromotropic acid.

TITRIMETRIC METHODS

These methods are not specific. The methods using sodium sulphite, ammonium chloride, potassium cyanide, and hydroxylamine hydrochloride are all dependent on the characteristic carbonyl-group reactions of aldehydes and ketones. Oxidation procedures based on alkaline hydrogen peroxide, and iodometric and mercurimetric methods, suffer interference from any other chemicals which can be oxidized under the test conditions.

The procedures are well described⁸ but have the limited sensitivity associated with most titrimetric methods. Although largely superseded, the bisulphite-iodine procedure remains the recommended National Institute for Occupational Safety and Health (NIOSH) procedure for evaluation of primary aqueous standards.¹²

SPECTROPHOTOMETRIC METHODS

A number of spectrophotometric methods have been developed for the determination of formaldehyde, many of them by Sawicki *et al.* Procedures involving spectrophotometric methods are summarized in Table 3.

Xanthylium dyes

In concentrated sulphuric acid, polynuclear xanthylium dyes are formed with chromotropic acid (1,8-dihydroxynaphthalene-3,6-disulphonic acid), J-acid (6-amino-1-naphthol-3-sulphonic acid) and phenyl J-acid (6-anilino-1-naphthol-3-sulphonic acid). The resulting chromogens are illustrated in Fig. 1.

The chromotropic acid method¹³ has been used for the determination of formaldehyde in air,^{14,15} and for environmental¹⁶ and occupational¹⁷ analyses. The use of concentrated sulphuric acid in the analysis is potentially hazardous, but it has the practical advantage that the heat of mixing with aqueous media facilitates the completion of colour formation.

A recently recommended method in the U.K.¹⁸ uses chromotropic acid but with 50% v/v sulphuric acid, thus reducing the potential hazard. We have noted, however, that the more dilute acid does not liberate formaldehyde quantitatively from the bisulphite complex. Aqueous ammonium acetate must be used as the collection medium, but this has a lower collection efficiency than sodium bisulphite solution. A large volume of the acid is required, which reduces the sensitivity of the method, and we have found the

Table 3. Spectrophotometric techniques

Reagent	Reference	λ_{max} , nm	$10^3 l \cdot mole^{-1} \cdot cm^{-1}$	ϵ , $l \cdot mole^{-1} \cdot cm^{-1}$	Beer's law range, $\mu g/ml$	Colour stability	Interferences
Chromotropic acid	21	578	15.7	15.7	0.2-4.0	> 24 hr	Formaldehyde-yielding compounds, acrolein, phenols
J-acid tervalent cation	23	468	21.0	21.0	0.15-3.2	> 24 hr	Formaldehyde-yielding compounds, acrolein
J-acid univalent cation	23	612	34	34	0.088-1.5	10 min	Formaldehyde-yielding compounds
Phenyl J-acid	23	660	51.4	51.4	0.056-1.3	> 24 hr	Formaldehyde-yielding compounds, acrolein
Phenylhydrazine	25	520	8.7	8.7	0.008-1.5	15 min	Aldehydes
HBT	26	582	48.0	48.0	0.062-1.25	20 min	Aliphatic aldehydes
MBTH	27	670	65.0	65.0	0.05-0.92	40 min	Aliphatic aldehydes, aromatic amines, imino heterocyclic compounds
Oxalylhydrazide + Cu(II)	28	628	50.0	50.0	0.03-1.72	12 min	Sulphur dioxide, hydrogen sulphide, carbon disulphide, aliphatic aldehydes
1-Ethylquinaldinium iodide	30	620	7.7	7.7	0.6-3.6	180 min	Aliphatic aldehydes
Acetylacetone	32	608	73	73	0.04-0.82	30 min	Aldehydes
Schiff's	33	412	8.0	8.0	0.37-8.7	> 24 hr	Aldehydes
	34	550	3.5	3.5	—	30 min	Sulphur dioxide

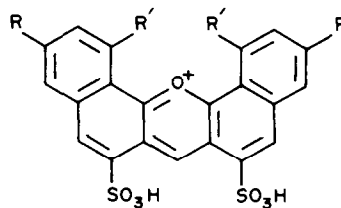
heating step required to complete colour formation rather time-consuming.

Although the older method has been widely used it has only recently been reported that the order of addition of reagents affects the extent of colour development.¹⁹ If a composite chromotropic acid/sulphuric acid reagent is added to an aqueous sample the calibration graph is markedly non-linear. We therefore recommend that the chromotropic acid is added first, followed by sulphuric acid.

Optimization of the chromotropic acid reaction²⁰ and the effect of interfering agents²¹ have been investigated in detail. Saturated aldehydes, ketones, ethanol and methanol do not interfere. Higher molecular weight alcohols, phenols, aromatic hydrocarbons and alkenes cause a negative error when present in excess. Of the unsaturated aldehydes, acrolein gives the greatest positive error, and oxides of nitrogen also interfere positively. We believe that the order of reagent addition affects the degree of interference.

In concentrated sulphuric acid medium, J-acid forms a stable, triply-charged yellow cation with formaldehyde.²² The reagent may be used with aqueous samples in an analogous way to chromotropic acid,²³ with slightly improved sensitivity. For personal sampling we prefer to use J-acid coated onto silica as a solid adsorbent for formaldehyde. For analysis, concentrated sulphuric acid is then added and the samples are left at room temperature. (We find that heating at this stage increases the colour intensity but not in relation to the formaldehyde concentration.) The absorbance is measured after filtering or centrifuging. This simplified collection and analytical procedure gives reproducible results comparable with those obtained by the chromotropic acid-impinger method. Dilution of the yellow sulphuric acid solution with water leads to the formation of an unstable, singly-charged blue cation. If aqueous ammonium acetate solution is used as the diluent the stability is improved sufficiently to allow absorbance measurement,²³ and acrolein does not interfere.

In concentrated sulphuric acid a mixture of singly and triply-charged cations is formed with phenyl J-acid, which on dilution gives only the singly-charged species ($\lambda_{max} = 660$ nm). The sensitivity is 2.5



Reagent: chromotropic acid J-acid phenyl J-acid
 R = SO₃H R = NH₃⁺ R = NHPH
 R' = OH R' = H R' = H

Fig. 1. Structures of the xanthylium dyes.

times that of the chromotropic acid method, but when the reagents are mixed and the colour developed the temperature must be carefully controlled.²³

Formazan dyes

Formazan dyes are formed by the reaction of formaldehyde with aromatic hydrazines and hydrazones in the presence of an oxidizing agent. The reaction is not specific and is essentially an aldehyde group method. Reaction of aldehydes with phenylhydrazine in the presence of potassium hexacyanoferrate(III) gives an unstable red dye²⁴ and this reaction has been applied to the determination of formaldehyde in air.²⁵

2-Hydrazinobenzothiazole (HBT) has been shown to be a suitable reagent for formaldehyde.²⁶ The reaction is thought to give a chromogen with the structure represented in Fig. 2. The procedure is more sensitive than the chromotropic acid method but the oxidation time is critical and the colour is stable for only 20 min after the final dilution step. We have found this restrictive when several samples have to be analysed.

3-Methyl-2-benzothiazole hydrazone hydrochloride (MBTH) undergoes an analogous reaction in the presence of iron(III) chloride-sulphamic acid mixture as oxidant. The resulting chromogen has two absorption maxima, and two procedures have been developed. One involves measurement at 670 nm where the molar absorptivity is high, but acetone must be added to overcome turbidity.²⁷ The second method does not require acetone as there is no problem of turbidity, but measures the lower absorption maximum at 627 nm.²⁸ The reagent is one of the most sensitive spectrophotometric reagents available as a group reagent for aldehydes. It suffers interferences from aromatic amines and imino heterocyclic compounds. In the presence of concentrated sulphuric acid the MBTH complex breaks down, and a technique has been proposed in which the MBTH and chromotropic acid methods are both applied to the same sample to determine total aldehydes and formaldehyde simultaneously.²⁹

Metal complexes

The formation of a hydrazone is suggested as the first step in a procedure using oxalyldihydrazide.³⁰ The hydrazone then forms a blue complex with copper(II) in aqueous solution, $\lambda_{\max} = 620$ nm. The formaldehyde:oxalyldihydrazide:Cu(II) reacting ratio is 2:2:1. The procedure is very simple but the pH must be carefully controlled, with ammonium acetate as buffer. Sulphur compounds, including hydrogen

sulphide, carbon disulphide, and sulphur dioxide, interfere. Other aliphatic aldehydes react but the wavelength of maximum absorption differs from that for the formaldehyde product.

A second spectrophotometric procedure involving formation of a metal complex is the reaction of formaldehyde with tryptophan in the presence of sulphuric acid and iron(III).³¹ A violet chromogen, $\lambda_{\max} = 575$ nm, is formed, which obeys Beer's law up to 3 $\mu\text{g/ml}$. The technique is more applicable to biological assays than air samples, and methanol, acetaldehyde, amino-acids, sugars and related compounds do not interfere. Other metal ions, notably Fe^{2+} , Ni^{2+} and Co^{2+} , may replace Fe^{3+} in the reaction and other 3-substituted indoles also give a colour. The disadvantages are the use of concentrated sulphuric acid and the time-consuming incubation period (heating at 70° for 90 min is optimal).

Trimethine dye

A trimethine dye is formed by 1-ethylquinaldinium iodide with formaldehyde on heating in basic solution.³² The molar absorptivity at 608 nm is high, but the reproducibility is poor and other aliphatic aldehydes interfere.

Hantzsch reaction

The Hantzsch reaction between acetylacetone, ammonia and formaldehyde to form 3,5-diacetyl-1,4-dihydropyridine ($\lambda_{\max} = 412$ nm) forms the basis of a spectrophotometric procedure.³³ The procedure requires pH adjustment with ammonium acetate and gentle warming to complete the reaction. The reaction is selective for aldehydes and although not as sensitive as some others it is useful on account of the mild conditions employed. It may be used in the presence of trioxan and other compounds which degrade to formaldehyde under strongly acidic conditions. The sensitivity may be increased by measuring the fluorescence spectrum.

Schiff's reagent

Finally, one of the earliest and most sensitive analytical reagents is the Schiff reagent. Modifications to this method have been published but the reaction employed is that of fuchsin or pararosaniline which, in the presence of sulphite and formaldehyde, yields a rose chromogen.³⁴ It has been applied to the determination of formaldehyde in urban air.³⁵ A modification of the reaction, involving scrubbing the air sample with sodium tetrachloromercurate(II) solution, has been established as a reference method for sulphur dioxide determination.³⁶ Simply varying the order of reagent addition allows this method to be used to determine formaldehyde.³⁷ A modification has eliminated the need for the toxic mercury complex³⁸ and has been compared with the chromotropic acid method. Despite these modifications the procedure is generally the most lengthy and complex of all those reviewed.

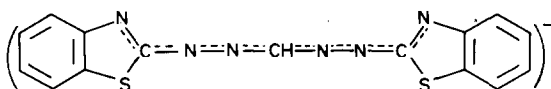


Fig. 2. Structure of the formazan dye formed with 2-hydrazinobenzothiazole ($\lambda_{\max} = 582$ nm).

The final absorbance is dependent on temperature and pH³⁹ and the reagent has poor stability.⁴⁰ The analogous reaction with *p*-aminoazobenzene⁴¹ has higher sensitivity but gives high blank values.

FLUORIMETRIC METHODS

Some of the spectrophotometric reagents can also be used for fluorimetric determination of formaldehyde. These methods are more difficult to use and tend to show poor reproducibility and fluorescence stability. They are, however, more sensitive and are summarized in Table 4.

GAS CHROMATOGRAPHY (GC)

Direct methods

No completely satisfactory GC method has been demonstrated, largely because most detectors, especially the widely used flame ionization detector (FID), have a poor response to formaldehyde. Several procedures have been developed to overcome this difficulty. In general they are methods for aldehydes, the individual components being separated on the column. For details of operational conditions the individual papers should be consulted but a summary is given in Table 5. A second difficulty is that formaldehyde is eluted from GC columns as a distorted peak, owing to interactions and polymerization on the column. Nevertheless GC has been used for analysis for free formaldehyde, and formaldehyde solutions,⁴² vapour,^{43,44} pollution sources⁴⁵⁻⁴⁷ and ambient air⁴⁸ have been analysed. Typically, porous polymers have been used as the stationary phase, with various detectors.

When a thermal conductivity detector (TCD) is used, a detection limit of approximately 1 µg of formaldehyde in the volume injected can be obtained.⁴² Temperatures above 100° and glass columns are recommended to reduce the tailing of peaks. Porous polymer column packings have been found to give satisfactory performance lasting over a year⁴³ and with reproducible retention times.^{43,46}

It is well established that the FID is insensitive to formaldehyde, but one report⁴⁴ quotes a detection limit of 70 mg/m³ in air by use of the FID without prior concentration. However, the methods used for

calibration and standard atmosphere generation were unreliable.

To improve the sensitivity of detection a micro-reductor may be fitted between the column and the FID.^{46,47} The formaldehyde is reduced to methane, to which the FID is more sensitive. The detection limit is then 5 mg/m³ of air, with approximately 3 ng injected into the chromatograph. Carbon dioxide, carbon monoxide and methanol are similarly reduced, but since they are separated from formaldehyde on the column the technique can be applied to exhaust gases.⁴⁷

Mass spectrometric analysis has been coupled with GC for determination of the components of ambient air, including formaldehyde.⁴⁸ Measurement of the peak heights for *m/z* = 29 and 30 enabled formaldehyde to be detected in nanogram quantities. The formaldehyde was first trapped on a solid adsorbent and then desorbed into the chromatograph, by which means a few µg/m³ could be detected. The technique is sensitive and selective but the equipment required militates against its widespread use.

The problems with analysis of formaldehyde vapour have led to most of the proposed GC methods being based on derivatives. Initial attack on the carbonyl group by a nucleophilic nitrogen centre leads to several possible derivatives.

Nitrogen derivatives

The 2,4-dinitrophenylhydrazine (2,4-DNPH) derivative has proved popular because of the selectivity of the reaction for carbonyl compounds and the efficiency of the reaction at room temperature. Early methods gave poor reproducibility, variable response factors and spurious peaks, but modifications have improved the method and made possible the determination of aldehydes in exhaust fumes.⁴⁹ Symmetrical carbonyl compounds give single peaks but other aldehydes form isomers which when eluted give rise to multiple peaks.⁵⁰ Use of an excess of 2,4-DNPH and a packed column was reported to cause deterioration of the column and necessitate frequent recalibration.⁴⁹ Nevertheless the method allowed detection down to the equivalent of 70 ng of formaldehyde injected, and good separation of the components from a combustion source.

Table 4. Fluorimetric techniques

Reagent	Reference	Excitation	Emission	Stability, <i>min</i>	Comments
		wavelength, <i>nm</i>	wavelength, <i>nm</i>		
I-acid	32	470	522	120	The detection limit is 1 ng/ml but the reproducibility is poor and acrolein interferences
Acetylacetone	80	410	510	90	The detection limit is 5 ng/ml; the excitation spectrum varies with concentration
	81				
Cyclohexane-1,3-dione	82	395	460	60	The reproducibility of both procedures is poor
		460	505	3	
Dimedone	82	395	460	30	The fluorescence spectra of the products are stable for a very limited period
		465	520	5	

Table 5. Gas chromatographic techniques

Derivative	Reference	Column conditions			Retention time,		Detector
		Length, m	Stationary phase	Temperature, °C	min	min	
None	42	1.96	Porapak N	120	~3.5	TCD	
None	45	2.0	Porapak Q	83	11.4	TCD	
None	45	2.0	Chromosorb 102	83	7.6	TCD	
None	48	1.96	Porapak T	30-150 at 16°/min	~8.5	MS	
2,4-DNPH	49	1.2	4% OV-17	150-300 at 7.5°/min	~11	FID	
2,4-DNPH	50	2.4	2% SE-30	200-270 at 4°/min	0.52	FID	
2,4-DNPH	50	1.5	12% F-60	225	0.38	ECD	
2,4-DNPH	53	20 (capillary)	SF-96	200-240	—	FID	
<i>O</i> -(2,3,4,5,6-pentafluorobenzyl)hydroxylamine	55	2	3% XE-60	90	~2.5	FID	
2-Benzylaminoethanol	56	25 (capillary)	Carbowax 20M	70-200 at 10°/min	~11	FID	
Dimedone	60	25 (capillary)	SE-30	270	—	FID/MS	
Thioethanol	61	2	3% OV-17	200	7.6	FID	

The method has been modified⁵⁰ to improve the sensitivity of the FID for the analysis of solutions containing 1.5 µg/ml of formaldehyde. The 2,4-DNPH derivatives were extracted from aqueous solution into carbon disulphide, and this solution was then injected; this saves a great deal of time since no purifying and drying of the derivatives is required, and the extraction is satisfactory. The relative merits of the FID and the electron-capture detector (ECD) have been evaluated.⁵¹ The ECD is very sensitive but has a limited response range (20–500 pg) whereas the FID is less sensitive but has a broad linear response range (10–10⁴ ng) to the 2,4-DNPH derivative.

The use of capillary glass columns and temperature programming facilitates the separation of carbonyl compounds as their 2,4-DNPH derivatives.^{52,53} The procedure has been applied to food samples,⁵² exhaust gases⁵³ and cigarette smoke.⁵³ We consider the collection procedure employed in the latter case⁵³ to be restrictive and the purification of derivatives needlessly slow. Extraction from aqueous solution into carbon disulphide is generally adequate, in view of the resolving power of a capillary column.

Pentafluorophenylhydrazine (PFPH) has been used as a reagent for preparing aldehyde derivatives for GC analysis,^{54,55} but separation of the carbonyl derivatives on packed columns was incomplete. The use of a capillary column or temperature programming might overcome this.

Oximes have been investigated as an alternative to the hydrazones. In particular, benzyloxamine has been used to form the *O*-benzyloximes of carbonyl compounds in cigarette smoke for subsequent GC analysis.² Pairs of isomers are formed from unsymmetrical carbonyl compounds, leading to additional peaks. Temperature programming on a capillary column was used to resolve these peaks, but the reproducibility was poor and the method is described as only semi-quantitative.

The pentafluoro compound *O*-(2,3,4,5,6-pentafluorobenzyl)hydroxylamine has also been used and compared with the analogous hydrazine derivative (PFPH),⁵⁵ over which it was found to have some advantages, but the reagent has poor stability in aqueous solution and a long reaction time is required for some carbonyl compounds.

Another proposed reagent containing a nucleophilic nitrogen centre is 2-benzylaminoethanol: with formaldehyde this forms 3-benzylloxazolidine, which is detectable by the FID. The reaction is fast enough for the reagent to have been proposed as a trapping agent on a solid sorbent,⁵⁶ but the desorption is time-consuming and difficult. The reaction is again not specific for formaldehyde, and although the higher aldehydes do not isomerize, the separation of the derivatives of carbonyl compounds is incomplete on packed columns. Analysis by split and splitless injections of solutions of the derivative into a temperature-programmed capillary column gives a linear and reproducible response over the range

6.6–56.5 μg of formaldehyde. This is a very limited range, especially in view of the need to vary the injection technique, and the detection limit is poor for industrial-hygiene analyses requiring short-term sampling. The limited sampling rate restricts the method largely to time-weighted average sampling. Furthermore there is some difficulty in preparing calibration standards, as pure 3-benzoyloxazolidine is not commercially available. However, there are no time-consuming purification and drying stages in the derivative preparation, and the method has been evaluated by NIOSH.⁵⁷

Carbon derivatives

Attack at the carbonyl group by a nucleophilic carbon centre can lead to formation of suitable derivatives. Dimedone (5,5-dimethylcyclohexane-1,3-dione) contains a nucleophilic carbon centre at C-2 and forms crystalline aldehyde derivatives, which can be used for infrared⁵⁸ or GC^{59,60} determination of aldehydes. The FID may be used but higher aldehydes may interfere; MS is therefore used in preference.⁶⁰ The method is restricted to use with capillary columns operated at above 220°C.

Sulphur derivatives

Thiols have been proposed as agents leading to formation of dithioacetal derivatives through reaction at the sulphur atom. Use of thioethanol has been proposed, on account of its odour being less offensive than that of simple thiols, and the trimethylsilyl derivatives of the complexes may be determined by GC.⁶¹ The method is a general one for aldehydes, but separation is possible on short packed columns, and the derivatives are eluted as single peaks. An FID was used⁶¹ but a flame photometric detector might give better sensitivity. No quantitative formaldehyde determination was reported and the derivative preparation is complex and lengthy, involving two reactions of 30-min duration. One of the reactions requires heating, so compounds which are thermally degraded to formaldehyde will interfere.

HIGH-PRESSURE LIQUID CHROMATOGRAPHY (HPLC)

Determination of carbonyl compounds by HPLC has been based exclusively on the 2,4-DNPH derivatives.^{62–67} The earliest technique⁶² used normal-phase liquid chromatography, which is suitable for formaldehyde determination, but some of the higher aldehydes are not fully resolved. The separation is improved by the use of reversed-phase liquid chromatography⁶⁴ and the two approaches have been compared.⁶⁵ Solvent programming also facilitates separation.^{65,66} The use of acetonitrile as solvent has eliminated the time-consuming filtration, extraction and drying steps from the work-up procedure, but involves either heating⁶⁵ for 30 min at 70° or the use of a catalyst.⁶⁶ The formaldehyde can be trapped from air on a solid support coated with 2,4-DNPH,

and this allows phenol to be co-sampled and determined by GC, the aldehydes being determined by HPLC.⁶⁷ The detection limit of the HPLC method is 1.8 ng of formaldehyde, by use of an ultraviolet detector operating at 254 nm or near 360 nm. The method is therefore comparable with gas chromatography in sensitivity, and the limiting factors for detection of atmospheric formaldehyde are the collection and work-up procedures.

ION CHROMATOGRAPHY

The formaldehyde is oxidized to formate on a treated charcoal sampling tube. After desorption with a solvent the formate is passed through ion-exchange columns, and detected as formic acid.⁶⁸ A detection range of 0.3–40 $\mu\text{g}/\text{ml}$ is claimed if a 10-ml desorption volume is used. The technique has a number of drawbacks. Formic acid and formate in the sample obviously interfere, as do acetate, acetaldehyde and acetic acid. The sample desorption requires ultrasonic treatment, and recent studies have shown significant loss of formaldehyde from the solid sorbent. Hence the NIOSH recommendation for this method has been withdrawn.⁶⁹

ELECTROCHEMICAL METHODS

Polarography has been used to determine formaldehyde, although the method has not proved popular. The Girard T derivative is used: its half-wave potential at a dropping mercury electrode is -0.99 V vs. a saturated calomel electrode.⁷⁰ The method lacks sensitivity, having a detection limit of 2 $\mu\text{g}/\text{ml}$, and other aldehydes interfere. The sensitivity can be improved to 1 $\mu\text{g}/\text{ml}$ by use of indirect differential pulse polarography,⁷¹ but the procedure is complicated.

An instrument for direct measurement of formaldehyde in air has been based on an electrochemical fuel cell.⁷² Clean air diffuses to the cathode of the cell, and the sample is passed to the anode, at which formaldehyde is oxidized. The resulting potential change is related to the formaldehyde concentration. The device is portable and simple to operate. It has a detection limit of 0.4 mg/m^3 but suffers severe interference from alcohols and phenols.

MISCELLANEOUS SPECTROSCOPIC METHODS

Chemiluminescence

A chemiluminescent method is based on the vigorous reaction between formaldehyde, alkaline hydrogen peroxide and 3,4,5-trihydroxybenzoic acid.⁷³ The resulting strong orange luminescence may be monitored by a photomultiplier; the detection limit is 3 ng/ml of formaldehyde, which is comparable to the sensitivity of the HPLC method. The luminescence lasts several minutes, and the analysis is rapid, but there are several interferences. Chemical interferences

include carbonyl compounds, particularly acetaldehyde, humic acids and some inorganic ions. The intensity of luminescence is also dependent on temperature and pressure.

The methods discussed below all involve direct analysis of gaseous samples and do not require a trapping medium.

Laser-induced fluorescence

Formaldehyde in clean air has been determined by using a pulsed frequency-doubled tunable dye-laser covering the region 320–345 nm.⁷⁴ The laser beam is passed through a cell containing the gaseous sample at reduced pressure; the detection limit is around 1 µg/ml. Nitrogen dioxide and sulphur dioxide do not interfere. It may be possible to improve on the sensitivity but the test of the method would be its application to ambient and polluted air.

Microwave spectroscopy

The microwave rotational spectral lines of small molecules at low pressures are very sharp and characteristic, and the absorbance is proportional to the concentration. The method has been used for determining formaldehyde by examining the microwave absorption spectra of polluted atmospheres.⁷⁵ The experimental detection limit was estimated to be 0.3 mg/m³ but theoretically this could be improved. Although the analysis time is short the instrument requires a recovery time of 20 min or ultrasonic treatment to eliminate carry-over between samples. The apparatus is expensive, requiring sophisticated electronic equipment to ensure high resolution, stability and sensitivity. It requires high power and use of a vacuum pump and is unsuitable as a field instrument, and the low operating pressure makes accurate gas sampling difficult.

Infrared spectroscopy

An infrared spectrometer tuned to the carbonyl absorption band can be used to detect atmospheric formaldehyde. Thus a portable Miran infrared monitor may be used, and a detection limit of 0.3 mg/m³ is claimed. However, the infrared spectrum of formaldehyde is not particularly characteristic and many compounds interfere.

Infrared spectroscopy has been used to monitor atmospheric pollutants over an extended period of time in California.⁷⁶ To determine concentrations of specific atmospheric pollutants a long path-length and a Fourier transform technique were used.⁷⁷ The method is a highly sensitive and selective technique for measuring most of the pollutants present in the atmosphere. The analysis is fast and the lower detection limit is approximately 1.2 µg/m³, but the equipment is highly specialized.

CONCLUSIONS

Increasing concern over the effects of prolonged

exposure to formaldehyde, coupled with the widespread use of the substance, makes it likely that the trend towards lower threshold limit values will continue. Epidemiological studies will require more information from monitoring surveys on exposure patterns.⁷⁸ Accurate and increasingly sensitive analytical techniques are therefore required, which should be simple and suitable for on-site testing.

Of the techniques reviewed, the chromotropic acid method is widely tested and will therefore remain popular. However, it can be used only for air samples collected by an impinger, and has limited sensitivity, and the use of concentrated sulphuric acid restricts its use in the laboratory; J-acid offers some advantages as an alternative.

High-pressure liquid chromatography is rapidly becoming a standard laboratory technique, and the sensitivity and short analysis time for the determination of formaldehyde suggest it will become more widely used for this purpose. No gas chromatographic method has proved to be without some drawback, though selected methods may be very suitable for particular applications. It is also the technique most likely to be applied on-site, if the difficulties of derivative preparation and solvent handling can be overcome. The methods utilizing direct analysis of gaseous samples require expensive and complex instrumentation which currently prevents their widespread use.

Acknowledgements—The authors wish to thank Dr. J. M. Thompson and Dr. R. Sithampanadarajah (Dutom Meditech), who with Dr. R. S. Barratt, Dr. A. J. Cochran and Mr. M. Piney (University of Aston) have given valuable advice in the compilation of this review.

REFERENCES

1. P. L. Magill and R. W. Benoiel, *Ind. Eng. Chem.*, 1952, **44**, 1347.
2. D. F. Magin, *J. Chromatog.*, 1980, **202**, 255.
3. *Current Intelligence Bulletin*, 34, NIOSH, Cincinnati, 1981.
4. *Guidance Note EH 40/84*, Health and Safety Executive, HMSO, 1984.
5. *Threshold Limit Values for Chemical Substances and Physical Agents in the Workroom Environment*, American Conference of Government Industrial Hygienists, Cincinnati, 1983.
6. R. J. Fielder, *Toxicity Review 2, Formaldehyde*, HMSO, 1981.
7. *The Assessment of Data on the Effect of Formaldehyde on Humans*, Technical Report 1, European Chemical Industries Ecology and Toxicology Centre, Brussels, 1982.
8. J. F. Walker, *Formaldehyde*, 3rd Ed., Reinhold, New York, 1964.
9. NIOSH, *Manual of Analytical Methods*, 2nd Ed., Vol. 1, p. 235. Cincinnati, 1977.
10. D. Grosjean and K. Fung, *Anal. Chem.*, 1982, **54**, 1221.
11. British Standards Institute, *B.S. 6069, Part 1*, 1981.
12. NIOSH, *Manual of Analytical Methods*, 2nd Ed., Vol. 1, p. 125. Cincinnati, 1977.
13. E. Eegriwe, *Z. Anal. Chem.*, 1937, **110**, 22.

14. W. E. MacDonald, *Am. Ind. Hyg. Assoc. Quart.*, 1954, **15**, 217.
15. P. W. West and B. Sen, *Z. Anal. Chem.*, 1956, **153**, 177.
16. N. A. Renzetti and R. J. Bryan, *J. Air Pollut. Control Assoc.*, 1962, **11**, 421.
17. C. W. Lee, Y. S. Fung and K. W. Fung, *Analyst*, 1982, **107**, 30.
18. *Formaldehyde in Air*, MDHS 19, Health and Safety Executive, HMSO, 1983.
19. G. W. Meadows and G. M. Rusch, *Am. Ind. Hyg. Assoc. J.*, 1983, **44**, 71.
20. S. N. Deming, in *Validation of the Measurement Process*, J. R. DeVoc (ed.), p. 162. American Chemical Society, Washington, 1977.
21. A. P. Altshuller, D. L. Miller and S. F. Sleva, *Anal. Chem.*, 1961, **33**, 621.
22. M. Kamel and R. Wizinger, *Helv. Chim. Acta*, 1960, **43**, 594.
23. E. Sawicki, T. R. Hauser and S. McPherson, *Anal. Chem.*, 1962, **34**, 1460.
24. R. W. Kersey, J. R. Maddocks and T. E. Johnson, *Analyst*, 1940, **65**, 203.
25. M. Tanenbaum and C. E. Bricker, *Anal. Chem.*, 1951, **23**, 354.
26. E. Sawicki and T. R. Hauser, *ibid.*, 1960, **32**, 1434.
27. E. Sawicki, T. R. Hauser, T. W. Stanley and W. Elbert, *ibid.*, 1961, **33**, 93.
28. T. R. Hauser and R. L. Cummins, *ibid.*, 1964, **36**, 679.
29. R. R. Miksch and D. W. Anthon, *Am. Ind. Hyg. Assoc. J.*, 1982, **43**, 362.
30. J. Nair and V. K. Gupta, *Talanta*, 1979, **26**, 962.
31. J. Chrasil and J. T. Wilson, *Anal. Biochem.*, 1975, **63**, 202.
32. E. Sawicki, T. W. Stanley and J. Pfaff, *Anal. Chim. Acta*, 1963, **28**, 156.
33. T. Nash, *Biochem. J.*, 1953, **55**, 416.
34. D. E. Kramm and C. L. Kolb, *Anal. Chem.*, 1955, **27**, 1076.
35. A. C. Rayner and C. M. Jephcott, *ibid.*, 1961, **33**, 627.
36. ASTM D2914-78, *Annual Book of ASTM Standards*, Part 26, American Society for Testing and Materials, Philadelphia, 1980.
37. G. R. Lyles, F. B. Dowling and V. J. Blanchard, *J. Air Pollut. Control Assoc.*, 1965, **15**, 106.
38. R. R. Miksch, D. W. Anthon, L. Z. Fanning, C. D. Hollowell, K. Revzan and J. Glanville, *Anal. Chem.*, 1981, **53**, 2118.
39. P. E. Georgiou, L. Harlick, L. Winsor and D. Snow, *ibid.*, 1983, **55**, 567.
40. A. T. J. M. Kuijpers, *ibid.*, 1983, **55**, 391.
41. P. Verma and V. K. Gupta, *Talanta*, 1983, **30**, 443.
42. E. Onsuka, J. Janák, S. Duras and M. Krcmarová, *J. Chromatog.*, 1969, **40**, 209.
43. R. S. Mann and H. W. Hahn, *Anal. Chem.*, 1967, **39**, 1314.
44. T. Dumas, *J. Chromatog.*, 1982, **247**, 289.
45. I. Otvos, G. Palyi, Z. Balthazar and B. Bartha, *ibid.*, 1971, **60**, 422.
46. M. B. Colket, D. W. Naegeli, F. L. Dryer and I. Glassman, *Environ. Sci. Technol.*, 1974, **8**, 43.
47. K. Bergmann and W. Schneider, *Chromatographia*, 1982, **15**, 631.
48. Y. Yokouchi, T. Fujii, Y. Ambe and K. Fuwa, *J. Chromatog.*, 1979, **180**, 133.
49. L. J. Papa and L. P. Turner, *J. Chromatog. Sci.*, 1972, **10**, 744.
50. H. Kallio, R. R. Linko and J. Kaitaranta, *J. Chromatog.*, 1972, **65**, 355.
51. R. R. Linko, H. Kallio and K. Rainio, *ibid.*, 1978, **155**, 191.
52. R. A. Smith and I. Drummond, *Analyst*, 1979, **104**, 875.
53. Y. Hoshika and Y. Takata, *J. Chromatog.*, 1976, **120**, 379.
54. K. Kobayashi, M. Tanaka, S. Kawai and T. Ohno, *ibid.*, 1979, **176**, 118.
55. K. Kobayashi, M. Tanaka and S. Kawai, *ibid.*, 1980, **187**, 413.
56. E. R. Kennedy and R. H. Hill, Jr., *Anal. Chem.*, 1982, **54**, 1739.
57. NIOSH, *Manual of Analytical Methods*, Vol. 7, p. 354. Cincinnati, 1981.
58. J. F. Thomas, E. N. Sanborn, M. Mukai and B. D. Tebbens, *Arch. Ind. Health*, 1959, **20**, 420.
59. A. Wenstrom and G. Samuelsson, *Odontol. Revy*, 1972, **23**, 79.
60. E. Janos, J. Balla, E. Tyihak and R. Gaborjanyi, *J. Chromatog.*, 1980, **191**, 239.
61. S. Honda, N. Tanimitsu and K. Kakehi, *ibid.*, 1980, **194**, 191.
62. L. J. Papa and L. P. Turner, *J. Chromatog. Sci.*, 1972, **10**, 747.
63. S. Selim, *J. Chromatog.*, 1977, **136**, 271.
64. R. Kuntz, W. Lonneman, G. Namie and L. A. Hull, *Anal. Lett.*, 1980, **13**, 1409.
65. G. Creech, R. T. Johnson and J. O. Stoffer, *J. Chromatog. Sci.*, 1982, **20**, 67.
66. F. Lipari and S. J. Swarin, *J. Chromatog.*, 1982, **247**, 297.
67. K. Andersson, C. Hallgren, J. O. Levin and C. A. Nilsson, *Scand. J. Work Environ. Health*, 1981, **7**, 282.
68. W. S. Kim, C. L. Gerachi and R. E. Kupel, *Am. Ind. Hyg. Assoc. J.*, 1980, **41**, 334.
69. D. L. Smith, M. Bolyard and E. R. Kennedy, *ibid.*, 1983, **44**, 97.
70. NIOSH, *Manual of Analytical Methods*, 2nd Ed., Vol. 4, S327, Cincinnati, 1978.
71. S. T. Sulaiman and D. Amin, *Microchem. J.*, 1983, **28**, 168.
72. P. M. Williams, I. R. Whiteside and T. P. Jones, *Intern. Environ. Saf.*, 1981, No. 4, 15.
73. D. Slawinska and J. Slawinski, *Anal. Chem.*, 1975, **47**, 2101.
74. K. H. Becker, U. Schurath and T. Tatarczyk, *Appl. Opt.*, 1975, **14**, 310.
75. H. Uehara and Y. Ijuuin, *Chem. Phys. Lett.*, 1974, **28**, 597.
76. E. C. Tuazon, A. M. Wincer, R. A. Graham and J. N. Pitts, Jr., *U.S. Gov. Repts. Announce Index*, 1981, **81**, 3671.
77. P. L. Hanst, *Opt. Quantum Electron.*, 1976, **8**, 87.
78. D. A. John, unpublished work.
79. T. G. Matthews and T. C. Howell, *Anal. Chem.*, 1982, **54**, 1495.
80. P. Bisgaard, L. Molhave, B. Reitz and P. Wilhardt, *Anal. Lett.*, 1983, **16**, 1457.
81. S. Belman, *Anal. Chim. Acta*, 1963, **29**, 120.
82. E. Sawicki and R. A. Carnes, *Mikrochim. Acta*, 1968, 148.

APPLICATION OF ICAP-AES FOR THE DETERMINATION OF Dy, Eu, Gd, Sm AND Th IN URANIUM AFTER CHEMICAL SEPARATION

T. K. SESHAGIRI, Y. BABU, M. L. JAYANTH KUMAR, A. G. I. DALVI, M. D. SASTRY and B. D. JOSHI

Radiochemistry Division, Bhabha Atomic Research Centre, Trombay, Bombay-400 085, India

(Received 25 March 1983. Revised 16 April 1984. Accepted 10 May 1984)

Summary—A method has been developed for the determination of Dy, Eu, Gd, Sm and Th in uranium (after chemical separation) by use of an inductively-coupled argon plasma in conjunction with a direct-reading spectrometer. The method can be used for the determination of Dy and Eu down to 0.02 $\mu\text{g/ml}$, Gd to 0.05 $\mu\text{g/ml}$, Sm to 0.1 $\mu\text{g/ml}$ and Th to 0.20 $\mu\text{g/ml}$.

The inductively-coupled argon plasma (ICAP) is finding increasing application as an excitation source for simultaneous multielement analysis by atomic-emission spectrometry (AES).¹⁻⁴ This system has high sensitivity, large dynamic range and exceptional stability and relative freedom from matrix effects, but use has not yet been made of it for trace metal determinations in matrices, such as uranium and plutonium, which have rich emission spectra. It is potentially of great use for analysis of such matrices for elements such as the rare earths, which themselves give a large number of emission lines. Brockaert *et al.*⁵ have reported the determination of rare earths in mineralogical samples by use of a low-power ICAP, and Brenner *et al.*⁶ have described a procedure for determination of rare earths in a large variety of geological materials, with a medium-power argon-nitrogen ICP coupled with a 3.4-m Ebert spectrophotograph.

Owing to their large neutron-absorption cross-sections, determination of Gd, Sm, Eu and Dy at sub-ppm levels is important in the quality-control of nuclear materials such as uranium. The well established d.c. arc carrier-distillation technique,^{7,8} though useful in the direct determination of volatile impurities in uranium, cannot be used for estimation of the rare earths at such low concentrations because of their refractory nature. When the ICAP source is used for this analysis, though matrix effects are not expected to be significant, the problem of spectral interference still exists and it is necessary to separate the rare earths from uranium before the determination.

This paper describes the use of an ICAP, coupled with a direct-reading spectrometer, for the determination of Dy, Eu, Gd, Sm and Th after their separation from uranium by solvent extraction^{9,10} from hydrochloric acid medium with 20% tri-*n*-octylamine solution in xylene.

EXPERIMENTAL

Equipment

A Jarrell-Ash Mark III Atomcomp direct-reading spectrometer and associated ICAP source were used. The main features of the equipment are summarized in Table 1. A pneumatic nebulizer with adjustable cross-flow was used for injection of the sample into the plasma.

Procedure

The separation procedure and the preparation of standards and samples were essentially similar to those described earlier⁹ except that 1M hydrochloric acid was used for the final dilution of the samples. For calibration, aqueous standards and also uranium standards that had been subjected to chemical separation were used.

RESULTS AND DISCUSSION

Optimization of plasma operating conditions

The parameters for each element were optimized for a 10- $\mu\text{g/ml}$ solution of the element in 1M hydrochloric acid, the signal-to-noise ratio being studied as a function of (i) the observation height above the work coil, (ii) the lateral position of the plasma observation zone, (iii) the radiofrequency (RF) power and (iv) the coolant-gas flow-rate.

The analytical signal was taken as the count in the analytical channel, corrected for the background count. The background was measured on either side of the analytical line, at a wavelength 0.26 Å away from the peak, by use of a spectrum shifter which can give the line profile over a 2-Å range by means of a quartz refractor plate. The optimum position of the spectrum shifter for background measurement was selected after the profiles of the relevant analytical lines had been obtained. The analytical signals for the 10- $\mu\text{g/ml}$ solution of the element and the reagent blank were taken as representing the signal and the noise respectively.

It was found from univariate studies that the

Table 1. Technical specifications of direct-reading spectrometer

<i>Optics</i>	
Rowland circle	0.75 M
Grating	
Ruling	2400 grooves/mm
Ruled area	30 × 40 mm
Blaze	2700 Å (first order)
Angle of incidence	42°
Length of focal curve	580 mm
Wavelength coverage	1899–5000 Å
	Additional optics for Na 5890 Å, Li 6707 Å and K 7664 Å channels
Reciprocal linear dispersion	5.3 Å/mm in first order
Working resolution	0.36 Å
Optical alignment	Hg profiling and refractor plate movement
<i>Excitation sources</i>	
ICAP (inductively-coupled argon plasma)	
RF generator frequency	27.12 MHz (crystal controlled)
Max. power	2 kW
<i>Detection system</i>	
Analytical channels	
	47, covering 33 elements
	Variable wavelength channel
	1 low-voltage test card
	1 Hg reference-channel for optical alignment
Temperature stability	15–35°C
<i>Data processing system</i>	
Spectrochemical controller	
	PDP-11/23 computer with 64 kbyte MOS memory CPU and dual RLO1 disk drive
Data storage	RLO1 hard disk with 5.2 Mbyte capacity
Input/Output device	High-speed LA-120 DEC writer with 180 characters/sec printing speed
Basic software	RSX-11M system
Analytical software	Jarrell-Ash SAIL III
Additional features	Variable wavelength ($N + 1$)th channel assembly with 0.5-m Ebert scanning monochromator Advanced automatic background correction facility available over a spectral region of 0.032–1 Å on either side of spectral line

variation of coolant flow-rate from 15 to 25 l./min had no significant effect on the analytical signal. Hence the coolant flow-rate was kept constant at 18 l./min in subsequent studies. The signal-to-noise ratio for the element studied was found to be maximum at an observation height of 8 mm above the work coil. The effect of lateral position was measured by taking the centre of the sample flow channel as the reference line. The maximum intensity was obtained

at the centre of the flow channel. The optimum observation height was found to be dependent on the torch dimensions and configuration. For two torches of different dimensions the optimum height was found to be 8 and 12 mm above the coil, but the optimum lateral position was the same in both cases. The optimum RF power was between 1.1 and 1.2 kW.

Because the effects of some of the plasma param-

Table 2. Optimized parameters for determination of rare-earth and thorium impurities in uranium by ICAP source

Coolant gas flow	18 l./min
Carrier argon gas flow	0.5 l./min
Power	1.10 kW
Observation height	8 mm above the work coil
Lateral position	0 (centre of sample flow channel)
Integration time	10 sec

Table 3. Results for synthetic samples

Sample	Element	Wavelength, <i>A</i>	Amount added,* <i>ppm</i>	Amount found,		RSD† %
				<i>μg/ml</i>	<i>ppm</i>	
A	Dy	3531	0.100	0.022	0.088	9.0
	Eu	4205	0.100	0.022	0.088	2.2
B	Dy	3531	0.500	0.123	0.49	1.7
	Eu	4205	0.500	0.125	0.50	2.5
	Gd	3796	0.500	0.154	0.62	13.3
	Sm	4424	0.500	0.129	0.52	11.5
	Dy	3531	1.00	0.49 ₃	0.99	0.9
C	Eu	4205	1.00	0.47 ₃	0.95	0.7
	Gd	3796	1.00	0.50 ₈	1.02	0.8
	Sm	4424	1.00	0.50 ₇	1.01	1.1
	Th	4019	1.00	0.55 ₂	1.10	2.6
	Dy	3531	2.0	0.92 ₆	1.85	0.3
D	Eu	4205	2.0	0.88 ₃	1.77	0.4
	Gd	3796	2.0	0.93 ₆	1.87	1.2
	Sm	4424	2.0	0.95 ₁	1.90	0.6
	Th	4019	2.0	0.92 ₄	1.85	1.3

*Based on a 5-g uranium sample. For samples A and B, the final volume after separation of impurities from uranium was 20 ml of 1M HCl, while for samples C and D, the final volume after separation was 10 ml of 1M HCl.

†Based on 12 replicate measurements.

ters may be interdependent, the observation height, lateral position and RF power were optimized simultaneously by the simplex method.^{11,12} The values obtained were found to be very similar to those from the univariate study, within the ranges of power and gas flow available with the instrument. The optimum operating conditions are listed in Table 2.

Analysis of synthetic samples

Four synthetic samples were prepared by adding known amounts of the rare earths and thorium to pure uranium to give concentrations ranging from 0.1 to 2 ppm. These elements were then separated from 5 g of sample by the solvent extraction technique. The aqueous phase containing the rare earths and thorium was made up to 20 ml in 1M hydrochloric acid medium and analysed. Aqueous standards were used, covering the range 0–10 $\mu\text{g/ml}$ for the element in 1M hydrochloric acid medium. Additionally, standards prepared from uranium and the test element, and subjected to the same chemical separation procedure as the sample, were also used. The results obtained for both types of standards agreed well within experimental error, so it was concluded that aqueous standards could be used for all the analytes investigated. The results of analysis of synthetic samples are shown in Table 3. There is good agreement

between the amounts added and the amounts estimated. The precisions (relative standard deviations) obtained at various concentration levels are also given in Table 3.

Effect of uranium

Because the aqueous phase from the separation will contain traces of residual uranium, it was important to examine the effect of uranium on the determination. This was done by aspirating a 1-mg/ml solution of uranium and measuring the emission signals at the wavelengths used for the analyte determinations. Uranium was found to affect the different analyte channels to varying degrees. The interference was found to be least for Eu and Dy, which appeared to tolerate a 1000- $\mu\text{g/ml}$ uranium level. The interference, however, was significant in the Gd and Sm channels, particularly before the background correction. The correction reduced the interference effects by about an order of magnitude, but the 1000- $\mu\text{g/ml}$ uranium level still gave signals in the Gd and Sm channels that were about 20 and 7 times those corresponding to the respective limits of detection. Therefore, the tolerance limit for uranium, if significant interference effects are to be avoided, is 10 $\mu\text{g/ml}$, and it was found that 25 extractions were necessary to bring the uranium concentration down

Table 4. Detection limits and estimation ranges

Element	Analytical line, <i>A</i>	Detection limit, ($X_L = \bar{X}_{bl} + 3\sigma_{bl}$) <i>μg/ml</i>	Sensitivity, <i>counts/ng</i>	Estimation range, <i>μg/ml</i>
Dy	3531	0.006	0.58	0.02–10
Eu	4205	0.006	2.39	0.02–10
Gd	3796	0.015	1.79	0.05–10
Sm	4424	0.035	0.68	0.10–10
Th	4019	0.063	3.92	0.20–10

to this level. The reasons for the interference are not clear, but spectral interference cannot be ruled out, since the uranium 3796.2 Å and 4423.7 Å lines are very close to the Gd 3796.4 Å and Sm 4424.3 Å lines used for measurement. In the previous work,⁹ the spectrographic buffer used suppressed the effect of uranium, so a much higher level of this element (0.5 mg/ml) could be tolerated and only five extractions were needed (a smaller sample was used).

Detection limits

The detection limits, calculated¹³ as the concentration corresponding to a signal equal to the blank signal plus three times its standard deviation, are given in Table 4. The practical limit for quantitative determination was taken to be the concentration corresponding to about three times the detection limit.² On this basis the lower limit of estimation is 0.02 µg/ml for Dy and Eu, 0.05 µg/ml for Gd, 0.1 µg/ml for Sm and 0.2 µg/ml for Th. The sensitivities are also given in Table 4.

CONCLUSION

The method described permits the determination by Dy and Eu at 0.02 µg/ml, Gd at 0.05 µg/ml, Sm at 0.1 µg/ml and Th at 0.2 µg/ml concentration levels. With 5 g of sample and a final volume of the sample, after extraction, of 10 ml, the corresponding concentrations in the sample are 0.04, 0.1, 0.2 and 0.4 ppm

respectively. The use of the ICAP source and direct-reading spectrometer provides faster analysis with better precision.

Acknowledgements—The authors are grateful to Dr. M. V. Ramaniah, Director, Radiological Group, and Dr. P. R. Natarajan, Head, Radiochemistry Division, for their keen interest and encouragement during the course of this work.

REFERENCES

1. V. A. Fassel and R. N. Kniseley, *Anal. Chem.*, 1974, **46**, 1110A, 1115A.
2. P. W. J. M. Boumans, *Z. Anal. Chem.*, 1979, **299**, 337.
3. R. M. Barnes, *CRC Crit. Rev. Anal. Chem.*, 1978, **7**, 203.
4. S. Greenfield, H. McD. McGeachin and P. B. Smith, *Talanta*, 1976, **23**, 1.
5. J. A. E. Brockaert, F. Leis and K. Laqua, *Spectrochim. Acta*, 1979, **34B**, 73.
6. I. B. Brenner, A. E. Watson, T. W. Steel, E. A. Jones and M. Goncalves, *ibid.*, 1981, **36B**, 785.
7. A. G. Page, S. V. Godbole, S. B. Deshkar and B. D. Joshi, *Bhabha At. Res. Centre*, 1976, 862.
8. A. G. I. Dalvi, C. S. Deodhar, T. K. Sheshagiri, M. S. Khalap and B. D. Joshi, *Talanta*, 1978, **25**, 665.
9. A. G. I. Dalvi, C. S. Deodhar and B. D. Joshi, *ibid.*, 1977, **24**, 143.
10. A. G. I. Dalvi, T. K. Sheshagiri, V. Natarajan, Y. Babu, M. K. Bhide, M. D. Sastry and B. D. Joshi, *Z. Anal. Chem.*, 1983, **315**, 353.
11. S. P. Terblanche, K. Visser and P. B. Zeeman, *Spectrochim. Acta*, 1981, **36B**, 293.
12. S. N. Deming and S. L. Morgan, *Anal. Chem.*, 1973, **45**, 278A.
13. IUPAC, *Appl. Spectrosc.*, 1977, **31**, 348.

USE OF ACTIVE NITROGEN IN ANALYTICAL CHEMILUMINESCENCE SPECTROMETRY

HEATHER JURGENSEN* and J. D. WINEFORDNER†

Department of Chemistry, University of Florida, Gainesville, FL 32611, U.S.A.

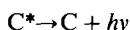
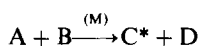
(Received 28 September 1983. Revised 26 April 1984. Accepted 7 May 1984)

Summary—Methods of obtaining active nitrogen plasmas at both reduced and atmospheric pressures are described. The mechanism of energy transfer from the excited states of nitrogen to metal atoms and to organic molecules and the subsequent emission of characteristic radiation is outlined. The application of these processes to the detection and determination of traces of metals and organic compounds is discussed and recent work on gas chromatographic detectors, based on these systems, is reviewed.

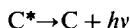
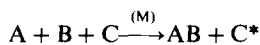
Chemiluminescence arises when a chemical reaction produces an electronically excited state which emits radiation upon return to the ground state. Previous reviews¹⁻⁹ on chemiluminescence give extensive discussions of analytical uses of chemiluminescence in the liquid phase, the gas phase and flames. The purpose of this review is to discuss the use of active nitrogen for analytical chemiluminescence spectrometry.

In order for chemiluminescence to occur, three conditions must be fulfilled: (i) sufficient energy must be produced in the reaction to populate an excited state; (ii) the reaction mechanism must favour the production of the excited state; (iii) the excited state formed must be able to emit a photon or transfer its energy to another species that can emit a photon. Chemi-excitation is unusual since most chemical reactions involve ground-state species.¹⁰ Any excess of energy is released as vibrational excitation of ground-state products and is detected as heat.

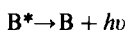
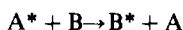
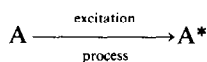
Direct chemiluminescence is defined as follows.¹¹



where M represents a third body and * indicates an excited state. Indirect chemiluminescence consists of:¹¹



as well as metastable-energy transfer:¹²



The production of chemiluminescence by active nitrogen (N_2^*) is an example of metastable-energy transfer.

Most studies of the analytical applications of active nitrogen have involved the detection of metals. Recent work on induction of chemiluminescence of metals by active nitrogen is discussed below and listed in Table 1. Lewis³⁴⁻³⁶ was the first to observe spectral lines corresponding to metallic electrode materials in an active-nitrogen afterglow. He also observed mercury lines due to the diffusion of mercury vapour from the pumping system into a nitrogen afterglow. Kenty^{14,21,22} conducted a series of experiments in which he examined the metal atomic emissions in an atmosphere of argon and nitrogen (at 300 and 10 mmHg pressure, respectively). He passed a condensed discharge through a gap between electrodes made from the metal of interest and detected the metal arc spectra. Later, Brennen and Kistiakowsky²³ studied the active nitrogen-induced chemiluminescence of metal carbonyls. Active nitrogen was produced by a microwave discharge at low pressure (1-5 mmHg) in a steady-flow apparatus. They discovered that $Ni(CO)_4$, $Fe(CO)_5$, $Cr(CO)_6$, $W(CO)_6$, $Mo_2(CO)_{10}$ and $Co(NO)(CO)_3$ reacted very rapidly to form metal atoms and produced intense flames due to neutral metal atomic emission spectra. The reaction mechanism was concluded to be a stepwise degradation: $Me(CO)_n + N \rightarrow Me(CO)_{n-1} + NCO$. The metal atoms were probably excited by collision with $N_2(A^3\Sigma_u^+)$ molecules.

The analytical potential of chemiluminescence induced by active nitrogen was clearly indicated in the study by Meyer *et al.*,²⁶ who observed the mercury emission line at 253.7 nm at concentrations of 10^9 atoms/cm³. They produced the active nitrogen with a microwave discharge and observed the Lewis-Rayleigh afterglow with a photomultiplier tube.

Capelle and Sutton³⁷ introduced bismuth vapour (produced in a resistively heated crucible) into a Lewis-Rayleigh afterglow. Argon was used to sweep the bismuth vapour into a viewing region in a quartz

*Present address: E. I. duPont de Nemours & Co., Atomic Energy Plant, Bldg. 723-A, Savannah River Plant, Aiken, SC 29808.

†Author to whom all correspondence should be sent.

Table 1. Detection of metals by use of active nitrogen

Metal	Date	Emission, nm	Other information*	Reference
Ag	1954	"Brush" flame	Produced by passing a condensed spark across Ag gaps in (300 mmHg Ar + 10 mmHg N ₂)	13
Ag	1982	328.1	Microwave-induced N ₂ [*] at low pressure; LOD 2 pg, LDR 10 ⁴ -10 ⁵	14
Al	1954	"Brush" flame	Produced by passing a condensed spark across Al gaps in (300 mmHg Ar + 10 mmHg N ₂)	13
Al	1969	396.2	Microwave-induced N ₂ [*] at low pressure	15
Au	1954	"Brush" flame	Produced by passing a condensed spark across Au gaps in (300 mmHg Ar + 10 mmHg N ₂)	13
As	1980	193.7	N ₂ [*] excited in an electrodeless ozonizer discharge at 1 atm; LOD 0.2 ng, LDR 10 ³	17
Ba	1969	Resonance lines Ba ⁺ at 493.4 and 455.4	Ba vapour added to N ₂ [*] afterglow produced by a weak discharge through Xe containing trace N ₂	18,19
Be	1954	Arc lines emitted in a "brush" flame	Produced by passing a condensed spark across Be gaps in (300 mmHg Ar + 10 mmHg N ₂)	13
Bi	1977	306.8	Microwave-induced N ₂ [*] at low pressure; 1.5 × 10 ⁴ atoms/cm ³ detected	20
Bi	1980	306.8	N ₂ [*] excited in an electrodeless ozonizer discharge at 1 atm; LOD < 0.1 ng, LDR 10 ²	17
Bi	1982	306.8	Microwave-induced N ₂ [*] at low pressure; LOD 300 pg, LDR 10 ⁴ -10 ⁵	14
Ca	1955	"Fountain" flame	Produced by low-current discharge through inert gas with trace N ₂	21,22
Ca	1969	393.4, 422.7	Impurity in N ₂	18
Cd	1955	"Fountain" flame	Produced by low-current discharge through inert gases containing trace N ₂	21,22
Cd	1973	321.6	Microwave-induced N ₂ [*] ; pressure-dependent with E _{max} at 10 mmHg	24
Cd	1982	326.1	Microwave-induced N ₂ [*] at low pressure; LOD 30 pg, LDR 10 ⁴ -10 ⁵	14
Co	1954	Co arc lines emitted from "brush" flame	Produced by passing a condensed spark across Co gaps in (300 mmHg Ar + 10 mmHg N ₂)	13
Co	1966	345.4	Microwave degradation and excitation of Co(NO)(CO) ₃	23
Cr	1954	Cr arc lines emitted from "brush" flame	Produced by passing a condensed spark across Cr gaps in (300 mmHg Ar + 10 mmHg N ₂)	13
Cs	1977	455.5	Cs impurity in a laser	20
Cu	1954	Cu lines emitted from "brush" flame	Produced by passing a condensed spark across Cu gaps in (300 mmHg Ar + 10 mmHg N ₂)	13
Cu	1982	324.7	Microwave-induced N ₂ [*] at low pressure; LOD 20 pg, LDR 10 ⁴ -10 ⁵	14
Cu	1963	324.8	Microwave degradation and excitation of Cu halides	25
Fe	1954	Fe arc lines emitted from violet "brush"	Produced by passing a condensed spark across Fe gaps in (300 mmHg Ar + 10 mmHg N ₂)	13
Fe	1966	372.0	Microwave degradation and excitation of Fe(CO) ₅	23
Ga	1955	"Fountain" flame	Produced by low-current discharge through inert gases containing trace N ₂	21,22
Ge	1980	265.1	N ₂ [*] generated in electrodeless ozonizer discharge at 1 atm; LOD 20 ng, LDR 10 ²	17
Hg	1967	253.7	Microwave-induced N ₂ [*] E _{max} at 10 mmHg; relative line intensity pressure-dependent	24
Hg	1972	253.7	Microwave-induced N ₂ [*] ; < 10 ⁹ atoms/cm ³ detected	26
Hg	1981	253.7	N ₂ [*] generated by dielectric discharge at low pressure; LOD 10 ⁷ atoms cm ³	27
Hg	1980	253.7	N ₂ [*] generated in electrodeless ozonizer discharge at 1 atm; LOD < 0.02 ng, LDR 10 ³	16,17
In	1955	"Fountain" flame	Produced by a low-current discharge through inert gases containing trace N ₂	21,22
Ir	1954	"Brush" flame	Produced by passing a condensed spark across Ir gaps in (300 mmHg Ar + 10 mmHg N ₂)	13
K	1973	404.4	Microwave-induced N ₂ [*] at low pressure; E _{max} at 0.7 mmHg	24
Li	1955	"Fountain" flame	Excited by a long-lived excited nitrogen species	21,22
Li	1960			
Li	1973	670.8	Microwave induced N ₂ [*] at low pressure; E _{max} at 0.7 mmHg	24
Mg	1937	Lines in 284.7-518.4 region	Mg wire cathode	28

Table 1.—Continued

Metal	Date	Emission, nm	Other information*	Reference
Mg	1955	"Fountain" flame	N ₂ * produced by low-current discharge through inert gases containing trace N ₂	21
Mg	1982	383.8	Microwave-induced N ₂ * at low pressure; LOD 80 pg, LDR 10 ⁴ –10 ⁵	23
Mn	1966	257.6	Microwave degradation and excitation of Mn ₂ (CO) ₁₀	23
Mo	1954	550.65 "blue" flame	Produced by passing a condensed spark across Mo electrodes in Ar containing trace N ₂	14,21
Na	1958	D-line emission	Detected in daytime in upper atmosphere at 90–110 km levels when Na was ejected from a rocket	28
Na	1973	589.0, 589.6, 330.2	Microwave-induced N ₂ *, E _{max} at 0.7 mmHg	24
Nb	1954	Yellow "brush" flame emitted	Produced by passing a condensed spark across Nb electrodes in Ar containing trace N ₂	13,21
	1955	Nb lines		
Ni	1954	Ni arc lines emitted from "brush" flame	Produced by passing a condensed spark across Ni gaps in (300 mmHg Ar + 10 mmHg N ₂)	13
Ni	1966	341.5	Microwave degradation and excitation of Ni(CO) ₄	23
Pb	1963	368.3, 405.8	Microwave degradation and excitation of Pb halides	29
Pb	1980	368.3	Microwave-induced N ₂ * at low pressure; LOD 0.2 ng	30
Pb	1980	283.3	N ₂ * generated in electrodeless ozonizer discharge at 1 atm; LOD 5 ng, LDR 10 ³	17
Pb	1982	368.3	Microwave-induced N ₂ * at low pressure; LOD 40 pg, LDR 10 ⁴ –10 ⁵	14
Pd	1954	Green "brush" flame	Produced by passing a condensed spark across Pd gaps in (300 mmHg Ar + 10 mmHg N ₂)	14,21
	1955			
Pt	1954	"Brush" flame	Produced by passing a condensed spark across Pt gaps in (300 mmHg Ar + 10 mmHg N ₂)	13
Re	1954	"Brush" flame	Produced by passing a condensed spark across Re gaps in (300 mmHg Ar + 10 mmHg N ₂)	13
Rh	1954	"Brush" flame	Produced by passing a condensed spark across Rh gaps in (300 mmHg Ar + 10 mmHg N ₂)	13
Sb	1952	206.8	Excitation by active nitrogen formed in thermal decomposition of silver azide	31
Sb	1980	206.8	N ₂ * generated in electrodeless ozonizer discharge at 1 atm; LOD 1 ng, LDR 10 ³	31
Se	1980	196.0	N ₂ * generated in electrodeless ozonizer discharge at 1 atm; LOD 5 ng, LDR 10 ³	17
Sn	1980	326.2	N ₂ * generated in electrodeless ozonizer discharge at 1 atm; LOD 20 ng, LDR 10 ²	17
Sr	1955	"Fountain" flame	Produced by low-current discharge through inert gases containing trace N ₂	21,22
	1960			
Ta	1954	Blue flame emission at 521.3	Produced by passing a condensed discharge spark across Ta gaps in (300 mmHg Ar + 10 mmHg N ₂)	23,32
Tc	1980	214.3	N ₂ * generated in electrodeless ozonizer discharge at 1 atm; LOD 50 ng, LDR 10 ²	17
Th	1954	535.1	Produced by passing a condensed spark across Th gaps in (300 mmHg Ar + 10 mmHg N ₂)	13
Ti	1954	Ti arc lines from "brush" flame	Produced by passing a condensed spark across Ti gaps in (300 mmHg Ar + 10 mmHg N ₂)	13
Tl	1963	258.0–535.0	Correlated N ₂ excited states with Tl transitions	25
Tl	1963	535.0	The efficiency of excitation of Tl atoms by active nitrogen was very low	33
Tl	1982	351.9	Microwave-induced N ₂ * at low pressure; LOD 5 pg, LDR 10 ⁴ –10 ⁵	14
U	1954	"Brush" flame	Produced by passing a condensed spark across U gaps in (300 mmHg Ar + 10 mmHg N ₂)	13
V	1954	Brilliant red "brush" flame	Produced by passing a condensed spark between V electrodes in Ar containing trace N ₂	13,22
	1955			
W	1954	Blue "brush" flame	Produced by passing a condensed spark across W gaps in (300 mmHg Ar + 10 mmHg N ₂)	13
W	1966	430.2	Microwave degradation and excitation of W(CO) ₆	23
Zr	1954	Zr arc lines produced from "brush" flame	Produced by passing a condensed spark across Zr gaps in (300 mmHg Ar + 10 mmHg N ₂)	13
Zn	1955	Zn line emission in "fountain" flame	Produced by low-current discharge through inert gases containing trace N ₂	21,22
	1960			
Zn	1973	308, 481, 472, 468	Microwave-induced N ₂ * at low pressure; E _{max} at 10 mmHg	24
Zn	1981	468	N ₂ * generated by dielectric discharge at low pressure; LOD 10 ⁸ atoms/cm ³ , LDR 10 ⁷	27

*LOD = limit of detection; LDR = linear dynamic range, E_{max} = excitation maximum, i.e., maximal emission.

tube. The active nitrogen was generated by a microwave discharge. Bismuth concentrations as low as 1.5×10^4 atoms/cm³ were measured.

In 1978, Capelle and Sutton³⁸ named this technique metastable transfer emission spectroscopy (MTES) and presented further uses for this low-pressure system for microwave discharge generation of active nitrogen. They introduced gas phase samples through a stainless-steel capillary into a flow tube where the sample was mixed with an active nitrogen-argon mixture at 1–5 mmHg. Germane (GeH₄) concentrations as low as 7×10^7 molecules/cm³ (corresponding to parts-in-10¹² levels in the gas) were detected.

The application of MTES for the determination of lead in water was demonstrated by Melzer *et al.*³⁰ The apparatus was an improvement on the one employed for the detection of bismuth³⁷ and the crucible was replaced by a small tantalum boat. A limit of detection of 0.2 ng of Pb was achieved.

The first analytical study of inorganic species with a nitrogen afterglow produced at atmospheric pressure was published by D'Silva *et al.*^{16,17} The active nitrogen was generated in an electrodeless discharge ozonizer operated at 20 kV and 1800 Hz. The hydrides of As, Bi, Ge, Pb, Sb, Se, Sn and Te were produced and mixed with the afterglow in the observation regions. Limits of detection for these elements (Table 1) were compared with those obtained by other spectrometric techniques employing hydride generation. The results were of the same order of magnitude as those obtained by atomic-absorption spectroscopy.

Another approach to the measurement of metals at low pressure was introduced by Dodge and Allen.^{27,40} This technique was called metastable energy transfer for atomic luminescence (METAL) and differed from that of Sutton and co-workers^{20,30,38} in respect of the method of active-nitrogen generation and the nitrogen emission system. The apparatus of Sutton and co-workers^{20,30,38} utilized a microwave discharge for the production of active nitrogen and the emission was the straw yellow Lewis-Rayleigh afterglow.²⁰ A microwave produces nitrogen plasmas with high concentrations of nitrogen atoms and a concentration³⁹ of N₂(A³Σ_u⁺) of the order of 5×10^9 molecules/cm³. The concentrations of N₂(A³Σ_u⁺) and vibrationally-excited ground-state N₂(X'³Σ_g⁺) are crucial, since they are the principal energy carriers.^{14,17} Many different mechanisms for metal excitation in active nitrogen have been suggested,^{14,27,52} but it is generally accepted that the N₂(A³Σ_u⁺) state is responsible for excitation of energy levels requiring >4.5 eV while the N₂(X'³Σ_g⁺) state is responsible for excitation of lower levels. Dodge and Allen^{27,40} generated active nitrogen by means of a dielectric discharge and the nitrogen emission they observed was the second positive system of nitrogen. The concentration of N₂(A³Σ_u⁺) was reported to be in the order of 10¹⁷ molecules/cm³. Detection limits of 10⁸ and 10⁷ atoms/cm³ were obtained for mercury and zinc, respectively. The

linear dynamic range for zinc was reported to be 7 orders of magnitude.

More recently, Na and Niemczyk¹⁴ measured a series of metals by MTES. Aqueous solutions of trace metals were dried and atomized in a tantalum boat. The metal vapour was mixed in a flow cell with active nitrogen generated by microwave discharge. Limits of detection for Ag, Bi, Cd, Cu, Mg, Pb and Tl ranged from 2 to 300 pg. The measurements were performed at 1–2.4 mmHg. The effect of various interferences in electrothermal-atomization metastable-emission spectrometry has also been examined.⁴¹ The anion effect on the analyte signal is an important parameter since in furnace atomic-absorption spectroscopy (FAAS), the magnitude of the analyte signal intensity depends strongly on sample composition.⁴¹ For example, cadmium and lead nitrates gave higher sensitivities than their chloride counterparts,^{42,43} and copper nitrate was found to give a sensitivity the same as or lower than that of copper chloride. Na and Niemczyk have shown that the anion effects of sulphate, nitrate and chloride on the signal intensities of Cu, Cd and Pb (detected by MTES) are minimal.⁴¹ Na and Niemczyk have also investigated the matrix effects of NH₄Cl, NH₄NO₃, NaCl, NaNO₃, MgCl₂ and Mg(NO₃)₂ on the analyte signals of Cd, Cu and Pb chlorides and nitrates. In general, there were no matrix effects detected except for negative interferences at high concentrations of matrix materials.

Active nitrogen-induced chemiluminescence of molecules, especially hydrocarbons, is a relatively new research topic. Recent work in this area is discussed below and Table 2 tabulates the results.

Two research groups, Sutton and co-workers^{46,49} and D'Silva and co-workers^{17,47,48} have examined the application of an active nitrogen-induced chemiluminescence gas-chromatographic detector. The system of Sutton *et al.*⁴⁶ involved a microwave-induced nitrogen plasma operated at 8–30 mmHg. A 0.05 mm bore stainless-steel capillary tube was used to couple the gas chromatograph (operated at 1 atmosphere) to the active-nitrogen detector. When small hydrocarbon molecules (7 carbon atoms or less) were mixed with active nitrogen, CN was produced and emission from the CN(B²Σ⁺ → X²Σ⁺) transition was detected. By monitoring the CN chemiluminescence at one wavelength, as the eluent from the gas chromatograph became mixed with the active nitrogen, a chromatogram could be obtained. To reduce the limits of detection, a 1% mixture of HCl in nitrogen was added to the nitrogen afterglow. The addition of HCl is known to catalyse the reaction of Group II hydrocarbons (simple saturated compounds) in active nitrogen and hence increase the production of CN; this is due to the catalytic effect of HCl on the residual polymerized CN present.⁵¹ Limits of detection of 10 pg for vinyl fluoride and 4 ng for CH₄ were obtained.⁴⁶ To make the detector specific for oxygen-containing compounds (as well as air leaks), either the NO(A²Σ⁺ → X²Π) bands or the

Table 2. Detection of molecular species with active nitrogen

Compound	Date	Emission, <i>nm</i>	Other information*	Reference
Al(CH ₃) ₃	1979	Al line	MTES system; no AFOM	45
AsH ₃	1978	As line	MTES system; no AFOM	45
Bi(CH ₃) ₃	1978	Bi line	MTES system; detected 10 ⁷ –10 ¹⁰ molecules/cm ³ , LDR 10 ⁵ –10 ⁶	45
Bi(CH ₃) ₃	1979	Bi line	MTES system; detected 10 ⁴ molecules/cm ³ , LDR 10 ⁶	38
CH ₄	1979	CN emission	MTES system; LOD 4 ng, LDR 10 ³ ; HCl added	46
CH ₃ OH	1980	OH and NO emission	MTES system; LOD < 0.1 μg	49
CH ₂ CHF	1979	CN emission	MTES system; LOD 100 pg, LDR 10 ⁴	46
GeH ₄	1978	Ge line	MTES system; LOD 10 ⁷ molecules/cm ³ , LDR 10 ⁵ –10 ⁶	45
GeH ₄	1978	Ge line	MTES system; LOD 7 × 10 ⁷ molecules/cm ³ , LDR 10 ⁵	38
Ge(C ₂ H ₅) ₄	1978	Ge line	MTES system; no AFOM	45
Hexadecane	1982	383.3 (CN)	APAN system; LOD 0.8 ng, LDR 10 ²	47
Hg(CH ₃) ₂	1981	Hg line	APAN system; LOD 2 pg, LDR 10 ⁵	47
Hg(CH ₃) ₂	1982	Hg line	APAN system; LOD 2 pg, LDR 10 ⁵	48
Hg(C ₂ H ₅) ₂	1982	Hg line	APAN system; LOD 5 pg, LDR 10 ⁵	48
Hg(C ₃ H ₇) ₂	1982	Hg line	APAN system; LOD 10 pg, LDR 10 ⁵	48
Hg(C ₄ H ₉) ₂	1982	Hg line	APAN system; LOD 20 pg	48
Hg(C ₆ H ₁₃) ₂	1982	Hg line	APAN system; LOD 30 pg	48
Hg(C ₈ H ₁₇) ₂	1982	Hg line	APAN system; LOD 50 pg	48
Hg(CH ₃)Cl	1982	Hg line	APAN system; LOD 50 pg	48
Naphthalene	1982	383.3	APAN system; LOD 2 ng	45
Pb(C ₄ H ₉) ₄	1981	Pb line	MTES system; LOD 100 pg, LDR 10 ³	47
PH ₃	1978	P line	MTES system; no AFOM	45
SiH ₄	1978	Si line	MTES system; no AFOM	45
Sn(C ₅ H ₁₁) ₄	1981	Sn line	APAN system; LOD 2 ng, LDR 10 ³	47
Anthracene	1983	445.5	Dielectric discharge; LOD 10 pg, LDR > 10 ³	52,53
Benzene	1983	274.2	Dielectric discharge; LOD 1 μg, LDR > 10 ²	52,53
3,4 Benzopyrene	1983	402.4	Dielectric discharge; LOD 50 pg, LDR > 10 ³	52,53
1,2 Benzopyrene	1983	386.8	Dielectric discharge; LOD 20 pg, LDR > 10 ³	52,53
1,12 Benzo- perylene	1983	471.5	Dielectric discharge; LOD 40 pg, LDR > 10 ³	52,53
Chrysene	1983	401.5	Dielectric discharge; LOD 30 pg, LDR > 10 ³	52,53
Corocne	1983	453.1	Dielectric discharge; LOD 100 pg, LDR > 10 ³	52,53
1,2:5,6	1983	391.7	Dielectric discharge; LOD 30 pg, LDR > 10 ³	52,53
Dibenzanthracene	1983	391.7	Dielectric discharge; LOD 30 pg, LDR > 10 ³	52,53
20-Methyl- cholanthrene	1983	414.7	Dielectric discharge; LOD 40 pg, LDR > 10 ³	52,53
Naphthacene	1983	504.4	Dielectric discharge; LOD 20 pg, LDR > 10 ³	52,53
Naphthalene	1983	330.0	Dielectric discharge; LOD 2 μg, LDR > 10 ²	52,53
Perylene	1983	436.4	Dielectric discharge; LOD 40 pg, LDR > 10 ³	52,53
Pyrene	1983	373.1	Dielectric discharge; LOD 40 pg, LDR > 10 ³	52,53
Toluene	1983	381.0	Dielectric discharge; LOD 1 μg, LDR > 10 ²	52,53

*MTES = metastable-transfer emission spectroscopy. The active nitrogen is microwave-induced at low pressure.
APAN = atmospheric-pressure active nitrogen. The active nitrogen is microwave-induced at 1 atm. AFOM = analytical figures of merit.

OH(A²Σ⁺ → X²Π) transition could be monitored. Selectivity was demonstrated⁴⁹ but no limits of detection other than those for methanol were obtained. Mach *et al.*⁵¹ have used high-resolution capillary gas-chromatography with MTES detection to separate and detect the carbon-, oxygen- and phosphorus-containing compounds in 0.5 μl of jet engine A fuel.

Rice *et al.*⁴⁸ have applied an atmospheric-pressure active-nitrogen afterglow (APAN) as a detector for gas chromatography. A glass-capillary transfer line was used to couple the gas chromatographic column to the APAN system previously described.¹⁷ Selective trace level detection of organo-mercury, -lead, and -tin compounds was achieved by monitoring the metal line emissions. Hexadecane and naphthalene were detected by observing the CN emission at

388.3 nm. Methods for determining methylmercury compounds in fish, water, urine and sediments, and dialkylmercury compounds in water with the GC-APAN system have been reported⁴⁷.

Jurgensen *et al.*^{52,53} have used the dielectric discharge^{27,40} to excite organic molecules. The excitation is sufficiently gentle to produce no apparent fragmentation. The resulting fluorescence spectra are similar to those obtained in both the liquid and gaseous state. They found that the electronic (iron 2-line method) temperature of the direct discharge was 3280 ± 132 K and that of the afterglow discharge was 3090 ± 70 K. The concentration of the metastable N₂ species (N₂A³Σ_u⁺) in the afterglow was found to be 10¹⁶ molecules/cm³ (2% of the N₂ molecules are in the A³Σ_u⁺ state). On the basis of these and

other diagnostic measurements, Jurgensen^{52,53} found that the afterglow background (and the direct discharge background) was due primarily to the transition $C^3\Pi_u \rightarrow B^3\Pi_g$ and the species responsible for excitation of the organic molecules was $A^3\Sigma_u^+$ (~ 6.3 eV energy). Detection limits were obtained in the subnanogram range for polycyclic aromatic hydrocarbons (Table 2) by using a large-aperture monochromator and either an RI66 or a 1P28A photomultiplier tube. All species (except benzene and naphthalene) were introduced into the afterglow by injecting $0.5 \mu\text{l}$ of 1–100 ppm solutions in hexane into a heated injection port. Benzene, toluene and naphthalene vapours were introduced continuously into the afterglow through an external heated chamber by a flow of nitrogen. Jurgensen *et al.*^{52,53} also interfaced a gas chromatograph to the dielectric discharge and used a silicon intensified target-vidicon (SIT) for spectral detection. The limits of detection were degraded by a factor of 10–100, and owing to the need to reduce the nitrogen carrier-flow, the separation characteristics were seriously impaired. This system needs further work to be of analytical use.

In conclusion, the dielectric discharge used by Dodge and Allen^{27,40} and the atmospheric-pressure active-nitrogen afterglow used by D'Silva *et al.*^{17,47,48} seem to be the most versatile low- and high-pressure means of producing active nitrogen. Both discharges are robust in terms of solvent and matrix introduction, simple to construct and operate and intense for both atomic and molecular species. In addition, the dielectric discharge has future application to identification and determination of molecular species in gas chromatography.^{52,53} Microwave-induced metastable-transfer emission spectroscopy (MTES) has been the most fully evaluated means of using active nitrogen for excitation of both atomic and small molecular species, and may ultimately be the method of choice, particularly as a gas-chromatographic detector.

REFERENCES

- U. Isacson and G. Wettermark, *Anal. Chim. Acta*, 1974, **68**, 339.
- W. Seitz and M. P. Neary, *Anal. Chem.*, 1974, **46**, 188A.
- D. Paul, *Talanta*, 1978, **25**, 377.
- J. H. Glover, *Analyst*, 1975, **100**, 449.
- M. A. DeLuca and W. D. McElroy, *Bioluminescence and Chemiluminescence*, Academic Press, New York, 1981.
- E. Schram and P. Stanley, *Proceedings of the International Symposium on Analytical Applications of Bioluminescence and Chemiluminescence*, State Printing and Publishing, Westlake Village, CA, 1979.
- W. R. Seitz and M. P. Neary, *Contemp. Top. Anal. Chem. Clin. Chem.*, 1977, **1**, 49.
- G. Nethemark, S. E. Brolin and S. Hjeketen, *Cell. Mol. Biol.*, 1977, **22**, 329.
- F. Gorus and E. Schram, *Clin. Chem.*, 1979, **25**, 512.
- M. G. Evans, H. Eyring and J. F. Kincaid, *J. Chem. Phys.*, 1938, **6**, 349.
- A. Fontijn, in *Chemiluminescence and Bioluminescence*, J. Lee, D. M. Hercules and M. L. J. L. Corneir, (eds.), Plenum Press, New York, 1973.
- M. M. Rauhut, *Kirk-Othmer Encyclopaedia of Chemical Technology*, 3rd Ed., 1979, **5**, 416.
- C. Kenty, *Phys. Rev.*, 1954, **93**, 651.
- H. C. Na and T. M. Niemczyk, *Anal. Chem.*, 1982, **54**, 1839.
- S. Rosenwaks and H. P. Broida, *J. Chem. Phys.*, 1969, **51**, 2764.
- A. P. D'Silva and V. A. Fassel, *Anal. Chem.* **44**, 2115 (1972).
- A. P. D'Silva, G. W. Rice and V. A. Fassel, *Appl. Spectrosc.*, 1980, **34**, 578.
- R. J. Oldman and H. P. Broida, *J. Chem. Phys.*, 1969, **51**, 2764.
- C. Kenty, *ibid.*, 1961, **35**, 2267.
- G. A. Capelle and D. G. Sutton, *Appl. Phys. Lett.*, 1977, **30**, 407.
- C. Kenty, *J. Chem. Phys.*, 1955, **23**, 1555.
- Idem*, *Rept. 20th Ann. M.I.T. Conf. Phys. Electron*, p. 192, 1960.
- W. R. Brennen and G. B. Kistiakowsky, *J. Chem. Phys.*, 1966, **44**, 2695.
- C. J. Duthler and H. P. Broida, *ibid.*, 1973, **59**, 1967.
- J. F. Phillips, *Can. J. Chem.*, 1963, **41**, 723.
- J. A. Meyer, D. W. Setser and W. G. Clark, *J. Phys. Chem.*, 1972, **76**, 1.
- W. B. Dodge and R. O. Allen, *Anal. Chem.*, 1981, **53**, 1279.
- J. E. Bedinger, E. R. Manring and S. N. Ghosh, *J. Geophys. Res.*, 1958, **63**, 19.
- M. F. Golde and B. A. Thrush, *Rep. Prog. Phys.*, 1973, **36**, 1285.
- J. E. Melzer, J. J. Jordan and D. G. Sutton, *Anal. Chem.*, 1980, **52**, 348.
- M. A. Finkelstein, *J. Chim. Phys.*, 1952, **49**, 196.
- J. E. Morgan, L. F. Phillips and H. I. Shiff, *Discuss. Faraday Soc.*, 1962, **33**, 118.
- L. F. Phillips, *Can. J. Chem.*, 1963, **41**, 2060.
- E. P. Lewis, *Ann. Phys. (Leipzig)*, 1900, **2**, 459.
- Idem*, *Astrophys. J.*, 1900, **12**, 8.
- Idem*, *Phys. Rev.*, 1904, **18**, 125.
- G. A. Capelle and D. G. Sutton, *Appl. Phys. Lett.*, 1977, **30**, 407.
- Idem*, *Rev. Sci. Instrum.*, 1978, **49**, 1124.
- R. R. Baker, *Can. J. Chem.*, 1971, **49**, 1671.
- W. B. Dodge, *Thesis*, Univ. of Virginia, 1980.
- H. C. Na and T. M. Niemczyk, *Anal. Chem.*, 1983, **55**, 1240.
- T. Takeuchi, M. Yanagisawa and M. Suzuki, *Talanta*, 1972, **19**, 465.
- W. G. Schrenk and R. T. Everson, *Appl. Spectrosc.*, 1975, **29**, 41.
- T. Maruta and T. Takeuchi, *Anal. Chim. Acta*, 1972, **62**, 253.
- D. G. Sutton, J. E. Melzer and G. A. Capelle, *Anal. Chem.*, 1978, **50**, 1247.
- D. G. Sutton, K. R. Westburg and J. E. Melzer, *ibid.*, 1979, **51**, 1399.
- G. W. Rice, J. J. Richard, A. P. D'Silva and V. A. Fassel, *ibid.*, 1981, **53**, 1519.
- Idem*, *ibid.*, in the press.
- J. E. Melzer and D. G. Sutton, *Appl. Spectrosc.*, 1980, **34**, 434.
- D. R. Safranry, P. Harteck and R. R. Reeves, Jr., *J. Chem. Phys.*, 1964, **41**, 1161.
- M. H. Mach D. G. Sutton and J. E. Melzer, *Appl. Spectrosc.*, 1982, **36**, 597.
- H. Jurgensen, T. Yu and J. D. Winefordner, *J. Can. Spectrosc.*, submitted.
- H. Jurgensen, *Ph.D. Dissertation*, University of Florida, Gainesville, FL, 1983.

KINETIC FLUORIMETRIC DETERMINATION OF CYANIDE BY MEANS OF ITS CATALYTIC EFFECT ON THE AERIAL OXIDATION OF PYRIDOXAL-5-PHOSPHATE OXALYLDIHYDRAZONE

S. RUBIO, A. GOMEZ-HENS and M. VALCARCEL

Department of Analytical Chemistry, Faculty of Sciences, University of Córdoba, Córdoba, Spain

(Received 9 January 1984. Revised 26 April 1984. Accepted 7 May 1984)

Summary—A highly specific determination of traces of cyanide is described, based on the catalytic effect of cyanide on the oxidation of pyridoxal-5-phosphate oxalyldihydrazone by dissolved oxygen. The reaction is monitored by measuring the fluorescence of the oxidation product (λ_{ex} 350, λ_{em} 420 nm), and allows determination of 3–180 ng/ml cyanide concentrations with relative standard deviations of 0.4–0.8%. The effect of 56 foreign ions has been investigated: 45 of them do not interfere, and only one, Hg(II), interferes when present at the same level as the cyanide. Its application to the determination of total cyanide in industrial and synthetic samples, without preliminary distillation, is reported.

It is well known that cyanide catalyses the oxidation of some aromatic aldehydes to acids, through formation of cyanohydrins,¹ and this has been utilized for spectrophotometric and fluorimetric determination of cyanide.²⁻⁵ The reaction between the cyanohydrin of *p*-nitrobenzaldehyde and *o*-dinitrobenzene to give a highly-coloured blue compound, the doubly-charged anion of *o*-nitrophenylhydroxylamine, has been used by Guilbault and Kramer.² The rate of reduction of the *o*-dinitrobenzene was followed spectrophotometrically at 560 nm. Cyanide could be determined in the range 45–450 ng/ml, and the method was highly specific.

The fluorimetric methods for determination of cyanide have been reviewed and critically studied.⁶ The reaction of pyridoxal with oxygen to give 4-pyridoxolactone, a highly fluorescent compound, is catalysed by cyanide.³⁻⁵ Factors affecting the reaction rate have been studied by Takanashi and Tamura.⁷ The reagents are mixed in phosphate medium at pH 7.4 and heated at 50° for 60 min. The fluorescence is measured at pH 10 (achieved by adding sodium carbonate). The calibration graph is linear from 4 to 180 ng/ml. This reaction is regarded as the most sensitive fluorimetric method for cyanide.⁸

Here, the analytical properties of a new compound, pyridoxal-5-phosphate oxalyldihydrazone (PPOH), are described for the first time, and its aerial oxidation is used for the kinetic fluorimetric determination of traces of cyanide by means of their catalytic effect on the oxidation reaction. Under the conditions proposed, the reaction is rapid, measurements being taken less than 7 min after the start. The method is very selective, no preliminary distillation is needed and cyanide concentrations as low as 3 ng/ml can be determined.

EXPERIMENTAL

Synthesis of the reagent

Pyridoxal-5-phosphate (0.6 g) dissolved in the minimum of hot water-ethanol (3:2 v/v) solution was mixed with 0.13 g of oxalyldihydrazone dissolved in hot water-ethanol mixture (1:1 v/v). The mixture was refluxed for 30 min, then let cool to room temperature. The yellow product was filtered off and washed with ethanol. Calculated for C₁₈H₂₂O₁₂N₆P₂, C 37.50%, H 3.82%; found C 37.5%, H 4.1%.

Reagents

Pyridoxal-5-phosphate oxalyldihydrazone (PPOH) solution 7 × 10⁻⁴M, in methanol. Several drops of 0.01M sodium hydroxide (enough to give an apparent pH of ~7) were added to dissolve the reagent. This solution is stable for at least one month.

Standard cyanide solution. Potassium cyanide (2.5 g, equivalent to 1 g of cyanide) was dissolved in 1 litre of 0.05M sodium hydroxide and standardized argentometrically.⁹

Ammonia-ammonium chloride 6M buffer solution, pH 9.8.
*Chloramine-T solution and pyridine-barbituric acid reagent.*¹⁰

Reagent-grade chemicals and pure solvents were used. All anions tested were added in the form of their sodium or potassium salts.

Apparatus

Spectrofluorimeter. A Perkin-Elmer fluorescence spectrophotometer, model MPF-43A, fitted with a device for kinetic measurement and with 1-cm quartz cells was used. The cell compartment of the spectrofluorimeter was kept at constant temperature by circulating water. The sensitivity was set at 3, and the excitation and emission slits were set to give 6-nm spectral band-pass. A set of fluorescent polymer samples was used daily to adjust the spectrofluorimeter to compensate for changes in source intensity.

*Cyanide distillation apparatus.*¹⁰

Air-sampling equipment. A constant-flow pump, Dupont model S2500; impingers, volume 30 ml; cellulose ester filters, 37 mm in diameter and 0.8 μm thick.

Procedure

To 10-ml standard flasks add 0.5 ml of $7 \times 10^{-4} M$ PPOH solution, 5 ml of $6 M$ ammonia-ammonium chloride buffer (pH 9.8), 2.5 ml of $4 M$ sodium chloride and appropriate volumes of cyanide sample to give a final concentration of cyanide between 3 and 180 ng/ml. Make up to volume with distilled water, mix and after 1 min transfer a portion to a 1-cm quartz cell kept at $62 \pm 0.1^\circ$. Wait 2 min before starting to record the fluorescence intensity (λ_{ex} 350, λ_{em} 420 nm) as a function of time. Run a blank with no cyanide present. Calculate the reaction rate from the difference in the slopes of the fluorescence-time plots for the sample and the blank.

RESULTS AND DISCUSSION

Analytical properties of the reagent

At room temperature, PPOH is highly soluble in water or in sodium hydroxide solution, moderately soluble in dimethylformamide or methanol and slightly soluble in ethanol. Aqueous solutions are unstable whatever their pH. A $3.5 \times 10^{-5} M$ solution in methanol-water (1:24 v/v) has an absorption maximum at 305 nm and a very small absorption band at 360 nm in acidic and neutral media. In alkaline medium it shows a broad band with an absorption maximum at 305 nm. PPOH solutions are fluorescent (λ_{ex} 365 nm, λ_{em} 510 nm in acid medium and λ_{ex} 400 nm, λ_{em} 510 nm in alkaline medium).

The stability of the PPOH solutions is critically dependent on the medium. The reagent is stable in organic solvents such as methanol. Aqueous PPOH solutions are unstable owing to the autoxidation of the reagent by dissolved oxygen. This difference in behaviour occurs because there is a hydrolysis step prior to the oxidation, and this is favoured in an aqueous medium. For this reason, neutral aqueous solutions are more stable than acid or basic ones, because H^+ and OH^- ions catalyse the hydrolysis. This autoxidation reaction occurs at pH values very close to that used for the determination of cyanide, which is why blanks are run.

The pK values for the dissociation in methanol-water (1:24 v/v) were found^{11,12} to be 3.9, 8.2 and 10.4.

The colour reactions of the reagent with 62 ions at various pH values were investigated; it reacts with Mg(II), Co(II), Ni(II), Mn(II), Fe(II) and Fe(III). Only the red Mg(II)-PPOH complex formed at pH 4.2 and 50° (acetic acid-sodium acetate buffer) is of any photometric analytical interest. The fluorescence reactions are not important. Only V(V) and Al(III) show fluorescence which is different from that of the reagent, but the sensitivity is low.

Oxidation of PPOH and catalytic action of cyanide

The excitation and emission spectra of PPOH show a hypsochromic change in basic (λ_{ex} 350 nm, λ_{em} 420 nm) and acid (λ_{ex} 320 nm, λ_{em} 395 nm) media in presence of such oxidizing agents as KIO_3 , H_2O_2 , $K_2S_2O_8$ and $NaIO_4$. Solutions of PPOH in ammonia-ammonium chloride buffer show identical

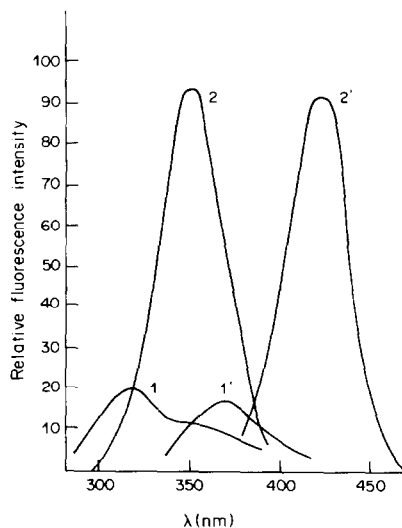


Fig. 1. Catalytic effect of cyanide on the oxidation of PPOH by dissolved oxygen. Excitation and emission spectra. 1,1': PPOH; 2,2': PPOH + CN^- . $[PPOH] = 8 \times 10^{-5} M$; $[CN^-] = 0.4 \mu g/ml$; $[NH_4Cl-NH_3] = 0.4 M$. Graphs were recorded after a reaction time of 1 hr. Temperature $50^\circ C$.

fluorescence maxima (λ_{ex} 350 nm, λ_{em} 420 nm) to those obtained in the presence of oxidants but the formation of the fluorescent product is so slow that it takes several days for a detectable amount to be produced. In the presence of traces of cyanide, the oxidation rate of PPOH by dissolved oxygen is accelerated. This effect is shown in Fig. 1. The catalytic nature of the cyanide reaction is revealed by the fact that it does not take place in an inert atmosphere. When oxidants are utilized, the reagent is oxidized immediately, and cyanide then does not have a catalytic effect.

Several tests have been made to characterize the oxidation product of PPOH and establish the mechanism of the reaction, with the following results

(a) The characteristic absorption peak at 305 nm of the Schiff's base formed between pyridoxal-5-phosphate and oxalylhydrazide disappears in the course of the reaction. This seems to be due to hydrolytic breaking of the azomethine group.

(b) The fluorescence maxima corresponding to the reagent (λ_{ex} 400 nm, λ_{em} 510 nm) disappear like the absorption maximum, but an intermediate product (λ_{ex} 320 nm, λ_{em} 370 nm) can be observed before the formation of the final product (λ_{ex} 350 nm, λ_{em} 420 nm). This intermediate is in equilibrium with PPOH and subsequently with the final product, and its fluorescence characteristics are the same as those of the pyridoxal-5-phosphate.¹³ This seems to corroborate the supposition of hydrolytic breaking.

(c) The fluorescence maxima of the oxidation product of PPOH are similar to those reported for a solution of pyridoxal-5-phosphate treated with hydrogen peroxide, which forms 4-pyridoxic acid.

From these observations it can be inferred that the likely oxidation mechanism consists of hydrolytic

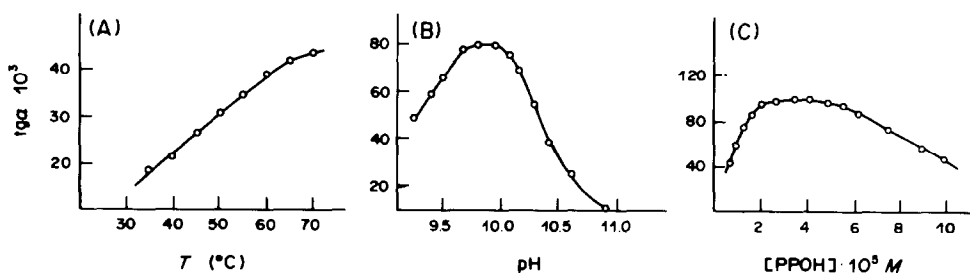


Fig. 2. Effect of the temperature (A), pH (B) and PPOH concentration (C) on the reaction rate of the PPOH-O₂-CN⁻ system.

breaking of the azomethine group and oxidation of the resulting compounds.

Several attempts have been made to isolate the highly water-soluble fluorescent species from mixtures of the parent reagent and cyanide, but without success. Evaporation yielded a reddish brown liquid which would not crystallize. Addition of ethanol produced a yellow solid, the excitation and emission spectra of which were identical to those obtained in the analytical test, but this solid was water-soluble and non-extractable by water-immiscible organic solvents, and was contaminated by the reagent, so meaningful ultraviolet and infrared spectra could not be obtained. Attempts to obtain a pure product by thin-layer chromatography were unsuccessful.

Influence of reaction variables on the oxidation

The temperature of the cell-holder was varied over the range 35–70° (Fig. 2A). The reaction rate increased linearly with temperature increase between 35 and 60° but less steeply at higher temperatures. A temperature of 62° was selected for use. From Arrhenius plots of $\ln k$ vs. reciprocal of the absolute temperature, the activation energy for the catalysed reaction was calculated to be 5.1 ± 0.1 kcal/mole.

The effect of pH on the reaction rate is given in Fig. 2B. The optimum pH is 9.7–10.0. The effect of the type of buffer (phosphate, carbonate, ammonia) was examined. The reaction develops only in the presence of ammonia–ammonium chloride buffer, and is linearly related to the buffer concentration up to at least 4M. A 3M concentration was chosen.

The influence of the PPOH concentration was tested in the range 5×10^{-6} – 10^{-4} M and is shown in Fig. 2C. A purely aqueous solution could not be used because of its instability, so a methanol solution was used. However, increasing the methanol content of the final aqueous methanol medium decreased the reaction rate, so its concentration in the solution measured was minimized.

The rate of reaction rises with increasing ionic strength up to 1M and then remains constant.

The fluorescence intensity vs. time curves for different cyanide concentrations were recorded. The initial slopes indicate a first-order reaction with respect to cyanide.

The various kinetic dependences on pH (Fig. 2B), reagent concentration (Fig. 2C) and buffer concen-

tration are summarized in Table 1, and the following equation is suggested for the oxidation of PPOH (3.5×10^{-5} M) by dissolved oxygen at pH 9.85 in the presence of 3M ammonia buffer and cyanide as catalyst:

$$d[\text{PPOH}]_{\text{ox}}/dt = k[\text{NH}_4\text{Cl-NH}_3]^{3/2}[\text{CN}^-]$$

in which $[\text{PPOH}]_{\text{ox}}$ is the concentration of oxidized reagent and k is the conditional rate constant. This equation does not include the effect of the uncatalysed reaction.

Calibration graphs

Three kinetic methods have been tested for the determination of cyanide: tangent ($[\text{CN}^-]$ 10–180 ng/ml), fixed-time ($[\text{CN}^-]$ 3–180 ng/ml) and variable-time ($[\text{CN}^-]$ 3–60 ng/ml).¹⁴ For the fixed-time method, measurements were made after 7 min. For the variable-time method, the inverse of the time necessary to obtain a relative fluorescence intensity of 30% was plotted against the cyanide concentration.

The relative standard deviation for 50 ng/ml cyanide ($P = 0.05$, $n = 11$) is smaller for the initial-rate method ($\pm 0.4\%$) than the fixed-time ($\pm 0.8\%$) and the variable-time ($\pm 0.7\%$) methods.

The initial-rate method is recommended when precision is the prime consideration and the fixed-time method when a low detection limit is the important factor.

Interferences

The effect of 35 anions and 21 cations on the determination of cyanide was tested. The tangent method was used because a change in slope could be more clearly detected than a change in a single data point. The tolerance limits for interfering ions are

Table 1. Summary of kinetic data

Dependence of V_0 on	Concentration range, M
$[\text{H}^+]$	4.5×10^{-11} – 7.9×10^{-11}
$[\text{H}^+]^0$	7.9×10^{-11} – 2.5×10^{-10}
$1/[\text{H}^+]$	2.5×10^{-10} – 5.0×10^{-10}
$[\text{PPOH}]^{1/2}$	10^{-5} – 2.2×10^{-5}
$[\text{PPOH}]^0$	2.2×10^{-5} – 5.0×10^{-5}
$[\text{PPOH}]^{-3/2}$	5.0×10^{-5} – 10^{-4}
$[\text{Buffer}]^{3/2}$	2.0–4.0

Table 2. Effect of various ions on the determination of 50 ng/ml of cyanide by the tangent method

Tolerance ratio, ion to CN ⁻	Ion added
100	SCN ⁻ , F ⁻ , Cl ⁻ , Br ⁻ , I ⁻ , NO ₃ ⁻ , CO ₃ ²⁻ , SO ₃ ²⁻ , S ₂ O ₃ ²⁻ , SO ₄ ²⁻ , ClO ₄ ⁻ , ClO ₃ ⁻ , BrO ₃ ⁻ , IO ₃ ⁻ , IO ₄ ⁻ , S ₂ O ₈ ²⁻ , PO ₄ ³⁻ , P ₂ O ₄ ⁴⁻ , P ₃ O ₁₀ ⁵⁻ , AsO ₂ ⁻ , AsO ₃ ³⁻ , SeO ₃ ²⁻ , VO ₃ ⁻ , MoO ₄ ²⁻ , WO ₄ ²⁻ , B ₄ O ₇ ²⁻ , acetate, tartrate, citrate, K ⁺ , Ca ²⁺ , Sr ²⁺ , Ba ²⁺ , Mg ²⁺ , Zn ²⁺ , Cd ²⁺ , Al ³⁺ , Cr ³⁺ , Bi ³⁺ , In ³⁺ , Sb ³⁺ , Tl ⁺ , Pb ²⁺ , Ti ⁴⁺ , Zr ⁴⁺
75	C ₂ O ₄ ²⁻ , NO ₂ ⁻
40	CrO ₄ ²⁻ , S ²⁻
20	Cu ²⁺ , Fe ³⁺
10	Ni ²⁺ , Fe(CN) ₆ ⁴⁻ , Fe(CN) ₆ ³⁻
5	Co ²⁺
1	Ag ⁺
less than 1	Hg ²⁺

summarized in Table 2; 45 of the ions tested did not affect the determination of cyanide when present in 100-fold ratio to it. Silver interferes when present at the same level as cyanide, but mercury(II) interferes at even lower concentrations. Hence, the method is highly specific.

Applications

The determination of microamounts of cyanide in industrial effluents is of interest owing to its toxicity. The pyridine-barbituric acid colorimetric method recommended¹⁰ has a detection limit of 4 ng/ml for cyanide. To determine cyanide in water samples by this method, it is necessary first to separate it from interfering substances by distillation of hydrocyanic acid from the acidified sample. It is well known,⁸ and has been verified by us, that when the equipment and conditions described¹⁰ for the distillation are used, the cyanide is not quantitatively recovered at levels below 1 µg/ml in the original sample. The reasons for this

have been investigated¹⁵ and it was found that the hydrocyanic acid is completely distilled but not totally absorbed in the collection solution. The distillation also takes about 90 min.

Because of its high selectivity, we have used the new method for determination of cyanide in several samples without preliminary distillation. Three types of sample were investigated.

Water and air from an electroplating factory. Several samples of water and air were analysed by both the fluorimetric and the standard colorimetric method, with and without distillation. As the true cyanide concentration in the samples was unknown, the distillation was included, on the assumption that the determination could be taken as free of interferences if the results obtained with and without distillation agreed. The air sample (90 litres) was aspirated at 1.5 l./min through three impingers connected in series, each containing 10 ml of 0.1M sodium hydroxide; the solutions were mixed for

Table 3. Determination of cyanide in water and air from an electroplating factory

Sample	Cyanide (Without preliminary distillation)		Cyanide, µg/ml (With preliminary distillation)	
	Fluorimetric method*	Standard method*	Fluorimetric method*	Standard method*
1	—	12.5 ± 0.4 ng/ml	—	—
2	7.2 ± 0.4 µg/ml	8.5 ± 0.3 µg/ml	7.1 ± 0.2	7.2 ± 0.1
3	4.1 ± 0.3 µg/ml	5.3 ± 0.5 µg/ml	4.2 ± 0.2	4.0 ± 0.3
4	2.5 ± 0.3 ng/ml	1.3 ± 0.6 ng/ml	—	—
5	0.10 ± 0.01 mg/m ³	0.10 ± 0.02 mg/m ³	—	—

*Average and standard deviation of five separate determinations.

Sample:

1. Water intake to the baths.
2. Water from the first washing of the silver-plated pieces.
3. Water from the second washing of the silver-plated pieces.
4. Waste-water from a plating factory with zinc-plating, silver-plating and chromium-plating baths.
5. Air from the workroom.

Table 4. Determination of cyanide in synthetic plating-baths

Plating-bath	Cyanide content, $\mu\text{g/ml}$	
	Added*	Found†
1	4.7	4.6 ± 0.1
2	5.8	5.8 ± 0.2
3	4.4	4.3 ± 0.1
4	4.1	3.9 ± 0.2
5	3.3	3.2 ± 0.1
6	4.8	5.0 ± 0.1
7	3.3	3.4 ± 0.1

*Initial concentration diluted 10,000-fold with potable water.

†Average and standard deviation of four separate determinations.

Sample:

1. Brass-plating bath: CuCN (3%), Zn(CN)₂ (0.9%), NaCN (4.9%), Na₂CO₃ (1.5%), NH₃ (0.015%).
2. Brass-plating bath: CuCN (2.025%), Zn(CN)₂ (5.0%), NaCN (3%), Na₂CO₃ (2.25%).
3. Brass-plating bath: CuCN (2.6%), Zn(CN)₂ (1.1%), NaCN (4.5%), Na₂CO₃ (1.5%).
4. Brass-plating bath: CuCN (3%), Zn(CN)₂ (2.6%), NaCN (3.8%), Na₂CO₃ (1.5%).
5. Copper-plating bath: CuCN (2.6%), NaCN (3.4%), Na₂CO₃ (1.5%), NaKC₄H₄O₆·4H₂O (3.6%).
6. Cadmium-plating bath: CdO (2.6%), NaCN (9%), Na₂CO₃ (1.5%).
7. Silver-plating bath: AgCN (0.4%), NaCN (6%), Na₂CO₃ (0.8%).

analysis. A cellulose ester filter was inserted in the sampling line to retain particulate matter.

The results obtained are shown in Table 3. No cyanide was detectable in the water entering the plating bath (sample 1). The value found by the standard method without distillation was probably due to positive interferences, which were also found in samples 2 and 3. The agreement of the values obtained for these samples by the fluorimetric method with and without distillation shows that this preliminary step is not necessary. Owing to the low

concentration of cyanide in sample 4, no results were obtained when distillation was used. The sample of air (sample 5) also contained a low amount of cyanide and gave the same results by the two methods.

Water from synthetic plating solutions. The results obtained with the fluorimetric method for the real samples described above agree with those obtained by the standard method with prior distillation, but, owing to the low concentration of cyanide in some of these samples, it was not possible to obtain reliable results for all of them by use of distillation. For this reason, several synthetic plating solutions were prepared.¹⁶ To obtain a final cyanide concentration similar to that in the waste-water from washing of plated pieces, these solutions were diluted 10000-fold with water. Table 4 shows the values obtained by the fluorimetric method without distillation, and the initial compositions of the solutions. The accuracy of the results proves that preliminary distillation is not necessary, at least for this type of sample.

Other synthetic samples. A series of synthetic samples containing several mixtures of ions which usually interfere in other methods for cyanide determination were prepared, in order to explore the application of the fluorimetric method. Cyanide was determined in several binary, ternary and quaternary mixtures, and the results are summarized in Table 5 and compared with those obtained by the colorimetric method. The standard colorimetric method gave higher errors than the fluorimetric method for all the samples.

Comparison with other methods

Comparison of the fluorimetric determination reported here with the fluorimetric procedures described in the literature leads to the following considerations. Only three other methods have determination limits similar to those in our method. They are based on (a) the catalytic action of cyanide on the

Table 5. Determination of 50 ng/ml cyanide in synthetic samples

Sample composition*	Relative error, %†	
	Fluorimetric method	Standard method
1 CN ⁻ 75 NO ₂ ⁻	+0.5	-69
1 CN ⁻ 40 S ²⁻	-1.2	-55
1 CN ⁻ 100 SCN ⁻	-0.4	≥ +100
1 CN ⁻ 100 Br ⁻	+1.0	-74
1 CN ⁻ 100 I ⁻	-0.7	-100
1 CN ⁻ 20 Fe(III)	+0.3	-7
1 CN ⁻ 10 Ni(II)	-0.5	-66
1 CN ⁻ 5 Co(II)	-0.8	-55
1 CN ⁻ 100 Br ⁻ 100 I ⁻	+1.2	-98
1 CN ⁻ 20 S ²⁻ 60 SCN ⁻	-0.9	≥ +100
1 CN ⁻ 60 NO ₂ ⁻ 80 SCN ⁻	+1.1	≥ +100
1 CN ⁻ 5 Ni(II) 6 Fe(III)	-0.8	-20
1 CN ⁻ 20 Cu(II) 200 Zn(II)	-1.2	-13
1 CN ⁻ 20 Cu(II) 100 Cd(II)	+0.6	-12
1 CN ⁻ 20 Cu(II) 1 Ag(I)	-0.3	-8
1 CN ⁻ 60 Br ⁻ 60 SCN ⁻ 60 I ⁻	-1.2	+79
1 CN ⁻ 60 SCN ⁻ 40 NO ₂ ⁻ 20 S ²⁻	-0.7	≥ +100

*Each number means the ion/cyanide concentration ratio.

†Average of five separate determinations.

oxidation of pyridoxal to 4-pyridoxolactone,⁶ (b) the ligand-exchange reaction between cyanide and the non-fluorescent complex Cu(II)-leucofluorescein,¹⁷ and (c) quenching of the fluorescence of 2-(*o*-hydroxyphenyl)benzoxazole by copper.¹⁸ The first of these involves two steps in the sample preparation and a period of 50 min for the final fluorescence development, whereas only 3–7 min reaction monitoring is needed in our method reported here. Furthermore, the oxidation of pyridoxal is not specific for cyanide, there being numerous interferences.⁷ The second method has a relative standard deviation of 10% for 5 ng/ml cyanide, and sulphide and strongly oxidizing and reducing anions must be absent. At this cyanide level our method has a relative standard deviation of only 4.4%. No data have been reported on the selectivity and precision of the third method. This method has also been proposed for the determination of sulphide, and therefore this ion must be absent. The pyridine-barbituric acid method is also not specific, and a preliminary distillation is necessary to avoid interference.

REFERENCES

1. R. T. Morrison and R. N. Boyd, *Organic Chemistry*, p. 656. Allyn and Bacon, Boston, 1973.
2. G. G. Guilbault and D. N. Kramer, *Anal. Chem.*, 1966, **38**, 834.
3. V. Bonavita, *Arch. Biochem. Biophys.*, 1960, **88**, 366.
4. S. Takanashi, Z. Tamura, A. Yoshino and Y. Lidaka, *Chem. Pharm. Bull.*, 1968, **16**, 758.
5. N. Oishi and S. Fukui, *Arch. Biochem. Biophys.*, 1968, **128**, 606.
6. A. Gómez-Hens and M. Valcárcel, *Analyst*, 1982, **107**, 465.
7. S. Takanashi and Z. Tamura, *Chem. Pharm. Bull.*, 1970, **18**, 1633.
8. M. Brebec, G. Delarue, B. Santoni and P. Sanat, *Analisis*, 1975, **4**, 127.
9. I. M. Kolthoff and E. B. Sandell, *Textbook of Quantitative Inorganic Analysis*, 2nd Ed., p. 574. Macmillan, New York, 1947.
10. *Standard Methods for the Examination of Water and Wastewater*, 15th Ed., APHA-AWWA-WPCF, Washington, 1980.
11. W. Stenström and N. Goldsmith, *J. Phys. Chem.*, 1926, **30**, 1683.
12. L. Sommer, *Folia Fac. Sci. Natn. Univ. Purkynianae Brno*, 1964, **5**, 1.
13. J. W. Bridges, D. S. Davies and R. T. Williams, *Biochem. J.*, 1966, **98**, 451.
14. K. B. Yatsimirskii, *Kinetic Methods of Analysis*, Chapter 3, Pergamon Press, Oxford, 1966.
15. P. D. Goulden, B. K. Afghan and P. Brooksbank, *Anal. Chem.*, 1972, **44**, 1845.
16. Kirk-Othmer, *Encyclopedia of Chemical Technology*, Uthea, Mexico.
17. D. E. Ryan and J. Holzbecher, *Int. J. Environ. Anal. Chem.*, 1971, **1**, 159.
18. F. Vernon and P. Whitham, *Anal. Chim. Acta*, 1972, **59**, 155.

VOLTAMMETRIC INTERPRETATION OF THE POTENTIAL AT AN ION-SELECTIVE ELECTRODE, BASED ON CURRENT-SCAN POLAROGRAMS OBSERVED AT THE AQUEOUS/ORGANIC SOLUTION INTERFACE*

SORIN KIHARA

Institute for Chemical Research, Kyoto University, Uji, Kyoto 611, Japan

ZENKO YOSHIDA

Analytical Chemistry Laboratory, Japan Atomic Energy Research Institute, Tokai, Ibaraki 319-11, Japan

(Received 12 March 1984. Accepted 7 May 1984)

Summary—The potential-generating process at ion-selective electrodes (ISE) of liquid-membrane types has been interpreted by comparing the ISE potential with the current-scan polarogram which indicates the transfer of a particular ion i^{z+} at the aqueous/organic solution (w/o) interface. The potential at zero current, $\Delta V_{I=0}$, in the composite polarogram observed with i^{z+} in both w and o , corresponds to the ISE potential. A stable potential giving Nernstian response to the concentration of i^{z+} in w is obtained at the ISE only when the w/o interface is depolarized by i^{z+} . The detection limits are controlled by the final rise and final descent of the residual current in the polarogram. The interference of a second ion, j^{z+} , in the ISE measurement of i^{z+} , and the role of an ionophore in the membrane of the ISE can be explained by considering the shift of $\Delta V_{I=0}$ in the composite polarogram of i^{z+} in the presence of j^{z+} in w or the ionophore in o . Equations which express the ISE potential, the interference at the ISE, and the effect of an ionophore on the ISE potential have been derived, connected with the polarographic equations for ion-transfer at the w/o interface.

In potentiometry the potential is measured at negligible current-flow, as is well known. This condition, however, does not necessarily mean that electron-transfer at the solution/electrode interface is negligibly small. The equilibrium potential in potentiometry is attained when the rate of the anodic reaction is equivalent to that of the cathodic reaction.¹ The potential at an ion-selective electrode (ISE) should also be interpreted in terms of the above-mentioned concept, although most of the electrode reaction at the solution/membrane interface of an ISE is attributed not to electron transfer but to ion-transfer as represented in equation (1):



where subscripts w and m indicate the ion i^{z+} in water and in the membrane, respectively.

Koryta^{2,3} and Fujinaga⁴ advocated that the potential at the ISE, and such important factors in the ISE measurement as Nernstian response, detection limit, and interference, must be explained on the basis of the voltammetry of the ion-transfer at the solution/membrane interface. To realize this idea Koryta presented various voltamperograms for the water/organic solution interface, which were

obtained by simulation from extraction data, with certain assumptions.

In a previous communication,⁵ we presented several polarograms obtained by polarography at the dropping aqueous-electrolyte electrode (DAEE) combined with the current-scan method⁶ and explained briefly the potential-generating process at the ISE on the basis of the polarographic results.

In the present paper, a quantitative interpretation of the potential-generation process is deduced from more detailed experimental results, and the role of the ionophore in the membrane of the ISE is also discussed.

EXPERIMENTAL

Polarographic measurement

The current-scan polarograms were recorded with use of a polarographic cell identical with that described previously.⁶ The aqueous electrolyte solution (w), containing 1M magnesium sulphate as supporting electrolyte, was forced upward dropwise into nitrobenzene solution (nb) containing 0.05M tetrabutylammonium tetraphenylborate (TBA^+TPhB^-) or 0.02M tetraphenylarsonium dipicryl-amine ($TPhAs^+DPA^-$) as supporting electrolyte, through a Teflon capillary (1.4 mm bore and 3 mm long) at a mean flow-rate of $m = 0.028$ ml/sec, the time per drop being about 2.1 sec. For the polarographic study, the current, I , applied at the w/nb interface was scanned at a rate v of 0.5 $\mu A/sec$. In order to detect the potential difference, ΔV , at the w/nb interface, a silver-silver chloride electrode (SSE) and a tetramethylammonium electrode (TMAE) were set in the aqueous and the nb solutions, respectively, close to the

*This paper is submitted in celebration of the award of the Talanta Gold Medal to Professor Taitiro Fujinaga.

interface. To compensate the ohmic-potential IR drop caused by the resistance, R , between the SSE and TMAE, a resistance R_c equivalent to R was put in series into the current-supplying circuit and the voltage, IR_c , generated by R_c was subtracted automatically from ΔV .⁶

The composition of the TMAE and the cell configuration for the potential measurement are as follows:

SSE (Ag-AgCl, 1M LiCl) (aqueous)	1M LiCl+ 10 ⁻³ M TMA ⁺ Br ⁻ (aqueous)	10 ⁻³ M TMA ⁺ TPhB ⁻ or 10 ⁻³ M TMA ⁺ DPA ⁻ (nitrobenzene)	i^{z+} (TPhB ⁻) _z + 0.05M TBA ⁺ TPhB ⁻ or i^{z+} (DPA ⁻) _z + 0.02M TPhAs ⁺ DPA ⁻ (nitrobenzene)	i^{z+} Br _z ⁻ or i^{z+} Cl _z ⁻ + 1M MgSO ₄ (aqueous, DAEE)	SSE (Ag-AgCl, 1M LiCl) (2) (aqueous)
Tetramethylammonium electrode (TMAE)					

where TMA⁺ and i^{z+} are the tetramethylammonium ion and the cation of charge $z +$ under investigation.

The potential of the TMAE is controlled by the Galvani potential difference, $\Delta_{nb}^w\phi$, at the w/nb interface, which can be expressed as

$$\Delta_{nb}^w\phi = \Delta_{nb}^w\phi_{TMA^+}^0 + (RT/F) \ln (a_{TMA^+,w}/a_{TMA^+,nb}) \quad (3)$$

where $\Delta_{nb}^w\phi_{TMA^+}^0$ is the standard Galvani potential for the transfer of TMA⁺ from w to nb , and a_{TMA^+} indicates the activity of TMA⁺. The value of $\Delta_{nb}^w\phi_{TMA^+}^0$ was found to be 0.035 V by Koryta *et al.*,⁷ by using the standard Gibbs energy for the transfer of TMA⁺, calculated from distribution data with the extrathermodynamic assumption of Parker⁸ and Popovych⁹ that the transfer energies of TPhAs⁺ and of TPhB⁻ across the w/nb interface are equal.

ISE measurement

The cell configuration for the measurement of the ISE potential is summarized in equation (4):

SSE (satd. KCl) (aqueous)	i^{z+} Br _z ⁻ or i^{z+} Cl _z ⁻ (aqueous, inner solution)	i^{z+} (TPhB ⁻) _z or i^{z+} (DPA ⁻) _z (nitrobenzene, liquid membrane)	i^{z+} Br _z ⁻ or i^{z+} Cl _z ⁻ (aqueous, test solution)	SSE (satd. KCl) (aqueous)	(4)
---------------------------------	--	--	--	---------------------------------	-----

For comparison of the results obtained by polarography with those by ISE measurement, the supporting electrolytes used in the polarographic study were also used in the aqueous inner and test solutions and the nb membrane solution in the ISE cell.

In order to prepare i^{z+} (TPhB⁻)_z or i^{z+} (DPA⁻)_z in nb , i^{z+} Br_z⁻ or i^{z+} Cl_z⁻ was mixed with Na⁺TPhB⁻ or Na⁺DPA⁻ in water and the precipitate produced was extracted into nb .

Sigma Chemical Co. valinomycin was used. All other reagents were of reagent grade and all measurements were made at 25 ± 1°.

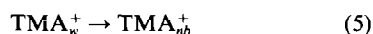
RESULTS

Current-scan polarograms of various ions at the w/nb interface

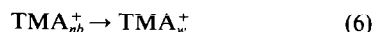
In the following, we define the transfer of a cation from w to nb or an anion from nb to w as the anodic reaction and that of an anion from w to nb or a cation from nb to w as the cathodic reaction.

The polarogram realized in curve 1 of Fig. 1 was obtained at the DAEE (containing 5 × 10⁻⁴M TMA⁺) transferring drops into an nb solution which did not contain TMA⁺. (For raw polarograms see references 5 and 6). The polarogram indicates the reversible transfer of TMA⁺ from w to nb [reaction (5)] and the limiting current is proportional to the concentration of TMA⁺ in the DAEE, over the range

$$2 \times 10^{-5} - 10^{-3}M.$$



Curve 2 shows the reversible transfer of TMA⁺ from nb to w [reaction (6)] and the limiting current is



proportional to the concentration of TMA⁺ in the nb solution, over the range from 5 × 10⁻⁵ to 10⁻³M.

Curve 3 is the composite polarogram obtained under the same conditions as curve 1 or 2, but with 5 × 10⁻⁴M TMA⁺ in both the DAEE and nb . The composite polarogram sharply intersects the potential axis where the current, I , is zero, suggesting that the w/nb interface is depolarized. The zero-current potential, $\Delta V_{I=0}$, of the composite polarogram becomes about 60 mV more negative when the concentration of TMA⁺ in the DAEE is increased by one order in the range between 5 × 10⁻⁵ and 5 × 10⁻¹M

(curves 3–7), and more positive when the concentration of TMA⁺ in the nb solution is increased by one order in the range between 5 × 10⁻⁵ and 5 × 10⁻³M, (e.g., curves 9 and 10). With more than 0.5M or less than 10⁻⁵M TMA⁺ in the DAEE the composite polarograms overlap the final descent or the final rise, respectively, of the residual current (curve 11).

By varying the concentration of TBA⁺TPhB⁻ and changing the supporting electrolyte from TBA⁺TPhB⁻ to TPhAs⁺DPA⁻, it was confirmed that the anodic final rise and the cathodic final descent in polarogram 11 in Fig. 1 were attributable to the transfer of TPhB⁻ and TBA⁺, respectively, from nb to w .

Polarogram 3 in Fig. 1 is reproduced as curve 1 in Fig. 2. Polarograms 2 and 3 in Fig. 2, which show the transfer of Cs⁺ and tetraethylammonium ion (TEA⁺) from w to nb solution were recorded under the same conditions as those for curve 1 in Fig. 1, but with 5 × 10⁻⁴M concentration of these ions instead of TMA⁺ in the DAEE. Curves 4 and 5 show composite polarograms recorded with the DAEE containing 5 × 10⁻⁴M Cs⁺ and TEA⁺, respectively, in addition to 5 × 10⁻⁴M TMA⁺, and nb solution containing 5 × 10⁻⁴M TMA⁺. The $\Delta V_{I=0}$ of the composite polarogram of TMA⁺ is hardly affected by the Cs⁺

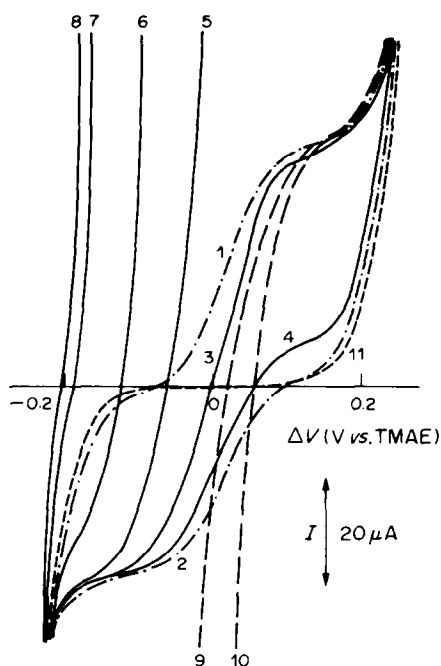


Fig. 1. Polarograms for the transfer of TMA^+ at the w/nb interface. Concentration of TMA^+Br^- in w (M): (1), (3), (9), (10), 5×10^{-4} ; (4), 5×10^{-5} ; (5), 5×10^{-3} ; (6), 5×10^{-2} ; (7) 5×10^{-1} ; (8), 5; (2), (11), 0. Concentration of $\text{TMA}^+\text{TPhB}^-$ in nb (M): (2)–(8), 5×10^{-4} ; (9), 1×10^{-3} ; (10), 5×10^{-3} ; (1), (11), 0. Supporting electrolyte in w : $1M \text{MgSO}_4$; in nb : $0.05M \text{TBA}^+\text{TPhB}^-$.

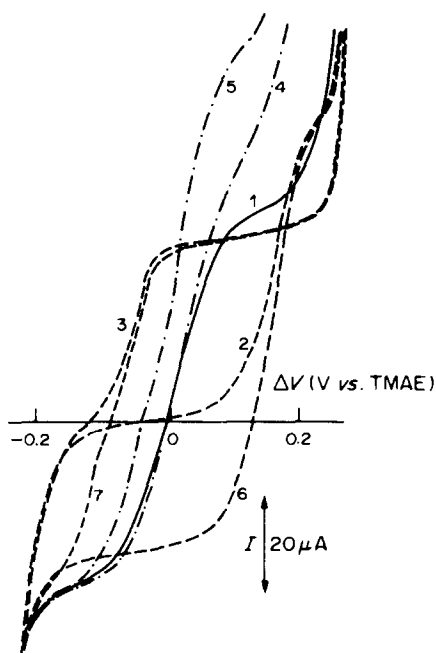


Fig. 2. Polarograms for the transfer of TMA^+ , Cs^+ , and TEA^+ at the w/nb interface. Depolarizer(s) ($5 \times 10^{-4}M$) in w : (1) TMA^+Br^- ; (2), (6), Cs^+Br^- ; (3), (7), TEA^+Br^- ; (4), $\text{TMA}^+\text{Br}^- + \text{Cs}^+\text{Br}^-$; (5) $\text{TMA}^+\text{Br}^- + \text{TEA}^+\text{Br}^-$. Depolarizer ($5 \times 10^{-4}M$) in nb : (1), (4), (5), $\text{TMA}^+\text{TPhB}^-$; (6) Cs^+TPhB^- ; (7) $\text{TEA}^+\text{TPhB}^-$; (2), (3) none. Supporting electrolyte in w : $1M \text{MgSO}_4$; in nb : $0.05M \text{TBA}^+\text{TPhB}^-$.

in the DAEE, whereas it is strongly influenced by TEA^+ .

The effect of supporting electrolyte on the residual current

The final rise or final descent of the residual-current polarogram appears at a different potential when the kind of supporting electrolytes and their concentration in the DAEE or the nb solution are changed, as shown in Fig. 3. The anodic final rise shifts to more negative potentials as the cations in w or the anions in nb are more easily transferred across the w/nb interface, and the cathodic final descent shifts to more positive potentials as the anions in w or the cations in nb are transferred more easily across the interface.⁷ The results in Fig. 3 indicate that the widest potential window is achieved in polarography with magnesium sulphate or sodium carbonate and $\text{TPhAs}^+\text{TPhB}^-$ or $\text{TPhAs}^+\text{DPA}^-$ as the supporting electrolytes in the DAEE and nb solution, respectively. The use of $\text{TPhAs}^+\text{TPhB}^-$ is, however, restricted because of its low solubility in nb .

Polarograms of K^+ and Na^+ in the absence and presence of valinomycin in the nb solution

The polarograms illustrated in Figs. 4 and 5 are obtained with the DAEE containing various concentrations of potassium chloride (Fig. 4) or sodium chloride (Fig. 5) and nb solution containing $2 \times 10^{-3}M \text{K}^+\text{TPhB}^-$ with or without valinomycin

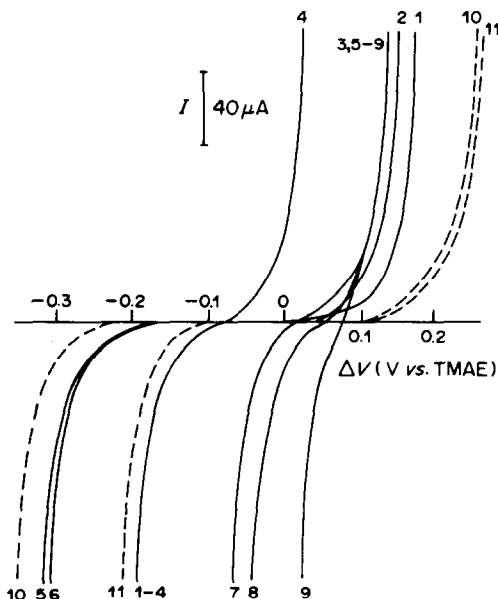


Fig. 3. Residual current in polarograms with various supporting electrolytes. Supporting electrolytes ($1M$) in w : (1), LiCl ; (2), HCl ; (3), NaCl ; (4), KCl ; (5), Na_2SO_4 ; (6), Na_2CO_3 ; (7), NaNO_3 ; (8), NaSCN ; (9), NaClO_4 ; (10), (11), MgSO_4 . Supporting electrolytes in nb : (1)–(10), $0.02M \text{TPhAs}^+\text{DPA}^-$; (11), $0.05M \text{TBA}^+\text{TPhB}^-$.

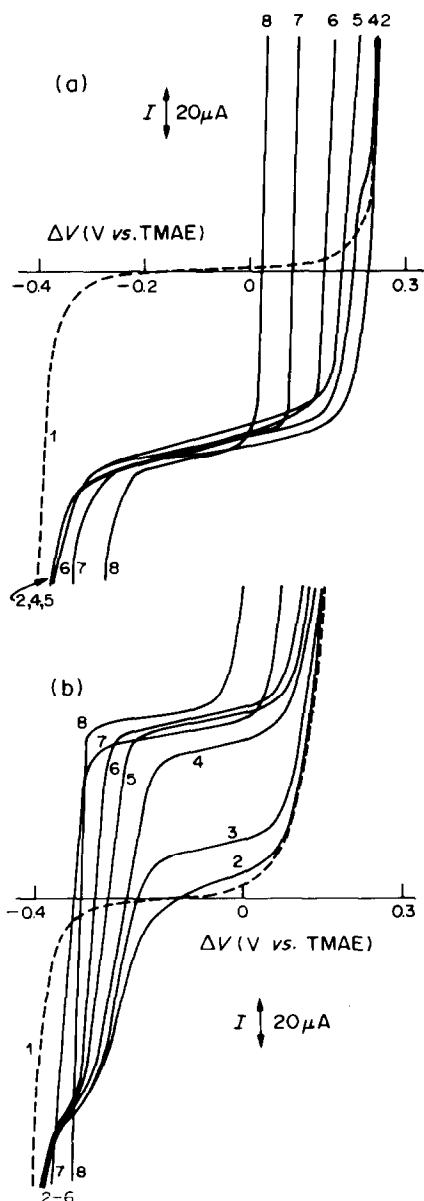


Fig. 4. Composite polarograms observed with K^+ in w and K^+ in nb in the absence (a) and presence (b) of $3.75 \times 10^{-3}M$ valinomycin in nb . Concentration of K^+Cl^- in w (M): (1), (2), 0; (3), 2×10^{-4} ; (4), 5×10^{-4} ; (5), 2×10^{-3} ; (6), 5×10^{-3} ; (7), 5×10^{-2} ; (8), 5×10^{-1} . Concentration of K^+TPhB^- in nb (M): (1), 0; (2)–(8) 2×10^{-3} . Supporting electrolyte in w : $1M$ $MgSO_4$; in nb : $0.02M$ $TPhAs^+DPA^-$.

($3.75 \times 10^{-3}M$). The presence of valinomycin in the nb solution facilitates the transfer of K^+ and Na^+ from w to nb . When the concentration of K^+ or Na^+ in the DAEE was larger than that of uncombined valinomycin in nb , the anodic limiting current controlled by the concentration of uncombined valinomycin was observed. The cathodic final descent shifted to more positive potential when the concentration of potassium chloride or sodium chloride in

the DAEE was $>10^{-2}M$. This shift is attributed to the transfer of Cl^- from w to nb .

The anodic final rise in the residual polarogram obtained with nb solution containing $3.75 \times 10^{-3}M$ valinomycin and aqueous solution containing no potassium or sodium chloride (curve 1 in Fig. 4b or 5b) shifted by about -130 mV from that obtained in the absence of valinomycin in the nb solution (curve 1 in Fig. 4a or 5a). This potential shift might be attributed to complex formation of valinomycin with magnesium.¹⁰

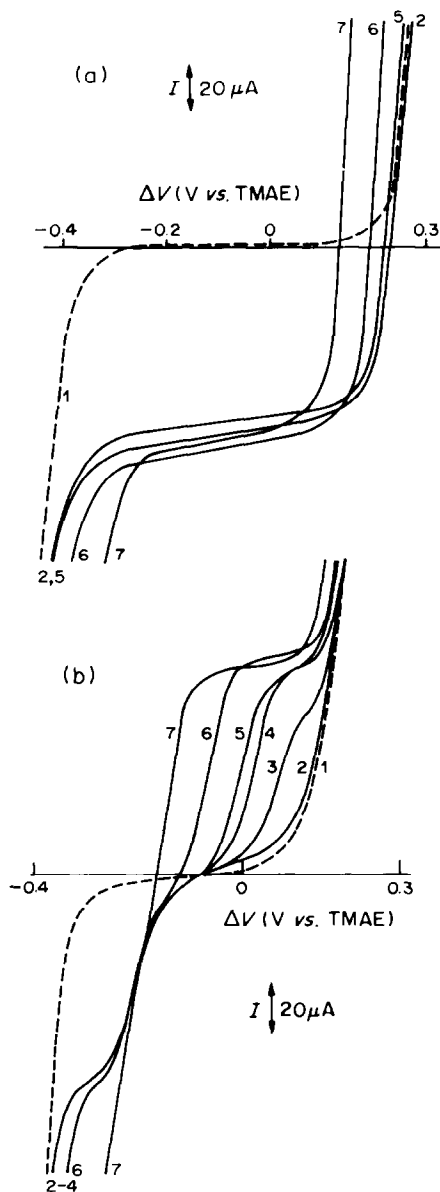


Fig. 5. Composite polarograms observed with Na^+ in w and K^+ in nb in the absence (a) and presence (b) of $3.75 \times 10^{-3}M$ valinomycin in nb . Concentration of Na^+Cl^- in w (M): (1), (2), 0; (3), 5×10^{-4} ; (4), 2×10^{-3} ; (5), 5×10^{-3} ; (6), 5×10^{-2} ; (7), 5×10^{-1} . Concentration of Na^+TPhB^- in nb (M): (1), 0; (2)–(7) 2×10^{-3} . Supporting electrolyte in w : $1M$ $MgSO_4$; in nb : $0.02M$ $TPhAs^+DPA^-$.

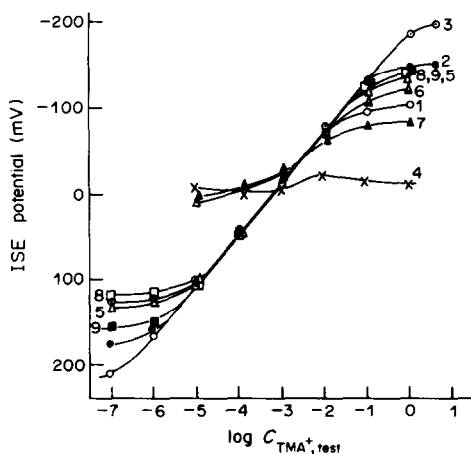


Fig. 6. Potential measured at the *nb* membrane ISE for TMA^+ . Concentration of $\text{TMA}^+\text{TPhB}^-$ in the membrane (M): (1), 5×10^{-5} ; (2), (5)–(9), 5×10^{-4} ; (3), 5×10^{-3} ; (4), 0. Concentration of TMA^+Br^- in the inner solution: $5 \times 10^{-4}M$. Supporting electrolyte in inner and test solutions: (1)–(4), none; (5), (8), (9), $1M \text{MgSO}_4$; (6), $1M \text{HCl}$; (7), $1M \text{NaNO}_3$; in the membrane: (1)–(7), none; (8), $0.05M \text{TBA}^+\text{TPhB}^-$; (9), $0.02M \text{TPhAs}^+\text{DPA}^-$.

The concentration ranges where $\Delta V_{I=0}$ shifts by -60 mV for increase of one order of magnitude in the concentration of K^+ or Na^+ in the DAEE are $>5 \times 10^{-4}M \text{K}^+$ and $>5 \times 10^{-2}M \text{Na}^+$ in the absence of valinomycin, but from 2×10^{-4} to $2 \times 10^{-2}M$ for K^+ and from 5×10^{-3} to $5 \times 10^{-1}M$ for Na^+ in the presence of $3.75 \times 10^{-3}M$ valinomycin in the *nb* solution.

Potentials measured at the liquid-membrane ISE

The relation between the concentration of TMA^+ in the test solution and the ISE potential measured at the ISE of equation (4) is shown in Fig. 6. Curves 1–3 were obtained with the ISE cell, in which the *nb* membrane and the inner solution contained various concentrations of $\text{TMA}^+\text{TPhB}^-$ and $5 \times 10^{-4}M \text{TMA}^+\text{Br}^-$, respectively, without any other electrolytes. When the concentration of TMA^+ in the membrane was $5 \times 10^{-5}M$, $5 \times 10^{-4}M$ or $5 \times 10^{-3}M$, the ISE potential was proportional to the logarithm of the concentration of TMA^+ in the test solution in the range from 10^{-7} to $10^{-2}M$, from 10^{-6} to $10^{-1}M$ or from 10^{-5} to $1M$, respectively. When the ISE was used without TMA^+ in the membrane, Nernstian response could not be obtained, as shown in curve 4. Adding such electrolytes as $1M$ magnesium sulphate, hydrochloric acid or sodium nitrate to the inner and to the test solutions or $0.05M \text{TBA}^+\text{TPhB}^-$ or $0.02M \text{TPhAs}^+\text{DPA}^-$ to the membrane, changed the upper or lower detection limits as shown in curves 5–9 in Fig. 6.

The ISE measurement of TMA^+ at a concentration $<5 \times 10^{-3}$ or $5 \times 10^{-5}M$ is interfered with by $5 \times 10^{-4}M \text{TEA}^+$ or $5 \times 10^{-4}M \text{Cs}^+$, respectively, in the test solution.

The relation between the concentration of potassium chloride in the test solution and the ISE potential was investigated by use of the ISE cell with a membrane containing $5 \times 10^{-4}M \text{K}^+\text{DPA}^-$ (curve 1 in Fig. 7). The lower detection limit for K^+ with this ISE cell is $10^{-3}M$. The presence of $0.5M$ sodium chloride in the test solution interferes in the ISE measurement of less than $0.02M \text{K}^+$. When $3.75 \times 10^{-3}M$ valinomycin is added to the membrane, the lower as well as the upper detection limits for K^+ are lowered, and it becomes possible to determine $5 \times 10^{-4}M$ – $5 \times 10^{-2}M \text{K}^+$ even in the presence of $0.5M$ sodium chloride.

DISCUSSION

Koryta *et al.*⁷ discussed the transfer of ions under Faradaic current-flow at the interface of two immiscible electrolyte solutions, by analogy with the transfer of metal ions at the solution/metal amalgam interface, as deduced by Delahay,¹¹ and derived an equation which expresses the polarographic wave observed at the DAEE for the reversible transfer of an ion i^{z+} from phase α to phase β . With α and β the aqueous and organic phases, respectively, and taking our definition of anodic and cathodic reactions into account, we obtain equations (7) and (8) for the Galvani potential difference at the α/β interface, $\Delta_\beta^z\phi$, and the average current, I , due to the transport of i^{z+} to the interface under the polarographic condition.

$$\Delta_\beta^z\phi = \Delta_\beta^z\phi_{i^{z+}}^0 - (RT/zF) \ln (a_{i^{z+},\alpha}^{x=0}/a_{i^{z+},\beta}^{x=0}) \quad (7)$$

$$\begin{aligned} I &= \kappa_{i^{z+},\alpha} (a_{i^{z+},\alpha} - a_{i^{z+},\alpha}^{x=0}) \\ &= \kappa_{i^{z+},\beta} (a_{i^{z+},\beta}^{x=0} - a_{i^{z+},\beta}) \end{aligned} \quad (8)$$

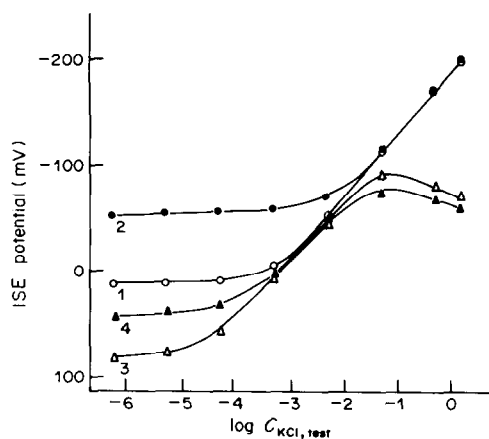


Fig. 7. Potential measured at *nb* membrane ISE for K^+ with and without valinomycin in the membrane. Concentration of K^+DPA^- in the membrane: $5 \times 10^{-4}M$. Concentration of valinomycin in the membrane: (1), (2), 0; (3), (4), $3.75 \times 10^{-3}M$. Concentration of Na^+Cl^- co-existing in the test solution: (1), (3), 0; (2), (4), $5 \times 10^{-1}M$.

where $\Delta_{\beta}^{\alpha}\phi_{i^{\pm}}^0$ is the standard Galvani potential difference for the ion transfer of i^{\pm} between α and β , $\kappa_{i^{\pm},\alpha}$ and $\kappa_{i^{\pm},\beta}$ are the coefficients of the Ilkovič equation, given by equations (9) and (10), and $a_{i^{\pm}}^{\alpha=0}$ and $a_{i^{\pm}}$ are the surface activity and the bulk activity of i^{\pm} in each phase, respectively.

$$\kappa_{i^{\pm},\alpha} = KzFD_{i^{\pm},\alpha}^{1/2} m^{2/3} t^{1/6} \quad (9)$$

$$\kappa_{i^{\pm},\beta} = KzFD_{i^{\pm},\beta}^{1/2} m^{2/3} t^{1/6} \quad (10)$$

Here, $D_{i^{\pm},\alpha}$ and $D_{i^{\pm},\beta}$ are the diffusion coefficients of i^{\pm} in the α and β phases, K is the Ilkovič constant, m is the volume flow-rate of the dropping electrolyte, and t is the electrolyte drop-time. The Ilkovič constant K had been determined by Samco *et al.*¹² to be 3.57, taking I , a , D , m and t in ampere, mole/ml, cm²/sec, ml/sec, and sec respectively. If i^{\pm} was originally present only in α or β , the polarogram can be described by equation (11) or (12), respectively. These equations are derived by using equations (7)–(10).

$$I_{a,i^{\pm}} = I_{ad,i^{\pm}}/[1 + (D_{i^{\pm},\alpha}/D_{i^{\pm},\beta})^{1/2} \exp\{-zF(\Delta_{\beta}^{\alpha}\phi - \Delta_{\beta}^{\alpha}\phi_{i^{\pm}}^0)/RT\}] \quad (11)$$

$$I_{c,i^{\pm}} = \frac{I_{cd,i^{\pm}} (D_{i^{\pm},\alpha}/D_{i^{\pm},\beta})^{1/2} \exp\{-zF(\Delta_{\beta}^{\alpha}\phi - \Delta_{\beta}^{\alpha}\phi_{i^{\pm}}^0)/RT\}}{[1 + (D_{i^{\pm},\alpha}/D_{i^{\pm},\beta})^{1/2} \exp\{-zF(\Delta_{\beta}^{\alpha}\phi - \Delta_{\beta}^{\alpha}\phi_{i^{\pm}}^0)/RT\}]} \quad (12)$$

where $I_{a,i^{\pm}}$ and $I_{c,i^{\pm}}$ are the average anodic and cathodic currents and $I_{ad,i^{\pm}}$ and $I_{cd,i^{\pm}}$ are the average anodic and cathodic limiting currents, which are given by equations (13) and (14):

$$I_{ad,i^{\pm}} = \kappa_{i^{\pm},\alpha} a_{i^{\pm},\alpha} \quad (13)$$

$$I_{cd,i^{\pm}} = -\kappa_{i^{\pm},\beta} a_{i^{\pm},\beta} \quad (14)$$

The electrical potential difference, ΔV , is given by

$$\Delta V + \text{const} = \Delta_{\beta}^{\alpha}\phi \quad (15)$$

The constant in equation (15) depends only on the composition of the solutions of the base electrolyte, on liquid-junction potentials, and on the reference electrodes, and is independent of the nature of the ion i^{\pm} .

Nernstian response at the ISE

The results gathered in Fig. 6 clearly indicate that the ISE displays a stable potential and gives Nernstian response to the concentration of TMA⁺ in the test solution, when the membrane contains TMA⁺.

From the polarograms presented in Fig. 1, it is also clear that when both the DAEE and the organic solution contain the analyte ion and the transfer of the ion at the aqueous/organic solution interface is very fast, the polarograms sharply intersect the potential axis at $\Delta V_{I=0}$, which is uniquely determined by the concentration of the ion in the DAEE or in the organic solution. From the ISE and polarographic results, we conclude that Nernstian response is

obtained at the ISE only when the test solution/membrane interface is depolarized by the analyte ions, as pointed out by Koryta^{2,3} and Fujinaga.⁴

Here, it should be stressed that zero current in the composite polarogram does not mean that there is no charge or mass transfer at the interface, but that the rate of transfer by the anodic reaction is equal to that by the cathodic reaction. That is to say,

$$I_{a,i^{\pm}} + I_{c,i^{\pm}} = 0 \quad (16)$$

By using equations (11)–(16), we obtain equation (17), which is similar to equation (7) but contains the bulk activities instead of surface activities of i_{α}^{\pm} and i_{β}^{\pm} .

$$\begin{aligned} \Delta V_{I=0} + \text{const} &= (\Delta_{\beta}^{\alpha}\phi)_{I=0} \\ &= \Delta_{\beta}^{\alpha}\phi_{i^{\pm}}^0 - (RT/zF) \\ &\quad \times \ln(a_{i^{\pm},\alpha}/a_{i^{\pm},\beta}) \end{aligned} \quad (17)$$

This equation suggests that $\Delta V_{I=0}$ in the polarogram or the ISE potential is controlled not only by the activity of i^{\pm} in the DAEE, $a_{i^{\pm},\text{DAEE}}$, or in the test solution, $a_{i^{\pm},\text{test}}$, but also by that in the organic solution, $a_{i^{\pm},\text{org}}$, or in the membrane, $a_{i^{\pm},\text{m}}$. In fact, $\Delta V_{I=0}$ given in Fig. 1 shifts by about +60 mV when the concentration of TMA⁺ in the *nb* solution is increased by a factor of 10, so the concentration in the DAEE remains constant. In the potential measured in the ISE cell of equation (4), the effect of $a_{i^{\pm},\text{m}}$ is not noticeable because the potential is measured as the difference between the potential at the inner solution/membrane interface and that at the test solution/membrane interface, and the effect cancels out. As mentioned later, however, the shift of the detection limit clearly indicates that the absolute potential at the individual interface changes, as a function of $a_{i^{\pm},\text{m}}$.

Detection limit in the ISE measurement

The composite polarogram and $\Delta V_{I=0}$ are affected by the anodic final rise or cathodic final descent of the residual current, when $a_{i^{\pm},\text{DAEE}}$ is sufficiently high or sufficiently low. Consequently, the shift of $\Delta V_{I=0}$ with $a_{i^{\pm},\text{DAEE}}$ is small in these concentration ranges. From comparison of the shift of $\Delta V_{I=0}$ in Fig. 1 with curve 8 in Fig. 6, it is clear that the dynamic concentration range detectable at the ISE is restricted by the same process as that which controls the shift of $\Delta V_{I=0}$.

The kind of supporting electrolytes and their concentration in the DAEE or in the organic solution

influence the final rise or the final descent in the polarogram. Hence, the detection limit at the ISE is affected by other salts present, as shown in Fig. 6.

The detection limit at the ISE is also controlled by $a_{i^z+,m}$ as indicated in Fig. 6, curves (1)–(3), because $\Delta V_{I=0}$ shifts towards more (or less) positive values and comes near to the anodic final rise (or the cathodic final descent) in the residual current with increase in the concentration of the analyte cation (or anion) in the organic solution (Fig. 1).

Interference in the ISE measurement

The polarogram for the transfer of j^{z+} from the α to the β phase is expressed by equation (18), similarly to equation (11) for i^{z+}

$$I_{a,j^z+} = I_{ad,j^z+} / [1 + (D_{j^z+,a} / D_{j^z+,\beta})]^{1/2} \times \exp\{-zF(\Delta_{\beta}^{\alpha}\phi - \Delta_{\beta}^{\alpha}\phi_{j^z+}^0) / RT\} \quad (18)$$

The interference from j^{z+} in the ISE measurement of i^{z+} can be explained by considering the effect of j^{z+} in the DAEE on $\Delta V_{I=0}$ in the composite polarogram for i^{z+} . The zero-current potential of the composite polarogram recorded in the presence of both i^{z+} and j^{z+} in the DAEE and i^{z+} in the organic solution is obtained when

$$I_{a,i^z+} + I_{a,j^z+} + I_{c,i^z+} = 0 \quad (19)$$

From equations (11), (12), (18) and (19), we obtain

$$\Delta V_{I=0} + \text{const} = \Delta_{\beta}^{\alpha}\phi_{i^z+}^0 - (RT/zF) \times \ln\{-B + (B^2 - 4AC)^{1/2}\} / 2A \quad (20)$$

where

$$A = (D_{i^z+,a} / D_{i^z+,\beta})^{1/2} (D_{j^z+,a} / D_{j^z+,\beta})^{1/2} D_{i^z+,\beta}^{1/2} a_{i^z+,\beta} \quad (21)$$

$$B = (D_{i^z+,a} / D_{i^z+,\beta})^{1/2} (D_{i^z+,\beta}^{1/2} a_{i^z+,\beta} - D_{j^z+,a}^{1/2} a_{j^z+,\alpha}) \times \exp\{-zF(\Delta_{\beta}^{\alpha}\phi_{j^z+}^0 - \Delta_{\beta}^{\alpha}\phi_{i^z+}^0) / RT\} \quad (22)$$

$$- (D_{j^z+,a} / D_{j^z+,\beta})^{1/2} D_{i^z+,a}^{1/2} a_{i^z+,\alpha}$$

$$C = - (D_{i^z+,a}^{1/2} a_{i^z+,\alpha} + D_{j^z+,a}^{1/2} a_{j^z+,\alpha}) \times \exp\{-zF(\Delta_{\beta}^{\alpha}\phi_{j^z+}^0 - \Delta_{\beta}^{\alpha}\phi_{i^z+}^0) / RT\} \quad (23)$$

The difference, $\Delta(\Delta V_{I=0})$, between equations (17) and (20) corresponds to the interference of j^{z+} in the ISE measurement of i^{z+} , and is given by

$$\Delta(\Delta V_{I=0}) = (RT/zF) \ln[(a_{i^z+,\beta} / a_{i^z+,\alpha}) \times \{-B + (B^2 - 4AC)^{1/2}\} / 2A] \quad (24)$$

The effect of Cs^+ and TEA^+ in the test solution on the ISE potential of $5 \times 10^{-4} M$ TMA^+ at the ISE

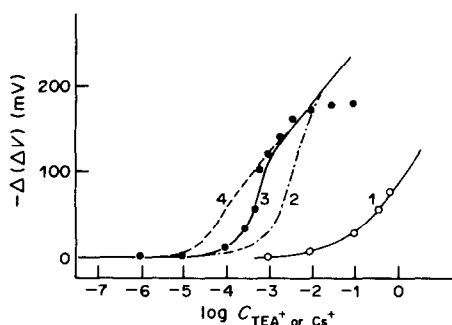


Fig. 8. Effect of Cs^+ or TEA^+ on the ISE potential of $5 \times 10^{-4} M$ TMA^+ . —, —, —; calculated, \odot , \bullet ; experimental. Foreign ion in the test solution: (1), Cs^+ ; (2)–(4), TEA^+ . Concentration of TMA^+ in the membrane (M): (1), (3), 5×10^{-4} ; (2), 5×10^{-3} ; (4), 5×10^{-5} . Constants used for the calculation: diffusion coefficients ($10^{-6} \text{ cm}^2/\text{sec}$): $D_{\text{TMA}^+,w}$ 6.4; $D_{\text{TMA}^+,nb}$ 3.3; $D_{\text{Cs}^+,w}$ 7.7; $D_{\text{Cs}^+,nb}$ 2.4; $D_{\text{TEA}^+,w}$ 5.1; $D_{\text{TEA}^+,nb}$ 2.8. Standard Galvani potential difference (V vs. TMAE): $\Delta_{nb}^w\phi_{\text{TMA}^+}^0$ 0; $\Delta_{nb}^w\phi_{\text{Cs}^+}^0 + 0.107$; $\Delta_{nb}^w\phi_{\text{TEA}^+}^0 - 0.105$.

(the nb membrane of which contains $5 \times 10^{-4} M$ TMA^+) are calculated according to equation (24) and illustrated as curves 1–4 in Fig. 8. In this calculation the diffusion coefficients of the ions in w and nb were estimated from the average limiting currents in the polarograms illustrated in Fig. 2, by use of equations (9), (10), (13) and (14), and the $\Delta_{\beta}^{\alpha}\phi^0$ values were determined from $\Delta V_{I=0}$ in the same polarograms and equation (17), assuming that the constant is negligible and the activity coefficient is unity. These values are given in Fig. 8. The experimental results obtained with the ISE cell of equation (4) are also plotted in Fig. 8. The accordance of the experimental with the calculated results in Fig. 8, especially in the lower concentration ranges, suggests that the interference should be estimated on the basis of equation (24). The deviation between the experimental and calculated values at higher concentrations of TEA^+ is attributable to the final descent in the residual current restricting the shift of $\Delta V_{I=0}$ in the composite polarogram for $\text{TMA}_w^+ \rightleftharpoons \text{TMA}_{nb}^+$ with $\text{TEA}_w^+ \rightarrow \text{TEA}_{nb}^+$.

From equation (24) it is obvious that the concentration of i^{z+} in the membrane is an important factor governing the magnitude of the interference.

With the aid of the conceptual polarograms in Fig. 9, the influence of the foreign ion, j^{z+} , on the ISE potential of i^{z+} , expressed by equation (24), can be intuitively understood. Curves 1–4 in Figs. 9a and 9b show polarograms for the transfer of j^{z+} in various concentrations from the aqueous (α) to the organic solution (β), $j_{\alpha}^{z+} \rightarrow j_{\beta}^{z+}$. Curve 5 is the composite polarogram of i^{z+} , $i_{\alpha}^{z+} \rightleftharpoons i_{\beta}^{z+}$, and curves 1'–4' are those in the presence of j^{z+} in the aqueous phase, $i_{\alpha}^{z+} \rightleftharpoons i_{\beta}^{z+}$ with $j_{\alpha}^{z+} \rightarrow j_{\beta}^{z+}$. Roughly speaking, the degree of interference of j^{z+} with the ISE potential of i^{z+} can be classified into two categories

- (i) $\Delta_{\beta}^{\alpha}\phi_{j^z+}^0 < \Delta_{\beta}^{\alpha}\phi_{i^z+}^0$, Fig. 9a.

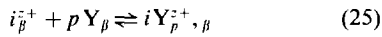
When $a_{j^+, \alpha}$ is small enough to give a smaller limiting current, $I_{ad, j^+, \alpha}$, than that of i^{z^+} in β , $I_{cd, i^+, \alpha}$, the deviation between $\Delta V_{I=0}$ in the presence of j^{z^+} , $\Delta V_{I=0(i^+ + i_{\beta} + j_{\alpha})}$, and that in the absence of j^{z^+} , $\Delta V_{I=0(i^+ + i_{\beta})}$, is small. At an $a_{j^+, \alpha}$ at which $I_{ad, j^+, \alpha}$ is equal to $I_{cd, i^+, \alpha}$, $\Delta V_{I=0}$ jumps from around $\Delta V_{I=0(i^+ + i_{\beta})}$ to around $\Delta V_{I=0(i_{\beta} + j_{\alpha})}$ (Fig. 9a). Here $\Delta V_{I=0(i_{\beta} + j_{\alpha})}$ is $\Delta V_{I=0}$ in the composite polarogram formed from the cathodic polarogram for $j^+ \rightarrow i^+$ and the anodic polarogram for $j^+ \rightarrow j^+$ when $I_{ad, j^+, \alpha}$ is slightly larger than $I_{cd, i^+, \alpha}$. At higher $a_{j^+, \alpha}$, $\Delta V_{I=0}$ shifts from $\Delta V_{I=0(i_{\beta} + j_{\alpha})}$ in almost Nernstian response to change in $a_{j^+, \alpha}$.

(ii) $\Delta_{\beta}^{\alpha} \phi_{j^+}^0 > \Delta_{\beta}^{\alpha} \phi_{i^+}^0$, Fig. 9b.

The interference of j^{z^+} is small and $\Delta V_{I=0}$ shifts monotonically with $a_{j^+, \alpha}$. When $a_{j^+, \alpha}$ is large enough, $\Delta V_{I=0}$ shifts in almost Nernstian response to change in $a_{j^+, \alpha}$.

The role of the ionophore in the ISE membrane

In the presence of the ionophore Y in β , i^{z^+} complexes with Y:



The stability constant, $K_{st, i^+ - Y}$, is

$$K_{st, i^+ - Y} = a_{iY_{p, \beta}^{z^+}} / a_{i^+, \beta} a_{Y, \beta}^p, \quad (26)$$

When $K_{st, i^+ - Y}$ is sufficiently large, $a_{i^+, \beta}$ is expressed as equation (27), using total activity of i^{z^+} and $i Y_{p, \beta}^{z^+}$, $a_{i^+, \text{total}, \beta}$,

$$a_{i^+, \beta} = a_{i^+, \text{total}, \beta} / (K_{st, i^+ - Y} a_{Y, \beta}^p) \quad (27)$$

Taking equations (7) and (27) into account, we obtain equations (28) and (29) for polarograms which show the transfer of i^{z^+} from α to β and from β to α , respectively, in the presence of Y in β .

$$I_{a, i^+} = I_{ad, i^+} / [1 + (D_{i^+, \alpha} / D_{iY_{p, \beta}^{z^+}})^{1/2} (K_{st, i^+ - Y} a_{Y, \beta}^p)^{-1} \exp \{-zF(\Delta_{\beta}^{\alpha} \phi - \Delta_{\beta}^{\alpha} \phi_{i^+}^0) / RT\}] \quad (28)$$

$$I_{c, i^+} = \frac{I_{cd, i^+} + (D_{i^+, \alpha} / D_{iY_{p, \beta}^{z^+}})^{1/2} (K_{st, i^+ - Y} a_{Y, \beta}^p)^{-1} \exp \{-zF(\Delta_{\beta}^{\alpha} \phi - \Delta_{\beta}^{\alpha} \phi_{i^+}^0) / RT\}}{[1 + (D_{i^+, \alpha} / D_{iY_{p, \beta}^{z^+}})^{1/2} (K_{st, i^+ - Y} a_{Y, \beta}^p)^{-1} \exp \{-zF(\Delta_{\beta}^{\alpha} \phi - \Delta_{\beta}^{\alpha} \phi_{i^+}^0) / RT\}]} \quad (29)$$

In these equations we assume that i^{z^+} diffuses from the bulk of the β phase to the interface as $i Y_{p, \beta}^{z^+}$, with diffusion coefficient $D_{iY_{p, \beta}^{z^+}}$, when $K_{st, i^+ - Y}$ is sufficiently large, and that formation of complexes of i^{z^+} in the α phase is negligible. $\Delta V_{I=0}$ in the composite polarogram recorded in the presence of i^{z^+} in both α and β , and of Y in β , occurs when $I_{a, i^+} + I_{c, i^+} = 0$:

$$\begin{aligned} \Delta V_{I=0} + \text{const} = & \Delta_{\beta}^{\alpha} \phi_{i^+}^0 - (RT/zF) \\ & \times \ln(a_{i^+, \alpha} / a_{i^+, \text{total}, \beta}) \\ & - (RT/zF) \ln(K_{st, i^+ - Y} a_{Y, \beta}^p) \quad (30) \end{aligned}$$

$\Delta V_{I=0}$ in the composite polarogram for the ion transfer,

$$(i_{\beta}^{z^+} \rightarrow i_{\alpha}^{z^+}) + (j_{\alpha}^{z^+} \rightarrow j_{\beta}^{z^+}),$$

in the presence of Y in β , can be expressed by equations (31)–(34), employing

$$I_{c, i^+} + I_{a, j^+} = 0.$$

Here, I_{a, j^+} is given by equation (28) modified by substituting j^{z^+} for i^{z^+} .

$$\begin{aligned} \Delta V_{I=0} + \text{const} = & \Delta_{\beta}^{\alpha} \phi_{j^+}^0 - (RT/zF) \\ & \times \ln\{[-L + (L^2 - 4MN)^{1/2}] / 2M\} \quad (31) \end{aligned}$$

where

$$\begin{aligned} L = & a_{i^+, \text{total}, \beta} (K_{st, i^+ - Y} a_{Y, \beta}^p)^{-1} D_{iY_{p, \beta}^{z^+}}^{1/2} \\ & \times (D_{i^+, \alpha} / D_{iY_{p, \beta}^{z^+}})^{1/2} (D_{j^+, \alpha} / D_{jY_{p, \beta}^{z^+}})^{1/2} \\ & \times (K_{st, j^+ - Y} a_{Y, \beta}^p)^{-1} \quad (32) \end{aligned}$$

$$\begin{aligned} M = & \{D_{iY_{p, \beta}^{z^+}}^{1/2} a_{i^+, \text{total}, \beta} - D_{j^+, \alpha}^{1/2} a_{j^+, \alpha}\} \\ & \times (D_{i^+, \alpha} / D_{iY_{p, \beta}^{z^+}})^{1/2} \\ & \times (K_{st, i^+ - Y} a_{Y, \beta}^p)^{-1} \\ & - \Delta_{\beta}^{\alpha} \phi_{i^+}^0 / RT \} \quad (34) \end{aligned}$$

From $\Delta V_{I=0}$ in the polarogram shown in Fig. 4a and equation (17), $\Delta_{nb}^w \phi_{K^+}$ is found to be +0.162 V vs. TMAE, and from equation (30) and $\Delta V_{I=0}$ in Fig.

4b, $K_{st, K^+ - val}$ is calculated to be 2.8×10^9 . Substituting $\Delta_{nb}^w \phi_{K^+}$, $K_{st, K^+ - val}$, and $\Delta V_{I=0}$ in the composite wave given as curve (7) in Fig. 5a, into equation (20) and taking $a_{i^+, \alpha}$ as zero, $\Delta_{nb}^w \phi_{Na^+}$ is found to be +0.290 V vs. TAME. From equations (31)–(34), $K_{st, Na^+ - val}$ is calculated to be 3.4×10^6 . Here, we assumed the diffusion coefficients of Na^+ and $Na^+ - val$ to be identical to those of K^+ and $K^+ - val$, respectively, as the solubility of Na^+ in nb is so low that it is difficult to get these values from the polarograms of Na^+ . Reported values^{10,13} for $\log K_{st, K^+ - val}$ are 6.82 in acetonitrile medium, 3.7–6.3 in ethanol, and 3.9–4.9 in methanol. Because a larger value for $K_{st, K^+ - val}$ in nb

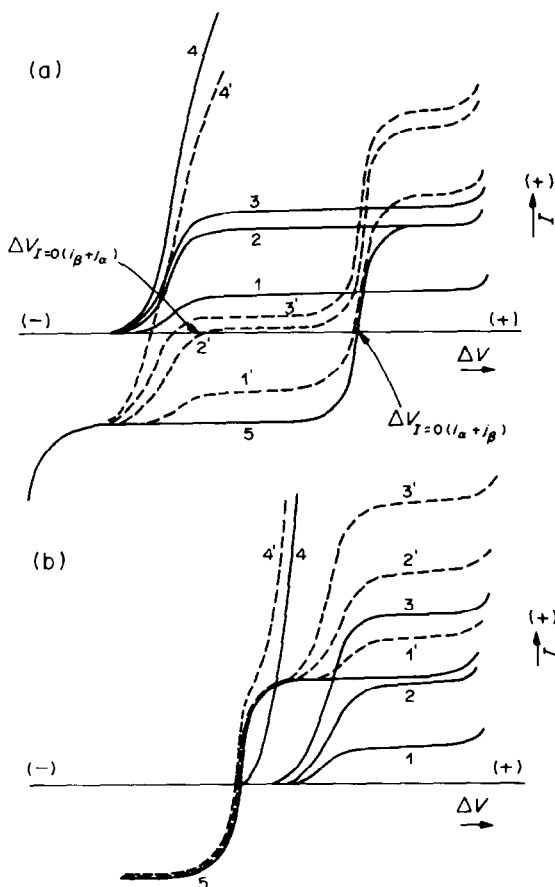


Fig. 9. The influence of j^{z+} in w on $\Delta V_{I=0}$ of the composite polarogram of $i_w^{z+} \rightleftharpoons i_{org}^{z+}$. (1)–(4), $j_w^{z+} \rightarrow j_{org}^{z+}$; (1')–(4'), $i_w^{z+} \rightleftharpoons i_{org}^{z+}$ with $j_w^{z+} \rightarrow j_{org}^{z+}$; (5), $i_w^{z+} \rightleftharpoons i_{org}^{z+}$.

was obtained in the present work, we consider that, taking the donor numbers¹⁴ (calculated value) of acetonitrile, ethanol and methanol to be 14.6, 30.4 and 33.8, respectively, solvation of K^+ in nb (which has a donor number of 8.4) may be considerably smaller than that in the other solvents, and consequently K^+ may easily complex with valinomycin in nb .

With regard to the role of the ionophore Y in the ISE measurements of i^{z+} it should be stressed not only that the interference from j^{z+} is reduced by the ionophore (depending on the values of $K_{st,i^+ - Y}$ and $K_{st,i^+ - Y}$), but also that the lower and upper detection limits are changed, depending on $K_{st,i^+ - Y}$. Considering that the lower and upper detection limits are determined by the anodic final rise and the cathodic final descent, respectively, of the residual current and

that $\Delta V_{I=0}$ in the composite polarogram for K^+ shifts by about -0.42 V in the presence of $3.75 \times 10^{-3} M$ valinomycin in nb , the detection limits are expected to be lowered by about seven orders of magnitude. In the presence of valinomycin, however, the lower detection limit is improved by only two orders of magnitude in the ISE measurement under the conditions of Fig. 7. This may be due to the negative shift of the anodic final rise in the residual current in the presence of valinomycin in nb .

As discussed above, it is possible to find a logical explanation for various essential points which have been empirically recognized in potentiometric ISE measurement, if we take the voltammetric current-potential relations into account.

In conclusion, although no experimental results are presented, we consider that the following may also be explained from the voltammetric viewpoint. (i) The diffusion current in the polarogram grows when the solution is stirred, resulting in a shift of $\Delta V_{I=0}$ in the composite polarogram and hence in the potential at the ISE. (ii) The super-Nernstian response in the ISE measurement may be attributed to irreversible ion transfer at the solution/membrane interface.

Acknowledgement—The authors thank Professor T. Fujinaga for his useful discussions and encouragement throughout the present work.

REFERENCES

1. G. Charlot, J. Badoz-Lambing and B. Trémillon, *Les réactions électrochimiques. Les méthodes électrochimiques d'analyse*, Masson, Paris, 1959.
2. J. Koryta, *Ion-selective Electrode Rev.*, 1983, **5**, 131.
3. *Idem.*, *Anal. Chim. Acta*, 1979, **111**, 1.
4. T. Fujinaga, *Phil. Trans. Roy. Soc.*, 1982, **305A**, 631.
5. T. Fujinaga, S. Kihara and Z. Yoshida, *Bunseki Kagaku*, 1982, **31**, E310.
6. S. Kihara, Z. Yoshida and T. Fujinaga, *ibid.*, 1982, **31**, E297.
7. J. Koryta, P. Vanysek and M. Brezina, *J. Electroanal. Chem.*, 1977, **75**, 211.
8. A. J. Parker, *Chem. Rev.*, 1969, **69**, 1.
9. O. Popovych, *Crit. Rev. Anal. Chem.*, 1970, **1**, 73.
10. Yu. A. Ovchinnikov, V. T. Ivanov and A. M. Shkrob, *Membrane Active Complexones*, p. 1. Elsevier, New York, 1974.
11. P. Delahay, *J. Phys. Chem.*, 1966, **70**, 2067.
12. Z. Samec, V. Marecek, J. Weber and D. Homolka, *J. Electroanal. Chem.*, 1979, **99**, 385.
13. W. Simon and W. E. Morf, in *Membranes, A Series of Advances, Vol. 2, Lipid Bilayers and Antibiotics*, G. Eisenman (ed.), p. 329. Dekker, New York, 1973.
14. V. Gutmann, *Co-ordination Chemistry in Non-aqueous Solutions*, pp. 19, 126. Springer Verlag, Vienna, 1968.

THE USE OF EMULSIONS IN THE PREPARATION OF SAMPLES AND STANDARDS FOR ANALYSIS BY ATOMIC-ABSORPTION SPECTROSCOPY DETERMINATION OF Cu AND Fe IN MIBK EXTRACTS OF THEIR APDC COMPLEXES

M. DE LA GUARDIA and M. T. VIDAL

Departamento de Química Analítica, Facultad de Ciencias Químicas, Universidad de Valencia, España

(Received 7 March 1983. Revised 5 November 1983. Accepted 7 May 1984)

Summary—The use of aqueous/organic emulsions is shown to give advantages in the AAS determination of Cu and Fe extracted as their pyrrolidinedithiocarbamate complexes into methyl isobutyl ketone. The emulsions are more stable than the extracts, and the standards can be prepared from aqueous solutions by emulsification, but without extraction.

In the last few years we have studied the application of the emulsion-formation technique to analysis for various metals in lipo-soluble matrices by atomic-absorption spectrometry, and by flame,² inductively coupled plasma³ and d.c. plasma⁴ emission photometry, with use of conventional aqueous solutions as standards. We have concluded that for emulsions to be employed successfully, the following requirements must be met.

- (1) The emulsions must be stable during the period of analysis.
- (2) The emulsions must be physically suitable for introduction into the atomization system.
- (3) Atomization of the samples and standards must match for identical concentrations of the analyte.

The first two conditions affect the method of preparing the emulsions, and for a particular matrix require selection of the surfactant, the proportions of the phases and the preparation procedure. The third condition depends essentially on the nature of the analyte compounds present in the matrix.

For example, in the determination of lead and manganese in gasolines^{1,5} the tetra-alkyl lead compounds and the tricarbonylmethylcyclopentadienyl-manganese must be previously mineralized with iodine or bromine to enable an emulsified aqueous solution to be used in the preparation of the standards, whereas in the determination of metallic additives in lubricating oils⁶ aqueous standards can be used directly for the analysis of oil samples emulsified with water.

However, owing to the complexity of the samples, clear conclusions about the behaviour of the emulsions cannot be deduced, so simple systems such as organic solutions of metallic complexes have been used for fundamental studies. Thus Berenguer *et al.*⁷ used oil-in-water (o/w) emulsions in the flame AAS

determination of copper and iron oxinates extracted into benzene and ethyl acetate. Later, we studied the use of o/w emulsions in the determination of aluminium by flame emission spectrometry of aluminium oxinate extracted into methyl isobutyl ketone (MIBK),² and also the use of different types of emulsified standards for the determination of magnesium oxinate in MIBK.⁸

In the present work, we examined the use of o/w and w/o (water in oil) emulsions for determination of Cu and Fe, extracted as their APDC complexes into MIBK, and compared the results with those obtained by use of direct aspiration of the organic extracts and of aqueous solutions, with respect to sensitivity and stability.

EXPERIMENTAL

Apparatus

Atomic-absorption measurements were made with a double-beam Perkin-Elmer Model 460 atomic-absorption spectrophotometer equipped with a single-slot burner for use with air/acetylene flame. The following operating parameters were employed:

	Cu	Fe
Wavelength, nm	324.8	248.3
Band-pass, nm	0.7	0.2
Lamp current, mA	15	30

Reagents

Standard 1000-ppm solutions of Cu and Fe.

Ammonium pyrrolidinedithiocarbamate (APDC). A freshly prepared 1% aqueous solution was purified by extraction with MIBK.

Nemol K 38. Nonyl phenol polyethylene glycol ether with 8 ethylene oxide units (Masso y Carol).

Tergitol XD. (Union Carbide), 1% aqueous solution.

Emulsogen LBH (Hoechst).

Procedure

APDC solution (1%, 1 ml) was added to 50 ml of an aqueous solution of a metal ion and the pH was adjusted to

Table 1. Extraction conditions

Element	Shaking time, <i>min</i>	pH for quantitative extraction	pH for optimum absorbance	Maximum concentration, <i>ppm</i>
Cu	2	0-10	2-10*	20
Fe	3	1-8	5-6	> 50

*Except at pH = 8.

a suitable value. The solution was transferred to a separatory funnel and shaken for a suitable time with 20 ml of MIBK (accurately measured). The two phases were then allowed to separate.

For preparation of the o/w emulsions, 10 ml of the organic extract were emulsified with 0.25 g of Nemol K 38 and 25 ml of a 1% aqueous solution of Tergitol XD, and enough distilled water to bring the total volume to 100 ml.

The w/o emulsions were prepared with 10 ml of the organic phase, 2.5 ml of distilled water and 3 ml of Emulsogen LBH, and enough MIBK to make the volume 25 ml.

Samples prepared in this manner were introduced into an air/acetylene flame and analysed under the optimum instrumental conditions. MIBK-in-water and water-in-MIBK emulsions were employed as standards. They were prepared in the same way, but the metal ion was introduced in the aqueous phase.

RESULTS AND DISCUSSION

Extraction conditions

Solvent extraction with APDC in MIBK is the most frequently employed system for determination of Cu and Fe by liquid-liquid extraction and atomic-absorption spectrometry.⁹⁻¹⁴ The optimum extraction conditions were described in a previous paper,¹⁵ and are summarized in Table 1.

Instrumental conditions

For each of the four different types of standard used, the flame profiles and instrumental conditions which give the best sensitivity were determined. From the data in Table 2 it can be seen that the presence

of the organic phase changes the flame profiles, and the optimum gas flows and heights of observation in the flame are modified accordingly.

However, there are some differences between the behaviour of the two elements. For iron, the optimum flow ratio (air to acetylene) is 4.1 for aqueous solutions and o/w emulsions, 8.3 for organic extracts and 5.3 for w/o emulsions; that is, the gas mixture is made richer in air as more organic solvent is introduced.

For copper, a different behaviour can be observed, the optimum gas ratio being the same for the aqueous standards and w/o emulsions, but lower for the o/w emulsions and again highest for the organic extracts.

For both elements the aspiration rate of the organic extracts was lower than that for the aqueous standards and greater than that for the o/w and w/o emulsions, so the apparently irregular behaviour of copper (with respect to flame composition) is not due to the rheological features of the emulsions (which were the same as those used for iron) but to the temperature and atomization conditions.

There are also very marked differences in the optimum positions of observation in the flame (*i.e.*, height above burner top) though the pattern is the same for the two elements.

Comparison between emulsified standards and emulsified extracts

One of the principal advantages of the use of emulsions in the AAS determination of metallic

Table 2. Optimum AAS instrumental parameters for maximum sensitivity

Element	Flame parameter	Samples			
		aqueous	extracts	emulsions o/w	emulsions w/o
Cu	air flow, <i>l./min</i>	17.5	29.5	13.4	17.5
	acetylene flow <i>l./min</i>	3.3	3.3	3.3	3.3
	height above burner top, <i>mm</i>	20	17.5	20	10
	aspiration rate, <i>ml/min</i>	6.8	6.5	5	3.8
Fe	air flow, <i>l./min</i>	13.4	27.5	13.4	17.5
	acetylene flow, <i>l./min</i>	3.3	3.3	3.3	3.3
	height above burner top, <i>mm</i>	17.5	12.5	17.5	7.5
	aspiration rate*, <i>ml/min</i>	6.8	6.5	5	3.8

*The aspiration rates have not been optimized, but were measured for identical nebulizer positions and are used in a comparative manner.

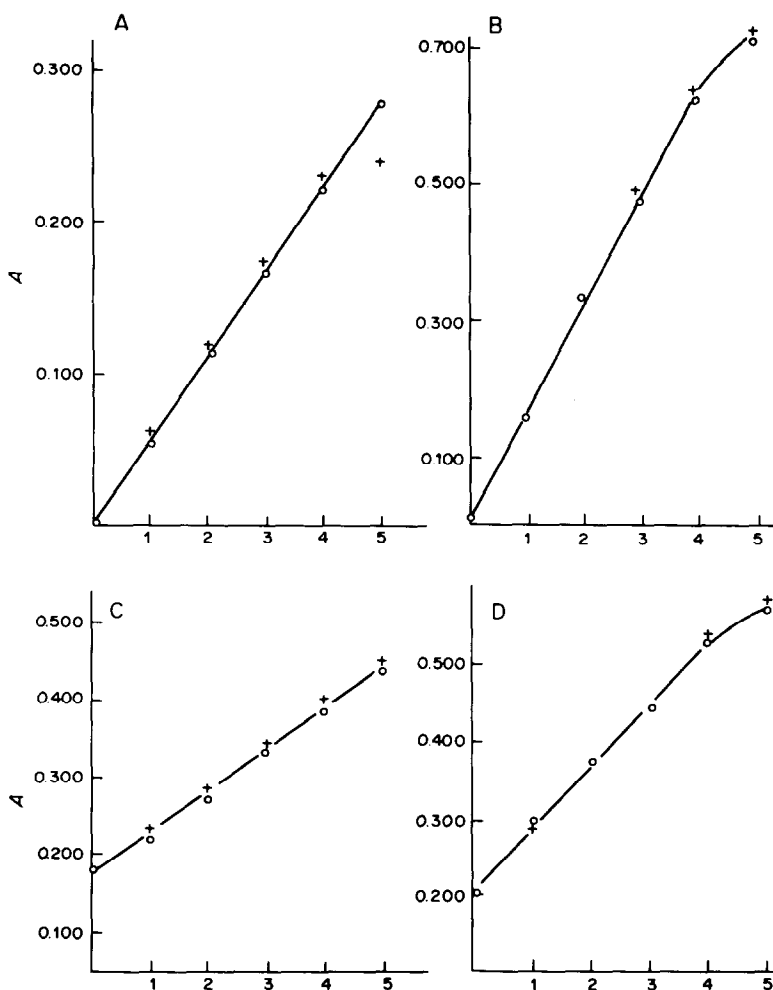


Fig. 1. Absorbance values for aqueous emulsified standards (○) and emulsified extracts (+) plotted vs. metal concentration: A, o/w emulsions Cu, $\psi = 0.08$; B, w/o emulsions Cu, $\psi = 0.08$; C, o/w emulsions Fe, $\psi = 0.17$; D, w/o emulsions Fe, $\psi = 0.05$.

elements in organic matrices is that aqueous solutions can be used for preparation of the standards.

To test whether aqueous copper and iron solutions emulsified with MIBK can be used as standards for the determination of these elements in extracts of their complexes with APDC in MIBK, calibration graphs were prepared from emulsified aqueous solutions and from aliquots of emulsified extracts. The results are shown in Fig. 1.

The agreement between the two sets of results was evaluated by means of Exner's parameter¹⁶ and found to be good to very good for all cases, except the iron o/w emulsions for which it was only fairly good.

The slightly greater absorbance obtained for the emulsified organic extracts may be due to the solubility of MIBK in water, although both phases were pre-equilibrated.¹⁵

Comparison of the different types of standards

Figures 2 and 3 show the calibration graphs obtained with each of the four types of standards

under optimum instrumental conditions. It can be noted that the introduction of an organic phase, alone or emulsified, produces a strong increase in the sensitivity. Although the use of organic extracts and emulsions decreases the feed-rate into the flame, this effect is largely offset by the contribution of the MIBK combustion to the flame temperature.

We have found that in some cases the use of an aspiration rate different from that usually used for aqueous solutions can make the sensitivity for emulsified samples and standards higher than that for direct introduction of organic extracts, but difficulty in reproducing the nebulizer position makes these results less easily reproducible. For that reason the results given here were all obtained at the aspiration rate usually used for aqueous solutions.

The important features of the calibration graphs are summarized and compared in Tables 3 and 4. An important aspect to be considered is the stability of the extracts, since this is one of the disadvantages that can appear in analysis by liquid-liquid extraction and

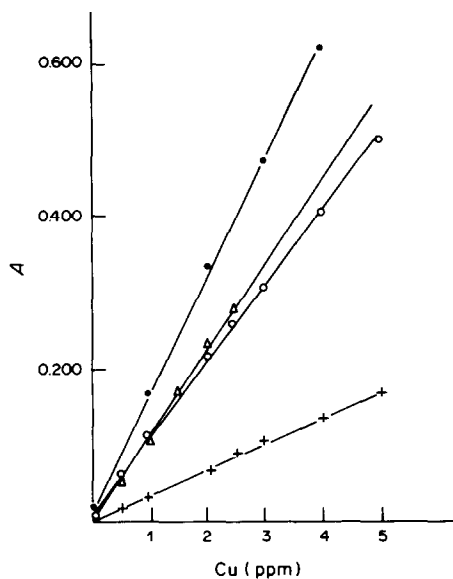


Fig. 2. Calibration curves for the different Cu standards: ○ extracts; ● w/o emulsions; Δ o/w emulsions; + aqueous.

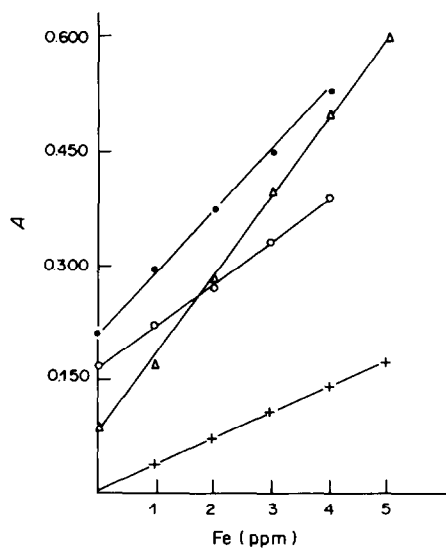


Fig. 3. Calibration curves for the different Fe standards: ● w/o emulsions; ○ extracts; Δ o/w emulsions; + aqueous.

AAS. For iron, whereas the extracts are only stable for 2 hr, the o/w and w/o emulsions are stable for 1 day and 3 weeks respectively.

For copper, however, there is less advantage, since the extracts are stable for 5 days, and o/w and w/o emulsions for 1 day and 8 days respectively.

Conclusions

Conversion of MIBK extracts of the APDC com-

plexes of iron and copper into aqueous/organic emulsions allows direct preparation of standards from aqueous solutions of the elements, but the solubility of MIBK in the aqueous phase may lead to systematic error unless the entire organic extract is converted into an emulsion. For iron, the emulsified extracts are appreciably more stable than the more commonly used simple organic extracts. The flame conditions should be optimized for the particular emulsion used.

Table 3. Comparison of copper standards

	aqueous	extracts	emulsions o/w	emulsions w/o
Sensitivity*	0.065	0.174	0.098	0.154
Relative sensitivity†	1	2.7	1.5	2.4
Detection limit, ppm ($K = 3$)	0.01	0.03	0.03	0.02
Applicability range, ppm	0.01-5	0.03-5	0.03-2	0.02-5
Stability	—	5 days	1 day	8 days

*Sensitivity is determined from the slope of the regression line.

†Relative sensitivity

$$= \frac{\text{Slope of the calibration line for the standard}}{\text{Slope of the calibration line for aqueous standards}}$$

Table 4. Comparison of iron standards

	aqueous	extracts	emulsions o/w	emulsions w/o
Sensitivity*	0.045	0.084	0.074	0.097
Relative sensitivity†	1	1.9	1.6	2.2
Detection limit, ppm ($K = 3$)	0.04	0.05	0.03	0.02
Applicability range, ppm	0.04-5	0.05-5	0.03-5	0.02-3
Stability	—	2 hr	1 day	3 weeks

*See footnotes to Table 3.

REFERENCES

1. V. Berenguer, J. L. Guiñon and M. de la Guardia, *Z. Anal. Chem.*, 1979, **294**, 416.
2. M. de la Guardia, V. Berenguer and J. L. Guiñon, *Analisis*, 1980, **8**, 166.
3. M. de la Guardia, G. Legrand, M. Druon and J. L. Louvrier, *ibid.*, 1982, **10**, 476.
4. M. de la Guardia, A. Salvador and V. Berenguer, *ibid.*, 1981, **9**, 74.
5. M. de la Guardia and M. J. Sanchez, *Atom. Spectrosc.*, 1982, **3**, 36.
6. L. C. Westwood, *Develop. Appl. Spectrosc.*, 1971, **9**, 235.
7. V. Berenguer, M. Esplá and J. Hernandez, *Anal. Chem.*, 1977, **31**, 329.
8. M. de la Guardia and V. Berenguer, *Afinidad*, 1982, **39**, 377.
9. S. R. Koirtyohann and J. W. Wen, *Anal. Chem.*, 1973, **45**, 1986.
10. K. Kremling and H. Peterson, *Anal. Chim. Acta*, 1974, **70**, 35.
11. T. K. Jan and D. R. Young, *Anal. Chem.*, 1978, **50**, 1250.
12. P. Pakalns and Y. J. Farrar, *Water Res.*, 1977, **11**, 145.
13. J. D. Kinrade and J. C. Van Loon, *Anal. Chem.*, 1974, **46**, 1894.
14. L. Danielsson, B. Magnusson and S. Westerlund, *Anal. Chim. Acta*, 1978, **98**, 47.
15. M. de la Guardia and M. T. Vidal, *Atom. Spectrosc.*, 1983, **4**, 40.
16. O. Exner, *Collection Czech. Chem. Commun.*, 1965, **31**, 3222.

SPECTROPHOTOMETRIC STUDY OF URANIUM(VI) CHELATE FORMATION WITH β -DIKETONES AND TRIBUTYL PHOSPHATE IN AQUEOUS, NONA(OXYETHYLENE) DODECYL ETHER SOLUTION

TOMITSUGU TAKETATSU

College of General Education, Kyushu University, Ropponmatsu, Chuo-ku, Fukuoka, Japan 810

(Received 24 March 1984. Accepted 2 May 1984)

Summary—The distribution ratio of uranium(VI) with 2-thenoyltrifluoroacetone, 2-furoyltrifluoroacetone and benzoyltrifluoroacetone in the presence and absence of tributyl phosphate between micellar and bulk phases in nona(oxyethylene) dodecyl ether solution was measured spectrophotometrically as a function of hydrogen-ion concentration. The thermodynamic constants for these reactions were evaluated from the variation of the equilibrium constants as a function of temperature. The entropy change contributes to the synergistic reaction.

It has been shown that uranium(VI)¹ and europium,^{2,3} terbium³ and samarium^{2,3} can be determined spectrophotometrically and spectrophotofluorimetrically, respectively, with 2-thenoyltrifluoroacetone (TTA) and trioctylphosphine oxide in micellar solutions of a non-ionic surfactant. The synergistic partition of metal ions with β -diketones and a neutral donor between organic and aqueous phases has been widely studied. Several investigators have estimated the thermodynamic constants for the purpose of explaining the mechanism of synergistic solvent extraction of uranium⁴ and europium⁵ with TTA and a neutral donor. However, the corresponding partition equilibria between micellar and bulk phases have been scarcely studied, because the estimation of the species in these phases is not always easy. In the present paper, the distribution ratios (D) for uranium(VI) with TTA, 2-furoyltrifluoroacetone (FTA) and benzoyltrifluoroacetone (BFA) in the presence and absence of TBP, between micellar and bulk phases in nona(oxyethylene) dodecyl ether (BL-9EX) solution have been determined as a function of hydrogen-ion concentration, assuming that the absorbance of the metal chelate corresponds to the concentration of metal ion in the micellar phase. The equilibrium constants for those chelates are evaluated from the slopes of plots of $\log D$ vs. $\log [H^+]$. Thermodynamic constants are calculated from the relationship between the equilibrium constants and temperature.

EXPERIMENTAL

Materials

TTA, FTA and BFA were obtained from Dojin Chemical Co., TBP and uranium acetate from Wako Chemical Co. and BL-9EX from Nikko Chemical Co. The solution of uranium acetate was standardized by titration with EDTA (Xylenol Orange as indicator). All chemicals used were of analytical-reagent grade.

Stock solutions

The concentrations in the mixed stock solution (pH 5.5–6.0) used were $4 \times 10^{-3} M$ TTA, FTA or BFA, $4 \times 10^{-5} M$ uranyl acetate, $0.01 M$ acetic acid, $0.2 M$ sodium chloride and 1% w/v BL-9EX. The concentration of TBP was $4 \times 10^{-3} M$.

Procedure

Ten ml of the mixed stock solution were placed in a beaker, adjusted to approximately the desired pH value with dilute hydrochloric acid, transferred to a 20-ml standard flask and made up to volume with water. The solution was poured into a 25-ml stoppered flask and the flask was shaken mechanically in a thermostat for at least 3 hr. The absorbance was measured at 385, 375 and 377 nm for TTA, FTA and BFA, respectively, both in the absence and presence of TBP. A reagent blank was used as reference solution.

RESULTS AND DISCUSSION

Figure 1 shows the absorption spectra of the UO_2^{2+} -TTA and UO_2^{2+} -TTA-TBP systems in the BL-9EX micellar solution. The absorption maxima are at 385 nm. A similar pattern was found at 375 nm for the FTA and FTA-TBP systems and at 377 nm for the BFA and BFA-TBP systems.

Figures 2 and 3 show the relationship between the absorbance at 385 nm and pH in the UO_2^{2+} -TTA and UO_2^{2+} -TTA-TBP systems, at different temperatures. It is seen that the absorbances are constant and maximal at pH > 4.0 for the TTA system and > 3.0 for the TTA-TBP system at all the temperatures tested. For the other systems, which behaved similarly, the critical pH values were 4.2 (FTA), 3.3 (FTA-TBP), 3.5 (BFA) and 2.8 (BFA-TBP).

In a previous paper,⁶ it was shown by a spectrophotometric method that most of the TTA exists outside the micelles, i.e., in the bulk phase. On the other hand, most of the β -diketone chelates and TBP

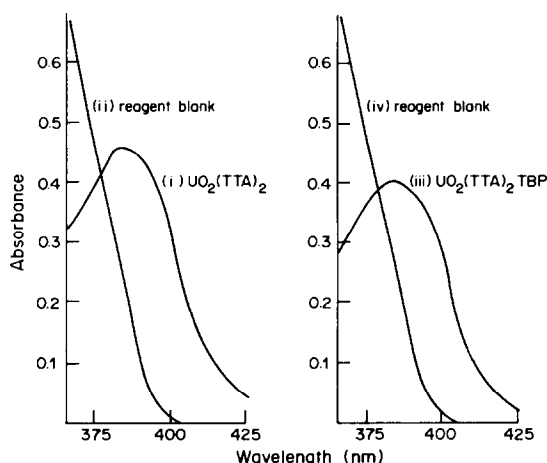
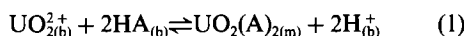


Fig. 1. Absorption spectra of $\text{UO}_2(\text{TTA})_2$ and $\text{UO}_2(\text{TTA})_2\text{TBP}$ chelates in micellar solution. $\text{UO}_2^{2+} 2 \times 10^{-5} M$, $\text{TTA} 2 \times 10^{-3} M$, $\text{TBP} 2 \times 10^{-3} M$ and $\text{BL-9EX} 0.5\%$. (i) $\text{UO}_2(\text{TTA})_2$ chelate, pH 4.16 and (ii) reagent blank; (iii) $\text{UO}_2(\text{TTA})_2\text{TBP}$ chelate, pH 4.06 and (iv) reagent blank.

seem to exist in the micellar phase, because the species are scarcely dissolved in an aqueous solution if the surfactant is not added. Also, the uranium chelates with β -diketones (HA) are known to be $\text{UO}_2(\text{A})_2(\text{H}_2\text{O})_x$,^{4,7} and $\text{UO}_2(\text{A})_2\text{TBP}$.^{4,7,8} For simplicity, the question of hydration of the chelate will be ignored for the moment, but discussed later. Then the chelate $\text{UO}_2(\text{A})_2$ is presumed to be formed by the reaction



the subscripts (b) and (m) referring to the mutually equilibrated bulk and micellar phases, respectively, and the equilibrium constant is defined by

$$k_1 = \frac{[\text{UO}_2(\text{A})_2]_{(m)} [\text{H}^+]_{(b)}^2}{[\text{UO}_2^{2+}]_{(b)} [\text{HA}]_{(b)}^2} \quad (2)$$

Equation (2) can be expressed as

$$\log D_1 + 2\log [\text{H}^+]_{(b)} - 2\log [\text{HA}]_{(b)} - \log k_1 = 0 \quad (3)$$

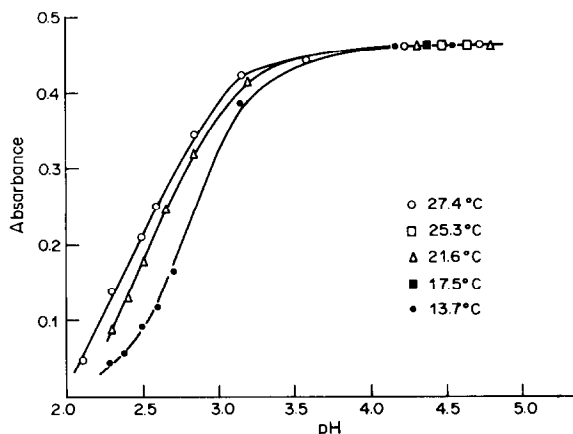


Fig. 2. Relationship between absorbance and pH for the UO_2^{2+} -TTA system at various temperatures. Concentrations as for Fig. 1, $\text{UO}_2^{2+} 2 \times 10^{-5} M$, $\text{TTA} 2 \times 10^{-3} M$ and $\text{BL-9EX} 0.5\%$.

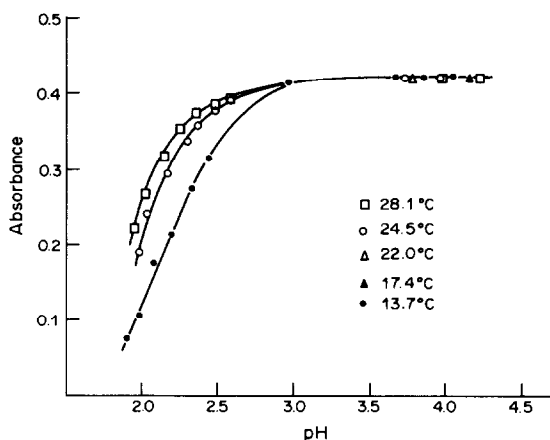


Fig. 3. Relationship between absorbance and pH for the UO_2^{2+} -TTA-TBP system at various temperatures. Concentrations as for Fig. 1.

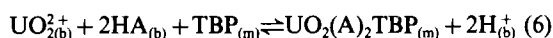
where

$$D_1 = \frac{[\text{UO}_2(\text{A})_2]_{(m)}}{[\text{UO}_2^{2+}]_{(b)}} \quad (4)$$

When equation (3) is differentiated with respect to $\log [\text{H}^+]_{(b)}$ at constant HA concentration,

$$\frac{d \log D_1}{d \log [\text{H}^+]_{(b)}} = -2 \quad (5)$$

is obtained; here, the concentration of HA can be assumed to be constant if there is a large excess of reagent relative to metal ion. The ionic strength is held constant at about 0.1. Similarly, the equilibrium for the adduct reaction is



for which

$$k_2 = \frac{[\text{UO}_2(\text{A})_2\text{TBP}]_{(m)} [\text{H}^+]_{(b)}^2}{[\text{UO}_2^{2+}]_{(b)} [\text{HA}]_{(b)}^2 [\text{TBP}]_{(m)}} \quad (7)$$

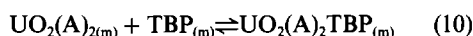
and

$$\frac{d \log D_2}{d \log [\text{H}^+]_{(b)}} = -2 \quad (8)$$

where

$$D_2 = \frac{[\text{UO}_2(\text{A})_2\text{TBP}]_{(m)}}{[\text{UO}_2^{2+}]_{(b)}} \quad (9)$$

Equation (11) for the reaction in equation (10) is derived from equations (2) and (7):



$$\beta = \frac{[\text{UO}_2(\text{A})_2\text{TBP}]_{(m)}}{[\text{UO}_2(\text{A})_2]_{(m)} [\text{TBP}]_{(m)}} = \frac{k_2}{k_1} \quad (11)$$

The following assumptions can be introduced from the results shown in Figs. 2 and 3: (i) the concentration of uranium(VI) in the micellar phase is linearly proportional to the absorbance, and (ii) almost all the uranium species exist in the micellar phase, in the pH range for which the absorbance is constant and maximal. Thus, the values of D_1 and D_2 were

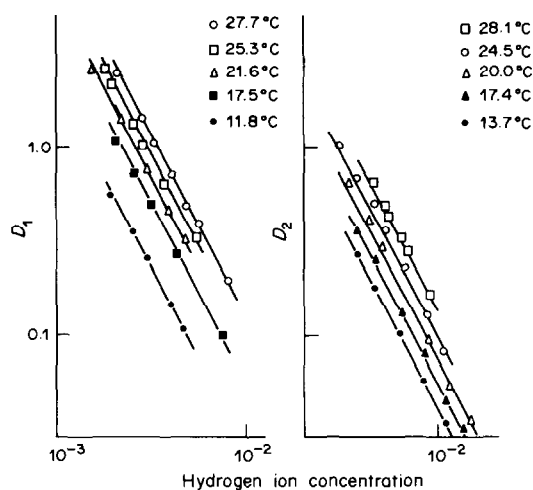


Fig. 4. Variation of distribution ratio in the UO_2^{2+} -TTA and UO_2^{2+} -TTA-TBP systems as a function of hydrogen-ion concentration at various temperatures. Concentrations as for Fig. 1.

calculated by using the spectrophotometric data described above.

Figure 4 shows that the slopes of the graphs of $\log D_1$ vs. $\log [\text{H}^+]_{(b)}$ and $\log D_2$ vs. $\log [\text{H}^+]_{(b)}$ for the UO_2^{2+} -TTA and UO_2^{2+} -TTA-TBP systems, respectively, are almost linear (about -2), irrespective of the temperatures used. Similar results are obtained in the other systems. The values of $\log k_1$ and $\log k_2$ can be estimated by using equations (2) and (7), respectively, and the values of $\log \beta$ by using equation (11). The values at 25° are given in Table 1. It is seen that $\log k_1$ and $\log k_2$ decrease in the orders $\text{UO}_2(\text{BFA})_2 > \text{UO}_2(\text{TTA})_2 > \text{UO}_2(\text{FTA})_2$ and $\text{UO}_2(\text{BFA})_2\text{TBP} > \text{UO}_2(\text{TTA})_2\text{TBP} > \text{UO}_2(\text{FTA})_2\text{TBP}$, respectively. The synergistic effect of TBP adduct formation is obvious for all the systems.

Akiba *et al.*⁹ measured the values of $\log \beta$ in various organic solvents for the UO_2^{2+} -TTA-TBP system by the solvent-extraction method. The values ranged from 4.42 for methylene chloride to 6.81 for

Table 1. Thermodynamic values for $\text{UO}_2(\text{A})_2$ and $\text{UO}_2(\text{A})_2\text{TBP}$ chelate formation

	$\log k_1$	$\Delta G,$ kJ/mole	$\Delta H,$ kJ/mole	$\Delta S,$ $\text{J. mole}^{-1}, \text{K}^{-1}$
TTA	0.29	-1.66	53.9	186
FTA	-0.46	2.63	51.3	165
BFA	1.08	-6.16	67.5	247
	$\log k_2$			
TTA	6.83	-39.0	64.7	348
FTA	5.86	-33.6	78.7	376
BFA	7.77	-44.4	68.8	379
	$\log \beta$			
TTA	6.54	-37.3	10.8	161
FTA	6.32	-36.1	27.4	211
BFA	6.69	-38.2	1.3	133

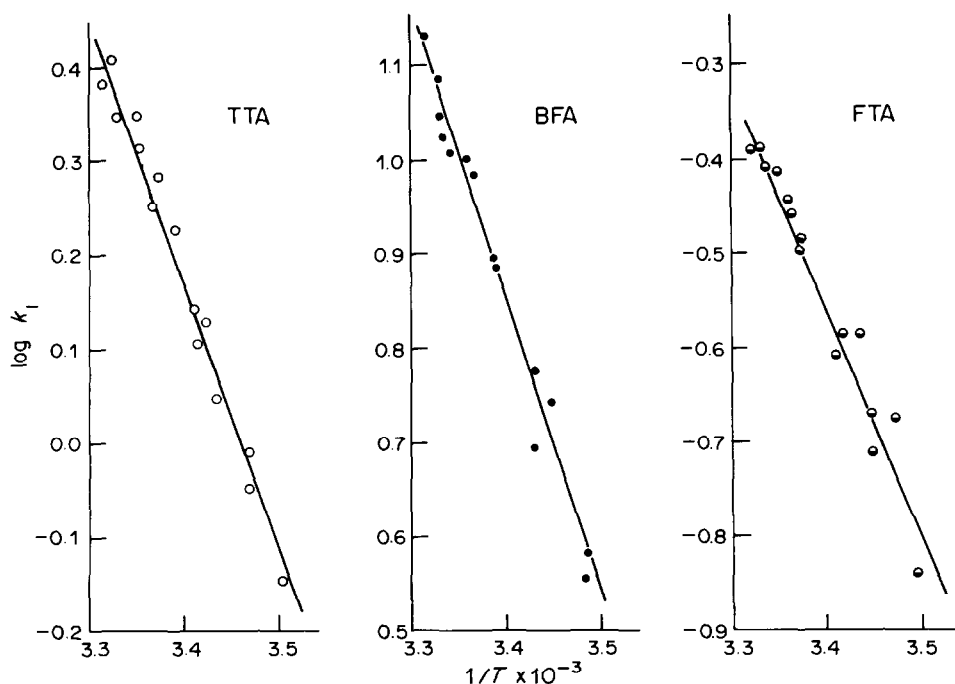


Fig. 5. Variation of $\log k_1$ with temperature. Concentrations as for Fig. 1 and $[\text{BFA}] = [\text{FTA}] = [\text{TTA}]$.

cyclohexane, corresponding to the solubility of water in the solvents. The value of 6.54 for the micellar system is about the same as that of 6.47 for the n-heptane system. This perhaps gives a clue to the state of the micellar microenvironment in which the adduct chelates exist.

Figure 5 shows the variation of $\log k_1$ with reciprocal of the absolute temperature for the simple systems, and the enthalpy changes ΔH were calculated from them by using the van't Hoff equation. The corresponding entropy changes were also evaluated. The values of ΔH for the UO_2^{2+} -TTA, UO_2^{2+} -FTA and UO_2^{2+} -BFA systems are 53.9, 51.3 and 67.5 kJ/mole, respectively. Endothermic reactions are common for chelate formation in which the hydration sheath of the metal ion is replaced by the chelating reagent. The values of ΔS are positive and large. It is thought that the reason for this is release of the water molecules from the $\text{HTTA}\cdot\text{H}_2\text{O}$ and $\text{UO}_2\cdot y\text{H}_2\text{O}$ species when the reagent reacts with uranyl ion according to equation (1) since the HTTA species that is dominant in the micellar system exists as the keto-hydrate in the bulk phase.

ΔH and ΔS for all the synergistic reactions are both positive, and ΔS is especially large. The large ΔS could be explained as due to release of water molecules from both the hydrated chelate $\text{UO}_2(\text{A})_2(\text{H}_2\text{O})_x$ and the $\text{TBP}\cdot\text{H}_2\text{O}$ dominant species that is in the micellar system, when the TBP adduct is formed. However, Subramanian *et al.*⁴ reported that the values of ΔH and ΔS were -21.8 kJ/mole and

-34 J.mole⁻¹.K⁻¹, respectively, for the UO_2^{2+} -TTA-TBP system with benzene as solvent. Choppin¹⁰ has stated that these negative values would imply no replacement of water molecules and no expansion of the co-ordination sphere of uranium(VI) in the adduct formation. This contrast in the values for the micellar and solvent-extraction systems could be explained by the degree of affinity of TBP for water. In the micellar system, the alkyl groups and oxygen atom of TBP perhaps orient to the oligophile and hydrophile parts of the micelle, respectively. Therefore, the environment of the TBP-water adduct is more hydrophilic than that in benzene and the adduct perhaps exists as $\text{TBP}\cdot\text{H}_2\text{O}$.

REFERENCES

1. T. Taketatsu, M. Aihara and Y. Kimoto, *Bunseki Kagaku*, 1981, **30**, 328.
2. T. Taketatsu and A. Sato, *Anal. Chim. Acta*, 1979, **108**, 429.
3. T. Taketatsu, *Talanta*, 1982, **29**, 397.
4. M. S. Subramanian and S. A. Pai, *J. Inorg. Nucl. Chem.*, 1970, **32**, 3677.
5. A. T. Kandil, H. F. Aly, M. Raieh and G. R. Choppin, *ibid.*, 1975, **37**, 229.
6. T. Taketatsu and A. Sato, *Bull. Chem. Soc. Japan*, 1980, **53**, 3713.
7. N. C. Li, S. M. Wang and W. R. Walker, *J. Inorg. Nucl. Chem.*, 1965, **27**, 2263.
8. K. Akiba, *ibid.*, 1973, **35**, 3323.
9. K. Akiba and N. Suzuki, *Bull. Chem. Soc. Japan*, 1971, **44**, 1043.
10. G. R. Choppin, *Sep. Sci. Technol.*, 1981, **16**, 1113.

RADIOCHEMICAL DETERMINATION OF TECHNETIUM-99

NORTON Y. CHU and JERRY FELDSTEIN*

Environmental Measurements Laboratory, U.S. Department of Energy, New York, NY 10014, U.S.A.

(Received 3 November 1983. Accepted 30 April 1984)

Summary—A procedure has been developed for the determination of ^{99}Tc in vegetation, by use of $^{95\text{m}}\text{Tc}$ as an internal tracer. The samples are wet-ashed, without significant loss of Tc. The Tc is separated from most other radionuclides by precipitation with calcium carbonate, and is purified by anion-exchange chromatography and electro-deposition. The radiochemical yield of Tc is determined by Ge(Li) gamma-ray spectrometry of the 204-keV photon peak of the $^{95\text{m}}\text{Tc}$ internal tracer, and the ^{99}Tc activity is determined by counting its 0.292-MeV beta-particles with a scintillation counter. The detection limit for ^{99}Tc in a sample weighing about 10 g is 0.1 pCi for a 3000-min count.

There has recently been considerable interest in measuring the environmental concentrations and distributions of ^{99}Tc ,¹⁻⁷ a potential toxic pollutant hazard originating from nuclear power plants and nuclear fuel reprocessing operations.⁴⁻¹³ This interest has led to the development of a number of methods for measuring this long-lived beta emitter. ^{99}Tc and the other major isotopes of Tc are listed in Table 1.

Isotope-dilution mass-spectrometry (IDMS), with a ^{97}Tc tracer, is the most sensitive analytical method for determining ^{99}Tc .^{1,8} Measurements of ^{99}Tc activities as small as 0.02 pCi have been achieved by this method. However, IDMS requires expensive sophisticated instrumentation and very thorough decontamination from ^{97}Mo , which causes interference. This interference problem can be eliminated by substituting resonance (laser-induced ionization) IDMS for the usual thermal-ionization IDMS, but at the cost of additional special apparatus.

^{99}Tc has also been determined by beta-counting with $^{97\text{m}}\text{Tc}$ as an internal tracer.⁹ The $^{97\text{m}}\text{Tc}$ yield is measured by counting its conversion electrons in a beta-counter. However, the beta radioassay of the ^{99}Tc requires that the conversion electrons from the $^{97\text{m}}\text{Tc}$ be screened out. This is accomplished with 14-mg/cm² aluminium absorbers,⁹ but the absorbers cause a severe reduction in the sensitivity of the method,^{9,14} and a decrease in precision. Because the ^{99}Tc and the $^{97\text{m}}\text{Tc}$ are both counted by the same detector, an unexpectedly high ^{99}Tc activity can interfere with the $^{97\text{m}}\text{Tc}$ count-rate measurement.⁹ (The $^{97\text{m}}\text{Tc}$ count rate is typically 30-40 cpm in a Geiger-Müller detector.⁹)

$^{95\text{m}}\text{Tc}$ has been used as an external tracer for the determination of ^{99}Tc by adding it to one of a pair of duplicate samples and attempting to analyse both in an identical manner. The unspiked duplicate was beta-counted, and it was assumed that its Tc chemical yield was the same as that of the spiked duplicate.

The reproducibility of the chemical recovery of Tc was found to depend primarily on the care taken by the analyst.^{14,15}

In the method presented here, $^{95\text{m}}\text{Tc}$ is used as an internal tracer for the measurement of ^{99}Tc . The yield of $^{95\text{m}}\text{Tc}$ is determined by measuring the tracer's 204-keV photon peak by Ge(Li) gamma-ray spectrometry. The activity of $^{95\text{m}}\text{Tc}$ tracer added is sufficient for a reasonably precise determination of the radiochemical yield by gamma-ray spectrometry. The interference by this very small amount of $^{95\text{m}}\text{Tc}$ tracer activity in the ^{99}Tc beta-counting is less than the beta-counter background and is corrected for in the calculations. Not only are absorbers unnecessary, but their use would be detrimental, because ^{99}Tc beta particles are attenuated more by absorbers than the $^{95\text{m}}\text{Tc}$ gamma-rays are. In addition, high levels of ^{99}Tc activity in a sample have no effect on the $^{95\text{m}}\text{Tc}$ yield determination by gamma-ray spectrometry.

The volatility of Tc is a unique aspect of its chemistry. Excessive temperatures should be avoided during sample dissolution, wet ashing, and evaporation.^{10,14,16,17} Some reports of the volatility of Tc from hot nitric acid solutions conflict with others.¹⁰ One report recommends that to avoid loss of Tc during evaporation of a solution of Tc in nitric acid, the temperature should not exceed 90°. ¹⁷ At its melting point (119.5°) Tc_2O_7 exhibits a vapour pressure of about 1.0 mmHg.¹⁹ We have found that wet-ashing of vegetation samples with nitric acid at moderate hot-plate temperature settings results in Tc losses of < 5%.

Tc can be separated from many other elements by treatment with carbonate. Tc remains in solution while actinides, radium, strontium, calcium, lead and transition metals precipitate.^{11,15,20}

The anion-exchange behavior of Tc has been extensively studied.^{9,17-19,21-25} Dowex 1 × 4 resin has been used successfully to separate Tc from most other elements. It sorbs Tc from alkaline or weakly acidic solutions, and the Tc is eluted with more strongly acidic solutions.

*Author for correspondence.

Table 1. Half-lives and decay modes of the major Tc isotopes^{32,33}

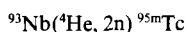
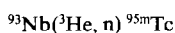
Nuclide	Half-life	Mode of decay	Energy of beta and photon emissions, keV
^{95m} Tc	61 days	95 + % electron capture 4% internal transition	204, 582, 835
⁹⁵ Tc	20 hours	electron capture	17, 20, 766
^{97m} Tc	91 days	internal transition	conversion electrons
⁹⁷ Tc	2.6 × 10 ⁶ years	electron capture	conversion electrons
⁹⁹ Tc	2.1 × 10 ⁵ years	beta	292

Electro-deposition of Tc^{9,14,17,19} provides additional decontamination from other elements and provides a convenient form for beta-counting and for tracer yield determination by gamma-ray spectrometry.

EXPERIMENTAL

Reagents

The ^{95m}Tc tracer was obtained from Argonne National Laboratory, where it was prepared by cyclotron bombardment of niobium with ³He or ⁴He nuclei:^{14,26}



When prepared in this manner the ^{95m}Tc is free from ^{97m}Tc. ⁹⁹Tc standard solutions were obtained from Amersham Radiochemicals, Arlington Heights, IL 60005. ⁹⁹Tc can also be obtained from Oak Ridge National Laboratory.¹⁴

The Dowex 1 × 4 (100–200 mesh) (Bio-Rad type AG) was prepared for use by washing 500 g of it successively with 1 litre of 3M sodium hydroxide, 1 litre of water, 2 litres of 6M hydrochloric acid, and finally with four 2-litre portions of water.

To prepare the anion-exchange column a plug of glass wool was positioned at the base of a 17-mm outside diameter glass tube (280 mm long), then a 10-ml volume of settled resin was transferred into the tube and 200 ml of 0.1M nitric acid were passed through it.

All other chemicals used were of analytical reagent grade.

Apparatus

The electro-deposition equipment comprised platinum discs (17.6 mm in diameter, 0.127 mm thick, one side mirror-finished), an electrolytic cell, a constant-current power supply and a voltage recorder. This system has been described elsewhere.^{27,28}

After the electro-deposition, the platinum discs are covered with a plastic scintillating phosphor and a 0.0254-mm thick film of mylar,²⁸ and mounted on a nylon ring-disc assembly²⁸ for beta-counting. The plastic scintillating phosphors²⁸ used were 2.4 cm in diameter (Nuclear Enterprises Ltd., Edinburgh, Scotland).

In the mercury-shielded low-level beta counters^{28,29} the phototube and sample were fitted into the well of a Phillips (or Amperex) hollow-anode Geiger tube operated in anti-coincidence. Tennelec scalers, clock and interface fed the data to a teletype paper punch and typewriter.

Chemical procedure

A measured amount of ^{95m}Tc tracer, sufficient to produce a 204-keV peak of about 1 cpm in a Ge(Li) gamma-ray spectrometer, was added to 10 g of vegetation in a 3-litre beaker, and 300 ml of concentrated nitric acid were added and the mixture was stirred. The mixture was wet-ashed until the decomposition of organic compounds was complete. The solution was evaporated to the smallest volume attainable without separation of salts, then allowed to cool; 800 ml of water were added and the mixture was stirred. The solution was then filtered through a 15-cm glass fibre filter and the silica and other insoluble material were discarded.

The filtrate was evaporated to a volume of about 200 ml. Then 200 mg of Ca²⁺, 100 mg of Ba²⁺, and 50 mg of Fe³⁺ (as nitrate solutions) were added, followed by 6M sodium hydroxide (with continuous stirring) until a pH of 10 was obtained. Then 60 ml of 2M sodium carbonate were added, with continuous mixing. The precipitate formed was allowed to settle, then filtered off on a glass fibre filter and discarded.

To prepare the filtrate for anion-exchange, 7.5M nitric acid was gradually added until the pH was 4–5, then 12 ml more of the acid were added and the solution was diluted with water to 870 ml. This final solution was 0.1M in nitric acid, and was heated gently to remove the carbon dioxide produced by acidification of the carbonate.

Anion-exchange was performed by passing the solution through a prepared Dowex 1 × 4 anion-exchange column, then washing the column with 500 ml of 0.1M nitric acid. The Tc was then eluted with 100 ml of 5M nitric acid. The eluate was evaporated to about 1 ml on a warm hot-plate and then left overnight at room temperature to evaporate to dryness.

Electro-deposition

An electrochemical cell containing a flamed platinum disc cathode was assembled. The Tc was dissolved in 1 ml of concentrated hydrochloric acid and transferred to the cell with three 1-ml water rinses. A drop of Methyl Red indicator (0.1% solution in alcohol) was added, followed by ammonia until the solution turned yellow. Then 2M hydrochloric acid was added until the solution turned red, and two drops in excess. The electrolysis cell was kept immersed in an ice-water bath during the electroplating, which was performed (with stirring) at a constant current of 1.2 A. After about an hour, the electro-deposition voltage increased abruptly, indicating completion of the electrolysis. The solution in the cell was quenched with 1 ml of concentrated ammonia solution, the current was turned off, and the cell was dismantled. The platinum cathode carrying the electro-deposited Tc was rinsed with water, then with ethanol, and dried on a hot-plate with gentle heat. The electroplated area on the platinum discs was 1.33 cm².

Radioassay

The electroplated platinum discs were beta-counted for at least 1000 min. To calibrate the beta-counters for ⁹⁹Tc radioassay, a known weight of standard ⁹⁹Tc solution was placed on a platinum disc; the solution was evaporated to dryness and the activity counted. To estimate the response of the beta-counters to the ^{95m}Tc emissions, aliquots of the ^{95m}Tc tracer were electrolysed with platinum discs. These electroplated ^{95m}Tc tracer disc standards were counted on a beta-counter and in a Ge(Li) gamma-ray spectrometer. The solutions remaining after the electro-deposition were gamma-counted with a sodium iodide crystal to correct for any unplated ^{95m}Tc.

To determine the radiochemical yield of a Tc determination, the electroplated platinum disc was counted for 1000 min in a Ge(Li) gamma-ray spectrometer. The area of the 204-keV photon peak of the ^{95m}Tc internal tracer was compared with the corresponding areas from the ^{95m}Tc

Table 2. ^{99}Tc analysis of a reference vegetation sample

Aliquot	Tc radiochemical recovery		^{99}Tc (s.d.) for each beta-counter, $\mu\text{Ci/g}$		
	%	s.d., %*	Beta 17	Beta 18	Beta 19
PG16	65.2	3.8	5.59 (0.21)	5.81 (0.22)	5.49 (0.21)
PG17	65.3	3.5	6.31 (0.22)	6.62 (0.23)	6.60 (0.23)
PG18	66.6	5.1	5.81 (0.30)	6.44 (0.33)	6.10 (0.31)
PG19	72.3	4.4	5.87 (0.26)	6.14 (0.27)	6.10 (0.27)
PG20	78.6	5.2	5.87 (0.31)	6.03 (0.31)	5.73 (0.30)
PG21	59.9	4.7	5.95 (0.28)	6.03 (0.28)	5.95 (0.28)
Mean	68.0	6.5	5.90 (0.24) (4.1%)	6.18 (0.30) (4.9%)	6.00 (0.38) (6.3%)

*s.d. standard deviation.

tracer electroplated disc standards, to obtain the radiochemical Tc yield. The gamma-spectrometry measurement of the $^{99\text{m}}\text{Tc}$ electroplated disc standards also provided the data needed to calculate the ratio of the beta and 204-keV gamma count-rates for $^{99\text{m}}\text{Tc}$.

Calculations

The ^{99}Tc activity in the sample is equal to the total beta activity, corrected for background and for the beta contribution from the $^{99\text{m}}\text{Tc}$ tracer, and adjusted for counting efficiency and chemical yield:

$$^{99}\text{Tc dpm} = (A - C)/(YE)$$

where A = net beta cpm of sample [corrected for background of counter (0.3 cpm)], C = beta cpm from $^{99\text{m}}\text{Tc}$, Y = chemical yield, and E = counting efficiency (about 40% on Environmental Measurements Laboratory, EML, beta-counters) and $C = GR$ where G = net 204-keV gamma cpm of sample [from the Ge(Li) spectrometer] decay-corrected to the time of the sample beta-count, and R = mean ratio of the net beta and 204-keV gamma count-rates of the $^{99\text{m}}\text{Tc}$ tracer standard discs, both activities being decay-corrected to the same time, (for the EML systems, this ratio is about 0.5).

DISCUSSION

One important requirement for preparing a plated source of a low-energy beta-emitter such as ^{99}Tc is that a very small mass is electro-deposited on the platinum surface. Therefore, our chemical separation procedure has been designed to separate, by means of an alkaline carbonate precipitation and anion-exchange, Tc from all elements that would also be electro-deposited, with the exception of chromium in chromate form. If barium is added before the solution is made alkaline for the carbonate precipitation, any chromate is precipitated as barium chromate. The removal of chromate is important because it interferes with the electro-deposition of Tc. When applied to pure $^{99\text{m}}\text{Tc}$ solutions our electro-deposition procedure plated 95% of the Tc onto platinum.

A blended, homogeneous stable sample of dried grass has been prepared by EML for use as an environmental-type reference material within the scientific community.³⁰ This material has been analysed by several expert international laboratories to certify its ^{99}Tc content.³⁰ To demonstrate the quality of our procedure, six aliquots of this vegetation sample were analysed. Each of the Tc electroplated

discs was counted in three different beta-counters. Three samples of distilled water were processed simultaneously to investigate ^{99}Tc contamination in the laboratory reagents. No detectable net activity was observed in any of these blanks. These results are presented in Table 2.

The chemical yield of the procedure, as evidenced by the recoveries of the six samples in Table 2, is good, averaging 68%. The beta activity in these samples was sufficiently high and the counting period long enough, for the relative standard deviation of the beta radioassay to be only $\pm 0.5\%$. For these samples the main uncertainty was due to the gamma-spectral analysis of the 204-keV photon peak of $^{99\text{m}}\text{Tc}$ in the determination of chemical recovery.

The results in Table 2 indicate the precision of the analysis. For any one aliquot, the results among counters agree within 1 standard deviation of the individual counting uncertainties. For any one beta counter, the results among the six aliquots agree within 2 standard deviations of the individual counting uncertainties, with the single exception of sample PG17 on counter Beta 19, which agrees within 3 standard deviations. This indicates that the main imprecision in the procedure is due to the stochastic nature of radioactivity.

The accuracy of the analysis is dependent upon the quality of the calibration of the beta counters, the completeness of equilibration of the $^{99\text{m}}\text{Tc}$ internal tracer with the ^{99}Tc of the sample during and subsequent to sample dissolution, and the radiochemical purity of the Tc electroplated onto the disc. The ^{99}Tc standard is certified within $\pm 1.2\%$. In addition, there is about 4% uncertainty in the actual calibration process, and this outweighs the smaller uncertainty in the certification value.

The radiochemical purity of the separated element is a quality-assurance requirement in every radiochemical procedure. This is difficult to demonstrate by decay-rate in the case of the long-lived ^{99}Tc . The most practical method is to show that the energy of the beta-particle emitted from the sample is equivalent to that of the ^{99}Tc beta-particles ($E_{\text{max}} = 292$ keV, $E_{\text{mean}} = 97$ keV).³¹ One way to accomplish this is to prepare a Harley-Halden plot²⁸ in which the log of the reduction in activity of a sample by selected

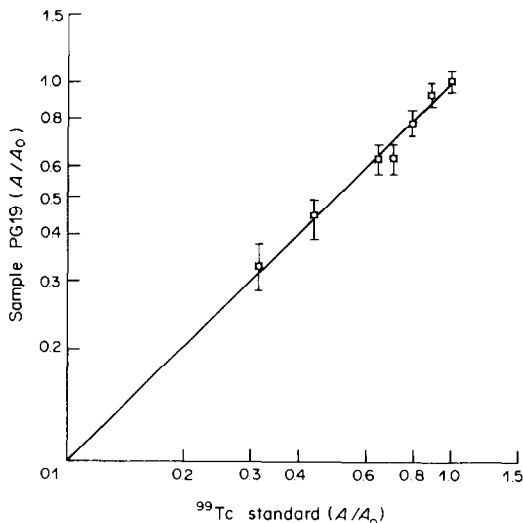


Fig. 1. Harley-Halden plot²⁸ of beta-counting with selected aluminium absorbers. The ranges around each data point represent one standard deviation for the count. The solid line is the theoretical line, slope = 1, for pure ^{99}Tc .

aluminium absorbers is plotted against the log of the reduction in activity of a ^{99}Tc standard by the same absorbers. If the reduction in the sample activity parallels the reduction in activity of a ^{99}Tc standard, the Harley-Halden plot will have a slope of unity. Such a logarithmic plot, with slope of unity, is shown in Fig. 1 for one of the ^{99}Tc electroplated discs from the reference vegetation analyses.

The good analytical precision obtained strongly suggests that complete equilibration of the $^{95\text{m}}\text{Tc}$ internal tracer and ^{99}Tc of the sample was accomplished. The correct analysis of an environmental reference material is an effective way to demonstrate this equilibration, along with other factors that determine analytical accuracy. Although the certified value for the reference vegetation has not yet been published, the mean of the 18 individual results in Table 2 (6.02 pCi/g, standard deviation 0.31) is within one standard deviation of the tentative value.³⁰ Consequently, there appears to be no demonstrable bias in the procedure.

The lower limit of detection for ^{99}Tc determination by this method is 0.1 pCi for a beta-counting time of 3000 min.²⁸ This limit is defined as the smallest amount of sample activity that will yield a net count rate for which there is 95% confidence that activity is present.

This study has demonstrated the utility of $^{95\text{m}}\text{Tc}$ as an internal tracer for the measurement of ^{99}Tc by beta-counting. A combination of alkaline carbonate precipitation, anion-exchange and electro-deposition provides good radiochemical isolation of ^{99}Tc and satisfactory recovery.

Acknowledgements—We thank Philip W. Krey of EML for his guidance and advice, Melvin S. Feiner of EML for the samples and intercomparison study data, Colin G. Sand-

erson of EML for gamma spectrometry, Norbert W. Golchert and Jacob Sedlet of Argonne National Laboratory for consultation, and John Hines and Clarence Ricklefs of Argonne National Laboratory for the $^{95\text{m}}\text{Tc}$ tracer.

REFERENCES

1. J. H. Kaye, M. S. Rapids and N. E. Ballou, *Proc. Third Intern. Conf. on Nuclear Methods in Environmental and Energy Research*, Columbia, MO, CONF-771072, 1977, pp. 211–224.
2. *Twenty-third Analytical Conference in Gatlinburg*, October 1979.
3. *Twenty-fourth Analytical Conference in Gatlinburg*, October 1980.
4. *Twenty-fifth Analytical Conference in Gatlinburg*, October 1981.
5. F. O. Hoffman, C. T. Garten, Jr., J. W. Huckabee and D. Lucas, *J. Environ. Qual.*, 1982, **11**, 134.
6. F. O. Hoffman, *Environmental Behavior of Technetium In Soil And Vegetation: Implications For Radiological Impact Assessment*, Oak Ridge Natl. Lab. Rept. ORNL-5856, 1982.
7. F. O. Hoffman, C. T. Garten, Jr., D. M. Lucas and J. W. Huckabee, *Environ. Sci. Technol.*, 1982, **16**, 214.
8. T. J. Anderson and R. L. Walker, *Anal. Chem.*, 1980, **52**, 709.
9. J. H. Kaye, J. A. Merrill, R. R. Kinnison, M. S. Rapids and N. E. Ballou, *ibid.*, 1982, **54**, 1158.
10. R. J. Meyer, R. D. Oldham and R. P. Larsen, *ibid.*, 1964, **36**, 1975.
11. T. L. Rucker and W. T. Mullins, *Radioanalysis of Technetium-99 At The Oak Ridge Gaseous Diffusion Plant*, pp. 95–100. Analytical Services Department, Technical Services Division, Oak Ridge, TN.
12. C. R. Walker, B. W. Short and H. S. Spring, *The Determination of Technetium-99 by Liquid Scintillation Counting*, Technical Division, Goodyear Atomic Corp., Piketon, OH.
13. B. G. Blaylock, M. L. Frank and D. L. DeAngelis, *Health Phys.*, 1982, **42**, 257.
14. N. W. Golchert and J. Sedlet, *Anal. Chem.* 1969, **41**, 669.
15. F. O. Hoffman, J. W. Huckabee, D. M. Lucas, C. T. Garten, Jr., T. G. Scott, R. L. Walker, P. S. Gouge and C. V. Holmes, *Sampling of Technetium-99 In Vegetation and Soils in the Vicinity of Operating Gaseous Diffusion Facilities*, Oak Ridge Natl. Lab. Rept., ORNL/TM-7386, 1980.
16. W. T. Smith, Jr., J. W. Cobble and G. E. Boyd, *J. Am. Chem. Soc.*, 1953, **75**, 5773.
17. G. E. Boyd, Q. V. Larson and E. E. Motta, *ibid.*, 1960, **82**, 809.
18. M. Pirs and R. J. Magee, *Talanta*, 1961, **8**, 395.
19. G. E. Boyd, *J. Chem. Educ.*, 1959, **36**, 3.
20. G. E. F. Lundell and J. I. Hoffman, *Outlines of Methods of Chemical Analysis*, Wiley, New York, 1938.
21. J. P. Faris and R. F. Buchanan, *Anal. Chem.*, 1964, **36**, 1157.
22. R. W. Atteberry and G. E. Boyd, *J. Am. Chem. Soc.*, 1950, **72**, 4805.
23. N. Hall and D. Johns, *ibid.*, 1953, **75**, 5787.
24. K. A. Kraus and F. Nelson, *Proc. 1st UN Intern. Conf. Peaceful Uses Atomic Energy*, Geneva, 1955, **7**, 113.
25. E. Anders, *The Radiochemistry of Technetium*, *Radiochemistry Monograph*, NAS-NS-3021, National Academy Research Council, Washington, D.C., 1960.
26. S. Fried, A. M. Friedman, D. Cohen, J. J. Hines and R. Strickert, *The Migration of Long-Lived Radioactive Processing Wastes In Selected Rocks*, Annual Report To The Office of Waste Handling, Project AN0115A. Argonne National Laboratory, Argonne, IL.

27. N. Y. Chu, *Anal. Chem.*, 1971, **43**, 449.
28. *EML Procedures Manual*, H. Volchok and G. de Planque (eds.), *U.S. Dept. Energy Rept.*, HASL-300, 25th Ed., New York, 1982.
29. J. H. Harley, N. A. Hallden and I. M. Fisenne, *Nucleonics*, 1962, **20**, 59.
30. M. S. Feiner, Environmental Measurements Laboratory, USDOE, NY, private communication, 1982.
31. E. Holm, I. Rioseco and R. B. R. Persson, *Surface Barrier Detectors for the Determination of ⁹⁹Tc By Beta Spectrometry*, IAEA-SM-252/16, 1981.
32. S. Fried, A. H. Jaffey, N. F. Hall and L. E. Glendinin, *Phys. Rev.*, 1951, **81**, 741.
33. G. Erdtmann and W. Soyka, *Die Gamma-Linien der Radionuclide*, Band I, Kernforschungs Anlage Julich, Zentralinstitut fur Analytische Chemie, 1974.

PLATINUM METALS—SOLUTION CHEMISTRY AND SEPARATION METHODS (ION-EXCHANGE AND SOLVENT EXTRACTION)

S. J. AL-BAZI and A. CHOW*

Department of Chemistry, University of Manitoba, Winnipeg, Manitoba, Canada

(Received 14 October 1983. Revised 6 February 1984. Accepted 20 April 1984)

Summary—The effects of knowledge of the solution chemistry of the platinum metals on their separation by solvent extraction and ion-exchange methods are reviewed, for the period 1950-1983. The review concentrates on the chloro-complexes of these metals and indicates those areas which need more investigation or interpretation to provide adequate separational methods.

The complex nature of the solution chemistry of the platinum metals has contributed to the difficulty of developing methods for their separation. With more knowledge of the complexes possible in solution, and of their stability and kinetic properties, the solvent extraction and ion-exchange methods should be better understood. The relationship between the solution chemistry of the platinum metals and the ion-exchange and solvent extraction methods used for their separation is therefore reviewed here, for the period 1950-1983. Because of the common use of the chloro-complexes of these metals in such investigations, the review is mainly restricted to these. In some publications, the solution chemistry has been extensively discussed, whereas in others it has been almost completely ignored. We have divided the methods into appropriate sections with illustrative examples and have tabulated similar procedures. An indication is given in each section of the areas which require additional investigation or interpretation. It is important that the chemistry be elucidated if progress is to be made in this difficult area of analytical chemistry.

ION-EXCHANGE

Ion-exchange methods have been developed for most of the platinum metals, based either on differences in the affinity of similar complexes for a resin or on larger differences caused by varying the solution constituents. The capacity of the resins used is usually large (up to 1 meq/g), which allows concentration of the metals, and the method is rapid and offers separation from a variety of other ions.

Electrostatic effects

Several studies¹⁻⁷ of the chloro-complexes of the platinum metals clearly indicate that the strength of interaction with anion-exchangers is highly dependent on the charge of the complex. Doubly-

charged complexes (PdCl_4^{2-} , PtCl_4^{2-} , PtCl_6^{2-} , IrCl_6^{2-} , RuCl_6^{2-} , OsCl_6^{2-}) were found to be strongly sorbed by the resins, whereas the triply-charged (IrCl_6^{3-} , RhCl_6^{3-} , RuCl_6^{3-}) were only weakly bound in static systems used for preconcentrating these metals. The sorption of the chloro-complexes of rhodium and ruthenium also depends on the age of the solution, mainly because of the labile character of these metals towards aquation;^{4,8-10} complexes of the type $[\text{MCl}_{6-x}(\text{H}_2\text{O})_x]^{x-3}$ ($x = 1-6$) are formed.¹¹⁻²⁶ This property might be useful in some separations but has mainly been considered a problem in dealing with solutions of rhodium and ruthenium. Several platinum metals have been separated with anion-exchange resins, on the basis of the relative strengths of electrostatic interaction (Table 1).

Palladium and platinum. Palladium and platinum in dilute acid are both sorbed strongly by anion-exchangers but it is possible to use the slight difference in interaction at high acid concentrations for sequential elution of palladium with concentrated hydrochloric acid and then platinum with perchloric acid.² Alternatively²⁷ palladium can be recovered with sodium hydroxide solution and platinum with dilute nitric acid.

Rhodium and iridium. By use of only the differences in the strength of electrostatic interaction with the anion-exchange resin, rhodium is typically eluted from the column first with a dilute acid or salt solution, and can be separated from palladium² and platinum.⁷ The separation of rhodium and iridium by anion-exchange often requires a suitable oxidizing agent to maintain iridium in the quadrivalent state, which is strongly sorbed by the resin.^{8,9} Selective reducing agents can reduce Ir(IV) to the non-extractable Ir(III) ($E^\circ = 1.02$ V),²⁸ which permits a separation from palladium² and platinum.^{5,27,29} Furthermore, by controlling the oxidation-reduction conditions it is possible to separate a multicomponent system. Table 1 outlines separations of rhodium and iridium from each other and from palladium and platinum.^{2,30}

*Author for correspondence.

Table 1. Ion-exchange separation based on electrostatic effects

Metals separated*	Medium	Exchanger	Eluent	Other information	Reference
Pd(II)-Pt(IV)	NaCl	Amberlite IRA-400(Cl ⁻)	Pd: 9-12M HCl Pt: 2.4M HClO ₄	Pd and Pt quantitatively sorbed	2
Pd(II)-Pt(IV)		Permutite ES(OH ⁻)	Pd: 1M NaOH Pt: 2.5M HNO ₃	Milligram amounts	27
Rh(III)-Pd(II)	2M HCl	Amberlite IRA-400(Cl ⁻)	Rh: 2M HCl Pd: 12M HCl	Quantitative separation; microgram amounts	2
Rh(III)-Pt(IV)	pH 2.1, 0.1M NaCl	Cellulose DEAE	Rh: 0.1M NaCl Pt: 1M HCl	Error 1% for 4.7 mg Pt, 3% for 2.5 mg Rh	7
Rh(III)-Ir(IV)	0.1M HCl, 2% NaCl	Amberlite IRA-400(Cl ⁻)	Rh: 2% NaCl in 0.1M HCl and 5% bromine water Ir: 5M NH ₄ OH followed by 6M HCl	Bromine water maintains iridium as Ir(IV)	8
Rh(III)-Ir(IV)	0.8M HCl, NaCl	Amberlite IRA-400(Cl ⁻)	Rh: Cerium(IV) solution Ir: Soxhlet extraction with 6M HCl Ir: 10M HCl	Cerium(IV) as oxidizing agent	9
Ir(III)-Pd(II) Ir(III)-Pt(IV) Ir(IV)-Pd(II)	10M HCl 2M HCl	Dowex-1(Cl ⁻) Amberlite IRA-400(Cl ⁻)	Ir: 2M HCl Pd: 12M HCl Ir: 1M NaOH Pt: 2.5M HNO ₃	99% Ir eluted: no attempt to recover Pd or Pt NH ₂ OH to reduce Ir(IV)	1 2
Ir(IV)-Pt(IV)		Permutite ES(OH ⁻)		Sodium oxalate to reduce Ir(IV) selectively	27

Ir(IV)-Pt(IV)	0.1M HCl	Cellulose DEAE(OH ⁻)	Ir: 0.1-0.4M NaCl in 0.01-0.1M HCl, 0.035M ascorbic acid Pt: 1M HCl Ir: 9M HCl Pt: 50% HClO ₄ Pd: 9M HCl Rh: 2M HCl Ir: Reduced with NH ₂ OH·HCl and eluted with 2M HCl Pt: 2.4M HClO ₄	Ascorbic acid to reduce Ir(IV) selectively	29
Ir(IV)-Pt(IV)	3M HCl	Dowex A-1(Cl ⁻)	Pt: 1M HCl Ir: 9M HCl	NH ₂ OH·HCl to reduce Ir(IV) selectively	5
Rh(III)-Ir(IV)-Pd(II)	2M HCl, NaCl	Amberlite IRA-400(Cl ⁻)	Pt: 50% HClO ₄ Pd: 9M HCl Rh: 2M HCl Ir: Reduced with NH ₂ OH·HCl and eluted with 2M HCl	Ir(IV) in mixture reduced with NH ₂ OH·HCl Ir(III) in effluent oxidized with cerium(IV) before recycling through column	2
Rh(III)-Ir(IV)-Pt(IV)	2M HCl, NaCl	Amberlite IRA-400(Cl ⁻)	Pt: 2.4M HClO ₄	Ir(IV) in mixture reduced with NH ₂ OH·HCl Rh and Ir separation as above	2
Rh(III)-Ir(IV)-Pd(II)-Pt(IV)	2M HCl, NaCl	Amberlite IRA-400(Cl ⁻)	Rh: 2M HCl Ir: 2M HCl Pd: 9M HCl Pt: 2.4M HClO ₄ Pt: 8% thiourea	Combination of the above two procedures used for separation	2
Ir(IV)-Pt(IV) Rh(III)-Pt(IV) Pd(II)-Pt(IV) Rh(III)-Ir(IV) Ir(IV)-Pd(II)-Pt(IV) Rh(III)-Ru(IV)	HBr	Dowex-1(Br ⁻)		Bromo-complexes separated; Br ₂ as oxidant, N ₂ H ₄ ·HCl as reductant	30
		Amberlite IRA-400(Cl ⁻)	Rh: 2M HCl Ru: Not possible even with 1% NH ₂ OH·HCl	Cerium(IV) to prevent Ru reduction by resin	2

*(-) means "separated from".

Table 2. Ion-exchange separation based on kinetic effects

Metals separated*	Medium	Exchanger	Eluent	Other information	Reference
Ir(IV)-Pd(II)	NH ₄ OH	Amberlite IR-100(NH ₄ ⁺)	Ir: 0.025M NH ₄ OH- 0.025M NH ₄ Cl Pd: 1M HCl	Pd retained as Pd(NH ₃) ₂ ²⁺ ; Ir as anionic chloride not sorbed	41
Pt(IV)-Pd(II)	NH ₄ OH	Amberlite IR-100(NH ₄ ⁺)		Similar procedure as above	40
Ir(IV), Pt(IV)-Pd(II)	NH ₄ OH	Amberlite IR-100(NH ₄ ⁺)	Pd: 1M HCl		40
Pd(II)-Rh(III)- Pt(IV)-Ir(IV)	NH ₄ OH	Amberlite IR-100(NH ₄ ⁺)	Pd: 1M HCl		40
[Rh(III)-Pt(IV)- Ir(IV)]		Dowex-2(Cl ⁻)	Rh, Pt: removed one after another with 0.025M NH ₄ OH-0.025M NH ₄ Cl	Effluent from cation-exchanger made acidic before passing through anion-exchanger; Ir not recovered	42
Pd(II)-Pt(IV)	NH ₄ OH	Silica gel	Pd: 0.5M HCl	Static system	43
Pt(IV)-Pd(II)	0.25M NH ₄ Ac	AG50W-X4(NH ₄ ⁺)	Pt: 0.25M NH ₄ Ac Pd: 0.1M HCl in 90% acetone	Heated for 10 min to ensure complete formation of Pd(NH ₃) ₂ ²⁺	43
Pd(II)-Pt(IV)	0.25M NH ₄ Ac	AG1-X8(Cl ⁻)	Pd: 0.25M NH ₄ Ac Pt: 0.01M HCl-0.1M thiourea mixture at 80°	Anion-exchanger sorbed PtCl ₆ ²⁻ but not Pd(NH ₃) ₂ ²⁺	43
Pt(IV)-Rh(III)	pH 2	Varion KS(H ⁺)	Pt: water	Made alkaline (pH 13) first with NaOH, then acidified with HNO ₃	44
Rh(III)-Pt(IV)	pH 3.5	Strongly basic anion- exchanger (Cl ⁻)	Rh: 1M HCl Pt: dilute NH ₄ OH	Made alkaline first with NaOH then acidified with HCl; 3.5% Rh left on column	45
Pd(II)-Rh(III)	pH 3.5, NaCl	Dowex 50(H ⁺)	Pd or Pt: water Rh: 6M HCl with heating at 60°	First made basic with NaOH and after 10 min made acidic with HCl	46

Ir(IV)-Rh(III)	pH 2.8	Dowex 50(H ⁺)	Ir: 10% chlorine water Rh: 6M HCl	Ir(IV) reduced with 1% hydroquinone before Rh precipitated and redissolved as cationic complex, then Ir(III) oxidized with chlorine gas Combination of the two procedures above used for separation of Rh from the mixtures	46
Rh(III)-Pt(IV), Pd(II)					46
Rh(III)-Pd(II), Ir(IV) Rh(III)-Pt(IV), Ir(IV)					47
Rh(III)-Pt(IV), Pd(II), Ir(IV) Ir(IV)-Rh(III)	Pyridine	KU-2(H ⁺)		Rh reacts 6.5 times faster than Ir to form (Mpy ₄ Cl ₃) ⁺ With excess Cl ⁻ , Ir(IV) forms (Irpy ₂ Cl ₄) ⁻ which is reduced with ascorbic acid to (Irpy ₂ Cl ₄) ⁻ Rh and Ir do not react with thiourea under these conditions	53
Ir(IV)-Rh(III)	Pyridine	KU-2(H ⁺)			48
Rh(III)/Ir(IV)- Pd(II)/Pt(IV)	0.5M HCl, 0.1M thiourea	AG50W-X4(H ⁺)	Rh or Ir: 0.5M HCl- 0.1M thiourea Pd or Pt: 4.5M HBr		49
Ir(IV)-Rh(III)	0.3M HCl, thiourea	Dowex 50W-X8(H ⁺)	Ir: 3M HCl Rh: 6M HCl at 74°	Heating for 1 hr on steam-bath permits complete formation of the cationic Rh-thiourea complex	50
Pt(IV)-Pd(II)	0.02M NH ₄ SCN, 2M HCl	Cellulose DEAE (SCN ⁻)	Pt: 0.02M NH ₄ SCN-2M HCl Pd: 0.05M thiourea	Separation done at below 5° Pd forms Pd(SCN) ₂ ⁻ and Pt remains as PtCl ₆ ²⁻	51
Pt(II)-Pd(II)	pH 2	Sulphonylguanidine	Pt: water Pd: 3-4M HCl	Sulphonylguanidine, which forms a neutral complex with Pd, was incorporated into a styrene-divinylbenzene copolymer	52
Rh(III)/Ir(III)- Pd(II), Pt(IV)	3M HCl	Styrene-8-aminoquino- line-based copolymer	Rh or Ir: 3M HCl	Sorbent exhibits both ion-exchange and complex-forming properties	

*(-) means "separated from"; (c) means "and"; (o) means "or"; [] indicates "a subsequent separation of these metals after the preliminary step shown above it".

Ruthenium and osmium. The only description found of an anion-exchange separation of Ru(IV) is for its separation from Rh(III), both being present as chloro-complexes.² The ease of reduction of Ru(IV) to Ru(III) by the resin made it essential to add cerium(IV) to maintain the higher oxidation state. However, because of the strong sorption of ruthenium on the resin, its complete recovery was impossible even with reducing agents such as hydroxylamine hydrochloride. If the ruthenium is reduced to Ru(III) in solution, no separation is possible from Rh(III) because of the similar low affinity of both trivalent metals for the exchanger.

No work has been reported on the sorption of the chloro-complexes of osmium by anion-exchange resins, although quantitative liquid ion-exchange extraction of the quadrivalent metal has been achieved.³¹⁻³⁷ No successful ion-exchange separation of osmium and ruthenium has been reported. The ease of reduction of Os(IV) and the reduction or partial hydrolysis of Ru(IV) prevent their quantitative separation.³⁸ However, liquid anion-exchangers have been used for the separation of the chloro-complexes of Ru(III) and Os(IV),^{34,39} as discussed later. Because the ion-exchange resins are usually less reducing than the liquid ion-exchangers, it would be expected that the resin separation of ruthenium and osmium should indeed be possible.

Kinetic effects

The differences in the labile character of the platinum metals in the formation of cationic, anionic, and neutral species has been used for their separation (Table 2). For example, the rate of formation of the cationic ammine complex of Pd(II) from its chloro-complex is sufficiently different from that for other metals⁴⁰⁻⁴³ to permit isolation of the complex. The rapid formation of $\text{Rh}(\text{H}_2\text{O})_6^{3+}$ through precipitation of the hydroxide and redissolution in dilute acid has been used in several ion-exchange procedures.⁴⁴⁻⁴⁶ Incomplete conversion and instability in more acid conditions [resulting in formation of other complexes, $\text{RhCl}_{6-x}(\text{H}_2\text{O})_x^{x-3}$] cause major problems with these methods.

Other studies on the separation of platinum metals have been reported where the differences in their labile character toward pyridine,⁴⁷ thiourea,^{48,49} thiocyanate,⁵⁰ sulphonylguanidine incorporated into a styrene-divinylbenzene copolymer,⁵¹ and styrene-8-aminoquinoline-based copolymer⁵² have played an important role.

Though several studies have indicated reasonable success in separation of several of the platinum metals, the advantage of the differences in their labile character could be further utilized.

SOLVENT EXTRACTION

Solvent extraction has been widely used for separation of the platinum metals.⁵⁴⁻⁵⁵ The difficulty in

developing extraction procedures for the individual metals is due to the slow reaction of the chloro-complexes. The solvent extraction methods for the separation of binary or multicomponent systems of these metals use the differences in their kinetic behaviour for the formation of extractable species, as well as the strength of electrostatic interaction of their chloro-complexes with liquid ion-exchangers or with oxygen-containing solvents.

Common binary mixtures

Electrostatic effects. The contribution of the charge of the complex and its labile character towards hydration has been useful in the separation of platinum metal mixtures. The inertness of the chloro-complexes of palladium and platinum toward aqution plays an important role in their extraction from acidic solution by an anion-exchange mechanism with organic bases such as amines, quaternary ammonium salts, antipyrines and other nitrogen-containing exchangers.^{34,36,56-63} However, because both metals are highly extractable as chloro-complexes their separation is difficult and has not been reported in the literature reviewed.

The chloride complex of Ir(IV) is highly extractable into organic solvents,^{34,36,57,59,62-69} whereas the Ir(III) form is much less extractable^{59,62,65,68} owing to the increase in the charge on the complex. On the other hand, the Rh(III) chloro-complex is also poorly extracted,^{34,36,57,59,63-66,69} which is due to the charge of the complex as well as its labile character toward aqution, *i.e.*, formation of $[\text{RhCl}_{6-x}(\text{H}_2\text{O})_x]^{x-3}$ ($x = 1-6$).

Ruthenium and osmium can also be separated as chloro-complexes because of their different affinities towards the extractant through either the anion-exchange or hydration-solvation mechanism. Ru(IV) is highly extractable but Ru(III) is not.^{34,36,59,76-79} The poor extraction of Ru(III), like that of Rh(III), is attributed to both the charge on the complex and to the ease of aqution to form $[\text{RuCl}_{6-x}(\text{H}_2\text{O})_x]^{x-3}$ ($x = 1-6$). Os(IV) behaves similarly to Ir(IV) and is inert toward aqution and is quantitatively extracted by anion-exchangers³¹⁻³⁷ or by oxygen-containing extractants.⁸⁰⁻⁸³

Several procedures (Table 3) have utilized these differences in behaviour of the chloro-complexes of these common binary mixtures of platinum metals for their separation by different types of organic solvents.

Although the separation of rhodium and iridium as their chloro-complexes has been widely investigated with the iridium kept in the quadrivalent state, the problem of recovery of the last traces of rhodium has not yet been solved. In addition, the nature of the extracted rhodium complex needs to be elucidated to provide the necessary information for developing efficient methods for its recovery.

Kinetic effects. The differences in the formation rate of the extractable anionic, neutral, or cationic species of the binary mixtures of Pd-Pt, Rh-Ir, and

Table 3. Solvent extraction based on electrostatic effects

Metals separated*	Aqueous phase	Organic phase	Other information	Reference
Rh(III)–Ir(IV)	6–7M HCl	Tri-n-butyl phosphate	Aqueous phase treated with H ₂ O ₂ to oxidize Ir, heated at 90° to destroy excess peroxide	70
Rh(III)–Ir(IV)	6M HCl saturated with NaCl	Tri-n-butyl phosphate	For quantitative separation, the oxidation of Ir by H ₂ O ₂ is necessary in each of the nine extraction stages required	71
Rh(III)–Ir(IV)	6MHCl	Tri-n-octylamine in benzene	Continuous treatment with chlorine gas to prevent Ir reduction by amine	72
Rh(III)–Ir(IV)	6M HCl	Tri-n-octylamine-loaded silicone rubber foam	In presence of free chlorine, 98% Ir extracted while 99% Rh remained	73
Rh(III)–Ir(IV)	HCl	Diantiprylpropylmethane in dichloroethane	Acidic solutions containing NaCl and H ₂ O ₂ evaporated to a moist salt before dissolving for extraction	34
Ru(IV)–Os(IV)	3–6M HCl	Diantiprylpropylmethane in dichloroethane	Solutions containing N ₂ H ₄ ·HCl or N ₂ H ₄ ·H ₂ SO ₄ heated to reduce Ru selectively to Ru(III)	34
Ru(III)–Os(IV)	0.1–0.3M HCl Ph ₄ AsCl	Chloroform	Os extracted as 2Ph ₄ As ⁺ ·OsCl ₆ ²⁻	74
Ru(III)–Os(IV)	0.058M HCl	Amberlite LA-1 in chloroform	Os extracted then Ru oxidized to RuO ₄ ⁻ and extracted with Ph ₄ AsCl in chloroform	39
Ru(III)–Os(IV)	6M HBr	Methyl isobutyl ketone	As bromo-complexes, Os extracted quantitatively whereas only 2% Ru was extracted	75
Ru(III)–Os(IV)	~ 5M HCl	Triphenylphosphine in 1,2-dichloroethane	A quantitative separation is possible	64

(–) means “separated from”.

Ru–Os with several complexing or chelating agents have been utilized for their separation from aqueous solution.

Palladium and platinum. These will be discussed in terms of charge type.

(i) *Anionic complexes.* The kinetically labile character of the chloro-complexes of palladium towards a number of hydrophobic anions allows the immediate formation of highly extractable anionic complexes at room temperature.^{84–86} Platinum, which reacts slowly under the same conditions,⁸⁷ may thus be separated from palladium. For example, milligram amounts of these metals in ammonium thiocyanate–hydrochloric acid solutions can be separated by the weakly basic diethylaminoethyl cellulose ion-exchanger.⁵⁰ The efficiency of separation increases with decreasing temperature, and below 5°, about 98% of the platinum (as PtCl₆²⁻) can be separated from palladium, which is quantitatively sorbed as Pd(SCN)₄²⁻. Because the palladium complex is highly extractable by oxygen-containing solvents whereas the PtCl₆²⁻ is not, it should also be possible to separate them by using extractants such as phosphates, alcohols, ketones, esters, ethers, etc.

(ii) *Neutral complexes.* Neutral complexes of the type MX_nL₂ (*n* = 2 for Pd and 2 or 4 for Pt) are formed by the reaction of palladium^{88–97} and platinum^{56,88,93,98,99} with suitable singly-charged anions (X) and organic bases (L) such as those containing N, S, P, As, Sb, etc. These complexes with ions such as halide or thiocyanate are soluble in carbon tetrachloride, chloroform, 1,2-dichloroethane, cyclohexane, benzene, etc. The extractable species of

Pd(II)^{64,92,99–102} are produced rapidly even at room temperature, whereas Pt(II) complexes form more slowly and Pt(IV) complexes often require heating^{93,100,102,103} or the use of a catalyst such as stannous chloride.^{64,93,99–101} Stannous chloride also acts by reducing Pt(IV) to the more reactive Pt(II) species. The rate of formation of the neutral complexes is in the order Cl⁻ < Br⁻ < I⁻ in the presence of excess of the halo-acid; this corresponds to the order of decreasing bond strength and increasing reduction potential. For example, there is no reaction with 2-mercaptobenzothiazole¹¹² or diphenylthiourea¹¹³ added to a hydrochloric acid solution of platinum, but a yellow precipitate is formed if potassium iodide is added to the solution either before or after the ligand. This can be attributed to reduction to Pt(II) and the subsequent formation of the more labile PtI₄²⁻ from the original PtCl₆²⁻. Also, palladium can be extracted as PdX₂(DOS)₂ [DOS = di-n-octyl sulphide] from acidic chloride, bromide or iodide solution with cyclohexane,¹⁰⁶ but platinum can only be extracted from iodide solution [probably as PtI₂(DOS)₂ rather than the reported PtI₄(DOS)₂].

The separation of platinum and palladium is best accomplished by extracting the palladium complex before formation of the extractable platinum complex becomes significant. This can be done by starting with the chloro-complexes of the metal in neutral solution at room temperature or below. A low salt concentration reduces the formation of PtCl_nL₂ and a weakly acidic solution restricts the extraction of PtCl₆²⁻ through the hydration–solvation or anion-extraction mechanism. To minimize the extraction of

platinum, it is best to start with Pt(IV) in the absence of any reducing agent, since this form is less labile, and the separation should be done quickly since the formation of PtX_nL_2 is kinetically slow.

On the basis of these differences in the behaviour of palladium and platinum toward different neutral ligands, several methods for their separation have been considered, some of which are indicated in Table 4.

Several sulphur-containing ligands,¹¹⁴⁻¹¹⁶ including dialkylsulphides and dialkylsulphoxides,^{107,117-119} have been used to extract palladium and may be efficient for its separation from platinum. Though several derivatives of dithiocarbamic acid have been used in chloroform to extract palladium and platinum individually, it would appear¹²⁰ that diphenyl-dithiocarbamic acid can be used for quantitative separation of palladium from platinum. This should be possible in solutions containing sodium sulphide as a reducing agent, even in up to 2M hydrochloric acid, though at such high acid concentrations it is customary to use a nitrogen-containing ligand as counter-anion in an ion-association extraction.

Some of the most promising ligands for the separation of palladium and platinum are dialkylsulphoxides, which can be used in oxidizing media, and dialkylsulphides, which can be used in basic or highly acidic solutions (>6M hydrochloric acid), whereas ligands containing sulphur and nitrogen and/or oxygen as donor atoms can be used only in dilute acid solutions. More detail is needed on the effect of branched substituents on the behaviour of the ligand and on whether the different extractable species formed with the sulphoxides in highly acidic solutions are neutral $PdX_2(R_2SO)_2$ or hydrated-solvated $2[H(R_2SO)(H_2O)_n]^+ \cdot [PdCl_4]^{2-}$ complexes. Also there may be sufficient differences in the kinetic behaviour of platinum and palladium with different amines to allow separation of these metals, since the tendency of the amines to form the neutral complexes decreases in the order $RNH_2 > R_2NH > R_3N$.

(iii) *Cationic complexes.* The significant difference in the rate of formation in ammoniacal medium of the ammine complexes $[M(NH_3)_n]^{m+}$ of palladium and platinum has been used for the separation of these metals.¹¹¹ High molecular-weight amines such as tri-n-hexylamine, tri-n-octylamine and primene, dissolved in chloroform or benzene, have been used as liquid anion-exchangers for the extraction separation of platinum from palladium, but careful timing was necessary to avoid significant formation of the platinum ammine complex. Other methods could be developed, based on the slower formation of the platinum-ammine, perhaps by enhancing the difference in the formation rates by using ammonium acetate rather than ammoniacal medium, or by use of different liquid anion- and cation-exchangers.

Rhodium and iridium. The chloride complexes of both rhodium^{61,64,65,70,87,93,121-125} and iridium^{64,65,93,100,101,103,115,124,126,127} react very slowly at room temperature

to form extractable anionic $(M_nCl_mX_p)^{k-}$ [$X = Br^-$, I^- , $SnCl_3^-$, $SnBr_3^-$, SCN^- , etc.] or neutral MCl_mL_n [$L =$ a neutral organic compound containing N, S, P, As, Sb] complexes. Heating the aqueous phase or introduction of a catalyst before extraction accelerates the formation of the extractable species. The relatively labile character of rhodium compared to iridium [$Rh(III) > Ir(III) > Ir(IV)$] in the formation of the extractable anionic¹²⁸⁻¹³⁰ or neutral^{64,98,99,131,132} complexes plays an important role in their separation; this commonly involves converting rhodium into the extractable form while maintaining iridium in the unextractable chloride form. In addition, the presence of excess of salt or stannous chloride affects the formation of the anionic and neutral complexes, respectively. Table 5 lists the separation of several rhodium and iridium complexes.

(i) *Anionic complexes.* Rhodium has been extracted in the form $Rh_nCl_mX_p^{k-}$ from solutions containing iridium, by oxygen-containing solvents. The addition of stannous bromide produces the rhodium complex much more rapidly than that of iridium in hydrochloric acid solution.¹³³ Isopentyl alcohol can be used to remove the rhodium-tin(II) bromide even in the presence of large amounts of sodium chloride, and from perchloric acid solution. The difference in the reaction rates means that the rhodium complex takes 2 hr to form at room temperature (although obviously the time could be shortened by warming the solution) whereas the iridium complex is formed only by heating the solution at 90° for at least 3 min (and even then gives inconsistent results).

Rhodium can also be extracted from iodide solution with tri-n-butyl phosphate in toluene.¹³⁴ The formation of the iodo-complex requires heating at 70° for 1 hr at pH 2. The complex is extracted from 1M sulphuric acid, probably through the hydration-solvation mechanism, and can be stripped with ammonia solution. The iridium complex is unlikely to be appreciably formed under these conditions and a separation of rhodium and iridium should be possible.

One of the difficulties in the extraction of rhodium and its separation from iridium is the labile character of the starting hexachloro-complex of rhodium towards aquation. With aging, species of the type $[RhCl_{6-x}(H_2O)_x]^{x-3}$ ($x = 1-6$) are formed, which react at different rates with a ligand and thus produce different complexes with varying extractability. To avoid this problem, rhodium can be converted into the hexachloro form by evaporating the solution to dryness in the presence of a chloride salt shortly before use.¹³³ An example of the effect of aging¹³⁵ is the extraction of rhodium as a thiocyanate complex by polyurethane foam; in this case a one-day old solution, containing mainly $[RhCl_5(H_2O)]^{2-}$, was 92% extracted, whereas a seven-month old solution containing mainly $RhCl_3(H_2O)_3$ was only 78% extracted.

The use of a chloride salt for stabilizing rhodium

Table 4. Solvent extraction of palladium and platinum, based on kinetic effects

Aqueous phase	Organic phase	Other information	Reference
<i>Neutral complexes</i> pH 2-5, alcoholic solution of <i>p</i> -nitrosodimethylaniline	Chloroform	Five min at room temperature for Pd- <i>p</i> -nitrosodimethylaniline complex formation; no Pt reaction for several hr	104
pH 4	Dimethylglyoxime-treated silicone fubber foam	Quantitative separation; Pd extracted was completely recovered with 8 <i>M</i> HNO ₃	105
HCl or HBr	Di- <i>n</i> -octyl sulphide in cyclohexane	Selectivity of the ligand for Pd permits its separation from Pt	106
HCl or HNO ₃	R ₂ S ₂ in benzene; R = Bu-C ₈ H ₁₇ , Ph	High efficiency of Pd extraction as PdX ₂ ·2R ₂ S (X = NO ₂ ⁻ or Cl ⁻) from HCl or HNO ₃ may isolate it from Pt	107
Up to 2 <i>M</i> HCl 6 <i>M</i> HCl	Di- <i>n</i> -octyl sulphoxide in benzene Di- <i>n</i> -heptyl sulphoxide in 1,1,2-trichloroethane	A separation factor of 10 ³ permits selective removal of Pd	108
pH 3	2-Mercaptobenzothiazole in chloroform	Simultaneous extraction of Pd and Pt and subsequent back-extraction of Pt with water and Pd with 10% dimethylamine can separate Pd and Pt in solution containing Rh and Ir	93
pH 6, 2-thenoyltrifluoroacetone	<i>n</i> -Butanol	Pd was quantitatively extracted and since 1.8% Pt was extracted, a separation was suggested	110
<i>Cationic complexes</i> NH ₄ OH, conc. HCl, SnCl ₂	Tri- <i>n</i> -hexylamine, tri- <i>n</i> -octylamine, or primene in benzene or chloroform	After Pd was extracted as PdCl ₂ ·L ₂ , solution was made 6 <i>M</i> in HCl and Pt extracted with butanol-acetophenone mainly through the hydration-solvation mechanism	111

Table 5. Solvent extraction of rhodium and iridium, based on kinetic effects

Aqueous phase	Organic phase	Other information	Reference
<i>Anionic complexes</i>			
SnBr_2 , HBr-HClO_4 , NaCl	Isopentyl alcohol	Extractable Rh-stannous bromide complex formed at room temperature; heating required for Ir	133
NaI , $1M \text{H}_2\text{SO}_4$ or HClO_4	Tri-n-butyl phosphate in toluene	Under optimum conditions for Rh-iodide complex formation (pH 2, heating at 70° for 1 hr), a distribution coefficient ratio of Rh/Ir of 650 suggests an efficient separation possible	134
$2 \times 10^{-3}M \text{KSCN}$, $2M \text{HCl}$	Polyurethane foam	Acid added after heating the solution at 90° for 4 hr; an average of 88% Rh extracted while 91% of Ir remained in aqueous phase	135
$2 \times 10^{-3}M \text{KSCN}$, $2M \text{HCl}$, $3M \text{LiCl}$	Polyurethane foam	Acid added after heating the solution at 90° for 30 min; an average of 93% Rh extracted; 95% Ir remained in aqueous phase	125
<i>Neutral complexes</i>			
$4-6M \text{HCl}$	2-Mercaptobenzothiazole in chloroform	Solution boiled for 7 min; quantitative for Rh, 6-10% Ir extracted	93
$0.25-2M \text{HCl}$, SnCl_2	2-Mercaptobenzothiazole in chloroform	Heating not required; quantitative for Rh; negligible Ir extraction	93
$1-2M \text{HCl}$, 4,5-dimethyl-2-mercaptothiazole	Chloroform	Vigorous boiling for 1 hr required for reduction and maximum formation of complex; both Rh and Ir extractable	136, 137
$3-9M \text{HCl}$, SnCl_2 , 4,5-dimethyl-2-mercaptothiazole	Chloroform	Reduction and formation of complex at room temperature; no interference by Ir	137
$1-6M \text{HCl}$, SnCl_2 , diphenylthiourea	3:2 v/v Chloroform-acetone mixture	Standing for 20 min at room temperature for complete Rh-diphenylthiourea complex formation; quantitative separation of Rh and Ir.	113
<i>Cationic complexes</i>			
$<0.05M \text{HCl}$	Dinonylnaphthalene-sulphonic acid in n-heptane	$\text{Rh}(\text{OH})_3$ precipitated by $6M \text{NaOH}$ and redissolved with $0.1M \text{HCl}$; 90% Rh extracted and recovered with $6M \text{HCl}$; 99% Ir in aqueous phase	138

as the hexachloro-complex in solutions is of considerable importance. Because rhodium solutions usually require heating to form the extractable species, the aquation of the rhodium complex is facilitated. The different aquation complexes react at various rates with a ligand, because the water molecule is less labile than the chloride ion, although eventually the same complex may be produced. When a chloride salt is present in a freshly-prepared rhodium solution, it ensures the rhodium is present as the hexachloro-complex, which is the most labile form.

The use¹²⁵ of 2*M* lithium chloride medium reduces the heating time for formation of $\text{Rh}(\text{SCN})_6^{3-}$ at 90° to 30 min from the 4 hr required in absence of the chloride. However, with iridium solutions even 4*M* lithium chloride does not decrease the required heating time of 4 hr and in fact decreases the extraction of the thiocyanate complex by polyurethane foam;^{125,135} this is due to the inertness of the hexachloroiridate towards aquation, resulting in a competition between the chloride and thiocyanate ions for iridium.

The tin(II) bromide complexes of rhodium and iridium, which are extracted by several nitrogen-containing solvents in chloroform,¹²⁹ are also affected by chloride ion. The presence of 4*M* chloride almost completely inhibits the formation of the extractable iridium-tin(II) bromide complex while not affecting the formation of the rhodium complex, for which these are the ideal formation conditions. In this case the competition between SnBr_3^- and Cl^- for iridium is the most likely reason for the decrease in formation of the bromostannate(II) complex.

The role of chloride in the reaction of iridium and in labilizing the formation of anionic complexes of rhodium with different hydrophobic anions, *e.g.* Br^- , I^- , SnCl_3^- , SnBr_3^- , *etc.* needs to be further studied and should be extended to neutral ligands containing N, S, P, As, Sb, *etc.*

(ii) *Neutral complexes.* Neutral sulphur-containing complexes of rhodium can be formed, and extracted by an organic solvent, while iridium is maintained as the unextractable chloro-complex. Heating is required to accelerate the formation of the rhodium complex and reduction to the more labile Rh(II) form, but this also results in the partial formation of an extractable iridium complex. Though quantitative extraction of rhodium has been obtained⁹³ by boiling a solution of rhodium and iridium with 2-mercaptobenzothiazole, cooling, and extracting with chloroform, 6–10% of the iridium was co-extracted.

To avoid co-extraction of the iridium with rhodium, acidic solutions of stannous chloride have been used to labilize formation of the rhodium complex. The catalytic behaviour of stannous chloride arises mainly because of its ability to reduce rhodium to Rh(II) and form relatively labile complexes of the type $\text{MCl}_m(\text{SnCl}_3)^{-(n+m)}$. The formation of the extractable neutral sulphur-containing complex (MCl_mL_n)

is facilitated by substitution of a sulphur-containing ligand (L) for the more labile SnCl_3^- rather than for Cl^- . In the presence of stannous chloride the rhodium complex forms rapidly and does not require heating, which would result in the simultaneous formation of a similar iridium complex. From acid solutions containing 2-mercaptobenzothiazole and stannous chloride, more than 99% of the rhodium can be extracted into chloroform, but no iridium.⁹³ It is possible that stannous bromide may be even more effective in accelerating the formation of an extractable rhodium complex, since it is a stronger reducing agent and is more labile than stannous chloride.

The use of sulphur-containing ligands has not been studied extensively and the effectiveness of several alkyl and aryl derivatives of thiourea which are now available should be considered. Dialkyl sulphides and other sulphur-containing reagents with a relatively high electron density should be examined, for example, since dibenzylthiocarbamate has been noted as introducing an extreme interference from rhodium in the extraction of palladium and platinum¹²⁰ because of an analogous rapid reaction. Other neutral-acceptor ligands which are weakly protonated in acidic media, *e.g.*, derivatives of phosphine, arsine and stibine, may also be useful for separations.

(iii) *Cationic complexes.* Liquid cation-exchangers have been used for the separation of the chloro-complexes of rhodium and iridium, utilizing the ease of formation of the cationic $\text{Rh}(\text{H}_2\text{O})_6^{3+}$ complex. This complex has usually been produced by precipitation of $\text{Rh}(\text{OH})_3$ and formation of $\text{Rh}(\text{H}_2\text{O})_6^{3+}$ by redissolution in dilute acid. The latter complex can be extracted with dinonylnaphthalenesulphonic acid in heptane.¹³⁸ These methods are limited because of incomplete $\text{Rh}(\text{OH})_3$ precipitation and instability of $\text{Rh}(\text{H}_2\text{O})_6^{3+}$ in hydrochloric acid, where neutral or anionic chloro-complexes can also be formed.

Ruthenium and osmium. The chloro-complexes of Ru(III or IV)^{98,99,116,139–141} and Os(IV)^{98,99,142} react with hydrophobic anions or neutral ligands to form extractable species. Several hours are required for the reaction of Ru(III or IV) chloride complex with hydrophobic¹⁴¹ and neutral complexing agents¹⁴³ at room temperature but only a few minutes with heating; the rate of reaction with Os(IV) chloride is much slower.^{144–146}

Excess of chloride also plays an important role in the separation, since the chloride complexes of Ru(III or IV), like those of Rh(III)¹⁴⁷ are labile toward aquation, whereas osmium is inert like iridium. Therefore the addition of chloride ions increases the rate of ruthenium reaction with hydrophobic or neutral complexing agents and decreases that of osmium.

(i) *Anionic complexes.* The maximum formation of $\text{Ru}(\text{SCN})_6^{3-}$ requires only 5 min heating at 90° while that of $\text{Os}(\text{SCN})_6^{3-}$ requires 3 hr. In addition, the presence of 3*M* lithium chloride increases the formation of the ruthenium complex and decreases

that of the osmium complex, so a 95% complete separation is possible.¹⁴² It would be useful to see the effect of other complexing agents in this type of separation.

(ii) *Neutral complexes.* The chloro-complexes of Ru(III or IV) and Os(IV) react with neutral organic compounds (L) such as those containing N, S, P, As, Sb, etc. to form neutral complexes of the type^{64,98,99,140} MCl_nL_m which are highly extractable into organic solvents (Table 6). The difference in formation of the complexes of ruthenium and osmium is mainly due to the reducing nature of the solution and has played an important role in their separation.

Osmium can be quantitatively extracted from 6M hydrochloric acid with triphenylphosphine in 1,2-dichloroethane.⁶⁴ Ruthenium is not extracted in the absence of stannous chloride, because of its low lability at room temperature. If stannous chloride is present, the extraction of osmium is reduced to less than 20%, while ruthenium becomes up to 95% extractable from 4M hydrochloric acid. Mojski suggested that in the presence of stannous chloride osmium is reduced to an oxidation state lower than the tervalent, and that this forms neither a stable chloride complex with phosphine nor stable negatively charged chloride complexes.

The presence of excess of chloride has a considerable effect on the separation of osmium and ruthenium, as noted¹⁴⁹ in the extraction from 2-mercaptobenzothiazole medium into chloroform. Osmium can be quantitatively extracted from solution at pH 3.5–5.0 after 15 min standing at room temperature. If the solutions are 3–6M in hydrochloric acid and boiled for even as little as 5 min, the extraction is reduced to only 0.4%,⁹³ this may be due to some reduction and/or the competition between the ligand and chloride for osmium. On the other hand, the chloride accelerates the formation of the extractable ruthenium complex in comparison to the aquated species.

Methods for the separation of osmium and ruthenium and their spectrophotometric determination

need to be developed on the basis of the effect of excess of halide and the reaction with organic compounds containing weak donor atoms. At present, the nature of the extractable species formed under reducing conditions is unclear and should be elucidated.

(iii) *Cationic complexes.* The reactions between thiourea and hexabromo-osmate¹⁵⁰ and hexachloro-osmate¹⁴⁶ are extremely slow at room temperature. However, though the osmium complex is not formed in 6.7M hydrobromic acid for at least 4 hr, the maximum formation of the cationic ruthenium–thiourea complex occurs in only 15 min.¹⁵¹ Solvent extraction and ion-exchange separation of osmium and ruthenium should thus be possible, although neither has been reported.

The labile nature of the chloride complex of ruthenium toward aquation to give $[RuCl_{6-x}(H_2O)_x]^{x-3}$ ($x = 1-6$), which is like that of rhodium, results in ruthenium interference in the extraction of rhodium by the liquid cation-exchanger dinonylnaphthalene-sulphonic acid,¹³⁸ and explains the sorption of some ruthenium on Dowex-50 cation-exchanger.¹⁰ Since, like that of iridium, the chloro-complex of osmium is kinetically inert toward aquation, the difference in the tendency for formation of cationic complexes may be used for separation by converting ruthenium into a cationic form while keeping osmium as an anion, in the manner used for the separation of rhodium and iridium.¹³⁸

Other effects used for separation of binary mixtures

Palladium and platinum. The photosensitive nature of platinum has been used¹⁵² to enhance the formation of the thiocyanate complex and the separation of palladium and platinum by extraction of the triphenylisopropylphosphonium salt into ethyl acetate. It would appear that in the absence of light that the palladium complex should still be formed, while the platinum remains as a chloro-complex, thus

Table 6. Solvent extraction of osmium and ruthenium, based on kinetic effects

Aqueous phase	Organic phase	Other information	Reference
<i>Anionic complexes</i>			
0.6M KSCN, 3M NH ₄ Cl pH ~ 3	Polyurethane foam	Heating the solution at 90° for 5 min was enough for maximum formation of $Ru(SCN)_6^{3-}$ while leaving Os as its unextractable chloro-complex	142
<i>Neutral complexes</i>			
~3M HCl	Triphenylphosphine in 1,2-dichloroethane	Presence of SnCl ₂ accelerates formation of extractable Ru–triphenylphosphine complex and reduces Os(IV) to lower states which form no stable complex with the ligand	64
6M HCl, 1,4-diphenylthiosemicarbazide	Chloroform	Heated at 100° for 10–15 min in presence of SnCl ₂ , Ru forms an extractable red-violet complex, but Os does not react with the organic reagent	148
6M HCl, 2-mercaptobenzothiazole	Chloroform	Aqueous phase boiled for 5 min; Ru extracted quantitatively; less than 0.4% Os extracted	93

permitting an extraction of $\text{Pd}(\text{SCN})_4^{2-}$ by several organic solvents.⁵²

The thiocyanate concentration has a considerable effect on the formation of $\text{Pt}(\text{SCN})_6^{2-}$: the rate of formation of the complex decreases up to 0.1M thiocyanate concentration and then increases. The rate is also inversely proportional to pH and the reaction is completely inhibited at pH 7.0. Because $\text{Pd}(\text{SCN})_4^{2-}$ is easily formed, at a rate relatively independent of thiocyanate concentration, a separation of these metals is possible, and extraction with polyurethane foam, which may be considered as an oxygen-containing solvent, has been reported.¹⁵³

The importance of solution acidity can be seen in the separation of Pd(II) and Pt(IV) from thiocyanate solution adjusted to pH 6.0 with pyridine, $\text{Pdpy}_2(\text{SCN})_2$ being extracted with methyl isobutyl ketone.⁸⁷ Platinum could only be extracted when the solution was adjusted to pH 2.0 with hydrochloric acid and heated at 90°.

The separation of palladium and platinum by simultaneously controlling more than one of the effects of light, pH, thiocyanate concentration and use of different oxygen-containing solvents, needs more investigation than has been reported in the papers listed in Table 7. In addition, hydrophobic complexing anions other than thiocyanate, such as bromide and iodide, with which replacement reactions with hexachloroplatinate are reported to be strongly photosensitive,^{160,161} also warrant study.

Ruthenium and osmium. One of the characteristic features of ruthenium and osmium is their ability to form the volatile non-polar tetroxides, which are extractable with several organic solvents such as carbon tetrachloride,^{154,162-165} chloroform^{154,166,167} and mepesine¹⁶⁸ (Table 7). Osmium can be selectively oxidized to the tetroxide and separated from ruthenium¹⁵⁴ by extraction into carbon tetrachloride.

Ruthenium and osmium can also be simultaneously oxidized and subsequently distilled as their tetroxides. A separation is possible because of the difference in the kinetics of reduction of the tetroxides. The reduction of OsO_4 to $[\text{OsO}_2\text{Cl}_4]^{2-}$ and then to OsCl_6^{2-} is slow and highly dependent on the hydrochloric acid concentration, temperature and reduction time, whereas that of RuO_4 to the corresponding anionic chloro-complexes is fast and takes place under much milder conditions.¹⁴⁷ For example,¹⁵⁵ ruthenium can be trapped by reduction in 10M, 4M or 3M hydrochloric acid while osmium is not, and instead is subsequently absorbed by 1:1 sulphuric acid-phenyldimethylamine mixture.

Several extraction-spectrophotometric determinations of osmium that start with the tetroxide are reported to suffer no interference from Ru(III) chloride, e.g., the anionic osmium-thiocyanate complex^{158,169} and the neutral 2-mercaptobenzothiazole¹⁴⁹ and 2-mercaptobenzimidazole¹⁷⁰ complexes. Alternatively,^{75,171} ruthenium may be extracted quantitatively as the cationic thiourea complex,

because in concentrated hydrobromic acid medium, the formation of an osmium-thiourea complex is inhibited.

The tetroxides of ruthenium^{157,172} and osmium^{144,158,169,170,173-175} have been used for their pre-concentration, and the difference in their tendency to form extractable species can play a major role in their separation by organic solvents (Table 7).

The thiocyanate concentration also appears important in the formation of the extractable complexes.¹⁵⁷ After distillation of the tetroxides and collection in 0.2M ammonium thiocyanate in 0.4M hydrochloric acid, osmium can be extracted quantitatively with diethyl ether containing hydrogen peroxide. If the conditions are then changed to 0.3M thiocyanate in 1M hydrochloric acid, ruthenium can then be quantitatively transferred into methyl isobutyl ketone. In the presence of 0.04M thiocyanate, the extraction of osmium does not require addition of hydrogen peroxide,¹⁶⁹ and although this was not reported, may in fact give a good separation from ruthenium.

The presence of chelating agent and excess of chloride ion increases the difference in the rate of formation of the extractable neutral species of osmium and ruthenium. For example, ruthenium can be separated from osmium by extraction into chloroform after the formation of a ruthenium-diphenylthiourea⁷⁴ or 2,4-thiosemicarbazide complex¹⁵⁹ at high hydrochloric acid concentration.

The effect of neutral organic ligands and hydrophobic anions such as Br^- , SnCl_3^- , SnBr_3^- , etc. on the labile nature of the complexes and its contribution to the extraction of ruthenium and osmium with oxygen-containing solvents and liquid anion-exchangers still needs investigation. The tendency of osmium tetroxide to form more than one extractable species with thiocyanate,^{157,158,169,176-179} whereas ruthenium forms only one, may also be potentially useful.

Other binary and multicomponent systems

Although Pd-Pt, Rh-Ir, and Ru-Os are the common pairs of platinum metals which often exhibit some difficulty in their separation, there are several other combinations which have been investigated, including those with multiple components. These separations use the electrostatic effects, kinetic effects, and selective oxidation, often in conjunction with one another for complex systems.

Tetroxides. Ruthenium and osmium are commonly separated first from any of the other platinum metals because of their easy removal from the system as their tetroxides. The selective oxidation of ruthenium and osmium to the tetroxides and subsequent extraction by chloroform or carbon tetrachloride has been utilized for the separation of these metals from the rest of the platinum metals. Furthermore, the differences in the kinetic behaviour of these tetroxides toward reduction in acidic solutions has been used for the separation of ruthenium and osmium as discussed

Table 7. Solvent extraction based on other effects

Aqueous phase	Organic phase	Other information	Reference
<i>Palladium and platinum</i>			
NaSCN	Ethyl acetate and methyl isobutyl ketone	Solution irradiated for 15 min with 500-W incandescent bulb; Pt extracted as ion-association complex $[(C_6H_5)_3C_3H_7P^+]_2 \cdot [Pt(SCN)_2^-]$ with ethyl acetate then Pd as $[(C_6H_5)_3C_3H_7P^+]_2 \cdot [Pd(SCN)_2^-]$ with methyl isobutyl ketone	152
0.15M KSCN, 0.5M HCl, H ₂ O ₂	Polyurethane foam	Under these conditions Pd is present as $Pd(SCN)_2^-$ and Pt as $PtCl_6^-$; 95% Pd extracted, but less than 2% Pt	153
KSCN	Methyl isobutyl ketone	Pd extracted as $Pdpy_2(SCN)_2$ at pH 6 fixed by pyridine; Pt extracted by adjusting the pH to 2 with HCl and heating the solution at 90° for 4 min	87
<i>Ruthenium and osmium</i>			
HNO ₃	Chloroform	Tetroxides of Ru and Os reduced with $(NH_4)_2Fe(SO_4)_2$; Os selectively oxidized with 5M HNO ₃ and extracted	154
HClO ₄		Ru and Os oxidized with HClO ₄ and distilled; RuO ₄ reduced in 10M, 4M, 3M HCl; OsO ₄ reduced with 1:1 sulphamic acid-phenylmethylamine mixture	155
HClO ₄		The tetroxide complexes passed into five flasks; RuO ₄ reduced with 1:1, 1:2, 1:3 HCl; OsO ₄ reduced with 10% NaOH and alcohol	156
0.2M NH ₄ SCN, 0.4M HCl	Peroxide-containing diethyl ether	5 min in a boiling water-bath then Os extracted; Ru was extracted with methyl isobutyl ketone from solution made 0.3M in NH ₄ SCN, 1M in HCl	157
0.03-0.06M NH ₄ SCN, 1.25-1.75M HCl	Hexamethylphosphoramide in chloroform	No interference in determination of the blue Os-SCN complex suggests a method for its separation from Ru	158
HClO ₄ , 1,5-diphenylcarbohydrazide in ethanol	Chloroform	With excess of chloride OsO ₄ is reduced to $OsCl_6^-$ which prevents its reaction with the ligand; Ru(III) is highly extractable and can be separated from Os	144
5-7M HCl, diphenylthiourea	Chloroform	Extraction of 30 μg/ml Ru as diphenylthiourea complex was not affected by 10 mg of Os	74
6M HCl, 2,4-thiosemicarbazide	Chloroform	Heating at 100° for 10-15 min produced extractable Ru complex; extraction not interfered with by Os	159

above. Some of these procedures are summarized in Table 8.

Electrostatic effects. The differences in the strength of interaction of the doubly and triply-charged chloride complexes of platinum metals towards extractants, either through the anion-exchange or hydration-solvation mechanism, have played an important role in the separation of binary and multiple mixtures of these metals. Examples in which liquid anion-exchangers, including amines, quaternary ammonium salts and other nitrogen-containing as well as oxygen-containing extractants, are used, are summarized in Table 9.

Kinetic effects. The differences in the kinetic behaviour of platinum metals in forming extractable species with hydrophobic anions and neutral ligands have also been very important in the separation of these metals. The labile character of the platinum metals decreases in the order $\text{Pd} > \text{Pt} > \text{Ru} > \text{Rh} > \text{Ir}$, with osmium between ruthenium and iridium, depending on the solution conditions. Several of the studies listed in Table 10 used these differences in the rate of formation of anionic and neutral species, and the tendency of rhodium for $\text{Rh}(\text{H}_2\text{O})_3^{3+}$ formation.

Combination effects. The separation of multi-component systems of platinum metals often uses a combination of more than one point of difference in the behaviour of their chloride complexes, such as the tendency to volatile oxides, the strength of interaction with anion-exchangers as well as oxygen-containing solvents, and lability in the formation of extractable anionic or neutral species. If osmium and ruthenium are present, they are commonly removed first by oxidation to their tetroxides. Several examples are tabulated in Table 11.

More extensive investigations of the separation of anionic chloride complexes of uncommon binary and multicomponent systems of platinum metals are needed, utilizing the differences in their strength of

interaction with quaternary ammonium salts and taking into account the effect of acidity, the oxidation-reduction nature of the aqueous phase, and the tendency to form cationic ammonium complexes. In addition, combinations of these effects in the back-extraction of platinum metals may provide more efficient methods. Several hydrophobic anions such as Br^- , I^- , SCN^- , SnCl_3^- , SnBr_3^- , *etc.* and neutral organic compounds containing N, P, S, As, Sb, *etc.* may alter the lability of the platinum metals in formation of extractable species. A combination of such studies should generate more efficient methods for the separation of platinum metals in any combination.

In the years since the review by Beamish,²⁰⁰ many investigators have provided new methods for isolating and separating the platinum metals. As he predicted, knowledge of the solution chemistry of these metals has allowed a somewhat more systematic approach to development in this area. However, there are still many reports which do not treat the platinum metal solution chemistry involved in the separations, or include methods where it is not clear. As suggested throughout this review, there still remain several areas of separation which need considerable investigation and many where the chemistry of the method requires clarification. We expect that the use of newer instrumental techniques in conjunction with the standard methods will facilitate these studies and that the growing knowledge of the solution chemistry of these metals will continue to offer new and exciting answers for their separation and isolation. This expectation seems justified by the recent report of the use of systematic solvent-extraction separation for production of high-purity platinum metals.²⁰¹

Acknowledgement—This work was financially supported by the Natural Sciences and Engineering Research Council of Canada.

Table 8. Solvent extraction of other platinum metal-mixtures, based on tetroxide extraction

Metals separated*	Oxidizing agent	Organic phase	Other information	Reference
Ru-Rh	Cl_2	Carbon tetrachloride	After RuO_4 extraction, Rh co-precipitated with $\text{Fe}(\text{OH})_3$, redissolved in 6M HCl and separated by the anion-exchanger Deacidite FF (Cl^-)	180
^{103}Ru - ^{103m}Rh	$\text{Ce}(\text{SO}_4)_2$	Carbon tetrachloride	From H_2SO_4 solution, 96.2% Ru and 6% Rh were extracted	181
^{103}Ru - ^{103m}Rh	NaOCl	Carbon tetrachloride	After $^{103}\text{RuO}_4$ extraction, the solution was boiled to eliminate the contamination resulting from droplets of CCl_4 containing $^{103}\text{RuO}_4$ and possibly some non-extractable tetroxide	182
Ru-Os in a mixture of Pt-metals	$\text{NaClO}_3 + \text{NaBrO}_3$	—	After simultaneous distillation of Ru and Os tetroxides, RuO_4 reduced selectively in HCl medium and OsO_4 redistilled and absorbed in ethanolic NaOH	183
Ru-Os in a mixture of Pt-metals	Na_2O_2 , NaOCl	Carbon tetrachloride	After simultaneous extraction of tetroxides at pH 5-7, Ru recovered with 6M HCl saturated with SO_2 and Os recovered with 6M NaOH	184

*Notation used: (—) means "separated from".

Table 9. Solvent extraction of other platinum metal mixtures, based on electrostatic effects

Metals separated*	Aqueous phase	Organic phase	Other information	Reference
Pt(IV)-Rh(III)	2M HCl	Tri-n-octylamine in toluene	Extraction twice to remove Pt quantitatively and Rh partially; Pt and Rh recovered with conc. HCl and extracted twice again; 99.8% Rh in aqueous phase; 99.8% Pt extracted	185
Pt(IV)-Rh(III)	0.1M HCl	Primene, tribenzylamine, tri-n-hexylamine or tri-n-octylamine in chloroform or benzene	Pt determined in the organic phase as an orange Pt(II)-Sn(II) complex; amount of Rh should not exceed that of Pt	111
Pt(IV)-Ru(III)		Tetraoctylammonium chloride in dichloroethane	Pt removed quantitatively; <0.05% Ru extracted	186
Pt(IV)-Rh(III)		(CH ₃) ₂ (PhCH ₂) ₂ RNCl (R = C ₁₂ -C ₁₄) in 5% iso-amyl alcohol in dichloroethane	Displacement of [Rh(H ₂ O)Cl ₅] ²⁻ from organic phase takes place easily with aqueous solution of PtCl ₆ ²⁻	187
Pd(II)-Ir(III) Pt(IV)-Ir(III)	2M HCl, tetraoctylammonium bromide	Caprylic acid (5-10%) in dichloroethane	Poor extraction of Rh(III) and Ru(III); their separation from Pt(IV) or Pd(II) may also be possible	188
Pd(II)-Rh(III) Pt(IV)-Rh(III)	1M HCl	Diantipyrilpropylmethane in dichloroethane	Six extraction stages required for milligram amounts; Pd and Pt recovered with HNO ₃	34
Pt(IV)-Rh(III)	3M HCl saturated with NaCl	Tri-n-butyl phosphate	Counter-current extraction; Rh and Ir separation not feasible, owing to reduction of Ir(IV) by the extractant	189
Pd(II), Pt(IV)-Rh(III)	3.5-6.5M HCl	Tri-n-octylamine in benzene	After Pd and Pt extraction, Rh extracted in presence of SnCl ₂ as Rh-SnCl ₂ complex by same extractant	61
Pt(IV)-Pd(II)-Rh(III)	4.38M HBr	Methyl isobutyl ketone	Counter-current extraction and recovery with 25% HNO ₃ saturated with NaNO ₃ ; 45 stages required for 95% separation	190

*Notation used: (-) means "separated from"; () means "and"; (/) means "or".

Table 10. Solvent extraction of other platinum metal mixtures, based on kinetic effects

Metals separated*	Aqueous phase	Organic phase	Other information	Reference
<i>Anionic complexes</i>				
Pd-Rh	pH 1, KSCN	Tri-n-butyl phosphate	Solutions heated for 10 min before extraction; effective separation of 95% of each metal with less than 10 equilibration stages	191
Pd-Ir				
Pt-Rh				
Pt-Ir				
Pd-Rh	4.38M HBr	Tri-n-butylphosphate (90%) in benzene	Metals extracted as bromo-complexes recovered with 2.5M HNO ₃ saturated with NaNO ₂ ; 10 equilibration stages separated 98.5% Pt-99.5% Rh, 98.5% Pd-98.2% Rh	190
Pt-Rh				
Ru-Rh	pH 2.5, 0.6M KSCN, 3M NH ₄ Cl	Polyurethane foam	Aqueous phase heated at 90° for 5 min; extracted for 1 hr	141
Pd-Ru	KSCN; pyridine	Methyl isobutyl ketone	Pd extracted as Pdp ₂ (SCN) ₂ at pH 11 adjusted with NaOH; Ru then extracted as thiocyanate complex from 2M HCl after heating to 90°	192
Pt-Ir	0.05-0.1M KI	Diantipyrylpropylmethane in chloroform	Forms extractable PtI ₄ ²⁻ whereas IrCl ₆ ²⁻ is reduced to unextractable IrCl ₂ ⁻ ; subsequent extraction of Ir by the same reagent in dichloroethane achieved after removing iodide and oxidizing to Ir(IV)	68
Pd/Pt/Rh-Ir	1M HBr-1.5M HClO ₄ , 0.15M SnBr ₂	Isoamyl alcohol	Pd, Pt react immediately at room temperature with SnBr ₂ ; Rh requires 1-2 hr; Ir does not react	128
Pd-Pt/Rh	α -Nitroso- β -naphthol, 2-3M HCl	Isoamyl alcohol	Pd forms complex with the ligand preferentially to Pt and Rh	128
<i>Neutral complexes</i>				
Pd/Ru/Os-Rh, Ir	NaSCN, H ₂ SO ₄	Diantipyryl methane in iso-butyl alcohol-benzene	Over 95% Pd, Ru, Os extracted; Rh and Ir did not form extractable thiocyanate complexes	193
Pd-Ru	pH 3.15, 3-phenyl-5-(2-furyl)pyrazoline dithiocarbamate	Chloroform	Pd extracted quantitatively; <1% Ru extracted	194
Pd-Ir	2M HCl, di-n-octylsulphoxide	Benzene	Extraction difference of 10 ⁵ ; separation should be possible	108

continued overleaf

Table 10. Solvent extraction of other platinum metal mixtures, based on kinetic effects

Metals separated*	Aqueous phase	Organic phase	Other information	Reference
Pd-Pt-Ir	Organic petroleum sulphide	Dichloroethane	Pd forms extractable species with sulphide at room temperature, Pt requires SnCl_2 , and Ir must be heated for 1.5 hr	101
Pd from the rest of Pt-metals	Di-n-octyl sulphide, decylmethyl sulphide or dihexyl sulphide		Selective extraction of Pd	195
Pd, Pt-Rh, Ir	Diethyldithiocarbamate, KI, HCl	Chloroform	Conversion of chloro-complexes of Pd, Pd into PdI_4^{2-} , PtI_4^{2-} accelerates the reaction with the ligand	104
[Pd-Pt]	pH 2-5, <i>p</i> -nitroso dimethylamine	Chloroform	Pd extraction after evaporation of extractant to dryness and mineralization of residue by HNO_3 and H_2O_2	
Pd-Pt, Rh, Ir	pH 5.6, 2-mercapto-benzothiazole	Carbon tetrachloride	Pd completely extracted; less than 1% Pt, Rh, Ir extracted; used for Pd in Pt-wire	196
Pd-Pt-Rh	2-Mercaptobenzothiazole	Weakly polar solvents	Differences in distribution at different temperatures and rate of attaining equilibrium can be utilized for separation	197
Pd-Pt-Rh-Ir	HCl, KI, 2-mercapto-benzothiazole	Chloroform	Separates Pd and Pt from Rh and Ir	112
[Pd-Pt]	Dimethylglyoxime	Chloroform	Pd separated from Pt	
[Rh-Ir]	HCl, SnCl_2 , 2-mercapto-benzothiazole	Chloroform	SnCl_2 accelerates formation of extractable Rh complex	
Pd-Pt-Rh-Ir	HCl, KI, diphenylthiourea	Chloroform	Separates Pd and Pt from Rh and Ir	113
[Rh-Ir]	HCl, SnCl_2 , diphenylthiourea	Chloroform	SnCl_2 accelerates formation of extractable Rh-diphenylthiourea complex	
<i>Cationic complexes</i>				
Rh-Pd	0.05M HCl	Dinonylnaphthalene-sulphonic acid in heptane	Solution made basic with NaOH to precipitate Rh, then acidic with HCl to dissolve the precipitate; poor separation from Ru	138
Rh-Pt				
Rh-Ir				
Rh-Ru				

*Notation used: (-) means "separated from"; () means "and"; () means "or"; [] indicates "a subsequent separation of these metals after the preliminary step shown above".

Table 11. Separation of multicomponent systems

Metals separated*	Aqueous phase	Organic phase	Other information	Reference
Pd-Pt-Rh-Ir	4.7M HCl, NaI	Tri-n-butyl phosphate in hexane	Pd and Pt simultaneously extracted as MCl_4^- ; Rh and Ir do not form extractable species at room temperature and Ir(IV) reduced to unextractable Ir(III) by the iodide medium	65
[Pd-Pt] [Rh-Ir]	<i>p</i> -Nitrosodimethylamine HCl	Chloroform Tri-n-butyl phosphate in hexane	Pd complex extracted After iodide destroyed with HNO_3 , Ir(III) oxidized to extractable Ir(IV) by H_2O_2	
Pd-Ir-Pt	1M HCl, H_2O_2	Dianthipyrilpropylmethane in chloroform	Simultaneous extraction of chloride complexes of Pd(II), Pt(IV), Ir(IV); back-extraction of Ir with NH_4OH and Pd with $N_2H_4 \cdot HCl$	62
Os-Ru-Pd-Pt-Rh-Ir	70% $HClO_4$		Simultaneous distillation of Ru, and Os and collection in 3% H_2O_2	198, 199
[Os-Ru] [Pd, Pt-Rh, Ir]	$H_2SO_4-H_2O_2$ mixture Diethyldithiocarbamate	Chloroform	Selective distillation of Os After evaporation of $HClO_4$ and conversion of metals into chloro-complexes, reagent added and Pd, Pt simultaneously extracted	
[Pd-Pt] [Rh-Ir]	<i>p</i> -Nitrosodimethylamine 1M HCl, Cu powder	Chloroform	Pd complex extracted Reduction and precipitation of Rh	
Os-Ru-Pd-Pt-Rh-Ir		Carbon tetrachloride	Simultaneous extraction of tetroxides of Os, Ru	109
[Ru-Os]			Ru recovered from CCl_4 with 6M HCl containing SO_2 ; Os recovered with 3M NaOH	
[Pd-Pt-Ir-Rh]	6M HCl, di-n-heptyl-sulphoxide (R_2SO)	1,1,2-Trichloroethane	Extraction of $PdCl_2$, $2R_2SO$ and $(R_2SOH^-)_2 MCl_6^{2-}$; [M = Pt(IV) or Ir(IV)]; Rh partially extracted	
[Pt-Ir]	1M HCl, di-n-heptyl-sulphoxide	1,1,2-Trichloroethane	After recovery of Pt and Ir with water, Ir(IV) reduced to Ir(III) with hydrazine or hydroquinone; 10 equilibration stages extract Pt	
[Pd, Rh]			Back-extraction of Pd with 10% dimethylamine and Rh with aqueous $NaNO_2$ at 70° and pH 7	

*Notation used: (-) means "separated from"; (.) means "and"; [] indicates "a subsequent separation of these metals after the preliminary step shown above it".

REFERENCES

1. K. A. Kraus, F. Nelson and G. W. Smith, *J. Phys. Chem.*, 1954, **58**, 11.
2. S. S. Berman and W. A. E. McBryde, *Can. J. Chem.*, 1958, **36**, 835.
3. R. Kuroda and N. Yoshikuni, *Talanta*, 1971, **18**, 1123.
4. C. Pohlandt, *Natl. Inst. Metall., Republ. S. Afr., Project No. 06476*, 28 April 1978.
5. D. D. Busch, J. M. Prospero and R. A. Naumann, *Anal. Chem.*, 1959, **31**, 884.
6. H. Shimojima, *Nippon Kagaku Zasshi*, 1960, **81**, 564; *Chem. Abstr.*, 1961, **55**, 18246d.
7. K. Brajter and B. Gankowski, *Talanta*, 1977, **24**, 761.
8. M. L. Cluett, S. S. Berman and W. A. E. McBryde, *Analyst*, 1955, **80**, 204.
9. S. S. Berman and W. A. E. McBryde, *Can. J. Chem.*, 1958, **36**, 845.
10. H. Zachariassen and F. E. Beamish, *Anal. Chem.*, 1962, **34**, 964.
11. C. K. Jørgensen, *Acta Chem. Scand.*, 1956, **10**, 500.
12. J. S. Forrester and G. H. Ayres, *J. Phys. Chem.*, 1959, **63**, 1979.
13. A. M. Kristjanson and M. Lederer, *J. Less-Common Met.*, 1959, **1**, 245.
14. W. C. Wolsey, C. A. Reynolds and J. Kleinberg, *Inorg. Chem.*, 1963, **2**, 463.
15. V. I. Shlenskaya, O. A. Efremenko, S. V. Oleinikov and I. P. Alimarin, *Izv. Akad. Nauk SSSR, Ser. Khim.*, 1969, 1643; *Chem. Abstr.*, 1969, **71**, 129432n.
16. H. H. Cady and R. E. Connick, *J. Am. Chem. Soc.*, 1958, **80**, 2646.
17. V. I. Paramonova and E. F. Latyshev, *Radiokhimiya*, 1959, **1**, 458; *Chem. Abstr.* 1960, **54**, 8405e.
18. R. E. Connick and D. A. Fine, *J. Am. Chem. Soc.*, 1960, **82**, 4187.
19. *Idem, ibid.*, 1961, **83**, 3414.
20. F. Pantani, *J. Less-Common Met.*, 1962, **4**, 116.
21. S. K. Shukla, *J. Chromatog.*, 1962, **8**, 96.
22. V. I. Shlenskaya and A. A. Biryukov, *Vestn. Mosk. Univ. Ser. II, Khim.*, 1963, **18**, 75; *Chem. Abstr.*, 1963, **59**, 13489h.
23. A. Ohyoshi, E. Ohyoshi, M. Senoo and M. Shinagawa, *J. Nucl. Sci. Technol.*, 1966, **3**, 237.
24. V. I. Shlenskaya, Z. A. Kuratashvili and I. G. Tikhonov, *Vestn. Mosk. Univ., Khim.*, 1973, **14**, 122; *Chem. Abstr.*, 1973, **78**, 164990j.
25. V. I. Shlenskaya, G. V. Pichug, V. P. Khvostova and I. P. Alimarin, *Izv. Akad. Nauk, SSSR, Khim.*, 1974, 268; *Chem. Abstr.*, 1974, **81**, 54938c.
26. V. I. Shlenskaya, A. A. Biryukov, V. M. Kadomtseva, *Zh. Neorgan. Chem.*, 1972, **17**, 1104; *Chem. Abstr.*, 1972, **77**, 10352v.
27. E. Blasius and U. Wachtel, *Z. Anal. Chem.*, 1954, **142**, 341.
28. L. G. Sillén and A. E. Martell, *Stability Constants of Metal-Ion Complexes*, Chemical Society, Spec. Publ. 17, London, 1971.
29. K. Brajter and K. Slonawska, *Chem. Anal. (Warsaw)*, 1979, **24**, 273.
30. R. Dyczynski and H. Maleszewska, *J. Radioanal. Chem.*, 1974, **21**, 229.
31. R. Neeb, *Z. Anal. Chem.*, 1956, **152**, 158.
32. *Idem, ibid.*, 1957, **154**, 23.
33. W. Geilmann and R. Neeb, *ibid.*, 1957, **156**, 411.
34. A. I. Busev and V. K. Akomov, *Talanta*, 1964, **11**, 1657.
35. H. Meier, E. Zimmerhackl, W. Albrecht, D. Bosche, W. Hecker, P. Menge, A. Ruckdeschel, E. Unger and G. Zeitler, *Mikrochim. Acta*, 1969, 826.
36. A. J. Radford, *Natl. Inst. Metall., Publ. S. Afr., Project No. 00674*, 12 May 1975.
37. O. Bozkov, L. Cermakova and M. Malat, *Anal. Lett.*, 1979, **12**, 1259.
38. F. E. Beamish, *Talanta*, 1960, **5**, 1.
39. G. Dinstl and F. Hecht, *Mikrochim. Acta*, 1963, 895.
40. W. M. MacNevin and W. B. Crummett, *Anal. Chem.*, 1953, **25**, 1628.
41. *Idem, Anal. Chim. Acta*, 1954, **10**, 323.
42. K. R. Kar and S. Singh, *Mikrochim. Acta*, 1970, 616.
43. F. V. S. Toerien and M. Levin, *J. S. Afr. Chem. Inst.*, 1974, **27**, 87.
44. K. Brajter, K. Kleyny and Z. Vorbrodt, *Talanta*, 1980, **27**, 433.
45. F. Coufalik and M. Svach, *Z. Anal. Chem.*, 1960, **173**, 113.
46. W. M. MacNevin and E. S. McKay, *Anal. Chem.*, 1957, **29**, 1220.
47. N. K. Pshenitsyn, K. A. Gladyshevskaya and L. M. Ryakhava, *Analiz Blagorod. Metal., Akad. Nauk, SSSR, Inst. Obschei Neorgan. Khim.*, 1959, 103; *Chem. Abstr.*, 1960, **54**, 16280i.
48. F. V. S. Toerien and M. Levin, *J. S. Afr. Chem. Inst.*, 1974, **27**, 91.
49. E. W. Berg and W. L. Senn, *Anal. Chem.*, 1955, **27**, 1255.
50. K. Ishida, T. Kiriyama and R. Kuroda, *Anal. Chim. Acta*, 1968, **41**, 537.
51. A. Gulko, H. Feigenbaum and G. Schmuckler, *ibid.*, 1972, **59**, 397.
52. G. V. Myasoedova, I. I. Antokol'skaya, L. I. Bol'shakova, O. P. Shvoeva and S. B. Savvin, *J. Anal. Chem. USSR*, 1974, **29**, 1807.
53. N. K. Pshenitsyn, K. A. Gladyshevskaya and L. M. Ryakhova, *Vopr. Analiza Blagorod. Metal. Sb.*, 1963, 72; *Chem. Abstr.*, 1964, **61**, 6364a.
54. F. E. Beamish, *The Analytical Chemistry of the Noble Metals*, Pergamon Press, Oxford, 1966.
55. F. E. Beamish and J. C. Van Loon, *Recent Advances in the Analytical Chemistry of the Noble Metals*, Pergamon Press, Oxford, 1972.
56. S. N. Ivanova, L. M. Gindin and L. Ya. Mironova, *Izv. Sib. Otd. Akad. Nauk SSSR, Ser. Khim. Nauk*, 1964, 35; *Chem. Abstr.*, 1965, **62**, 4682b.
57. L. M. Gindin, P. I. Bobikov and E. F. Kouba, *ibid.*, 1961, 84; *Chem. Abstr.*, 1962, **56**, 9779c.
58. C. M. Davidson and R. F. Jamieson, *Trans. Faraday Soc.*, 1965, **61**, 133.
59. E. N. Gil'bert, V. A. Pronin, I. M. Ivanov, S. N. Ivanova, A. A. Vasil'eva, P. I. Artyukhin and L. M. Gindin, *Zh. Neorgan. Khim.*, 1968, **13**, 1055.
60. A. A. Vasil'eva, L. M. Gindin, G. N. Pelina and G. D. Mal'chikov, *Izv. Sib. Otd. Akad. Nauk, SSSR, Ser. Khim. Nauk*, 1969, 40; *Chem. Abstr.*, 1970, **72**, 71221v.
61. M. A. Khattak and R. J. Magee, *Anal. Chim. Acta.*, 1969, **45**, 297.
62. V. P. Ionov, S. A. Potapova, Z. N. Dubrovina and N. M. Zharoronkov, *J. Anal. Chem. USSR*, 1975, **30**, 802.
63. C. Pohlandt, *Natl. Inst. Metall., Republ. S. Afr., Project No.*, 03276, 28 March 1977.
64. M. Mojski, *Talanta*, 1980, **27**, 7.
65. G. H. Faye and W. R. Inman, *Anal. Chem.*, 1963, **35**, 985.
66. R. Neeb, *Z. Anal. Chem.*, 1957, **154**, 17.
67. V. F. Borbat and O. B. Tikhomirov, *Tsvet. Metal.*, 1967, **40**, 30; *Chem. Abstr.*, 1967, **67**, 66695v.
68. N. P. Rudenko and V. O. Kordyukevich, *J. Anal. Chem. USSR*, 1968, **23**, 929.
69. O. S. Shelkovich, A. V. Nikolaev and R. I. Novoselov, *Izv. Sib. Otd. Akad. Nauk SSSR, Ser. Khim. Nauk*, 1975, 50; *Chem. Abstr.*, 1976, **84**, 35885d.
70. R. B. Wilson and W. D. Jacobs, *Anal. Chem.*, 1961, **33**, 1650.
71. E. W. Berg and W. L. Senn, *Anal. Chim. Acta*, 1958, **19**, 109.
72. G. A. Kanert and A. Chow, *ibid.*, 1974, **69**, 355.

73. A. Baghai and H. J. M. Bowen, *Analyst*, 1976, **101**, 661.
74. W. Geilmann and R. Neeb, *Z. Anal. Chem.*, 1957, **156**, 420.
75. E. W. Berg and H. E. Moseley, *Anal. Chim. Acta*, 1969, **47**, 360.
76. N. M. Sinitsyn, F. Ya. Rovinskii and V. F. Travkin, *Izv. Sib. Otd. Akad. Nauk SSSR, Ser. Khim. Nauk*, 1970, **101**; *Chem. Abstr.*, 1971, **74**, 80395y.
77. K. A. Bol'shakov, N. M. Sinitsyn, V. V. Borisov, V. I. Efanov, and N. A. Pantyukhina, *Uchen. Zap. Mosk. Inst. Tonkoi Khim. Technol.*, 1970, **1**, 35; *Anal. Abstr.*, 1972, **23**, 310.
78. K. A. Bol'shakov, N. M. Sinitsyn, V. V. Borisov and S. M. Vaseneva, *Zh. Neorgan. Khim.*, 1971, **16**, 1968.
79. A. Bol'shakov, N. M. Sinitsyn, T. M. Bustaeva and A. P. Ivchenko, *Dokl. Akad. Nauk SSSR*, 1980, **251**, 1406; *Anal. Abstr.*, 1981, **40**, 1B167.
80. H. Meier, D. Bosche, E. Zimmerhackl, W. Albrecht, W. Hecker, P. Menge, A. Ruckdeschel, E. Unger and G. Zeitler, *Microchim. Acta*, 1969, 1083.
81. H. Meier, E. Zimmerhackl, W. Albrecht, D. Bosche, W. Hecker, P. Menge, A. Ruckdeschel, E. Unger and G. Zeitler, *ibid.*, 1969, 557.
82. S. Kalyanaraman and S. M. Khopkar, *Anal. Chim. Acta*, 1975, **78**, 231.
83. A. G. Saed, B. Z. Iofa and A. N. Nesmeyanov, *Vestn. Mosk. Univ. Khim.*, 1978, **33**, 222.
84. A. M. Golub and G. V. Pomerants, *Ukr. Khim. Zh.*, 1965, **31**, 104; *Chem. Abstr.*, 1965, **62**, 13822b.
85. P. K. Paria and S. K. Majumdar, *Indian J. Chem.*, 1976, **14A**, 820.
86. S. J. Al-Bazi and A. Chow, *Talanta*, 1983, **30**, 487.
87. J. H. W. Forsythe, R. J. Magee and C. L. Wilson, *ibid.*, 1960, **3**, 330.
88. *Ion-Exchange and Solvent Extraction*, J. A. Marinsky and Y. Marcus (eds.), Vol. 8, p. 311. Dekker, New York, 1981.
89. P. Senise and F. Levi, *Anal. Chim. Acta*, 1964, **30**, 422.
90. *Idem*, *ibid.*, 1964, **30**, 509.
91. W. J. Holland, R. A. Dimenna and R. J. Walker, *Mikrochim. Acta*, 1972, 183.
92. R. J. Walker and W. J. Holland, *ibid.*, 1973, 591.
93. A. Diamantatos, *Anal. Chim. Acta*, 1973, **66**, 147.
94. V. A. Pronin, M. V. Usol'tseva, Z. N. Shastina, N. K. Gusanova, E. P. Vylykh, S. V. Amosova and B. A. Trofimov, *Zh. Neorgan. Khim.* 1973, **18**, 1921.
95. V. K. Akimov, G. P. Rudzit, G. L. Dzhishkariani and A. I. Busev, *J. Anal. Chem. USSR*, 1974, **29**, 693.
96. P. K. Paria and S. K. Majumdar, *Indian J. Chem.*, 1977, **15A**, 158.
97. P. Dunn and W. J. Holland, *Mikrochim. Acta*, 1977, **1**, 363.
98. O. M. Petrukhin, V. N. Shevchenko, I. A. Zakharova and V. A. Prokhorov, *J. Anal. Chem. USSR*, 1977, **32**, 703.
99. Yu. A. Zolotov, O. M. Petrukhin, V. N. Shevchenko, V. V. Dunina and E. G. Ruhkadze, *Anal. Chim. Acta*, 1978, **100**, 613.
100. E. E. Rakovskii, N. V. Shvedova and L. D. Berliner, *J. Anal. Chem. USSR*, 1974, **29**, 1933.
101. E. E. Rakovskii and M. I. Starozhitskaya, *ibid.*, 1974, **29**, 1799.
102. V. K. Akimov, A. I. Busev and K. V. Kodua, *ibid.*, 1978, **33**, 1851.
103. E. E. Rakovskii and B. S. Rabinovich, *Izv. Sib. Otd. Akad. Nauk SSSR, Ser. Khim. Nauk*, 1970, 98; *Chem. Abstr.*, 1971, **74**, 80383t.
104. J. H. Yoe and J. J. Kirkland, *Anal. Chem.*, 1954, **26**, 1335.
105. D. C. Gregoire and A. Chow, *Talanta*, 1975, **22**, 453.
106. M. Mojski, *Talanta*, 1978, **25**, 163.
107. V. G. Torgov, V. N. Andrievskii, E. N. Gil'bert, I. L. Kotlyarevskii, V. A. Mikhailov, A. V. Nikolaev, V. N. Pronin and D. D. Trotsenko, *Izv. Sib. Otd. Akad. Nauk SSSR, Ser. Khim. Nauk*, 1969, 148; *Chem. Abstr.*, 1970, **72**, 93804q.
108. A. V. Nikolaev, V. G. Torgov, E. N. Gil'bert, V. A. Mikhailov, V. A. Pronin, L. G. Stadnikova and I. L. Kotlyarevskii, *ibid.*, 1967, 120; *Chem. Abstr.*, 1968, **69**, 90385f.
109. P. A. Lewis, D. F. C. Morris, E. L. Short and D. N. Waters, *J. Less-Common Met.*, 1976, **45**, 193.
110. A. K. De and M. S. Rahaman, *Analyst*, 1964, **89**, 795.
111. M. A. Khattak and R. J. Magee, *Talanta*, 1965, **12**, 733.
112. A. Diamantatos, *Anal. Chim. Acta*, 1973, **67**, 317.
113. A. Diamantatos and A. A. Verbeek, *ibid.*, 1977, **91**, 287.
114. V. M. Shul'man and T. V. Zagorskaya, *Izv. Sib. Otd. Akad. Nauk SSSR, Ser. Khim. Nauk*, 1971, 142; *Chem. Abstr.*, 1972, **76**, 104448n.
115. E. E. Rakovskii and G. M. Baevskaia, *J. Anal. Chem. USSR*, 1971, **26**, 1602.
116. V. M. Shul'man and L. A. Kosareva, *Izv. Sib. Otd. Akad. Nauk SSSR, Ser. Khim. Nauk*, 1973, 137; *Chem. Abstr.*, 1974, **80**, 7594g.
117. A. V. Nikolaev, V. G. Torgov, V. A. Nikhailov, V. N. Andrievskii, K. A. Bakovets, M. F. Bondarenko, E. N. Gil'bert, I. L. Kotlyarevskii, G. A. Mardezhova and S. S. Shatskaya, *ibid.*, 1970, 54; *Chem. Abstr.*, 1971, **74**, 80400w.
118. V. A. Mikhailov, V. G. Torgov, E. N. Gil'bert, L. N. Mazalov and A. V. Nikolaev, *Proc. Intern. Solvent Extn. Conf.* 1971, **2**, 1112; *Chem. Abstr.*, 1975, **83**, 137660y.
119. M. Mojski, *Chem. Anal. (Warsaw)*, 1979, **24**, 207.
120. J. T. Pyle and W. D. Jacobs, *Anal. Chem.*, 1964, **36**, 1796.
121. V. F. Borbat and E. F. Kouba, *Tsvet. Metal.*, 1967, **40**, 33; *Chem. Abstr.*, 1968, **69**, 5674g.
122. S. K. Kalinin, G. S. Katykhin, M. K. Nikitin and G. A. Yakovleva, *J. Anal. Chem. USSR*, 1970, **25**, 459.
123. M. Di Casa and R. Stella, *Radiochem. Radioanal. Lett.*, 1972, **10**, 331.
124. N. A. Borshch and O. M. Petrukhin, *J. Anal. Chem. USSR*, 1978, **33**, 1672.
125. S. J. Al-Bazi and A. Chow, *Talanta*, 1984, **31**, 431.
126. E. E. Rakovskii, M. I. Starozhilskaya and P. Ya. Yampolskii, *J. Radioanal. Chem.*, 1972, **11**, 5.
127. T. I. Shurupova and V. M. Ivanov, *J. Anal. Chem. USSR*, 1982, **37**, 1455.
128. F. Pantani and G. Piccardi, *Anal. Chim. Acta*, 1960, **22**, 231.
129. A. T. Pilipenko, V. N. Danilova and S. L. Lisichenko, *J. Anal. Chem. USSR*, 1970, **25**, 998.
130. D. J. Nicolas, *Natl. Inst. Metall., Repub. S. Afr., Project No. 01374*, 5 Dec 1974.
131. J. R. Stokely and W. D. Jacobs, *Anal. Chem.*, 1963, **35**, 149.
132. G. A. Vorob'eva, Yu. A. Zolotov, L. A. Izosenkov, A. V. Karyakin, L. I. Pavlenko, O. M. Petrukhin, I. V. Seryakova, L. V. Simonova and V. N. Shevchenko, *J. Anal. Chem. USSR*, 1974, **29**, 425.
133. G. G. Tertipis and F. E. Beamish, *Anal. Chem.*, 1962, **34**, 623.
134. R. Stella and M. Di Casa, *J. Radioanal. Chem.*, 1973, **16**, 183.
135. S. J. Al-Bazi and A. Chow, *Anal. Chem.*, 1981, **53**, 1073.
136. D. E. Ryan, *Analyst*, 1950, **75**, 557.
137. *Idem*, *Can. J. Chem.*, 1961, **39**, 2389.
138. M. A. Khan and D. F. C. Morris, *J. Less-Common Met.*, 1967, **13**, 53.

139. Y. Oka and T. Kato, *Nippon Kagaku Zasshi*, 1963, **84**, 249; *Chem. Abstr.*, 1964, **60**, 3542e.
140. A. T. Pilipenko, I. P. Sereda and E. P. Semenyuk, *J. Anal. Chem. USSR*, 1970, **25**, 1682.
141. S. J. Al-Bazi and A. Chow, *Talanta*, 1984, **31**, 189.
142. *Idem*, *Anal. Chim. Acta*, 1984, **157**, 83.
143. T. D. Avtokratova, *Analytical Chemistry of Ruthenium*, p. 19. Ann Arbor-Humphrey Science Publishers, Ann Arbor, 1969.
144. G. Goldstein, D. L. Manning, O. Menis and J. A. Dean, *Talanta*, 1961, **7**, 307.
145. W. J. Allan and F. E. Beamish, *Anal. Chem.*, 1952, **24**, 1608.
146. R. D. Sauerbrunn and E. B. Sandell, *J. Am. Chem. Soc.*, 1953, **75**, 3554.
147. W. P. Griffith, *The Chemistry of the Rarer Platinum Metals*, Interscience, London, 1967.
148. T. Hara and E. B. Sandell, *Anal. Chim. Acta*, 1960, **23**, 65.
149. B. C. Bera and M. M. Chakrabartty, *Microchem. J.*, 1966, **11**, 420.
150. F. P. Dwyer and N. A. Gibson, *Analyst*, 1951, **76**, 104.
151. E. W. Berg and H. E. Moseley, *Anal. Lett.*, 1969, **2**, 259.
152. P. Senise and L. R. M. Pitombo, *Talanta*, 1964, **11**, 1185.
153. S. J. Al-Bazi and A. Chow, *Anal. Chem.*, 1983, **55**, 1094.
154. R. D. Sauerbrunn and E. B. Sandell, *Anal. Chim. Acta*, 1953, **9**, 86.
155. V. G. Sil'nichenko and Yu. V. Dolinina, *Zavodsk. Lab.*, 1969, **35**, 1159; *Chem. Abstr.*, 1970, **72**, 62487j.
156. W. R. Schoeller and A. R. Powell, *The Analysis of Minerals and Ores of the Rarer Elements*, 3rd Ed., p. 344. Hafner, New York, 1955.
157. Z. Marczenko and M. Balcerzak, *Anal. Chim. Acta*, 1979, **109**, 123.
158. B. K. Pal, R. P. Chowdhury and B. K. Mitra, *Talanta*, 1981, **28**, 62.
159. W. Geilmann and R. Neeb, *Z. Anal. Chem.*, 1956, **152**, 96.
160. R. L. Rich and H. Taube, *J. Am. Chem. Soc.*, 1954, **76**, 2608.
161. D. R. Stranks and G. R. Wilkins, *Chem. Rev.*, 1957, **57**, 808.
162. F. S. Martin, *J. Chem. Soc.*, 1954, 2564.
163. W. L. Belew, G. R. Wilson and L. T. Corbin, *Anal. Chem.*, 1961, **33**, 886.
164. J. W. T. Meadows and G. M. Matlack, *ibid.*, 1962, **34**, 89.
165. G. Goldstein, *Inorg. Chem.*, 1963, **2**, 425.
166. G. Goldstein, D. L. Manning, O. Menis and J. A. Dean, *Talanta*, 1961, **7**, 296.
167. *Idem*, *ibid.*, 1961, **7**, 301.
168. W. Smulek, *Radiochem. Radioanal. Lett.*, 1969, **2**, 265.
169. J. H. Wiersma and P. F. Lott, *Anal. Chem.*, 1967, **39**, 674.
170. B. C. Bera and M. M. Chakrabartty, *ibid.*, 1966, **38**, 1419.
171. A. D. Westland and F. E. Beamish, *ibid.*, 1954, **26**, 739.
172. Y. Oka and T. Kato, *Nippon Kagaku Zasshi*, 1966, **87**, 580; *Chem. Abstr.*, 1966, **65**, 8088d.
173. E. L. Steele and J. H. Yoe, *Anal. Chem.*, 1957, **29**, 1622.
174. I. Hoffman, J. E. Schweitzer, D. E. Ryan and F. E. Beamish, *ibid.*, 1953, **25**, 1091.
175. Z. Marczenko and J. Uscinska, *Anal. Chim. Acta*, 1981, **123**, 271.
176. S. J. Al-Bazi, *Ph.D. Thesis*, University of Manitoba, 1983.
177. M. Qureshi and K. N. Mathur, *Z. Anal. Chem.*, 1968, **242**, 159.
178. V. I. Shlenskaya and V. P. Khvostova, *J. Anal. Chem. USSR*, 1968, **23**, 193.
179. U. Muralikrishna, K. V. Bapanaiah, N. S. N. Prasad and P. Kannarao, *Indian J. Chem.*, 1976, **14A**, 291.
180. D. F. C. Morris and M. A. Khan, *Radiochim. Acta*, 1966, **6**, 110.
181. C. E. Epperson, R. R. Landolt and W. V. Kessler, *Anal. Chem.*, 1976, **48**, 979.
182. J. Chiu, R. R. Landolt and W. V. Kessler, *ibid.*, 1978, **50**, 670.
183. S. T. Payne, *Analyst*, 1958, **85**, 698.
184. M. A. Khan and D. F. C. Morris, *Sep. Sci.*, 1967, **2**, 635.
185. L. M. Gindin and S. N. Ivanova, *Izv. Sib. Otd. Akad. Nauk SSSR Ser. Khim. Nauk*, 1964, **28**; *Chem. Abstr.*, 1965, **62**, 4681h.
186. S. N. Ivanova, L. M. Gindin and I. Ya. Mironova, *ibid.*, 1967, **97**; *Chem. Abstr.*, 1967, **67**, 68134k.
187. L. M. Gindin, S. N. Ivanova, A. A. Mazurova, A. A. Vasil'eva, L. Ya. Mironova, A. P. Sokolov and P. P. Smirnov, *ibid.*, 1967, **89**; *Chem. Abstr.*, 1967, **67**, 68138q.
188. A. A. Vasil'eva, L. M. Gindin, S. N. Ivanova, L. Ya. Mironova and G. I. Smirnova, *ibid.*, 1967, **174**; *Chem. Abstr.*, 1967, **67**, 121960e.
189. E. W. Berg and W. L. Senn, *Anal. Chim. Acta*, 1958, **19**, 12.
190. E. W. Berg and J. R. Sanders, *ibid.*, 1967, **38**, 377.
191. E. W. Berg and E. Y. Lau, *ibid.*, 1962, **27**, 248.
192. J. H. W. Forsythe, R. J. Magee and C. L. Wilson, *Talanta*, 1960, **3**, 324.
193. A. T. Pilipenko and P. F. Ol'khovich, *Izv. Sib. Otd. Akad. Nauk SSSR, Ser. Khim. Nauk*, 1970, **87**; *Chem. Abstr.*, 1971, **74**, 80399c.
194. A. I. Busev, V. M. Byr'ko, A. G. Kvesitadze and V. N. Simonova, *J. Anal. Chem. USSR*, 1972, **27**, 1635.
195. R. I. Edwards, *S. African Natl. Inst. Metallurgy Rept.*, 7405, 109, 9 Feb. 1976; *Chem. Abstr.*, 1977, **87**, 121008p.
196. E. G. Koleva and T. H. Ngat, *J. Anal. Chem. USSR*, 1979, **34**, 1713.
197. A. V. Nikolaev, V. M. Shul'man, L. M. Gindin, S. V. Larionov, P. I. Aryukhin, L. Ya. Mironova, T. V. Zagorskaya, L. I. Tyuleneva and L. A. Il'ina, *Izv. Sib. Otd. Akad. Nauk, SSSR, Ser. Khim. Nauk*, 1970, **60**; *Chem. Abstr.*, 1971, **74**, 80394x.
198. J. G. S. Gupta and F. E. Beamish, *Am. Mineral.*, 1963, **48**, 379.
199. J. G. S. Gupta, *Anal. Chim. Acta*, 1968, **42**, 481.
200. F. E. Beamish, *Talanta*, 1967, **14**, 991.
201. L. R. P. Reavill, *Platinum Met. Rev.*, 1984, **28**, 2.

SHORT COMMUNICATIONS

DETERMINATION OF THE STABILITY CONSTANT OF THE TERNARY COMPLEX FORMED IN THE COPPER-BIPYRIDYL-ERIOCHROME CYANINE R SYSTEM, BY AN ISOSBESTIC POINT-SPECTROPHOTOMETRIC METHOD

SHI-FU ZOU and WEI-AN LIANG

Department of Chemistry, Shandong University, Jinan, Shandong, People's Republic of China

(Received 23 March 1983. Revised 23 June 1983. Accepted 13 May 1984)

Summary—This paper reports a new method for determining the stability constants of ternary complexes, based on analysis of isosbestic points. First, it is necessary to determine the absolute molar absorptivities of the various species concerned, then their concentrations and the stability constant. In this method, the approximate treatment of classical photometric methods is not required. The conditional constant can be calculated directly from the measured data.

Most spectrophotometric methods¹⁻³ for the determination of the stability constants of complexes are based on measurements made at an absorption peak. The parameters estimated by these methods are not always sufficiently accurate and are unsuitable for application to complicated systems,^{2,4-8} so it seems desirable to find new methods based on other characteristics.

The system⁹ copper-bipyridyl-Eriochrome Cyanine R (Cu-Bpy-ECR) was chosen as the subject of investigation, because there are two different complexes (1:1:1 and 1:1:2) formed and it is not possible to obtain the stability constants by classical methods.

The method suggested is based on analysis of the isosbestic points of the absorption spectra, from which the absolute molar absorptivities and the concentrations of the species concerned can be obtained.

EXPERIMENTAL

Apparatus

A Hitachi recording spectrophotometer, model 340, and a model pHs-2 pH-meter were used.

Reagents

The Eriochrome Cyanine R (ECR) was purified according to Dixon's procedure,¹⁰ by dextran column chromatography, slightly modified,^{11,12} and was used to prepare a $2 \times 10^{-3}M$ standard solution with a final hydrochloric acid concentration of $0.008M$. The other chemicals used were either of guaranteed grade or analytically pure.

Precipitates are readily formed in the Cu-Bpy-ECR system. In order to prevent this precipitation, Ishida *et al.*⁹ added the non-ionic surfactant Triton X-100 as solubilizer. In our experience, this is ineffective when the [Cu-Bpy]:[ECR] ratio is greater than 3:4, or when the pH

is lower than 9.6. We used an anionic surfactant (sodium dodecyl sulphate) instead. This gives a stable solution, even at pH somewhat lower than 9.

Procedure

To each of ten 50-ml standard flasks add a small amount of water, 5 ml of 0.1% surfactant solution, 4 ml of $5 \times 10^{-4}M$ ECR, followed by various amounts of Cu-Bpy mixture (1:1 v/v, each $5 \times 10^{-4}M$) and 20 ml of buffer solution. Dilute the solutions to volume with water, mix well, and allow to stand for 10 min. Record the absorption spectra (with water as reference; 1-cm cells) over the wavelength region 400-620 nm. The ionic strength of the solution is controlled at $0.08M$ by the buffer solution. The pH is redetermined as a check after the measurement of absorbance.

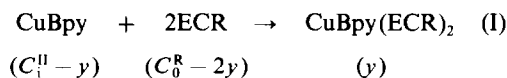
In this way the pH and concentrations of ECR (C_0^R) and surfactant (C_0^S) are kept constant, and the concentration of CuBpy (C_0^I) is increased gradually so as to obtain a set of absorption spectra (Fig. 1). Table 1 compares the data with literature values.

CALCULATIONS AND DISCUSSION

The composition of the complexes was studied in detail by earlier workers,⁹ and we did not repeat their work.

Analysis of absorption spectra

According to references 13 and 14, the isosbestic point E in Fig. 1 results from incorporation of ECR (with CuBpy) into a 1:1:2 complex. The chemical reaction should be:



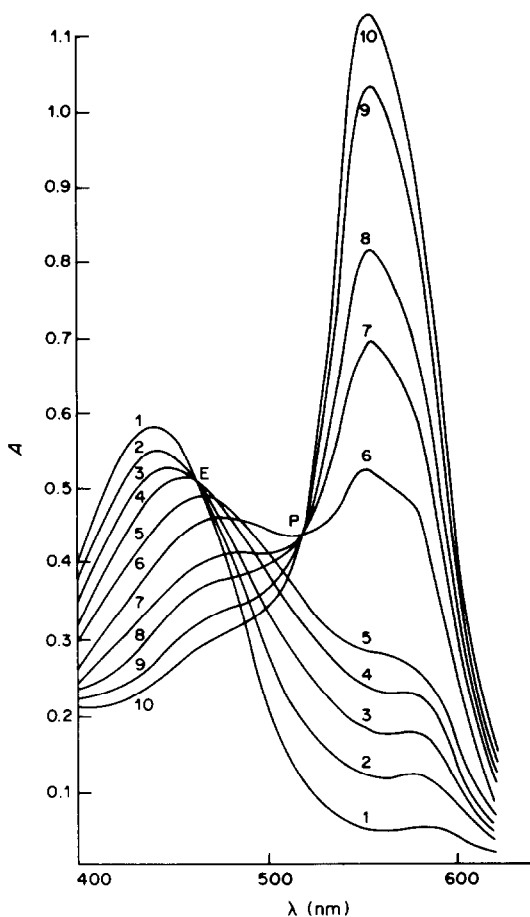


Fig. 1. Absorption spectra for the Cu-Bpy-ECR system. pH = 10.41; $\mu = 0.08M$; $T = 24 \pm 1^\circ$; $C_0^R = 4.00 \times 10^{-5}M$; $C_0^S = 0.01\%$; $C_1^H (\times 10^{-5}M)$ for the curves: 1—0, 2—0.500, 3—1.00, 4—1.50, 5—2.00, 6—3.00, 7—3.50, 8—4.00, 9—4.50, 10—5.00.

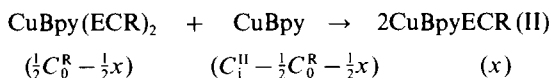
Charges on the ions are omitted and y represents the concentration of the 1:1:2 complex at equilibrium. Then the absorbance is

$$A_1 = (\epsilon^y - 2\epsilon^R)y + \epsilon^R C_0^R \quad (1)$$

where ϵ^y and ϵ^R are the molar absorptivities of the 1:1:2 complex and ECR respectively. The absorbance of CuBpy is practically zero in this region of the spectrum.

At the wavelength of the isosbestic point (λ_E), $\epsilon^y = 2\epsilon^R$. Therefore A_1 is constant and independent of y . Hence an isosbestic point appears (E).

Correspondingly, the isosbestic point P is formed by the transformation of the 1:1:2 complex into the 1:1:1. The reaction is



where $\frac{1}{2}C_0^R$ represents the concentration of CuBpy- $(\text{ECR})_2$ when CuBpy and ECR have been mixed in exactly 1:2 ratios and x is the concentration of the 1:1:1 complex at equilibrium for reaction (II). The absorbance is

$$A_2 = (\epsilon^x - \frac{1}{2}\epsilon^y)x + \frac{1}{2}\epsilon^y C_0^R \quad (2)$$

where ϵ^x represents the molar absorptivity of the 1:1:1 complex. At λ_P A_2 is constant and independent of x , because $\epsilon^x = \frac{1}{2}\epsilon^y$.

Deduction and calculation of the absolute molar absorptivity of the 1:1:2 complex

Two isosbestic points appear consecutively in Fig. 1 (E comes before P), which shows that reaction (I) takes place before (II). If these two reactions take place strictly in this order, then the equivalence point of reaction (I) must also be the starting point of reaction (II). Thus equations (1) and (2) both apply at the equivalence point. This is an oversimplification, of course, because it assumes that there is no overlap of the two equilibria (or that any overlap makes a negligible contribution to the data). In this case, $y = \frac{1}{2}C_0^R$ (i.e., $x = 0$). Substituting into equations (1) and (2) respectively, we obtain

$$A_1 = A_2 = \frac{1}{2}\epsilon^y C_0^R \quad (3)$$

A_1 and A_2 have the same form and can be used for any wavelength. That is to say, in principle the absorption spectrum of a solution of composition corresponding to the equivalence point will pass through both of the isosbestic points. It is very important to prove this relationship, since the absorbance at an isosbestic point can be determined accurately. The value of C_0^R is known, so ϵ^y and ϵ^x can be calculated from equation (3). For example, at point P, in Fig. 1, $A = 0.435$ and $\epsilon^y = A/\frac{1}{2}C_0^R = 2.18 \times 10^4 \text{ l. mole}^{-1} \cdot \text{cm}^{-1}$. It should be pointed out that such an absorption spectrum cannot be obtained in practice, for some dissociation of the complex will always occur. Thus, the absolute values of ϵ^y and ϵ^x at other wavelengths are difficult to obtain.

Table 1. Comparison of spectral characteristics with literature values

Reference	Pure ECR		Isosbestic point				Complex 1:1:1 λ_{\max} , nm
	λ_{\max} , nm	A	ECR \rightarrow 1:1:2	1:1:2 \rightarrow 1:1:1	1:1:2 \rightarrow 1:1:1	Complex 1:1:1	
	λ , nm	A	λ , nm	A	λ , nm	A	
This paper	440	0.580	460	0.510	515	0.435	550
9	440	0.420	460	0.360	515	0.370	550

Table 2. Values of β_2 from the various curves ($C_0^R = 4 \times 10^{-5} M$; $\epsilon^y = 3.18 \times 10^4 \text{ l. mole}^{-1} \cdot \text{cm}^{-1}$; $\epsilon^R = 3 \times 10^3 \text{ l. mole}^{-1} \cdot \text{cm}^{-1}$)

Curve	A	C_i^H, M	y, M	β_2
2	0.193	3.00×10^{-6}	4.62×10^{-6}	1.3×10^{10}
3	0.263	1.00×10^{-5}	9.05×10^{-6}	2.0×10^{10}
4	0.322	1.50×10^{-5}	1.28×10^{-5}	2.8×10^{10}

Calculation of the overall stability constant β_2 of the 1:1:2 complex

As discussed previously, all curves passing through point E correspond to reaction (I), and therefore obey equation (1). If equation (1) is rearranged to give

$$y = (A - \epsilon^R C_0^R) / (\epsilon^y - 2\epsilon^R) \quad (4)$$

then ϵ^y is known, ϵ^R can be calculated from curve 1, and A is a measured value of each curve at λ_p . Then y can be found. Since

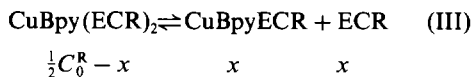
$$\beta_2 = \frac{[\text{CuBpy}(\text{ECR})_2]}{[\text{CuBpy}][\text{ECR}]^2} = \frac{y}{(C_i^H - y)(C_0^R - 2y)} \quad (5)$$

substitution of y and the corresponding C_i^H from each curve leads to a set of values of β_2 . These are listed in Table 2. The mean value of β_2 is taken to be 2×10^{10} .

Calculation of the stepwise stability constants K_1 and K_2

Since β_2 is known, and $\beta_2 = K_1 K_2$, then if either K value is known, the other can be found.

At the equivalence point there must be some degree of dissociation. Therefore curve 5 does not pass through the two isosbestic points but below them. In that case we can write the reaction as



The absorbance is

$$A' = \epsilon^y \left(\frac{1}{2} C_0^R - x \right) + x \epsilon^x + x \epsilon^R$$

$$= x (\epsilon^x + \epsilon^R - \epsilon^y) + \frac{1}{2} \epsilon^y C_0^R$$

At λ_p , $\epsilon^x = \frac{1}{2} \epsilon^y$, so

$$A' = \frac{1}{2} \epsilon^y C_0^R + x (\epsilon^R - \frac{1}{2} \epsilon^y) \quad (6)$$

*The conditional constants derived from curves 2-4 in Fig. 2a¹⁴ are 1.1×10^9 , 3.9×10^9 and 1.6×10^{10} respectively. The constant calculated from Nazarenko's results (*Zh. Analit. Khim.*, 1969, **24**, 536) is 9.6×10^9 .

or

$$A_{\text{isos}} - A' = x (\frac{1}{2} \epsilon^y - \epsilon^R) \quad (7)$$

This gives $x = 1.08 \times 10^{-5} M$. Then, since

$$K_2 = \frac{[\text{CuBpy}(\text{ECR})_2]}{[\text{CuBpy}][\text{ECR}]}$$

$$K_2 = 8.0 \times 10^4 \text{ and } K_1 = 2.5 \times 10^5$$

Thus, all the stability constants of the two complexes in this system have been obtained.

Finally, it is worth noting that the values of β_2 given in Table 2 increase with the ratio $[\text{CuBpy}]:[\text{ECR}]$. When the same method is applied to a similar system—the binary complexing system of stepwise complexes¹⁴—the same result is obtained.* Although conditional constants may vary somewhat with variation in the conditions, such a regularity merits further study.

REFERENCES

1. F. J. C. Rossotti and H. Rossotti, *The Determination of Stability Constants*, Chapters 3, 5 and 13. McGraw-Hill New York, 1961.
2. H. M. Shi and X. W. He. *Anal. Chem. (China)*, 1979, **7**, 228.
3. E. Asmus, *Z. Anal. Chem.*, 1960, **178**, 104.
4. W. A. E. McBryde, *Talanta*, 1974, **21**, 979.
5. J. S. Adsul and P. S. Ramanathan, *Anal. Chim. Acta*, 1978, **101**, 157.
6. K. Momoki, J. Sekino, H. Sato and N. Yamaguchi, *Anal. Chem.*, 1969, **41**, 1286.
7. P. S. Ramanathan & A. P. Walvekar, *Z. Phys. Chem.*, 1976, **257**, 801.
8. X. L. Zhang, *Chemistry of Complexing*, p. 172. Metallurgical Ind. Pub. House, Beijing, 1979.
9. R. Ishida, H. Narita and K. Tonasaki, *Bull. Chem. Soc. Japan*, 1978, **51**, 1951.
10. E. J. Dixon, L. M. Grisley and R. Sawyer, *Analyst*, 1970, **95**, 945.
11. E. J. Langmyhr and T. Stumpe, *Anal. Chim. Acta*, 1965, **32**, 535.
12. H. G. C. King and G. Pruden, *Analyst*, 1967, **92**, 83.
13. S. F. Zou and L. J. Dai, *Acta Chimica Sinica*, 1982, **40**, 39.
14. W. A. E. McBryde and G. F. Atkinson, *Can. J. Chem.* 1961, **39**, 510.

SPECTROPHOTOMETRIC DETERMINATION OF ZINC WITH PHENYLFLUORONE IN THE PRESENCE OF HEXADECYLPYRIDINIUM BROMIDE AND PYRIDINE

SATORU SAKURABA

Industrial Research Institute of Aomori Prefecture, Fukuro-machi, Hirosaki-shi, 036 Japan

(Received 9 January 1984. Accepted 7 May 1984)

Summary—Phenylfluorone reacts with zinc in the presence of hexadecylpyridinium bromide and pyridine to form a water-soluble red chelate. The absorption maximum of the chelate is at 585 nm and its absorbance is constant in the pH range 7.7–8.2. At this wavelength, Beer's law is obeyed up to $1.53 \times 10^{-5} M$ zinc. The sensitivity is very high and the molar absorptivity is $8.0 \times 10^4 \text{ l. mole}^{-1} \text{ cm}^{-1}$. The chelate has been utilized in the determination of zinc at the microgram level. The ratio of zinc to phenylfluorone in the complex is 1:1.

Various 2,3,7-trihydroxyfluorone dyes substituted at the C₉ carbon atom have been reported as colour reagents for spectrophotometric determination of metal ions; they include 2,3,7-trihydroxy-9-phenyl-6-fluorone (phenylfluorone).¹⁻³ The reactions of the dye molecule with vanadium(IV) at different pH values have been reported.⁴ Phenylfluorone and its metal chelates are soluble in ethanol, but the solutions are not stable, as a turbidity develops. When a cationic surfactant and a unidentate ligand such as pyridine or nitrite is added the turbidity does not appear. We have applied this reaction to the determination of cobalt,⁵ nickel⁶ and copper.⁷ Zinc reacts with phenylfluorone in the presence of hexadecylpyridinium bromide and pyridine or nitrite to form a water-soluble red chelate. Pyridine is the more favourable because it gives a molar absorptivity that is nearly twice that obtained with nitrite. The spectrophotometric determination of zinc by means of this colour reaction is described in this communication. The molar absorptivity is $8.0 \times 10^4 \text{ l. mole}^{-1} \text{ cm}^{-1}$ at the wavelength of maximum absorption (585 nm), about 2.5 times that of the dithizone or zincon complex. Moreover, this method is much simpler than the dithizone method since no extraction is required.

EXPERIMENTAL

Reagents

A standard stock zinc solution was prepared by dissolving 4.40 g of analytical-reagent grade zinc sulphate in water and diluting to 1 litre, and diluted as required to give working solutions. A standard solution of phenylfluorone (PF) was prepared by dissolving a known amount of the reagent (Merck) in ethanol containing a few drops of concentrated hydrochloric acid. Aqueous $2.0 \times 10^{-2} M$ hexadecylpyridinium bromide (HPB) and $2.48 M$ pyridine (Py) solutions were prepared. A borate buffer was used. All the other reagents were of analytical-reagent grade. Demineralized water was used.

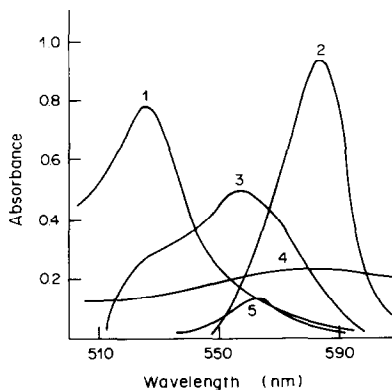


Fig. 1. Absorption spectra of zinc complex and reagent. Concentrations of Zn(II), HPB, Py and PF $1.22 \times 10^{-5} M$, $2 \times 10^{-3} M$, $0.149 M$ and $3 \times 10^{-5} M$, respectively; pH 7.9; 1, reagent blank vs. water; 2, Zn-HPB-Py-PF; 3, Zn-Py-PF; 4, Zn-PF; 5, Zn-HPB-PF. Reference, 2-5 reagent blank.

Procedure

Two ml of buffer solution, 2.5 ml of HPB solution, 1.5 ml of Py solution and 0.75 ml of PF solution were added to the sample solution, in that order. The absorbance was measured at 585 nm against reagent blank after the solution had stood for 30 min at 25°.

RESULTS AND DISCUSSION

Absorption spectra

The absorption spectra of the reagent blank and the zinc complex in the four-component system at pH 7.9 are shown in Fig. 1. For comparison, the spectra for other combinations of zinc with the reagents at the same pH are also given. Zinc reacts with PF to form a red complex (λ_{max} 585 nm) in the presence of HPB and Py. A solution containing the Zn-PF complex is turbid, but addition of HPB and Py clarifies it. The red complex is formed only if both HPB and Py are added to the Zn-PF complex

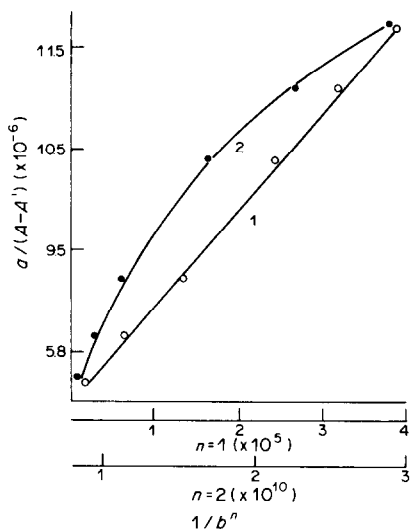


Fig. 2. Relationship between $a/(A - A')$ and $1/b^n$. Concentrations of Zn(II), HPB, Py and PF $6.12 \times 10^{-6}M$, $2 \times 10^{-3}M$, $0.149M$ and $7 \times 10^{-6} - 4 \times 10^{-5}M$, respectively. \circ — \circ $n = 1$; \bullet — \bullet $n = 2$; measured at 585 nm.

solution, and in the absence of either, the absorbance was only about a tenth of that of the red complex (Fig. 1, curves 3–5). The absorbance is maximal and nearly constant over the pH range 7.7–8.2.

The calibration graph made under optimum conditions is linear up to $1.53 \times 10^{-5}M$ zinc concentration. The molar absorptivity at 585 nm is 8.0×10^4 l. mole $^{-1}$. cm $^{-1}$.

The Benesi and Hildebrand method⁸ was used for finding the composition of the complex. For a ZnL_n complex ($L =$ ligand) the following relationship may be derived:

$$a/(A - A') = \{1/(\epsilon_1 - n\epsilon_2)\} + \{K'/(\epsilon_1 - n\epsilon_2)b^n\}$$

where A is the absorbance of the solution measured against the reagent blank, a and b are the initial concentrations of zinc and reagent respectively. The values of ϵ_1 and ϵ_2 ($\epsilon_2 b = A'$), are the molar absorptivities of the complex and reagent blank respectively at a constant pH value. Then if $\log a/(A - A')$ is plotted against $\log 1/b$, the slope will be n . In Fig. 2, $a/(A - A')$ is plotted against $1/b^n$ for 585 nm. A straight line is obtained for $n = 1$. When a similar plot is made for varied concentration of Py (0.05–0.3M), a straight line is obtained for $n = 2$.

Therefore it is concluded that a 1:1:2 complex is formed between zinc, PF and Py.

Interferences

Table 1 shows that alkali-metal, alkaline-earth metal, halide, sulphate and nitrate ions do not interfere. Vanadium(V), iron(III), cobalt, nickel, copper(II), aluminium and tin(IV) ions give some errors.

Table 1. Influence of foreign ions on determination of 10.0 μ g of zinc

Foreign ion	Amount added, μ g	Zn found, μ g
Na ⁺	10.0	10.0
K ⁺	10.0	10.0
Mg ²⁺	10.0	10.1
Ca ²⁺	10.0	10.1
Ba ²⁺	10.0	9.9
Co ²⁺	10.0	8.4
Co ²⁺ †	10.0	9.8
Ni ²⁺	10.0	8.7
Ni ²⁺ †	10.0	10.1
Cu ²⁺	10.0	8.0
Cu ²⁺ *	10.0	10.3
Al ³⁺	10.0	17.5
Fe ²⁺	10.0	9.6
Fe ³⁺	10.0	7.2
Sn ⁴⁺	10.0	16.8
V(V)	10.0	6.5
Mo(VI)	10.0	9.1
NO ₃ ⁻	10.0	9.9
Cl ⁻	10.0	9.9
F ⁻	10.0	9.6
SO ₄ ²⁻	10.0	9.8
PO ₄ ³⁻	10.0	9.3

*1 ml of 10% hydroxylamine hydrochloride solution was added.

†In the presence of nitrite instead of pyridine, measurement at 565 nm.

Iron(III) and copper(II) can be masked by reducing with hydroxylamine hydrochloride before colour development. Use of nitrite instead of Py completely eliminates the interference of cobalt and nickel (Table 1) but the sensitivity is lower. The absorption maximum of the nitrite complex is at 565 nm and the molar absorptivity 4.4×10^4 l. mole $^{-1}$. cm $^{-1}$.

Acknowledgements—The author is sincerely grateful to Dr. Masuo Kojima, of the National Chemical Laboratory for Industry, for his advice, and Professor Kengo Uchida of Hirosaki University for his kind encouragement throughout this study.

REFERENCES

1. J. Gillis, J. Hoste and A. Claeys, *Anal. Chim. Acta*, 1947, **1**, 302.
2. E. B. Sandell, *Colorimetric Determination of Traces of Metals*, 3rd Ed., p. 862. Interscience, New York, 1959.
3. C. L. Luke and M. E. Campbell, *Anal. Chem.*, 1956, **28**, 1273.
4. J. P. Verema, O. Prakash and S. Mushra, *Anal. Chim. Acta*, 1970, **52**, 357.
5. S. Sakuraba and M. Kojima, *Nippon Kagaku Kaishi*, 1976, 345.
6. *Idem, ibid.*, 1978, 208.
7. *Idem, ibid.*, 1980, 209.
8. H. A. Benesi and J. H. Hildebrand, *J. Am. Chem. Soc.*, 1949, **71**, 2703.

DETERMINATION OF ISOCYANO GROUPS ON POLYMER SUPPORTS BY BROMINATION

REZA ARSHADY and IVAR UGI

Organisch-Chemisches Institut, der Technischen Universität München, 8046 Garching, Lichtenbergstr. 4, BRD

(Received 31 March 1983. Revised 2 November 1983. Accepted 7 May 1984)

Summary—The isocyno content of several cross-linked polymer samples, carrying *ca.* 0.5–3.0 mmole of isocyanide groups per gram, was determined by reacting the resins with excess of bromine in chloroform, then treating the unreacted bromine with potassium iodide and titrating the liberated iodine with thiosulphate. The method is not suitable for titration of soluble isocyanides, but for the determination of insoluble macromolecular isocyanides is more satisfactory than the thiocyanic acid method.

Recently we have reported the synthesis of several types of isocyno polymer supports.¹ These resins are currently employed for synthesis of peptides by four-component condensation² and immobilization of transition-metal complexes,³ and are potentially useful for enzyme-immobilization and general organic synthesis. Quantitative determination of functional groups on a polymer support⁴ is generally complicated, because of problems such as polymer swelling and partial inaccessibility of the reactive sites, as well as the technical difficulties in the monitoring of a reaction on a cross-linked polymer. However, the isocyno group can undergo many reactions,⁵ so there are many potential methods for its determination⁶ on a polymer support. This report gives the details of the determination of polymer-bound isocyanides by bromination, and suggests alternative methods based on transition metal coordination.

EXPERIMENTAL

Preparation of thiocyanic acid in chloroform

A solution of 1.25 g (20 mmoles) of ammonium thiocyanate in 20 ml of water is stirred with 15 ml of chloroform in an ice-bath, then 10 ml of 2*M* sulphuric acid are added dropwise. The chloroform solution is separated, and the aqueous solution is extracted with three 10-ml portions of chloroform. The combined chloroform solution is dried over anhydrous magnesium sulphate, and stored in a dark bottle. Titration of the chloroform solution with 0.1*M* triethylamine in ethyl acetate shows a thiocyanic acid concentration of 0.35*M*. This decreases to 0.255*M* within 24 hr and to 0.228*M* in 48 hr, but then remains practically unchanged.

Determination of isocyno polymers with thiocyanic acid

The polymer (100 mg) is added to the thiocyanic acid solution in chloroform (5 ml were used for samples 1–3 and 1 ml was used for 4 and 5) and is allowed to react for 2 hr. The mixture is then diluted with ethyl acetate and dimethylformamide (5 ml of each were used for samples 1–3, and 1 ml of each for samples 4 and 5). An indicator (four drops of 0.2% Neutral Red/0.2% Methylene Blue in methanol) is

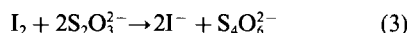
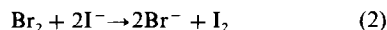
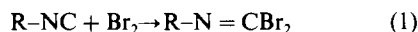
added, and the mixture is titrated with 0.1*M* triethylamine to a green colour.

Determination of isocyno polymers by bromination

The polymer (100 mg) is swollen in 5 ml of chloroform for about 10 min, then bromine (up to 3.5 ml of 0.1*M* solution in chloroform) is added, and the mixture is stirred for 30 min. Potassium iodide solution (5%, 5–7 ml) is added, and the mixture is stirred vigorously for 30 min, and then titrated with 0.1*M* sodium thiosulphate to a pale yellow colour. The indicator (two drops of 0.5% starch solution) is added and the titration continued (usually over a period of about 30–40 min) with vigorous stirring until the starch-iodine colour persists for about 5 min. The formamide precursor of the isocyno resin is treated similarly.

RESULTS AND DISCUSSION

The reaction of isocyanides with bromine was described by Nef⁷ in 1882 and shown to proceed according to equation (1) without any side-reactions. In principle this reaction is ideal for determination of polymer-bound isocyno groups, since the polymer can be treated with excess of bromine, followed by titrimetric determination of unreacted bromine [see equations (2) and (3)].⁸



The method is not suitable for determination of soluble isocyanides because the starch-iodine end-point is obscured by the colour of the brominated product, but is particularly useful for determination of polymer-bound isocyanides, because the reaction can be done in chlorinated solvents such as chloroform, which are good solvents for practically all types of isocyno polymer supports. The brominated polymer is insoluble and does not interfere with the end-point. The method is not altogether satisfactory, however, because both bromine and iodine are sorbed by the cross-linked resin. A further complication

is the reaction of bromine with residual double bonds of the polymer backbone; this can cause consumption of up to about 0.5 mmole of bromine per gram of polymer. The first problem is overcome by vigorous mixing and allowing longer times for the oxidations and reductions and the second problem is solved by titration of the formamide precursor of the isocyanato resin.

A procedure reported previously,⁶ based on the simpler reaction of isocyanides with thiocyanic acid in ethyl acetate, was found to be less suitable, because most isocyanato polymers¹ do not swell adequately in ethyl acetate. Modification of this procedure by using chloroform as the solvent also appears to be less satisfactory, primarily because of the low solubility of thiocyanic acid in chloroform (see below).

The results of estimation of the isocyanato content of five polymer samples by the two methods are given in Table 1. The bromine method is somewhat laborious, but according to the results presented in Table 1, it provides a highly reliable method for determination of polymer-bound isocyanato groups. In the case of the thiocyanic acid method, more satisfactory data are obtained for polymers with low degrees of substitution. It should also be noted that the infrared spectra of the resin samples reacted with thiocyanic acid were not always consistent with the single reaction pathway observed in the case of soluble isocyanides.⁶

Polymer-bound isocyanato groups are readily coordinated by various transition metals.³ For example, when resin sample 1 is reacted with excess of K_2PdCl_4 or $Pd(PhCN)_2Cl_2$, the corresponding bis-co-ordinated palladium derivative is obtained.³ This complexation by palladium(II) (and probably by other metals) may provide a more convenient route for the deter-

Table 1. Titration of polymer-bound isocyanides

Resin*	NC content, mmole/g		
	Theory	Br ₂ method	HSCN method
1	2.58	2.60	2.84
2	2.00	2.00	2.23
3	2.86	3.00	—
4	0.57	0.50	0.43
5	0.51	0.47	0.47

*Prepared by copolymerization of dimethylacrylamide, 3-formamidopropyl acrylate, and bis-acrylamide cross-linkers, followed by treatment with tosylchloride in pyridine (*cf.* ref. 1).

mination of polymer-bound isocyanide through either determination of the excess of metal in solution, or of the metal complexed by the polymer. This method has been examined for samples 1 and 2, and has been found to give fairly good agreement with the theoretical values and those of the bromine method.

REFERENCES

1. R. Arshady and I. Ugi, *Angew. Chem.*, 1982, **94**, 367; *Angew. Chem. Int. Ed. Engl.*, 1982, **21**, 374; *Angew. Chem. Suppl.*, 1982, 761.
2. *Idem*, *Z. Naturforsch.*, 1982, **36b**, 1202.
3. R. Arshady and B. C. Corain, *Transition Met. Chem.*, 1983, **8**, 182.
4. See, *e.g.*, *Polymer-supported Reactions in Organic Synthesis*, P. Hodge and D. C. Sherrington (eds.), Wiley, Chichester, 1980.
5. *Cf. Isonitrile Chemistry*, I. Ugi (ed.), Academic Press, New York, 1971.
6. D. S. Arora, E. v. Hinrichs and I. Ugi, *Z. Anal. Chem.*, 1974, **269**, 124; see also E. v. Hinrichs, *Dissertation*, Techn. Univ., München, 1974.
7. J. U. Nef, *Annalen*, 1882, **270**, 267.
8. *Cf. Treatise on Analytical Chemistry*, Part II, Vol. 7, I. M. Kolthoff and P. J. Elving (eds.), Wiley-Interscience, New York, 1961.

MICRODETERMINATION OF IRON IN WATER BY ION-EXCHANGER COLORIMETRY WITH FERROZINE

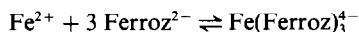
LI SHI-YU and GAO WEI-PING

Department of Chemistry, Beijing University, Beijing, China

(Received 7 September 1982. Revised 4 April 1984. Accepted 2 May 1984)

Summary—The use of ion-exchanger colorimetry for determination of microamounts of iron in water with 3-(2-pyridyl)-5,6-bis(4-phenylsulphonic acid)-1,2,4-triazine disodium salt as colour reagent is described. The advantages are the high sensitivity, ease of operation, good reproducibility, and simplicity of apparatus. Also, because of concentration by the ion-exchanger resin the detection limit of the method may be as low as the $\mu\text{g/ml}$ level.

3-(2-Pyridyl)-5,6-bis(4-phenylsulphonic acid)-1,2,4-triazine disodium salt ("Ferrozine", abbreviated to PPST) is a highly sensitive reagent for iron(II), usable even in strongly alkaline medium.¹ It is easily soluble in water, in which it is fully dissociated.² At pH 4-9 it reacts with iron(II) to form a stable magenta complex which is very soluble in water. The reaction may be expressed as



The complex has its absorption peak at 562 nm, the molar absorptivity being $2.79 \times 10^4 \text{ l. mole}^{-1} \text{ cm}^{-1}$.

The complex anion can be quantitatively sorbed by an anion-exchange resin, which provides the possibility of determining iron(II) by a direct colorimetric method.³ For determination of total iron any iron(III) must be reduced to iron(II); hydroxylamine hydrochloride can be used for this purpose.

EXPERIMENTAL

Reagents

Standard iron(II) stock solution (1 mg/ml). Dissolve 0.1000 g of pure iron wire with 10 ml of hydrochloric acid (1 + 1) and dilute the solution to volume in a 100-ml standard flask.

Standard iron(II) solution (10 $\mu\text{g/ml}$). Dilute 1 ml of the standard iron(II) stock solution to volume in a 100-ml standard flask with water after addition of 2 ml of hydrochloric acid (1 + 1).

PPST solution, 0.5%.

Hydroxylamine hydrochloride solution, 10%

Anion-exchange resin. The resin (20-40 mesh, Cl^- form) used was no. 717, produced by the Shanghai Resin Factory; it is a strong-base resin, equivalent to Dowex 1 or Deacidite FF. When new resin is to be used it should be soaked in water for 24 hr and then washed repeatedly. All small particles and inclusions should be removed and the resin dried with filter paper and stored in a polyethylene container.

Analytical-grade chemicals and demineralized water should be used.

Procedure for determination of iron(II)

Take 100 ml of sample solution containing not less than 0.5 μg of iron(II) and at pH 4-9 in a 250-ml Erlenmeyer flask fitted with a ground-glass or plastic stopper. Add 1 ml

of 0.5% PPST solution and mix. After 10 min the solution will be magenta in colour. Then add 1.5 g of anion-exchange resin and shake the flask mechanically for 30 min. The resin will take up the magenta colour. Withdraw the resin with a dropper and put it into a 0.5-cm glass cell, ensuring that it is evenly packed. Measure the absorbance at 575 nm against a resin blank.

Determination of iron in drinking water

Take a series of six equal samples of water (containing not less than 0.5 or more than 5 μg of iron) in 500 ml Erlenmeyer flasks fitted with ground-glass or plastic stoppers. Add 1.5 ml of 10% hydroxylamine hydrochloride solution to each to reduce iron(III). Adjust the pH to 4-9 if necessary. Add 0, 1, 2, 3, 4, 5 μg of iron(II), dilute to 250 ml, add 1 ml of PPST solution to each flask, and let the colour develop. Shake each solution with 1.5 g of resin for 30 min and complete the determination as above. Plot the absorbance against weight of iron(II) added and determine the iron(II) in the sample by extrapolation in the usual way for the standard-additions method.

Seriously polluted water samples should be digested with 5 ml of hydrochloric acid (1 + 1) for every 30 ml of water sample, then filtered before determination of the iron.

RESULTS AND DISCUSSION

Figure 1 shows that the wavelength of maximum absorption is 575 nm, a 13-nm displacement from

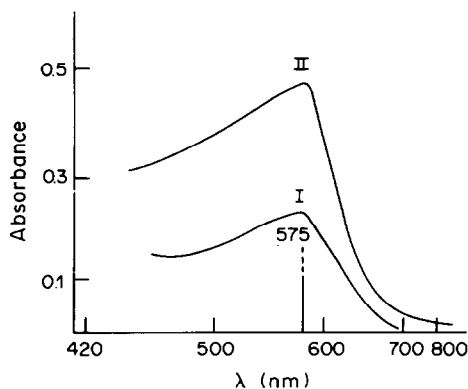


Fig. 1. Absorption spectra of Fe^{2+} -PPST by ion-exchange colorimetry. I, 5 μg of Fe^{2+} ; II, 10 μg of Fe^{2+} ; $\lambda_{\text{max}} = 575 \text{ nm}$.

Table 1. Effect of foreign ions on determination of 5.0 μg of iron(II)

Ion	Added, mg	Fe ²⁺ found, μg
—	—	5.0
Cr ³⁺	0.40	4.9
	0.80	5.0
Mn ²⁺	0.80	5.0
	1.00	4.9
Co ²⁺	0.20	5.3
Cu ²⁺	0.20	5.0
Zn ²⁺	0.20	4.9
	0.40	4.9
Cd ²⁺	1.00	5.0
Pb ²⁺	0.20	5.0
	1.00	4.9
Al ³⁺	0.10	5.2
Ca ²⁺	10.0	5.0
Mg ²⁺	10.0	5.0

λ_{max} for the complex in solution.² Figure 2 indicates that the ion-exchange step takes 30 min to reach completion. Figure 3 shows that the absorbance obtained is practically independent of pH over the range 4–9, the range needed for forming $\text{Fe}(\text{Ferroz})_3^-$ in aqueous solution. The calibration graph is linear up to an iron(II) concentration of 0.1 $\mu\text{g}/\text{ml}$ in the sample solution.

The effect of various metal ions is given in Table 1. When more than 50 μg of nickel is present the colour is unevenly distributed on the resin and the measurement is adversely effected. Silver interferes if

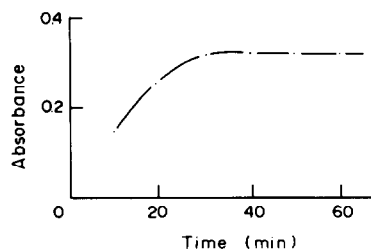


Fig. 2. Effect of shaking time.

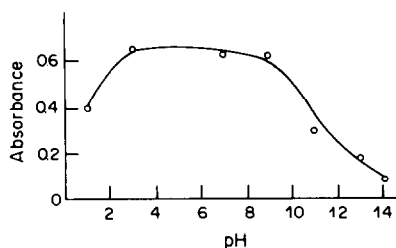


Fig. 3. Effect of pH on the ion-exchange.

silver chloride is precipitated by the chloride released in the ion-exchange.

By this method the minimum iron content detectable is 1–2 ng/ml in the test solution. The recovery exceeds 98%.

REFERENCES

1. L. Stookey, *Anal. Chem.* 1970, **42**, 719.
2. J. Kellen and B. Jaselskis, *ibid.*, 1976, **48**, 1538.
3. E. Yoshimura and S. Ohashi, *Talanta*, 1978, **25**, 103.

ESTIMATION OF URANIUM IN COLUMBITE-TANTALITE SAMPLES: A METHOD FOR SAMPLE SOLUTION PREPARATION FOR FLUORIMETRIC ESTIMATION

B. K. BALAJI, A. PREMADAS and G. V. RAMANAIHAH

Chemical Laboratory, Atomic Minerals Division, Department of Atomic Energy, 'Patan Bhavan', Race
Course Road, Bangalore-560 001, India

(Received 14 December 1983. Accepted 30 April 1984)

Summary—A method has been developed for obtaining a clear solution of columbite-tantalite samples in nitric acid medium before the fluorimetric estimation of uranium. Ammonium hydrogen fluoride is used to keep tantalum, niobium and titanium dissolved in the acid medium. The excess of fluoride is complexed with boric acid. The method has been successfully applied to a number of synthetic and natural columbite-tantalite samples.

The fluorimetric method for the determination of uranium is widely used because of its high sensitivity. The published methods^{1,2} for the determination of uranium in columbite-tantalite samples involve separation of the uranium by filtration from the gelatinous hydrous tantalum, niobium and titanium oxides that are formed in acid solution. This is a time-consuming step and there is risk of loss of uranium by retention in the precipitate. It was observed that the occluded uranium cannot be completely removed by washing. This prompted us to seek a new approach by which the tantalum, niobium and titanium would be kept in solution in the acid medium. Since all three elements form soluble fluoro-complexes, ammonium hydrogen fluoride is added to obtain a clear solution of the columbite-tantalite sample after its fusion with sodium peroxide and taking up of the cooled melt with nitric acid. The excess of fluoride is complexed with boric acid, and the uranium content is then determined by the fluorimetric method^{2,3} after its separation by ethyl acetate extraction from a solution saturated with aluminium nitrate as salting-out agent.

EXPERIMENTAL

Procedures

Conventional extraction fluorimetric method. A 0.500-g synthetic sample was treated with 15 ml of concentrated hydrofluoric acid and 5 ml of nitric acid in a platinum dish, and the solution evaporated to dryness. The residue was digested with dilute nitric acid, the solution filtered and the residue washed and then ignited at 650–700°. The product was fused with 8 g of sodium peroxide and the cooled melt taken up with the original filtrate. The solution yielded a hydrolysed precipitate on acidification. This mixture was boiled for 15 min and filtered, the residue being repeatedly washed with hot 5% nitric acid (about 300 ml) in batches of 15–20 ml in order to remove the uranium from the precipitate. The filtrate was concentrated and nearly neutralized with ~7M ammonia solution, then acidified with concentrated nitric acid to give a final acidity of ~1.6M (~10% v/v nitric acid) when diluted to a standard volume. The

uranium was extracted by shaking a 3-ml portion of this solution for 2 min with 10 ml of ethyl acetate after addition of 15 ml of saturated aluminium nitrate solution as salting-out agent. The uranium was determined fluorimetrically^{2,3} as follows.

About 5 ml of the ethyl acetate layer was filtered through a Whatman No. 40 filter paper (7 cm) to free it from traces of moisture. Aliquots of 0.1 of this solution were taken in 5 small platinum dishes (capacity 0.5 ml, diameter 1 cm) containing a drop of water, and dried under an infrared lamp. Each residue was fused at ~670° with a 0.4 g pellet of finely powdered flux (NaF, Na₂CO₃ and K₂CO₃ in w/w ratio 1:5:5) for 3 min in a muffle furnace. The dishes were then cooled in a desiccator to room temperature (15 min). The fluorescence of the button was measured in a fluorimeter (exciting radiation 365 nm, fluorescence radiation 555 nm) and compared with that of standard buttons (0.01–0.1 µg of uranium) prepared in a similar way. Corrections were made for the fluorescence of the flux.

Proposed method. A 0.500-g sample was fused with 8 g of sodium peroxide in a nickel crucible to give a clear red melt. The cooled fused mass was taken up in 40 ml of 8M nitric acid. This process resulted in hydrolysis of the tantalum, niobium and titanium present. The solution and precipitate, after boiling, were transferred into a polythene beaker and treated with just sufficient ammonium hydrogen fluoride to dissolve the hydrolysis products. The solution was warmed on a water-bath for 10 min. It was then nearly neutralized with ~7M ammonia solution, and 5 ml of saturated boric acid solution were added, followed by concentrated nitric acid to give a final acidity of ~1.6M after dilution to standard volume. This solution was analysed for uranium fluorimetrically, as described above.

RESULTS AND DISCUSSION

Preliminary studies to determine whether the amount of fluoride required to keep niobium and tantalum in solution would affect the extraction of uranyl nitrate into ethyl acetate from 1.6M nitric acid containing saturated aluminium nitrate as salting-out agent, showed that up to 10% of ammonium hydrogen fluoride would not interfere in the extraction of at least 130 µg of uranium. Under these conditions, at least 5 mg of tantalum, 2 mg of niobium, 1 mg each of iron(III) and manganese(II) and 0.5 mg of

Table 1. Recovery of uranium from synthetic tantalite* and columbite† samples

U ₃ O ₈ taken, %	U ₃ O ₈ found, %					
	Tantalite samples			Columbite samples		
	Conventional method	Analysis of the residue	Proposed method	Conventional method	Analysis of the residue	Proposed method
0.010	0.010	0.001	0.010	0.010	0.001	0.010
0.040	0.037	0.004	0.040	0.036	0.003	0.039
0.200	0.187	0.013	0.201	0.196	0.005	0.202
0.500	0.451	0.040	0.492	0.453	0.016	0.490
0.750	0.734	0.015	0.750	0.720	0.020	0.747
1.000	0.779	0.183	0.950	0.926	0.062	1.020

*Approximate composition (%) 53.5 Ta₂O₅, 27.2 Nb₂O₅, 11.9 Fe₂O₃, 5.7 MnO₂, 0.3 WO₃, 0.1 SnO₂ and 1.0 TiO₂.

†Approximate composition (%) 55.5 Nb₂O₅, 22.1 Ta₂O₅, 8.1 Fe₂O₃, 12.5 MnO₂, 0.5 WO₃ and 1.0 TiO₂.

Table 2. Analyses of six natural columbite-tantalite samples by conventional and proposed methods

No.	Contents, %			U ₃ O ₈ found, %	
	Ta ₂ O ₅	Nb ₂ O ₅	TiO ₂	Conventional method	Proposed method
	1.	49.2	26.0	1.0	0.048
2.	8.0	61.9	1.3	0.164	0.186
3.	22.7	36.2	2.6	0.197	0.214
4.	54.9	26.6	1.0	0.056	0.060
5.	17.3	45.4	3.0	0.191	0.230
6.	24.2	42.5	1.5	1.550	1.610

titanium(IV), which are usually found in columbite-tantalite minerals, can be present during the extraction step, either individually or in combination, without causing significant error in the result. Furthermore, boric acid can be used to complex the excess of fluoride without interfering in the extraction of uranium. In the presence of fluoride and boric acid, the solution becomes slightly turbid on addition of the aluminium nitrate solution, but this does not affect the extraction.

Tables 1 and 2 show the results obtained when the proposed method was applied to a series of synthetic⁴ columbite and tantalite samples, in which the added uranium was varied from 0.01 to 1%, and to natural samples, respectively. They also show the results obtained by the conventional ethyl acetate extraction method. The results show that the proposed method gives slightly higher results, which we ascribe to losses in the conventional method owing to occlusion of uranyl species in the gelatinous hydrolysis products. This was further confirmed by analysis of the residue for uranium, after dissolution in ammonium hydrogen fluoride solution. The occlusion found was higher for tantalite samples than for columbite samples. The

higher retention of uranyl ion by the hydrated tantalum pentoxide can be attributed to the greater cation-exchange behaviour of the latter.⁵ Similar behaviour was also exhibited in the analysis of the natural columbite-tantalite samples (Table 2).

Replicate analysis, by the proposed method, of a natural sample of columbite-tantalite containing 0.183% U₃O₈, gave a standard deviation of 0.004%.

Acknowledgement—We are highly thankful to Mr B. N. Tikoo and Dr K. M. V. Jayaram for their encouragement to do the work.

REFERENCES

1. Pe-Nien Yu, *J. Chinese Chem. Soc.*, 1948, **15**, 170.
2. F. S. Grimaldi, I. May, M. H. Fletcher and J. Titcomb, *U.S. Geol. Survey Bull.* 1006, 1954.
3. M. D. Hassialis and R. C. Musa, *Proc. Intern. Conf. Peaceful Uses of Atom. Energy Geneva*, Vol. VIII, 216, 1955.
4. C. Palache, H. Berman and C. Frondel *Dana's System of Mineralogy*, Vol. I, Wiley, New York, 1944.
5. B. E. Chidley, F. L. Parker and E. A. Talbot, *U.K. At. Energy Auth. Res. Group Rept.*, AERER 5220, October 1966.

SPECTROPHOTOMETRIC DETERMINATION OF TELLURIUM AFTER ADSORPTION OF ITS MORPHOLINE-4-CARBODITHIOATE ON MICROCRYSTALLINE NAPHTHALENE

C. L. SETHI, ASHOK KUMAR, M. SATAKE*
and B. K. PURI†

Department of Chemistry, Indian Institute of Technology, New Delhi 110016, India

(Received 5 August 1982. Revised 12 April 1984. Accepted 30 April 1984)

Summary—A rapid spectrophotometric method has been developed for microdetermination of Te(IV) after co-precipitation of its morpholine-4-carbodithioate complex on microcrystalline naphthalene and subsequent dissolution in chloroform. The molar absorptivity at 415 nm is $9.18 \times 10^3 \text{ l. mole}^{-1} \text{ cm}^{-1}$. Beer's law is obeyed over the range 5–75 μg of Te(IV); 25.0 μg of Te(IV) in 10.0 ml of final solution gives a mean absorbance of 0.180 with a relative standard deviation of 0.55%. The method has been tested for determination of tellurium in some alloys and synthetic mixtures.

Morpholine-4-carbodithioate was suggested as an analytical reagent by Beyer and Ott¹ for spectrophotometric^{2,3} and titrimetric⁴ determination of certain metals. In this communication, a spectrophotometric method for the determination of tellurium after adsorption of its morpholine-4-carbodithioate on microcrystalline naphthalene is described. In comparison with extraction into molten naphthalene,⁵ the method is rapid, sensitive, more convenient and less expensive.

EXPERIMENTAL

Reagents

A solution of analytical grade potassium tellurite was prepared in distilled water and standardized.⁶ Potassium morpholine-4-carbodithioate was prepared by the method given by Marcotrigiano *et al.*⁷ and used as a 0.2% solution in distilled water. Naphthalene and chloroform of reagent grade were checked spectrophotometrically before use. Dilute solutions of ammonia and perchloric acid, and 0.2M acetate buffer, were used for pH adjustment.

Procedure

In a stoppered Erlenmeyer flask take a volume of sample solution containing up to 75 μg of Te, add 1.0 ml of 0.2% reagent solution, 2.0 ml of 0.2M buffer solution of pH 5.1, dilute to about 30 ml and add 5 ml of 1M potassium nitrate. Then add 2 ml of 20% solution of naphthalene in acetone in a fast stream and shake the mixture vigorously for 1–2 min. Collect the solid on a Whatman (No. 1042) filter paper, wash it two or three times with distilled water, drain it dry, dissolve it in chloroform and make up the solution to volume in a 10-ml standard flask. Dry the solution with 2 g of anhydrous sodium sulphate and measure the absorbance at 415 nm against a reagent blank prepared in a similar manner.

RESULTS AND DISCUSSION

The absorption spectra of the reagent and its tellurium complex in naphthalene/chloroform solution measured against water and a reagent blank respectively, are shown in Fig. 1. The Te(IV) complex absorbs at 415 nm, but the reagent absorbs negligibly at this wavelength. The absorbance remains constant for only 2 hr, so measurements should be made within that period. Co-precipitation of the tellurium complex, with microcrystalline naphthalene, is quantitative over the pH range 4.0–6.4 (Fig. 2), and for 25.0 μg of Te(IV) under optimum conditions a minimum of 0.1 ml of 0.2% reagent solution is necessary, but the volume of the aqueous phase

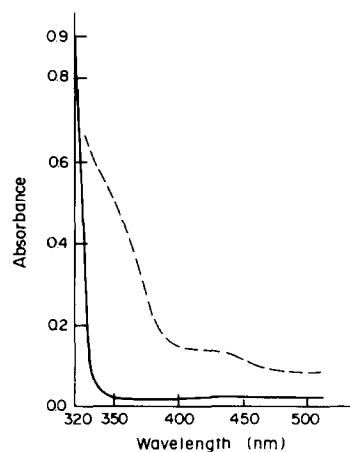


Fig. 1. Absorption spectra of reagent measured against water (—) and Te(IV) morpholine-4-carbodithioate complex in naphthalene/chloroform solution measured against reagent solution in water (---). Te 25.0 μg , 2.0 ml of 0.2% reagent solution, aqueous phase volume 30 ml, pH 5.16, 2.0 ml of 20% naphthalene solution in acetone.

*Faculty of Engineering, Fukui University, Fukui 910, Japan.

†Author for correspondence.

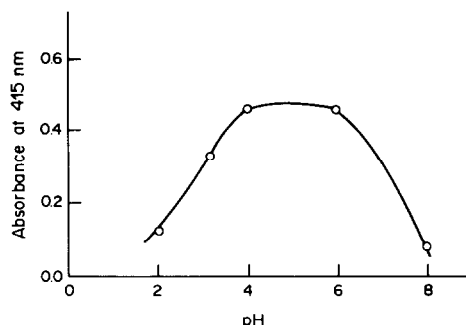


Fig. 2. Effect of pH. Conditions as for Fig. 1.

should not exceed 30 ml. The co-precipitation of the complex with microcrystalline naphthalene is practically instantaneous. Hence a shaking time of at least 15 sec should be adequate, but shaking for 1–2 min is recommended for safety.

Effect of electrolytes

For quantitative co-precipitation the presence of an inert electrolyte such as sodium chloride, perchlorate or acetate, or potassium nitrate, seems essential. An electrolyte concentration of 0.05M is adequate, and higher concentrations have no further effect, so addition of 5 ml of 1M inert-electrolyte solution is recommended.

Under the optimum conditions the calibration graph is linear over the concentration range 5.0–75 μg of Te(IV) in 10.0 ml of the final solution.

Effect of diverse ions

The following (in the amounts shown in parentheses) do not interfere: Pb, Cd, Hg(II), Bi, As(III), Sb(III), Pd(II), Co(II) and Cr(III) (0.8 mg each); Mg, Zn, Ru, Rh, W, Mo, U(VI), Au(III), Pt(IV), V(V)

Table 1. Determination of tellurium in synthetic mixture

Te taken, μg	Foreign ions added, mg	Te found,* μg
8.0	Se 5.0 Zn 800 Mg 300 SiO ₃ ²⁻ 500	7.9–8.1 (8.0)
10.0	Se 10.0 Zn 800 Mg 800 SiO ₃ ²⁻ 800	9.9–10.1 ₅ (10.0)
20.0	Se 60.0 Zn 1000 Mg 800 VO ₃ ⁻ 800	19.7 ₅ –20.1 ₅ (19.9)
25.0	Se 500 Zn 1000 VO ₃ ⁻ 500 SiO ₃ ²⁻ 300	24.8 ₅ –25.3 (25.1)
35.0	Se 50.0 Mg 500 SiO ₃ ²⁻ 500 Al 1000	34.8 ₅ –35.4 (35.1)

*Range of 5 determinations (mean in brackets).

Table 2. Determination of tellurium in synthetic samples (Te 0.65%, Cu 5.75%, Ni 12.2%, Co 5.5%, S 9.0%, P 1.6%, Na 14.1%, Fe 51.2%)*

Te taken, μg	Te found,† μg
10.0	10.0 (9.8 ₅ –10.1 ₅)
15.0	15.5 (14.8 ₅ –15.2)
20.0	19.9 (19.7 ₅ –20.1)
25.0	25.1 (24.8–25.2 ₅)
30.0	30.1 (29.8 ₅ –30.2 ₅)

*Stock solution standardized by atomic-absorption spectrophotometry.

†Average of 5 determinations, range given in brackets.

Table 3. Analysis of copper alloys for tellurium

Sample	Tellurium content, %	
	Present method*	Certified value
1	1.08 ± 0.007	1.06
2	0.492 ± 0.005	0.51
3	0.098 ± 0.002	0.10

*Mean and standard deviation of ten replicates.

and Ag (1.0 mg each); Se (0.1 mg); Fe(III) (0.5 mg). Ni and Cu interfere but can be masked by adding 15 ml of 10% sodium cyanide solution before the co-precipitation. Sodium chloride, oxalate, acetate and sulphate and potassium bromide and tartrate (35 mg each), potassium iodide and sodium carbonate (50 mg each), sodium dihydrogen phosphate (40 mg), potassium thiocyanate and sodium citrate (30 mg each), sodium fluoride (23 mg) and disodium EDTA (10 mg) are also tolerated.

Analysis of alloys

Dissolve a 0.1–0.2 g sample of the alloy by heating for 20–30 min with 20 ml of concentrated nitric acid or of *aqua regia* (3:1 HCl–HNO₃), cool, dilute with water, filter, and make up to volume in a 200-ml standard flask.

Take an aliquot of this solution, containing up to 75 μg of tellurium, and adjust it to pH 5.2 with 2.0 ml of the acetate buffer and dilute ammonia solution. Add 15 ml of 10% sodium cyanide solution to mask copper (if present). Dilute to 30 ml, add 5 ml of 1.0M potassium nitrate and 2.0 ml of 0.2% reagent solution and complete the determination as already described.

Acknowledgement—The sincere thanks of the authors are due to the University Grants Commission (India), for financial assistance to one of them (CLS).

REFERENCES

- W. Beyer and R. D. Ott, *Mikrochim. Acta*, 1965, 1130.
- W. Beyer and W. Likussar, *ibid.*, 1967, 621.

3. W. Likussar, W. Beyer and O. Wawshinek, *ibid.*, 1968, 575.
4. W. Beyer, R. D. Ott and G. Pokorny, *ibid.*, 1967, 575.
5. B. K. Puri, *ibid.*, 1979 I, 515.
6. A. I. Vogel, *A Text Book of Quantitative Inorganic Analysis*, 3rd Ed., Longmans, London, 1969.
7. G. M. Marcotrigiano, G. C. Pallacani, C. Preti and G. Tosi, *Bull. Chem. Soc. Japan*, 1975, **48**, 1018.

QUALITY CONTROL IN CLINICAL CHEMISTRY: CHARACTERIZATION OF REFERENCE MATERIALS

ROBERT REJ and RICHARD W. JENNY

Wadsworth Center for Laboratories and Research, New York State Department of Health,
Albany, NY 12201, U.S.A.

JEAN-PIERRE BRETAUDIÈRE

Department of Pathology and Laboratory Medicine, The University of Texas Medical School,
Houston, TX 77025, U.S.A.

(Received 24 May 1984. Accepted 12 June 1984)

Summary—Reference serum preparations are key components of internal and external quality-control programmes. These materials are often poorly characterized, and use of inappropriate specimens may result in erroneous conclusions regarding quality of laboratory data. Several techniques are described that characterize specimens used in the quality-control or calibration of laboratory procedures. A characteristic approach requires detailed study of a few fundamental characteristics of reference preparations—such as steady-state kinetic properties of an enzyme—and comparison with the same parameters determined for patient specimens. Descriptive techniques—ratio methods and the multivariate statistical procedure of correspondence analysis—are used for further description of the interactions of materials in a variety of assay methods. The applications of these procedures to two clinical analytes—theophylline and alkaline phosphatase—are described.

The fundamental objective of statistical quality-control programmes in the clinical laboratory is to characterize the analytical process accurately and thereby provide information regarding the quality of results reported for clinical specimens. This information may be used for a number of purposes. An internal quality-control programme may provide information about the routine performance of an analytical technique—and thereby serve as a basis for selection of one among many procedures available—or give on-line monitoring of an analytical process in which acceptance of a result depends on whether it falls within predetermined limits. External quality-control provides a basis for independent characterization of laboratory performance and gives information on the reliability of test procedures in various locations and in laboratories with different backgrounds. External quality-control programmes serve, in some instances, for the determination of acceptability, licensing, or eligibility for reimbursement for laboratory services.

The reliability of this assessment of quality is dependent on a variety of factors, but the key to the success of all these schemes is that the reference materials used simulate as closely as possible the clinical specimens analysed. This facet of quality control is often (incorrectly) assumed or (equally erroneously) overlooked in both internal and external quality-control programmes. The scope of this paper is the review of criteria for materials used in clinical laboratory quality-control programmes and to pro-

vide a basis on which their acceptability can be judged.

Various types of reference materials are currently used in quality control programmes,¹⁻⁹ and differ in their basic composition and physical character. Specimens may be prepared from human serum, plasma that has been “converted” into a serum-like state, various animal sera, albumin solutions, or synthetic substances, and are distributed in the dry or liquid state. Because stability is a prime requirement for such specimens, most are in lyophilized form. Unfortunately, freeze-drying alters certain physicochemical properties of biological materials;¹⁰⁻¹² for example, human lipoproteins are irreversibly denatured, and consequently serum viscosity may be changed, serum turbidity increased,^{13,14} and the spectral properties altered.¹⁵ Removal of lipoproteins prior to lyophilization,^{14,16} or addition of sucrose¹⁷ in order to minimize specimen turbidity, also results in materials that are fundamentally altered. Other typical treatments of quality-control sera include dialysis and addition of matrix expanders, preservatives, antimicrobial agents, surfactants, and clarifying agents.¹⁸⁻²⁰

Concentrations of constituents are also often altered by attempts to obtain reference specimens with analyte concentrations outside the “normal” ranges. Such specimens, usually prepared by dilution or by addition of pure materials to a normal specimen, may differ from the sample sera because metabolites or other substances are lacking. Therefore, in use of a non-specific method that is influenced by one or several metabolites, the results for such a supplemented quality-control material will not be affected in the same way as those for a patient’s serum. Such

Portions of the introductory material in this paper were included in a paper in *Clin. Chem.*, 1981, 27, 798 and are adapted here with permission.

effects are related to the *matrix* of the reference material—a term which in this article will be used to describe the principal constituents of the material. The major components of the matrix (serum; specific serum proteins, such as albumin; synthetic expanders such as polyvinylpyrrolidone) may differ from native serum in viscosity, physical interaction of low molecular-weight substances with proteins, and Donnan and other charge-related phenomena.^{21,22} Finally, the pH of some lyophilized control materials differs significantly from that of normal or patients' sera.^{9,23} Differences between the matrixes of commonly used lyophilized materials and clinical specimens are evident in Table 1.

In addition to the matrix, the analyte in the reference material may be quite different from that in the clinical specimen. Enzymes of animal origin are often added to such control preparations²⁶⁻³³ and the properties of at least a portion of these enzymes are known to differ from those of human serum enzymes with respect to optimal substrate concentrations, pH, effects of inhibitors, and related factors. A simple example of errors introduced by such differences is provided in Fig. 1, where the hypothetical response of the activity of three enzymes to an assay parameter is presented. If the assay concentration of this parameter were increased by the increment shown, each material would respond differently. A negligible decrease is found for enzyme A; enzyme B (here for discussion purposes considered to be the response of the enzyme found in human serum) shows a moderate decrease, and enzyme C an exaggerated decrease. Use of enzyme A in a control material would tend to mask the effects of assay variables and would be least appropriate for quality-control reference preparations. The ideal control material would have a response similar to that of enzyme B in order to provide an accurate monitor of results obtained for patients' specimens. Use of a material characterized by enzyme C would indicate results that were "out of control"

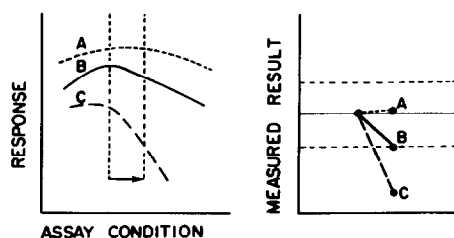


Fig. 1. *Left*—hypothetical response of activity of three enzyme preparations to a change in an assay variable. *Right*—typical quality-control chart representation of measured response due to change in analytical conditions shown by the arrow at the left. Dashed lines represent limits of acceptability. If response B is representative of the enzyme in patient-specimens, responses A and C are inappropriate and the enzyme materials are not suitable in a routine quality-control programme.

for this material, though results for patients might be unaffected by a slight change in the assay variable. In these days of laboratory cost-effectiveness, this material might be considered by some to be equally inappropriate as material A. Certainly it does not authentically represent the clinical specimen. However, as we have suggested previously,²⁷ if this property of the control material was recognized by the analyst, this exaggerated response would be useful in an internal quality-control programme because of the increased sensitivity to change, and might indicate an unsuspected error that could be corrected by the laboratory before any results for patients' samples were affected.

In an external quality-control programme—where many different analytical techniques are examined—it is clear that only materials giving the same response as enzyme B would provide a fair assessment of interlaboratory results. This would also be the case for an internal quality-control programme in an institution where several methods are used for the determination of a single analyte (*e.g.*, back-up pro-

Table 1. Effects of lyophilization on properties* of human and bovine serum

	Bovine serum		Human serum		Human serum reference values†
	Frozen	Lyophilized	Frozen	Lyophilized	
Osmolality, <i>mOsm/kg</i>	280	254	297	268	281–297
Density, <i>g/ml</i>	1.027	1.025	1.025	1.023	1.025–1.029
Surface tension, <i>dyne/cm</i> , 22°	49.3	46.6	47.1	46.4	56.2
Viscosity‡, 22°	1.962	1.942	1.706	1.670	—
pH	8.30	8.96	8.18	9.05	7.38–7.42
Particles, 10 ⁶ / <i>l.</i>	11	58	34	221	—
Particle size‡, μm	<0.5	<0.5	1.0	0.5–5.0	—
<i>A</i> _{600nm} , 10-mm cell	0.761	0.803	0.551	1.247	—

*Normally collected bovine and human serum were frozen in 10.0-ml aliquots at -60° ; representative aliquots were lyophilized and reconstituted with 10.0 ml of water (this would result in a volume slightly different from the original 10 ml).

†Reference values for normal human serum are from Diem and Lentner²⁴ and are 95% confidence intervals; the mean value is shown for surface tension.

‡Values of 1.80 and 1.62 have been obtained for commercially available lyophilized control sera; 3.82 was determined for a liquid material based on ethylene glycol.²⁵

§Particle sizes $>20 \mu\text{m}$ have been found for commercial serum preparations.¹³

cedures, "stat" or emergency-room techniques, different analytical instruments used on different shifts) and the internal quality-control programme takes on many aspects of external surveys.

Peptide hormones and specific serum proteins also exhibit such behavioural differences between species and demonstrate effects similar to those described above.^{34,35}

It is clear that such differences from clinical specimens can affect the use of reference materials in quality-control programmes. Many clinical laboratory procedures use reference materials as calibration solutions and differences between specimens and calibration standards are all the more important, since all the analytical results obtained are potentially affected by these differences. A dozen years ago, a report from our laboratory²⁷ pointed out these potential sources of error and we drew distinctions between the properties of reference materials that are important for their potential application in calibration (standards), and as control materials for intermethod studies (exemplified by external quality-control), intramethod controls, and precision controls. The properties of reference materials would differ in importance according to the intended use. Among the variables we considered were the effects of the matrix and the source of the enzyme. One of the properties that we suggested as important for materials used as intermethod controls and for calibration was *commutability*—a term that we coined to refer to the ability of a material to show interassay properties comparable to those of human serum. At the time we suggested that this was an indispensable property of materials used for calibration and external quality-control but an unnecessary one for within-method studies. Though this is basically true, this property is also necessary for intramethod-control materials when they are used to reflect the precision and accuracy of analysis of patients' specimens rather than as specialized tools for the analyst.

The term commutability has been accepted by others,^{9,36-41} and the term *fidelity* has been suggested as a synonym for commutability.²³ There has been a suggestion by one group^{28,42} that as analytical methods become more homogeneous around the world—in part because of the introduction of reference methods—the principle of commutability is no longer needed and they suggest that *representativeness* of these materials be used instead. However, they define this term in much the same way as we originally defined commutability. Furthermore, although methodology has become more uniform for some test procedures, it has become more diverse for others, owing to new technology. For example, dry-reagent systems require a much larger sample volume fraction than classical techniques do, thus exaggerating matrix effects.^{36,43} It is likely that the property of commutability will become more, rather than less,

important in the future. Wilding and Wilkes⁴¹ have attempted to quantify this property by describing a *commutability index* whereby the range of results from a variety of techniques for an analyte of a reference material is compared with an overall mean value—the larger the index value the less commutable the material for that analyte.

Another term that we have applied to describe the properties of reference materials is *behaviour*.⁴⁴ This term, formally defined as "the response to the whole range of factors constituting its environment" seems well suited to describe the interaction of materials (whether reference materials or clinical specimens) with assay variables. Thus poor reference materials would show behaviour considerably different from that of clinical specimens, whereas satisfactory materials—those that demonstrate commutability—would have given similar behaviour.

The characterization of quality-control material behaviour is crucial for a true estimate of the quality of results and an accurate evaluation of analytical methods. Otherwise, artificial biases, not encountered with patients' specimens, will also be detected, or biases existing with patients' sera will not be observed.

How should the behaviour of these reference materials be assessed? We recognize that many techniques are possible but have found three that are particularly useful and efficient.

Characteristic approach

This technique involves the descriptive characterization of the variable measured in the reference material—usually an enzyme, protein, or peptide hormone—in comparison with the same entity in human serum. This fundamental approach is of value in that the characteristics found for this analyte are relatively stable, and predictions of interassay behaviour can be made on the basis of small amounts of data such as steady-state kinetic constants for substrate and inhibitor, optimal pH, ligand affinity, *etc.* As new assay techniques are introduced, their relative bias for clinical specimens and reference materials can be predicted on the basis of assay conditions. In addition, the underlying cause for differences among assay techniques, observed for some reference materials, can be explained in terms of these fundamental differences among the species determined.

We have characterized a reference material for aspartate aminotransferase* measurements by such an approach.^{31,45,46} In terms of substrate affinity, optimal pH and temperature effects, the enzyme purified from human erythrocytes has properties that are indistinguishable from those of the enzyme native to human serum. This purified material could thus serve well as a reference preparation for the quality control or calibration of aspartate aminotransferase assays. There have been several attempts to characterize similarly other human enzyme reference preparations.^{39,47} Gruber *et al.*²⁶ systematically compared

*EC 2.6.1.1, L-aspartate: 2-oxoglutarate aminotransferase.

the catalytic properties of various purified enzymes of animal origin and those purified from human tissues in order to judge their acceptability as control materials. There have been several other investigations characterizing individual properties of control sera in order to assess their suitability.^{28,33,48}

Although these studies provide useful and fundamental information, they are limited to characterization of the catalytic, immunochemical or molecular properties of a limited number of analytes. Matrix effects—a major source of differences in behaviour or lack of commutability—are not often demonstrated by these studies. There have been some attempts at describing the protein matrix of control materials. Clark *et al.*⁴⁹ have described a two-dimensional gel technique as a method for characterizing the matrix of specimens, and patterns obtained for control sera were compared with those of fresh human serum. This approach has also been recommended by Bais *et al.*,⁵⁰ who used a one-dimensional electrophoretic procedure.

The following techniques compensate for any shortcomings of the characteristic approach, but are purely descriptive so the underlying cause of differences must be obtained by other means (such as the characteristic approach) or by a thorough examination of variables affecting the analytical procedures.

Ratio methods

These procedures compare ratios of analyte concentrations for control materials (found by different techniques) with those similarly found for patients' specimens. As an example, simulated data are presented in Table 2 representing average patient-results and results for six quality-control specimens, by four analytical methods (A, B, C, and D). Method A is considered as the reference method, and all other results are expressed as percentages of those obtained with this method. Figure 2 shows a graphic representation (linear ratio, also called a commutability diagram)³⁶ for the simulated data given in Table 2. Results obtained by the four methods are displayed on a horizontal scale for each specimen or group of specimens. The positions for the reference method—

Table 2. Simulated results for an analyte in patients' specimens and six quality-control sera, as measured by four methods

Specimen	Method			
	A	B	C	D
Patients' sera, mean	100	102	106.8	102.8
SD		0.8	0.8	0.6
Quality-control sera				
1	100	102.0	107.0	103.0
2	100	102.0	103.5	103.0
3	100	106.5	107.0	103.0
4	100	102.0	110.0	103.0
5	100	100.0	105.1	101.0
6	100	102.0	103.0	107.0

Results for each method were generated by random selection ($n = 200$) from Gaussian distributions with the following characteristics: method B, mean 102, SD = 0.9; method C, mean 107, SD = 0.8; method D, mean = 103, SD = 0.7. (Adapted from reference 44, by permission).

or selected comparison method—are aligned vertically for each scale to aid in comparison of the profiles. The average intermethod bias demonstrated by the four analytical methods for patients' specimens is shown by the position of their respective letters on the reference scale (patients' specimens) in Fig. 2. Variability among the patients' specimens themselves for each method is shown by the shaded bars at each letter; in this example the bar represents ± 2 standard deviations. The behaviour pattern—reflected in the positions of the methods—for each quality-control specimen is also shown in Fig. 2 and should be compared with the corresponding pattern on the reference scale. Acceptable method-bias in this example is considered to be $\leq 5\%$, so results from methods B and D are considered reliable for assay of patients' specimen, but method C is not.

For a candidate reference specimen to be useful in a laboratory control programme, results obtained for it should give a pattern identical to that of the patients' specimens. An acceptable quality-control specimen will produce positions within the dispersion ranges given in the reference scale, for all the methods used.

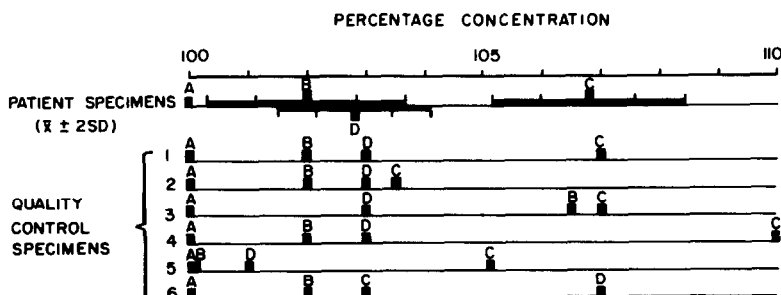


Fig. 2. Linear ratio representation of hypothetical data presented in Table 2. The reference scale is the range of intermethod bias found with patient specimens. Adapted from reference 44 with permission.

Quality-control specimen 1 demonstrates an inter-method bias identical to that of the typical patients' specimens, but the pattern shown by quality-control specimen 6 is aberrant for methods C and D (Fig. 2). The behaviour pattern of quality-control specimen 2 differs from the behaviour of patients' specimens in such a way that the large bias of method C is lost. If this specimen were to be used in an interlaboratory quality-control program, those laboratories using method C would incorrectly be considered to give results equivalent to those of method A. The reverse situation is shown in the case of quality-control specimen 3, where an exaggerated bias is shown for method B. Use of this material in a quality-control survey would incorrectly characterize this method as one which gives unacceptable results.

Quality-control specimen 4 shows an exaggerated bias for method C, but unlike the case for the previous specimens, this difference might be considered useful in that it amplifies the already unacceptable bias of method C. However, the magnitude of this bias is greater than that shown for any patients' specimen, making the behaviour of this specimen different from that of the reference population. Quality-control specimen 5 likewise differs from the reference population because it shows a reduced bias for all methods, but it maintains the pattern of acceptability: methods B and D are acceptable in comparison with the reference technique, while method C is not.

The use of linear regression statistics offers another ratio approach to the assessment of control-material behaviour. An assumption in the linear regression model is that each of the y -populations is distributed normally and with equal variances and that the standard error of estimate (SEE) is a measure of the dispersion of data points around the least-squares line. In our application, one method is selected as a comparative or reference procedure and regression statistics are determined for each of the other methods, from data obtained from the analysis of clinical specimens. Deviation of control-material data from the least-squares line is then determined from the ratio, residual/SEE, where "residual" is the perpendicular distance between a control-material data-point and the regression line. At the 95% confidence

level, the ratio should be within ± 2.0 if the control-material behaviour is similar to that of clinical specimens. This analysis was performed with the simulated data of Table 2 and is presented in Table 3. Control specimens 3 and 5, when analysed by method B, clearly do not conform to the distribution of the clinical-specimen data, so these materials are not considered to be representative of authentic patient-samples when analysed by this method. Likewise, quality control specimens 2, 4, 5 and 6, when analysed by method C and specimens 5 and 6 when analysed by method D do not behave like clinical specimens.

This application of regression parameters was first proposed by van Helden *et al.*³⁷ Conclusions drawn from the linear ratio analysis of control-material acceptability are reinforced by this least-squares technique. Since these parameters are easily calculated, this procedure lends itself particularly well to micro-computer application.

Multivariate statistical analysis

When numerous patient-specimens are examined by several analytical methods, the ratio techniques cannot adequately and simultaneously present comparisons of specimens and methods. These data, however, can be processed by a variety of multivariate statistical techniques. The most appropriate statistical procedure would be a descriptive method that is not based on a preconceived model. It should also be able to characterize potential differences in behaviour among the clinical specimens themselves, and provision should be made for the treatment of quality-control specimens as inactive elements if desired, so that they will not distort the patterns shown by the clinical specimens as active elements.

The two statistical techniques that best meet these criteria are principal-components analysis and correspondence analysis. These procedures are frequently utilized in the social sciences and for applications in interpretation of data such as political polls⁵¹ but are only now being actively explored by analytical scientists for their power to predict, classify and reveal the underlying structure of large data bases.⁵² Although there is a similarity between these methods, we have described in detail the application of correspondence analysis⁴⁴ and our rationale for preferring it over principal-components analysis.

When the data of Table 2 are subjected to correspondence analysis the cluster diagram presented in Fig. 3 is obtained, where the data are projected onto the factorial plane established by the two most significant factors. The positioning of an individual specimen on the plane described by these two factors is representative of its behaviour. In such representations, specimens with similar behaviour are projected near one another. The twenty patient-specimens form a well-defined cluster that includes control material 1—as indicated above, it is a material exhibiting commutability. Note, however,

Table 3. Deviation (number of standard deviations) of hypothetical quality-control serum analyte concentration from the respective method regression lines determined by using patient-data of Table 2

Quality control serum	Deviation		
	Method B	Method C	Method D
1	0	0.2 ₄	0.3 ₁
2	0	-4.0 ₂	0.3 ₁
3	5.4 ₂	0.2 ₄	0.3 ₁
4	0	3.9	0.3 ₁
5	-2.4 ₁	-2.0 ₇	-3.1 ₃
6	0	-4.6 ₃	6.5 ₆

that specimen 5, which has been shown to have some properties different from those of patient-specimens (Table 3, Fig. 2), is also projected near the centre of the projections for patients. This is due to the similar *profile* of intermethod response and demonstrates the need to apply more than one procedure to the characterization of material behaviour. Control materials 2, 3, 4 and 6 are projected far from the patient-samples, indicating a behaviour different from those of the patient-specimens. Correspondence analysis has the advantage of simultaneously projecting variables (here the analytical methods) onto the factorial plane. Proximity of the projections for method and material indicates an interaction between the two that often aids interpretation.

We have applied these techniques to characterize the behaviour of α -amylase* and aspartate aminotransferase reference materials in several analytical methods.^{29,53} Here we describe two new applications to different areas of clinical chemistry analysis—therapeutic drug monitoring (theophylline) and enzyme assays (alkaline phosphatase†).

Case 1—Theophylline

In this application, the effects of specimen preparation, preservation, and matrix were examined. Nineteen specimens, selected at random from serum samples delivered to the laboratory for routine theophylline monitoring, were used to characterize the analytical systems included in this study; the theophylline concentration range was 6.5–18.6 mg/l.

Control materials were prepared by using commercially available normal human serum and bovine serum. Treatments of the serum included: precipitation of β - and pre- β -lipoproteins by the procedures of Proksch and Bonderman¹⁴ (treatment A) and of Bais *et al.*⁵⁰ (treatment B); precipitation of α - and β -lipoproteins¹⁶ (treatment C); and lyophilization. Theophylline was added to all pooled materials, to give concentrations of approximately 15.5 mg/l. The nature, treatment, and coding of control materials is outlined in the first column of Table 4.

The theophylline concentration in authentic patient and control specimens was determined by five methods, each differing in principle. The techniques used were: (a) the enzyme-multiplied immunoassay technique (EMIT); the Syva Emit and Theophylline Assay reagent kit was used with a Gilford Stasar III spectrophotometer controlled by a System 5 Clinical Analyzer; (b) fluorescent polarization immunoassay (FPIA); the Abbott TDx Theophylline Reagent Pack was used with the TDx Direct Reading Fluorescence Polarization Immunoassay Analyzer; (c) substrate-labelled fluorescent immunoassay (SLFIA); Optimate theophylline reagents were used with the Ames/Gilford Optimate Automated TDA and Chem-

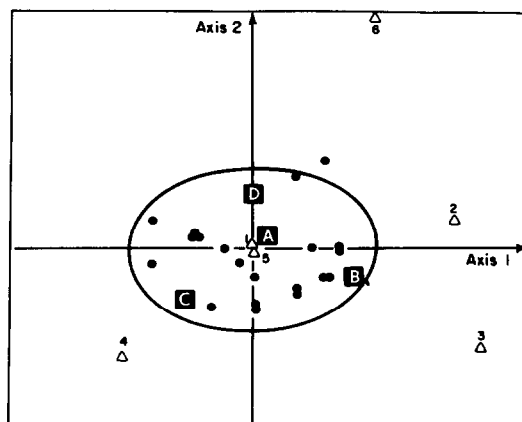


Fig. 3. Correspondence analysis of hypothetical data given in Table 2. Projection onto the plane described by the two most significant factors. Projections on the plane are: patients' specimens (●); quality-control specimens (△) numbered as in Table 2; the four analytical methods (lettered boxes). The ellipse defines the 95% confidence area describing the multivariate variability in behaviour of the patients' specimens with respect to the four methods. Adapted from reference 44 with permission.

istry Analyzer; (d) rate-inhibition nephelometry (NIIA); Beckman theophylline reagents were used with the ICS II analyser; (e) high-pressure liquid chromatography (HPLC); the liquid chromatograph consisted of a Beckman Instruments Model 100A and a Model 110A pump, Model 210 injection valve fitted with 20- μ l sample loop, a 15 cm \times 4.6 mm Ultrasphere-ODS column, and a Model 155-40 variable wavelength UV-VIS detector. HPLC was used as the reference method.

All techniques exhibited excellent correlation with the reference method for results obtained from clinical specimens with the exception of NIIA, where the relative error exceeded 30%. When the buffer-diluted samples were centrifuged prior to analysis, as is recommended if the specimen has been frozen or lyophilized, the relative error was decreased to 19%.

The regression analysis parameters were used to assess the relative behaviour of control materials by determining the "closeness-of-fit" of results for control specimens to the clinical specimen regression line (Table 4). Theophylline concentrations in lyophilized control materials analysed by FPIA were found to give greater error than the frozen sample in each treatment pair. At the 95% confidence level, controls 1L, 4L, 6L, 7L and 8L were significantly distant from the regression line defined by the clinical samples. SLFIA analysis of human-serum control specimens, both frozen and lyophilized, also resulted in significant error while bovine-serum materials all gave results within acceptable limits. The behaviour of all control materials in the EMIT assay was similar to that of clinical specimens, as was also the case with NIIA except for sample 8F.

*EC 3.2.1.1, 1,4- α -D-glucan glucanohydrolase.

†EC 3.1.3.1, orthophosphoric monoester phosphohydrolase (alkaline optimum).

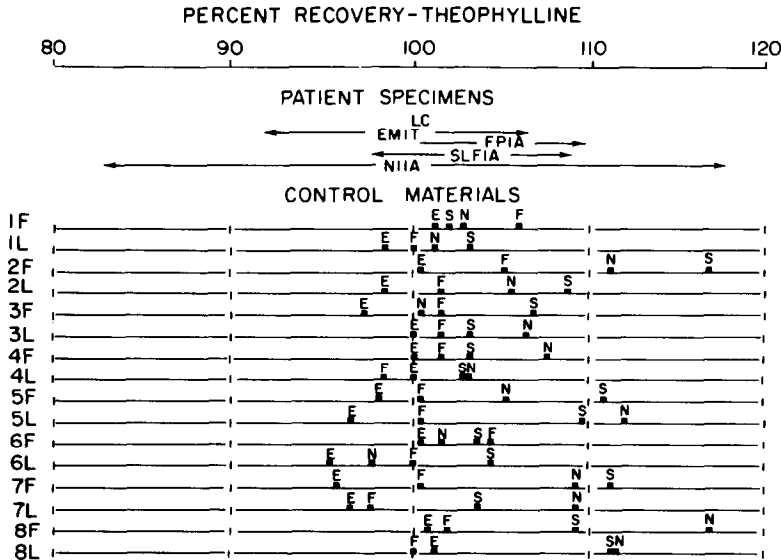


Fig. 4. Linear ratio presentation of theophylline method bias relative to HPLC. The mean recovery and 95% confidence interval for patient-specimens is represented by the method code and horizontal bars respectively. With HPLC results representing target concentrations, the recovery of theophylline from patients' and control specimens is presented for the EMIT (E), FPIA (F), SLFIA (S), and NIIA (N) methods.

These data are presented in the linear-ratio format in Fig. 4, where results are expressed as a percentage of those obtained by HPLC. The mean recovery and 95% confidence interval for each method were determined by using the data for patient specimens. Recovery of theophylline from the control material should be within the respective ranges for the methods if matrix effects are negligible. The significantly higher theophylline recovery from human-serum con-

trols for SLFIA is clearly observed. Also, the FPIA theophylline recovery from 1L, 4L, 7L and 8L is lower than that for clinical specimens.

Correspondence analysis of these data was performed with patient-results as active elements (Fig. 5). Since the intermethod bias between NIIA and the other analytical systems was considerable, patient-data obtained from NIIA were treated as inactive elements to allow evaluation of the more subtle

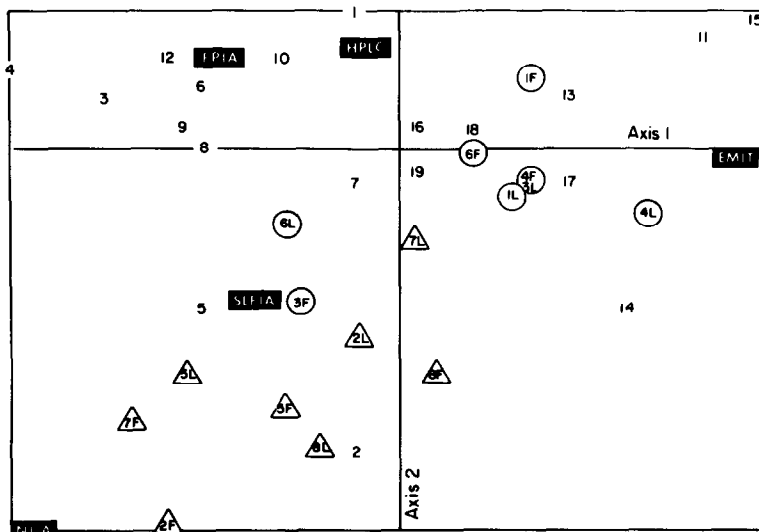


Fig. 5. Correspondence analysis of theophylline data. The coded rectangles are projections of the five theophylline methods; projections of bovine (O) and human (Δ) serum control materials are identified by the enclosed codes. Projections of the patient-data are identified by the patients' numbers (1-19).

differences among the EMIT, SLFIA, FPIA and HPLC results. Data projected onto the plane determined by factorial axes 1 and 2 accounted for 59 and 41% respectively of the information contained in the data matrix. Along the most significant axis 1, EMIT is well-separated from the projections for SLFIA, FPIA and HPLC. Evaluation of the patient-data revealed a consistent positive bias of FPIA and SLFIA results relative to HPLC. EMIT results, on the other hand, for the cluster of patient-specimens with projections on the left of axis 1 were lower than HPLC results. Concentrations determined by EMIT were higher than those obtained by HPLC for those patient-specimens with projections on the right of axis 1. The position of the method projections on axis 1 is consistent with the intermethod bias of patient-results noted from regression analysis, and this axis probably reflects the intermethod bias of the theophylline results. Axis 2 is largely determined by the differences in behaviour of patients 2, 5 and 14 from that of patients 1, 11 and 15, and the method responsible for the dissimilarity in behaviour is SLFIA. The mean theophylline recovery from patients 2, 5 and 14 by SLFIA was 111.2%, which is significantly higher than the 100.1% recovery from specimens 1, 11 and 15. Figure 5 also demonstrates a separation of bovine-serum from human-serum materials along axis 2. As noted with the other techniques, a significant matrix effect existed in the

human-serum control material when analysed by SLFIA. Theophylline recovery from the human-serum controls by SLFIA averaged 114% and was therefore projected on axis 2 along with the results for patients 2, 5 and 14.

Of the methods currently used in clinical toxicology, NIIA appears to be most sensitive to the presence of endogenous particulate matter. These particles may conceivably act as centres at which immunocomplexes are formed, resulting in larger but fewer immunocomplexes than would occur in the absence of particulate matter. In this situation, falsely elevated drug concentrations are reported. Centrifugation of the buffer-diluted clinical specimens to remove cryoprecipitates prior to analysis resulted in improved accuracy and precision, but significant bias remained. The behaviour of control materials was similar to that of patients' serum, with the exception of the frozen human serum, which appears to have been rectified by treatment with dextran and "Aerosil" (Table 4).

Correspondence analysis dramatically illustrates the unique behaviour of human-serum control specimens when analysed by SLFIA. At least a portion of the bias is due to background fluorescence of the control specimens. The manufacturer claims that background fluorescence is rarely found in authentic clinical specimens, and that specimen blanks need not be routinely run in the clinical laboratory.⁵⁴

Table 4. Deviation* of control material theophylline concentration from the respective HPLC-method regression line for clinical specimens

Control material	Deviation			
	FPIA	SLFIA	EMIT	NIIA†
Bovine serum, untreated				
Frozen (1F)	0.7 ₇	-0.5 ₁	0.5 ₄	-0.6 ₇
Lyophilized (1L)	-2.3 ₂	0	0.5 ₄	-0.9 ₄
Human serum, treatment B				
Frozen (2F)	0.7 ₇	5.4 ₀	0.2 ₇	1.2 ₁
Lyophilized (2L)	-1.1 ₆	2.0 ₆	-0.5 ₄	0
Bovine serum, treatment C				
Frozen (3F)	-1.5 ₄	1.5 ₄	-1.0 ₉	1.0 ₈
Lyophilized (3L)	-1.5 ₄	0	0	0.1 ₃
Bovine serum, treatment B				
Frozen (4F)	-1.5 ₄	0	0	0.4 ₀
Lyophilized (4L)	-3.4 ₇	-0.2 ₆	0	-0.6 ₇
Human serum, treatment A				
Frozen (5F)	-1.9 ₃	3.0 ₈	-0.8 ₂	-0.1 ₃
Lyophilized (5L)	-1.9 ₃	2.5 ₇	-1.6 ₃	1.3 ₅
Bovine serum, treatment A				
Frozen (6F)	0.3 ₉	0.2 ₆	0.2 ₇	-0.8 ₁
Lyophilized (6L)	-2.3 ₁	0.5 ₁	-1.9 ₁	-1.7 ₃
Human serum, treatment C				
Frozen (7F)	-1.9 ₃	3.3 ₄	-1.9 ₁	0.6 ₇
Lyophilized (7L)	-3.8 ₆	0.2 ₆	-1.6 ₃	0.6 ₇
Human serum, no treatment				
Frozen (8F)	-1.5 ₄	2.5 ₇	0.2 ₇	2.2 ₉
Lyophilized (8L)	-2.3 ₂	3.3 ₄	-0.5 ₄	1.2 ₁

*Deviation, expressed in number of standard deviations, was determined from the expression, residual/SEE, where residual is the perpendicular distance between the control-material data point and the regression line derived from clinical specimen data.

†The buffer-diluted samples were centrifuged at 8000 g for 5 min before analysis.

Correspondence analysis, however, demonstrates that 3 of the 19 patient-samples used in this study behaved similarly to the processed human-serum controls, suggesting that background fluorescence may frequently occur in clinical specimens.

Lyophilization appeared to have an adverse effect on specimen behaviour in analysis by FPIA. Mean theophylline recovery from patient-specimens, frozen and lyophilized controls was 105, 103 and 100% respectively. In the FPIA system, the extent of tracer polarization is inversely proportional to the concentration of endogenous drug.⁵⁵ Analytical variables which may increase rotational relaxation time, and hence decrease apparent analyte recovery, are decreased temperature and increased viscosity of the medium.⁵⁶ Temperature control is well maintained in the TDx analyser and control materials were dispersed among clinical samples in the analytical runs. The viscosity of the control material is increased both by lyophilization and by addition of dextran or colloidal silica, but the sample dilution factor in this assay is over 1000-fold, which minimizes the variability of viscosity between specimens. It is evident that the bias introduced by lyophilization, though measurable, was not of sufficient magnitude to exceed the limits of acceptability likely to be used in an interlaboratory quality-control programme. In the New York State programme, the coefficient of variation of the collective theophylline data averages 10%, and 80–120% recovery of drug is considered acceptable. The lyophilization effect, however, may contribute to an overestimation of this method's imprecision by external quality control.

Case 2—Alkaline phosphatase

The selection of a source of alkaline phosphatase for supplementing the activity of quality-control

specimens is difficult, since it is not practical to use the two isoenzymes of clinical importance—those from human liver and bone. At present, manufacturers often add the enzyme derived from human placenta or intestinal enzyme of calf or chicken origin.^{32,57} The purpose of this experiment was to seek an alternative source of alkaline phosphatase that would mimic more closely the behaviour of alkaline phosphatase from human liver and patient-specimens with respect to the most widely used methods of determination.

Twelve methods were chosen for measuring the alkaline phosphatase activity; essential details of these methods, and the three-letter abbreviation codes used for them in this article, are summarized in Table 5. Unless specified, these methods were applied exactly as described or according to the manufacturer's recommendations. The method of Kind and King (K&K)⁵⁸ was used in the Price and Woodman⁵⁹ adaptation using Technicon Auto-Analyzer equipment with dialysis. Three different modifications of the method of Bowers *et al.*⁶⁰ were used. The procedures coded AMD and AMZ followed the procedure as described⁶⁰ but the 2-amino-2-methyl-1-propanol used was pretreated; in method AMD it was distilled under reduced pressure and in method AMZ it was pretreated by addition of zinc ions with removal of the excess by cation-exchange as described previously.⁶¹ The third modification (code CPS) used 0.1M CAPS [3-(cyclohexylamino)propanesulphonate] as the buffer⁶² instead of 2-amino-2-methyl-1-propanol, since it is not transphosphorylated. Other methodological details will be reported separately.⁶³

The methods were chosen to represent a wide spectrum of analytical principles characteristic of methods used in clinical chemistry laboratories throughout the world. In addition, the effects of

Table 5. Methods used for determination of alkaline phosphatase activity*

Code	Buffer	Substrate	Determination†	Temperature °	Reference or manufacturer
AMD	2A2M1P	4-NPP	Kinetic	30	Bowers <i>et al.</i> ⁶⁰
AMZ	2A2M1P	4-NPP	Kinetic	30	Bowers <i>et al.</i> ⁶⁰
BMC	DEA	4-NPP	Kinetic	37	Boehringer Mannheim Diagnostics
WOR	2A2M1P	4-NPP	Kinetic	30	Worthington Diagnostics
HYC	2A2M1P	TMPP	Two-point	37	Hycel
COU	Tris	TMPP	Two-point	37	Coulter
SMA	2A2M1P	4-NPP	Kinetic	37	Technicon (SMAC)
BEC	2A2M1P	4-NPP	Kinetic	30	Beckman (liquid)
CPS	CAPS	4-NPP	Kinetic	30	Bowers <i>et al.</i> , ⁶⁰ modified
K&K	Bicarbonate	Phenylphosphate	Two-point	37	Kind and King ⁵⁸ Price and Woodman ⁵⁹
ATE	2A2M1P	PPMP	Two-point	30	General Diagnostics (Phosphastrate)
ABS	Tris	PPDP	Two-point	37	General Diagnostics (Phosphatabs)

*Abbreviations used: 2A2M1P, 2-amino-2-methyl-1-propanol; DEA, diethanolamine; CAPS, 3-(cyclohexylamino)propanesulphonate; Tris, tris(hydroxymethyl)aminomethane; 4-NPP, 4-nitrophenylphosphate; TMPP, thymolphthalein monophosphate, PPMP, phenolphthalein monophosphate; PPDP, phenolphthalein diphosphate.

†Kinetic refers to continuous monitoring of the reaction rate, except for method SMA where the reaction rate is calculated by using three measured points.

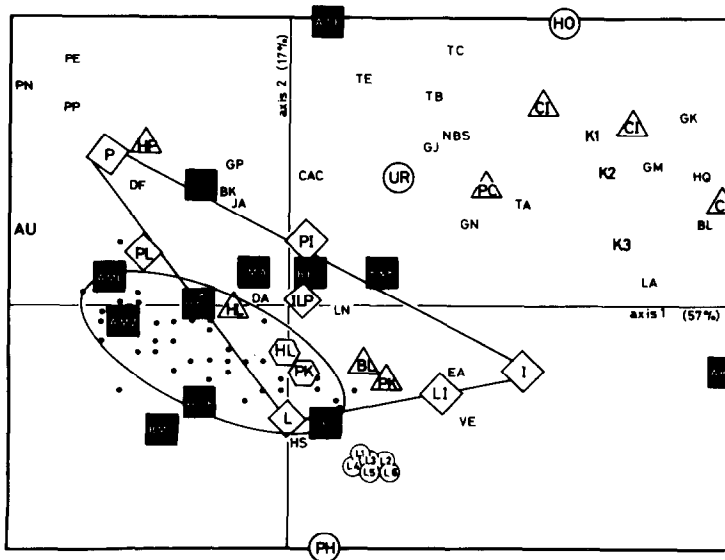


Fig. 6. Correspondence analysis of alkaline phosphatase measurements. Projection on the plane described by axes 1 and 2. The large squares are projections of the analytical methods identified by the three-letter codes given in Table 5. Other symbols are: patient-specimens (●); purified isoenzymes (△) identified as given in the text; letter-coded points without symbols are quality-control specimens. Large circles represent projections of results for alkaline phosphatase determined in the presence of inhibitors (see text).

homoarginine (code HO), urea (code UR), and L-phenylalanine (code PH)—all inhibitors of certain alkaline phosphatase isoenzymes—were examined under the conditions of the method coded CPS in order to better characterize the patient-specimens and candidate materials.

Patient-specimens were selected from a hospital population by use of criteria that we have described previously⁴⁴ and represented a variety of normal and pathological states with both normal and abnormal activities of alkaline phosphatase—they are shown as solid dots on the multivariate map (Fig. 6). Candidate quality-control materials were obtained commercially (shown by two- or three-character codes) or were prepared specifically for this study. These latter specimens made use of three kinds of matrixes: a native human-serum pool (shown as hexagons), a denatured human-serum pool (shown as open diamonds), and a native bovine-serum pool (shown as triangles). Enzymes of various tissue and species origin were used to supplement the matrixes. These included enzymes from calf intestine (code CI), beef liver (BL), pig kidney (code PK), and human enzymes purified from liver (code HL or L), intestine (code I), and human placenta (code P). Specimens L1–L6 (Fig. 6) differed with respect to alkaline phosphatase activity but were otherwise identical. They were made of human liver enzyme in an artificial matrix composed of polyvinylpyrrolidone, albumin and buffer.⁵⁷

Results were processed by correspondence analysis and the projection of these data on the plane formed by factorial axes 1 and 2 is shown in Fig. 6. These two axes represent 57 and 17% respectively of the infor-

mation contained in the data, as calculated from their eigenvalues. The aggregate clustering of the patients' specimens, surrounded by the 95% confidence ellipse is in sharp contrast to most of the quality-control specimens, which have their projections outside this ellipse. A remarkable result is the similar projection of the diamond-coded specimens, which can be used as an alternative reference of behaviour. They contain either one pure human isoenzyme (code I, L or P), determining the corners of a triangle, or equal-activity mixtures of two of them (code PI, LI or PL), positioned at the middle of each corresponding side, or an equal-activity mixture of all three (code ILP), located at the centre of gravity of the triangle. The relative positions of the ellipse and the triangle are consistent with the fact that most alkaline phosphatase activity encountered in patient-specimens is of liver origin.

As we have described earlier, the differences in behaviour are directly related to the intermethod biases for different kinds of specimens. It is possible to conclude that in this experiment, a lack of correlation between methods cannot be accounted for by any biases, since the projections for the specimens L1–L6 are near each other, irrespective of the concentration.

Most quality-control specimens situated in the upper right corner of the map apparently contain intestinal alkaline phosphatase either from chicken or calf. It is interesting that they differ significantly from those containing the enzyme of human origin. This was verified for some of the control materials known to contain one of the non-human intestinal

enzymes, including that coded as NBS in Fig. 6, which is the U.S. National Bureau of Standards reference material SRM-909, for which enzyme data are available.⁶⁴ Our data suggest that this material has an intermethod behaviour demonstrably different from that of patient-specimens and is therefore of limited usefulness in intermethod comparisons. Similarly, commercial specimens PE, PP, PN, containing human placental enzymes in a semi-artificial matrix, are all located near the P diamond. Conversely, some of the commercially available specimens (*e.g.*, DA or HS) display a behaviour similar to that of the patient-specimens, since their projections are close to the ellipse. These specimens were manufactured from human plasma to which no supplemental alkaline phosphatase was added. Finally, the behaviour of prepared specimens containing pig kidney or beef liver show a behaviour very similar to that of patient-specimens when the matrix is a denatured human-serum pool. Minor departure from behaviour can be observed when native bovine serum is supplemented with these enzymes (see triangles on the right of the ellipse in Fig. 6).

As a conclusion from this study, we recommend the use of pig kidney or beef liver alkaline phosphatase as an adequate source of the enzyme for simulating intermethod behaviour of patient-specimens.

CONCLUSIONS

The success of any statistical quality-control program is dependent in large part on the characteristics of the specimens used to evaluate the analytical system(s). In external programmes it is essential that the material has properties similar to those of patient-specimens in the methods tested. The procedures that we have outlined—and applied to two cases here—are relatively simple yet highly informative for the evaluation of control-material commutability. Correspondence analysis, in particular, is a powerful descriptive tool. It also clearly presents information regarding the interaction of patient-specimens with the analytical methods, so that matrix effects that may also influence results for certain types of patient-specimens will also be characterized (Fig. 4). Such matrix effects may be a significant source of error for patient-specimens.⁶⁵ Jansen⁶⁶ has used an alternative multivariate technique for similarly classifying methods, but possible non-commutability of the control specimens was not considered in that application.

Recognition of the limitations of certain control materials should help in the interpretation of interlaboratory quality-control data. Procedures such as those described here will help in the design of more effective materials for quality-control in the future.

REFERENCES

1. J. Büttner, R. Borth, J. H. Boutwell, P. M. G. Broughton and R. C. Bowyer, *Clin. Chem.*, 1977, **23**, 1784.
2. G. A. Uriano and C. C. Gravatt, *CRC Crit. Rev. Anal. Chem.*, 1977, **6**, 361.
3. D. Stamm, *J. Clin. Chem. Clin. Biochem.*, 1979, **17**, 283.
4. G. F. Grannis and W. G. Miller, *Clin. Chem.* 1976, **22**, 500.
5. C. G. Fraser, A. N. Fudge and L. A. Penberthy, *Ann. Clin. Biochem.*, 1978, **15**, 121.
6. G. N. Bowers, Jr., R. W. Burnett and R. B. McComb, *Selected Methods Clin. Chem.*, 1977, **8**, 21.
7. W. Gerhardt, A. Louderback and J. Waldenström, *Clin. Chem.*, 1982, **28**, 719.
8. G. J. Proksch and D. P. Bonderman, *ibid.*, 1981, **27**, 468.
9. C. G. Fraser and M. J. Peake, *CRC Crit. Rev. Clin. Lab. Sci.*, 1980, **12**, 59.
10. W. Pichel, *Am. Soc. Heat. Refrig. Aircond. Eng. J.*, 1965, **7**, 68.
11. A. P. MacKenzie and B. J. Luyet, *Nature*, 1967, **251**, 83.
12. N. Hanafusa, *Freezing and Drying of Microorganisms*, p. 117. University of Tokyo Press, Tokyo, 1969.
13. J. G. Atwood and H. W. Marshall, *Lab. Med. Newslett.*, 1973, **5**, 6.
14. G. J. Proksch and D. P. Bonderman, *Clin. Chem.*, 1976, **22**, 456.
15. B. W. Steele, D. F. Koehler, T. P. Blaszkowski and M. Azar, *ibid.*, 1975, **21**, 1812.
16. W. Stephan and L. Roka, *Z. Klin. Chem. Klin. Biochem.*, 1968, **6**, 186.
17. H. Wieland and D. Seidel, *Clin. Chem.*, 1982, **28**, 1335.
18. B. Klein and M. Weissman, *ibid.*, 1958, **4**, 194.
19. W. J. Frajola and J. Maurukas, *Health Lab. Sci.*, 1976, **13**, 25.
20. R. L. Rush and D. L. Vlastelica, *U.S. Patent*, 3,853,465, 1974.
21. R. Rej and R. E. Vanderlinde, *Clin. Chem.*, 1974, **20**, 454.
22. P. Suter and J. P. Rosenbusch, *Anal. Biochem.*, 1977, **82**, 109.
23. A. L. Louderback, in G. Anido, S. B. Rosalki, E. J. van Kampen and M. Rubin (eds.), *Quality Control in Clinical Chemistry*, p. 385. De Gruyter, New York, 1975.
24. K. Diem and C. Lentner, *Scientific Tables*, p. 557. Ciba-Geigy, Basle, 1972.
25. R. J. Elin and B. A. Gray, *Clin. Chem.*, 1984, **30**, 129.
26. W. Gruber, H. Möllering and L. Perras, *J. Clin. Chem. Clin. Biochem.*, 1977, **15**, 565.
27. C. F. Fasce, Jr., R. Rej, W. H. Copeland and R. E. Vanderlinde, *Clin. Chem.*, 1973, **19**, 5.
28. K. Jung, K. D. Grützmann, C. Fechner, M. Pergande and E. Egger, *Clin. Chim. Acta*, 1979, **97**, 171.
29. J.-P. Bretauiere, R. Rej, P. Drake, A. Vassault and M. Bailly, *Clin. Chem.*, 1981, **27**, 806.
30. J.-P. Bretauiere and M. Bailly, in N. W. Tietz, A. Weinstock and D. O. Rodgerson (eds.), *Proc. 2nd Intern. Symp. Clin. Enzymol.* p. 227. American Association for Clinical Chemistry, Washington, 1976.
31. R. Rej, C. F. Fasce, Jr. and R. E. Vanderlinde, *Clin. Chem.*, 1975, **21**, 1141.
32. G. N. Bowers, Jr., M. L. Kelley and R. B. McComb, *ibid.*, 1967, **14**, 595.
33. M. D. O'Donnell and K. F. McGeeney, *ibid.*, 1983, **29**, 510.
34. R. S. Yalow, *Adv. Clin. Chem.*, 1978, **29**, 1.
35. C. B. Reimer and S. E. Maddison, *Clin. Chem.*, 1976, **22**, 577.
36. P. M. S. Clark, L. J. Kricka and T. P. Whitehead, *Clin. Chim. Acta*, 1981, **113**, 293.
37. W. C. H. van Helden, R. W. J. Visser, F. A. J.-T. M. van den Bergh and J. H. M. Souverijn, *ibid.*, 1979, **93**, 335.
38. H. Büttner, in G. Anido, E. J. van Kempen and S. B. Rosalki (eds.), *Progress in Quality Control in Clinical Chemistry*, p. 243. Huber, Bern, 1973.

39. E. J. Sampson, P. H. Duncan, D. M. Fast, V. S. Whitner, S. S. McKneally, M. A. Baird, M. L. MacNeil and D. D. Bayse, *Clin. Chem.*, 1981, **27**, 714.
40. N. S. Lawson, G. T. Haven and G. W. Williams, *CRC Crit. Rev. Clin. Lab. Sci.*, 1982, **17**, 1.
41. P. Wilding and B. Wilkes, *J. Clin. Chem. Clin. Biochem.*, 1981, **19**, 876.
42. K. Jung, K. D. Grützmann, E. Egger and C. Fechner, *Clin. Chim. Acta*, 1977, **79**, 515.
43. P. M. S. Clark, I. M. Surplice, P. M. G. Broughton and D. G. Bullock, *Clin. Chem.*, 1983, **29**, 578.
44. J.-P. Breaudiere, G. Dumont, R. Rej and M. Bailly, *ibid.*, 1981, **27**, 798.
45. R. Rej, R. E. Vanderlinde and C. F. Fasce, Jr., *ibid.*, 1972, **18**, 374.
46. R. Rej and R. E. Vanderlinde, in N. W. Tietz, A. Weinstock and D. O. Rodgerson (eds.), *Proc. 2nd Intern. Symp. Clin. Enzymol.*, p. 249. American Association for Clinical Chemistry, Washington, 1976.
47. P. H. Duncan, S. S. McKneally, M. L. MacNeil, D. M. Fast and D. D. Bayse, *Clin. Chem.*, 1984, **30**, 93.
48. G. R. Warnick, C. Mayfield and J. J. Albers, *ibid.*, 1981, **27**, 116.
49. P. M. S. Clark, L. J. Kricka, A. R. Z. Gomo, T. P. Whitehead, D. G. Bullock and H. Saidi, *Clin. Chim. Acta*, 1980, **103**, 219.
50. R. Bais, P. D. O'Loughlin, J. C. Philcox and J. B. Edwards, *Pathology*, 1983, **15**, 15.
51. B. G. Tabachnick and L. S. Fidell, *Using Multivariate Statistics*, Harper and Row, New York, 1983.
52. D. L. Massart and L. Kaufman, *The Interpretation of Analytical Chemical Data by the Use of Cluster Analysis*, Wiley, New York, 1983.
53. R. Rej, J.-P. Breaudiere and M. Hørdler, in D. M. Goldberg and M. Werner (eds.), *Progress in Clinical Enzymology*, Vol. 2, p. 25. Masson, New York, 1983.
54. L. A. Flynn, S. L. Hammock and D. R. Parker, *Clin. Chem.*, 1983, **29**, 1209.
55. S. R. Popelka, D. M. Miller, J. T. Holen and D. M. Kelso, *ibid.*, 1981, **27**, 1198.
56. G. Weber, *Adv. Protein Chem.*, 1953, **8**, 415.
57. R. Rej, *Clin. Chem.*, 1977, **23**, 1903.
58. P. R. N. Kind and E. J. King, *J. Clin. Pathol.*, 1954, **7**, 322.
59. C. P. Price and D. D. Woodman, *Clin. Chim. Acta*, 1971, **35**, 265.
60. G. N. Bowers, Jr., R. B. McComb and M.-L. Kelley, *Selected Methods Clin. Chim.*, 1977, **8**, 31.
61. R. Rej, J.-P. Breaudiere, R. W. Jenny and K. Y. Jackson, *Clin. Chem.*, 1981, **27**, 1401.
62. J.-P. Breaudiere and R. Rej, *ibid.*, 1978, **24**, 1001.
63. *Idem*, in preparation.
64. G. N. Bowers, Jr., R. Alvarez, J. P. Cali, K. R. Eberhardt, D. J. Reeder, R. Schaffer, G. A. Uriano, R. Elser, L. M. Ewen, R. B. McComb, R. Rej and L. M. Shaw, *The Measurement of the Catalytic (Activity) Concentration of Seven Enzymes in NBS Human Serum SRM 909*, U.S. National Bureau of Standards, Washington, DC, 1983.
65. W. Stein and J. Bohner, *Clin. Chem.*, 1984, **30**, 238.
66. R. T. P. Jansen, *Ann. Clin. Biochem.*, 1983, **20**, 41.

SOLID-PHASE CHEMISTRY: ITS PRINCIPLES AND APPLICATIONS IN CLINICAL ANALYSIS

ADAM ZIPP

Ames Division, Miles Laboratories Inc., Elkhart, Indiana, U.S.A.

W. E. HORNBY

Ames Division, Miles Laboratories Ltd., Stoke Court, Stoke Poges, Bucks, England

(Received 5 May 1984. Accepted 2 July 1984)

Summary—A review is given of the development of solid-phase reaction systems (test papers, impregnated-fibre systems, multi-layer film systems) for rapid field and laboratory testing in clinical analysis.

Anyone who has worked or been taught in a chemical laboratory is very familiar with the use of indicator papers for the rapid and approximate estimation of the pH of a solution. Likewise, most people who have been associated with clinical biochemistry are equally aware of the use of other types of reagent strips for the rapid estimation of certain urinary constituents such as glucose and protein. In the more specialized area of diabetology, the usefulness of reagent strips for the measurement of whole blood glucose has been recognized for more than a decade, and more recently, attention has been drawn to the use of yet more sophisticated reagent strips for the quantitative measurement of a much wider range of analytes in serum and plasma, such as enzymes, metabolites and drugs. All these test papers or reagent strips are types of solid-phase reagents which may thus be looked upon as self-contained analytical devices.

A common denominator underlying the use of these solid-phase reagents is the need to be able to perform rapid and convenient analyses without the encumbrances or impedimenta that are often associated with more conventional analytical techniques. While it is recognized today that convenience is one of the principal driving forces behind the use of solid-phase reagents, it is not widely known that such considerations prompted similar interest in and use of solid-phase reagents a century ago. Thus, in reporting on the use of test papers for the detection of urinary glucose, George Oliver in 1883 wrote "All busy practitioners must admit the clinical utility and importance of accurate, time-saving and portable tests. . .".¹

Since the development and manufacture today of solid-phase reagents is tightly bound up with modern and advanced technology, it is generally thought that these analytical tools are artefacts of the twentieth century and inventions of the companies which have pioneered their application in diagnostics. This is not strictly true, since solid-phase reagents of one type or another have been used as diagnostic tools for the best part of two centuries. Indeed, many of the

precepts governing the use of solid-phase reagents in diagnostics were developed during the last century and it is worthwhile to note a few of the landmarks in their evolution, before reviewing in more detail the latest developments.

Among the earliest accounts is that by Prout in 1817² reporting the use of litmus paper for testing the alkalinity of urine. Further applications of litmus paper, this time for measuring the alkalinity of mucus, were recorded by Babington in 1837, who reported that "bibulous paper tinged with litmus and reddened by simple exposure or by a very dilute acid solution is restored to its blue colour by fresh mucus". It is interesting that as early as 1837 Babington was able to recognize the importance of the nature of the matrix of the solid-phase reagent and the effect this can have on the performance of the test system. He reported that the sensitivity of the mucus test was modulated when the type of paper was changed: "In the shops they commonly tinge writing paper for use; but the size it contains, which cannot be soaked out by cold water, diminishes its delicacy as a test".³ A few years later, in 1850, Maumené extended the range of application of solid-phase reagents when he described the detection of urinary glucose with test strips woven from white merino wool and impregnated with stannous chloride.⁴ Maumené, too, recognized the role of the solid-phase matrix itself, and pointed out that the glucose test strips should not be made from paper, since the paper itself developed a false-positive reaction with the stannous chloride.

Another variant of solid-phase reagent was developed and reported by Oliver¹ in an attempt to render more portable and convenient some of the tests then commonly carried out by general practitioners. Oliver used reagent-impregnated papers as reagent carriers and reconstituted the liquid tests systems by leaching the reagents out of the strips immediately before their use. In this way, he managed to obviate the need to transport bulky and corrosive liquid reagents, and developed a range of assays⁵ which

included tests for urinary glucose based upon its reaction with indigo carmine, and for albumen based upon its precipitation by solutions of potassium and mercuric iodides.

In this paper we will describe the principles of modern solid-phase chemistry, emphasize impregnated fibre and multi-layer film systems and attempt to convey a basic understanding of the theoretical and practical aspects of their use. We will describe in some detail the characteristics of the most popular systems and discuss future applications of this new and exciting area of clinical chemistry.

GENERAL CONSIDERATIONS

From the manner in which they are used, solid-phase reagents can be regarded as self-contained analytical devices. This description may be expanded in order to define these tools more fully. Thus, they can be described more precisely as integral analytical elements which typically take the form of thin pads or films, and contain all of the reagents required for the performance of an assay, distributed in a dry form within the pad or film. These component reagents may be distributed either homogeneously throughout the matrix of the element or may be organized, or compartmentalized, into specific domains within the infra-structure of the matrix. In either case, regardless of the geometric distribution of the component reagents in the solid-phase device, the *modus operandi* may be described schematically as follows: the analyte-containing solution, which may be urine, whole blood, serum or plasma, is applied to one of the surfaces of the solid-phase element, where it diffuses into the matrix of the element and, in so doing, dissolves the component reagents dispersed therein, as shown in Fig. 1. When the dry reagents have dissolved, they react with the analyte to give products which are used as a measure of the analyte concentration, generally through the use of chromogenic reagents and either visual or instrumental measurement of the colour generated in and on the surface of the solid-phase element. Thus, in operational terms, these analytical devices may be considered as unitized reagents that make possible the performance of certain assays, without the need to prepare, dispense and mix the component reagents of the system.

As described above, solid-phase reagents conform, in general, to one of two principal types, which will be referred to as the fibre-impregnated systems and the multilayer film systems respectively. From the standpoint of use, both systems have many features in common and in general operate as shown schematically in Fig. 1. They differ significantly, however, structurally and in composition, and accordingly will be treated separately in later sections of this review.

Solid-phase reagents of the fibre-impregnated type have been used in their current format for many years^{6,7} and form the basis of the rapid diagnostic test

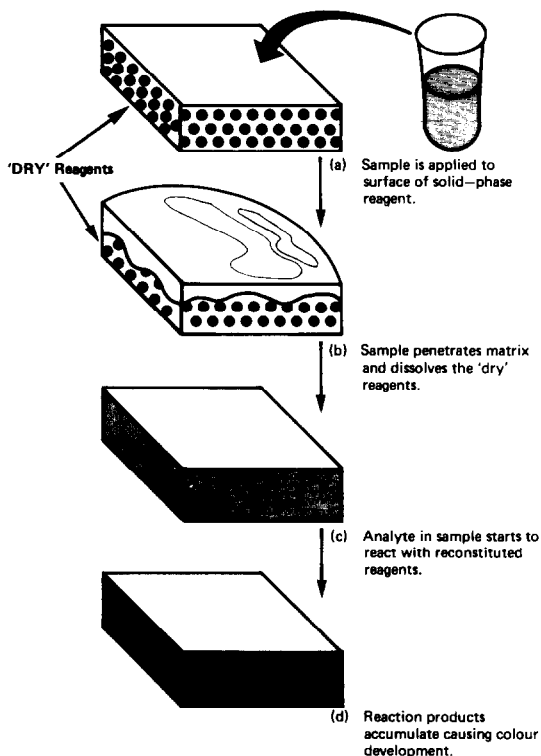


Fig. 1. Schematic representation of the operation of a simple solid-phase reagent.

systems commonly used in urine analysis⁸ and now used routinely for the determination of whole blood glucose.⁹ On the other hand, the multilayer film type of device has been in evidence for only a few years and forms the basis of a new fully-automated clinical chemistry analyser.¹⁰ Interestingly, there is already an apparent slight divergence in the manner of application and the locus of use of these two types of solid-phase reagent. The fibre-impregnated type of system traditionally appears to have been associated more with rapid diagnostic testing away from the central laboratory, whereas the multilayer film system so far appears to have been mainly used in large central analytical laboratories, though there have been recent reports of their use in group practices and even by individual physicians. Reasons underlying their application in analysis are common and perhaps should be enumerated at this point as justification of our interest in them.

Besides their obvious advantages of simplicity and convenience, already mentioned above, the solid-phase reagents also afford a useful and efficient vehicle for stabilizing some labile analytical reagents. Because of their dry form, and also the stabilizing influence sometimes generated by the solid-phase matrix itself, some of these systems, particularly those employing cellulose fibre supports, have prolonged storage stability, often for up to two years, even at room temperature. Obviously such extended and simplified storage features further increase the convenience to the user.

At the time of writing this review, interest in solid-phase reagents is being further stimulated by extensions and improvements in the technologies of their manufacture and use, which suggest the generation of new analytical systems and novel applications employing these devices. Of particular interest is the potential development of systems for quantitative clinical analysis outside the laboratory, so that testing can be done closer to the patient.

FIBRE-IMPREGNATED SYSTEMS

General considerations

Fibre-impregnated systems have been in use for many years. Hence they represent the largest and most diverse type of solid-phase reagent, certainly in terms of the assortment of assays that can be performed with them. Even though there is an abundance of reports in the literature that both review their performance and describe their evaluation, and a wide selection of diagnostic products that utilize this technology is commercially available, there is a remarkable dearth of reports that either describe their preparation or detail their make-up and characteristics. This is not surprising, since virtually all of the research and development work on fibre-impregnated systems has been performed by industry and for obvious reasons such activities have been subject to a degree of secrecy. Consequently it is often very difficult to extract specific details describing fully many of these solid-phase devices, and in a review such as this it is equally hard to report in depth on some aspects of their make-up and characteristics. In order to try to compensate for this sparsity of information, an attempt will be made here to describe in general terms the preparation and properties of typical fibre-impregnated systems.

In general, the fibre-impregnated solid-phase systems consist of a sheet of cellulose matrix which is either porous or semi-permeable with respect to solute diffusion. In this type of solid-phase reagent, the components of the assay system, which might comprise such diverse species as group-specific chemical reagents, indicator enzymes, co-enzymes, activators and buffer salts, are distributed in a dry form both in the interstices of the cellulose matrix and on the surface of its integral structural fibres.

In the simplest form of the fibre-impregnated solid reagent, the components of the assay system are distributed homogeneously throughout the matrix, with no attempt made to segregate the different components into separate compartments within the matrix. Further insight into the make-up of this simple type of fibre-impregnated reagent is gleaned from the manner of its manufacture: the cellulose matrix, which might be a porous paper, is immersed in a single solution of the various assay components and then removed and dried under controlled conditions; upon evaporation of the solvent, the dry reagents become uniformly trapped in the matrix of

the solid-phase. From an operational viewpoint, this type of solid-phase reagent is described by the schematic in Fig. 1.

Design and manufacture

In reality, most fibre-impregnated solid-phase reagents, such as the systems described by Greyson¹¹ and Zipp,¹² are somewhat more complicated and sophisticated in their design and composition than that just used to illustrate the concept of these reagents, in which there was no compartmentalization of the component reagents within the matrix of the solid-phase element. Such a configuration is not suitable for a solid-phase reagent that incorporates an assay system composed of mutually incompatible component reagents. With some analytical reactions, it is necessary to introduce into the system a degree of compartmentalization, either to segregate mutually incompatible reagents, or to separate sequentially particular steps of the overall analytical reaction. Such compartmentalization can be built very efficiently into the design of the fibre-impregnated reagent. Obviously, in order to achieve this, the manufacturing process necessarily becomes both more complicated and sophisticated.

A schematic outline of a manufacturing process for the production of a fibre-impregnated reagent that allows for the compartmentalization of the different reagents is depicted in Fig. 2, which throws some light on the structure of this more complicated type of device. In this scheme, the native matrix, which might be paper-based and in the form of an extended sheet, is fed continuously from a storage spool through a sequence of operational work stations, wherein the various unit operations that make up the overall manufacturing process take place. Thus, for example, the matrix is fed at a carefully controlled speed through the first work station, where it is steeped in a solution of some of the components of the assay system, and these components become uniformly distributed in solution throughout its structure. After passing through this station, the matrix is dried in the course of its passage through the second work station, under drying conditions which are carefully controlled by regulating the temperature, relative humidity and laminar air flow. The sheet, now dry, is then fed through the third work station, where it is soaked in a solution of the remaining components of the assay system, in a solvent different from that used during the first impregnation stage. The solvent for this stage is carefully selected so that it does not dissolve the first set of reactants already deposited in the matrix of the paper during the first impregnation stage. Thus the second set of reactants is layered on top of the first set in the matrix in the course of evaporation of the second solvent during the second drying stage. The process, as described, allows for two reagent systems to be layered separately in the matrix of the cellulose, each effectively in a separate "reagent compartment". Clearly, if more reagent

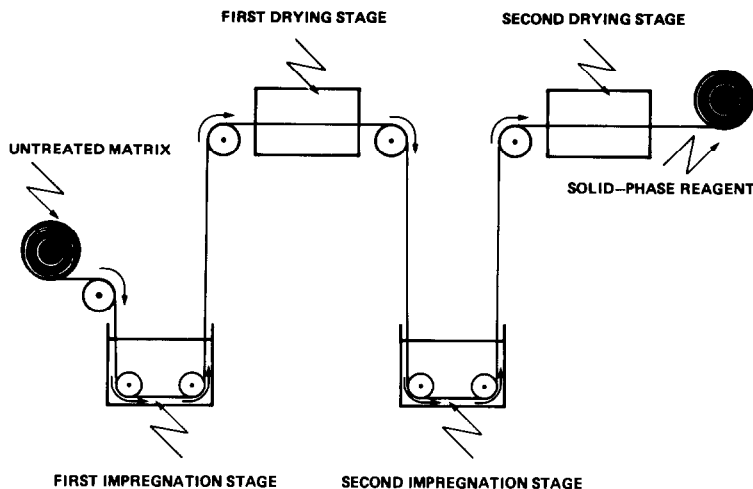


Fig. 2. Schematic representation of a typical process for the continuous manufacture of a fibre-impregnated solid-phase reagent incorporating two separate reagent compartments.

compartments are required, because of a multiplicity of reagents and/or the need for segregated reaction steps, they can be accomplished by adding extra impregnation and drying work stations to the continuous process shown in Fig. 2.

Further insight into the make-up of this more complicated type of fibre-impregnated system is best gleaned, perhaps, by consideration of a specific example. Such a reagent was first reported by Turk and Zipp¹³ for the quantitative measurement of urea in serum. In this example, the analyte, urea, is measured in a two-stage reaction as shown in Fig. 3 in which urea (II) first couples with the group-specific reagent *o*-phthalaldehyde (I) to form dihydroxyisoindoline (III).^{14,15} Then in the second reaction the dihydroxyisoindoline is complexed in strongly acidic conditions with the indicator 3-hydroxy-1,2,3,4-tetrahydrobenzo-(h)-quinoline to form a blue adduct, the concentration of which is determined photometrically.

The translation of the reaction sequence shown in Fig. 3 into the format of a fibre-impregnated reagent requires the solution of two problems. The first relates to the need to separate the indicator from the *o*-phthalaldehyde, because of their mutual reactivity, while the second relates to the need to overcome the known instability of cellulose in the strongly acidic conditions that prevail in the second part of the

reaction sequence. The particular configuration of solid-phase reagent developed by Turk and Zipp for the solution of these problems is depicted schematically in Fig. 4 and is achieved by a process of the type illustrated in Fig. 2, but involving three sequential impregnation and drying stages. The problem relating to the provision of acidic conditions without destroying the cellulose matrix is overcome by the incorporation into the cellulose of a cation-exchange resin, which dissociates when hydrated by the sample, thus generating strongly acidic conditions. In this way, the dry or unreacted form of the reagent is not exposed to strong acid and hence the integrity of the cellulose is preserved. The problem of segregating the two mutually incompatible reagents, indicator and *o*-phthalaldehyde, is resolved by depositing three layers concentrically around the cellulose fibres of the solid-phase matrix. The first, or proximal layer, which is adjacent to the fibres and contains the indicator, is laid down in the first impregnation stage and is separated from the *o*-phthalaldehyde, which is in the distal layer and is laid down in the third impregnation stage, by a polymeric separation layer, which is deposited in the second impregnation stage. When sample is applied to the surface of this solid-phase reagent it diffuses into the distal layer, where any urea in it reacts with the *o*-phthalaldehyde. Further diffusion of the sample within the infra-

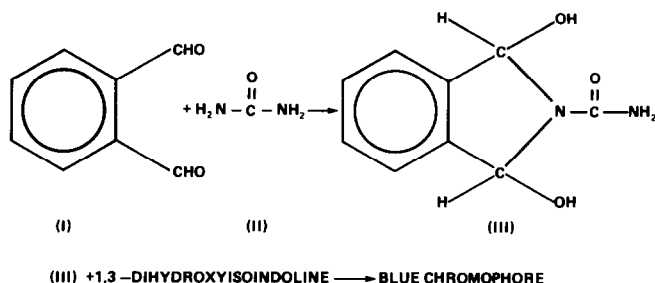


Fig. 3. Reactions involved in the measurement of urea according to Turk and Zipp.¹³

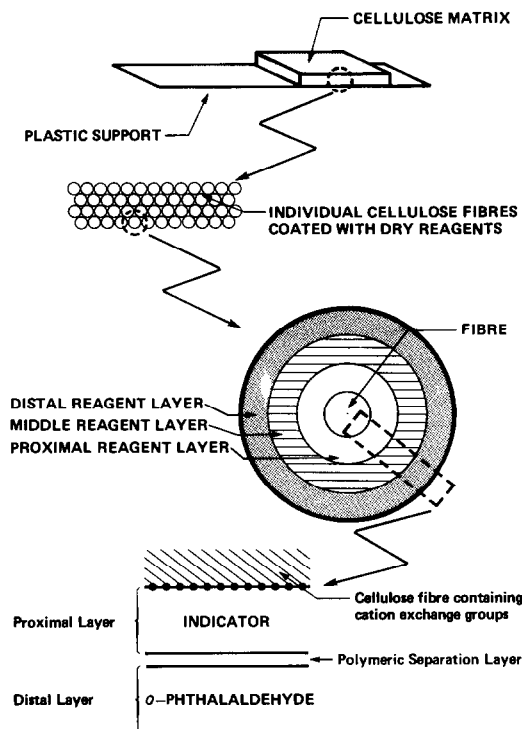


Fig. 4. Schematic breakdown of a fibre-impregnated solid-phase reagent containing three reagent compartments. The system shown is that for measurement of urea.¹³

structure causes disruption of the polymeric separation layer and thus permits the dihydroxyisourea to gain access to the proximal layer. Thereafter complexing with the indicator takes place in the now strongly acidic conditions brought about by the dissociation of the cation-exchange resin in the water of the sample.

The nature of the matrix

Reference has already been made to the long-standing recognition^{3,4} of the importance of selecting the correct type of matrix for a solid-phase reagent.

Today most solid-phase reagents of the fibre-impregnated type utilize cellulose-based materials such as paper for the support matrix. Arguably this decision was made some 25 years ago, and more than likely emanated from familiarity with the common laboratory spot-test devices, such as pH indicator papers, which can therefore be considered as the forebears of the present day solid-phase reagents. Even though the selection of cellulose in the form of paper was more by accident than design, nevertheless it turned out to be a very good choice, as will now be seen.

It will be recalled that one reason for interest in solid-phase reagents stemmed from the opportunities that these devices offer for the stabilization of some analytical reagents. It has been known for some time now that polyhydric alcohols can have a stabilizing effect on the structure of proteins. Indeed, in the industry, certain polyols are often used to stabilize

labile protein preparations.¹⁶ Owing to its polyhydric character, cellulose also can exert a stabilizing influence on neighbouring proteins, perhaps by forming hydrogen bonds with them in such a way that a greater degree of stability is conferred upon the protein structure. Consequently, experience has shown that some biochemical systems have enhanced stability when included in solid-phase cellulose matrices,¹⁷ Thus it is not surprising that many cellulose-based solid-phase reagents, perhaps containing labile component enzymes, are stable for many months, even when stored at room temperature.

Another factor which is associated with the cellulosic nature of the fibre-impregnated systems and which also contributes significantly to their good stability, is the high degree to which cellulose can be dried. Thus, under carefully controlled conditions, such as those prevailing during the manufacture of the fibre-impregnated systems, cellulose matrices, such as paper, can be dried to an extremely low residual water content. Since the denaturation of enzymes is a solution phenomenon, this process is dramatically arrested when these proteins are stored in the dry state, especially when they are in close proximity to the stabilizing influence of a polyhydric alcohol such as cellulose.

Cellulose also proves to be an effective and useful dry-phase matrix because of its strongly hydrophilic character, since dry cellulose structures will therefore tend to hydrate very rapidly and efficiently. The ease with which the dry cellulose structures can be wetted means that when the sample is applied, it spreads evenly and thus promotes homogeneous diffusion of analyte and reactants and results in uniform colour development.

The measurement process

Figure 1 described schematically the *modus operandi* of a typical fibre-impregnated system. With this type of solid-phase reagent, the extent of the reaction, and hence the concentration of the analyte, is determined by measuring the colour change that accompanies the reaction in the solid-phase matrix. This is done either visually by comparison of the colour of the reacted matrix with a standardized colour chart, or by recording instrumentally the reflectance of light of a defined wavelength, from the surface of the solid-phase element.

For the visual measurement, the comparison standard colour scales are typically made up of a number of discrete colour blocks, each of which corresponds to a different concentration of the analyte, and the colour of the reacted matrix is matched to that of a particular block, or interpolated between the colours of two adjacent blocks. Clearly the quality of the result depends on the ease and certainty with which the observer can discriminate between the component colour blocks of the scale. To optimize this discrimination, the colour blocks must be distinctly different

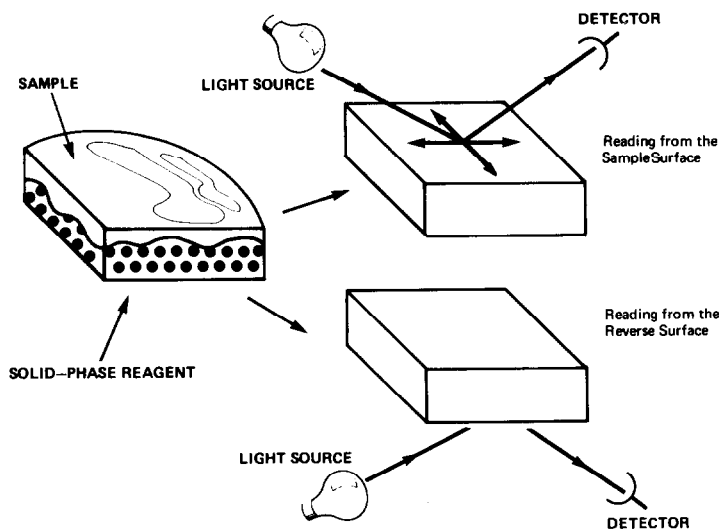


Fig. 5. Instrumental methods used for the measurement of the colour of reacted solid-phase reagents by reflectance photometry.

but the concentration steps must be close enough for the results to be clinically meaningful.

In order to achieve this goal, the analytical reaction used must produce coloured products, the concentration and spectral characteristics of which both must change with the analyte concentration. In this way, both the intensity and wavelengths of light reflected from the reacted solid-phase reagent will change with analyte concentration and thereby maximize the visual discrimination between colours corresponding to different analyte concentrations. In practice, this can sometimes be achieved by using combinations of different chromogenic reagents or by inclusion in the solid-phase reagent of background dyes which interact spectrally with the product chromophores to achieve the desired effect.

Obviously, instrumental measurement of the colour change in the solid-phase matrix will improve the quality of the results by removing the subjective component of the visual method, but it is fair to point out that the price of better quantification has to be paid in the currency of convenience. Thus, to achieve a precision comparable with that of traditional solution-based analytical procedures, the solid-phase techniques have to forfeit their freedom from instrumental encumbrances. However, this lost benefit can be offset by decreasing the size and complexity of the instrument used. A conspicuous trend in the evolution of fibre-impregnated systems is the development of such instrumentation.

Because of the opacity of the solid-phase reagent, the colour developed can only be measured by reflectance spectrophotometry. This technique involves measuring the intensity of light reflected and scattered from a surface of the solid-phase reagent when that surface is irradiated with light of a wavelength which is absorbed by the reaction products. In principle, this is performed in one of two ways, as illustrated schematically in Fig. 5.

In the first way, the sample is applied to the top surface of the solid-phase reagent and after it has permeated into the reagent and the reaction has occurred, the resulting colour is determined by measuring the reflectance from the same surface. This approach has been the one adopted so far for measuring instrumentally the colours of reacted solid-phase reagents of the fibre-impregnated type. In the second way, the sample is applied to the top surface of the solid-phase reagent and, after the ensuing reaction, the colour is measured by monitoring the reflectance from the reverse side of the element, as shown in Fig. 5. This is the approach that has been used for measuring the reaction colours of the multi-layer film systems that are described later in the review.

As shown in Fig. 5, the concentration of the reaction products formed in the fibre-impregnated systems is determined instrumentally by measuring the reflectance of light from the top side of the analytical element. In essence, this process involves irradiating the top surface of the matrix with light and measuring the intensity of light of that wavelength as it is reflected from the same surface. In reality, the light is not reflected only from the top surface, as would be the case with an ideal reflector or mirror, but penetrates into the solid-phase matrix, as shown in Fig. 6. Inside the solid-phase system the light is affected separately by the solid and liquid components of the heterogeneous matrix. Thus, the solid components, such as the fibres, scatter part of the light, and the liquid component, which contains the reaction products, absorbs part of the light. These events take place both before and after the light is reflected from the interface of the matrix and the plastic support on its lower surface; in other words, throughout the passage of the light through the solid-phase reagent. To relate the concentration of the reaction products to the intensity of the light

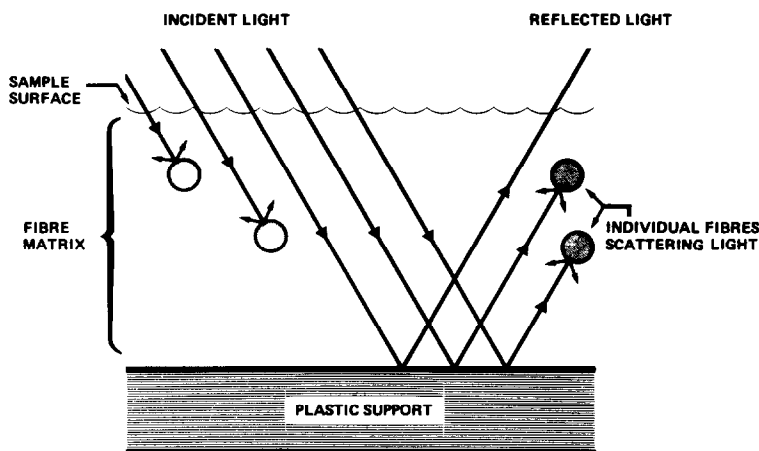


Fig. 6. Schematic representation of the events occurring when a light-beam irradiates a typical fibre-impregnated solid-phase reagent.

leaving the matrix, it is necessary to take all events into account. Kubelka and Munk¹⁸ studied this model of a diffuse reflector and developed an equation which related the concentration of the light-absorbing species (C) in the reflector to the measured reflectance (R) of the light. In its simplest form:

$$C = \frac{S(1 - R)^2}{2ER} \quad (1)$$

where S is a scattering coefficient for the effect of the solid component and E is the absorption coefficient for the liquid component, the relation pertains to a reflector with thickness such that the light is either absorbed or scattered before it can reach the lower reflected surface. In other words, equation (1) approximates the behaviour of a diffuse reflector in those cases when the difference in intensity between the incident and reflected beams is independent of the thickness of the structure. This happens to be the case with most fibre-impregnated systems and hence this equation often approximates their behaviour.

The reflectance is the ratio of the intensity of the reflected beam to that of the incident beam, and may be regarded as equivalent to the transmittance term (T), in the Lambert-Beer relation [equation (2), where L is the path-length].

$$C = \frac{\log(1/T)}{EL} \quad (2)$$

Figure 7 shows graphically the qualitative similarity between these two relationships and suggests that reflectance measurements approach transmittance measurements in precision. A more detailed treatment of the behaviour of diffuse reflectors, together with a critical analysis of quantitative reflectometry, has been presented by Kealey.^{19,20}

We should emphasize that the model developed by Kubelka and Munk provides only an approximate description of the interaction of light with a solid-phase matrix. The mathematical relationships derived from experimental data can take functional forms

different from those derived by Kubelka and Munk. A more detailed discussion of this has been given by Greyson.¹¹

Clearly, the measurement potential of solid-phase reagents, predicted above, can only be realized if appropriate instrumentation is developed. Figure 6 shows what happens when the surface of a diffuse reflector, such as a fibre-impregnated solid-phase reagent, is irradiated with light. Owing to the random nature of the light-scattering events, both the incident *and* the reflected beams are dispersed in all directions, and hence only part of the reflected light is collected by a simple unidirectional detector such as that shown in Fig. 5. To improve the efficiency of the measuring process, the more sophisticated types of reflectance analysers use a device called an integrating sphere, the operation of which is shown schematically in Fig. 8.

In the optical arrangement shown in Fig. 8, the light issuing from the lamp undergoes multiple

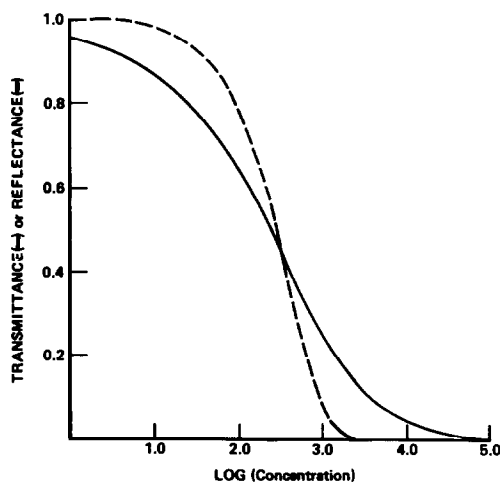


Fig. 7. Relationship between transmittance and concentration (---) and between reflectance and concentration (—) as predicted by equations (1) and (2) respectively for $S/E = 1/EL = 1000$.

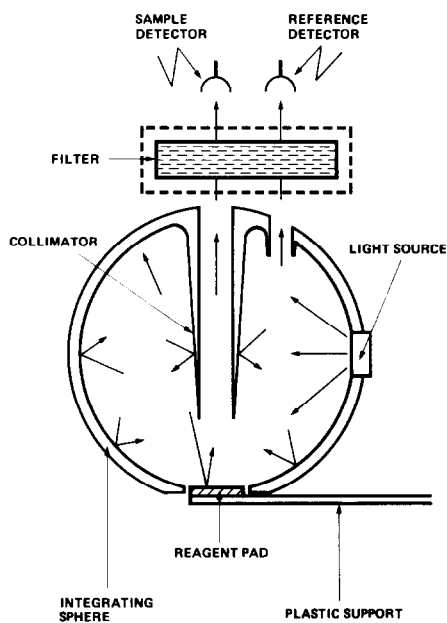


Fig. 8. Optical arrangement for measuring the colour of a reacted solid-phase reagent by reflectance photometry with an integrating sphere.

internal reflections from the inside surface of the sphere and so irradiates the surface of the reagent pad uniformly from all directions. Thus, by measuring the intensity of the reflected light normal to the pad, the same effect is achieved as would have been obtained had the pad been irradiated unidirectionally and the light reflected in all directions been collected equally.

Figure 8 also shows some other features of a reflectance photometer, such as a filter for wavelength selection, and a split-beam arrangement to compensate for variations in the intensity of the light source. Such features are incorporated in the reflectance analyser described by Zipp¹² and are essential for obtaining the type of results discussed in the next section.

Applications and performance

Visual and single-analyte systems. Although urine test papers were manufactured and sold as diagnostic devices nearly a century ago,²¹ their widespread use and acceptance as analytical tools in rapid testing was not really established until the second half of this century. Without doubt, the emergence of solid-phase reagents as routine analytical tools some 25 years ago was catalysed by industry, which developed both new and improved solid-phase systems and made them widely available. Today, solid-phase reagents of the fibre-impregnated type are used for the measurement of a wide assortment of analytes, such as enzymes, metabolites and proteins in urine, whole blood, serum and plasma.

The first of the new fibre-impregnated systems, Clinistix[®] reagent strip and Tes-Tape[®], were developed by the American companies, Ames Division, Miles Laboratories Inc., and Eli Lilly respectively,

and both made their appearance in 1956 as tools for the measurement of urinary glucose. Free *et al.*⁶ described the former system, which used the enzymes glucose oxidase and peroxidase, together with the chromogenic substrate *o*-tolidine, and a basic red background dye, and Comer⁷ reported on the latter system, which used the same enzymes and substrate, but with a basic yellow background dye (Tartrazine, C.I. 19140).

Further tests making possible the measurement of a wider range of urinary analytes, such as protein,²² pH,²³ blood,²⁴ ketones,²⁵ bilirubin,²⁶ leucocytes²⁷ and specific gravity²⁸ have been developed in more recent years and are now widely used in routine urine analysis.^{8,29}

The possibility that solid-phase reagents could also be used for the measurement of blood analytes was explored by Kohn³⁰ who showed that the fibre-impregnated Clinistix[®] reagent strips, hitherto used for the determination of urinary glucose, could also be used for measuring the same analyte in whole blood. Thereafter, fibre-impregnated systems appeared which were tailor-made for the measurement of whole blood glucose. The first of these (Dextrostix[®] reagent strip) again used the enzymes glucose oxidase and peroxidase, together with a combination of three ancillary chromogenic indicators to generate the required visual discrimination between various glucose concentrations. The performance of this system and its utility for the measurement of blood glucose in the management of diabetes was reported by Marks and Dawson.³¹

To improve visual discrimination, more recent solid-phase reagents for blood glucose incorporate more sophisticated colour scales. Thus Kerner *et al.*³² reported the use of Visidex[®], which uses two different reaction systems to generate two separate colour scales that measure glucose in the concentration ranges 1.1–10 mM and 11.1–44.4 mM respectively. The lower concentration scale utilizes the glucose oxidase-peroxidase system, together with the chromogenic substrate tetramethylbenzidine, and the higher concentration scale uses a Trinder-type reaction³³ involving the substrates 4-aminoantipyrine and 3,5-dichloro-2-hydroxybenzene sulphonic acid. This reagent system has recently been improved and is marketed under the trade name Visidex II[®].

All the solid-phase reagents mentioned above were initially designed to be read visually, and various reflectance meters were subsequently developed along the lines and principles already discussed. One of the first of these instruments was developed for use with Dextrostix[®] reagent strips and the improvement in results achieved by use of this instrument-reagent system was reported by Jarrett *et al.*³⁴ As the usefulness of solid-phase reagents for measuring blood glucose became more widely accepted, development of cheaper and smaller yet more sophisticated meters progressed at a rapid pace. Webb *et al.* have reported on the performance of a number of these new

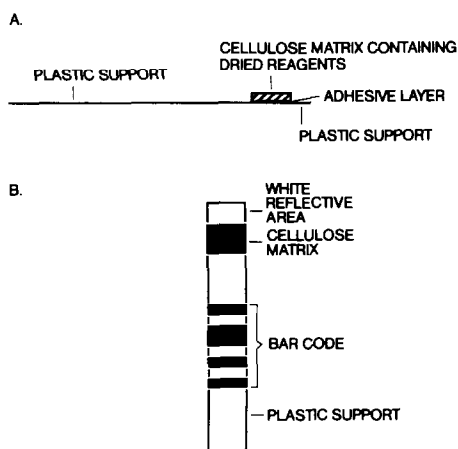


Fig. 9. Schematic of Seralyzer[®] solid-phase reagent strip. A; Side view. B; Front view.

systems.³⁵ With continuing advances in micro-electronics, it is expected that newer generations of meters will be even cheaper and smaller, yet more powerful in their overall capability and performance.

Multi-analyte systems: the Seralyzer[®] reflectance photometer. More recently, the sphere of application of the fibre-impregnated systems has been extended to a wider range of analytes, including serum enzymes and metabolites, by the development of integrated systems comprising the solid-phase reagents together with appropriate dedicated instrumentation. The first such system (the Ames Seralyzer[®] reflectance photometer)¹³ was reported by Turk and Zipp in 1978 for the measurement of urea and later described in greater detail by Greyson¹¹ and Zipp.¹² This system now consists of a reflectance photometer along with solid-phase reagents for 10 traditional blood analyses [glucose, urea, uric acid, cholesterol, bilirubin, creatinine, whole blood haemoglobin, triglycerides, lactic dehydrogenase (LDH), creatine phosphokinase (CPK)], is suitable for use in any location, and does not need a skilled operator. It is also applicable as a "stat" or back-up instrument in clinical laboratories.

The solid-phase reagent strip used with the Seralyzer[®] system is shown in Fig. 9. A cellulose matrix is impregnated with the reagents, dried, and then bonded with a special adhesive layer onto a plastic support. A white reflective area is incorporated under the cellulose matrix to improve the reflectance efficiency. A barcode, printed directly onto the plastic support, is read by the instrument upon insertion of the strip, to avoid improper matching of reagent strip and module (see Fig. 11, below).

The Seralyzer[®] optical system is shown in Fig. 10. The light source is a xenon flash-tube which produces a high-intensity flash covering the entire spectral region. In particular, it provides high intensity at 340 nm, so enzyme reactions can be monitored in the ultraviolet region. The reagent strip sits on a constant-temperature table which is pushed into the integrating sphere after application of the sample.

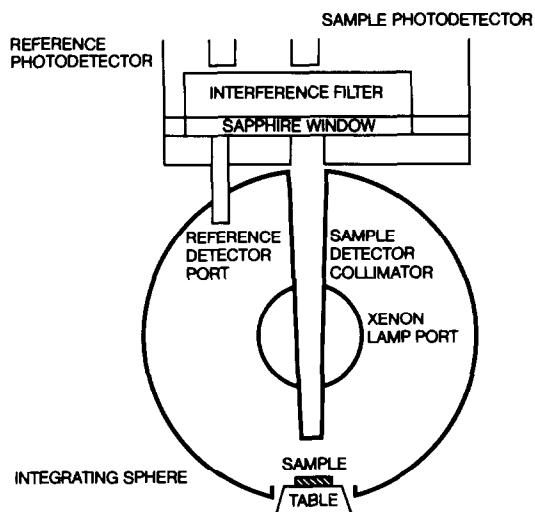


Fig. 10. Cross-section of Seralyzer[®] optical system.

The environment of the sphere is also thermostatically controlled. The collimator collects the reflected light and directs it through an interference filter to a solid-state detector.

The reference detector port directs light scattered from the sphere wall to the reference detector. The reflectance is the ratio of the sample and reference detector signals. This arrangement eliminates error due to changes in light intensity from flash to flash. The sapphire window which covers the sample and reference detector ports minimizes evaporation from the pad surface. The interference filter is contained in a plug-in module which is specific for each serum test and also contains a read-only memory chip which programs the processing of the reflectance signals. The module and its relationship to the optical system are shown in Fig. 11. The microprocessor also runs a series of checks and balances on system performance so that any malfunctions or operator error can be easily detected. For example, on completion of the calibration, the microprocessor checks the calibration slope to determine its validity. If the slope is

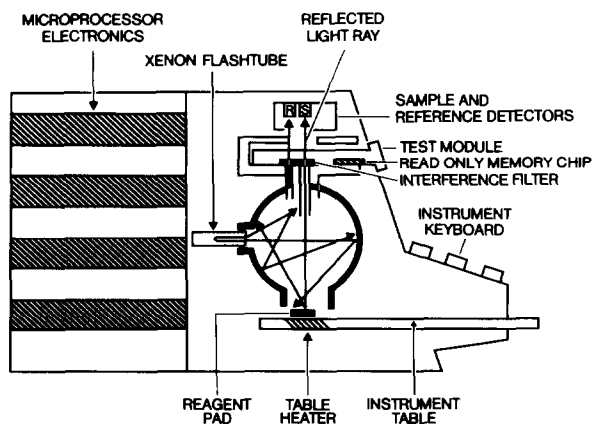


Fig. 11. Cross-section of Seralyzer[®] reflector photometer showing relationship between test module and optical system.

Table 1. Precision of the Seralyzer[®] system and that of various comparative methods, for analysis of control sera

Analyte	Seralyzer			Comparative method				
	Mean†	CV, %		Method	Mean†	CV, %		
		Within runs	Between runs			Within runs	Between runs	
Glucose	66.3	4.4	6.3	Beckmann	66.1	3.1	6.5	
	214.9	2.5	1.7		195.9	1.0	2.4	
	301.9	3.1	2.4		310.2	1.0	0.9	
Blood urea nitrogen	12.1	3.8	4.1	SMA 6/60	12.2	1.8	2.5	
	31.5	3.9	5.0		30.4	0.7	1.5	
	54.3	4.4	3.6		54.3	0.8	1.0	
Uric acid	4.3	4.8	4.9	SMA 12/60	4.4	2.7	1.9	
	8.4	4.4	4.5		8.8	5.7	3.3	
	Total	0.64	4.3		8.3	SMA 12/60	0.69	11.9
bilirubin	1.4	2.9	3.0	AA II	1.5	5.9	3.8	
	4.3	2.5	4.9		4.3	2.2	2.8	
	Cholesterol	286	2.9		3.4	300	1.3	3.6
LDH	399	3.4	3.1	Rotochem	426	1.7	1.5	
	949 IU/l.	4.6	6.3		1140 IU/l.	2.4	4.3	
	251 IU/l.	4.6	4.1		226 IU/l.	2.4	3.4	
Creatinine	404 IU/l.	3.4	4.1	SMAC—Jaffé reaction	381 IU/l.	2.3	4.1	
	1.07	6.0	5.4		1.16	4.5	7.7	
	2.63	3.0	4.7		2.32	3.1	5.2	
CPK§	5.95	2.2	4.8	SMAC—Jaffé reaction	5.35	2.3	2.2	
	51 IU/l.	3.4	5.8		Rotochem	1140 IU/l.	2.4	4.3
	180 IU/l.	4.8	4.6			226 IU/l.	2.4	3.4
399 IU/l.	1.9	3.7	381 IU/l.	2.3		4.1		
Haemoglobin‡	8.2 g/dl	NA	3.4	SMAC—Jaffé reaction	1.16	4.5	7.7	
	14.6 g/dl	NA	2.8		2.32	3.1	5.2	
	21.3 g/dl	NA	3.2		5.35	2.3	2.2	
Triglycerides§	64	3.2	4.6	SMAC—Jaffé reaction	1.16	4.5	7.7	
	202	1.6	1.4		2.32	3.1	5.2	
	359	1.8	2.4		5.35	2.3	2.2	

*Data extracted from Karmen and Lent³⁷ unless otherwise noted.

†All values in mg/100 ml unless otherwise noted.

§Independent study at South Bend Indiana Medical Foundation.

‡Khabbaza and Lott, *Clin. Chem.*, 1983, **29**, 1212.

outside specification, an error message is given. Such conditions as improper dilution or operating procedures or loss of reagent activity or thermal control will be recognized by the instrument and an appropriate error message flashed on the instrument display.

A complete description of the system has been published elsewhere¹².

The performance of this system has been reported by Thomas *et al.*³⁶ and by Karmen and Lent³⁷. Tables 1 and 2 summarize typical results and show that the precision is comparable to that of traditional laboratory methods and of other automated analysers.

Recent reports³⁸ indicate that the enzyme assays ALT (alanine aminotransferase) and AST (aspar-

Table 2. Correlation between Seralyzer[®] solid-phase chemistry system and various comparative methods

Analyte	Number of samples	Correlation coefficient	Slope	Intercept†	Comparative method
Glucose	134	0.99	1.01	12.8	Rotochem: hexokinase
	106	0.98	1.00	12.5	Beckman Glucose Analyzer
Blood urea nitrogen	185	0.97	0.95	1.28	SMA 6/60
Uric acid	184	0.94	0.96	0.25	SMA 12/60
Total bilirubin	194	0.94	0.98	0.02	SMA 12/60
Cholesterol	120	0.97	0.97	6.9	AA II
	114	0.97	1.01	3.0	SMAC
Lactate					
Dehydrogenase (LDH)	196	0.95	0.96	5.6	Rotochem
Creatinine	154	0.99	1.06	0.004	SMAC—Jaffé Reaction
CPK§	87	0.99	0.97	5.54	Dupont ACA
Haemoglobin‡	96	0.99	1.03	0.31	Coulter-S
Triglycerides§	214	0.98	0.95	11.3	Centrifichem

*All data extracted from Karmen and Lent³⁷ unless otherwise noted.

†All values in mg/100 ml except for LDH and CPK which are in IU/l. and haemoglobin which is in g/100 ml.

§Independent study at South Bend Indiana Medical Foundation.

‡Khabbaza and Lott, *Clin. Chem.*, 1983, **29**, 1212.

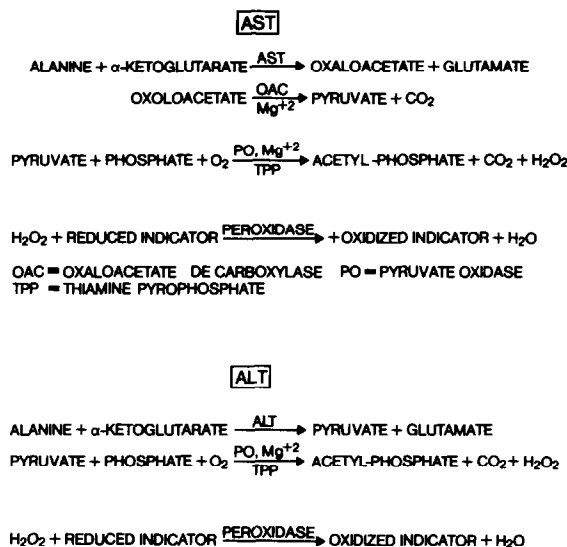


Fig. 12. Chemistries for Seralyzer[®] ALT and AST determinations.

tate aminotransferase) will soon be added to the Seralyzer[®] system. The chemistry for these two assay systems is shown in Fig. 12. In contrast to the more conventional ultraviolet assays for these enzymes, colorimetric assays are used, based on the oxidation of an indicator system by peroxide. The choice of colorimetry stems from the sensitivity limitations encountered in use of substrates such as NADH, which have comparatively low molar absorptivities; these limitations are most apparent when reflectance spectroscopy is used, since it is inherently less sensitive than absorbance measurement. Table 3 shows some precision and correlation data for the ALT and AST assays.

Immunochemistry. Greenquist *et al.*³⁹ have reported on the performance of a number of solid-phase immunoassays utilizing the substrate-labelled fluorescent immunoassay technique first described by Burd *et al.*⁴⁰ Tyhach *et al.*⁴¹ have described attempts to incorporate immunoreagents for the measurement of theophylline and phenytoin, into solid-phase matrices. This early work has been significantly extended, resulting in the recent report of Greenquist *et al.*⁴² of a colorimetric solid-phase theophylline assay utilizing the ARIS[™] immunoassay system. This system, first described by Morris *et al.*⁴³ is based on a competitive protein-binding reaction in which the analyte competes with an analyte-conjugate for a limited number of antibody binding-sites that are specific for the analyte. The conjugate consists of the analyte covalently linked to the prosthetic group of glucose oxidase, flavine adenine dinucleotide (FAD). In the absence of analyte, the conjugate binds to the antibody and is unavailable for further reaction. In the presence of analyte, a corresponding proportion of the conjugate remains in solution because of the competitive binding, and FAD liberated from it reacts with apoglucose oxidase to reconstitute glucose

Table 3. Precision and correlation results for Seralyzer[®] AST and ALT assay systems applied to control sera*

Assay	Mean, IU/l.	CV, %	
		Within runs	Between runs
AST	35.0	2.2	2.7
	50.5	2.1	1.9
	82.1	2.1	1.5
	201.8	2.3	2.0
	300.3	2.2	2.3
ALT	26	2.9	3.3
	51	2.0	1.3
	121	1.8	1.2
	231	1.7	2.3
	330	2.6	3.7
		AST	ALT
Slope		1.0	0.96
Intercept, IU/l.		0.3	1.9
Correlation coefficient		0.99	0.99
S _{y,x} , IU/l.		0.3	6.4
N		95	81

S_{y,x} = Standard error of the estimate.

N = Number of samples.

*From Zipp *et al.*³⁸

oxidase, which is then detected through a coupled reaction with peroxidase to yield a coloured product. The theophylline assay described by Greenquist *et al.*⁴² utilizes monoclonal theophylline antibody to ensure reproducibility of the immunochemical response.

Figure 13 shows the correlation between HPLC and Seralyzer[®] results for solid-phase theophylline assay. The precision is reported to be about 5%, and thus comparable to that of the "wet methods".^{39,42}

Litman *et al.*⁴⁴ have recently described a solid-phase immunoassay system for morphine detection, based on the enzyme-channelling technique. A glucose oxidase and horseradish peroxidase enzyme-pair is used to generate an insoluble coloured reaction product of an immunospecific reaction on the test strip surface. The authors claim a potential sensitivity of 5–10 µg/l., with a 20-min assay time. Although this assay time is significantly longer than that, for exam-

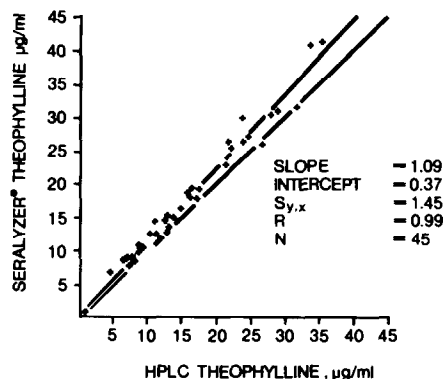


Fig. 13. Correlation of Seralyzer[®] theophylline assay with the HPLC reference method for 45 clinical specimens. The regression line statistics are given in the figure. The dashed line represents $y = x$.

Table 4. Solid-phase reagent systems available for whole-blood glucose determination

Name	Measurement method	Manufacturer
Dexstrostix [®] /Glucometer [®]	Instrumental	Ames Div. Miles Labs
Dexstrostix [®] /Dextrometer	Instrumental	Ames Div. Miles Labs.
Glucoscan [™]	Instrumental	Lifescan
Stat-Tek [™]	Instrumental	Boehringer-Mannheim Corp
Reflocheck [™]	Instrumental	Boehringer-Mannheim Corp
Chemstrip bG [®] /Accu-check	Instrumental	Boehringer-Mannheim Corp
Chemstrip bG [®]	Visual	Boehringer-Mannheim Corp
Glucopat [™]	Visual	Kyoto Daiichi
Visidex [™]	Visual	Ames Div. Miles Labs.
Visidex II [™]	Visual	Ames Div. Miles Labs.

ple, for the Seralyzer[®] theophylline assay (80 sec), these enzyme-channelled systems should be useful when assay time is not critical and high sensitivity is demanded.

Solid-phase immunoassays, like their blood-chemistry counterparts, offer significant advantages over comparable wet systems. No reagent mixing or manipulation is required and assay times are short. These reagents are extremely stable (1 year at room temperature for Seralyzer[®] theophylline), require low sample volumes and only a minimum of skill. Hence therapeutic-drug assay testing may soon be as common and easy to perform as simple glucose determinations.

Whole blood. The multi-analyte solid-phase systems just described are used primarily with serum as the sample. Those systems designed for whole-blood samples are generally for glucose assays in diabetes cases. Some of these systems have already been briefly mentioned and a summary of those most commonly used is given in Table 4.

Although glucose is so far the only analyte conveniently measured in whole blood, a multi-analyte fibre-impregnated solid-phase system utilizing whole blood as the sample has recently been announced.⁴⁵ This system—the Reflotron/Refloquant[™]—uses a complex reagent strip on which plasma is separated from the red cell components by a glass filter. For several analytes the system is claimed to give good correlation with other methods, but extensive field evaluation has not yet taken place.

MULTI-LAYER FILM SYSTEMS

The multi-layer film systems first appeared in the literature five years ago, when Curme *et al.*¹⁰ described a multi-layer film reagent for measurement of glucose in serum. At the same time, Spayd *et al.*⁴⁶ reported similar types of reagent for measurement of urea, amylase, bilirubin and triglycerides. Multi-layer films are used in the same way as impregnated fibre systems, and differ from them only in construction. As the name implies, the multi-layer film systems are laminated, with the different reagents deposited in flat strata. The support material is protein-based instead of polysaccharide-based, and in most systems so far is gelatin.

The simplest configuration of a multi-layer film system is shown schematically in Fig. 14. The sample is applied to the exposed surface of the top layer (which typically is made of titanium dioxide, in order to facilitate reflectance measurements from the reverse surface), spreads quickly through its porous structure, then penetrates into the reactant layer, hydrating its contents and initiating the analytical reaction. Additional layers can be added to keep incompatible reagents separate or to provide a sequence of reactions. Such a multi-layer film is depicted in Fig. 15, which shows schematically the system described by Spayd *et al.*⁴⁶ for measurement of urea in serum, by the reaction sequence (Fig. 16) in which urea is hydrolysed by urease in a strongly buffered solution at pH 8.0, and the free ammonia formed then reacts with a protonated merocyanine dye, and changes its colour to that of the unprotonated dye.

The urease and buffer are located in a gelatin-based reagent layer (Fig. 15) which is immediately below the

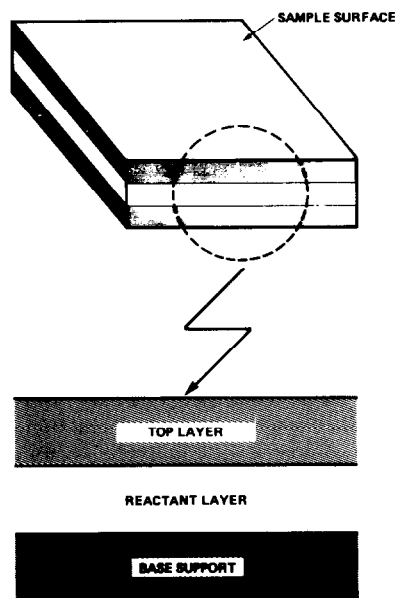


Fig. 14. Schematic representation of a simple multi-layer film solid-phase reagent. The sample is applied on the top layer and then diffuses into the reactant layer, where reaction takes place. Typically, the colour is measured by reflectance photometry from the reverse side and through the base support.

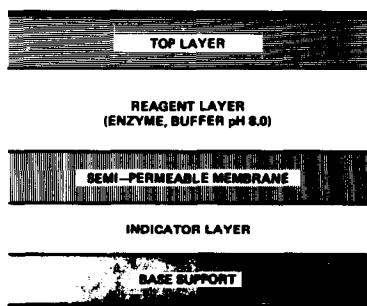


Fig. 15. Reactions involved in the measurement of urea with the multi-layer film solid-phase reagent described by Spayd *et al.*⁴⁶

porous titanium dioxide layer, and separated from the indicator layer by a semi-permeable cellulose acetate/butyrate membrane. The ammonia produced diffuses through the semi-permeable membrane, which forms a barrier to other basic species such as the hydroxide ion, and finally into the last layer which comprises an indicator in a film of cellulose acetate. This type of multi-layer element is used in the Eastman Kodak Ektachem[®] system.

The multi-layer film approach has been further developed by Ohkubu *et al.*,⁴⁷ who described a multi-layer element that could be used with whole blood. The device differs from those reported by Spayd *et al.*⁴⁶ and Curme *et al.*¹⁰ mainly in the make-up of the surface layers. The top layer consists of a finely woven thin web, which may be cellulose-based. This layer is reported to act as a coarse filter which removes platelets and red cells as the sample diffuses through it. The sample then diffuses through a semi-permeable "blocking layer" which allows the glucose, now free from blood proteins, to gain access to the reactant layer, which is next to the base support material.

Use of the system for determination of whole-blood urea nitrogen is shown in Fig. 17. This reagent system is used in the Fuji Drichem[®] 1000 analyser, which is not yet commercially available, and is packaged as slides which are operationally equivalent to the Kodak elements described above.

Measurement

With multi-layer film systems, the reflectance measurement is made on the surface opposite to that of sample application. The optics of such a system are rather more complicated than those for the simpler systems already described. Williams and Clapper⁴⁸ constructed a mathematical model of the system,

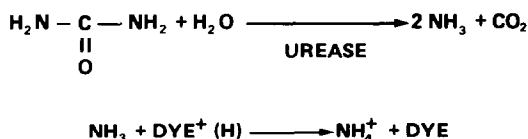


Fig. 16. Schematic representation of the multi-layer film solid-phase reagent described by Spayd *et al.*⁴⁶ for the measurement of urea.

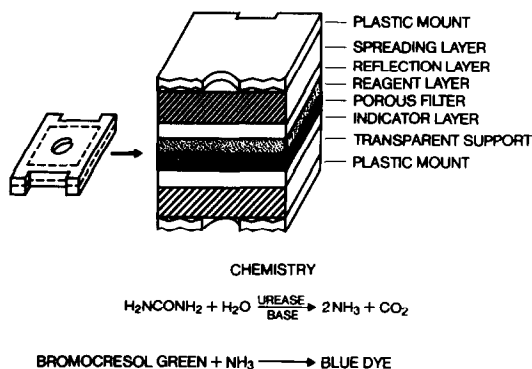


Fig. 17. Schematic representation of the Fuji Drichem[®] slide for determination of whole-blood urea nitrogen. Note the "filter" layer for screening out interfering substances.

which leads to the equation

$$D_R = \log R_0 / (R_{\text{test}} - R_f) \quad (3)$$

where D_R is the so-called reflective density of the film element, which is analogous to absorbance in transmission spectroscopy, R_0 is the intensity of light reflected from a standard reflector (*e.g.*, a barium sulphate surface) in the beam, R_f is a correction factor for non-linear effects and R_{test} is the intensity for the test film. Like R in the Kubelka–Munk equation, D_R is a non-linear function of concentration. However, D_R can be transformed into a function D_T which is linearly related to concentration by the equation:

$$C = B (D_T - D_B) = B \left\{ \text{tr} \left[\log \left(\frac{R_0}{R_{\text{test}} - R_f} \right) \right] - D_B \right\} \quad (4)$$

where C is the analyte concentration, tr represents the Williams–Clapper transformation, B is proportional to reciprocal absorptivity and D_B is the reflective density for the blank (*i.e.*, $C = 0$). The effect of the transformation is shown in Fig. 18. B , D_B and D_T are

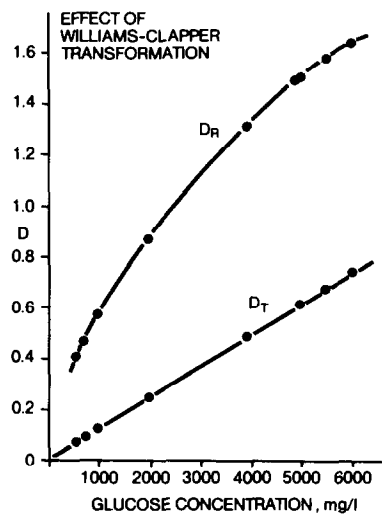


Fig. 18. Reflective density (D) as a function of glucose concentration for a multi-layer film system. D_R represents the reflective density before and D_T that after application of the Williams–Clapper transformation;⁴³ From Curme *et al.*¹⁰

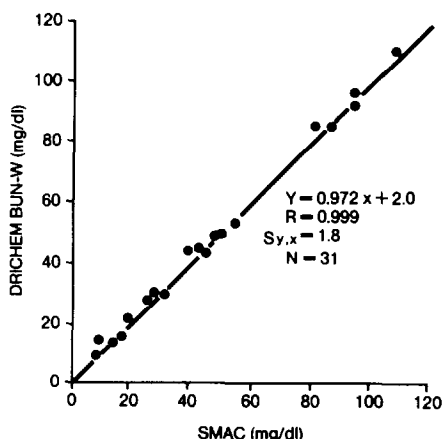


Fig. 19. Correlation of Fuji Drichem[®] whole-blood blood-urea nitrogen assay with SMAC comparative method. Regression statistics are given in the figure.

determined with a three-point calibration technique. The need for three points is in contrast to the case for diffuse reflectance systems (Kubelka–Munk theory) such as an impregnated fibre, for which linear response regions can be developed and a two-point calibration is all that is required¹². The Williams and Clapper approach is valid for both the Kodak and Fuji systems since both rely on basically the same technology.

Performance

The laboratory performance of Ektachem[®] clinical chemistry slides has been extensively reported by Warren *et al.*⁴⁹ and Dappen *et al.*⁵⁰ Recent reports have given the assay performance for a number of new enzyme determinations.^{51,52} In general the performance is excellent, with coefficients of variation < 2% for some assays and good correlation with reference methods. It is interesting that multi-layer films appear to be less susceptible than impregnated-fibre systems to serum interferences, presumably because the various polymeric spreading and filtering layers serve as effective screens for some interfering substances.

The performance of the Fuji Drichem[®] whole-blood glucose assay has been reported and appears excellent.⁴⁷ Figure 19 shows correlation data for the Fuji whole-blood urea nitrogen assay, which indicate performance comparable to that of impregnated-fibre or other multi-layer film systems for serum analysis, but as, like the Reflotron/Refloquant[™] system, the Fuji Drichem 1000 analyser is not yet commercially available, final judgement must await extensive field testing.

COMPARISON OF MULTI-LAYER FILM AND IMPREGNATED-FIBRE SYSTEMS

Besides the obvious structural differences between impregnated-fibre and multi-layer film systems, the differences in the nature of the matrices for these two systems can lead to significant differences in their

physical properties. Thus, Haeckel *et al.*⁵⁴ have reported that there is an apparent dependence of the response of multi-layer film systems on the viscosity of the sample. In contrast, the fibre-impregnated systems appear to be less affected by added protein and sample viscosity, as was shown by Greyson.¹¹ A further difference arises from the nature of the polymer used as the matrix for the reactant layers. Most fibre-impregnated systems are cellulose-based, whereas multi-layer film systems tend to be gelatin-based. Gelatin cannot be dried as thoroughly as cellulose and the residual water content in the gelatin-based reactant layers is about 10%. Consequently, the reagents are not totally dry and any protein components are prone to solution denaturation. This property of the multi-layer films perhaps accounts for the need to store them under refrigeration for maximum stability. This higher water content may also lead to decreased stability for multi-layer film systems because of diffusion effects as well as denaturation effects. The typical “coupler–developer” type of indicator systems used in these films can react prematurely if the components come into too close contact before the main reaction has begun. This inactivation would appear as a decrease in reactivity with time for these film systems.

OTHER FILM SYSTEMS

In addition to the multi-layer film devices described above, other analytical films comprising only a single film layer have been reported and used successfully for some years. The best-known of these is the Chemstrip bG[®] product of Boehringer Mannheim GmbH, which is used for the visual determination of whole blood glucose.⁵⁵ The system consists of a polymer film containing the appropriate reagents, coated onto a plastic support. The blood sample can be removed after a given reaction time and there is good colour stability after sample removal.⁵⁶ The Ames Division of Miles Laboratories has recently introduced Visidex[®] II reagent strips for the determination of whole-blood glucose. This product is a combination of impregnated-fibre and film technology. A hardened gelatin film is coated over the cellulose matrix to impart “wipe-off” properties to the system as a whole. The blood sample can be removed by either wiping or blotting, and the system is directly competitive with the Chemstrip bG[®] product.

Film systems have also been designed for electrolyte determination. The most common are the Ektachem[®] slide systems for Na⁺, K⁺, CO₂ and Ca²⁺, which utilize potentiometric measurement in combination with ion-selective membranes.¹⁰ Charlton *et al.*⁵⁷ have reported a solid-phase analytical element for the determination of serum potassium. It consists of a poly(vinyl chloride) film which contains a plasticizer and valinomycin. The serum sample is diluted with an anionic dye solution and

pipetted onto the film surface. The dye molecules then partition into the film layer in order to maintain electrical neutrality. After removal of excess of dye, the resulting colour can be measured by standard absorption or reflectance techniques.

CONCLUSIONS

It is clear that the technology of solid-phase analytical systems has moved extremely rapidly in the last five years. From the initial application to blood analysis, the applications have been extended to drug detection and electrolyte determination. It might reasonably be expected that even broader applications will emerge in the years ahead as the potential of these systems for convenient testing is more fully realized, and ultimately clinical chemistry may be brought to the bedside.

REFERENCES

1. G. Oliver, *Lancet*, 1883, **I**, 858.
2. L. Wershub, *Urology from Antiquity to the Twentieth Century*, p. 139, Green, St. Louis, 1970.
3. B. G. Babington, *Guys Hosp. Repts.*, 1837, **2**, 534.
4. M. Maumené, *Compt. Rend.*, 1850, **30**, 314.
5. G. Oliver, *On Bedside Urine-Testing*, 2nd Ed., Lewis, London, 1884.
6. A. H. Free, E. C. Adams, M. L. Kercher, H. M. Free and M. H. Cook, *Abstracts International Congress of Clinical Chemistry*, New York, 1956, p. 236.
7. J. P. Comer, *Anal. Chem.*, 1956, **28**, 1748.
8. D. Kutter, *Rapid Clinical Diagnostic Test*, Urban and Schwarzenberg, Munich, 1977.
9. M. L. Reeves, S. E. Forhan, J. S. Skyler and C. M. Peterson, *Diabetes Care*, 1981, **4**, 404.
10. H. Curme, R. L. Columbus, G. M. Dappen, T. W. Eder, W. D. Fellows, J. Figueras, C. P. Glover, C. A. Goffe, D. E. Hill, W. H. Lawton, E. J. Muka, J. E. Pinney, R. N. Rand, K. J. Sanford and T. W. Wu, *Clin. Chem.*, 1978, **24**, 1335.
11. J. Greyson, *J. Autom. Chem.*, 1981, **3**, 66.
12. A. Zipp, *ibid.*, 1981, **3**, 71.
13. R. Turk and A. Zipp, *Clin. Chem.*, 1981, **24**, 1018.
14. R. R. Reynolds, D. L. Arendsen, D. F. Guanci and R. F. Wickman, *J. Org. Chem.*, 1970, **35**, 3940.
15. D. Jung, H. Biggs, J. Erikson and P. N. Ledyard, *Clin. Chem.*, 1975, **21**, 1136.
16. I. E. Modrovich, *U.S. Patent*, No. 4277562, 1981.
17. W. E. Hornby, M. D. Lilly and E. M. Crook, *Biochem. J.*, 1966, **98**, 420.
18. B. Kubelka and F. Munk, *Z. Tech. Phys.*, 1931, **12**, 593.
19. D. Kealey, *Talanta*, 1972, **19**, 1563.
20. *Idem*, *ibid.*, 1974, **21**, 475.
21. Wilson and Son, *Brit. Med. J.*, 1886, **1**, 160.
22. A. H. Free and O. E. Fancher, *Abstracts Am. Chem. Soc. Div. Biol. Chem. Meeting San Francisco*, 1958, 140.
23. H. M. Free, G. F. Collins and A. H. Free, *Clin. Chem.*, 1960, **6**, 352.
24. J. M. Yoder, E. C. Adams and A. H. Free, *Am. J. Med. Tech.*, 1965, **31**, 285.
25. A. J. Bradley, *Practitioner*, 1969, **202**, 558.
26. G. M. Bradley, *Med. Clin. N. Am.*, 1971, **55**, 1457.
27. E. Vormittag, P. Bruhl, T. Fuchs, R. Kattermann, D. Hannak, A. Peracino, H. Oldenzel, A. P. M. Van Oudheusden, F. Zekert, K. Bergstroem, R. Jagenburg, J. P. Colombo, E. Peheim and D. Kutter, *Dtsch. Med. Wochenschr.*, 1979, **104**, 1236.
28. A. E. Burkhardt, K. H. Johnston, C. E. Waszak, C. E. Jackson and S. R. Shafer, *Clin. Chem.*, 1984, in the press.
29. J. P. Colombo and R. Richterich, *Die einfache Urinuntersuchung*, Huber, Bern, 1977.
30. J. Kohn, *Lancet*, 1957, **II**, 119.
31. V. Marks and A. Dawson, *Brit. Med. J.*, 1965, **I**, 293.
32. W. Kerner, C. Rosak, I. Navascues, P. H. Althoff, A. Torres, E. Jungmann, H. Zier, K. Schoeffling, E. F. Pfeiffer, W. Plischke and G. Storz, *Dtsch. Med. Wochenschr.*, 1982, **107**, 1346.
33. D. Barham and P. Trinder, *Analyst*, 1972, **97**, 142.
34. R. J. Jarrett, H. Keen and C. Hardwick, *Diabetes*, 1970, **19**, 724.
35. D. J. Webb, J. M. Lovesay, A. Ellis and A. H. Knight, *Brit. Med. J.*, 1980, **280**, 362.
36. L. T. Thomas, W. Plischke and G. Storz, *Ann. Clin. Biochem.*, 1982, **19**, 214.
37. A. Karmen and R. Lent, *J. Clin. Lab. Autom.*, 1982, **2**, 284.
38. A. Zipp, B. Walter, W. Wilcox, R. Co, L. Berreth and G. Makowski, XII World Congress of Anatomic and Clinical Pathology, 10-14 October 1983, Tokyo, Japan.
39. A. C. Greenquist, B. Walter and T. M. Li, *Clin. Chem.*, 1981, **27**, 1614.
40. J. F. Burd, R. J. Carrico, M. C. Fetter, R. T. Buckler, R. D. Johnson, R. C. Boguslaski and J. E. Christner, *Anal. Biochem.*, 1977, **77**, 56.
41. R. H. Tyhach, P. A. Rupchock, J. H. Pendergrass, A. C. Skjold, P. J. Smith, R. D. Johnson, J. P. Albarella and J. A. Profitit, *Clin. Chem.*, 1981, **27**, 1499.
42. A. C. Greenquist, P. Pupchock, R. Tyhach and A. Zipp, *ibid.*, 1984, in the press.
43. D. L. Morris, P. B. Ellis, R. J. Carrico, F. M. Yeager, H. R. Schroeder, J. P. Albarella, R. C. Boguslaski, W. E. Hornby and D. Rawson, *Anal. Chem.*, 1981, **53**, 658.
44. D. S. Litman, R. H. Lee, H. J. Jeong, H. K. Tom, S. N. Stiso, N. C. Sizto and E. Fullman, *Clin. Chem.*, 1983, **29**, 1598.
45. W. Gruber, *ibid.*, 1983, **29**, 1212.
46. R. W. Spayd, B. Bruschi, B. A. Burdick, G. M. Dappen, J. N. Elkenberry, T. W. Esders, J. Figueras, C. T. Goodhue, D. D. LaRossa, R. W. Nelson, R. N. Rand and T.-W. Wu, *ibid.*, 1978, **24**, 1343.
47. A. Ohkubo, S. Kamei, M. Yamauka, F. Arai, M. Kitasima and A. Kondo, *ibid.*, 1981, **27**, 1287.
48. F. C. Williams and F. R. Clapper, *J. Opt. Soc. Am.*, 1953, **43**, 595.
49. K. Warren, N. P. Kubasik, B. B. Brody, H. E. Sine and J. P. D'Souza, *Clin. Chem.*, 1980, **26**, 133.
50. G. M. Dappen, P. E. Cumbo, C. T. Goodhue, S. Y. Lynn, C. C. Morganson, B. F. Nellis, D. M. Sablauskas, J. R. Schaeffer, R. M. Schubert, R. E. Snoke, G. M. Underwood, C. D. Warburton and T.-W. Wu, *ibid.*, 1982, **28**, 1159.
51. J. B. Findlay, R. Searle, A. Thunberg and R. Schubert, *ibid.*, 1983, **29**, 1211.
52. K. Slickers, R. Coolen, W. Erickson, G. Green, G. Norton, J. Novros, D. Powers and C. Stanton, *ibid.*, 1983, **29**, 1211.
53. Fujii Film Corp., private communication.
54. R. Haeckel, O. Sonntag and K. Petry, *J. Autom. Chem.*, 1982, **1**, 273.
55. D. O. Frey, L. Thomas, W. Tritschler and W. Bablock, *München. Med. Wochenschr.*, 1979, **121**, 1545.
56. R. S. Worth, K. Harrison, J. Anderson, D. G. Johnston and K. G. M. M. Alberti, *Diabetes Care*, 1981, **4**, 407.
57. S. C. Charlton, R. L. Fleming and A. Zipp, *Clin. Chem.*, 1982, **28**, 1857.

FLOW-INJECTION ANALYSIS IN CLINICAL CHEMISTRY

CLIFFORD RILEY

Post-graduate Division of Biomedical Engineering, University of Sussex, Falmer, Brighton, England

BERNARD F. ROCKS and ROY A. SHERWOOD

Biochemistry Department, Royal Sussex County Hospital, Brighton, England

(Received 20 December 1983. Accepted 1 June 1984)

Summary—Flow-injection is the most recent addition to the techniques used in automatic analysis. In the simplest form, the sample is injected as a discrete slug into a stream of reagent flowing in a narrow-bore tube. Various sampling valves have been used in order to achieve full mechanization, but are not ideal for clinical analyses since they are wasteful of sample. An economical alternative has been developed which is based on the precise aspiration of sample by a probe. Applications of FIA and this modification in particular to clinical chemistry are discussed.

In technological societies innovations commonly appear in response to an obvious need. Thus it was that in 1957 Skeggs¹ introduced his bubble-segmented continuous-flow automatic analyser. This was developed in response to the intolerable pressure, caused by exponentially rising workloads, experienced by clinical laboratories all over the Western world. Soon after this the discrete analyser appeared. This was a simple concept which, despite some daunting problems in small-scale chemical engineering, was successfully developed. Subsequently, in 1969, in answer to the specific need for simultaneous analyses of cell fractions, the centrifugal analyser was developed² and this was soon modified for clinical work. The latest system to appear, flow-injection analysis, was developed simultaneously by Stewart and his co-workers in the United States³ and by Růžicka and Hansen in Denmark.⁴ From very simple beginnings the technique has advanced rapidly. This progress has been reviewed recently by Stewart⁵ and Růžicka.⁶

Unlike the techniques mentioned earlier FIA has not found immediate favour with clinical chemists though it has been received enthusiastically by analytical chemists working in industry.

This indifference on the part of clinical chemists, which ignores the enormous potential of the method, arises because of the changed expectations of this group of workers. They have become used to purchasing dedicated machines with methodology fully developed and comprehensive data-handling systems included. So far no manufacturer has offered such a package based on FIA.

The preparation of a brief review such as this, aimed at two widely disparate sections of the scientific community, is difficult. The clinical chemist would possibly prefer a simple account of practical possibilities. The analytical chemist would undoubtedly prefer something more sophisticated.

In classical bubble-segmented continuous-flow systems the samples are divided and separated by gas (usually air) bubbles; at any one time several specimens are moving one behind the other through the same pipeline and the flow is to some extent turbulent.

In flow-injection the approach is quite different. The sample is injected as a discrete slug or bolus into a stream of reagent moving under conditions of laminar flow in a narrow-bore tube. No air is admitted, so the slug, flowing along the so-called reactor tube, remains intact throughout and is normally cleared completely from the system before another sample is introduced. When fast reactions are used, throughput can be high, and indeed Tijssen⁷ has reported that under special conditions analytical rates of 900/hr can be achieved. Slower reactions must be dealt with differently; use is made of the lack of elasticity in the system and the sample is arrested to allow the reaction to proceed, but this of course limits the throughput. A limiting factor on throughput is the preparation of samples, if preliminary treatment is necessary.

The behaviour of the slug of sample as it travels through the reactor tubing is of cardinal importance. Since it generally moves under conditions of laminar flow it may be thought of as having the classical parabolic velocity profile, progressively adopting a bullet-shaped form with a hollow tail as shown in Fig. 1. If this were the only phenomenon involved the slug would rapidly disperse into the reagent stream, but the behaviour of the slug is greatly modified by radial diffusion. The tip of the slug continually diffuses outwards, entering slower moving streams of reagent and thus being retarded; conversely, the tail of the slug diffuses inwards into more rapidly moving streams and is thus accelerated. Apart from limiting the longitudinal dispersion of the slug this must also

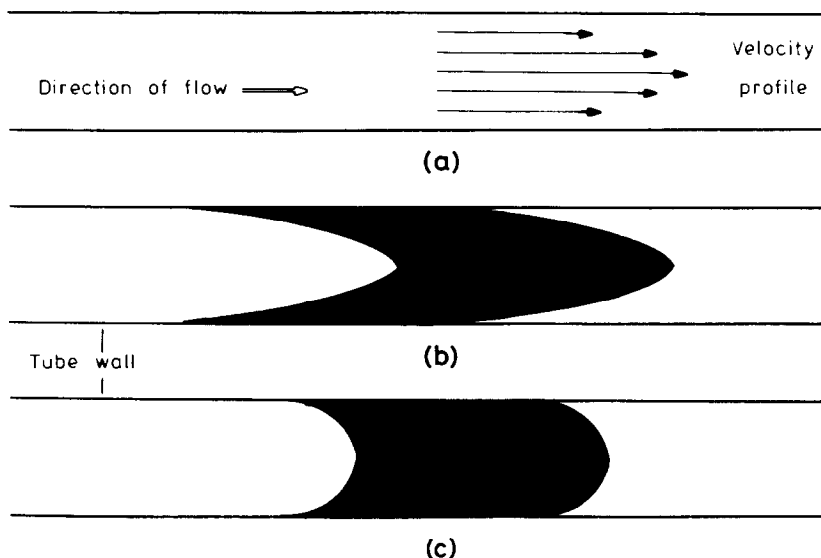


Fig. 1. Convection/diffusion-induced dispersion of a sample slug in a flowing stream. (a) Laminar-flow velocity profile; (b) dispersion of sample slug caused by convection; (c) sample zone modified by molecular diffusion. (The drawing is not to scale; a $10\text{-}\mu\text{l}$ sample injected into a 0.5-mm bore tube would occupy a length of about 5 cm before dispersion.)

modify its shape. Vanderslice *et al.*⁸ show some estimates of shapes at various stages of development of the moving bolus. Most figures of this kind, including our own Fig. 1, are misleading in that they suggest that the slug is short and compact; in fact, a $25\text{-}\mu\text{l}$ slug injected into a 0.5-mm bore tube is immediately over 125 mm long and it may well be ten times as long by the time it leaves the system. The radial diffusion ensures efficient mixing with the reagent: the moving slug is continuously exposed to fresh boundary layer and since this is composed of undiluted reagent the latter diffuses rapidly into the slug until equilibrium is approached. These processes are rapid because of the small diameters employed. Linear diffusion has very little effect and in fact the slug can be held stationary for prolonged periods without significant sample-spreading occurring.

The classical work on the behaviour of liquids flowing in narrow-bore pipes is that of Taylor^{9,10} and much of the theoretical discussion used in FIA is based on his work.

The dispersion, or spread, of the slug as it travels along the tube has been defined by Růžička and Hansen¹¹ as the ratio of the concentrations of the sample before and after the dispersive process has taken place. In practice this is easily determined by injecting a slug of sample and measuring the peak height obtained with the read-out device being used. The sample is then pumped continuously, without carrier solution, and the peak height at steady state measured. The dispersion coefficient $D = H^0/H$ where H^0 is the peak height at steady state and H is the peak height given by the injected slug. This is a

practical working formula, but it describes only the maximum concentration of sample in the slug.

Several factors govern the degree of dispersion.

(1) Size of sample. Large samples give smaller dispersions than small samples; the ultimate limitation is the steady state, when the sample is infinitely large and the dispersion is 1.0.

(2) Length of reactor tubing. All other things being equal, the dispersion is proportional to the square root of the length of the reactor tubing. In practice, most work is done with tube lengths of $<1\text{ m}$.

(3) Tube diameter. The larger the diameter, the greater the dispersion, which increases approximately with the square of the radius. The upper limit for the internal diameter is perhaps 1.0 mm ; with larger diameters it becomes difficult to maintain the integrity of the slug. The lower limit is determined by practical difficulties (high pumping pressures, tendency to blockage and so on). Tijssen⁷ has worked with tubing of only $20\text{ }\mu\text{m}$ bore. In practice, tubes of internal diameter $0.5\text{--}0.8\text{ mm}$ are most commonly used.

(4) Flow velocity. The effects of this appear to have been insufficiently investigated. In our work with 0.5-mm tubing, the dispersion increased with flow-rate up to about 0.5 ml/min ; above that rate, the dispersion decreased.

There are two other factors which should be mentioned. First, if the reactor tubing is tightly coiled the dispersion is decreased. It has been suggested that this

is a centrifugal effect, but this is not a wholly satisfying explanation. Secondly, the effect of turbulent flow can be exploited. Although most work has been done under conditions of laminar flow, Tijssen⁷ and Reijn *et al.*¹² argue that the flat velocity profile obtained under conditions of turbulent flow should give reduced dispersion, and, working with reactor tubes packed with glass beads, have shown this to be true.

The behaviour of the travelling slug is obviously very complex; all the possible variables in the system interact with each other and are probably modified in their turn by the chemical reaction itself.¹³

Important contributions to the theory have been made by Reijn *et al.*¹⁴ and Vanderslice *et al.*⁸ These largely mathematical treatments do not, however, explain some of the phenomena encountered when working with the technique. For example, with intensely coloured samples it is occasionally possible to see the main body of the slug preceded by a fine thread; again, insoluble matter appears to travel more rapidly than material in solution, perhaps under the influence of factors suggested by Repetti and Leonard¹⁵ for red blood cells; then, for what it is worth, there is some anecdotal evidence that a substance can pass forward through the slug without reacting with it. There seems to be a good case for making photographic studies.

Notwithstanding the uncertainty of these variables, the behaviour of the slug remains remarkably reproducible provided that the system, once set up, is undisturbed.

In general, limited dispersion ($D = 1-3$) is used where high local concentrations of sample are required, for example, with measurements by ion-selective electrodes, whereas medium dispersions ($D = 3-10$) are needed for many of the reactions used in clinical chemical analyses; however, several important clinical determinations require systems designed to produce large dispersion ($D > 10$).

FIA is remarkably versatile, and there are a number of modes in which it may be used which are particularly useful in clinical chemistry. The most fundamentally useful manoeuvre is "stopped-flow". Because the system is inelastic, when the pump is

stopped the slug is immobilized and its integrity remains preserved for long periods. This is exploited in two ways. First, when a period of incubation is required, the slug can be arrested in the reaction tubing for as long as necessary; this, of course, limits the throughput. However, with careful choice of reactor tubing it is possible to arrest two or three samples, separated by uncontaminated carrier liquid. Secondly, when kinetic studies are required, the slug can be arrested in the flow-through cell of the detector and the changes recorded during the appropriate time. "Stopped-flow" operation requires precise timing.

A disadvantage of the basic system is that reagent consumption can be large (though still small in comparison with other methods). This problem has been overcome by Bergamin *et al.*¹⁶ with a technique which they have named "merging zones." In this technique, the carrier liquid is distilled water, and two streams of it are pumped. A bolus of sample and a larger one of reagent are injected simultaneously into the respective streams, which join downstream at a T-junction in such a fashion that the reagent slug overlaps the sample. Once set up, this arrangement is remarkably stable, but it does give larger dispersions than the conventional approach. Other techniques reported which are applicable to clinical work include solvent extraction,¹⁷⁻²¹ gas transfer²² and dialysis.²³ In the case of dialysis, it should be possible to operate in a counter-current mode, with greater efficiency than obtainable with the unidirectional flowing streams required by gas-segmented systems. However, in our hands, attempts to operate with counter-flowing streams have been disappointing.

FIA IN PRACTICE

Simple flow-injection systems can be easily assembled from items of equipment usually available in clinical laboratories. A basic system requires no more than a means of propelling the stream of reagent, a coil of reactor tubing, some means of injecting the sample, and a detector with a flow-through cell together with some means of recording the output (Fig. 2).

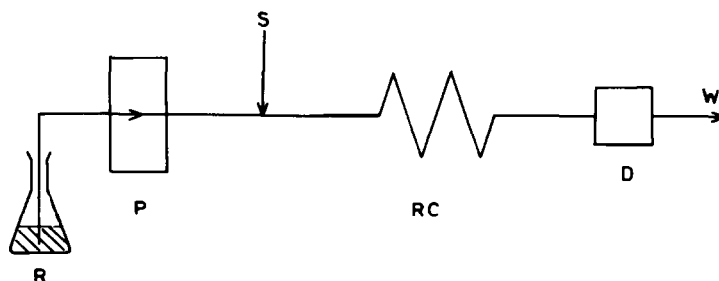


Fig. 2. Configuration of a simple FIA system based on reaction between the sample (S) and the reagent (R). A pump (P) propels the stream through the reaction coil (RC), through the detector (D) and to waste (W). These symbols are also used in Figs. 3-6.

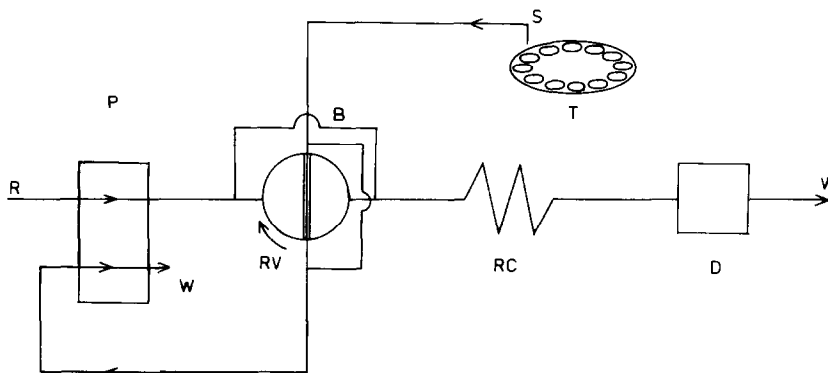


Fig. 3. Automated FIA. The sample is drawn from the sample turntable (T) into the bore of a motorized rotary valve (RV). The valve then rotates through 90° and "injects" the sample into the reagent stream. The valve is fitted with by-pass tubes (B) to allow flow of reagent when the valve is in the "fill" position.

The stream of reagent may be propelled in a variety of ways. In their original apparatus Stewart *et al.*³ used a pressurized reservoir. This has the merit of simplicity and also provides non-pulsatory flow. Mechanical constant-flow pumps intended for HPLC have been used by some workers, for example Rocks *et al.*²⁴ Whilst these arrangements work well, a separate pump or reservoir is needed for each flowing stream. Peristaltic pumps do not have this disadvantage, but the severe pulsation produced by some models is undesirable. Least pulsation is given by pumps which have closely spaced rollers, together with platens which are designed so that the rollers lift off them gradually. Some workers have used pulse-suppressing devices^{25,26} but Vanderslice *et al.*⁸ suggest that a slight degree of pulsation may be beneficial.

The sample can be injected in a variety of ways, of which the simplest is direct injection by means of a syringe, either through a septum^{4,24} or a "flap" valve.^{27,28} Injection septa of the type designed for HPLC are very suitable. However, the majority of workers have favoured some form of valve capable of transferring an accurately measured volume of sample into the flowing stream of reagent. The basic principle is indicated in Fig. 3; the hole in the key of a stopcock provides the volumetric measure, and when filled with sample is rotated into the flowing stream. A by-pass is necessary to avoid interrupting the flow of reagent and this must be arranged so that it provides greater resistance to flow than the hole in the key does. A considerable number of variations on this theme have been described. Perhaps the first to be used was the slide valve activated by compressed air, devised by Stewart *et al.*³ A similar principle, in a manually operated valve, was employed by Bergamin *et al.*¹⁶ Most workers have preferred to use rotary valves; custom-built valves of this type have been described by Růžička and Hansen,²⁸ Mindegaard²⁹ and Anderson.³⁰ Riley *et al.*³¹ have described a motorized version. Rocks *et al.*^{32,33} have successfully used commercially available manually operated laboratory stopcocks, whilst a number of

workers, for example Pardue and Fields,³⁴ Fogg *et al.*³⁵ and Strohl and Curran³⁶ have used loop sampling-valves of the type manufactured for use in HPLC.

In the case of the custom-built rotary valves, the hole in the rotor, or alternatively a separate loop of tubing, provides the volumetric measurement of the sample. Sample is either injected into the sample valve by means of a syringe, or is passed through it by means of the peristaltic pump. If the latter approach is coupled with a motorized valve, a completely automatic system is possible³¹ (Fig. 3). Rotary valves have disadvantages; the sliding surfaces are very vulnerable to wear, a problem which particularly affects the custom-built valves already mentioned, in which the stators are generally made of acrylic polymer and the rotors of PTFE. It is in any case a formidable task to machine a really flat surface on a PTFE rotor.

The introduction of injection valves greatly complicated what is fundamentally an extremely simple system. As an alternative, Růžička and Hansen³⁷ have proposed a technique they have named "hydrodynamic injection". The essential features are shown in Fig. 4. Two pumps are required, one pumping reagent and the other pumping sample. In practice, the reagent pump, P1, is stopped and the sample pump, P2, is started to draw sample through the side-arms and fill length *L* of the reactor line. The sample pump is then stopped and the reagent pump started, and the segment of sample held in length *L* moves on into the reactor coil.

Harrow and Janata³⁸ have proposed a modification of this arrangement in which the sample introduction pump is replaced by a hand-operated vacuum pump. Solenoid pinch-valves are used to stop and start the carrier flow and to allow sample to be drawn into the reactor tube. By control of the operating time of the valves, different sample volumes may be drawn into the system. This method of injection is claimed to be more precise than either the use of injection valves or "hydrodynamic injection".

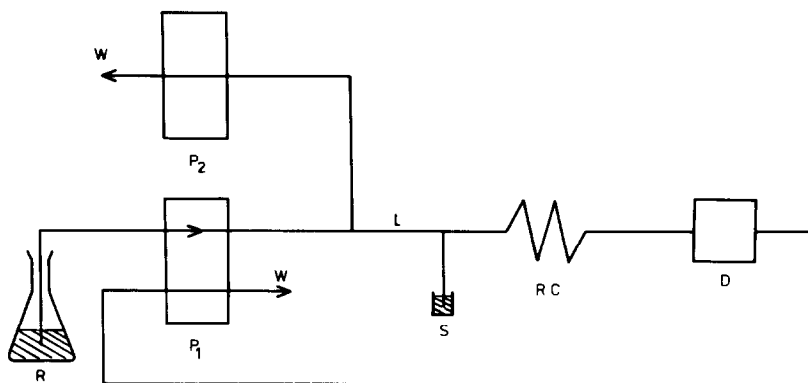


Fig. 4. Sample introduction by "hydrodynamic injection". A second pump (P₂) is used to draw sample into the section of the reaction tube marked L.

This approach, and the previously mentioned systems employing rotary valves, all suffer from a common fault; not only must the entry and exit tubes be filled with sample over and above the volume required to fill the sample-measuring space, but also an excess of sample must be used to flush out the residue of the previous specimen. This is unacceptable in clinical chemistry, where the size of the specimen is always limited, and sample volumes of less than 50 μl are the aim. This requirement of strict economy of sample prompted Riley *et al.*³⁹ to adopt a different approach, which they call "Controlled Dispersion Flow Analysis". The simplest form of this is indicated in Fig. 5. In this system the peristaltic pump is driven by a stepping motor controlled by a microcomputer. The sample probe normally rests in a reagent container, R, so reagent is pumped through the system between samples. When a sample is offered to the machine, the pump is stopped and the probe is transferred to the sample container, S. The pump then rotates through a precise predetermined angle, and again stops. The probe is returned to the reagent container and the pump restarted. The sample slug travels up the probe, through the pump and onwards into the reactor tubing and finally the detector, no part of the sample being wasted. When this system was first constructed it was expected that the journey through the pump would increase the dispersion of the sample slug. This was tested by measuring the dispersion in the new system and

comparing it with the dispersion obtained with the pump sited downstream of the detector. Surprisingly, appreciably *less* dispersion occurred when the slug travelled through the pump.

Economy in use of expensive reagents is of only slightly less importance than economy of sample and therefore the system was subsequently modified to make use of the merging zone technique. As indicated in Fig. 6, the dipping mechanism is fitted with two probes and two pump tubes, one each for sample and reagent respectively. The probes normally rest in a container of distilled water, C. When a sample is offered to the machine the sample probe is transferred to the sample container. As in the previous example, the pump makes a precise angular movement, but this time both a sample and a reagent slug are created and subsequently pumped onwards to meet at a T-junction downstream from the pump. Typically, sample volumes of 10–20 μl and reagent volumes of 50–150 μl are used. It is, of course, possible to use two or more reagent probes, merging the sample and reagents either simultaneously or one after the other at predetermined time intervals.⁴⁰

The earliest model of this machine was operated effectively under the control of a simple cam timer, but this was soon replaced by a microcomputer. The enormous benefits conferred by computer control make the additional expense and complications worthwhile. In particular, computer control, by feeding exactly the correct number of pulses to the

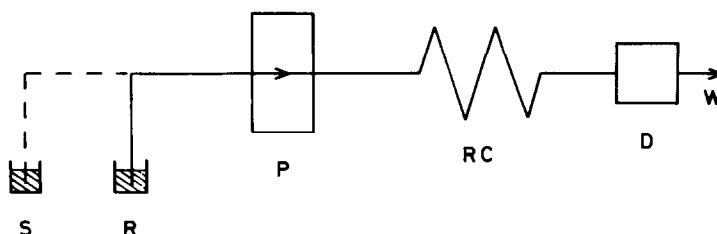


Fig. 5. Basic "controlled dispersion" analyser. The broken line represents probe movements.

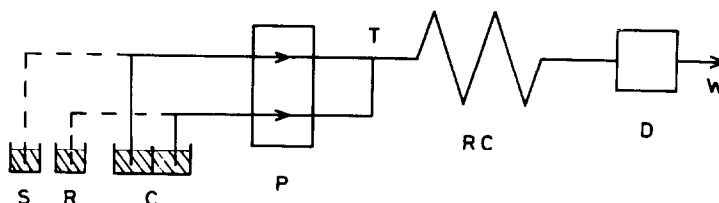


Fig. 6. Merging-zone "controlled dispersion" analyser. Sample and reagent are simultaneously aspirated into independent carrier streams (C) of demineralized water. Sample and reagent zones merge at a T-connector (T).

stepping motor, ensures maximum sampling precision. The same pulse-counting technique is invaluable in stopped-flow work, ensuring that successive samples are treated identically; a peak-identification programme enables the correct conditions for stopped-flow to be set and can verify at any time that these conditions are being maintained. In addition to its control functions, the computer can deal effectively with the data output of the system.

Detectors

In clinical chemistry, most requirements for sample detectors are met by relatively simple flow-through photometers. An important requirement is that the volume of the flow-through cuvette is small; the type of cell used in HPLC detectors, typically $8 \mu\text{l}$ in volume, meets most needs. Refractive-index effects can be a problem with the small diameter light-paths used in these cells, especially if zones of liquid with widely different temperatures pass through the cell. These effects can be minimized by maintaining the reactor coil and cuvette at the same temperature. Anderson³⁰ suggests that refractive-index effects are unimportant at absorbances >0.05 , but with the wide range of values commonly encountered in clinical chemistry, measurements at such low levels sometimes have to be made.

FIA has been used with considerable success in clinical chemistry as a means of feeding samples to various other detectors (see Table 1).

The output signal generated by the detector is conveniently displayed with a fast-response chart recorder. Because the response curves do not reach the steady-state plateau and the sample zone passes through the detector relatively quickly, the recorder trace has the form of sharp peaks (Fig. 7).

The most convenient method of calibration is to use peak heights, *i.e.*, the peak maximum is taken as the reference point from which the read-out is obtained. However, any other point on the output signal may also be used, provided all readings are taken at exactly the same place. In practice this is accomplished by taking the readings at a fixed time after sample injection. By monitoring several points on the trailing edge of the peak a multipoint calibration curve may be constructed from a single injection of sample.⁶

From the clinical chemist's point of view a useful feature of all FIA systems is that start-up and close-down times are very short. Except for detector warm-up time the FIA system is ready for operation almost as soon as the pump has been started. When the work is finished, reagent and sample are easily and quickly removed from the conduits by pumping distilled water for a short period. Hence FIA should be very suitable for stand-by or emergency applications.

Sample viscosity

When we first began to investigate FIA we became concerned that the variation in viscosity between different biological specimens would make the technique unsuitable for clinical use. In fact FIA has been used to estimate viscosity.⁴¹⁻⁴³ The greater the viscosity of the solutions the less they disperse into the carrier solution. However, in most of the assays that we have investigated, viscosity effects have not been a problem, although when manual injection techniques are used,^{24,44} the rate of injection can be

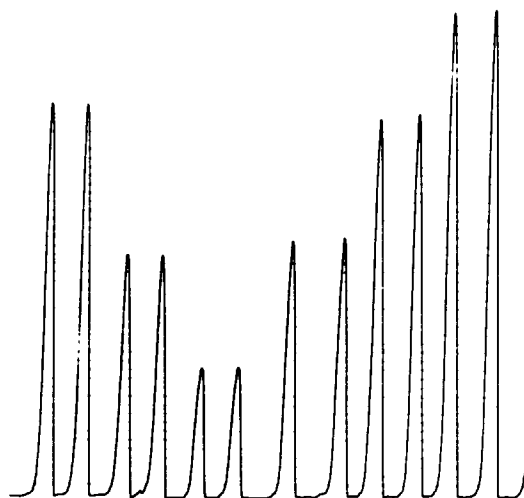


Fig. 7. Recorder trace showing the characteristic shape of FIA peaks. The peaks resulted from the duplicate injection of (right to left) 0.5, 1.0, 1.5 and 2.0mM magnesium standards followed by two serum samples, into an atomic-absorption spectrophotometer by means of a simple FIA system.³³

influenced by the viscosity of the sample, and in this case aqueous standards should be modified to have a viscosity near to that of the sample to be assayed.

There are no literature reports of viscosity problems encountered when using injection valves. In systems designed to give high dispersion, the sample soon becomes diluted with the carrier and any difference in viscosity between samples and/or standards soon becomes negligible. In low-dispersion systems, differences in viscosity may have a greater effect and aqueous and serum-based standards may not always yield comparable results.

APPLICATION OF FIA TO CLINICAL ANALYSES

Many of the most frequently requested assays in clinical chemistry laboratories can be done by FIA. Table 1 is a compilation of determinations performed on clinical specimens. Although interesting, some of the determinations involve esoteric methods and would be most unsuitable for routine hospital use. Additionally, many of these report results only for standard solutions, or a very small number of samples taken from patients (*i.e.*, real specimens), and consequently should be regarded as feasibility studies. As a crude guide to clinical usefulness, we have indicated (by an asterisk) those determinations in which more than ten different clinical specimens were assayed. We have not included systems incorporating mixing chambers or columns of immobilized enzymes, since in such systems laminar flow does not predominate. Lists of clinically relevant species determined by FIA, but not all in clinical specimens, have been previously compiled by Růžička and Hansen²⁸ and by Rocks and Riley.⁴⁵

In the simplest system the sample is injected into a stream of demineralized water (or buffer) and swept by the moving stream to a detector such as an atomic-absorption spectrophotometer or an ion-selective electrode. The sample size and flow conditions can be adjusted to produce the desired degree of sample dispersion (dilution) before it reaches the detector. For example, zinc in serum is easily determined by using this approach.⁴⁴ The analytical peak is available 8 sec after injection of the 50- μ l sample.

Rapid colorimetric tests can be performed by injecting the sample into a flowing stream of reagent and recording the colour intensity of the resulting products. Assays in this category include albumin, total protein, calcium and chloride. These determinations require FIA systems capable of producing high dispersion ($D > 40$). High dispersion is best achieved by using the smallest sample size consistent with adequate sensitivity. Increasing the dispersion by increasing the reactor tube length and/or radius produces peak broadening and reduces the sampling rate. However, the injection of very small volumes imposes great demands on valve design and in prac-

tice most FIA valves have a minimum delivery volume of between 5 and 10 μ l. This means that most simple FIA systems work most efficiently, in terms of sampling rate and reagent consumption, when $D < 10$. A common way round this problem is to dilute the specimen appropriately before injecting it into a conventional FIA system (see Table 1 for examples). Another approach, useful for small molecules, is to use dialysis as a means of rejecting the bulk of the sample.⁴⁶ Converging streams can also be used to perform an "on-line" dilution of the sample before it encounters the reagent stream.^{47,48}

Mindegaard²⁹ has described a novel method of dealing with concentrated samples, based on the merging-zone principle. The sample and reagent zones are put slightly out of synchronization so that when the streams converge the reagent zone overlaps the relatively dilute tail of the sample zone. By this method albumin was measured, without predilution, at a rate of 300 samples per hour.

The sample introduction system described by Riley *et al.*³⁹ has an advantage over the valve system, in that the sample volume is more easily varied and volumes of less than 1 μ l can be easily and reproducibly sampled when required.⁴⁰ Moreover, in this system the pump tubes may be chosen to give different flow-rates, the reagent usually being pumped at a higher flow-rate than the sample. Hence the sample zone will be further diluted by the reagent zone when they meet at the mixing point. Thus this system offers a greater range of dispersion coefficients than is possible with conventional FIA.

As mentioned earlier, slower reactions are best monitored by stopping the slug of sample in the cuvette and observing the initial rate of reaction. Additionally, the amount of expensive reagents needed can be minimized by the use of merging zones. Rocks *et al.*⁴⁰ have used the combined techniques of stopped flow and synchronous merging zones to determine plasma triglycerides. The procedure used 7.5 μ l of plasma and 115 μ l of reagent. The sample-reagent zone was held in the cuvette for 30 sec while the rate of reaction was recorded.

For analyses involving incubations longer than about 1 min, gas-segmented flow analysis will generally yield a higher sample throughput than an equivalent FIA system. However, if a scarce or expensive reagent is involved, and sampling rate is not a priority, then FIA may still be appropriate for use with reactions requiring relatively long incubation periods. Lim *et al.*⁴⁹ have used FIA to minimize reagent consumption in a homogeneous energy-transfer fluorimmunoassay for albumin. Sample and reagent (both 36 μ l) were brought together by the merging-zones technique and the carrier flow was stopped for a 6-min period before measurement. (We are not, of course, advocating this approach to routine plasma albumin estimation; the method shows that relatively long incubations are possible when necessary.)

Table 1. Assay of clinical specimens by FIA

Determination	(ref.)	Type of FIA	Carrier/reagent	Detection mode
<i>Albumin</i> in serum	(47)*	C	Bromocresol Green	Photometric
	(29)	M	Bromocresol Green	Photometric
in prediluted serum	(40)*	C (CDA)	Bromocresol Green	Photometric
	(31)*	F	Bromocresol Purple	Photometric
	(45)	F	Bromocresol Green	Photometric
	(56)	F	8-Anilino-1-naphthalene sulphonic acid	Fluorimetric
	(49)	M	8-Anilino-1-naphthalene sulphonic acid	Fluorimetric
	(49)	M/S	Fluorescein-labelled albumin and Rhodamine-labelled antibody	Fluorimetric (Homogenous energy-transfer immunoassay)
<i>Alcohol</i> in prediluted whole blood and serum	(57)	C/S	Alcohol dehydrogenase + NAD ⁺	Photometric (NADH)
<i>Ammonia</i> in whole blood and plasma	(50)*	C/G	Donor alkali; recipient pH indicator dye	Photometric
	(58)	C/G	Donor: Tris buffer, pH 7.5; recipient: Tris buffer, pH 8.5	Potentiometric (ammonia selective electrode)
<i>Calcium</i> in serum	(59)	F	EDTA	Flame atomic absorption
	(33)*	F	Acidic lanthanum chloride	Flame atomic absorption
	(60)	F	Tris buffer	Potentiometric (calcium ion-selective electrode)
in prediluted serum	(60)	C	<i>o</i> -Cresolphthalein complexone	Photometric
<i>Chloride</i> in serum	(46)	C/D	Mercuric thiocyanate/ferric nitrate	Photometric
	(39)*	M (CDA)	Mercuric thiocyanate/ferric nitrate	Photometric
<i>Total CO₂</i> in plasma	(22)*	G	Donor acid; recipient pH indicator dye	Photometric
<i>Copper</i> in serum	(44)*	F	Water	Flame atomic absorption
in deproteinated serum	(61)*	R	Ferric thiosulphate	Photometric
<i>Glucose</i> in serum	(62)*	R	Glucose oxidase	Amperometric
	(23)	F;C;D	Glucose dehydrogenase/NAD ⁺	Photometric (NADH)
in prediluted serum	(63)	M	Glucose dehydrogenase/NAD ⁺	Photometric (NADH)
	(64)	C	Glucose oxidase/potassium ferricyanide/luminol	Luminometric
<i>γ-Glutamyl transferase</i> in serum	(39)*	M/S (CDA)	L-γ-Glutamyl-3-carboxy-4-nitroanilide	Photometric
<i>pH</i> of serum	(60)	F	Tris buffer	Potentiometric (pH electrode)
<i>Immunoglobulin, IgG</i> , in prediluted serum	(65)	C	HRP labelled antibody/LDADCF, H ₂ O ₂	Fluorimetric
<i>Iron</i> in deproteinated serum	(32)*	F	Deminerlized water	Flame atomic absorption
<i>Lithium</i> in serum	(24)*	F	Deminerlized water	Flame atomic absorption
<i>Lactate dehydrogenase</i> in serum	(31)*	F/S	Pyruvate/NADH	Photometric
	(66)	F	Tris buffer	Amperometric (pyruvate sensor)
<i>Lactate</i> in deproteinated serum	(67,68)*	F	Lactate dehydrogenase NADH	Fluorimetric
<i>α₂-Macroglobulin</i> in prediluted serum	(31)*	F	<i>N</i> -α-Benzoyl-L-arginine ethyl ester	Photometric
<i>Magnesium</i> in serum	(59)	F	EDTA	Flame atomic absorption
	(33)	F	EDTA	Flame atomic absorption
<i>Phosphate</i> (inorganic) in serum	(46)	C	Molybdate/ascorbic acid	Photometric (molybdenum blue)
<i>Potassium</i> in serum	(69)	F	Tris buffer	Potentiometric (ion-selective electrode)
	(70)	F	Deminerlized water	Flame atomic absorption

Table 1—continued

Determination	(ref.)	Type of FIA	Carrier/reagent	Detection mode
Protein (total) in serum	(48)*	C	Biuret reagent	Photometric
Sodium in serum	(70)	F	Demineralized water	Flame atomic absorption
Sulphate (inorganic) in urine	(71)*	D	Donor water; recipient acidic barium chloride solution	Turbidimetric
Theophylline in serum, therapeutic levels	(40)	M/S(CDA)	EMIT reagent	Photometric
Triglycerides in serum	(40)*	M/S(CDA)	"Triglyceride enzymatic" reagent	Photometric
Urea in serum	(72)	C	Urease/hypochlorite/phenol	Photometric (Indophenol blue)
in prediluted serum	(73)	F	Urease	Potentiometric (pH electrode used to measure pH change)
Zinc in serum	(44)*	F	Demineralized water	Flame atomic absorption
in deproteinated serum	(74)	F	Demineralized water	Flame atomic absorption
in prediluted serum, simultaneously determined with sodium, potassium, calcium, magnesium, lithium, iron and copper	(75)	F	Demineralized water	Plasma atomic emission

Type of system:

F = single-line FIA

M = merging zones

G = gas transfer

D = dialysis

C = confluent streams

S = stopped flow

R = recirculating reagent

CDA = controlled-dispersion
analysis

NADH = Nicotinamide adenine dinucleotide

EDTA = Disodium ethylenediaminetetra-acetate

HRP = Horseradish peroxidase

LDADCF = leuco-diacetyldichlorofluorescein

EMIT = enzyme multiplied immunoassay technique

*Publications in which more than 10 assays are reported.

Gas-transfer methods have some applications in clinical chemistry. For example, an FIA method for total CO₂ in plasma has been described.²² The sample is injected into a stream of dilute sulphuric acid and some of the liberated carbon dioxide diffuses through a gas-permeable membrane into a stream containing a pH-sensitive indicator dye. The change in colour of the recipient stream is monitored by a photometer. Ammonia in whole blood and plasma has also been determined by a similar technique in which the sample is first made alkaline to convert all ammonium ions into ammonia.⁵⁰

In addition to its applications listed in Table 1, FIA has been used in other ways which could be of value to the clinical chemist. For example, it has been used as an interface between a high-pressure liquid chromatograph and an atomic-absorption instrument.⁵¹ Abdullahi *et al.*⁵² have used FIA as a convenient method of studying drug-protein binding interactions and a generalized method has been proposed⁵³ for assessing the extent of interference by

a foreign species in a given chemical reaction. Inherent in the FIA dispersion equations⁸ is the ability to determine reaction-rate constants⁵⁴ and molecular-diffusion coefficients.^{43,55} Gerhardt and Adams⁵⁵ have used these equations for rapid determination of diffusion coefficients of biogenic amine compounds related to neurotransmitters.

CONCLUSIONS

Despite their success in industrial applications and their very obvious potential, flow-injection instruments have so far found little use in routine hospital laboratories. There are two reasons for this. First, the sampling valves universally used in currently available machines are wasteful of sample. Secondly these machines do not possess the sophisticated sample-handling and data-processing facilities that clinical chemists have come to expect, and the pressures on the clinical chemist are such that he no longer has the time to adapt unsuitable machines. The potential is

there—rapid production of results, low reagent consumption and mechanical simplicity; what is needed is the commercial manufacture of machines specifically designed for clinical work.

REFERENCES

1. L. T. Skeggs, *Am. J. Clin. Path.*, 1957, **28**, 311.
2. N. G. Anderson, *Anal. Biochem.*, 1969, **31**, 272.
3. K. K. Stewart, G. R. Beecher and P. E. Hare, *ibid.*, 1976, **70**, 167.
4. J. Růžicka and E. H. Hansen, *Anal. Chim. Acta*, 1975, **78**, 145.
5. K. K. Stewart, *Anal. Chem.*, 1983, **55**, 931A.
6. J. Růžicka, *ibid.*, 1983, **55**, 1040A.
7. R. Tijssen, *Anal. Chim. Acta*, 1980, **114**, 71.
8. J. T. Vanderslice, K. K. Stewart, A. G. Rosenfeld and D. J. Higgs, *Talanta*, 1981, **28**, 11.
9. G. Taylor, *Proc. Roy. Soc. A*, 1953, **219**, 186.
10. *Idem*, *ibid.*, 1954, **223**, 446.
11. J. Růžicka and E. H. Hansen, *Anal. Chim. Acta*, 1978, **99**, 37.
12. J. M. Reijn, W. E. Van der Linden and H. Poppe, *ibid.*, 1981, **123**, 229.
13. C. C. Paintner and H. A. Mottola, *ibid.*, 1983, **154**, 1.
14. J. M. Reijn, W. E. Van der Linden and H. Poppe, *ibid.*, 1981, **126**, 1.
15. R. V. Repetti and E. F. Leonard, *Trans. Am. Soc. Artif. Int. Organs*, 1964, **10**, 311.
16. H. Bergamin, E. Zagatto, F. Krug and B. F. Reis, *Anal. Chim. Acta*, 1978, **101**, 17.
17. B. Karlberg and S. Thelander, *ibid.*, 1978, **98**, 1.
18. B. Karlberg, A. Johansson and S. Thelander, *ibid.*, 1979, **104**, 21.
19. H. F. Bergamin, J. X. Mcdeiras, B. F. Reis and A. G. Zagatto, *ibid.*, 1978, **101**, 9.
20. J. Kawase, A. Nakae and M. Yamanaka, *Anal. Chem.*, 1979, **51**, 1640.
21. J. Kawase, *ibid.*, 1980, **52**, 2124.
22. H. Baadenhuijsen and H. E. H. Seuren-Jacobs, *Clin. Chem.*, 1979, **25**, 443.
23. E. H. Hansen, J. Růžicka and B. Reitz, *Anal. Chim. Acta*, 1977, **89**, 241.
24. B. F. Rocks, R. A. Sherwood and C. Riley, *Clin. Chem.*, 1982, **28**, 440.
25. K. K. Stewart, *Anal. Chem.*, 1977, **49**, 2125.
26. H. Bergamin, B. F. Reis and E. A. Zagatto, *Anal. Chim. Acta*, 1978, **97**, 427.
27. D. Betteridge, *Anal. Chem.*, 1978, **50**, 832A.
28. J. Růžicka and E. H. Hansen, *Flow Injection Analysis*, Wiley, New York, 1981.
29. J. Mindegaard, *Anal. Chim. Acta*, 1979, **104**, 185.
30. L. Anderson, *ibid.*, 1979, **110**, 123.
31. C. Riley, B. F. Rocks, R. A. Sherwood, L. H. Aslett and P. R. Oldfield, *J. Autom. Chem.*, 1983, **5**, 32.
32. B. F. Rocks, R. A. Sherwood, Z. J. Turner and C. Riley, *Ann. Clin. Biochem.*, 1983, **20**, 72.
33. B. F. Rocks, R. A. Sherwood and C. Riley, *ibid.*, 1984, **21**, 51.
34. H. L. Pardue and B. Fields, *Anal. Chim. Acta*, 1981, **124**, 39.
35. A. G. Fogg, N. K. Bsebsu and M. A. Abdalla, *Analyst*, 1982, **107**, 1040.
36. A. N. Strohl and D. J. Curran, *Anal. Chem.*, 1979, **51**, 1045.
37. J. Růžicka and E. H. Hansen, *Anal. Chim. Acta*, 1983, **145**, 1.
38. J. J. Harrow and J. Janata, *Anal. Chem.*, 1983, **55**, 2461.
39. C. Riley, L. H. Aslett, B. F. Rocks, R. A. Sherwood, J. D. McK. Watson and J. Morgon, *Clin. Chem.*, 1983, **29**, 332.
40. B. F. Rocks, R. A. Sherwood and C. Riley, *Analyst*, In the press.
41. D. Betteridge and J. Růžicka, *Talanta*, 1976, **23**, 409.
42. D. Betteridge, W. C. Cheng, E. C. Dagless, P. David, T. B. Goad, D. R. Deans, D. A. Newton and T. B. Pierce, *Analyst*, 1983, **108**, 1.
43. *Idem*, *ibid.*, 1983, **108**, 17.
44. B. F. Rocks, R. A. Sherwood, L. M. Bayford and C. Riley, *Ann. Clin. Biochem.*, 1982, **19**, 338.
45. B. F. Rocks and C. Riley, *Clin. Chem.*, 1982, **28**, 409.
46. E. H. Hansen and J. Růžicka, *Anal. Chim. Acta*, 1976, **87**, 353.
47. B. W. Renoe, K. K. Stewart, G. R. Beecher, M. R. Wills and J. Savory, *Clin. Chem.*, 1980, **26**, 331.
48. E. C. Shideler, K. K. Stewart, J. Crump, M. R. Wills, J. Savory and B. W. Renoe, *ibid.*, 1980, **26**, 1454.
49. C. S. Lim, J. N. Miller and J. W. Bridges, *Anal. Chim. Acta*, 1980, **114**, 183.
50. G. Svensson and T. Anfält, *Clin. Chim. Acta*, 1982, **119**, 7.
51. B. W. Renoe, C. E. Shideler and J. Savory, *Clin. Chem.*, 1981, **27**, 1546.
52. G. L. Abdullahi, J. N. Miller, H. N. Sturley and J. W. Bridges, *Anal. Chim. Acta*, 1983, **145**, 109.
53. E. H. Hansen, J. Růžicka, F. J. Krug and E. A. G. Zagatto, *ibid.*, 1983, **148**, 111.
54. J. T. Vanderslice, G. R. Beecher and A. G. Rosenfeld, *Anal. Chem.*, 1984, **56**, 268.
55. G. Gerhardt and R. N. Adams, *Anal. Chem.*, 1982, **54**, 2618.
56. J. I. Braithwaite and J. N. Miller, *Anal. Chim. Acta*, 1979, **106**, 395.
57. P. J. Worsfold, J. Růžicka and E. H. Hansen, *Analyst*, 1981, **106**, 1309.
58. M. E. Meyerhoff and Y. M. Fraticelli, *Anal. Lett.*, 1981, **14**, 415.
59. J. L. Burguera, M. Burguera, M. Gallagnani and O. M. Alarcán, *Clin. Chem.*, 1983, **29**, 568.
60. E. H. Hansen, J. Růžicka and A. K. Ghose, *Anal. Chim. Acta*, 1978, **100**, 151.
61. S. M. Ramasamy and H. A. Mottola, *ibid.*, 1981, **127**, 39.
62. C. Wolff and H. A. Mottola, *Anal. Chem.*, 1978, **50**, 94.
63. J. Růžicka and E. H. Hansen, *Anal. Chim. Acta*, 1980, **114**, 183.
64. C. Ridder, E. H. Hansen and J. Růžicka, *Anal. Lett.*, 1982, **15**, 1751.
65. T. A. Kelly and G. D. Christian, *Talanta*, 1982, **29**, 1109.
66. N. Minoura and S. Yamada, *Anal. Chim. Acta*, 1982, **135**, 355.
67. U. Rydevik, L. Nord and F. Ingram, *Intern. J. Sports Med.*, 1982, **3**, 47.
68. J. Karlsson, I. Jacobs, B. Sjödin, P. Tesch, P. Kaiser, O. Sahl and B. Karlberg, *ibid.*, 1983, **4**, 52.
69. J. Růžicka, E. H. Hansen and E. A. Zagatto, *Anal. Chim. Acta*, 1977, **88**, 1.
70. J. L. Burguera, M. Burguera and M. Gallagnani, *An. Acad. Brasil. Cienc.*, 1983, **55**, 209.
71. J. F. Van Staden and W. D. Basson, *Lab. Pract.*, 1980, **29**, 1279.
72. J. Růžicka and E. H. Hansen, *Anal. Chim. Acta*, 1980, **114**, 19.
73. J. Růžicka, E. H. Hansen, A. K. Ghose and H. A. Mottola, *Anal. Chem.*, 1979, **51**, 199.
74. A. S. Attiyat and G. D. Christian, *Clin. Chim. Acta*, 1984, **137**, 151.
75. C. W. McLeod, P. J. Worsfold and A. G. Cox, *Analyst*, 1984, **109**, 327.

ENZYME-LINKED IMMUNOSORBENT ASSAY (ELISA) OF ANTIBODIES TO EIGHT COMMON NEUROTROPIC VIRUSES

J. A. P. EARLE, N. V. MCFERRAN and G. B. WISDOM*

Department of Biochemistry, The Queen's University of Belfast, Medical Biology Centre, Belfast, U.K.

(Received 5 January 1984. Accepted 2 May 1984)

Summary—Enzyme-linked immunosorbent assay (ELISA) methods were developed for determining serum levels of antibodies to adenovirus, cytomegalovirus, Epstein-Barr virus, herpes simplex type I virus, measles virus, mumps virus, rubella virus, and varicella zoster virus. The assays were evaluated for specificity, range, precision and accuracy and found to give satisfactory performances. Serum samples from 76 blood donors were assayed for the different antibodies. The antibodies to adenovirus and the members of the Herpesviridae had wide concentration ranges, with a significant minority of the samples having zero or very low levels, whereas the antibodies to measles, mumps and rubella had narrower distributions, with very few samples having levels below the detection limit of the ELISA.

As part of an investigation of the viral aetiology of psychiatric diseases we wished to measure the levels of the antibodies to eight common neurotropic viruses in the serum of a large number of patients and controls. The enzyme-linked immunosorbent assay (ELISA) technique of Engvall and Perlmann¹ appeared to be ideally suited to this purpose. In this technique the antigen is immobilized on a solid phase, a dilution of test serum is incubated with this solid phase, and any antibody present binds to the immobilized antigen. Non-bound serum components are removed by washing, and an anti-immunoglobulin/enzyme conjugate is then added. The conjugate binds to the immunoglobulin attached to the solid phase and, after removal of excess of conjugate by washing, the amount bound is determined by measuring the product formed by incubation with substrate for the enzyme label.

ELISA has been used to identify and measure many types of antibody.^{2,3} The major advantages of the technique are that it is objective, quantitative, sensitive and precise, the reagents are stable and non-hazardous, and it is relatively easy and inexpensive to apply to a large number of samples.

We decided to develop ELISA methods for the antibodies to adenovirus, cytomegalovirus, Epstein-Barr virus, herpes simplex type I virus, measles virus, mumps virus, rubella virus, and varicella zoster virus. Microtitre plates (MTPs) were chosen as the solid phase because they offered several advantages, particularly for handling large numbers of samples.⁴ Alkaline phosphatase was selected as the enzyme label because of its stability and high activity and because it can be easily attached to antibody molecules with glutaraldehyde.¹ The viral antigens were prepared

from cell cultures grown in our laboratory or purchased commercially. The eight assays were evaluated for their specificity, range, precision and accuracy, and applied to serum samples from blood donors.

EXPERIMENTAL

Sera

Serum samples used for assay evaluation were obtained from blood donors aged 20-65 (Blood Transfusion Service, Belfast, Northern Ireland).

Standard sera (positive and negative) for different viral antibodies were obtained from Dynatech Laboratories Ltd. (Billingshurst, Sussex, England) or Flow Laboratories Ltd. (Irvine, Ayrshire, Scotland).

Control sera for routine use in the assay were: positive control—pool of 200 human serum samples (Department of Haematology, Royal Victoria Hospital, Belfast, Northern Ireland); negative control—newborn-calf serum (Gibco Bio-Cult, Glasgow, Scotland).

Sera were stored in small portions at -70° .

Assay solutions

Coating buffer. A 0.05M sodium carbonate buffer, pH 9.6, containing 0.02% sodium azide.

Phosphate-buffered saline/Tween (PBS/T). A 0.02M sodium phosphate buffer, pH 7.2, 0.15M in sodium chloride and containing 0.05% Tween 20, and 0.02% sodium azide.

Substrate solution. A 0.05M sodium carbonate buffer, pH 9.8, containing 1 mg/ml *p*-nitrophenyl disodium phosphate, and 1mM magnesium chloride.

Conjugate

Rabbits were immunized with pure human immunoglobulin G (IgG) and the monospecific antiserum was purified by treatment with an Ultrogel AcA34-human IgG adsorbent.⁵ The antibodies were conjugated to calf-intestine alkaline phosphatase of high specific activity (type VIII; Sigma Chemical Co. Ltd., Poole, Dorset, England) by use of glutaraldehyde in a one-step procedure.¹ Conjugates were stored at 4° in 2% bovine serum albumin solution containing 0.02% sodium azide.

The activity of different batches of conjugate was evaluated by reacting dilutions of conjugate with MTP wells coated with 100 μ l of human IgG (5 μ g/ml of coating buffer)

*Requests for reprints should be addressed to this author.

for 3 hr at 37°. Unbound material was washed out and the amount of bound conjugate was determined by incubation with substrate solution for 5 min as described below.

Microtitre plates

Microtitre plates (M129A; Dynatech Laboratories) were used as the solid phase. The binding characteristics of samples from each box of 50 plates were evaluated by coating the wells with 100 μ l of human IgG (5 μ g/ml of coating buffer) for 3 hr at 37°. The wells were washed and 100 μ l of conjugate (1:500 dilution in PBST) were incubated at 4° for 18 hr. The amount of bound conjugate was determined as described below.

Antigens

Adenovirus types 3, 4 and 7 CF antigen (in Vero cells), varicella zoster strain 2591G CF antigen (in Vero cells), Epstein-Barr virus micro-ELISA antigen (in P3HR1 cells), and Vero cell control antigen were obtained from Dynatech Laboratories.

Cytomegalovirus strain AD169 CF antigen (in human embryonic fibroblast cells) and the corresponding control antigen were purchased from Flow Laboratories.

Rubella HA antigen (in baby-hamster kidney cells) and the corresponding control antigen were obtained from Wellcome Laboratories Ltd. (Beckenham, Kent, England).

Measles virus Edmonston strain, mumps virus Belfast strain and herpes simplex virus type I were grown in Vero cells supplied with Eagles BHK medium (Wellcome Laboratories). Infected cell suspensions were washed 5 times in 0.02M sodium phosphate buffer, pH 7.2, 0.15M in sodium chloride (phosphate-buffered saline, PBS), incubated in 4% paraformaldehyde solution in PBS at 4° for 15 min and washed as before. The suspension was subjected to ultrasonic radiation at 4° for four 30-sec periods. Uninfected Vero cells were used as the control antigen for these three viruses.

The antigens from commercial sources were reconstituted in 0.15M sodium chloride. Protein concentrations were determined by the Lowry method,⁶ with bovine serum albumin as the standard, and the antigens were stored, in 500- μ l portions, at -70°.

Each antigen preparation was screened for non-specific effects before use in the ELISA. Endogenous alkaline phosphatase activity was determined by coating MTP wells at 37° for 3 hr with 100 μ l of antigen at 50 μ g/ml concentration. The wells were washed, substrate solution was added, the mixture incubated at 26° for 1 hr and the product measured as described below. Non-specific binding of conjugate was measured by treating antigen-coated wells (as above) with 100 μ l of conjugate (1:100 dilution in PBS/T) at 4° for 18 hr. The amount of bound conjugate was determined as before.

ELISA

To minimize variation, the edge wells of the MTPs were not used.⁷ Each assay was performed in triplicate and each

half-plate (30 wells) contained positive and negative control sera together with 8 test sera. During incubation the MTP was tightly sealed with cellophane film. The concentrations of antigen preparation, serum sample and conjugate used in each assay are listed in Table 1. The procedure is as follows.

Each MTP well was treated with antigen in coating buffer (100 μ l) by incubation at 37° for 3 hr. The wells were washed free from unbound material by flooding three times with PBST, followed by a 15-min soak in the same solution, and then inverted and tapped on a paper towel until dry. A 100- μ l portion of a serum dilution in PBST was added to each of the coated wells, and incubated at 37° for 3 hr. Unbound serum components were washed from the wells as before and rabbit anti-human IgG/alkaline phosphate conjugate diluted in PBST (100 μ l) was added to each well and incubated at 4° for 18 hr. Excess of conjugate was removed by washing as before and substrate solution (200 μ l) was added and incubated at 26° for 30 min (or 60 min in the case of adenovirus, Epstein-Barr virus and varicella zoster virus antibodies). The reaction was stopped by the addition of 50 μ l of 3M sodium hydroxide. The absorbance of a 100- μ l sample from each well was measured at 405 nm (A_{405}) with a Vitatron DCP photometer fitted with a flow-through cell of 5 mm path-length; the measurements were semi-automated by use of an MSE Microelisa reader (MSE Scientific Instruments Ltd., Crawley, Sussex, England) connected to an Apple II microcomputer (Apple Computer Inc., Cupertino, California, U.S.A.).

Each individual absorbance measurement was transferred to the Apple microcomputer for storage on magnetic disc. The microcomputer produced a tabulated record of the assays from each MTP, each serum assay being reported as the corrected mean absorbance value and its coefficient of variation (CV). The corrected mean absorbance value was calculated by subtracting the mean value of the negative control serum from the mean test serum value and expressing the results as a percentage of the similarly corrected positive control for that particular half-plate. A suite of programs was written to allow editing of the data-base of raw absorbances and gathering together in a single record the mean absorbance values for all the viral antibodies appropriate to a particular test serum. Mean absorbances stored on disc were then converted into concentration units for each antibody, relative to the positive control values, by using a polynomial fitting procedure for the calibration data and linear interpolation between the calibration points. The resultant data-base could be interrogated to produce either the complete spectrum of responses present in a single individual or the overall population pattern of response to each viral antigen.

Evaluation of the ELISA methods

Specificity. Each assay was performed with positive and negative standard sera and with antigen and control antigen (control antigen for Epstein-Barr virus was not available).

Range. The positive control (pooled human serum) was assayed at dilutions from 1:6.25 to 1:6400.

Table 1. Concentrations of antigen preparation, serum sample and conjugate used in the ELISAs

Virus	Antigen (μ g protein/ml)	Serum (dilution)	Conjugate (dilution)
Adenovirus	128	1:100	1:100
Cytomegalovirus	79	1:50	1:200
Epstein-Barr	3	1:50	1:100
Herpes simplex	28	1:500	1:200
Measles	35	1:50	1:200
Mumps	48	1:100	1:200
Rubella	80	1:100	1:200
Varicella zoster	126	1:200	1:100

Precision. Test sera with high, medium or low levels of each antibody were assayed 5 times simultaneously, and on 5 different days for the medium level.

Accuracy. Sets of 10 test sera with ELISA values covering the whole range were assayed by either a neutralization test⁸ or an immunofluorescence titration using rabbit anti-human IgG and fluorescein-labelled sheep anti-rabbit IgG.⁹

RESULTS

Several batches of conjugate were used during the course of these experiments, and the preparation procedure was found to give reproducibly active conjugates. These conjugates lost a negligible amount of activity during storage at 4° for one year. The different batches of MTPs used were found to be satisfactory although the reproducibility of binding, as determined by the degree of adsorption of IgG (5 µg/ml), could have CVs as large as 8.8% for between plate measurements.

The viral antigens and control antigens employed showed negligible endogenous alkaline phosphate activity and very low direct conjugate binding.

The concentrations of the assay components (antigen preparation, serum sample and conjugate) were varied (Table 1) together with the incubation times, to optimize the assay conditions. The aim was to saturate the solid phase with antigen and to use a combination of serum and conjugate dilutions which would give: (a) the best discrimination between positive and negative serum samples, (b) a response in the appropriate range, (c) the most economical use of reagents. Incubation times and temperatures were chosen so as to allow the reactions to approach or reach equilibrium. In the case of the conjugate incubation, for convenience, 18 hr at 4° was selected rather than 3 or 4 hr at 37°.

The performance of each of the 8 ELISAs was evaluated. The *specificity* was tested by using positive and negative standard sera together with antigen and control (negative) antigen. The results (Table 2)

showed that the assays could clearly distinguish between positive and negative samples. The positive and negative control sera incorporated routinely in the assays also gave the expected responses, which were stable during regular use of the 8 assays over a period of 6 months. The possibility of rheumatoid factor cross-linking the viral antibody to the conjugate was investigated by the addition of sera having high titres of rheumatoid factor to sera with known levels of viral antibody; no increase in conjugate binding was found. The ELISAs had effective *ranges* of at least two orders of magnitude and gave linear log-log calibration graphs of corrected absorbance *vs.* concentration of the positive control serum (except those for herpes simplex and mumps, which were convex with respect to the abscissa). The *precision* was determined by using sera with high, medium and low levels of antibody. The CVs found for the mid-range replicates (Table 2) had a mean of 4.8% for within-day and 7.6% for between-day assays. The CVs for within-day assays at low and high levels were larger, with means of 6.9 and 5.6% respectively. The *accuracy* was evaluated by comparison with the antibody levels found in serum samples by a neutralization test or by immunofluorescence titration. The correlation coefficients obtained (Table 2) ranged between 0.78 and 0.95.

The methods were applied to sera from a group of 76 blood donors and the distributions of the 8 viral antibody levels were determined. Two basic patterns were seen. Adenovirus and the members of the Herpesviridae (cytomegalovirus, Epstein-Barr, herpes simplex, varicella zoster) had wide concentration ranges, with a significant minority of the group having zero or very low antibody levels and a smaller minority having relatively high levels. The other viruses (measles, mumps, rubella) had narrower ranges, which contained few, if any, values that were below the detection limit of the assay. Examples of the distributions are shown in Fig. 1.

Table 2. Specificity, precision and accuracy of the ELISAs: specificity was determined by assaying positive and negative standard sera, and antigen and control antigen; precision was estimated by assaying replicates ($n = 5$); accuracy is presented as the correlation coefficient of the ELISA results for a set of samples with those of a neutralization test (*) or an immunofluorescence titration (†); ND = not determined

Virus	Specificity (A_{405})				Precision (CV, %)		Accuracy (correlation coefficient)
	Antigen		Control antigen		Within-day	Between-day	
	Positive serum	Negative serum	Positive serum	Negative serum			
Adenovirus	1.090	0.319	0.335	0.324	5.4	8.0	0.88†
Cytomegalovirus	1.103	0.143	0.198	0.121	5.1	10.6	0.89†
Epstein-Barr	1.073	0.255	ND	ND	4.5	7.4	0.89†
Herpes simplex	0.429	0.152	0.101	0.114	1.5	4.9	0.95*
Measles	0.655	0.236	0.143	0.157	3.5	7.4	0.80*
Mumps	0.722	0.224	0.061	0.140	5.5	7.2	0.83*
Rubella	0.433	0.110	0.107	0.096	7.0	11.1	0.78†
Varicella zoster	0.982	0.302	0.129	0.117	5.7	4.2	0.81†

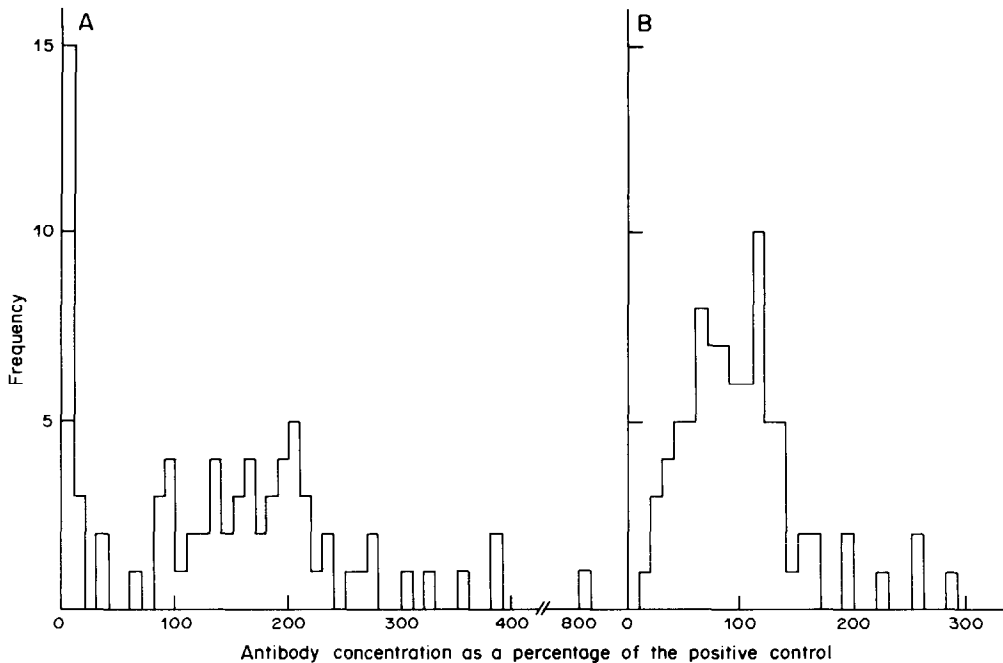


Fig. 1. Frequency distributions of viral antibody levels in serum samples from blood donors: A, herpes simplex type 1 virus; B, measles virus.

DISCUSSION

The ELISAs described measured antibodies to viruses belonging to four groups: Adenoviridae, Herpesviridae, Paramyxoviridae (measles, mumps) and Togaviridae (rubella). They all gave satisfactory performance. The ranges were sufficiently wide for a single dilution of most sera to give results falling on the calibration curve. The occasional sample having a high antibody level could be analysed by assaying a higher dilution. For all the antibodies very low levels could not be distinguished from each other or from zero. The specificity of the assays, as judged by the responses given by control (negative) antigen and by positive and negative standard sera, was high despite the use of antigen preparations in which virus-specific polypeptides probably made up only a small percentage of the total protein. The positive standard sera for herpes simplex, measles and rubella did not give high ELISA values and this probably reflects relatively low levels of the antibody in these sera, as many test sera gave greater responses. The negative standard sera gave somewhat higher values than the negative control (bovine) serum used routinely in the assay; this is probably due to a small amount of non-specific binding of IgG and, in some cases, to the sensitivity of the ELISA allowing detection of low levels of antibody in sera which are negative in other tests. (The bovine serum was used as negative control in preference to control antigen or negative human serum for reasons of economy.) Interference by rheumatoid factor and other proteins did not present problems with the antigens employed. A few commercial antigens, especially rubella anti-

gens, did not give good discrimination between positive and negative sera and they were not used in this investigation. Assay precision was adequate and only a small number of assays required repetition. This was signalled by the computer when the MTPs were read, if (a) the CV of the difference between the positive and negative control sera exceeded 10%, in which case that half-plate of assays was rejected, or (b) the CV of the triplicate determinations exceeded 15%, in which case the individual assay was rejected. The accuracy of immunoassays can be difficult to determine, as different methods may have different biases; however, in the comparisons reported here the ELISA results showed reasonably high correlation with those from the alternative method of measuring antibody level.

The assays are easy to perform. The small amounts of serum required mean that many assays can be done on 1 ml of blood and the use of MTPs makes the handling of large numbers of assays relatively easy, even with only a partially automated system for reading the absorbances (with our apparatus the MTP had to be moved manually for reading the wells). Although the MTPs were coated with antigen and used immediately, pretreatment of MTPs may allow the antigen-coated solid phase to be stored before use.¹⁰ This, together with the stability of the conjugates, adds to the convenience of ELISAs which are required for only occasional use during a period of many months. The ELISA procedures described here take a little over a day to complete, but could be accelerated if required, and viral antibody ELISAs may be completed in as little as 2 hr.¹¹

Although the assays reported here and elsewhere^{2,3} are already useful methods, recent developments promise to increase the scope and performance of ELISAs. High-capacity MTPs with more reproducible adsorption properties have become available and antigen preparations specifically for use in highly sensitive ELISAs are now being produced commercially. This is very important, as the quality of the antigen determines, to a large extent, the quality of the assay. Anti-immunoglobulin conjugates specific for different immunoglobulin heavy chains and with different enzyme labels are currently produced by many different firms. They are usually of high activity and can be measured by use of fluorogenic substrates, as well as the conventional ones, to give increased sensitivity. Automation of the technique has developed extensively in recent years and machines which can load, wash and read MTPs are available from several sources. In addition, ELISA kits for the determination of several important viral antibodies are now being marketed.¹²

While no extensive comparisons of ELISA with other methods for determining antibody levels were made in this study, previous reports indicate that ELISAs usually equal or exceed the sensitivity of most alternative techniques and are generally more convenient.^{2,3} Our experience indicates that ELISAs can easily be set up for viral antibodies, with reagents which are available commercially, and these assays have performances adequate for most research and routine investigations.

Acknowledgements—We wish to thank Prof. S. J. Martin and Dr. B. K. Rima for advice on the growth of viruses, and Dr. D. J. King, Dr. S. J. Cooper and Dr. W. M. McClelland for arranging the supply of blood-donor samples. This work was supported by a grant from the Department of Health and Social Services, Northern Ireland.

REFERENCES

1. E. Engvall and P. Perlmann, *J. Immunol.*, 1972, **109**, 129.
2. A. Voller, D. E. Bidwell and A. Bartlett, *The Enzyme Linked Immunosorbent Assay (ELISA)*, Dynatech Europe, Guernsey, 1979.
3. A. Voller and D. Bidwell, *The Enzyme Linked Immunosorbent Assay (ELISA)*, Vol. 2, MicroSystems Ltd., Guernsey, 1980.
4. A. Voller, D. Bidwell, G. Hult and E. Engvall, *Bull. Wild. Hlth. Org.*, 1974, **51**, 209.
5. J.-L. Guesdon and S. Avrameas, *J. Immunol. Methods*, 1976, **11**, 129.
6. E. Layne, *Methods in Enzymology*, 1957, **3**, 447.
7. L. J. Kricka, T. J. N. Carter, S. M. Burt, J. H. Kennedy, R. L. Holder, M. I. Halliday, M. E. Telford and G. B. Wisdom, *Clin. Chem.*, 1980, **26**, 741.
8. G. D. Johnson, E. J. Holborow and J. Dorling, in D. M. Weir, *Handbook of Experimental Immunology*, 3rd Ed., p. 15.16. Blackwell, Oxford, 1978.
9. D. A. J. Tyrell, *ibid.*, p. 40.9.
10. I. J. Skurrie and G. L. Gilbert, *J. Clin. Microbiol.*, 1983, **17**, 738.
11. D. J. Kiefer, D. A. Phelps and S. P. Halbert, *ibid.*, 1983, **18**, 33.
12. G. B. Wisdom, *The Ligand Review*, 1981, **3**, 44.

DEVELOPMENT OF A SENSITIVE ENZYME IMMUNOASSAY FOR PLASMA AND SALIVARY STEROIDS

A. RODA*, S. GIROTTI, S. LODI and S. PRETI

Istituto di Scienze Chimiche, Facoltà di Farmacia, Università degli Studi di Bologna, Bologna, Italy

(Received 4 January 1984. Accepted 1 June 1984)

Summary—The development of an enzyme-labelled immunoassay (EIA) of sufficient range and sensitivity for determination of plasma and salivary steroids is described. The method is based on competition in the solid phase. A fixed amount of a specific antibody is immobilized on polystyrene beads, its amount being enough to bind about 50% of a steroid-enzyme conjugate (covalently linked steroid/horseradish peroxidase conjugate). The initial incubation at 25° of serum sample or extract with the conjugate in presence of the immobilized antibody is followed by washing and the addition of a substrate for measurement of the enzyme activity either colorimetrically by the H₂O₂/o-phenylenediamine method or by the luminescence reaction based on the use of H₂O₂/luminol. The method is precise and accurate (CV < 10% for both the intra- and inter-assay studies). The sensitivity of the colorimetric determination is similar to that of radioimmunoassay, but the luminescence method is more sensitive. Radioimmunoassay and EIA gave results in good agreement ($r > 0.97$). The method has also been applied to salivary steroids: the procedure is direct and only a few μ l of saliva are required. The levels of these steroids in saliva are only about a tenth of those in serum but directly correlated with them ($r > 0.85$). The enzyme immunoassay proposed is sensitive and precise enough to measure these steroids accurately in saliva and plasma.

All steroids of diagnostic significance in the routine assessment of endocrine function can now be measured accurately both in plasma and urine samples thanks to the development of sensitive and accurate radioimmunoassays (RIA). Several methods have been described based on the use of radiolabelled tracers such as ³H and ¹²⁵I.^{1,2} These assays are mostly based on a competitive principle and require separation of the antigen-antibody complex. The results obtained on biological samples have been validated by comparison with independent methods such as GC-MS³ and the data agree well. Most procedures still require a preliminary liquid extraction of the steroids from the serum matrix. Several kits are commercially available and wide applications have been reported.

Some problems related to methodology still remain. Data derived from different laboratories for the same specimen sometimes disagree and this seems related to differences in antibody heterogeneity and recovery in the extraction.

A factor limiting widespread application of tests using radioactive materials is the need for expensive equipment and consequently the use of these methods is mainly limited to hospital laboratories.

The limited half-life of some radioisotopes (e.g. ¹²⁵I) used in such assays is another drawback when these tests are used in small laboratories where only a few samples are analysed per day.

Alternative methods to RIA have recently been proposed, including enzyme immunoassay,⁴ amplified

enzymatic methods⁵ and fluorescence⁶ (FIA) or luminescence⁷ (LIA) immunoassay. Until now few of them have fulfilled the requisites of sensitivity and accuracy shown by RIA and few commercial kits for steroid analysis are available.

In addition, the exact definition of endocrine function requires the measurement of such steroids in urine collected over a 24-hr period or the use of dynamic tests with consequent collection of several plasma samples.

Recently Riad-Fahmy *et al.*⁸ reported the measurement of steroids in saliva and demonstrated its validity by comparing the results with those obtained for plasma. They concluded that all steroids, including cortisol, oestriol, testosterone, progesterone, *etc.*, can be accurately measured in saliva and that their levels are independent of the saliva flow-rate (over a range with the highest rate 4-6 times the lowest) and reflect those in the free fraction present in plasma. A direct method without preliminary extraction from the matrix can be developed for saliva even for those steroids which require a solvent extraction from plasma samples.

For the clinician the use of saliva sampling simplifies the work and reduces stress for the patient. These factors, together with a considerable reduction in cost, make this test attractive.

Salivary levels of most steroids are very low, between about a tenth and a twentieth of those in serum. Consequently an analytical method applicable to saliva has to be highly sensitive and accurate to detect disease-related variations at picomolar levels.

*To whom correspondence should be addressed.

In the present paper we report the development of a highly sensitive enzyme immunoassay based on a competitive principle, able to measure steroids in plasma and saliva samples.

The method is based on the use of steroid labelled with horseradish peroxidase (HRP) as a "label" and a steroid-specific antibody immobilized on a solid support (polystyrene beads). The method is extremely simple and rapid and can be performed in a single tube. The enzymatic activity of the HRP-steroid conjugate can be measured by conventional colorimetric detection with H_2O_2 /*o*-phenylenediamine (OPD) as substrate or by a luminescence reaction using H_2O_2 /luminol as substrate.

The general method reported here shows a sensitivity comparable to that of RIA and sometimes better, mainly when luminescence detection is used. Here we describe the general scheme of the assay and its application in the development of sensitive immuno-enzymatic assays for progesterone, testosterone, oestriol, cortisol and conjugated lithocholate (CLCA). Comparison with RIA and validation with saliva and serum samples, by an extraction procedure or a direct method, is also reported.

EXPERIMENTAL

Reagents

All the reagents used were of analytical grade and used without further purification. Steroid-carboxymethylxime derivatives (CMO) were obtained from Makor Chemical Ltd., Jerusalem, Israel, or synthesized in our laboratory by published methods.⁹

The purity of such derivatives and steroid standards was assessed both by TLC and HPLC and found better than 98%. Horseradish peroxidase (HRP) was obtained from Boehringer GmbH, Mannheim, West Germany (Grade 1). Sephadex G-100 was obtained from Pharmacia, Uppsala, Sweden. Polystyrene beads (6.5 mm diameter) were purchased from Precision Plastic Balls, Chicago, U.S.A., and luminol from LKB, Bromma, Sweden. Tritium-labelled steroids (specific activity 80–110 Ci/mmmole) were obtained from the Radiochemical Centre, Amersham, U.K. Tritium-labelled glycolithocholic acid (specific activity 17 Ci/mmmole) was obtained from NEN, Worcester, Mass., U.S.A.

Antibodies

Antisera were produced in rabbits against (CMO)-bovine serum albumin (BSA) conjugated steroids; these derivatives were prepared by the previously described mixed anhydride method¹⁰ and in the case of conjugated lithocholic acid the antigen was prepared by direct conjugation of glycolithocholic acid with BSA, by a carbodi-imide method, at the C-24 carboxyl group.¹¹ The molar ratio of steroid to bovine serum albumin, evaluated by adding ³H-labelled steroids to the reaction mixture, ranged from 15 to 20. Unbound steroid was removed by gel-exclusion chromatography on a Sephadex G-100 column and dialysis against three changes of 0.1M phosphate buffer, pH 7.0.

The immunization technique was similar to that previously reported,¹² and antisera with adequate titre, affinity and specificity were obtained 3–5 months after the first immunization. BSA (0.3%) was first added to the rabbit sera in order to eliminate any anti-BSA present, by precipitation. The IgG-rich fraction was isolated by salting-out precipitation with anhydrous sodium sulphate, following a slight modification of the method described by Axen *et al.*¹³ The

IgG were then extensively dialysed against 0.1M phosphate buffer, pH 7.0.

Immobilization. The purified antibody was immobilized on polystyrene beads (6.4 mm diameter) previously washed with distilled water. An appropriate dilution of IgG was incubated with the beads (1 mg/100 beads) in 0.1M phosphate buffer (pH 8) for 4 hr at 4°. The solution was removed and BSA solution containing 0.01% of thiomersal was added and incubated for 2 hr. The solution was discarded and the beads were washed with doubly distilled water, dried under vacuum and stored at 4° until use.

Enzyme-steroid conjugate

The mixed anhydride method was selected to conjugate the steroid-CMO derivative with HRP by a slight modification of the method originally described by Erlanger *et al.*¹⁰ The conjugate was freed from unreacted steroids by gel-exclusion chromatography on Sephadex G-100 and the eluate dialysed against three changes (1 litre) of 0.1M phosphate buffer, pH 7.0, at 4°. The molar ratio of steroid to HRP was evaluated by adding ³H-labelled steroid-CMO to the reaction mixture. In the case of lithocholic acid, which already contained a carboxyl group, the reaction was performed with a water-soluble carbodi-imide as previously reported.¹¹

Samples

The method developed is directly applicable to plasma samples only for cortisol and CLCA. For the other steroids a preliminary liquid extraction is still required for plasma samples. The plasma sample (500 μ l) was extracted with 5 ml of diethyl ether. The ether phase was decanted and evaporated to dryness. The residue was then dissolved in 5 ml of 0.1M phosphate buffer (pH 7.0) and 100- μ l aliquots of solution were used for the assay. In order to validate the method saliva samples were also run, with and without extraction. In the case of saliva 1-ml aliquots were extracted with 10 ml of diethyl ether. The aqueous phase was quick-frozen and the ether phase decanted off and evaporated to dryness. The residue was dissolved in 1 ml of phosphate buffer and 100- μ l aliquots of solution were used for the assay.

Assay procedure

The assay buffer used was 0.05M phosphate/EDTA buffer (pH 7.5) containing 0.1% BSA. A 100- μ l portion of steroid-HRP conjugate (diluted 10³-fold) was added to the assay tube containing 100 μ l of sample prepared as described above, or a standard solution. The final volume was adjusted to 500 μ l with assay buffer. The immobilized antibody was then added to the tube. The tubes were incubated for 3 hr at 25°.

At the end of incubation the beads (bound fraction) were washed twice with 4 ml of water. The enzyme activity of the bound fraction was measured by adding 2 ml of "substrate solution" (0.1M phosphate buffer, pH 6.0, containing 2 mg of OPD and 1 μ l of 30% H_2O_2) to each tube. After incubation for 30 min in the dark at 25° the reaction was stopped with 200 μ l of 4M sulphuric acid and the absorbance at 492 nm recorded.

The luminescence detection was based on the use of the luminol/ H_2O_2 system. The washed beads were added to a tube containing the "luminescence solution" (1 ml of 0.01M phosphate buffer, pH 7.0; 0.1 ml of 0.01M luminol; 0.5 ml of 0.01M H_2O_2). The light emission occurs in a few seconds and is stable for 30–40 sec. The peak light emission was measured with an LKB luminometer, model 1250, and the output signal recorded on an LKB potentiometer recorder, model 2210.

RIA

The radioimmunoassay procedures employed for obtaining comparison results have already been published elsewhere. The main characteristics in terms of sensitivity and

Table 1. Comparison between colorimetric, luminescence and radioimmunological methods for steroid analysis

Steroid	Colorimetry			Luminescence			RIA		
	Sensitivity, pg/tube	CV, %	Recovery, %	Sensitivity, pg/tube	CV, %	Recovery, %	Sensitivity, pg/tube	CV, %	Recovery, %
Progesterone	10	8-11	98-102	5	9-11	96-101	10	6-9	95-101
Testosterone	3	6-9	96-104	1	9-12	100-104	2	8-10	100-105
Oestriol	20	8-12	97-102	8	10-12	96-100	10	9-12	97-101
Cortisol	9	9-13	98-102	5	8-10	100-104	10	7-11	96-102
CLCA	500	7-9	96-98	100	10-12	98-104	1,000	7-10	98-102

CV = coefficient of variation.

precision are reported in Table 1. The same antibodies were used both for RIA and immunoenzymatic assay.

RESULTS

Antibodies

The specificities of the antibodies used are reported in Table 2. As far as the CLCA assay is concerned, the antibody is specific both for glycolithocholic and tauro lithocholic acid. The cross-reactivity of the unconjugated bile acid is 5%, but other bile acids do not cross-react. The antibody titre is extremely high for all the assays: the final dilution of the antibody at 50% binding is about $1:10^5$ and the affinity constant is around 10^{10} l./mole. The stability of the immobilized antibody was checked by weekly assays of the same standard at both 4° and 25° . Figure 1 shows the results for two representative steroids, cortisol and oestriol. The reproducibility of the immobilization procedure was assessed by adding ^3H -labelled steroid (10 pg/tube, 10^4 dpm) to the beads and measuring the bound radioactivity after 3-hr incubation. The same procedure was repeated several times. For all immobilized antibodies the coefficient of variation was less than 5%, showing that the same amount of antibody was bound to each polystyrene bead.

Enzyme label

Approximately 1 mole of HRP is bound to 2-3 moles of steroid, as calculated by measuring the radioactivity of the ^3H -labelled CMO-steroid added to the reaction mixture. At the final dilution of this label in the assay tube, not more than 20 pg of steroid is present and the maximum absorbance recorded at 412 nm is between 1.0 and 2.0. When luminescence detection is used it is possible to reduce the dilution to 5 pg/tube.

These "labels" are highly stable when stored in concentrated form (1 mg/ml), at 4° and in presence of 0.1M gelatine. Once diluted for the assay (1 $\mu\text{g}/\text{ml}$) they are drastically reduced in stability, as shown in Fig. 2.

Immunoassay

A linear response was obtained over a wide concentration range when the fraction of antigen bound was plotted against the concentration in a logit-log plot. Representative calibration graphs obtained by colorimetric detection are shown in Fig. 3.

The detection limit, defined as the concentration resulting in a response equal to twice the standard deviation of the zero dose response, is reported in Table 1 for both detection systems used. In all assays the luminescence EIA was more sensitive than RIA and the colorimetric EIA.

The intra- and inter-assay reproducibility, expressed as the coefficient of variation, was obtained from 20 replicate determinations at low and high concentrations. In addition, various amounts of standard steroids were added to plasma and the mixtures

Table 2. Specificity of the antisera used both in the RIA and enzyme immunoassays

	Cross-reactivity, %			
	Cortisol	Oestriol	Testosterone	Progesterone
Cortisol	100	—	—	—
Corticosterone	9	—	—	—
Cortisone	4.8	—	—	—
11 α -Deoxycortisol	5.2	—	—	—
Deoxycorticosterone	0.6	—	—	—
20 α -Dihydroprogesterone	0.3	—	—	—
Aldosterone	0.1	—	—	—
Oestriol	—	100	—	—
17 β -Oestradiol	—	0.2	—	—
Oestrone	—	0.02	—	—
Testosterone	—	—	100	—
5 α -Dihydroxytestosterone	—	—	36.6	—
5 α -Androstan-3 α ,17 β -diol	—	—	7.4	—
5 α -Androstan-3 β ,17 β -diol	—	—	6.3	—
Androstendione	—	—	1.4	—
5-Androstene-3 β ,17 β -diol	—	—	1.5	—
Progesterone	—	—	—	100
11 α -Hydroxyprogesterone	—	—	—	85
11- β -Hydroxyprogesterone	—	—	—	17
6 α -Hydroxyprogesterone	—	—	—	<1
6 β -Hydroxyprogesterone	—	—	—	<1
14 α -Hydroxyprogesterone	—	—	—	<1

assayed by the three methods. The recovery is expressed as the mean range of five determinations.

Comparison of methods

Figure 4 shows the results obtained by using the colorimetric or luminescence EIA, compared with those obtained by RIA for 25 extracted plasma testosterone samples with normal or pathological levels of this steroid. The other steroid assays behave in a similar fashion. The agreement was good at both low and high levels, as shown by the correlation coefficient ($r > 0.88$).

When the plasma and salivary levels measured by EIA or LIA methods were compared, a good correlation was found, suggesting that variations in the saliva levels reflect those in the plasma (Fig. 5). The salivary levels are lower than those in plasma by a factor of 10–20.

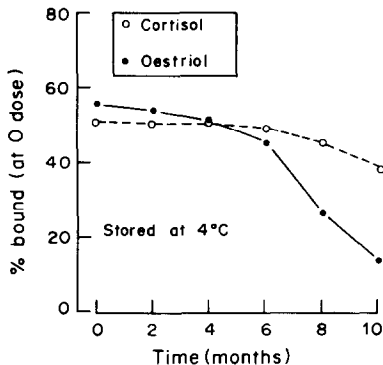


Fig. 1. The stability of the immobilized antibodies when stored dry at 4°. Each point is the mean value from five experiments.

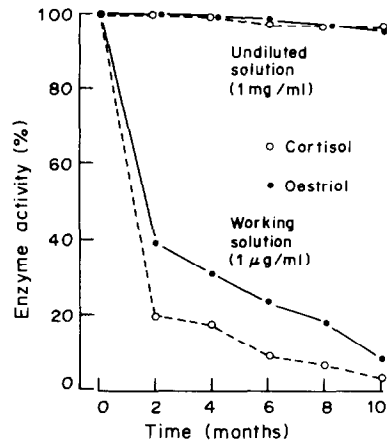


Fig. 2. Fraction of enzymatic activity retained by the conjugate as a function of time when stored concentrated (1 mg/ml) or diluted (1 µg/ml) at 4°.

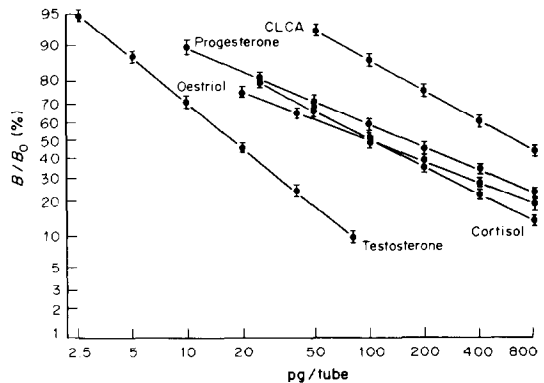


Fig. 3. Dose vs. response plots for the steroids determined by enzyme immunoassay, with colorimetric detection of the enzyme activity. B , Antibody-bound enzyme-labelled steroid; B_0 , antibody-bound enzyme-steroid at zero dose of unlabelled steroid.

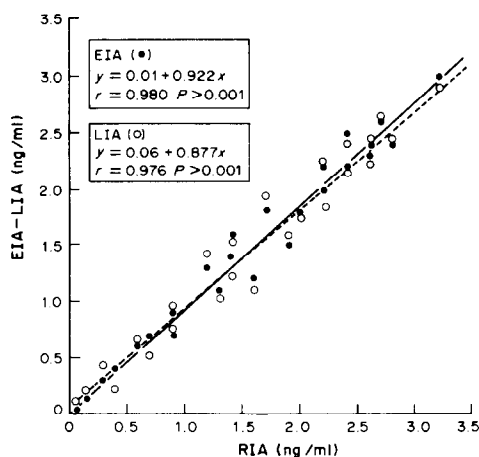


Fig. 4. Relationship between testosterone plasma levels as measured by colorimetric EIA and luminescence LIA, enzyme immunoassay, and radioimmunoassay (RIA).

DISCUSSION

The solid-phase immunoenzymatic assay described here appears to be a useful alternative to RIA for measuring steroids in plasma and saliva. Its sensitivity is comparable to that of RIA and in some cases higher. For example, the RIA developed for CLCA has a sensitivity lower by a factor of 1000, probably because of the low specific activity of the ^3H -tracer used (17 Ci/mmol). The uncontrolled adsorption of the antibody on the solid beads when a non-covalent binding is chosen is improved by careful selection of the coating conditions, such as ionic strength, pH, antibody purity and pre-coating treatment of the plastic beads. The high specificity and affinity of the antibodies used seems a key parameter. Once treated with BSA so that all the remaining possible specific adsorptive sites on the bead surface are occupied, the beads are very stable, either wet or dry if stored at 4° . The non-specific binding is very low (less than 1%) and increases to only a limited extent during 2–3 months of storage.

The HRP-steroid conjugates have high specific activity, allowing them to be used at high dilution in the assay tube, with consequent increased sensitivity of the assay. The conjugates can be used at a final dilution at least 10–100 times greater than that for other conjugates.¹⁴

When luminescence detection is used, an even greater dilution of the conjugate is possible, and as little as 2 pg of steroid (or even less) can be assayed. The method is precise and accurate (Table 1) and the use of polystyrene beads seems ideal when colorimetric, and particularly luminescence, detection is used. The main advantages are as follows.

(1) The beads are easily washed, with consequent removal of all possible non-specific interferences in the colorimetric and luminescence reactions.

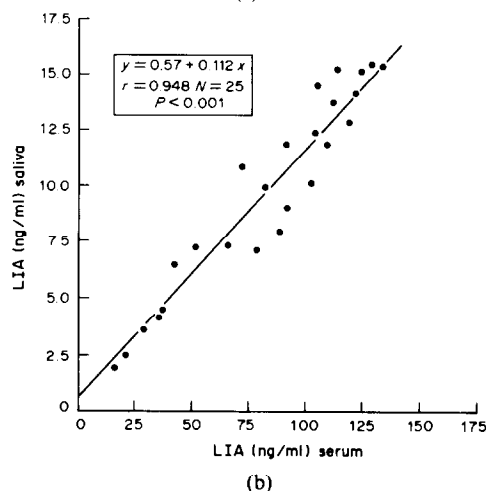
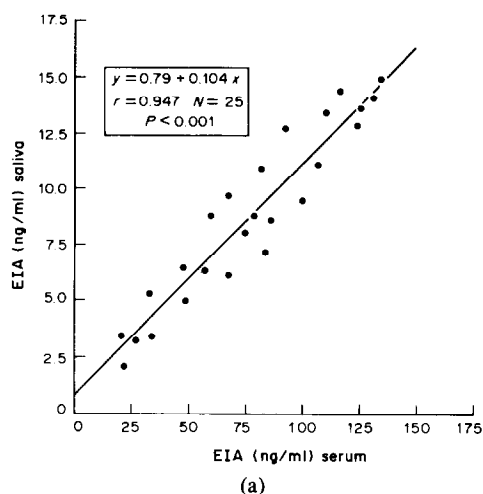


Fig. 5. Relationship between plasma and saliva levels of cortisol as measured by colorimetric (a) and luminescence (b) enzyme immunoassay.

(2) The washing difficulties and bacterial growth experienced in methods using Sepharose beads¹⁴ are resolved.

(3) With $\text{OPD}/\text{H}_2\text{O}_2$ as the detection-system substrate, the sensitivity is adequate to measure disease-related variations in both plasma and saliva. The luminescence detection is faster and much more sensitive but requires the use of a luminometer, which is not widely available in clinical chemistry laboratories.

Both assays are easy to perform and require only inexpensive equipment. The reagents used, such as the enzyme-steroid conjugate and the immobilized antibody are very stable, thus simplifying storage and shipment of kits. The preliminary results reported here on the correlation between salivary and plasma levels of oestriol are in agreement with those previously published. The combination of this enzyme immunoassay with saliva sampling will make steroid tests more practicable.

REFERENCES

1. G. E. Abraham, *Acta Endocrinol.*, 1974, **74**, 183.
2. V. H. T. James and S. L. Jeffcate, *Br. Med. Bull.*, 1974, **30**, 50.
3. S. J. Gaskell and A. K. Griffiths, *Steroids*, 1980, **36**, 219.
4. S. L. Scharpe, W. M. Coorcman, W. J. Blomme and G. M. Laekeman, *Clin. Chem.*, 1976, **22**, 733.
5. J. C. Nicolas, A. M. Boussioux, B. Descamps and A. Crastes De Paulet, *Clin. Chim. Acta*, 1979, **92**, 1.
6. R. C. Aalberse, *ibid.*, 1973, **48**, 109.
7. T. P. Whitehead, L. J. Kricka, T. J. N. Carter and G. H. G. Thorpe, *Clin. Chem.*, 1979, **25**, 1531.
8. D. Riad-Fahmy, G. F. Read, R. F. Walker and K. Griffiths, *Endocrine Rev.*, 1982, **3**, 367.
9. B. F. Erlanger, F. Borek, S. M. Beiser and S. Lieberman, *J. Biol. Chem.*, 1957, **228**, 713.
10. *Idem, ibid.*, 1959, **234**, 1090.
11. A. Roda, E. Roda, D. Festi, R. Aldini, G. Mazzella, C. Sama, and L. Barbare, *Steroids*, 1978, **32**, 13.
12. A. Roda and G. F. Bolelli, *J. Steroid Biochem.*, 1980, **13**, 449.
13. R. Axén, J. Porath and S. Ernback, *Nature*, 1967, **214**, 1302.
14. K. M. Rajkowski, N. Cittanova, B. Desfosses and M. F. Jayle, *Steroids*, 1977, **29**, 701.

LUMINESCENT IMMUNOASSAY (LIA) METHODS FOR STEROID HORMONES

M. PAZZAGLI, G. MESSERI, R. SALERNO, A. L. CALDINI,
A. TOMMASI, A. MAGINI and M. SERIO

Endocrinology Unit, University of Florence, Viale Morgagni 85, 50134 Florence, Italy

(Received 4 January 1984. Accepted 25 May 1984)

Summary—The application of luminescence to the development of non-isotopic immunoassay methods for steroids and urinary steroid metabolites is reviewed. On-line computer analysis of the light emission is particularly useful, as it reveals the interfering effects of biological compounds on the reaction and this can improve the quality of luminescence immunoassay (LIA) methods. The main characteristics of chemiluminescent tracers are stability, safety, speed and sensitivity of detection, and reliability. Homogeneous methods, not requiring phase separation, have also been reported and validated. Heterogeneous methods which use dextran-coated charcoal or solid-phase techniques can be used for direct determination of urinary steroids in unextracted samples.

Many compounds of clinical interest are currently determined at low levels by protein-binding assays with radioactive labels. Although radioimmunoassay (RIA) methods are sensitive and reasonably specific, they possess certain disadvantages inherent in the use of radioactive material, such as problems of stability of the tracer, radioactive waste disposal, and the availability of expensive instrumentation and reagents.

Other analytical procedures have been developed which take full advantage of the specificity and sensitivity that result from the use of an antibody, but do not employ an isotopically labelled antigen. These include the use of an enzyme and a fluorescent or chemiluminescent molecule as a label.

In this paper we survey the use of such labels in immunoassay methods for steroid hormones.

THE ANALYTICAL SIGNAL OF A CHEMILUMINESCENCE REACTION

Luminescence may be defined as the chemical production of light and involves the emission of photons from excited molecules during their return to a lower energy state. Luminescence can be applied in a wide variety of assays of biological interest and more information on the characteristics of bioluminescence (BL) and chemiluminescence (CL) reactions, instrumentation, and applications in clinical chemistry can be found in several recent reviews^{1,2} and books.^{3,4} Here we describe how some compounds giving chemiluminescence reactions can be used as labels for the development of luminescence immunoassay (LIA) methods for steroids.

The main difference between LIA and radioimmunoassay (RIA) procedures lies in the measure-

ment of the tracer; in the case of LIA, the tracer measurement has the following characteristics:

(i) the chemiluminescence of the tracer must be activated before it can be measured, and this requires an additional step, *viz.* an oxidation reaction,⁵ which can be a source of variability; radioisotopes emit spontaneously beta or gamma radiation;

(ii) the signal of a CL reaction is not easily definable in absolute terms of light emission⁶ and the luminometer (the instrument used for luminescence measurements) records values in arbitrary light units; microprocessor-controlled beta- and gamma-counters can automatically evaluate efficiency and convert cpm into dpm values;

(iii) the CL signal is time-dependent whereas radioisotope tracers give an effectively constant signal which is more easily quantifiable (Fig. 1).

Consequently the measurement of the chemiluminescent tracer in LIA methods is a more critical step than the measurement of radioactivity in RIA. Further, beta- or gamma-counters are usually quite sophisticated instruments in comparison to the commercially available luminometers, which are com-

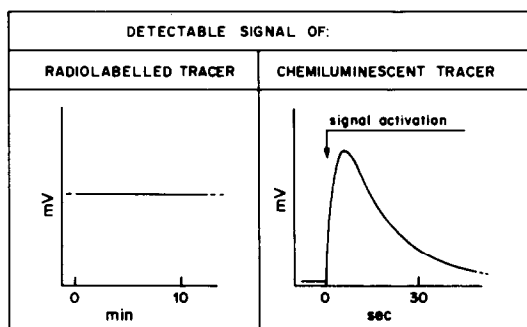


Fig. 1. Comparison between the analytical signal of a radiolabelled or a chemiluminescent tracer.

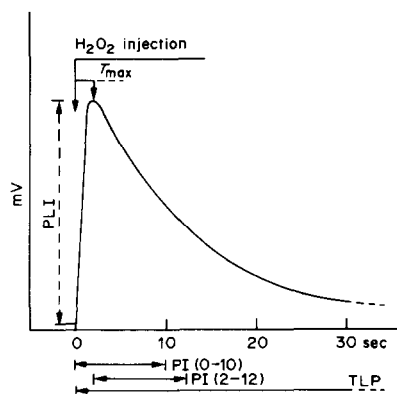


Fig. 2. Time-course of the light signal obtained on oxidation of a CL tracer with the H_2O_2 -microperoxidase system at pH 13, and some of the most used measurement parameters. TLP (total light production). The integrated value of the photon emission reaching the detector during the total time of emission. PLI (peak light intensity). A fast measurement parameter often related to PI. PI (portion integration for 0–10 or 2–12 sec or other intervals). An integration value for a fixed time interval. T_{max} . Time interval from the oxidant injection to PLI. This is a "shape" index which can often reveal changes in the CL kinetics due to interfering compounds (see reference 8).

monly equipped with inadequate injection devices and crude light measurement systems.

To minimize errors due to the chemiluminescent tracer measurement, the following factors should be optimized.

Choice of the measurement parameter. The CL reaction, because of its time-dependence, can be quantified in various ways (see Fig. 2) which possess different characteristics in terms of time, reproducibility, linearity, signal to-noise ratio *etc.*⁷ The most suitable method for the measurement depends of the kind of CL compound used and on the reaction conditions.

Evaluation of the CL kinetics. The reaction conditions (*viz.* pH, buffers, the relative concentrations of the oxidant and catalyst, and in particular the presence of materials of biological origin such as plasma or urine) can modify the kinetics and consequently the measured light output.⁷ Consequently it is necessary to have a criterion for evaluating the shape or pattern of the signal. In fact, quenching corrections, analogous to dead-time corrections in radioisotope counting, can be developed by using a detailed analysis of the time course of the CL signal.

In an attempt to improve the present methods of

Table 1. Typical cortisol LIA data; table of significant parameters, one row for each CL reaction, computed by using the program GRAFST2 (sample rate 10/sec; acquisition time 10 sec; 50 tubes)

Tube	No.	PLI, <i>cps</i>	T_{max} , <i>sec</i>	PI, 0–10 sec	PI, 2–10 sec	5/10 ratio	B/B_0 , %
background	1	30	0.70	204	168	0.62	
	2	40	0.80	214	177	0.62	
aspecific	3	820	0.60	2983	1887	0.58	
	4	830	0.70	2959	1893	0.56	
total	5	21,070	0.60	76,287	47,432	0.61	
	6	20,350	0.60	77,717	49,643	0.57	
zero	7	9290	0.60	31,697	19,614	0.62	100
	8	9040	0.60	30,759	19,436	0.61	
7.8 pg/tube	9	8430	0.60	29,903	18,415	0.60	96.0
	10	8641	0.60	30,310	18,917	0.61	
15.6 pg/tube	11	8540	0.60	27,850	16,820	0.62	89.6
	12	8521	0.60	28,710	17,341	0.63	
31.2 pg/tube	13	7720	0.60	26,899	16,457	0.62	83.6
	14	7830	0.60	26,304	16,329	0.63	
62.5 pg/tube	15	6130	0.60	22,428	13,853	0.63	70.2
	16	6540	0.60	23,179	14,472	0.60	
125 pg/tube	17	5120	0.60	18,950	11,799	0.60	57.0
	18	5420	0.60	19,211	11,850	0.60	
250 pg/tube	19	4300	0.60	14,890	9299	0.61	41.8
	20	3950	0.60	14,674	9182	0.61	
500 pg/tube	21	2740	0.60	10,522	6598	0.61	27.6
	22	2930	0.60	11,018	6923	0.60	
1000 pg/tube	23	2610	0.60	9169	5749	0.60	20.9
	24	2300	0.60	8583	5373	0.60	
2000 pg/tube	25	2010	0.60	7412	4788	0.60	15.4
	26	2050	0.60	7288	4603	0.60	
sample 1	27	4170	0.60	15,573	9833	0.59	45.2
	28	4320	0.60	15,956	9958	0.60	
sample 2	29	2810	0.60	10,501	6549	0.59	25.9
	30	2850	0.60	10,074	6323	0.60	
sample 3	31	4389	0.66	13,660	8860	0.49	rejected
	32	4255	0.65	13,567	8756	0.50	

* = value calculated as mean of duplicates and using the PI 0–10 sec values.

measurement of CL reactions with commercial luminometers, we have interfaced a microcomputer to operate on-line with a luminometer (Packard PICO-LITE model 6200). The signal from the photomultiplier of the luminometer is processed by the interface to become acceptable for the parallel port of the computer, and is then analysed in terms of light emission and shape of the signal. Details of this approach have been reported.⁸

The use of on-line computer analysis of CL reactions facilitates selection of the most suitable method of measurement and can characterize the reaction kinetics. Table 1 gives an example of the computer output of the most significant signal parameters of an LIA method for cortisol.

We believe that on-line use of the computer with the luminometer allows us both to monitor the CL reaction and identify and eliminate some sources of error, and thus improve the quality and consistency of LIA methods. In addition, we use the computer for routine analysis of RIA and LIA dose-response curves, using a weighted four-parameter logistic method.⁹

CHEMILUMINESCENT TRACERS FOR STEROIDS

Several compounds which produce chemiluminescence can be used as labelling reagents. In par-

ticular some aminophthalylhydrazides (luminol, isoluminol and isoluminol derivatives) participate in simple oxidation reactions (*e.g.* the hydrogen peroxide-microperoxidase reaction at pH 8.6–13) to produce light with relatively high quantum efficiency¹⁰ and thus can be used as universal labels for both antigens¹¹ and haptens.¹²

Some isoluminol derivatives have been conjugated to steroid molecules and the resulting steroid-CL tracer conjugates have been investigated in terms of both their affinity for the homologous antibody and their CL characteristics. The results of this study¹² can be summarized as follows.

(1) The preparation of the steroid-CL tracer conjugate is a simple conjugation reaction, such as a carbodi-imide reaction, similar to those used in the synthesis of steroid-protein immunogens. Purification can be done on silica gel TLC plates and the identity of the final compound confirmed by mass spectrometry. An example of the structure of a steroid-CL tracer conjugate is shown in Fig. 3.

(2) The CL efficiency of the conjugates is mainly determined by the isoluminol derivative used and is not significantly affected by the steroid molecule. Some isoluminol derivatives (AEEI or ABEI) are more efficient than others, and always produce CL tracers detectable at picomolar level (range 0.1–0.4 fmole/tube).

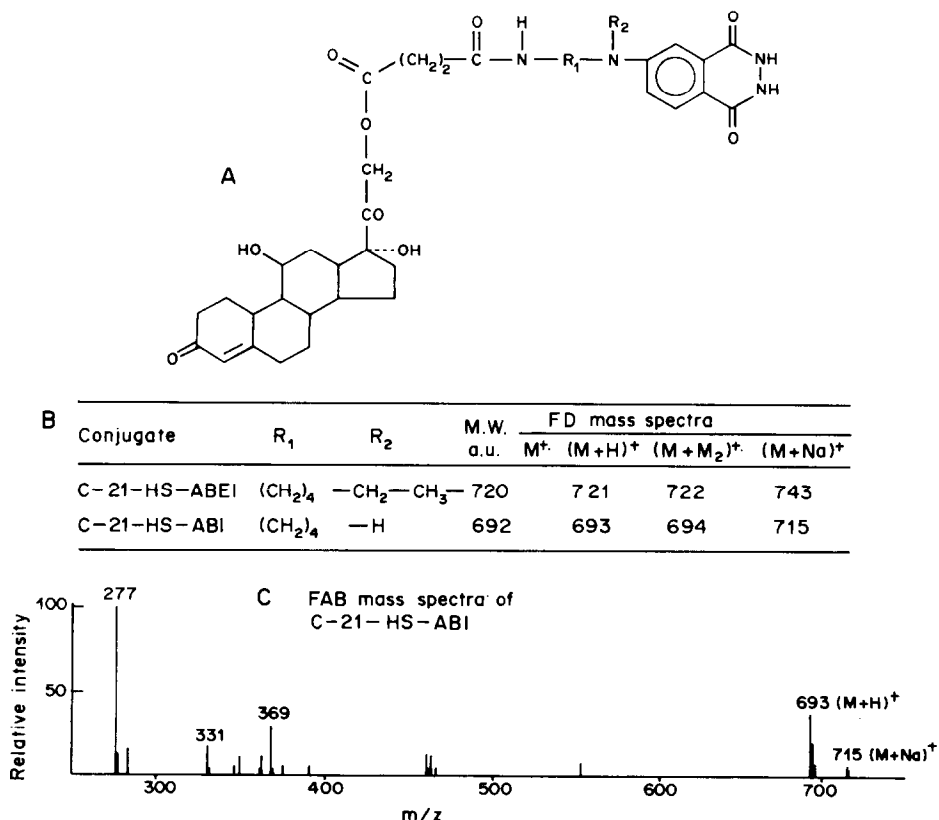


Fig. 3. Example of the structure of a steroid CL tracer (A) and of the mass spectrum data obtained by the field desorption (FD; B) or the fast-atom bombardment (FAB; C) ionization techniques.

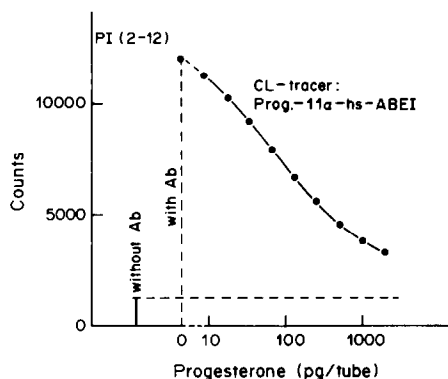


Fig. 4. Homogeneous LIA for progesterone: standard curve. The continuous vertical bar represents the 2–12 sec PI value of the CL tracer in absence of antibody, and the dotted line at the zero point the PI value in presence of the homologous antibody. The enhancement phenomenon is evident. The effect of adding increasing amounts of cold progesterone to the reaction mixture, on the enhancement, is also shown.

(3) The affinity of the steroid–CL tracer conjugate for the homologous antibody can be affected by the ability of the antibody to recognize both the steroid and the bridge between the steroid and the CL molecule (*e.g.*) the carboxymethyloxime or the hemisuccinate bridge). Consequently the affinity can be higher or lower than that of the native steroid, or similar to it, and this can affect the sensitivity and specificity of the assay.^{13,14} However, most of the steroid–CL tracer conjugates possess suitable affinity for use in LIA methods.

THE LUMINESCENT IMMUNOASSAY METHOD

Within the last few years, LIA methods have been reported for several compounds of biological and clinical interest.⁴ In this paper we will discuss several types of steroid immunoassay based on monitoring chemiluminescence; these include homogeneous methods, which do not require a phase separation, and heterogeneous methods using dextran-coated charcoal or solid-phase separation systems.

Homogeneous LIA

The steroid–CL tracer conjugate emits light on oxidation by the hydrogen peroxide–microperoxidase system at pH 8.6–13.0. Use of pH 8.6 is compatible with monitoring of competitive protein-binding reactions in homogeneous medium when the presence of the specific antibody affects the light-yield from the conjugate.

A homogeneous LIA for progesterone has been developed.¹⁵ In this assay, the homologous antibody raised in rabbits by use of an anti-progesterone-11 α -hemisuccinate–BSA as the immunogen, causes an increase of the light-yield of the progesterone-11 α -hemisuccinate–ABEI during oxidation. The addition of unaltered homologous steroid (progesterone) to

the reaction mixture competitively inhibits the light production and this is the basis for the assessment of the standard curve in the homogeneous phase (Fig. 4).

This approach has been used for developing homogeneous LIA methods for progesterone,¹⁵ cortisol,^{12,16} and oestriol-16 α -glucuronide^{16,17} which have sensitivity and specificity similar to those of conventional RIA methods. However, an extraction of the biological sample (plasma or urine) was introduced into the procedure in order to remove non-specific compounds interfering in the CL reaction.

Recently we have developed a homogeneous LIA for total urinary oestrogens in diluted hydrolysed urine samples,¹⁸ this direct assay was possible because only 0.5 μ l of samples was used for the assay, a quantity small enough not to interfere in the CL reaction.

Homogeneous LIA methods are attractive because they can allow full automation of the assay; however, they do have some disadvantages, mainly due to incomplete knowledge of the mechanism of the antibody-enhanced chemiluminescence. Several factors are involved in the enhancement phenomenon, including the chemical structure of the tracer and the immunological characteristics of the antibody.¹⁵ Consequently, it appears that different procedures have to be chosen according to the antibody or labelled ligand used, and this is not practical for routine work, but the situation should improve as well standardized reagents become available (especially monoclonal antibodies).

Heterogeneous LIA

In contrast to homogeneous LIA, heterogeneous LIA does not utilize the light-enhancement properties of the specific antibody, but introduces a phase-separation step into the procedure.

An example of the dose–response curves for cortisol obtained by LIA and RIA procedures is shown in Fig. 5, and a comparison between the working ranges and detection limits is given in Fig. 6.

Some heterogeneous LIA methods have been described for cortisol,¹⁹ progesterone²⁰ and testosterone⁹

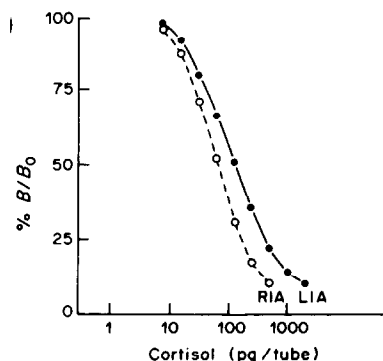


Fig. 5. Representative standard curves for cortisol, obtained by an LIA and an RIA procedure.

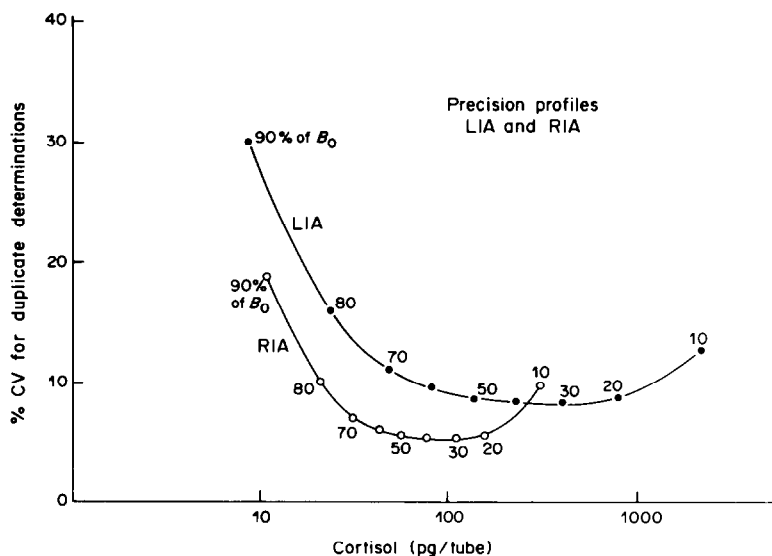


Fig. 6. Precision profiles of LIA and RIA for cortisol. Relationship between dose and precision (CV for duplicate determinations) as calculated from five LIA and RIA standard curves by a weighted four-parameter logistic analysis (program RIA004; see reference 9).

which use dextran-coated charcoal for separation of bound and free forms of the ligand, and can be readily introduced into clinical laboratories. However, this kind of phase separation step cannot always remove interfering compounds from biological samples and consequently most of these assays, like the homogeneous LIA methods, require a preliminary extraction step.

In attempts to develop simple and reliable LIA methods for plasma steroids and urinary steroid metabolites, we have explored the possibility of using solid-phase techniques. The solid-phase separation systems can obviate the need for prior purification of the sample since non-specific compounds, which may interfere in the CL reaction, are removed by washing after the binding reaction.

A number of solid supports (polystyrene tubes, etched polystyrene beads and antibodies covalently linked to polyacrylamide beads) have been used, and solid-phase LIA methods have been developed for progesterone²¹ and oestradiol²² in plasma and for oestriol-16 α -glucuronide,²³ testosterone-17-glucuronide,²⁴ oestrone-3-glucuronide²⁵ and pregnanediol-3-glucuronide²⁶ in urine.

These solid-phase LIA methods for urinary steroid glucuronides appear promising and the use of specific antibodies raised against urinary steroid metabolites (glucuronides) together with solid-phase techniques can avoid both the hydrolysis and the purification of urine samples, which are time-consuming and impractical methodological steps. The determination of urinary steroid metabolites can be an important tool in the investigation of several physiopathological conditions. For example, determination of oestriol-16 α -glucuronide can be used in monitoring of foetal

well-being,^{23,27} and testosterone-17-glucuronide is a useful index of the total androgenic secretion in man and woman in both normal conditions and under specific suppressive therapies.²⁴ Oestrone-3-glucuronide and pregnanediol-3-glucuronide can be used in monitoring the menstrual cycle^{28,29} and in this case only daily samples of early-morning urine are required, instead of 24-hr pooled collection. An example of monitoring of a normal menstrual cycle by LIA of urinary steroid metabolites is shown in Fig. 7.

DISCUSSION

In this paper we have reviewed the application of luminescence in the development of non-isotopic immunoassays for steroids. The analytical signal from the chemiluminescent tracer can be perturbed by interfering compounds of biological origin, present in the assay tube, and this reduces the reliability of the LIA methods. On-line computer analysis of the CL reactions seems particularly useful for identifying and eliminating these sources of error.

The main characteristics of the steroid-CL tracer conjugates are stability, safety, speed and sensitivity of detection. LIA methods based on use of such reagents possess sensitivity, specificity, accuracy and precision comparable to those commonly obtained with the equivalent RIA methods. Moreover, LIA methods which use solid-phase techniques allow the direct determination of steroids in unextracted samples, making the procedures simple and easy to introduce into clinical laboratories without problems of licensing and safety.

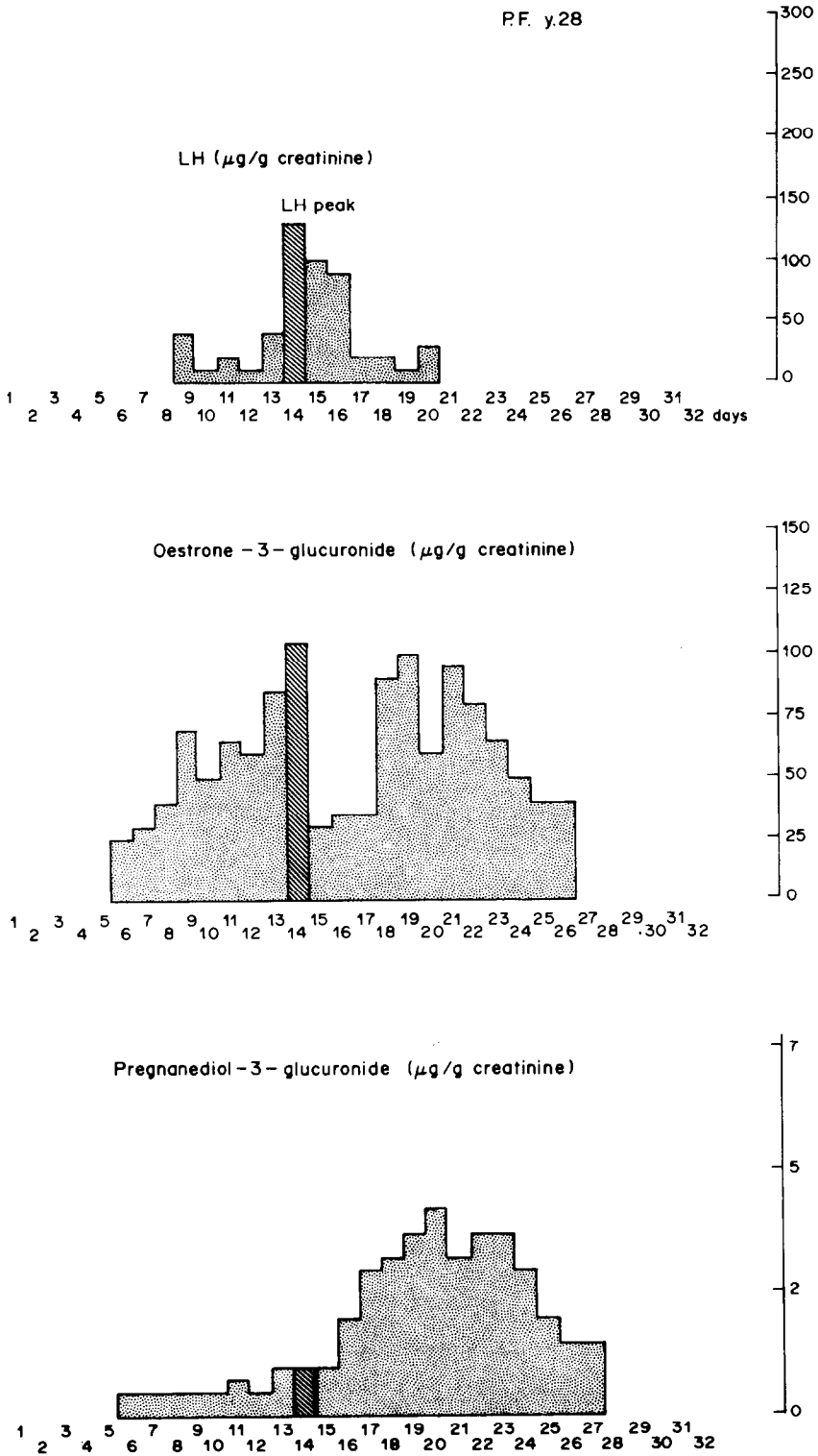


Fig. 7. Daily excretion of pregnanediol-3-glucuronide and oestrone-3-glucuronide through a normal menstrual cycle, as measured in early morning urine samples by solid-phase LIA methods. Urinary LH was measured by RIA.

In conclusion, the application of luminescence to non-isotopic immunoassays is a very promising technique, and would be more widely used if the commercial availability of well standardized reagents and of automated instrumentation for CL reactions improved.

Acknowledgements—This work is supported by a Grant of the University of Florence (ITEM X/02) and of the National Research Council, Italy "Progetto Finalizzato Tecnologie Biomediche e Sanitarie". R. Salerno is a fellow of the Lega Italiana per la Lotta contro i Tumori, Sez. di Firenze. We thank Bouty Diagnostici S.p.A., Milan, Italy, for technical assistance.

REFERENCES

1. T. P. Whitehead, L. J. Kricka, T. J. N. Carter and G. H. G. Thorpe, *Clin. Chem.*, 1979, **25**, 1531.
2. F. Gorus and E. Schram, *ibid.*, 1979, **25**, 512.
3. M. De Luca, *Bioluminescence and Chemiluminescence, Methods in Enzymology*, Vol. LVII. Academic Press, New York, 1978.
4. M. Serio and M. Pazzagli, *Luminescent Assays: Perspectives in Endocrinology and Clinical Chemistry*, in *Serono Symposia Publications*, Vol. 1, Raven Press, New York, 1982.
5. L. R. Faulkner, *Chemiluminescence from Electron-transfer Processes*. In Ref. 3, pp. 494–526.
6. H. H. Seliger, *Excited States and Absolute Calibrations in Bioluminescence*. In Ref. 3, pp. 560–600.
7. M. Pazzagli, J. B. Kim, G. Messeri, F. Kohen, G. F. Bolelli, A. Tommasi, R. Salerno, G. Moneti and M. Serio, *J. Steroid Biochem.*, 1981, **14**, 1005.
8. M. Pazzagli, M. Damiani, A. Tommasi, R. Salerno and M. Serio, *On-line Computer Analysis of the Kinetics of Chemiluminescent Reactions: Application to Luminescent Assays*, in *Computers in Endocrinology*, D. Rodbard and G. Forti (eds.), Serono Symposia Publications, Vol. 14, pp. 163–169. Raven Press, New York, 1984.
9. M. Pazzagli, M. Serio, P. Munson and D. Rodbard in *Radioimmunoassay and Related Procedures in Medicine—1982*, pp. 747–755. International Atomic Energy Agency, Vienna, 1982.
10. H. R. Schroeder and F. M. Yeager, *Anal. Chem.*, 1978, **50**, 1114.
11. H. R. Schroeder, in *Luminescent Assays: Perspectives in Endocrinology and Clinical Chemistry*, M. Serio and M. Pazzagli (eds.), pp. 129–146. Raven Press, New York, 1982.
12. M. Pazzagli, G. Messeri, A. L. Caldini, G. Moneti, G. Martinazzo and M. Serio, *J. Steroid Biochem.*, 1983, **19**, 407.
13. R. Malvano, *Radioimmunoassay in Principles of Competitive Protein-binding Assays*, W. D. Odell and P. Franchimont (eds.), pp. 161–204. Wiley, Chichester, 1983.
14. R. M. Allen and M. R. Redshaw, *Steroids*, 1978, **32**, 467.
15. M. Pazzagli, G. F. Bolelli, G. Messeri, G. Martinazzo, A. Tommasi, R. Salerno and M. Serio, in *Luminescent Assays*, M. Serio and M. Pazzagli (eds.), Vol. 1, Serono Symposia Publications, Raven Press, New York, 1982.
16. F. Kohen, M. Pazzagli, J. B. Kim and H. R. Lindner, *Steroids*, 1981, **36**, 421.
17. F. Kohen, J. B. Kim, G. Barnard and H. R. Lindner, *ibid.*, 1980, **36**, 405.
18. G. Messeri, A. L. Caldini, A. Tommasi, M. Pazzagli, G. F. Bolelli and M. Serio, *Clin. Chem.*, 1984, in the press.
19. M. Pazzagli, J. B. Kim, G. Messeri, F. Kohen, G. F. Bolelli, A. Tommasi, R. Salerno and M. Serio, *J. Steroid Biochem.*, 1981, **14**, 1181.
20. M. Pazzagli, J. B. Kim, G. Messeri, G. Martinazzo, F. Kohen, F. Franceschetti, A. Tommasi, R. Salerno and M. Serio, *Clin. Chim. Acta*, 1981, **115**, 287.
21. F. Kohen, J. B. Kim, H. R. Lindner and W. P. Collins, *Steroids*, 1981, **38**, 73.
22. J. B. Kim, G. J. Barnard, W. P. Collins, F. Kohen, H. R. Lindner and Z. Eshhar, *Clin. Chem.*, 1982, **28**, 1120.
23. G. Barnard, W. P. Collins, F. Kohen and H. R. Lindner, *J. Steroid Biochem.*, 1981, **14**, 941.
24. P. L. Vannucchi, G. Messeri, G. F. Bolelli, M. Pazzagli, A. Masala and M. Serio, *ibid.*, 1983, **18**, 625.
25. D. A. Weerasekera, J. B. Kim, G. J. Barnard, W. P. Collins, F. Kohen and H. R. Lindner, *Acta Endocrinol.*, 1982, **101**, 254.
26. Z. Eshhar, J. B. Kim, G. Barnard, W. P. Collins, S. Gilad, H. R. Lindner and F. Kohen, *Steroids*, 1981, **38**, 89.
27. A. L. Caldini, M. Pazzagli, G. Messeri, G. F. Bolelli, P. Buzzoni, A. Borri, G. Moneti and M. Serio, In *RIA 83: Progress in Perinatal Medicine*, 1983, Abstract No. 50.
28. World Health Organization, *J. Steroid Biochem.*, 1982, **17**, 695.
29. H. R. Lindner, F. Kohen, Z. Eshhar, J. B. Kim, G. Barnard and W. P. Collins, *ibid.*, 1982, **15**, 131.

DETERMINATION OF HORMONES BY TIME-RESOLVED FLUOROIMMUNOASSAY

TIMO LÖVGREN, ILKKA HEMMILÄ, KIM PETTERSSON,
JARKKO U. ESKOLA and ERIC BERTOFT
Wallac Biochemical Laboratory, P.O. Box 10, SF-20101 Turku 10, Finland

(Received 3 May 1984. Accepted 4 June 1984)

Summary—Immunoassays based on europium labels and time-resolved fluorescence as the detection method, have been developed. The specific activity of the label is several orders of magnitude higher than that of radioactive labels. Consequently, the technique provides great potential, especially in the determination of analytes which require high sensitivity. Both competitive and immunometric assays which use labelled antibodies have been worked out. In competitive assays the antigen is immobilized on a solid phase with a protein carrier. The antigen in the standard or sample then competes with the labelled antibody in solution. Separation is done simply by washing the wells in the microtitre strip where the assays are performed. Model systems are described for the measurement of testosterone and cortisol. Immunometric assays of human thyrotropin (hTSH) and luteotropin (LH) were performed with monoclonal antibodies, by either a one-step (hTSH) or two-step (LH) incubation procedure. These assays, which exploit the specific activity of the label, give a very high sensitivity and good reproducibility. The standard curves are linear and the dynamic range is at least 1000-fold. Because of the properties of the europium label and the simple assay design, the immunoassays based on time-resolved fluorescence are expected to gain wide application both in research and in routine determinations.

Since the development of RIA and related saturation assay techniques by Berson and Yalow¹ and Ekins² in the late 1950s, the assays have been extensively applied to numerous analytes in routine work as well as in research. The basic procedure in RIA has been refined, but at least in clinical chemistry it is still the most widely used immunoassay technique. The wide use of radioactive labels in immunoassays has, however, increased awareness of the problems involved, e.g., health hazards associated with the use and disposal of radioactive material, and the limited shelf-life of the labelled reagents due to the short half-life of the radioactive label and to radiolysis. A number of alternative non-isotopic techniques have been tested with the purpose of avoiding the disadvantages of radioimmunoassays without any decrease in the potential of the immunoassay technique as such. At present the most promising alternatives to RIA are enzyme immunoassay, chemiluminescence immunoassay and fluoroimmunoassay.

The sensitivity of most fluoroimmunoassay methods reported to date is, however, far lower than that of radioimmunoassay.³ The limited sensitivity is caused by the high background signal which is always obtained in conventional fluorometric determinations, and which seriously limits the possibilities for exploiting the inherent sensitivity of the measurement principle. A tremendous increase in sensitivity is achievable by utilizing the difference in the fluorescence lifetime of the signal originating from different fluorescent compounds.^{4,5} All conventional fluorescence, including that causing the high background which limits the sensitivity, has a half-life of

decay in the range 10^{-8} – 10^{-9} sec. Consequently, if a europium chelate with a fluorescence decay time of 10^{-3} – 10^{-6} sec is chosen as label and its specific fluorescence is measured after the background signal has decayed, an excellent sensitivity can be achieved. When time-resolved fluorescence is used, europium concentrations as low as $5 \times 10^{-14}M$ can be measured.^{5,6}

The present communication describes immunoassay methods based on the use of europium as label and time-resolved fluorescence as the technique for determining it. The new immunoassay technique has been applied both in competitive and reagent-excess measurements on systems involving labelled antibodies. Model assays using solid-phase antigens or antibodies have been worked out for steroids and peptides. The advantage of the high specific activity of the label is obvious in the reagent-excess system, as an increased sensitivity can be achieved.

EXPERIMENTAL

Materials

Eu_2O_3 was obtained from Fluka. EuCl_3 was prepared by dissolving the oxide in hydrochloric acid and evaporating the excess of acid. Isothiocyanatophenyl-EDTA-Eu and other corresponding polycarboxylic acid derivatives were synthesized from the amino-derivatives of the europium chelate by condensation with thiophosgene in a water-chloroform mixture. After this the chloroform was removed and the isothiocyanate derivative was recovered from the aqueous phase mixture. The aminophenyl derivative of EDTA was synthesized by a modification of the Sundberg method.⁷ The enhancement solution used for europium determination by time-resolved fluorescence⁸ and the assay buffer consisting of 0.05M Tris-HCl, pH 7.7,

containing 0.9% sodium chloride, 0.05% sodium azide, 0.5% bovine serum albumin, 0.05% bovine globulin, 0.01% Tween 40 and 20 μM diethylenetriaminepenta-acetic acid, were obtained from LKB-Wallac, Turku, Finland. The monoclonal antibodies used in the peptide assays were obtained from Medix Laboratories Ltd., Kauniainen, Finland, and the polyclonal antibodies used in steroid assays came from Farnos Diagnostica, Turku, Finland.

The europium fluorescence was measured with a 1230 Arcus time-resolved fluorometer⁴ (LKB-Wallac, Turku, Finland). In all assays polystyrene microtitre strips (Lab-systems Oy, Helsinki, Finland) were used.

Labelling of antibodies

Depending on the conjugation conditions and the antibody preparations, a 50–300-fold molar excess of europium isothiocyanatophenylcomplexonate was used in conjugations performed in phosphate buffer at pH 9.0–9.3 and 4°, overnight. The europium-labelled antibody was separated from excess of label by gel-filtration on a Sepharose-6B column (1.5 \times 70 cm) and eluted with 0.05M Tris-HCl buffer, pH 7.4, containing 0.9% sodium chloride and 0.05% sodium azide. The number of europium ions incorporated per immunoglobulin molecule was determined by measuring the fluorescence in comparison to that of known EuCl₃ standards.⁶ On the average, 5–15 europium ions were incorporated per protein molecule. Bovine serum albumin (1 mg/ml) was added as carrier to the labelled antibody solutions.

Coating of microtitre strips

In immunometric assays the wells of polystyrene microtitre strips were coated with the antibodies, whereas in competitive assays protein-bound haptens were used.

Coating with antibody was performed by physical adsorption. Individual wells were treated with 0.2 ml of antibody preparation (5 $\mu\text{g}/\text{ml}$) in 0.1M phosphate buffer, pH 4.9, for 20 hr at room temperature, washed three times with saline, then saturated by treatment for 2 hr with 0.3 ml of 0.05M Tris-HCl buffer, pH 7.4, containing 0.9% sodium chloride, 0.05% sodium azide, 0.5% bovine serum albumin. The coated and saturated strips were washed twice with saline and stored humid at 4° until used.

Coating with protein-bound haptens was performed with cortisol- or testosterone-3-CMO-ovalbumin conjugates (CMO = carboxymethylloxime) prepared as described by Hosoda *et al.*⁸ Individual wells were coated by treatment with 0.25 ml of protein-bound hapten preparation (0.05 $\mu\text{g}/\text{ml}$) in 0.1M sodium carbonate buffer, pH 9.3, overnight at room temperature. After coating, the wells were washed three times with 0.15M saline solution containing 0.05% sodium azide, after which they were ready for use.

Measurement of europium fluorescence

When the immunoreaction is complete, the label is dissociated from the antibody bound to the solid by adding an enhancement solution (200 μl) consisting of 0.1M acetate buffer adjusted to pH 3.2 with potassium hydrogen phthalate, and containing 15 μM 2-naphthoyltrifluoroacetone, 50 μM tri-n-octylphosphine oxide and 0.1% Triton X-100.⁶

RESULTS

Immunometric assay of peptide hormones

Monoclonal antibodies for different gonadotropic hormones have recently become available, and have been applied in combination with europium labels and time-resolved fluorometric detection. These antibodies suit immunometric assays well, as the two-site concept can be utilized in tests which require either

one or two incubation steps.⁹ In addition, it is possible to use the reagent-excess technique,¹⁰ as the supply of antibody is unlimited.

In the assay of hTSH two β -chain specific monoclonal antibodies are used. The hTSH sample or standard is reacted with a β -chain specific monoclonal antibody immobilized on the surface of microtitre-strip wells. The europium-labelled second monoclonal antibody, specific against a different site on the β -subunit, is added simultaneously with the analyte. Thus the whole assay requires only one incubation step. After thorough washing of the strip, the added enhancement solution dissociates into solution the europium ions from the labelled second antibody bound to the solid phase. In solution the europium ion forms a new and highly fluorescent chelate, and the fluorescence is directly measured in the microtitre strip well. The assay procedure is outlined in Fig. 1A and a typical standard curve is shown in Fig. 2. The dose-response curve is linear after the background of the zero standard has been subtracted, and the fluorescence intensity is directly proportional to the antigen concentration over the whole standard range, which extends from 0.25 to 324 $\mu\text{U}/\text{ml}$.

A precision profile calculated from 12 replicates of each hTSH concentration is also shown in Fig. 2. The whole working range of the assay is covered by a coefficient of variation (CV) that is 5% or smaller. The minimum detection limit, defined as the hTSH concentration corresponding to the mean fluorescence signal of 12 replicates of the zero standard plus 3 times the standard deviation, is 0.03 $\mu\text{U}/\text{ml}$ —far below the lowest standard concentration used in the assay.

Cross-reactions obtained for the two monoclonal antibodies separately (RIA) and in combination (time-resolved fluoroimmunoassay), are given in Table 1.

Figure 3 shows the correlation between the time-resolved immunofluorometric assay and a conventional competitive RIA for samples with hTSH levels either above (A) or below (B) 4 $\mu\text{U}/\text{ml}$. At concentrations above 4 $\mu\text{U}/\text{ml}$ correlation between the two procedures is excellent whereas samples with hTSH levels below 4 $\mu\text{U}/\text{ml}$ give poor correlation. Furthermore, in a number of samples the hTSH levels were not detectable by the RIA procedure. Only 3 samples among the 27 with hTSH levels below 1 $\mu\text{U}/\text{ml}$ gave a negative result in the immunometric procedure.

The LH assay is performed with β -chain and α -chain specific monoclonal antibodies, respectively. The assay is performed in either one or two steps. The two-step assay procedure is outlined in Fig. 1B and a typical standard curve is shown in Fig. 4.

The fluorescence intensity is directly proportional to the LH concentration within a range from 1 to 125 IU/l. and the standard curve is linear after subtraction of the zero standard. The CV over the whole

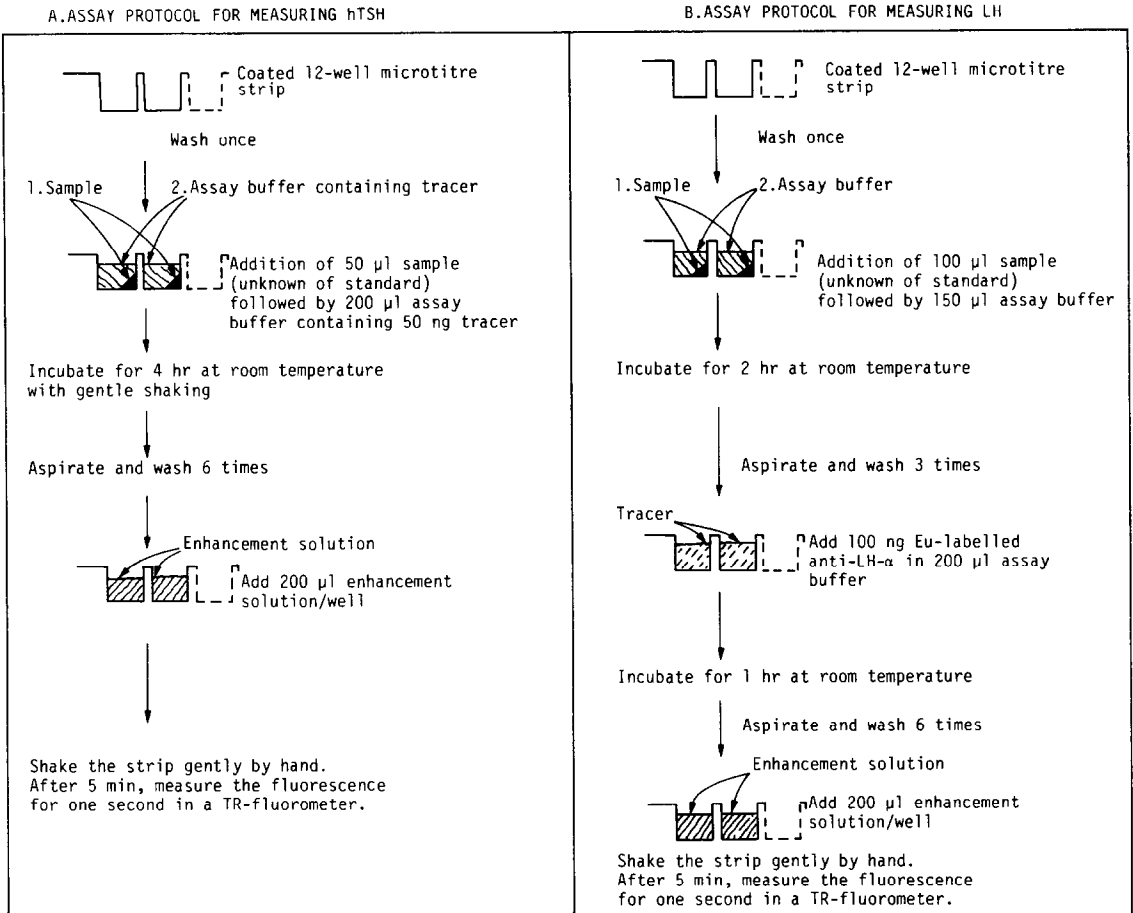


Fig. 1. Immunometric assay procedures for hTSH (A) and LH (B), using antibody-coated microtitre-strip wells, europium-labelled antibodies and time-resolved fluorescence.

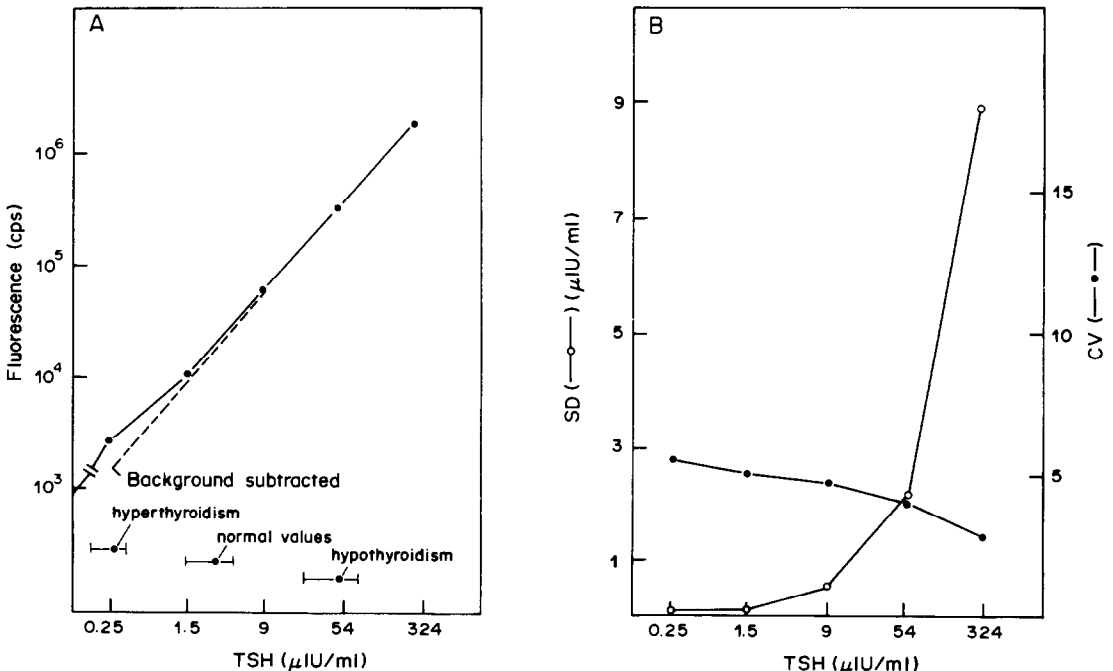


Fig. 2. Standard curve (A) and precision profile (B) for the one-step hTSH assay, performed according to Fig. 1A. The reference values were measured by Imagura *et al.*¹² by enzyme immunoassay with fluorescent detection.

Table 1. The cross-reactivities of the two β -specific monoclonal antibodies (I = solid-phase antibody, II = used for labelling) used in the hTSH assay, when measured separately (RIA) or in combination (TR-FIA)

Hormone	Cross-reactivity, %		
	I (RIA)	II (RIA)	I + II (TR-FIA)
hTSH	100	100	100
hLH	<0.4	0.5	2.3
hCG	<0.1	<0.02	<0.001
hTSH β -subunit	195	<1.0	1.8
hFSH	—	—	1.8

assay range is below 8%. The detection limit (mean of the zero sample + 3 standard deviations) was found to be 0.04 IU/l. when a 100- μ l sample volume was used. Table 2 shows the cross-reactivity of the two monoclonal antibodies employed, when measured separately in a conventional RIA and in combination by the assay procedure described in Fig. 1B. Cross-reactivity with hCG is rather high, and the clinical situation has to be taken into account when the assay results are evaluated. In the process of ovulation the hCG level is virtually zero and a rapid increase in the LH level occurs. There is good correlation between the time-resolved fluorescence method and a conventional RIA for LH.

Competitive steroid assays with labelled antibodies

To avoid the need to label different antigens with a europium chelate and with the intention of making the separation step required in competitive assay procedures as simple as possible, the conventional assay design was abandoned and an antibody-labelled competitive technique was designed. In this technique a known amount of antigen is immobilized on the solid phase. The standard or sample is added immediately before the labelled antibody. The immo-

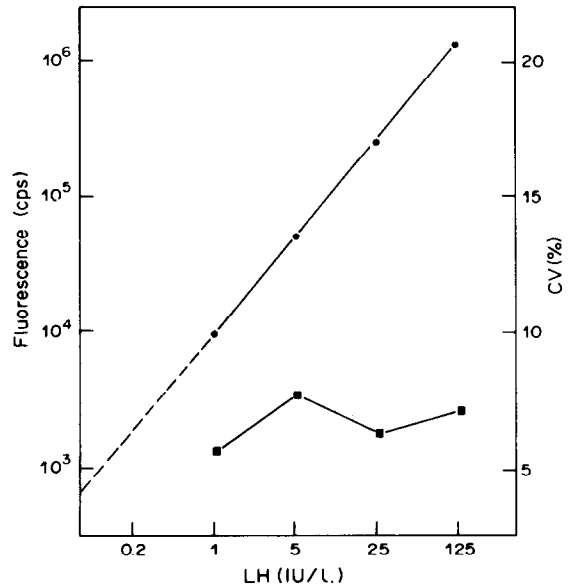


Fig. 4. Standard curve (●) and precision profile (■) for the two-step LH assay done according to Fig. 1B. The reading of the zero-standard (550 cps) has been subtracted from all standards.

bilized and free antigen will then compete for the binding sites on the labelled antibody. After a 1-hr incubation at room temperature, the microtitre strip wells where the assay is performed are washed, and the amount of europium-labelled antibodies bound to the solid phase is determined by adding the enhancement solution and measuring the europium fluorescence by time-resolved fluorometry. The assay design is outlined in Fig. 5. A standard curve similar to that obtained in a conventional competitive RIA is constructed and the analyte concentration of the samples is read. Assays as described above have been worked out for both testosterone and cortisol.

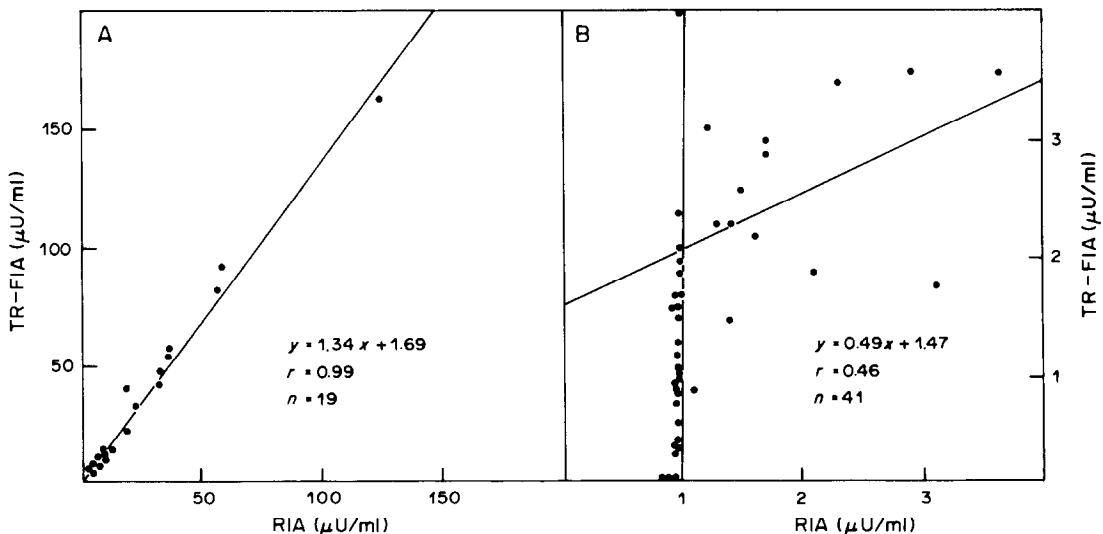


Fig. 3. Correlation between RIA and time-resolved assays of hTSH in serum samples with an hTSH concentration above (A) or below (B) 4 μ U/ml.

Table 2. The cross-reactivities of the β - and α -chain specific monoclonal antibodies used in the LH assay, when measured separately (RIA) or in combination (TR-FIA)

Hormone	Cross-reactivity, %		
	Anti- β (RIA)	Anti- α (RIA)	Both antibodies (TR-FIA)
LH	100	100	100
hCG	62	28	62
hTSH	14	24	10

The effect of the amount of the solid-phase antigen and labelled antibody in the testosterone assay has been investigated in detail. Figure 6A illustrates a typical result when the amount of testosterone immobilized by physical adsorption as a testosterone-3-CMO-ovalbumin conjugate on the solid phase, is varied. A constant amount of labelled antibody was used, in the absence (B_0) and presence (B) of free steroid in solution. In absence of free testosterone, the solid phase is saturated with the steroid conjugate at a concentration of about 2 pmole per well. The signal from the europium-labelled antibody bound to the solid-phase antigen reaches a constant level. In the presence of a free testosterone concentration corresponding to the level of the highest standard in an actual assay, the signal increases as the amount of immobilized antigen on the solid phase increases. If the fraction bound is plotted against the immobilized-antigen concentration, it becomes obvious that the best replacement is obtained at a relatively low amount of antigen on the solid phase (Fig. 6B) which favours competition between the amounts of bound and free antigen. At low solid-phase antigen concentrations various amounts of labelled antibody can be used without any critical effect on the performance of the assay. A testosterone-3-CMO-ovalbumin concentration of 0.05 $\mu\text{g/ml}$ for coating the microtitre-strip well and 25 ng of europium-labelled antibody preparation per well were found optimal.

A standard curve and a precision profile for the testosterone assay covering the range of clinical inter-

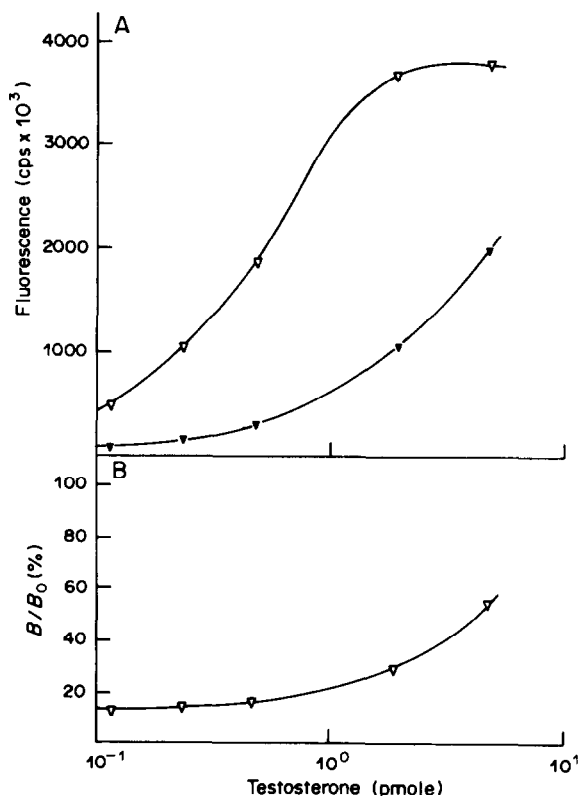


Fig. 6. (A) The effect of different amounts of testosterone immobilized on the solid phase (as a testosterone-3-CMO-ovalbumin conjugate) on the fluorescence signal obtained with a constant amount (25 ng, 5 Eu/IgG) of labelled antibody. The assay was done in the absence (Δ) and presence (\blacktriangle , 300 nM, 50 μl sample volume) of free testosterone in solution. The total volume was 200 μl and the incubation time 90 min at room temperature. (B) The effect of the immobilized testosterone concentration on the fraction of labelled antibody bound to the solid-phase antigen in the presence of 300 nM free testosterone.

est is shown in Fig. 7. The precision over the assay range lies between 18 and 6%. Correlation between the new time-resolved fluorescence assay and conventional RIA was found to be good when extracted serum samples were used (Fig. 8).

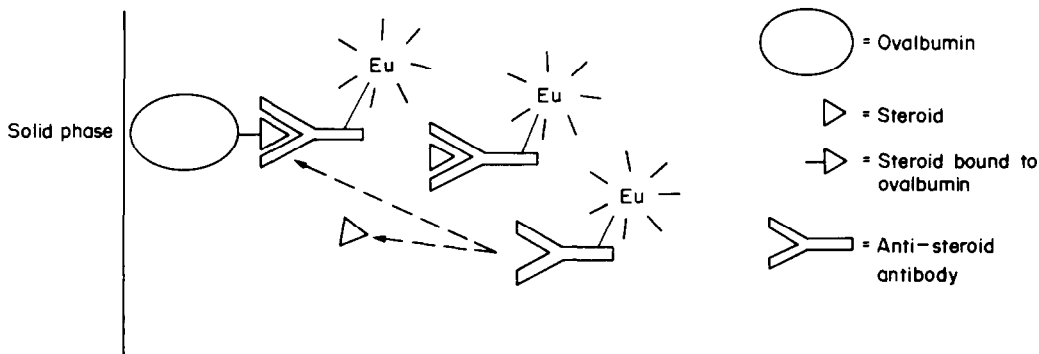


Fig. 5. The principle of the competitive time-resolved fluoroimmunoassay of steroids, based on a europium-labelled antibody assay and a constant amount of immobilized steroid on the wall of microtitre-strip wells. After the competitive immunoreaction has been completed, the label is released into solution by addition of the enhancement solution.

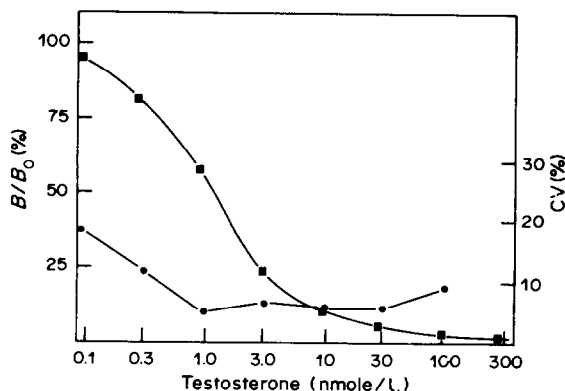


Fig. 7. Dose-response curve (■) and precision profile (●) for the time-resolved fluoroimmunoassay of testosterone. The assay conditions were as described in Fig. 6A and a solid-phase antigen concentration of 0.23 pmole of testosterone per well was used.

A similar assay procedure has also been developed for cortisol. However, it is a direct test and thus no pretreatment of the serum samples is required. The assay has been optimized in the same way as the testosterone assay. Figure 9 shows the effect of three different amounts of the cortisol-3-CMO-ovalbumin conjugate on the shape of the standard curve for cortisol within the clinically relevant range. The fraction bound (B/B_0) at different standard concentrations decreases as the amount of antigen bound to the solid phase is reduced, as will of course the actual amount of labelled antibody bound to the solid phase at each concentration. The fluorescence signal level in the assay is dependent on the number of europium

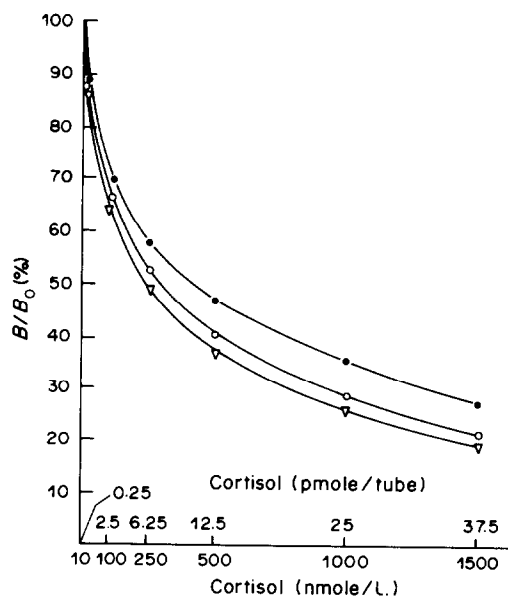


Fig. 9. Standard curves for a competitive time-resolved fluoroimmunoassay of cortisol with three different amounts of cortisol-3-CMO-ovalbumin immobilized on the walls of microtitre strips: ● 3.5, ○ 1.7 and △ 0.9 pmole of cortisol per well. The assays were done with a sample volume of 20 μ l and a total volume of 120 μ l, with 50 ng of labelled antibody (5 Eu/IgG) in the assay buffer. Incubation was 1 hr at room temperature. B_0 was 4.05×10^5 , 2.30×10^5 and 1.33×10^5 cps, for the three solid-phase antigen levels (in order of decreasing concentration).

ions conjugated to the labelled antibody, but the level can be further adjusted by varying the amount of labelled antibody within a certain limit. Consequently, the fluorescence signal in the assay is modified by varying the parameters during the optimization of assay conditions.

Figure 10 shows the correlation between a conventional RIA and the time-resolved fluoroimmunoassay of cortisol with labelled antibodies. The coefficient of variation (CV) within the assay range was below 11%.

DISCUSSION

The results obtained in immunometric and competitive assays, both of them based on a labelled-antibody technique, show that sensitive, rapid and simple assays can be developed with europium as the label and time-resolved fluorescence as the detection method. The long decay time of the europium label is utilized to eliminate the background problem which previously limited the applicability of fluorescent labels in assays requiring high sensitivity. In the assays, the europium ion is actually bound to the antibody as a non-fluorescent chelate.⁶ Consequently, only the chelated metal ion is used as the label during the immunoreaction, and the europium fluorescence is developed after the ion is released by dissociation in the presence of an enhancement solu-

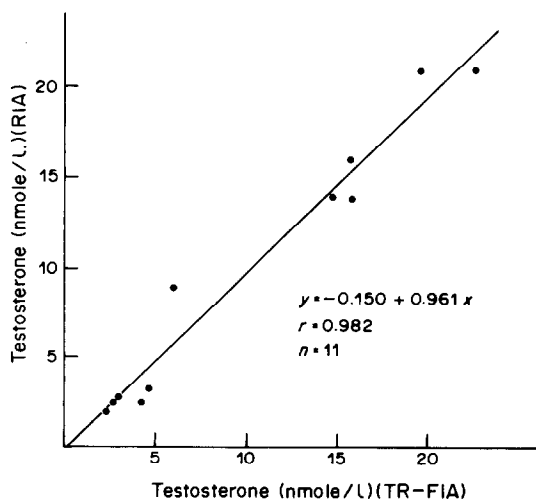


Fig. 8. Correlation between RIA and time-resolved fluoroimmunoassay of testosterone. Serum-based standards of unknown samples (100 μ l) were extracted for 15 min with 1 ml of freshly prepared diethyl ether-ethyl acetate mixture (9:1 v/v); a 400- μ l portion of the ether phase was evaporated under a stream of air, after which 120 μ l of assay buffer were added and the sample was left for at least 30 min before duplicate 50- μ l samples were taken for the measurement.

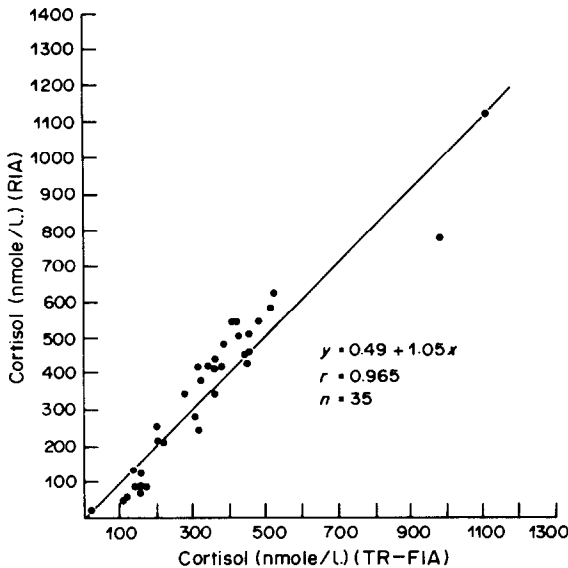


Fig. 10. Correlation between RIA and time-resolved fluoroimmunoassay of cortisol. Serum-based standards and unknowns (20 μ l) were used in accordance with the assay conditions described in the caption to Fig. 9.

tion which contains the energy-absorbing ligands required for the formation of a fluorescent chelate. The situation is very favourable in regard to the measurement of fluorescence because excitation and emission occur in solution and not on a solid phase. In solution, europium concentrations as low as $5 \times 10^{-14} M$ have been determined by use of the present systems, and as a number of europium ions can be coupled per antibody molecule, prospects for obtaining assays with even higher sensitivity exist.^{5,6} The specific activity of the label, calculated on the basis of the measurement in solution, is actually 10^6 times that for ^{125}I , which is most commonly used in assays employing radioactive labels.⁴

The europium label can be used as in both competitive and immunometric assays. The competitive assays are based on a labelled-antibody technique to avoid the need to label every separate antigen, and hence avoid the difficulties involved in such steps. Furthermore, the use of the immobilized-antigen technique in competitive assays greatly simplifies the procedure, and all stability problems connected with the solid phase are eliminated. The performance characteristics are at least as good as those of conventional competitive techniques employing radioactive labels.

The immunometric assay design benefits more extensively from the properties of the europium label. As shown before, assays with a higher sensitivity than that normally achieved with radioactive labels are obtained, for the same assay principle. The reason for the improved performance can be traced back to (a) the labelling, which does not affect the properties of the antibody, (b) the high specific activity of the label, and (c) the large excess of labelled antibody that can

be used in the assays with no increase in non-specific binding. Of these causes, the last is probably the most important. In principle it should be possible to obtain similar performance characteristics with the same immunocomponents by using a radioactive label such as ^{125}I , but a tremendous amount of radioactivity would have to be added, which in practice would cause several undesirable effects. The experimental results are consistent with the theoretical optimization of immunoradiometric assays.¹¹

Besides high sensitivity, the immunometric assays based on europium labels have a number of other benefits. The europium concentration can be measured over a wide dynamic range and as the capacity of the antibody immobilized on the solid phase is large and a considerable excess of the labelled antibody is used, an assay with an extraordinarily wide dynamic range is obtained. The benefit of the wide range is, of course, dependent on the degree of variation in the analyte concentration in clinical samples. It will, however, be of greater importance in the future as improved sensitivity in the assays widens the detectable concentration range for a number of analytes and facilitates important research on their clinical importance; hTSH is a typical analyte belonging to this category, because in conventional methods difficulties arise in measurement of concentrations at normal levels and below.

The standard curve in immunometric assays is linear after the background signal has been subtracted. Because of this it becomes possible to reduce the number of standards required. Assays can even be performed with only one standard and a blank. This property can be utilized to full extent when a stable label-preparation is used. However, replication of the standard will improve the precision.

Both the competitive and immunometric assays have been based on use of the wells of polystyrene microtitre strips as the solid phase. In each case handling becomes simpler, since the separation step in the solid-phase assays is accomplished by washing the wells, which can be done with a variety of commercially available devices designed for the purpose. The only additional step [apart from the incubation(s) and washing] currently needed in the time-resolved fluorescence assays is the addition of enhancement solution before the 1-sec measurement in the fluorometer. The total assay time, including the immunoreaction(s), is dependent on the quality of the antibodies used. Several of the assays can be done in 1 hr or less, as the fast and easy handling eliminates the error caused by slight variations in incubation times when equilibrium is not reached. In practice, however, the number of tests in fast assays must be limited to 1 microtitre plate (8 strips). Monoclonal antibodies contribute to the simplicity of the procedure in immunometric assays, as some of the tests can often be performed with a single incubation, with all the components required added in one step. A one-incubation, multi-site, solid-phase assay of

human pancreatic phospholipase A₂, based on time resolved fluorescence, has been developed recently, and was successful even though a polyclonal antibody was used.¹³

CONCLUSIONS

Europium ions as labels and time-resolved fluorometry as the detection method have been shown to provide an alternative of high potential in the field of non-isotopic immunoassays. The high specific activity, which exceeds that of radioactive labels, makes the europium label ideal in assays requiring high sensitivity. The label can be applied both in competitive assays using a labelled-antibody technique, and in immunometric assays. In both types of assay high sensitivity and excellent precision have been obtained, and the immunometric assays give a linear range of at least 1000-fold.

The combination of solid-phase assay with the stable label and fast and sensitive detection principle results in rapid tests that are easy to handle. The technique is predicted to have a wide application in a variety of immunoassays in both research and routine determinations in the near future.

REFERENCES

1. R. S. Yalow and S. A. Berson, *Clin. Invest.*, 1960, **39**, 1157.
2. R. P. Ekins, *Clin. Chim. Acta*, 1960, **5**, 453.
3. J. Landon and R. S. Kamel, in A. Voller, A. Bartlett and D. Bidwell, *Immunoassays for the 80's*, p. 91. MTP Press, Lancaster, 1981.
4. E. Soini and H. Kojola, *Clin. Chem.*, 1983, **29**, 65.
5. T. Lövgren, I. Hemmilä, K. Petterson and P. Halonen, in W. P. Collins, *Alternative Immunoassays*, Wiley, Chichester, 1984, in the press.
6. I. Hemmilä, S. Dakubu, V.-M. Mikkala, H. Siitari and T. Lövgren, *Anal. Biochem.*, 1984, **137**, 335.
7. M. W. Sundberg, C. F. Meares, D. A. Goodwin and C. J. Diamanti, *J. Med. Chem.*, 1974, **17**, 1304.
8. H. Hosoda, Y. Sakai, H. Yoshida and T. Nambara, *Chem. Pharm. Bull.*, 1979, **27**, 2147.
9. E. D. Sevier, G. S. David, J. Martinis, W. J. Desmond, R. M. Bartholomew and R. Wang, *Clin. Chem.*, 1981, **27**, 1797.
10. R. P. Ekins, in A. Voller, A. Bartlett and D. Bidwell, *Immunoassays for the 80's*, p. 5. MTP Press, Lancaster, 1981.
11. T. M. Jackson, N. J. Marshall and R. P. Ekins, in W. M. Hunter and J.E.T. Corrie, *Immunoassays for Clinical Chemistry*, 2nd Ed., p. 557. Churchill Livingstone, Edinburgh, 1983.
12. M. Imagawa, E. Ishikawa, S. Yoshitake, K. Tanaka, H. Kan, M. Inada, H. Imura, H. Kurosaki, S. Tachibana, M. Nishiura, N. Nakazawa, H. Ogawa, Y. Tsunetoshi and K. Nakajima., *Clin. Chim. Acta*, 1982, **126**, 227.
13. J. U. Eskola, T. J. Nevalainen and T. N-E. Lövgren, *Clin. Chem.*, 1983, **29**, 1777.

IMMUNOASSAYS IN AQUEOUS TWO-PHASE SYSTEMS

TORBJÖRN G. I. LING and BO MATTIASSON

Pure & Applied Biochemistry, Chemical Centre, P.O. Box 740, S-220 07 Lund, Sweden

(Received 24 January 1984, Accepted 13 April 1984)

Summary—Aqueous two-phase systems provide a novel and convenient method for separating bound from free fractions in a binding assay. The ease of automation of this type of procedure makes it particularly attractive for separations based on immobilized ligands or binders or on adsorbents.

In order to determine the degree of binding in a ligand:binder assay, the amount of free and/or bound reactant must be measured. This generally requires a separation step. There are exceptions to this rule, but there is no general method that avoids separation. In an effort to meet at least some of the requirements for a fast and simple assay we have developed the so-called "partition-affinity ligand assay" (PALA). The method involves a binding reaction and subsequent separation by partition in an aqueous two-phase system.

In aqueous two-phase systems, both phases contain 85–95% water together with a water-soluble polymer or a salt. The systems based on poly(ethylene glycol) (PEG), and dextran have been studied extensively. In these systems the PEG is mainly in the upper phase, and the denser phase is rich in dextran. The systems are biocompatible because of their high water content and the extremely low surface tension (in many cases less than 0.1 dyne/cm).

When a substance is added to a two-phase system, it will partition between the phases according to the surface properties of its molecules. The partition behaviour is characterized by the partition coefficient, K_{part} , which is the ratio of the concentrations in the top phase to that in the bottom phase.

The principle for studying direct binding reactions in aqueous two-phase systems is schematically illustrated in Fig. 1. The composition of the phase system is chosen so that the antigen partitions into one phase (Fig. 1a) and the antibody into the other (Fig. 1b). The degree of binding is then a function of the displacement of antigen when antibodies are added to the system and antigen is moved to the phase into which the antibodies partition (Fig. 1c). In practice, neither reactant is completely partitioned into one of the phases, but the two partition coefficients give the range for the calibration curve.

The separation step in a binding assay must be highly reproducible and preferably fast as well. This means that when phase systems are used for separation, the effects of salts and other substances that influence partitioning should be minimized. It also means that long multi-step procedures should be

avoided. Both these requirements imply the use of an effective separation procedure and can be met by employing an antibody with strongly selective partitioning into one of the phases and thus low sensitivity to change in the composition of the phase system.

Requirements for separation

Proper partitioning of the antibody can be accomplished by choosing a proper phase system,^{1,2} or if necessary, by modifying the surface structure of the antibody³⁻⁵ in order to make it partition practically exclusively into one of the phases. Such modified binding structures have been called *separator molecules*.

Partition-affinity ligand assays can only be set up when the differences in partition behaviour between the reactants are sufficiently large. The character of the label used and the binding characteristics of the antigen-antibody interaction, as well as the reactant concentrations influence the overall partitioning. In general terms, however, when the ratio of the partition coefficients is greater than 10 it is possible to set up a manually interpreted assay. In this case the partition coefficient can be regarded as an approximation of the bound/free ratio. As will be discussed later, even small differences in the partition coefficients may be sufficient if an evaluation method

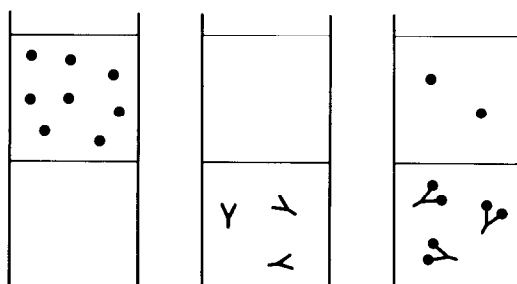


Fig. 1. Schematic representation of a direct binding assay between antigen and antibody. (A) The antigen partitions into the top phase and (B) the antibody partitions into the bottom phase. (C) Binding is observed as a displacement of antigen from the top phase to the bottom phase.

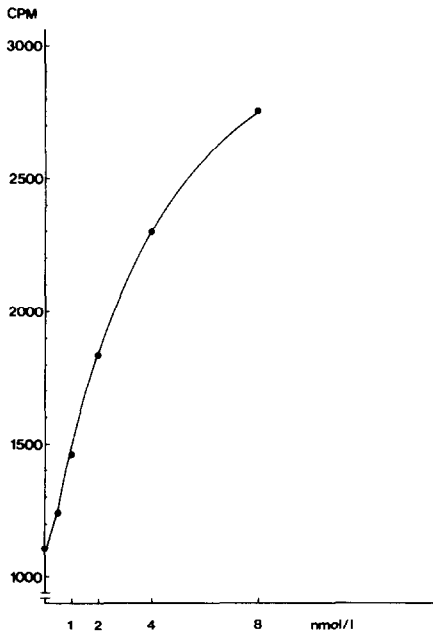


Fig. 2. Calibration curve for a competitive assay of digoxin. Native and iodine-labelled digoxin partitioned into the top phase, whereas the antibodies partitioned into the bottom phase. The radioactivity in the top phase is given as a function of added native digoxin. (From Mattiasson,¹ by permission of the copyright holders.)

that compensates for the incomplete separation is utilized.

In assays of haptens favouring the top phase, a very favourable situation occurs. In the case of digoxin, for example, the partition coefficient for the digoxin is 4.0 and for the antibody against digoxin 0.30. Furthermore, the reactants differ in size

sufficiently for the complex formed to partition in the same way as the native antibody. By measurement of the decrease in label concentration in the top phase and/or the concomitant increase in the bottom phase at constant concentration of antibodies and labelled digoxin, the concentration of the native digoxin can be obtained by interpolation in a calibration curve.

A typical calibration curve is shown in Fig. 2. Several haptens behaving like digoxin have been determined (Table 1). When the molecules are equally large and/or favour the same phase as the antibodies do, a much more complicated situation occurs. In such cases one of the reactants has to be modified in order to change its partition behaviour. Several possibilities for overcoming this problem are discussed in the following section.

In a study of molecules of similar molecular weights (less than one order of magnitude difference) and similar partition behaviour, the interaction between the lectin concanavalin A (Con A) and the glycoenzyme, horseradish peroxidase (HRP), was examined. The system was designed to study binding of sugars in a competitive assay where the carbohydrate competed with the carbohydrate entities of the peroxidase molecule for binding to Con A. The enzyme part of the glycoprotein was thus utilized as an enzyme label on the carbohydrate. In the phase system used, K_{part} for HRP was 0.12 and for Con A 0.031.

In order to solve the separation problem, a rather drastic change in the partition behaviour of one of the entities was necessary. The aim, besides changing K_{part} , was to make the complexes formed by binding partition into the same phase as the modified reactant. The binder, Con A, was modified, because modification of the carbohydrate was inconvenient.

Table 1. Partition-affinity ligand assay—immunoassays of different antigens

Type of antigen	Antigen	Separator	Other reactant	Label	Type	Time, min		Range	Reference
						I	S		
Hydrophobic hapten	Digoxin	(Ab)	Ab/digoxin*	¹²⁵ I	Comp	5	5	1–8nM	1
Hydrophobic hapten	T ₃	(Ab)	Ab/T ₃ *	¹²⁵ I	Comp	30	30	1–6nM	2
Hydrophobic hapten	T ₄	(Ab)	Ab/T ₄ *	¹²⁵ I	Comp	120	15	50–200nM	16
Hydrophobic hapten	Digoxin	Dextran Ab	Digoxin*	¹²⁵ I	Comp	120	39	1–8nM	1
Hydrophilic hapten	Glucose	PEG-Con A	Glucose*	HRP	Comp	10–30	10	20–1000μM	3
Protein	β ₂ -Microglobulin	PEG-Ab	β ₂ m*	¹²⁵ I	Comp	20	15	3–96 μg/l.	5
Protein	β ₂ -Microglobulin	PEG-Staph.	β ₂ m*/Ab	¹²⁵ I	Comp	20	15	3–96 μg/l.	5
Cells	Staphylococci	(Staph)	IgG*	¹²⁵ I	Dir	30	120	10 ⁶ –10 ⁷	4
Cells	Staphylococci	PEG-Staph	IgG*	¹²⁵ I	Comp	30	120	10 ⁵ –10 ⁷	4
Cells	Streptococci	(Ab*)	Ab*	HRP	Dir	30, 60	60	2.5 × 10 ³ –10 ⁵	7
Cells	Streptococci	PEG-Strep	Ab*	¹²⁵ I	Comp	30, 60	60	2.5 × 10 ⁴ –10 ⁵	7

*Labelled reactant.

Label: HRP = Horseradish peroxidase.

Type: Comp = competitive assay; Dir = direct binding assay.

Time: I = reaction period (at room temperature); S = time allowed for phase separation.

Table 2. Methods used for activation of PEG

Activating agent	Time for activation	Coupling		Reference
		Time, hr	pH range	
Triazine	1 hr	3	8.7	8
Tresyl	15 min	16	7.5–9.5	9
Epichlorohydrin	16 hr	3	8.5–11.0	17
Carbonyl di-imidazole	15 min	3–5	5.5–8.5	18

The modification strategy was to introduce groups onto the surface of the molecule to make it favour one of the phases.

Modification has mostly been effected by covalent attachment of a polymer, *e.g.*, PEG, to make the substance partition into the PEG-rich top phase.^{3–5} To prevent the formation of cross-linked complexes of the binder, a monomethoxy-PEG was used. Several methods for PEG-activation and coupling to the protein have been tried (Table 2). On the other hand, addition of dextran in the form of the single polymer⁶ or cross-linked in Sephadex particles,¹ enables the substance to partition into the dextran-rich (or salt-rich) bottom phase. Organic moieties such as phenyl groups and alkyl chains (octyl, dodecyl) have also been used for modification.⁶ The formation of an antibody–enzyme conjugate can also be regarded as a modification of the antibody, since it is possible to change its partitioning in this way.⁷

The methods for modification with PEG have been developed at various laboratories since PEG-modification of various biological macromolecular structures became important. Abuchowski *et al.*⁸ introduced triazine activation of PEG, a method we have used in many of our applications. The tresyl-modification method has also been successfully applied and is now our routine process.⁹

When antibodies are modified by attachment of PEG, their surface properties are altered, giving them a higher partition coefficient. However, the PEG molecules may sterically hinder binding reactions. Highly modified antibodies have a significantly decreased binding capacity and if PEG-modified antibodies are to be used in an assay, they should be able to partition predominantly into the top phase and also retain a fair amount of their binding capacity. Each batch of modified antibodies has, therefore, been tested for the ability to bind antigen and move it to the top phase.^{3–5} This ability has been called the *transport capacity*. For most types of binding structures, the degree of modification has an optimum.

Optical properties

If the partition assay is to be done with limited facilities (*e.g.*, in the field), it should be advantageous to use a phase system that is optically clear in order to permit use of a colorimetric assay for direct registration of the enzyme activity in one of the phases. With conventional systems, it is possible to obtain one clear phase by changing the volume ratio of the phases. It is also possible, by careful selection

of polymers, to set up a system that separates directly into two optically clear phases.¹⁰

Immunoassay procedure

An immunoassay for use in the field must be simple, quick and easy to operate. How does the PALA method meet these demands?

A typical test is performed in a test-tube, in which the labelled antigen (in a small volume of buffer) is mixed with the sample to be assayed. A fixed amount of antibodies is added and binding takes place. The kinetics of the binding reaction are difficult to alter, but since the assay procedure involves a quick separation step, it is possible to terminate the binding step long before equilibrium is attained, without degrading the analytical result. Phase separation takes place within seconds after addition of the fine dispersion of the two phases.

If the assay is to be performed by direct reading of the distribution of enzyme activity in the phase system, then the substrates must be added with the phase system. Ultimately, all the steps—binding, separation and reading—can take place in the same test-tube. If only semiquantitative results are required, visual determination of the activity in the two phases might be enough.

Otherwise an aliquot of either phase may be removed, mixed with substrate and assayed. There are few manual steps involved in the process. In theory, at least, this should give good accuracy and also easy automation, as discussed later.

Binding analysis

The art of performing binding analyses is often the art of separating free and bound antigen. Most of the separation methods used in biochemistry have also been used in binding analyses. A good separation method must be able to separate the reactants without perturbing the binding reaction. This statement may sound superfluous, but the perturbation effect is not always easy to avoid and its consequences may be difficult to establish.

After the degree of binding has been determined in an analysis, the data may be used for calculation of the association constant or stoichiometry of the reaction. The interaction between a protein, P, and a ligand L, produces a complex, PL.



If the complex is completely isolated during the separation process, the complex will dissociate

slightly and after some time establish equilibrium. In practice, complete separation does not occur, but many methods are designed to remove most of the free reactants and thus introduce risk of dissociation of the complex. Another factor that governs the dissociation is, of course, the magnitude of K_{ass} . However, even if the complex is not thermodynamically stable, it may be kinetically stable (*i.e.*, the dissociation is slow).

It is thus evident that a separation method that is to be used in analytical procedures must not only be highly reproducible but may also have to be precisely timed.¹¹

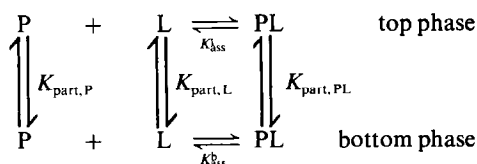
Another problem that may occur involves interactions between the reactants and the material used in the separation process. Many binding reactions are studied in a very low concentration range (pM – μM) and are thus very sensitive to perturbations, *e.g.*, adsorption on plastic reaction vessels, ultrafiltration membranes,^{12,13} or gel-filtration media. Thus the commonly used method of equilibrium dialysis has an inherent weak point. This method is often used for determining binding between a protein and a low molecular-weight ligand. Many of the ligands studied are rather hydrophobic in nature, have low solubility in aqueous buffer solutions and are prone to adsorption on the dialysis membrane. Such adsorption may be strong enough to completely distort the outcome of a binding analysis.^{12,14} Problems of this kind are not very often discussed in the literature. The interpretation of binding data from equilibrium dialysis experiments has, however, been found in some cases to be inadequate.¹³

The preparation of bound and free reactant in aqueous two-phase systems has, in this respect, two advantages.

1. The degree of separation can be controlled. It is reproducible between different batches of phase systems¹⁵ and is not time-dependent after equilibrium has been reached.

2. There are generally no problems with adsorption of biomolecules. However, particles and very large protein aggregates may be adsorbed at the interface.

We have used a method evaluating results from binding analyses where neither reactant is completely partitioned into one phase. It is, however, required that the reactants are preferentially partitioned into different phases and that their partition coefficients are known. The interaction of a ligand, L, with a protein, P, in a two-phase system can be represented by the following scheme (the stoichiometry is not considered at this point):



The partition coefficient, K_{part} , is defined as the ratio of the concentrations in the top and bottom phases:

$$K_{\text{part}} = C^t/C^b \quad (1)$$

The superscript t denotes the top phase and b the bottom phase. After the total amount of label in each phase has been determined the evaluation can start.

$$C_{\text{L,tot}}^t = C_L^t + C_{\text{PL}}^t \quad (2)$$

$$C_{\text{L,tot}}^b = C_L^b + C_{\text{PL}}^b \quad (3)$$

The total concentration of complex and concentration of free ligand are now to be determined. The following set of equations is used and solved by iteration.^{5,10} As an initial approximation, $C_{\text{L,tot}}^t$ is used instead of C_L^t in equation (1).

$$C_L^b = C_{\text{L,tot}}^t / K_{\text{part,L}} \quad (4)$$

$$C_{\text{PL}}^b = C_{\text{L,tot}}^b - C_L^b \quad (5)$$

$$C_{\text{PL}}^t = C_{\text{PL}}^b \times K_{\text{part,PL}} \quad (6)$$

$$C_L^t = C_{\text{L,tot}}^t - C_{\text{PL}}^t \quad (7)$$

In equation (7) a new value of C_L^t is obtained and can be used in equation (4). The calculations proceed until the same values are obtained in two successive steps.

This method has been used to evaluate binding analyses of the interactions between serum albumin and Cibacron Blue¹² and in competitive immunoassays involving binding of β_2 -microglobulin to antibodies.⁵ A more detailed description of the evaluation procedure has been published.^{5,12} The method is only a basic concept and can be further developed for calculations involving more complicated binding situations.

AUTOMATION

A particular advantage of using aqueous two-phase systems for separation in analysis is that the steps of the assay are mechanically simple. The separation is initiated by the mixing of the phase components and terminated by withdrawal of a sample from one of the phases. The steps of the PALA are as follows.

1. Mixing of the reactants for the binding reaction (*e.g.*, sample, antibody and antigen–enzyme conjugate).

2. Addition of the phase system. Enzyme substrates might be included. Mixing.

3. Withdrawal of sample from one of the phases for determination of enzyme activity. The sample is mixed with substrate if this was not done in the previous step.

Steps 1 and 2 are necessary for the assay. In some cases step 3 may be excluded and the result read directly, *e.g.*, by visual determination. Each step can be automated without loss of control of the process.

Commercial equipment available can easily be adapted for use with the PALA-technique. A disadvantage is that such equipment is dedicated and unnecessarily sophisticated and expensive. It is, however, also possible to assemble an automatic PALA analyser from equipment commonly available in biochemical laboratories.

Design

The PALA analyser consists of a conveyor belt (or a fraction collector) having three stations, three dual-channel peristaltic pumps, a photometer and a microcomputer.

The three steps mentioned above can be executed in the following way. The samples are manually distributed in test-tubes and put on the conveyor belt. At the first pump station, antibody and antigen-enzyme conjugate are added by delivery of a controlled volume of each. After a predetermined time, set by the speed of the belt and the number of test-tube positions between the stations, the test-tube arrives at the second station. Here, the phase components are added by dual-channel pump. Each piece of tubing has a narrow outlet, thus giving a fine jet which hits the liquid forcefully, resulting in instantaneous mixing. After a second time interval, which is long enough to allow the phases to settle, the test-tube comes to the last station, where a sampling needle is brought down into one of the phases. If necessary, a dual-channel pump can be used, so that the aliquot taken can be mixed with buffer and enzyme substrate, or other reagents.

Equipment

Conveyor belts are commercially available, but rather expensive. A modified fraction collector, can be used instead. A fraction collector of carousel type, having all the test-tubes in a circle, is advantageous, since this makes it easy to have the stations in the proper positions. The timer in the collector can be used for initiating the operations at the different stations.

Pumps

Almost any type of peristaltic pump can be used. It should be checked that it can be controlled externally by a microcomputer and that tubing with diameter suitable to allow flow of the somewhat viscous phase components is available.

Photometer

Any simple spectrophotometer and many filter photometers can be used, provided the instrument can be equipped with a flow cuvette and that it has a connector for external read-out. Depending on the intended use, ruggedness of the model may be a more important consideration.

Microcomputer

Many microcomputers that can be used for control and data-acquisition are available. Important factors when choosing a system are portability, data-storage capacity and availability of interface cards for connection of external equipment. We have used an ABC80 (Luxor AB, Motala, Sweden), equipped with one interface card for controlling the conveyor belt and the pumps and one A/D-converter for reading the photometer.

REFERENCES

1. B. Mattiasson, *J. Immunol. Meth.*, 1980, **35**, 137.
2. B. Mattiasson and H. Eriksson, *Clin. Chem.*, 1982, **28**, 680.
3. B. Mattiasson and T. G. I. Ling, *J. Immunol. Meth.*, 1980, **38**, 217.
4. B. Mattiasson, T. G. I. Ling and M. Ramstorp, *ibid.*, 1981, **41**, 105.
5. T. G. I. Ling and B. Mattiasson, *ibid.*, 1983, **59**, 327.
6. B. Mattiasson and T. G. I. Ling, U.S. Patent 4312944, 1982.
7. T. G. I. Ling, M. Ramstorp and B. Mattiasson, *Anal. Biochem.*, 1982, **122**, 26.
8. A. Abuchowski, T. van Es, N. C. Palczuk and F. Davis, *J. Biol. Chem.*, 1976, **252**, 3578.
9. T. G. I. Ling and K. Nilsson, in preparation.
10. T. G. I. Ling and B. Mattiasson, Patent pending, 1983.
11. H. Eriksson, B. Mattiasson and J. I. Thorell, *J. Immunol. Meth.*, 1981, **42**, 105.
12. T. G. I. Ling and B. Mattiasson, *J. Chromatog.*, 1982, **252**, 159.
13. H. L. Behm and J. G. Wagner, *Res. Commun. Chem. Pathol. Pharmacol.*, 1979, **26**, 145.
14. V. P. Shanbhag, R. Södergård, H. Cartensson and P.-Å. Albertsson, *J. Steroid Biochem.*, 1973, **4**, 537.
15. P.-Å. Albertsson, *Partition of Cell Particles and Macromolecules*, Almqvist & Wiksell, Uppsala, 1971.
16. H. Eriksson, J. Nilsson and B. Mattiasson, *Appl. Biochem. Biotechnol.*, 1983, **8**, 1.
17. S. Hjertén, J. Rosengren and S. Pählman, *J. Chromatog.*, 1974, **101**, 281.
18. G. S. Bethell, J. S. Ayers, W. S. Hancock and M. T. W. Hearn, *J. Biol. Chem.*, 1979, **254**, 2572.

DEVELOPMENT OF A LIGHT-SCATTERING IMMUNOASSAY FOR THYROXINE-BINDING PREALBUMIN IN PLASMA OR SERUM

K. SPENCER

Department of Biochemistry, Oldchurch Hospital, Romford, Essex, England

(Received 8 December 1983. Accepted 2 May 1984)

Summary—This paper describes the development of an assay for the measurement of thyroxine binding prealbumin in plasma or serum, based on the technique of fixed-time kinetic immunoturbidimetry with the Cobas Bio centrifugal analyser. The assay has good precision (coefficient of variation < 5%) and a detection limit of 15 mg/l. The assay is rapid, economical, and the results compare well with those obtained by an established procedure. The technique has wide applicability to instruments which can make kinetic measurements and could prove useful in the clinical monitoring of patients receiving nutritional support and in the identification of nutritionally-at-risk groups prior to surgery. The assay further emphasises the sensitivity and usefulness of kinetic immunoturbidimetry for the measurement of low concentrations of proteins.

In the last decade there has been an increasing interest in the nutritional status of patients in hospital, both by the doctors looking after them and the pharmaceutical industry providing nutritional products. Recent North American surveys have indicated that up to 50% of such patients may be suffering from clinical and subclinical malnutrition.^{1,2} Evidence directly linking malnutrition with increased morbidity and mortality is not hard to find, since loss of weight and combined nitrogen may be rapid after injury or during any illness, because of a combination of increased breakdown of body tissue and insufficient food intake. Some of this evidence has been recently reviewed by Woolfson.³ Clearly, for a whole range of different medical and surgical conditions there are distinct advantages in improving nutrition by assisting, or replacing the patient's ordinary diet.

Total parenteral nutrition is increasingly used in the correction of nutritional deficiencies, but is expensive. Clearly a practical and sensitive method for the early detection of subclinical protein and energy malnutrition and for assessing the adequacy of dietary treatment and nutritional support, would be useful.

Measuring plasma albumin has been the mainstay of nutritional screening in clinical practice, but the long half-life (19 days) limits its usefulness in following the rapid nutritional changes that need to be monitored in patients receiving total parenteral nutrition. Plasma transferrin is also reduced in severe protein and energy malnutrition, but its usefulness in the detection of subclinical malnutrition is limited because of its relatively long half-life (8 days), the effect of iron status, its "acute phase" response to infection and stress, and the buffering ability of a good nutritional state.⁴

The use of rapid-turnover transport proteins such as thyroxine-binding prealbumin (TBPA)⁴⁻⁶ and

retinol-binding protein (RBP),⁴⁻⁶ with biological half-lives of 48 and 12 hr respectively, has been shown to be very sensitive to changes in both dietary protein and energy over very short time periods.^{4,6} It appears that these proteins will prove useful in the assessment of nutritional support and in the early detection of subclinical protein and energy malnutrition.

It must be borne in mind, however, that changes in both liver disease and chronic renal disease may influence the levels of such proteins. Furthermore TBPA is also a negative acute-phase reactant and care may be needed in some situations in interpreting the data.

The protein TBPA has a molecular weight of 5.5×10^4 and migrates faster than albumin in cellulose acetate electrophoresis. The protein also binds the smaller (m.w. 2.1×10^4) RBP and thyroxine. TBPA has usually been measured by a variety of time-consuming or imprecise immunological techniques which include radial immunodiffusion⁵ and electroimmunoassay.^{6,7} More recently, light-scattering immunoassay has proved to be a sensitive, precise, rapid, easily automated alternative to these time-honoured gel-precipitation methods for proteins.^{8,9} The technique of light-scattering immunoassay has been based on use of dedicated analysers employing nephelometric detection⁸⁻¹⁰ or on use of kinetic analysers and spectrophotometers, with turbidimetric detection.^{8,9,11} The kinetic turbidimetric approach has much to commend it in terms of flexible use of equipment, superior precision, less effect of analyser and reagent noise, and comparable sensitivity.¹² In particular, "enzyme analysers" such as the LKB reaction-rate analyser have proved very useful,¹³⁻¹⁷ as have centrifugal analysers.^{11,18-20}

The precision and sensitivity of immunoturbidimetry now seem comparable with those of nephelometry (unless some form of sample pre-

treatment is used),^{8,9,12} thus raising the question of the need for dedicated nephelometric instruments. Centrifugal analysers seem very well suited for the purpose, with their very precise control of timing, mixing and temperature, and the use of sophisticated micro-processor or computer facilities for analysing kinetic data.²¹ One such commercial instrument (Cobas Bio) has a novel optical system in which absorbance measurements are made with the cuvettes lying longitudinally in the light-beam, and the light-source is a pulsing xenon tube.²² The advantages of this type of optical arrangement over other types of photometric system have been outlined.²³

This paper outlines the development of a fixed-time kinetic immunoturbidimetric method for the measurement of thyroxine-binding prealbumin with the Cobas Bio centrifugal analyser.

EXPERIMENTAL

Instrumentation

The Cobas Bio Centrifugal Analyser (Roche Diagnostics, P.O. Box 8, Welwyn Garden City, Hertfordshire, U.K.) was used to collect absorbance data. Data-processing of absorbances and calibration curve-fitting were done with a third-order polynomial routine on an Apple II computer.

Reagents

All reagents were obtained from British Drug Houses, Poole, Dorset, and were of "AnalaR" grade or equivalent except where stated.

Phosphate-buffered saline. Prepared by dissolving 5.85 g of sodium chloride, 9.10 g of dipotassium ethylenediaminetetra-acetate dihydrate, 7.16 g of disodium hydrogen phosphate and 1.33 g of potassium dihydrogen phosphate in 950 ml of distilled water, adjusting to pH 7.40 ± 0.02 and diluting to 1 litre with distilled water. The buffer was stable for at least three months when stored at 4°. Its composition is 0.05M phosphate, 0.1M sodium chloride and 0.0225M EDTA. The EDTA minimizes variation in the effect of calcium and magnesium.^{8,9}

Phosphate buffer with polyethylene glycol 6000. Prepared by dissolving 40 g of polyethylene glycol 6000 (PEG) in 800 ml of phosphate-buffered saline and diluting to 1 litre with the saline. This solution was stable at 4° for at least three months.

Stock antihuman thyroxine-binding prealbumin antiserum. Rabbit antihuman thyroxine-binding prealbumin was obtained from Hoechst Pharmaceuticals, Hounslow, Middlesex, U.K. (Product Number ORCA 05). To produce a working antiserum solution, the required volume of antiserum was appropriately diluted with phosphate-buffered PEG reagent. After 15 min at room temperature the working reagent was centrifuged (1750 g, 10 min) to remove any precipitate formed.

Standards and quality-assurance materials. A stabilized standard human serum (Hoechst Pharmaceuticals, Product Number ORDT 07) was diluted stepwise with 0.1M sodium chloride, to provide a series of five standards covering the range 35–560 mg/l. Protein standard serum B (Hoechst Pharmaceuticals, Product Number OTFG 07) was used for quality-control of the assay.

Procedures

Kinetic immunoturbidimetry. Table 1 summarizes the final assay conditions, including the instrument settings for the Cobas Bio analyser. The antiserum was diluted 1:9 with phosphate-buffered PEG. The sample, diluent and reagent volumes and all other variables of the analyser were set by

Table 1. Cobas Bio parameter listing for thyroxine-binding prealbumin assay

1	Units	DA
2	Calculation factor	1000
3	Standard 1 conc.	0
4	Standard 2 conc.	0
5	Standard 3 conc.	0
6	Limit	0
7	Temperature (°C)	25.0
8	Type of analysis	5
9	Wavelength (nm)	290
10	Sample volume (μl)	6
11	Diluent volume (μl)	50
12	Reagent volume (μl)	200
13	Incubation time (sec)	0
14	Start reagent volume (μl)	0
15	Time of first reading (sec)	1.0
16	Time interval (sec)	10
17	Number of readings	30
18	Blanking mode	1
19	Print-out mode	1

the microprocessor when the required program was called. Cuvette 1 contained a reagent blank and cuvettes 2–6 contained appropriate standards. The analyser, operating at 25° and 290 nm, took absorbance measurements every 10 sec after mixing and the change in absorbance between 1 and 300 sec after mixing was multiplied by 1000 and printed out for each cuvette.

The absorbance data from the Cobas Bio were manually fed into a microcomputer and the calibration curve computed by using a third-order polynomial; the results for test samples were then calculated from this standard curve. Alternatively the results can be calculated graphically.

Radial immunodiffusion (RID). Radial immunodiffusion assay was done with Hoechst M Partigen immunodiffusion plates (Product Number OTBW 03). The diffusion rings were evaluated with a calibration graph obtained by plotting the square of the diameter against concentration of thyroxine-binding prealbumin for standard solutions.

RESULTS

Study of immunokinetic assay conditions

Factors likely to affect the antigen–antibody reaction and its kinetics have been described in detail elsewhere.^{8,9,13} The reaction of TBPA with the antiserum was studied in relation to the following variables.

pH. In contrast to previous experience^{13–15} which showed no significant pH optima, the TBPA system had a distinct optimum pH of 7.40.

Sodium chloride. The ionic strength of the reaction medium and the charge-density of the ions present significantly affect the kinetics of the antigen–antibody reaction.⁹ Previous studies^{13–16} have demonstrated the chaotropic effect of chloride ions; increasing the chloride ion concentrations decreases the rate of reaction. The addition of sodium chloride to the TBPA system increased the absorbance change, the effect being maximum at 0.1M sodium chloride concentration in the buffered PEG. Further increase in sodium chloride concentration resulted in a marked decrease in the absorbance change.

Temperature. The effect of temperature on antibody-antigen reactions has been investigated by several authors but no clear picture has emerged. Price and Spencer,²⁴ in a study of over 35 antisera against 8 antigens, found temperature coefficients (Q_{10}) varying from +40% to +120% increase in reaction rate for a 10° temperature rise from 25°. The data for the TBPA assay indicate a significantly increased sensitivity if the assay is run at 25°, with a Q_{10} (25–35°) of +89% for the Hoechst antiserum.

Enhancement by polymer. The effect of PEG 6000 on the antigen-antibody reaction was studied by diluting the antiserum with PEG reagents of increasing concentration. The possibility of kinetic blank-reactions¹⁶ was also investigated by studying the response in the absence of antiserum with a saline blank as reference. The results indicated an optimum PEG reagent concentration of 60 g/l. (46.9 g/l. in the final reaction mixture); however, at this concentration, non-specific precipitation, contributing to a kinetic sample-blank, was observed. It was therefore decided to choose a PEG concentration of 40 g/l. (31.3 g/l. in the final reaction mixture) since the sensitivity was reduced by only 15% and no non-specific precipitation could be detected.

Antiserum dilution. Previous experience has shown that performance characteristics given for antiserum by the manufacturer do not always provide helpful information on the use of the antiserum in a kinetic assay. Batches of antisera must therefore be tested to ascertain the dilution necessary to obtain the required sensitivity. Figure 1 shows the precipitin curve at various dilutions of the antiserum used in this study. It was decided to use a dilution of 1 part of antiserum with 8 parts of diluent in the TBPA assay. This dilution represents a compromise between the need to operate with excess of antibody and to reduce assay costs, while still maintaining adequate sensitivity and precision.

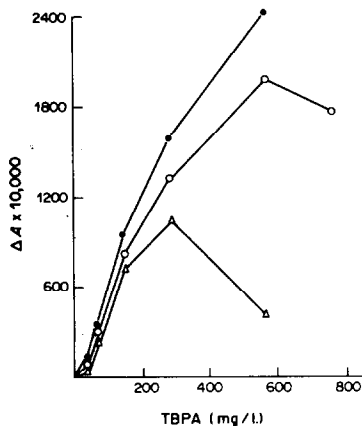


Fig. 1. Hoechst antiserum precipitin curves at various dilutions in PEG 6000 (40 g/l). ●—● dilution 1:6; ○—○ dilution 1:9; △—△ dilution 1:15.

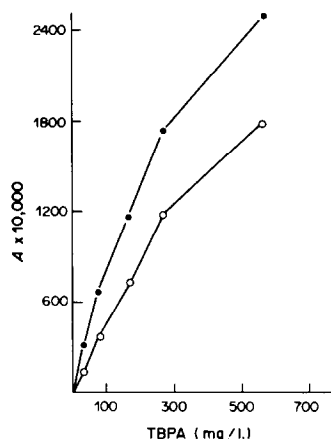


Fig. 2. Calibration curve changes at two detector wavelengths ●—● at 290 nm; ○—○ at 340 nm.

Wavelength. One factor influencing assay sensitivity is the wavelength used to measure the scattered light.^{9,12} The Cobas Bio, unlike many automated kinetic analysers, uses a grating monochromator, so the influence of wavelength on the assay could be studied. Rayleigh's law of light-scattering indicates that the scattering intensity varies as the reciprocal of the fourth power of the wavelength of the incident light. Therefore, if this wavelength is decreased the intensity of the scattered light increases, hence the sensitivity increases. However, it must also be borne in mind that antibodies and proteins themselves are of sufficient size to scatter light and hence the serum and reagent blank signals will also increase. A further consideration in the choice of assay wavelength is the instrument noise at various wavelengths.¹²

The TBPA assay system was set so that a set of standards for the calibration curve was run first, followed by 20 saline samples. The absorbance data at 340 and 290 nm were collected in the usual way. The data from the 20 saline samples were used to obtain a measure of instrument noise and the absorbance changes for the calibration curve were plotted graphically (Fig. 2).

Although the initial absorbance of the reagent blank was 0.120 at 340 nm but 1.480 at 290 nm (because of the Rayleigh law effect), the instrument noise, expressed as the standard deviation (sd) of the absorbance of the 20 saline blank samples, increased only from 0.011 to 0.013. This minimal shift in instrument noise compared with the 40-fold increase in sensitivity, suggested 290 nm as the wavelength of choice.

ASSAY PERFORMANCE

Detection limits

The detection limit is the smallest value (for a single analysis) which can be distinguished with a stated probability from a suitable blank. For light-scattering assays, assuming equality of absolute pre-

cision in measuring blanks and samples with concentrations near the detection limit, the detection limit will be equal to the mean blank result plus 3 sd.⁸ The data from the wavelength experiment with saline samples as blanks were subjected to curve fitting and the sd (and hence the detection limit) was calculated. For the assay at 290 nm the detection limit was found to be 15 mg/l., corresponding to an absorbance change of 0.018 in 5 min. This is equivalent to a concentration of 90 ng per cuvette and compares well with previously published data.^{8,9,12-18}

Within and between batch precision

Within-batch precision of the assay system was assessed in the usual way by measuring replicates of three samples at different TBPA levels (Table 2). Between-batch precision was assessed by running the assay on 20 separate occasions, with freshly thawed aliquots of the three samples. On each occasion a fresh dilution of the stock antiserum was prepared. Table 2 shows the precision data.

Relative accuracy

The kinetic immunoturbidimetric assay was compared with the well-established standard technique of radial immunodiffusion, for analysis of samples from patients. The regression parameters obtained according to the Deming procedure were $y(\text{RID}) = 5.141 + 1.019 \times (\text{immunokinetic})$; $r = 0.9864$, $n = 50$.

Reference range

Heparinized plasma samples taken from 45 healthy volunteers (23 female, 22 male; mean age 31.7 years) were submitted for analysis by the new procedure. The results showed a Gaussian distribution with a mean level of 277 mg/l, and a ± 2 sd range of 160–390 mg/l. There was no difference between the population mean for women and men. This range is in close agreement with those previously obtained by use of RID⁶ and electroimmunoassay;⁷ however, one brief report²⁵ on light-scattering immunoassay with a Beckman Rate Nephelometer indicated a reference range as wide as 151–503 mg/l. (This paper also reported much wider levels for the RID technique: 131–487 mg/l.)

Excess of antigen

The various methods for detection of excess of antigen have been outlined elsewhere.^{8,9} In this partic-

ular assay kinetic equivalence occurs at 600 mg/l., so only samples with antigen levels greater than this will cause problems; such high levels are extremely unlikely in clinical situations. Many authors have used the change in reaction kinetics on change from antigen excess to antibody excess as a means of detecting antigen excess. This method proves very practical for analysers with analogue recorder output, but is less practical for analysers that only store the data readings. For instances of suspected antigen excess the data points must then be plotted manually. More recently, kinetic analysers with additional computational facilities have allowed presentation of raw data for inspection on a VDU and various computations and algorithms for real-time detection of this condition have been investigated.

CONCLUSION

Turbidimetric assays for the measurement of specific proteins in clinical chemistry have been realized by use of various analytical systems, including centrifugal analysers. The potential of these analysers for multiple data-point collection allows the use of kinetic techniques, and their ability to read the absorbance at the start of the reaction allows measurement of sample blanks. Accurate timing of the data of the data collection means that the reactions do not have to run to completion and sample throughput can therefore be increased.

The assay described for TBPA is a rapid assay making use of instrumentation which is widely available in clinical chemistry departments. The precision and speed of the assay are far superior to those of conventional assays such as RID and electroimmunoassay, and also superior to those of more recently outlined kinetic nephelometric²⁵ and enzyme immunoassay²⁶ methods. The detection limit of the assay, about 100 ng in the sample in the cuvette, is comparable to that reported for use of kinetic analysers^{8,9} and indicates that the novel optical arrangement of the Cobas Bio introduces no advantages or disadvantages in terms of assay sensitivity. However, the ability to use small volumes has an obvious cost implication.

Preliminary clinical studies with the TBPA assay indicate that TBPA and other short half-life proteins have considerable potential for monitoring of nutritional status in a wide range of conditions.

Table 2. Within and between batch precision ($n = 20$) for the kinetic immunoturbidimetric TBPA method

	Within batch			Between batch		
	Mean, mg/l.	sd, mg/l.	CV, %	Mean, mg/l.	sd, mg/l.	CV, %
A	91.8	2.9	3.2	92.9	4.2	4.5
B	231.8	6.0	2.6	229.7	8.7	3.8
C	399.7	7.2	1.8	401.1	11.6	2.9

REFERENCES

1. C. E. Butterworth and G. L. Blackburn, *Nutr. Today*, 1975, **10**, 8.
2. B. R. Bistran, G. L. Blackburn, E. Hollowell and R. Heddle, *J. Am. Med. Assoc.* 1974, **230**, 858.
3. A. M. J. Woolfson, *Brit. Med. J.* 1983, **287**, 1004.
4. P. S. Shetty, K. E. Watrasiewicz, R. T. Jung and W. P. T. James, *Lancet*, 1975 (2), 230.
5. Y. Ingenbleek, M. De Visscher and P. De Nayer, *ibid.*, 1972 (2), 106.
6. Y. Ingenbleek, H-G. Van Den Schrieck, P. De Nayer, and M. De Visscher, *Clin. Chim. Acta*, 1975, **63**, 61.
7. P. Douville, J. Talbot, R. Lapointe and L. Belanger, *Clin. Chem.*, 1982, **28**, 1706.
8. C. P. Price, K. Spencer and J. T. Whicher, *Ann. Clin. Biochem.*, 1983, **20**, 1.
9. J. T. Whicher, C. P. Price and K. Spencer, *CRC Crit. Rev. Clin. Lab. Sci.*, 1983, **18**, 213.
10. J. C. Sternberg, *Clin. Chem.*, 1977, **23**, 1456.
11. I. Deverill, in *Centrifugal Analysers in Clinical Chemistry*, C. P. Price and K. Spencer (eds.), p. 109. Praeger, Eastbourne, 1980.
12. K. Spencer and C. P. Price, *U.V. Spectrosc. Group Bull.*, 1981, **8**, 38.
13. *Idem*, *Clin. Chim. Acta*, 1979, **95**, 263.
14. K. Spencer, C. P. Price, F. Anthony and P. J. Wood, *ibid.*, 1979, **99**, 177.
15. K. Spencer and C. P. Price, *Clin. Chem.*, 1980, **26**, 1531.
16. C. P. Price and K. Spencer, *ibid.*, 1981, **27**, 882.
17. K. Spencer, E. J. Coombes and P. J. Wood, *J. Clin. Chem. Clin. Biochem.*, 1963, **21**, 133.
18. K. Spencer and C. P. Price, In *Centrifugal Analysers in Clinical Chemistry*, C. P. Price and K. Spencer (eds.), p. 457. Praeger, Eastbourne, 1980.
19. P. R. Wenham and D. B. Horn, In *Centrifugal Analysers in Clinical Chemistry*, C. P. Price and K. Spencer (eds.), p. 477. Praeger, Eastbourne, 1980.
20. G. J. Marell and P. J. Brombacker, *J. Clin. Chem. Clin. Biochem.*, 1981, **19**, 67.
21. T. O. Tiffany, In *Centrifugal Analysers in Clinical Chemistry*, C. P. Price and K. Spencer (eds.), p. 3. Praeger, Eastbourne, 1980.
22. H. G. Eisenwiener and M. Keller, *Clin. Chem.*, 1979, **25**, 117.
23. H. G. Eisenwiener, J. M. Kindbeiter, M. Keller and K. Gutlin, In *Centrifugal Analysers in Clinical Chemistry*, C. P. Price and K. Spencer (eds.), p. 29. Praeger, Eastbourne, 1980.
24. C. P. Price and K. Spencer, *U.V. Spectrosc. Group Bull.*, 1980, **8**, 29.
25. R. A. Jacobs and N. Gorman, *Clin. Chem.*, 1982, **28**, 1619A.
26. E. J. Shrawder and M. D. Cinelli, *ibid.*, 1982, **28**, 1619A.

PHARMACEUTICAL AND CLINICAL ANALYSIS BY TANDEM MASS SPECTROMETRY

RICHARD A. YOST,* ROBERT J. PERCHALSKI,† HARRY O. BROTHERTON,§
JODIE V. JOHNSON and MARY BETH BUDD

Department of Chemistry, University of Florida, Gainesville, FL 32611, USA

(Received 11 April 1984. Accepted 7 May 1984)

Summary—Tandem mass spectrometry (MS/MS) is a promising technique for trace determination of compounds in complex mixtures. The application of triple-quadrupole MS/MS to clinical and pharmacological studies has been investigated with major emphasis on rapid screening and determination of drugs and biomolecules in physiological fluids and tissues. These techniques have been applied to a range of problems, including the determination of chlorinated compounds in humans, subpicogram analysis of neurochemicals and the detection of illegal drugs in racing animals. A new technique for determining the structures of all the metabolites of a particular drug has also been developed. It is possible to identify in a single sample all molecular ions which contain substructures characteristic of the parent drug. The structure of each metabolite can then be determined by obtaining the MS/MS spectrum of the molecular ion.

Tandem mass spectrometry (MS/MS) is a relatively new analytical technique based upon mass spectrometers that can provide two (or more) stages of mass separation in sequence. This capability makes possible the integration of the two basic operations of chemical analysis, separation and identification, in one instrumental technique. Because both operations are based upon mass analysis, the technique is rapid, sensitive and selective. Here we describe the application of MS/MS to problems in pharmaceutical and clinical analysis.

TANDEM MASS SPECTROMETRY

A conceptual diagram of a tandem mass spectrometer is illustrated in Fig. 1 and compared with the familiar gas chromatograph/mass spectrometer combination (GC/MS). Although several instrumental approaches have been employed for mass analysis in GC/MS and MS/MS, the quadrupole mass filter shown is by far the most common. Tandem mass spectrometry has its roots in the early studies of ion-molecule reactions¹ and metastable ions.² The earliest applications of MS/MS for mixture analysis employed double-focusing mass spectrometers.^{3,4} The development of the triple-quadrupole mass spectrometer⁵ made possible routine analytical applications of MS/MS and led the way to commercial introduction of MS/MS instruments.⁶ Instrumentation for tandem mass spectrometry has been reviewed recently.⁷

Tandem mass spectrometry has a wide range of applicability for chemical analysis, as illustrated by the wide range of applications presented in the first book devoted to the subject.⁸ These range from trace mixture analysis to structure elucidation. Here we will concentrate on clinical and pharmaceutical applications that employ the mixture-analysis capabilities of MS/MS. Before discussing those applications, however, it is important to consider why MS/MS is advantageous for trace analysis.

The unique position of mass spectrometry for trace analysis was presented recently by Cairns,⁹ as shown in Table 1. The extreme sensitivity of mass spectrometric analysis provides detectable signals for minute quantities of analyte. For trace analysis, however, sensitivity is not the most critical figure of merit; rather it is the limit of detection, as shown in Table 2. The response of the detector in mass spectrometry is rarely the limiting factor; indeed, detecting a single ion is commonplace. To take advantage of this sensitivity, high selectivity must be achieved, so that the signal from the analyte can be differentiated from that due to other compounds in the sample or the mass spectrometer background. The practical figure of merit, therefore, is limit of detection, a function of both sensitivity and selectivity. The increase in selectivity provided by two stages of mass analysis in MS/MS can lead to improved (lower) limits of detection compared to traditional MS, even though some sensitivity is inevitably lost in the second stage.

The benefits of multiple stages of analysis in MS/MS were first elucidated by Cooks.³ He pointed out that the signal due to chemical interferences is essentially "chemical noise", and that the use of two or more sequential analytical stages or "gates" can be highly effective in filtering out this noise. Figure 2

*Author to whom correspondence should be addressed.

†Medical Research Service, Veterans Administration Medical Center, Gainesville, FL 32602 and Department of Medicinal Chemistry, University of Florida.

§Current address: Department of Chemistry, Northeast Louisiana University, Monroe, LA 71209.

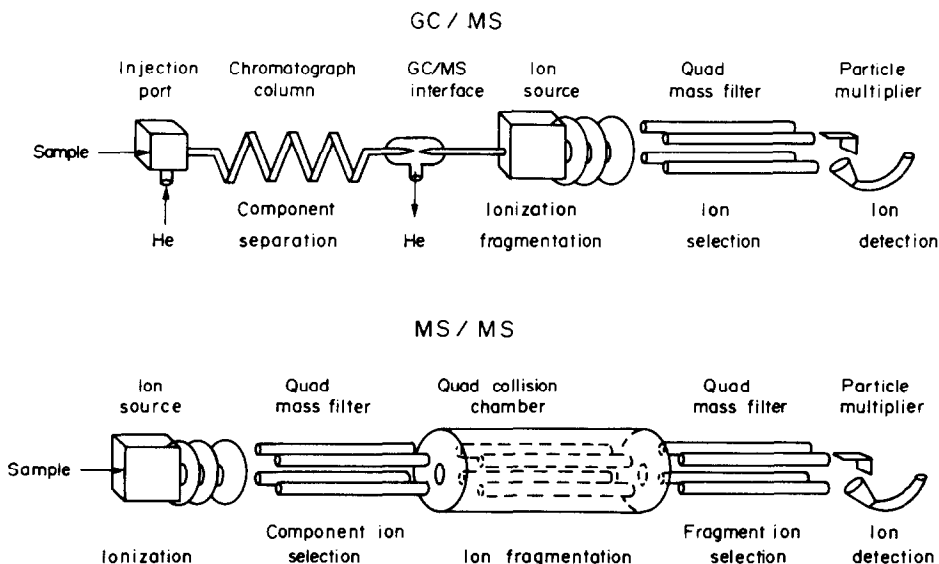


Fig. 1. Conceptual diagrams of the triple-quadrupole tandem mass spectrometer (MS/MS) and a traditional gas chromatograph/quadrupole mass spectrometer (GC/MS).

illustrates this concept. It is apparent that, as long as the signal is not decreased to the point that it cannot be detected, increasing the number of analytical stages increases the signal-to-noise ratio, and thereby improves the limit of detection. The added stages of analysis can include the second stage of mass analysis in MS/MS, the chromatographic separation in GC/MS, or both in GC/MS/MS.

A further benefit of the sensitivity and selectivity of tandem mass spectrometry is the potential for rapid analysis. This results primarily from the ability either to eliminate the chromatographic separation step, or to use rapid, limited chromatographic separation with short packed or capillary columns. The loss in chromatographic selectivity is compensated for by the gain in mass spectrometric (MS/MS) selectivity. Speed is also gained since it is often possible to

analyse complex mixtures with little or no sample preparation.

Because of the potential for rapid, sensitive and selective trace mixture analysis, MS/MS is finding increased use in pharmaceutical and clinical applications. In the sections below, we present some of these applications, taken from work in our own laboratory.

SCREENING AND TRACE ANALYSIS

Many problems in pharmaceutical and clinical analysis are best solved by a two-step screening/confirmation procedure. In this process, a rapid screening step is used to identify samples which may contain the analyte (positives) and to eliminate those which do not (negatives). The screening step should be sensitive enough to prevent false negatives,

Table 1. Trace analysis and its technological implications

Amount to be detected	Weight, g	Trace contamination, w/w	Instrumental technique required
Milligram (mg)	10^{-3}	1 ppth	Titrimetric
Microgram (μ g)	10^{-6}	1 ppm	Spectrophotometric
Nanogram (ng)	10^{-9}	1 ppb	Gas chromatographic
Picogram (pg)	10^{-12}	1 ppt	Mass spectrometric
Femtogram (fg)	10^{-15}	1 ppqua	Mass spectrometric
Attogram (ag)	10^{-18}	1 ppqui	Yet to be discovered
(Mologram)?	10^{-21}	1 ppsex	

Table 2. Figures of merit for analytical methods

$$\text{Sensitivity} = \left[\frac{\text{Slope of calibration curve}}{\text{d (Amount)}} \right] = \frac{\text{d (Signal)}}{\text{d (Amount)}}$$

$$\text{Limit of detection} = \left[\frac{\text{Amount for which signal/noise} = 3}{\text{Sensitivity}} \right] = 3 \left(\frac{\text{Noise}}{\text{Sensitivity}} \right)$$

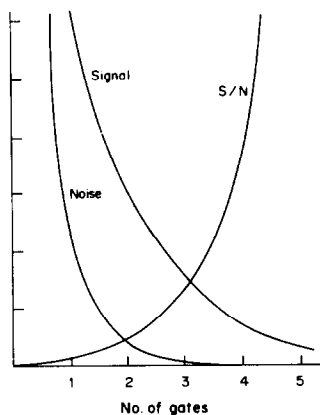


Fig. 2. Effect of multiple gates (sequential stages of analysis) on the signal, noise and signal-to-noise ratio of a measurement. Calculated for the case where each successive stage reduces the signal by a factor of 2 and the noise by 6.

but will generally lack the selectivity to prevent false positives. All positives are then subjected to a second, more selective, confirmation step in order to identify those samples which do contain the analyte. If the rapid screening step effectively reduces the number of samples which must be subjected to the more time-consuming confirmation step, then this two-step procedure saves time and expense. Typically, the two steps employ two different analytical techniques. Tandem mass spectrometry offers the advantage of being able to perform both steps with the same instrument.

As an example of such an analytical problem, consider the testing of athletes (both animal and human) for illegal drugs. This type of analysis is traditionally performed by use of a thin-layer chro-

matographic screening step followed by a GC/MS confirmation step.¹⁰ We have developed an MS/MS procedure for these analyses.¹¹ Screening for up to 50 drugs in a serum or urine sample is accomplished by selected-reaction monitoring (SRM) of one parent-ion/daughter-ion pair for each compound [analogous to selected-ion monitoring (SIM) in MS]. Alternatively, selected neutral losses or daughter ions characteristic of particular classes of drugs can be monitored. Any positives are then confirmed by obtaining complete daughter spectra for the suspected parent ions and matching the resulting spectra with a library of daughter spectra for standards. This procedure is illustrated in Fig. 3, in which a horse serum sample, spiked with 25 ppm procaine, is screened for four drugs.

The ion-current for each selected reaction is monitored as a 1- μ l sample, inserted into the chemical ionization source on a direct insertion probe, is heated to 325° in 100 sec. The screening in Fig. 3 indicated a positive for procaine. The presence of this drug is confirmed by heating a second 1- μ l sample while obtaining the complete daughter spectrum for the compound's protonated molecular ion, as shown in Fig. 4. The library match (Fig. 4) confirms the presence of procaine. This procedure permits the screening of 12 serum or urine samples per hr, with detection limits in the range 0.1–100 ppm for most drugs in serum, urine, or extracts thereof. This procedure permits the sensitive and selective screening and confirmation of illegal drugs rapidly and with minimal sample preparation.

The enhanced selectivity of MS/MS over traditional MS also makes possible trace analysis with extremely low limits of detection. For example, we

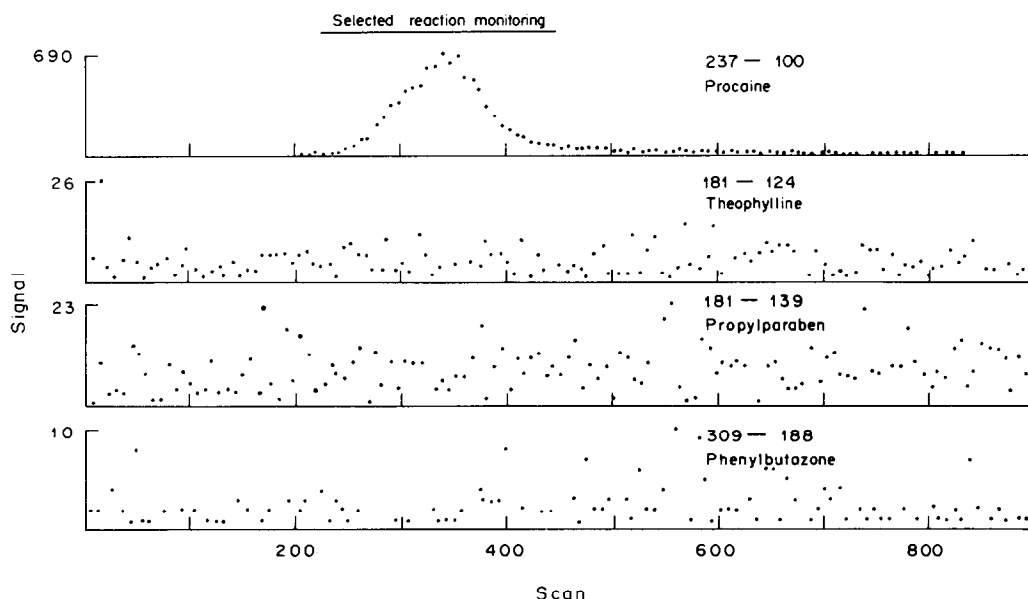


Fig. 3. Screening for four drugs in horse serum spiked with 25 ppm procaine. Results are positive for procaine, negative for the other three drugs.

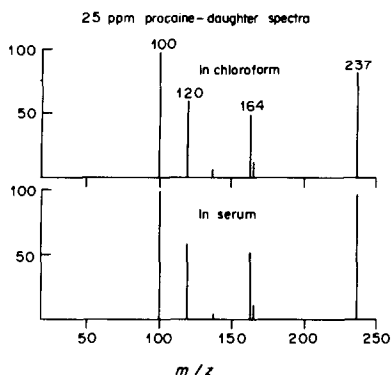


Fig. 4. Comparison of daughter spectrum of procaine in serum with reference library daughter spectrum (for procaine in chloroform).

have demonstrated the ability to detect hexachlorobenzene and trichlorophenol in extracts of human serum and urine with detection limits of 0.05 pg and 0.25 pg, respectively, at a rate of 100 sample injections/hr.¹² The low detection limits were made possible by the use of a short GC column for sample introduction, negative chemical ionization (NCI), and selected-reaction monitoring MS/MS. The use of the 50 cm \times 0.1 cm GC column provides short retention times (<30 sec) for rapid analysis.

A similar approach has been applied to trace analysis for neurochemicals (tryptolines in rat brain extract¹³ and octopamines and synephrines in human serum and urine).¹⁴ In order to take advantage of the sensitivity of NCI, the compounds are converted into their perfluorinated propionic or butyric acid derivatives. This approach provides extremely low limits of detection (Table 3) in standard solutions. When real brain-tissue, urine, or blood serum are analysed, however, large numbers of compounds, many present at levels significantly higher than the analytes, also form derivatives. The short GC column is not adequate to resolve these compounds from the analyte, leading to severe quenching in the electron-capture NCI process and difficulty in detecting even 10 ng of the analyte. Indeed, not even the selectivity possible in the MS/MS analysis can correct for competitive ionization and quenching from interferences in the NCI source.

One solution to this problem would be to switch to positive CI, which is much less sensitive to ionization interferences, albeit with a significant loss in sensitivity. Alternatively, longer capillary columns could be used to separate the analyte derivative from those of other sample components. This latter approach provides detection limits similar to those achieved with the short column, but with longer retention times (*ca.* 10 min) and therefore less rapid analysis. The real value of selected-reaction monitoring MS/MS compared to selected-ion monitoring MS, even with capillary GC separation, is illustrated in Fig. 5. Figure 5a shows the GC/MS (SIM) and 5b the

GC/MS/MS (SRM) chromatograms for a crude rat-brain extract spiked with 35 ppb of methtryptoline. The SIM chromatogram shows numerous compounds producing the m/z 362⁻ ion, while the SRM chromatogram for m/z 362⁻ \rightarrow m/z 179⁻ shows only methtryptoline. Expansion of the chromatogram time-scale in the area of the methtryptoline peak (Figs. 5c and 5d) shows that in the SIM analysis, the methtryptoline is actually an unresolved shoulder on the side of a large interference peak. SRM eliminates this interference.

Preliminary experiments¹³ with 1- μ l injections of crude brain extracts (corresponding to 10 mg of tissue) show tryptoline levels of 50 pg/g in rat brain. The combination of a 20-m cross-linked methyl silicone capillary column with MS/MS has provided isomer-specific detection of the *o*-, *m*-, and *p*- octopamines and synephrines at the 1 ppb level. The use of deuterium-labelled internal standards has permitted precise (\pm 5%) determination in urine and serum extracts.¹⁴

These studies illustrate the potential for rapid, sensitive, and selective analysis of clinical and pharmaceutical samples. Rapid screening and confirmation is possible for large numbers of targeted compounds at the ppb–ppm level in complex mixtures, with minimal sample preparation. Trace analysis at sub-ppb levels is possible by combination of the sensitivity of negative CI with the selectivity of capillary GC/MS/MS.

DRUG METABOLISM STUDIES

The combination of gas chromatography with mass spectrometry has long been used to determine structures of drug metabolites. The methods generally involve some pretreatment of the sample to free conjugated or protein-bound species, followed by extraction to separate basic, acidic and neutral components and endogenous interferences. Since many metabolites are polar molecules, derivatives may be employed to increase volatility, thermal stability and

Table 3. Calculated instrumental sensitivity and limits of detection for tryptoline standards

<i>Sensitivity</i>	
Ion source efficiency (NCI)	10 ⁻³
Transmission (Q1/Q2/Q3)	10 ⁻²
CID efficiency (348 ⁻ \rightarrow 179 ⁻)	10 ⁻¹
Data system sensitivity*	2 counts/ion
Overall sensitivity 2 counts/10 ⁶ molecules	
<i>Limit of detection</i>	
Blank	300 counts
3 \times blank	900 counts
	= 4 \times 10 ⁸ molecules
	= 700 attomoles
	= 200 femtograms
	= 200 ppt† (1 μ l sample)

*EM gain = 10⁵.

†See Table 1.

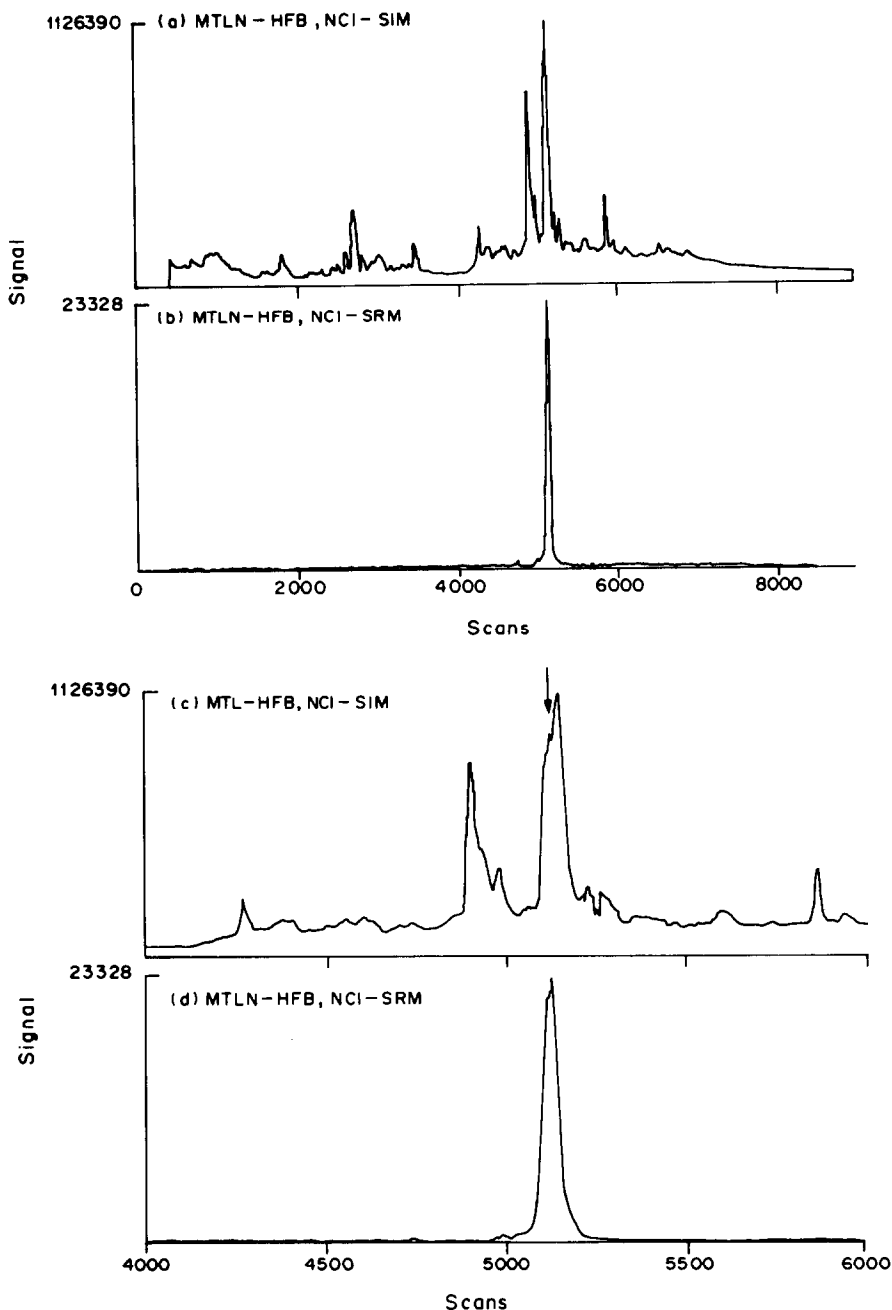


Fig. 5. Chromatograms for a crude rat-brain extract spiked with 35 ppb of methtryptoline, obtained with a 23-m DB-5 fused silica capillary column and negative chemical ionization. (a) Selected-ion monitoring for the $(M-HF)^-$ ion, m/z 362; (b) selected-reaction monitoring for the $362^- \rightarrow 179^-$ fragmentation; (c) enlargement of SIM chromatogram in (a) in the area of the methtryptoline peak (arrow); (d) enlargement of the SRM chromatogram in (b).

chromatographic compatibility. This final item is important because compounds that have dissimilar functional groups may not all be detectable under a single set of chromatographic conditions. Therefore, in a metabolite search in which the compounds sought are unknown, use of only one set of conditions may preclude the discovery of one or more species, while development of multiple chromatographic systems takes considerable time.

The capabilities of MS/MS make it ideally suited to the determination of structures of drug metabolites. Since most metabolites retain a relatively large part of the parent drug structure, it is reasonable to assume that their daughter spectra will contain peaks corresponding to one or more of the fragment ions or neutral fragments characteristic of the pure drug. Therefore, if an extract of urine or plasma from a person taking a particular drug is analysed for these

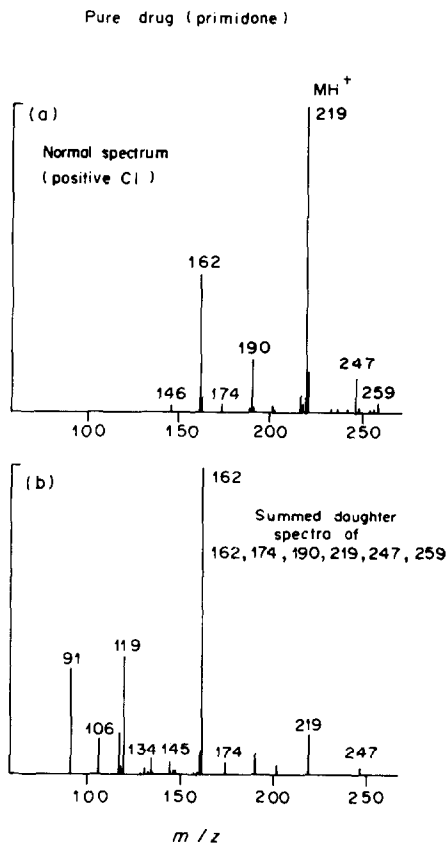


Fig. 6. Spectra obtained in a study of the metabolites of the drug primidone: (a) the positive (CH_4) CI mass spectrum of the pure drug showing the $(\text{M} + \text{H})^+$ ion at m/z 219 as well as $(\text{M} + 29)^+$, $(\text{M} + 41)^+$, and fragment ions; (b) the summed daughter spectra of six ions in (a).

characteristic fragment ions or neutral fragments, the resulting spectrum should contain molecular ions which correspond to potential metabolites of the drug. To identify the compounds, complete daughter spectra are obtained. Because all components of a sample are ionized under a single set of conditions, there is no need to spend time developing chromatographic methods or waiting for components of interest to be eluted.

We have described a method that allows determination of metabolite structure from one extract of urine (2 ml) or plasma (1 ml) in as little as 30 min.¹⁵ As an example, Figs. 6 and 7 illustrate the steps involved in determining the metabolites of the anti-epileptic drug primidone. First a normal (positive or negative ion) CI mass spectrum of the pure drug is obtained, as shown in Fig. 6a. Secondly characteristic substructures of the drug, both daughter ions and neutral fragments, are identified by recording daughter spectra of the molecular ions and major fragment ions in the CI mass spectrum. Figure 6b shows the sum of the daughter spectra of six of these ions. Next, for a sample of serum, urine, or tissue, all ions that contain the drug's characteristic substructures are

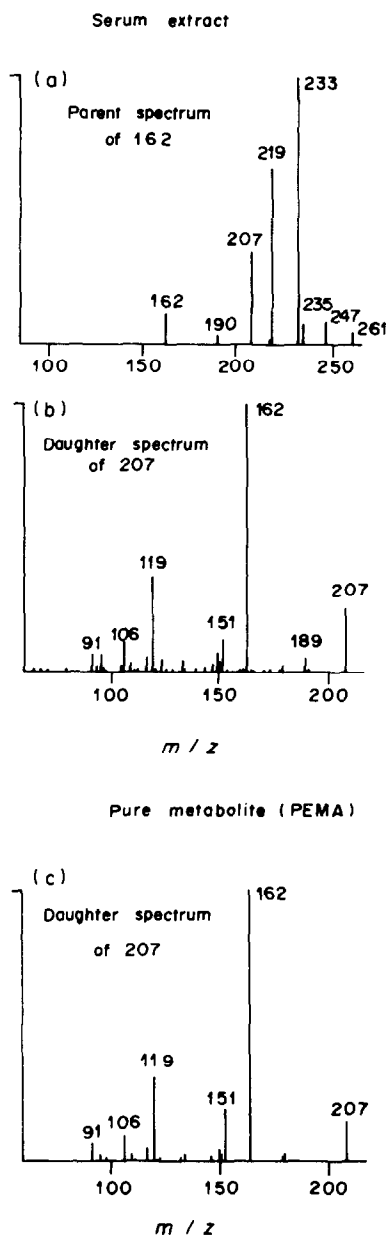


Fig. 7. (a) Parent spectrum of an extract of a patient's serum for the m/z 162 daughter ion characteristic of primidone, showing $(\text{M} + \text{H})^+$ ions for the drug (m/z 219) and two metabolites (m/z 207 and m/z 233); (b) the daughter spectrum of the m/z 207 ion from the serum extract; (c) the daughter spectrum of the m/z 207 ion from pure phenylethylmalonamide (PEMA) for comparison with (b).

identified by acquiring a parent spectrum for each selected daughter ion and a neutral fragment spectrum for each selected neutral fragment. Each of the parent ions seen in these scans corresponds to a potential metabolite. Figure 7a shows one such scan, a parent spectrum for the characteristic 162 daughter ion, from an extract of serum from a patient being treated with the drug. The $(\text{M} + \text{H})^+$ ions are seen for the parent drug at m/z 219, and two possible metab-

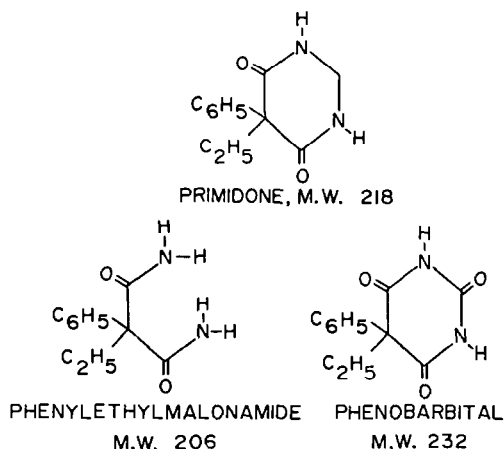


Fig. 8. Primidone and its metabolites identified in serum by MS/MS.

olites at m/z 207 and 233. In addition, the $(M + 29)^+$ and $(M + 41)^+$ ions are observed for each compound. Finally, a daughter spectrum corresponding to the molecular ion of each potential metabolite is obtained in order to determine the metabolite structure. The daughter spectrum of the m/z 207 ion is shown in Fig. 7b. It may be interpreted directly, or compared with the daughter spectrum of the authentic metabolite (Fig. 7c) in order to confirm the structure. In this case two metabolites, phenylethylmalonamide and phenobarbital, are identified, as shown in Fig. 8. This example demonstrates the potential of MS/MS for rapid metabolite identification in a single physiological sample.

CONCLUSION AND FUTURE TRENDS

These studies have demonstrated that tandem mass spectrometry is a powerful tool for clinical and pharmacological studies. Rapid screening and determination at the ppb level and below are possible, since the selectivity of tandem mass spectrometry reduces the need for high selectivity in sample clean-up and chromatographic separation. Furthermore, the unique capabilities of MS/MS offer new analytical techniques, such as the metabolite identification method presented here.

Tandem mass spectrometry is a rapidly evolving field, with dramatic advances particularly apparent in

instrumentation. Although the first commercial triple-quadrupole instruments appeared barely three years ago, sophisticated MS/MS instruments are now being sold by nearly every MS manufacturer. Perhaps the most important advance in MS/MS instrumentation will involve those developments necessary to make low-cost (\$50,000–150,000) instruments available. This will make tandem mass spectrometry even more attractive for rapid screening, trace analysis and metabolite studies.

Acknowledgements—The reported work done at the University of Florida was supported by the National Science Foundation, the Petroleum Research Fund of the American Chemical Society, the National Institutes of Health Biomedical Research Support program, the Medical Research Service of the Veterans Administration and the Epilepsy Research Foundation of Florida. We are grateful for the collaborative assistance of Clyde Williams and B. J. Wilder of the Veterans Administration Medical Center (Gainesville), Ron Gronwall of the University of Florida School of Veterinary Medicine and Kym Faull of the Stanford University School of Medicine.

REFERENCES

1. J. H. Futrell and T. O. Tiernan, in *Ion-Molecule Reactions*, J. L. Franklin (ed.), Chap. 11. Plenum Press, New York, 1972.
2. R. G. Cooks, J. H. Beynon, R. M. Caprioli and G. R. Lester, *Metastable Ions*, Elsevier, Amsterdam, 1973.
3. R. W. Kondrat and R. G. Cooks, *Anal. Chem.*, 1978, **50**, 81A.
4. F. W. McLafferty and F. M. Bockhoff, *ibid.*, 1978, **50**, 69.
5. R. A. Yost and C. G. Enke, *ibid.*, 1979, **51**, 1251A.
6. J. R. B. Slayback and M. S. Story, *Ind. Res. Dev.*, 1981, No. 2, 128–133.
7. R. A. Yost and D. D. Fetterolf, *Mass Spectrom. Rev.*, 1983, **2**, 1.
8. F. W. McLafferty, (ed.), *Tandem Mass Spectrometry*, Wiley, New York, 1983.
9. T. Cairns and W. M. Rogers, *Anal. Chem.*, 1983, **55**, 54A.
10. T. Tobin, *J. Equine Med. Surg.*, 1978, **2**, 518.
11. H. O. Brotherton and R. A. Yost, *Anal. Chem.*, 1983, **55**, 549.
12. R. A. Yost, D. D. Fetterolf, J. R. Hass, D. J. Harvan, A. F. Weston, P. A. Skotnicki and N. A. Simon, *ibid.*, in the press.
13. J. V. Johnson, R. A. Yost and K. F. Faull, *ibid.*, 1984, **56**, 1655.
14. M. B. Budd, R. A. Yost and C. M. Williams, *ibid.*, in the press.
15. R. J. Perchalski, R. A. Yost and B. J. Wilder, *ibid.*, 1982, **54**, 1466.

PERTURBATION OF LABORATORY TEST RESULTS BY ANALYTICAL INTERFERENCES AND DRUG EFFECTS

M. M. GALTEAU and G. SIEST

Centre du Médicament, 30 Rue Lionnois, 54000 Nancy, France
Centre de Médecine Préventive, 2 Avenue du Doyen Jacques Parisot,
54500 Vandoeuvre-les-Nancy, France

(Received 2 May 1984. Accepted 12 June 1984)

Summary—An account is given of ways in which drug treatment can influence the results of laboratory tests for certain species of clinical importance, and of methods of detecting such interferences or effects.

When interpreting laboratory test results, clinical chemists and physicians meet various problems that are due to drug intake by the test subjects. It is now well known that some drugs are able to perturb laboratory tests in two ways.^{1,2} *Analytical*, in which the drug and/or its metabolites can interfere, at any stage, with the assay of a constituent. In clinical chemistry, the term "analytical interference" can be reserved for this *in vitro* effect. *Biological*, in which the drug provokes a change in a biological constituent by a physiological, pharmacological or toxicological mechanism (*in vivo* effect). This aspect includes both the primary desirable effects and also the undesirable so-called "side-effects".

In this paper we describe recent results obtained in our laboratory on both analytical interference and the biological effects of drugs on the most commonly performed routine tests.

ANALYTICAL INTERFERENCES

The studies were performed in two steps, using the procedures developed by the IFCC Expert Panel on "Drug Effects in Clinical Chemistry".³ The first step is the detection of possible analytical interference, the second is its determination. The methods and materials used are listed in Table 1. The sample consists of one pool of sera drawn from supposedly healthy subjects taking no drug. This pool is lyophilized in 25-ml vials. Before use, two vials are reconstituted with (a) 25 ml of a solution in which the active principle is dissolved (this is the spiked sample) and (b) 25 ml of the solvent used to dissolve the drug (the control sample). The contents of the two vials are stirred for 30 min and then dispatched to the laboratory and the tests performed.

We have studied 39 active principles and the interference is considered as significant when the

Table 1. Techniques used for the study of analytical interferences

<i>SMA II</i>	
Albumin	Bromocresol Green
Total bilirubin	Sulphanilic acid
Total calcium	Cresolphthalein
Total cholesterol	Cholesterol-oxidase/4-aminoantipyrine
Creatinine	Picric acid
Glucose	Glucose oxidase/peroxidase
Alkaline phosphatase	4-Nitrophenylphosphate as substrate
Phosphates	Phosphomolybdate complex
Total proteins	Biuret
Urates	Phosphotungstate
Urea	Diacetylmonoxime
<i>GSA II</i>	
Gamma-glutamyltransferase	Gamma-L-glutamyl-3-carboxy-4-nitroanilide/ glycylglycine
Triglycerides	Lipase/esterase
<i>ROTOCHEM II</i>	
Aspartate aminotransferase	Aspartate/2-oxoglutarate/pyridoxal phosphate
Alanine aminotransferase	Alanine/2-oxoglutarate/pyridoxal phosphate

Table 2. Analytical interferences of 34 drugs with laboratory test results (from Gosset⁴)

Active principle	Maximal concentrations used,*		Interference: difference, %			
	mM	mg/l.	0	5-10	10-20	>20
Digoxin	0.01	10	0			
Dihydroergotamine	0.01	10	0			
Clorazepate	0.02	10	0			
Glibenclamide	0.02	10	0			
Nicergoline	0.02	10	0			
Ethinyl oestradiol	0.03	10	0			
Norgestrel	0.03	10	0			
Lorazepam	0.03	10	0			
Oxazepam	0.03	10	0			
Clonidine	0.04	10	0			
Chlordiazepoxide	0.05	16	0			
Amiodarone	0.07	50	0			
Isoniazid	0.10	20	0			
Amitriptyline	0.11	30		Glucose -6 Bilirubin +6		
Methyldopa	0.12	30		Cholesterol -7 Urates +9		Bilirubin +22
Diazepam	0.17	50	0			
Furosemide	0.20	80	0			
Phenobarbital	0.20	50	0			
Acebutolol	0.30	100		Glucose -5		Creatinine +44
Troleandomycin	0.30	200			Phosphates +17	
Carbamazepine	0.40	100	0			
Disopyramide	0.60	200		Phosphates +6 Triglycerides +9		
Propranolol	0.90	100				
Meprobamate	0.92	200	0			
Cimetidine	1.20	300	0			
Acetaminophen	1.30	200		Urates +6		
Allopurinol	1.50	200	0			
Thiamine	1.50	500	0			
Caffeine	2.60	500	0			
Doxepin	4.30	1200		AP +9	GGT +19 Bilirubin -19 Phosphates -16	
Theophylline	5.50	1000				AP -77
Ascorbic acid	5.70	1000		Phosphates -5	Creatinine +17	Glucose -100 Cholesterol -97 Urates +85
Valproic acid	6.00	1000		AP +10		
Metformin	23.00	3000		Glucose -6		

*These concentrations correspond to 10 times the maximal therapeutic levels.

AP = alkaline phosphatase.

Table 3. Interferences of different concentrations of ascorbic acid, methyldopa and theophylline in laboratory tests

Concentration, mM	Glucose	Cholesterol	Effects, % on		Bilirubin	AP
			Urates	Creatinine		
<i>Ascorbic acid</i>						
0.85	-18.0	-11.4	+7.5	+14.3		
0.55	-13.0	-7.0	+4.5	n.d.		
0.34	-8.0	n.d.	+2.8	+7.2		
0.28	-5.6	-4.6	n.d.	+5.4		
0.22	-2.8	-1.9	+1.8	+6.0		
0.17	-2.2	-1.2	n.d.	n.d.		
0.11	-2.0	-0.2	+1.0	+2.9		
<i>Methyldopa</i>						
0.04		-1.5	+4.4		+4.0	
0.02		n.d.	+3.1		n.d.	
<i>Theophylline</i>						
0.28						-15.0
0.22						-6.4
0.16						-5.0
0.11						-3.4

n.d. = not determined.

results for the spiked and unspiked samples differ by more than 5% for chemical constituents and 10% for enzymes.

The results are given in Table 2.

Among the 39 drugs tested, 3 are insoluble in the solvents used, *i.e.*, water, 0.002*M* sodium hydroxide, or water-ethanol (98:2-90:10 v/v). These three drugs are fenofibrate, dipyridamole and glafenine, and they were not studied.

Of the 36 drugs left, 23 give no interference with the methods assayed, and 13 of these do not interfere when added at a concentration of less than 0.1 *mM*. It is logical to think that the higher the drug concentration, the more likely it is to produce an interference, and conversely, the lower the constituent level, the more a drug at a higher concentration can interfere, but we found no correlation between the levels of blood constituents and the concentrations at which drugs interfered. The other 13 active principles produce an analytical interference with at least one serum constituent when they are tested at concentrations 10 times the maximal therapeutic level.

To measure the interferences quantitatively, we performed a new series of tests with decreasing concentrations of the 13 interfering substances. At least two of these levels were within the therapeutic range.

Only 3 drugs, ascorbic acid, methyl dopa and theophylline, still produced an analytical interference with some constituents. The results are given as a function of the concentrations in Table 3.

We found that ascorbic acid interferes with determination of glucose, cholesterol, urates and creatinine, but the interference decreases with dose level. The interference of ascorbic acid in determination of glucose and cholesterol was expected, as these tests were performed by enzymatic methods involving a

Trinder reaction (peroxidase).⁵ Villatte⁶ has shown that the lack of specificity of the peroxidase reaction is responsible not only for these analytical interferences with glucose and cholesterol determination but also with that of urates, phospholipids and triglycerides (Fig. 1).

Although the risk of interference is reduced by the development of more specific methods, it is always necessary to assess the possible interference of commonly used drugs in the application of new techniques, especially in measurement of very low concentrations of hormones or other molecules. Analytical interferences are particularly important in measurement of urinary constituents.

BIOLOGICAL EFFECTS

We have studied certain drugs suspected of having secondary cholestatic effects, in particular some neuroleptics, minor tranquillizers, anabolic steroids, anti-diabetics and oral contraceptives. From the biological tests performed at the Centre for Preventive Medicine, we selected those using enzymes which can reflect a hepatic effect, *e.g.*, gamma-glutamyltransferase (GGT), alkaline phosphatase (AP) and alanine aminotransferase (ALT).

The "samples" were subjects who had undergone a health examination at the Centre for Preventive Medicine in Vandoeuvre-Les-Nancy (France). The test population comprised subjects being treated with at least one drug, generally on a long-term basis. The control population was composed of subjects matching the treated subjects in sex, age and weight, but taking no medication. Information concerning drug intake was collected by means of questionnaires filled up by pharmacists and nurses when blood samples were drawn, and was then computerized by classes, subclasses and trade names.⁴ In some cases, the control subjects presented the same pathological characteristics as the test subjects. The 50th centiles from the two populations were compared. The methods used for measuring the enzymatic activities of GGT, ALT and AP are briefly described in Table 1.

Table 4 summarizes the results obtained for certain classes of drugs. In some cases, we have differentiated the results according to sex. Of the 3 enzymes studied, GGT is the most liable to suffer interference. The ingestion of drugs does not systematically increase the enzyme activities, and some medications are able to decrease plasma enzymes.

The procedure described is sometimes not appropriate. The example of antihypertensive agents is interesting. In this case, it is impossible to compare the treated subjects with supposedly healthy people to detect the effect of drug intake. Instead it is necessary to compare the results obtained for the treated population with those for hypertensive non-treated subjects. The results of such a study are presented in Table 5.

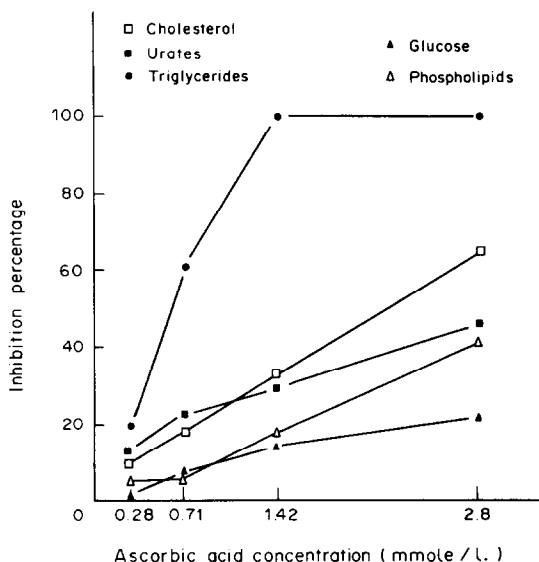


Fig. 1. Interference by ascorbic acid in tests (from Villatte⁶).

Table 4. Effect of long-term drug intake on plasma enzyme activities (per cent difference, calculated on 50th centiles and referred to control values)

	GGT			ALT			AP	
	M + F	M	F	M + F	M	F	M	F
Analgesics ⁷		0	+1		0	+3	+2	+9
Antianginals ⁷		0	+41		-3	+12	-5	+10
Anticoagulants ⁷		-16	0		+1	0	0	+40
Anticonvulsant ⁸		+200	+220		+72	+36	+24	+70
Phenobarbital	+100			-5				
Phenobarbital + phenytoin	+245			+19				
Antidiabetic ⁷		+21	0		+7	+11	-5	+20
Anti-gout		+27	0		+7	0	-1	0
Anti-inflammatory agents ⁴								
Diclofenac	0			0				
Indomethacine	0			0				
Oxyphenbutazone	0			0				
Neuroleptics ^{3,9}	+38							
Imipramine		+14	+59	+4				
Oral contraceptives ^{10,11}			+32			+32		-10
Normo			+29			0		-11
Mini-diphasic			+20			+5		-9
Mini-monophasic			+25			0		-9
Oral contraceptives + imipramine ⁹			+140			-16		
Tranquilizers		+2	+15		-3	+10	-4	0
Chlordiazepoxide		0	0					
Clorazepate						-10		-11
Diazepam							-12	
Vasoconstrictor agents ⁷					+3	-2	+5	+5
Vasodilator agents ⁷		-4	-2		-2	+8	+2	+10

M + F: total population (males + females), M: males, F: females.

The ALT and AP activities do not show large variations after antihypertensive treatments. In contrast, plasma GGT is affected by each drug to an extent varying between -40 and -80%. On the basis of these results, the GGT activity is proposed as a useful test for monitoring antihypertensive drug therapy.¹²

Most of the variations described above are important and indisputable. However, in certain cases the effects of drugs are less clear, and comparison with a control population is not easy. For example, we have examined the effect of 2 hypolipidemic drugs, *viz.* fenofibrate and clofibrate, on GGT, ALT and AP activities.

The 50th centile of a population undergoing treatment was compared with that of a presumably healthy untreated control group (Table 6). Subjects were paired according to sex, age and weight. We also compared these centiles with those of a sample population in a "reference state", consisting of 20-30 year old subjects, taking no drugs and with none overweight.

Comparison of the results for the fenofibrate-treated patients with those for the controls, shows a decrease in the GGT and AP activities for the 50th centiles. For the clofibrate-treated patients this decrease is even bigger. For ALT, the effect is dependent on sex. In men fenofibrate produces a slight decrease, but clofibrate has no effect. On the contrary, in women the ALT activity increases after either treatment.

In contrast, if the results are compared with those for the reference state, the GGT activity increases in males and females treated with fenofibrate. No significant modification occurs with clofibrate. The ALT activity seems to be very much increased by the

Table 5. Effect of antihypertensive agents on plasma enzyme activities (per cent difference, calculated on 50th centile, referred to untreated subjects)¹²

Antihypertensive agent	GGT		ALT		AP	
	M	F	M	F	M	F
Guanoxan	-47	-73	-15	-11	-1	-13
Methyldopa	-51	-75			+7	+3
Atenolol	-39	-80			+1	+13
Bendroflumethiazide + reserpine	-50	-63	-3	-19	-31	-19

Table 6. Variation of plasma enzyme activities after fenofibrate and clofibrate treatment (percentages of variation calculated in centile 50)^{13,14}

Drug	GGT		ALT		AP	
	T/C	T/RS	T/C	T/RS	T/C	T/RS
Fenofibrate						
Males	-5	+49	-10	+44	-18	-30
Females	-25	+37	+25	+92	-18	-12
Clofibrate						
Males	-31	+10	0	+33	-20	-32
Females	-45	0	+21	+76	-28	-16

T = treated; C = control; RS = reference state.

treatment, and the AP activity is decreased. This example illustrates the difficulties in interpretation, particularly when the dispersion of the control distribution is large. These results could be due to inclusion of overweight individuals in the control group, or to age.

Drugs can affect enzymes *in vivo* by modifying either their activity or their concentration. It is impossible to distinguish between the two effects, since only the activity is measured. The activities of plasma enzymes can be modified by a direct effect of the drug on the enzyme (either inhibitive or enhancing) or indirectly by action on a co-enzyme or on a cation necessary for the enzymatic reaction.

The changes in enzyme levels are due to more complex effects: change in enzyme metabolism by inductive processes, repression, acceleration of metabolism or catabolism. The well-known effect of anticonvulsant drugs, especially phenobarbital, on GGT results from the increase of synthesis of this enzyme in the liver. However, the change in plasma enzyme levels due to drugs can be independent of enzyme synthesis. For example, cholestatic effects of drugs can increase alkaline phosphatase. This also seems to be the case for antiepileptic drugs. Another general mechanism of drug-enzyme interactions is an effect on membrane structures.

Some results can be explained in terms of the mechanism of actions of drugs, but most of the *in vivo* effects remain unexplained. Moreover, it is difficult to interpret these effects. They must be related to other physiological variations of enzymes.¹⁵ It is now well known that plasma GGT or ALT varies with age, sex, overweight.

CONCLUSION

As it is impossible to remember all the *in vitro* interferences, and the *in vivo* effects and simultaneously the physiological variations for each biological constituent, data banks are absolutely necessary to help clinical chemists and physicians in interpreting laboratory test results. In Nancy, we have constituted such a bank, entitled INTER-MEDIC.^{2,16,17} It contains information from our own results obtained at the Centre for Preventive Medicine or from the existing literature. Two other computerized drug information systems exist in Europe; a Swedish one (SWEDIS)¹⁸ and a British one¹⁹ (at the University of Surrey). The first data bank on drug effects was established by Young *et al.*²⁰

Acknowledgement—This work was supported by a grant of the Caisse Nationale d'Assurance Maladie des Travailleurs Salariés: contract "Effets analytiques et pharmacologiques des médicaments sur les examens de laboratoire".

REFERENCES

1. G. Siest (ed.), *Drug Effects on Laboratory Tests Results*, Nijhoff, The Hague, 1980.
2. G. Siest, S. J. Dawkins and the IFCC Expert Panel on Drug Effects in Clinical Chemistry, *J. Clin. Chem. Clin. Biochem.*, 1984, **22**, 271.
3. M. M. Galteau, G. Siest and the IFCC Expert Panel on Drug Effects in Clinical Chemistry, *ibid.*, **22**, 275.
4. J. Gosset, *Thèse 3ème cycle*, Biochimie Pharmacologie, Nancy, 1983.
5. G. Siest, W. Appel, G. B. Blijenberg, B. Capolaghi, M. M. Galteau, C. Heusghem, M. Hjelm, B. Le Perron, V. Loppinet, C. Love, R. J. Royer, C. Tognoni and P. Wilding, *J. Clin. Chem. Clin. Biochem.*, 1978, **16**, 103.
6. S. N. Villatte, *Thèse d'Etat en Pharmacie*, Clermont-Ferrand, 1982.
7. F. Schiele, J. L. Neumann, B. Le Perron, M. M. Galteau and G. Siest, in *Drug Measurement and Drug Effects in Laboratory Health Science*, G. Siest and D. S. Young (eds.), pp. 185–193. Karger, Bâle, 1980.
8. D. Bagrel, A. Bagrel, B. Le Perron and G. Siest, in *Drug Effects on Laboratory Tests Results*, G. Siest (ed.), pp. 261–273. Nijhoff, The Hague, 1980.
9. A. Tazi, M. M. Galteau and G. Siest, in *Drug Effects on Laboratory Tests Results*, G. Siest (ed.), pp. 312–322. Nijhoff, The Hague, 1980.
10. F. Schiele, T. Mikstacki and G. Siest, *Ann. Biol. Clin.*, 1982, **40**, 526.
11. F. Schiele and G. Siest, in *Drug Effects on Laboratory Tests Results*, G. Siest (ed.), pp. 274–294. Nijhoff, The Hague, 1980.
12. J. Hitz, J. Henny, J. Steinmetz and G. Siest, *J. Suivi. Therap., Paris*, 1983, **9**.
13. J. Henny, G. Siest, F. Schiele and J. Steinmetz, in *Gamma-glutamyltransferases. Advances in Biochemical Pharmacology*, G. Siest and C. Heusghem (eds.), pp. 209–213. Masson, Paris, 1982.
14. J. Steinmetz, E. Gaspard and D. Notter, in *Drug Effects on Laboratory Tests Results*, G. Siest (ed.), pp. 295–303. Nijhoff, The Hague, 1980.
15. G. Siest, J. Henny and F. Schiele, *Interprétation des examens de laboratoire; variations biologiques et valeurs de référence*, Karger, Bâle, 1981.
16. M. M. Galteau, D. Notter, J. Gosset, B. Le Perron, A. Floc'h, R. Gueguen and G. Siest, in *Topics in Clinical Chemistry*, pp. 849–856. De Gruyter, Berlin, 1982.
17. G. Siest, M. M. Galteau and S. J. Dawkins, *J. Pharm. Biomed. Anal.*, 1983, **1**, 247.
18. N. Tryding, S. G. Johansson and P. Manell, in *Drug Effects on Laboratory Tests Results*, G. Siest (ed.), pp. 27–35. Nijhoff, The Hague, 1980.
19. J. G. Salway and S. J. Dawkins, System for reporting drug-diagnostic test interactions to clinicians, *XI Intern. Cong. Clin. Chem.*, Vienna, 1981 (abstract).
20. D. S. Young, L. C. Pestaner and V. Gibberman, *Clin. Chem.*, 1975, **21**, No. 5.

DETERMINATION OF MICRO AMOUNTS OF URANIUM BY A MOLYBDENUM BLUE METHOD

V. K. BHARGAVA, M. S. OAK, A. R. JOSHI and V. B. SAGAR

Radiochemistry Division, Bhabha Atomic Research Centre, Trombay, Bombay-400 085, India

(Received 22 July 1983. Revised 22 May 1984. Accepted 1 June 1984)

Summary—A new and highly sensitive spectrophotometric method has been developed for the determination of micro amounts of uranium by a molybdenum blue method. The method is based on the observation that at low acidities uranium(IV) reduces ammonium molybdate to molybdenum blue, the absorbance of which is proportional to the amount of uranium present. The variables affecting development of the colour have been investigated and the conditions optimized. Beer's law is found to hold good for uranium concentrations between 1 and 20 ppm, with a precision of 2%. The effect of diverse ions has been studied. The method is useful for the determination of uranium present as an impurity (down to 0.1%) in plutonium, neptunium or thorium.

Several methods are available for the determination of micro amounts of uranium. These include spectrophotometric methods¹⁻⁴ which involve the formation of highly sensitive coloured complexes. Fission-track registration^{5,6} has also been used for the determination of micro quantities of uranium in various matrices. In all these methods plutonium interferes, if present, and a preliminary separation is needed. The present paper describes a spectrophotometric method for the determination of uranium at micro level, valid in the presence of plutonium, neptunium or thorium, by formation of molybdenum blue. The results of preliminary investigations were reported earlier.⁷

It has long been known that heteropolymolybdates of As, P, Si *etc.*, on reduction produce a blue colour which can be used either to determine the central atom incorporated in the complex or to determine the amount of reductant.⁸ The blue colour is also reported to be developed when an acidified solution of molybdate is reduced by mild reducing agents.⁹ It was thought of interest to see whether U(IV) [$E^\circ = 0.33$ V for the U(VI)/U(IV) couple] could be used to reduce either the heteropolymolybdates of As, P, Si *etc.* or ammonium molybdate to form a blue colour. Attempts to reduce the heteropoly compounds did not yield the desired results, but U(IV) was found to reduce ammonium molybdate to a molybdenum blue at low acidities. The variables affecting development of the blue colour have therefore been investigated and the conditions optimized. The effect of diverse ions has been studied and is discussed.

EXPERIMENTAL

Reagents

All reagents used were of analytical-reagent grade.

Ammonium molybdate solution, 10%. Prepared in doubly distilled water and allowed to stand for 3 hr for complete dissolution.

Sulphuric acid. A 2M stock solution was prepared in doubly distilled water and used for controlling the acidity.

Ti(III) solution. Titanium sponge was dissolved in 2M sulphuric acid and the saturated solution obtained was filtered and used as the reductant.

Preparation of pure uranium solution. Nuclear-purity UO₃ was dissolved in 8M nitric acid and converted into sulphate form by repeated evaporation with 4M sulphuric acid and finally transferred with 1M sulphuric acid to a dry weighed flask, which was then weighed again. The uranium content in the stock solution was determined by the Davies and Gray method.¹⁰

Uranium in the stock solution was reduced to U(IV) with Ti(III) in a medium consisting of a mixture of sulphuric acid, sulphamic acid and nitric acid.

Preparation of pure plutonium solution. Plutonium(IV) oxalate was converted into the oxide by heating in a platinum boat at 900°. The absence of impurities such as vanadium and iron was checked by emission spectrography. The oxide was dissolved in concentrated nitric acid containing 0.05 mole of hydrofluoric acid per litre, in a platinum dish. The solution was evaporated to dryness, then the residue was taken up in concentrated nitric acid; this step was repeated twice more to ensure complete removal of hydrofluoric acid. The solution was then repeatedly evaporated with 4M sulphuric acid to convert the plutonium into sulphate form and finally transferred with 1M sulphuric acid to a dry weighed flask, which was then weighed again. The plutonium content of this stock solution was determined by the Drummond and Grant method.¹¹ Absence of uranium in the stock solution was ascertained by the present method.

Apparatus

All spectra were recorded on a Cary model 14 spectrophotometer, with 1-cm quartz cells. For studying the effect of diverse ions, temperature and time, the absorbance measurements were made with a Brinkman DC 800 probe colorimeter, with appropriate filters.

Procedure

Take the solution containing uranium in a 25-ml standard flask for reduction. Add 0.5 ml of a reaction mixture consisting of sulphamic acid (0.25M), nitric acid (1M) and sulphuric acid (0.5M), followed by the titanium(III) solution until its colour persists. The excess of titanium(III) is slowly oxidized to titanium(IV) by the nitric acid present, and the titanium(IV) does not absorb in the wavelength span of interest. Add 5 ml of 2M sulphuric acid, ~10 ml of distilled water and 7.5 ml of 10% ammonium molybdate solution, and then make up to volume with distilled water, giving a final acidity of 0.4M sulphuric acid and an ammo-

mium molybdate concentration of 3%. After 20 min, measure the absorbance at 600 nm in a 1-cm cell against a reagent blank. Prepare a calibration graph in a similar way.

RESULTS AND DISCUSSION

It was observed that when U(IV) is added to an acidified ammonium molybdate solution, a blue colour is produced, the intensity of which varies with the amount of U(IV) added. The absorption spectrum of this blue solution is dependent on the acidity and on the amount of ammonium molybdate present. A systematic study was therefore made, to optimize the conditions.

Influence of acidity and selection of wavelength

Figure 1 shows the change in the spectrum with acidity. At low acidity, *i.e.*, 0.02–0.1M sulphuric acid, λ_{\max} is between 820 and 800 nm, then gradually shifts to 600 nm at an acidity of $\sim 0.18M$ sulphuric acid. At acidities between 0.18 and 0.5M sulphuric acid, λ_{\max} remains fairly constant at 600 nm but the absorbance decreases at higher acidities. At sulphuric acid concentrations $>0.5M$, the blue colour changes to green. Beer's law is obeyed at λ_{\max} at all acidities in the range 0.02–0.5M. The molar absorptivities at 0.04, 0.2 and 0.4M sulphuric acid concentration have been calculated for 820, 660 and 600 nm for comparison, and are shown in Table 1. The molar absorptivity is highest at 820 nm but the dependence of λ_{\max} on acidity is very critical, making this wavelength unsuitable for quantitative work. An acidity range of 0.2–0.4M is optimal but an acidity of 0.4M sulphuric

Table 1. Molar absorptivities at different acidities and wavelengths (measurement after 20 min colour development)

λ , nm	Molar absorptivity, $10^4 \text{ l. mole}^{-1} \text{ cm}^{-1}$		
	[H ₂ SO ₄] 0.04M	0.20M	0.40M
600	0.7	1.3	1.2
660	1.1	1.1	1.1
820	2.0	0.7	0.7

acid is preferred, at the cost of sensitivity, as the tolerance limit for various ions is then higher and there is no precipitation. When the acidity is not accurately known, the absorbance measurements should be made at 660 nm.

Effect of ammonium molybdate concentration

Figure 2 shows the change in the spectrum with variation in molybdate concentration. At lower concentrations, *i.e.*, from 1.8 to 2.2%, λ_{\max} is at ~ 700 nm, and gradually shifts to 600 nm with increasing concentration of molybdate up to 2.8%. Though the absorbance at 600 nm increases with increasing molybdate concentration, high concentrations cause precipitation on standing. A concentration of 3% is therefore recommended.

Influence of sequence of addition of reagents, time and temperature

The order of addition of the reagents is immaterial. To study the effect of time and temperature, two

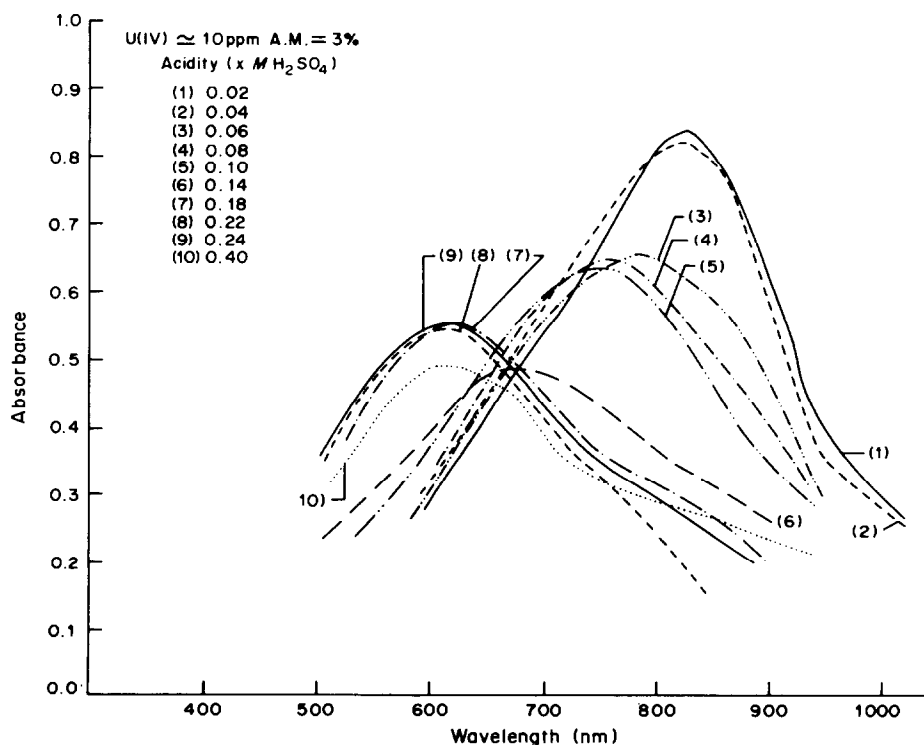


Fig. 1. Change in absorption spectrum of Mo blue with acidity (A.M. = ammonium molybdate)

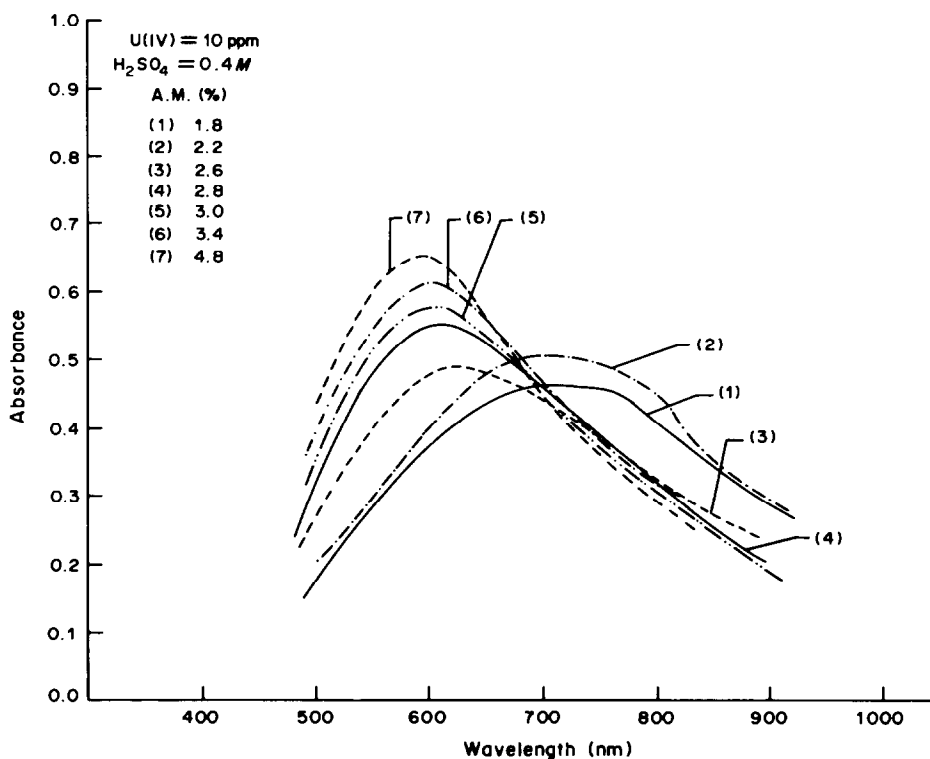


Fig. 2. Change in absorption spectrum of Mo blue with ammonium molybdate (A.M.) concentration.

solutions were prepared, containing about 12 ppm of U(IV) and 3% ammonium molybdate in (A) 0.04M and (B) 0.4M sulphuric acid, and the absorbance was measured as a function of time (Fig. 3). Maximal absorbance is attained after ~20 min, and remains constant for ~12 hr. These solutions were also heated after constant absorbance had been reached (Fig. 4). No appreciable change in absorbance was observed until a temperature of 35° was reached. At higher temperatures the absorbance of solution (A) increased whereas that of solution (B) decreased. At above 70° the blue colour changed into green.

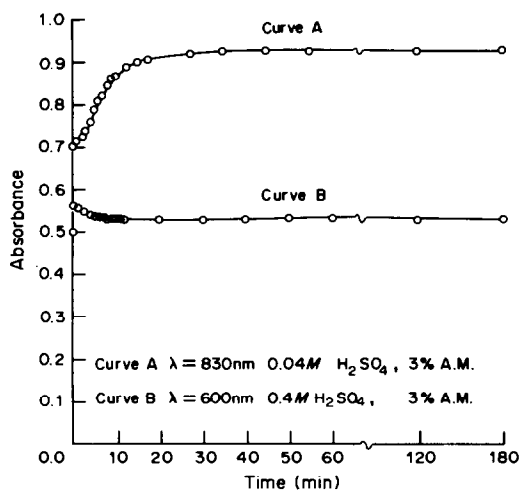


Fig. 3. Time dependence of absorbance.

Beer's law, sensitivity and precision

Beer's law was obeyed at all acidities from 0.04 to 0.5M sulphuric acid and at 820, 660 and 600 nm. The precision of the method was determined with 10 aliquots of an 898- $\mu\text{g/g}$ stock solution of U(IV); the mean found was 911 $\mu\text{g/g}$, with a relative standard deviation of $\pm 1.6\%$.

Determination in presence of plutonium

Since the method is suitable for determination of uranium in the ppm range, it was of interest to see whether it could be exploited for the determination of uranium as an impurity in plutonium samples. Synthetic mixtures of U and Pu were prepared, and analysed for uranium by the procedure described. Identical amounts of uranium were taken in separate flasks and the colour developed. Comparison of the absorbances of the two sets showed that plutonium does not interfere. In principle, as little as 5 μg of uranium can be determined in the presence of 2500 μg of plutonium per 25 ml of solution, but larger amounts of plutonium cause precipitation.

Effect of diverse ions

A known amount of potentially interfering ion was added to a known amount of uranium, the blue colour was developed by the procedure described and the absorbance compared with that of a pure uranium solution. A change of 3%, twice the relative standard deviation, in the absorbance was taken as

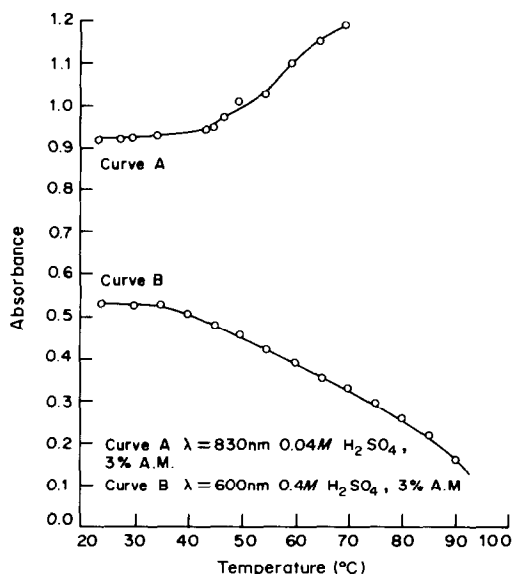


Fig. 4. Temperature dependence of absorbance.

the tolerance limit. Table 2 lists the ions that cause interference. The most serious interference was caused by Ru, Ta, Te, Se, Si, As, Ce, V, Fe, PO_4^{3-} and F^- . A few cations, *e.g.*, Pb, Ba, Sr, Ca, were precipitated as the sulphates. Palladium(II) was reduced to the metal and precipitated, but the blue colour could still be produced, though with reduced intensity. Vanadium and iron interfere quantitatively

by forming blue solutions themselves; their lower oxidation states [V(III), Fe(II)] are capable of reducing isopolymolybdates to molybdenum blue. Thorium, plutonium and neptunium up to 100 $\mu\text{g/ml}$ did not interfere, but higher concentrations resulted in precipitation. Alkali metals and most of the rare-earth metals did not interfere. Anions such as SCN^- , NO_3^- , Cl^- , ClO_4^- , CH_3COO^- , $\text{C}_2\text{O}_4^{2-}$, NH_2SO_3^- did not interfere.

Acknowledgements—The authors thank Dr. P. R. Natarajan, Head, Radiochemistry Division, for constant encouragement during the course of this work.

REFERENCES

1. J. Y. Hsieh and B. Jaselskis, *Talanta*, 1979, **26**, 141.
2. J. A. Bustamante and F. P. Delgado, *Analyst*, 1971, **96**, 407.
3. S. C. Dubey and M. N. Nadkarni, *Talanta*, 1977, **24**, 266.
4. T. Yamamoto, *Anal. Chim. Acta*, 1973, **65**, 329.
5. G. R. Mahajan, N. K. Chaudhuri, R. Sampathkumar and R. H. Iyer, *Nucl. Instr. Meth.*, 1978, **153**, 253.
6. R. H. Iyer, M. L. Sagu, R. Sampathkumar and N. K. Chaudhuri, *ibid.*, 1973, **109**, 453.
7. V. K. Bhargava, M. S. Oak, A. R. Joshi and V. B. Sagar, Paper Anal-60, Annual Convention of Chemists, Madras, India, December 1981.
8. G. A. Parker, in *Treatise on Analytical Chemistry*, I. M. Kolthoff and P. J. Elving (eds.), Part II, Vol. 10, p. 352. Wiley-Interscience, New York, 1978.
9. F. A. Cotton and G. Wilkinson, *Advanced Inorganic Chemistry*, 2nd Ed., p. 934. Wiley, New Delhi, 1970.
10. W. Davies and W. Gray, *Talanta*, 1964, **11**, 1203.
11. J. L. Drummond and R. A. Grant, *ibid.*, 1966, **13**, 477.

Table 2. Interference studies* (absorbance at 600 nm = 0.86 for $[U] = 200 \mu\text{g}/25 \text{ ml}$)

Ion	Added as	Concentration, $\mu\text{g}/25 \text{ ml}$	Absorbance at 600 nm	Error, %
Ba^{2+} , Ca^{2+} , Sr^{2+}	Nitrates	1000	—	pptn
VO^{2+}	Sulphate	200	—	forms Mo blue
Ta^{5+}	Chloride	500	0.383	-55
Fe^{2+}	Sulphate	200	—	forms Mo blue
Co^{2+}	Nitrate	1000	0.916	+6.5
Ni^{2+}	Chloride	1000	0.940	+9.3
Ru^{3+}	Chloride	500	0.49	-43.0
Pd^{2+}	Chloride	500	—	pptn
Pt^{4+}	Chloride	500	0.690	-19.7
Cu^{2+}	Chloride	1000	0.820	-4.7
Ag^+	Nitrate	1000	0.801	-6.9
Zn^{2+}	Acetate	1000	0.904	+5.1
Ga^{2+}	Chloride	500	0.725	-15.7
SiO_3^{2-}	Sodium silicate	500	0.628	-27.0
Ge^{4+}	Chloride	500	0.921	+7.1
Sn^{2+}	Chloride	500	—	forms Mo blue
Pb^{2+}	Acetate	1000	—	pptn
PO_4^{3-}	Phosphate	—	—	masks blue colour
As^{3+}	Chloride	500	0.616	-2.8
Ce^{4+}	Ceric ammonium nitrate	1000	0.655	23.8
F^-	Sodium fluoride	100	—	masks blue colour

*All interference studies were made in presence of uranium.

MULTIPARAMETRIC CURVE FITTING—V THE GENERAL PROGRAM 'ABLET', A SYSTEM FOR REGRESSION ANALYSIS IN STUDIES OF SOLUTION EQUILIBRIA

MILAN MELOUN

Department of Analytical Chemistry, College of Chemical Technology, 532 10 Pardubice, Czechoslovakia

JOSEF ČERMÁK

Computing Centre, College of Chemical Technology, 532 10 Pardubice, Czechoslovakia

(Received 22 July 1983. Revised 12 May 1984. Accepted 1 June 1984)

Summary—The general program ABLET is a system of subprograms for non-linear regression analysis of experimental data to find an appropriate model. The structure of ABLET provides a suitable organizational framework in which just two specific subroutines have to be supplied by the user. The resulting program can estimate non-linear model parameters with their standard deviations, test the agreement between experimental data and a mathematical model, test the accuracy and reliability of the parameters found, and simulate synthetic data for preselected parametric values. Heuristic, and/or algorithmic minimization strategies aid examination of the local and overall minima. The method of construction of the program for a particular system is discussed.

The original LETAGROP VRID of Sillén and Ingri^{1,2} has been rewritten in the form of the subroutine LETAG in autocode MOST F 13 for the ODRA 1013 computer,³ in Fortran for the Hewlett-Packard 2116B,⁴ and in Fortran IV for the EC 1040 or EC 1033 computers.⁵ Various programs⁶⁻¹⁵ have been based on LETAG and applied to studies of protonation and complex-formation equilibria and determination of stability constants.^{7,16-27}

More than ten years of experience with the use of LETAG, and critical comparison with other up-to-date minimization algorithms, have led to the improved version, ABLET, and revision of all our previous programs based on it. Adaptation of the ABLET system to a particular equilibrium problem is now much easier. The ABLET system also makes a statistical test of the reliability of the estimated parameters, plots a curve-fitting graph by a printer routine, and provides three minimization strategies for finding not only the global minimum but also any selected one. Minimization may be done algorithmically or by trial-and-error or by a combination of the two.

The seven programs of the ABLET family^{28,29} are (1) DHLET for determination of thermodynamic dissociation constants and parameters of the extended Debye-Hückel equation, (2) DCLET for determination of dissociation constants and molar absorptivities,³⁰ (3) NCLET for determination of stability constants from competitive titration equilibria,¹¹ (4) MRLET for determination of ligand purity and the stability constant of a predominant

complex from mole-ratio data,³¹ (5) SPLET for determination of stability constants and parameters of a chemical model from absorbance data,²⁸ (6) EXLET for analysis of extraction/photometric data,²⁸ and (7) POLET for determination of stability constants and complex stoichiometry from potentiometric titration.²⁸

The ABLET system allows the minimization subroutine to be changed from LETAG to another subroutine from the library.

THEORY

Modus operandi of the ABLET system

In studies of chemical equilibria it is often necessary to fit a function $f(x; \beta)$ to a set of experimental data. Unknown parameters are estimated by minimizing the difference between the experimental and calculated data:

$$U = \sum_{i=1}^n w_i (y_{\text{exp},i} - y_{\text{calc},i})^2 = \text{minimum} \quad (1)$$

where w_i represents the statistical weight, $y_{\text{exp},i}$ is a single observation made for x_i , and $y_{\text{calc},i} = f(x_i; \beta_1, \beta_2, \dots, \beta_m)$ is the functional relationship assumed to exist. Each observed y_i for a given x_i is related to the calculated value of y_i by the equation $y_i = f_i + \epsilon_i$ where ϵ_i represents a random error. Random (or observational) errors are assumed to follow a Gaussian (normal) distribution expressed as

$$f(\epsilon_i) = \frac{\exp[-\epsilon_i^2/2s^2(y)]}{\pi \sqrt{2}s(y)} \quad (2)$$

where $s^2(y)$ is the variance of y . Theoretically, the assumption that the model giving minimum U is the best fit is justified only if (i) the correct form of the equation for y_{calc} is known and used, (ii) there are no errors other than random errors in y , (iii) the random errors in y have a Gaussian distribution, and (iv) w_i is an exact indication of the inherent accuracy of y_i . None of these conditions is usually strictly fulfilled, but $U = \text{minimum}$ is still widely used as a criterion because there is no better alternative.

A computer program for analysing data from equilibrium studies may usefully be constructed from logical units, each consisting of one or more sub-routines. The division of the program into logical units aids the understanding of the functional structure of the whole program, Fig. 1.

The MASTER unit contains the main part of the program. The INPUT unit reads and checks data, and makes some preliminary calculations. The RESIDUAL-SQUARE SUM unit formulates the sum of squared residuals, *i.e.*, the squares of the differences between experimental and calculated values of the dependent variable. The relevant mathematical model in the form of an explicit or implicit functional relationship must be available.

Example. The dissociation equilibrium of HL^z , $\text{HL}^z \rightleftharpoons \text{L}^{z-1} + \text{H}^+$, is characterized by the thermodynamic (activity) dissociation constant $K_a^T = a_{\text{H}} a_{\text{L}} / a_{\text{HL}}$. The dependence of the mixed dissociation constant $K_a = a_{\text{H}} [\text{L}] / [\text{HL}]$ on ionic strength, assuming that both ions HL^z and L^{z-1} have roughly

the same ion-size parameter \hat{a} (10^{-10} m) and that the overall salting-out coefficient is given by $C = C_{\text{HL}} - C_{\text{L}}$, is expressed by the Debye-Hückel equation in the form

$$\text{p}K_a = \text{p}K_a^T - AI^{1/2}(1 - 2z)/(1 + B\hat{a}I^{1/2}) + CI \quad (3)$$

where

$$A = 0.5112 \text{ mole}^{-1/2} \cdot \text{l}^{1/2} \cdot \text{K}^{3/2}$$

and

$$B = 0.3291 \text{ mole}^{-1/2} \cdot \text{m}^{-1} \cdot \text{l}^{1/2} \cdot \text{K}^{1/2} \cdot 10^{10}$$

for aqueous solutions and 25° . The mixed dissociation constant $\text{p}K_a$ represents a dependent variable and the ionic strength I is taken as the independent variable, because it can be adjusted precisely so that its random error is less than that of the dependent variable $\text{p}K_a$. The three unknown parameters $\text{p}K_a^T$, \hat{a} and C are to be estimated by minimization of U :

$$U = \sum_{i=1}^n w_i (\text{p}K_{a,\text{exp},i} - \text{p}K_{a,\text{calc},i})^2 \quad (4)$$

The program used is DHLET.⁸

The MINIMIZATION unit contains the least-squares curve-fitting algorithm LETAG³⁻⁵ which estimates unknown parameters by the minimization of a residual-square sum function. LETAG is based on the approach developed by Sillén and Ingri^{1,2} which approximates the residual-square sum as a possible or proposed. The statistical analysis of re-

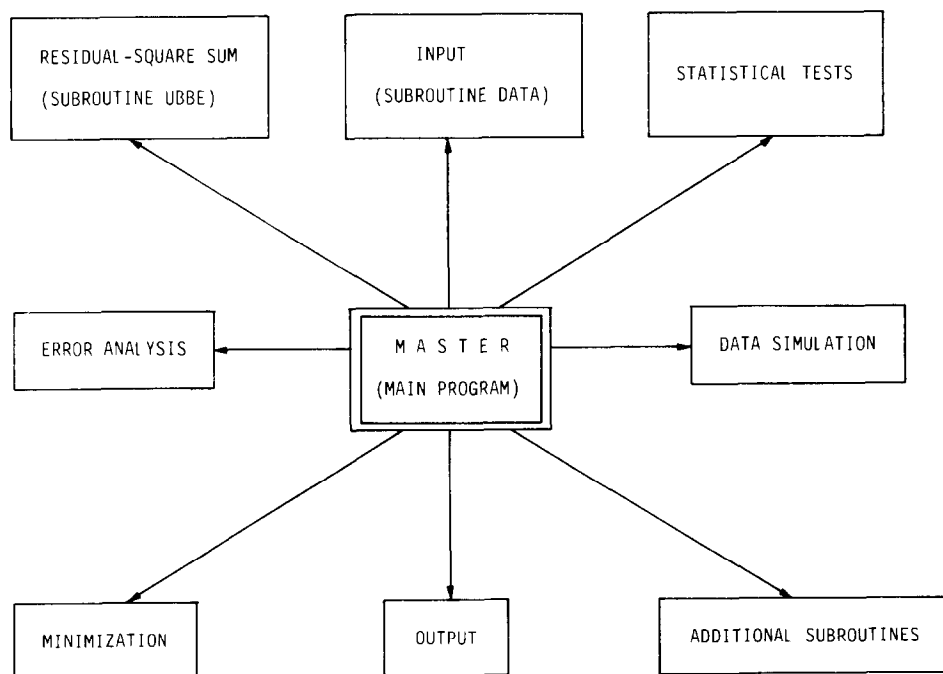


Fig. 1. The functional units of the general ABLET program. The three units to be written by the user are SUBROUTINE UBBE, SUBROUTINE DATA, MAIN PROGRAM. The rest of the ABLET system is identical for all programs.

Table 1. Shortened form of LETAG minimization process for input data listed in Table 3

DHLET PROGRAM				
DHLET: SIMULATED DATA SET				
xxxxxx RURIK = 7 xxxxxx LASK (INITIAL GUESS):				
NUMBER OF ESTIMATED PARAMETERS = 3				
NUMBER OF POSITIVE PARAMETERS = 3				
NUMBER OF TWIST MATRIX ELEMENTS = 0				
INITIAL GUESS OF THE FIRST PARAMETER (PKT) = 4.9				
THE SECOND PARAMETER (A) = 5.0				
THE THIRD PARAMETER (C) = 0.15				
xxxxxx RURIK = 3 xxxxxx STEG (STEP OF PARAMETERS):				
1 0.12 2 0.45 3 0.15				
xxxxxx RURIK = 2 xxxxxx UTTAG (RESIDUAL-SQUARE SUM):				
U = 7.67215E-01 4.90000 5.00000 0.15000				
xxxxxx RURIK = 5 xxxxxx SKOTT (SHOT):				
U = 7.67215E-01 4.90000 5.00000 0.15000				
U = 3.16076E-01 5.02000 5.00000 0.15000				
U = 1.79436E 00 4.78000 5.00000 0.15000				
U = 6.36359E-01 4.90000 5.45000 0.15000				
U = 9.31824E-01 4.90000 4.55000 0.15000				
U = 1.38683E-01 4.90000 5.00000 0.30000				
U = 2.35673E 00 4.90000 5.00000 0.00000				
U = 2.46029E-01 5.02000 5.45000 0.15000				
U = 3.62017E-02 5.02000 5.00000 0.30000				
U = 1.14367E-01 4.90000 5.45000 0.30000				
MINUSGROP (MINUS PIT)				
KBOM (PARAMETERS)	NUMBER	VALUE	DARR1	DARR2
	1	4.98758E 00	-1.00000	-1.00000
	2	5.17657E 00	-1.00000	-1.00000
	3	2.76862E-01	-1.00000	-1.00000
PROVA (TESTING)				
U = 1.85920E-03	4.98758E 00	5.17657E 00	2.76862E-01	
1 ITERATION	U = 1.85920E-03	4.98758E 00	5.17657E 00	2.76862E-01
2 ITERATION	U = 1.55934E-03	4.99138E 00	5.04157E 00	2.76862E-01
3 ITERATION	U = 3.07154E-04	4.99590E 00	4.55719E 00	2.98522E-01
4 ITERATION	U = 3.03922E-04	4.99606E 00	4.55890E 00	2.98029E-01
5 ITERATION	U = 3.03919E-04	4.99605E 00	4.55925E 00	2.98007E-01
6 ITERATION	U = 3.03919E-04	4.99605E 00	4.55925E 00	2.98007E-01

second-degree surface of an elliptical paraboloid for one of the two parameters (i.e., $m = 2$) in $(m + 1) = 3$ -dimensional space. For more parameters than two ($m > 2$), it deals with a hyperparaboloid in $(m + 1)$ -dimensional space.

Table 1 gives an example of a DHLET output which estimates three parameters, pK_a^T , \hat{a} and C [from 20 data points (pK_a, I)] from Table 2. Key 7 calls the block LASK, which reads the initial guessed values for the parameters. Key 3 calls block STEG which reads the size of the initial minimization steps. Key 2 calls block UTTAG which calculates the residual-square sum function for an actual parameter value. Then a systematic search of parameters by block LETA, called by key 5, begins.

The minimization process starts with a “central” set $\vec{\beta}_c$ equal to initial guessed values for the parameters, supplied by the user, and calculates U for $\vec{\beta}_c$ and for sets where one or two elements in $\vec{\beta}_c$ have been changed by steps h_i . In the heuristic (trial-and-error) strategy, these steps are always supplied by the user, but in the algorithmic strategy they are supplied by the user only for the first iteration; for subsequent iterations they are calculated by the program.

From the U values for $(m + 1)(m + 2)/2$ systematically chosen points, the coefficients of the equation for a second-degree surface through these points are calculated, and hence the position $\vec{\beta}_0$ of the minimum on that surface. For brevity, the procedure described so far will be referred to as a “shot”. The $\vec{\beta}_0$ obtained from the first shot may be used as the central value for the next shot, and so on. The co-ordinates of the pit, the lowest point of function U , are computed from the coefficients of the equations describing the approximate surface.

This pit-mapping method can also be employed when the parameters are inhomogeneous (e.g., stability constants, molar absorptivities, concentrations, etc.). The U surface is very often distorted and not symmetrical. With such a cleft-like surface (a “skew pit”), or if there is a high degree of correlation between the β_i parameters, difficulties arise in the calculations. When the steps chosen are too large and the pit is deep and skew, the points are high up on the wall of the “cleft”, and terms of third and higher degree become important. On the other hand, if the steps are too small, rounding errors in the computer can cause rounding errors in the calculation of $\vec{\beta}_0$.

Table 2. Shortened form of the last part of the output from DHLET, printed after termination of the minimization process from Table 1

7 ITERATION U = 3.03919E-04 4.99605E 00 4.55925E 00 2.98007E-01				
xxxxxx SKRIK (OUTPUT) xxxxxx				
PARAMETERS AND THEIR STANDARD DEVIATIONS:				
FIRST (PKT):		4.99605		±0.00112
SECOND (A):		4.55925		±0.03784
THIRD (C):		0.29801		±0.00212
I	I(EXP)	PK(EXP)	PK(CALC)	RESIDUAL
1	0.0100	4.8646	4.8656	-0.0010
2	0.0400	4.7752	4.7719	0.0033
3	0.0900	4.7019	4.7054	-0.0035
4	0.1600	4.6661	4.6602	0.0059
5	0.2500	4.6407	4.6322	0.0085
6	0.3600	4.6145	4.6188	-0.0043
7	0.4900	4.6084	4.6182	-0.0098
8	0.6400	4.6318	4.6289	0.0029
9	0.8100	4.6484	4.6499	-0.0015
10	1.0000	4.6726	4.6804	-0.0078
11	1.2100	4.7179	4.7198	-0.0019
12	1.4400	4.7769	4.7677	0.0093
13	1.6900	4.8213	4.8236	-0.0023
14	1.9600	4.8896	4.8873	0.0023
15	2.2500	4.9522	4.9585	-0.0063
16	2.5600	5.0424	5.0370	0.0054
17	2.8900	5.1242	5.1226	0.0015
18	3.2400	5.2178	5.2152	0.0026
19	3.6100	5.3129	5.3147	-0.0019
20	4.0000	5.4196	5.4210	-0.0014
STATISTICAL ANALYSIS OF RESIDUALS:				
RESIDUAL MEAN = 1.52E-06				
MEAN RESIDUAL = 0.0041				
STANDARD DEVIATION = 0.0050				
SKEWNESS = 0.022				
KURTOSIS = 2.390				
PEARSON CHI SQUARE = 3.20 and SHOULD BE 12.60				
(FOR 6 D.F. AND 0.95 PROBABILITY LEVEL)				
R-FACTOR = 0.00103				

The values of parameters are varied along the main axis of the pit instead of parallel to the original co-ordinate axes, in the second and subsequent refinement cycles.

For equilibrium constants and certain other types of parameters such as concentrations, a negative value has no physical meaning. LETAG⁵ contains a number of safeguards to prevent such parameters from becoming negative during a shot, and at the same time to check that the calculation is not carried too far from the minimum.

If the calculated minimum $\bar{\beta}_0$ gives negative values for such parameters, they are set equal to zero, and the computer searches for the minimum of the "reduced pit". The block performing this operation, MIKO, searches the calculated second-degree surface systematically for the set $\bar{\beta}$ that gives the lowest value for U while no member of $\bar{\beta}$ is negative.

MIKO can also be used to find the set $\bar{\beta}$ that gives the lowest U value, subject to the restriction that each member β_i should have a value of either zero or not less than its standard deviation $s(\beta_i)$ multiplied by a selected factor F_s .

The ERROR ANALYSIS unit calculates the standard deviations of the estimated parameters and

dependent variable. LETAG⁵ is used for calculating the residual-square sum function for the pit found, U_{\min} , and the standard deviation of y , $s(y)$, which is denoted by SIGY in the output in Table 1 and is the square root of U_{\min} divided by the square root of the number of degrees of freedom $[(n - m)$ where n is the number of data points and m the number of parameters]:

$$s(y) = \sqrt{U_{\min}/(n - m)}. \quad (5)$$

For defining the standard deviations $s(\beta_i)$ of the parameters, the term "D-boundary" was introduced by Sillén^{1,2}. It is the curve or supercurve on which $U = U_{\min} + s^2(y)$. The "D-boundary" is sometimes called the U contour. The standard deviation of each parameter $s(\beta_i)$ has a parabolic distribution and is calculated as the maximum difference between the value for β_i at any point on the "D-boundary" and the value for β_i at the minimum, $s(\beta_i) = D_i = [(\beta_D - \beta_0)_i]_{\max}$. In the output of Table 1, $s(\beta_i)$ is printed under the heading DARR2 if it is available in the minimization process, otherwise -1.0 is printed.

The STATISTICAL TESTS unit identifies the "best" model when more than one hypothesis is

siduals involves examination of the differences between the experimental and calculated values of the dependent variable, $r_i = y_{\text{exp},i} - y_{\text{calc},i}$. The assumptions necessary for the least-squares treatment have already been mentioned. If the model represents the data adequately, the residuals should possess characteristics that satisfy or at least do not contradict the basic assumptions: thus the residuals should be randomly distributed about y_{calc} . Systematic departures from randomness indicate that the model is not satisfactory. The examination of plots of the residuals vs. x may assist numerical and/or graphical aids in the analysis of residuals. A study of the signs of the residuals (+ or -) and sums of signs can also be used.

For the analysis of residuals, graphical presentation is extremely helpful for the following tests: (i) detection of an outlier (an extreme residual), (ii) detection of a trend in the residuals, (iii) detection of sign changes, (iv) detection of an abrupt shift level of the experiment, (v) examination of residuals for normal distribution. A relative frequency plot should give approximately the familiar bell-shaped curve about a mean of zero.

For a more objective statistical analysis,³² the set of residuals can be described by its four moments (cf. Table 2) and may be used for hypothesis testing.

(i) The first moment is the arithmetic mean of residuals $m_{r,1} = \bar{r}$, which should be equal to zero.

(ii) The second moment is the variance

$$m_{r,2} = \left(\sum_{i=1}^n r_i^2 / n \right) - \left(\sum_{i=1}^n r_i / n \right)^2$$

and its square root is the standard deviation, which should have a value similar to the experimental error in the dependent variable y , $s_{\text{inst}}(y)$. The same rule is applied to the mean of the residuals which is calculated as the arithmetic mean of the absolute values of the residuals.

(iii) The third moment, the coefficient of symmetry (skewness) gives information about the symmetry of the residual distribution curve;

$$m_{r,3} = \sum_{i=1}^n (r_i - \bar{r})^3 / nm_{r,2}^{3/2}$$

is equal to zero for a Gaussian distribution.

(iv) The fourth moment, the coefficient of kurtosis, characterizes the "peakedness" of the residual distribution curve and is defined by

$$m_{r,4} = \sum_{i=1}^n (r_i - \bar{r})^4 / nm_{r,2}^2.$$

For a normal Gaussian shape it has the value 3.

(v) A goodness-of-fit statistic χ^2 (Pearson test) is derived from the difference between the observed and calculated probability distribution. The residuals may be divided into eight classes, each of which should contain 12.5% of all residuals. These classes are defined by the limits $-\infty, -1.15s, -0.675s,$

$-0.319s, 0.0, 0.319s, 0.675s, 1.15s, +\infty$. Since the residuals standard deviation s is calculated from the residuals themselves, the total χ^2 has 6 degrees of freedom. A fit can be accepted at the appropriate confidence level if the experimental value χ^2 is less than the value expected.

(vi) The Hamilton R -factor is defined by the expression

$$R = \left[\frac{\sum_{i=1}^n w_i (y_{\text{exp},i} - y_{\text{calc},i})^2}{\sum_{i=1}^n w_i y_{\text{exp},i}^2} \right]^{1/2}.$$

This value is compared with the limiting value R_{lim} calculated by saying $r_i = y_{\text{exp},i} - y_{\text{calc},i}$ is the residual in the i th equation calculated from pessimistic estimates of the errors in all experimental quantities, by using the error-propagation rules. To test alternative hypotheses, the R -factor ratio test can be applied. If, for example, a particular hypothesis H_0 gives an R -factor of R_0 and an alternative hypothesis H_1 gives the value R_1 , then H_1 can be rejected at the α -significance level if $R_1/R_0 > R_{m,n-m,\alpha}$ where m is the number of parameters that have been refined and $(n - m)$ is the number of degrees of freedom of the least-squares adjustment. The value of $R_{m,n-m,\alpha}$ is found from statistical tables.³³

Table 2 gives an example of a goodness-of-fit test for the data from Table 3 and the minimization process of Table 1.

The DATA SIMULATION unit calculates a simulated curve by the addition of generated random errors to the calculated precise curve. To test the reliability of a written program and the validity of the parameters estimated from a given type of experimental curve, simulated data are often used initially.

The user supplies values for the parameters, their standard deviations if available, the values of parametric weights if the conditioning of a particular parameter in the model is bad, and the values of the standard deviation of the dependent variable $s_{\text{inst}}(y)$, denoted by SINST. A set of n values of the independent variable x should also be given. The program then calculates precise values of "theoretical points" along the exact curve $y = f(x; \beta_1, \beta_2, \dots, \beta_m)$. Each theoretical point is then converted into a simulated "experimental" one by the addition of a Gaussian error generated by a random-number generator. The four statistical moments, Pearson χ^2 test and Hamilton R -factor test are then applied to the "experimental" curve points, in order to check whether the errors are normally distributed.

The weight for each curve point, w_i , is calculated for m parameters

$$\vec{\beta} = (\beta_1, \beta_2, \dots, \beta_m),$$

a vector of their standard deviations

$$\vec{s}(\vec{\beta}) = [s(\beta_1), s(\beta_2), \dots, s(\beta_m)]$$

and a vector of their parametric weights

$$\vec{w}(\vec{\beta}) = [w(\beta_1), w(\beta_2), \dots, w(\beta_m)]$$

Table 3. Simulation of pK_a - I curve points for pre-selected values of parameters, their standard deviations, their weights and errors $s_{\text{inst}}(pK_a)$ for the dissociation $HL^- = L^{2-} + H^+$. Statistical analysis of the set of errors generated tests whether a distribution is Gaussian [$z = -1$, $(z - 1)^2 - z^2 = 3$]

PRESELECTED VALUES:					
INSTRUMENTAL ERROR = 0.0050					
	STANDARD				
PARAMETER	DEVIATION	WEIGHT			
5.000	0.020	0.010			
4.500	0.300	0.980			
0.300	0.010	0.010			
xxxxxx DATA xxxxxx					
NUMBER OF POINTS = 20					
THE CONSTANT A = 0.5115					
THE CONSTANT B = 0.3291					
THE CHARGE OF IONS $(Z - 1)**2 - Z*2 = 3$					
SIMULATION OF PK-I CURVE					
I	I(EXP)	PK(ACCUR)	ERROR	PK(LOADED)	WEIGHT
1	0.0100	4.869341	-0.004709	4.864632	8.371428
2	0.0400	4.775226	-0.000053	4.775172	2.681057
3	0.0900	4.708259	-0.006368	4.701891	1.488267
4	0.1600	4.662537	0.003544	4.666080	1.023263
5	0.2500	4.634170	0.006563	4.640733	0.786365
6	0.3600	4.620485	-0.005943	4.614542	0.646007
7	0.4900	4.619591	-0.011206	4.608385	0.554365
8	0.6400	4.630105	0.001697	4.631802	0.490324
9	0.8100	4.650997	-0.002646	4.648351	0.443288
10	1.0000	4.681484	-0.008908	4.672576	0.407440
11	1.2100	4.720958	-0.003016	4.717941	0.379244
12	1.4400	4.768940	0.007988	4.776928	0.356556
13	1.6900	4.825051	-0.003786	4.821265	0.337922
14	1.9600	4.888982	0.000621	4.889603	0.322366
15	2.2500	4.960482	-0.008307	4.952174	0.309191
16	2.5600	5.039344	0.003041	5.042385	0.297890
17	2.8900	5.125397	-0.001236	5.124161	0.288112
18	3.2400	5.218496	-0.000682	5.217814	0.279560
19	3.6100	5.318518	-0.005667	5.312851	0.272021
20	4.0000	5.425362	-0.005801	5.419560	0.265330
STATISTICAL ANALYSIS OF GENERATED ERRORS:					
ERROR MEAN = -2.24E-03					
MEAN ERROR = 0.0046					
STANDARD DEVIATION = 0.0055					
SKEWNESS = -0.869					
KURTOSIS = 2.145					
PEARSON CHI SQUARE = 6.40 AND SHOULD BE 12.60 (FOR 6 D.F. AND 0.95 PROBABILITY LEVEL)					
R-FACTOR = 0.00113					

according to the general scheme

$$y_{i,0} = f(x_i; \beta_1, \beta_2, \dots, \beta_m) \quad (6)$$

$$y_{i,1} = f[x_i; \beta_1 + s(\beta_1), \beta_2, \dots, \beta_m] \quad (7.1)$$

$$y_{i,2} = f[x_i; \beta_1, \beta_2 + s(\beta_2), \dots, \beta_m] \quad (7.2)$$

.....

$$y_{i,m} = f[x_i; \beta_1, \beta_2, \dots, \beta_m + s(\beta_m)] \quad (7.m)$$

$$P_j = 1 \left/ \sum_{i=1}^n (y_{i,j} - y_{i,0})^2 \right. \quad (8)$$

$$w_j = \sum_{j=1}^m P_j w(\beta_j) |y_{i,j} - y_{i,0}| \quad (9)$$

The value of the parametric weight $w(\beta_j)$ serves to increase the sensitivity of the j th parameter in the model. When all the parameters are well-conditioned in a model, their parametric weights are equal.

Table 3 demonstrates a data simulation for the

program DHLET. The parametric values are $\beta_1 = 5.0$ ($= pK_a^T$), $\beta_2 = 4.5$ ($= \hat{a}$), $\beta_3 = 0.3$ ($= C$). The standard deviations of the parameters can be set at any desired values; in this case the values were $s(\beta_1) = 0.02$, $s(\beta_2) = 0.3$, $s(\beta_3) = 0.01$. The statistical weight for each parameter can also be set to a suitable value to improve the sensitivity of the parameter in the model. Therefore $w(\beta_1) = 0.01$, $w(\beta_2) = 0.98$ and $w(\beta_3) = 0.01$. As the ion-size parameter \hat{a} is ill-conditioned in the model and its estimate is not so precise as the estimate of the other two parameters, its parametric weight was set at a value 98 times the parametric weights for the thermodynamic constant and salting-out coefficient. Statistical weights for each point on the pK_a - I curve are calculated according to the scheme above.

The OUTPUT unit displays the estimated results in various graphical ways: deconvolution of the experimental absorbance curve into the absorbance curves

for individual species, distribution diagrams for all the complex species in equilibrium, curves of molar absorptivities of requested species, curve fitting, fitness tests, *etc.* are possible.

The ADDITIONAL SUBROUTINES unit contains various mathematical subprograms, format-free reading subroutines, subroutines of matrix calculus, *etc.*

CONSTRUCTION OF AN ABLET PROGRAM

An ABLET program is constructed from (1) three specific units formulated by the user for the particular mathematical model of the equilibrium study and (2) six permanent units which are the same for all ABLET family programs.

Units formulated by the user

The MASTER unit contains the MAIN PROGRAM which reads in some of the organization data, keys, termination criteria, *etc.* SINST is set such that either synthetic data (SINST > 0) or experimental data (SINST = -1.0) are treated. The present version of ABLET allows up to N = 50 curve points and M = 8 unknown parameters. Enlargement of arrays for M in single precision may lead to instability in the least-squares algorithm LETAG, and is at the risk of the user. An array for the parametric vector XK(M), parametric standard deviations SIGXK(M) and parametric weights WEI(M) should be declared. Variable arrays are transferred by COMMON/FUNC/. This contains a vector for the independent variable XEXP(50), a vector for the dependent variable YEXP(50), a vector for the generated random error ERR(50), a vector for the calculated variable YCAL(50) and a vector of weight for each curve point W(50). The input channel number NI is transferred by COMMON/KANAL/ and four numerical constants for printer-plotting subroutine PLOTT and seven keys are transferred by COMMON/PLOT/ and COMMON/ISW/.

```

MAIN
DIMENSION XK(8),SIGXK(8),WEI(8)
COMMON/FUNC/XEXP(50),YEXP(50),ERR(50),
YCAL(50),W(50)/KANAL/NI
COMMON/PLOT/MY,MX,NLS,NCL,DUMMY
(1930)/ISW/ISSW(7)
...
...
STOP
END
    
```

The INPUT unit should contain a version of SUBROUTINE DATA(IOU,NB) written for the particular equilibrium problem. The subroutine reads the experimental data and does some preliminary calculations. It has two arguments: IOU is an output channel number and NB the number of curve points. All variables are transferred by labelled COMMON

blocks. The preliminary calculations must be specified by the user.

```

SUBROUTINE DATA(IOU,NB)
COMMON/FUNC/XEXP(50),YEXP(50),ERR(50),
YCAL(50),W(50)/KANAL/NI
CALL READI(NB,1)
...
...
RETURN
END
    
```

The RESIDUAL-SQUARE SUM unit should contain a subroutine UBBE(U,NK,XK,NB) which uses the parametric vector XK(M) and the independent variable vector XEXP(N) to calculate a dependent variable vector YCAL(N) and then the sum of squared residuals

$$\sum_{i=1}^n W(I) * [YEXP(I) - YCAL(I)]^2$$

The arguments for UBBE are NB, the number of curve points; NK, the number of parameters; XK, the parametric vector; and U, the residual-square sum function. Other variables are transferred by a labelled COMMON.

```

SUBROUTINE UBBE(U,NK,XK,NB)
DIMENSION XK(NK)
COMMON/FUNC/XEXP(50),YEXP(50),ERR(50),
YCAL(50),W(50)
U = 0.0
DO 1 I = 1,NB
...
...
YCAL(I) = ...
1 U = U + W(I) * (YEXP(I) - YCAL(I)) ** 2
RETURN
END
    
```

Permanent parts of the ABLET program

The MINIMIZATION unit contains SUBROUTINE LETAG(IOU,NAUT,NK,NB,XK,UMIN,ISSW,DARK2,DATA,UBBE,SKRIK),⁵ which performs a search for parameters XK and their standard deviations SIGXK. The LETAG subroutine is divided into independent logical blocks, use of which is controlled by the value of IRUR. Its arguments are IOU, the output channel number; NK, the number of parameters; NB, the number of curve points; ISSW, the vector of keys; subroutines DATA, UBBE and SKRIK; NAUT, a key; XK, a parametric vector; DARK2, a vector of parametric standard deviations calculated in LETAG; and UMIN, the minimum of U achieved.

The STATISTICAL TEST unit contains SUBROUTINE STATS(IOU,NK,NB,X,Y,EPS) which is adapted from the program MINQUAD.³²

The DATA SIMULATION unit contains three subprograms, SIMUL, NORAND and FUNCTION RANDOL. In the SUBROUTINE SIMUL

(X,YC,YM,NB,ISTART) X is the vector of the independent variable; YC the vector of dependent variable calculated precisely; YM the vector of dependent variable loaded with an error generated by $YM(I) = YC(I) + SINST * EPS(I)$ where $EPS(I)$ is the random error generated by subroutine NORAND,³⁴ SINST is the standard deviation of the dependent variable; ISTART is a starting value for generation of random numbers. SUBROUTINE NORAND(D1,D2,IS) is the routine³⁴ for generation of random numbers and calls internal FUNCTION RANDOL(IS).

The OUTPUT unit contains SUBROUTINE SKRIK(NB,NK,IOU,IRUR,XK,SIGXK) and outputs the estimated parameters and their standard deviations, a statistical analysis of residuals, and a printer-plot of the curve-fitting done by subroutine PLOTT.³⁵

The ADDITIONAL SUBROUTINES unit contains seven subroutines: WEIGHT, PLOTT, READI, READR, INVERT, PINUS and MULLE. SUBROUTINE WEIGHT(UBBE,NB,XK,SIGXK,WEI) calculates weights for simulated curve points. SUBROUTINE PLOTT(XX,YY,NDATA,NDMAX,ISYMBL,NF,XLINE,MX,YLINE,MY,NLS,NCL,MM,LL,AREA,YSCALE) makes a line-printer plot.³⁵ SUBROUTINE READI(I,N) and SUBROUTINE READR(A,N) are used for format-free input. I is the identifier of the variable or array to contain N integers, and A is the identifier of the variable or array to contain N reals. The input channel is defined by COMMON/KANAL/NI, e.g., NI = 5. As separator between two numbers, blank(s) or comma(s) may be used, or any symbol(s) which cannot be interpreted as numbers by READI or READR (e.g., 1E7 is interpreted by READR as 1.0×10^7 but by READI as two different integers 1 and 7). When r numbers of the same value are to be read in, the form r * number may be used, e.g., 5.52, 5.52, 5.52 may be written as 3*5.52. The form 5*b, where b is one blank, causes READI or READR to skip the next readings, leave the corresponding variables at their previous values.

Three internal subroutines of LETAG are SUBROUTINE INVERT for matrix inversion,² SUBROUTINE PINUS for multiplication of a vector by a matrix,² and SUBROUTINE MULLE for multiplication of a matrix by a matrix.²

CONCLUSION

Many problems in a wide variety of fields of analysis can be reduced to the problem of finding a correct mathematical model and its unknown parameters by minimizing the difference between experimental and calculated data. ABLET is a system of subprograms to solve such problems. Since in prin-

ciple ABLET is designed to handle any function $y = f(x; \beta)$ it is quite general, and it may suit the needs of quite different users, not only in the study of solution equilibria.

A listing of the ABLET system and data input instructions are available on request.

REFERENCES

1. L. G. Sillén, *Acta Chem. Scand.*, 1964, **18**, 1085.
2. N. Ingri and L. G. Sillén, *Ark. Kemi*, 1964, **23**, 97.
3. J. Čermák and M. Meloun, *Sb. Věd. Pr., Vys. Šk. Chemickotechnol., Pardubice*, 1974, **32**, 37.
4. *Idem*, 2nd Symposium on Algorithms in Computation Technique, High Tatras 1974, *Knižnica algoritmov*, Vol. 2, SVTS Bratislava, 1974.
5. *Idem*, *Sb. Věd. Pr., Vys. Šk. Chemickotechnol., Pardubice*, 1978, **39**, 41.
6. *Idem*, *ibid.*, 1973, **30**, 31.
7. M. Meloun and S. Kotrlý, *Collection Czech. Chem. Commun.*, 1977, **42**, 2115.
8. M. Meloun and J. Čermák, *Sb. Věd. Pr., Vys. Šk. Chemickotechnol., Pardubice*, 1973, **30**, 49.
9. V. Říha, M. Meloun, M. Franz and J. Čermák, *ibid.*, 1975, **33**, 39.
10. M. Meloun and J. Čermák, *ibid.*, 1974, **32**, 57.
11. *Idem*, *Talanta*, 1976, **23**, 15.
12. J. Havel, M. Vrchlabský, J. Sekaninová and J. Komárek, *Scripta Fac. Sci. Nat. Univ. Purkynianae Brunensis*, 1979, **9**, 51.
13. L. Müllerová, M. Vrchlabský and J. Havel, *ibid.*, 1980, **10**, 13.
14. E. Mikanová, M. Bartušek and J. Havel, *ibid.*, 1980, **10**, 3.
15. M. Suchánek and L. Šůcha, *Sb. Věd. Pr., Vys. Šk. Chemickotechnol., Praha*, 1978, **H13**, 41.
16. M. Meloun and J. Pancl, *Collect. Czech. Chem. Commun.*, 1976, **41**, 2365.
17. M. Meloun and J. Chýlková, *ibid.*, 1979, **44**, 2815.
18. M. Meloun, *Iraqi J. Sci.*, 1981, **22**, 26.
19. M. Meloun, J. Chýlková and J. Pancl, *Collection Czech. Chem. Commun.* 1978, **43**, 1027.
20. M. Meloun and J. Pancl, *ibid.*, 1979, **44**, 2032.
21. J. Voštová and L. Sommer, *ibid.*, 1976, **41**, 1137.
22. L. Jančář, J. Havel, V. Kubán and L. Sommer, *ibid.*, 1982, **47**, 2654.
23. P. Voznica, J. Havel and L. Sommer, *ibid.*, 1980, **45**, 54.
24. J. Komárek, J. Havel and L. Sommer, *ibid.*, 1979, **44**, 3241.
25. J. Votava and M. Bartušek, *ibid.*, 1975, **40**, 2050.
26. E. Mikanová, M. Mikešvá and M. Bartušek, *ibid.*, 1980, **46**, 701.
27. A. Mikan, J. Havel and M. Bartušek, *Scripta Fac. Sci. Nat., Univ. Purkynianae Brunensis*, 1980, **10**, 23.
28. M. Meloun and J. Havel, *Computation of Solution Equilibria. I. Spectrophotometry*, Folia Fac. Sci. Nat., Univ. Purkynianae Brunensis, Brno, 1983.
29. J. Havel and M. Meloun, in *Computational Methods for the Determination of Stability Constants*, D. J. Leggett (ed.), Plenum Press, New York, 1983.
30. M. Meloun and J. Čermák, *Talanta*, 1979, **26**, 569.
31. M. Meloun and M. Javůrek, *ibid.*, in press.
32. A. Sabatini, A. Vacca and P. Gans, *ibid.*, 1974, **21**, 53.
33. W. C. Hamilton, *Statistics in Physical Science*, Ronald Press, New York, 1964.
34. J. R. Bell, *Commun. ACM*, 1968, **11**, 498, Algorithm 334.
35. C. F. Moore, *Comp. Phys. Commun.*, 1971, **2**, 53.

A NEW PROCEDURE FOR SEPARATION OF THE ENAMEL AND DENTIN OF HUMAN TEETH

BRUCE R. SMITH, CAROLE YOUNGBERG, DENNIS FINTON,
DAVID WILLEY and THEODORE R. WILLIAMS*
Chemistry Department, The College of Wooster, Wooster, Ohio 44691, U.S.A.

JANET B. VAN DOREN
University of Akron, Akron, Ohio 44325, U.S.A.

(Received 20 June 1983. Revised 19 March 1984. Accepted 1 June 1984)

Summary—A new method for the separation of enamel and dentin in various types of human teeth is proposed. The separated enamel and dentin samples have been analysed for thirteen elements by inductively-coupled plasma emission-spectroscopy and also for fluoride.

Many of the recent reports on trace metals in biological tissues merely report the bulk concentrations for the sample. Such is the case with most studies involving the analysis of human teeth. There have, however, been a few efforts to separate teeth into their various components before analysis. One method¹ involves a bromoform-acetone flotation process based on the differences in density of the various components of teeth. Another involves a mechanical separation of enamel and dentin with a diamond saw.^{2,3} A third suggests the use of a dental burr⁴ to section the teeth. All three have significant limitations. In the flotation procedure, some of the sample tends to adhere to the bromoform surface, and there is considerable risk of contamination when the mechanical separation is used.

There have been only a few reports of multiple-element analysis of human teeth and none involves the separate analysis of dentin and enamel. Oehme *et al.*⁵ determined copper, lead, cadmium and zinc in whole teeth, by anodic-stripping voltammetry, and Curzon and Crocker⁶ analysed over 300 whole enamel samples for 29 elements by spark-source mass spectrometry. Our study was undertaken to develop a method for separating the enamel and dentin of human teeth before analysis for trace metals or fluoride, and to minimize the risk of sample contamination.

In our preliminary work, attempts were made to separate the enamel and dentin by mechanical means. Our experiences indicated that it was very easy to contaminate the sample when grinding or chipping techniques were used. A number of earlier studies employed the freeze-thaw technique, but, in our opinion, they do not offer any advantages over our newly proposed procedure. The freeze-thaw method requires subjecting the tooth to temperature extremes

over a 2-day period, followed by mechanically chipping the tooth to separate the enamel and dentin. The cementum can only be separated from the dentin by chipping the tooth under the microscope at 40× magnification. The new method avoids this problem and the various solutions obtained are ready for immediate analysis. Several teeth can be dealt with simultaneously, so the effective working time required to separate the enamel and dentin is less than 1 hour per tooth. The solutions obtained are analysed by plasma emission-spectrometry for twelve metallic elements and boron, and by ion-selective electrode for fluoride.

EXPERIMENTAL

Tooth samples

Intact, non-carious permanent human teeth were obtained from Defiance, Ohio and the suburban Cleveland area. Following extraction, the teeth were immediately placed in polyethylene vials and frozen to retard contamination. Before analysis, extraneous blood, tissue, bone, and collagenous material were removed from each tooth by agitation in 5 ml of 3% reagent-grade hydrogen peroxide (Fisher Scientific Company) for 5 min. Next the teeth were rinsed with distilled demineralized water and any remaining tissues were removed by scraping with a Teflon spatula. The samples were rinsed again in distilled demineralized water, air-dried overnight and stored at -15° in Falcon 2070 plastic tubes until they were prepared for analysis.

Reagents

Digestion reagents. A protective coating material of "Total" denture rebase power (autopolymerizing) and "Total" acrylic rebase liquid (self-curing) was supplied by Stratford-Cookson Company of College Park, Georgia. These materials gave no appreciable trace metal signals.

Nitric acid, 0.6M, was prepared from "Suprapur" (Matheson-Coleman and Bell) or "Baker Instra-Analyzed" reagents which are designed for trace metal analysis.

Metal standards. Standard solutions were prepared in Nalgene standard flasks and then stored in Falcon 2070 polyethylene tubes. Most were prepared from Matheson Coleman and Bell 1000-ppm atomic-absorption standards, and the others from atomic-absorption standards available from Anderson Laboratories Inc., Fort Worth, Texas.

*Author for correspondence.

Solutions for fluoride determination. Sodium fluoride standards down to $10^{-5}M$ were prepared by serial dilution of a 0.1M stock solution made by dissolving the Baker "Analyzed grade" material in 0.6M nitric acid ("Suprapur"). The total ionic strength adjustment buffer (TISAB) was prepared by dissolving 57 ml of glacial acetic acid (Baker "Analyzed"), 58 of sodium chloride (Baker "Analyzed"), and 4 g of diaminocyclohexanetreta-acetic acid (ICN Pharmaceutical, Inc., Plainview, N.Y.) in 500 ml of distilled demineralized water, adjusting to pH 5.0-5.5 with 5M sodium hydroxide (Baker "Analyzed"), and diluting to 1 litre with distilled demineralized water.

Apparatus

Analysis for metals and boron. An ARL ICPO-137 inductively-coupled plasma spectrometer was used, under standard operating procedures.

Digestion. Parr A 238 Teflon containers and lids were used. Each container was inserted into a Parr 4745 acid-digestion bomb or an aluminium jacket before heating on a Corning PC-35 hot-plate. Before use, all the Teflon caps and lids were cleaned with 25% nitric acid (Fisher Reagent Grade) in a Bransonic B-12 ultrasonic cleaner, and rinsed several times with distilled demineralized water.

Fluoride determination. A fluoride ion-selective electrode (Orion Model 94-09) and a silver-silver chloride reference electrode (Sargent-Welch, Model 30080-10C, platinum junction) were used in conjunction with a digital Corning 135 pH/ion-meter.

Selective sectioning procedure. To dissolve the various layers of the tooth, several acids already used for the purpose were tried. Although lactic acid, hydrochloric acid^{2,8} and acetic acid² have been reported to be effective in achieving the separation, none was as effective as the 0.6M nitric acid.

Several protective coatings were tried in the initial work, including spray acrylic, paraffin wax and lucite. Dental rebase mixture, which is used as a temporary liner for dentures, was found to be the most effective. Disposable surgical gloves were worn whenever handling the teeth. Tweezers and spatulas coated with Teflon or Parafilm were used for handling the teeth, to prevent contamination.

The sample teeth were thawed at room temperature and allowed to dry in air, under a tissue-paper cover. The dry teeth were weighed and then coated with denture rebase mixture (over the cementum only). Each of the Teflon containers was inserted into the metal jacket of a Parr 4745 acid-digestion bomb and the bombs were placed on the Corning PC-35 hot-plate; 15 ml of 0.6M "Suprapur" nitric acid were added to each Teflon container and the lids were replaced. The acid was given 15 min to reach a steady temperature of approximately 90°, at which the enamel was to be digested. The coated sample teeth were then inserted into the Teflon containers (one in each) and these were then recapped. The temperature was kept constant throughout the digestion.

In the preliminary work, X-rays were taken to check the completeness of enamel removal. The digestion times for the dissolution of the enamel depend on the type of tooth (Table 1). Once the enamel is removed, the digestion time for the dentin is the same for all teeth.

On completion of removal of the enamel layer, the remains of the teeth were extracted from the containers with Teflon-covered forceps and the enamel solutions were poured into polyethylene tubes which were immediately transferred to a freezer (at -15°) to await elemental analysis. The coated tooth remains were placed in an oven at $\sim 140^{\circ}$ for 5-10 min to soften the denture rebase. The coating was then peeled off with a Teflon-coated spatula and the remaining tooth parts were weighed and placed in polyethylene tubes.

The next step involved the removal of residual enamel and

Table 1. Enamel-digestion times for various tooth groups

Tooth group	Digestion time, min
Upper incisors	40
Lower incisors	20
Cuspids	30
Bicuspid	30
Molars	60

cementum, leaving just the dentin. By the same procedure as for the enamel digestion, excepting the addition of 20 ml of 3M "Suprapur" nitric acid, the Teflon containers and lids were cleaned and placed on the hot-plate. After addition of the tooth remains, the capped containers were heated at 90° for 10-15 min, and then examined to see whether the remaining tooth parts floated. Flotation of the tooth remains indicated a change in density which was attributed to having only the dentin left unconsumed. However, if the surviving tooth sections did not float, the bombs were recapped and digestion continued for an additional 5 min. The additional heating consistently produced flotation. This flotation proved reproducible.

The dentin remnants were removed from the Teflon (Parr acid-digestion) containers and placed in polyethylene tubes, air-dried, and weighed. The Teflon containers were then cleaned, and the dentin samples put back into them along with 7.5 ml of 1.2M "Suprapur" nitric acid, preheated to 100°. The containers were placed in the Parr bombs, which were then tightly capped, and heated for 75 min on the hot-plate at 90°. After this time the dentin was completely in solution. The resultant solutions were diluted to 15 ml with distilled demineralized water and poured into polyethylene tubes, in which they were then frozen (at $\sim 15^{\circ}$) and stored at the same constant temperature until analysis.

Procedure for metals and boron. Without further dilution, the whole 15 ml of solution was thawed and analysed with the ICP. This procedure results in approximately a 1:15 dilution of the original material. The enamel portion is approximately 0.6-0.8 g and the dentin 0.2-0.4 g.

Procedure for fluoride. A 2-ml portion of the 15 ml of diluted digest was pipetted into a Falcon 2076 graduated 50-ml plastic tube. Enough TISAB (6-9 ml) was added to bring the pH to 4.8-5.0 and the solution was diluted to the 15-ml mark with distilled demineralized water. The fluoride content was then measured with the ion-selective electrode.

In the early work the dilution was done by weight on a top-loading balance, but later the dilution was done as described above, when it was found that the reproducibility was adequate (2%).

RESULTS

Table 2 summarizes the results for samples obtained from the northeast Ohio area. The technique was also applied to the determination of fluoride in samples obtained from the northwest Ohio area (Table 3). Both sets of samples came from both fluoridated and non-fluoridated communities.

DISCUSSION

Most of our values are somewhat lower than those obtained in earlier studies. This may be partially due to the lower risk of contamination. In particular, the earlier values are much higher than ours for potas-

Table 2. Comparison of experimental and literature values (mg/g)

Element	Experimental						Literature				
	Enamel			Dentin			Enamel		Dentin		Reference
	Mean	Std. devn.	Range	Mean	Std. devn.	Range	Mean	Range	Mean*		
K	178	43	104-298	159	47	54-273	961	60-4056	—	6	
Mg	1670	344	973-2703	4670	1109	2670-9082	2800	—	8700	9	
							3200	—	7700	10, 11	
Fe	10.1	8.3	2.5-38.8	10.4	8.90	1.40-48.8	3600	—	7200	10, 12	
							28.0	0-157	93.4	6, 9	
Zn	104	30	42-184	100	25.4	58.7-161	38.6	—	42.1	13	
							153	9.9-806	199	6, 12	
Cu	2.4	1.7	0.9-9.3	2.5	2.1	0.5-9.9	263	—	173	9	
							1.50	0.0-30	149	13	
Mn	0.84	0.48	0.39-3.1	0.58	0.41	0.20-2.24	10.9	—	7.3	6, 10	
							11.5	—	0.21	12, 14	
B	0.891	0.241	0.431-1.61	0.84	0.22	0.471-1.81	0.60	0.0-6.7	0.6	6, 9	
	6.6	2.41	3.81-21.8	5.1	1.3	3.0-9.5	0.59	—	—	9	
Co	0.72	0.40	0.18-2.3	Below detection limits	Below detection limits	Below detection limits	0.45	0.0-18	2	6, 9	
							0.27	0.0-1.5	1.11	6, 9	
Al	8.4	1.6	5.1-12.5	Below detection limits	Below detection limits	Below detection limits	0.13	—	—	6, 9	
							22.9	0.0-510	68.6	9	
Na	5490	1127	3210-8540	4870	925	2670-7670	86.1	—	—	9	
	44.3	16.6	15.9-126	39.4	13.2	21.0-80.1	7000	—	5500	9	
Sr							157	13.0-1400	94.3	6, 9	
							111	—	—	9	
Ba	2.48	1.24	0.49-7.0	4.2	2.3	1.4-9.0	18.3	0.0-510	129	6, 9	
							125	—	96	6, 11	

*No ranges given for literature values.

Table 3. Comparison of experimental and literature values for fluoride (mg/g); references are given in parentheses

Present study	
Enamel	Dentin
$X_F = 487 + 219$	$X_F = 77 + 311$
$X_{NF} = 323 + 93$	$X_{NF} = 753 + 262$
$X_t = 442 + 206$	$X_t = 769 + 295$
Previous work*	
12.5 + 9.52 (5)	71.9 + 39.4 (5)
32-1247 (15)	200-8000 (15, 16)
32-1247 (17)	175.6 (13)
293 + 34 (18)	
130.27 (6)	
79.5 + 6.04 (19)	
248.0 + 20.0 (14)	
104.6 (13)	

F = fluoridated source; NF = non-fluoridated source; t = total of all samples; results expressed as mean + standard deviation or as range.

*References in brackets.

sium, sodium, iron and boron, which are normally contaminants from glassware. The use of Teflon containers for the digestion process eliminates the introduction of such elements.

Clearly, there are advantages in analysing the enamel and dentin separately. Only limited reports on the composition of these portions of human teeth exist. Often only mean values are given, with no indication of the range of the data. Table 2 provides values for some elements for which no previous results are available.

The most remarkable differences in the composition of the enamel and dentin are for magnesium, fluoride and aluminium. The magnesium concentrations were considerably greater in the dentin than in the enamel. The dentin is much more porous than the enamel, thus enabling the systemic introduction of elements. Magnesium is able to substitute easily for calcium in the structure of the tooth, which is primarily hydroxyapatite.

The fluoride levels are also much higher for the dentin than the enamel, by a factor of at least three. The literature shows almost no relation between fluoride levels in enamel and dentin. It appears that a great deal of the fluoride which is ingested from water supplies and toothpastes is concentrated in the teeth. Although aluminium is present in many foods, the levels in dentin suggest that it is not systemically concentrated in the body.

Comparison of the values from previous work with ours shows certain clear differences. The samples from the Ohio area gave somewhat higher chromium values than those of other workers. A possible explanation is that the concentration of this element in the water supplies varies with the different regions. Similar considerations apply to strontium, the content of

which, in minerals, varies considerably, depending on the region of the United States.²⁰ This may account for the wide range of values previously found for this element in the enamel.

Several questions are raised by this study. One important issue is which elements are associated with the fluoride ingested from water or fluoride-containing dental materials. A second concern is whether there is any relationship between the number of cavities and the metal content in a person's teeth. Both of these questions are at present under study in our laboratory. A third problem is that of considerable skewness in the distributions for iron, copper, manganese, chromium, strontium and barium in both enamel and dentin. Correlations between unusually high levels of different elements would also be of interest, but were not looked for in the present work.

Acknowledgements—This study was supported by the Wilson Fund of the College of Wooster. Appreciation is expressed to Louis d'Angelo who performed the initial experiments on this project. The authors wish to express their appreciation to the Research Extension Analytical Laboratory for making their ICP available for this work.

REFERENCES

1. I. L. Shannon, *J. Dent. Child.*, 1980, **94**, 17.
2. F. Brudevold, R. Aasenden, B. N. Srinivasian and Y. Bakhos, *J. Dent. Res.*, 1977, **56**, 1165.
3. V. Michelich, D. H. Pashley and G. M. Whitford, *ibid.*, 1978, **57**, 1019.
4. M. L. Swartz, R. W. Philips, H. E. Clark, R. D. Norman and R. Potter, *ibid.*, 1980, **59**, 1596.
5. M. Oehme, W. Lund and J. Jonsen, *Anal. Chim. Acta*, 1978, **100**, 389.
6. M. E. J. Curzon and D. C. Crocker, *Arch. Oral Biol.*, 1978, **23**, 647.
7. I. L. Shannon and E. J. Edmonds, *Gen. Dent.*, 1977, **82**, 49.
8. M. Knwittila, R. Lappalainen and V. Kontturi-Narhi, *Scand. J. Dent. Res.*, 1979, **87**, 192.
9. D. H. Retief, P. E. Cleaton-Jones, J. Turkstra and W. J. DeWet, *Arch. Oral Biol.*, 1971, **16**, 1257.
10. N. L. Derise, S. J. Ritchey and A. Furr, *J. Dent. Res.*, 1974, **53**, 847.
11. A. Helle and K. Haavikko, *Finn. Dent. Soc.*, 1977, **73**, 87.
12. R. Soremark and K. Samsahl, *Arch. Oral Biol.*, 1961, **6**, 275.
13. N. L. Derise and S. J. Ritchey, *J. Dent. Res.*, 1974, **53**, 853.
14. F. L. Losee, M. E. J. Curzon and M. F. Little, *Arch. Oral Biol.*, 1974, **19**, 467.
15. G. W. Jenkins and J. Speirs, *Physiol. (London)*, 1953, **121**, 21.
16. S. Yoon, F. Brudevold, D. E. Gardner and F. A. Smith, *J. Dent. Res.*, 1960, **39**, 845.
17. F. Brudevold, D. E. Gardner and F. A. Smith, *ibid.*, 1956, **35**, 420.
18. F. L. Losee, T. W. Cutress and R. Brown, *Caries Res.*, 1974, **8**, 112.
19. M. E. J. Curzon, F. L. Losee and A. D. MacAlister, *New Zealand Dent. J.*, 1974, **71**, 80.
20. F. L. Losee and B. L. Adkins, *Nature*, 1968, **219**, 530.

EXTRACTIVE SEPARATION AND SPECTROPHOTOMETRIC DETERMINATION OF PALLADIUM AND PLATINUM WITH DITHIZONE IN THE PRESENCE OF STANNOUS CHLORIDE

Z. MARCZENKO, S. KUŚ and M. MOJSKI

Department of Analytical Chemistry, Technical University, Warsaw, Poland

(Received 15 December 1983. Accepted 1 June 1984)

Summary—The conditions [acid used, presence of chloride and tin(II)] for the extractive separation and spectrophotometric determination of palladium and platinum as the dithizonates Pd(HDz)₂ and Pt(HDz)₂ have been examined. In the absence of stannous chloride platinum does not undergo extraction. Conditions for the separation and determination of these metals in the presence of mercury, gold and copper, which are also extracted with dithizone into carbon tetrachloride or chloroform under the conditions suitable for palladium (1M sulphuric acid/0.1M hydrochloric acid), have been defined. The mercury and gold dithizonates are formed quickly and can be removed before the palladium and platinum compounds have had time to form. They can be decomposed with iodide. Copper dithizonate is decomposed by reduction with tin(II). The proposed procedure has been applied to the determination of palladium in technical platinum metal.

The methods of separation of platinum metals are of considerable importance in the chemical analysis of these metals because of substantial similarities in their chemical properties. These separation methods have been reviewed.¹⁻³ Among the organic reagents that can be applied for extractive separation of palladium from platinum, dithizone is worthy of attention.⁴⁻⁶ Several papers have been published on the spectrophotometric determination of palladium⁷⁻¹¹ and platinum^{7,12,13} with dithizone, but some aspects of this subject still require more clarification.

The study described here was devoted mainly to extractive separation of palladium from platinum with dithizone. In solving this problem attention has been paid to the advantages of introducing stannous chloride into the aqueous phase, since for a number of other extractive reagents, e.g., thiourea derivatives,¹⁴ dioctyl sulphide,¹⁵ triphenylphosphine,¹⁶ the use of stannous chloride in the extraction system has made it possible to separate the platinum metals effectively.

EXPERIMENTAL

Reagents

Standard palladium solution (1 mg/ml) was prepared by dissolving 0.84 g of palladium(II) chloride in 10 ml of concentrated hydrochloric acid and diluting to volume with water in a 500-ml standard flask. The solution was standardized gravimetrically with dimethylglyoxime. Working solutions (e.g., 10 µg/ml) were obtained by suitable dilution of the stock solution with water.

Standard platinum solution (1 mg/ml) was prepared by dissolving 0.5000 g of suitably pure platinum metal in 20 ml of *aqua regia*. Oxides of nitrogen were removed by three successive evaporations (almost to dryness) with hydrochloric acid. The residue was dissolved in 10 ml of concen-

trated hydrochloric acid, and the solution was transferred to a 500-ml standard flask and diluted to volume with water. Working solutions were obtained by suitable dilution of the stock solution with water.

Dithizone (H₂Dz), 0.01% solution in carbon tetrachloride or chloroform, was standardized by extractive titration of standard silver solution.³

A 1M stannous chloride solution in 2M hydrochloric acid was used.

Procedure

Separation and determination of palladium. From the acid test solution, ca. 1M with respect to sulphuric acid and 0.1M with respect to hydrochloric acid (volume ca. 20 ml), containing platinum and not more than 50 µg of palladium, extract palladium with two portions of 2×10^{-4} M dithizone in carbon tetrachloride (shaking for 2 min), and reserve the aqueous phase for platinum determination. Shake the combined extracts for 30 sec with 5 ml of 4M hydrochloric acid plus one drop of 1M stannous chloride. Separate the phases and shake the organic extract with two 5-ml portions of dilute ammonia solution (1 + 50). Separate, and dilute the extract to volume with carbon tetrachloride in a 10-25 ml standard flask, according to the amount of palladium. Measure the absorbance of the Pd(HDz)₂ solution at 635 nm against carbon tetrachloride.

Determination of platinum. To the aqueous phase reserved from separation of palladium, add 1 ml of hydrochloric acid (1 + 1) and 0.2 ml of 1M stannous chloride. Extract the platinum with two portions of 2×10^{-4} M dithizone in chloroform (shaking for 1 min). Wash the combined extracts first with 5 ml of 1M hydrochloric acid, and then with 5 ml of ammonia solution (1 + 50). Dilute the organic phase with chloroform to a known volume (standard flask), suitable for the amount of platinum. Measure the absorbance of the Pt(HDz)₂ solution at 710 nm against chloroform.

RESULTS AND DISCUSSION

Extraction and determination of palladium

When an acidic aqueous solution of palladium(II) is shaken with excess of dithizone solution in carbon

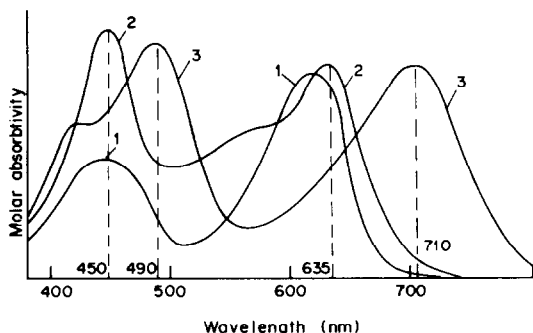


Fig. 1. Absorption spectra of: 1—dithizone, 2— $\text{Pd}(\text{HDz})_2$, 3— $\text{Pt}(\text{HDz})_2$ (in carbon tetrachloride).

tetrachloride or chloroform, grey-green palladium dithizonate is formed. The absorption spectrum of $\text{Pd}(\text{HDz})_2$ in carbon tetrachloride has absorption maxima at 450 and 635 nm (Fig. 1).

The concentration of sulphuric acid or perchloric acid present should not exceed $4M$. It is not advisable to use nitric acid of concentration higher than $1M$, because it would readily oxidize the dithizone. The concentration of hydrochloric acid (alone or in the presence of the above-mentioned acids) should not exceed $0.1M$. As the concentration of chloride increases, the formation of $\text{Pd}(\text{HDz})_2$ becomes more and more difficult because of the inertness of PdCl_4^{2-} towards dithizone, and the necessary shaking time for complete extraction becomes longer.

Palladium dithizonate in carbon tetrachloride or chloroform is stable in time and when formed is resistant to hydrochloric acid (1 + 1), sulphuric acid (1 + 1) and ammonia solution (up to $3M$). A single shaking for 30 sec with dilute ammonia solution (1 + 50) will remove the excess of dithizone from the organic phase.

The completeness of extraction of palladium dithizonate is a function of the concentration of dithizone in the organic phase, the shaking time, and the nature of the aqueous medium, as shown in Figs. 2 and 3.

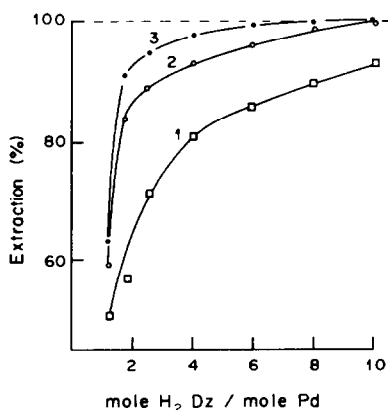


Fig. 2. Dependence of palladium extraction on dithizone concentration, from: 1— $1M$ HCl, 2— $1M$ H_2SO_4 , 3— $0.05M$ HCl; $20 \mu\text{g}$ of Pd.

The rate of extraction of palladium is considerably increased by the presence of small amounts of stannous chloride in the solution, because SnCl_3^- ions replace chloride ions in the chloride complex of palladium (which is rather inert towards reaction with dithizone) and are themselves easily displaced by dithizonate ligands.

The calibration graph obtained under the conditions given in the procedure is linear up to a palladium concentration of $2.5 \mu\text{g}/\text{ml}$. The molar absorptivity is $3.55 \times 10^4 \text{ l. mole}^{-1} \text{ cm}^{-1}$ at 635 nm.

Extraction and determination of platinum

Platinum(IV) in acid solutions (0.1 – $4M$ hydrochloric, sulphuric, or perchloric acid) does not form a dithizonate when shaken with dithizone solution in carbon tetrachloride or chloroform, and can oxidize the dithizone. Nor is platinum extracted with dithizone in the presence of ascorbic acid or sulphite, even though these reducing agents transform platinum(IV) into platinum(II). If stannous chloride is added, however, brown-yellow platinum(II) dithizonate is rapidly extracted. As can be seen from Figs. 4 and 5, the optimum conditions for the extraction of platinum are *ca.* $1M$ sulphuric acid and $0.1M$ stannous chloride or 1 – $2M$ hydrochloric acid and 0.01 – $0.05M$ stannous chloride. For a mixed medium ($1M$ sulphuric acid/ $0.5M$ hydrochloric acid) a lower concentration of stannous chloride ($0.01M$) is sufficient. It is best to use chloroform as solvent, because platinum dithizonate is more soluble in it than in carbon tetrachloride.

Platinum dithizonate is stable in time and resistant to ammonia, which can therefore be used for removing the excess of dithizone from the extract. Before the treatment with ammonia, however, it is necessary to wash the extract with $1M$ hydrochloric acid to decompose the red tin(II) dithizonate, which forms in the pH range 5 – 9 .⁴

The absorption spectrum of platinum dithizonate (Fig. 1) has maxima at 490 and 710 nm. Dithizone does not absorb light of the latter wavelength.

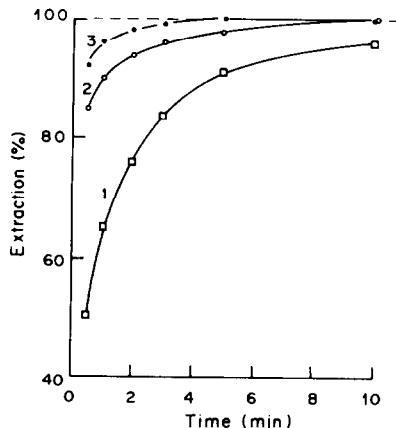


Fig. 3. Dependence of palladium extraction on shaking time, from: 1— $1M$ HCl, 2— $1M$ H_2SO_4 , 3— $0.05M$ HCl.

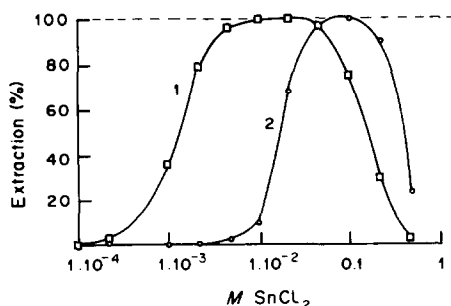


Fig. 4. Dependence of platinum extraction on stannous chloride concentration, from: 1—1M HCl, 2—1M H₂SO₄.

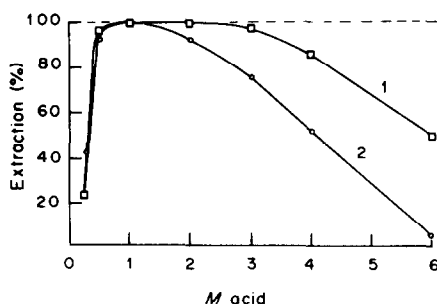


Fig. 5. Dependence of platinum extraction on acid concentration: 1—HCl (and 0.01M SnCl₂), 2—H₂SO₄ (and 0.1M SnCl₂).

Unlike palladium (which would form the pink secondary dithizonate¹⁰), at high Pt:H₂Dz ratio platinum can be extracted stepwise with successive small portions of dithizone solution. This fact allows the composition of the platinum dithizonate to be determined by the spectrophotometric titration method; the compound is found to be 1:2 (Pt:HDz).

As ternary complexes of platinum metals are known which contain SnCl₃⁻ as a ligand, it was necessary to check whether the platinum compound extracted in the presence of stannous chloride contained any tin. After evaporation of the solvent and mineralization of the residue with concentrated sulphuric and nitric acids, the spectrophotometric method for determination of tin with phenylfluorone³ was applied but no tin was found. The correctness of the result was verified by analysing the extracts after addition of known amounts of tin before the mineralization. The tin introduced was completely recovered. Therefore platinum dithizonate can be ascribed the formula Pt(HDz)₂. The stannous chloride used in the procedure performs a double function: it reduces Pt(IV) to Pt(II), and then transforms the platinum chloro-complex (rather inert towards dithizone) into the more labile complex with SnCl₃⁻ as ligand.

The calibration graph obtained according to the procedure is linear up to a platinum concentration of 5 μg/ml. The molar absorptivity is 3.50 × 10⁴ l. mole⁻¹. cm⁻¹ at 710 nm, and 3.75 × 10⁴ l. mole⁻¹. cm⁻¹ at 490 nm.

Separation of palladium from platinum

It follows from the investigations described above, that palladium can be separated from platinum with dithizone. The palladium can first be extracted with dithizone from ca. 1M sulphuric acid medium. In the absence of stannous chloride platinum remains in the aqueous phase. Low concentrations of stannous chloride (below 0.001M in the aqueous phase) would increase the rate of extraction of palladium and prevent dithizone from being oxidized by platinum(IV) and aerial oxygen, but would also result in extraction of small quantities of platinum. It is therefore better to extract the palladium in the absence of stannous chloride and then to wash the extract with a highly dilute stannous chloride solution in 4M hydrochloric acid; the tin(II) reduces the dithizone oxidation products back to dithizone, which can then be removed from the extract by washing with ammonia. Furthermore, any copper(II) dithizonate which may be present in the extract is decomposed by reduction of the Cu(II) to Cu(I) by the Sn(II).

Various mixtures of palladium and platinum were analysed by the proposed procedure. The results in Table 1 show good precision and accuracy, and indicate the possibility of determining palladium in the presence of large quantities of platinum.

Other platinum metals do not react with dithizone under the conditions used.^{4,5} Silver, mercury, gold and copper can also be extracted with dithizone from acidic media, but silver does not form a dithizonate in the presence of chloride. The orange-yellow mercury(II) dithizonate forms quickly; shaking for several seconds is enough. Hence, any mercury can be preliminarily separated by extraction with small portions of dithizone solution in carbon tetrachloride. These extractions are continued until there is a change in colour between one portion of dithizone extract and the next. Any mercury in this last portion of extract can be removed by brief shaking with a dilute acid solution of potassium iodide containing a little ascorbic acid (to prevent oxidation of iodide to iodine), and the organic phase added to the subsequent palladium extracts.

Brown-yellow gold dithizonate is also extracted quickly. For larger amounts of gold it is better to use a chloroform solution of dithizone, in which gold

Table 1. Results of the separation and determination of palladium and platinum with dithizone

Added, μg		Found, μg			
Pd	Pt	Pd		Pt	
20.0	20.0	20.0	19.7	20.0	20.8
10.0	50.0	10.0	9.9	49.5	50.0
50.0	10.0	48.1	48.9	10.1	10.0
5.0	50.0	5.1			
10.0	1000	10.1	10.1		
10.0	2500	10.3			
10.0	5000	10.6			
10.0	10,000	11.0			

Table 2. Determination of palladium (20 μg) and platinum (20 μg) with dithizone in solutions containing copper, mercury and gold

Added			Found, μg			
Cu, mg	Hg, μg	Au, μg	Pd		Pt	
1			19.7	19.3	18.9	19.3
10			18.9	19.2	18.0	19.0
	20		19.8	20.1	19.1	19.3
	100		19.2	18.9	17.9	18.6
		20	20.3	19.7	19.9	19.3
		100	18.9	19.0	18.9	19.4
		500	19.1	18.0	19.3	19.3
0.1	20	20	19.8	19.9	18.9	19.8
1	50	50	19.3	19.8	19.3	20.1
10	100	100	18.7	19.3	17.9	19.2

dithizonate is more soluble. The procedure is the same as that for removal of mercury, including the washing with potassium iodide solution.

Copper(II) (especially in larger quantities) reacts with dithizone faster than palladium does, forming a violet dithizonate. However, if the extraction is prolonged (*e.g.*, to 5 min), palladium displaces copper from its dithizonate, because palladium dithizonate is more stable than copper dithizonate.⁵ As explained above, any copper present in the palladium extract can be removed by shaking with 4M hydrochloric acid containing a little stannous chloride.

A series of solutions containing (besides palladium and platinum) known quantities of copper, mercury and gold, separately or simultaneously, was analysed, the procedure being modified as already indicated, by prior separation of mercury and gold by shaking with small portions of dithizone solution (for a few seconds) until there was a change in colour from one extract to the next, and the last of these extracts was then washed with 5 ml of 2% potassium iodide/0.1% ascorbic acid solution in 1M sulphuric acid, and added to the subsequent extracts containing palladium and copper. The results shown in Table 2 were satisfactory.

The proposed method was applied to determination of palladium in technical platinum metal.

The sample was dissolved in *aqua regia* and the product was subjected to alternating evaporation almost to dryness and addition of hydrochloric acid. The residue was dissolved in 2M sulphuric acid. The palladium was extracted and determined in aliquots corresponding to 5 mg of the sample. The palladium content found was $0.12 \pm 0.01\%$ (for 6 determinations). The recovery was checked by addition of 5 μg of palladium to the test solution, and re-analysis, and found to be 95%.

REFERENCES

1. F. E. Beamish and J. C. Van Loon, *Recent Advances in the Analytical Chemistry of the Noble Metals*, Pergamon Press, Oxford, 1972.
2. S. I. Ginzburg, N. A. Ezerskaya, I. Y. Prokof'eva, N. V. Fedorenko, V. I. Shlenskaya and N. K. Belskii, *Analytical Chemistry of Platinum Metals* (in Russian), Izdat. Nauka, Moscow, 1972.
3. Z. Marczenko, *Spectrophotometric Determination of Elements*, Horwood, Chichester, 1976.
4. G. Iwantscheff, *Das Dithizon und seine Anwendung in der Mikro- und Spurenanalyse*, 2nd Ed., Verlag Chemie, Weinheim, 1972.
5. H. M. N. H. Irving, *Dithizone*, The Chemical Society, London, 1977.
6. E. B. Sandell and H. Onishi, *Photometric Determination of Traces of Metals, General Aspects*, 4th Ed., Wiley, New York, 1978.
7. R. S. Young, *Analyst*, 1951, **76**, 49.
8. Z. Marczenko and M. Krasiejko, *Chem. Anal. (Warsaw)*, 1964, **9**, 291.
9. D. A. Beardsley, G. B. Briscoe, J. Růžička and M. Williams, *Talanta*, 1966, **13**, 328.
10. J. Minczewski, M. Krasiejko and Z. Marczenko, *Chem. Anal. (Warsaw)*, 1970, **15**, 43.
11. G. B. Briscoe and S. Humphries, *Talanta*, 1971, **18**, 39.
12. V. G. Goryushina and E. Ya. Gailis, *Zavodsk. Lab.*, 1954, **20**, 14.
13. W. Kemula, W. Brachaczek and A. Hulanicki, *Chem. Anal. (Warsaw)*, 1958, **3**, 913.
14. Yu. A. Zolotov, O. M. Petrukhin, V. N. Shevchenko, V. V. Dunina and E. G. Rukhadze, *Anal. Chim. Acta*, 1978, **100**, 613.
15. M. Mojski, *Warsaw Techn. Univ., Rept.*, No. 21, 1980.
16. *Idem*, *Talanta*, 1980, **27**, 7.

EXTRACTION OF COBALT FROM THIOCYANATE SOLUTIONS WITH POLYURETHANE FOAM

R. F. HAMON and A. CHOW

Department of Chemistry, University of Manitoba, Winnipeg, Manitoba, Canada

(Received 23 December 1983. Revised 6 April 1984. Accepted 26 May 1984)

Summary—The extraction of cobalt (II) from aqueous thiocyanate solutions with polyurethane foam has been extensively investigated. The extraction is enhanced by high thiocyanate concentration, high ionic strength and low temperature. A pH of 1.0–9.0 can be used for efficient extraction. Cobalt can be extracted at low concentration and the distribution coefficient is independent of foam weight. Several foam types and foam pretreatments have been examined. The effect of various substances added to the cobalt thiocyanate solutions has been investigated. Some of these substances caused either enhanced or decreased extractions by interacting with the polyurethane foam or by changing the solution chemistry.

The thiocyanate complex has been used for several decades as a means of extracting cobalt into organic solvents.¹ The sorption of cobalt by flexible polyurethane foam from thiocyanate solutions has been reported,²⁻⁷ although no very detailed studies were undertaken. The present paper outlines a systematic investigation of the extraction of cobalt, which was used to provide precise information on the sorption process under a wide variety of conditions. Throughout this work, cobalt-60 was used as a tracer so as to provide the most precise data possible, and extreme care was taken to eliminate or correct for as many sources of error as possible.

EXPERIMENTAL

Apparatus

Radiometric counting was done with a Baird-Atomic model 530A gamma spectrometer and spectrophotometric measurements with a Unicam model SP800B recording spectrophotometer. Pyrex cells for distribution studies were designed so that 150 ml of solution could be equilibrated with a foam sample by squeezing, this action causing reasonable stirring and minimal splashing of the sample. These cells consisted of a lower section with a side-arm and stopper for removal of samples, and an upper section with a central sleeve and glass plunger. A mechanical squeezer was made with plungers driven up and down in the extraction cells by means of large glass tubes on brass cams mounted eccentrically on a motor-driven rod. This system gave the plungers a 5-cm stroke at a rate of 25 cycles/min. A controlled-temperature cabinet was made, fitted with a heater and cooler, and a fan for circulation of the air in the system. The temperature was maintained within $\pm 0.05^\circ$ of the preset value, and the difference between cell temperatures was approximately $\pm 0.01^\circ$. Details of the cells and squeezing apparatus are available on request.

Standard flasks were calibrated to contain 150 ml $\pm 0.06\%$. The Pyrex test-tubes used for gamma-counting were numbered and calibrated to contain 15.0 ml. A counting error of only $\pm 0.07\%$ was caused by a variation of 0.1 ml in volume, since the sample extended well beyond the detector crystal. Slight differences in counting geometry of the tubes were corrected for by using a radioactive tracer calibration solution to obtain a correction factor (maximum 2%).

All chemicals were reagent grade and the water was doubly distilled and then demineralized. A stock solution of 1000 ppm (17 mM) Co(II) was prepared from $\text{CoCl}_2 \cdot 6\text{H}_2\text{O}$ in $10^{-5}M$ hydrochloric acid. Tracer ^{60}Co (ICN Nuclear), obtained as CoCl_2 solution, was mixed with concentrated hydrochloric acid and evaporated to dryness, then the residue was taken up in 0.001M hydrochloric acid for storage. A 2.5M sodium acetate/acetic acid buffer (pH ~ 4.7) was used.

Polyether-type polyurethane foam (# 1338 from G. N. Jackson Ltd., Winnipeg, Canada) was used for all experiments except those investigating the effect of foam type. All foams were cut into cubes (1.3 cm edge), cleaned by soaking in 1M hydrochloric acid for 12 hr, washed in distilled water, washed in a Soxhlet apparatus with acetone for 6 hr, and dried. A foam weight of 50 ± 2 mg was generally used, with the weight measured to 0.01 mg after any static charge had been allowed to dissipate in a grounded metal container. To avoid any bias from the sample cells or position, the ten solutions were randomized with respect to numbered sample location. Observed evaporation losses of 1.8% over 24 hr were reduced to 0.3% by using a latex rubber seal over the plunger and cell neck.

Sample solutions were prepared as required and 30 or 40 μl of ^{60}Co tracer added. After rough dilution and mixing, the solutions were left overnight for temperature and solution equilibration before the final volume adjustment and mixing. A 15-ml aliquot was withdrawn from each sample, counted on the gamma-spectrometer for ten 100-sec periods, and carefully returned to its original flask. The sample was then placed in a distribution cell, with 99.70–99.75% of the 150 ml actually transferred. All gamma-spectrometer data were corrected for both background and detector drift. The background was obtained from one hundred 100-sec counting periods. A solid ^{60}Co standard was used with every counting sequence to determine any detector drift. Calibration indicated that the detector had a linear response over the normal counting-rate range.

In all cases the equipment was washed and dried before use, to prevent sample loss or dilution. Samples were usually taken after 6, 12 and 24 hr since this gave information on when equilibrium was obtained and the relative rates of equilibration.

It should be noted that in many experiments, in order to obtain meaningful data it was necessary to use conditions which were not optimum, since the distribution coefficient was so large. Calculations of the distribution coefficient (D , l./kg) and degree of extraction ($\%E$) were done as previously discussed.⁸

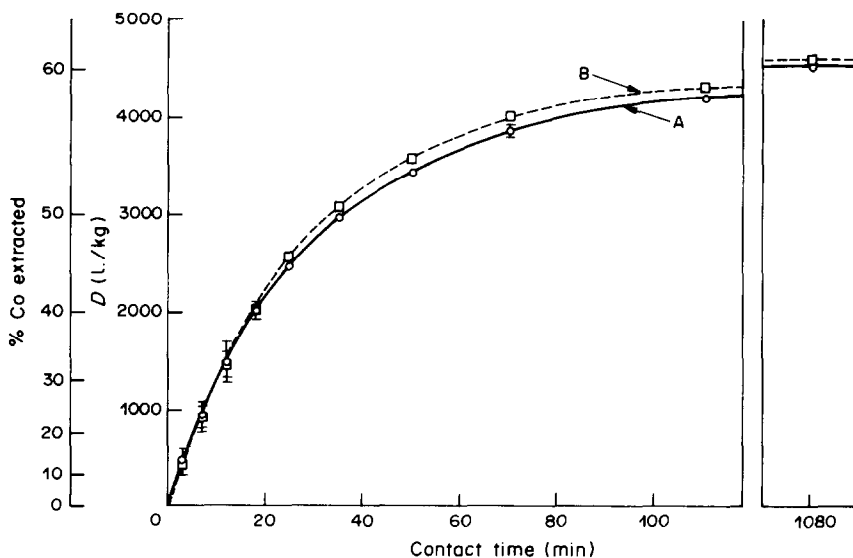


Fig. 1. Time dependence of cobalt sorption. Conditions: 0.05 g of foam; 150 ml of solution $1.7 \times 10^{-6} M$ in Co(II), 0.10M in NaSCN, ionic strength 3.00M, pH 4.8, 25.00°. Duplicate experiments, A and B.

RESULTS AND DISCUSSION

Time dependence

A $1.7 \mu M$ Co(II) solution at pH 4.8 containing ^{60}Co tracer, 0.10M sodium thiocyanate, 1.90M sodium and chloride and 1.00M sodium acetate/acetic acid buffer was used to determine the time required for equilibration between the cobalt solution and polyurethane foam. One experiment mainly evaluated the first 2 hr of extraction, and a second experiment extended the time up to 48 hr. Typical results shown in Fig. 1 indicate that equilibrium is approached fairly slowly with the small amount of foam used. The extraction increased from 90% of its final value after 2 hr to 97% after 24 hr. The final value determined after 48 hr may be affected by small evaporation

losses which cause a gradual increase in D due to increasing thiocyanate and ionic strength. This experiment was deliberately done under conditions which ensured only a moderate extraction. Under more appropriate conditions (e.g. 1.0M thiocyanate and 0.4 g of foam) 99.99% extraction can be obtained, with 90% extraction in less than 2min.

Effect of pH

The pH of $1.7 \mu M$ Co(II) containing ^{60}Co tracer and 0.10M sodium thiocyanate was adjusted with hydrochloric acid or sodium hydroxide as required and the ionic strength fixed at 3.00M with sodium chloride. After initial pH measurement, the solutions were equilibrated with 50 mg of foam for up to 24 hr and the pH redetermined. It was noted that at

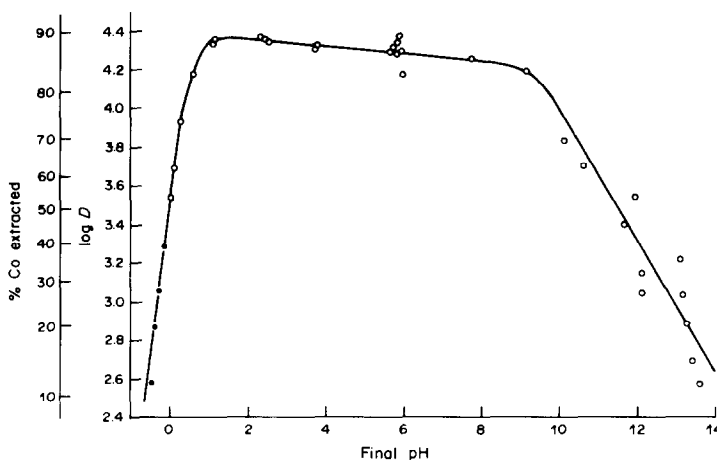


Fig. 2. Effect of pH on cobalt sorption. Conditions: 0.050 g of foam; 150 ml of solution $1.7 \times 10^{-6} M$ in Co(II), 0.1M in NaSCN, pH adjusted with HCl or NaOH, NaCl added to maintain 3.00M ionic strength. Equilibrium pH values: measured \circ ; calculated \bullet .

solution acidities between 0.5M acid and pH 4, the foam developed a red to red-brown colour due to the presence of small specks of iron inhomogeneously distributed in the reagent-grade sodium chloride. This extraction of iron by polyurethane foam has been reported before,^{3,5-7} and the iron either does not affect the cobalt extraction or is easily displaced by the cobalt species. At an acidity greater than 1M, a yellow colour quickly developed, accompanied by the smell of H₂S. On standing overnight a small amount of yellow precipitate formed, and there was a return of cobalt to the solution from the polymer. These observations are consistent with the reported⁹ instability of HSCN in acid solution, resulting in hydrolysis to give H₂S or polymerization to give the yellow isoperthiocyanic acid. At pH > 11, a precipitate was formed which was assumed to be Co(OH)₂.¹⁰

The pH values before and after the extraction were practically the same except in the range 7–11.5, where changes of up to two units occurred, probably due to decomposition of SCN⁻ or sorption of acid by the foam.

From the results in Fig. 2, the sorption of cobalt is quite insensitive to pH from 1 to 9. Hydrogen-ion concentrations greater than 0.1M affect the cobalt extraction because the available thiocyanate concentration is reduced in fairly acid solution by protonation¹¹ ($pK_a \sim -2.0$). In addition the decomposition of HSCN in acid further shifts the equilibrium and results in the observed decrease in cobalt extraction with time. In more basic solutions the sorption gradually decreases and there is considerably more scatter in the results, owing to the formation of Co(OH)₂.

Therefore most experiments were done in the middle of the optimum pH range, with sodium acetate/acetic acid buffer.

The lack of sensitivity to hydrogen-ion concentration indicates that either hydrogen ion is available in vast excess or it is involved in formation of neither the extractable species nor weakly basic anion-exchange sites on the foam (by protonation). That cobalt can be sorbed from mildly basic solutions makes it unlikely that the mechanism involves protonation of the polymer sites to form a weak-base anion-exchanger (as suggested by Bowen¹²). In addition, the small changes in pH indicate that the largest amount of hydrogen ion which could have been released from the foam is not sufficient to account for the large amount of cobalt extracted.

Effect of thiocyanate

Cobalt(II) solutions (1.7 μM) containing ⁶⁰Co tracer, 0.88M sodium acetate/1.00M acetic acid buffer and various sodium thiocyanate concentrations were adjusted with sodium chloride to a total ionic strength of 2.88M. Extraction with 50 mg of polyurethane for up to 24 hr showed that *D* rises to 10⁵ at 0.25M thiocyanate and to 3.3 × 10⁶ at 2.00M thiocyanate.

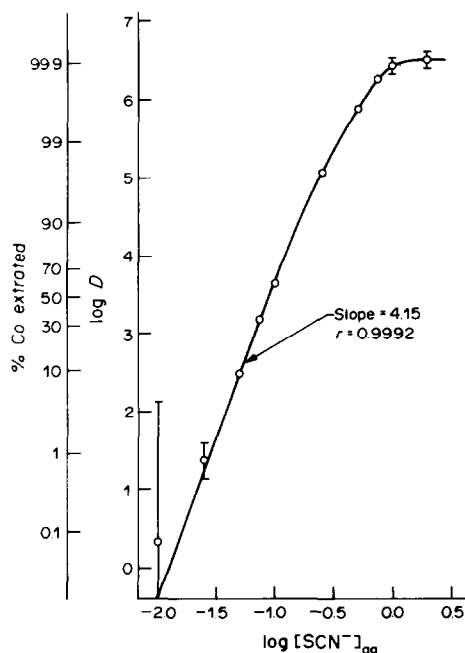


Fig. 3. Effect of thiocyanate on cobalt sorption. Conditions: 0.050 g of foam; 150 ml of solution $1.7 \times 10^{-6}M$ in Co(II), 2.88M ionic strength, pH 4.7, 25.00°.

The latter value is equivalent to 99.9% sorption of cobalt from 3000 litres of solution by a kilogram of foam. Figure 3 shows the near linearity of a $\log D$ vs. $\log [SCN^-]$ plot, at the lower thiocyanate concentrations; the slope of about 4 indicates that four SCN⁻ ligands are involved in the extractable species.

Control of the thiocyanate concentration provides very wide flexibility in the sorption and desorption of cobalt. Some degree of selectivity may be possible by careful choice of the thiocyanate concentration and other solution parameters, in column chromatographic or batch extraction separations.

Effect of cobalt concentration

Initial cobalt concentrations from tracer only ($\sim 1.7 \times 10^{-10}M$) to 1.7mM were used to evaluate their effect on cobalt extraction in 24 hr from solutions containing 1.00M sodium acetate/acetic acid buffer, 0.10M sodium thiocyanate and 1.90M sodium chloride. A second series of experiments used 0.25M thiocyanate, 1.00M buffer and 1.75M sodium chloride.

The colours of the equilibrated polyurethane foams ranged from off-white through various shades of green to a dark blue-green, in parallel with the amount of cobalt sorbed. The foam pieces containing the largest amounts of cobalt became brittle and broke apart on squeezing, which has been interpreted as supporting the cation chelation mechanism for the extraction.⁸

Figure 4 shows that the distribution ratio, *D*, is markedly affected by thiocyanate concentration, as expected, but the fraction of cobalt extracted is

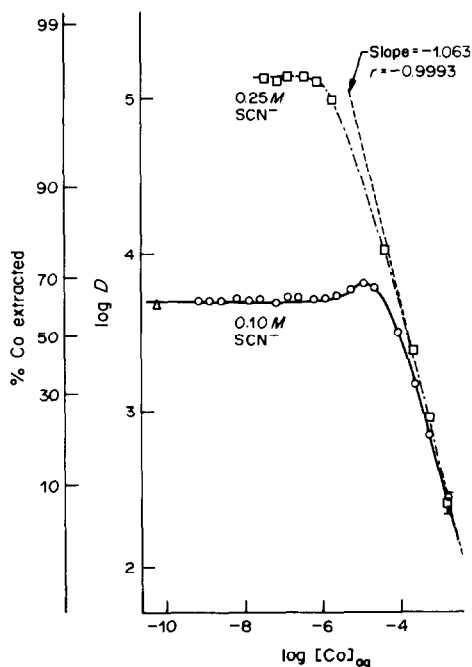


Fig. 4. Effect of cobalt concentration on distribution ratio. Conditions: 0.050 g of foam; 150 ml of solution, 3.00M ionic strength, at 25.00°. ○ 0.10M NaSCN; □ 0.25M NaSCN; △ ^{60}Co tracer only.

essentially independent (slope = 0) of the amount of cobalt present (at low concentrations), which indicates¹³ that a mononuclear complex is extracted. Moreover, at high cobalt concentration, the slope is about -1.0 , indicating that nearly all additional

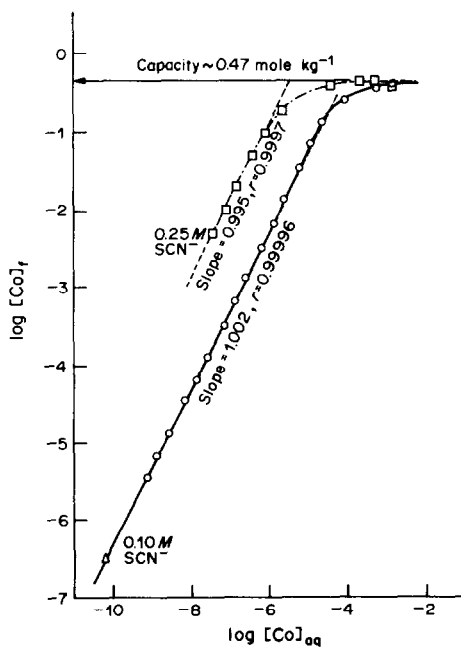


Fig. 5. Effect of cobalt concentration on extraction. Conditions: 0.050 g of foam; 150 ml of solution, 3.00M ionic strength, 25.00°. ○ 0.10M NaSCN; □ 0.25M NaSCN; △ ^{60}Co tracer only.

cobalt added remains in the aqueous phase. Figure 5 displays the results in a different way, showing the maximum concentration of cobalt in the foam is ~ 0.47 mole/kg. Since a typical polyurethane foam has a surface area¹⁴ of 81 m²/kg and the cross-sectional area¹⁵ of a Co^{2+} ion is about 1.63×10^{-20} m², the sorption process must involve the whole bulk of the polymer and be akin to a solvent extraction or ion-exchange process rather than solely a surface adsorption phenomenon.

It is apparent that the degree of cobalt extraction does not decrease even at very low cobalt concentrations, which makes polyurethane foam and thiocyanate useful either for the preconcentration of very low levels of cobalt for analysis or for the complete recovery of cobalt from radioactive wastes or spills. Further, since the distribution ratio remains constant until the foam is almost saturated, reasonably symmetrical elution peaks are expected when the system is used in column chromatography. The relatively high capacity of polyurethane foam [0.47 mole of $\text{Co}(\text{SCN})_4^{2-}$ and hence 0.94 mole of Na^+ /kg] is of the same order of magnitude as that of many commercially available ion-exchange resins and its cost is competitive.

Effect of phase ratio

A wide range of phase ratios was studied, to test the assumption that D is constant for different relative amounts of aqueous phase and foam. Because of the experimental difficulties in using small sample volumes for extraction, the study was done by using a wide variation in foam weight. Solutions containing 0.10M sodium thiocyanate, 0.88M sodium acetate/1.00M acetic acid buffer, 1.90M sodium chloride, 0.10 ppm Co(II) and ^{60}Co tracer were equilibrated with 1–1000 mg pieces of foam for 48 hr. Special care was taken to eliminate the effect of static charge on weighing the smaller pieces of foam and to ensure that these had the entrapped air removed by manual squeezing before the normal mechanical squeezing.

From Table 1 it appears that D remains nearly

Table 1. Effect of phase ratio on distribution coefficient

Foam weight, mg	$D \times 10^{-3}$		
	12 hr	24 hr	36 hr
1029.75	4.6 ± 0.6	4.7 ± 0.6	4.7 ± 0.6
390.17	4.62 ± 0.16	4.73 ± 0.16	4.71 ± 0.15
209.594	4.73 ± 0.09	4.81 ± 0.10	4.76 ± 0.10
108.312	4.69 ± 0.05	4.74 ± 0.05	4.77 ± 0.05
46.473	4.71 ± 0.05	4.81 ± 0.05	4.83 ± 0.05
24.546	4.85 ± 0.03	4.94 ± 0.04	4.96 ± 0.03
10.974	4.98 ± 0.06	5.04 ± 0.06	5.08 ± 0.06
4.233	4.84 ± 0.07	4.71 ± 0.14	4.76 ± 0.12
1.780	4.84 ± 0.22	4.71 ± 0.21	4.58 ± 0.23
0.967	5.0 ± 0.5	4.4 ± 0.5	4.3 ± 0.4

Conditions: 150 ml of solution 1.7×10^{-6} M in Co(II), 0.10M in NaSCN, with ionic strength 2.88M and pH 4.7; foam squeezed for 12.0, 24.0 and 36.0 hr at 25.00°.

constant, considering the 1000-fold range of foam weight, but there are some changes. With the larger foam pieces there is some increase in D with time whereas for the smallest foam pieces D decreases with increasing time.

It can be shown¹³ that these effects can be caused by losses of water through evaporation, and that

$$D_{\text{apparent}} = D^{\circ} \left(\frac{V^{\circ}}{V^{\circ} - \Delta V} \right)^4 - \frac{\Delta V}{W}$$

where D° is the actual distribution coefficient, D_{apparent} the apparent distribution coefficient, V° the initial sample volume, ΔV the volume loss, and W the foam weight.

If the distribution ratio, D , is assumed to be completely independent of foam weight, then if even minor evaporative losses of solvent occur, small increases in the apparent distribution ratio will be observed at high foam weights and fairly large decreases will be seen at low foam weights, as was observed.

Two 0.50-g amounts of foam, in one case as a single piece and in the second as 222 small pieces, were equilibrated for 48 hr with the same solution as that above and gave D values of 4688 and 4686 l./kg respectively in spite of the drastic difference in piece sizes. Thus the squeezing behaviour, air entrapment and other physical factors associated with the various sizes of foam pieces used, did not affect the extraction.

The distribution ratio is essentially independent of cobalt concentration (when this is below the saturation limit) and of the relative quantities of the two phases. Thus large volumes of solutions may be

extracted with small weights of polyurethane with no decrease in efficiency.

Effect of temperature

The extraction of cobalt was studied over the temperature range 0–95° after preliminary observations had revealed that even a 0.2° change due to normal laboratory fluctuations caused a 10% variation in D . Maloney *et al.*⁶ have reported the large variation in cobalt extraction from 0.4M potassium thiocyanate when the temperature changes from 20° to 90°.

Five series of potassium thiocyanate solutions (0.010, 0.050, 0.25, 1.00 and 5.00M) that were 1.7μM in Co(II) were prepared, with ⁶⁰Co tracer. The ionic strength was adjusted to 3.00M for the 0.050M SCN⁻ series, 5.88M for the 5.00M SCN⁻ and 2.88M for the remainder, with sodium acetate/acetic acid buffer. Samples were extracted with 50 mg of foam in water-jacketed distribution cells for 6 hr, then the temperature was recorded and an aliquot removed for measurement (after return to room temperature). To minimize any effect of foam deterioration, or loss or contamination of the solution, the temperature of a single sample was raised in 10° increments in successive runs and then lowered to intermediate values. The data for ascending and descending temperature matched, showing the absence of such effects.

The data in Fig. 6 indicate that the cobalt sorption is very sensitive to temperature, but less so at high thiocyanate concentrations. These data can be used to help interpret the extraction process, as discussed in detail elsewhere.¹³ Since D increases sharply with decrease in temperature the solution concentration of

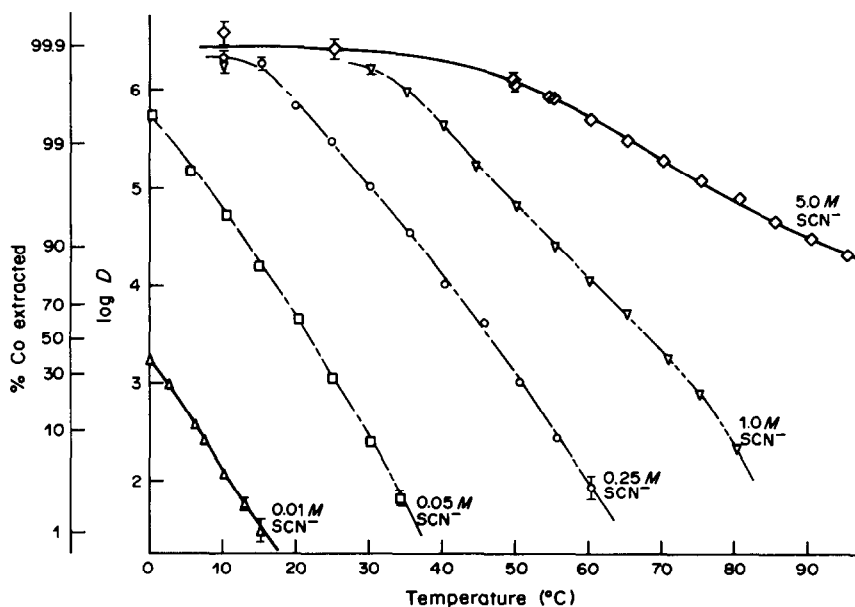


Fig. 6. Effect of temperature on cobalt extraction. Conditions: 0.050 g of foam; 150 ml of solution 1.7×10^{-5} M in Co(II). Δ 0.010M KSCN, 2.88M ionic strength; \square 0.050M KSCN, 3.00M ionic strength; \circ 0.25M KSCN, 2.88M ionic strength; ∇ 1.00M KSCN, 2.88M ionic strength; \diamond 5.00M KSCN, 5.88M ionic strength.

Table 2. Effect of ionic strength

[NaCl],* M	Ionic strength,* M	Cobalt extracted, %	log <i>D</i>
0.000	0.200	10.5 ± 0.4	2.536 ± 0.018
0.100	0.300	11.0 ± 0.4	2.571 ± 0.014
0.300	0.500	12.17 ± 0.34	2.615 ± 0.012
0.500	0.700	14.4 ± 0.4	2.731 ± 0.012
0.800	1.000	21.2 ± 0.5	2.911 ± 0.010
1.800	2.000	56.0 ± 0.4	3.608 ± 0.005
2.801	3.001	88.5 ± 0.4	4.360 ± 0.014
3.80	4.00	97.38 ± 0.32	5.08 ± 0.05
4.80	5.00	99.38 ± 0.32	5.70 ± 0.22

Conditions: 150 ml of solution, $1.7 \times 10^{-6}M$ in Co(II), 0.10M in NaSCN, 0.10M in HCl; 0.050 g foam; 24 hr extraction.

* ± 1%.

the extractable species must correspondingly increase markedly. At low temperatures *D* assumes the same large value of 3×10^6 l./kg for thiocyanate concentrations of 0.25, 1.00 and 5.00M. This suggests that the species in solution is either co-ordinatively saturated with the ligand [*i.e.*, Co(SCN)₄²⁻ aq is formed] or does not contain any thiocyanate (which is improbable in view of the very high thiocyanate dependence at low cobalt concentrations).

Hence cooling the system can create considerable economy in large scale operations, and the temperature effect may be used to shift the equilibrium either to increase cobalt sorption or aid in its recovery from the foam.

Effect of ionic strength

Preliminary studies of cobalt extraction in the presence of a variety of sodium salts indicated that the extraction was somewhat enhanced by 1.0M sodium chloride, bromide, nitrate or acetate, somewhat decreased by sodium iodide, greatly decreased by sodium carbonate, and made slower but otherwise unchanged, by sodium sulphate. Sodium chloride was used in various amounts as an "inert" salt and 1.7μM Co(II) solutions containing ⁶⁰Co tracer, 0.10M sodium thiocyanate and 0.10M hydrochloric acid were extracted with 50 mg of polymer for 24 hr.

The increase in extraction (Table 2) is quite large and is due to three effects. One is the increase in dielectric constant of the aqueous phase, which favours the extraction of less polar and more hydrophobic species such as Co(SCN)₄²⁻. The second is the decrease in water activity¹⁶ as a result of solvating the added solute ions; this decreases the solubility of Co(SCN)₄²⁻ and shifts the equilibrium towards its production. Finally, if the cobalt is sorbed as an ion-association complex of Co(SCN)₄²⁻ with two sodium ions, as is apparently the case at high pH, then any sodium salt should increase the extraction (which would not be the case for an ion-exchange type of mechanism).

The addition of salts significantly improves the extraction of cobalt and suggests that cobalt could be

extracted efficiently from brine solutions containing small amounts of thiocyanate.

Effect of type of polyurethane foam

Several different polyurethane foams were tested for extraction of cobalt from its 1.7μM solutions containing ⁶⁰Co tracer, 0.100M sodium thiocyanate, 0.10M sodium acetate/acetic acid buffer and 2.80M sodium chloride. As usual, the colour of the foams developed rapidly, darkening during several hours in parallel with the measured sorption of cobalt.

The most striking observation from the data shown in Table 3 is that the only polyester-type polyurethane foam gave negligible sorption of cobalt, compared to the polyether-type foams under the conditions used, indicating that the polyol portion of the polymer must be very important in the sorption of cobalt and that polyesters must be largely unsuitable.

Several unknown polyether-type foams (of the kind used for upholstery) as well as one containing carbon black, showed remarkable consistency of extraction. Hypol® polyether foams, which were prepared by the manufacturer from mixtures of prepolymer and water, gave lower *D* values.

One difficulty in evaluating the polyurethane-foam extraction process is the general lack of simple foams with no additives and of known composition. In one case a pair of foams made from a polyethylene oxide (PEO)/polypropylene oxide (PPO) co-polymer together with a styrene/acrylonitrile co-polymer showed a 12% larger *D* value for the foam with the larger fraction of PEO/PPO, although the polyether content was 33% greater. Although the polyether content of the polymer is important in sorption, site accessibility or the positional requirements of the polyether may also be important. With three foams that were similar except for PPO content the cobalt extraction increased as the PEO content increased, showing that the polyethylene oxide must play an important chemical role in the sorption phenomenon.

Effect of foam pretreatment

A systematic study of foam pretreatment was made with 1.7μM Co(II) solutions with ⁶⁰Co tracer in 0.100M sodium thiocyanate at pH 4.8 (0.10M sodium acetate/acetic acid buffer) and ionic strength 3.00M (adjusted with 2.8M sodium chloride). The 50-mg pieces of foam were squeezed in a solution of the given reagent and then left in contact with it for 18 hr, after which they rinsed with an appropriate solvent to remove excess of reagent, squeezed dry in filter paper and finally dried for 12 hr in a vacuum desiccator.

The results are given in Table 4. Saturated chlorine water turned the foam into a sticky mass and 45% w/w boron trifluoride solution in diethyl ether caused immediate swelling and subsequent dissolution of the foam. In the presence of several oxidizing and reducing agents there were no appreciable increases or decreases in *D* so preliminary

Table 3. Absorption of cobalt by various types of polyurethane foam

Foam designation	Foam type	Supplier	Cobalt extracted, %	<i>D</i> , l./kg
# 1122 BFG	unknown polyether	G. N. Jackson Ltd., Winnipeg	85.9 ± 0.5	1.83 ± 0.06 × 10 ⁴
# 1338 BFG	unknown polyether	G. N. Jackson Ltd., Winnipeg	84.5 ± 0.8	1.63 ± 0.08 × 10 ⁴
# 1338 BFG	unknown polyether	G. N. Jackson Ltd., Winnipeg	84.6 ± 0.4	1.69 ± 0.05 × 10 ⁴
# 1338 BFG	unknown polyether	G. N. Jackson Ltd., Winnipeg	84.8 ± 0.5	1.72 ± 0.06 × 10 ⁴
# 1338 M	unknown polyether	G. N. Jackson Ltd., Winnipeg	85.7 ± 0.6	1.80 ± 0.07 × 10 ⁴
# 1538 BFG	unknown polyether	G. N. Jackson Ltd., Winnipeg	86.28 ± 0.30	1.86 ± 0.04 × 10 ⁴
# 1831 BFG	unknown polyether	G. N. Jackson Ltd., Winnipeg	89.4 ± 0.8	2.49 ± 0.18 × 10 ⁴
# 2331 BFG	unknown polyether	G. N. Jackson Ltd., Winnipeg	88.6 ± 0.6	2.34 ± 0.12 × 10 ⁴
Qualux*	unknown polyether	G. N. Jackson Ltd., Winnipeg	70.5 ± 0.6	7.17 ± 0.14 × 10 ³
Black	unknown polyether containing carbon black	unknown	84.3 ± 0.5	1.60 ± 0.05 × 10 ⁴
A	60% PEO/PPO co-polymer with 40% styrene/acrylonitrile co-polymer	Union Carbide Corp.	70.6 ± 0.3	7.26 ± 0.09 × 10 ³
B	80% PEO/PPO co-polymer with 20% styrene/acrylonitrile co-polymer	Union Carbide Corp.	73.2 ± 0.4	8.12 ± 0.14 × 10 ³
D2931A	unknown polyether with 14% tris-(2,3-dibromopropyl) phosphate flame retardant added	Union Carbide Corp.	74.6 ± 0.5	9.05 ± 0.17 × 10 ³
27CGS44-2A	100% PPO polyether	Union Carbide Corp.	25.9 ± 0.5	1.047 ± 0.023 × 10 ³
27CGS44-1	8% PEO/92% PPO polyether	Union Carbide Corp.	70.8 ± 0.6	7.26 ± 0.17 × 10 ³
27CGS44-3	14% PEO/86% PPO polyether	Union Carbide Corp.	87.7 ± 0.4	2.16 ± 0.07 × 10 ⁴
Hypol (9030-43-1)	unknown polyether (FHP 3000 prepolymer)	W. R. Grace & Co.	55.2 ± 0.5	3.69 ± 0.05 × 10 ³
Hypol (9131-13-1)	unknown polyether (FHP 3000 prepolymer)	W. R. Grace & Co.	63.4 ± 0.6	5.17 ± 0.10 × 10 ³
Hypol (9131-33-8)	unknown polyether (FHP 2000 prepolymer)	W. R. Grace & Co.	67.6 ± 0.5	6.42 ± 0.11 × 10 ³
Hypol (9131-32-11)	unknown polyether (FHP 2000 prepolymer)	W. R. Grace & Co.	63.7 ± 0.6	5.24 ± 0.10 × 10 ³
Hypol (9131-6-1)	unknown polyether (FHP 3000 prepolymer)	W. R. Grace & Co.	62.6 ± 0.4	4.96 ± 0.06 × 10 ³
Hypol (9281-2-B)	unknown polyether (FHP 3000 prepolymer)	W. R. Grace & Co.	61.3 ± 0.4	4.72 ± 0.06 × 10 ³
DiSPo*	unknown polyether	Scientific Products Ltd.	0.2 ± 0.5	6 ± 15 × 10 ⁰

Conditions: 150 ml of solution $1.7 \times 10^{-6}M$ in Co(II), 0.10M in NaSCN, with ionic strength 3.00M and pH 4.8; 0.050 g of foam squeezed for 24 hr (* for 48 hr) at 25.00°.

observations which had shown changes with hydroxylamine and hydrogen peroxide were probably showing solution phenomena. It appears that amine-type sites on the foam are either not present in significant numbers or not involved in the sorption of cobalt, and a weak base anion-exchange type of mechanism seems doubtful.

The sorption of cobalt from solution was made markedly slower by the boron trifluoride treatment (more noticeably so with those foams exposed to the

most concentrated solutions). Since BF₃ is a particularly good Lewis acid for sites such as polyether oxygen atoms, this delay must reflect strong interaction of BF₃ with the key sorption sites in the polyurethane until it is slowly displaced by other Lewis bases (e.g., water). The equilibrium value of *D* was increased by this treatment, however, perhaps by the generation or freeing of more sites or even formation of an adduct. Silicon tetrachloride does not have the same effect, because of its easy hydro-

Table 4. Effect of foam pretreatment

Foam pretreatment	Visible changes in foam	Weight change on treatment, %	Cobalt extracted, %	log <i>D</i>
None	—	0	84.6 ± 0.6	4.225 ± 0.017
30% H ₂ O ₂ in water	none	+0.3	84.4 ± 0.8	4.206 ± 0.022
0.01 <i>M</i> Ce(SO ₄) ₂ in 1 <i>M</i> HCl, rinse with 0.1 <i>M</i> HCl	yellowed, slightly sticky	-2.6	83.30 ± 0.33	4.192 ± 0.009
Cl ₂ saturated solution in water	yellowed, collapsed, very sticky	—	—	—
1.0 <i>M</i> NH ₂ OH.HCl in water	none	+0.5	83.9 ± 0.5	4.201 ± 0.013
8.5% H ₂ NNH ₂ in water	none	+0.3	84.5 ± 0.5	4.220 ± 0.015
2% TiCl ₃ in 0.1 <i>M</i>	became deep	+0.1	83.7 ± 0.5	4.199 ± 0.014
HCl, rinse with 0.1 <i>M</i> HCl	purple			
99.8% SiCl ₄ , rinse with ether	yellowed, slightly sticky	+5.0	83.7 ± 0.5	4.179 ± 0.013
9% BF ₃ in diethyl ether, ³ rinse with ether	greyed, slightly sticky	-6.4	87.1 ± 0.4	4.341 ± 0.012
6.5% HPF ₆ in water	browned	+0.4	84.1 ± 0.6	4.224 ± 0.016
0.1 <i>M</i> NaB(C ₆ H ₅) ₄ in water	none	+24.0	43.4 ± 0.5	3.280 ± 0.006
0.1 <i>M</i> NaB(C ₆ H ₅) ₄ in acetone	slightly stiff	+0.2	85.6 ± 0.6	4.246 ± 0.018
0.001 <i>M</i> NaB(C ₆ H ₅) ₄ in solution rather than on foam	—	—	0.9 ± 0.5	1.44 ± 0.25

Conditions: 150.0 ml of solution $1.7 \times 10^{-6}M$ in Co(II), 0.10*M* in NaSCN with ionic strength 3.00*M* and pH 4.8: 0.050 g of foam rinsed and dried after pretreatment, then squeezed for 48.0 hr at 25.00°.

lysis and subsequent removal from the foam in the presence of water.

When sodium tetraphenylborate was used to pretreat the foam, or more notably, added to the solution, there was a considerable decrease in the extraction. This can be interpreted as the strongly preferential sorption of B(C₆H₅)₄⁻ in place of Co(SCN)₄²⁻ at some form of cationic site in the foam. The failure of PF₆⁻ to interfere similarly at these sites is probably because it is not a bulky, hydrophobic and highly polarizable anion [as both Co(SCN)₄²⁻ and B(C₆H₅)₄⁻ are] and so is not readily accommodated in polyurethane.

Effect of added substances

In order to simplify interpretation of the results of this study, no sodium chloride was added to the samples, although the resulting low ionic strength necessitated using 0.50*M* thiocyanate to obtain a reasonable cobalt extraction. The 1.7 μ*M* Co(II) solutions with ⁶⁰Co tracer were buffered with 0.1*M* sodium acetate/acetic acid. High concentrations of the test chemicals were used initially and then progressively lower amounts tried until the observed effect was small. In some cases where there was a significant change, the trial was repeated with 1.7*mM* Co(II) and the absorption spectra were taken shortly

after preparation and again after 24 hr in order to simulate the normal sample-solution preparation.

The effect of the sodium salts of various anions on the cobalt extraction by polyurethane foam is shown in Table 5. Part of the effect observed will be due to increases in ionic strength and to the presence of the additional extractable cation, Na⁺. However, the remainder may result from competitive reactions between added ligands and SCN⁻ to form other cobalt complexes [which are more or less extractable than Co(SCN)₄²⁻] destruction of the SCN⁻ ligand by chemical reaction, competitive sorption of species other than Co(SCN)₄²⁻ onto the foam or alteration of some important solution parameter such as pH. For example, sodium nitrate, chlorate and perchlorate do not alter the cobalt equilibria but do decrease the extraction from that expected for solutions with the same ionic strength. Large polarizable anions such as perchlorate are likely to be extractable and interfere by competition for sorption sites.

Stronger interferences were noted for several anions which produce stable cobalt complexes which are not extracted.

The effects of many metal ions were examined at the 1000-ppm level and at levels as low as 1 ppm if there was an interference. The results are collected in a periodic table (Fig. 7). In general the group IIa metals cause a minor increase in sorption but Be(II) forms

Table 5. Effect of anions on cobalt absorption

Anion	Source	Concentration, M	D, l./kg	Observations
None		—	1.225×10^4	solution colourless; foam blue-green
F ⁻	NaF	1.00	3.26×10^4	two-phase solution little or no change in spectra; Co equilibria unaltered
Cl ⁻	NaCl	1.00	1.5×10^5	
Br ⁻	NaBr	1.00	1.5×10^5	
I ⁻	NaI	1.00	1.49×10^5	
NO ₃ ⁻	NaNO ₃	1.00	9.8×10^4	
NO ₂ ⁻	NaNO ₂	0.100	1.19×10^4	
HCO ₃ ⁻	NaHCO ₃	0.100	1.53×10^4	
ClO ₃ ⁻	NaClO ₃	1.00	1.21×10^5	
ClO ₄ ⁻	NaClO ₄ ·H ₂ O	1.00	9.0×10^4	
H ₂ PO ₄ ⁻	NaH ₂ PO ₄ ·H ₂ O	1.00	9.1×10^4	
CN ⁻	NaCN	0.0100 0.00100	1.0×10^1 1.13×10^4	some decrease in Co(SCN) ₄ ²⁻ formation
SO ₃ ²⁻	Na ₂ SO ₃	1.00	7.02×10^3	new unextractable complex formed
SO ₄ ²⁻	Na ₂ SO ₄	1.00	1.7×10^5	new unextractable complexes formed
S ₂ O ₃ ²⁻	Na ₂ S ₂ O ₃ ·5H ₂ O	1.00	2.9×10^5	white precipitate
S ²⁻	Na ₂ S·9H ₂ O	0.100	4.06×10^2	precipitation; new extractable complexes and/or physical trapping
CrO ₄ ²⁻	Na ₂ CrO ₄	1.00	3.39×10^3	solution turns yellow then colourless; foam remains white
CH ₃ COO ⁻	NaC ₂ H ₃ O ₂ ·3H ₂ O	1.00	7.1×10^4	possible decomposition of SCN ⁻
C ₂ O ₄ ²⁻	Na ₂ C ₂ O ₄	0.0100 0.00103	7.55×10^2 6.51×10^3	some new extractable complex formation
Tartrate	Na ₂ C ₄ H ₄ O ₆ ·2H ₂ O	0.100	6.53×10^3	new complex formed
Citrate	Na ₃ C ₆ H ₅ O ₇ ·2H ₂ O	0.100 0.00100	5.1×10^1 8.44×10^3	foam green; small amount of new complex
EDTA	Na ₂ C ₁₀ H ₁₄ O ₈ ·N ₂ ·2H ₂ O	1.00×10^{-5} 1.00×10^{-6}	9.1×10^1 8.06×10^3	new unextractable complex formed

Conditions: 0.050 g of foam squeezed for 24.0 hr at 25.00°; 150 ml of solution $1.7 \times 10^{-6}M$ in Co(II), 0.10M in NaSCN, with initial pH 4.8 and ionic strength 0.6M, plus the added salt.

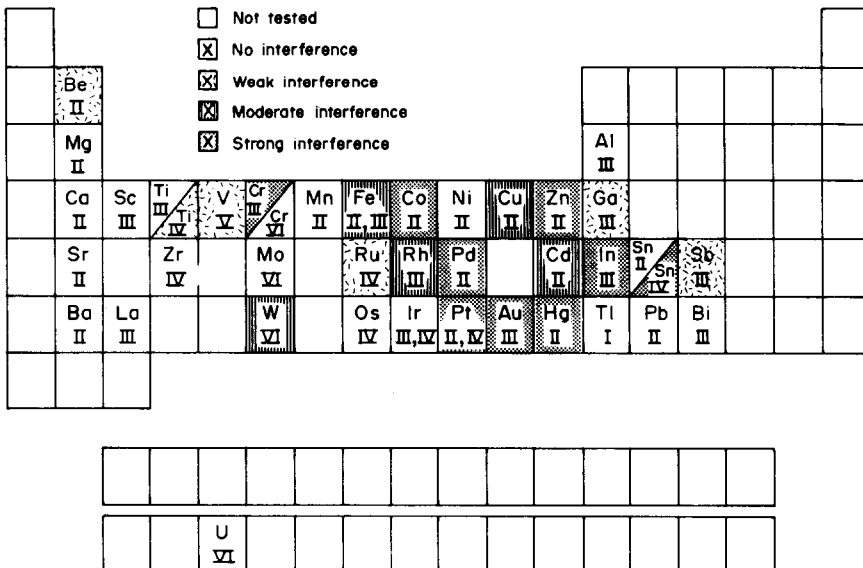


Fig. 7. Summary of interference studies with various metal ions.

an extractable red thiocyanate complex which interferes with the cobalt sorption. The apparent increase caused by $V(V)$ was due to the ammonium ion from the salt used.

The group VIa metals differ considerably in their effect, owing to formation of extractable thiocyanate complexes.¹⁷

The group VIII metals give a variety of results, because of competition for the foam sites or formation of extractable complexes.

Gold causes a significant interference with the cobalt sorption even at 1 ppm. The group IIb metals form thiocyanate complexes and compete for foam sites. Of the group IIb metals, Al(III) and Tl(I) enhance the extraction slightly, and Ga(III) interferes somewhat. Indium forms a highly extractable thiocyanate complex and greatly reduces the cobalt sorption.

Sn(IV) interferes strongly by co-precipitating cobalt with gelatinous $\text{SnO}_2 \cdot x\text{H}_2\text{O}$.

Many metals can be extracted as thiocyanate complexes under these conditions but a thorough examination would be required to optimize specific separations or particular co-extractions.

The effect of several nitrogen-containing compounds was tested, since cobalt forms a fairly large number of complexes with this type of ligand and a

number of extraction procedures make use of both SCN^- and a protonated nitrogen-containing compound. Most of these test compounds are stronger bases than acetate and so will exist in the protonated cationic form in the sample solutions (near pH 4.5 with the acetate buffer). A few, such as tetramethylammonium bromide, are ionic at any pH, and a few such as *N*-methylformamide are very weak bases and essentially neutral under these conditions. Pyridine and aniline are borderline cases and so both forms will be present.

The data obtained are recorded in Table 6. With 1.0M ammonium chloride and hydroxylamine hydrochloride an enhancement occurs, but there is no change in the spectra of these solutions so the effect must be related to some sorption characteristic of the added ions themselves. Most probably NH_4^+ and NH_3OH^+ are more extractable as counter-ions with $\text{Co}(\text{SCN})_4^{2-}$ than is Na^+ .

The progressive substitution of methyl groups in the ammonium ion leads to a steady trend from a substantial enhancement with 0.10M NH_4^+ to a slight depression with 0.10M $(\text{CH}_3)_4\text{N}^+$. Since the spectra show no substantial difference, this again suggests that NH_4^+ has some special effect on the solvation process. When n-butyl groups are substituted in the NH_4^+ , the opposite effect (from that for the methyl

Table 6. Effect of nitrogen-containing compounds and cations on cobalt absorption

Compound/cation	Source	$\text{p}K_{\text{HB}}$	Concentration, M	D , l./kg
None	—	—	—	1.225×10^4
NH_4^+	ammonium chloride	9.95	1.00	3.9×10^5
NH_3OH^+	hydroxylammonium chloride	5.96	1.00	2.4×10^5
CH_3NH_3^+	methylammonium chloride	10.68	0.100	1.52×10^4
$(\text{CH}_3)_2\text{NH}_2^+$	dimethylammonium chloride	10.77	0.100	1.17×10^4
$(\text{CH}_3)_3\text{NH}^+$	trimethylammonium chloride	9.80	0.100	1.13×10^4
$(\text{CH}_3)_4\text{N}^+$	tetramethylammonium chloride	strong base	1.00	3.51×10^3
$\text{CH}_3\text{CH}_2\text{NH}_3^+$	ethylammonium chloride	10.63	0.100	1.54×10^4
$\text{H}_3\text{NCH}_2\text{NH}_3^+$	ethylenediamine	{ 1st 6.85 2nd 9.93 }	0.050 9.90×10^{-3}	1.4×10^1 1.20×10^4
$\text{CH}_3(\text{CH}_2)_3\text{NH}_3^+$	n-butylamine	10.01	0.100	3.21×10^4
$\text{CH}_3\text{CH}_2\text{CH}(\text{CH}_3)\text{NH}_3^+$	sec-butylamine	10.60	0.100	1.70×10^4
$(\text{CH}_3)_3\text{CNH}_3^+$	tert-butylamine	10.83	0.100	1.43×10^4
$[\text{CH}_3(\text{CH}_2)_2]_2\text{NH}_2^+$	di-n-butylamine	11.25	0.100	1.3×10^5
$[\text{CH}_3(\text{CH}_2)_3]_2\text{NH}^+$	tri-n-butylamine	11.04	$\ll 0.100$	2×10^6
$[\text{CH}_3(\text{CH}_2)_3]_4\text{N}^+$	tetra-n-butylamine	strong base	$\ll 0.100$ 0.0100	4.7×10^3 6×10^5
$\text{CH}_3(\text{CH}_2)_5\text{NH}_3^+$	n-hexylamine	10.56	0.100	2.6×10^5
$\text{C}_5\text{H}_5\text{N}/\text{C}_5\text{H}_5\text{NH}^+$	pyridine	5.23	0.100	7.76×10^3
$\text{C}_6\text{H}_5\text{NH}_2/\text{C}_6\text{H}_5\text{NH}_3^+$	aniline	4.60	0.100	5.1×10^4
CH_3CONH_2	formamide	small	0.100	1.33×10^4
$\text{CH}_3\text{CONH}(\text{CH}_3)$	<i>N</i> -methylformamide	small	0.100	1.26×10^4
$(\text{CH}_3)_2\text{HNCONH}(\text{CH}_3)$	<i>N,N'</i> -dimethylurea	small	0.100	1.26×10^4
$\text{H}_2\text{NCOOCH}_2\text{CH}_3$	urethane	small	0.100	1.27×10^4

Conditions: 0.050 g of foam squeezed for 24.0 hr at 25.00°; 150 ml of solution $1.7 \times 10^{-6}M$ in Co(II), 0.5M in NaSCN with initial pH 4.8 and ionic strength 0.6M, plus the added salt.

compounds) is seen, because two phases form in these solutions, and also these *n*-butylamines can act as liquid ion-exchangers. This effect is also seen with other substances, such as aniline. Ethylenediamine interferes since it is a good complexant of cobalt, and pyridine interferes by precipitating cobalt, probably as $\text{Co}(\text{C}_3\text{H}_5\text{N})_4(\text{SCN})_2$.

A group of very weak bases (formamide, *N*-methylformamide, *N,N*-dimethylurea and urethane) which might mimic types of *N*-containing groups in polyurethane foam, showed no detectable effect, indicating that the foam-nitrogen ligands are not involved in the sorption process.

In general, substances interfere with the extraction by formation of less extractable cobalt complexes, by decreasing the concentration of available thiocyanate ion, by occupying or destroying sorption sites on the foam, and/or by affecting the formation of $\text{Co}(\text{SCN})_4^{2-}$. An enhancement of extraction occurs when more extractable cobalt complexes are formed, when the concentration of more extractable cations is increased, and/or the solution ionic strength is increased.

CONCLUSION

Cobalt(II) is extracted very efficiently from aqueous thiocyanate solutions by polyether-type polyurethane foam. Using high thiocyanate concentration, high ionic strength, low temperature and a pH between 1.0 and 9.0 gives distribution coefficients as high as 3×10^6 l./kg. The high distribution coefficient, reasonably large capacity, high flow-through, and low cost suggest that polyurethane

foam may find several industrial and analytical applications for the extraction of cobalt and other thiocyanate complexes.

Acknowledgement—This work was supported by the Natural Science and Engineering Research Council of Canada.

REFERENCES

1. N. S. Bayliss and R. W. Pickering, *Ind. Eng. Chem., Anal. Ed.* 1946, **18**, 446.
2. T. Braun, A. B. Farag and M. P. Maloney, *Anal. Chim. Acta*, 1977, **93**, 191.
3. T. Braun and A. B. Farag, *ibid.*, 1978, **98**, 133.
4. T. Braun and M. N. Abbas, *ibid.*, 1980, **119**, 113.
5. M. P. Maloney, G. J. Moody and J. D. R. Thomas, *Proc. Chem. Soc. Anal. Div.*, 1977, **14**, 244.
6. *Idem*, *Analyst*, 1980, **105**, 1087.
7. G. J. Moody, J. D. R. Thomas and M. A. Yarmo, *Anal. Proc.*, 1983, **20**, 132.
8. R. F. Hamon, A. S. Khan and A. Chow, *Talanta*, 1982, **29**, 313.
9. A. A. Newman, *Chemistry and Biochemistry of Thiocyanic Acid and its Derivatives*, Academic Press, London, 1975.
10. R. B. Fischer and D. G. Peters, *Quantitative Chemical Analysis*, 3rd Ed., Saunders, Philadelphia, 1968.
11. L. G. Sillén, *Stability Constants of Metal-Ion Complexes*, Supplement No. 1, Part 1, Spec. Publ. No. 25, The Chemical Society, London, 1971.
12. H. J. M. Bowen, *J. Chem. Soc. A*, 1970, 1082.
13. R. F. Hamon, *Ph.D. Thesis*, University of Manitoba, 1981.
14. G. A. Horsfall, *M.Sc. Thesis*, University of Manitoba, 1977.
15. R. C. Weast, *Handbook of Chemistry and Physics*, 48th Ed., Chemical Rubber Co., Cleveland, 1967.
16. V. P. Ionov and Yu. A. Zolotov, *Dokl. Phys. Chem.*, 1975, **223**, 807.
17. Z. Kh. Sultanova, L. K. Chuckalin, B. Z. Iofa and Yu. A. Zolotov, *J. Anal. Chem. USSR*, 1973, **28**, 369.

DETERMINATION OF DIPHENYLTIN AND DIALKYLtin HOMOLOGUES BY HPLC WITH MORIN IN THE ELUENT

WENCHE LANGSETH

Department of Chemistry, The University of Oslo, Blindern, 0315 Oslo 3, Norway

(Received 28 February 1984. Accepted 25 May 1984)

Summary—A sensitive and selective method has been developed for the simultaneous determination of diphenyltin and dialkyltin compounds. The compounds were separated by HPLC on a cyanopropyl-bonded silica column with toluene containing 1–5% acetic acid, 1–5% ethanol or methanol and 0.0015% morin. The organotins were eluted as morin complexes and detected by a fluorescence spectrophotometer. Detection limits ranged from 1 to 4 pg. Data reported include capacity factors, separation efficiencies and linearity of detection.

Organotin compounds have found widespread commercial use as pesticides, fungicides and stabilizers of plastics.^{1,2} Dialkyltin compounds, especially, have been used to stabilize certain plastics against heat and light. Studies have shown that both the number and kind of organic groups covalently attached to tin in the organotin species affect the toxicity.^{3,4} The need for better analytical methods capable of trace specification of various organotin compounds is apparent.

A variety of analytical techniques and procedures have been applied for the determination of organotin species. These include atomic-absorption spectrophotometry,^{5,6} gas chromatography (GC)^{7,8} and HPLC.^{9,10} Adsorption and decomposition of dialkyltin compounds is found to be a problem in GC.^{11,12} HPLC appears to be the most versatile method for these compounds. The most common and generally sensitive HPLC detectors are the spectrophotometer and fluorimeter, but in most cases these are not directly applicable to alkytin compounds. HPLC is therefore often combined with an element-specific detector such as an atomic-absorption spectrophotometer,^{13,14} flame photometer or inductively-coupled plasma-emission spectrophotometer (ICP).^{15,16} These approaches need expensive equipment, however, and are often far too complicated. The separation and determination of metals in the form of chelates by HPLC, with ultraviolet or fluorescence detection, have found increased application.¹⁷ The metal complexes can be formed either prior to injection,¹⁸ on the column¹⁹ or post-column.²⁰ Separation of dialkyltin dichlorides and post-column reaction with morin to give a fluorescent product has been described,²¹ but post-column reactors are complicated and not available in most laboratories.

The aim of this study was to separate trace amounts of dialkyltin and diphenyltin compounds with ordinary HPLC equipment. This paper describes

a method requiring only a single HPLC pump and a fluorimetric or photometric detector.

EXPERIMENTAL

Reagents

Dibutyltin dichloride was obtained from Fluka AG (Switzerland). Diphenyltin dichloride, diethyltin dichloride and dimethyltin dichloride were purchased from the Alfa Division, Ventron Corporation. When necessary, the alkytin chlorides were purified by recrystallization from light petroleum (b.p. 40–60°). Morin (2',3,4',5,7-pentahydroxyflavone) was obtained from Fluka AG and 3-hydroxyflavone from Eastman Kodak Ltd. The toluene used was of glass-distilled grade from Rathburn Chemicals. All HPLC solvents and the morin and 3-hydroxyflavone solutions were filtered through 0.45- μ m Millipore filters.

Apparatus

The HPLC equipment consisted of a Perkin-Elmer dual pump module (Series 2) with a Rheodyne injector, model 7105, a Perkin-Elmer LC-75 spectrophotometer and a Kontron spectrophotometer, model SFM-23.

Two prepacked cyanopropyl-bonded silica (5.0 μ m particle size) columns were used in this study, both obtained from Brownlee Labs; one stainless-steel column 250 \times 4.6 mm i.d. and one MPLC™ cartridge 100 \times 4.6 mm i.d. The guard column, 30 \times 4.6 mm i.d., also containing cyanopropyl-bonded silica (5 μ m particle size), was of the MPLC™ type. The solvent flow-rate was 1.0 ml/min.

Procedure

The diphenyltin and dialkyltin dichlorides were injected as hexane solutions (normally 10 μ l). They were eluted with toluene containing 1–5% v/v acetic acid, 1–5% v/v methanol or ethanol and 0.0015% morin. Morin is stable in alcohol for weeks, and its alcoholic solution was added to the eluent. The excitation wavelength of the fluorescence detector was set at 420 nm and the emission wavelength at 500 nm.

RESULTS AND DISCUSSION

The use of post-column derivative formation before detection requires a reaction chamber or mixer of high quality. Considerable band-broadening and a high noise level are often observed when a con-

ventional reaction coil is used. Alkyltin chlorides or similar compounds are easily adsorbed by residual silanol groups on bonded-phase columns, making tailing hard to avoid. The tin atom is, however, considerably reduced in reactivity in chelates where it is six-co-ordinated.

Complex formation in HPLC separations can be done either prior to injection or on the column. If the ligand is not incorporated in the eluent, the complex has to be very stable. No dialkyltin complexes suitable for ultraviolet or fluorescence detection were found to be stable enough.

Organotin chelates are generally unstable and nearly insoluble in aqueous media. Mobile phases containing organic solvents are therefore preferred. Cyanopropyl-bonded phase columns have found increased applicability when normal silica packing is unsuitable because of strong adsorption effects. It was therefore decided to try a cyanopropyl-bonded stationary phase. Recent works have shown that these columns are suitable for separations of alkyltins²¹ and other organometallic compounds.²²

Basic studies of the complexes formed between dialkyltins and 3-hydroxyflavone²³ and morin²⁴ revealed that both reagents could be used as complexing agents. Preliminary studies showed that both formed dialkyltin complexes that were sufficiently stable for HPLC determination, when the ligand was incorporated in the mobile phase. Morin was selected for further work because of the high fluorescence intensity of the complexes, giving better selectivity and sensitivity.

Toluene was found to be the best major component of the mobile phase. The sensitivity for the alkyltin complexes when hexane or methanol was used instead, was only 1 or 10%, respectively, of that when toluene was used. Toluene containing small amounts of acetic acid, methanol or ethanol and morin was found to give good selectivity, high resolution and high sensitivity.

An eluent with 0.0015% morin gave reproducible peak heights, which was not the case when only 0.0010% morin was incorporated in the eluent. Use of 0.002% did not increase the sensitivity.

Experiments proved that acetic acid was essential in the mobile phase. Hardly any selectivity was obtained for dioctyl-, dibutyl- and dipropyltin when only ethanol (containing 4% water) was used, and the peaks became broad and undetectable with water-free ethanol. The retention volume decreased with increasing amount of acetic acid for all the diorganotin chlorides examined, as shown in Fig. 1.

The alcohol was necessary to obtain reasonable sensitivity, which was found to decrease appreciably for ethanol content <1%. A high degree of tailing was observed when the alcohol was replaced by another modifier such as ethyl acetate.

Table 1 shows the capacity factors and resolutions when methanol, ethanol and propan-1-ol were used as modifiers of the mobile phase. A high degree of

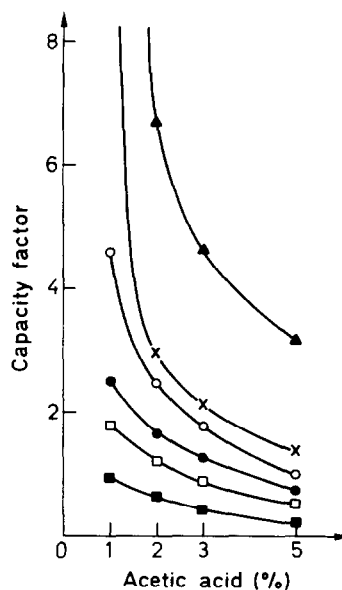


Fig. 1. Effect of the acetic acid content in the mobile phase on the separation of diphenyl- and dialkyltin compounds. Column: 30 × 4.6 mm bore + 250 × 4.6 mm bore cyanopropyl-bonded column (Brownlee Labs.) Mobile phase: toluene, x% acetic acid, 3% ethanol (4% water), 0.0015% morin. ■, Oc₂SnCl₂; □, Bu₂SnCl₂; ●, Pr₂SnCl₂; ○, Ph₂SnCl₂; ×, Et₂SnCl₂; ▲, Me₂SnCl₂.

tailing and low sensitivity were observed for diethyltin and especially for dimethyltin with propan-1-ol. Methanol and ethanol (4% water) gave about the same resolution (Figs. 2 and 3), but the sensitivity was about 50% higher with methanol, except for

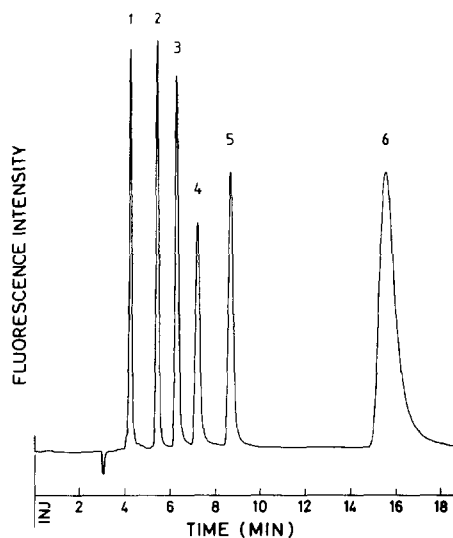


Fig. 2. Chromatogram of diphenyl- and dialkyltin compounds. Column as for Fig. 1. Mobile phase: toluene, 3% acetic acid, 2% methanol, 0.0015% morin, flow-rate 1.0 ml/min. Peaks: 1 = Oc₂SnCl₂ (60 ng); 2 = Bu₂SnCl₂ (60 ng); 3 = Pr₂SnCl₂ (60 ng); 4 = Ph₂SnCl₂ (20 ng); 5 = Et₂SnCl₂ (60 ng); 6 = Me₂SnCl₂ (120 ng). Amounts of each compound injected are given in parentheses.

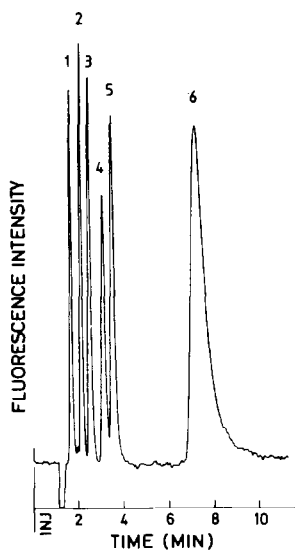


Fig. 3. Chromatogram of diphenyl- and dialkyltin compounds. Column: 30 × 4.6 mm bore + 100 × 4.6 mm bore cyanopropyl-bonded column (Brownlee Labs.). Mobile phase: toluene, 3% acetic acid, 2% ethanol (water-free), 1% ethanol (4% water), 0.0015% morin, flow-rate 1.0 ml/min. Peaks: 1 = Oc_2SnCl_2 (3 ng); 2 = Bu_2SnCl_2 (3 ng); 3 = Pr_2SnCl_2 (3 ng), 4 = Ph_2SnCl_2 (1 ng); 5 = Et_2SnCl_2 (3 ng); 6 = Me_2SnCl_2 (8 ng). Amounts injected are given in parentheses.

dimethyltin, for which a threefold increase in peak height was observed. The capacity factor for diphenyltin was particularly sensitive to the water content. Maximum resolution can be obtained by regulation of the water content, though the optimal conditions may vary from one column to another, even with the same packing material. Change in the resolution is also observed with both methanol and ethanol after prolonged use of the column.

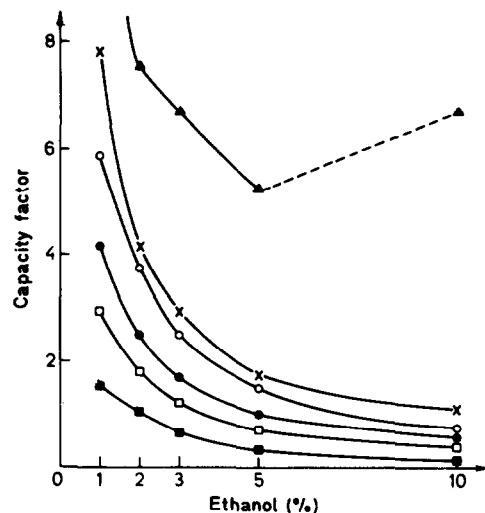


Fig. 4. Effect of the ethanol content of the mobile phase on the separation of diphenyl- and dialkyltin compounds. Column as for Fig. 1. Mobile phase: toluene, 2% acetic acid, x% ethanol (4% water), 0.0015% morin. ■, Oc_2SnCl_2 ; □, Bu_2SnCl_2 ; ●, Pr_2SnCl_2 ; ○, Ph_2SnCl_2 ; ×, Et_2SnCl_2 ; ▲, Me_2SnCl_2 .

The retention volume decreased with increasing ethanol content for all the diorganotin chlorides examined, except dimethyltin (Fig. 4). The capacity factor for dimethyltin was halved when the ethanol level was raised from 1 to 2% (2% acetic acid). With higher ethanol content less reduction was observed, and the retention volume increased again at ethanol concentrations above about 5%.

Very good resolution of diphenyltin and all the dialkyltins examined can be achieved within less than 10 min with isocratic elution on a 10-cm analytical column containing only 2700 theoretical plates (Fig.

Table 1. Chromatographic parameters for different mobile phase modifiers (mobile phase: toluene, 3% acetic acid, x% alcohol, 0.0015% morin)

Diorganotin dichloride	3% n-Propanol		3% Ethanol (0.03% H_2O)		3% Ethanol (0.12% H_2O)		2% Methanol	
	k' *	R_s †	k'	R_s	k'	R_s	k'	R_s
Oc_2SnCl_2	0.30	3.6	0.30	3.3	0.40	4.2	0.40	4.0
Bu_2SnCl_2	0.63	1.4 ^a	0.63	2.2	0.83	3.0	0.80	2.6
Pr_2SnCl_2	0.90	0.8	0.87	0.9	1.20	3.8	1.10	2.6
Ph_2SnCl_2	0.80	4.6 ^b	0.97	4.3	1.77	2.4	1.43	3.8
Et_2SnCl_2	1.90	6.8	1.53	5.7	2.13	7.4	1.93	7.4
Me_2SnCl_2	5.73 ^c		3.90 ^d		5.10		4.27	

$$*k' = \frac{V_R - V_0}{V_0}; V_0 = 3.0 \text{ ml}$$

$$†R_s = \frac{V_{n+1} - V_n}{1/2(V_{w_{n+1}} + V_{w_n})}$$

^a R_s between Bu_2SnCl_2 and Ph_2SnCl_2 .

^b R_s between Pr_2SnCl_2 and Et_2SnCl_2 .

^c Extremely broad band.

^d Quite broad band.

Table 2. Relative fluorescence intensities and relative peak heights for some diorganotin dichlorides (mobile phase: toluene, 5% acetic acid, 3% ethanol, 0.0015% morin, sample injected 100 ng)

Diorganotin dichloride	Relative fluorescence intensity*		Relative peak heights	
	per g	per mole	per g	per mole
Oc ₂ SnCl ₂	30.3	36.7	51.0	61.7
Bu ₂ SnCl ₂	34.9	30.8	52.1	46.0
Pr ₂ SnCl ₂	36.9	29.6	48.5	38.9
Ph ₂ SnCl ₂	100.0	100.0	100.0	100.0
Et ₂ SnCl ₂	39.8	28.7	42.3	30.5
Me ₂ SnCl ₂	51.4	32.8	16.0	10.2

*Injected without use of any column.

†30 × 4.6 mm bore + 250 × 4.6 mm bore cyanopropyl-bonded column (Brownlee Labs).

3), (flow-rate 1.0 ml/min). Increasing the flow-rate to 2.0 ml/min gave band-broadening. Better resolution within the same time can be obtained with gradient elution, with increasing acetic acid content of the mobile phase. A broad band is often observed, however, because of the alteration of the equilibrium of adsorbed morin on the column.

Thorough deaeration of the mobile phase is normally recommended, when using fluorescence detection, because of the quenching effect of oxygen, but it increased the noise-level in this case, because of an increase in the fluorescence intensity of the morin, so deaeration was omitted.

The relative fluorescence intensities of the diphenyltin- and dialkyltin-morin complexes are given in Table 2. The dialkyltin complexes all produced about the same fluorescence per mole, but only about 30% of that of the diphenyltin complex.

The linearity of the calibration graphs was checked by injecting 10 µl of standard mixtures of diphenyltin and dialkyltin chlorides (0.001–100.0 µg/ml) in hexane. They were linear up to at least 1 µg. The correlation coefficients were in all cases found to be >0.998.

Detection limits ranged from 1.0 pg for diphenyltin dichloride to 4.0 pg for dimethyltin dichloride, when the "High HV" mode of the detector was used and the detection limit taken as twice the noise level. An MPLCTH 10-cm cartridge was then used with a mobile phase of toluene, 3% acetic acid, 2% water-free ethanol, 1% ethanol (4% water) and 0.0015% morin.

The dialkyltin dichloride solution could be prepared in hexane or toluene. Hexane seemed to be the best choice. The solvent peak was then well separated from the dioctyltin peak. This was not the case for toluene, the capacity factor being close to that for dioctyltin. No higher sensitivity or better resolution could be observed when the morin complexes were prepared before injection. The complexes seemed to remain stable for days, except the diphenyltin com-

plex, which decomposed after some hours. Hexane solutions of diphenyltin and dialkyltin chlorides, (1000 µg/ml), however, were stable for weeks.

Conclusion

The proposed method using an eluent containing morin or some other complexing agent appears to have considerable potential for the examination of different organotin compounds. No special equipment is required, only a single HPLC pump, an injector and a fluorescence detector (or ultraviolet detector). The utilization of a cyano-bonded silica stationary phase and normal-phase elution allows complete resolution of diphenyltin and dialkyltin homologues. The dialkyltins are eluted in order of decreasing molecular weight. The selectivity offered by the reported HPLC conditions, coupled with the linearity of the calibration graph and the detection limits of a few picograms, demonstrates the possibility of trace analysis for diphenyltin and dialkyltins.

REFERENCES

1. W. T. Piver, *Environ. Health Perspect.*, 1963, **61**, June 1963.
2. L. A. Hobbs and P. J. Smith, *Tin, Its Uses*, 1982, No. 131, 10.
3. W. N. Aldridge, *Organomet. Coord. Chem., Germanium, Tin, Lead, Plenary Lect. Inst. Conf. 2nd*, 1978, **9**, 30.
4. J. S. Thayer, *J. Organomet. Chem.*, 1974, **76**, 265.
5. V. F. Hodge, S. L. Seidel and E. D. Goldberg, *Anal. Chem.*, 1979, **51**, 1256.
6. H. L. Trachman, A. J. Tyberg and P. D. Branigan, *ibid.*, 1977, **49**, 1090.
7. D. R. Hansen, T. J. Gilfoil and H. H. Hill, *ibid.*, 1981, **53**, 857.
8. M. D. Mueller, *Z. Anal. Chem.*, 1984, **317**, 32.
9. E. B. Jessen, K. Taugbøl and T. Greibrokk, *J. Chromatog.*, 1979, **168**, 139.
10. E. J. Parks, R. B. Johannesen and F. E. Brinckman, *ibid.*, 1983, **255**, 439.
11. Y. Arakawa, O. Wada, T. H. Yu and H. Iwai, *ibid.*, 1981, **207**, 237.
12. *Idem, ibid.*, 1981, **216**, 209.
13. F. E. Brinckman, W. R. Blair, K. L. Jewett and W. P. Iverson, *J. Chromatog. Sci.*, 1977, **15**, 493.
14. D. T. Burns, F. Glockling and M. Harriott, *Analyst*, 1981, **106**, 921.
15. L. Ebdon, R. W. Ward and D. A. Leathard, *Anal. Proc.*, 1982, **19**, 110.
16. D. Bushee, I. S. Krull, R. N. Savage and S. B. Smith, *J. Liq. Chromatog.*, 1982, **5**, 463.
17. A. R. Timerbaev, O. M. Petrikhin and Yu. A. Zolotov, *J. Anal. Chem. USSR*, 1981, **36**, 811.
18. R. C. Gurira and P. W. Carr, *J. Chromatog. Sci.*, 1982, **20**, 461.
19. R. M. Smith and L. E. Yankey, *Analyst*, 1982, **107**, 744.
20. P. Jones, P. J. Hobbs and L. Ebdon, *Anal. Chim. Acta*, 1983, **149**, 39.
21. T. H. Yu and Y. Arakawa, *J. Chromatog.*, 1983, **258**, 189.
22. D. J. Mazzo, Z. B. Cheng, P. C. Uden and M. Rausch, *ibid.*, 1983, **269**, 11.
23. W. Langseth, *Inorg. Chim. Acta*, 1984, 90.
24. Y. Arakawa, O. Wada and M. Manabe, *Anal. Chem.*, 1983, **55**, 1901.

INTERFERENCES IN THE DETERMINATION OF TOTAL NITROGEN IN NATURAL WATERS BY PHOTO-OXIDATION TO NITRATE-NITRITE MIXTURE

LILLY GUSTAFSSON

Department of Analytical Chemistry, University of Uppsala, P.O. Box 531, S-751 21 Uppsala, Sweden

(Received 9 January 1984. Revised 10 April 1984. Accepted 18 May 1984)

Summary—The method proposed by Armstrong, Williams and Strickland for the photo-oxidation of total nitrogen in sea-water to nitrate and nitrite has been studied in some detail, to extend its use to fresh and brackish waters, applying a more accurate method for the determination of the reaction products. Variables influencing the yield of nitrate and nitrite are irradiation time, pH and type of buffer, kind of nitrogen compound and its concentration, and the concentrations of oxygen, carbon dioxide, organic matter and salts, especially bromides, even at the low concentrations found in brackish waters. All these variables interact in a rather complicated way. Interferences from halides, organic matter and carbon dioxide are considerably reduced by ensuring that the pH is kept at 8.5-9 during the irradiation. Because pure solutions of many substances give quantitative yields ($\geq 98\%$) in the pH-range 7-9 usually recommended, whereas others require lower pH for maximal oxidation, a method has been developed involving photo-oxidation first at pH 2.1 and then at pH 8.5-9. In the absence of interfering concentrations of halides the relative increase in yield by an initial irradiation at low pH is especially large (10-36%) for proteins, organic nitrogen in fresh waters, uric acid and urea. A comparison is made between determination of total nitrogen in some natural waters by using photo-oxidation and by a Kjeldahl method modified to give total nitrogen. By making use of the optimal conditions presented in this paper, a negative error of less than 8% is expected in the determination of total nitrogen in fresh waters. For saline waters the error will probably be larger, at least at a high ratio of organic to inorganic nitrogen.

Armstrong *et al.*¹ proposed a method for the determination of nitrogen and phosphorus in sea-water, based on photo-oxidation of the sample by ultraviolet radiation from a 1200-W high-pressure mercury-arc lamp. In the presence of an excess of oxygen ensured by addition of hydrogen peroxide, ammonia and many organic nitrogen compounds were quantitatively oxidized after 3 hr of irradiation, to give a mixture of nitrate and nitrite. Strickland and Parsons² recommend this method for sea-water "even although there are some inherent errors and a doubt exists as to its applicability to certain nitrogenous compounds". Photo-oxidation by means of a mercury-arc lamp of lower power (380 W) was studied by Armstrong and Tibbitts.³ They reported 98% oxidation of the nitrogen compounds in sea-water after irradiation for 12 hr. Henriksen⁴ adapted the photo-oxidation method to the determination of nitrogen, phosphorus and iron in fresh water. Also working with fresh water, Afghan *et al.*⁵ observed that certain nitrogen compounds were quantitatively oxidized within a reasonable time only in acid solution, while others required an alkaline medium. This led to the development of methods^{5,6} based upon irradiation in two steps, first in acid and then in alkaline solution. Contrary to these authors, Manny *et al.*⁷ irradiated the samples only at pH 4 and made separate determinations of the oxidation products formed, ammonia, nitrite and nitrate.

Some problems arose when we wanted to apply the photo-oxidation method to brackish water. There

seemed to be some interferences not observed by other authors.¹⁻⁷ We soon found that the large range of pH recommended by Strickland and Parsons (6-8.5) and Henriksen⁴ (6.5-9) may lead to large errors because the interference from some substances is very dependent on pH. We also wanted to know whether the method mentioned above, using irradiation in two steps, could be adapted to sea-water analysis. Using a thoroughly investigated method^{8,9} for the determination of the nitrate-nitrite mixture formed we undertook a detailed investigation of the factors influencing the photo-oxidation and made a comparison between irradiation at a certain pH and the more laborious method involving irradiation first in acid and then in alkaline medium.

EXPERIMENTAL

Equipment

The photo-oxidation was performed with equipment similar to that described by Henriksen, consisting of a 900-W high-pressure mercury-arc lamp mounted axially in an aluminium-sheet cylinder provided with a cooling fan at its lower end. Twelve silica tubes (27 mm outside diameter), each containing 100 ml of sample, were placed in a circle about 70 mm from the lamp. The temperature stabilized at 80-85° in the upper part of the solutions after prolonged irradiation.

Reagents

Water. For dilution of solutions intended for irradiation the ordinary distilled water was further purified by passing it through a column of Dowex 50 W cation-exchanger, H⁺-form. Its nitrogen (N) concentration was thus reduced from 0.4 to 0.15 μM .

"Double sea-water" (DSW). This was prepared from specially purified reagents and had the following composition: 0.960M Na⁺, 0.0212M Ca²⁺, 0.109M Mg²⁺, 0.0227M K⁺, 1.121M Cl⁻, 0.060M SO₄²⁻ and 0.00168M Br⁻. Diluting this solution with an equal volume of water gives a synthetic sea-water of 3.5% salinity, containing the major constituents except strontium, bicarbonate, borate and fluoride.

Hydrogen peroxide, 30%. Perhydrol, Merck No. 7210, stabilized for higher storage temperature was preferred to the ordinary reagent grade, No. 7209, because it had a considerably lower nitrogen content, only 0.016–0.025 μ mole of N per ml compared to 0.29 μ mole of N per ml in Perhydrol No. 7209. The nitrogen content was determined after decomposition of the hydrogen peroxide by boiling an acid solution (5 ml of Perhydrol in 40 ml of 0.002M sulphuric acid) for about 1 hr in the presence of a platinum grid.

Regarding solutions used in the reduction of nitrate and the spectrophotometric determination of nitrite, see Nydahl.^{8,9} In solutions of undefined substances, e.g. meat peptone and proteins, the nitrogen content was determined by Kjeldahl digestion according to the A.O.A.C.¹⁰ before the final dilution. Tests of the Kjeldahl procedure on *p*-aminobenzoic acid and glycine gave relative errors within $\pm 0.2\%$.

Blanks. The total blank for the whole procedure (Method A) was 0.026 μ mole of N ($s = 0.006$, $n = 14$) with use of purified water and 0.039 μ mole of N ($s = 0.012$, $n = 8$) with synthetic sea-water of 3.5% salinity.

Procedures

Method A—One-step photo-oxidation. To each of the samples, generally containing 2 μ moles of N, were added 50 μ moles of borax and 0.30 ml of Perhydrol, followed by dilution to 95 ml and mixing. The tubes were then covered with glass caps, irradiated for 3 hr, and allowed to cool to room temperature. The solutions were quantitatively transferred to 100-ml standard flasks each containing 1 mmole of Tris-buffer and the calculated amount of alkali or acid to adjust the pH to 8.2, and were diluted to volume. The nitrate–nitrite mixture produced was then analysed according to Nydahl,^{8,9} with use of electrolytically precipitated cadmium for the reduction of nitrate to nitrite before the differential spectrophotometric determination.^{8,11} The absorbance of the solutions was measured against a standard nitrate solution, usually 20 μ M, which contained the same buffer and salts as the samples and was reduced in the same column.

Method B—Two-step photo-oxidation. The irradiation was performed in two steps, first at pH 2.1 (0.50 mmole of sulphuric acid added) for 1 hr and then at pH 9 for 3 hr after addition of 0.30 ml of Perhydrol and a buffer solution containing 50 μ moles of borax and enough sodium hydroxide to neutralize the previously added sulphuric acid and the acids (H₂CO₃, etc.) formed during the irradiation. The analysis was continued as in Method A.

RESULTS AND DISCUSSION

Reduction-step errors

To obtain rapid photo-oxidation it is essential to use an adequate amount of hydrogen peroxide in order to produce a high concentration of oxygen. Irradiation accelerates the decomposition of the hydrogen peroxide; it was found that less than 0.01% remained after 1 hr. Notwithstanding the high temperature the solution may remain supersaturated with oxygen even after prolonged irradiation time and this large excess must be removed before the reduction in the cadmium column. Otherwise the reduction of

oxygen would lead to a deleterious production of cadmium ions, and cadmium hydroxide would precipitate and decrease the efficiency of the column (cf. Nydahl⁸). With use of 0.30 ml of Perhydrol and an irradiation time of 3 hr, interfering concentrations of oxygen were occasionally observed if the solutions were rapidly cooled after irradiation and immediately analysed for nitrate and nitrite, but if the solutions were left in the reactor until the next day no such problems arose. If necessary, an excess of oxygen can easily be removed by shaking and aeration. Contrary to other authors,^{2,4} it was found that reagent-grade hydrogen peroxide may contain significant concentrations of nitrogen compounds.

Without due attention to pH, chloride concentration and flow-rate, the errors introduced in the reduction step may be quite large (cf. Nydahl⁸), especially for copperized cadmium, which is commonly used on account of its high rate of reduction. Differences in composition (pH, concentration of chloride and nitrite) between the irradiated sample and the nitrate standard used for calibrating the reduction step may lead to errors, positive or negative depending on the differences and on the flow-rate used. The thoroughly investigated reduction method used in the present paper gave for both nitrate and nitrite a nitrite yield of $\geq 99.5\%$ at low salt content, and about 99% for synthetic ocean water. The error in the determination of nitrate + nitrite did not exceed 0.3% for 1–2 μ moles of nitrogen and any larger errors found can therefore be attributed to the photo-oxidation step.

One-step photo-oxidation

Effect of pH and buffer type. In our experiments, generally with boric acid–borax buffer, irradiation for 3 hr gave quantitative ($\geq 98\%$) yields from ammonia, glycine, EDTA, 8-hydroxyquinoline and *n*-butylamine within the pH-range 7–9, but the yield was reduced at lower pH. Other substances, e.g., urea and *p*-aminobenzoic acid, required lower pH for quantitative oxidation and therefore gave large negative errors at pH > 7. Nitrogen compounds containing nitrogen-to-nitrogen bonds gave extremely low yields—Methyl Orange only 35% (and hydrazine sulphate only 5% by Method B)—presumably on account of losses as free nitrogen. Natural waters, however, are not likely to contain significant concentrations of such compounds. The behaviour of urea is particularly interesting. Armstrong *et al.*,¹ who performed the irradiation of sea-water at pH 8, state that urea is only partly oxidized to give nitrate. Using a similar apparatus, Semenov *et al.*,⁶ found that urea was 80% oxidized at pH 4, whereas hardly any nitrate–nitrite mixture was formed at pH 9. The remarkable resistance of urea to photo-oxidation is also shown by Armstrong and Tibbitts,³ who report that urea required 24 hr for nearly complete oxidation, double the time necessary for other nitrogen compounds. We obtained quantitative oxidation

of urea at pH 4–6, but low and erratic yields at higher pH. The great influence of pH in the presence of halides is described later on.

It is usually recommended to buffer the solution with sodium bicarbonate. For some substances (urea, creatinine and guanidine) the yields were 15–45% lower with 50–100 μ moles of this buffer than with borax buffer of the same pH.

Effect of organic matter. Organic matter may interfere in various ways. Apart from a conceivable specific effect, it consumes oxygen, which may lower the oxidation rate, and carbon dioxide is formed which lowers the pH, the more so the more poorly the solution is buffered; at low pH carbon dioxide also lowers the oxidation rate, as shown by other experiments. It might be expected that addition of still more hydrogen peroxide would increase the oxidation rate, partly on account of the higher concentration of oxygen and partly by partial removal of carbon dioxide with the excess of oxygen escaping from the hot solution.

To test these predictions some experiments were performed with sucrose as model organic matter. The results are given in Fig. 1. Theoretically, 0.30 ml of Perhydrol should be sufficient for the complete oxidation of as much as 120 μ moles of sucrose. In spite of the large excess of oxygen there was a decrease in yield for the oxidation of glycine in the presence of even moderate amounts of sucrose (curve A). The effect of increasing the irradiation time to 5 hr (curve B) was slight, but if at the same time the amount of Perhydrol was doubled (curve C), the

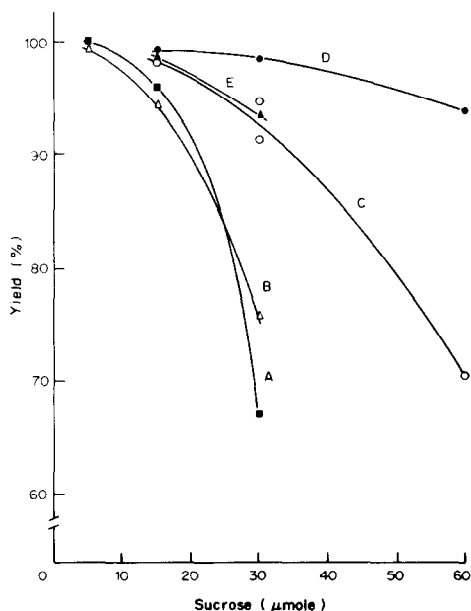


Fig. 1. Effect of sucrose on the photo-oxidation of 2 μ moles of glycine (10 μ moles of sucrose in 95 ml corresponds to a COD of 40 mg of oxygen per litre). Curves A and B: 0.30 ml of Perhydrol, 50 μ moles of borax; (A) 3 hr, (B) 5 hr irradiation. Curves C and D: 0.60 ml of Perhydrol, 5 hr irradiation; (C) 50 μ moles, (D) 150 μ moles of borax. Curve E: 0.30 ml of Perhydrol, 150 μ moles of borax, 3 hr irradiation.

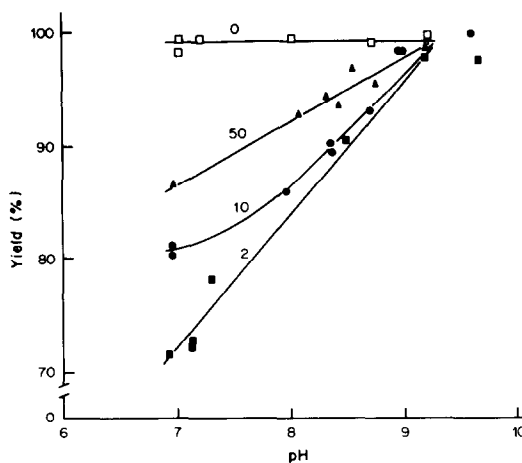


Fig. 2. Effect of salt concentration and pH on the photo-oxidation of 2 μ moles of ammonium chloride. DSW added: 0, 2, 10 and 50 ml.

values became considerably higher. Still more sucrose could be tolerated if the pH was kept higher during the irradiation by using 150 instead of 50 μ moles of borax (curve D). Unfortunately it is possible to use this large quantity of borax only in samples low in calcium and magnesium, e.g., most lake waters, because at higher levels their borates will precipitate. Further experiments showed that the interference from sucrose was similar for meat peptone and also for glycine in synthetic sea-water of 3.5% salinity.

Effect of bromide and chloride. In this study five test substances were chosen as representatives of different groups of nitrogen compounds in natural waters (meat peptone as a representative of the decomposition products of proteins). Different dilutions of DSW were used to obtain solutions of various salinities.

(i) **Ammonia.** As shown in Fig. 2, the yield was very dependent on pH in saline solutions. Pure solutions of ammonium chloride gave quantitative yields in the whole pH-range tested. In saline solutions the yield was about 98% at pH 9–9.5 at all three dilutions of DSW, but the yield decreased with decreasing pH, the more the lower the salinity. Obviously, there must be a salinity that will cause a minimum in yield in the lower pH-range. Figure 3B shows that such a minimum was obtained at a salinity of about 0.15% (2 ml of DSW added) when irradiation was performed at pH 7. In Fig. 3 a comparison is made between the yields found at pH 7 and 9 for sodium chloride solutions and synthetic sea-waters. At pH 9 the yield was fairly independent of the salt concentration but at pH 7 large negative errors were obtained, especially in the presence of DSW.

Experiments proved that these low yields were caused by losses of nitrogen, presumably as free nitrogen, and not by a decrease in the rate of photo-oxidation. The difference between the effects of sodium chloride and synthetic sea-water are fully explained by the bromide content of the latter. Figure

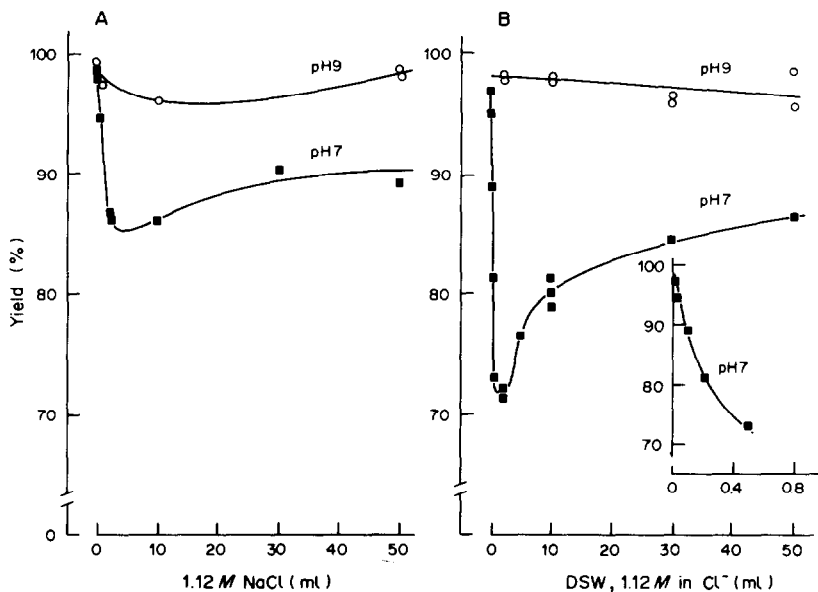


Fig. 3. Photo-oxidation of 2 μ moles of ammonium chloride at pH 7.0 and 9.0 in the presence of 0.02–50 ml of 1.12M NaCl (A) or DSW, 1.12M in Cl⁻ (B). The insert is an enlargement of the first part of curve B, pH 7.

4 shows the yields obtained when 2 μ moles of ammonium chloride were irradiated in solutions of chloride and bromide. Generally a certain concentration of bromide caused increased losses of ammonia-nitrogen as the chloride content decreased. The values agree well (within 2%) with the corresponding yields obtained in the presence of synthetic sea-water of the same halide content. Thus the other salts in synthetic sea-water have insignificant effect in this respect. At least part of the negative errors obtained without any addition of potassium bromide may be attributed to traces of bromide in the sodium chloride reagent used. It is well known that hypobromite may oxidize ammonia and amino groups to free nitrogen and it seems probable that a similar reaction may cause the losses found here. At the minimum shown in Fig. 3B, the concentrations of bromide and nitrogen are of the same order of magnitude. Hydrogen peroxide had no specific effect on the bromide-nitrogen reaction, as shown by irradiating saline solutions saturated with oxygen as a substitute for addition of hydrogen peroxide. This gave about the same losses at pH 7 as in the presence of hydrogen peroxide.

The necessity of maintaining sufficiently high pH during the irradiation of saline waters is less pronounced at lower concentration of ammonia, as demonstrated in Fig. 5 where the yields for 0.1–2 μ mole amounts of ammonia at pH 7.2 and 9.0 are shown.

(ii) *Glycine*. The influence of halides and nitrogen concentrations at different pH-values (7 and 9) on glycine was similar to that on ammonia, although the minimum in yield at pH 7 for a salinity of 0.15% was less pronounced (78% compared to 73% for ammonia).

(iii) *Meat peptone*. The photo-oxidation of meat peptone in synthetic sea-water was fairly independent of pH and of the concentration of peptone-nitrogen (Fig. 5).

(iv) *Urea*. In contrast to other substances investigated, urea gave much higher yields at pH 7 than at pH 9 in the presence of halides. At pH 7 the negative influence of halides was smaller, the lower the concentration of urea. As with meat peptone, there was a general decrease in yield with increasing salinity; no minimum was observed.

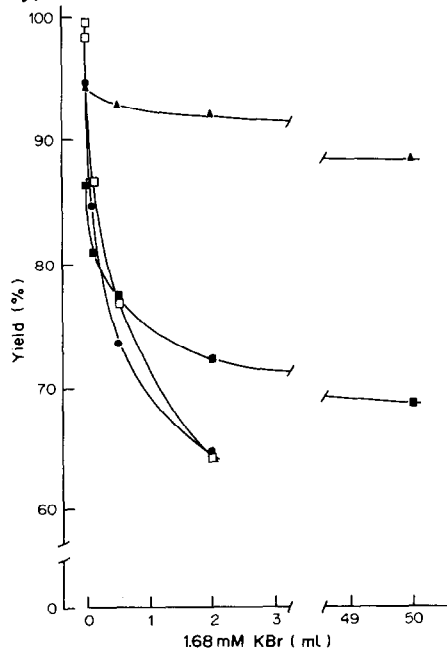


Fig. 4. Effect of chloride and bromide on the photo-oxidation of 2 μ moles of ammonium chloride at pH 7; 1.12M NaCl added: 0 (\square), 0.5 (\bullet), 2 (\blacksquare) and 50 (\blacktriangle) ml.

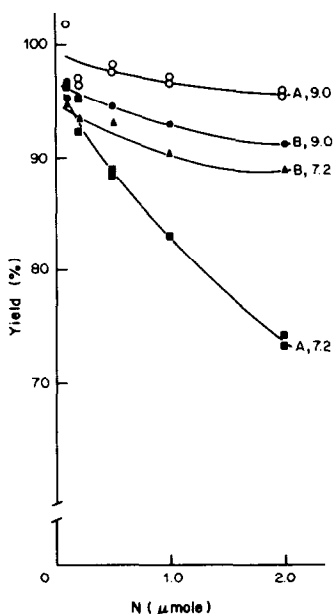


Fig. 5. The yield as function of the nitrogen concentration in the presence of 2 ml of DSW; 0.1–2 μ mole amounts of ammonia-nitrogen (A) or peptone-nitrogen (B) irradiated at pH 7.2 and 9.0.

(v) *Nitrate*. For nitrate, small losses of nitrogen, proportional to the irradiation time, were observed in spite of the high oxygen content. These losses (1% for irradiation for 4 hr) were independent of salinity.

Two-step photo-oxidation

Method A with irradiation for 3 hr at pH 9 gave low yields (85–88%) for some proteins (gelatine, milk, white of a hen's egg, pepsin). This is of special interest, as to a large extent organic nitrogen compounds in natural waters may be proteins or their decomposition products. Attempts to increase the yield by using longer irradiation times, more hydrogen peroxide or pH 7 instead of pH 9 were unsuccessful, nor did dilution of the samples (0.2 μ mole of N taken) significantly increase the yield.

Preliminary experiments. Preliminary experiments on gelatine showed that it was possible to increase the yield by performing the irradiation in two steps, first in acid medium and then at pH 9 for 3 hr after addition of hydrogen peroxide. When the first irradiation (for 1 hr) was performed in the presence of 0.01, 0.05, 0.1, 0.2 or 0.5 mmole of sulphuric acid, the final yields were 92.8, 94.6, 95.1, 94.5 and 97.2%, respectively. The positive effect of a decreasing pH in the first step was still more pronounced if the solution contained halides. At a salinity of 0.15% acidification with 0.05, 0.2 and 0.5 mmole of sulphuric acid gave final yields of 70.5, 85.0 and 90.8%. Other experiments showed that not much was gained by using still larger amounts of acid. For practical reasons 0.5 mmole of sulphuric acid was therefore found to be adequate. Addition of hydrogen peroxide before the

irradiation in acid medium decreased the yield if halides were present.

Reaction products found after irradiation at pH 2.1. Ammonia, glycine, *N*-acetylglycine, meat peptone and caffeine were irradiated for 1 or 3 hr at pH 2.1 (0.5 mmole of sulphuric acid added) in the absence or presence of hydrogen peroxide (29 experiments). After cooling, the solutions were analysed for ammonia by an indophenol blue method,¹² and for nitrate and nitrite. Only 0.3% of the nitrogen added was found as nitrite. Ammonia remained as such. Glycine-nitrogen was mostly converted into ammonia; only 2–5% was found as nitrate. When the amino group was protected by acetylation (*N*-acetylglycine) the yield of nitrate was increased to 27–33%. The sum of inorganic nitrogen was 98–100% for ammonia, glycine and *N*-acetylglycine, the higher values generally being obtained with the longer irradiation time. For the more complicated substances caffeine and meat peptone, the formation of ammonia and nitrate proceeded more slowly, their relative amounts varied, and the sum of inorganic nitrogen was only 84–95%.

These experiments show that nitrogen remaining after irradiation in acid medium is present as ammonium, nitrate and incompletely mineralized organic nitrogen. A second irradiation at high pH is therefore necessary (Method B).

Comparison between Method A and Method B

In Table 1 a comparison is made between methods A and B for some well-defined chemical compounds and for some proteins or their partial decomposition products in the absence of interfering substances. In all cases method B gave higher yields, the relative increase being especially large for caffeine (35%), uric acid (31%), urea (36%) and proteins (about 10%). Experiments proved that the lower yield obtained with method A could not be caused by the shorter total irradiation time.

As might be expected from our earlier results (one-step photo-oxidation) an initial irradiation in acid medium caused large losses of ammonia-nitrogen if halides were present (see Table 2). These losses could be prevented by the addition of 1 μ mole of sucrose and it seems probable that organic matter present in natural waters is also beneficial in this respect. For the other substances listed in Table 2 the yields were about the same with both methods (A and B) in the presence of halides.

Experiments not recorded here showed large interference from halides if hydrogen peroxide was added before the irradiation at pH 2.1.

In order to elucidate the applicability of photo-oxidation to natural waters, some samples, filtered through 0.45- μ m Millipore filters, were analysed by both photo-oxidation and a Kjeldahl method¹³ modified to give the sum of nitrate, nitrite, ammonia and organic nitrogen. The principal features of this method were: oxidation of nitrite to nitrate with bromate, added before the sulphuric acid, reduction

Table 1. Comparison between methods A and B in the absence of interfering substances: 2 μ moles of N taken; *s* indicates standard deviation, *n* number of determinations

Irradiated substance	Method A			Method B		
	Mean yield, %	<i>s</i>	<i>n</i>	Mean yield, %	<i>s</i>	<i>n</i>
Gelatine	85.2	2.9	7	97.2	0.4	2
White of hen's egg	87.8	0.8	3	94.5	0.7	4
Milk, 0.5% fat	87.8	1.5	3	95.1	0.7	4
Pepsin, Merck 1:3000	86.9	1.2	3	95.5	1.6	3
Meat peptone, Merck	93.6	0.7	2	97.1	0.7	2
Caffeine	70.0	1.6	2	94.2	1.6	3
Creatinine	90.6	3.9	2	94.6	2.0	2
2,2'-Bipyridyl	94.3	—	1	97.8	0.6	3
Hexamethylenetetramine	86.9	—	1	97.6	—	1
Uric acid	49.3	1.2	2	64.6	1.4	2
Urea	73	22	3	99.2	0.2	2
<i>p</i> -Aminobenzoic acid	90.5	2.2	2	97.3	0.1	2

of nitrate to ammonia with Cr(II)-Ti(III) in the absence of oxygen, evaporation and Kjeldahl digestion. As the method permitted large samples to be taken, the ammonia formed could be determined by acidimetric titration after distillation. The results are presented in Table 3, which also includes values for Cl^- , COD, NH_4^+ , NO_3^- and NO_2^- . For two of the samples (10 and 14) it was found that addition of 0.05 ml of Perhydrol before irradiation at pH 2.1 increased the yield considerably but, as expected from earlier experiments, such an addition led to rather large relative losses of nitrogen for the brackish samples. Compared to the values for total nitrogen obtained with the thoroughly tested Kjeldahl method used, photo-oxidation gave for the fresh water samples a mean yield of 89.7% with method A and 95.4% with method B modified by addition of 0.05 ml of Perhydrol before the irradiation at pH 2.1 (method B* in Table 3). As the fresh water samples are essentially

of the same kind it is possible to treat the results obtained for them statistically. Applying the *t*-test shows that the photo-oxidation methods gave significantly lower values (confidence level about 99%) than the modified Kjeldahl method. Besides, the difference between the means obtained by method B* and either of methods A and B is significant at the 95% confidence level. For the brackish samples, which were very low in ammonia and nitrate, the relative errors were larger with both photo-oxidation methods. If the effect on organic nitrogen is considered, the advantage of method B* for fresh waters is even more apparent. The mean relative change in yield of organic nitrogen by use of method B* instead of method A was +13% for the fresh water samples in Table 3. As it is possible to determine ammonia and nitrate + nitrite with fairly high accuracy, the error in organic nitrogen will mostly depend on the analysis for total nitrogen.

Table 2. Effect of salinity on methods A and B; 2 μ moles of N taken

Irradiated substance	DSW added, ml	Yield, %			
		Method A*		Method B Sucrose added	
				none	1 μ mole
Ammonium chloride	0	98.7	99.3	99.4	—
	2	98.2	97.9	71.3	96.5
	50	95.1	98.5	77.7	95.7
Glycine	0	100.5	—	99.3	—
	2	97.9	96.5	95.1	—
	50	95.4	97.4	95.7	95.9
Urea	0	93.1	55.5	99.2	99.1
	2	62.7	45.1	69.4	39.6
	50	49.8	51.1	—	—
Meat peptone	0	93.2	94.0	97.1	—
	2	92.1	91.5	91.6	90.3
	50	86.8	89.8	—	—
Gelatine	0	85.2	—	97.2	93.5
	2	88.1	—	90.8	91.1
	50	87.0	—	89.9	91.0
<i>p</i> -Aminobenzoic acid	0	90.5	—	97.3	—
	2	—	—	95.1	—
	50	—	—	—	—
Hexamethylenetetramine	0	86.9	—	97.6	—
	2	85.3	—	89.4	—

*No sucrose added, separate determinations.

Table 3. Comparison between photo-oxidation (sample volume 13–75 ml containing about 2 μ moles of N) and the modified Kjeldahl method for total nitrogen (sample volume 175–800 ml) applied to some natural waters; the yields obtained with the photo-oxidation methods are expressed as percentages of total nitrogen; the modified Kjeldahl method is reported¹³ to give a mean yield of 99.5% ($s = 0.6\%$, $n = 16$) when applied to synthetic waters containing glycine or meat peptone together with ammonium, nitrate and nitrite

Sample No.	Cl ⁻ , mM	COD, mmole O/l.	NH ₄ ⁺ , μ M	NO ₃ ⁻ , μ M	NO ₂ ⁻ , μ M	Total N, μ M	Yield, %		
							Method A	Method B	Method B*
10	< 0.5	1.8	2.7	13.8	0.2	53.7	85.5 89.2	87.3 88.5	94.6 93.9
11	< 0.5	2.3	12.2	51.9	0.6	109.6	91.8 93.7	94.2 96.0	94.8
12	< 0.5	2.0	0.5	1.0	0.4	36.9	83.7	—	93.5 93.2
13	< 0.5	2.0	3.1	103.5	1.4	152.8	94.2	—	97.8 96.3
14	< 0.5	1.7	4.9	11.8	≤ 0.2	47.1	87.5	89.2	96.6 96.0
15	< 0.5	2.2	1.4	60.9	0.6	109.9	91.9	—	97.7
16	84	—	0.3	0.5	≤ 0.1	21.6	78.2	79.6	66.7
17	96	—	0.2	0.4	≤ 0.1	16.5	83.6	81.2	73.9
Mean yield with confidence interval (95% level) for the fresh water samples 10–15							89.7 \pm 3.2	91.0 \pm 4.8	95.4 \pm 1.0

*As for method B but with addition of 0.05 ml of Perhydrol before irradiation at pH 2.1.

The water samples analysed in Table 3 were about 20 μ M in total nitrogen when irradiated. A greater dilution before irradiation would presumably have led to higher yields.

CONCLUSIONS

Experimental conditions such as intensity and spectral composition of the radiation, as well as pH and concentration of nitrogen and salts, especially halides, in the irradiation step have a large influence on the yields of the photo-oxidation. It is therefore difficult to compare results obtained by different authors, especially as the information given about the parameters used is often incomplete.

The low results obtained when solutions of proteins, urea and some other substances were irradiated according to method A led to the development of method B. In the absence of interfering concentrations of halides method B gave considerably higher yields for many of the substances investigated. A drawback of method B, however, is the difficulty in adjusting the pH before the final irradiation, as the form of the irradiation vessels prohibits the use of a glass electrode. Because only small amounts of borax can be used, the relatively large quantity of sulphuric acid requires that the amount of sodium hydroxide added should be adequate to increase the pH to the desired value, due regard being given to the extra acids (H₂CO₃, etc.) formed by oxidation. Other authors^{5,6} have also used irradiation in two steps, but at pH 4 and 9. For fresh waters it might be advantageous to do the first irradiation at pH 4 instead of 2.1, because the adjustment to pH 9 before the final irradiation would be less difficult. In our experience, however, the losses caused by even rather low concen-

trations of halides are far larger in solutions of lower acidity than pH 2.1.

Provided the concentration of halides is sufficiently low, a small addition of hydrogen peroxide before the first irradiation (at pH 2.1) is recommended. The gain in yield may be considerable, especially at high concentrations of organic nitrogen and/or organic matter.

If the concentration of nitrogen is high it is advisable to dilute the sample to $\leq 20 \mu$ M in N before irradiation, thus also reducing the concentrations of any interfering substances that may be present.

It is evident from the results of this investigation that the different variables interact in a rather complicated way. The method chosen must be a compromise, and dependent on the kind of water sample and also on the accuracy desired. To minimize interferences from halides and organic matter the final irradiation should be performed at fairly high pH, 8.0–8.5 for sea-waters and 8.7–9 for samples low in calcium and magnesium. Borax was chosen as buffer because the generally recommended bicarbonate buffer led to low results for some compounds. In practice, however, naturally occurring bicarbonates must be tolerated and may then, if in sufficient concentration, as in ocean water and hard waters, serve as the buffer; addition of borax is then preferably omitted, as involving a certain risk of formation of precipitates.

In the absence of interfering concentrations of halides the advantage of an initial irradiation at pH 2.1 according to method B is clearly shown. For saline solutions, however, the gain in yield by using method B instead of method A is usually slight and may not warrant the extra work involved. For practical reasons it may therefore be preferable to analyse brackish and sea-waters with method A.

On account of the low blank and the high sensitivity of the spectrophotometric finish, the photo-oxidation method is particularly suitable for samples (fresh as well as saline waters) of low nitrogen content.

From the results obtained it seems probable that the determination of total nitrogen in filtered fresh waters according to method B may have a negative error of 2–8%, the larger error being expected for samples relatively high in organic nitrogen. For saline samples the errors will probably be larger, at least at high ratio of organic nitrogen to inorganic nitrogen.

The photo-oxidation of particulate matter was not investigated.

Acknowledgements—The author wishes to express her thanks to Professors F. Nydahl and Å.Olin for valuable discussions and to Professor B. Nygård for the facilities put at her disposal.

REFERENCES

1. F. A. J. Armstrong, P. M. Williams and J. D. H. Strickland, *Nature*, 1966, **211**, 481.
2. J. D. H. Strickland and T. R. Parsons, *A Practical Handbook of Seawater Analysis*, 2nd Ed., Fisheries Research Board of Canada, Ottawa, 1972.
3. F. A. J. Armstrong and S. Tibbitts, *J. Mar. Biol. Assoc. U.K.*, 1968, **48**, 143.
4. A. Henriksen, *Analyst*, 1970, **95**, 601.
5. B. K. Afghan, P. D. Goulden and J. F. Ryan, *Paper presented at the Technicon International Congress*, New York, 1970.
6. A. D. Semenov, V. G. Soier, V. A. Bryzgalo and L. S. Kosmenko, *Zh. Analit. Khim.*, 1976, **31**, 2030.
7. B. A. Manny, M. C. Miller and R. Wetzel, *Limnol. Oceanogr.*, 1971, **16**, 71.
8. F. Nydahl, *Talanta*, 1976, **23**, 349.
9. *Idem*, *Water Res.*, 1978, **12**, 1123.
10. A.O.A.C., *Official Methods of Analysis*, 12th Ed., §2.049. Washington DC, 1975.
11. K. Bendschneider and R. J. Robertsson, *J. Mar. Res.*, 1952, **11**, 87.
12. Sveriges standardiseringskommission, *Svensk Standard, SIS 028134*, Utgåva 1, 1976.
13. F. Nydahl, *University of Uppsala, Institute of Chemistry, Central Analytical Laboratory, Rept. No. 1*, 1980.

CONTRIBUTIONS TO THE THEORY OF CATALYTIC TITRATIONS—I*

COMPLEXOMETRIC CATALYTIC TITRATIONS

FERENC F. GAÁL and BILJANA F. ABRAMOVIĆ

Institute of Chemistry, Faculty of Sciences, University of Novi Sad, V. Vlahovića 2, YU-21000 Novi Sad,
Yugoslavia

(Received 2 December 1983. Revised 5 March 1984. Accepted 15 May 1984)

Summary—Complexometric catalytic titrations with both volumetric and coulometric addition of the titrant have been simulated. By taking into consideration the equilibrium concentration of the catalyst during the titration, general mathematical equations have been set up. The influence of several factors on the shape of the simulated catalytic titration curve has been investigated and is discussed. The work also deals with the conditions under which the approximate mathematical expressions (equilibrium concentration of the catalyst being neglected) can be applied to simulate the catalytic titration curves with a satisfactory accuracy.

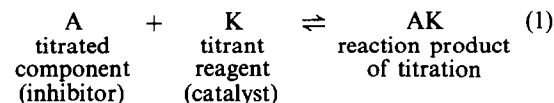
As with other analytical procedures, in the development of catalytic titrations the methodological and experimental foundations were laid before the corresponding theoretical relations were derived. From our own research in the field^{1,2} and the results of other authors,³⁻⁹ it seems that the experimental conditions have hitherto been chosen on the basis of extensive experimentation, which is a rather tedious job. However, by further development of the theory of catalytic titrations it should be possible, in a relatively easy way (with the aid of computers), to determine the optimal titration conditions. It should also be possible, on the basis of the reaction kinetics, to decide in advance whether a certain indicator reaction would be suitable for determination of particular analytes. After an experimental check, simulated catalytic titration curves might also be used for determination or revision of the indicator reaction kinetics, as well as for determination of all other quantities influencing the shape of the catalytic titration curves.

In catalytic titrations the titrant can be added either continuously or discontinuously, but in both cases the titration curve is obtained by plotting the change in some physical parameter (which is a function of an indicator-reaction rate, *i.e.*, the catalytic activity of a component of the solution to be titrated) against the amount of titrant added. Since methods with a continuous addition of the titrant are of greater importance, and experimentally much simpler, their mathematical interpretation has attracted more attention.

In 1970 Mottola¹⁰ gave the first mathematical treatment of catalytic titration curves, starting from some general expressions, but without particular

solutions for the titration curves. Goizman¹¹ in 1971 derived equations for the catalytic thermometric curves, but his work was restricted to volumetric addition of the titrating reagent, and the volume change of the solution during titration was neglected. Simpson¹² in 1973 was the first to simulate catalytic spectrophotometric titration curves by using a computer, introducing a new quality into these investigations, but he, also, neglected the solution volume changes during titration. Gaál¹ in 1977 formulated some general mathematical equations as a basis for interpretation of the shape of catalytic titration curves, obtained by means of different techniques, for both coulometric and volumetric addition of the titrating reagent.

However, all these authors have assumed that the catalyst concentration before the equivalence point can be neglected. This approximation is acceptable provided the reaction product formed in reaction (1)



is, for example, a sparingly soluble compound with a very low solubility product, or a complex with a very high stability constant. This is not always the case, however. For this reason we have formulated a mathematical description of catalytic titration curves, taking into account the equilibrium concentration of catalyst in the course of titration. In this article we derive the mathematical expressions for simulation of complexometric catalytic titration curves for both volumetric and coulometric addition of the titrant. We consider indicator reactions of first or pseudo-first and second order. Since the mathematical expressions obtained in this way are rather complex, we have also determined the conditions under which the equilibrium concentration of catalyst can be neglected.

*Dedicated to Professor. V. J. Vajgand, Faculty of Sciences, University of Belgrade, on the occasion of his 60th birthday.

THEORY

To simplify derivation of the mathematical expressions, we consider it advisable to introduce several approximations, namely

- (1) titrant is added to the ideally stirred solution;
- (2) temperature changes during titration do not affect the thermodynamics and kinetics of the reactions;
- (3) the indicator reaction has an incubation period short enough to be neglected;
- (4) the rate constant of the titration reaction is high, and need not be taken into account;
- (5) changes caused in the measured parameter by the titration reaction are negligibly small compared to the changes due to the indicator reaction.

The procedure for obtaining expressions for simulation of catalytic complexometric titrations consists of deriving an equation for the catalyst concentration during the titration. The expression obtained is then introduced into the one for the rate of the indicator reaction and, this expression is integrated for the limiting conditions.

In deriving the equation for the catalyst concentration in the course of titration, we start from the expression for the instability constant K_N of the catalyst-inhibitor complex (assumed to have 1:1 stoichiometry):

$$K_N = \frac{c(K)c'(A)}{c(AK)} \quad (2)$$

where $c(K)$ is the molar concentration of catalyst K, $c'(A)$ that of inhibitor A and $c(AK)$ that of the complex AK.

After introduction of the appropriate expressions for $c'(A)$ and $c(AK)$ into expression (2), a relation is obtained for the equilibrium concentration of the catalyst during the titration.

Simulation of volumetric complexometric catalytic titrations

If $c'(A)$ and $c(AK)$ during the titration are taken as

$$c'(A) = \frac{V_r c(A)}{V_r + jt} - c(AK) \quad (3)$$

and

$$c(AK) = \frac{jt c(T)}{V_r + jt} - c(K) \quad (4)$$

where $c(A)$ is the initial molar concentration of the inhibitor, $c(T)$ the concentration of the titrant, V_r the initial volume of the titrated solution (l.), j the rate of addition of titrant (l./sec), and t is time (sec), then introducing these expressions into equation (2) gives the following relation for the catalyst concentration during the titration:

$$c(K) = \frac{[c(T) - K_N]jt - E_k^{1/2} + (E_k + F_k t + G_k t^2)^{1/2}}{2(V_r + jt)} \quad (5)$$

where

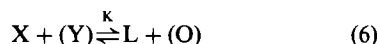
$$E_k = \{V_r[c(A) + K_N]\}^2;$$

$$F_k = 2V_r j \{K_N[c(A) + K_N] - c(T)[c(A) - K_N]\};$$

$$G_k = j^2[c(T) + K_N]^2$$

In order to obtain equations for the catalytic titration curves we start (similarly to other authors^{1,10-12}) from the corresponding expressions for the rates of the indicator reactions.

First-order indicator reaction. If the indicator reaction



proceeds according to first or pseudo-first order kinetics with respect to the indicator reaction component X, then its rate can be expressed as:

$$-\frac{dc(X)}{dt} = [k'_0 + k'_k c(K)]c(X) + \frac{c(X)j}{V_r + jt} \quad (7)$$

where k'_0 is the rate constant of the first-order spontaneous reaction (sec^{-1}), k'_k the rate constant of the first-order catalysed reaction ($\text{l.mole}^{-1}.\text{sec}^{-1}$) and $c(X)$ the molar concentration of the indicator reaction component. The last term in equation (7) describes the change in the rate of the indicator reaction due to the increase in volume of the reaction mixture during the titration.

With the catalyst concentration expressed by equation (5) and integration of equation (7) for the limiting conditions $c(X) = c_0(X)$ at $t = 0$, an expression is obtained for describing the concentration of component X at time t :

$$c(X) = c_0(X) \frac{V_r}{V_r + jt} \exp(-M_k) \quad (8)$$

where $c_0(X)$ is the initial molar concentration of the indicator reaction component, and

$$M_k = k'_0 t - \frac{k'_k V_r}{2j} [c(A) + c(T)] \ln \frac{V_r + jt}{V_r} + \frac{k'_k t}{2} [c(T) - K_N] + \frac{k'_k}{2j} R_k \quad (9)$$

in which

$$\begin{aligned} R_k = & [A_k + B_k(V_r + jt) + C_k(V_r + jt)^2]^{1/2} - (A_k + B_k V_r + C_k V_r^2)^{1/2} \\ & + \frac{B_k}{2C_k^{1/2}} \ln \frac{2C_k(V_r + jt) + B_k + 2\{C_k[A_k + B_k(V_r + jt) + C_k(V_r + jt)^2]\}^{1/2}}{2C_k V_r + B_k + 2\{C_k(A_k + B_k V_r + C_k V_r^2)\}^{1/2}} \\ & - A_k^{1/2} \ln \frac{V_r \{2\{A_k[A_k + B_k(V_r + jt) + C_k(V_r + jt)^2]\}^{1/2} + B_k(V_r + jt) + 2A_k\}}{(V_r + jt)\{2[A_k(A_k + B_k V_r + C_k V_r^2)]^{1/2} + B_k V_r + 2A_k\}} \end{aligned} \quad (10)$$

where

$$\begin{aligned} A_k &= \{V_r[c(A) + c(T)]\}^2; \\ B_k &= 2V_r\{K_N[c(A) - c(T)] - c(T)[c(A) + c(T)]\}; \\ C_k &= [c(T) + K_N]^2 \end{aligned}$$

Since the concentrations of the reaction products are often measured during the titration, it can be suitable to express the reaction rates as a function of these concentrations. If product L is formed from component X in equation (6), in 1:1 ratio, then the concentration of X remaining at time t will be:

$$c(X) = c_0(X) \frac{V_r}{V_r + jt} - c(L) \quad (11)$$

where $c(L)$ is the molar concentration of the indicator-reaction product.

On the basis of equations (8) and (11) it follows that the concentration of L at time t is:

$$c(L) = c_0(X) \frac{V_r}{V_r + jt} [1 - \exp(-M_k)] \quad (12)$$

Second-order indicator reaction. If the indicator reaction is second order, the reaction rate will be maximal when the initial concentrations of the reacting components, $c(X)$ and $c(Y)$, are equal. The rate of the indicator reaction can then be written in the form:

$$-\frac{dc(X)}{dt} = [k_0 + k_k c(K)]c(X)^2 + \frac{c(X)j}{V_r + jt} \quad (13)$$

where k_0 is the rate constant for the second-order spontaneous reaction ($l. \text{mole}^{-1} \cdot \text{sec}^{-1}$), and k_k the rate constant for the second-order catalytic reaction ($l^2 \cdot \text{mole}^{-2} \cdot \text{sec}^{-1}$).

After introduction of equation (5), describing the catalyst concentration, and integration of equation (13), the following expression is obtained for the concentration of component X at time t :

$$c(X) = \frac{c_0(X) V_r}{[1 + c_0(X)Q_k](V_r + jt)} \quad (14)$$

where

$$Q_k = \frac{k_0 V_r}{j} \ln \frac{V_r + jt}{V_r} + \frac{k_k V_r}{2j} [c(T) - K_N] \left(\ln \frac{V_r + jt}{V_r} - \frac{jt}{V_r + jt} \right) - \frac{k_k V_r^2}{2j} [c(A) + K_N] \left(\frac{1}{V_r} - \frac{1}{V_r + jt} \right) + \frac{k_k V_r}{2j} S_k \quad (15)$$

in which

$$\begin{aligned} S_k &= \frac{-[A_k + B_k(V_r + jt) + C_k(V_r + jt)^2]^{1/2}}{V_r + jt} + \frac{(A_k + B_k V_r + C_k V_r^2)^{1/2}}{V_r} \\ &+ C_k^{1/2} \ln \frac{2C_k(V_r + jt) + B_k + 2\{C_k[A_k + B_k(V_r + jt) + C_k(V_r + jt)^2]\}^{1/2}}{2C_k V_r + B_k + 2\{C_k(A_k + B_k V_r + C_k V_r^2)\}^{1/2}} \\ &- \frac{B_k}{2A_k^{1/2}} \ln \frac{V_r \{2\{A_k[A_k + B_k(V_r + jt) + C_k(V_r + jt)^2]\}^{1/2} + B_k(V_r + jt) + 2A_k\}}{(V_r + jt)\{2[A_k(A_k + B_k V_r + C_k V_r^2)]^{1/2} + B_k V_r + 2A_k\}} \end{aligned} \quad (16)$$

The concentration of product L is

$$c(L) = \frac{c_0^2(X)Q_k V_r}{[1 + c_0(X)Q_k](V_r + jt)} \quad (17)$$

Simulation of coulometric complexometric catalytic titrations

The concentrations of the inhibitor, $c'(A)$, and of complex, $c(AK)$, in coulometric addition of the titrant are:

$$c'(A) = c(A) - c(AK) \quad (18)$$

$$c(AK) = \frac{It}{nFV_r} - c(K) \quad (19)$$

where I is the generating current (A), F the Faraday constant (C/mole), n the number of electrons in the half-reaction for electrochemical generation of the titrant, and their introduction into expression (2) leads to an equation for the catalyst concentration:

$$c(K) = \frac{It - (E'_k)^{1/2} + [E'_k + F'_k t + (It)^2]^{1/2}}{2nFV_r} \quad (20)$$

where

$$E'_k = \{nFV_r[c(A) + K_N]\}^2;$$

$$F'_k = 2nFV_r I [K_N - c(A)]$$

First-order indicator reaction. In coulometric addition of the titrant the rate of an indicator reaction of first or pseudo-first order with respect to component X is given by

$$-\frac{dc(X)}{dt} = [k'_0 + k'_k c(K)]c(X) \quad (21)$$

Expression (21) differs from (7) by the absence of the term describing the volume changes during the titration.

After introduction of equation (20) into (21), and integration for the limiting conditions $c(X) = c_0(X)$ at $t = 0$, expression (22) is obtained for the concentration of component X at time t :

$$c(X) = c_0(X) \exp(-M'_k) \quad (22)$$

where

$$\begin{aligned} M'_k &= k'_0 t + \frac{k'_k I t^2}{4nFV_r} - \frac{k'_k [c(A) + K_N] t}{2} \\ &+ \frac{k'_k}{2nFV} R'_k \end{aligned} \quad (23)$$

in which

$$R'_k = \frac{(2I^2t + F'_k)[E'_k + F'_kt + (It)^2]^{1/2} - F'_k(E'_k)^{1/2}}{4I^2} + \frac{4E'_kI^2 - (F'_k)^2}{8I^3} \ln \times \frac{2I[E'_k + F'_kt + (It)^2]^{1/2} + 2I^2t + F'_k}{2I(E'_k)^{1/2} + F'_k} \quad (24)$$

From the relation

$$c(L) = c_0(X) - c(X) \quad (25)$$

and (22), an expression is obtained for the concentration of product L at time t :

$$c(L) = c_0(X)[1 - \exp(-M'_k)]. \quad (26)$$

Second-order indicator reaction. The expression for the rate constant of the second-order indicator reaction in coulometric addition of the titrant [$c(X) = c(Y)$] is

$$-\frac{dc(X)}{dt} = [k_0 + k_k c(K)]c(X)^2 \quad (27)$$

and combination of this with relation (20) for the catalyst concentration during the titration, gives, after integration of equation (27) for the limiting conditions $c(X) = c_0(X)$ $t = 0$, the following relations for the concentration of component X and product L:

$$c(X) = \frac{c_0(X)}{1 + c_0(X)Q'_k} \quad (28)$$

$$c(L) = \frac{c_0^2(X)Q'_k}{1 + c_0(X)Q'_k} \quad (29)$$

where Q'_k is analogous to M'_k in equation (23) but with constants k_0 and k_k instead of k'_0 and k'_k .

Calculations

As can be seen, the equations obtained for simulation of catalytic titration curves are rather complex, so to treat the data numerically it is necessary to use a computer. We have employed a Univac 1100 and a Varian 73, with FORTRAN IV as the programming language. Also, the expressions to be used for calculation of the concentration of the indicator-reaction product depend on the nature of the indicator reaction [equations (12) and (17), or (26) and (29)]. Moreover, we have planned to simulate precipitation, redox and neutralization catalytic titration curves in our further work. For this reason we wished to construct a program by means of which we could simulate all types of catalytic titration curves, regardless of the order of the indicator reaction and the type of titration reaction. We have achieved this in the following way: we have written a program which in fact contains two programs. The flow-diagrams of both are given in Figs. 1 and 2. As can be seen, the first program (Fig. 1) contains a great number of subroutines (one for each type of catalytic titration). Therefore we first introduce the "number of the

subroutine", IP, in order to supply the computer with the information on the type of catalytic titration and which subroutine, PP_i, is to be used in the calculations. We then introduce the data on the number of curves as well as all necessary data for calculation of the concentration of the indicator-reaction product at various stages of the titration. The results are then calculated with the derived expressions (by calling for the corresponding subroutine) and tabulated on a disc. We have constructed this program in such a way that besides putting the data on a disc, we can simultaneously list them with the corresponding headings, on the basis of which it is possible to recognize the particular catalytic titration. From such a list it is then possible to plot the catalytic titration curves. Since hand-plotting is time-consuming we have constructed a program to do it. This program (Fig. 2) is written in such a way that after introducing the data from the disc, the text for figure headings and the co-ordinates of the figures, besides listing the results, the computer prints the graph of the corresponding simulated catalytic titration curves together with the headings containing all the pertinent data: type of catalytic titration curve, order of the indicator

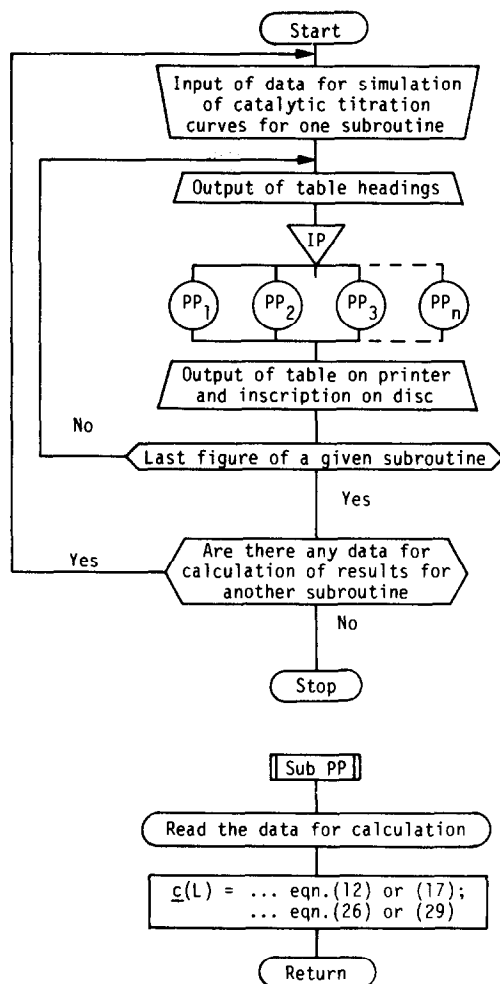


Fig. 1. Flow diagram for program.

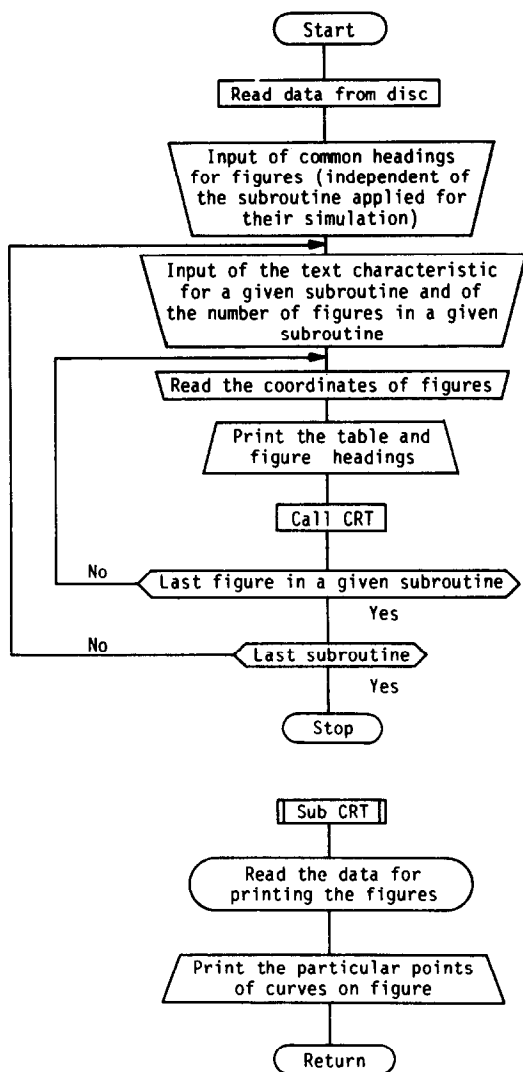


Fig. 2. Flow diagram for program.

reaction, concentrations of the titrant and titrand, concentration of the indicator-reaction component, initial volume of the solution, rate constants for both the spontaneous and the catalysed reaction, the equilibrium constant, rate of addition of the titrant in the volumetric method or the generating current in a coulometric determination, as well as the number of electrons in the equation for the electrochemical generation of the titrant (in the coulometric method). On each graph several catalytic titration curves are plotted, differing only in the value for the parameter being investigated. The listings of the programs are available on request.

RESULTS AND DISCUSSION

As pointed out in the introduction, by simulation of catalytic titration curves it is possible to choose, in a relatively simple way, the optimal experimental conditions. Therefore the effect of a number of

factors affecting the shape of simulated titration curves is discussed below.

Effect of the complex instability constant

One of the most interesting effects, which has not been considered in previous works (Fig. 3, curves 1-4), is certainly that of the value of the complex instability constant. As can be seen from Fig. 3, determination of the titration end-point is difficult when the complex instability constant is $>10^{-7}$ (curve 2) under the given working conditions. However, if the rate constant of the catalysed reaction is lower, it may be possible to determine the end-point even for values of the complex instability constant $>10^{-7}$.

It is also interesting to find the limiting value for the complex instability constant for which it is necessary to apply the derived expressions, *i.e.*, the lowest value of the constant, for which the catalyst ions are practically not present in the solution before the equivalence point. It is evident from Fig. 3 that with decrease in the complex instability constant, the differences between complexometric catalytic titration curves become smaller and smaller. Thus, for example, for values of 10^{-8} and 10^{-10} for the complex instability constant (curves 3 and 4) the difference in shape of the titration curves is very small. Furthermore, with further decrease of the constant, the differences between the simulated curves practically disappear. Hence, it can be concluded that for complex instability constants of about 10^{-8} or below, it is possible to use an approximative expression, neglecting the equilibrium concentration of the catalyst. The error will be relatively small, as will be shown later on.

Since the approximative equations are much simpler (see Appendix 1) we have examined and presented graphically a broad range of conditions for which it is possible to neglect the equilibrium concentration of the catalyst. The procedure was as follows: the curves obtained on the basis of the complete and the approximative expressions were compared, and the conditions determined for which the difference in shape of the titration curves, *i.e.*, in the concentrations of component X and product L, respectively, does not exceed a prescribed value. We have examined the conditions for which the approximation error is not higher than $0.03c_0(X)$ or $0.05c_0(L)$. Since these calculations were also relatively complex, we wrote suitable programs in FORTRAN IV and used a Univac 1100. Figures 4 and 5 present the diagrams for deciding in advance whether it is necessary to apply the complete expression or an approximative one for simulation of the volumetric complexometric catalytic titration with a first-order indicator reaction, so that the error does not exceed $0.03c_0(X)$ (Fig. 4) or $0.05c_0(L)$ (Fig. 5).

It is necessary to use the complete expression for all conditions on the left-hand side of each curve, but not for those on the right-hand side. Thus, for

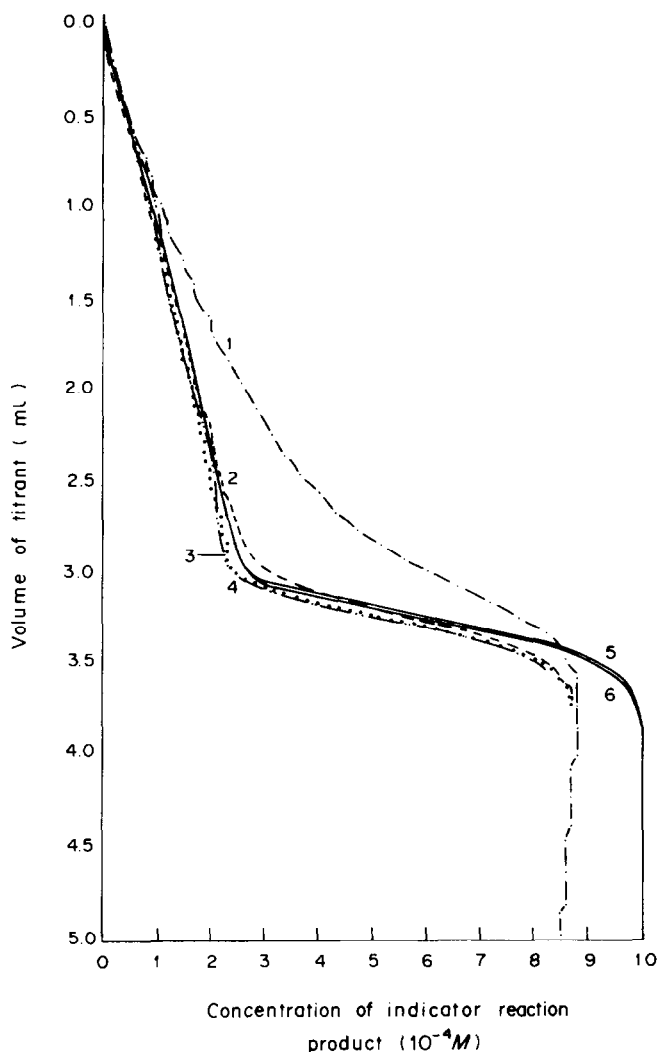


Fig. 3. Simulated curves for catalytic complexometric titrations obtained with volumetric addition of titrant and a first or pseudo-first order indicator reaction, under the following conditions: $V_r = 3 \times 10^{-2}$ l.; $c_0(X) = 10^{-3}M$; $k'_0 = 10^{-3} \text{ sec}^{-1}$; $k'_k = 10^3 \text{ l. mole}^{-1} \cdot \text{sec}^{-1}$; $c(T) = 5 \times 10^{-3}M$; $c(A) = 5 \times 10^{-4}M$; $j = 10^{-3} \text{ l./sec}$. Curves 1-4—equilibrium catalyst concentration taken into account [according to equation (12)]; 5—on the basis of the expressions obtained by Goizman¹¹ and Simpson;¹² 6—according to the expressions obtained by Gaál.¹ Values for K_N are: 1, 10^{-6} ; 2, 10^{-7} ; 3, 10^{-8} ; 4, 10^{-10} . Equivalence point 3.00 ml.

example, if K_N is 10^{-9} , $k'_0 = 10^{-4} \text{ sec}^{-1}$, $k'_k = 10^4 \text{ l. mole}^{-1} \cdot \text{sec}^{-1}$, $c(A) = 5 \times 10^{-4}M$ and $c(T) = 5 \times 10^{-3}M$, it is possible to use the approximative expression, for an approximation error $< 0.03c_0(X)$, because the point is on the right-hand side of the corresponding curve (Fig. 4, curve 2'). However, if we choose an error not exceeding $0.05c(L)$, then use of the approximative expression is not possible, because the point is on the left-hand side of the corresponding straight line (Fig. 5, curve 2').

Similar diagrams have been obtained for a second-order indicator reaction with the rate constants of both the spontaneous and the catalysed reaction 1000 times those for a first-order reaction. This will be discussed further, below.

Very similar diagrams have been obtained for the case of coulometric addition of the titrant, so the same diagrams can be applied (under the given working conditions) regardless of the mode of titrant addition.

Figure 3 also shows catalytic titration curves obtained on the basis of the approximative expressions derived by Goizman¹¹ and Simpson¹² (curve 5) and Gaál¹ (curve 6). As mentioned before, curves 1-4 differ from curves 5 and 6 by taking into account the concentration changes of the indicator-reaction product, due to dilution, and the equilibrium concentration of the catalyst during the titration. These two parameters have opposite effects, *i.e.*, the first causes a decrease and the second an increase in the concen-

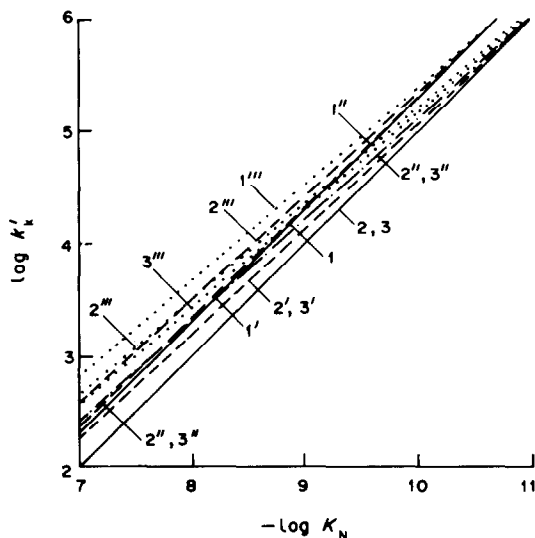


Fig. 4. Range of applicability of approximative equations for simulation of volumetric complexometric catalytic titrations with an approximation error not exceeding $0.03c_0(X)$ (first-order indicator reaction) under the following conditions: $V_t = 3 \times 10^{-2}$ l.; $c_0(X) = 10^{-3}M$; $j = 10^{-5}$ l./sec. 1–3, $c(A) = 5 \times 10^{-3}M$; $c(T) = 5 \times 10^{-2}M$; 1'–3', $c(A) = 5 \times 10^{-4}M$; $c(T) = 5 \times 10^{-3}M$; 1''–3'', $c(A) = 5 \times 10^{-5}M$; $c(T) = 5 \times 10^{-4}M$; 1'''–3''', $c(A) = 5 \times 10^{-6}M$; $c(T) = 5 \times 10^{-5}M$; 1, 1', 1'', 1''', $k_0' = 10^{-3} \text{ sec}^{-1}$; 2, 2', 2'', 2''', $k_0' = 10^{-4} \text{ sec}^{-1}$; 3, 3', 3'', 3''', $k_0' = 10^{-5} \text{ sec}^{-1}$.

tration of L, as could be expected. Which of the two effects will prevail depends on the value of the complex instability constant and the concentration of the titrant. If, for example, the instability constant is 10^{-7} or higher (for given other conditions), the effect of the equilibrium concentration of the catalyst is larger in the period before the equivalence point. Consequently, curves 1 and 2 are then above curves 5 and 6. On the other hand, if the complex instability constant is below 10^{-8} the effect of dilution of the solution has a greater influence, hence curves 3 and 4 lie below curves 5 and 6. However, after the equivalence point, when the indicator-reaction components have completely reacted, curves 1–4 have the same shape, *i.e.*, only the effect in volume increase of the reacting mixture is noticeable, so that all the curves, irrespective of the complex instability constant, are below curves 5 and 6. It is evident that when the concentration of the titrant is ten times that of the titrand it is necessary to take into account the concentration changes of the indicator-reaction product, due to dilution of the solution.

However, it should be mentioned again that under certain working conditions (for example, at a small value of the instability constant and at a high ratio of the concentration of titrant to that of titrand) satisfactory agreement is obtained between the experimental and simulated catalytic titration curves even when the expressions derived by Goizman,¹¹ Simpson¹² and Gaál¹ are used.

Effect of initial concentrations of the indicator reaction components

In the case of the first-order indicator reaction, the reaction rate, *i.e.*, the rate at which the measured parameter changes during the titration, is a linear function of the initial concentrations of the indicator-reaction components. This can be concluded on the basis of equations (12) and (26) and of the experimental results. A further conclusion is that increasing the initial concentrations of the indicator-reaction components or decreasing the sensitivity of the monitoring instrument (or *vice versa*) will have the same effect on the shape of the titration curve. Whether a higher or lower concentration is chosen in the experimental work depends on the measuring instrument (recorder) available. If we have a sensitive recorder we shall certainly choose a lower starting concentration of the indicator-reaction components. In the case of the second-order indicator reaction this effect is somewhat more complex. As can be concluded on the basis of equations (17) and (29), under given working conditions the dependence on this parameter can vary from linear to quadratic (limiting cases). If $c_0(X)Q_k < 1$ or $c_0(X)Q_k' < 1$, which happens either at a low $c_0(X)$ or $k_0, k_k, c(K)$, or t (all these last four quantities being included in Q_k and Q_k'), the dependence is practically quadratic. However, with increase in $c_0(X)Q_k$ or $c_0(X)Q_k'$ it becomes less and less quadratic with a tendency to linearity (which is achieved in the limiting case). Since Q_k (or Q_k') is also changing during the titration [the values for both t and $c(K)$ show an increase] the effect of changing $c_0(X)$ on the rate of the indicator reaction (*i.e.*, on the shape of the titration curve) is decreasing. The optimal starting concentration of the indicator-reaction components depends on several factors. If the value for k_0 is small, curves of a better shape will be obtained with higher starting concentrations of the indicator-reaction components, especially if the value for k_k is small. However, for a higher k_0 value, it will be more convenient to use a lower starting concentration of the indicator-reaction components, which is in agreement with the experimental results.

Effect of the mode of titrant addition

If complexometric catalytic titration curves obtained by volumetric and coulometric addition of the titrant are compared, it can be noticed that (under the working conditions as in Fig. 3) they are similar to each other in the period before the equivalence point. With decrease of the titrant concentration and the generating current, respectively, the differences in shape of the titration curves, and hence, the concentration changes for the indicator-reaction component in coulometric addition of the titrant, will become larger and larger. However, in the pretitration period a significant difference is noticeable even at a titrant concentration ten times that of the titrand. This is because there is no volume change during the

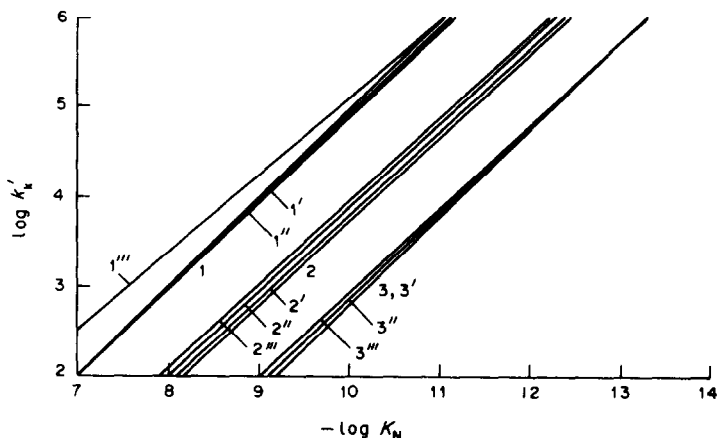


Fig. 5. Range of applicability of approximative equations for simulation of volumetric complexometric catalytic titrations with an approximation error not exceeding $0.05c(L)$ (first-order indicator reaction) under the following conditions: $V_t = 3 \times 10^{-2}$ l.; $c_0(X) = 10^{-3}M$; $j = 10^{-5}$ l./sec. 1-3 $c(A) = 5 \times 10^{-3}M$; $c(T) = 5 \times 10^{-2}M$; 1'-3' $c(A) = 5 \times 10^{-4}M$; $c(T) = 5 \times 10^{-3}M$; 1''-3'' $c(A) = 5 \times 10^{-5}M$; $c(T) = 5 \times 10^{-4}M$; 1'''-3''' $c(A) = 5 \times 10^{-6}M$; $c(T) = 5 \times 10^{-5}M$; 1, 1', 1'', 1''', $k'_0 = 10^{-3}$ sec $^{-1}$; 2, 2', 2'', 2''', $k'_0 = 10^{-4}$ sec $^{-1}$; 3, 3', 3'', 3''', $k'_0 = 10^{-5}$ sec $^{-1}$.

coulometric titration so that the concentration of product L at some moment becomes equal to the initial concentration of component X. After that, with further generation of the titrant, there is no change in the concentration of product L. However, in the volumetric addition method, owing to the dilution of the solution the concentration of product L cannot reach the value for the starting concentration of the indicator-reaction component X, so a maximum appears on the titration curve, after which the concentration of product L decreases with further addition of the titrant. For this reason, the total concentration change of product L is somewhat larger in the coulometric method and hence this mode is more suitable, especially in titration of smaller amounts of substances, and when higher generating currents are used. Since we are considering further development of coulometric complexometric catalytic titrations, the conclusions derived from this work may be of great help in choosing the proper experimental conditions.

Effect of the rate constant of the catalysed reaction

An increase in the rate of the catalysed reaction (Fig. 6) does not show a significant effect before the equivalence point (under the given working conditions), but has a very pronounced effect after the equivalence point. However, for higher values of the instability constant, the effect is more conspicuous in the period before the equivalence point. It can also be concluded that the titration end-point can be easily determined when k'_k is > 10 l. mole $^{-1}$. sec $^{-1}$ (curve 4), for given other conditions. If $c(T)$ or j is larger, it might also be possible to employ an indicator reaction with a somewhat lower value for k'_k . On the basis of Fig. 6, it can be concluded that the best way of determining the end-point is by direct graphical

extrapolation of the linear parts of the titration curve before and after the equivalence point, since the concentration of L changes gradually. However, the results obtained in this way would be slightly higher than the theoretical values, so it is necessary to correct them with the corresponding results from blank titrations. Simulation of these titrations will be described in a future article.

However, if the indicator reaction is second order, it is possible to determine the titration end-point in a satisfactory way if k_k is $> 10^4$ l 2 . mole $^{-2}$. sec $^{-1}$, under the same working conditions as in the case of the first-order indicator reaction. These differences in the effect of the k_k values on the shape of the catalytic titration curves can be easily understood by comparing expression (12) with (17), and (26) with (29), respectively.

Under such conditions, in the case of the second-order indicator reaction the dependence of $c(L)$ on $c_0(X)$ is practically quadratic. For this reason it is necessary to have a thousandfold higher Q_k in order to obtain a curve of the same shape as in the case of the first-order indicator reaction. This is best achieved by a thousandfold increase in k_k .

Effect of the rate constant of the spontaneous reaction

This effect is very significant, even in the period before the equivalence point (under the same working conditions, Fig. 6), which is quite understandable. Under the given experimental conditions, which are those most often used in practice, it is possible to determine satisfactorily the titration end-point if $k'_0 \leq 10^{-3}$ sec $^{-1}$ in the case of a first-order indicator reaction, and $k_0 < 1$ l. mole $^{-1}$. sec $^{-1}$ in the case of a second-order indicator reaction. These differences in the maximal values for k'_0 and k_0 can be explained in the same way as in the case of k_k .

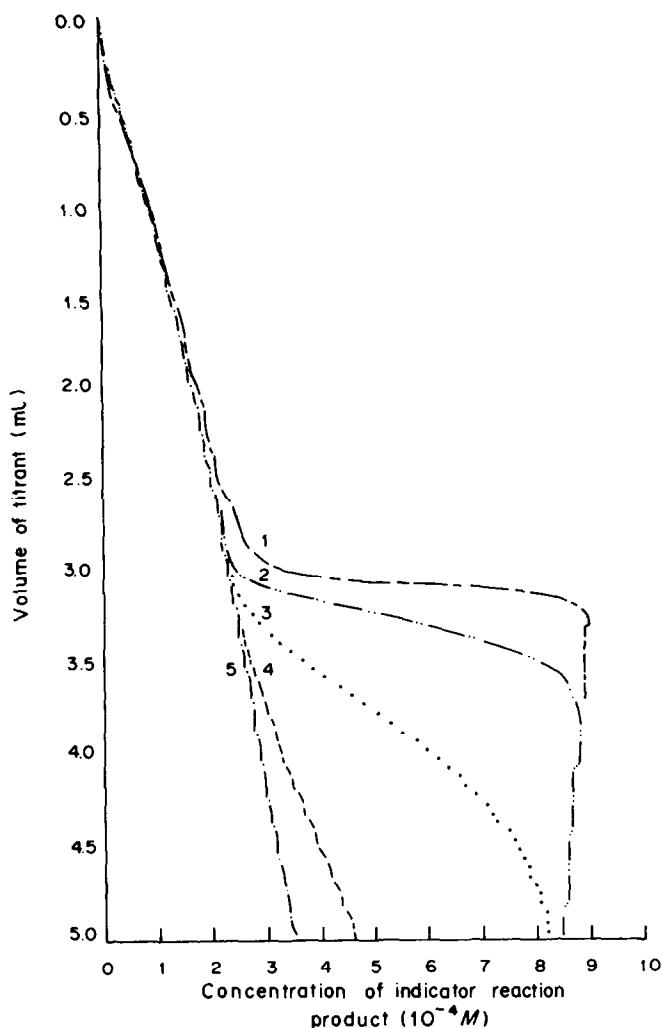


Fig. 6. Effect of rate constant for the first, or pseudo-first order catalysed reaction, k'_k , on the shape of the simulated volumetric complexometric catalytic titration curves obtained under the following conditions: $V_r = 3 \times 10^{-2}$ l.; $c_0(X) = 10^{-3}M$; $k'_0 = 10^{-3} \text{ sec}^{-1}$; $c(T) = 5 \times 10^{-3}M$; $c(A) = 5 \times 10^{-4}M$; $j = 10^{-5}$ l./sec; $K_N = 10^{-8}$. Values for k'_k (l. mole $^{-1}$. sec $^{-1}$) are: 1, 10^4 ; 2, 10^3 ; 3, 10^2 ; 4, 10; 5, 1. Equivalence point 3.00 ml.

Effect of concentrations of the titrant and titrand

It appears possible to determine the titration endpoint if the concentrations of the titrant and titrand are not lower than 5×10^{-4} and $5 \times 10^{-5}M$ respectively (under the same working conditions as in simulated curve 2, Fig. 6). If the rate constant for the catalysed reaction were higher, it would be possible to titrate even more dilute solutions and with a more dilute titrant, but the complex instability constant would have to be lower, in order to have a reaction proceeding quantitatively at the equivalence point.

Other effects

The following effects have been also investigated: rate of titrant addition, magnitude of the generating current, and the number of electrons involved in the electrochemical generation of the titrant. These pa-

rameters all had the expected effect on the shape of the simulated titration curves.

The conclusions reached in this work explain and confirm, to a great extent, our experimental results, as well as those of other investigators in the field. Also, the optimal experimental conditions have been predicted for realization of further experimental studies on the subject.

Acknowledgements—The authors are grateful to Prof. Dr. Ivan Gutman for his valuable suggestions. The authors thank the SIZ for Research of SAP Vojvodina for partial financial support of the work.

REFERENCES

1. F. F. Gaál, *Ph.D. Thesis*, University of Belgrade, 1977.
2. B. F. Abramović, *Ph.D. Thesis*, University of Novi Sad, 1982.
3. H. A. Mottola, *Talanta*, 1969, **16**, 1267.

4. H. Weisz, *Allgem. Prakt. Chem.*, 1971, **22**, 98.
5. H. Weisz and S. Pantel, *Z. Anal. Chem.*, 1973, **264**, 389.
6. T. P. Hadjiioannou, *Rev. Anal. Chem.*, 1976, **3**, 82.
7. R. L. Parry-Jones, *Educ. Chem.*, 1976, **13**, 76.
8. E. J. Greenhow, *Chem. Rev.*, 1977, **77**, 835.
9. Y. Rugu, *Chin. J. Pharm. Anal.*, 1981, **1**, 54.
10. H. A. Mottola, *Anal. Chem.*, 1970, **42**, 630.
11. M. S. Goizman, *Zavodsk. Lab.*, 1971, **10**, 1164.
12. B. E. Simpson, *M.Sc. Thesis*, Oklahoma State University, 1973.

APPENDIX

Approximative expressions for simulation of catalytic titrations

Mode	Order of indicator reaction	Period of titration	Concentration of catalyst	Concentration of the product of indicator reaction
Volumetric	First	$t \leq t_e$	$c(\text{K}) = 0$	$c(\text{L}) = c_0(\text{X}) \frac{V_r}{V_r + jt} [1 - \exp(-k'_0 t)]$
	First	$t \geq t_e$	$c(\text{K}) = \frac{j(t - t_e)c(\text{T})}{V_r + jt}$	$c(\text{L}) = c_0(\text{X}) \frac{V_r}{V_r + jt} \left\{ 1 - \exp \left[-k'_0 t - k'_k c(\text{T})(t - t_e) + k'_k c(\text{T}) \left(\frac{V_r}{j} + t_e \right) \ln \frac{V_r + jt}{V_r + jt_e} \right] \right\}$
	Second	$t \leq t_e$	$c(\text{K}) = 0$	$c(\text{L}) = \frac{c_0^2(\text{X}) Q^* V_r}{[1 + c_0(\text{X}) Q^*](V_r + jt)}$ where $Q^* = \frac{k_0 V_r}{j \ln \frac{V_r}{V_r - V_r}}$
	Second	$t \geq t_e$	$c(\text{K}) = \frac{j(t - t_e)c(\text{T})}{V_r + jt}$	$c(\text{L}) = c_0(\text{X}) \frac{V_r}{V_r + jt} - \frac{c_e(\text{X})(V_r + jt_e)}{[1 + c_e(\text{X}) Q''](V_r + jt)}$ where $c_e(\text{X}) = \frac{c_0(\text{X}) V_r}{[1 + c_0(\text{X}) Q^*](V_r + jt_e)}$ and $Q'' = \frac{k_0(V_r + jt_e)}{j} \ln \frac{V_r + jt}{V_r + jt_e} + \frac{k_k(V_r + jt_e)c(\text{T})}{j} \left(\ln \frac{V_r + jt}{V_r + jt_e} + \frac{V_r}{V_r + jt} - \frac{V_r}{V_r + jt_e} \right) + k_k c(\text{T})(V_r + jt_e) \left(\frac{1}{V_r + jt} - \frac{1}{V_r + jt_e} \right) t_e$
Coulometric	First	$t \leq t_e$	$c(\text{K}) = 0$	$c(\text{L}) = c_0(\text{X}) [1 - \exp(-k'_0 t)]$
	First	$t \geq t_e$	$c(\text{K}) = \frac{I(t - t_e)}{nFV_r}$	$c(\text{L}) = c_0(\text{X}) \left\{ 1 - \exp \left[-k'_0 t - \frac{k'_k I}{2nFV_r} (t - t_e)^2 \right] \right\}$
	Second	$t \leq t_e$	$c(\text{K}) = 0$	$c(\text{L}) = \frac{k_0 c_0^2(\text{X}) t}{1 + k_0 c_0(\text{X}) t}$
	Second	$t \geq t_e$	$c(\text{K}) = \frac{I(t - t_e)}{nFV_r}$	$c(\text{L}) = \frac{c_0^2(\text{X}) [2k_0 nFV_r + k_k I(t - t_e)^2]}{2[1 + k_0 c_0(\text{X}) t] nFV_r + k_k I c_0(\text{X}) (t - t_e)^2}$

 t_e = time at the equivalence point.

SPECTROPHOTOMETRIC DETERMINATION OF GERMANIUM IN ORES, CONCENTRATES, ZINC-PROCESSING PRODUCTS AND RELATED MATERIALS WITH PHENYLFLUORONE AND CETYLTRIMETHYLAMMONIUM BROMIDE AFTER SEPARATION BY IRON COLLECTION AND HEPTANE EXTRACTION OF GERMANIUM TETRACHLORIDE

ELSIE M. DONALDSON

Mineral Sciences Laboratories, Canada Centre for Mineral and Energy Technology, Department of Energy, Mines and Resources, Ottawa, Canada

(Received 13 March 1984. Accepted 14 May 1984)

Summary—A method for determining $\sim 0.2 \mu\text{g/g}$ or more of germanium in ores, concentrates, zinc-processing products and related materials is described. The sample is decomposed by fusion with sodium peroxide and the cooled melt is dissolved in dilute sulphuric acid. Silica, if $> 50 \text{ mg}$, is removed by volatilization with hydrofluoric acid. Germanium is separated from sodium salts by co-precipitation with hydrous ferric oxide, the precipitate is dissolved in $3M$ hydrochloric acid and germanium is subsequently separated from iron(III) and other co-precipitated elements by a single heptane extraction of germanium tetrachloride from $\sim 9.4M$ hydrochloric acid. The extract is washed with $12M$ hydrochloric acid to remove residual iron(III), then germanium is stripped with water and determined spectrophotometrically with phenylfluorone in a $1.4M$ hydrochloric acid- $0.002M$ cetyltrimethylammonium bromide medium in the presence of ascorbic acid as a reductant for co-extracted chlorine. The apparent molar absorptivity of the complex is $1.71 \times 10^4 \text{ l. mole}^{-1} \cdot \text{mm}^{-1}$ at 507 nm , the wavelength of maximum absorption. Up to 5 mg of tin(IV), 10 mg of antimony(V) and tungsten(VI) and $\sim 50 \text{ mg}$ of silica do not interfere. Germanium values are given for some Canadian certified reference ores, concentrates and iron-formation samples and for a metallurgical dust.

A current long-term CANMET project involves a study of the behaviour, form and distribution of silver in conventional hydrometallurgical processes or circuits designed to recover metallic zinc from zinc ores and concentrates. The objective of this project is to increase the recovery of silver in Canadian zinc plants. As part of this project, solvent extraction/atomic-absorption spectrophotometric (AAS) methods^{1,2} and a direct AAS³ method have been developed for the determination of small and moderate amounts of silver, respectively. In addition, an improved solvent extraction/flame atomic-emission method⁴ has been developed for the determination of indium, which is also a valuable by-product and which affects the behaviour of silver in the zinc circuit. Because the intermediate products from the processing of zinc ores are a primary source of germanium,⁵ which might also affect the recovery of silver, a reliable, simple and reasonably rapid method was required for the routine determination of microgram-quantities of germanium in these and related materials.

In the past, the two most widely used methods for the determination of small amounts of germanium were those based on its separation by distillation or

extraction of germanium tetrachloride from strongly acidic hydrochloric acid media, followed by spectrophotometric measurement of its complex with phenylfluorone or other chromogenic reagents.⁵⁻⁷ Currently, however, the extraction method has almost completely replaced the distillation method because of its greater selectivity, convenience, speed and simplicity and because the germanium can be more readily concentrated into a small volume.^{7,8} Furthermore, the distillation method yields low results in the presence of large amounts of sodium chloride and insoluble material such as lead sulphate and amorphous silica.^{5,6} In recent years the AAS determination of germanium by electrothermal atomization⁹ and by hydride-evolution techniques coupled with both flame¹⁰⁻¹³ and electrothermal finishes¹⁴ has been studied and direct methods have been reported for coal¹⁴ and coal ash.¹¹ However, these methods are strongly subject to interference from matrix elements^{10-12,14} and, although the finishes used are relatively sensitive, they are more complicated and time-consuming than a simple spectrophotometric phenylfluorone finish. Several investigators have found that with these finishes the accurate determination of trace amounts of germanium necessitates its preliminary separation from matrix elements by extraction as the chloride.^{9,12} The

literature shows that most of the published methods for the determination of germanium in ores, concentrates and related materials appear in obscure Soviet and other journals not readily accessible to Western readers. Recently, however, methods published up to ~mid-1971 were reviewed by Nazarenko.^{15a} Most of these and the later methods¹⁶⁻²⁰ involve spectrophotometric finishes, usually with phenylfluorone and generally after the separation of germanium by a double or triple extraction of the tetrachloride into carbon tetrachloride. Some also involve a preliminary collection step with iron to separate germanium from large amounts of zinc or from sodium salts resulting from decomposition of the sample by fusion with an alkaline flux. In most of these methods, gum arabic, gelatin and poly(vinyl alcohol)^{15b} are used as dispersing agents to stabilize the suspension of the germanium-phenylfluorone complex. However, Shijo and Takeuchi²¹ found that cetyltrimethylammonium bromide (CTAB) acts as a surface-active agent and greatly increases the sensitivity and rate of the reaction between germanium and phenylfluorone. Since the publication of their work, other quaternary ammonium salts and analogous compounds have been found to react in a similar manner.²²⁻²⁴ Because of the simplicity and speed of the spectrophotometric phenylfluorone finish and the high sensitivity obtained in the presence of these surfactants, it was considered that this type of finish would be advantageous for the routine determination of small amounts of germanium in diverse ores, concentrates, zinc-processing products and related materials after suitable separation of germanium from the matrix elements.

The proposed method, which is a modification of other published methods,^{15a} involves the separation of germanium from sodium salts, introduced during fusion of the sample, by co-precipitation with hydrous ferric oxide from an ammoniacal medium, followed by its separation from iron and other co-precipitated matrix elements by a single heptane extraction of germanium tetrachloride from ~9.4*M* hydrochloric acid. The germanium is stripped from the extract with water and determined spectrophotometrically with phenylfluorone in ~1.4*M* hydrochloric acid in the presence of CTAB. Some potential sources of error in existing methods are described and germanium values are given for some Canadian certified reference materials.

EXPERIMENTAL

Reagents

Standard germanium solution, 100 $\mu\text{g}/\text{ml}$. Dissolve 0.1441 g of pure germanium dioxide by heating gently with 20 ml of 2% sodium hydroxide solution (Note 1). Transfer the solution to a 1-litre standard flask and dilute to volume with water. Prepare a 10- $\mu\text{g}/\text{ml}$ solution by diluting 10 ml of this stock solution to 100 ml with water. Prepare this diluted solution fresh as required.

Phenylfluorone, 0.001*M* solution. Transfer 0.160 g of 2,6,7-trihydroxy-9-phenylisoxanthene-3-one (9-phenyl-2,3,7-

trihydroxy-6-fluorone) to a 400-ml beaker containing a Teflon-coated magnetic stirring bar. Add ~200 ml of ethanol and 2 ml of concentrated hydrochloric acid, stir on a magnetic stirrer until the reagent has dissolved, then transfer the solution to a 500-ml standard flask and dilute to volume with ethanol. This solution is stable for at least one month.

CTAB, 0.9% solution. Add ~300 ml of water to 4.5 g of CTAB, mix thoroughly and place the beaker in a pan of warm water (Note 2). When the salt has dissolved, dilute the solution to 500 ml with water. Prepare a fresh solution every 4 weeks.

Iron(III) sulphate solution, 10 mg of iron/ml. Dissolve 25 g of ferric sulphate nonahydrate in ~300 ml of hot water containing 5 ml of concentrated sulphuric acid, cool and dilute to 500 ml with water.

Ascorbic acid, 10% solution. Prepare a fresh solution every 2 days.

Sulphuric acid, 50% v/v.

Hydrochloric acid, 25% v/v. Store in a plastic squeeze-type wash bottle.

Ammonia, 5% v/v solution. Store in a wash-bottle.

Heptane. Analytical reagent-grade.

Calibration curves

Transfer a 20-ml aliquot of 10- $\mu\text{g}/\text{ml}$ standard germanium solution to a 250-ml separatory funnel and add 15 ml of water, 150 ml of cold (~0°) (Note 3) concentrated hydrochloric acid and 75 ml of heptane. Stopper the funnel and shake it for 2 min. Allow the layers to separate, then drain off and discard the lower (aqueous) layer. Wash the heptane phase by shaking it gently for ~30 sec with 5 ml of cold concentrated hydrochloric acid. Drain off and discard the acid layer and wash the stem of the funnel with water. Add 10 ml of water to the extract, stopper the funnel and shake it for 1 min. Allow the layers to separate, then drain the lower (aqueous) layer into a 200-ml standard flask with the aid of a small funnel placed in the neck of the flask. Wash the stem of the separatory funnel with water and collect the washings in the flask. Repeat the stripping step twice more by shaking the extract for ~30 sec each time with 10-ml portions of water. Wash the stem of the separatory funnel with water each time. Dilute the solution to volume with water and mix thoroughly.

From a burette, add 1, 2, 3, 4, 5 and 6 ml of the resulting 1- $\mu\text{g}/\text{ml}$ germanium solution to six 25-ml standard flasks and dilute each solution to ~10 ml with water. Add 10 ml of water to a seventh flask, to prepare the blank. To each flask, add in succession 2 ml of 10% ascorbic acid solution, 3 ml of concentrated hydrochloric acid and 2 ml of 0.9% CTAB solution, mixing thoroughly after each addition, then add 2 ml of 0.001*M* phenylfluorone solution, dilute to volume with water and mix. Add 5, 10, 15, 20 and 25 ml of the 1- $\mu\text{g}/\text{ml}$ germanium solution to five 100-ml standard flasks and dilute each solution to ~50 ml with water. Add 2 ml of 10% ascorbic acid solution to each flask, then proceed with the complex formation as described above, but with four times the volumes of concentrated hydrochloric acid and CTAB and phenylfluorone solutions (Note 4). Allow the resulting solutions to stand for ~5 min to complete the complex formation, then measure the absorbance, at 507 nm, of the blank and each of the six solutions in the first series against water as the reference solution, using 10-mm cells. Measure the absorbance of each of the five solutions in the second series in a similar manner. Correct the absorbance value obtained for each germanium-phenylfluorone solution by subtracting that obtained for the blank. Plot μg of germanium *vs.* absorbance for each series of measurements.

Analysis of ores, concentrates, zinc processing products and related materials

Silica ≤ 50 mg. Depending on the expected germanium content, transfer up to 0.5 g of powdered sample, containing

not more than 200 μg of germanium and up to ~ 150 mg of iron (Note 5), to a 50-ml zirconium crucible. Add 4 g of sodium peroxide, mix thoroughly (Note 6) and cautiously fuse the mixture over a low-temperature flame (Note 7) and keep it molten for ~ 30 sec to ensure complete decomposition (Note 8). Allow the melt to cool for several min, then transfer the crucible to a covered 400-ml beaker containing ~ 80 ml of water and 20 ml of 50% sulphuric acid. When the melt has dissolved, remove the crucible after washing it thoroughly with water, then cover the beaker (Note 9), boil the solution vigorously and allow it to evaporate to ~ 100 ml to ensure the complete destruction of hydrogen peroxide. Cool to room temperature, then add 5 ml of concentrated hydrochloric acid and, if necessary, add sufficient iron(III) sulphate solution for at least 100 mg of iron to be present.

Add sufficient concentrated ammonia solution to precipitate iron as the hydrous oxide, then add 5 ml in excess and boil the solution for ~ 1 min to coagulate the precipitate. Allow it to settle, then filter (Whatman No. 541 paper) and wash the beaker twice with 5% ammonia solution. Wash the paper and precipitate twice with the ammonia solution, followed by water, then discard the filtrate and washings. Place the funnel containing the precipitate in the neck of a 250-ml separatory funnel marked at 50 ml. Wash down the sides of the precipitation beaker with ~ 10 ml of cold (Note 3) 25% hydrochloric acid added from a plastic squeeze-type wash-bottle and add the solution to the funnel containing the precipitate. Carefully, to avoid tearing the paper, break up the gelatinous precipitate with a glass rod to aid dissolution. Wash the beaker twice more with ~ 5 -ml portions of cold 25% hydrochloric acid, then wash the paper at least three times with small portions of the acid solution to dissolve any remaining precipitate. Discard the paper and, if necessary, dilute the solution to the mark with cold 25% hydrochloric acid. Add 135 ml of cold concentrated hydrochloric acid (Note 3) and 75 ml of heptane, stopper the funnel, then proceed with the extraction of germanium as described for the calibration. Wash the heptane phase with 5 ml of cold concentrated hydrochloric acid as described above, then drain off and discard the acid phase.

If the sample contains ~ 5 μg or less of germanium, add 5 ml of water to the extract, stopper the funnel and shake it for ~ 1 min. Allow the layers to separate, then carefully, without washing the stem of the funnel after the draining step, collect the aqueous phase in a 25-ml standard flask with the aid of a small funnel placed in the neck of the flask (Note 10). Wash the extract twice by shaking it for ~ 30 sec with 3 ml and then with 1 ml of water and add the washings to the flask (Note 11). Remove the small funnel from the flask and proceed with the addition of ascorbic acid solution and the subsequent determination of germanium as described above.

If the sample contains between 5 and 25 μg of germanium, shake the extract with three 10-ml portions of water as described for the calibration. Collect the solutions in a 100-ml standard flask, dilute to ~ 50 ml with water and proceed with the determination of germanium as described above.

If the sample contains more than 25 μg of germanium, strip the extract with three 10-ml portions of water as described above and dilute the resulting solution to volume with water in a 100-ml standard flask. Transfer a suitable aliquot (up to 50 ml) of the solution to a 100-ml standard flask, dilute to ~ 50 ml with water, if necessary, and proceed with the determination of germanium as described above.

Silica > 50 mg. Decompose a suitable weight of sample as described above and dissolve the melt as described, using a covered 400-ml Teflon beaker. Evaporate the solution to ~ 100 ml, then remove the cover, add 10 ml of concentrated hydrofluoric acid and evaporate the solution until copious fumes of sulphur trioxide are evolved. Cool, wash down the sides of the beaker with water and evaporate the solution to

fumes of sulphur trioxide again to ensure the complete removal of hydrofluoric acid. Cool, add ~ 100 ml of water and heat to dissolve the salts. Cool the solution, add 5 ml of concentrated hydrochloric acid and, if necessary, add sufficient iron(III) sulphate solution for at least 100 mg of iron to be present, then proceed with the co-precipitation, extraction and determination of germanium as described above.

Notes

1. If the germanium dioxide does not dissolve completely, the standard solution can be prepared by fusing the compound with ~ 4 g of sodium carbonate in a covered platinum crucible, with a high-temperature blast burner. The cooled melt should be dissolved in water and the resulting solution should be diluted as described.

2. The beaker should not be placed in hot water or on a hot-plate because a gelatinous substance, not readily soluble, forms under these conditions. If crystals form in the solution on standing they can be readily redissolved by placing the container in a pan of warm water.

3. The concentrated hydrochloric acid used for extraction and the 25% solution employed for the dissolution of the hydrous ferric oxide precipitate are most conveniently kept in a freezer. The extraction should be done without too much delay because germanium may be lost by volatilization as the chloride if the solution is allowed to warm to room temperature.^{7,13a}

4. A second blank can be prepared in a similar manner or the first can be used for correction purposes. In this work the absorbance of the blank for the same batch of phenylfluorone varied from ~ 0.14 to 0.16.

5. More than ~ 0.5 g of sample is not recommended, because the amount of iron(III) used in the co-precipitation step may not be sufficient for the complete co-precipitation of germanium if the total concentration of other co-precipitated elements is too great. Samples containing more than 150 mg of iron can be taken but the filtration and/or dissolution steps may become unduly slow because of the bulk of the precipitate.

6. It is not necessary to run a reagent blank.

7. A bunsen burner, not a high-temperature blast burner, should be used. Too hot a flame causes the molten sodium peroxide to attack the crucible and results in the presence of too much zirconium in the final solution. This can cause difficulty in the co-precipitation step.

8. Ores containing very little sulphide minerals may be decomposed more readily by fusion with ~ 4 g of sodium carbonate as described in Note 1. The cooled melt should subsequently be dissolved in dilute sulphuric acid as described.

9. The solution should be kept almost completely covered during the initial evaporation, to avoid loss by spray.

10. Care should be taken that no heptane accompanies the aqueous phase, or the final solution obtained after the addition of phenylfluorone solution may be cloudy.

11. The heptane can be used continually for subsequent extractions if the stripped extracts are combined in a large separatory funnel and washed once by shaking with ~ 100 ml of water.

RESULTS AND DISCUSSION

Spectrophotometric determination of germanium with phenylfluorone

Recent work has shown that various quaternary ammonium salts and compounds [benzalkonium chloride,²² dodecyltrimethylammonium bromide (DTAB)²³ and sodium lauryl sulphate²⁴] other than CTAB, which is a commonly used surfactant, also sensitize and hasten the formation of the neutral 1:2

complex formed between $\text{Ge}(\text{OH})_2^{2+}$ and phenylfluorone.^{15c} However, none of these reagents appears to offer any particular advantages over CTAB. Consequently, CTAB was used in this work. Initial tests with 1M hydrochloric acid media showed that, for up to $\sim 0.25 \mu\text{g}$ of germanium per ml, the optimum concentration of CTAB required for rapid complex formation is $\geq 0.0016M$. The optimum range of hydrochloric acid concentration is $\sim 1\text{--}1.8M$. Therefore, CTAB and hydrochloric acid concentrations of 0.002 and 1.4M, respectively, were chosen for subsequent work. Under these conditions, the optimum concentrations of phenylfluorone and ethanol, which is required to keep the reagent in solution, are $\sim 8 \times 10^{-5}M$ and $\sim 8\%$ v/v, respectively. Except for the phenylfluorone concentration, these conditions are in good agreement with those reported by Shijo and Takeuchi.²¹ More than $\sim 12\%$ v/v ethanol inhibits the reaction. Higher concentrations of phenylfluorone are not recommended because of the magnitude of the reagent blank; at lower concentrations the reaction is incomplete. Beer's law is obeyed for up to $\sim 0.25 \mu\text{g}$ of germanium per ml. Complex formation is complete in 2 or 3 min and the absorbance of the complex remains constant for at least 4 hr.

Except for the greater intensity of the main spectral band for a given amount of germanium, the spectrum of the complex formed in the presence of CTAB is essentially the same as the spectra obtained in the presence of poly(vinyl alcohol) and other dispersing agents.²¹ The apparent molar absorptivity of the complex is $1.71 \times 10^4 \text{ l. mole}^{-1} \cdot \text{mm}^{-1}$ at 507 nm, the wavelength of maximum absorption. This is in excellent agreement with the value reported by Shijo and Takeuchi,²¹ viz. $1.71 \times 10^4 \text{ l. mole}^{-1} \cdot \text{mm}^{-1}$ at 505 nm, and with that reported recently by Kurihara and Kuwabara²³ for the complex formed in the presence of a similar compound, DTAB, viz. $1.72 \times 10^4 \text{ l. mole}^{-1} \cdot \text{mm}^{-1}$ at 503 nm. However, neither the results obtained in this work nor those obtained by the investigators above agree with those reported for CTAB by Burns and Dadgar.²⁴ These investigators found that in the presence of CTAB ~ 2 hr were required for complex formation and that the wavelength of maximum absorption shifted from 504 to 528 nm. Because the use of surfactants or other dispersing agents does not cause a significant shift in the absorption maximum of the germanium-phenylfluorone complex,^{15b} this suggests that either the reagent used by these workers was not CTAB or that its composition had altered in some manner. Burns and Dadgar recommend the use of sodium lauryl sulphate as a dispersing agent. However, the apparent molar absorptivity value they obtained in the presence of this compound ($1.18 \times 10^4 \text{ l. mole}^{-1} \cdot \text{mm}^{-1}$) shows that it is not nearly as effective a solubilizing agent as CTAB, DTAB or benzalkonium chloride (which gives a molar absorptivity of $1.81 \times 10^4 \text{ l. mole}^{-1} \cdot \text{mm}^{-1}$).

Separation of germanium by co-precipitation with hydrous ferric oxide

Acid attack involving the use of hydrofluoric and sulphuric acids or hydrofluoric and phosphoric acids, in the absence or presence of nitric acid, has been recommended for the decomposition of ores and related materials containing germanium before its separation by extraction as the tetrachloride and ultimate determination with phenylfluorone or other chromogenic reagents. However, under these conditions, if the sample contains an appreciable amount of chloride some germanium be lost by volatilization as the tetrachloride. In addition if the decomposition is incomplete, some germanium may remain in the insoluble residue.^{7,15a} Furthermore, as mentioned later, phosphoric acid inhibits the extraction of germanium, and evaporation with sulphuric acid can produce low results. Because fusion with an alkaline flux, which usually results in complete decomposition of the sample, causes no loss of germanium as the tetrachloride,^{7,15a} fusion with sodium peroxide was chosen for this work. However, because the large amount of sodium chloride formed when the hydrochloric acid concentration of the solution is adjusted to $\geq 9M$ before the extraction step interferes mechanically with the extraction of germanium,^{15a,17,25} it is necessary to make a preliminary separation of germanium from the sodium salts by co-precipitation with hydrous ferric oxide from ammoniacal medium (pH $\sim 7\text{--}10$) as recommended by many previous investigators.^{6,15a,15d} However, in initial tests involving $5\text{--}50 \mu\text{g}$ of germanium and 50 mg of iron(III) (as sulphate), low results ($\sim 85\text{--}90\%$ recovery) were obtained when the precipitates were dissolved in cold (0°) $\geq 9M$ hydrochloric acid before the extraction step, as recommended by some previous workers.^{15a,18,26-28} Some of these investigators also obtained low results under these conditions.^{18,26,28} Ultimately, tests in which germanium was completely recovered when the precipitate was dissolved in 10% hydrochloric acid, followed by the direct determination of germanium in the resulting solution, showed that the loss when $\geq 9M$ hydrochloric acid was used occurred in the dissolution step. Presumably, the local heat generated during the dissolution of the precipitate, even in very cold $9\text{--}12M$ hydrochloric acid, results in some loss of germanium by volatilization as the tetrachloride. Tests showed that there is no advantage in using a hydrobromic acid system for the extraction. Although germanium tetrabromide is considered to be less volatile than the tetrachloride because of its higher boiling point, low results ($\sim 85\text{--}95\%$ recovery), which were not due to incomplete extraction, were also obtained when the hydrous oxide precipitate was dissolved in concentrated hydrobromic acid before the extraction step. Further work showed that no loss by volatilization occurs if the precipitate is dissolved in $\sim 3M$ hydrochloric acid, followed by the adjustment of the hydrochloric

acid concentration of the resulting solution to $\sim 9.4M$ with cold concentrated hydrochloric acid just before the extraction step.

Previous investigators²⁹ showed that for the quantitative co-precipitation of germanium with the hydrous oxides of trivalent metallic elements, which results in the formation of the corresponding germanates, the metal ion to germanium ratio should be greater the lower the concentration of germanium. For the co-precipitation of $\sim 0.01 \mu\text{g}$ of germanium per ml with hydrous ferric oxide, this ratio should not be less than $\sim 1000:1$.^{15d} Although, as determined experimentally with pure germanium solutions, the amount of iron(III) (50 mg) used in the initial tests was sufficient for the complete co-precipitation of $\leq 1 \mu\text{g}$ of germanium, subsequent work showed that this amount is not sufficient when germanium is co-precipitated in the presence of ≥ 50 mg of aluminium, 25 mg of arsenic(V) or vanadium(V) or moderately large amounts of other co-precipitated elements and compounds such as antimony(V) and silica. This is because they compete with germanium to form ferric aluminates, arsenates, vanadates, antimonates and silicates.^{15d} In further work 100 mg of iron(III) was found to be suitable for co-precipitation purposes. Under these conditions, up to 0.5 g of sample containing moderate amounts of aluminium and other co-precipitated elements can be used.

Separation of germanium by extraction as the tetrachloride

Carbon tetrachloride is the most commonly used solvent for the extraction of germanium tetrachloride and most investigators recommend a double or triple extraction to ensure complete extraction.^{7,15a,15c,30} Extraction from $\geq 8M$ hydrochloric acid is reported to be essentially complete under these conditions.^{15e,25,30,31} However, Luke and Campbell³² found that germanium is only $\sim 95\%$ extracted in one extraction from $\sim 8.5M$ hydrochloric acid when the volume ratio of organic to aqueous phase is $\sim 1:1$ and that additional extractions do not improve the recovery. These findings were confirmed in the present work, with carbon tetrachloride, benzene and heptane as extractants. Presumably this loss of germanium could be due to its volatilization as the tetrachloride before or during extraction. However, a more probable explanation is that the $\text{Ge}(\text{OH})_2^{2+}$ present in the initial solution is not all completely converted into GeCl_4 when the hydrochloric acid concentration of the solution is adjusted to $\geq 8M$ before the extraction step. According to previous investigators,^{33,34} some germanium can be present as an unextractable, partly hydrolysed anionic oxychloride complex under these conditions. Similar results (~ 98 and 0% recovery for the first and second extractions, respectively), which also suggest the formation of such species, were obtained when germanium was extracted as the less volatile tetrabromide from $8.6M$ hydrobromic acid into heptane.

On the basis of these findings, it was considered that one extraction with a non-polar solvent of specific gravity < 1 would be advantageous for the separation of germanium from iron and other co-precipitated elements after its separation by collection with hydrous ferric oxide. Unlike extraction with carbon tetrachloride and other heavy solvents, which requires the use of three separatory funnels for the extraction and subsequent washing and stripping steps, this would result in a quicker and simpler method because all these operations could be carried out in the same funnel. Although many non-polar solvents of low specific gravity can be used to extract germanium tetrachloride, heptane was chosen because it is readily available and has a favourable extraction capacity with respect to germanium tetrachloride.^{15e} It is also not as unpleasant to use as benzene or cyclohexane. Tests showed that up to at least $200 \mu\text{g}$ of germanium is $\sim 98\%$ extracted from $\geq 9M$ hydrochloric acid in one extraction with heptane in 1:1 or 2:1 aqueous/organic phase-volume ratio. To avoid error in the germanium result, the loss of germanium must be compensated for in the calibration curve. This is usually accomplished by taking all the solutions used for calibration purposes through the extraction step.³² However, it is only necessary to extract one solution of relatively high germanium content (e.g., $200 \mu\text{g}$) and then to use the resultant strip solution for the preparation of the calibration curve.

Effect of diverse ions

Previous investigators found that only arsenic(III) as the chloride, and osmium and ruthenium as the tetroxides, are co-extracted into carbon tetrachloride from high concentrations of hydrochloric acid.^{5,15e,30,33} Osmium and ruthenium are rarely present in ores and related materials in amounts sufficient to interfere during complex formation and, after sample decomposition by fusion with sodium peroxide, arsenic will be present in the quinquevalent state. However, it was considered necessary to investigate the possible interference effects of various elements that would be completely or partly co-precipitated with germanium or occluded by the precipitate during the iron collection step. These tests showed that, when 100 mg of iron(III) is used for co-precipitation, up to at least 75 mg of phosphate, 50 mg of aluminium, 25 mg of bismuth, manganese(II), molybdenum(VI), titanium(IV), arsenic(V) and vanadium(V) and 2 mg of selenium(VI) and tellurium(VI) can be present during the co-precipitation step without interfering in the co-precipitation or subsequent extraction of germanium. More than 10 mg of antimony(V) and tungsten(VI) will cause low results for germanium and more than ~ 5 mg of tin(IV) causes a high result. The interference of tin is due to its reaction with phenylfluorone³² because, at the 5-mg level, tin(IV) is $\sim 0.6\%$ co-extracted under the conditions used for the extraction of germanium. More than ~ 50 mg of

Table 1. Recovery of germanium from synthetic zinc concentrates*

Matrix and nominal composition, %	Total	
	Ge present, $\mu\text{g/g}$	Ge found, $\mu\text{g/g}$
Zn concentrate CZN-1 (44.7 Zn, 30.2 S, 10.9 Fe, 7.5 Pb, 1.0 SiO ₂)	4.4 ₀	4.3 ₆
	6.4 ₀	6.3 ₀
	12.4	12 ₆
	22.4	22 ₃
	42.4	41 ₉
	102.4	102 ₈
	202.4	200 ₀

*The mean value for germanium in CZN-1 by the proposed method is 2.4₀ $\mu\text{g/g}$ (cf. Table 4). From 1 to 100 μg of germanium was added to 0.5-g samples.

silica causes a low result. Presumably, it interferes by competing with germanium to form ferric silicate and by forming a silicic acid gel when the hydrous oxide precipitate is dissolved in 3M hydrochloric acid before the extraction step. This gel adsorbs germanium and prevents its extraction as the tetrachloride.^{15d} Interference from silica can readily be avoided by volatilizing it with hydrofluoric acid after dissolution of the melt in dilute sulphuric acid. However, under these conditions, more than microgram-quantities of chloride should not be present, because some germanium will be lost by volatilization as the chloride when the solution is evaporated to fumes of sulphur trioxide to remove the excess of hydrofluoric acid. At the 50- μg level, the loss of germanium in the presence of 1 mg of chloride is ~10–20%. Conversely, if the hydrofluoric acid treatment is not required, up to at least 2 g of chloride can be present in the solution of the melt without causing loss of germanium when the

solution is boiled to destroy the hydrogen peroxide produced.

Interference from co-extracted chlorine, which oxidizes phenylfluorone, is avoided by reducing it with ascorbic acid just before complex formation. This also reduces any iron(III) remaining after the extract is washed with concentrated hydrochloric acid. In the presence of the recommended amount of ascorbic acid, up to at least 5 mg of iron(III) will not interfere during complex formation.

Applications

Table 1 shows that the results obtained by the proposed method for a series of synthetic zinc concentrates in which the added germanium was varied from 2 to 200 $\mu\text{g/g}$ agree favourably with the calculated amount present. Similarly, Table 2 shows that the results obtained for five diverse Canadian Certified Reference Materials Project (CCRMP) ores

Table 2. Recovery of germanium from synthetic ores, concentrates and zinc-processing products

Sample	Nominal composition, %	Ge found, $\mu\text{g/g}$	Total Ge present	
			after addition of Ge, $\mu\text{g/g}$ *	Ge found after addition, $\mu\text{g/g}$
CCRMP-SU-1 Nickel copper-cobalt ore†	22.9 Fe, 5.0 Al, 12.1 S, 16.2 Si, 1.5 Ni, 0.9 Cu, 0.5 Ti	1.5 ₈ , 1.4 ₀	3.4 ₉	3.1 ₆
			41.5	40 ₈
			101.5	101 ₃
CCRMP-HV-1 Copper molybdenum ore†	1.9 Fe, 6.6 Al, 0.3 S, 33.9 Si, 0.5 Cu, 0.2 Ti	2.3 ₈ ‡	4.3 ₈	4.4 ₆
			42.4	42 ₁
			102.4	101 ₈
CCRMP-CCU-1 Copper concentrate	24.7 Cu, 3.2 Zn, 30.8 Fe, 35.6 S, 2.6 SiO ₂	0.4 ₉ , 0.6 ₉	2.5 ₉	2.4 ₀
			40.6	40 ₄
			100.6	101 ₀
CCRMP-CPB-1 Lead concentrate	64.7 Pb, 4.4 Zn, 8.4 Fe, 17.8 S, 0.7 SiO ₂ , 0.4 Sb	0.5 ₅ , 0.4 ₆	2.5	2.4 ₆
			40.5	40 ₅
			100.5	101 ₀
Nickel concentrate	33.3 Ni, 37.2 Fe, 4.5 Cu, 32.1 S, 0.3 Co, 0.2 As	0.1 ₀ , N.D.§	2.0 ₅	1.9 ₆
			40.1	39 ₉
			100.1	99 ₈
No. 1 Roaster bed overflow	~60 Zn, ~10 Fe, ~2 S	4.1 ₉ , 4.2 ₅	6.2 ₂	6.2 ₆
			44.2	43 ₆
			104.2	104 ₀
Jarosite precipitate	32.2 Fe, 1.3 Pb, 25.6 SO ₄	7.0 ₄ , 7.2 ₃	9.1 ₄	9.2 ₆
			47.1	47 ₄
			107.1	108 ₀
Combined calcine to leach	61.1 Zn, 9.8 Fe, 2.0 S	4.0 ₄ , 4.1 ₄	6.0 ₉	6.1 ₆
			44.1	43 ₈
			104.1	105 ₀

*Values include mean value for germanium present in the sample plus that added to a 0.5-g sample, viz. 1, 20 or 50 μg .

†Silica removed by volatilization with hydrofluoric acid.

‡Mean value shown in Table 4.

§N.D. means none detected.

Table 3. Determination of germanium in CCRMP iron-formation samples

Sample	Nominal composition, %	Ge found, $\mu\text{g/g}$	
		Abbey <i>et al.</i> "usable values"*	Proposed method
FeR-1	17.0 SiO ₂ , 0.5 Al ₂ O ₃ , 49.8 Fe ₂ O ₃ , 23.5 FeO, 3.3 CaO, 2.4 P ₂ O ₅	3	2.7, 2.6
FeR-2	48.9 SiO ₂ , 5.2 Al ₂ O ₃ , 22.6 Fe ₂ O ₃ , 15.3 FeO, 2.1 MgO, 2.2 CaO, ~0.01 Cl	6	7.1, 7.0
FeR-3	53.2 SiO ₂ , 29.4 Fe ₂ O ₃ , 13.7 FeO, 1.0 MgO	4	4.5, 4.5
FeR-4	50.0 SiO ₂ , 1.7 Al ₂ O ₃ , 22.9 Fe ₂ O ₃ , 15.6 FeO, 1.4 MgO, 2.2 CaO, ~0.01 Cl	5	6.4, 6.5

*Approximate mean of two sets of values.³⁵

and concentrates and for three typical zinc-processing products, to which 2–100 $\mu\text{g/g}$ of germanium was added, are also in good agreement with the calculated values. In these tests, the required volumes of appropriate standard alkaline germanium solution were added to the zirconium crucibles and the solutions were gently evaporated to dryness before the addition of the sample and sodium peroxide. Table 3 shows that the results obtained for four CCRMP iron-formation samples agree reasonably well with the "usable" germanium values reported by Abbey *et al.*³⁵ These "usable" values, which are the approximate means of the sets of values obtained by automated d.c. arc optical emission and spark-source mass spectrometry, are only approximate interim germanium values because too few data were reported during the interlaboratory certification programme for firm values to be assigned.

Table 4 shows that the precision for germanium at about 2–26 $\mu\text{g/g}$ is reasonably good. The non-ferrous dust, PD-1, is a composite of metallurgical dusts collected on electrostatic precipitators from zinc and copper roaster stacks.

In many existing methods for the determination of germanium in silicates and related materials, in which the extraction step follows the decomposition step, mixtures of hydrofluoric and sulphuric acids and

hydrofluoric and phosphoric acids, in the absence or presence of nitric acid, are recommended for the decomposition of the sample.^{6,7,15a,30} This is followed by the evaporation of the solution to fumes of sulphur trioxide and to a syrupy state, respectively, to ensure the complete removal of the excess of hydrofluoric acid which interferes in the extraction of germanium. Although these methods yield reasonably accurate results for samples containing microgram-quantities of germanium, tests in which solutions containing 100 μg were evaporated to fumes of sulphur trioxide as described above, followed by the extraction of germanium, yielded considerably low results. Presumably, this could be caused by the formation, during prolonged evaporation with sulphuric acid, of crystalline germanium dioxide which is insoluble in hot water or cold 9M hydrochloric acid. Heating with hydrochloric acid is required for its dissolution.^{15a,36} In the proposed method for samples of high silica content, in which silica is removed by evaporation with hydrofluoric and sulphuric acids, the large amount of sodium salts present after fusion of the sample possibly inhibits the formation of this insoluble compound. Low results were obtained in similar tests with phosphoric acid, which was found to inhibit the extraction of germanium. As mentioned previously, a further disadvantage of both methods of acid attack is that the decomposition may not be complete.^{7,15a}

The proposed method has several advantages over older methods based on carbon tetrachloride extraction and a phenylfluorone finish. It is quicker and simpler because only one extraction is required and because the extraction, washing and stripping steps are all done in the same separatory funnel. In addition, sample decomposition is complete and the phenylfluorone finish in the presence of CTAB is more rapid and about twice as sensitive as finishes involving the use of gelatin, gum arabic or poly(vinyl alcohol) as dispersing agents. The method is suitable for samples containing ~0.2 $\mu\text{g/g}$ or more of germanium. It should also be directly applicable to zinc-

Table 4. Precision for germanium in a CCRMP ore, concentrate and non-ferrous dust

	Ge, $\mu\text{g/g}$		
	HV-1*	CZN-1	PD-1†
	2.40	2.46	25.7
	2.39	2.43	26.0
	2.39	2.48	25.9
	2.29	2.34	26.1
	2.44	2.31	26.0
	2.38	2.40	25.9
Mean (standard deviation)	0.06	0.08	0.15

*Silica removed by volatilization with hydrofluoric acid.
†The approximate percentage chemical composition of PD-1 is 35.9 Zn, 12.2 Fe, 8.2 S, 7.0 Cu, 3.1 Si, 2.8 Pb and 0.8 As.

process solutions. The mean values obtained for the CCRMP materials in Tables 2-4 should be of value to analysts for comparison purposes.

REFERENCES

1. E. M. Donaldson, *Talanta*, 1982, **29**, 1069.
2. *Idem, ibid.*, 1984, **31**, 443.
3. *Idem, ibid.*, 1984, **31**, 89.
4. *Idem, CANMET Report 83-4E*, Canada Centre for Mineral and Energy Technology, Department of Energy, Mines and Resources, Ottawa, Canada, 1983.
5. F. D. Snell and L. S. Ettre, *Encyclopedia of Industrial Chemical Analysis*, Vol. 13, pp. 375-389. Interscience, New York, 1971.
6. J. Korkisch, *Modern Methods for the Separation of Rarer Metal Ions*, pp. 345-356. Pergamon, Oxford, 1969.
7. I. M. Kolthoff and P. J. Elving (eds.), *Treatise on Analytical Chemistry*, Part II, Vol. 2, pp. 215-235. Interscience, New York, 1962.
8. D. P. Shcherbov and R. N. Plotnikova, *Zh. Analit. Khim.*, 1972, **27**, 740.
9. Y. Gao and Z. Ni, *Huaxue Xuebao*, 1982, **40**, 1021; *Chem. Abstr.*, 1983, **98**, 64806y.
10. A. E. Smith, *Analyst*, 1975, **100**, 300.
11. J. R. Castillo, J. Lanaja and J. Aznárez, *ibid.*, 1982, **107**, 89.
12. K. Jin, H. Terada and M. Taga, *Bull. Chem. Soc. Japan*, 1981, **54**, 2934.
13. M. Ikeda, J. Nishibe and T. Nakahara, *Bunseki Kagaku*, 1981, **30**, 548; *Chem. Abstr.*, 1981, **95**, 143504q.
14. T. Inui, S. Terada, H. Tamura and N. Ichinose, *Z. Anal. Chem.*, 1983, **315**, 598.
15. V. A. Nazarenko, *Analytical Chemistry of Germanium*, (a) pp. 191-199, (b) 146-156, (c) 41, (d) 76-77, (e) 82-88. Israel Program for Scientific Translations, Jerusalem, 1974 (and references therein).
16. G. V. Flyantikova and V. A. Nazarenko, *Fiz.-Khim. Metody Anal. Kontr. Proizvod., Mater. Konf. Rab. Vuzov (Vyssh. Uch. Zaved.) Zavodsk. Lab. Yugo-Vostoka SSSR*, 4th, 1971, 3831; *Chem. Abstr.*, 1974, **80**, 103517e.
17. B. J. Shelton, E. Komarkova, M. Josephson, E. B. T. Cook and K. Dixon, *Natl. Inst. Metall., Johannesburg Rept.*, No. 1857, 1977.
18. K. Dixon, H. Holan, E. A. Jones, E. Komarkova, R. C. Mallett, E. J. Ring, R. V. D. Robért, G. M. Russell and B. J. Shelton, *ibid.*, No. 1911, 1977.
19. G. V. Flyantikova, L. I. Korolenko, L. I. Vinarova and T. N. Chekirda, *Zh. Analit. Khim.*, 1977, **32**, 1028.
20. H.-C. Hsieh, Y.-T. Cheng and C.-M. Cheng, *Fen Hsi Hua Hsueh*, 1979, **7**, 485; *Chem. Abstr.*, 1981, **94**, 57429s.
21. Y. Shijo and T. Takeuchi, *Bunseki Kagaku*, 1967, **16**, 51; *Chem. Abstr.*, 1967, **67**, 39825f.
22. H. Kurihara, H. Kuwabara and T. Kurihara, *ibid.*, 1980, **29**, 560; *Chem. Abstr.*, 1980, **93**, 214882h.
23. H. Kurihara and H. Kuwabara, *ibid.*, 1982, **31**, 50; *Chem. Abstr.*, 1982, **96**, 134948f.
24. D. T. Burns and D. Dadgar, *Analyst*, 1980, **105**, 75.
25. V. A. Nazarenko, N. V. Lebedeva and R. V. Ravitskaya, *Zavodsk. Lab.*, 1958, **24**, 9.
26. J. D. Burton, F. Culkin and J. P. Riley, *Geochim. Cosmochim. Acta*, 1959, **16**, 151.
27. A. V. Shpak and N. I. Isaenko, *Metody Anal. Khim. Reaktiv. Prep.*, 1971, **20**, 101; *Chem. Abstr.*, 1973, **79**, 100170e.
28. T. I. Denisova and G. E. Kislinskaya, *Khim. Tekhnol. (Kiev)*, 1975, **4**, 14; *Chem. Abstr.*, 1976, **85**, 201539m.
29. I. V. Tananaev and M. Ya. Shpirt, *Russ. J. Inorg. Chem.*, 1962, **7**, 602.
30. W. A. Schneider, Jr. and E. B. Sandell, *Mikrochim. Acta*, 1954, 263.
31. Gh. Sauvenier and G. Duyckaerts, *Anal. Chim. Acta*, 1957, **16**, 592.
32. C. L. Luke and M. E. Campbell, *Anal. Chem.*, 1956, **28**, 1273.
33. G. O. Brink, P. Kafalas, R. A. Sharp, E. L. Weiss and J. W. Irvine, Jr., *J. Am. Chem. Soc.*, 1957, **79**, 1303.
34. F. A. Cotton and G. Wilkinson, *Advanced Inorganic Chemistry*, 1st Ed., p. 355. Interscience, New York, 1962.
35. S. Abbey, C. R. McLeod and W. Liang-Guo, *Geol. Surv. Canada Paper*, 83-19, Geological Survey of Canada, Department of Energy, Mines and Resources, Ottawa, Canada, 1983.
36. H. Nishiba, *Bunseki Kagaku*, 1957, **6**, 654; *Chem. Abstr.*, 1958, **52**, 15336h.

SHORT COMMUNICATIONS

CONSTRUCTION AND EVALUATION OF A POTASSIUM-SELECTIVE TUBE-MOUNTED MEMBRANE ELECTRODE

R. E. FARRELL and A. D. SCOTT

Department of Agronomy, Iowa State University, Ames, Iowa 50011, U.S.A.

(Received 6 March 1984. Accepted 4 June 1984)

Summary—A simple procedure for the rapid construction of inexpensive potassium-selective electrodes with valinomycin-based PVC membranes is described. Potassium-selective membranes were formed on the end of Parafilm- or Tygon-covered glass tubes by dipping the tubes into a mixture of PVC, valinomycin, and dioctyl sebacate dissolved in tetrahydrofuran. Small internal Ag/AgCl reference electrodes were made with silver wire and placed inside the tubes with AgCl-saturated potassium chloride solution. This procedure yields tube-mounted membrane electrodes that perform as well as commercially available potassium-selective electrodes in terms of their response characteristics and practical applications with soil extracts. Moreover, it facilitates the evaluation of membranes with different compositions, for making ion-selective electrodes.

Potassium-selective electrodes incorporating the neutral carrier valinomycin in PVC membranes have become extremely popular during the past decade.^{1,2} These electrodes, which can be constructed with either an internal reference solution^{3,4} or a solid internal contact,⁵ have proved to be both reliable and versatile. Construction of these electrodes, however, can be quite cumbersome and, in some instances, may require specially designed membrane housings.^{4,5} Furthermore, although potassium-selective PVC membrane electrodes are commercially available from several manufacturers,^{6,7} they are relatively expensive, as are the membrane replacements periodically required. Here, we report on a simple, rapid and inexpensive method of constructing potassium-selective tube-mounted membrane electrodes with valinomycin-based PVC membranes and Ag/AgCl internal reference elements.

EXPERIMENTAL

Electrodes

The membrane material was a PVC-valinomycin-plasticizer mixture⁴ prepared by dissolving 5 mg of valinomycin in 0.92 ml of dioctyl sebacate (DOS) in a screw-cap centrifuge tube, adding 150 mg of PVC and 2 ml of tetrahydrofuran (THF) as solvent, and mixing thoroughly with a vortex mixer. Twenty or more electrodes can be prepared from this amount of material, which, if refrigerated, will keep for several months.

The Ag/AgCl internal reference electrodes were prepared by a modification of the procedure described by Bailey.⁸ A 2.5-cm length of 20-gauge silver wire was welded to a 20-cm length of 18-gauge copper wire, dipped into a solution of PVC (500 mg dissolved in 3-4 ml of THF) several times, and air-dried. Approximately 1.5 cm of the PVC coating was removed from the tip end of the silver wire, which was then dipped into concentrated ammonia solution for 30 sec, rinsed with demineralized water, dipped into 50% nitric acid until an even white colour developed (~60 sec), and rinsed again. With a 500-k Ω , 10-turn, 0.75-W potentiometer to regulate the current from a 9-V battery, the silver wire was

first made cathodic (platinum anode) in 0.1M hydrochloric acid for 15-30 sec at a current density that just produced bubbles at the cathode (~0.3 mA/mm²). The battery connections were then reversed, and the same current density held for 5-10 min. Properly prepared electrodes had a uniform purple-grey colour and were stored in AgCl-saturated 10⁻³M potassium chloride.

The membrane electrodes were constructed as follows. Membranes were formed on the ends of glass tubes (2 mm bore) by dipping the tubes in the PVC mixture and air-drying overnight. Because of the poor adhesion between glass and PVC and the non-availability of rigid small-diameter PVC tubing, a 5-mm length of the end to be dipped was wrapped with Parafilm or covered with Tygon tubing (3 mm bore) before dipping. The THF in the PVC mixture dissolved enough of the Parafilm or Tygon to glue the PVC to the glass covering and thereby achieve a good seal between the membrane and the tube. When the membranes had dried, the tubes were partly filled with AgCl-saturated 10⁻³M potassium chloride, in which the internal Ag/AgCl reference electrodes were then immersed, and the upper ends of the tubes were sealed with Parafilm. The electrodes thus prepared were conditioned in 10⁻⁵M potassium chloride for 1-2 hr and calibrated.

An Orion (model 93-19) and a Corning (model 476132) potassium-selective electrode were similarly conditioned and calibrated. An Orion (model 90-02) double-junction sleeve-type reference electrode with a saturated lithium acetate salt bridge was used in the calibration.

Measurements

Cell e.m.f. values (E) were measured with a Corning (model 135) pH/Ion meter and recorded when the rate of change was ≤ 0.1 mV/min. All measurements were performed at $22.0 \pm 0.1^\circ$ in plastic beakers, with the test solutions mixed at constant speed. The potassium-selective electrodes were stored in 10⁻³M potassium chloride when they were not to be used for periods of 2 days or more, and otherwise in 10⁻⁵M potassium chloride. Calibration measurements were made in sequence from dilute to more concentrated solutions, the electrodes being rinsed with 10⁻⁶M potassium chloride and lightly blotted dry between measurements. Before and after each complete calibration sequence, the electrodes were soaked in 10⁻⁶M potassium chloride for 15-20 min.

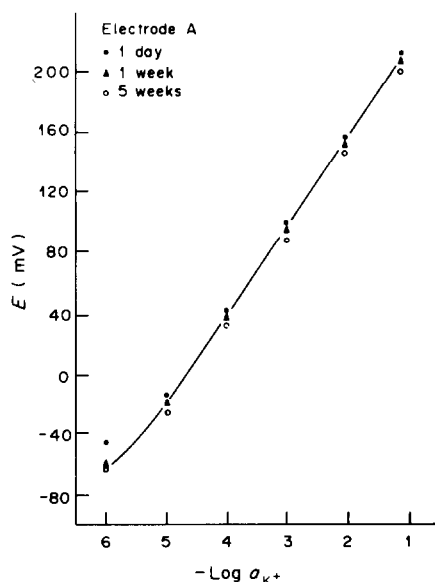


Fig. 1. Calibrations with tube-mounted membrane electrode A, 1 day, 1 week and 5 weeks after construction.

RESULTS AND DISCUSSION

Typical calibration results are shown in Fig. 1. The cell e.m.f. decreased by ~ 1.5 mV/day during the first week, then at only ~ 0.2 mV/day over the next month. Most of the rapid initial change was due to

drift in the potential of the internal Ag/AgCl reference electrode as it equilibrated with the internal solution. This drift can be eliminated by equilibrating the Ag/AgCl electrode in AgCl-saturated $10^{-3}M$ potassium chloride for 3–5 days before use. The later changes are probably due to the effect of aging on the asymmetry potential of the PVC membrane. Similar but smaller changes were observed with the Orion and Corning electrodes.

The response characteristics of our electrodes (after 1 week of use) were very similar to those of the Orion and Corning electrodes (Table 1). The variations in cell constants (E°) are presumably due to differences between various internal reference solutions and asymmetry potentials. The response times, *i.e.*, the times needed for ΔE to become ≤ 0.1 mV/min, for the electrodes were about the same: 3–5 min at low ($\leq 10^{-5}M$) potassium concentrations and 1–2 min at higher concentrations. The characteristics of all the electrodes were relatively unaffected by changes in pH from 5 to 11.

Our electrodes performed as well as or better than the commercial electrodes in practical determinations of potassium in soil extracts. A comparison of the results obtained for potassium determinations in 0.5M barium chloride extracts of 10 soil samples with our electrode C (TM-C), the Orion electrode, and standard atomic-absorption (AAS) procedures is given in Table 2.

Our electrode provides an excellent alternative to

Table 1. Experimentally determined response characteristics of various valinomycin-based potassium-selective electrodes

Electrode type	E° *, mV	Slope, mV/pK	LLR†		L_D ‡		$\log k_{KX}$ §		
			μM	mg/l.	μM	mg/l.	NH_4^+	Na^+	Ba^{2+}
Tube-mounted A	270.0	57.6	8.9	0.35	1.1	0.043	-1.95	-4.38	-4.92
Tube-mounted B	236.9	57.9	10	0.39	1.7	0.066	—	—	—
Tube-mounted C	226.4	58.4	6.1	0.24	0.86	0.034	-1.96	-4.93	-5.78
Orion 93-19	81.2	58.6	6.8	0.27	0.89	0.035	-1.94	-4.11	-4.90
Corning 476132	223.7	57.7	10	0.39	1.6	0.063	-1.95	-4.66	-4.99

*Cell constant (sum of potential of the cell when $a_{K^+} = 1$, the potentials of the internal and external reference electrodes, and the liquid-junction and asymmetry potentials).

† K^+ concentration at the lower limit of linear response.

‡Limit of detection.⁹

§ k_{KX} is the selectivity coefficient as determined by the mixed solution method⁸ and X is NH_4^+ (0.01M), Na^+ (0.1M) or Ba^{2+} (0.1M).

Table 2. Comparison of the results obtained with potassium-selective electrodes and atomic-absorption for K^+ in $BaCl_2$ extracts of soil

Method	Soil K^+ extracted,* $\mu g/g$	No. of replicates	CV,† %	R^2 §		
				AAS	Orion	TM-C
AAS	109	3	2.7	1	0.962	0.994
Orion electrode	111	3	1.0	—	1	0.987
TM-C electrode	106	3	0.5	—	—	1

*Mean for 10 soil samples.

†Coefficient of variation.

§Square of correlation coefficient.

the more expensive commercial electrodes, especially when the risk of damage to the membrane is high. Since the tube holding the membrane is quite small and can be even smaller, the electrodes are well suited for determination of potassium in small samples. Furthermore, many electrodes can be prepared at one time and the membranes can be easily removed and replaced. Accordingly, our technique for construction of PVC membrane electrodes is particularly useful when a variety of membranes with different compositions is to be prepared and compared for specific applications.

Acknowledgement—Journal Paper No. J-11385 of the Iowa Agriculture and Home Economics Experimental Station, Ames, Iowa. Project No. 2311. This project was supported in part by the Potash and Phosphate Institute.

REFERENCES

1. A. K. Covington, *Crit. Rev. Anal. Chem.*, 1974, **3**, 355.
2. J. Koryta, *Anal. Chim. Acta*, 1982, **139**, 1.
3. L. Jaikonen and R. Virtanen, *Anal. Lett.*, 1981, **14**, 479.
4. R. E. Dohner and W. Simon, *ibid.*, 1979, **12**, 205.
5. M. Trojanowicz, Z. Augustowska, W. Matuszewski, G. Moraczewska, and H. Hulanicki, *Talanta*, 1982, **29**, 113.
6. Orion Research Inc., *Instruction Manual—Potassium Ion Electrode Model 93-19*. Orion Research Inc., Cambridge, Massachusetts, 1979.
7. Corning Medical and Scientific, *Potassium Electrode—Operating Instructions and Technical Specifications*, Corning Glass Works, Medfield, Massachusetts, 1980.
8. P. L. Bailey, *Analysis with Ion-Selective Electrodes*, p. 20. Heyden, London, 1978.
9. IUPAC Analytical Chemistry Division, Commission on Analytical Nomenclature, *Pure Appl. Chem.*, 1976, **48**, 127.

DETERMINATION OF NICKEL BY FLAME ATOMIC-ABSORPTION SPECTROPHOTOMETRY AFTER SEPARATION BY ADSORPTION OF ITS NIOXIME COMPLEX ON MICROCRYSTALLINE NAPHTHALENE

TOHRU NAGAIRO and BAL KRISHAN PURI

Himeji Institute of Technology, 2167, Shosha, Himeji-shi, Hyōgo, Japan

MOHAN KATYAL and MASATADA SATAKE

Faculty of Engineering, Fukui University, Fukui 910, Japan

(Received 31 December 1983. Accepted 1 June 1984)

Summary—A method has been developed for the determination of nickel in alloys by flame atomic-absorption spectrophotometry after formation of a water-insoluble complex, its adsorption on microcrystalline naphthalene, and dissolution of the complex and naphthalene in nitric acid and xylene.

Nioxime forms a water-insoluble, thermally stable red complex with nickel, which can be determined spectrophotometrically in the presence of gum arabic in aqueous medium,^{1,2} but the complex is only partially soluble in the common organic solvents and so cannot be determined by extraction and spectrophotometry. Like many other complexes,³⁻⁸ nickel nioximate is readily and quantitatively adsorbed on microcrystalline naphthalene, however, and thus easily separated from the aqueous phase. The nickel can then be stripped by dissolving the solid with nitric acid and xylene, and determined by atomic-absorption.

EXPERIMENTAL

Reagents

- Standard nickel solution, 5 ppm.
- Nioxime solution in ethanol, 0.1%.
- Acetic acid/ammonium acetate buffer, 1M, pH 4.0.
- Naphthalene solution in acetone, 20%.

Procedure

To a known volume (up to 40 ml) of sample solution containing 5–100 µg of nickel, in an 80-ml stoppered Erlenmeyer flask, add 2.0 ml of pH 4.0 buffer and 1.5 ml of nioxime solution, mix, then after a few minutes add 2.0 ml of naphthalene solution and shake the mixture vigorously for 30 sec. Filter off the naphthalene on a filter paper (No. 5C, Toyo Roshi Co., Japan) placed flat on a perforated Teflon disc (3 cm in diameter) placed in an ordinary filter funnel or on a sintered glass filter (porosity 2). Wash with water, then add 13 ml of 3M nitric acid and 2 ml of xylene to the filter to dissolve the naphthalene and nickel complex. The nickel is then in the aqueous phase and the naphthalene in the xylene. Filter the aqueous phase into a 20-ml standard flask, and wash the paper with water until the solution is diluted to the mark. Aspirate the solution into an air-acetylene flame and measure the absorbance at 232.0 nm, using a nickel hollow-cathode lamp.

RESULTS AND DISCUSSION

The optimum pH range is 3.2–11.2. The adsorption of the complex is quantitative with use of 0.3–6.0 ml

of the nioxime solution, and 1–5 ml of buffer can be used. The nickel complex forms completely in a few minutes. Adsorption is complete with 0.5–4.0 ml of the naphthalene solution and takes only a few seconds of shaking. Mineral acids of various concentrations were tried for dissolution of the nickel complex and 3M nitric acid was found the most suitable. The adsorption yield with the 0.4 g of naphthalene is constant for aqueous phase volumes up to 200 ml, but decreases for larger volumes. Beer's law is obeyed for nickel up to 5 µg/ml in the final aqueous solution. For ten replicate determinations of 40 µg of nickel, the relative standard deviation was less than 1.4%.

Effect of diverse ions

In determination of 40 µg of nickel the following compounds did not interfere, even at the 100-mg level: KI, NaClO₄, KNO₃, NaCl, CH₃COONa·3H₂O, NH₄Cl, sodium tartrate, Na₂SO₄, KSCN, NaF, KH₂PO₄·12H₂O. Only relatively low amounts (1 mg) of sodium citrate and oxalate could be tolerated. EDTA and KCN interfered seriously. Mg, Mo(VI), Ca, W(VI), Mn(II), Pb, Cd, Hg(II) and Ag (adsorbed at pH 11.2), could be tolerated even at the 1000-mg level. Pd(II) can be removed by prior extraction into molten naphthalene at pH 1.0. The following metal ions (amounts, mg, in parentheses) could be tolerated: Al (150), V(V) (100), Zn (50), Cr(VI) (20), Pt(VI) (15), Bi(III) (2), Fe(III) (1.5) and Co (0.1). Cu(II) (4 mg) could be completely masked with 5 ml of 5% thiourea. In analysis of steels, if the iron concentration is higher than the tolerance limit, it can be lowered by extraction from 6M hydrochloric acid medium with methyl isobutyl ketone or diethyl ether. Generally, metal ions such as Fe(III), Co and Cu(II), which form complexes, interfere with the determination, and hence they must be eliminated with masking agents or by prior extraction with organic solvents.

Table 1. Determination of nickel in samples

Sample	Composition, %	Nickel certified value %	Nickel content, %	
			Present method	Direct AAS
N.B.S. SRM-163 Low alloy	C:0.933, Mn:0.897 P:0.007, S:0.027 Si:0.488, Cu:0.087 Cr:0.982, Mo:0.029 N:0.007	0.081	0.085, 0.082, 0.082, 0.085, 0.082	0.082
N.B.S., SRM-171 Magnesium alloy	Mn:0.45, Si:0.0118 Cu:0.0112, Al:2.98 Pb:0.0033, Fe:0.0018 Zn:1.05	0.0009	0.0007, 0.0007 0.0008, 0.0007 0.0006	0.0008
N.B.S., SRM-85 Aluminium alloy	Cu:3.99, Mg:1.49 Mn:0.61, Cr:0.21 Si:0.18, Fe:0.24 Zn:0.03, Ti:0.022 Pb:0.021, Ga:0.019 V:0.006	0.084	0.089, 0.093 0.089, 0.090 0.087	0.085
JSS 157-3 Carbon steel	C:0.21, Si:0.21 S:0.025, Al:0.017 Mn:0.61, P:0.020 Cr:0.10, Cu:0.10	0.11	0.10, 0.10, 0.10 0.11, 0.11	0.11
JSS 503-4 Nickel- chromium steel	C:0.33, Si:0.27 S:0.020, N:0.0115 Cu:0.084, V:0.004 Mn:0.63, P:0.029 Cr:0.70, Mo:0.013	1.24	1.28, 1.28, 1.27 1.26, 1.27	1.34
JSS 505-4 Ni-Cr-Mo steel	C:0.20, Si:0.30 S:0.0086, N:0.0061 Cu:0.10, Al:0.026 Mn:0.64, P:0.02 Cr:0.50, Mo:0.22	1.82	1.72, 1.75, 1.72 1.76, 1.76	1.93
CoSO ₄ ·7H ₂ O*	—	—	0.009, 0.009, 0.009 0.010, 0.010	0.010, 0.010, 0.011 0.010, 0.010
Co(NO ₃) ₂ ·6H ₂ O*	—	—	0.030, 0.031, 0.030 0.030, 0.031	0.030, 0.030, 0.031 0.030, 0.031

*Cobalt was removed from 8M HCl medium by extraction with three 30-ml portions of 5% tri-n-octylamine solution in xylene.⁹

Analysis of alloys

This method has been successfully applied to the analysis of nickel-containing alloys and metal salts. The results (Table 1) are in reasonable agreement with the certified values or those obtained by direct AAS determination. The method is not really suitable for alloys containing > ~2% nickel, on account of the comparatively high relative standard deviation.

REFERENCES

1. R. B. Singh, B. S. Garg and R. P. Singh, *Talanta*, 1979, **26**, 425.
2. R. C. Ferguson and C. V. Banks, *Anal. Chem.*, 1951, **23**, 448.
3. T. Fujinaga, Y. Takagi and M. Satake, *Bull. Chem. Soc. Japan*, 1979, **52**, 2556.
4. M. Satake, Y. Matsumura and M. C. Mehra, *Mikrochim. Acta*, 1980 **I**, 455.
5. M. Satake and M. C. Mehra, *Microchem. J.*, 1982, **27**, 182.
6. M. Satake, M. C. Mehra and T. Fujinaga, *Bull. Chem. Soc. Japan*, 1982, **55**, 2079.
7. M. Satake and H. B. Singh, *Defence Science J.*, 1982, **32**, 201.
8. M. Satake, M. C. Mehra, H. B. Singh and T. Fujinaga, *Bunseki Kagaku*, 1983, **32**, E165.
9. G. Nakagawa, *Nippon Kagaku Zasshi*, 1961, **82**, 1042.

COMPARISON OF TWO DIGESTION METHODS USED IN THE DETERMINATION OF SELENIUM IN MARINE BIOLOGICAL TISSUES BY GAS CHROMATOGRAPHY WITH ELECTRON-CAPTURE DETECTION

K. W. MICHAEL SIU* and SHIER S. BERMAN

Division of Chemistry, National Research Council of Canada, Montreal Road, Ottawa, Ontario, Canada

(Received 14 February 1984. Revised 7 May 1984. Accepted 25 May 1984)

Summary—The performance of two decomposition procedures, with (a) nitric/perchloric/sulphuric acid and (b) nitric acid/magnesium nitrate, in the determination of selenium in marine biological tissues by gas chromatography with electron-capture detection was compared. Both methods were found satisfactory and performed equally well for sample dissolution, but method (b) was judged to be more convenient.

Selenium is an essential element. During the course of analyses in establishing a reliable value for it in the newly issued lobster hepatopancreas reference material for trace metals, TORT-1, it was felt necessary to compare some existing digestion methods and evaluate their relative merits for use in conjunction with gas-chromatographic determination. Two decomposition procedures, namely with nitric/perchloric/sulphuric acid and nitric acid/magnesium nitrate, were chosen because of their popularity and success with other types of materials.

Acid digestion is generally used for decomposing biological materials for selenium determination. Within this category, nitric/perchloric acid digestion with or without sulphuric acid is most widely employed.¹⁻⁴ It has been used in conjunction with a variety of instrumental methods, including gas chromatography with electron-capture detection.² Nitric acid/magnesium nitrate digestion has also been used with the gas-chromatographic determination of selenium.^{5,6} It was the preferred decomposition method in one study and reportedly yielded cleaner chromatograms.⁵

Gas chromatography with electron-capture detection has been used to determine selenium in a variety of materials, after its reaction with *o*-phenylenediamine and conversion into piazselenol.⁷ In this study, the commercially available 4-nitro-*o*-phenylenediamine was selected as reagent. It reacts with selenium(IV) to form 5-nitropiazselenol. This reaction is highly selective and suffers from few, if any, known interferences.

TORT-1 is issued by the National Research Council of Canada's Marine Analytical Chemistry Standards Program. The material was prepared from commercial edible tomalley paste, considered a gas-

tronomic delight by many. The sample was homogenized, spray-dried, extracted with acetone, vacuum-dried, sieved, blended, bottled, and sterilized with gamma-radiation. The metal levels in tomalley are relatively high, and even more so in TORT-1 because of the concentration factors inherent in the processing steps.

EXPERIMENTAL

Instrumentation

A Varian 6000 gas chromatograph equipped with a constant-current electron-capture detector was used. The column was a 12-m fused silica capillary coated with SE-30. Splitless injection was used. Nitrogen (oxygen content < 10 ppm), further purified by passage through molecular sieve 5A and a heated oxygen-scavenger unit (Supelco), was used as carrier and make-up gas, at flow-rates of about 1 and 60 ml/min respectively. The injector temperature was held at 220°. In the temperature programme, the column was held at 120° for 2 min, and then heated at 20°/min to 200°, and held at that temperature for 11 min. The detector temperature was 300°.

Reagents

All reagents were of analytical grade. To minimize contamination, acids were further purified by sub-boiling distillation.⁸ Demineralized distilled water (DDW) was produced by passing distilled water through a demineralizer consisting of a charcoal cartridge and two mixed-bed demineralizers (Cole-Palmer). Toluene was "distilled-in-glass" grade (Caledon).

A 1000-ppm selenium(IV) stock solution was prepared by dissolving sodium selenite (B.D.H.) in 1M hydrochloric acid, and standardized gravimetrically by precipitation of selenium with sulphur dioxide.⁹ Similarly, a 1000-ppm selenium(VI) stock solution in 2M nitric acid was prepared from sodium selenate (B.D.H.). Working solutions were made by dilution of the Se(IV) and Se(VI) stock solutions with 1M hydrochloric acid and 2M nitric acid, respectively.

A 1% 4-nitro-*o*-phenylenediamine hydrochloride solution in 1M hydrochloric acid was prepared as previously described.¹⁰

Sample digestions

In addition to TORT-1, another reference material, NBS-1566 oyster tissue, was used. They were both vacuum-dried before weighing, as recommended.

*Author for correspondence.
NRCC 23549.

Nitric/perchloric/sulphuric acid digestion. Approximately 1 g of sample was weighed and placed in a 100-ml glass beaker, 25 ml of concentrated nitric acid were added and the beaker was covered. The mixture was allowed to stand for at least 2 hr. Then 5 ml each of concentrated perchloric and sulphuric acids were added, plus a few glass spheres to minimize bumping. The beaker was placed on a hot-plate and gradually heated until the nitric acid boiled gently. When the volume was reduced to about 25 ml, the temperature was raised to drive off nitric acid rapidly. The beaker was removed from the hot-plate when the volume had been reduced to 15 ml, and allowed to cool for 1 min. Then 3 ml of concentrated nitric acid were added. The digest was heated until dense white fumes of perchloric acid appeared and its volume was reduced to 5 ml. The solution was cooled and 5 ml of 10M hydrochloric acid were added. It was then heated to 95° for 15 min, cooled, transferred into a 50-ml standard flask and diluted to the mark with DDW.

Nitric acid/magnesium nitrate digestion. Ten ml of concentrated nitric acid and 4 g of magnesium nitrate hexahydrate were added to a 1-g sample in a 100-ml beaker. The mixture was allowed to stand at room temperature for at least 2 hr. The beaker was then put on a hot-plate and heated at 95° for 3 hr, after which the contents were slowly evaporated to dryness overnight. The next morning, the hot-plate was kept at its maximum temperature until volatilization of nitrogen dioxide ceased. The beaker was then placed in a cold muffle furnace, heated up to 500° and held at that temperature for 30 min. The beaker was cooled, 5 ml of 10M hydrochloric acid were added and the solution was heated at 95° for 15 min. The digest was allowed to cool and transferred into a 50-ml standard flask. Finally 5 ml of 40% urea solution were added, followed by dilution to volume with DDW.

Analytical procedure

Determinations were done by the method of standard additions. A 0.1-ml portion of the digest solution and the appropriate amount of Se(IV) spike were allowed to stand with 0.1 ml of 1% 4-nitro-*o*-phenylenediamine hydrochloride solution in a 5-ml "Reacti-vial" (Chromatographic Specialties Ltd.) for 2 hr, then 1 ml of toluene was added. The vial was shaken vigorously for 5 min to extract the 5-nitropiazselenol into the organic phase, and 1 μ l of the toluene layer was injected into the chromatograph. The injection was repeated at least three times for each extract, and the average taken.

RESULTS AND DISCUSSION

Figure 1 shows chromatograms resulting from both digestion methods. They were all reasonably clean, with the piazselenol peak the most prominent; the extra peaks were due to excess of 4-nitro-*o*-phenylenediamine, its reaction side-products, and impurities in the toluene. In this respect both procedures were equally satisfactory. This apparently contradicts an earlier report which judged the nitric acid/magnesium nitrate digestion the more favourable.⁵ However, that comparison was made with a nitric acid and a nitric/perchloric/sulphuric acid/hydrogen peroxide digestion, and the experimental conditions were different from ours.

In terms of convenience and ease of use, the nitric acid/magnesium nitrate digestion is preferred. It requires minimal attention, and because the digest is taken to dryness, constant volume checks are not necessary, in contrast to the nitric/perchloric/sulphuric acid decomposition, where the digest vol-

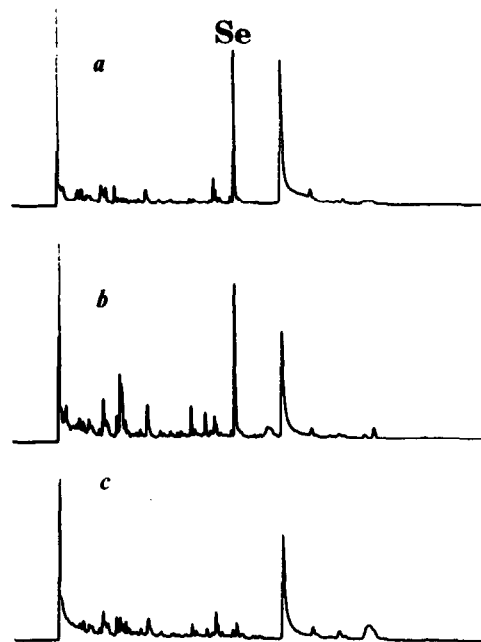


Fig. 1. Chromatograms of piazselenol prepared from acid digest of TORT-1: (a) nitric/perchloric/sulphuric acid digestion; (b) nitric acid/magnesium nitrate digestion; (c) blank for (b).

ume at each stage is moderately critical (control to $\pm 20\%$ is needed). Further, unattended overnight heating reduces the man-hours of labour.

In both decomposition procedures, the temperature and its rate of change were controlled to minimize charring, which usually results in low selenium recoveries.^{3,5,7} Heating with 10M hydrochloric acid was used to convert Se(VI) into Se(IV) [necessary because only Se(IV) reacts to form the piazselenol].

Both digestion methods were judged satisfactory for selenium determination by gas chromatography. Table 1 shows both decomposition procedures gave

Table 1. Selenium concentrations in marine biological tissues

Sample	Digestion method*	Se concentration, μ g/g	
		Found†	Certified values‡
TORT-1	a	$7.3_8 \pm 0.4_5$	6.88 ± 0.47
	b	$7.0_7 \pm 0.4_8$	
NBS-1566	a	$2.1_6 \pm 0.2_5$	2.1 ± 0.5
	b	$2.2_3 \pm 0.2_6$	

*a = nitric/perchloric/sulphuric acid digestion; b = nitric acid/magnesium nitrate digestion.

†Mean \pm standard deviation ($n = 5$).

‡Mean \pm 95% confidence limit. Certified values were derived from results of at least two independent analytical techniques: for TORT-1, atomic-absorption spectrometry, isotope-dilution spark-source mass spectrometry and gas chromatography; for NBS-1566, atomic-absorption spectrometry, isotope-dilution spark-source mass spectrometry and neutron-activation analysis.

results in good agreement with the certified values, with no significant difference between them.

A limited recovery study with 10 μg of Se(IV) or Se(VI) added to 1 g of biological material before the digestion showed quantitative recovery of both [$98 \pm 5\%$ for Se(IV) and $102 \pm 6\%$ for Se(VI), 8 replicates for each]. No organoselenium compounds were tested for recovery, but the results in Table 1 suggest that decomposition of such compounds would be complete.

The gas chromatographic determination was simple but sensitive, the detection limit, calculated as twice the reagent blank, being 0.5 pg of injected Se, or 250 ng per g of sample. The latter figure could easily be lowered by increasing the volume ratio of digest to toluene in the extraction. The precision for 15 pg of injected Se was better than 7%; the main source of variation was drift in the detector sensitivity.

Both methods were found to decompose the samples satisfactorily (giving accurate results and quan-

titative recoveries) and yield clean chromatograms. Convenience is the only criterion in which they differ, the nitric acid/magnesium nitrate digestion being superior.

REFERENCES

1. M. Verlinden, *Talanta*, 1982, **29**, 875, and references therein.
2. H. Uchida, Y. Shimoishi and K. Toei, *Analyst*, 1981, **106**, 757.
3. R. J. Mailer and J. E. Pratley, *ibid.*, 1983, **108**, 1060.
4. W. A. Mahler, *Anal. Lett.*, 1983, **16**, 801.
5. C. F. Poole, N. J. Evans and D. G. Wibberley, *J. Chromatog.*, 1977, **136**, 73.
6. T. P. McCarthy, B. Brodie, J. A. Milner and R. F. Beville, *ibid.*, 1981, **225**, 9.
7. K. Toei and Y. Shimoishi, *Talanta*, 1981, **28**, 967, and references therein.
8. R. Dabeka, A. Mykytiuk, S. S. Berman and D. S. Russell, *Anal. Chem.*, 1976, **48**, 1203.
9. A. I. Vogel, *A Text-book of Quantitative Inorganic Analysis*, 3rd Ed., pp. 508-509. Longmans, London, 1961.
10. K. W. M. Siu and S. S. Berman, *Anal. Chem.*, 1983, **55**, 1603.

A SENSITIVE SPECTROPHOTOMETRIC METHOD FOR THE DETERMINATION OF HYDROXYLAMINE BY USE OF *p*-NITROANILINE AND *N*-(1-NAPHTHYL)-ETHYLENEDIAMINE

PRATIMA VERMA and V. K. GUPTA*

Department of Chemistry, Ravishankar University, Raipur, 492010 India

(Received 3 October 1983. Revised 26 April 1984. Accepted 26 May 1984)

Summary—A sensitive method for the spectrophotometric determination of hydroxylamine is described, based on known diazotization and coupling reactions. Hydroxylamine is oxidized by iodine in acetic acid medium to nitrite which then diazotizes *p*-nitroaniline to form a diazonium salt which is later coupled with *N*-(1-naphthyl)ethylenediamine to give a purple dye which has an absorption maximum at 545 nm, with a molar absorptivity of 6.6×10^4 l.mole⁻¹.cm⁻¹. Beer's law is obeyed over the hydroxylamine concentration range 0–8 µg/25 ml (0.0–0.32 ppm) in the final solution.

The determination of hydroxylamine is important in studies of biological processes and for industrial purposes. It has been detected in bacterial media and in the tissue of a number of organisms. It is produced during the reduction of nitrites.¹ Hydroxylamine is often found in biological materials in combined forms, e.g., as hydroxamic acids or oximes.² The toxicity of hydroxylamine and its derivatives has been described.³

Earlier methods for the spectrophotometric determination of hydroxylamine were based either on the Griess–Ilosvay reaction,^{4,5} after oxidation to nitrite⁶ or on direct reaction with hydroxylamine.⁷ Other spectrophotometric methods reported^{8–11} are less sensitive and suffer from common interferences. Titrimetric methods^{12–14} reported are generally based on oxidation of hydroxylamine. Electrochemical methods^{15–17} utilize the redox properties of hydroxylamine. A coulometric method¹⁵ is based on reduction of Fe³⁺ to Fe²⁺ by hydroxylamine. There is a potentiometric titration¹⁶ of Fehling's solution with hydroxylamine, and also a chronopotentiometric method.¹⁷

The present communication describes a sensitive method based on combination of two well-tried reactions: oxidation of hydroxylamine to nitrite by iodine in acetic acid medium,⁶ and nitrite determination with *p*-nitroaniline (PNA) and *N*-(1-naphthyl)ethylenediamine dihydrochloride (NEDA).¹⁸ The purple product has an absorption maxima at 545 nm. The reaction is very sensitive and Beer's law is obeyed over the hydroxylamine range 0–8 µg/25 ml of the final solution (0.0–0.32 ppm). The molar absorptivity is $(6.60 \pm 0.01) \times 10^4$ l.mole⁻¹.cm⁻¹.

EXPERIMENTAL

Reagents

Standard hydroxylamine solution, 4 µg/ml. Prepared by appropriate dilution of stock solution.

Sodium acetate solution, 2.5%.

p-Nitroaniline solution, 0.05%.

Iodine reagent. Iodine (1.3 g) dissolved in 100 ml of glacial acetic acid.

Sodium thiosulphate solution, 2.5%.

N-(1-Naphthyl) ethylenediaminedihydrochloride (NEDA) solution, 0.2%.

All reagents used were of analytical grade, and doubly distilled water was used throughout.

Procedure for hydroxylamine

To an aliquot of sample solution containing 0–8 µg of hydroxylamine, in a 25-ml standard flask, add 1 ml of sodium acetate solution, 1 ml of *p*-nitroaniline solution and 0.5 ml of iodine reagent, shake and allow to stand for 2–5 min. Remove the residual iodine by dropwise addition of sodium thiosulphate solution (avoid excess). Add 2 ml of *N*-(1-naphthyl)ethylenediamine solution and let stand for 10 min for complete development of the purple colour, then make up to the mark with 25% v/v acetic acid solution. Measure the absorbance at 545 nm against a reagent blank.

Procedure for benzohydroxamic acid

To 1 ml of sample solution containing 10–80 µg of benzohydroxamic acid in a 25-ml standard flask add 0.5 ml of sodium acetate solution, 1 ml of *p*-nitroaniline solution, and 0.2 ml of iodine solution, shake and let stand for 2–5 min. Then add thiosulphate solution dropwise and continue as for hydroxylamine.

RESULTS AND DISCUSSION

The absorption spectrum of the product shows λ_{\max} at 545 nm. The absorbance was maximal and independent of pH in the range 2.2–3.0. This pH range is obtained by adding 0.5 ml of the iodine reagent and subsequently diluting with 25% acetic acid solution. (The colour is not stable if water is used for the final dilution.)

*To whom correspondence should be sent.

Table 1. Effect of foreign species on determination of 0.16 ppm of hydroxylamine

Tolerance limits*, ppm	
Phenylhydrazine, 2000	Hydrazine, 2000
2,4-Dinitrophenylhydrazine, 2250	Hydrocarbons, 5000
Alcohols, 2000	Aldehydes, 1500
Cd ²⁺ , 2000	Pb ²⁺ , 2000
Zn ²⁺ , 2500	Hg ²⁺ , 1500
Cu ²⁺ , 600	Fe ³⁺ , 1000
Ca ²⁺ , 600	Mg ²⁺ , 650

*Concentration which causes a 2% error.

The oxidation of hydroxylamine to nitrite is fast, and complete in 2 min. The excess of iodine should be removed within the next 5 min, or lower absorbances will be obtained. Sodium thiosulphate solution is added dropwise to remove the iodine, but excess must be avoided or low absorbances will be obtained. However this effect can be prevented by addition of bromobenzene solution, as reported by Lee and Roughan.¹⁹

The time required for full colour development at pH 2.2–3.0 is 10 min after addition of the NEDA solution. The best results are obtained if the reaction is done at 10–30°. Higher temperatures reduce the rate of the reaction.

The colour system was found to obey Beer's law over the hydroxylamine concentration range 0–8 µg/25 ml (0.0–0.32 ppm) in the final solution. The reproducibility of the method was determined by 10 replicate determinations of 4 µg of hydroxylamine over a period of 10 days. The mean absorbance was 0.400, standard deviation 0.0037. The molar absorptivity was found to be 6.60×10^4 l. mole⁻¹. cm⁻¹.

Effect of foreign species

Hydroxylamine (4 µg) was determined in the presence of known amounts of various species likely to accompany it. Excess of hydrazine, 2,4-dinitrohydrazine and phenylhydrazine did not interfere provided sufficient excess of iodine was used in the oxidation. Several common organic species and several metal ions also did not interfere. The tolerance limits are shown in Table 1. Nitrite interfered

but could be removed by adding 1 ml of 3% sulphamic acid solution before the iodine oxidation.

Application to determination of benzohydroxamic acid

Primary hydroxamic acids are quantitatively oxidized to nitrite by the iodine reagent. Benzohydroxamic acid is directly oxidized to nitrite by iodine at pH 5.0–6.5. At pH 2.2–3.0 no colour is formed. Benzohydroxamic acid is oxidized at pH ~5.5, then estimated by following the procedure described earlier. Beer's law is obeyed in the range 0.0–80.0 µg of benzohydroxamic acid/25 ml of solution. The molar absorptivity (referred to benzohydroxamic acid) is 2.50×10^4 l. mole⁻¹. cm⁻¹. For 40 µg/25 ml concentration the mean absorbance is 0.281, standard deviation 0.003.

Acknowledgements—The authors thank the Head, Department of Chemistry, Ravishankar University, Raipur, for providing laboratory facilities, and the University Grants Commission, New Delhi, for the award of fellowship to one of them (PV).

REFERENCES

1. A. I. Virtanen and T. Z. Csaky, *Nature*, 1948, **161**, 814.
2. D. Lewis, *Biochem. J.*, 1951, **49**, 149.
3. F. A. Patty, *Industrial Hygiene and Toxicology*, 2nd Ed., Vol. II, p. 2106. Interscience, New York, 1962.
4. F. Feigl, *Spot Tests in Inorganic Analysis*, 6th Ed., p. 345. Elsevier, Amsterdam, 1972.
5. Y. Kobayashi, *Anal. Chem.*, 1966, **38**, 917.
6. J. Blom, *Ber.*, 1926, **59**, 121.
7. D. P. Johnson, *Anal. Chem.*, 1968, **40**, 64.
8. K. K. Verma, *Talanta*, 1979, **26**, 257.
9. F. Dias and A. S. Olojla, *ibid.*, 1979, **26**, 47.
10. D. S. Frear and R. C. Burrell, *Anal. Chem.*, 1955, **27**, 1664.
11. A. A. Schilt and A. M. Cresswell, *Talanta*, 1966, **13**, 911.
12. S. R. Cooper and J. B. Morris, *Anal. Chem.*, 1952, **24**, 1360.
13. B. R. Sant, *Anal. Chim. Acta*, 1959, **20**, 371.
14. K. Burger and E. Schulek, *Talanta*, 1960, **5**, 97.
15. T. Takahashi and H. Sakurai, *ibid.*, 1962, **9**, 189.
16. H. T. S. Britton and M. Konigstein, *J. Chem. Soc.*, 1940, 673.
17. D. G. Davis, *Anal. Chem.*, 1963, **35**, 1603.
18. A. K. Baveja and V. K. Gupta, *Proc. First Intern. Conf. Industr. Pollution and Control*. Vol. 1, Singapore, 1983.
19. D. F. Lee and I. A. Roughan, *Analyt.*, 1971, **96**, 798.

SIMULTANEOUS DETERMINATION OF DEXTROPROPOXYPHENE NAPSYLATE, CAFFEINE, ASPIRIN AND SALICYLIC ACID IN PHARMACEUTICAL PREPARATIONS BY REVERSED-PHASE HPLC

I. M. JALAL

Al-Hikma Pharmaceuticals, P.O. Box 182400, Amman, Jordan

S. I. SA'SA'

Yarmouk University, Irbid, Jordan

(Received 10 January 1984. Revised 18 April 1984. Accepted 26 May 1984)

Summary—The official compendial method for the determination of dextropropoxyphene napsylate, caffeine, aspirin and salicylic acid involves a lengthy extraction by gas chromatography and spectrophotometry. The analytical scheme reported here provides a fast, sensitive, and stability-indicating reversed-phase HPLC assay for all these components concurrently. The total elution time is 10 min. The accuracy of the method has been tested on commercial products. The method can easily detect low levels of salicylic acid.

Dextropropoxyphene napsylate (DPN) is a widely prescribed analgesic for mild to moderate pain, either alone or in combination with caffeine, aspirin or acetaminophen. Several methods for the detection of DPN have been reported. The colorimetric^{1,2} and TLC³ methods lack the sensitivity necessary for determination of low concentrations. In biological fluids, DPN has been determined by gas chromatography (GC),⁴⁻⁸ but there have been conflicting opinions about the stability of DPN under various GC conditions. The amounts of decomposition have been found to be dependent on column temperature, sample size and flow-rate.⁹ Numerous methods have been reported for the determination of aspirin, including colorimetry,¹⁰ fluorimetry¹¹ and GC.^{12,13} Aspirin in combination with caffeine, phenacetin or acetaminophen has been determined by HPLC.^{14,15} Determination of DPN and aspirin by the National Formulary (13th Ed.) method (NF XIII) involves conventional extraction of the two drugs. The concentration of each is then determined by infrared spectrometry. DPN and aspirin have also been determined by ultraviolet spectrophotometry after separation by partition chromatography.¹⁶ A mixture of propoxyphene hydrochloride, aspirin, caffeine and phenacetin has been analysed similarly¹⁷ but the method is slow.

The current official method¹⁸ for determining DPN, caffeine, aspirin and salicylic acid in a mixture involves separation of salicylic acid by column partition chromatography followed by ultraviolet spectrophotometry, separation by gas chromatography with nitrogen as carrier gas for determination of

DPN and caffeine, and colorimetry for aspirin. This method, while specific, is lengthy and requires three samples. The analytical scheme described in this paper provides a fast, sensitive and reliable reversed-phase HPLC method for simultaneous separation of the four compounds.

EXPERIMENTAL

Reagents

Glacial acetic acid, salicylic acid (B.D.H) and sodium pentane sulphonate (Fluka) were reagent grade. HPLC-grade methanol (Fluka) and distilled demineralized water were used. Standard DPN (Siegfried, Basle), caffeine (Boehringer, Ingelheim, West Germany), and aspirin (Graesser Salicylates, Deeside, England), were used as received; their purities were certified as 99.7, 99.9 and 99.85%, respectively. The Varian 5000 LC HPLC system, equipped with a Valco manual loop injector (Valco Instruments Co., Houston, Texas) was connected to a Varian UV-50 variable wavelength detector (λ 229 nm) and Varian 9176 chart recorder. A 300 × 4 mm reversed-phase octadecylsilane column (Varian Micropak MCH-10) was used.

Chromatographic conditions

The mobile phase was prepared by dissolving 0.1922 g of sodium pentane sulphonate in 700 ml of water and 300 ml of methanol and adjusted to pH 3.9 with glacial acetic acid. It was always filtered through a Gelman 0.45- μ m filter and degassed by vacuum before use. The flow-rate was 2.0 ml/min and pressure about 2000 psi. The detector sensitivity was 0.1 absorbance full-scale for DPN, caffeine and aspirin and 0.02 for salicylic acid. The chart speed was 0.5 cm/min.

Standard preparation

A four-component standard methanolic solution was prepared containing 50 μ g of DPN, 30 μ g of caffeine, 375 μ g of aspirin and 3.75 μ g of salicylic acid per ml. The solution was filtered through a 0.45- μ m filter before use.

Sample preparation

Twenty capsules were emptied and their contents weighed. The average content per capsule was weighed out and dissolved in 100 ml of methanol. The solution was filtered through a 0.45- μ m filter, and 5 ml of the filtrate were diluted to 50 ml with methanol.

Assay method

Equal volumes (10 μ l) and approximately equal concentrations of freshly prepared standard and sample preparations were injected into the HPLC and chromatographed under the conditions described above. The peak heights were measured for each component in both samples and standards, and the content in the sample was calculated by simple proportion. The quantity of each component injected was always within the linearity range.

RESULTS AND DISCUSSION

Calibration standard solutions of DPN, caffeine, aspirin and salicylic acid were prepared and the following quantities of each compound were injected: 0.2, 0.4, 0.6, 0.8, 1, 2, 3, 4 and 5 μ g. A plot of peak height *vs.* amount injected was linear up to 3 μ g for DPN, and up to 5 μ g for the other three, with correlation coefficients of 0.999 or better.

Each standard was doped with pharmaceutical excipients and subjected to HPLC analysis. In all cases, satisfactory recoveries and reproducibility of peak heights were obtained (Table 1). No interference due to excipients was detected in the chromatograms produced.

The specificity of the method is shown by the complete separation of DPN, salicylic acid, aspirin and caffeine, with retention times of 2.5, 4.3, 5.5 and 9.4 min, respectively (Fig. 1).

The detection limit was determined by diluting the standard solution with methanol and injecting 1 μ l of each solution into the column. The amounts that produced a signal equal to twice the noise were 4.8, 30, 6, and 7 ng, for DPN, caffeine, aspirin and salicylic acid, respectively.

The reproducibility was checked by analysing a commercial product on four separate days. The results listed in Table 2 show reproducibility with no statistical difference at the 5% level, and the accuracy is shown by the agreement between the amounts nominally present ("label claim") and those found.

Stability studies

To determine the stability-indicating capability of the procedure, samples of caffeine and aspirin, and also samples of a commercial product, were stored in tubes at 50° in a humid atmosphere. A sample was

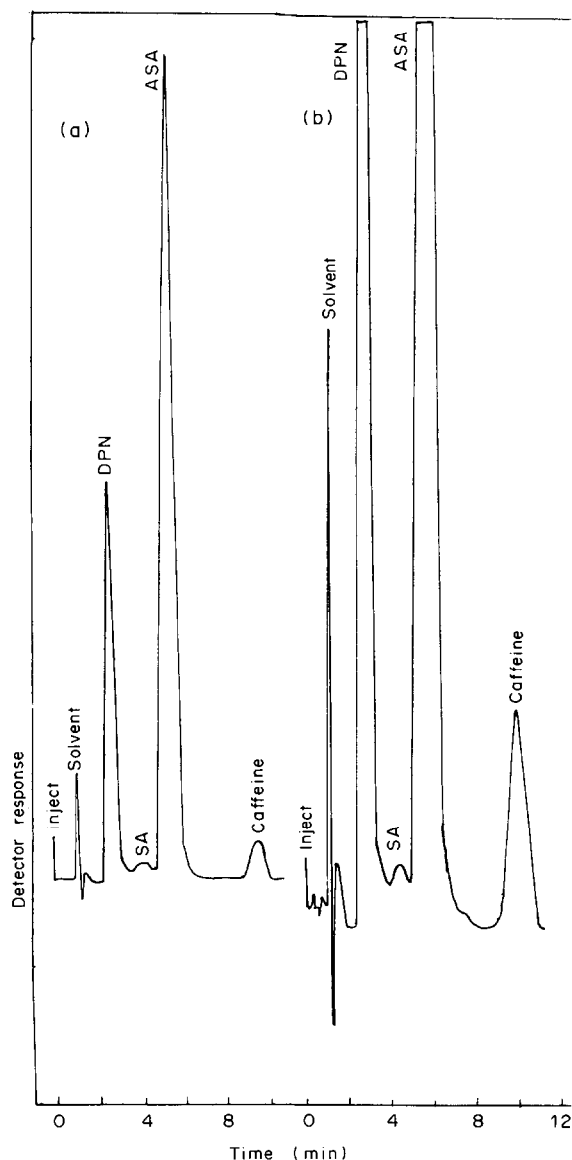


Fig. 1. (a) A typical chromatogram for a 10 μ l injection of a synthetic mixture containing 0.50, 0.01, 3.75, and 0.30 μ g of DPN, salicylic acid (SA), aspirin (ASA) and caffeine, respectively. Full-scale deflection = 0.10 absorbance. (b) The same chromatogram with full-scale deflection = 0.02 absorbance. Chromatographic conditions as described in the text.

taken daily and assayed. It should be noted that DPN was not studied individually because it had been shown in an earlier study to be stable.¹⁹

The results in Table 3 show the stability of caffeine and the partial degradation of aspirin, with an increase in salicylic acid content after seven days. Moreover, the results in Table 4 show that when the commercial product is stored for the same period of time it yields essentially the same results. This clearly illustrates that the method is specific. In conclusion, the HPLC method described here is applicable to individual bulk drugs as well as commercial combina-

Table 1. Recovery studies

Standard	Recovery, %*
DPN	100.4 \pm 1.8
Caffeine	99.5 \pm 2.1
Aspirin	99.4 \pm 1.9
Salicylic acid	102.1 \pm 10.7

*Mean \pm RSD for 8 determinations.

Table 2. Precision studies on Doloxene Compound-50 (lot 60631 AE, E. Lilly, England)

Day	% of label claim \pm RSD*		
	DPN	Caffeine	Aspirin
1	100.4 \pm 0.9	100.0 \pm 2.6	100.7 \pm 1.4
2	99.4 \pm 2.1	100.0 \pm 0.0	100.1 \pm 1.7
3	100.1 \pm 1.2	100.9 \pm 2.1	100.2 \pm 1.0
4	100.2 \pm 1.2	101.9 \pm 0.0	100.1 \pm 1.2
$\bar{X} \pm$ RSD†	100.1 \pm 1.4	100.7 \pm 1.7	100.3 \pm 1.2

*Mean \pm RSD for 5 determinations on each day.†Mean \pm RSD for all 20 determinations.

Table 3. Stability studies for individual standards

Period elapsed days	% of label claim \pm RSD (6 samples)		
	Aspirin		
	Caffeine	Aspirin	Salicylic acid
1	99.7 \pm 0.3	99.5 \pm 0.4	0.3 \pm 0.0
7	100.7 \pm 1.0	100.0 \pm 0.3	0.9 \pm 0.2

Table 4. Stability studies on Doloxene Compound-50 (lot 60631 AE, E. Lilly, England)

Period elapsed days	% of label claim \pm RSD (6 determinations)			
	DPN	Caffeine	Aspirin	Salicylic acid
1	99.6 \pm 1.0	101.3 \pm 1.8	98.5 \pm 1.0	0.4 \pm 0.0
7	100.0 \pm 1.0	99.2 \pm 2.5	99.5 \pm 0.9	1.0 \pm 0.1

tions, with minimum sample manipulation. The total elution time is 10 min. As shown above, the method is accurate, fast and stability-indicating.

Acknowledgements—The financial support provided by Yarmouk University is gratefully acknowledged. The authors would also like to thank Al-Hikma Pharmaceuticals, Amman, Jordan, for providing the materials and standards.

REFERENCES

- C. E. Stevenson and L. Comer, *J. Pharm. Sci.*, 1968, **57**, 1227.
- N. R. Kuzel, *ibid.*, 1968, **57**, 852.
- J. L. Emmerson and R. A. Anderson, *J. Chromatog.*, 1965, **17**, 497.
- W. R. Maynard, R. B. Bruce and G. G. Fox, *Anal. Lett.*, 1973, **6**, 1005.
- J. F. Nash, I. F. Bennet, R. J. Boop, M. K. Brunson and H. R. Sullivan, *J. Pharm. Sci.*, 1975, **64**, 429.
- K. Verbely and C. E. Inturrisi, *J. Chromatog.*, 1973, **75**, 195.
- R. L. Wolen and C. M. Gruber, *Anal. Chem.*, 1968, **40**, 1243.
- M. Cleeman, *J. Chromatog.*, 1978, **132**, 287.
- C. M. Sparacino, E. D. Pellizzari, C. E. Cook and M. W. Wall, *ibid.*, 1973, **77**, 413.
- P. A. Harris and S. Riegelman, *J. Pharm. Sci.*, 1967, **56**, 713.
- R. G. Baum and F. F. Cantwell, *ibid.*, 1978, **67**, 1066.
- J. G. Nickerly, *Anal. Chem.*, 1964, **36**, 2248.
- Y. K. Tam, D. S. L. Au and F. S. Abbott, *J. Chromatog.*, 1979, **1974**, 239.
- P. P. Ascione and J. P. Chrekrian, *J. Pharm. Sci.*, 1975, **64**, 1029.
- V. D. Gupta, *ibid.*, 1980, **69**, 110.
- C. G. Cunningham and S. Barkan, *J. Assoc. Off. Anal. Chem.*, 1973, **56**, 667.
- Idem*, *ibid.*, 1974, **57**, 728.
- U.S. Pharmacopeia XX*, Mack Publishing, Easton, U.S.A.
- S. Sa'sa', I. Jalal and A. Rashid, *Talanta*, 1984, **31**, 397.

TITRIMETRIC MICRODETERMINATION OF SILVER, LEAD AND CADMIUM WITH THIOGLYCOLLIC ACID AND OF MERCURY(II) WITH 2-MERCAPTOPROPANOIC ACID

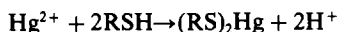
K. K. TIWARI and R. M. VERMA*

Department of Post-Graduate Studies and Research in Chemistry, University of Jabalpur, Jabalpur
(M.P.), 482001, India

(Received 25 November 1983. Revised 27 April 1984. Accepted 15 May 1984)

Summary—A simple and rapid titrimetric method is described for the microdetermination of Ag^+ , Cd^{2+} and Pb^{2+} , based on their formation of mercaptides with a measured excess of 2-mercaptopropanoic acid, and similar determination of Hg^{2+} with thioglycollic acid. Univalent and bivalent metal ions release one and two thiol protons respectively, which along with the carboxyl protons of the thiol reagent are titrated with standard alkali. The difference from the blank titration gives the increase in acidity which is a function of the metal-ion concentration. The proposed procedure is applicable to samples containing 0.025–0.25 mmole of these ions, the average deviation being in the range 0.2–0.5%.

Silver and mercury(II) have been extensively used as reagents in the determination of mercaptans.¹ Organomercuric salts have generally been employed but some authors have recommended the use of mercuric chloride.^{2,3} Though a number of titrimetric procedures are available for determining ionized mercuric salts,⁴ these fail when applied to weakly ionized Hg(II) salts such as mercuric chloride. The latter is usually determined by titration with potassium iodide or by reduction to mercury(I) chloride, which can be collected and weighed,⁵ or titrated with iodine⁴ or potassium iodate.⁶ It was, therefore, thought worthwhile to study the reaction of mercuric chloride with certain mercaptans with a view to developing a rapid and convenient titrimetric procedure for its determination. Our earlier work⁷ on the determination of certain mercaptans was based on their treatment with an excess of mercuric chloride and titration of the acid liberated. Under these conditions the molar reacting ratio was 1:1. If the mercaptan is in excess, however, a 1:2 reacting ratio was observed:



This reaction has now been utilized in a simple and accurate method for determining mercuric chloride. A micro procedure has been evolved for determining mercury(II), and also silver, cadmium and lead. 2-Mercaptopropanoic acid is suitable for the mercury determination, but gives an insoluble mercaptide with silver, cadmium and lead, and this interferes

with detection of the end-point. Though thioglycollic acid also gives a precipitate with these three metals, the precipitate dissolves just before the equivalence point during the titration, and does not impair the phenolphthalein end-point. The dissolution of the precipitate can serve as a guide to the approach of the end-point. In the blank titration only the carboxyl proton is titrated, whereas for the samples the protons released from the thiol group and the carboxyl protons of the reagent are titrated. The difference in the volume of alkali used (ΔV ml, molarity M) corresponds to the metal concentration in the test solution:

$$\text{mg of metal ion} = \left(\frac{\text{atomic weight}}{\text{ionic charge}} \right) M \Delta V$$

EXPERIMENTAL

Reagents

All solutions were prepared with analytical-reagent grade chemicals and conductivity water.

2-Mercaptopropanoic acid. Standardized with potassium iodate solution,⁸ and diluted to give 0.025, 0.020, 0.0125 and 0.01M solutions.

Thioglycollic acid. Standardized by titration with iodine solution⁹ and diluted to give 0.05, 0.025, 0.0125 and 0.01M solutions.

Sodium hydroxide. Standardized with oxalic or preferably furoic acid solution; 0.05, 0.025 and 0.0125M solutions were prepared by dilution.

Phenolphthalein. A 1% solution in 1:1 v/v ethanol–water mixture.

Metal salt solutions. Silver nitrate and mercuric chloride solutions were prepared by dissolving a known weight of the salt and diluting to known volume with water. Solutions of lead nitrate and cadmium sulphate were standardized by titration with EDTA⁶ and then suitably diluted.

*Address for correspondence: Dr. R. M. Verma, 226, Napier Town, Jabalpur 482001, India.

Table 1. Determination of some metal salts with mercaptans

Compound	Amount of metal, mg		Average deviation, %	Relative standard deviation, %
	Taken	Recovered*		
Silver nitrate	26.97	27.02	0.2	0.2
	13.49	13.54	0.4	0.3
	6.74	6.77	0.5	0.3
Mercuric chloride	20.06	20.10	0.2	0.1
	10.03	10.06	0.3	0.2
	5.01	5.03	0.4	0.2
Cadmium sulphate	22.48	22.55	0.3	0.2
	11.24	11.27	0.3	0.2
	5.62	5.64	0.4	0.3
Lead nitrate	25.90	25.95	0.2	0.1
	10.36	10.40	0.4	0.2
	5.18	5.20	0.4	0.3

*Average of 6 determinations.

Procedure

Pipette 5 or 10 ml of metal salt solution containing 0.025–0.25 mmole of the substance and add about 100% excess of mercaptan solution (2-mercaptopropanoic acid for mercuric chloride and thioglycolic acid for silver, cadmium and lead salts). With mercuric chloride a precipitate appears initially but eventually dissolves when all the reagent has been added and the mixture is shaken. With silver, cadmium and lead salts, the dissolution of the mercaptide occurs just before the end-point.

Add 5–10 drops of phenolphthalein solution and titrate with standard sodium hydroxide solution. Run a blank with the same volume of mercaptan solution as that added to the sample. From the difference between the volumes of alkali needed for the blank and sample calculate the amount of metal: 1 ml of 0.02M sodium hydroxide \equiv 2.006 mg of mercury, 2.158 mg of silver, 1.124 mg of cadmium or 2.072 mg of lead.

RESULTS AND DISCUSSION

Silver nitrate, mercuric chloride, cadmium sulphate and lead nitrate were used for testing the proposed method at three concentration levels between 0.005 and 0.025M. The results recorded in Table 1 are the averages of six determinations. The recovery studies showed that the average deviation is between 0.2 and 0.5% and the relative standard deviation between 0.1 and 0.3%.

Several gravimetric methods have been proposed for the determination of mercury(II) but the most suitable weighing form is the sulphide.¹⁰ However, it is difficult to keep volatilization losses within reasonable limits.⁴ Titrimetric methods for determining mercury(II) involve neutralization, precipitation or redox reactions. The Volhard titration with thiocyanate, using iron(III) as indicator,¹¹ has the disadvantage that the reaction is not quite stoichiometric,¹² and halides interfere. The EDTA titration can be done in presence of chloride and even small amounts of bromide, with Eriochrome Black T as indicator, at pH \geq 10. Because the mercury cannot be kept initially in solution at such high pH values without the aid of auxiliary complex-forming substances (which will interfere in the EDTA titration)¹³ a back-

titration method is generally used. Most of these titrimetric procedures are applicable only to ionized mercury salts and cannot be used for determining mercuric chloride. Most of the redox methods involve reduction of mercury(II) to mercury(I), followed by oxidimetric titration of the latter, which is time-consuming.

The most extensively used methods for the determination of silver are precipitation as silver chloride or bromide, or the so-called¹⁴ Volhard titration, which is satisfactory only at macro levels. Several organic reagents have been used for gravimetric determination of cadmium, and there are several procedures in which cadmium is precipitated by suitable reagents and the precipitate analysed titrimetrically. In most cases cadmium has to be separated from interfering elements before a titrimetric method is feasible. Only the EDTA complex is suitable for the direct titrimetric determination of cadmium, but there is extensive interference from other elements. However, a combination of pH control and masking reactions will eliminate most interferences.¹⁵ The gravimetric determination of lead is based on its precipitation as sulphate, chromate, molybdate, iodate, salicylaldoximate *etc.* The chromate precipitate can be analysed iodometrically. The best titrimetric method is with EDTA.

The procedure proposed here is simple, rapid and accurate. No unusual reagent or indicators are required and the reaction conditions are not critical. It has been observed that addition of 100–300% excess of mercaptan solution or letting the mixture stand for 2–30 min before the titration does not affect the results. There will obviously be interference by the presence of any metals which react with mercaptans.

Acknowledgement—The authors are thankful to University Grants Commission, New Delhi, for financial assistance to one of them (KKT).

REFERENCES

1. M. R. F. Ashworth, *The Determination of Sulphur-*

- Containing Groups*, Vol. 2, pp. 56–129. Academic Press, London, 1976.
2. J. R. Sampey and E. E. Reid, *J. Am. Chem. Soc.*, 1932, **54**, 3404.
 3. F. Ratkovic and P. Szepesvary, *Magy. Kem. Folyoirat*, 1958, **64**, 472.
 4. I. M. Kolthoff and P. J. Elving (eds.), *Treatise on Analytical Chemistry*, Part II, Vol. 3, pp. 198–286. Interscience, New York, 1961.
 5. H. M. El-Badry and C. L. Wilson, *Analyst*, 1952, **77**, 596.
 6. A. I. Vogel, *A Text Book of Quantitative Inorganic Analysis*, 3rd Ed., pp. 265–444. Longmans, London, 1968.
 7. K. K. Tiwari and R. M. Verma, *Talanta*, 1981, **26**, 397.
 8. *Idem*, *Microchem. J.*, in press.
 9. I. M. Kolthoff and R. Belcher, *Volumetric Analysis*, Vol. III, p. 38. Interscience, New York, 1957.
 10. H. Flaschka and H. Jakobljevich, *Anal. Chim. Acta*, 1951, **5**, 152.
 11. J. J. Lingane and R. S. Kline, *ibid.*, 1956, **15**, 410.
 12. I. M. Kolthoff and J. J. Lingane, *J. Am. Chem. Soc.*, 1935, **57**, 2377.
 13. G. Schwarzenbach, *Complexometric Titrations*, 1st Ed., Interscience, New York, 1957.
 14. F. Szabadváry, *History of Analytical Chemistry*, p. 255. Pergamon Press, Oxford, 1966.
 15. R. Přibil, *Applied Complexometry*, Pergamon Press, Oxford, 1982.

STUDIES ON THE APPLICATION OF Fe-Zr MIXED HYDROUS OXIDE MEMBRANES IN ION-SELECTIVE POTENTIOMETRY

S. K. SRIVASTAVA and C. K. JAIN

Department of Chemistry, University of Roorkee, Roorkee-247667, India

(Received 30 September 1983. Revised 5 March 1984. Accepted 15 May 1984)

Summary—A solid membrane electrode selective to chloride ions has been prepared from Fe-Zr mixed hydroxide (with iron as a major constituent) with polystyrene as binder. Although the response of the electrode is non-Nernstian it can be utilized to estimate chloride in the concentration range 10^{-4} – $10^{-1}M$. The potentials generated across the membrane are reproducible within ± 0.2 mV and the response time is a few seconds. The standard deviation of the potential measurements is 0.4 mV at the 0.1M level. The useful pH range is 4–7 and the electrode can also be used in partially non-aqueous systems. The electrode exhibits fairly good selectivity for chloride.

Hydrous oxides of zirconium, thorium, tin *etc.*, are known to possess anion- as well as cation-exchange properties, depending on the pH of the environment. These oxides can be used as ion-sensors when combined with an appropriate membrane and suitable support matrix,¹ because they have fixed ionic groups in their structure, ensuring selective ion-exchange reactions. Various ion-selective electrodes are available for the determination of chloride in milk,² boiler water,³ gaseous mixtures,⁴ water and industrial wastes,^{5–10} but do not have high precision and accuracy at very low chloride levels, and are susceptible to interference by various ions.

We have been working on the sorption characteristics of some mixed oxide systems and have also investigated the electrochemical performance of membranes made with them. We have found that a mixed hydroxide of iron and zirconium (with iron as a major constituent) exhibits much greater capacity for anion uptake than either the pure iron or zirconium oxide. Polystyrene-based membranes made with this product also possess better anion-selectivity than those made with the individual oxides. Earlier, we described the use of a zirconium oxide membrane for estimation of molybdate,¹¹ and here we report the use of the mixed oxide membrane as an ion-selective electrode for chloride.

EXPERIMENTAL

All reagents were of analytical grade.

Preparation of mixed and doped oxides

Iron(III) chloride (0.2M) and zirconyl chloride (0.2M) solutions were mixed in 8:1 volume ratio, then 1.0M ammonia solution was added with constant stirring; the precipitate obtained was aged in the mother liquor for two days at room temperature, then filtered off, washed with water and dried at 80° for 24 hr.

A doped oxide was prepared by adding 50 ml of a solution containing 0.075 g of tin(II) chloride to 450 ml of the 8:1

mixed iron/zirconium solution, and precipitating *etc.* as just described.

Preparation of the ion-selective membrane

Unsupported membranes of the oxides could not be prepared, but membranes made with polystyrene as binder were found to be quite stable. They were obtained by thoroughly mixing 1.275 g of the oxide with 0.225 g of polystyrene and heating the mixture in a 2.5-cm diameter die at 120° under a pressure of 6500–7000 psi. By this method, membranes that were both mechanically and chemically stable were obtained and were checked under an electron microscope for deformities or cracks. Membranes thus obtained were equilibrated in 0.1M sodium chloride for 2–3 days, the solution being changed four or five times at intervals during this period. The minimum equilibration time was determined in a preliminary investigation, and it was observed that membranes equilibrated for shorter times did not give stable potentials.

Potential measurements

The electrode assembly used for potential measurements was the same as that reported earlier¹² and the reference solution was 0.1M sodium chloride. Ionic strength was adjusted by adding 5 ml of saturated potassium nitrate solution to 50 ml of test solution. All e.m.f. measurements were made at $25 \pm 0.1^\circ$ with a Radiometer (model PHM64) millivoltmeter coupled with a Servoscribe recorder. Ceramic-junction calomel reference electrodes were used.

RESULTS AND DISCUSSION

The response of the electrode is relatively fast. The response time (static) was found to be 15 sec for dilute solutions ($10^{-3}M$) and a little more (20 sec) for concentrated solutions (0.1M), the potentials reaching a value constant within ± 0.2 mV, with no deviation for 30 min, after which a slow drift in potential occurred. Ten replicates at two concentration levels gave a standard deviation of 0.4 mV in the higher concentration range (0.1M) and 0.5 mV in the lower concentration range ($10^{-3}M$).

The potentials obtained with mixed and doped

Table 1. Selectivity coefficient values for Fe-Zr and Sn(II)-doped Fe-Zr mixed hydrous oxide membrane electrodes at $10^{-3}M$ concentration of interfering ion, determined by the fixed interference method

Ion	$k_{A,B}^{pot}$	
	Mixed oxide membrane	Doped oxide membrane
Br^-	1.75×10^{-2}	1.34×10^{-2}
I^-	1.64×10^{-2}	1.29×10^{-2}
NO_3^-	1.05×10^{-2}	1.01×10^{-2}
ClO_4^-	1.07×10^{-2}	1.02×10^{-2}
SCN^-	1.14×10^{-2}	1.08×10^{-2}
$S_2O_4^{2-}$	1.29×10^{-3}	1.12×10^{-3}
$C_2O_4^{2-}$	6.44×10^{-4}	6.23×10^{-4}
SO_4^{2-}	8.5×10^{-4}	8.25×10^{-4}
WO_4^{2-}	1.13×10^{-3}	1.02×10^{-3}
MoO_4^{2-}	1.16×10^{-3}	1.08×10^{-3}
PO_4^{3-}	9.79×10^{-4}	9.42×10^{-4}
AsO_4^{3-}	4.36×10^{-4}	4.12×10^{-4}
$Fe(CN)_6^{3-}$	7.65×10^{-4}	7.43×10^{-4}
$Fe(CN)_6^{4-}$	3.36×10^{-5}	3.18×10^{-5}

oxide membranes in contact with chloride ions are shown in Fig. 1. In both cases the potential response is linear in the range 10^{-4} – $10^{-1}M$ chloride, with a non-Nernstian slope of 29.5 mV/decade. Coetzee and Basson have reported an even lower response for a caesium-electrode based on caesium phospholybdate.¹³

The effect of pH was investigated at two chloride concentrations (Fig. 2). The useful pH range was found to be 4–7. Below pH 4 hydrogen ions interfere and above pH 7 hydroxide ions interfere.

The membrane electrodes can also be applied to the determination of chloride concentration in an aqueous medium containing up to 25% v/v ethanol, methanol or acetone, the response being the same as in purely aqueous medium. The stability of response decreases at higher levels of the non-aqueous component and there is a drift in potential.

The performance of the electrode in the presence of other ions has been assessed and the selectivity coefficients determined by the fixed interference¹⁴ method (Table 1). The selectivity is fairly good.

The effect of cations was also examined. The potential values for chloride were independent of the presence of various cations such as Na^+ , K^+ , Li^+ , Ca^{2+} , Ba^{2+} , Sr^{2+} , Mg^{2+} , Zn^{2+} , Al^{3+} at concentrations equivalent to that of the chloride, but Ag^+ , Hg^{2+} and Pb^{2+} interfere at levels at which they will decrease the

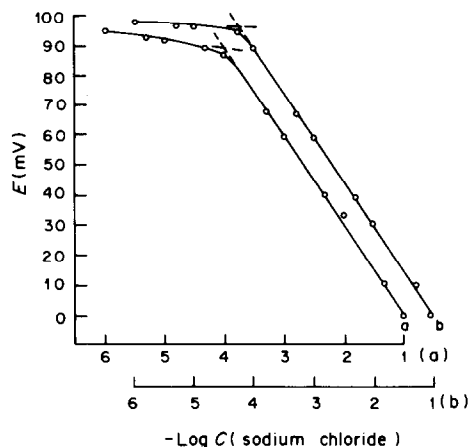


Fig. 1. Potential vs. $-\log[Cl^-]$ with the mixed oxide membrane (a), and doped oxide membrane (b).

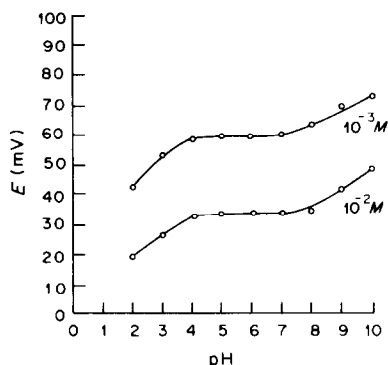


Fig. 2. Variation of membrane potential with pH.

chloride concentration by precipitation or complex formation.

The electrode system is also tolerant of the presence of low concentrations ($10^{-4}M$) of cationic surfactants (cetyltrimethylammonium bromide or cetylpyridinium chloride). Proteins (albumin, gelatin), if present in traces (10^{-5} – $10^{-6}M$) also do not cause any disturbance but higher levels ($10^{-3}M$) of proteins poison the membrane surface. Anionic surfactants (sodium dodecyl sulphate) cause significant interference, but if the membrane is preconditioned by soaking for 4 hr in a solution of the anionic surfactant, this effect disappears (Table 2).

The membrane electrode can be used in the temperature range 20–40° without correction to the potential. The electrode can be used for 4 months

Table 2. Potentials for sodium chloride and SDS ($10^{-4}M$) mixtures

[Cl ⁻], M	Potential from calibration plot, mV	Potential when SDS is also present, mV	
		Original membrane	Membrane treated with SDS
10^{-2}	32.9	39.8	33.0
10^{-3}	59.0	67.1	59.1
10^{-4}	85.0	97.6	85.2

without showing any drift in potential, but the linear range and slope decrease slowly after continuous use for about 6 months. If contamination occurs, it can be removed by equilibrating the membrane with 0.1M sodium chloride for 2–3 days. If this treatment fails, it is advisable to discard the electrode and prepare a new one.

Acknowledgement—One of the authors (C.K.J.) is grateful to CSIR, New Delhi, India for financing this research project.

REFERENCES

1. C. J. Coetzee, *Ion-Selective Electrode Rev.*, 1981, **3**, 105.
2. A. W. M. Sweetsur, *Analyst*, 1974, **99**, 690.
3. G. B. Marshall and D. Midgley, *ibid.*, 1978, **103**, 438.
4. T. G. Lee, *Anal. Chem.*, 1969, **41**, 391.
5. I. Sakerka, J. F. Lechner and R. Wales, *Water Research*, 1975, **9**, 663.
6. M. Mascini and A. Liberti, *Anal. Chim. Acta*, 1969, **47**, 339.
7. J. Růžička and G. G. Lamm, *ibid.*, 1971, **54**, 1.
8. K. Torrance, *Analyst*, 1974 **99**, 203.
9. J. C. Van Loon, *ibid.*, 1968, **93**, 788.
10. *Idem*, *Anal. Chim. Acta*, 1971, **54**, 23.
11. S. K. Srivastava, A. K. Sharma and C. K. Jain, *Talanta*, 1983, **30**, 285.
12. S. K. Srivastava, R. P. Singh and S. Agarwal, *J. Chem. Tech. Biotech.*, 1977, **27**, 680.
13. C. J. Coetzee and A. J. Basson, *Anal. Chim. Acta*, 1971, **54**, 478.
14. G. G. Guilbault, *Ion-Selective Electrode Rev.*, 1979, **1**, 139.

DUAL-WAVELENGTH SPECTROPHOTOMETRIC DETERMINATION OF TRACE SULPHIDE IN DOMESTIC WATER THROUGH ITS LIGAND-EXCHANGE REACTION WITH SILVER-CADION 2B-TRITON X-100

WEI FU-SHENG, TENG EN-JIANG and RUI KUI-SHENG
China National Environmental Monitoring Centre, Beijing, China

(Received 13 January 1984. Accepted 15 May 1984)

Summary—Trace amounts of S^{2-} can be determined by means of the exchange reaction with the Ag^+ -Cadion 2B complex in presence of Triton X-100 and $Na_2B_4O_7$ solution, by dual-wavelength spectrophotometry. Beer's law is obeyed for the sulphide range 0–2.0 $\mu g/25$ ml. The apparent molar absorptivity is 2.65×10^5 l.mole $^{-1}$.cm $^{-1}$. The effect of diverse ions in the presence of EDTA has been studied. The interferences produced by some anions in water samples can be eliminated by precipitation with zinc acetate.

In the presence of Triton X-100 and sodium tetraborate solution (pH 9.2), Ag^+ forms a purplish red complex with Cadion 2B which has been used for determination of silver and cyanide in water.^{1,2} In those experiments we noticed that sulphide can discharge the purplish red of the Ag^+ -Cadion 2B complex. This paper reports the exchange reaction of S^{2-} with the Ag^+ -Cadion 2B complex and the optimum conditions for the determination of trace amounts of sulphide in water. By the dual-wavelength method the apparent molar absorptivity for sulphide is 2.65×10^5 l.mole $^{-1}$.cm $^{-1}$. The method is more sensitive than the standard Methylene Blue method³ and the other indirect spectrophotometric methods for the determination of sulphide with Ag^+ -phen-BPR,^{4,5} Cu^{2+} -DDTC,⁶ Cu^{2+} -STTA,⁷ Cu^{2+} -(2'-amino-3'-hydroxypyridyl-4'-azo)-benzene-4-sulphonic acid (AHD-4S),⁸ Cu^{2+} -oxine,⁹ Hg^{2+} -chloranilic acid,¹⁰ Hg^{2+} -DPC,¹¹ Hg^{2+} -AHD-4S,¹² Fe^{2+} -bathophen.¹³ The accuracy and precision of this method are quite good.

EXPERIMENTAL

Reagents

Standard silver solution, 1.000 mg/ml. Dissolve 0.1578 g of analytical-reagent grade silver nitrate in distilled water and dilute to 100 ml.

Standard sulphide solution, 1.0 mg/ml. Use $Na_2S \cdot 9H_2O$ of analytical-reagent grade, and standardize it.³ Before use dilute it with cooled boiled water to give a 1.00- $\mu g/ml$ working standard.

Cadion 2B solution, 0.04%, in ethanol.

Triton X-100 solution, 5%, in distilled water.

Sodium tetraborate solution, 5%, in distilled water.

Coloured complex solution. To a 200-ml standard flask containing 400 μg of Ag^+ , add 40 ml of the sodium tetraborate solution, 20 ml of the Triton X-100 solution and 30 ml of the Cadion 2B solution, dilute to volume with distilled water and mix well.

General procedure

To a 25-ml standard flask add a known volume of sample containing less than 2.0 μg of sulphide and then 10.0 ml of the coloured complex solution, dilute to volume with distilled water, and mix well. After 10 min, measure the absorbance at 446 nm for the sample and 556 nm for the reference (1-cm cells) with a dual-wavelength double-beam recording spectrophotometer (e.g., a Shimadzu model UV 3000).

Procedure for determination of the sulphide in domestic sewage

Pipette an aliquot of water sample containing less than 2.0 μg of sulphide into a beaker, dilute to 25 ml with water, then add 1 ml of 1% zinc acetate solution and 1.25 ml of 0.1M sodium hydroxide and mix well. Allow the precipitated ZnS and $Zn(OH)_2$ to settle out, and then decant the supernatant liquid. Wash the precipitate with sufficient distilled water and separate again. Add 1.5 ml of 0.05M EDTA, and mix well. After 3 min, add 10.0 ml of the coloured complex solution and dilute to 25 ml with distilled water. Measure the absorbance according to the procedure above.

RESULTS AND DISCUSSION

The principle of the method and selection of wavelength

The absorption spectra of Cadion 2B, and of Ag^+ -Cadion 2B complex alone and in the presence of sulphide at pH 9.2 in borax buffer solution, are shown in Fig. 1. The absorbance of the Ag^+ -Cadion 2B system at 556 nm is decreased by the presence of sulphide and that at 446 nm is increased. The sensitivity for sulphide will be increased by measuring the difference in absorbance at these wavelengths by dual-wavelength spectrophotometry.

Experiments showed that the best linearity for the calibration graph was obtained by taking 446 nm as the "sample" wavelength and 556 nm as the "reference" wavelength. The apparent molar absorptivity for sulphide is 2.65×10^5 l.mole $^{-1}$.cm $^{-1}$.

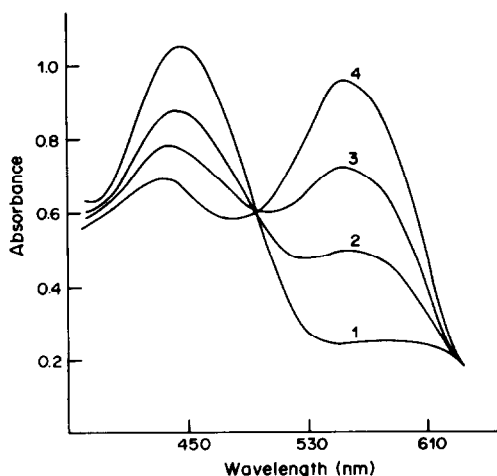


Fig. 1. Absorption spectra: 1, $1.6 \times 10^{-3} M$ Cadion 2B; 2, 10.0 ml of the coloured soln. + $2.0 \mu\text{g}$ of S^{2-} ; 3, 10.0 ml of the coloured soln. + $1.0 \mu\text{g}$ of S^{2-} ; 4, 10.0 ml of the coloured soln. (water as reference).

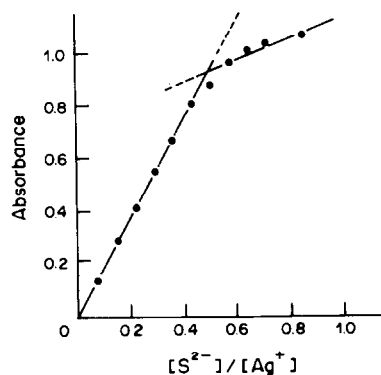
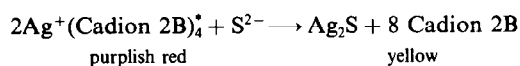


Fig. 2. The molar ratio method: $[\text{Ag}^+] = 7.4 \times 10^{-6} M$.

Figure 2 shows the reacting molar ratio of sulphide to silver in this system is 1:2.

The apparent molar absorptivity of the Ag^+ -Cadion 2B complex is $1.41 \times 10^5 \text{ l. mole}^{-1} \text{ cm}^{-1}$ by the dual-wavelength method, approximately half that for the sulphide.

The basis of the method is obviously the ligand exchange reaction



Effect of the amount of Ag^+ -Cadion 2B coloured complex

It does not matter whether the sulphide is added before or after formation of the silver-Cadion 2B complex. To simplify operations and reduce error, use of the coloured complex solution was selected. The effect of the amount of coloured complex solution used is given in Fig. 3. Beer's law is obeyed in

*See Reference 1 for the molar ratio of silver to Cadion 2B.

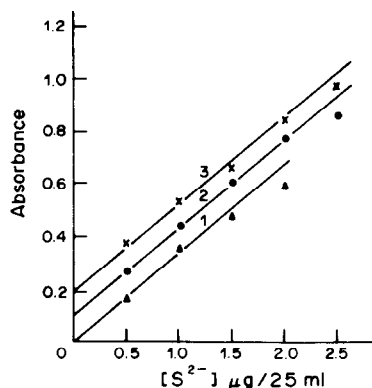


Fig. 3. Effect of the amount of the coloured complex solution: 1, 7.0 ml; 2, 10.0 ml; 3, 13.0 ml.

the sulphide range 0–80 ng/ml for 10.0 ml of the coloured complex solution, and the only effect of adding more or less reagent is to shift the calibration graph along the absorbance axis.

Effect of other ions and elimination of interferences

All the anions that react with Ag^+ to form stable compounds would interfere and so would all metal ions that form coloured complexes with Cadion 2B or hydrolyse under the conditions used, so the effects produced by some ions generally present in water samples, on determination of $1.0 \mu\text{g}$ of sulphide in the presence of EDTA, were examined. The following ions [in the amounts (μg) given in parentheses] do not interfere: PO_4^{3-} (1000), SO_4^{2-} (1000), NO_3^- (1000), Cu^{2+} (100), Fe^{2+} (50), Pb^{2+} (25), Ni^{2+} (25), Cd^{2+} (25), Al^{3+} (25), Cr^{3+} (25), Cl^- (10), Br^- (10). Cyanide and iodide cannot be tolerated at all.

To separate sulphide from large amounts of Cl^- , and from SO_3^{2-} , $\text{S}_2\text{O}_3^{2-}$, I^- , CN^- , which may appear in some water samples, it is precipitated with zinc acetate. The recovery is between 95 and 104% (shown by adding standard sulphide solution to distilled water and tap water, see Table 1).

Table 1. Recovery obtained by adding standard sulphide solution

No.	System	Added, μg	Found, μg
1	25 ml of distilled water	0.50	0.50
2		1.00	0.99
3		2.00	1.91
4	25 ml of tap water	2.00	1.96
5		2.00	2.08

Table 2. Analysis of water samples

No.	Source	Concentration of S^{2-} , mg/l.	
		Present method	Methylene Blue method
1	Domestic sewage	0.009	Undetected
2		0.018	0.017
3		0.084	0.088
4	Waste water	0.55	0.54
5		2.00	2.07

Precision

The coefficient of variation obtained according to the procedure above was 5% for 0.21 $\mu\text{g}/25\text{ ml}$ (8 determinations) and 1.4% for 0.91 $\mu\text{g}/25\text{ ml}$ (6 determinations).

Results for water samples analysed

Some domestic sewage samples were analysed by the new method and the results compared well with those of the Methylene Blue method (Table 2).

REFERENCES

1. F. S. Wei and F. Yin, *Talanta*, 1983, **30**, 190.
2. Y. R. Zhu, F. S. Wei and F. Yin, *ibid.*, 1983, **30**, 795.
3. *Standard Methods for the Examination of Water and Wastewater*, 14th Ed., p. 503, American Public Health Association, American Water Works Association and Water Pollution Control Federation, 1976.
4. F. S. Wei, Y. R. Zhu, F. Yin and N. K. Shen, *Talanta*, 1981, **28**, 853.
5. J. H. Hwang and Y. S. Guo, *Zhonshan Daxue Xuebao (Ziran Kexueban)*, 1983, No. 1, 140.
6. N. Toshio, *Bunseki Kagaku*, 1973, **22**, 691.
7. D. Masakazu and K. Akihide, *ibid.*, 1978, **27**, 527.
8. O. S. Chauhan, I. Singh, B. S. Garg and R. P. Singh, *Chem. Anal. (Warsaw)*, 1981, **26**, 477.
9. M. Román Ceba, F. Vinagre Jara and J. A. Muñoz Leyva, *Analyst*, 1982, **107**, 781.
10. R. E. Humphrey and W. Hinze, *Anal. Chem.*, 1971, **43**, 1100.
11. T. Okutani and S. Utsumi, *Bull. Chem. Soc. Japan*, 1967, **40**, 1386.
12. O. S. Chauhan, Y. S. Varma, I. Singh, B. S. Garg and R. P. Singh, *Acta. Chim. Acad. Sci. Hung.*, 1981, **108**, 351.
13. N. K. Shen, F. S. Wei and N. X. Chen, *Zhonguo Kexue Jishu Daxue Xuebao*, 1982, **12**, 62.

DETERMINATION OF QUINONES BY A CHEMILUMINESCENCE REACTION IN SOLUTION

J. L. BURGUERA and M. BURGUERA

Departamento de Química, Facultad de Ciencias, Universidad de Los Andes, Apartado Postal 542, Mérida 5101-A, Venezuela

(Received 25 January 1984. Accepted 19 March 1984)

Summary—Oxidation of *p*-benzoquinone by hydrogen peroxide in an alkaline medium gives chemiluminescence emission with maximum intensity at 660 and 560 nm. 1,4-Naphthaquinone gives only a single maximum at 660 nm. These emissions can be used for the determination of μg amounts of the quinones. The interference effect of some organic compounds is described.

Quinones present in waste waters from the paper industry¹ and in airborne diesel-engine exhaust particulate samples² are considered to be potential warfare agents, because of their high toxicity to mammals^{3,4} and insects.⁵ Accordingly, analytical methods for the detection of such compounds should be as sensitive as possible. The methods recommended are based on polarographic measurements,⁶ reaction with substrates and detection by thin-layer chromatography,⁷ determination by ion-selective electrode and a Gran plot,⁸ and reaction with 8-hydroxyquinoline and colorimetric measurements.⁹ All these methods may be applied for the detection, identification or determination of quinones, but are not satisfactory in all respects. For example, the polarographic method is reproducible but time-consuming, and the thin-layer chromatographic method is sensitive but most quinones produce similar colours.

The chemiluminescence accompanying redox reactions of some quinones has been observed on reacting *p*-benzoquinone and adrenochrome with hydrogen peroxide in concentrated alkaline solutions.¹⁰ Although some kinetic studies have been made of these systems, no analytical applications have yet been reported. A number of quinones were therefore tested for chemiluminescence emission with hydrogen peroxide in alkaline medium to evaluate the analytical potentialities. Some mono and binuclear quinones, soluble in alkaline media, were tested for chemiluminescence emission in the wavelength range 400–700 nm. No emission was observed from tetrafluoro-1,4-benzoquinone, tetrahydroxy-1,4-quinone and 1,2-naphthaquinone-4-sulphonic acid, but emission was given by *p*-benzoquinone and 1,4-naphthaquinone. This paper describes the use of these observations for determining these two compounds.

EXPERIMENTAL

Apparatus

A standard Bausch & Lomb Spectronic 20 spectrophotometer with a working range from 340 to 950 nm,¹¹

was converted for measuring chemiluminescence by the pulse technique.¹² The signal was recorded on a Hewlett-Packard 680M chart recorder. The experimental technique used was that described previously.¹³

Reagents

All reagents were analytical grade, unless otherwise stated. The water was twice distilled from an all-glass apparatus.

Hydrogen peroxide (1.2–0.1M). Prepared by appropriate dilution of 100-volume hydrogen peroxide with water.

Stock quinone solutions ($10^{-2}M$). Prepared daily in 3mM phosphate buffer. Working solutions were prepared before use by appropriate dilution with buffer solution of the chosen pH.

Procedure

The quinone solution (1.2 ml) was injected into the hydrogen peroxide solution (1.2 ml). The emission intensity was recorded at 560 or 660 nm for *p*-benzoquinone and at 660 nm for 1,4-naphthaquinone, over a period of 65 sec. Each measurement was repeated 3–5 times. The same procedure was used for calibration or the determination of unknown samples.

RESULTS

Injections of a quinone solution into an alkaline hydrogen peroxide solution produces a chemiluminescence emission after ~35 sec. Typical emission *vs.* time curves for the two quinones studied are shown in Fig. 1. The spectral distribution of the chemiluminescence emission for *p*-benzoquinone and 1,4-naphthaquinone in the alkaline hydrogen peroxide system is shown in Fig. 2. The spectra were obtained by measuring the emission intensity produced at various wavelengths by a constant amount of quinone. The spectrum from the 1,4-naphthaquinone system has not hitherto been reported; it reveals a strong emission band in the spectral range from 600 to 700 nm with a maximum at 660 nm, indicating the formation of a single emitter. The spectrum from the *p*-benzoquinone system showed two broad bands in the range 400–700 nm with maxima at 560 and 660 nm, indicating the formation of two emitters. This spectrum resembled that obtained previously by Slawinska.¹⁰ Although

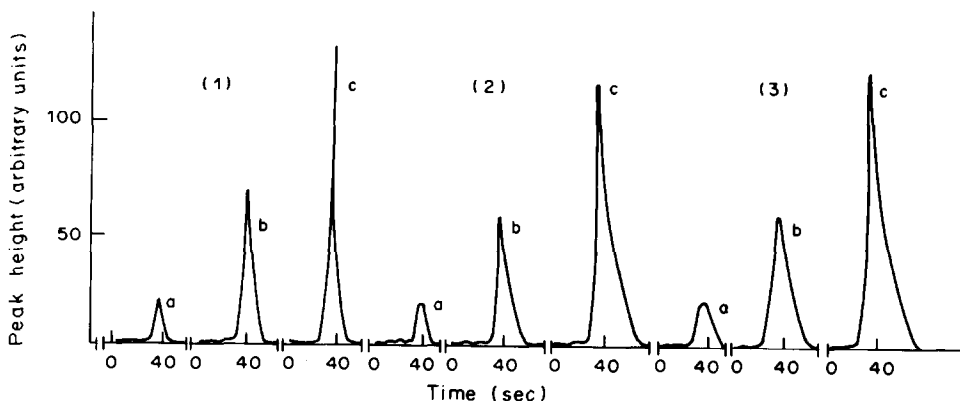


Fig. 1. Intensity vs. time profile obtained for (1) *p*-benzoquinone at 660 nm, (2) *p*-benzoquinone at 560 nm, (3) 1,4-naphthaquinone at 660 nm. a, b and c refer to quinone concentrations, in the final solution, of 4.5, 13.6 and 27.3 $\mu\text{g/ml}$. pH 12.0; 0.3M H_2O_2 ; 1.2 ml of sample and of hydrogen peroxide solution.

the spectra give no evidence on the nature of the emitters, it is likely that the chemiluminescence observed from both quinones at 660 nm is due to emitters of similar structure. This emission may arise by addition of O_2^- to the quinone, followed by decomposition to an excited orthoquinone. The chemiluminescence at 560 nm from *p*-benzoquinone could be attributed to the formation of a different excited complex between a *p*-benzoquinone free radical and a sensitized quinone molecule.¹⁴⁻¹⁶

The effect of hydrogen peroxide concentration on the maximum intensities is shown in Fig. 3. The chemiluminescence intensity at 660 nm increases with hydrogen peroxide concentration up to 0.3M for both quinones. The chemiluminescence intensity at 560 nm (from *p*-benzoquinone) shows similar behaviour up to a final hydrogen peroxide concentration of 0.4M. In all cases excess of hydrogen peroxide (up to 0.6M) produces no further increase in chemiluminescence intensity.

The effect of pH (8.0–13.0) on the chemiluminescence intensity is shown in Fig. 4, and was the same irrespective of the quinone and wavelength of maximum emission. The greatest intensity was observed at pH 12.0, which was therefore used in subsequent studies.

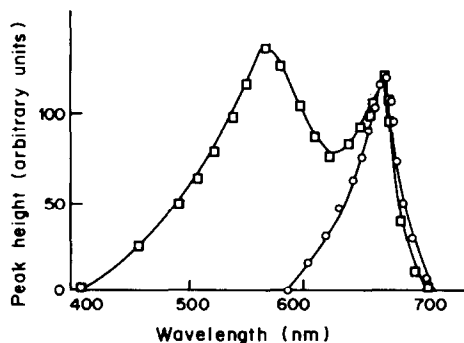


Fig. 2. Chemiluminescence spectra of (\square) *p*-benzoquinone and (\circ) 1,4-naphthaquinone. Quinone concentration 27.3 $\mu\text{g/ml}$. Other conditions as in Fig. 1.

Calibration graphs for both quinones were linear and had the equations: $I_1 = 1.008 + 0.498X_1$, $r_1 = 0.9995$; $I_2 = 1.087 + 0.419X_2$, $r_2 = 0.9999$; $I_3 = -0.163 + 0.442X_3$, $r_3 = 0.9991$, where I_1 , I_2 and I_3 are the intensities (in arbitrary units) for *p*-benzoquinone at 660 nm, *p*-benzoquinone at 560 nm, and 1,4-naphthaquinone at 660 nm, respectively, X_1 and X_2 are the *p*-benzoquinone concentrations in the

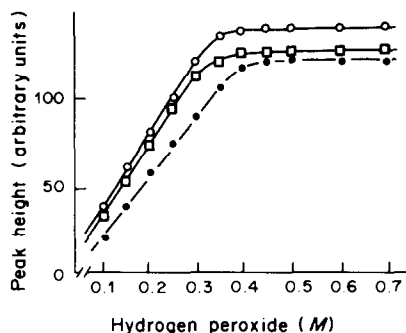


Fig. 3. Effect of hydrogen peroxide concentration on the chemiluminescence emission intensities. (\circ) 1,4-Naphthaquinone at 660 nm, (\square) *p*-benzoquinone at 660 nm, (\bullet) *p*-benzoquinone at 560 nm. Quinone concentration 27.3 $\mu\text{g/ml}$. Other conditions as in Fig. 1.

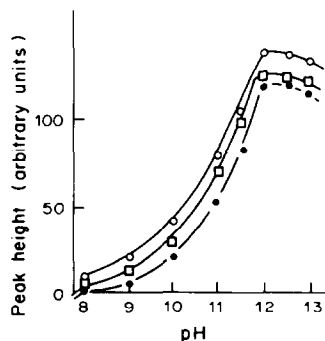


Fig. 4. Effect of pH on the chemiluminescence intensity. (\circ) 1,4-Naphthaquinone at 660 nm, (\square) *p*-benzoquinone at 660 nm, (\bullet) *p*-benzoquinone at 560 nm. Other conditions as in Fig. 3.

Table 1. Effect of hydrogen peroxide concentration on interference by organic compounds*

Interferent	Chemiluminescence intensity (arbitrary units)†														
	H ₂ O ₂ 0.3M			H ₂ O ₂ 0.4M			H ₂ O ₂ 0.5M			H ₂ O ₂ 0.6M			H ₂ O ₂ 0.7M		
	I	II	III	I	II	III	I	II	III	I	II	III	I	II	III
No interferent	145	135	146	125	135	145	128	137	148	123	135	144	126	138	
8-Hydroxyquinoline	72	69	89	65	90	112	95	122	146	122	134	145	122	134	
1,2-Chloranilic acid	136	129	142	119	130	147	123	135	148	124	137	146	126	136	
Hydroquinone	87	81	101	100	112	120	115	126	147	122	134	146	125	137	
Tetrahydroxy-1,4-quinone	124	108	130	98	122	135	117	130	146	122	135	146	123	134	
Tetrafluoro-1,4-benzoquinone	132	122	137	118	127	140	120	131	148	121	133	143	123	135	
Formaldehyde	188	162	170	168	150	165	147	146	158	132	142	156	131	140	
Gallic acid	170	156	165	135	154	163	130	148	152	127	141	150	129	140	
2,6-Dimethylbenzoquinone	158	148	156	136	146	156	134	144	153	132	143	150	130	143	

*Quinone concentration 27.2 µg/ml, interferent concentration 54.4 µg/ml.

†Concentration in final solution.

§I, II, III indicate values for *p*-benzoquinone at 660 and 560 nm, and for 1,4-naphthaquinone at 660 nm, respectively. pH 12.0, sample and hydrogen peroxide solution volumes 1.2 ml each.

ranges 1.8–36.4 and 2.3–29.5 µg/ml, respectively, and X_3 is the naphthaquinone concentration (3.2–27.3 µg/ml), and r_1 , r_2 and r_3 are the correlation coefficients (10 results). The detection limits were 1.0, 1.5 and 3 µg/ml for *p*-benzoquinone at 660 and 560 nm, and 1,4-naphthaquinone at 660 nm, respectively. The coefficients of variation for 6 measurements at the 9.1 µg/ml level were 3.0, 3.1 and 3.4% for *p*-benzoquinone (at 660 and 560 nm), and 1,4-naphthaquinone at 660 nm, respectively.

Interferences

The effects of some organic compounds on the chemiluminescence intensity from both quinones were investigated. An interference is defined as significant if it causes a change of more than two standard deviations in the chemiluminescence emission intensity. The results are shown in Table 1. Several organic compounds depress the emission from both quinones (e.g., 8-hydroxyquinoline, 1,2-chloranilic acid, hydroquinone, tetrahydroxy-1,4-quinone and tetrafluoro-1,4-benzoquinone), whereas others increase the chemiluminescence emission (e.g., formaldehyde, gallic acid and 2,6-dimethylbenzoquinone). These effects can be reduced or eliminated by increasing the hydrogen peroxide concentration to 0.6M. The depressive effects are reduced probably because at high concentrations of hydrogen peroxide there are sufficient O₂⁻ radicals present for the two quinones to be oxidized despite quenching by the inhibitors.¹⁷ The strong stimulating effect of formaldehyde and gallic acid is less sensitive to hydrogen peroxide concentration, possibly due to the intervention of other processes of sensitized chemiluminescence.^{18–20}

Conclusion

The chemiluminescence measurements have demonstrated the possibility of the determination of *p*-benzoquinone and 1,4-naphthaquinone at µg/ml level. The method is simple and rapid (1 measurement/min) and the detection limits are simi-

lar to those for many other techniques.^{6,7,9} The equipment used is simple and may be adapted to flow-injection analysis.^{21–23}

REFERENCES

- D. I. Stom, S. N. Suslov and V. N. Kurochkin, *Vopr. Prognoz. Biol. Rezhima Ust'-Ilim. Vodokhran.*, 1975, **14**, 111.
- K. Morita and K. Fukamachi, *Eisei Kagaku*, 1981, **27**, 169.
- D. I. Stom, S. S. Timofeeva and S. N. Suslov, *Gidrobiol. Ikhtiol. Isslev. Vost Sib.*, 1979, **3**, 157.
- V. V. Labunskii and V. A. Volodchenko, *Tr. Khar'k. Gos. Med. Inst.* 1976, **124**, 5.
- D. K. Reed, M. Jacobson, L. Jurd and B. Freedman, *Tech. Bull. U.S. Dept. Agric.*, 1981, No. 1641, 13.
- D. I. Stom, S. S. Timofeeva, N. F. Kashim, L. I. Bedykh, S. N. Suslov, U. V. Butorov and M. S. Apartsin, *Acta Hydrochim. Hydrobiol.* 1980, **8**, 204.
- H. Thielemann, *Sci. Pharm.*, 1979, **47**, 246.
- S. S. M. Hassan and M. B. Elsayed, *Mikrochim. Acta*, 1978 **II**, 333.
- V. Rani, M. Sugumaran, N. Appaji Rao and C. S. Vaidyanathan, *J. Indian Inst. Sci.*, 1978, **60**, No. 4, 43.
- D. Slawinska, *Photochem. Photobiol.*, 1978, **28**, 453.
- The Bausch & Lomb Spectronic 20 Colorimeter/Spectrophotometer*, Cat. Nos. 33-29-59, 33-29-61-65 and 33-29-95-01; 14th Ed., Bausch & Lomb, Rochester, New York.
- J. L. Burguera and A. Townshend, *Talanta*, 1979, **26**, 795.
- Idem, ibid.*, 1981, **28**, 731.
- S. A. Wilson and J. H. Weber, *Anal. Lett.*, 1977, **10**, 75.
- D. Slawinska, K. Lichszeld and T. Michaeska, *Pol. J. Chem.*, 1978, **52**, 1729.
- I. B. Afanas'ev and N. I. Polozova, *Zh. Org. Khim.*, 1979, **15**, 1802.
- C. S. Foote, R. W. Denny, L. Weaver, Y. Chang and J. Peters, *Ann. N.Y. Acad. Sci.*, 1970, **171**, 139.
- J. L. Burguera, M. Burguera and A. Townshend, *Acta Cient. Venez.*, 1981, **32**, 115.
- J. L. Burguera and M. Burguera, *ibid.*, 1983, **34**, 45.
- D. Slawinska and J. Slawinski, *Anal. Chem.*, 1975, **47**, 2101.
- J. L. Burguera and A. Townshend, *Proc. Anal. Chem.*, 1979, **16**, 263.
- J. L. Burguera, A. Townshend and S. Greenfield, *Anal. Chim. Acta*, 1980, **114**, 209.
- J. L. Burguera, M. Burguera and A. Townshend, *Rev. Roum. Chim.*, 1982, **27**, 879.

ANALYTICAL DATA

SOLVENT EXTRACTION OF THE ION-PAIRS OF CHROMIUM(VI) AND MOLYBDENUM(VI) WITH TRIOCTYLMETHYLAMMONIUM CHLORIDE AND BENZYLDIMETHYLCETYLAMMONIUM CHLORIDE

KOUSABURO OHASHI, KEIKO SHIKINA, HIROYUKI NAGATSU,
IZUMI ITO and KATSUMI YAMAMOTO

Department of Chemistry, Faculty of Science, Ibaraki University, Mito 310, Ibaraki, Japan

(Received 19 September 1983. Accepted 1 June 1984)

Summary—The number of capriquat molecules per chromium(VI) atom in the chromate–capriquat ion-association complex has been found to be between one and two. The distribution ratio in the extraction of chromium(VI) with capriquat is dependent on the dielectric constant of the organic solvent, with a minimum at a dielectric constant of about 8. The absorption spectra of the ion-pair extracted into cyclohexane, carbon tetrachloride, benzene and n-butanol are very similar to that of chromate in aqueous solution. The absorption spectra of the chromium(VI)–capriquat extracts in these organic solvents gradually change to an absorption spectrum similar to that of HCrO_4^- in aqueous solution. Chromium(VI)–capriquat extracted into chloroform and 1,2-dichloroethane gives absorption spectra similar to that of HCrO_4^- in aqueous medium. The chromium(VI)–capriquat species extracted into 1,2-dichloroethane may be $(\text{Q}^+)_2 \cdot \text{CrO}_4^{2-} (\text{H}_2\text{O})_n$. In contrast, chromium(VI) is extracted with capriquat into the other organic solvents from ammoniacal medium as a mixture of $(\text{Q}^+)_2 \cdot \text{CrO}_4^{2-} (\text{H}_2\text{O})_n$ and $\text{Q}^+ \cdot \text{NH}_4^+ \cdot \text{CrO}_4^{2-} (\text{H}_2\text{O})_n$. The spectral change is ascribed to the change of the extracted species from $(\text{Q}^+)_2 \cdot \text{CrO}_4^{2-} (\text{H}_2\text{O})_n$ and $\text{Q}^+ \cdot \text{NH}_4^+ \cdot \text{CrO}_4^{2-} (\text{H}_2\text{O})_n$ to $\text{Q}^+ \cdot \text{HCrO}_4^- (\text{H}_2\text{O})_{n-1}$. The chromium(VI)–zephiramine species extracted is formulated as $(\text{Q}^+ \cdot \text{NH}_4^+)_2 \cdot \text{CrO}_4^{2-} (\text{H}_2\text{O})_n \cdot (\text{Q}^+ \cdot \text{Cl}^-)_m$. Molybdenum(VI) is extracted with capriquat into the same organic solvents as a mixture of $(\text{Q}^+)_2 \cdot \text{MoO}_4^{2-} (\text{H}_2\text{O})_n$ and $\text{Q}^+ \cdot \text{NH}_4^+ \cdot \text{MoO}_4^{2-} (\text{H}_2\text{O})_n$.

Several studies have been made of the solvent extraction of ion-association complexes of chromium(VI)¹⁻³ and molybdenum(VI)⁴⁻⁷ with organic cations, to obtain detailed information about the complexes and the extraction mechanism, because chromium(VI) and molybdenum(VI) exist as various species in aqueous solution. The study of the extraction of chromium(VI) from weakly acid solution with organic cations (Q^+) such as triphenyltetrazolium,³ tetraphenylarsonium³ and n-propyltriphenylphosphonium³ suggested that chromium(VI) was extracted as an ion-pair ($\text{Q}^+ \cdot \text{HCrO}_4^-$). Winkhaus and Uhring² found that chromium(VI) was extracted in the pH range 1–3 with the di- π -cyclopentadienyltitanium cation (Q^{2+}) as $\text{Q}^{2+} \cdot \text{CrO}_4^{2-}$. In this pH range the main species of chromium(VI) is probably HCrO_4^- . They proposed that extraction of the 1:1 ion-pair is more favourable.

There have been few detailed investigations of the mechanism of solvent extraction of chromium(VI) with long-chain quaternary ammonium ions. The solvent extraction of low concentrations of chromium(VI) from alkaline solution with capriquat and zephiramine is described here.

Most of the work on the extraction of molybdenum(VI) with amines and quaternary ammonium

salts has been done in acid media, and the influence of acidity and diluents on the extraction investigated.^{6,7}

The extraction of molybdenum(VI) from alkaline solution with capriquat and zephiramine has therefore also been investigated, to compare it with that of chromium(VI).

EXPERIMENTAL

Apparatus

A Hitachi 170-30 type atomic-absorption spectrophotometer was used for determination of chromium(VI) and molybdenum(VI). A Hitachi EPS-3 type spectrophotometer was used to measure the absorption spectra. A Hitachi Horiba F-7 type pH-meter was used for pH measurements.

Reagents

Standard 0.1M chromium(VI) solution was prepared from potassium chromate and redistilled water. Standard 0.1M molybdenum(VI) solution was made by dissolving sodium molybdate in sodium hydroxide solution (pH 9). Working solutions were prepared by diluting these stock solutions with redistilled water, and buffered with ammonia/ammonium chloride solution.

Capriquat (Kanto Co. Ltd.) and zephiramine (Dojin Co. Ltd. GR grade) were used without further purification. Organic solvents were distilled before use. All other reagents were of analytical grade.

Procedure

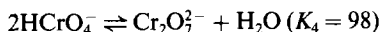
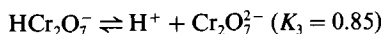
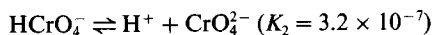
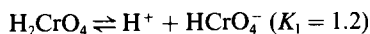
A 10-ml portion of $1.50 \times 10^{-5} M$ chromium(VI) and 10 ml of a given concentration of quaternary ammonium chloride in the selected organic solvent were pipetted into a 50-ml separatory funnel. A shaking time of 10 min gave a constant degree of extraction. After separation of the phases, chromium(VI) in the aqueous phase was determined. The pH of the aqueous phase was measured after the extraction, and found to change negligibly during the extraction. The number of quaternary ammonium ions per chromium(VI) atom in the ion-pair was determined from the slope of the straight line obtained by plotting $\log D$ vs. $\log [Q^+ \cdot Cl^-]$, where D and $[Q^+ \cdot Cl^-]$ are the distribution ratio and the concentration of free quaternary ammonium chloride. A large excess of quaternary ammonium chloride was used, so that the amount extracted could be neglected and $[Q^+ \cdot Cl^-]$ taken as the concentration added.

RESULTS AND DISCUSSION

Extraction of chromium(VI) with capriquat

The plots of $\log D$ vs. $\log [Q^+ \cdot Cl^-]$ for extraction of chromium(VI) with capriquat into the organic solvents were linear up to 90% extraction. Table 1 gives the number (n) of capriquat ions per chromium(VI) atom in the ion-pairs extracted into cyclohexane, carbon tetrachloride, benzene, chloroform, n-butanol, 1,2-dichloroethane and methyl isobutyl ketone (MIBK); n varied between 1.3 and 2.0.

The equilibria for the proton-dissociation and dimerization of chromium(VI) in aqueous solution are well characterized and are as follows:⁸



At a chromium(VI) concentration of $10^{-4} M$, CrO_4^{2-} is the main species in alkaline solution. The fact that the number of capriquat ions per chromium(VI) atom is between 1.3 and 2.0 in these extractions suggests that chromium(VI) may be extracted as a mixture of $(Q^+)_2 \cdot CrO_4^{2-}$ and other ion-pair species.

Absorption spectra of extracted chromium(VI)-capriquat species

Figures 1 and 2 show the absorption spectra of the chromium(VI)-capriquat species extracted into cyclohexane and carbon tetrachloride, and Fig. 3 the spectra of CrO_4^{2-} and $HCrO_4^-$ in aqueous solution. The spectrum of the extracted chromium(VI)-capriquat species, measured immediately after sepa-

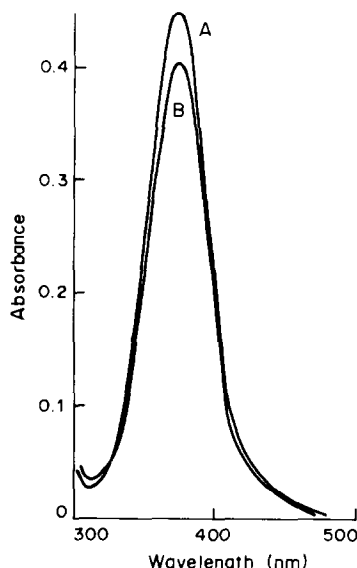


Fig. 1. Absorption spectra of the chromium(VI)-capriquat species extracted into cyclohexane. $[Cr(VI)]: 1.00 \times 10^{-4} M$; $[capriquat]: 0.1 M$; pH 9.2; 94% extraction; 17 hr standing after extraction; spectra (A) and (B) were measured 3 min and 100 hr, respectively, after separation.

ration, is very similar to that of CrO_4^{2-} in aqueous solution. When benzene and n-butanol were used, similar absorption spectra were obtained. On the other hand, the absorption spectra of

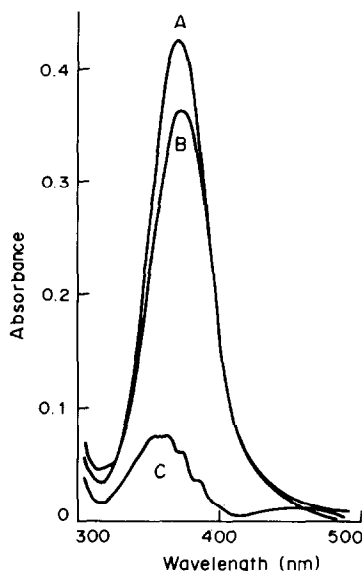


Fig. 2. Absorption spectra of the chromium(VI)-capriquat species extracted into carbon tetrachloride. Conditions as for Fig. 1; 90% extraction; 4 hr standing after extraction; spectra (A), (B) and (C) were measured 3 min, 11 hr and 62 hr, respectively, after separation.

Table 1. Number (n) of capriquat ions bonded per chromium(VI) atom, as a function of the dielectric constant (ϵ) of the organic solvent (extraction at pH 9.2)

Solvent	CCl_4	C_6H_6	C_6H_{12}	$CHCl_3$	$1,2-C_2H_4Cl_2$	MIBK	$n-C_4H_9OH$
n	1.5	1.5	1.3	1.5	2.0	2.0	1.6
ϵ	2.2	2.3	2.3	4.9	10.4	13.1	16.4

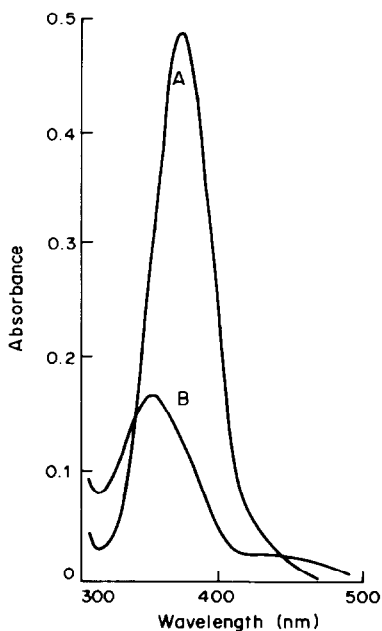


Fig. 3. Absorption spectra of $1.00 \times 10^{-4} M$ chromium(VI) in aqueous solution: (A) pH 9.5, (B) pH 3.0.

chromium(VI)-capriquat species extracted into 1,2-dichloroethane (Fig. 4) and chloroform are very similar to that of HCrO_4^- in aqueous solution. The absorption spectra of the chromium(VI)-capriquat species extracted into benzene, cyclohexane, carbon tetrachloride and *n*-butanol gradually changed into an absorption spectrum similar to that of HCrO_4^- in aqueous solution. The rate of the spectral change increases in the order cyclohexane < benzene < carbon tetrachloride < *n*-butanol < MIBK. The molar absorptivity and wavelength of maximum absorption for the cyclohexane extract are in good agreement with those of CrO_4^{2-} in aqueous solution, suggesting that the chromium(VI) species in the ion-pair is CrO_4^{2-} . The number of capriquat ions extracted per chromium(VI) atom with cyclohexane was 1.3. As an ammonia buffer was used to adjust the pH, ammonium ions may also participate in the

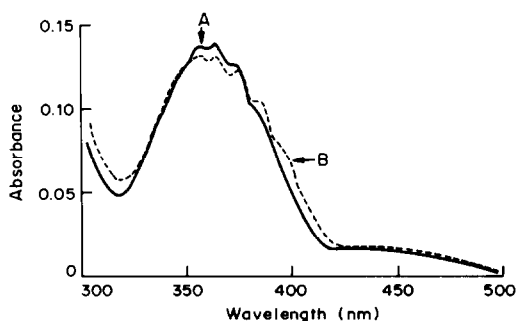


Fig. 4. Absorption spectra of the chromium(VI)-capriquat species extracted into 1,2-dichloroethane. $[\text{Cr(VI)}]: 1.00 \times 10^{-4} M$; [capriquat]: $0.05 M$; pH 9.2; 84% extraction; 3 min standing time after shaking; (A) and (B) measured 3 min and 15 hr, respectively, after separation.

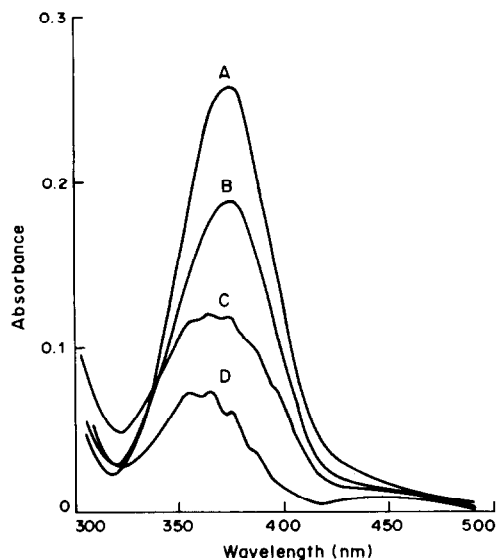


Fig. 5. Absorption spectra of the chromium(VI)-zephiramine species extracted into chloroform. $[\text{Cr(VI)}]: 1.00 \times 10^{-4} M$; [zephiramine]: $0.05 M$; 79% extraction; pH 9.2; 2 hr standing after separation; (A), (B), (C) and (D) measured 2 min, 1 hr, 6 hr and 13 hr, respectively, after separation.

extraction, and the chromium(VI) be extracted as a mixture of $(\text{Q}^+)_2 \cdot \text{CrO}_4^{2-}$ and $\text{Q}^+ \cdot \text{NH}_4^+ \cdot \text{CrO}_4^{2-}$. The same could apply to the benzene, carbon tetrachloride and *n*-butanol systems, although the molar absorptivities for these extracts are slightly smaller than that of CrO_4^{2-} in aqueous medium. The corresponding data for the 1,2-dichloroethane system ($n = 2.0$, absorption spectrum, immediately after separation, similar to that of HCrO_4^- in aqueous solution) suggest that $(\text{Q}^+)_2 \cdot \text{CrO}_4^{2-}$ is extracted but rapidly changes into $\text{Q}^+ \cdot \text{HCrO}_4^-$, the proton possibly coming from a water molecule attached to the chromium(VI) in the ion-pair.

Extraction of chromium(VI) with zephiramine

The plots of $\log D$ vs. $\log [\text{zephiramine}]$ were linear with a slope of 2.7. The absorption spectrum of the species extracted into chloroform is shown in Fig. 5. The spectrum measured immediately after the separation is very similar to that of CrO_4^{2-} in aqueous medium and changes much more slowly than that of the chromium(VI)-capriquat species in chloroform. The chromium(VI) may be extracted with zephiramine as $(\text{Q}^+, \text{NH}_4^+)_2 \text{CrO}_4^{2-} (\text{H}_2\text{O})_n \cdot (\text{Q}^+ \cdot \text{Cl}^-)_m$ where $(\text{Q}^+, \text{NH}_4^+)$ indicates vicarious substitution of NH_4^+ for Q^+ . The spectral change may be ascribed to the formation of $\text{Q}^+ \cdot \text{HCrO}_4^- (\text{H}_2\text{O})_{n-1}$.

Chromium(VI) has been found² to be extracted at pH 1-3 with the di- π -cyclopentadienyltitanium cation (Q^{2+}) into chloroform as $\text{Q}^{2+} \cdot \text{CrO}_4^{2-}$, though the dominant species of chromium(VI) in aqueous solution at pH 1-3 is HCrO_4^- .

In the present work, it was found spectrophotometrically that the chromium(VI)-capriquat species extracted into organic solvents as

Table 2. Number (n) of capriquat ions bonded to one molybdenum(VI) atom

Solvent	CCl ₄	C ₆ H ₆	C ₆ H ₁₂	CHCl ₃	1,2-C ₂ H ₄ Cl ₂	n-C ₄ H ₉ OH
n	1.3	1.4	1.1	1.0	1.5	1.8
ϵ	2.2	2.3	2.3	4.9	10.4	16.4

$Q^+ \cdot NH_4^+ \cdot CrO_4^{2-} \cdot (H_2O)_n$ and/or $(Q^+)_2 \cdot CrO_4^{2-} \cdot (H_2O)_n$ changes to $Q^+ \cdot HCrO_4^- \cdot (H_2O)_{n-1}$. It therefore seems likely that there are thermodynamic factors that favour extraction of 1:1 charge-matched species rather than 2:1 species formed from components with different charges.

Extraction of molybdenum(VI) with capriquat and zephiramine

The number of capriquat ions per molybdenum(VI) in the molybdenum(VI)–capriquat species extracted was determined by the procedure used for chromium(VI). As shown in Table 2, n for the capriquat system was between 1.0 and 1.8. For the zephiramine system it was 2.7. The extraction of molybdenum(VI) from alkaline solution with capriquat and zephiramine seems essentially the same as the extraction of chromium(VI) with capriquat and zephiramine. At pH 9.2, molybdenum(VI) exists as MoO_4^{2-} because the proton-dissociation constant (pK_a) of $HMoO_4^-$ is 4.1, and polymerized species can be neglected for $10^{-4}M$ Mo(VI) in alkaline medium. The ion-association species of $(Q^+)_2 \cdot MoO_4^{2-} \cdot (H_2O)_n$ and $Q^+ \cdot NH_4^+ \cdot MoO_4^{2-} \cdot (H_2O)_n$ are proposed for the capriquat system and $(Q^+, NH_4^+)_2 MoO_4^{2-} \cdot (H_2O)_n \cdot (Q^+ \cdot Cl^-)_m$ for the zephiramine system.

The absorption spectra of the molybdenum(VI)–capriquat and molybdenum(VI)–zephiramine species extracted were not obtained, because of their very small molar absorptivities.

Effect of organic solvent on the distribution ratio

Figure 6 shows the relationship between $\log D$ and the dielectric constant of the organic solvents for the

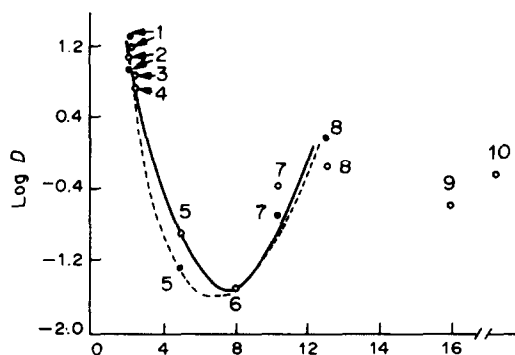


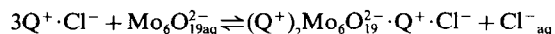
Fig. 6. Relationship between $\log D$ and the dielectric constant (ϵ) of the organic solvent. O: $5.00 \times 10^{-5}M$; Cr(VI); pH 9.2; 0.01M capriquat. ●: $1.00 \times 10^{-4}M$; Mo(VI); pH 10.5; 0.01M capriquat. Organic solvent: 1, cyclohexane; 2, carbon tetrachloride; 3, benzene; 4, toluene; 5, chloroform; 6, tributyl phosphate; 7, 1,2-dichloroethane; 8, MIBK; 9, n-butanol; 10, nitrobenzene.

extraction of chromium(VI) and molybdenum(VI) with capriquat. The value of $\log D$ exhibits a minimum at a dielectric constant of about 8. Though the dielectric constants of n-butanol and nitrobenzene are 16.1 and 34.8 respectively, the distribution ratios are not very different. Similar solvent effects were obtained for the molybdenum(VI)–capriquat system.

The degree of extraction of chromium(VI) with triphenyltetrazolium at pH 4.0–4.2 decreases according to the solvent used, in the order³ nitrobenzene > chloroform > benzene > carbon tetrachloride > cyclohexane. It is noteworthy that the long-chain quaternary ammonium ion seems to have a different effect from that of triphenyltetrazolium ion on the extraction of chromium(VI).

The influence of organic solvents on the extraction of molybdenum(VI) with tri-iso-octylamine from hydrochloric acid has been reported.⁶ The degree of extraction of molybdenum(VI) from 1.0M hydrochloric acid decreases according to the solvent used, in the order 1,2-dichloroethane > 1,2-dichlorobenzene > carbon tetrachloride. In contrast, the distribution ratio for the extraction of molybdenum(VI) with capriquat into carbon tetrachloride is larger than that for use of 1,2-dichloroethane (Fig. 6). The molybdenum(VI) species extracted with tri-iso-octylamine was reported⁶ to be $MoO_2Cl_4^{2-}$ or MoO_2Cl_2 . We cannot discuss these results in detail, because of the limited number of studies of the solvent effect on these extraction systems.

As mentioned above, the number of zephiramine ions bonded per molybdenum(VI) is greater than that needed to give electroneutrality with MoO_4^{2-} . A similar result was obtained for the extraction of molybdenum(VI) with capriquat into kerosene at pH 2.2–2.5,⁷ and it was proposed that for $[Mo(VI)] > [Q^+ \cdot Cl^-]$ the reaction was



The same process was proposed for the extraction into chloroform.

Sato *et al.*⁹ investigated the extraction of molybdenum(VI) with capriquat from sodium hydroxide solution into benzene and suggested the extracted species had the composition $Q^+ : Mo(VI) : H_2O = 2 : 1 : 14$. It is interesting that it was proposed that molybdenum(VI)–capriquat is solvated with water. The molybdenum(VI)–capriquat species extracted into carbon tetrachloride, n-butanol, 1,2-dichloroethane, chloroform and benzene from an alkaline ammonia buffer may also be solvated with water.

We have therefore examined the extraction of chromium(IV) and molybdenum(VI) with capriquat from sodium hydroxide medium. Extraction of

chromium(VI) into chloroform or 1,2-dichloroethane gave a solution with an absorption spectrum similar to that for CrO_4^{2-} in aqueous medium, in contrast to the spectra of extracts from ammoniacal medium. The number of capriquat ions bound per chromium(VI) or molybdenum(VI) in the extracts from sodium hydroxide medium (pH 11.7; 0.01M NaOH) is shown in Table 3. The result for molybdenum(VI) differs from that found by Sato *et al.*,⁹ but this may be due to differences in experimental conditions. However, it appears that sodium ions may be involved in this extraction of chromium(VI) and molybdenum(VI).

Table 3. Number (n) of capriquat ions bonded per Cr(VI) or Mo(VI) atom

Solvent	CCl_4	C_6H_6	CHCl_3	1,2- $\text{C}_2\text{H}_4\text{Cl}_2$
n for Cr(VI)	2.0	2.0	0.9	1.5
n for Mo(VI)	1.0	1.2	1.4	1.1

REFERENCES

1. R. Bock and C. Hummel, *Z. Anal. Chem.*, 1963, **198**, 176.
2. G. Winkhaus and H. Uhring, *ibid.*, 1964, **200**, 14.
3. J. Hála, O. Navrátil and V. Nechuta, *J. Inorg. Nucl. Chem.*, 1966, **28**, 553.
4. G. B. Fasolo, R. Malvano and A. Massaglia, *Anal. Chim. Acta*, 1963, **29**, 569.
5. R. Kollar, V. Plichon and J. Saulnier, *Bull. Soc. Chim. France*, 1969, 2193.
6. A. S. Vieux, N. Rutagengwa and V. Noki, *Inorg. Chem.*, 1976, **15**, 722.
7. L. Karagiozov and Kh. Vasilev, *J. Inorg. Nucl. Chem.*, 1981, **43**, 199.
8. J. Y. Tong and E. L. King, *J. Am. Chem. Soc.*, 1953, **75**, 6180.
9. T. Sato and H. Watanabe, Paper presented at the 11th Chiubu Kagaku Rengo Meeting, 1980 (meeting Abstracts, p. 137).

THE SOLUBILITY OF ALKALI-METAL FLUORIDES IN NON-AQUEOUS SOLVENTS WITH AND WITHOUT CROWN ETHERS, AS DETERMINED BY FLAME EMISSION SPECTROMETRY

DAVID A. WYNN*, MARIE M. ROTH and BRUCE D. POLLARD†
Chemistry Department, Marquette University, Milwaukee, WI 53233, U.S.A.

(Received 17 April 1984. Accepted 15 May 1984)

Summary—The solubilities of LiF, NaF, KF, RbF and CsF in acetonitrile, acetone, tetrahydrofuran, dimethylformamide, benzene and cyclohexane have been determined with and without a crown ether (usually 0.1M 18-crown-6) present. Flame emission spectrometry was the determination method. Three procedures, selected according to the miscibility of the solvent with water, and the solubility of the fluoride, are described. Samples, standards and blanks were matrix-matched. The precision varied between 1 and 10% RSD. Although extensive drying procedures were applied, moisture present in the solvents and salts had some effect on the results.

The solubility of inorganic salts in non-aqueous media, though usually very low, is of concern in corrosion and wear studies,^{1,2} in environmental and toxicological problems and in studies of organic reactions in which the rate or outcome of the reaction is affected by traces of salts. Reliable solubility data, obtained by methods carefully designed to give good reproducibility and accuracy, are essential for interpretation of these studies.

Fluoride ions are useful in organic synthesis for cleavage of carbon-silicon bonds,^{3,4} in displacement and elimination reaction⁵⁻⁷ and as catalysts,⁸ but the low solubility of metal fluorides in organic solvents⁹ is a problem. The addition of crown ethers which form complexes with alkali-metal cations can enhance the solubility of alkali-metal fluorides in organic solvents.^{5,10} The resultant increased availability of fluoride ion may affect its reactivity as a participating reagent or as a catalyst.^{11,12} Solubility data for alkali-metal fluorides in organic solvents in the presence of crown ethers must be considered when interpreting and optimizing the effect of fluoride ion on the reactions.

In the present study, flame spectrometry was applied to the determination of solubilities of alkali-metal fluorides in non-aqueous media in the absence and presence of crown ethers. Flame spectrometry is a convenient, rapid and accurate method for these determinations if several conditions are met. The solubility must be sufficient to provide signals in the high-precision part of the linear calibration. The matrix for the standards and blanks must match the sample matrix exactly, because the analyte signal is

not only a direct function of the nebulization flow-rate, which depends on the physical properties, e.g., viscosity, of the solution, but is also governed by the degree of atomization and ionization produced at the flame temperature (which is modified by the combustibility of the organic solvent in the matrix). Standards should bracket the concentration of the sample so that a linear signal/concentration relationship is ensured.

If a suitable matrix can be found, aqueous standards are the most convenient to use. An aqueous/organic solvent mixture must be a true solution to be suitable for nebulization and combustion in the burner. A water-miscible solvent presents no problem; if the solvent is not miscible with water, addition of a common solvent to produce a single-phase system is sometimes possible. Non-aqueous solutions can be analysed directly but present problems with flame techniques, and require organometallic standards which are not always available or may be difficult to handle.

The solubilities reported here for alkali-metal fluorides in particular organic solvents have been obtained by procedures based on flame spectrometric determination. The procedures can be extended to other salts and solvents and adapted for use whenever trace metals in solvents must be determined.

EXPERIMENTAL

Equipment

Alkali-metal concentrations were determined with an IL 251 flame atomic spectrophotometer (Instrumentation Laboratory, Andover, MA) in the atomic-emission mode. Wavelengths (nm) used were: Li, 670.8; Na, 589.0; K, 766.5; Rb, 780.0; Cs, 852.1. A special red-sensitive photomultiplier (R446, Hamamatsu, Middlesex, NJ) was installed because several of the wavelengths were outside the range of the original photomultiplier of the equipment. The standard

*Present address: American Cyanamid Co., Chemical Research Center, Stamford, CT 06904.

†Author to whom correspondence should be addressed.

slot-burner was operated off-axis and carefully cleaned after each series of determinations. The acetylene/air flame was slightly fuel-rich and had a typical fuel/oxidant flow ratio of 5.5/19. For each element/solvent system the instrumental parameters, including slit-width, flame position, nebulization rate and integration time, were optimized on the basis of signal-to-noise ratios.

Samples and reagents

The salts [lithium fluoride (Aldrich Chem., Milwaukee, WI, 99.999% pure), sodium fluoride (Fisher Scientific, certified A.C.S.), potassium fluoride (Allied Chem., reagent grade), rubidium fluoride (Cerac, Milwaukee, WI, 99.9% pure), and caesium fluoride (Alfa, Danvers, MA, 99.9% pure)] were dried for two days at 120° under vacuum and stored over phosphorus pentoxide in a desiccator.

A solution of 25 g³ of 1,4,7,10,13,16-hexaoxacyclooctadecane (18-crown-6)¹³ (Aldrich Chem., Milwaukee, WI) in 200 ml of dichloromethane was dried overnight with 2 g of anhydrous magnesium sulphate in a nitrogen atmosphere and pressure-filtered under nitrogen. After distillation of the dichloromethane, the residue was dried at 76 mmHg pressure. 1,4,7,10-Tetraoxacyclododecane (12-crown-4) and 1,4,7,10,13-pentaoxacyclopentadecane (15-crown-5) (Aldrich Chem., Milwaukee, WI) were used without further purification.

Acetonitrile (reagent grade dried with calcium hydride and filtered, or Aldrich gold label 99+% pure) was fractionally distilled from phosphorus pentoxide in a nitrogen atmosphere, stored over 3A molecular sieve and freshly distilled before use. Benzene was fractionally distilled under nitrogen from sodium/benzophenone ketyl and stored over 3A molecular sieves. Tetrahydrofuran (THF) was fractionally distilled under nitrogen from sodium-potassium/benzophenone ketyl and used immediately. Dimethylformamide (DMF) was shaken with potassium hydroxide, fractionally distilled from barium oxide under reduced pressure and stored over 3A molecular sieve. Cyclohexane (<0.002% water) and acetone (<0.2% water) were of spectrophotometric grade (MCB Mfg. Chemists Omnisolv Reagents).

All water used was ultrapure, prepared from distilled water and demineralized by passage through a SYBRON/Barnstead Nanopure water system (Model 02782). Stock solutions of standards (1000 ppm) were prepared from the dry solid alkali-metal fluorides; the

lithium fluoride solution was also 0.3M in hydrochloric acid. Aqueous standards in the proper concentration ranges were prepared by dilution.

General procedure

Saturated solutions of the metal fluorides were prepared by stirring an excess of the salt (usually less than 0.2 g) with 15 ml of solvent for 30 min in a closed system at a constant measured temperature ($\pm 0.2^\circ$). It was important that the salt was as dry as possible; otherwise, the care in solvent preparation was negated. The suspension was decanted and centrifuged* at 5000 rpm (International Equipment Co., Clinical Centrifuge, Model CL) for 10–15 min. Varying periods of refluxing, stirring and ultrasound treatment were evaluated as methods for ensuring saturation and found to give identical results. For water-miscible solvents (acetonitrile, acetone, THF and DMF), 1-ml aliquots of centrifugate were transferred to 50-ml beakers and diluted with 5 ml of water to give a sample with a 16.7% solvent/83.3% water matrix. One-ml amounts of pure solvent diluted with 5 ml of aqueous standard or water provided matrix-matched standards and blanks, respectively. Use of PMP (poly-methylpentene) beakers was preferred, to avoid exchange of metallic ions with a glass surface, and improved the reproducibility of the results. Kimax-glass beakers were used for cyclohexane solutions, however, since cyclohexane causes immediate decomposition of the PMP beakers.

For solubility systems which, by the procedure above, gave samples with concentrations below the limit of detection, a known volume (6 ml) of the saturated solution was preconcentrated by evaporation and the residue was dissolved in 1 ml of water to provide a sample for direct comparison with aqueous standards. Blanks for this procedure were prepared from a similar volume of pure solvent, evaporated in a similar vessel.

When the solvent was immiscible with water (benzene, cyclohexane), a modification employing a common solvent in the matrix was employed. For benzene, dilution of the 1 ml of centrifuge to 20 ml with 95% ethanol gave a sample in a 5% benzene/90% ethanol/5% water matrix. For cyclohexane, dilution of the 1-ml aliquot of centrifuge with 5 ml of 95% ethanol produced a sample in a 16.7% cyclohexane/79.2% ethanol/4.2% water matrix. Blanks and standards were matched to these matrices.

In studies on the effect of crown ethers on saturation solubility, similar procedures were followed, with the crown ether added at a known concentration to the solvent used for the preparation of the saturated solution and the corresponding blanks and standards. It was important to match the matrix exactly, because the crown ether caused noticeable broad-band enhancement of the blank signal, which was attributed to a change in flame conditions.

*The very fine suspensions settled with difficulty. Repetition of decantation and centrifugation resulted in more complete removal of suspended solid metal fluoride, and the later centrifugates did not show higher alkali-metal concentrations.

Table 1. Solubility of alkali-metal fluorides in organic solvents in the absence and presence of crown ethers

Salt	Solvent	Crown ether/M	Solubility, mM	Temperature °C	Literature values, mM
LiF	CH ₃ CN	—	0.09 ± 0.01	24	
		18-crown-6/0.10	0.10 ± 0.01	24	
	acetone	—	0.10 ± 0.01	24	0.00010/18°, 0.00012/37° ¹⁴
		12-crown-4/0.10	0.12 ± 0.01	24	
		18-crown-6/0.12	0.10 ± 0.01	24	
		—	0.09 ± 0.01	24	
	THF	—	0.09 ± 0.01	24	
		18-crown-6/0.10	0.10 ± 0.01	24	
	DMF	—	0.10 ± 0.01	24	0.0505/25° ¹⁵
		18-crown-6/0.10	0.10 ± 0.01	24	
	benzene	—	0.011 ± 0.002†	25	
		12-crown-4/0.10	0.023 ± 0.001†	25	
18-crown-6/0.10		0.027 ± 0.001†	25		
cyclohexane	—	<0.0002*†	24		
	18-crown-6/0.10	<0.0002*†	24		

Table 1. Solubility of alkali-metal fluorides in organic solvents in the absence and presence of crown ethers

Salt	Solvent	Crown ether/M	Solubility, mM	Temperature °C	Literature values mM	
NaF	CH ₃ CN	—	0.029 ± 0.007	25	0.50/25 ^{o16,17} , 0.30/18 ^{o16} , 2.71/25 ^{o18}	
		18-crown-6/0.10	0.026 ± 0.006	25		
	acetone	—	0.013 ± 0.002	25	0.00046/18 ^o , 0.00050/37 ^{o14}	
		15-crown-5/0.10	0.018 ± 0.002	25		
		18-crown-6/0.11	0.052 ± 0.003	25		
	THF	—	0.018 ± 0.004	24		
		18-crown-6/0.10	0.081 ± 0.004	24		
	DMF	—	0.031 ± 0.002	24	0.0440/25 ^{o15}	
		18-crown-6/0.10	0.13 ± 0.01	24		
	benzene	—	0.0054 ± 0.0005†	25		
		15-crown-5/0.10	0.012 ± 0.002†	25		
		18-crown-6/0.12	0.0060 ± 0.0007†	25		
	cyclohexane	—	< 0.0001*†	24		
		18-crown-6/0.10	< 0.0001*†	24		
KF	CH ₃ CN	—	0.031 ± 0.004	24	0.32 ¹⁷ , 0.32/25 ^{o16} , 0.48/18 ^{o16} 0.318/25 ^{o10}	
		18-crown-6/0.11	0.94 ± 0.02	24		
	acetone	—	0.034 ± 0.003	24	0.0030/18 ^o , 0.0033/37 ^{o14}	
		18-crown-6/0.10	1.26 ± 0.06	24		
	THF	—	0.13 ± 0.01	24		
		18-crown-6/0.10	2.00 ± 0.02	24		
	DMF	—	0.12 ± 0.01	24		
		18-crown-6/0.10	1.57 ± 0.06	24		
	benzene	—	0.0026 ± 0.0001†	24	14/0.34M/25 ^o , 52/1.01M/25 ^{o10}	
		18-crown-6/0.10	0.51 ± 0.03§	24		
	cyclohexane	—	< 0.00009*†	24		
		18-crown-6/0.10	0.0051 ± 0.0002†	24		
	RbF	CH ₃ CN	—	0.159 ± 0.001	25	
			18-crown-6/0.10	11.2 ± 0.1	25	
acetone		—	0.038 ± 0.003	24	0.027/18 ^o , 0.29/37 ^{o14}	
		18-crown-6/0.10	3.4 ± 0.2	24		
THF		—	0.008 ± 0.002	24		
		18-crown-6/0.10	0.51 ± 0.02	24		
DMF		—	1.05 ± 0.05	24		
		18-crown-6/0.10	6.4 ± 0.1	24		
benzene		—	0.000017 ± 0.000001†	24		
		18-crown-6/0.10	0.68 ± 0.02 ^b	24		
cyclohexane		—	< 0.00004*†	24		
		18-crown-6/0.10	0.057 ± 0.004§	24		
CsF		CH ₃ CN	—	0.25 ± 0.02	25	1.65/20 ^o , 1.90/30 ^{o19}
			18-crown-6/0.10	3.50 ± 0.04	25	
	acetone	—	0.065 ± 0.004	24	0.040/18 ^o , 0.044/37 ^{o14}	
		18-crown-6/0.10	9.7 ± 0.8	24		
	THF	—	0.093 ± 0.008	24	0.97/20 ^o , 1.25/30 ^{o19}	
		18-crown-6/0.10	0.97 ± 0.04	24		
	DMF	—	0.60 ± 0.03	24		
		18-crown-6/0.10	5.95 ± 0.03	24		
	benzene	—	< 0.00005*†	24		
		18-crown-6/0.10	1.14 ± 0.08§	24		
	cyclohexane	—	< 0.00006*†	24		
		18-crown-6/0.10	0.0063 ± 0.0004†	24		

*Limit of detection.

†Evaporation method.

§Common solvent method.

RESULTS AND DISCUSSION

The present method produced consistent solubility data (Table 1), with good standard deviations, for

alkali-metal fluorides in several organic solvents in the presence and absence of crown ethers. In general, the values obtained were lower than the solubilities previously reported, which differed over a wide range.

Evaluation of the results must take account of how the sample was prepared and how the solubility was measured. The importance of controlled procedures and reproducibility cannot be overemphasized.

High values for the solubility of very slightly soluble salts can result from traces of very finely divided solid present in the saturated solution samples. In investigations of solubility in non-aqueous solvents, trace amounts of water present in the solvents used or introduced during the preparation of the saturated solutions can increase the amount of solute dissolved. Inconsistent and inaccurate data can also result if standards are improperly matched; in flame spectrometry, organic solvents and other components can affect the flame temperature and rate of nebulization and thereby the degree of ionization. The present method has provided for separation of the solution from the finely divided solid phase, and for the use of dry solvents in a controlled atmosphere. The standards were chosen to provide an identical matrix and to bracket sample concentrations in a range of linear response.

The effect of traces of moisture is probably the major factor influencing such solubility data.²⁰ The results in Table 1 represent the solubilities in dry solvents under laboratory working conditions normal for moisture-sensitive materials. The effect of moisture on the solubility of potassium fluoride in acetonitrile is illustrated by the following comparison. For one group of samples extreme precautions were taken to ensure dryness; the acetonitrile was dried for several days over phosphorus pentoxide and redistilled under nitrogen immediately before use;²¹ its moisture content was monitored by modified coulometric Karl Fischer titration;^{22,23} the potassium fluoride was dried under vacuum at 120° for 2 hr; refluxing, cooling to room temperature, two-step centrifugation and Acro-disc® filtration were all performed in a closed system (glove-bag) under dry nitrogen. This resulted in a $0.014 \pm 0.002M$ saturated solution of potassium fluoride in acetonitrile with a water content of $100 \pm 20 \mu\text{g/ml}$, which may be compared with the value $0.031 \pm 0.004mM$ obtained for a saturated solution of potassium fluoride in normally dried acetonitrile containing $400 \pm 40 \mu\text{g/ml}$ water. Obviously, the solubility of potassium fluoride in the organic solvent is dependent on the amount of water present. Although it would be possible to extrapolate to a solubility at zero water content, this would represent a condition that does not exist under experimental conditions. The solubility of real experimental significance is that obtained under normal anhydrous operating conditions, such as those employed for the solubilities reported in Table 1.

The solubilities recorded in the literature for alkali-metal fluorides in acetone¹⁴ are lower than those obtained by the present method for lithium, sodium and potassium fluorides. These literature values were obtained by conductance measurements, which de-

pend on free ions in solution; any ion-pair formation or solvation would result in lower apparent solubility. The solubilities of the more soluble rubidium and caesium fluorides were probably determined by weight, but no details were given; they are in agreement with the values obtained by our flame photometric method.

The ability of a crown ether to enhance solubility in non-aqueous solvents depends not only on the cavity size of the crown ether and the cation radius but also on the inherent solubility of the particular inorganic salt in the pure solvent.¹⁰ 18-Crown-6 was found to enhance the solubility of potassium, rubidium and caesium fluorides in all the solvents tested—acetonitrile, acetone, THF, DMF, benzene and cyclohexane; a smaller degree of enhancement was observed for sodium fluoride in acetone, THF, DMF and benzene, and only a very slight enhancement for lithium fluoride in benzene, with no enhancement in the other solvents. The cavity diameter in 18-crown-6 (2.6–3.2 Å)¹⁰ can accommodate the potassium ion (ionic diameter 2.66 Å) or rubidium ion (2.94 Å) in a 1:1 complex. The increased solubility of a caesium fluoride can be attributed to the caesium ion being sandwiched between two 18-crown-6 molecules in a 1:2 complex. The smaller sodium ion (1.94 Å) and lithium ion (1.36 Å) can be complexed by 18-crown-6 but the poorer fit of ion to cavity results in a smaller degree of complex formation and less enhancement of solubility.

The effect of the smaller crown ethers, 15-crown-5 (cavity diameter 1.7–2.2 Å¹⁰ or 1.72–1.84 Å²⁴) and 12-crown-4 (cavity diameter 1.2–1.5 Å¹⁰) on the solubility of sodium and lithium fluorides, respectively, was investigated since these would seem to provide good cavity sizes for complexing the cations, but the result is not always as expected.²⁵ For benzene as solvent, in which 18-crown-6 had caused a slight enhancement of lithium fluoride solubility, only the same degree of enhancement was observed with 12-crown-4, although it would seem to give an ideal fit for lithium ions. Neither crown ether produced any enhancement of the solubility of lithium fluoride in acetone. The sodium ion may be slightly large for the 15-crown-5 ether cavity but there a slight enhancement of the solubility of its fluoride in both benzene and acetone was found. The 18-crown-6 ether was found to be ineffective with sodium fluoride in benzene, but was more effective than 15-crown-5 in acetone. A similar anomaly in effect of crown cavity size on effectiveness of ion-complexing was noted by Hopkins and Norman²⁵ who observed that the equilibrium constants for complexation with a fixed concentration of lithium iodide were in the order 18-crown-6 > 15-crown-5 > 12-crown-4.

CONCLUSIONS

The solubilities of alkali-metal fluorides in non-aqueous solvents have been determined with and

without crown ether present. The results compare favourably with those in the literature. A discussion of the solubilities, based on ion-size, ion-pair formation and solvent donor-power can be found elsewhere.²⁶ Water present in the solvent, air and salts has a marked influence on the solubility. Crown ethers increase the solubility of some alkali-metal fluorides, particularly when the ion-size matches the cavity in 18-crown-6. The methods of determination, based on flame emission spectrometry, are simple and result in good precision. The importance of matrix-matching samples, standards and a proper blank, cannot be overemphasized.

REFERENCES

1. C. S. Saba and K. J. Eisentraut, *Anal. Chem.*, 1977, **49**, 454.
2. S. Sprague and W. Slavin, *At. Absorp. Newslett.*, 1965, **4**, 367.
3. T. H. Chan and B. S. Ong, *J. Org. Chem.*, 1978, **43**, 2994.
4. E. Vedejs and G. R. Martinez, *J. Am. Chem. Soc.*, 1979, **101**, 6452.
5. C. L. Liotta and H. P. Harris, *ibid.*, 1974, **96**, 2250.
6. F. Naso and L. Ronzini, *J. Chem. Soc. Perkin Trans. 1*, 1974, 340.
7. P. Ykman and H. K. Hall, *Tetrahedron Lett.*, 1975, **16**, 2429.
8. S. E. Cremer and C. Blankenship, *ibid.*, 1980, **21**, 2979.
9. J. H. Clark, *Chem. Rev.*, 1980, **80**, 429.
10. R. M. Izatt and J. J. Christensen, *Synthetic Multidentate Macrocyclic Compounds*, Chaps. 1, 3. Academic Press, New York, 1978.
11. D. J. Sam and H. F. Simmons, *J. Am. Chem. Soc.*, 1972, **94**, 4024.
12. I. M. Kolthoff, *Anal. Chem.*, 1979, **51**, 1R.
13. G. W. Gokel, D. J. Cram, C. L. Liotta, H. P. Harris and F. L. Cook, *J. Org. Chem.*, 1974, **39**, 2445.
14. A. Lannung, *Z. Phys. Chem.*, 1932, **161**, 255.
15. C. M. Criss and E. Kusksha, *J. Phys. Chem.*, 1968, **72**, 2966.
16. T. Pavlopoulos and H. Strehlow, *Z. Phys. Chem. Leipzig*, 1954, **202**, 474.
17. W. F. Linke and A. Seidell, *Solubilities of Inorganic and Metal Organic Compounds*, 4th Ed., American Chemical Society, Washington, D.C., 1958 (Vol. 1), 1965 (Vol. 2).
18. D. V. S. Jain, B. S. Lark and P. K. Naygar, *Indian J. Chem.*, 1970, **8**, 73.
19. G. M. Tyul'ga, V. A. Gubanov, I. G. Popova, L. A. Petrukhno, B. M. Volkhovets, P. E. Trovchanskaya and I. M. Dolgopolshii, *J. Org. Chem. USSR*, 1978, **14**, 2158.
20. A. Lannung, *Z. Phys. Chem.*, 1932, **161**, 269.
21. D. R. Burfield, K.-H. Lee and R. H. Smithers, *J. Org. Chem.*, 1977, **42**, 3060.
22. E. Scholz, *Am. Lab.*, 1981, **13**, No. 8, 89.
23. *Idem*, *Z. Anal. Chem.*, 1980, **303**, 203.
24. J. D. Lamb, R. M. Izatt, C. S. Swain and J. J. Christensen, *J. Am. Chem. Soc.*, 1980, **102**, 475.
25. H. P. Hopkins and A. B. Norman, *J. Phys. Chem.*, 1980, **84**, 309.
26. D. A. Wynn, *M.S. Thesis*, Marquette University, 1981.

2-(8-QUINOLYLAZO)-7-PHENYLAZOCHROMOTROPIC ACID AS AN ANALYTICAL REAGENT*

RU-QIN YU, ZHI-HUA ZHANG and YA-WEN LI

Department of Chemistry and Chemical Engineering, Hunan University, Changsha, People's Republic of China

(Received 11 April 1983. Revised 7 May 1984. Accepted 22 June 1984)

Summary—2-(8-Quinolylazo)-7-phenylazochromotropic acid (QAPAC) has been synthesized by coupling diazotized 8-aminoquinoline with 2-phenylazochromotropic acid as well as by coupling diazotized aniline with 2-(8-quinolylazo)chromotropic acid. The properties of QAPAC and the spectrophotometric characteristics of some metal-QAPAC complexes are reported.

Quinolylazo derivatives are promising analytical reagents for spectrophotometric determination of trace elements. So far the number of published works on reagents derived from diazotized 8-aminoquinoline is limited.¹⁻⁵ We have tested 23 compounds derived from this compound and find that 2-(8-quinolylazo)-7-phenylazo-1,8-dihydroxynaphthalene-3,6-disulphonic acid [2-(8-quinolylazo)-7-phenylazochromotropic acid, QAPAC] has the best analytical characteristics. Our studies on its synthesis and properties are now reported.

EXPERIMENTAL

Synthesis of the reagent

Dissolve 7.9 g of 8-aminoquinoline in 60 ml of 2M hydrochloric acid and cool to 0°. With stirring, add dropwise 60 ml of ice-cold water containing 4.2 g of sodium nitrite. Cool the mixture for 1 hr in an ice-bath. In a separate vessel suspend 42.5 g of calcium oxide in 200 ml of hot water. Dissolve about 45 g of Chromotrope 2R (disodium salt of phenylazochromotropic acid) in the minimum amount of water and chromatograph it on a Polyamide 6 column with water as effluent. Collect the red fraction and pour it into the cooled calcium hydroxide suspension. To this mixture add the diazotized 8-aminoquinoline solution, followed by 63 g of sodium chloride. Stir the mixture for 1 hr, then dilute with 1 litre of water. Add 100 ml of concentrated hydrochloric acid to precipitate the QAPAC. Collect the precipitate and wash it with hydrochloric acid of decreasing concentration, then with water. Dry the crude product under vacuum at 45° (yield 12.9 g). Dissolve the product in 1M sodium hydroxide, and reprecipitate it three times with concentrated hydrochloric acid. For further purification, prepare a chromatographic column of Polyamide 6 sorbent (6-7 cm in length, 2-4 cm diameter). Dissolve the crude product in the minimum amount of 1M sodium hydroxide, apply it to the column, elute with 0.2M sodium hydroxide and discard the red fraction of the eluate. Collect the blue fraction and precipitate QAPAC from it with concentrated hydrochloric acid. Filter off under suction and dry under vacuum. Evaluate the purity of the product

by paper chromatography with 2:1:1 (v/v) butan-1-ol-glacial acetic acid-water. The best product shows a blue spot remaining at the start. Analysis: C₂₅H₁₇O₈N₅S₂ requires 12.08° N, 11.06° S; found 12.0° N, 10.7° S. The principal infrared bands are at 1030, 1190, 1275 and 1445 cm⁻¹.

RESULTS AND DISCUSSION

Purification and identification of QAPAC

The commercially available Chromotrope 2R contained blue impurities which were left on the Polyamide 6 column when the red fraction was eluted with water. When QAPAC was precipitated with hydrochloric acid, most of the unreacted phenylazochromotropic acid remained in solution. For the chromatographic separation of QAPAC from impurities on a Polyamide 6 column, ammonia or sodium hydroxide solutions of various concentration were tried as eluents, and 0.2M sodium hydroxide was found to be the best.

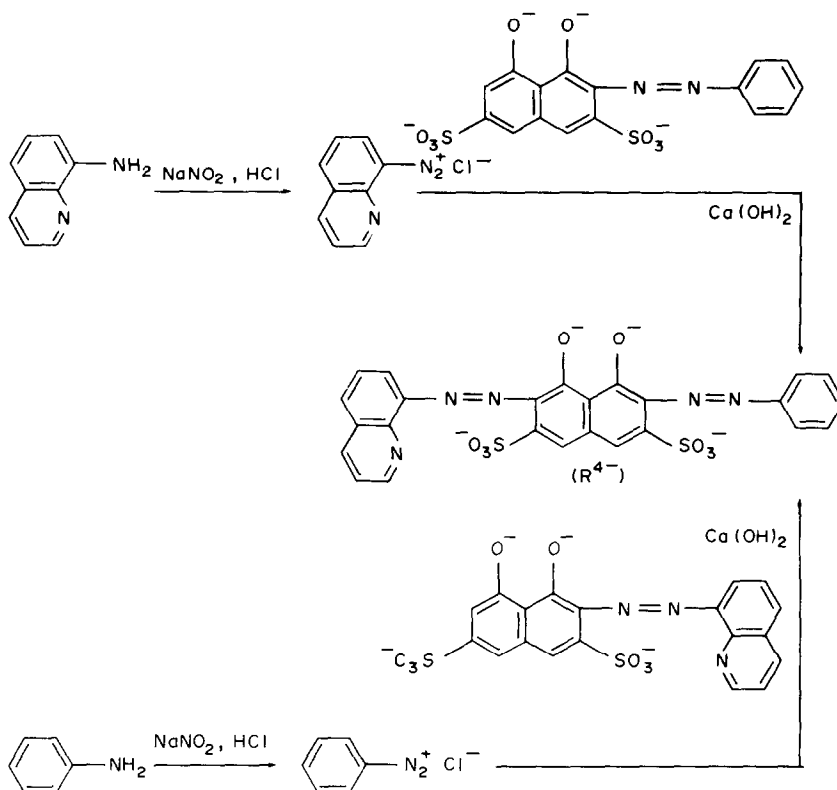
Theoretically, QAPAC can be synthesized by two different routes (an example of so-called "meeting synthesis"⁶) (Scheme 1).

Both routes were used, in order to confirm the nature of the product obtained. Diazotized 8-aminoquinoline was first coupled with chromotropic acid in sodium carbonate medium to give 2-(8-quinolylazo)-1,8-dihydroxynaphthalene-3,6-disulphonic acid. The second coupling reaction was done in calcium hydroxide medium with diazotized aniline. The crude product was reprecipitated and further purified by column chromatography. QAPAC obtained in this way was examined by paper chromatography and infrared spectroscopy, and gave the same results as the product obtained by the first reaction route.

Properties of QAPAC

QAPAC is a dark-purple amorphous powder, slightly soluble in water and ethanol, readily soluble

*Research supported by Chem. Grant No. 566 of Science Foundation, Academia Sinica, PRC.



Scheme 1.

in *N,N*-dimethylformamide and strongly acidic or alkaline solutions.

In strongly alkaline solutions QAPAC is assumed to exist in a blue dissociated form (R^{4-} , $\lambda_{\max} = 630$ nm). The absorption spectrum of QAPAC shows a

$$*k_i = \frac{[H_i R^{i-4}]}{[H^+][H_{i-1} R^{i-5}]}$$

hypsochromic shift when the pH is decreased. The protonation data for R^{4-} were obtained by means of pH-absorbance measurements.⁷ The protonation constants found for the two naphthol oxygen atoms and the quinolyl nitrogen atom are: $\log k_1 = 14.30$; $\log k_2 = 11.27$; $\log k_3 = 1.66$.^{*} The $\log k$ value for protonation of the quinolyl group is fairly close to that for 1-(8-quinolylazo)-2-hydroxy-

Table 1. Spectrophotometric characteristics of metal-QAPAC complexes

Ion	Auxiliary agents added*	pH	λ_{\max} , nm	$\Delta\lambda$, nm	Molar absorptivity† at λ_{\max} , l.mole ⁻¹ .cm ⁻¹
Ca(II)		4.5	726	170	2.46×10^5
	DDMAA + phen	5.6	726	170	2.10×10^5
Sr(II)	DDMAA + phen	5.6	716	160	1.00×10^5
La(III)	DDMAA + phen	8.0	710	154	4.90×10^4
Y(III)	DDMAA + phen	8.0	710	154	4.00×10^4
V(V)		4.2	630	74	2.74×10^4
Fe(II)	CTMAB + Triton X-100	2.7	670	114	2.80×10^4
		2.7	680	124	2.16×10^4
Co(II)	CTMAB + Triton X-100	5.0	670	114	1.03×10^5
		5.0	650	94	7.40×10^4
Cu(I)	SLS + NH ₂ OH	5.0	650	94	9.47×10^4
Cu(II)		1.0-1.5	694	138	4.65×10^4
Pd(II)		1.4	660	104	4.10×10^4
	DDMAA	2.4M HCl	600	44	6.00×10^4
Hg(II)		9.2	700	144	8.50×10^3
Ga(III)		4.0	600	44	2.72×10^4

*CTMAB = cetyltrimethylammonium bromide; DDMAA = dodecyldimethylaminoacetic acid; phen = 1,10-phenanthroline; SLS = sodium lauryl sulphate.

†With excess of QAPAC present.

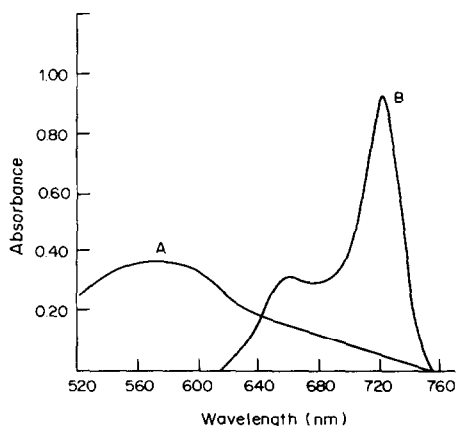


Fig. 1. Absorption spectra. A: QAPAC, $1.36 \times 10^{-5} M$, against water; B: Ca-QAPAC complex, $[Ca^{2+}] = 3.75 \times 10^{-6} M$, $[QAPAC] = 3.40 \times 10^{-5} M$, against reagent blank. pH 4.5, 1-cm cells.

naphthalene-3,6-disulphonic acid (1.48) reported by Basargin *et al.*³

Colour reactions of QAPAC with metal ions

QAPAC forms water-soluble, intensely coloured complexes with various metal ions. The reaction conditions and spectrophotometric characteristics of the complexes are presented in Table 1. The photometric sensitivity for certain metals is higher than that with other reagents. Calcium, for instance, can be determined with excellent sensitivity, the molar absorptivity of the 1:1 Ca-QAPAC complex in the absence of sensitizing agents being 2.46×10^5 l.mol⁻¹.cm⁻¹ at 726 nm. In the presence of dodecyl-dimethylaminoacetic acid and 1,10-phenanthroline the molar ratio of Ca and QAPAC in the complex changes from 1:1 to 1:2, with better colour stability

and broader optimum pH-range (pH 4–10 instead of pH 4.3–4.9 in the absence of auxiliary agents), but the molar absorptivity falls slightly to 2.1×10^5 . The selectivity is comparable with that of the Arsenazo III method. The QAPAC method has been applied to the determination of calcium in rain and snow samples; the experimental details are described elsewhere.⁸

Savvin *et al.* have described three types of colour reactions of alkaline-earth metal and some other elements with 2,7-bisazo derivatives of chromotropic acid. The absorption curve of the Ca-QAPAC complexes exhibits two humps at 726 and 660 nm (Fig. 1) and is quite similar to those of the third type of colour complexes reported by Savvin *et al.*^{9,10} These authors interpreted the presence of two absorption maxima in the metal-complex spectrum as a consequence of a 1:2 sandwich structure, with two isolated reagent molecules in the complex.¹⁰ However, according to our experimental results, QAPAC forms calcium complexes with a metal to ligand ratio of 1:1. Hence, in this instance the mechanism of the colour development requires to be examined further.

REFERENCES

1. L. A. Okhanova, L. I. Bolshakova and S. B. Savvin, *Zh. Analit. Khim.*, 1968, **23**, 1562.
2. N. N. Basargin, A. V. Kadomtseva and V. I. Petrashen, *Zavodsk. Lab.*, 1969, **35**, 16.
3. *Idem*, *Zh. Analit. Khim.*, 1970, **25**, 34.
4. *Idem*, *ibid.*, 1970, **25**, 285.
5. S. B. Savvin, *Organic Reagents of the Arsenazo III Group*, pp. 30–38, Atomizdat, Moscow, 1971.
6. *Idem*, *op. cit.*, p. 79.
7. A. Albert and E. P. Serjeant, *Ionization Constants of Acids and Bases*, pp. 69–92, Methuen, London, 1962.
8. R. Q. Yu, Y. W. Li and Z. H. Zhang, *Fenxi Huaxue*, 1984, **12**, 254.
9. T. V. Petrova and S. B. Savvin, *Zh. Analit. Khim.*, 1969, **24**, 490.
10. S. B. Savvin, E. L. Kuzin, T. V. Petrova and N. Khakimkhodzhaev, *ibid.*, 1969, **24**, 1325.

DETERMINATION OF SCANDIUM, YTTRIUM AND LANTHANIDES IN SILICATE ROCKS AND FOUR NEW CANADIAN IRON-FORMATION REFERENCE MATERIALS BY FLAME ATOMIC-ABSORPTION SPECTROMETRY WITH MICROSAMPLE INJECTION

J. G. SEN GUPTA

Geological Survey of Canada, Ottawa, Ontario, Canada

(Received 14 February 1984. Revised 26 May 1984. Accepted 23 June 1984)

Summary—Enhancement of sensitivity by factors of up to 1.5 by use of the microsampling technique, coupled with the advantage of using small samples in small solution volumes, permits rapid flame AAS determination of traces of Sc, Y, Nd, Eu, Dy, Ho, Er, Tm and Yb in ultramafic and most other rocks of low rare-earth content, which would be either impossible or very difficult to analyse by direct aspiration because of the need for much larger sample weights and solution volumes. The rare-earths are separated by a modified ion-exchange or a double calcium oxalate and single hydrous ferric oxide co-precipitation procedure, and ultimately determined in an ethanolic perchlorate solution, buffered with 1% lanthanum, by the flame microsample injection technique, with a nitrous oxide-acetylene flame. The results obtained by this technique for six international reference rocks SY-2 (syenite), BCR-1 (basalt), BHVO-1 (Hawaiian basalt), SCo-1 (cody shale), MAG-1 (marine mud) and STM-1 (syenite) are compared with those obtained previously by the direct aspiration method and with other reported data. Results are given for four new Canadian iron formation reference materials FeR-1 to FeR-4.

Abundance-studies on the rare-earths for petrogenetic modelling require their rapid determination in a variety of igneous and sedimentary rocks and rock-forming minerals. An earlier publication¹ described an atomic-absorption spectrometric (AAS) method for the determination of Y, Nd, Eu, Dy, Ho, Er, Tm and Yb in some minerals and rocks, by direct aspiration of the sample solution (in ethanolic perchlorate medium containing 1% lanthanum as spectroscopic buffer) into a nitrous oxide-acetylene flame. The rare-earth elements (REE) were separated from a relatively large sample (3–10 g) by double co-precipitation with calcium oxalate followed by a co-precipitation with hydrous iron oxide to remove calcium. Although this method is applicable to rare-earth minerals and to certain rocks of relatively high rare-earth content (*e.g.*, syenites, carbonatites, tuffs, foyaites, some basalts and granites), it is not suitable for ultramafic and some common rocks and rock-forming minerals (*e.g.*, peridotites, gabbros, basic gneisses, anorthosites, tonalites, certain shales and altered granites, atzites, sandstones, iron formations and pyroxenes) containing only a few ppm of REE, because of the difficulties in the decomposition and subsequent handling of the large amount (10–15 g) of sample required for preconcentration of the rare-earths. Use of a smaller sample (2–3 g) for the flame AAS determination of these rare-earth elements in these materials would require a small final solution volume (2–3 ml) after preconcentration of the ele-

ments as described previously,^{1,2} so use of a flame microsample injection technique³⁻⁵ has been investigated. This AAS finish has not been used before for the determination of the rare-earths in rocks. The ion-exchange procedure used previously for britholite² was modified in this work by using smaller volumes and higher concentrations of hydrochloric acid for rapid elution.

The microsampling method is easier to use than the graphite-furnace AAS technique normally favoured for trace element determinations, suffers less interference from associated elements and is much faster for routine work. The results obtained for six international reference rocks by this technique are compared with those obtained previously by the direct-aspiration flame method and with other reported data. Results are also given for four new Canadian iron-formation reference materials, FeR-1, FeR-2, FeR-3 and FeR-4.

EXPERIMENTAL

Apparatus

A Techtron model AA-3 spectrometer fitted with a Goguel-type water cooled burner¹ and a variable-flow nebulizer with an uptake rate of 4 ml/min, and equipped with some Techtron model AA-5 accessories such as a modulated lamp-current supply (Type MLS-5), lamp turret assembly and an indicating module (Type IM-5), was used for atomic-absorption measurements. Eppendorf multivolume micropipettes (100–1000 μ l) and a Varian model 66 micro-sampler were used for sample dilution and for dispensing solutions into the flame. Up to 10-fold scale expansion on the IM-5 unit was used and the absorbance peaks were recorded on a Varian model 9176 strip-chart recorder with

Table 1. Operating parameters and sensitivities of scandium, yttrium and certain rare-earths in the nitrous oxide—acetylene flame by microsample injection*

Element	Wavelength, nm	Spectral bandwidth, nm	Westinghouse lamp current, mA	Sensitivity, ppm/1% absorption		Sensitivity enhancement factor (DA/MS)
				Micro sampling (MS)*	Direct aspiration (DA)†	
Sc	391.18	0.2	5	0.22	0.25‡	1.1
Y	410.24	0.5	5	3.2	3.2	1.0
Nd	492.45	0.2	10	7.7	9.4	1.2
Eu	459.40	0.2	5	0.35	0.35	1.0
Dy	421.17	0.2	10	0.36	0.40	1.1
Ho	410.38	0.2	5	0.47	0.67	1.4
Er	400.80	0.5	5	0.32	0.46	1.4
Tm	371.79	0.5	10§	0.14	0.21	1.5
Yb	398.80	0.5	5	0.048	0.07	1.5

*200- μ l injections of absolute ethanolic perchlorate solutions of the elements, buffered with 1% La.

†Sen Gupta.¹

‡Sen Gupta.⁹

§Varian hollow-cathode lamp.

a chart-speed of 200 cm/hr. The supply of compressed air or nitrous oxide and acetylene to the burner head was controlled by a Beckman gas-control unit.

Sensitivities and instrumental operating parameters are given in Table 1. An improvement of sensitivity by factors of up to 1.5 for most elements was obtained by using microsample injection instead of direct aspiration.

Ion-exchange column. Pack a 30-cm long Dowex 50W-X8 cation-exchange resin (50–100 mesh) column in the borosilicate glass apparatus shown in Fig. 1. Wash the column with 6M hydrochloric acid until the effluent is free from Fe³⁺ (test with ammonium thiocyanate solution), and then

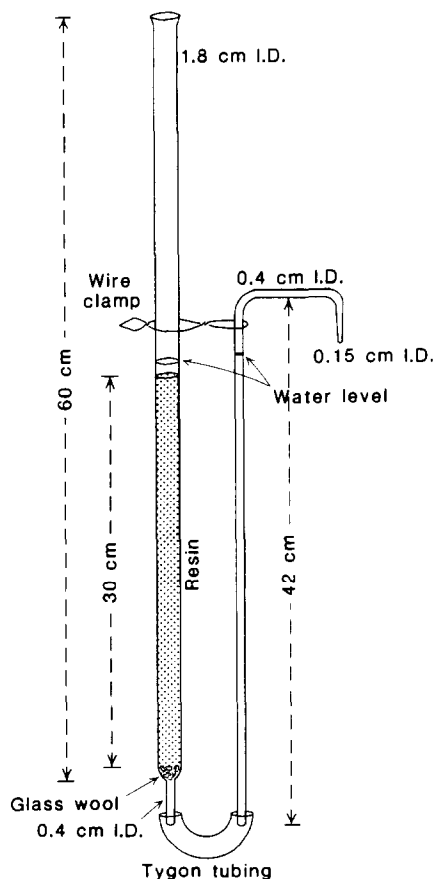


Fig. 1. Ion-exchange column.

with demineralized water until the washings are neutral to blue litmus paper.

Reagents

Standard solutions. Prepare stock solutions (1000 ppm) of Sc, Y and the lanthanides by dissolving appropriate quantities of the pure oxides in hot dilute nitric acid. Remove the excess of acid by evaporation, dilute the solutions to known volume with 1M nitric acid and store them in Nalgene bottles. To standardize, transfer 5 ml to a 10-ml platinum crucible previously ignited to constant weight at 1000°, evaporate to dryness on a steam-bath, heat the crucible gently with a low Bunsen flame until no more fumes are evolved, then strongly with the full flame, and finally ignite in a muffle furnace at 1000° for 30 min. Cool in a desiccator for 30 min and weigh. Prepare working solutions (0.1–100 ppm) by appropriate dilution of the stock solution with 0.1M nitric acid and store them in Nalgene bottles.

Lanthanum buffers, 5% solutions. Prepare an aqueous solution by dissolving 5.85 g of high-purity lanthanum oxide in hot dilute nitric acid. Dilute to 100 ml with demineralized water and store in a 125-ml Nalgene bottle. To prepare an ethanolic solution, evaporate 25 ml of the aqueous solution to dryness on a hot-plate, add 10 ml of concentrated perchloric acid, evaporate to a moist residue, cool the covered beaker to room temperature, and add 10–15 ml of absolute ethanol. Warm on a steam-bath and stir to dissolve the salts, then transfer the solution to a 25-ml standard flask, dilute to volume with ethanol and store in a 30-ml Nalgene bottle.

Other reagents. Ferric nitrate solution (Fe 5 mg/ml in 1M nitric acid); ferric perchlorate solution (Fe 5 mg/ml in absolute ethanol); 10% nitric acid—5% hydrogen peroxide solution; 1.85M and 6M hydrochloric acid; 0.1M and 1M nitric acid.

Procedures

Calibration solutions. Using 100-ml standard flasks, prepare three stock standard solutions, diluted to volume with 1M nitric acid, containing Sc, Y, Th and the REE in amounts approximating those found in a 25-g sample of the international reference rocks GA (granite^{6,7}), SY-2 and SY-3 (both syenites^{7,8}) (see Table 2 and Note 1). Store the solutions in Nalgene bottles.

To 20-ml beakers, transfer 5, 10 and 15 ml of synthetic standard GA solution, 2.5, 5 and 7.5 ml of synthetic standard SY-2 solution, and 2, 3 and 4 ml of synthetic standard SY-3 solution. Add 1 ml of aqueous 5% lanthanum buffer solution to each beaker, evaporate the solutions to dryness, then add 2 ml of concentrated perchloric acid and evaporate to a moist residue. Cool each beaker, cover with a watch-glass

and dissolve the salts in 2–3 ml of absolute ethanol, stirring with a glass rod. Transfer the solutions to 5-ml standard flasks, dilute to volume with ethanol, then transfer to 8-ml glass vials and close the screw-caps tightly.

Prepare a blank for correction purposes after the ion-exchange separation of the rare earths, by diluting 1 ml of ethanolic 5% lanthanum buffer solution to volume in a 5-ml standard flask with absolute ethanol. Prepare a similar blank containing 6–10 mg of iron(III), as perchlorate, for correction purposes after the separation of the rare earths by co-precipitation. Transfer to 15-ml glass vials and close the screw-caps tightly.

Sample decomposition. Depending on the type of sample and the quantity available, transfer 2–3 g, accurately weighed, of the finely powdered sample to a 50- or 100-ml platinum dish and moisten with water. Cover the dish with a platinum lid and gradually, while stirring with a platinum rod, add 10–20 ml of concentrated hydrofluoric acid. Heat on a steam-bath for 2–3 hr, then remove the lid and rinse it in with water, and evaporate the solution to dryness. Add 10–20 ml of concentrated nitric acid to the residue, stir to break up any lumps, and evaporate to dryness.*

Add 15–20 ml of concentrated perchloric acid, stir the mixture until a thin slurry is produced, then cover the dish, and heat gently on a sand-bath until fumes of perchloric acid start to appear. Remove the lid, rinse in with water, stir to mix, then evaporate the solution to a syrupy consistency.

Cool the dish, add 25 ml of 10% nitric acid–5% hydrogen peroxide solution, cover and, with occasional stirring, heat on a steam-bath to dissolve the salts. Transfer the solution to a 400-ml beaker, rinse the dish thoroughly with water, cover the beaker with a watch-glass and boil vigorously to decompose the excess of hydrogen peroxide. If insoluble material is present or a precipitate forms on cooling, filter the solution through a Whatman No. 40 paper, wash with hot 10% nitric acid–5% hydrogen peroxide solution, then transfer the paper and residue to a platinum crucible and burn off the paper at $\sim 400^\circ$ in a muffle furnace. Ignite the residue at $\sim 800^\circ$ for 15 min, cool the crucible and, depending on the quantity of residue, add 0.5–1 g of potassium pyrosulphate. Mix thoroughly, then fuse the mixture over an open flame and keep the melt at red heat for a short time to ensure complete decomposition. Cool the crucible, add 15 ml of water, loosen the cake with a glass rod, then transfer to a 50-ml beaker. Heat on a hot-plate and add 50% sulphuric acid dropwise, if necessary, until a clear solution is obtained. Add this solution to the main solution.

Ion-exchange separation. Using a pH-meter, adjust the pH of the solution to 1.2 ± 0.2 by dilution with demineralized water, then transfer the solution to a 250-ml separatory funnel clamped at the top of the cation-exchange resin column. Pass the solution through the column at about 2.5 ml/min. Wash the beaker three times with 10-ml portions of acidulated water (pH 1.2 ± 0.2) and add the washings to the column.

Elute the common ions from the column with 250–300 ml of 1.85M hydrochloric acid (at 2.5 ml/min) until the effluent is free from Fe^{3+} (test with ammonium thiocyanate solution). Discard the effluent.

Elute the rare-earths, scandium and yttrium by passing 500 ml of 6M hydrochloric acid through the column at 2.5 ml/min. Collect the eluate in a 600-ml beaker, and evaporate it to about 5 ml. Transfer the solution to a 20-ml beaker, rinsing the original beaker with hot 6M hydrochloric acid. Evaporate the solution to a syrupy liquid on a hot-plate and finally to dryness on a steam-bath. Add 5 ml of concentrated nitric acid and 1 ml of 30% hydrogen

peroxide, cover the beaker with a watch-glass and heat on a steam-bath to decompose any resin and convert the chlorides into the nitrates. When the reaction has subsided, raise the watch-glass by means of glass hooks and evaporate the solution to dryness. Repeat the nitric acid–peroxide treatment and subsequent evaporation twice more to ensure complete decomposition of the organic material and conversion of the salts into nitrates. Dissolve the final residue in 5 ml of 0.1M nitric acid by stirring and warming briefly on a steam-bath, then transfer to a 10-ml standard flask and dilute to the mark with 0.1M nitric acid. If necessary, filter the 5 ml of solution through a 5.5-cm glass-fibre paper in a 58° funnel 35 mm in diameter, rinsing the beaker and washing the paper with 0.1M nitric acid, collecting the filtrate and washings in a 10-ml standard flask. This 10 ml of solution is Solution A.

Alternative preconcentration by oxalate and hydroxide co-precipitations. Preconcentrate the rare-earths by double oxalate co-precipitation with 0.2 g of added calcium, followed by a single hydrous oxide co-precipitation with 5 mg of added iron to remove the calcium.¹ After destruction of the paper containing the hydrous oxide residue, by three evaporations with concentrated nitric acid and 30% hydrogen peroxide, evaporate the solution to dryness on a steam-bath. Dissolve the salts in 5 ml of 0.1M nitric acid, stirring with a glass rod and briefly warming on a steam-bath, and make up to volume with the same acid in a 10-ml standard flask (filtering *etc.*, if necessary, as just described) to obtain Solution A.

Preparation of ethanolic perchlorate solution. If the sample weight was 3 g, transfer 8 ml (Note 2) of Solution A to a 10-ml beaker, add 0.6 ml of aqueous 5% lanthanum buffer solution and evaporate to dryness, then add 2 ml of concentrated perchloric acid and evaporate on an asbestos-covered hot-plate to a moist residue. Cool until no fumes are visible, then cover the beaker with a watch-glass. Add 1 ml of absolute ethanol and stir the mixture with a small glass rod to dislodge the solids and dissolve the salts. Transfer the solution to a 3-ml standard flask (available from Mandel Scientific Co. Ltd., Rockwood, Ontario), dilute to volume with absolute ethanol, then transfer the solution to a 5-ml glass vial and close the screw-cap tightly (Note 3).

If the original sample weight was <3 g, transfer 8 ml of Solution A to a 10-ml beaker, add 0.4 ml of aqueous 5% lanthanum buffer solution and evaporate with perchloric acid as above. Dissolve the salts in 1 ml of absolute ethanol, transfer the solution to a 2-ml standard flask, dilute to volume with ethanol, then transfer the solution to a 5-ml glass vial. In order to have sufficient volume for determination of the specified elements, transfer 0.5 ml to a 1-ml standard flask, add 0.1 ml of ethanolic 5% lanthanum buffer solution, dilute to volume with absolute ethanol, then transfer the solution to a 5-ml glass vial (Note 4). Close the screw-caps tightly to prevent evaporation losses.

AAS determination of Sc, Y, Nd, Eu, Dy, Ho, Er, Tm and Yb by flame microsample injection. After adjustment of the solution uptake into the lean nitrous oxide–acetylene flame (3–4 cm red feather) to 4 ml/min, with absolute ethanol as the test liquid, and optimization of the vertical and horizontal burner positions with 10-fold scale expansion and an ethanolic perchlorate solution of the appropriate element (containing ethanolic lanthanum buffer), connect one end of the uptake tubing to the burner nebulizer and the other end to the bottom of the injection funnel of the micro-sampler, which is firmly held on the vial tray by a mounting bracket.

With the AAS instrument set at 10-fold scale expansion and the strip-chart recorder at appropriate sensitivity, successively aspirate (Note 5) 200- μl portions of the blank, calibration and sample solutions by means of the injection funnel, in the following order: blank, low calibration solution (*e.g.*, synthetic GA), sample solution, blank, high calibration solution (*e.g.*, synthetic SY-2 or SY-3). Between each aspiration, wash the funnel and the capillary tube with

*For shale samples of high carbon content (2–8%), place the dish on a silica triangle supported on a tripod, cover and heat gently with a Bunsen burner until all acid fumes are expelled and all organic material is destroyed. Heat briefly to red heat, cool, then proceed as described.

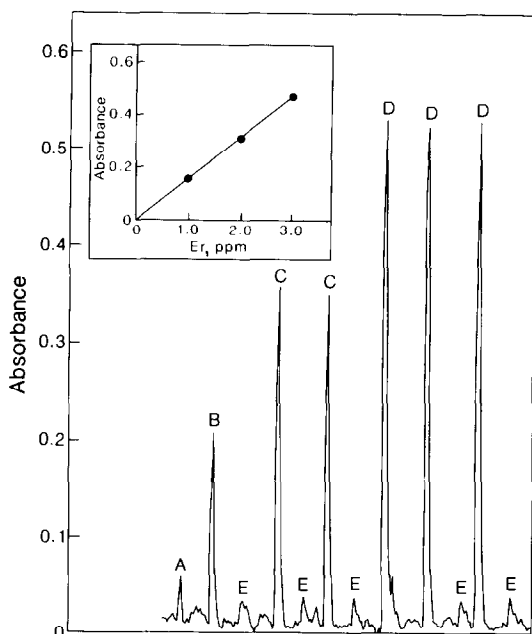


Fig. 2. Absorbance peaks and calibration curve (inset) for erbium: A, blank (1% La buffer solution); B, 1 ppm Er; C, 2 ppm Er; D, 3 ppm Er; E, capillary tube and spray chamber cleaned with absolute ethanol between injection of samples. Approximately 10-fold scale expansion was used.

a jet of absolute ethanol from a wash bottle until the flame shows no colour due to sample salts and lanthanum. Use a fresh pipette tip for each solution (Note 6).

Correct the absorbance value obtained for each calibration solution and plot absorbance of the particular rare-earth element *vs.* its concentration. Determine the corresponding rare-earth content of the sample solution by reference to the calibration curve, after correction for the blank. Monitor the recovery by determination (in the same run) of the same element in two international reference rocks for which "usable values"⁷ for the REE are available.

Notes

1. Since in the flame AAS determination of REE there are no interelement interferences among the rare-earths in

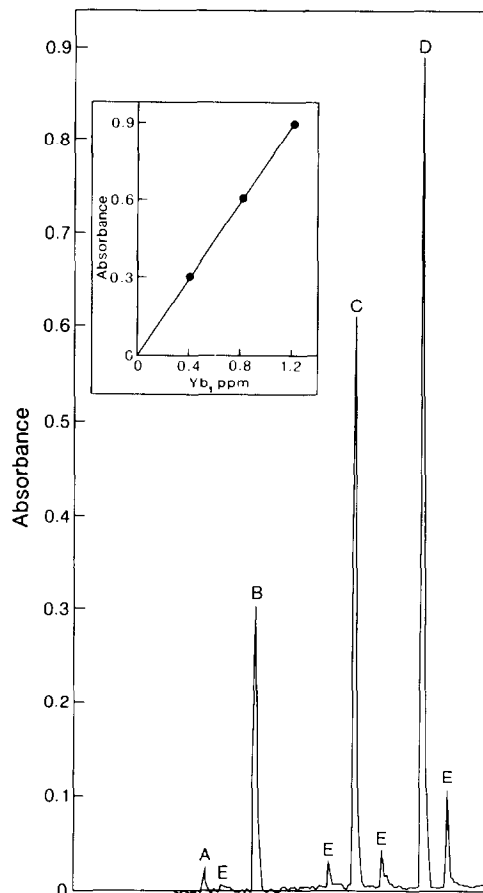


Fig. 3. Absorbance peaks and calibration curve (inset) for ytterbium: A, blank (1% La buffer solution); B, 0.4 ppm Yb; C, 0.8 ppm Yb; D, 1.2 ppm Yb; E, capillary tube and spray chamber cleaned with absolute ethanol between injection of samples. Approximately 10-fold scale expansion was used.

the presence of 1% lanthanum spectroscopic buffer,¹ such solutions provide handy standards for the specified elements for preparation of calibration curves.

Table 2. Recovery of Sc, Y and seven rare-earth elements from synthetic solutions* used for calibration purposes, after preconcentration by double calcium oxalate and single hydrous ferric oxide co-precipitations

Element	Concentration, ppm					
	GA (Granite)		SY-2 (Syenite)		SY-3 (Syenite)	
	Taken	Found	Taken	Found	Taken	Found
Sc	7	7	7	7	11	11
Y	17	17	120	120	600	600
Nd	20	19	75	73	700	680
Eu	0.83	0.8	2.3	2.3	14	14
Dy	2.7	2.8	21	22	118	119
Ho	0.5	<1	7	6.8	22	21
Er	1.5	1.5	13	13	52	52
Tm	0.21	0.2	2.5	2.4	10.5	10
Yb	1.4	1.45	16	15.9	55	53

*The synthetic solutions contained the amounts of scandium, yttrium and rare-earth elements shown, plus the following elements (in ppm): GA—38 La, 70 Ce, 7 Pr, 5.2 Sm, 3 Gd, 0.5 Tb, 0.3 Lu and 17.6 Th. SY-2—88 La, 210 Ce, 16 Pr, 17 Sm, 11 Gd, 2.7 Tb, 3 Lu and 370 Th. SY-3—1250 La, 2000 Ce, 125 Pr, 108 Sm, 53 Gd, 15 Tb, 8 Lu and 980 Th.

Table 3. Determination of Sc, Y and seven rare-earth elements in U.S.G.S. reference rocks (concentrations in ppm)

Element	BCR-1 (Basalt)			BHVO-1 (Hawaiian basalt)			SCO-1 (Cody shale)			MAG-1 (Marine mud)			STM-1 (Syenite)		
	This work*	Other values	This work	Other values	This work	Other values	This work	Other values	This work	Other values	This work	Other values	This work	Other values	
Sc	30	33†	25*	(32.33 ^b)‡	10.4*	(10.11 ^b)‡	15*	(17.18 ^b)‡	1	0.74 ^a					
Y		32.8 ± 2.2‡	25‡	31†	10‡	11†	19‡	17†		0.77†					
	37	33 ^d	27*	(28.27 ^c) ^f	32*	(24.25 ^c) ^f	28*	29 ^g	50	0.678 ± 0.002 ^c					
		40†	30‡	27†	28‡	24†	33‡	27†		(50.445 ^e) ^f					
Nd	25	38.7 ± 6.6‡	25*	28 ± 2 ^c	28*	26 ^c	42*	25-57 ^c	88	53 ^c					
		22 ^d	28‡	(28.26 ^c) ^f	24‡	27†	34‡	(38.42 ^c) ^f		(67.475 ^c) ^f					
Eu	2	26†	2*	24 ± 6 ^c	1.3*	26 ± 2 ^c	1.6*	41,144 ± 3 ^c	3.8	78,182 ± 5 ^c					
		1.7 ^d	2†	26 ± 7 ^c	1.2‡	1.2 ^a	1.6*	34 ± 7 ^c		78 ± 15 ^c					
Dy	7	1.98 ± 0.1‡	2.7‡	2†	1.2‡	1.2†	1.5‡	1.8 ^a		3.2 ^a					
		4.9 ^d	5.2*	2.0 ± 0.4 ^c	5*	1.2 ± 0.2 ^c	5.6*	1.6 ± 0.2 ^c	9	3.6 ± 0.4 ^c					
Ho	1.2	6.35 ± 0.31‡	6‡	5.3 ^a	4.5‡	4.2†	5‡	4.3 ^a		8 ^a					
		1.0 ^d	0.9*	4.8 ± 0.2 ^c	1*	1.0 ^b	1*	3.8 ^c		7.8 ^c					
Er	3.8	1.25 ± 0.14‡	1‡	0.95 ^a	1‡	0.9†	1‡	0.9†		1.5 ^b					
		3.5 ^d	2.5*	0.94 ^c	1‡	0.93 ^c	1‡	0.92 ^c		2.1 ^c					
Tm	0.5	3.5†	2.4‡	2.5 ^a	2.6*	2.5 ^a	4*	2.8 ^a	4.4	3.8 ^a					
		3.6 ± 0.19‡	0.3*	2 ± 0.3 ^c	3‡	2.5†	3.5‡	3.16 ^b		4.4 ^c					
Yb	3.3	0.576 ± 0.06‡	0.3‡	0.3 ^b	0.4*	0.4 ^b	0.45*	0.4 ^b	0.7	0.6 ^b					
		3.2 ^d	0.3‡	0.3†	0.4‡	0.5†	0.4‡	0.44 ^c		<1 ^c					
	3.4†	0.576 ± 0.06‡	2*	0.31 ± 0.04 ^c	2.2*	(2.3 ^a 2.5 ^c) ^f	2.7*	0.54 ^d	4.4	1.6 ^d					
	3.37 ± 0.27‡	3.4†	2.5‡	2.1 ± 0.5 ^c	2.4‡	2.2†	2.7‡	(2.5, 2.7 ^c) ^f		4.3†					
								3.0 ± 0.3 ^c		4.4 ± 0.4 ^c					

*Preconcentrated by double calcium oxalate and single hydrous ferric oxide co-precipitations.

†“Usable value” reported in a compilation of data by Abbey.⁷

‡Mean value ± standard deviation reported in a compilation of data by Gladney and Burns.¹⁵

§Preconcentrated by ion-exchange.

¶Sen Gupta.⁹

^aDirect aspiration flame AAS value.

^bGraphite furnace AAS value.

^cMean value ± standard deviation reported in a compilation of data by Gladney and Goode.¹⁶

^dSen Gupta.¹³

^eEmission spectrographic value.

^fSen Gupta.¹⁴

^gChurch (ICP-AES value).¹⁷

^hMcLennan and Taylor (spark-source mass-spectrographic value).¹⁸

ⁱRosenberg and Zilliacus (instrumental neutron-activation value).¹⁹

Table 4. Determination of Sc, Y and seven rare-earth elements in Canadian reference materials (concentrations in ppm)

Element	SY-2 (Syenite)			FeR-1 (Iron formation)			FeR-2 (Iron formation)			FeR-3 (Iron formation)			FeR-4 (Iron formation)		
	This work	Other values	This work*	Other values	This work*	Other values	This work*	Other values	This work*	Other values	This work*	Other values	This work*	Other values	
Sc	6*	7 [†] , 8 [†] , 7 ^{‡a}	0.9	0.7-1 ^b 0.8 ^c	6	4-6.7 ^b 6 ^c	0.6	(0.497, 0.58, 2) ^b	1.4	1.29-2 ^b 1.5 ^c					
Y	131*	120 ^{†, d} (125, 8117 ^e) ^f	18	11-46 ^b	16	12-19 ^b 15 ^c	5	2-6 ^b 6 ^c	9	4-10 ^b 8 ^c					
Nd	70*	130 ^a 75 ^{†, d}	10	—	12.5	15 ^b	5	—	10	—					
	75 [†]	(81, 884 ^e) ^f 71 ^{†g}													
Eu	2.6*	2.3 ^{†, §, d, f} 2.4 ^{†g}	2.8	0.76-3.1 ^b	1.3	1.1-1.32 ^b	0.25	0.18-0.24 ^b	0.8	0.61-0.77 ^b					
Dy	20*	21 ^{†, d} 208 [†]	2.5	1.76 ^b	2.5	2.36 ^b	0.8	0.34 ^b	1.3	1.05 ^b					
	20.8 [†]	207 ^{†a}													
Ho	5*	7 ^{†, d} 58 [†]	0.5	0.33 ^b	0.6	0.6 ^b	<0.3	0.08 ^b	0.3	0.22 ^b					
	5 [†]	2.9-7 ^g													
Er	15*	13 ^{†, d, f} 11-24 ^g	1.5	—	1.6	—	0.4	—	0.7	—					
	16 [†]	127 ^{†a}													
Tm	2.4*	2.5 ^{†, §, d, f} 1.6-2.5 ^g	0.2	—	0.2	—	0.1	—	<0.1	—					
	2.3 [†]	27 ^{†a}													
Yb	17.7*	16 ^{†, d} 158 ^{†, e, f}	1	0.98-1 ^b 1 ^c	1.5	1.2-1.7 ^b 1.3 ^c	0.29	0.19-0.36 ^b 0.2 ^c	0.7	0.3-0.76 ^b 0.5 ^c					
	17 [†]	17 ^{†a}													

*Preconcentrated by double calcium oxalate and single hydrous ferric oxide co-precipitations.

†Preconcentrated by ion-exchange.

‡Direct aspiration flame AAS value.

§Graphite furnace AAS value.

¶Sen Gupta.⁹^aUsable value" reported in a compilation of data by Abbey.⁷^bReported in a compilation of data by Abbey *et al.*²⁰^cUsable value" reported in a compilation of data by Abbey *et al.*²⁰^dSen Gupta.¹^eEmission spectrographic value.^fSen Gupta.¹⁰^gReported in a compilation of data by Abbey.⁸

2. The remaining 2 ml of Solution A can be used for the determination of other rare-earths by electrothermal AAS.⁹⁻¹²

3. For a sample of high scandium or REE content it may be necessary to dilute the initial solution to a suitable volume with absolute ethanol before the AAS determination. Sufficient ethanolic 5% lanthanum solution must be added for the final concentration of lanthanum to be 1% by weight.

4. The determination of Sc (see Note 3 above), Dy and Yb should be completed from this diluted solution, and the original sample solution should be used for determination of Y, Nd, Eu, Ho, Er and Tm.

5. For recording absorbances of most standards and sample solutions use the recorder set at 10 mV full-scale deflection. Additional scale expansion may be obtained by using 5 mV full-scale deflection (useful for very low Nd, Eu and Ho contents).

6. Do not discard the blue pipette tips after use. Wash them thoroughly in tap water, followed by demineralized water, then dry at room temperature overnight.

RESULTS

Figures 2 and 3 show that for the concentration ranges tested the absorbance peaks obtained for erbium and ytterbium with the microsampling technique are reasonably reproducible, and linear calibration graphs are obtained. Similar results were obtained for Sc, Y, Nd, Eu, Dy, Ho and Tm in suitable concentration ranges.

The reliability of the proposed method was tested by applying it to the analysis of the synthetic GA, SY-2 and SY-3 solutions prepared for calibration purposes. It was also applied to various Canadian and U.S.G.S. reference rocks for which published data on the REE are available for comparison, and to four new Canadian iron formation reference materials FeR-1, FeR-2, FeR-3 and FeR-4. The results of these determinations are given in Tables 2-4.

DISCUSSION

Table 2 shows that complete recovery ($100 \pm 5\%$) of the added REE was obtained after their separation by double calcium oxalate and hydrous ferric oxide co-precipitation. Tables 3 and 4 show that the results obtained for six international reference rocks, in which the REE were preconcentrated by double calcium oxalate and hydrous ferric oxide co-precipitation for all six and by ion-exchange for four of them, are in reasonably good agreement with those obtained by the author by direct-aspiration flame AAS.^{1,9,13,14} There is also satisfactory agreement with the author's graphite-furnace AAS and emission spectrographic values,^{9,10,14} and the "usable values" reported in compilations of data by Abbey^{7,8} (the value with a question mark indicates uncertainty about the "usable value" because it represents the median of only 5-9 available results⁷) and the "mean values \pm standard deviations" reported in compilations of data by Gladney *et al.*^{15,16} Where sufficient values are not available in such com-

pilations, other published values¹⁷⁻¹⁹ are included for comparison purposes.

The results obtained by the proposed method for the Canadian iron formation reference materials either compare well with the "usable value?" reported in a recent compilation of data by Abbey *et al.*²⁰ or fall within the range of other values (Table 4). Values for neodymium (except FeR-2), erbium and thulium have not hitherto been reported.

Although the results obtained by the two separation methods are in good agreement with each other and with published values, the ion-exchange method is somewhat the faster. The proposed method is also applicable to the determination of large amounts of lanthanum and samarium in some rocks rich in rare-earths. It is considerably quicker than methods based on direct aspiration of the sample solution, particularly for ultramafic and other common rocks containing trace rare-earths, because of the saving of time in preconcentration of REE from a relatively small sample. It has been applied to the routine determination of the specified REE in shales and mafic dykes.

The use of the microsampling technique has resulted in significant saving of time and simplification of the sample dissolution and preconcentration procedures for the determination of traces of rare-earths in ultramafic and many common rocks and rock-forming minerals. The results are in reasonably good agreement with those of direct flame aspiration and graphite-furnace AAS methods which require a much longer time for such determinations.

Acknowledgement—The author is indebted to Mrs. E. M. Donaldson of Canada Centre for Mineral and Energy Technology for critical reading of the manuscript.

REFERENCES

1. J. G. Sen Gupta, *Talanta*, 1976, **23**, 343.
2. M. R. Hughson and J. G. Sen Gupta, *Am. Mineralogist*, 1964, **49**, 937.
3. E. Sebastiani, K. Ohls and G. Riemer, *Z. Anal. Chem.*, 1973, **264**, 105.
4. H. Berndt, J. Messerschmidt, F. Alt and D. Sommer, *ibid.*, 1981, **306**, 385.
5. H. Urbain and N. Martin, *At. Spectrosc.*, 1981, **2**, 127.
6. M. Roubault, H. de La Roche and K. Govindaraju, *Sci. de La Terre*, 1968, **13**, 379.
7. S. Abbey, *Geol. Surv. Can. Paper*, 1983, 83-15.
8. *Idem*, *Canmet Report*, 1979, 79-35.
9. J. G. Sen Gupta, *Anal. Chim. Acta*, 1982, **138**, 295.
10. *Idem*, *Talanta*, 1981, **28**, 31.
11. *Idem*, *ibid.*, 1984, **31**, 1053.
12. *Idem*, *ibid.*, 1984, in press.
13. *Idem*, *Geostds. Newsl.*, 1977, **1**, 149.
14. *Idem*, *ibid.*, 1982, **6**, 241.
15. E. S. Gladney and C. E. Burns, *ibid.*, 1983, **7**, 3.
16. E. S. Gladney and W. E. Goode, *ibid.*, 1981, **5**, 31.
17. S. E. Church, *ibid.*, 1981, **5**, 133.
18. S. M. McLennan and S. R. Taylor, *Chem. Geol.*, 1980, **29**, 333.
19. R. J. Rosenberg and R. Zilliacus, *Geostds. Newsl.*, 1980, **4**, 191.
20. S. Abbey, C. R. McLeod and W. Liang-Guo, *Geol. Surv. Can. Paper*, 1983, 83-19.

DETERMINATION OF CERIUM IN SILICATE ROCKS BY ELECTROTHERMAL ATOMIZATION IN A FURNACE LINED WITH TANTALUM FOIL

APPLICATION TO 19 INTERNATIONAL GEOLOGICAL REFERENCE MATERIALS

J. G. SEN GUPTA

Geological Survey of Canada, Ottawa, Ontario, Canada

(Received 8 December 1983. Revised 26 May 1984. Accepted 22 June 1984)

Summary—A 40-fold increase in sensitivity obtained by using a tantalum foil lining in a pyrolytically-coated graphite furnace permitted determination of low ppm levels of cerium in most silicate rocks. A preliminary preconcentration by oxalate and hydroxide co-precipitations was used before determination by use of a Varian GTA-95 atomizer coupled with an AA-475 spectrometer. The results for 3 synthetic and 19 international reference materials, including 4 new Canadian iron-formation reference materials, showed good recovery and satisfactory agreement with other published values.

The determination of cerium by atomic-absorption spectrometry has always been a baffling problem because of the low sensitivity for the element, whether a flame or a graphite furnace is used. Attempts to determine this element by use of an oxy-acetylene¹ or nitrous oxide-acetylene flame² were not successful. The detection limit of 150 ppm of Ce obtained by Thomas³ by use of a fuel-rich $N_2O-C_2H_2$ flame is of hardly any use in rock analysis. This poor detection limit was attributed to the complexity of the low-intensity cerium spectra, more than 60% ionization of the cerium atoms, and the tendency to form CeO molecules in the gas phase.³ When the graphite furnace is used, there is difficulty in volatilizing cerium because of the formation of its carbide or an interlayer compound with graphite. Although L'vov and Pelieva⁴ noted a significant increase in sensitivity for most rare-earth elements when a graphite furnace lined with tantalum foil was used, cerium was not included in that study. In a subsequent publication⁵ these authors reported a detection limit of 3–5 ng for cerium by use of the furnace lined with tantalum foil, after evaporation of the cerium and excess of lanthanum from a tungsten probe. Although mention was made of the application of a tungsten probe soaked in a solution of iron, in the determination of 0.05–0.23% cerium in some low-alloy steels, no data were reported. No other information is available on the application of a tungsten probe or simply a tantalum-foil lined furnace to the determination of cerium in geological materials.

After our acquisition of a Varian graphite-tube atomizer (GTA-95) and a Westinghouse hollow-cathode cerium lamp, it was possible to test the

sensitivity for cerium by electrothermal atomization. With use of an argon gas purifier and a tantalum foil lining to the furnace, an average sensitivity of 5 ng was obtained at 567.0 nm and a temperature of 2600°. In concurrence with the observation of L'vov and Pelieva,⁵ the 567.0 nm line was found to be slightly more sensitive than the 520.1 nm line and relatively free from incandescence effects from the furnace at 2600°. However, addition of lanthanum (2.5 µg) to enhance the cerium signal and linearize the calibration, as done by L'vov and Pelieva,⁵ complicated the problem of determination of very small amounts of cerium, because the lanthanum gave significant absorption at 567.0 nm. Therefore, all determinations were done without addition of lanthanum.

The method developed was tested with synthetic solutions and a number of international reference samples of established cerium contents, and applied to the determination of cerium in four new Canadian iron-formation reference materials.

EXPERIMENTAL

Apparatus and operating parameters

A Varian graphite-tube atomizer (GTA-95) equipped with a programmable sample dispenser and memory storage for 8 operating-parameter programmes, and coupled with a Varian AA-475 spectrometer fitted with IEEE communication, was used for all atomic-absorption studies. Other accessories included an Epson MX-82 Type III printer with IEEE interface, pyrolytically-coated tubes, tantalum foil (99.95% pure, 0.05 mm thick, A.D. Mackay, Darien, Conn., U.S.A.), argon gas (99.999% pure) connected through a gas purifier (Matheson, Model 6406), and a Radiometer 22 pH-Meter.

The AA-475 spectrometer was operated on single beam with restricted 0.5-nm bandpass, in the peak-height mode; a 1-sec integration-time was used in setting zero absorbance

Table 1. Operating parameters of GTA-95 with Ta-foil lined furnace (5–20 μ l sample solution)

Step	Temperature, °C	Time, sec	Argon gas flow, l./min	Read
1	75	15	3	
2	90	60	3	
3	120	60	3	
4	850	10	3	
5	1800	10	3	
6	1800	2	0	
7	2600	1.3	0	*
8	2600	2	0	*
9	2600	1	3	

on the instrument. A Westinghouse cerium hollow-cathode lamp was used, operated at 10 mA. The signal, at 567.0 nm, was maximized in the usual way. Other operating parameters are given in Tables 1 and 2.

Preparation of furnace lined with tantalum foil

A 2-mm hole was drilled in a 12 \times 14 mm piece of tantalum foil (Fig. 1). The foil was wrapped on a 4-mm glass rod as a former (short side parallel to the rod) and the tube thus made was inserted into the centre of a new pyrolytically-coated graphite tube (PCGT) so that the holes in both tubes coincided. A metal rod (3 mm diameter) was inserted into the tube, and firmly rolled inside it (on the bench top) to attach the tantalum foil smoothly to the inner lining of the graphite tube, over the "hump" at the centre of the tube. This was the only way found for fitting the liner so that no blockage of the light-path was caused by distortion of the foil on heating. A further step to prevent distortion (and embrittlement of the foil) was a careful annealing. For this, the tantalum-lined graphite tube was placed in the GTA-95, and before first use, it was heated in a current of argon according to the following programme. The tube was brought to 1000° in 10 sec, held at that temperature for 10 sec, and then cooled down in 16 sec. This

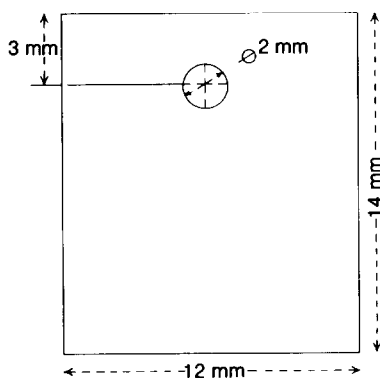


Fig. 1. Shape and dimensions of the tantalum foil.

Table 2. Auto sample dispenser parameters for tantalum-foil lined furnace

Samples and standards			Blank* volume, μ l
Type	Location	Volume, μ l	
Blank	—		20
STD 1	46	5	15
STD 2	46	10	10
STD 3	46	15	5
STD 4	46	20	0
Samples	—	20	0

*0.1M nitric acid.

operation was repeated for temperatures of 1500° and 2000°, followed by a blank run according to the heating programme in Table 1.

Sensitivity

The characteristic amounts found for cerium (*i.e.*, weight producing 1% absorption) are given in Table 3. The memory effect after atomization from the tantalum surface at 2600° for 4.3 sec was negligible. Although atomization at 2700° gave a further increase in sensitivity, there was more rapid deterioration of the liner so 2600° is recommended as the maximum temperature to be used.

Reagents

Stock solution of cerium (~1000 ppm). Prepared by dissolving an accurately weighed quantity of CeO₂ (99.999% pure, Spex Industries Inc.) in hot dilute nitric acid with the addition of few drops of 30% hydrogen peroxide. The solution was evaporated to dryness on a steam-bath, and the salts were dissolved in 1M nitric acid and diluted to known volume with the same acid. A 5-ml aliquot was evaporated in a 10-ml weighed platinum crucible on a steam-bath, the nitrate was decomposed by gentle heating with a Bunsen burner, and finally the crucible and contents were ignited to constant weight at 1000° to determine the CeO₂ content. Solutions of lower concentration (100 or 10 ppm) were prepared by appropriate dilution with 0.1M nitric acid.

Stock solutions of other rare-earth elements. Prepared by dissolving the high-purity oxides (Spex Industries Inc.) in dilute nitric acid, and standardized as for the cerium solution.

Synthetic standard mixtures. Synthetic standard mixtures approximating the compositions (except for the common elements) of three international reference samples [GA (granite), SY-2 (syenite) and Sy-3 (syenite)] were prepared by mixing the standard solutions in appropriate amounts (see Table 4).

Interferences

In order to determine cerium in rocks it was necessary to separate the rare earths from common elements. Although no interference from the associated rare earths from common rocks was noticed, addition of 2.5 μ g of lanthanum (as recommended⁵ for enhancing the cerium signal) was found

Table 3. Sensitivities for cerium in pyrolytically-coated and tantalum-foil lined furnace (GTA-95)

Atomization temperature, °C	Sensitivity*		Sensitivity enhancement factor (PCGT/TaF)
	Pyrolytically-coated graphite tube (PCGT)	Ta-foil lined furnace (TaF)	
2500	3×10^{-7}	10×10^{-9}	30
2600	2×10^{-7}	5×10^{-9}	40

*Defined as the weight of the element in g which produces a change, compared to pure solvent or blank, of 0.0044 absorbance unit.

Table 4. Concentrations of Sc, Y, Th and the rare-earth elements in synthetic mixtures of GA, SY-2 and SY-3 (in ppm)*

Element	GA (Granite)	SY-2 (Syenite)	SY-3 (Syenite)
Sc	7	7	11
Y	17	120	600
La	38	88	1250
Ce	70	210	2000
Pr	7	16	125
Nd	20	75	700
Sm	5.2	17	108
Eu	0.83	2.3	14
Gd	3	11	53
Tb	0.5	2.7	15
Dy	2.7	21	118
Ho	0.5	7	22
Er	1.5	13	52
Tm	0.21	2.5	10.5
Yb	1.4	16	55
Lu	0.3	3	8
Th	17.6	370	980

*These values were derived from the author's own published and unpublished works as well as those found in the literature.

to increase the signal at 567.0 nm because of absorption by the lanthanum. Since this complicated the problem of determination of very small amounts of cerium (0.1–0.6 μg) because of uncertainty as to the cerium contribution to the total absorbance value, no additional lanthanum was added in this work. The La:Ce ratio in most rocks is about 1:2, but it was found that lanthanum could be tolerated up to a ratio to cerium of 1:1. No interferences were noticed from the presence of relatively large amounts of iron (up to 500 ppm). Therefore, rare earth concentrates obtained by double oxalate co-precipitation with calcium, followed by a hydroxide co-precipitation with iron,⁶⁻⁸ were found to be suitable for

the electrothermal atomic-absorption determination of cerium.

Recommended procedure

Decompose a 3-g sample and separate the lanthanides from the common elements by double co-precipitation with calcium oxalate and then from excess of calcium by single co-precipitation as hydroxide with 5 mg of iron, as described earlier.⁶⁻⁸ Destroy the filter paper by heating with concentrated nitric acid and 30% hydrogen peroxide and evaporating to dryness on the steam-bath, then dissolve the salts in 0.1M nitric acid and, depending on the concentration of cerium expected, dilute the solution to exactly 5 or 10 ml with the same acid. For solutions containing higher amounts of cerium (e.g., for samples of SY-3 type) dilute further with 0.1M nitric acid to bring the cerium concentration within the range 10–30 ppm. Store all sample solutions in glass vials tightly closed with screw-caps. Using the operating parameters mentioned earlier and those in Tables 1 and 2, prepare the calibration graph by atomization of 0.1–0.6 μg of cerium in the furnace lined with tantalum foil. Use up to 5 \times scale-expansion, and take the average reading from two atomizations.

RESULTS AND DISCUSSION

The results for 3 synthetic solutions and 19 international reference rocks are given in Table 5 and compared with the expected or published values. Quantitative recoveries were obtained for the synthetic solutions and the results for the reference samples either agreed with the recommended values or fell within the mid-range of other values.

The condition of the tantalum-foil liner was checked by running a standard after every five samples, and if necessary a correction was applied to the adjacent sample. The tantalum foil was changed after

Table 5. Determination of cerium in synthetic solutions and international geological reference samples by electrothermal atomization in a tantalum-foil lined furnace

Synthetic or reference sample	Ce, ppm			Reference sample	Ce, ppm	
	Taken	Found (this work)	Other values		This work	Other values
Synthetic GA	70	69		U.S.G.S.		
Synthetic SY-2	210	200		Basalt BCR-1	59	53a
Synthetic SY-3	2000	1900		Basalt BHVO-1 (Hawaiian)	49	49 ^e , 41 \pm 4 ^b , 46 \pm 3 ⁱ
<i>Canadian</i>						
Syenite SY-2		210	210 ^g a	Nepheline syenite STM-1	251	258 ^e , (226–354) ^h
Syenite SY-3		2162	2200 ^a			260 ^a
Iron formation FeR-1		24	11, 21.38 ^b	Cody shale SCo-1	69	66 ^e , 62 \pm 6 ^h
Iron formation FeR-2		26	11–32.12 ^b	Rhyolite RGM-1	47	49 ^e , 48 ^a
Iron formation FeR-3		8	5 ^b	Diabase W-2	26	26 ^j , 26 \pm 3 ^k
Iron formation FeR-4		19	7.33–14.48 ^b	Diabase DNC-1	15	15 ^j , 15 \pm 4 ^k
<i>CRPG (France)</i>						
Granite MA-N		9	10 ^c			
Anorthosite AN-G		8	4.7 ^c			
Basalt BE-N		196	110–247 ^d			
<i>South African</i>						
Granite NIM-G		200	200 ^a			
Tuff NIM-35/71		2500	2540 ^e , 2650 ^f			
Red Syenite NIM-37/71		890	926 ^e , 700 ^f , 880 ^g			

^aAbbey,⁹ ^bAbbey;¹⁰ ^cGovindaraju's proposed value;¹¹ ^dGovindaraju;¹¹ ^eSen Gupta (optical-emission spectroscopic value on the concentration);¹² ^fBrenner *et al.*;¹³ ^gdirect-reader optical-emission spectroscopic value without preconcentration;¹⁴ ^hGladney and Goode;¹⁵ ⁱChurch;¹⁶ ^jSen Gupta (optical-emission spectroscopic value on the concentrate);⁷ ^kGladney and Burns.¹⁷

about 30 firings. The drying temperatures given in Table 1 were found adequate for up to 20 μ l of sample solution. Larger volumes required either a longer drying time or multiple injections (of not more than 20 μ l each) with drying after each injection. The pyrolytically-coated tube was replaced after about 60 firings.

REFERENCES

1. V. G. Mossotti and V. A. Fassel, *Spectrochim. Acta*, 1964, **20**, 1117.
2. M. D. Amos and J. B. Willis, *ibid.*, 1966, **22**, 1325.
3. P. E. Thomas, *Resonance Lines*, 1969, **1**, 6.
4. B. V. L'vov and L. A. Pelieva, *Can. J. Spectrosc.*, 1978, **23**, 1.
5. *Idem*, *Zh. Analit. Khim.*, 1979, **34**, 1744; *J. Anal. Chem. U.S.S.R.*, 1980, **34**, 1354.
6. J. G. Sen Gupta, *Talanta*, 1976, **23**, 343.
7. *Idem*, *ibid.*, 1981, **28**, 31.
8. *Idem*, *Anal. Chim. Acta*, 1982, **138**, 295.
9. S. Abbey, *Geol. Surv. Can. Paper*, 1983, 83-15.
10. *Idem*, *ibid.*, 1983, 83-19.
11. K. Govindaraju, *Geostds. Newsl.*, 1980, **4**, 49.
12. J. G. Sen Gupta, *ibid.*, 1982, **6**, 241.
13. I. B. Brenner, A. E. Watson, T. W. Steele, E. A. Jones and M. Goncalves, *Spectrochim. Acta*, 1981, **36B**, 785.
14. W. H. Champ, *Geol. Surv. Can.*, personal communication, 1979.
15. E. S. Gladney and W. E. Goode, *Geostds. Newsl.*, 1981, **5**, 31.
16. S. E. Church, *ibid.*, 1981, **5**, 133.
17. E. S. Gladney and C. E. Burns, *ibid.*, 1983, **7**, 3.

ETUDE DE LA CAPACITE COMPLEXANTE DES EAUX DE L'ESTUAIRE ET DE LA BAIE DE SEINE

JEAN-CLAUDE FISCHER, RENÉ NGANOU et MICHEL WARTEL

Université des Sciences et Techniques de Lille, Laboratoire de Chimie Analytique et Marine,
Bâtiment C 8, Station Marine de Wimereux, 59655 Villeneuve d'Ascq Cedex, France

(Reçu le 15 mai 1984. Accepté le 23 juin 1984)

Résumé—Le dosage des métaux Cd, Pb et Cu dans l'estuaire et en Baie de Seine a été effectué. Le site a été choisi en raison du régime macrotidal fortement marqué qui régit les déplacements des masses d'eau. Une répartition des métaux en trois classes est proposée (métal libre, métal engagé dans des complexes détruits par abaissement du pH, métal engagé dans des complexes stables détruits par irradiation ultraviolette en milieu acide). Les propriétés particulières du cuivre ont été utilisées afin d'établir une capacité complexante apparente des différentes eaux étudiées. En faisant l'hypothèse simplificatrice de l'existence d'un équilibre du type (charges omises)



(L symbolisant le ligande), les concentrations totales du ligande ainsi que les constantes de stabilité des complexes CuL ont été déterminées. Les résultats obtenus sont discutés.

Notre attention s'est portée, dans ce travail, sur le comportement du cadmium, du plomb et surtout du cuivre dissous dans les eaux de l'estuaire de la Seine, afin de contribuer à une meilleure connaissance des modes de transport et du devenir des métaux lourds au sortir d'un fleuve débouchant dans une mer soumise à un régime macrotidal. Peu de mers, à l'échelle planétaire, possèdent des amplitudes et des circulations de marée aussi importantes.

La répartition du métal entre ses différentes formes solubles influence non seulement la biodisponibilité de ce métal, mais joue également un rôle important dans son devenir en raison de l'existence de complexes qui peuvent induire des phénomènes de copécipitation, des retards à la précipitation... etc., et entraîner ainsi des modifications des temps de résidence.

Il nous a donc paru judicieux d'établir un classement des divers complexes dans lesquels sont engagés les métaux étudiés. Dans l'état actuel des connaissances des processus qui permettent au milieu marin de conserver son équilibre, il est illusoire de prétendre établir un classement rigoureux rendant compte de tous les phénomènes. C'est la raison pour laquelle notre choix s'est porté sur une méthode simple qui a de plus l'avantage de limiter les risques de pollution accidentelle.¹ C'est ainsi que nous avons, par la technique de redissolution anodique en mode impulsif différentiel, effectué les analyses des métaux cadmium, plomb et cuivre dans les différents échantillons au pH naturel, puis en milieu acide avant et après irradiation ultraviolette. Nous pouvons ainsi proposer un classement du type:

—métal "libre"

—métal engagé dans des complexes détruits par abaissement du pH

—métal engagé dans des "complexes stables" détruits par irradiation ultraviolette en milieu acide.

Un tel classement met bien en évidence le relargage des métaux lors du mélange des eaux douces et salées.

Dans un second temps, nous nous sommes intéressés à la capacité complexante apparente des eaux étudiées. Le métal, retenu pour cette étude, a été le cuivre en raison de sa faculté de former généralement des complexes avec la quasi-totalité des ligandes organiques présents dans les eaux naturelles, plus stables que ceux formés par les autres métaux étudiés. La méthode employée de détermination de la capacité complexante apparente des eaux de l'estuaire de la Seine est dérivée de celles proposées dans la littérature.^{2,4}

PARTIE EXPERIMENTALE

Quatre sites de prélèvements ont été choisis en Seine et dans l'estuaire de la Seine: Saint-Aubin (en amont de la ville de Rouen), Quilleboeuf, Honfleur et au Cap de la Hève (Figure 1). Tous les prélèvements ont été effectués en septembre 1982 à 1 m au-dessous de la surface. Les échantillons ont été filtrés sur membrane Sartorius de porosité 0,45 μm . La conservation a été assurée par acidification à l'aide d'acide nitrique (pH \sim 1,0) et par congélation pour les eaux non acidifiées. Tous les récipients utilisés sont en polyéthylène haute densité et ont été conditionnés avant utilisation.

Les métaux cadmium, plomb et cuivre ont été dosés par redissolution anodique en mode impulsif différentiel (technique analytique parmi les plus sensibles^{5,6}) à l'aide de l'ensemble (Tacussel) suivant: unité polarographique UAP 4, potentiostat PRT 20.2X, unité Polaromax, électrode tournante EDI CVJ à disque de carbone vitreux (le film de mercure est formé in situ: addition de nitrate mercurique préparé par attaque de mercure métallique), cellule de mesure étanche en quartz.

Toutes les manipulations sont effectuées sous une hotte à flux laminaire.

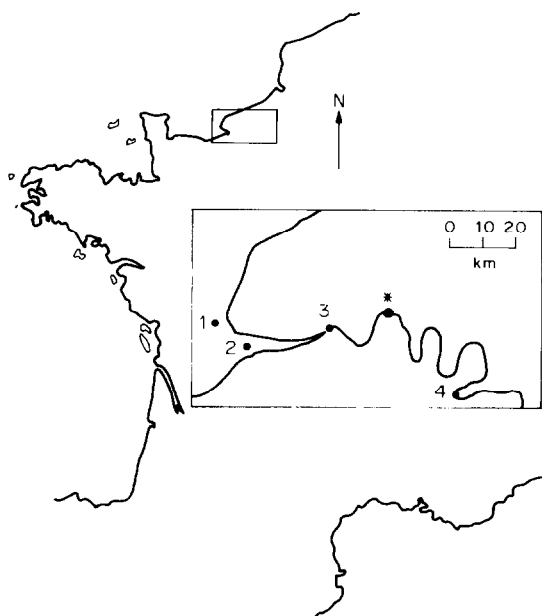


Fig. 1. Sites de prélèvements. ①: Cap de la Hève ②: Honfleur ③: Quilleboeuf ④: Saint-Aubin *: limite amont de l'intrusion saline.

L'irradiation ultraviolette des échantillons a été effectuée à l'aide d'un appareillage construit au laboratoire selon le modèle décrit par Gillain.¹ Cet appareillage comporte une série de tubes de quartz horizontaux entourés de lampes ultraviolettes (lampes Philips, 15 W puissance maximum entre 2482 et 2753 Å). Les tubes de quartz, contenant l'échantillon (1/3 du volume du tube), sont soumis à une lente rotation afin d'augmenter le rendement de l'irradiation (formation d'un film de liquide sur les parois du tube). La durée d'exposition est de 12 hr. Une addition de peroxyde d'hydrogène Normapur Prolabo est effectuée avant irradiation (0,025 ml pour 50 ml d'échantillon).

Pour la préparation des échantillons destinés à l'étude de la capacité complexante, nous avons respecté la méthode suivante:

- additions de cuivre en quantité connue et croissante dans différents échantillons (généralement 10) provenant d'un même site le plus rapidement possible après le prélèvement et la filtration;

- congélation dans l'attente de l'analyse;

- décongélation programmée avant l'analyse, afin de laisser aux échantillons le même temps de mise à l'équilibre; chaque échantillon a ainsi été analysé 24 hr après la décongélation.

RESULTATS ET DISCUSSION

Parmi les diverses méthodes de classement des métaux en leurs différentes formes solubles décrites dans la littérature,^{7,8} nous avons retenu celle qui nécessite le moins de manipulations de l'échantillon et le moins d'additions de réactifs afin de minimiser les risques de pollution.¹ Cette technique de spéciation consiste à doser les métaux Cd, Pb et Cu contenus dans la colonne d'eau (échantillons filtrés sur membrane 0,45 μm) au pH naturel puis en milieu acide avant et après irradiation ultraviolette (l'acidification des échantillons est faite sur les lieux du prélèvement).

Nous avons reporté dans le Tableau I les résultats d'analyse, par redissolution anodique en mode impulsionnel différentiel, des métaux Cd, Pb et Cu pour les différents sites de prélèvement. La colonne I représente la concentration en métal dit libre, c'est-à-dire directement accessible par la méthode de dosage. Il est clair que cette concentration dépend de la technique analytique choisie et dans notre cas particulier, elle dépend également de la valeur du potentiel appliqué à l'électrode indicatrice pendant la phase de dépôt ($-1,2$ V par rapport à l'électrode au calomel pour le dosage du plomb et du cadmium et $-0,8$ V pour le dosage du cuivre). La répartition que l'on pourra déduire par la suite ne pourra donc être qu'arbitraire. On peut noter que pour les sites de Saint-Aubin, de Quilleboeuf et de Honfleur, aucun pic de redissolution n'a pu être détecté au pH naturel, c'est-à-dire qu'aucun complexe métallique n'a été détruit pendant la phase de dépôt. Nous avons là un premier indice du caractère complexant marqué de ces eaux naturelles. La colonne II donne les valeurs des concentrations métalliques obtenues en milieu acide (acide nitrique, pH $\sim 1,0$). La différence entre ces deux colonnes permet d'obtenir la quantité de métal engagé dans des complexes détruits par un abaissement du pH. Pour les sites de Saint-Aubin et de Quilleboeuf, les dosages manquent de reproductibilité. L'accroissement des teneurs métalliques peut être dû:

- à la dissolution d'oxydes (comme MnO_2) ou d'hydroxydes (surtout ceux de fer), composés jouant un rôle important dans le transport des métaux en raison de leur forte capacité d'adsorption;

- à la désorption de colloïdes d'origine minérale ou organique;

- à la protonation de certains complexes organiques.

La colonne III donne les teneurs métalliques après irradiation ultraviolette en milieu acide. Nous observons une nouvelle augmentation des concentrations des différents métaux, augmentation imputable à la destruction par l'irradiation ultraviolette de formes non électroactives essentiellement d'origine organique. Les teneurs métalliques figurant dans cette dernière colonne sont considérées comme représentatives de la concentration totale des différents métaux.⁹

Nous avons reporté sur la Figure 2 la répartition du cadmium, du plomb et du cuivre dans les trois classes:

- métal "libre";

- métal engagé dans des complexes détruits par abaissement du pH (origine minérale essentiellement);

- métal engagé dans des complexes détruits par irradiation ultraviolette en milieu acide (principalement d'origine organique).

Ce classement, bien que dépendant de la technique analytique utilisée, montre bien le relargage des métaux d'amont en aval. Pour les sites de Saint-

Tableau 1. Dosage des métaux Cd, Pb et Cu par redissolution anodique. (I) pH in situ; (II) pH ~ 1; (III) irradiation ultraviolette en milieu acide. (a) non détecté; (b) manque de reproductibilité. S = salinité ‰

	Cd, µg/l.			Pb, µg/l.			Cu, µg/l.			S
	(I)	(II)	(III)	(I)	(II)	(III)	(I)	(II)	(III)	
Saint Aubin	(a) (pH = 7,9)	(b)	0,21 ± 0,05	(a) (pH = 7,9)	(b)	0,20 ± 0,06	(a) (pH = 7,9)	(b)	3,54 ± 0,80	< 1
Quilleboeuf	(a) (pH = 8,0)	(b)	0,08 ± 0,02	(a) (pH = 8,0)	(b)	0,45 ± 0,03	(a) (pH = 8,0)	(b)	1,42 ± 0,18	< 1
Honfleur	(a) (pH = 7,9)	0,06 ± 0,01	0,09 ± 0,02	(a) (pH = 7,9)	0,21 ± 0,03	0,33 ± 0,08	(a) (pH = 7,9)	1,70 ± 0,20	1,95 ± 0,30	4
Cap de la Hève	0,12 ± 0,02 (pH = 8,1)	0,22 ± 0,04	0,31 ± 0,05	1,08 ± 0,13 (pH = 8,1)	2,56 ± 0,07	2,62 ± 0,34	0,13 ± 0,02 (pH = 8,1)	0,27 ± 0,08	0,54 ± 0,19	31

Aubin et de Quilleboeuf, la distinction des différents groupes n'a pu être réalisée en raison du caractère très complexant des eaux. C'est la raison pour laquelle nous avons, pour ces deux sites, regroupé les deux classes:

—métal engagé dans des complexes détruits par acidification;

—métal engagé dans des complexes détruits par irradiation en milieu acide.

Ces résultats nous ont conduit à étudier l'évolution de la capacité complexante apparente des eaux le long de l'estuaire de la Seine (la limite amont de l'intrusion saline est située bien au-delà du site de Quilleboeuf), et à nous intéresser plus particulièrement à la dernière classe de complexes: les complexes métalliques détruits par irradiation en milieu acide. En effet, ces derniers sont directement liés à la quantité des complexants organiques dissous, principaux responsables du pouvoir complexant des eaux naturelles. Pour effectuer cette étude, nous avons, comme de nombreux auteurs, utilisé le cuivre qui a la propriété de former des complexes stables avec la plupart des ligandes organiques.¹⁰ Nous avons donc considéré l'équilibre $Cu + L \rightleftharpoons CuL$, où L symbolise le ligande organique susceptible de former le complexe CuL "stable". Les charges ont été omises pour plus de clarté. La concentration du cuivre "libre" supposée accessible par la technique analytique utilisée (redissolution anodique en mode impulsif différentiel) a été suivie lors d'ajouts connus de cuivre à différents échantillons provenant d'un même site de prélèvement. Le cuivre ajouté a été laissé en contact 24 hr avec la solution afin de permettre aux équilibres de s'établir (voir partie expérimentale). Nous avons reporté sur la Figure 3 les courbes obtenues en traçant concentration de cuivre trouvée en fonction de la concentration ajoutée de cuivre, pour les différents sites de prélèvement. Toutes les courbes tendent vers une asymptote (droite dont la pente est égale à l'unité—droite en pointillés sur la figure). Nous avons déterminé les points d'intersection des différentes asymptotes avec l'axe des abscisses par la méthode décrite par Plavsic *et al.*¹¹ En posant $K = [CuL]/[Cu][L]$, $(Cu)_T$ = concentration totale en cuivre, c'est-à-dire concentration initiale + concentration ajoutée, et $(L)_T$ = concentration totale en ligande, on montre que:

$$\frac{[Cu]}{(Cu)_T - [Cu]} = \frac{[Cu]}{(L)_T} + \frac{1}{K(L)_T}$$

Nous avons reporté, sur la Figure 4, les courbes obtenues en traçant:

$$\frac{[Cu]}{(Cu)_T - [Cu]} = f[Cu]$$

Nous obtenons des droites dont la pente permet de déterminer $(L)_T$ et l'ordonnée à l'origine le produit $K(L)_T$. Cette méthode permet donc également de déterminer les constantes de stabilité K. Les concen-

Tableau 2. Concentrations en ligande et constantes de stabilité du complexe du cuivre pour les différents sites étudiés. R = coefficient de corrélation

	$(L)_T, 10^{-7}M$	K	$K(L)_T$	R
Cap de la Hève	$1,8 \pm 0,2$	$(5,5 \pm 0,2) \cdot 10^7$	9,9	0,96
Honfleur	$3,8 \pm 0,4$	$(5,9 \pm 0,6) \cdot 10^7$	22,4	0,95
Quilleboeuf	$3,4 \pm 0,3$	$(12,7 \pm 2,7) \cdot 10^7$	43,2	0,97
Saint Aubin	$3,7 \pm 0,2$	$(3,8 \pm 1,3) \cdot 10^8$	140,6	0,80
Manche Orientale	1,6	$3,2 \cdot 10^7$	5,1	0,98
Mer Adriatique ¹¹	1,5	$6,4 \cdot 10^7$	9,6	—
Lac Huron ⁴	2,0	$1,6 \cdot 10^9$	320	0,70
Onaping river ⁴	3,8	$4,0 \cdot 10^8$	152	0,95

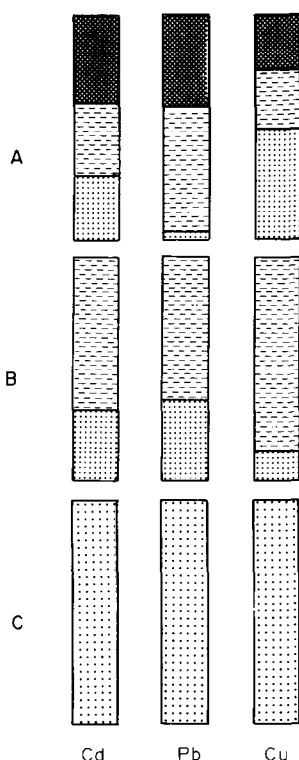


Fig. 2. Répartition des métaux Cd, Pb et Cu dans les sites de prélèvements: A: Cap de la Hève; B: Honfleur; C: Quilleboeuf et Saint-Aubin. Métal engagé dans des complexes non différenciables détruits par abaissement du pH et par irradiation ultraviolette. Métal engagé dans des complexes détruits par irradiation ultraviolette en milieu acide. Métal engagé dans des complexes détruits par abaissement du pH. Métal libre.

trations des ligandes et les différentes constantes ainsi déterminées sont reportées dans le Tableau 2. Il faut noter que les valeurs des coefficients de corrélation relatifs aux droites obtenues confirment la validité de l'approximation faite quant à la formation d'un complexe 1:1 du type CuL .

Les valeurs des concentrations totales de ligande $(L)_T$ trouvées permettent de tracer les asymptotes aux courbes de la Figure 2. Ce sont ces valeurs que retiennent certains auteurs comme estimation de la capacité complexante des eaux naturelles.³ Pour notre part, nous avons préféré utiliser un autre critère. En effet, l'examen des valeurs de $(L)_T$ semblerait montrer que les eaux du site de Honfleur sont, des eaux

étudiées, les plus complexantes, ce qui est en désaccord avec les résultats obtenus lors de notre ébauche de "spéciation" (Tableau 1 et Figure 2). Nous avons préféré utiliser à la fois la concentration du ligande et la valeur de la constante de stabilité du complexe correspondant. Nous avons donc reporté dans le Tableau 2 les valeurs du produit $K(L)_T$. Nous obtenons ainsi un classement des capacités complexantes apparentes en accord avec nos résultats de spéciation. Dans les sites étudiés, en général la concentration initiale en cuivre est petite devant la concentration totale en ligande, ce qui entraîne:

$$K(L)_T \sim [CuL]/[Cu]$$

Le produit $K(L)_T$ nous renseigne donc directement, dans la plupart des cas, sur la valeur du rapport: métal complexé/métal libre.

Nous avons reporté également dans le Tableau 2 les valeurs, concernant d'autres sites, calculées à partir de résultats relevés dans la bibliographie.¹¹ Les concentrations de ligande et les constantes de stabilité relatives aux sites "Lac Huron" et "Onaping river" ont été déterminées par une méthode basée sur l'adsorption des métaux par le dioxyde de manganèse. Il faut noter que les résultats obtenus ne semblent pas dépendre de la méthode utilisée, tout au

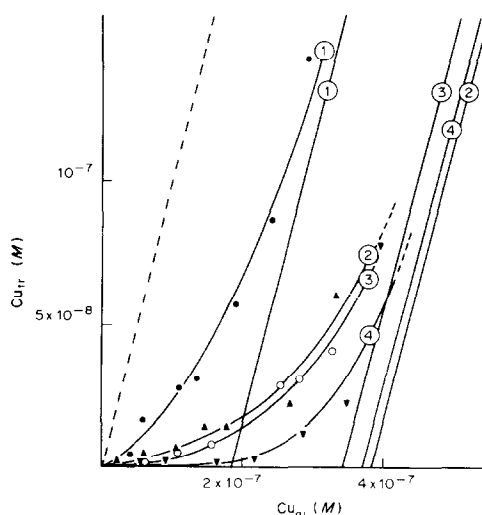


Fig. 3. Courbes obtenues en traçant: Cu trouvé en fonction de Cu ajouté (indices des courbes: voir légende de la figure 1) la droite en pointillés correspond à la droite de pente égale à l'unité. Détermination des asymptotes: voir texte.

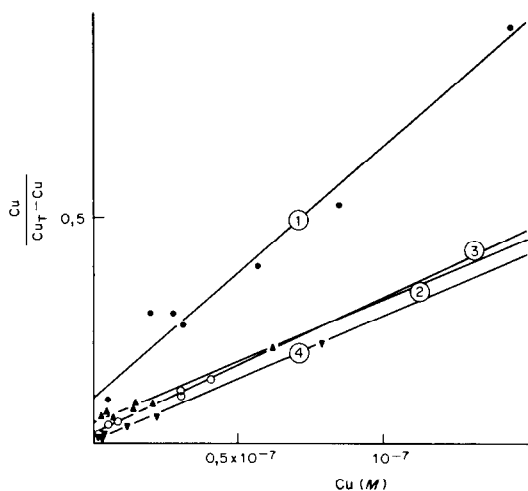


Fig. 4. Représentation de la fonction $[Cu]/\{(Cu)_T - Cu\} = f[Cu]$ permettant de déterminer la concentration totale du ligand $(L)_T$ et la constante de stabilité (K) du complexe correspondant (indices des courbes voir légende de la Figure 1).

moins en ce qui concerne les eaux de rivière "Onaping river" et "Saint Aubin". Pour ces derniers sites les capacités complexantes sont tout à fait comparables.

CONCLUSION

L'étude du comportement des métaux Cd, Pb et Cu dans la colonne d'eau de l'estuaire de la Seine a été effectuée par redissolution anodique en mode impulsif différentiel. Les différentes formes métalliques solubles ont pu être classées en trois groupes: métal libre et métal engagé dans des complexes détruits en milieu acide avec ou sans irradiation

ultraviolette. La répartition obtenue le long de l'estuaire montre que dans la détermination de la capacité complexante apparente des eaux étudiées, on ne peut se limiter à la seule détermination de la concentration totale du ligande comme l'ont préconisé certains auteurs. Il est nécessaire de tenir compte de la valeur de la constante de stabilité du complexe formé. Nous proposons donc d'utiliser le produit de la concentration du ligande par la constante de stabilité du complexe comme grandeur définissant la capacité complexante apparente.

Nous nous proposons, dans un prochain travail, d'étudier l'influence des particules en suspension sur le pouvoir complexant des eaux naturelles.

Remerciements—Nous tenons à remercier le Centre National de la Recherche Scientifique pour l'aide financière apportée à ces travaux (A.T.P. n° 9-83-38 Gréco-Manche), ainsi que Messieurs Guéguénat et Gandon du Laboratoire d'Ecologie Marine (Commissariat à l'Energie Atomique, la Hague) pour les discussions fructueuses et leur concours dans la réalisation matérielle de cette étude.

LITTÉRATURE

1. G. Gillain, *Thèse*, Liège, 1980.
2. B. T. Hart, *Environ. Technol. Lett.*, 1981, **2**, 95.
3. Y. K. Chau, R. Gachter et K. Lum-Shue-Chan, *J. Fish. Res. Board Can.*, 1974, **31**, 1515.
4. C. M. G. van den Berg et J. R. Kramer, *Anal. Chim. Acta*, 1979, **106**, 113.
5. A. M. Bond et B. S. Grabaric, *Anal. Chem.*, 1979, **51**, 337.
6. A. M. Bond, *ibid.*, 1980, **52**, 1318.
7. T. M. Florence et G. E. Batley, *Talanta*, 1977, **24**, 151.
8. P. Figura et B. McDuffie, *Anal. Chem.*, 1980, **52**, 1433.
9. F. A. J. Armstrong, P. M. Williams et J. D. H. Strickland, *Nature*, 1966, **211**, 481.
10. R. L. Schmidt, *Crit. Rev. Environ. Control*, 1978, **1**, 151.
11. M. Plavsic, D. Krznaric et M. Branica, *Marine Chem.*, 1982, **11**, 17.

Summary—Analyses for the metals Cd, Pd and Cu in the estuary and bay of the Seine have been made. The site was chosen because of the very high tides, which produce considerable water displacement. For the purpose of analysis the metals have been divided into three categories: free metals, metals forming complexes that are unstable at low pH, and metals forming stable complexes that are destroyed in an acidic medium by ultraviolet radiation. The special properties of copper have been used to establish a "complexing capacity" of the different water samples studied. By making the simple hypothesis of the existence of an equilibrium of the type $Cu + L \rightleftharpoons CuL$, where L represents the ligand, the total ligand concentration, as well as the stability constants of the CuL complexes, has been determined. These results are presented and discussed.

PRECISE AND ACCURATE DETERMINATION OF HIGH CONCENTRATIONS OF SULPHUR BY ISOTOPE-DILUTION THERMAL-IONIZATION MASS-SPECTROMETRY

W. R. KELLY and P. J. PAULSEN

Center for Analytical Chemistry, National Bureau of Standards, Washington, D.C. 20234, U.S.A.

(Received 24 May 1984. Accepted 19 June 1984)

Summary—An isotope-dilution thermal-ionization mass-spectrometric procedure has been developed for the accurate and precise determination of sulphur in steels and organic-based materials. The sample and isotopically enriched sulphur spike are dissolved in a sealed tube to prevent loss of sulphur and the sulphur isotopes are measured as AsS^+ ions, with silica gel as an emitter. This technique has been applied to the determination of sulphur in 13 NBS Standard Reference Materials ranging in concentration from 0.03 to 5% S. The relative uncertainty for a single determination is typically 0.5% (95% confidence interval) and arises primarily from the uncertainty in the spike calibration and from sample inhomogeneity.

The precise and accurate determination of the total sulphur (S) content in some materials is of great importance. The S content in coal is important because many states have laws which forbid the burning of coal which has more than a certain S content, typically 1%. The S concentrations in the SRM coals reported here cover the range typical of coals used in industry and power generation. The S content of fly-ash is important for the measurement and control of particulate S emissions. The S content of plants can reflect their exposure to atmospheric SO_2 .¹⁻³ The determinations of S in the diverse materials in this study provide the S standards needed for calibration of automated S analysers and provide quality assurance for these important environmental measurements.

We have recently reported on a new procedure for the determination of S at concentrations below 0.01% in copper and iron-based materials.⁴ In this procedure ^{34}S enriched tracer is added to a sample and all the S is oxidized to sulphate in a closed system. Subsequently, the sulphate is reduced to H_2S and the sulphur precipitated as As_2S_3 . A small portion of an ammoniacal solution of this compound, equivalent to 1.5 μg of S, is added to a flat rhenium filament coated with silica gel, used as an emitter. The S isotopes are measured as the AsS^+ ions. We showed that the analytical blank of about 0.3 μg of S was the largest source of uncertainty in the determination of low S concentrations.⁴ In this study these techniques have been applied to materials of high S concentration.

The inherent high precision of thermal ionization makes this technique the method of choice for accurate and precise S determinations at high levels where the uncertainty due to the blank is negligible. The chemical procedure for isolating S is matrix-independent.^{4,5} Once the samples have been dissolved, they are all processed identically to obtain the As_2S_3 precipitate. In this paper we demonstrate the wide application of this technique by determining high S concentrations in such diverse materials as steels, coal, fly-ash, bovine liver, powdered milk and citrus leaves.

EXPERIMENTAL

Reagents

NBS sub-boiling distilled nitric acid and hydrochloric acid were used to dissolve samples. The reducing solution consisted of ACS reagent grade hypophosphorous acid (61 ml), hydriodic acid (125 ml) and hydrochloric acid (205 ml), as described by Thode *et al.*⁵

The ^{34}S -enriched spike in the form of elemental S was obtained from Mound Laboratory (Monsanto Research Corporation*). Standard solutions of known S concentration were prepared from high-purity anhydrous sodium sulphate and potassium sulphate. Aqueous ammonia solution was prepared by bubbling high-purity ammonia into distilled water. An As(III) solution (1000 $\mu\text{g}/\text{ml}$) was prepared by dissolving NBS SRM 83c (As_2O_3) in aqueous ammonia solution.

The silica gel used for the mass-spectrometric loading was premixed with phosphoric acid and this mixture was neutralized with aqueous ammonia solution. The details of the preparation of these reagents and solutions were reported earlier.⁴

Apparatus

All glassware and the modified Carius tubes were made of borosilicate glass. The reduction apparatus consisted of a 100-ml flask fitted with a 15-cm water-cooled condenser, a 25-ml bubbler and a Pasteur pipette. The flask had a side-arm through which nitrogen was injected into the flask to sweep the H_2S from the reducing solution in the flask, through the condenser, into the bubbler, and then into the centrifuge tube containing 1 ml of the As(III) solution.

*Certain commercial equipment, instruments, or materials are identified in this report to specify adequately the experimental procedure. Such identification does not imply recommendation or endorsement by the National Bureau of Standards, nor does it imply that the materials or equipment identified are necessarily the best available for the purpose.

The sample-loading for mass spectrometry was performed with a 5-cm length of 0.76 mm bore intermedic tubing attached to a 21-gauge hypodermic needle fixed to a syringe. Flat filaments were fabricated from zone-refined rhenium. Samples were loaded in a small glove box in a dry nitrogen atmosphere. Isotopic ratio measurements were performed with a single-sector 12-in. radius mass spectrometer of NBS design. Ion currents were measured with a Cary 401 MR vibrating-reed electrometer and a Faraday cup detector.

Procedure

The same chemical procedure was used for all samples and has been discussed in detail by Paulsen *et al.*,⁶ Burke *et al.*⁷ and Paulsen and Kelly.⁴ A brief outline of the procedure is given below and any changes are noted.

Preparation of spike. The ³⁴S-enriched spike in the form of elemental S was oxidized to sulphate in a sealed Carius tube. High-purity sodium carbonate was added to yield an Na/S atom ratio of 4. The spike was stored in 2M hydrochloric acid. The S content of the spike was calibrated by comparison with gravimetrically prepared solutions of high-purity sodium and potassium sulphates.

Spiking and dissolution of samples. Sample, spike and nitric and hydrochloric acids were added to a Carius tube. The typical sample size was 0.1–0.2 g for the organic samples. This sample size was used to conserve spike and minimize the internal pressure produced in the Carius tube from CO₂ and NO₂ formed during oxidation. Sample sizes for steels were about 0.5 g. Approximately 1 μg of ³⁴S-enriched spike was added for every 3 μg of S in the sample.

The sealed Carius tubes were placed in closed steel shells with approximately 50 g of solid CO₂ to equalize the pressure. The organic samples were heated to 240° for 24 hr to ensure complete oxidation of organic matter and equilibration of the S isotopes. In all cases clear solutions were obtained, except for the coal and fly-ash samples which contained residues. Small portions of these residues were analysed by spark-source mass-spectrometry and shown to be silicate material inherent in the samples. Steel samples were heated for 12 hr. The solutions were repeatedly heated with hydrochloric acid and evaporated to dryness under a nitrogen atmosphere to destroy nitrates.

Reduction of sulphate to H₂S and conversion into As₂S₃. The dried samples were dissolved in 5 ml of hydrochloric acid and an aliquot equivalent to approximately 500 μg of total S was reduced in the reduction apparatus to H₂S. The H₂S was trapped in an ammoniacal As(III) solution cooled in an ice-water bath, then precipitated as As₂S₃ by the addition of hydrochloric acid and the As₂S₃ precipitate was

washed repeatedly with distilled water. The chemical yield of these steps is greater than 80%.⁴ The As₂S₃ was dissolved in ammoniacal As(III) solution to yield an S concentration of 100 μg/ml with an As/S atom ratio of 2. This solution was stored at –16° and not used until at least 16 hr had elapsed.

Mass spectrometry. A small portion of the solution prepared as just described, equivalent to 1.5 μg of total S, was added to an outgassed flat rhenium filament coated with ~100 μg of silica gel and phosphoric acid. The sample and silica gel were dried, heated to 700° for 5 sec and immediately loaded into the mass spectrometer. When a pressure of 2 × 10⁻⁷ mmHg was obtained, the filament was heated to 800° (time = 0). The temperature was increased by 50° each time at 5-min intervals until a temperature of 950° was obtained. After 30 min the ³²S/³⁴S ratio was measured at *m/z* 107 and 109 for the AsS⁺ ions. The total ion current rose typically to 3–5 × 10⁻¹¹ A and then decayed. Three sets of 5 ratios were obtained, with a 15-sec integration time. The observed change in the ratio during data collection was less than 0.1%. Typical precision for 3 sets was 0.1% relative standard deviation (r.s.d.).

Sulphur concentrations were calculated from the measured ³²S/³⁴S ratios by using the equation:

$$S\% = \frac{WK(A_{sp} - B_{sp}R)}{m(BR - A)} \times 10^4 \quad (1)$$

where *R* is the measured ³²S/³⁴S ratio, *A*_{sp} and *B*_{sp} are the ³²S and ³⁴S abundances in the spike, *A* and *B* are the natural abundances of ³²S and ³⁴S in the sample, *W* is the amount of S spike (in μg) added to the sample, *m* is the sample weight (g), and *K* is the ratio of the atomic weight of natural S to the atomic weight of the S spike.

Caution. Great care should be used in handling the pressurized tubes. The Carius tubes should be annealed at 560° and checked for fire cracks before use. A small hole in the tube is potentially very dangerous. When a tube with a leak is used, the CO₂ in the closed steel shell will equilibrate with the atmosphere inside the tube. If this occurs, liquid CO₂ will be visible in the tube at room temperature when the tube is removed from the steel shell, and indicates that the internal pressure is at least 60 atm. Such tubes should be isolated and not handled until the liquid CO₂ phase has bled off, which may take several days. The most common cause of a leak is improper sealing of the neck of the tube after addition of the sample. After sealing, the Carius tube should be handled behind a blast shield. Before opening with a torch the tube should be cooled to 0° or below.

Hypophosphorous acid and some metals can form an explosive mixture if taken near to dryness. The refluxing of our reduction mixture has never resulted in any measurable loss of volume, but this could occur during prolonged heating or breakage of the flask.

Table 1. Measured S isotopic ratios in high-purity reagents and NBS SRMs

Sample	³² S/ ³⁴ S	³³ S/ ³⁴ S
Na ₂ SO ₄	22.598	0.1775
K ₂ SO ₄	22.775	0.1787
NBS SRMs		
133b (Cr-Mo Steel)	22.868	0.1787
891 (White Cast Iron)	22.538	0.1771
1138a (Cast Steel)	22.538	0.1778
1549 (Powdered Milk)	22.624	0.1779
1577a (Bovine Liver)	22.555	0.1776
1577b (Bovine Liver)	—	—
2682 (Coal)	22.699	0.1783
2683 (Coal)	22.364	0.1769
2684 (Coal)	22.726	0.1782
2685 (Coal)	22.546	0.1777
1635 (Coal)	22.546	0.1778
1633a (Coal Fly Ash)	22.641	0.1781
1572 (Citrus Leaves)	22.631	0.1781

RESULTS AND DISCUSSION

From equation (1) it is seen that only isotopic ratios need to be measured for an accurate S determination. For almost all elements, the natural isotopic abundances are invariant. Sulphur is one of a few elements which shows measurable variations in composition as a result of isotopic fractionation, principally during the biological oxidation and reduction of sulphur.⁸ Therefore the isotopic composition of S in all samples and calibration solutions was measured to preclude bias from this source, which could be 1% or greater if IUPAC values were assumed for all compositions.⁹ The measured S isotopic ratios for all samples are given in Table 1.

Table 2. Calibration of ^{34}S spike

Natural sulphur*	Concentration of S determined in ^{34}S spike, $\mu\text{g/g}\dagger$
Na_2SO_4	
Mix 1	313.85
Mix 2	314.26
Mix 3	314.04
	Mean 314.05 ± 0.21
K_2SO_4	
Mix 1	314.63
Mix 2	314.80
	Mean 314.72 ± 0.12
	Mean of 5 mixes 314.32 ± 0.40

*The mixes are independent weighings of spike and natural S.

†Given as total μg of S per g of solution. Mean \pm standard deviation.

Table 3. Sulphur concentration in NBS SRM 133b (Chromium-Molybdenum Steel) determined by thermal-ionization mass-spectrometry

Bottle	Sample weights, g	Sulphur, $\mu\text{g/g}$	Mean S, $\mu\text{g/g}$
1	0.62499	3350	3350
2	0.43932	3339	
2	0.66457	3325	3337
2	0.50733	3346	
3	0.66824	3359	
3	0.56377	3350	
3	0.61242	3340	3350
4	0.60806	3319	
4	0.57478	3301	3313
4	0.62711	3320	
5	0.49587	3355	3355
6	0.47834	3358	3358
			Mean = 3344 ± 17 (0.51%, r.s.d)*

*Uncertainty computed for the mean of the six values. Total uncertainty given in Table 4.

The relative abundances of ^{32}S , ^{33}S and ^{34}S were calculated from these data, assuming the abundance of ^{36}S to be 0.015%. Since the ^{36}S abundance is very low, its variability has a negligible effect on the calculated abundances of the other isotopes. The

calculated ^{32}S and ^{34}S abundances for each material were used in equation (1) to calculate the sulphur concentration.

Calibration of ^{34}S -enriched spike

The ^{34}S spike was calibrated against solutions prepared from two high-purity sulphates. Previously, it was shown that solutions gravimetrically prepared from these salts yielded a spike calibration value within a few parts in 10^4 of that determined from three different solutions of coulometrically titrated sulphuric acid.⁴ Therefore these two salts can be used reliably as primary S standards. About 300 μg of S from a solution of natural S composition was accurately weighed into a Teflon beaker along with a known weight of spike solution. The resulting solution was mixed thoroughly, added to the reduction flask and treated in the same way as a sample. The S concentration determined in the spike for the individual mixes is given in Table 2. The uncertainty (r.s.d.) for the grand mean is 0.13%. For the high S concentrations reported in this paper, the uncertainty in the spike calibration is a significant source of uncertainty in the values for homogeneous SRMs.

S determinations in steel

The S concentration was determined in three SRM steels, which were in the form of chips. The individual values are given in Table 3 for replicate determinations on SRM 133b. The 1.4% (relative) range observed for the six bottles indicates sample inhomogeneity among bottles, since much smaller ranges have been observed for materials of comparable S concentration (see Table 6). Three separate samples were taken from bottles 2, 3 and 4. The range in S concentration in all three bottles was about 0.6% relative and may indicate slight sample inhomogeneity within individual bottles. A one-way analysis of variance of the twelve replicates, grouped according to their bottle designation, showed that there was a statistically significant difference ($\alpha = 0.03$) among the bottles. The significant difference is caused by the low values for bottle No. 4. Table 4 summarizes the S determinations on steels analysed in this study. The S values determined

Table 4. Sulphur concentrations in NBS Fe-based alloys

Sample	% S, w/w	
	Certified value (date)*	Value from this study†
SRM 133b (Cr-Mo steel)	0.328 ± 0.004 (8/12/81)	0.3344 ± 0.0056
SRM 891 (White cast iron, Ni Hard I)	0.029 (6/82)	0.0284 ± 0.0002
SRM 1138a (Cast steel)	0.056 ± 0.001 (1/20/77)	0.0541 ± 0.0005

*Isotope-dilution values determined in this study were used in the certification of SRM 891 only.

†The total uncertainty is computed as the linear sum of the uncertainty (ts , 95% confidence interval) in the spike calibration, the sample reproducibility, and the absolute value of the blank divided by the sample weight. The contribution of the blank was negligible for SRMs 133b and 1138a.

Table 5. Replicate sulphur determinations on NBS SRM 1572, Citrus leaves

Sample*	Weight loss, %	Sample weight, g	S found, %		Mean S, %
1U	5.566	0.20583	0.4044		
1D		0.19018	0.4068		
1D		0.17277	0.4078		0.4063
2U	5.423	0.23267	0.4073		0.4073
3U	5.056	0.22655	0.4056		
3D		0.19210	0.4072		
4U	5.068	0.19064	0.4069		0.4069
5U	5.336	0.17863	0.4074		
5D		0.19027	0.4051		
Mean			0.4063	0.4067	0.4066
s.d.			±0.0013	±0.0012	±0.0004†
r.s.d.			(±0.32%)	(±0.30%)	(±0.11%)

*"D" samples were determined after drying. "U" samples were determined on undried material and the weights corrected to a dry weight basis.

†Total uncertainty given in Table 6.

for SRMs 133b and 1132a are in good agreement with previously certified values.

S determinations in organic-based materials

Sulphur was determined in a number of organic Standard Reference Materials ranging from powdered milk (0.35%) to a bituminous coal (4.8%). All organic materials measured in this study had to be dried to remove moisture. The drying procedure must effectively reduce all materials to the same dry weight basis. Two approaches have commonly been used at NBS. One involves drying a sample from each bottle to determine the weight loss, but performing the actual analysis on an undried sample. The weight loss from the dried material is then used to correct the data obtained from the undried material. The second method uses the dried material directly for the analysis. Because of the possibility that sulphur could be lost during the drying, both dried and undried SRM 1572 (Citrus Leaves) was analysed. Replicate determinations on five bottles of SRM 1572 are shown in Table 5. Five weighing bottles containing citrus leaves were dried at 85° for 2 hr as instructed in the certificate. The weight losses given in column 2 have an average value of approximately 5%. Samples denoted by "U" were taken directly from the SRM bottle without drying, and the corresponding drying weight-loss correction was applied. Dried samples, denoted by "D" were taken from the weighing bottles that had been heated. A comparison of the S content of the undried and dried material by a one-sided *t*-test indicates no detectable S loss during drying for this material. The mean S value for each bottle is given in the last column. The total range in S content was 0.25% relative, which is much smaller than the 9% spread in weight loss. This indicates that in spite of large differences in moisture content, the drying procedure reduces all bottles to the same dry weight basis. The standard deviation for the means of the five bottles was 0.098% relative. This small uncertainty in the mean demonstrates the high precision

capability of this technique and indicates that this SRM is homogeneous for S to this degree or better for the sample weights analysed.

Table 6 summarizes the thermal-ionization determinations of S in the organic materials. In all cases sample sizes were 0.1–0.3 g of the dried material, except for SRM 1572 (Citrus Leaves) where both dried and undried material was analyzed (see Table 5). In all cases the samples were spiked with ³⁴S-enriched tracer and decomposed in a sealed Carius tube; an aliquot equivalent to 300–500 µg of total S was reduced. Blank corrections were negligible in all cases. The relative observed ranges for single determinations from six different bottles are shown in the last column. The powdered milk, bovine liver and citrus leaves show very small S ranges, indicating good sample homogeneity for S, and the high precision of this technique. For these three SRMs, the spike calibration uncertainty is a large component (approximately half) of the total uncertainty given in the penultimate column.

The relatively large uncertainties for the coal determinations are a result of sample inhomogeneity, which in turn is primarily responsible for the large ranges observed. The certified values for SRM coals 2682, 2683, 2684 and 2685 are based on three independent techniques: gravimetry, ion chromatography and the isotope-dilution values from this study.

S determinations in SRM 1633a, Fly Ash

Sulphur was determined in four different bottles of Fly Ash SRM 1633a, with sample sizes of about 0.2 g of dried material. This particular fly-ash has the following major element composition (%): Si 22.8, Al 14, Fe 9.4, K 1.88, Ca 1.11. After sealed-tube dissolution with hydrochloric and nitric acids, the insoluble portion of two unspiked samples was centrifuged, washed repeatedly with distilled water and dissolved in 10 ml of concentrated nitric acid and 1 ml of concentrated hydrofluoric acid in a Teflon jar equipped with a threaded cap (Savillex Corporation).

Table 6. Sulphur concentrations in non-metallic NBS SRMs

Sample*	S, %		Range in S concentration in this study, % <i>rel.</i>
	Certified† value (date)	Mean value from this study‡	
SRM 1549 (Powdered Milk)	‡	0.3514 ± 0.0029	0.48
SRM 1577a (Bovine Liver)	0.78 ± 0.01 (6/15/82)	0.7845 ± 0.0046	0.25
SRM 1577b (Bovine Liver)	‡	0.7846 ± 0.0061	0.52
SRM 2682 (Coal)	0.47 ± 0.03 (12/14/82)	0.494 ± 0.011	1.93
SRM 2683 (Coal)	1.85 ± 0.06 (12/14/82)	1.896 ± 0.037	1.79
SRM 2684 (Coal)	3.00 ± 0.13 (12/14/82)	3.076 ± 0.090	2.70
SRM 2685 (Coal)	4.62 ± 0.18 (12/14/82)	4.76 ± 0.19	3.84
SRM 1635 (Coal)	0.33 ± 0.03 (8/22/82)	0.354 ± 0.014	1.44
SRM 1572 (Citrus Leaves)	0.407 ± 0.009 (2/22/82)	0.4066 ± 0.0022	0.25

*Sample sizes were 0.1–0.3 g of dried material.

†Isotope-dilution values determined by this technique were used with values from other techniques to arrive at the values given here.

‡SRMs not yet certified.

§The concentration given for each SRM is the mean of a single determination for dried material from six different bottles except for citrus leaves (see Table 5). The total uncertainty is computed as the linear sum of the uncertainty (*ts*, 95% confidence interval) in the spike calibration, the sample reproducibility, and the absolute value of the blank divided by the sample weight. The contribution from the blank was negligible.

The S concentrations found in the two fractions are given in Table 7. The insoluble residues represented 47.7% and 46.0% of the total sample. The sum of the values for the soluble and insoluble fractions gives the total S content per gram of fly-ash. A comparison of the values shows that more than 99% of the S in this fly-ash is present in the soluble fraction, but this may not be the case for other fly-ash samples.

CONCLUSIONS

The sealed-tube chemical procedure and the isotope-dilution thermal-ionization mass-spectro-

Table 7. Sulphur concentration in NBS SRM 1633a, Fly ash

Bottle	S, µg/g
Insoluble portion*	
1	6.9
3	9.8
	Mean 8.4
Soluble portion†	
1	1769
2	1765
3	1756
4	1770
	Mean 1765 ± 6§
	Corrected mean 1773 ± 32‡

*Residue from HNO₃/HCl sealed-tube digestion, washed, spiked and dissolved in HF/HNO₃.

†Sulphur extracted during sealed-tube digestion.

‡The total uncertainty was computed as the linear sum of the uncertainty (*ts*, 95% confidence interval) in the spike calibration, the sample reproducibility and the absolute value of the blank divided by the sample weight and twice the observed range between the insoluble residues.

§Mean ± s.d. for 4 determinations.

metric technique described in this paper satisfy the need for a highly precise and accurate technique for producing certified S standards and for the measurement of S concentrations in environmental samples. For materials that are sufficiently homogeneous, this method can determine the S concentration with a total relative uncertainty of 0.5% (95% confidence interval) or better. The capability now exists to certify standards with total uncertainties that are smaller than the measurement precision of the automated instruments that use them for calibration. Therefore, investigators making S determinations will be in the favourable position of having accurate standards with uncertainties that have a negligible effect on the overall measurement uncertainty.

The high precision of this technique allows small changes in S concentration to be observed. This capability could be useful for the detection of small changes in S content in plants living in SO₂-polluted environments. For example, a relative increase of 0.5% S content in leaves could be easily detected in sample sizes of 0.1 g or less.

The upper limit to the amount of sulphur that can be determined by this technique is governed by the cost of the enriched spike. Sample sizes of high-sulphur materials have been kept at the 0.1-g level to conserve spike. The recent availability of less expensive spike in large quantities makes the cost factor less prohibitive. The lower limit on sample size is governed by the homogeneity of the sample for S.

REFERENCES

1. G. R. Ricks and R. J. H. Williams, *Environ. Pollut.*, 1974, **2**, 57.
2. R. J. H. Williams, M. M. Lloyd and G. R. Ricks, *ibid.*, 1971, **6**, 87.
3. K. Killham and M. Wainwright, *ibid.*, 1981, **2**, 81.

4. P. J. Paulsen and W. R. Kelly, *Anal. Chem.*, 1984, **56**, 708.
5. H. G. Thode, J. Monster and H. B. Dunford, *Geochim. Cosmochim. Acta*. 1961, **25**, 159.
6. P. J. Paulsen, R. W. Burke, E. J. Maienthal and G. M. Lambert, *Am. Soc. Test. Mater., Spec. Tech. Publ.* 747, 1982, p. 113.
7. R. W. Burke, P. J. Paulsen, E. J. Maienthal and G. M. Lambert, *Talanta*, 1982, **29**, 809.
8. H. R. Krouse, *Sulfur Isotopes in Our Environment*. In *Handbook of Environmental Isotope Geochemistry*, Vol. 1, *The Terrestrial Environment*, Elsevier, New York, 1980.
9. N. E. Holden, R. L. Martin and I. L. Barnes, *Pure Appl. Chem.*, 1983, **55**, 1119.

DIRECT DETERMINATION OF SUB-NANOMOLAR LEVELS OF ZINC IN SEA-WATER BY CATHODIC STRIPPING VOLTAMMETRY

CONSTANT M. G. VAN DEN BERG

Department of Oceanography, University of Liverpool, Liverpool, England

(Received 19 March 1984. Revised 3 May 1984. Accepted 19 June 1984)

Summary—A novel technique for the determination of nanomolar levels of zinc in aqueous solution is presented. The zinc complex with ammonium pyrrolidine dithiocarbamate is adsorbed on a hanging mercury-drop electrode and the reduction current of zinc is measured by voltammetry. The detection limit for zinc is $3 \times 10^{-11}M$, with 10-min collection time. A procedure is suggested for the simultaneous determination of Ni and Zn in a single sample.

The conventional electrochemical determination of trace amounts of zinc in aqueous solution is by anodic stripping voltammetry (ASV). The working electrode is then either a hanging mercury-drop electrode (HMDE), or a solid electrode covered with a mercury film.^{1,2} The limit of detection for zinc is $2-4 \times 10^{-9}M$ after a plating time of 15–60 min with an HMDE,^{3,4} and lower by a factor of about ten if a rotating disk electrode (RDE) is used, with *in situ* plating of mercury.⁵ The determination of zinc is adversely affected by the formation of intermetallic compounds with Cu, Ni and Co,^{1,6} especially when thin-film techniques are used. The half-wave potential of Zn^{2+} is at $-1.1V$ (*vs.* SCE) in non-complexing electrolytes,⁶ so the solution needs to be maintained at $pH > 4$ to prevent masking of the zinc oxidation current by the hydrogen wave.

Recently it has been found possible to determine low concentrations of several trace metals in aqueous solution by means of adsorption voltammetry (AV). This technique is based on the tendency of certain complexes to adsorb on the surface of the HMDE. The reduction current of the metal ions in the adsorbed complex is used as a sensitive measure of the solution concentration. Thus low concentrations of Cu(II), U(VI), V(V) and Fe(III) can be determined by complexation with catechol,^{7,8} and of Ni(II) and Co(II) by complexation with dimethylglyoxime (DMG),^{9,10} with limits of detection typically near $10^{-10}M$.

The results of a study of the possible determination of trace quantities of Zn in sea-water by means of AV are reported in this paper. Several complexing ligands were tested in preliminary experiments and it was found that reduction peaks for both zinc and nickel in sea-water are obtained with 8-hydroxyquinoline as complexing agent. However, the concentration–reduction current relationship was non-linear for both metals, although the sensitivity (reduction current/metal concentration) was sufficient for analysis of unpolluted sea-water. Com-

plexes of zinc with catechol were also found to adsorb on the HMDE but the sensitivity was low (no peak from clean sea-water). Aqueous solutions of ammonium pyrrolidine dithiocarbamate (APDC) were found to produce a marked reduction peak in the presence of low concentrations of zinc. It is proposed in this paper to use this property for the detection of dissolved zinc in water and sea-water.

EXPERIMENTAL

Equipment

Voltamperograms were recorded with a PAR 174 A polarograph in conjunction with a PAR 303 static mercury-drop electrode in the stationary-drop mode; the surface area of the mercury drop was 2.83 mm^2 . The internal clock of the polarograph was altered to allow for a faster pulse rate of 10 Hz. The reference electrode was Ag/saturated AgCl, KCl. For some experiments a home-made water-jacketed electrochemical cell was used, containing 60 ml of liquid, which allowed simultaneous pH-measurement. The solution was stirred with a Teflon-coated magnetic stirring bar. The pH was measured with a Radiometer PHM 64 Research pH-meter with a combined pH/calomel reference electrode, calibrated for the free hydrogen-ion scale with a solution of 0.01M hydrochloric acid in 0.69M sodium chloride. The experiments were performed in a "clean room", equipped with filtered-air conditioning.

Reagents

An aqueous 0.1M APDC ("Spectrosol", BDH) stock solution (100 ml) was prepared and traces of metal ions were removed by extraction with three 10-ml portions of 1,1,2-trichlorotrifluoroethane. A stock aqueous 0.1M DMG solution was prepared in 0.2M sodium hydroxide. Buffer solutions were prepared from *N*-2-hydroxyethylpiperazine-*N'*-2-ethane sulphonic acid (HEPES), piperazine-*N,N'*-bis(2-ethane sulphonic acid) (monosodium salt) (PIPES), and *N,N'*-bis(2-hydroxyethyl)-2-aminoethane sulphonic acid (BES): each stock buffer solution contained 1 mole of buffer agent and 0.5 mole of ammonia ("Aristar") per litre. Metal contamination in these buffers was removed by addition of $10^{-3}M$ APDC and extraction with 1,1,2-trichlorotrifluoroethane. A stock buffer solution (1M boric acid/0.4M ammonia; pH 8.5) was used without further purification. Stock aqueous solutions of zinc, nickel and cobalt were prepared by dilution of BDH atomic-absorption ("Spectrosol") standard solutions. Sea-water used for these

experiments was collected from the Menai Straits (and filtered through a $0.45 \mu\text{m}$ Oxoid filter) and from the eastern North Atlantic (used unfiltered, supplied by courtesy of I. Butler, M.B.A., Plymouth). Distilled water was produced by a quartz double-distillation unit. Interfering dissolved organic material was removed from the sea-water by ultra-violet irradiation.⁷

Procedure

A 10-ml sample is pipetted into the electrochemical cell and 0.1 ml of $0.1M$ APDC and 0.075-ml of $1M$ BES are added; the solution is then purged with argon to remove oxygen. The magnetic stirrer is switched on and a new mercury drop is extruded; this is the beginning of the collection period of 2 min. The collection potential (E_{col}) is set at -1.3 V, and the scan is started at -0.9 V: the "hold" facility of the polarograph is therefore used during the collection period. The stirrer is stopped, then after 10 sec the potential is switched to -0.9 V ("initial potential" setting) and after a further 20 sec the potential scan is started. The scanning parameters are: differential pulse modulation 25 mV, 10 pulses/sec, scan-rate 10 mV/sec. The scan is stopped at -1.3 V by using the "hold" facility. The procedure is repeated after standard additions of zinc. The reduction-current/Zn-concentration relationship is linear up to about $10^{-7}M$ Zn under the given conditions. Zinc concentrations greater than about $5 \times 10^{-8}M$ can best be determined by using a reduced collection period (1 min or less), and a higher solution pH (boric acid buffer, pH 8.5): at this pH the sensitivity is slightly reduced and the hydrogen wave is shifted to more negative potentials. At high zinc concentrations ($> 5 \times 10^{-8}M$) the analysis time can be further reduced by using a linear sweep (LS) potential scan of 50 mV/sec instead of the DP modulation.

RESULTS

A potential scan from -0.1 V in the negative direction, with an HMDE in an aqueous $10^{-3}M$ APDC solution (pH 7.3), is characterized by a large reduction current between -0.5 and -0.8 V. This wave is caused by reduction of adsorbed APDC molecules and its magnitude is not affected by varying the zinc concentration. At potentials more negative than about -0.8 V the background current is very low until the hydrogen wave is reached. A reduction peak for the adsorbed zinc complex is present at -1.18 V. The reduction of APDC takes place in at least two steps, as revealed by the presence of two major, irregularly shaped peaks at -0.5 and -0.6 V (current measurements by adsorption linear sweep voltammetry, ALSV, after 1.5 min collection at -0.1 V, with stirring, scan-rate 50 mV/sec). The peak at -0.5 V is predominant until an APDC concentration of $\sim 10^{-4}M$ is reached (Fig. 1), whereas the second peak becomes predominant at higher concentrations. In $10^{-3}M$ APDC medium the reduction current of APDC is about 25 times that of $4 \times 10^{-8}M$ zinc; reduction of APDC therefore produces a massive background current between -0.4 and -0.85 V.

Adsorption of zinc on the HMDE depends on the APDC concentration, as shown in Fig. 1: the experimental solution was irradiated sea-water (UV-SW) containing $3 \times 10^{-8}M$ Zn and $0.01M$ BES (pH 7.3). Each scan was preceded by collection for 1.5 min while the potential was held at -0.3 V, and the

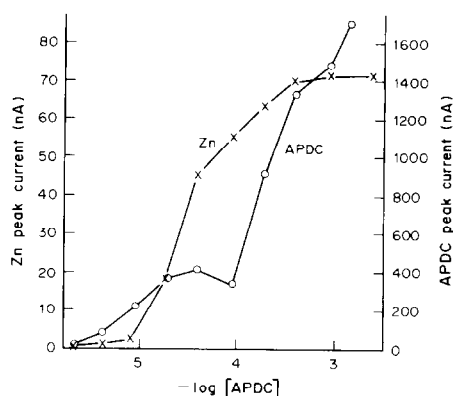


Fig. 1. Reduction currents of Zn and APDC as a function of APDC concentration.

reduction of Zn was measured by ADPV (10 pulses/sec and 10 mV/sec). It was found that the adsorption of zinc (as indicated by the reduction current) continued to increase with the APDC concentration up to $\sim 10^{-3}M$. This concentration was therefore selected for the following experiments.

Effect of variation of pH

Adsorption of $3 \times 10^{-8}M$ Zn was measured as a function of the pH of UV-SW that had been made $10^{-3}M$ in APDC. The collection time was 1 min at a potential of -0.3 V. The reduction current was measured by ALSV at a sweep-rate of 50 mV/sec. It was found (Fig. 2) that the peak height was maximal at about pH 6.8. The zinc peak is preceded by that for nickel at -1.12 V, the reduction current for which, as a function of pH, is also shown in Fig. 2.

The peak-height for zinc was greatest at pH 6.3–6.8. It was found, however, that addition of a pH buffer in this range (such as PIPES at pH 6.9) caused the hydrogen wave to shift in the positive direction and tests showed that the baseline was sufficiently flat for low concentrations of Zn to be determined at pH 7.3 in the presence of BES buffer, whereas $0.01M$ HEPES (pH 7.8) shifted the hydrogen

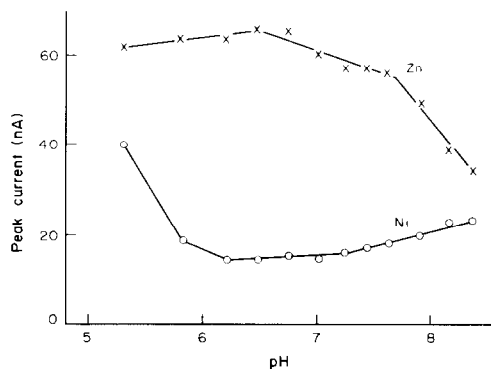


Fig. 2. AV reduction currents of Zn and Ni as a function of pH. Experimental conditions: sea-water containing $3 \times 10^{-8}M$ Zn, $1 \times 10^{-8}M$ Ni, $10^{-3}M$ APDC; stirred collection during 1 min at -0.3 V, sweep-rate 50 mV/sec.

wave to more positive potentials. BES buffer was therefore selected for the following experiments.

Effect of variation of collection time

The reduction current of zinc in sea-water medium buffered at pH 7.3 with 0.01M BES and containing $10^{-3}M$ APDC was measured by ALSV (scan-rate 50 mV/sec) as a function of the collection period. It was found (Fig. 3) that the reduction current increased linearly with the collection time up to about 7 min for $3 \times 10^{-8}M$ zinc, but only up to a collection time of 3 min for $2 \times 10^{-7}M$ zinc. The maximum in the reduction current for $2 \times 10^{-7}M$ zinc ($\sim 3 \mu A$), obtained after collection for 7 min was similar to the maximum current obtainable by increasing the zinc concentration and using a fixed collection period of 1.5 min. This means that the electrode was then completely covered with zinc-APDC complex. Increasing the collection period decreased the current, indicating that some of the adsorbed zinc was displaced, probably by other metals present as traces in the sample (APDC is a general complexing agent). A similar effect has been shown for the AV determination of Cu and Fe with catechol.^{7,8}

Effect of variation of the collection potential

The adsorbed film of metal-APDC complex can form in two ways: (a) the metal ions react with APDC molecules that are already adsorbed on the mercury surface, or (b) the complex species is formed in solution and then adsorbed. The potential of the HMDE during the collection period is important, since it determines the sign of the electrical charge on the electrode surface. The charge is zero at the electrocapillary maximum (ecm) which is located at ~ -0.52 V in electrolyte solutions similar to sea-water.

The effect of the electrical surface charge was studied by measuring the reduction current for both $3 \times 10^{-8}M$ zinc and $1 \times 10^{-8}M$ nickel in irradiated sea-water by ALSV after collection for 1.5 min at various potentials, at pH 7.3 (0.01M BES buffer), with $10^{-3}M$ APDC (scan-rate 50 mV/sec). Scans with collection potentials more negative than -0.9 V were

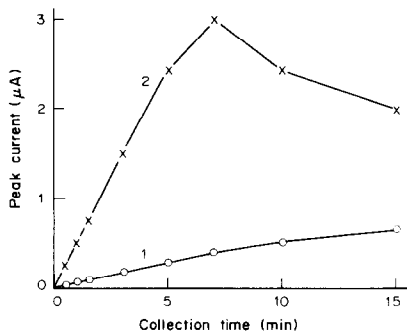


Fig. 3. Adsorption of Zn on the HMDE as a function of collection time. Experimental conditions: sea-water containing $3 \times 10^{-8}M$ Zn (1) and $2.3 \times 10^{-7}M$ Zn (2), $10^{-3}M$ APDC, 0.01M BES (pH 7.3); ALSV, sweep-rate 50 mV/sec.

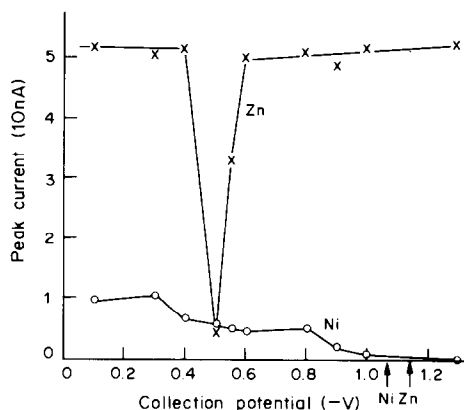


Fig. 4. Adsorption of Zn and Ni on the HMDE as a function of collection potential. Current measurement by ALSV, 50 mV/sec sweep-rate after 1.5 min collection, from sea-water containing $3 \times 10^{-8}M$ Zn, $1 \times 10^{-8}M$ Ni, $10^{-3}M$ APDC and 0.01M BES (pH 7.3); peak potentials of Zn and Ni are indicated on the x-axis.

initiated at -0.9 V as described in the experimental section. It was found (Fig. 4) that the effect of the surface charge on the adsorption was generally small, except for the sharp drop in adsorption of zinc at ~ -0.5 V where the surface charge reverses, which suggests that (b) is the operative mechanism. The dip in the curve at the ecm could possibly be explained by the dipolar nature of the Zn-APDC complex(es). This property is useful as it allows for selective collection of nickel with respect to zinc.

The peak potentials for zinc and nickel are also indicated in Fig. 4. The metallic zinc produced by reduction is amalgamated and diffuses into the mercury drop when the collection potential is kept more negative than the reduction potential (-1.14 V). When the potential is switched to -0.9 V the amalgamated zinc is oxidized, then is complexed by the adsorbed APDC and remains at the surface of the HMDE. This procedure permits selective collection of zinc without interference by nickel and high concentrations of cobalt (as shown below).

Maximum adsorption capacity of the HMDE

At any given collection time the relationship between the reduction current of zinc and its concentration in solution is linear only until a certain maximum degree of surface coverage has been reached. A linear response was found, for instance, up to $2 \times 10^{-7}M$ zinc, with a collection period of 1 min. The maximum adsorption capacity of the HMDE was determined by measuring the total charge (in μC) corresponding to the reduction of zinc, as a function of its concentration in irradiated sea-water, in a collection period of 1.5 min. This charge was calculated from the area under the Zn peak obtained by ALSV, with a scan-rate of 50 mV/sec and a collection potential of -0.3 V. The results were fitted to a linear form of the Langmuir equation.⁷ It was found that under saturation conditions the

charge was $2.3 \mu\text{C}$, equivalent to adsorption of 4.1×10^{-10} mole of zinc complex per cm^2 of surface (calculated from $\text{charge}/2 \times F \times \text{surface area}$, where F is the Faraday constant). This adsorption density is approximately twice that of the complex of Cu(II) with catechol (2×10^{-10} mole/ cm^2),⁷ but less than half that of the Ni(II) complex with DMG (1×10^{-9} mole/ cm^2).¹⁰

Interferences

Metal ions can interfere with the determination of Zn if their complexes are adsorbed on the electrode and their reduction potential is near that of zinc. It was found by making standard additions of Cu, Fe, V, U, Ni, Pb and Co, that only Ni(II) and Co(II) produced reduction peaks near that of zinc. The sensitivity for cobalt was only about a tenth of that for zinc and nickel, so it is not expected to interfere, as its concentration is of the order of $10^{-10}M$ in unpolluted sea-water,¹¹ whereas the concentrations of nickel and zinc in sea-water are in the range 10^{-9} – $10^{-8}M$.¹² The zinc concentration can be determined selectively by using a collection potential of -1.3 V (Fig. 4) and differential pulse (DP) modulation. The height of the zinc reduction peak was found to be increased by a factor of about 10 relative to that of nickel by use of DP modulation (10 pulses/sec), as a result of the irreversible reduction of nickel.¹³

Natural waters are known to contain low concentrations of surface-active organic material. Such material may reduce the sensitivity of this technique by competitive adsorption onto the HMDE. The reduction currents of zinc and nickel in irradiated sea-water were therefore measured before and after additions of Triton-X-100, a non-ionic surfactant which has been used as a calibration standard for surfactant activities in natural waters.¹⁴ It was found that the coastal sea-water samples had a surfactant activity equivalent to a 0.01–0.5 mg/l. concentration of Triton-X-100. When this surfactant was added to irradiated sea-water (containing $10^{-3}M$ APDC and $0.01M$ BES) the peak-heights for zinc and nickel were reduced by 40 and 80% respectively, by a 0.5-mg/l. level of surfactant, and both by about 90% by a 1-mg/l. level. The sensitivity for Zn was found to be lower in untreated water from the Irish Sea than for an irradiated sample, whereas no significant effect was observed for water from the N. Atlantic. It is therefore advisable to irradiate samples which may be suspected to contain significant amounts of surfactants.

Organic complexing material present in natural water samples could interfere by competition for dissolved zinc. The concentrations of such ligands are normally low (10^{-8} – $10^{-7}M$), but their zinc complexes are about as strong as the Zn–EDTA complex.^{15,16} Addition of 10^{-6} , 10^{-5} , 3×10^{-5} and $7 \times 10^{-5}M$ EDTA to irradiated sea-water (containing $3.9 \times 10^{-8}M$ Zn, $8.88 \times 10^{-4}M$ APDC, and $0.01M$

BES, pH 7.3) reduced the ALSV peak height of zinc by 0, 11, 45 and 86% respectively. At the APDC concentration ($8.88 \times 10^{-4}M$) used, the effect was therefore significant only at ligand concentrations much greater than those normally present in natural waters. Ultraviolet irradiation of water samples, as recommended for the removal of surfactants, should also remove high concentrations of strongly complexing ligands possibly occurring in interstitial waters.

The stability constant of the zinc–APDC complex is not known, but can be estimated from the competitive effect of EDTA. A 50% reduction in the ALSV peak height of zinc in the presence of $8.88 \times 10^{-4}M$ APDC should be caused by the presence of $3.47 \times 10^{-5}M$ EDTA (calculated by interpolation in the data above). Under these conditions the concentration ratio of zinc complex to free zinc must be the same for both complexes, so $C_{\text{EDTA}}K'_{\text{ZnEDTA}} = C_{\text{APDC}}K'_{\text{ZnAPDC}}$ where C_{EDTA} and C_{APDC} are the concentrations of free EDTA and APDC respectively and K'_{ZnEDTA} and K'_{ZnAPDC} are the conditional stability constants for the complexes. For sea-water medium at pH 7.3 it can be calculated that $\log K'_{\text{ZnEDTA}} = 7.71$ (from the stability constants quoted by Martell and Smith¹⁷) so K'_{ZnAPDC} is approximately 2×10^6 . A $10^{-4}M$ concentration of APDC in sea-water would give an α -coefficient for the side-reaction with zinc ($\alpha_{\text{ZnAPDC}} = 1 + K'_{\text{ZnAPDC}}C_{\text{APDC}}$) of about 200, and for $10^{-3}M$ APDC, $\alpha_{\text{ZnAPDC}} \sim 2000$. These values can be compared with those (40–100) for complexes of zinc with natural organic complexing material in sea-water and interstitial waters,¹⁵ and with that (2) for inorganic complexes.¹⁸ No significant interference by natural organic complexing material is therefore to be expected when $10^{-3}M$ APDC is used.

Determination of zinc in sea-water

From the experiments reported it was concluded that optimal sensitivity was obtained by using a solution containing $0.01M$ BES buffer (pH 7.3) and $10^{-3}M$ APDC, but that a better baseline at higher zinc concentrations would be obtained at pH 8.5. The effects of various experimental conditions on the peak current are shown in Fig. 5. The zinc peak is much reduced (scan 3) after collection at -0.5 V (see also Fig. 4), and the peaks of nickel and cobalt at -1.08 and -1.2 V respectively are readily discernible. The nickel and zinc peaks are both improved by collection at -0.1 V, whereas cobalt is completely, and nickel substantially, masked by collection at -1.3 V (scan 1). The reduction current of zinc is much increased by using differential pulse modulation (scan 4). By standard additions it was found that the zinc concentration was $3 \times 10^{-8}M$ in the sample from the N. Atlantic. This concentration was confirmed by DPASV at pH 4.5 with the HMDE.

The detection limit was evaluated from scan 5 in Fig. 5. The peak-height of 5 nA for $2 \times 10^{-9}M$ zinc had a relative standard deviation (RSD) of 2.3% (8

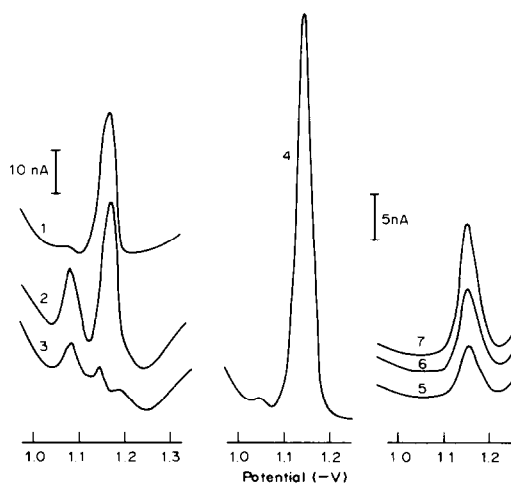


Fig. 5. ALSV and ADPV scans of water containing $3 \times 10^{-8} M$ Zn and $10^{-3} M$ APDC after 1.5 min collection. Scans 1-4: sea-water, pH 8.5; scans 1-3: ALSV, sweep-rate 50 mV/sec, collection potentials of 1, -1.3 V; 2, -0.1 V; 3, -0.5 V; scan 4: ADPV, 10 pulses/sec, sweep-rate 10 mV/sec, collection at -1.3 V. Scans 5-7: $10^{-3} M$ APDC in distilled water, pH 7.3; 1.5 min collection at -1.3 V; ADPV with 10 pulses/sec and sweep-rate 10 mV/sec; 5, $2 \times 10^{-9} M$ Zn; 6, $3.8 \times 10^{-9} M$ Zn; 7, $6.9 \times 10^{-9} M$ Zn.

degrees of freedom). The detection limit was calculated as 3 times this standard deviation, giving a value of $1.4 \times 10^{-10} M$. This limit was obtained with a collection period of only 1.5 min. A collection period of 10 min would reduce the limit of detection to about $3 \times 10^{-11} M$. This is comparable to that for nickel by similar AV techniques,^{7,10} but about a hundredth of that for determination of zinc by DPASV with an HMDE,^{3,4} and a tenth of that by DPASV with an RDE.⁵ Application of this technique allows determination of zinc in sea-water with a collection period of only 1-2 min, with an HMDE. This type of electrode is easier to handle than the RDE, as its surface is readily renewed before each measurement and no polishing is needed.

Simultaneous determination of nickel and zinc

Peaks for both elements are obtained from a single ALSV scan of sea-water containing $10^{-3} M$ APDC, but the sensitivity for nickel is much lower than that for zinc. Comparative measurements on sea-water at pH 8.5 showed that about 10 times better sensitivity was obtained for nickel with $2 \times 10^{-5} M$ DMG than with $10^{-3} M$ APDC. DMG is selective for Ni,¹⁰ and at $2 \times 10^{-5} M$ concentration in $10^{-3} M$ APDC medium has no effect on the peak-height for zinc. Hence

nickel can be determined first by addition of $2 \times 10^{-5} M$ DMG and use of a collection potential of -0.7 V, followed by determination of zinc by addition of $10^{-3} M$ APDC and use of a collection potential of -1.3 V. The solution is buffered at pH 8.5 with $0.01 M$ boric acid. A pH of 8.5 is selected rather than 9.2 as recommended for nickel,¹⁰ because of the possible precipitation of magnesium hydroxide and because of the lower sensitivity for zinc at a higher pH. DP modulation was used in both cases (10 pulses/sec, 10 mV/sec) and a collection period of 1.5 min. A reduction current of 57 nA was obtained for $10^{-8} M$ nickel (RSD 2%) and a limit of detection of $6 \times 10^{-10} M$. The sensitivity under the given conditions is therefore sufficient to determine Ni and Zn simultaneously, given that the levels of these metals in unpolluted sea-water are typically 10^{-9} - $10^{-8} M$.^{3,12}

Acknowledgement—The author is grateful for assistance with some of the experiments by Z. Q. Huang.

REFERENCES

1. M. I. Abdullah, B. Reusch Berg and R. Klimek, *Anal. Chim. Acta*, 1976, **84**, 307.
2. G. E. Batley and T. M. Florence, *J. Electroanal. Chem.*, 1974, **55**, 23.
3. A. Zirino and M. L. Healy, *Limnol. Oceanog.*, 1971, **16**, 773.
4. G. Gillain, G. Duyckaerts and A. Disteché, *Anal. Chim. Acta*, 1979, **106**, 23.
5. M. Landy, *ibid.*, 1980, **121**, 39.
6. R. Neeb, *Inverse Polarographie und Voltammetrie*, p. 191. Verlag Chemie, Weinheim, 1969.
7. C. M. G. van den Berg, *Anal. Chim. Acta*, 1984, in press.
8. C. M. G. van den Berg and Z. Q. Huang, *J. Electroanal. Chem.*, 1984, in press.
9. Kh. Z. Brainina, *Stripping Voltammetry in Chemical Analysis*, p. 121. Wiley, New York, 1974.
10. B. Pihlar, P. Valenta and H. W. Nürnberg, *Z. Anal. Chem.*, 1981, **307**, 337.
11. L.-G. Danielsson, *Mar. Chem.*, 1980, **8**, 199.
12. K. W. Bruland and R. P. Franks, in *Trace Metals in Sea Water*, C. S. Wong, E. Boyle, K. W. Bruland, J. D. Burton and E. D. Goldberg (eds.), p. 395. Plenum Press, London, 1983.
13. I. M. Kolthoff and J. J. Lingane, *Polarography*, 2nd Ed., Vol. 2, p. 487. Interscience, London, 1952.
14. B. Cosovic and V. Vojvodic, *Limnol. Oceanog.*, 1982, **27**, 361.
15. C. M. G. van den Berg and S. Dharmvanij, *ibid.*, 1984, in the press.
16. K. Hirose, Y. Dokiya and Y. Sugimura, *Mar. Chem.*, 1982, **11**, 343.
17. A. E. Martell and R. M. Smith, *Critical Stability Constants*, Vol. 1, p. 204. Plenum Press, New York, 1974.
18. D. R. Turner, M. Whitfield and A. G. Dickson, *Geochem. Cosmochim. Acta*, 1981, **45**, 855.

1,2- AND 1,3-CYCLOHEXANEDIONE BIS(2-HYDROXYBENZOYLHYDRAZONE)S AS ANALYTICAL REAGENTS

M. GALLEGO, M. SILVA and M. VALCARCEL

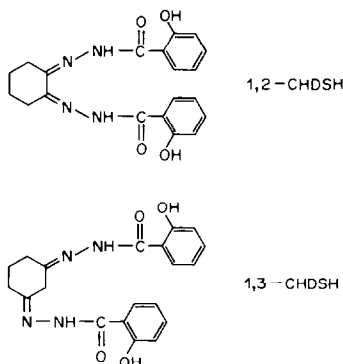
Department of Analytical Chemistry, Faculty of Sciences, University of Córdoba, Córdoba, Spain

(Received 13 February 1984. Revised 2 May 1984. Accepted 19 June 1984)

Summary—The synthesis, characteristics and analytical properties of 1,2- and 1,3-cyclohexanedione bis(2-hydroxybenzoylhydrazone)s are described. Spectral characteristics, p*K* values, hydrolysis resistance, reactions with common cations and their potential use in kinetic analysis are reported.

Hydrazones have been widely used for spectrophotometric and spectrofluorimetric determination of metal ions, and their analytical applications have been reviewed^{1,2}. Bis(arylhyazone)s have recently been proposed as analytical reagents. Lever³ reported the photometric and fluorimetric properties of the bis(4-hydroxybenzoylhydrazone)s of glyoxal, methylglyoxal and dimethylglyoxal. The photometric reactions of other bis(arylhyazone)s with several metal ions have been investigated by us.⁴⁻⁸

In this paper, studies of the synthesis and properties of the 1,2-cyclohexanedione and 1,3-cyclohexanedione bis(2-hydroxybenzoylhydrazone)s (1,2-CHDSH and 1,3-CHDSH respectively) and their reactions with common cations and use in kinetic analysis are described.



EXPERIMENTAL

Reagents

All reagents were of analytical-reagent grade and all solutions were prepared with distilled water. The 1,2- and 1,3-cyclohexanedione bis(2-hydroxybenzoylhydrazone)s were used as 0.1% solutions in dimethylformamide; the solutions were stable for at least 1 week.

Procedures

Synthesis of bis(arylhyazone)s. The 1,2- or 1,3-cyclohexanedione (0.37 g) and the stoichiometric amount of

2-hydroxybenzoylhydrazine (1.00 g) were dissolved in 15 ml of absolute ethanol, several drops of concentrated hydrochloric acid were added and the mixture was heated under reflux for 15 min for synthesis of 1,2-CHDSH and for 30 min for 1,3-CHDSH. After cooling to room temperature, the products were filtered off and recrystallized from ethanol. The melting points were 243° and 253° respectively. Elemental analysis gave C 62.9%, H 5.4%, N 14.5% for 1,2-CHDSH, C 63.2%, H 5.4%, N 14.8% for 1,3-CHDSH; C₂₀H₂₀N₄O₄ requires C 63.16%, H 5.26%, N 14.74%.

Photometric reactions. The solutions were prepared in 25-ml standard flasks from appropriate amounts of the cation, 5 ml of 0.1% reagent solution in dimethylformamide, 10 ml of dimethylformamide, and enough dilute hydrochloric acid or sodium hydroxide solution to give the selected pH value, and diluted to volume with distilled water. The absorbances were measured at 350–500 nm against a blank solution.

Oxidation reactions. The reactions with several oxidizing agents and the catalytic effects of several cations were investigated. To a solution containing 0.5 ml of reagent solution in dimethylformamide, in a 10-ml standard flask, were added 2 ml of oxidizing agent solution (0.3% v/v hydrogen peroxide, 0.1*M* potassium persulphate or 0.1*M* sodium periodate) and 2 ml of 0.14*M* ammonia solution, and the mixture was made up to the mark with distilled water. In the study of the catalysed reactions appropriate amounts of the catalysts were also added. The absorbances were measured at 350–500 nm and the spectrofluorimetric measurements were made in the range 200–500 nm.

RESULTS AND DISCUSSION

The synthesis of these bis(arylhyazone)s is very easy and the reaction needs only slight heating. Bright yellow crystals appear when the reagents are mixed.

The solubilities of the two reagents were found to be very low in organic solvents except for dimethylformamide (Table 1). Therefore, water–dimethylformamide (4:6 v/v) mixtures were used. The most important characteristics of the reagents in several solvents are shown in Table 1.

The infrared spectra (potassium bromide discs) were analogous, with bands assigned to the stretching vibrations of NH (3200 cm⁻¹), C=N (1650 cm⁻¹),

Table 1. Characteristics of both compounds in several solvents

Solvent	1,2-CHDSH			1,3-CHDSH		
	Solubility, g/l.*	λ_{\max} , nm	Molar absorptivity, $10^3 \text{ l. mole}^{-1} \text{ cm}^{-1}$	Solubility, g/l.*	λ_{\max} , nm	Molar absorptivity, $10^3 \text{ l. mole}^{-1} \text{ cm}^{-1}$
Ethanol	1.26	350	16.6	0.70	385	29.5
Acetone	2.04	350	16.2	1.05	390	29.5
Dimethylformamide	4.64	400	15.7	54.17	430	49.5
Chloroform	1.08	350	17.6	0.40	385	30.4
Benzyl alcohol	1.84	350	15.2	0.20	385	30.4
Amyl alcohol	1.38	350	17.6	0.42	385	30.0
Benzene	0.56	350	17.6	0.30	385	29.9
Ethyl acetate	0.34	350	19.0	0.57	385	30.4
IBMK	0.36	350	16.6	0.15	385	30.9

*Measured by the method of Wittenberger.¹⁰

OH (1310 cm^{-1}) and *ortho*-substitution in the aromatic ring (760 cm^{-1}).

The ultraviolet spectra of the reagents show analogous absorption maxima at 300 and 310 nm (Fig. 1) with bathochromic shifts in alkaline medium (λ_{\max} 350 nm). Aqueous solutions of 1,2-CHDSH do not fluoresce at any pH, but alkaline solutions of 1,3-CHDSH exhibit a blue fluorescence (λ_{ex} 350 nm, λ_{em} 430 nm). This behaviour can be attributed to interaction between the two aroylhydrazone chains, enhancing the rigidity and planarity of this compound. This effect could also explain the reactivity of this reagent relative to that of 1,2-CHDSH (see Table 2).

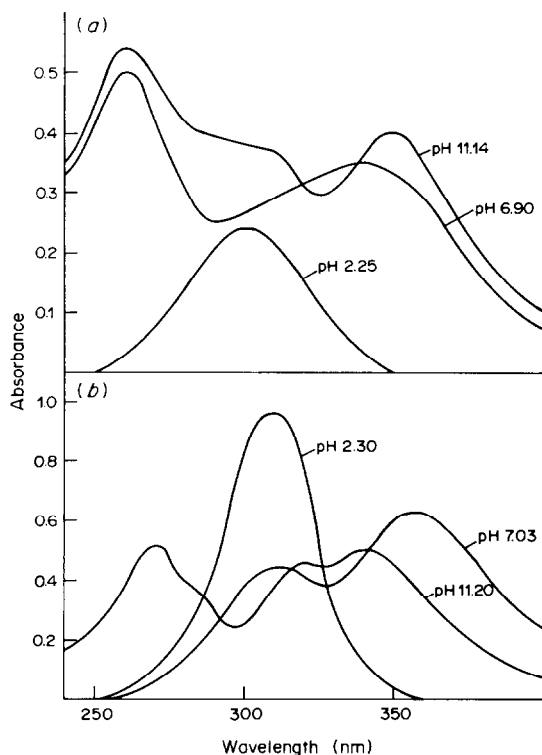


Fig. 1. Absorption spectra of the reagents in aqueous solutions at various pH values. (a) 1,2-CHDSH reagent and (b) 1,3-CHDSH reagent. $C_{\text{reagent}} = 5.2 \times 10^{-5} \text{ M}$.

A combined potentiometric and photometric method⁹ was used to determine the ionization constants, the first for ionization of the enolic hydroxyl group and the second for the ionization of the phenolic group. The ionization constants of 1,3-CHDSH have also been calculated from the fluorescence measurements. The average pK values are:

	1,3-CHDSH		
	1,2-CHDSH	Photometric	Fluorimetric
pK ₁	6.3 ± 0.1	5.6 ± 0.1	6.3 ± 0.1
pK ₂	10.8 ± 0.1	10.1 ± 0.1	10.1 ± 0.1

Solutions of these compounds in dimethylformamide are stable for at least one week and the reagents are resistant to hydrolysis at any pH.

The characteristics of the chelates formed in water-dimethylformamide (4:6 v/v) medium are shown in Table 2. 1,2-CHDSH is superior in sensitivity, but in both cases preliminary separations or masking reactions must be used to improve selectivity. However, molybdenum(VI), titanium(IV) and tin(II) react with 1,2-CHDSH at much lower pH than the other cations do, and it should be possible to

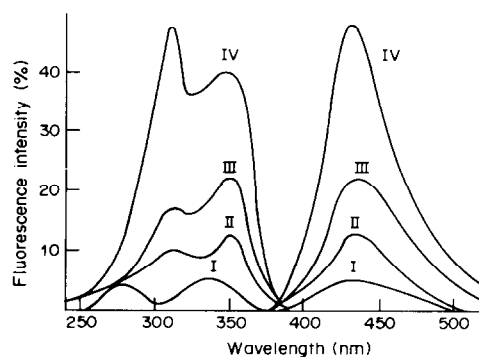


Fig. 2. Excitation and emission spectra of $1.3 \times 10^{-4} \text{ M}$ 1,2-CHDSH (pH = 10.4). Sensitivity $\times 0.3$. In the presence of: I, dissolved oxygen; II, 0.02M sodium periodate; III, 0.02M potassium peroxodisulphate and IV, 0.017M hydrogen peroxide. $C_{\text{NH}_3} = 0.028 \text{ M}$; reaction time 24 hr. Temperature 25°C .

Table 2. Photometric characteristics of complexes in solution

Metal ion	1,2-CHDSH			1,3-CHDSH		
	λ_{\max}, nm	pH range	Molar absorptivity, $10^4 l. mole^{-1}. cm^{-1}$	λ_{\max}, nm	pH range	Molar absorptivity, $10^4 l. mole^{-1}. cm^{-1}$
Ti(IV)	450-470	HCl 1M-5.2	1.42			
V(V)				410	4.0-5.1	1.02
Mn(II)	435	7.9-9.1	3.04	480	9.1-11.5	0.66
Fe(II)	440	7.2-8.6	2.85	470	6.4-8.1	0.16
Fe(III)	440	6.9-9.5	2.73	475	5.8-12.1	0.34
Co(II)	405-435	3.2-4.5; 6.5-8.4	2.0; 1.54	480	9.4-11.9	0.75
Ni(II)	435	5.8-8.3	0.93	485-530	8.2-12.3	1.32; 0.71
Cu(II)	405	3.4-4.0	3.47	475	7.7-9.8	0.67
Zn(II)	435	6.4-7.6	4.24	475	7.3-10.8	0.46
Zr(IV)	450	4.2-9.3	2.01			
Mo(VI)	470	2.0-4.7	1.65			
Pd(II)				475	9.8-11.1	0.85
Cd(II)	430	6.4-8.4	7.38	475	7.7-9.8	0.67
In(III)	435-455	4.3-4.9; 6.1-9.4	5.86; 2.56			
Sn(II)	445	HCl 1M-5.7	2.74			
Sn(IV)	445	4.2-9.3	2.05			
La(III)	415	7.6-9.1	5.32			
Pb(II)	450	6.8-8.5	4.31			
Th(IV)	435	5.8-7.9	7.27			

determine both tin(II) and tin(IV) in a mixture. No fluorescence was found for any of the complexes, but the fluorescence of 1,3-CHDSH is quenched by the cations that react with this reagent.

Oxidation studies

Ammoniacal solutions of 1,2-CHDSH do not show native fluorescence, but when treated with an oxidizing agent such as hydrogen peroxide, potassium persulphate or sodium periodate exhibit a blue fluorescence (λ_{ex} 310 nm and 350 nm, λ_{em} 430 nm). Figure 2 shows this behaviour as well as the slight

effect of dissolved oxygen on this compound in ammoniacal medium. If alkali-metal hydroxides are used for the pH adjustment, the effect of these oxidants is less. Potassium persulphate produces a brown oxidation product (λ_{max} 420 nm) after 48 hr, which is not fluorescent.

The most important catalytic effect on the oxidative production of fluorescence from 1,2-CHDSH is that of manganese(II) (Fig. 3a), when hydrogen peroxide, potassium persulphate or dissolved oxygen is the oxidant. The effect of dissolved oxygen was confirmed by measurements in an inert atmosphere

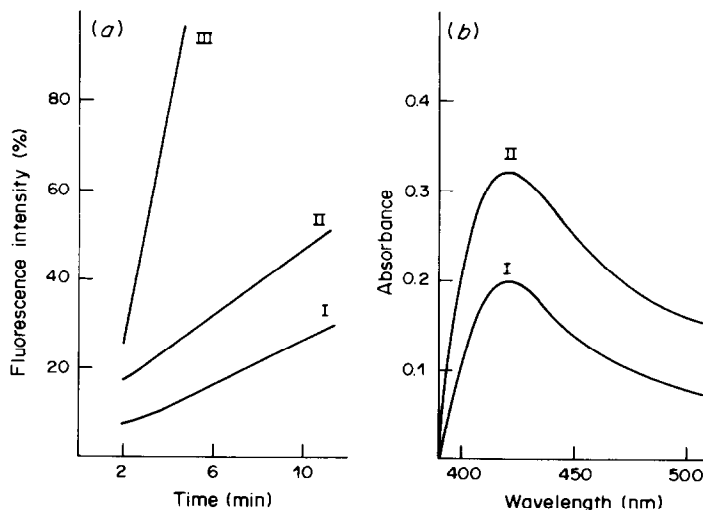


Fig. 3. (a) Plots of fluorescence vs. time for the kinetic determination of manganese at the 5.0 ng/ml level in the presence of several oxidants: I, potassium peroxodisulphate; II, dissolved oxygen and III, hydrogen peroxide. ($1.3 \times 10^{-4} M$ 1,2-CHDSH, $8.8 \times 10^{-3} M$ H_2O_2 or $10^{-2} M$ $K_2S_2O_8$, $0.4 M$ ammonia, $25^\circ C$, sensitivity $\times 0.3$). (b) Absorption spectra of 1,2-CHDSH in the presence of several oxidants, catalysed by manganese(II) (100 ng/ml): I, potassium peroxodisulphate and II, dissolved oxygen. Conditions as described in the procedure. In both cases, the reagent blank was negligible.

Table 3. Influence of iron(III) and silver(I) on the kinetic determination of Mn at the 5.0 ng/ml level

Metal ion	Tolerance ratio, [Ion]/[Mn ²⁺]*		
	Hydrogen peroxide	Potassium persulphate	Dissolved oxygen
Iron(III)	20	10	20
Silver(I)	100	8	50

*Experimental conditions as for Fig. 3a.

on solutions made with oxygen-free reagent solutions. The reagent blanks do not show fluorescence. The catalytic effect of manganese(II) is maximal with hydrogen peroxide as the oxidant, and manganese can be determined at sub-ng/ml levels. Iron(III) and silver(I) are the only other cations to show catalytic action (at about the $\mu\text{g/ml}$ level) with hydrogen peroxide and potassium persulphate as the oxidant. The tolerance levels for these ions are shown in Table 3. Hydrogen peroxide is the oxidant of choice for the catalytic determination of manganese, owing to the greater sensitivity and selectivity.

In the photometric study and when potassium persulphate or dissolved oxygen is the oxidant, only the catalytic effect of manganese(II) has been found. This behaviour is shown in Fig. 3b.

1,3-CHDSH is similarly oxidized, to a product with blue fluorescence (λ_{ex} 315 nm, λ_{em} 415 nm). Only manganese(II) and iron(III) show a catalytic effect (a slight one) when hydrogen peroxide is the oxidant.

1,2-CHDSH is of more potential use than 1,3-CHDSH in kinetic analysis.

REFERENCES

1. M. Katyal and Y. Dutt, *Talanta*, 1975, **22**, 151.
2. R. B. Singh, P. Jain and R. R. Singh, *ibid.*, 1982, **29**, 77.
3. E. Lever, *Anal. Chim. Acta*, 1973, **65**, 311.
4. M. Silva and M. Valcárcel, *Ann. Quim.*, 1980, **76**, 129.
5. *Idem*, *Analyst*, 1980, **105**, 193.
6. *Idem*, *Microchem. J.*, 1980, **25**, 117.
7. *Idem*, *ibid.*, 1980, **25**, 289.
8. M. Silva, M. Gallego and M. Valcárcel, *Talanta*, 1980, **27**, 615.
9. J. A. Muñoz-Leyva and F. Pino, *Quim. Anal.*, 1973, **27**, 67.
10. W. Wittenberger, *Chemische Laboratoriumstechnik*, 4th Ed., p. 101. Springer, Vienna, 1950.

SYNTHESIS AND PROPERTIES OF A CHELATING RESIN CONTAINING TRIAZOLETHIOL GROUPS

ATSUSHI SUGII, NAOTAKE OGAWA and YOSHIHISA HAGIWARA

Faculty of Pharmaceutical Sciences, Kumamoto University, Kumamoto 862, Japan

(Received 8 January 1982. Revised 24 January 1984. Accepted 19 June 1984)

Summary—A macroreticular poly(acrylic acid)-based resin with triazolethiol as the functional group has been synthesized. The stability of the resin in acidic media and the behaviour in sorption and desorption of various metal ions have been investigated and compared with those of the acylthiosemicarbazide resin which is an intermediate in synthesis of the triazolethiol resin. Both resins show high affinity for copper(II) silver, cadmium and mercury(II), and high selectivity for silver and mercury(II) at low pH (1–2), and even at pH 7 if EDTA is present. The triazolethiol resin sorbs metal ions faster than the acylthiosemicarbazide resin does and sorbs mercury(II) from high concentrations of acids and neutral salt solutions. This resin has been applied to the concentration of silver and mercury(II) from sea-water samples by column operation.

Chelating resins having a sulphur atom in their functional group should show high affinity for "soft" metal ions, and several have been synthesized and investigated. In particular, the chelating resins containing thiol groups^{1–15} have been extensively investigated because of their high reactivity towards heavy metal ions. The thiol groups, however, are likely to be oxidized by oxygen during usage and/or storage of the resin, resulting in decrease in capacity, so it is worthwhile trying to synthesize new chelating resins having stable thiol groups. The present paper describes a resin containing triazolethiol groups, which is resistant to air-oxidation. The characteristics of the acylthiosemicarbazide resin which is an intermediate in the synthesis of the triazolethiol resin are also described.

EXPERIMENTAL

Apparatus and reagents

The infrared spectra and surface properties of the resins, and the radioactivity of the tracers used, were measured with the apparatus described earlier.¹⁶ A Shimadzu AA-610S atomic-absorption spectrophotometer was used for the determination of nickel, copper and silver. The stock metal ion solutions, approximately 0.1M, were standardized by complexometric titration. The solutions used for the sorption studies were prepared by diluting aliquots of the stock solutions with the desired background acid (hydrochloric acid or nitric acid in 1M acetic acid) or buffer solution (1M acetic acid–sodium acetate). The radioisotopes ⁶⁰Co, ⁶⁵Zn, ¹⁰⁹Cd, ^{110m}Ag and ²⁰³Hg, as nitrate or chloride, were obtained from the New England Nuclear Corp. and the Radiochemical Centre, Amersham.

Preparation of resins

Resin I. To 450 ml of 0.5% aqueous hydroxyethylcellulose solution containing 45 g of sodium chloride, 120 ml of ethyl acrylate, 30 ml of 50% divinylbenzene solution and 150 ml of iso-octane, 2.25 g of benzoyl peroxide were added, and the mixture was stirred. After dispersion of the monomers, the mixture was heated to 70–75° and kept at this temperature for 8 hr with constant stirring. The product was

filtered off and washed with hot water and methanol. After drying in a vacuum desiccator, the 35–60 mesh fraction was collected.

Resin II. To 60 g of resin I, 220 ml of anhydrous hydrazine were added and the mixture was heated at 120° for 10 hr, then the reaction mixture was poured into 2 litres of water, and the product was filtered off, and washed with water and methanol. After vacuum drying, about 55 g of a white resin was obtained.

Resin III. To 200 ml of 50% aqueous ethanol, 50 g of resin II and 30 g of methyl isothiocyanate were added, and the mixture was refluxed for 8 hr with stirring. The reaction product was filtered off, washed with methanol, and dried under vacuum. A white resin (about 73 g) was obtained.

Resin IV. Resin III (50 g) was suspended in 400 ml of 50% aqueous dioxan containing 30 g of potassium hydroxide, and the mixture was refluxed for 8 hr with stirring. The product was filtered off, washed with water, 10% acetic acid, water and methanol, and finally dried under vacuum. A white resin (about 46 g) was obtained.

Stability of resins

Portions (1 g) of resins III and IV were shaken with 50 ml of acid solutions of various concentrations (1–5M) for 5 days, then filtered off and washed with water, 1M sodium hydroxide, 1M acetic acid and water until the washings were neutral. After vacuum drying, the nitrogen and sulphur contents were determined.

Sorption of metal ions by batch operation

Unless otherwise stated, aliquots (10 or 100 ml) of 0.01M metal ion solutions were mechanically shaken with 100 mg of dry resin III or IV for a selected time at room temperature. The amount of metal ion sorbed was determined by radiochemical or spectrophotometric measurement of equal portions of the solution, before and after sorption of the metal ions.

Recovery of metal ions

Resins III and IV, loaded with metal ions, were shaken with various desorbents for 3 hr, then filtered off, and the amounts of the metal ions in the filtrates were determined.

Breakthrough

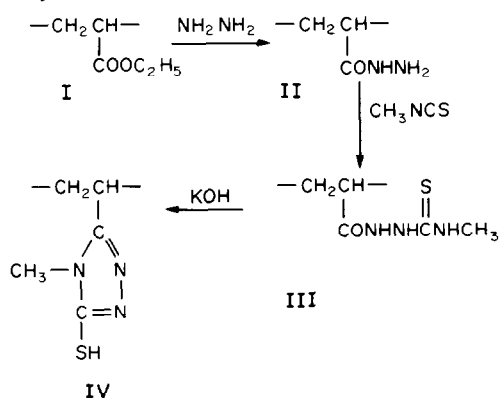
The metal solution (0.2 mg/ml, pH 7) was passed through a glass tube packed with 1 g of resin III or IV (0.5 × 15 cm)

at a flow-rate of 2 ml/min, and the effluent fractions were analysed for the metal.

RESULTS AND DISCUSSION

Preparation and stability of resins

The resins were synthesized from macroreticular (MR) poly(ethyl acrylate) cross-linked with 10% divinylbenzene as shown in Scheme 1.



The elemental analyses of resins II–IV are shown in Table 1. Resins III and IV contain nitrogen and sulphur in 3:1 molar ratio and the higher nitrogen and sulphur content of resin IV corresponds to the dehydration of resin III. The absorption band at 1680 cm^{-1} ($\nu_{\text{C}=\text{O}}$) observed for resins II and III is absent for resin IV. These facts suggest that the conversion from resin II into resin IV proceeds almost quantitatively.

The physical properties of the resins are listed in Table 2; resins III and IV show the characteristic MR structure. The specific surface area of both resins is nearly the same, but the pore volume and diameter of resin III are larger than those of resin IV. It is also clear that the thiol group in resin IV increases the hydrophilicity.

The chemical stability of resins III and IV was assessed from the change in nitrogen and sulphur content on exposure to acids. Resin IV was stable in 1–5M hydrochloric acid but not in 1M nitric acid, which caused about 97% desulphurization of the original resin (*cf.* preparation of 1,2,4-triazole from its thiol derivative¹⁷). The thiol groups of resin IV were stable for about a year on exposure to air, however. Resin III, which contains acylthiosemicarbazide groups, was stable in both nitric and hydrochloric acid media.

Sorption of metal ions

Metal chelates with 1,2,4-triazole-5-thiol have been

Table 1. Analytical data of resins

Resin	Nitrogen, % (mmole/g)	Sulphur, % (mmole/g)	Molar ratio N:S
II	17.31 (12.36)	—	—
III	18.13 (12.95)	13.65 (4.26)	3.04
IV	19.86 (14.19)	15.14 (4.72)	3.01

characterized by Gupta *et al.*¹⁸ and the usefulness of thiosemicarbazide derivatives in inorganic analysis has also been reviewed.¹⁹ It was expected that resins III and IV would have the same reactivity as their monomeric compounds towards metal ions. The sorption of metal ions on resins III and IV at various pH values was investigated, and the results are shown in Fig. 1. The sorption of silver and mercury(II) was similar on both resins at pH below 7, but for copper(II) and cadmium the affinity of resin IV was higher than that of resin III.

The maximum capacities for the four metal ions which showed the highest affinity in the preliminary experiment are listed in Table 3. The order of sorption is $\text{Ag} > \text{Hg} > \text{Cu} > \text{Cd}$ on both resins. The sorption mechanism is still not completely elucidated. The high capacity for silver, however, suggests that the nitrogen atom as well as the sulphur atom in the functional group contributes to the sorption of metal ions. This was confirmed experimentally; the capacity at pH 7 of resin IV (desulphurized with 1M nitric acid) for copper and silver was still 1.87 and 3.50 mmole/g, respectively.

The rate of sorption was determined for copper, silver, cadmium and mercury at pH 7 by batch operation with resins III and IV, and the results are shown in Fig. 2. The equilibration is faster on resin IV; the times required for 50% uptake of copper, silver, cadmium and mercury were 15, 2, 20 and 6 min, respectively.

The effect of diverse ions on the sorption of the four metal ions with resins III and IV was studied. The presence of $10^{-2}M$ chloride, nitrate, thiocyanate, thiosulphate and sulphate did not interfere with sorption of metal from 10 ml of $1 \times 10^{-3}M$ metal solution (pH 4) except for mercury(II) in thiosulphate solution, in which the mercury was reduced. Figure 3 shows that mercury(II) is effectively sorbed in the presence of high concentrations of various acids and salts. This suggests that resin IV is applicable to the concentration of mercury from highly saline solutions and/or acids widely used as reagents. The presence of 100-fold amount of cobalt(II), nickel, copper(II), zinc, cadmium, lead and iron(III) showed no significant interference with the sorption of silver(I) and mercury(II) with resins III and IV at pH 7.

Table 2. Physical properties of resins

Resin	Specific surface area, m^2/g	Pore volume, ml/g	Average pore diameter, nm	Water regain, g/g
III	39.4	0.109	111	0.98
IV	40.0	0.081	81	1.09

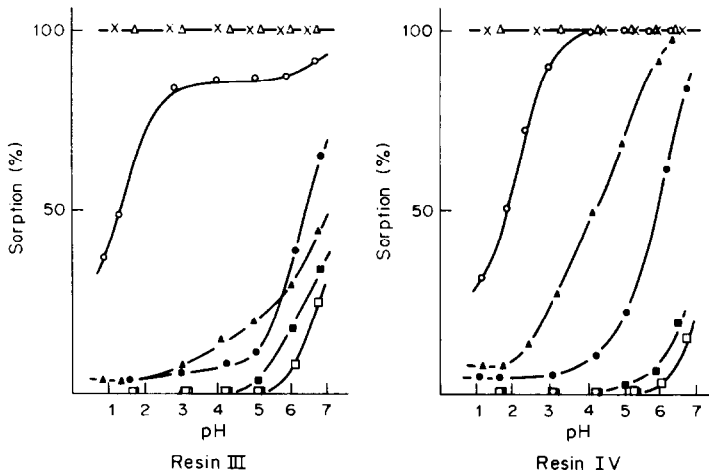


Fig. 1. Effect of pH on the sorption of metal ions with resins III and IV. Resin: 100 mg. Metal solutions: 0.01M, 10 ml. Shaking time; 24 hr. □: Co; ■: Ni; ○: Cu; ●: Zn; △: Ag; ▲: Cd; ×: Hg.

Mercury(II) was found to be 99.9% sorbed on resin IV in the presence of silver (in 100:1 ratio to mercury) in 0.001M nitric acid medium. The amounts of silver and mercury used corresponded to 10 and 0.1 mmole per g of resin IV, respectively, so the result indicates that the resin thiol group has much higher affinity for mercury(II) than for silver.

Table 4 shows the degree of sorption of the four metal ions in the presence of EDTA, selected as a typical chelating agent. The results suggest that the resins may be useful for the concentration and recovery of silver and mercury from natural water, which contains several chelating substances. The time required for 50% uptake of silver and mercury is not affected by the presence of EDTA. As shown in Fig. 1, resin IV sorbs mercury and silver selectively at

low pH but the selectivity decreases with increasing pH. When EDTA is present, however, resin IV sorbs only mercury and silver.

In general, desorption of the metal ions from the resins was rather difficult, probably because of formation of stable metal complexes with the functional groups on the resin matrix. Quantitative recovery was achieved only by using 0.1M hydrochloric acid containing 1-10% thiourea.

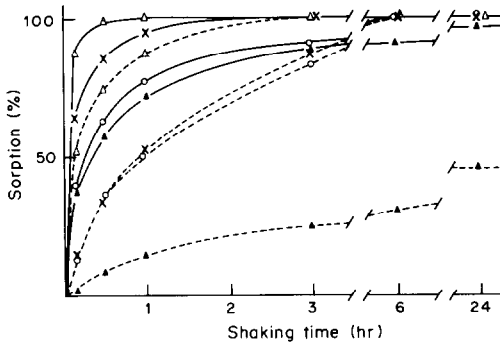


Fig. 2. Effect of shaking time on the sorption of metals in acetate buffer (pH 7). Resin: 100 mg. Metal solutions: 0.01M, 10 ml. Symbols are the same as those in Fig. 1. - - -: resin III —: resin IV.

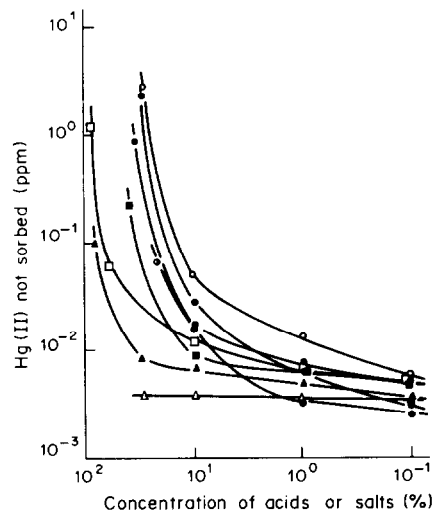


Fig. 3. Sorption of mercury(II) from acids and neutral salts solutions with resin IV. Resin: 100 mg. Sample solution: Hg 100 ppm, 10 ml. Shaking time: 12 hr. ●: HCl; ○: HNO₃; ■: CH₃COOH; □: H₂SO₄; ▲: H₃PO₄; △: NaNO₃; ○: NaCl; ○: NaSCN.

Table 3. Total capacity (mmole/g) for copper, silver, cadmium and mercury

Resin	Cu(II)		Ag(I)		Cd(II)		Hg(II)	
	pH 3	pH 7	pH 3	pH 7	pH 3	pH 7	pH 3	pH 7
III	0.91	1.85	6.39	7.56	0.49	0.61	3.97	3.23
IV	1.05	2.81	7.13	7.77	0.42	1.89	3.76	3.70

Metal solutions: 0.01M, 100 ml. Shaking time: 24 hr.

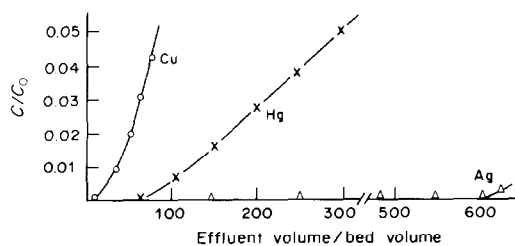


Fig. 4. Breakthrough curves with resin IV column.

The breakthrough curves for copper, silver and mercury on resin IV are shown in Fig. 4. About 20, 70 and 600 bed-volumes of 200-ppm copper, mercury and silver solutions respectively could pass through the column without leakage into the effluent. With resin III, however, leakage of mercury was observed after passage of about 3–5 bed-volumes of the feed solution. Although resin III is superior to resin IV in stability, its rate of equilibration is too slow for use in column work.

Resin IV was applied to concentration of mercury and silver from sea-water. Mercury was concentrated on a resin IV column from 1 litre of sea-water spiked with mercury tracer (^{203}Hg) under the same conditions as in the breakthrough experiment, and was recovered quantitatively with less than 8 bed-volumes of 0.1M hydrochloric acid containing 10% thiourea. Silver was also concentrated on a resin IV column (resin 1 g, 1×3.7 cm) from 15 litres of sea-water at a flow-rate of 20 ml/min. The silver retained

was eluted with 20 ml of 0.1M hydrochloric acid containing 1% thiourea, and determined by atomic-absorption spectrophotometry. It was found that the sea-water contained 0.02–0.05 μg of silver per litre, in reasonable agreement with published data (0.04 $\mu\text{g/l.}$)²⁰

Acknowledgement—The authors thank the members of the Central Research Laboratory, Sumitomo Chemical Co., Osaka, Japan for measurement of the surface properties of the resins.

REFERENCES

1. J. R. Parrish, *Chem. Ind. (London)*, 1956, 137.
2. M. Okawara, T. Nakagawa and E. Imoto, *Kogyo Kagaku Zasshi*, 1957, **60**, 73.
3. M. Okawara and Y. Sumitomo, *ibid.*, 1958, **61**, 1508.
4. G. J. De Jong and C. J. N. Rekers, *J. Chromatog.*, 1974, **102**, 443.
5. M. J. Benes, J. Stamberg, J. Peska, M. Tichy and M. Cikrt, *Angew. Makromol. Chem.*, 1975, **44**, 67.
6. E. M. Moyers and J. S. Fritz, *Anal. Chem.*, 1976, **48**, 1117.
7. K. Hayakawa and H. Yamakita, *J. Appl. Polym. Sci.*, 1977, **21**, 665.
8. K. Kaeriyama, T. Rokusha and K. Naomi, *ibid.*, 1978, **22**, 3075.
9. R. J. Phillips and J. S. Fritz, *Anal. Chem.*, 1978, **50**, 1504.
10. T. Saegusa, S. Kobayashi, K. Hayashi and A. Yamada, *Poly. J.*, 1978, **10**, 403.
11. Z. Slovák, M. Smrž, B. Dočekal and S. Slováková, *Anal. Chim. Acta*, 1979, **111**, 243.
12. H. Egawa, Y. Jogo and H. Maeda, *Nippon Kagaku Kaishi*, 1979, 1760.
13. Z. Slovák and B. Dočekal, *Anal. Chim. Acta*, 1980, **117**, 293.
14. A. Deratani and B. Seville, *Anal. Chem.*, 1981, **53**, 1742.
15. M. Nakayama, M. Chikuma and H. Tanaka, *Talanta*, 1982, **29**, 503.
16. A. Sugii, N. Ogawa and H. Hashizume, *ibid.*, 1980, **27**, 627.
17. C. Ainsworth, *Org. Synth.*, 1960, **40**, 99.
18. B. K. Gupta, D. S. Gupta and U. C. Agarwala, *Bull. Chem. Soc. Japan*, 1978, **51**, 2724.
19. R. B. Singh, B. S. Garg and R. P. Singh, *Talanta*, 1978, **25**, 619.
20. P. G. Brewer, *Chemical Oceanography*, J. P. Riley and G. Skirrow (Eds.), 2nd Ed., Vol. 1, p. 418. Academic Press, London, 1975.

Table 4. Sorption of metal ions from acetate buffer (pH 7) in the presence of EDTA with resin IV

[EDTA] [Metal]	Metal sorption, %			
	Cu(II)	Ag(I)	Cd(II)	Hg(II)
—	100	99.9	100	99.9
1	11.3	100	4.0	99.9
3	1.3	100	0	99.9
5	0	100	0	99.9
10	0	99.9	0	99.8

Metal solutions: $1 \times 10^{-3}M$, 10 ml. Shaking time: 24 hr.

MULTIPARAMETRIC CURVE FITTING—VI. MRFIT AND MRLET, COMPUTER PROGRAMS FOR ESTIMATION OF THE STABILITY CONSTANT OF THE PREDOMINANT M_pL_q COMPLEX AND THE LIGAND PURITY BY ANALYSIS OF PHOTOMETRIC TITRATION CURVES

MILAN MELOUN

Department of Analytical Chemistry, College of Chemical Technology, 532 10 Pardubice, Czechoslovakia

and

MILAN JAVŮREK

Computing Centre, College of Chemical Technology, 532 10 Pardubice, Czechoslovakia

(Received 23 September 1983. Revised 12 May 1984. Accepted 1 June 1984)

Summary—MRFIT and MRLET, two FORTRAN computer programs, can analyse a photometric mole-ratio curve (photometric titration curve) to estimate the stability constant β_{pq} of the predominant complex M_pL_q , the ligand concentration factor f_L , the extrapolated absorbance A_{ext} and the stoichiometric coefficient q (p is usually 1). MRFIT uses algorithmic minimization of a residual-square sum to reach, usually, the global minimum or the lowest of several local ones. MRLET, an ABLET system program based on LETAG, allows algorithmic and/or heuristic minimization. A local minimum described by parametric co-ordinates with a definite physical meaning might be found by the heuristic process.

The mole-ratio method introduced by Yoe and Jones^{1,2} for spectrophotometric investigation of complex-formation equilibria has been frequently used,³⁻⁹ and is known as photometric titration in analytical chemistry. It is based on graphical interpretation of the absorbances observed when the concentration of one component of the complex is varied while that of the other is held constant.

If the system forms a sufficiently stable complex, such a plot gives a sharp break and the mole ratio at the break corresponds to the composition of the complex. If, however, a weak complex is formed, only a curved plot results (Fig. 1). Previous papers in this area have been reviewed by Momoki *et al.*⁹ who also suggested a new generalized approach to the mole-ratio method to allow computer-assisted treatment.

We introduce here two FORTRAN programs that use different mathematical approaches to the minimization of a residual-square sum function. The program MRFIT is easy to apply because its algorithmic strategy works completely automatically, and minimization always leads to the global minimum or to the lowest of several minima. The parametric co-ordinates of the minimum always have mathematical meaning, although in some cases they may have no physical one.

The program MRLET, part of the ABLET system,¹⁰ allows application of an algorithmic strategy or a heuristic strategy, or a combination of the two.

This makes it possible to find a local minimum with parametric co-ordinates with definite physical meaning.¹⁰ Heuristic minimization requires some intervention by the user, to set the initial size of the minimization steps, the initial guesses for the parameters to be estimated or the value of the parametric steps for the final refinement of parameters.

THEORY

Mathematical model—equation of a photometric titration curve

A photometric titration curve is a graphical representation of the mole-ratio method. It shows how the

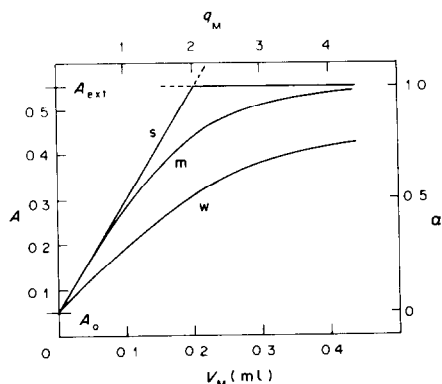
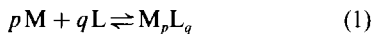


Fig. 1. Photometric mole-ratio curves shown in original (A ; V_M) and normalized (α ; q_M) co-ordinates for complex M_2L . Curves for strong (s), medium (m) and weak (w) complexes are shown.

absorbance changes as the mole ratio of the two components M and L of the complex M_pL_q is changed when the concentration of one is varied and the concentration of the other is held constant. Let us consider the formation of a single complex M_pL_q by the reaction



with (concentration) formation constant

$$\beta_{pq} = [M_pL_q]/([M]^p[L]^q) \quad (2)$$

$$\beta_{pq} = [M_pL_q]/\{(c_M - p[M_pL_q])^p (c_L - q[M_pL_q])^q\} \quad (3)$$

If the total concentrations of M and L are denoted by c_M and c_L , the mass-balance equations are

$$c_M = [M] + p[M_pL_q] = c_{M,b}V_M/V_0 \quad (4)$$

$$c_L = [L] + q[M_pL_q] = c_{L,w}f_L \quad (5)$$

where $c_{M,b}$ is the molar concentration and V_M the volume of the metal-ion solution added from the burette, V_0 is the initial titrand volume, $c_{L,w}$ is the nominal ligand concentration, calculated from the weight of reagent used and volume of solution made from it, and f_L is a concentration factor to allow for impurity in the reagent.

The mole ratio is $q_M = c_M/c_L$ and the normalized absorbance α is defined by the expression⁹

$$\alpha = [A(1 + V_M/V_0) - A_0]/(A_{ext} - A_0) \quad (6)$$

where A_0 is the initial absorbance and A_{ext} is the absorbance of a solution in which an excess of metal ion has been added to suppress dissociation of the complex. For constant ligand concentration the following function may be derived:

$$F = \alpha p/q + \alpha^{1/p}/[q\beta_{pq}c_L^{(p+q-1)/p}(1-\alpha)^{p/q}] - q_M = 0 \quad (7)$$

This describes the experimental relation $A = f(q_M)$ or the photometric titration curve $A = f(V_M)$. This mathematical model contains the dependent variable (A), the independent variable (V_M), and three unknown parameters, the overall stability constant (β_{pq}), the absorbance of the complex M_pL_q (A_{ext}), and the ligand concentration factor (f_L). The two stoichiometric coefficients of the complex, p and q , are usually suggested by the user and then validated by calculation; p is usually 1.

The relationship between absorbance and mole ratio is measured for constant total ligand concentration, and varied metal ion concentration, so the method is known as the "metal-changing method" (MCh). When the ligand concentration is varied and the metal-ion concentration is kept constant, the method is known as the "ligand-changing method" (LCh).⁹

If only one complex is formed (and it is very stable), the graph of $A = f(q_M)$ consists of two intersecting lines (Fig. 2). The ratio of the total concentrations of metal and ligand at the point of inter-

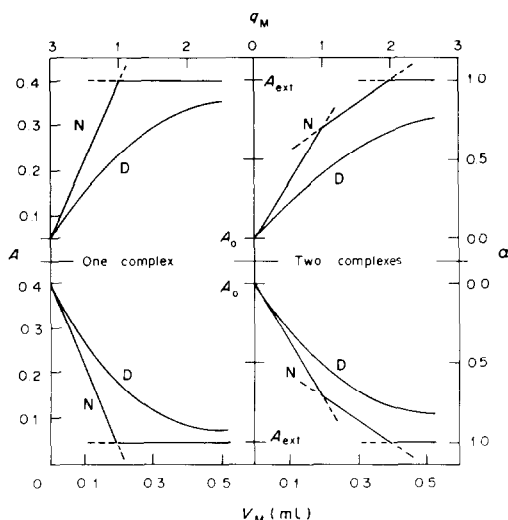


Fig. 2. Photometric mole-ratio curves shown in original (A ; V_M) and normalized (α ; q_M) co-ordinates for a single prevailing complex ML in solution (left half of figure) and a mixture of complexes ML and M_2L (right half), for strong (N) and weak (D) complexes in solution. The photometric titration curve is shown for the wavelength at which the complex absorbs (upper part) or at which the ligand absorbs (lower part).

section gives the metal-to-ligand ratio in the complex. If the complex is only moderately stable, a steep curve is obtained and the intersection of tangents to the initial and final sections can still give this ratio, but the uncertainty increases with decreasing stability. For weak complexes, this simple graphical method fails to give any reliable information. If N complexes are formed and the successive formation constants are sufficiently high for there to be little overlap of the equilibria, the curve consists of $(N + 1)$ segments. If a single complex predominates, regression evaluation of the mole-ratio curve can be used to estimate the three parameters β_{pq} , f_L , and A_{ext} .

Regression analysis

Regression analysis consists of the estimation of unknown parameters by minimizing the difference between experimental and calculated data. The theoretical justification for the procedure has recently been discussed.¹⁰

The experimental error in reading the burette is usually less than the error in the absorbance reading. Because an explicit expression of the absorbance $A = f(V_M)$ is not possible, the calculated absorbance A_{calc} is obtained by the Müller approximation¹¹ in both MRLET and MRFIT. The sum of weighted squared residuals

$$U = \sum_{i=1}^n w_i (A_{exp,i} - A_{calc,i})^2 = \text{minimum} \quad (8)$$

where w_i is the statistical weight, usually taken as unity, can be minimized by use of the least-squares procedure LETAG¹² for MRLET, and FIT¹³ for

MRFIT. The FIT subroutine uses only algorithmic minimization, and always finds the global minimum. The normal equations are linearized in FIT and transformed to the principal axis system. The subroutine contains a main loop for calculating alterations to parameters from the eigenvalues and eigenvectors of the normal equations, with reduction of the alterations if the linearity range is exceeded, and a minor loop for reducing the linearity ranges if it is found that the squared error obtained with the new parameters is greater than that for the old ones. The termination criterion is tested only in normal iterations.

The MRLET program, from the ABLET system,¹⁰ uses the pit-mapping algorithm LETAG,¹² and does the minimization with heuristic (steps controlled by the user) or algorithmic (steps controlled automatically by the program) control. Heuristic minimization may reach a local minimum with definite physical meaning, but the algorithmic process always finds the global minimum or lowest minimum of several, but this does not necessarily have a physical meaning. In the heuristic process, the user must decide whether it is sufficient to know the location of some local minimum or whether knowledge of the global minimum is required. The user has to supply initial guesses of the values of the parameters and the minimization steps, and an organizational framework to control the process from iteration to iteration.

For all the parameters involved here, a negative value has no physical meaning. For such parameters the MRLET program contains a safeguard to stop them from becoming negative during the minimization, and at the same time to check that the calculations are not carried too far from the minimum. The block doing this is called MIKO; it searches systematically, over the calculated second-degree surface, for the set of three parameters that gives the lowest value for U with no parameter negative.

DATA INPUT INSTRUCTIONS

MRFIT

The data cards required for MRFIT are as follows, and each photometric titration requires this sequence of cards.

1. *Title card*: TITLE (20A4)
2. *Termination card*: STOP, SINST.
3. *Titration conditions card*: NB, CMB, VO, AL, CLW, CORM, ALFMIN, ALMAX, P, Q.
4. *Data card*: for simulated data set: VM(I), I = 1, NB; for experimental data set: VM(I), AEX(I), I = 1, NB.
5. *Initial guess card*: BETAO, FLO, AEXTO.
6. *Simulation card*: for a simulated data set: BETA, FL, AEXT; for an experimental data set this card is omitted.

The *termination card* contains STOP values (the algorithm FIT terminates when the sum of squares of parameter alterations divided by their variances is less than the STOP value), and SINST, the standard deviation of the absorbances measured with the spectrophotometer used: SINST > 0 indicates that a simulated data set is used, and SINST ≤ 0 that the experimental data are used.

The *titration conditions card* contains ten experimental quantities: NB is the number of data points, CMB is the

molar concentration of metal solution in the burette, $c_{M,b}$, VO is the initial volume of titrand solution V_0 , AL is the initial absorbance of the ligand in the titrand before the titration is started, CLW is the total molar concentration of the ligand in the titrand, $c_{L,w}$, CORM is a correction factor relating the burette volumes $V_{M,i,read}$ to true volumes delivered [so $V_{M,i} = VM(I) \cdot CORM$], ALFMIN is the lower limit α_{min} of the curve interval to be analysed numerically and ALFMAX is the upper limit α_{max} , and P and Q are stoichiometric coefficients p and q of the complex M_pL_q .

The *data card* contains experimental pairs of titration-curve points; VM(I) is the volume $V_{M,i,read}$ of metal solution added and AEX(I) is the measured absorbance (when NB is written with a minus sign, transmittance is read in instead of absorbance). With simulated data, only the independent variable VM(I) is read here, and the dependent variable, absorbance, is generated by MRFIT.

The *initial guess card* contains the initial guesses of the three parameters to be estimated: $\beta_{pq}^{(0)}$, $f_L^{(0)}$, $A_{ext}^{(0)}$.

The *simulation card* contains preselected values BETA, FL, AEXT for the parameters β_{pq} , f_L , and A_{ext} . For experimental data, this card is omitted.

MRLET

Programs of the ABLET system all use similar data decks, as discussed previously.¹⁰ Only the three specific cards (the *simulation card*, *titration conditions card* and *data card*) are commented on in detail here.

1. *Title card*: TITLE (20A4).
2. *Keys card*: ISSW(I), I = 1, 6.
3. *Termination card*: EPS, PSI, SINST.
4. *Simulation card*: for a simulated data set: (XK(I), I = 1, 4), (SIGXK(I), I = 1, 4), (WEI(I), I = 1, 4). For an experimental data set this card is omitted.
5. *Titration conditions card*: for a simulated data set: NB, CMB, VO, AL, CLW, CORM, ALFMIN, ALFMAX, P, Q, FLO, AEXTO; for an experimental data set: 6, plus the same deck as for a simulated data set.
6. *Data card*: for a simulated data set: VM(I), I = 1, NB; for an experimental data set: VM(I), AEX(I), I = 1, NB.
7. *Initial guess card*: 7, 4, 4, AEXTO, FLO, LBETAO, QO.
8. *Matrix card*: ISKIN, (I(K), J(K), S(I(K), J(K))), K = 1, ISKIN.
9. *Step card*: 3, N, (I(K), STEK(I(K))), K = 1, N).
10. *Process card*: IRUR, IRUR, IRUR, ... (e.g., 2, 5, 13).

This set of cards constitutes one data block, and as many data blocks as desired may be executed, one after the other. The *simulation card* reads preselected values of four parameters in sequence (A_{ext} , f_L , $\log \beta_{pq}$, q) followed by their standard deviations $s(A_{ext})$, $s(f_L)$, $s(\log \beta_{pq})$, $s(q)$ and their weights $w(A_{ext})$, $w(f_L)$, $w(\log \beta_{pq})$, $w(q)$.

The *titration conditions card* contains the same quantities as for MRFIT. FLO and AEXTO here represent the initial guesses $f_L^{(0)}$, $A_{ext}^{(0)}$. For an experimental data set, this card must begin with the integer key 6.

The *data card* has the same content as for MRFIT.

The *initial guess card* contains the key 7 followed by the number of parameters to be refined and the number of positive parameters. Values of the initial guesses for particular parameters in the sequence $A_{ext}^{(0)}$, $f_L^{(0)}$, $\log \beta_{pq}^{(0)}$, $q^{(0)}$ follow.

The remaining cards have been described previously.¹²

EXPERIMENTAL

Photometric titration techniques

The mole-ratio curve for a complex-forming system may be measured by two methods.

(1) *The MCh (metal-changing) method*. The concentration of the ligand in the titration vessel is kept constant

and this solution is titrated with the metal-ion solution added from a burette.

(2) *The LCh (ligand-changing) method.* The concentration of metal-ion solution in the titration vessel is kept constant and the amount of ligand is gradually increased by addition from a burette.

There are two distinct experimental techniques for doing photometric titrations.

(1) *Titration done in the cell (internal MCh technique).* A known volume of ligand solution (2–30 ml) is placed in the spectrophotometer cell. For the total increase in volume during the titration to be small enough for the ionic strength and some equilibrium properties not to be seriously affected, the volume of metal solution added should be in the range 100–300 μ l. A stirrer and the capillary tip of the microburette are inserted in the cell (and a glass electrode if it is desired to check the pH during the titration). The geometric arrangement should be unchanged throughout the titration. If necessary, polyethylene inlet tubes are also inserted into the cap to allow the cell to be flushed with a solvent-saturated stream of inert gas.

(2) *Titration done outside the cell (external MCh technique).* A 150-ml double jacket titration vessel is connected to the photometer cell by polyethylene tubes or glass capillary tubes fitted with glass ball-joints. Tubes pass through the Teflon cell-stopper, one of them connecting the bottom of the cell to a 100-ml glass syringe. The titration of the ligand solution is done in this titration vessel, the reagents being mixed by passage of inert gas or by a mechanical stirrer. After each addition of metal ion solution and establishment of equilibrium, some solution is transported into the cell by overpressure of inert gas or by use of a syringe. The cell is rinsed several times with the solution from the titration vessel, the absorbances at various wavelengths are measured, and the solution is transported back into the vessel. The concentration of metal is then changed by adding solution from a microburette and the whole procedure is repeated.

APPLICATIONS

Some examples are given below of systems in which a predominant complex exists at equilibrium, and which were studied with the aid of MRFIT and MRLET.

Example 1. SNAZOXS–zinc complex, studied by the internal MCh technique.

The stability constant of the ML_2 complex and the ligand concentration factor are estimated by the MCh data-evaluation procedures of MRFIT and MRLET. The two minimization strategies, algorithmic and heuristic, are illustrated.

Experimental conditions. An initial volume of 4.00 ml (= VO) of $1.65 \times 10^{-4} M$ (= CLW) SNAZOXS, was titrated with $2.0 \times 10^{-3} M$ (= CMB) zinc added from a home-made microburette having a correction factor of 0.988 (= CORM). The titration was done in acetate buffer at pH 5.5, with $I = 0.1$ ($NaClO_4$), with measurement at 575 nm in a 1.000 cm cell at 25°; these experimental conditions are given in the title card. The absorbance before the titration was started was 0.670 (= AL).

Input data for MRFIT (Table 1). Program MRFIT will test the proposed chemical model and verify or reject the existence of complex ML_2 , the input data being $P = 1$, $Q = 2$, and the initial guesses $\beta_{12}^{(0)} = 10^8$ (= BETAO), $f_L^{(0)} = 1.0$ (= FLO), and $A_{ext}^{(0)} = 0.01$ (= AEXTO). Selected points from the total 24 (= NB) points of the photometric titration curve, between $\alpha_{min} = 0.01$ (= ALFMIN) and $\alpha_{max} = 0.99$ (= ALFMAX) will be used. The experimental data are executed, so SINST must be equal to -1 . The MRFIT algorithmic minimization is limited to 100 iterations (program code) or by the termination criterion 10^{-9} (= STOP) in the input.

Input data for MRLET (Tables 2 and 3). Program MRLET can perform an algorithmic (Table 2) or a heuristic (Table 3) minimization. In each iteration a print of the parameter values and the residual-square sum function is requested [ISSW(1) = 1] and also a print of the elements of the twist matrix [ISSW(2) = 1] and the determinant [ISSW(3) = 1]. When an algorithmic process is used, [ISSW(6) = 0], the minimization step in the next iteration is calculated either as a PSI fraction (PSI = 0.3) of the previous step [STEP(I) = PSI * STEP(I)], in which case ISSW(4) is equal to 0, or as a PSI fraction of the parametric standard deviation DARK2(I) calculated in the previous iteration [STEP(I) = PSI * DARK2(I)], in which case ISSW(4) is equal to 1. The key ISSW(5) is used for simulated data only. The minimization process is terminated when $|(U^{(i)} - U^{(i+1)})/U^{(i)}| \leq EPS$ (here $EPS = 10^{-6}$) or when 40 iterations have been performed. As experimental data are to be used, SINST is -1.0 . When no twist matrix elements are available, ISKIN is equal to 0 and the rest of the card may be omitted. The step card contains IRUR = 3 which calls the block STEG,

Table 1. MRFIT input data for Example 1

Card	Content of card
1. Title card	ZN + SNAZOXS, PH = 5.5, I = 0.1, 575 NM, 1.000 CM,
2. Termination card	1.0E-9, -1.0 ,
3. Titration conditions	24, 0.002, 4.0, 0.670, 1.65E-4 0.988, 0.01, 0.99, 1, 2,
4. Data card	0.0100, 0.628, 0.0296, 0.547, 0.0494, 0.468, 0.0692, 0.392, 0.0889, 0.318, 0.0988, 0.286, 0.1087, 0.255, 0.1136, 0.241, 0.1186, 0.227, 0.1235, 0.214, 0.1284, 0.202, 0.1334, 0.195, 0.1383, 0.182, 0.1433, 0.174, 0.1482, 0.164, 0.1531, 0.159, 0.1581, 0.151, 0.1680, 0.141, 0.1704, 0.138, 0.1754, 0.138, 0.1778, 0.139, 0.1877, 0.121, 0.1976, 0.117, 0.2075, 0.110,
5. Initial guess card	1.0E8, 1.0, 0.01,
6. Simulation card	For experimental data this card is omitted.

Table 2. MRLET input data for Example 1 (algorithmic minimization)

Card	Content of card
1. Title card	ZN + SNAZOXS, PH = 5.5, I = 0.1, 575 NM, 1.000 CM, ALGORITHMIC STRATEGY, MRLET
2. Keys card	1, 1, 1, 0, 1, 0,
3. Termination card	1.0E-6, 0.3, -1.0,
4. Titration conditions card	6, 24, 2.0E-3, 4.0, 0.670, 1.65E-4, 0.988,, 0.01, 0.99, 1, 2, 0.9, 0.01,
5. Data card	the same as Data card in Table 1.
6. Initial guess card	7, 4, 4, 0.01, 0.9, 9.0, 2.0,
7. Matrix card	0,
8. Step card	3, 3, 1, 0.04, 2, 0.01, 3, 0.2,
9. Process card	2, 5, 13,

Table 3. MRLET input data for Example 1 (heuristic minimization)

Card	Content of card
1. Title card	ZN + SNAZOXS, PH = 5.5, I = 0.1, 575 NM, 1.000 CM, HEURISTIC STRATEGY, MRLET
2. Keys card	1, 1, 1, 0, 1, 1,
3-7. The same as corresponding cards in Table 2.	
8. Step card + process card	3, 1, 3, 0.06, 2, 5,
9. Step card + process card	3, 3, 1, 0.04, 2, 0.01, 3, 0.2, 2, 5,
10. Final card	-1,

followed by the number of parameter steps ($N = 3$) and the number, $I(K)$, and numerical value $STEK(I(K))$ of each parameter step. This $STEK(I(K))$ step value is used in the first iteration only; in following iterations it is calculated as indicated above. The process card lists three IRUR numbers (2, 5, 13) which call three blocks; 2 calls UTTAG, *i.e.*, the starting value of the first central point of the residual-square sum function; 5 calls LETA for systematic variation of parameters and the minimization process; 13 calls SKRIK for output of the results and fitness test.

When a heuristic minimization is required the key ISSW(6) is set equal to 1 (*cf.* Table 3), and minimization steps and process keys IRUR are read from data cards in each iteration. One iteration is executed after reading in IRUR = 5, which calls the block LETA. The parameters do not all need to be refined at once. They are estimated one at a time, then in the final iteration all are refined together. This heuristic strategy is recommended, for example, when there are some ill-conditioned parameters in the model or when the pit-shape is skew or plate-like.

Example 2. The 7-(2-carboxyphenylazo)-8-hydroxyquinoline-5-sulphonic acid-copper(II) complex studied by the external MCh technique.

The stability constant of ML and the ligand correction factor are estimated by MRFIT analysis of mole-ratio curves measured at various wavelengths.

Experimental conditions. An initial volume of 20.00 ml (= VO) of $1.102 \times 10^{-4} M$ (= CLW) ligand solution, was titrated with $3.39 \times 10^{-3} M$ (= CMB) copper(II) added from a home-made syringe microburette with a correction factor of 0.01947 ml/mm (= CORM). The titration was done in acetate buffer at pH = 4.901, and $I = 0.1$ (NaClO₄) with measurement at 510 nm in a 1.000-cm cell at 25°. The initial absorbance was 1.210 (= AL).

Input data for MRFIT (Table 4). MRFIT will test the proposed chemical model ML, the parameters being $P = 1$, $Q = 1$, $\beta_{11}^{(0)} = 10^6$ (= BETAO), $f_1^{(0)} = 0.9$ (= FLO), $A_{ext}^{(0)} = 0.56$ (= AEXTO). Selected points from the total of 13 (= NB) on the photometric titration curve between $\alpha_{min} = 0.01$ (= ALFMIN) and $\alpha_{max} = 0.99$ (= ALFMAX) will be used for curve fitting. Because experimental data are used, SINST is

Table 4. MRFIT input data for Example 2

Card	Content of card
1. Title card	OB + CU, PH = 4.901, I = 0.1, 510 NM, 1.000 CM,
2. Termination card	1.0E-9, -1.0,
3. Titration conditions card	13, 3.39E-9, 20.0, 1.210, 1.102E-4, 0.01947, 0.01, 0.99, 1, 1,
4. Data card	2.22, 1.162,, 8.89, 1.019, 11.12, 0.971, 13.33, 0.924, 15.57, 0.878, 17.79, 0.831, 20.00, 0.785, 22.24, 0.738, 24.46, 0.694, 26.68, 0.652, 28.91, 0.620, 31.12, 0.592, 35.57, 0.559,
5. Initial guess card	1.0E6, 0.9, 0.56,
6. Simulation card	For experimental data this card is omitted.

Table 5. MRFIT input data for Example 3 (simulated data)

Card	Content of card
1. Title card	SIMULATED DATA SET, EXAMPLE 3,
2. Termination card	1.0E-9, 0.006,
3. Titration conditions card	28, 1.0E-3, 20.0, 0.0001, 1.0E-5, 1.000, 0.01, 0.99, 1, 1,
4. Data card	0.0222, 0.0355, 0.0450, 0.0569, 0.0686, 0.0808, 0.0934, 0.1064, 0.1200, 0.1344, 0.1405, 0.1500, 0.1533, 0.1566, 0.1601, 0.1636, 0.1671, 0.1708, 0.1746, 0.1785, 0.1825, 0.1866, 0.1910, 0.1954, 0.2001, 0.2049, 0.2100, 0.2153,
5. Initial guess card	1.5E6, 0.9, 0.95,
6. Simulation card	1.000E6, 1.0, 1.0,

– 1.0. The MRFIT minimization is algorithmic, limited to 100 iterations or by the termination criterion 10^{-9} (= STOP).

Example 3. Data simulation. The influence of the instrumental error of the spectrophotometer used, $s_{\text{inst}}(A)$, on the estimated parameters can be investigated by the use of simulated data, by MRFIT.

Experimental conditions. For parameters $\beta_{11} = 10^6$, $f_L = 1.0$, $A_{\text{ext}} = 1.0$ and various preselected values of the instrumental error, viz. $s_{\text{inst}}(A) = 10^{-6}$, 10^{-4} , 10^{-3} , 0.002, 0.004, 0.006, (= SINST), and with the rest of the experimental conditions kept constant (NB = 28, CMB = 0.001, VO = 20.0, AL = 0.0001, CLW = 0.00001, CORM = 1.0, ALFMIN = 0.01, ALFMAX = 0.99, P = 1, Q = 1, BETA0 = 1.5E6, FLO = 0.9, AEXT0 = 0.95) six mole-ratio curves are generated. After data simulation, a MRFIT minimization is done. The input data for simulation and minimization process are given in Table 5.

DISCUSSION

Table 6 shows the MRFIT output for Example 1. The first part lists the experimental conditions and the calculation conditions. All 24 experimental points are used in the regression analysis because they lie between α_{min} and α_{max} . TITRATION DATA lists the original co-ordinates $\{V_{M,\text{read}}, A_{\text{read}}\}$ of the photometric titration points and SELECTED POINTS lists the transformed co-ordinates $\{c_M; A\}$, the i th point having the co-ordinates $c_{M,i} = c_{M,b} * V_{M,\text{read},i} * \text{CORM} / V_0$ and $A_i = A_{i,\text{read}} (1 + V_{M,i,\text{read}} * \text{CORM} / V_0)$. MRFIT solves equation (7) by using equations (5) and (6) and the mole-ratio curve in transformed co-ordinates $\{c_M; A\}$.

INTERMEDIATE RESULTS gives the residual-square sum for the initial guesses of the parameters and for the fitted values found at the end of minimization.

OUTPUT lists the values of the parameters and their absolute and relative standard deviations. When the elements of the covariance matrix are negative, they are not printed, and the standard deviations of the parameters are also not defined. CURVE FITTING lists the experimental and calculated points of the photometric titration curve in the original $\{c_M; A\}$ and normalized $\{q_M; \alpha\}$ co-ordinates. The re-

siduals demonstrate the quality of the fit achieved. The degree of fit is tested objectively by the statistical analysis of the residuals.

MRFIT verified the proposed chemical model, that the ML_2 complex is formed in the photometric titration of zinc with SNAZOXs, when excess of ligand is present. The statistical tests show that the calculated and experimental points are very close: the mean value of the absorbance residuals is only 0.0012 (i.e., the arithmetic mean of the absolute values of the residuals), less than the instrumental error for the spectrophotometer used [$s_{\text{inst}}(A) = 0.002$ for the Zeiss VSU2-G spectrophotometer], and the standard deviation 0.0020 of the residual mean is of the same magnitude as the instrumental error. The other statistical tests also prove that the degree of fit is sufficiently good for the parameter estimates found to be considered reliable.

The statistical test of the degree of fit used here is an efficient diagnostic tool when a chemical model is sought, and it may be used as a criterion for comparison and selection of the best model from several plausible proposed ones.

From the numerical analysis of the photometric titration of zinc with SNAZOXs, it may be concluded that for the range from excess of ligand in solution to nearly equimolar solutions ($q_L = c_L/c_M = 31.6\text{--}1.54$) the ML_2 complex prevails in solution. This complex has a stability constant $\beta_{12} = 3.05 \times 10^9$, the concentration factor of SNAZOXs is $f_L = 0.947$ (this means that the SNAZOXs has a purity of 94.7%) and the extrapolated absorbance is $A_{\text{ext}} = 0.01205$ (Table 6).

Table 8 shows a MRLET output for Example 1. Experimental conditions and curve-point selection are the same as for MRFIT. Most of the MRLET output is self-explanatory, but some comments are appropriate. The control label RURIK indicates the sequence of operations in the minimization process. RURIK = 6 introduces block DATA, which reads the titration conditions card and data card and prints their content in the output. RURIK = 7 calls block LASK which reads the initial guesses of the four parameters to be refined, and RURIK = 3 reads and writes the minimization steps for the first iteration. RURIK = 2 causes calculation of the residual-square sum U_c for the central point in the first iteration, i.e., for the initial guesses of the parameters.

Table 6. Shortened MRFIT output for Example 1 (Table 1)

MRFIT PROGRAM							
MRFIT-TITLE: ZN + SNAZOXS, PH = 5.5, I = 0.1,575 NM, 1.000 CM,							
TYPE OF INPUT: EXPERIMENTAL DATA							
TITRATION VESSEL: TOTAL LIGAND CONCENTRATION (MOL/L) = 0.000165							
INITIAL VOLUME (ML) = 4.00							
INITIAL ABSORBANCE = 0.670							
BURETTE: FACTOR OF MICROBURETTE (ML PER 1 MM) = 0.988							
METAL STOCK SOLUTION(MOL/L) = 0.00200							
CURVE FITTING: SEGMENT OF CURVE TAKEN TO REGRESSION							
FROM ALPHAMIN = 0.0100							
TO ALPHAMAX = 0.9900							
TESTED STOICHIOMETRY OF COMPLEX P = , Q = ,							
NUMBER OF POINTS OF THE WHOLE TITRATION CURVE = 24							
NUMBER OF POINTS OF THE CURVE SEGMENT TAKEN TO REGRESSION = 24							
TERMINATION CRITERIA: MAXIMUM NUMBER OF ITERATIONS DECL. = 100							
PRECISION WHEN COVARIATION MATRIX IS CALCULATED = 1.0E-9							
INITIAL GUESS OF FIRST PARAMETER (STABILITY CONSTANT, K) = 1.0E8							
INITIAL GUESS OF SECOND PARAMETER (LIGAND FACTOR, FL) = 1.000							
INITIAL GUESS OF THIRD PARAMETER (ABSORBANCE EXTRAPOLATED) = 0.010							
INTERMEDIATE RESULTS:							
IN 23 ITERATIONS THE NORMAL EQUATIONS WERE ILL CONDITIONED							
IN 24 ITERATIONS THE CALCULATED ALTERATION OF PARAMETERS WAS GREATER THAN THE							
ESTIMATED LINEARITY RANGE							
RESIDUAL-SQUARED SUM/DEGREES OF FREEDOM WITH INITIAL GUESS: 4.283E-02 AND WITH FITTED							
PARAMETERS: 4.684E-06							
OUTPUT:							
	VALUE OF PARAMETER		VALUE OF STANDARD DEVIATION				
	GUESSED	FITTED	ABSOLUTE	RELATIVE			
K	1.0E08	3.0525E09	NOT FOUND	NOT FOUND			
FL	1.0000	0.94708	NOT FOUND	NOT FOUND			
AEXT	0.0100	0.01205	NOT FOUND	NOT FOUND			
CURVE FITTING IN ORIGINAL COORDINATES:				IN NORMALIZED COORDINATES:			
		ABSORBANCE				MOLE	RATIO
I	METAL	MEASURED	CALCUL.	RESIDUAL	ALPHA	(M/L)	(L/M)
1	4.94E-6	0.6296	0.6296	0.0000	0.0615	0.0316	31.6332
2	1.45E-5	0.5510	0.5510	0.0000	0.1809	0.0926	10.7963
3	2.41E-5	0.4736	0.4724	0.0012	0.3003	0.1543	6.4822
4	3.37E-5	0.3986	0.3966	0.0020	0.4155	0.2159	4.6315
5	4.34E-5	0.3249	0.3248	0.0001	0.5246	0.2779	3.5990
6	4.82E-5	0.2929	0.2920	0.0009	0.5745	0.3065	3.2411
7	5.31E-5	0.2618	0.2614	0.0004	0.6210	0.3395	2.9454
8	5.55E-5	0.2477	0.2472	0.0004	0.6425	0.3550	2.8169
9	5.79E-5	0.2336	0.2342	-0.0006	0.6624	0.3702	2.7014
10	6.03E-5	0.2205	0.2215	-0.0010	0.6817	0.3860	2.5908
11	6.27E-5	0.2083	0.2102	-0.0018	0.6989	0.4012	2.4928
12	6.51E-5	0.2013	0.1995	0.0019	0.7151	0.4167	2.4001
13	6.75E-5	0.1881	0.1897	-0.0016	0.7300	0.4321	2.3141
14	6.99E-5	0.1801	0.1809	-0.0009	0.7433	0.4473	2.2356
15	7.23E-5	0.1699	0.1728	-0.0028	0.7557	0.4628	2.1607
16	7.47E-5	0.1649	0.1653	-0.0004	0.7670	0.4783	2.0908
17	7.72E-5	0.1568	0.1586	-0.0017	0.7773	0.4939	2.0252
18	8.20E-5	0.1468	0.1468	0.0000	0.7952	0.5245	1.9068
19	8.32E-5	0.1437	0.1437	0.0000	0.7998	0.5324	1.8785
20	8.56E-5	0.1439	0.1439	0.0000	0.7996	0.5478	1.8253
21	8.68E-5	0.1450	0.1371	0.0079	0.8100	0.5554	1.8004
22	9.16E-5	0.1265	0.1288	-0.0023	0.8225	0.5864	1.7053
23	9.64E-5	0.1226	0.1219	0.0008	0.8331	0.6171	1.6206
24	1.01E-4	0.1156	0.1159	-0.0003	0.8422	0.6481	1.5431
FITNESS TEST BY THE STATISTICAL ANALYSIS OF RESIDUALS:							
RESIDUAL MEAN = 8.799E-5							
MEAN RESIDUAL = 0.0012							
STANDARD DEVIATION = 0.0020							
SKEWNESS = 2.348							
KURTOSIS = 10.281							
PEARSON'S CHI-SQUARE OBSERVED = 8.00							
THEORETICAL = 12.60 (FOR 6 D.F. AND 0.95							
PROBABILITY LEVEL)							
HAMILTON'S R-FACTOR = 0.007256							

Table 7. Results calculated for Example 2 [$r = 10^3(A_{\text{exp}} - A_{\text{calc}})$]

Wavelength (in nm)	510					520			540		
A_0	1.210					1.200			0.550		
i	$v_M(\text{ml})$	$c_M \times 10^5$	q_M	α	A_{exp}	r	A_{exp}	r	A_{exp}	r	
1	0.0432	0.733	0.0727	0.0728	1.162	0.0	1.134	0.0	0.516	0.0	
2	0.1731	2.934	0.2911	0.2888	1.019	1.5	0.937	2.4	0.414	0.4	
3	0.2165	3.670	0.3641	0.3609	0.971	1.1	0.872	3.0	0.381	1.2	
4	0.2595	4.399	0.4364	0.4322	0.924	0.9	0.806	1.6	0.347	0.4	
5	0.3031	5.138	0.5098	0.5041	0.878	1.9	0.742	2.5	0.314	0.9	
6	0.3464	5.871	0.5824	0.5749	0.831	1.1	0.677	1.2	0.281	0.8	
7	0.3894	6.600	0.6548	0.6446	0.785	0.4	0.613	-0.3	0.248	0.2	
8	0.4330	7.340	0.7281	0.7141	0.738	-1.5	0.549	-2.0	0.214	-1.5	
9	0.4762	8.072	0.8008	0.7808	0.694	-2.2	0.488	-3.1	0.183	-1.2	
10	0.5195	8.805	0.8735	0.8433	0.652	-3.3	0.430	-4.2	0.153	-1.6	
11	0.5629	9.541	0.9465	0.8975	0.620	1.6	0.384	1.0	0.131	2.5	
12	0.6059	10.270	1.0188	0.9364	0.592	2.2	0.347	4.1	0.110	0.8	
13	0.6925	11.740	1.1356	0.9665	0.559	-1.1	0.301	-1.6	—	—	
$\beta_{11} \times 10^{-6}$						1.651 ± 0.278	1.743 ± 0.314			3.043 ± 1.064	
f_L						0.938 ± 0.005	0.941 ± 0.005			0.911 ± 0.009	
A_{ext}						0.5576 ± 0.0050	0.2832 ± 0.0069			0.0932 ± 0.0073	
Residual mean						2.041E-4	3.553E-4			1.163E-4	
Mean residual						0.0014	0.0021			0.0009	
Standard deviation						0.0017	0.0024			0.0011	
Skewness						-0.354	0.075			0.536	
Kurtosis						2.001	1.924			2.617	
Pearson's chi-square observed						2.38	4.85			2.67	
theoretical						12.60	12.60			12.60	
Hamilton's R-factor						0.00199	0.00353			0.00385	

Table 8. Shortened MRLET output for Example 1 (Table 3)

MRLET PROGRAM					
MRLET-TITLE: ZN + SNAZOXS, pH = 5.5, I = 0.1, 575 NM, 1.000 CM, HEURISTIC S.					
TYPE OF INPUT: EXPERIMENTAL DATA					
xxxxxx RURIK - 6 xxxxxx DATA					
EXPERIMENTAL CONDITIONS:					
METAL—TOTAL CONCENTRATION IN BURETTE (MOL/L):					0.002000
LIGAND—TOTAL CONCENTRATION IN VESSEL (MOL/L):					0.000165
INITIAL ABSORBANCE:					0.6700
INITIAL VOLUME (ML):					4.000
FACTOR OF MICROBURETTE (ML PER MM):					0.988
CURVE SEGMENT LIMITS—ALPHAMIN:					0.0100
—ALPHAMAX:					0.9900
TESTED STOICHIOMETRIC COEFFICIENTS P = ..., Q = ...,					1 2
POINTS OF EXPERIMENTAL A-V CURVE:					
TITRATION DATA			SELECTED POINTS OF SEGMENT		
I	V(ML)	A READ	J	METAL(MOL/L)	A CORRECTED
1	0.0099	0.6280	1	0.00000494	0.6296
2	0.0289	0.5470	2	0.00001447	0.5510
3	0.0482	0.4680	3	0.00002411	0.4736
4	0.0675	0.3920	4	0.00003374	0.3986
5	0.0868	0.3180	5	0.00004342	0.3249
6	0.0964	0.2860	6	0.00004821	0.2929
7	0.1061	0.2550	7	0.00005306	0.2618
8	0.1110	0.2410	8	0.00005548	0.2477
9	0.1157	0.2270	9	0.00005785	0.2336
10	0.1206	0.2140	10	0.00006032	0.2205
11	0.1254	0.2020	11	0.00006269	0.2083
12	0.1302	0.1950	12	0.00006511	0.2013
13	0.1351	0.1820	13	0.00006753	0.1881
14	0.1398	0.1740	14	0.00006990	0.1801
15	0.1446	0.1640	15	0.00007232	0.1699
16	0.1495	0.1590	16	0.00007474	0.1649
17	0.1543	0.1510	17	0.00007716	0.1568
18	0.1639	0.1410	18	0.00008195	0.1468

Table 8 (contd.)

19	0.1664	0.1380	19	0.00008319	0.1437
20	0.1712	0.1380	20	0.00008561	0.1439
21	0.1736	0.1390	21	0.00008680	0.1450
22	0.1833	0.1210	22	0.00009164	0.1265
23	0.1929	0.1170	23	0.00009643	0.1226
24	0.2025	0.1100	24	0.00010127	0.1156

xxxxxx RURIK = 7 xxxxxx LASK (INITIAL GUESS):

NUMBER OF ESTIMATED PARAMETERS = 4
 NUMBER OF POSITIVE PARAMETERS = 4
 NUMBER OF TWIST MATRIX ELEMENTS IN DATA = 0
 INITIAL GUESS OF THE FIRST PARAMETER (AEXT) = 0.01
 INITIAL GUESS OF THE SECOND PARAMETER (FL) = 0.90
 INITIAL GUESS OF THE THIRD PARAMETER (LOG K) = 9.00
 INITIAL GUESS OF THE FOURTH PARAMETER (Q) = 2

xxxxxx RURIK = 3 xxxxxx STEG (STEPS OF PARAMETERS):

3 0.06

xxxxxx RURIK = 2 xxxxxx UTTAG (RESIDUAL-SQUARE SUM):

U = 4.14349E-02 PARAMETERS = 0.01000 0.90000 9.00000 2.00000

xxxxxx RURIK = 5 xxxxxx SKOTT (SHOT):

DET = 1.48072E-03

SIGY (STANDARD DEVIATION IN Y): 1.8379E-02

KBOM (PARAMETERS)	NUMBER	VALUE	DARR1	DARR2
	3	9.28609E0	2.86574E-02	2.86574E-02

xxxxxx RURIK = 3 xxxxxx STEG (STEPS OF PARAMETERS):

1 0.04 2 0.01 3 0.2

xxxxxx RURIK = 2 xxxxxx UTTAG (RESIDUAL-SQUARE SUM):

U = 2.19640E-02 PARAMETERS = 0.01000 0.90000 9.28609 2.00000

xxxxxx RURIK = 5 xxxxxx SKOTT (SHOT):

DET = 1.41416E-09

SIGY (STANDARD DEVIATION IN Y): 2.9333E-03

KBOM (PARAMETERS)	NUMBER	VALUE	DARR1	DARR2
	1	2.29424E-03	2.25108E-03	2.25108E-03
	2	9.26916E-01	5.13708E-03	5.13708E-03
	3	9.37156E 00	1.19959E-02	1.19959E-02

DET = 5.91280E-07

SIK (TWIST MATRIX ELEMENTS)

1 2 -1.74808E-01
 1 3 1.55984E-01
 2 3 -1.11772E-01

xxxxxx RURIK = 2 xxxxxx UTTAG (RESIDUAL-SQUARE SUM):

U = 3.37861E-04 PARAMETERS = 0.00249 0.92692 9.37156 2.00000

ALGORITHMIC PROCESS:

1 ITERATION	U = 3.37861E-04	PAR. = 0.00249	0.92692	9.37156	2.00000
2 ITERATION	U = 1.20580E-04	PAR. = 0.00110	0.94758	9.47373	2.00000
..
17 ITERATION	U = 5.40662E-06	PAR. = 0.01337	0.94569	9.49520	2.00000

xxxxxx RURIK = 13 xxxxxx SKRIK (OUTPUT):

PARAMETERS AND THEIR STANDARD DEVIATIONS:

AEXT = 0.01337 ± 0.00012
 FL = 0.94569 ± 0.00013
 LOG K = 9.49520 ± 0.00009
 Q = 2.00000 ± -1.00000

CURVE FITTING IN ORIGINAL AND NORMALIZED COORDINATES:

I	V(EXP)	A(EXP)	A(ACAL)	RESIDUAL	METAL	M/L	ALPHA
1	0.00988	0.6296	0.6296	0.0000	4.94E-6	0.0317	0.0616
2	0.02895	0.5510	0.5510	0.0000	1.45E-5	0.0928	0.1813
3	0.04821	0.4736	0.4724	0.0012	2.41E-5	0.1545	0.2990
4	0.06748	0.3986	0.3966	0.0020	3.37E-5	0.2162	0.4133
5	0.08685	0.3249	0.3247	0.0002	4.34E-5	0.2783	0.5256
6	0.09643	0.2929	0.2918	0.0011	4.82E-5	0.3090	0.5743
7	0.10611	0.2618	0.2612	0.0006	5.31E-5	0.3400	0.6217
8	0.11095	0.2477	0.2470	0.0007	5.55E-5	0.3555	0.6432
9	0.11569	0.2336	0.2339	-0.0003	5.79E-5	0.3707	0.6647
10	0.12063	0.2205	0.2212	-0.0007	6.03E-5	0.3866	0.6846

Contd.

Table 8 (contd.)

11	0.12538	0.2083	0.2099	-0.0015	6.27E-5	0.4017	0.7031
12	0.13022	0.2013	0.1992	0.0021	6.51E-5	0.4173	0.7137
13	0.13506	0.1881	0.1894	-0.0013	6.75E-5	0.4328	0.7338
14	0.13980	0.1801	0.1807	-0.0006	6.99E-5	0.4480	0.7461
15	0.14464	0.1699	0.1725	-0.0026	7.23E-5	0.4635	0.7616
16	0.14948	0.1649	0.1651	-0.0002	7.47E-5	0.4790	0.7692
17	0.15433	0.1568	0.1584	-0.0015	7.72E-5	0.4945	0.7815
18	0.16391	0.1468	0.1468	0.0000	8.20E-5	0.5252	0.7968
19	0.16638	0.1437	0.1437	0.0000	8.32E-5	0.5331	0.8015
20	0.17122	0.1439	0.1392	0.0047	8.56E-5	0.5486	0.8012
21	0.17359	0.1450	0.1371	0.0079	8.68E-5	0.5562	0.7995
22	0.18327	0.1265	0.1288	-0.0022	9.16E-5	0.5873	0.8276
23	0.19286	0.1226	0.1219	0.0007	9.64E-5	0.6180	0.8336
24	0.20254	0.1156	0.1159	-0.0003	1.01E-4	0.6490	0.8444

FITNESS TEST BY THE STATISTICAL ANALYSIS OF RESIDUALS:

RESIDUAL MEAN	= 8.241E-05
MEAN RESIDUAL	= 0.0010
STANDARD DEVIATION	= 0.0015
SKEWNESS	= 1.063
KURTOSIS	= 5.002
PEARSON'S CHI-SQUARE OBSERVED	= 4.00
THEORETICAL	= 12.60 (FOR 6 D.F. AND 0.95
	PROBABILITY LEVEL)
HAMILTON'S R-FACTOR	= 0.005379

Systematic variation of m particular parameters is done in block LETA, called by RURIK = 5. The label SKOTT introduces the "shots" fired for individual parameters in a particular step, and the relevant values of U are printed in tabular form. In each iteration ($m + 1$) ($m + 2$)/2 shots are performed, and after each iteration, current estimates of the parameters and statistics are printed: SIGY means the value of the standard deviation of the dependent variable $s(A)$ in the given iteration, KBOM lists the refined values of the parameters, and DARR2 their standard deviations.

The twist matrix is interpreted as a rotation of the axis to coincide with the long axis of the ellipse. When parameters are varied along the direction of the main axes of the ellipsoidal cross-section of the pit, the convergence will be improved. For this purpose the axes of the trial parameters must be transformed, and the elements above the diagonal of a new (twist) matrix are printed after the label SIK. The PROVA block performs a test of the U value reached in a particular iteration. The lowest value of U , once found, is stored. If the calculated set of trial parameters in the i th iteration gives a lower value of the U function than any previously found, it is accepted as the best set; if, however, the preceding ($i - 1$)th iteration gave a lower value of U , this previous set is accepted and printed by the label GAMLA KONSTANTER. If some earlier iteration gave the lowest U value, then that set of parameters is accepted and printed by the label SLUMPSKOTT.

The most efficient minimization strategy seems to be a combination of a heuristic and an algorithmic process. The ill-conditioned parameters, for example, are heuristically refined at the beginning of the minimization, and later an algorithmic refinement of all the parameters is performed.

When one of the termination criteria is fulfilled, the minimization process terminates. Label SKRIK produces a table of final estimates of the refined parameters, with their standard deviations and the degree-of-fit table produced by the statistical analysis of residuals. These tables are the same as in MRFIT.

The purpose of studying simulated data is (1) investigation of the influence of the instrumental error of the spectrophotometer used on the estimates of parameters refined, or (2) investigation of ill-conditioned parameters, or (3) testing the program validity and the reliability of parameter estimation. In the simulated data, the random error generated is used to load precise absorbance values. The resulting spread of points along the A vs. q_M curve is a good representation of real experimental data.

Table 9 shows how the calculated estimates of the three parameters depend on the simulated instrumental error, $s_{\text{inst}}(A)$. The set of generated random errors is statistically tested in order to find whether its distribution is Gaussian. The reliability of the calculated parameter estimates may be classified according to the agreement between the statistical characteristics of the set of random errors and the set of residuals. The original mole-ratio curve, along which the random errors are spread, should be identical with the calculated mole-ratio curve, so each residual should be of the same magnitude as the corresponding random error of the particular point but of opposite sign.

Because all the computational conditions were kept constant, and only $s_{\text{inst}}(A)$ was changed, Table 9 illustrates the effect of randomization. Well-conditioned parameters are estimated accurately within the tolerance of their standard deviations but ill-conditioned parameters are estimated with a great deal of uncertainty and not accurately. This illus-

Table 9. Influence of the instrumental error of the spectrophotometer on the values found for the parameters (Example 3)

$s_{\text{inst}}(A)$	1.0E-6	0.0001	0.001	0.002	0.004	0.006
DEVIATION MEAN	4.26E-9	3.43E-6	3.47E-5	6.94E-5	1.39E-4	2.08E-4
MEAN DEVIATION	6.00E-7	6.50E-5	0.00065	0.00129	0.00258	0.00387
STAND. DEVIATION	8.00E-7	7.80E-5	0.00078	0.00156	0.00312	0.00468
SKEWNESS	0.445	0.550	0.551	0.551	0.551	0.551
KURTOSIS	3.06	3.05	3.05	3.05	3.05	3.05
CHI-SQUARE (to be 12.6)	1.71	4.57	4.57	4.57	4.57	4.57
RESIDUAL-SQUARE SUM AT ACHIEVED PIT						
U	3.20E-10	6.43E-8	6.34E-7	2.53E-6	1.01E-5	2.37E-5
$s(A)$	3.58E-6	5.07E-5	0.00016	0.00032	0.00064	0.00097
VALUES OF ESTIMATED PARAMETERS						
$\beta_{11} \times 10^{-6}$	0.997 ± 0.000	0.999 ± 0.004	1.021 ± 0.044	1.045 ± 0.089	1.096 ± 0.185	1.218 ± 0.306
f_L	1.000 ± 0.000	1.000 ± 0.000	0.996 ± 0.006	0.996 ± 0.006	0.993 ± 0.012	0.988 ± 0.017
A_{ext}	1.000 ± 0.000	1.000 ± 0.000	0.992 ± 0.014	0.992 ± 0.014	0.983 ± 0.028	0.966 ± 0.039
STATISTICAL ANALYSIS OF RESIDUALS						
RESIDUAL MEAN	7.11E-7	2.85E-6	2.87E-6	3.83E-6	8.10E-6	-5.94E-5
MEAN RESIDUAL	3.73E-6	5.96E-5	0.000588	0.00117	0.00235	0.00367
STAND. DEVIATION	5.34E-6	7.58E-5	0.000752	0.00150	0.00300	0.00459
SKEWNESS	1.384	0.283	0.178	0.173	0.173	0.122
KURTOSIS	6.14	3.01	3.09	3.09	3.09	2.91
CHI-SQUARE (to be 12.6)	8.57	4.57	3.43	3.43	2.86	5.71
R-FACTOR	0.000009	0.00013	0.00129	0.00258	0.00516	0.00789

Table 10

	LETAGROP-SPEFO ¹⁴	MRLET	MRFIT
(1) Mathematical model	Mass-balance equations and Beer-Lambert Law	Recursive expression for photometric titration curve	
(2) Parameters refined			
Stability constants β_{pq} of:	All consecutive complexes	One prevailing complex ML_q	
Molar absorptivities ϵ_{pq} of:	All consecutive complexes	One prevailing complex ML_q	
Stoichiometric coefficients p, q :	For each complex by means of SPECIES SELECTOR ¹⁴	$p = 1$, q to be estimated	p and q are known constants
Effective concentration factor of ligand used, f_L	No	Yes	Yes
(3) Minimization procedure	LETAGROP program ¹⁴	LETAG routine ¹⁰	FIT routine ¹³
(4) Strategy of minimization process	Heuristic only	Heuristic and/or algorithmic	Algorithmic only
(5) Estimation reliability of parameters			
Statistical tests	No	Yes	Yes
(6) Simulation of experimental data	No	Yes	Yes
(7) Plot of fitted mole-ratio graph	No	Yes	Yes

trates the danger of applying algorithmic non-linear regression to experimental data, when the true values of the parameters sought are unknown.

CONCLUSIONS

The programs MRLET and MRFIT offer considerable advantages over LETAGROP-SPEFO,¹⁴ the most obviously comparable program. Table 10 compares and contrasts some of the features of the three programs.

REFERENCES

- J. H. Yoe and A. L. Jones, *Ind. Eng. Chem., Anal. Ed.*, 1944, **16**, 111.
- J. H. Yoe and A. E. Harvey, *J. Am. Chem. Soc.*, 1948, **70**, 648.
- A. S. Meyer and G. H. Ayres, *ibid.*, 1955, **77**, 2671.
- M. Bobtelsky and J. Jordan, *ibid.*, 1945, **67**, 1824.
- Idem*, *ibid.*, 1947, **69**, 2286.
- A. S. Meyer and G. H. Ayres, *ibid.*, 1957, **79**, 49.
- A. E. Harvey and D. L. Manning, *ibid.*, 1950, **72**, 4488.
- H. Diehl and F. Lindstrom, *Anal. Chem.*, 1959, **31**, 414.
- K. Momoki, J. Sekino, H. Sato and N. Yamaguchi, *ibid.*, 1969, **41**, 1286.
- M. Meloun and J. Čermák, *Talanta*, 1984, **31**, 947.
- S. D. Conte and C. D. Boor, *Elementary Numerical Analysis*, 2nd Ed., McGraw Hill, New York, 1972.
- J. Čermák and M. Meloun, *Sb. Věd. Pr., Vys. Šk. Chemickotechnol., Pardubice*, 1978, **39**, 41.
- J. Lang and R. Müller, *Computer Physics Commun.*, 1971, **2**, 79.
- L. G. Sillén and B. Warnqvist, *Acta Chem. Scand.*, 1968, **22**, 3032.

A NEW EXPERIMENTAL TECHNIQUE FOR VALIDATING EXCHANGE MODELS OF CARBON DIOXIDE BETWEEN THE ATMOSPHERE AND SEA-WATER

SAM BEN-YAAKOV and HUGO GUTERMAN

Department of Electrical and Computer Engineering, Ben-Gurion University of the Negev, Beer-Sheva, Israel

(Received 1 February 1984. Accepted 26 May 1984)

Summary—The mechanism of CO₂-exchange between the atmosphere and sea-water was re-examined by simultaneously measuring pH and pO₂ in artificial sea-water exposed to CO₂ and air atmospheres. The data were fitted to an exchange model by using both the differential and integral forms of the diffusion equation. It was found that the pH and pO₂ data support the assumption that the exchange for these gases is driven by the gradient of the partial pressure of the gas across the imaginary solution-gas boundary layer (the *z* layer) and is not affected by chemical reaction or hydration rate under the experimental conditions used, *viz.* 1–100 meq/l., alkalinity, pH 4.5–8.3 and *z*-layer thickness 2–500 μm. It is concluded that the rate of hydration of CO₂ plays an insignificant role in the exchange mechanisms between the atmosphere and the oceans.

Exchange of CO₂ between the gas and liquid phases is a fundamental process in many scientific and technological disciplines. The process is crucial in regulating CO₂ concentration in the oceans and atmosphere, a topic which has recently been of much concern in connection with the very high production of CO₂ due to the utilization of fossil fuel by modern technology.^{1,2} The fact that dissolved CO₂ undergoes hydration to produce carbonic acid and that the acid further dissociates into bicarbonate and carbonate ions, raises the question of possible effects of these reactions on the exchange process. The simplified model generally used to describe gas exchange between the gas and liquid phases is the film model.³ It consists of an imaginary stagnant solution layer (the *z* layer) separating the gas phase from the bulk of solution, both of which are assumed to be well mixed. The exchange process between the two phases is thus assumed to be controlled by molecular diffusion of the dissolved gas through the *z* layer. In the case of CO₂, this simple model is complicated by the fact that CO₂ reacts with the water and the transport process might therefore be dependent on the hydration kinetics as well as the migration rates of a number of species, such as HCO₃⁻ and CO₃²⁻. A number of investigators have studied this question analytically and experimentally. The proposed methods differ with regard to the assumptions made concerning the carbonate chemistry within the layer. Bolin,⁴ and Hoover and Berkshire⁵ assumed the pH to be constant within the layer, Quinn and Otto⁶ assumed electroneutrality, whereas Emerson's approach^{7,8} permitted alkalinity and ionic gradients within the *z* layer. The different models predict similar behaviour: a transport rate which is dependent on pH and the thickness of the boundary layer. Attempts to verify

the proposed models experimentally were made by Hoover and Berkshire⁵ and Liss.⁹ In both cases exchange of CO₂ was monitored by tagging the dissolved CO₂ with ¹⁴C and monitoring the residual radioactivity in solution after loss of CO₂ to the atmosphere. The experiments were done with solutions buffered at low and high pH (~5 and ~8 respectively).

It is questionable whether the experimental procedures used in previous studies are capable of simulating natural processes, for at least two reasons. First, it is unknown whether a tracer diffusion (¹⁴CO₂) is indeed quantitatively equal to bulk diffusion of CO₂.¹⁰ Secondly, application of a buffer to control the pH introduces an artificial restriction not found in natural environments such as oceans and lakes, in which the pH is mainly controlled by the carbonate system.¹⁰ A constant pH implies a constant H₂CO₃/HCO₃⁻ ratio independent of total CO₂ in sea-water, which is contrary to the behaviour of the oceans. Consequently, the results of these experiments may not reflect the actual behaviour of a solution such as sea-water in which the carbonate system is the main buffer. The purpose of the present study was to examine the process of CO₂ exchange between the atmosphere and sea-water over a large pH range under solution-chemistry conditions which simulate those of the oceans. This was accomplished by measuring simultaneously the partial pressures of CO₂ and O₂ in sea-water solutions which were exposed to overlying atmospheres of air and CO₂. The purpose of simultaneously monitoring pO₂ and pCO₂ was to permit the comparison of an inert gas (O₂ under these exchange conditions) and a chemically reactive gas (CO₂).

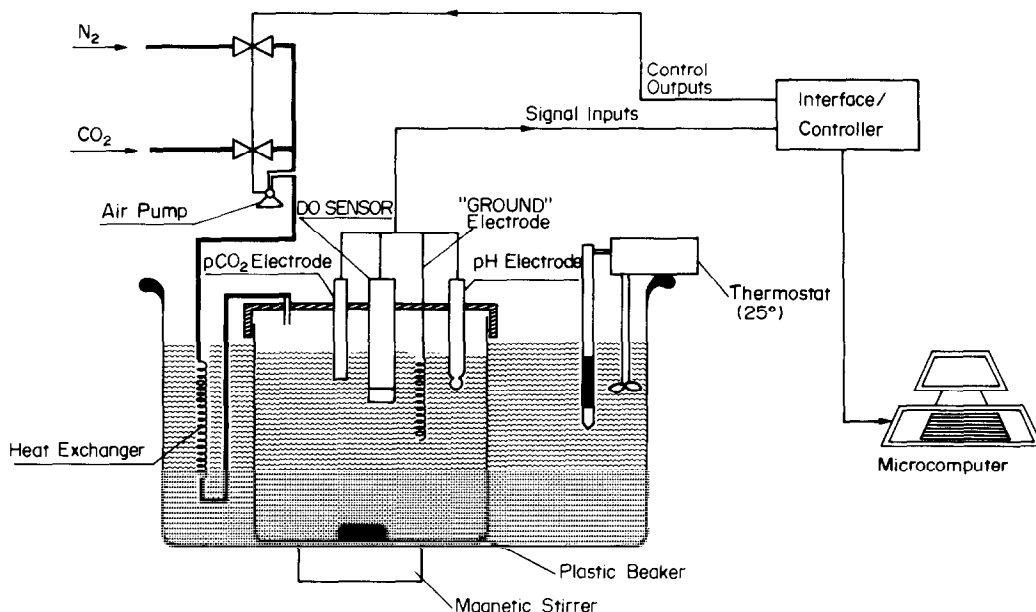


Fig. 1. Experimental assembly (DO SENSOR = dissolved oxygen sensor).

EXPERIMENTAL

The apparatus (Fig. 1) consisted of a covered beaker kept at constant temperature, pH and dissolved-oxygen electrodes, and a computerized data-acquisition system.¹¹ The experiments were done at 25° on 2-litre samples of artificial Mediterranean sea-water¹² with alkalinity in the range 1–100 meq/l. The solutions, stirred by a magnetic stirrer, were exposed to a CO₂ and air atmosphere at atmospheric pressure (*ca.* 980 mbar) and the resulting changes in pH and dissolved O₂ were monitored, with reading every 0.5–2 min. In some experiments, the exchange between the gas and liquid phases was accelerated by bubbling the gas through the solution. The pH change during the experimental runs was from pH 4.5 to pH 8.3. The dissolved-oxygen electrode was similar in design to the one described earlier.^{13,14} The membrane was a 2.4×10^{-3} cm (1 mil) thick Teflon film.

In some experiments pCO₂ was also measured directly with a membrane electrode (ORION, type 9502), but the results were not used in the regression analysis.

RESULTS AND DISCUSSION

The partial pressure of CO₂ (pCO₂) and concentration of total CO₂ (TCO₂) solution, during the experimental runs, were calculated from the carbonate alkalinity and pH by using the apparent constants of the carbonate system at the given salinity:¹⁰

$$p\text{CO}_2 = \frac{CA \times a_{\text{H}}^2}{K_1 \alpha_s [a_{\text{H}} + 2K_2]} \quad (1)$$

and

$$\text{TCO}_2 = CA \left[\frac{a_{\text{H}} K_1 + K_1 K_2 + a_{\text{H}}^2}{a_{\text{H}} K_1 + 2K_1 K_2} \right] \quad (2)$$

where CA = carbonate alkalinity; K_1 = first apparent dissociation constant of carbonic acid, K_2 = second apparent dissociation constant of carbonic acid, α_s = solubility of CO₂, a_{H} = hydrogen-ion activity.

The CO₂ and O₂ data for the transition from low to high pH (Fig. 2), were fitted to the simple gas-exchange model:³

$$\frac{dC}{dt} = -\frac{D_c}{z} (pc_b - pc_s) \alpha_c A / V \quad (3)$$

where C = concentration of the gas (mole/ml), D_c = diffusion coefficient of the gas c (cm²/sec), z = thickness of stagnant diffusion layer (cm), α_c = solubility of the gas c (mole.cm⁻³.atm⁻¹), pc = partial pressure of gas c (atm), A = area of the solution (cm²) in direct contact with the atmosphere, V = volume of solution (cm³) and the subscripts b and s denote the bulk solution and boundary layer respectively.

The model assumes that the driving force of the exchange process is dependent on the partial-pressure gradient of the pertinent gas across the z layer (or the

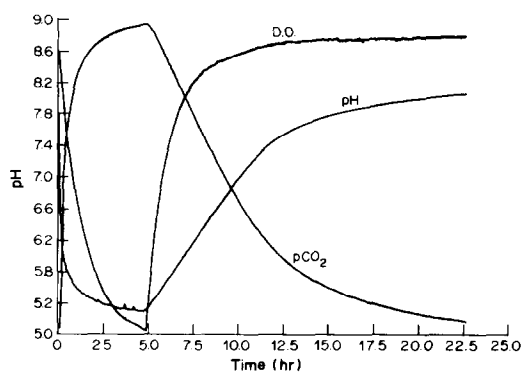


Fig. 2. Typical response of pH, pO₂ and pCO₂ of solutions to a change in the overlying atmosphere, in the sequence air-CO₂-air.

concentration gradient of $H_2CO_3^* = [CO_2(aq) + H_2CO_3]$ and neglects kinetic effects, and migration of ionized species such as HCO_3^- . It is also assumed that pCO_{2s} at any instant can be calculated from the pH and carbonate alkalinity. That means that hydration and ionization-rate effects are assumed to be insignificant in comparison with the overall time constant of the exchange process, *i.e.*, the carbonate system in the bulk solution can be considered to be in equilibrium at any instant.

The explicit equations for O_2 and CO_2 exchange are:

$$\frac{dO_2}{dt} = -\frac{D_{O_2}\alpha_{O_2}}{zh} pO_{2b} + \frac{D_{O_2}\alpha_{O_2}}{zh} pO_{2s} \quad (4)$$

$$\frac{dTCO_2}{dt} = -\frac{D_{CO_2}\alpha_{CO_2}}{zh} pCO_{2b} + \frac{D_{CO_2}\alpha_{CO_2}}{zh} pCO_{2s} \quad (5)$$

where

$$O_2 = pO_{2b}\alpha_{O_2} \quad (6)$$

and h = height of solution in beaker (Fig. 1).

The parameters D/z and pc_s were estimated for each experimental run by fitting the data to the linear equation:

$$y = ax + b \quad (7)$$

where $y = dTCO_2/dt$, $x = pc_b$, $a = -D_c\alpha_c/zh$, $b = D_c\alpha_c pc_s/zh$, from which we obtain

$$\frac{D_c}{z} = \frac{ah}{\alpha_c}$$

and

$$pc_s = b/a$$

where c denotes O_2 or TCO_2 .

The derivatives for each point were obtained by using a modified numerical differentiation method with an inherent smoothing effect,^{15,16} to reduce differentiation noise. The equation for the i th value for a backward numerical differentiation was established as

$$\frac{dC}{dt}(i) = \frac{1}{10t_s} [-2C(i-2) - C(i-1) + C(i+1) + 2C(2+i)] \quad (8)$$

where t_s is the sampling time.

A second approach to reduce the fitting scatter further was also used. It was based on the integral form of equations (4) and (5), which can be represented by:

$$TC = -\frac{D\alpha_c}{zh} \int pc_b dt + \frac{D\alpha_c}{zh} pc_s \int dt \quad (9)$$

or, in its numerical form:

$$TC_i = -\frac{D\alpha_c}{zh} \sum_0^i pc_b i + \frac{D\alpha_c}{zh} pc_s \sum_0^i i \quad (10)$$

In this case, the data were fitted to a two-variable

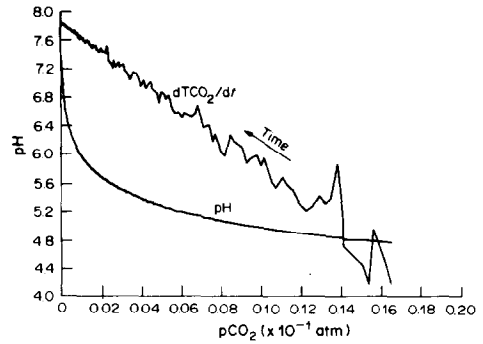


Fig. 3. Typical regression of $dTCO_2/dt = f(pCO_{2b})$ in the derivative form.

equation of the form:

$$y = ax_1 + bx_2 \quad (11)$$

with

$$y_i = TC_i,$$

$$x_{1i} = \sum_0^i pc_{b,i}$$

$$x_{2i} = \sum_0^i i,$$

$$a = D\alpha_c/zh,$$

$$b = D\alpha_c pc_s/zh.$$

Typical fitting curves for the differential and integral forms are depicted in Figs. 3 and 4.

The data from all the experiments were found to fit the simple model of equation (1) for both O_2 and CO_2 , which assumes that the flux is controlled solely by the partial-pressure gradient between the solution and gas phases (Tables 1 and 2). The excellent fit of the data to the model suggests that kinetic effects associated with the hydration rate of CO_2 are negligible over the range of conditions used in the experiments. It was found that by using this model along with the derived numerical values of D_{CO_2}/z for a given experiment, the change in TCO_2 during the experimental cycle can be accurately simulated (Fig.

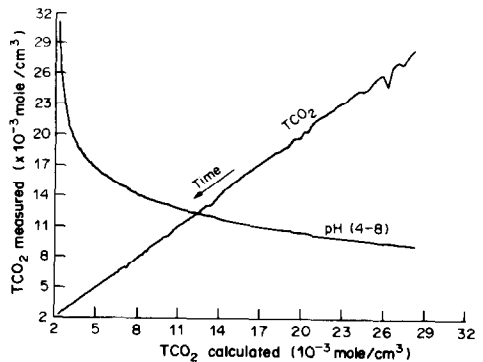


Fig. 4. Measured TCO_2 vs. predicted (TCO_2 calculated) during a typical experimental run.

Table 1. Summary of experimental results for O₂ exchange

Experiment	Gas		Alkalinity meq/l.	pH range	D_{O_2}/z^* , $10^{-3}cm/sec$	Correlation coefficient, R^2	Confidence limits†, %	$z\$,$ μm
	Atmosphere	Flow						
1	Air	Surface	10	5.4-7.0	2.88 ± 0.04	0.9918	> 99	73.6
1	CO ₂	Surface	10	5.6-7.8	2.62 ± 0.22	0.9920	> 20	80.9
2	Air	Surface	1	4.7-6.4	2.80 ± 0.07	0.9731	> 95	75.7
2	CO ₂	Surface	1	4.8-4.9	3.13 ± 0.37	0.9395	> 80	67.7
3	Air	Bubbles	1	4.4-5.7	38.7 ± 1.0	0.9930	> 90	5.56
3	CO ₂	Bubbles	1	4.4-7.4	45.6 ± 0.8	0.9976	> 80	4.64
4	Air	Bubbles	10	5.4-7.1	70.3 ± 4.6	0.9795	> 50	3.01
4	CO ₂	Bubbles	10	5.4-6.5	104.4 ± 2.9	0.9924	> 99	2.03
5	Air	Surface	100	6.6-7.8	3.95 ± 0.06	0.9940	> 98	53.7
5	CO ₂	Surface	100	6.6-7.1	7.53 ± 0.13	0.9968	> 80	28.2

* Limits are $\pm 2\sigma$.† Based on χ^2 test.§ Assuming $D_{O_2} = 2.12 \times 10^{-5} cm^2/sec$.

4). We conclude therefore that this model represents to a high degree of accuracy the process of gas exchange for both CO₂ and O₂. It is also found that the diffusion coefficients of the two gases (when expressed as a function of partial pressures) is numerically identical, within 3% (Table 3).

Rigorous statistical analysis of typical experimental runs did not reveal any significant difference between the data points at low pH and those at high

pH (Table 4). Such a difference should have been observed if previously suggested models were accepted.^{4,5}

The results of the present study seem to conflict with the conclusions of previous investigations although a direct comparison between our data and previous results is impossible owing to the difference in the experimental techniques used. Previous studies seem to suggest that a kinetic enhancement should be

Table 2. Summary of experimental results for CO₂ exchange

Experiment	Gas		Alkalinity meq/l.	pH range	D_{CO_2}/z^* , $10^{-3}cm/sec$	Correlation coefficient, R^2	Confidence limits†, %	$z\$,$ μm
	Atmosphere	Flow						
1	Air	Surface	10	5.4-8.0	2.63 ± 0.02	0.9926	> 90	73.6
1	CO ₂	Surface	10	5.6-7.8	3.16 ± 0.47	0.8224	> 0.1	80.9
2	Air	Surface	1	4.7-7.8	2.64 ± 0.02	0.9890	> 99	75.7
2	CO ₂	Surface	1	4.8-4.9	5.24 ± 1.60	0.6930	> 80	67.7
3	Air	Bubbles	1	4.3-7.6	35.2 ± 0.11	0.9990	> 98	5.56
3	CO ₂	Bubbles	1	4.4-7.4	48.6 ± 2.2	0.9984	> 95	4.64
4	Air	Bubbles	10	5.4-8.3	69.7 ± 0.25	0.9990	> 99	3.01
4	CO ₂	Bubbles	10	5.4-6.5	113.9 ± 3.1	0.9926	> 50	2.03
5	Air	Surface	100	6.6-8.3	3.71 ± 0.03	0.9906	> 95	53.6
5	CO ₂	Surface	100	6.6-7.1	5.38 ± 0.63	0.8809	> 5	28.1
6	Air	Surface	2.4	4.9-7.9	0.41 ± 0.001	0.9999	> 99	485†

* Limits are $\pm 2\sigma$.† Based on χ^2 test.§ Calculated from O₂ data assuming $D_{O_2} = 2.12 \times 10^{-5} cm^2/sec$.‡ Assuming $D_{CO_2} = 1.97 \times 10^{-5} cm^2/sec$.Table 3. Calculated ratio of O₂ and CO₂ diffusion coefficients

Experiment	Gas		Alkalinity meq/l.	$D_{O_2}/D_{CO_2}^*$	$z\$,$ μm
	Atmosphere	Flow			
1	Air	Surface	10	1.09 ± 0.02	73.6
1	CO ₂	Surface	10	0.82 ± 0.14	80.9
2	Air	Surface	1	1.06 ± 0.02	75.7
2	CO ₂	Surface	1	0.59 ± 0.20	67.7
3	Air	Bubbles	1	1.08 ± 0.03	5.56
3	CO ₂	Bubbles	1	0.93 ± 0.05	4.64
4	Air	Bubbles	10	1.00 ± 0.07	3.01
4	CO ₂	Bubbles	10	0.91 ± 0.04	2.03
5	Air	Surface	100	1.06 ± 0.02	53.7
5	CO ₂	Surface	100	1.39 ± 0.17	28.2

* Limits are $\pm 2\sigma$.† Assuming $D_{O_2} = 2.12 \times 10^{-5} cm^2/sec$.

Table 4. Statistical analysis of data sections of experiments 1 and 2, for surface flow of air, to examine possible variation of D as a function of pH.

Experiment	Alkalinity, meq/l.	No. of points	pH range	D_{CO_2}/z , 10^{-3} cm/sec	Correlation coefficient, R^2	Confidence limits,† %	F -test, %	z ‡, μm
1	10	150	5.4–6.9	2.62 ± 0.05	0.9880			73.6
1	10	150	6.9–7.8	2.70 ± 0.05	0.9862			73.6
1	10	150	7.8–8	2.34 ± 0.60	0.2883			73.6
1	10	450	5.4–8	2.62 ± 0.03	0.9880	> 90	< 10	73.6
2	1	160	4.7–6.4	2.64 ± 0.06	0.9828			75.7
2	1	160	6.4–7.3	2.61 ± 0.06	0.9809			75.7
2	1	160	7.3–7.8	3.64 ± 1.37	0.1524			75.7
2	1	480	4.7–7.8	2.64 ± 0.03	0.9828	> 95	< 10	75.7

* Limits are $\pm \sigma$.

† Based on χ^2 test.

‡ Assuming $D_{\text{O}_2} = 2.12 \times 10^{-5}$ cm²/sec.

observed at high pH for experiments with a z layer about 300 μm thick. Our results do not support such a conjecture, as we did not observe any difference between the results for high and low pH even for a z layer about 500 μm thick. Therefore, the question of kinetic enhancement can be excluded in discussion of CO_2 exchange between the atmosphere and the oceans, for which the z layer has been estimated to be in the range 30–70 μm thick.^{17,18} Hence the only CO_2 flux that should be considered in this case is the one directly associated with, and linearly proportional to, the pCO_2 gradient across the z layer. However, the time constant of the response of the oceans to change in atmospheric pCO_2 will none the less be dependent on the chemical reactivity of CO_2 in sea-water.¹⁹ As a result of hydration of CO_2 and subsequent ionization, the increase in pCO_2 due to CO_2 invasion is much smaller for the pH range of normal sea-water than the increase at low pH. It can be calculated, for example, that at pH 8.2 an increase of 1 $\mu\text{mole/l.}$ in the TCO_2 concentration in sea-water will result in an increase of 2.2 ppm in pCO_2 , whereas the same increase in TCO_2 will cause a change of 36 ppm in pCO_2 at pH 5. Consequently, the decrease in CO_2 flux due to increase in TCO_2 in the ocean will be slower, reducing the time required for reaching equilibrium.

Although the experimental results of the present study disagree with the results of previous investigations, the general conclusion concerning the minor effect of hydration rate on exchange of CO_2 between the atmosphere and the oceans, has already been stated by a number of investigators. The estimated thickness of the z layer in the oceans is about 70 μm , for which previous models also suggest a negligible kinetic enhancement. However, augmentation of the hydration rate could be important in other areas. It has been suggested, for example, that reflux of CO_2 from the urinary tract to the blood could be highly dependent on the kinetics of hydration of CO_2 .²⁰ In this case, the thickness of the

membranes through which the CO_2 diffuses is considerably larger than that of the z layer in the oceans, and the effect of rate of hydration could be important. A better assessment of the exchange mechanism may be obtainable when more experimental data for thick diffusion layers are available.

Acknowledgement—We wish to thank Neli Grinberg for laboratory assistance. The study was supported by a research grant from the Ministry of Energy and Infrastructure.

REFERENCES

1. J. Wehmiller, in *The Encyclopedia of Geochemistry and Environmental Sciences*, R. W. Fairbridge (ed.), pp. 125–129. Van Nostrand Reinhold, New York, 1972.
2. W. S. Broecker and T. Takahashi, in *The Fate of Fossil Fuel CO_2 in the Oceans*, N. R. Andersen and A. Malahoff (eds.), pp. 213–241. Plenum Press, New York, 1977.
3. P. V. Danckwerts, *Gas-Liquid Reactions*, McGraw-Hill, New York, 1970.
4. B. Bollin, *Tellus*, 1960, **12**, 274.
5. T. E. Hoover and D. C. Berkshire, *J. Geophys. Res.*, 1969, **74**, 456.
6. J. A. Quinn and N. C. Otto, *ibid.*, 1971, **76**, 1539.
7. S. Emerson, *Limnol. Oceanogr.*, 1975, **20**, 743.
8. *Idem*, *ibid.*, 1975, **20**, 754.
9. P. S. Liss, *Deep-Sea Res.*, 1973, **20**, 221.
10. G. Skirrow, in *Chemical Oceanography*, J. P. Riley and G. Skirrow (eds.), Vol. II. Academic Press, London, 1975.
11. S. Ben-Yaakov, R. Raviv, H. Guterman, A. Dayan and B. Lazar, *Talanta*, 1982, **29**, 267.
12. O. Amit and Y. K. Bendor, *Chem. Geol.*, 1971, **7**, 307.
13. S. Ben-Yaakov and E. Ruth, *Talanta*, 1980, **27**, 391.
14. S. Ben-Yaakov, *Bamidgeh*, 1979, **31**, 69.
15. F. Schied, *Numerical Analysis*, McGraw-Hill, New York, 1968.
16. R. Raviv and S. Ben-Yaakov, *Biotechnol. Bioeng.*, in the press.
17. J. Kanwisher, *Deep-Sea Res.*, 1962, **10**, 195.
18. W. S. Broecker and T. H. Peng, *Earth Planet. Sci. Lett.*, 1971, **11**, 99.
19. W. S. Broecker, Y. H. Li and T. H. Peng, in *Impingement of Man on the Oceans*, D. H. Hood (ed.), pp. 287–324. Wiley-Interscience, New York, 1971.
20. G. Malnic, *Am. J. Physiol.*, 1980, **239**, F307.

BEITRÄGE ZUR FRAGE DER EXISTENZ EINES TAUTOMERENGLEICHGEWICHTES IN LÖSUNGEN VON DITHIZON IN ORGANISCHEN SOLVENZIEN—I

DIE KORRELATION ZWISCHEN DEN LÖSUNGSMITTELABHÄNGIGEN REAKTIONSUNTERSCHIEDEN IN DEN SYSTEMEN PALLADIUM/DITHIZON UND KUPFER/DITHIZON UND DEN LÖSUNGSMITTELABHÄNGIGEN UNTERSCHIEDEN DER SPEKTREN DER DITHIZONLÖSUNGEN

H. WAGLER und H. KOCH

Zentralinstitut für Isotopen- und Strahlenforschung der AdW der DDR, Leipzig, DDR

(Eingegangen am 20. Dezember 1983. Revidiert am 23. April 1984. Angenommen am 7. Mai 1984)

Zusammenfassung—Beim Einsatz substöchiometrischer Reagenzmengen zeigten signifikante lösungsmittel- und milieuabhängige Reaktionsunterschiede in den Systemen Palladium/Dithizon und Kupfer/Dithizon differenziertes Reaktionsverhalten von Dithizon gegenüber Metallen an, was zunächst qualitativ auf die Existenz eines Tautomerenpaares in Dithizonlösungen hindeutet. Die Reaktionsunterschiede korrelieren eindeutig mit den Unterschieden in den Spektren der Dithizonlösungen. Gestützt auf diese Differenzen konnten die Aussagen zur Tautomerie über ein mathematisches Optimierungsverfahren zur Bandentrennung quantifiziert werden und erstmalig die Einzelspektren der beiden tautomeren Formen ermittelt werden.

Dithizon (Diphenylthiocarbazon, H_2Dz) wurde von Fischer¹ als photometrisches Reagens für Schwermetallspuren in die Analytik eingeführt und ist seitdem ein bekanntes und bewährtes Reagens geworden,² obwohl einige grundlegende Fragen des Reaktionsverhaltens bis heute noch nicht endgültig geklärt sind.

Die Frage bezüglich möglicher Tautomerie in Lösungen von Dithizon in organischen Solvenzien wurde von Irving³ noch unter die Rubrik der ungelösten Probleme eingeordnet.

Fischer⁴ hatte auf Grund des Reaktionsverhaltens von Dithizon gegenüber Metallen Thioketo-Thiol-Tautomerie angenommen, wogegen die Ergebnisse von IR-Untersuchungen, MO-Berechnungen, NMR-Untersuchungen und das Fehlen einer signifikanten Temperaturabhängigkeit der Spektren als Hinweis bzw. Beweis für das Vorliegen nur einer Spezies angesehen werden.⁵⁻⁹

Jedoch ist und bleibt die auffällige mit bekannten tautomeren Systemen korrelierende Lösungs-mittelabhängigkeit der Spektren der Dithizonlösungen (Abb. 1) bei Verneinung eines Tautomerengleichgewichtes *das* Problem,^{3,8-10} so daß die Frage bezüglich möglicher Tautomerie weiter im Disput ist.

Auf die Problematik der Tautomerie in Lösungen von Dithizon in organischen Solventien wurden wir beim Einsatz von Dithizon als Chelatbildner für substöchiometrische Abtrennungen aufmerksam.¹¹

Ausgangspunkt war die Aufgabenstellung gewesen, Kupferspuren in Halbleitermaterialien und Palladiumspuren in Katalysatormaterialien mittels quantitativer Isotopenverdünnungsanalyse durch Solventextraktion von Metallchelaten zu bestimmen.

Voraussetzungen für diese radiochemische Methode sind das Vorhandensein eines Radionuklides hoher spezifischer Aktivität des zu bestimmenden Elementes und eines Reagenses, das im Spurenbereich noch zu quantitativ einheitlichem und exakt stöchiometrischem Umsatz mit den Metallionen befähigt ist. Im Gegensatz zur Photometrie wird bei dieser Methode mit substöchiometrischen Reagenzmengen gearbeitet. Es gibt nur wenige geeignete Reagenzien für substöchiometrische Abtrennungen. Dithizon wurde von Růžicka und Starý als geeignetes Reagens empfohlen und auch schon vielfach bei substöchiometrischen Bestimmungen angewandt,¹²⁻¹⁵ wobei stillschweigend vorausgesetzt wurde, daß Dithizon quantitativ einheitlich reagiere, das heißt, kein Tautomerengleichgewicht vorliege bzw. die Reaktivität gegenüber Metallen auf die Thiol-Form beschränkt sei.

Bei unseren Voruntersuchungen zu den substöchiometrischen Bestimmungen deuteten Besonderheiten im System Palladium/Dithizon (siehe Tabelle 1) und signifikante Reaktionsunterschiede zu dem System Kupfer/Dithizon auf differenziertes Reaktionsverhalten von Dithizon gegenüber Metallen hin, so daß zunächst der Frage der Tautomerie

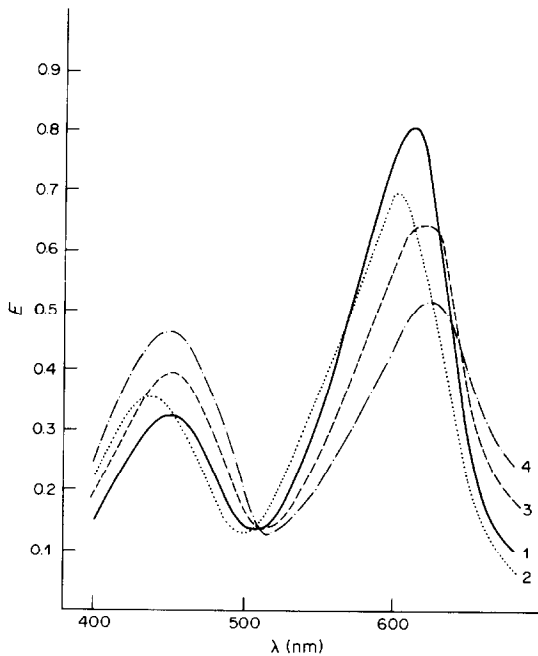


Abb. 1. Spektren $2 \cdot 10^{-5} M$ Dithizonlösungen: 1, H_2Dz in Chloroform; 2, H_2Dz in 2-Propanol; 3, H_2Dz in Tetrachlorkohlenstoff; 4, H_2Dz in Cyclohexan.

nachgegangen werden mußte, bevor die Erarbeitung fundierter substöchiometrischer Bestimmungen in Angriff genommen werden konnte; wobei vor allem die substöchiometrische Pd-Bestimmung mit Dithizon nicht unproblematisch ist.¹⁶

EXPERIMENTELLES

Reaktionsunterschiede in den Systemen Pd/ H_2Dz und Cu/ H_2Dz

Da auch geringe Reaktionsunterschiede erfaßt werden sollten, ergaben sich hohe Reinheitsanforderungen an alle verwendeten Glasgeräte und Chemikalien.

Für die *Reinigung von Dithizon* und das Herstellen der Stammlösungen hat sich die folgende Prozedur bewährt: Lösen des Dithizons in Chloroform, Reextrahieren mit

verdünnter Ammoniaklösung, Wiederausfällen durch Einleiten von SO_2 (unter Kühlung), Neutralwaschen des Dithizon-Niederschlags mit bidest. Wasser und Wasserfreiwaschen mit gekühltem Methanol. Anschließend wird mit dem organischen Solvenz methanolfrei gewaschen, das zur Bereitung der Stammlösung verwendet werden soll (gekühltes Lösungsmittel!), und die Stammlösung hergestellt. Die Arbeitslösungen, meist $2 \cdot 10^{-5} M$, wurden unmittelbar für jede Versuchsserie durch Verdünnen bereit.

Die Titerbestimmung erfolgte photometrisch und radiometrisch unter Einsatz von ^{110m}Ag . Für die photometrische Titerbestimmung wurden nicht nur die Extinktionen im Maximum aufgenommen, sondern das gesamte Spektrum zwischen 400 und 670 nm.¹¹

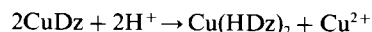
Die Stammlösungen wurden im Kühlschrank aufbewahrt und bis zu 14 Tagen verwendet. In dieser Zeit wurden keinerlei Titerverschiebungen beobachtet. In den verdünnten Arbeitslösungen konnten dagegen zum Teil Veränderungen (nicht oxydativer Art) beobachtet werden: bei H_2Dz in CCl_4 zu $E_{620}/E_{450} < 1.65$ und bei H_2Dz in C_6H_{12} zu "Rosa-Dithizon" mit λ_{max} bei 530 nm.²⁵

ERGEBNISSE

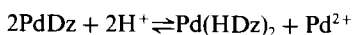
Zu den Reaktionsunterschieden in den Systemen Palladium/Dithizon und Kupfer/Dithizon

Auf deutliche Unterschiede in den beiden Systemen wiesen bereits Meriwether und Mitarbeiter²⁶ hin.

Die milieuhängige Gleichgewichtsverschiebung zwischen dem 1:2 und dem 1:1 Cu-Dithizonat verlief quantitativ:



wegen die Umwandlung des 1:1 Pd-Dithizonates durch Veränderung des pH-Wertes nur partiell und die des 1:2 Pd-Dithizonates in das 1:1 Pd-Dithizonat überhaupt nicht gelang:



nur zu ca. 25% (H_2Dz in $CHCl_3$)

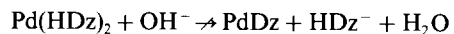


Tabelle 1. Beobachtete Besonderheiten im System Palladium/Dithizon (detailliertere Angaben in Zitat 11)

Besonderheiten im System Palladium/Dithizon	Literaturzitate ähnlicher Effekte im System Pd/ H_2Dz bzw. in anderen Me/ H_2Dz -Systemen
Schwierigkeiten bei der Festlegung der Stöchiometrie der Reaktion.	17-21
Differenzen zwischen radiometrisch und photometrisch ermittelten Pd-Gehalten der organischen Phase bei Zugabe stöchiometrischer und/oder überschüssiger Dithizonmengen → Abweichungen vom Beer'schen Gesetz.	21-23
Abweichungen beim Mischen äquimolarer Lösungen.	24
Komplexzusammensetzung nach der Job-Methode, saures Medium: photometrische Werte nicht interpretierbar, die radiometrischen Werte wiesen das Reaktionsoptimum für H_2Dz in $CHCl_3$ bei 0.69 Teilen Pd^{2+} und 0.81 Teilen H_2Dz und für H_2Dz in CCl_4 bei 0.525 Teilen Pd^{2+} und 0.975 Teilen H_2Dz aus.	
Im alkalischen Medium existiert kein 1:1 Pd-Dithizonat.	

Tabelle 2. Die umgekehrt proportional verlaufende Milieu- und Lösungsmittelabhängigkeit in den Systemen Pd/H₂Dz und Cu/H₂Dz

Organische Solvenzien für Dithizon	$\frac{E_{\max 1}}{E_{\max 2}}$	Extraktionszunahme für		Medium der wäßr. Phase
		Palladium	Kupfer	
Chloroform	2.5	↑	↓	sauer
Tetrachlorkohlenstoff	1.65			alkalisch
Cyclohexan	1.1			

Tautomerengleichgewichtsverschiebung
zugunsten der
Thioketo- Thiol-Form

Meriwether und Mitarbeiter fanden auch charakteristische Unterschiede in den IR-Spektren der 1:1 Dithizonate. Im IR-Spektrum des 1:1 Cu-Dithizonates konnte keine NH-Bande gefunden werden, wogegen im IR-Spektrum des 1:1 Pd-Dithizonates noch eine NH-Bande nachweisbar war.

Wie wir feststellen konnten, passen die Reaktionen zwischen Pd²⁺ und Dithizon, im Gegensatz zu denen von Cu²⁺ und Dithizon, nicht in das allgemeine Schema, das Iwantschew² für alle zweiwertigen Schwermetalle angibt: saures Medium und Reagensüberschuß → Bildung der 1:2 Dithizonate; alkalisches Medium und Reagensmangel → Bildung der 1:1 Dithizonate.

Meriwether und Mitarbeiter gehen davon aus, daß alle 1:1 Dithizonate zweiwertiger Metalle Verbindungen des Dianions von Dithizon seien, während Iwantschew beschreibt alle 1:1 Dithizonate mit einem Anion als Zweitligand.

Bei den 1:1 Dithizonaten müssen aber zwei Komplextypen unterschieden werden:

die Sub-Dithizonate: Beteiligung von Anionen an der Komplexbildung bei Reagensmangel, saures Medium, z.B. PdHDzX,

die sekundären Dithizonate: Verbindungen des Dianions, Bildung im alkalischen Milieu bei Reagensmangel, z.B. CuDz.

Die intensiven Studien zum Extraktionsverhalten in den Systemen Pd/H₂Dz in der Kombination Radiotracer-technik/Photometrie bei Vorgabe substöchiometrischer Reagensmengen (Einsatz äquimolarer Lösungen von Dithizon in verschiedenen organischen Solvenzien) bestätigten das differenzierte Reaktionsverhalten von Dithizon gegenüber Metallen. Die Milieu- und Lösungsmittelabhängigkeit verläuft umgekehrt proportional, woraus gefolgert werden kann, daß die beiden Metalle mit verschiedenen Tautomeren von Dithizon reagieren (Tabelle 2).

Auf Grund des chemischen Verhaltens von Dithizon, gestützt auf eigene NMR-Untersuchungen und unter Einbeziehen der Literaturangaben, wurde eine Zuordnung der Reaktionen zu denen der Thioketo- und denen der Thiol-Form möglich.¹¹

Im alkalischen Milieu liegt das Tautomerengleichgewicht ganz auf der Seite der Thiol-

Form, im sauren Medium verschiebt es sich zugunsten der Thioketo-Form.^{11,16} (Signifikante Strukturunterschiede der Säure-Base-Formen des Dithizons wurden kürzlich auch über Raman-spektroskopische Untersuchungen offenkundig.²⁷)

Schlußfolgerungen aus den Reaktionsunterschieden

Die Reaktionsunterschiede in den Systemen Palladium/Dithizon und Kupfer/Dithizon korrelieren eindeutig und unverkennbar mit dem Intensitätsverhältnis der beiden Maxima der VIS-Spektren der Dithizonlösungen (Abb. 1); demnach muß das Intensitätsverhältnis $R = E_{610}/E_{450}$ eine charakteristische Größe für die Tautomerenteilung sein.^{11,17,28,29}

Präzisierung der Tautomerenteilung in Lösungen von Dithizon in Chloroform, Tetrachlorkohlenstoff, Cyclohexan und 2-Propanol über die VIS-Spektren

Zu qualitativen als auch zu quantitativen Aussagen bezüglich der Lage eines Tautomerengleichgewichtes können chemische und verschiedene physikalische Methoden herangezogen werden. Konkrete Aussagen zu erhalten bereitet jedoch Schwierigkeiten, da durch chemische Reaktionen das Tautomerengleichgewicht verschoben werden kann und auch nicht alle physikalischen Methoden, wie z.B. IR-, NMR- und UV/VIS-Spektrometrie für jedes tautomere System mit gleichem Erfolg eingesetzt werden können.

Sowohl IR- als auch NMR-Untersuchungen bleiben für Dithizon auf Chloroformlösungen beschränkt, da die Löslichkeit in den anderen Lösungsmitteln zu gering ist (in Cyclohexan nur ~0,05 mM, in Tetrachlorkohlenstoff ~2mM und in Chloroform ~70mM). Allein die VIS-Spektrometrie bietet gute Untersuchungsmöglichkeiten.

Ausgehend von den charakteristischen lösungsmittelabhängigen Unterschieden in den VIS-Spektren können Aussagen zur Lage des Tautomerengleichgewichtes gewonnen werden.

Bisher wurde bei Annahme der Existenz eines Tautomerengleichgewichtes in Dithizonlösungen je eine Bande des sichtbaren Spektrums je einem Tautomeren zugeordnet.^{3,10,28-32}

Tabelle 3. Tautomerenverteilung nach der (in diesem Fall unbefriedigende Ergebnisse liefernden) Methode von Fabian

Organische Solvenzien für Dithizon	$\lambda_{\max 1}$, nm	$\epsilon_{\max 1}$, l. mole ⁻¹ . cm ⁻¹	$\lambda_{\max 2}$, nm	$\epsilon_{\max 2}$, l. mole ⁻¹ . cm ⁻¹	ϵ_1/ϵ_2	Thioketo-Form, %
Chloroform	605	4.0×10^4	445	1.6×10^4	2.5	71.9 (1)
2-Propanol	600	3.5×10^4	440	1.75×10^4	2.0	66.4 (2)
Tetrachlorkohlenstoff	620	3.3×10^4	450	2.0×10^4	1.65	62.1 (3)
Cyclohexan	630	2.6×10^4	450	2.35×10^4	1.1	52.6 (4)

Berechnungsversuch der Tautomerenverteilung bei Zuordnung je einer Bande zu je einem Tautomeren

In Anlehnung an die Berechnung des Prozentgehaltes an Enol in Monothioacetylaceton in verschiedenen organischen Solvenzien, wie sie von Fabian³³ ausgeführt wurde, soll die Berechnung über die Extinktionen der Maxima erfolgen. Für Dithizon müßte die Zuordnung des Maximums 1 (ϵ_1) zur Thioketo-Form und des Maximums 2 (ϵ_2) zur Thiol-Form erfolgen. Es ergäbe sich:

$$\% \text{ Thioketo-Form} = \epsilon_{\max 1} / (\epsilon_{\max 1} + \epsilon_{\max 2}).$$

Fabian weist darauf hin, daß diese Berechnungsmethode nur dann befriedigende Ergebnisse liefert, wenn 3 Voraussetzungen erfüllt sind.

1. Bei den einzelnen Maxima darf nur eine tautomere Form absorbieren.
2. Die molaren Extinktionskoeffizienten beider Tautomerer müssen gleich sein.
3. Die lösungsmittelabhängigen Unterschiede in der molaren Absorption jedes einzelnen Tautomerer müssen vernachlässigbar sein.

Zur Überprüfung der Gültigkeit der in die Rechnung eingegangenen Voraussetzungen wurden die nach der Formel von Fabian berechneten Prozentgehalte an Thioketo-Form (Tab. 3) in Abhängigkeit der Extinktionen in den Maxima (für $1 \cdot 10^{-3} M$ Lösungen)

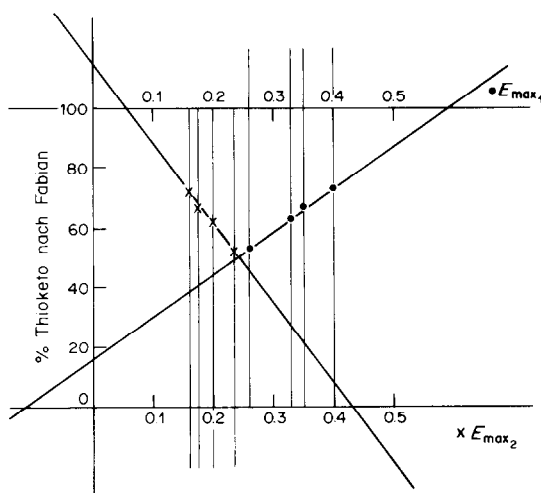


Abb. 2. Überprüfung der Zuordnungsmöglichkeit je einer Bande der VIS-Spektren von Dithizonlösungen zu je einem Tautomeren.

aufgetragen (Abb. 2), wobei sich zeigt, daß die ersten beiden Voraussetzungen nicht erfüllt sind, da die Geraden in Abb. 2 weder durch Null noch durch 100% (Koordinatenursprung) gehen, noch die Achsen bei gleichen Extinktionen schneiden.

Die Zuordnung je einer Bande zu je einem Tautomeren ist demnach für Dithizon nicht zulässig und die somit berechneten Prozentgehalte sind unkorrekt.

MATHEMATISCHES OPTIMIERUNGSVERFAHREN ZUR BANDENTRENNUNG

Berechnung der prozentualen Tautomerenverteilung in den vier verwendeten Dithizonlösungen und Ermittlung der Einzelspektren der Thioketo- und der Thiol-Form

Die VIS-Spektren der Dithizonlösungen werden hierbei als Linearkombination der entsprechenden Anteile der Einzelspektren der Thioketo- und der Thiol-Form aufgefaßt. In die Rechnung werden die Extinktionswerte der vier verwendeten Dithizonlösungen ($2 \cdot 10^{-5} M$) zwischen 400 und 670 nm in Schritten von 10 nm (28 Meßwerte) eingegeben, gesucht sind die Extinktionen für die Einzelspektren und die prozentuale Verteilung der beiden tautomeren Formen in den vier Dithizonlösungen.

In die Berechnung geht nur noch die eine Annahme ein, daß die Unterschiede in der molaren Absorption jedes Tautomerer in den verschiedenen organischen Lösungsmitteln vernachlässigbar sind.

Wären die molaren Absorptionen sowohl der Thioketo- als auch der Thiol-Form in allen organischen Lösungsmitteln voll identisch, müßten die Spektren verschiedener äquimolarer Lösungen exakt ausgeprägte isosbestische Punkte aufweisen.

Die Spektren der Lösungen von Dithizon in Chloroform, Tetrachlorkohlenstoff und Cyclohexan weisen auch zwei isosbestische Punkte auf (Abb. 1), wobei allerdings der Punkt um 630 nm etwas verschoben ist, da er sich in diesem Bereich aus Schnittpunkten von 3 Kurven mit etwa gleich großem $dE/d\lambda$ zusammensetzt und demzufolge sowohl gegen Abweichungen in E als auch in λ sehr empfindlich ist.

Dagegen wird deutlich, daß das gesamte Spektrum von Dithizon in 2-Propanol zu kleineren Wellenlängen hin verschoben ist. Wird eine entsprechende Korrektur vorgenommen (Verschieben des gesamten Spektrums um 10 nm), geht auch dieses Spektrum durch die isosbestischen Punkte (Abb. 3). In die Rechnung wurden für Dithizon in 2-Propanol diese korrigierten Extinktionswerte eingegeben. Als Richt-

werte für entsprechende Korrekturen solcher "reinen" Lösungsmittelleffekte kann der isosbestische Punkt im Minimum dienen.

Zur Verfügung stehen die folgenden Gleichungen:

$$E_{400}(\text{CHCl}_3) = E_{400}(\text{keto}) \cdot C_{\text{keto}}(\text{CHCl}_3) + E_{400}(\text{thiol}) \cdot C_{\text{thiol}}(\text{CHCl}_3)$$

$$E_{410}(\text{CHCl}_3) = E_{410}(\text{keto}) \cdot C_{\text{keto}}(\text{CHCl}_3) + E_{410}(\text{thiol}) \cdot C_{\text{thiol}}(\text{CHCl}_3)$$

$$\vdots$$

$$E_{670}(\text{CHCl}_3) = E_{670}(\text{keto}) \cdot C_{\text{keto}}(\text{CHCl}_3) + E_{670}(\text{thiol}) \cdot C_{\text{thiol}}(\text{CHCl}_3)$$

$$E_{400}(\text{CCl}_4) = E_{400}(\text{keto}) \cdot C_{\text{keto}}(\text{CCl}_4) + E_{400}(\text{thiol}) \cdot C_{\text{thiol}}(\text{CCl}_4)$$

$$\vdots$$

$$E_{670}(\text{CCl}_4) = E_{670}(\text{keto}) \cdot C_{\text{keto}}(\text{CCl}_4) + E_{670}(\text{thiol}) \cdot C_{\text{thiol}}(\text{CCl}_4)$$

$$E_{400}(\text{C}_6\text{H}_{12}) = E_{400}(\text{keto}) \cdot C_{\text{keto}}(\text{C}_6\text{H}_{12}) + E_{400}(\text{thiol}) \cdot C_{\text{thiol}}(\text{C}_6\text{H}_{12})$$

$$\vdots$$

$$E_{670}(\text{C}_6\text{H}_{12}) = E_{670}(\text{keto}) \cdot C_{\text{keto}}(\text{C}_6\text{H}_{12}) + E_{670}(\text{thiol}) \cdot C_{\text{thiol}}(\text{C}_6\text{H}_{12})$$

$$E_{400}(\text{2-Prop.}) = E_{400}(\text{keto}) \cdot C_{\text{keto}}(\text{2-Prop.}) + E_{400}(\text{thiol}) \cdot C_{\text{thiol}}(\text{2-Prop.})$$

$$\vdots$$

$$E_{670}(\text{2-Prop.}) = E_{670}(\text{keto}) \cdot C_{\text{keto}}(\text{2-Prop.}) + E_{670}(\text{thiol}) \cdot C_{\text{thiol}}(\text{2-Prop.})$$

Verallgemeinert mit $C_{\text{thiol}} = 1 - C_{\text{keto}}$, ergibt sich

$$E_{ij} = E_{ik} \cdot C_{kj} + E_{ith} \cdot (1 - C_{kj})$$

wobei i = Wellenlängen von 400 bis 670 nm; j = Lösungsmittel (CHCl_3 , CCl_4 , C_6H_{12} , 2-Propanol); k = Thioketo-Form; th = Thiol-Form.

In diesen Gleichungen sind also zunächst sowohl die C_{kj} -Werte (Prozentgehalte Thioketo-Form in den verschiedenen Lösungsmitteln) als auch die E_{ik} - und E_{ith} -Werte (Extinktionen der Einzeltautomeren bei verschiedenen Wellenlängen) unbekannt.

Anhand unserer chemischen Experimente können Richtwerte gewisser Varianzbreite für die Prozentgehalte an Thioketo-Form vorgegeben werden (Tab. 4), so daß man für je eine Wellenlänge ein lineares Gleichungssystem aus 4 Gleichungen mit den beiden Koeffizienten E_{ik} und E_{ith} erhält. Dieses Gleichungssystem läßt sich nach der Methode der kleinsten Fehlerquadrate lösen, wobei die beiden Koeffizienten E_{ik} und E_{ith} allerdings noch von den vorgegebenen Prozentgehalten an Thioketo-Form abhängen. Die Aufgabe besteht nun darin, solche prozentuale Verteilungen der Tautomeren für die 4 Dithizonlösungen zu finden, die für den gesamten betrachteten Spektralbereich eine befriedigende Übereinstimmung zwischen den gemessenen Spektren und den aus den Einzelspektren der Thioketo- und der Thiol-Form und den entsprechenden Prozentgehalten berechneten Spektren ergeben.

Läßt sich ein eindeutiges Minimum der Fehlerquadratsumme S_G

$$S_G = \sum_{i=1}^{28} \sum_{j=1}^4 [E_{ij} - (E_{ik} \cdot C_{kj} + E_{ith} \cdot (1 - C_{kj}))]^2$$

finden, was gleichbedeutend mit bestmöglicher Übereinstimmung der berechneten und gemessenen Spektren ist, gilt als bewiesen, daß die Spektren der Dithizonlösungen in verschiedenen Lösungsmitteln eine Linearkombination der entsprechenden Anteile

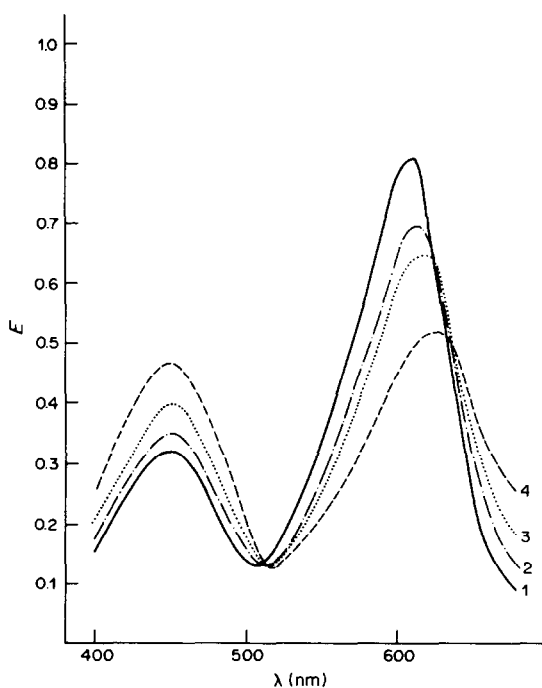


Abb. 3. Spektren $2 \cdot 10^{-5} M$ Dithizonlösungen. 1, H_2Dz in Chloroform; 2, H_2Dz in 2-Propanol, Korrektur um 10 nm; 3, H_2Dz in Tetrachlorkohlenstoff; 4, H_2Dz in Cyclohexan.

der zwei verschiedenen Spektren der Einzeltautomeren sind.

Mit Hilfe eines Optimierungsverfahrens (parabolisches Extrapolationsverfahren nach Jacob³⁴) wurden die C_{kj} -Werte für den vorgegebenen Pro-

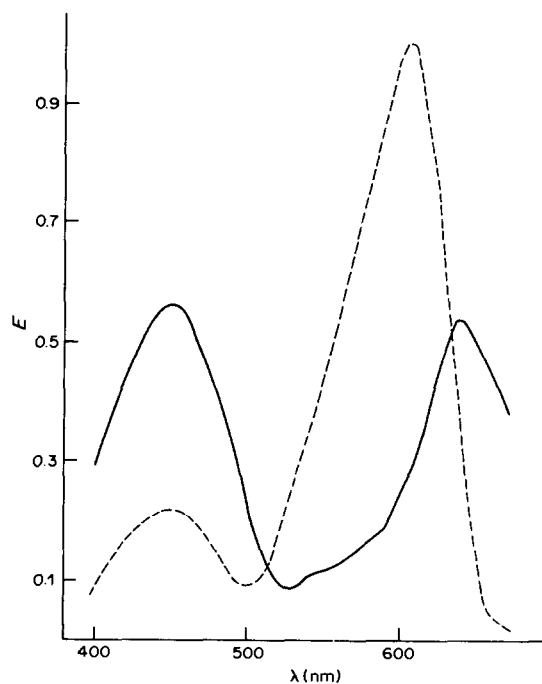


Abb. 4. Berechnete Einzelspektren der beiden tautomeren Formen ($2 \cdot 10^{-5} M$). ---- Spektrum der Thioketo-Form; — Spektrum der Thiol-Form.

Tabelle 4. Richtwerte für den Thioketo-Anteil, abgeleitet aus Reaktionsabstufungen¹¹

H ₂ Dz, gelöst in	Richtwert für Thioketo-Anteil, %	vorgegebene Varianzbreite, %
Cyclohexan	ca. 25	20–30
Tetrachlorkohlenstoff	ca. 47,5	45–55
Chloroform	ca. 75	70–80
2-Propanol	ca. 60	55–65

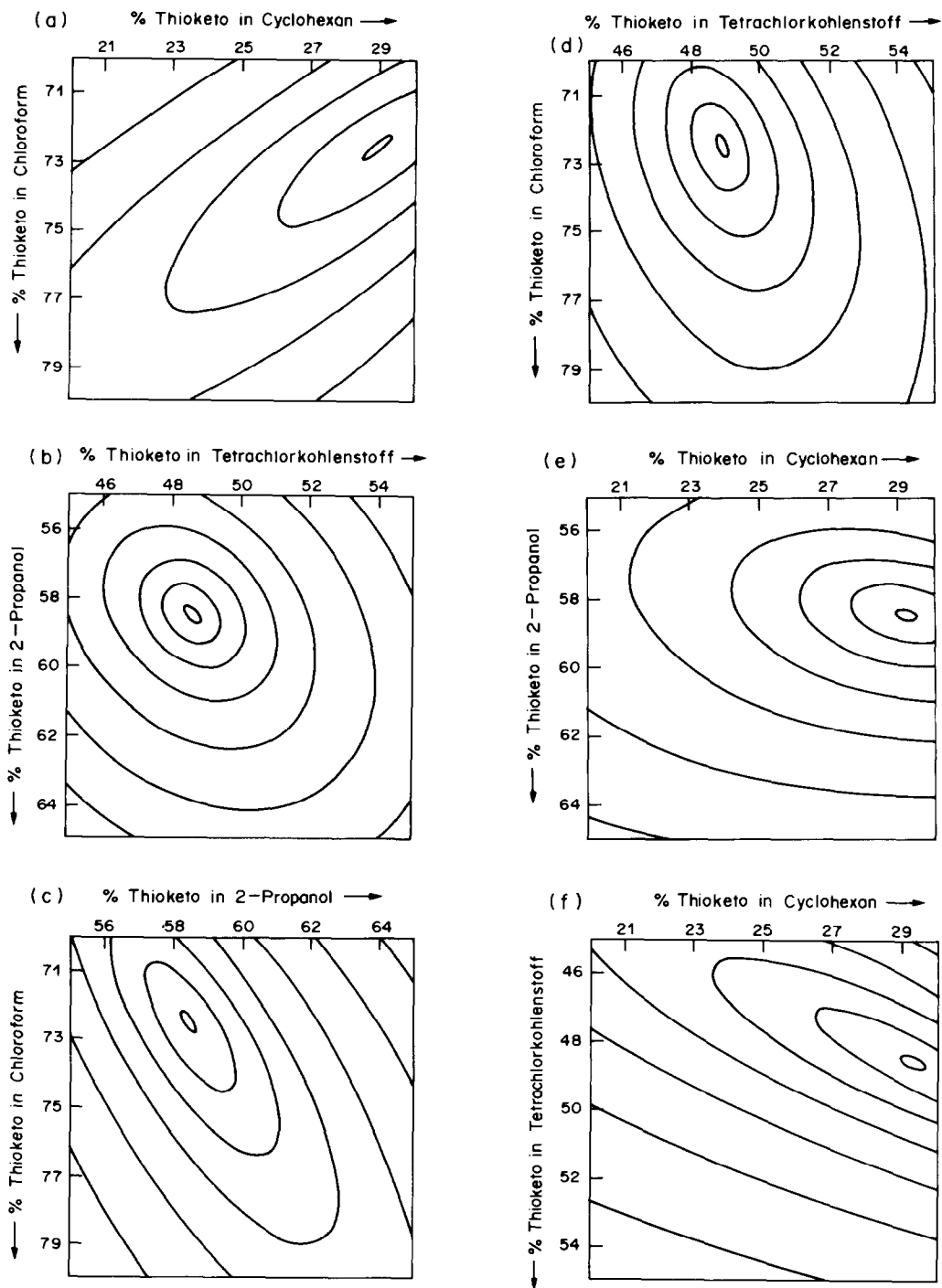


Abb. 5. Abhängigkeit der globalen Fehlerquadratsumme von den Prozentgehalten an Thioketo-Form.

Tabelle 5. Berechnete Tautomererverteilung

	Thioketo-Anteil, %	Thiol-Anteil, %
H ₂ Dz in Chloroform	72.5	27.5
H ₂ Dz in 2-Propanol	58.5	41.5
H ₂ Dz in Tetrachlorkohlenstoff	48.5	51.5
H ₂ Dz in Cyclohexan	29.3	70.7

zentbereich systematisch so verändert, daß die globale Fehlerquadratsumme (S_G) über das gesamte Spektrum minimiert wird.

Als Lösung erhält man sowohl die Einzelspektren E_k und E_{th} der beiden tautomeren Formen (Abb. 4) als auch die prozentuale Verteilung der Tautomeren in den 4 verwendeten Dithizonlösungen (Tab. 5).

In Abb. 5 wird veranschaulicht, daß die Optimierungsprozedur das Minimum der Fehlerquadratsumme gefunden hat. In den Abbildungen ist die Fehlerquadratsumme S_G als Funktion von je zwei Prozentgehalten C_{kj} dargestellt, wobei die Prozentgehalte für 2 Lösungsmittel variiert und für die übrigen 2 Lösungsmittel die optimalen Prozentgehalte eingesetzt werden. Die Niveaulinien geben von innen nach außen folgende Fehlerquadratsumme wieder: $6.3 \cdot 10^{-3}$; $6.5 \cdot 10^{-3}$; $7.0 \cdot 10^{-3}$; $8.0 \cdot 10^{-3}$; $1.0 \cdot 10^{-2}$; $1.4 \cdot 10^{-2}$ und $2.0 \cdot 10^{-2}$.

Durch die Tatsache, daß die berechneten Prozentgehalte innerhalb der vorgegebenen Varianzbreite liegen, wird bestätigt, daß die über chemische Methoden (Einsatz unterstöchiometrischer Reagensmengen) ermittelten Prozentgehalte gute Richtwerte darstellten. Die sehr gute Übereinstimmung der gemessenen Spektren mit den aus den

Einzelspektren und den Prozentgehalten berechneten Spektren wird in Abb. 6 an zwei Beispielen gezeigt.

DISKUSSION DER ERGEBNISSE

Neben der prozentualen Verteilung der Tautomeren in den vier betrachteten Dithizonlösungen konnten auch die Einzelspektren der Thioketo- und Thiol-Form ermittelt werden. Beiden tautomeren Formen kommt ein VIS-Spektrum mit zwei Maxima zu. Im Wellenlängenbereich zwischen 600 und 640 nm überlagern sich die Banden der beiden Tautomeren dargestellt, daß das Maximum 1 der Dithizonspektren sich mit steigendem Thiol-Gehalt zu höheren Wellenlängen hin verschiebt und die Bande bei Verlust an Höhe breiter wird.

Bisher dominierten bei der Interpretation der VIS-Spektren 2 Varianten.

Bei Variante 1 wurde der Charakter der Dithizonspektren als gleich definiert, da die Spektren aller grünen Dithizonlösungen zwei ausgeprägte Maxima aufweisen. Die markanten Unterschiede im Intensitätsverhältnis der Maxima der Spektren wurden als "reine" Lösungsmittelleffekte angesehen und das gesamte Spektrum einer Spezies zugeordnet. Als Schlußfolgerung aus dieser Interpretationsvariante ergeben sich unzulässige Verallgemeinerungen der Einzelergebnisse, so z.B. die Schlußfolgerungen aus den MO-Berechnungen von Spěváček und Spěváčková⁶ und die der IR-Untersuchungen von Kemula und Mitarbeiter.⁵

Bei Variante 2 wurde dagegen gerade das Auftreten dieser zwei gut ausgeprägten Maxima als Hinweis für das Vorliegen eines Tautomerenspaars gewertet, wobei dann Zuordnung je einer Bande zu je einem Tautomeren erfolgte.^{3,28-32} Widersprachen experimentelle Details dieser Zuordnungsmöglichkeit je einer Bande zu je einem Tautomeren, wurde dann als Schlußfolgerung die Existenz eines Tautomerenspaars verneint.

Die signifikante Korrelation zwischen den lösungsmittelabhängigen Reaktionsunterschieden in den Systemen Palladium/Dithizon und Kupfer/Dithizon und den charakteristischen lösungsmittelabhängigen Unterschieden in den VIS-Spektren, sowie die Tatsache, daß die Dithizonspektren als Linearkombination der entsprechenden Anteile an Thioketo- und Thiol-Form aufgefaßt werden können, sprechen dafür, daß sich die Bindungen der Dithizonmolekel (hochsymmetrische Struktur mit weitestgehend delokalisierten π -Elektronen³⁵) in organischen Lösungsmitteln entsprechend

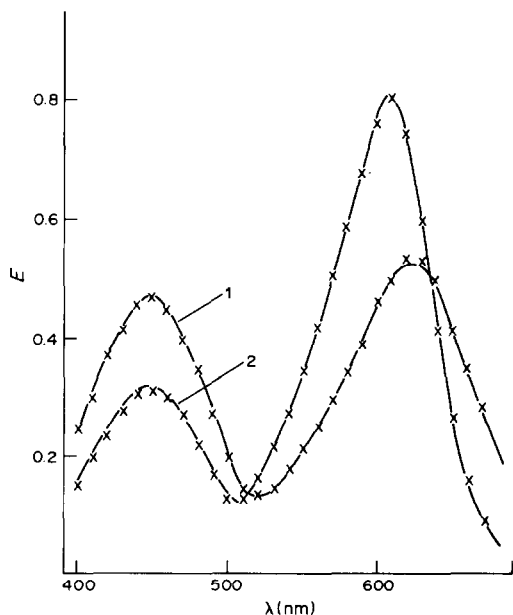
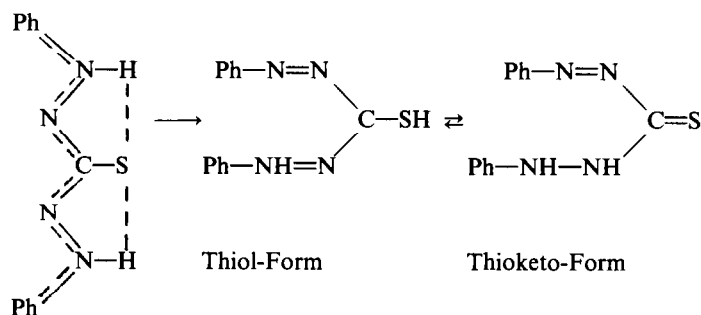


Abb. 6. Beispiele für die gute Übereinstimmung der am Cary 118 gemessenen Spektren (—) von Dithizon und den aus den entsprechenden Anteilen der Einzeltautomeren berechneten Spektren ($\times \times \times$). (1) H₂Dz in Cyclohexan; (2) H₂Dz in Chloroform.

der Polarität der Lösungsmittel lokalisieren und Tautomerie vorliegt:



Festschubstanz in organischen Lösungsmitteln

Unter Berücksichtigung der neuen Erkenntnisse über die Einzelspektren der Thioketo- und der Thiol-Form (Abb. 4) und der Milieu- und Lösungsmittelabhängigkeit des Tautomerengleichgewichtes (Tab. 2) ergeben sich für viele experimentelle Daten neue Interpretationsvarianten und Tatsachen, die bisher als widersprüchlich angesehen wurden, fügen sich in das Gesamtbild ein.^{5-10,36-40}

LITERATUR

- H. Fischer, *Wiss. Veröff. Siemens-Konzern*, 1925, **4**, 158.
- G. Iwantscheff, *Das Dithizon und seine Anwendung in der Mikroanalyse*, 2nd Ed., Verlag Chemie, Weinheim, 1972.
- H. M. N. H. Irving, *Dithizone*, Chem. Soc. London, 1977; U.S. Mahnot, *Ph.D. Thesis*, Leeds, 1966.
- H. Fischer, *Angew. Chem.*, 1934, **47**, 685.
- W. Kemula, T. Ganko und A. Janowski, *Bull. Acad. Pol. Sci. Ser. Sci. Chim.* 1971, **19**, 325.
- V. Spěváček und V. Spěváčková, *J. Inorg. Nucl. Chem.*, 1976, **38**, 1299.
- A. T. Hutton und H. M. N. H. Irving, *Chem. Commun.*, 1981, **15**, 735.
- H. M. N. H. Irving und A. T. Hutton, *Anal. Chim. Acta*, 1982, **141**, 311.
- Idem, ibid.*, 1981, **128**, 261.
- H. M. N. H. Irving, N. F. Naqvi und C. G. Tilley, *ibid.*, 1978, **100**, 597.
- H. Wagler, *Dissertation*, Karl-Marx-Univ., Leipzig, 1981.
- J. Růžicka und J. Starý, *Substoichiometry in Radiochemical Analysis*, Pergamon Press, Oxford, 1968.
- K. Kudo und N. Suzuki, *J. Radioanal. Chem.*, 1975, **26**, 328.
- J. Růžicka und J. Starý, *Talanta*, 1961, **8**, 228; 1962, **9**, 617.
- G. B. Briscoe und S. Humphries, *ibid*, 1971, **18**, 39.
- H. Wagler, *Isotopenpraxis*, 1983, **19**, 307.
- B. A. H. G. Jütte, J. Agterdenbos und R. A. van der Welle, *Talanta*, 1971, **18**, 965.
- H. Irving und J. J. Cox, *J. Chem. Soc.*, 1961, 1470.
- R. Litman, E. T. Williams und H. L. Finston, *Anal. Chem.*, 1977, **49**, 983.
- F. Ingman, *Talanta*, 1971, **18**, 744.
- P. A. Beardsley, G. B. Briscoe, J. Růžicka und M. Williams, *Talanta*, 1966, **13**, 328.
- J. Minczewski, M. Krasienko und Z. Marczenko, *Chem. Anal. (Warsaw)*, 1970, **15**, 45.
- R. S. Young, *Analyst*, 1951, **76**, 49.
- H. M. N. H. Irving, A. H. Nabils und S. S. Sahota, *Anal. Chim. Acta*, 1973, **67**, 135.
- H. Wagler, H. Koch und J. Flachowsky, *Z. Chem.*, 1984, **24**, 98.
- L. S. Meriwether, E. C. Breitner und C. L. Sloan, *J. Am. Chem. Soc.*, 1965, **87**, 4441.
- J. E. Pemberton und R. P. Buck, *J. Raman Spectrosc.*, 1982, **12**, 76.
- P. S. Pelkis und R. G. Dubenko, *Dokl. Akad. Nauk USSR* 1953, **88**, 999.
- Idem, Ukr. Khim. Zh.* 1957, **23**, 748.
- P. S. Pelkis, *ibid.*, 1951, **17**, 93.
- A. T. Pilipenko, *Usp. Khim.*, 1956, **25**, 1402.
- A. H. Corwin und G. R. Jackson, *J. Am. Chem. Soc.*, 1949, **71**, 3698.
- J. Fabian, *Tetrahedron*, 1973, **29**, 2449.
- H. G. Jacob, *XVIII Intern. Wiss. Koll., TH, Ilmenau*, 1973, **3**, 43.
- P. A. Alsop, *D. Phil. Thesis*, London, 1971; M. Laing, *J. Chem. Soc. Perkin Trans.*, 1977, **10**, 1248.
- H. Irving und C. F. Bell, *J. Chem. Soc.*, 1954, 4253.
- R. A. Coleman, W. H. Foster, J. Kazan und M. Manson, *J. Org. Chem.*, 1970, **35**, 2039.
- A. H. Nabils, *Ph.D. Thesis*, Leeds, 1972.
- K. S. Math, Q. Fernando und H. Freiser, *Anal. Chem.*, 1964, **36**, 1762.
- H. M. N. H. Irving, A. M. Kiwan, D. C. Rupainwar und S. S. Sahota, *Anal. Chim. Acta*, 1971, **56**, 205.

Summary—Significant differences have been observed in the reactions of substoichiometric amounts of reagent for the extraction of palladium dithizonate and of copper dithizonate. These differences depend on both the organic solvent and the composition of the aqueous phase, and suggest that dithizone can react with metals in two ways, and can exist as a mixture of tautomeric forms in organic solvents. Moreover the differences in the reactions show a clear correlation with the differences in the visible absorption spectra of dithizone in various organic solvents. A mathematical analysis of these spectra has allowed calculation of the spectra of the individual thione and thiol forms of dithizone, and also estimation of the position of the tautomeric equilibrium in the different solvents.

SHORT COMMUNICATIONS

POTENTIOMETRIC DETERMINATION OF PLUTONIUM BY SODIUM BISMUTHATE OXIDATION

M. M. CHARYULU, V. K. RAO and P. R. NATARAJAN

Radiochemistry Division Bhabha Atomic Research Centre Trombay, Bombay-400085, India

(Received 24 June 1983. Revised 24 April 1984. Accepted 30 June 1984)

Summary—A potentiometric method for the determination of plutonium is described, in which the plutonium is quantitatively oxidized to plutonium(VI) with sodium bismuthate in nitric acid medium, the excess of oxidant is destroyed chemically and plutonium(VI) is reduced to plutonium(IV) with a measured excess of iron(II), the surplus of which is back-titrated with dichromate. For 3–5 mg of plutonium the error is less than 0.2%. For submilligram quantities of plutonium in presence of macro-amounts of uranium the error is below 2.0%.

Plutonium in mg amounts is usually determined by titrimetric methods based on the Pu(III)/Pu(IV) and Pu(IV)/Pu(VI) couples.^{1–4} Methods based on oxidation of plutonium to plutonium(VI) with silver(II) oxide are widely used. The method of Rao *et al.*⁵ is more versatile than those reported by Drummond and Grant⁶ and by Milner *et al.*⁷ However, a disadvantage of the method is that the excess of iron(II) added for reduction of the plutonium(VI) is rather critical. Linder and Baeckman⁸ reported that addition of more than 50% excess of iron(II) causes a positive error due to reduction of silver(I) to metallic silver.

This paper describes an alternative method based on the use of sodium bismuthate to oxidize the plutonium to the hexivalent state.^{9,10} The excess of bismuthate is destroyed chemically before the usual back-titration procedure for plutonium, in which a considerable excess of iron(II) can be tolerated.

EXPERIMENTAL

Reagents

Analytical grade reagents were used. Potassium dichromate solutions (0.05 and 0.001 meq/g) were prepared by dissolving accurately weighed amounts of the reagent (dried at 110°) in doubly distilled water. Ammonium ferrous sulphate (~0.1M) was prepared, and standardized by potentiometric weight titration with standard dichromate solution.

Standard plutonium nitrate solution was prepared by dissolving high-purity plutonium dioxide in concentrated nitric acid plus a few drops of 0.05M hydrofluoric acid, followed by repeated evaporation to remove hydrogen fluoride and final dilution to known weight with 1M nitric acid. The solution was standardized by mass spectrometry and by the silver(II) oxide method.⁵ The fluoride concentration in the plutonium standard was measured with an ion-selective electrode and found to be less than that in the reagent blank. Standard uranium solution was prepared by dissolving the oxide in nitric acid and standardized by a modification of the Davies and Gray method.¹¹

Apparatus

The potentiometric titrations were performed with a digital potentiometer with a readability of 1 mV. A 50-ml

beaker was used as titration cell, with a saturated calomel electrode and platinum working electrode. The standard potassium dichromate and iron(II) solutions were added from polythene weight-burettes with suitably finely drawn jets.

Recommended procedure

A suitable accurately known weight (~0.2 g) of sample solution containing 3–4 mg of plutonium in 1M nitric acid medium was transferred to the titration cell with 5 ml of 1M nitric acid solution, and sodium bismuthate powder (80–100 mg) was added and stirred with the sample for 5 min to oxidize the plutonium quantitatively to plutonium(VI). Then 2 ml of 6M hydrochloric acid were added and the mixture was stirred for 10 min to ensure complete destruction of the excess of bismuthate. Ten ml or 2M sulphuric acid were then added followed by a drop or two of 1.5M sulphamic acid solution to destroy any nitrous acid. Finally enough iron(II) solution was added to give a potential of ~450 mV, indicating complete reduction to plutonium(IV), and the excess of iron(II) was titrated potentiometrically with dichromate, first with the more concentrated solution and then with the dilute titrant when the end-point was near.

The amount of plutonium (mg) present was calculated from the expression

$$\text{Pu} = [W_1 A - (W_1 + W_{II} B)] C_1 E$$

where W_1 is the weight of iron(II) solution added, A is the weight of concentrated dichromate solution equivalent to 1 g of iron(II) solution, W_1 and W_{II} are the weights used of the concentrated and dilute dichromate solutions respectively, B is the concentration ratio of dilute to concentrated dichromate solution, C_1 is the concentration (meq/g) of the concentrated dichromate solution and E is half the atomic weight of plutonium.

RESULTS AND DISCUSSION

Oxidation of plutonium with sodium bismuthate

Sodium bismuthate is a powerful oxidant in acidic medium, with $E^\circ = 1.6$ V for reduction to Bi(III).¹² The conditional potential for the Pu(IV)/Pu(VI) couple¹³ in 1M nitric acid is 1.054 V, so bismuthate will quantitatively oxidize Pu(IV) to Pu(VI). Hindman and Holland¹⁴ reported that the oxidation in 5M nitric acid medium is quantitative at room temperature. In sulphuric acid medium, however, it is

essential to heat the solution to complete the oxidation.^{9,10} We have found that in 1M nitric acid medium, the oxidation to plutonium(VI) is complete at room temperature in 5 min with 80–100 mg of bismuthate per 3–5 mg of plutonium.

Destruction of excess of sodium bismuthate

The excess of sodium bismuthate had to be destroyed before the titration. Markov⁹ removed the excess by filtration but this is undesirable in high-precision work because the slight solubility of sodium bismuthate in acidic solutions leads to positive bias. A chemical method was therefore sought. Of several reagents tried, 6M hydrochloric acid was found to be the most effective. It reduces the bismuthate in nitric acid medium at room temperature in less than 3 min, with liberation of chlorine.¹⁵ Most of the chlorine escapes as gas and the residual amount does not affect the subsequent titration significantly. This was established by adding a known amount of iron(II) to nitric acid in which bismuthate had previously been destroyed with hydrochloric acid, and titrating with dichromate; the amount found agreed within 0.01–0.04% with the amount found by direct titration of the same amount of iron(II).

Reduction of plutonium(VI) by iron(II), and back-titration

Direct titration of plutonium(VI) with iron(II) is sluggish, which is why a back-titration procedure is invariably used. The end-point was detected from the maximum of the first derivative. Analysis of 20 replicate samples of standard plutonium solution gave a relative standard deviation of 0.2% and zero bias for 3–5 mg of plutonium. Determination of 50–200 μ g of plutonium (20 replicates) by the same method [but with more dilute iron(II) and dichromate solutions] gave an RSD of 2.0%.

The advantage of using sodium bismuthate instead of silver(II) oxide is that much larger quantities of iron(II) are tolerated. Amounts corresponding to as much as 1000% excess had no effect on the plutonium values found.

Effect of uranium

The method has been tested for the determination of plutonium in presence of uranium. Up to 28-fold w/w ratio of uranium to plutonium had no significant effect on the results.

Interference of various impurities

The effect of the relevant impurities has been investigated. The cations examined were those likely to be associated with plutonium, e.g., high-yield fission products such as Sr(II), Ru(III), Zr(IV) and Mo(VI) or impurities such as Al(III), Ni(II) and Hg(II). Corrosion products such as Cr(III), Mn(II) and V(IV) were found to interfere quantitatively because of their oxidation by sodium bismuthate.

Among the anions, fluoride is of most interest,

Table 1. Study of interferences

Substance	Amount added to 3–5 mg of plutonium, mg	Error, %
Strontium(II)	2.0	–0.2
Cadmium(II)	2.0	–0.1
Ruthenium(III)	2.0	–0.2
Zirconium(IV)	2.0	+0.2
Molybdenum(VI)	1.0	+0.1
Aluminium(III)	28.8	+0.2
Nickel(II)	5.0	+0.2
Copper(II)	1.6	+0.1
Mercury(II)	8.4	+0.1
Fluoride	0.005	+0.2
	0.010	–5.9
	0.130	–20.8
Nitrate	3200	–0.2
Sulphate	19.6	–1.5

since preparation of standard plutonium nitrate solution involves the use of a little hydrofluoric acid. Hydrogen fluoride is quantitatively driven off by repeated evaporation, however, and its concentration in the plutonium working standards was found to be negligible. Tests showed that up to 5 μ g of fluoride had no effect on the plutonium determination. The amount present in the test solutions prepared as described was less than 2 μ g per aliquot used.

Tests showed that up to 50 mmoles of nitric acid in 5 ml of sample solution (which includes the aliquot and wash solution) can be tolerated. It may be noted that the volume of the solution is about 17 ml before the addition of iron(II) solution, which means that such a solution would be about 3M in nitric acid at this stage. Our observation shows that nitric acid of higher concentration would oxidize iron(II) and therefore lead to positive error.

Regarding chloride, small amounts in the sample would cut down the amount of bismuthate available for the plutonium oxidation, but the plutonium should be oxidized preferentially according to the potentials involved. However, larger amounts of chloride would interfere unless the sample has already been subjected to repeated evaporation, which is normally the case to remove the small quantities of fluoride added when the solution is prepared from plutonium oxide.

Sulphate was found to inhibit the oxidation of plutonium to plutonium(IV) at room temperature. Table 1 gives the tolerance limits for the interfering ions studied.

Acknowledgements—The authors wish to express their sincere thanks to Dr. M. V. Ramaniah, Director of the Radiological Group, for his interest in the work. The assistance rendered by Dr N. K. Chaudhuri and Shri M. V. R. Prasad in determining the fluoride content of the plutonium nitrate standard solutions is gratefully acknowledged. Thanks are also due to Dr R. A. Chalmers of University of Aberdeen for valuable suggestions in the preparation of the manuscript.

REFERENCES

1. C. P. Metz and G. R. Waterbury, in *Treatise on Analytical Chemistry*, I. M. Kolthoff and P. J. Elving (eds.), Part II, Vol. 9, pp. 296-352. Interscience, New York, 1962.
2. *Analytical Chemistry of Nuclear Fuels*, IAEA, Vienna, 1972.
3. C. J. Rodden, *US At. Energy Comm. Rept.*, TID-7029, 1972.
4. M. V. Ramaniah, P. R. Natarajan and P. Venkataramana, *Radiochim. Acta*, 1975, **22**, 199.
5. C. L. Rao, G. M. Nair, Singh, M. V. Ramaniah and N. Srinivasan, *Z. Anal. Chem.*, 1971, **254**, 126.
6. J. L. Drummond and R. A. Grant, *Talanta*, 1966, **13**, 477.
7. G. W. C. Milner, A. J. Wood and G. E. Cassie, *UK At. Energy Authority Rept.*, AERE-R-4975, 1965.
8. L. Linder and A. E. Baeckmann, *Karlsruhe Rept*, KFK-701, 1967.
9. V. K. Markov, *Safeguards Techniques*, Proceedings of Symposium, Karlsruhe, Vol, pp. 3-26, IAEA, Vienna, 1970; *U.S. At. Energy Comm. Rept.*, LA-TR-71-24, p.3, 1970.
10. M. S. Milyukova, N. I. Gusev, I. G. Sentyunin and I. S. Skylarenko, *Analytical Chemistry of Plutonium*, pp. 152-153. Israel Program for Scientific Translations, Jerusalem, 1967.
11. A. R. Eberle, M. W. Lerner, C. G. Goldbeck and C. J. Rodden, *US At. Energy Comm., Rept.*, NBL-252, 1970.
12. M. C. Sneed and R. C. Brasted, *Comprehensive Inorganic Chemistry*, Vol. V, p. 149. Van Nostrand, Princeton, 1956.
13. J. M. Cleveland, *The Chemistry of Plutonium*, p.20. Gordon and Breach, New York, 1970.
14. *The Actinide Elements*, G. T. Seaborg and J. J. Katz (eds.), p. 254. McGraw-Hill, New York, 1954.
15. H. Martin-Frère, *Compt. Rend.*, 1946, **213**, 436.

SPECTROPHOTOMETRIC DETERMINATION OF IRON(II) AFTER SEPARATION BY ADSORPTION OF ITS COMPLEX WITH 3-(4-PHENYL-2-PYRIDYL)-5,6-DIPHENYL-1,2,4-TRIAZINE AND TETRAPHENYLBORATE ON MICROCRYSTALLINE NAPHTHALENE

TOHRU NAGAIRO and KATSUYA UESUGI

Himeji Institute of Technology, 2167, Shosha, Himeji-shi, Hyōgo, Japan

M. C. MEHRA

Chemistry Department, Université de Moncton, Moncton, Canada

MASATADA SATAKE[®]

Faculty of Engineering, Fukui University, Fukui-910, Japan

(Received 28 April 1983. Revised 4 June 1984. Accepted 19 June 1984)

Summary—Trace iron(II) is determined spectrophotometrically after adsorption of its ternary complex with 3-(4-phenyl-2-pyridyl)-5,6-diphenyl-1,2,4-triazine and tetraphenylborate on microcrystalline naphthalene at pH 5.1–7.4. The absorption maximum is at 567 nm; the molar absorptivity is 2.9×10^4 l. mole⁻¹. cm⁻¹.

Extractive spectrophotometric determination of iron(II) with 3-(4-phenyl-2-pyridyl)-5,6-diphenyl-1,2,4-triazine (PPDT) has been reported by Schilt and Hoyle¹. The complex Fe(PPDT)₃²⁺ is only slightly soluble in water, but soluble in ethanol, ethanol-water, isoamyl alcohol, benzene and nitrobenzene. The complex forms slowly at room temperature, but rapidly in presence of perchlorate or relatively large amounts of ethanol. The perchlorate salt of the complex is extremely insoluble in water but readily extracted into isoamyl alcohol.

The spectrophotometric determination of metals after adsorption of their complexes on microcrystalline naphthalene is now well established.²⁻⁹ In the present work the technique is applied to the ion-association complex produced by Fe(PPDT)₃²⁺ and tetraphenylborate (TBP), which is not extractable into the usual organic solvents. The complex is quantitatively adsorbed on microcrystalline naphthalene and is freely soluble in dimethylformamide and acetonitrile, which are miscible with water.

EXPERIMENTAL

Reagents

Standard iron(III) solution, 2 ppm. Prepared by diluting 1000-ppm standard iron(III) solution with water.

PPDT solution in ethanol, 0.04%.

Hydroxylammonium chloride solution, 2%.

TPB solution, 1%.

Naphthalene solution in acetone, 20%.

Buffer solutions, 1M. Acetic acid/ammonium acetate; ammonia/ammonium acetate.

Procedure

Place the sample solution [containing 1–20 μg of iron(III)]

in an 80-ml stoppered Erlenmeyer flask and dilute it to about 40 ml with water. Add 1.0 ml of 2% hydroxylammonium chloride solution, 3.0 ml of 0.04% PPDT solution, and 2.0 ml of acetate buffer (pH 5.8) and mix. Add 3.0 ml of 1% TPB solution. Heat on a water-bath (60°) for 50 min to precipitate the complex completely. Cool to room temperature, add 2.0 ml of 20% naphthalene solution and shake vigorously for 30 sec. Collect the naphthalene on a filter paper (Toyo Roshi No 5C) placed flat on a Teflon plate in a funnel, or on a sintered-glass filter (porosity 2). Wash it with water and dry it at 55–60°. Dissolve the mixture in dimethylformamide and dilute with the solvent in a 10-ml standard flask. Measure the absorbance at 567 nm against a reagent blank.

RESULTS AND DISCUSSION

The complex has its absorbance maximum at 567 nm, where there is practically no absorption due to the reagent blank. The absorbance is unaffected by the pH of precipitation in the range 5.1–7.4; pH 5.8 is a convenient choice for the buffer. The absorbance is constant when 1.5–8.0 ml of 0.04% PPDT solution and 0.01–6.0 ml of 1% TPB solution are used. From 0.1 to 10 ml of 2% hydroxylammonium chloride and 1.0–5.0 ml of pH 5.8 buffer solution can be used.

The formation of the complex is relatively slow at room temperature, but considerably faster above 60°, and the complex is stable for a considerable period. A digestion time of 30–90 min is enough for complete formation of the complex.

As usual, 0.4 g of naphthalene is convenient for the adsorption and shaking for 30 sec is adequate.

The volume of the aqueous phase can be varied in the range 20–60 ml without effect on the absorbance,

Table 1. Tolerance limits for diverse salts and ions in determination of 10 μg of iron

Salt	Tolerance limit	Ion	Tolerance limit
NaI	11 g	Mg ²⁺	48 mg
KNO ₃	6 g	Mn ²⁺	19 mg
NaCl	1 g	Ca ²⁺	14 mg
KH ₂ PO ₄	0.6 g	Al ³⁺	480 μg
Na ₂ SO ₄	0.5 g	Cr ⁶⁺	970 μg
NaClO ₄ · H ₂ O	15 g	Pb ²⁺	480 μg
KSCN	0.1 g	Hg ²⁺	480 μg
Sodium tartrate · 2H ₂ O	85 mg	Cd ²⁺	470 μg
Sodium citrate · 2H ₂ O	3 mg	Sn ²⁺	480 μg
NH ₄ Cl	10 g	Zn ²⁺	270 μg
Na ₂ C ₂ O ₄	80 μg	Pt ⁴⁺	80 μg
CH ₃ COONa · 3H ₂ O	14 g	Bi ³⁺	17 μg
		Ni ²⁺	7 μg
		Co ²⁺	8 μg
		Cu ²⁺	5 μg

Table 2. Comparative analysis for iron in various samples

Sample	Composition of alloy, %	Iron, certified value, %	Iron content*		
			Present method	TPTZ method ^{10,11}	1,10-Phenanthroline method ¹²
N.B.S. SRM-85b Al alloy	Cu: 3.99, Cr: 0.21 Mn: 0.61, Ni: 0.089 Si: 0.18, Ti: 0.022 Zn: 0.03, Ga: 0.019 V: 0.006, Pb: 0.021	0.24	0.236 ± 0.003	0.252 ± 0.002	0.247 ± 0.002
N.B.S. SRM-158a Silicon-Bronze alloy	Cu: 90.93, Si: 3.03 Zn: 2.08, Mn: 1.11 Ti: 0.96, Al: 0.46 Pb: 0.097, Ni: 0.001 P: 0.026	1.23	1.25 ± 0.02	1.24 ± 0.02	1.24 ± 0.02
Metallic magnesium (powder)	—	—	0.0022 ± 0.0001	0.0023 ± 0.0001	0.0023 ± 0.0002
Metallic aluminum (powder)	—	—	0.148 ± 0.002	0.151 ± 0.002	0.152 ± 0.002
CoSO ₄ · 7H ₂ O (solid)	—	—	0.0034 ± 0.0002	0.0036 ± 0.0002	0.0036 ± 0.0002
Lake water	—	—	0.35 ± 0.02†	0.36 ± 0.01†	0.35 ± 0.02†
River water	—	—	0.137 ± 0.003†	0.141 ± 0.002†	0.146 ± 0.002†
Hot springs	—	—	82 ± 2§	84 ± 2§	78 ± 2§

*Average of five determinations.

† $\mu\text{g}/\text{ml}$.§ ng/ml .

but with 60 ml a digestion time of 60 min and a shaking time of 2 min are recommended. The mixture of the complex and naphthalene can be dissolved in dimethylformamide, acetonitrile, dimethyl sulphoxide or propylene carbonate. Dimethylformamide is preferred and the complex is stable in it for 60 min.

The calibration graph is linear over the range 0.1–2.0 μg of iron per ml of dimethylformamide. The molar absorptivity is $2.90 \times 10^4 \text{ l. mole}^{-1} \text{ cm}^{-1}$. Ten replicate determinations of 10 μg of iron gave a mean absorbance of 0.523 with a relative standard deviation of 1.3%.

Effect of diverse ions

The tolerance limits (error < 2%) for various ions

in determination of 10 μg of iron are summarized in Table 1. If the iron content in practical samples is low and interfering metal ions are present, a preliminary extraction of iron with methyl isobutyl ketone (MIBK) or diethyl ether from 6M hydrochloric acid is necessary.

Analysis of practical samples

The results in Table 2 are in reasonably good agreement with those obtained spectrophotometrically with 2,4,6-tri(2-pyridyl)-1,3,5-triazine^{10,11} and 1,10-phenanthroline.¹² The aluminium alloy (1-g sample) was dissolved with 40 ml of hydrochloric acid (1 + 1) and 2 ml of 30% hydrogen peroxide, then the excess of peroxide was decomposed by heating. After

cooling, the solution was made up accurately to 500 ml with water, a 2-ml aliquot was transferred to a 100-ml separatory funnel, 40 ml of hydrochloric acid (1 + 1) were added, and the iron was extracted by vigorous shaking for 5 min with 20 ml of MIBK. The iron was stripped with 25 ml of water, and determined by the proposed method.

The standard silicon bronze alloy (100 mg) was dissolved with 10 ml of hydrochloric acid (1 + 1), 1 ml of concentrated nitric acid and 3 ml of concentrated sulphuric acid. The excess of acid was evaporated and the residue dissolved and diluted accurately to 1000 ml with water. An aliquot was analysed.

Magnesium powder (10 g) and aluminium powder (2 g) were analysed in the same way as the aluminium alloy.

Water samples, made 0.1M in nitric acid immediately after collection, were filtered through paper to remove suspended particulates, and the filtrates were analysed for total iron as described above.

REFERENCES

1. A. A. Schilt and W. C. Hoyle, *Anal. Chem.*, 1967, **39**, 114.
2. M. Satake, Y. Matsumura and M. C. Mehra, *Mikrochim. Acta*, 1980 **I**, 455.
3. *Idem*, *Analisis*, 1981, **9**, 389.
4. A. Kumar, M. F. Hussain, M. Satake and B. K. Puri, *Bull. Chem. Soc. Japan*, 1982, **55**, 3455.
5. M. Satake, M. C. Mehra and T. Fujinaga, *ibid.*, 1982, **55**, 2079.
6. M. Satake, *Anal. Chim. Acta*, 1977, **92**, 423.
7. M. Satake, T. Suzuki and N. Yoshida, *Mem. Fac. Eng. Fukui Univ.*, 1979, **27**, 287.
8. M. Satake and M. C. Mehra, *Microchem. J.*, 1982, **27**, 182.
9. M. Satake and Y. Matsumura, *Mem. Fac. Eng. Fukui Univ.*, 1980, **28**, 87.
10. P. F. Collins and H. Diehl, *Anal. Chim. Acta*, 1960, **22**, 125.
11. P. F. Collins, H. Diehl and G. F. Smith, *Anal. Chem.*, 1959, **31**, 1862.
12. *Standard Methods for the Examination of Water and Waste Water*, p. 189. American Public Health Assoc., 1971.

DETERMINATION OF URANIUM IN PHOSPHOGYPSUM

HELENA GÓRECKA and HENRYK GÓRECKI

Institute of Inorganic Technology and Mineral Fertilizers, Technical University of Wrocław, Poland

(Received 16 January 1984. Revised 28 May 1984. Accepted 19 June 1984)

Summary—A method for determination of uranium in phosphogypsum is based on extraction of uranium from phosphoric acid in which hydration transformations of calcium sulphate hydrates have occurred. The uranium is extracted with a kerosene solution of a mixture of mono- and dinonylphenylphosphoric acids, then stripped with concentrated phosphoric acid, and determined spectrophotometrically with Arsenazo III.

Production of wet phosphoric acid, which is in common use for the production of phosphate and mixed fertilizers, is associated with the creation of very large amounts of phosphogypsum waste (in about 2:1 weight ratio to the phosphate raw material used). About 4.5–6 tons of phosphogypsum waste are created in producing one ton of P_2O_5 in fertilizer products.¹ On account of its enormous amount, its mineral impurities and high water content, the waste is at present utilized only to a very small degree.² Phosphogypsum is generally stored near fertilizer works or dumped in rivers or the oceans. This is of danger to the natural environment since the waste contains toxic components such as fluorine, uranium and radium. Utilization of the waste for the production of building materials requires reduction of the amount of these contaminants, as well as of the phosphorus compounds.²

Uranium is recovered on a commercial scale more and more often from wet phosphoric acid,^{3–5} and requires increased efficiency of the uranium recovery process.

A chemical analysis of the uranium content of phosphogypsum waste will make it possible to determine the proper conditions for the production of wet phosphoric acid with simultaneous uranium recovery, and allow control of the uranium content of phosphogypsum that is to be used as a raw material or an intermediate in the production of building materials.

Physicochemical reasons for presence of uranium in phosphogypsum

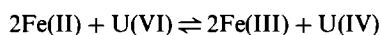
The uranium content of phosphogypsum depends on the type of the phosphate raw material, the technology of decomposition, and on crystallization of the phosphogypsum as well as on various technological parameters.

The uranium balance in the wet method is generally thought to depend on the liquid phase composition when the calcium sulphate crystallizes.^{5–9} The uranium content depends mainly on the degree of hydration of the calcium sulphate.⁶ The phos-

phogypsum obtained as calcium sulphate dihydrate contains 5–25 μg of U per g. A much greater amount of uranium (50–110 $\mu\text{g/g}$) is contained in phosphogypsum produced by applying the hemihydrate method (the main component is $\alpha\text{-CaSO}_4 \cdot \frac{1}{2}\text{H}_2\text{O}$). The reason for this large difference lies in the different structure of the unit cells, the fact that the hemihydrate forms agglomerates and clusters, and that the co-ordination of uranium depends on the temperature and the concentration of phosphoric acid.

A significant role is also played by the relative concentrations of U(IV) and U(VI) in the liquid phase. It is thought⁶ that in phosphate raw materials about 40–91% of the uranium (mean about 65%) is in the quadrivalent form.

In the decomposition of phosphate raw materials with sulphuric acid U(IV), U(VI), Fe(II) and Fe(III) are transferred into the liquid phase, where the equilibrium



is established. Fe(III) and U(IV) form stable co-ordination compounds with F^- and HPO_4^{2-} ions, which is why the liquid phase contains more U(IV) than was in the raw material.¹⁰

Many authors have proved^{6–8} that the higher the U(IV) content (*i.e.*, under strongly reducing conditions), the higher the amount of uranium in the phosphogypsum. Under oxidizing conditions, up to 90% of the uranium can pass to the liquid phase, and even 95% if some nitric acid is added.⁸

Decomposition under the usual technological conditions transfers about 25–30% of the uranium into the phosphogypsum, whereas addition of a large amount of iron(II) increases this to as much as 80%.

The uranium is transferred into the phosphogypsum by substitution of U^{4+} for Ca^{2+} in the crystal lattice of calcium sulphate, the probability of substitution being 3.75×10^{-5} . The process is possible because of the similarity in the ionic radii of U^{4+} (0.97 Å) and Ca^{2+} (0.99 Å). This substitution is dependent on the course of the calcium sulphate crystallization, and thus on the local concentrations

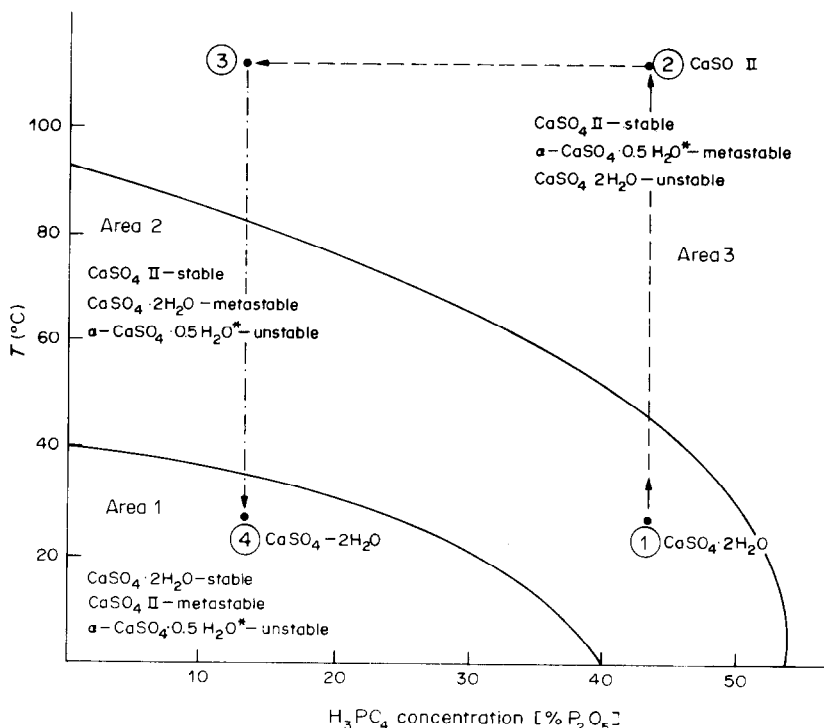


Fig. 1. The recrystallization scheme used in the analysis of phosphogypsum, shown as a phase scheme comprising domains of existence of calcium sulphate in various hydration forms in phosphoric acid solution.

of Ca^{2+} , SO_4^{2-} , HPO_4^{2-} , and F^- , as well as on the hydrodynamic conditions. It is also presumed that the presence of organic compounds in the phosphate raw material and application of organic defoamers to lower the stability of the foam in the decomposition process will increase the uranium content in the phosphogypsum. It has been experimentally proved that calcination may reduce the uranium content in phosphogypsum by about 30%.⁸

Another process significantly affecting the uranium content in phosphogypsum is adsorption of uranium(VI) as UO_2HPO_4 on the surface of the gypsum or by substitution of one UO_2^{2+} ion for 2Ca^{2+} ions in the terminal nodes of the crystal lattice.⁶

We have proved experimentally⁹ that phosphogypsum particles with average weight $< 10 \mu\text{g}$ contain 30–40% more uranium than particles with mean weight $> 50 \mu\text{g}$.

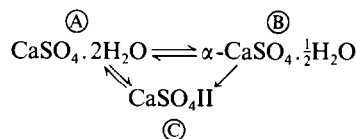
Principle of the analysis method

During the crystallization of phosphogypsum there is a non-uniform distribution of the uranium: about 80–90% in the liquid phase, and the remainder in the phosphogypsum. The distribution can be controlled by making a slight addition of oxidizing reagents, which results in a lower uranium content in the phosphogypsum.

Thus if phosphogypsum recrystallizes in a pure phosphoric acid solution, the liquid phase is separated and the recrystallization repeated, then at least

96% of the uranium can be removed from the phosphogypsum.

Depending on the phosphoric acid concentration and the temperature, there are three phase areas delimited by the lines of the phase transition. From Fig. 1 it appears that only 2 stable modifications exist: $\text{CaSO}_4 \cdot 2\text{H}_2\text{O}$ (area 1) and CaSO_4 (areas 2 and 3). Particular hydrate forms may undergo changes according to the temperature and concentration conditions:¹



For the analysis the phase transition $\text{A} \rightarrow \text{C}$ is used. The metastable transition $\text{A} \rightleftharpoons \text{B}$ is utilized in the production of wet phosphoric acid by the dihydrate–hemihydrate or hemihydrate–dihydrate methods.¹ This transition requires exact adjustment of the technological conditions.

In the analysis, the sample of dry phosphogypsum is placed in a 0.1% w/w solution of sodium chlorate in concentrated phosphoric acid (this corresponds to point 1 in Fig. 1) and heated to 90–100°, which results in transformation of $\text{CaSO}_4 \cdot 2\text{H}_2\text{O}$ into $\text{CaSO}_4 \text{ II}$ (point 2 in Fig. 1) with 75–85% of the uranium passing into the liquid phase. After filtering off from the concentrated acid, the wet phosphogypsum is added to a volume of water that is half that of the concentrated acid introduced initially. This lowers the concentration of P_2O_5 in solution and the

$\text{CaSO}_4\cdot\text{II}$ is transformed back into $\text{CaSO}_4\cdot 2\text{H}_2\text{O}$ (point I in Fig. 1) with simultaneous further release of uranium compounds to the liquid phase. After filtration and washing, the two filtrates and the washings are combined, and the uranium is extracted with a kerosene solution of a mixture of mono- and dinonylphenylphosphoric acids (NPPA). The aqueous phase should contain 20–30% P_2O_5 and ferrous sulphate. The uranium is stripped from the organic phase with 10M phosphoric acid containing sodium chlorate.^{11,12} The uranium content of the strippings is determined by the Korkisch spectrophotometric method with Arsenazo III.^{13,14}

EXPERIMENTAL

Reagents

Kerosene solution of NPPA, 0.2M.

Phosphoric acid, 85% H_3PO_4 , pure for analysis.

Calcium sulphate dihydrate. Pure for analysis, for preparing the calibration curve.

Procedure

Prepare 100 ml of phosphoric acid of 40% P_2O_5 content (about 55% H_3PO_4) and 0.1% sodium chlorate. Weigh the sample of phosphogypsum (about 50 g) into a beaker and add the phosphoric acid. Heat to 90–100° and keep at temperature for about 1 hr. Check by examination under the microscope that transformation to $\text{CaSO}_4\cdot\text{II}$ has taken place, and if it has, filter the suspension hot on a Buchner funnel and wash with 10 ml of water. Return the sediment to the beaker, add 50 ml of water, and let stand for at least 12 hr for reversion into $\text{CaSO}_4\cdot 2\text{H}_2\text{O}$. When the change is complete (microscopic observation), filter the suspension and combine the filtrates.

Add 2 g of $\text{FeSO}_4\cdot\text{H}_2\text{O}$ to the combined filtrates. Shake the solution with 10 ml of 0.2M NPPA solution in kerosene at 20–30° for 1 hr. After phase separation, strip the kerosene phase at 55° with three 25-ml portions of 10M phosphoric acid containing 0.2% sodium chlorate, shaking for 30 min in each extraction. Combine the three extracts and analyse for uranium spectrophotometrically as for uranium in wet phosphoric acid.¹¹

The calibration graph is prepared by adding known amounts of UO_2SO_4 to 50-g samples of pure calcium sulphate, and analysing as just described.

CONCLUSIONS

The procedure permits chemical analysis for uranium in phosphogypsum samples arising from the production of wet phosphoric acid. The method

makes use of change in pattern of the distribution of uranium between the liquid and solid phases when calcium sulphate is recrystallized from phosphoric acid of different concentrations. The effect is utilized by applying a double recrystallization and knowledge of the phase transitions of particular forms of calcium sulphate. In this way 92–96% of the uranium originally present in the phosphogypsum is extracted, and then determined by extraction with a mixture of mono- and dinonylphenylphosphoric acids, and use of a modified spectrophotometric method with Arsenazo III.

Test analyses gave an error of $\pm 6\%$ in determination of uranium in phosphogypsum in the range 4–100 $\mu\text{g/g}$, the relative standard deviation being 9% at the 18.8 $\mu\text{g/g}$ level.

Twenty samples of phosphogypsum containing 30–60 μg of U per g were analysed by the method described and by X-ray fluorescence. The results obtained by the latter method were higher by an average of 2%.

Use of the phase equilibrium diagram for calcium sulphate in phosphoric acid makes it possible to apply the procedure for analysis of the phosphogypsum produced in the hemihydrate and anhydrite methods.

REFERENCES

1. A. V. Slack, *Phosphoric Acid*, Dekker, New York, 1968.
2. *Phosph. Potass.*, 1977, **87**, 37; 1977, **89**, 36; 1977, **94**, 24; 1978, **96**, 30.
3. *Ibid.*, 1980, **108**, 20; 1981, **111**, 31.
4. K. Kouloheris, *Chem. Age (India)*, 1980, **31**, 1.
5. H. Górecka and H. Górecki, *Przem. Chem.*, 1981, **60**, 373.
6. F. J. Hurst and W. D. Arnold, *Proc. Intern. Symp. Phosphogypsum*, Buena Vista, USA, 1980, Vol. 2, p. 424.
7. G. K. Show, *Report Dow Chemical Co.*, Dow-III, 1954.
8. E. W. Stolz, *Proc. Intern. Conf. Peaceful Uses Atomic Energy, Geneva*, 1958, **3**, 234.
9. H. Górecka and H. Górecki, *Pr. Nauk. AE we Wrocławiu*, 1980, **159**, 262.
10. C. F. Baes, Jr., *J. Phys. Chem.*, 1956, **60**, 805.
11. H. Górecki and H. Górecka, *Talanta*, 1984, **31**, 459.
12. *Idem*, *Pol. Pat. Appl.*, P-237275, 1982.
13. J. Korkisch and D. Dimitriadis, *Talanta*, 1973, **20**, 1199.
14. J. Korkisch and H. Hubner, *ibid.*, 1976, **23**, 283.

STANDARD-ADDITION PROCEDURE FOR THE DETERMINATION OF TRACES OF LEAD IN SOLID SAMPLES BY X-RAY FLUORESCENCE SPECTROMETRY

NIELS PIND

Department of Chemistry, Aarhus University, Langelandsgade 140, 8000 Aarhus C, Denmark

(Received 12 March 1984. Accepted 19 June 1984)

Summary—A standard-addition procedure for analysis of powdered solid samples by energy-dispersive X-ray fluorescence is described. Different amounts of the element to be determined are added to 4-6 specimens of the unknown sample. The spiked samples are prepared by mixing the powdered sample with an aqueous standard solution and drying the mixture. Homogeneously spiked samples are thus obtained with analyte and spike concentrations at the ppm level. The procedure has been investigated theoretically, and it is found suitable for the quantitative determination of lead at the ppm level. The accuracy of the technique for traces of lead has been tested on solid reference materials for the determination of lead. The quantitative results obtained compare well with those found by potentiometric stripping analysis.

X-Ray fluorescence spectrometry (XRF) is well suited for direct elemental analysis of solid samples. Quantitative analysis, however, is often hampered by interelement effects.¹ Ways of correcting for these effects can be divided into two main groups: (1) mathematical methods, *e.g.*, those based on fundamental parameters or "influence coefficients", which are applicable when a complete elemental analysis is done; (2) comparative methods, *e.g.*, those using an external standard, internal standard, double dilution or standard addition. The comparative methods are better suited for partial analysis of a sample. For single-element determinations, a comparative method is often chosen. In trace element determination, the dilution technique should be avoided, in order not to decrease the count-rate of the analyte line. Thus the main methods left for single-element determination are those using (1) an external standard; (2) an internal standard; (3) standard addition.

With the external-standard method, the general sample composition is assumed to be constant for all specimens of nearly identical composition. This allows the use of a calibration graph. However, the production of single-element calibration graphs requires a large number of standards of known composition, which must be close to that of the sample. Therefore, this approach can be quite cumbersome.

With the internal-standard and the standard-addition (spiking) methods, a known amount of a standard is added to the sample. For the internal-standard method, the element added must not be present in the sample. Thus problems arise when the internal-standard method is to be applied to complex samples, *e.g.*, coal fly-ash. Furthermore, the difficulty is increased if more than one internal standard is used.

The standard-addition method uses addition of the analyte itself and is frequently used in conjunction

with instrumental methods of trace analysis. In principle, the technique can be applied to any sample and in effect produces its own calibration graph. However, for successful application of the method, the spiked samples must be homogeneous. This condition is easy to meet for liquid samples and standards. Thus, standard addition is often used in conjunction with flame atomic-absorption spectrometry and electroanalytical techniques. The method has also been used in an XRF study on sulphur in gasoline.² The sulphur standard used in this investigation was di(*tert*-butyl)disulphide in sulphur-free iso-octane, which could be dissolved in the gasoline samples. When the sample is a solid, it is less easy to employ the standard-addition technique. If the analyte concentration is low, only minute amounts of standard should be added, and an even distribution within the sample volume can then be difficult to achieve. To determine the germanium content of low-germanium coal-ash, Campbell *et al.*³ used a solid standard for spiking. This standard was a germanium-rich lignite ash with a known content of germanium. These workers were thus able to obtain results accurate to within $\pm 10\%$ relative for ashes with a germanium-content exceeding 0.1%. For lower concentrations the accuracy decreased, probably because of non-homogeneous distribution of the solid spike.

The present paper describes a spiking procedure for quantitative XRF determination of trace elements in powdered solid samples: a dilute aqueous solution of the standard is mixed with the powdered sample, and the mixture is dried. In this manner, an even distribution of the spike is obtained. Apparently, despite its simplicity, this approach has not yet been reported in the literature. The procedure has been used for the XRF determination of lead in a number of solid materials, and accurate results have been obtained.

THEORY

The X-ray fluorescence intensity, I , of an analyte line excited by monoenergetic radiation, from a specimen of infinite thickness, can be expressed as:⁴

$$I = GA(1 + H)W$$

where G includes the primary intensity for the exciting radiation, the geometry factor and the detection efficiency for the analyte, A corrects for absorption of both excitation and fluorescence radiation, and H corrects for enhancement effects. Both A and H depend on the excitation energy and the specimen composition. W is the concentration of the analyte, expressed as a weight fraction.

The analyte concentration of a spiked specimen is given by

$$W = W_0W_p + W_s$$

where W_0 is the analyte concentration of the original sample, and W_p and W_s are the weight fractions of the original sample and of the pure elemental standard in the spiked specimen. The standard-addition procedure is based on the assumption that $GA(1 + H)$ is an unknown constant K . Since $W_p + W_s = 1$, there is a linear relationship between the intensity and the concentration of analyte in the spiked specimen:

$$I = B_0 + B_1W_s \quad (1)$$

where $B_0 = KW_0$ and $B_1 = K(1 - W_0)$. For each sample several spiked specimens with known W_s are prepared. Hence a set of fluorescence intensities and added concentrations is obtained. This set of intensities and corresponding weight fractions is used to establish a set of simultaneous equations of type (1), from which B_0 and B_1 are found by a least-squares procedure. The concentration of analyte in the original sample is then:

$$W_0 = B_0/(B_0 + B_1) \quad (2)$$

EXPERIMENTAL

Apparatus

The X-ray spectrometer used is equipped with a DTG Si(Li) detector with pulsed optical feed-back (crystal dimensions 30 mm² × 4 mm, resolution 160 eV at 5.9 keV). The main amplifier is a Canberra model 2020 spectroscopy amplifier with pulse pile-up rejection, and the analogue-to-digital converter is a Canberra model 2070. The digitized signals are stored by a Motorola 68000 microcomputer, which also performs on-line control of the spectrometer, data-acquisition, spectrum-display and data-transmission to the central computer, a VAX 11/780.

Samples were excited by the $K\alpha$ and $K\beta$ radiation of a secondary target, which was irradiated by an X-ray tube powered by a Philips PW 1732/10 high-voltage generator (60 kV, 80 mA, maximum power 4 kW). The irradiation chamber contained six secondary targets (Ti, Se, Mo, Ag, Te and Gd), which allow effective excitation of a wide range of fluorescence energies. Except for a few minor changes, the chamber is that described in detail by Christensen *et al.*⁵

For the determination of lead the spectrometer was operated at 40 kV, the Mo secondary target being used. The

current was set at 20–45 mA and chosen so that the dead-time of the detector system was less than 40% of the total measurement time. The counting time was 200–600 sec and chosen to give about 10⁴ counts for the Pb- $L\beta$ line for the unspiked samples. For each specimen, the spectrum was recorded three times, and the Pb- $L\beta$ line intensity was calculated by a simple summation procedure, with linear background subtraction. The Pb- $L\beta$ line was used because the As- $K\alpha$ line interferes with the Pb- $L\alpha$ line.

Reagents

Prepare standard solutions of lead (100 and 1000 ppm) by diluting a commercial standard solution (*e.g.*, Merck Titrisol No. 9969) with triply distilled water.

Preparation of spiked samples

Weigh accurately approximately 1 g of powdered solid sample. Transfer it into a 25-ml polyethylene test-tube, add the appropriate amount of standard solution, and mix carefully. Dry the spiked sample in a desiccator. Add four glass beads (5 mm diameter) to the dried sample and shake for 10 min. Finally, transfer the powder to the XRF sample-holder.

For each unknown sample, prepare 4–6 spiked specimens, such that the spiked sample with the highest analyte concentration will yield an analytical signal which is about three times the signal for the unspiked sample. Typically, 1–10 ml of 100-ppm lead solution should be added to a 1-g sample.

Measurements and calculations

Measure, at constant spectrometer settings, the analytical signals (Pb- $L\beta$ line-intensities) for the unspiked and spiked samples. For each measurement, set up an equation of type (1). From the resulting set of simultaneous equations, determine the constants B_0 and B_1 by linear regression. Finally, calculate W_0 from equation (2).

RESULTS AND DISCUSSION

Maximum amount of spike

The standard-addition method is valid provided that equation (2) holds, *i.e.*, the analytical signal is linearly proportional to the concentration of analyte in the spiked sample. The maximum amount of spike which can be added and still result in a linear signal/concentration relationship was estimated as follows. The procedure outlined by Christensen and Pind⁶ was used to calculate the Pb- $L\beta$ line intensity, I , for a spiked fly-ash. The standard chosen was elemental lead. The elemental composition of a representative model coal fly-ash was established in the following manner. The element concentrations certified by the National Bureau of Standards for NBS SRM 1633a trace elements in coal fly-ash were used, and the non-certified concentrations were taken to be correct. The remainder was arbitrarily assumed to be the oxygen in the ash. The compositions of samples made by spiking this were calculated. Hence for any ash of these spiked samples W_s was known, and the analytical signal, I , could be calculated. In this manner, a number of simultaneous equations of type (1) were established, and solved for B_0 and B_1 by a least-squares procedure. The quantity W_0 could then be found from equation (2). From the linear range of the relationship between concentration and intensity for this model fly-ash it was found that an

Table 1. Concentrations of lead (*ppm*) in solid materials found by XRF and the proposed standard-addition technique; the results are compared with those obtained with potentiometric stripping analysis (PSA) and, for the reference material, the NBS certified value

Sample	XRF	PSA	NBS Value
NBS SRM 1571 Orchard Leaves	44 42	43 ± 2	45 ± 3
NBS SRM 1632a Trace Elements in Coal, Bituminous	13.7 13.7	12.9 ± 1.7	12.4 ± 0.6
NBS SRM 1633a Trace Elements in Coal Fly-Ash	77.0 74.5	72 ± 3*	72.4 ± 0.4
Coal Fly-Ash, 1	225 227	231 ± 16	
Coal Fly-Ash, 2	71.5 63.8	58 ± 7	
Oil Fly-Ash	231 225 221	219 ± 16	

*Christensen *et al.*⁹

accurate value for W_0 could be obtained by spiking with not more than 5 times the amount of lead present in the sample itself.

The lead in the standard solution added is in practice most probably deposited in the sample as lead nitrate. The maximum amount of solid material derived from the added spike is small (<0.1% of the sample weight), so the change in sample weight and the change in the Pb- $L\beta$ intensity caused by the nitrate and other species in the spike will be negligible; in other words, the addition of the standard lead solution is equivalent to spiking with elemental lead.

The standard-addition procedure described above was used to determine the lead content of NBS SRM 1571 orchard leaves, NBS SRM 1632a trace elements in coal (bituminous), NBS SRM 1633a trace elements in coal fly-ash, two unspecified coal fly-ashes (1 and 2) and one unspecified oil fly-ash. For all materials, linear calibration relationships were obtained (correlation coefficient better than 0.99). Table 1 shows the lead concentrations found by the proposed method, and the certified concentrations. Potentiometric stripping analysis⁷ has recently been used to determine the amount of lead in the materials investigated here,^{8,9} and the results found are also given in Table 1.

The results in Table 1 indicate that an aqueous standard solution is suitable as spiking agent in the XRF determination of lead (and, by inference, of

other trace elements) at the ppm level in solid powdered samples. The results presented here were obtained with an energy-dispersive spectrometer and secondary target excitation. However, equation (2) is valid even when direct excitation and a wavelength-dispersive spectrometer are used, and the standard-addition method ought to perform equally well for quantitative work with such equipment.

Acknowledgements—The author is grateful to the Danish National Technical Research Council for financial support (grant nos. 16-0193, 16-1792 and 16-1866), to the Cement Laboratory at Aalborg Portland for supplying samples, to J. K. Christensen and L. Kryger for doing the potentiometric stripping analysis, to J. Marcussen for programming the Motorola, and to S. E. Rasmussen for his advice on the preparation of this paper.

REFERENCES

1. R. Tertian and F. Claisse, *Principles of Quantitative X-Ray Fluorescence Analysis*, Heyden, London, 1982.
2. R. A. Jones, *Anal. Chem.*, 1961, **33**, 71.
3. W. J. Cambell, H. F. Carl and C. E. White, *ibid.*, 1957, **29**, 1009.
4. C. J. Sparks, Jr., *Adv. X-Ray Anal.*, 1976, **19**, 19.
5. L. H. Christensen, S. E. Rasmussen, N. Pind and K. Henriksen, *Anal. Chim. Acta*, 1980, **116**, 7.
6. L. H. Christensen and N. Pind, *X-Ray Spectrom.*, 1981, **10**, 156.
7. D. Jagner, *Analyst*, 1982, **107**, 1275.
8. J. K. Christensen, L. Kryger and N. Pind, *Anal. Chim. Acta*, 1982, **136**, 39.
9. J. K. Christensen, L. Kryger and N. Pind, *ibid.*, 1982, **141**, 131.

ANALYTICAL DATA

PYROCATECHOLSULPHONPHTHALEIN COMPLEXAN AS AN ANALYTICAL REAGENT*

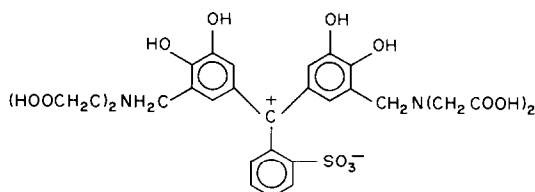
RU-QIN YU, ZHENG-QI ZHANG and ZHI-HUA ZHANG

Department of Chemistry and Chemical Engineering, Hunan University, Changsha, People's Republic of China

(Received 10 May 1983. Revised 7 May 1984. Accepted 22 June 1984)

Summary—Pyrocatecholsulphonphthalein complexan (PSC) has been synthesized from Pyrocatechol Violet (PV), iminodiacetic acid and formaldehyde by Mannich condensation. Its acid dissociation equilibria have been studied potentiometrically. Some characteristic properties of Xylenol Orange (XO) and PV are found in PSC, which is slightly superior to XO and PV in sensitivity as a chromogenic reagent for bismuth. The spectrophotometric characteristics of some metal ion-PSC complexes are reported.

Körbl *et al.*¹ reported that a number of chelating agents can be obtained from Pyrocatechol Violet (PV), Pyrogallol Red and rosolic acid by condensation with iminodiacetic acid and formaldehyde according to the procedure described by Schwarzenbach *et al.*,² but the synthesis and analytical application of these products have not been described. The acid-base indicator Cresol Red, from which Xylenol Orange (XO) is derived, is structurally related to PV. The structure of the product derived from condensation of PV and iminodiacetic acid therefore seems likely to be



Scheme 1.

This compound, pyrocatecholsulphonphthalein complexan (PSC), is in essence XO with its methyl groups replaced by phenolic groups, so PSC has the functional groups of both XO and PV. The question then is whether PSC possesses the characteristic properties of both XO and PV. For complexometric titration of bismuth, a mixture of PV and XO has been recommended as the indicator.³ PSC may therefore give even better results for such titrations. In this paper the synthesis of PSC and its characteristic properties as an analytical reagent are reported.

EXPERIMENTAL

Synthesis of PSC

Finely powdered PV (4.0 g) and iminodiacetic acid (5.4 g) were dissolved in 15 ml of water containing 3.2 g of sodium hydroxide, and 80 ml of glacial acetic acid were added, with

stirring. The mixture was transferred into a 250-ml three-necked, round-bottomed flask fitted with a reflux condenser, stirrer and dropping funnel containing 40% aqueous formaldehyde. After addition of 2.4 ml of formaldehyde the mixture was heated at 55–60° for 12 hr, with stirring. A further 2.4 ml of formaldehyde were added and the mixture was stirred for a total of 7 days at 55–60°. The formation of PSC was checked before proceeding further. To do this, a few drops of reaction mixture were added to 5 ml of acetone; the dark-green precipitate produced was separated and dissolved in a small amount of water. The solution gave a purple-red colour with La(III) in acetate buffer at pH 5.0. Completion of the Mannich reaction was identified by paper chromatography with butan-1-ol-glacial acetic acid-water (3:1:1, v/v). The reaction was considered complete if the chromatogram showed only a green spot at $R_f = 0$. The hot reaction mixture was then filtered by suction, and the filtrate was poured into 1 litre of acetone, with stirring. After standing for 1 hr the dark-green precipitate was filtered off under suction and washed with a small amount of acetone. The product was dried at 40° under vacuum. The yield was about 5.6 g of crude product (56%).

Purification and analysis of PSC

A 2.0-cm bore chromatographic column 80 cm long was prepared with Polyamide 6 (Beijing). About 5 g of the crude product was dissolved in the minimum amount of water, applied to the top of the column, and eluted with water at a flow-rate of 0.5 ml/min. The green fraction of the eluate (*ca.* 50 ml) was evaporated to dryness at 40° under vacuum. The product was evaluated by paper chromatography as described above, and also by thin-layer chromatography. A 9:1 w/w mixture of Polyamide 6 and cellulose powder slurried with methanol was spread on a 6.5 × 18 cm glass plate to give a layer 0.3–0.5 mm thick. The sample, dissolved in water, was applied to the air-dried plate and the chromatogram developed with 0.05M sodium hydroxide ($R_f = 0.83$). The product was a dark green hygroscopic solid with metallic lustre. Analysis: C₂₉H₁₈N₂O₁₅S requires 4.08%N, 4.66%S; found, 4.2%N, 4.5%S. The principal infrared bands were at 525, 700, 900, 1380, 1590, 2980 and 3350 cm⁻¹.

Solutions

All solutions were prepared with demineralized water and analytical-reagent grade chemicals unless otherwise stated.

The stock solution of 10⁻²M PSC was prepared from the purified reagent and diluted as required. Cetyltrimethylammonium bromide (CTMAB, Fluka) was used

*Research supported by Chem. Grant No. 566 of Science Foundation, Academia Sinica, PRC.

without further purification. Standard solutions of rare-earth ions were prepared from the corresponding spectrally pure oxides (except La_2O_3 , 99.99% and Y_2O_3 , 99.999% pure). Solutions of other metal ions were standardized, when necessary, by EDTA titration. The carbonate-free hydroxide solutions used in the potentiometric titrations

$$\bar{n} = \frac{K_{a,1}[\text{H}^+] + 2K_{a,1}K_{a,2}[\text{H}^+]^2 + \dots + 11K_{a,2}K_{a,2}\dots K_{a,11}[\text{H}^+]^{11}}{1 + K_{a,1}[\text{H}^+] + K_{a,1}K_{a,2}[\text{H}^+]^2 + \dots + K_{a,1}K_{a,2}\dots K_{a,11}[\text{H}^+]^{11}} \quad (1)$$

were prepared by passing 0.2M potassium chloride through a column (8 mm bore, 10 mm long) of Zerolit FF (OH^- form, 200 mesh). The potassium hydroxide solution obtained was collected in a flask protected with a soda-lime tube, and standardized by acid-base titration.

Potentiometric studies of dissociation equilibria

PSC solutions were potentiometrically titrated with potassium hydroxide under an atmosphere of nitrogen.⁴ The flow of nitrogen was stopped during readings. The degree of neutralization a and average number of bound protons \bar{n} were calculated and the \bar{n} -pH curves constructed. The ionization constants were calculated by the Bjerrum method.⁵

RESULTS AND DISCUSSION

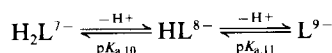
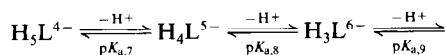
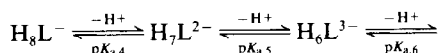
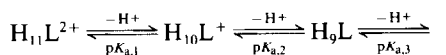
Synthesis and purification of PSC

Preliminary experiments showed that in aqueous alcohol medium the Mannich reaction was difficult to control, owing to the tendency to polymerization. Of the tested reaction media, glacial acetic acid gave the best yield. The paper chromatography described showed that the spot of crude product remained at the starting point ($R_f = 0$) and did not contain unreacted PV ($R_f = 0.45$).

For the separation on the Polyamide 6 column, water was used as the eluent to avoid introducing alkali-metal ions. A blue fraction of impurities appeared before the green fraction for some batches of crude product. The blue fraction was discarded and only the green fraction collected. The main part of the impurities (brown in colour) remained on the column.

Dissociation of PSC

Under strongly acidic conditions PSC can take up two protons to give a form that will be represented by $\text{H}_{11}\text{L}^{2+}$. The acid-base equilibria of PSC are:



The dissociation of the sulphonate group and the two

protonated tertiary amino groups ($K_{a,1}$ - $K_{a,3}$) takes place in acidic medium. The constants $K_{a,4}$ - $K_{a,11}$ are related to the dissociation of the carboxyl and phenol groups. The Bjerrum formation function \bar{n} for the protonation of L^{9-} may be written as

and can be calculated from the equation:⁶

$$\bar{n} = \frac{(9-a)T_{\text{psc}} + [\text{OH}^-] - [\text{H}^+]}{T_{\text{psc}}} \quad (2)$$

where T_{psc} is the total PSC concentration and a is the degree of neutralization, defined as ratio of moles of sodium hydroxide added to moles of PSC taken.

The formation curves for protonation of L^{9-} in the absence and presence of CTMAB ($1.5 \times 10^{-3}M$) are shown in Fig. 1. The $pK_{a,i}$ values calculated are presented in Table 1.

The presence of CTMAB inhibits the dissociation of the first carboxylic acid group ($K_{a,4}$), but promotes the remaining steps.

Figure 2 shows the absorption spectra of PSC at various pH values. The equilibrium corresponding to constant $K_{a,7}$ is mainly responsible for the colour change of the indicator from yellow to blue. On addition of CTMAB to the yellow PSC solution at pH 5.0, the $K_{a,7}$ value increases remarkably and the solution turns blue. The values of $K_{a,7}$ and $K'_{a,7}$ can easily be determined spectrophotometrically. From the pH-absorbance curves at 620 nm (for $K_{a,7}$) or 610 nm (for $K'_{a,7}$), $pK_{a,7}$ and $pK'_{a,7}$ have been found to be 5.36 and 4.49, respectively. These values are in good agreement with those obtained from potentiometric measurements.

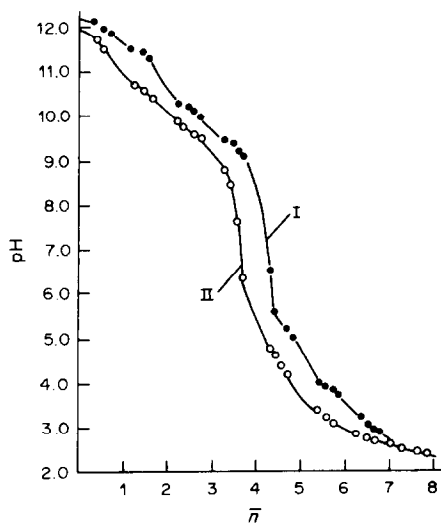


Fig. 1. The formation curves for protonation of PSC (L^{9-}): I, in the absence of CTMAB; II, in the presence of CTMAB ($1.5 \times 10^{-3}M$).

Table 1. Acid dissociation constants of PSC

<i>i</i>	4	5	6	7	8	9	10	11
$pK_{a,i}$	2.03	3.08	3.92	5.40	9.36	10.20	11.40	12.15
$pK'_{a,i}$	2.60	2.95	3.30	4.50	8.25	9.65	10.60	11.70

$K_{a,i} = \frac{[H_{11-i}L][H^+]}{[H_{11-i+1}L]}$; ionic strength = 0.1 (KCl); the $K'_{a,i}$ values are the apparent acid dissociation constants determined in the presence of CTMAB.

Colour reactions of PSC with metal ions

PSC forms intensely coloured water-soluble complexes with many metal ions. The characteristics of these reactions are summarized in Table 2.

The complexation reaction of Bi(III) with PSC has been taken as an example for more detailed investigation. In 0.10M nitric acid medium, at least two Bi(III)-PSC complex species are formed. In the presence of excess of Bi(III), a blue 1:1 complex is formed, with absorption maximum at 620 nm. When PSC is in excess, a red complex with metal:ligand ratio of 1:2 is formed, with an absorption maximum at 505 nm. The stepwise stability constants of the 1:1 and 1:2 complexes, determined by the method of corresponding solutions modified by Guan *et al.*⁷ are $\log K_1 = 5.45$ and $\log K_2 = 3.89$ (in 0.1M nitric acid/0.1M potassium nitrate medium). The apparent molar absorptivity of the 1:2 complex is 2.15×10^4

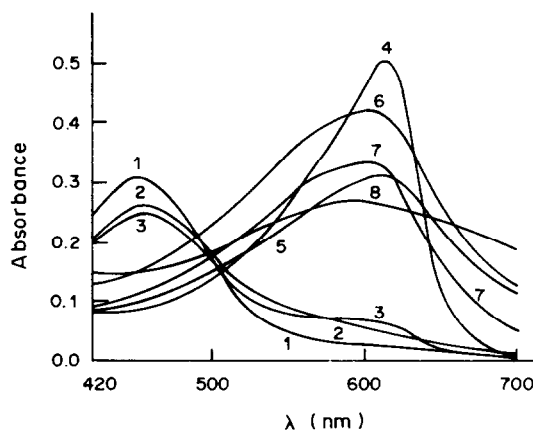


Fig. 2. Absorption spectra of PSC at various pH values: 1, 2.41; 2, 3.30; 3, 4.00; 4, 6.10; 5, 9.46; 6, 10.50; 7, 11.80; 8, 13.00.

$l \cdot \text{mole}^{-1} \cdot \text{cm}^{-1}$. The sensitivity of PSC as a colorimetric reagent for Bi(III) is better than that of XO ($\epsilon_{530} = 1.6 \times 10^4 l \cdot \text{mole}^{-1} \cdot \text{cm}^{-1}$)⁸ or PV ($\epsilon_{580} = 1.37 \times 10^4 l \cdot \text{mole}^{-1} \cdot \text{cm}^{-1}$).⁹ PSC is a useful indicator for the EDTA titration of bismuth, giving a colour change from blue to yellow in 0.5M nitric acid medium. A transient purple-red colour develops just before the equivalence point, and is a useful signal of the approaching end-point. The relative standard devi-

Table 2. Spectrophotometric characteristics of metal-PSC complexes formed with excess of PSC

Metal ion	pH*	λ_{max} , nm	ϵ , $10^4 l \cdot \text{mole}^{-1} \cdot \text{cm}^{-1}$
Al(III)	4.0	530	0.26
Be(II)	5.0	500	0.32
Bi(III)	0.1M HNO ₃	505	2.15
Cd(II)	5.0	580	0.70
Ce(III)	4.2	550	1.50
Co(III)	5.0	560	0.94
Cr(III)	4.0†	530	1.31
Cu(III)	5.0	560	1.06
Er(III)	4.20	550	1.09
Fe(II)	5.0	570	1.20
Fe(III)	3.6	530	1.84
Ga(III)	1.5 (HNO ₃)	520	0.55
Gd(III)	4.20	550	1.28
Hg(II)	5.0	510	0.54
La(III)	4.20	580	1.81
Mg(II)	10.0	550	1.25
Mn(II)	5.0	530	0.51
Nb(V)	2.4 (ClCH ₂ COOH-HCl)	530	1.50
Nd(III)	4.20	550	0.93
Ni(II)	5.0	620	1.23
Pb(II)	5.0	540	1.20
Pr(III)	4.20	550	1.00
Sm(III)	4.20	550	0.95
Sn(II)	4.0	530	1.00
Sn(IV)	0.1M HCl	530	1.87
V(V)	3.6‡	540	0.86
Y(III)	4.20	560	1.85
Zn(II)	5.0	550	1.70
Zr(IV)	0.1M H ₂ SO ₄	530	1.80

*HOAc-NaOAc buffer unless otherwise stated.

†HOAc-NaOAc buffer containing ascorbic acid. The colour develops after heating in a boiling water-bath for 10 min.

‡Heating in a boiling water-bath for 5 min.

ation is found to be 0.06%. Details will be published elsewhere.

In acetate solution buffered at pH 4.2, lanthanum(III) forms a 1:2 red complex with PSC, apparent stability constant 1.23×10^9 (pH 4.2, ionic strength 0.1M). Similarly, yttrium give a 1:2 complex with an apparent stability constant of 6.17×10^7 (pH 4.2, ionic strength 0.1M). In the presence of CTMAB, lanthanum and yttrium form blue ternary complexes with PSC, the molar absorptivities of the La(III) and Y(III) complexes being 6.5×10^4 (650 nm) and 7.31×10^4 l. mole⁻¹. cm⁻¹ (640 nm), respectively (for [metal] = $1 \times 10^{-5}M$, [PSC] = $3.5 \times 10^{-4}M$). A preliminary investigation shows that the increase in sensitivity seems to be the formation of complexes with unusual metal-to-ligand molar ratios. It is interesting that addition of an organic solvent such as ethylene glycol depresses the formation of the lanthanum ternary complex but remarkably enhances the absorptivity of the Y(III)-PSC-CTMAB species. This effect can be utilized for the determination of yttrium in the presence of lanthanum.

When PSC solution is mixed with an aged zirconium(IV) solution, a slow complexation reaction takes place. Trace amounts of fluoride catalyse this reaction, even at a fluoride concentration as low as $5.0 \times 10^{-10}M$. This provides a promising means of kinetic assay of traces of fluoride. It is difficult to detect fluoride in water at levels below $10^{-7}M$ with a

lanthanum fluoride electrode, because traces of fluoride are released from the membrane surface itself into the test solution, and the PSC-Zr(IV) reaction will easily distinguish between two samples of demineralized water, one of which has been in brief contact with a lanthanum fluoride electrode. This is a very sensitive qualitative test, but its analytical characteristics depend on the history of the zirconium solution, and quantitative application will require further investigation.

Acknowledgement—The authors are grateful to Professor Shu-Chuan Liang, Institute of Chemistry, Academia Sinica, Beijing, for valuable comments and encouragement.

REFERENCES

1. J. Körbl, V. Svoboda and D. Terziska, *Chem. Ind. London*, 1958, 1232.
2. G. Anderegg, H. Flaschka, R. Sallmann and G. Schwarzenbach, *Helv. Chim. Acta*, 1954, **37**, 113.
3. N. Zhou, *Huaxue Shiji*, 1979, 273.
4. A. Albert and E. P. Serjeant, *Ionization Constants of Acids and Bases*, pp. 16–68. Methuen, London, 1962.
5. J. Bjerrum, *Metal Amine Formation in Aqueous Solution*. Haase, Copenhagen, 1941.
6. J. Inczedy, *Analytical Applications of Complex Equilibria*, p. 98, Horwood, Chichester, 1976.
7. Y. W. Guan and G. X. Xu, *Acta Chim. Sinica*, 1963, **29**, 37.
8. B. Buděšínský, in *Chelates in Analytical Chemistry*, H. A. Flaschka and A. J. Barnard (eds.), Vol. 1, p. 21. Dekker, New York, 1967.
9. M. Malát, *Z. Anal. Chem.*, 1962, **186**, 418.

ETUDE DE LA PURETE DES ECHANTILLONS COMMERCIAUX D'EOSINE

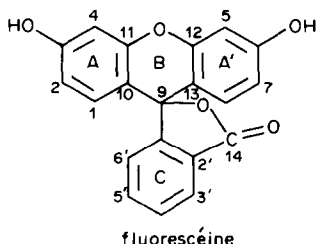
D. FOMPEYDIE et P. LEVILLAIN

Laboratoire de Chimie Analytique, UER des Sciences Pharmaceutiques et Biologiques,
4, avenue de l'Observatoire, 75270 Paris Cedex 06, France

(Reçu le 15 mai 1984. Accepté le 15 juin 1984)

Résumé—L'étude de 8 échantillons commerciaux d'éosine montre que l'utilisation de ce colorant comme médicament se heurte à 3 problèmes: hydratation et teneur en composés minéraux très variables selon les échantillons, mais surtout complexité importante de la fraction xanthénique qui peut contenir jusqu'à 8 constituants. Cette étude a nécessité la mise au point d'un certain nombre de méthodes d'analyse décrites dans cet article.

Deux colorants xanthéniques ont été inscrits comme médicaments à différentes Pharmacopées. La fluorescéine y figure depuis longtemps sous diverses formes¹⁻³ et des critères de pureté ont également été définis par l'Association of Official Analytical Chemists.⁴ Enfin il est possible de s'en procurer des échantillons commerciaux suffisamment purs.⁵



Par contre, l'éosine (tétrabromo-2,4,5,7 fluorescéine) n'a été inscrite que récemment à la IXe édition de la Pharmacopée Française, et Marshall⁵ a déjà signalé l'hétérogénéité des échantillons commerciaux de ce colorant.

Lors d'études antérieures sur les propriétés des colorants xanthéniques,⁶⁻¹⁰ l'obtention d'éosine pure s'est révélée difficile. Il peut donc être intéressant de rapporter les résultats observés lors de l'étude d'échantillons commerciaux d'éosine, ces résultats différant notablement de ceux déjà publiés et pouvant aider à mieux cerner les problèmes de la monographie de la Pharmacopée.

PARTIE EXPERIMENTALE

Préparation des colorants bromés sur le cycle xanthénique

Les dérivés bromés sur le cycle xanthénique sont préparés par action du mélange bromate-bromure sur la fluorescéine en milieu mixte eau-acétone acide. Cette technique évite la formation d'esters du groupement carboxylique.¹¹ On utilise une quantité de bromate double de celle stoechiométriquement nécessaire pour obtenir le dérivé recherché. On obtient un mélange de colorants qu'on sépare sur colonne d'échangeurs d'ions DEAE Trisacryl M¹² à

l'aide d'un gradient eau-méthanol puis méthanol-acide formique.

Préparation des esters des colorants xanthéniques bromés

Ils peuvent être obtenus par deux voies. (1) Préparation et purification de l'éthylfluorescéine par synthèse en milieu acide dans l'alcool correspondant,¹³ puis bromation et séparation chromatographique du mélange obtenu selon les techniques décrites au paragraphe précédent. (2) On peut estérifier individuellement chacun des colorants xanthéniques en milieu alcoolique acide.¹³ Il reste toujours une petite quantité de colorant xanthénique non estérifié qu'on peut éliminer par chromatographie sur Sephadex LH 20, en éluant au méthanol, ou sur DEAE Trisacryl M, à l'aide du mélange utilisé pour la séparation du colorant xanthénique correspondant.¹²

Préparation des produits bromés sur le cycle C

Nous avons préparé le bromo 3'-4'-5'-6' fluorescéine par action du résorcinol sur l'anhydride phtalique tétrabromé selon la méthode classique de préparation de la fluorescéine.¹⁴ La bromation du cycle xanthénique et la séparation des colorants formés s'effectuent comme précédemment, l'éluant de la colonne étant réalisée par un gradient de 0 à 15% d'acide formique dans le méthanol.

Caractérisation des produits formés

La caractérisation des produits formés a été obtenue:

—par RMN¹H à 270 MHz sur un appareil Bruker WH 270 FT;

—par détermination des maximums d'absorption dans le visible sur un appareil Beckmann Acta III;

—par détermination du R_M en chromatographie sur couche mince de gel de silice avec un mélange éluant toluène-acide acétique (65:35 v/v) en cuve saturée.

Etude de la pureté des échantillons commerciaux

L'étude de l'hydratation des échantillons a été effectuée par dessiccation à 135°. La fraction minérale a été étudiée par la méthode des cendres sulfuriques de la Pharmacopée et le sodium dosé par photométrie de flamme. Le pourcentage en colorant dans les échantillons a été obtenu par précipitation en milieu acide puis dessiccation du précipité.⁴ La séparation chromatographique a été effectuée sur couche mince de gel de silice avec un mélange toluène-acide acétique (65:35 v/v) en cuve saturée.¹⁵

En HPLC, nous avons utilisé une colonne de silice greffée C₁₈ (longueur 10 cm) avec un appareil Varian 5000 équipé d'un détecteur Varichrom. Le mélange éluant est constitué

d'un gradient méthanol-eau (allant de 10 à 20% d'eau) renfermant une concentration constante 0,05M d'acide perchlorique.

L'analyse qualitative des échantillons a été effectuée par chromatographie sur couche mince par comparaison des R_f avec ceux obtenus pour des produits purs de référence.

Le dosage des fractions a été effectué:

(1) après séparation chromatographique sur couche mince — par densitométrie des taches à l'aide d'un intégrateur Sebia "Cellomatic" par rapport à un étalon interne d'érythrosine;

— par élution des spots dans l'ammoniaque à 0,5% et mesure de l'absorption à l'aide d'un spectrophotomètre Beckmann Acta III;

(2) par HPLC, en étalonnant l'appareil à l'aide des produits de référence;

(3) par spectrophotométrie des solutions à l'aide d'un appareil Hewlett-Packard 8450 A. Le calcul des concentrations est effectué par rapport à des solutions étalons des différents constituants des mélanges et à partir des courbes dérivées.

Le brome a été dosé par le laboratoire de microanalyse du CNRS. L'étude a été effectuée sur huit échantillons commerciaux d'éosinate de différentes origines: éosinate de sodium 1, Y RAL n° 18; 2, Aldrich (numéro de lot non précisé); 3, Merck 25 89282; 4, Flucka 19637187; 5, RAL extra cristallisée; 6, Merck 2520149; 7, Flucka (lot non précisé); 8, éosinate de potassium RAL.

Deux échantillons ont été étudiés dès l'ouverture du flacon (n° 3 et 4) alors que les autres étaient plus anciens.

Nous avons également analysé un échantillon de dibromo 4,5 fluorescéine moléculaire, Koch and Light, n° 65491.

RESULTATS

Caractéristiques des produits purs

Les caractéristiques des produits obtenus sont rassemblés dans le tableau 1 pour la RMN ^1H dans le DMSO d_6 et dans le tableau 2 pour les propriétés d'absorption dans le visible. En RMN ^1H on observe en outre deux signaux à $\delta = 0,89$ et 4,05 ppm pour les esters éthyliques.

La figure 1 représente les courbes reliant les R_M , en

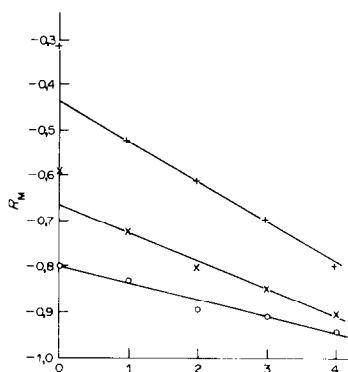


Fig. 1. R_M de la fluorescéine et de ses dérivés en fonction du nombre d'atomes de brome fixés sur le cycle xanthénique: *fluorescéine; + éthylfluorescéine; O fluorescéine bromée sur le cycle C.

chromatographie sur couche mince, au nombre d'atomes de brome fixé sur le cycle xanthénique.

Pureté des échantillons commerciaux

Le tableau 3 regroupe les résultats d'ensemble obtenus pour les échantillons étudiés.

DISCUSSION

Préparation des produits de référence

Les produits purs de référence ont été obtenus par application ou modification de méthodes classiques de synthèse, les mélanges obtenus étant séparés sur échangeur d'ion DEAE Trisacryl M. La pureté de ces produits a été vérifiée par chromatographie sur couche mince. La nature des colorants isolés peut être déduite de la réaction ayant servi à les préparer et vérifiée par des propriétés simples.

Pour les produits substitués sur le cycle xanthénique, la RMN ^1H montre la disparition progressive des protons en fonction du nombre

Tableau 1. Déplacements chimiques δ ppm obtenus en RMN ^1H pour les colorants xanthéniques dans le DMSO d_6

	H ₁	H ₂	H ₄	H ₅	H ₇	H ₈	H ₉	H ₄	H ₅	H ₆
Fluorescéine (Fl)	6,60	6,47	6,47	6,47	6,47	6,60	7,96	7,68	7,76	7,23
Bromo-4 Fl	6,67	6,50	—	6,52	6,50	6,67	7,94	7,65	7,74	7,24
Bromo-4,5 Fl	6,72	6,54	—	—	6,54	6,72	7,96	7,69	7,77	7,32
Bromo-2,4,5 Fl	6,73	—	—	—	6,53	6,82	7,96	7,70	7,77	7,35
Eosine	6,85	—	—	—	—	6,85	8,00	7,73	7,81	7,47

Tableau 2. Caractéristiques des spectres électroniques des colorants xanthéniques, de leurs esters et des dérivés bromés sur le cycle C (solvant NH_4OH 0,5%)

	Fluorescéine (Fl)	Bromo-4 Fl	Bromo-4,5 Fl	Bromo-2,4,5 Fl	Eosine
λ_{max} , nm	490	496	504	510	516
ϵ , $l \cdot \text{mole}^{-1} \cdot \text{cm}^{-1}$	$1,00_4 \cdot 10^5$	$9,24 \cdot 10^4$	$8,54 \cdot 10^4$	$9,07 \cdot 10^4$	$1,02_4 \cdot 10^5$
ester éthylique					
λ_{max} , nm	494	500	508	514	520
dérivés bromés en C					
λ_{max} , nm	510	517	525	531	539

Tableau 3. Résultats (exprimés en % de la prise d'essai) obtenus pour différents échantillons commerciaux et dibromofluorescéine

échantillon	perte à la dessiccation	Na	rendres sulfuriques*	colorant précipité	éosine	tribromo fluorescéine	dibromo fluorescéine	bromo fluorescéine	fluorescéine	éthyl éosine	méthyl éosine	éthyltribromo fluorescéine	éthylidibromo fluorescéine	bromo éosine	nombre de Br par molécule	rappor absorbance 516/490 nm
1	9,2	6,50	6,40	79,5	54	17,6	2,6	—	—	4,9	—	0,4	—	—	3,54	2,32
2	14,4	5,83	6,30	78	47,5	25,5	1,7	†	†	1,4	—	0,5	—	1,4	3,55	2,22
3	2,5	6,57	7,20	88,2	59	15,3	8,3	—	—	4,8	—	0,8	†	—	3,27	2,09
4	3,95	6,35	6,90	86,7	61,7	22,4	0,1	—	—	2,5	—	—	—	—	3,39	2,36
5	9,6	7,53	—	78,5	58,7	17,1	2,1	—	—	—	0,6	—	—	—	3,60	2,49
6	11,75	5,96	5,90	80,2	64,6	11,1	5,5	—	—	—	—	—	—	—	3,62	2,54
7	9,35	6,72	—	80,1	49,5	25,4	0,5	—	—	3,8	—	0,9	—	—	3,57	2,45
8	11,8	8,18	—	73,6	70	3,6	—	—	—	—	—	—	—	—	3,64	2,63
Bromo 4,5 Fl	2,2	0	0,20	97,5	7,5	21	36	24	9	—	—	—	—	—	—	—

*Exprimées en sodium.

†Traces non quantifiables.

d'atomes de brome fixés en 4,5 puis en 2,7 (tableau 1). Le spectre des esters possède en outre les signaux du groupement éthyle ($\delta = 0,89$ et 4,05 ppm). Enfin pour les dérivés bromés sur le cycle C, on observe la disparition des massifs situés entre 7 et 8 ppm en même temps qu'un déblindage des protons H_{1-8} sous l'influence de la modification du noyau C.

En chromatographie sur couche mince, la courbe reliant le R_M au nombre d'atomes de brome fixés sur le cycle xanthénique est sensiblement une droite pour les trois classes de composés. Comme prévu d'après la valeur de l'énergie d'adsorption du brome sur silice ($Q = -0,17^{16}$) l'augmentation de la teneur en cet élément entraîne une accélération de la migration du colorant (figure 1).

Les spectres d'absorption dans le visible sont d'aspect semblable. Leur maximum subit un effet bathochrome lié à la présence de brome sur le noyau xanthénique. L'estérification entraîne en outre un déplacement de +4 nm alors que la bromation du cycle C augmente de 20 nm la position du maximum (tableau 2).

Pureté des échantillons commerciaux

Cette étude met en évidence l'importance et la variabilité de la teneur en eau des éosinates, teneur qui peut atteindre 15% pour des échantillons anciens. D'autre part, la conservation des sels augmente fortement leur hydratation: pour l'échantillon n° 3 la perte à la dessiccation passe de 2,5 à 6,6% après deux mois de conservation. Enfin les formes moléculaires sont beaucoup moins solvatées que les sels: nous les vérifions ici pour la dibromofluorescéine étudiée, comme nous l'avons observé pour la fluorescéine.⁷ Ce caractère fortement hygroscopique des sels pose le problème de leur conservation.

La concentration en sodium, supérieure à celle attendue de la teneur réelle en colorant, est liée à l'existence d'impuretés minérales et de dérivés moins

bromés que l'éosine renfermant un pourcentage plus important de cet ion. Enfin, par différence avec les résultats obtenus par photométrie de flamme, les rendres sulfuriques—dont les résultats sont ici exprimés en sodium—montrent que les échantillons contiennent sans doute de faibles quantités d'autres cations.

La teneur globale en colorant, déterminée par gravimétrie de la forme moléculaire précipitée en milieu acide, dépend essentiellement de l'hydratation. La somme des concentrations en sodium et en colorant et de la perte à la dessiccation est en effet assez proche de 100%, montrant ainsi que la teneur en éléments minéraux est généralement faible.

L'analyse qualitative de la fraction xanthénique, effectuée par chromatographie sur couche mince, montre la complexité des produits étudiés, le nombre de composants pouvant varier de 2 à 8. Il semble donc difficile d'obtenir des échantillons commerciaux purs. On peut noter que le rapport des absorbances à 516 et 490 nm—égal à 2,81 pour un échantillon d'éosine pure—paraît constituer un test valable de la pureté de l'éosine (tableau 3).

L'étude quantitative des différentes fractions a été effectuée sur trois échantillons, par quatre techniques différentes avec une bonne concordance des résultats. Les valeurs du tableau 3 ont été obtenues par chromatographie sur couche mince suivie d'élution et mesure de l'absorbance des solutions. Les résultats montrent que la teneur globale en éosine est généralement faible et comprise entre 50 et 70% des échantillons. On peut remarquer que la complexité des échantillons rend inapplicable la méthode de spectrophotométrie à trois longueurs d'onde proposée par Marshall⁵ car elle ne prend en compte que trois colorants (éosine, tribromofluorescéine, fluorescéine) qui ne reflètent pas la composition de la plupart des échantillons.

Cette complexité des éosinates commerciaux

confirme que la bromation de la fluorescéine est très délicate: elle présente en effet deux difficultés importantes. Selon la densité électronique calculée sur le cycle xanthénique⁷ la bromation s'effectue en 4,5 puis en 2,7 enfin beaucoup plus difficilement sur le cycle C désactivé par le groupement carboxylique. Toutefois les réactions sont assez lentes et la vitesse diffère notablement selon la position. L'excès de réactif peut donc attaquer le produit formé avant que le produit initial ait entièrement réagi. On retrouve donc systématiquement dans le milieu plusieurs composés à différents stades de bromation (fluorescéine, dérivés mono, di, tri et tétrabromés sur le cycle xanthénique et, en présence d'un excès important de brome destiné à accélérer la réaction, dérivés de l'éosine bromés sur le cycle C). Ceci est confirmé par la teneur moyenne en brome par molécule, toujours inférieure à 4 (tableau 3). Par ailleurs la réaction se produit plus régulièrement en milieu acide mais alors les colorants sont insolubles dans l'eau. On évite leur précipitation en ajoutant au milieu un solvant organique miscible à l'eau. Ce sont les alcools qui sont le plus souvent employés mais leur présence entraîne la formation d'esters du groupement carboxylique qui augmente la complexité des produits commerciaux.

CONCLUSION

La complexité des échantillons commerciaux d'éosinate de sodium pose le problème de la pureté des produits à utiliser en pharmacie. Il est certes possible de synthétiser de l'éosine très pure¹¹ ou de

séparer par chromatographie les produits commerciaux¹² mais le prix de revient devient alors très élevé. Il semble donc nécessaire de préciser la nature et la teneur limite en impuretés admissibles, en tenant compte des difficultés de la synthèse et en se basant sur leur efficacité thérapeutique et leur toxicité éventuelle.

LITTÉRATURE

1. *British Pharmacopoeia*, London, 1973.
2. *Deutsches Arzneibuch*, 7e Ed., Bd. 3, Berlin, 1964.
3. *U.S. Pharmacopoeia*, XIX, Washington, 1975.
4. *Official Methods of Analysis of the Association of Official Analytical Chemists*, 13e Ed., Horwitz (ed.), Washington, 1980.
5. P. N. Marshall, *Stain Technol.*, 1975, **50**, 107.
6. J.-P. Dubost, J.-M. Léger, J.-C. Colleter, P. Levillain et D. Fompeydie, *Compt. Rend.*, 1981, **292**, **II**, 965.
7. D. Fompeydie, *Thèse d'Etat ès Sciences Pharmaceutiques*, Paris, 1978.
8. D. Fompeydie, F. Onur et P. Levillain, *Bull. Soc. Chim. France*, 1979, 1-375.
9. D. Fompeydie et P. Levillain, *ibid.*, 1980, 1-459.
10. D. Fompeydie, A. Rabaron, P. Levillain et R. Bourdon, *J. Chem. Res. (M)*, 1981, 4052.
11. D. Fompeydie, F. Onur et P. Levillain, *Bull. Soc. Chim. France*, 1982, II-5.
12. D. Fompeydie et P. Levillain, *J. Chromatog.*, sous presse.
13. A. I. Vogel, *A Text Book of Practical Organic Chemistry*, 3e Ed. Longmans, London, 1961.
14. M. V. Liebig, *J. Prakt. Chem.*, 1915, **88**, 26.
15. M. B. Naff et A. S. Naff, *J. Chem. Ed.*, 1963, **40**, 534.
16. L. R. Snyder, *Principles of Adsorption Chromatography*, Dekker, New York, 1968.

Summary—Eight commercial samples of eosin have been analysed. Three problems were encountered in selecting material for use as a drug: the degree of hydration, the inorganic content and, above all, the composition of the xanthene moiety, which could contain up to 8 dyes.

SPECTROPHOTOMETRIC DETERMINATION OF FORMATION CONSTANTS OF 1:1 COMPLEXES OF LANTHANIDES WITH 4-(2-PYRIDYLAZO)RESORCINOL (PAR)

EMIKO OHYOSHI

Yatsushiro College of Technology, Hirayamashinmachi 2627, Yatsushiro, Kumamoto, 866 Japan

(Received 7 February 1984. Revised 23 April 1984. Accepted 25 May 1984)

Summary—Complex formation (1:1) between lanthanides(III) and 4-(2-pyridylazo)resorcinol (PAR or H₂R) has been studied by spectrophotometry. The method is based on indirect estimation of the protonated (MHR) and the normal (MR) complexes by measuring the absorbance at the peak for the ligand, which decreases with increasing metal concentration at a constant pH. Similar experiments were made at various pH values. Both MHR and MR complexes were found to be formed in the pH range 5–6. Their formation constants, $\log K_{\text{MHR}}$ and $\log K_{\text{MR}}$, determined by graphical analysis, ranged from 3.78 ± 0.02 (Ce) to 4.39 ± 0.02 (Lu), and from 9.61 ± 0.06 (Ce) to 10.70 ± 0.05 (Lu), respectively. The acidity of the MHR complexes parallels the order of stability of the MR complexes.

4-(2-Pyridylazo)resorcinol (PAR or H₂R) forms intensely coloured complexes with many metal ions and is widely used in analytical chemistry.^{1,2} The formation of these complexes is known to be very dependent on pH but little information on the complexation equilibria has been obtained. Such information will aid in choosing experimental conditions so as to increase the selectivity. The system is rather complicated because of simultaneous formation of the protonated and normal type of complexes with many metal ions. In a previous paper³ we proposed a method for facilitating the spectrophotometric analysis of these two types of 1:1 complex, and applied it to the zinc and lanthanum PAR complexes. The results showed that the method was more applicable to the lanthanum system because a larger variation in absorbance with change in metal concentration could be obtained, owing to the lower absorptivity of LaHR at the absorption peak for the free ligand, PAR. This suggests that the method should also be applicable to the system of PAR and the other lanthanides(III). Sommer and Novotna⁴ have studied the PAR complexes of several lanthanides(III) and found no simple relation between the stability of the complexes and the atomic number or radius of the lanthanide ions. To establish such a relationship the complexation should be studied for all the lanthanides(III).

In the present work, we investigated the complexation of PAR with all the lanthanides(III) by applying the method developed previously,³ and have compared the results with those reported by Sommer and Novotna.⁴

EXPERIMENTAL

Reagents

All chemicals used were of analytical-reagent grade. PAR was obtained from Dojindo Chemical Co., and purified by

recrystallization. The purity was checked by thin-layer chromatography.⁵ The concentration of PAR in its aqueous stock solution was calculated from its weight. The lanthanide(III) nitrate solutions, except for cerium(III), were prepared by dissolving the calculated amounts of the respective oxides in nitric acid. The cerium(III) nitrate solution was prepared by dissolving Ce(NO₃)₃·2(NH₄NO₃)·4H₂O in 0.01M nitric acid, and standardized by EDTA titration. Sodium acetate and hexamine solutions (0.02M) were used to maintain the pH in the range 4.8–6.3. The ionic strength was maintained at 0.1 with sodium nitrate.

Procedure

The metal solution was added in small increments (50 μ l), by μ l pipette, to 10 ml of buffered PAR solution (2.0 – $3.0 \times 10^{-5}M$), to give concentrations increasing from 10^{-4} to $5 \times 10^{-3}M$. Before and after each addition of metal the absorbance at the wavelength for the absorption peak of PAR (which depends on the pH, and varies from 390 to 413 nm) was measured with a Shimadzu UV 200s spectrophotometer. No precipitation occurred under these experimental conditions.

RESULTS AND DISCUSSION

Absorption spectra of the complexes

The absorption spectra of PAR solutions containing excess of each lanthanide(III) were measured over the range 350–600 nm. The variation in the spectrum with metal concentration (C_M) was investigated at constant pH values in the range 4.8–6.3. The absorbance at the peak for PAR was observed to decrease with increasing C_M . After addition of sufficient metal there was no observable change in the spectra, indicating practically complete formation of the 1:1 complexes. The spectra varied according to the lanthanide(III) used and the pH. The spectra obtained for different lanthanides(III) at pH 4.83 showed two maxima, at 410 and 495 nm. The apparent molar absorptivities at 410 nm decreased from 1.48 to 1.28×10^4 l.mole⁻¹.cm⁻¹ and those at 495 nm in-

creased from 0.95 to $1.15 \times 10^4 \text{ l. mole}^{-1} \cdot \text{cm}^{-1}$ with atomic number of the lanthanide. The isosbestic points also varied from 428 to 442 nm . As the pH increased, the peak at 410 nm decreased and the one at 495 nm (which was slightly shifted to 500 nm at pH 6.3) increased remarkably with atomic number. To study the latter peak more extensively we further increased the pH by adding a small amount of $1.0M$ sodium hydroxide. As a result, the peak was further shifted to 505 nm and showed nearly the same limiting absorptivity of $3.0 \times 10^4 \text{ l. mole}^{-1} \cdot \text{cm}^{-1}$ for all the lanthanides, though this value was reached at different pH values for the different lanthanides, ranging from pH 6.7 (Lu) to 7.5 (Ce). From these facts, the peaks at 410 nm and 495 nm are attributed to the MHR complex and that at 505 nm is attributed to the MR complex.

Determination of the formation constants of MHR and MR

As described previously,³ the stability constants of the metal complexes of PAR (H_2R), MHR and MR, can be indirectly estimated by utilizing the ligand absorption peak. The absorbance at the peak for the free ligand, measured in the absence (A_0) and the presence (A) of the metal, under conditions where $C_M \gg C_R$ ($C_R =$ ligand concentration), can be related to the formation constants, K_{MHR} and K_{MR} , of the 1:1 complexes MHR and MR assumed to be formed as follows (charges are omitted for simplicity):

$$C_R = [\text{MHR}] + [\text{MR}] + [\text{R}'] \quad (1)$$

$$A = \epsilon_{\text{MHR}}[\text{MHR}] + \epsilon_{\text{MR}}[\text{MR}] + \epsilon_{\text{R}'}[\text{R}'] \quad (2)$$

where R' is the free ligand not combined with any metal, and ϵ_{MHR} , ϵ_{MR} and $\epsilon_{\text{R}'}$ are the molar absorptivities of MHR, MR and R' respectively, at the wavelength of the free-ligand peak. With the aid of

the formation constants, $K_{\text{MHR}} = [\text{MHR}]/[\text{M}][\text{HR}]$ and $K_{\text{MR}} = [\text{MR}]/[\text{M}][\text{R}]$, the acid dissociation constants of H_2R , $K_1 = [\text{H}][\text{HR}]/[\text{H}_2\text{R}]$ and $K_2 = [\text{H}][\text{R}]/[\text{HR}]$, and the Ringbom α -coefficient,⁶ $\alpha_R = [\text{R}']/[\text{R}]$, equations (1) and (2) can be converted into the following expressions:

$$[\text{M}](K_{\text{MHR}}K_1[\text{H}] + K_{\text{MR}}K_1K_2)/(\alpha_R K_1 K_2) = C_R/[\text{R}'] - 1 \quad (3)$$

$$A/\epsilon_{\text{R}'} = [\text{R}'] \{ 1 + (\epsilon_{\text{MHR}}K_{\text{MHR}}K_1[\text{H}] + \epsilon_{\text{MR}}K_{\text{MR}}K_1K_2)[\text{M}]/(\epsilon_{\text{R}'}\alpha_R K_1 K_2) \} \quad (4)$$

Combining equation (3) with equation (4), and substituting C_M for $[\text{M}]$ (since $C_M \gg C_R$), and A_0 for $C_R\epsilon_{\text{R}'}$, we obtain

$$\frac{K_{\text{MHR}}K_1[\text{H}] + K_{\text{MR}}K_1K_2}{\alpha_R K_1 K_2} - \frac{\epsilon_{\text{MHR}}K_{\text{MHR}}K_1[\text{H}] + \epsilon_{\text{MR}}K_{\text{MR}}K_1K_2}{\epsilon_{\text{R}'}\alpha_R K_1 K_2} \times \frac{A_0}{A} = (A_0/A - 1)/C_M \quad (5)$$

From equation (5), a linear relation between $(A_0/A - 1)/C_M$ and A_0/A should be obtained at constant pH (where $\epsilon_{\text{R}'}$ remains constant). The product of the intercept y_0 on the y -axis [$y = (A_0/A - 1)/C_M$], at a fixed pH, and $\alpha_R K_1 K_2$ is a function of $[\text{H}]$:

$$y_0 \alpha_R K_1 K_2 = K_{\text{MHR}}K_1[\text{H}] + K_{\text{MR}}K_1K_2 \quad (6)$$

According to equation (6), a plot of the left-hand side of equation (6) vs. $[\text{H}]$ should be linear in a pH-range where no hydrolysis of the metal ion occurs. From the slope and the intercept of the line, both K_{MHR} and K_{MR} can be determined.

From the measured absorbance decreases at the peak for PAR with increasing metal concentrations and constant pH, we plotted the relation expressed by equation (5). All the plots at different pH values for the different lanthanides(III) were linear with a negative slope as expected. The intercepts on the y -axis, which indicate the degree of complex formation, increased with either increasing pH or atomic number. There is no observable difference in the values for Lu(III) and Yb(III) and for Tb(III), Gd(III), Eu(III) and Sm(III) at any pH studied, and for Er(III), Ho(III) and Dy(III) at relatively low pH values in the range studied. The intercept x_0 on the x -axis (A_0/A) at pH 4.83 , which might be nearly equal to the ratio $\epsilon_{\text{R}'}/\epsilon_{\text{MHR}}$ at 390 nm at such a low pH, slightly increased with atomic number (from 1.5 to 1.7). This is in accord with the decrease in the molar absorptivities of the MHR complexes at 410 nm with atomic number (1.48 – $1.28 \times 10^4 \text{ l. mole}^{-1} \cdot \text{cm}^{-1}$). At the higher pH of 5.70 , as illustrated in Fig. 1, both the x_0 and y_0 values increase with atomic number to a greater extent, to give some detectable differentiation between Er(III), Ho(III) and Dy(III). This would be

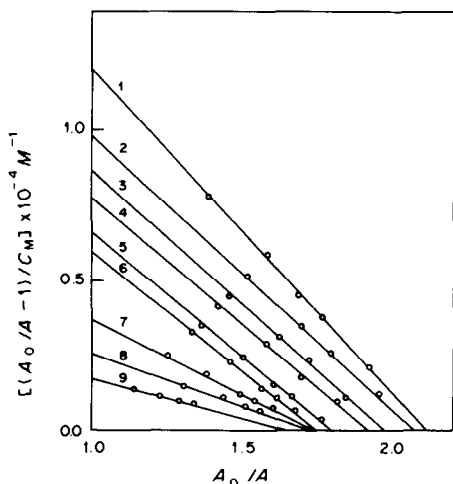


Fig. 1. Plots according to equation (5) for the system of PAR and different lanthanides(III) at a constant pH of 5.70 . (1) Lu, Yb; (2) Tm; (3) Er; (4) Ho; (5) Dy; (6) Tb, Gd, Eu, Sm; (7) Nd; (8) Pr; (9) Ce.

Table 1. Formation constants of lanthanide-PAR complexes, K_{MHR} and K_{MR} , and the proton dissociation constants of MHR, $K_{\text{MHR}}^{\text{H}}$ (0.1M NaNO₃, 25°C)

Element	log K_{MHR} , this work	log K_{MR}		
		This work	Sommer and Novotna ⁴	$\text{p}K_{\text{MHR}}^{\text{H}}$, this work
Ce(III)	3.78 ± 0.02	9.61 ± 0.06		6.47
Pr(III)	3.95 ± 0.02	9.78 ± 0.06	9.3	6.47
Nd(III)	4.07 ± 0.02	10.02 ± 0.06	9.8	6.35
Sm(III)	4.28 ± 0.03	10.25 ± 0.07	10.1	6.33
Eu(III)	4.28 ± 0.03	10.25 ± 0.07		6.33
Gd(III)	4.28 ± 0.03	10.25 ± 0.07		6.33
Tb(III)	4.28 ± 0.03	10.25 ± 0.07		6.33
Dy(III)	4.29 ± 0.03	10.36 ± 0.06	10.6	6.23
Ho(III)	4.29 ± 0.03	10.47 ± 0.06		6.12
Er(III)	4.31 ± 0.03	10.52 ± 0.06	10.1	6.09
Tm(III)	4.34 ± 0.02	10.57 ± 0.05		6.07
Yb(III)	4.39 ± 0.02	10.70 ± 0.05	10.2	5.99
Lu(III)	4.39 ± 0.02	10.70 ± 0.05		5.99

due to formation of MR complexes as well as the MHR complexes. The stabilities of the MR complexes of the heavy lanthanides(III) must differ more than those of the MHR complexes. The slope given by $-(\epsilon_{\text{MHR}}K_{\text{MHR}}K_1[\text{H}] + \epsilon_{\text{MR}}K_{\text{MR}}K_1K_2)/(\epsilon_{\text{R}}\alpha_{\text{R}}K_1K_2)$ varies with the K_{MHR} value if it can be assumed that $\epsilon_{\text{MHR}} \gg \epsilon_{\text{MR}}$ and $\epsilon_{\text{MHR}} \sim \epsilon_{\text{M'HR}}$ (M and M' being different lanthanides), suggesting that the K_{MHR} values for Sm(III)–Tm(III) are not so much different from each other.

To determine the formation constants of the MHR and MR complexes we plotted the relationship expressed by equation (6), for various lanthanides(III). The values, $K_1 = 10^{-5.50}$ and $K_2 = 10^{-12.30}$,⁷ were used for calculation of $\alpha_{\text{R}}K_1K_2$. All the plots were linear, with intercepts indicating the presence of both the MHR and MR complexes. It was generally observed that the greater the slope of the line the greater the intercept, and that both increased with atomic number, though the extent of the two increases was not the same. The lanthanides heavier than Sm(III) showed greater difference in the intercept than in the slope. The slopes for Sm(III)–Er(III) were very similar, as is to be expected. Table 1 shows the formation constants of K_{MHR} and K_{MR} obtained from the slope and intercept of the plot of equation (6), and the proton dissociation constant of MHR, $K_{\text{MHR}}^{\text{H}}$, calculated from $K_{\text{MHR}}^{\text{H}} = K_2K_{\text{MR}}/K_{\text{MHR}}$. The values were obtained by the least-squares method. For comparison the values reported in the literature⁴ are included. Sommer and Novotna⁴ assumed existence of the protonated complexes, MRH* where H* denotes the proton of the *p*-hydroxy group of PAR, and calculated the K_{MRH}^* values by using K_3 as an approximation to K_2^* , where K_1 is the dissociation constant of H_3R^+ . The resulting values for K_{MRH}^* were larger than those for K_{MR} . However, Chalmers⁸ has stated that the use of k_2 is preferable to use of K_3 for the approximation, because the *o*-hydroxy group should be regarded intrinsically as at least as acidic as the *p*-hydroxy group, its lower acidity being due to internal hydrogen-bonding. For the MR complexes,

our results mostly agree with those reported by Sommer and Novotna. Although they offered no explanation for the unusual relation between complex stability and atomic number, this could result from the different values of the molar absorptivity of MR ($1.48\text{--}4.1 \times 10^4 \text{ l. mole}^{-1}\text{.cm}^{-1}$ at 530 nm) estimated for the different lanthanides(III). From our results, however, the ϵ values of MR at 505 nm are nearly the same ($3.0 \times 10^4 \text{ l. mole}^{-1}\text{.cm}^{-1}$) for all the lanthanides(III).

Comparison of complexation trends of HR^- and R^{2-}

The dependence of the formation constants, K_{MHR} and K_{MR} on the reciprocal of the ionic radius r is plotted in Fig. 2. The two curves show a similar complexation trend for the light lanthanides(III). For the heavy lanthanides(III), however, there are different trends between the HR^- and the R^{2-} ligands. These two trends are often observed in lanthanide chemistry. According to Moeller *et al.*⁹, who divided the ligands into three types showing different complexation trends, the R^{2-} and the HR^- ligand belong to the first and the second group, respectively. Although the similarity among the li-

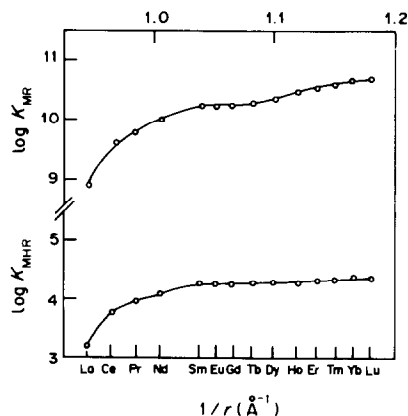


Fig. 2. Plots of the formation constants of the lanthanide(III)-PAR complexes, MHR and MR, vs. the reciprocal of the radius of the metal ions.

gands in the respective groups has not been clearly indicated, the ligands in the first group are capable of forming at least one chelate ring in the complexes.

In an attempt to elucidate the co-ordination structure of the protonated and the normal type of PAR complexes, detailed studies on extraction of the 1:2 Ni-PAR complexes were made by Hoshino *et al.*¹⁰ They suggested that in the chelation of Ni(HR)₂·2H₂O and NiR₂²⁻, the ligands, HR⁻ and R²⁻, are acting as bidentate and terdentate, respectively. They stated that the basic change of the chelate structure from Ni(HR)₂·2H₂O to NiR₂²⁻ and deprotonation of HR⁻ ligand both caused a remarkable increase in the absorptivity (from 3.73 × 10⁴ to 8.08 × 10⁴ l.mole⁻¹.cm⁻¹). Although the lanthanide-PAR complexes (1:1) differ in type from the Ni-PAR complexes, a considerable increase in the absorptivity (from 0.95–1.15 × 10⁴ to 3.0 × 10⁴ l.mole⁻¹.cm⁻¹) was similarly observed with increasing pH. The LnR complexes (Ln = lanthanide) may have a more stable chelate structure which gives rise to a larger difference in stability between the heavy lanthanides(III) than that for the LnHR complexes. The acidity of the LnHR complexes parallels the stability order of the LnR complexes (Table 1).

CONCLUSIONS

The complexes MHR and MR can be differentiated by spectrophotometric means and their formation constants, K_{MHR} and K_{MR} , determined. Both values regularly increase with increasing atomic number up to Sm(III). For the heavy lanthanides(III), the K_{MR} values also increase but the K_{MHR} values are nearly the same.

REFERENCES

1. R. G. Anderson and G. Nickless, *Analyst*, 1967, **92**, 207.
2. S. Shibata, in *Chelates in Analytical Chemistry*, A. J. Barnard Jr. and H. Flaschka (eds.), Vol. 3, Dekker, New York, 1972.
3. E. Ohyoshi, *Anal. Chem.*, 1983, **55**, 2404.
4. L. Sommer and H. Novotna, *Talanta*, 1967, **14**, 457.
5. F. H. Pollard, G. Nickless, T. J. Samuelson and R. G. Anderson, *J. Chromatog.*, 1964, **16**, 231.
6. A. Ringbom, *Complexation in Analytical Chemistry*, Interscience, New York, 1963.
7. W. J. Geary, G. Nickless and F. H. Pollard, *Anal. Chim. Acta*, 1962, **27**, 71.
8. R. A. Chalmers, *Talanta*, 1967, **14**, 527.
9. T. Moeller, D. F. Martin, L. C. Thompson, R. Ferrus, G. R. Feistel and W. J. Randall, *Chem. Rev.*, 1965, **65**, 1.
10. H. Hoshino, T. Yotsuyanagi and K. Aomura, *Anal. Chim. Acta*, 1976, **83**, 317.

ZINC AND NICKEL FERROCYANIDES: PREPARATION, COMPOSITION AND STRUCTURE

C. LOOS-NEKOVIC

Laboratoire d'Analyse par Activation Pierre Sûe, C.E.N./SACLAY, 91191 Gif-sur-Yvette, France

M. FEDOROFF

Centre d'Etudes de Chimie Métallurgique, 15 rue Georges Urbain, 94400 Vitry-sur-Seine, France

E. GARNIER and P. GRAVEREAU

Laboratoire de Cristalchimie Minérale, Université de Poitiers, 40, Avenue du Recteur Pineau,
86022 Poitiers Cedex, France

(Received 12 March 1984. Accepted 25 May 1984)

Résumé—Revue sur les ferrocyanures de nickel et de zinc durant la période 1922–1983, avec une attention particulière à leur composition et leur structure en relation avec les méthodes de préparation.

During the last two decades, inorganic ion-exchangers have attracted chemists because they seemed to be very useful in separative chemistry. A rapid development in nuclear energy, hydro-metallurgy, and recovery of valuable materials from industrial wastes has enforced attempts to synthesize highly selective ion-exchange materials resistant to chemicals and ionizing radiation.^{1,2} Among them, insoluble ferrocyanides have been studied mainly in connection with the removal of caesium in decontamination of radioactive liquid wastes.³ The ferrocyanides of bivalent metals have been the most extensively studied. It has been shown that zinc^{4,5} and nickel ferrocyanides⁶ in particular have an exceptionally strong affinity for caesium ions.

Before undertaking a systematic study of the exchange properties of these ferrocyanides, we needed a good knowledge of their chemical composition and structure in relation to the methods used for their preparation. We therefore made a thorough literature survey, and tried to make a synopsis of what was published on these topics, which we hope will be helpful to all those who want to use these products for laboratory studies or industrial applications. In order to make appraisal easier, the collected information is summarized in Table 1 for zinc ferrocyanides and in Table 2 for nickel ferrocyanides.

PREPARATION METHODS

The main purpose of this survey was to specify which preparation procedure should be used in order to obtain a product of controlled composition and structure. In the first three columns of Tables 1 and 2 we indicate the main experimental features, when details are available. In most cases the ferrocyanide

precipitate is obtained by mixing a ferrocyanide solution (alkali-metal ferrocyanide or ferrocyanic acid) with a solution of a nickel or zinc salt. Sometimes a solution of another alkali-metal salt is also added. The ratio of cations to ferrocyanide ions is an important factor. In some cases it varies continuously during the preparation, when one of the solutions is slowly added to the other. In other cases it remains constant, when the solutions are added simultaneously at the same rate.

The grain size of the precipitates and even the preparation yield are seldom indicated in the literature, so we cannot give any precise indications on these subjects. With such sparingly soluble products as zinc and nickel ferrocyanides, the particles are always very small and may even be colloidal. Most authors suggest dropwise addition of the solutions, because it should avoid formation of too small particles. According to some authors the proportion of colloidal particles depends on the reactant ratio. The colloidal character of nickel ferrocyanide is said to decrease when the Ni/Fe ratio increases from 1 to 1.5.⁷ Kourim⁸ recommends a 50% excess of zinc in order to avoid colloidal $Zn_2Fe(CN)_6$. In contrast, Kawamura⁴ recommends using the stoichiometric ratio, in order to obtain a well crystallized $Na_2Zn_3[Fe(CN)_6]_2$ precipitate. Aging of the precipitate in the solution is used by some authors to increase the grain size.

We also indicate the conditions for drying the precipitate, whenever they were given. They vary widely: the temperature ranges from ambient to 140° and the drying is done in air or in vacuum. The drying conditions may influence the structure and composition of the ferrocyanide.

The exchange properties of the ferrocyanides have

Table 1. Preparation, formulae and structure of zinc ferrocyanides

Reagents	Reagent ratio	Experimental procedure	Formula	Structure	Reference
A = $2.5 \times 10^{-3} M$ ZnSO ₄ B = $0.033 M$ K ₄ Fe(CN) ₆	$\frac{Zn}{Fe} \geq 1.5$	B poured into A 0.2 M HCl at 60°	K ₂ Zn ₃ [Fe(CN) ₆] ₂ and K ₂ ZnFe(CN) ₆ (?) ^a		
A = $5 \times 10^{-3} M$ ZnSO ₄ B = $0.033 M$ Na ₄ Fe(CN) ₆	$\frac{Zn}{Fe} \geq 2$	B poured into A neutral pH at 65°	Zn ₂ Fe(CN) ₆ ^a		
A = $2.5 \times 10^{-3} M$ ZnSO ₄ B = $0.033 M$ Na ₄ Fe(CN) ₆	$\frac{Zn}{Fe} \geq 1.5$	B poured into A + C in excess, 0.2 M HCl at 70°	K ₂ Zn ₃ [Fe(CN) ₆] ₂ ^a		22
C = KCl	$\frac{K}{Fe} \geq 20$				
A = $5 \times 10^{-3} M$ ZnSO ₄ B = $0.03 M$ K ₄ Fe(CN) ₆ C = Cs ₂ CO ₃	$\frac{Zn}{Fe} \geq 1.5$	B poured into A + C in excess, 0.2 M HCl at 60°	Cs ₂ ZnFe(CN) ₆ ^a		
A = $5 \times 10^{-5} M$ ZnSO ₄ B = $2.5 \times 10^{-5} M$ K ₄ Fe(CN) ₆	$\frac{Zn}{Fe} \geq 1$	B poured into A + C 0.04 N H ₂ SO ₄	Cs ₂ ZnFe(Cn) ₆ ^b		
C = $10^{-4} M$ CsCl	$\frac{Cs}{Fe} \geq 4$				
A = $5 \times 10^{-5} M$ ZnSO ₄ B = $2.5 \times 10^{-5} M$ Na ₄ Fe(CN) ₆	$\frac{Zn}{Fe} \geq 2$	B poured into A 0.04 N H ₂ SO ₄	Zn ₂ Fe(CN) ₆ ^a		
or Mg ₂ Fe(CN) ₆ or Ca ₂ Fe(CN) ₆	$\frac{Zn}{Fe} \leq 2$ 1		$\begin{cases} Na_2Zn_3[Fe(CN)_6]_2 \\ MgZn_3[Fe(CN)_6]_2 \\ CaZn_3[Fe(CN)_6]_2 \end{cases}$ ^a		19
A = ZnSO ₄ B = (NH ₄) ₄ Fe(CN) ₆	$\frac{Zn}{Fe} \geq 1$	B poured into A 0.04 N H ₂ SO ₄	(NH ₄) ₂ Zn ₃ [Fe(CN) ₆] ₂ ^a		
A = ZnSO ₄ B = H ₄ Fe(CN) ₆	$\frac{Zn}{Fe} \geq 1$	B poured into A	H ₂ Zn ₃ [Fe(CN) ₆] ₂ ^a		

A = $2.5 \times 10^{-2} M$ ZnSO ₄ B = 0.1 M K ₄ Fe(CN) ₆	$\frac{Zn}{Fe} \geq 5$	B poured into A	Zn ₂ Fe(CN) ₆ · 0.1 K ₄ Fe(CN) ₆ ^c	42
	$1 \leq \frac{Zn}{Fe} \leq 1.5$		Zn ₂ Fe(CN) ₆ · 0.33 K ₄ Fe(CN) ₆ ^c	
		pH ≤ 7	K ₂ Zn(CN) ₆ or K ₂ Zn ₃ [Fe(CN) ₆] ₂ ^d	23
		pH > 7 in presence of ammonia	Zn ₂ Fe(CN) ₆	non-cubic
A = 0.02 M ZnSO ₄ B = 0.1 M K ₄ Fe(CN) ₆	$\frac{Zn}{Fe} \leq 1.54$	A poured into B. Gel centrifuged. Supernatant liquid analysed for zinc and ferrocyanide	K ₂ Zn ₃ [Fe(CN) ₆] ₂ (?) ^c	43
	$\frac{Zn}{Fe} \leq 5$		Zn ₂ Fe(CN) ₆ (?)	non-cubic, X-ray spectra given
A = Zn salt B = 0.001 M Fe(CN) ₆ ⁴⁻ C = radioactive Cs	$\frac{Zn}{Fe} = 2$	Radioactive Cs co-precipitated with zinc and ferrocyanide ions in 2.5 M HNO ₃ . Precipitate allowed to digest at 80° and centrifuged	Cs ₂ ZnFe(CN) ₆ · 2H ₂ O	26
A = 0.1 M Zn(NO ₃) ₂ B = 0.1 M Na ₄ Fe(CN) ₆	$\frac{Zn}{Fe} \geq 3$	B poured into A. Filtration, washing with 0.3 M NaNO ₃ , water. Drying 1 hr at 110°	Zn ₂ Fe(CN) ₆	8 44
A = 0.2 N (ZnCl ₂ + M ¹ Cl) M ¹ = Na, K, NH ₄ , Rb, Cs B = 0.025 M Na ₄ Fe(CN) ₆	various ratios	A + B mixture shaken for 24 hr Precipitate centrifuged	M ₃ Zn _{1-x} [ZnFe(CN) ₆] Na, K, NH ₄ ; 0 ≤ x ≤ 0.5 Rb, Cs; 0 ≤ x ≤ 1	6
A = 0.026 M ZnSO ₄ B = H ₄ Fe(CN) ₆	$5 \leq \frac{Zn}{Fe} \leq 10$	A poured into B or B poured into A with or without 1.1 M H ₂ SO ₄	Zn ₂ Fe(CN) ₆ · xH ₂ O	
	Zn = 1.5 Fe		H ₂ Zn ₃ [Fe(CN) ₆] ₂ · xH ₂ O	21

continued

Table 1—continued

Reagents	Reagent ratio	Experimental procedure	Formula	Structure	Reference
	$1.5 \leq \frac{\text{Zn}}{\text{Fe}} \leq 5$		$\text{Zn}_2\text{Fe}(\text{CN})_6 \cdot x\text{H}_2\text{O}$ and $\text{H}_2\text{Zn}_3[\text{Fe}(\text{CN})_6]_2 \cdot x\text{H}_2\text{O}$		
A = 0.025 M Zn^{2+} (Cl^- , NO_3^- or SO_4^{2-})	$\frac{\text{Zn}}{\text{Fe}} = 1$	A + B + C mixed 30 min, aged 16 hr, washed with water and air-dried	$\text{Cs}_3\text{ZnFe}(\text{CN})_6 \cdot x\text{H}_2\text{O}$	cubic, space group P4_332 or P2_13 $a = 10.34 \text{ \AA}$ or $a = 10.37 \text{ \AA}$	27
B = 0.25 M $\text{Na}_4\text{Fe}(\text{CN})_6$	$\frac{\text{Cs}}{\text{Fe}} = 2$				45
C = 0.8 M Cs^+ (NO_3^- or Cl^-)	$\frac{\text{Zn}}{\text{Fe}} = 1.33$		$\text{Cs}_4\text{Zn}_4[\text{Fe}(\text{CN})_6]_3 \cdot x\text{H}_2\text{O}$	$a = 10.32 \text{ \AA}$	8
	$\frac{\text{Cs}}{\text{Fe}} = 1.33$		$0 \leq x \leq 5$	or $a = 10.31 \text{ \AA}$	
			$\text{Zn}_2\text{Fe}(\text{CN})_6$ $\text{Zn}_2\text{Fe}(\text{CN})_6 \cdot 2\text{H}_2\text{O}$	X-ray spectra given	46
A = 0.1 M $\text{Zn}(\text{NO}_3)_2$	$\frac{\text{Zn}}{\text{Fe}} \geq 4$	B poured into A. Precipitate washed and air-dried at 130°			47
B = 0.1 M $(\text{NH}_4)_4\text{Fe}(\text{CN})_6$					
A = 0.5 M $\text{Zn}(\text{NO}_3)_2$	$0 \leq \frac{\text{Zn}}{\text{Fe}} \leq 1.5$	A poured into B. Aging 1 day at room temp. Precipitate washed, air- dried 2 hr at 140°	$\text{K}_2\text{Zn}_3[\text{Fe}(\text{CN})_6]_2$	^a	20
B = 0.5 M $\text{K}_4\text{Fe}(\text{CN})_6$					
A = 0.1 M $\text{Zn}(\text{NO}_3)_2$	$\frac{\text{Zn}}{\text{Fe}} = 3$	A and B poured simultane- ously. Aging 2 hr at 100° and 1 day at room temp. Precipitate washed and dried 24 hr at 60°	$\text{Zn}_2\text{Fe}(\text{CN})_6$	^a X-ray spectra given	4
B = 0.1 M $\text{K}_4\text{Fe}(\text{CN})_6$					

A = 0.1 M ZnSO ₄ B = 0.1 M K ₄ Fe(CN) ₆	A poured into B. Then CH ₃ COONa and H ₂ O ₂ added. Heating at 100° until colour change yellow to white. Aging 1 day. Precipitate washed and dried 1 day at 60°		$K_2Zn_3[Fe(CN)_6]_2$	^h	X-ray spectra given	4
A = 0.1 M Zn(NO ₃) ₂ B = 0.1 M Na ₄ Fe(CN) ₆	A and B poured simultaneously. Aging 2 hr at 100° and 1 day at room temp. Precipitate washed and air-dried 1 day at 60°	$\frac{Zn}{Fe} = 0.66$ or 1	$Na_2Zn_3[Fe(CN)_6]_2$		X-ray spectra given	9
A = Zn ₂ Fe(CN) ₆ solid B = 0.01 or 0.1 M CsCl	A exchanged by B. Solid washed free from excess of Cs ⁺	$\frac{Zn}{Fe} = 3$	Zn ₂ Fe(CN) ₆			
A = 5×10^{-3} M - 1.3×10^{-3} M ZnSO ₄	B poured into A	$\frac{Zn}{Fe} \geq 2$	Zn ₂ Fe(CN) ₆		X-ray spectra given	17
B = 0.125 M K ₄ Fe(CN) ₆	A poured into B	$1 \leq \frac{Zn}{Fe} \leq 1.5$ $\frac{Zn}{Fe} \geq 2$	$K_2Zn_3[Fe(CN)_6]_2$ Zn ₂ Fe(CN) ₆	^a ^a		34
A = Zn ²⁺ B = K ₄ Fe(CN) ₆	A + B mixed. Precipitate washed and air-dried	$\frac{Zn}{Fe} = 1$	K ₂ ZnFe(CN) ₆	ⁱ		25
A = Zn ²⁺ B = 0.1 M K ₄ Fe(CN) ₆	B poured into A		$K_{0.5}Zn_{1.15}Fe(CN)_6$	^j	tetragonal $a = 10.09 \text{ \AA}$ $c = 12.32 \text{ \AA}$	12
A = 0.1 M Zn(NO ₃) ₂ B = 0.1 M Na ₄ Fe(CN) ₆	B poured into A. Mixture heated 2 hr on a boiling water-bath. Precipitate washed with 0.1 M NaNO ₃ and water. Dried under vacuum at room temp.	$\frac{Zn}{Fe} \geq 3$	Zn ₂ Fe(CN) ₆ · 2.5H ₂ O	^k	orthorhombic $a = 11.510 \text{ \AA}$ $b = 13.167 \text{ \AA}$ $c = 9.898 \text{ \AA}$	10 11

continued

Table 1—continued

Reagents	Reagent ratio	Experimental procedure	Formula	Structure	Reference
A = $Zn_2Fe(CN)_6 \cdot 2.5H_2O$ B = 0.25 M $CsNO_3$		A exchanged by B	$Cs_2ZnFe(CN)_6$	cubic $a = 10.20 \text{ \AA}$	
A = 1 M $ZnSO_4$ B = 1 M $K_4Fe(CN)_6$	$\frac{Zn}{Fe} = 4$	A and B poured simultaneously. Precipitate aged 7 days and dried at 70°	$K_2Zn_3[Fe(CN)_6]_2 \cdot xH_2O$		5
A = $K_2Zn_3[Fe(CN)_6]_2$ B = 0.1 M $CaCl$		A exchanged by B	$Cs_2Zn_3[Fe(CN)_6]_2 \cdot xH_2O$		5
A = 0.118 M $Zn(NO_3)_2$ B = 0.1 M $Na_4Fe(CN)_6$	$\frac{Zn}{Fe} \geq 3$	B poured into A. Precipitate washed with 0.1 M $NaNO_3$ and water. Air-dried at room temp. or 2 hr at 150°	$Zn_3Fe(CN)_6 \cdot 2H_2O$	trigonal, space group $D_{3d}^5 - P\bar{3}m1$ $a = 7.598 \text{ \AA}$ $c = 5.756 \text{ \AA}$	18
A = 0.15 M $ZnSO_4$ B = 0.08 M $K_4Fe(CN)_6$ C = 0.3 M NH_4Cl D = 12 M NH_3	$\frac{Zn}{Fe} \geq 2$ $\frac{NH_4}{Fe} \geq 10$	B + D added to A + C + D	$Zn_3Fe(CN)_6 \cdot 2NH_3$	trigonal, space group $D_{3d}^5 - P\bar{3}m1$ $a = 7.509 \text{ \AA}$ $c = 5.939 \text{ \AA}$	
A = 0.05 M $ZnCl_2$ B = 0.05 M $K_4Fe(CN)_6$		A and B introduced in opposite limbs of a U-tube filled with silica gel enriched in potassium	$K_2Zn_3[Fe(CN)_6]_2 \cdot xH_2O$ single crystals, zeolitic water: $0 < x < 9$	rhombohedral, $R\bar{3}c$ $a = 12.960 \pm 0.004 \text{ \AA}$ $\alpha = 57.83 \pm 0.01^\circ$	14 24 38
A = 5×10^{-3} M $ZnCl_2$ B = 5×10^{-3} M $Na_4Fe(CN)_6$		A and B introduced in opposite limbs of a U-tube filled with silica gel enriched in sodium	$Na_2Zn_3[Fe(CN)_6]_2 \cdot xH_2O$ single crystals, zeolitic water	rhombohedral, $R\bar{3}c$ $a = 13.126(3) \text{ \AA}$ $\alpha = 56.71(2)^\circ$	15
A = 0.1 M $CsCl$ B = $Na_2Zn_3[Fe(CN)_6]_2$ single crystals		B exchanged by A. Washed and dried at 40°	$Cs_2Zn_3[Fe(CN)_6]_2 \cdot xH_2O$ single crystals, zeolitic water	rhombohedral, $R\bar{3}c$ $a = 13.140(3) \text{ \AA}$ $\alpha = 56.80(2)^\circ$	16

been used by some authors for changing the composition of already precipitated products.⁹⁻¹³ In some cases, the structure is also modified during this process.⁹

Single crystals of composition $M_2^1Zn_3[Fe(CN)_6]_2$ have been prepared by slow diffusion of $M_4^1Fe(CN)_6$ ($M^1 = Na$ or K) and $ZnCl_2$ through silica gel.^{14,15} This preparation took about three months and led to 0.05 mm crystals, which were used for accurate X-ray analysis. The analogous $Cs_2Zn_3[Fe(CN)_6]_2$ single crystals were obtained by ion-exchange of $Na_2Zn_3[Fe(CN)_6]_2$ crystals with caesium ions.¹⁶

COMPOSITION AND STRUCTURE

We first looked at the methods used for determination of the chemical formulae, and in the tables have indicated these methods in footnotes. Often, however, the methods were not given by the authors and we do not know whether the formulae given were based on analysis or simply assigned from theoretical assumptions. The methods that are given may be divided into two types: (1) chemical analysis of the products or the residual solutions; (2) potentiometric or conductimetric measurements during the precipitation. It should be noted that the formulae deduced from measurements of the second type do not necessarily reflect the composition of the product which is achieved after filtration and drying. The crystallographic structures were deduced from X-ray diffraction work.

Zinc ferrocyanides

The compositions obtained are summarized in Fig. 1. We first notice that a stoichiometric formula is nearly always given for all the series. Pure zinc ferrocyanide $Zn_2Fe(CN)_6$ is produced when the ratio of zinc cations to ferrocyanide anions used is >2 , in presence of either sodium or hydrogen ions. According to Bellomo¹⁷ this also holds when potassium ferrocyanide is used. It should be noted, however, that this author did not analyse the product obtained, but used potentiometric measurements during the precipitation. More recent studies,^{5,14} with accurate analyses of the precipitates, indicated that with potassium ferrocyanide, pure $Zn_2Fe(CN)_6$ ferrocyanide could not be obtained even with high Zn/Fe ratios and concentrated solutions.

The structure of this compound was found to be orthorhombic by Cola and Ganzerli-Valentini.¹⁰ A more recent study by Siebert *et al.*¹⁸ finds a trigonal lattice for the $Zn_2Fe(CN)_6 \cdot 2H_2O$ hydrate and gives an explanation for the earlier interpretation.

If the Zn/Fe ratio used is <1.5 , in the presence of sodium,^{19,20} ammonium^{6,19} or hydrogen^{19,21} ions, a mixed ferrocyanide is obtained. The formula assigned is $M_2^1Zn_3[Fe(CN)_6]_2$ where M^1 is the alkali-metal ion. In presence of potassium ions, according to

- a* Potentiometric measurements.
b Non-stoichiometric compound. Possibility of ferrocyanide ions.
c Conductivity measurements.
d Electron diffraction from deposited colloidal solution.
e No definite salt: may contain less $K_4Fe(CN)_6$ than in the formula.
f Zn determined in supernatant solution by complexometry.
g Air-dried at 140° or under vacuum at 100°.
h Chemical analysis given for Zn, Fe(CN)₆ and alkali metals.
i Chemical analysis given for Zn, Fe, C.
j See procedure given.⁴¹
k Chemical analysis given for Zn, Fe, H₂O, Cs, K.
l The X-ray diffraction pattern corresponds to those given by Kawamura *et al.*⁴⁹
m Formula deduced from radio-tracer and atomic-absorption measurements.
n Chemical analysis given for Zn, Fe, C, N, H, NH₃.
o Powders of the same compounds were obtained according to Vlasselaer *et al.*⁵ and Kawamura *et al.*⁹ X-ray spectra of powders are consistent with single-crystal structures.

Table 2. Preparation, formulae and structure of nickel ferrocyanides

Reagents	Reagents ratio	Experimental procedure	Formula	Structure	Reference
A = $5 \times 10^{-3} M$ NiSO ₄ B = $0.033 M$ Li ₄ Fe(CN) ₆			Ni ₂ Fe(CN) ₆ ^a		
A = $5 \times 10^{-3} M$ NiSO ₄ B = $0.033 M$ Na ₄ Fe(CN) ₆	$\frac{Ni}{Fe} \geq 1$	B poured into A at 55°	Na ₂ Ni ₃ [Fe(CN) ₆] ₂ ^a		31
A = $5 \times 10^{-3} M$ NiSO ₄ B = $0.033 M$ K ₄ Fe(CN) ₆		B poured into A at 65°	K _{1.68} Ni _{1.16} Fe(CN) ₆ ^a		
A = $0.025 M$ NiSO ₄		B poured into A at 25°	Ni ₂ Fe(CN) ₆ · xK ₄ Fe(CN) ₆ x = 0.5 and 0.78 ^b		42
B = $0.1 M$ K ₄ Fe(CN) ₆	$\frac{Ni}{Fe} \geq 1$	A + various quantities of B mixed for 1 day	Ni ₂ Fe(CN) ₆ · xK ₄ Fe(CN) ₆ 0.56 ≤ x ≤ 1.22 ^c		
A = NiSO ₄	$\frac{Ni}{Fe} \geq 2$	A + B mixed	Ni ₂ Fe(CN) ₆	f.c.c. a = 10.00 ± 0.05 Å	23
B = K ₄ Fe(CN) ₆	$\frac{Ni}{Fe} \ll 1$		K ₂ NiFe(CN) ₆	f.c.c. a = 9.96 ± 0.05 Å	
A = $0.02 M$ NiSO ₄	$\frac{Ni}{Fe} = 5$;	A poured into B at 25°	Ni ₂ Fe(CN) ₆ · xK ₄ Fe(CN) ₆ 0.56 ≤ x ≤ 1.22 ^d	Solid solutions with identical structure	43
B = $0.1 M$ K ₄ Fe(CN) ₆	1.2; 0.8			X-ray spectra given	
A = $1.12 \times 10^{-2} M$ NiSO ₄ B = $0.0436 M$ Li ₄ Fe(CN) ₆	$1.83 \leq \frac{Ni}{Fe} \leq 4$		Ni ₂ Fe(CN) ₆ ^a		
A = $1.12 \times 10^{-2} M$ NiSO ₄ B = $0.04649 M$ Na ₄ Fe(CN) ₆	$1.78 \leq \frac{Ni}{Fe} \leq 8$	B poured into A at 25°. Aged 3 hr	Ni ₂ Fe(CN) ₆ · xNa ₄ Fe(CN) ₆ solid solution and Na ₂ Ni ₃ [Fe(CN) ₆] ₂ ^d		28
A = $1.12 \times 10^{-2} M$ NiSO ₄ B = $0.04582 M$ K ₄ Fe(CN) ₆	$1.33 \leq \frac{Ni}{Fe} \leq 8$		Ni ₂ Fe(CN) ₆ · xK ₄ Fe(CN) ₆ solid solution and K ₄ Ni ₄ [Fe(CN) ₆] ₃ ^a		

A = 0.025 M Ni(NO ₃) ₂ B = 5 × 10 ⁻³ M Li ₄ Fe(CN) ₆ C = 0.025 M TiNO ₃	$\frac{\text{Ni}}{\text{Ti}} = 1$ $1.14 \leq \frac{\text{Ni}}{\text{Fe}} \leq 5$	B poured into a mixture of A + C. Mixed for 4 hr at 25°	Tl _x Ni ₄ [Fe(CN) ₆] _h	48	^a ^c
A = 0.025 M Ni(NO ₃) ₂ B = 1.25 × 10 ⁻² M Li ₄ Fe(CN) ₆ C = 5 × 10 ⁻³ M TiNO ₃	$\frac{\text{Ni}}{\text{Fe}} = 2$ $0 \leq \frac{\text{Ti}}{\text{Fe}} \leq 4$		Tl _{1.2x} Ni _{2-x} Fe(CN) ₆ $0 \leq x \leq 0.4$		^d ^e
A = 0.001 M Ni ²⁺ B = 0.005 M Fe(CN) ₆ ⁻ C = 10 ⁻⁴ M Cs ⁺ 1 M HNO ₃	$\frac{\text{Ni}}{\text{Fe}} = 2$	A + B added simultaneously to a radioactive Cs solution of the indicated composition, stirred, allowed to digest at room temp. for 1 hr and centrifuged	Cs ₂ Ni ₃ [Fe(CN) ₆] _h	26	
A = 1 M Ni(NO ₃) ₂ B = 0.5 M Na ₄ Fe(CN) ₆	$\frac{\text{Ni}}{\text{Fe}} \geq 3$	B poured into A. Precipitate dried at 80–110°. Filtered material impregnated with 4% aqueous poly(vinyl alcohol) and dried for 4 hr at 95°		8	
A = 0.2 N (NiCl ₂ + M'Cl) M' = Na, K, NH ₄ , Rb, Cs B = 0.025 M Na ₄ Fe(CN) ₆	Various ratios	A + B mixture shaken for 24 hr. Precipitate centrifuged	M' _{2x} Ni _{1-x} [NiFe(CN) ₆] M' = Na 0.1 ≤ x ≤ 0.8 M' = K, NH ₄ , Rb x ~ 0.8 M' = Cs 0.8 ≤ x ≤ 1.2	6	^d
A = 0.1 M Ni(NO ₃) ₂ B = 0.1 M (NH ₄) ₄ Fe(CN) ₆	$\frac{\text{Ni}}{\text{Fe}} \geq 4$	B poured into A at room temp. Aged for 24 hr. Precipitate washed with distilled water, filtered and dried at 130°		47	
A = 0.1 M Ni(NO ₃) ₂ B = 0.1 M Na ₄ Fe(CN) ₆ + xRbCl	$\frac{\text{Ni}}{\text{Fe}} \geq 1.33$ $\frac{\text{Rb}}{\text{Fe}} = 1.33$	A + B poured simultaneously with stirring. Precipitate washed, cooled to 2.5° and dried at room temp.	Rb _{1.25} K _{0.01} Na _{0.06} Ni _{1.34} Fe(CN) ₆	49	

continued

Table 2—continued

Reagents	Reagents ratio	Experimental procedure	Formula	Structure	Reference
A = 0.1 M Ni(NO ₃) ₂ B = 0.1 M K ₄ Fe(CN) ₆		A + B poured simultaneously with stirring. Precipitate washed, cooled to -10°	K ₄ Ni ₄ [Fe(CN) ₆] ₃		50
A = 0.1 M Ni(NO ₃) ₂ B = 0.1 M Na ₄ Fe(CN) ₆ + x RbCl			Rb ₄ Ni ₄ [Fe(CN) ₆] ₃		
A = Rb ₄ Ni ₄ [Fe(CN) ₆] ₃ see Kolesova and Vol'khin ⁴⁹ B = RbNO ₂		B poured into A until equilibrium reached	Rb _{4.5} Ni _{6.75} [NiFe(CN) ₆] ₃ · n RbNO ₂ n = 0, 1, 2, 3, 4		51
A = Ni ²⁺ solution B = 0.1 M K ₄ Fe(CN) ₆		see Kolesova and Vol'khin ⁴⁹	K _{1.50} Ni _{1.25} Fe(CN) ₆		
A = K _{1.50} Ni _{1.25} Fe(CN) ₆		A exchanged by Na ⁺ solution	Na _{1.50} Ni _{1.25} Fe(CN) ₆		
		A exchanged by Rb ⁺ solution	Rb _{1.47} Ni _{1.26} Fe(CN) ₆	cubic a = 10.12 Å	12
A = M _{1.50} Ni _{1.25} Fe(CN) ₆ M ¹ = Na, K, Rb		A exchanged by Cs ⁺ solution	Cs _{0.75} M _{0.75} Ni _{1.25} Fe(CN) ₆		
		Direct precipitation in presence of Cs ⁺	Cs _{1.50} Ni _{1.25} Fe(CN) ₆		
A = KNi _{1.50} Fe(CN) ₆ B = 0.02 N TiNO ₃		A exchanged by B	Tl _{1.10} Ni _{1.45} Fe(CN) ₆		
A = KNi _{1.50} Fe(CN) ₆ B = 0.02 N Ti ₂ SO ₄		A exchanged by B	Tl _{1.10} Ni _{1.45} Fe(CN) ₆ · 0.25Ti ₂ SO ₄		13
			NaNi _{1.5} Fe(CN) ₆ KNi _{1.5} Fe(CN) ₆ Rb _{1.24} Ni _{1.38} Fe(CN) ₆ Cs _{1.42} Ni _{1.39} Fe(CN) ₆ Tl _{1.10} Ni _{1.45} Fe(CN) ₆	f.c.c., Fm3m	32

A = NiSO ₄	Ni Fe	≪ 2	A added dropwise to a large excess of B. Precipitate washed and dried in vacuum at room temp.	$K_{2.15}Ni_{0.92}Fe(CN)_6 \cdot 3H_2O$	^g _k	f.c.c. a = 10.07 Å (sample dried at 200°)	37
B = K ₄ Fe(CN) ₆							
A = NiSO ₄	Ni Fe	> 1	A + B mixed in different ratios at various pH. Precipitate centrifuged and washed, dried at 100°. 4 < pH < 10	$K_xNi_yFe(CN)_6 \cdot K_n[Fe(CN)_6]_m$	ⁱ	cubic a = 10.15 Å	7
B = K ₄ Fe(CN) ₆				$\frac{Ni}{Fe} \leq 1.4$			
colloidal product							
A = NiCl ₂ or $\left\{ \begin{array}{l} Ni(NO_3)_2 \\ NiSO_4 \end{array} \right.$	Ni Fe	= 2	A + B added simultaneously. Final Ni concentration 0.01 M	Ni ₂ Fe(CN) ₆ · 5H ₂ O		f.c.c., Fm3m a = 9.90 ± 0.03 Å	29
B = 0.25 M Na ₄ Fe(CN) ₆			<i>Idem</i> , dried at 140° in air	Ni ₂ Fe(CN) ₆		f.c.c., Fm3m a = 10.18 ± 0.02 Å	
A = 0.025 M $\left\{ \begin{array}{l} NiCl_2 \\ Ni(NO_3)_2 \\ NiSO_4 \end{array} \right.$	Ni Fe	= 1	A + B + C mixed in stoichiometric amounts, aged 16 hr, washed with water, dried in air	C ₈ Ni ₄ Fe(CN) ₆ · 4.26H ₂ O	^g	simple cubic a = 10.32 ± 0.05 Å possible space group P4 ₃ 32 or P2 ₁ 3	
B = 0.25 M Na ₄ Fe(CN) ₆	C ₈ Fe	= 2	<i>Idem</i> , dried in air at 135–140° and in vacuum at 100°	C ₈ Ni ₄ Fe(CN) ₆	^g	a = 10.25 ± 0.05 Å	27
C = 0.8 M CsNO ₃ or CsCl	Ni Fe	= 1.33	A + B + C mixed in stoichiometric amounts, aged 16 hr, washed with water, dried in air	C ₈ Ni ₄ [Fe(CN) ₆] ₃ · 10H ₂ O	^g	a = 10.17 ± 0.05 Å	
	C ₈ Fe	= 1.33	<i>Idem</i> , dried in air at 135–140° and in vacuum at 100°	C ₈ Ni ₄ [Fe(CN) ₆] ₃	^g	a = 10.19 ± 0.05 Å	

continued

Table 2—continued

Reagents	Reagents ratio	Experimental procedure	Formula	Structure	Reference
A = Ni ²⁺ B = K ₄ Fe(CN) ₆		A + B mixed. Precipitate washed with water, 95% ethanol and diethyl ether, air-dried	K ₂ NiFe(CN) ₆ · 3H ₂ O	f.c.c. $a = 10.08 \pm 0.02 \text{ \AA}$	25
A = 0.05 M Ni(NO ₃) ₂ + 0.3 M HCl B = 0.05 M K ₄ Fe(CN) ₆	$\frac{\text{Ni}}{\text{Fe}} = 1$	B poured into A. Precipitate filtered off, washed with KCl solution. Dried 72 hr under vacuum at room temp. then 24 hr at 60°	K ₂ NiFe(CN) ₆ (approximate formula)	f.c.c., Fm3m $a = 9.96 \text{ \AA}$	53
A = $5 \times 10^{-4} M$ or $10^{-3} M$ Ni ²⁺ B = $0.25 \times 10^{-3} M$ $2 \times 10^{-3} M$ K ₄ Fe(CN) ₆	$\frac{\text{Ni}}{\text{Fe}} \geq 1$	B added to A	K ₂ Ni ₃ [Fe(CN) ₆] ₂ K ₄ Ni ₄ [Fe(CN) ₆] ₃	^a ^g	
C = 0.5 M K ⁺	$\frac{\text{K}}{\text{Fe}} \geq 4$	B added to A + C	K ₄ Ni ₄ [Fe(CN) ₆] ₃	^a ^g	33
	$\frac{\text{Ni}}{\text{Fe}} \leq 2$	A added to B	K ₁₂ Ni ₆ [Fe(CN) ₆] ₇ K ₄ Ni ₄ [Fe(CN) ₆] ₃ K ₂ Ni ₃ [Fe(CN) ₆] ₂	^a ^g	34
	$\frac{\text{Ni}}{\text{Fe}} \leq 2$ $\frac{\text{K}}{\text{Fe}} \geq 4$	A added to B + C	K ₁₂ Ni ₆ [Fe(CN) ₆] ₇	^a ^g	
A = 0.1 M Ni(NO ₃) ₂ B = 0.1 M Na ₄ Fe(CN) ₆	$\frac{\text{Ni}}{\text{Fe}} = 10:3:3:2:1$ $\frac{\text{Ni}}{\text{Fe}} = 0:1$	A + B mixed in different ratios. Precipitate heated 2 hr on a boiling water-bath, allowed to stand for 24 hr, filtered off, washed, dried at room temp.	Ni ₂ Fe(CN) ₆ Na ₂ NiFe(CN) ₆	^j ^j	30

A = 0.4 M NiSO ₄			
B = 0.4 M H ₄ Fe(CN) ₆	B poured into A. Aging 24 hr. Precipitate washed, air-dried 16 hr at 80°	Ni ₂ Fe(CN) ₆	52
A = 0.4 M NiSO ₄	$\frac{\text{Ni}}{\text{Fe}} \geq 1$		
B = 0.4 M Na ₄ Fe(CN) ₆		Na _{1.30} Ni _{1.35} Fe(CN) ₆	cubic $a = 10.19 \pm 0.01 \text{ \AA}$

- a* Potentiometric measurements.
b Conductivity measurements.
c From the conductivity curves, the authors deduced the following compounds: K_{1.47}Ni_{1.27}Fe(CN)₆ and K_{2.14}Ni_{1.09}Fe(CN)₆.
d Composition determined by titration of the supernatant solutions.
e TI⁺ determined in the supernatant solution.
f Analysis for Rb⁺ and NO₂⁻ in the supernatant solution.
g Chemical analysis.
h Thermogravimetric analysis.
i Potentiometry, conductivity, electrophoresis, chemical analysis, radiometry.
j Chemical analysis performed, but no results given.

the most recent studies, a mixed ferrocyanide is obtained whatever the Zn/Fe ratio. In most cases the formula K₂Zn₃[Fe(CN)₆]₂ is assigned.^{5,17,20,22,23} MgZn₃[Fe(CN)₆]₂ and CaZn₃[Fe(CN)₆]₂ belong to the same series.¹⁹

The structure of this series was accurately determined by X-ray diffraction methods with powder and single crystals.^{14,15,16,24} It belongs to the rhombohedral system R $\bar{3}$ c. The parameters vary very slightly according to which alkali metal is present.

For the products obtained in presence of potassium ions, other compositions are sometimes given: cubic K₂ZnFe(CN)₆ by Rigamonti²³ and Ayers *et al.*²⁵ or tetragonal K_{0.5}Zn_{1.75}Fe(CN)₆ by Vol'khin *et al.*¹².

Precipitation in the presence of caesium ions leads to a product with formula Cs₂ZnFe(CN)₆.^{19,22,26,27} and a cubic structure.^{10,26,27}

Kuznetsov *et al.*²⁷ proposed another composition, also with a cubic structure.

Ion-exchange has been used in order to obtain mixed zinc-caesium ferrocyanides. Starting from Zn₂Fe(CN)₆, the exchange leads to Cs₂ZnFe(CN)₆.^{9,11} Starting from the M $\frac{1}{2}$ Zn₃ series (M¹ = Na, K), the exchange leads to Cs₂Zn₃[Fe(CN)₆]₂ which belongs to the same R $\bar{3}$ c space group.^{5,16}

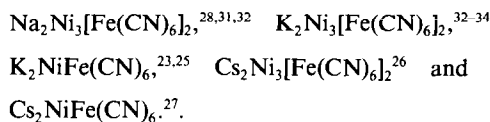
According to Ganzerli-Valentini *et al.*,¹¹ sodium ions cannot be retained on Zn₂Fe(CN)₆ by ion-exchange.

Nickel ferrocyanides

The compositions found in the literature are reported in Fig. 1. In contrast to zinc, the compounds are mostly non-stoichiometric.

Pure Ni₂Fe(CN)₆, nickel ferrocyanide, was prepared by Tananaev,²⁸ Kuznetsov,²⁹ and Kawamura³⁰ with the aid of lithium or sodium ferrocyanide and a nickel:ion ratio close to 2. Rigamonti²³ recommends the use of potassium ferrocyanide.

In general, however, products made in the presence of an alkali-metal ion contain various proportions of the starting cations. Some examples of the variations observed are given in Table 3. Owing to the wide range of compositions, most of the proposed stoichiometric formulae are included in the limits given in Table 3:



A few compositions do not have the general formula, such as Na₂NiFe(CN)₆ found by Kawamura.³⁰ The alkali-metal ion content increases in the order Na < K < Rb < Cs.

The preparation of nickel ferrocyanides by exchange has been studied by only one group.^{12,13} According to these investigators, the exchange does not alter the alkali-metal to nickel ratio.

All the investigators who have studied the crystallographic structure of nickel ferrocyanides have

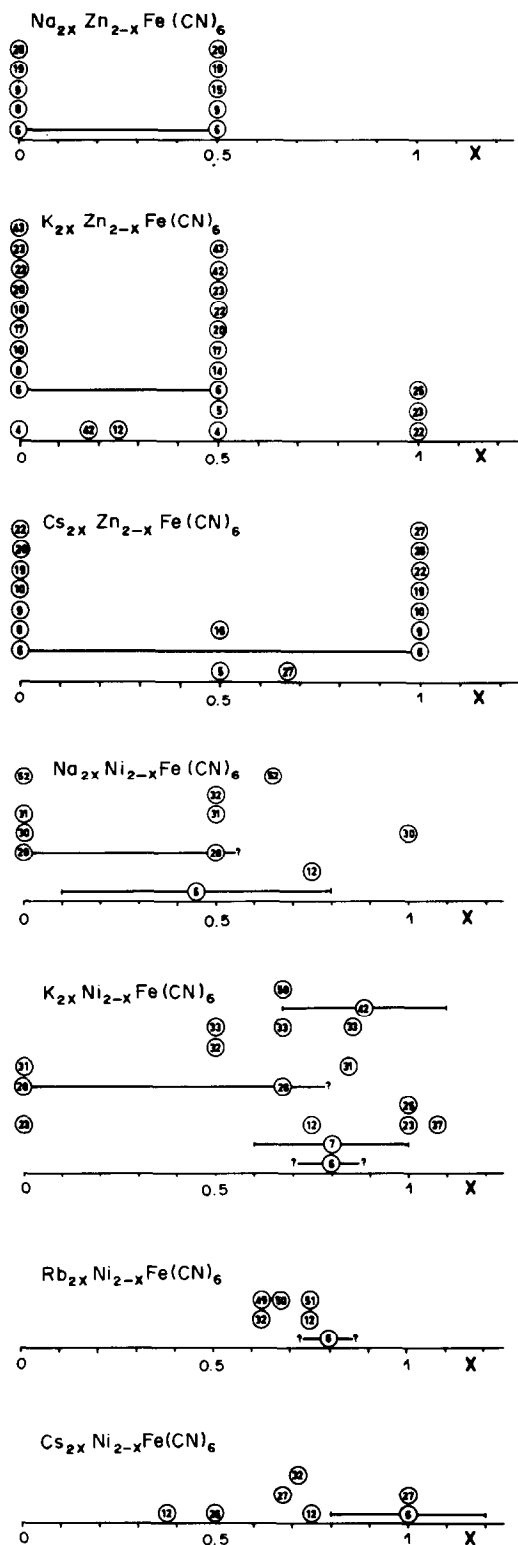


Fig. 1. Composition of ferrocyanides, according to various authors. The formula is taken as $M^I_x M^{II}_{2-x} Fe(CN)_6$, where M^I is an alkali metal and M^{II} is Zn or Ni. The number refers to the literature and is placed at the x value indicated in the paper referred to. If x varies, its range is indicated by a straight line.

Table 3. Domain of validity of the formula $A_{2x}Ni_{2-x}Fe(CN)_6$ for various alkali-metal ions (A)

Element	x , range	\bar{x}
Na	0.1–0.8	0.52
K	0.5–1.1	0.82
Rb	—	0.70
Cs	0.66–1.2	0.84

found a cubic cell, whatever the composition. The unit cell parameter is between 9.9 and 10.2 Å.

Water content

The water content received little attention in the earlier studies and there are discrepancies between values reported.^{5,10,25–27,29,35–37} No general conclusion was reached concerning the occurrence of definite hydrates.

Recently the problem was more accurately studied for some zinc ferrocyanides. Siebert *et al.*¹⁸ showed that heating $Zn_2Fe(CN)_6 \cdot xH_2O$ leads to a compound with two molecules of water per formula unit. In the $M^I_2Zn_3[Fe(CN)_6]_2$ series ($M^I = Na, K, Cs$) the water is zeolitic.^{14–16,24,38} The uptake of water may reach a very high value (9 molecules per formula unit for $M^I = Na$) in agreement with the microporous character of the structure.

CONCLUSIONS

Too rapid an approach to the literature on ferrocyanides could lead to a very confused idea of their composition. However, after a more systematic and synoptic review, certain general features may be found. First, the two types of ferrocyanides dealt with here appear to be quite different in composition and structure. Almost all zinc ferrocyanides seem to belong to two families, having definite formulae: $Zn_2Fe(CN)_6 \cdot xH_2O$ and $M^I_2Zn_3[Fe(CN)_6]_2 \cdot xH_2O$. The methods leading to each of these two types of compound are well defined. In contrast, nickel ferrocyanides seem not to have definite formulae, but always belong to the cubic system.

However, many points cannot be fully understood even after this review, and should be the subject of further investigations. It would be interesting to examine the conditions for existence of some zinc ferrocyanides departing from the two families mentioned, such as $Cs_2ZnFe(CN)_6$ and $K_2ZnFe(CN)_6$. In the case of nickel, the stability domains of the $M^I:Ni$ ratio should be studied for each alkali metal, as well as the nature of the water molecules bound in the compounds. A more accurate knowledge of the structure should be obtained by using single crystals, as already done for the $M^I_2Zn_3[Fe(CN)_6]_2$ series.

A very important point is the preparation of products usable as ion-exchangers. The ferrocyanides generally obtained have very small particle size and cannot be easily used for column work. Some au-

thors have made attempts to prepare products more suitable for that purpose.

Better mechanical properties have been obtained by mixing the ferrocyanide with silica gel³⁹ or an organic binding agent.⁴⁰ In both cases the capacity for caesium is lowered. Another attempt consisted in growing nickel ferrocyanide crystals at low temperature.⁴¹

The development of the use of ferrocyanides seems to depend on the low-cost manufacture of a product suitable for industrial applications.

REFERENCES

1. V. Veselý and V. Pekárek, *Talanta*, 1972, **19**, 219, 1245.
2. A. K. De and A. K. Sen, *Seprn, Sci. Technol.*, 1978, **13**, 517.
3. H. Loewenschuss, *Radioactive Waste Management*, 1982, **2**, 327.
4. S. Kawamura, K. Kurotaki and M. Izawa, *Bull. Chem. Soc. Japan*, 1969, **42**, 3003.
5. S. Vlasselaer, W. D'Olieslager and M. D'Hont, *J. Inorg. Nucl. Chem.*, 1976, **38**, 327.
6. J. Doležal and V. Kourim, *Radiochem. Radioanal. Lett.*, 1969, **1**, 295.
7. J. Des Ligneris, *Thèse Docteur-Ingénieur*, Clermont-Ferrand, 1969.
8. V. Kourim, J. Rais and B. Million, *J. Inorg. Nucl. Chem.*, 1964, **26**, 1111.
9. S. Kawamura, H. Kuraku and K. Kurotaki, *Anal. Chim. Acta*, 1970, **49**, 317.
10. M. Cola and M. T. Ganzerli-Valentini, *Inorg. Nucl. Chem. Lett.*, 1972, **8**, 5.
11. M. T. Ganzerli-Valentini, S. Meloni and V. Maxia, *J. Inorg. Nucl. Chem.*, 1972, **34**, 1427.
12. V. V. Vol'khin, E. A. Shul'ga and M. V. Zil'berman, *Izv. Akad. Nauk SSSR, Neorgan. Mater.*, 1971, **7**, 77.
13. A. V. Kaliuzhnyi, V. V. Vol'khin and M. V. Zil'berman, *Izv. Vyssh. Uchebn. Zaved.*, 1977, **5**, 45.
14. P. Gravereau, E. Garnier and A. Hardy, *Acta Cryst.*, 1979, **B35**, 2843.
15. E. Garnier, P. Gravereau and A. Hardy, *ibid.*, 1982, **B38**, 1401.
16. P. Gravereau and E. Garnier, *Rev. Chim. Min.*, 1983, **20**, 68.
17. A. Bellomo, *Talanta*, 1970, **17**, 1109.
18. H. Siebert, B. Nuber and W. Jentsch, *Z. Anorg. Allg. Chem.*, 1981, **474**, 96.
19. I. M. Kolthoff and E. J. A. H. Verzijl, *Rec. Trav. Chim. Pays-Bas*, 1924, **43**, 389.
20. S. Kawamura, K. Kurotaki, H. Kuraku and M. Izawa, *J. Chromatog.*, 1967, **26**, 557.
21. I. V. Tananaev and A. P. Korolkov, *Izv. Akad. Nauk SSSR, Neorgan. Mater.*, 1965, **1**, 100.
22. W. D. Treadwell and D. Chervet, *Helv. Chim. Acta*, 1922, **5**, 633.
23. R. Rigamonti, *Gazz. Chim. Ital.*, 1938, **68**, 803.
24. A. Renaud, P. Cartraud, P. Gravereau and E. Garnier, *Thermochim. Acta*, 1979, **31**, 243.
25. J. B. Ayers and W. H. Waggoner, *J. Inorg. Nucl. Chem.*, 1971, **33**, 721.
26. G. B. Barton, J. L. Hepworth, E. D. McClanhan Jr., R. L. Moore and H. H. Van Tuyl, *Ind. Eng. Chem.*, 1958, **50**, 212.
27. V. G. Kuznetsov, Z. V. Popova and G. B. Seifer, *Zh. Neorgan. Khim.*, 1970, **15**, 2105; *Russian J. Inorg. Chem.*, 1970, **15**, 1084.
28. I. V. Tananaev and M. I. Levina, *Zh. Analit. Khim.*, 1946, **1**, 224.
29. V. G. Kuznetsov, Z. V. Popova and G. B. Seifer, *Zh. Neorgan. Khim.*, 1970, **15**, 1860.
30. S. Kawamura, S. Shibata and K. Kurotaki, *Anal. Chim. Acta*, 1976, **81**, 91.
31. W. D. Treadwell and D. Chervet, *Helv. Chim. Acta*, 1923, **6**, 550.
32. V. V. Vol'khin, *Izv. Akad. Nauk SSSR, Neorgan. Mater.*, 1979, **15**, 1086.
33. A. Bellomo, D. De Marco and A. Casale, *Talanta*, 1972, **19**, 1236.
34. *Idem*, *Ann. Chim. (Roma)*, 1973, **63**, 477.
35. G. B. Seifer, *Russian J. Inorg. Chem.*, 1959, **4**, 841.
36. *Idem*, *ibid.*, 1963, **8**, 607.
37. P. J. Gellings, *Z. Phys. Chem. (Frankfurt)*, 1967, **54**, 296.
38. P. Cartraud, A. Cointot and A. Renaud, *J. Chem. Soc. Faraday Trans.*, 1981, **77**, 1561.
39. C. Konecny and R. Caletka, *J. Radioanal. Chem.*, 1973, **14**, 255.
40. J. Stejskal, J. Soukup, J. Doležal and V. Kourim, *J. Radioanal. Chem.*, 1974, **21**, 371.
41. V. V. Vol'khin, B. I. L'vovich, S. A. Kolesova, G. V. Leont'eva, A. F. Kalashnikova, Yo. I. Nalimov and A. G. Kubareva, *Izv. Vyssh. Ucheb. Zaved. Tsvein. Met.*, 1966, **4**, 28.
42. H. T. S. Britton and E. N. Dodd, *J. Chem. Soc.*, 1933, 1543.
43. H. B. Weiser, W. O. Milligan and J. B. Bates, *J. Phys. Chem.*, 1938, **42**, 945.
44. V. Kourim and B. Million, *Collection Czech. Chem. Commun.*, 1965, **30**, 2848.
45. V. G. Kuznetsov and S. I. Maksimova, *Zh. Strukt. Khim.*, 1973, **14**, 849.
46. V. G. Kuznetsov, Z. V. Popova and G. B. Seifer, *Zh. Neorgan. Khim.*, 1970, **15**, 2077; *Russian J. Inorg. Chem.*, 1970, **15**, 1071.
47. B. Gorenc and L. Kosta, *Z. Anal. Chem.*, 1966, **223**, 410.
48. I. V. Tananaev and M. A. Glushkova, *Zh. Neorgan. Khim.*, 1957, **2**, 586.
49. S. A. Kolesova and V. V. Vol'khin, *Izv. Akad. Nauk SSSR, Neorgan. Mater.*, 1966, **11**, 1110.
50. V. V. Vol'khin and S. A. Kolesova, *Zh. Prikl. Khim.*, 1967, **40**, 342.
51. *Idem*, *Zh. Fiz. Khim.*, 1969, **43**, 1834.
52. C. Loos-Neskovic, M. Fedoroff and G. Revel, *Radiochem. Radioanal. Lett.*, 1976, **26**, 17.
53. D. F. Shriver, S. A. Shriver and S. E. Anderson, *Inorg. Chem.*, 1965, **4**, 725.

Summary—A review is given of work on nickel and zinc ferrocyanides during the period 1922–1983 with an emphasis on their compositions and structures in relation to the methods of preparation.

ANNOTATIONS

ALKALI-METAL ION COMPLEXATION WITH LARIAT ETHERS POSSESSING A CHROMOGENIC GROUP

B. P. BUBNIS and G. E. PACEY

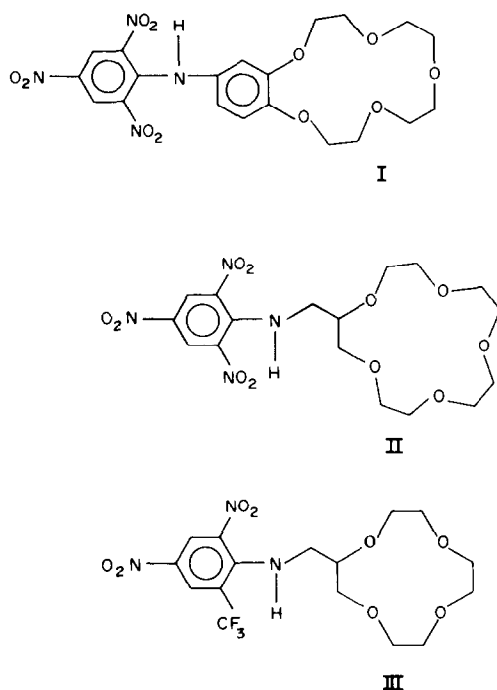
Department of Chemistry, Miami University, Oxford, Ohio 45056, U.S.A.

(Received 28 February 1984. Accepted 25 June 1984)

Summary—The extraction and complexation abilities of chromogenic alkyl crown-ether reagents were compared with those of their chromogenic benzo crown ether analogues. Improvements in the extraction efficiency and stability of the complexes were observed, and can be attributed to various factors such as increased lipophilic character and decreased charge separation. The spectral separation caused by the deprotonation of the amine-group was significantly decreased, so the usefulness of these compounds will be limited, until improved spectral separation can be achieved.

Ion-pairing with picrate as counter-ion was the first method used for colorimetric determination by means of complexation with crown ethers. Later, Ueno reported the synthesis and complexation behaviour of a chromogenic crown ether (I) which formed an intramolecular ion-pair with alkali-metal ions.¹ This molecule incorporated a secondary amino-group, which conferred acid/base character on the chromogenic crown ether. When the extraction system was buffered at a sufficiently high pH, the protonated ligand (HL) dissociated, resulting in a shift in λ_{\max} and an increase in the molar absorptivity (ϵ). The dissociated crown ether species (L^-) complexed alkali-metal ions in the aqueous phase and the complex was extracted into chloroform. Absorbance measurements at an appropriate wavelength were linear with respect to $[K^+]$ from 10 to 700 ppm in the presence of 2300 ppm Na^+ . The selectivity of the reagent for K^+ in the presence of a large excess of Na^+ made it ideally suited for K^+ determinations in blood serum.^{1,2}

Alkali-metal ion complexation by crown ethers has been shown to be governed largely by the relative fit of the alkali-metal ion in the crown ether cavity.³⁻⁵ Experimental evidence has shown that other factors need to be considered when developing new crown ether molecules to be used for alkali-metal ion determination.² For example, changing the chromogenic tag altered the complexation behaviour of these new analytical reagents.² The replacement of the *p*-nitro group in compound I with a cyano group shifted λ_{\max} of HL to longer wavelengths (390→420 nm) and decreased ϵ_{\max} ($1.3 \times 10^4 \rightarrow 1.1 \times 10^4$ l. mole⁻¹. cm⁻¹). $\Delta\lambda_{\max}$ [*i.e.*, $\lambda_{\max}(L^-) - \lambda_{\max}(HL)$] was increased from 55 to 130 nm, and the formation constant for the potassium complex (K_{ML}) was lowered (80.5→22.5). Interestingly, this evidence showed that the chromophore structure also had an effect on the strength of the metal-ligand complex.



Scheme 1.

Our experience with chromogenic crown ether reagents in extraction analysis has led us to conclude that to improve the extraction efficiency an increase in the lipophilic nature of the compound is needed. Hence reagents II and III were prepared from the aminomethyl derivatives of 15-crown-5 and 12-crown-4.

This paper reports data on the visible spectra, extraction constants, dissociation constants, and formation constants for complexes of compounds II and III with alkali-metal ions.

EXPERIMENTAL

The dichloromethane and chloroform used were of spectral analysis quality. All water was distilled, and demineralized with Barnstead Nanopure system. All alkali-metal salts were purchased from Alfa Chemical Co. and dried at 110°. Absorption spectra were recorded with a Hewlett-Packard 8450-A spectrophotometer. All pH measurements were made with a Corning 12 pH-meter.

The aminomethyl derivatives were synthesized in good yield from the hydroxymethyl precursors described in the literature.⁶ The aminomethyl crown ether molecules were synthesized from the hydroxymethyl molecules by either of two pathways: (1) the use of thionyl chloride and subsequent reaction of the product with the potassium salt of phthalimide; (2) generation of a phosphonium salt intermediate by the addition of an equivalent each of triphenylphosphine, diethylazodicarboxylate, and phthalimide to an equivalent of the hydroxymethyl compound. Both methods yielded the phthalimidomethyl compounds which was then reacted with hydrazine hydrate. Details of the synthesis have been given elsewhere.⁷

General method for the preparation of chromogenic lariet ethers

Approximately 2 mmoles of the appropriate aminomethyl crown ether hydrochloride were placed in 25 ml of tetrahydrofuran (THF) containing one equivalent of sodium hydroxide and the mixture was stirred at room temperature for 1 hr. An equivalent of chromophore [4-chloro-3,5-dinitrobenzotrifluoride (Aldrich) or 1-chloro-2,4,6-trinitrobenzene (Fairfield)] was then added along with an additional equivalent of base. The stirring was continued for 1 hr. The solution was filtered and the THF removed in a rotary evaporator. Water (25 ml) was then added to the residue and the mixture was extracted with three 30-ml portions of chloroform. The extracts were dried over anhydrous magnesium sulphate and filtered, and the chloroform was removed in a rotary evaporator. The products were obtained as yellow powders in 60% yield following recrystallization from ethanol. 2,4,6-Trinitrophenylaminomethyl-15-crown-5 hydrochloride (II), m.p. 187–188°, C₁₇H₂₅N₃O₁₁Cl requires 41.09% C, 5.07% H, 11.27% N; found 41.8% C, 5.5% H, 11.3% N. 2,4-Dinitro-6-trifluoromethylphenylaminomethyl-12-crown-4 (III), m.p. 86–88°, C₁₆H₂₀F₃N₃O₈ requires 43.74% C, 4.58% H, 12.97% F, 9.56% N; found 43.8% C, 4.6% H, 13.0% F, 9.4% N.

Visible region spectra

Spectra for II and III were obtained for solutions in 20%

acetonitrile/80% water mixture. Two spectra were recorded, one at pH 2 and the other at a pH at which the amine proton was dissociated.

Determination of extraction constants

A 5-ml portion of 0.1M alkali-metal ion solution was extracted with 5 ml of 1M triethylamine solution in chloroform, which contained a known concentration of crown ether. The organic and aqueous layers were analysed spectrophotometrically.

Determination of K_a, K_{ML}, K_{MHL}

The crown ether reagent was dissolved in a 40% acetonitrile/60% water mixture to give a final concentration of approximately 2.5 × 10⁻⁴M. A 10-ml portion was diluted to 25 ml with demineralized water. K_a was determined experimentally with the diluted solution containing a constant concentration of the alkali-metal ion which does not readily complex with the crown ether. K_a^{app}, K_{ML}, and K_{MHL} were determined experimentally by varying the concentration of the alkali-metal salt (0.1, 0.08, 0.06M) in the solution. The absorbance was measured at the wavelength of maximum apparent molar absorptivity, at varying [H⁺], with hydrochloric acid and a weakly or non-complexing alkali-metal hydroxide to adjust the pH.⁸

RESULTS AND DISCUSSION

Visible region spectra

The spectral data for reagents II and III are given in Table 1. The Δλ_{max} resulting from dissociation of the monobasic amine proton was relatively small (2 and 12 nm), because an extended conjugated system was not created by the deprotonation. The changes in molar absorptivity ((Δε) at λ_{max} for II and III were 1.52 × 10³ and 4.96 × 10³ l.mole⁻¹.cm⁻¹, and the largest Δε for reagent III was found to be at 377 nm (Δε = 6.47 × 10³ l.mole⁻¹.cm⁻¹). The visible-region spectra for both reagents indicate that their usefulness as alkali-metal ion sensors would be limited, since there was extensive spectral overlap of the (HL) and (L⁻) species. This was confirmed when reagent III was tested for determination of potassium. Although the Δε was adequate for extraction analyses,¹

Table 1. Wavelengths of maximum absorption and molar absorptivities of the test compounds

Compound	HL		L ⁻	
	λ _{max} , nm	ε, 10 ⁴ l.mole ⁻¹ .cm ⁻¹	λ _{max} , nm	ε, 10 ⁴ l.mole ⁻¹ .cm ⁻¹
I	390	1.30	445	2.00
II	355	1.24	357	1.40
III	350	1.43	362	1.93

Table 2. Extraction constants for alkali-metal ions (pK_{ext})^{*}

Compound	Solvent	Li ⁺	Na ⁺	K ⁺	Rb ⁺	Cs ⁺
I†	CHCl ₃	—	10.00	7.55	8.50	10.40
II	CHCl ₃	7.10 ± 0.08	7.41 ± 0.09	6.10 ± 0.08	8.00 ± 0.10	7.30 ± 0.05
	CH ₂ Cl ₂	6.80 ± 0.06	6.50 ± 0.06	6.40 ± 0.05	6.40 ± 0.05	—
II‡	CHCl ₃	7.40 ± 0.08	6.19 ± 0.08	5.86 ± 0.05	6.50 ± 0.05	7.64 ± 0.07

*1.0M triethylamine buffer system.

†From Takagi *et al.*

‡Calculated for 1:2 metal-ligand complex, except for Li⁺.

Table 3. A comparison of benzo and alkyl crown ether acid dissociation constants and formation constants

Compounds	I ²	II	III	2",4"-Dinitro-6"-trifluoromethylphenyl 4'-aminobenzo-15-crown-5
pK _a	10.5	11.6 ± 0.05	11.4 ± 0.05	10.2 ± 0.05
pK' _a	9.5	10.3–11.1*	9.8–10.9*	9.5
log K _{MD} †	1.91	2.28 ± 0.02	2.93 ± 0.08	2.11 ± 0.02
log K _{MHL} †	0.98	1.12 ± 0.01	1.33 ± 0.01	1.41 ± 0.01

*pK'_a varied according to which metal was complexed.

†For the K⁺ complex.

the very small $\Delta\lambda_{\max}$ on deprotonation reduced the analytical usefulness of the larger $\Delta\epsilon$.

Extraction

The selectivity of chromogenic crown ethers for alkali-metal ions can be described in terms of their extraction constants. The appropriate plot gave a straight line with slope equal to the extraction constant, K_{ext} .¹

Table 2 lists the pK_{ext} values. The alkyl chromogenic crown ethers exhibited better overall extraction of alkali-metal ions. This could be partly due to the absence of the benzene ring giving the molecule a more lipophobic nature and better solubility in water. Also, the charge separation between the intramolecular ion-pair was smaller than in the case of reagent I. A tight ion-pair or chelate-type interaction between the anion and metal ion would improve extraction. Although the improvement in extraction efficiency was beneficial, there was also reduced selectivity. An additional change was that the alkyl reagents extracted lithium. It is interesting that the 15-crown-5 molecule (II) extracted lithium better than the 12-crown-4 reagent did. The hydrated lithium ion is larger than the unhydrated ion and therefore requires a larger cavity. The data in Table 2 also indicate that solvent interaction plays an important role in the ability of crown ethers to extract alkali-metal ions into an organic phase. Comparison of the extraction constants for reagent II revealed that dichloromethane improved the extraction efficiency in most cases, although the gain in efficiency was offset by a significant loss in selectivity.

The selectivity sequence with I was found to be K⁺ > Rb⁺ > Na⁺ ~ Cs⁺. The selectivity (Table II) for the alkyl analogue under the same experimental conditions was K⁺ > Li⁺ > Cs⁺ > Na⁺ > Rb⁺. In each case K⁺ was the alkali-metal ion extracted most efficiently. The reported data for I indicate that the preferred stoichiometry is the 1:2 metal-ligand complex.¹ The selectivity data for reagent II showed that factors other than cation/cavity diameters need to be considered in order to explain the experimental results. If cation/cavity diameters were solely responsible for complexation then the extraction selectivity would be K⁺ > Li_{aq}⁺ > Rb⁺ > Na⁺ ~ Cs⁺.

Although the degree of extraction of Na⁺ and Cs⁺ were similar, Rb⁺ was extracted less efficiently than either.

The predicted selectivity of the 12-crown-4 analogues, based solely on cation/cavity diameters, is Na⁺ > K⁺ > Li_{aq}⁺ > Rb⁺ > Cs⁺. The experimentally determined extraction selectivity of III was K⁺ > Na⁺ > Rb⁺ > Li_{aq}⁺ > Cs⁺. This experimental evidence, along with the 15-crown-5 data, indicated that the nature of the ligand (aryl *vs.* alkyl, side-chains, *etc.*) was also a factor, though to a lesser degree, in the selectivity of crown ethers towards alkali-metal ions.

Complexation in aqueous medium

K_a, K'_a, K_{ML} and K_{MHL} values for II and III were experimentally determined, by use of equations previously reported.²

The pK_a values for reagents I–III and 2",4"-dinitro-6"-trifluoromethylphenyl-4'-aminobenzo-15-crown-5 are given in Table 3. The pK_a value for II was determined with rubidium hydroxide used to adjust the pH; for III lithium hydroxide was used. Dilute hydrochloric acid was used to lower the pH in both cases. These hydroxides were chosen because the extraction data in Table I indicated that these metal cations interacted the least with the respective reagents. The experimentally determined pK_a values were 11.6 for II and 11.4 for III, 1.0 pK_a unit higher than those for the benzo type crown ethers were in both cases. These experimentally determined data agreed with the theoretical prediction that the pres-

Table 4. Formation constants for complexes of reagents II and III

	Reagent	Li ⁺	Na ⁺	K ⁺	Rb ⁺
log K _{ML}	II	2.28	2.05	2.28	
log K _{MHL}	II	1.09	1.47	1.12	
pK' _a	II	10.3	11.01	10.4	
log K _{ML}	III		1.66	2.93	1.64
log K _{MHL}	III		1.17	1.33	1.01
pK' _a	III		10.9	9.8	10.8

ence of a benzene ring adjacent to an amino group should decrease the pK_a of the dissociable proton.⁹

Table 3 also shows the effect of presence of the benzene ring on alkali-metal complexation. With potassium reagent I had a formation constant of $10^{1.91}$. The reagent without the benzene ring gave a formation constant of $10^{2.28}$, in agreement with the literature¹⁰ in showing that the introduction of a benzo-group in the crown ether ring decreased the stability of the metal complex.

The complexation data for aqueous medium were in good agreement with the extraction data presented in Table 2. The extraction efficiencies with reagent II were $K^+ > Li^+ > Na^+$. The order of strengths of the crown ether-alkali-metal ion complexes, from the formation constants, was $K^+ \sim Li^+ > Na^+$. Similarly, with reagent III the extractability order was $K^+ > Na^+ > Rb^+$, and the formation constants followed the same trend. The K_{ML} values were larger than the K_{MHL} values, indicating that the overall negative charge of the molecule was influencing the formation of the metal complex. The selectivity of complexation also agreed with the literature in that the interaction was not strictly a charge-interaction.⁸

The absence of the benzene ring also had an effect on the pK'_a values of the molecule. When the benzene ring was present, as in the case of I, the complexation of various alkali-metal ions in the crown-ether cavity had little effect on the pK'_a value. The benzene ring acted as an insulator which protected the monobasic amine proton from the electron-withdrawing effects of the complexed cation. Removing the ring produced pK'_a values which depended on the cation and the strength of the complex. Table 3 indicates that as the formation constants (K_{ML}) increase, the pK'_a values decrease.

CONCLUSION

Complexation with crown ethers is a selective and sensitive method for determining alkali metals. The usefulness of these reagents is determined largely by the spectral characteristics of the molecule. Future attempts to use crown ether chromogenic reagents must deal with the problem of the large spectral overlap for reagent and complex or suffer from exceptionally high blank values.

The extraction and complexation data are better for the alkyl reagents than for their benzo analogues. The improvement can be attributed to numerous factors. As expected, the chromogenic activity does not appear to be useful in current methods of determination of alkali metals, but the knowledge gained has encouraged us to investigate alkyl crown ethers which incorporate fluorogenic tags.

REFERENCES

1. M. Takagi, H. Nakamura and K. Ueno, *Anal. Lett.*, 1977, **10**, 1115.
2. B. P. Bubnis, J. L. Steger, Y. P. Wu, L. A. Meyers and G. E. Pacey, *Anal. Chim. Acta*, 1982, **139**, 307.
3. C. J. Pederson, *J. Am. Chem. Soc.*, 1967, **89**, 7017.
4. C. J. Pederson and H. K. Frensdorff, *Angew. Chem. Intern. Ed. Engl.*, 1972, **11**, 16.
5. N. S. Poonia and M. R. Truter, *J. Chem. Soc. Dalton Trans.*, 1973, 2062.
6. T. Miyazaki, S. Yanagida, A. Itoh and M. Okahara, *Bull. Chem. Soc. Japan*, 1982, **55**, 2005.
7. B. P. Bubnis and G. E. Pacey, *Tetrahedron Lett.*, 1984, in the press.
8. H. Nakamura, M. Takagi and K. Ueno, *Anal. Chem.*, 1980, **52**, 1668.
9. H. House, *Modern Synthetic Reactions*, 2nd Ed., Benjamin, Phillipines, 1972.
10. J. J. Christensen, D. J. Eatough and R. M. Izatt, *Chem. Rev.*, 1974, **74**, 351.

DISSOLUTION OF GEOLOGICAL MATERIAL WITH ORTHOPHOSPHORIC ACID FOR MAJOR-ELEMENT DETERMINATION BY FLAME ATOMIC-ABSORPTION SPECTROSCOPY AND INDUCTIVELY-COUPLED PLASMA ATOMIC-EMISSION SPECTROSCOPY

PHILIP HANNAKER and HOU QING-LIE*

Department of Geology, School of Earth Sciences, University of Melbourne, Victoria 3052, Australia

(Received 16 January 1984. Accepted 24 June 1984)

Summary—An analytical procedure has been developed for the determination of major elements in geological material by both flame atomic-absorption spectrometry and inductively-coupled plasma atomic-emission spectrometry. Condensed phosphoric acid was used for the decomposition of 70 natural minerals containing sulphide, oxide, silicate or carbonate constituents. The results were compared with those obtained when a perchloric acid and orthophosphoric acid mixture was used for the decomposition, to ensure dissolution of even the most acid-resistant minerals. The procedure can be applied to rocks, ores, soils, slags and refractory material as a means of rapid and complete dissolution for the analysis of even the most insoluble material.

Atomic-absorption spectrometry (AAS) is now widely used to analyse a wide range of geological material for major and trace elements.¹⁻⁵ Recent years have seen an impressive increase in the application of inductively-coupled plasma atomic-emission spectroscopy (ICP-AES) for the determination of major, minor and trace elements in geological material.^{6,7} One of the advantages of ICP-AES is its speed, which is due to simultaneous measurement of several elements. When automated AAS⁸⁻¹¹ and ICP-AES are used, the slowest step in the analysis is dissolution of the sample.

The usual procedure for dissolution of geological material¹ involves evaporation to dryness with a mixture of hydrofluoric, nitric and perchloric acids, followed by two evaporations with perchloric acid and dissolution of the resulting residue in dilute hydrochloric or nitric acid; this procedure, however, is both time-consuming, as it requires at least 20 hr of continuous heating, and incomplete, as certain minerals such as chromite and ilmenite are very resistant to such acid mixtures.

More rapid dissolution techniques using reagents such as nitric acid,¹² nitric acid-hydrogen peroxide,¹³ hydrochloric acid-nitric acid^{13,14} or ammonium acetate^{15,16} to leach soluble material generally produce low results on account of incomplete attack on silicate material, and possibly high results (when AAS is used) due to light scattering by suspended particles in the solution.

Many analysts have found it necessary to resort to fusion techniques for the complete dissolution of geological material and the determination of silica

(which is lost by volatilization with hydrofluoric acid, when this is used in acid dissolution techniques).

Fusion with alkaline mixtures such as sodium hydroxide/sodium peroxide,¹⁷ however, produces a high salt concentration, with consequent light-scattering,¹⁸ which is a considerable disadvantage with AAS. It has also been reported that the plasma torch is easily fouled when solutions with high salt concentrations are used.¹⁹ The use of these mixtures also presents difficulties because of the formation of colloidal silicic acid when the solutions are acidified. Fusion with sodium carbonate results in similar problems with the precipitation of silicic acid, and completeness of decomposition of certain refractory oxides has been questioned.²⁰

Heating with hydrofluoric acid under pressure gives rapid dissolution of silicate material,²²⁻²⁴ but the excess of hydrofluoric acid must be complexed with boric acid, again resulting in high light-scattering, owing to the aspiration of highly concentrated salt solutions. Also, the technique has been observed to give incomplete decomposition of minerals such as tourmaline and of some titanium and aluminium compounds, which limits its use for geological samples.²⁵

To reduce the errors associated with determination of the major components of geological material, alternative dissolution techniques have been investigated.

Use of condensed phosphoric acid

On heating, orthophosphoric acid undergoes a succession of condensation reactions, giving pyrophosphoric acid ($H_4P_2O_7$), tetrapolyphosphoric acid ($H_6P_4O_{13}$) and metaphosphoric acid ($H_4P_4O_{12}$). It is convenient to call the product "condensed" phos-

*Visiting Research Fellow from Baiyin Research Institute of Mining and Metallurgy, Lanzhou, China.

phoric acid (the Japanese workers^{26,27} who first developed its use called it "strong phosphoric acid").

Because of the complexing ability and the strength of the condensed phosphoric acid, and its ability to form a stable soluble silica compound SiP_2O_7 ,²⁸ heating with this acid should dissolve a large number of geologically interesting materials.

In the 1930s phosphoric acid was used to dissolve chrome²⁹ and iron ores.³⁰ Also at this time concentrated phosphoric acid was used to dissolve many silicates such as kaoline, mica and feldspar from clay minerals.³¹ Perchloric and phosphoric acid mixtures have been studied for the dissolution of iron ores.³² A mixture consisting of equal volumes of these two acids was found to be superior to hydrochloric acid when iron was determined by titration after reduction.

So far, condensed phosphoric acid has found limited use in the analysis of chrome ores³³ and some of the more difficultly soluble refractory oxides.³⁴ The potential of this acid used alone or combined with other acids as a means of dissolution for rapid major and trace multi-element analysis in geological material has been underestimated by many workers.

Condensed phosphoric acid was fully investigated in these laboratories for the solution and subsequent determination of major element components for oxide, silicate, sulphide and carbonate materials of a geological nature.

EXPERIMENTAL

Reagents

The reagents used were of analytical reagent grade and all water used was distilled and demineralized (DDW).

Standard solutions

Appropriate metals or stoichiometric salts were dissolved to prepare stock 1000-ppm standard solutions. The working standards for AAS contained 10% v/v orthophosphoric acid, and those for ICP-AES calibration and analysis contained 5% v/v orthophosphoric acid.

Instrumentation

The ICP-AES system is described in Table 1. The working conditions are listed in Table 2. A Techtron Model AA-3 with Varian Techtron 1m-6D indicator module was used for all AAS determinations.

Dissolution of minerals with condensed phosphoric acid

Natural minerals of oxide, silicate, sulphide and carbonate type (150-mg samples) were treated with 10 ml of orthophosphoric acid in a platinum crucible at a temperature of 290° on a hot-plate, with swirling at regular intervals.

The reaction mixtures were inspected at 15-min intervals to check completeness of dissolution. For rapid dissolution, in most cases it was found necessary to grind the sample in a mortar and pestle to 300 mesh grain-size. Finely ground silicate, oxide and carbonate minerals were rapidly dissolved, but attack on sulphides was slow, and in some cases (Cu_2FeS_4 , CuFeS_2 , MoS_2 , FeS_2) dissolution was still incomplete after continuous heating for 3 hr, reflecting the poor oxidizing power of phosphoric acid. The combined use of

Table 1. ICP-AES instrumentation

RF generator:	air-cooled, 3-kW rating, 27.12 MHz
Spectrometer:	ARL 34000, grating ruled 1080 lines/mm; primary slit-width 20 μm
Nebulizer:	glass pneumatic concentric nebulizer designed by ARL
Torch:	quartz, 18 mm outer diameter, two-turn coil surrounding the torch

0.5 ml of 70% perchloric acid with 10 ml of 85% phosphoric acid, however, provided a strongly oxidizing solution capable of dissolving the most resistant sulphide material in 45 min.

Table 3 illustrates the usefulness of phosphoric acid, especially in combination with perchloric acid, for rapid dissolution of natural minerals, including the more acid-resistant minerals such as ilmenite, chromite and tourmaline.

Dissolution of standard rocks, ores, slags and refractory materials

Each of a series of 5 NIM standard rocks and 5 BCS standard materials was treated with 10 ml of 85% phosphoric acid as described above. The solutions obtained were cooled, and then diluted to 100 ml (for AAS) or 200 ml (for ICP) with DDW. The major elements (Al, Ca, Fe, Si, Mg, Na, Ti) were determined by both ICP-AES and flame AAS, calibration being done with standards prepared in a similar manner. The experiment was repeated with the perchloric-phosphoric acid mixture (see above) for further comparison of the two acid treatments.

The completeness of dissolution was established by comparing the experimental values with the certified values for the standard material.

All materials tested were completely dissolved in less than 1 hr, without precipitation on cooling or dilution. However, for higher Ti concentrations in the prepared standards a precipitate appeared on standing, probably $\text{Ti}(\text{OH})\text{PO}_4$, which can be eliminated by the addition of 0.5 ml of 30% w/w hydrogen peroxide before dilution.

Tables 4 and 5 show the completeness of attack for all material tested.

Precision

An internal department rock standard, DCB-1 (basalt), was used for checking the reproducibility of the method. Table 6 shows the results. The coefficients of variation ranged from 0.5% (Mn) to 3.6% (K).

Note

It should be noted that phosphoric acid, especially in the presence of perchloric acid, may slightly attack platinum crucibles at elevated temperatures. This will only become of consequence if heating is prolonged.

For samples containing high levels of organic carbon, care is needed to avoid possible explosive reactions in the presence of perchloric acid. When analysing such samples it is always advisable to pretreat the samples with concentrated nitric acid.

Table 2. ICP-AES working parameters

Incident power:	1600 W
Flush time:	30 sec
Integration time:	10 sec
Integration cycle:	3
Observation height:	division 2 (14 mm above the coil)

Table 3. Effect of H₃PO₄ and H₃PO₄/HClO₄ on the dissolution time for 150 mg of 300-mesh natural minerals

Mineral	Max. dissolution time, min		Max. dissolution time, min		Mineral	Max. dissolution time, min	
	H ₃ PO ₄	H ₃ PO ₄ /HClO ₄	H ₃ PO ₄	H ₃ PO ₄ /HClO ₄		H ₃ PO ₄	H ₃ PO ₄ /HClO ₄
Alabandite	45	30	45	45	Prolusite	30	30
Allinite	45	45	15	15	Psilomelane	30	30
Amblygonite	30	30	30	30	Pyrite	195a	30
Amphibole	30	30	15	15	Pyrolusite	30	30
Anhydrite	15	15	30	30	Pyroxene	45	45
Apatite	30	30	15	15	Pyrrhotite	75	30
Apophyllite	15	15	15	15	Rhodocrosite	15	15
Azurite	15	15	135	45	Serpentine	30	30
Bornite	195*	30	45	45	Siderite	15	15
Calcite	15	15	165	45	Smithsonite	15	15
Cerussite	15	15	30	30	Sphalerite	15	15
Chalcanthite	15	15	75	75	Spinel	30	30
Chalcopyrite	195*	30	60	60	Staurolite	120	120
Chinochlore	30	30	15	15	Stiibite	15	15
Chromite	150	30	15	15	Talc	90	90
Chrysolite	45	45	15	15	Tetrahedrite	195	15
Colemanite	30	30	15	15	Tourmaline	150	150
Corundum	180	180	15	15	Wavellite	30	30
Cryolite	30	30	105	30	Wernerite	30	30
Cuprite	15	15	195*	45	Wolframite	30	30
Datolite	15	15	105	105	Wollastonite	30	30
Emboelite	15	15	60	60	Zincite	15	15
Enstatite	45	45	30	30	Zircon	150	150
			30	30			

*Incomplete dissolution

Table 4. Major components (%) in NIM standard rocks

Component	NIM-S		NIM-D		NIM-P		NIM-N		NIM-L	
	Measured value	Quoted value*	Measured value	Quoted value*	Measured value	Quoted value	Measured value	Quoted value	Measured value	Quoted value
Al ₂ O ₃	17.1†	17.33	0.46†	0.46	4.33†	4.38	16.6†	16.64	13.6†	13.93
	17.4§		0.41§		4.32§		16.7§		13.7§	
CaO	17.6‡	0.70	0.15†	0.31	3.94‡	2.68	16.5‡	11.55	13.6‡	3.03
	0.78		0.65		2.85		11.9		3.80	
Fe ₂ O ₃	0.83	1.40	0.36	16.97	2.72	12.29	12.9	9.00	4.05	9.77
	0.67		0.23		2.47		11.39		3.10	
MgO	1.50	0.48	16.63	43.30	12.17	25.19	9.08	7.43	9.64	0.36
	1.29		41.5		25.12		8.76		9.81	
MnO	1.40	0.01	43.3	0.20	24.06	0.21	7.10	0.17	0.23	0.71
	0.22		42.66		24.06		7.10		0.23	
SiO ₂	0.39	63.67	0.19	38.86	0.17	50.88	0.14	52.52	0.46	52.52
	0.017		0.22		0.21		0.19		0.78	
TiO ₂	0.01	0.05	0.21	0.04	0.20	0.20	0.16	0.19	0.52	0.51
	0.01		0.02		0.20		0.16		0.52	
Na ₂ O	62.1	0.43	38.8	0.10	50.1	0.37	51.0	2.44	52.7	8.27
	61.5		38.5		50.6		51.2		51.4	
K ₂ O	61.7	15.34	38.7	0.04	47.5	0.10	52.3	0.26	51.4	5.54
	0.06		0.05		0.24		0.22		0.51	
	0.07	0.07	0.04	0.23	0.20	0.23	0.19	0.55	0.51	
	0.06	0.02	0.02	0.30	0.20	0.23	0.19	0.76	0.51	
	0.55‡	0.43	0.02	0.10	0.32	0.37	2.54	2.44	8.59	8.27
	14.96‡	15.34	0.04	0.04	0.14	0.10	0.26	0.26	5.33	5.54

*Flanagan³⁵.†H₃PO₄ dissolution.§H₃PO₄-HClO₄ dissolution.

‡Measured by ICP-AES.

Table 5. Major components (%) in BCS standard materials

Component	BCS No. 370 Magnesite/chrome		BCS No. 309 Sillimanite		BCS 174/1 Basic slag		BCS 175/2 Nimba iron		BCS 381 Basic slag	
	Measured value	Quoted value	Measured value	Quoted value	Measured value	Quoted value	Measured value	Quoted value	Measured value	Quoted value
Al ₂ O ₃	12.2	12.2	60.0	61.1	1.78	1.72	1.16	1.08	0.67*	0.67
CaO	12.3*	1.54	59.9*	0.34	1.52*	44.8	0.84*	0.08	48.8	49.0
	1.85		0.38		45.0		0.13			
Fe ₂ O ₃	1.44	7.24	0.23	1.51	45.6	12.10	12.17	92.1	94.50	18.31
	7.25		1.52		12.17		12.10		92.1	
MgO	7.47	61.8	1.41	0.17	7.20	7.13	0.03	0.03	0.90	1.03
	60.9		0.12		7.20		7.13		0.03	
MnO	63.6	0.11	0.14	0.03	7.37	5.11	0.03	0.14	3.24	3.16
	0.10		0.025		5.12		5.11		0.12	
SiO ₂	0.12	3.01	0.05	34.1	5.07	14.69	0.16	2.58	7.91	8.78
	3.40		35.1		14.6		14.69		2.44	
TiO ₂	3.09	0.12	34.1	1.92	14.6	0.70	2.44	0.09	7.91	8.78
	0.13		2.44		1.92		0.84		0.70	
Na ₂ O	0.20	0.06	0.45	0.34					0.49	0.35
K ₂ O		0.03	0.42	0.46						

*Measured by ICP-AES

Table 6. Statistical evaluation for H₃PO₄ dissolution (II variates)

	Na ₂ O	K ₂ O	MgO	CaO	Fe ₂ O ₃	Al ₂ O ₃	SiO ₂	TiO ₂	MnO
Mean, %	3.23	1.14	7.20	9.01	10.44	14.76	49.18	2.01	0.14
Standard deviation, %	0.06	0.014	0.16	0.21	0.24	0.13	0.97	0.014	0.006
RSD, %	1.8	1.2	2.2	2.3	2.3	0.87	2.0	2.1	0.5
Quoted value*, %	3.05	1.01	7.43	9.01	10.67	14.69	51.65	1.81	0.15

*Mean of 50 XRF determinations

REFERENCES

1. F. N. Ward, H. M. Nakagawa, T. F. Harms and G. H. Van Sickle, *U.S. Geol. Surv. Bull.*, 1969, No. 1289, 1.
2. S. Abbey, *Geol. Surv. Canada*, 1967, **67** (37), 1.
3. A. Mazzucotelli, R. Frache, A. Dadone and F. Baffi, *Talanta*, 1976, **23**, 879.
4. F. W. E. Strelow, C. J. Liebenberg and A. H. Victor, *Anal. Chem.*, 1974, **46**, 1409.
5. R. T. T. Rantala and D. H. Loring, *At. Absorp. Newsl.*, 1975, **14**, 117.
6. M. Ødegård, *J. Geochem. Explor.*, 1981, **14**, 119.
7. H. Uchida, T. Uchida and C. Iida, *Anal. Chim. Acta*, 1980, **116**, 433.
8. H. J. Gitelman, *At. Absorp. Newsl.*, 1979, **18**, 99.
9. M. J. Fishman and D. E. Erdmann, *ibid.*, 1970, **9**, 88.
10. C. Falinower, *ibid.*, 1975, **14**, 145.
11. L. T. Blouin, C. V. Dostie, W. L. Bloom and F. J. Low, *Anal. Chem.*, 1970, **42**, 1298.
12. J. Doležal, P. Povondra and Z. Šulcek, *Decomposition Techniques in Inorganic Analysis*, p. 46. Iliffe, London; Elsevier, New York, 1968.
13. K. V. Krishnamurty, E. Shpirt and M. M. Reddy, *At. Absorp. Newsl.*, 1976, **15**, 68.
14. A. S. G. Jones, *Marine Geol.*, 1973, **14**, M1.
15. H. L. Kahn, F. J. Fernandez and S. Slavin, *At. Absorp. Newsl.*, 1972, **11**, 42.
16. I. I. Petrov, D. L. Tsalev and A. J. Barsev, *At. Spectrosc.*, 1980, **1**, 47.
17. J. A. Maxwell, *Rock and Mineral Analysis*, p. 98. Wiley, New York, 1968.
18. G. K. Billings, *At. Absorp. Newsl.*, 1965, **4**, 357.
19. R. K. Winge, V. A. Fassel, R. N. Knisely, E. Dekalb and W. J. Haas, *Spectrochim. Acta*, 1977, **32B**, 327.
20. C. W. Sill, in *Accuracy in Trace Analysis, Sampling, Sample Handling, Analysis*, p. 463. Natl. Bur. Stds., Washington DC, 1976.
21. B. Bernas, *Anal. Chem.*, 1968, **40**, 1682.
22. F. J. Langmyhr and E. Sveen, *Anal. Chim. Acta*, 1965, **32**, 1.
23. F. J. Langmyhr and P. E. Paus, *ibid.*, 1968, **43**, 397.
24. H. Agemian and A. S. Y. Chau, *Anal. Chim. Acta*, 1975, **80**, 61.
25. F. Bea Barredo and L. Polo Diez, *Talanta*, 1976, **23**, 859.
26. T. Kiba, T. Takagi, Y. Yoshimura and I. Kishi, *Bull. Chem. Soc. Japan*, 1955, **28**, 641.
27. T. Kiba, I. Akaza and N. Sugishita, *ibid.*, 1957, **30**, 972.
28. E. J. Holmyard and W. G. Palmer, *A Text Book of Theoretical and Inorganic Chemistry*, Revised Ed., p. 587. Dent, London, 1956.
29. G. F. Smith and C. A. Goetz, *Ind. Eng. Chem., Anal. Ed.*, 1937, **9**, 378.
30. H. H. Willard and J. J. Thompson, *ibid.*, 1931, **3**, 399.
31. H. Hirsch and W. Dawihl, *Ber. Deut. Keram. Ges.*, 1932, **13**, 54.
32. C. A. Goetz and E. P. Wadsworth, *Anal. Chem.*, 1956, **28**, 375.
33. R. P. Lucas and B. C. Ruprecht, *ibid.*, 1971, **43**, 1013.
34. T. Mizoguchi and H. Ishii, *Talanta*, 1979, **26**, 33.
35. F. J. Flanagan, *Geochim. Cosmochim. Acta*, 1973, **33**, 1189.

Talanta

The International Journal of Pure and Applied Analytical Chemistry



The illustration of a Greek balance from one of the Hope Vases is reproduced here by kind permission of Cambridge University Press

Editor-in-Chief

DR R.A. CHALMERS, Department of Chemistry, University of Aberdeen, Old Aberdeen, Scotland

Assistant Editors

DR J.R. MAJER, University of Birmingham, England

DR I.L. MARR, University of Aberdeen, Scotland

Computing Editor

DR MARY R. MASSON, University of Aberdeen, Scotland

Regional Editors

PROFESSOR I.P. ALIMARIN, Vernadsky Institute of Geochemistry and Analytical Chemistry, U.S.S.R. Academy of Sciences, Vorobievskoe Shosse 47a, Moscow V-334, U.S.S.R.

PROFESSOR E. BLASIUS, Institut für Analytische Chemie und Radiochemie der Universität des Saarlandes, D-6600 Saarbrücken 15, GFR

MR H.J. FRANCIS JR, Pennwalt Corporation, 900 First Avenue, King of Prussia, PA 19406, U.S.A.

PROFESSOR J.S. FRITZ, Department of Chemistry, Iowa State University, Ames, IA 50010, U.S.A.

PROFESSOR T. FUJINAGA, Department of Chemistry, Kobe-Gakuin University, Tarumi, Kobe, Japan

DR M. PESEZ, Roussel-Uclaf, 102 et 111 route de Noisy, F-93, Romainville (Seine), France

PROFESSOR E. PUNGOR, Institute for General and Analytical Chemistry, Technical University, Gellért tér 4, 1502 Budapest XI, Hungary

PROFESSOR J.D. WINEFORDNER, Department of Chemistry, University of Florida, Gainesville, FL 32611, U.S.A.

Consulting Editor

DR M. WILLIAMS, Oxford, England

Editorial Board

DR R.A. CHALMERS, *Editor-in-Chief*

DR M. WILLIAMS, *Consulting Editor*

DR I.L. MARR, *Assistant Editor*

DR J.R. MAJER, *Assistant Editor*

MR H.J. FRANCIS JR, *representing Regional Editors*

MR G.F. RICHARDS, *Managing Director, Pergamon Press Ltd*

Annual Subscription Rates (1984)

US\$300.00 (2-yr rate US\$570.00)—For libraries, government laboratories, research establishments, manufacturing houses and other multiple-reader institutions. Price includes postage and insurance. Published monthly, 1 volume per annum.

Specially Reduced Rate for Individuals

In the interests of maximizing the dissemination of the research results published in this important international journal we have established a two-tier price structure. Any individual, whose institution takes out a library subscription, may purchase a second or additional subscriptions for personal use at the much reduced rate of US\$55.00 per annum.

Microform Subscriptions and Back Issues

Back issues of all previously published volumes are available in the regular editions and on microfilm and microfiche. Current subscriptions are available on microfiche simultaneously with the paper edition and on microfilm on completion of the annual index at the end of the subscription year.

Publishing Office

Pergamon Press Ltd, Hennock Road, Marsh Barton, Exeter, Devon EX2 8RP, England (Tel. Exeter (0392) 51558; Telex 42749).

Subscription Enquiries and Advertising Offices

North America: Pergamon Press Inc., Maxwell House, Fairview Park, Elmsford, NY 10523, U.S.A.

Rest of the World: Pergamon Press Ltd, Headington Hill Hall, Oxford OX3 0BW, England (Tel. Oxford (0865) 64881).

Copyright © 1984 Pergamon Press Ltd

It is a condition of publication that manuscripts submitted to this journal have not been published and will not be simultaneously submitted or published elsewhere. By submitting a manuscript, the authors agree that the copyright for their article is transferred to the publisher if and when the article is accepted for publication. However, assignment of copyright is not required from authors who work for organizations which do not permit such assignment. The copyright covers the exclusive rights to reproduce and distribute the article, including reprints, photographic reproductions, microform or any other reproductions of similar nature and translations. No part of this publication may be reproduced, stored in a retrieval system or transmitted in any form or by any means, electronic, electrostatic, magnetic tape, mechanical, photocopying, recording or otherwise, without permission in writing from the copyright holder.

Photocopying information for users in the U.S.A.

The Item-Fee Code for this publication indicates that authorization to photocopy items for internal or personal use is granted by the copyright holder for libraries and other users registered with the Copyright Clearance Center (CCC) Transactional Reporting Service provided the stated fee for copying beyond that permitted by Section 107 or 108 of the U.S. Copyright Law is paid. The appropriate remittance of \$3.00 per copy per article is paid directly to the Copyright Clearance Center Inc., 21 Congress Street, Salem, MA 01970. The copyright owner's consent does not extend to copying for general distribution, for promotion, for creating new works or for resale. Specific written permission must be obtained from the publisher for such copying. In case of doubt please contact your nearest Pergamon office. The Item-Fee Code for this publication is: 0039-9140/84 \$3.00 + 0.00

PAPERS RECEIVED

- Determination of trace elements in American cigarette paper by neutron-activation analysis:** F. Y. ISKANDER, T. L. BAUER and D. E. KLEIN. (25 September 1984)
- Spectrophotometric determination of iron and copper in milk, foodstuffs and body tissues with 1-(2-quinolyazo)-2,4,5-trihydroxybenzene:** ISHWAR SINGH, MRS. POONAM and P. S. KADYAN. (26 September 1984)
- Performance characteristics of differential pulse polarography and voltammetry with an automated microprocessor-based polarograph and a static mercury drop electrode:** WEE TEE TAN and GAIK SEE TAN. (26 September 1984)
- Contributions to the theory of catalytic titrations—IV: Neutralization catalytic titrations:** FERENC F. GAÁL and BILJANA F. ABRAMOVIĆ. (26 September 1984)
- Determination of gold, indium, tellurium and thallium in the same sample digest of geological materials by atomic-absorption spectroscopy after a two-step solvent extraction:** A. E. HUBERT and T. T. CHAO. (27 September 1984)
- A modified oxygen-flask combustion technique:** THURAYAH M. KARADAKHI, FADHIL M. NAJIB and FAHMI A. MOHAMMAD. (27 September 1984)
- A selective method of qualitative analysis for the copper-tin group cations:** SALAH M. SULTAN. (1 October 1984)
- A method for the determination of vanadium and iron oxidation states in naturally occurring oxides and silicates:** RICHARD B. WANTY and MARTIN B. GOLDBABER. (21 September 1984)
- Formation equilibria of copper(II) complexes with some pyridinols in various solvents:** R. BUCCI, V. CARUNCHIO, A. M. GIRELLI and A. MESSINA. (2 October 1984)
- Reversed-phase liquid chromatographic retention behaviour of catechol amino-acids:** T. ISHIMITSU, S. HIROSE and H. SAKURAI. (3 October 1984)
- A new fluorogenic thiol-selective reagent: *N*-{*p*-[2-(6-dimethylamino)benzofuranyl]phenyl}maleimide:** KENICHIRO NAKASHIMA, HIROYUKI AKIMOTO, KEN'ICHI NISHIDA, SHIN'ICHI NAKATSUJI and SHUZO AKIYAMA. (3 October 1984)
- The synthesis and complexing ability of fluorogenic crown ethers:** J. L. STEGER and G. E. PACEY. (4 October 1984)
- Automated flow-injection pseudotitrations of strong and weak acids, ascorbic acid and calcium, with a microcomputer controlled analyser: Catalytic pseudotitrations of aminopolycarboxylic acids:** M. A. KOUPPARIS, P. ANAGNOSTOPOULOU and H. V. MALMSTADT. (5 October 1984)
- Calculation of equilibrium constants from multiwavelength spectroscopic data—II. SPECFIT: two user-friendly programs in basic and standard FORTRAN 77:** HARALD GAMPP, MARCEL MAEDER, CHARLES J. JEYER and ANDREAS D. ZUBERBÜHLER. (5 October 1984)

PAPERS RECEIVED

- The manganese(IV) oxide electrode as a manganese(II) sensor:** DEREK MIDGLEY and DENNIS E. MULCAHY. (13 July 1984)
- Acid-base titrations in methanol: Acetylsalicylic acid:** ROBERT D. BRAUN and SCOTT A. RESWEBER. (26 June 1984)
- The use of di-2-pyridinyl-methylene-2-furoylhydrazone as a fluorogenic reagent for the determination of low concentrations of aluminium:** M. SALGADO ORDOÑEZ, A. GARCIA DE TORRES and J. M. CANO PAVON. (17 July 1984)
- Ion-exchanger phase absorptiometry for trace analysis:** KAZUHISA YOSHIMURA and HIROHIKO WAKI. (17 July 1984)
- A timed solenoid injector for flow analysis:** S. D. ROTHWELL and A. A. WOOLF. (17 July 1984)
- A chemical phase-analysis method for the oxidation states of uranium in phosphate samples:** L. A. GUIRGUIS. (20 July 1984)
- Corrosion measurements by potential-step chronoamperometry:** R. VON WANDRUSZKA, S. W. ORCHARD and A. GREEFF. (20 July 1984)
- 2-(2-Picolyliminomethyl)pyrrole: A new analytical reagent:** F. CAPITAN, L. F. CAPITAN-VALLVEY, F. MOLINA and P. ESPINOSA. (23 July 1984)
- Studies on the extraction of the mercury(II)-phenanthroline-Rose Bengal ternary system—selective separation of mercury(II) from various bivalent metal ions:** Y. ANJANEYULU, P. CHANDRAMOULI, K. CHANDRA SEKHAR and M. RAVI PRAKASA REDDY. (23 July 1984)
- Fluorimetric determination of tautomeric equilibria in 8-aminoquinolines:** PEDRO J. ZAVALA, MARC D. RADCLIFFE and STEPHEN G. SCHULMAN. (28 June 1984)
- The application of tetrazolium salts in analytical chemistry:** ALEXANDER V. ALEXANDROV. (24 July 1984)
- New metal ion buffer for standardization of copper ion-selective electrode:** H. A. AZAB, R. M. HASSAN and S. A. IBRAHIM. (24 July 1984)
- Application of pyrolysis-chemical ionization mass spectrometry to lichenology:** JOSEPH B. ADDISON. (24 July 1984)
- Express automatic potentiometric method for analytical control in the manufacture of extraction phosphoric acid:** GEORGI VELINOV. (25 July 1984)
- Spectrophotometric determination of oxyphenbutazone by a chelate-forming reaction:** SAIED BELAL, AFAF A. ELKHEIR and ABDULLA M. ELSHANWANI. (25 July 1984)
- Spectrophotometric determination of silicon in silicates by flow-injection analysis:** ROKURO KURODA, IWAO IDA and HIDEKI KIMURA. (25 July 1984)
- Application of dicarbollycobaltate(III) anion in the water-nitrobenzene extraction system:** EMANUEL MAKRLÍK and PETR VAŇURA. (25 July 1984)
- Application of organic solvent-soluble membrane filters to the preconcentration and determination of trace elements:** Spectrophotometric determination of phosphorus as phosphomolybdenum blue: SHIGERU TAGUCHI, EYUKI ITO-OKA, KEIKO MASUYAMA, ISSEI KASAHARA and KATSUMI GOTO. (25 July 1984)
- Deconvolution techniques for rapid flow-injection analysis:** JAMES T. DYKE and QUINTUS FERNANDO. (28 May 1984)
- The fluorometric determination of biacetyl: A promising method for the determination of biacetyl in foodstuffs:** A. J. MAROULIS, A. N. VOULGAROPOULOS and C. P. HADJANTONIOU-MAROULIS. (1 August 1984)
- A software package for computer-controlled flow-injection analysis:** L. T. M. PROP, P. C. THIJSEN and L. G. G. VAN DONGEN. (1 August 1984)
- Fluorometric determination of the complexation of amino crown ethers with alkali-metal ions:** G. E. PACEY and B. P. BUBNIS. (1 August 1984)
- Phosphate determination using molybdoantimonylphosphoric acid on polyurethane foam:** A. S. KHAN and A. CHOW. (1 August 1984)
- The role of thiourea as additive for medium modification problems in potentiometric stripping analysis (P.S.A.):** C. LABAR and L. LAMBERTS. (2 August 1984)

LOUIS GORDON MEMORIAL AWARD



Presentation of the Louis Gordon Memorial Award for 1982 to Mr. N. A. Dimmock (right) and Dr. D. Midgley (centre) by Dr. R. A. Chalmers. (See *Talanta* 1982, **29**, 557.)

PAPERS RECEIVED

- Solid membrane electrode for the determination of La(III) in presence of other rare-earth cations:** P. S. THIND and S. K. MITTAL. (9 May 1984)
- Ionic-strength dependence of formation constants—V: Protonation constants of some cationic acids at different temperatures and ionic strengths:** PIER G. DANIELE, CARMELO RIGANO and SILVIO SAMMARTANO. (9 May 1984)
- The effect of EDTA/NaF solutions on the Cu(II) ion electrode:** H. F. STEGER. (9 May 1984)
- Determination of fluorine in mineral samples through decomposition with alkali-metal hydroxides and spectrophotometric analysis:** J. V. GIMENO ADELANTADO, V. PERIS MARTINEZ, A. CHECA MORENO and F. BOSCH REIG. (9 May 1984)
- Amperometric titration of cadmium, copper, lead, mercury and zinc with diethyldithiocarbamate at zero applied voltage with a rotated platinum-wire micro electrode:** MAHMOUD GHANDOUR. (10 May 1984)
- Pollution profile of Damodar River sediment in Raniganj-Durgapur Industrial Belt, West Bengal, India:** ANIL K. DE, ASIT K. SEN, MD. REAZUL KARIM, K. J. IRGOLIC, DIPANKAR CHAKRABORTY and R. A. STOCKTON. (14 May 1984)
- Etude de la pureté des échantillons commerciaux d'éosine:** D. FOMPEYDIE and P. LEVILLAIN. (15 May 1984)
- Etude de la capacité complexante des eaux de l'estuaire et de la Baie de Seine:** JEAN-CLAUDE FISCHER, RENÉ NGANOU and MICHEL WARTEL. (15 May 1984)
- Analysis of some phenolic co-polymer mixtures by electrometric titration techniques:** S. K. CHATTERJEE and ANITA KATYAL. (15 May 1984)
- Determination of iron and cyanides in cyanoferrate complexes:** NICOLETTA BURGER. (16 May 1984)
- Derivatives of imidazole as spectrophotometric analytical reagents:** C. F. PEREIRA and J. GASCH. (16 May 1984)
- Fluorimetric determination of μg of boron:** J. M. MIR and M. C. MARTÍNEZ. (16 May 1984)
- Thionalide as titrant for several metals:** J. O. N. REIS, A. M. M. AMORIM and A. C. SPÍNOLA COSTA. (17 May 1984)
- Comment on "Laser-excited fluorescence line-narrowing: An analytical study":** J. D. WINEFORDNER. (2 March 1984)
- The determination of simple and complex iodides with ferric chloride: an alternative to Andrews titration;** M. CARTWRIGHT and A. A. WOOLF. (18 May 1984)
- Extraction of cadmium with poly(acrylonitrile) and acrylonitrile-charcoal composite:** M. A. DIAB, M. A. KABIL, A. M. ABDALLAH and Y. A. AGGOUR. (18 May 1984)
- Highly sensitive and selective microdetection of iron(III) with desferrioxamine B by the "resin spot test" technique:** SVJETLANA LUTEROTTI and VLADIMIR GRDINIĆ. (21 May 1984)
- Chemical destruction of carcinogenic aromatic amines in laboratory wastes, monitored by HPLC with electrochemical detection:** JIŘÍ BAREK, VĚRA PACÁKOVÁ, KAREL ŠTULÍK and JIŘÍ ZIMA. (21 May 1984)
- Effects of microscopic surface roughening on the voltammetric response of gold electrodes:** KENNETH W. PRATT. (21 May 1984)
- Thin-layer technique in spark-source mass spectrometry:** I. R. SHELPKOVA, A. I. SAPRYKIN, T. A. CHANYSHOVA and I. G. YUDELEVICH. (22 May 1984)
- Highly sensitive micellar solubilization spectrophotometric method for determination of microamounts of titanium(IV) with the system Ti-phenylfluorone-Triton X-305-emulsifier op:** QIANFENG WU. (23 May 1984)
- Bidentate pyrimidine-2-thiols as spectrophotometric reagents for palladium and osmium. Determination in alloys, minerals and catalysts:** AJAI K. SINGH, BANI ROY and R. P. SINGH. (24 May 1984)
- Organic ion-exchange beads as indicators in acid-base titration:** M. F. EL-HADI and M. S. METWALLY. (24 May 1984)
- Spectrophotometric determination of triacetyloleandomycin and some tetracyclines with 2,3,5-triphenyltetrazolium chloride:** EL-SEBAI IBRAHIM, M. ABDEL SALAM, Y. BELTAGY and M. KHOLIEF. (24 May 1984)
- Precise and accurate determination of high concentrations of sulphur by isotope-dilution thermal-ionization mass spectrometry:** W. R. KELLY and P. J. PAULSEN. (24 May 1984)

PAPERS RECEIVED

- Investigations for trace analysis of A^{III}B^V semiconductor microsamples by atomic spectroscopy—VII: Investigations for trace and thin-layer analysis of doping elements (Ag, Au, Bi, Cd, Sn, Tl) in InAs by atomic absorption with electrothermal evaporation:** K. DITTRICH, W. MOTHE, I. G. JUDELEWITSCH and T. S. PAPIA. (9 April 1984)
- The effect of organic colloids on the ASV signals of Cd, Pb and Cu:** T. UGAPO and W. F. PICKERING. (10 April 1984)
- Determination of the rare earths, yttrium and scandium in silicate rocks and four new geological reference materials by electrothermal atomization from graphite and tantalum surfaces:** J. G. SEN GUPTA. (11 April 1984)
- Studies on the electroanalytical chemistry of rare-earth elements—XVII: Polarographic study on Sm(III)–tetracycline complex:** XIANZHEN YE and XIAOXIA GAO. (11 April 1984)
- Studies on the electroanalytical chemistry of rare-earth elements—XVIII: Polarographic study on Eu(III)–tetracycline complex:** ZIWEI JIANG and XIAOXIA GAO. (11 April 1984)
- Pharmaceutical and clinical analysis by tandem mass spectrometry:** RICHARD A. YOST, ROBERT J. PERCHALSKI, HARRY O. BROTHERTON, JODIE V. JOHNSON and MARY BETH BUDD. (11 April 1984)
- Complexometric determination of citric acid by use of a specific copper(II) indicator:** E. SZEKELY. (13 April 1984)
- Formation of ternary complexes of Pb(II) with Pyrocatechol Violet and cetyltrimethylammonium bromide:** JOSÉ VALERO. (13 April 1984)
- Calculation scheme for acid–base titration:** YOSHITSUGU HASEGAWA and NAOYA NAKAGAWA. (13 April 1984)
- N-Chlorophthalimide as a new oxidimetric titrant for potentiometric determination in aqueous acetic acid medium:** N. JAYASREE and P. INDRASENAN. (16 April 1984)
- Classification of experimental methods in solution chemistry:** PATRICK MACCARTHY. (14 November 1983)
- The solubility of alkali metal fluorides in non-aqueous solvents with and without crown ethers, as determined by flame emission spectrometry:** DAVID A. WYNN, MARIE M. ROTH and BRUCE D. POLLARD. (17 April 1984)
- Studies on semicrystalline tin(IV) selenophosphate—II: Separation and determination of chromium, nickel and iron in super alloys:** SYED ASHFAQ NABI and ZIA MAHMOOD SIDDIQI. (18 April 1984)
- Spectrophotometric determination of palladium with 4,4'-bis(diethylamino)thiobenzophenone and Triton X-100:** YUN-XIANG CI, WEN-BAO CHANG and FENG-JI YAO. (19 April 1984)
- A simple titrimetric method for determination of aldehydes and ketones:** EMTITHAL EL-SAWI and NADIA KANDILE. (24 April 1984)
- Optimization of parameters in the determination of iron and vanadium in petroleum fractions by atomic-absorption spectrophotometry with a graphite furnace:** M. C. GONZALEZ, A. R. RODRIGUEZ and V. GONZALEZ. (24 April 1984)
- AC Polarographic assay of penicillin V benzathine:** J. A. SQUELLA, M. M. SILVA and LUIS J. NUNEZ-VERGARA. (4 April 1984)
- Preparation and analytical characterization of 1-(2-pyridylazo)-2-naphthol-coated chelating resin:** J. CHWASTOWSKA and E. MOZER. (25 April 1984)
- Electrochemical studies on the oxidation of oxohydroxotetracyano-molybdate(IV) and -tungstate(IV) with Ce(IV), Cr(VI) and Mn(VII):** S. I. ALI and SEEMA SHARMA. (26 April 1984)
- A novel and sensitive spot-test for *m*-dinitroaromatics and their derivatives with sodium sulphite and dimethylsulphoxide:** SAEDUZZAFAR QURESHI, PUSHKIN M. QURESHI and SEEMA HAQUE. (27 April 1984)
- Fluorimetric determination of sulphate ion by ternary complex formation with zirconium and diacetylmonoxime nicotinylhydrazone:** S. RUBIO, A. GOMEZ-HENS and M. VALCARCEL. (30 April 1984)
- Arsenic speciation in soil pore waters from mineralized and unmineralized areas of South West England:** STEPHEN J. HASWELL, PETER O'NEILL and KEITH C. C. BANCROFT. (1 May 1984)
- Analytical interferences and drug effects on laboratory test results:** M. M. GALTEAU and G. SIEST. (2 May 1984)
- New chelate-forming sorbents for noble metals:** G. V. MYASOEDOVA, I. I. ANTOKOLSKAYA and S. B. SAVVIN. (2 May 1984)
- A new method for the determination of total lead blended as lead alkyls in motor spirit, by atomic-absorption spectroscopy:** SAMARESH BANERJEE. (2 May 1984)
- Relationship of pH and potential:** K. L. CHENG. (3 May 1984)
- Determination of hormones by using time-resolved fluoroimmunoassay:** TIMO LÖVGREN, ILKKA HEMMILÄ, KIM PETTERSSON, JARKKO U. ESKOLA and ERIC BERTOFT. (3 May 1984)
- Solvent extraction separation of rubidium with dicyclohexeno-18-crown-6:** B. S. MOHITE and S. M. KHOPKAR. (8 May 1984)

PAPERS RECEIVED

- Determination of thermodynamic ionization constants for eight medicinal benzylimidazolines:** J. E. KOUNOURELLIS, N. POPADOPOULOS and A. RAPTOULI. (19 March 1984)
- Direct determination of sub-nanomolar levels of zinc in sea-water by cathodic stripping voltammetry:** C. M. G. VAN DEN BERG. (19 March 1984)
- Positive feed-back compensation of iR-drop in modified normal pulse polarography of sodium ion in acid solution:** MINORU HARA. (19 March 1984)
- Spectrofluorimetric assay of tetracycline and anhydrotetracycline in combination:** M. ABDEL-HADY ELSAYED, M. E. BARARY and H. MAHGOUR. (19 March 1984)
- A new polarographic catalytic method for the determination of micro quantities of tungsten (VI):** H. RAMACHANDRA MURTHY, G. VENUGOPAL and V. SURYANARAYANA RAO. (19 March 1984)
- Reversed-phase partition high-pressure liquid chromatography of trace amounts of inorganic and organic mercury with silver diethyldithiocarbamate;** SADANOBU INOUE, SUWARU HOSHI and MUTSUYA MATSUBARA. (24 March 1984)
- Determination of rare-earth elements in geological samples by thin-film X-ray fluorescence and inductively-coupled plasma atomic-emission spectrometry:** HOU QING-LIE, T. C. HUGHES, MAUNU HAUKKA and PHILIP HANNAKER. (24 March 1984)
- Construction and evaluation of a potassium-selective tube-mounted membrane electrode:** R. F. FARRELL and A. D. SCOTT. (6 March 1984)
- Investigation of industrial di(alkylphenyl)dithiophosphoric acids:** ZS. WITTMANN, Z. DÉCSY and E. PUDMER. (26 March 1984)
- Rapid spectrophotometric determination of some phenothiazine derivatives with *N*-chlorosuccinimide:** RANGASWAMY, H. S. YATHIRAJAN, P. NAGARAJA, JAYARAMA and B. M. MOHAN. (26 March 1984)
- Calculation of the formation constants of the Cu(II)-thiosemicarbazone complexes by a modification of the Deford and Hume method applicable to quasi-reversible and irreversible processes:** M. ARGÜESO, M. DOLORES LUQUE DE CASTRO and MIGUEL VALCARCEL. (27 March 1984)
- Pyridylazo compounds as analytical reagents: A review:** ALI Z. ABU-ZUHRI. (27 March 1984)
- 5,5'-(2-Pyridyl)-1,2,4-triazine-5,6-diyl-bis-2-furan-sulphonic acid, disodium salt, as a novel chromogenic reagent for ruthenium:** M. C. MEHRA and A. ARSENEAU. (28 March 1984)
- Photometric complex-formation titration of submicromole amounts of uranium:** J. KRAGTEN and W. OZINGA. (28 March 1984)
- Study on the synergistic extraction of cobalt(II) with lower fatty acids in the presence of heterocyclic amines, and some metal-ion separations:** S. K. GOGIA, D. SINGH, O. V. SINGH and S. N. TANDON. (29 March 1984)
- The application of internal electrolysis to determination of the equivalence point of a reaction, based on the variation in the current flowing: precipitation determination of chloride and chromate:** W. RZESZUTKO and E. SOMOGYI. (29 March 1984)
- Spectrophotometric study of the interaction of tris-[2,4,6-(2-hydroxy-4-sulpho-1-naphthylazo)]-s-triazene, trisodium salt, with silver, and use of the silver complex for indirect determination of bromide and iodide:** ISHWAR SINGH and PRATAP SINGH KADYAN. (30 March 1984)
- Indirect determination of trace phenol in water by atomic-absorption spectrophotometry:** XU BO-XING, XU TONG-MING, SHEN MING-YENG and FANG YU-ZHI. (30 March 1984)
- Atomic-absorption and flame-photometric analysis of Nigerian crude oils and the associated water, for sodium, potassium, calcium, magnesium and arsenic:** C. A. NWADINIGWE and P. C. ACHLIKE. (2 April 1984)
- Rapid and selective chelatometric titration of aluminium in non-ferrous alloys:** ZHOU NAN, GU YUAN-XIANG, LU ZHI-REN and CHEN WEI-YONG. (4 April 1984)
- Indirect spectrophotometric determination of silicate:** I-WEN SUN and FREDRICK BET-PERA. (4 April 1984)
- The solubility and acid dissociation constants of fluorescein in water solution:** HARVEY DIEHL and RICHARD MARKUSZEWSKI. (4 April 1984)
- Fluorimetric determination of catecholamines:** FATMA B. SALEM and I. W. MOHAMED. (6 April 1984)
- Analytical applications of semicarbazones and thiosemicarbazones: Recent advances:** AJAI K. SINGH. (6 April 1984)
- Potentiometric studies on the chelates of Al(III), Ga(III) and In(III) with some disubstituted pyridines:** R. S. SINDHU and R. P. SINGH. (6 April 1984)

PAPERS RECEIVED

- A new and very rapid indirect method for determination of stability constants of 1:1 complexes:** P. H. TEDESCO, V. B. DE RUMI, L. B. DE CORDO, A. PIRO and A. IGEA. (3 January 1984)
- Sensitive flotation-spectrophotometric determination of gold, based on the gold(I)-iodide-Methylene Blue system:** Z. MARCZENKO and K. JANKOWSKI. (18 February 1984)
- Spectrophotometric and potentiometric determination of the protonation constants of dithiocarbazates: Studies on some of their metal chelates:** A. IZQUIERDO, J. GUASCH and F. X. RIUS. (22 February 1984)
- Analytical application of a macroreticular hydroxamic acid resin:** CHUEN-YING LIU. (22 February 1984)
- Spectrophotometric determination of nitrate and nitrite in natural water and sea-water:** S. J. BANJIC and B. JASELSKIS. (24 February 1984)
- Reaction of iron(III) with tiron in the presence of ferrozine, and determination of tiron:** N. SIMONZADEH and B. JASELSKIS. (24 February 1984)
- The spectrophotometric determination of the platinum metals—VIII: Highly sensitive extraction determination of palladium with 4-(2-pyridylazo)-resorcinol in the presence of cetylpyridinium bromide:** O. COUFALOVÁ and L. ČERMÁKOVÁ. (24 February 1984)
- The determination of chlorpromazine and thioridazine by differential pulse voltammetry in acetonitrile medium:** N. ZIMOVÁ and I. NĚMEC. (24 February 1984)
- Chromatic evaluation of pyridine-2-aldehyde and 6-methylpyridine-2-aldehyde-*p*-nitrophenylhydrazones as indicators:** A. M. CAMEAN FERNANDEZ, J. BATISTA PALOMA and M. GUZMAN CHOZAS. (1 February 1984)
- Alkali-metal ion complexation with lariat ethers possessing a chromogenic group:** B. P. BUBNIS and G. E. PACEY. (28 February 1984)
- Determination of diphenyltin and dialkyltin homologues by high-performance liquid chromatography incorporating morin in the eluent:** W. LANGSETH. (28 February 1984)
- Critical study of some metallochromic indicators for lead:** J. CACHO, C. NERIN and A. GARNICA. (28 February 1984)
- Flow-injection analysis in clinical chemistry:** C. RILEY, B. F. ROCKS and R. A. SHERWOOD. (20 December 1983)
- The development of a light-scattering immunoassay for plasma thyroxene binding prealbumin:** K. SPENCER. (8 December 1983)
- Enzyme-linked immunosorbent assay (ELISA) of antibodies to eight common neurotropic viruses:** J. A. P. EARLE, N. V. MCFERRAN and G. B. WISDOM. (5 January 1984)
- Luminescent immunoassay (LIA) methods for steroids:** M. PAZZAGLI, G. MESSERI, A. L. CALDINI, P. L. VANNUCCHI, A. TOMMASI and M. SERIO. (4 January 1984)
- Immunoassays in aqueous two-phase systems:** TORBJÖRN G. I. LING and BO MATTIASSON. (24 January 1984)
- Development of a sensitive enzyme immunoassay for plasma and salivary steroids:** A. RODA, S. GIROTTI, S. LODI and S. PRETI. (4 January 1984)
- Zinc and nickel ferrocyanides: preparation, composition and structure:** C. LOOS-NEKOVIC, M. FEDOROFF, E. GARNIER and P. GRAVEREAU. (12 March 1984)
- Thermodesorptive analysis of GaAs and ZnSe surfaces:** I. A. KIROVSKAYA, G. M. ZELYEVA and A. V. YURYEVA. (12 March 1984)
- Thin-layer chromatography of some aliphatic aldehyde-MBHT derivatives:** V. CARUNCHIO, G. DE ANGELIS, A. M. GIRELLI and A. MESSINA. (12 March 1984)
- Simultaneous determination of arsenic, selenium, tin and mercury by non-dispersive atomic-fluorescence spectrometry:** A. D'ULIVO, R. FUOCO and P. PAPOFF. (12 March 1984)
- Catalytic titration of iodide, bromide and thiocyanate by use of the silver-catalysed phloxin-persulphate reaction:** C. SANCHEZ-PEDRENO, M. HERNANDEZ CORDOBA and P. VINAS. (12 March 1984)
- A kinetic method for trace mercury determination:** K. MALLIKARJUNA RAO, T. SREENIVASULU and S. BRAHMAJI RAO. (12 March 1984)
- Spectrophotometric determination of aliphatic primary and secondary amines by reaction with *p*-benzoquinone:** SAAD S. M. HASSAN, K. L. ISKANDER and N. E. NASHED. (12 March 1984)
- Voltammetric interpretation of potential at the ion-selective electrode, based on current-scan polarograms observed at the aqueous/organic solution interface:** S. KIHARA and Z. YOSHIDA. (12 March 1984)
- Polarographic behaviour of some substituted arylhydrazones of acetylacetone:** K. RAM and S. BRAHMAJI RAO. (12 March 1984)
- Extractive spectrophotometric determination of molybdenum as an ion-association complex with thiocyanate and Adogen:** F. SALINAS, J. J. BERZAS NEVADO and M. I. ACEDO VALENZUELA. (12 March 1984)
- Ultraviolet spectral structure correlations of five amidines of pharmaceutical interest:** JOHN E. KOUNTOURELLIS and JOHN T. R. OWEN. (12 March 1984)
- Hydroxide complexes of lanthanides—VII: neodymium(III) in perchlorate medium:** J. KRAGTEN and L. G. DECNOP-WEEVER. (12 March 1984)
- A comparative study of some hydroxyanthraquinones as acid-base indicators:** J. BARBOSA, E. BOSCH and R. CARRERA. (12 March 1984)
- Standard addition procedure for the determination of traces of lead in solid samples by X-ray fluorescence spectrometry:** NIELS PIND. (12 March 1984)
- Spectrophotometric determination of germanium in ores, concentrates, zinc processing products and related materials with phenylfluorone and cetyltrimethylammonium bromide after separations by iron collection and heptane extraction of germanium tetrachloride:** ELSIE M. DONALDSON. (13 March 1984)
- The stability of metal complexes with 8-mercaptoquinoline and alkyl-substituted 8-mercaptoquinolines in dimethylformamide:** N. A. ULAKHOVICH, H. C. BUDNIKOV, T. S. CORBUNOVA and A. P. STURIS. (13 March 1984)
- Synthesis and characterization of 1,2-cyclohexanedione bis-benzoylhydrazone and its application to the determination of titanium in minerals and rocks:** M. GARCIA-VARGAS, S. TREVILLA and M. MILLA. (13 March 1984)

PAPERS RECEIVED

- The spectrophotometric evaluation of acidity constants: The double incomplete colour change:** A. G. ASUERO, M. J. NAVAS and D. ROSALES. (26 November 1984)
- Urea as basic component in pyridine-free Karl Fischer reagent:** M. BOS. (6 December 1983)
- Comment on laser-excited fluorescence line-narrowing: An analytical study:** J. M. HAYES and G. J. SMALL. (7 December 1983)
- Factors that influence the first-order kinetics and completeness of deposition in the electro-deposition of trace amounts of metals:** RAGNAR BYE. (8 December 1983)
- Determination of cerium in silicate rocks by electrothermal atomization in a furnace lined with tantalum foil: Application to 19 international geological reference materials:** J. G. SEN GUPTA. (8 December 1983)
- Estimation of uranium in columbite-tantalite samples: A method for sample-solution preparation for fluorometric estimation:** B. K. BALAJI, A. PREMDAS and G. V. RAMANAIAH. (14 December 1983)
- Study of the potential response of solid-state chloride electrodes in low concentration ranges:** E. G. HARSÁNYI, K. TÓTH, E. PUNGOR, YOSHIO UMEZAWA and SHIZUO FUJIWARA. (14 December 1983)
- A new colorimetric determination of DDA: 2,2-bis(4-chlorophenyl) acetic acid:** B. D. BANERJEE, M. RAMACHANDRAN and Q. Z. HUSSAIN. (15 December 1983)
- Extractive separation and spectrophotometric determination of palladium and platinum with dithizone in the presence of stannous chloride:** Z. MARCZENKO, S. KUŚ and M. MOJSKI. (15 December 1983)
- Chemiluminescent reaction of lucigenin with reducing sugars:** ROBERT L. VEAZEY, HOWARD NEKIMKEN and TIMOTHY A. NIEMAN. (15 December 1983)
- Use of a simple monitored thermometric technique for reaction-rate determination of inorganic species: System based on the iodide-catalysed cerium(IV)-arsenic(III) reaction:** F. GRASES, R. FORTEZA, J. G. MARCH and V. CERDA. (20 December 1983)
- Étude polarographique du niobium dans les mélanges eau-fluorure d'hydrogène en présence d'ions tétraalkylammonium:** HUGHES MÉNARD and RÉJEAN BEAUDOIN. (28 June 1983)
- Extraction of cobalt from thiocyanate solutions with polyurethane foam:** R. F. HAMON and A. CHOW. (23 December 1983)
- A partial deproteinization technique for simplifying whole-blood and related matrices for flame atomic spectrometry:** E. J. EKANEM. (31 December 1983)
- Spectrophotometric determination of cyanide by unsegmented flow methods:** A. RIOS, M. D. LUQUE DE CASTRO and M. VALCARCEL. (31 December 1983)
- Ion-pair extraction of lithium ion with cryptand 211 and resazurin:** YUN PEI WU and GILBERT E. PACEY. (31 December 1983)
- Determination of nickel by flame atomic-absorption spectrophotometry after separation by adsorption of its nioximate on microcrystalline naphthalene:** TOHRU NAGAIRO, BAL KRISHAN PURI, MOHAN KATYAL and MASATADA SATAKE. (31 December 1983)
- Precipitate-polished electrode: New voltammetric method with the solid electrode:** TAITIRO FUJINAGA and TAKASHI KIMOTO. (6 January 1984)

PAPERS RECEIVED

- Titrimetric determination of aminobenzoic acids:** D. AMIN, F. M. EL-SAMMAN and H. ABDULAHED-MALALLA. (7 November 1983)
- Extraction-spectrophotometric determination of small amounts of boron in copper metal and copper-base alloys with Methylene Blue:** ZDENĚK ČÍŽEK and VLASTA ŠTUDLAROVÁ. (7 November 1983)
- Exchange equilibria between bicarbonate, carbonate, chloride, and bromide on Dowex 1-x8:** ULLA LUNDSTRÖM and ÅKE OLIN. (8 November 1983)
- Standard-addition ammonia-electrode determination of nitrogen in coal:** T. D. RICE, V. SWEENEY, R. SEMITEKOLOS and G. J. RHYDER. (8 November 1983)
- Selective complexometric determination of tin, with mercaptans as masking agents: Its estimation in alloys:** K. N. RAOOT and SARALA RAOOT. (9 November 1983)
- Preparation of a new complexing resin modified by SPADNS:** MARIA LUISA MARINA, VENERANDO GONZÁLEZ and ADELA ROSA RODRÍGUEZ. (9 November 1983)
- Application of anion-exchange technique to the determination of traces of molybdenum in sea-water:** TETSUYA KIRIYAMA and ROKURO KURODA. (9 November 1983)
- Radiochemical determination of technetium-99:** NORTON Y. CHU and JERRY FELDSTEIN. (3 November 1983)
- Linear titration plots for the resolution of mixtures of three weak acids or bases:** DEREK MIDGLEY and COLIN MCCALLUM (14 November 1983)
- Signal-to-noise characteristics of optical polarimeters:** JOUKO J. KANKARE and ROGER STEPHENS. (17 November 1983)
- Differential pulse polarographic determination of molybdenum after separation by 8-hydroxyquinoline extraction into dichloromethane:** YUKIO NAGAOSA and KATSUNORI KOBAYASHI. (21 November 1983)
- Potentiometric studies on the chelates of Al(III), Ga(III) and In(III) with 2'-hydroxychalkone:** R. S. SINDHU and R. P. SINGH. (24 November 1983)
- Ultraviolet spectrophotometric determination of lead and bismuth with ammonium 1-pyrrolidinecarbodithioate:** YOSHIKAZU YAMAMOTO, HIDENAO SAITO and KAZUMASA UEDA. (24 November 1983)
- Effect of surface-active compounds on voltammetric stripping analysis at the mercury film electrode:** JOSEPH WANG and DEN-BAI LUO. (24 November 1983)
- Spectrophotometric determination of lead with 2-(5-bromo-2-pyridylazo)-5-diethylaminophenol and cetyltrimethylammonium bromide:** ALI Z. ABU-ZUHRI and JAMAL SHALABI. (25 November 1983)
- Solvent extraction of zirconium(IV) from acidic sulphate-acetate medium with bis-(2-ethylhexyl) phosphoric acid in benzene:** R. K. BISWAS and M. A. HAYAT. (25 November 1983)
- Titrimetric microdetermination of Ag(I), Hg(II), Cd(II) and Pb(II) with 2-mercaptopropanoic acid and thioglycollic acid:** K. K. TIWARI and R. M. VERMA. (25 November 1983)
- Polyurethane foam for the extraction of rhodium and its separation from iridium:** S. J. AL-BAZI and A. CHOW. (28 November 1983)
- Electro-deposition of traces of metals applied for analytical preconcentration and prepreparation:** ROMAN E. SIODA. (29 November 1983)
- Protonation constants of some organic acids:** ZS. WITTMANN. (29 November 1983)
- Chromatographic analysis of phospholipid and cholesterol oxidation:** ULRICH J. KRULL, MICHAEL THOMPSON and ANITA ARYA. (29 November 1983)
- Extraction of arsenic(III) from chloride-iodide solutions by diphenyl-2-pyridyl methane/benzene:** M. EJAZ, R. SIDDIQUE and SUHAIL AHMED. (1 December 1983)
- Colorimetric determination of carazolol with 3-methyl-2-benzothiazolone hydrazone hydrochloride:** M. A. KORANY, F. A. EL-YAZBI and M. H. ABDEL-HAY. (2 December 1983)
- Contribution to the theory of catalytic titrations—I: Complexometric catalytic titrations:** FERENC F. GAÁL and BILJANA F. ABRAMOVIĆ. (2 December 1983)
- Voltammetric study of the redox behaviour of the Hg(II)/Hg(I)/Hg system at a rotating metal-ring/glass-carbon disk electrode:** P. KIEKENS, E. TEMMERMAN and F. VERBEEK. (5 December 1983)
- Ion chromatographic determination of chloride and fluoride in electrolyte from the halogen tinning process:** W. KORTH and J. ELLIS. (5 December 1983)
- Lead sulphide as a sorbent for preconcentration of mercury from air and determination of mercury by atomic-emission spectroscopy:** S. ALEXANDROV. (5 December 1983)

PAPERS RECEIVED

- The pK_a values of imidazole in water-ethanol mixtures:** JANUSZ OSZCZAPOWICA and MAŁGORZATA CZURYZOWSKA. (11 October 1983)
- Extraction of zinc with the high molecular-weight amine Amberlite LA-2:** UDAY SANKAR RAY and SUNIL BARAN KAR. (13 October 1983)
- Effect of pH on chromium(VI) species in solution:** R. K. TANDON, P. T. CRISP, J. ELLIS and R. S. BAKER. (14 October 1983)
- Platinum metals—solution chemistry and separation methods: Ion-exchange and solvent extraction:** SARGON J. AL-BAZI and ARTHUR CHOW. (14 October 1983)
- A comparison of cationic polymerization and esterification for end-point detection in the catalytic thermometric titration of organic bases:** EDWARD J. GREENHOW and PILAR VIÑAS. (17 October 1983)
- Determination of Ni in serum of occupationally exposed workers, by means of flame atomic-absorption spectroscopy—I: The analytical method:** ANNA MARIA GHE, MARIA TERESA LIPPOLIS and LUCIANA PASTORELLI. (19 October 1983)
- Determination of Ni in serum of occupationally exposed workers, by means of flame atomic-absorption spectroscopy—II: Study of some interferences:** ANNA MARIA GHE, LUCIANA PASTORELLI and MARIA TERESA LIPPOLIS. (19 October 1983)
- Method for the prediction of the behaviour of a single flow-injection manifold:** MIGUEL ANGEL GOMEZ-NIETO, MARIA DOLORES LUQUE DE CASTRO, ANTONIO MARTIN and MIGUEL VALCARCEL. (19 October 1983)
- Simultaneous separation of copper, cadmium and cobalt in sea-water by co-flotation with octadecylamine and ferric hydroxide as collectors:** L. M. CABEZON, M. CABALLERO, R. CELA R and J. A. PEREZ-BUSTAMANTE. (20 October 1983)
- Reactivity and chelate effect of triethanolamine complexes derived from cobalt(II), nickel(II) and copper(II) salts:** MAMDOUH S. MASOUD and MOHAMED A. EL-DESSOUKY. (20 October 1983)
- Use of ammonium molybdate in the colorimetric assay of cephalosporins:** M. M. ABDEL-KHALEK and M. S. MAHROUS. (20 October 1983)
- Sulphuric acid extraction of chlorinated hydrocarbons from marine organisms:** VITTORIO CONTARDI, BIANCA COSMA, MARILISA MATTACE RASO and GILDA ZANICCHI. (25 October 1983)
- Determination of cadmium by differential pulse anodic-stripping voltammetry after salting-out extraction with acetonitrile as solvent:** YUKIO NAGAOSA and TOSHIHIRO YAMADA. (26 October 1983)
- Studies on extraction of thorium from nitrate solutions by quaternary ammonium halides:** I. S. EL-YAMANI and E. I. SHABANA. (28 October 1983)
- Studies on extraction of indium(III) by tributyl phosphate from thiocyanate solutions:** I. S. EL-YAMANI and E. I. SHABANA. (28 October 1983)
- Flow-injection analysis: Epidemiology and origin of a revolution within a revolution:** T. BRAUN and W. S. LYON (1 November 1983)
- Separation and determination of arsenic(V) and arsenic(III) in sea-water by solvent extraction and atomic-absorption spectrophotometry by the hydride-generation technique:** SAMUEL A. AMANKWAH and JAMES L. FASCHING. (25 October 1983)
- 2-[2-(5-Chloropyridyl)azo]-5-dimethylaminophenol as indicator for the complexometric determination of zinc:** E. MARCHEVSKY, R. OLSINA and C. MARONE. (13 October 1983)
- The colours of co-ordination compounds: Methods of classification:** FRANZ LUDWIG WIMMER and LAURENCE PONCINI. (2 November 1983)
- Diffusion coefficients and complex equilibria in solution—IV: Experimental determination and manipulation of diffusion data:** D. R. CROW. (4 November 1983)

PAPERS RECEIVED

- Polarographic determination of zirconium at trace levels:** Y. CASTRILLEJO, R. PARDO, E. BARRADO and P. SANCHEZ BATANERO. (16 August 1984)
- Spectrophotometric determination of some 1,4-benzodiazepines by use of orthogonal polynomials:** M. A. KORANY, F. A. EL-YAZBI and M. H. ABDEL-HAY. (16 August 1984)
- Application of microcomputers in the analytical laboratory—III: On-line monitoring of a blue-green algae (*spirulian platensis*) culture:** HUGO GUTERMAN and SAM BEN-YAAKOV. (20 August 1984)
- Nuclear magnetic resonance spectrometry of chemically and physically altered porous silica surfaces under gas chromatographic conditions:** R. K. GILPIN and M. E. GANGODA. (20 August 1984)
- Fluorometric determination of nitrite:** P. DAMIANI and G. BURINI. (20 August 1984)
- A new polarographic catalytic method for the determination of micro quantities of tungsten(VI):** R. RAMACHANDRA MURTHY and V. SURYANARAYANA RAO. (20 August 1984)
- The effects of heating temperature, heating time and sample size during wet digestion in the determination of Ca, Fe, Cu and Na in some processed meats:** S. A. THOMAS and A. O. FADIRAN. (20 August 1984)
- Some factors in the determination of calcium, iron, copper and sodium from plant and soil samples by mixed-acid digestion:** S. A. THOMAS and A. JOB. (20 August 1984)
- Determination of trace amounts of copper, lead and zinc in cements by X-ray fluorescence spectrometry after precipitation-separation with hexamethylene ammonium hexamethylenedithiocarbamate:** YOSHIKAZU YAMAMOTO, YASUHIRO NISHINO and KAZUMASA UEDA. (22 August 1984)
- Further developments in the high-precision coulometric titration of uranium:** TATSUHIKO TANAKA, GEORGE MARINENKO and WILLIAM F. KOCH. (2 August 1984)
- Studies with an inorganic ion-exchange membrane exhibiting selectivity to Pb(II) ions:** SURESH K. SRIVASTAVA, SATISH KUMAR, CHAKRESH K. JAIN and SURENDER KUMAR. (22 August 1984)
- Determination of carbonate alkalinity and apparent dissociation constants in a multipyrolytic system:** ZVI-HAI BURBEA, CIDIO HAIMOVITZ and SAM BEN-YAAKOV. (22 August 1984)
- Ruthenium determination in synthetic Purex waste solutions by AAS:** W. HEINIG and K. MAUERSBERGER. (24 August 1984)
- Differential-pulse stripping voltammetry for the determination of nickel and cobalt in simulated PWR coolant:** K. TORRANCE and C. GATFORD. (24 August 1984)
- Spectrophotometric methods for the determination of thiobarbiturates:** C. S. P. SASTRY, P. SATYANARAYANA and M. K. TUMMURU. (24 August 1984)
- MICMAC—un programme général et rigoureux d'affinement multiparamétrique pour la détermination de constantes d'équilibre à partir de méthodes physiques variées:** ANDRÉ LAOUEAN and ÉLISABETH SUET. (9 August 1984)
- Dosage thermométrique et potentiométrique de l'aluminium par l'hydroxyde de sodium en présence de divers cations et anions:** PHILIPPE BOUDEVILLE. (9 August 1984)
- Caractérisation des jus pyrolytiques en provenance de différents procédés de conversion du bois:** H. MÉNARD, D. BÉLANGER, G. CHAUVETTE, A. GABOURY, J. KHORAMI, M. GRISÉ, A. MARTEL, E. POTBIN, C. ROY and R. LANGLOIS. (9 August 1984)
- N-Acetylmuramoyl-L-alanyl-D-isoglutamine determination in liposomes by HPLC:** E. POSTAIRE, M. HAMON, E. SPONTON, D. PRADEAU and R. LARCHEE. (9 August 1984)
- Backplane bus structures and systems:** V. KARANASSIOS and G. HORLICK. (27 August 1984)
- Smart backplanes—I: The Apple II:** V. KARANASSIOS and G. HORLICK. (27 August 1984)
- Smart backplanes—II: The IBM PC:** V. KARANASSIOS and G. HORLICK. (27 August 1984)
- Investigation of the effect of dilution and number of points in the performance of a linear method of potentiometric titration of weak bases:** L. M. ALEIXO, O. E. S. GODINHO and W. F. DA COSTA. (29 August 1984)
- Sorption and permeation behaviour of metal thiocyanate complexes on cellulose acetate polymers:** TAKASHI HAYASHITA and MAKOTO TAKAGI. (28 August 1984)
- Extraction-spectrophotometric determination of boron and antimony in carbon steel and low alloys with mandelic acid and Malachite Green:** SHIGEYA SATO. (31 August 1984)
- Spectrophotometric determination of cyanide in biological samples with a new reagent:** S. SUNITA and V. K. GUPTA. (31 August 1984)
- A kinetic study of the 1,3,5-triphenyl- Δ^2 -pyrazoline-Tc(VII) system, and its usefulness for measurement of technetium:** F. GRASES, J. G. MARCH, F. MATA and A. PENAFIEL. (4 September 1984)
- Injection analysis in flow-gradient systems: A new approach to unsegmented flow techniques:** ANGEL RIOS, MARIA DOLORES LUQUE DE CASTRO and MIGUEL VALCARCEL. (4 September 1984)
- Mathematical optimization in the determination of the dissociation constants of a tribasic organic acid with ^{13}C NMR spectroscopy:** ANNE-MARIE SALONEN. (6 September 1984)
- Studies of the solubilized metal-dithizone-surfactants system—I: Spectrophotometric determination of zinc in food and water samples:** WEN-BIN QI and WEI-QIANG GUO. (6 September 1984)
- Extraction of manganese(II), iron(II), cobalt(II), nickel(II), copper(II), zinc(II) and cadmium(II) into 1,2-dichloroethane with 4,7-diphenyl-1,10-phenanthroline and perchlorate ion:** TAKAHARU HONJO, AKIKO OKAZAKI, KIKUO TERADA and TOSHIYASU KIBA. (6 September 1984)
- Analytical investigations of cephalosporins—I: Two spectrophotometric methods for the determination of ceftriaxone in pharmaceutical formulations:** FATMA INCI SENGÜN and KÖKSAL ULAS. (7 September 1984)
- Preparation and properties of a chelating polymer containing the dithiocarboxylate group:** C. O. GIWA. (7 September 1984)
- A study on the polarography of the alkaline-earth metals—II: The polarographic adsorptive wave of magnesium-Eriochrome Black T and its application:** JINGRU AN, JINKUI ZHOU and XIAODAN WEN. (11 September 1984)
- Effect of acidity on the extraction and kinetic stability of the copper(II)/APCD/IBMK system in strongly acidic media:** MASAHIKO MURAKAMI and TAKEO TAKADA. (11 September 1984)

- Discussion on the possibility of reducing systematic error in trace analysis of metals by the SSMS methods:** WOJCIECH VIETH. (13 September 1984)
- Characterization of sediment reference materials by X-ray photoelectron spectroscopy:** M. SOMA, H. SEYAMA and K. OKAMOTO. (17 September 1984)
- Spectrophotometric assay of some tranquilizers in pure and dosage forms:** P. G. RAMAPPA and K. BASAVIAH. (18 September 1984)
- Electrolytic preconcentration: Preliminary step in instrumental analysis:** ROMAN E. SIODA, GRAEME E. BATLEY, WALTER LUND, JOSEPH WANG and STEVEN C. LEACH. (18 September 1984)
- Influence of acetate medium on the extraction of Co(II) by di-2-ethylhexylphosphoric acid:** P. BENEITEZ, S. J. ORTIZ and J. ORTEGA. (18 September 1984)
- Study on the glycopyrrolate selective electrodes:** SHOU-ZHUO YAO and GIANG-HUA LIU. (18 September 1984)
- Methods of preconcentration of organic pollutants: Determination of sorption capacity of solids:** JACEK NAMIEŚNIK. (19 September 1984)
- Determination of neodymium and boron in iron-neodymium-boron alloys by direct-current plasma atomic-emission spectrometry:** NOEL M. POTTER and HARRY E. VERGOSEN, III. (20 September 1984)
- Stability constants of the ternary complexes of CuDTPA, NiDCTA, CrEDTA, CoHEEDTA, NiHEEDTA and CuHEEDTA with OH⁻:** J. KORSE, G. A. J. LEURS and P. W. F. LOUWRIER. (20 September 1984)

PAPERS RECEIVED

- Spectrophotometric determination of paracetamol with iodylbenzene:** KRISHNA K. VERMA and ARCHANA JAIN. (29 May 1984)
- Determination of copper in blood serum with *o*-hydroxyphenylthiourea by a kinetic method:** S. JAGADESWARA RAO, G. SIVA REDDY, J. KRISHNAKUMARI and J. KRISHNA REDDY. (30 May 1984)
- Multiparametric curve fitting—VII: Determination of a number of complex species by factor analysis of potentiometric data:** JOSEF HAVEL and MILAN MELOUN. (30 May 1984)
- Platinum-graphite biamperometry in non-aqueous medium: Determination of iron (II), thioglycolic acid and ascorbic acid in *N,N*,-dimethylformamide with copper(II) chloride as the oxidant:** D. GHOSH and B. B. PRASAD. (31 May 1984)
- Aquametric microdetermination of hydration of ion-exchange resins: Measurement of the water content in anion-exchanges, derivation of hydration isotherms, relationship to hydration and the amount of pre-adsorbed moisture:** F. B. SHERMAN, B. M. KATZ and G. N. EVENKO. (31 May 1984)
- The use of certified reference materials in the verification of analytical data and methods:** R. SUTARNO and H. F. STEGER. (1 June 1984)
- Analytical chemistry of uranium in the phosphoric acid wet process:** SRBOBRAN RAJIĆ. (1 June 1984)
- Polarographic study of mixed ligand (glycoldimercaptopropionate-oxalate/citrate/tartrate/glutamate) complexes of cadmium(II) and lead(II):** K. C. GUPTA and KALPANA K. SHARMA. (4 June 1984)
- Studies on fluorescein—III: The acid strengths of fluorescein as shown by potentiometric titration:** HARVEY DIEHL, NAOMI HORCHAK, ALTA J. HEFLEY, LINDA ANN FREYTAG MUNSON and RICHARD MARKUSZEWSKI. (4 June 1984)
- Beiträge zur Frage der Existenz eines Tautomerengleichgewichtes in Lösungen von Dithizon in organischen Solventien:** H. WAGLER, H. KOCH and J. FLACHOWSKY. (26 April 1984)
- Differential determination of antimony(III) and antimony(V) by solvent extraction-spectrophotometric determination with mandelic acid and Malachite Green, based on the difference in reaction rates:** SHIGEYA SATO. (6 June 1984)
- Indirect determination of thallium by differential pulse polarography:** ALI H. BAZZI and BRIAN R. KERSTEN. (6 June 1984)
- Studies on extraction of manganese(II) with 1-phenyl-3-methyl-4-acyl-5-pyrazolone:** Y. AKAMA, H. YOKOTA, K. SATO and T. NAKAI. (7 June 1984)
- Calculation of equilibrium constants from multiwavelength spectroscopic data—I: Mathematical considerations:** HARALD GAMPP, MARCEL MAEDER, CHARLES J. MEYER and ANDREAS D. ZUBERBÜHLER. (7 June 1984)
- Studies on determination of fluoride in zinc and lead concentrates by using a fluoride ion electrode:** S. C. S. RAJAN, L. M. BHANDARI and B. R. L. ROW. (8 June 1984)
- Potentiometric determination of stability constants of Cu(II), Ni(II), Co(II) and Zn(II) complexes with SPADNS:** M. L. MARINA, V. GONZALEZ and A. R. RODRIGUEZ. (11 June 1984)
- Thermodynamic parameters and stability constants of binary complexes of the lanthanons with acenaphthenequinone monothiosemicarbazone (AQTS):** S. K. SINGH, R. K. SHARMA and S. K. SINDHWANI. (11 June 1984)
- Differential pulse polarography in the alternating pulse mode:** CSABA URBANICZKY. (11 June 1984)
- Preparation of a new complexing resin modified by SPADNS: Application to separation of metal ions:** M. L. MARINA, V. GONZALEZ and A. R. RODRIGUEZ. (13 June 1984)
- Kinetic determination of cysteine traces by their inhibitory effect on the silver-catalysed phloxin-persulphate reaction:** M. HERNANDEZ CORDOBA, P. VINAS and C. SANCHEZ-PEDRENO. (13 June 1984)
- Application of ion-exchange reactions between membranes and resins:** JAMES A. COX and NOBUYUKI TANAKA. (13 June 1984)
- Copper(I) electrode function of two types of ion-selective electrodes for copper(II):** M. NESHKOVA and H. SHEYTANOV. (13 June 1984)
- The behaviour of two types of copper ion-selective electrodes in different copper(II)-ligand systems:** M. NESHKOVA and H. SHEYTANOV. (13 June 1984)
- Quality control in clinical chemistry: Characterization of reference materials:** ROBERT REJ, RICHARD W. JENNY and JEAN-PIERRE BRETAUDIERE. (24 May 1984)
- Solid-phase chemistry: Its principles and applications in clinical analysis:** ADAM ZIPP and W. E. HORNBY. (5 May 1984)
- Formation constants for the complexes of orthophosphate with magnesium(II) and hydrogen ions:** PETER W. LINDER and JOHN C. LITTLE. (14 June 1984)
- Anionic interferences with copper ion-selective electrodes: The chloride and bromide interferences:** A. LEWENSTAM, T. SOKALSKI and A. HULANICKI. (14 June 1984)
- An inexpensive and robust conductance electrode:** J. P. LORIMER, K. JAGIT and TIMOTHY J. MASON. (18 June 1984)
- Determination of manganese in steels by atomic-absorption spectrophotometry:** L. P. PANDEY, P. DASGUPTA, N. N. CHATTERJEE and S. N. JHA. (22 June 1984)
- A chemical amplification method for the sequential estimation of phosphorus, arsenic and silicon at ng/ml levels by dc polarography:** R. KANNAN, T. V. RAMAKRISHNA and S. R. RAJAGOPALAN. (22 June 1984)
- Extractive spectrophotometric determination of zirconium as zirconium(IV) ferronate:** S. P. ARYA and VEENA SLATHIA. (26 June 1984)
- Spectrophotometric determination of saccharin in different materials by a solvent extraction method using Nile Blue as reagent:** M. HERNANDEZ CORDOBA, I. LOPEZ GARCIA and C. SANCHEZ-PEDRENO. (26 June 1984)
- Separation of iron-52 from chromium cyclotron targets on the 2% cross-linked anion-exchange resin AG1-X2 in hydrochloric acid:** TJAART N. VAN DER WALT, FRANZ W. E. STRELOW and FLORIS J. HAASBROEK. (26 June 1984)
- Asymmetric derivatives of carbonylhydrazide and thiocarbonylhydrazide as analytical reagents:** DANIEL ROSALES, GUSTAVO GONZALEZ and JOSE L. GOMEZ ARIZA. (26 June 1984)
- Presence of unreacted alcohol in *n*-alkyl ethoxylates used in spin finish lubricant formulations:** H. A. ANDERSON, D. L. BRYDON and C. D. TAYLOR. (27 June 1984)
- Consistent sub-micromolar traces of phosphate in doubly demineralized and demineralized-distilled water:** VINCENT P. GUTSCHICK. (12 May 1984)

A sensitive method for the fluorometric determination of lithium with a "crowned" benzothiazolyphenol: KENICHIRO NAKASHIMA, SHIN'ICHI NAKATSUJI, SHUZO AKIYAMA, ISAMU TANIGAWA, TAKAHIRO KANEDA and SOICHI MISUMI. (25 June 1984)

Contributions to the theory of catalytic titrations—II: Precipitation catalytic titrations: BILJANA F. ABRAMOVIĆ and FERENC F. GAÁL. (3 July 1984)

Contributions to the theory of catalytic titrations—III: Redox catalytic titrations: BILJANA F. ABRAMOVIĆ, FERENC F. GAÁL and DJURA Ž. PAUNIĆ. (3 July 1984)

Influence of some metal ions on NADH oxidation and on the formation of the superoxide anion O_2^- radical during the enzymatic catalysis of E.C. 1.2.3.2. xanthine oxidase: ANNA MARIA GHE, CLAUDIO STEFANELLI, PAGONA TSINTIKI and GABRIELE VESCHI. (3 July 1984)

Use of enzymatic catalysis with E.C. 1.2.3.2 xanthine oxidase for the kinetic determination of V(V) at low concentrations: ANNA MARIA GHE, CLAUDIO STEFANELLI, GIUSEPPE CHIAVARI and PAGONA TSINTIKI. (3 July 1984)

Determination of trace amounts of molybdenum in plant tissue by solvent extraction—atomic-absorption and direct-current plasma emission spectrometry: LAURI H. J. LAJUNEN and AARO KUBIN. (3 July 1984)

Extractive spectrophotometric determination of trace amounts of cobalt with benzyltriethylammonium chloride: K. C. BAYAN and H. K. DAS. (3 July 1984)

Precipitation of cobalt and iron with alkali metal hydroxide and oxides: C.O. GIWA. (3 July 1984)

Homogeneous immunoassay of phenobarbital by phase-resolved fluorescence spectroscopy: FRANK V. BRIGHT and LINDA B. MCGOWN. (11 June 1984)

Computer interfacing of intelligent instrumentation by means of keyboard emulation: P. M. WIEGAND and S. R. CROUCH. (11 June 1984)

Determination of polyethylene glycols by precipitation with I_2 : M. FRANCOIS and R. DE NEVE. (5 July 1984)

Effect of container material, storage time and temperature on determination of cadmium levels in human urine: KUNNATH S. SUBRAMANIAN, JEAN-CHARLES MÉRANGER and JOHN CONNOR. (6 July 1984)

Polarographic determination of the stability constants of cadmium and lead ternary complexes with thiosemicarbazide and thiosulphate: MAHMOUD A. GHANDOUR, AHMAD A. EL SAMAHY and ZANATI KOMY. (10 July 1984)

Phosphorus-31 nuclear magnetic resonance chemical shifts of phosphoric acid derivatives: Zs. WITTMAN and Zs. KOVÁCS. (11 July 1984)

Fluorimetric determination of dissociation constants and pH-controlled fluorescence analysis of purines and pyrimidines: DIARIATOU GNINGUE and JEAN JACQUES AARON. (11 July 1984)

Spectrophotometric determination of some ketosteroid drugs: MAGDA M. AYAD, SAIED F. BELAL, SOBHI M. EL ADL and AFAF A. EL KHEIR. (11 July 1984)

PAPERS RECEIVED

- Spectrophotometric determination of zinc(II) with phenylfluorone in the presence of hexadecylpyridinium bromide and pyridine:** SATORU SAKURABA. (9 January 1984)
- Pyrimidinethiol, a new reagent for extraction spectrophotometric determination of gold(III):** M. A. ANUSE, S. R. KUCHEKAR, N. A. MOTE and M. B. CHAVAN. (9 January 1984)
- Kinetic fluorimetric determination of cyanide by its catalytic effect on the aerial oxidation of pyridoxal 5-phosphate oxalyldihydrazone:** S. RUBIO, A. GOMEZ-HENS and M. VALCARCEL. (9 January 1984)
- Interferences in the determination of total nitrogen in natural waters by photo-oxidation to nitrate and nitrite:** LILLY GUSTAFSSON. (9 January 1984)
- Analytical applications of copper(II) and copper(I) in acetonitrile: Potentiometric and spectrophotometric determination of dithiocarbamates:** BALBIR CHAND VERMA, SAROJ CHAUHAN, ANITA SOOD, D. K. SHARMA and H. S. SIDHU. (9 January 1984)
- Determination of sulpha-drugs with ion-selective membrane electrodes—II:** G. E. BAIULESCU, GÖNÜL KANDEMİR, M. S. IONESCU and C. CRISTESCU. (10 January 1984)
- Gel speciation studies—II: An extension of earlier studies of the protonation equilibria of cross-linked carboxymethyl dextran:** SALVADOR ALEGRET, MARIA-TERESA ESCALAS and JACOB A. MARINSKY. (10 January 1984)
- Simultaneous determination of dextropropoxyphene napsylate, caffeine, aspirin and salicylic acid in pharmaceutical preparations by reversed-phase HPLC:** I. M. JALAL and S. I. SA'SA'. (10 January 1984)
- Untersuchungen zur Anwendung ternärer Komplexe in der Photometrie—III: Die Bestimmung des Titanium(IV) mit Brompyrogallolrot in Gegenwart von Nitrilotriessigsäure bzw. Ethylendiamintetraessigsäure:** S. KOCH, G. ACKERMANN and H. MOSLER. (10 January 1984)
- Testing the adequacy of equilibrium models for complex formation: Complexation between molybdate and oxalate revisited:** ERIK SYLVEST JOHANSEN and OLE JØNS. (11 January 1984)
- Colorimetric determination of some phenothiazine derivatives and chlorprothexine with different oxidizing agents:** EL-SEBAI A. IBRAHIM, A. S. ISSA, M. A. ABDEL SALAM and M. S. MAHROUS. (11 January 1984)
- The macrocyclic crown ether and cryptand mediated extraction of potassium *p*-nitrophenoxide from aqueous medium into diverse organic solvents: A systematic evaluation:** E. BUNCEL, H. S. SHIN, R. A. B. BANNARD, J. G. PURDON and B. G. COX. (13 December 1983)
- Determination of poly(oxyethylene) non-ionic surfactants by two-phase titration:** MASAHIRO TSUBOUCHI and YOSHIKO TANAKA. (11 January 1984)
- The polarographic determination of malononitrile:** D. PH. ZOLLINGER, M. BOS, A. M. W. VAN VEEN-BLAAUW and W. E. VAN DER LINDEN. (11 January 1984)
- Synthesis and analytical properties of monobutyl esters of α (*N*-benzylamino)salicylphosphonic acid and α (*N*-*p*-chlorobenzylamino)salicylphosphonic acid:** JERZY SIEPAK. (13 January 1984)
- Dual-wavelength spectrophotometric determination of trace sulphide in domestic water through its ligand-exchange reaction with silver—Cation 2B—Triton X-100:** FU-SHENG WEI, EN-JIANG TENG and KUI-SHENG RUI. (13 January 1984)
- Orthophosphoric acid dissolution of geological material and flame atomic-absorption spectroscopy and inductively-coupled plasma atomic-emission spectroscopy for major element determinations:** PHILIP HANNAKER and HOU QING-LIE. (16 January 1984)
- Determination of uranium in phosphogypsum:** HELENA GÓRECKA and HENRYK GÓRECKI. (16 January 1984)
- Simultaneous kinetic determination of copper, cobalt and nickel by means of interchange of $>C=N-$ groups:** A. RIOS and M. VALCARCEL. (16 January 1984)
- Determination of beryllium in Pt-Be alloy by atomic-absorption spectrometry and preliminary ion-exchange separation:** KRYSZYNA BRAJTER and KRZYSZTOF KLEJNY. (17 January 1984)
- Beiträge zur Frage der Existenz eines Tautomerengleichgewichtes in Lösungen von Dithizon in organischen Solventien—I: Die Korrelation zwischen den lösungsmittelabhängigen Reaktionsunterschieden in den Systemen Palladium/Dithizon und Kupfer/Dithizon und den lösungsmittelabhängigen Unterschieden der VIS-Spektren der Dithizonlösungen:** H. WAGLER and H. KOCH. (17 January 1984)
- An improved titrimetric method for the determination of oxygen to metal ratio in uranium oxide:** FAHMIDA KHATOON and C. SUBBA RAO. (18 January 1984)
- Cadmium-113 and carbon-13 nuclear magnetic resonance spectrometry of cadmium peptide complexes:** SHUI-MEI WANG and ROGER K. GILPIN. (14 November 1983)
- Polarographic determination of amoxicillin in certain pharmaceutical preparations:** M. M. AYAD, A. M. A. MORSI and M. YOUSEF. (23 January 1984)
- Aerosol collection on a tungsten wire:** KEIJO HAAPAKKA and ROGER STEPHENS. (24 January 1984)
- Determination of silver in doré metal by weight titration with equivalence point detection by differential electrolytic potentiometry (DEP):** PABLO COFRE and GEORGIAN COPIA. (25 January 1984)
- Determination of certain quinones by a chemiluminescence reaction in solution:** J. L. BURGUERA and M. BURGUERA. (25 January 1984)
- A chelate-forming resin prepared from sulphonated dithizone and an anion-exchange resin and its application to collection of heavy metal ions:** MASAHIKO CHIKUMA, MORIO NAKAYAMA, KUNICHI KUNIMASA, YUNIKO SUZUKI, YORIKO KURISAKA and HISASHI TANAKA. (26 February 1984)
- Detection of uranium in aqueous media by using X-ray photoelectron spectroscopy:** DALE L. PERRY and LEON TSAO. (27 January 1984)
- Studies on synthetic inorganic ion exchangers—X: Synthesis and physicochemical properties of crystalline zirconium selenite:** PRITAM SINGH THIND and HARBANS SINGH. (27 January 1984)
- Elucidation of the redox behaviour of ethyl 2,3-dioxobutylate-2-phenylhydrazono 3-semicarbazone by polarographic and voltammetric techniques:** R. N. GOYAL and ASHWANI MINOCHA. (27 January 1984)

- Non-extractive spectrophotometric determination of trace amounts of thallium with 7-(4,5-dimethylthiazolyl-2-azo)-8-oxime-5-sulphonic acid: Determination of thallium in metals and ores:** GAO JIALONG, GU GANG, LIU XILIN and CHEN TONGYUE. (30 January 1984)
- A new experimental technique for validating models of carbon dioxide exchange between the atmosphere and sea-water:** SAM BEN-YAAKOV and HUGO GUTERMAN. (1 February 1984)
- Spectrophotometric determination of molybdenum in steel alloys after separation by adsorption of its trifluoroethylxanthate on naphthalene:** M. F. HUSSAIN, B. K. PURI, R. K. BANSAL and M. SATAKE. (1 February 1984)
- A versatile low-cost laboratory computer network:** R. L. A. SING and ERIC D. SALIN. (3 February 1984)
- The determination of the heavy-metal content of fluvial sediments:** STEPHEN B. BRADLEY. (6 February 1984)
- Differential pulse polarography as a tool for determining trace levels of nicotinamide adenine dinucleotide (NAD⁺) and nicotinamide adenine dinucleotide phosphate (NADP⁺) in aqueous solution:** S. T. SULAIMAN. (6 February 1984)
- Basic studies and analytical applications of Nb(V)-Bromopyrogallol Red complexation in micellar media:** M. E. DIAZ GARCIA and A. SANZ-MEDEL. (6 February 1984)
- Spectrophotometric determination of formation constants of 1:1 complexes of lanthanides with 4-(2-pyridylazo)resorcinol (PAR):** EMIKO OHYOSHI. (7 February 1984)
- Oxidation of PGR by chromium(VI): Kinetic-spectrophotometric determination:** J. MEDINA-ESCRICHE, A. SEVILLANO-CABEZA and M. DE LA GUARDIA-CIRUGEDA. (9 February 1984)
- Solvent extraction separation of tantalum from niobium on macro scale with di(2-ethyl hexyl)phosphoric acid as the extractant:** S. N. BHATTACHARYYA and B. (NANDI) GANGULY. (10 February 1984)
- Application of some colorimetric methods for the spectrophotometric determination of some antipyretic and antirheumatic drugs:** A. S. ISSA, Y. A. BELTAGY, M. GABR KASSEM and H. G. DAABEES. (10 February 1984)
- 1,2 and 1,3-cyclohexandione bis(2-hydroxybenzoylhydrazones)s as analytical reagents:** M. GALLEGO, M. SILVA and M. VALCARCEL. (13 February 1984)
- Determination of scandium, yttrium and seven lanthanides in silicate rocks and four new Canadian iron-formation reference materials by flame micro-sample injection atomic-absorption spectrometry:** J. G. SEN GUPTA. (14 February 1984)
- Comparison of two digestion methods used for the determination of selenium in marine biological tissues by gas chromatography with electron capture detection:** K. W. MICHAEL SIU and SHIER S. BERMAN. (14 February 1984)

**EDITORIAL:
SOFTWARE SURVEY SECTION**

In order to encourage the open exchange of information on software for use in analytical chemistry, TALANTA is to introduce a new Software Survey Section. Alongside the rapid penetration of computers into academic and industrial institutions has come a parallel increase in the number of scientists and researchers designing their own software. The existence of much of this software remains unknown to many who could greatly benefit from its use. We believe that it would be extremely useful to our readers to have such information made available, and that a professional journal is the best place for doing it. We therefore invite you to consider making a contribution to the Section.

The two-page questionnaire on the following pages is designed to assist you in reporting on software that you have developed or are in the process of developing. The information you supply will then be published; thus it will reach thousands of your colleagues who may benefit from your work and possibly offer suggestions for enhancement of your software. If you are interested, please complete the form and return it to our Computing Editor:

Dr M R Masson
Dept of Chemistry
University of Aberdeen
Old Aberdeen, Scotland

We do not intend to comment on or review the material submitted, which will be published "as received" (apart from any editing needed for clarity and uniformity) in order to expedite its publication. Any comments or suggestions you may have will be welcome. The Software Description Form will appear in all future issues.

THE EDITORS

NAME OF JOURNAL TALANTA

PERGAMON PRESS
SOFTWARE DESCRIPTION FORM

Title of software package: _____

It is: Application program Utility Other _____

Specific area _____
(e.g. stability constants, calibration, pattern recognition, optimization)

Software developed for [name of computer(s)] _____

in [language(s)] _____

to run under [operating system] _____

and available on:

Floppy disk/diskette.

Size _____ Density _____ Single-sided Double-sided

Magnetic tape.

Size _____ Density _____ Character set _____

Distributed by: _____

Minimum hardware configuration required: _____

Memory required: _____ User friendly?: Yes No

Documentation: None Minimal Self-documenting
 Extensive external documentation

Source code available: Yes No

Level of development: Design complete Coding complete
 Fully operational Collaboration would be welcomed

Is software being currently used? Yes No
If yes, how long? _____ If yes, how many sites? _____

Contributor is willing to deal with enquiries?: Yes No

(continued)

PERGAMON PRESS
Maxwell House, Fairview Park, Elmsford NY 10523, USA
Headington Hill Hall, Oxford OX3 0BW, England

[This Software Description Form may be photocopied without permission]

Description of what software does [200 words maximum; use separate sheet if necessary]:

Potential users: _____

Fields of interest: _____

#####

Name of contributor: _____

Institution: _____

Address: _____

Telephone number: _____

#####

Reference No. [Assigned by Journal Editor] _____

RETURN THIS FORM TO:

Dr M R Masson
Dept of Chemistry
University of Aberdeen
Old Aberdeen, Scotland

SUBJECT INDEX

Abundance ratio, of Zr and Hf	621
Acetaminophen, Determination, by HPLC	397
Acid-base indicator, Chromaticity parameters	279
Acidic substances, Determination, thermometric	218
Acidity constants, spectrophotometric evaluation	233
Acids and bases, weak, linear titration plots	409
Activity, pharmacological, of phenylpropionic acid derivatives	144
Aerosol collection, by tungsten wire electrode	679
Alkali metals, Complexes with crown ethers	1149
—, —, Ion-pair extractions	165
—, —, Pulse polarography	105
— fluorides, Solubility	1036
Aluminium, Determination, fluorimetric	253
Amines, aromatic, Determination, spectrophotometric	295
Amplification procedure, Determination of phenols	283
Analysis, of simultaneous protolysis equilibria	113
Analytical processes, Information power and selectivity	162
Anion-exchange, Separation of Mo	472
— resins, Extraction of organic dyestuffs	401
—, —, Separation of Se(IV)	269
Antibodies, Detection of	375
—, Anticardiolipin, Immunoassay for	889
Antimony, Determination, by AAS	367
—, —, by FAAS	709
—, —, by isotopic-dilution analysis	509
Argon plasma, Determination of rare metals	773
Aromatic hydrocarbons, polycyclic, Determination by GC	49
Arsenic, Determination, by XRF	304
Aspirin and other drugs, Determination by HPLC	1015
Atomic-absorption spectrometry (AAS), Calibration technique	9
—, —, Determination of Ag	443
—, —, — of cyanide	141
—, —, — of major elements	1153
—, —, — of Ni	1008
—, —, — of organic compounds	15
—, —, — of Sb, Bi and Hg	367
—, —, — of Sc, Y and lanthanides	1045
—, —, — of Zn	347
—, —, Twin-spray	367
—, —, Use of emulsions	799
—, —, /Fire assay, Determination of Ag	89
—, —, flameless (FAAS), combined with extraction, Review	449
—, —, —, Determination of Ce	1053
—, —, —, — of heavy metals	561
—, —, —, — of In and Tl	133
—, —, —, — of Sb	709
—, —, —, — of Sn	73, 573
—, —, —, — of Tl	150
Atomic hyperfine structures, Determination, by optogalvanic spectroscopy	659
Barium, Complex with Thorin	479
1,4-Benzodiazepines, Determination by HPLC	1
Benzylimidazolines, Dissociation constants	730
Beryllium, Determination, spectrophotometric	249
Bicarbonate, Exchange equilibria with other anions	521
Binary mixtures, Analysis	298
Bis(diphenyldithiophosphine)disulphide, Determination, electrochemical	69
Bismuth, Adsorption on lead dioxide	292
—, Chelates, polarographic behaviour	379
—, Determination, by AAS	367
—, —, potentiometric	212
Boron, Determination, spectrophotometric	547
Bromide, Determination by MAS	39
—, Enrichment, chromatographic	45
—, Exchange equilibria with other anions	521

Cadmium, Determination, by ASV	221, 371
—, —, titrimetric	1018
—, Separation from sea-water	597
Calibration technique, for AAS	9
Carbon dioxide, Air-sea-water exchange model	1095
— monoxide, Determination, spectrophotometric	33
Carbonate, Exchange equilibria with other anions	521
Carboxymethyl-dextran, Protonation equilibria	683
Catalysis, enzymatic, with xanthine oxidase	241
Catechol Violet, Extraction with anion-exchangers	401
Cation-exchange gels, Dissociation constants	199
Cephalosporins, Determination, spectrophotometric	635
Cerium, Determination by FAAS	1053
Chelating resin, Separation of Mo(VI) and W(VI)	353
—, —, Synthesis and properties	1079
Chemiluminescence, Determination of quinones	1027
Chloramphenicol, Determination, spectrophotometric	289
Chloride, Determination, by ion-chromatography	467
—, —, by MAS	341
—, Exchange equilibria with other anions	521
—, Ion-selective electrode for	79, 579, 1021
Cholesterol oxidation, Analysis by TLC and GC	489
Chromaticity parameters, of acid-base indicator	279
Chromatography, gas (GC), Determination of phospholipids and cholesterol	489
—, —, —, of polycyclic aromatics	49
—, —, —, of Se	1010
—, high-pressure liquid (HPLC), Determination of acetaminophen and dextropropoxy- phene	397
—, —, —, — of aspirin and other drugs	1015
—, —, —, — of 1,4-benzodiazepines, Review	1
—, —, —, — of diphenyltin and dialkyltin homologues	976
—, —, —, — of trifluoroacetate	147
—, ion-, Determination of chloride and fluoride	467
—, —, — of sulphony anions	331
—, ion-exchange, of U, Ti, Nb and rare-earth elements	185
—, paper (PC), Purification of Xylenol Orange	645
—, thin-layer (TLC), of phospholipids and cholesterol	489
Chrome Azurol S, Extraction with anion-exchangers	401
Chromium(VI) species, Effect of pH	227
— and molybdenum(VI), Extraction of ion-pairs	1031
Classification, of colours of co-ordination compounds	651
Clinical analysis, Applications of solid-phase chemistry	863
—, —, by tandem MS	929
—, —, Quality control	851
—, —, Use of flow-injection	879
Cobalt, Extraction, from sea-water	597
—, —, with polyurethane foam	963
Co-flotation, Separation of Cu, Cd and Co	597
Colour, of co-ordination compounds, Classification	651
— change limits, of acid-base indicator	279
Complex equilibria and diffusion coefficients	421
— formation, polarographic study	155
Complexes, Stoichiometry by computer	97
Complexing capacity, of Seine water	1057
Computer network, versatile low-cost	565
— program, for estimation of stability constants	1083
— software survey section	No. 8, I
Copper, Composition of Alizarin S complexes	101
—, Determination, by AAS	799
—, Electrodeposition	135
—, Extraction, from sea-water	597
—, —, with dithizone	1101
—, Stability constants, of ternary complexes	837
Copper(II), Determination, spectrophotometric	325
CuInS ₂ semiconductor, analytical characterization	253
Curve fitting, multiparametric	947, 1083
Cyanide, Determination, by AAS	141
—, —, kinetic fluorimetric	783
—, —, spectrophotometric	85, 673
Data acquisition, binary	275
DeFord and Hume method, Calculation of formation constants	379
Dentin, Separation from tooth enamel	955
Dextropropoxyphene, Determination by HPLC	397
Diffusion coefficients and complex equilibria	421

Digestion methods for Se, Comparison	1010
Diphenyltin and dialkyltin homologues, Determination by HPLC	976
Dissociation constants, of benzylimidazolines	730
—, of cation-exchange gels	199
—, of 2-mercaptopropenoic acids	475
—, of organic acids	734
Drug effects, on laboratory test results	937
Electrode, gold, Determination of cadmium	221
—, ion-selective, Detection of anticardiolipin antibodies	375
—, —, for ammonia	607
—, —, for bismuth	212
—, —, for chloride	79, 579, 1021
—, —, for potassium	1005
—, —, Potential interpretation	789
—, mercury-film, for ASV	703
—, precipitate-polished, for voltammetry	720
—, rotating ring-disc, for voltammetry	693
—, tungsten-wire, for aerosol collection	679
Elements, toxic, Determination in biological samples	307
Emulsions, Use in AAS	799
End-point detection, in catalytic thermometric titrations	611
Enthalpimetry, Determination of glucose	131
Enzymes, immobilized bioluminescent	173
Eosin, Purity of commercial samples	1125
Equilibrium in heme model systems, Analysis	224
Eriochrome Cyanine R, Extraction with anion-exchangers	401
Esterification, for end-point detection	611
Exchange equilibria, between bicarbonate and other anions	521
— model, air-sea-water, for carbon dioxide	1095
Extraction, of Ag	89, 443
—, of alkali metals	165
—, of bromide	39
—, of chloride	341
—, of Co	963
—, of Cr(VI) and Mo(VI) ion-pairs	1031
—, of Cu and Pd	1101
—, of Fe complexes	525
—, of Ge as tetrachloride	997
—, of In with tributyl phosphate	630
—, of Mo	265, 593
—, of noble metals	755
—, of Pd and Cu	1101
—, of phosphate	235
—, of potassium <i>p</i> -nitrophenoxide	585
—, of Ru thiocyanate	189
—, of Th with quaternary ammonium halides	627
—, of Zn	215
—, combined with FAAS, Review	449
Flavonols, Determination, polarographic	615
Flow-injection analysis, Determination of cyanide	673
—, in clinical analysis	879
—, —, voltammetric detection	387
Fluorescence line narrowing, laser-excited	741, 753
Fluoride, Determination by ion-chromatography	467
Fluorimetry, Determination of cyanide	777
—, — of Li	749
—, — of Mn	29
—, — of Pb ultratraces	515
Fluoroimmunoassay, for hormones	909
Formaldehyde traces, Determination, Review	763
Formation constants, Calculation by DeFord and Hume method	379
—, of lanthanide complexes	1129
Germanium, Determination, spectrophotometric	997
Glucose, Determination, enthalpimetric	131
Graphite furnace, for FAAS	73
—, for MAS	39
Hafnium, Determination, gravimetric	621
Heavy metals, Determination by FAAS	561
Heme model systems, Analysis of equilibrium	224
Heroin, Determination	138
Hexacelsian, Determination by infrared spectroscopy	550
High-voltage breakdown, in spark-source MS	177

Hormones, Fluoroimmunoassay	909
—, Immunoassay.	901
Humic acids, Determination, polarographic.	207
Hydrolysis products of tetrahydrozoline, Identification	229
Hydroxide complexes, of Nd.	731
Hydroxylamine, Determination, spectrophotometric	1013
8-Hydroxyquinoline derivatives, Determination, spectrophotometric	648
Imidazole, protonated, pK_a values	559
Immunoassay, for antibodies.	889
—, for hormones.	901
—, for plasma and salivary steroids	895
—, for prealbumins	923
—, in two-phase systems	917
Indicator, acid–base, Evaluation	279
Indium, Determination, by FAAS	133
—, Extraction with tributyl phosphate	630
Indoles, Reaction with <i>N</i> -chlorosuccinimide	642
Information power, of analytical processes	162
Injection, of microsamples into gaseous carrier	463
Instrumentation with BCD-coded output	275
Intercomparison studies between water analysis laboratories	537
Interferences, in laboratory test results	937
Ion-exchange, Enrichment of bromide	45
—, Separation of Pt metals	815
Ion-exchanger, lanthanum arsenate	195
Iridium, Separation from Rh	431
Iron, Complexes with PAR	525
—, Determination, by AAS	799
—, —, spectrophotometric	844
Iron(II), Determination, spectrophotometric	1112
Iron(III), Determination, spectrophotometric	715
Isocyano groups, Determination on polymer supports	842
Isosbestic points, of ternary Cu complexes	837
Isotope dilution analysis (IDA), Determination of Sb	509
Karl Fischer reagent, pyridine-free.	553
Khelline, Oxidation with vanadate.	655
Laboratory test results, Interferences and drug effects	937
Lanthanides, Determination, by AAS.	1045
—, Formation constants of complexes	1129
Lanthanum arsenate, as ion-exchanger	195
Laser-excited fluorescence line narrowing	741, 753
Lead, Determination, by XRF	1118
—, —, fluorimetric	515
—, —, titrimetric.	1018
Ligand-exchange, Separation of phenolic compounds	357
Light-emission, Detection, photographic	173
Lithium, Determination, fluorimetric	749
Louis Gordon Memorial Award	No. 9, I
Lucigenin, Reaction with reducing sugars	603
Malonic acid, oxidation with Tl(III)	209
Malononitrile, Determination, polarographic	723
Manganese, Determination, fluorimetric	29
—, —, kinetic.	437
—, —, spectrophotometric	109
Material consumption, in spark-source MS.	177
Matrix, Acetone, Determination of water	82
—, Air, Determination of methanol	394
—, Atmospheric particulates, Determination of sulphate	479
—, Biological samples, Determination of 1,4-benzodiazepines	1
—, —, — of Hg	307
—, Blood plasma, Determination of Zn	347
—, Coal, Determination of N	607
—, Columbite–tantalite, Determination of U	846
—, Cu metal and alloys, Determination of B	547
—, Environmental materials, Determination of nitrate	319
—, Ethanol, Determination of water	82
—, Foodstuffs, Determination of Mn.	109
—, Geochemical samples, Determination of Sb, Bi and Hg	367
—, Geological materials, Determination of major elements	1153
—, —, — of Sn	73
—, Iron ores, Determination of P	301

—, Metamict minerals, Determination of U, Ti, Nb and rare-earth elements	185
—, Ores, Determination of Ag	443
—, —, — of Zr	638
—, — and concentrates, Determination of Ge.	997
—, Natural water, Determination of N	979
—, Organic solvents, Determination of water	556
—, Pharmaceutical preparations, Determination of acetaminophen and dextropropoxy- phene	397
—, —, — of aspirin and other drugs	1015
—, Phosphogypsum, Determination of U	1115
—, Phosphoric acid, Determination of U	459
—, Plasma, Determination of trifluoroacetate	147
—, —, Immunoassay for prealbumins	923
—, Reference ores and concentrates, Determination of Ag	89
—, River and sea-water, Determination of phosphate	235
—, Sea-water, Determination of Cu, Cd and Co	597
—, —, — of Mo	472
—, —, — of Zn	1069
—, Sediments, Determination of heavy metals.	561
—, Serum, Determination of Zn	347
—, —, Immunoassay for prealbumins	923
—, Silicate rocks, Determination of Ce	1053
—, —, — of Sc, Y and lanthanides	1045
—, Silicates, Determination of Be	249
—, Soil, Determination of nitrite	391
—, Steel reference materials, Verification of S contents.	311
—, Tin-plating solutions, Determination of chloride and fluoride	467
—, Uranium, Determination of rare metals.	773
—, Urine, Determination of Se	497
—, —, — of trifluoroacetate	147
—, Vegetation, Determination of ⁹⁹ Tc	809
—, Water, Determination of bromide.	45
—, —, — of cyanide	141
—, —, — of Fe	844
—, —, — of methanol.	394
—, —, — of nitrite	391
—, —, — of sulphide	1024
—, —, — of Tl	150
—, Wine, Determination of acidic substances	218
Mercury, Determination, by AAS	367
—, —, in biological samples	307
Mercury(II), Determination, titrimetric	1018
—, Reduction at glassy-carbon electrode	693
Metal complexes with 8-mercaptoquinolines, Stability	727
— ions, Role in enzymatic catalysis	241
Metals, Determination of ultratraces by MS	55
Methanol, Determination, spectrophotometric	394
Microsamples, injection into gaseous carrier	463
Molybdate, Complexes with oxalate	743
Molybdenum, Determination, polarographic	593
—, —, spectrophotometric	265, 472
Molybdenum(VI), Separation with chelating resin	353
— and chromium(VI), Extraction of ion-pairs.	1031
Multiparametric curve fitting.	947
Neodymium, Hydroxide complexes	731
Nickel, Determination by AAS	1008
— and zinc ferrocyanides, Review	1133
Niobium, Determination, polarographic	417
—, —, spectrophotometric	185
—, surfactant-sensitized reaction	361
Nitrate, Determination, polarographic	319
Nitrite, Determination of ultratraces	391
Nitrogen, Determination by ion-selective electrode	607
—, — in water	979
—, active, Use in chemiluminescence spectroscopy	777
Nitrosamines, Determination by chemical ionization MS	615
Organic acids, Dissociation constants.	734
— compounds, Determination of ultratraces by MS.	55
—, —, indirect determination by AAS.	15
Osmium, Determination, catalytic	61
—, —, spectrophotometric	205
Palladium, Complexes with TTHA	153

—, Determination, spectrophotometric	959
—, Extraction by formazans	755
—, Extraction with dithizone	1101
Pentacyanoferrate(III), Complexes with <i>N</i> -heterocyclic aldoximes	169
pH, Effect on Cr(VI) species	227
Pharmaceutical analysis, by tandem MS	929
Phase equilibria, liquid-liquid, analytical applications	298
Phenol, Determination, titrimetric	283
Phenolic compounds, Separation by ligand-exchange	357
Phenothiazines, Determination, spectrophotometric	289
— derivatives, Determination, titrimetric	287
Phenylhydrazine, Determination, spectrophotometric	466
Phenylpropionic acid derivatives, Titration, coulometric	144
Phloroglucinol, Determination, titrimetric	283
Phosphate, Determination, spectrophotometric	235
Phospholipid oxidation, Analysis by TLC and GC	489
Phosphorus, Determination, spectrophotometric	301
pK_a values, of protonated imidazole	559
Plasma, Immunoassay for	895
Platinum, Determination, spectrophotometric	959
—, Extraction by formazans	755
— metals, Separation	815
Plutonium, Determination, potentiometric	1109
Polarimeters, optical, shot-noise limit	689
Polarography, Determination of bis(diphenyldithiophosphine)disulphide	69
—, — of flavonols	615
—, — of Nb	417
—, — of Zr traces	638
—, differential pulse, Determination of Bi	292, 379
—, —, — of malononitrile	723
—, —, — of Mo	593
—, —, — of nitrite	319
—, pulse, of alkali metals	105
—, —, of Cu complexes	101
—, —, of humic acid fractions	207
—, Study of complex formation	155
Polymerization, for end-point detection	611
Polythionate, Determination by ion-chromatography	331
Polyurethane foam, for extraction of Rh	431
Potassium, Extraction as <i>p</i> -nitrophenoxide	585
—, Ion-selective electrode for	1005
Prealbumins, Immunoassay	923
Programmable stepper-motor controller	117
Protolysis equilibria, Analysis	113
Protonation equilibria, of carboxymethyl dextran	683
Pulsed-current potentiometric technique	123
Pyridine, Determination, spectrophotometric	325
Quality control, in clinical analysis	851
Quinones, Determination, by chemiluminescence	1027
Rare-earth metals, Determination, by argon plasma	773
—, —, spectrophotometric	185
Reagent, Alizarin S, Complexes with Cu	101
—, <i>n</i> -Alkanediaminotetra-acetic acids, for V(VI)	525
—, 8-Amino-1-hydroxynaphthalene-3,6-disulphonic acid, for aromatic amines	295
—, Ammonium molybdate, for cephalosporins	635
—, Azomethine derivatives of 2-benzoylpyridine, for Bi	379
—, Benzothiazolylphenol, for Li	749
—, Bromopyrogallol Red, for Ti	667
—, Cacotheline, for phenylhydrazine	466
—, Chloranil, for tranexamic acid	77
—, <i>N</i> -Chlorosuccinimide, for indoles	642
—, 12-Crown-4, Extraction of alkali metals	165
—, 18-Crown-6, for Pb	515
—, Crown ethers, for alkali metals	1149
—, —, for extraction of K	585
—, Cyanocuprate(I), for Os	61
—, Cyclohexanedione bis(2-hydroxybenzoylhydrazones), for metals	1075
—, DCTA, for V(IV)	717
—, 2-(3,5-Dibromo-2-pyridylazo)-5-diethylaminophenol, for Zn	624
—, 4-H-Diethylenetriamines, for Ag	735
—, 1,4-Dihydroxyanthraquinone, Acid-base indicator	279
—, β -Diketones, for U(VI)	805
—, Dithizone, for Pd and Cu	1101

—, —, for Pd and Pt	959
—, Eosin, for Pb	515
—, Ethyl xanthate, Extraction of Zn	215
—, Ferricyanide, for phenothiazine	287
—, Ferrozine, for Fe	844
—, Formazans, Extraction of noble metals	755
—, <i>N</i> -Heterocyclic aldoximes, for pentacyanoferrate(III)	169
—, 2-Hydroxy-1-naphthaldehyde <i>p</i> -methoxybenzoylhydrazone, for Al	253
—, 8-Hydroxyquinoline-5-sulphonic acid, for Nb	361
—, Malachite Green, for phosphate	235
—, 2-Mercaptopropanoic acid, for Hg(II)	1018
—, 2-Mercaptoquinolines, Complexes with metals	727
—, Methylene Blue, for B	547
—, Molybdate, Extraction of phosphate	235
—, Molybdenum Blue, for U	943
—, Morin, for diphenyltin and dialkyltin homologues	976
—, <i>N</i> -(1-Naphthyl)ethylenediamine, Coupling agent	295
—, 3-(1-Naphthyl-2-mercaptopropenoic acids, Dissociation constants	475
—, <i>p</i> -Nitroaniline, for hydroxylamine	1013
—, Oxalate, Complexes with molybdate	743
—, Phenylfluorone, for Ge	997
—, —, for Zn	840
—, 3-(4-Phenyl-2-pyridyl)-5,6-diphenyl-1,2,4-triazine, for Fe(II)	1112
—, 1-Phenyl-4,4,6-trimethyl-(1 <i>H</i> ,4 <i>H</i>)-2-pyrimidinethiol, for Os	205
—, Potassium morpholine-4-carbodithioate, for Te	848
—, 4-(2-Pyridylazo)resorcinol (PAR), for Fe	525
—, —, for lanthanides	1129
—, Pyrocatecholsulphonphthalein complexan, for metals	1121
—, 2-(8-Quinolylazo)-7-phenylazochromotropic acid, Synthesis	1041
—, 1-(2-Quinolylazo)-2,4,5-trihydroxybenzene, for Mn(II)	109
—, Ru(II) octaethylporphyrin	33
—, Sodium cobaltinitrite, for phenothiazines and other compounds	289
—, — 4,8-diamino-1,5-dihydroxyanthraquinone-2,6-disulphonate, for Mn	437
—, 3-Styryl-2-mercaptopropenoic acid, Dissociation constants	475
—, Thallium(III), for malonic acid	209
—, Thioglycollic acid, for Ag, Pb and Cd	1018
—, Thorin, for Ba	479
—, Tiron, for Fe(III)	715
—, Tributyl phosphate, extraction of In	630
—, Triethylenetetraminehexa-acetic acid, for Tl	153
—, Triphenyltin hydroxide, Extraction of bromide	39
—, —, — of chloride	341
—, 4-Unsubstituted 5-pyrazolones, for Mo	265
—, Vanadate, for khelline	655
—, Xylenol Orange, for Zr	645
Reference materials, Characterization	851
Resorcinol, Determination, titrimetric	283
Review, Determination of formaldehyde traces	763
—, Extraction combined with FAAS	449
—, Structure of Zn and Ni ferrocyanides	1133
Rhodium, Extraction with polyurethane foam	431
Ruthenium thiocyanate, Extraction	189
Salivary steroids, Immunoassay	895
Scandium, Determination, by AAS	1045
Schiff's bases, Fluorescence properties	29
Seine water, complexing capacity	1057
Selectivity, of analytical processes	162
Selenium, Determination, by different methods	497
—, —, by GC	1010
Selenium(IV), Collection by anion-exchange	269
Semiconductor CuInS ₂ , analytical characterization	253
Shot-noise limit, of optical polarimeters	689
Silver, Determination, by AAS	443
—, —, by AAS/fire assay	89
—, —, titrimetric	1018
—, Electro-deposition	135
Silver(I), Extraction by formazans	755
—, Stability of complexes	735
Solid-phase chemistry, Applications in clinical analysis	863
Solubility, of alkali-metal fluorides	1036
Spectrometry, chemiluminescence, Use of active nitrogen	777
—, differential, Determination of Cu complexes	101
—, flame emission, Determination of alkali-metal fluoride	1036
—, infrared, Determination of hexacelsian	550

—, mass, chemical ionization, of nitrosamines	619
—, —, isotope-dilution, Determination of S	311
—, —, —, thermal ionization, Determination of S	1063
—, —, negative chemical ionization, for ultratrace analysis	55
—, —, spark-source, in analysis	177
—, —, tandem, for pharmaceutical and clinical analysis	929
—, molecular absorption (MAS), Determination of bromide	39
—, —, — of Cl traces	341
—, optogalvanic, for hyperfine structures	659
—, Plasma atomic emission, Determination of Cu and Ag	135
—, —, —, of major elements	1153
—, X-ray fluorescence (XRF), Determination of As	304
—, —, —, of Pb	1118
Spectrofluorimetry, Determination of trace water	556
Stable-isotope ratio analysis	659
Stability, of metal complexes with 8-mercaptoquinolines	727
— constants, Computer program for estimation	1083
—, —, of ternary Cu complexes	837
Stepper-motor controller, programmable	117
Stoichiometry of complexes, by computer	97
Sugars, reducing, reaction with lucigenin	603
Sulphacetamide sodium, Titration, non-aqueous	285
Sulphate, Determination, by ion-chromatography	331
—, —, complexometric	479
Sulphide, Determination of traces, spectrophotometric	1024
Sulphite, Determination by ion-chromatography	331
Sulphur, Determination by MS	1063
Surfactants, Effect on ASV	703
—, non-ionic, Determination	633
—, sensitized reaction of Nb	361
Talanta Advisory Board	No. 1, III
Tchnetium-99, Determination, radiochemical	809
Tellurium, Determination, spectrophotometric	848
Ternary complexes, Applications in photometry	667
Tetracyclines, Determination, spectrophotometric	289
Tetrahydrozoline, Identification of hydrolysis products	229
Thallium, Determination, by FAAS	133, 150
Theory of catalytic titrations	987
Thiosulphate, Determination by ion-chromatography	331
Thorium, Extraction with quaternary ammonium halides	627
Tin, Determination, by FAAS	73, 573
—, —, complexometric	469
Tiron, Determination, spectrophotometric	715
Titanium, Determination, spectrophotometric	185, 667
Titration, of phenol, resorcinol and phloroglucinol	283
—, of phenothiazine derivatives	287
—, catalytic, of Os	61
—, — thermometric, End-point detection	611
—, complexometric, of Sn	469
—, —, of sulphate	479
—, —, of V(IV)	717
—, — catalytic, Theory	987
—, coulometric, acid-base and other systems	315
—, —, of metal ions	123
—, —, of phenylpropionic acid derivatives	144
—, enthalpimetric, of water	82
—, non-aqueous, of sulphacetamide sodium	285
—, photometric, of phenylhydrazine	466
—, potentiometric, of Bi	212
—, —, of Pu	1109
—, thermometric, of acidic substances	218
—, two-phase, Determination of surfactants	633
— plots, linear, of weak acids and bases	409
Tooth enamel, separation from dentin	955
Tranexamic acid, Determination, spectrophotometric	77
Trifluoroacetate, Determination, by HPLC	147
Tungsten(VI), Separation with chelating resin	353
Ultratrace analysis, by negative chemical ionization MS	55
Uranium, Determination, fluorimetric	846
—, —, in phosphoric acid	459
—, —, spectrophotometric	185, 943, 1115
Uranium(VI), Chelates with β -diketones	805
Uranyl, Complexes with n-alkanediaminotetra-acetic acids	531

Urea, as component of Karl Fischer reagent	553
Vanadium(IV), Determination, complexometric	717
Verification of S contents in steel reference materials	311
Voltammetry, anodic stripping, Determination of Cd	221, 371
—, —, —, Effect of surfactants	703
—, background-current subtraction	387
—, cathodic stripping, Determination of Zn	1069
—, Determination of Hg(II)	693
—, Interpretation of potentials	789
—, with precipitate-polished electrode	720
Water, Determination, enthalpimetric	82
—, —, spectrofluorimetric	556
— analysis laboratories, Intercomparison studies	537
Wet ashing, of biological materials	307
Xanthine oxidase, enzymatic catalysis.	241
Yttrium, Determination, by AAS	1045
Zinc, Determination, by AAS	347
—, —, by cathodic SV	1069
—, —, spectrophotometric	624, 840
—, Extraction	215
— and nickel ferrocyanides, Review	1133
Zirconium, Complex with Xylenol Orange	645
—, Determination, gravimetric	621
—, —, polarographic	638

LIST OF CONTENTS

JANUARY

<i>Talanta Advisory Board</i>	III
Anil C. Mehta	1 High-pressure liquid chromatographic determination of some 1,4-benzodiazepines and their metabolites in biological fluids: a review
J. F. Tyson and J. M. H. Appleton	9 A continuous-dilution calibration technique for flame atomic-absorption spectrophotometry
E. R. Clark and El-Sayed A. K. Yacoub	15 Indirect determination of organic compounds by atomic-absorption spectrophotometry
J. Vazquez Ruiz, A. Garcia de Torres and J. M. Cano-Pavon	29 Fluorescence properties of some Schiff's bases derived from 3-hydroxypyridine-2-aldehyde and of their metal chelates. Fluorimetric determination of manganese based on its catalytic effect on the oxidation of these compounds with hydrogen peroxide
A. Corsini, A. Chan and H. Mehdi	33 Spectrophotometric determination of carbon monoxide with ruthenium(II) octaethylporphyrin
K. Dittrich, B. Ya. Spivakov, V. M. Shkinev and G. A. Vorob'eva	39 Molecular absorption spectrometry (MAS) by electrothermal evaporation in a graphite furnace—IX. Determination of traces of bromide by MAS of AlBr after liquid-liquid extraction of bromide with triphenyltin hydroxide
Ulla Lundström, Åke Olin and Folke Nydahl	45 Determination of low levels of bromide in fresh water after chromatographic enrichment
Michael J. Avery, John J. Richard and Gregor A. Junk	49 Simplified determination of polycyclic aromatic hydrocarbons
I. K. Gregor and M. Guilhaus	55 Detection limits and surface interactions in quantitative negative chemical-ionization mass spectrometry. Ultratrace determination of metals and organic compounds by means of their complexes
I. N. C. Ling and G. Svehla	61 Determination of traces of osmium by the catalysed hydrogen peroxide-cyanocuprate(I) reaction
Angel Schischkov, Shivko Dentshev und Christina Malakova	69 Elektrochemische Untersuchung von bis(Diphenyldithiophosphin) Disulfid
<i>Short Communications</i>	
Liyi Zhou, T. T. Chao and A. L. Meier	73 Determination of total tin in geological materials by electrothermal atomic-absorption spectrophotometry using a tungsten-impregnated graphite furnace
Abdel-Aziz M. Wahbi, Essam A. Lotfi and Hassan Y. Aboul-Enein	77 Spectrophotometric determination of tranexamic acid with chloranil
G. Subramanian, Navin Chandra and G. Prabhakara Rao	79 Estimation of chloride in oxidizing media by means of ion-selective electrodes
Wallace A. de Oliveira and Celio Pasquini	82 Determination of water in ethanol and acetone by direct injection enthalpimetry based on the heat of dilution
M. Blanco and S. Maspoeh	85 Determination of cyanide by a highly sensitive indirect spectrophotometric method
<i>Annotation</i>	
Elsie M. Donaldson, E. Mark and Maureen E. Leaver	89 Comparison of silver results for Canadian reference ores and concentrates and zinc-processing products by acid decomposition, tribenzylamine/chloroform extraction and fire-assay combined with atomic-absorption spectrophotometry
<i>Papers Received</i>	i
<i>Errata</i>	iii
<i>Notice</i>	iv

FEBRUARY

Th. Prange, U. Lechner-Knoblauch and F. Umland	97	Ein neues Graphisches Auswerteverfahren zur Ermittlung stöchiometrischer Faktoren gelöster Komplexe
Th. Prange, H. D. Sommer and F. Umland	101	Differenzspektroskopische und pulspolarographische Untersuchungen zur Zusammensetzung der Kupfer-Alizarin S-Komplexe
Minoru Hara and Noboru Nomura	105	Modified normal pulse polarography of alkali-metal ions in acid solution
Ishwar Singh and Mrs. Poonam	109	Spectrophotometric determination of Mn(II) with 1-(2-quinolyazo)-2,4,5-trihydroxybenzene and microdetermination of Mn in foodstuffs
Jürgen Polster	113	Spectrophotometric analysis of simultaneous protolysis equilibria
F. Papoff and D. Ricci	117	A programmable positioning stepper-motor controller with a Multibus/IEEE 796 compatible interface
Theologos Andronidis, Anna Maria Ghe, Cesare Pagura and Sergio Valcher	123	Coulometric titration by means of a controlled-potential-pulsed-current potentiometric technique—I. Metal ions by electro-deposition
<i>Short Communications</i>		
Nobutoshi Kiba, Tosimitsu Tomiyasu and Motohisa Furusawa	131	Flow enthalpimetric determination of glucose, based on oxidation by 1,4-benzoquinone and use of an immobilized glucose oxidase column
Du Yan, Zhang Yan, Guang-shen Cheng and An-mo Li	133	Determination of indium and thallium by hydride generation and atomic-absorption spectrometry
Roman E. Sioda	135	Electro-deposition of Cu and Ag from solutions of ppm concentration, followed by inductively-coupled plasma spectrometry
Giovanna Bertocchi, Giovanni Gottarelli and Romano Prati	138	Determination of heroin by means of the pitch of induced cholesteric mesophases
Xu Bo-Xing, Xu Tong-Ming and Fang Yu-Zhi	141	Indirect determination of cyanide in water by atomic-absorption spectrophotometry
G. Kanoute, E. Nivaud, B. Paulet et P. Boucly	144	Dosage de dérivés de l'acide phénylpropionique à activité pharmacologique par titrage coulométrique
M. Imbenotte, A. Brice, F. Erb and J. M. Haguenoer	147	Determination by HPLC of trifluoroacetate levels in plasma and urine of patients anaesthetized with halothane
Shan Xiao-quan, Ni Zhe-ming and Zhang Li	150	Application of matrix-modification in determination of thallium in waste water by graphite-furnace atomic-absorption spectrometry
<i>Analytical Data</i>		
Aldo Napoli	153	Palladium complexes with triethylenetetraminehexa-acetic acid
<i>Annotations</i>		
P. H. Tedesco and J. Martinez	155	Polarographic study of simple and mixed-ligand complex formation
J. Inczédy	162	Some remarks on the information power and selectivity of analytical processes
<i>Papers Received</i>	i	
<i>Publications Received</i>	iii	
<i>Notes for Authors</i>	v	

MARCH

- | | |
|--|---|
| G. E. Pacey and Y. P. Wu | 165 Ion-pair extractions with 12-crown-4 and its analogues |
| Nicoletta Burger and
Vinka Karas-Gašparec | 169 Spectrophotometric studies of the reactions of pentacyanoferrate(II) complexes with three <i>N</i> -heterocyclic aldoximes |
| K. Green, L. J. Kricka,
G. H. G. Thorpe and
T. P. Whitehead | 173 Rapid assays based on immobilized bioluminescent enzymes and photographic detection of light-emission |
| J. Van Puymbroeck,
J. Verlinden,
K. Swenters and R. Gijbels | 177 Study of high-voltage breakdown and material consumption in spark-source mass spectrometry and their significance in analytical applications |
| A. Mazzucotelli, R. Vannucci,
S. Vannucci and
E. Passaglia | 185 Chemical analysis of uranium and titanium niobotantalate metamict minerals by ion-exchange chromatography and spectrophotometric procedures |
| Sargon J. Al-Bazi and
Arthur Chow | 189 Extraction of ruthenium thiocyanate and its separation from rhodium by polyurethane foam |
| Ashis K. Mukherjee and
Suchitra K. Mandal | 195 Studies on the lanthanum arsenate ion-exchanger: preparation, physicochemical properties and applications |
| Yves Merle and
Jacob A. Marinsky | 199 Gel speciation studies—I. The intrinsic dissociation constant of weakly acidic cation-exchange gels |
| <i>Short Communications</i> | |
| A. Wasey, R. K. Bansal,
B. K. Puri and
A. L. J. Rao | 205 Spectrophotometric determination of osmium with 1-phenyl-4,4,6-trimethyl-(1H,4H)-2-pyrimidinethiol and extraction into molten naphthalene |
| Maria Teresa Lippolis,
Vittorio Concialini
and Giuseppe Chiavari | 207 Pulse polarography of nitrosated GPC fractions of humic acids |
| S. R. Sagi, K. Appa Rao
and M. S. Prasada Rao | 209 Thallimetric oxidations—IV. Estimation of malonic acid |
| Walenty Szczepaniak and
Maria Ren | 212 Determination of bismuth(III) by direct potentiometry and potentiometric titration, with an electrode sensitive to Bi ³⁺ |
| A. K. Chakravarti, S. Mukherjee,
H. K. Saha and T. Chakrabarty | 215 Liquid-liquid extraction of zinc(II) as its ethyl xanthate |
| O. E. S. Godinho, J. A. Coelho,
A. P. Chagas and L. M. Aleixo | 218 Investigation of the use of thermometric titrimetry for the determination of acidic substances in wine |
| Cui Chunguo | 221 Determination of cadmium(II) at a gold electrode in the presence of selenium(IV) by anodic-stripping voltammetry with enhancement by iodide ion |
| Luiz A. Morino and
Henrique E. Toma | 224 Analysis of equilibrium in heme model systems, by a successive linear regression method |
| <i>Analytical Data</i> | |
| R. K. Tandon, P. T. Crisp,
J. Ellis and R. S. Baker | 227 Effect of pH on chromium(VI) species in solution |
| <i>Annotation</i> | |
| A. Nicolas, M. Mirjolet et
J. M. Ziegler | 229 Séparation et identification des produits d'hydrolyse de la tétryzoline |
| <i>Letter to the Editor</i> | |
| A. G. Asuero, M. J. Navas
and D. Rosales | 233 The spectrophotometric evaluation of acidity constants: the double incomplete colour change |
| <i>Papers Received</i> | i |
| <i>Publications Received</i> | iii |
| <i>Notices</i> | v |

APRIL

Shoji Motomizu, Toshiaki Wakimoto and Kyoji Tôei	235	Solvent extraction-spectrophotometric determination of phosphate with molybdate and Malachite Green in river water and sea-water
Anna Maria Ghe, Claudio Stefanelli and Daniela Carati	241	Influence and role of metal ions in enzymatic catalysis with E.C. 1.2.3.2. xanthine oxidase. Application to trace analysis
Alfred Sauerer and Georg Troll	249	Spectrophotometric determination of trace amounts of beryllium in silicate materials
P. C. Ioannou and P. A. Siskos	253	Fluorimetric kinetic studies and sub- μM determination of aluminium with 2-hydroxy-1-naphthaldehyde <i>p</i> -methoxybenzoylhydrazone
C. F. Hung, P. Y. Chen, L. Y. Weng, H. L. Huang and M. H. Yang	259	Analytical characterization of CuInS ₂ semiconductor material
A. Ahmad, F. Ik. Nwabue and G. E. Ezeife	265	Extractive-spectrophotometric determination of molybdenum with 4-unsubstituted-5-pyrazolones
Morio Nakayama, Kazuo Itoh, Masahiko Chikuma, Hiromu Sakurai and Hisashi Tanaka	269	Anion-exchange resin modified with bismuthiol-II, as a new functional resin for the selective collection of selenium(IV)
L. Lampugnani, D. Guidarini and N. Fanelli	275	Binary data acquisition from instrumentation with BCD-coded output: a hardware converter and an example of the relative software control
J. Barbosa, J. Sanchez and E. Bosch	279	Study of 1,4-dihydroxyanthraquinone as an acid-base indicator in iso-propyl alcohol medium. Evaluation of colour-change limits through complementary chromaticity parameters
<i>Short Communications</i>		
D. Amin and W. A. Bashir	283	Titrimetric determination of phenol, resorcinol and phloroglucinol
Sobhi A. Soliman, Saled Belal and Mona Bediar	285	Improvement of end-point detection in the non-aqueous titration of sulphacetamide sodium
A. S. Issa and M. S. Mahrous	287	Titrimetric determination of some phenothiazine derivatives, with ferricyanide
M. S. Mahrous and M. M. Abdel-Khalek	289	Spectrophotometric determination of phenothiazines, tetracyclines and chloramphenicol with sodium cobaltinitrite
Shinichi Ito, Toshio Matsuda and Toyoshi Nagai	292	Adsorption of bismuth on hydrous lead dioxide from bismuth-EDTA solution
George Norwitz and Peter N. Keliher	295	Further application of the diazotization-coupling spectrophotometric technique to the determination of aromatic amines with 8-amino-1-hydroxynaphthalene-3,6-disulphonic acid and <i>N</i> -(1-naphthyl)ethylenediamine as coupling agents
S. K. Suri and Mohinder Pal	298	Analytical applications of liquid-liquid phase equilibria: analysis of binary mixtures of chemically similar components
Om P. Bhargava and Michael Gmitro	301	Rapid photometric determination of phosphorus in iron ores and related materials as phosphomolybdenum-blue
A. S. Khan and A. Chow	304	Determination of arsenic by polyurethane foam extraction and X-ray fluorescence
H. F. Haas and V. Krivan	307	Open wet ashing of some types of biological materials for the determination of mercury and other toxic elements
<i>Annotation</i>		
Kazuo Watanabe	311	Verification of certified sulphur values in steel reference materials by isotope-dilution mass spectrometry, and characterization of sulphur present on the solid samples
<i>Papers Received</i>	i	
<i>Publications Received</i>	iii	
<i>Notice</i>	iv	

MAY

Editorial	III
Theologos Andronidis, Anna Maria Ghe and Sergio Valcher	315 Coulometric titration by a controlled-potential pulsed-charge potentiometric technique—II. Acid–base, precipitation and homogeneous redox systems
Hirotochi Hemmi, Kiyoshi Hasebe, Kunio Ohzeki and Tomihito Kambara	319 Differential pulse polarographic determination of nitrate in environmental materials
F. Salinas López, J. J. Berzas Nevado and A. Espinosa Mansilla	325 Kinetic–spectrophotometric determination of Cu(II) and pyridine by use of the aerial oxidation of dimedone bisguanyldiazone
Carl O. Moses, D. Kirk Nordstrom and Aaron L. Mills	331 Sampling and analysing mixtures of sulphate, sulphite, thiosulphate and polythionate
K. Dittrich, B. Ya. Spivakov, V. M. Shkinev and G. A. Vorob'eva	341 Molecular absorption spectrometry by electrothermal evaporation in the graphite furnace—X. Determination of chloride traces by AlCl ₃ MA in graphite cuvettes after liquid–liquid extraction of chloride with triphenyltin hydroxide
M. J. Soriano and M. De La Guardia	347 A comparative study of flame atomic-absorption methods for determination of zinc in serum and blood plasma
Chuen-Ying Liu and Peng-Joung Sun	353 Separation and concentration of molybdenum(VI) and tungsten(VI) with chelating ion-exchange resins containing sulphur ligands
B. M. Petronio, A. Laganà and G. D'Andrea	357 Applications of ligand-exchange—III. Preparation and properties of phenol–formaldehyde-based resin in the iron(III) form
J. I. García Alonso, M. E. Díaz García and A. Sanz Medel	361 The surfactant-sensitized analytical reaction of niobium with 8-hydroxyquinoline-5-sulphonic acid
Yu Xian-an, Dong Gao-Xiang and Li Chun-xue	367 Twin-spray flame atomic-absorption spectrometric determination of antimony, bismuth and mercury in geochemical samples
Yukio Nagaosa and Toshihiro Yamada	371 Determination of cadmium by differential pulse anodic-stripping voltammetry after salting-out extraction into acetonitrile
Yoshio Umezawa, Susumu Sofue and Yoshiaki Takamoto	375 Thin-layer ion-selective electrode detection of anticardiolipin antibodies in syphilis serology
M. A. Gómez-Nieto, J. L. Cruz Soto, M. D. Luque de Castro and M. Valcárcel	379 Application of the DeFord and Hume method modified for quasi-reversible and irreversible processes to the chelates of Bi(III) with azomethine derivatives of 2-benzoylpyridine
Joseph Wang and Howard D. Dewald	387 Background-current subtraction in voltammetric detection for flow-injection analysis
<i>Short Communications</i>	
Abha Chaube, Anil K. Baveja and V. K. Gupta	391 Determination of ultra trace concentrations of nitrite in polluted waters and soil
Pratima Verma and V. K. Gupta	394 A sensitive spectrophotometric method for the determination of methyl alcohol in air and water
S. Sa'sa', A. Rashid and I. Jalal	397 Simultaneous determination of acetaminophen and dextropropoxyphene napsylate in pharmaceutical preparations by reverse phase HPLC
<i>Papers Received</i>	i
<i>Publications Received</i>	iii
<i>Notice</i>	v
<i>Errata</i>	vi

JUNE

- | | | |
|--|-----|---|
| S. Przeszlakowski and
H. Wydra | 401 | Extraction of Catechol Violet, Chrome Azurol S and Eriochrome Cyanine R with chloroform solutions of liquid anion-exchangers |
| Derek Midgley and
Colin McCallum | 409 | Linear titration plots for the analysis of mixtures of three weak acids or bases |
| Hugues Menard et Rejean Beaudoin | 417 | Etude polarographique du niobium dans les mélanges eau-fluorure d'hydrogène en présence d'ions tetraalkylammonium |
| D. R. Crow | 421 | Diffusion coefficients and complex equilibria in solution—IV. Experimental determination and manipulation of diffusion data |
| S. J. Al-Bazi and A. Chow | 431 | Polyurethane foam for the extraction of rhodium and its separation from iridium |
| A. Navas and
F. Sanchez Rojas | 437 | Photometric and fluorimetric kinetic determination and manganese by means of the oxidation of sodium 4,8-diamino-1,5-dihydroxy-anthraquinone-2,6-disulphonate |
| Elsie M. Donaldson | 443 | Improved tribenzylamine-silver bromide extraction/atomic-absorption spectrophotometric method for the determination of silver in ores, related materials and zinc process solutions |
| A. B. Volynsky, B. Ya. Spivakov
and Yu. A. Zolotov | 449 | Solvent extraction-electrothermal atomic-absorption analysis |
| Helen Górecka and
Henryk Górecki | 459 | Determination of uranium in wet phosphoric acid |
| <i>Short Communications</i> | | |
| Abdulrahman S. Attiyat and
Gary D. Christian | 463 | Discrete microsample injection into a gaseous carrier |
| N. Krishna Murty,
V. Jagannadha Rao and
N. V. Srinivasa Rao | 466 | Detection and determination of phenylhydrazine |
| W. Korth and J. Ellis | 467 | Ion-chromatographic determination of chloride and fluoride in electrolyte from the halogen tin-plating process |
| K. N. Raoot and Sarala Raoot | 469 | Selective complexometric determination of tin, with mercaptans as releasing agents |
| Tetsuya Kiriya and
Rokuro Kuroda | 472 | Application of anion-exchange techniques to the determination of traces of molybdenum in sea-water |
| <i>Analytical Data</i> | | |
| A. Izquierdo, E. Bosch
and J. L. Beltran | 475 | Dissociation constants, neutralization enthalpies and reactions of 3-styryl-2-mercaptopropenoic and 3-(1-naphthyl)-2-mercaptopropenoic acids |
| <i>Papers Received</i> | | |
| | i | |
| <i>Publications Received</i> | | |
| | iii | |

JULY

- | | | |
|---|-----|--|
| P. Bruno, M. Caselli,
A. Traini and A. Zuffianò | 479 | A contribution to the use of Thorin as an analytical reagent: spectrophotometric study of its complexation with barium and application to sulphate determination in atmospheric particulates |
| Ulrich J. Krull, Michael Thompson
and Anita Arya | 489 | Chromatographic analysis of phospholipid and cholesterol oxidation |
| H. J. Robberecht and
H. A. Deelstra | 497 | Selenium in human urine. Determination, speciation and concentration levels |

H. Yoshioka and T. Kambara	509	Comparison of the sub- and super-equivalence and substoichiometric methods of isotope dilution analysis for the determination of a trace amount of antimony
A. Sanz-Medel, D. Blanco Gomis, E. Fuente and S. Arribas Jimeno	515	Extractive fluorimetric determination of ultratraces of lead with 18-crown-6 and eosin
Ulla Lundström and Åke Olin	521	Exchange equilibria between bicarbonate, carbonate, chloride, and bromide on Dowex 1 × 8
Hitoshi Hoshino and Takao Yotsuyanagi	525	Spectrophotometric studies on ion-pair extraction equilibria of the iron(II) and iron(III) complexes with 4-(2-pyridylazo)resorcinol
M. L. Simões Gonçalves, A. M. Almeida Mota and J. J. R. Fraústo da Silva	531	Uranyl complexes of n-alkanediaminotetra-acetic acids
R. Smith	537	Organization and evaluation of interlaboratory comparison studies among southern African water analysis laboratories
<i>Short Communications</i>		
Zdeněk Čížek and Vlasta Študlarová	547	Extraction-spectrophotometric determination of small amounts of boron in copper metal and copper-base alloys with Methylene Blue
M. Carmen Guillem Villar and Claudio Guillem Monzonis	550	Determination of hexacelsian by infrared spectroscopy
M. Bos	553	Urea as the basic component in pyridine-free Karl Fischer reagent
Ci Yunxiang and Jia Xin	556	Determination of trace water in organic solvents by a spectrofluorimetric method
<i>Analytical Data</i>		
Janusz Oszczapowicz and Małgorzata Czuryłowska	559	The pK_a values of the conjugate acid of imidazole in water-ethanol mixtures
<i>Annotation</i>		
M. J. T. Carrondo, F. Reboredo, R. M. B. Ganho and J. F. S. Oliveira	561	Analysis of sediments for heavy metals by a rapid electrothermal atomic-absorption procedure
<i>Papers Received</i>	i	
<i>Notice</i>	iii	
AUGUST		
Editorial	I	
Questionnaire	II	
R. L. A. Sing and Eric D. Salin	565	A versatile low-cost laboratory computer network
János Fazakas	573	Critical study of the determination of tin by electrothermal atomic-absorption spectrometry using resonance and non-resonance lines
E. G. Harsányi, K. Tóth, E. Pungor, Yoshio Umezawa and Shizuo Fujiwara	579	Study of the potential response of solid-state chloride electrodes at low concentration ranges
E. Buncel, H. S. Shin, R. A. B. Bannard, J. G. Purdon and B. G. Cox	585	Extraction of potassium <i>p</i> -nitrophenoxide with macrocyclic crown ethers and cryptands from aqueous medium into diverse organic solvents: a systematic evaluation
Yukio Nagaosa and Katsunori Kobayashi	593	Differential pulse polarographic determination of molybdenum after separation by 8-hydroxyquinoline extraction into dichloromethane
L. M. Cabezon, M. Caballero, R. Cela and J. A. Pérez-Bustamante	597	Simultaneous separation of copper, cadmium and cobalt from sea-water by co-floitation with octadecylamine and ferric hydroxide as collectors

Robert L. Veazey, Howard Nekimken and Timothy A. Nieman	603	Chemiluminescent reaction of lucigenin with reducing sugars
T. D. Rice, V. Sweeney, R. Semitekolos and G. J. Rhyder	607	Standard-addition determination of nitrogen in coal with an ammonia-sensitive electrode
Edward J. Greenhow and Pilar Viñas	611	A comparison of cationic polymerization and esterification for end-point detection in the catalytic thermometric titration of organic bases
F. Fahrat, M. Kallel, A. Caiola, D. Cantin et J. Alary	615	Détermination polarographique de facteurs vitaminiques P (rutine et ses dérivés)
<i>Short Communications</i>		
Yin Fang, Ding Jiahua and Liu Shili	619	Chemical ionization mass spectrometry of nitrosamines
Tomitaro Ishimori, Masatomi Sakamoto and Tadao Watanabe	621	Gravimetric determination of the abundance ratio of zirconium and hafnium, based on the <i>in situ</i> thermal decomposition of $K_4[(Zr,Hf)(C_2O_4)_4] \cdot 5H_2O$
Tan Zhe and Shui-Sheng Wu	624	Spectrophotometric determination of zinc with 2-(3,5-dibromo-2-pyridylazo)-5-diethylaminophenol in the presence of anionic surfactant
I. S. El-Yamani and E. I. Shabana	627	Studies on extraction of thorium from nitrate solutions with quaternary ammonium halides
I. S. El-Yamani and E. I. Shabana	630	Studies on extraction of indium by tributyl phosphate from thiocyanate solutions
Masahiro Tsubouchi and Yoshiko Tanaka	633	Determination of poly(oxyethylene) non-ionic surfactants by two-phase titration
M. M. Abdel-Khalek and M. S. Mahrous	635	Use of ammonium molybdate in the colorimetric assay of cephalosporins
Ye Hua-Li and He You-Hua	638	Polarographic determination of traces of zirconium in ores by use of complex-forming compounds adsorbable at the dropping mercury electrode
Imadul Islam, D. D. Misra, R. N. P. Singh and J. P. Sharma	642	A study of the reaction of <i>N</i> -chlorosuccinimide with indoles and its analytical application
V. Michaylova, L. Šúcha and M. Suchánek	645	Purification of Xylenol Orange by preparative paper chromatography, and examination of its zirconium complex
F. Belal	648	Spectrophotometric determination of halogenated 8-hydroxyquinoline derivatives
<i>Letter to the Editor</i>		
Franz Ludwig Wimmer and Laurence Poncini	651	The colours of co-ordination compounds: methods of classification
<i>Papers Received</i>	i	
<i>Erratum</i>	iii	

SEPTEMBER

Louis Gordon Memorial Award	I	
J. E. Hila, M. Tsitini-Souleau, M. Hamon et M. Chastagnier	655	Oxydation vanadique de la khelline: applications analytiques
William G. Tong and Edward S. Yeung	659	Stable-isotope ratio analysis based on atomic hyperfine structure and optogalvanic spectroscopy

- S. Koch, G. Ackermann und
H. Mosler 667 Untersuchungen zur Anwendung ternärer Komplexe in der Photometrie—
III. Die Bestimmung des Titanium(IV) mit Brompyrogallolrot in Gegen-
wart von Nitritotriessigsäure bzw. Ethylenediamintetraessigsäure
- A. Ríos, M. D. Luque de Castro
and M. Valcárcel 673 Spectrophotometric determination of cyanide by unsegmented flow
methods
- Keijo Haapakka and
Roger Stephens 679 Aerosol collection and RF plasma volatilization on a tungsten wire
electrode
- Salvador Alegret,
Maria-Teresa Escalas and
Jacob A. Marinsky 683 Gel speciation studies—II. An extension of earlier studies of the pro-
tonation equilibria of cross-linked carboxymethyl-dextran
- Jouko J. Kankare and
Roger Stephens 689 Shot-noise limit for optical polarimeters
- P. Kiekens, E. Temmerman
and F. Verbeek 693 Voltammetric study of the redox behaviour of the Hg(II)/Hg(I)/Hg system
at a rotating metal-ring/glassy-carbon disc electrode
- Joseph Wang and Den-bai Luo 703 Effect of surface-active compounds on voltammetric stripping analysis at
the mercury film electrode
- Lauri H. J. Lajunen,
Timo Merkkiniemi
and Hannu Häyrynen 709 Influence of volatile hydride-forming elements on antimony determination
by atomic-absorption spectrometry with hydride-generation
- Short Communications*
- Ninus Simonzadeh and
Bruno Jaselskis 715 Reaction of iron(III) with Tiron in the presence of ferrozine, and
determination of Tiron
- Ram Parkash, Kuldip Singh,
Jitendra Pal Kaur and
R. L. Singhal 717 Titrimetric determination of vanadium(IV) with DCTA
- Taitiro Fujinaga and
Takashi Kimoto 720 The polished precipitate electrode: a new voltammetric method with the
solid electrode
- D. Ph. Zollinger, M. Bos,
A. M. W. van Veen-Blaauw and
W. E. van der Linden 723 Polarographic determination of malononitrile
- Analytical Data*
- N. A. Ulakhovich, H. C. Budnikov,
T. S. Gorbunova and A. P. Sturis 727 The stability of metal complexes with 8-mercaptoquinoline and alkyl-
substituted 8-mercaptoquinolines in dimethylformamide
- J. E. Kountourellis,
N. Papadopoulos and
A. Raptouli 730 Determination of thermodynamic ionization constants for eight medicinal
benzylimidazolines
- J. Kragten and
L. G. Decnop-Weever 731 Hydroxide complexes of lanthanides—VII. Neodymium(III) in
perchlorate medium
- Zs. Wittman 734 Dissociation constants of some organic acids
- J. Yperman, J. Mullens,
J.-P. François and L. C. Van Poucke 735 Potentiometric investigation of the stability of silver(I) complexes of some
N-methyl substituted 4-H-diethylenetriamines in aqueous solution
- Annotations*
- J. M. Hayes and G. J. Small 741 Comment on laser-excited fluorescence line-narrowing: an analytical study
- Erik Sylvest Johansen and
Ole Jøns 743 Testing the adequacy of equilibrium models for complex formation.
Complexation between molybdate and oxalate revisited
- Preliminary Communication*
- Kenichiro Nakashima,
Shin'ichi Nakatsuji,
Shuzo Akiyama, Isamu Tanigawa,
Takahiro Kaneda and Soichi Misumi 749 A sensitive method for the fluorometric determination of lithium with a
"crowned" benzothiazolylphenol
- Letter to the Editor*
- J. D. Winefordner 753 Comment on "Laser-excited fluorescence line-narrowing: an analytical
study"

<i>Papers Received</i>	i
<i>Notes for Authors</i>	iii
<i>Notices</i>	v
<i>Questionnaire</i>	vii

OCTOBER (A)

M. Grote, U. Hüppe and A. Ketrup	755	Solvent extraction of noble metals by formazans—I. Comparative study on the extractability of Pt(IV), Pd(II) and Ag(I) by formazans combined with a liquid anion-exchanger
A. D. Pickard and E. R. Clark	763	The determination of traces of formaldehyde
T. K. Seshagiri, Y. Babu, M. L. Jayanth Kumar, A. G. I. Dalvi, M. D. Sastry and B. D. Joshi	773	Application of ICAP–AES for the determination of Dy, Eu, Gd, Sm and Th in uranium after chemical separation
Heather Jurgensen and J. D. Winefordner	777	Use of active nitrogen in analytical chemiluminescence spectrometry
S. Rubio, A. Gómez-Hens and M. Valcárcel	783	Kinetic fluorimetric determination of cyanide by means of its catalytic effect on the aerial oxidation of pyridoxal-5-phosphate oxalyldihydrazone
Sorin Kihara and Zenko Yoshida	789	Voltammetric interpretation of the potential at an ion-selective electrode, based on current-scan polarograms observed at the aqueous/organic solution interface
M. de la Guardia and M. T. Vidal	799	The use of emulsions in the preparation of samples and standards for analysis by atomic-absorption spectroscopy. Determination of Cu and Fe in MIBK extracts of their APDC complexes
Tomitsugu Taketatsu	805	Spectrophotometric study of uranium(VI) chelate formation with β -diketones and tributyl phosphate in aqueous nona(oxyethylene) dodecyl ether solution
Norton Y. Chu and Jerry Feldstein	809	Radiochemical determination of technetium-99
S. J. Al-Bazi and A. Chow	815	Platinum metals—solution chemistry and separation methods (ion-exchange and solvent extraction)
<i>Short Communications</i>		
Shi-Fu Zou and Wei-An Liang	837	Determination of the stability constant of the ternary complex formed in the copper–bipyridyl–Eriochrome Cyanine R system, by an isosbestic point–spectrophotometric method
Satoru Sakuraba	840	Spectrophotometric determination of zinc with phenylfluorone in the presence of hexadecylpyridinium bromide and pyridine
Reza Arshady and Ivar Ugi	842	Determination of isocyanato groups on polymer supports by bromination
Li Shi-yu and Gao Wei-ping	844	Microdetermination of iron in water by ion-exchanger colorimetry with ferrozine
B. K. Balaji, A. Premadas and G. V. Ramanaiah	846	Estimation of uranium in columbite–tantallite samples: a method for sample solution preparation for fluorimetric estimation
C. L. Sethi, Ashok Kumar, M. Satake and B. K. Puri	848	Spectrophotometric determination of tellurium after adsorption of its morpholine-4-carbodithioate on microcrystalline naphthalene

<i>Papers Received</i>	i
<i>Publications Received</i>	iii
<i>Questionnaire</i>	v

ANALYTICAL METHODS IN CLINICAL CHEMISTRY

- | | |
|--|---|
| L. J. Kricka | V Foreword |
| Robert Rej, Richard W. Jenny
and Jean-Pierre Breaudiere | 851 Quality control in clinical chemistry: characterization of reference materials |
| Adam Zipp and W. E. Hornby | 863 Solid-phase chemistry: its principles and applications in clinical analysis |
| Clifford Riley, Bernard F. Rocks
and Roy A. Sherwood | 879 Flow-injection analysis in clinical chemistry |
| J. A. P. Earle, N. V. McFerran
and G. B. Wisdom | 889 Enzyme-linked immunosorbent assay (ELISA) of antibodies to eight common neurotropic viruses |
| A. Roda, S. Girotti, S. Lodi
and S. Preti | 895 Development of a sensitive enzyme immunoassay for plasma and salivary steroids |
| M. Pazzagli, G. Messeri, R. Salerno,
A. L. Caldini, A. Tommasi,
A. Magini and M. Serio | 901 Luminescent immunoassay (LIA) methods for steroid hormones |
| Timo Lövgren, Ilkka Hemmilä,
Kim Pettersson, Jarkko U. Eskola
and Eric Bertoft | 909 Determination of hormones by time-resolved fluoroimmunoassay |
| Torbjörn G. I. Ling and Bo Mattiasson | 917 Immunoassays in aqueous two-phase systems |
| K. Spencer | 923 Development of a light-scattering immunoassay for thyroxine-binding prealbumin in plasma or serum |
| Richard A. Yost, Robert J. Perchalski,
Harry O. Brotherton,
Jodie V. Johnson
and Mary Beth Budd | 929 Pharmaceutical and clinical analysis by tandem mass spectrometry |
| M. M. Galteau and G. Siest | 937 Perturbation of laboratory test results by analytical interferences and drug effects |

NOVEMBER

- | | |
|---|--|
| V. K. Bhargava, M. S. Oak,
A. R. Joshi and V. B. Sagar | 943 Determination of micro amounts of uranium by a molybdenum blue method |
| Milan Meloun and Josef Čermák | 947 Multiparametric curve fitting—V. The general program ABLET, a system for regression analysis in studies of solution equilibria |
| Bruce R. Smith, Carole Youngberg,
Dennis Finton, David Willey,
Theodore R. Williams and
Janet B. Van Doren | 955 A new procedure for separation of the enamel and dentin of human teeth |
| Z. Marczenko, S. Kuś and
M. Mojski | 959 Extractive separation and spectrophotometric determination of palladium and platinum with dithizone in the presence of stannous chloride |
| R. F. Hamon and A. Chow | 963 Extraction of cobalt from thiocyanate solutions with polyurethane foam |
| Wenche Langseth | 975 Determination of diphenyltin and dialkyltin homologues by HPLC with morin in the eluent |
| Lilly Gustafsson | 979 Interferences in the determination of total nitrogen in natural waters by photo-oxidation to nitrate-nitrite mixture |
| Ferenc F. Gaál and
Biljana F. Abramović | 987 Contributions to the theory of catalytic titration—I. Complexometric catalytic titrations |

Elsie M. Donaldson	997	Spectrophotometric determination of germanium in ores, concentrates, zinc-processing products and related materials with phenylfluorone and cetyltrimethylammonium bromide after separation by iron collection and heptane extraction of germanium tetrachloride
<i>Short Communications</i>		
R. E. Farrell and A. D. Scott	1005	Construction and evaluation of a potassium-selective tube-mounted membrane electrode
Tohru Nagahiro, Bal Krishan Puri, Mohan Katyal and Masatada Satake	1008	Determination of nickel by flame atomic-absorption spectrophotometry after separation by adsorption of its nioxime complex on microcrystalline naphthalene
K. W. Michael Siu and Shier S. Berman	1010	Comparison of two digestion methods used in the determination of selenium in marine biological tissues by gas chromatography with electron-capture detection
Pratima Verma and V. K. Gupta	1013	A sensitive spectrophotometric method for the determination of hydroxylamine by use of <i>p</i> -nitroaniline and <i>N</i> -(1-naphthyl)ethylenediamine
I. M. Jalal and S. I. Sa'sa'	1015	Simultaneous determination of dextropropoxyphene napsylate, caffeine, aspirin and salicylic acid in pharmaceutical preparations by reversed-phase HPLC
K. K. Tiwari and R. M. Verma	1018	Titrimetric microdetermination of silver, lead and cadmium with thio-glycollic acid and of mercury(II) with 2-mercapto-propanoic acid
S. K. Srivastava and C. K. Jain	1021	Studies on the application of Fe-Zr mixed hydrous oxide membranes in ion-selective potentiometry
Wei Fu-sheng, Teng En-jiang and Rui Kui-sheng	1024	Dual-wavelength spectrophotometric determination of trace sulphide in domestic water through its ligand-exchange reaction with silver-Cadion 2B-Triton X-100
J. L. Burguera and M. Burguera	1027	Determination of quinones by a chemiluminescence reaction in solution
<i>Analytical Data</i>		
Kousaburo Ohashi, Keiko Shikina, Hiroyuki Nagatsu, Izumi Ito and Katsumi Yamamoto	1031	Solvent extraction of the ion-pairs of chromium(VI) and molybdenum(VI) with trioctylmethylammonium chloride and benzyldimethylcetylammmonium chloride
David A. Wynn, Marie M. Roth and Bruce D. Pollard	1036	The solubility of alkali-metal fluorides in non-aqueous solvents with and without crown ethers, as determined by flame emission spectrometry
Ru-Qin Yu, Zhi-Hua Zhang and Ya-Wen Li	1041	2-(8-Quinolylazo)-7-phenylazochromotropic acid as an analytical reagent
<i>Papers Received</i>	i	
<i>Publications Received</i>	iii	
<i>Questionnaire</i>	v	

DECEMBER

J. G. Sen Gupta	1045	Determination of scandium, yttrium and lanthanides in silicate rocks and four new Canadian iron-formation reference materials by flame atomic-absorption spectrometry with microsample injection
J. G. Sen Gupta	1053	Determination of cerium in silicate rocks by electrothermal atomization in a furnace lined with tantalum foil. Application to 19 international geological reference materials
Jean-Claude Fischer, René Nganou et Michel Wartel	1057	Etude de la capacité complexante des eaux de l'estuaire et de la baie de Seine
W. R. Kelly and P. J. Paulsen	1063	Precise and accurate determination of high concentrations of sulphur by isotope-dilution thermal-ionization mass-spectrometry

Constant M. G. van den Berg	1069	Direct determination of sub-nanomolar levels of zinc in sea-water by cathodic stripping voltammetry
M. Gallego, M. Silva and M. Valcárcel	1075	1,2- and 1,3-cyclohexanedione bis(2-hydroxybenzoylhydrazone)s as analytical reagents
Atsushi Sugii, Naotake Ogawa and Yoshihisa Hagiwara	1079	Synthesis and properties of a chelating resin containing triazoethiol groups
Milan Meloun and Milan Javůrek	1083	Multiparametric curve fitting—VI. MRFIT and MRLET, computer programs for estimation of the stability constant of the predominant M_pL_q complex and the ligand purity by analysis of photometric titration curves
Sam Ben-Yaakov and Hugo Guterman	1095	A new experimental technique for validating exchange models of carbon dioxide between the atmosphere and sea-water
H. Wagler und H. Koch	1101	Beiträge zur Frage der Existenz eines Tautomerengleichgewichtes in Lösungen von Dithizon in organischen Solvenzien—I. Die Korrelation Zwischen den Lösungsmittelabhängigen Reaktionsunterschieden in den Systemen Palladium/Dithizon und Kupfer/Dithizon und den Lösungsmittelabhängigen Unterschieden der Spektren der Dithizonlösungen
<i>Short Communications</i>		
M. M. Charyulu, V. K. Rao and P. R. Natarajan	1109	Potentiometric determination of plutonium by sodium bismuthate oxidation
Tohru Nagahiro, Katsuya Uesugi, M. C. Mehra and Masatada Satake	1112	Spectrophotometric determination of iron(II) after separation by adsorption of its complex with 3-(4-phenyl-2-pyridyl)-5,6-diphenyl-1,2,4-triazine and tetraphenylborate on microcrystalline naphthalene
Helena Górecka and Henryk Górecki	1115	Determination of uranium in phosphogypsum
Niels Pind	1118	Standard-addition procedure for the determination of traces of lead in solid samples by X-ray fluorescence spectrometry
<i>Analytical Data</i>		
Ru-Qin Yu, Zheng-Qi Zhang and Zhi-Hua Zhang	1121	Pyrocatecholsulphonphthalein complexan as an analytical reagent
D. Fompeydie et P. Levillain	1125	Etude de la pureté des échantillons commerciaux d'éosine
Emiko Ohyoshi	1129	Spectrophotometric determination of formation constants of 1:1 complexes of lanthanides with 4-(2-pyridylazo)resorcinol (PAR)
C. Loos-Neskovic, M. Fedoroff, E. Garnier and P. Gravereau	1133	Zinc and nickel ferrocyanides: preparation, composition and structure
<i>Annotations</i>		
B. P. Bubnis and G. E. Pacey	1149	Alkali-metal ion complexation with lariat ethers possessing a chromogenic group
Philip Hannaker and Hou Qing-Lie	1153	Dissolution of geological material with orthophosphoric acid for major-element determination by flame atomic-absorption spectroscopy and inductively-coupled plasma atomic-emission spectroscopy
<i>Papers Received</i>	i	
<i>Questionnaire</i>	iii	

ERRATUM

In the letter to the editor, on pages 233 and 234 in the March 1984 issue of *Talanta*, an error in interpretation led to an error in the letter. The second paragraph should read:

“Linear equations in four terms and three unknowns³ can be used to evaluate the pK_a of a monoprotic acid:

$$\frac{[H]_i \underline{A}_i}{K_a} - \frac{[H]_i A_{HR}}{K_a} - \underline{A}_R = -\underline{A}_i$$

in which \underline{A}_i is the absorbance of a solution containing a mixture of HR and R, A_{HR} and A_R are the unknown absorbances for pure HR and R respectively at a concentration equal to $[HR]_i + [R]_i$ for the solution measured, and charges are omitted for simplicity . . .”

In equations (2) and (3) and the line above them, ϵ_{HR} and ϵ_R should be replaced by \underline{A}_{HR} and \underline{A}_R respectively. In reference 3, Rossenblatt should be Rosenblatt.

NOTICE

1985 PITTSBURGH CONFERENCE CALL FOR PAPERS

The Pittsburgh Conference takes great pride in providing a scientific forum for authors from diverse backgrounds—from the Nobel Laureate to the novice. We invite you to join our distinguished array of invited speakers in presenting papers at the 1985 Pittsburgh Conference and Exposition.

Papers may be contributed in all areas of the disciplines of Analytical Chemistry and Applied Spectroscopy.

Those authors wishing to present papers at the 1985 Pittsburgh Conference should submit four (4) copies of a 300-word abstract to:

Mrs. Linda Briggs, Program Secretary
Pittsburgh Conference, Department J-029
437 Donald Road
Pittsburgh, PA 15235, U.S.A.

The abstract should be complete and show:

- a. The title of the paper.
- b. The name of the author(s), the organization(s) in whose laboratory the work was done, and the address(es). Provide the **COMPLETE** mailing address of each author, including department and any other mailing code.
- c. The name of the author who will present the paper must be underlined.
- d. Sign and date the abstract page in verification that the paper and all material therein has not been published or previously presented.

The final date for receipt of abstracts is 15 August 1984. Abstracts received after this date cannot be guaranteed consideration for inclusion in the 1985 Technical Program.

Exposition of modern laboratory equipment

In 1984 the Modern Laboratory Equipment presented at the Conference totalled 636 exhibitors occupying 1607 booths and seminar rooms in which was displayed the latest equipment available in the areas of Analytical Chemistry and Spectroscopy. Anyone desiring to reserve exhibit space or to obtain additional information regarding the 1985 Exposition should contact:

Mr. Peter Castle, Exposition Chairman
Pittsburgh Conference
437 Donald Road
Pittsburgh, PA 15235, U.S.A.

PUBLICATIONS RECEIVED

Atomic Absorption Spectrometry: JOHN E. CANTLE (ed.), Elsevier, Amsterdam, 1982. Pp. xvi + 448 \$97.75, Dfl. 210.

It is always interesting, when looking at a new text on atomic-absorption spectroscopy, to see what the author(s) feel they have to offer that makes their particular text different from the many already published. In this instance the book is really a collection of specialized reviews, drawing on the expertise of more than twenty contributors. The price paid is that there are substantial differences in quality and style, and inconsistencies in choice of units, from section to section. This is most noticeable in the figures, which often look distinctly "second hand". Moreover there is little cross-referencing. However these are minor criticisms, and the coverage of the selected topics in the applications section is generally good.

The first chapter in the book, one on basic principles, is disappointing. In several places a novice in the field could acquire ideas which are basically wrong. It might perhaps have been improved by stricter editing. Chapters 2 and 3, on instrumentation and practical techniques, are more helpful, but unfortunately devoid of references to the literature. Chapter 4, the applications chapter, is undoubtedly the most useful. The areas covered include water and effluents, marine samples, airborne particulates, foodstuffs, ferrous and non-ferrous metallurgy, geochemistry, petroleum products, glasses and ceramics, medicine, forensic science and miscellaneous chemicals. These sections contain much useful material, and generally, with two or three exceptions, include extensive references, at least to the pre-1978 literature. The index is, to put it politely, pathetically inadequate, and the reader will find the detailed contents pages far more useful.

If the book happens to cover your particular field of specialization in its applications section, then it is well worth reading. However, its future probably depends on purchase by libraries rather than by individual users.

MALCOLM S. CRESSER

An Introduction to Chemical Equilibrium and Kinetics: LOUIS MEITES, Pergamon Press, Oxford, 1981. Pp. xii + 549. Hard cover \$75.00, £31.00; Flexicover \$19.95, £8.95.

This book is the first of the Pergamon Series in Analytical Chemistry and is intended for first and second year students. It deals with the equilibria and rates of chemical reactions, along with the various methods for their study. It is beautifully organized and written with great clarity. Each of the fifteen chapters starts with a brief introduction, and every subsection begins with a summary of the material discussed. All chapters contain a number of worked mathematical problems, followed by some for the reader to solve.

The first chapter tells what the book is about, and the next two introduce chemical thermodynamics, equilibrium and kinetics in a simple but comprehensive manner. The next five chapters deal with different types of chemical equilibria and the study of reaction rates. These chapters are well written but could have been further improved by inclusion of more graphical representations. Chapter 9 discusses gravimetric and titrimetric analysis, right from sample preparation to the stoichiometric calculation of the results, and Chapter 10 deals with the mechanism of precipitation and co-precipitation, and also the various factors that affect the physical properties and the rates of formation and growth of precipitates. The next chapter deals with titration curves and contains a number of graphical representations of different chemical equilibria, and this makes the subject easier to understand.

Chapter 12 is on errors in scientific measurements. The author is successful in presenting the basic statistics in a simple way, a task which is often difficult to achieve. The next chapter, on activity and activity coefficients, is the best written in the book. It deals with the effect of ionic strength on activity coefficients and with the Debye-Hückel limiting law and its various extended forms.

The last two chapters deal with the most common techniques for studying chemical equilibria and reaction rates, viz. potentiometry and spectrometry, and convey the essentials necessary for a working knowledge of both techniques. In the chapter on potentiometry, however, the last of a detailed section on use of ion-selective electrodes is a notable omission, since these have become essential tools for the chemist working in the field of potentiometry.

Overall, in spite of a few printing errors, the book is well illustrated and informative. It successfully serves its purpose of introduction of chemical equilibria and kinetics to a beginner in analytical chemistry. The standard of printing and binding is good, and the price of the flexicover edition well within the reach of students.

MAHMOUD I. FAROOQI

Quantitative Analysis of Steroids: S. GÖRÖG, Elsevier, Amsterdam, 1983. Pp. 440. US \$86.50 (U.S.A. and Canada); Dfl. 225.00 (Rest of World).

Görög's latest book provides a comprehensive and readable account of the quantitative aspects of the analytical methods currently used in the steroid field. All the major classes of steroids are covered in crisp and critical fashion, from the sex hormones and their metabolites (including conjugates), through corticoids, cholesterol and other sterols, the vitamin D group, bile acids, cardiac glycosides, sapogenins and ecdysones, to steroid alkaloids. Techniques covered range from the spectroscopic methods (ultraviolet, infrared, nmr, etc.) through chromatographic methods, particularly gas chromatography and high-pressure thin-layer liquid chromatography, to biochemical methods such as radioimmunoassay and enzyme immunoassay. Only the very recent chemiluminescence methods are omitted. In the discussion of gas chromatography the superior resolving power of capillary columns over packed columns for the profiling of complex mixtures is clear, but clean-cut comparisons for a given sample mixture are lacking. Sample preparation procedures for analysis of steroids from various types of biological fluids are covered in detail.

Thankfully, the book does not follow the recent sinister trend for review books to have only an author index (or at most an author index and a token subject index)—instead there is a most useful index of the substances dealt with.

ALAN B. TURNER

EDITORIAL

“THE EDITOR REGRETS...”

It is always a difficult and unpleasant task to reject a paper submitted for publication, and it is not easy to avoid offending the author(s). Nevertheless, standards must be maintained, for the sake of the author as much as the reader and the reputation of the journal, and papers that fall into the category of “futile” (see the Editorial in the February 1979 issue of *Talanta*) or are incorrect in their chemistry, or unacceptable for other reasons, must be firmly but politely rejected. Judging by the Editorial in the January 1984 issue of *Analytical Chemistry*, rejection can produce rather startling reactions from authors, presumably those most urgently in need of publications to support claims for tenure or promotion. Such authors might well reflect that besides the “publish or perish” situation, there is also “publish *and* perish” if the papers are of inadequate standard. Our policy in *Talanta* has always been to explain to the author exactly why his paper is not being accepted, and often to suggest ways in which the work might be improved. Sometimes we have gone so far as to edit the paper in order to help him if he decides to try his luck elsewhere. Some papers, however, are so poor that *no* journal can be found that will accept them. Very occasionally an author will have had a paper rejected by so many journals that he has forgotten which ones he has tried, and sends it back (unaltered!) to the journal he tried first.

We are glad to say that the problem of writing the rejection letter has now been solved, and by courtesy of *World Medicine* (where we found the solution on p. 45 of the issue for 21 January 1984) we can share the solution with our readers. The letter was said to be written by the editor of a Chinese medical journal, and reads as follows.

“Dear Dr. —,

We have read your manuscript with boundless delight. If we were to publish your paper it would be impossible for us to publish any work of lower standard. And as it is unthinkable that, within the next thousand years, we shall see its equal we are, to our great regret, compelled to return your divine composition, and to beg you a thousand times to overlook our short sight and timidity.”

Now who could want a better letter than that (or even write one)?

PUBLICATIONS RECEIVED

Soil Analysis—Instrumental Techniques and Related Procedures: K. A. SMITH (ed.), Marcel Dekker, New York, 1983. Pages 562 + xii. SFr. 198.

This text goes a long way towards filling a conspicuous gap in the literature of analytical chemistry, in providing a useful and comprehensive account of most of the major instrumental techniques that find widespread use in soil science. Eleven chapters from 16 established authorities cover atomic-absorption and flame emission spectroscopy, ion-selective electrodes, automation, XRF, isotope techniques (including ^{15}N determination), neutron-activation analysis, gas chromatography, and high-pressure liquid chromatography.

A consistent style has been maintained throughout the book. Each chapter covers fundamental principles, instrumentation and practical aspects of analysis, with many references to the original literature up to 1978. Unfortunately, in most of the contributions very little more recent work has been included, creating the impression that the book was a long time in the writing, with sometimes reluctance to update contributions.

Nevertheless the end-product has benefited from a wealth of first-hand experience, and provides excellent coverage of the topics selected. The material is presented at a level which makes it useful to the complete newcomer to a technique, or to experienced users who simply require more background information. The book will be useful both to soil scientists needing to use analytical techniques and to analysts whose work includes soil samples.

The title of the book is rather more all-embracing than the contents, which are primarily concerned with elemental analysis. Instrumental methods of mineralogical analysis are therefore excluded. This must have been necessary to keep length and costs at a reasonable level. It would, however, still have been possible to write another volume of the same length covering topics which are omitted, including for example conductivity measurement and other electrochemical techniques, ion analysers, autotitrators, sub-sampling techniques, etc. Generally the book can be strongly recommended.

MALCOLM S. CRESSER

Recent Advances in Capillary Gas Chromatography, Volumes 1–3: W. BERTSCH, W. G. JENKINS and R. E. KAISER (eds). Hüthig Verlag, Heidelberg, 1981–2. Vol. 1, pp. XII + 592, DM 75.00, \$38.00; Vol. 2, pp. XII + 557, DM 75.00, \$38.00; Vol. 3, pp. XII + 590, DM 75.00, \$38.00.

These volumes are published as a trilogy reflecting the worldwide growth of the development of modern capillary chromatography and its application to a very wide range of chemical problems. It is a particularly unusual series in that it republishes papers already in print in the *Journal of High Resolution Chromatography and Chromatographic Communications*. However, rather than giving a wasteful proliferation of mediocre information the editors have wisely and carefully selected papers which reflect the major innovations made in capillary gas chromatography during the years when this technique took a quantum step forward. This selection and exclusive focus on capillary chromatography will make this series invaluable to the legion of modern chromatographers. Such a dedicated series is very timely and should do much to dispel any lingering concern, not in academia, but in industrial analytical services, about the reliability and accuracy of analyses by capillary gas chromatography.

The three volumes have a similar format of subject areas, each volume covering the development of the subject chronologically. There are eight chapters in each volume and each begins with a series of reviews. The review subjects covered are: (Vol. I) Techniques in Two Dimensional High Resolution Gas Chromatography (HRGC); Performance of Gas Chromatograph (GC) Detectors with Glass Capillary Columns; Twenty years of Glass Capillary Columns; Practical Capillary GC—a Systematic Approach; (Vol. II) Evolution and Application of the Fused Silica Column; (Vol. III) Glass Surfaces as Support Phases in GC; Analysis of Drugs and Related Compounds; Surface Modification in Glass Capillary GC.

There are 4 papers on Theoretical Considerations, 39 covering the Preparation, Deactivation and Repair of Columns, and 10 dealing with Testing, Selection and Efficiency of Columns. The section covering Column Installation, Conversion of Apparatus for Capillary GC has 13 papers, Sampling; Special Conditions and Techniques of Sampling has 18, Applications has 48 and the final section on Detection Conditions: Separation and Detection Optimization and Data Handling has 8.

The series spans some 1700 pages and encompasses the work of 240 authors, who collectively cover a number of major themes which encourage the reader to adopt a lateral approach to each subject. There is the continuing search for the utopian column having maximum activity and efficiency for every conceivable sample type. One fruit of this apparently endless search has been the successful emergence of the polyimide-coated fused silica column, which now has cross-linked (chemically bonded) phases to enhance stability and prevent liquid phase from being stripped by the solvent during injection. The development, rigorous testing and applications of these columns have been fully documented and comparisons made with their glass predecessors. Considerable attention has also been given to methods of sample introduction, with a number of designs for on-column injection highlighting the need for a "cold" injection, and expansion of the various hypotheses advanced to explain cold-trapping and solvent effects. There are a number of sophisticated separation procedures, involving column switching, two-dimensional chromatography and multidetection techniques, some of which are no more than an academic exercise, while others have already found some practical everyday use.

Volume 3 contains the cumulative author and subject index for the series, while the first two books have just their own indexes. Such a trilogy will be ideal for scientists new to the field. The set should become well thumbed handbooks for the practising chromatographer and an excellent review source for future authors developing these subjects.

D. E. WELLS

PUBLICATIONS RECEIVED

Computers in Analytical Chemistry: PHILIP BARKER, Pergamon Press, Oxford, 1983. Pages xvi + 472. £37.50, \$75.00.

Although some of its chapters contain well-presented useful information, I feel that this book as an entity is not totally satisfactory, and that a more appropriate title might have been chosen, since most of the emphasis of the book is on the use of computers in association with analytical instrumentation. The long-established use of computers for calculations and predictions of classical analytical equilibria is scarcely mentioned: the review by Childs *et al.* (*Talanta*, 1969, 16, 629, 1119), the program HALTAFALL (*Talanta*, 1967, 14, 1261) and the book by Dyrssen, Jagner and Wenglein (*Computer Calculation of Ionic Equilibria and Titration Procedures*, Almqvist and Wiksell, Stockholm, 1968) are not referred to at all. It is rather unusual to make this criticism, but I think that the author has placed far too much emphasis on very recent literature, to the detriment of earlier material.

As an analytical chemist, I found the first three chapters, What is Analysis?, Analytical techniques, and Instrumentation, almost totally superfluous. They made me wonder just who the author wrote the book for. Chapter 4 gives a good brief description of computers and their function, but I felt that it was rather too brief for the real novice. I also felt that the author had been rather selective in his choice of microprocessors and microcomputers for detailed consideration. For example, he does not mention the Apple II computer, which has found very wide application.

Chapters 5-8, on Data Collection, Interfaces and Principles of Interfacing, Communication Channels, and Automation in the Laboratory, I found much more satisfactory—the real meat of the book. The chapter on interfacing gives a great deal of detailed information, and is likely to be the most useful one to an analytical chemist who is actually trying to hitch up his instruments to computers.

Of the remaining chapters, Chapter 9 gives a rather superficial picture of Data-Processing Methods, and Chapter 10 gives a useful introduction to Data Bases and Data Centres. Chapter 11, Information Services, could well have been omitted, since the topic has been discussed in detail elsewhere (*e.g.*, by Ash and Hyde, *Chemical Information Systems*, Horwood, Chichester, 1974) and is one with which all chemists should be concerned, not just analytical chemists. The final chapter, on Computer Networks, is probably timely, but much of the detailed information would be of more use to computer experts than to the average working analytical chemist.

MARY MASSON

Metal Vapours in Flames: C. TH. J. ALKEMADE, T.J. HOLLANDER, W. SNELLEMAN and P. J. TH. ZEEGERS. Pergamon Press, Oxford, 1982. Pages xxii + 1033. £50.00, \$95.00.

The book is devoted to all aspects of metal-vapour behaviour in combustion flames. It contains a great deal of material of interest for those who work in spectrochemical analysis, plasma physics and high-temperature chemistry of metal compounds. The volume is very helpful as a summary of the multitude of works scattered throughout the literature on emission, absorption and fluorescence spectroscopy. It was a titanic work for the authors to systematize so huge and so varied an amount of material. The tremendous merit of Professor Alkemade is that he managed to organize for the task a group of experts who actively research in this field.

It must be mentioned that the professional interests of the authors in emission and fluorescence spectroscopy manifest themselves in the scope of the topics covered. As a result the authors pay relatively small attention to the chemistry of the carbon-rich flames, which are of little interest for emission and fluorescence, and the two-line atomic-absorption method of temperature measurement is altogether out of the scope of the book. At the same time, the authors' own rich experience has made it possible to select the most reliable and proved data for the book.

This has resulted in a volume of more than 1000 pages. The literature cited comprises about 2000 works. Chapters I and II deal with fundamentals of the structure and interaction of atoms and molecules, and general experimental methods which give rapid information about the material in question. The authors have avoided excessive use of mathematical expressions, which is why the book is of great value for both the expert and the beginner in the field. The topics are covered very thoroughly and the practical experience of the authors is evident throughout the volume. The system of cross-references throughout the text and the detailed subject index (including about 3500 items) make the book the real encyclopaedia on laboratory flames.

Undoubtedly, the book should be a part of the personal libraries of theoreticians and experimentalists interested in the fundamentals and the analytical application of flame spectroscopy.

B. V. L'VOV

TALANTA ADVISORY BOARD

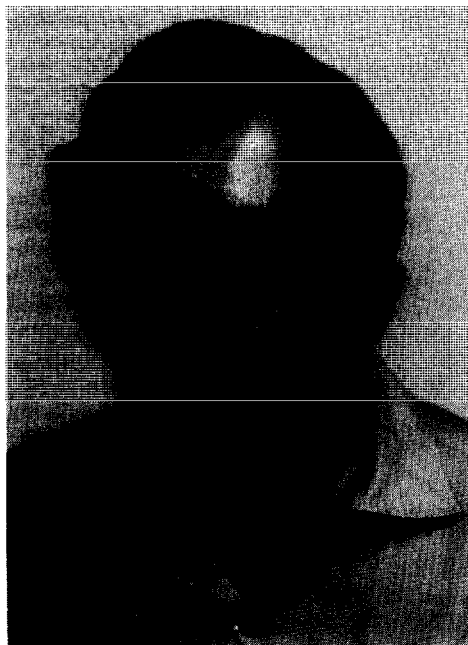
The Editorial Board and the Publisher of *Talanta* take pleasure in welcoming the following new member of the Advisory Board of the journal.

KAREL ŠTULÍK

They also wish to record their sincere thanks for the help given by

R. PŘIBIL H. SANKE GOWDA

who retire from the Advisory Board. They are particularly grateful to Dr. Přibil, who has been associated with *Talanta* from its inception.



Dr. Štulík was born in Kolín, Czechoslovakia in 1941, and graduated in chemistry in 1963 from the Faculty of Technical and Nuclear Physics, at the Czech Technical University in Prague. His postgraduate studies in electroanalytical chemistry at the J. Heyrovský Polarographic Institute, Czechoslovak Academy of Sciences, Prague, from 1964 to 1968 led to his Ph.D. degree in 1967. Since then he has been a research worker and lecturer at the Department of Analytical Chemistry, Charles University, Prague, except for the year 1968–1969, which he spent as assistant lecturer in the Department of Pure and Applied Chemistry, University of Strathclyde, Glasgow, Scotland. His research interests include polarography, electrochemical stripping analysis, ion-selective electrodes, and combination of electrochemistry with separation techniques, chiefly HPLC. He has published about 80 research and review papers and several university texts. He is co-author of "Electrochemical Stripping Analysis" and "Analysis with Ion-Selective Electrodes", published by Ellis Horwood in 1968 and 1969; the former has been translated into Russian and published by Mir, Moscow (in 1980). He is co-author with Professor J. Koryta, of "Ion-Selective Electrodes", to be published by Cambridge University Press. He is a member of the Czechoslovak Chemical Society.

ERRATA

In the paper by P. A. Michalik and R. Stephens, *Talanta*, 1983, **30**, 819, the symbol ∇ should be replaced by \triangle in the captions of Figs 2, 3 and 5.

In the paper by D. F. Grant and D. Eastwood, *Talanta*, 1983, **30**, 825, the following corrections should be made.

In Fig. 6 the y -axis should be labelled "Absorbance".

In Fig. 7 the labels "1.0-2.0(O.D.)" and "0-1.0(O.D.)" in the middle of the scales on the left- and right-hand y -axes should be deleted, and so should the second sentence in the caption.

PUBLICATIONS RECEIVED

Liquid Chromatography in Environmental Analysis: Edited by JAMES F. LAWRENCE. Humana Press, Clifton, New Jersey, 1984. Pages xiv + 382. \$55 (\$65 outside USA).

Success in chromatography comes with experience: acquiring the instrument and learning the theory are just the first steps. It can help to work alongside an old hand and be guided round some of the pitfalls, but not every beginner is so fortunate. So if you are thinking of setting up for HPLC this book might be the next best thing. Individual chapters are written by specialists, e.g., on Polycyclic aromatics, Pesticide residues, and Surfactants. Probably fewer people will intend to determine trace metals by HPLC, but the review here is certainly welcome. The chapter on ion chromatography should please many readers, and remind them that there is a choice of columns for difficult combinations of anions, as in sea-water or acid extracts. Other chapters balance the picture by covering Quality assurance programmes, Injection and switching, and HPLC as a clean-up technique, but basic theory and instrumentation are not discussed. I was surprised to find so little attention given to HPLC/MS considering that this combination is now commercially available. However, what is covered is done in a readable text with many references from the literature up to 1981, and frequent inclusion of experimental details: recommended.

IAIN L. MARR

Reversed Phase High-Performance Liquid Chromatography: ANTE M. KRSTULOVIC and PHYLLIS R. BROWN. Wiley, New York, 1982. Pages xi + 296. \$27.00.

The choice of title for this book—and therefore the bias of the subject matter—strikes me as slightly odd. But then, just as Molière's character was surprised to find he had been speaking prose all his life, we may need to be reminded that most HPLC users are actually using RPLC. Would it not have been better to include an additional section on columns and another on applications of normal HPLC to complete the picture? But let us look at what is included. I find this a very lucid account of HPLC—a combination of theoretical and practical aspects with much useful information for the newcomer intending to set up for HPLC. On the other hand I wonder why the tabular comparison of detection systems covers only polarographic, conductimetric and fluorimetric devices, so that they are not so easily seen in relation to the very widely used UV and RI systems. And should not there be some mention of element-selective detection by, e.g., plasma spectroscopy, and of diode-array “instant-scan” spectrometers which are now available from several manufacturers? Attention is, however, given to columns, solvents, and the difficulties of characterizing unknown peaks, and a final chapter summarizes a wide range of biochemical applications of RPLC, serving to illustrate the scope and power of the technique. There is much to commend in this book: possibly the omissions are compensated by the smooth continuity of the text resulting from close co-operation between the authors, which has resulted in a readable and useful book.

IAIN L. MARR

Solvation, Ionic and Complex Formation Reactions in Non-Aqueous Solvents: K. BURGER, Elsevier, Amsterdam, 1983. Pages 286. DFR 145; \$61.75

This rather specialized monograph is concerned with properties of solvents and with the various interactions of solvents with various kinds of solutes. Thus, solvent-solute interactions, donor-acceptor interactions, effects of solvents on metal complexes in solution, effects of solvents on kinetics and mechanism of co-ordination reactions, and interactions in solvent mixtures are some of the topics included. A survey of the various theories of such systems is given, but the main emphasis of the book is on experimental methods for study of complex systems and for the characterization of solvents. (Sixteen possible techniques for study of complex systems are discussed.) There is an extensive wide-ranging bibliography.

MARY MASSON

The Practice of Ion Chromatography: F. C. SMITH, JR. and R. C. CHANG, Wiley, New York, 1983. Pages xxiv + 218. £43.95.

This is an outstanding “how-to-do-it” book, written by two very experienced workers in the field. It traces the history of Ion Chromatography from the original Dow patents in 1975, which led to the exploitation by Dionex of suppressor IC, and also the later development of non-suppressor systems. The merits of suppressor and non-suppressor IC are discussed without bias, and the various sorts of instrumentation that can be used are described. The rest of the book deals with practical IC, giving first of all standard conditions for the various variants of the technique, then offering suggestions as to the procedure for finding conditions for some particular problem. There is a useful discussion of chromatogram anomalies, such as the so-called “water dip”. The chapter on applications gives some idea of very wide range of applications of IC that have been developed, and should be of considerable use to the potential IC user (331 references are included).

MARY MASSON

Wilson and Wilson's Comprehensive Analytical Chemistry, Vol. XV: G. SVEHLA (ed.). Methods of Organic Analysis: L. MAZOR, Elsevier, Amsterdam, 1983. Pages xxii + 529. Dfl 325, \$138.25.

As befits a title in “Wilson and Wilson”, this book might well have been entitled “Comprehensive Organic Analysis”, because of the wide scope of the contents. The main chapters cover the topics “Preliminary Tests”, “Qualitative Elemental Analysis”, “Determination of Physical Constants”, “Qualitative Functional Group Analysis”, “Micro Reactions for the

Detection of Certain Important Organic Compounds", "Instrumental Methods in Organic Chemical Analysis", "Quantitative Elemental Analysis", "Quantitative Functional Group Analysis", and finally "Automatic Analysis". The chapter on "Instrumental Methods" is short and gives only a general introduction to the use of these methods. Thus, most of the book is devoted to review, discussion, and detailed descriptions of chemical methods of qualitative and quantitative analysis. It is difficult to say much more about a book so packed-full of useful information, except perhaps to recommend that a copy should be available for use in every organic analytical laboratory. The one disappointing feature is that the only reference I could find after 1976 was a 1979 one to the author's own work.

MARY R. MASSON

PUBLICATIONS RECEIVED

Computer Applications in Chemistry: S. R. HELLER and R. POTENZONE, JR., (eds.), Analytical Chemistry Symposia Series, Vol. 15, Elsevier, Amsterdam, 1983. Pages xii + 394. US\$89.25. Dfl.210.

It is very difficult to give a general review of a book like this, covering as it does such a wide range of topics as Macromolecular Structure Representation, Computer Networks, Computerized Standard Reference Data, Chemical Information Systems, Structure Elucidation, and Computer-Aided Drug Design. The seventeen full papers included were presented at the 6th International Conference on Computers in Chemical Research and Education (ICCCRE), held in Washington, DC, July 1982. Also included are the abstracts of 63 poster papers, and a list of those attending the meeting. The most novel paper included is the one on "The Chemistry in Future Molecular Computers", by F. L. Carter, and this paper is also the one that contains the most "meat". Many of the other papers are very general in content. I was impressed, however, by the introductory paper, on "The Neglected Ingredient in Chemical Computer Systems". In this the author, E. Hyde, discusses the problems met by non-chemists seeking chemical information from chemical computer databases. He suggests that chemists use a sign language and unpronounceable words to maintain a mystique that non-chemists cannot penetrate. He criticizes the *Chemical Abstracts* computer files, in that they are convenient for the indexer but not for the user, be he a chemist or non-chemist, who is interested in relationships between compounds. He points out the futility of the CA Registry Numbers, but then goes on to suggest how improvements might be made. I cannot recommend this volume for purchase by individuals (other than conference participants), but it probably does deserve a place in most chemical libraries.

MARY MASSON

Environmental Chemical Analysis: L. L. MARR and M. S. CRESSER, International Textbook Company, Glasgow, 1983. pp. xii + 258. £21.00.

This book is an effort to compile and present the complex of knowledge on a variety of analytical methods in such a form that it will be useful to students, teachers, analysts and even experts in other fields. It demonstrates a new approach to teaching analytical chemistry and shows how chemical analysis can yield reliable data which are valuable to other scientists. The authors underline the difficulties facing the analyst who deals with environmental chemical analysis and show how he chooses methods and techniques appropriate to the situation. They gave some insight not just into the working tools of the environmental analyst, but also into the types of problems he may be called upon to help in solving. The authors have also tried to indicate why a certain line of approach or choice of methods may be needed for attacking the problem in hand.

The methods developed and the results obtained by analytical chemists are used by many other scientists. This book will give them some background knowledge and appreciation of the subject to avoid possible pitfalls or errors. It will help all readers, both practitioners and customers, to get most out of their analysis by taking time to think, to check and then to analyse.

A. KHALONIN

Practical Absorption Spectrometry: A. KNOWLES and C. BURGESS (eds.), Chapman and Hall, London, 1984. Pp. xxii + 234. £18.00.

The Ultraviolet Spectrometry Group have produced another invaluable volume in their series on Techniques in Visible and Ultraviolet Spectrometry. The book is both a guide to the practice of absorption spectrometry, and a succinct account of the relevant theory. Much of the information provided is not found in standard texts nor in the manufacturers' handbooks, yet it is vital for the user, in order that instruments can be used correctly and to their best advantage. A copy of this book should be in every laboratory that uses absorption spectrometers.

MARY MASSON

Electrochemistry: Principles, Methods and Applications: ALLEN J. BARD, LARRY R. FAULKNER; R. ROSSET and D. BAUER (eds.), Masson, Paris, 1983. pp. XXX + 791. FFfr. 350.

At the present time the importance of electrochemistry in solving various scientific problems and for characteristic chemical systems in research areas is rapidly increasing. The present book, now in French translation, will prove to be very useful for modern education in the field of electroanalytical chemistry. There is a full systematic treatment of both the fundamental theory of electrochemistry and the basic aspects and techniques of up-to-date electroanalytical methods, complete with mathematical interpretations and equations.

The book contains 14 chapters and 3 appendixes. Chapters 1-4 cover the general thermodynamic and kinetic properties of electrode processes. The main attention is focused on the theoretical grounds of electrochemistry, which are useful for mastering various electrochemical methods, in particular the problems of mass transfer at the electrode-electrolyte interfaces and the kinetics of electrochemical reactions at electrode surfaces.

Chapters 6–10 deal with the theory of modern electrochemical methods, including micro- and macro-electrolyses, hydrodynamic and impedance methods, methods with voltage- and current-control *etc.*

Chapters 11 and 12 give details of electrochemical reactions coupled with chemical reactions in a homogeneous phase. It gives the treatment of the double electrical layer structure and adsorption processes on the electrodes.

Chapters 13 and 14 describe in detail various electrochemical techniques developed or widely used during recent years.

Unlike other books on electroanalytical chemistry it devotes special attention to the interpretation of all electrochemical processes with the help of exact mathematical descriptions. Complete references and also special exercises and chemical tasks are given for each chapter, helping successful assimilation of the contents.

This book is highly recommended to students and teachers at universities and institutes. It contains much useful information and should be of interest to all chemists who use electroanalytical methods in research and would like to explore the practical possibilities of electrochemistry.

L. K. SHPIGUN

PUBLICATIONS RECEIVED

Treatise on Analytical Chemistry, 2nd Ed., Part I, Vols. 3, 10, 12: I. M. KOLTHOFF and PHILIP L. ELVING (editors), Wiley/Interscience, New York, 1983-1984. Volume 3: pp. xxi + 592; £66.50. Volume 10: pp. xxvii + 533; £61.75. Volume 12: pp. xxvii + 603; £71.25.

These three volumes continue the second edition of "Kolthoff and Elving", and maintain the standards now expected of the series as a matter of course. There are certain surprises, however. For instance, the reader of Volume 3 may wonder whether some of the authors had read Volume 2, since they discuss certain aspects of solution of equilibria without cross-reference to Högfeldt's chapter there, on graphical representation of equilibria, and do not seem to have heard of Ringbom's classic work on complexation effects and use of conditional constants *etc.*, or at any rate do not choose to mention it. Nevertheless, the volume contains authoritative and useful accounts of redox equilibria, the application of surface chemistry in analysis, precipitation methods, solubility (although some comment on the effect of pressure on the solubility of solids in liquids would have been a welcome addition), and the role of reactive groups in reagents.

Volume 10 (with Dr. M. M. Bursey as associate editor) covers proton and carbon-13 nuclear magnetic resonance, electron spin resonance and nuclear quadrupole resonance and their applications, Mössbauer spectroscopy and secondary ion mass spectrometry (SIMS). Volume 12 (with C. B. Murphy as associate editor) deals with some thermal techniques used in analysis, ranging from temperature measurement, constant-temperature baths, calorimetry, thermochemistry, and thermal analytical methods, to evolved gas analysis, measurement of thermal expansion, electrothermal analysis (based on the effect of temperature on conductivity) and thermoacoustic methods (based on the effect of temperature changes on sound waves transmitted by the sample).

As with the other volumes in the second edition, it at once becomes evident that the last two decades have seen an extraordinarily rapid and fruitful development of physical and instrumental methods of analysis, many of which owe their existence as routine methods to the introduction of reliable and sensitive transducers systems. As Professor Pimentel observed at the 1984 Pittsburgh Conference, we now have the tools available for exploring systems that were hitherto completely inaccessible to experimentation, and the resulting greater understanding of the fundamental processes of physics and chemistry should allow us to make greater progress in industry and technology. Such progress is urgently needed in view of the ever more rapid depletion of natural resources by that most rapacious of animals—man.

These volumes, together with the others in the series, will undoubtedly play an important role in these future researches.

R. A. CHALMERS

Aquametry, 2nd Ed., Part II: DONALD MILTON SMITH and JOHN MITCHELL, JR., Wiley/Interscience, New York, 1984. Pages xii + 1352. \$165.00

The long-awaited final volume of this monumental treatise on the determination of water has at last appeared, though unhappily after the death of one of its authors (to whom it is dedicated). This volume alone is more than twice the size of the first edition of the whole work, which shows the great strides made in advancement of the subject. It deals with the measurement of water by means of capacitance determination (259 pages), conductivity measurements (255 pages), coulometry (601 pages) and microcoulometry (218 pages). The book is full of practical hints and tips, critical and informed comment on the extraordinarily widespread and varied literature, and is written in a most lucid and refreshing style. It should be made required reading for all authors of papers submitted to the scientific journals—they could learn so much from it about conciseness achieved without loss of information. Together with Parts I and III it is an essential part of any chemical library worthy of the name, and well worth the price.

R. A. CHALMERS

Mass Spectrometry Advances 1982, Parts A,B and C,D in two volumes: E. R. SCHMIDT, K. VARMUZA and I. FOGY (editors) Elsevier, Amsterdam, 1983. Part A XLI + 379, Part B XVII + 544, Part C XVII + 544, Part D XVI + 461; \$361.75.

This is a record of the 9th Triennial International Mass Spectrometry Conference held in Vienna 30 August-3 September 1982. The great value of such published accounts of scientific conferences is that they provide an accurate picture of the state of the discipline under review at the time of the meeting. At the most elementary level, the size of the conference is a reasonable indication of the well-being of the scientific enterprise. By this criterion the technique of mass spectrometry is still expanding and attracting interest, the accounts of its three-yearly conferences having grown from the modest books of the fifties to the substantial two-volume work reviewed here.

All the familiar aspects of the subject are covered in a series of plenary lectures collected together in Part A. The analytical possibilities of the technique, both qualitative and quantitative, and its use in the determination of molecular structure are included, together with the applications to environmental and geological studies. Other aspects under discussion range from isotopic analysis to data processing. Part B deals with instrumentation and reveals the success which has been achieved in devising methods of ionizing large molecules and of recording their mass spectra. Another preoccupation has been with the coupling of mass spectrometry with chromatographic techniques such as HPLC to provide ever more versatile and sensitive analytical systems. Advances in the construction of "tandem" mass spectrometers and triple quadrupoles and their application to specific problems are also discussed. Theoretical aspects of ionization and dissociation are given some attention and there are a large number of papers concerned with the newer methods of producing both positive and negative ions from a wide variety of samples. In particular, the analytical potentialities of fast-atom bombardment ion sources, laser desorption, pyrolysis and secondary-ion mass spectrometry are well illustrated in many contributions. Some authors have devoted their attention to the physical chemistry of ion fragmentation and kinetic energy release and to the interactions

of ions and molecules. In contrast to previous meetings, the interest in the analysis of solid samples by spark-source mass spectrometry has waned and there are comparatively few papers describing specific investigations.

The subject of the mechanism of the fragmentation of positive ions which has proved so fascinating to organic chemists is represented in Section C by the largest number of papers and in addition there are many contributions detailing the processing of such information by computers.

Part D is exclusively confined to applications of the technique and it is an indication of the ever widening uses of mass spectrometry that this part contains no less than 100 papers covering the fields of gas analysis, biochemical problems, environmental studies, geological specimens and nuclear chemistry. This is an excellent production and is recommended to the libraries of all scientific institutes, particularly those where analysis by physical methods is a prime concern.

J. R. MAJER

The Analysis of Gases by Chromatography: C. J. COWPER and A. J. DEROSE. Pergamon Press, Oxford, 1983. Pages xii + 147. £14.00

From time to time a book comes along which is so much needed that it finds a space empty on the reader's bookshelf waiting for it. This is such a book, though to be fair, the space has not been totally vacant since Jeffery and Kipping's monograph has been the gas analyst's pocket chromatography book for many years and will remain alongside this newcomer. The marvel is that two people who have spent so much time doing gas analyses have found the time to write about their subject, because only experienced practitioners can make the contribution which Cowper and DeRose are offering us.

The gas analyst is accustomed to solving each new problem from scratch: how to sample, how to match the plumbing, how to condition the column (after deciding which stationary phase), how to prepare the reference standards how to quantify the results. This volume combines all this blended with recent applications from the literature and spiced with those invaluable tips which are learned only by long experience. The gas analyst is of course also accustomed to using other than chromatographic techniques, and this book frequently points out that gas chromatography may not be the best approach for some particular problems.

I must confess to having been surprised by the statement that "measurement of a major component by difference is considerably more precise and usually more accurate (than direct measurement)" since I have been accustomed to quoting a value by difference only when the customer likes the results to add up to exactly 100%. Perhaps the authors might have stressed that the difference method works when it is known what all the impurities are likely to be. But this is after all a small quibble and the authors have the results to prove their point.

Do you know what might give rise to a small peak between nitrogen and methane for a sample of contaminated air run on a 5A molecular sieve column? The cost of this book will be a cheap price to pay for at least one colleague of mine who has this problem, and for anyone concerned with gas analysis the purchase of this book must get high priority.

IAIN L. MARR

Sample Preparation for Gas Chromatographic Analysis: W. G. JENNINGS and A. RAPP, Hüthig Verlag, Heidelberg, 1983. Pages 104. DM 46.00.

This small monograph sets out to describe sample preparation for gas chromatography, but in only 90 pages or so, it can hardly be expected to cover such a wide subject completely. What it does do, and that very well, is to give a lucid and useful account of direct injection procedures, and some isolation and concentration techniques. The chapter on direct injection I found very good, covering split, splitless, on-column and various headspace techniques. The isolation and concentration chapter I found less satisfactory, largely because the authors give very little practical detail of the more novel and hence interesting techniques. The final short chapter on specific application I felt did not match the standard of the rest of this small book, and is extremely sketchy in its treatment. For me, the most useful 7 pages in the 22 of this section was the reproduction of the NIOSH/OSHA air sampling standards. The book is well produced and bound, and is pleasant to handle and to read. It is marred by a few proof-reading errors; I noted one point where μl is used where ng is meant and another where an equation as written would be acceptable as a statement in BASIC but is a nonsense as a statement in simple mathematics. There is a consistent misuse of "analyte" to mean the solution being analysed, and a description of detection limits as lower when poorer is meant, but these are minor flaws in an otherwise nice little book.

R. C. ROONEY

PUBLICATIONS RECEIVED

Ion-Selective Electrode Reviews, Volume 3: J. D. R. Thomas (editor), Pergamon Press, Oxford, 1982. 257 pages. \$62.00

Volume 3 continues this now well-established series of reviews on ion-selective electrodes, edited by one of the most prolific authors in the field. The volume under scrutiny contains five chapters, a compilation of recent literature, a couple of book reviews by the editor, and indexes. The five chapters are primarily concerned with analytical applications of electrodes and will be most appreciated by professional analysts responsible for developing and improving the use of electrodes in their own special areas.

In the first chapter Birch and Cockcroft open with some general comments on surfactant analysis with a view to introducing immobilized liquid membranes, mostly supported in inactive poly(vinyl chloride), containing a surfactant complex as sensor. Details are given for the preparation of several types and the effects of different constituents are described. Dip, flow and coated-wire electrodes are dealt with. The discussion principally concerns their use as titration end-point indicators and it is clearly proved that the results obtained are the same as those given by the conventional two-phase dye-indicator method. Finally, a number of practical cases are dealt with in which surfactants at high and at trace concentrations have to be determined. The reviewer is not aware of any more complete or recent review of this topic.

The second and fifth chapters are closely related. Midgley deals with the detection limits of ion-selective electrodes and Moody and Thomas consider ways of extending the linear range. Both chapters make it evident that there is no substitute for painstaking care in seeking ideal responses from electrodes. Midgley includes a scholarly account of the definition and determination of the lower detection limit. He gives a theoretical analysis of the factors that affect the limit and this shows how to work reliably close to the limit and how to improve matters in the future. Moody and Thomas describe in a practical way what can be done to extend the linear range of the main types of electrodes currently in use. Both chapters contain a great deal of information on how to get the best out of particular electrodes and so will be welcomed by users.

A chapter on the use of inorganic ion-exchangers in electrodes, by Coetzee, shows that, despite a good deal of hard work, rather few have been found useful. These are mostly heterogeneous membrane electrodes in which the inorganic ion-exchanger is embedded in a polymeric binder. Their main value is as end-point indicators in titrations.

Kakabadse has reviewed his own work and that of others on ion-selective electrodes used in non-aqueous and mixed aqueous and non-aqueous solvents. It appears that, given some precautions, inorganic and glass electrodes will function well in such solvents although liquid and polymeric membrane electrodes usually will not. There are, however, many incompletely understood changes in the response characteristics with changes of solvent composition, and these limit the range of uses in non-aqueous media. This is a long chapter with 242 references and covers many individual electrodes as well as discussing wider issues.

Finally, Moody and Thomas have listed systematically 40 pages of new titles in the literature on ion-selective electrodes but this must surely overlap with similar compilations in *Anal. Chem.*

This is not really a book for reading but it is a necessary addition to the analyst's library.

P. MEARES

Analytical Techniques for Heavy Metals in Biological Fluids: S. FACCHETTI (editor), Elsevier, for the Commission of the European Communities, Amsterdam, 1983.

Analytical Techniques for Heavy Metals in Biological Fluids contains a series of lectures given during a course held at the Ispra Establishment of the Joint Research Centre of the European Communities in June 1981, and updated in 1982. It is a most useful textbook both for people involved in research on the biomedical aspects of toxic (and/or essential) substances, especially the heavy metals, and for those concerned with the preservation of human health in industrial areas, where exposure of workers to toxic metals poses a real threat to their physical and mental well-being.

This volume gives an *instructive introduction* to the epidemiological, biological and medical aspects of human exposure to heavy metals, while also summarizing the analytical chemistry that underlies the results by means of which these are studied. It can be divided into two main sections, dealing with the biomedical and the analytical aspects of the subject, respectively. The first five chapters cover the biomedical aspects. A review of the objectives of and requirements for biological monitoring, as well as of the currently available monitoring possibilities, is incorporated in the description of WHO and CEC projects on biological monitoring in environmental and occupational health. Although the main focus is on biomedical features, attention is also paid to preanalytical quality assurance (sampling conditions, sampling materials, quality control, sample composition, spiking procedures, storage and transport guidelines), statistical analyses and laboratory performance. The most illustrative examples of biological indicators of metals in occupational health are presented in Chapter 3. Alessio and Bertelli elucidatively review a number of important concepts in the field of biological monitoring. Lead, cadmium and arsenic serve as examples to illustrate the indicators of *internal dose* (dose, exposure, accumulation) and of *effect* (indicators of critical effect, dose-effect relationship). The periodic surveillance of workers who are exposed to a noxious agent requires the use of biological indicators *in the field*. The pros and cons of screening tests are discussed.

The rationale for biological monitoring as based on the identification and quantification of toxic agents and the prevention of their impact on man requires the availability of accurate and precise analytical techniques, and knowledge of the pharmacokinetic and metabolic behaviour of the toxic agents, as illustrated by lead (Chapter 4) and arsenic (Chapter 5).

Two-thirds of the book deal with analytical aspects of biological monitoring of heavy metals. An excellent, comprehensive and critical update of mineralization procedures that can be used in the pretreatment of biological samples for biological monitoring, is given by Sansoni and Panday. It may be rather detailed for the biomedical profession, but to the analyst in charge of the quantification of metals and their metabolites, in general, it undoubtedly represents one of the most useful,

practical, complete and guiding parts of the book. It links the first part of the book to the second in a logical way. Analytical methods suitable for determinations on biological materials are selected on the basis of a number of criteria such as accuracy, precision, sensitivity, single or multielement analysis, cost, *etc.* Requirements for these will differ according to the specific purpose of a trace element analysis, as illustrated in Chapter 6 by lead, cadmium and nickel analysis. Spectrochemical techniques are used in the majority of cases in analytical practice. A very general introduction on spectrochemical techniques, their indicators of analytical performance (limit of detection, noise, analytical range) and the newer methodologies such as Zeeman correction, wavelength modulation and inductively coupled emission spectroscopy precedes a detailed evaluation of atomic absorption and emission spectrometric techniques for heavy-metal determinations. Voltammetry techniques, however, have a number of advantages over the latter. The best known example may well be the determination of lead in blood by inverse voltammetry or anodic stripping voltammetry (Chapter 11). Mass spectrometric isotope dilution analysis is dealt with in the Ispra course as a technique capable of determining absolute quantities of heavy metals.

The combination of a review on the state-of-the-art of sample pretreatment procedures with accounts of the fundamental aspects of different analytical techniques uncovers the potentialities of specific methods that are currently available to both physician and analyst, and that are capable of guaranteeing the technical reliability, accuracy and precision that render biological monitoring of metals sensible. A number of errors leading to bias need to be excluded or accounted for. This necessitates a regular assessment of quality-control performance. In the last chapter of the book, the methods by which the latter is established are introduced to the reader.

MARLEEN VERLINDEN

NOTICE

FLOW ANALYSIS III—AN INTERNATIONAL CONFERENCE ON FLOW ANALYSIS

Birmingham, Great Britain, 5–8 September, 1985

The Third International Conference on Flow Analysis will be held in Birmingham, Great Britain, from 5 to 8 September, 1985. It will be organized by the Midlands Region of the Analytical Division of the Royal Society of Chemistry. The scope of the Conference will be similar to that of the Flow Analysis Conferences held in Amsterdam, 1979, and Lund, 1982, and will cover research on all aspects of continuous flow analysis. The scientific programme will consist of plenary and invited lectures, submitted research papers and posters, and working demonstrations. An exhibition of commercial equipment will be organized. As with the earlier conferences, proceedings will be published in a special issue of *Analytica Chimica Acta*.

The Conference will be held in the Department of Chemistry, University of Birmingham; accommodation will be available in the University Halls of Residence.

For further information, contact: Flow Analysis III, Dr. A. M. G. Macdonald, Department of Chemistry, The University, P.O. Box 363, Birmingham B15 2TT, England.

NOTICE

INTERNATIONAL SYMPOSIUM ON QUANTITATIVE LUMINESCENCE SPECTROMETRY IN BIOMEDICAL SCIENCES

An international symposium on quantitative luminescence spectrometry in biomedical sciences, sponsored by the Faculty of Pharmaceutical Sciences of the State University of Ghent, the National Foundation of Scientific Research (N.F.W.O.—F.N.R.S.), and the Ministry of Education, will be held in Ghent, Belgium, 3–6 September 1984, at the Farmaceutisch Instituut.

Contributed papers (20-minute lectures or poster communications) will cover the following topics: drug and bioanalysis by fluorescence and phosphorescence (LTP, RTP, micellar); fluorescence and chemiluminescence immunoassays; detection techniques in chromatography (fluorescence, RTPL, . . .); solid surface luminescence methods; chemical derivatization methods; luminescence applications and drug metabolism, clinical chemistry, biochemistry, pharmacokinetics, toxicology, ecology, protein tagging. The Conference will be conducted in English and no simultaneous translation will be provided. Facilities for technical exhibitions will be arranged.

Five plenary lectures will be presented by outstanding specialists in the field of quantitative luminescence spectrometry: R. P. Ekins (fluoroimmunoassays, Institute of Nuclear Medicine, The Middlesex Hospital Medical School, London, U.K.); R. W. Frei (detection techniques, Vrije Universiteit Amsterdam, The Netherlands); G. G. Guilbault (fluorescence techniques, University of New Orleans, Louisiana, U.S.A.); J. N. Miller (solid surface methods, University of Technology, Loughborough, U.K.); J. S. Woodhead (chemiluminescence immunoassays, University of Wales, Cardiff, U.K.).

Before and after the Symposium all correspondence should be sent to: Dr. W. Baeyens, Symposium Chairman, Laboratoria voor Farmaceutische Chemie en voor Ontleding van Geneesmiddelen, Rijksuniversiteit Gent, Harelbekestraat 72, B-9000-Gent, Belgium, from whom full details can be obtained.

FOREWORD

This "Paper Symposium" deals with selected analytical aspects of modern day clinical chemistry. Clinical chemistry is concerned with the analysis of biological specimens as an aid to the detection, diagnosis and management of disease. The precision and accuracy of analytical results is of vital importance and considerable attention is paid to quality control of analytical procedures (p. 851) and also to detecting possible interferences, *e.g.*, by drugs (p. 937). Many different analytical methods have been utilized by the clinical chemist, and these include flow-injection analysis (p. 879), turbidimetry (p. 923), methods based on reagent strips (p. 863), and immunoassays employing labelled reagents. This last method, because of its great sensitivity, has assumed particular importance, and a range of labels have been used, *e.g.*, radioisotopes (p. 917), enzymes (p. 889), fluorophores (p. 909), and chemiluminescent molecules (p. 901). In the quest for new tests with improved sensitivity and specificity, clinical chemists have investigated many analytical methods. The penultimate paper in this symposium reviews a new development, the application of tandem mass spectrometry to clinical analysis.

L. J. KRICKA

NOTICE

FACSS 11
ELEVENTH ANNUAL MEETING
FEDERATION OF ANALYTICAL CHEMISTRY
AND SPECTROSCOPY SOCIETIES

SEPTEMBER 16-21, 1984

PHILADELPHIA MARRIOTT HOTEL
CITY LINE AVENUE AND MONUMENT ROAD
PHILADELPHIA, U.S.A

The Eleventh Annual FACSS meeting will once again be held in Philadelphia—this year at the Philadelphia Marriott Hotel. The Philadelphia Marriott Hotel is conveniently located on City Line Avenue at the edge of Philadelphia's Main Line. There is direct public limousine service from Philadelphia International Airport and express bus service from downtown Philadelphia. The Marriott has fine conference facilities with up to twelve meeting rooms, 705 accommodation rooms, seven restaurants and lounges, indoor/outdoor pools, platform tennis, and a games room. There is ample parking with no charge for any parking. The Marriott is within easy walking distance of the Bala Cynwyd Shopping Centre and several fine area restaurants.

Information on the technical programme from:

Dr. Patricia B. Roush
Perkin-Elmer Corporation
M/S-903
901 Ethan Allen Highway
Ridgefield, CT 06877

General information from:

Dr. D. Bruce Chase
DuPont Experimental Station
CRD E328
Wilmington, DE 19898

NOTICES

SYMPOSIUM ON ANALYTICAL METHODS IN FORENSIC CHEMISTRY AND TOXICOLOGY

MIAMI, FLORIDA
29 April–2 May 1985

CALL FOR PAPERS

This symposium is sponsored by the American Chemical Society Division of Analytical Chemistry and will be held in conjunction with the 189th ACS National Meeting in Miami, Florida (28 April–3 May 1985). The scientific programme will comprise invited lectures and contributed papers dealing with the state-of-the-art of analytical methodology in forensic chemistry and toxicology. Topics such as the following will be covered: novel optical and spectroscopic methods, analytical separation and chromatographic methods; electro-analytical methods; biological and immunological methods; automated systems; computer-aided methods; luminescence methods; electrophoresis; drug analysis; explosives analysis; gunshot residue, arson and bloodstain investigations; trace-evidence detection; other recent advances in forensic analytical chemistry and analytical toxicology.

You are invited to submit abstracts for presentation. Papers submitted for consideration may be reviews or original research papers. Abstracts (150 words on ACS standard abstract forms) should be sent to Dr. M. H. Ho, Department of Chemistry, University of Alabama in Birmingham, Birmingham, Alabama 35294, phone 205-934-4747, by *November 30, 1985*. Publication of the proceedings as a hard-cover book in the ACS Symposium Series is planned.

ISM-10 10th INTERNATIONAL SYMPOSIUM ON MICROCHEMICAL TECHNIQUES

ANTWERP, BELGIUM
25–29 August 1986

This Symposium is the next in the series of triennial conferences, the last three of which were held in Amsterdam (1983), Graz (1980) and Davos (1977). As with the preceding Symposia, ISM-10 will cover both pure and applied micro- and trace-analysis. Special attention will be paid to the application of modern techniques such as microbeam analysis methods. A special workshop on laser microprobe mass analysis is planned, and a special session in co-operation with the Association of Official Analytical Chemists will deal with trace-analysis of food. The Symposium language will be English, and no simultaneous translation will be provided. Contributions for presentation in either oral or poster sessions are invited. A second announcement will appear early in 1985, and can be obtained by writing to

Dr. R. Dewolfs,
University of Antwerp (UIA),
Department of Chemistry,
Universiteitsplein 1,
B-2610 Wilrijk,
Belgium.

CHROMATOGRAPHIC COURSE AT KENT STATE UNIVERSITY

KENT, OHIO 44242, U.S.A.

3-7 December 1984

The course, entitled "Fundamentals of Chromatographic Analysis", is co-sponsored by the KSU Chemistry Department, IBM Instruments and the University Conference Bureau. It will provide a coherent overview of chemical separations by chromatographic methods, and will be directed towards beginning and intermediate chromatographers, with material on gas, liquid and thin-layer methods. The course will treat the three techniques as complementary rather than competing processes, and will be a blend of fundamental information on theory and instrumentation, with applications. In addition to lecture sessions, accompanying laboratory sessions will provide intensive "hands-on" training in the various techniques discussed.

The lecturers will be Dr. Roger K. Gilpin (Kent State University), Dr. Neil D. Danielson (Miami University) and Mr. Ronald L. Lewis of IBM Instruments.

Information and registration through Carl J. Knauss, Chromatographic Course Coordinator, Chemistry Department, Kent State University, Kent, Ohio 44242, U.S.A. (telephone 216/672-2327).

NOTICES

THIRD INTERNATIONAL CONGRESS ON ANALYTICAL TECHNIQUES IN ENVIRONMENTAL CHEMISTRY

21-23 November 1984

This International Congress, to be held in conjunction with the 14th Annual Symposium on the Analytical Chemistry of Pollutants, will take place at the Congress Centre, Barcelona, Spain, 21-23 November 1984. The Congress will be devoted to invited plenary lectures, invited and submitted research lectures, and poster presentations, covering the whole field of environmental analytical chemistry.

Further details, together with registration form and preliminary programme, may be obtained from: Dr. J. Albaiges, Expoquimia, Avenida Reina Ma, Cristina, Barcelona 4, Spain.

First International World Congress

NEW COMPOUNDS IN BIOLOGICAL AND CHEMICAL WARFARE: TOXICOLOGICAL EVALUATION

21-23 May 1984

State University of Ghent—Belgium
Department of Toxicology
Chairman: Professor A. Heyndrickx

Scientific Programme

Human and medical factors

New evidence; effects of chemicals, the methods of detection, mortality and morbidity rates, environmental problems, defensive needs, protection.

Diagnosis, treatment, influence

Methods of diagnosis, assignment to treatment modalities.

Action Programme

International legislation and rules, enforcement, sanctioning strategies, interaction between public information and enforcement. Evidence of chemical warfare in SE Asia and Afghanistan.

All information can be obtained from:

Professor A. Heyndrickx
Head of the Department of Toxicology
State University of Ghent
Hospitaalstraat 13
B-9000 Ghent
Belgium
(Telex: 11.558 A.Z. Gent—Toxicology)

THE EASTERN ANALYTICAL SYMPOSIUM

NEW YORK PENTA HOTEL, NEW YORK CITY, 13-16 NOVEMBER 1984

A limited number of oral and poster presentations on new developments in analytical chemistry will be accepted for the 1984 Eastern Analytical Symposium. These presentations will be grouped into several sessions to complement the Symposium's invited technical sessions. Prospective authors should submit a 50-100 word abstract before the deadline, 1 April 1984, indicating preference for oral or poster format, to: Mr. Thomas Kometani, EAS Program Chairman, Bell Laboratories RM1A-378, 600 Mountain Avenue, Murray Hill, NJ 07974, telephone (201) 582-6559. Care should be exercised in considering the title and authors of the proposed presentation; if the presentation is accepted, both title and authors will be considered final. Authors of accepted presentations will receive forms for submission of a 200-300 word abstract which will appear in the final programme.

For details contact:

Dr. S. David Klein
EAS Publicity
Merck & Co., Inc.
P.O. Box 2000/R80L-106
Rahway, NJ 07065, U.S.A.

ERRATA

In the paper by A. C. Mehta, *Talanta*, 1984, 31, 1, the following corrections are needed:
Page 3, right-hand column, paragraph 2, line 23, for "chlodiazepoxide" read "chlordiazepoxide"
Page 5, Table 2, below "Fluazepam" in column 1, for "††" read "‡‡"

AUTHOR INDEX

- Abdel-Khalek M. M., 289, 635
 Aboul-Enein H. Y., 77
 Abramović B. F., 987
 Ackermann G., 667
 Ahmad A., 265
 Akiyama S., 749
 Alary J., 615
 Al-Bazi S. J., 189, 431, 815
 Alegret S., 683
 Aleixo L. M., 218
 Almeida Mota A. M., 531
 Amin D., 283
 Andronidis T., 123, 315
 Appa Rao K., 209
 Appleton J. M. H., 9
 Arribas Jimeno S., 515
 Arshady R., 842
 Arya A., 489
 Asuero A. G., 233
 Attiyat A. S., 463
 Avery M. J., 49

 Babu Y., 773
 Baker R. S., 227
 Balaji B. K., 846
 Bannard R. A. B., 585
 Bansal R. K., 205
 Barbosa J., 279
 Bashir W. A., 283
 Baveja A. K., 391
 Beaudoin R., 417
 Bediar M., 285
 Belal F., 648
 Belal S., 285
 Beltran J. L., 475
 Ben-Yaakov S., 1095
 Berg C. M. G. van den, 1069
 Berman S. S., 1010
 Bertocchi G., 138
 Bertoft E., 909
 Berzas Nevado J. J., 325
 Bhargava Om P., 301
 Bhargava V. K., 943
 Blanco M., 85
 Blanco Gomis D., 515
 Bos M., 553, 723
 Bosch E., 279, 475
 Boucly P., 144
 Breaudiere J.-P., 851
 Brice A., 147
 Brotherton H. O., 929
 Bruno P., 479
 Bubnis B. P., 1149
 Budd M. B., 929
 Budnikov H. C., 727
 Buncel E., 585
 Burger N., 169
 Burguera J. L., 1027
 Burguera M., 1027

 Cabellero M., 597
 Cabezon L. M., 597
 Caiola A., 615
 Caldini A. L., 901
 Cano-Pavon J. M., 29
 Cantin D., 615
 Carati D., 241
 Carrondo M. J. T., 561
 Caselli M., 479
 Cela R., 597

 Čermák J., 947
 Chagas A. P., 218
 Chakrabarty T., 215
 Chakravarti A. K., 215
 Chan A., 33
 Chandra N., 79
 Chao T. T., 73
 Chastagnier M., 655
 Charyulu M. M., 1109
 Chaube A., 391
 Chen P. Y., 259
 Cheng Guang-shen, 133
 Chiavari G., 207
 Chikuma M., 269
 Chow A., 189, 304, 431
 815, 963
 Christian G. D., 463
 Chu N. Y., 809
 Chunguo C., 221
 Ci Yunxiang, 556
 Čížek Z., 547
 Clark E. R., 15, 763
 Coelho J. A., 218
 Concialini V., 207
 Corsini A., 33
 Cox B. G., 585
 Crisp P. T., 227
 Crow D. R., 421
 Cruz Soto J. L., 379
 Czuryłowska M., 559

 Dalvi A. G. I., 773
 D'Andrea G., 357
 Decnop-Weever L. G., 731
 Deelstra H. A., 497
 Dentschev S., 69
 Dewald H. D., 387
 Diaz García M. E., 361
 Ding Jiahua, 619
 Dittrich K., 39, 341
 Donaldson E. M., 89, 443, 997
 Dong Gao-Xiang, 367

 Earle J. A. P., 889
 Ellis J., 227, 467
 El-Yamani I. S., 627, 630
 Erb F., 147
 Escalas M.-T., 683
 Eskola J. U., 909
 Espinosa Mansilla A., 325
 Ezeife G. E., 265

 Fahrat F., 615
 Fanelli N., 275
 Fang Yu-Zhi, 141
 Farrell R. E., 1005
 Fazakas J., 573
 Fedoroff M., 1133
 Feldstein J., 809
 Finton D., 955
 Fischer J.-C., 1057
 Fompeydie D., 1125
 François J.-P., 735
 Fraústo da Silva J. J. R. 531
 Fuente E., 515
 Fujinaga T., 720
 Fujiwara S., 579
 Furusawa M., 131

 Gaál F. F., 987
 Gallego M., 1075
 Galteau M. M., 937
 Ganho R. M. B., 561
 Gao Wei-ping, 844
 García Alonso J. I., 361
 Garcia de Torres A., 29
 Garnier E., 1133
 Ghe A. M., 123, 241, 315
 Gijbels R., 177
 Girotti S., 895
 Gmitro M., 301
 Godinho O. E. S., 218
 Gómez-Hens A., 783
 Gómez-Nieto M. A., 379
 Gorbunova T. S., 727
 Górecka H., 459, 1115
 Górecki H., 459, 1115
 Gottarelli G., 138
 Gravereau P., 1133
 Green K., 173
 Greenhow E. J., 611
 Gregor I. K., 55
 Grote M., 755
 Guardia M. de la, 799
 Guidarini D., 275
 Guilhaus M., 55
 Guillem Monzonis C., 550
 Guillem Villar M. C., 550
 Gupta V. K., 391, 394, 1013
 Gustafsson L., 979
 Guterma H., 1095

 Haapakka K., 679
 Haas H. F., 307
 Hagiwara Y., 1079
 Haguenoer J. M., 147
 Hamon M., 655
 Hamon R. F., 963
 Hannaker P., 1153
 Hara M., 105
 Harsányi E. G., 579
 Hasebe K., 319
 Hayes J. M., 741
 Häyrynen H., 709
 He You-Hua, 638
 Hemmi H., 319
 Hemmilä I., 909
 Hila J. E., 655
 Hornby W. E., 863
 Hoshino H., 525
 Hou Qing-Lie, 1153
 Huang H. L., 259
 Hung C. F., 259
 Hüppe U., 755

 Imbenotte M., 147
 Inczédy J., 162
 Ioannou P. C., 253
 Ishimori T., 621
 Ishwar S., 109
 Islam I., 642
 Issa A. S., 287
 Ito I., 1031
 Ito S., 292
 Itoh K., 269
 Izquierdo A., 475

- Jagannadha Rao V., 466
 Jain C. K., 1021
 Jalal I. M., 397, 1015
 Jaselskis B., 715
 Javůrek M., 1083
 Jenny R. W., 851
 Jia Xin, 556
 Johansen E. S., 743
 Johnson J. V., 929
 Jøns O., 743
 Joshi A. R., 943
 Joshi B. D., 773
 Junk G. A., 49
 Jurgensen H., 777
- Kallel M., 615
 Kambara T., 319, 509
 Kaneda T., 749
 Kankare J. J., 689
 Kanoute G., 144
 Karas-Gašparec V., 169
 Katyal M., 1008
 Kaur J. P., 717
 Keliher P. N., 295
 Kelly W. R., 1063
 Kettrup A., 755
 Khan A. S., 304
 Kiba N., 131
 Kiekens P., 693
 Kihara S., 789
 Kimoto T., 720
 Kiriyama T., 472
 Kobayashi K., 593
 Koch H., 1101
 Koch S., 667
 Korth W., 467
 Kountourellis J. E., 730
 Kragten J., 731
 Kricka L. J., 173, V (No. 10B)
 Krishna Murty N., 466
 Krivan V., 307
 Krull U. J., 489
 Kumar A., 848
 Kumar M. L. J., 773
 Kuroda R., 472
 Kuš S., 959
- Laganà A., 357
 Lajunen L. H. J., 709
 Lampugnani L., 275
 Langseth W., 975
 Leaver M. E., 89
 Lechner-Knoblauch U., 97
 Levillain P., 1125
 Li An-mo, 133
 Li Chun-xue, 367
 Li Shi-yu, 844
 Li Ya-Wen, 1041
 Liang Wei-An, 837
 Linden W. E. van der, 723
 Ling I. N. C., 61
 Ling T. G. I., 917
 Lippolis M. T., 207
 Liu Chuen-Ying, 353
 Liu Shili, 619
 Lodi S., 895
 Loos-Neskovic C., 1133
 Lotfi E. A., 77
 Lövgren T., 909
 Lundström U., 45, 521
 Luo Den-bai, 703
 Luque de Castro M. D., 379, 673
- Magini A., 901
 Mahrous M. S., 287, 635
 Malakova C., 69
 Mandal S. K., 195
 Marzenko Z., 959
 Marinsky J. A., 199, 683
 Mark E., 89
 Martinez J., 155
 Maspoeh S., 85
 Matsuda T., 292
 Mattiasson B., 917
 Mazzucotelli A., 185
 McCallum C., 409
 McFerran N. V., 889
 Mehdi H., 33
 Mehra M. C., 1112
 Mehta A. C., 1
 Meier A. L., 73
 Meloun M., 947, 1083
 Menard H., 417
 Merkkiniemi T., 709
 Merle Y., 199
 Messeri G., 901
 Michaylova V., 645
 Midgley D., 409
 Mills A. L., 331
 Mirjolet M., 229
 Misra D. D., 642
 Misumi S., 749
 Mojski M., 959
 Morino L. A., 224
 Moses C. O., 331
 Mosler H., 667
 Motomizu S., 235
 Mukherjee A. K., 195
 Mukherjee S., 215
 Mullens J., 735
- Nagahiro T., 1008, 1112
 Nagai T., 292
 Nagaosa Y., 371, 593
 Nagatsu H., 1031
 Nakashima K., 749
 Nakatsuji S., 749
 Nakayama M., 269
 Napoli A., 153
 Natarajan P. R., 1109
 Navas A., 437
 Navas M. J., 233
 Nekimken H., 603
 Nganou R., 1057
 Ni Zhe-ming, 150
 Nicolas A., 229
 Nieman T. A., 603
 Nivaud E., 144
 Nomura N., 105
 Nordstrom D. K., 331
 Norwitz G., 295
 Nwabue F. Ik., 265
 Nydahl F., 45
- Oak M. S., 943
 Ogawa N., 1079
 Ohashi K., 1031
 Ohyoshi E., 1129
 Ohzeki K., 319
 Olin Å., 45, 521
 Oliveira J. F. S., 561
 Oliveira W. A. de, 82
 Oszczapowicz J., 559
- Pacey G. E., 165, 1149
 Pagura C., 123
 Pal M., 298
 Papadopoulos N., 730
 Papoff P., 117
 Parkash R., 717
 Pasquini C., 82
 Passaglia E., 185
 Paulet B., 144
 Paulsen P. J., 1063
 Pazzagli M., 901
 Perchalski R. J., 929
 Pérez-Bustamante J. A., 597
 Petronio B. M., 357
 Pettersson K., 909
 Pickard A. D., 763
 Pind N., 1118
 Pollard B. D., 1036
 Polster J., 113
 Poncini L., 651
 Poonam (Mrs.), 109
 Prange Th., 97, 101
 Prati R., 138
 Premadas A., 846
 Preti S., 895
 Przeszlakowski S., 401
 Pungor E., 579
 Purdon J. G., 585
 Puri B. K., 205, 848, 1008
- Ramanaiah G. V., 846
 Rao A. L. J., 205
 Rao G. P., 79
 Rao M. S. P., 209
 Rao N. V. S., 466
 Rao V. K., 1109
 Raoot K. N., 469
 Raoot S., 469
 Raptouli A., 730
 Rashid A., 397
 Reboredo F., 561
 Rej R., 851
 Ren M., 212
 Rhyder G. J., 607
 Ricci D., 117
 Rice T. D., 607
 Richard J. J., 49
 Riley C., 879
 Rios A., 673
 Robberecht H. J., 497
 Rocks B. F., 879
 Roda A., 895
 Rosales D., 233
 Roth M. M., 1036
 Rubio S., 783
 Rui Kui-sheng, 1024
 Ruiz J. V., 29
- Sagar V. B., 943
 Sagi S. R., 209
 Saha H. K., 215
 Sakamoto M., 621
 Sakuraba S., 840
 Sakurai H., 269
 Salerno R., 901
 Salin E. D., 565
 Salinas López F., 325
 Sanchez J., 279
 Sanchez Rojas F., 437
 Sanz Medel A., 361, 515
 Sa'sa' S., 397, 1015
 Sastry M. D., 773

- Satake M., 848, 1008, 1112
 Sauerer A., 249
 Schischkov A., 69
 Scott A. D., 1005
 Semitekolos R., 607
 Sen Gupta J. G., 1045, 1053
 Serio M., 901
 Seshagiri T. K., 773
 Sethi C. L., 848
 Shabana E. I., 627, 630
 Shan Xiao-quan, 150
 Sharma J. P., 642
 Sherwood R. A., 879
 Shikina K., 1031
 Shin H. S., 585
 Shkinev V. M., 39, 341
 Siest G., 937
 Silva M., 1075
 Simões Gonçalves M. L., 531
 Simonzadeh N., 715
 Sing R. L. A., 565
 Singh K., 717
 Singh R. N. P., 642
 Singhal R. L., 717
 Sioda R. E., 135
 Siskos P. A., 253
 Siu K. W. M., 1010
 Small G. J., 741
 Smith B. R., 955
 Smith R., 537
 Sofue S., 375
 Soliman S. A., 285
 Sommer H. D., 101
 Soriano M. J., 347
 Spencer K., 923
 Spivakov B. Ya., 39, 341, 449
 Srivastava S. K., 1021
 Stefanelli C., 241
 Stephens R., 679, 689
 Študlarová V., 547
 Sturis A. P., 727
 Subramanian G., 79
 Šúcha L., 645
 Suchánek M., 645
 Sugii A., 1079
 Sun Peng-Joung, 353
 Suri S. K., 298
 Svehla G., 61
 Sweeney V., 607
 Swenters K., 177
 Szczepaniak W., 212
 Takamoto Y., 375
 Taketatsu T., 805
 Tanaka H., 269
 Tanaka Y., 633
 Tandon R. K., 227
 Tanigawa I., 749
 Tedesco P. H., 155
 Temmerman E., 693
 Teng En-jiang, 1024
 Thompson M., 489
 Thorpe G. H. G., 173
 Tiwari K. K., 1018
 Tōei K., 235
 Toma H. E., 224
 Tomiyasu T., 131
 Tommasi A., 901
 Tong W. G., 659
 Tóth K., 579
 Traini A., 479
 Troll G., 249
 Tsubouchi M., 633
 Tsitini-Souleau M., 655
 Tyson J. F., 9
 Uesugi K., 1112
 Ugi I., 842
 Ulakhovich N. A., 727
 Umezawa Y., 375, 579
 Umland F., 97, 101
 Valcárcel M., 379, 673, 783, 1075
 Valcher S., 123, 315
 Van Doren J. B., 955
 Vannucci R., 185
 Vannucci S., 185
 Van Poucke L. C., 735
 Van Puymbroeck J., 177
 Veazey R. L., 603
 Veen-Blaauw A. M. W. van, 723
 Verbeek F., 693
 Verlinden J., 177
 Verma P., 394, 1013
 Verma R. M., 1018
 Vidal M. T., 799
 Viñas P., 611
 Volynsky A. B., 449
 Vorob'eva G. A., 39, 341
 Wagler H., 1101
 Wahbi A.-A. M., 77
 Wakimoto T., 235
 Wang J., 387, 703
 Wartel M., 1057
 Wasey A., 205
 Watanabe K., 311
 Watanabe T., 621
 Wei Fu-sheng, 1024
 Weng L. Y., 259
 Whitehead T. P., 173
 Willey D., 955
 Williams T. R., 955
 Wimmer F. L., 651
 Winefordner J. D., 753, 777
 Wisdom G. B., 889
 Wittman Zs., 734
 Wu Shui-Sheng, 624
 Wu Y. P., 165
 Wydra H., 401
 Wynn D. A., 1036
 Xu Bo-Xing, 141
 Xu Tong-Ming, 141
 Yacoub E.-S. A. K., 15
 Yamada T., 371
 Yamamoto K., 1031
 Yan Du, 133
 Yan Zhang, 133
 Yang M. H., 259
 Ye Hua-Li, 638
 Yeung E. S., 659
 Yin Fang, 619
 Yoshida Z., 789
 Yoshioka H., 509
 Yost R. A., 929
 Yotsuyanagi T., 525
 Youngberg C., 955
 Yperman J., 735
 Yu Ru-Qin, 1041, 1121
 Yu Xian-an, 367
 Zhang Li, 150
 Zhang Zheng-Qi, 1121
 Zhang Zhi-Hua, 1041, 1121
 Zhe Tan, 624
 Zhou L., 73
 Ziegler J. M., 229
 Zipp A., 863
 Zollinger D. Ph., 723
 Zolotov Yu. A., 449
 Zou Shi-Fu, 837
 Zuffianò A., 479